

Regular and Young Investigator Award Abstracts

Biomarkers, Immune Monitoring, and Novel Technologies

1 DISSECTING β -CATENIN ASSOCIATED INFLAMMATION IN PATIENTS WITH DESMOID FIBROMATOSIS TO IDENTIFY PROGNOSTIC BIOMARKERS

Laura Bergamaschi, Federica Perrone, Francesca Rini, Licia Rivoltini, Chiara Castelli, Alessandro Gronchi, Chiara Colombo, Viviana Vallacchi*. *Fondazione IRCCS Istituto Nazionale Nazionale dei Tumori, Milan, Italy*

Background Desmoid fibromatosis (DF) is a locally aggressive rare tumor with high recurrence rate after surgery and unpredictable clinical course. Standard of care for DF patients is active surveillance; however, 30% of patients will progress and need active treatments. Biomarkers discriminating aggressive forms of DF are not available and prediction of progressing patients remains challenging. DF harbors mutations in β -catenin and a transcriptional 'inflammatory phenotype'. Cancer-associated inflammation is fostered by systemic factors and detectable in circulating immune cells. Blood leukocytes thus represent a promising source of prognostic biomarkers for DF patients. In this study we investigate phenotypic and functional features of peripheral blood immune cells and molecular profile of DF biopsies to identify DF patients at risk of progression and guide tailored therapeutic approaches.

Methods This is a prospective observational study enrolling patients with primary sporadic desmoid fibromatosis under active surveillance (n=80). Tumor and blood samples collected at diagnosis and during active surveillance will be studied by 1. transcriptomic analysis of DF biopsies; 2. multiparametric flowcytometry and functional profiling of blood cells; 3. RNA profiling of whole blood; 4. evaluation of plasma levels of cyto/chemokine and ctDNA of β -catenin variants. Levels of blood analytes will be correlated with patients' clinical outcome and integrated with immunological parameters.

Results Peripheral blood immune profile of 42 cases and 17 healthy donors (HD) shows that DF patients display at baseline an altered myeloid profile compared to HD, which is maintained in a subset of patients during the first year of active surveillance. An increase in immunosuppressive activated granulocytes and granulocytic myeloid-derived suppressor cells, defined by differential co-expression of CD15, CD11b, CD16 and LOX1, is observed, concomitantly, with a boost of monocyte subsets, defined by co-expression of CD33, CD11b, CD14, CD16, HLA-DR and PDL1. Immunosuppressive low density granulocytes are increased in progressing patients compared to HD and regressors. Of note, a significant up-regulation of immunosuppressive PMN-MDSC (defined as CD15+LOX-1+) is observed in DF harboring T41A mutation, but not in S45 mutated DF. Transcriptomic data of DF biopsies and of plasma analytes are ongoing.

Conclusions Systemic alterations of immunosuppressive and inflammatory myeloid cell subsets in peripheral blood of DF patients indicate that the inflammatory status detected at tumor site is reflected at systemic level. The altered myeloid profile supports the involvement of the immune system in DF onset and may represent a marker of disease aggressiveness.

Acknowledgements Supported by Italian Ministry of Health (RF-2016-02362609).

Trial Registration Not applicable.

REFERENCES

Not applicable.

Ethics Approval The study was conducted according to the guidelines of the Declaration of Helsinki, and approved by the Ethics Committee of Fondazione IRCCS Istituto Nazionale dei Tumori di Milano (protocol code INT85/10).

Consent Written informed consent was obtained from the patient for publication of this abstract. A copy of the written consent is available for review by the Editor of this journal.

<http://dx.doi.org/10.1136/jitc-2021-SITC2021.001>

2

QUANTITATION OF CD137 AND NECTIN-4 EXPRESSION ACROSS MULTIPLE TUMOR TYPES TO SUPPORT INDICATION SELECTION FOR BT7480, A *BICYCLE* TUMOR-TARGETED IMMUNE CELL AGONIST™ (*BICYCLE* TICA™)

¹Heather Cohen*, ¹Carly Campbell, ¹Kristen Hurov, ¹Johanna Lahdenranta, ¹Tara Gelb, ²David Galbraith, ²Dan Rozelle, ³Mate Nagy, ³Qingyan Au, ³Erinn Parnell, ¹Phil Brandish, ¹Sebastien Hazard, ¹Dominic Smethurst, ¹Nicholas Keen, ¹Stephen Blakemore. ¹*Bicycle Therapeutics, Lexington, MA, USA*; ²*Rancho Bio Sciences, San Diego, USA*; ³*NeoGenomics Laboratories, Aliso Viejo, USA*

Background *Bicycles* are fully synthetic constrained peptides with antibody-like affinities that target selectively, readily penetrate tumor tissue, have relatively short half-lives, and can be chemically linked together to generate multifunctional molecules. BT7480 is a *Bicycle* TICA™ that binds both CD137 on immune cells and Nectin-4 on cancer cells to deliver a potent anti-tumor immune signal in Nectin-4 expressing tumors. Nectin-4 has been reported to be highly expressed in a wide range of human solid tumors, however the expression of CD137, abundance and localization of CD137+ immune cells in Nectin-4+ tumors are unknowns. A translational and informatics pipeline was established to interrogate the human tumor microenvironment to identify patient populations most likely to benefit from BT7480, which is being developed as a potential first-in-class molecule for the treatment of high unmet need cancers associated with Nectin-4 expression.

Methods TCGA RNAseq data for Nectin-4 and CD137 were analyzed from ~10,000 samples across 36 human cancers. Using a proprietary Nectin-4 mAb and MultiOmyx™ technology, a 19-plexed immunofluorescence assay was developed to simultaneously quantify the presence of Nectin-4+ and CD137+ cells, identify immune cell subsets and their spatial topography in 43 human tumor FFPE samples from HNSCC, lung, bladder, and breast cancers. Each FFPE slide was presented to a pathologist for tissue annotation and selection of regions of interest for image analysis. Proprietary deep learning-based workflows were applied to identify stroma and tumor regions, individual cells and perform cell classification for phenotypes of interest.

Results RNA expression analysis indicated co-expression of Nectin-4 and CD137 in several tumor types with >50% tumors within NSCLC, HNSCC, breast, esophageal, and ovarian cancers expressing high levels of both targets. Spatial proteomic studies in HNSCC, lung, breast and bladder cancer samples demonstrated that Nectin-4 and CD137 co-expression at the protein level (>1% positive cells) was detected in 74% samples tested. CD137+ cells in Nectin-4+ tumors were identified as CD4+ T cells (37.6%), CD8+ T cells (16.8%) and CD68+ macrophages (5.9%). A subset of CD137+ cells (32.7%) were found to be deeply tumor penetrant and within close proximity of Nectin-4+ tumor cells across all indications tested.

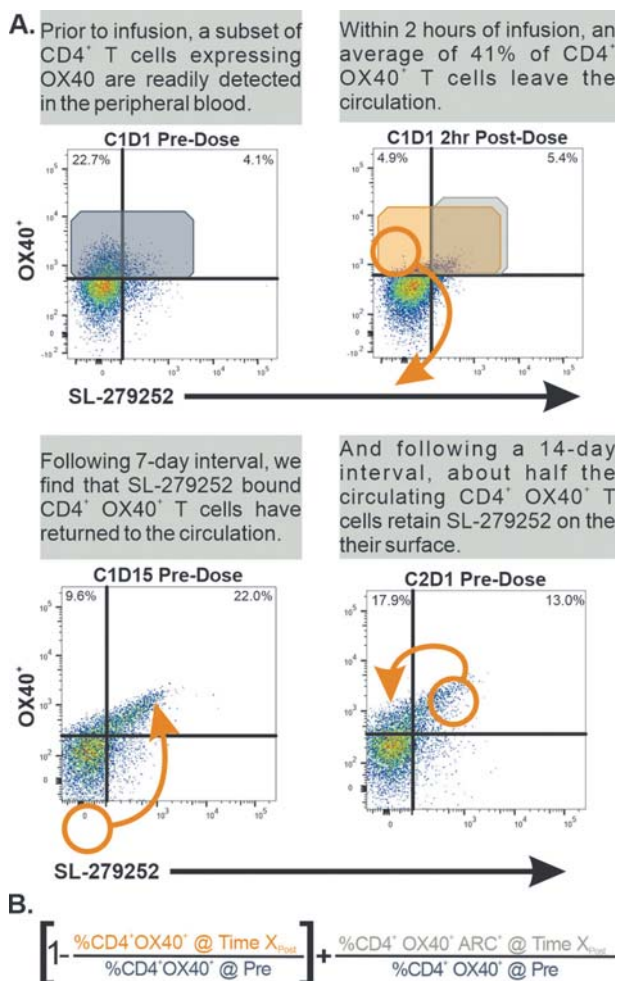
Conclusions Results from this study support prioritization of indications for BT7480 clinical development and the utility of the MultiOmyx™ assay to monitor Nectin-4 and CD137 expression and to demonstrate proof-of-mechanism for the BT7480 FIH clinical trial expected to start in 2H-2021.

<http://dx.doi.org/10.1136/jitc-2021-SITC2021.002>

3 DEVELOPMENT OF AN INTEGRATED METHOD TO QUANTIFY RECEPTOR OCCUPANCY FOR AGONIST IMMUNOTHERAPEUTICS THAT STIMULATE TARGET CELLS TO MIGRATE FROM THE PERIPHERAL BLOOD

Louis Gonzalez*, Bo Ma, Robert Hernandez, Hannah McKay, Fatima Rangwala, Lini Pandite, Taylor Schreiber. *Shattuck Labs, Durham, NC, USA*

Background One of the pharmacodynamic measures of biologic compounds is an assessment of target receptor/ligand occupancy (RO). If the primary mechanism for drug clearance is through target binding, drug exposure may increase once RO is saturated. SL-172154 (SIRP α -Fc-CD40L) and SL-279252 (PD1-Fc-OX40L) are two bi-functional fusion proteins in phase I clinical trials (NCT04406623 and NCT03894618). The binding interaction between a biologic compound and its targets (CD47 or PD-L1) typically does not stimulate migration from the blood, allowing direct measurement of drug and target. Evaluation of RO for immune agonists (CD40 and OX40) is challenging because agonists can stimulate lymphocytes to rapidly extravasate from the peripheral blood following infusion, thus precluding direct RO measurement as target cells are no longer present in the blood (figure 1a).



Abstract 3 Figure 1 CD4⁺ OX40⁺ T cells and SL-279252

Methods To assess full receptor engagement of CD40 or OX40, the formula shown in figure 1b was derived. The formula captures cells that rapidly migrated from the blood, combined with those that remained in the blood within 2

hours post infusion using multiparameter FACS analysis. SAS JMP was used to calculate and visualize all parameters.

Results Within 2 hours of SL-172154 infusion at 1 mg/kg (n=3), CD40⁺ B cell counts decreased from a pre-dose average by 87%. Of the CD40⁺ B cells remaining in the blood, ~95% were bound with SL-172154. CD40⁺ B cell counts recovered in the blood by the next dose, and as counts increased so did the proportion of cells that were bound with SL-172154. Similarly, within 2 hours of SL-279252 infusion at 1 mg/kg (n=10), CD4⁺OX40⁺ T cell counts decreased from a pre-dose average by 41.5% (range 0 – 70%). Of the CD4⁺OX40⁺ cells remaining in the blood, ~32% were bound with SL-279252. CD4⁺OX40⁺ cells returned to pre-treatment numbers over a 7-day interval and nearly all cells remained bound with SL-279252. Taken together, these data demonstrate that a large proportion of CD40⁺ (SL-172154) or OX40⁺ (SL-279252) cells bind drug immediately post infusion, migrate from the blood, and slowly return to the blood with drug still bound to the cell surface.

Conclusions Administration of SL-172154 (CD40) and SL-279252 (OX40) stimulated rapid egress of target cells from the blood. An integrated assessment, termed ‘receptor engagement’, was developed to derive RO both on circulating cells and those that rapidly marginated. When CD40⁺ or OX40⁺ cells returned to the blood, they remained drug-bound, indicating that the compounds may piggy-back on target cells into tissues.

Acknowledgements Thanks are extended to study participants; Takeda Pharmaceutical Company, Boston, MA, United States; Cathrine Leonowens, PhD, Nuventra Pharma Sciences, Durham, NC, United States and Cadence Communications and Research, Thousand Oaks, CA, United States. This study is funded by Shattuck Labs, Inc. Austin, TX and Durham, NC, USA

Ethics Approval This study is being conducted in full conformity with the Declaration of Helsinki and was approved by all IRBs/ethics committees from each clinical site participating in the study. Specific approval numbers can be provided upon request.

<http://dx.doi.org/10.1136/jitc-2021-SITC2021.003>

3D COCULTURE PLATFORM REVEALS INSIGHTS INTO PATIENT AUTOLOGOUS IMMUNE CELL-TUMOR INTERACTION AND IMMUNE MODULATION IN VITRO

Garima Kaushik*, Amy Wesa. *Champions Oncology, Rockville, MD, USA*

Background Understanding tumor microenvironment (TME) and immune microenvironment are vital to devising therapeutic interventions against tumors. Robust models that mimic patient-specific immune interactions in vitro become necessary with the recent promise of immunotherapeutics. Organoid models recapitulate patient tumor morphology and 3D architecture but fall short in recapitulating complex immune biology of native human tumors. Infiltrating immune populations, especially tumor-infiltrating lymphocytes (TIL), vastly impact patients' response to therapies. Here we describe a co-culture platform of patient-derived xenograft (PDX) derived organoids (PDXO) with autologous TIL to simulate the tumor-specific immune response and immune modulation *ex vivo*. The described model allows high throughput screening of immunomodulatory therapies on anti-tumor T cell functions.

Methods Primary patient tumor fragments simultaneously implanted in NOG mice to establish PDX and in parallel were placed in culture to expand primary TIL *ex vivo*. PDXO established from resected xenograft tumors were characterized for cancer marker expression and tumor histology. Expanded TIL were characterized by flow cytometry. A 3D autologous co-culture using fluorescently labeled PDXO and matching labeled patient TIL were incubated for four days with and without anti-PD1 treatment. High content imaging was used to measure T cell infiltration and tumor-specific cytotoxicity. Flow cytometry analysis was used to further evaluate T cell function with and without immunomodulatory therapy.

Results PDXO were established and characterized to mimic *in vivo* tumor biology and histology. TIL were successfully expanded and characterized to express memory, inhibitory, activation, and regulatory T cell markers. In cocultures, TIL infiltration in PDXO was observed by high content imaging and confirmed using immunofluorescence detection of CD8+ T cells within the PDXO. Immune infiltration in the PDXO and resultant tumor cell killing were quantified in response to immunotherapeutic intervention. Treatment with immune-modulatory therapeutics impacted T cell infiltration and tumor cytotoxicity. Flow cytometry analysis further elucidated the impact of co-culture and drug treatment on T cell phenotype and functional activity.

Conclusions This autologous, patient-derived, 3D *ex vivo* platform provides an improved model for evaluating therapeutic efficacy and pharmacodynamics of therapeutic drugs, while simultaneously providing a window into T cell-tumor cell interactions constrained within the existent patient T cell repertoire and autologous MHC restriction.

<http://dx.doi.org/10.1136/jitc-2021-SITC2021.004>

5 **CD274 (PD-L1) GENE EXPRESSION AND THE 27-GENE IMMUNO-ONCOLOGY (IO) ASSAY ARE ASSOCIATED WITH EFFICACY TO IMMUNE CHECKPOINT INHIBITOR TREATED PATIENTS WITH NON-SMALL CELL LUNG CANCER (NSCLC)**

¹Tyler Nielsen*, ¹Matthew Varga, ¹Kim McGregor, ¹Douglas Ross, ¹Brock Schweitzer, ¹Rob Seitz, ²Gregory Vidal. ¹Oncocyte Corporation, Nashville, TN, USA; ²West Cancer Center and Research Institute, Germantown, TN, USA

Background Immune checkpoint inhibitors (ICIs) have become standard of care in NSCLC. Programmed death ligand-1 (PD-L1) as measured by immunohistochemistry (IHC) is an accepted biomarker for predicting response but has many limitations. We previously described the 27-gene IO assay as a classifier of the tumor immune microenvironment (TIME) and its association with response to immune checkpoint inhibitor (ICI) therapy in multiple tumor types. We explore here the utility of CD274 expression as a biomarker and determine its contribution with the 27-gene IO assay in terms of their association with efficacy to ICI therapy in NSCLC.

Methods Fifty-nine late-stage NSCLC FFPE specimens were obtained with one-year PFS and PD-L1 IHC tumor proportion score (TPS-22c3) status. The CLIA-validated 27-gene RT-qPCR IO assay was run to produce the IO score^{1 2} and CD274 mRNA expression was quantified by RT-qPCR. A generalized linear model was created using CD274 expression and PD-L1 IHC positivity ($\geq 1\%$), then plotted to measure AUC. The optimal threshold for CD274 expression was determined by the Closest-to-left method. Cox proportional hazard ratios (HRs) were calculated for IO score, PD-L1 IHC, and binary CD274. A model combining IO score and CD274 at the 100% specificity threshold was also analyzed.

Results The optimal CD274 threshold was found at 82% sensitivity by AUC. The IO score and the CD274, but not PD-L1 IHC, were significantly associated with 1-year PFS (IO score, HR=0.24; p=0.001, 32/59 positive; CD274, HR=0.33; p=0.009, 46/59 positive; PD-L1 IHC HR=0.76; p=0.6; 45/59 positive). Both CD274 and PD-L1 IHC were approximately 77% positive with 75% agreement between classifiers. In a bivariate analysis of IO score and CD274, only the IO score retained significance (HR=0.28, p=0.01; HR=0.48, p=0.12, respectively), demonstrating IO score independence from CD274 expression. Modeling of an algorithm combining IO score with the CD274 mRNA threshold set at 100% specificity (to minimize the false-positive rate), added 3 patients to the responder category (HR=0.22; p=0.0003; 35/59 positives).

Conclusions Quantification of CD274 mRNA expression is correlated with PD-L1 IHC expression. Although the CD274 model outperformed PD-L1 IHC for one-year PFS, it failed to retain significance with IO score. Combining IO score with a more stringent CD274 threshold led to modest improvement in its association with one-year PFS. Together, these data demonstrate measuring CD274 mRNA may help to better inform clinical decision making and help contribute to a better understanding of the TIME.

REFERENCES

1. Nielsen TJ, et al. A novel immuno-oncology algorithm measuring tumor microenvironment to predict response to immunotherapies. *Heliyon* 2021;7(3):e06438.
2. Saltman A, et al. Prostate cancer biomarkers and multiparametric MRI: is there a role for both in prostate cancer management? *Ther Adv Urol* 2021;13:1756287221997186.

<http://dx.doi.org/10.1136/jitc-2021-SITC2021.005>

6 IMMUNE CORRELATES OF CLINICAL BENEFIT IN PATIENTS WITH HPV-ASSOCIATED MALIGNANCIES TREATED WITH BINTRAFUSP ALFA

Yo-Ting Tsai*, Renee Donahue, Nicole Toney, Julius Strauss, James Gulley, Jeffrey Schlom.
NIH, Bethesda, MD, USA

Background The safety and efficacy of bintrafusp alfa, a first-in-class bifunctional fusion protein targeting TGF β and PD-L1 pathways, have been demonstrated in patients with HPV-related cancers in an open-label, multicenter phase 1 trial (NCT02517398), and an open-label, single-center phase 2 trial (NCT03427411). The current study aimed to identify immune related biomarkers prior to and following 1 cycle of bintrafusp alfa that associate with clinical benefit.

Methods Immune parameters were compared in patients (n=65) deriving clinical benefit from bintrafusp alfa (defined as BOR of stable disease (SD) or better, which included SD, mixed, partial, and complete responses) versus patients with a BOR of progressive disease (PD). Peripheral blood was obtained from patients before and after 1 cycle of therapy, and evaluated for complete blood counts, plasma cytokines/soluble factors, 158 immune subsets, and T cells specific for HPV-16 E6 and E7.

Results Prior to therapy, patients who developed a BOR of SD or better had lower counts of neutrophils, monocytes, and platelets, lower levels of TGF- β 1 and sCD73, and higher levels of sCD27:sCD40L than patients with a BOR of PD. Lower baseline frequencies of MDSCs, monocytes, naïve CD4+ and CD8+ T cells, and CD8+ T cells that express CD73, an immune checkpoint associated with adenosine metabolism, were detected in patients with a BOR of SD or better than those with PD. Following 1 cycle of treatment, lymphocyte counts were reduced, while neutrophil counts and the NLR were increased, in patients with PD compared to those with a BOR of SD or better. IL-8, a cytokine involved in tumor progression and associated with reduced clinical benefit to immune checkpoint inhibitors, was increased in patients with PD compared to those with a BOR of SD or better, while conventional dendritic cells and CD8+ T cells expressing the proliferative marker ki67 were increased in patients with a BOR of SD or better compared to those with PD. Greater increases in the frequency and magnitude of HPV-16 specific CD8+ T-cells were also detected in individuals with a BOR of SD or better compared to PD.

Conclusions Immune profiling identified specific measures prior to therapy, as well as changes induced early after therapy (preceding restaging), that may serve as predictive biomarkers to identify patients with HPV-related cancers most likely to benefit from bintrafusp alfa. These findings also provide the rationale to combine bintrafusp alfa with other therapies including HPV-targeted therapeutic vaccines and agents that block IL-8 signaling.

Acknowledgements This research was supported by the Intramural Research Program of the Center for Cancer Research, NCI, National Institutes of Health, and through a Cooperative Research and Development Agreement with EMD Serono Research & Development Institute and GSK.

Ethics Approval The study protocol was approved by ethics committees at all participating institutions, and each patient provided written informed consent before study enrollment.

<http://dx.doi.org/10.1136/jitc-2021-SITC2021.006>

7

ANALYTICAL COMPARISON OF A PD-L1 22C3 ANTIBODY LABORATORY-DEVELOPED TEST PROTOCOL ON THE BENCHMARK XT AND PD-L1 IHC 22C3 PHARMDX: PAN-TUMOR AND TRIPLE-NEGATIVE BREAST CANCER SAMPLES

¹Gilad Vainer, ¹Ghadeer Zatar, ²Lingkang Huang, ²Shanthy Nuti*, ²Shanthy Nuti, ²Kenneth Emancipator. ¹Hadassah-Hebrew University Medical Center, Jerusalem, Israel; ²Merck and Co., Inc., Westfield, NJ, USA

Background PD-L1 IHC 22C3 pharmDx is an FDA-approved companion diagnostic for pembrolizumab across multiple tumor types designed for use on the Autostainer Link 48 (AL48). Many pathology laboratories do not have access to the AL48 and therefore do not use PD-L1 IHC 22C3 pharmDx but instead assess PD-L1 using laboratory-developed tests (LDTs) on the Ventana BenchMark platform. We compared our PD-L1 22C3 antibody-based LDT on the BenchMark XT platform with PD-L1 IHC 22C3 pharmDx using cervical cancer (CC), head and neck squamous cell carcinoma (HNSCC), urothelial carcinoma (UC), esophageal SCC (ESCC), and triple-negative breast cancer (TNBC) samples.

Methods Tumor specimens from patients with CC, HNSCC, UC, ESCC, and TNBC were stained with the 22C3 antibody, scored using the LDT on the BenchMark XT as previously described,¹ and compared with PD-L1 IHC 22C3 pharmDx scored by a trained pathologist, who measured PD-L1 with the use of combined positive score (CPS) and standard cutoffs (HNSCC and CC, ≥ 1 ; UC, ESCC, and TNBC, ≥ 10). Agreement in PD-L1 CPS as determined using the LDT and the PD-L1 IHC 22C3 pharmDx was evaluated.

Results 423 samples with CC (n = 77), HNSCC (n = 126), UC (n = 121), ESCC (n = 80), and TNBC (n = 19) were evaluated in this study. The pan-tumor (CC, HNSCC, UC, and ESCC) intraclass correlation coefficient (ICC) of PD-L1 CPS as a continuous variable was 0.95 (95% CI, 0.94–0.96%); Spearman correlations were 0.95. ICC (95% CI) was 0.92 (0.88–0.95) for CC, 0.97 (0.96–0.98) for HNSCC, 0.95 (0.92–0.97) for UC, and 0.92 (0.88–0.95) for ESCC; Spearman correlation was 0.93, 0.96, 0.92, and 0.89, respectively. The overall percentage agreement at the respective CPS cutoff was 96% (CC), 96% (HNSCC), 96% (UC), and 90% (ESCC). Staining patterns by 22C3 LDT and PD-L1 IHC 22C3 pharmDx were also very similar in our TNBC pilot study; however, correlation was not calculated because of the small sample numbers.

Conclusions The PD-L1 22C3 antibody-based LDT on the BenchMark XT demonstrated high concordance with PD-L1 IHC 22C3 pharmDx. These findings suggest the comparability of PD-L1 IHC 22C3 pharmDx with an LDT based on the 22C3 antibody across several tumor types. Further validation for TNBC is ongoing to confirm the data from the pilot run.

REFERENCE

1. Neuman T, et al. *J Thorac Oncol*. 2016;**11**:1863–1868.

<http://dx.doi.org/10.1136/jitc-2021-SITC2021.007>

8 MULTIPARAMETER CHARACTERIZATION OF CAR T CELLS

¹Xueting Wang, ¹Christina Pitzka, ¹Daniela Rheindorf, ¹Nadine Mockel-Tenbrinck, ¹Tatjana Holzer, ¹Anne Richter, ²Toni Cathomen, ¹Cesar Evaristo*. ¹Miltenyi Biotec B.V. and Co. KG, Bergisch Gladbach, Germany; ²Medical Center – University of Freiburg, Freiburg im Breisgau, Germany

Background Adoptive cell transfer of chimeric antigen receptor (CAR) modified T cells has demonstrated great therapeutic success against certain hematological malignancies. However, a substantial number of patients experienced relapse at some point after treatment with the underlying mechanisms not fully understood. Emerging data suggest that the undesired clinical outcome is related to different aspects, which include: the tumor heterogeneity, the tumor microenvironment, as well as intrinsic characteristics of the CAR T cells. In this work, we aimed to understand the diversity of CAR T cells generated from different donors, using multiparameter in vitro characterization.

Methods Leukapheresis from healthy donors were collected to generate CAR T cells using the GMP-compliant CliniMACS Prodigy[®] platform, enabling an automated and closed engineering of CAR T cells in a highly reproducible manner. We performed an in-depth characterization of the resulting CAR T cells by exploring differences in the immunophenotype, cell fitness and effector function of the freshly prepared as compared to frozen CAR T cell samples. Specifically, we designed several flow cytometry panels for the extensive characterization of immunophenotypes of interest such as: proliferative capacity, differentiation, activation and exhaustion. Cell fitness status was determined by the rate at which cells undergo apoptosis following stress. Finally, effector function was determined by the ability of the activated CAR T cells to secrete proinflammatory cytokines including IFN- γ , TNF- α and IL-2. The associations between these different parameters were analyzed using comprehensive statistical approaches.

Results With our established workflow, over 20 healthy-donor derived CAR T cells were generated and characterized. We have observed donor-dependent variations and responses for most of the explored parameters. In general, the freezing and thawing process negatively affected cell fitness and effector function of the CAR T cells and resulted in altered immunophenotypes. Additionally, correlations between certain immunophenotypes and cell fitness/effector function were identified.

Conclusions Collectively, we established a workflow for multiparameter characterization of CAR T cells and assessed the intrinsic variability of CAR T cells for both research and clinical application.

<http://dx.doi.org/10.1136/jitc-2021-SITC2021.008>

9

BRAF MUTATIONS ARE ASSOCIATED WITH T-HELPER CELL INFILTRATION AND POLARIZATION IN MELANOMA

Michael Ware*, Bhavana Pavuluri, Aubrey Smith, Megan Wyatt, Guillermo Rangel Rivera, Anna Cole, Chrystal Paulos. *Winship Cancer Institute of Emory, Atlanta, GA, USA*

Background BRAF mutations are highly prevalent in patients with melanoma (50–65%), and mark tumors which are responsive to combination immune checkpoint inhibition (ICI) with nivolumab (α PD-1) and ipilimumab (α CTLA-4). Interestingly, this combination does not improve outcomes over nivolumab alone for patients with BRAF wild-type melanoma.¹ We propose that BRAF mutations shape the immunological response to ICI through tumor derived cytokines and chemokines. While BRAF mutations can influence cytokine production and myeloid cell infiltration, the influence of BRAF mutations on tumor infiltrating CD4+ T-helper cells is underexplored in all tumor types. However, one study described a unique association between BRAF mutant melanoma and signatures of Th17 biology using transcriptomic analysis.² We hypothesize that BRAF mutations create a unique cytokine and chemokine milieu which support the infiltration and polarization of Th17 cells.

Methods To address this hypothesis we employed the congenic BRAF wild-type murine melanoma lines B16F10 and YUMM4.1, and the BRAF mutant line YUMM1.7. These cell lines were implanted subcutaneously into female C57BL/6 mice. Blood cytokines, splenocytes and tumor infiltrating lymphocytes were analyzed at 1 week and 3 weeks post tumor implantation to simulate both early stage and late-stage tumors respectively. Flow cytometry was used to define T-helper cell and myeloid cell phenotypes. In vitro analysis of chemokines and cytokines produced by each cell line were conducted via array and confirmed by ELISA.

Results Th1 and Th17 cells preferentially infiltrated early stage (1 week) BRAF wild-type and mutant tumors respectively while the CD4+ compartment of all tumors was dominated by an overwhelming Treg presence. The CD4+ compartment of endpoint (3 week) B16F10 tumors were almost entirely dominated by Tregs, while YUMM1.7 tumors were infiltrated by a diverse array of T-helper cells. In parallel with these results, we found YUMM1.7 tumors contained more dendritic cells and F4/80hiMHC-II+ macrophages as a percentage of the CD45+ infiltrate. Unique chemokine profiles were associated with each cell line, highlighted by relatively high expression of CXCL10 by BRAF wild-type lines and CXCL12 by both YUMM4.1 and YUMM1.7 cell lines.

Conclusions This work indicates the mutational landscape of melanoma can dynamically impact CD4+ T cell responses to melanoma. This ongoing work is directly translatable and will aid the development of novel cellular therapies tailored to specific immunological phenotypes of patients. Further, this work may help explain disparities in the response to ICI observed between patient populations with defining mutational signatures.

Acknowledgements We would like to acknowledge Emory University, The Winship Shared Resource, and the Pediatrics/Winship Flow Cytometry Core

REFERENCES

1. Ma VT, Daignault-Newton S, Waninger JJ, Journey S, Chopra Z, Tezel A, Redman BG, Fecher LA, Green MD, Alva AS, Lao CD. The impact of BRAF mutation status on clinical outcomes with anti-PD-1 monotherapy versus combination ipilimumab/nivolumab in treatment-naïve advanced stage melanoma. *Pigment Cell Melanoma Res.* 2021 May;**34**(3):629–640.

2. Tomei S, Bedognetti D, De Giorgi V, Sommariva M, Civini S, Reinboth J, Al Hashmi M, Ascierto ML, Liu Q, Ayotte BD, Worschech A, Uccellini L, Ascierto PA, Stronck D, Palmieri G, Chouchane L, Wang E, Marincola FM. The immune-related role of BRAF in melanoma. *2015 Mol Oncol Jan*;**9**(1):93–104.

Ethics Approval All animal studies were conducted under the approval of the Emory Institutional Animal Care and Use Committee and ethical guidelines established by this committee were strictly adhered to.

<http://dx.doi.org/10.1136/jitc-2021-SITC2021.009>

10

TERTIARY LYMPHOID STRUCTURE IN PANCREATIC DUCTAL ADENOCARCINOMA; A POTENTIAL TARGET IN AN IMMUNOLOGICALLY INERT MALIGNANCY

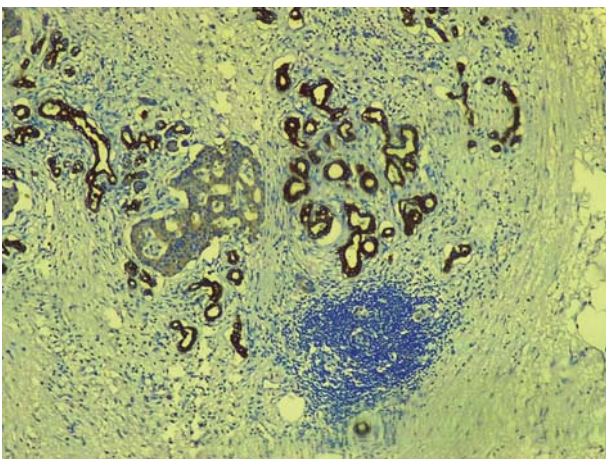
¹Kasimu Adoke*, ²Sanusi Haruna. ¹Department of Pathology Federal Medical Center Birnin Kebbi, Kebbi, Nigeria; ²Department of Morbid Anatomy and Forensic Medicine UDUS Sokoto, Kebbi, Nigeria

Background Tertiary lymphoid structure (TLS) are immune aggregates with various degrees of organization that forms outside of secondary lymphoid organ in response to chronic inflammation, infection or tumours.^{1 2} TLS like secondary lymphoid organ, has defined T cell zones, B cell zones, high endothelial venules (HEV) and matured dendritic cells. They have been shown to correlate with increase patient survival in many tumours. Pancreatic ductal carcinoma (PDAC) is generally believed to be immunologically inert, low tumour mutation burden (TMB) and poor response to checkpoint blockade. Recent findings in some patients with PDAC shows significant intratumoral cytotoxic T cell infiltration and a high Inflammatory signature. Since current immunotherapy aim to enhance CD 8+ T cells, we aim to investigate the contribution of humoral immunity in patients with TLS in PDAC.

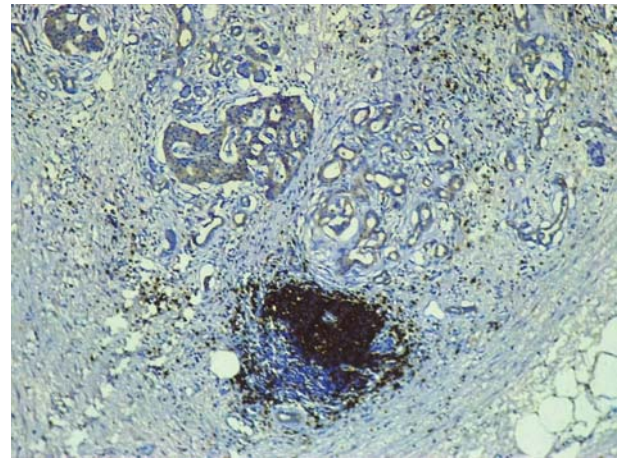
Methods Tissue blocks were obtained from departmental archive and sections were cut and stained with routine H&E of all patients who underwent surgery for pancreatic cancer from 2015–2021 at Federal Medical Centre Birnin Kebbi. Serial sections were done at 5µ and four immunohistochemical stains CD 3, CD8, CD20 and PD-L1 were used. Statistical analysis was done using spss version 24.

Results A total of nine cases of PDAC were diagnosed during the period with a Male Female ratio of 1:1.25 with an age range of 40–68 years and a mean age of 57.7±8.4. Five cases (55.6%) of PDAC showed TLS with marked expression of CD20 B+ cells seen in all five cases (figures 1 and 2). Also expressed are CD 8+ cytotoxic T cells and PD-L1. Prognosis was better in patients with TLS compare with those without TLS.

Conclusions TLS can be a potential therapeutic target to explore in the future for treatment of some cancers including PDAC through induction of TLS formation in inert tumours or B lymphocyte specific target.



Abstract 10 Figure 1 TLS in pancreatic ductal adenocarcinoma.



Abstract 10 Figure 2 CD 20 stain in TLS

REFERENCES

1. Pitzalis C, Jones GW, Bombardieri M, Jones S. Ectopic lymphoid like structures in infection, cancer and autoimmunity. *Nat Rev Immunol* 2014; **14**: 447–462.
2. Neyt K, Perros F, Geurtsvan C, Hammad H, Lambrecht B. Tertiary lymphoid organs in infection and autoimmunity. *Trends Immunol* 2012; **33**: 297–305.

Ethics Approval Ethical Approval was obtained for this study with Ethics number KSHREC Registration Number:104:6/2019
Consent N/A

<http://dx.doi.org/10.1136/jitc-2021-SITC2021.010>

MOLECULAR CHARACTERIZATION OF NATURALLY OCCURRING COLORECTAL AND BREAST CANCER IN NON-HUMAN PRIMATES TO MODEL HUMAN IMMUNOTHERAPEUTIC AGENTS

¹Simon Deycmar*, ¹Brendan Johnson, ²Declan Ryan, ¹William Sills, ¹David Caudell, ¹Greg Dugan, ¹Kiran Solingapuram Sai, ³Michael Hettich, ³Bruno Gomes, ³Maurizio Ceppi, ¹Mark Cline. ¹Wake Forest University School of Medicine, Winston Salem, NC, USA; ²University of California, Davis, CA, USA; ³Roche Innovation Center Basel, Basel, Switzerland

Background Non-human primates (NHP) with naturally occurring cancers (also called tumor-bearing monkeys or TBM) are a proposed model for translational cancer immunotherapy (CIT) research.¹ TBM spontaneously develop cancers with progression patterns similar to humans, potentially bridging the gap between preclinical models and cancers in patients. Interventional CIT trials recently conducted in colorectal (CRC) and breast cancer (BC)-bearing NHP, have generated relevant proof-of-mechanism evidence for three different CIT agents.^{1–3} To further validate these animals as translational models for CIT, we conducted a deep molecular characterization of tumors at baseline and reverse translated biomarker assays employed in human patients.

Methods Our cohort (n=19) consisted of Indian-origin rhesus macaques (*Macaca mulatta*) with naturally occurring CRC (n=14, female=9, male=5) and BC (n=5, female=5). Clinical examination, imaging (contrast-enhanced CT, PET) and biopsy to confirm cancer histology were performed. Molecular characterization was done by IHC for CRC-associated mismatch repair (MMR) proteins MLH1, MSH2, MSH6, and PMS2 and BC markers ER, PR, and HER2. We assessed microsatellite instability (MSI) by PCR and electrophoresis, and for selected cases somatic tumor mutations and tumor mutational burden (TMB) by whole exome sequencing.

Results Deficiency in MMR proteins determines eligibility for PD-1 blockade therapy, is observed in approximately 15% of human CRCs, and surprisingly in 100% (14/14) of our NHP CRCs. The absence of MLH1 (14/14), MSH2 (1/14), MSH6 (0/14) and PMS2 (14/14) observed in NHP CRCs clearly exceeds the frequencies reported in human CRCs ranging from 2–15% for each individual MMR protein.^{4 5} Moreover, we have documented MSI cases in some NHP CRCs, as described in human CRCs. We sequenced 3 CRCs and observed mutations in KRAS (G12D & A59T), WNT7A (V238M), IDH2 (R362Q), AKT3 (R388H), and TMB of 4.27, 22.95, and 29.3 mut/Mbp. Regarding breast, we found hormone receptor positive (Luminal A), HER2 positive, and TNBC, as in human BC patients. Sequencing of 2 BCs revealed mutations in PTEN (G251V), TGFBR2 (L162P), and ERBB4 (R1250Q), and TMB of 2.32 and 17.22 mut/Mbp.

Conclusions NHP cancers can be similarly characterized as human cancers, both macroscopically and molecularly. In this study we demonstrated an overrepresentation of MMR deficiency in NHP CRCs. Receptor expression in NHP BCs revealed similar subtypes as in human BCs. Cancer-associated mutations described in humans are also evident in TBM. This work highlights the possible translatability of naturally occurring NHP cancers for human cancer immunotherapy research, and can be further explored in future TBM trials.

REFERENCES

1. Ceppi M, Hettich M, Teichgraeber V, Driessen W, Tuerck D, *et al.* Tumor-bearing non-human primates: an unrivaled model for translational cancer immunology research. Proceedings: AACR Annual Meeting 2020.

- Claus C, Ferrara C, Xu W, Sam J, Lang S, Uhlenbrock F, *et al.* Tumor-targeted 4-1BB agonists for combination with T cell bispecific antibodies as off-the-shelf therapy. *Sci Transl Med* 2019;**11**(496).
- Waldhauer I, Gonzalez-Nicolini V, Freimoser-Grundschober A, Nayak TK, Fahrni L, *et al.* Simlukasfusp alfa (FAP-IL2v) immunocytokine is a versatile combination partner for cancer immunotherapy. *MAbs* 2021;**13**(1).
- Parc Y, Gueroult S, Mourra N, Serfaty L, Flejou J-F, Tiret E, Parc R. Prognostic significance of microsatellite instability determined by immunohistochemical staining of MSH2 and MLH1 in sporadic T3N0M0 colon cancer. *Gut* 2004;53.
- Chen L, Chen G, Zheng X, Chen Y. Expression status of four mismatch repair proteins in patients with colorectal cancer: clinical significance in 1238 cases. *Int J Clin Exp Pathol* 2019;**12**(10).

Ethics Approval Wake Forest University is accredited by the Association for the Assessment and Accreditation of Laboratory Animal Care, International (AAALAC) and registered with the United States Department of Agriculture (USDA) to conduct research in laboratory animals. The protocols and any subsequent amendments are reviewed and approved by the Wake Forest Institutional Animal Care and Use Committee (IACUC) and in compliance with the U.S. Animal Welfare Act, the *Guide for the Care and Use of Laboratory Animals*, the Office of Laboratory Animal Welfare, and public health service regulations.

<http://dx.doi.org/10.1136/jitc-2021-SITC2021.011>

KEY PHARMACOKINETIC AND PHARMACODYNAMIC PARAMETERS THAT CORRELATE WITH THE ANTI-TUMOR ACTIVITY OF A BISPECIFIC PD-L1 CONDITIONAL 4-1BB AGONIST

Heather Kinkead*, Chelsie Macedo, Angelica Sanabria, Garrett Cyprus, Rajay Pandit, James Kalabus, Bryan Becklund, Florian Sulzmaier, John Timmer, Quinn Deveraux, Brendan Eckelman, Analeah Heidt. *Inhibrx, La Jolla, CA, United States*

Background 4-1BB is a costimulatory molecule that is predominantly expressed on activated CD8+ T cells and is induced upon T cell receptor mediated activation.¹ Within the tumor microenvironment, 4-1BB-expressing T cells are enriched for anti-tumor reactivity²; thus, 4-1BB agonism provides an opportunity for selective activation of anti-cancer immune effector cells. Early efforts to develop 4-1BB targeted agonists were limited by poor tolerability (Urelumab) or insufficient efficacy (Utomilumab). INBRX-105 is a bispecific antibody that aims to overcome these prior limitations through induction of 4-1BB agonism specifically at sites of PD-L1 expression. Preclinical models have defined pharmacokinetic (PK) and pharmacodynamic (PD) parameters that are correlated with maximal INBRX-105-specific immune responses and anti-tumor activity.

Methods INBRX-105 was generated by linking 2 humanized single-domain antibody binding domains targeting human PD-L1 and 4-1BB, fused to an effector-silenced human IgG1 constant domain (Fc). A bispecific, anti-mouse PD-L1x4-1BB surrogate molecule, INBRX-105-a, was engineered to match the function and target affinities of INBRX-105. This surrogate was tested for in vivo activity in non-tumor-bearing and MC-38 tumor-bearing animals, including measurements of serum exposure, PD-L1 receptor occupancy, immunophenotyping of peripheral blood and intra-tumoral immune cell populations.

Results INBRX-105-a was shown to be an appropriate anti-mouse surrogate for INBRX-105 in a variety of in vitro assays. Comparable potencies of activity were demonstrated in a PD-L1 dependent 4-1BB reporter assay, as well as in cytokine induction through co-stimulation of primary T cells. In vivo, INBRX-105-a showed robust induction of mouse CD8+ T effector memory populations (CD8+ TEM) at dose levels that achieved \geq 96 hours of PD-L1 receptor occupancy. A serum concentration of 800 ng/mL at 96 hours, achieved by a dose of 2 mg/kg in mice, was sufficient to provide the requisite occupancy for maximal pharmacodynamics. CD8+ TEM responses were dependent on 4-1BB agonism and were more efficiently induced by PD-L1 localization, as opposed to 4-1BB multivalent clustering alone. Optimal tumor responses, including complete responses and demonstration of immunological memory, were observed when maximal 4-1BB driven pharmacodynamics were paired with extended PD-1/PD-L1 pathway blockade, provided either by an orthogonal molecule or increased exposure of INBRX-105.

Conclusions Preclinical receptor occupancy and pharmacokinetic determinations have defined a dose of INBRX-105-like activity that induces maximal pharmacodynamics. Additional PD-1 checkpoint inhibition does not change the pharmacodynamic profile of INBRX-105-a, but does allow for optimal efficacy. INBRX-105 is currently being evaluated in patients with advanced solid tumors in a first-in-human trial (NCT03809624).

Trial Registration INBRX-105 is currently being evaluated in patients with advanced solid tumors in a first-in-human trial (NCT03809624).

REFERENCES

1. Vinay DS, Kwon BS. 4-1BB (CD137), an inducible costimulatory receptor, as a specific target for cancer therapy. *BMB Reports*; 2014;**47**:122–129.
2. Ye Q, Song D-G, Poussin M, *et al.* CD137 accurately identifies and enriches for naturally occurring tumor-reactive T cells in tumor. *Clin Cancer Res*; 2014;**20**:44–55.

Ethics Approval The care and use of all animals were reviewed and approved by Explora BioLabs' IACUC # SP17-010-013 and conducted in accordance with AAALAC regulations.

<http://dx.doi.org/10.1136/jitc-2021-SITC2021.012>

13

**DEXTER™ MICROFLUIDIC PLATFORM COUPLING
SINGLE-CELL RESOLUTION OF DYNAMIC TUMOR-
IMMUNE INTERACTION WITH AI FOR ELUCIDATING
MECHANISTIC MODULATION IN CANCER
IMMUNOTHERAPY**

¹Pradip Majumder, ²Biswanath Majumder, ¹Ranjeet Singh, ³Abhay Sane, ³Rushil Manglik, ³Ravi Keshari, ³M Mohanasundaram, ¹Ashwin Lal*. ¹Shilps Sciences Pvt Ltd, Chestnut Hill, MA, USA; ²Bugwroks, Bangalore, India; ³Shilps Sciences, Bangalore, India

Background Immunotherapies in recent years emerged as effective treatment modalities for primary and metastatic tumors. However, a durable response besides a high objective response rate (ORR) is still elusive. Limitations of predictive functional platforms in providing spatial and temporal mechanistic insights into tumors and their dynamic immune proximity at the single-cell level critically highlight the challenges of modeling successful therapy outcomes. Here we describe the development of a novel microfluidic platform integrated with AI that incorporates single-cell sorting and functional interactions between different immune cells and tumors.

Methods The Dexter™ microfluidic platform involves the generation of a large number of nanoliter droplets (> 10,000) and mechanical dispensing of sorted droplets in a spatially defined array of nano-wells and achieves high throughput (> 1,000) independent nano bioreactors. Its open design concept illustrates simple workflow, easy perfusion through a gas permeable oil, sufficient nutrient availability, and offers a protective cushion around the cell for minimizing any impending stress during the downstream process. Indeed, the droplets in the array are spatially segregated to avoid any cross-talk. The platform is integrated with a multicolor fluorescence and bright field imager equipped with a culture stage and precise motion robotic arm in proximity to the droplet of interest for its efficient aspiration and release into mapped well.

Results To demonstrate the applications of this platform for functional modulation, we used differentially labeled immune cells like CD45, CD4, CD8 and detected cytokines like IFN γ and granzyme B at single-cell level; antigen uptake by dextran-FITC endocytosis. We further quantified the functionalities critical for immune-immune interactions, tumor-immune synapse formation, and killing of target tumor cells in a dynamic PBMC and tumor (breast, colon, and head and neck cancer cells) coculture setting. Longitudinal imaging showed the ability of the platform to capture the dynamic state of the antigen uptake and presentation, functional activation of driver phenotypes like CD8+cytotoxic T cells, and subsequent directed killing of tumor cells upon reinvigoration of effector phenotypes. Further coupling of AI-guided matrix with features from polyfunctional modulation accurately demonstrated the mechanistic shift choreographed upon immune activation.

Conclusions Together, these findings illustrate the preclinical relevancy of a therapy agonist multimodality correlative platform integrating a controllable microfluid system and AI for real-time tracking of dynamic tumor-immune interplay at the level of single-cell resolution. Further validation of this system will offer opportunities for identifying driver modulation linked to predicted therapy response and modeling next-generation cell-based immunotherapies.

<http://dx.doi.org/10.1136/jitc-2021-SITC2021.013>

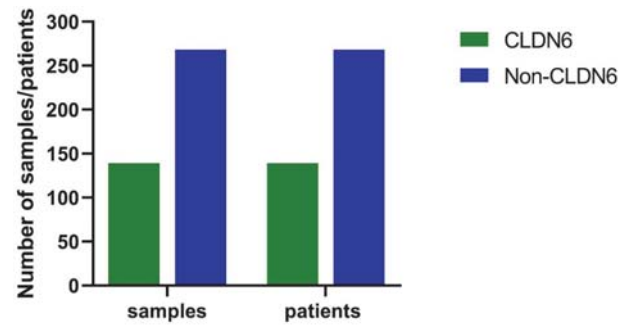
14 **CLAUDIN-6 AFFECTS THE CELL CYCLE AND P53 SIGNALING IN GASTRIC CANCER**

Sanyog Dwivedi*. *Cinvestav IPN, Mexico City, Mexico*

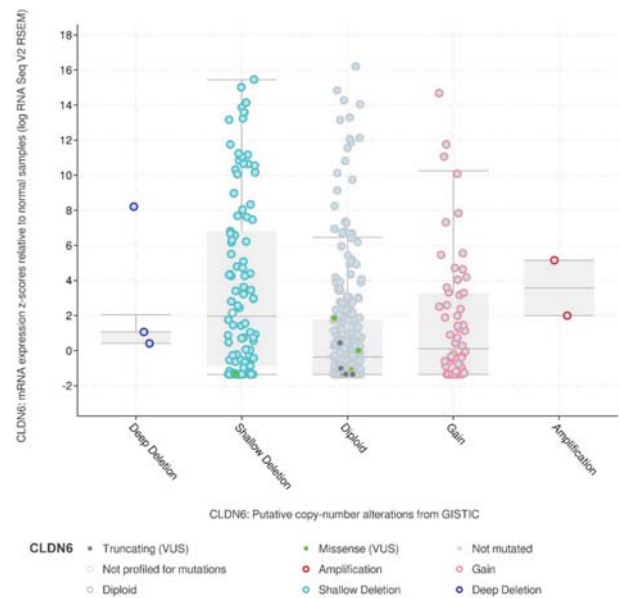
Background Claudin-6 (CLDN6) differentially overexpressed in Gastric Cancer (GC) is associated with poor prognosis and survival of patients. Uncovering affected pathways and genes associated with CLDN6 in GC can help in the identification of novel prognostic targets.

Methods CBioPortal^{1,2} was used to extract and analyze The Cancer Genome Atlas (TCGA) Stomach Adenocarcinoma Pan-Cancer Atlas Data (STAD). FunRich tool³ and Gene Ontology molecular signature database of Gene Set Enrichment Analysis (GSEA) were used for functional enrichment. CBioPortal was used to identify differentially expressed genes between groups. Graph pad Prism 8 was used to generate the graphics.

Results TCGA STAD PanCancer Atlas data was analyzed in terms of alterations in CLDN6. 34% of the GC samples (141 samples) were assigned to the CLDN6 alteration group while the rest of the samples (299) were assigned to the non-CLDN6 alteration group (figure 1). Major alterations of CLDN6 in GC included shallow deletion, diploid, gain, and differentially expressed mRNA (figure 2). Differentially overexpressed genes in the CLDN6 group with log-ratio cutoff ≥ 1 were used for functional enrichment in different biological pathway categories (figure 3); 18.1% of genes were associated with the transport of small molecules through the membrane, 14.6% mediated transmembrane transport and 12.5% were associated with lipid metabolism (figure 4). The Gene ontology molecular signature database of GSEA also confirmed that these genes were involved in lipid metabolism, transport activity, and epithelium development processes (table 1). Moreover, GC samples with CLDN6 alterations have higher mutations in p53 signaling (29% in TP53, 7% in CDKN2A) gene signature (figure 5) over samples in the non-CLDN6 alteration group (figure 6). Similarly, genes related with cell cycle control like CCNE1, MYC, SRC, and STAT3 showed higher mutations in the CLDN6 alteration group while JAK1 and E2F8 showed lower mutations than non-CLDN6 GC samples (figure 7). These observations indicate that CLDN6 in GC affects the transport of small molecules and lipid metabolism and that it is associated to tumors with higher mutations in p53 and cell cycle-related genes.



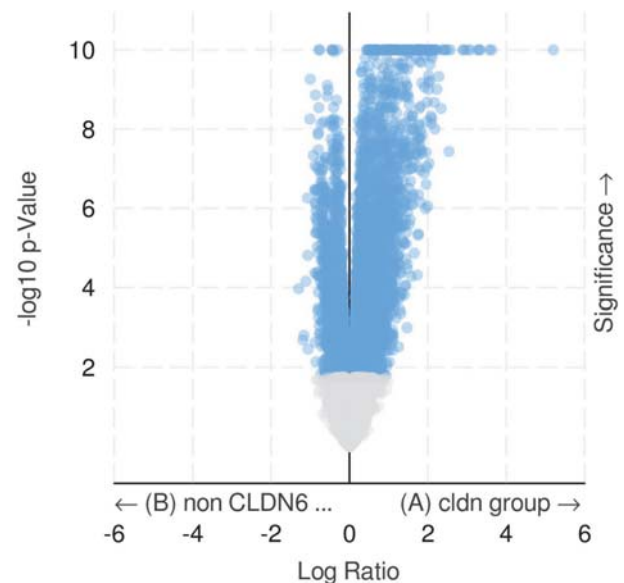
Abstract 14 Figure 1 Distribution of GC samples and patients of TCGA STAD data between CLDN6 and non CLDN6 alteration groups



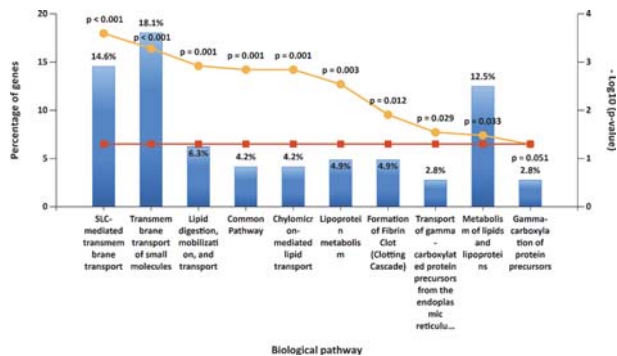
Abstract 14 Figure 2 Major alterations in CLDN6 in GC (TCGA STAD data)

Abstract 14 Table 1 Functional enrichment of differentially expressed genes (log-ratio ≥ 1) in CLDN6 group GC samples in Gene ontology molecular signature database of GSEA

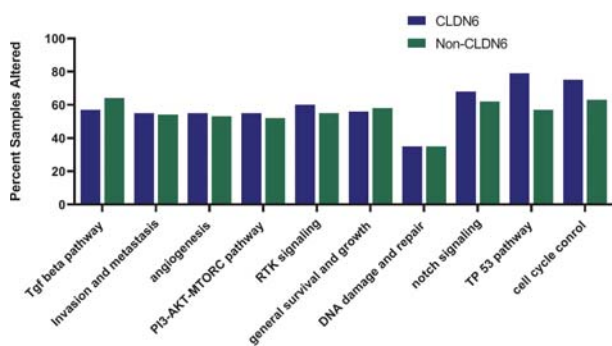
Gene Set Name [# Genes (K)]	# Genes in Overlap (k)	p-value	FDR q-value
GOBP EPITHELIUM DEVELOPMENT [1275]	60	9.32 e ⁻²¹	9.49 e ⁻¹⁷
GOCC APICAL PLASMA MEMBRANE [351]	31	1.33 e ⁻¹⁸	6.76 e ⁻¹⁵
GOCC APICAL PART OF CELL [414]	33	2.25 e ⁻¹⁸	7.66 e ⁻¹⁵
GOCC CLUSTER OF ACTIN BASED CELL PROJECTIONS [156]	22	6.87 e ⁻¹⁸	1.75 e ⁻¹⁴
GOMF TRANSPORTER ACTIVITY [1168]	52	4.5 e ⁻¹⁷	9.16 e ⁻¹⁴
GOBP LIPID METABOLIC PROCESS [1426]	57	1.49 e ⁻¹⁶	2.54 e ⁻¹³
GOCC BLOOD MICROPARTICLE [146]	20	3.93 e ⁻¹⁶	5.72 e ⁻¹³
GOCC BRUSH BORDER [101]	17	1.88 e ⁻¹⁵	2.4 e ⁻¹²
GOCC PLASMA MEMBRANE REGION [1208]	50	3.32 e ⁻¹⁵	3.36 e ⁻¹²
GOBP EMBRYO DEVELOPMENT [992]	45	3.43 e ⁻¹⁵	3.36 e ⁻¹²



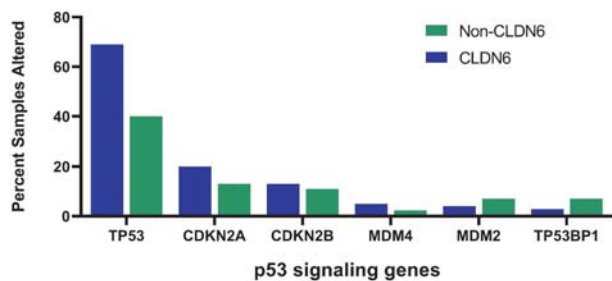
Abstract 14 Figure 3 Volcano plot of differentially expressed genes in CLDN6 and non CLDN6 groups. Log10 p-Value cutoff ≥ 2



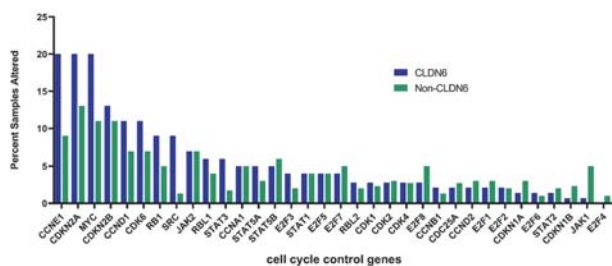
Abstract 14 Figure 4 Functional enrichment of differentially expressed genes (log-ratio ≥ 1) in biological process category



Abstract 14 Figure 5 Overall mutations in several important gene signatures involved in cancer between CLDN6 and non-CLDN6 GC samples



Abstract 14 Figure 6 Total mutations in p53 signaling genes



Abstract 14 Figure 7 Total mutations in genes involved in cell cycle control between CLDN6 and non-CLDN6 GC samples

Conclusions CLDN6 alterations in GC affect the cell cycle and p53 signaling pathways with higher mutations in TP53, CDKN2A, CCNE1, MYC, SRC, and STAT3 genes.

Acknowledgements This research was supported by CONACYT CVU grant 871712.

REFERENCES

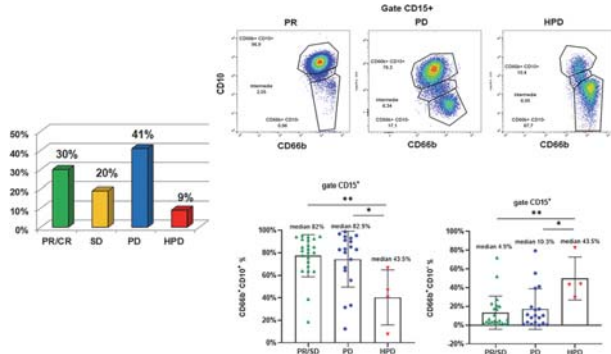
1. Cerami E, Gao J, Dogrusoz U, Gross BE, Sumer SO, Aksoy BA, et al. The cBio cancer genomics portal: an open platform for exploring multidimensional cancer genomics data. *Cancer Discov* 2012;**2**:401–4.
2. Gao J, Aksoy BA, Dogrusoz U, Dresdner G, Gross B, Sumer SO, et al. Integrative analysis of complex cancer genomics and clinical profiles using the cBioPortal. *Sci Signal* 2013;**6**:11.
3. Pathan M, Keerthikumar S, Ang C-S, Gangoda L, Quek CYJ, Williamson NA, et al. FunRich: An open access standalone functional enrichment and interaction network analysis tool. *2015PROTEOMICS*;15:2597–601.

<http://dx.doi.org/10.1136/jitc-2021-SITC2021.014>

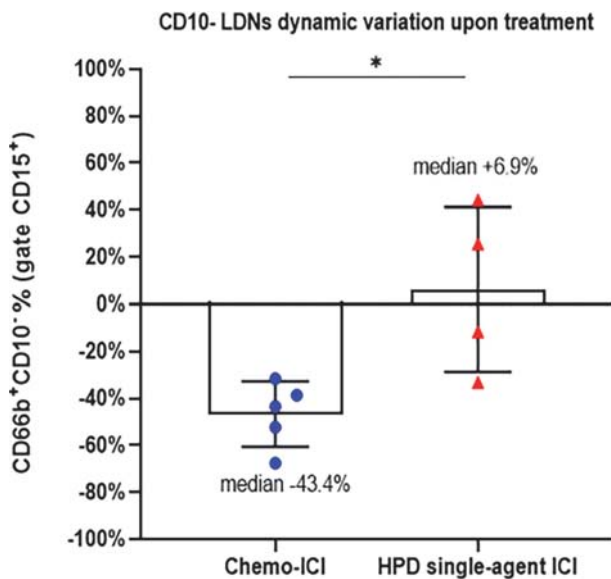
15 FIRST-LINE PLATINUM-BASED CHEMOTHERAPY COMBINED WITH PD-1/PD-L1 INHIBITORS (ICI) PREVENTS HYPERPROGRESSION IN NON-SMALL CELL LUNG CANCER (NSCLC) PATIENTS BY REDUCING CIRCULATING IMMATURE NEUTROPHILS

Roberto Ferrara*, ¹Giuseppe Lo Russo, ¹Elena Jachetti, ¹Giuseppina Calareso, ¹Claudia Proto, ¹Arsela Prelaj, ¹Giulia Galli, ²Diego Signorelli, ¹Marta Brambilla, ¹Alessandro De Toma, ¹Mario Occhipinti, ¹Sara Manglaviti, ¹Giulia Apollonio, ¹Laura Mazzeo, ¹Monica Ganzinelli, ¹Antonia Martinetti, ¹Filippo De Braud, ³Marina Garassino, ¹Mario Paolo Colombo, ¹Sabina Sangaletti. ¹Istituto Nazionale dei Tumori di Milano, Milano, Italy; ²Ospedale Niguarda, Milan, Italy; ³University of Chicago, Chicago, USA

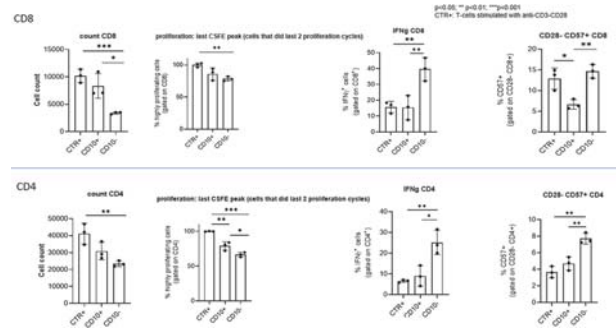
Background Hyperprogression (HPD) has been described in 14–26% of NSCLC patients upon single-agent ICI¹ and has not been reported upon ICI and platinum-based chemotherapy (PCT) combinations. Both high circulating neutrophils² and senescent T-cells³ correlated with HPD, however the exact neutrophils-T-cells interplay and the role of specific neutrophils subsets in driving HPD is unknown.



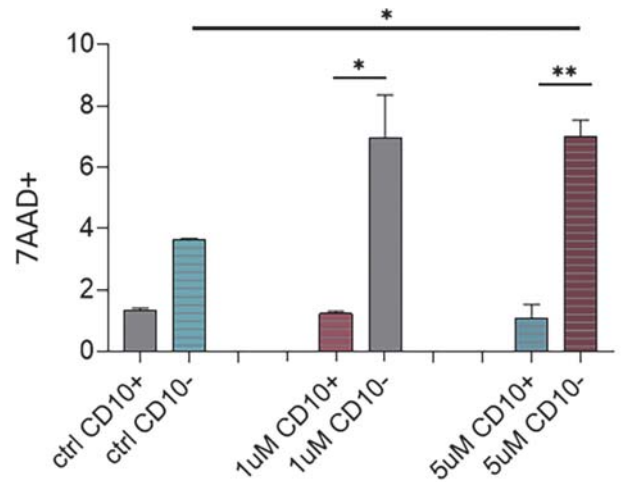
Abstract 15 Figure 1 Patterns of response, progression and hyperprogression to single-agent ICI and correlation with mature (CD10+) or immature (CD10-) LDNs' subtypes



Abstract 15 Figure 2 Neutrophils dynamic variation upon treatment (5 patients with high baseline CD10- LDNs and PD/SD to chemo-ICI vs 4 patients with HPD upon single-agent ICI)



Abstract 15 Figure 3 Mature (CD10+) and immature (CD10-) LDNs in coculture with T-cells from a healthy donor differently influence CD8 and CD4 T-cells survival, proliferation, IFN-gamma production and expression of a senescent (CD28- CD57+) phenotype.



7-Aminoactinomycin D: cell death marker

Abstract 15 Figure 4 Cisplatin in-vitro treatment at different concentration (1 uM and 5 uM) increases necrotic (7AAD expression) cell death preferentially of immature (CD10-) rather than mature (CD10+) LDNs

Methods NSCLC patients treated with 1st line ICI as single-agent or in combination with PCT were assessed for HPD and circulating neutrophils' phenotype. HPD required 3 assessment (2 before ICI, 1 upon ICI) and was defined as delta tumor growth rate (TGR) (TGR upon ICI – TGR before ICI) >50% and/or TGR ratio (TGR upon ICI/TGR before ICI) ≥2. Circulating low density neutrophils (LDNs) subtypes were assessed by flow cytometry on peripheral blood mononuclear cells (PMBCs). LDNs were defined as CD66b+CD15+ cells among CD11b+ PMBCs. Immature subtypes were defined as CD10- LDNs. T-cells were isolated from healthy donors and cocultured with patients' LDNs to characterize the neutrophils-T-cells interplay. LDNs subtypes were isolated from patients and treated in-vitro with cisplatin to assess cell death.

Results 46 NSCLC patients were treated with single-agent ICI and 17 with PCT+ICI (table 1). In the ICI single-agent cohort, PD and HPD occurred in 21 (41%) and 4 (9%) patients. Before ICI start, HPD patients had significantly higher median% of circulating immature CD10- LDNs neutrophils [43.5 (min 29.5; max 82.6) vs 10.3 (min 0.1; max

79.4), $p=0.01$] compared to PD patients (figure 1). In the ICI-PCT cohort no HPD was reported. 5 patients had baseline CD10- LDNs $\geq 43.5\%$ (median% of CD10- LDNs in HPD patients upon single-agent ICI), 2 of them had stable disease and 3 PD upon ICI-PCT. In these 5 patients, CD10- LDNs significantly decreased during ICI-PCT compared to what observed in HPD patients upon single-agent ICI [median variation -43.4 (min -67.6, max -31.6) vs +6.9 (min -33, max +44), $p= 0.03$] (figure 2). After 7 days of coculture with T-cells, immature CD10- LDNs significantly reduced T-cells survival and promoted a T-cell senescent phenotype (CD28 loss, CD57 gain) impairing T-cells proliferation and increasing IFN-gamma production (figure 3). Cisplatin treatment significantly increased necrotic cell death among CD10- LDNs compared to CD10+ LDNs (figure 4).

Abstract 15 Table 1 Patients characteristics in the single-agent ICI and PCT+ICI cohorts

	Single-agent ICI	PCT + ICI
Patients Characteristic	N=46 (%)	N=17 (%)
Age		
≥ 70 years	21 (46%)	6 (35%)
< 70 years	25 (54%)	11 (65%)
Sex		
Male	29 (63%)	11 (65%)
Female	17 (37%)	6 (35%)
Histology		
Adenocarcinoma	32 (69%)	15 (88%)
Squamous	8 (17%)	0 (0%)
NSCLC-Other	6 (13%)	2 (12%)
Smoking status		
Never	4 (9%)	3 (18%)
Former	25 (54%)	8 (47%)
Current	17 (37%)	6 (35%)
N° met sites ICI baseline		
0-2	34 (74%)	10 (59%)
> 2	12 (26%)	7 (41%)
Performance status		
0-1	40 (87%)	16 (94%)
≥ 2	6 (13%)	1 (6%)
PD-L1 IHC (dako 22c3)		
< 1	2 (4%)	7 (41%)
1-49%	31 (67%)	8 (47%)
≥ 50%	13 (28%)	1 (6%)
Unknown	0 (0%)	1 (6%)
Molecular Status		
KRAS mut	12 (26%)	4 (23%)
Wild type*	25 (55%)	6 (36%)
Targetable §	2 (4%)	4 (23%)
Unknown	7 (15%)	3 (18%)

*wild type for EGFR, ALK, ROS1, § 2 MET ex 14 mutation, 1 BRAF V600E mutation, 1 ALK fusion, 2 EGFR mutations

Conclusions Higher baseline immature CD10- LDNs impair T-cell survival and promote T-cell senescence being a circulating biomarker of HPD upon single-agent ICI. The addition of PCT prevents HPD by inducing immature neutrophils cell death.

REFERENCES

- Ferrara R, Mezquita L, Texier M, Lahmar J, Audigier-Valette C, Tessonier L, et al. Hyperprogressive disease in patients with advanced non-small cell lung cancer treated with pd-1/pd-l1 inhibitors or with single-agent chemotherapy. *JAMA Oncol* 2018;**4**:1543–52. <https://doi.org/10.1001/jamaoncol.2018.3676>
- Kim Y, Kim CH, Lee HY, Lee S-H, Kim HS, Lee S, et al. Comprehensive clinical and genetic characterization of hyperprogression based on volumetry in advanced non-small cell lung cancer treated with immune checkpoint inhibitor. *J Thorac Oncol* 2019;**14**:1608–18. <https://doi.org/10.1016/j.jtho.2019.05.033>
- Ferrara R, Naigeon M, Auclin E, Duchemann B, Cassard L, Jouniaux JM, et al. Circulating T-cell immunosenescence in advanced non-small cell lung cancer patients treated with single agent PD-1/PD-L1 inhibitors or platinum-based chemotherapy. *Clin Cancer Res* 2020. <https://doi.org/10.1158/1078-0432.CCR-20-1420>.

Ethics Approval Patients blood was obtained after signature of informed consent and within an observational prospective study (INT 22_15) approved by local Institutional Ethical Committee.

<http://dx.doi.org/10.1136/jitc-2021-SITC2021.015>

16 **TUMOR GROWTH INHIBITION MEDIATED BY A SINGLE DOSE OF INTRATUMORAL TRANSCON™ TLR7/8 AGONIST WAS ASSOCIATED WITH ACTIVATED CIRCULATING T AND B CELLS AND SUSTAINED LOW LEVELS OF SYSTEMIC CYTOKINES**

Amer Mirza*, Luis Zuniga, Karan Uppal, Kathy Bang, Enping Hong, Simran Sabharwal, Yuchi Lee, Salomon Martinez, David Rosen, Juha Punnonen. *Ascendis Pharma, Redwood City, CA, USA*

Background TLR agonists can elicit anti-tumor activity by activating innate immune cells and promoting a proinflammatory microenvironment. Local delivery of TLR agonists has shown encouraging preclinical and clinical anti-tumor activity. However, intratumoral (IT) delivery of naked TLR agonists such as resiquimod, a TLR7/8 agonist, can lead to rapid efflux from the tumor, resulting in acute high systemic drug exposure and transient but high level of peripheral proinflammatory cytokines, thus limiting anti-tumor benefit and increasing risk of cytokine-driven adverse effects.

Methods TransCon™ TLR7/8 Agonist was designed to elicit a sustained and local release of resiquimod following IT administration of a hydrogel depot. In the syngeneic murine CT26 tumor model, a single IT injection of TransCon TLR7/8 Agonist monotherapy was sufficient to induce potent tumor growth inhibition. Following treatment, the induction of key cytokines and chemokines associated with innate immunity was determined.

Results Proinflammatory cytokines (IL-1b, IL-6, and TNF α) were induced following IT TransCon TLR7/8 Agonist treatment, but in contrast to free resiquimod, peak levels were more than 10-fold lower than those observed with an equimolar dose of free resiquimod. The circulating levels of these cytokines were sustained above control alone through Day 21. TH1-associated IFN γ was induced with levels increased at Day 1 and maintained at Day 7. Additionally, expression of myeloid-associated chemokines (KC/GRO α /CXCL1, MCP-1/CCL2, IP-10/CXCL10, and MIP-1a/CCL3) were induced and sustained in a largely dose-dependent manner through Day 21. The sustained increase in cytokines was consistent with an increase in circulating innate immune cells, such as NK and myeloid cells. Furthermore, evidence of adaptive immune cell activation was observed as indicated by expression of Ly6C, ICOS and Ki67, which were increased on CD8+ T cells, CD4+ T cells (Ki67, ICOS), and B cells (Ly6C).

Conclusions These data show that a single IT injection of TransCon TLR7/8 Agonist can elicit sustained expression of key cytokines and chemokines, promote innate immune cell mobilization, activate adaptive immune cells, and mediate robust anti-tumor activity. The levels of the cytokines remained relatively low through the observation period of 21 days, suggesting a low risk of systemic cytokine-associated adverse events. The increase in activated B, T, and NK cells in blood was associated with induction of a potent anti-tumor response, further supporting TransCon TLR7/8 Agonist as a novel and potentially efficacious PRRA therapy. A clinical trial to evaluate its safety and efficacy in cancer patients is currently underway (transcendIT-101; NCT04799054).

Ethics Approval The animal studies described were performed in accordance with the 'Guide for the Care and Use of Laboratory Animals: Eighth Edition' and approved by the institutional animal care and use committee (IACUC).

<http://dx.doi.org/10.1136/jitc-2021-SITC2021.016>

PREDICTIVE SOLUBLE BIOMARKERS OF IMMUNE RESPONSE TO CHECKPOINT BLOCKADE IN NON-SMALL CELL LUNG CANCER (NSCLC) PATIENTS

Afsheen Raza*, Reyad Mohsen, Aladdin Kanbour, Abdul Rehman Zar Gul, Anite Philip, Suma Vijayakumar, Shereena Hydrose, Maysaloun Merhi, Varghese Inchakalody, Shahab Uddin, Mohammed Ussama Al Homsy, Said Dermime. *Hamad Medical Corporation, DOHA, Qatar*

Background There is limited data on the predictive biomarkers of response to immune checkpoint blockade (ICB) treatment of non-small cell lung cancer (NSCLC) patients. The main aim of this prospective study was to understand the utility of pre-treatment soluble immune checkpoint markers as surrogate markers for tissue PD-L1 and as predictors of response in locally advanced/metastatic NSCLC patients treated with ICBs.

Methods The study was conducted at the National Center for Cancer Care and Research (NCCCR), HMC, Qatar. A total of 30 patients on Pembrolizumab/Nivolumab were enrolled and blood samples were collected before treatment. 17 Healthy controls were also included in the study. Multiplex Magnetic Bead Panel kits for soluble immune checkpoint markers was utilized to measure the concentrations of 24 soluble markers including BTLA, GITR, HVEM, IDO, LAG-3, PD-1, PDL-1, PDL-2, TIM-3, CD28, CD80, 4-1BB, CD27, CTLA-4, ICOS Ligand, CD276, VISTA, B7-H6; CD47 (IAP), BLAST-1, Galectin-9, TIMD-4; OX40 and S100A8/A9. Mann-Whitney test was used to evaluate a) the difference in median values between healthy controls and pre-treatment samples b) compare soluble markers with tissue PD-L1 status and c) response to treatment 4 months after treatment via PET CT imaging data.

Results The results showed significant changes in the pre-treatment plasma concentrations of soluble markers in the NSCLC patients compared to healthy controls. Significant upregulation was observed in the immune suppression markers: S100A8/A9 ($<0.0001^{***}$), PDL-2 ($<0.006^{**}$), LAG-3 ($<0.006^{**}$), PD-1 ($<0.008^{*}$), TIM-3 ($<0.002^{*}$), CD80 ($<0.001^{*}$) and Galactin 9 ($<0.023^{*}$). Significant upregulation was observed for the immune stimulatory markers: TIMD4 ($<0.0001^{***}$), CD137/4-1BB ($<0.007^{*}$), CD134/OX40 ($<0.006^{**}$) in NSCLC patients compared to healthy controls. When soluble markers were compared with tissue PD-L1, significant upregulation of CD276/B7-H3 ($<0.039^{*}$) and VISTA ($<0.034^{*}$) was observed in patients expressing $>50\%$ of PD-L1 in their tissues. We then correlated the pre-treatment soluble markers expression with the clinical response of the patients to Pembrolizumab/Nivolumab using imaging (PET CT) data obtained 4 months after treatment. Interestingly, significant upregulation of GITR ($<0.0005^{***}$), PD-L1 ($<0.002^{**}$) and HVEM ($<0.006^{**}$) was observed in responding patients.

Conclusions The study demonstrates that 10 markers show differences in NSCLC patients as compared to healthy controls; 2 markers as surrogates for tissue PDL-1 and 3 markers as predictive biomarkers of response to ICB treatment.

Acknowledgements We would like to thank all enrolled subjects for their participation in the study.

Ethics Approval The study was approved by Hamad Medical Corporation, Medical Research Center Ethics Board; approval number MRC-01-20-507

<http://dx.doi.org/10.1136/jitc-2021-SITC2021.017>

18 SYSTEMIC IMMUNE PROFILING OF ADVANCED BILIARY TRACT CANCER PATIENTS DEFINES ALTERED CYTOKINES AND IMMUNE CELL POPULATIONS

¹Amanda Ruggieri*, ²Mark Yarchoan, ¹Yuan Liu, ¹Subir Goyal, ³Elad Sharon, ³Helen Chen, ¹Brian Olson, ¹Shishir Maitel, ¹Bassel El-Rayes, ²Nilofer Azad, ¹Gregory Lesinski. ¹Emory University, Atlanta, GA, USA; ²Johns Hopkins University, Baltimore, MD, USA; ³National Cancer Institute, Bethesda, MD, USA

Background Biliary tract cancers (BTCs) are aggressive malignancies often refractory to chemotherapy and immunotherapy. There is urgent need to identify novel, data-driven therapeutic targets to change the course of disease. It is also challenging to procure substantial quantities of tissue for research from patients with advanced or metastatic disease. Thus, we posit that peripheral blood holds particular value for exploring immune landscapes in patients with advanced BTC. We hypothesized actionable immunotherapy targets can be identified from blood that are suited to improve outcomes for BTC patients.

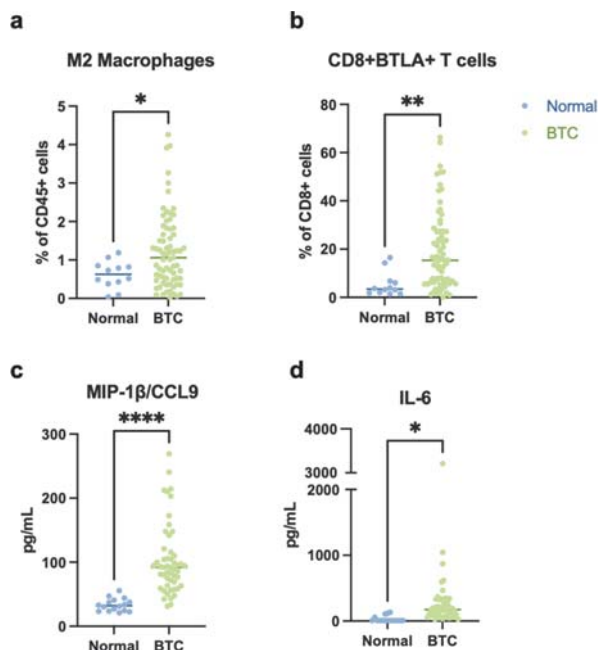
Methods We examined a comprehensive panel of immune biomarkers in pre-treatment blood from 79 patients with advanced BTC on a national, randomized Phase II clinical trial of atezolizumab ± cobimetinib in advanced metastatic BTC (NCI10139). A cohort of 12 healthy donors was obtained as a comparator. Blood was processed via ficoll and density gradient centrifugation. PBMCs and plasma were cryopreserved prior to analysis by bioplex assay and multiparameter flow cytometry (n=23 colors). Analysis of 45 peripheral soluble factors was performed on a Luminex 100. Flow cytometric analysis was conducted on a Cytex Aurora and analyzed using FlowJo software. Comparisons of normal versus BTC patient samples were conducted via unpaired two-tailed t tests.

Results Bioplex analysis of 45 peripheral soluble factors revealed significant elevations in BTC plasma compared to normal donors for several factors including IL-6, IL-18, eotaxin/CCL11, IP-10/CXCL10, MIP-1β/CCL9, IFN-γ, PDGF-BB, PIGF-1, and SCF (p's<0.01). Our comprehensive flow panel captured 27 phenotypically defined cell populations encompassing T/B lymphocytes, monocytes, NK cells, and myeloid cells. Only 6 cell populations were significantly different between BTC patients and normal donors (figure 1). Patients with advanced BTC had higher frequencies of T cells expressing inhibitory checkpoint molecules compared to healthy donors. Namely, higher frequencies of CD4+PD-1+ T cells, CD8+PD-1+ T cells, CD4+BTLA+ T cells, and CD8+BTLA+ T cells (p's<0.01) were evident. In addition, BTC patients had more monocytes (CD11b+CD11c+CD14+CD16-HLA-DR+), and M2 macrophages (CD11b+CD11c+CD16+CD33+CD14+) (p's<0.03) versus healthy donors. Ongoing analysis will determine associations between biomarkers and overall survival in the patient cohort using the Cox proportional hazard model for time-to-event outcomes.

Conclusions To our knowledge, this work represents the most comprehensive analysis of peripheral immune biomarkers in BTC patients to date. These data suggest that cytokine mediators and/or distinct immune checkpoints deserve further investigation as actionable targets in patients with BTC.

Ethics Approval Patient samples were collected as part of a study approved by the National Cancer Institute's (NCI) Cancer Therapy Evaluation Program (CTEP), as well as central and local institutional review boards (IRBs). All patients and healthy donors gave informed consent before participation in these studies.

<http://dx.doi.org/10.1136/jitc-2021-SITC2021.018>



Abstract 18 Figure 1 Several immune biomarkers are elevated in the peripheral blood of biliary tract cancer patients compared to normal donors, including (a) percent of CD45% cells that are phenotypically defined as M2 macrophages (CD11b+CD11c+CD16+CD33+CD14+), (b) percent of CD45% cells that are BTLA+CD8+ T cells, (c) soluble MIP-1β/CCL9, and (d) soluble IL-6.

EXOME-SCALE LIQUID BIOPSY CHARACTERIZATION OF EMERGING IMMUNE RESISTANCE MECHANISMS IN TREATMENT-RESISTANT GIST

¹Charles Abbott*, ²Niamh Coleman, ¹Jing Wang, ¹Josette Northcott, ¹Fabio Navarro, ¹Lee McDaniel, ¹Eric Levy, ¹Rachel Pyke, ²Filip Janku, ¹Richard Chen, ¹Sean Boyle. ¹Personalis, Inc., Menlo Park, CA, USA; ²MD Anderson Cancer Center, Houston, TX, USA

Background Metastatic gastrointestinal stromal tumors (GIST) are lethal tumors of the GI tract characterized by gain of function mutations in KIT or PDGFR β . Transient first-line control is achieved through the inhibition of tyrosine kinase signaling using the KIT inhibitor imatinib, though most patients progress after 2–3 years. Progression through successive lines of therapy results in a molecularly heterogeneous disease with diverse subtypes, driven by distinct collections of exon-specific KIT mutations which directly inform therapy decisions. To address the unmet need of comprehensive understanding of GIST, we used tumor-informed whole exome liquid biopsy to identify and track the evolution of multiple concurrent heterogeneous resistance mechanisms in individual patients receiving tyrosine kinase inhibitors (TKIs).

Methods Baseline matched tumor, normal and longitudinal plasma samples were obtained from 15 metastatic, heavily pre-treated GIST patients. Following baseline sample collection, all patients received systemic TKI therapy, and were monitored until disease progression. Paired tumor and normal samples were profiled using the ImmunoID NeXT Platform®, an augmented exome/transcriptome platform and analysis pipeline which generates comprehensive tumor and immune information. Exome-scale cfDNA profiling of matched plasma samples was performed using the NeXT Liquid Biopsy™ platform to detect somatic variants.

Results Baseline solid tumor WES confirmed primary sensitizing KIT mutations in all 15 (100%) patients, and secondary KIT mutations in 7/15 patients (47%). Serial plasma whole exome sequencing identified evolution and expansion of clones harboring newly formed, druggable, exon-specific KIT mutations which evolved prior to identification of tumor progression using standard imaging techniques. In addition to these variants, we detected node-specific enrichment of PI3K-AKT and MAPK pathway mutations in plasma of patients with shorter overall survival (OS), which may contribute to the observed immune evasion. Accompanying these changes, we also detected significant association between gene copy-number profiles and duration of OS ($P = 0.0097$). Investigation of immune signatures using univariate cox modeling revealed a significant association between TCR β diversity and reduced OS (HR = 2.55, log rank $P = 0.04$).

Conclusions Comprehensive genomic profiling (WES and RNA-Seq) of paired tumor tissue and WES of serially collected ctDNA identified evolving druggable KIT mutations and other molecular alterations which preceded clinical disease progression. These findings suggest liquid biopsy-based monitoring of late-stage GIST malignancies may be useful for early identification of treatment resistance, providing treatment guidance prior to traditional approaches.

Ethics Approval Ethics approval was granted by the MD Anderson Human Research Protection Program, and all participants gave informed consent prior to participation.

<http://dx.doi.org/10.1136/jitc-2021-SITC2021.019>

TUMOR-INFORMED LIQUID BIOPSY MONITORING OF EVOLVING THERAPEUTIC RESISTANCE MECHANISMS IN HEAD AND NECK SQUAMOUS CELL CARCINOMA PATIENTS RECEIVING ANTI-PD-1 THERAPY

¹Charles Abbott*, ²Nikita Bedi, ¹Jing Wang, ¹Josette Northcott, ¹Rachel Pyke, ¹Robin Li, ¹Lee McDaniel, ¹Eric Levy, ³Mena Mansour, ²Dimitrios Colevas, ¹John Lyle, ²John Sunwoo, ¹Sean Boyle, ¹Richard Chen. ¹Personalis, Inc., Menlo Park, CA, USA; ²Stanford University, Stanford, CA, USA; ³Washington University in St. Louis, St. Louis, USA

Background Typical liquid biopsy panels offer a limited understanding of tumor biology, potentially under-representing the heterogeneity of resistance in late-stage cancers. Here, diminished scope can result in undetected, therapeutically-relevant biomarkers which respond dynamically to treatment, as well as potentially missed resistance mechanisms and pathway-level events. To address the challenges associated with identifying multiple concurrent heterogeneous resistance mechanisms in individual patients, we evaluated longitudinal exome-scale tumor-informed cell-free DNA (cfDNA) data from head and neck squamous cell carcinoma (HNSCC) patients receiving anti-PD1 therapy.

Methods Pre- and post-intervention matched tumor, normal and plasma samples were retrospectively obtained from 15 stage II-IV HNSCC patients. Following baseline sample collection, all patients received a single dose of nivolumab or pembrolizumab. The primary tumor was then resected approximately one month later when possible, or a second biopsy collected where resection was impractical. Paired tumor and normal samples were then profiled using Immunoid NeXT Platform®, an augmented exome/transcriptome platform and analysis pipeline. Exome-scale cfDNA profiling of matched plasma samples was performed using the NeXT Liquid Biopsy™ platform to detect somatic variants.

Results Patient neoantigen presentation score (NEOPSTM) rapidly and significantly contracted following therapy ($p=.00098$). Novel neoantigens arising post-treatment which were predicted to be presented on lost HLA alleles were significantly higher in patients with longer overall survival ($p=.019$). Variant detection across same-patient serial cfDNA samples revealed significantly correlated VAFs ($R=.62$, $p<.0001$) despite significant contraction of mutational burden in solid tumor ($p=.0039$), suggesting complex clonal/subclonal dynamics. Investigation of the evolving tumor and cfDNA subclonal architecture revealed significant association between decreasing cellular prevalence and NOTCH signaling ($q=.001$) and the innate immune system ($q=.002$), while increasing cellular prevalence was associated with p53 signalling ($q=.02$) and hypoxia ($q=.02$). These findings were complimented by transcriptomic data which showed significant enrichment of multiple immune pathways across treatment.

Conclusions We found that immune checkpoint blockade precipitates rapid evolution of the HNSCC tumor microenvironment. By leveraging comprehensive, tumor-informed liquid biopsy data we were able to identify contracting cellular populations enriched for NOTCH pathway mutations. Longer OS following either intervention was associated with an expansion of novel neoantigens predicted to be presented by lost HLA alleles. Our results suggest that tumor-informed liquid biopsy provides a more robust understanding of therapeutic response and resistance mechanisms than that attainable with typical liquid biopsy panels alone.

Ethics Approval This study obtained ethics approval from Human Subjects Research at Stanford University. ID number is

40425. All participants gave informed consent prior to enrollment.

<http://dx.doi.org/10.1136/jitc-2021-SITC2021.020>

21 **NEUTROPHIL EXTRACELLULAR TRAPS (NETS) CAN BE MEASURED NON-INVASIVELY WITH CPA9-HNE – BIOMARKER POTENTIAL ACROSS DIFFERENT SOLID TUMOR TYPES IN THE IMMUNO-ONCOLOGY SETTING**

Christina Jensen*, Jeppe Thorlacius-Ussing, Joachim Mortensen, Morten Karsdal, Nicholas Willumsen. *Nordic Bioscience, Herlev, Denmark*

Background Serological predictive biomarkers to anti-PD-1 therapy across different solid tumor types represent an unmet medical need. High neutrophil activity is associated with poor response to immune checkpoint inhibitor therapy, amongst others due to the release of neutrophil extracellular traps (NETs) that have been shown to protect tumor cells against cytotoxic attacks. Human neutrophil elastase (HNE) and calprotectin are the major NETs constituents. We have previously shown that high levels of a serum calprotectin assay, which quantifies a specific HNE generated calprotectin fragment (CPa9-HNE), as a measure of neutrophil activity, associate with poor response to anti-PD-1 therapy in metastatic melanoma patients. The aim of this study was to investigate the performance of CPa9-HNE in serum from patients with other solid tumor types.

Methods HNE mediated degradation of calprotectin (CPa9-HNE) was measured in pretreatment serum from 223 patients with bladder cancer (n=20), breast cancer (n=20), colorectal cancer (n=20), head and neck cancer (n=20), kidney cancer (n=20), liver cancer (n=3), lung cancer (n=20), melanoma (n=20), ovarian cancer (n=20), pancreatic cancer (n=20), prostate cancer (n=20), and stomach cancer (n=20), and compared to age-matched healthy controls (n=33). Statistical differences were analyzed using the Kruskal-Wallis test adjusted for Dunn's multiple comparisons test.

Results CPa9-HNE serum levels were significantly elevated in patients with bladder cancer ($p < 0.0001$), breast cancer ($p < 0.0001$), colorectal cancer ($p < 0.0001$), head and neck cancer ($p < 0.0001$), kidney cancer ($p < 0.0001$), lung cancer ($p < 0.0001$), melanoma ($p = 0.0001$), ovarian cancer ($p < 0.0001$), pancreatic cancer ($p < 0.0001$), prostate cancer ($p = 0.0009$), and stomach cancer ($p < 0.0001$) compared to healthy controls. In all solid tumor types, a large patient-to-patient variation was observed. CPa9-HNE was also significantly elevated in stage IV cancer patients compared to stage I cancer patients ($p = 0.044$).

Conclusions The novel serological biomarker CPa9-HNE measuring HNE mediated degradation of calprotectin is significantly elevated in patients with different solid tumor types suggesting that these patients have high neutrophil activity. As high neutrophil activity is associated with poor response to anti-PD-1 therapy, CPa9-HNE may be used as a biomarker for anti-PD-1 therapy across different solid tumor types.

Ethics Approval The serum samples in this study was obtained from the commercial vendor Proteogenex and BioIVT, and according to the vendors, sample collection was approved by an Institutional Review Board or Independent Ethical Committee and patients gave their informed consent (Protocol numbers PG-ONC 2003/1 and WIRB® Protocol #20161665). All investigations were carried out according to the Helsinki Declaration.

<http://dx.doi.org/10.1136/jitc-2021-SITC2021.021>

THE POTENTIAL OF SERUM AUTOANTIBODIES AGAINST TYPE III COLLAGEN IN CANCER

Christina Jensen*, Jeppe Thorlacius-Ussing, Patryk Drobinski, Morten Karsdal, Anne-Christine Bay-Jensen, Nicholas Willumsen. *Nordic Bioscience, Herlev, Denmark*

Background Autoantibodies are classically associated with autoimmune diseases but have recently emerged as attractive cancer biomarkers as they can be easily assessed in serum. Certain autoantibodies have been shown to promote cancer while others contribute to the body's defense against it. Cancer progression is associated with excessive remodeling of the extracellular matrix (ECM) and collagen, but little is known about the role of autoantibodies against collagen in cancer. To investigate autoreactivity against collagen in cancer, we developed a novel biomarker assay to quantify autoantibodies against type III collagen products in serum from patients with various solid tumor types and compared levels with those found in healthy controls.

Methods The presence and levels of autoantibodies against denatured type III collagen were measured in pretreatment serum from 223 patients with bladder cancer (n=20), breast cancer (n=20), colorectal cancer (n=20), head and neck cancer (n=20), kidney cancer (n=20), liver cancer (n=3), lung cancer (n=20), melanoma (n=20), ovarian cancer (n=20), pancreatic cancer (n=20), prostate cancer (n=20), and stomach cancer (n=20), and compared to age-matched healthy controls (n=33). Statistical differences were analyzed using the Kruskal-Wallis test adjusted for Dunn's multiple comparisons test.

Results Serum levels of autoantibodies against type III collagen were significantly lower in patients with bladder cancer (p=0.0007), breast cancer (p=0.0002), colorectal cancer (p<0.0001), head and neck cancer (p=0.0005), kidney cancer (p=0.005), liver cancer (p=0.030), lung cancer (p=0.0004), melanoma (p<0.0001), ovarian cancer (p<0.0001), pancreatic cancer (p<0.0001), prostate cancer (p<0.0001), and stomach cancer (p<0.0001) compared to healthy controls. This autoimmunity biomarker could discriminate between cancer and healthy controls with an AUROC value of 0.88 (p<0.0001).

Conclusions In this study, we observed that cancer patients with different solid tumor types have downregulated levels of circulating autoantibodies directed against type III collagen compared to healthy controls suggesting that autoantibodies against type III collagen and tumor fibrosis may be important for tumor control and eradication. This autoimmunity biomarker may have the potential for studying and monitoring the close relationship between autoimmunity and cancer such as the risk of developing cancer on rheumatoid arthritis immunosuppressant or the risk of developing immune-related adverse events on cancer immunotherapy.

Ethics Approval The serum samples in this study were obtained from the commercial vendor Proteogenex and Bio-IVT, and according to the vendors, sample collection was approved by an Institutional Review Board or Independent Ethical Committee and patients gave their informed consent (Protocol numbers PG-ONC 2003/1 and WIRB® Protocol #20161665). All investigations were carried out according to the Helsinki Declaration.

<http://dx.doi.org/10.1136/jitc-2021-SITC2021.022>

VALIDATION OF PD-L1 DYNAMIC EXPRESSION ON EXTRACELLULAR VESICLES AS A PREDICTOR OF RESPONSE TO IMMUNE-CHECKPOINT INHIBITORS AND SURVIVAL IN NON-SMALL CELL LUNG CANCER PATIENTS

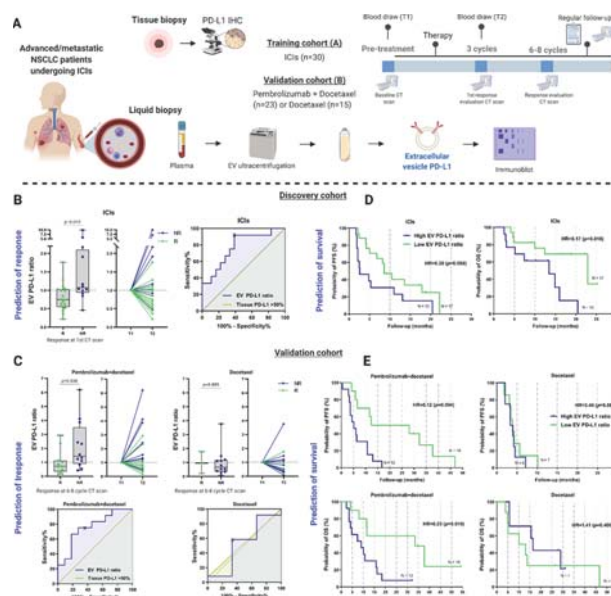
¹Diego de Miguel Perez*, ²Feliciano Barrón, ³Alessandro Russo, ²Luis Lara-Mejía, ⁴Muthukumar Gunasekaran, ⁵Andrés Cardona, ⁶Christine Peterson, ⁷Rivka Colen, ⁶Aung Naing, ⁸Philip Mack, ⁸Fred Hirsch, ⁹Vincenzo Adamo, ²Oscar Arrieta, ¹Christian Rolfo. ¹Tisch Cancer Institute and Icahn School of Medicine, Mount Sinai, NY and Marlene and Stewart Greenebaum Comprehensive Cancer Center, University of Maryland School of Medicine, New York, NY, USA; ²Instituto Nacional de Cancerología (INCAN), Mexico city, Mexico; ³A.O. Papardo and Department of Human Pathology, University of Messina and Marlene and Stewart Greenebaum Comprehensive Cancer Center, University of Maryland School of Medicine, Messina, Italy; ⁴University of Maryland School of Medicine, Baltimore, MD, USA; ⁵Clinica del Country, Bogota, Colombia; ⁶The University of Texas MD Anderson Cancer Center, Houston, TX, USA; ⁷University of Pittsburgh, Pittsburgh, PA, USA; ⁸Tisch Cancer Institute and Icahn School of Medicine, Mount Sinai, NY, New York, NY, USA; ⁹A.O. Papardo and Department of Human Pathology, University of Messina, Messina, Italy

Background Immune-checkpoint inhibitors (ICIs) revolutionized the treatment of advanced non-small cell lung cancer (NSCLC).^{1–3} To date, tissue PD-L1 immunohistochemistry is one of the leading biomarkers for prediction of ICIs response but has several limitations.^{4–5} Extracellular vesicles (EVs) are cell-derived structures involved in cell communication and represent a potential minimally invasive alternative to predicting ICI response.^{6–9} Based on this and our preliminary results presented at SITC 2020,¹⁰ we hypothesize that EV PD-L1 predicts response to ICIs in NSCLC.

Methods This study evaluates an exploratory cohort of advanced/metastatic NSCLC patients receiving ICIs (cohort A) and a validation cohort receiving Pembrolizumab+docetaxel or docetaxel alone (PROLUNG Phase 2 randomized trial) (cohort B).¹¹ Plasma samples were collected pre-treatment (T1) and at 3 treatment cycles (T2) (figure 1A). Response was assessed by computed-tomography scan at 3 (cohort A) and 6–8 treatment cycles (cohort B) according to mono- or chemotherapy combination therapy. Patients were classified as responders (partial, stable, or complete response) or non-responders (progressive disease) by RECISTv1.1.¹² EVs were isolated by serial ultracentrifugation and characterized following ISEV recommendations.^{13,14} Tissue PD-L1 expression was measured by standardized immunohistochemistry (SP263, 22C3, or 28–8 clones)⁵ and EV PD-L1 expression by immunoblot and its ratio was calculated as EV PD-L1 T2/T1. Cut-offs from the exploratory cohort were applied to the validation cohort, being EV PD-L1 ratio <0.85 = Low.

Results Paired samples from 30 ICIs, 23 pembrolizumab+docetaxel, and 15 docetaxel treated patients were analyzed. In cohort A, non-responders showed higher EV PD-L1 ratio than responders ($p=0.012$) (figure 1B) with an area-under-the-curve (AUC) of 77.3%, 83.3% sensitivity, and 61.1% specificity, while the tissue PD-L1 was not predictive (AUC=50%). As a validation, pembrolizumab+docetaxel treated non-responders showed higher EV PD-L1 ratio ($p=0.036$) than responders with an AUC=69.3%, sensitivity=75%, and specificity=63.6%, outperforming the tissue PD-L1 (figure 1C). No statistically significant differences were observed in the docetaxel group ($p=0.885$). Moreover, ICIs patients with higher EV PD-L1 ratio showed shorter progression-free survival (PFS) (HR=0.30, $p=0.066$) and overall survival (OS) (HR=0.17, $p=0.016$) (figure 1D) which was also observed in the pembrolizumab+docetaxel cohort with shorter PFS (HR=0.12,

$p=0.004$) and OS (HR=0.23, $p=0.010$) (figure 1E). EV PD-L1 ratio did not predict survival in docetaxel-treated patients.



Abstract 23 Figure 1 (A) Study design and methodology. (B) EV PD-L1 ratio predicts response to ICIs in 30 NSCLC patients from the discovery cohort A and outperforms tissue PD-L1. (C) EV PD-L1 ratio is predictive for response to pembrolizumab+docetaxel in 23 NSCLC patients but not in 15 patients receiving docetaxel alone from cohort B. (D) Higher EV PD-L1 ratio predicts shorter PFS and OS in 30 patients from the discovery cohort A treated with ICIs. (E) Higher EV PD-L1 ratio is associated with shorter PFS and OS in 23 patients treated with pembrolizumab+docetaxel but not in patients treated with docetaxel alone. Abbreviations: CT: Computed tomography, EV: Extracellular vesicle; HR: Hazard Ratio; ICIs: Immune-checkpoint Inhibitors; IHC: Immunohistochemistry; NR: Non-Responders; OS: Overall Survival; p: p-value; PFS: Progression-free survival; R: Responders [Created with BioRender].

Conclusions We demonstrated that treatment-associated changes in EV PD-L1 levels are predictive of response and survival in advanced NSCLC patients treated with ICIs. This model, if confirmed in a large prospective cohort, could have important clinical implications, guiding treatment decisions and improving the outcome of patients receiving ICIs.

Acknowledgements We would like to extend our gratitude to the all the patients that participated in the study.

REFERENCES

- Borghaei H, Paz-Ares L, Horn L, Spigel DR, Steins M, Ready NE, *et al.* Nivolumab versus Docetaxel in Advanced Nonsquamous Non-Small-Cell Lung Cancer. *N Engl J Med* 2015;**373**:1627–39.
- Herbst RS, Baas P, Kim DW, Felip E, Pérez-Gracia JL, Han JY, *et al.* Pembrolizumab versus docetaxel for previously treated, PD-L1-positive, advanced non-small-cell lung cancer (KEYNOTE-010): A randomised controlled trial. *Lancet* 2016;**387**:1540–50.
- Ruiz-Patiño A, Arrieta O, Cardona AF, Martín C, Raez LE, Zatarain-Barrón ZL, *et al.* Immunotherapy at any line of treatment improves survival in patients with advanced metastatic non-small cell lung cancer (NSCLC) compared with chemotherapy (Quijote-CLICaP). *Thorax Cancer* 2020;**11**:353–61.
- Doroshov DB, Bhalla S, Beasley MB, Sholl LM, Kerr KM, Grnjatic S, *et al.* PD-L1 as a biomarker of response to immune-checkpoint inhibitors. *Nat Rev Clin Oncol* 2021;**18**:345–362.
- Hirsch FR, McElhinny A, Stanforth D, Ranger-Moore J, Jansson M, Kulangara K, *et al.* PD-L1 immunohistochemistry assays for lung cancer: results from phase 1

- of the blueprint PD-L1 IHC assay comparison project. *J Thorac Oncol* 2017;**12**:208–222.
6. Poggio M, Hu T, Pai CC, Chu B, Belair CD, Chang A, et al. Suppression of exosomal PD-L1 induces systemic anti-tumor immunity and memory. *Cell* 2019;**177**:414–427.e13.
 7. Cordonnier M, Nardin C, Chanteloup G, Derangere V, Algros MP, Arnould L, et al. Tracking the evolution of circulating exosomal-PD-L1 to monitor melanoma patients. *J Extracell Vesicles* 2020;**9**:1710899.
 8. Del Re M, Cucchiara F, Rofi E, Fontanelli L, Petrini I, Gri N, et al. A multiparametric approach to improve the prediction of response to immunotherapy in patients with metastatic NSCLC. *Cancer Immunol Immunother* 2020;**70**:1667–1678.
 9. Chen G, Huang AC, Zhang W, Zhang G, Wu M, Xu W, et al. Exosomal PD-L1 contributes to immunosuppression and is associated with anti-PD-1 response. *Nature*. 2018;**560**:382–6.
 10. 10 de Miguel Perez D, Russo A, Gunasekaran M, Cardona A, Lapidus R, Cooper B, et al. 31 Dynamic change of PD-L1 expression on extracellular vesicles predicts response to immune-checkpoint inhibitors in non-small cell lung cancer patients. *2020J Immunother Cancer*;8(Suppl 3):A30–A30.
 11. Arrieta O, Barrón F, Ramírez-Tirado LA, Zatarain-Barrón ZL, Cardona AF, Díaz-García D, et al. Efficacy and safety of pembrolizumab plus docetaxel vs docetaxel alone in patients with previously treated advanced non-small cell lung cancer: the PROLUNG phase 2 randomized clinical trial. *2020JAMA Oncol*;6:856–864.
 12. Eisenhauer EA, Therasse P, Bogaerts J, Schwartz LH, Sargent D, Ford R, et al. New response evaluation criteria in solid tumours: Revised RECIST guideline (version 1.1). *2009Eur J Cancer*;45:228–47.
 13. Reclusa P, Verstraelen P, Taverna S, Gunasekaran M, Pucci M, Pintelon I, et al. Improving extracellular vesicles visualization: From static to motion. *2020Sci Rep*;10:6494.
 14. Théry C, Witwer KW, Aikawa E, Alcaraz MJ, Anderson JD, Andriantsitohaina R, et al. Minimal information for studies of extracellular vesicles 2018 (MISEV2018): a position statement of the International Society for Extracellular Vesicles and update of the MISEV2014 guidelines. 2018/*J Extracell Vesicles*;7:1535750

Ethics Approval Patients consented to Institutional Review Board–approved protocol, A.O. Pappardo, Messina, Italy for cohort A and Thoracic Oncology Unit, Instituto Nacional de Cancerología (INCan), México City, México in case of the cohort B. Biological material was transferred to the University of Maryland School of Medicine, Baltimore for EV analysis under signed MTA between institutions MTA/2020–13111 & MTA/2020–13113.

<http://dx.doi.org/10.1136/jitc-2021-SITC2021.023>

NIVOLUMAB SERUM CONCENTRATION IN METASTATIC MELANOMA PATIENTS COULD BE RELATED TO ANTI-TUMOR ACTIVITY GENE AND OUTCOME

¹Domenico Mallardo*, ¹Maria Grazia Vitale, ²Diana Giannarelli, ³Giusy Trillò, ¹Assunta Esposito, ¹Mariaelena Capone, ¹Maria Antonietta Isgrò, ¹Gabriele Madonna, ¹Grazia D'Angelo, ¹Lucia Festino, ¹Vito Vanella, ¹Claudia Trojaniello, ¹Alessandro Manzoni, ⁴Andrew White, ⁴Michael Bailey, ¹Ester Simeone, ¹Corrado Caracò, ¹Piera Maiolino, ¹Nicola Normanno, ⁴Sarah Warren, ¹Ernesta Cavalcanti, ¹Paolo Ascierto. ¹Istituto Nazionale Tumori IRCCS Pascale, Naples, Italy; ²IRCCS Regina Elena, Rome, Italy; ³Università degli studi di Napoli Federico II, Naples, Italy; ⁴NanoString Technologies, Seattle, WA, USA

Background Nivolumab (nivo) is a monoclonal antibody that targets programmed death-1 (PD-1) molecule and has been approved for the treatment of several solid tumors; in the treatment of adjuvant and metastatic melanoma had better efficacy compared with chemotherapy or ipilimumab (anti-CTLA4).¹⁻⁴ The classical dosage of nivo tested in the phase III trials was 3 mg/kg every 2 weeks (Q2W). However, in order to make easier the administration, it was introduced the flat dosage at 240mg every 2 weeks (Q2W) or 480mg every 4 weeks (Q4W).⁵⁻⁶ The purpose of this study was to investigate retrospectively the relationships between the different nivo dosages and their serum concentration; in addition, we also investigated possible relationship with the expression of pro/antitumor activity genes.

Methods From July 2016 to December 2018 at INT IRCCS Pascale, Naples, we collected serum and RNA samples from 88 patients with metastatic melanoma at week 12 from the first administration of nivo. All patients have appropriately signed informed consent. The ORR among the 88 patients was 25% (patients baseline characteristics are listed in table 1). Commercial ELISA assay were performed in 96 well plates following the protocol procedures. Gene expression profiling was performed using NanoString[®] IO360 panels on 37 patients (CR: 4, PR: 10, SD: 11, PD: 12). Statistical analysis was performed through the Student's t-test and via Spearman's rho correlation coefficient. Gene profiling analysis was performed via Bonferroni correction.

Results We observed that patients with complete response (CR) have a higher nivo concentration ($p=0.003$) compared to other groups. No correlation was observed with the most important markers of renal and hepatic function: eGFR, creatinine, AUC, albumin, ALT, AST and gamma GT. Data from gene expression profile shown that patients with CR had a higher expression of anti-tumor and immune activation genes such as: TAPBP, CD47, HDC, IL12RB2 and HLA-DQA1 ($P < 0.05$). Furthermore, genes with pro-tumor or immunosuppressive activity such as MMP9, GOR160, HK2 and LILRA5 ($P < 0.05$) were found to be inversely related with drug concentration while CD1C, a T-cell surface glycoprotein involved in antigen-presenting, it is directly related ($p=0.005$).

Conclusions In this retrospective study we found that higher serum concentration of nivo was correlated with a better outcome and higher frequency of CR. Moreover, in patients with a CR there was an enhancing of the immune activation with an increase of HLA-DQA, TAPBP and IL12RB2. Further investigations are needed to get additional information.

Acknowledgements The study was supported by the Institutional Project 'Ricerca Corrente' of Istituto Nazionale Tumori IRCCS Fondazione 'G. Pascale' of Napoli, Italy.

Abstract 24 Table 1 Patients clinical parameters

Table 1. patients clinical parameters.

Patients Characteristic	N = 88
Median age	60 (range 27-91)
Gender: female/male, n (%)	45 (51)/43(49)
Melanoma AJCC Stage 8 ed.	
Stage IV, n (%)	84 (96)
Stage IIIC, n (%)	3 (3)
Stage IIIB, n (%)	1 (1)
CNS metastases at baseline, n (%)	25 (22)
BRAF Status	
Wilde type, n (%)	57 (65)
Mutation, n (%)	26 (29)
NA, n (%)	5 (6)
BMI	
Normal weight ($18.5 < \text{BMI} \leq 24.9$), n (%)	24 (27)
Overweight ($25 < \text{BMI} \leq 29.9$), n (%)	36 (41)
Obese ($\text{BMI} \geq 30$), n (%)	28 (32)
Response rate at 1° assessment	
Complete response (CR), n (%)	6 (7)
Partial response (PR), n (%)	16 (18)
Stable disease (SD), n (%)	30 (34)
Progression disease (PD), n (%)	36 (41)
Nivolumab dosage	
Flat dose 240 mg, n (%)	11 (12)
Flat dose 480 mg, n (%)	19 (22)
Dose 3 mg /Kg, n (%)	58 (66)
LDH level	
High	30 (34)
Normal	33 (38)
NA	25 (28)

REFERENCES

- James Larkin, Vanna Chiarion-Sileni, Rene Gonzalez *et al.* Combined nivolumab and ipilimumab or monotherapy in untreated melanoma. *N Engl J Med* 2015 Jul 2;**373**(1):23–34.
- Robert C, Long GV, Brady B *et al.* Nivolumab in previously untreated melanoma without BRAF mutation. *N Engl J Med* 2015 Jan 22;**372**(4):320–30.
- Weber JS, D'Angelo SP, Minor D *et al.* Nivolumab versus chemotherapy in patients with advanced melanoma who progressed after anti-CTLA-4 treatment (CheckMate 037): a randomised, controlled, open-label, phase 3 trial. *Lancet Oncol* 2015 Apr;**16**(4):375–8.

4. Weber J, Mandala M, Del Vecchio M, Gogas HJ, Arance AM, Cowey CL, Dalle S, Schenker M, Chiarion-Sileni V, Marquez-Rodas I et al. CheckMate 238 Collaborators. Adjuvant nivolumab versus ipilimumab in resected stage III or IV melanoma. *N Engl J Med* 2017 Nov 9;**377**(19):1824–1835.
5. Zhao X, Suryawanshi S, Hruska M et al. Assessment of nivolumab benefit-risk profile of a 240-mg flat dose relative to a 3-mg/kg dosing regimen in patients with advanced tumors. *Ann Oncol* 2017 Aug 1;**28**(8):2002–2008.
6. Long GV, Tskodi SS, Schneider JG et al. Assessment of nivolumab exposure and clinical safety of 480?mg every 4 weeks flat-dosing schedule in patients with cancer. *Ann Oncol* 2018 Nov 1;**29**(11):2208–2213.

Ethics Approval The study was approved by the internal ethics board of the Istituto Nazionale Tumori IRCCS Fondazione ‘G. Pascale’ of Napoli Italy, approval number of registry 33/17 OSS.

Consent Written informed consent was obtained from the patient for publication of this abstract and any accompanying images. A copy of the written consent is available for review by the Editor of this journal.

<http://dx.doi.org/10.1136/jitc-2021-SITC2021.024>

25 **POTENTIAL ROLE OF SERUM PROTEOME IN PREDICTING IMMUNE-RELATED ADVERSE EVENTS FROM IMMUNOTHERAPY IN NON-SMALL CELL LUNG CANCER**

¹Leeseul Kim*, ²Young Kwang Chae, ²Dong-Uk Lee. ¹AMITA health Saint Francis Hospital Evanston, Chicago, IL, USA; ²Developmental Therapeutics Northwestern Medicine, Chicago, IL, USA

Background Predicting immune-related adverse events (irAEs) in early stage is being emphasized even more. Host response to disease is reflected in serum proteome level and that allows serum proteome level as a new marker to explore response to immunotherapy. With the help of a serum-based proteomics test, Primary Immune Response (PIR), we are accessing the correlations between developing irAEs and immunotherapy in non-small cell lung cancer (NSCLC) patients.

Methods Data of 48 consented NSCLC patients with baseline PIR test done within one week prior to the start of immunotherapy were collected. Samples were grouped into either sensitive or intermediate/resistant (not sensitive) by PIR classification. We analyzed the durations from the immunotherapy initiation to the first episode of irAE. IrAEs were graded according to Common Terminology Criteria for Adverse Events (CTCAE) v5.0.

Results Among the 48 NSCLC patients, 19 patients (39%) experienced one or more irAEs with the majority classified as either grade 1 (n=7, 36%) or grade 2 (n=10, 52%). PIR-sensitive group showed no difference in irAE free period compared to PIR-not sensitive (p=0.92, HR=0.95, 95% CI=0.3212 to 2.834). The median 'Time to first irAE' were undefined and 24 in PIR-sensitive and PIR-not sensitive, respectively.

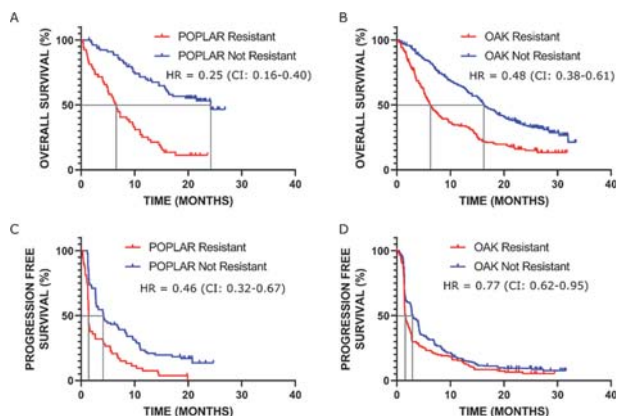
Conclusions Our results demonstrated PIR-sensitive patients are not likely to tolerate immunotherapy longer without developing irAEs.

<http://dx.doi.org/10.1136/jitc-2021-SITC2021.025>

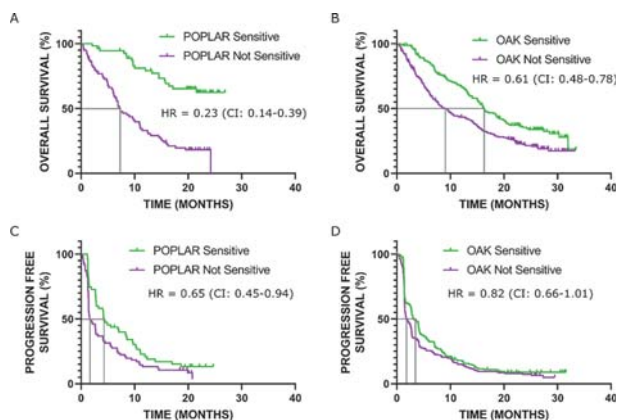
VALIDATION OF THE PRIMARY IMMUNE RESPONSE (PIR) TEST IN ADVANCED NON-SMALL CELL LUNG CANCER (NSCLC): BLINDED RETROSPECTIVE ANALYSES FROM THE POPLAR AND OAK TRIALS

¹Heinrich Roder*, ¹Laura Maguire, ¹Senait Asmellash, ¹Steven Rightmyer, ¹Patrick Norman, ²Mark McClelland, ³Wei Zou, ³Minu Srivastava, ¹Lelia Net, ¹Thomas Campbell, ³David Shames, ¹Robert Georgantas, ¹Joanna Roder. ¹Biodesix, Inc., Boulder, CO, USA; ²Former employee of Genentech, South San Francisco, CA, USA; ³Genentech, South San Francisco, CA, USA

Background Biomarkers of immune checkpoint inhibitor (ICI) efficacy can be used for patient selection. PD-L1 expression in tumor tissue is used to determine eligibility for combination or monotherapy in 1st line NSCLC.^{1, 2} The liquid-biopsy mass spectrometry-based PIR test was developed to capture the role of patient biology on ICI outcomes.³ The test, stratifying patients into Resistant, Intermediate, and Sensitive groups, was associated with outcome on nivolumab treatment in 2nd line NSCLC patients.³ In this study, we blind validated PIR classifications in two large clinical studies (POPLAR⁴ and OAK⁵) of advanced NSCLC patients treated in the second or third line with atezolizumab.



Abstract 23 Figure 1 Kaplan-Meier plots of OS and PFS by test classification Resistant vs Not Resistant for the POPLAR and OAK cohorts



Abstract 23 Figure 2 Kaplan-Meier plots of OS and PFS by test classification Not Sensitive vs Sensitive for the POPLAR and OAK cohorts

Methods Pretreatment serum samples from patients assigned to receive atezolizumab in the two studies (POPLAR (NCT01903993) and OAK (NCT02008227)) underwent PIR testing blinded to all clinical data. Association of test classification, as Sensitive vs Not Sensitive (Resistant+Intermediate) and Resistant vs Not Resistant (Sensitive+Intermediate), with overall survival (OS) and progression-free survival (PFS) was investigated using Cox proportion hazards models in univariate and multivariate analysis.

Results PIR classifications were generated for 133 (POPLAR) and 403 (OAK) samples; the remaining available samples failed test QC, mainly due to hemolysis. PIR classified the POPLAR samples as 53 (40%) Resistant, 25 (19%) Intermediate, 55 (41%) Sensitive and the OAK samples as 154 (38%) Resistant, 89 (22%) Intermediate, and 160 (40%) Sensitive. In both cohorts, OS and PFS were better in the Not Resistant vs Resistant group (figure 1). OS and PFS were superior in the Sensitive vs Not Sensitive group in the POPLAR cohort, while OS was better and PFS showed indications of superiority in the OAK cohort (figure 2). Multivariate analysis within the OAK cohort showed that test classification predicted OS when adjusted for baseline factors, including PD-L1 negative vs positive, with hazard ratio 0.51 (95% confidence interval (CI) 0.40–0.65) for Resistant vs Not Resistant and 0.65 (CI: 0.50–0.83) for Sensitive vs Not Sensitive.

Conclusions The PIR test stratified outcomes for patients treated with atezolizumab in second and third line NSCLC even when adjusted for PD-L1 expression. The combination of both tumor and host biomarkers appears to provide a more specific prognosis of NSCLC treated with ICIs.

Trial Registration clinicaltrials.gov NCT01903993 and NCT02008227

REFERENCES

- Roy S Herbst, Giuseppe Giaccone, Filippo de Marinis et al. Atezolizumab for first-line treatment of PD-L1-selected patients with NSCLC. *N Engl J Med* 2020 Oct 1;**383**(14):1328–1339
- Tony S K Mok, Yi-Long Wu, Iveta Kudaba et al. Pembrolizumab versus chemotherapy for previously untreated, PD-L1-expressing, locally advanced or metastatic non-small-cell lung cancer (KEYNOTE-042): a randomised, open-label, controlled, phase 3 trial. *Lancet* 2019 May 4;**393**(10183):1819–1830.
- Muller M, Hummelink K, Hurkmans D, et al. A serum protein classifier identifying patients with advanced non-small cell lung cancer who derive clinical benefit from treatment with immune checkpoint inhibitors. *Clin Cancer Res* 2020;**26**(19):5188–5197.
- Fehrenbacher L, Spira A, Ballinger M, et al. Atezolizumab versus docetaxel for patients with previously treated non-small-cell lung cancer (POPLAR): a multicentre, open-label, phase 2 randomised controlled trial. *Lancet* 2016;**387**(10030):1837–1846.
- Rittmeyer A, Barlesi F, Waterkamp D, et al. Atezolizumab versus docetaxel in patients with previously treated non-small-cell lung cancer (OAK): a phase 3, open-label, multicenter randomized controlled trial. *Lancet* 2017;**389**(10066):255–265.

Ethics Approval The OAK study was done in 194 academic medical centers and community oncology practices across 31 countries worldwide. The study was done in full accordance with the guidelines for Good Clinical Practice and the Declaration of Helsinki. All patients gave written informed consent. The POPLAR trial was done at 61 academic medical centers

and community oncology practices across 13 countries in Europe and North America. The study was done in full accordance with the guidelines for Good Clinical Practice and the Declaration of Helsinki. Protocol (and modification) approval was obtained from an independent ethics committee for each site. Patients gave written informed consent.

<http://dx.doi.org/10.1136/jitc-2021-SITC2021.026>

CYTOKINE SIGNATURE OF PD-1, CXCL10, AND TNF-ALPHA PREDICTS RESPONSE TO NIVOLUMAB AND IPILIMUMAB

¹Jesper Pedersen*, ¹Mateo Sokac, ¹Nicolai Birkbak, ²Trine Øllegaard, ¹Martin Jakobsen. ¹Aarhus University, Aarhus, Denmark; ²Aarhus University Hospital, Aarhus, Denmark

Background Checkpoint inhibitors have significantly improved treatment of metastatic melanoma. Yet, 40–60% of the patients do not achieve a long-term benefit from such immunotherapy. Thus, there is an urgent need to identify biomarkers that can predict response to immunotherapy to guide patients for the best possible treatment. Here, we evaluate an unsupervised machine learning approach to identify potential cytokine signatures from liquid biopsies that predict response to immunotherapy in melanoma.

Methods Blood samples were drawn from 74 patients diagnosed with unresectable advanced-stage melanoma undergoing treatment with first-line nivolumab/ipilimumab or pembrolizumab between August 2017 – July 2019 at Aarhus University Hospital, Denmark. Blood samples were tested for plasma levels of PD-1, PD-L1, IFN-beta, IFN-gamma, CCL20, CXCL5, CXCL10, IL6, IL8, IL10, MCP1, and TNF-alpha by Meso Scale ELISA assays. Healthy controls were used to compare general cytokine levels in plasma. A bioinformatic workflow consisting of Uniform Manifold Approximation and Projection (UMAP) dimension reduction method and k-means clustering analysis was applied to define clusters based on the cytokine profile, followed by survival analysis of the clusters.

Results UMAP analysis demonstrated that the cytokine profile at baseline was similar for healthy controls and patients, regardless of treatment. Upon treatment initiation, the cytokine profile changed in a treatment-dependent way to be significantly different between patient groups. Clustering defined by the cytokine profile measured early during treatment in nivolumab/ipilimumab treated patients identified two clusters associated with superior progression-free survival (PFS) (log-rank $p=0.018$). We identified that these cluster were characterized by significantly higher levels of PD-1, CXCL10, and TNF-alpha. UMAP analysis of the cytokine level as fold change over baseline level, confirmed that nivolumab/ipilimumab patients with superior PFS were characterized by higher levels of PD-1, CXCL10, and TNF-alpha. Cox regression analysis revealed high fold change of PD-1 as a strong predictor for superior PFS (HR=0.29; 95% CI 0.12–0.66; $p=0.0032$). However, a similar cytokine profile was not associated to superior PFS in patients receiving pembrolizumab, suggesting that the cytokine signature is specific for nivolumab/ipilimumab treatment.

Conclusions Using unsupervised machine learning we identified a cytokine signature of high PD-1, CXCL10, and TNF-alpha to be associated with superior PFS in advanced-stage melanoma patients treated with nivolumab/ipilimumab but not pembrolizumab, with high fold change of PD-1 being a strong individual predictor for PFS.

Acknowledgements We thank the medical laboratory technicians who collected blood samples and the patients who participated in the study.

Ethics Approval The study was approved by Central Denmark Region Committees on Biomedical Research Ethics, approval number 1-10-72-374-15.

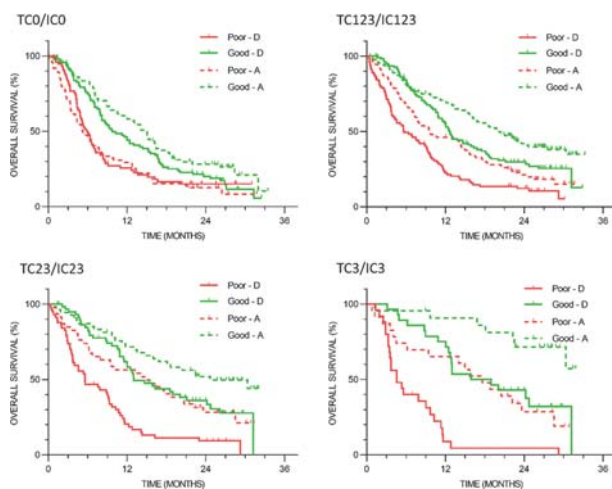
<http://dx.doi.org/10.1136/jitc-2021-SITC2021.027>

PREDICTIONS OF OUTCOMES AND BENEFIT OF IMMUNE CHECKPOINT INHIBITOR TREATMENT IN NSCLC REQUIRE INFORMATION ON BOTH TUMOR AND HOST BIOLOGY

¹Joanna Roder*, ¹Thomas Campbell, ¹Senait Asmellash, ¹Steven Rightmyer, ¹Patrick Norman, ¹Robert Georgantas, ²Mark McClelland, ³Wei Zou, ⁴Minu Srivastava, ¹Lelia Net, ¹Laura Maguire, ¹Heinrich Roder, ³David Shames. ¹Biosix, Boulder, CO, USA; ²Former employee of Genentech, South San Francisco, CA, USA; ³Genentech, South San Francisco, CA, USA

Background Immunotherapy has become a key element in the arsenal of treatments for advanced non-small cell lung cancer (NSCLC). The anti-PD-L1 Response Test (ART), based on mass spectrometry of pretreatment serum, captures the effect of host biology on outcomes after atezolizumab (A) therapy. It stratified outcomes on A and was predictive of benefit of A over docetaxel (D) in a blinded, retrospective study of 2nd and 3rd line NSCLC patients in the POPLAR Ph2 clinical study.¹ Our current work applies the test to the larger OAK NSCLC Ph3 clinical study² to investigate the interplay between tumor PD-L1 expression and ART classifications in predicting outcomes and benefit from A therapy.

Methods Pretreatment serum samples from 823 of the 850 patients in the OAK study (NCT02008227) were analyzed with ART blinded to all clinical data. The ART assigns a result of Good or Poor corresponding to better or worse outcomes on A. Association of test classification with overall survival (OS) within and between treatment arms was investigated using Cox proportion hazards models overall and within PD-L1 subgroups defined by SP142 assay.³



Abstract 28 Figure 1 Kaplan-Meier plots of OS by test classification, Good and Poor, and treatment arm, A and D, within PD-L1 subgroups

Abstract 28 Table 1 Hazard ratios between A and D by test classification group and PD-L1 subgroup

PD-L1 subgroup	Poor Classification Subgroup HR (CI)	Good Classification Subgroup HR (CI)
TC=0 and IC=0	1.12 (0.79-1.59)	0.74 (0.53-1.04)
TC=1/2/3 or IC=1/2/3	0.63 (0.46-0.85)	0.67 (0.49-0.93)
TC=2/3 or IC=2/3	0.46 (0.30-0.73)	0.57 (0.35-0.94)
TC=3 or IC=3	0.31 (0.16-0.62)	0.30 (0.12-0.72)

Results Test classifications were generated for 786 (96%) samples; the remaining samples failed test QC, mainly due to hemolysis. A Good classification was assigned to 359 (46%) samples and a Poor classification to 427 (54%) samples. Overall, OS was better for the Good subgroup than the Poor subgroup within both arms, arm A (hazard ratio (HR)=0.52 (95% Confidence Interval (CI): 0.41–0.66)) and arm D (HR=0.54 (CI:0.43–0.68)). The test was not predictive of benefit of A over D, but was prognostic for both A and D. Patients classified as Good had better outcomes than those classified as Poor in both treatment arms for all PD-L1 subgroups investigated (figure 1). Benefit of A vs D was found in both test classification groups for PD-L1 positive patients (table 1).

Conclusions Information on both tumor and host are essential to predict outcomes of immunotherapy and chemotherapy in NSCLC patients.

Trial Registration ClinicalTrials.gov NCT02008227

REFERENCES

- Kowanetz M, Leng N, Roder J, et al. Evaluation of immune-related markers in the circulating proteomic and their association with atezolizumab efficacy in patients with 2L+ NSCLC. *J Immunother Cancer* 2018;**6**(Suppl1):114.
- Rittmeyer A, Barlesi F, Waterkamp D, et al. Atezolizumab versus docetaxel in patients with previously treated non-small-cell lung cancer (OAK): a phase 3, open-label, multicenter randomized controlled trial. *Lancet* 2017;**389**(10066):255–265.
- Herbst R, Giaccone G, de Marinis F, et al. Atezolizumab for first-line treatment of PD-L1-selected patients with NSCLC. *N Engl J Med* 2020;**383**:1328–1339.

Ethics Approval The OAK study (NCT02008227) was done in 194 academic medical centres and community oncology practices across 31 countries worldwide. The study was done in full accordance with the guidelines for Good Clinical Practice and the Declaration of Helsinki. All patients gave written informed consent.

<http://dx.doi.org/10.1136/jitc-2021-SITC2021.028>

ELEVATED FLT3L PREDICTS LONG-TERM SURVIVAL IN PATIENTS WITH HIGH-GRADE GASTROENTEROPANCREATIC NEUROENDOCRINE NEOPLASMS

¹Katharina Detjen, ²Raik Otto, ¹Yvonne Giesecke, ¹Lukas Geisler, ¹Pamela Riemer, ¹Henning Jann, ¹Carsten Grötzinger, ¹Christine Sers, ³Tom Luedde, ²Ulf Leser, ¹Bertram Wiedenmann, ¹Michael Sigal, ¹Frank Tacke, ³Christoph Roderburg, ¹Linda Hammerich*. ¹Charité Universitätsmedizin Berlin, Berlin, Germany; ²Humboldt-Universität zu Berlin, Berlin, Germany; ³University Hospital Düsseldorf, Duesseldorf, Germany

Background Gastroenteropancreatic neuroendocrine neoplasms (GEP-NEN) are a rare and heterogeneous family of tumors arising from the disseminated neuroendocrine system of the gastrointestinal tract and pancreas. Clinical management of high-grade GEP-NEN is challenging due to disease heterogeneity, illustrating the need for reliable biomarkers facilitating patient stratification and guiding treatment decisions. FMS-like tyrosine kinase 3 ligand (Flt3L) is emerging as a prognostic or predictive surrogate marker of host tumoral immune response and might enable stratification of patients with otherwise comparable tumor features.

Methods We used RNAseq data from human foregut-derived pancreatic and gastric GEP-NEN to evaluate Flt3L gene expression in tumor tissue. The data set (n=54) represented the full range of NEN grades and differentiation, and expression levels were compared to healthy control tissue as well. We also analyzed circulating Flt3L levels in serum samples of a separate cohort of G2/G3 GEP-NEN (n=59) and healthy controls (n=4). The study was approved by the local ethics committee at Charité Universitätsmedizin Berlin, Germany (ethical approval number EA1/229/17) and patient informed consent was obtained.

Results We detected a prominent induction of Flt3L gene expression in individual G2 and G3 NEN, but not in G1 neuroendocrine tumors (NET). Flt3L mRNA expression levels in tumor tissue predicted disease related survival of patients with highly proliferative G2 and G3 NEN more accurately than the conventional criteria of grading or NEC/NET differentiation. High level Flt3L mRNA expression was associated with increased expression of genes related to immunogenic cell death, lymphocyte effector function and dendritic cell maturation, suggesting a less tolerogenic (more proinflammatory) phenotype of tumors with Flt3L induction. Importantly, circulating levels of Flt3L were also elevated in high grade NEN and correlated with patients' progression-free and disease-related survival, thereby reflecting the results observed in tumor tissue.

Conclusions Our results suggest Flt3L as a surrogate marker of an inflammatory tumor microenvironment. Therefore, we propose Flt3L as a prognostic biomarker for high grade GEP-NEN. Flt3L measurements in serum, which can be easily be incorporated into clinical routine, may hold the promise to guide patient stratification and tailor treatment decisions and should be further evaluated, especially in the context of immunotherapies.

Ethics Approval The study was approved by the local ethics committee at Charité Universitätsmedizin Berlin, Germany (ethical approval number EA1/229/17) and patient informed consent was obtained.

<http://dx.doi.org/10.1136/jitc-2021-SITC2021.029>

BLOOD-BASED GLYCOPROTEIN SIGNATURES IN ADVANCED NON-SMALL-CELL LUNG CARCINOMA (NSCLC) RECEIVING FIRST-LINE IMMUNE CHECKPOINT BLOCKADE

¹Klaus Lindpaintner*, ²Michael Cheng, ³Jillian Prendergast, ³Karl Normington, ¹Maurice Wong, ¹Gege Xu, ¹Xini Cong, ¹Rachel Rice, ²Marissa Lawrence, ²Kesi Michael, ¹Daniel Serie. ¹InterVenn, Concord, NH, USA; ²DFCI, Boston, MA, USA; ³Palleon, Waltham, MA, USA

Background Immune checkpoint blockade is an integral component of first-line therapy for most patients with advanced non-small cell lung cancer (NSCLC), however individual patient outcomes are highly variable and improved biomarkers are needed. Protein glycosylation is an emerging mechanism of immune evasion in cancer. We examined blood-based glycopeptide signatures in a cohort of advanced NSCLC patients treated with first-line immune checkpoint blockade.

Methods Pretreatment blood samples were obtained from 46 advanced NSCLC patients treated with first line pembrolizumab or pembrolizumab + carboplatin + pemetrexed. All patients provided written informed consent to the institutional review board-approved protocols (#02-180 and 13-367) at the Dana-Farber/Harvard Cancer Center (Boston, MA), and the study was conducted in accordance with the Declaration of Helsinki. Samples were analyzed using an advanced glycoproteomics platform (Inter-Venn Biosciences) that combines ultra-high-performance liquid chromatography coupled to triple quadrupole mass spectrometry with a proprietary neural-network-based data processing engine. 409 individual glycopeptide (GP) signatures derived from 67 abundant serum proteins were analyzed and correlated with overall survival (OS) and other clinical outcomes.

Results We identified 30 GPs with abundance differences using a False Discovery Rate (FDR) threshold of 0.05. Using the 5 most predictive GP markers, we created a multivariable model for OS by generating leave-one-out cross-validation (LOOCV) scores and determining an optimized cutoff value of -0.83 (range: -2.2 - 3.4) for these scores using Harrell's concordance index. The median overall survival was 2.8 years for patients (n=14) whose GP classifier value was above the cutoff and 0.8 years for patients (n=32) whose GP classifier value was below the cutoff (HR 7.4, 95% CI 1.7-32.1, p=0.007) The model's performance was not affected by sex, age, or treatment regimen.

Conclusions Blood-based glycopeptide signatures may represent novel, non-invasive biomarkers of clinical outcome to first-line immune checkpoint blockade in advanced NSCLC. Additional research is needed to validate these findings in larger cohorts and to explore potential applications relevant to clinical decision-making.

Ethics Approval The study obtained ethics approval from the institutional review board (approved protocol #02-180 and 13-367) at the Dana-Farber/Harvard Cancer Center (Boston, MA), and the study was conducted in accordance with the Declaration of Helsinki.

Consent All patients provided written informed consent to the institutional review board-approved protocols (#02-180 and 13-367) at the Dana-Farber/Harvard Cancer Center (Boston, MA), and the study was conducted in accordance with the Declaration of Helsinki.

<http://dx.doi.org/10.1136/jitc-2021-SITC2021.030>

SERUM LAG-3 IS ASSOCIATED WITH IMPROVED PATIENT PROGNOSIS IN HIGH GRADE SEROUS OVARIAN CANCER

¹Nicole James*, ¹Katrin Eurich, ¹Erin Lips, ²Payton De La Cruz, ¹Morgan Woodman, ¹Jennifer Ribeiro. ¹Women and Infants Hospital, Providence, RI, USA; ²Brown University, Providence, RI, USA

Background High grade serous ovarian cancer (HGSOC) is a lethal gynecologic malignancy with a five-year survival rate of only 39 percent.¹ Despite the fact that ovarian tumors are considered immunologic, HGSOC patients respond poorly to PD-1 based immunotherapy. Hence, the need to identify novel prognostic and therapeutic immunologic factors is crucial. Our previous investigation uncovered intratumoral levels of immune co-inhibitory receptor LAG-3 as a marker of improved HGSOC patient survival. For this current study we sought to evaluate the prognostic utility of serum-based LAG-3, as well as determine how these circulating levels change in response to HGSOC standard of care therapy.

Methods This study was approved by the Women and Infants Institutional Review Board; approval number 1057626. HGSOC serum samples were obtained from the Department of Special Testing and the Program in Women's Oncology Gynecologic Tissue Bank at Women and Infants Hospital. A total of 43 HGSOC treatment naïve serum samples were tested for serum LAG-3 and in 20 of these patients, samples from on- and post- frontline platinum-based chemotherapy were also analyzed. A commercially available ELISA kit was employed to detect serum LAG-3.

Results There was no statistically significant change in pre-, on-, and post- serum LAG-3 levels following frontline chemotherapy, however median levels of LAG-3 decreased once patients initiated therapy and remained stable post-treatment. Spearman Rank Correlation analysis revealed a significant relationship between progression-free survival (PFS) and pre-treatment serum LAG-3 levels ($r=0.36$, $p=0.017$). Furthermore, it was found that patients with a PFS of 6 months or less exhibited a significantly ($p=0.0031$) lower mean rank of pre-treatment serum LAG-3 levels, compared to patients with a PFS of 18 months or longer. Finally, Kaplan Meier curve analysis revealed a statistically significant association between longer patient PFS and higher pre-treatment LAG-3 concentrations, when stratified by both median ($HR=0.4916$, \log -rank $p=0.022$) and quartile LAG-3 serum levels ($HR=0.2679$, \log -rank $p=0.0031$).

Conclusions This study demonstrates for the first time that circulating immune checkpoint receptors have prognostic capabilities in ovarian cancer. Our findings suggest that LAG-3 is a marker for improved patient PFS. Future directions include an expansion of this original cohort in order to validate and further assess the clinical prognostic utility of serum LAG-3 in HGSOC.

REFERENCE

1. Survival Rates for Ovarian Cancer, American Cancer Society, [<https://www.cancer.org/cancer/ovarian-cancer/detection-diagnosis-staging/survival-rates.html>]

<http://dx.doi.org/10.1136/jitc-2021-SITC2021.031>

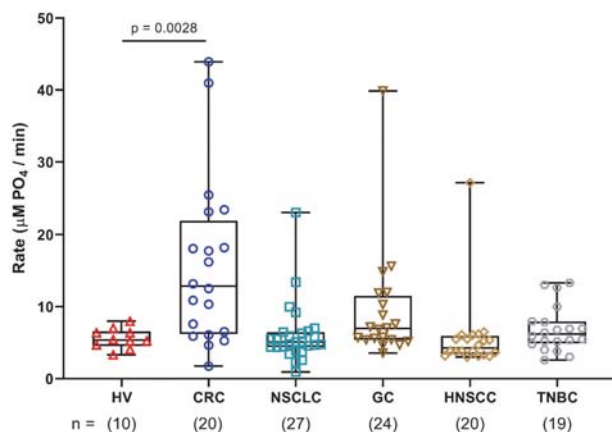
32

MEASURING SOLUBLE CD73 ACTIVITY IN HIGH CONCENTRATIONS OF HUMAN PLASMA TO ASSESS PHARMACODYNAMICS OF CD73 INHIBITORS

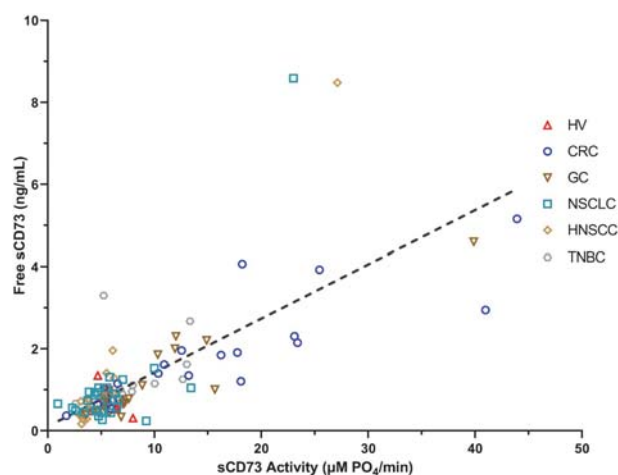
Rick Sorensen*, Marianna Zavodovskaya, Ping Cheng Yi, Michael Lee, Audrey Goddard, Matthew Peach. *Gilead Sciences, Seattle, WA, USA*

Background Inhibiting ecto-5'-nucleotidase (CD73) to reduce immunosuppressive adenosine in the tumor microenvironments is an anti-tumor strategy currently explored in clinical trials. Measuring soluble CD73 (sCD73) activity in plasma to evaluate pharmacodynamics of CD73 inhibitors is appealing. Quantifying phosphate in plasma after adding exogenous adenosine monophosphate (AMP) can be used to determine sCD73 activity.¹ Maintaining high plasma concentration to prevent dilution of endogenous sCD73 when quantifying its activity is desirable. High protein concentrations in plasma, however, can affect accurate phosphate quantitation. By precipitating plasma proteins prior to phosphate quantitation, we developed and qualified a method to determine sCD73 activity in 95% plasma.

Methods Platelet poor heparinized plasma (PPP), AMP, tissue nonspecific alkaline phosphatase inhibitor (TNAPi), recombinant CD73, malachite green, adenosine 5'- (α , β -methylene) diphosphate (APCP), and recombinant alkaline phosphatase (ALP) were procured commercially. sCD73 concentrations were measured by ELISA and total protein concentration was quantified by BCA. sCD73 activity was measured by combining PPP, TNAPi, and AMP at 37°C. Reactions were terminated with trichloroacetic acid (TCA) at various timepoints to generate a kinetic readout. After protein precipitation, phosphate concentrations were measured by malachite green and enzymatic rates calculated as change in free phosphate concentration per minute.



Abstract 32 Figure 1a sCD73 activity in HV and cancer patient plasma. sCD73 activity in patient plasma from healthy volunteers and solid tumor indications. Abbreviations: HV, healthy volunteer; CRC, colorectal cancer; NSCLC, non-small cell lung cancer; GC, gastric cancer; HNSCC, head and neck squamous cell carcinoma; TNBC, triple-negative breast cancer.



Abstract 32 Figure 1b sCD73 activity correlates to sCD73 concentration. Correlation of plasma sCD73 activity and free sCD73 concentrations in patient plasma from healthy volunteers and solid tumor indications. Spearman correlation: $r = 0.75$, $p < 0.0001$, $n = 135$. Abbreviations: HV, healthy volunteer; CRC, colorectal cancer; NSCLC, non-small cell lung cancer; GC, gastric cancer; HNSCC, head and neck squamous cell carcinoma; TNBC, triple-negative breast cancer.

Abstract 32 Table 1 Plasma sCD73 activity assay qualification limits

Parameter	Result
Range	1.09 – 133 $\mu\text{M PO}_4/\text{min}$
Limits	LOD: 0.74 $\mu\text{M PO}_4/\text{min}$ LLOQ: 1.09 $\mu\text{M PO}_4/\text{min}$ ULOQ: 133 $\mu\text{M PO}_4/\text{min}$
Precision	Intra-assay: 4.33 – 17.2 %CV Inter-assay: 10.2 – 18.4 %CV
Freeze/Thaw stability (80% - 120% expected)	4 Freeze/Thaw cycles: 90.2% – 108.0%
Parallelism (80% - 120% expected)	92.6% - 112.5%
Specificity (maximum inhibition by APCP)	APCP: 93.7% - 103.1%
Plasma stability	3 hours at room temperature
Phosphate stability	164 hours at 4°C
Longitudinal variation (Day 1 and Day 8)	1.1 – 12.5 %CV

Results Incubating TCA-terminated reaction mixtures at 4°C for ≥ 3 hours reduced protein in supernatants to below lower limits of quantitation and eliminated interference in phosphate detection. Plasma sCD73 activity was dependent on AMP concentrations ($K_m = 612 \mu\text{M}$), proportional to sCD73 in the sample and could be fully inhibited by APCP. 500 μM TNAPi, an inhibitor of non-CD73 AMPase activity, fully blocked 670 IU/L of recombinant human ALP activity. sCD73 activity in PPP from colorectal carcinoma (CRC) patients was higher ($p = 0.0028$) than in healthy volunteers (HV). sCD73 activity in some individuals with gastric cancer (GC), non-small cell lung cancer (NSCLC), and triple-negative breast cancer (TNBC) were also numerically higher than in healthy volunteers (figure 1a). sCD73 activity was correlated to sCD73 concentrations in these samples (figure 1b). The method was qualified for use in clinical studies (table 1).

Plasma sCD73 activity assay characterization and fit-for-purpose qualification. Abbreviations: LOD, limit of detection; LLOQ, lower limit of quantitation; ULOQ, upper limit of quantitation; APCP, adenosine 5'- (α , β -methylene) diphosphate.

Conclusions A method to quantify sCD73 activity in 95% plasma to evaluate pharmacodynamics of CD73 inhibitors in clinical samples was developed and qualified. Plasma sCD73 activity was dependent on AMP concentration and inhibited by APCP. Plasma sCD73 activity was significantly elevated in CRC patients and selected patients with GC, NSCLC, and TNBC and was proportional to sCD73 concentration.

REFERENCE

1. Morello S, Capone M, Sorrentino C, Giannarelli D, Madonna G, Mallardo D, Grimaldi AM, Pinto A, Ascierto PA. Soluble CD73 as biomarker in patients with metastatic melanoma patients treated with nivolumab. *J Transl Med* 2017 Dec 4;15(1):244. doi: 10.1186/s12967-017-1348-8. PMID: 29202855; PMCID: PMC5716054.

<http://dx.doi.org/10.1136/jitc-2021-SITC2021.032>

33 DEVELOPMENT OF A CLINICAL *EX VIVO* ASSAY FOR THE ASSESSMENT OF THERAPEUTIC CD28 COSTIMULATORY PATHWAY ENGAGEMENT

Chelsea Gudgeon*, Mark Maurer, Gary Means, Sherri Mudri, Lori Blanchfield, Jing Yang, Stacey Dillon, Pamela Holland, Zelanna Goldberg, Stanford Peng. *Alpine Immune Sciences, Inc., Seattle, WA, USA*

Background Preclinical evidence supports combining checkpoint inhibition (CPI) with T cell costimulatory agonism to improve the breadth and durability of anti-tumor responses relative to CPI alone. Currently, there are a number of therapeutic approaches combining costimulatory receptor agonists (e.g. CD28, 4-1BB, OX40L, etc.) with tumor targeting agents and/or CPI. Identification of a pharmacodynamically-justified therapeutic dose can be challenging because traditional duration of target occupancy does not necessarily correlate with immunological activity in the case of costimulatory molecules, and an ‘always on’ dose risks immune exhaustion. ALPN-202, a variant CD80 vIgD-Fc fusion protein that mediates PD-L1-dependent CD28 costimulation and inhibits the PD-L1 and CTLA-4 checkpoints, is in development for the treatment of multiple advanced malignancies. To assess clinical CD28 agonism in the context of ALPN-202 treatment, we developed a novel, *ex vivo* whole blood target-dependent costimulation (TDC) assay.

Methods A TDC assay was developed using clinical samples from NEON-1 (NCT04186637), an ongoing dose escalation and expansion clinical trial of ALPN-202 for patients with advanced malignancies. The assay uses patient blood stimulated with paraformaldehyde-fixed, artificial antigen presenting cells (aAPC) expressing both cell-surface anti-CD3 and PD-L1. Pre-dose and end-of-infusion (EOI) blood was drawn from trial participants and co-cultured for 24 hours with the aAPCs in a pre-made assay plate. Plasma was collected and secreted IL-2 was quantified and used as a measure of PD-L1-dependent CD28 costimulation. Nonlinear regression was used to calculate area under the curve (AUC) for each condition, and sample AUC values were compared to a positive control (pre-dose blood stimulated with a fixed concentration of ALPN-202). Serum concentration of ALPN-202 and CD28 target saturation analyses were conducted concurrently to evaluate the exposure-response relationship.

Results Using the *ex vivo* TDC assay, ALPN-202 demonstrated PD-L1-dependent T cell costimulation at all dose levels tested to date in the NEON-1 clinical trial, consistent with preclinical assay development data. Similarly, CD28 target saturation levels on circulating T cells correlated with serum concentration of ALPN-202.

Conclusions We have developed a novel *ex vivo* assay to assess induction of PD-L1-dependent CD28 costimulation in a therapeutic setting. This assay has been successfully employed to monitor controlled CD28 costimulation by the CD28 agonist therapeutic candidate ALPN-202, helping to establish a PK/PD relationship that is consistent with preclinical data. More broadly, this type of cell-based, *ex vivo* TDC assay could be adapted to assess costimulatory receptor engagement, particularly target-dependent costimulation, for other therapeutic agonists in clinical development.

Ethics Approval This study was approved by WCG IRB’s Human Subjects Review, approval number: 20211877.

<http://dx.doi.org/10.1136/jitc-2021-SITC2021.033>

SELECTIVE INFILTRATION OF ANTIBODY-DEPENDENT CELLULAR CYTOTOXICITY (ADCC) MEDIATING IMMUNE CELLS IN RESPONSE TO TREATMENT IN A HUMAN TUMOR HISTO-CULTURE PLATFORM

<http://dx.doi.org/10.1136/jitc-2021-SITC2021.034>

¹Satish Sankaran, ¹Nandini Pal Basak*, ¹Sindhu Govindan, ²BV Prakash, ³BV Manjula, ⁴MS Ganesh, ⁴Amritha Prabha, ¹Kowshik Jaganathan, ¹K Vasanth, ¹K Gowri Shankar, ¹A Manimaran, ¹M Rajashekar, ¹Ritu Malhotra, ¹M Oliyarsi, ¹Rachita Rao. ¹Farcast BioSciences Pvt Ltd, Bangalore, India; ²Sri Lakshmi Multi Speciality Hospital, Bangalore, India; ³Bangalore Baptist Hospital, Bangalore, India; ⁴Vydehi Multi Speciality Hospital, Bangalore, India

Background A 3D histo-culture platform provides a near native Tumor immune Micro-Environment (TiME), making it best suited for evaluating response to immunotherapy drugs. Farcast™ TiME is a human 3D tumor histo-culture platform that preserves TiME and maintains functional fidelity of intratumoral immune cells (IIC). In this study we investigated the utility of this platform in demonstrating treatment induced Antibody-Dependent Cellular Cytotoxicity (ADCC) mechanism driven by IICs alone versus co-culture with autologous peripheral blood immune cells.

Methods Head and neck squamous cell carcinoma tissue samples (n=5) along with matched blood from consented patients were used in this study. All Peripheral Blood Nucleated Cells (PBNCs) including lymphocytes, monocytes, NK cells and neutrophils were isolated and stained with a tracking dye to distinguish them from IICs. Tumor tissues were processed to generate explants, treated with 184 µg/ml Cetuximab (anti-EGFR) or vehicle control, and cultured with or without PBNCs for 72 hrs. Response was evaluated using flow cytometry and cytokine release assay.

Results Amount of infiltrated autologous PBNCs showed a strong negative correlation (R2=0.98) with the amount of IICs in the absence of drug treatment. The proportions of infiltrated immune cell sub-populations were similar to the composition of PBNCs added in culture. Cetuximab treatment, however, led to enhanced infiltration of the effector cells for ADCC driven tumor killing, namely NK cells, macrophages, neutrophils, and cytotoxic T cells (CTLs). Notably the unique infiltration pattern of effector cell populations observed in each sample was reflected in the secretion of specific cytokine/chemokines associated with that cell population. NK cell increase (fold change: 1.6 ± 0.8) was observed in all samples with a concomitant increase in MCP-1 secretion (fold change: 1.7 ± 0.9). Granzyme-B expressing NK cells increased (>1.7 fold) in a subset of samples. Samples showing increase in neutrophil infiltration exhibited increased MMP9 secretion, involved in neutrophil infiltration via stromal remodeling. Sample with highest increase in infiltration of CD16+ Monocyte/Macrophages (>2.4 fold) showed maximum increase in Granzyme-B secretion with respect to the untreated arm. Increase in fold secretion (>1.4) of CXCL9/CXCL10 was associated with the sample that showed highest fold increase of Granzyme-B expressing CTL in comparison to untreated arm. IICs alone were not sufficient in eliciting optimal ADCC response.

Conclusions The study demonstrated ADCC response in the explant/PBNC co-culture platform leading to specific infiltration of effector sub-populations. Farcast™ TiME thus provides a unique platform to explore for heterologous adoptive cell and CAR-T therapies that involve immune cell infiltration.

Ethics Approval All samples included in the study were approved by institutional review boards of the centers providing the samples.

CHEMOKINE-DRIVEN SPATIAL ORGANIZATION OF IMMUNE CELL MICROAGGREGATES MARKS OROPHARYNGEAL SQUAMOUS CELL CARCINOMAS CONTAINING TUMOR-SPECIFIC T CELLS

¹Ziena Abdulrahman*, ¹Saskia Santegoets, ²Gregor Sturm, ³Pornpimol Charoentong, ⁴Marieke Ijsselsteijn, ⁴Antonios Somarakis, ⁴Thomas Höllt, ²Francesca Finotello, ²Zlatko Trajanoski, ⁴Sylvia van Egmond, ⁵Dana Mustafa, ¹Marij Welters, ⁴Noel de Miranda, ¹Sjoerd van der Burg. ¹Leiden University Medical Center, Oncode Institute, Leiden, Netherlands; ²Medical University of Innsbruck, Innsbruck, Austria; ³University Hospital Heidelberg, Heidelberg, Germany; ⁴Leiden University Medical Center, Leiden, Netherlands; ⁵Erasmus University Medical Center, Rotterdam, Netherlands

Background Oropharyngeal squamous cell carcinoma (OPSCC) is the most prevalent type of head and neck cancer. The survival of patients with OPSCC is tightly linked to the intratumoral presence of tumor-specific CD4+ and CD8+ T cells. Yet, immunotherapy is currently far from effective in OPSCC partly due to our limited understanding of its immune microenvironment.

Methods Here a multi-modal, high-dimensional approach was used to dissect the immune landscape in a unique cohort of pre-therapy OPSCC patient samples (n=20) in which intratumoral tumor-specific T cells were either detected (immune response positive, IR+) or not (IR-). This included imaging mass cytometry (Hyperion) for high-dimensional phenotyping, spatial localization and interaction analyses of the cells in the tumor microenvironment with our newly developed imaging processing pipeline employing machine learning, Nanostring PanCancer IO360 panel analysis of immune signaling pathways, and combined single-cell gene expression profiling and T cell receptor sequencing (scRNAseq) to characterize the transcriptional states of clonally expanded tumor-infiltrating T cells.

Results Immune cell infiltration in IR+ tumors is stronger and highly coordinated, with a distinct spatial phenotypic signature characterized by microaggregates of tumor-resident (CD103+) CD8+ and CD4+ T cells and dendritic cells within the tumor cell beds, which retained after permutation based correction for differences in cell frequencies. Furthermore, the increased expression of CXCL12 and LTB produced by CD4+ T cells, both involved in the spatial organization of immune cell infiltration, and the clonal expansion of CD8+ T cells producing the DC-attracting chemokines CCL4 or XCL1 in IR+ OPSCC, indicate that tumor-reactive T cells act as a positive feedback loop in the formation of these aggregates. The impact of these chemokines on local immunity and clinical outcome was confirmed in an independent TCGA OPSCC cohort. In contrast, the IR- OPSCC signature comprised spatial interactions between lymphocytes and different subpopulations of immunosuppressive myeloid cells.

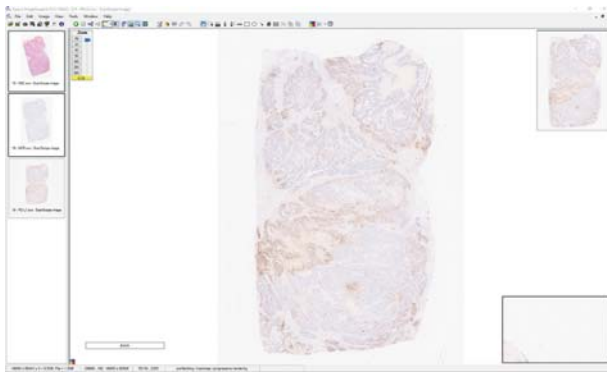
Conclusions Our study reveals that the chemokine-driven spatial immune signature of OPSCC has strong potential as a prognostic and predictive biomarker. While the immune signature of IR+ OPSCC suggests potential benefit from neoadjuvant immunotherapeutic approaches to limit the side effects of current radio(chemo)therapy, that of IR- OPSCC calls for strategies focused on stimulating T cells and counteracting immune suppressive mechanisms.

<http://dx.doi.org/10.1136/jitc-2021-SITC2021.035>

36 DIGITAL WHOLE SLIDE IMAGE (WSI) SCORING IS EQUIVALENT TO MICROSCOPE GLASS SLIDE SCORING FOR EVALUATION OF PROGRAMMED DEATH-LIGAND 1 (PD-L1) EXPRESSION ACROSS MULTIPLE TUMOR INDICATIONS

Micki Adams*, Deanna Moquin, Joshua Littrell, Jay Milo, Stephanie Hund, Angeliki Apostolaki. *Agilent Technologies, Inc., Santa Barbara, CA, USA*

Background The COVID-19 pandemic brought a host of new challenges, including the immediate need for digital solutions addressing the lack of remote options available to pathologists in the field of immunohistochemistry (IHC)-based companion diagnostics for Programmed Death-Ligand 1 (PD-L1) expression evaluation in tumor tissues. Agilent Technologies, Inc. investigated concordance of PD-L1 expression results recorded by trained pathologists between stained glass slides and digital whole slide images (WSIs). Formalin-fixed, paraffin-embedded (FFPE) specimens of eleven tumor indications (table 1) were evaluated in this study. Specimens were stained using the qualitative IHC assay PD-L1 IHC 22C3 pharmDx on Autostainer Link 48 and scored using TPS (Tumor Proportion Score) or CPS (Combined Positive Score) algorithms at six validated cut-offs.¹ The objective was to demonstrate equivalency between digital WSI and microscope glass slide scoring.



Abstract 36 Figure 1 Digital WSI of a triple-negative breast carcinoma (TNBC) specimen stained with PD-L1 IHC 22C3 pharmDx primary antibody and viewed on Aperio ImageScope software with corresponding H&E and NCR WSIs for use as aids in the interpretation of PD-L1 staining.*

*Tissue sample supplied by BioIVT (Hicksville, NY, USA)

Abstract 36 Table 1 Algorithm-cutoff pairs tested

Algorithm	Cutoff	# of Tumor Indications Tested	Tumor Indications Tested/ # of Specimens Tested from Each Indication
CPS	1	8	Urothelial carcinoma (UC): 30 Head and neck squamous cell carcinoma (HNSCC): 32 Cervical cancer: 34 Breast carcinoma (BC) including triple-negative breast carcinoma (TNBC): 37 Renal cell carcinoma (RCC): 30 Biliary tract adeno cancer (BTAC): 32 Small cell lung cancer (SCLC): 30 Colorectal carcinoma (CRC): 38
	10	5	Esophageal cancer: 30 UC: 30 Cervical cancer: 34 BC (including TNBC): 30 BTAC: 32
	20	1	HNSCC: 122
	50	1	HNSCC: 122
TPS	1%	2	Non-small cell lung cancer (NSCLC): 90 NSCLC cytology: 30
	50%	3	HNSCC: 68 NSCLC: 40 NSCLC cytology: 30

Abstract 36 Table 2 Minimum computer monitor requirements for viewing WSIs on Aperio ImageScope

Component	Aperio Image Hub	eSlide Manager and Aperio Image Analysis Workstation
Display type	LCD (flat panel)	LCD (flat panel)
Screen Resolution	1680(h) x 1050(v) pixels	1680(h) x 1050(v) pixels
Screen size	24-inch	24-inch
Color depth	24-bit	24-bit
Brightness	250cd/m ² or greater	250cd/m ² or greater
Contrast ratio	500:1	500:1

Abstract 36 Table 3 Glass slide vs. digital WSI NPA/PPA/OA results summary for the six algorithm-cutoff pairs tested

Algorithm	Cutoff	Total Comparisons	Performance Criteria	Point Estimate	95% Confidence Interval (Bootstrap)	
					Lower-bound: 2.5%	Upper-bound: 97.5%
CPS	1	358	NPA	96.6%	94.521	98.003
		425	PPA	97.9%	96.487	99.061
		784	OA	97.3%	95.802	98.599
CPS	10	223	NPA	93.3%	89.091	96.847
		243	PPA	95.1%	91.968	97.561
		466	OA	94.2%	91.845	96.360
CPS	20	164	NPA	91.5%	86.310	95.808
		197	PPA	88.3%	83.505	92.746
		361	OA	89.8%	85.912	93.333
CPS	50	179	NPA	91.6%	87.069	95.652
		180	PPA	90%	84.153	95.055
		359	OA	90.8%	86.944	94.167
TPS	1%	171	NPA	90.6%	85.965	94.767
		188	PPA	97.3%	94.149	99.479
		359	OA	94.2%	91.365	96.657
TPS	50%	230	NPA	91.7%	87.611	95.575
		180	PPA	93.9%	89.617	97.340
		410	OA	92.7%	89.731	95.400

Abstract 36 Table 4 Number of PD-L1 expression level discordances in HNSCC CPS ≥20 study for predefined negative, near-cutoff (NCO) negative, NCO positive, and positive categories based on specimen screening data assigned by one or more Agilent pathologists prior to the study

Specimen Category with CPS ≥20 Cutoff	# of Discordances Generated by Glass Slide Scoring	# of Discordances Generated by Digital WSI Scoring
Negative	10	8
Negative NCO	15	10
Positive NCO	3	6
Positive	6	5

Abstract 36 Table 5 Number of PD-L1 expression level discordances in HNSCC CPS ≥50 study for predefined negative, NCO negative, NCO positive and positive categories based on specimen screening data assigned by one or more Agilent pathologists prior to the study

Specimen Category with CPS ≥50 Cutoff	# of Discordances Generated by Glass Slide Scoring	# of Discordances Generated by Digital WSI Scoring
Negative	2	6
Negative NCO	10	9
Positive NCO	10	13
Positive	2	4

Methods Three Agilent-certified pathologists evaluated specimen PD-L1 expression level (positive/negative) using CPS and/or TPS at relevant cutoff(s) for each indication (table 1) using two scoring modalities for the same specimen sets: 1) light microscope, and, 2) digital monitor (WSI) with a minimum 14-day washout period between glass slide and WSI reads. WSIs were generated using Leica's Aperio AT2 scanner and evaluated using Aperio ImageScope software (figure 1) on appropriate monitors (table 2). Concordance between specimen glass slide (reference condition) and WSI PD-L1 expression results was assessed per cutoff on pooled data from all applicable indications using negative percent agreement (NPA),

positive percent agreement (PPA) and overall agreement (OA) with 95% two-sided percentile bootstrap confidence intervals (CI); the acceptance criteria for equivalency at each cutoff were set at CI lower-bounds (CILBs) $\geq 85\%$. Discordant comparisons with respect to specimen screening data generated prior to inclusion in the study were also analyzed where applicable.

Results NPA/PPA/OA CILBs for the CPS ≥ 1 , CPS ≥ 10 , TPS $\geq 1\%$, and TPS $\geq 50\%$ cutoffs were $\geq 85\%$ (table 3). NPA and OA CILBs at CPS ≥ 20 and CPS ≥ 50 were $\geq 85\%$; PPA CILBs were 83.2% and 84.2%, respectively. Discordant comparisons analysis for CPS ≥ 20 and CPS ≥ 50 suggested that WSI is not more prone to discordances in PD-L1 expression level than glass slide scoring when compared to specimen screening data (tables 4 and 5).

Conclusions Glass slide and WSI scoring are equivalent across multiple validated cutoffs and tumor indications tested for PD-L1 expression using PD-L1 IHC 22C3 pharmDx with CPS and/or TPS algorithms and are, thus, considered interchangeable scoring modalities.

Acknowledgements < i >We would like to thank our colleagues at Agilent Technologies, Inc. and all of the pathologists involved in study specimen scoring for their valuable contributions to this study. Samples/tissue supplied by Conversant Biologics. Tissue samples supplied by BioIVT (Hicksville, NY, USA) The data and biospecimens used in this project were provided by Centre Hospitalier Universitaire (CHU) de Nice (Nice, France), Contract Research Ltd (Charlestown, Nevis), National BioService LLC (Saint Petersburg, Russia), Sofia Bio LLC (New York, NY, USA), US Biolab (Gaithersburg, MD, USA), Nottingham University Hospitals NHS Trust (Nottingham, UK), Gundersen Medical Foundation Center Biobank (La Crosse, WI, USA), LLC Biomedica CRO (Kyiv, Ukraine), Clinfound Clinical Research Services Pvt Ltd (Idukki, Kerala, India), SageBio LLC (Sharon, MA, USA), GLAS (Winston-Salem, NC, USA), Hospices Civils de Lyon (Lyon, France), IOM Ricerca (Viagrande, Italy), Clin-Path Diagnostics (Tempe, AZ, USA), Centre Antoine Lacassagne (CAL; Nice, France), CHU de Bordeaux (Biobank ID: BB-0033–00036; Bordeaux, France) and contributions by clinical personnel from Centre de ressources biologiques, and SELARL DIAG (Nice, France) with appropriate ethics approval and through Trans-Hit Biomarkers Inc. Biological materials were provided by the Ontario Tumour Bank, which is supported by the Ontario Institute for Cancer Research (Toronto, Ontario, Canada) through funding provided by the Government of Ontario. Tissue samples were provided by the Cooperative Human Tissue Network which is funded by the National Cancer Institute. Other investigators may have received specimens from the same subjects. < /i >

Trial Registration N/A

REFERENCE

1. P02893/13 Instructions for Use (IFU) for PD-L1 IHC 22C3 pharmDx Human Cancer (SK00621-4) Package Insert

Ethics Approval N/A

Consent N/A

<http://dx.doi.org/10.1136/jitc-2021-SITC2021.036>

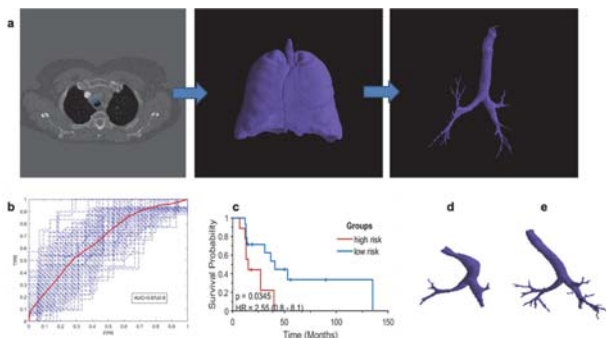
37

QUANTITATIVE LUNG AIRWAY MORPHOLOGY (QUALM) FEATURES ON CHEST CT SCANS ARE ASSOCIATED WITH RESPONSE AND OVERALL SURVIVAL IN LUNG CANCER PATIENTS TREATED WITH CHECKPOINT INHIBITORS

¹Mehdi Alilou*, ¹Thomas Patton, ²Pradnya Patil, ²Nathan Pennell, ¹Kaustav Bera, ³Amit Gupta, ¹Pingfu Fu, ⁴Vamsidhar Velcheti, ¹Anant Madabhushi. ¹Case Western Reserve University, Beachwood, OH, USA; ²Cleveland Clinic, Cleveland, OH, USA; ³University Hospitals, Cleveland, OH, USA; ⁴NYU Langone, New York, NY, USA

Background Immune checkpoint inhibitors (ICI) have revolutionized the management of lung tumors decreasing mortality rates. However, the response rates to these ICI drugs are limited, and identifying those patients who are most likely to benefit remains a clinical challenge. Due to the complex nature of the host immune response, tissue-based biomarker development for immunotherapy (IO) is challenging. Consequently, there is a critical unmet need to develop accurate, validated imaging biomarkers to predict which Non-Small Cell Lung Cancer (NSCLC) patients will benefit from IO. Airway deformations such as central airway obstruction can be considered an important manifestation of cancer aggressiveness or metastatic disease and may have a significant impact on therapeutic refractoriness. In this study, we sought to evaluate whether quantitative measurements of lung airway morphology (QualM) on baseline CT scans are associated with response and overall survival in NSCLC patients treated with ICI.

Methods In this retrospective study, 80 cases who underwent 2–3 cycles of PD1/PD-L1 ICI therapy (nivolumab/pembrolizumab/atezolizumab) were included. RECIST v1.1 was used to define ‘responders’ and ‘non-responders’. Patients were randomly divided into a training (n=40) and a test set (n=40). A region growing algorithm is applied to the trachea, identified by Hough transform, to segment bronchi and bronchioles (figure 1a). 14 QualM features were extracted from segmented airway on CT scans. Wilcoxon ranksum test is used to identify the predictive QualM features. The top 4 QualM features in conjunction with a linear discriminant machine learning classifier were used to predict the response to IO. We also built a QualM risk score using the least absolute shrinkage and selection operator (LASSO) Cox regression model to predict overall survival (OS).



Abstract 37 Figure 1 a) The pipeline of airway segmentation includes trachea identification, segmenting the lung regions from surrounding anatomy, and segmenting the airway by applying a region-growing algorithm. b) ROC curve of QualM model for predicting IO response from baseline CT scans. c) Kaplan Meier curve analysis reveals dichotomization of patients into low risk and high-risk groups with distinct survival patterns based off QualM features. d,e) An example airway structure of a non-responder and a responder to ICI.

Abstract 37 Table 1 Predictive airway features that found to be significantly different among responders and non-responders to IO

Feature	Description	P-value
Major Axis Length	A measure of the axis on the ROI-enclosing ellipsoid which is longest.	0.010
Maximum 2D Diameter Column	The largest pairwise Euclidean distance between surface mesh vertices in the row-slice.	0.046
Maximum 3D Diameter	The largest pairwise Euclidean distance between any two vertices.	0.048
Sphericity	A measure of the roundness of the tumor region relative to a sphere	0.007

Results The response prediction model trained with top QualM features (table 1) predicts responders to ICI with an area under research operating characteristic curve (ROC AUC) of 0.67 ± 0.08 (figure 1.b) in the training (St) and $AUC=0.63$ in the test set (Sv). The airway radiomics risk-score was found to be significantly associated with OS in St (HR=2.34, 95% CI:[1.08–5.07], P=0.008) and Sv (HR=2.55, 95% CI:[0.8–8.1], P=0.034) (figure 1.c).

Conclusions QualM features were able to distinguish responders from non-responders and also were found to be associated with OS for NSCLC patients treated with ICI. With additional validation, QualM could potentially serve as an imaging biomarker of ICI response assessment for NSCLC patients. This could allow the selection of NSCLC patients who will benefit from IO and help design more rational clinical trials with a combination of IO.

<http://dx.doi.org/10.1136/jitc-2021-SITC2021.037>

SPATIAL IMMUNE PROFILING OF HUMAN GLIOBLASTOMA TISSUE REVEALS THE PRESENCE OF AGGREGATED LYMPHOID NICHES IN THE TUMOR MICROENVIRONMENT

¹Todd Bartkowiak*, ¹Asa Brockman, ¹Sierra Barone, ¹Madeline Hayes, ¹Caroline Roe, ¹Justine Sinnaeve, ²Akshikumar Mistry, ¹Nalin Leelatian, ¹Allison Greenplate, ²Bret Mobley, ²Lola Chambless, ²Reid Thompson, ²Kyle Weaver, ¹Rebecca Ihrle, ¹Jonathan Irish. ¹Vanderbilt University, Nashville, TN, USA; ²Vanderbilt University Medical Center, Nashville, TN, USA

Background Glioblastomas (GBM) account for 60% of adult primary brain tumors. With few advances in therapeutics, median overall survival remains 15-months post-diagnosis. Immunotherapies may provide therapeutic benefit in GBM patients; however, no predictive immune features currently inform therapeutic stratification in GBM. We have shown that, independently of known prognosticators, radiographic tumor contact with the lateral ventricle (C-GBM) correlates with 7-months worse survival prognosis compared to patients with ventricle non-contacting GBM (NC-GBM). This study sought to characterize the GBM immune microenvironment and identify targetable mechanisms of immunosuppression correlating with worse outcomes in C-GBM.

Methods Twelve patients presented with pathologically confirmed primary, IDH wildtype C-GBM and thirteen with NC-GBM. Multiplex immunohistochemistry (mxIHC) was performed on formalin-fixed paraffin embedded (FFPE) tissue for each patient interrogating 8 predictive immune markers (CD3, CD4, CD8, FOXP3, CD68, IBA1, PD-1, and PD-L1). Machine learning tools characterized tumor-infiltrating immune populations and identified biomarkers correlating with C-GBM and patient survival. K-means clustering identified immunological neighborhoods within the tissue and a log odds ratio was used to quantify the likelihood of cell-cell interactions in the tissue.

Results C-GBM tumors were enriched in monocyte-derived macrophages (MDM) compared to NC-GBM ($19 \pm 8\%$ vs. $6 \pm 2\%$; $p < 0.001$) and depleted in lymphocytes ($2.9 \pm 1\%$ vs. $7.6 \pm 2\%$; $p < 0.001$) and tissue-resident microglia ($1.8 \pm 0.3\%$ vs. $7 \pm 3\%$; $p < 0.001$). Further, T cells in C-GBM co-expressed the checkpoint receptors PD-1, suggesting T cell exhaustion in the C-GBM tumor microenvironment. K-means clustering identified 10 immunological niches prevalent in GBM tissue. Macrophage-tumor niches were most common niche in the tissue accounting for 17.93% of all niches, followed by T cell-microglia-tumor niches (17.72%). Conversely, tumor-tumor niches were the least prevalent, accounting for only 2.51% of niches. Within niches, T cell-T cell interactions occurred more frequently than expected by random chance (log odds ratio = 0.90) whereas T cell-macrophage interactions occurred less frequently than expected by random chance (log odds ratio = -1.61). Pathological assessment of the tissue confirmed the presence of lymphoid aggregates in regions of myeloid exclusion in the tissue.

Conclusions These findings suggest that factors within the periventricular space may influence antitumor immunity within GBM, and have identified clinically targetable immune biomarkers in glioblastoma. The prevalence of T cell niches in GBM tumors suggests the establishment tertiary lymphoid aggregates may be targetable to improve patient outcomes. Lastly, radiologic assessment of lateral ventricle contact by standard-of-care MRI may guide clinical trial design for immunotherapies in neuro-oncology.

Acknowledgements This study was funded by NIH/NCI grant K00 CA212447 and supported by the Translational Pathology Shared Resource at Vanderbilt University (P30 CA068485).

Ethics Approval Primary glioblastoma tumors obtained in accordance with the Declaration of Helsinki and with institutional IRB approval (#131870) along with patient written informed consent.

<http://dx.doi.org/10.1136/jitc-2021-SITC2021.038>

A MULTI-MODAL ANALYSIS APPROACH LEVERAGING MULTIPLEXED SPATIAL PHENOTYPING AND MULTI-OMICS ANALYSIS TO BETTER UNDERSTAND THE PROGNOSTIC VALUE OF TERTIARY LYMPHOID STRUCTURES IN NSCLC

¹Julie Berthe*, ¹Sriram Sridhar, ¹Felix Segerer, ¹Marco Testori, ¹Megha Saraiya, ¹Lorenz Rognoni, ¹Harald Hessel, ¹Alma Andoni, ¹Anatoliy Shumilov, ¹Andreas Spitzmüller, ¹Mari Heininen-Brown, ¹Jorge Blando, ¹Felicia Ng, ¹Emma Jones, ¹Sophie Willis, ¹Michael Surace, ²Rieneke van de Ven, ²Tanja de Gruij, ¹Helen Angell. ¹AstraZeneca, Cambridge, UK; ²Cancer Center Amsterdam, Amsterdam, Netherlands

Background Tertiary Lymphoid Structures (TLS) are highly organized ectopic lymphoid structures found in inflamed or tumor tissues, acting as sites of lymphoid recruitment and immune activation. A high TLS density within the tumor is commonly associated with an increased prognostic effect of TILs and with an improved disease free survival and overall survival for patients.¹ However, the existence of conflicting studies suggest that multiple TLS features should be taken into account when assessing their prognostic value, such as their location, cellular composition, maturation stage and spatial organisation, as those may affect their functionalities.²

Methods With the aim of gaining insights into TLS biology and evaluating the prognostic role of TLS in Non-Small Cell Lung Carcinoma according to their multiple features, we developed a TLS multiplex immunofluorescent (mIF) panel that includes T cells (CD3, CD8), B cells (CD20), Follicular Dendritic cells (CD21, CD23) and mature dendritic cells (DC-LAMP) markers. We deployed this panel across a cohort of primary tumors from NSCLC patients (n=408) and established a mIF image analysis workstream to assess the status and spatial location of each cell within the tissue. A H&E staining of the same tissue section was performed to evaluate mIF spatial data in relation to the tumor context. Additional multi-omics assessments were conducted across the same cohort including; whole exome sequencing, NanoString transcriptomics, and immunohistochemistry (e.g. PD-L1, FOXP3, Nkp46, LKB1, CTLA4). We have leveraged clinical metadata, including demographics (e.g. age, sex, smoking status) and clinical risk factors (e.g. stage, grade, Standard of Care treatment) with clinical follow up (e.g. OS, PFS) for prevalence analysis, novel biomarker identification, and survival association.

Results Assessment of the prevalence of each cell phenotype within the tumor tissue and TLS, the cell-cell interactions, the distance between each cell type, and the distance of non-TLS immune cells to the closest TLS will be described, demonstrating the different types of lymphoid aggregates and TLS and their functional status. An integrative analysis combining spatial biology data with multi-omics and clinical data will be presented evaluating the prognostic value of TLS composition, maturation status and spatial organization, in correlation with additional biomarkers and clinical characteristics.

Conclusions This exploratory study using cutting-edge technologies enables us to better understand how TLS orchestrate an organised anti-tumour response, defining TLS spatial biomarker signatures, TLS gene signatures, and TLS features associated with patient outcomes to evaluate in the clinic.

REFERENCES

1. Marie-Caroline Dieu-Nosjean, Jérémy Goc, Nicolas A Giraldo, Catherine Sautès-Fridman, Wolf Herman Fridman. Tertiary lymphoid structures in cancer and beyond. *Trends Immunol* 2014;**35**(11):571–580.
2. Catherine Sautès-Fridman, Florent Petitprez, Julien Calderaro, Wolf Herman Fridman. Tertiary lymphoid structures in the era of cancer immunotherapy. *Nat Rev Cancer* 2019;**19**(6):307–325.

Ethics Approval The study was approved by AstraZeneca.

<http://dx.doi.org/10.1136/jitc-2021-SITC2021.039>

40

**PRECISE SPATIAL MULTIPLEXING FOR IMMUNE
PROFILING IN NON-SMALL CELL LUNG CANCER FFPE
SAMPLES WITH CHIPCYTOMETRY**

Thomas Campbell*, Arne Christians, Adam Northcutt, Crystal Winkeler, Kevin Gamber.
Canopy Biosciences – A Bruker Company, Saint Louis, MO, USA

Background Emergent data indicate that highly multiplexed spatial biomarker analysis has the potential to advance precision medicine in immuno-oncology and inform the discovery of novel biomarkers.

Methods Here we present the analysis of clinical FFPE samples from non-small cell lung cancer patients using ChipCytometry, a novel precise spatial multiplexing technology which combines iterative immuno-fluorescent staining with high-dynamic range imaging to facilitate quantitative phenotyping with single-cell resolution. Standard FCS files are generated from multichannel OME-TIFF images, enabling identification of cellular phenotypes via flow cytometry-like hierarchical gating. In this study, a 27-plex assay was used to identify and quantify more than 30 cellular phenotypes and subtypes in FFPE samples.

Results The results show precise expression levels for each marker in the assay in each individual cell in the sample, maintaining spatial information about each cell. Spatial analysis of the samples reveals quantifiable heterogeneity of immune cell infiltration within the tumor samples, demonstrating the utility of the ChipCytometry platform for the in-depth immune profiling in clinical samples.

Conclusions N/A

<http://dx.doi.org/10.1136/jitc-2021-SITC2021.040>

ASSESSMENT OF THE SPATIAL DISTRIBUTION OF CD4+ T CELLS SUBPOPULATIONS IN THE TUMOR MICROENVIRONMENT BY BRIGHTPLEX[®], A SEQUENTIAL CHROMOGENIC MULTIPLEX ASSAY

¹Aurelie Collignon, ¹Alex Trinh, ¹Marion Olive, ¹Clémence Jaume, ¹Maité Chamourin, ¹Nour Sfeir, ¹Dylan Anselmo, ¹Raana Ramouz-Charpentier, ¹Georgia Culey, ¹Christophe Haond*, ²Jerome Galon, ¹Jacques Fieschi-Meric. ¹HaliDx, Marseille, France; ²INSERM, Paris, France

Background Cancer immunotherapy reinvigorates tumor-specific T cell responses of CD8+ cytotoxic T lymphocytes that detect intracellular antigens that are presented by MHC class I molecules expressed by all tumor cell types. Because most tumors do not express MHC class II, the potential antitumor protective role of CD4 T cells, which bind MHC class II molecules on target cells, has been less studied. However, CD4+ T cells are also required for efficacious antitumor immunity; they are core components of adaptive immunity that differentiate into lineages responsible for effector activities. Both TH1 and TH2 cell types mediate antitumor immunity, although TH1 cells may be more potent due to the production of large amounts of IFN- γ , as well as chemokines that enhance the priming and expansion of CD8 cells. TH1 cells help in recruiting natural killer cells and type I macrophages to tumor sites, which can act in concert toward tumor eradication. The ability of TH2 cells to mobilize innate cells, may represent a general pathway for their impact on the host antitumor response. Tumor infiltrating TFH cells play a key role in immune cell recruitment to the tumor and in the formation of intratumoral follicular structures, which correlate with a positive prognosis. On the contrary, cells from the TH17 subset induces inflammatory responses resulting in a tumor-promoting environment. CD4+ Tregs which are critically important for the maintenance of self-tolerance, impede effective immunity against the tumor when they are present in the tumor microenvironment (TME). Therefore, beyond the detection of total CD4+ T cells within the TME, it is of critical importance to determine to which subpopulation each CD4+ T cell belongs to decipher their roles in tumor rejection.

Methods We have developed a multiplex 7-plex panel of antibodies against biomarkers to identify main types of CD4+ T cells

Results On a single FFPE tissue section, main types of CD4+ T cells: TH1, TH2, TFH, TH17 and Tregs are identified by a combination of antibodies against transcription factors and membrane proteins. Following images registration, complex cells phenotypes can be detected and quantified. Furthermore, digital pathology tools allow the evaluation of the spatial distribution of CD4+ T cells within the TME.

Conclusions This new tool unravels the diversity of CD4+ T cells in TME and could help clinical researchers to design more effective immunotherapies in cancer treatment. Integrated into an Immunogram, this new Brightplex[®] Panel will also be critical to understand the immune contexture of tumors.

<http://dx.doi.org/10.1136/jitc-2021-SITC2021.041>

THE ROLE OF TISSUE STIFFNESS IN PREDICTING THE IMMUNOTHERAPY RESPONSE IN HEPATOCELLULAR CARCINOMA

Betul Gok Yavuz*, Elshad Hasanov, Lianchun Xiao, Yehia Mohamed, Sunyoung Lee, Asif Rashid, Ahmed Kaseb, Aliya Qayyum. *UT MD Anderson Cancer Center, Houston, TX, USA*

Background Currently, there is no standard biomarker that predict immunotherapy response in hepatocellular carcinoma (HCC). Here, we aim to investigate the role of tissue stiffness measured by magnetic resonance elastography (MRE) in predicting neoadjuvant immunotherapy response in patients with resectable HCC.

Methods This was a study of 15 patients with HCC treated with immune checkpoint blockade (ICB) therapy, nivolumab ± ipilimumab, followed by surgical resection. HCC MRE assessment was performed at baseline and after 6 weeks of therapy. HCC stiffness (kPa) was measured on MRE elastograms (liver stiffness maps). Baseline stiffness and changes in stiffness were compared with treatment response to ICB. Treatment response was defined as a tumor with more than 60% necrosis which was the major pathological response. Analysis was performed using descriptive statistics, Fisher's exact test, and Wilcoxon rank sum test; p-value <0.05 was considered statistically significant.

Results Fifteen patients were evaluable for MRE assessment. The median age was 67 years. Etiology of liver disease was NASH (n=4), HCV (n=3), HBV (n=2) and unknown (n=6). Three out of 15 patients (20%) achieved a major pathological response (MPR). Median baseline HCC stiffness and change in stiffness were 4.6 kPa and -0.2 kPa, respectively. Among the 4 patients with stiffness increase, 3 (75%) of them achieved MPR and 1 (25%) did not achieve MPR. Among the patients without stiffness increase, none of them achieved MPR. Fisher's exact test indicates that increase in stiffness was associated with a higher chance to achieve MPR than patients without stiffness increase (p=0.0088). Median baseline HCC stiffness for responders and non-responders was 6.8 (5.4, 9) kPa and 3.9 (2.2, 9.7) kPa, respectively (p=0.09). The median change in HCC stiffness for responders and non-responders was 1 (1, 1.4) kPa and -0.4 (-2.2, 0.7) kPa, respectively (p=0.02).

Conclusions Patients who achieved MPR inclined to have a higher baseline stiffness than patients who did not achieve MPR. Regarding the changes in stiffness between the two arms, patients with MPR group had a greater increase than that in the non-MPR group. In conclusion, baseline and change in MRE stiffness may be a useful biomarkers in predicting response to ICB therapy in HCC.

Ethics Approval This was an Institutional Review Board approved study (MDACC 2017-0972). All patients provided written informed consent.

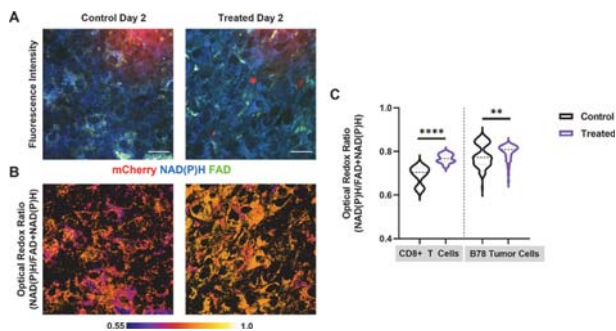
<http://dx.doi.org/10.1136/jitc-2021-SITC2021.042>

43

INTRAVITAL MULTIPHOTON IMAGING OF INFILTRATING CD8 T CELL AND TUMOR CELL METABOLISM DURING IMMUNOTHERAPY IN A MURINE MELANOMA MODEL

¹Alexa Heaton*, ²Anna Hoefges, ³Peter Rehani, ²Angelica Lopez, ²Nathaniel Burkard, ²Alexander Rakhmievich, ²Amy Erbe, ²Paul Sondel, ¹Melissa Skala. ¹Morgridge Institute for Research and University of Wisconsin, Madison, WI, USA; ²University of Wisconsin, Madison, WI, USA; ³Morgridge Institute for Research, Madison, WI, USA

Background Intravital multiphoton microscopy (IMM) provides single cell imaging within intact living systems. IMM of the autofluorescent metabolic co-enzymes NAD(P)H and FAD, optical metabolic imaging (OMI), provides *in vivo* label-free imaging of metabolic changes. The metabolism of tumor and immune cells is closely associated with cancer progression and tissue site,^{1–4} so we aim to study metabolic trends during administration of an effective, triple-combination immunotherapy within murine melanoma tumors.⁵ This therapy includes external beam radiation, intratumoral hu14.18-IL2 immunocytokine (anti-GD2 mAb fused to IL2), and intraperitoneal anti-CTLA-4 leading to *in situ* vaccination and cure of GD2+ murine tumors.⁵ Previous work has shown that a T cell response is critical to the efficacy of this therapy,^{5–6} so we created an mCherry-labeled T cell mouse model to study this response. Here, IMM was used to image concurrent tumor and CD8+ T cell metabolic trends during administration of immunotherapy.



Abstract 43 Figure 1 *In vivo* multiphoton images of immune and tumor cell populations during immunotherapy. A) Representative *in vivo* fluorescence intensity images of B78 melanoma tumors growing in control and treated CD8 mCherry reporter mice show mCherry-labeled CD8+ T cells (red) infiltrating tumor tissue as well as autofluorescent metabolic coenzymes NAD(P)H (blue) and FAD (green) expressed by the tumor and T cells. Scale bar 25 μ m. B) Corresponding *in vivo* optical redox ratio intensity images show redox balance within the tumor microenvironment. Treated tumors exhibit an increased optical redox ratio which may indicate increased glycolytic activity during immunotherapy. C) Quantified single-cell B78 tumor (n = 353) and CD8 T cell (n = 18) autofluorescence data. Both CD8 T cells (p<0.0001) and tumor cells (p<0.0034) exhibit significantly increased optical redox ratio with treatment (n = 2 mice, median – center bold dashed line, 3rd quartile – upper dashed line, 1st quartile – lower dashed line, Mann-Whitney U Test).

Methods We created an mCherry-labeled CD8+ T cell mouse model through CRISPR/Cas9 knock-in. We then implanted syngeneic B78 (GD2+) melanoma cells into the flanks of these reporter mice to induce measurable tumors. Mice were anesthetized, skin flap surgery performed, and tumors imaged at several time points. IMM was performed using 750–1040 nm to excite NAD(P)H, FAD, and mCherry through a 40X (1.15 NA) objective. Fluorescence lifetime data was collected

using time correlated single photon counting electronics. Murine tissues were harvested and analyzed via flow cytometry and multiplex immunofluorescence to corroborate IMM findings and characterize the immune infiltrate.

Results Here we demonstrate the feasibility of our IMM platform to capture single cell metabolic changes during immunotherapy administration. Through our intravital imaging we show that CD8 T cell and tumor cell redox ratio (intensity of NAD(P)H/intensity of NAD(P)H + FAD) is significantly increased in treated compared to control mice (figure 1), possibly indicating increased glycolytic activity. We also show differences in protein binding within both CD8 T cells and tumor cells during treatment. Overall, this technology enables analysis of metabolic changes in CD8 T cells and tumor cells *in vivo* during administration of our immunotherapy regimen.

Conclusions These results provide additional support that the combination of intravital imaging with OMI allows for concurrent imaging of T cell infiltration and metabolic trends. Specifically, OMI enabled us to probe single cell metabolic changes occurring during our immunotherapy regimen. With continued work, this imaging platform may be leveraged to develop new combinations of immunotherapies.

Acknowledgements This work is supported by the Morgridge Institute for Research (Interdisciplinary Fellowship awarded to A.R.H.) and the NIH (R01 CA205101 and R35 CA197078). The authors thank the University of Wisconsin Carbone Cancer Center (UWCCC) Support Grant P30 CA014520, the UWCCC Translational Research Initiatives in Pathology laboratory - supported by the UW Department of Pathology and Laboratory Medicine and the Office of The Director NIH (S10OD023526), the UWCCC Flow Cytometry Laboratory, and the Genome Editing and Animal Models Laboratory for core services. The authors also thank Tiffany M. Heaster for training and thoughtful discussions as well as Dan Pham for cell isolation help.

REFERENCES

- Renner K, Singer K, Koehl GE, Geissler EK, Peter K, Siska P J, Kreutz M. Metabolic Hallmarks of Tumor and Immune Cells in the Tumor Microenvironment. *Front Immunol* 2017, 8 Mar: 1–11.
- Mockler MB, Conroy MJ, Lysaght J. Targeting T Cell Immunometabolism for Cancer Immunotherapy; Understanding the Impact of the Tumor Microenvironment. *Front Oncol* 2014, 4 May: 1–11.
- Ghesquière B, Wong BW, Kuchnio A, Carmeliet P. Metabolism of stromal and immune cells in health and disease. *Nature* 2014; **511**(7508):167–176.
- Heaster TM, Heaton AR, Sondel PM, Skala MC. Intravital metabolic autofluorescence imaging captures macrophage heterogeneity across normal and cancerous tissue. *Front Bioeng Biotechnol* 2021, **9**(April): 1–10.
- Morris ZS, Guy EI, Francis DM, Gressett MM, Werner LR, Carmichael LL, Yang RK, Armstrong EA, Huang S, Navid F, Gillies SD, Korman A, Hank JA, Rakhmievich AL, Harari PM, Sondel PM. In situ tumor vaccination by combining local radiation and tumor-specific antibody or immunocytokine treatments. *Cancer Res* 2016; **76** (13): 3929–3941.
- Morris ZS, Guy EI, Werner LR, Carlson PM, Heinze CM, Kler JS, Busche SM, Jaquish AA, Sriramaneni RN, Carmichael LL, Loibner H, Gillies SD, Korman AJ, Erbe AK, Hank JA, Rakhmievich AL, Harari PM, Sondel PM. Tumor-specific inhibition of *in situ* vaccination by distant untreated tumor sites. *Cancer Immunol Res* 2018; **6**(7): 825–834.

Ethics Approval All animal work was approved by the University of Wisconsin Institutional Animal Care and Use Committees.

<http://dx.doi.org/10.1136/jitc-2021-SITC2021.043>

44

DETECTION OF MEMORY B CELLS CROSS-REACTIVE AGAINST POLYMORPHIC MALARIA ANTIGENS USING A MULTIPLEX FLUOROSPOT ASSAY

¹David Spezzano*, ²Peter Jahnmatz, ¹Evan Johnson. ¹Mabtech, Inc., Boston, MA, USA; ²Mabtech, Stockholm, Sweden

Background Antigenic diversity of the malaria parasite *Plasmodium falciparum* is a major challenge for vaccine development. Identifying cross-reactive antibodies to polymorphic antigens linked with protection, eg merozoite surface protein 2 (MSP2), could further guide vaccine design. Circulating malaria-specific antibodies are generally short-lived and analysis of memory B-cells (MBC) may therefore better reflect responses of importance for immunity. The B-cell FluoroSpot assay enables a sensitive analysis of antigen-specific B cells, in addition, it allows also for analysis of cross-reactivity displayed by single B cells.

Methods Patients treated for *P. falciparum* malaria at Karolinska University Hospital in Stockholm Sweden were followed prospectively with repeated sampling over one year. PBMCs were analyzed using a B-cell FluoroSpot assay including *P. falciparum* antigens MSP-1(19), MSP-3, AMA-1 and different variants of MSP2. The gene coding for the polymorphic region of MSP-2 from the patient's own parasite was amplified, sequenced and recombinantly expressed together with a peptide tag that enabled detection in the FluoroSpot assay. Combinations of MSP2 variants were tested for homologous and heterologous responses.

Results Preliminary results show that the FluoroSpot assay was able to simultaneously detect single MBCs specific against the different merozoite antigens in the same well including either one of the antigen variant of MSP-2 in patients with single or repeated exposure to malaria (figure 1). Cross-reactivity displayed by single B cells to different MSP2 antigens was detected in variants within the two respective allelic families FC27 and 3D7 but not between allelic families. Further analyses are ongoing involving additional antigens as well as individuals with different degree of pre-existing immunity. **Conclusions** Preliminary results suggest that this novel multiplex B-cell FluoroSpot assay could be a powerful tool to analyze antigen-specificity and antibody cross-reactivity to polymorphic merozoite antigens and its association with previous exposure and immunity.

<http://dx.doi.org/10.1136/jitc-2021-SITC2021.044>

Detection of memory B cells cross-reactive against polymorphic malaria antigens using a multiplex FluoroSpot assay

Peter Jahnmatz¹, David Spezzano², Evan Johnson¹, Marjeh Hata Hormaez, Victor Yman, Ariana Soreli, Nilsas Hagg, & Peter Farnert¹
¹Division of Infectious Diseases, Department of Medicine Solna, Karolinska Institutet, Stockholm, Sweden, ²Mabtech AB, Nacka Strand, Sweden
³Department of Infectious Diseases, Karolinska University Hospital, Stockholm, Sweden

Introduction

Antigenic diversity of the malaria parasite *Plasmodium falciparum* is a major challenge for vaccine development. Identifying cross-reactive antibodies to polymorphic antigens linked with protection, e.g. merozoite surface protein 2 (MSP-2), could further guide vaccine design. Circulating malaria-specific antibodies are generally short-lived and analysis of memory B cells (MBCs) may therefore better reflect responses of importance for immunity. The B-cell FluoroSpot assay enables a sensitive analysis of antigen-specific B cells, in addition, it allows also for analysis of cross-reactivity displayed by single B cells.

Aim

The aim was to evaluate the utility of the B-cell FluoroSpot assay to study cross-reactivity displayed by single MBCs towards the polymorphic region of MSP-2 from the allelic families 3D7 and FC27.

Material

P. falciparum parasites were isolated from patients treated for a malaria infection in Sweden. The gene coding for the polymorphic region of MSP-2 from the patient's own parasite was amplified using nested PCR and then sequenced using capillary electrophoresis. The MSP-2 sequence was recombinantly expressed together with a peptide tag that enabled detection in the FluoroSpot assay.

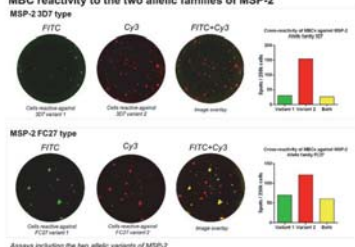
B-cell FluoroSpot assay

IgG secreted from single MBCs was captured by immobilized anti-IgG antibodies and then exposed to two variants of polymorphic MSP-2 antigen tagged with separate peptide tags. Using fluorescent anti-tag reagents with separate fluorophores, the antigen-specific MBCs were detected and their position could be visualized as fluorescent spots on the membrane. IgG antibodies that bind both antigens, i.e. that cross-react, will give rise to co-positioned spots from both detection systems and can be visualized as a mixture of spot colors. Spot analysis was made using Mabtech FRSTM with RAWispotTM technology.

Results

The results show that the FluoroSpot assay was able to detect single MBCs reactive to either one allelic antigen variant of MSP-2, or two. Furthermore, cross-reactivity of single B cells could be detected against variants from both allelic families FC27 and 3D7 but not between allelic families (data not shown).

MBC reactivity to the two allelic families of MSP-2



Conclusions

The novel assay described can be a powerful tool to analyze the broadness of antibody cross-reactivity and its association with clinical manifestation. This assay will now be used in a larger study involving individuals with different degree of pre-existing immunity in order to further analyze cross-reactivity against polymorphic malaria antigens.



Karolinska Institutet
 Peter Jahnmatz
 PhD Student - Department of Medicine Solna
 Karolinska University Hospital, Huddinge
 141 77 Stockholm, Sweden

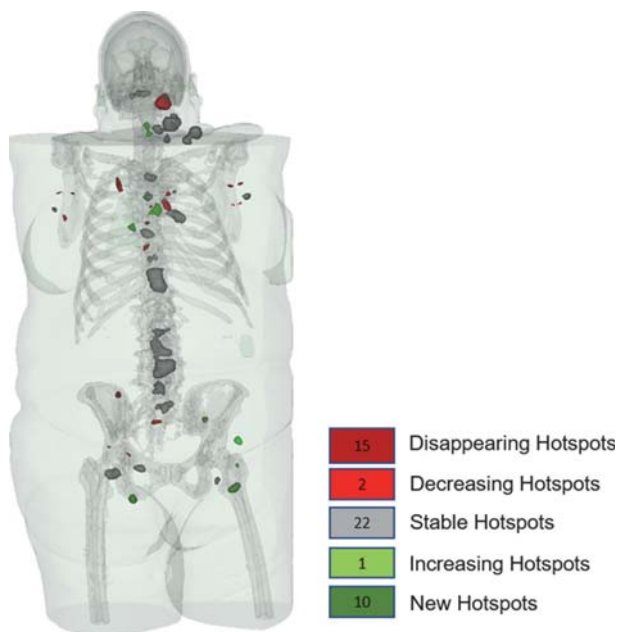


Abstract 44 Figure 1 Detection of memory B cells cross-reactive against polymorph. Detection of memory B cells cross-reactive against polymorphic malaria antigens using a multiplex FluoroSpot assay

AI-ASSISTED WHOLE-BODY ASSESSMENT OF IMMUNOTHERAPY RESPONSE USING [18F]F-ARAG, A PET AGENT FOR ACTIVATED T CELLS

¹Jelena Levi*, ²Timothy Perk, ¹Lyna Huynh, ¹Juliet Packiasamy, ³Serena Cheng, ³John Sunwoo, ³A Dimitrios Colevas. ¹CellSight Technologies, San Francisco, CA, USA; ²AIQ Solution, Inc., Madison, WI, USA; ³Stanford University, Palo Alto, CA, USA

Background Patterns of response to immunotherapy differ from traditional cytotoxic drugs, making clinical decisions concerning response evaluation more challenging. Radiological response criteria, such as iRECIST, updated to address response patterns unique to immunotherapeutics, focus only on changes in the tumor burden.¹ An 18F labeled nucleoside analog, [18F]F-AraG was developed as a PET agent for imaging activated T cells,²⁻⁵ critical components of immune response and the common target of immunotherapies. Whole body assessment of [18F]F-AraG uptake that indicates presence of activated T cells might allow for analysis of complex immunologic processes and provide early indication of treatment response as well as off-target side effects. Here, we employ AIQ Solutions' TRAQinform IQ software to analyze [18F]F-AraG scans and assess activation of T cells in head and neck squamous cell carcinoma (HNSCC) patients undergoing anti-PD-1 therapy.



Abstract 45 Figure 1 TRAQinform IQ assessment of the SUVmean [18F]F-AraG signal change in a HNSCC patient two weeks after a single dose of anti-PD-1 antibody. Quantification of the differences in the [18F]F-AraG uptake in the baseline and on-treatment scan revealed 17 hotspots with disappearing or decreasing signal, 22 hotspots with the stable signal and 11 hotspots with increasing or new signal post therapy.

Methods Four treatment-naïve HNSCC patients were imaged using [18F]F-AraG before and 2–3 weeks after a single dose of anti-PD-1 antibody. [18F]F-AraG PET scans of six healthy subjects were used to define areas of increased [18F]F-AraG

uptake in patients. The regions of uptake in the baseline and on-treatment scans were registered and matched using articulated registration.^{6,7} Standardized uptake values, SUVmax, SUVmean and SUVtotal were extracted from all areas of tracer uptake in both scans and changes in signal calculated to assess therapy effects. The change in signal was analyzed in the context of the patient's clinical status and changes in T cell infiltration in the primary lesion when biopsy specimens were available.

Results TRAQinform IQ whole body evaluation of [18F]F-AraG PET revealed heterogeneity in the signal range and extent of signal change both between different patients and between different areas of tracer uptake within the same patient (figure 1). The post-therapy whole-body [18F]F-AraG signal change trended with patients' outcome. The patients with areas where the signal disappeared or decreased post therapy, indicative of the lack of T cell activation, had shorter overall survival than the patients with areas with stable and increasing signal. The change in infiltration of activated T cells in the primary lesion tissue did not correspond to the patient survival, reflecting limitations of serial biopsy in evaluating therapy response.

Conclusions TRAQinform IQ analysis and quantification of [18F]F-AraG PET provides patient-level assessment of tracer uptake and may allow for better understanding of heterogeneity of T cell activation and potentially offer a more comprehensive evaluation of response to immunotherapy than the standard, tumor-centric, radiologic methods.

REFERENCES

1. Nishino M, et al. Monitoring immune-checkpoint blockade: response evaluation and biomarker development. *Nat Rev Clin Oncol*. 2017.
2. Namavari M, et al. Synthesis of 2'-deoxy-2'-[18F]fluoro-9-beta-D-arabinofuranosyl-guanine: a novel agent for imaging T-cell activation with PET. *Mol Imaging Biol* 2011; 13(5):812–8.
3. Ronald JA, et al. A PET imaging strategy to visualize activated T cells in acute graft-versus-host disease elicited by allogeneic hematopoietic cell transplant. *Cancer Res* 2017; 77(11):2893–2902.
4. Levi J, et al. Imaging of activated T cells as an early predictor of immune response to anti-PD-1 Therapy. *Cancer Research* 2019; 79(13):3455–3465.
5. Levi J, et al. (18)F-AraG PET for CD8 profiling of tumors and assessment of immunomodulation by chemotherapy. *J Nucl Med* 2021; 62(6):802–807.
6. Yip S, T Perk, and R Jeraj, Development and evaluation of an articulated registration algorithm for human skeleton registration. *Phys Med Biol* 2014; 59(6):1485–99.
7. Yip S. and R Jeraj. Use of articulated registration for response assessment of individual metastatic bone lesions. *Phys Med Biol* 2014; 59(6): 1501–14.

Ethics Approval The study was approved by Stanford University Ethics Board, approval number 40425.

<http://dx.doi.org/10.1136/jitc-2021-SITC2021.045>

PROXIMITY BETWEEN CYTOTOXIC ANTIGEN-EXPERIENCED T CELLS AND TUMOR CELLS IS ASSOCIATED WITH IMPROVED CLINICAL OUTCOMES IN EARLY-STAGE NSCLC

Qianyun Luo*, Edwin Parra, Marcelo Negrao, Neal Akhave, Erin Bayley, Kyle Mitchell, Jianjun Zhang, John Heymach, Boris Sepesi, Ignacio Wistuba, Don Gibbons, Alexandre Reuben. *The University of Texas MD Anderson Cancer Center, Houston, TX, United States*

Background While the development of immunotherapies has improved the treatment of non-small cell lung cancer (NSCLC), most patients still fail to respond. Immune cell densities have been utilized to predict clinical responses but have largely failed to do so. However, the spatial distribution and interaction of these cells at the tissue level have been less studied. Here, we performed spatial analysis of the cells within the tumor immune microenvironment in order to evaluate their relationship with clinical outcomes in early-stage NSCLC.

Methods Multiplex immunofluorescence was performed on 123 early-stage NSCLC patients from the ICON (Immunogenomic profiling of non-small cell lung cancer) cohort including Cytokeratin (CK), CD3, CD8, CD45RO, FoxP3, CD68, CD20, CD57, Granzyme B (GzmB), PD-1, and PD-L1. Area under the curve (AUC) was calculated using Ripley's L function, which evaluates the degree of spatial proximity of two cell populations, with a high AUC indicating clustering and low AUC indicating scattering. Findings were integrated with clinical parameters.

Results Adenocarcinomas demonstrated CD3+PD1+ T cells were closer to CK+ tumor cells ($n=60$, $p=0.035$), and B cells were closer to cytotoxic T cells ($n=43$, $p=0.03$) than in squamous cell carcinoma. Higher AUC was observed between CD3+PD1+ T cells ($n=56$, $p=0.035$), with cytotoxic antigen-experienced T cells (CD45RO+GzmB+) closer to tumor cells ($n=35$, $p=0.017$) in stage I and II compared to stage III tumors. Untreated patient tumors exhibited higher proximity between CD20+ B cells and CD57+ NK cells ($n=59$, $p=0.012$), CD3+ T cells and PD-L1+ tumor cells ($n=56$, $p=0.027$), and CD68+ macrophages and PD-L1+ tumor cells ($n=52$, $p=0.016$) than neoadjuvant chemotherapy-treated patients. Patients with no recurrence presented higher AUC in antigen-experienced CD45RO+GzmB+ T cells and tumor cells ($n=36$, $p=0.006$), while those with improved survival demonstrated greater proximity between CD68+ macrophages and PD-L1+ tumors ($n=52$, $p=0.016$), CD20+ B cells and GzmB+ cells ($n=49$, $p=0.03$), and antigen-experienced CD45RO+GzmB+ T cells and tumor cells ($n=36$, $p=0.047$). Lastly, patients with improved survival also displayed greater proximity between CD3+CD8+ cytotoxic T cells and PD-L1- epithelial cells ($n=76$, $p=0.04$) in tumors versus matched adjacent lungs.

Conclusions Overall, our findings shed light on some of the potential cell interactions at play in the tumor microenvironment of early-stage NSCLC patients and suggest cell distributions could be utilized to predict clinical outcomes in early-stage NSCLC patients.

<http://dx.doi.org/10.1136/jitc-2021-SITC2021.046>

TERTIARY LYMPHOID STRUCTURES (TLS) IN DESMOPLASTIC MELANOMAS (DM) DIFFER FROM NON-DM-ASSOCIATED TLS BY THEIR INTRATUMORAL LOCATION AND ENHANCED IMMUNE ACTIVITY

¹Ileana Mauldin*, ²Anne Stowman, ³Alexandra Hickman, ¹Adela Mahmutovic, ¹Alejandro Gru, ¹Kevin Lynch, ¹Samuel Young, ¹Max Meneveau, ¹Nolan Wages, ¹Victor Engelhard, ¹Craig Slingluff. ¹University of Virginia, Charlottesville, VA, USA; ²The University of Vermont, Burlington, VT, USA; ³Washington University School of Medicine, St. Louis, MO, USA

Background Tertiary lymphoid structures (TLS) are ectopic lymphoid organs that are localized near tumors and other sites of inflammation, and are commonly believed to support anti-tumor immunity. We previously published studies that show that most desmoplastic melanomas contain TLS, and that TLS in cutaneous metastatic melanomas varied widely in maturation state, in proportions of proliferating T and B cells, and in markers of B cell function, including AID and CD21. Thus, we hypothesized that there may be diversity in TLS function, or immunologic activity, among melanomas. To address this hypothesis, we evaluated TLS in primary desmoplastic melanomas (DM), and non-desmoplastic melanomas (non-DM) for markers of cell proliferation which are indicative of early immune activity.

Methods DM and non-DM tumor specimens, which included primary melanomas (PM), and cutaneous metastatic melanomas (CMM), were evaluated for TLS by multiplex Immunofluorescence histology, by staining for CD20, CD8, PNA⁺, Ki67, FoxP3, and DAPI. Lymphoid aggregates were identified in 20x spectrally unmixed images by visual inspection and identified as TLS if possessing organized T-cell and B-cell regions in addition to high endothelial venule-like vasculature (PNA⁺). TLS were identified in 30 out of 64 screened (48%) CMM, 4/4 non-DM PM, and 8 out of 11 screened (73%) DM. Immune cells localized in TLS were enumerated using Halo software (Indica Labs). Mann-Whitney tests were used for statistical assessments.

Results DM commonly contain a dense network of fibroblasts and associated stroma, which are not typical for other non-DM (PM and CMM). TLS in DM are located throughout the tumors, intratumorally, in sharp distinction from the peritumoral location of TLS in non-DM. Furthermore, when compared to TLS of non-DM (PM and CMM), TLS of DM contain increased densities of CD20⁺ B cells (PM $p=0.007$; CMM $p<0.0001$) and CD8⁺ T cells (PM $p=0.017$; CMM $p=0.0006$), and a higher proportion of proliferating (Ki67⁺) CD20⁺ B cells (PM $p=0.04$; CMM $p=0.009$).

Conclusions Recently published studies have identified tumor-associated fibroblasts as the likely initiating cells for TLS formation in murine melanomas. The intratumoral location of TLS in DM puts them in close proximity to the dense fibroblasts and desmoplastic stroma in these tumors, which may be responsible for their intratumoral location. The increased density of B and T cells, and higher proportion of proliferating (Ki67⁺) B cells, in DM than in non-DM, suggests that there may be greater immune activation, increased germinal center maturation, or less regulation in TLS of DM.

Ethics Approval Approval was obtained for these studies under IRB protocol #'s 10598 and 19694.

<http://dx.doi.org/10.1136/jitc-2021-SITC2021.047>

48 IMMUNE ENVIRONMENT CORRELATES WITH NSCLC AND CRC PATIENT SURVIVAL

Dannah Miller*, Huong Nguyen, Kate Hieber, Charles Caldwell, Roberto Gianani. *Flagship Biosciences, Broomfield, CO, USA*

Background Immune cells within the tumor microenvironment (TME) play a vital role in regulating tumor progression. Therefore, immunotherapies that stimulate anti-tumor responses are of great interest for the treatment of various cancers. PD-L1 expression on immune cells is positively correlated with increased patient survival. Our hypothesis is that non-small cell lung carcinoma (NSCLC) and colorectal cancer (CRC) patients with high immune infiltration and greater amounts of anti-tumor immune cells within the tumor compartment have an increased time of survival compared to cancers with immune excluded or immune desert environments.

Methods One NSCLC and one CRC tumor microarray (TMA) containing primary tumors, metastases, and normal tissue were stained via multiplex immunofluorescence (mIF) for 6 different immune markers: CD3, CD8, CD56, CD68, CD163, and PD-L1. This multiplex panel was designed to evaluate the immune cell population as well as tumor and immune cell PD-L1 status to aid in research for immunotherapies, specifically anti-PD-L1 therapies. The stained TMAs were analyzed utilizing Flagship Biosciences' proprietary image analysis platform. Machine learning algorithms stratified cells as belonging to the tumoral or stromal space based on their cellular features. Core level expression data was pulled and represented on a whole-cohort basis. All staining and image analysis outputs were reviewed by a board-certified, MD pathologist. Kaplan-meier curves were generated based on survival data in relation to the levels of immune cells present within the tumor cores as well as the percentage of immune cells infiltrating into the tumor.

Results There is a clear correlation between patient survival and the presence or absence of various types of immune cells, including helper T cells, cytotoxic T cells, M1 macrophages, M2, macrophages, NK cells, as well as PDL1 expression on tumor and immune cells. Specifically, the increased presence of anti-tumor immune cells as well as increased expression of PD-L1 on immune cells within the tumor compartment correlates with an increase in patient survival.

Conclusions Data generated through Flagship Biosciences' image analysis platform showed a strong relationship between immune cell presence and localization and NSCLC and CRC patient survival. Altering the immune cells within the tumor to an anti-tumor immune environment could increase patient survival times. Combining immune checkpoint inhibitors with current FDA approved therapies for NSCLC and CRC are of interest to further extend patient survival. Further, utilizing Flagship Biosciences' image analysis software to understand cancer immune microenvironments should be further utilized to aid in diagnosis and treatment decisions.

<http://dx.doi.org/10.1136/jitc-2021-SITC2021.048>

HIGHLY MULTIPLEXED DETECTION OF CRITICAL IMMUNE CHECKPOINTS AND IMMUNE CELL SUBTYPES IN CANCEROUS FFPE TISSUES USING CODEX

Olive Shang*, Judi Gordon, Nadya Nikulina*, Sejal Mistry, Jasmine Singh, Hailing Zong, Jessica Yuan, Trillium Blackmer, Darren Locke, Oliver Braubach, Julia Kennedy-Darling, Peter Miller. *Akoya Biosciences, Menlo Park, CA, USA*

Background There is growing consensus that spatial biology is the key to unlocking the underlying mechanisms of cancer immunotherapy and to predicting patient outcomes. Indeed, a recent example using the Akoya Phenoptics technology revealed a unique phenotypic signature of CD8/Foxp3 positive cells embedded within the tumor microenvironment of patients that responded favorably to PD-1 checkpoint inhibition.¹ In this case, the combination of both multiparameter and spatial readouts was required to correlate significantly with outcome. As the number of treatment options expands and knowledge regarding cell types that contribute to treatment mechanisms improves, so too do the number of markers required to analyze responses that enable discovery of new signatures.

Methods Here, we present data from the analysis of human FFPE cancer tissues using an expanded CODEX antibody catalog targeting a variety of immune, immune checkpoint and transcription factors. CODEX enables the highly multiplexed detection of more than 40 targets within the same tissue sample, with single cell resolution and without degradation of the sample.

Results Our expanded target list enables detection of key macrophage populations, T and B cell subtypes, granulocytes, dendritic cells, natural killer cells, stromal, tumor and epithelial cells. Additionally, the activation state of these immune and tumor cell types can be measured through detection of key immune checkpoints, including PD-1 and PD-L1. Through the addition of these critical markers, both cells known to contribute to treatment outcome and new biomarker signatures can be identified.

Conclusions Continued expansion of spatial biology discovery capabilities will be critical to continuing to improve patient outcomes and to develop new treatment options of solid tumors using cancer immunotherapies.

REFERENCE

1. Berry S, Taube J, et al. Analysis of multispectral imaging with the AstroPath platform informs efficacy of PD-1 blockade. *Science*. 2021; 372: 6547.

<http://dx.doi.org/10.1136/jitc-2021-SITC2021.049>

IN-SITU VISUALIZATION AND MEASUREMENT OF TUMOR-INFILTRATING LYMPHOCYTES (TILS) ON INTACT FFPE RENAL CELL CARCINOMA (RCC) TISSUE USING THE SPATIAL MOLECULAR IMAGER (SMI)

¹Evan Newell, ²Youngmi Kim*, ¹Heeju Ryu, ¹Shamin Li, ²Michael Leon, ²Sean Kim, ²Mark Gregory, ²Patrick Danaher, ²Joseph Beechem. ¹Fred Hutchinson Cancer Research Center, Seattle, WA, USA; ²Nanostring Technologies, Seattle, WA, USA

Background Although cancer immunotherapies can effectively restore T cell-mediated immunity leading to sustained clinical responses, these responses are unpredictable partly due to highly heterogeneous phenotypes of tumor-infiltrating lymphocytes (TILs) between patients. Thus, understanding such TILs and their roles in the context of tumor microenvironments (TME) may lead to developing better immunotherapy solutions. The spatial molecular imager (SMI) is a novel spatial transcriptomics platform that allows spatially resolved high-dimensional cellular phenotyping for comprehensive TIL profiling. SMI uses fluorescent molecular barcodes to enable in-situ measurement of biological targets on an intact tissue sample. Here, we characterize comprehensive TIL phenotypes and visualize landscape of TILs directly on intact formalin-fixed paraffin-embedded (FFPE) tissues using a 1000+-plex RNA panel.

Methods To build multi-omics TIL profiling data sets for renal cell carcinoma (RCC) tissues, we employed scRNA-seq, mass cytometry (CyTOF) and SMI. Peripheral blood mononuclear cells and dissociated cells from matched RCC tumor and adjacent normal tissues were analyzed by CyTOF and single-cell sequencing. Then, SMI profiling of matching FFPE tissues was used to visualize TILs in the context of the TME and to understand relationships between high-dimensional cellular heterogeneity and the spatial organization of cells within a tumor tissue.

Results CyTOF and scRNA-seq analysis of dissociated cells was used to determine the gene expression profiles of numerous cellular subsets. TCR sequencing was also used to assess the extent of clonal expansion and clonotypic relationships between blood and tumor. Consistent with our previous reports, T cell populations could be segregated based on markers associated with chronic T cell receptor signaling and many T cells with an exhausted phenotype were clonally expanded in the tumor but not the blood. In contrast, T cell clonotypes with bystander phenotypes in the tumor were readily detected as expanded clones in the blood, supporting notion that not all tumor-infiltrating T cells are specific for tumor antigens. SMI analysis of matched tumor tissue was used to accurately quantify the densities and to determine the spatial organization of all T cell subsets. In addition, computational methods were used to describe distinct cellular niches within tumors with accurately defined cellular compositions.

Conclusions High dimensional cellular profiling highlights the abundance of bystander T cell infiltration of RCC tumors. Comprehensive spatial profiling by SMI provides spatial context to the highly diverse immune cell composition of tumor infiltrates.

Ethics Approval Fully anonymous human material was obtained from Northwest Biotrust and given IRB designation of non-human subjects research.

<http://dx.doi.org/10.1136/jitc-2021-SITC2021.050>

**A NOVEL CROSS-SITE ANALYSIS OF VECTRA®
POLARIS™ MULTIPLEX FLUORESCENCE PD-1/PD-L1
IMMUNOHISTOCHEMISTRY ON COLORECTAL CANCER
WITH HIGH AND LOW MICROSATELLITE INSTABILITY**

¹Sara Pollan, ²Bethany Remeniuk, ¹Arezo Hanifi, ²Kristin Roman, ²Bei Hopkins, ²Natalie Monteiro, ¹Harry Nunns, ¹Erinn Parnell, ¹Josette William, ¹Qingyan Au*. ¹NeoGenomics Laboratories Inc., Aliso Viejo, CA, USA; ²Akoya Biosciences, Marlborough, MA, USA

Background Colorectal cancer (CRC) is the third most diagnosed cancer in the United States with a projected 52,980 deaths in 2021.¹ Microsatellite instability-high (MSI-H) CRCs with deficiencies in mismatch repair (MMR) are significantly associated with positive response to immunotherapy and improved outcomes when treated with immune checkpoint inhibitors. Programmed cell death ligand-1 (PD-L1) is an effective biomarker of MSI-H status to identify CRC patients who will respond to treatment, however, reproducible quantification of programmed cell death receptor-1 (PD-1)/PD-L1 in the tumor microenvironment (TME) across laboratory sites has been under-reported.²⁻³ In this study, our group directly addressed this issue by interrogating PD-1/PD-L1 cross-site at Akoya Biosciences and NeoGenomics Laboratories by employing the MOTiF™ PD-1/PD-L1 Panel kit along with the Vectra Polaris imaging system.

Methods Serial sections from 40 CRC samples with known MSI status were stained at Akoya and NeoGenomics Laboratories using a modified MOTiF PD-1/PD-L1 Lung Panel Kit on the Leica BOND RX. Sections were scanned using the Vectra Polaris imaging system at both sites. Inter-site staining reproducibility was assessed using image analysis algorithms developed with inForm tissue analysis software. Cell counts and densities were calculated using the R-script package Phenoptr. Reports and correlations were plotted per marker.

Results The average signal intensity for all markers/Opal fluorophores was within the recommended ranges of 10–30 normalized counts, with the exception of Polaris 780, which has an advised range of 1–10. This indicates the protocol stained successfully and reproducibly across all serial sections at both sites. Inter-site concordance analysis of cell densities for each marker yielded an average R2 value of ≥ 0.70 . H-Score of PD-L1 quantified at the cell membrane trended with MSI status (stable/high).

Conclusions This study demonstrated that the MOTiF PD-1/PD-L1 Panel kit imaged in conjunction with the Vectra Polaris is not only a reliable assay that can be run across different sites, based on the concordant cross-site data, but that re-optimization of the kit allows for the assay panel to be successfully adapted to other cancers, such as CRC, which can then capture biological differences across a multitude of samples.

REFERENCES

1. American Cancer Society <https://www.cancer.org/cancer/colon-rectal-cancer/about/key-statistics.html>
2. Yi M, Jiao D, Xu H, Liu Q, Zhao W, Han X, et al. Biomarkers for predicting efficacy of PD-1/PD-L1 inhibitors. *Mol Cancer* 2018;**17**(1):129
3. Lemery S, Keegan P, Pazdur R. First FDA approval agnostic of cancer site - when a biomarker defines the indication. *N Engl J Med* 2017;**377**(15):1409–12.

<http://dx.doi.org/10.1136/jitc-2021-SITC2021.051>

**CHARACTERIZATION OF THE TUMOR
MICROENVIRONMENT IN MELANOMA USING
MULTIPLEXED ION BEAM IMAGING (MIBI)**

¹Jason Ptacek*, ²Matthew Vesely, ²David Rimm, ¹Monirath Hav, ¹Murat Aksoy, ¹Ailey Crow, ¹Jessica Finn. ¹Ionpath, Inc, Menlo Park, CA, USA; ²Yale University School of Medicine, New Haven, CT, USA

Background The complexity of the tumor microenvironment (TME) necessitates the application of high-dimensional methods that can spatially resolve the phenotypic heterogeneity that exists within tumors. MIBI, which combines time-of-flight secondary ion mass spectrometry (ToF-SIMS) with metal labeled antibodies to simultaneously image 40+ proteins at subcellular spatial resolution, was used to classify cell populations and their expression of immunoregulatory proteins within 54 melanoma samples.

Methods A tissue microarray (TMA) comprised of 0.6 mm FFPE melanoma cores was stained with a panel of 30 metal labeled antibodies. The tissue was imaged using MIBI and multi-step processing was performed to create images of the samples. Single cell segmentation enabled enumeration of 32 cell populations and quantitative analyses were performed of both immune checkpoint expression and the spatial relationships between cells of different types.

Results Tumor cells and immune cells represented 62% (1.4% - 92.2%) and 24% (2.0% - 92.1%), respectively, of the segmented cells from the melanoma samples. Fibroblasts, lymphatics, and blood vessels were also present at varying densities. Within the immune compartment, M2 macrophages, M2 monocytes, and monocyte-derived dendritic cells (mDCs) were most abundant, representing 36.3% (4.9% - 79.3%), 7.0% (0.0% - 30.6%), and 9.8% (0.0% - 34.6%), respectively, of the total immune cell infiltrate. Rare populations such as myeloid-derived suppressor cells (MDSCs) and regulatory T cells were at greater than 100 cells/mm² in six samples and four samples, respectively. The presence of immune checkpoint markers (IDO-1, LAG3, PD-1, PD-L1, TIM-3) varied between populations and between samples. A minority of the samples showed expression of IDO-1 and PD-L1 on myeloid populations. Interestingly, among the myeloid subsets, M2 macrophages and monocyte-derived dendritic cells showed the most abundant PD-L1 expression. Although many samples had few T cell infiltrates, those that did showed expression of PD-1, LAG-3, and TIM-3 on T cell populations.

Conclusions MIBI offers high-parameter tissue imaging, at sensitivity and resolution suited to understanding the complex tumor immune landscape, including the spatial relationships of immune and tumor cells and the expression of immunoregulatory proteins. Datasets that quantify population densities and immune checkpoint expression levels across tumor samples, such as the present one, can be used to test for associations to clinical variables and further understand the TME at the cellular level.

<http://dx.doi.org/10.1136/jitc-2021-SITC2021.052>

**UNIQUE INSIGHTS INTO PDAC DEVELOPMENT
REVEALED BY BOTH INSITUPLEX[®] AND IMAGING MASS
CYTOMETRY**

¹Andrew Quong, ²Mark Rees, ²Kirsteen Maclean, ²Mael Manesse, ¹Jordan Nieto*,
¹Amanda Esch, ²Devan Fleury, ²Keith Wharton, ²Gourab Chatterjee. ¹*Fluidigm, South San
Francisco, USA*; ²*Ultivue, Huntington, NY, USA*

Background Pancreatic cancer remains a deadly disease due to difficulties hindering its early diagnosis, giving way to metastasis of the tumor and resulting in poor prognosis. While there are many neoplasms of the pancreas, pancreatic invasive ductal adenocarcinoma (PDAC) is the most common and treatment options are few, with poor overall survival. Aggressive surgeries such as the Whipple procedure coupled to systemic chemotherapy is one of the few treatment options. Recently, several publications have demonstrated improved outcomes with the inclusion of immunotherapy to cytotoxic drug combinations in some patients, however optimally selecting patients as candidates for immunotherapy-chemotherapy combinations remains a critical challenge. The complexities of the tumor microenvironment have been implicated in the failure of chemotherapy, radiation therapy, and immunotherapy. The tumor microenvironment of PDAC is especially rich with multiple interactions between pancreatic epithelial/cancer cells, stromal cells, immune cells and the extracellular matrix (ECM). PDACs are characterized by a complex ECM of desmoplastic reaction consisting of an extensive and dense fibrotic stroma that surrounds and infiltrates clusters of malignant epithelial cells, together with the loss of basement membrane integrity and an abnormal vasculature.

Methods In the present study we demonstrate a tissue phenotyping workflow combining three complementary methods that can unravel novel insights in the complex tumor microenvironment. This novel translational workflow delivers tissue morphology information, spatial phenotyping of immune cell population on whole slides, and high dimensional imaging in selected regions of interest (ROI), by combining H&E, multiplex immunofluorescence (mIF), and Imaging Mass Cytometry (IMC[™]).

Results The use of the InSituPlex[®] UltiMapper[®] I/O PD-L1 kit enabled the streamlined combination and alignment of H&E and mIF data, leading to the strategic selection of relevant ROIs, while utility of IMC technology enabled downstream imaging of 35 protein markers associated with the ECM in the selected ROIs to provide a deeper understanding of the tumor microenvironment.

Conclusions The incorporation of advanced multiplex imaging platforms such as mIF and IMC with routine H&E workflow in tumor biology can deliver some of the much-needed insight into tumor morphology, cellular composition, cellular functions, and cell-cell interactions and paves the way for potentially improved clinical prognosis and efficacy prediction in patients with cancer.

<http://dx.doi.org/10.1136/jitc-2021-SITC2021.053>

A STRATEGY TO QUANTITATIVELY ASSESS THE ACCURACY AND PRECISION OF MULTIPLEX IMMUNOFLUORESCENCE ASSAYS – APPLICATION TO ULTIVUE INSITUPLEX® PD-L1, T-ACT AND APC PANELS

Sripad Ram*, Eric Powell. *Pfizer, Inc., San Diego, CA, USA*

Background Multiplex immunofluorescence assays represent an essential tool in immuno-oncology research. The recent past has witnessed the introduction of several multiplexing methodologies to detect multiple biomarkers on a single tissue section. The quantitative assessment of the accuracy and precision of multiplex panels is of paramount importance for their widespread use in clinical samples. While there have been numerous reports providing qualitative characterization of multiplex panels, there is a paucity of data concerning the quantitative validation of these panels.

Methods Ultivue Insituplex® T-act, PD-L1 and APC panels, which are 4-plex assays, were evaluated using breast tumor resections with varying levels of T-cell infiltration. For each panel, accuracy and precision was evaluated through a concordance and a reproducibility test, respectively. In the concordance test, five serial sections from each tumor specimen were cut and the 3rd (middle) serial section was immunolabeled with the 4-plex assay whereas the remaining sections were immunolabeled for the individual biomarkers (1-plex) that comprised the 4-plex assay. In the reproducibility test, five serial sections from each tumor specimen were immunolabeled with the 4-plex assay in separate, independent runs. The coefficient of variation (CV) of the density of different cell phenotypes was quantified from the serial sections and was used to assess the precision of that multiplex panel. All whole-slide image analysis was performed in QuPath software (version 0.2.3).

Results The results of the concordance test revealed that the relative difference in the single-biomarker cell density between 1-plex and 4-plex assays for the biomarkers in the 3 panels was typically less than 25%. Results of the precision test revealed that the CV for most cell phenotypes was typically less than 30%. We also identified special phenotypes such as CD3+PanCK+ cells and CD3+CD68+ cells, which exhibited unexpected combinations of biomarkers. Additional analysis revealed that these special phenotypes were in fact pairs of touching cells that were positive for the corresponding individual biomarkers (e.g., CD3+ cell touching a PanCK+ cell), and that this was due to limitations in the image analysis software package to segment the touching nuclei as two separate entities.

Conclusions Our results demonstrated that the Ultivue panels evaluated here had satisfactory accuracy and precision in breast tumor resections. The identification of special cell phenotypes in our data revealed the potential shortcomings of image analysis software and underscored the importance of performing a comprehensive evaluation of the multiplex assay as well as the image analysis workflow.

Ethics Approval The biospecimens used in the study were anonymized specimens which were collected with written patient consent, processed and distributed in full ethical and regulatory compliance with the Sites from which they were collected. This includes independent ethical review, Institutional Review Board approval (where appropriate), and independent regulatory review.

<http://dx.doi.org/10.1136/jitc-2021-SITC2021.054>

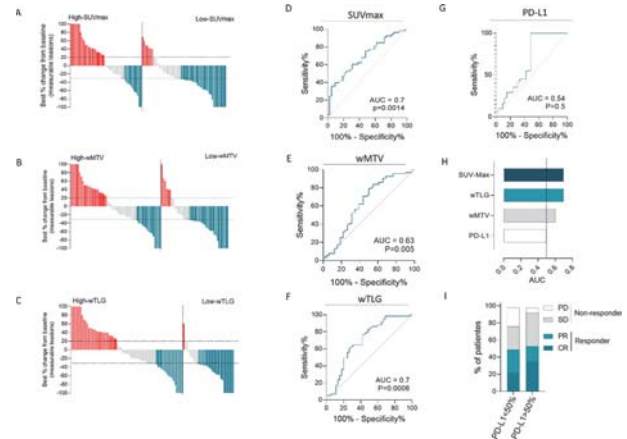
BASELINE GLYCOLYTIC TUMOR BURDEN PREDICTS RESPONSE AND SURVIVAL IN NSCLC AND MELANOMA PATIENTS TREATED WITH IMMUNE CHECKPOINT INHIBITORS

¹Saulo Silva*, ¹Carlos Wagner Wanderley, ²Jose Flavio Marin, ²Mariana De Macedo, ²Ellen Nascimento, ²Fernanda Antonacio, ¹Fernando Cunha, ²Gilberto de Castro. ¹Faculdade de Medicina de Ribeirão Preto – Universidade de São Paulo, Ribeirão Preto, Brazil; ²Hospital Sírio-Libanês, São Paulo, Brazil

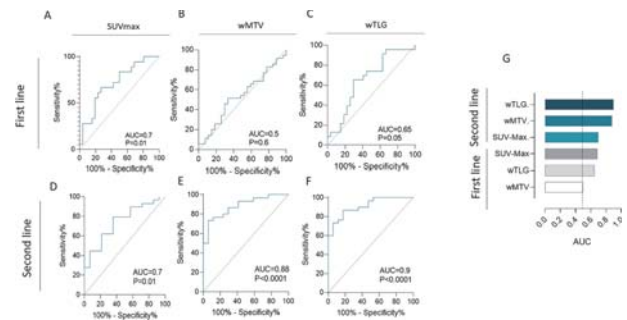
Background Tumor metabolic remodeling is considered one of the hallmarks of cancers and has been implicated in immune evasion. Highly glycolytic tumors can lead to immune suppression by both nutrient competition and toxic metabolite accumulation. Immune checkpoint inhibitors (ICIs) are essential in treating melanoma and non-small cell lung cancer (NSCLC) patients, but novel predictive biomarkers can significantly contribute to clinical practice. Herein we analyzed the predictive and prognostic value of baseline metabolic tumor volumes in NSCLC and melanoma patients treated with ICIs.

Methods This retrospective, single-center study includes patients with metastatic NSCLC or melanoma and a baseline 18F-FDG-PET/CT (PET) performed before ICI. PET studied parameters were SUV (maximum standardized uptake value), wMTV (whole metabolic tumor value), and wTLG (whole total lesion glycolysis). Best response rates were analyzed through RECIST. High or low glycolytic tumor burden (GTB) patients were defined according to SUV, wMTV, and wTLG cut-offs that best discriminate progressive disease. Overall survival (OS) and progression-free survival (PFS) were estimated using the Kaplan-Meier method, and curves were compared with log-rank.

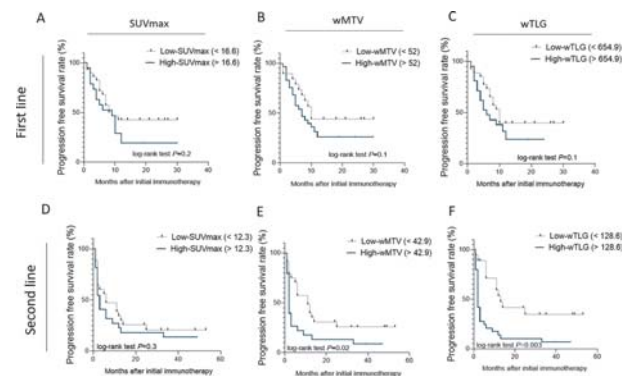
Results Among 151 patients included, 107 had NSCLC and 44 melanoma. Regarding NSCLC patients, there was a significant correlation between GTB and responses among all PET parameters (figure 1). Noteworthy, only one patient with a low wTLG (<146) showed progressive disease after ICIs (figure 2C). In regard to the potential in predicting response to ICIs, the area under the curve (AUC) obtained for each glycolytic parameter was higher than that for PD-L1 expression (figure 2D-H). Furthermore, when patients were categorized according to ICI exposure (1st or ≥ 2nd line), AUC for glycolytic parameters was higher in ≥ 2nd line versus 1st line (figure 3). Lastly, a low GTB was associated with improved PFS (figure 4) and OS (figure 5). Regarding melanoma patients, wMTV and wTLG were significantly associated with response (figure 6), and a low GTB was significantly associated with improved PFS and OS (figure 7).



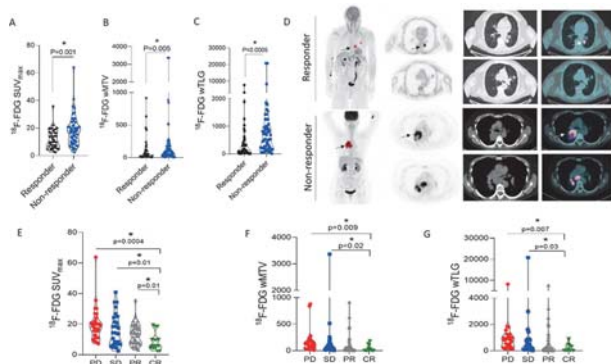
Abstract 55 Figure 2



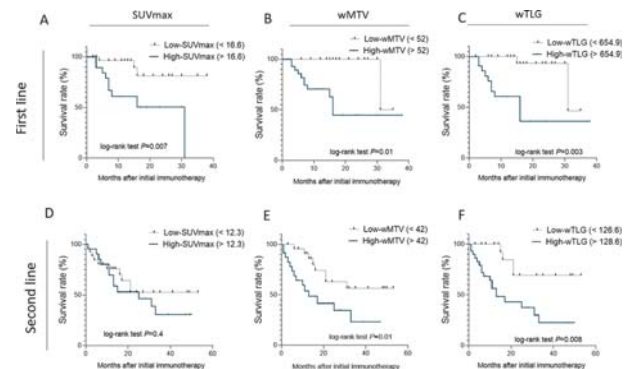
Abstract 55 Figure 3



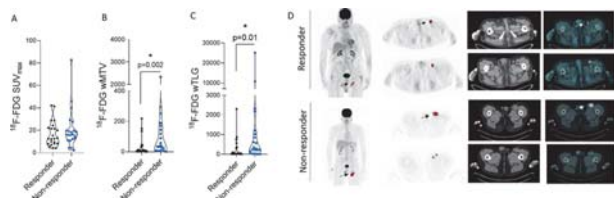
Abstract 55 Figure 4



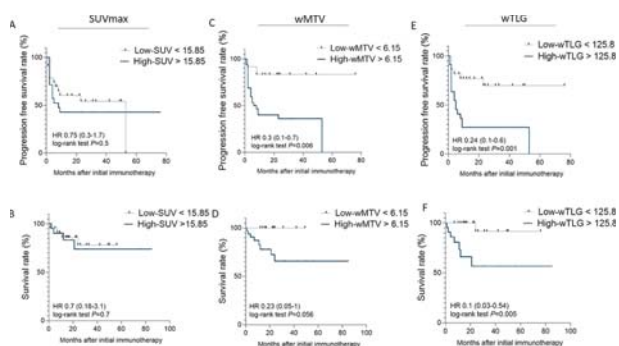
Abstract 55 Figure 1



Abstract 55 Figure 5



Abstract 55 Figure 6



Abstract 55 Figure 7

Conclusions GTB accessed through a baseline PET is associated with survival and response to ICIs in NSCLC and melanoma patients, suggesting that the tumor metabolism might impact immune responses and be a promising predictive tool.

Ethics Approval The study obtained ethics approval by Sírío-Libanês Hospital institutional review board. Study participants were not required to give an informed consent before taking part.

<http://dx.doi.org/10.1136/jitc-2021-SITC2021.055>

QUANTITATIVE EVALUATION OF THE TISSUE MICRO-ENVIRONMENT BY HIGH-RESOLUTION 17-PLEX IMMUNOFLOUORESCENCE REVEALS DISTINCT CELL POPULATIONS

¹Kyla Teplitz, ¹Daniel Campton, ¹Erin McCarty, ¹Jeremy Cooper, ²Anne Hellebust, ²Donald Allen, ²Kimberly Collins, ²Kate Lillard, ¹Eric Kaldjian, ¹Tad George*. ¹RareCyte, Seattle, WA, USA; ²Indica Labs, Albuquerque, NM, USA

Background Inflammatory tumor micro-environments contain cells of various types and sub-types. The composition and spatial location of the cell populations reflects the host reaction to the inflammatory stimulus and increasingly is understood to influence responsiveness to tumor immunotherapies. Multiplexed imaging technologies allow identification of cell types and states within the spatial context of tissue architecture. We present here a prototype workflow that combines rapid high-resolution, whole-slide highly multiplexed immunofluorescence imaging with advanced image analysis tools for 1) segmenting tissues, cells, and quantifying cellular phenotypes based on multiple markers and 2) determining regional densities and proximity between cells. We apply the workflow to comparative assessment of three lymphoid tissues: tonsil (follicular hyperplasia); lymph node (quiescence); lymphoma (architectural effacement).

Methods Formalin-fixed, paraffin-embedded 5 micron sections of tonsil, lymph node and chronic lymphocytic leukemia/small lymphocytic lymphoma were deparaffinized, subjected to alkaline pH epitope retrieval, and then manually stained with a 17-plex panel including CD45 (leukocytes); CD20 (B cells); CD3d, CD4, CD8 (T cells); FOXP3 (T reg cells); CD68, CD163 (macrophages); CD45RO (activated cells); PD-L1, PD-1 (checkpoint markers); CD31 (vascular and lymphatic endothelial cells); cytokeratin, E-cadherin (epithelial cells); PCNA, Ki-67 (proliferating cells); and a nuclear dye. Stained slides were coverslipped and imaged on the Orion Instrument (RareCyte) generating .ome tiff image files. The HighPlex FL module of the HALO image analysis platform from Indica Labs with embedded HALO AI performed nuclear and cell segmentation, nuclear phenotyping, and user-defined thresholds were applied to each of the biomarkers to define positivity for the appropriate subcellular localization (nuclear, cytoplasmic, and/or membrane) for phenotypic analysis. H & E images from either the same or serial sections were integrated with the multiplex images using the HALO Serial Stain module.

Results Regional masks that were defined by predominance of B-cells (CD20) or T-cells (CD3d) matched known lymphoid micro-anatomy of follicles and inter-follicular cortex respectively. Within the regions, populations and sub-populations of B-cells, T-cells, macrophages and vessels were measured, and their densities calculated and compared between tissues. Rare cell types of potential importance in immuno-oncology were investigated. The results demonstrate differences between the tissues at a phenotypic level that correspond to the morphologic differences seen by light microscopy.

Conclusions Orion imaging combined with HALO image analysis provides a powerful and intuitive workflow for visualization and quantification of distinct microenvironment populations for use in translational and clinical research.

<http://dx.doi.org/10.1136/jitc-2021-SITC2021.056>

57 **ASSESSMENT OF THE SPATIAL DISTRIBUTION OF B CELLS SUBPOPULATIONS IN THE TUMOR MICROENVIRONMENT AND TERTIARY LYMPHOID STRUCTURES BY BRIGHTPLEX®, A SEQUENTIAL CHROMOGENIC MULTIPLEX ASSAY**

¹Alex Trinh, ¹Aurélie Collignon, ¹Marion Olive, ¹Clémence Jaume, ¹Maité Chamourin, ¹Nour Sfeir, ¹Dylan Anselmo, ¹Raana Ramouz-Charpentier, ¹Georgia Culey, ¹Christophe Haond*, ²Jerome Galon, ¹Jacques Fieschi-Meric. ¹*HaliDx, Marseille, France*; ²*INSERM, Paris, France*

Background Density and localization of T cells within the tumor microenvironment (TME) is critical to control tumor growth. Immunotherapy with antibodies against immune checkpoint inhibitors (ICI), which aim to reinvigorate exhausted T cells, despite inducing long-term response in many cancer types, remains ineffective for most patients. Other factors present in the TME may participate in the control of tumors, among several candidates, the role of B cells has been underestimated. Publications revealed that B-cells are associated with good prognosis in several indications. However, there are no general rules since neutral or even deleterious impact of the presence of B-cells in the tumor was reported. Among other hypotheses, we can suppose that the level of activation and isotype switch will be important to mediate activation of NK cells or ADCC within the tumor and will have a favorable impact on the prognosis. In addition, the spatial distribution of B-cells may be important since, in the TME, they are mostly located in Tertiary Lymphoid Structures (TLS) which are ectopic lymphoid organs. Mature TLSs contain zones where dendritic cells (DC) present antigen to T-cells and others where proliferating B-cells undergo class switch and maturation toward plasma cells. Antigen presentation by B cells to T cells is supported by DCs, therefore, the presence of these three types of cells within the TLS allows T cell activation in the TME. If B-cells are major players in the therapeutic efficacy of ICI antibodies, not all subtypes of tumor infiltrating B-cells are likely to participate in response to immunotherapy.

Methods To decipher the roles of B cells, new tools are needed to identify the differentiation and activation status of individual B cells. We have developed a 7-plex panel of antibodies against biomarkers that allow the identification of main types of B cells.

Results On a single FFPE tissue section: naïve, unswitched memory, switched memory, activated, plasmablast and plasma B cells, as well as T cells and DC are identified. Following images registration, complex cells phenotypes can be detected and quantified. Furthermore, digital pathology tools allow the evaluation of the spatial distribution within the TME of subtypes of B cells especially in association with TLSs.

Conclusions This new tool unravels the heterogeneity of B cells in TME and could help clinical researchers to understand their contribution to the response to immunotherapy. Integrated into an Immunogram, this new Brightplex® Panel will be critical to understand the immune contexture of the tumor.

<http://dx.doi.org/10.1136/jitc-2021-SITC2021.057>

**ANALYTICAL VALIDATION OF A NOVEL
IMMUNOHISTOCHEMISTRY ASSAY TO DETERMINE
NUCLEAR AHR EXPRESSION IN HUMAN BLADDER
CANCER**

Lei Wang*, Marta Sanchez-Martin, Steve Tirrell, Nerymar Ortiz-Otero, Michelle Zhang. *Ikena Oncology, Boston, MA, USA*

Background Aryl hydrocarbon receptor (AHR) is a ligand-activated transcription factor that translocates to the nucleus upon ligand binding, and activates a target gene expression program, contributing to the immunosuppressive state of the tumor microenvironment.¹ IK-175 is a selective, oral, potent AHR antagonist that has demonstrated strong immune modulation, and robust tumor growth inhibition, either as a single agent or in combination with anti-PD-1, in mouse models. IK-175 is being evaluated in an ongoing phase 1 clinical study as a single agent and in combination with nivolumab for bladder cancer patients (NCT04200963). We hypothesized that nuclear AHR protein expression in tumors is an indicator of activated AHR signaling, and thus a potential predictive biomarker for the clinical response to IK-175. To test this hypothesis, we have developed a novel AHR immunohistochemistry (IHC) assay and analytically validated it in a Clinical Laboratory Improvement Amendments (CLIA) certified lab. We have successfully implemented it in our ongoing phase 1b clinical trial of IK-175 for prospective patient enrollment.

Methods The AHR IHC assays were developed in collaboration with Flagship Biosciences and Neogenomics on a Leica Bond RX and a CDx-compatible Leica Bond III platform, respectively. AHR expression pre-characterized cell lines, xenografts, and human bladder cancer samples were used to optimize the IHC conditions for specific and sensitive detection of nuclear AHR protein. The Neogenomics assay was further analytically validated for accuracy, sensitivity, specificity, and precision. The IHC assay developed in Flagship was used as an orthogonal comparator for accuracy testing. A cutoff value for AHR nuclear positivity was also determined by assessing n=200 human bladder cancer specimens.

Results To determine the prevalence of nuclear AHR expression in human bladder cancer, two hundred unique human bladder cancer specimens, including sixty bladder cancer blocks and 2 tumor microarrays, were analyzed. A cutoff of 65% tumor cells positive for 2+/3+ nuclear AHR was determined to enable a targeted enrollment of 1 in 3 to 5 patients screened. Assay accuracy, sensitivity, specificity, and precision were assessed, and reached 96%, 100%, 95%, and 100% respectively. The intra-pathologist concordance was also assessed to be 90% concordant. The assay passed the pre-defined acceptance criteria (>85%) in all parameters.

Conclusions A novel and robust nuclear AHR IHC assay for bladder cancer was developed and analytically validated in a CLIA certified lab and showed $\geq 95\%$ accuracy, specificity, sensitivity, and precision, enabling its implementation in an IK-175 Ph1b clinical study (NCT04200963) for prospective patient enrichment.

Trial Registration NCT04200963

REFERENCE

1. Campesato L, Budhu S, Tchaicha J, et al. Blockade of the AHR restricts a Treg-macrophage suppressive axis induced by L-Kynurenine. *Nature Communications* 2020; **11**:4011

<http://dx.doi.org/10.1136/jitc-2021-SITC2021.058>

ASSOCIATIONS BETWEEN KIR/KIR-LIGAND GENOTYPES AND CLINICAL OUTCOME FOR PATIENTS WITH ADVANCED SOLID TUMORS RECEIVING BEMPEG PLUS NIVOLUMAB COMBINATION THERAPY IN THE PIVOT-02 TRIAL

¹Arika Feils*, ¹Amy Erbe, ¹Jen Birstler, ¹KyungMann Kim, ²Ute Hoch, ²Sue Currie, ²Tuan Nguyen, ²Danni Yu, ³Arlene Siefker-Radtke, ³Nizar Tannir, ⁴Matthew Hellmann, ⁵Sara Tolaney, ³Adi Diab, ¹Paul Sondel. ¹University of Wisconsin-Madison, Madison, WI, USA; ²Nektar Therapeutics, San Francisco, CA, USA; ³The University of Texas, Houston, TX, USA; ⁴Memorial Sloan Kettering Cancer Center, New York, NY, USA; ⁵Harvard Medical School, Boston, MA, USA

Background High-dose IL2 therapy has shown clinical benefit in metastatic melanoma and renal cell carcinoma, however only in a select subset of patients. Bempegaldesleukin (BEMPEG), a novel CD122-preferential IL2 pathway agonist, preferentially binds the heterodimeric IL2 β γ R predominantly expressed on NK and CD8 T cells and minimizes binding to the IL2 α R expressed on immunosuppressive Tregs. BEMPEG monotherapy in Phase I clinical trials induced proliferation and activation of NK cells in the blood and tumor microenvironment.¹ NK activation is dependent on the balance of inhibitory and excitatory signals transmitted by NK receptors, including Fc-gamma receptors (FC γ Rs) and killer immunoglobulin-like receptors (KIRs) along with their KIR-ligands. The repertoire of KIRs/KIR-ligands an individual inherits and the single-nucleotide polymorphisms (SNPs) of FC γ Rs can influence NK cell function and affect responses to immunotherapies.²⁻⁴ Thus, we sought to investigate whether distinct immunogenotypes are associated with clinical response of patients enrolled in PIVOT-02, a Phase II study of BEMPEG plus nivolumab.

Methods 200 patients with advanced solid tumors enrolled in PIVOT-02 who were not previously treated with immunotherapy (immunotherapy-naïve, 'IO') had DNA available for genotyping and clinical data for correlative analyses. All patients received 0.006mg/kg BEMPEG plus 360mg nivolumab every 3 weeks.⁵ KIR/KIR-ligand gene status was assessed by real-time SYBR green PCR melt-curve analyses and PCR-SSP. FC γ R SNP status was determined using Taqman primers/probes for FC γ R2A, and FC γ R3A and FC γ R2C were determined using RNaseH primers/probes.⁶ Clinical outcome parameters included objective response rate (ORR), progression-free survival (PFS), and tumor shrinkage (TS, defined as best objective response <0% by RECIST). Preliminary statistical analyses were done using a chi-square test, log-rank test, and Wilcoxon rank-sum test, respectively.

Results KIR2DL2+/C1+ IO patients observed significantly greater TS (p=0.015) and a trend towards improved ORR (p=0.060) and increased PFS (p=0.058) compared to IO patients who were not KIR2DL2+/C1+. IO patients who were KIR2DL2+/C1+/KIR3DL1+/Bw4+ showed significantly improved ORR (p=0.014) and greater TS (p=0.044) compared to IO patients who were not KIR2DL2+/C1+/KIR3DL1+/Bw4+, with no significance found for PFS in these patients. FC γ R polymorphisms did not influence ORR/PFS/TS.

Conclusions NK cells may play an important role in the anti-tumor efficacy of BEMPEG plus nivolumab, and NK activation is influenced by certain immunogenotypes. Similar to previous findings,²⁻⁴ the status of KIR2DL2+/C1+ and KIR2DL2+/C1+/KIR3DL1+/Bw4+ was associated with the response to BEMPEG plus nivolumab treatment in the PIVOT-02 trial. The potential to utilize these genotypes in clinical decision-

making for immunotherapy treatment requires further investigation.

Trial Registration ClinicalTrials.gov NCT02983045

REFERENCES

1. Benteibibel S-E, et al. A first-in-human study and biomarker analysis of NKTR-214, a Novel IL2 β -Biased cytokine, in patients with advanced or metastatic solid tumors. *Cancer Discov* 2019;**9**:711–21.
2. Erbe AK, et al. Follicular lymphoma patients with KIR2DL2 and KIR3DL1 and their ligands (HLA-C1 and HLA-Bw4) show improved outcome when receiving rituximab. *J Immunother Cancer* 2019;**7**(1):70.
3. Erbe AK, et al. Neuroblastoma patients' KIR and KIR-Ligand genotypes influence clinical outcome for dinutuximab-based immunotherapy: A report from the Children's Oncology Group. *Clin Cancer Res* 2018;**24**(1):189–96.
4. Erbe AK, et al. FCGR polymorphisms influence response to IL2 in metastatic renal cell carcinoma. *Clin Cancer Res* 2017;**23**(9):2159–68.
5. Diab A, et al. Bempegaldesleukin (NKTR-214) plus nivolumab in patients with advanced solid tumors: Phase I dose-escalation study of safety, efficacy, and immune activation (PIVOT-02). *Cancer Discov* 2020;**10**:1–16.
6. Erbe AK, et al. Genotyping single nucleotide polymorphisms and copy number variability of the FCGRs expressed on NK cells. *Methods Mol Biol* 2016;**1441**:43–56.

Ethics Approval The study was conducted in accordance with Good Clinical Practice guidelines and the Declaration of Helsinki. The Protocol (online only) was approved by independent ethics committees and the relevant institutional review board at each site. All patients provided written informed consent.

<http://dx.doi.org/10.1136/jitc-2021-SITC2021.059>

USE OF THE COMBINED POSITIVE SCORE (CPS) WITH THE COMPANION DIAGNOSTIC PD-L1 IHC 22C3 PHARMDX PROVIDES PRECISE EVALUATION OF PD-L1 EXPRESSION ACROSS MULTIPLE TUMOR INDICATIONS AND CUTOFFS

Francisco Ponce*, Stephanie Hund, Lindsay Peltz, Chris La Placa, Monika Vilardo, Brittany Watts, Siena Tabuena-Frolli, Grant Toland, Alex Posch, Jay Milo, Karina Kulangara, Angeliki Apostolaki. *Agilent Technologies, Carpinteria, CA, USA*

Background The Combined Positive Score (CPS)¹ algorithm includes tumor and immune cells for determination of Programmed Death-Ligand 1 (PD-L1) protein expression in tumor tissues and has been analytically and clinically validated for use with PD-L1 IHC 22C3 pharmDx across multiple indications and cutoffs.² PD-L1 22C3 IHC pharmDx is a qualitative immunohistochemical assay using anti-PD-L1, Clone 22C3 to detect PD-L1 in formalin-fixed, paraffin-embedded (FFPE) tumor tissues using Autostainer Link 48. PD-L1 IHC 22C3 pharmDx is FDA-approved as an aid in identifying patients for treatment with KEYTRUDA[®] for six tumor indications at clinically validated CPS diagnostic cutoffs²: gastric or gastroesophageal junction (GC/GEJ) adenocarcinoma (CPS \geq 1), cervical cancer (CPS \geq 1), urothelial carcinoma (CPS \geq 10), head and neck squamous cell carcinoma (HNSCC) (CPS \geq 1), esophageal squamous cell carcinoma (ESCC) (CPS \geq 10)³, and triple-negative breast cancer (TNBC) (CPS \geq 10).

Methods Precision of PD-L1 IHC 22C3 pharmDx using CPS was assessed for all six indications at the corresponding clinically validated diagnostic cutoffs and at additional exploratory cutoffs under normal, day-to-day testing conditions. Precision testing included Combined Precision (inter-instrument/operator/run (day)), Intra-Run Repeatability, and Observer (inter-/intra) Scoring Reproducibility studies. FFPE specimens were stained with PD-L1 IHC 22C3 pharmDx and scored using CPS as described in the package insert.² Four CPS cutoffs were evaluated: CPS \geq 1 (GC/GEJ, urothelial carcinoma, ESCC, cervical cancer, HNSCC, TNBC), CPS \geq 10 (GC/GEJ, urothelial carcinoma, ESCC, TNBC), CPS \geq 20 (HNSCC), and CPS \geq 50 (HNSCC). Data were analyzed using negative percent agreement (NPA), positive percent agreement (PPA), and overall agreement (OA) with two-sided 95% percentile bootstrap confidence intervals (CIs) based on PD-L1 binary status at the applicable cutoff(s). For each study, data from each CPS cutoff-indication pair were individually analyzed. Meta-analyses were also performed by pooling data from all indications per (i) study and cutoff, and (ii) per study for all tested cutoffs.

Results Nearly all agreement analyses (142/144) for each CPS cutoff-indication pair showed NPA/PPA/OA point estimates (PE) \geq 90% and CI lower bounds (CILB) \geq 85%. Meta-analyses showed PE \geq 90% for NPA/PPA/OA and CILB \geq 85% per study and cutoff, and per study for all tested cutoffs. Discordant comparisons accounted for <5% of total comparisons performed for each study type.

Conclusions CPS used with PD-L1 IHC 22C3 pharmDx provides precise evaluation of PD-L1 expression across multiple tumor indications and cutoffs under normal, day-to-day testing conditions.

Acknowledgements We thank the IUSCC Cancer Center at Indiana University School of Medicine, for the use of the Tissue Procurement and Distribution Core, which provided Dako North America, Inc. service. The data and biospecimens used in this project were provided by US Biolab (Gaithersburg, MD, USA), Sofia Bio LLC (New York, NY, USA), Contract

Research Ltd (Charlestown, Nevis), and Centre Hospitalier Universitaire (CHU) de Nice (Nice, France) with appropriate ethics approval and through Trans-Hit Biomarkers Inc. Tissue samples were provided by the Cooperative Human Tissue Network which is funded by the National Cancer Institute. Other investigators may have received specimens from the same subjects. Tissue samples supplied by BioIVT (Hicksville, NY, USA).

Trial Registration N/A

REFERENCES

1. CPS = (# PD-L1 staining cells (tumor cells, lymphocytes, macrophages))/(Total # viable tumor cells) \times 100
2. PD-L1 IHC 22C3 pharmDx [Instructions for Use]. Available at: www.agilent.com/library/eifu. Code SK006. Accessed July 2, 2021
3. ESCC was analytically validated as a subtype of esophageal cancer [2].

Ethics Approval N/A

Consent N/A

<http://dx.doi.org/10.1136/jitc-2021-SITC2021.060>

61

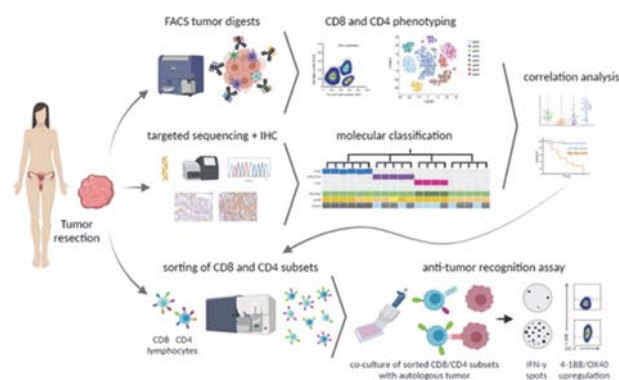
BIOMARKERS OF FAVORABLE PROGNOSIS GUIDES THE IDENTIFICATION OF TUMOR REACTIVE CD4+ AND CD8+ TILS IN ENDOMETRIAL CANCER

¹Jara Palomero*, ¹Carla Panisello, ²August Vidal, ²Jordi Ponce, ¹Ana Vivancos, ²Josep Maria Piulats, ²Xavier Matias-Guiu, ¹Alena Gros. ¹Vall D'Hebron Institute of Oncology (VHIO), Barcelona, Spain; ²Bellvitge University Hospital, Barcelona, Spain

Background Endometrial cancer (EC) is the most prevalent gynecological cancer and it can be categorized into four molecular subtypes; ultramutated POLE, hypermutated MSI, CNL and CNH. To date, the prevalence, specificity and phenotype of tumor infiltrating lymphocytes (TILs), and their exact role in EC remain controversial. Thus, a thorough investigation deciphering the phenotypic landscape of EC-infiltrating T lymphocytes and their anti-tumor reactivity is still missing.

Methods In order to study the implications of the T-cells infiltrating EC for prognosis or susceptibility to immune checkpoint inhibitors, we analyzed the phenotypic traits of CD8 and CD4 EC-resident T cells from single-cell suspensions (n=47) by multicolor flow cytometry (19 biomarkers). Correlation analyses between the phenotype of the TILs, EC molecular subgroups and the survival of the patients were performed to identify biomarkers that could predict prognosis or survival. This identification guided the isolation of specific CD8 and CD4 subpopulations based on the differential expression of the selected biomarkers to evaluate their ability to recognize tumor (figure 1).

Results Our analysis evidenced the presence of CD8+ and CD4+ T cells with distinct levels of PD-1 expression: cells that did not express PD-1 (PD-1-), cells expressing intermediate (PD-1dim) or high (PD-1hi) levels of PD-1. We found that TIM-3+, CD39+, CXCL13+, BCL6+ or Ki67+ cells frequently co-expressed almost exclusively on the PD-1hi, but not on the PD-1- or dim CD8+ TILs. On the other hand, CD4+ TILs displayed co-expression of TIM-3, CD103, CD39, CD38, HLA-DR, CXCL13, BCL6, CXCR5 or Ki67 within the PD-1hi, but also PD-1dim cells. Importantly, our data shows that the frequency of PD-1hi or CD39+ CD8+ EC TILs, and of PD-1hi but not CD39+ CD4+ TILs was associated with improved survival. Of the 5 predominant CD8 + tumor-resident subpopulations observed (PD-1-CD39-, PD-1dimCD39-, PD-1dimCD39+, PD-1hiCD39- and PD-1hiCD39+) the PD-1hiCD39+, but not the PD-1hiCD39- lymphocytes, harbored the highest frequency of autologous tumor-reactive lymphocytes in all four EC tumors studied. However, both the CD4+ PD-1hiCD39+ and the PD-1hiCD39- contained autologous tumor-reactive lymphocytes in all four tumors screened; being the PD-1hiCD39+ cells the subpopulation containing the majority of tumor-reactive CD4+ cells.



Abstract 61 Figure 1 Schematic workflow of the study. A section of a primary EC tumor resection is digested and stained with specific antibodies to characterize the phenotype of CD8 and CD4 TILs by flow cytometry (upper panel). Targeted sequencing and IHC including typically altered genes in EC are performed in order to molecularly classify the patient's cohort into different disease subgroups. Combining the data generated by flow cytometry, targeted sequencing and IHC, specific biomarkers on CD8 and CD4 TILs are investigated for their potential role in predicting molecular subtypes or survival (middle panel). CD8 and CD4 TILs are isolated from the tumor digest based on the differential expression of PD-1 and CD39 and the specific isolated CD8 and CD4 subpopulations are cultured in vitro to expand them to large numbers. The expanded CD8 and CD4 subpopulations are subsequently screened for tumor recognition by co-culturing the isolated subpopulations with autologous tumor cell lines. Tumor recognition is assessed by measuring the up-regulation of the activation markers 4-1BB or OX40 on CD8+ or CD4+ T cells, respectively, by flow cytometry, and by measuring IFN- γ production by ELISPOT.

Conclusions Overall, our data suggest that CD39 expression on CD8+PD-1hi EC-resident T cells defines a tumor-reactive population that plays an important role in protecting patients from recurrence after surgery. However, PD-1 expression but not CD39 on CD4+ TILs, better guides the identification of lymphocyte subsets with enriched tumor-recognition potential that contribute to improved clinical benefit in EC.

Ethics Approval This study was approved by the 'Comité de Ética de Investigación con Medicamentos del Hospital Universitario Vall d'Hebron' institution's Ethics Board; approval number PR(AG)537/2019.

<http://dx.doi.org/10.1136/jitc-2021-SITC2021.061>

APPLYING MACHINE VISION TO EMPOWER PRECLINICAL DEVELOPMENT OF CELL ENGAGER AND ADOPTIVE CELL THERAPEUTICS IN PATIENT-DERIVED ORGANOID MODELS OF SOLID TUMORS

Sonal Khare*, Chi-Sing Ho, Madhavi Kannan, Brian Larsen, Brandon Mapes, Jenna Shaxted, Jagadish Venkataraman, Ameen Salahudeen. *Tempus Labs, Chicago, IL, USA*

Background Cell engager and adoptive cell therapeutics have emerged as efficacious and durable treatments in patients with B-cell malignancies. Though many analogous strategies are under development in solid tumors, none have received approval. Preclinical development of these therapies requires cell labeling of immortalized cell lines and/or primary expanded T cells to distinguish target and effector cells. However, cell engager and adoptive cell therapies have had limited evidence of reproducibility in primary patient-derived models such as tumor organoid cultures thus far. Here, we build upon our tumor organoid platform¹ to measure organoid specific responses to these therapies. Utilizing machine vision coupled with time-lapse-microscopy, we obtain multiparameter kinetic readouts of patient-derived tumor organoid cell killing and allogeneic MHC-matched primary peripheral blood mononuclear cells (PBMCs).

Methods The patient-derived tumor organoids were co-cultured with PBMCs in the presence of engagers/activators and vital dyes and incubated for 96 hrs. Cell death was measured by quantifying the caspase 3/7 vital dye pixel intensities at different time points using high throughput imaging. As a first step, a fully convolutional neural network was trained to segment out organoids from brightfield images comprised of organoids, immune cells and potential background artifacts. This segmentation mask was then transferred over to registered caspase 3/7 images to quantify tumor cell specific phenotypes in a rapid and automated manner.

Results The time-lapse imaging assay allowed for both the tracking of the organoid growth over time as well as the quantification of the kinetics of engagers/activators in comparison to controls resulting in accurate and precise technical reproducibility. Further, this assay allowed for the co-localization of the organoids and the immune cells over time, thus, enabling a spatiotemporal summary of dose dependent efficacy of candidate therapeutics.

Conclusions We demonstrate the scalability and throughput of a machine vision tumor organoid immune co-culture platform across multiple unique patient-derived tumor organoid lines bearing a target of interest, enabling future discovery of biomarkers of therapeutic response and resistance.

REFERENCE

1. Larsen B, Kannan M, Langer LF, Khan AA, Salahudeen AA, A pan-cancer organoid platform for precision medicine. *Cell Reports* 2021; **36**:109429

<http://dx.doi.org/10.1136/jitc-2021-SITC2021.062>

A CLONING AND EXPRESSION SYSTEM OF THE NEOANTIGEN-SPECIFIC TCRs FROM TUMOR-INFILTRATING LYMPHOCYTES BY SINGLE-CELL SEQUENCING OF PAIRED TCR α AND TCR β CHAINS

¹Yukari Kobayashi*, ¹Koji Nagaoka, ²Kaori Kubo, ²Toshikazu Nishie, ²Sachiko Okamoto, ²Tatsuji Enoki, ²Junichi Mineno, ³Yasuyoshi Sato, ³Shunji Takahashi, ⁴Jun Nakajima, ¹Kazuhiro Kakimi. ¹The University of Tokyo Hospital, Bunkyo-ku, Japan; ²Takara Bio Inc., Shiga, Japan; ³The Cancer Institute Hospital of JFCR, Tokyo, Japan; ⁴The University of Tokyo, Tokyo, Japan

Background T-cells that target tumor neoantigens arising from cancer mutations are the primary mediators of cancer immunotherapies. Identifying neoantigens and T-cells that recognize them is essential for T-cell-based immunotherapy. However, neoantigen-reactive Tumor-infiltrating lymphocytes (TILs) are highly differentiated or exhausted with a limited proliferative capacity; it is challenging to expand them for a sufficient number to probe their specificity. Therefore, we developed a novel cloning and expression system to examine TCRs discovered by single-cell sequencing of TILs for their neoantigen-specificity.

Methods TILs of lung cancer and sarcoma were analyzed. Surgically removed tumors were divided into several pieces. They were enzymatically digested to prepare fresh tumor digest (FTD) and cryopreserved. They were used to generate TIL cultures and perform WES and RNA-Seq to identify tumor-specific mutations. MHCflurry was used to predict the binding affinity of potential epitopes arising from these mutations to HLA class I. Peptides that were predicted to bind to patients' own MHC class I molecules strongly were then synthesized. Single TILs isolated with the ICELL8[®] cx system (Takara Bio) were dispensed into a nanowell TCR chip containing pre-printed barcodes. Barcoded cDNAs were PCR-amplified in-chip, pooled off-chip, and used as a template in the TCR-specific PCR or for the whole transcriptome library generation of 5' ends of all transcripts. Based on single-cell transcriptome data and TCR profiles of TILs, we predict and prioritize neoantigen-specific TCRs and cloned them into siTCR[®] retrovirus vectors. These TCRs were transduced into SUP-T1-based reporter cells in which ZsGreen fluorescent protein expression is controlled by AP-1 and NFAT binding sites. TCR-expressing reporter cells were cocultured with patient autologous APCs pulsed with a pool of candidate neoantigen peptides. ZsGreen expression indicates that TCRs match their cognate neoantigens.

Results In a lung cancer patient, we set up 18 TIL cultures and obtained 12 TILs. TILs were cocultured with FTD; IFN- γ production was measured by ELISA to evaluate their reactivity to the autologous tumor. NGS identified 197 somatic mutations, 4 fusion genes, and 8 highly expressed cancer-testis antigens. Among them, 339 candidate peptides were synthesized and screened. In addition, we cloned 3 pairs of TCR $\alpha\beta$ chains from most expanded TIL cultures and 4 TCRs from ex vivo TILs with exhausted phenotype. Two reporter cells that express TCRs from exhausted TILs responded to the same neoantigen peptide.

Conclusions Generating TCR expressing cell lines facilitated the identifying neoantigens and their cognate TCR sequences from patients.

Ethics Approval G3545

<http://dx.doi.org/10.1136/jitc-2021-SITC2021.064>

IDENTIFICATION OF FREQUENTLY PRESENTED NON-MUTATED TUMOR-SPECIFIC IMMUNOGENS FOR THE DEVELOPMENT OF BOTH OFF-THE-SHELF AND PERSONALIZED VACCINES WITHOUT NEED FOR TUMOR BIOPSY

Orsolya Lorincz*, Levente Molnar, Zsolt Csiszovszki, Eszter Somogyi, Jozsef Toth, Katalin Pantya, Peter Pales, Eniko Toke. *Treos Bio Ltd., London, UK*

Background Vaccines have little chance of destroying heterogeneous tumor cells since they rarely induce polyclonal T-cell responses against the tumor. The main challenge is the accurate identification of tumor targets recognizable by T cells. Presently, 6–8% of neoepitopes selected based on the patients' tumor biopsies are confirmed as real T cell targets.^{1 2}. To overcome this limitation, we developed a computational platform called Personal Antigen Selection Calculator (PASCAL) that identifies frequently presented immunogenic peptide sequences built on HLA-genetics and tumor profile of thousands of real individuals.³ Here we show the performance of PASCAL for the identification of both shared and personalized tumor targets in metastatic colorectal cancer (mCRC) and breast cancer subjects.

Methods Expression frequency of the tumor-specific antigens (TSAs) ranked in PASCAL's database (based on 7,548 CRC specimen) was compared to the RNA-sequencing data of CRC tumors obtained from TCGA. Using PASCAL, 12 shared PEPs (epitopes restricted to at least 3 HLA class I alleles of a subject from an in silico cohort) derived from 7 TSAs were selected as frequent targets (calculated probability: average 2.5 [95%CI 2.4–2.8] TSAs/patient). Spontaneous immune responses against each of the twelve 9mer peptides were determined by ELISpot using PBMCs of 10 mCRC subjects who participated in the OBERTO-101 study.⁴ PEPs selected for a breast cancer subject based on her HLA genotype were also tested.

Results Each of the 106 tumors analyzed expressed at least 13, average 15 of the 20 top-ranked TSAs in PASCAL's database confirming their prevalence in CRC. 7/10 subjects had spontaneous CD8+ T-cell responses against at least one peptide selected with PASCAL. Each peptide (12/12) was recognized by at least one patient. Patients' T-cells reacted with average 3.6/12 (30%) peptides confirming the expression of average 2.8 [95%CI 1.0–4.6] TSAs (n=10). After HLA-matching, among the subjects for whom we could select at least 4 PEPs (average 5) from the list of 12 peptides (n=6), average 2.5 (50%) peptides were positive. Of the 12 PEPs selected with PASCAL for a breast cancer subject, we detected spontaneous T-cell responses against 9 PEPs, indicating that at least 75% of the selected peptides were present in the subject's tumor and were recognized by T-cells.

Conclusions PASCAL platform accommodates both tumor- and patient heterogeneity and identifies non-mutated tumor targets that may trigger polyclonal cytotoxic T-cell responses. It is a rapid tool for the design of both off-the-shelf and personalized cancer vaccines negating the need for tumor biopsy.

REFERENCES

1. Wells DK, van Buuren MM, Dang KK, et al. Key parameters of tumor epitope immunogenicity revealed through a consortium approach improve neoantigen prediction. *Cell* 2020;**183**(3):818–34.e13.
2. Bulik-Sullivan B, Busby J, Palmer CD, et al. Deep learning using tumor HLA peptide mass spectrometry datasets improves neoantigen identification. *Nat Biotech* 2018;**37**:55–63.

3. Somogyi E, Csiszovszki Z, Lorincz O, et al. 1181PD Personal antigen selection calculator (PASCAL) for the design of personal cancer vaccines. *Annal Oncol* 2019;**30** (Supplement_5):v480-v81.
4. Hubbard J, Cremolini C, Graham R, et al. P329 PolyPEP1018 off-the shelf vaccine as add-on to maintenance therapy achieved durable treatment responses in patients with microsatellite-stable metastatic colorectal cancer patients (MSS mCRC). *J ImmunoTher Cancer* 2019;**7**(1):282.

<http://dx.doi.org/10.1136/jitc-2021-SITC2021.065>

66

PROGNOSTIC AND PREDICTIVE VALUE OF PRE-TREATMENT T-CELL RECEPTORS (TCR) REPERTOIRE IN NON-SMALL CELL LUNG CANCER (NSCLC) PATIENTS TREATED WITH SINGLE AGENT IMMUNOTHERAPY

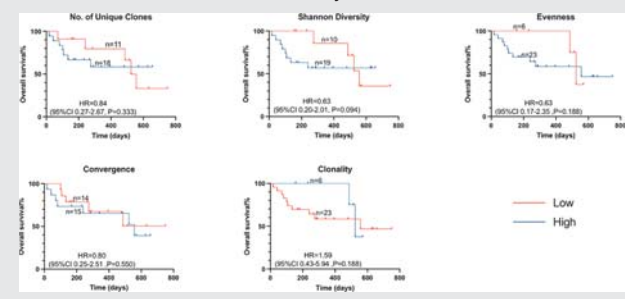
¹Afaf Abed*, ¹Elin Gray, ²Michael Millward. ¹Edith Cowan University, Joondalup, Australia; ²Linear clinical research, Perth, Australia

Background TCR repertoire plays a key role on the orchestration of the immune response. In particular, reduced pre-treatment Shannon diversity, increase clonality and increase convergence of TCRs have been suggested to reflect clonal expansion of antigen-specific T-cells in the tumour microenvironment. These are thought to be correlated with better response rate, improved progression free survival (PFS) and overall survival (OS). Here we aim to explore the above TCR repertoire features in peripheral blood of NSCLC patients (with PDL1 \geq 50%) treated with single agent pembrolizumab in the first line setting; and correlate them with overall response rate (ORR), PFS and OS.

Methods We prospectively collected baseline blood from 48 NSCLC patients treated with first line pembrolizumab. High quality DNA was extracted from white blood cells and used for TCR sequencing using the Oncomine TCR Beta-SR Assay (Thermo Fisher). TCR clonality and convergence were calculated for each individual and correlated with survival using Kaplan-Meier curves and survival statistics. Multivariate analysis was carried out controlling for other variable that may influence the association of TCR repertoire and outcomes such as age, sex, ECOG, smoking status and pre-treatment neutrophil to lymphocyte ratio (NLR).

Results Our data matured for 29 patients only with a follow-up of at least 6 months. We observed a trend towards increased pre-treatment TCR clonality in patients with objective response to pembrolizumab and statistically significant reduced Shannon diversity ($P = 0.042$). Convergence did not seem to affect ORR in our cohort. Moreover, there was a significantly longer PFS in patients with reduced number of pre-treatment clones (HR = 0.40, 95%CI 0.14–1.17, $P = 0.031$), reduced Shannon diversity (HR = 0.44, 95%CI 0.16–1.21, $P = 0.041$), reduced Evenness (HR = 0.31, 95%CI 0.11–0.94, $P = 0.033$) and elevated clonality (HR = 3.18, 95%CI 1.06–9.53, $P = 0.033$) (table 1). Reduced rather than increased convergence was correlated with a trend towards improved PFS. None of these parameters were statically significant in relation to OS (table 2).

Abstract 66 Table 2 TCR diversity and OS



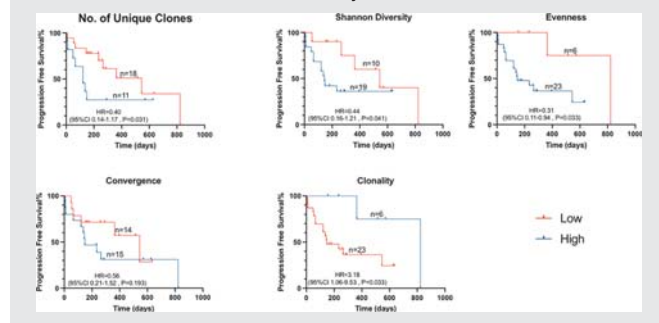
Conclusions Increased pre-treatment TCR clonality and reduced diversity are associated with improved ORR and PFS, but not OS in NSCLC patients with high PD-L1 treated with pembrolizumab monotherapy. Further maturation of this cohort will demonstrate whether the circulating pre-treatment TCR repertoire is a prognostic factor for immunecheckpoint inhibition.

Ethics Approval The proposed project has already received approval by the Human Research Ethics Committees and Research Governance at Fiona Stanley Hospital, Sir Charles Gairdner Hospital and Edith Cowan University [ECU (No. 18957) and SCGH (RGS0000003289)].

Consent Written informed consent was obtained from the patient for publication of this abstract and any accompanying images. A copy of the written consent is available for review by the Editor of this journal.

<http://dx.doi.org/10.1136/jitc-2021-SITC2021.066>

Abstract 66 Table 1 TCR diversity and PFS



67

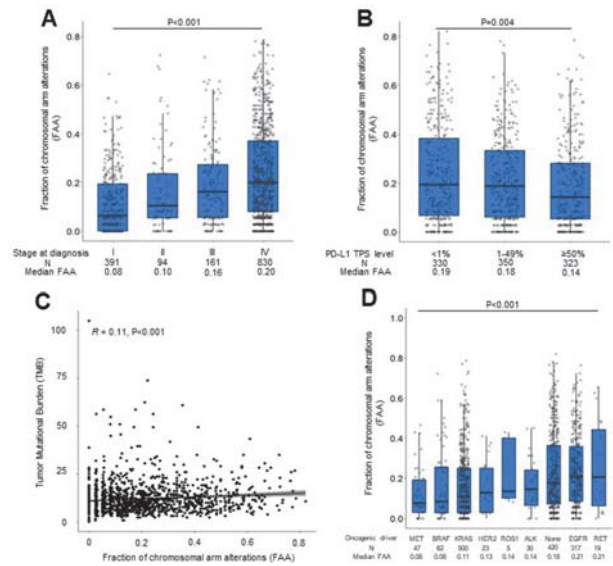
CANCER ANEUPLOIDY IS ASSOCIATED WITH A DISTINCT TUMOR IMMUNE MICROENVIRONMENT AND IMPACTS OUTCOMES TO IMMUNE CHECKPOINT INHIBITION IN NONSQUAMOUS NON-SMALL CELL LUNG CANCER

¹Joao Victor Alessi*, ¹Biagio Ricciuti, ¹Yvonne Lin-Liu, ¹Hersh Gupta, ²Xinan Wang, ¹Giuseppe Lamberti, ¹Gonzalo Recondo, ¹Victor Vaz, ¹Adriana Barrichello, ¹Mizuki Nishino, ¹Andrew Cherniack, ¹James Lindsay, ¹Bijaya Sharma, ¹Kathleen Pfaff, ¹Kristen Felt, ³Scott Rodig, ¹Mark Awad. ¹DFCI, Boston, MA, USA; ²Harvard School of Public Health, Boston, MA, USA; ³Brigham and Women's Hospital, Boston, MA, USA

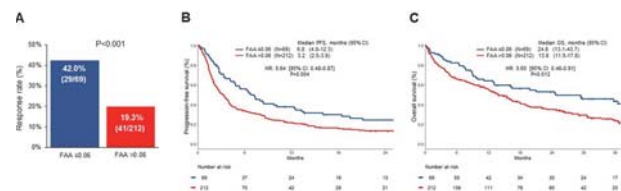
Background Cancer aneuploidy, an unbalanced number of chromosomes, is associated with somatic mutation rate, expression of proliferative genes, and altered immune signaling. Whether aneuploidy correlates with a distinct tumor immunophenotype or impacts clinical outcomes to immune checkpoint inhibitors (ICIs) in NSCLC is unclear.

Methods Among nonsquamous NSCLCs which underwent targeted next-generation sequencing, we retrospectively quantified aneuploidy using the fraction of chromosomal arm alterations (FAA), defined as the number of aneuploid chromosome arms divided by the number of chromosome arms assessed. An unbiased recursive partitioning algorithm was used to investigate an FAA level which best discriminated responders from non-responders to ICIs. Multiplexed immunofluorescence to quantify CD8, FOXP3, and PD-1-positive cell counts, as well as PD-L1 expression was performed on a separate cohort of nonsquamous NSCLCs to determine differences in tumor immune cells subsets according to FAA levels.

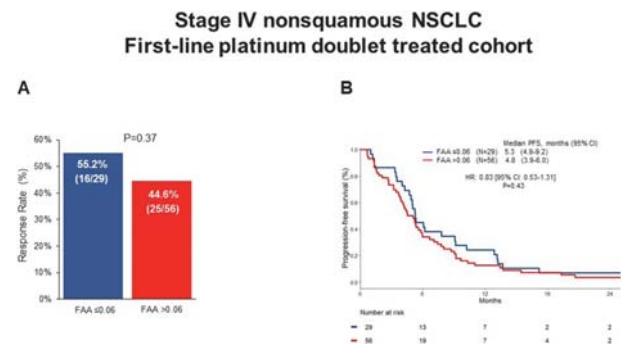
Results Among 1426 nonsquamous NSCLCs identified, FAA increased along with the increase of pathologic stage, and was highest among tumors harboring EGFR mutations and RET fusions, and lowest among those with KRAS, BRAF, and MET mutations. FAA inversely correlated with PD-L1 expression levels, and positively correlated with tumor mutational burden (TMB) (figure 1A-D). Among 281 NSCLCs treated with ICIs, the median FAA was significantly lower among patients with a partial response to ICI compared to those with stable or progressive disease (0.11 vs 0.21, P=0.006). A fractional aneuploidy level of 0.06 (representing the lowest quartile of FAA) was identified as an optimal cutpoint to discriminate responders from non-responders to ICI. Compared to pts with an FAA >0.06 (N=212), pts with FAA ≤0.06 (N=69) had a significantly higher ORR (42.0% vs 19.3%, P<0.001), longer median progression-free survival (mPFS 6.8 vs 3.2 months, HR: 0.64, P=0.004), and longer median overall survival (mOS 24.8 vs 13.8 months, HR: 0.65, P=0.012) with ICIs (figure 2). After adjusting for performance status, PD-L1 expression, TMB, and line of treatment, FAA retained a significant association with improved PFS (HR: 0.66, P=0.018) and OS (HR: 0.66, P=0.041) to immunotherapy. FAA had no impact on clinical outcomes among pts who received first-line platinum doublet chemotherapy without ICI (figure 3). Among 239 nonsquamous NSCLCs profiled by multiplex immunofluorescence, cancers with a low FAA (≤25th percentile) were significantly enriched in CD8+ T cells and had a higher CD8+ to FOXP3+ ratio compared to those with high FAA (>25th percentile) (figure 4).



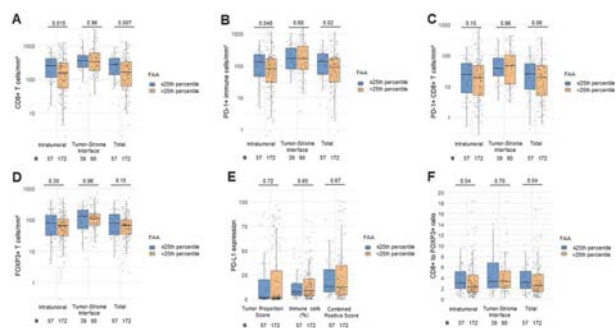
Abstract 67 Figure 1 (A) Median fraction of chromosomal alterations (FAA) are shown for stages I, II, III, and IV NSCLCs. (B) Tumors with negative (<1%), low (1–49%), and high PD-L1 tumor proportion score (TPS) (≥50%) expression. (C) Pearson’s correlation coefficient between FAA and tumor mutational burden (TMB). (D) Median FAA distribution across a set of 8 targetable driver mutations (ALK, BRAF, EGFR, HER2, KRAS, MET, RET and ROS1) and none identified alteration.



Abstract 67 Figure 2 (A) Objective response rate, (B) progression-free survival, and (C) overall survival, in patients with a fraction of chromosomal arm alterations (FAA) ≤0.06 versus >0.06 in the immunotherapy-cohort.



Abstract 67 Figure 3 (A) Objective response rate and (B) progression-free survival (PFS) in patients with a fraction of chromosomal arm alterations (FAA) ≤0.06 versus >0.06 in the chemotherapy-cohort.



Abstract 67 Figure 4 (A) CD8+, (B) PD-1+, (C) PD-1+ CD8+ (D), FOXP3+ cells/mm², and (E) PD-L1 distribution in nonsquamous NSCLCs with an fraction of arm-level altered (FAA) low (≤ 25 th percentile) versus high (> 25 th percentile). (F) CD8+ to FOXP3+ ratio in tumors with FAA low versus FAA high.

Conclusions Nonsquamous NSCLCs with low aneuploidy have a distinct immune microenvironment and more favorable outcomes to ICIs.

<http://dx.doi.org/10.1136/jitc-2021-SITC2021.067>

68 **RAPID DETECTION OF SOMATIC VARIANTS IN HUMAN LEUKOCYTE ANTIGEN CLASS 1 GENES FROM SOLID TUMOR SAMPLES**

¹Ramit Bharanikumar*, ²Karl Beutner, ²Aly Khan, ²Jason Perera. ¹Tempus Labs, Chicago, IL, USA; ²Tempus, Chicago, IL, USA

Background Human Leukocyte Antigens (HLA) class 1 proteins are important for recognizing tumor specific mutations (neoantigens) and presenting them to CD8+ T-cells. Somatic mutations in HLA genes can potentially reduce the set of neoantigens available for presentation to T-cells, providing a possible immune escape mechanism for tumors. The presence of mutations in HLA genes may thus affect an individual's response to Immune Checkpoint Blockade therapy but calling somatic variants in HLA genes is challenging given high degrees of polymorphism and the presence of pseudogenes in HLA loci. Here, we present a rapid, modular algorithm to detect somatic variants in HLA class 1 genes from next-generation sequencing data.

Methods Our method takes as input matched tumor and normal sequencing (BAM) files and a patient's HLA type. Our first step involves mapping and aligning reads to the full-length HLA class 1 genes of an individual patient. Next, we filter reads to minimize sequencing errors and process them to account for potential cross-mapping between genes in the broader HLA locus. Our algorithm uses the final set of processed reads from matched tumor and normal sequencing files to call somatic variants. The final set of variants are then provided with a genetic variant annotation that summarizes their functional effect.

Results We validated the efficacy of our approach using TCGA samples that were previously known to contain somatic HLA mutations. Out of a total of 46 mutations previously characterized from 41 samples, our algorithm detected 43 mutations with the correct functional annotation and did so with a computational run-time that is an order of magnitude faster than the current gold-standard approach. Eight of these mutations were previously validated using PacBio long-read sequencing, and all of these validated mutations were detected by our method. Additionally, we analyzed transcriptomic data in samples containing nonsense mutations and detected a transcriptomic signature in RNA-seq data that corresponded to the Nonsense Mediated Decay pathway.

Conclusions Our findings show that our algorithm can reliably and rapidly detect somatic mutations in HLA class 1 classical genes. We leveraged multi-modal TCGA data and modules developed at Tempus to link samples with nonsense mutations to the nonsense mediated decay pathway. This allowed us to posit a possible biological mechanism that could result in increased resistance to immunotherapy because of somatic HLA mutations. Finally, we emphasize that our approach is modular and can be extended to call somatic variants in other non-classical and class 2 HLA genes.

<http://dx.doi.org/10.1136/jitc-2021-SITC2021.068>

69 IMMUNOPHENOTYPING OF TCR AND BCR CLONOTYPES

Alex Chenchik*, Michael Makhanov, Russell Darst, Tianbing Liu, Lester Kobzik. *Collecta, Inc., Mountain View, CA, USA*

Background T-cell receptor (TCR) and B-cell receptor (BCR) repertoire profiling holds great potential for understanding disease mechanisms and for the development of new therapeutics in infectious diseases, autoimmunity and in immuno-oncology. However, this potential could be greatly improved by combining information about receptor clonotypes with immunophenotypes of T and B cells.

Methods To facilitate these studies, we developed a novel technology for combined profiling of all human TCR and BCR variable regions and phenotypic characterization of immune cells in bulk and at the single-cell level in PBMC and immune cell fraction samples. The developed TCR/BCR Immunophenotyping method involves multiplex RT-PCR amplification and sequencing of CDR3 regions of TCR and BCR genes and a set of the most informative T- and B-cell phenotyping genes. Bioinformatics analysis of NGS data allows profiling of TCR/BCR clonotypes, and identification of major immune cell subtypes and their activation status.

Results Data will be presented showing how combined TCR/BCR clonotype analysis combined with targeted expression profiling of immune cells can be applied for large-scale discovery of novel cell typing and activation biomarkers in several immune-responsive model systems.

Conclusions Preliminary studies demonstrate the assay has unparalleled throughput, sensitivity, and improved cost-effectiveness for high-throughput immunity biomarker discovery applications.

<http://dx.doi.org/10.1136/jitc-2021-SITC2021.069>

NOVEL IMMUNOTHERAPEUTIC TARGETS IN CANCER OF UNKNOWN PRIMARY (CUP)

¹Mary Nesline, ²Paul DePietro, ¹Yong Hee Lee*, ¹Zachery Bliss, ¹RJ Seager, ¹Erik Van Roey, ¹Shuang Gao, ¹Vincent Giamo, ¹Blake Burgher, ¹Sean Glenn, ¹Shengle Zhang, ¹Sarabjot Pabla, ¹Roger Klein, ¹Jeffrey Conroy. ¹OmniSeq, Inc., Buffalo, NY, USA; ²OmniSeq, Buffalo, NY, USA

Background Cancer of unknown primary (CUP) is a rare tumor type accounting for 2% of solid cancers. In the subset of CUP cases where tumor of origin is posited and treated as such, no clear clinical benefit has been demonstrated. Furthermore, CUP patients treated by empiric platinum-based regimens have low response and survival rates of approximately 20%.¹⁻² Support of tissue-agnostic marker-directed immunotherapy is growing because it targets the immune system rather than the tumor, with some efficacy evidence emerging for CUP.³ Identifying new targets for immunotherapeutic opportunities in this heterogeneous and difficult to treat patient group is a critical unmet need.

Methods Comprehensive genomic and immune marker profiling by NGS⁴ was performed on FFPE tissue for CUP tumors (n=298) as indicated by physicians' test orders from >100 clinical practice sites. Histology was verified by a molecular pathologist as part of pre-analytic test quality control, with cases representing tumors with adenocarcinoma (58%), carcinoma (26%), squamous (10%), and neuroendocrine (6%) histologic features. RNA-expression levels of immune genes that are current targets in non-CUP immunotherapy clinical trials (n=36) were ranked against a reference population (≥ 75 th percentile=high), and described by histologic type, along with PD-L1 IHC (22C3) expression, tumor mutational burden (TMB) and genomic variants.

Results 90% of all CUP tumors had at least 1 highly expressed immune gene target in active immunotherapy trials, with the most frequent being TGFB1 (47%) and CCL2 (39%). 55% of CUP tumors were PD-L1 IHC 22C3 positive ($\geq 1\%$ TPS), and 21% had high TMB (≥ 10 mut/Mb) in CUP tumors with neuroendocrine (32%), carcinoma (30%), squamous cell (21%), and adenocarcinoma (17%) histologic features. Overall, 26% of CUP patient tumors, mostly adenocarcinomas (28%) and carcinomas (27%), harbored genomic variants (n=77) with FDA approved targeted therapies in other tumor types. The most frequently immunogenic CUP tumors were carcinomas, showing high RNA-seq expression of 26/36 genes in at least 20% of patients, most represented by CD20, CD27, TLR8, and PD-L1. High expression of CD40, CSF1R, TIM3, and VISTA was most common in adenocarcinomas. Squamous cell carcinomas were relatively immunogenic, with frequent high expression of 17/36 immune genes, uniquely including MAGEA4. Neuroendocrine tumors were the least immunogenic, with frequent high expression in only 4/36 genes, including ADORA2A (42%) and MAGEA1 (37%).

Conclusions CUP tumors diversely express both standard marker and novel immunotherapeutic targets based on histology and may benefit from selective access to clinical trials for these therapies.

REFERENCES

1. National Comprehensive Cancer Network. NCCN Clinical Practice Guidelines in Oncology (NCCN Guidelines[®]) Occult Primary (Cancer of Unknown Primary [CUP]), Version 2.2021. Fort Washington, Pennsylvania: National Comprehensive Cancer Network; 2021. https://www.nccn.org/professionals/physician_gls/pdf/occult.pdf.

2. Laprovitera N, Riefolo M, Ambrosini E, Klec C, Pichler M, Ferracin M. Cancer of unknown primary: Challenges and progress in clinical management. *Cancers (Basel)* 2021;**13**(3):1–30. doi:10.3390/cancers130304513.
3. Naing A, Meric-Bernstam F, Stephen B, et al. Phase 2 study of pembrolizumab in patients with advanced rare cancers. *J Immunother Cancer* 2020;**8**(1):e000347. doi:10.1136/jitc-2019-000347.
4. Conroy JM, Pabla S, Glenn ST, et al. Analytical validation of a next-generation sequencing assay to monitor immune responses in solid tumors. *J Mol Diagnostics* 2018;**20**(1):95–109. doi:10.1016/j.jmoldx.2017.10.001

<http://dx.doi.org/10.1136/jitc-2021-SITC2021.070>

71

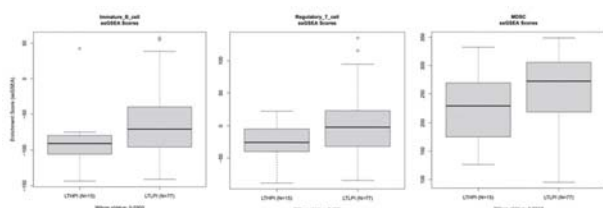
TUMORS WITH HIGHER HETEROGENEITY WERE ASSOCIATED WITH SUPERIOR SURVIVAL OUTCOME AMONGST STAGE I LUNG CANCER PATIENTS WITH LOW TUMOR MUTATIONAL BURDEN (TMB)

¹Stanislav Fridland*, ²Young Kwang Chae. ¹Northwestern University Feinberg School of Medicine, Chicago, IL, USA; ²NU Feinberg School of Medicine, Chicago, IL, USA

Background Tumor mutational burden (TMB) has been shown to predict response to immune checkpoint inhibitors.¹ Furthermore, the FDA has approved the use of TMB as a biomarker for response to pembrolizumab in solid tumors.² Simultaneously, the relationship between tumor heterogeneity and outcome has been studied across a range of cancer indications and has shown predictive value.³ For Lung Squamous Cell Carcinoma (LUSC) the utility of heterogeneity metrics has not been established. To study this relationship we used both TMB and tumor heterogeneity to stratify patients, compare outcomes, explore differences in immune cell enrichment, and predict driver genes.

Methods We obtained Tumor Cancer Genome Atlas (TCGA) LUSC SNP, CNV, and RNASeq data from the GDC Data Portal⁴ and clinical data from the PanCancer Atlas dataset through cBioPortal.⁵ TMB was calculated by dividing the number of mutations by 38 to yield a mut/Mb value. To estimate tumor heterogeneity we ran PyClone, an algorithm that estimates the number of tumor clones.⁶ PyClone uses a random seed and output for the same sample may differ. We ran each sample in triplicate on three separate days yielding 9 runs per sample, yielding an average PyClone clone number. Clones with >2 mutations were counted. Using p-value minimization we chose 5 for the TMB cutoff and 4.6 for the PyClone cutoff. This yielded 4 groups: HTHP, HTLP, LTHP, and LTLT, where H - high, L- low, T-TMB, and P-PyClone. Immune cell enrichment analysis was accomplished with ssGSEA via the GenePattern platform.⁷ Driver gene prediction was performed with OncoDriveClust⁸ via the R package maftools.⁹

Results A statistically significant difference was found in progression free survival (PFS) between stage I LTHP (LTHPI, N = 15) and stage I LTLT (LTLPI, N = 77) patients (51.27 months vs. 25.4 months, p-value = 0.0059). Intriguingly, highly heterogeneous tumors revealed superior survival outcomes compared to less heterogeneous tumors in this subgroup. LTLPI patients were enriched for immature B cells, regulatory T cells, and myeloid derived suppressor cells (figure 1). Three driver genes were predicted for the LTLPI cohort (NFE2L2, PIK3CA, and TP53), while none were predicted for the LTHPI cohort.



Abstract 71 Figure 1 Immune Cell Gene Set Enrichment

Conclusions Contrary to previous literature, superior survival outcomes were observed in high tumor heterogeneity, low TMB Stage I LUSC patients. Early stage patients can be

stratified using heterogeneity metrics like PyClone. Given the presence of specific driver genes and an immunosuppressive tumor microenvironment, this population warrants further investigation for therapeutic implications.

Acknowledgements This research was supported in part through the computational resources and staff contributions provided by the Genomics Compute Cluster which is jointly supported by the Feinberg School of Medicine, the Center for Genetic Medicine, and Feinberg's Department of Biochemistry and Molecular Genetics, the Office of the Provost, the Office for Research, and Northwestern Information Technology. The Genomics Compute Cluster is part of Quest, Northwestern University's high performance computing facility, with the purpose to advance research in genomics.

Trial Registration N/A

REFERENCES

- Samstein RM, Lee C-H, Shoushtari AN, Hellmann MD, Shen R, Janjigian YY, et al. Tumor mutational load predicts survival after immunotherapy across multiple cancer types. *Nature Genetics* 2019;**51**(2):202–6.
- Center for Drug Evaluation and Research. FDA approves pembrolizumab for adults and children With TMB-H solid tu [Internet]. U.S. Food and Drug Administration. FDA; [cited 2021 Jul 28]. Available from: <https://www.fda.gov/drugs/drug-approvals-and-databases/fda-approves-pembrolizumab-adults-and-children-tmb-h-solid-tumors>
- Morris LGT, Riaz N, Desrichard A, Şenbabaoğlu Y, Hakimi AA, Makarov V, et al. Pan-cancer analysis of intratumor heterogeneity as a prognostic determinant of survival. *Oncotarget* 2016;**7**(9):10051–63.
- GDC. [cited 2021Jul28]. Available from: <https://portal.gdc.cancer.gov/>
- cBioPortal for cancer genomics [Internet]. cBioPortal for Cancer Genomics. [cited 2021Jul28]. Available from: <https://www.cbioportal.org/>
- Roth A, Khattra J, Yap D, Wan A, Laks E, Biele J, et al. PyClone: Statistical inference of CLONAL population structure in cancer. *Nature Methods* 2014;**11**(4):396–8.
- GenePattern [Internet]. GenePattern sign in. [cited 2021Jul28]. Available from: <https://cloud.genepattern.org/gp/pages/index.jsf>
- Tamborero D, Gonzalez-Perez A, Lopez-Bigas N. OncodriveCLUST: Exploiting the Positional clustering of somatic mutations to identify CANCER GENES. *Bioinformatics*. 2013;**29**(18):2238–44.
- Mayakonda A, Lin D-C, Assenov Y, Plass C, Koeffler HP. Maftools: Efficient and comprehensive analysis of somatic variants in cancer. *Genome Research* 2018;**28**(11):1747–56.

Ethics Approval N/A

Consent N/A

<http://dx.doi.org/10.1136/jitc-2021-SITC2021.071>

SPATIAL WHOLE TRANSCRIPTOME PROFILING OF THE TUMOR MICROENVIRONMENT IN PROSTATE CARCINOMAS

Naishitha Anaparthi*, Valeria Giangarra, Sarah Taylor, Mesruh Turkekul, Stephen Williams, Paulius Mielinis, Caroline Gallant. *x Genomics, Pleasanton, CA, USA*

Background Despite years of studies and effort, the best strategies for treating prostate cancer and minimizing the complications of treatment remain unanswered questions. This gap in knowledge is partially due to the inability to dissect the complex heterogeneous tumor microenvironment (TME) and immune compartment. Spatially resolved molecular profiling of tumor sections will enhance our understanding of these complexities; However, it has been particularly challenging to do spatial molecular profiling in formalin-fixed paraffin-embedded (FFPE) tissues due to RNA degradation associated with this tissue-embedding method, which is routinely used in oncology workflows. The 10x Genomics Visium Spatial Gene Expression Solution for FFPE tissue overcomes these limitations, enabling spatial gene expression analysis of FFPE tissues combined with classical histology staining techniques such as Hematoxylin & Eosin (H&E) staining and immunofluorescence.

Methods We used the 10x Genomics Visium Spatial Gene Expression Solution for FFPE tissue to analyze and resolve tumorigenic profiles in sections of normal and adenocarcinoma prostate samples. This assay incorporates ~5,000 molecularly barcoded, spatially encoded capture probes in spots over which the tissue is placed, imaged, and permeabilized. Imaging and sequencing data are processed together, resulting in a spatially resolved transcriptional readout.

Results We profiled the whole transcriptome in normal, invasive adenocarcinoma, and acinar cell carcinoma FFPE human prostate tissues. Unsupervised clustering of the whole transcriptome data from normal, invasive adenocarcinoma, and acinar cell prostate carcinoma FFPE sections enabled the identification of 2 different regions, which had a well defined spatial distribution within the tissues. Well known prostate gland and prostate-cancer markers were over-expressed in the corresponding healthy and cancerous portions of the tissue, validating the performance of this method. We found that, while in healthy tissues basal cells and luminal cells are spatially organized, this pattern is lost in tumor samples, where luminal cells are greatly expanded in the invasive carcinoma region and do not colocalize with basal cells. Moreover, T lymphocytes are dispersed throughout the whole tissue section in the adenocarcinoma, while plasma B cells are located in the peritumoral region which could impact prognosis.

Conclusions Spatial whole transcriptome analysis opens new opportunities for better understanding the TME which can not only help discover novel predictive tumor biomarkers, but also enable identifying cell type and tumor region specific drug targets.

<http://dx.doi.org/10.1136/jitc-2021-SITC2021.072>

**CHARACTERIZATION OF TUMOR-INFILTRATING T-CELL
REPERTOIRE IN HUMAN CANCERS**

Taylor Harding*, Qidi Yang, Brittany Mineo, Jenna Malinauskas, Jason Perera, Karl Beutner, Denise Lau, Aly Khan. *Tempus, Chicago, IL, USA*

Background TCR and BCR repertoire profiling is a promising technique that can provide a clinically useful window into the complex interactions between tumor cells and infiltrating lymphocytes. Despite recent advances in repertoire sequencing methods, the characterization of tumor-infiltrating T-cell repertoires has been limited to small sample sizes due to technical and material constraints. In this study, we constructed a large multidimensional database of repertoire data covering a diverse landscape of HLA genotypes and tumor neoantigens from routine clinical sequencing. We present a descriptive summary of repertoire profiles derived from tens of thousands of tumor samples from over fifty different cancer cohorts and characterize the associations between T-cell repertoires and various clinical and molecular features.

Methods To enrich immune receptor transcripts detected by the Tempus RNA-sequencing workflow, hybrid capture probes tiling TCR and BCR genes were used. Repertoire profiling reads were aligned, assembled, and annotated against IMGT reference sequences. Repertoires are profiled as a component of Tempus|xT RNA sequencing and are summarized here for >25 thousand tumor samples from over 50 different cancer cohorts.

Results We demonstrate that the use of TCR/BCR hybrid capture probes is an effective method for enriching immune receptor transcripts in RNA-sequencing data without interfering with downstream transcriptomic analysis. These repertoires were profiled as part of a larger, multimodal DNA/RNA-sequencing pipeline that quantifies a variety of tumor clinical and molecular features. We explored the correlation between high-level repertoire metrics like richness (the number of unique receptor clonotypes in a given repertoire) and clonality/evenness (Shannon entropy) against both gene expression-based metrics (i.e. immune cell infiltration estimates, etc.) and mutational patterns (mutational burden and neoantigen load). Finally, we observed that the repertoire clonality of B-cell and T-cell driven cancers frequently exhibits clear monoclonal dominance for the tumor cells' lymphoid receptors.

Conclusions TCR/BCR repertoire profiling can be incorporated into high-volume clinical RNA sequencing to generate a diverse multimodal dataset for studying the tumor-immune microenvironment. By creating a large-scale database of TCR/BCR repertoire profiles from a variety of tissue, HLA genotypes, and mutational contexts, we can better resolve the molecular and clinical correlates of cancer with host adaptive immunity.

<http://dx.doi.org/10.1136/jitc-2021-SITC2021.073>

TUMOR MICROENVIRONMENT BASED ON PD-L1 AND CD8 T-CELL INFILTRATION CORRELATED WITH THE RESPONSE OF MSS MCRC PATIENTS TREATED VACTOSERTIB IN COMBINATION WITH PEMBROLIZUMAB

¹Tae Won Kim*, ²Keun-Wook Lee, ³Joong Bae Ahn, ⁴Young Suk Park, ⁵Chan-Young Ock, ⁵Hyejoo Park, ⁵Jiyeon Ryu, ⁵Bitna Oh, ⁵Bo-Kyoung Kim, ⁵Sunjin Hwang, ⁵Ki Baik Hahm, ⁵Seong-jin Kim. ¹Asan Medical Center, University of Ulsan College of Medicine, Seoul, Korea, Republic of; ²Seoul National University Bundang Hospital, Seoul National University College of Medicine, Seoul, Korea, Republic of; ³Yonsei Cancer Center, Yonsei University College of Medicine, Seoul, Korea, Republic of; ⁴Samsung Medical Center, Sungkyunkwan University School of Medicine, Seoul, Korea, Republic of; ⁵MedPacto, Inc., Seoul, Korea, Republic of

Background The expression of PD-L1 and tumor-infiltrating CD8 T cells were reported to have a decisive effect on the immunotherapy response (PMID: 26819449). Microsatellite stable (MSS) metastatic colorectal cancer (mCRC) shows a limited clinical benefit to immunotherapy alone known to be having an ‘immune-cold’ microenvironment. To understand the basis of the clinical responses to anti-PD-1 and TGF- β inhibitor combination therapy in MSS mCRC, we conducted a comprehensive analysis of survival outcome, whole transcriptome sequencing (WTS) data, and multiplex immunohistochemistry (mIHC) data from a combination treatment of vactosertib and pembrolizumab.

Methods Clinical outcomes were evaluated by RECIST v1.1 and iRECIST. Tumor tissue biopsy samples for WTS and mIHC were obtained in screening and cycle 2 post-treatment time point. CD274(PD-L1) and CD8A expression cut-off were calculated as a median value in the merged data set of TCGA Pan-cancer and MP-VAC-204 study. Having over median value defined as a high group and under median value as a low group. Tumor immune status by a combination of gene expression (high or low) was classified into four subtypes (1: CD274 high, CD8A high; 2: CD274 low, CD8A low; 3: CD274 high, CD8A low; 4: CD274 low, CD8A high). Tumor tissue slides stained with PD-L1, CD8, and granzyme B (GZB) in tumor nest and stroma.

Results Among 43 patients whose WTS data are available, thus included in the analysis, 9 patients were responders (7 PRs and 2 iPRs). Subtype 2 showed a major proportion in the MP-VAC-204 CRC patients (1: 14%, 2: 58%, 3: 12%, 4: 16%). Responders were observed in subtype 2 and 4 (24% and 14%, RECIST). The CD8A expression and median overall survival (mOS) showed a significantly positive correlation (**P=0.0028) and there was no significance in the correlation of CD274 and mOS. mOS was significantly longer in high expression of CD8A patients (*P=0.0083, Not reached vs 9.9 months, hazard ratio 8.812 [95% CI 3.19–24.31]). After the combination treatment, CD8 and GZB positive T cells were increased significantly in both tumor nest and stroma.

Conclusions Our study suggests a high level of CD8 T cells, even in the case of low PD-L1 expression, is significantly correlated with the improved clinical outcomes in MSS mCRC patients treated with vactosertib and pembrolizumab. The increases in CD8 T cells both in tumor nest and stroma after the combined inhibition of PD-1 and TGF- β pathway may contribute to the survival benefit. Further clinical investigations are warranted. (Clinical trial information: NCT03724851)

<http://dx.doi.org/10.1136/jitc-2021-SITC2021.074>

COMPREHENSIVE PROFILING OF THE TUMOR-IMMUNE MICROENVIRONMENT USING AN AUGMENTED TRANSCRIPTOME

Eric Levy*, Pamela Milani, Fabio Navarro, Gabor Bartha, Charles Abbott, Jose Jacob, Rena McClory, Robin Li, John West, John Lyle, Sean Boyle, Richard Chen. *Personalis, Inc., Menlo Park, CA, USA*

Background Comprehensive profiling of both the tumor and tumor microenvironment (TME) can help further our understanding of tumor progression and response to treatment. Many immune features can be extracted from transcriptomic data, including characterization of the immune infiltrate and profiling the diversity of immune receptors. To address this, we have developed multiple TME profiling features as part of the ImmunoID NeXT Platform®, an augmented, immunoncology-optimized exome/transcriptome platform designed to provide comprehensive information regarding the tumor and TME from a single FFPE tumor sample. These features including quantification of immune cell infiltration and profiling of the T-cell receptor (TCR) and B-cell receptor (BCR).

Methods To develop our immune infiltrate quantification method, we profiled the transcriptomes of eight purified immune cell types using ImmunoID NeXT™ to develop platform-specific gene sets, and compared our transcriptome quantification to immune cell quantification with IHC. For TCR and BCR methods, we analyzed the reproducibility of clone results, and compared top clones to standalone TCR and BCR sequencing approaches. In addition, we characterized the immune content of over 800 tumor samples across 14 cancer types. Finally, we analyzed the immune features in a cohort of melanoma patients who underwent PD-1 blockade.

Results We observe significant concordances between cell fractions by IHC and ImmunoID NeXT's transcriptome-based scores in tumor FFPE samples for B cells, CD8+ T cells, and macrophages ($R_2 > 0.82$, $R_2 > 0.75$, and $R_2 > 0.52$, respectively). For TCR and BCR methods, abundances of clones shared between subsequent curls of a tumor FFPE sample have very high concordances ($R_2 > 0.89$, $R_2 > 0.92$, and $R_2 > 0.76$ for TRB, IgG, and IgA, respectively). Compared to the standalone approaches, we identify 100% of the top 500 TRB clones and 95% of the top 500 IgG clones, with highly concordant abundances ($R_2 > 0.94$ and $R_2 > 0.82$ for TRB and IgG, respectively) in a PBMC sample. We identify biologically-relevant immune signatures across tumor types by characterizing the immune features across over 800 tumor samples. Finally, in a melanoma cohort, TRB clonality and CD8+ T cell scores are significantly different in responders to checkpoint inhibition.

Conclusions RNA sequencing can be used as a scalable approach to profile the immune composition in tumors. Such analysis can add to our understanding of the tumor-immune interaction, including studies of response to immunotherapy. We show that immune infiltrate quantification and TCR and BCR profiling – all part of the ImmunoID NeXT Platform – are able to accurately and effectively evaluate the composition and diversity of tumor-infiltrating immune cells.

<http://dx.doi.org/10.1136/jitc-2021-SITC2021.075>

SPATIAL MAPPING OF T CELL RECEPTORS AND TRANSCRIPTOMES IN RENAL CELL CARCINOMA FOLLOWING IMMUNE CHECKPOINT INHIBITOR THERAPY

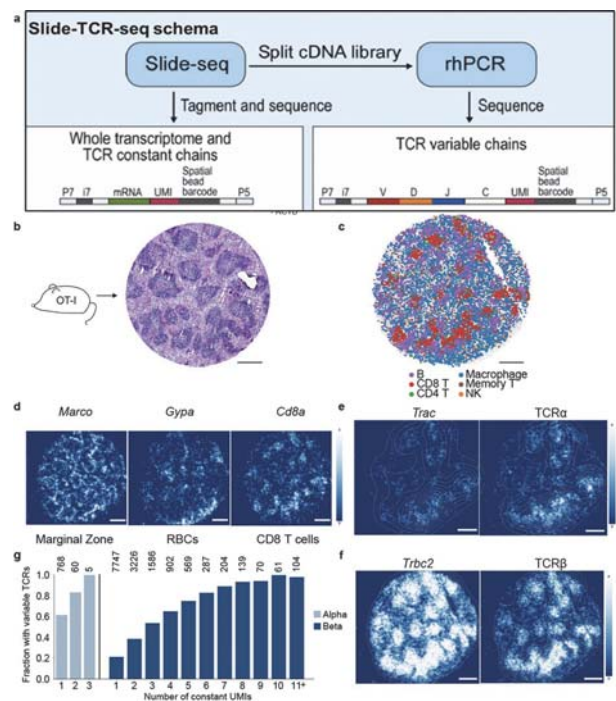
¹Sophia Liu, ²Bryan Iorgulescu*, ³Shuqiang Li, ¹Julia Morris, ³Mehdi Borji, ¹Evan Murray, ³David Braun, ³Kenneth Livak, ³Catherine Wu, ¹Fei Chen. ¹Broad Institute, Cambridge, USA; ²Dana-Farber Cancer Institute, Boston, MA, USA; ³DFCI, Cambridge, MA, USA

Background Because conventional single-cell strategies rely on dissociating tissues into suspensions that lose spatial context,¹ we developed Slide-TCR-seq to sequence both whole transcriptomes and TCRs with 10µm-spatial resolution, & applied it to renal cell carcinoma (ccRCC) treated with immune checkpoint inhibitors (ICI).

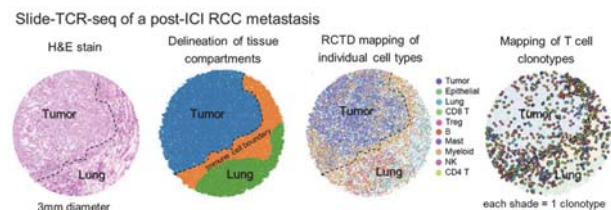
Methods Slide-TCR-seq combines Slide-seqV2^{2,3}—a 10µm-resolution spatial approach utilizing mRNA capture and DNA-barcoded beads—with sensitive targeted capture of TCR sequences (rhTCRseq,⁴ previously developed by our group), thereby enabling amplification of segments extending from upstream of CDR3 to the 3'-end of the TCR transcript (figure 1A). We tested Slide-TCR-seq first on OT-I murine spleen and then applied this methodology to 3 patients' pre-αPD-1 ccRCC samples⁵ and a post-αPD-1 metastasis to investigate the spatial, functional, and clonotypic organization of T cells in relationship to tumor using RCTD,⁶ spatial enrichment, and spatial expression analyses.

Results Using Slide-TCR-seq, we first recapitulated native spatial structure of OT-I mouse spleen (figure 1B-G). TCRα/β CDR3 sequences were detected on 37.1% of beads with Trac/Trbc2 constant sequences—comparable to other scTCRseq methods. Because the clonal and spatial context of TILs have been increasingly implicated in immunotherapy resistance, we used Slide-TCR-seq to analyze a lung ccRCC metastasis following αPD-1 therapy. We employed unsupervised clustering to delineate the tumor, intervening boundary, and lung compartments, and RCTD analyses to spatially map individual cell types; together recapitulating the architecture observed in corresponding histology (figure 2). We identified 1,132 unique clonotypes, with distinct spatial distributions spanning the tissue compartments. Eight clonotypes were significantly enriched in tumor, whereas 5 were depleted (all $p < 0.05$) (figure 3). We then analyzed the relationships between the T cells' clonotype, gene expression, and tumor infiltration depth among clonotypes. Using a T-cell geneset associated with poor response to ICI,⁷ we dichotomized T-clonotype beads by geneset expression, and found spatial segregation of this geneset's expression both within and across clonotypes (figure 4). TCR-4—the most significantly tumor-enriched clonotype—and TCR-2 displayed high expression of the poor ICI response geneset near the tumor's edge, but low expression deeper in the tumor compartment; indicating that there are transcriptionally distinct subpopulations of these clonotypes, which depended on the extent of their tumor infiltration.

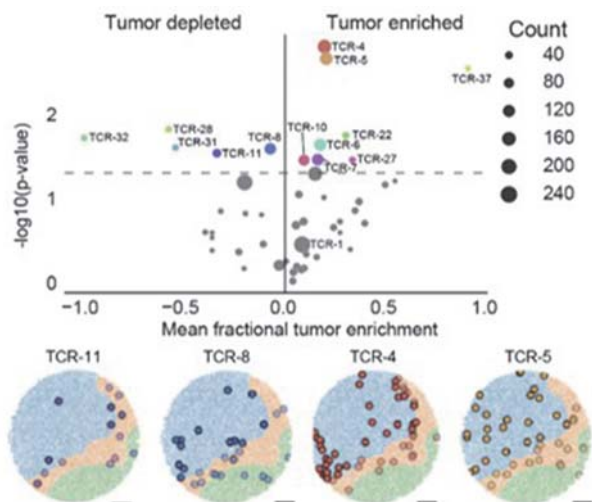
Conclusions Slide-TCR-seq effectively integrates spatial transcriptomics with TCR detection at 10µm resolution, thereby relating T cells' clonality and gene expression to their spatial organization in tumors. Our findings suggest that a clonotype's T cells may exhibit mixed responses to ICI depending on their spatial localization. The heterogeneity among clonotypes, in both gene expression and organization, underscores the importance of studying the TCR repertoire with spatial resolution.



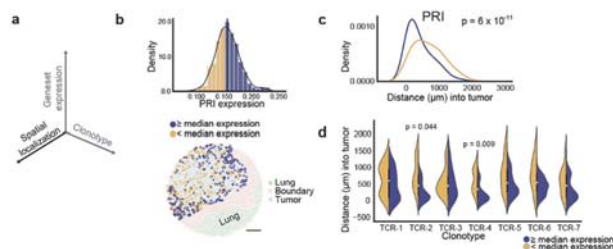
Abstract 76 Figure 1 Slide-TCR-seq spatially localizes T cell receptors and transcriptome information. a. Schematic of Slide-TCR-seq, in which tissue is placed onto an in situ barcoded bead array. cDNA libraries prepared with Slide-seqV2 are split prior to fragmentation with one portion used for targeted amplification via rhTCRseq optimized for use with Slide-seq libraries. Slide-TCR-seq provides gene expression, cell type, and clonotype information in space. b. Serial sections of the OT-I mouse spleen with hematoxylin and eosin stain show characteristic architecture of red pulp and white pulp separation. c. Spatial reconstruction of Slide-TCR-seq array for a corresponding section of OT-I mouse spleen, with RCTD immune cell type assignment. NK = natural killer. d. Gene expression gaussian-filtered heatmap for visualizing the spatial distribution of gene markers for marginal zone (Marco), red blood cells (RBCs; Gypa), and CD8 T cells (Cd8a). e and f. Comparing the spatial distribution of constant (left) and variable (right) sequences for TCRα (e) and TCRβ (f), with superimposed density plot. g. The fraction of beads that capture CDR3 variable sequences (y-axis) when constant UMIs are captured (x-axis) for TCRα (left, light blue) and TCRβ (right, dark blue), with the number of corresponding beads along the top axis. All scale bars: 500 µm.



Abstract 76 Figure 2 Slide-TCR-seq identifies spatial differences between T cell clonotypes in renal cell carcinoma. (a) H&E stain of a ccRCC metastasis to the lung following PD-1 blockade therapy. (b) The compartment assignment of lung (green), immune cell boundary (orange), and tumor (blue) by applying K-nearest neighbors to cell types determined by unsupervised clustering from Slide-TCR-seq of a sequential tissue section. (c) Spatial reconstruction of cell type identified using RCTD analysis of the Slide-TCR-seq data. (d) Spatial localization of T cell clonotypes (n=447 clonotypes, colored by clonotype) from the Slide-TCR-seq data.



Abstract 76 Figure 3 Top: y-axis Significance of clonotype spatial distributions compared against all other clonotypes with at least ten beads per array from the ccRCC lung metastasis plotted against an x-axis of magnitude of tumor enrichment or depletion (data from $n=3$ replicate arrays, two one-tailed K-S tests). Bottom: Visualization of selected significant clonotypes, ordered by tumor enrichment, in tissue compartments for a single array (T cells within the tumor compartment are displayed as opaque, T cells within other compartments are displayed as translucent).



Abstract 76 Figure 4 Spatial and molecular heterogeneity in clonotype gene expression and tumor infiltration. a. The three axes — spatial localization, gene expression, and T cell clonotype — that Slide-TCR-seq can relate. b. Top: distribution of poor response to immune checkpoint inhibitor treatment ('PRI') geneset⁷ expression across all clonotypes in the tumor region of the same post-PD1 inhibitor RCC lung metastasis from figures 2–3 (from a single replicate) with kernel density estimation. Yellow = clonotypes with lower than median PRI expression; purple = clonotypes with PRI expression greater than or equal to the median value. Bottom: localization of low (yellow) and high (purple) PRI geneset expression clonotypes within the tumor region (light blue) from the Slide-TCR-seq array shows their distinct spatial separation (light blue = tumor region, orange = boundary region, green = lung region). Scale bar: 500 μm . c. Smoothed histograms comparing the distance infiltrated into tumor by two-tailed K-S test comparing low (yellow) and high (purple) expression clonotypes, as dichotomized by median expression of PRI. d. Comparing distance infiltrated into tumor by two-tailed K-S test between low and high PRI expression T cells across those clonotypes with at least 20 beads ($n=7$ clonotypes).

Acknowledgements We are grateful to Irving A. Barrera-Lopez, Zoe N. Garcia, and Aziz Al'Khafaji for technical assistance.

REFERENCES

- Gohil S, Iorgulescu JB, Braun D, Keskin D, Livak K. Applying high-dimensional single-cell technologies to the analysis of cancer immunotherapy. *Nat Rev Clin Oncol* 2021; **18**:244–256.
- Stickels RR, Murray E, Kumar P, Li J, Marshall JL, Di Bella DJ, Arlotta P, Macosko EZ, Chen F. Highly sensitive spatial transcriptomics at near-cellular resolution with Slide-seqV2. *Nat Biotechnol* 2021 Mar; **39**(3):313–319.
- Rodrigues SG, Stickels RR, Goeva A, Martin CA, Murray E, Vanderburg CR, Welch J, Chen LM, Chen F, Macosko EZ. Slide-seq: A scalable technology for measuring genome-wide expression at high spatial resolution. *Science* 2019 Mar 29; **363**(6434):1463–1467.
- Li S, Sun J, Allesøe R, Datta K, Bao Y, Oliveira G, Forman J, Jin R, Olsen LR, Keskin DB, Shukla SA, Wu CJ, Livak KJ. RNase H-dependent PCR-enabled T-cell receptor sequencing for highly specific and efficient targeted sequencing of T-cell receptor mRNA for single-cell and repertoire analysis. *Nat Protoc* 2019 Aug; **14**(8):2571–2594.
- Braun DA, Street K, Burke KP, Cookmeyer DL, Denize T, Pedersen CB, Gohil SH, Schindler N, Pomerance L, Hirsch L, Bakouny Z, Hou Y, Forman J, Huang T, Li S, Cui A, Keskin DB, Steinharter J, Bouchard G, Sun M, Pimenta EM, Xu W, Mahoney KM, McGregor BA, Hirsch MS, Chang SL, Livak KJ, McDermott DF, Shukla SA, Olsen LR, Signoretti S, Sharpe AH, Irizarry RA, Choueiri TK, Wu CJ. Progressive immune dysfunction with advancing disease stage in renal cell carcinoma. *Cancer Cell* 2021 May 10; **39**(5):632–648.
- Cable DM, Murray E, Zou LS, Goeva A, Macosko EZ, Chen F, Irizarry RA. Robust decomposition of cell type mixtures in spatial transcriptomics. *Nat Biotechnol* 2021 Feb 18. doi: 10.1038/s41587-021-00830-w. Epub ahead of print. PMID: 33603203.
- Sade-Feldman M, Yizhak K, Bjorgaard SL, Ray JP, de Boer CG, Jenkins RW, Lieb DJ, Chen JH, Frederick DT, Barzilay-Rokni M, Freeman SS, Reuben A, Hoover PJ, Villani AC, Ivanova E, Portell A, Lizotte PH, Aref AR, Eliane JP, Hammond MR, Vitzthum H, Blackmon SM, Li B, Gopalakrishnan V, Reddy SM, Cooper ZA, Pawletz CP, Barbie DA, Stemmer-Rachamimov A, Flaherty KT, Wargo JA, Boland GM, Sullivan RJ, Getz G, Hacohen N. Defining T Cell States Associated with Response to Checkpoint Immunotherapy in Melanoma. *Cell* 2018 Nov 1; **175**(4):998–1013

Ethics Approval This study was approved by MGB/DFCI/Broad institution's Ethics Board; approval number 2019P000017.

<http://dx.doi.org/10.1136/jitc-2021-SITC2021.076>

PREVALENCE OF SECONDARY IMMUNOTHERAPEUTIC TARGETS IN THE ABSENCE OF ESTABLISHED IMMUNE BIOMARKERS IN SOLID TUMORS

Paul DePietro*, Mary Nesline, Yong Hee Lee, RJ Seager, Erik Van Roey, Shuang Gao, Vincent Giamo, Blake Burgher, Sean Glenn, Shengle Zhang, Roger Klein, Sarabjot Pabla, Jeffrey Conroy. *OmnSeq, Inc., Buffalo, NY, USA*

Background Immune checkpoint inhibitor-based therapies have achieved impressive success in the treatment of several cancer types. Predictive immune biomarkers, including PD-L1, MSI and TMB are well established as surrogate markers for immune evasion and tumor-specific neoantigens across many tumors. Positive detection across cancer types varies, but overall ~50% of patients test negative for these primary immune markers.¹ In this study, we investigated the prevalence of secondary immune biomarkers outside of PD-L1, TMB and MSI. **Methods** Comprehensive genomic and immune profiling, including PD-L1 IHC, TMB, MSI and gene expression of 395 immune related genes was performed on 6078 FFPE tumors representing 34 cancer types, predominantly composed of lung cancer (36.7%), colorectal cancer (11.9%) and breast cancer (8.5%). Expression levels by RNA-seq of 36 genes targeted by immunotherapies in solid tumor clinical trials, identified as secondary immune biomarkers, were ranked against a reference population. Genes with a rank value ≥ 75 th percentile were considered high and values were associated with PD-L1 (positive $\geq 1\%$), MSI (MSI-H or MSS) and TMB (high ≥ 10 Mut/Mb) status. Additionally, secondary immune biomarker status was segmented by tumor type and cancer immune cycle roles.

Results In total, 41.0% of cases were PD-L1+, 6.4% TMB+, and 0.1% MSI-H. 12.6% of cases were positive for >2 of these markers while 39.9% were triple negative (PD-L1-/TMB-/MSS). Of the PD-L1-/TMB-/MSS cases, 89.1% were high for at least one secondary immune biomarker, with 69.3% having ≥ 3 markers. PD-L1-/TMB-/MSS tumor types with $\geq 50\%$ prevalence of high secondary immune biomarkers included brain, prostate, kidney, sarcoma, gallbladder, breast, colorectal, and liver cancer. High expression of cancer testis antigen secondary immune biomarkers (e.g., NY-ESO-1, LAGE-1A, MAGE-A4) was most commonly observed in bladder, ovarian, sarcoma, liver, and prostate cancer ($\geq 15\%$). Tumors demonstrating T-cell priming (e.g., CD40, OX40, CD137), trafficking (e.g., TGFB1, TLR9, TNF) and/or recognition (e.g., CTLA4, LAG3, TIGIT) secondary immune biomarkers were most represented by kidney, gallbladder, and sarcoma ($\geq 40\%$), with melanoma, esophageal, head & neck, cervical, stomach, and lung cancer least represented ($\geq 15\%$).

Conclusions Our studies show comprehensive tumor profiling that includes gene expression can detect secondary immune biomarkers targeted by investigational therapies in ~90% of PD-L1-/TMB-/MSS cases. While genomic profiling could also provide therapeutic choices for a percentage of these patients, detection of secondary immune biomarkers by RNA-seq provides additional options for patients without a clear therapeutic path as determined by PD-L1 testing and genomic profiling alone.

REFERENCE

1. Huang R S P, Haberberger J, Severson E, et al. A pan-cancer analysis of PD-L1 immunohistochemistry and gene amplification, tumor mutation burden and microsatellite instability in 48,782 cases. *Mod Pathol* 2021;**34**: 252–263.

<http://dx.doi.org/10.1136/jitc-2021-SITC2021.077>

NOVEL RNA-SEQ PLATFORM IMPROVE PATIENT OUTCOME IN CLINICAL ONCOLOGY AND ENABLE IMPLEMENTATION OF AI IN THE CLINIC

¹Vy Nguyen, ²Gitte Pedersen*, ²Morten Pedersen. ¹*Genomic Expression, Beverly, MA, USA;* ²*Genomic Expression, Inc., Beverly, MA, USA*

Background Only 1 out of 4 cancer treatments prolongs life while expenditure for cancer treatment is greater than \$100 billion/year. RNA-sequencing has allowed researchers to gain insight into the transcriptome of human cancers. However, RNA-sequencing remains widely unused in clinical oncology. We address this issue through the development and CLIA validation of OneRNA—an RNA-sequencing platform for cancer diagnostics and the design of new treatments. The development of OneRNA had to overcome the two main hurdles for implementation of RNA sequencing in the clinic: 1) clinical samples are typically embedded in FFPE which results in highly fragmented RNA making sequencing of these samples difficult. 2) how to interpret aberrant gene expression events and translate these results into clinical action. We demonstrate how OneRNA[®] would enable the design of sophisticated combinatorial clinical studies. An example is combining immune targeting agents such as checkpoint inhibitors with mRNA vaccines. OneRNA also supports the integration of gene expression algorithms because of its ability to interrogate the entire sample transcriptome. OneRNA[®] has been CLIA certified using FFPE, FF, blood, and saliva samples. Furthermore, the sample preparation method has demonstrated >95% concordance between FF and FFPE and 5–10X the sensitivity compared to Truseq.

Methods This study aims to demonstrate the clinical utility of OneRNA in detecting aberrant gene expression events and connecting these to already approved drugs that targets these events to offer truly individualized treatment options.

Results We show that OneRNA has the ability to predict results for not only validated biomarkers used in standard of care such as ER, PR and HER2 in breast cancer, but also provide insight into biomarkers for response to already approved drugs independent of tissue type and with no standard test. Finally, we demonstrate the reproducibility of OneRNA in predicting IHC status in ER, PR and HER2.

Conclusions These results demonstrate that OneRNA has applications in both cancer research, drug discovery and development, development of companion diagnostic algorithms and implementation of truly individualized treatment.

<http://dx.doi.org/10.1136/jitc-2021-SITC2021.078>

79 EXTENSIVELY VALIDATED HLA LOH ALGORITHM DEMONSTRATES AN ASSOCIATION BETWEEN HLA LOH AND GENOMIC INSTABILITY

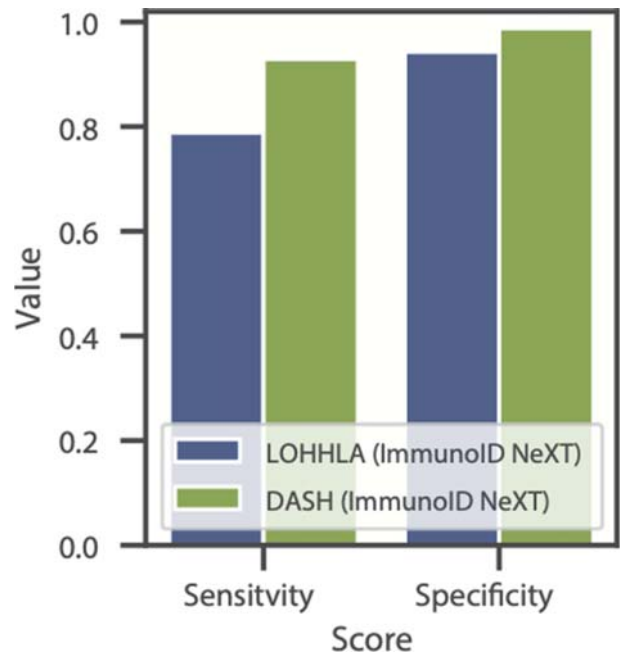
¹Rachel Pyke*, ¹Steven Dea, ¹Dattatreya Mellacheruvu, ²Charles Abbott, ¹Simo Zhang, ¹Lee McDaniel, ¹Eric Levy, ¹Gabor Bartha, ¹John West, ³Michael Snyder, ¹Richard Chen, ¹Sean Boyle. ¹Personalis, Oakland, USA; ²Personalis, Menlo Park, CA, USA; ³Stanford University, Menlo Park, USA

Background Human Leukocyte Antigen (HLA) genes are critical for the presentation of neoantigens to the immune system by cancer cells. Deletion of HLA alleles, known as HLA loss of heterozygosity (LOH), has been highlighted as a key immune escape mechanism. Validated algorithms to detect HLA LOH from sequencing data are critical for exploring the biological impact of HLA LOH and assessing its utility as a clinical biomarker.

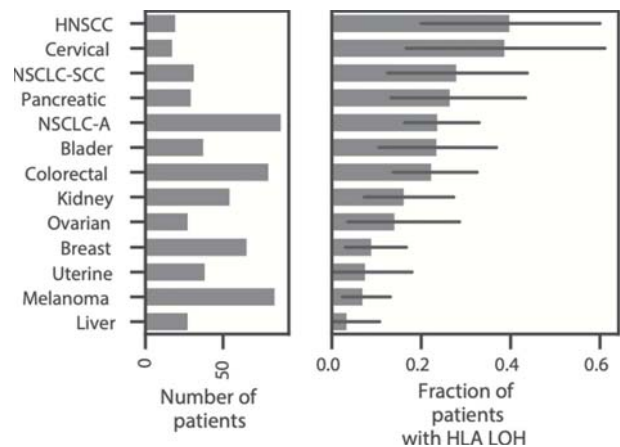
Methods We developed DASH (Deletion of Allele-Specific HLAs), a machine learning algorithm trained on data from 279 patients on the ImmunoID NeXT Platform using features that account for probe capture variability between alleles and incorporate information from the regions flanking each HLA gene. To understand the contribution of boosted sequencing in the HLA region of the ImmunoID NeXT Platform, we performed an in silico downsampling analysis. To assess DASH's performance at variable tumor purities and HLA LOH sub-clonalities we identified three tumor-normal cell lines with HLA LOH and created in silico mixtures. Furthermore, after designing patient-specific primers for 21 patients that target specific alleles, we applied digital PCR (dPCR) to validate the HLA allele copy number status of the patients. Finally, we applied DASH to 611 patients spanning 15 tumor types.

Results In cross validation analyses across patient samples, DASH achieved 98.7% specificity and 92.9% sensitivity while LOHHLA, a widely used algorithm, only reached 94.3% and 78.8%, respectively (figure 1). Downsampling analyses demonstrated that DASH benefits significantly from the boosted HLA sequencing on the ImmunoID NeXT Platform, dropping 0.06 in F-score after downsampling to the sequencing depth of other exome platforms. In cell line mixture analyses, DASH demonstrates greater than 99% specificity across all tumor purity and sub-clonality levels and greater than 98% sensitivity for above 27% tumor purity. Moreover, DASH demonstrated 100% sensitivity and specificity in dPCR experiments across 21 tumor samples with stable controls. We applied DASH to a large pan-cancer cohort and found that 18% of patients had HLA LOH (figure 2). We identified strong associations between HLA LOH and genomic instability. Moreover, we demonstrated relationships between HLA LOH and markers of immune pressure, such as a correlation with CD274 (PD-1) expression and allele-specific neoantigen enrichment for deleted HLA alleles.

Conclusions DASH, a highly sensitive HLA LOH algorithm that has been extensively validated using cross validation, in silico downsampling, cell line mixtures and dPCR, has demonstrated the widespread impact of HLA LOH in a large pan-cancer cohort.



Abstract 79 Figure 1 Bar plots showing the sensitivity and specificities scores across ImmunoID NeXT cross validation samples between LOHHLA (blue) and DASH (green).



Abstract 79 Figure 2 Bar plots denoting the number of patients and the frequency of HLA LOH in each tumor type cohort. 95% confidence intervals are shown with the thin dark grey bars. Only cohorts with at least 10 patients are shown

<http://dx.doi.org/10.1136/jitc-2021-SITC2021.079>

CANCER TESTIS ANTIGEN BURDEN: A NOVEL PREDICTIVE BIOMARKER FOR IMMUNOTHERAPY IN SOLID TUMORS

Sarabjot Pabla*, RJ Seager, Yong Hee Lee, Erik Van Roey, Shuang Gao, Vincent Giamo, Blake Burgher, Paul DePietro, Mary Nesline, Sean Glenn, Shengle Zhang, Jeffrey Conroy. *OmnSeq, Inc., Buffalo, NY, USA*

Background When expressed in cancer cells, cancer testis antigens (CTAs) are highly immunogenic and have the capacity to elicit cancer-specific immune responses in diverse malignancies. With their expression limited to tumor cells, CTAs have become a prime target of natural T cell response, immune cell-based therapy, and cancer vaccines. In this study, we investigated CTA burden in real-world clinical tumors spanning multiple histologies, revealing a novel prognostic gene expression-based biomarker.

Methods Targeted RNA-seq was performed on 5450 FFPE tumors representing 39 histologic types, predominantly composed of lung cancer (40.4%) followed by colorectal cancer (10.6%) and breast cancer (8.6%). Using an amplicon-based NGS approach, expression levels of 17 CTA genes were ranked against a reference population. Cancer Testis Antigen Burden (CTAB) was calculated as the sum of the gene expression rank for each CTA gene. The median CTAB of ≥ 171 was used as cutoff for CTAB High versus Low classification. We estimated Pearson's correlation for all CTA genes to discover co-expression patterns between CTAs and histologies. Overall survival (OS) analysis was performed using CoxPh regression model whereas response analysis was performed using logistic regression model with p-values reported.

Results Within the tumor samples, CTAB values ranged from 0–1700, with kidney cancer demonstrating overall lowest mean CTAB (110) and melanoma the highest (550). NSCLC had an average CTAB of 283. In an immune checkpoint blockade treated retrospective cohort of 110 NSCLC patients, High CTAB showed better OS compared to Low CTA (HR: 0.55, $p=0.07$). Additionally, when combined with tumor inflammation and cell proliferation biomarkers, highly inflamed but poorly proliferative tumors with High CTAB had improved OS (HR: 0.27, $p=0.05$). No significant association with response was detected.

Conclusions Our studies show that co-expression of multiple CTA genes occurs in many tumor types and can be reliably detected using a targeted RNA-seq approach. Utilization of this co-expression pattern to calculate CTAB reveals tumor-type associated signatures, which in a small NSCLC cohort is associated with the overall survival. The findings suggest that these immunogenic antigens expose the tumor cells to natural or immunotherapy augmented cell-based immune response, and that CTAB is a potential predictive marker for therapeutic response to checkpoint inhibitors. Further studies are needed to establish the predictive value in other tumor types, as well as the role of CTAB in immune cell therapies and vaccinations.

<http://dx.doi.org/10.1136/jitc-2021-SITC2021.080>

SINGLE-CELL RNA SEQUENCING AND CITE-SEQ ANALYSIS OF BLADDER CANCER PATIENT URINE WITH MATCHED TUMOR AND PERIPHERAL BLOOD SUGGESTS URINE AS A WINDOW INTO THE TUMOR IMMUNE MICROENVIRONMENT

Michelle Tran* Adam Farkas, Kristin Beaumont, Timothy O'Donnell, Reza Mehrazin, Amir Horowitz, Peter Wiklund, Matthew Galsky, John Sfakianos, Nina Bhardwaj. *Icahn School of Medicine at Mount Sinai, New York City, NY, USA*

Background FDA-approved immunotherapies for early and advanced stage bladder cancer have response rates of 15–65% in bladder cancer, suggesting that tumor-associated resistance mechanisms undermine their efficacy. Accordingly, there is an unmet need to identify accessible biomarkers that predict response. Urine, which is in direct contact with urothelial tumors, represents an easily accessible patient material that may reflect cellular and/or genetic signatures related to immune resistance. It has been demonstrated that urine from bladder cancer patients contains not only tumor cells, which are routinely assessed by clinical urinalyses, but also immune cells that previous studies suggest may reflect the tumor microenvironment (TME).¹ However, the concordance between cells in the urine and those in bladder tumors is unknown. Here, we characterized patient urine in an unbiased fashion by performing the first single-cell RNA sequencing (scRNAseq) and Cellular Indexing of Transcriptomes and Epitopes by Sequencing (CITE-seq) on matched bladder cancer patient urine, tumor, and peripheral blood.

Methods Matched tumor tissue, urine, and peripheral blood were collected from bladder cancer patients (n=7) during surgery; either trans-urethral resection of bladder tumor or cystectomy. All three tissues were processed to single-cell suspensions and sequenced using the 10X Genomics platform (scRNAseq: 17 samples, CITE-seq: 3 samples). These sequencing approaches permitted quantification of both transcriptomic and surface protein expression of 54,469 cells total.^{2–3} Analysis was performed using Seurat, Enrichr, and Monocle packages and platforms.^{4–6}

Results scRNAseq of urine from bladder cancer patients revealed several immune populations including CD4+ and CD8+ T cells, Treg cells, NK cells, B cells, neutrophils, dendritic cells, monocytes, and macrophages in addition to non-hematopoietic lineages including bladder epithelial cells, neuronal cells, prostate epithelial cells, fibroblasts, myofibroblasts, and endothelial cells. The composition and transcriptional profiles of urine immune cells were more similar to TME immune cells than to peripheral blood immune cells. Urine immune cells expressed gene signatures associated with hypoxia, anergy, pro-inflammation, and glucose deprivation that were more similar to tumor immune cells than those in the peripheral blood.

Conclusions Our work represents the first scRNAseq and CITE-seq profiling of cancer patient urine. Our study suggests several viable immune cells shed in bladder cancer patient urine that look more transcriptionally and phenotypically similar to the TME than peripheral blood cells. This important finding has several implications for future research and clinical applications as urine can be sampled non-invasively in scenarios when tumor resection may not be feasible.

REFERENCES

1. Wong YNS, Joshi K, Khetrpal P, et al. Urine-derived lymphocytes as a non-invasive measure of the bladder tumor immune microenvironment. *Journal of Experimental Medicine*. 2018; **215**:2748–59.

- Zheng GXY, Terry JM, Belgrader P, et al. Massively parallel digital transcriptional profiling of single cells. *Nature Communications* 2017; **8**.
- Stoeckius M, Hafemeister C, Stephenson W, et al. Simultaneous epitope and transcriptome measurement in single cells. *Nature Methods* 2017; **14**, 865–68.
- Butler A, Hoffman P, Smibert, P, et al. Integrating single-cell transcriptomic data across different conditions, technologies, and species. *Nature Biotechnology* 2018; **36**: 411–20.
- Xie Z, Bailey A, Kuleshov MV, et al. Gene set knowledge discovery with Enrichr. *Current Protocols* 2021.
- Trapnell C, Cacchiarelli D, Grimsby J, et al. The dynamics and regulators of cell fate decisions are revealed by pseudotemporal ordering of single cells. *Nature Biotechnology* 2014; **32**: 381–6.

Ethics Approval The study was approved by Mount Sinai Institution's Ethics Board, approval number 10–1180. Participants gave informed consent before taking part in the study.

<http://dx.doi.org/10.1136/jitc-2021-SITC2021.082>

SPATIALLY RESOLVED TRANSCRIPTOMIC AND PROTEOMIC INVESTIGATION OF BREAST CANCER AND ITS IMMUNE MICROENVIRONMENT

Jennifer Chew*, ¹Cedric Uytingco, ¹Rapolas Spalinskas, ¹Yifeng Yin, ¹Joe Shuga, ¹Benton Veire, ¹Naishitha Anaparthi, ¹Ryo Hatori, ¹Anna-Maria Katsor, ¹Layla Katiraei, ¹Alexander Hermes, ¹Jun Ding Chiang, ¹Patrick Roelli, ¹Stephen Williams, ¹William Nitsch, ¹Neil Weisenfeld, ¹Dan Walkser, ¹Jason Koth, ²Subham Basu, ²Will Howat, ¹Karthik Ganapathy, ¹Marlon Stoeckius. ¹10X Genomics, Pleasanton, CA, USA; ²Abcam, Cambridge, UK

Background The tumor microenvironment (TME) is composed of highly heterogeneous extracellular structures and cell types such as endothelial cells, immune cells, and fibroblasts that dynamically influence and communicate with each other. The constant interaction between a tumor and its microenvironment plays a critical role in cancer development and progression and can significantly affect a tumor's response to therapy and capacity for multi-drug resistance. High resolution analyses of gene and protein expression with spatial context can provide deeper insights into the interactions between tumor cells and surrounding cells within the TME, where a better understanding of the underlying biology can improve treatment efficacy and patient outcomes. Here, we demonstrated the ability to perform streamlined multi-omic tumor analyses by utilizing the 10X Genomics Visium Spatial Gene Expression Solution for FFPE with multiplex protein enablement. This technique simultaneously assesses gene and protein expression to elucidate the immunological profile and microenvironment of different breast cancer samples in conjunction with standard pathological methods.

Methods Serial (5 μ m) sections of FFPE human breast cancer samples were placed on Visium Gene Expression (GEX) slides. The Visium GEX slides incorporate ~5,000 molecularly bar-coded, spatially encoded capture spots onto which tissue sections are placed, stained, and imaged. Following incubation with a human whole transcriptome, probe-based RNA panel and an immuno-oncology oligo-tagged antibody panel, developed with Abcam conjugated antibodies, the tissues are permeabilized and the representative probes are captured. Paired GEX and protein libraries are generated for each section and then sequenced on an Illumina NovaSeq at a depth of ~50,000 reads per spot. Resulting reads from both libraries are aligned and overlaid with H&E-stained tissue images, enabling analysis of both mRNA and protein expression. Additional analyses and data visualizations were performed on the Loupe Browser v4.1 desktop software.

Conclusions Spatial transcriptomics technology complements pathological examination by combining histological assessment with the throughput and deep biological insight of highly-multiplexed protein detection and RNA-seq. Taken together, our work demonstrated that Visium Spatial technology provides a spatially-resolved, multi-analyte view of the tumor microenvironment, where a greater understanding of cellular behavior in and around tumors can help drive discovery of new biomarkers and therapeutic targets.

<http://dx.doi.org/10.1136/jitc-2021-SITC2021.083>

COMPARATIVE ANALYSIS OF IMMUNOID NEXT™ AND ACE IMMUNOID™ NEXT GENERATION SEQUENCING PLATFORMS FOR INVESTIGATING TUMOR-IMMUNE INTERACTIONS TO ENABLE PRECISION ONCOLOGY DRIVEN BIOMARKER DISCOVERY

¹Danyi Wang*, ²Juergen Scheuenpflug, ¹Zheng Feng, ¹EMD Serono Research and Development Institute, Inc., Billerica, MA, USA; ²Merck KGaA, Darmstadt, Gibraltar

Background ImmunoID NeXT is a comprehensive enhanced whole exome and whole transcriptome scale platform, that provides a multidimensional view of the molecular tumor microenvironment from a single tumor sample with augmented coverage and specific targeting.¹ As ImmunoID NeXT is based on Accuracy and Content Enhanced (ACE) technology to further supplement gaps in all 20,000 human genes and target unique genomic regions for immuno-oncology, we assessed key sequencing metrics between the platforms to assure smooth platform migration.

Methods Fifteen FFPE samples from late-stage, treatment-naive colorectal cancer patients were processed on both ACE ImmunoID and ImmunoID NeXT platforms. Specimens were evaluated using the same input criteria including the minimum 4 unstained slides per FFPE sample with 5–10 micro-meter thick sections, 25mm² surface area each section, ≥ 20% tumor content. ACE ImmunoID sequencing was performed using ACE enrichment including library preparation and 2x150bp sequencing on the NovaSeq. Whereas, ImmunoID NeXT exome sequencing was performed using NeXT enrichment including library preparation and 2x150bp sequencing on the NovaSeq. We assessed the concordance of the assays in overlapping features with respect to sequencing quality metrics, somatic variant calling, tumor mutational burden, and gene expression. Tumor mutation burden (TMB) from the two platforms was re-computed to align with the FOCR guidelines, counting exome-wide non-synonymous somatic variants over the coding sequence footprint of each assay.

Results The sequencing average base quality (Q score) is equivalent (exome-Seq: NeXT = 36.17 vs. ACE = 36.02; Transcriptome-Seq: NeXT = 35.79 vs. ACE = 35.90;) and alignment coverage consistent with the platform design. To look at somatic variant concordance, the ACE ImmunoID and ImmunoID NeXT .bed files were intersected, and the analysis was focused on the overlapping target region. The following filters were applied to the variants detected with ACE ImmunoID: allelic frequency of >10%, read depth of >50, and a population frequency filter where any variant over 1% was excluded. The same population frequency filter was also applied to variants detected with ImmunoID NeXT. We observed a concordance of 89–98% in high confidence calls between the two platforms. Focused on the overlapping coding region in the intersection of ACE and NeXT, the consistent TMB results were achieved with both platforms.

Conclusions It is demonstrated that both ImmunoID NeXT and ACE ImmunoID are high-performance platforms with consistently strong sequencing QC metrics. Collectively, ImmunoID NeXT, as the universal cancer immunogenomics platform, could provide end-to-end solution for immune/precision oncology clinical biomarker discovery.

REFERENCES

1. Zheng Feng, Danyi Wang, Mengyao Tan, Juergen Scheuenpflug. Whole-exome sequencing based immunogenomic profiling with potential clinical applicability in circulating cell-free DNA and tissue from advanced stage colorectal cancer patients [abstract]. In: Proceeding of the Annual Meeting of the Society for

Immunotherapy for Cancer 2020; Nov 11–14: SITC; J Immunother Cancer 2020; 8 (16 Suppl 3): Abstract nr 19.

Ethics Approval The study protocol was in accordance with the tenets of the Declaration of Helsinki. Commercial samples used in this study were procured from BioIVT and BioChain following protocols approved by the local Institutional Review Board (IRB) committee. Informed consent forms were obtained from all the human subjects in this study.

Consent Written informed consent was obtained from the patient for publication of this abstract and any accompanying images. A copy of the written consent is available for review by the Editor of this journal.

<http://dx.doi.org/10.1136/jitc-2021-SITC2021.084>

DETECTION OF HUMAN ANGIOTENSIN-CONVERTING ENZYME 2 RECEPTOR (HACE2R) ON HUMAN CANCER CELL LINES

Tarsem Moudgil*, Bernard Fox, Hong-Ming Hu. *E.A.Chiles Research INST, Portland, OR, USA*

Background SARS-CoV-2 infections have delayed administration of treatments for some patients with cancer, increasing the number of avoidable deaths. However, we hypothesized that infection of cancer cells with SARS-CoV-2 might increase the immunogenicity of those cancer cells. Here we sought to determine whether non-small cell lung cancer (NSCLC) and head and neck squamous cell cancer (HNSCC) cell lines could be a potential target of SARS-CoV-2, which binds and infects host cells via interactions between the viral spike glycoprotein and the human angiotensin-converting enzyme 2 receptor (hACE2) receptor. Through an institutional research tissue protocol, our lab has established a panel of cancer cell lines of various histologies. Here we set out to identify whether HNSCC and NSCLC cell lines expressed the hACE2R. We also investigated the expression of neuropilin-1, a molecule reported to facilitate SARS-CoV-2 cell entry.

Methods Established cell lines were phenotyped by flow cytometric analysis utilizing the anti-hACE2R antibody from Novus Biologicals. Cell lines were also stained with mIgG1 and anti-CD3 antibodies as negative staining controls.

Results We identified that three of eight NSCLC cell lines expressed the hACE2R and two of these had strong expression of neuropilin-1. Evaluation of HNSCC cell lines identified seven of seven cell lines expressed detectable levels of hACE2R but only one of seven HNSCC cell lines expressed substantial levels of neuropilin-1. Preliminary evaluation of a renal cell carcinoma (RCC) cell line revealed strong staining for hACE2R.

Conclusions Our study found that a majority of HNSCC cell lines (100% n=7) and approximately a third of the NSCLC cell lines (37.5%, n=8) tested express the hACE2R. Some cell lines express both hACE2R and neuropilin-1, potentially increasing their susceptibility for infection with SARS-CoV-2. While these studies were performed with cultured cell lines that may have modulated expression of hACE2R, it is possible that in vivo these tumors express the ACE2R and could serve as a target and possible reservoir for SARS-CoV-2.

Acknowledgements

Support The Chiles foundation, Nancy Lematta

<http://dx.doi.org/10.1136/jitc-2021-SITC2021.085>

EXTENSIVE FAP EXPRESSION ANALYSIS IN 23 TUMOR INDICATIONS AND POTENTIAL APPLICATION IN DEFINING THE PATIENT POPULATION IN FAP-TARGETING CANCER IMMUNOTHERAPIES

Sebastian Dziadek*, Anton Kraxner, Wei-Yi Cheng, Mike Flores, Tai-Hsien, Noah Theiss, Tsu-Shuen Tsao, Emilia Andersson, Suzana Vega Harring, Gabriele Gabriele Hoelzlzimmer, Ann-Marie Broeske, Maurizio Ceppi, Jehad Charo. *Roche/Genentech, Basel, Switzerland*

Background Fibroblast activation protein alpha (FAP) is frequently over-expressed in the tumor microenvironment (TME) while exhibiting limited expression in normal tissues. FAP expression was reported to be immunosuppressive in tumor mouse models and generally associated with worse prognosis in clinical studies. Therefore, it is important to understand the context in which FAP both exhibits immunosuppressive characteristics and be a useful target for immunotherapy.

Methods Comprehensive immunohistochemistry (IHC) analyses on formalin-fixed paraffin-embedded tissue specimens with emphasis on lymph nodes and primary and metastatic tumor lesions spanning a wide range of indications were undertaken in this study. FAP staining of tumor tissues was performed with an optimized IHC robust-prototype-assay (RPA) and manually scored. The area (normal stroma & neoplastic) staining positively relative to the total tumor area at each intensity level was recorded and an H-score calculated (FAP-intensity score). These were supplemented by gene expression analysis using public as well as Roche phase 1, 2 and 3 cancer immunotherapy (CIT) clinical trial data sets.

Results Analysing FAP expression on normal tissue confirmed the general absence of FAP apart from a subset of pancreatic islet cells. Unlike the more homogenous expression of typical protein targets on tumor cells, FAP expression in the TME is heterogeneous in both pattern and intensity, requiring the analysis of a large sample set. Therefore, we evaluated 1216 samples from 23 tumor indications and 70 sub-indications. FAP expression exhibited a significant spread ranging from indications with highly abundant expression to those with low coverage. Using data from matching IHC and gene expression samples we confirmed FAP mRNA expression to significantly correlate with RPA H-scores (Spearman correlation: 0.62) (N=289, P=1.2E-31). Gene expression data from 12 atezolizumab clinical studies, including standard of care (SOC) randomized studies, with more than 6000 samples from 4 major indications were interrogated for the association between FAP expression and clinical response as evaluated by overall and progression free survival. This analysis suggests that FAP expression is generally associated with higher hazard ratios across all atezolizumab-treated samples (OS: 95% CI 1.04–1.09; PFS: 1.04–1.08), with the highest effect observed in Renal Cell Carcinoma (OS: 95% CI 1.08–1.31; PFS: 1.05–1.21), indicating a potential role of FAP in limiting CIT.

Conclusions Data from these analyses can tailor indication and patient enrichment strategies for achieving optimal FAP-targeting. We propose to select indications with FAP-levels that are high enough to enable drug accumulation, yet low enough to reduce immunosuppressive effects that can hamper successful immunotherapy.

<http://dx.doi.org/10.1136/jitc-2021-SITC2021.086>

87

ENHANCED IMMUNOGENICITY WITHIN THE TUMOR MICROENVIRONMENT AND THE CIRCULATION OF HIGH-RISK MELANOMA PATIENTS WITH UNKNOWN PRIMARY COMPARED TO THOSE WHOSE PRIMARY MELANOMA IS KNOWN

¹Ahmad Tarhini*, ¹Aik Choon Tan, ¹Issam El Naqa, ²Sandra Lee, ³F Stephen Hodi, ⁴Lisa Butterfield, ⁵William LaFramboise, ⁶Walter Storkus, ¹Jose Conejo-Garcia, ¹Patrick Hwu, ⁷Howard Streicher, ¹Vernon Sondak, ⁸John Kirkwood. ¹H. Lee Moffitt Cancer Center and Research Institute, Tampa, FL, USA; ²Harvard Medical School, Dana Farber Cancer Institute, ECOG-ACRIN Biostatistics Center, Boston, MA, USA; ³Dana-Farber/Harvard Cancer Center, Boston, MA, USA; ⁴Parker Institute for Cancer Immunotherapy, San Francisco, CA, USA; ⁵Allegheny General Hospital, Pittsburgh, PA, USA; ⁶University of Pittsburgh, Pittsburgh, PA, USA; ⁷National Cancer Institute, Chevy Chase, MD, USA; ⁸UPMC Hillman Cancer Center, Pittsburgh, PA, USA

Background We recently reported data supporting the unknown primary status as a potentially distinct prognostic group among high-risk melanoma patients treated with ipilimumab and high dose interferon-alfa (HDI) in the ECOG-ACRIN E1609 trial (N=1670) with improved RFS and OS outcomes compared to known primary. Therefore, we investigated differences in candidate immune biomarkers in the circulation and tumor microenvironment (TME) of patients with unknown compared to those with known primary melanoma enrolled in this trial that tested adjuvant ipilimumab at 3 and 10 mg/kg versus HDI.

Methods Gene expression profiling (GEP) was performed on the tumor biopsies of 718 (102 unknown, 616 known primary) melanoma patients. The primary endpoint was mRNA expression profiling using U133A 2.0 Affymetrix gene chips. Raw microarray data sets were normalized by using the Robust Multi-array Average (RMA) method using Affymetrix Power Tools (APT) as previously published. Multiple probe sets representing the same genes were collapsed by using the probe with maximum gene expression. Gene set enrichment analysis (GSEA) was performed by comparing the unknown and known primary tumor samples, and gene sets with FDR q-value <0.1 were deemed as significant. Similarly, peripheral blood (serum and PBMC) samples were tested for soluble (Luminex) and cellular (multicolor flow cytometry) immune biomarkers in a subset of patients (N=321; 66 unknown and 255 known primary). All patients provided an IRB-approved written informed consent.

Results Unknown primary melanoma cases represented 12.8% of the total E1609 study population (N=1670) including 11.7% on the ipilimumab arms and 14.7% on the HDI arm. Stratifying by stage, relapse free survival (RFS) (P=0.001) and overall survival (OS) (P=0.009) were significantly better for patients with unknown primary tumor compared to known primary. Including only ipilimumab-treated patients, RFS (P=0.005) and OS (P=0.023) were significantly better in favor of the unknown primary status. Among the cohort of patients with tumor GEP data (N=718), GEP identified pathways and genes related to autoimmunity, inflammation, immune cell infiltration and immune activation that were significantly enriched in the unknown primary tumors compared to known primaries (table 1). Among the subset of patients tested for circulating biomarkers, patients with unknown primary melanoma had significantly higher circulating levels of IL-2R than those with known primary (P=0.04).

Abstract 87 Table 1 Immune pathways enriched in unknown primary melanoma

Pathways	P-value	FDR q-value	Pathways	P-value	FDR q-value
CIBERSORT_MACROPHAGES_M1	0	0	KEGG_ANTIGEN_PROCESSING_AND_PRESENTATION	0	0
CIBERSORT_B_CELLS_MEMORY	0	0	KEGG_AUTOIMMUNE_THYROID_DISEASE	0	0
CIBERSORT_T_CELLS_GAMMA_DELTA	0	0	KEGG_ALLOGRAFT_REJECTION	0	0
CIBERSORT_B_CELLS_NAIVE	0	0	KEGG_SYSTEMIC_LUPUS_ERYTHEMATOSUS	0	0
CIBERSORT_PLASMA_CELLS	0	0	KEGG_INTESTINAL_IMMUNE_NETWORK_FOR_IgA_PRODUCTIION	0	1.62E-04
CIBERSORT_T_CELLS_CD8	0	0	KEGG_GRAFT_VERSUS_HOST_DISEASE	0	1.35E-04
CIBERSORT_T_CELLS_CD4_MEMORY_RESTING	0	0	KEGG_LEISHMANIA_INFECTION	0	7.42E-04
CIBERSORT_NK_CELLS_RESTING	0	0	KEGG_PRIMARY_IMMUNODEFICIENCY	0	0.003084
CIBERSORT_NK_CELLS_ACTIVATED	0	0	KEGG_TYPE1_DIABETES_MELLITUS	0	0.00115
CIBERSORT_T_CELLS_CD4_MEMORY_ACTIVATED	0	0	KEGG_DNA_REPLICATION	0.00974	0.038615
CIBERSORT_T_CELLS_REGULATORY_TREGS	0	2.39E-04	KEGG_TOLL_LIKE_RECEPTOR_SIGNALING_PATHWAY	0	0.038395
HISTONES	0	2.39E-04	KEGG_VIRAL_MYOCARDITIS	0.003067	0.034207
CIBERSORT_T_CELLS_FOLLICULAR_HELPER	0	2.02E-04	KEGG_PANTOTHENATE_AND_COA_BIOSYNTHESIS	0.02005	0.033828
CIBERSORT_DENDRITIC_CELLS_ACTIVATED	0	3.96E-04	KEGG_PRION_DISEASES	0.008432	0.05644
CIBERSORT_MACROPHAGES_M2	0.002623	0.006049	KEGG_NATURAL_KILLER_CELL_MEDIATED_CYTOTOXICITY	0.002963	0.053087
CIBERSORT_MHCI	0.006579	0.008082	KEGG_PROTEIN_EXPORT	0.018771	0.05286
CIBERSORT_MONOCYTES	0	0.008812	KEGG_ASTHMA	0.022337	0.06327
CIBERSORT_DENDRITIC_CELLS_RESTING	0.001681	0.010999	KEGG_STARCH_AND_SUCROSE_METABOLISM	0.016129	0.073731
CIBERSORT_MACROPHAGES_M0	0.008738	0.03623	KEGG_COMPLEMENT_AND_COAGULATION_CASCADES	0.014151	0.077393
			KEGG_CELL_ADHESION_MOLECULES_CAMS	0.035294	0.126863

Conclusions Unknown primary high-risk melanoma patients had significantly better prognosis and evidence of significantly enhanced immune activation within the TME and the circulation, supporting the designation of unknown primary melanoma as a distinct prognostic marker in patients with high-risk melanoma.

Acknowledgements We are grateful to the patients and family members who participated in the E1609 trial and the E1609 trial investigators. This study was conducted by the ECOG-ACRIN Cancer Research Group (Peter J. O'Dwyer, MD and Mitchell D. Schnall, MD, PhD, Group Co-Chairs) and supported by the National Cancer Institute of the National Institutes of Health under the following award numbers: U10CA180794, U10CA180820, U10CA180888, UG1CA233180, UG1CA233184. Biomarkers studies were supported under the following award number: P50CA12197310 (Tarhini and Kirkwood). The content is solely the responsibility of the authors and does not necessarily represent the official views of the National Institutes of Health.

Trial Registration NCT01274338

Ethics Approval The E1609 study protocol was approved by the institutional review board of each participating institution and conducted in accordance with Good Clinical Practice guidelines as defined by the International Conference on Harmonization. All patients provided an IRB-approved written informed consent.

Consent Not applicable.

<http://dx.doi.org/10.1136/jitc-2021-SITC2021.087>

EVIDENCE OF ENHANCED IMMUNE ACTIVATION WITHIN THE TUMOR MICROENVIRONMENT AND THE CIRCULATION OF FEMALE PATIENTS WITH HIGH-RISK MELANOMA COMPARED TO MALES

¹Mariam Saad, ²Aik Choon Tan, ²Issam El Naqa, ³Sandra Lee, ⁴F Stephen Hodi, ⁵Lisa Butterfield, ⁶William LaFramboise, ⁷Walter Storkus, ²Jose Conejo-Garcia, ²Patrick Hwu, ⁸Howard Streicher, ²Vernon Sondak, ⁹John Kirkwood, ²Ahmad Tarhini*. ¹American University of Beirut, Beirut, MI, USA; ²H. Lee Moffitt Cancer Center and Research Institute, Tampa, FL, USA; ³Harvard Medical School, Dana Farber Cancer Institute, ECOG-ACRIN Biostatistics Center, Boston, MA, USA; ⁴Dana-Farber/Harvard Cancer Center, Boston, MA, USA; ⁵Parker Institute for Cancer Immunotherapy, San Francisco, CA, USA; ⁶Allegheny General Hospital, Pittsburgh, PA, USA; ⁷University of Pittsburgh, Pittsburgh, PA, USA; ⁸National Cancer Institute, Chevy Chase, MD, USA; ⁹UPMC Hillman Cancer Center, Pittsburgh, PA, USA

Background Sex differences in tumor immunity and response to immunotherapy were shown in murine models and descriptive analyses from recent clinical trials. We recently reported that female gender is a favorable prognostic marker for survival benefit following ipilimumab and high dose interferon- α (HDI) adjuvant therapy of high-risk melanoma in the ECOG-ACRIN E1609 trial (N=1670). Therefore, we investigated differences in candidate immune biomarkers in the circulation and tumor microenvironment (TME) of female and male patients.

Methods Gene expression profiling (GEP) was performed on the tumor biopsies of 718 (454 male, 264 female) patients. The primary endpoint was mRNA expression profiling using U133A 2.0 Affymetrix gene chips. Raw microarray data sets were normalized by using the Robust Multi-array Average (RMA) method using Affymetrix Power Tools (APT) as previously published. Multiple probe sets representing the same genes were collapsed by using the probe with maximum gene expression. Gene set enrichment analysis (GSEA) was performed by comparing the female and male tumor samples, and gene sets with FDR q-value <0.1 were deemed as significant. Similarly, peripheral blood (serum and PBMC) samples were tested for soluble (Luminex) and cellular (multicolor flow cytometry) prognostic biomarkers in a subset of patients (N=321; 109 female and 212 male). All patients provided an IRB-approved written informed consent.

Results Among the subset of patients tested for circulating biomarkers, females were significantly younger than males (P=0.03). Testing PBMCs, the percentages of CD3+ T cells (P=0.04) and CD3+CD4+ helper T cells (P=0.0005) were significantly higher in female patients compared to males. Also, there were trends toward higher levels of proinflammatory cytokines IL1beta (P=0.07) and IL6 (P=0.06) in females. On the other hand, males had significantly higher percentages of monocytes (P=0.03). Further, there were trends toward higher percentages of CD3+/CD4+/CD25hi+/Foxp3+ (P=0.1) and CD3+/CD4+/CD25+/CD127low+ (P=0.1) T-reg in male patients compared to females. Among the cohort of patients (N=718) with tumor GEP data, females were significantly younger than males (P=0.0009). GEP identified pathways and genes related to immune cell infiltration and activation that were significantly enriched in the tumors of females compared to males (table 1).

Abstract 88 Table 1 Immune pathways significantly enriched in tumors of females

Pathways	P-value	FDR q-value
CIBERSORT_T_CELLS_GAMMA_DELTA	0.005199	0.11409
CIBERSORT_NK_CELLS_ACTIVATED	0.010187	0.060707
CIBERSORT_NK_CELLS_RESTING	0.011824	0.055186
CIBERSORT_DENDRITIC_CELLS_ACTIVATED	0.010638	0.046483
CIBERSORT_T_CELLS_REGULATORY_(TREGS)	0.008547	0.050286
CIBERSORT_DENDRITIC_CELLS_RESTING	0.013986	0.063591
CIBERSORT_T_CELLS_CD8	0.027027	0.082961
CIBERSORT_MACROPHAGES_M1	0.016393	0.082415
CIBERSORT_T_CELLS_CD4_NAIVE	0.029412	0.093233

Conclusions Female gender was associated with adjuvant immunotherapeutic benefits and female patients were more likely to have evidence of immune activation within the TME and the circulation, supporting a potentially important role for female related factors in the immune response against melanoma, and these require further investigation.

Acknowledgements We are grateful to the patients and family members who participated in the E1609 trial and the E1609 trial investigators. This study was conducted by the ECOG-ACRIN Cancer Research Group (Peter J. O'Dwyer, MD and Mitchell D. Schnall, MD, PhD, Group Co-Chairs) and supported by the National Cancer Institute of the National Institutes of Health under the following award numbers: U10CA180794, U10CA180820, U10CA180888, UG1CA233180, UG1CA233184. Biomarkers studies were supported under the following award number: P50CA12197310 (Tarhini and Kirkwood). The content is solely the responsibility of the authors and does not necessarily represent the official views of the National Institutes of Health.

Trial Registration NCT01274338

Ethics Approval The E1609 study protocol was approved by the institutional review board of each participating institution and conducted in accordance with Good Clinical Practice guidelines as defined by the International Conference on Harmonization. All patients provided an IRB-approved written informed consent.

Consent Not applicable.

<http://dx.doi.org/10.1136/jitc-2021-SITC2021.088>

THE IMMUNE MARKER LAG-3 INCREASES THE PREDICTIVE VALUE OF CD38⁺ IMMUNE CELLS FOR SURVIVAL OUTCOME IN IMMUNOTHERAPY-TREATED HEPATOCELLULAR CARCINOMA

¹Chun Chau Lawrence Cheung*, ²Yong Hock Justin Seah, ²Juntao Fang, ³Nicole Orpilla, ⁴Justina Nadia Li Wen Lee, ⁵Han Chong Toh, ⁵Su Pin Choo, ¹Kiat Hon Lim, ⁵Wai Meng David Tai, ⁴Joe Yeong. ¹Singapore General Hospital, Singapore, Singapore; ²National University of Singapore, Singapore, Singapore; ³Temasek Polytechnic, Singapore, Singapore; ⁴Institute of Molecular and Cell Biology, Singapore, Singapore; ⁵National Cancer Centre Singapore, Singapore, Singapore

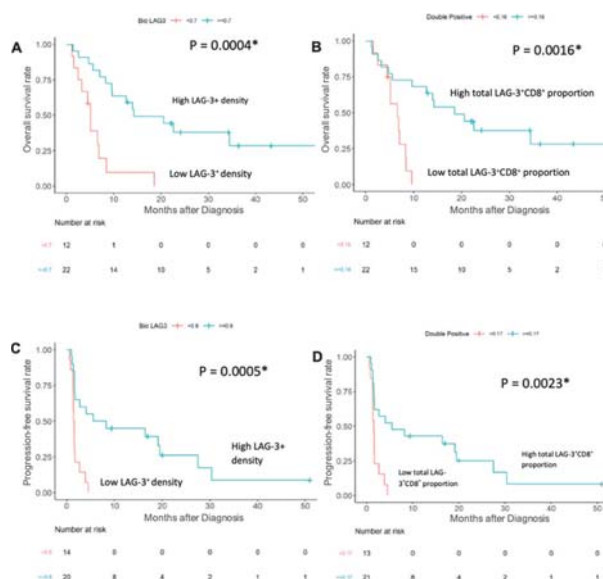
Background Immune check-point blockade (ICB) is one of the emerging therapeutic options for advanced hepatocellular carcinoma (HCC). However, low response rates amongst patients necessitates the development of robust predictive biomarkers that identify patients who likely benefit from ICB. Previously our group found that immunohistochemical scoring of CD38 in the tumour microenvironment predicts responsiveness to anti-PD-1/anti-PD-L1 immunotherapy in HCC.¹ Recently BMS 4-gene inflammatory signature, comprising the 4 genes CD8, PD-L1, LAG-3 and STAT1, has been shown to be associated with better overall response to immunotherapy in various cancer types.²⁻⁴ In the present study, we examined the relationship between tissue expression of BMS 4-gene inflammatory signature and the responsiveness of HCC to immunotherapy, and whether BMS 4-gene inflammatory signature increases the predictive power of CD38.

Methods HCC tissue samples from 124 Asian patients that underwent conventional treatment and from 49 Asian patients that underwent ICB were analysed for CD8, PD-L1, LAG-3, STAT1, CD38 and CD68 tissue expression using immunohistochemistry and multiplex immunohistochemistry, followed by survival and statistical analysis.

Results Survival analysis of the 124 samples showed that high LAG-3 tissue expression was associated with shorter progression-free survival (PFS). On the other hand, immunohistochemical analyses on the 49 patient samples treated with ICB revealed that high LAG-3 density and high total LAG-3⁺CD8⁺ T cell proportion were associated with improved response to ICB (figure 1). However, CD8, PD-L1 and STAT1 levels did not significantly correlate with improved survival. The addition of total LAG-3⁺ cell proportion to total CD38⁺ cell proportion significantly increased the predictive value for both PFS (DeltaLRChi²=9.97; P=0.0016; table 1) and overall survival (OS) (DeltaLRChi²=8.84; P=0.0021; table 1), compared with total CD38⁺ cell proportion alone. Similarly findings were obtained after adding total LAG-3⁺CD8⁺ cell proportion to total CD38⁺ cell proportion (PFS: DeltaLRChi²=7.21; P=0.0072; OS: DeltaLRChi²=8.06; P=0.0045; table 1), compared with total CD38⁺ cell proportion alone. Lastly, when the total LAG-3⁺CD8⁺ cell proportion was added to total CD38⁺ and CD38⁺CD68⁺ cell proportion, the predictive value of the biomarker was significantly increased (PFS: DeltaLRChi²=6.10; P=0.0136; OS: DeltaLRChi²=6.18; P=0.0129; table 1). Ongoing works include further validation of the findings in various cohorts, and correlating with clinical outcome of the patients.

Abstract 89 Table 1 Log-likelihood of models with added predictive terms

Variables	Progression-free Survival		Overall Survival	
	ΔLRχ ²	P-value	ΔLRχ ²	P-value
CD38 ⁺ + CD38 ⁺ CD68 ⁺ proportion vs CD38 ⁺ proportion	3.78	0.0519	4.55	0.0329
CD38 ⁺ + PD-L1 proportion vs CD38 ⁺ proportion	0.77	0.3813	0.15	0.7010
CD38 ⁺ + CD8 ⁺ proportion vs CD38 ⁺ proportion	1.30	0.2541	2.89	0.0890
CD38 ⁺ + STAT-1 proportion vs CD38 ⁺ proportion	2.58	0.1083	2.48	0.1153
CD38 ⁺ + LAG-3 proportion vs CD38 ⁺ proportion	9.97	0.0016	8.84	0.0029
CD38 ⁺ + LAG-3 ⁺ CD8 ⁺ proportion vs CD38 ⁺ proportion	7.21	0.0072	8.06	0.0045
CD38 ⁺ cells + CD38 ⁺ CD68 ⁺ + LAG-3 ⁺ CD8 ⁺ proportion vs CD38 ⁺ + CD38 ⁺ CD68 ⁺ proportion	6.10	0.0136	6.18	0.0129



Abstract 89 Figure 1 HCC patients' response to ICB in relation to LAG-3 density. (A) Kaplan-Meier curve showing the association between a high LAG-3 density and improved overall survival after treatment with ICB. (B) Kaplan-Meier curve showing the association between a high total LAG-3⁺CD8⁺ T cell proportion and improved overall survival after treatment with ICB. (C) Kaplan-Meier curve showing the association between a high LAG-3 density and improved progression-free survival after treatment with ICB. (D) Kaplan-Meier curve showing the association between a high total LAG-3⁺CD8⁺ T cell proportion and improved progression-free survival after treatment with ICB.

Conclusions High LAG-3 expression on tissue-infiltrating immune cells predicted greater response to ICB. LAG-3⁺ and LAG-3⁺CD8⁺ cell proportion added predictive value to CD38⁺ cells for predicting survival outcome in immunotherapy-treated HCC. LAG-3 may be used in conjunction with CD38 to predict responsiveness to ICB in HCC.

REFERENCES

1. Ng HHM, Lee RY, Goh S, et al. Immunohistochemical scoring of CD38 in the tumor microenvironment predicts responsiveness to anti-PD-1/PD-L1 immunotherapy in hepatocellular carcinoma. *J Immunother Cancer* 2020;**8**.
2. Hodi FS, Wolchok JD, Schadendorf D, et al. Abstract CT037: Genomic analyses and immunotherapy in advanced melanoma. *AACR* 2019.
3. Lei M, Siemers NO, Pandya D, et al. Analyses of PD-L1 and Inflammatory Gene Expression Association with Efficacy of Nivolumab ± Ipilimumab in Gastric Cancer/Gastroesophageal Junction Cancer. *Clinical Cancer Research* 2021;**27**:3926–35.
4. Sangro B, Melero I, Wadhawan S, et al. Association of inflammatory biomarkers with clinical outcomes in nivolumab-treated patients with advanced hepatocellular carcinoma. *J Hepatol* 2020.

Ethics Approval This study was approved by the Centralised Institutional Review Board of SingHealth (CIRB ref: 2009/907/B).

Consent Written informed consent was obtained from the patient for publication of this abstract and any accompanying images. A copy of the written consent is available for review by the Editor of this journal.

<http://dx.doi.org/10.1136/jitc-2021-SITC2021.089>

UNBIASED PROTEOMIC PROFILING LEADS TO THE DISCOVERY OF A NOVEL NON-INVASIVE BLOOD-BASED PROTEIN PANEL WITH SIGNIFICANT POSITIVE PREDICTIVE VALUE IN PANCREATIC AND COLORECTAL CANCERS

Kristina Beeler*, Roland Bruderer, Marco Tognetti, Kamil Sklodowski, Sebastian Mueller, Dominique Kamber, Lukas Reiter. *Biognosys, Schlieren, Switzerland*

Background Mass spectrometry-based discovery proteomics has recently emerged as a high-throughput method for the proteomic profiling in biofluid samples from large clinical and population screening cohorts. Despite this progress, a significant fraction of the plasma proteome is currently not covered by state-of-the-art discovery approaches and therefore not accessible for biomarker discovery. To close this analytical gap, we present a novel workflow combining automated plasma depletion and FAIMS-DIA-MS to bridge both sensitivity and scalability. We demonstrate the applicability of this workflow to support biomarker discovery and subject stratification in precision oncology in a case-control cohort.

Methods The plasma samples were depleted in 96-well format using an automated MARS-14 depletion system. The depleted samples were processed to tryptic peptides and analyzed using a Thermo Scientific Orbitrap Exploris 480 equipped with a FAIMS Pro device. Data processing and analysis were performed using Biognosys' SpectroMine and Spectronaut software.

Results Using the unbiased discovery workflow, we investigated a cohort comprising of 180 plasma samples from healthy donors and subjects diagnosed with pancreatic, breast, prostate, colorectal and lung (NSCLC) cancer at either early or late stage of the disease. Overall, the optimized FAIMS-DIA-MS quantified 2,741 proteins across all samples and 1,849 proteins on average per sample measurement. Based on estimated plasma protein concentrations (Human Protein Atlas), quantified proteins span across 8 orders of magnitude, down to single digit pg/mL. Within this dynamic range, we could interrogate the tissue leakage proteome, interleukins and signaling proteins. Using classification algorithms, we were able to select candidates to build protein panels which provide significant positive predictive values associated with different disease stages, especially in the sub-cohorts for pancreatic and colorectal cancer.

Conclusions We demonstrate the capabilities of a novel discovery workflow for deep, quantitative profiling of plasma samples at large scale, providing a rich proteomic resource for precision oncology.

<http://dx.doi.org/10.1136/jitc-2021-SITC2021.090>

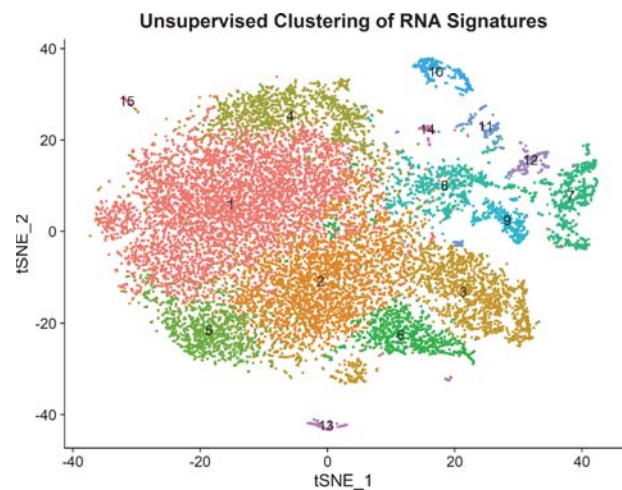
IMPACT OF ULTRA-FAST 'FLASH' RADIOTHERAPY ON SINGLE CELL IMMUNOGENOMICS IN DIFFUSE INTRINSIC PONTINE GLIOMA (DIPG)

¹Oscar Padilla*, ¹Hanna Minns, ¹Hong-Jian Wei, ¹Andrea Webster-Carrion, ¹Masih Tazhibi, ¹Nicholas McQuillan, ¹Xu Zhang, ¹Zhiguo Zhang, ¹Raul Rabadan, ¹Peter Canoll, ¹Luca Szalontay, ¹Jovana Pavisic, ¹Guy Garty, ¹Stergios Zacharoulis, ²Claire Vanpouille-Box, ¹Vilas Menon, ¹Marta Olah, ¹Cheng-Chia Wu, ¹Robyn Gartrell. ¹Columbia University Medical Center, New York, NY, USA; ²Weill Cornell Medicine, New York, NY, USA

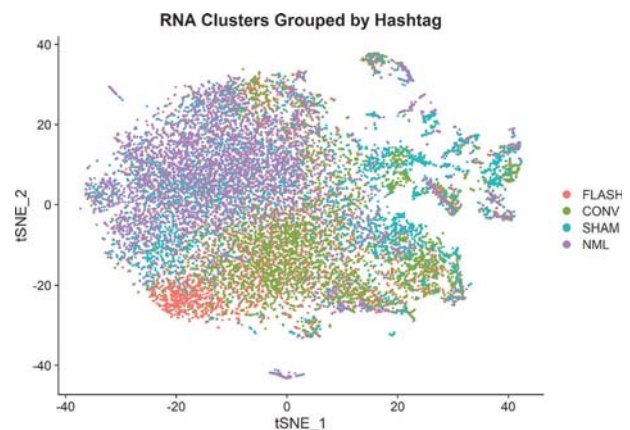
Background Diffuse intrinsic pontine gliomas (DIPG's) are immunologically inert tumors with a median survival of 9–15 months. Radiation therapy (RT) is the mainstay treatment for DIPG but is associated with immunodepletion of the tumor microenvironment (TME) at high dose ranges. FLASH, or ultra-fast dose rate RT, represents a novel ablative technique that may spare TME immune responses while decreasing tumor burden. Here, we present single-cell immune profiling of DIPG tumors treated with FLASH, conventional dose rate RT (CONV) or no RT (SHAM).

Methods Murine H3.3K27M mutant DIPG cells were stereotactically injected and tumor induction confirmed by magnetic resonance imaging (MRI) 15 days later. DIPG-bearing mice were randomly assigned to one of three treatment groups (n=4/group), FLASH, CONV or SHAM. A fourth group with no tumor (NML) was included as a negative biological control. A modified linear accelerator was used to deliver 15 Gy of electron RT to the brainstem at dose rates of 90 Gy/second and 2 Gy/minute, for the FLASH and CONV groups, respectively. Four days post-RT, mice brainstems were harvested, homogenized, stained for CD45 and tagged with a hashtag antibody specific to each group. CD45+ immune cells were isolated and sequenced using the 10X Genomics chromium single-cell 3' platform. After processing and alignment of the reads using Cell Ranger with default parameters, the data was quality checked and filtered before hashtag demultiplexing, unsupervised clustering and downstream analysis was implemented following the Seurat R package. Differential expression analysis evaluated based on the non-parametric Wilcoxon rank sum test. Key genes determined by an adjusted p value of < 0.05 based on bonferroni correction and $|\text{avg log}_2\text{FC}| > 0.8$.

Results Preliminary analysis identifies 15 clusters with distinct CD45 immune phenotypes (figure 1). Differential gene expression analysis by hashtag antibody (treatment group) reveals 14 clusters differentially expressing key genes, including 3 clusters upregulated in DIPG compared to NML, and 2 clusters upregulated in irradiated tumors compared to SHAM and NML (figure 2). Notably, analysis demonstrates an individual cluster upregulated in FLASH versus all other groups ($p = 3.07\text{E-}171$). Further deconvolution of specific immune phenotypes represented by each cluster is ongoing.



Abstract 91 Figure 1 tSNE plot based on clustering of RNA signatures, grouped by RNA



Abstract 91 Figure 2 tSNE plot based on clustering of RNA signatures, grouped by hashtag antibody

Conclusions Our preliminary analysis shows differential immune responses among DIPG tumors compared to NML. We also find several immune cell subsets that are unique to DIPG treated with CONV or FLASH compared to unirradiated samples. Most notably, we identify a single immune cell subset that is exclusive to FLASH alone, indicating that FLASH elicits a unique immune response in murine DIPG.

<http://dx.doi.org/10.1136/jitc-2021-SITC2021.091>

SINGLE CELL AND SPATIAL MULTIPLEX PROFILING OF IMMUNE CELL MARKERS IN FFPE TUMOR TISSUES USING THE NOVEL RNASCOPE™ HIPLEX V2 IN SITU HYBRIDIZATION ASSAY

Sayantani Basak*, Anushka Dikshit, Ming Yu, HaYeun Ji, Ching-Wei Chang, Bingqing Zhang. *Advanced Cell Diagnostics, Bio-Techne, Newark, CA, USA*

Background The tumor microenvironment (TME) is highly complex, comprised of tumor cells, immune cells, stromal cells, and extracellular matrix. Understanding spatial interactions between various cell types and their activation states in the TME is crucial for implementing successful immunotherapy strategies against various types of cancer. This study demonstrates a highly sensitive and specific multiplexed technique, the RNAscope HiPlex v2 in situ hybridization (ISH) assay for spatial and transcriptomic profiling of target genes to assess immune regulation in human lung, breast, cervical and ovarian FFPE tumor tissues.

Methods We have expanded our current RNAscope HiPlex assay capability of iteratively multiplexing up to 12 targets in fixed and fresh frozen samples to include formalin fixed paraffin embedded (FFPE) tissues. The novel FFPE reagent effectively reduces background autofluorescence, improving the signal to noise ratio. We have leveraged this technology to investigate spatial expression of 12 oncology and immunology target genes, including tumor markers, immune checkpoint markers, immunosuppression markers, immune cell markers and secreted chemokine RNA expression profile within the TME. The targets were simultaneously registered using HiPlex image registration software v2 that enables background subtraction.

Results We visualized T cell infiltration and identified T cell subsets within tumors using CD3 and CD8 expression and activated T cells by IFNG expression. We further identified subsets of pro- and anti-inflammatory macrophages by CD68 and CD163 expression as well effector cells which secrete chemokines and cytokine. We also detected the hypoxia markers HIF1A and VEGF to elucidate the immunosuppressive state of tumor cells. Preliminary analysis and quantification of the HIF1A expression using HALO® image analysis software showed higher copy numbers in the lung tumor as compared to the other tumors, demonstrating the sensitivity of the assay through differential expression. We additionally showed the differential expression of immune checkpoint markers PDCD1, and CD274 within the TME.

Conclusions Using a highly sensitive multiplexed RNAscope HiPlex v2 ISH assay, we have demonstrated the capability of this technique to spatially resolve 12 targets in four different tumor types. The FFPE reagent efficiently quenched background autofluorescence in the tissues and identified immune cell signatures within the TME. Quantification of immunosuppressive markers further depicted a differential expression among various tumors. This technology is highly beneficial for investigating complex and spatial tumor-stroma interactions in basic science and translational research. The assay can also provide valuable understanding of the biological crosstalk among various cell types in complex and heterogeneous tissues.

<http://dx.doi.org/10.1136/jitc-2021-SITC2021.092>

COMPUTATIONAL BIOLOGY AND TISSUE-BASED APPROACHES TO INFORM INDICATION SELECTION FOR A NOVEL AHR INHIBITOR

Marta Sanchez-Martin*, Lei Wang, Jeffrey Ecsedy, Karen MCGovern, Michelle Zhang. *Ikena Oncology, Boston, MA, USA*

Background Aryl Hydrocarbon Receptor (AHR) is a ligand-activated transcription factor that regulates the activities of multiple innate and adaptive immune cell types. Multiple ligands such as kynurenine bind to AHR driving its nuclear translocation and transcriptional activation, leading to an immunosuppressive tumor microenvironment.^{1 2} AHR activation is implicated in tumor development in multiple cancer types. In addition, high levels of serum kynurenine are associated with resistance to checkpoint inhibitors.³ To overcome AHR-mediated immunosuppression in cancers, we developed a selective oral AHR inhibitor IK-175 and took a combined computational and tissue-based approach to select cancer indications for its clinical development.

Methods The aim of this work is to identify tumor indications dependent on AHR signaling and design patient selection strategies based on a proprietary transcriptional signature, mRNA and protein detection assays to evaluate AHR pathway activation in tumors.

Results Genomic profiling of solid and hematological cancers from TCGA and Project GENIE databases identified bladder and esophageal tumors among others, as frequently harboring AHR gene amplifications. A proprietary gene signature of AHR activation was developed integrating literature, pathway analysis, RNAseq and nanostring data from PBMC, T-cells and cell lines upon AHR inhibition. Transcriptional analysis of the TCGA data using this signature demonstrated bladder cancer has the highest expressions of AHR and AHR signature genes, suggesting increased pathway activity in bladder cancer relative to other cancer types. Increased AHR signature gene expression was associated with worse overall survival in the TCGA bladder cancer cohort. Furthermore, RNAscope analysis of a tissue microarray containing 10 different tumor types revealed bladder cancer had one of the highest AHR transcript expression in the tumor compartment. Finally, nuclear localization of AHR protein was assessed as an indicator of pathway activation through the development of a novel IHC method. Extensive TMA screening of AHR protein in 15 different indications demonstrated bladder cancer as the tumor type with the highest prevalence of AHR nuclear expression.

Conclusions In summary, we demonstrated high prevalence of nuclear AHR protein expression, AHR gene amplification and target gene expression in bladder cancer, suggesting aberrant AHR activation may play an important role in the progression of this tumor type. This study provides rationale for therapeutic targeting of AHR in bladder cancer patients. Ikena is currently evaluating the anti-tumor activity of IK-175 as a single agent and in combination with nivolumab in bladder cancer in a Phase 1a/1b clinical study (NCT04200963).

REFERENCES

1. Quintana FJ, Sherr DH. Aryl hydrocarbon receptor control of adaptive immunity. *Pharmacol Rev* 2013 Aug 1;**65**(4):1148–61.
2. Murray IA, Patterson AD, Perdew GH. Aryl hydrocarbon receptor ligands in cancer: friend and foe. *Nat Rev Cancer* 2014 Dec;**14**(12):801–14.
3. Li, Haoxin et al. 'Metabolomic adaptations and correlates of survival to immune checkpoint blockade.' *Nature Communications* 2019 Sep 25;**10**:1–4346.

<http://dx.doi.org/10.1136/jitc-2021-SITC2021.093>

EFFECTS OF CHEMOIMMUNOTHERAPY ON THE PERIPHERAL BLOOD: INSIGHTS FROM IMMUNE MONITORING OF A PHASE IB TRIAL OF PEMBROLIZUMAB AND PACLITAXEL OR CAPECITABINE FOR TRIPLE-NEGATIVE BREAST CANCER (TNBC)

¹Brie Chun*, ¹Joanna Pucilowska, ²Shu Ching Chang, ³Isaac Kim, ¹Benjamin Nikitin, ¹Yoshinobu Koguchi, ¹William Redmond, ¹Brady Bernard, ¹Venkatesh Rajamanickam, ⁴Nathan Polaske, ⁴Paul Fields, ¹Valerie Conrad, ¹Mark Schmidt, ¹Walter Urba, ¹Alison Conlin, ⁵Heather McArthur, ¹David Page. ¹EACRI, Providence Cancer Institute, Portland, OR, USA; ²Providence St. Joseph Health, Portland, OR, USA; ³EACRI, Providence Cancer Center, Portland, OR, USA; ⁴Adaptive Biotechnologies, Seattle, WA, USA; ⁵Cedars-Sinai Medical Center, Los Angeles, CA, USA

Background Pembrolizumab plus curative-intent dose-dense anthracycline-based chemotherapy (ddAC) is associated with improved outcome in PD-L1-negative TNBC,¹ whereas in the metastatic setting, clinical benefit of chemoimmunotherapy (taxane or gemcitabine/carboplatin) is restricted to PD-L1-positive patients.² We hypothesize that this discordance could be related to immunomodulatory differences of the various chemotherapies. On-treatment serial monitoring of peripheral blood and tumoral T cells can be used to compare the effects of various regimens. We also hypothesize that T cell clonal expansion may differ across the regimens, and that tumor-enriched T cell clones are more likely to be tumor-reactive and expand following chemoimmunotherapy.

Methods Blood and tumor samples were collected from patients enrolled in a phase Ib clinical trial of palliative pembrolizumab and paclitaxel or capecitabine for metastatic TNBC, and from a contemporaneous cohort of patients treated with ddAC. T-cells were characterized using fresh whole blood flow cytometry and T-cell receptor (TCR) immunosequencing (immunoSEQ, Adaptive Biotechnologies) of DNA digests. Longitudinal regression was used to test the hypothesis that tumor-enriched T-cell clonotypes are more likely to expand in peripheral blood following therapy.

Results When combined with pembrolizumab, paclitaxel versus capecitabine had similar effects on T-cells, resulting in a time-dependent lymphodepletion across all major T cell subsets (average CD3+ T cell fold-change capecitabine: -0.42, paclitaxel: -0.56, $p = 0.80$ t-test), whereas ddAC was associated with more profound lymphodepletion (CD3+ average fold-change: -1.21). Notably, ddAC was associated with higher odds of novel clonotype detection compared to capecitabine (odds ratio (OR): 3.42, 95% CI: 3.34–3.5) as well as compared to paclitaxel (OR: 1.53, 95% CI: 1.47–1.60). Significant expansion of tumoral clonotypes occurred in five patients receiving chemoimmunotherapy (average 4.2 unique clonotypes per patient, range 2–11). These clonotypes did not significantly expand over time in the blood. Similarly, T-cell clonotypes that were enriched within tumor did not exhibit measurable differences in serial trend within the peripheral blood.

Conclusions Effects to T cell subsets and clonotypes are similar between capecitabine and paclitaxel when combined with pembrolizumab. ddAC was more profoundly lymphotoxic, but resulted in greater clonotype expansion. These findings offer mechanistic insight onto the differences in clinical activity observed with chemoimmunotherapy in early stage versus metastatic TNBC. We observed no strong association between tumor clonotype enrichment and peripheral clonotype expansion, highlighting the unmet need to develop methods of monitoring tumor-reactive T cell clones in the context of immunotherapy.

Acknowledgements The authors would like to acknowledge collaborators at the Earle A. Chiles Research Institute and Adaptive Biotechnologies for mentorship and guidance. Support for the clinical trial (NCT02734290), which comprised the metastatic cohort was provided by Merck and the Providence Opportunity Fund. Laboratory services were provided at no cost by Adaptive Biotechnologies

Trial Registration NCT02734290

REFERENCES

- Schmid P, Cortes J, Pusztai L, et al. Pembrolizumab for early triple-negative breast cancer. *N Engl J Med* 2020 Feb 27;**382**(9):810–821. doi: 10.1056/NEJMoa1910549.
- Cortes J, Cescon DW, Rugo HS, et al. Pembrolizumab plus chemotherapy versus placebo plus chemotherapy for previously untreated locally recurrent inoperable or metastatic triple-negative breast cancer (KEYNOTE-355): a randomised, placebo-controlled, double-blind, phase 3 clinical trial. *Lancet* 2020;**396**(10265):1817–1828. doi:10.1016/S0140-6736(20)32531-9

Ethics Approval All patients provided written, informed consent. The study protocols for the collection of specimens from the early-stage breast cancer cohort and from the metastatic TNBC clinical trial were separately approved by independent review boards at Providence Portland Medical Center and Cedars Sinai Medical Center (mTNBC clinical trial only).

<http://dx.doi.org/10.1136/jitc-2021-SITC2021.094>

MAGE-A1 PROTEIN EXPRESSION PATTERN IN > 5,000 TUMOR AND HEALTHY TISSUE SAMPLES: VALIDATION OF MAGE-A1 AS AN IDEAL TARGET FOR TCR-BASED CELL THERAPY

¹Jennifer Oduro, ²Ronald Simon, ²Natalia Gorbokov, ²Christoph Fraune, ¹Julia Bluhm, ¹Vivian Scheuplein, ¹Elisa Kieback, ³Matthias Obenaus, ⁴Thomas Blankenstein, ¹Eugen Leo*. ¹T-knife Therapeutics Inc., Berlin, Germany; ²University Hospital Hamburg-Eppendorf, Hamburg, Germany; ³Charite University Hospital, Berlin, Germany; ⁴Max Delbrück Center, Berlin, Germany

Background Cancer testis antigens (CTAs) are considered attractive targets for T cell receptor (TCR)-based cellular therapies as their expression in healthy adults is considered restricted to the immune-privileged testis. However, low-level expression of some CTAs in healthy tissue has been observed, resulting in significant on-target/off-cancer toxicity. Melanoma associated antigen 1 (MAGE-A1) is a member of the MAGE-A CTA family, whose members are known to influence cellular signaling pathways through their E3 ubiquitin ligase-binding MAGE homology domain. MAGE-A proteins are frequently expressed in different cancer types, have been linked to oncogenic activity and their expression has been associated with poor prognosis.¹ Literature data suggest that in healthy tissues MAGE-A1 is detected in testis, only, with one exception suggesting MAGE-A1 RNA expression in cerebellum and cerebrum.² Therefore, to evaluate MAGE-A1 as a potential target for cellular immunotherapies, an in-depth analysis of MAGE-A1 expression in > 70 different healthy tissue types and > 5,000 cancer biopsies was conducted, aiming to assess if MAGE-A1 represents a valid and safe target.

Methods A MAGE-A1 antibody with high specificity (TK-AbMA1P) was identified and characterized for immunohistochemistry. A large panel of > 70 different healthy tissue types and > 5,000 tumor biopsies was explored and scored for MAGE-A1 expression by tissue microarray. Identified cancer entities with relevant MAGE-A1 expression were further investigated to assess spatial intratumoral MAGE-A1 expression distribution and expression consistency between primary tumor and lymph node/distant metastases.

Results Characterization of TK-AbMA1P demonstrated fully paralog-selective staining for MAGE-A1. Analysis of MAGE-A1 expression in over 70 different healthy tissues confirmed strictly selective expression of MAGE-A1 in testis. An extended analysis of various CNS tissues including cerebellum and cerebrum did not reveal any expression in CNS. The analysis of > 5,000 tumor biopsies showed significant MAGE-A1 expression in distinct subgroups of multiple major tumor types with high unmet medical need. Substantial expression was detected for example in non-small-cell lung cancer, various breast cancer subtypes, gastrointestinal and urogenital cancers, among others. Extended analysis of the MAGE-A1 positive tumors demonstrated highly homogenous and consistent spatial intratumoral distribution of MAGE-A1 expression as well as between primary tumor and metastases.

Conclusions This analysis confirms that MAGE-A1 is a highly selectively expressed CTA and demonstrates relevant expression in various indications with high unmet medical need, suggesting that MAGE-A1 is an ideal target for highly potent TCR-based adoptive cell therapy.

REFERENCES

1. Weon JL, Potts PR. The MAGE protein family and cancer. *Curr Opin Cell Biol* 2015;**37**:1–8.
2. Morgan RA, Chinnsamy N, Abate-Daga D, Gros A, Robbins PF, Zheng Z, Dudley ME, Feldman SA, Yang JC, Sherry RM, Phan GQ, Hughes MS, Kammula US,

Miller AD, Hessman CJ, Stewart AA, Restifo NP, Quezado MM, Alimchandani M, Rosenberg AZ, Nath A, Wang T, Bielekova B, Wuest SC, Akula N, McMahon FJ, Wilde S, Mosetter B, Schendel DJ, Laurecot CM, Rosenberg SA. Cancer regression and neurological toxicity following anti-MAGE-A3 TCR gene therapy. *J Immunother* 2013;**36**(2):133–51.

Ethics Approval This study was approved by the Ethics Commission of the Ärztekammer Hamburg; approval number WF-049/09. Participants gave informed consent before taking part.

<http://dx.doi.org/10.1136/jitc-2021-SITC2021.095>

THE IMPACT OF RADIOGRAPHIC TUMOR THICKNESS ON THE COMPLEXITY OF THE TUMOR IMMUNE MICROENVIRONMENT IN MALIGNANT PLEURAL MESOTHELIOMA

Katarzyna Tomczak*, Jacqueline Lizabeth Oliva, Nicolas Zhou, Carlos Ramos, Nathaniel Deboeve, Hope Feldman, Percy Lee, Chad Strange, Annikka Weissferdt, David Rice, Reza Mehran, Jianjun Zhang, Anne Tsao, Boris Sepesi, Cara Haymaker. *The University of Texas MD Anderson Cancer Center, Houston, TX, USA*

Background Malignant pleural mesothelioma (MPM) is a rare and aggressive cancer associated with exposure to asbestos with limited treatment strategies and poor prognosis.¹ There is no curative treatment for MPM, and patients follow standard treatment options.^{2,3} Radiographic tumor thickness (TT) has recently emerged as a surrogate marker associated with overall survival,⁴ however, the influence of TT on the complexity of the immune component within tumor microenvironment is unknown. Our aim was to perform comprehensive profiling of the tumor immune microenvironment (TIME) relative to the TT to understand of this relationship to guide the design of novel treatment strategies.

Methods Tumor specimens (n=29) were obtained from surgically managed MPM patients. Analysis was performed based on the median tumor thickness of 80mm, which defined thick vs thin groups. Additional analysis used TT as a continuous variable for correlations with immune features. The immune cell composition in the TIME was determined by flow cytometry (n=23). Transcriptomic profiling (n=20) was assessed using Nanostring nCounter Tumor Signaling 360 panel. Expanded tumor-infiltrating lymphocytes (TIL) were utilized for further characterization by 10x Genomics single cell RNA-seq profiling (n=8) and cytotoxicity assays (n=18). Level of significance was determined using unpaired non-parametric statistical test.

Results Fresh tumor tissue cytometry showed substantial differences in the immune profiles for thick versus thin tumors, highlighting a relationship of the TT and its immune composition. Thin tumors contained more Tregs, and higher OX40 expression (p=0.081 for non-Treg CD4+ and p<0.05 for CD8+ T cells), CTLA4, LAG3, TIGIT and Ki67 in TIL, while PD-1 expression was not associated with TT. Gene expression profiling suggested an impaired adaptive immune response in thin tumors compared to thick tumors characterized by the exhausted CD8 score (p=0.0252), T-cell co-stimulation score (p=0.0387) and TNF superfamily member score (p=0.0159) and a subset with a myeloid immune evasion score (p=0.0387). TIL expansion was not impacted by baseline TT. However, TIL cytotoxicity, as measured in a redirected lysis assay, showed IFN-gamma response was negatively correlated with baseline TT (p=0.023, R2=0.28). Expanded TIL clustering based upon single cell profiling is underway.

Conclusions Utilizing multi-platform immune profiling approaches, we observed a distinct relationship between the TT and immune signatures. Understanding underlying immune signatures underpinning the biology of thick versus thin MPM tumors provides insights to potential responsiveness to immune-based therapies and may inform on the design for future novel strategies relative to the disease extent based on TT.

REFERENCES

1. Bibby AC, Tsim S, Kanellakis N, Ball H, Talbot DC, Blyth KG, Maskell NA, Psallidas I. Malignant pleural mesothelioma: an update on investigation, diagnosis and treatment. *Eur Respir Rev* 2016;**25**(142):472–86.

2. Faig J, Howard S, Levine EA, Casselman G, Hesdorffer M, Ohar JA. Changing pattern in malignant mesothelioma survival. *Transl Oncol* 2015;**8**(1):35–9.
3. Alpert N, van Gerwen M, Taioli E. Epidemiology of mesothelioma in the 21st century in Europe and the United States, 40 years after restricted/banned asbestos use. *Transl Lung Cancer R* 2020;**9**:S28-S38.
4. de Perrot M, Dong Z, Bradbury P, Patsios D, Keshavjee S, Leighl NB, Hope A, Feld R, Cho J. Impact of tumour thickness on survival after radical radiation and surgery in malignant pleural mesothelioma. *Eur Respir J* 2017;**49**(3).

Ethics Approval This study was approved by the University of Texas MD Anderson Cancer Center's IRB; approval number LAB08-0380; participants gave informed consent before taking part.

<http://dx.doi.org/10.1136/jitc-2021-SITC2021.096>

Cellular Therapies

97 HIGH THROUGHPUT SCREENING OF HPV-ANTIGEN PEPTIDES AND EXPANSION OF TUMOR-SPECIFIC T CELLS FOR ADOPTIVE CELL THERAPY OF HPV-ASSOCIATED MALIGNANCIES

David Langan*, Jourdain Lemaster, Lauren Suarez, Pratima Kunwar, Sojung Kim, Mathias Oelke. *NexImmune, Gaithersburg, MD, USA*

Background NexImmune is developing highly differentiated immunotherapies to target, activate and expand tumor antigen-specific T cells using the proprietary Artificial Immune Modulation (AIM™) nanotechnology platform. The AIM nanoparticle (AIM-np) technology functions as synthetic dendritic cells capable of directing a specific T cell-mediated immune response. By mimicking natural T cell biology, NexImmune's cellular therapy product candidates (AIM ACT) are designed to combine the attributes of cellular precision, potency, and persistence with reduced potential for undesired toxicities. Human papilloma virus (HPV) is responsible for >45,000 cancers yearly in the United States, according to the CDC. From 2013–2017 an estimate 79% of cervical, vulva, penis, vaginal, anus, and oropharyngeal cancers were attributed to HPV and of these about 80% were associated with high-risk HPV types 16 and 18. Although multivalent vaccines against high-risk HPV infections exist, significant clinical challenges remain. A limited vaccination rate means many remain vulnerable and vaccination does not treat pre-existing HPV infections or malignancies.

Methods Therefore, NexImmune is employing its AIM-np technology to generate an adoptive cell therapy (ACT) using its proprietary enrichment and expansion (E+E) ex vivo process to expand clinically relevant numbers of CD8+ T cells that recognize the HPV16 and HPV18 oncogenic antigens (i. e., E6 and E7) expressed by malignant cells of head and neck, cervical, and anal cancers. Using the Immune Epitope Database and Analysis Resource (IEDB), 44 HLA-A2 restricted peptides were identified as potential immunogenic targets for preclinical screening. Using PBMCs from healthy donor-derived apheresis material, different combinations of these peptides were used in the E+E process to expand HPV-cancer specific CD8+ T cells.

Results After multiple E+E experiments were concluded, 5 peptides were identified that consistently elicited the strongest T cell responses. Furthermore, these CD8+ T cells were predominantly from the central memory (CD62L+CD45RA-) and effector memory (CD62L-CD45RA-) phenotype (sum total 82.18 ± 8.29 [Mean \pm SEM]) suggesting their in vivo functionality and persistence will combine anti-tumor activity with long-term immunologic memory.

Conclusions A similar E+E screening is being conducted with PBMCs isolated from HPV+ cancer patients. A comparison of the CD8+ T cell responses from healthy donor and cancer patient cells will provide critical preclinical data to support a planned FIH trial for HPV-associated malignancies. The current study demonstrates the ability for high-throughput peptide screening to identify clinically relevant peptide cocktails capable of expanding multi-antigen tumor-specific CD8+ T cell populations within 2 weeks.

<http://dx.doi.org/10.1136/jitc-2021-SITC2021.097>

NX-0255, A SMALL MOLECULE CBL-B INHIBITOR, EXPANDS AND ENHANCES TUMOR INFILTRATING LYMPHOCYTES (TIL) FOR USE IN ADOPTIVE CANCER IMMUNOTHERAPY

Sarah Whelan*, Jennifa Gosling, Monisha Mani, Frederick Cohen, Austin Tenn-McClellan, Janine Powers, Gwenn Hansen, Michael Lotze, Arthur Sands. *Nurix Therapeutics, San Francisco, CA, USA*

Background Adoptive cell transfer (ACT) of TIL effects durable responses in patients with melanoma and some epithelial tumors. It is thought that poor in vitro cell expansion and inefficient T-cell migration to the tumor limits the broader application of this approach. The E3 ubiquitin ligase, Casitas B-lineage lymphoma b (CBL-B) is expressed in T-cells where it functions as a regulator of immune cell activation, in part by requiring CD28 co-stimulation in addition to T-cell receptor activation. We have developed NX-0255, a highly potent small molecule inhibitor of CBL-B, demonstrating its ability to increase T-cell derived cytokine secretion and proliferation in the presence or absence of co-stimulation. Here, we investigated the effects of NX-0255 on the ex vivo growth and characteristics of human TIL to create drug-enhanced TIL (DeTIL-0255) as an ACT product for treating patients with cancer.

Methods TIL from ovary, colon, lung, head and neck, breast, and vulva carcinomas were cultured with IL-2 and compared in two experimental groups: NX-0255 without IL-2, or NX-0255 in combination with IL-2. Following 22 days of culture, cell number, and phenotype were assessed by flow cytometry and single-cell transcriptomics.

Results Culturing of TIL in the presence of NX-0255 alone resulted in the expansion of cells, with numbers comparable to that of conventionally cultured TIL with IL-2. The addition of NX-0255 in combination with IL-2 significantly increased the number of cells expanded compared to TIL (n=16, p=0.004). Flow cytometric analysis demonstrated that DeTIL-0255 were significantly less exhausted compared to TIL, as shown by the significant reduction of CD8+ T-cells expressing PD-1 (p=0.02), and co-expressing PD-1+TIM-3+ (p=0.03) and PD-1+LAG-3+ (p=0.03). Furthermore, upon stimulation, the functional capacity of DeTIL-0255 was differentially enhanced, with significant increases in the absolute numbers of CD8+ T-cells expressing intracellular perforin (p=0.001), granzyme-B (p=0.005) and CD107a (p=0.01) when comparing DeTIL-0255 to TIL. An increase of CD8+ T-cells expressing CD137/4-1BB, a biomarker of CD8+ T-cell tumor reactivity was also observed (p=0.03). TCR repertoire and single-cell sequencing analysis demonstrated that DeTIL-0255 had increased TCR diversity and enhanced expression of genes associated with stemness (CD127+,CCR7+,CD62L+) and cytotoxicity (GNLY+,GZMB+,NKG7+).

Conclusions Collectively, these data suggest that DeTIL-0255 increases the proportion and absolute numbers of less exhausted CD8+ memory T-cells, enhancing cytolytic T-cell function. Adoptive transfer of DeTIL-0255 may increase persistence and exhibit broader functional activity than conventional TIL, potentially conferring improved anti-tumor activity. Taken together, these data support the clinical development of DeTIL-0255 for the treatment of patients with cancer.

<http://dx.doi.org/10.1136/jitc-2021-SITC2021.098>

T CELL IMMUNOTHERAPIES TRIGGER NEUTROPHIL ACTIVATION TO ELIMINATE TUMOR ANTIGEN ESCAPE VARIANTS

¹Daniel Hirschhorn*, ¹Sadna Budhu, ¹David Schröder, ¹Lukas kraehenbuehl, ¹Anne-Laurent Flammar, ¹Andrew Chow, ¹Isabell Schulze, ¹Sara Schad, ¹Jacob Ricca, ¹Billel Gasm, ¹Olivier De Henau, ¹Levi Mangarin, ²David Redmond, ¹Czrina Cortez, ¹Cailian Liu, ¹Aliya Holland, ¹Mathieu Gigoux, ¹Asrhi Arora, ¹Katherine Panageas, ³Gabrielle Rizzuto, ⁴Jean Albregues, ⁴Mikala Egeblad, ¹Jedd Wolchok, ¹Taha Merghoub. *Memorial Sloan Kettering Cancer Center, New York, NY, USA; ²Cornell Medical School, New York, USA; ³University of California San Francisco, San Francisco, USA; ⁴Cold Spring Harbor Laboratories, Cold Spring Harbor, NY, USA*

Background Targeted immune-based therapies such as adoptive T cell transfer (ACT) are often ineffective because tumors evolve over time and under selective pressure display antigen loss variant clones. A classic example in melanoma is de-differentiation and loss of expression of antigenic proteins. Therapies that activate multiple branches of the immune system may eliminate such escape variants

Methods Here we show that melanoma-specific CD4+ ACT therapy in combination with OX40 co-stimulation or CTLA-4 blockade can eradicate large melanoma tumors with clonal escape variants.

Results Early on-target recognition of melanoma antigens by adoptively transferred tumor-specific CD4+ T cells was required. Surprisingly, however, complete tumor eradication was partially dependent on neutrophils. Supporting these findings, extensive neutrophil activation and neutrophil extracellular traps were found in mouse tumors and in biopsies of melanoma patients treated with immune checkpoint blockade.

Conclusions Our findings uncover a novel interplay between T cells mediating the initial tumor- and tissue-specific immune response, and neutrophils mediating tumor destruction of antigen loss variants.

Ethics Approval All tissues were collected at MSKCC following study protocol approval by the MSKCC Institutional Review Board. All mouse procedures were performed in accordance with institutional protocol guidelines at Memorial Sloan-Kettering Cancer Center (MSKCC) under an approved protocol.

<http://dx.doi.org/10.1136/jitc-2021-SITC2021.099>

REDIRECTING GLUCOSE FLUX DURING IN VITRO EXPANSION IMPROVES THE IN VIVO PERFORMANCE OF ADOPTIVE T CELL THERAPIES FOR CANCER

¹Andrew Frisch*, ¹Yiyang Wang, ¹Yupeng Wang, ²Konstantinos Lontos, ¹Dayana Rivadeneira, ¹Greg Delgoffe. ¹University of Pittsburgh, Pittsburgh, PA, USA; ²UPMC, Pittsburgh, PA, USA

Background Adoptive cell therapy (ACT) has shown great promise as a cancer therapeutic in some hematologic malignancies. However, several barriers prevent widespread use of cellular therapies in other cancers, including the need for T cells to perform and persist within the nutrient-poor tumor microenvironment (TME). Extensive in vitro culture is required for all current forms of ACT, but current culture strategies favor the energetic needs of T cells for rapid and robust expansion while ignoring their metabolic requirements within the TME. Here we demonstrate that the deleterious effects of in vitro culture can be mitigated by redirecting T cell glycolysis away from terminal lactate production to more energetically efficient OXPHOS during initial expansion. This in vitro metabolic shift drastically improves anti-tumor efficacy in vivo and establishes long-term memory without any further modifications, thus demonstrating an easily applied improvement for all forms of ACT.

Methods Antigen-specific T cells were activated in culture with their cognate peptide or in vivo in response to cognate antigen. The pyruvate dehydrogenase kinase (PDHK1) inhibitor dichloroacetate (DCA) was used to redirect glucose flux during cell expansion. Mouse experiments were performed with gp100-specific pmel-1 TCR-Tg T cells transferred into B16 melanoma-bearing mice. Human experiments were performed with anti-hCD19 CAR-T cells transferred into NSG mice bearing hCD19-A549 lung cancer cells.

Results Identical, antigen-specific T cells stimulated with typical in vitro culture conditions or responding to cognate antigen in vivo differ not in effector function but heavily in their metabolism: typical T cell activation and culture heavily favors aerobic glycolysis. The PDHK1 inhibitor DCA allows for glucose uptake and metabolism but shunts glucose into the mitochondria, maintaining mitochondrial health. In vitro expansion of T cells in the presence of DCA improves their pre-infusion metabolic profile, cytokine production, and survival in low nutrient culture media. Expansion in the presence of DCA results in striking improvements in ACT in both murine TCR-Tg and human CAR-T cells.

Conclusions Current culture strategies do not prepare T cells for performance within the TME. DCA shunts glycolysis in a manner that re-directs metabolism to a more oxidative state. This small redirection improves the phenotype of T cells pre-infusion and better prepares them for the lack of nutrients in vivo. By generating more functional T cells for infusion, we are able to metabolically enhance their in vivo performance in a manner potentially synergistic with other more engineered improvements.

<http://dx.doi.org/10.1136/jitc-2021-SITC2021.100>

EXPANSION OF TUMOR-INFILTRATING LYMPHOCYTES (TIL) USING STATIC BAG FOR THE CLINICAL MANUFACTURING RAPID EXPANSION PROTOCOL (REP) PROCESS

Kenneth Onimus*, Adrian Wells, Nermin Gerges, Courtney Herman, Shwetha Lakshmpathi, Viktoria Gontcharova, Joe Wypych, Arvind Natarajan, Anand Veerapathran. *Iovance Biotherapeutics, Inc., San Carlos, CA, USA*

Background Lifileucel (LN-144) and LN-145, adoptive cell therapies using autologous tumor-infiltrating lymphocytes (TIL), have demonstrated encouraging efficacy with acceptable safety in a variety of tumor types.¹⁻⁴ The lifileucel Gen 2 clinical manufacturing process uses gas-permeable rapid expansion (G-Rex[®], Wilson Wolf, Saint Paul, MN) bioreactors for TIL expansion.⁵ Static gas-permeable cell culture bags (EXP-Pak[™], Charter Medical, Winston-Salem, NC) are alternate bioreactors that have been used for clinical manufacturing of T cells.⁶ In this study, TIL product characteristics were compared after expansion at small- and full-scale using EXP-Pak bags and G-Rex bioreactors.

Methods Cryopreserved pre-REP TIL were cultured with OKT-3 and irradiated peripheral blood mononuclear cells in either small-scale (G-Rex 5M flasks or EXP-50 bags) or full-scale (G-Rex 500MCS or EXP-5L bags) conditions. The same culture media formulation was used throughout the process. Final harvested TIL products were characterized for the following quality attributes: total viable cells (TVC), purity (% viability), identity (% CD45⁺CD3⁺), and activity (IFN-gamma release). Additional characterization was performed to determine the TIL differentiation, central and effector memory subsets, activation, exhaustion status, and impurities using multi-color flow cytometry. The T-cell receptor (TCR) repertoires of the final products were assessed for unique CDR3 (uCDR3) counts and shared clones using RNA-seq.

Results The median (range) TVC from 6 small-scale runs of G-Rex condition was 90.8×10⁹ (26.9×10⁹–98.6×10⁹) cells, and the corresponding TVC of EXP-Pak bag condition was 119×10⁹ (63.2×10⁹–141×10⁹) cells. Full-scale runs (n=3) yielded similar TVC for G-Rex and EXP-Pak bag conditions. Both conditions had comparable purity, identity, and activity (table 1). 91–99% of TCR Vbeta clones of EXP-Pak bag TIL were present in G-Rex (table 2). Cell proliferation, cell cycle, and mitochondrial function of TIL generated from EXP-Pak bags and G-Rex flask methodologies will be presented.

Abstract 101 Table 1 Summary of final TIL product attributes

Testing Parameter, median (range)	Small-scale (N=6)		Full-scale (N=3)	
	G-Rex	EXP-Pak	G-Rex	EXP-Pak
TVC, × 10⁹	90.8 (26.9 – 98.6) ¹	119 (63.2 – 141) ¹	47.9 (44.2 – 51.8) ²	48.1 (42.8 – 64.4) ²
Purity (% viability)	88.8 (83.2 – 95.1)	92.7 (78.3 – 95.7)	86.9 (84.4 – 92.4)	86.1 (79.1 – 91.6)
Identity (% CD45⁺/CD3⁺)	99.4 (98.7 – 99.8)	99.3 (98.4 – 99.6)	99.7 (99.6 – 99.7)	99.8 (99.8 – 99.9)
Activity (IFN-γ release)	3986 (435 – 5305)	5069 (484 – 16,457)	2354 (2205 – 3308)	1830 (1134 – 3312)

¹TVC were extrapolated to full scale. ²Pre-LOVO TVC count are reported.
TIL, tumor-infiltrating lymphocytes; TVC, total viable cells.

Abstract 101 Table 2 Common uCDR3 clones and % overlap of TCR clones

Full-scale Run Number	REP Condition	Number of Common uCDR3, (% Overlap)	
		G-Rex	EXP-Pak
1	G-Rex	10,584 (100)	5784 (97 ¹ , 91 ²)
	EXP-Pak	- ³	20,212 (100)
2	G-Rex	11,701 (100)	4607 (93 ¹ , 96 ²)
	EXP-Pak	- ³	14,934 (100)
3	G-Rex	3792 (100)	2122 (99 ¹ , 99 ²)
	EXP-Pak	- ³	4152 (100)

¹Percentage of uCDR3 clones in G-Rex found in EXP-Pak condition.
²Percentage of uCDR3 clones in EXP-Pak found in G-Rex condition.
³Not applicable.
REP, rapid expansion protocol; TCR, T-cell receptor; uCDR3, unique CDR3.

Conclusions The final TIL product generated in the EXP-Pak bag condition did not differ from cells produced in the G-Rex flask functionally or phenotypically and demonstrated similar growth profiles. These data support further evaluation of EXP-Pak bags for potential use in clinical and potential commercial TIL cell therapy manufacturing applications.

Acknowledgements This study and analysis were funded by Iovance Biotherapeutics, Inc. (San Carlos, CA, USA). Editorial support was provided by Amanda Kelly (Iovance).

REFERENCES

- Sarnaik AA, et al. *J Clin Oncol.* 2021; doi: 10.1200/JCO.21.00612.
- Thomas SS, et al. *J Clin Oncol.* 2021;39 (suppl; abstract 9537).
- Jazaeri A, et al. *J Clin Oncol.* 2019;37 (suppl; abstract 2538).
- Jimeno A, et al. *J Immunother Cancer.* 2020;8 (suppl; abstract A378).
- Wardell S, et al. *J Immunother Cancer.* 2019;7 (suppl 1; abstract P226).
- BioProcess International. 2014 [white paper]. <https://bioprocessintl.com/sponsored-content/efficacy-utility-new-exp-pak-closed-system-disposable-cell-expansion-bags-designed-cell-therapy-applications/> Accessed July 23, 2021.

<http://dx.doi.org/10.1136/jitc-2021-SITC2021.101>

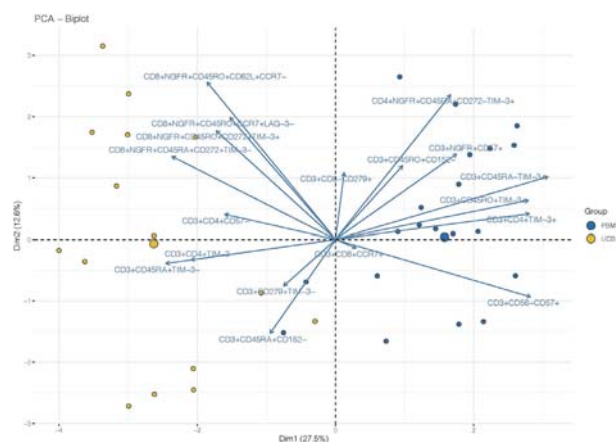
THE DEEP PHENOTYPE CHARACTERIZATION OF 'OFF-THE-SHELF' CD19-CHIMERIC ANTIGEN RECEPTOR (CAR) T CELLS ALLOWS TO IDENTIFY THEIR SUBSET COMPLEXITY AND TO OPTIMIZE THEIR MANUFACTURING

¹Cristina Maccalli*, ¹Asma Al-Sulaiti, ¹Mohammed El-Anbari, ¹Moza Al Khulaifi, ¹Mohammed Toufiq, ¹Rebecca Mathew, ¹Chiara Cugno, ¹Sara Deola, ¹Suruchi Mohan, ¹Damilola Olagunju, ³Chiara Bonini, ²Monica Casucci, ¹Sara Tomei, ¹Damien Chaussabel. ¹Sidra Medicine, Doha, Qatar; ²San Raffaele Hospital, Milano, Italy

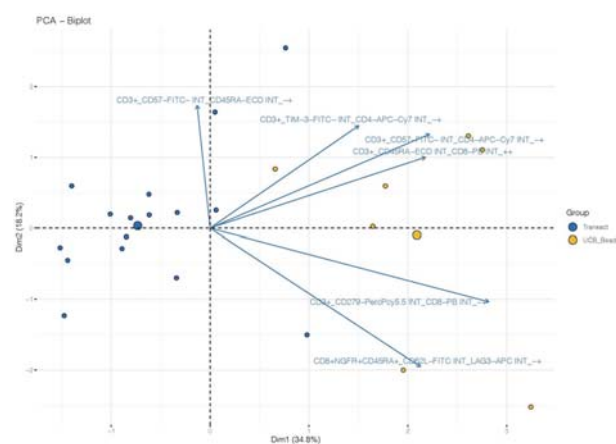
Background Umbilical cord blood (UCB) represents a promising source of T cells for the generation of 'off-the-shelf' T cells engineered to express a chimeric antigen receptor (CAR). This study is aimed at understanding the composition of T cell subsets within UCB-CAR-T cells.

Methods T cells, either from UCB or peripheral mononuclear cells (PBMCs) of healthy donors, were activated in vitro with CD3/CD28 mAbs either conjugated to magnetic beads (Dyna-beads) or to a colloidal polymeric nanomatrix (TransAct; Miltenyi Biotec). T cells were then transduced with lentiviral vectors encoding for CD19-CD28z or CD19-4-1BBz CARs. The deep phenotype analyses of the CD19-CAR-T cells (N=32) was performed through a multidimensional flow cytometry to assess the expression/co-expression of T cell-associated markers (N=29). The NGFR was utilized as probe for the expression of CD19-CAR. To select the pertinent markers characterising the different groups, we applied a machine learning technique called L0-regularized logistic regression,^{1,2} and implemented in the R package L0Learn. 5-fold cross-validation (CV) was used to select the optimal values of the tuning parameters. CD19-CAR-T cells have been also characterized for the transcriptomic profile by parallel quantitative PCR using the high throughput BioMark HD platform and for cytokines, perforin and granzyme B release upon the co-culture with CD19 expressing or not target cells.

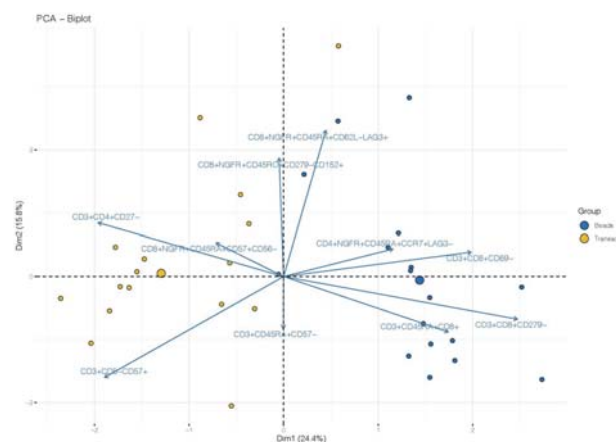
Results T lymphocytes UCB showed efficient expression of the CARs (40–70% of positive cells). Different T cell subsets could discriminate the composition of T cells activated with either Beads or TranAct. CD4+NGFR+CD45RA+ or CD8+NGFR+CD45RA+ T cells associated with different combinations of CCR7, CD62L, LAG3, CD57, CD56 could discriminate between cells activated with Beads vs. TranAct (figures 2–3). CD8+NGFR+CD45RO+CD279–CD152+ T cells were also differentially expressed in TranAct vs. Beads. The PCA analyses also highlighted differences in terms of CD19-CAR-T cell subsets (such as CD8+NGFR+CD45RO+CD62L+, CD8+NGFR+CD45RO+CCR7+, CD8+NGFR+CD45RO+CD272+TIM–3+, CD8+NGFR+CD45RO+CD272+TIM–3+, CD8+NGFR+CD45RA+CD272+TIM–3– and CD4+NGFR+CD45RA+CD272–TIM–3+) in PBMCs vs. UCBs (figure 1). In addition, bystander T cells with different phenotype not expressing the CARs were also detected within the populations of T cells with different origins. Similarly, different T subsets were found in relationship with the sources of T cells. These CD19-CAR-T cells were also characterized for the anti-tumor activity and transcriptomic profiling.



Abstract 102 Figure 1 PCA of CAR-T cells from UCB vs. PBMCs



Abstract 102 Figure 2 PCA of CAR-T cells from UCB to compare TransAct vs. beads



Abstract 102 Figure 3 PCA of CD19-CAR-T cells to compare TransAct vs. Beads irrespective of the source of the T cells

Conclusions The combination of deep phenotype characterization with novel statistical tools allowed to identify the complexity of subsets in the engineered T cells in relationship with the starting material and the methods for the activation of the lymphocytes. These findings have important implications for the optimization of the manufacturing of CD19-CAR-T cells.

REFERENCES

1. Antoine Dedieu, Hussein Hazimeh, and Rahul Mazumder. Learningsparse classifiers: Continuous and mixed integer optimization perspectives. *Journal of Machine Learning Research* 2021.
2. Hussein Hazimeh and Rahul Mazumder. Fast best subset selection: Coordinated descent and local combinatorial optimization algorithms. *Operations Research* 2020;68(5):1517–1537.

Ethics Approval Sidra Medicine's Ethics Board approval, #1812044429

<http://dx.doi.org/10.1136/jitc-2021-SITC2021.102>

103

QUALITY IMPROVEMENT OF ANTI-CD38-JAK/STAT CAR-T CELLS BY SUPPRESSING CD38 EXPRESSION AND INHIBITION OF TYROSINE KINASE

¹Yasunori Amaishi*, ¹Izumi Maki, ¹Maiko Sugizaki, ²Kenichiro Mihara, ¹Sachiko Okamoto, ¹Junichi Mineno. ¹Takara Bio Inc., Kusatsu, Shiga, Japan; ²Fujita Health University, Toyoake, Aichi, Japan

Background CAR-T cell therapy has shown highly effective clinical results in several diseases, but further improvement is necessary to target a wider range of antigens and tumors. In particular, excessive activation of CAR-T cells leads to cell exhaustion and reduction of naive/memory T cells' population, which are important for long-term immune response. Therefore, suppressing non-antigen-specific activity is necessary for CAR-T cell production. However, when targeting tumor-related antigens that are also expressed on T cells, CAR-T cells recognize the antigens on the T cells, resulting in fratricide, poor cell growth, differentiation, and exhaustion during cell production process. In this study, we investigated a method for producing CAR-T cells targeting CD38 antigen that is common to T cells and tumor cells. CD38 is a suitable target antigen for CAR-T cell therapy because it is highly expressed in lymphocyte malignant tumors including B-cell non-Hodgkin's lymphoma and multiple myeloma. However, as it is also intermediately expressed in normal blood cells, unwanted activation of CAR-T cells may be caused.

Methods We tried to suppress the expression of CD38 in CAR-T cells by co-expressing CD38 siRNAs, and prevent activation during cell production by modifying the signal domain of anti-CD38-CAR to the newly developed JAK/STAT-CAR. JAK/STAT-CAR contains the intracellular domain of the IL-2 receptor β chain and the STAT3 binding motif, which have been shown to improve the proliferation of CAR-T cells and suppresses differentiation compared to conventional second-generation CAR-T cells. For further improvement, CAR-T cells were prepared in the presence of the tyrosine kinase inhibitor Dasatinib to suppress activation during the cell manufacturing process.

Results CD38 siRNA co-expressing CAR-T cells showed decreased expression of CD38 and exhaustion markers, and the further reduction of exhaustion marker expression was observed in JAK/STAT CAR-T cells. However, compared to CAR-T cells targeting other antigens, CD38-CAR-T cells tended to be more exhausted and differentiated. As Dasatinib treatment maintained a high proportion of naive/memory T cells and was able to suppress exhaustion, combination of these approaches (CD38 siRNA-expressing CD38-JAK/STAT CAR-T cells with Dasatinib treatment) showed long-term persistence of antitumor activity in in vitro re-challenge assay.

Conclusions CD38 siRNA co-expressing CD38-JAK/STAT CAR-T cells produced in the presence of a tyrosine kinase inhibitor are expected to be suppressed excessive activation and maintain long-term antigen-specific activity. This approach is also expected to be applied to other CAR-T cell therapies targeting tumor-related antigens expressed on T cells.

<http://dx.doi.org/10.1136/jitc-2021-SITC2021.103>

DEVELOPMENT AND CHARACTERIZATION OF HUMAN CHIMERIC ANTIGEN RECEPTOR MONOCYTES (CAR-MONO), A NOVEL CELL THERAPY PLATFORM

Daniel Blumenthal*, Linara Gabitova, Brett Menchel, Patricia Reyes-Uribe, Andrew Best, Michael Lynch, Sotheavy Chhum, Maggie Schmierer, Sascha Abramson, Michael Klichinsky. *Carisma Therapeutics, Philadelphia, PA, USA*

Background Engineered cell therapies have demonstrated significant clinical activity against hematologic malignancies, but solid tumors remain an intractable challenge. We have previously developed a human chimeric antigen receptor macrophage (CAR-M) platform for adoptive cell therapy and shown potent anti-tumor activity in pre-clinical solid tumor models.¹ CAR-M overcome critical solid tumor challenges such as tumor infiltration, immunosuppression within the tumor microenvironment, lymphocyte exclusion, and target antigen heterogeneity. Currently, CAR-M are generated in a week-long ex-vivo process in which peripheral blood monocytes are differentiated into macrophages prior to genetic manipulation. Here, we demonstrate the production feasibility, phenotype, pharmacokinetics, cellular fate, specificity, and anti-tumor activity of human CD14⁺ CAR monocytes.

Methods Using the chimeric adenoviral vector Ad5f35, we engineered primary human CD14⁺ monocytes to express a CAR targeted against human epidermal growth factor receptor 2 (HER2) (CAR-mono). Using a partially automated approach, we established a process that allowed for same day manufacturing (from Leukopak to cryopreserved CAR-mono cell product).

Results CAR expression and cell viability exceeded 90%, and cells efficiently differentiated into CAR-expressing macrophages. The adenoviral based gene modification method led to pre-conditioning of CAR-mono cells resulting in a strong M1 phenotype upon differentiation, and potent anti-tumor activity regardless of exposure to GM-CSF, M-CSF, or immunosuppressive factors. Treating CAR-mono cells with GM-CSF and IL-4 resulted in their differentiation to monocyte-derived CAR-DCs, indicating that these cells retain their myeloid differentiation potential. In vivo, CAR-mono treatment induced anti-tumor activity in various HER2⁺ solid tumor xenograft models. Following intravenous administration, CAR-mono demonstrated the ability to traffic to both GM-CSF^{high} and GM-CSF^{low} expressing tumors. Notably, CAR-mono showed long-term CAR expression and persistence (>100 days) in both NSG and NSG-S mouse models, demonstrating lasting persistence irrespective of human cytokine support.

Conclusions The CAR-mono platform allows for a rapid, same-day manufacturing process while maintaining the key characteristics of CAR-M therapy. Ad5f35 engineered human monocytes are primed toward M1 macrophage differentiation and produce a cell population highly similar to our established CAR-M platform. Collectively, these findings provide strong pre-clinical support to advance the CAR-mono platform into clinical testing.

REFERENCE

1. Klichinsky M, et al. Human chimeric antigen receptor macrophages for cancer immunotherapy. *Nature Biotechnology* March 2020.

<http://dx.doi.org/10.1136/jitc-2021-SITC2021.104>

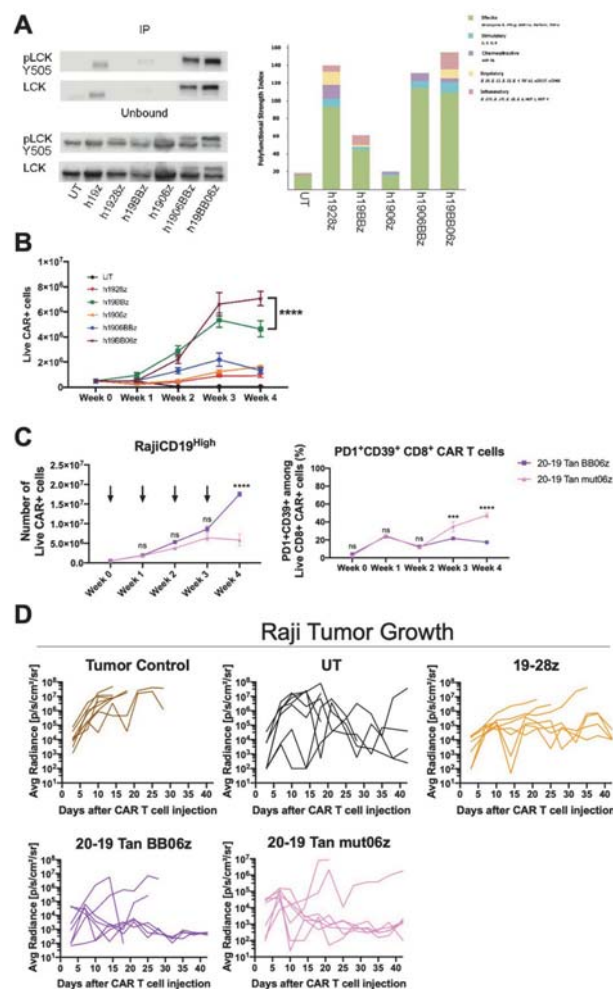
4-1BB AND OPTIMIZED CD28 CO-STIMULATION ENHANCES FUNCTION OF HUMAN MONO- AND BI-SPECIFIC THIRD-GENERATION CAR T CELLS

¹Emiliano Roselli*, ¹Justin Boucher, ¹Gongbo Li, ¹Hiroshi Kotani, ¹Kristen Spittle, ¹Kayla Reid, ²Yannick Bulliard, ¹Nhan Tu, ¹Sae Bom Lee, ¹Bin Yu, ¹Frederick Locke, ¹Marco Davila. ¹H. Lee Moffitt Cancer Center, Tampa, FL, USA; ²Atara Biotherapeutics, Thousand Oaks, USA

Background Co-stimulatory signals regulate the expansion, persistence, and function of chimeric antigen receptor (CAR) T cells. Most studies have focused on the co-stimulatory domains CD28 or 4-1BB. CAR T cell persistence is enhanced by 4-1BB co-stimulation leading to NF- κ B signaling, while resistance to exhaustion is enhanced by mutations of the CD28 co-stimulatory domain.

Methods We hypothesized that a third-generation CAR containing 4-1BB and CD28 with only PYAP signaling motif (mut06) would provide beneficial aspects of both. We designed CD19-specific CAR T cells with 4-1BB or mut06 together with the combination of both (BB06). We evaluated their immune-phenotype, cytokine secretion, real-time cytotoxic ability and polyfunctionality against CD19-expressing cells. We analyzed LCK recruitment by the different constructs by immunoblotting. We further determined their ability to control growth of Raji cells in NSG mice. Additionally, we engineered bi-specific CARs against CD20/CD19 combining 4-1BB and mut06 and performed repeated in vitro antigenic stimulation experiments to evaluate their expansion, memory phenotype and phenotypic (PD1+CD39+) and functional exhaustion. Bi-specific CAR T cells were transferred into Raji or Nalm6-bearing mice to study their ability to eradicate CD20/CD19-expressing tumors.

Results Co-stimulatory domains combining 4-1BB and mut06 confers CAR T cells with an increased polyfunctionality and LCK recruitment to the CAR (figure 1A), after repeated-antigen stimulation these cells expanded significantly better than second-generation CAR T cells (figure 1B). A bi-specific CAR targeting CD20/CD19, incorporating 4-1BB and mut06 co-stimulation, showed enhanced antigen-dependent in vitro expansion with lower exhaustion-associated markers (figure 1C). Bi-specific CAR T cells exhibited improved in vivo anti-tumor activity with increased persistence and decreased exhaustion (figure 1D).



Abstract 105 Figure 1 A. pLCK is increased in h19BB06z CAR T cells and associated with the CAR. CAR T cells were stimulated with irradiated 3T3-hCD19 cells at a 10:1 E:T ratio for 24hr. Cells were lysed and CAR bound and unbound fractions were western blotted. A single-cell measure of polyfunctional strength index (PSI) of CAR T cells. B. h19BB06z CAR T cells have the highest proliferation after repeated antigen stimulations. 5×10^5 CAR T cells were stimulated with 1×10^5 irradiated 3T3-hCD19 cells. After 1 week, half of the cells were enumerated by flow cytometry and the other half was re-stimulated with 1×10^5 fresh irradiated 3T3-hCD19 cells. This was repeated for a total of 4 weeks. C. 5×10^5 CAR T cells were co-cultured with 5×10^5 target cells (Raji-CD19High). After 1 week half the cells were harvested enumerated and stained by flow cytometry while the other half was re-stimulated with 5×10^5 fresh target cells (indicated by arrows). This was repeated for a total of 4 weeks. Frequency of PD1+CD39+ cells within CD8+ CAR T cells. D. Raji-FFLuc-bearing NSG mice were treated with 1×10^6 CAR T cells 5 days after initial tumor cell injection. Tumor burden (average luminescence) of mice treated with bi-specific or monospecific CAR T cells, UT and tumor control. Each line represents an individual mouse. (n = 7 mice per group).

Conclusions These results demonstrate that co-stimulation combining 4-1BB with an optimized form of CD28 is a valid approach to optimize CAR T cell function. Cells with both mono- and bi-specific versions of this design showed enhanced in vitro and in vivo features such as expansion, persistence and resistance to exhaustion. Our observations validate the approach and justify clinical studies to test the efficacy and safety of this CAR in patients.

<http://dx.doi.org/10.1136/jitc-2021-SITC2021.105>

TREATMENT WITH CC-99282 ENHANCES ANTITUMOR FUNCTION OF THE ANTI-CD19 CAR T CELL THERAPY LISOCABTAGENE MARALEUCEL (LISO-CEL)

Archana Brahmmandam*, Jim Qin, Susan Kim, Yue Jiang, Brook Barajas, Soraya Carrancio, Leanne Peiser. *Bristol Myers Squibb, Seattle, WA, USA*

Background Liso-cel, an autologous, CD19-directed, defined composition, 4-1BB CAR T cell product administered at equal target doses of CD8+ and CD4+ CAR+ T cells, has demonstrated efficacy and a favorable safety profile in adult patients with third-line or later large B-cell lymphoma. Clinically, disease relapse or progression may be due partly to CAR T cell exhaustion. Combination therapies promoting sustained CAR T cell pharmacologic function may increase the rate, depth, and durability of responses. CC-99282 is a novel cereblon E3 ligase modulator (CELMoD[®]) compound capable of co-opting cereblon to induce the recruitment and subsequent ubiquitin-mediated degradation of Ikaros/Aiolos, resulting in therapeutic effects, including enhanced antitumor activity and augmentation of T cell function. We examined CC-99282 in combination with liso-cel in acute activation and chronic stimulation assays to assess the effect of CC-99282 on liso-cel activation, exhaustion onset, and exhaustion rescue.

Methods Liso-cel produced from healthy donor T cells was subjected to acute activation (up to 72 hours) or chronic stimulation (6–7 days) to recapitulate CAR T cell exhaustion and assess effects of CC-99282 on liso-cel in a concurrent or rescue setting after CAR T cells achieved a hypofunctional exhausted state. Functional activity was measured by proliferation, cytotoxicity, effector cytokine production, and gene signature analyses after further culture of liso-cel with CD19+ non-Hodgkin lymphoma (NHL) cells or tumor spheroids.

Results In acute activation assays, CC-99282 degraded Ikaros/Aiolos in liso-cel after 24 hours and uncoupled liso-cel proliferation from cytokine production after 72 hours, demonstrated by a simultaneous increase in interferon-gamma and slowed proliferation. Concurrent incubation of liso-cel with low concentrations (nM) of CC-99282 during chronic stimulation limited liso-cel exhaustion onset with increased cytokine production and cytotoxicity against CD19+ NHL spheroids. Furthermore, incubation of CC-99282 with exhausted liso-cel in the rescue setting resulted in enhanced cytokine production and cytotoxicity compared with control. Gene expression analysis by RNA-seq confirmed that CC-99282 modulated gene signatures associated with liso-cel hypofunctionality. Interestingly, transient dosing with higher CC-99282 concentrations further alleviated T cell exhaustion, enhancing liso-cel-mediated cytotoxicity against CD19+ NHL cells and preserving a less differentiated CAR T cell memory phenotype.

Conclusions At clinically relevant concentrations, CC-99282 enhanced liso-cel antitumor activity and reduced liso-cel exhaustion in in vitro CD19+ NHL models. The combination may improve efficacy of liso-cel, including response duration, in the treatment of CD19+ NHL. Additionally, CC-99282 substrate potency may support an intermittent dosing regimen for CC-99282 and liso-cel combination treatment, which could potentially improve tolerability.

Acknowledgements We would like to thank Michael Ports for contributions to the study design and data interpretation, Shailaja Kasibhatla for contributions to the study concept and critical review, and the patients, caregivers, investigators, and study personnel. This study was funded by Bristol Myers Squibb. All authors contributed to and approved the abstract;

writing and editorial assistance were provided by Allison Green, PhD, of The Lockwood Group (Stamford, CT, USA), funded by Bristol Myers Squibb.

Ethics Approval The authors are accountable for all aspects of the work in ensuring that questions related to the accuracy or integrity of any part of the work are appropriately investigated and resolved. All procedures performed in studies involving human participants were in accordance with the ethical standards of the institutional and/or national research committee(s) and with the Helsinki Declaration. Written informed consent was obtained from the healthy donor subjects.

<http://dx.doi.org/10.1136/jitc-2021-SITC2021.106>

ARMORING NKG2D CAR T CELLS WITH IL-18 IMPROVES IN VIVO ANTI-TUMOR ACTIVITY

Eytan Breman, Ann-Sophie Walravens, Isabelle Gennart, Amelie Velghe, Thuy Nguyen, Benjamin Violle, Fanny Huberty, Nancy Ramelot, Laure Twyffels, Emilie Gauthy, Hannes Iserentant, David Gilham*. *Celyad Oncology, Mont-Saint-Guibert, Belgium*

Background Whilst delivering impressive clinical efficacy in certain hematological malignancies, Chimeric Antigen Receptor (CAR) T cell therapy has yet to deliver significant clinical impact across a broader array of cancer indications. Armoring CAR T through the co-expression of immune modifying cytokines is an approach that may aid anti-cancer activity but is currently at an embryonic stage of development. In this study, the potential benefit of expressing IL-18 alongside a NKG2D CAR was assessed.

Methods A series of retroviral vectors encoding the NKG2D CAR (a fusion of NKG2D with CD3z), a cell surface tag to facilitate cell selection and tracking (truncated CD19) either with or without full length IL-18 were compared. In certain vectors, a single shRNA targeting CD3z was included to generate allogeneic CAR T versions. All transgenes were delivered as a single vector expressed under the control of the retroviral promoter with individual 2A elements ensuring equimolar levels of protein expression. T cells transduced with the individual vectors were challenged in vitro and in vivo to determine the impact of IL-18 upon NKG2D CAR directed function.

Results Armored NKG2D CAR T cells that included the IL-18 transgene showed high levels of IL-18 secretion in culture and increased levels of interferon gamma secretion upon antigen challenge as compared to non-armored NKG2D CAR T cells. Armored NKG2D CAR T cells also showed prolonged sequential target cell killing as compared to non-armored CAR T versions. Importantly, in an in vivo stress test where the dose of non-armored NKG2D T cells was reduced to a level where minimal anti-tumor activity and survival above control was seen using an established THP-1 model, armored CAR T cells showed enhanced anti-tumor activity (as determined by bioluminescence) and overall survival. Interestingly, at high doses of armored CAR T cells, toxicity was seen in some tumor bearing models. This toxicity was abrogated by systemic infusion of human IL-18 binding protein (IL-18BP).

Conclusions Armoring NKG2D CAR T cells with IL-18 resulting in increased in vitro and in vivo target-dependent anti-tumor activity. The transient toxicity observed with high doses of the armored CAR T in tumor bearing models was eliminated by IL-18BP. Together, these observations imply that armoring NKG2D CAR T cells with IL-18 is likely to drive improved anti-tumor activity of the CAR T cell in line with previous publications^{1 2} while the presence of systemic IL-18BP³ should negate possible toxicities arising from high level constitutive expression of the cytokine.

REFERENCES

1. Chmielewski M, Abken H. *Cell Reports* 2017;**21**(11): 3205–32192.
2. Hu B, Ren J, Luo Y, Keith B, Young R, Scholler J, Zhao Y, June C. *Cell Reports* 2017; **20**(13): 3025–30333.
3. Dinarello C, Novick D, Kim S, Kaplanski G. *Frontiers in Immunology* 2013;**4**:289

<http://dx.doi.org/10.1136/jitc-2021-SITC2021.107>

FAST AND ACCURATE PREDICTION OF OPTIMAL CAR T-CELL FUNCTION USING Z-MOVI[®] CELL AVIDITY ANALYZER

Will Singletary*, Andrea Candelli, Rogier Reijmers, Jens Eberlein. *LUMICKS, Waltham, MA, USA*

Background Affinity between himeric antigen receptors (CARs) to their target has shown to be a poor predictor of functional capacity of T cells. Recent studies have revealed that the overall binding strength (or avidity) between T cells and tumor cells represents a crucial parameter for identifying and developing potent cancer immunotherapies. Compared with affinity, cell avidity provides a more complete and physiologically relevant picture that reflects the bona fide interaction between T cells and tumor cells. Therefore, this interaction could better predict cellular responses in vitro, drive better, more informed decisions and potentially improve clinical outcome. However, one of the main obstacles in the process of measuring avidity is the lack of fast, specific, and accurate technologies to assess cellular avidity.

Methods The z-Movi[®] Cell Avidity Analyzer is a novel and unique instrument for direct measurement of cell–cell interaction strength using acoustic forces. This new technology provides predictive, reproducible, and fast high-throughput results at a single-cell level.

Results In this poster we will demonstrate that data obtained with the z-Movi Cell Avidity Analyzer correlates strongly with standard in vitro assays, such as cytokine release and cytotoxicity measurements. We will review the simple principles behind the z-Movi, the workflow to set up an experiment consisting of multiple runs, and how the intuitive software package will assist in getting precise cell avidity information of hundreds of cells simultaneously. Finally, we will demonstrate the great potential of the z-Movi for accelerating the development of CAR T immunotherapy against cancer.

Conclusions Finally, we will demonstrate the great potential of the z-Movi for accelerating the development of CAR T immunotherapy against cancer.

<http://dx.doi.org/10.1136/jitc-2021-SITC2021.108>

IL-2 VARIANT IMPROVES CAR-T FUNCTIONALITY AND EFFICACY AGAINST SOLID TUMORS

Qi Dong*, Wenjie Yin, Pengfei Jiang, Manli Yin, Tao Wang, Ping Wang, Xinxin Wang, William Wei Cao, Lianjun Shen. *Gracell Biotechnologies, Shanghai, China*

Background Solid tumors remain a challenge for chimeric antigen receptor T (CAR-T) cell therapy due to lack of tumor-specific antigens, often-hard-to-penetrate tumor structure, and hostile tumor microenvironment (TME) for T-cell activation and survival. Interleukin (IL)-2 is an essential cytokine central to the initiation and maintenance of T-cell-mediated immune responses, which is usually downregulated in TME. IL-2 has been shown to improve the effectiveness of various T-cell-based therapies for solid tumors. However, systemic administration of IL-2 has been shown to elicit immunosuppression through regulatory T cells and cause capillary leak syndrome, both of which limit its use in T-cell immunotherapies, such as CAR-T. To improve the resistance of CAR-T to TME and to enhance its persistence, expansion and efficacy *in vivo*, we designed novel second generation mesothelin (MSLN)-specific CAR constructs (MSLN-CAR-T-IL-2tb) that incorporate secretory form of IL-2 variants (IL-2tb). IL-2tb produced by MSLN-CAR-T-IL-2tb improves cell viability, expansion, and potency, and reduces immunosuppression which could also potentially stimulate endogenous polyclonal tumor-infiltrating lymphocytes in solid tumors.

Methods MSLN-CAR-T-IL-2tb and MSLN-CAR-T cells were generated by lentiviral transduction. To assess *in vitro* proliferation, CAR-T cells were repeatedly cocultured with MSLN-expressing tumor cell lines and CAR⁺ T cells were enumerated. CAR-T cell apoptosis, memory phenotype and exhaustion were monitored by flow cytometry at various time points. MSLN-CAR-T-IL-2tb and MSLN-CAR-T cell resistance to TME was tested *in vitro*. Cytotoxicity was determined using RTCA- or luciferase-based assays. CAR-T tumoricidal activity *in vivo* was evaluated in human cell line-derived xenograft models using severe immunodeficient mice.

Results MSLN-CAR-T-IL-2tb and MSLN-CAR-T demonstrated comparable efficacies in short-term tumor killing assays *in vitro* against multiple tumor cell lines expressing varying levels of MSLN in the presence of exogenous IL-2. However, when cultured in the absence of IL-2, MSLN-CAR-T-IL-2tb was much longer-lasting than MSLN-CAR-T in terms of CAR-T cell viability, proliferation, and persistence. MSLN-CAR-T-IL-2tb was more cytotoxic against multiple MSLN-expressing tumor cells, including MDA-MB-231 and HCC70 (triple-negative breast cancers) and OVCAR-3 (ovarian cancer). Moreover, in multiple xenograft mouse models, MSLN-CAR-T-IL-2tb showed very potent and durable anti-tumor responses.

Conclusions MSLN-CAR-T cells expressing a secretory form of IL-2 variant were able to maintain long-term proliferation and cytotoxicity which could be partly due to the reduced immunosuppression in the TME. Autocrine and paracrine loops of IL-2 can further improve CAR-T functionality in solid tumor and could be a promising strategy for clinical application.

Ethics Approval All animal experiments were conducted in facilities accredited by the service providers' Institutional Review Boards.

<http://dx.doi.org/10.1136/jitc-2021-SITC2021.110>

**ARMORED CAR T CELLS SECRETING 4-1BB LIGAND
CROSSLINKED TO PD-1 CHECKPOINT INHIBITOR FOR
ENHANCED SOLID TUMOR EFFICACY**

Zachary Dunn*, Yun Qu, Melanie MacMullan, Xianhui Chen, Gunce Cinay, Pin Wang.
University of Southern California, South Pasadena, CA, USA

Background Chimeric antigen receptor (CAR) T cell therapy has transformed the treatment of hematological malignancies but has yet to achieve similar success in solid tumors due to a lack of persistence and function in the tumor microenvironment. We previously reported the augmentation CAR T cell therapy in an engineered solid tumor model through the secretion of anti-PD-1 scFv, as shown by enhanced CAR T cell antitumor efficacy, expansion, and vitality.¹ We have since matured the platform to create a superior cellular product – CAR T cells secreting single-chain trimeric 4-1BB ligand crosslinked to anti-PD-1 scFv (α PD1-41BBL). 4-1BB signaling promotes cytotoxic T lymphocytes proliferation and survival but targeting 4-1BB with agonist antibodies in the clinic has been hindered by low antitumor activity and high toxicity. CAR T cells using 4-1BB endodomain for costimulatory signals have demonstrated milder anti-tumor response and longer persistence compared to CAR T cells costimulated by CD28 endodomain. We have, for the first time, engineered CAR T cells to secrete a fusion protein containing the soluble trimeric 4-1BB ligand.

Methods We hypothesized that crosslinking the current anti-PD-1 scFv with 4-1BB ligand would provide additional benefits to CAR T cells and is potentially of translational value in the management of tumors resistant to PD-1 blockade due to lack of T cell function. Therefore, we engineered CAR T cells to secrete a novel immunomodulatory fusion protein consisting of anti-PD-1 scFv crosslinked to a single-chain format of trimeric 4-1BB ligand, in which three extracellular domain units of 41BBL are connected with polypeptide linkers. The CAR T cells were then characterized in vitro and subcutaneous tumor models.

Results In vitro and in vivo, CAR19. α PD1-41BBL T cells exhibited reduced inhibitory receptor upregulation, enhanced persistence and proliferation, and a less differentiated memory status compared to CAR T cells without additional 4-1BB:4-1BBL costimulation. Accordingly, CAR19. α PD1-41BBL T cell-treated mice displayed significantly improved tumor growth control and overall survival. Spurred on by our preclinical success targeting CD19 as a model antigen, we produced mesothelin-targeting CAR T cells and confirmed the enhanced solid tumor efficacy and persistence of α PD1-41BBL secreting CAR T cells.

Conclusions Given the significantly better therapeutic efficacy of α PD1-41BBL expressing T cells over α PD1 expressing T cells, we believe that it is of high translational value to adopt secretion of α PD1-41BBL fusion protein to improve CAR T cell solid tumor efficacy, especially given the large number of patients that are PD1/PD-L1 therapy resistant.

REFERENCES

1. Li S, Siriwon N, Zhang X, Yang S, Jin T, He F, et al. Enhanced cancer immunotherapy by chimeric antigen receptor–modified T cells engineered to secrete checkpoint inhibitors. *Clin Cancer Res* 2017;23(22):6982–92.

<http://dx.doi.org/10.1136/jitc-2021-SITC2021.111>

TUMOR-SPECIFIC REACTIVITY AND EFFECTOR FUNCTION OF CHIMERIC ANTIGEN RECEPTOR ENGINEERED MACROPHAGES TARGETING MUC1

Seth Eisenberg*, Amy Powers, Jason Lohmueller, James Luketich, Rajeev Dhupar, Adam Soloff. *University of Pittsburgh School of Medicine, Pittsburgh, PA, USA*

Background Chimeric antigen receptors (CAR) have demonstrated remarkable efficacy in licensing T cells for antitumor responses against hematopoietic malignancies but have had limited success against solid tumors. Macrophages, both archetypic phagocytes and professional antigen presenting cells, may exert profound effector functions which complement adaptive cellular immunity.¹ Recently, it was shown that human macrophages engineered to express CARs (CAR-Ms) demonstrated antigen-specific phagocytosis, inhibited solid xenograph tumors, and induced an inflammatory tumor microenvironment boosting antitumor T cell responses.² Kimura et al. previously completed the first prophylactic cancer vaccine trial based on a non-viral antigen, tumor-associated hypoglycosylated Mucin 1 (MUC1).³ A panel of fully-human affinity-matured MUC1-specific antibodies raised in healthy subjects following immunization was identified from these patients.⁴ Using these MUC1-specific scFv domains for CAR generation, we have now engineered MUC1-targeting CAR-Ms that may potentially possess reduced off-target specificities.

Methods Lentiviral CAR expression vectors containing the scFv domains of three unique hypoglycosylated MUC1-specific antibodies or a CD20-specific antibody, the CD3zeta signaling domain, and CD28 and OX40 co-stimulatory domains were constructed. The human monocyte/macrophage U937, SC, and THP-1 lines were stably transduced and flow-sort purified to generate MUC1- or CD20-specific CAR-Ms. CAR-Ms were differentiated into macrophages via 48 hour PMA treatment, and subsequently evaluated for antigen-specific function against MUC1- and/or CD20-expressing K562, ZR-75-1, and Raji cells or cancer cells isolated from solid lung tumors or malignant pleural effusions. CAR-M phenotype was evaluated by flow cytometry following in vitro differentiation and polarization with conventional 'M1' and 'M2' stimuli. Phagocytosis and lysosomal processing of phagocytosed cargo were evaluated by fluorescence microscopy of GFP/CellTrace labeled targets or detection of pH-sensitive pHrodo expression following CAR-M and tumor cell co-culture, respectively. Antigen-specific cytokine production was determined via cytometric bead array following co-culture of CAR-Ms with MUC1- or CD20-expressing tumor cells or 100mer MUC1 peptide.

Results Differentiated CAR-Ms possessed an inflammatory phenotype expressing IL-8 and CD86 which was further enhanced by IFN γ or LPS treatment and was resistant to 'M2' polarization with conventional stimuli. CAR-Ms exhibited phagocytosis and subsequent lysosomal processing in an antigen-specific manner, with minimal reactivity against tumor cell targets in the absence of the corresponding MUC1 or CD20 antigen. MUC1-specific CAR-Ms stimulated with MUC1 peptide or MUC1+ tumor cells secreted robust levels of pro-inflammatory IL-8, TNF α , and IL-1 β , but not immunosuppressive IL-10.

Conclusions MUC1-targeting CAR-Ms exert potent tumor-restricted effector function in vitro and may provide a novel treatment strategy either alone or in potential synergistic combination with T cell-mediated immunotherapies.

Acknowledgements The authors would like to thank Dr. Olivera J. Finn for generously providing reagents and guidance

and Dr. Michael T. Lotze for his mentorship. This study was supported by funding from the University of Pittsburgh's Department of Cardiothoracic Surgery to ACS and RD.

REFERENCES

- Williams CB, Yeh ES, Soloff AC. Tumor-associated macrophages: unwitting accomplices in breast cancer malignancy. *Npj Breast Cancer* [Internet]. Breast Cancer Research Foundation/Macmillan Publishers Limited; 2016;**2**:15025. Available from: <http://dx.doi.org/10.1038/npjbcancer.2015.25>
- Klichinsky M, Ruella M, Shestova O, Lu XM, Best A, Zeeman M, et al. Human chimeric antigen receptor macrophages for cancer immunotherapy. *Nat Biotechnol* 2020;**38**:947–53.
- Kimura T, McKolanis JR, Dzubinski LA, Islam K, Potter DM, Salazar AM, et al. MUC1 Vaccine for Individuals with Advanced Adenoma of the Colon: A Cancer Immunoprevention Feasibility Study. *Cancer Prev Res [Internet]* 2013;**6**:18–26. Available from: <http://cancerpreventionresearch.aacrjournals.org/content/6/1/18.abstract>
- Lohmueller JJ, Sato S, Popova L, Chu IM, Tucker MA, Barberena R, et al. Antibodies elicited by the first non-viral prophylactic cancer vaccine show tumor-specificity and immunotherapeutic potential. *Sci Rep* 2016;**6**:31740.

Ethics Approval The study was approved by the University of Pittsburgh's Institutional Review Board approval number CR19120172-005.

<http://dx.doi.org/10.1136/jitc-2021-SITC2021.112>

113

CISH GENE-KNOCKOUT ANTI-CD70-CAR NK CELLS DEMONSTRATE POTENT ANTI-TUMOR ACTIVITY AGAINST SOLID TUMOR CELL LINES AND PROVIDE PARTIAL RESISTANCE TO TUMOR MICROENVIRONMENT INHIBITION

Chao Guo*, Yanying Fan, Alexander Aronov, Luxuan Buren, Ming-Hong Xie, Ivan Chan, Sasha Lazetic, James Trager. *NKARTA THERAPEUTICS, South San Francisco, CA, USA*

Background Peripheral blood natural killer (NK) cells are attractive candidates for adoptive cell therapy. NK cells possess innate ability for tumor cell killing and are also amenable to genomic engineering for enhanced functions. Moreover, NK cells possess an inherent capacity for allogeneic, off-the-shelf therapy since, unlike T cells, they are neither HLA-restricted nor known to cause graft-versus-host disease. Cytokine inducible SH2-containing protein (CISH) is a negative regulator of interleukin 15 (IL-15) signaling in natural killer (NK) cells. Here we show the potential application of CISH gene-knockout CAR NK cells targeting CD70 and expressing a membrane-bound form of IL-15. CD70 is an antigen that is aberrantly expressed in a variety of malignant settings, including renal cell carcinoma (RCC), while its expression in normal tissues is restricted to a subset of lymphoid cell types.

Methods To target CD70 on RCC cells, we generated CD70-CAR NK cells with CISH deletion. Using the CRISPR/Cas9 system, we knocked out CISH expression in isolated peripheral blood NK cells from healthy donors. Since CD70 expression is present on activated NK cells, we also targeted CD70 for CRISPR knockout to avoid fratricide. We then expanded these edited NK cells by using IL-2 and stimulation using NKSTIM, a modified K562 stimulatory cell line expressing membrane-bound form of IL-15 (mbIL-15) and 4-1BBL. IL-12 and IL-18 were added during expansion to drive memory-like NK cell differentiation. We transduced the expanded NK cells to express engineered CD70-targeted CAR and mbIL-15. We assessed CAR expression, NK cell persistence, and NK cell activity against RCC target cells using end-point cytotoxicity assays and IncuCyte.

Results CISH gene-knockout CD70-CAR NK cells could be produced efficiently and exhibited extended persistence in culture. After engineering and expansion, CD70-CAR transduction efficiency was 60–80%. CD70-CAR NK cells displayed potent cytotoxicity against CD70-expressing renal cancer derived cell lines. Interestingly, cytotoxicity assays demonstrated that CISH gene-knockout CD70-CAR NK cells were partially resistant to TGF β and adenosine inhibition of cytotoxicity. Furthermore, CISH gene-knockout CD70-CAR NK cells maintained their activity during prolonged culture.

Conclusions In summary, we show CISH gene-knockout CD70-CAR NK cells demonstrate potent anti-tumor activity against relevant solid tumor cell lines and partially provide resistance to tumor microenvironment inhibition. These data support the further exploration of CISH gene-knockout CD70 CAR NK cells for clinical application.

<http://dx.doi.org/10.1136/jitc-2021-SITC2021.113>

AN NFAT PROMOTER BASED FLUORESCENT JURKAT CELL PLATFORM FOR HIGH-THROUGHPUT SCREENING OF CHIMERIC ANTIGEN RECEPTOR (CAR) CONSTRUCTSBrikena Gjenci*, Sadik Kassim, Julian Scherer. *Vor Biopharma, Cambridge, MA, USA*

Background CAR T-cells have exhibited efficacious treatment of hematological malignancies, such as Acute Myeloid Leukemia (AML). Upon antigen binding, CARs initiate Ca²⁺-dependent signaling pathways, leading to an increased intracellular concentration of nuclear factor of activated T cells (NFAT), which stimulates downstream T cell effector functions.^{1 2} However, an objective high-throughput platform to compare CAR-induced T cell activity has been lacking. Here, we report on a CAR screening platform that utilizes an NFAT-sensitive promoter driving fluorescent protein expression in Jurkat T cells. This approach, termed 'IL-2 Reporter System' (IRS), is employed for the identification of functional CD33CARs to improve AML CAR T-cell therapies.

Methods Lentiviral transduction of two fluorescent proteins (mOrange2 and mTurquoise2) under either the constitutively active EF1alpha (FP1) or the NFAT-sensitive minimal IL-2 promoter (FP2) into Jurkat cells resulted in two IRS cell lines. IRS cell function was confirmed by treatment with phorbol myristate acetate (PMA) and ionomycin to induce activation and thus the expression of FP2. To screen CARs with previously described potential in AML therapy, IRS cells were transduced with eight distinct CD33CAR constructs and cocultured with CD33+ cells (MOLM13-WT) and CD33 knock-out (MOLM13-CD33KO) cells. IRS cell analysis was performed using flow cytometry, fluorescent microscopy, and IncuCyte live cell imaging.

Results As expected, live cell fluorescence imaging revealed that PMA/ionomycin treatment induced expression of FP2. Peak expression occurred at 12–15 hours post-treatment and consistent, high FP2 signal was detected for 24h in both cell lines. Flow cytometry analysis 24hr post treatment determined that 60–80% of transduced IRS cells expressed FP2. Normalized FP2 expression was comparable between both IRS cell lines but varied across the eight CD33CARs. Six of the eight CD33CAR constructs resulted in significant increases (up to 8-fold) in FP2 signal upon exposure to CD33+ cells compared to control CD33KO cells.

Conclusions Our results indicate that IRS cells can be used as an objective, fast, and reliable reporter system for CD33CAR activity. The constitutively expressed FP1 eliminates false negative outcomes and verifies successful transduction of the reporter construct. FP2 expression, driven only in activated cells, represents antigen recognition by and activity of the CAR. Importantly, the use of IRS cells is not restricted to just CD33CARs but provides a platform for CAR and recombinant TCR screenings against any antigen. Additionally, efforts are underway to adapt this platform entirely to microplates and a liquid handling system, allowing for high-throughput screens of several AML-targeting CAR constructs.

REFERENCES

1. Hogan PG. Calcium–NFAT transcriptional signaling in T cell activation and T cell exhaustion. *Cell Calcium* 2017;**63**:66–9.
2. Chow C-W, Rincón Mercedes, Davis RJ. Requirement for Transcription Factor NFAT in Interleukin-2 Expression. *Molecular and Cellular Biology* 1999;**19**(3):2300–7.

<http://dx.doi.org/10.1136/jitc-2021-SITC2021.115>

DEVELOPMENT OF LOGIC GATED CAR-NK CELLS FOR THE TREATMENT OF SOLID TUMORS

Alba Gonzalez Junca*, Nicholas Frankel, Marcus Gainer, Alyssa Mullenix, Miguel Palermo, Derrick Lee, Frances Liu, Russell Gordley, Chen-Ting Lee, Assen Roguev, Niran Almudhfar, Mengxi Tian, Gary Lee. *Senti Biosciences, Inc., South San Francisco, CA, USA*

Background CAR-based therapies have transformed the treatment of several cancers, but this progress has not translated into solid tumors. One challenge of CAR-mediated therapies for solid tumors is the lack of specific tumor-associated antigens (TAA's) that are only expressed on cancer cells and not on healthy cells, thereby posing a risk for on-target off-tumor toxicities. This presents a unique opportunity to use Logic Gates to expand the universe of cancer targets that may be treated with CAR-based cell therapies. CEA, a widely expressed tumor antigen, found in >90% of colorectal cancer (CRC), is also expressed in healthy gastrointestinal and lung epithelial cells. Clinical experience targeting CEA resulted in severe dose-limiting toxicities,^{1,2} highlighting the need for healthy tissue protection. Logic-gated gene circuits can prevent off-tumor toxicities by pairing a CEA activating-CAR (aCAR) with an inhibitory-CAR (iCAR) that recognizes a safety antigen (SA) uniquely expressed in healthy epithelial cells.

Methods We developed a bioinformatics-driven antigen paired discovery platform using single-cell transcriptomics to discover and prioritize TAA's and pair them with SA's that are selectively expressed on the membrane of healthy cells. TAA's and SA's were validated in primary cancer and healthy tissue samples using IHC. We constructed aCAR/iCAR gene circuits and tested their function in NK cells.

Results Our bioinformatics platform identified VSIG2 to be co-expressed with CEA in healthy gastrointestinal and lung epithelial cells. IHC confirmed the expression of VSIG2 on the membrane of healthy colon (N=72 samples) and lung (N=24 samples) epithelial cells. Using our Design-Build-Test-Learn platform, we screened >250 CAR constructs targeting CEA. CAR-NK cells were generated and tested for anti-tumor activity against CRC CEA+ cells and lead candidates were selected based on NK cell performance. A single dose of CEA-CAR-NK cells had anti-tumor activity in a human CRC xenograft model, reducing tumor burden in >33% of the treated mice. We identified iCARs with different intracellular domains derived from native domains containing immunoreceptor tyrosine-based inhibitory motifs. These iCARs suppressed >50% of aCAR-mediated killing ($p < 0.05$) and significantly reduced TNF α secretion ($p < 0.0005$) in a SA-specific manner.

Conclusions We are developing Logic-Gated CAR-NK cell therapies aimed at reducing on-target off-tumor toxicities, to spare healthy cells in a SA-dependent manner. SENTI-401 will focus on targeting CEA+ CRC tumors with a NOT gate that recognizes the SA VSIG2 in the colon and lungs.

REFERENCES

1. Parkhurst M, et al. T cells targeting carcinoembryonic antigen can mediate regression of metastatic colorectal cancer but induce severe transient colitis. *Mol Ther* 2011; Mar; **19**(3):620–6.
2. Thistlethwaite FC, et al. The clinical efficacy of first-generation carcinoembryonic antigen (CEACAM5)-specific CAR T cells is limited by poor persistence and transient pre-conditioning-dependent respiratory toxicity. *Cancer Immunol Immunother* 2017 Nov; **66**(11):1425–1436.

<http://dx.doi.org/10.1136/jitc-2021-SITC2021.116>

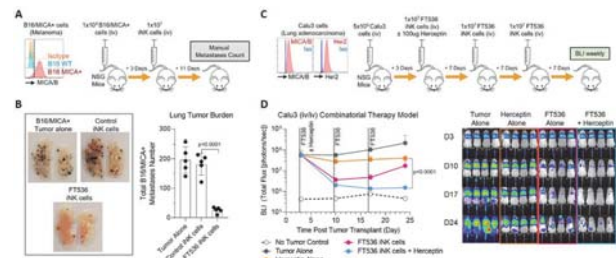
FT536 PATH TO IND: UBIQUITOUS TARGETING OF SOLID TUMORS WITH AN OFF-THE-SHELF, FIRST-OF-KIND MICA/B-SPECIFIC CAR-INK CELLULAR IMMUNOTHERAPY

¹John Goulding, ¹Bryan Hancock*, ¹Robert Blum, ¹Moyar Ge, ¹Svetlana Gaidarova, ¹Paul Rogers, ¹Sajid Mahmood, ¹Rina Mbofung, ¹Wen-I Yeh, ¹Bi-Huei Yang, ¹Chia-Wei Chang, ¹Brian Groff, ¹Soheila Shirinbak, ¹Joy Grant, ¹Martin Hosking, ¹Mochtar Pribadi, ¹Yijia Pan, ¹Hui-Yi Chu, ¹Shohreh Sikaroodi, ¹Lauren Fong, ¹Nicholas Brookhouser, ¹Fernanda Rodrigues Cugola, ¹Ramzey Abujarour, ¹Janel Huffman, ¹Pei-Fang Tsai, ¹Antonio Fernandez-Perez, ¹Karina Palomares, ¹Natalie Marquez-Solorzano, ¹Riya Kanherkar, ¹Andrew Burns, ¹Aidan Keefe, ¹Samvel Nazaretyan, ¹Christine Chen, ¹Raedun Clarke, ¹Thomas Dailey, ¹Miguel Meza, ¹Jason O'Rourke, ¹Jerome Bressi, ¹Tom Lee, ¹Ryan Bjordahl, ²Lucas Ferrari de Andrade, ³Kai Wucherpfennig, ¹Bahram Valamehr. ¹Fate Therapeutics, San Diego, CA, USA; ²Icahn School of Medicine at Mount Sinai, New York, NY, USA; ³Dana-Farber Cancer Institute, Boston, MA, USA

Background Chimeric antigen receptor (CAR)-T cell therapy has revolutionized cancer treatment, but it is associated with significant dose-limiting toxicities, restricted tumor targeting (limited by specific antigen expression), and, notably, a lack of multi-antigen targeting capability to mitigate tumor associated immune evasion and heterogeneity. Furthermore, dysfunctional starting material, product inconsistency, and small manufacturing lot size limits the application and on-demand availability of CAR-T cell therapy.

Methods To overcome these considerable limitations, we have developed FT536, a first-of-kind, induced pluripotent stem cell (iPSC)-derived NK (iNK) cell with a novel CAR that ubiquitously targets cancer cells through canonical stress ligand recognition. We have previously reported FT536 recognizes the conserved $\alpha 3$ domain of the pan-tumor associated antigens MICA and MICB (MICA/B), and is derived from a renewable master iPSC line that contains multiplexed genetic edits to enhance effector cell functionality, persistence, and multi-antigen targeting capabilities via high affinity non cleavable CD16 (hnCD16) mediated antibody dependent cellular cytotoxicity (ADCC). Here we preview the nonclinical study for the investigational new drug (IND) application for FT536.

Results Utilizing a manufacturing process analogous to pharmaceutical drug product development, we demonstrate FT536 can be consistently and uniformly produced with a greater than 4×10^7 fold cellular expansion per manufacturing campaign. Furthermore, FT536 can be cryopreserved at clinical scale to support off-the-shelf clinical application, with rapid product thaw and immediate patient infusion in an out-patient setting. Functional evaluation demonstrated that FT536 uniquely possesses potent and persistent antigen specific cytolytic activity against an array of solid and hematological tumor lines. Through its hnCD16 modality, FT536 can be utilized in combination with monoclonal antibodies to provide multi-antigen targeting capabilities and in conjunction with chemotherapeutics and/or radiation that augment surface MICA/B expression. In addition, directly thawed and infused FT536 demonstrated significant tumor growth inhibition in multiple solid and liquid in vivo xenograft models, in which tumor control was further enhanced in combination with a therapeutic antibody (figure 1). Finally, ongoing studies utilizing a lung adenocarcinoma model have highlighted the sustained persistence of FT536 in lung tissue up to 33 days following a single dose infusion without the need for exogenous cytokine support.



Abstract 117 Figure 1 FT536 provides statistically significant in vivo anti-tumor activity which is enhanced in combination with ADCC active monoclonal antibody therapy. (A-B) FT536 significantly reduced the number of lung and liver (not shown) metastases compared to CAR negative iNK control cells in a murine metastatic melanoma model using B16-F10 cells engineered to overexpress human MICA. (C-D) FT536 alone, and in combination with Herceptin, demonstrate significant tumor growth inhibition (TGI) compared to Herceptin alone in an orthotopic xenograft model of human lung adenocarcinoma.

Conclusions Collectively, these studies demonstrate that FT536 is a highly potent, multi-tumor targeting CAR-iNK cell product that is uniform in composition and can be effectively and safely used off-the-shelf for on-demand treatment of multiple solid and hematological malignancies. An IND submission is planned for 2021, with an initial Phase 1 clinical trial to follow.

<http://dx.doi.org/10.1136/jitc-2021-SITC2021.117>

118 DEVELOPMENT OF CLAUDIN 18.2 TAC T CELLS FOR THE TREATMENT OF GASTRIC CANCER

Christopher Helsen*, Tania Benatar, IP Philbert, Stacey Xu, Laura Shaver, Thanyashanthi Nitya-Nootan, Andreas Bader, Prabha Lal. *Triumvira Immunologics, Hamilton, Canada*

Background The T cell antigen coupler (TAC) is a novel, proprietary chimeric receptor that facilitates the re-direction of T cells to tumor cells and activates T cells by co-opting the endogenous T cell receptor complex with the goal to elicit a safe and durable anti-tumor response. In preclinical models of cancer, TAC-engineered T cells effectively eradicate tumor cells in vitro and in vivo without TAC-related toxicities. TAC01-HER2, a first-in-class TAC T product targeting HER2 (ERBB2), has recently entered a phase I/II clinical trial in patients with HER2-positive solid tumors. Here, we present the development of a new TAC T product targeting Claudin 18.2 (CLDN18.2) to treat gastric cancer. CLDN18.2 belongs to a family of Claudin tight junction proteins whose expression is naturally exclusive to normal stomach. In gastric cancer cells, however, cell polarity is perturbed, leading to tumor-selective surface expression of CLDN18.2. Thus, CLDN18.2 is a preferred antigen for the specific targeting of tumor cells via TAC T cells.

Methods The functionality of the CLDN18.2-TAC receptor was characterized using a variety of in vitro and in vivo assays. In vitro assays were based on flow cytometric analysis of TAC surface staining and cytokine release. Cytotoxicity was assessed via luminescence-based co-culture assays and real-time microscopy. In vivo studies examined the anti-tumor effect of TAC-engineered T-cells against established CLDN18.2 expressing tumor xenografts.

Results T cells virally transduced with the CLDN18.2-TAC transgene demonstrated satisfactory surface expression of the TAC receptor and showed increased cytokine production when activated by CLDN18.2 expressing target cells in vitro. Secretion of IL2, IFN γ and TNF α were comparable with cytokine levels produced by activated HER2-TAC T cells used as a positive control. In vitro cytotoxicity assays demonstrated a strong anti-CLDN18.2 response and killing of CLDN18.2 expressing target cell lines. No increases in cytokine levels and no cytotoxicity were observed in non-transduced T cells and CLDN18.2-TAC T cells co-cultured with CLDN18.2-negative target cells, indicating that the T cell response is specific to the CLDN18.2 antigen. Intravenous administration of CLDN18.2-TAC T cells in mice carrying CLDN18.2-positive tumor xenografts led to a sustained anti-tumor response.

Conclusions The in vitro and in vivo data confirm strong and specific activity of CLDN18.2-targeted TAC T cells against CLDN18.2-expressing cancer cells and highlight the versatility of the TAC platform for therapeutic applications in solid tumors.

<http://dx.doi.org/10.1136/jitc-2021-SITC2021.118>

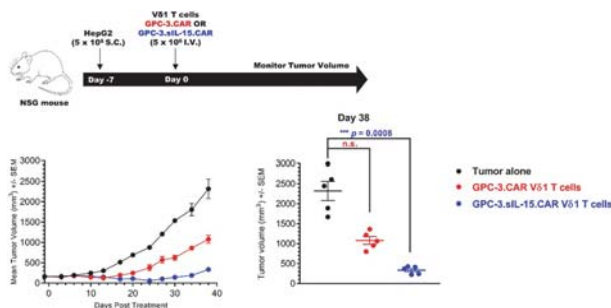
119

ADI-002: AN IL-15 ARMORED ALLOGENEIC 'OFF-THE-SHELF' V δ 1 GAMMA DELTA CAR T CELL THERAPY FOR SOLID TUMORS TARGETING GLYPICAN-3 (GPC3)

Amani Makkouk, Xue (Cher) Yang, Taylor Barca, Anthony Lucas, Mustafa Turkoz, Jonathan Wong, Kevin Nishimoto, Mary Brody, Maryam Tabrizi, Smitha Gundurao, Lu Bai, Arun Bhat, Zili An, Stewart Abbot, Daulet Satpayev, Marissa Herrman*. *Adicet Therapeutics, South San Francisco, CA, USA*

Background Glypican-3 (GPC-3) is an oncofetal protein that is highly expressed in various solid tumors including hepatocellular carcinoma (HCC) but is rarely expressed in healthy adult tissues and serves as a therapeutic target of interest. Autologous $\alpha\beta$ chimeric antigen receptor (CAR) T cell therapy has established clinical benefit in hematologic malignancies but limited success in solid tumors due to numerous challenges including poor T cell homing, heterogenous antigen expression, and hostile tumor microenvironments.¹ These challenges may be overcome by the V δ 1 subset of gamma delta T cells due to their natural peripheral tissue tropism and ability to recognize and kill tumor cells through MHC-independent antigens upregulated under stress.² Allogeneic V δ 1 T cells engineered with CARs can have enhanced intrinsic antitumor activity and overcome challenges of allogeneic $\alpha\beta$ T cells, including graft-versus-host disease (GvHD). Here, we describe the first preclinical evaluation of ADI-002, a next-generation allogeneic CAR V δ 1 T cell therapy targeting GPC-3 and armored with IL-15, for the treatment of solid tumors.

Methods V δ 1 T cells were expanded from healthy donor PBMCs and transduced to express a 4-1BB/CD3z CAR against GPC-3 that encodes constitutively-secreted IL-15 (sIL-15), which we hypothesized could sustain proliferation and antitumor activity of intratumoral GPC-3.CAR V δ 1 T cells. In vitro characterization included co-culture with HCC targets expressing high (HepG2) and low (PLC/PRF/5) GPC-3, phenotypic analysis by flow cytometry, and cytokine production by multiplexed immunoassay. For in vivo assessment, immunodeficient NSG mice were subcutaneously injected with HepG2 tumor cells and treated with a single dose of GPC-3.CAR V δ 1 T cells. Tissues were harvested 7 days post transfer and analyzed for V δ 1 T cell tissue homing and proliferation, or at study end and analyzed for GvHD by immunohistochemistry.



Abstract 119 Figure 1 In vivo antitumor efficacy in a subcutaneous HepG2 tumor model in NSG mice

Results GPC-3.sIL-15.CAR V δ 1 T cells expanded over 10,000-fold and routinely reached >80% purity. Expanded V δ 1 T cells showed a primarily naïve-like phenotype (CD45RA⁺CD27⁺) with minimal exhaustion receptor expression and

displayed robust proliferation, cytokine production, and cytotoxic activity against HCC cell lines in vitro. In vivo, GPC-3.sIL-15.CAR V δ 1 T cells primarily accumulated and proliferated in tumors, and a single dose could efficiently control tumor burden without causing GvHD. When compared to GPC-3.CAR V δ 1 T cells lacking sIL-15, GPC-3.sIL-15.CAR V δ 1 T cells displayed greater tumor-specific proliferation that resulted in enhanced tumor control (figure 1).

Conclusions Expanded V δ 1 T cells engineered with GPC-3.CAR and sIL-15 represent a promising approach for safe and effective off-the-shelf treatment of HCC and support further investigation in the clinical setting.

REFERENCES

1. Labanieh L, Majzner RG, Mackall CL. Programming CAR-T cells to kill cancer. *Nat Biomed Eng* 2018;**2**(6):377–91.
2. Sebestyen Z, Prinz I, Déchanet-Merville J, Silva-Santos B, Kuball J. Translating gammadelta ($\gamma\delta$) T cells and their receptors into cancer cell therapies. *Nat Rev Drug Discov* 2020;**19**(3):169–84.

Ethics Approval All mouse experiments were performed in accordance with the Guide for the Care and Use of Laboratory Animals and followed all institutional and national guidelines and after appropriate approvals.

<http://dx.doi.org/10.1136/jitc-2021-SITC2021.119>

CHEMOKINE RECEPTOR ENGINEERING ENHANCES TRAFFICKING AND HOMING OF PRIMARY AND IPSC-DERIVED CAR-T CELLS TO SOLID TUMORS

Martin Hosking*, Soheila Shirinbak, Joy Grant, Yijia Pan, Angela Gentile, Amit Mehta, Bjoern Gaertner, Bishwas Shrestha, Mochtar Pribadi, Jason ORourke, Alec Witty, Tom Lee, Bob Valamehr. *Fate Therapeutics, Inc., San Diego, CA, USA*

Background Chimeric antigen receptor (CAR)-T cells for solid tumors have shown modest effectiveness as compared to hematologic malignancies, a consequence of antigen heterogeneity, the immuno-suppressive tumor microenvironment (TME), limited cell persistence, and perhaps most notably, the trafficking of the CAR-T cell to the tumor itself. Early detection of CAR-T cells within a solid tumor has been associated with better outcomes across several clinical trials in diverse tumor settings, suggesting that strategies focused on enhancing CAR-T cell homing to and infiltration into the tumor can yield therapeutic benefit.

Methods Here, we demonstrate that following irradiation or exposure to common chemotherapy drugs, selected tumor cell lines (breast, ovarian, and prostate) specifically upregulate several chemokines, notably the CXCR2 ligand, interleukin (IL)-8, up to 4-fold over baseline control (e.g. 24ng/ml increased to 79ng/ml for SKOV3; 2.9ng/ml increased to 12.5ng/ml for MDA-MB-231). To leverage the upregulation of IL-8 as a mechanism of directing CAR-T cells to the tumor site, we initially engineered primary CAR-T cells to express CXCR2 and demonstrated functional migration, in a dose-dependent manner, to recombinant IL-8 in an in vitro transwell chemotaxis assay; maximal migration of approximately 2-fold over baseline was observed with 10ng/ml of rhIL-8. Similarly, supernatant from pre-conditioned tumor lines also elicited functional enhancements in migration (up to 4-fold specific migration). In addition, ovarian tumors were sub-optimally treated with paclitaxel in vivo, which promoted infiltration of CXCR2+ CAR-T cells and demonstrated enhanced tumor control.

Results We then incorporated these findings into our off-the-shelf, iPSC-derived CAR-T cell product platform. Induced pluripotent stem cells (iPSCs) were precisely engineered to co-express CAR and CXCR2 and subsequently differentiated to T cells to generate iPSC-derived CAR-T cells (CAR-iT cells). Like their primary CAR-T cell counterparts, functional chemotaxis of CXCR2+ CAR-iT cells was also observed in response to recombinant IL-8 and preconditioned tumor media. Importantly, CXCR2 expression did not limit CAR-dependent cytolytic function and the specificity of CAR-iT cells, underscoring the compatibility of this approach. Further in vitro and in vivo studies are ongoing and will be presented.

Conclusions Collectively, these data demonstrate that rational engineering of unique chemokine receptors to deliver the ideal chemokine/chemokine receptor match between tumors and effector cells can be leveraged to enhance tumor targeting and trafficking of CAR-iT cells for more effective treatment of solid tumors.

Ethics Approval These studies were approved by Fate Therapeutics Institutional Animal Care and Use Committee and were carried out in accordance with the National Institutes of Health's Guide for the Care and Use of Laboratory Animals.

<http://dx.doi.org/10.1136/jitc-2021-SITC2021.120>

ICAM-1-SPECIFIC AFFINITY TUNED CAR T CELLS EXPRESSING SSTR2 FOR REAL-TIME IMAGING

¹Jingmei Hsu, ²Eric von Hofe*, ¹Michael Hsu, ¹Koen Van Besien, ¹Thomas Fahey, ¹Jana Ivanidze, ²Janusz Puc, ²Karrie Du, ¹Moonsoo Jin. ¹Weill Cornell Medicine, New York, NY, USA; ²AffyImmune Therapeutics, Natick, MA, USA

Background The use of CAR T cells for solid tumors has a number of challenges, such as lack of tumor-specific targets, CAR T cell exhaustion, and the immunosuppressive tumor microenvironment. To address these challenges, AffyImmune has developed technologies to affinity tune and track CAR T cells in patients. The targeting moiety is affinity tuned to preferentially bind to tumor cells overexpressing the target while leaving normal cells with low basal levels untouched, thereby increasing the therapeutic window and allowing for more physiological T cell killing. The CAR T cells are designed to express SSTR2 (somatostatin receptor 2), which allows for the tracking of CAR T cells *in vivo* via PET/CT scan using FDA-approved DOTATATE.

Methods AIC100 was generated by affinity tuning the I-domain of LFA-1, the physiological ligand to ICAM-1. Various mutants with 10⁶-fold difference in affinity were evaluated for affinity. This allowed structure activity relationships to be conducted using CAR T cells expressing the various affinity mutants against targets with varying antigen densities. The variant with micromolar affinity was clearly the most effective in non-clinical animal models. AIC100 is currently being evaluated to assess safety, CAR T expansion, tumor localization, and preliminary activity in patients with advanced thyroid cancer in a phase I study (NCT04420754). Our study uses a modified toxicity probability interval design with three dosage groups of 10 x 10⁶, 100 x 10⁶, and 500 x 10⁶ cells.

Results Preclinical studies demonstrated greater *in vivo* anti-tumor activity and safety with lower affinity CAR T cells. A single dose of AIC100 resulted in tumor elimination and significantly improved survival of animals. AIC100 activity was confirmed in other high ICAM-1 tumor models including breast, gastric, and multiple myeloma. In a Phase I patient given 10-million CAR T cells, near synchronous imaging of FDG and DOTATATE revealed preliminary evidence of transient CAR T expansion and tumor reduction at multiple tumor lesions, with the peak of CAR T density coinciding with the spike in CAR T numbers in blood.

Conclusions We have developed affinity tuned CAR T cells designed to selectively target ICAM-1 overexpressing tumor cells and to spatiotemporally image CAR T cells. Near-synchronous FDG and DOTATATE scans will enhance patient safety by early detection of off-tumor CAR T activity and validation of tumor response. We anticipate that our ‘tune and track’ technology will be widely applicable to developing potent yet safe CAR T cells against hard-to-treat solid cancers.

Trial Registration NCT04420754

Ethics Approval

IRB number 19-12021154IACUC (animal welfare): All animal experiments were performed in accordance with the National Institute of Health’s Guide for the Care and Use of Laboratory Animals. Animal handling protocols were approved by the Institutional Laboratory Animal Use and Care Committee of Weill Cornell Medicine (Permit Number: 2012–0063).

<http://dx.doi.org/10.1136/jitc-2021-SITC2021.121>

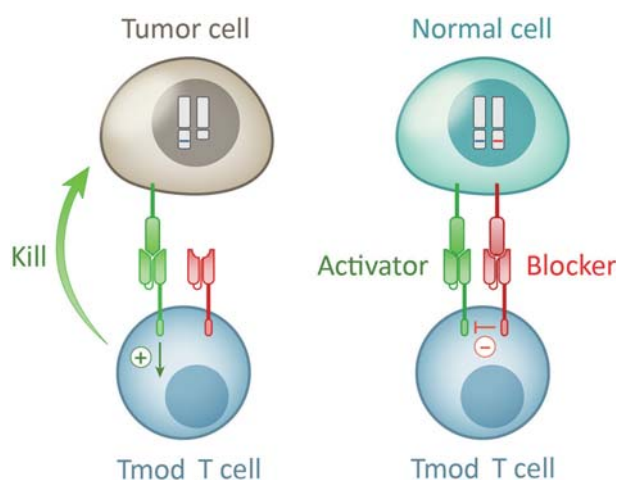
A POWERFUL, PRECISE TARGETING SYSTEM CONTROLLED BY TUMOR DELETIONS TRANSFORMS CEA AND MSLN CAR-T CELLS INTO TUMOR-SELECTIVE AGENTS

Agnes Hamburger, Han Xu, Yuta Ando, Grace Asuelime, Kristian Bolanos-Ibarra, Mark Daris, Kiran Deshmukh, Breanna DiAndreth, Fernando Fisher, Grant Gabrelow, Maria Imun, David Ju, Wen-Hua Lee, Chuck Li, Edwin Liu, Aaron Martin, Michele Mcelvain, Jee-Young Mock, Daniel Nampe, Martin Naradikian, Mark Sandberg, Sanam Shafaattalab, Shruti Sharma, Talar Tokatlian, Dora Toledo-Warshaviak, Xueyin Wang, Lu-Min Wong, Alexander Kamb*. *A2 Biotherapeutics, Agoura Hills, CA, USA*

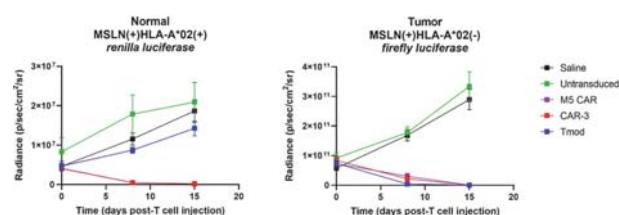
Background Mesothelin (MSLN) and carcinoembryonic antigen (CEA) are classic tumor-associated antigens that are expressed in many solid tumors including the majority of lung, colorectal and pancreatic cancers. However, both MSLN and CEA are also expressed in vital normal organs. This normal expression creates risk of serious inflammation for CEA- or MSLN-directed therapeutics. To date all active CEA- or MSLN-targeted investigational therapeutics have been toxic when administered systemically.

Methods We have developed a safety mechanism to protect normal tissues without abrogating sensitivity of cytotoxic T cells directed at MSLN(+) or CEA(+) tumors in a subset of patients with defined loss of heterozygosity (LOH) in their tumors (figure 1). This dual-receptor (Tmod^{>TM}) system exploits common LOH at the HLA locus in cancer cells, allowing T cells to recognize the difference between tumor and normal tissue.^{1 2} T cells engineered with specific Tmod constructs contain: (i) a MSLN- or CEA-activated CAR; and, (ii) an inhibitory receptor gated by HLA-A*02. HLA-A*02 binding blocks T cell cytotoxicity, even in the presence of MSLN or CEA. The Tmod system is designed to treat heterozygous HLA class I patients, selected for HLA LOH. When HLA-A*02 is absent from tumors selected for LOH, the CARs are predicted to mediate potent killing of the A*02(-) malignant cells.

Results The Tmod system robustly protects surrogate normal cells even in mixed-cell populations in vitro while mediating robust cytotoxicity of tumor cells in xenograft models (see example in figure 2). The MSLN CAR can also be paired with other blockers, supporting scalability of the approach to patients beyond HLA-A*02 heterozygotes.



Abstract 122 Figure 1 Illustration of the Tmod T cell engaging with tumor cells with somatic loss of HLA-A*02 and with normal cells.



Abstract 122 Figure 2 Bioluminescence measurements show the average difference between the size of the MSLN(+)/A*02(+) 'normal' graft compared to the MSLN(+)/A*02(-) tumor graft on the two flanks of mice after T cell infusion. Both tumor and normal grafts are destroyed by CAR-Ts (CAR-3 and M5 benchmark) while the MSLN Tmod cells kill the tumor but not the normal graft.

Conclusions The Tmod mechanism may provide an alternative route to leverage solid-tumor antigens such as MSLN and CEA in safer, more effective ways than previously possible.

REFERENCES

- Hamburger AE, DiAndreth B, Cui J, et al. Engineered T cells directed at tumors with defined allelic loss. *Mol Immunol* 2020;**128**:298–310.
- Hwang MS, Mog BJ, Douglass J, et al. Targeting loss of heterozygosity for cancer-specific immunotherapy. *Proc Natl Acad Sci U S A* 2021;**118**(12): e2022410118.

<http://dx.doi.org/10.1136/jitc-2021-SITC2021.122>

P-MUC1C-ALLO1: A FULLY ALLOGENEIC STEM CELL MEMORY T CELL (TSCM) CAR-T THERAPY WITH BROAD POTENTIAL IN SOLID TUMOR

Yan Zhang*, Anna Kozłowska, Jacqueline Fritz, Yingying Zhao, Claudia Palomino La Torre, Stacey Cranert, Steven Wang, Rebecca Codde, Elvira Argus, Samad Ibitokou, Vanitra Richardson, Sumiti Jain, Maximilian Richter, Deepak Patil, Yening Tan, Min Tong, Lu Yao, Majid Ghoddusi, Eric Ostertag, Julia Coronella, Devon Shedlock. *Poseida Therapeutics, Inc, San Diego, CA, USA*

Background While CAR-T have demonstrated potent activity against hematologic tumors, less success has been seen with solid tumors. Here we report generation of TSCM-enriched allogeneic MUC1-C-specific CAR T cells, P-MUC1C-ALLO1, with potential for a broad range of solid tumors. The proliferative capacity and metabolic profile of TSCM CAR-T are well-suited to activity in the solid tumor setting. MUC1 is comprised of an N-terminal subunit (MUC1-N) tethered to a C-terminal subunit (MUC1-C), forming a stable complex on the cell surface. During tumorigenesis, MUC1 becomes both over-expressed and hypo-glycosylated on many carcinomas. Furthermore, MUC1 undergoes proteolytic cleavage in the tumor microenvironment, leaving behind a proteolytic ‘stump’ of MUC1-C that is over-represented in cancer, making it an attractive therapeutic target.

Methods P-MUC1C-ALLO1 is manufactured using the piggy-Bac[®] DNA Delivery System for CAR insertion and the Cas-CLOVER[™] Gene Editing System to knockout both the TCR and MHC class I proteins. The addition of a selectable marker within the transposon allows for selection of a fully CAR-positive population while any residual TCR-positive cells are removed at the end of production to prevent TCR-mediated GvHD. Lastly, inclusion of a proprietary ‘booster molecule’ in our allogeneic process further improves cell expansion, along with phenotype and function, and enables the production of up to hundreds of patient doses from a single manufacturing run.

Results Significant doses of P-MUC1C-ALLO1 products made from multiple healthy donors were achieved and comprised of an exceptionally high-percentage of desirable TSCM cells. Pre-clinical evaluation of these products showed potent tumor killing and cytokine secretion against MUC1-C-positive breast and ovarian tumor cell lines. P-MUC1C-ALLO1 demonstrates potent cytotoxicity against tumor cells, and minimal killing of normal MUC1-C-positive human primary cells. In a triple negative breast cancer xenograft model, MUC1C CAR-T eliminated established MDA-MB-468 tumor cells, mounted robust T cell expansion in peripheral blood and maintained a favorable TSCM percentage over time. Likewise, in an orthotopic ovarian cancer xenograft model, intraperitoneally administered MUC1C CAR-T eliminated established OVCAR3 cells to levels below the limit of detection. All together, these data demonstrated the efficacy of the MUC1C CAR-T cells and the robustness of the allogeneic platform.

Conclusions P-MUC1C-ALLO1 is an allogeneic TSCM CAR-T therapy that has a potential to treat multiple MUC1-expressing indications. P-MUC1C-ALLO1 displayed specificity for tumor vs. normal cells as well as in vivo efficacy against xenograft models of breast and ovarian cancer. This allogeneic cell therapy is advancing rapidly towards the clinic.

<http://dx.doi.org/10.1136/jitc-2021-SITC2021.123>

FUNCTIONALIZING CAR T CELLS FOR SELECTIVE PROLIFERATION AND DUAL-TARGETING USING THE MEDITOPE TECHNOLOGY

Cheng-Fu Kuo*, Yi-Chiu Kuo, Miso Park, Zhen Tong, Brenda Aguilar, Agata Xella, Vanessa Salvary, Stephen Forman, John Williams, Christine Brown. *City of Hope, Duarte, CA, USA*

Background Meditope is a small cyclic peptide that was identified to bind to cetuximab within the Fab region. The mediotope binding site can be grafted onto any Fab framework, creating a platform to uniquely and specifically target monoclonal antibodies. Here we demonstrate that the mediotope binding site can be grafted onto chimeric antigen receptors (CARs) and utilized to regulate and extend CAR T cell function. We demonstrate that the platform can be used to overcome key barriers to CAR T cell therapy, including T cell exhaustion and antigen escape.

Methods Meditope-enabled CARs (meCARs) were generated by amino acid substitutions to create binding sites for mediotope peptide (meP) within the Fab tumor targeting domain of the CAR. meCAR expression was validated by anti-Fc FITC or meP-Alexa 647 probes. In vitro and in vivo assays were performed and compared to standard scFv CAR T cells. For meCAR T cell proliferation and dual-targeting assays, the mediotope peptide (meP) was conjugated to recombinant human IL15 fused to the CD215 sushi domain (meP-IL15:sushi) and anti-CD20 monoclonal antibody rituximab (meP-rituximab).

Results We generated meCAR T cells targeting HER2, CD19 and HER1/3 and demonstrate the selective specific binding of the mediotope peptide along with potent meCAR T cell effector function. We next demonstrated the utility of a meP-IL15:sushi for enhancing meCAR T cell proliferation in vitro and in vivo. Proliferation and persistence of meCAR T cells was dose dependent, establishing the ability to regulate CAR T cell expansion using the mediotope platform. We also demonstrate the ability to redirect meCAR T cells tumor killing using meP-antibody adaptors. As proof-of-concept, meHER2-CAR T cells were redirected to target CD20+ Raji tumors, establishing the potential of the mediotope platform to alter the CAR specificity and overcome tumor heterogeneity.

Conclusions Our studies show the utility of the meCAR platform for overcoming key challenges for CAR T cell therapy by specifically regulating CAR T cell functionality. Specifically, the meP-IL15:sushi enhanced meCAR T cell persistence and proliferation following adoptive transfer in vivo and protects against T cell exhaustion. Further, meP-rituximab can redirect meCAR T cells to target CD20-tumors, showing the versatility of this platform to address the tumor antigen escape variants. Future studies are focused on conferring additional 'add-on' functionalities to meCAR T cells to potentiate the therapeutic effectiveness of CAR T cell therapy.

<http://dx.doi.org/10.1136/jitc-2021-SITC2021.124>

CO-OPTING IL-8 TO ENHANCE EFFICACY OF B7H3 CAR T CELLS AGAINST PEDIATRIC SARCOMA

Jessica Lake*, ²Kevin Winkler, ²Alexander Harrant, ²Ashley Yingst, ²Kristin Schaller, ²Eric Hoffmeyer, ²Madeline Larson, ²Dejene Tufa, ²Laura Cobb, ²Dallas Jones, ²Michael Verneris. ¹University of Colorado Anschutz Medical Campus, Aurora, CO, USA; ²University of Colorado, Aurora, CO, USA

Background The 5-year disease-free survival for children and young adults with metastatic sarcoma at diagnosis or recurrent disease after front-line therapy is 20–30%.^{1–2} Cellular immunotherapy using chimeric antigen receptor (CAR) T cells has shown dramatic benefits in leukemia, but only limited success in solid tumors.^{3–4} One limitation of CAR T cell therapy has been poor trafficking into solid tumors.^{5–7} Chemokines are small, secreted, cytokine-like molecules that mediate lymphocyte homing and migration.⁸ In this study, we discovered that both osteosarcoma (OS) and rhabdomyosarcoma (RMS) cells significantly increase expression of the chemokine IL-8 after clinically achievable doses of radiation, but not at rest. Given that CAR T cells do not express the receptor for IL-8, we created a construct with an IL-8 receptor (CXCR2) and a B7H3 CAR in T cells to improve CAR T homing and to create an effective new immunotherapy for patients with sarcoma.

Methods Multiple OS and RMS cell lines were irradiated at 10 Gy and IL-8 was measured by ELISA. We created retroviral constructs, B7H3 CAR-T2a-CXCR2 and B7H3 CAR. Peripheral blood T lymphocytes were stimulated with IL-2 and anti-CD3/28 antibodies for 48 hours prior to transduction with the retroviral vectors. Surface expression of the scFv (by L protein) and CXCR2 (mAb) were assessed using flow cytometry. In vitro cytotoxicity assays using sarcoma tumor spheroids were conducted using Incucyte. INF- γ and IL-2 production were measured by ELISA. NSG mice injected orthotopically with an IL-8 overexpressing RMS cell line were treated 4–7 days later with the B7H3 CAR-CXCR2 T cells or B7H3 T cells (control) and followed weekly with bioluminescent imaging.

Results Irradiated (10 Gy) sarcoma cells express 2–9x higher IL-8 than non-irradiated sarcoma. T cells were transduced with efficiencies of 60–90%. INF- γ production was equivalent between the B7H3 CAR-T2a-CXCR2 T cells and B7H3 CAR T cells, but IL-2 production was significantly higher in the dual expressing CAR T cells. In vitro cytotoxicity with sarcoma spheroids was measured by Incucyte and showed faster and greater killing by B7H3 CAR-T2a-CXCR2 T cells than B7H3 CAR T cells. Furthermore, when sarcoma tumor bearing mice were treated with B7H3 CAR-T2a-CXCR2 T cells, tumors resolved completely by 4–5 weeks and had long-lasting remission.

Conclusions Chemokine receptor expressing CAR T cells showed superior cytokine production and T cell activation/cytotoxicity compared to a CAR T construct alone. These findings lead to better efficacy in animal models and suggest a promising approach for pediatric sarcoma.

REFERENCES

1. Luetke A, Meyers PA, Lewis I, Juergens H. Osteosarcoma treatment - where do we stand? A state of the art review. *Cancer Treat Rev* 2014;**40**:523–32.
2. Bleyer A, Barr R, Hayes-Lattin B, et al. The distinctive biology of cancer in adolescents and young adults. *Nat Rev Cancer* 2008;**8**:288–98.
3. Buechner J, SA G, SL M, et al. Global Registration Trial of Efficacy and Safety of CTL019 in Pediatric and Young Adult Patients with Relapsed/Refractory (R/R) Acute Lymphoblastic Leukemia (ALL): Update to the interim analysis. 2017 European Hematology Association Annual Meeting: Madrid, Spain 2017.

4. Maude SL, Laetsch TW, Buechner J, et al. Tisagenlecleucel in Children and Young Adults with B-Cell Lymphoblastic Leukemia. *N Engl J Med* 2018;**378**:439–48.
5. Gill S, Maus MV, Porter DL. Chimeric antigen receptor T cell therapy: 25 years in the making. *Blood Rev* 2016;**30**:157–67.
6. Fousek K, Ahmed N. The Evolution of T-cell Therapies for Solid Malignancies. *Clin Cancer Res* 2015;**21**:3384–92.
7. Newick K, Moon E, Albelda SM. Chimeric antigen receptor T-cell therapy for solid tumors. *Mol Ther Oncolytics* 2016;**3**:16006.
8. Nagarsheth N, Wicha MS, Zou W. Chemokines in the cancer microenvironment and their relevance in cancer immunotherapy. *Nat Rev Immunol* 2017;**17**:559–72.

Ethics Approval The animal experiments discussed in the abstract were approved by the University of Colorado IACUC, protocol #00251.

<http://dx.doi.org/10.1136/jitc-2021-SITC2021.125>

REGIONAL ADMINISTRATION OF IL-12 ENDOWED CAR T CELLS EFFECTIVELY TARGETS SYSTEMIC DISEASE

Hee Jun Lee*, Cody Cullen, John Murad, Jason Yang, Wen-Chung Chang, Stephen Forman, Saul Priceman. *City of Hope, Duarte, CA, USA*

Background While chimeric antigen receptor (CAR) T cell therapy has shown impressive clinical efficacy for hematological malignancies,¹ efficacy remains limited for solid tumors due in large part to the immunosuppressive tumor microenvironment.² Tumor-associated glycoprotein 72 (TAG72) is an aberrantly glycosylated protein overexpressed on ovarian cancer³ and is an exciting target for CAR T cell immunotherapy. Our lab previously developed a second-generation TAG72 CAR T cell product and showed its potency against TAG72-expressing ovarian tumor cells both in vitro and in preclinical mouse models.⁴ We report here further modification of our TAG72 CAR T cells, with incorporation of interleukin-12 (IL-12) and interleukin-15 (IL-15), and evaluate the therapeutic benefits in peritoneal ovarian tumor models.

Methods In this preclinical study, we build upon our earlier work with in vitro and in vivo evaluation of 9 different second-generation TAG72 CAR constructs varying in single-chain variable fragment, extracellular spacer, transmembrane, and intracellular co-stimulatory domains. We then engineer CAR T cells with two types of cytokines – IL-12 and IL-15 – and put these engineered cells against challenging in vivo tumor models.

Results Through in vitro and in vivo studies, we identify the most optimal construct with which we aim to evaluate in a phase 1 clinical trial targeting TAG72-positive ovarian cancer in 2021. Despite thorough optimizations to the CAR backbone, CAR T cells can be additionally engineered for improved anti-tumor response. Therefore, we further engineered CAR T cells with IL-12 or IL-15 production that greatly improves the effectiveness of TAG72-CAR T cells in difficult-to-treat in vivo tumor models. We observed that modification of CAR T cells with IL-15 displayed toxicity when regionally delivered in vivo, yet introduction of IL-12 not only demonstrated safe and superior therapeutic responses, but also allowed the regional administration of CAR T cells to address systemic disease. We are now expanding these findings by evaluating these therapies using syngeneic immunocompetent mouse tumor models.

Conclusions The tumor microenvironment (TME) harbors various factors that thwart the killing of tumor cells by CAR T cells. Thus, CAR T cells will likely require further engineering to overcome this barrier. We show that amplifying cytokine pathways is one way to overcome the TME and improve the efficacy of CAR T cell therapy for solid tumors.

REFERENCES

1. Maude SL, Teachey DT, Porter DL, Grupp SA. CD19-targeted chimeric antigen receptor T-cell therapy for acute lymphoblastic leukemia. *Blood* 2015 Jun 25;**125**(26):4017–23.
2. Priceman SJ, Forman SJ, Brown CE. Smart CARs engineered for cancer immunotherapy. *Curr Opin Oncol* 2015 Nov;**27**(6):466–74.
3. Chauhan SC, Vinayek N, Maher DM, Bell MC, Dunham KA, Koch MD, Lio Y, Jaggi M. Combined Staining of TAG-72, MUC1, and CA125 Improves Labeling Sensitivity in Ovarian Cancer: Antigens for Multi-targeted Antibody-guided Therapy. *J Histochem Cytochem* 2007 Aug;**55**(8):867–75.
4. Murad JP, Kozłowska AK, Lee HJ, Ramamurthy M, Chang WC, Yazaki P, Colcher D, Shively J, Cristea M, Forman SJ, Priceman SJ. Effective Targeting of TAG72+ Peritoneal Ovarian Tumors via Regional Delivery of CAR-Engineered T Cells. *Front Immunol* 2018 Nov 19;**9**:2268.

<http://dx.doi.org/10.1136/jitc-2021-SITC2021.126>

127

CAR T CELLS TARGETING THE INTEGRIN ALPHA V BETA 3 EXHIBIT ROBUST ANTI-TUMOR RESPONSES AGAINST DIFFUSE INTRINSIC PONTINE GLIOMA AND GLIOBLASTOMA

Dustin Cobb*, Jacopo de Rossi, Lixia Liu, Erin An, Daniel Lee. *University of Virginia, Charlottesville, VA, USA*

Background Diffuse intrinsic pontine glioma (DIPG) and glioblastoma (GBM) are two highly aggressive and mostly incurable gliomas with little therapeutic advancements made in the past several decades. Despite immense initial success of chimeric antigen receptor (CAR) T cells for the treatment of leukemia and lymphoma, significant headway into the application of CAR T cells against solid tumors, including gliomas, is still forthcoming. The integrin complex alpha v beta 3 (avb3) is present on multiple and diverse solid tumor types and tumor vasculature with limited expression throughout most normal tissues, qualifying it as an appealing target for CAR T cell-mediated immunotherapy.

Methods Patient-derived diffuse intrinsic pontine glioma (DIPG) cells and glioblastoma (GBM) cell lines were evaluated by flow cytometry for surface expression of avb3. Second-generation CAR T cells expressing an anti-avb3 scFv were generated by retroviral transduction containing either a CD28 or 4-1BB co-stimulatory domain and CD3zeta. CAR T cells were evaluated by flow cytometry for CAR expression, memory phenotype distribution, and inhibitory receptor profile. DIPG and GBM cell lines were orthotopically implanted into NSG mice via stereotactic injection and monitored with bioluminescent imaging to evaluate avb3 CAR T cell-mediated anti-tumor responses.

Results We found that patient-derived DIPG cells and GBM cell lines express high levels of surface avb3 by flow cytometry, while avb3 is minimally expressed on normal tissues by RNA sequencing and protein microarray. Second-generation CAR T cells expressing an anti-avb3 single-chain variable fragment (scFv) were designed and generated by retroviral transduction containing either a CD28 or 4-1BB co-stimulatory domain and CD3zeta. avb3 CAR T cells demonstrated efficient, antigen-specific tumor cell killing in both cytotoxicity assays and in in vivo models of orthotopically and stereotactically implanted DIPG and GBM tumors into relevant locations in the brain of NSG mice. Tumor responses were rapid and robust with systemic CAR T cell proliferation and long-lived persistence associated with long-term survival.

Conclusions These results highlight the potential of avb3 CAR T cells for immunotherapeutic treatment of deadly brain tumors with reduced risk of on-target, off-tumor mediated toxicity due to the restricted nature of avb3 expression in normal tissues.

Acknowledgements We would like to acknowledge the following core facilities at the University of Virginia: The Research Histology Core, the Biorepository and Tissue Research Facility, and the Molecular Imaging Core which are supported by the University of Virginia School of Medicine and through the University of Virginia Cancer Center National Cancer Institute P30 Center Grant. We would also like to acknowledge the University of Virginia Center for Comparative Medicine for providing animal care and services.

<http://dx.doi.org/10.1136/jitc-2021-SITC2021.127>

KIR HAPLOTYPE CAN INFORM DONOR SELECTION PRODUCTION OF ALLOGENEIC MEMORY-LIKE CAR NK CELLS FOR CLINICAL APPLICATION

Hadia Lemar*, Anmol Vohra, Ming-Hong Xie, Ivan Chan, Sasha Lazetic, James Trager.
NKarta Therapeutics, South San Francisco, CA, USA

Background NK cells expanded on membrane-bound (mb) IL-15 and 41BBL expressing K562 stimulatory cells (NKSTIM) for clinical use can be genetically modified to express activating chimeric receptors.^{1 2 3} NK cells activated in the presence of IL-12, IL-15 and IL-18 develop cytokine induced memory-like (CIML) phenotype and function; these cells have shown clinical promise.⁴ Additionally, HSCT AML transplants using NK KIR Haplotype Group B donors with better and best Group B profiles (≥ 2 activating genes) show better survival.⁵ ⁶ Here we investigate whether KIR profiles impact healthy allogeneic donor NK cell function and phenotype when these cells are expanded on NKSTIM in the presence of IL-12 and IL-18 (12–18).

Methods Healthy donor PBMC NK were genotyped for HLA and KIR and expanded on K562-mbIL15-41BBL stimulatory cells with IL-2 alone or with IL-2 plus IL-12 and IL-18 (12–18). Expanded NK were transduced with CAR constructs including CD19, and then evaluated for NK cell expansion, cytokine secretion, RNA profiles, cytotoxicity against tumor lines, and cell surface phenotypes. Expanded CD19 NK donors with varying numbers of activating KIR vs inhibitory KIR were tested for effector function, and these donors were then tested for *in vivo* efficacy and pharmacokinetics. A KIR ranking score was developed by considering both the number of activating and inhibitory KIR genes expressed by each donor. This score was correlated with functional properties of CAR NK cells.

Results Addition of 12–18 to the K562-mbIL15-41BBL stimulatory cells improves CD19-CAR NK potency 2-fold relative to the stimulatory cell line alone ($P=0.02$) while NK cell expansion is unchanged. 12–18 also drove an increase in effector cytokine accumulation on exposure of CAR-NK to CD19 tumor. CIML CAR NK cells from donors with higher KIR scoring also had higher cytotoxicity (Pearson's $R=0.74$, $P=0.006$); this correlation was not observed following expansion in the absence of 12–18. 12–18 also drove more potent *in vivo* activity against tumor with an increased presence of circulating NK cells over 4 weeks in the mice.

Conclusions CIML CAR NK cells derived from donors with favorable KIR scoring have greater cytotoxic activity, effector cytokine production, and *in vivo* pharmacokinetics and efficacy. These findings may provide an important criterion for donor selection in the development of more robust and potent engineered NK cells for clinical use.

REFERENCES

1. Lapteva N, Durett AG, Sun J, Rollins LA, Huye LL, Fang J, Dandekar V, Mei Z, Jackson K, Vera J, Ando J, Ngo MC, Coustan-Smith E, Campana D, Szmania S, Garg T, Moreno-Bost A, Vanrhee F, Gee AP, Rooney CM. Large-scale *ex vivo* expansion and characterization of natural killer cells for clinical applications. *Cytotherapy* 2012;**14**(9):1131–1143.
2. Chihaya I, Iwamoto S, Campana D. Genetic modification of primary natural killer cells overcomes inhibitory signals and induces specific killing of leukemic cells. *Blood* 2005;**106**:376–383.
3. Yang Y, Connolly J, Shimasaki N, Mimura K, Kono K, Campana D. A Chimeric Receptor with NKG2D Specificity Enhances Natural Killer Cell Activation and Killing of Tumor Cells. *Cancer Res* 2013;**73**(6):1777–1786.
4. Romee R, Rosario M, Berrien-Elliott MM, Wagner JA, Jewell BA, Schappe T, Leong JW, Abdel-Latif S, Schneider SE, Willey S, Neal CC, Yu L, Oh ST, Lee YS, Mulder A, Claas F, Cooper MA, Fehniger TA. Cytokine-induced memory-like

natural killer cells exhibit enhanced responses against myeloid leukemia. *Sci Transl Med* 2016;**8**(357): 357ra123.

5. Cooley S, Weisdorf DJ, Guethlein LA, Klein JP, Wang T, Le CT, Marsh SGE, Geraghty D, Spellman S, Haagenson MD, Ladner M, Trachtenberg E, Parham P, and Miller JS. Donor selection for natural killer cell receptor genes leads to superior survival after unrelated transplantation for acute myelogenous leukemia. *Blood* 2010;**116**(14):2414–2419.
6. Cooley S, Weisdorf DJ, Guethlein LA, Klein JP, Wang T, Marsh SGE, Spellman S, Haagenson MD, Saetern K, Ladner M, Trachtenberg E, Parham P, and Miller JS. Donor Killer Cell Ig-like Receptor B Haplotypes, Recipient HLA-C1, and HLA-C Mismatch Enhance the Clinical Benefit of Unrelated Transplantation for Acute Myelogenous Leukemia. *JL*, 2014;**192**(10):4592–600.

Ethics Approval Animal studies were conducted with IACUC approval.

<http://dx.doi.org/10.1136/jitc-2021-SITC2021.128>

DEVELOPMENT OF AB-201, A NOVEL ALLOGENEIC ANTI-HER2-SPECIFIC CAR-NK CELL THERAPY FOR THE TREATMENT OF HER2+ TUMORS

¹Hoyong Lim, ²Amanda Medcalf, ²Lisa Guerrettaz, ¹Eun Ji Choi, ¹Hansol Kim, ¹Bitna Yang, ¹Eun Ji Kim, ¹Eun-Sol Lee, ¹Jeong Min Kim, ¹Yusun Kim, ¹Bokyung Min, ¹Sang-Min Paik, ¹Hyeong Jin Nam, ¹Seungryel Han, ²Srinivas Somanchi, ²Eugene Helsel, ²Jason Litten, ²Peter Flynn, ²Heather Raymon*, ¹Yu-Kyeong Hwang. ¹GC LabCell, Yongin, Republic of Korea; ²Artiva Biotherapeutics, San Diego, CA, USA

Background Human Epidermal Growth Factor Receptor 2 (HER2), is a receptor tyrosine kinase that is highly expressed on the surface of many solid tumors. While many patients derive meaningful benefit from the approved HER2-directed therapies, most will eventually suffer relapse or progression of their disease highlighting the need for additional treatment options. Currently there are no FDA-approved cellular therapies targeting HER2. Over the past decade, however, cellular therapy has been shown to be a viable treatment option in different cancer types. Here we present AB-201, an off-the-shelf, cryopreserved cord blood (CB)-derived HER2 chimeric antigen receptor (CAR)-natural killer (NK) cell therapy as a safe, active, and readily available option for patients with HER2+ solid tumors.

Methods AB-201 is comprised of ex vivo expanded allogeneic CB-derived NK cells that have been genetically modified to express a HER2-directed CAR and presented as a cryopreserved infusion-ready product. The manufacturing process utilizes a feeder-cell line engineered to express factors specifically identified as supportive to NK cell expansion and a lentiviral transduction step to introduce the HER2 CAR construct. In vitro characterization of AB-201 included evaluation of the purity and expression of cell surface markers by flow cytometry and short- (4 hour) and long-term (over 5 days) cytotoxicity assays in the presence of HER2+ tumor cell lines at various effector to target ratios. In addition, AB-201 efficacy was assessed in vivo in established ovarian (intraperitoneal, SKOV-3), breast (intraperitoneal, HCC1954) and gastric (subcutaneous, N87) xenograft models in NSG mice.

Results HER2 CAR expression was detected in 93.1% of AB-201 cells. AB-201 is 97.9% CD3-/CD56+ cells and 94.6% CD56+/CD16+. Further characterization of AB-201 demonstrated high expression of NK activating receptors such as NKG2D, NKp30, NKp46, and DNAM-1 and expression of the chemokine receptor, CXCR3. AB-201 demonstrated concentration-dependent and HER2 targeted short-term cytotoxic activity and sustained long-term cell killing against the tumor cell lines SKOV-3, HCC1954, and NCI-N87. Efficacy, as evidenced by a significant reduction in bioluminescent signal or tumor volume, was observed in all xenograft models. A significant survival benefit over non-transduced NK cells or trastuzumab controls was demonstrated in the HCC1954 model.

Conclusions Data presented herein suggests that AB-201, a highly pure and readily expandable HER2-directed CAR NK cell product, has potential to be an effective therapy in the treatment of HER2+ tumors.

Ethics Approval The animal studies were conducted in accordance with an Institutional Animal Care and Use Committee-approved protocol and with the approval of an IACUC committee at each center where the studies took place

<http://dx.doi.org/10.1136/jitc-2021-SITC2021.129>

130 **ENGINEERED NATURAL KILLER CELLS REACTIVELY BLOCK TIGIT AND CD73 IN THE GBM MICROENVIRONMENT**

Kyle Lupo*, Sandro Matosevic. *Purdue University, Lafayette, IN, USA*

Background Natural killer (NK) cells have emerged as promising effectors to target GBM and other solid tumors through genetic modifications and ex vivo manipulation. However, immunosuppressive conditions within the tumor microenvironment (TME) and interactions between NK cell activating and inhibitory receptors further complicate NK cell-based treatments. In particular, the T cell immunoreceptor with Ig and ITIM domains (TIGIT) is expressed on NK cells and interacts with CD155 to induce immunosuppression of NK cell cytolytic functions.¹⁻² Although CD155 also binds with activating receptors DNAM-1 and CD96 on NK cells, spurring NK cell activity, TIGIT has predominantly been reported as having an inhibitory effect on NK cells.³⁻⁵ Further, tumor cells release of high levels of ATP extracellularly. While intracellular ATP is necessary for cell metabolism, extracellular ATP is converted into adenosine (ADO) by ectonucleotidases CD39 and CD73, both overexpressed on GBM and other solid tumors.⁶ Extracellular ADO induces immunometabolic suppression of NK cells through binding with A2A adenosine receptors (A2ARs) on NK cells, suppressing cytokine secretion, proliferation, and other functional activities.⁷⁻⁹ We found that TIGIT and CD73 are effective combination targets in GBM for both primary and iPSC-derived NK cells.

Methods In order to effectively target immunometabolic reprogramming induced by CD73-produced adenosine and the immunosuppressive TIGIT-CD155 axis, we have engineered NK cells to concomitantly target CD155 and CD73-induced immunosuppression on GBM using a tumor-responsive genetic construct based on the synNotch signaling system. The construct is capable of blocking the immunosuppressive CD155/TIGIT interaction, and, upon binding, release a CD73-blocking scFv to inhibit the accumulation of extracellular ADO and mitigate immunosuppression of NK cells. Such localized response enhances specificity and reduces off-target effects of NK-based targeting.

Results Primary NK cells and iPSC-derived NK cells were successfully engineered to express the synthetic TIGIT-synNotch construct, measured through expression of TIGIT. To evaluate the functionality of engineered NK cells against GBM targets, we tested the cytotoxicity of our engineered NK cells against a primary, patient-derived GBM cell line, GBM43. Overall, cytolytic function of engineered NK cells against GBM was significantly higher than that of non-engineered NK cells, with or without CD73 (10 ug/mL) and TIGIT (50 ug/mL) antibodies, for E:T ratios of 5:1 and 10:1, demonstrating the functional efficacy of our genetic construct.

Conclusions Overall, we have shown that co-targeting CD155 and CD73 in a localized, responsive manner can dampen immunosuppression and significantly enhance the killing potential of engineered NK cells against aggressive patient-derived GBM tumors.

REFERENCES

1. Zhang B, et al. Immunoreceptor TIGIT inhibits the cytotoxicity of human cytokine-induced killer cells by interacting with CD155. *Cancer Immunol Immunother* 2016;**65**:305–314.
2. Lupo KB & Matosevic S. CD155 immunoregulation as a target for natural killer cell immunotherapy in glioblastoma. *J Hematol Oncol* 2020;**13**:76.

3. Hung AL, et al. TIGIT and PD-1 dual checkpoint blockade enhances antitumor immunity and survival in GBM. *Oncimmunology* 2018; e1466769. doi:10.1080/2162402X.2018.1466769.
4. Mahnke K & Enk, AH. TIGIT-CD155 Interactions in Melanoma: A Novel Co-Inhibitory Pathway with Potential for Clinical Intervention. *Journal of Investigative Dermatology* 2016; **136**, 9–11.
5. Stanitsky N, et al. Mouse TIGIT inhibits NK-cell cytotoxicity upon interaction with PVR: Innate immunity. *Eur J Immunol* 2013; 43:2138–2150.
6. Chambers AM, et al. Adenosinergic Signaling Alters Natural Killer Cell Functional Responses. *Front Immunol* 2018;**9**:2533.
7. Chambers AM, Lupo KB & Matosevic S. Tumor Microenvironment-Induced Immunometabolic Reprogramming of Natural Killer Cells. *Front Immunol* 2018;**9**:2517.
8. Chambers AM, et al. Adenosinergic Signaling Alters Natural Killer Cell Functional Responses. *Front Immunol* 2018;**9**:2533.
9. Wang J, Lupo KB, Chambers AM & Matosevic S. Purinergic targeting enhances immunotherapy of CD73+ solid tumors with piggyBac-engineered chimeric antigen receptor natural killer cells. *J Immunotherapy Cancer* 2018;**6**:136.

Ethics Approval Primary human NK cells were obtained from healthy adult donors approved under Purdue University's Institutional Review Board (IRB) (IRB-approved protocol #1804020540). Donors gave written informed consent prior to taking part in the study.

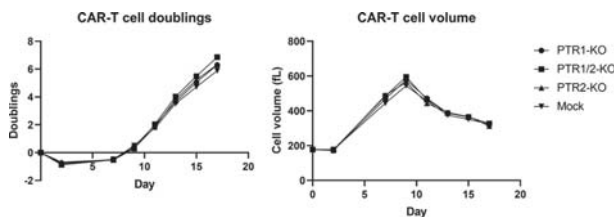
<http://dx.doi.org/10.1136/jitc-2021-SITC2021.130>

GENETIC DISRUPTION OF NEGATIVE IMMUNE REGULATORS TO ENHANCE CAR-T EFFICACY AGAINST SOLID TUMORS

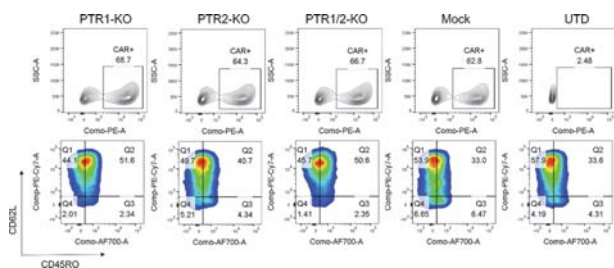
David Mai*, Omar Johnson, Carl June. *University of Pennsylvania, Philadelphia, PA, USA*

Background CAR-T cell therapy has demonstrated remarkable success in hematological malignancies but displays limited efficacy in solid tumors, which comprise most cancer cases. Recent studies suggest that CAR-T cell failure via T cell exhaustion is characterized by decreased surface CAR expression, cytotoxicity, and Th1 cytokine production, leading to reduced antitumor functionality.^{1 2 3} To address these issues, studies have turned to genetically knocking out or overexpressing targets associated with an exhaustion or effector phenotype, such as PD-1 knockout (KO) and c-Jun overexpression, among other candidates that are typically receptors or transcription factors.^{4 5 6} However, there are other underexplored factors that mediate various aspects of immune regulation. While genome-wide CRISPR screens may discover such factors, they are unlikely to reveal phenotypes for genes whose function is partially redundant, therefore promising candidates may be missed. Such candidates include post-transcriptional regulators (PTRs) that coordinate immune responses, which are less well-studied in the context of CAR-T cell function. We hypothesized that KO of these PTRs may increase CAR-T cell cytokine activity, phenotype, and persistence, potentially under long-term or exhaustion-inducing conditions, leading to increased tumor control. Ultimately, disruption of negative immune regulators could produce CAR-T cells with enhanced activity and persistence, narrowing the gap between efficacy in hematological and solid tumors.

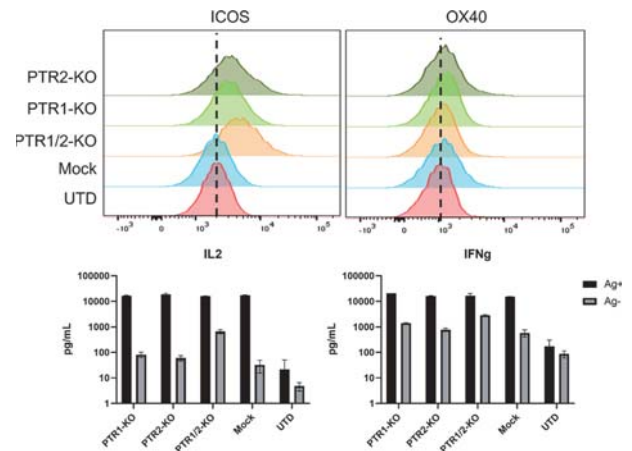
Methods To explore whether the disruption of two target PTRs improves solid tumor efficacy, we used CRISPR-Cas9 to genetically delete one or both PTRs in mesothelin-targeting human CAR-T cells and assayed their function in vitro and in vivo in NSG mice.



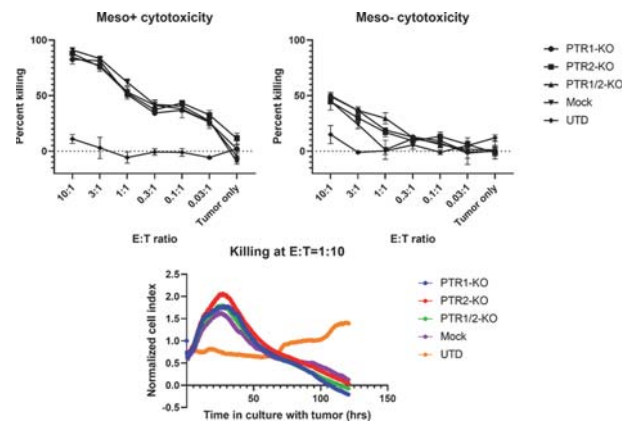
Abstract 131 Figure 1 Expansion kinetics of KO CAR-T cells



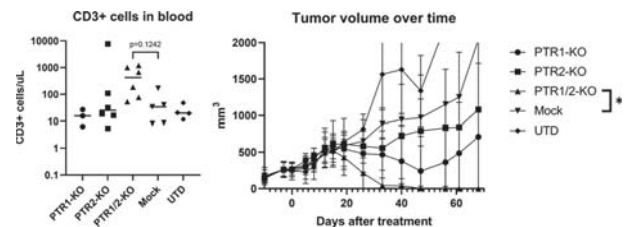
Abstract 131 Figure 2 Transduction efficiency and baseline phenotype of KO CAR-T cells



Abstract 131 Figure 3 Costimulatory receptor and cytokine expression of KO CAR-T cells



Abstract 131 Figure 4 In vitro cytotoxicity of KO CAR-T cells



Abstract 131 Figure 5 In vivo activity of KO CAR-T cells

Results We show successful genetic deletion of these genes in post-thymic human T cells and that their disruption does not affect primary expansion (figure 1) or transduction efficiency (figure 2). These KO CAR-T cells display increased expression of co-stimulatory receptors and various cytokines (figure 3). While KO CAR-T cells are functionally similar to WT CAR-T cells in in vitro assays (figure 4), KO CAR-T cells demonstrate superior activity in vivo and can clear large, established tumors compared to WT CAR-T cells at low dose (figure 5).

Conclusions These results indicate that KO of our target PTRs may improve the potency of CAR-T cells in solid tumors and may have important implications on the development of effective solid-tumor cell therapies.

REFERENCES

1. JE Wherry and M Kurachi, Molecular and cellular insights into T cell exhaustion, *Nature Reviews Immunology* 2015;**15**:486–499.
2. EW Weber, et al. Transient rest restores functionality in exhausted CAR-T cells through epigenetic remodeling. *Science* 2021;**372**:6537.
3. S Kuramitsu et al. Induction of T cell dysfunction and NK-like T cell differentiation in vitro and in patients after CAR T cell treatment. *Cell*, in revision.
4. BD Choi et al, CRISPR-Cas9 disruption of PD-1 enhances activity of university EGFRvIII CAR T cells in a preclinical model of human glioblastoma. *Journal for ImmunoTherapy of Cancer* 2019;**7**:304.
5. RC Lynn et al. c-Jun overexpression in CAR T cells induces exhaustion resistance. *Nature* 2019;**576**:293–300.
6. LJ Rupp et al. CRISPR/Cas9-mediated PD-1 disruption enhances anti-tumor efficacy of human chimeric antigen receptor T cells. *Scientific Reports* 2017;**7**:737.

<http://dx.doi.org/10.1136/jitc-2021-SITC2021.131>

HLA-INDEPENDENT T CELL RECEPTORS EFFECTIVELY TARGET LOW ABUNDANCE ANTIGENS

¹Jorge Mansilla-Soto*, ¹Justin Eyquem, ¹Sascha Haubner, ¹Mohamad Hamieh, ¹Judith Feucht, ²Noémie Paillon, ²Andres Zucchetti, ¹Zhuoning Li, ¹Maria Sjöstrand, ¹Pieter Lindenbergh, ¹Michelle Saetersmoen, ²Mathieu Maurin, ¹Archana Iyer, ¹Anton Dobrin, ¹Andreina Garcia Angus, ¹Matthew Miele, ¹Zeguo Zhao, ¹Theodoros Giavridis, ¹Sjoukje van der Stegen, ¹Fella Tamzalit, ¹Morgan Huse, ¹Ronald Hendrickson, ²Claire Hivroz, ¹Michel Sadelain. ¹MSKCC, New York, NY, USA; ²Institute Curie, Paris, France

Background Chimeric antigen receptors (CARs) engage antigen independently of HLA and enable sustained T cell proliferation when they are endowed with both activating and costimulatory functions. While remission rates have been noticeably elevated in numerous clinical trials targeting CD19, CD22 or BCMA, relapses are common. One of the several underlying relapse mechanisms is antigen escape, which refers to a relapsing tumor that is either negative for the targeted antigen or expresses the latter at a low level. Failure to eliminate antigen-low tumors raises questions about the sensitivity of CARs and the minimum antigen density that is required for effective tumor eradication. Unlike CARs, TCRs engage antigen in an HLA-dependent manner, and they do so with high sensitivity. We hypothesized that a TCR/CD3 complex containing the same heavy and light immunoglobulin chains as a CAR will display increased sensitivity to the target antigen.

Methods We edited the TRAC locus in human primary T cells to establish a novel antigen receptor structure, termed HLA-independent TCR or HIT receptor, by incorporating into the TCR/CD3 complex the same heavy and light chains as those of a corresponding CAR. We assessed their antigen sensitivity against a panel of cell lines expressing different antigen levels, analyzing their cytotoxicity, cytokine secretion, signaling response and degranulation activity. HIT and CAR T cells were further evaluated for their anti-tumor response using established ALL and AML mouse models.

Results CD19-TRAC-HIT and CD19-TRAC-CAR T cells lysed wild-type NALM6 (~27,000 CD19 molecules) and NALM6 variants with 100-fold less CD19. As CD19 levels decreased further, CAR T cells no longer killed their target, in contrast to HIT T cells. HIT T cells showed increased expression of IFN-gamma, IL-2 and TNF-alpha upon exposure to NALM6 cells expressing ~20 CD19 molecules per cell, compared to CAR T cells. This increased sensitivity of HIT receptors correlated to their greater signaling response, upon exposure to the low-antigen-density NALM6. Phospho-proteomic analyses further confirmed this increased response of HIT T cells to low antigen levels. Altogether, these results confirm that HIT receptors endow T cells with greater antigen sensitivity than canonical CARs. We further showed that HIT T cells have higher in vivo anti-tumor activity compared to CAR T cells in mice bearing low-antigen-density ALL or AML.

Conclusions HIT receptors consistently afford high antigen sensitivity and mediate tumor recognition beyond what current CARs can provide. HIT receptors open new prospects for targeting cell surface antigens of low abundance.

Ethics Approval Eight- to 12-week-old NOD/SCID/IL-2Rgamma-null (NSG) male mice (Jackson Laboratory) were used under a protocol approved by the MSKCC Institutional Animal Care and Use Committee.

<http://dx.doi.org/10.1136/jitc-2021-SITC2021.132>

133

CRISPR/CAS9 GENE-EDITED ALLOGENEIC CAR-T CELLS TARGETING CD33 SHOW HIGH PRECLINICAL EFFICACY AGAINST AML WITHOUT LONG-TERM HEMATOPOIETIC TOXICITY

¹Jonathan Terrett, ²Brigid Mcewan, ²Daniel Hostetter*, ²Luis Gamboa, ²Meghna Kuppuraju, ²Mohammed Ghonime, ²Robert Chain, ²Zinkal Padalia, ²Demetrios Kalaitzidis. ¹*Crispr Therapeutics, Cambridge, MA, USA*; ²*CrisprTx, Cambridge, MA, USA*

Background CD33 is the most consistently expressed antigen in AML, with high levels and homogeneous expression observed in malignant AML cells from most patients, including those with relapsed disease. Normal myelomonocytic cell lineages and a percentage of hematopoietic progenitors also express CD33, and the extreme myeloablation caused by the CD33-targeted antibody-drug conjugate (ADC) gemtuzumab ozogamicin reinforced concerns about targeting this antigen with more potent agents such as T-cell engaging bispecific antibodies and CAR-T cells. We have shown previously that allogeneic CRISPR/Cas9 gene-edited CAR-T cells targeting CD33 with TRAC disruption to reduce GvHD and B2M disruption to reduce allogeneic host rejection could eliminate tumors in xenograft models of AML.

Methods Given that off-target activity of the toxin could contribute to the myeloablation seen with CD33-targeted ADCs, we created in vitro and in vivo models to examine reconstitution of the myeloid compartment following treatment of CD33-targeted allogeneic CAR-T cells.

Results Although co-culture of CD34+ stem cells in vitro with our CD33-targeted allogeneic CAR-T cells did significantly deplete the cell population, colonies still formed after removal of the CAR-T cells as the presumably CD33-negative stem/progenitor cells expanded and differentiated. A similar phenomenon was observed in vivo with CD34 humanized mice bearing an AML tumor (THP-1 cells) and treated with the CD33-targeted allogeneic CAR-T cells. The CAR-T cells completely eradicated the THP-1 tumor but did not lead to long-term myelosuppression or B cell aplasia.

Conclusions Thus, allogeneic CRISPR/Cas9 multiplex gene-edited CD33-targeted CAR-T cell therapy may be both efficacious and tolerable in AML.

<http://dx.doi.org/10.1136/jitc-2021-SITC2021.133>

IDENTIFICATION AND CHARACTERIZATION OF AN ALLOGENEIC iNKT-CAR TARGETING BCMA

Xavier Michelet*, Eleni Chantzoura, Efrat Altman-Sharoni, Martyna Popis, Reed Masakyan, Paul Ibbett, Deborah Wright, Moira Pinzan Rossi, Marc Van Dijk. *MNK Therapeutics, Lexington, MA, USA*

Background Chimeric antigen receptor (CAR) T cell therapy has shown outstanding benefit in hematological malignancies with three autologous CAR-T therapies commercially available and several in clinical development. The use of autologous T cells to manufacture CAR therapies has several disadvantages including production time, cost, lengthy time to treatment and dependence on patient T cell functionality. An allogeneic off the shelf CAR product can overcome these issues. We use invariant natural killer T (iNKT) cells as basis for our allogeneic cell therapy platform. Invariant NKT cells are innate-like lymphocytes that bridge innate and adaptive immune response to promote anti-cancer immunity. iNKT cells share characteristics of T cells and Natural Killer (NK) cells, expressing both an invariant T Cell Receptor (iTCR) and canonical NK receptors. They can be activated by recognition of lipid antigens through the iTCR, pro-inflammatory cytokines and recognition of stress ligands. Moreover, iNKT do not cause Graft versus Host Disease making them an ideal platform for allogeneic CAR cell therapy. Here we describe a novel allogeneic iNKT-CAR product targeting BCMA designed to promote effective anti-cancer immunity

Methods Our proprietary CARDIS™ platform is a 2-stage discovery process where screening of highly diverse scFv libraries via phage display is followed by selection of potent CARs using mammalian display platform. Using this high throughput approach, we can interrogate large cell-based CAR libraries for specific binding and activation simultaneously, as well as eliminate tonic signaling at an early stage. This novel platform enabled rapid identification of a candidate CAR (agent-F6) for the targeting of BCMA. Anti-cancer efficacy of stably expressed BCMA CAR in expanded iNKT cells has been tested

Results Agent-F6 expressed at high levels in iNKT cells. Functional characterization demonstrated potent cytotoxic activity of agent-F6 expressing iNKT cells against human hematologic tumor cell lines expressing BCMA in vitro. Activated agent-F6 iNKT cells display a pro-inflammatory phenotype when challenged with tumor cell lines. Furthermore, using a multiple myeloma in vivo xenograft model, infusion of agent-F6 iNKT cells showed comparable tumor control to a clinical-stage BCMA CAR reference.

Conclusions MiNK therapeutics is developing the next generation allogeneic CAR-iNKT therapies by using 1) a CAR discovery platform that allows more rapid and efficient identification of antigen-specific and biologically potent CAR candidates and 2) an iNKT cell platform naturally lacking alloreactivity that allows rapid engineering and expansion of an off-the-shelf CAR product.

Ethics Approval All procedures performed in studies involving human participants were in accordance with the ethical standards of the institutional and/or national research committee and with the 1964 Helsinki declaration and its later amendments or comparable ethical standards

<http://dx.doi.org/10.1136/jitc-2021-SITC2021.135>

136

ATA3271: AN ARMORED, NEXT-GENERATION OFF-THE-SHELF, ALLOGENEIC, MESOTHELIN-CAR T CELL THERAPY FOR SOLID TUMORS

Xianhui Chen*, Jiangyue Liu, Shuai Yang, Amogh Oke, Sarah Davies, Bryan Ruiz-Juarez, Yannick Bulliard, Cokey Nguyen. *Atara Biotherapeutics, Thousand Oaks, CA, USA*

Background Mesothelin (MSLN) is a GPI-anchored membrane protein with high expression levels in an array of malignancies including mesothelioma and is an attractive target antigen for tumor surface antigen-targeting therapies. Regional administration of autologous, 2nd generation MSLN-targeted CAR-T cells for malignant pleural mesothelioma has shown promise in early clinical evaluation.^{1 2} More recently, a next-generation MSLN-targeted, autologous CAR T therapy leveraging 1XX CAR signaling and PD1DNR is currently under investigation for advanced mesothelioma [NCT04577326]. Although autologous MSLN CAR-T holds promise, an allogeneic approach may have more widespread application. EBV T-cells represent a unique, non-gene edited approach for allogeneic T-cell therapy. EBV-specific T-cells are currently in a phase 3 trial for EBV-positive post-transplant lymphoproliferative disease [NCT03394365] and, to-date, have demonstrated a favorable safety profile with no evidence for GvHD and cytokine release syndrome attributable to EBV T-cells. Clinical proof-of-principle studies for CAR transduced CD19-targeted allogeneic EBV T-cell therapies have shown acceptable safety and durable response.³ The first preclinical evaluation of ATA3271 was reported last year.⁴ Here, we describe updated preclinical data for this potential off-the-shelf, allogeneic cell therapy.

Methods We engineered MSLN CAR+ EBV T-cells (ATA3271) with a novel 1XX signaling domain that is associated with strong effector function and favorable persistence, as well as armored with PD1DNR to provide intrinsic checkpoint blockade.⁵ Anti-tumor effect of ATA3271 was assessed using a MSTO-211H-derived tumor cell line overexpressing MSLN and PDL1.

Results Upon MSLN engagement, ATA3271 showed proliferation, efficient tumor cell lysis in the presence of high-level cell-surface PD-L1 expression and secretion of effector cytokines [IL-2, TNF- α , granzyme B]. In a 16-day serial stimulation assay, with PD-L1+ tumor cells added every 2–3 days, ATA3271 expanded 4 to 45-fold without the need for external cytokines, and retained comparable antitumor function as CD3/CD28-stimulated ‘autologous’ CAR-T cells. In an orthotopic mouse model of pleural mesothelioma, ATA3271 demonstrated anti-tumor efficacy without toxicities. Memory markers [CD62L, CCR7] play a key role for T-cell persistence in vivo. We identified donor-to-donor variability in memory marker expression on ATA3271 and optimized our process to maximize their expression. Memory marker expression impact on ATA3271 potency, both in vitro and in vivo, will be presented.

Conclusions Overall, these in vitro and in vivo data show potent anti-tumor activity without evidence of toxicity, suggesting that ATA3271 may be a promising approach for the treatment of MSLN-positive cancers that warrants further clinical investigation.

REFERENCES

1. Adusumilli Prasad S, et al. Abstract CT036: A phase I clinical trial of malignant pleural disease treated with regionally delivered autologous mesothelin-targeted CAR T cells: Safety and efficacy. *Cancer Res* 2019;79(13 Suppl):Abstract CT036.
2. Adusumilli Prasad S, et al. A phase I trial of regional mesothelin-targeted CAR T-cell therapy in patients with malignant pleural disease, in combination with the anti-PD-1 agent pembrolizumab. *Cancer Discov* 2021.

3. Curran Kevin J, et al. Durable remission following ‘off-the-shelf’ chimeric antigen receptor (CAR) T-cells in patients with relapse/refractory (R/R) B-cell malignancies. *Biol Blood Marrow Transplant* 2020;26.3: S89.
4. Liu Jiangyue, et al. 98 ATA3271: an armored, next-generation off-the-shelf, allogeneic, mesothelin-CAR T cell therapy for solid tumors. *JITC* 2020;8.
5. Feucht Judith, et al. Calibration of CAR activation potential directs alternative T cell fates and therapeutic potency. *Nat Med* 2019;25.1: 82–88.

<http://dx.doi.org/10.1136/jitc-2021-SITC2021.136>

DEVELOPMENT OF ANTI-MUCIN1 CAR-T AGAINST SOLID TUMORS

Jihyun Lee*, Aream Park, Jungwon Choi, Dae Gwan Yi, Hee Jung Yang, Hae-youn Lee, Eurim Song, Sung Woong Jang, Hyoju Yi, Heedong Park, Eun-ji Jeun, Minjeong Park, Peter Hong. *LGChem, Gangseo-gu, Seoul, Korea, Republic of*

Background Chimeric antigen receptor (CAR) -T cell therapies have proven to be effective against various liquid tumors. However, the development of CAR-T against solid tumors has been challenging due to insufficient efficacy and potential on-target off-tumor toxicities caused by low expression of tumor antigens on normal tissues. Testing various affinities of CARs has demonstrated that lower affinity CARs maintain its anti-tumor effect while minimizing safety concerns (1). In order to develop a CAR-T against solid tumors expressing Mucin1, we have screened for Mucin1 binding antibodies and tested their anti-tumor effect in vitro and in vivo. The potential of on-target off-tumor toxicity was also measured in vitro.

Methods Anti-Mucin1 human single chain variable fragments (scFv) were obtained via screening against a scFv display library. Anti-Mucin1 scFvs were incorporated into CARs and in vitro, in vivo functions against various tumor cells expressing Mucin1 were tested. For in vivo studies, tumor bearing NOG mice (HCC1954 cells) received anti-Mucin1 CAR-T cells. Therapeutic efficacy was evaluated by measuring tumor volumes. Potential on-target off-tumor toxicity against Mucin1 on normal cells was tested by investigating the killing effect of anti-Mucin1 CAR-T against cancer cell line (HCC70) and non-tumorigenic breast epithelial cell line (MCF-10A) in co-culture systems

Results In vitro activity of anti-Mucin1 CAR-T cells that displayed a range of affinities for Mucin1 (27nM to 320nM) showed similar cytokine secretion levels and cytotoxicity against Mucin-1 expressing tumor cell lines (HCC70 and T47D). Robust anti-tumor activity was also demonstrated in vivo against large tumors (400~500 mm³) with relatively small numbers of CAR-T cells (0.5 x 10⁶ CAR-T cells per mouse). In vivo expansion of CAR-T cells were observed in all scFv-CAR-T cases and accompanied by close to complete regression of tumors within 25 days post CAR-T cell injection. Of the 4 scFv CAR-Ts, 2H08 (with a Kd of 94nM) was tested for activity against normal breast epithelial cells. When 2H08-CAR-T was cocultured with a mixture of HCC70 and MCF-10A cells, they preferentially killed only the Mucin1 overexpressing HCC70 cells leaving MCF-10 cells intact.

Conclusions Our study demonstrates anti-tumor activity of a novel scFv-derived CAR-T recognizing Mucin1 and its effectiveness in large pre-established tumors in vivo. We also demonstrate that 2H08-CAR-T can distinguish between target overexpressing cancer cells and normal epithelial cells, which suggests that by toning down the affinity of CAR against antigen one can improve the safety profile of solid tumor antigen targeting CAR-T cell therapies.

REFERENCE

1. Castellarin M, Sands C, Da T, Scholler J, Graham K, Buza E, Fraietta J, Zhao Y, June C. A rational mouse model to detect on-target, off-tumor CAR T cell toxicity. *JCI Insight* 2020; 5:e136012

Ethics Approval All experiments were done under protocols approved by the Institutional Animal Care and Use Committee (IACUC) (Study#LGME21-011).

Consent Written informed consent was obtained from the patient for publication of this abstract and any accompanying

images. A copy of the written consent is available for review by the Editor of this journal.

<http://dx.doi.org/10.1136/jitc-2021-SITC2021.137>

SYNTHETIC RE-DIRECTION OF TGF β RECEPTORS AS A NOVEL STRATEGY TO ENHANCE THE ANTI-TUMOR ACTIVITY OF CAR-T CELLS IN SOLID TUMORS

Eigen Peralta*, Emily Carron, Hui-Yi Chu, Lorraine Loter, Natalie Navarrete, Arvin Tam, Amit Mehta, Dan Lu, Philip Chu, Kenyon Lyon, Yijia Pan, Mochtar Pribadi, Alec Witty, Tom Lee, Bob Valamehr. *Fate Therapeutics, Inc., San Diego, CA, USA*

Background Transforming growth factor beta (TGF β) is an immuno-suppressive cytokine present in the tumor microenvironment (TME) that creates considerable challenges for the treatment of solid tumors. Small molecule inhibitors targeting TGF β exist, but the pleiotropic nature of TGF β signaling suggests that a more targeted approach is preferential, especially in the context of cellular therapy. We hypothesized that primary T cells and iPSC-derived chimeric antigen receptor-T cells (CAR-iT cells) would benefit not only from blockade of TGF β signaling, but also from re-direction of the signaling event toward specific cytokine pathways that activate cell function. Here we discuss novel synthetic TGF β redirector constructs that overcome TME limitations and enhance CAR-iT cell function for improved efficacy in treating solid tumors.

Methods To identify activation pathways for redirection of TGF β signaling, we screened a panel of cytokines for their effect on the anti-tumor activity of CAR-iT cells. We then developed synthetic redirector receptors where a TGFBR2 ectodomain was fused to the top selected cytokine receptor endodomains. Redirection of TGF β signaling was confirmed by phospho-flow of key signaling proteins. Anti-tumor activity of CAR-iT cells expressing these synthetic redirector constructs was tested in serial restimulation assays in the absence of cytokine support and in the presence of recombinant TGF β (rTGF β).

Results A dose-dependent decrease in CAR-iT cell cytolytic capacity in the presence of rTGF β was observed, with the activity of CAR-iT cells rescued in the presence of unique cytokines. We designed and tested synthetic TGF β redirector constructs and demonstrated a rTGF β -dependent increase in pSTAT5 positive cells (2.8-fold over control). The serial stimulation assay was then used to test CAR-iT cells engineered with synthetic TGF β redirector receptors. After three rounds of restimulation, an increase in tumor cell numbers for non-engineered and dominant negative TGFBR2 CAR-iT cell controls was observed (41-fold and 32-fold increase over base input, respectively). In contrast, the synthetic TGF β redirector receptor improved the ability of CAR-iT cells to control tumor cell growth with remarkable efficiency, limiting tumor growth to only 1.5-fold over three rounds of restimulation.

Conclusions These studies demonstrate that a novel synthetic construct comprised of fusion of cytokine endodomains to a TGFBR2 ectodomain can be deployed to hijack the immuno-suppressive signal of TGF β often found in the TME and activate CAR-iT cells for enhanced anti-tumor activity in solid tumors. Additional studies are underway to assess the temporal expression and activity of these synthetic redirector receptors in various preclinical models which will be further discussed.

<http://dx.doi.org/10.1136/jitc-2021-SITC2021.138>

CHIMERIC ANTIGEN RECEPTOR MACROPHAGES (CAR-M) ELICIT A SYSTEMIC ANTI-TUMOR IMMUNE RESPONSE AND SYNERGIZE WITH PD1 BLOCKADE IN IMMUNOCOMPETENT MOUSE MODELS OF HER2+ SOLID TUMORS<http://dx.doi.org/10.1136/jitc-2021-SITC2021.139>

Stefano Pierini*, Michael Klichinsky, Rashid Gabbasov, Alison Worth, Ilyssa Ramos, Daniel Blumenthal, Linara Gabitova, Sascha Abramson, Thomas Condamine, Michael Ball, Yumi Ohtani. *Carisma Therapeutics, Philadelphia, PA, USA*

Background Despite the remarkable efficacy achieved by CAR-T therapy in hematologic malignancies, application in solid tumors has been challenging. We previously developed human CAR-M and demonstrated that adoptive transfer of CAR-M into xenograft models of human cancer controls tumor progression and improves overall survival.¹ Given that CAR-M are M1-polarized macrophages with the potential to remodel the tumor microenvironment (TME) and act as professional antigen presenting cells, we developed an immunocompetent animal model to evaluate the interaction of CAR-M with the TME and the adaptive immune system.

Methods Murine bone marrow-derived macrophages were engineered to express an anti-HER2 CAR using the chimeric adenoviral vector Ad5f35. To evaluate the safety and efficacy of CAR-M therapy, immunocompetent mice were engrafted with HER2+ tumors and treated with syngeneic CAR-M monotherapy or in combination with a PD1 blocking antibody. Tumors were collected at various time points and dynamic changes in the TME were assessed using flow cytometry, immunohistochemistry, and gene expression analysis.

Results In addition to efficient gene delivery, Ad5f35 transduction promoted a pro-inflammatory (M1) phenotype in murine macrophages. CAR-M, but not control macrophages, phagocytosed and killed HER2-overexpressing tumor cell lines. CAR-M induced MHC-I expression on tumor cells and enhanced the cytotoxicity of CD8+ T cells. In vivo, CAR-M led to significant tumor regression and improved overall survival in multiple syngeneic models. Analysis of the TME showed that CAR-M led to increased infiltration of intratumoral CD4+ and CD8+ T, NK, and dendritic cells – as well as an increase in T cell responsiveness to tumor-associated antigens, indicating enhanced epitope spreading. Given the impact of CAR-M on the endogenous adaptive immune system, we evaluated the combination of CAR-M with anti-PD1 in the CT26-HER2 model, which is resistant to anti-PD1 monotherapy, and found that the combination further reprogrammed the TME, enhanced tumor control, and improved overall survival compared to monotherapy with either agent. Mice that achieved complete responses (CRs) after CAR-M therapy were protected against antigen-negative relapse, indicating long-term anti-tumor immunity. Finally, the combination of CAR-M with anti-PD1 did not trigger sustained elevations of any serum analyte associated with cytokine release syndrome (CRS) and was well tolerated across numerous safety assessments.

Conclusions These results demonstrate that CAR-M reprogram the TME, induce epitope spreading, and orchestrate a systemic immune response against solid tumors. Moreover, our findings provide rationale for the combination of CAR-M with immune checkpoint inhibitors for the treatment of solid tumors.

REFERENCE

1. Klichinsky M, Ruella M, Shestova O, et al. Human chimeric antigen receptor macrophages for cancer immunotherapy. *Nat Biotechnol* 2020;**38**(8):947–953

ALLOGENEIC CAR T CELLS WITH DEOXYCYTIDINE KINASE KNOCKDOWN DEMONSTRATE RESISTANCE TO FLUDARABINE

Michelle Pires*, Aaron Martin. *Precision Biosciences, Inc., Durham, NC, USA*

Background Clinical outcomes in CAR T therapy correlate with engraftment, expansion, and persistence of CAR T cells. In order to facilitate engraftment and expansion, a lymphodepleting regimen consisting of cyclophosphamide and fludarabine precedes CAR T infusion. This creates niches for infused CAR T cells and stimulates beneficial homeostatic cytokine production. As these compounds are also toxic to CAR T cells, administering the proper doses of both the conditioning drugs and the cell therapies with appropriate timing can be a challenge.

Methods To protect CAR T cells from fludarabine toxicity, we have knocked down deoxycytidine kinase (dCK), which converts fludarabine from the prodrug form to an active compound. This was accomplished using an RNAi sequence featuring a dCK-specific shRNA sequence embedded into a micro-RNA backbone. The resulting RNAi sequence demonstrated the potency of shRNA and the stability of a micro-RNA. Using Precision BioSciences' ARCUS® gene editing technology and AAV-mediated targeted transgene insertion strategy, we disrupted the endogenous T cell receptor and inserted a transgene encoding a CD19-specific CAR and a dCK-specific RNAi sequence. Cells produced in this manner were exposed to CD19+ target cells in vitro and in immunodeficient mice and CAR T proliferation and target killing were monitored in the presence and absence of fludarabine.

Results We observed that the inclusion of the RNAi feature resulted in 70% reduction in dCK mRNA abundance, and conferred resistance to fludarabine in vitro. Moreover, treatment of tumor-bearing mice with fludarabine and dCK knock-down CAR T cells resulted in enhanced tumor clearance and survival compared to mice receiving CAR T cells alone or fludarabine plus dCK replete CAR T cells.

Conclusions CAR T cells expressing a dCK-specific RNAi gene exhibited resistance to fludarabine in vitro and in vivo. This drug resistance feature may enable allogeneic CAR-T cells to be simultaneously administered with fludarabine, suppressing rejection of CAR T and improving CAR T engraftment and expansion. This synergy between conditioning and CAR T therapy may improve clinical outcomes by enhancing effector persistence and tumor clearing.

Acknowledgements I would like to thank Aaron J. Martin, PhD and Daniel T. Macleod, PhD for their excellent mentorship and the Precision Biosciences Vivarium team for their support during this study.

REFERENCES

1. Macleod DT, et al. Integration of a CD19 CAR into the TCR Alpha Chain Locus Streamlines Production of Allogeneic Gene-Edited CAR T Cells. *Mol Ther* 2017; **25**(4):949–961.
2. Fellmann C, et al. An Optimized microRNA Backbone for Effective Single-Copy RNAi. *Cell Reports* 2013; **5**:1704–1713.

Ethics Approval The animal study conducted was approved by the Institutional Animal Care and Use Committee (IACUC) of Mispro Biotech.

<http://dx.doi.org/10.1136/jitc-2021-SITC2021.140>

**ENHANCED ANTITUMORAL ACTIVITY OF HER2-CAR-TS
IN COMPARISON TO TRASTUZUMAB IN A LIVE CELL
IMAGING SUPPORTED 3D ASSAY**

¹Katharina Schaich, ²Gemma Moiset, ²Sophie Vermond, ²Monique Hazenoot, ¹Kanstantsin Lashuk, ¹Eva Oswald, ³Sanne Holt, ¹Julia Schuler*, ¹Charles River Research Services Germany, Freiburg, Germany; ²Charles River, Leiden, Netherlands; ³Merus N.V., Leiden, Netherlands

Background Although most breast cancer patients are treated these days with a curative intention, there are still many patients progressing to metastatic disease. The advent of anti-HER2 therapy has prominently prolonged the time of disease progression and survival for those patients, where a decent proportion is suffering from a HER2+ tumor. Beside classical approaches via antibodies against HER2, the use of Chimeric Antigen Receptor T (CAR-T) cells also in a solid cancer context is getting more and more attention.

Methods In our study we evaluated the efficacy of Trastuzumab and HER2+ targeting CAR-T cells in a panel of human cancer cell lines (SK-OV3, Hs578T and JIMT-1) with different HER2 expression levels. The tumor cells were seeded in the presence or absence of different immune cells (PBMC, monocytes, NK cells or T cells) and cultured as 3D spheroids in a matrix-based system. The tumor growth and if applicable the invasion of the immune cells was measured via fluorescence-based live cell imaging. On the last experiment day, a metabolic read-out (CellTiter-Glo, CTG assay) was performed.

Results Trastuzumab inhibited the tumor growth in a dose-dependent manner in the HER2+ cell line SK-OV3. The efficacy was increased specifically when NK cells were added to the culture. The HER2 positive cell line JIMT-1 was resistant to Trastuzumab treatment, which is in line with published data. The model was derived from a Trastuzumab-refractory patient. Interestingly, the addition of NK cells induced a marked increase of activity in this model as well. The HER2 targeted CART cells eradicated the 3D spheroids of SK-OV3 as well as JIMT-1 in a dose-dependent manner. The untransduced control T cells did not influence the tumor growth at all. The HER2- cell line Hs578T served as a negative control in the Trastuzumab as well as in the CAR-T cell experiments, and proved to be resistant to any treatment in this study. Taken together the 3D live cell imaging platform proved to be a feasible tool for efficacy testing of biologics as well as cellular therapies.

Conclusions Our in house developed HER2 CAR-T cells proved to be specific and effective in eradicating the targeted cancer cells. The mechanism behind the modulated sensitivity of the HER2+ JIMT-1 cells against HER2-targeted treatment will help to shed some light in possible resistance mechanism and hopefully have some translational value for patients suffering from this disease.

<http://dx.doi.org/10.1136/jitc-2021-SITC2021.142>

143

MESOTHELIN (MSLN) TARGETING ALLOGENEIC CAR T CELLS ENGINEERED TO OVERCOME TUMOR IMMUNOSUPPRESSIVE MICROENVIRONMENT

Cecile Schiffer-Mannioui, Sophie Leduc, Isabelle Chion-Sotinel, Diane le Clerre, Valérie Guyot, Marco Rotondi, Roman Galetto*, Agnès Gouble. *Cellectis SA, Paris, France*

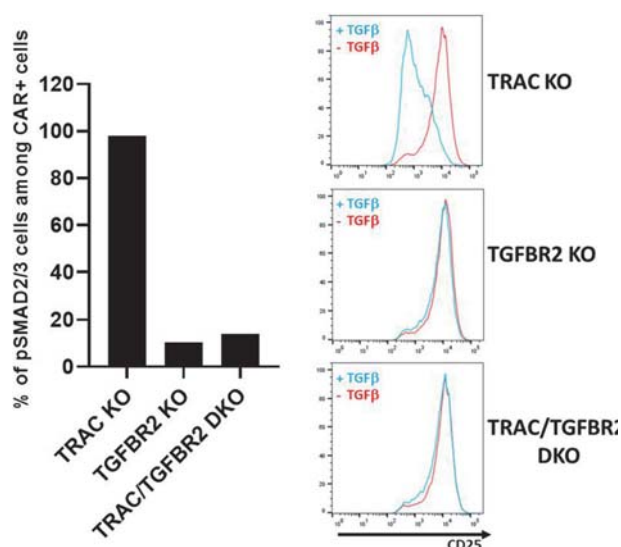
Background Chimeric Antigen Receptor (CAR) T cell therapy is emerging as a potential treatment for solid tumors, even if only limited activity has been observed for CAR T therapies to date. Cellular therapies face indeed many hurdles in solid tumors, such as the immunosuppressive microenvironment. TGF β is an important growth factor of the tumor microenvironment and has been shown to suppress anti-tumor immunity. Gene editing represents a powerful way to enhance properties of CAR T cells and can be used to circumvent the effect of TGF β signaling. The tumor associated antigen mesothelin (MSLN) is an attractive target for cellular therapy; being expressed at high levels in several tumor types (e.g., pleural mesothelioma and pancreatic cancer) while only modestly expressed in healthy tissues.

Methods UCARTMeso, an allogeneic CAR T cell product targeting MSLN expressing cells is being developed by Cellectis. UCARTMeso bears an anti-MSLN CAR and a triple gene knock-out (KO) for TRAC, CD52 and TGFBR2 genes, all generated using TALEN[®] gene-editing technology. TRAC KO limits the risk of GvHD, while CD52 KO allows the use of alemtuzumab in the preconditioning regimen. The additional KO of TGFBR2 confers resistance to the immunomodulatory effects of TGF β within the solid tumor microenvironment.

Results Preclinical studies showed high specificity of the anti-MSLN CAR, as well as potent anti-tumor activity in vitro against different cell lines expressing MSLN. In addition, this activity was confirmed in mouse studies against pancreatic and pleural mesothelioma tumor models, with comparable activities observed in the latest model upon i.v. or intra-pleural administration of UCARTMeso. Also, we observed that TGFBR2 edited anti-MSLN CAR T cells displayed a blockade in the TGF β signaling pathway, being able to respond to antigen stimulation in the presence of TGF β (figure 1).

Conclusions Altogether, we have demonstrated potent antitumor activity in vitro and in vivo, and that addition of the third knock-out of TGFBR2 gene provide valuable additional properties to UCARTMeso cells, representing a very attractive strategy for their use in the treatment of solid tumors.

<http://dx.doi.org/10.1136/jitc-2021-SITC2021.143>



Abstract 143 Figure 1 Left panel: TGF β -induced SMAD2/3 phosphorylation in anti-MSLN CAR T cells. UCARTMeso cells were stained with mesothelin recombinant protein for CAR detection and anti-pSMAD2/3 one hour post exposure to TGF β . The lack of SMAD2/3 phosphorylation in TGFBR2 KO cells indicates that they are unable to trigger TGF β signaling. Right panel: Antigen-induced anti-MSLN CAR T cell activation in the presence (blue histogram) or absence (red histogram) of TGF β . CAR T cells were stained with anti-CD25 antibody and analyzed by flow cytometry 5 days post exposure to antigen \pm TGF β . The data shows that cells not edited at the TGFBR2 locus are unable to be activated upon target exposure in the presence of TGF β , while edited cells were activated in the presence of TGF β , triggering CD25 expression at similar levels as those of cells activated in the absence of TGF β .

SIRP α DEFICIENT CAR-MACROPHAGES EXHIBIT ENHANCED ANTI-TUMOR FUNCTION AND BYPASS THE CD47 IMMUNE CHECKPOINT

Chris Sloas*, Rashid Gabbasov, Nicholas Anderson, Sascha Abramson, Michael Klichinsky, Yumi Ohtani. *Carisma Therapeutics, Philadelphia, PA, USA*

Background Adoptive macrophage cell therapy represents a novel approach for cancer immunotherapy. Macrophages engineered to express chimeric antigen receptors (CAR-M) have shown promising pre-clinical results against solid tumors by improving tumor clearance, overall survival and facilitating the remodeling of the tumor microenvironment to induce a potent adaptive immune response. CD47 is a well-established macrophage immune checkpoint molecule that is over-expressed on tumor cells. CD47 binds to the macrophage signal regulatory protein α (SIRP α) to limit phagocytosis and macrophage effector functions. In this study we evaluated the impact of CD47 on CAR-M activity and showed that CD47-resistant targeted macrophage cell therapy mediates enhanced anti-tumor activity.

Methods CRISPR/Cas9 was used to deplete the cognate receptor SIRP α from primary human macrophages (>90% efficiency and >90% viability) to increase CAR-M function. To assess anti-tumor activity of CAR-M, *in vitro* co-culture assays were established with an anti-human epidermal growth factor receptor 2 (HER2) CAR and HER2+ tumor cell lines. Macrophage killing and phagocytosis of target cells were quantified in real-time using a genetically encoded fluorophore (to monitor tumor cell growth) or a pH-sensitive dye (to monitor phagocytic acidification). In parallel, phenotypic characterization of surface molecules, cytokine secretion levels, biochemical analysis of downstream signaling molecules and response to purified HER2 and CD47 protein stimulation were evaluated.

Results SIRP α knockout (KO) alone failed to induce tumor phagocytosis and cytotoxicity but enhanced targeted CAR-M anti-tumor activity. This was demonstrated by a reduced time required to kill 50% of tumor cells and a 2-fold increase in phagocytic activity, indicating synergy between SIRP α KO and CAR stimulation. Furthermore, in the absence of SIRP α , enhanced cytokine/chemokine secretion, macrophage polarization, and downstream signaling were observed.

Conclusions We show for the first time the feasibility of generating gene edited primary human CAR macrophages for therapeutic purposes, and demonstrate that SIRP α deletion enhances the targeted anti-tumor activity of CAR-M.

<http://dx.doi.org/10.1136/jitc-2021-SITC2021.144>

COMPARISON OF CAR-T CELL MANUFACTURING PLATFORMS REVEALS DISTINCT PHENOTYPIC AND TRANSCRIPTIONAL PROFILES

Hannah Song*, Lipei Shao, Michaela Prochazkova, Adam Cheuk, Ping Jin, David Stroncek, Javed Khan, Steven Highfill. *National Institutes of Health, Bethesda, MD, USA*

Background With the clinical success of chimeric antigen receptor (CAR)-T cells against hematological malignancies, investigators are looking to expand CAR-T therapies to new tumor targets and patient populations. To support translation to the clinic, a variety of cell manufacturing platforms have been developed to scale manufacturing capacity while using closed and/or automated systems. Such platforms are particularly useful for solid tumor targets, which typically require higher CAR-T cell doses that can number in the billions. Although T cell phenotype and function are key attributes that often correlate with therapeutic efficacy, it is currently unknown whether the manufacturing platform itself significantly influences the output T cell phenotype and function.

Methods Static bag culture was compared with 3 widely-used commercial CAR-T manufacturing platforms (Miltenyi CliniMACS Prodigy, Cytiva Xuri W25 rocking platform, and Wilson-Wolf G-Rex gas-permeable bioreactor) to generate CAR-T cells against FGFR4, a promising target for pediatric sarcoma. Selected CD4+CD8+ cells were stimulated with Miltenyi TransAct, transduced with lentiviral vector, and cultured out to 14 days in TexMACS media with serum and IL2.

Results As expected, there were significant differences in overall expansion, with bag cultures yielding the greatest fold-expansion while the Prodigy had the lowest (481-fold vs. 84-fold, respectively; G-Rex=175-fold; Xuri=127-fold; average of N=4 donors). Interestingly, we also observed considerable differences in CAR-T phenotype. The Prodigy had the highest percentage of CD45RA+CCR7+ stem/central memory (Tscm)-like cells at 46%, while the bag and G-Rex cultures had the lowest at 16% and 13%, respectively (average N=4 donors). In contrast, the bag, G-Rex, and Xuri cultures were enriched for CD45RO+CCR7- effector memory cells and also had higher expression of exhaustion markers PD1 and LAG3. Gene clustering analysis using a CAR-T panel of 780 genes revealed clusters of genes enriched in Prodigy/de-enriched in bag, and vice versa. We are currently in the process of evaluating T cell function.

Conclusions This is the first study to our knowledge to benchmark these widely-used bioreactor systems in terms of cellular output, demonstrating that variables inherent to each platform (such as such as nutrient availability, gas exchange, and shear force) significantly influence the final CAR-T cell product. Whether enrichment of Tscm-like cells in the final infusion product correlates with response rate, as has been demonstrated in the setting of CD19 CAR-Ts, remains to be seen and may differ for FGFR4 CAR-Ts and other solid tumors. Overall, our study outlines methods to identify the optimal manufacturing process for future CAR-T cell therapies.

<http://dx.doi.org/10.1136/jitc-2021-SITC2021.145>

146 **EVOLVING MULTIPLEXED SHRNA TO GENERATE
TAILORED CAR T CELL THERAPY**

Mikhail Steklov, Benjamin Lecalve, Jerome Marijse, Fanny Huberty, Nancy Ramelot, Celine Jacques-Hespel, Hannes Iserentant, Eytan Breman*, David Gilham. *Celyad Oncology, Mont Saint Guibert, Belgium*

Background Manipulating protein expression to generate cells with a specific desired phenotype is one of the central goals of engineered cell therapy. Short Hairpin RNA (shRNA) is a well-established approach to reduce protein expression through the targeted degradation of messenger RNA transcripts. However, the use of shRNA in the Chimeric Antigen Receptor (CAR) T cell therapy has been limited. We have recently shown that single shRNA incorporated into a CAR expression vector can knockdown expression of the target antigen when expressed on the CAR T itself to avoid fratricide or expression of some elements of the T cell receptor (TCR) to generate allogeneic CAR T cells. An attraction of the shRNA approach is to express multiple shRNA from the same vector that can regulate protein expression thereby optimizing CAR T cell phenotype.

Methods Retroviral vectors encoding a CAR targeting a well-studied antigen (generally BCMA) co-expressing a tag for cell enrichment and identification along with shRNA multiplexed were generated. The shRNA multiplexed were inserted within a microRNA (miR) framework to enable expression from a single PolII promoter (the retroviral LTR promoter). Functional assessment of target knockdown target in T cells along with retroviral titers was determined

Results Our products in ongoing clinical development have employed a miR196a2 scaffold enabling the expression of the desired shRNA driven by the same promoter as that used for the CAR and other transgenes. Multiplexing the miR196a2 scaffold to express multiple shRNA (targeting CD247, beta 2 Microglobulin and CD95) was successful in terms of target knockdown but an obvious reduction in retroviral titer was observed. These titer reductions were variable between the duplex and triplex shRNA constructs examined but were uniformly low when considering clinical development. A proprietary scaffold was developed that coupled expression of duplexed and triplexed shRNA while also elevating vector titer by at least 2-3x.

Conclusions Multiplexing shRNA within a single vector format with scaffolds that ensure co-linked expression of the shRNA with therapeutic transgenes is a highly attractive approach to generate CAR T cells with bespoke, desired phenotypes. However, simply multiplexing shRNA using a currently clinical-used scaffold (miR196a2) resulted in reductions in vector titer. Engineering further proprietary scaffolds were produced that maintained shRNA expression but elevated retroviral titer to a level which does not preclude clinical development. These developments now provide the opportunity to develop second generation clinical candidates using shRNA multiplexed technology.

<http://dx.doi.org/10.1136/jitc-2021-SITC2021.146>

147

MEMORY PHENOTYPE IN ALLOGENEIC ANTI-BCMA CAR-T CELL THERAPY (P-BCMA-ALLO1) CORRELATES WITH IN VIVO TUMOR CONTROL

Hubert Tseng*, Yan Zhang, Stacey Cranert, Maximilian Richter, Karl Marquez, Jing Qiu, Benjamin Cho, Yening Tan, Min Tong, Christine Domingo, Leslie Weiss, Elvira Argus, Jessica Sparks, Eric Ostertag, Julia Coronella, Devon Shedlock. *Poseida Therapeutics, San Diego, CA, USA*

Background The emergence of CAR-T cell therapy has transformed the treatment of refractory/relapsed multiple myeloma (MM). Yet, autologous CAR-T cells suffer from many manufacturing challenges including mainly consistency, toxicity, and cost. To address these issues, we engineered a fully allogeneic anti-BCMA CAR-T cell candidate for MM from healthy donors (P-BCMA-ALLO1). Herein, we demonstrate that this therapy maintains a stem cell memory T cell (TSCM) phenotype through editing which correlates with in vivo antitumor efficacy.

Methods Using Poseida's non-viral piggyBac® (PB) DNA Delivery System in combination with the high-fidelity Cas-CLOVER™ (CC) Site-Specific Gene Editing System and a proprietary 'booster molecule', we generated P-BCMA-ALLO1 from healthy donor T cells. We used CC to eliminate surface expression of both the TCR and MHC class I to make fully allogeneic CAR-T cells. In addition to the CAR molecule, PB enables the delivery of a selectable marker allowing the generation of a final cell product that is >95% CAR-positive. The inclusion of the 'booster molecule' in the manufacturing process improves the expansion of gene-edited cells without compromising memory phenotype or function. This process can produce up to hundreds of patient doses from a single manufacturing run which significantly reduces manufacturing cost per dose. We characterized the memory phenotype of P-BCMA-ALLO1 by assessing the mRNA and protein expression profiles of rested and activated CAR-T cells by flow cytometry and Nanostring analysis. We also assessed the antitumor capabilities of these cells using cytotoxicity assays and performed serial in vitro restimulation to assess the ability of P-BCMA-ALLO1 to undergo multiple rounds of activation and expansion. We then evaluated the relationship of these characteristics with in vivo efficacy, as defined by control of tumor in an immunodeficient RPMI-8226 subcutaneous murine tumor model.

Results P-BCMA-ALLO1 is comprised of a high frequency of TSCM. It has potent in vivo antitumor activity, which is comparable to non-edited autologous anti-BCMA CAR-T cell therapy. Expression of memory markers at both mRNA and protein levels across individual lots significantly correlates with in vivo tumor control. Conversely, suboptimal research products with worse in vivo outcomes expressed an exhausted gene expression profile. Moreover, CAR-T products that are more effective in vivo are also more viable, cytotoxic, and proliferative following multiple rounds of restimulation in vitro.

Conclusions P-BCMA-ALLO1 is a highly potent and safe allogeneic anti-BCMA CAR with a manufacturing process that consistently maintains a TSCM phenotype, which correlates with antitumor efficacy. P-BCMA-ALLO1 is advancing rapidly towards the clinic (NCT04960579).

<http://dx.doi.org/10.1136/jitc-2021-SITC2021.147>

148 PRIMARY OR IPSC-DERIVED CELL-BASED CYTOTOXICITY ASSAYS TO ASSESS POTENTIAL SAFETY RISKS OF ENGINEERED T CELL THERAPIES *IN VITRO*

Sophie Vermond*, Monique Hazenoot, Rene McLaughlin, Sabrina de Munnik, Marco Guadagnoli, Gemma Moiset, Sanne Holt, Marijn Vlaming. *Charles River Laboratories, Leiden, Netherlands*

Background Engineered T cell therapies, such as Chimeric Antigen Receptor (CAR) T cell therapies offer great promise in becoming a new wave of highly specific therapies against solid tumors. Solid tumors generally lack the expression of tumor specific target antigens. The alternatively selected target antigens are often expressed at low levels in healthy tissues throughout the human body as well, which poses the risk of activation of engineered T cell therapies against these tissues resulting in severe side effects. Therefore, assessing the safety of engineered T cell therapies is a critical step during early development and before filing for Investigational New Drug (IND) status.

Methods Using a set of assays, we have generated an *in vitro* safety profile for CAR-T cells targeting the 'Human Epidermal growth factor Receptor 2' (HER2) which is amplified and/or overexpressed in 20–30% of invasive breast carcinomas and ovarian cancers. To determine which tissues are most at risk for unwanted CAR-T cell reactivity, *in silico* analysis for expression of the HER2 gene was performed. Subsequently, HER2 protein expression in various tissues was validated by flow cytometry using a HER2 targeting antibody. Primary tissues and hiPSC-derived cells with high and low HER2 protein expression were selected, characterized, and utilized for *in vitro* co-culture assays to evaluate on-target off-tumor and/or off-target cytotoxicity of CAR-T cells. As readout we measured target cell viability by flow cytometry and/or high content analysis and T cell activation by cytokine release.

Results Our study generated high quality data that provided insight into the safety of the HER2 targeting CAR-T cells. Cytotoxicity of HER2 CAR-T cells against low HER2 expressing human healthy cardiomyocytes and renal cells was observed with a clear E:T ratio dependent effect which was confirmed by IFN γ secretion. HER2 negative neurons showed a clear absence of CAR-T response. This data suggests a safety risk of our HER2 targeting CAR-T cells against heart and renal tissue.

Conclusions Engineered T cell therapies have the capacity to fill tremendous unmet medical needs and are moving into the clinic at a high pace. Shortening the timeframe towards clinical application, requires assay panels which can be conducted quickly and in are in line with the rigorous safety tests required before FDA approval. Our strategy of using primary tissues and hiPSC derived cells to generate a safety profile for these therapies *in vitro* is robust and can be applied during both early-stage development and late-stage testing of the therapeutic product.

<http://dx.doi.org/10.1136/jitc-2021-SITC2021.148>

IN VITRO EFFICACY STUDIES TO SUPPORT ENGINEERED T CELL THERAPIES

Sabrina de Munnik*, Monique Hazenoot, Sophie Vermond, Rene McLaughlin, Marco Guadagnoli, Gemma Moiset, Sann Holt, Marijn Vlaming. *Charles River, Leiden, Netherlands*

Background Cell therapies such as Chimeric Antigen Receptor T cells (CAR-T) and T Cell Receptor (TCR) T cells are immune-therapeutic approaches showing great momentum in research and the clinic. To date, four anti-CD19 CAR-T products and one anti-BCMA CAR-T products have been approved by the FDA for the treatment of lymphoid malignancies. Many more CAR-T cell products are currently being explored, targeting a wide variety of tumor antigens directed towards both liquid and solid tumors as well other clinical indications. In early-stage pre-clinical development, the use of *in vivo* animal models has presented significant hurdles in translatability of cell therapies. As a result, the establishment of high-quality *in vitro* efficacy and safety studies to foster the development of such therapies has become critical. The purpose of this study was to develop several *in vitro* efficacy experiments aimed at determining cell therapy activity, specificity and potency.

Methods We have generated CAR-T cells targeting the Human Epidermal growth factor Receptor 2 (HER2) as a model system. *In vitro* cytotoxicity co-culture assays were developed using flow cytometry-, high content analysis- or impedance-based read-outs.

Results HER2 CAR-T cells efficiently reduced the viability of the HER2-positive cell line ZR-75-30 in an effector:target cell ratio-dependent manner but had a limited effect on the viability of the HER2-negative cell line MDA-MB-468, confirming the activity and selectivity of the T cell therapy. A more complex three-way co-culture system (HER2 CAR-T cells co-cultured with both HER2-positive and -negative target cells) confirmed HER2 CAR-T specificity under activating conditions. Finally, following several rounds of antigen stimulation, the HER2 CAR-T cells persistently killed HER2-positive tumor cells, indicative of 'cellular fitness'.

Conclusions To conclude, we developed several *in vitro* proof of concept assays for the assessment of cell therapy activity, specificity, and potency during early-stage development. (Three-way) co-culture or repeated antigen stimulation assays can be used to aid cell therapy discovery research and lead optimization. These *in vitro* assays will provide the possibility to select the best therapies to further progress to clinic.

<http://dx.doi.org/10.1136/jitc-2021-SITC2021.149>

TARGETED DELIVERY OF A PD-L1-BLOCKING SCFV BY CAR-NK CELLS SHOWS POTENTIAL AS A NEW APPROACH TO IMMUNOTHERAPY FOR GLIOBLASTOMA

Jiao Wang*, Sandro Matosevic. *Purdue University, West Lafayette, IN, USA*

Background Despite advances in treatment, glioblastoma (GBM) remains an incurable primary brain tumor with a median survival of only 15 months, highlighting the need for new therapeutic approaches. Natural killer (NK) cells, innate cytotoxic effectors, are showing potential for cancer immunotherapy including GBM. Even though GBM tumors are infiltrated by NK cells.¹ However, their antitumor activities are impaired by the immunosuppressive tumor microenvironment (TME) via various mechanisms, including adenosine-mediated downregulation of NKG2D.² Therefore, it is critical to understand more about how the TME in GBM modulates the NK cell-mediated immunity so that we can develop novel NK cell-based therapies specifically for GBM.

Methods We isolated human peripheral blood NK cells from healthy volunteer donors. U87MG and GBM43 were used as GBM targets. We co-cultured NK cells with GBM cells and measured the PD-L1 expression on the NK cells. We built a transwell co-culture system to evaluate the crosstalk between NK and GBM cells on the PD-L1 expression on GBM target cells. We then generated gene-modified NK cells expressing an NKG2D.CAR which secretes anti-PD-L1 scFv locally in the TME. These NK cells are being evaluated for their efficacy against GBM both in vitro and in vivo.

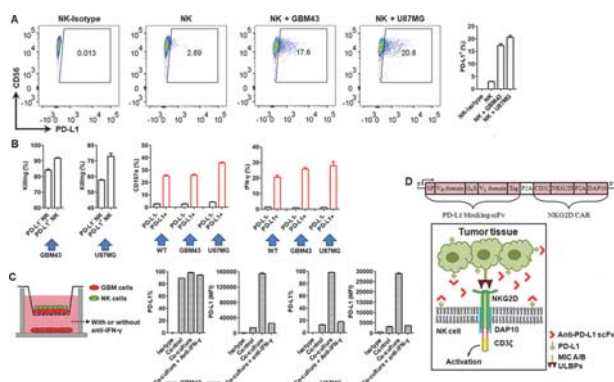
secretable PD-L1-blocking scFv and a CAR redirected against ligands for NKG2D (figure 1D).

Conclusions After direct contact with GBM cells, the increased population of PD-L1+ NK cells with superior cytolytic functions have been found for the first time. Also, NK cells co-cultured with GBM cells can further trigger PD-L1 upregulation on GBM cells. Stimulated by these results, we have been generating NK cells that can, at once, secrete the PD-L1-blocking scFv to target PD-L1 both expressed on NK and GBM cells, and express the NKG2D.CAR to specifically target its ligands on GBM cells. We are currently testing the in vitro and in vivo therapeutic efficacy of these engineered NK cells, which we believe could be used as a promising immunotherapy for GBM.

REFERENCES

1. Wang J, Matosevic S. NT5E/CD73 as correlative factor of patient survival and natural killer cell infiltration in glioblastoma. *J Clin Med* 2019;**8**(10):1526.
2. Wang J, Lupo KB, Chambers AM, Matosevic S. Purinergic targeting enhances immunotherapy of CD73+ solid tumors with piggyBac-engineered chimeric antigen receptor natural killer cells. *J Immunother Cancer* 2018;**6**(1):136.

<http://dx.doi.org/10.1136/jitc-2021-SITC2021.150>



Abstract 150 Figure 1 (A) PD-L1 expression on human primary NK cells after co-incubation with different types of cancer target cells, including U87MG (human glioblastoma cell line) and GBM43 (a human patient-derived glioblastoma cell line) cells at a E/T ratio of 10 for 24 h, respectively; (B) In vitro anti-GBM activities of PD-L1- NK cells vs PD-L1+ NK cells, including killing, degranulation (CD107a), and IFN- γ secretion; (C) Setup of transwell system for evaluation of PD-L1 expression on GBM target cells upon co-culture with NK cells; (D) Multifunctional genetically-engineered NK cells for GBM immunotherapy. Data are presented as the mean \pm SEM

Results We have found that GBM target cells can upregulate PD-L1 expression on NK cells (figure 1A). And induced PD-L1+ NK cells present better in vitro anti-GBM activity, including higher killing, degranulation and IFN- γ release (figure 1B). We have revealed that the expression of PD-L1 on GBM cells gets further boosted after crosstalk with NK cells, which is dependent on the induced IFN- γ release (figure 1C). Accordingly, we have designed and synthesized a multifunctional CAR construct that enables NK cells to express a

POTENTIATING THE LARGE-SCALE EXPANSION AND ENGINEERING OF PERIPHERAL BLOOD-DERIVED CAR NK CELLS FOR OFF-THE-SHELF APPLICATION

Michael Whang*, Ming-Hong Xie, Kate Jamboretz, Hadia Lemar, Chao Guo, Nafees Rahman, Ivan Chan, Erik Whiteley, Ralph Brandenberger, Sasha Lazetic, James Trager. *Nkarta Therapeutics, South San Francisco, CA, USA*

Background Peripheral blood natural killer (NK) cells are mature cytotoxic innate lymphocytes possessing an inherent capacity for tumor cell killing, thus making them attractive candidates for adoptive cell therapy. These NK cells are also amenable to CRISPR and chimeric antigen receptor (CAR) genomic engineering for enhanced functions. Moreover, NK cells possess an inherent capacity for off-the-shelf therapy since they are not known to cause graft-versus-host disease, unlike T cells. Presently, approved CAR cell therapy is custom-made from each patient's own T cells, a process that can limit patient pool, narrow therapeutic window, and contribute to product variability. In this study, we investigate whether peripheral blood NK cells from a selected donor can be edited, engineered, and expanded sufficiently for off-the-shelf use in a wide patient population.

Methods Using the CRISPR/Cas9 system, we knocked out CISH expression in isolated peripheral blood NK cells from 3 healthy donors. Subsequently, we expanded edited NK cells by using IL-2 and sequential stimulations using NKSTIM, a modified K562 stimulatory cell line expressing membrane-bound form of IL-15 (mbIL-15) and 4-1BBL. IL-12 and IL-18 were added twice during expansion to drive memory-like NK cell differentiation. We transduced the expanded NK cells to express engineered CD19-targeted CAR and mbIL-15 during an interval between the first and second NKSTIM pulses. We assessed NK cell cytotoxicity against Nalm6 target cells by IncuCyte.

Results Isolated peripheral blood NK cells from 3 healthy donors were successfully edited using CRISPR/Cas9, engineered to express high levels of CAR, extensively expanded using a series of NKSTIM pulses in the presence of IL-2, and differentiated into memory-like NK cells using IL-12 and IL-18. Interestingly, NK cells from the 3 donors exhibited distinct outcomes. NK cells from one donor reached a peak expansion limit of approximately 7-million-fold before undergoing contraction whereas NK cells from two donors continued to expand over the length of the study surpassing 100-million-fold expansion, without appearing to have reached a terminal expansion limit. At the end of the study, NK cells from one donor exceeded 1-billion-fold expansion and maintained 88% cytolytic activity compared to Nkarta's standard process control in a 72-hour IncuCyte assay.

Conclusions In this study, we demonstrate that healthy donor-derived peripheral blood NK cells are capable of expanding over billion-fold while maintaining potency. These results provide a rationale for the development of off-the-shelf CAR NK cell therapies using NK cells from donors selected to provide optimal product characteristics.

Ethics Approval Human samples were collected with written informed consent by an approved vendor.

<http://dx.doi.org/10.1136/jitc-2021-SITC2021.151>

COMMON TRAJECTORIES OF HIGHLY EFFECTIVE ANTI-CD19 CHIMERIC ANTIGEN RECEPTOR-MODIFIED T CELLS IDENTIFIED BY ENDOGENOUS T CELL RECEPTOR LINEAGES

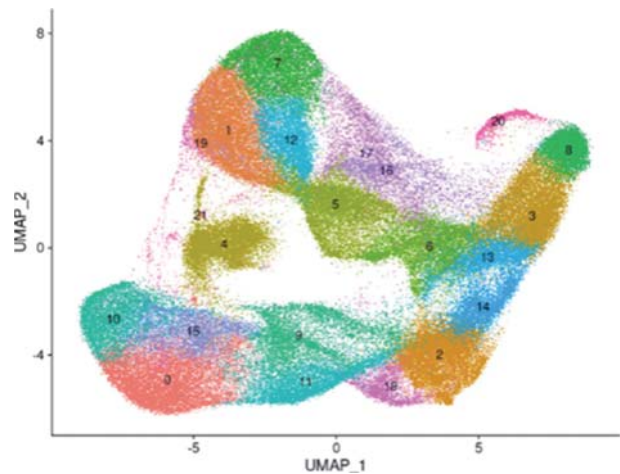
Taylor Wilson*, Hyunjin Kim, Jeremy Crawford, Ching-Heng Chou, Deanna Langfitt, E Kaitlynn Allen, Timothy Lockey, Michael Meagher, Aimee Talleur, Stephen Gottschalk, Paul Thomas. *St. Jude Children's Research Hospital, Memphis, TN, USA*

Background Chimeric antigen receptor modified (CAR) T cells have revolutionized the treatment of blood cancers, though some patients still show a poor response in either CAR expansion, effector response, or persistence.¹ In this study, we determined the features of pre-infusion CAR-transduced T cells that generated optimally functional responses after infusion.

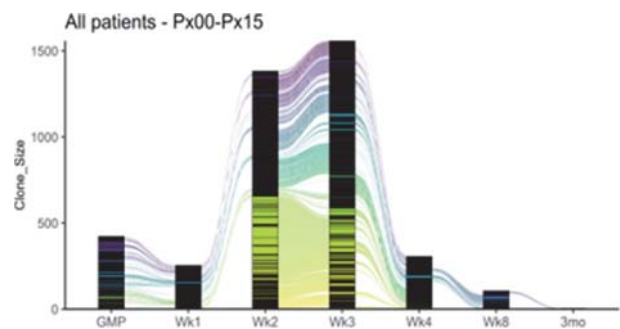
Methods Using both the pre-infusion product and PBMCs isolated at weeks 1–4, 8, and 3-months post-infusion from 15 patients undergoing experimental anti-CD19 CAR T cell treatment for refractory or relapsed B-ALL, we generated a comprehensive single cell gene expression and T cell receptor (TCR) sequencing dataset on over 180,000 CAR T cells (figure 1).

Results As expected, pre-infusion CAR T cells tend to highly express genes associated with proliferation, while post-infusion CARs show signs of either cytotoxic effector differentiation or dysfunctional terminal differentiation. Sequencing of the endogenous TCR, at the single cell level, allows us to track the trajectories of clonally and transcriptionally related cells (figure 2). Post-infusion cells with significant cytotoxic effector function share TCRs with a statistically defined subset of CARs in the pre-infusion sample (figure 3). Using a machine learning approach, we found that potent effector precursor CAR T cells have a specific transcriptional profile distinct from the other pre-infusion CAR T cells, including markers of early effector function such as increased EOMES, GNLY, GZMH, GZMK, KLRD1, and IFN γ . Formalizing this signature, we have developed a robust classifier that can predict with 82.8% accuracy whether a CAR T is likely to become a favorable effector based on its pre-infusion profile (figure 4). This prediction model can be used to evaluate the extent to which a patient's generated CAR product will be able to mount a robust response after encountering its target. Additionally, there are a number of genes, as a part of this signature, that are expressed on the cell surface and can be utilized as a method to differentiate the effector precursor pre-infusion CAR T cells from other pre-infusion CARs, including CD52, CD74, CD86, and LAG3, among others.

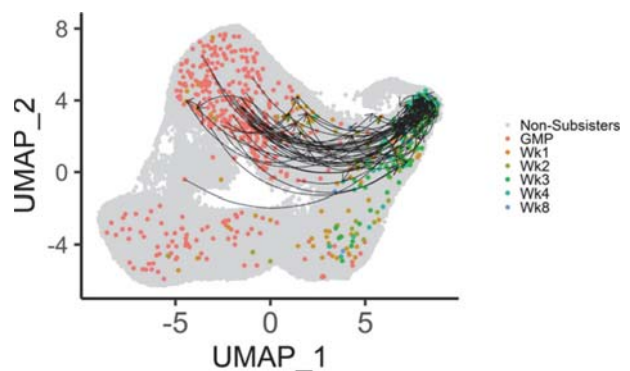
Conclusions Our findings suggest a therapeutic approach that enriches these cells prior to infusion resulting in superior per cell CAR effector activity.



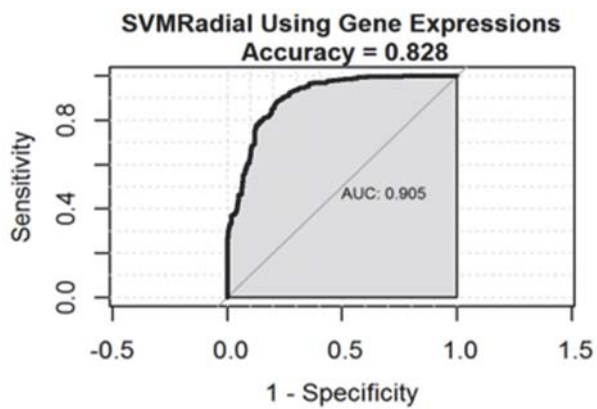
Abstract 152 Figure 1 Clustering of 184,791 CAR-transduced T cells based on gene expression



Abstract 152 Figure 2 Alluvial plot depicting CAR T cell lineage tracing using the endogenous T cell receptor



Abstract 152 Figure 3 Visualization of CAR T cell clusters with arrows indicating the shared TCRs between pre-infusion and post-infusion cells



Abstract 152 Figure 4 Machine learning classifier of pre-infusion, early effector CAR T cell phenotype

REFERENCE

1. Xu X, Huang S, Xiao X, Sun Q, Liang X, Chen S, et al. Challenges and Clinical Strategies of CAR T-cell Therapy for Acute Lymphoblastic Leukemia: Overview and Developments. *Front Immunol* 2020;**11**:569117.

Ethics Approval This study was approved by St. Jude Children's Research Hospital's Institutional Review Board (IRB); IRB number Pro00007661. All patients consented to the use of materials for the research study.

<http://dx.doi.org/10.1136/jitc-2021-SITC2021.152>

NANOSCALE, ANTIGEN-DEPENDENT, IL-12 DELIVERY BY CAR T CELLS PLUS PD-L1 BLOCKADE FOR CANCER TREATMENT

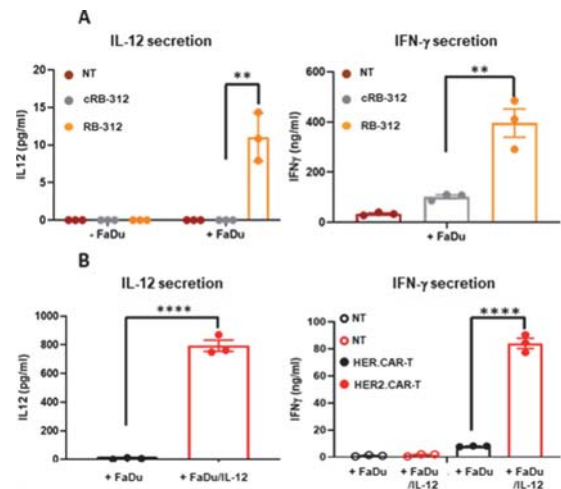
¹Zhifen Yang*, ²Francesco Marincola. ¹Refuge Biotech, Menlo Park, CA, USA; ²Refuge Biotech, currently Gilead/Kite, Santa Monica, CA, USA

Background Interleukin(IL)-12 activates T cells pivoting the switch that turns lingering inflammation into acute inflammation and cancer rejection. However, its clinical utilization is limited by severe systemic toxicity. IL-12 is a potent inducer of PD-1 expression in T cells. Here, we present a conditional, antigen-dependent, non-editing CRISPR-activation (CRISPRa) circuit (RB-312) that delivers nanoscale doses of IL-12 for autocrine activation of CAR-T cells. RB-312 was also tested in combination with PD-L1 blocking antibody (atezolizumab).

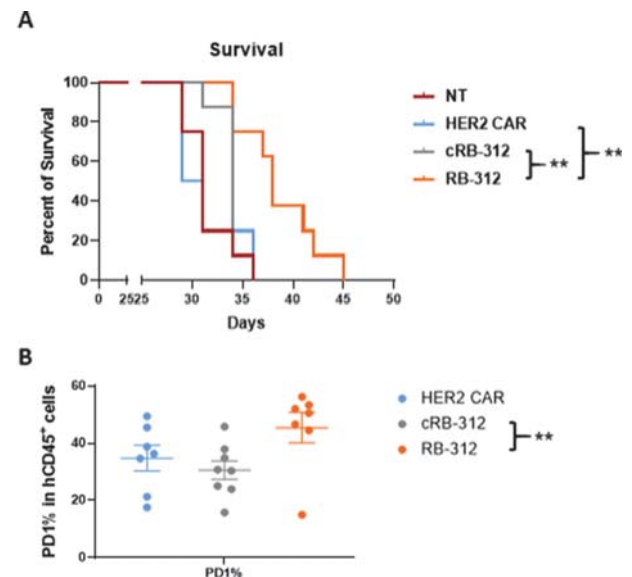
Methods RB-312 is a CAR T cell engineered to express the IL-12 heterodimer via conditional transcription of its two endogenous subunits p35 and p40. The circuit includes two lentiviral constructs with one encoding HER2-specific chimeric antigen receptor and two sgRNAs targeting IL-12A or IL-12B and the other encoding linker for activation of T cells, complexed to dead Cas9 (dCas9)-VP64-p65-Rta transcriptional activator (VPR) (LdCV). Activation of CAR allows the release of dCas9 for nuclear localization and hence conditionally and reversibly induces the secretion of IL-12 p70 heterodimer.

Results RB-312 induced low concentrations of IL-12 upon exposure to HER2+ FaDu cancer cells engineered to overexpress PD-L1 and this resulted in significantly enhanced production of IFN- γ , cytotoxicity and CAR-T proliferation (figure 1A). These effects were comparable to co-culturing conventional HER2 CAR with FaDu cells modified to express high doses of IL-12 (figure 1B). In vivo administration of RB-312 significantly enhanced survival of mice carrying FaDu xenografts compared to mice treated with the respective conventional HER2 CAR or cRB-312 (control lacking the IL-12 sgRNAs, figure 2A). RB-312 induced a strong upregulation of PD-1 in CAR-T cells in vivo (figure 2B). The critical role of the PD-1/PD-L1 interaction was demonstrated in vitro by comparing RB-312 proliferation when exposed to FaDu overexpressing PD-L1 or PD-L1 knock out cells (figure 3A). Indeed, combined treatment of RB-312 and atezolizumab resulted in significant reduction in tumor growth (figure 3B and C) and significantly enhanced survival (figure 3D).

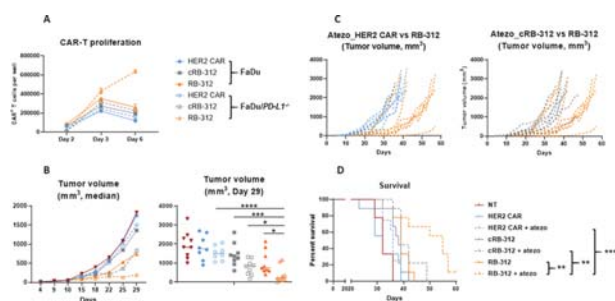
Conclusions We concluded that addition of a Th1 polarizing component such as IL-12 exponentially increases the efficacy of reprogrammed CAR-T cells by combining enhancement of effector functions to cellular fitness. The autocrine effects of nanoscale IL-12 production limit the risk of off-tumor leakage and systemic toxicity. Here, we tested the combination of PD-1/PD-L1 blockade with IL-12-induced CAR-T cell activation demonstrated dramatic synergistic effects. We are currently evaluating the intrinsic combination of IL-12 delivery and PD-L1 resistance for the next generation of RB-312 product eliminating the need for systemic checkpoint blockade.



Abstract 153 Figure 1 Conditional autocrine release of nanoscale-dose p70/IL-12 by RB-312 resulting in enhanced IFN- γ production in vitro after three days of exposure to HER2+ FaDu cells (figure 1A), and the level of IFN- γ production was comparable to co-culturing conventional HER2-specific CAR-T cells with a modified FaDu cell line engineered to constitutively express high doses of IL-12 (FaDu/IL-12, figure 1B)



Abstract 153 Figure 2 Intra-tumoral administration of RB-312 extended survival in mice carrying FaDu xenografts compared to NT (non-transduced T cells), HER2 CAR (conventional HER2 CAR-T cells) and cRB-312 CAR-T cells missing the sgRNAs for the two IL-12 subunits (figure 2A). Analysis of necropsy material demonstrated that PD-1 expression was dramatically increased in RB-312 compared with the respective control cRB-312 (figure 2B)



Abstract 153 Figure 3 RB-312 cellular function in vivo. PD-L1 expression by FaDu cell lines is a critical mechanism of repression of RB-312 function. In vitro CAR-T proliferation of RB-312 upon stimulation with FaDu tumor cells (orange solid lines) or FaDu/PD-L1 knockout tumor cells (orange dashed lines) over 6-day time course (figure 3A). In vivo efficacy of intra-tumoral RB-312 against FaDu tumor cells with (orange solid lines) or without (orange dashed lines) addition of PD-L1 blocking antibody atezolizumab (administered intravenously at 5 mg/kg twice per week), as shown by tumor growth followed till day 29 and scatter plot at day 29 (figure 3B), tumor growth spider plots (figure 3C) and Kaplan-Meier survival curve (figure 3D)

<http://dx.doi.org/10.1136/jitc-2021-SITC2021.153>

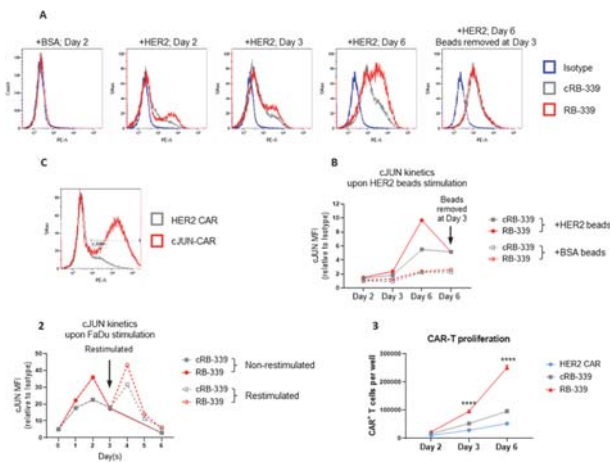
CONTEXT-DEPENDENT REVERSIBLE MODULATION OF cJUN EXPRESSION BY CAR T CELLS FOR CANCER TREATMENT

¹Zhifen Yang*, ²Francesco Marincola. ¹Refuge Biotech, Menlo Park, CA, USA; ²Refuge Biotech, currently Gilead/Kite, Santa Monica, CA, USA

Background Overexpression of canonical AP-1 factor cJUN was shown to prevent CAR T cell exhaustion and improve anti-tumor potency in vivo (1). However, its clinical utilization is limited by potential for transformation and oncogenic risk. Here, we present a conditional, antigen-dependent, non-editing CRISPR-activation (CRISPRa) circuit (RB-339) that delivers context-dependent upregulation of endogenous cJUN increasing CAR-T cell resistance to exhaustion.

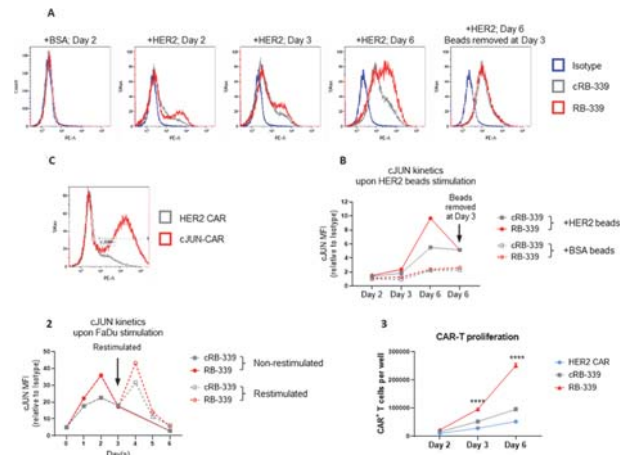
Methods RB-339 is a CAR T cell engineered to conditionally turn on the transcription of the cJUN endogenous gene. The circuit includes a lentiviral construct encoding an anti-HER2 (4D5) single chain variable fragment, with CD28 and CD3 ζ co-stimulatory domains linked to a tobacco etch virus (TEV) protease and a single guide RNA (sgRNA) targeting the promoter region of cJUN. A second construct encodes linker for activation of T cells, complexed to nuclease-deactivated/dead Cas9 (dCas9)-VP64-p65-Rta transcriptional activator (VPR) via a TEV-cleavable linker (LdCV). Activation of CAR allows the release of dCas9 for nuclear localization and conditionally and reversibly induces the expression of cJUN. RB-339 was compared in vitro to control (cRB-339, lacking the cJUN sgRNA) and CAR-T cells engineered to constitutively express cJun.

Results RB-339 induced cJUN upregulation upon stimulation with HER2-coated beads and this resulted in significantly elevated expression over a 6-day time course compared to the control cRB-339 (figure 1A-B). When HER2-coated beads were removed at day 3, cJUN expression returned to baseline parallel to cRB-339. The conditional upregulation of cJUN in RB-339 contrasted with the constitutive overexpression in the transgene carrying cells that was irrespective of antigen stimulation (figure 1C). Upon exposure to HER2+ FaDu cancer cells, RB-339 peaked at day 2 and declined afterwards when FaDu cells were killed at day 3; cJUN increased again at day 4 upon restimulation with FaDu cells at day 3 (figure 2). Such a dynamic induction of cJUN resulted in significantly enhanced CAR-T cells proliferation in RB-339 compared to the respective conventional CAR-T cells or cRB-339 (figure 3).

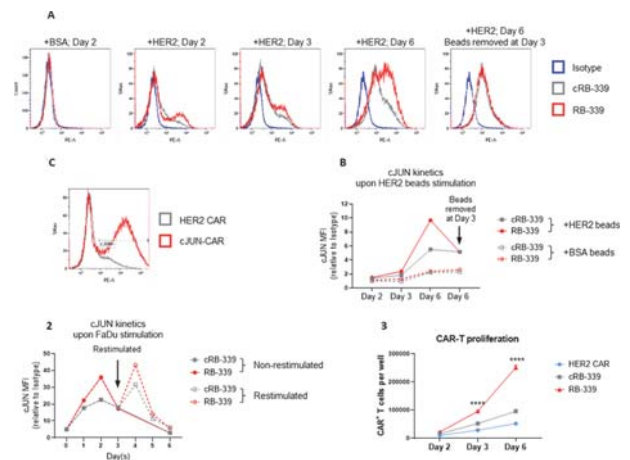


Abstract 154 Figure 1 Conditional upregulation of cJUN by RB-339 in vitro. RB-339 and its control cRB-339 were stimulated by HER2-coated or BSA-coated beads for either six days or three days followed

by removal of beads at day 3 (figure 1A-B). Intracellular expression of cJUN was detected at indicated time points. Intracellular cJUN expression in overexpressed cJUN-CAR (figure 1C)



Abstract 154 Figure 2 Kinetics of cJUN upregulation in RB-339 upon exposure to HER2+ FaDu tumor cells. RB-339 and its control cRB-339 were stimulated by FaDu tumor cells for six days with or without restimulation at day 3



Abstract 154 Figure 3 Conditional upregulation of cJUN resulted in enhanced CAR-T proliferation in RB-339 in vitro after 6-day co-culture with FaDu tumor cells, compared to conventional HER2 CAR or cRB-339

Conclusions We conclude that CAR-T engineered to conditionally express the canonical AP-1 factor cJUN increases expansion potential similarly to CAR-T cells engineered to constitutively express the cJun transgene. However, the context-dependent upregulation of cJUN limits the risk of oncogenic transformation. We are currently combining inducible and reversible cJUN and IL-12 upregulation for the generation of the next RB-339 product.

REFERENCE

- Lynn RC, Weber EW, et al. c-Jun overexpression in CAR T cells induces exhaustion resistance. *Nature* 2019; **576**(7786):293-300.

<http://dx.doi.org/10.1136/jitc-2021-SITC2021.154>

CD5 KNOCKOUT ENHANCES THE POTENCY OF MULTIPLEX BASE-EDITED ALLOGENEIC ANTI-CD5 CAR T-CELL THERAPY FOR THE TREATMENT OF T-CELL MALIGNANCIES

Yinmeng (Amy) Yang*, Ryan Murray, Adam Camblin, Faith Musenge, Lindsey Coholan, MarkVic Naniong, David Sweezy, Scott Haskett, Lauren Young, Yingying Zhang, Amanda Costa, Hui Wu, Alden Ladd, Luis Barrera, Lisa Schlehuber, Sarah Smith, Yeh-Chuin Poh, Giuseppe Ciaramella, Jason Gehrke. *Beam Therapeutics, Boston, MA, USA*

Background T-cell lymphomas and leukemias are a class of diseases lacking durable effective therapies, where median survival for patients suffering from relapsed/refractory disease is often measured in months. Translation of B-cell targeting CAR-T therapeutic success to T-cell malignancies comes with significant challenges. Notably, the shared expression of target antigens on malignant T-cells and in the T-cell product itself results in CAR-T activation and fratricide during manufacturing. To overcome the challenges associated with creating CD5-targeting CAR-Ts, we developed a process to simultaneously base edit five target genes, including CD5 and PD1, to produce potency-enhanced allogeneic anti-CD5 CAR T-cells for use as an off-the-shelf treatment for T-cell malignancies.

Methods Anti-CD5 CAR-Ts were produced in a GMP-compatible process using T-cells isolated from healthy human donors. T-cells were modified using base editing technology to simultaneously knock-out five target genes in a single electroporation step. Edited T-cells were transduced with a lentivirus encoding a second-generation anti-CD5 CAR. Knockout frequencies were evaluated by flow cytometry and next-generation sequencing. Anti-CD5 CAR-Ts were then characterized for their specificity in vitro and potency in in vivo xenograft tumor models.

Results Simultaneous base editing at five genomic loci resulted in anti-CD5 CAR-Ts edited with 94–98% efficiency at each target gene, greatly diminishing the likelihood of GvHD, CAR-T rejection, fratricide, and checkpoint inhibitor activation. In addition, CD5 has an established role as a negative regulator of TCR signaling, and T cells lacking CD5 have enhanced proliferative capacity.¹ Anti-CD5 CAR T-cells with or without CD5 KO demonstrated equally potent cytotoxicity and cytokine production in vitro against CD5 expressing tumor lines. However, CD5 KO greatly improved in vivo efficacy of anti-CD5 CAR-Ts in a murine model of T-ALL against established tumor xenografts. Mice previously cleared of tumor underwent a second tumor challenge to assess the persistence of anti-CD5 CAR-T cells and were cleared of tumor a second time, indicating extended persistence of functional anti-CD5 CAR-T cells in vivo.

Conclusions Our approach addresses current technological limitations in developing and applying CAR-Ts that target T-cell malignancies and demonstrates that simultaneous multiplex base editing of up to five targets can create universally compatible, fratricide-resistant, therapeutically active anti-CD5 CAR-Ts. We further demonstrate that CD5 knockout produces CAR-T cells with enhanced potency capable of clearing multiple tumor challenges in vivo. We are progressing this CD5-targeting CAR-T cell product towards potential clinical development for the treatment of T cell malignancies and other CD5+ hematological tumors.

REFERENCE

- Guillaume V, Peredo G, Romain R. CD5, an Undercover Regulator of TCR Signaling. *Frontiers in Immunology* 2018;**9**:2900.

Ethics Approval All animal studies were performed according to the guidelines and approval of the Institutional Animal Care and Use Committee.

<http://dx.doi.org/10.1136/jitc-2021-SITC2021.155>

RBC-DERIVED, ACTIVATING ANTIGEN CARRIERS (SQZ AACs) PRIME POTENT T CELL RESPONSES AND DRIVE TUMOR REGRESSION IN VIVO

Katarina Blagovic*, Carolyne Smith, Lindsay Moore, Emrah Ilker Ozay, Armon Sharei, Howard Bernstein, Scott Loughhead. *SQZ Biotechnologies, Watertown, MA, USA*

Background T cell responses are at the core of checkpoint inhibitor success in treating cancer; however, generating targeted antigen presentation to stimulate T cell responses remains challenging. Here, we take advantage of the natural process of eryptosis by professional antigen presenting cells (APCs) to drive antigen presentation and T cell activation in human and mouse models. Through the delivery of tumor antigen and adjuvant to red blood cells (RBCs) using the Cell Squeeze® platform, we generate activating antigen carriers (AACs) for use in tumor-specific cancer vaccines.

Methods Following intravenous AAC administration, we measured clearance kinetics of AACs and characterized the site and cell type of AAC uptake. We investigated upregulation of activation markers on phagocytes that engulf AACs, and the effect of priming and boosting on endogenous T cell responses. To determine the ability of AACs to control implanted tumors, we measured tumor growth rates in mice therapeutically treated with AACs. Tumor growth of AAC-treated mice in combination with a chemotherapy treatment was also assessed. Additionally, the in vitro uptake of adjuvant loaded human AACs and resultant maturation of monocyte-derived dendritic cells (MoDCs) was measured to qualify adjuvant delivery. Peptide antigen delivery to human AACs was measured with flow cytometry and fluorescence microscopy.

Results Squeezing effectively loads AACs with antigen and adjuvant and leads to exposure of phosphatidylserine on the AAC membrane. When administered into a mouse, mouse AACs were cleared from circulation within one hour and were engulfed by professional phagocytes in both the spleen and liver. In vivo, AACs induced upregulation of maturation markers on endogenous dendritic cells (DCs) and macrophages. Therapeutic AACs administration significantly slowed growth of the HPV-associated tumor, TC-1, and extended survival of treated animals. These anti-tumor responses correlated with >500-fold increase in antigen-specific CD8+ tumor-infiltrating lymphocytes compared to untreated mice. Boosting enhanced endogenous T cell responses and enhanced the efficacy of low dose vaccinations in a tumor model. Combination with early (days 7 and 9) or late (days 17 and 24) treatment with a chemotherapeutic agent cleared tumors in treated animals. In an in vitro human system, the intracellular delivery of peptide antigen and adjuvant to human AACs induced MoDC maturation and stimulated E7-specific CD8+ T cell responses.

Conclusions AACs loaded with antigen and adjuvant can effectively drive antigen presentation and prime a potent anti-tumor response in mice. These preclinical data support the further study of SQZ AACs as an immunotherapy for cancer treatment.

Ethics Approval All methods were performed in accordance with the relevant guidelines and regulations. Animal studies were approved by the Institutional Animal Care and Use Committee (IACUC) at SQZ Biotechnologies, using the recommendations from the Guide for the Care and Use of Laboratory Animals of the National Institutes of Health and the Office of Laboratory Animal Welfare. All activities were also

conducted in accordance with Public Health Service (PHS) Policy on Humane Use and Care of Laboratory Animals.

<http://dx.doi.org/10.1136/jitc-2021-SITC2021.156>

LYMPH NODE TARGETED BOOSTING WITH COGNATE AMPHIPHILE-PEPTIDE VACCINES ENHANCES TCR-T CELL THERAPY TO ERADICATE SOLID TUMORS

Dylan Drakes*, Abdulraouf Abbas, Jacqueline Shields, Peter DeMuth. *Elicio Therapeutics, Boston, MA, USA*

Background Clinical results from TCR-T Cell therapies demonstrate anti-tumor efficacy, although therapeutic benefits remain transient due to suboptimal T Cell functional persistence and tumor infiltration alongside antigen escape mechanisms.^{1 2 3 4}

⁵ Amphiphile (AMP) vaccines improve lymph node targeting of cancer immunogens, stimulating an enhanced endogenous anti-tumor response.^{6 7} We describe an approach to generate robust and durable anti-tumor responses by combining AMP lymphatic targeting with TCR-T Cell therapy. AMP cognate peptides traffic to lymph nodes and improve TCR-T Cell activation, persistence, and function compared to soluble (SOL) peptide vaccination or TCR-T Cells alone, inducing a superior anti-tumor effect.

Methods C57BL/6J mice were subcutaneously implanted with B16F10 10 days prior to transduced pmel-1 T cell transfer or 75 days after T cell treatment for rechallenge experiments. Tumor-bearing mice received 5 doses, 2x/week of AMP-GP100/AMP-CpG, SOL-GP100/SOL-CpG, or PBS by tail-base vaccination. Caliper measurements determined tumor progression and overall survival. TCR-T Cell persistence was assessed bi-weekly through retro-orbital bleeds. Tumors and lymph nodes from treated mice were excised and analyzed by Nanostring for differential gene expression and flow cytometry for TCR-T Cell functional persistence and T cell epitope spread. Human T Cells (HTCs) and Dendritic Cells (DCs) were isolated from autologous PBMCs, transduced with KRAS-specific TCRs, and cultured with AMP-KRAS-peptide pulsed DCs before assaying T Cell boosting.

Results We demonstrate that AMP vaccination expands tumor specific TCR-T Cells in vivo up to 46-fold while enhancing the activation, cytokine secretion, and pro-inflammatory gene expression of tumor-infiltrating TCR-T Cells. Endogenous tumor-infiltrating T cells from AMP vaccinated mice produced up to 17-fold greater cytokine secretion following re-stimulation with non-targeted tumor epitopes. These results correspond to the eradication of established B16F10 tumors and a resistance to secondary tumor challenge in cured mice. Providing clinical relevance, HTCs transduced with KRAS-specific TCRs and boosted with AMP-KRAS-peptide pulsed DCs exhibited enhanced T cell activation, Th1 cytokine secretion, and cytolytic capacity compared to HTCs exposed to unlabeled DCs.

Conclusions AMP vaccination delivers cognate peptides to lymph nodes providing in vivo activation of tumor-specific TCR-T Cells which amplifies anti-tumor potency of such adoptively transferred cells. AMP vaccination significantly enhanced TCR-T Cell anti-tumor response and led to durable cures of solid tumors in an established, syngeneic tumor model. Additionally, AMP-peptide pulsed autologous DCs enhanced the function of clinically relevant KRAS-specific TCR-T cells in vitro. Taken together, these studies provide direct rationale and evidence for the combination of AMP vaccination with TCR-T Cell therapies to augment clinical responses.

REFERENCES

1. Robbins PF, Morgan RA, Feldman SA, Yang JC, Sherry RM, Dudley ME, Wunderlich JR, Nahvi AV, Helman LJ, Mackall CL, et al. Tumor regression in patients

with metastatic synovial cell sarcoma and melanoma using genetically engineered lymphocytes reactive with NY-ESO-1. *J Clin Oncol* 2011;**29**:917–924. doi: 10.1200/JCO.2010.32.2537.

2. Rapoport AP, Stadtmauer EA, Binder-Scholl GK, Golubeva O, Vogl DT, Lacey SF, Badros AZ, Garfall A, Weiss B, Finklestein J, et al. NY-ESO-1-specific TCR-engineered T cells mediate sustained antigen-specific antitumor effects in myeloma. *Nat Med* 2015;**21**:914–921. doi: 10.1038/nm.3910.
3. Doran SL, Stevanovic S, Adhikary S, Gartner JJ, Jia L, Kwong MLM, Faquin WC, Hewitt SM, Sherry RM, Yang JC, et al. T-Cell Receptor Gene Therapy for Human Papillomavirus-Associated Epithelial Cancers: A First-in-Human, Phase III Study. *J Clin Oncol* 2019;**37**:2759–2768. doi: 10.1200/JCO.18.02424.
4. Chandran SS, Klebanoff CA. T cell receptor-based cancer immunotherapy: Emerging efficacy and pathways of resistance. *Immunol Rev* 2019;**290**:127–147. doi: 10.1111/imr.12772.
5. D'Angelo SP, Melchiori L, Merchant MS, Bernstein D, Glod J, Kaplan R, Grupp S, Tap WD, Chagin K, Binder GK, et al. Antitumor Activity Associated with Prolonged Persistence of Adoptively Transferred NY-ESO-1 (c259)T Cells in Synovial Sarcoma. *Cancer Discov* 2018;**8**:944–957. doi: 10.1158/2159-8290.CD-17-1417.
6. H Liu, KD Moynihan, Y Zheng, GL Szeto, AV Li, B Huang, DS Van Egeren, C Park, DJ Irvine. Structure-based programming of lymph-node targeting in molecular vaccines. *Nature* 2014;**507**: 519–522. doi: 10.1038/nature12978.
7. KD Moynihan, CF Opel, GL Szeto, A Tzeng, EF Zhu, JM Engreitz, RT Williams, K Rakhra, MH Zhang, AM Rothschilds, S Kumari, RL Kelly, BH Kwan, W Abraham, K Hu, NK Mehta, MJ Kauke, H Suh, JR Cochran, DA Lauffenburger, KD Wittrup, DJ Irvine. Eradication of large established tumors in mice by combination immunotherapy that engages innate and adaptive immune responses. *Nat Med* 2016;**22**: 1402–1410. doi: 10.1038/nm.4200.

<http://dx.doi.org/10.1136/jitc-2021-SITC2021.157>

CHEMOTHERAPY RESISTANT GAMMA DELTA T-CELL IMMUNOTHERAPY CAN LEVERAGE SYNERGISTIC LIGAND EXPRESSION THROUGH COMBINATIONAL CHEMOTHERAPY AND PARP-INHIBITOR USE TO ENHANCE TUMOR CELL RECOGNITION & KILLING

¹Kate Rochlin*, ²Amber Jones, ¹Lawrence Lamb, ²Anita Hjelmeland. ¹IN8bio Inc, New York, NY, USA; ²University of Alabama Birmingham, Birmingham, AL, USA

Background Cellular Immunotherapies, which have been transformative in the treatment of liquid tumors, have had extremely limited efficacy in solid tumors to-date, in part due to the challenges of efficiently targeting the tumor heterogeneity. Gamma-delta T cells recognize and immediately respond to stress-induced Natural Killer Group D Ligands (NKG2DL) which can thereby differentiate between healthy and malignant tissue. We designed methylguanine-DNA methyltransferase (MGMT) expressing gamma-delta T cells engineered to be TMZ resistant (DeltEx Drug Resistant Immunotherapy or DRI) which can be administered concurrently with alkylating chemotherapy. This leverages the brief but substantial upregulation of NKG2DL from the pharmacokinetic activity of the chemotherapy. We and others have shown checkpoint inhibitors improve gamma-delta T cell function and can be combined with chemotherapy to target checkpoint mediated tumor cell escape. Further, this approach can be used with DNA damage response (DDR) inhibitors, such as PARP-inhibitors or ATM kinase inhibitors to enhance the upregulation of NKG2DL and amplify the chemotherapy-induced vulnerability of tumor cells.

Methods Glioblastoma cells isolated from patient derived xenografts (PDX) were used to determine if TMZ and blood brain barrier penetrant DDR inhibitors could enhance NKG2D ligands. Three PDX with distinct subtypes and genetic profiles were utilized. GBM PDX-derived cells were propagated with epidermal growth factor (EGF) and fibroblast growth factor (FGF) but without serum to best model parental tumors in vitro. Quantitative real-time PCR was used to determine expression of a panel of NKG2DL under hypoxic and normoxic conditions

Results We found a heterogeneous induction of NKG2DL expression with the combination of niraparib + TMZ. While the combinatorial treatment induced stress responses in all cells tested, the specific mRNAs induced, the extent of induction, and the effect of hypoxia varied. Niraparib and TMZ induced >10-fold induction of MICA and MICB in GBM456 cells or ULBP1 in GBM39 cells. The cell type specific inductions of these three targets were reduced by hypoxia and low glucose conditions, suggesting microenvironmental regulation will be important in vivo.

Conclusions This approach holds promise for solid tumor treatment leveraging the ability of the gamma-delta T cells complex polyclonal receptor repertoire to identify and kill tumor cells with combinational therapeutic treatment to drive increases in NKG2DL. The broad utility of alkylating chemotherapies in solid tumor treatment, suggests that this mechanism could be applicable across multiple indications to drive tumor cell immunogenicity in combination with DeltEx DRI cells to increase cytotoxicity and tumor cell killing.

<http://dx.doi.org/10.1136/jitc-2021-SITC2021.158>

DEVELOPING PLACENTAL CD34+-DERIVED NATURAL KILLER CELLS WITH HIGH AFFINITY CLEAVAGE RESISTANT CD16 (CYNK-101) AND CETUXIMAB FOR ENHANCED THERAPY OF EGFR+ NON-SMALL CELL LUNG AND HEAD AND NECK CANCERS

Irene Raitman*, John Fitzgerald, Valentina Rousseva, Salvatore Rotondo, Xuan Guo, Hemlata Rana, Andrea DiFiglia, Tanel Mahlakoiu, Shuyang He, Lin Kang, Robert Hariri, Xiaokui Zhang. *Celularity, Florham Park, NJ, USA*

Background Natural killer (NK) cells are key mediators of antibody dependent cellular cytotoxicity (ADCC) via the CD16 Fc receptor. NK cellular therapies can effectively be targeted to tumor antigens when combined with tumor specific antibodies. Celularity Inc. is developing human placental CD34+-derived, cryopreserved, off-the-shelf, allogenic NK cells (CYNK-101) with high IgG binding affinity proteinase cleavage resistant CD16 variant (CD16VP) for cancer treatment. We hypothesize that expressing CD16VP augments anti-tumor ADCC activity. Here, we report the results of evaluating CYNK-101 in combination with Cetuximab, an anti-EGFR antibody, against EGFR+ non-small cell lung cancer (NSCLC) and head and neck squamous cell carcinomas (HNSCC).

Methods Human placental CD34+ cells were transduced with lentivirus expressing CD16VP and expanded in the presence of cytokines to generate CYNK-101 cells. The anti-tumor activity of CYNK-101 in combination with Cetuximab was assessed against EGFR+ NSCLC and HNSCC cell lines. The PI3K kinase inhibitor Wortmannin was used to investigate the molecular mechanisms underlying cytotoxicity of CYNK-101.

Results In vitro ADCC activity of CYNK-101 against NSCLC and HNSCC targets was assessed in combination with Cetuximab. At 4h at the effector to target (E:T) ratio of 2.5:1, CYNK-101 displayed increased cytotoxicity against NSCLC lines SK-MES-1 and NCI-H226 at $78.7 \pm 11.4\%$ and $58.3 \pm 10.0\%$ with Cetuximab vs. $44.9 \pm 9.2\%$ and $41.7 \pm 5.0\%$ with IgG control, respectively (n=5 donors, p<0.01). For HNSCC targets the cytolysis with Cetuximab compared to IgG control was $57.0 \pm 14.1\%$ vs. $23.3 \pm 6.2\%$ for CAL-27, $69.6 \pm 13.7\%$ vs. $34.0 \pm 12.5\%$ for FaDu, $41.6 \pm 22.6\%$ vs. $22.9 \pm 14.9\%$ for A-253, and $25.8 \pm 29.1\%$ vs. $4.2 \pm 8.0\%$ for SCC-25 (n=6 donors, p<0.005 for first 3 targets). CYNK-101 (n=6 donors) in the presence of Cetuximab secreted higher levels of GM-CSF (p<0.01), IFN- γ (p<0.05), and TNF- α (p<0.05) when co-cultured with the HNSCC lines A-253, FaDu, and SCC-25; and higher GM-CSF and IFN- γ levels (p<0.01) when co-cultured with NCI-H226 compared to that of IgG control. The enhanced cytotoxicity of CYNK-101 was PI3K pathway-dependent as at an E:T ratio of 2.5:1 Wortmannin significantly decreased the cytotoxicity for NCI-H226 from $49.2 \pm 18.1\%$ to $27.7 \pm 18.1\%$ (p<0.005) and for CAL-27 from $41.6 \pm 20.7\%$ to $19.4 \pm 13.0\%$ (p<0.05) (n=4 donors).

Conclusions Our results demonstrate that CYNK-101 have enhanced Cetuximab-mediated ADCC activity against EGFR+ NSCLC and HNSCC tumor cell lines. Further development of the combinational therapy for these solid tumor indications is warranted.

<http://dx.doi.org/10.1136/jitc-2021-SITC2021.159>

EVALUATION AND DEVELOPMENT OF DUAL AND TRIPLE ANTIGEN TARGETING CAR-T ENGAGER PROTEINS FOR HER2-POSITIVE CNS METASTASES AND SOLID TUMORS

Paul Rennert*, Lan Wu, Lihe Su, Roy Lobb, Christine Ambrose. *Aleta Biotherapeutics, Natick, MA, USA*

Background Solid tumors display pronounced antigen heterogeneity and clinical studies have shown that antigen escape from therapy occurs rapidly, limiting the persistence and efficacy of CAR T cells. Here we present dual and triple-antigen binding proteins that bridge CAR T cells to multiple antigens, allowing a simultaneous attack on tumor antigens by a single CAR T antibody domain. We call these CAR T Engager proteins. CAR T Engager proteins can be encoded into lentiviral vectors for secretion from CAR T cells, can be encoded into oncolytic viral vectors for secretion from transduced tumor cells, or can be engineered as biologics for injection.

Methods CAR T Engagers contain a protein target for a CAR T cell, eg. an anti-CD19 CAR T cell. We have previously presented a Her2-binding CAR T Engager protein with potent in vivo activity against solid tumors. We used this CAR T Engager as the basis for building dual and triple antigen binding proteins. Specifically, we mapped antigen expression for Her2-positive solid tumors, Her2-positive metastases, and primary CNS tumors. Our analysis identified expression patterns of two and three antigens that would essentially saturate the cellular composition of specific solid tumors, greatly reducing the chance of antigen escape from therapy. We created the corresponding CAR T Engagers and have developed single, dual and triple antigen expression cells lines to model the activity and potency of these novel proteins, administered alongside CAR T cells.

Results CAR T cells plus dual antigen CAR T Engagers that recognize and target Her2 and B7H3 demonstrate potent cytotoxicity against either antigen alone, and synergistic potency (2 pM) if both antigens are expressed. Similarly, triple antigen CAR T Engagers show single antigen binding and potent cytotoxicity which is enhanced when multiple antigens are expressed on a target cell. All of the cytotoxicity is mediated through one CAR domain expressed on the primary T cells. T cells can be pre-loaded with multi-antigen CAR T Engagers and retain cytotoxic activity. Because the underlying CAR is an anti-CD19 CAR, cell persistence and fitness is further enhanced in the presence of normal B cells.

Conclusions The CAR T Engager platform is a robust and modular solution for the multi-antigen targeting of solid tumors. Diverse antigens can be readily targeted for diverse indications. Examples of other functional modalities that can be added will be presented.

Acknowledgements We thank Cancer Research UK for their ongoing support.

<http://dx.doi.org/10.1136/jitc-2021-SITC2021.160>

161

ANTI-MYELOID POLY-PHARMACY COMBINED WITH FGFR4-TARGETED CHIMERIC ANTIGEN RECEPTORS (CARs) EFFECTIVELY TREATS ORTHOTOPIC RHABDOMYOSARCOMA, MODELING CAR EFFECTIVENESS FOR SOLID TUMORS

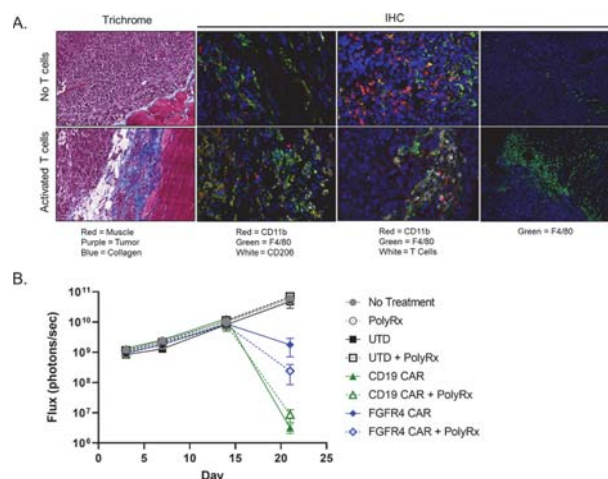
¹Peter Sullivan*, ¹Rajesh Kumar, ²Wei Li, ¹Lingyang Wang, ¹Yue Zhang, ³Adam Cheuk, ³Javed Khan, ²Dimitar Dimitrov, ⁴Rimas Orentas. ¹Seattle Children's Research Institute, Seattle, WA, USA; ²University of Pittsburgh, Pittsburgh, PA, USA; ³NCI, CCR, National Institutes of Health, Bethesda, USA; ⁴University of Washington, Seattle, WA, USA

Background Rhabdomyosarcoma (RMS) is the most common soft tissue cancer in children. Treatment outcomes have not improved in decades, especially for relapsed/refractory or metastatic disease. Previous work identified Fibroblast Growth Factor Receptor 4 (FGFR4, CD334) as being specifically upregulated in RMS, making it a candidate for targeting by CAR-T cells. A previous CAR designed to target FGFR4 showed in vitro efficacy, and some tumor control in a metastatic (intravenous) RMS model, but failed to control orthotopic (intramuscular, i.m.) disease in vivo. Impressively, even in the NSG mouse model system, i.m. disease is characterized by a collagen-rich stroma, replete with myeloid cells, that is induced by T cell therapy (figure 1A).

Methods A large-scale screening campaign for antibody-based binding domains, using the membrane proximal domain of FGFR4 as the bait molecule, yielded a number of candidates, that when expressed in the context of a CAR, exceed the activity of previous binders in vitro. CARs were ranked by direct detection on the T cell surface with recombinant target antigen, cytotoxicity, and cytokine production upon co-culture with target cell lines. Top candidate binders were then tested against orthotopic RMS tumors in NSG mice using the RMS cell line RH30, engineered to express truncated CD19. The presence of M2 macrophages (CD11b+, CD206+) and MDSC (F4/80-, CD11b+) was analyzed by immunohistochemical analysis of i.m. tumors from treated and untreated NSG mice. The presence of target antigen on the RH30_19 cell lines was quantified by flow cytometry using standardized bead assays.

Results The two highest ranking anti-FGFR4 CAR-T candidates failed to control i.m. RH30_19 on their own. Considering the low expression of target antigen present on tumors in vivo (700 FGFR4 per cell), we tested CD19 CAR-T (95,000 molecules per cell). Anti-CD19 CAR-T also failed. Gene expression analysis of RH30 identified several potential mechanisms of tumor resistance to CAR T therapy. Based on this data, the abundant presence of M2 macrophages, and the known presence of MDSC in NSG mice, we devised a pharmacologic strategy to augment CAR-T activity. The exposure of mice to anti-myeloid polypharmacy (targeting MDSC via ATRA, M2 macrophages via the CSF1R, IDO1, iNOS, MIF, TGFbeta, and PDL1) allowed both FGFR4 CAR-T and CD19 CAR-T to successfully clear orthotopic RMS tumors (figure 1B).

Conclusions RMS tumors can be cleared using an FGFR4-targeted CAR in combination with anti-myeloid poly-pharmacy, demonstrating that even extremely low copy number targets can be targeted by CAR-T by reversing an immunosuppressive microenvironment.



Abstract 161 Figure 1 T Cells induce myeloid-rich stroma in RMS which can be overcome with anti-myeloid poly-pharmacy. A. NSG mice with intramuscular RH30 tumors were left untreated (No T Cells) or received activated T Cells. Tumors were excised and stained as described in the figure. Upon T Cell treatment, a collagen-rich stroma forms, and is populated by M2-polarized macrophages (F4/80+CD206+), effectively excluding T Cells from the lesion. B. Anti-myeloid polypharmacy (PolyRx) treatment paired with CD19 or FGFR4 targeted CAR T therapy is able to control orthotopic RMS tumors.

Ethics Approval Animal experiments were conducted in an AAALAC accredited facility, following Seattle Children's Research Institute institutional animal care and use committee (IACUC) approval of procedures (IACUC00417).

<http://dx.doi.org/10.1136/jitc-2021-SITC2021.161>

NICOTINAMIDE REJUVENATES EX-VIVO EXPANDED NATURAL KILLER CELLS AND ENHANCES THEIR TUMOR KILLING CAPACITY

¹Aviad Pato*, ¹Astar Hailu, ¹Nurit Brickman, ¹Dima Yackoubov, ²Frank Cichocki, ³Amnon Peled, ¹Ronit Simantov, ¹Tracey Lodie, ¹Julia Rifman, ¹Yona Geffen, ¹Orit Berhani-Zipori, ¹Avishay Edri. ¹Gamida-Cell, Jerusalem, Israel; ²University of Minnesota, Minneapolis, MN, USA; ³Hadassah Medical Center, Jerusalem, Israel

Background Adoptive transfer of Natural Killer cells (NKs) is a growing area of innovation in cancer immunotherapy. Nicotinamide (NAM), an allosteric inhibitor of NAD-dependent enzymes, has been shown to preserve cell function and prevent differentiation in ex vivo culture of NK (NAM-NK) and other cells. Clinical responses were observed in a Phase 1 trial of NAM-NK (GDA-201) in patients with refractory non-Hodgkin lymphoma (Bachanova, et. al., Blood 134:777, 2019). We now characterize the mechanisms underlying the activity of NAM-NK by exploring their phenotype, functionality, and antitumor activity.

Methods CD56 positive cells obtained from healthy donors were cultured for 14 days with IL-15 in the presence or absence of NAM (7 mM). Cell-surface antigens were characterized using flow cytometry (FACS). Mitochondrial reactive oxygen species (ROS) were measured using MitoSox-based FACS. In vitro killing of tumor cells was evaluated by FACS after co-culture of NAM-NK with HER-2-positive A549 (lung adenocarcinoma) or SKOV-3 (ovarian cancer) cells in the presence or absence of trastuzumab; NK cell CD107a and intracellular IFN γ , TNF α , and GM-CSF were also measured by FACS. In vivo activity was determined using a subcutaneous tumor model in NSG mice injected with A549 cells (5x10⁶ cells) and treated with NAM-NK cells (20x10⁶ cells ip/day) on Day 9–12 with IL-2 (300 ug ip), with or without trastuzumab (100ug ip).

Results Characterization of cell surface markers revealed elevated CD56, CD62L, and CD49a and decreased CD16, CD57, and Nkp80 in NAM-NK compared to NK cultured without NAM. CD200R and LAG3 were decreased. NAM-NKs also demonstrated decreased mitochondrial superoxide formation triggered by H₂O₂ oxidative stress. NAM-NK co-cultured with A549 and SKOV-3 cells had increased expression of the degranulation marker CD107a and the proinflammatory cytokines INF- γ , TNF- α , and GM-CSF compared to NK without NAM, and demonstrated increased cytotoxicity in the presence and absence of trastuzumab. Finally, NAM-NK inhibited A549 tumor growth in vivo; tumor growth inhibition was potentiated in the presence of trastuzumab and greater than with trastuzumab alone.

Conclusions These data suggest that NAM rejuvenates cultured NK, generating activated and potent NK cells. NAM-NK (GDA-201) display a distinct phenotype similar to cytokine-induced memory like (CIML) NK, but with downregulation of immune checkpoint inhibitors such as CD200R and LAG3. In addition, NAM-NK are greatly resistant to ROS—a known mechanism of tumor resistance—and highly cytotoxic in in vitro and in vivo assays. The promising potential of GDA-201 as an anticancer immunotherapy is being explored further in clinical trials

Ethics Approval We hereby declare that the collection of the Apheresis units in the three participating institutes (sites) has been done under an approved clinical study that meets the following requirements: 1. Ethics approval has been obtained from the local EC at each of the sites, prior to any study related activities. 2. The working procedures of the EC at the

sites for conduct of clinical studies are in due compliance with local regulations (Israeli Ministry of Health) and provisions of Harmonized International Guidelines for Good Clinical Practice, namely: ICH-GCP.3. Sites follow EC conditions & requirements in terms of submissions, notifications, and approval renewals. 4. Participants gave Informed Consent (approved by the EC) before taking part in the study. 5. Informed Consent has been approved by the ECs. The Israeli template of Informed Consent is in used and it includes study specific information (e.g. study goal, design, method, duration, risks, etc.). Name of the Institute Name of the EC/IRB EC Study No. Hadassah Medical Center Helsinki Committee 0483-16-HMORambam Health Care Campus Helsinki Committee 0641-18-RMBIchilov Sourasky Medical Center Tel-Aviv Helsinki Committee 0025-17-TLVAnimal study- All experiments were approved by the Animal Care and Use Committee of the Hebrew University. MD 19-15815-5.

<http://dx.doi.org/10.1136/jitc-2021-SITC2021.162>

163 IMPROVED ANTI-TUMOR ACTIVITY OF NEXT-GENERATION TCR-ENGINEERED T CELLS THROUGH CD8 CO-EXPRESSION

Gagan Bajwa, Justin Gunesch, Inbar Azoulay-Alfaguter, Melinda Mata, Ali Mohamed, Mamta Kalra*, Steffen Walter. *Immatics US Inc, Houston, USA*

Background Successful targeting of solid tumors with TCR-engineered T cells (TCR-T) will require eliciting of antigen-specific, multi-dimensional, sustained anti-tumor immune response by infused T cells while overcoming the suppressive tumor microenvironment. First-generation TCR-T approaches have demonstrated clinical efficacy in some solid cancers. However, effective treatment across several solid tumor indications may require engineered T cells with enhanced anti-tumor activity. Here, we show pre-clinical data from one of the engineering approaches currently being developed for next-generation ACTengine® TCR-T product candidates. We evaluated the impact of co-expression of different CD8 co-receptors on functionality of CD4+ and CD8+ T cells genetically modified with an HLA class I-restricted TCR and determined the depth and durability of anti-tumor response in vitro.

Methods Here, we used a PRAME-specific TCR currently being tested in the ACTengine® IMA203 clinical trial. T cells expressing either the TCR alone or co-expressing the TCR and CD8 α homodimer (TCR.CD8 α) or CD8 $\alpha\beta$ heterodimer (TCR.CD8 $\alpha\beta$) were characterized for transgene expression, antigen-recognition, and functional efficacy in vitro. Comprehensive evaluation of CD4+ T cells expressing TCR.CD8 α or TCR.CD8 $\alpha\beta$ was performed focusing on cytotoxic potential and the breadth of cytokine response against target-positive tumor cell lines.

Results Introduction of CD8 α or CD8 $\alpha\beta$ enabled detection of transgenic TCR on the surface of CD4+ T cells via HLA multimer-guided flow cytometry otherwise lacking in the TCR only transduced T cells. Co-expression of either form of CD8 co-receptor endowed CD4+ T cells with the ability to recognize and kill target positive tumor cells; however, genetic modification with TCR.CD8 $\alpha\beta$ led to more pronounced CD4+ T cell activation as compared to TCR.CD8 α . Most distinct differences were observed in the breadth and magnitude of cytokine responses, less in cytotoxic activity against tumor cells. T cells expressing TCR.CD8 $\alpha\beta$ showed superior induction of Th1 cytokines e.g. IFN γ , TNF α , IL-2, GM-CSF in vitro upon antigen stimulation as compared to TCR.CD8 α -T cells. Additionally, TCR.CD8 $\alpha\beta$ T cells demonstrated more efficient engagement with antigen-presenting cells and consequently, modulation of cytokine response than TCR.CD8 α -T cells.

Conclusions Our findings illustrate that engaging CD4+ T cells via CD8 co-expression potentiates anti-tumor activity of HLA class I restricted TCR-T cells in vitro. The pleiotropic effects mediated by activated CD4+ T cells including acquired cytotoxicity may potentially improve outcomes in solid tumor patients when applied clinically. In addition, the differential functional profile of TCR-T cells co-expressing either CD8 α or CD8 $\alpha\beta$ suggests that optimizing the type of co-receptor is relevant to maximize anti-tumor response.

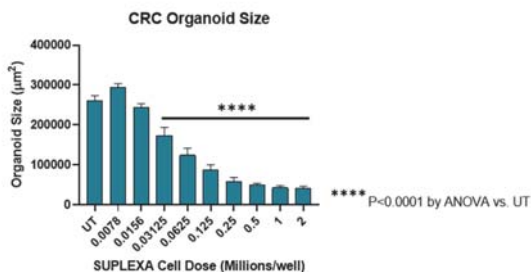
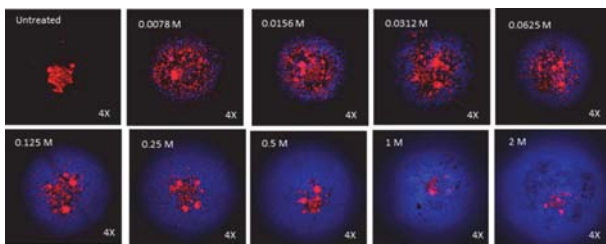
<http://dx.doi.org/10.1136/jitc-2021-SITC2021.163>

164 POTENT TUMOR ORGANOID INFILTRATION AND KILLING BY PBMC-DERIVED EFFECTOR CELLS

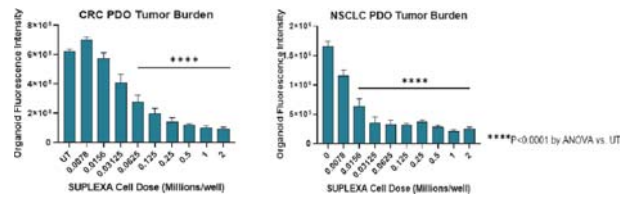
¹Frank Borriello*, ¹Joshua Keegan, ²James Lederer. ¹Alloplex Biotherapeutics, Inc., Woburn, MA, USA; ²BWH Harvard Medical School and Alloplex, Millis, MA, USA

Background Alloplex Biotherapeutics has developed a novel autologous cellular therapy for cancer that uses ENgineered Leukocyte ImmunoSTimulatory cell lines called ENLIST cells to activate and expand a heterogeneous population of tumor killing effector cells from human peripheral blood mononuclear cells (PBMCs). The 2-week manufacturing process from PBMCs consistently results 300-fold expansion of NK cells, CD8+ T cells, gamma/delta T cells, NKT cells and some CD4+ T cells, collectively called SUPLEXA therapeutic cells. SUPLEXA cells will be delivered back to cancer patients via intravenous administrations on a weekly schedule as an autologous adoptive cellular immunotherapy for cancer. In this study, we tested SUPLEXA cells developed from normal healthy volunteer PBMCs for their ability to infiltrate and kill patient-derived tumor organoids (PDO) as a pre-clinical assessment for potency against 2 different types of tumor organoids.

Methods Tumor organoids derived from colorectal cancer (CRC) or non-small cell lung carcinoma (NSCLC) patients were labeled with cell-trace red dye and plated at equal density in a 96-well plate. After 3 days culture, SUPLEXA cells were thawed (82.8% viable), labeled with cell-trace violet dye, and added to PDO at 1:2 serial diluted numbers ranging from 2 million to 7,800 cells per well. Fluorescent images were captured at 24 hours after adding SUPLEXA cells to PDO models to measure PDO size, tumor infiltration, and PDO killing.



Abstract 164 Figure 1 CRC organoid infiltration and killing by SUPLEXA. A representative fluorescent image of CRC organoid killing with addition of increasing SUPLEXA cell numbers and a plot showing statistical analysis of 6 replicate wells for changes in CRC organoid size in relation to SUPLEXA cell number additions



Abstract 164 Figure 2 Dose-dependent killing in CRC and NSCLC PDO models. CRC and NSCLC organoids were detected by total red fluorescence at 24 hours after adding the indicated numbers of SUPLEXA cells. Loss of red fluorescence after adding SUPLEXA is a measure of overall tumor cell killing/burden in organoids. Data is plotted as mean ± SEM for n=6 replicates per group.

Results Adding SUPLEXA cells to PDO from CRC and NSCLC resulted in significant infiltration and killing of organoids by 24 hours as shown by the fluorescent images and the organoid size plot for the CRC PDO model (figure 1). Significant reduction in PDO size was observed by adding 31,240 SUPLEXA cells. Similar results were observed with the NSCLC PDO model with significant reduction in PDO size by adding 15,600 SUPLEXA cells. Obvious organoid infiltration was observed in both PDO models and organoid fluorescence was significantly reduced by addition of SUPLEXA cells in both PDO models to suggest that SUPLEXA cells were able to reduce tumor burden (figure 2).

Conclusions SUPLEXA cells infiltrated and killed tumor cells in patient-derived organoids within 24 hours of culture at low cell concentrations indicating potent tumor killing activity. The observed activity in both colorectal and lung cancer organoid models support broad anti-tumor killing activity by SUPLEXA. These results provide further evidence that PBMCs from cancer patients can be activated and expanded by our approach as a novel autologous cellular immunotherapy for cancer.

<http://dx.doi.org/10.1136/jitc-2021-SITC2021.164>

165 **GENERATING ENHANCED TUMOR INFILTRATING
LYMPHOCYTES THROUGH MICROFLUIDIC CELL
SQUEEZING**

¹Devin Bridgen*, ¹Arindam Bhattacharjee, ²Colin Thalhofer, ²Ryan Montler,
²Andrew Weinberg, ¹Armon Sharei, ¹Jonathan Gilbert. ¹SQZ Biotech, Watertown, MA, USA;
²AgonOx, Portland, OR, USA

Background Tumor Infiltrating Lymphocyte (TIL) therapies have shown significant solid tumor activity in patients, but current TIL compositions require patient lymphodepletion and high dose IL-2 after cell infusion to support clinical activity. Removing this requirement through ex vivo engineering of the TIL product with mRNA could enhance potency, expand the potential patient population, and potentially allow for repeat dosing and concomitant treatment with checkpoint therapies.

Methods To transiently overexpress both membrane-bound cytokines and costimulatory molecules, we used microfluidic cell squeezing (Cell Squeeze[®]) to deliver mRNA directly to the cytosol of expanded tumor reactive CD8 human TILs (AGX-148). After mRNA delivery, the TILs were cultured in media with varying levels of exogenous IL-2 and characterized by flow cytometry.

Results We demonstrated that multiple mRNA constructs delivered simultaneously by microfluidic cell squeezing to human TILs are highly expressed (>80% of cells) for multiple days while maintaining high viability (>80%) in vitro. Membrane bound cytokines are able to support cell expansion in the absence of exogenous IL-2 at rates comparable to control cells incubated with a high concentration of IL-2 for up to 3 days. Furthermore, we have identified a membrane-bound cytokine that alters the TIL phenotype as quantified by multiple markers, including increased L-selectin (CD62L), which is an indicator of central memory T cells.

Conclusions Through microfluidic cell squeeze delivery of mRNAs, we have created enhanced TILs with high levels of membrane-bound cytokines and/or costimulatory molecules in vitro. These cells are able to proliferate without exogenous IL-2 and have an improved phenotype.

<http://dx.doi.org/10.1136/jitc-2021-SITC2021.165>

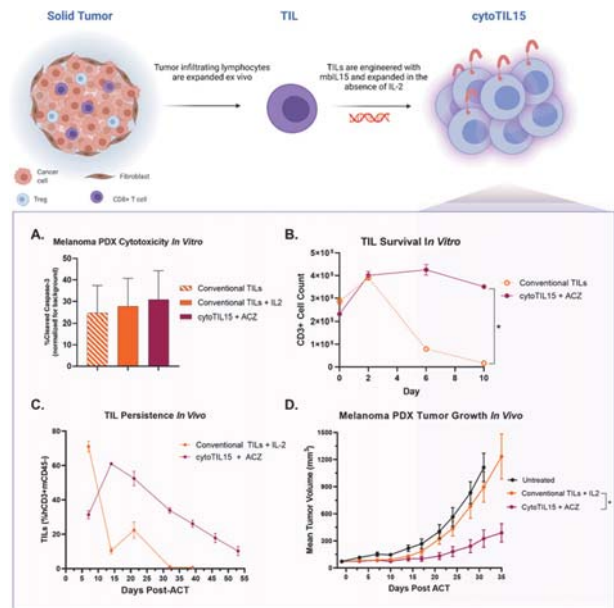
GENETICALLY ENGINEERED TUMOR-INFILTRATING LYMPHOCYTES (CYTOTIL15) EXHIBIT IL-2-INDEPENDENT PERSISTENCE AND ANTI-TUMOR EFFICACY AGAINST MELANOMA IN VIVO

Rachel Burga*, Mithun Khattar, Scott Lajoie, Kyle Pedro, Colleen Foley, Alonso Villasmil Ocano, Jack Tremblay, Benjamin Primack, Meghan Langley, Dan Thornton, Stanley Tam, Emily Brideau, Theresa Ross, Gwen Wilmes, Sunandan Saha, Gabriel Helmlinger, Jeremy Tchaicha, Dhruv Sethi, Michelle Ols, Gary Vanasse, Shyam Subramanian, Jan ter Meulen. *Obsidian Therapeutics, Cambridge, MA, USA*

Background Adoptive cell therapy with tumor-infiltrating lymphocytes (TILs) has demonstrated tremendous promise in clinical trials for patients with solid or metastatic tumors.¹ However, current TIL therapy requires systemic administration of IL-2 to promote TIL survival, and IL-2-associated toxicities greatly limit patient eligibility and reduce the long-term clinical benefit of TIL therapy.²⁻³ Unlike IL-2, which promotes T cell exhaustion, IL-15 maintains antigen-independent TIL persistence through homeostatic proliferation and supports CD8+ T cell anti-tumor activity without stimulating regulatory T cells. We designed genetically engineered TILs to express a regulated form of membrane-bound IL-15 (mbIL15) for tunable long-term persistence, leading to enhanced efficacy and safety for the treatment of patients with solid tumors.

Methods Obsidian's cytoDRIVE™ platform includes small human protein sequences called drug responsive domains (DRD)s that enable regulated expression of a fused target protein under control of FDA-approved, bioavailable small molecule ligands. cytoTIL15 contains TILs engineered with mbIL15 under the control of a carbonic-anhydrase-2 DRD, controlled by the ligand acetazolamide (ACZ). After isolation from tumors, TILs were transduced and expanded in vitro through a proprietary TIL expansion process. cytoTIL15 were immunophenotyped and assessed for in vitro antigen-independent survival and co-cultured with tumor cells to assess polyfunctionality and cytotoxicity. In vivo TIL persistence and anti-tumor efficacy was evaluated through adoptive transfer of TILs into immunodeficient NSG mice, either naïve or implanted with subcutaneous patient-derived-xenograft (PDX) tumors.

Results cytoTIL15 and conventional IL2-dependent TILs isolated from melanoma tumor samples expanded to clinically relevant numbers over 14 days. Throughout expansion, cytoTIL15 were enriched for CD8+ T cells and acquired enhanced memory-like characteristics, while maintaining diverse TCRVβ sub-family representation. cytoTIL15 demonstrated enhanced potency over conventional TILs, as measured by increased polyfunctionality and cytotoxicity against tumor and PDX lines in vitro (figure 1A). In a 10-day antigen-independent in vitro assay, cytoTIL15 persisted at greater frequencies than conventional TILs in the absence of IL-2 (figure 1B; *p<0.05). cytoTIL15 adoptively transferred into naïve NSG mice demonstrated ACZ-dependent long-term persistence without antigen or exogenous IL-2, whereas conventional TILs were undetectable >30 days following adoptive cell transfer (figure 1C). Importantly, cytoTIL15 achieved significant tumor control in a human PDX model (figure 1D), which correlated with increased TIL accumulation in secondary lymphoid organs.



Abstract 166 Figure 1 cytoTIL15 demonstrate superior persistence. cytoTIL15 is an engineered TIL product expressing regulatable mbIL15. (A) cytoTIL15 demonstrate enhanced in vitro cytotoxicity after co-culture with melanoma tumor lines (representative data from 3 TIL donors). (B) cytoTIL15 have improved persistence in antigen- and IL2- independent culture conditions in vitro compared to conventional TILs cultured in the absence of IL-2 as well as (C) in vivo compared to conventional TILs supplemented with IL-2, when engrafted into NSG mice (in vitro: representative data from 1 TIL donor, performed in >3 replicate donors, in vivo: n=5/group, representative of 1 TIL donor, performed in >3 replicate donors). (D) cytoTIL15 (with 200mg/kg ACZ PO QD) demonstrate enhanced anti-tumor efficacy in a xenograft melanoma model as compared to conventional TILs (with 50000 IU IL-2 q8h BID, IP for 5 days) (n=8/group, representative of 1 TIL donor, performed in >2 replicate donors; ACT = adoptive cell transfer).

Conclusions Taken together, the superior persistence and potency of cytoTIL15 in the complete absence of IL-2 highlights the clinical potential of cytoTIL15 as a novel TIL product with enhanced safety and efficacy for patients with melanomas, and other solid tumors.

Acknowledgements The authors wish to acknowledge the Cooperative Human Tissue Network for their supply of human tumor tissue, and the MD Anderson Cancer Center for technical support; schematic created with BioRender.com.

REFERENCES

- Chandran SS, Somerville RPT, Yang JC, Sherry RM, Klebanoff CA, Goff SL, Wunderlich JR, Danforth DN, Zlott D, Paria BC, Sabesan AC, Srivastava AK, Xi L, Pham TH, Raffeld M, White DE, Toomey MA, Rosenberg SA, Kammula US. Treatment of metastatic uveal melanoma with adoptive transfer of tumour-infiltrating lymphocytes: a single-centre, two-stage, single-arm, phase 2 study. *Lancet Oncol* 2017 Jun;**18**(6):792–802. doi: 10.1016/S1470-2045(17)30251-6. Epub 2017 Apr 7. PMID: 28395880; PMCID: PMC5490083.
- Yang JC. Toxicities associated with adoptive T-cell transfer for Cancer. *Cancer J* 2015;**21**:506–9.
- Schwartz RN, Stover L, Dutcher JP. Managing toxicities of high-dose interleukin-2. *Oncology (Williston Park)* 2002 Nov;**16**(11 Suppl 13):11–20. PMID: 12469935.

<http://dx.doi.org/10.1136/jitc-2021-SITC2021.166>

167

HIGH-EFFICIENCY CAPTURE OF ANTI-TUMOR NEOANTIGEN-REACTIVE T CELL RECEPTORS FROM TUMOR DIGEST

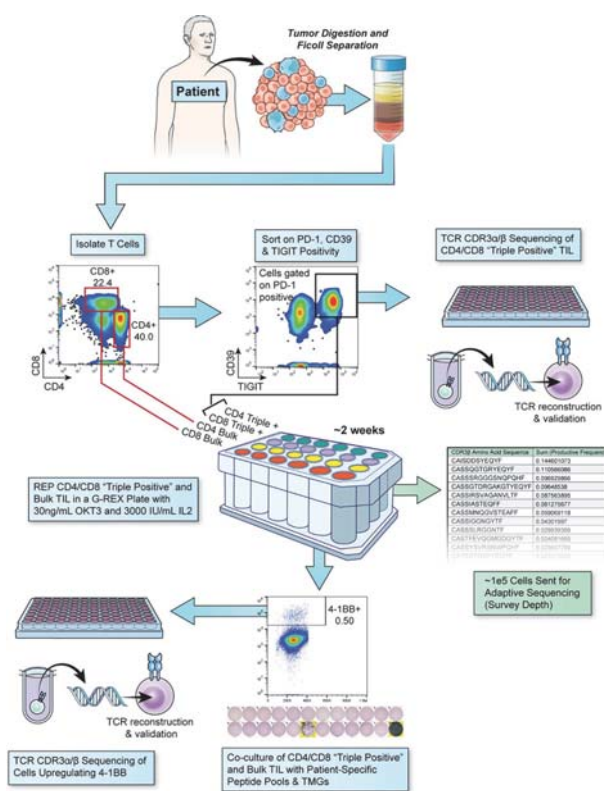
Praveen Chatani*, Frank Lowery, Neilesh Parikh, Rami Yossef, Victoria Hill, Zhiya Yu, Todd Prickett, Jared Gartner, Biman Paria, Satyajit Ray, Maria Florentin, Paul Robbins, Sri Krishna, Steven Rosenberg. *NCI, Bethesda, MD, USA*

Background As cellular immunotherapies utilizing genetically engineered T cells become a more significant focus of clinical investigation, identification of patient-specific neoantigen-reactive T cell receptors (TCRs) in a practical and efficient manner is a top priority. Using high-dimensional single-cell analysis, we recently identified a common gene expression signature in anti-tumor, neoantigen-reactive tumor-infiltrating lymphocytes (TIL) from patients with metastatic cancer, which included high gene expression of cell-surface markers of exhaustion.¹ Furthermore, analyses of intra-tumoral T cell populations have shown that neoantigen-specific TIL are enriched in subsets defined by cell-surface markers of exhaustion, likely secondary to oligoclonal expansion that occurs upon tumor antigen recognition in vivo.^{2–5} In this study we describe an efficient method to prospectively capture and reconstruct neoantigen-reactive T cell receptors from tumor digest based on co-expression of CD39, PD-1, and TIGIT.

Methods We evaluated the ability of PD-1+, CD39+, and TIGIT+ TIL (TIL-TP) to enrich for neoantigen-reactivity by sorting, sequencing, and reconstructing high-frequency TCR alpha/beta pairs from tumor digest in 5 patients with metastatic epithelial cancers. We then tested the ability of PD-1/CD39/TIGIT co-expressing TILs to sustain reactivity to patient-specific tumor neoantigens following in vitro expansion under similar conditions to our current clinical trial protocols (figure 1).

Results We prospectively reconstructed TIL-TP TCRs to identify additional novel TCRs, with 35% of prospectively screened TCRs being neoantigen- or tumor-reactive. Including both previously known and newly predicted TCRs, TIL-TP demonstrated enrichment for neoantigen-reactivity in 4 of 5 patients, with a median of at least 26.8% of sequenced TIL-TP cells being neoantigen-reactive (range: 11.9 – 88.4%). TIL-TP TCR isolation demonstrated a high degree of correlation with single-cell transcriptomic approaches to identification of neoantigen-reactive TCRs, though TIL-TP TCRs represent a more cost-effective and widely available approach compared to those utilizing more advanced technologies. However, despite their substantial enrichment for neoantigen-reactive TCR clonotypes, the majority of TIL-TP populations failed to demonstrate neoantigen-reactivity following in vitro expansion and exhibited loss of neoantigen-reactive clones as well as functional impairment.

Conclusions TIL-TP serve as a highly efficient and reliable source of tumor-reactive TCRs. While direct utilization of these TIL-TP as a source for cellular therapy presents significant challenges, sorting for TIL-TP offers a streamlined approach using readily available and affordable technology to identify neoantigen-reactive TCRs that may be used to design TCR engineered cellular immunotherapies.



Abstract 167 Figure 1

REFERENCES

- Lowery, FJ, et al. Single cell mapping of tumor infiltrating lymphocytes enables neoantigen-reactive T cell identification in metastatic human cancer [abstract]. In: Proceedings of the American Association for Cancer Research Annual Meeting 2021; 2021 Apr 10–15 and May 17–21. Philadelphia (PA): AACR; Cancer Res 2021;81(13_Suppl):Abstract nr 127.
- Duhen, T. et al. Co-expression of CD39 and CD103 identifies tumor-reactive CD8 T cells in human solid tumors. *Nat Commun* 2018;9:2724, doi:10.1038/s41467-018-05072-0.
- Gros A, et al. PD-1 identifies the patient-specific CD8(+) tumor-reactive repertoire infiltrating human tumors. *J Clin Invest* 2014;124:2246–2259, doi:10.1172/JCI173639.
- Pasetto, A. et al. Tumor- and Neoantigen-Responsive T-cell Receptors Can Be Identified Based on Their Frequency in Fresh Tumor. *Cancer Immunol Res* 2016;4:734–743, doi:10.1158/2326-6066.CCR-16-0001.
- Yossef, R. et al. Enhanced detection of neoantigen-reactive T cells targeting unique and shared oncogenes for personalized cancer immunotherapy. *JCI Insight* 2018;3: doi:10.1172/jci.insight.122467.

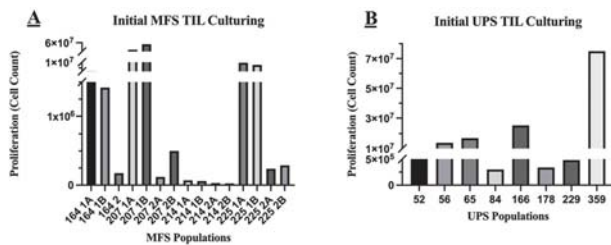
<http://dx.doi.org/10.1136/jitc-2021-SITC2021.167>

EXPANDING AND CHARACTERIZING TUMOR INFILTRATING LYMPHOCYTES FROM MYXOFIBROSARCOMA AND UNDIFFERENTIATED PLEOMORPHIC SARCOMA

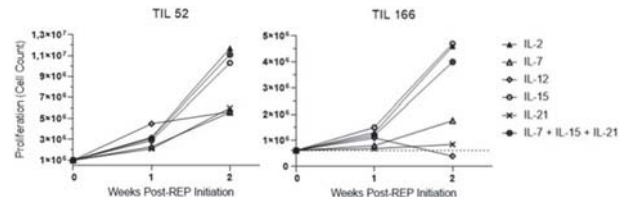
¹Jacky Chen*, ²Jay Wunder, ²Kim Tsoi, ¹Nalan Gokgoz, ¹Irene Andrusis. ¹Lunenfeld Tanenbaum Research Institute, Toronto, Canada; ²Sinai Health System, Toronto, Canada

Background Sarcoma is a group of rare bone and soft tissue tumors with over 50 distinct subtypes. Survival rate ranges widely due to the lack of efficacious treatments. Immunotherapy, such as adoptive cell therapy (ACT), has drawn significant interest due to its minimal toxicity. In ACT, tumor infiltrating lymphocytes (TILs) are isolated from patients, expanded, and autologously infused back. We recently observed TILs' presence in Undifferentiated Pleomorphic Sarcoma (UPS) and Myxofibrosarcoma (MFS) tumors and found that tumor's PD-L1 overexpression is correlated with better clinical outcome in UPS but not MFS.¹ The Th1 anti-tumoral inflammatory pathway was highly activated in the former cohort, which may explain the favorable outcome. We hypothesize that there are phenotypic and functional differences between TILs of UPS with differential PD-L1 expression, which may be related to clinical outcomes. However, sarcoma TILs are rare and challenging to culture, which significantly impedes their studies. We first aim to robustly expand sarcoma TILs to sufficient numbers.

Methods Tumors' PD-L1 expression was determined by RT-qPCR (table 1). To initiate the tumor-fragment (TF) method of TIL culturing, primary tumors were fragmented and cultured in IMDM, IL-2, and 10% HSA. We further optimized the TF protocol to expand rare sarcoma TILs. Rapid expansion protocol (REP) with anti-CD3/anti-CD28 co-stimulating beads was employed for additional expansion. During REP, TILs were co-treated with gamma-chain cytokines (IL-2, 7, 15, 21).



Abstract 168 Figure 1 Initial TIL Culturing with Tumor Fragment Method. **Figure A.** The traditional tumor fragment protocol was used to expand TILs of four MFS cases. TILs were cultured and expanded from primary tumor fragments in IL-2 (6000IU/mL) supplemented complete media (CM) over four weeks in duration. Fifteen TIL populations were derived from the four MFS cases. Populations were categorized based on their growth rates and labeled as '1' or '2' representing 'fast' or 'slow' growing TILs, respectively. Additional populations 'A' and 'B' represent biological replicates. Population TIL164 '2' had no replicates. At Week 4, populations' cell counts were determined via hemocytometer. As shown, only 6 out of 15 populations achieved > 1x10⁶ cells (40% success rate). **Figure B.** An optimized tumor fragment protocol was used to expand TILs of eight UPS cases. Optimization includes shortening the culturing duration from four weeks to two weeks, reducing frequency of cell culture disruption, and adjusting cell culture environments. TILs were expanded from primary tumor fragments in CM over two weeks in duration. At Week 2, populations' cell counts were determined via hemocytometer. As shown, 5 out of 8 cases achieved >1x10⁶ cells (62.5% success rate).



Abstract 168 Figure 2 Gamma-chain cytokine treatments of UPS TILs. Gamma-chain cytokine treatments of UPS TILs with CD3/CD28 stimulation. Magnetic Dynabeads coated with CD3 and CD28 monoclonal antibodies were used to stimulate cells at a bead to cell ratio of 1:3. In ACT, IL-2 is a gold-standard cytokine that facilitates potent T-cell growth. However, it is known to cause activation-induced cell death. Resulting TIL population also possesses an exhausted-effector phenotype with low durability. UPS TIL Case 52 and Case 166 were treated with various interleukins during two weeks of REP, including gamma-chain IL-7, 15, 21 and inflammatory IL-12. IL-7, IL-12, and IL-21 individually did not elicit significant T-cell growth. IL-15 alone and in combination with IL-7 and IL-21 yield growth comparable to IL-2. IL-2 was obtained from Novartis (50ng/mL). All other cytokines were obtained from PeproTech (25ng/mL).

Abstract 168 Table 1 Tumor PD-L1 RNA Expression. Four MFS and eight UPS cases were processed. Tumors' PD-L1 RNA expression was determined via RT-qPCR and evaluated as a ratio with the housekeeping gene STAM2. TIL359's PD-L1 status has yet to be evaluated.

MFS Cases	PD-L1/STAM2	UPS Cases	PD-L1/STAM2
TIL164	0.43	TIL 52	0.1
TIL207	0.094	TIL 56	0.81
TIL214	0.37	TIL 65	0.52
TIL225	0.143	TIL 84	0.16
		TIL 166	3.25
		TIL 178	2.49
		TIL 229	0.26
		TIL 359	n/a

Results Of the 15 MFS TIL populations expanded, only 40% achieved sufficient growth (1x10⁶) for analysis (figure 1A). Our optimized TF protocol expanded TILs from 8 UPS cases with a 62.5% success rate (figure 1B). UPS TILs were further stimulated with REP and various gamma-chain cytokine treatments. In ACT, prolonged culturing with IL-2 is known to cause activation-induced cell death, problematic in clinical treatments. We demonstrated that treatments with a Trio-cocktail (IL-7, 15, and 21) or IL-15 alone can achieve TIL proliferation comparable to that of IL-2 (figure 2).

Conclusions Sarcoma infiltrates are difficult to culture, and their roles remain largely unstudied. By optimizing the TF protocol in conjunction with anti-CD3/CD28 treatments, we developed a robust in vitro pipeline to expand rare sarcoma TILs, enabling downstream characterization. We also demonstrated the potential for alternate gamma-chain cytokines to favorably replace IL-2 during TIL expansion. Future phenotypic and functional evaluation of UPS TILs would elucidate the impact of tumors' differential PD-L1 expression on UPS patients' prognoses. These findings would inform the implementation of ACT in sarcoma treatments.

REFERENCES

1. Wunder J, Lee M, Nam J, Lau B, Dickson B, Pinnaduwage D, Bull S, Ferguson P, Seto A, Gokgoz N, Andrulis I. Osteosarcoma and soft-tissue sarcomas with an immune infiltrate express PD-L1: relation to clinical outcome and Th1 pathway activation. *Onco Immunology* 2020;**9**: e1737385-1- e1737385-13.

Ethics Approval Patients provided signed consent before study entry, as approved by Mount Sinai Hospital's Ethics Board (REB#01-0138-U).

<http://dx.doi.org/10.1136/jitc-2021-SITC2021.168>

169

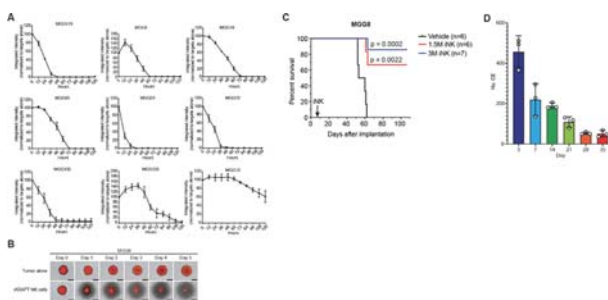
OFF-THE-SHELF, ENGINEERED iPSC-DERIVED NK CELLS MEDIATE POTENT CYTOTOXIC ACTIVITY AGAINST PRIMARY GLIOBLASTOMA CELLS AND PROMOTE DURABLE LONG-TERM SURVIVAL IN VIVO

¹Frank Cichocki, ¹Jianfang Ning, ¹Zachary Davis, ¹Hongbo Wang, ¹Katie Tuininga, ²Ryan Bjordahl, ²Paul Rogers, ²Moyar Ge, ²Tom Lee, ²Bob Valamehr, ¹Clark Chen, ¹Jeffrey Miller*. ¹University of Minnesota, Minneapolis, MN, USA; ²Fate Therapeutics, San Diego, CA, USA

Background Glioblastoma multiforme (GBM) is a primary brain tumor with a high mortality rate and median survival of ~14 months. Although progress has been made in the development of available therapies, the treatment of GBM remains palliative.¹ Emerging results from preclinical studies support the concept that GBM cells may be highly susceptible to natural killer (NK) cell cytotoxicity.²⁻³ However, sourcing donor-derived NK cells for adoptive cell therapy is limited by cell number and quality. To overcome these barriers, we developed a robust manufacturing system for the generation of high-quality off-the-shelf NK cells derived from induced pluripotent stem cells (iPSCs).⁴

Methods We generated triple gene-edited iPSCs designed for mass production of NK cells expressing a high affinity, non-cleavable version of the Fc receptor CD16a and a membrane-bound IL-15/IL-15R fusion protein along with knockout of the nicotinamide adenine dinucleotide (NAD⁺) hydrolase CD38. NK cells derived from these uniformly engineered iPSCs, termed iADAPT NK cells, displayed enhanced metabolic fitness, resistance to oxidative stress, broad natural cytotoxicity, and robust antibody-dependent cellular cytotoxicity (ADCC). To assess the cytotoxic capacity of iADAPT NK cells, we performed 3-dimensional (3-D) live imaging assays where iADAPT NK cell infiltration and cytotoxicity in response to 9 different primary, patient derived GBM spheroids was measured in real time over the course of 5 days. The in vivo persistence and antitumor function of iADAPT NK cells were also assessed using xenogeneic adoptive transfer models.

Results In 3-D live imaging assays, iADAPT NK cell efficiently infiltrated and eliminated patient-derived GBM spheroids (figure 1A, B). These in vitro results were recapitulated in vivo in xenogeneic experiments where human GBM cells were implanted intracranially into immunodeficient mice (n=19) followed by adoptive transfer of either 1.5x10⁶ or 3x10⁶ iADAPT NK cells. We show that adoptive transfer of iADAPT NK cells promoted survival in a dose-dependent manner (figure 1C). Importantly, we also found that iADAPT NK cells persisted at high levels in the brain for at least 21 days in the absence of exogenous cytokine support (figure 1D).



Abstract 169 Figure 1

Conclusions Triple gene-edited iPSCs can be used to robustly manufacture iADAPT NK cells. These off-the-shelf engineered NK cells exhibit potent cytotoxicity against primary, patient derived GBM cells. Work is in progress to further engineer iADAPT NK cells with chimeric antigen receptors incorporating defined targeting motifs to further enhance cytotoxicity against GBM cells. Our preclinical data provides proof-of-concept for a planned phase I clinical trial.

REFERENCES

- Jin J, Grigore F, Chen CC, Li M. Self-renewal signaling pathways and differentiation therapies of glioblastoma stem cells (Review). *Int J Oncol* 2021;**59**:45.
- Castriconi R, Daga A, Dondero A, Zona G, Luigi Poliani P, Melotti A, Griffiro F, Marubbi D, Spaziante R, Bellora F, et al. NK cells recognize and kill human glioblastoma cells with stem cell-like properties. *J Immunol* 2009;**182**:3530–3539.
- Shiam H, Shanley M, Basar R, Daher M, Gumin J, Zamler DB, Uprety N, Wang F, Huang Y, Gabrusiewicz K, et al. Targeting the αv integrin/TGF- β axis improves natural killer cell function against glioblastoma cells. *J Clin Invest* 2021;**131**: e142116.
- Cichocki F, Bjordahl R, Gaidarova S, Mahmood S, Abujarour R, Wang H, Tuininga K, Felices M, Davis ZB, Bendzick L, et al. iPSC-derived NK cells maintain high cytotoxicity and enhance in vivo tumor control in concert with T cells and anti-PD-1 therapy. *Sci Transl Med* 2020;**12**:eaaz5618.

Ethics Approval This project has been approved by the University of Minnesota IACUC. Approval ID: 1812-36595A

<http://dx.doi.org/10.1136/jitc-2021-SITC2021.169>

NOVEL GENE EDITING APPROACH TO ENHANCE CD38-DIRECTED ANTITUMOR ACTIVITY OF PRIMARY HUMAN NATURAL KILLER CELLS

Joseph Clara*, Emily Levy, Robert Reger, Mala Chakraborty, David Allan, Richard Childs.
National Institutes of Health, Bethesda, MD, USA

Background Natural killer (NK) cells play an important role in the antitumor responses of therapeutic monoclonal antibodies (mAbs) by mediating antibody-dependent cellular cytotoxicity (ADCC). ADCC occurs when tumor-ligated mAbs trigger NK cell killing by engaging CD16 on NK cells. Further, infusions of ex vivo expanded NK cells to potentiate the antitumor effects of mAbs is a promising immunotherapeutic approach. Daratumumab (DARA) is an anti-CD38 mAb used in the treatment of multiple myeloma (MM) that efficiently induces NK-mediated ADCC. However, CD38 is also expressed on NK cells, which leads to DARA-mediated NK cell destruction and impaired ADCC against MM. Harnessing NK cells to fully exploit the ADCC mechanism of DARA has the potential to improve DARA's efficacy.

Methods We developed a novel approach to maximize DARA-mediated ADCC against MM by protecting NK cells from DARA targeting while simultaneously boosting their ADCC capacity. We designed a CRISPR/Cas9-based gene editing platform to couple the disruption of CD38 expression with site-specific insertion of a gene encoding a high-affinity variant of CD16 at the CD38 locus in ex vivo expanded NK cells. To achieve this, we delivered a ribonucleoprotein composed of a single guide RNA and Cas9 nuclease to induce a double strand break within CD38, followed by infection with engineered AAV particles to deliver a homology directed repair template encoding either a truncated CD34 reporter or a FLAG-tagged high-affinity CD16 to be integrated at the site of CD38 gene disruption. Gene editing and insertion efficiency were assessed by flow cytometry for CD38, CD34, and/or FLAG. Transgene integration was confirmed by junction PCR.

Results High CD38 knockout efficiency was achieved ($90.1 \pm 4.1\%$). Using an EF-1 alpha promoter-containing CD34 donor template, stable CD34 expression was seen in $90.2 \pm 5.1\%$ NK cells. Insertion of high-affinity CD16, as assessed by FLAG expression, was observed in $47.7 \pm 6.1\%$ of edited NK cells. NK cells modified to express high-affinity CD16 also exhibited a higher number of CD16-positive NK cells compared to unedited control NK cells ($10.94 \pm 1.8\%$). Functionally, CD38 knockout NK cells expressing high-affinity CD16 demonstrated augmented degranulation in ADCC assays and killing of daratumumab-treated MM cells compared to unedited control and CD38 knockout NK cells.

Conclusions Novel gene editing techniques can be successfully applied to generate NK cells with enhanced antitumor capabilities. We established an efficient gene editing platform that can be utilized to produce NK cells optimized for adoptive combination with daratumumab.

<http://dx.doi.org/10.1136/jitc-2021-SITC2021.170>

171 TARGETING THE IMMUNOMODULATORY ROLES OF T-CELL IMMUNOGLOBULIN- AND MUCIN DOMAIN-CONTAINING (TIM)-3 ON NATURAL KILLER CELLS IN GLIOBLASTOMA

Tram Dao*, Sandro Matosevic. *Purdue University, West Lafayette, IN, USA*

Background Natural killer (NK) cells have emerged as a viable alternative to T cells in adoptive cell transfer for cancer treatment. NK cell activity is driven by the balance between inhibitory and activating receptors, many of which remain elusive. In addition, NK cell metabolism is also a driver of NK cell fitness in tumor settings, where changes in NK metabolic states with the tumor microenvironment *in vivo*, or with stimulants *ex vivo*, further confounds the NK cells' cytotoxic function in cancer settings. One receptor that lies at the intersection between NK cell function and metabolism is TIM-3, with its expression having consequences on NK cell cytokine production and glucose metabolism. However, the contribution of TIM-3 to NK cell anti-tumor immunity is unclear and its role in driving NK cell function so far not fully defined.

Methods NK cells were isolated from healthy adult peripheral blood and expanded in feeder-cell media. NK cell metabolism and function were evaluated by different flow cytometric assays to measure glucose uptake, cytotoxicity, degranulation, and cytokine production. TIM-3 knock-out cells were generated using the CRISPR-Cas9 system. Patient samples, including whole blood and tumor, were also processed and phenotyped to compare expression level with healthy donor samples.

Results Previously, we discovered that TIM-3 downregulation was associated with decreased cytokine production and target cytotoxicity, and that maintenance of expression above a certain threshold was needed for NK cell function. As cytokine production reflects immune cell metabolic state, we hypothesized that TIM-3 participates in regulation of *ex vivo*-activated NK cell metabolism, which in turn affect the production of the cytokine IFN- γ to sensitize cancer targets to NK cell-mediated lysis. Here, we report the consequences of glucose starvation on TIM-3 expression, and how knock-out of TIM-3 on human NK cells affects NK cell metabolism and functionalities against glioblastoma targets. We also cross-reference TIM-3 expression level with glioblastoma patient samples, which provide clinical context for microenvironmental cues and nutrient deprivation.

Conclusions Our findings suggest that TIM-3 expression is associated with both *ex vivo*-activated NK cell glucose metabolism and cytotoxic function against glioblastoma. As *ex vivo*-activated NK cells are considered to be highly glycolytic, and as such associated with higher cytotoxicity, TIM-3's involvement with glucose uptake could prove crucial in sustaining NK cytotoxic phenotype in the tumor microenvironment. This information is shedding further light on the immunomodulatory roles of TIM-3, and aiding in leveraging this receptor usage in future NK cell-based immunotherapies.

Ethics Approval All procedures performed in studies involving human participants were approved by Purdue University's Institutional Review Board (IRB) in August 2018 (#1804020540). All institutional safety and biosecurity procedures were adhered to.

<http://dx.doi.org/10.1136/jitc-2021-SITC2021.171>

OVERCOMING IMMUNOSUPPRESSIVE TGF- β SIGNALING IN HUMAN OVARIAN CANCER-DERIVED TUMOR INFILTRATING LYMPHOCYTES VIA NON-VIRAL CRISPR ENGINEERING

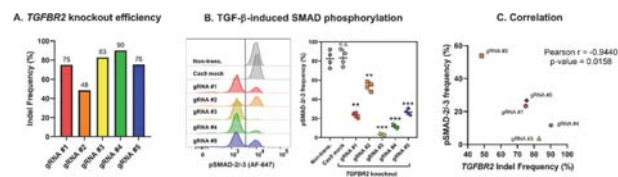
¹Samantha Fix*, ¹Marie-Andr e Forget, ¹Donastas Sakellariou-Thompson, ¹Yunfei Wang, ¹Ana Lucia Dominguez, ¹Rafet Basar, ²Christopher Reyes, ²Sanjay Kumar, ¹Larissa Meyer, ¹Patrick Hwu, ¹Chantale Bernatchez, ¹Amir Jazaeri. ¹MD Anderson Cancer Center, Houston, TX, USA; ²Thermo Fisher Scientific, Carlsbad, CA, USA

Background Our ongoing clinical trial for the treatment of melanoma with TGF- β -resistant tumor-infiltrating lymphocytes (TIL) [TGF- β dominant negative receptor 2 (TGF β DNR2) transduced-TIL] has yielded long-term responses in checkpoint refractory patients (NCT01955460). Building on this success, we sought to extend the impact of TGF- β -resistant TIL therapy to additional cancers while optimizing a non-viral alternative to transduction with a TGF β DNR2. Ovarian cancer (OvCa), which is characterized by an abundance of TGF- β , a dysfunctional immune infiltrate, and a paucity of novel treatment options, is an ideal candidate for TGF- β -resistant TIL therapy. Here, we present an optimized and clinically-scalable method for CRISPR/Cas9-mediated deletion of the TGF- β receptor (TGFB2) in OvCa TIL.

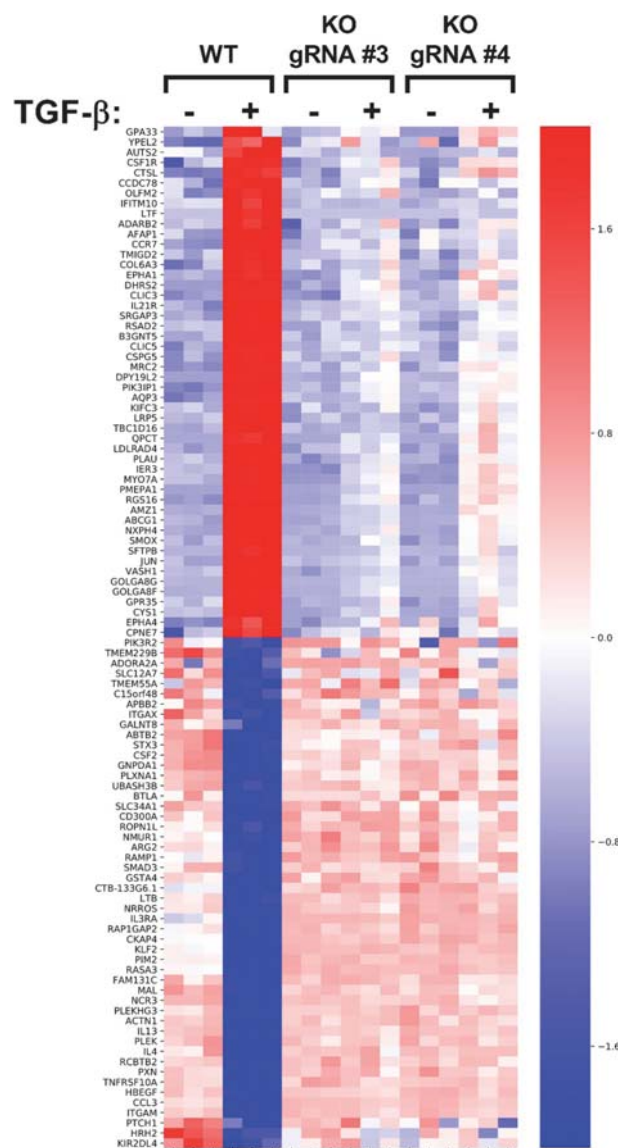
Methods OvCa TIL were generated from tumor fragments¹ and subjected to CRISPR-mediated knockout of TGFB2 before going through a rapid expansion protocol. Resistance of TGFB2-knockout TIL to TGF- β signaling was evaluated via quantification of downstream SMAD-2/3 phosphorylation, global transcriptional changes upon TGF- β exposure, and cytokine release following TCR stimulation in the presence of TGF- β . The impact of CRISPR modification on TIL expansion and TCR clonal diversity was evaluated. Finally, the risk of off-target CRISPR activity throughout the genome was evaluated using Target Enriched GUIDE-seq (TEG-seq)² followed by next generation sequencing (NGS) validation of putative off-target sites.

Results Using five TGFB2-directed guide RNAs (gRNAs), we achieved gene disruption efficiencies ranging from 48%–90%, which correlated inversely with the degree of SMAD phosphorylation after TGF- β exposure ($r=-0.9440$, $p=0.0158$, $n=4$ donors) (figure 1A-C). TGF- β exposure induced a strong transcriptional response in wild-type TIL but had little to no effect on TGFB2-knockout TIL (figure 2). TGFB2-knockout TIL functioned well in the presence of exogenous TGF- β as evidenced by equally strong secretion of pro-inflammatory cytokines in the presence and absence of TGF- β (figure 3). CRISPR-modification did not hamper the ex vivo expansion efficiency nor the TCR clonal diversity of expanded OvCa TIL (figure 4). Using TEG-seq, we identified ≤ 5 low-probability off-target sites for gRNA-#3 and gRNA-#4, each of which were attributed to background sequencing artifacts upon further validation by NGS of specific amplicons (figure 5).

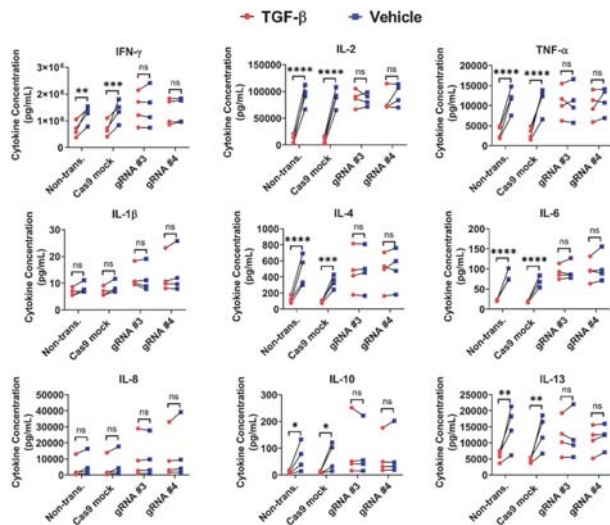
Conclusions CRISPR/Cas9-mediated knockout of TGFB2 is feasible and efficient in patient-derived OvCa TIL using clinically-scalable methods that yield little to no evidence of off-target activity. This study lays the groundwork for clinical translation of CRISPR-modified, TGF- β -resistant TIL for OvCa treatment, which will not only provide a novel immunotherapy for OvCa patients but also a platform for engineering more potent TIL therapies in general.



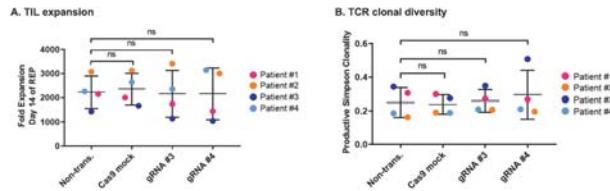
Abstract 172 Figure 1 (A) Genomic-level TGFB2 knockout efficiency using 5 different gRNAs as evidenced by NGS of specific amplicons ($n=1$ TIL donor). (B) SMAD-2 and SMAD-3 phosphorylation in TGFB2 knockout TIL vs. control TIL after 30 min exposure to TGF- β 1. The left panel shows representative histograms of phospho-SMAD staining, and the right panel shows quantification of cells positive for phospho-SMAD-2/3 after TGF- β exposure ($n=4$ TIL donors). The statistical significance of each experimental condition compared to the non-transfected control is shown. (C) Inverse correlation of TGFB2 knockout efficiency and TGF- β -mediated SMAD phosphorylation.



Abstract 172 Figure 2 Top 100 differentially expressed genes in non-transfected (WT) TIL exposed to TGF- β . TGFB2 knockout (KO) TIL display minimal gene expression changes upon TGF- β exposure ($n=3$ technical replicates).



Abstract 172 Figure 3 TIL were collected after 14 days of expansion and re-stimulated with 300 ng/mL plate-bound anti-CD3 in the presence of 3000 IU/mL IL2 and 10 ng/mL human TGF-β1 or vehicle. Cell culture supernatant was collected after 72 hrs of stimulation and assayed for the presence of 10 proinflammatory cytokines (IFN-γ, IL-1β, IL-2, IL-4, IL-6, IL-8, IL-10, IL-12p70, IL-13, and TNF-α). For TIL with intact TGFBR2 (non-transfected and Cas9 mock transfected TIL), the production of many pro-inflammatory cytokines decreased significantly in the presence of TGF-β. Conversely, TGFBR2 knockout TIL (generated using gRNA #3 or gRNA #4) retain cytokine secretion in the presence of TGF-β. IL-12p70 was below the limit of detection in this assay and is therefore not presented.



Abstract 172 Figure 4 (A) Control and CRISPR-modified OvCa TIL expand with equal efficiency during a 14-day rapid expansion protocol. Fold expansions ranging from 1000x - 3000x were observed across 4 independent patient samples. (B) The TCR clonal diversity of TIL after 14-day expansion was assessed by TCRB sequencing. Productive Simpson Clonality was equivalent in CRISPR-modified TIL compared to control TIL samples.

gRNA #3 binding site		TEG-Seq results				Validation by NGS		Conclusion
Site	Sequence	Replicate #1 (gRNA)		Replicate #2 (gRNA)		On target probability	Tag insertion	Large deletion (>1bp)
		Forward	Reverse	Forward	Reverse			
gRNA #3_010	CCCTTCCCTCCCTCCCTCCCTCCCT	12075	27912	2202	8213	On target	YES	YES
gRNA #3_010	CCCTTCCCTCCCTCCCTCCCTCCCT	120	0	10	0	Low	NO	NO
gRNA #3_012	CCCTTCCCTCCCTCCCTCCCTCCCT	0	0	0	0	Low	NO	NO
gRNA #3_019	CCCTTCCCTCCCTCCCTCCCTCCCT	0	0	0	0	Low	NO	NO

gRNA #4 binding site		TEG-Seq results				Validation by NGS		Conclusion
Site	Sequence	Replicate #1 (gRNA)		Replicate #2 (gRNA)		On target probability	Tag insertion	Large deletion (>1bp)
		Forward	Reverse	Forward	Reverse			
gRNA #4_010	CCCTTCCCTCCCTCCCTCCCTCCCT	4269	1039	12112	10012	On target	YES	YES
gRNA #4_010	CCCTTCCCTCCCTCCCTCCCTCCCT	0	0	0	0	Low	NO	NO
gRNA #4_012	CCCTTCCCTCCCTCCCTCCCTCCCT	0	0	0	0	Low	NO	NO
gRNA #4_014	CCCTTCCCTCCCTCCCTCCCTCCCT	219	0	0	0	Low	NO	NO
gRNA #4_019	CCCTTCCCTCCCTCCCTCCCTCCCT	0	0	0	0	Low	NO	NO

*Note: Indel spectrum similar to that of non-transfected control cells and therefore not likely due to CRISPR/Cas9 cleavage. Lack of TEG-seq Tag insertion supports the conclusion of "no CRISPR activity".

Abstract 172 Figure 5 TEG-seq revealed 3 putative off-target sites for gRNA #3 and 5 putative off-target sites for gRNA #4. The aligned sequences show similarities and differences between the gRNA sequence and the reference genome site. Dots represent exact matches in the reference genome compared to the gRNA sequence. Dashes represent missing bases, lower-case letters represent extra bases, and upper-case letters represent a base mismatch. Validation by NGS of specific amplicons confirmed the presence of TEG-seq Tag integration and large indels at the on-target cleavage sites for gRNA #3 and #4,

indicating successful Cas9 editing and Tag integration in our experiment. NGS validation revealed that all putative low probability off-target sites were background artifacts as evidenced by the lack of Tag identification and lack of large indels.

REFERENCES

1. Sakellariou-Thompson D, Forget MA, Hinchcliff E, Celestino J, Hwu P, Jazaeri AA, et al. Potential clinical application of tumor-infiltrating lymphocyte therapy for ovarian epithelial cancer prior or post-resistance to chemotherapy. *Cancer Immunology, Immunotherapy: CII* 2019;**68**(11):1747–57.
2. Tang PZ, Ding B, Peng L, Mozhayskiy V, Potter J, Chesnut JD. TEG-seq: an ion torrent-adapted NGS workflow for in cellulo mapping of CRISPR specificity. *Bio Techniques* 2018;**65**(5):259–67.

Ethics Approval All procedures performed were in accordance with the 1975 Helsinki declaration. Ethical approval and tissue from surgical resections used to expand TIL were both obtained under protocols (PA16-0912 and LAB02-188) approved by the Institutional Review Board of The University of Texas MD Anderson Cancer Center. Written informed consent was obtained from all individual participants included in the study for their specimens and data to be used in research and for publication.

<http://dx.doi.org/10.1136/jitc-2021-SITC2021.172>

173

EXPRESSION OF A MEMBRANE-TETHERED IL-15/IL-15 RECEPTOR FUSION PROTEIN ENHANCES THE PERSISTENCE OF MSLN-TARGETED TRUC-T CELLS

Michelle Fleury, Derrick McCarthy*, Holly Horton, Courtney Anderson, Amy Watt, Adam Zieba, Lindsay Webb, Jian Ding, Robert Tighe, Robert Hofmeister, Dario Gutierrez. *TCR2 Therapeutics, Cambridge, MA, USA*

Background Adoptive cell therapies have shown great promise in hematological malignancies but have yielded little progress in the context of solid tumors. We have developed T cell receptor fusion construct (TRuC[®]) T cells, which are equipped with an engineered T cell receptor that utilizes the full complement of TCR signaling subunits and recognizes tumor-associated antigens independent of HLA. In clinical trials, mesothelin (MSLN)-targeting TRuC-T cells (TC-210 or gavo-cel) have shown unprecedented results in patients suffering from advanced mesothelioma and ovarian cancer. To potentially increase the depth of response, we evaluated strategies that can promote intra-tumoral T cell persistence and function. Among the common $\gamma\delta$ -chain cytokines, IL-15 uniquely supports the differentiation and maintenance of memory T cell subsets by limiting terminal differentiation and conferring resistance to IL-2 mediated activation-induced cell death (AICD). In the studies described here, we evaluated the potential of IL-15 as an enhancement to TRuC-T cell phenotype, persistence and function against MSLN+ targets.

Methods Primary human T cells were activated and transduced with a lentiviral vector encoding an anti-MSLN binder fused to CD3 ϵ alone or co-expressed with a membrane-tethered IL-15 α /IL-15 fusion protein (IL-15fu). Transduced T cells were expanded for 9 days and characterized for expression of the TRuC, IL-15 α and memory phenotype before subjecting them to in vitro functional assays to evaluate cytotoxicity, cytokine production, and persistence. In vivo efficacy was evaluated in MHC class I/II deficient NSG mice bearing human mesothelioma xenografts.

Results In vitro, co-expression of the IL-15fu led to similar cytotoxicity and cytokine production as TC-210, but notably enhanced T-cell expansion and persistence upon repeated stimulation with MSLN+ cell lines. Furthermore, the IL-15fu-enhanced TRuC-T cells sustained a significantly higher TCF-1 + population and retained a stem-like phenotype following activation. Moreover, the IL-15fu-enhanced TRuCs demonstrated robust in vivo expansion and intra-tumoral accumulation as measured by ex vivo analysis of TRuC+ cells in the tumor and blood, with a preferential expansion of CD8+ T cells. Finally, IL-15fu-enhanced TRuC-T cells could be observed in the blood long after the tumors were cleared.

Conclusions These pre-clinical studies suggest that the IL-15fu can synergize with TC-210 to increase the potency and durability of response in patients with MSLN+ tumors.

Ethics Approval All animal studies were approved by the respective Institutional Animal Care and Use Committees.

<http://dx.doi.org/10.1136/jitc-2021-SITC2021.173>

COMBINED IL-2, AGONISTIC CD3 AND 4–1BB STIMULATION PRESERVE CLONOTYPE HIERARCHY IN PROPAGATED NON-SMALL CELL LUNG CANCER TUMOR-INFILTRATING LYMPHOCYTES

Meredith Frank*, Parin Shah, Marie Andree Forget, Lorenzo Federico, Peixin Jiang, Roohussaba Khairullah, Ignacio Wistuba, Chi-Wan Chow, Yan Long, Junya Fujimoto, Shiaw-Yih Lin, Anirban Maitra, Marcelo Negro, Kyle Mitchell, Annika Weissferdt, Ara Vaporciyan, Tina Cascone, Jack Roth, Jianjun Zhang, Boris Sepesi, Don Gibbons, John Heymach, Cara Haymaker, Daniel McGrail, Chantale Bernatchez, Alexandre Reuben. *The University of Texas MD Anderson Cancer Center, Houston, TX, USA*

Background While immune checkpoint blockade is regarded as standard of care for treatment of non-small cell lung cancer (NSCLC), up to 50% of patients with metastatic NSCLC do not achieve an optimal response.^{1–3} Previous work by our group and others in adoptive cell therapy (ACT) of metastatic melanoma (MM) has shown that infusion of a CD8+ TIL product significantly improved clinical outcomes, yet traditional IL-2 expansion methods have resulted in a predominantly CD4+ NSCLC TIL expansion product.^{7–12} This preclinical study explores the feasibility of producing a tumor-specific, CD8+-enriched NSCLC TIL product for ACT with an improved culture method.

Methods TIL from resected NSCLC tumors were cultured using 1) the traditional method using IL-2 alone in 24-well plates (TIL 1.0) or 2) IL-2 in combination with agonistic antibodies against CD3 and 4-1BB (Urelumab) in a G-Rex flask (TIL 3.0). Expanded TIL were phenotyped using flow cytometry for CD4 and CD8 subset assessment and the CDR3-beta variable region of the T-cell receptor (TCR) involved in antigen binding was sequenced to assess the T-cell repertoire.

Results In a shorter manufacturing time (median of 14 days vs 27.5 days), TIL 3.0 expanded on average 5.3-times more NSCLC TIL (95% CI= 4.3–6.2, $p < 0.0001$) and achieved a higher expansion success rate than the traditional TIL 1.0 method (100% vs 62.5%, respectively, $p < 0.0001$). Additionally, TIL 3.0 greatly enriched for CD3+CD8+ TIL (81.8% vs 36.9%, $p = 0.001$) and expanded a larger breadth of clonotypes ($p = 0.039$) which shared greater homology with the total clonotypes found in the repertoire of the resected tumor ($p = 0.0007$), and contained a greater fraction of the clones found at high frequency in the tumor ($p < 0.00001$). TIL 3.0 also retained a higher proportion of putative tumor-specific TCR when compared to TIL 1.0 ($p = 0.0039$), defined based on exclusion of known viral-specific TCR and other TCR found in the paired uninvolved lung tissue.

Conclusions This study reports the feasibility of using the TIL 3.0 methodology to robustly expand a CD8+ T-cell repertoire which maintains the respective clonal hierarchy in NSCLC tumors and enriches for putative tumor-specific TIL clones. The robustness and speed of the new process may facilitate testing and implementing effective TIL ACT in NSCLC.

REFERENCES

- Garon EB, Rizvi NA, Hui R, Leigh N, Balmanoukian AS, Eder JP, et al. Pembrolizumab for the treatment of non-small-cell lung cancer. *N Engl J Med* 2015;**372**(21):2018–28.
- Borghaei H, Paz-Ares L, Horn L, Spigel DR, Steins M, Ready NE, et al. Nivolumab versus Docetaxel in Advanced Nonsquamous Non-Small-Cell Lung Cancer. *N Engl J Med* 2015;**373**(17):1627–39.
- Gettinger S, Horn L, Jackman D, Spigel D, Antonia S, Hellmann M, et al. Five-Year Follow-Up of Nivolumab in Previously Treated Advanced Non-Small-Cell Lung Cancer: Results from the CA209–003 Study. *J Clin Oncol* 2018;**36**(17):1675–84.
- Melioli G, Ratto G, Guastella M, Meta M, Biassoni R, Semino C, et al. Isolation and in vitro expansion of lymphocytes infiltrating non-small cell lung carcinoma: functional and molecular characterisation for their use in adoptive immunotherapy. *Eur J Cancer* 1994;**30A**(1):97–102.
- McGranahan N, Furness AJ, Rosenthal R, Ramskov S, Lyngaa R, Saini SK, et al. Clonal neoantigens elicit T cell immunoreactivity and sensitivity to immune checkpoint blockade. *Science* 2016;**351**(6280):1463–9.
- Rosenberg SA, Yang JC, Sherry RM, Kammula US, Hughes MS, Phan GQ, et al. Durable complete responses in heavily pretreated patients with metastatic melanoma using T-cell transfer immunotherapy. *Clin Cancer Res* 2011;**17**(13):4550–7.
- Besser MJ, Shapira-Frommer R, Treves AJ, Zippel D, Itzhaki O, Hershkovitz L, et al. Clinical responses in a phase II study using adoptive transfer of short-term cultured tumor infiltration lymphocytes in metastatic melanoma patients. *Clin Cancer Res* 2010;**16**(9):2646–55.
- Pilon-Thomas S, Kuhn L, Ellwanger S, Janssen W, Royster E, Marzban S, et al. Efficacy of adoptive cell transfer of tumor-infiltrating lymphocytes after lymphopenia induction for metastatic melanoma. *J Immunother* 2012;**35**(8):615–20.
- Radvanyi LG, Bernatchez C, Zhang M, Fox PS, Miller P, Chacon J, et al. Specific Lymphocyte Subsets Predict Response to Adoptive Cell Therapy Using Expanded Autologous Tumor-Infiltrating Lymphocytes in Metastatic Melanoma Patients. *Clinical Cancer Research* 2012;**18**(24):6758–70.
- Forget MA, Haymaker C, Hess KR, Meng YJ, Creasy C, Karpinetz T, et al. Prospective Analysis of Adoptive TIL Therapy in Patients with Metastatic Melanoma: Response, Impact of Anti-CTLA4, and Biomarkers to Predict Clinical Outcome. *Clin Cancer Res* 2018;**24**(18):4416–28.
- Ben-Avi R, Farhi R, Ben-Nun A, Gorodner M, Greenberg E, Markel G, et al. Establishment of adoptive cell therapy with tumor infiltrating lymphocytes for non-small cell lung cancer patients. *Cancer Immunol Immunother* 2018;**67**(8):1221–30.
- Ma Y, Ou J, Lin T, Chen L, Wang J, Qiao D, et al. Phenotypic analysis of tumor-infiltrating lymphocytes from non-small cell lung cancer and their potential application for adoptive cell therapy. *Immunopharmacol Immunotoxicol* 2020;**42**(4):319–29

Ethics Approval This study was performed on NSCLC tumor tissue resected from 16 patients enrolled, following informed consent, in the Immunogenomic profiling of early-stage NSCLC (ICON) project. This study was approved by the University of Texas MD Anderson Cancer Center's Institutional Review Board (protocol number PA15-1112_MODCR001).

<http://dx.doi.org/10.1136/jitc-2021-SITC2021.174>

175

HIGH-DOSE TIL PRODUCT WITH IMPROVED PHENOTYPE AND FUNCTIONALITY

Christina Friese, Christina Heeke, Nikolaj Kirketerp-Møller*, Sandra Færch, Maria Juul Nielsen, Amalie Hey, Ulrik Cordes. *Cbio, Søborg, Denmark*

Background Adoptive cell transfer (ACT) with autologous tumor-infiltrating lymphocytes (TILs) has proven to be one of the most successful immune therapies with overall response rates of around 50% in patients with metastatic melanoma including complete responses in up to 20% of the patients. Current protocols combine a first expansion of TILs from tumor fragments or tumor digest with high-dose IL-2, followed by further expansion with a rapid-expansion-protocol (REP) using allogeneic feeder cells, α CD3 and IL-2. Following this protocol, TIL production takes 4–7 weeks, and many patients deteriorate before they can receive therapy. With success rates of TIL expansion ranging from 70–90%, a TIL product cannot be generated for every patient. Furthermore, clinical response to TIL therapy is lower in other solid tumors such as ovarian cancer, likely due to a lower number of expanded TILs and lower frequencies of tumor reactive CD8 + T cells. Therefore, there is a clinical need for improvement of current TIL expansion protocols to make this therapy available to more cancer patients.

Methods In this project, TILs from tumor fragments of patients with various solid tumors have been cultured under two different conditions using novel culture vessels. TIL yield, viability, composition, phenotype, reactivity and expansion time were compared to TILs expanded following the standard protocol.

Results Using the two novel culture conditions, success rates of expansion across all tumor types increased from 70% to >95%. Additionally, significantly higher frequency and total numbers of viable CD8+ T cells per fragment were obtained compared to standard expansion with IL-2 alone. The majority of these CD8+ T cells exhibit an effector memory phenotype with elevated levels of exhaustion markers. A third of CD8+ T cells can be activated unspecifically and express any combination of the cytotoxicity markers IFN γ , TNF α or CD107a. Overall, the initial expansion time could be reduced from 2–5 weeks to 10–14 days and the rapid expansion time from 2 weeks to 8–12 days. Thus, the total culture time was shortened from 4–7 weeks to 18–26 days. As the REP TILs still comprise a majority of CD8+ T cells (~75%), the clinical dose would contain a total number of 3–10 billion functional CD8+ T cells.

Conclusions With this study, we show that by improving the initial culture conditions, we can shorten expansion time while simultaneously improving the characteristics of the TIL product with a high dose of functional CD8+ T cells with potential anti-tumor activity.

<http://dx.doi.org/10.1136/jitc-2021-SITC2021.175>

SUCCESSFUL GENERATION OF TUMOR-INFILTRATING LYMPHOCYTE (TIL) PRODUCT FROM RENAL CELL CARCINOMA (RCC) TUMORS FOR ADOPTIVE CELL THERAPY

¹Brian Halbert, ¹David Einstein, ¹David McDermott, ¹Emanuelle Andrianopoulos, ¹Mamta Gupta, ¹Virginia Seery, ²Kenneth Onimus, ²Courtney Herman, ²Adrian Wells, ²Shwetha Lakshminpathi, ²Arvind Natarajan, ²Anand Veerapathran, ¹Rupal Bhatt, ¹Brian Halbert*. ¹BIDMC, Boston, MA, USA; ²Iovance Biotherapeutics, San Carlos, CA, USA

Background Patients with RCC may achieve remission with immune-checkpoint inhibitors (ICI); however, most patients will progress. Adoptive cell therapy with autologous TIL allows for expansion of T-cells from tumor tissue leading to a polyclonal T-cell product with a diverse T-cell receptor repertoire capable of recognizing an array of tumor antigens. TIL therapy with centrally manufactured lifileucel demonstrated a 36% overall response rate in patients with ICI-refractory melanoma.¹ We present our preclinical experience of TIL production in RCC.

Methods This study was approved by the DF/HCC Institutional Review Board. Fresh tumor samples (≥ 1.5 -cm) were harvested from consented patients undergoing resection for RCC. TIL were manufactured using pre-rapid expansion (1/10th scale) and rapid expansion (1/100th scale) protocol for 22 days. Characterization (total viable cells [TVC], % viability, identity, and potency) was performed on the final TIL product. TIL purity, differentiation, memory, activation, and exhaustion status were characterized using multi-color flow cytometry.

Results Baseline characteristics of 11 recruited patients are shown in table 1. Clear cell was the most common histology (73%). Two patients had previously treated metastatic disease with samples harvested from the lung and adrenal gland; one patient had prior cryoablation with adjacent local recurrence. The remainder were treatment-naïve primary nephrectomy samples. Eight products (73%) showed acceptable TIL product attributes (table 2). Median (range) TVC, viability, and identity (CD45+CD3+%) for the final TIL product were 74×10^9 (18×10^9 – 133×10^9), 95% (86%–97%), and 98% (94%–99%), respectively. Median (range) percentage of CD4+ cells was 69% (21%–97%) and CD8+ cells was 27% (2%–72%). The non-T-cell population, including B cells, monocytes, and NK cells, was <7%. The final TIL product was functional, and responded to polyclonal bead stimulation; the median (range) IFN γ and granzyme B were 8834 (3319–12,957) pg/mL and 34,329 (15,565–65,521) pg/mL, respectively. Acceptable TIL product was generated from both metastatic lesions and primary tumor samples. Of the 3 tumor samples that did not demonstrate acceptable TIL product attributes, one (ID 1) was from a patient treated with a CXCR4 inhibitor <1 month before resection, another (ID 4) was from a patient previously treated with ocrelizumab (CD20-directed cytolytic antibody) for multiple sclerosis, and the final (ID 8) was harvested from the cryoablated tumor nodule rather than the adjacent recurrent tumor.

Conclusions These feasibility data suggest that TIL can be successfully expanded ex vivo from RCC samples (including pre-treated and metastatic tumors) and support potential clinical investigation of TIL in patients with RCC.

Abstract 176 Table 1 Baseline demographics and tumor characteristics

N = 11	
Age, years, median (IQR)	59 (52-68)
Sex, n (%)	
Male	10 (91)
Race, n (%)	
White	9 (82)
Histology, n (%)	
Clear cell	8 (73)
Papillary	2 (18)
Chromophobe	1 (9)
Tumor site, n (%)	
Kidney	9 (82)
Adrenal	1 (9)
Lung	1 (9)

Abstract 176 Table 2 Summary of product attributes. 1, No CD3 + subset. 2, Product not available to test

Tumor ID	Histology	Tumor	Acceptance Criteria	TVC ($\times 10^9$)	Viability (%)	CD45 ⁺ CD3 ⁺ (%)	CD4 ⁺ (%)	CD8 ⁺ (%)	CD4 ⁺ CD8 ⁺
1	Clear cell	Lung	Not met	1	64	0		- ¹	
2	Clear cell	Primary	Met	77	97	99	48	34	1
3	Clear cell	Primary	Met	96	95	96	21	72	0
4	Clear cell	Primary	Not met	2	67	0		- ¹	
5	Clear cell	Primary	Met	71	91	99	77	18	4
6	Papillary	Primary	Met	63	95	98	58	29	2
7	Papillary	Primary	Met	81	94	99	97	2	49
8	Clear cell	Primary	Not met	1	92	75		- ²	
9	Chromophobe	Primary	Met	27	91	94	72	25	3
10	Clear cell	Primary	Met	113	95	99	65	29	2
11	Clear cell	Adrenal	Met	18	86	94	80	18	4

REFERENCES

- Sarnaik AA, Hamid O, Khushalani NI, Lewis KD, Medina T, Kluger HM, Thomas SS, Domingo-Musibay E, Pavlick AC, Whitman ED, Martin-Algarra S, Corrie P, Curti BD, Oláh J, Lutzky J, Weber JS, Larkin JMG, Shi W, Takamura T, Jagasia M, Qin H, Wu X, Chartier C, Graf Finckenstein F, Fardis M, Kirkwood JM, Chesney JA. Lifileucel, a Tumor-Infiltrating Lymphocyte Therapy, in Metastatic Melanoma. *J Clin Oncol* 2021 May 12;JCO2100612. doi: 10.1200/JCO.21.00612. Epub ahead of print. PMID: 33979178.

Ethics Approval This study was approved by the DF/HCC Institutional Review Board protocol # 06-105.

<http://dx.doi.org/10.1136/jitc-2021-SITC2021.176>

TREATMENT OUTCOMES WITH UNSELECTED AUTOLOGOUS TUMOR INFILTRATING LYMPHOCYTES IN PATIENTS WITH CHECKPOINT INHIBITION–REFRACTORY ADVANCED CUTANEOUS MELANOMA

¹Robert Hawkins*, ²Yizhou Jiang, ³Paul C Lorigan, ⁴Fiona C Thistlethwaite, ³Manon Pillai, ²Martine Thomas, ²Natalia Kirillova, ²John S Bridgeman, ²Gray Kueberuwa, ²Ryan D Guest, ²Zachary J Roberts. ¹*Instil Bio, Inc., Dallas, TX, USA and The Christie, NHS Foundation Trust and University of Manchester, Manchester, TX, UK;* ²*Instil Bio, Inc., Dallas, TX, USA;* ³*The Christie, NHS Foundation Trust, Manchester, UK;* ⁴*The Christie, NHS Foundation Trust, Manchester, UK and University of Manchester, Manchester, UK*

Background Tumor infiltrating lymphocyte (TIL) products made from tumor digests showed a high overall response rate (ORR; 67%) and complete response (CR) rate (19%) and a safety profile consistent with lymphodepletion and high-dose interleukin (IL)-2 in a retrospective analysis of a single center experience of TILs for compassionate use treatment of advanced cutaneous melanoma (n=21; Hawkins, et al. AACR 2021. ePoster LB150). This subanalysis assesses outcomes for patients who received TILs after prior checkpoint inhibition, a subset with limited treatment options.

Methods Patients with advanced cutaneous melanoma and no standard of care treatment options received lymphodepleting chemotherapy (cyclophosphamide ×2 days; fludarabine ×5 days) followed by TIL infusion and post TIL high-dose IL-2. Safety was assessed by clinically significant adverse events (AEs). Efficacy assessments included ORR, CR rate, and overall survival (OS).

Results Of 21 patients who underwent treatment between October 2011 and August 2019, median age was 45 years, median number of disease sites was 4, 100% of patients had M1c or M1d disease (33% with M1d), average number of prior therapies was 3 (any checkpoint inhibitor, 91%; BRAF inhibitor [BRAFi], 52%; and MEKi, 24%), and 52% were BRAF-mutated. Twelve patients received prior PD-1i therapy and are reported herein. Baseline characteristics were similar between the overall and prior PD-1i subgroup populations. All patients in the prior PD-1i subgroup received prior CTLA-4i, and all BRAF-mutated patients received prior BRAFi alone ± MEKi. The most commonly reported AEs post-TIL infusion were consistent between the overall and prior PD-1i subgroup populations and included thrombocytopenia (62% and 75%, respectively), pyrexia (57% and 50%), and rigors (43% and 50%). No treatment-related deaths occurred. With a median follow-up of 45.5 months, the ORR and CR rate for the prior PD-1i subgroup were 58% and 8%, respectively. At data cutoff, 2 of 12 patients (17%) had durable ongoing responses (>30 months post-TIL infusion). Median OS in the prior PD-1i subgroup and overall population was 21.3 months.

Conclusions In this subanalysis of patients with relapsed advanced melanoma after both PD-1i and CTLA-4i, and for some, BRAFi, outcomes of unselected autologous TILs were similar to those observed in all treated patients, with high response rates and a safety profile consistent with that of TIL therapy. Unselected TILs may address the unmet medical need for the poor-risk subset of patients with advanced melanoma who experience disease progression following checkpoint inhibition and, if applicable, targeted therapy.

Acknowledgements The authors would like to thank all the staff within The Christie NHS Foundation Trust and The Christie Clinic who worked tirelessly to provide high-quality care to all the patients in this report. Medical writing support was provided by Christopher Waldapfel, PharmD, of Instil

Bio, Inc. and Jennifer Yang, PhD, of Nexus GG Science, with funding from Instil Bio, Inc.

Ethics Approval As a compassionate use study, the treatment was approved by institutional review board and National Health Service commissioning.

<http://dx.doi.org/10.1136/jitc-2021-SITC2021.177>

EXPANSION OF TUMOR-INFILTRATING LYMPHOCYTES AND MARROW-INFILTRATING LYMPHOCYTES FROM PEDIATRIC MALIGNANT SOLID TUMORS

¹Jonathan Metts*, ²Jonathan Hensel, ²Alejandro Alfaro, ²Brook Olmo, ²Shari Pilon-Thomas, ²John Mullinax, ¹Ivanna Leon. ¹Johns Hopkins All Children's Hospital, St Petersburg, FL, USA; ²Moffitt Cancer Center, Tampa, FL, USA

Background High-risk non-CNS pediatric malignant solid tumors (pMST) have unsatisfactory outcomes, and novel therapies are warranted. Adoptive cellular therapy (ACT) using tumor-infiltrating lymphocytes (TIL) has produced durable responses in melanoma, and improvements in TIL expansion have made ACT-TIL feasible for other solid tumors.¹⁻³ Preclinical mouse models suggest that T-cells from bone marrow (marrow-infiltrating lymphocytes, MIL) have antitumor reactivity offering another source for ACT.^{4, 5} To demonstrate feasibility of ACT in pMST we hypothesized that TIL/MIL can be expanded from these patients.

Methods Patients ≤21 years old undergoing standard-of-care pMST resection were enrolled on an IRB approved protocol. Fresh tumor (≥1 cm³) was collected and bone marrow (10 mL) was obtained when accessible from standard of care procedures. TIL/MIL were cultured in media containing IL-2 (6000 IU/mL). TIL were expanded from tumor fragment cultures (TFC, >1 mm³) or tumor digest. Select TIL samples were further expanded using a rapid expansion protocol (REP). Phenotype of expanded TIL (CD3, CD4, CD8 and CD56) was evaluated using flow cytometry. IFN- γ secretion, measured by ELISA assay, measured tumor-specific reactivity after co-culture with autologous tumor and TIL.

Results Twenty samples were obtained between March 2019-May 2021. Two samples were ineligible (final pathology not pMST), leaving 18 samples for analysis. Five marrow samples were collected. TIL were expanded from 14/18 samples (78%) through TFC with median 5.17×10^6 cells (range 1.86×10^6 – 3.21×10^8). Average phenotype (%) of TFC-TIL were CD3 (63.17), CD4 (21.46), CD8 (46.19) and CD56 (32.68). 9/10 (90%) of samples successfully underwent REP with median 9.35×10^7 cells (range 2.49×10^7 – 5.86×10^8) final viable TIL and average fold-change 718.6 (median 458.6). Average phenotype (%) of post-REP TIL were CD3 (96.04), CD4 (75.04), CD8 (19.17) and CD56 (0.43). TIL were expanded from TFC of therapy-naïve (8/10, 80%) and pretreated (chemotherapy and checkpoint immunotherapy) samples (5/8, 63%). Seven samples had sufficient tissue to test tumor-specific reactivity; all were non-reactive. MIL pre-REP was expanded from four samples with median 9.55×10^6 cells (range 8.00×10^5 – 1.00×10^7). Average phenotype of expanded MIL (%) were CD3 (45.17), CD4 (24.46), CD8 (36.15) and CD56 (28.21) (table 1).

Results of TIL and MIL expansion from 18 pMST samples. Abbreviations: Dx: diagnosis, pre-REP: pre-rapid expansion protocol, post-REP: post-rapid expansion protocol, PBMC: peripheral blood mononuclear cells, GNB: ganglioneuroblastoma, WT: Wilms tumor, OS: osteosarcoma, NB: neuroblastoma, IMT: inflammatory myofibroblastic tumor; ASPS: alveolar soft part sarcoma, SS: synovial sarcoma, ERMS: embryonal rhabdomyosarcoma, N: no systemic therapy, C: chemotherapy, I: immunotherapy, DNG: did not grow, N/A: not applicable, NR: non-reactive

Abstract 178 Table 1 Expansion of TIL from pMST

Sample	Dx	Age (years)	Staging	Diagnosis	Sampling	Sample Source	Prior Therapy	Tumor Infiltration Culture (cells)	post-REP (cells)	Digest (cells)	MIL (cells)	Reactivity
1	GNB	3	Localized	Initial	Uplift resection	Abdomen, primary site	N	DNG	N/A	none available	1.92×10^7 post-REP, 5.2×10^6 post-REP	NR
2	WT	2	IV, favorable histology	Initial	Uplift resection	Abdomen, primary site	N	4.68×10^6	N/A	1.63×10^8	N/A	NR
3	WT	1	IV, favorable histology	Initial	Uplift resection	Abdomen, primary site	N	3.20×10^6	4.01×10^7	1.60×10^8	N/A	NR
4	OS	15	Metastatic	Relapse	After salvage chemotherapy	Lung, metastatic site	C	6.00×10^6	5.46×10^7	7.24×10^8	N/A	N/A
5	WT	7	IV, unfavorable histology	Initial	Uplift resection	Abdomen, lymph node	N	2.50×10^6	DNG	8.43×10^6	N/A	N/A
6	NB	7	IV, high-risk	Relapse	At relapse	CNS, metastatic site	C	5.63×10^6	3.17×10^8	4.23×10^8	N/A	NR
7	WT	14	Localized	Initial	Uplift resection	Lung, Primary site	N	3.21×10^6	N/A	3.00×10^7	N/A	N/A
8	NB	16	Stage II	Initial	Uplift resection	Lower Extremity, Primary site	N	1.80×10^6	N/A	1.00×10^8	N/A	N/A
9	OS	14	Metastatic	Initial	After neoadjuvant chemotherapy	Lower Extremity, Primary site	C	4.90×10^7	N/A	none available	9.10×10^6 post-REP	N/A
10	ASPS	20	Metastatic	Relapse	After salvage therapy	CNS, metastatic site	I	DNG	N/A	2.00×10^8	N/A	N/A
11	OS	13	Metastatic	Relapse	After salvage therapy	Lung, metastatic site	C	DNG	N/A	3.20×10^8	N/A	N/A
12	ASPS	20	Metastatic	Relapse	After salvage therapy	CNS, metastatic site	I	DNG	N/A	5.53×10^7	N/A	N/A
13	NB	7	IV, high-risk	Initial	Diagnostic biopsy	Abdomen, primary site	N	4.00×10^6	9.10×10^7	used in co-culture	7.28×10^7 (post-REP only)	NR
14	SS	13	Stage II	Initial	Uplift resection	Lower Extremity, Primary site	N	3.10×10^6	3.98×10^7	used in co-culture	N/A	NR
15	ERMS	3	Stage III, group 2	Initial	Uplift resection	Abdomen, primary site	N	1.10×10^6	3.22×10^8	used in co-culture	N/A	NR
16	OS	14	Localized	Initial	After neoadjuvant chemotherapy	Lower Extremity, Primary site	C	1.37×10^6	4.47×10^8	none available	8.00×10^6 post-REP	N/A
17	WT	4	Stage IV, favorable histology	Initial	Diagnostic biopsy	Abdomen, Primary site	N	5.40×10^7	9.80×10^8	8.92×10^7	N/A	N/A
18	OS	12	Localized	Initial	After neoadjuvant chemotherapy	Lower Extremity, Primary	C	3.50×10^6	2.49×10^7	4.00×10^8	1.90×10^7 post-REP, 1.40×10^6 post-REP	N/A

Conclusions This study demonstrates feasibility of pMST TIL expansion ex vivo. Due to tissue volume constraints inherent in pMST sampling, anti-tumor reactivity testing was not feasible for most patients. Determining optimal strategy for TIL-ACT in pMST will require further investigation regarding techniques for expanding tumor-specific TIL.

Acknowledgements The authors would like to thank Swim Across America (www.swimacrossamerica.org) and the Ocala Royal Dames (www.ocalaroyaldames.org) for their generous support of this work.

REFERENCES

- Rosenberg SA, Restifo NP. Adoptive cell transfer as personalized immunotherapy for human cancer. *Science* 2015;**348**(6230):62–68.
- Hall M, Mullinax JE, Royster E, et al. Expansion and characterization of tumor-infiltrating lymphocytes from human sarcoma. *Journal of Immunotherapy of Cancer* 2015;**3**(Suppl. 2):19.
- Mullinax JE, Hall M, Beatty M, et al. Expanded tumor-infiltrating lymphocytes from soft tissue sarcoma have tumor-specific function. *J Immunother* 2021;**44**(2):63–70.
- Feuerer M, Beckhove P, Bai L, et al. Therapy of human tumors in NOD/SCID mice with patient-derived reactivated memory T cells from bone marrow. *Nat Med* 2001;**7**(4):452–458.
- Feuerer M, Rocha M, Bai L, et al. Enrichment of memory T cells and other pro-found immunological changes in the bone marrow from untreated breast cancer patients. *Int J Cancer* 2001;**92**(1):96–105.

Ethics Approval This study was approved by the Johns Hopkins All Children's Hospital IRB (#IRB00193453). Consent was obtained from the patient or parent, as appropriate for age, prior to participating in this study.

<http://dx.doi.org/10.1136/jitc-2021-SITC2021.178>

179

CD8+CD69+ EXPANDED TUMOR INFILTRATING LYMPHOCYTES FROM SOFT TISSUE SARCOMA HAVE INCREASED TUMOR-SPECIFIC FUNCTIONAL CAPACITY

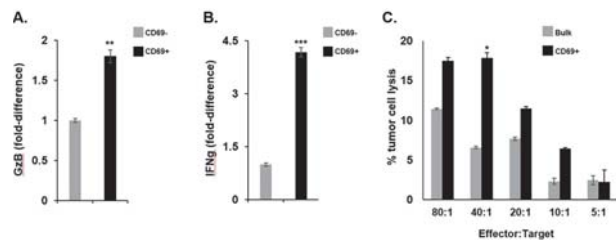
Jonathan Hensel, Alejandro Alfaro, Mary Rau, Patricio Perez-Villarroel, Zachary Sannasardo, Shari Pilon-Thomas, John Mullinax*. *H. Lee Moffitt Cancer Center, Tampa, FL, USA*

Background Adoptive cell therapy (ACT) utilizing tumor infiltrating lymphocytes (TIL) has demonstrated durable responses in patients with metastatic melanoma and offers potential for other solid tumors. Preclinical experience with expanded TIL from soft tissue sarcoma (STS) demonstrates less frequent tumor-specific reactivity compared to melanoma samples, limiting the potential for efficacy.¹ We hypothesized that CD69+ TIL have increased tumor-specific reactivity, which can be manipulated in culture, thereby offering an opportunity to enhance the antitumor effect of this cellular immunotherapy product.

Methods Patients were enrolled on an IRB-approved protocol and TIL were expanded from fresh surgical specimens. After enzymatic digestion, tumor single cell suspensions were cultured in media containing 10% human serum and IL-2 (6000IU/mL). Expanded TIL were then enriched for CD8+ using magnetic bead isolation and CD69+ by flow cytometry cell sorting (FACS). After co-culture with autologous tumor digest, functional capacity was compared between bulk TIL and enriched TIL by evaluation of IFN-gamma (IFN γ) and Granzyme B (GzB) secretion. Capacity for direct tumor cytotoxicity was assessed by Cr51 assay after co-culture of autologous immortalized cell lines with expanded TIL subpopulations after enrichment.

Results Following co-culture with autologous tumor digest, CD69+ TIL demonstrated increased IFN γ secretion compared to CD69- TIL in 6 samples (1.4–4.2x, $p < 0.05$). CD8+ enriched TIL (75% compared to bulk) had higher relative IFN γ secretion in both CD69+ and CD69- subsets (4.2 and 5.8x, respectively, $p < 0.001$). Maximal IFN γ secretion was seen from TIL that were both CD69+ sorted and CD8+ enriched, demonstrating a synergistic effect (16.3x vs Bulk CD69-, 4.2x vs Bulk CD69+, 2.8x vs CD8 enriched CD69-; $p < 0.001$). Functional capacity was also assessed by GzB secretion with similar results. CD69+ TIL had increased relative secretion (1.8–2.2x) compared to CD69- TIL ($p < 0.01$). CD8+ enriched TIL had increased relative GzB secretion in both CD69- and CD69+ sorted fractions (1.4x, 1.2x, respectively, $p < 0.05$). CD69+ sorted and CD8+ enriched TIL demonstrated an additive effect (2.6x vs Bulk CD69-, $p < 0.01$; 1.2x vs Bulk CD69+, $p < 0.05$; 1.8x vs CD8 enriched CD69-, $p < 0.01$). CD8+ enriched CD69+ sorted TIL had greater relative cytotoxicity (3x, $p < 0.05$) at 40:1 E:T ratio against autologous tumor cell lines compared to bulk expanded TIL (figure 1).

Conclusions TIL expanded from STS demonstrate greater tumor-specific functional capacity and cytotoxicity after CD8 enrichment and CD69+ FACS compared to bulk expanded TIL. These data validate the strategy to enhance CD8+CD69+ TIL during culture to yield a more efficacious cellular immunotherapy product.



Abstract 179 Figure 1 Functional capacity of CD69+ TIL is demonstrated by increased secretion of GzB (A) and IFN γ (B) after co-culture with autologous tumor digest. CD69+ TIL have greater cytotoxicity against autologous immortalized cell lines compared to bulk TIL at 40:1 E:T ratio (C).

Acknowledgements This work was funded by NIH K08CA252642

Trial Registration n/a

REFERENCE

1. Mullinax JE, Hall M, Beatty M, Weber AM, Sannasardo Z, Svrldin T, Hensel J, Bui M, Richards A, Gonzalez RJ, Cox CA, Kelley L, Mulé JJ, Sarnaik AA, Pilon-Thomas S. Expanded Tumor-infiltrating Lymphocytes From Soft Tissue Sarcoma Have Tumor-specific Function. *J Immunother* 2021 Feb-Mar 01;44(2):63–70.

Ethics Approval Abstract cites IRB-approved protocol in methods section.

Consent n/a

<http://dx.doi.org/10.1136/jitc-2021-SITC2021.179>

T CELL PHENOTYPE DRIVES RESTRUCTURING OF TUMOR MICROENVIRONMENT TO BALANCE T CELL LONGEVITY AND TUMOR CONTROL: INSIGHTS FROM MULTIPLEXED IMAGING AND MULTI-SCALE AGENT BASED MODELING

John Hickey*, Garry Nolan, Markus Covert, Eran Agmon, Nina Horowitz, John Sunwoo.
Stanford University, Stanford, CA, USA

Background Immune cell therapies continue to have success in treatment of cancers yet face challenges of complexity, cost, toxicity, and low solid-tumor efficacy. Much work has focused on the phenotype characterization and control of ex vivo expanded cells; however, little is known about its relationship to changes in the tumor microenvironment in vivo. Thus, we imaged tumors treated with different phenotype tumor-specific CD8+ T cells with CODEX multiplexed imaging¹⁻⁴ that is able to visualize 42 antibodies at the same tissue in the tissue (figure 1A). To further probe this data in a systems immunology approach we created a multiscale agent-based model including critical circuits from the T cell-tumor microenvironment interactions (figure 1B).

Methods We initialized our agent-based models various percentages of either PD1+, PD1-, PDL1+, or PDL1- phenotypes and ran simulations for 72 hours. We also treated PMEL CD8 + T cells with or without 2 hydroxycitrate as a metabolic inhibitor during activation to achieve different input phenotypes of CD8+ T cells for therapeutic adoptive transfer on day 10 following B16-F10 tumors had been established. We performed neighborhood analysis on CODEX multiplexed imaging data by clustering neighboring cell types using a sliding window for neighborhood analysis.

Results Interestingly, the agent-based modeling indicated that the tumor phenotype switch to decrease proliferation was more effective than direct T cell killing. We observed spatially restricted inflammatory immune fronts when simulating with different initial percentages of PD1+ T cells and also from our CODEX multiplexed imaging. Quantitatively we observe that there is a drastic increase in the PDL1+, MHC1+, Ki67-tumor phenotype that increases with metabolically inhibited T cells. Neighborhood analysis indicated that metabolically treated T cells were able to create distinct immune cell environments that supported productive T cell-tumor interactions and also helped maintain T cell phenotype.

Conclusions This indicates there is a balance for therapeutic T cell to mitigate chronic tumor exposure while controlling tumor growth through killing and by changing tumor phenotype. We observe T cells create distinct tumor microenvironments that differs significantly based on the starting T cell phenotype. Controlling T cell phenotype to promote productive immune-tumor structures will be critical to maintain T cell functionality and efficacy. In the future we will investigate T cell recruitment of immune structures by similar systems biology technologies.

Acknowledgements J.W.H. is funded by an ACS Postdoctoral Fellowship (PF-20-032-01-CSM).

REFERENCES

1. Goltsev Y, Samusik N, Kennedy-Darling J, Bhate S, Hale M, Vazquez G, Black S and Nolan GP, Deep profiling of mouse splenic architecture with CODEX multiplexed imaging. *Cell*, 174(4):968–981.
2. Schürch CM, Bhate SS, Barlow GL, Phillips DJ, Noti L, Zlobec I, Chu P, Black S, Demeter J, McIlwain DR and Samusik N. Coordinated cellular neighborhoods orchestrate antitumoral immunity at the colorectal cancer invasive front. *Cell* 182 (5):1341–1359.

3. Black S, Phillips D, Hickey JW, Kennedy-Darling J, Venkatarahaman VG, Samusik N, Goltsev Y, Schürch CM. and Nolan GP. CODEX multiplexed tissue imaging with DNA-conjugated antibodies. *Nature Protocols* 1–36.
4. Kennedy-Darling J, Bhate SS, Hickey JW, Black S, Barlow GL, Vazquez G, Venkatarahaman VG, Samusik N, Goltsev Y, Schürch CM and Nolan GP. Highly multiplexed tissue imaging using repeated oligonucleotide exchange reaction. *European Journal of Immunology* 51(5):1262–1277.

Ethics Approval All studies involving mice were approved under Stanford's APLAC protocol 33502.

<http://dx.doi.org/10.1136/jitc-2021-SITC2021.180>

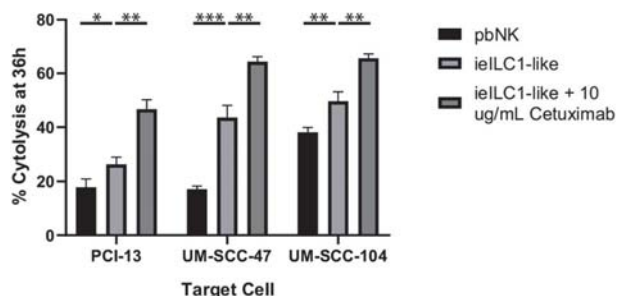
181 INTRAEPITHELIAL GROUP 1 INNATE LYMPHOID CELLS GENERATED *IN VITRO* EXHIBIT ENHANCED CYTOTOXICITY AND INFILTRATION INTO SOLID TUMOROIDS

Nina Horowitz*, John Hickey, John Sunwoo. *Stanford University, Stanford, CA, USA*

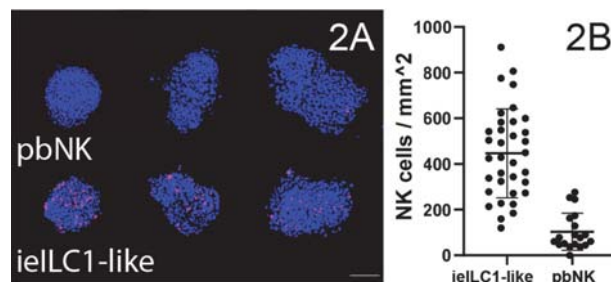
Background Immunotherapy approaches have shown striking success in the liquid tumor setting but have been unable to demonstrate similar efficacy against solid tumors. Cell-based therapies, in particular, struggle to overcome the harshly immunosuppressive tumor microenvironment. Additionally, cells for adoptive therapy are often generated from immune cells circulating in the peripheral blood of patients or healthy donors, rather than isolating them from solid tissues. Designing immunotherapies using insights from tissue-resident cells represents a novel method for enhancing trafficking into and retention within solid tumors.¹ To this end, we developed methodology for differentiating peripheral blood natural killer cells (pbNKs) into cells resembling intraepithelial group 1 innate lymphoid cells (ieILC1s) *in vitro* and assessed their potential for immunotherapy.

Methods We co-cultured irradiated squamous cell carcinoma (SCC) cells and pbNKs, isolated from blood of healthy human donors, to generate cells exhibiting an ieILC1 phenotype. We assessed the differentiation using traditional flow cytometry and further profiled the cells using cytometry by time of flight (CyTOF)² to obtain higher-dimensional data about their surface and intracellular phenotypes. We then tested the cells for their cytotoxicity against a variety of target cell lines using the xCELLigence platform. Next, we grew three-dimensional tumoroids from single-cell suspensions of SCC cell lines in basement membrane extracts and added fluorescently labeled pbNKs and ieILC1s to them. We assessed their infiltration capacity into the tumoroids using confocal microscopy.

Results The ieILC1-like cells generated *in vitro* had a comparable surface and intracellular phenotype to ieILC1s in healthy tissue. These cells exhibited significantly increased cytotoxicity against multiple SCC cell lines and were also capable of antibody-dependent cellular cytotoxicity, which we tested using anti-epidermal growth factor receptor (EGFR) antibody (figure 1). Importantly, the ieILC1-like cells efficiently infiltrated the tumoroids in a manner consistent with their tissue-resident phenotype (figure 2A) and at higher rates than the conventional pbNKs (figure 2B).



Abstract 181 Figure 1 Cytotoxicity of pbNKs and ieILC1-like cells was compared using the xCELLigence platform to monitor killing of adherent SCC target cells over 36 hours. Cells were cultured at a 1:4 E:T ratio with or without 10 ug/mL cetuximab.



Abstract 181 Figure 2 Tumoroid infiltration rates of pbNKs and ieILC1-like cells were compared using confocal microscopy. A: Representative cross-sections of tumoroids, with nuclei labeled with DAPI (blue) and infiltrating cells labeled with CellTrace Far Red (pink). B: Infiltrating cells within each tumoroid were counted and then normalized to the area of the tumoroid.

Conclusions Our data show that ieILC1-like cells can be generated from pbNKs using a co-culture system with irradiated epithelial tumor cells. These ieILC1-like cells provide a novel platform for adoptive cell therapy, as they exhibit strong natural cytotoxicity and ADCC against multiple cell lines. Finally, the ieILC1-like cells have an enhanced capacity for infiltration into solid tumoroids. Future work will include *in vivo* modeling of tumor infiltration and efficacy as well as optimization of the co-culture platform to maximize expansion and cytotoxicity of the cells as they differentiate.

Acknowledgements N.B.H. is funded by the Stanford Bio-X Fellowship. The laboratory of J.B.S. is funded by NIH R35 DE030054.

REFERENCES

- Milner J, Toma C, Yu B, Zhang K, Omilusik K, Phan A, Wang D, Getzler A, Nguyen T, Crotty S, Wang W, Pipkin M, Goldrath A. Runx3 programs CD8+ T cell residency in non-lymphoid tissues and tumours. *Nature* 2017;**552**:253–257.
- Bendall S, Simonds E, Qiu P, Amir E, Krutzik P, Finck R, Bruggner R, Melamed R, Trejo A, Ornatsky O, Balderas R, Plevritis S, Sachs K, Pe'er D, Tanner S, Nolan G. Single-Cell mass cytometry of differential immune and drug responses across a human hematopoietic continuum. *Science* 2011;**332**:687–696.

Ethics Approval The studies reported here were approved by the Stanford Institutional Review Board (IRB 11402) and the Stanford Administrative Panel on Laboratory Animal Care (APLAC 20547).

<http://dx.doi.org/10.1136/jitc-2021-SITC2021.181>

THERAPEUTIC T CELLS EXHIBIT DISTINCT VULNERABILITY TO GLUCOSE DEPRIVATION IN TUMORS WHICH CAN BE OVERCOME WITH AN ENGINEERED GLUCOSE TRANSPORTER

¹Jessica Jana*, ²Yiyang Wang, ¹Ashley Menk, ¹Andrew Frisch, ¹Greg Delgoffe. ¹University of Pittsburgh, Pittsburgh, PA, USA; ²Tsinghua University, Pittsburgh, PA, USA

Background While checkpoint blockade cancer immunotherapies reawaken dormant antitumor immunity, adoptive cell therapies (ACT) bolster an immune response through infusion of expanded tumor infiltrating lymphocytes (TIL), or healthy T cell redirected to tumors via chimeric antigen receptor (CAR), or T cell receptor (TCR) expression. However, the harsh, nutrient depleted tumor microenvironment (TME) creates metabolic barriers for T cell persistence and effector function. We and others have shown that glucose availability is key for T cell effector functions through multiple non-redundant mechanisms. We thus asked whether therapeutic T cells harbor increased sensitivity for glucose and whether this could be mitigated to increase efficacy.

Methods B16 and Pten deficient, *Braf* mutant melanomas were used as models in C57BL/6 mice. Tumor cell glucose uptake was inhibited using stable expression of shRNA to *Slc2a1*, encoding Glut1. Glut1 was retrovirally overexpressed in therapeutic, Pmel-1 (gp100-specific) T cells, and phosphomimetic mutations were engineered (S226D) into Glut1, stabilizing cell surface trafficking. Glucose uptake and glycolysis were measured using fluorescent glucose tracers and Seahorse analysis, respectively.

Results Here we sought to equip glucose sensitive therapeutic T cells with heightened ability to compete for glucose within the TME. Murine therapeutic T cells, expanded in hyperglycemic conditions *in vitro*, that infiltrate solid tumors compete poorly for glucose tracers compared to endogenous T cells. Knockdown or deletion of Glut1 in tumor cells sensitizes tumors to T cell therapies, but not checkpoint blockade, highlighting a role for glucose competition specifically in ACT. Overexpression of WT Glut1 in therapeutic T cells yields only modest increased glucose competition due to various modes of Glut1 regulation. We thus engineered a cell surface stabilized Glut1 construct. This construct's competitive advantage manifests robust increases in glucose uptake and glycolytic capacity, leading to superior effector functions even in extremely hypoglycemic conditions. This enhanced effector function manifests in therapeutic efficacy in highly glycolytic melanomas and with heightened competition for glucose tracers, tumor infiltration, and effector function *in vivo*.

Conclusions Our study suggests that, due to the hyperglycemic conditions of their *ex vivo* expansion, therapeutic T cells display a distinct metabolic disadvantage when they enter the nutrient poor TME in comparison to their endogenous counterparts. Overexpression of our surface engineered Glut1 in these therapeutic T cells rescues their ability to compete with highly glycolytic tumor cells for glucose, resulting in robust glycolytic metabolism and curative response to immunotherapy for cancer.

<http://dx.doi.org/10.1136/jitc-2021-SITC2021.183>

184 **ADOPTIVE T CELL THERAPIES TARGETING COMMON P53 NEOANTIGENS IN HUMAN SOLID CANCERS**

Peter Kim*, Steven Rosenberg, Nolan Vale. *NCI, Bethesda, MD, USA*

Background Adoptive cell therapies (ACT) targeting neoantigens arising from somatic mutations in cancer cells can successfully treat advanced solid cancers. Most neoantigens are rare and targeting them via ACT would require highly individualized therapies. Instead, we focused on p53 mutations shared among a broad range of patients. In this study, we have identified tumor infiltrating lymphocytes (TILs) and T cell receptors (TCR) recognizing p53 mutations and evaluated the efficacy of ACT targeting p53 neoantigens.

Methods Patient TILs were screened for reactivity against p53 mutations. Twelve patients with positive p53 neoantigen screening received autologous TIL ACT. One patient received TCR-engineered peripheral blood lymphocytes (PBL) ACT.

Results From 77 patient samples, TILs recognizing both ‘hot-spot’ and ‘non-hotspot’ p53 mutations were detected in 21 patient TILs (table 1). ACT using an HLA-A*02-restricted TCR targeting p53(R175H) led to regression of TYK-nu ovarian cancer cells that were p53(R175H)+ and HLA-A*02+ in NSG mice. Treatment of 12 patients with chemo-refractory epithelial cancers with autologous TILs targeting p53 neoantigens resulted in limited clinical responses (2 partial responses). We detected low frequencies, exhausted phenotypes, and poor persistence of the infused mutant p53-reactive TILs (table 2). Alternatively, we engineered peripheral blood lymphocytes (PBL) to express anti-mutant p53 TCRs. We retrovirally expressed the HLA-A*02:01-restricted anti-p53(R175H) TCR that had been tested preclinically in patient 4349’s autologous PBL. This approach improved anti-mutant p53 TCR expression and T cell persistence relative to the autologous TIL treatments. Patient 4349 with chemo-refractory breast cancer received 5.3e10 cells and, at 14-weeks post-ACT, she experienced significant regression of the metastases in the pericardium and chest wall, as well as the subcutaneous tumor deposits based on RECIST criteria (down 55%). Single cell RNA sequencing of PBLs at 6 weeks post-ACT revealed a cluster of circulating T cells with a central-memory and stem cell-like phenotype that expressed SELL (CD62L), IL7R, TCF7 (TCF1) and LEF1, suggesting long-term immunity against the p53 neoantigen. The patient recurred at 6 months post-ACT with a metastasis that exhibited loss of heterozygosity of a portion of chromosome 6 that included HLA-A*02.

Conclusions We have established a library of anti-mutant p53 TCRs that could potentially be used to treat 7.3% of patients with solid cancers that express the corresponding p53 mutation and HLA. One breast cancer patient treated with TCR-engineered PBLs targeting p53R175H experienced an objective response lasting 6 months. Collectively, our data demonstrate the feasibility of targeting shared p53 neoantigens by ACT for the treatment of solid cancers.

Abstract 184 Table 1 Anti-mutant p53 TCR library

TCR source	TP53 mutation	TP53 mutation frequency (%) ^a	HLA restriction	HLA frequency (%) ^b	Potentially treatable patient (%)
4141; 4196	R175H	5.530	A*02:01	47.40	2.621
4273	R248W	3.218	DPB1*02:01	27.30	0.878
4259	Y220C	1.790	A*02:01	47.40	0.848
4149; 4343	Y220C	1.790	DRB3*02:02	32.80	0.587
4285	R175H	5.530	DRB1*13:01	10.00	0.553
4386	R273C	2.259	DPB1*04:02	24.2 ^c	0.547
4127	G245S	1.598	DRB3*02:02	32.80	0.524
4259	Y220C	1.790	DRB1*04:01	17.30	0.310
4266	R248W	3.218	A*68:01	6.38	0.205
4316	C135Y	0.426	DRB1*07:01	26.84	0.114
4304	M237I	0.426	DRB1*01:01	14.60	0.062
4316	C135Y	0.426	A*29:02	7.06	0.030
4350	L111R	0.011	A*11:01	60% in Chinese populations	0.006
4324	T211I	0.032	C*06:02	18.64	0.006
4414	Y220D	0.011	A*02:01	47.40	0.005
4114	C135R	0.043	DRB1*11:01	10.9	0.005
4350	L111R	0.011	DRB1*08:03	7-20% in Chinese populations	0.004
4356	Q331H	0.011	B*40:01	11.00	0.001
4293	Y236S	0.011	DRB3*02:01	0.33	0.0003
Sum					7.305

Abstract 184 Table 2 Characteristics of 12 TIL and 1 TCR-engineered ACT

Patient ID	Tumor type	p53 mutation	Preselected TIL	HLA restriction	Number of IL2	Number of pembrolizumab	% mut-p53 positive cells in infusion product ^a	Total number of cells given to patients	Number of mutant p53 reactive cells given to patients	% persistence at 4 weeks post-ACT ^b	% PD1 ^{hi} in infusion product	% TIM3 ^{hi} in infusion product	% CD39 ^{hi} in infusion product	% CD62L ^{hi} in infusion product	Response (months)
4114	Pancreatic	C135R	Selected TIL (NCI-119 C-0160)	DRB1*11:01	2	0	18.9	2.14E+10	4.04E+09	Not detected	43.1	28.5	15.83	20.92	NR
4127	Ovarian	G245S	Selected TIL (NCI-119 C-0160)	DRB3*02:02	5	2	2.8	1.43E+11	4.00E+09	Not detected	16.66	33.83	71.8	15.94	PR (4)
4141	Colon	R175H	Selected TIL (NCI-119 C-0160)	A*02:01	4	4	2.2	6.90E+10	1.52E+09	0.05	46.2	32	87.4	29.24	NR
4149	Ovarian	Y220C	Selected TIL (NCI-119 C-0160)	DRB3*02:02	5	4	11.1	3.71E+10	4.12E+09	Not detected	58.7	15.27	93.2	6.8	SD (5)
4196 ^c	Colon	R175H	Selected TIL (NCI-119 C-0160)	A*02:01	0	4	3.3	9.18E+10	3.03E+09	0.02	NA	NA	NA	NA	SD (3)
4266	Colon	R248W	Selected TIL (NCI-119 C-0160)	A*68:01	6	0	50.8	1.01E+11	5.13E+10	0.19	64	89.5	98.8	0.89	NR
4273	Rectal	R248W	Selected TIL (NCI-119 C-0160)	DPB1*02:01	2	2 ^d	6.75	1.17E+11	7.90E+09	NA	28.4	42.7	96.3	4.03	NR
4285	Colon	R175H	Selected TIL (NCI-119 C-0160)	DRB1*11:01	6	0	2.43	6.96E+10	1.69E+09	Not detected	55.9	56.5	76.11	2.08	NR
4304	Colorectal	M237I	Selected TIL (NCI-119 C-0160)	DRB1*01:01	4	4	13 (3 TCRs)	8.97E+10	1.17E+10	0.01	30.6	19.32	97.4	2.79	NR
4324	Colorectal	T211I	Selected TIL (NCI-119 C-0160)	C*06:02	3	4	48 (2 TCRs)	8.49E+10	3.82E+10	1.45	29.8	75.7	29.8	5.02	SD (3)
4343	Breast	Y220C	Selected TIL (NCI-119 C-0160)	DRB3*02:02	4	4	1 ^e	7.68E+10	7.68E+08	0.002	63.2	NA	97.1	9.73	PR (6)
4350	Colon	L111R	Selected TIL (NCI-119 C-0160)	A*11:01	5	2	11	6.69E+10	7.34E+09	0.15	30.9	3.37	94.2	3.37	NR
4349	Breast	R175H	Allogeneic R175H TCR (NCI-114 C-0049)	A*02:01	0	1 ^f	64 ^g	5.30E+10	3.39E+10	14.4 ^h	13	21.7	52	51.5	PR (6)

Ethics Approval This study was approved by the Investigational Review Board at the National Cancer Institute in accordance with an assurance filed with and approved by the U.S. Department of Health and Human Services and was registered at <https://clinicaltrials.gov> under NCT00068003, NCT01174121 and NCT03412877.

<http://dx.doi.org/10.1136/jitc-2021-SITC2021.184>

EX VIVO EFFICACY OF ADOPTIVE T CELL THERAPY USING AUTOLOGOUS CD8+ T CELLS ISOLATED BY PD-1 POSITIVITY FROM PERIPHERAL BLOOD MONONUCLEAR CELLS IN SOLID TUMORS

¹Sungkyu Lee*, ²Yong Wha Moon. ¹Seoul National University, Seoul, Korea, Republic of; ²CHA University, Seongnam, Korea, Republic of

Background Tumor-infiltrating lymphocytes have been shown to display an antitumor activity in solid tumors including melanoma. Previously the proof of concept was developed that CD8+ T cells isolated by programmed cell death-1 (PD-1) receptor positivity from peripheral blood mononuclear cells (PBMCs), recognized tumor-specific antigens and neoantigens, and thus were reactive to tumors. We evaluated ex vivo efficacy of autologous, tumor-reactive CD8+ T cells isolated by PD-1 positivity from PBMCs of breast cancer and leiomyosarcoma patients.

Methods Fresh tumor tissues were cultured in RPMI supplemented with 20% FBS. PD-1 positive CD8+ T cells were isolated from PBMCs of the patients and expanded with Dynabeads human T-Activator CD3/CD28 in RPMI supplemented with 10% FBS and IL-2. Antitumor activity of PD-1-positive CD8+ T cells was tested by performing cytotoxic T lymphocyte (CTL) assay with the cultured autologous tumor cell targets. Specifically, the CTL assay was carried out by culturing tumor cells in multi-well plates overnight, and then adding the PD-1+CD8+ T cells to the plates. After 2 days, tumor cells were harvested from the wells and stained for CD45, CD8 and Live/Dead (ThermoFisher Scientific) to determine the killing activity of PD-1+CD8+ T cells. The results were compared to ones obtained with PD-1-CD8+ T cells.

Results We have successfully established ex vivo models for adoptive cell therapy using autologous PD-1+CD8+ T cells from three breast cancer and one leiomyosarcoma patients. Two breast cancer patients were hormone-receptor-positive and one was triple-negative. Stages were IA (n=1) or IIB (n=2). One leiomyosarcoma patient was in stage IV. All tumor and peripheral blood samples were obtained at chemotherapy-naïve status. CTL assays demonstrated that PD-1+CD8+ T cells efficiently killed target cells compared to PD-1-CD8+ T cells in all the breast cancer and leiomyosarcoma models. More and detailed results will be presented and discussed.

Conclusions Autologous PD-1+CD8+ T cells isolated from PBMCs of a few cancer patients displayed efficient antitumor activity in our established ex vivo models for adoptive cell therapy. Our results warrant further clinical development for adoptive T cell therapy in various types of cancers.

<http://dx.doi.org/10.1136/jitc-2021-SITC2021.185>

DEVELOPMENT OF KSQ-001, AN ENGINEERED TIL (ETIL) THERAPY FOR SOLID TUMORS THROUGH CRISPR/CAS9-MEDIATED EDITING OF SOCS1

Karrie Wong*, Sharon Lin, Christopher Wrocklage, Katri Sofjan, Leila Williams, Mallory Brady, Nicholas Colletti, Noah Tubo, Hugh Gannon, Robert LaMothe, Tianlei Xu, Tracy VandenBerg, Sol Shenker, Caroline Dugopolski, Frank Stegmeier, Louise Cadzow, Michael Schlabach, Micah Benson. *KSQ Therapeutics, Cambridge, MA, USA*

Background Adoptive cell therapy with ex vivo expanded tumor infiltrating lymphocytes (TIL) offers a potentially curative treatment for cancer. However, the immunosuppressive tumor microenvironment limits the effectiveness of TIL therapy. To address this medical need, we used our Immune-CRISPRomics® Platform to perform a series of genome-wide CRISPR/Cas9 screens to identify targets enhancing the ability of T cells to infiltrate and kill solid tumors in an in vivo setting. These screens identified SOCS1 as a top target that restrains T cell anti-tumor immunity. Based on these findings, we developed KSQ-001, an engineered TIL (eTIL) therapy created via CRISPR/Cas9-mediated editing of SOCS1 for the treatment of solid tumors.

Methods Genome-wide CRISPR/Cas9 screens were conducted in in vitro primary human T cells and TIL cultures and in in vivo primary mouse OT1 and PMEL-TCR-Tg T cells in syngeneic tumor models. The efficacy of surrogate murine KSQ-001 (mKSQ-001), in which the SOCS1 gene is inactivated by CRISPR/Cas9 in OT1 or PMEL-TCR-Tg T cells, was evaluated in both the B16-Ova and CRC-gp100 syngeneic tumor models, with memory formation and efficacy evaluated both in the presence and absence of cyclophosphamide-mediated lymphodepletion. KSQ-001 was manufactured from human TIL using SOCS1-targeting sgRNAs selected for therapeutic use based on potency and selectivity, with KSQ-001 characterized for in vitro function and in vivo anti-tumor efficacy.

Results Upon adoptive transfer of a single dose into solid tumor-bearing hosts, mKSQ-001 was found to robustly enhance anti-tumor efficacy and eradicate tumors in 7/10 mice in the PD1-sensitive OT1/B16-Ova model and to drive responses in the PD-1 refractory PMEL/CRC-gp100 syngeneic tumor model. mKSQ-001 also showed a ten-fold increase in anti-tumor potency in vivo compared to unengineered T-cell product and established durable anti-tumor memory by persisting in the form of T central memory cells detectable at high frequency in the peripheral blood of complete responder mice. In the setting of lymphodepletion, mKSQ-001 also displayed heightened anti-tumor potency, accumulation, and memory formation in comparison to inactivation of PD-1. Importantly, human KSQ-001 displayed a transcriptional signature indicative of increased anti-tumor function, produced increased amounts of pro-inflammatory cytokines, exhibited a hypersensitivity to IL-12 signaling, and demonstrated increased anti-tumor function both in vitro and in vivo solid tumor models.

Conclusions Based on insights from our Immune-CRISPRomics® platform and demonstrated efficacy across multiple pre-clinical tumor models, we have developed KSQ-001, a novel eTIL therapy. These preclinical data support clinical testing of KSQ-001 in a variety of solid tumor indications.

<http://dx.doi.org/10.1136/jitc-2021-SITC2021.186>

MULTI-OMIC SINGLE-CELL PROFILING DEMONSTRATES THAT COMPETITION FOR FATTY ACIDS AND FATTY ACID OXIDATION ENABLES TUMOR-INFILTRATING LYMPHOCYTE FUNCTION AND SURVIVAL

¹Melisa Angela Paniagua*, ²Cara Haymaker, ¹Jay R Adolacion, ¹Xingyue An, ²Caitlin Creasy, ¹Mohsen Fathi, ¹Ali Rezvan, ³Tamar Geiger, ³Michal Harel, ⁴Jonathan Robinson, ¹Amit Amritkar, ²Scott Woodman, ²Patrick Hwu, ²Chantale Bernatchez, ¹Navin Varadarajan. ¹University of Houston, Houston, TX, USA; ²UT MD Anderson Cancer Center, Houston, TX, USA; ³Tel Aviv University, Israel, Israel; ⁴Chalmers University of Technology, Sweden, Sweden

Background Adoptive transfer of ex vivo expanded tumor-infiltrating lymphocytes (TIL) have shown durable responses in metastatic melanoma, yet these responses are unpredictable. Bioenergetics dictates the function and fate of adoptively transferred human T cells within the tumor microenvironment but the nature of metabolic competition leading to T-cell function and dysfunction are incompletely understood.

Methods We integrated the profiling of TIL co-cultured with their autologous primary tumor cells with the aid of a suite of high-throughput single-cell functional assays, transcriptional, and proteomic assays. We validated the results of the model using flow cytometry and confocal microscopy. Association of functional features with clinical outcome was assessed.

Results Timelapse Imaging Microscopy In Nanowell Grids (TIMING) demonstrated that while TIL frequencies in killing autologous tumor cells are equivalent across the donors, R-TIL had a significantly higher survival rate than NR-TILs. Tumor cells from NR patients had higher motility and showed increased elongation compared to R-tumors. RNA-sequencing (RNA-seq) and proteomics showed that NR-tumors were enriched in pathways associated with utilization of fatty acids (FAs) and adipogenesis, as well as cancer cell metastasis, cellular motility, adhesion, and migration. Candidate genes associated with amoeboid migration (MYH9, MYH2; WNT5B and SERPINE1) and FA utilization (CD36 and PPARG) were enriched in the NR-tumors. Flow cytometry and confocal microscopy confirmed that NR-tumors showed increased CD36 expression and FA uptake compared to R-tumors. To simulate metabolic competition, we co-cultured the TIL with autologous tumors and sorted TIL for RNAseq. The R-TIL were enriched in pathways related to mitochondrial and carbohydrate metabolism; fatty acid oxidation (FAO), and long-chain FAs with a direct enrichment in fatty acyl CoA biosynthesis and both peroxisomal and mitochondrial FAO. Since patient-derived TILs were limiting for metabolomics type assays, we utilized genome-scale metabolic models to infer relevant metabolic pathways by comparison to the human metabolic Atlas (HMR2). At the level of individual metabolites, the significantly enriched metabolites within R TILs were dominated by peroxisome and mitochondria derived fatty acyl-CoA: e.g. palmitoyl-CoA, linoleoyl-CoA, and oleoyl-CoA. We utilized flow cytometry and confocal microscopy to perform pulse-chase assays with FAs for validation. R-TILs showed an increased accumulation of FA into the mitochondria confirming a direct role for TIL FAO.

Conclusions Efficient competition for FAs is a key attribute of T-cell efficacy in ACT. R-TILs are able to utilize FAs via FAO when in competition with autologous tumor cells whereas NR tumors effectively uptake and store FAs preventing T-cell function.

Acknowledgements This abstract was supported by the NIH (R01CA174385); CPRIT (RP180466); MRA Established Investigator Award to NV (509800), Welch Foundation (E1774);

NSF (1705464); CDMRP (CA160591); Owens Foundation (NV). We would like to acknowledge the MDACC Flow Cytometry and Cellular Imaging Core facility for the FACS sorting (NCI P30CA16672), UH Seq-n-edit core for RNA-seq, Intel for the loan of computing cluster, and the UH Center for Advanced Computing and Data Systems (CACDS) for high-performance computing facilities.

Trial Registration protocol (2004-0069)

Ethics Approval Approved by the Institutional Review Board (IRB) of the MD Anderson Cancer Center (Houston, TX) and an FDA- approved Investigational New Drug (IND) application (NCT00338377)

<http://dx.doi.org/10.1136/jitc-2021-SITC2021.187>

DEVELOPMENT OF WU-NK-101, A FEEDER CELL-FREE EXPANDED ALLOGENEIC MEMORY NK CELL PRODUCT WITH POTENT ANTI-TUMOR ACTIVITY

¹Ryan Sullivan*, ¹Mary Mather, ¹Jennifer Govero, ¹John Dean, ¹Andrew Martens, ¹You Zhou, ¹Malik Darwech, ¹Brunda Tumala, ¹Alex Vessoni, ¹Alexander Hamil, ¹Tom Leedom, ¹Corey Johnson, ²Melissa Berrien-Elliott, ²Mark Foster, ²Michelle Becker-Hapak, ²Ethan McClain, ²Carly Neal, ²Todd Fehniger, ³Niraj Shrestha, ³Mike Dee, ³Hing Wong, ¹Ayman Kabakibi, ¹Matthew Cooper, ¹Ken Chrobak. ¹Wugen, Saint Louis, MO, USA; ²Washington University in St. Louis, St. Louis, USA; ³HCW Biologics, Miramar, FL, USA

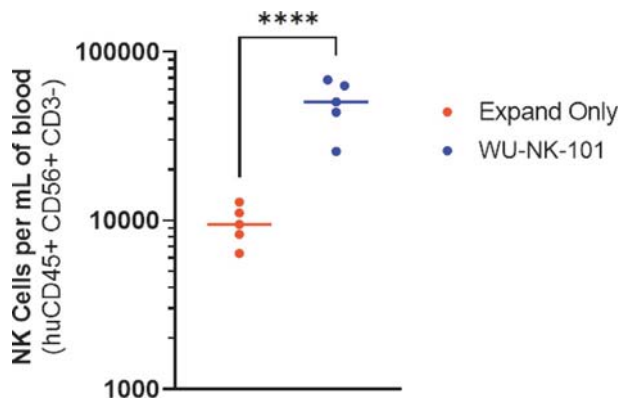
Background Allogeneic Natural Killer (NK) cells are emerging as a safe and effective modality for the treatment of cancer, overcoming several limitations associated with adoptive T cell therapies. Cytokine induced memory-NK cells offer several advantages over conventional NK cells, including enhanced functional persistence, efficacy, and metabolic fitness. Additionally, unlike iPSC and cord blood derived NK cells, they do not require engineering to enable functionality. Here we describe the use of WU-PRIME, a GMP-grade fusion protein complex to generate memory NK cells, and WU-EXPAND, a feeder cell free expansion system to expand memory-NK cells and create WU-NK-101. Further cryopreservation enables the large-scale, off-the-shelf manufacture of memory NK for cancer immunotherapy, with high anti-tumor activity.

Methods NK cells derived from healthy donor leukopheresate were either activated with WU-PRIME and then expanded with WU-EXPAND to form WU-NK-101 or immediately expanded with WU-EXPAND as controls and then cryopreserved. We compared NK cell expansion as well as post-thaw NK cell functionality as assessed by cytokine secretion and short-term and long-term anti-tumor functionality, long-term persistence in NSG mice, as well as anti-tumor activity in vivo.

60). Notably, this functionality is maintained long-term upon repeated challenge. In vivo, WU-NK-101 cells, compared to expanded NK cells have improved in vivo persistence (figure 1; 50,290 v. 9,623, $p < 0.0001$). In vivo anti-tumor activity was also assessed in leukemia models, where Memory NK cells demonstrate superior anti-tumor activity compared to expanded NK cells.

Conclusions The data demonstrate that WU-NK-101 generated using a feeder cell-free expansion system has a memory phenotype and improved in vitro and in vivo anti-tumor activity compared to conventional NK cells. This activation and expansion platform will enable the development and clinical translation of multiple allogeneic NK cell therapies.

<http://dx.doi.org/10.1136/jitc-2021-SITC2021.188>



Abstract 188 Figure 1 NK cell persistence in tumor-bearing mice. 10^6 cryopreserved NK cells were injected into K562 tumor-bearing mice, and supported with 50,000IU human IL-2 every other day. After 9 days, blood was harvested by cheek bleed and assessed for NK cells (hCD45+, CD56+, CD3) in the blood by flow cytometry.

Results NK cells activated with WU-PRIME followed by WU-EXPAND (WU-NK-101), expand robustly in large-scale reactions, over 250-fold in 14 days. The cells maintain durable expression of CD25 after expansion, as well as several other hallmarks of the memory-NK phenotype as assessed by mass cytometry. As compared to cells expanded with WU-EXPAND only, WU-NK-101 cells have improved in vitro activity against K562 cells, as well as AML cell lines (TF-1, THP-1, and HL-

TARGETING A NOVEL SHARED TUMOR-SPECIFIC ANTIGEN WITH T CELL RECEPTOR TRANSDUCED T CELLS FOR THE TREATMENT OF OVARIAN CANCER

¹Justyna Ogonek*, ¹Tiziana Franceschetti, ¹Andreas Acs, ¹Alexander Schmidt, ¹Alexandra Kuhlenkamp, ²Krystal Vincent, ²Claude Perreault, ¹Barbara Loesch, ¹Adriana Turqueti Neves, ¹Slavoljub Milosevic, ¹Dolores Schendel, ¹Daniel Sommermeyer. ¹Medigene Immunotherapies GmbH, Planegg-Martinsried, Germany, ²Université de Montréal, Montreal, Canada

Background Transgenic T cell receptor (TCR)-based T cell therapies are a powerful treatment for cancer. However, one of the greatest remaining challenges is the successful identification of tumor-specific antigens (TSAs) that are shared between patients and tumor entities and elicit strong T cell responses. The non-coding region of the genome has become a promising source of such novel TSAs. Previously, we have identified ten immunogenic shared TSAs, derived from the translation in canonical and non-canonical reading frames of non-mutated non-coding genomic regions like introns, intergenic regions and 5'-untranslated regions. In the following process, we identified several TCRs specific for these TSAs. Here we aimed at the validation of two TSA-specific TCRs in a model of ovarian cancer-derived organoids.

Methods Freshly collected ovarian tumor and normal ovarian tissue expressing the HLA of interest were mechanically disrupted, enzymatically digested and cryopreserved. Expression of the TSA of interest in the primary tumor tissue was confirmed with RNA sequencing and mass spectrometry. Thawed single cell suspensions were used to generate tumor organoids and 2D-growing normal ovarian cell lines. To validate the generated cell lines, the presence or absence of two previously identified tumor-specific mutations was investigated by targeted Sanger sequencing in the genome of the tumor organoids, normal cell lines and primary tissues. Two TSA-specific TCRs were retrovirally transduced into CD8+ T cells of three healthy donors. Expanded TSA-specific CD8+T cells were co-cultured 24 hours with single cell suspensions of IFN- γ pre-stimulated, tumor organoids or the 2D-growing normal ovarian cell line. IFN- γ ELISA was used to assess activation of TSA-specific T cells upon co-culture.

Results The TSA of interest was detected both at the transcriptomic and proteomic level in the primary ovarian tumor tissue. Using frozen single cell suspensions of this tumor and corresponding normal tissue, tumor organoids and 2D-growing normal cell lines were successfully established and their integrity was confirmed. Both TSA-specific TCRs were efficiently expressed on CD8+ T cells from three donors. TCR-transgenic T cells showed activation upon co-culture with tumor organoids without recognition of normal ovarian cell lines. Normal cells were only recognized after loading with the specific target peptide.

Conclusions In conclusion, the high relevance of two TCRs identified to be specific for a novel shared tumor-specific antigen was confirmed in a model of ovarian cancer organoids. The findings support further development of these TCRs for cancer immunotherapy and implementation of tumor organoids as a relevant tool for the characterization of TSA-specific TCRs.

Ethics Approval 'The tumor and normal tissue samples were purchased at a Biobank, collected in compliance with all applicable EU regulations and were pseudonymized.'

<http://dx.doi.org/10.1136/jitc-2021-SITC2021.189>

PATIENT-DERIVED TUMOR ORGANOID REVEAL MECHANISMS OF IMMUNE EVASION WHICH CAN GUIDE DECISIONS IN ADOPTIVE CELL THERAPY FOR COMMON EPITHELIAL CANCERS

Anup Parikh*, Maria Parkhurst, Paul Robbins, Steven Rosenberg, James Yang. *NCI, Bethesda, MD, USA*

Background Adoptive cellular transfer (ACT) of autologous tumor-infiltrating lymphocytes (TIL) is capable of inducing durable clinical responses in patients with advanced solid malignancies,¹ however response rates are low. Limitations in personalized cancer modeling have been obstacles to understanding tumor-specific mechanisms of immune evasion. Patient-derived tumor organoids (PDTO) can be efficiently grown from common solid tumors and show genetic fidelity to whole exomic sequencing (WES) of the source tumor. We investigated their use in evaluating patient-specific immune responses in vitro and selecting T-cells for adoptive cellular immunotherapy.

Methods PDTO were established from metastatic deposits from patients with colorectal, breast, and pancreatic cancers and with their tumors of origin, were subjected to WES and RNAseq. They were then included in immunologic recognition assays with autologous TIL and cloned T-cell receptors (TCR) against shared mutations. TIL neoantigen reactivity was defined by screening against mutations using minigenes or synthetic peptides expressed by autologous antigen presenting cells.

Results PDTO were successfully grown from 18/22 tumors from 15 patients. These cultures demonstrated a high degree of genetic fidelity to their parental tumors with near-complete retention of clonally expressed mutations. Organoid lines from 11 of these patients were utilized in recognition screening with autologous TIL or PBL transduced with relevant TCRs. TIL recognized 5/7 organoids tested, and this allowed the isolation and cloning of many of the TCRs responsible. Nineteen available TCRs predicted to be reactive with patient-specific neoantigens were also tested against relevant organoids, and only nine were found to be reactive. In most instances where such TCRs could not recognize organoid, tumor-specific defects in neoantigen processing or presentation or HLA-LOH events were either functionally or genetically identified.

Conclusions To improve response rates to neoantigen-directed adoptive T-cell therapy, a better understanding of tumor immune evasion mechanisms is needed. The inability to grow autologous tumor lines from common epithelial cancers has been a major obstacle. We demonstrate that PDTO can be efficiently established and are genetically representative of their parental tumors. Importantly, these organoids can reveal defects in neoantigen processing or surface presentation as well as HLA loss-of-heterozygosity that would preclude immune recognition. PDTO may be a valuable tool for screening for tumor reactivity and selecting T-cells and TCRs for clinical use.

Trial Registration The study protocol was registered under <https://clinicaltrials.gov> under NCT00068003.

REFERENCE

1. Zacharakis N, Chinnasamy H, Black M, et al. Immune recognition of somatic mutations leading to complete durable regression in metastatic breast cancer. *Nat Med.* 2018;**24**:724–730.

Ethics Approval All samples were derived from study participants who granted written, informed consent to be enrolled

on a clinical protocol approved by the Institutional Review Board at the NCI (Bethesda, MD).

<http://dx.doi.org/10.1136/jitc-2021-SITC2021.190>

GAPDH KNOCK-IN OF HIGH AFFINITY CD16 IN IPSC DERIVED NK CELLS DRIVES HIGH-LEVEL EXPRESSION AND INCREASED ANTI-TUMOR FUNCTION

Rithu Pattali, Kaitlyn Izzo, Edward Goncz, Steven Sexton, Kevin Wasko, John Zuris, Michael Nehil, Kate Zhang, Mark Shearman, Kai-Hsin Chang, Alexander Allen*. *Editas Medicine, Cambridge, MA, USA*

Background Natural killer (NK) cells have emerged as an alternative cell type for clinical utility given the low propensity for graft-versus-host disease, thereby making NK cells a potential off-the-shelf cell therapy. One critical pathway NK cells use to target tumor cells is through expression of Fc gamma receptor III alpha (CD16). Antibodies that bind tumor antigens are recognized by CD16 on NK cells, promoting NK-mediated tumor cell killing. High-affinity CD16 variants in the human population correlate with better clinical outcome and anti-tumor response. One mechanism tumors use to evade NK cell recognition is through down-regulation of CD16 expression on the NK cell surface. After being activated, CD16 is cleaved by A Disintegrin and Metalloprotease-17 (ADAM-17). By using a highly-active engineered AsCas12a to knock-in high-affinity CD16 (hCD16KI) at the GAPDH locus, hCD16 is constitutively expressed, continuously replacing hCD16, thereby allowing for repeated ADCC mediated killing.

Methods iPSCs were edited at the GAPDH locus with an engineered AsCas12a along with the CD16 donor construct. The bulk edited population was then plated at clonal density and single clones were selected and screened. iPSC clones were then differentiated into NK cells. A 3D tumor spheroid killing assay was used to demonstrate NK cell cytotoxicity against an ovarian cancer cell line (SKOV-3). In addition, a serial killing assay was used to better model NK cell serial killing.

Results Bi-allelic CD16KI iPSC clones were successfully generated. These iPSCs exhibited normal morphology and were able to differentiate into iNK cells. hCD16KI iNK cells showed normal differentiation and surface marker expression, such as CD45/CD56, compared to unedited iNK cells. CD16KI iNK cells demonstrated significantly increased cytotoxicity in the presence of antibody against tumor cells when compared with unedited iNK cells, as measured by reduction in tumor spheroid size in a 3D tumor spheroid killing assay. Importantly, enhanced surface expression of hCD16 on iNK cells after tumor exposure was detected, demonstrating the replenishment of cleaved hCD16. Notably, hCD16KI iNK cells demonstrated prolonged and enhanced tumor cell killing after being subjected to repeated tumor cell exposure in a serial killing assay.

Conclusions This work demonstrates a powerful new method to drive high-level constitutive hCD16 expression on the surface of iNK cells through transgene knock-in at the GAPDH locus using an engineered AsCas12a. The high level constitutive hCD16 expression enhances ADCC of iNK cells and enables enhanced serial tumor killing and is expected to exert enhanced anti-tumor activity in the clinic.

<http://dx.doi.org/10.1136/jitc-2021-SITC2021.191>

POOLED T CELL RECEPTOR SCREENING (POTS) PROVIDES UNBIASED, HIGH-THROUGHPUT METHOD FOR TCR DISCOVERY

¹Jack Reid*, ¹Shihong Zhang, ²Ariunaa Munkhbat, ³Matyas Ecsedi, ¹Megan McAfee, ¹Aude Chapuis, ¹Fred Hutchinson Cancer Research Center, Seattle, WA, USA; ²Bristol Myers Squibb, Seattle, WA, USA; ³Takeda Oncology, Cambridge, MA, USA

Background T Cell Receptor (TCR)-T cell therapies have shown some promising results in cancer clinical trials, however the efficacy of treatment remains suboptimal. Outcomes could potentially be improved by utilizing highly functional TCRs for future trials. Current TCR discovery methods are relatively low throughput and rely on synthesis and screening of individual TCRs based on tetramer binding and peptide specificity, which is costly and labor intensive. We have developed and validated a pooled approach relying on directly cloned TCRs transduced into a fluorescent Jurkat reporter system (figure 1). This approach provides an unbiased, high-throughput method for TCR discovery.

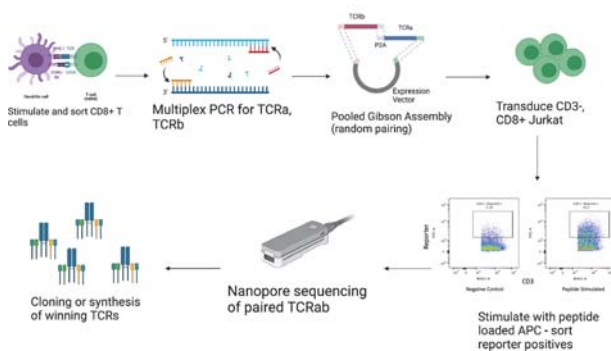
Methods As a model for POTS, T cells specific for a peptide derived adenovirus structural protein were sorted on tetramer and subjected to 10x single cell VDJ analysis. Pools of randomly paired TCR alpha and beta chains were cloned from the 10x cDNA into a lentiviral vector and transduced into a Jurkat reporter cells. Consecutive stimulations with cognate antigen followed by cell sorts were performed to enrich for functional TCRs. Full length TCRab pools were sequenced by Oxford Nanopore Technologies (ONT) and compared to a 10x dataset to find naturally paired TCRs.

Results Comparison between the ex vivo single cell VDJ sequencing and ONT sequencing of the transduced antigen specific TCRs showed more than 99% of the TCR pairs found in reporter positive Jurkat cells were naturally paired TCRs. The functionality of 8 TCR clonotypes discovered using POTS were compared and clone #2 showed the strongest response. Of the selected clonotypes, clone #2 showed a low frequency of 0.9% in the ex vivo single cell VDJ sequencing. After the first round of stimulation and sequencing, clone #2 takes up of 5% of all reporter-positive clones. The abundance of clone #2 further increased to 17% after another round of stimulation, sorting and sequencing, suggesting this method can retrieve and enrich for highly functional antigen specific TCRs.

Conclusions POTS provides a high-throughput method for discovery of naturally paired, high-avidity T cell receptors. This method mitigates bias introduced by T cell differentiation state by screening TCRs in a clonal reporter system. Additionally, POTS allows for screening of low abundance clones when compared with traditional TCR discovery techniques. Pooled TCRs could also be screened in vivo with primary T cells in a mouse model to screen for the most functional and physiologically fit TCR for cancer treatment.

<http://dx.doi.org/10.1136/jitc-2021-SITC2021.192>

20210727 POTS Workflow



Abstract 192 Figure 1 Outline of the POTS workflow.

THE ACHILLES VELOS™ PROCESS 2 BOOSTS THE DOSE OF HIGHLY FUNCTIONAL CLONAL NEOANTIGEN-REACTIVE T CELLS FOR PRECISION PERSONALIZED CELL THERAPIES

¹Eleni Kotsiou*, ¹Joe Robinson*, ¹Amber Rogers, ¹Daisy Melandri, ¹Amy Baker, ¹Anabel Ramirez Aragon, ¹Sidra Nawaz, ¹Michael Epstein, ¹Shreenal Patel, ¹Jennine Mootien, ¹Andrew Craig, ¹Satwinder Kaur-Lally, ¹Hinal Patel, ²Andreas Schmitt, ³Farah Islam, ³Mariam Jamal-Hanjani, ³David Lawrence, ³Martin Foster, ⁴Samra Turajlic, ¹Sergio Quezada, ¹Katy Newton. ¹*Achilles Therapeutics, London, UK*; ²*Royal Marsden Hospital, London, UK*; ³*University College London Hospital, London, UK*; ⁴*The Francis Crick Institute, London, UK*

Background Adoptive transfer of ex-vivo expanded tumor-infiltrating lymphocytes (TIL) has shown promise in the clinic. However, the non-specific expansion of TIL and the lack of understanding of the active component of TIL has resulted in poor correlation between clinical response and dose as well as poor understanding of response and resistance mechanisms. The VELOS™ manufacturing process generates a precision and personalized treatment modality by targeting clonal neoantigens with the incorporation of an antigen-specific expansion step to enrich the product for these specificities. Achilles has developed a second generation manufacturing process (VELOS™ Process 2) to boost the neoantigen-reactive cell dose while maintaining key qualitative features associated with function. Here we report the in-depth characterization of clonal neoantigen-reactive T cells (cNeT) products expanded using the two VELOS™ processes.

Methods Matched tumors and peripheral blood from patients undergoing routine surgery were obtained from patients with primary NSCLC or metastatic melanoma (NCT03517917). TIL were expanded from tumor fragments and peptide pools corresponding to the clonal mutations identified using the PELEUS™ bioinformatics platform were synthesized. cNeT were expanded by co-culture of TIL with peptide-pulsed autologous dendritic cells, with an optimized cytokine cocktail and co-stimulation for Process 2. Neoantigen reactivity was assessed using our proprietary potency assay with peptide pool re-challenge followed by intracellular cytokine staining. Single peptide reactivities were identified using ELISPOT and flow cytometric analysis for in-depth phenotyping of cNeT was performed.

Results CD3⁺ T cells displayed higher fold expansion in Process 2 (median 77.4) compared to Process 1 (median 3.8) (n=5). Both processes showed similar CD3⁺ T cell content (median Process 1=91.3%, Process 2=96.9% n=5) and contained both CD4⁺ and CD8⁺ T cells showing reactivity to clonal neoantigens. Proportion of cells responding to neoantigen re-challenge was similar across both processes (median Process 1=19.9% and Process 2=18.2%) leading to higher reactive dose when coupled with higher T cell doses in Process 2. Phenotypically T cells were predominantly effector memory for both processes and Process 2 had lower frequencies of terminally differentiated T cells.

Conclusions Achilles' proprietary potency assay enables the optimization of new processes that deliver high cNeT doses to patients by detecting the active drug component. We have generated proof of concept data that supports the transfer of the VELOS™ Process 2 to clinical manufacture for two first-in-human studies for the treatment of solid cancers.

Ethics Approval The samples for the study were collected under an ethically approved protocol (NCT03517917)

<http://dx.doi.org/10.1136/jitc-2021-SITC2021.193>

STIMULATION OF TUMOR INFILTRATING B-CELLS IMPROVES EX-VIVO TIL EXPANSION FOR MELANOMA IMMUNOTHERAPY

Renata Rossetti*, Leticia Tordesillas, Matthew Beatty, Yian Ann Chen, Dongliang Du, Amod Sarnaik, Shari Pilon-Thomas, Daniel Abate-Daga. *H. Lee Moffitt Cancer Center and Research Institute, Tampa, FL, USA*

Background The immunogenic nature of melanoma has been exploited for the development of adoptive transfer of ex-vivo expanded tumor infiltrating lymphocytes (TIL). This adoptive cell transfer therapy has overall response rates of around 50%. Multiple factors may determine the quality of the TIL product including components of the tumor microenvironment. B-cells are frequently found in melanoma metastasis, and display signs of antigen experience. Recently, B-cell tumor infiltration has been associated with improved clinical responses to immune checkpoint inhibitors,^{1 2} but their role in TIL therapy remains unexplored. Considering the potential role of B cells, we aim to develop strategies to enhance the quality of TIL products through B-cell stimulation during ex-vivo TIL expansion.

Methods We stimulated melanoma infiltrating B-cells using human recombinant CD40L on the first day of ex-vivo TIL expansion. Thirteen samples were expanded from melanoma tumor single cell suspensions, in high dose IL-2 alone (standard protocol), or in high dose IL-2 plus CD40L. After up to four weeks of expansion, the TIL phenotype was analyzed by flow cytometry.

Results The expansion success rate from the frozen tumor digests was 69% (95% CI: 38.6–90.9%) in the CD40L treatment condition compared to 23% with the standard protocol. Also, TILs cultured in the presence of CD40L expanded to higher numbers than with the standard protocol ($P = 0.02$). Interestingly, most of the samples expanded with CD40L had a significant increase in the percentage of CD4+ T cells ($P = 0.03$), but not to the detriment of the absolute number of CD8+ T cells. Treatment with CD40L increased the percentage of effector memory-like T cells ($P = 0.03$) and of CD39-CD69- T cells ($P < 0.05$), which were recently associated with response to TIL therapy.³

Conclusions This preliminary work demonstrates that the stimulation with CD40L at the initiation of TIL culture leads to enhanced TIL expansion and an increase in CD4+ T cells with an effector memory-like and stem-like phenotype. Our group and others have previously described cases of patients who had tumor regression after receiving TIL therapy that were predominantly CD4+ T cells, suggesting that expansion of the CD4+ TIL repertoire may enhance TIL therapy.⁴

Acknowledgements This work has been supported in part by the Flow Cytometry, Genomics and Biostatistics and Bioinformatics Core Facilities at Moffitt Cancer Center, an NCI designated Comprehensive Cancer Center (P30-CA076292). We acknowledge Moffitt's Melanoma Center of Excellence for the financial support.

REFERENCES

1. Cabrita R, Lauss M, Sanna A. Tertiary lymphoid structures improve immunotherapy and survival in melanoma. *Nature* 2020;**577**:561–565.
2. Petitprez F, de Reynies A, Keung EZ. B cells are associated with survival and immunotherapy response in sarcoma. *Nature* 2020;**577**:556–560.
3. Krishna S, Lowery FJ, Copeland AR. Stem-like CD8 T cells mediate response of adoptive cell immunotherapy against human cancer. *Science* 2020;**370**:1328–1334.
4. Friedman KM, Prieto PA, Devillier LE. Tumor-specific CD4+ melanoma tumor-infiltrating lymphocytes. *J Immunother* 2012;**35**:400–408.

Ethics Approval The study was approved by Advarra IRB, approval number MCC20559.

<http://dx.doi.org/10.1136/jitc-2021-SITC2021.195>

**TLR9-ACTIVATED B CELLS DIRECTLY LICENSE
ADOPTIVELY TRANSFERRED CD8+ T CELLS WITH
POTENT TUMOR IMMUNITY**

¹Aubrey Smith*, ³Hannah Knochelmann, ²Megan Wyatt, ²Guillermo Rangel Rivera, ²Brandon Ware, ²Amalia Rivera Reyes, ³Connor Dwyer, ³David Neskey, ³Mark Rubinstein, ³Bei Liu, ³Jessica Thaxton, ⁴Eric Bartee, ²Chrystal Paulos. ¹Medical University of South Carolina, Charleston, SC, USA; ²Emory University, Decatur, GA, USA; ³Emory University, Decatur, GA, USA; ³Medical University of South Carolina, Charleston, SC, USA; ⁴University of New Mexico, Albuquerque, NM, USA

Background The use of immunotherapies such as immune checkpoint blockade or adoptive cell therapy has substantially improved outcomes for many patients with advanced malignancies. However, a majority of these patients still do not respond or relapse. Thus, extensive efforts are being made to improve these therapies. We and others have demonstrated that adoptive cell therapy can be improved by the co-administration of TLR agonists intratumorally. TLR agonists have also been administered to patients alongside a number of other immunotherapies, but often induce toxic side effects that may be exacerbated by cell therapy. We hypothesized that TLR agonists could alternatively be used in ex vivo cell culture to propagate a more potent cell therapy product.

Methods To address our question, we used a transgenic mouse model of tumor-infiltrating lymphocyte (TIL) therapy, pmel-1, in which CD8+ T cells express a TCR specific for a melanoma/melanocyte antigen. We activated CD8+ pmel-1 T cells with APCs and the Toll-like receptor 9 agonist, CpG. Cell therapy efficacy was determined against mice bearing established B16F10 melanoma. Mechanisms underlying TLR-improved T cell products were determined using ex vivo cell depletion strategies and blocking antibodies.

Results CpG-expanded pmel-1 T cell products were much more effective against B16F10 melanoma in vivo than traditionally expanded T cells; they conferred more durable antitumor responses and improved survival of mice. CD8+ T cells generated in the presence of CpG also had heightened engraftment and persistence in the mice. We found that CpG did not act directly on T cells in culture, but on B cells, as depletion of B cells alone (not DCs, macrophages, NK cells, or CD4 cells) ablated the effects of CpG. B cells in CpG-treated cultures expressed a unique cytokine profile and upregulated several costimulatory markers on their cell surface, so we next questioned whether CpG improved the B cell/T cell axis via a direct or indirect (soluble) factor. Together, cell supernatant transfer experiments and costimulatory blockade experiments revealed that the direct interaction between B and T cells was required for the CpG-mediated improvement of the T cell product.

Conclusions Our findings reveal a novel role for B cells in the generation of potent CD8+ T cell therapies against an aggressive solid tumor. These findings highlight a unique way B cells can become powerful APCs for generating effective antitumor CD8+ T cells and can be directly translated to improve cell therapy products for patients with advanced malignancies.

Ethics Approval All animal procedures performed at the Medical University of South Carolina or Emory University were approved by each university's Institutional Animal Care & Use Committee, protocol number 0488 or 201900225, respectively.

<http://dx.doi.org/10.1136/jitc-2021-SITC2021.196>

NOVEL FCYR RECOMBINANT FUSION FACILITATES ANTIBODY ARMING OF ENGINEERED IPSC-DERIVED NK CELLS TO ENHANCE TARGETING AND KILLING OF OVARIAN CANCER CELLS

¹Kristin Snyder*, ¹Kate Dixon, ²Melissa Khaw, ²Zachary Davis, ³Paul Rogers, ³Martin Hosking, ³Ryan Bjordahl, ³Bahram Valamehr, ¹Jianming Wu, ¹Bruce Walcheck. ¹University of Minnesota, College of Veterinary Medicine, Saint Paul, MN, USA; ²University of Minnesota, Minneapolis, MN, USA; ³Fate Therapeutics, San Diego, CA, USA

Background Ovarian cancer is a leading cause of cancer-related deaths among women due to the development of therapeutic resistance. Natural killer (NK) cells are cytotoxic lymphocytes that can kill neoplastic cells without prior sensitization. A key anti-tumor function of human NK cells is antibody-dependent cell-mediated cytotoxicity (ADCC), mediated exclusively by the IgG Fcγ (FcγR) receptor CD16A. The mechanism of action of several clinically successful antitumor therapeutic monoclonal antibodies (mAbs) involves ADCC; however, their therapeutic efficacy is reduced due to regulatory checkpoints of CD16A, which include its low IgG binding affinity and rapid downregulation upon NK cell activation by the membrane metalloprotease ADAM17.^{1–3} CD64, the highest affinity FcγR, is expressed on myeloid-derived cells and not lymphocytes and is also not cleaved by ADAM17. To enhance ADCC, we generated CD64/16A, a novel recombinant FcγR consisting of extracellular CD64 and intracellular and transmembrane CD16A to mediate high affinity IgG binding and potent cell signaling.^{4 5}

Methods Engineered NK cells expressing CD64/16A were derived from human induced pluripotent stem-cells (iPSCs), referred to here as iNKs, which are clonal and clinically scalable NK cells. ADCC and natural cytotoxicity of three ovarian cancer cell lines were measured in vitro using Delfia EuTDA and IncuCyte cytotoxicity assays, and production of anti-tumor cytokines was determined via flow cytometry. Finally, tumor cell killing was assessed in vivo using a human xenograft mouse model of peritoneal metastatic ovarian cancer.

Results Our data show that iNK-CD64/16A cells uniquely facilitate mAb absorption, robustly produce IFN-γ and TNF-α, and kill several ovarian cancer cell lines in the presence of the therapeutic mAbs trastuzumab or cetuximab, which target HER2 or EGFR, respectively. We found that iNK-CD64/16A cells can capture soluble mAbs and retain antibody arming and ADCC efficacy after cryopreservation. Additionally, iNK-CD64/16A cells robustly mediate ADCC and reduce overall tumor burden of HER2+ tumor cells in vivo in the described metastatic ovarian cancer xenograft model.

Conclusions Our findings provide new insights into using high affinity Fc receptor-based adoptive NK cell therapies and lay the preclinical foundation necessary for developing an ‘off-the-shelf’ cellular therapy that can be combined with therapeutic tumor-targeting mAbs for the treatment of ovarian cancer. Importantly, iNK-CD64/16A cells can serve as a docking platform for therapeutic antibodies that can be switched and mixed for universal tumor antigen targeting to treat multiple malignancies.

Acknowledgements

Grant support NIH R01CA203348, HHMI Medical Research Fellows Program/Burroughs Wellcome Fund

REFERENCES

1. Jing Y, Ni Z, Wu J, et al. Identification of an ADAM17 cleavage region in human CD16 (Fcγ₃RIII) and the engineering of a non-cleavable version of the receptor in NK cells. *PLoS One* 2015;**10**(3):e0121788.

2. Wu J, Mishra HK, Walcheck B. Role of ADAM17 as a regulatory checkpoint of CD16A in NK cells and as a potential target for cancer immunotherapy. *J Leukoc Biol* 2019;**105**(6):1297–303.
3. Dixon KJ, Wu J, Walcheck B. Engineering Anti-Tumor Monoclonal Antibodies and Fc Receptors to Enhance ADCC by Human NK Cells. *Cancers (Basel)* 2021;**13**(2).
4. Snyder KM, Hullsiek R, Mishra HK, et al. Expression of a Recombinant High Affinity IgG Fc Receptor by Engineered NK Cells as a Docking Platform for Therapeutic mAbs to Target Cancer Cells. *Front Immunol* 2018;**9**:2873.
5. Walcheck B, Wu J. iNK-CD64/16A cells: a promising approach for ADCC? *Expert Opin Biol Ther* 2019;**19**(12):1229–32.

Ethics Approval This study was approved by the University of Minnesota’s Institutional Animal Care and Use Committee, protocol number 1902–36768A.

<http://dx.doi.org/10.1136/jitc-2021-SITC2021.197>

COSTIMULATORY ANTIGEN RECEPTOR (COSTAR): A NOVEL PLATFORM THAT ENHANCES THE ACTIVITY OF TUMOR INFILTRATING LYMPHOCYTES (TILS)

Sujita Sukumaran*, Milena Kalaitidou, Michelle Mojadidi, Clare Yarka, Yong (Stella) Ouyang, Eric Gschweng, Gray Kueberuwa, John Bridgeman, Bob Hawkins, Rubén Alvarez-Rodríguez. *Instil Bio, Inc., Dallas, TX, USA*

Background Major limiting factors for cell therapy in solid tumors include clonal heterogeneity and the related lack of universally expressed tumor-specific antigens. As the only truly polyclonal cell product in advanced development, tumor infiltrating lymphocytes (TILs) offer the broadest diversity of tumor reactivity but can be limited by suboptimal effector function in situ. Here we present a novel platform designed to leverage the diverse TCR repertoire of TILs while amplifying their anti-tumor activity via a synthetic costimulatory antigen receptor (CoStAR).

Methods A CoStAR molecule encoding an extracellular folate receptor alpha (FOLR1)-targeting single-chain fragment variable (scFv) and intracellular CD28 and CD40 signaling sequences was transduced into peripherally harvested T cells (healthy donor) and primary ovarian cancer TILs. Coculture experiments were performed with engineered cell lines and autologous tumor digests expressing varying levels TCR-stimulus and/or FOLR1. Cytolytic activity, activation markers, proliferation and cytokine secretion were measured.

Results Anti-FOLR1 CoStAR T cells activated with TCR stimulation and FOLR1 displayed increased activation markers (eg, CD137, > 50% increase), improved cytolytic activity, cytokine production (eg, IL-2, >15-fold) and ~7-fold increased proliferation when compared to either unmodified cells or when stimulated via TCR alone. Importantly, no T cell effector function, as measured by cytolytic activity, cytokine secretion, upregulation of activation markers or proliferation, was observed when CoStAR T cells were cocultured with targets expressing only FOLR1, underscoring the costimulation-only mechanism of action and reliance on native TCR repertoire for tumor recognition. Furthermore, increased activity was also observed when primary ovarian cancer anti-FOLR1 CoStAR TILs were cocultured with autologous tumor.

Conclusions CoStAR is a novel platform that leverages synthetic biology and T-cell-intrinsic circuits to create a product with markedly increased functional activity including cytotoxicity, proliferation, and cytokine expression while retaining broad, patient-specific neoantigen recognition to limit both antigen escape and off-tumor toxicity. Instil plans to initiate its first-in-human clinical trial with ITIL-306, an investigational anti-FOLR1 CoStAR TIL product in 1H 2022. Additional scFv targets are being evaluated for clinical application across a broad range of solid tumor histologies.

<http://dx.doi.org/10.1136/jitc-2021-SITC2021.198>

POTENT T CELL COSTIMULATION MEDIATED BY A NOVEL COSTIMULATORY ANTIGEN RECEPTOR (COSTAR) WITH DUAL CD28/CD40 SIGNALING DOMAINS TO IMPROVE ADOPTIVE CELL THERAPIES

Martina Sykorova, Leyuan Bao, Cynthia Chauvin-Fleurence, Milena Kalaitidou, Michelle Le Brocq, Robert Hawkins, Gray Kueberuwa, John Bridgeman*, Rubén Alvarez-Rodríguez. *Instil Bio, Inc., Dallas, TX, USA*

Background Costimulatory signals are a critical component to mount an effective anti-tumor response. Prolonged TCR stimulation in the absence of costimulatory signals can lead to T cell anergy and dysfunction. The tumor microenvironment evades immune surveillance by creating a suppressive environment characterized by high expression of coinhibitory receptors and lack of antigen presenting cells providing costimulatory signals. Third-generation CAR-T therapies containing two costimulatory domains have improved performance in animal models over second-generation CAR-T designs containing a single costimulatory domain, indicating the additive nature of some of these signaling pathways. Here we describe a synthetic CoStAR containing dual CD28 and CD40 domains designed to enhance the activity of T cells in the context of adoptive cell therapy.

Methods Healthy donor T cells were transduced with CoStAR receptors targeting the tumor-associated antigen CEA. Anti-CEA CoStAR T cells were then challenged with CEA+ tumor cells expressing a membrane anchored anti-CD3 antibody to provide signal 1 through TCR/CD3 complex cross linking. CoStAR signaling domains consisted of CD28 alone or a fusion of CD28 and CD40. Activity was measured by quantifying expression of activation markers, cytokine secretion, proliferation, and analysis of gene expression profiles.

Results Anti-CEA CoStAR-expressing T cells containing both CD28 and CD40 domains displayed increased cell activation, proliferation (>400-fold improvement over a 42-day serial coculture), and cytokine expression (eg, IL-2, ~14-fold; TNF α , ~2-fold) when compared to T cells expressing either CD28-only CoStAR or no CoStAR. Immunosuppressive cytokines (eg, IL-10 and IL-4) did not increase beyond levels observed with CD28-only CoStAR.

Conclusions The combination of CD28 and CD40 in the synthetic costimulatory antigen receptor CoStAR gives rise to superior T cell activity when compared to receptors consisting of a CD28 domain alone, including improvement in secretion of pro-inflammatory cytokines and long-term proliferative capacity. The novel design of the CoStAR molecule, including CD28 and CD40 signaling motifs, may further improve the performance of T-cell-based therapies, including tumor-infiltrating lymphocytes (TIL). Similar observations with an analogous anti-FOLR1 CoStAR have been observed, indicating broad applicability of the CoStAR platform across target molecules and tumor indications. Instil plans to initiate its first-in-human clinical trial with ITIL-306, an investigational anti-FOLR1 CoStAR TIL product in 1H 2022.

<http://dx.doi.org/10.1136/jitc-2021-SITC2021.199>

200

TGF β -ARMORING BOOSTS POTENCY AND PERSISTENCE OF ENGINEERED TCR T CELLS, UNLOCKING SUPERIOR EFFICACY AGAINST HPV-POSITIVE SOLID TUMORS

Gail Turner, Gabriela Diaz, Andreia Costa, Yeonjoo Oh, Jianguo Huang, Jenna Bailey, Cyr De Imus, Stephanie Busch, Teresa Foy, Pallavur Sivakumar, Ruth Salmon, Cédric Cleyrat*. *Bristol Myers Squibb, Seattle, WA, USA*

Background Adoptive transfer of chimeric antigen receptor (CAR)-expressing T cells targeting cell surface antigens has shown remarkable success in hematological malignancies. However, only limited success has been achieved to date with CAR T cells, or their engineered T cell receptor (eTCR) counterparts, in the context of solid tumors. This is largely due to: 1) challenges in identifying highly expressed, tumor-specific antigens and; 2) the immune-suppressive tumor microenvironment mediated by cellular and secreted factors such as TGF β , known to suppress intra-tumoral immunity and notably elevated in many human cancers, including in human papilloma virus (HPV)-associated cancers (e.g. head and neck squamous cell carcinoma and cervical cancers). Here, we describe the generation of highly potent, TGF β -armored, engineered T cells expressing a novel fully human, natural TCR $\alpha\beta$ sequence that is HLA-A*02:01-restricted, CD8 coreceptor-independent and targets the tumor-restricted HPV-16 E7(11–19) onco-peptide.

Methods Donor-derived T cells were genetically engineered using high efficiency CRISPR-Cas9 editing as follows: 1) TRAC domain knock-out (KO) to prevent endogenous TCR expression; 2) knock-in of an HPV-specific eTCR at the TRAC locus; and 3) KO of TGFBR2 to prevent TGF β signaling. Functional evaluation of edited T cells was performed in vitro using 3D serial spheroid stimulation as well as in vivo using NSG mouse tumor xenografts and against two cancer lines, SCC-152 and CasKi.

Results Under chronic antigen stimulation and in the presence of high TGF β at optimal effector-to-target (E:T) ratio, HPV eTCR WT (control) and HPV eTCR TGFBR2 KO cells demonstrated robust and comparable cytotoxic functions in vitro. However, when tested at suboptimal E:T ratio, HPV eTCR TGFBR2 KO cells demonstrated superior expansion (>5-fold difference), cytotoxicity and an improved functional phenotype, suggesting that TGF β -Armoring may decouple T cell expansion and the onset of exhaustion. In vivo studies demonstrated significant inhibition of tumor growth ($p < 0.0001$) and survival advantage ($p < 0.05$) in HPV eTCR TGFBR2 KO treated NSG mice when compared to HPV eTCR WT treated animals at a suboptimal dose of eTCR-positive cells. Additionally, in all conditions tested, T cell expression of CD103 (a pharmacodynamic marker of TGF β -induced signaling) was ablated in TGFBR2 KO groups. Both in vitro and in vivo data robustly reproduced across donors and tumor models.

Conclusions Pharmacology studies demonstrate that the HPV eTCR armoring strategy aimed at overcoming TGF β -mediated immune-suppression is highly effective in suboptimal conditions. Additionally, TGF β -armored eTCR cells presented with improved pharmacodynamic and phenotypic characteristics, paving the way for effective clinical applications in solid tumors.

Acknowledgements Ribonucleoprotein complexes designed specifically for the editing of human TRAC and TGFBR2 loci were provided by Editas Medicine.

<http://dx.doi.org/10.1136/jitc-2021-SITC2021.200>

BNT221, AN AUTOLOGOUS NEOANTIGEN-SPECIFIC T-CELL PRODUCT FOR ADOPTIVE CELL THERAPY OF METASTATIC OVARIAN CANCER

¹Christina Arieta*, ¹Diana Velez, ¹Susan Hannes, ¹Shirisha Meda, ¹Brian McCarthy, ¹Divya Lenkala, ¹Dewi Harjanto, ¹Prerna Suri, ¹Jessica Kohler, ¹Jonathan McGee, ¹Daniel Kallin, ¹Paul Turcott, ²Cynthia Nijenhuis, ²Maarje Rohaan, ²Gabe Sonke, ²John Haanen, ¹Mark DeMario, ¹Richard Gaynor, ¹Marit Van Buuren. ¹BioNTech US, Cambridge, USA; ²Netherlands Cancer Institute, Amsterdam, Netherlands

Background Neoantigens are tumor-specific antigens that are important in the anti-tumor immune response. These antigens are not subject to central immune tolerance and are therefore potentially more immunogenic than tumor-associated antigens. Here, we present the results of a proof-of-concept, pre-clinical study with multiple successful patient material runs generating a neoantigen-specific T-cell product (BNT221/NEO-PTC-01) using leukaphereses from patients with ovarian cancer. These products contain specific T-cell responses targeting multiple neoantigens from each individual patient's tumor.

Methods Leukapheresis and tumor biopsy samples were obtained from multiple patients with ovarian cancer and metastatic melanoma cancer under IRB approval using the N16NEON protocol at the Netherlands Cancer Institute subsidized by BioNTech US. Patient-specific neoantigens from the patient's biopsy were predicted using our RECON[®] bioinformatics platform and the best scoring neoantigens were encoded into synthetic peptides or mRNA molecules and were utilized in our ex vivo stimulation protocol, NEO-STIM[®], which is used to prime, activate, and expand memory and de novo T-cell responses from both the CD4+ and the CD8+ compartment. High-throughput flow cytometric analysis was performed to characterize the specificity and functionality (cytokine production and cytolytic capacity) of the induced T-cell responses.

Results NEO-STIM generates T-cell products specific to neoantigens from the peripheral blood of patients. Data will be presented showing the successful induction of 2–10 CD8+ and 4–13 CD4+ T-cell responses per patient, generated using peripheral blood mononuclear cells from patients with ovarian cancer using our NEO-STIM platform. We extensively characterized these T-cell responses and demonstrate that these responses are polyfunctional, specific and have the capacity to degranulate. T cells in the induced product are of effector memory and central memory phenotypes.

Conclusions NEO-STIM is a novel platform that generates ex vivo T-cell responses to high-quality neoantigen targets. Efforts are ongoing to upscale the manufacturing process and move this into a phase I study. BNT221, the neoantigen-specific T cell product generated from this process, is a potent adoptive cell therapy targeting multiple immunogenic neoantigens in patients with metastatic ovarian cancer.

Ethics Approval Leukapheresis and tumor biopsy samples were obtained from multiple patients with ovarian cancer and metastatic melanoma cancer under IRB approval using the N16NEON protocol at the Netherlands Cancer Institute subsidized by BioNTech US.

<http://dx.doi.org/10.1136/jitc-2021-SITC2021.201>

IN VIVO AND IN VITRO CHARACTERIZATION OF AIM ACT, A NOVEL NANOPARTICLE-BASED TECHNOLOGY, EXPANDED MART-1 SPECIFIC T CELLS

Ruipeng Wang*, Lauren Suarez, Emily Lu, Pratima Kunwar, Daniel Dembrow, Sojung Kim, Mathias Oelke. *Nelmmune, Gaithersburg, MD, USA*

Background NexImmune is developing highly differentiated immunotherapies to target, activate and expand tumor antigen-specific T cells using the proprietary Artificial Immune Modulation (AIM™) nanotechnology platform. The AIM nanoparticle (AIM-np) technology functions as synthetic dendritic cells capable of directing a specific T cell-mediated immune response. By mimicking natural T cell biology, NexImmune's non-genetically engineered cellular therapy product candidates (AIM ACT) are designed to combine the attributes of cellular precision, potency, and persistence with reduced potential for undesired toxicities.

Methods Here we present an example of AIM ACT expanded MART-1 specific T cells and their phenotypic and functional characterization in vitro and in vivo. Leukopaks from healthy donors were used to produce AIM ACT T cell products with our proprietary AIM ACT enrichment and expansion (E+E) manufacturing process and antigen peptide-loaded AIM-nanoparticles.

Results The final MART1 T cell products include up to 62.8% (20.8% in average) MART-1-specific CD8+ T cells as determined by MART1 peptide (ELAGIGILTV)-loaded multimer staining. MART1-specific T cells were tested in flow cytometry-based and live cell imaging-based cytotoxicity assays using HLA-A2 positive MART1 peptide-loaded target cells. The AIM ACT-generated T cells showed potent cytotoxicity to MART1 peptide-loaded target cells in vitro, while unloaded control cells were not killed. In over 30 independent AIM ACT E+E clinical scale runs, the expanded T cells consisted of a combined average of 91.7% T stem cell like, central and effector memory T cells, as determined by CD62L, CD45RA and CD95 staining. These phenotypes have been associated with long term in vivo persistence and anti-tumor efficacy. In a human melanoma PDX model, we confirmed that transfusion of AIM ACT T cells resulted in long term survival in vivo and significant reduction of tumor growth with complete tumor clearance in 6 out of 15 animals.

Conclusions The results demonstrate that AIM ACT MART1 T cells have long term persistence and anti-tumor activity in solid tumors such as melanoma, and that the AIM ACT E+E approach is a reproducible clinical scale manufacturing process for non-genetically engineered antigen-specific T cells. The AIM ACT platform is currently being used for generating T cell products for our current clinical trials, NEXI-001 (NCT04284228) and NEXI-002 (NCT04505813), and our pre-clinical development for HPV-associated malignancies. The findings support initiating Phase I trials of adoptive T cell therapy in solid tumors.

Ethics Approval The study was approved by the Institutional Animal Care and Use Committee (IACUC).

<http://dx.doi.org/10.1136/jitc-2021-SITC2021.202>

A MEMBRANE-TETHERED IL-15/IL-15 RECEPTOR FUSION PROTEIN ENHANCES THE PERSISTENCE AND EFFICACY OF CD70-TARGETED TRUC-T CELLS

Jian Ding*, Lindsay Webb, Troy Patterson, Michelle Fleury, Adam Zieba, Holly Horton, Robert Hofmeister, Dario Gutierrez, Robert Tighe. *TCR2 Therapeutics, Cambridge, MA, USA*

Background Adoptive cell therapies have shown great promise in hematological malignancies. To realize the potential of T cell therapies in solid tumors, we have developed T cell receptor fusion construct (TRuC[®]) T cells, which are equipped with an engineered T cell receptor that utilizes all TCR signaling subunits and recognizes tumor-associated antigens independent of HLA. Previously, we have described the discovery and pre-clinical efficacy of fratricide-resistant TRuC-T cells targeting CD70, a tumor antigen overexpressed in various solid and hematological malignancies. As a strategy to enhance T cell effector function and persistence in the hostile tumor microenvironment, we engineered anti-CD70 TRuC-T cells to co-express a membrane-bound IL15Ra-IL15 fusion protein (IL-15fu). IL-15 is a common γ chain cytokine that promotes the differentiation, maintenance, and effector function of memory CD8⁺ T cell subsets and confers resistance to IL-2-mediated activation induced cell death (AICD).

Methods T cells were activated by CD3/CD28 stimulation and lentivirally transduced with a T2A-containing bicistronic vector encoding the anti-CD70 CD3 γ -TRuC and the IL-15fu proteins; the cells were further expanded for 9 days in media containing IL-7/IL-15. Surface co-expression of the TRuC and IL-15fu proteins and the T cell memory phenotype was assessed by flow cytometry. In vitro persistence was tested in a repeated stimulation assay in which T cells were challenged by addition of fresh CD70⁺ target cells every four days with longitudinal assessment of T-cell expansion, phenotype, cytokine production, and cytotoxicity. In vivo, the antitumor efficacy of the anti-CD70 TRuC/IL-15fu T cells was evaluated in MHC class I/II deficient NSG mice bearing human tumor xenografts.

Results The anti-CD70 TRuC and IL-15fu proteins showed high transduction efficiency and robust co-expression on the surface of T cells. The IL-15fu significantly increased the proportion of naïve cells within the TRuC-T cell product, most dramatically in the CD8⁺ subset. In vitro, TRuC-T cells bearing the IL-15fu showed greatly enhanced expansion and persistence upon repeated stimulation with CD70⁺ target cells. Moreover, the IL-15fu enhanced T-cell survival and persistence under unstimulated, cytokine-free conditions. In vivo, the antitumor activity of CD70-targeted TRuC-T cells was significantly improved by IL-15fu in multiple tumor models and was associated with enhanced intratumoral T-cell accumulation and a preferential expansion of CD8⁺ T cells.

Conclusions The addition of the IL-15fu improved the phenotype, persistence, and anti-tumor activity of CD70-targeted TRuC-T cells, potentially increasing the likelihood of clinical benefit in patients with CD70 overexpressing solid and liquid cancers.

Ethics Approval All animal studies were conducted by TCR2 Therapeutics staff at the Charles River Laboratories CRADL facility under a protocol approved by the Charles River Laboratories Institutional Animal Care and Use Committee.

<http://dx.doi.org/10.1136/jitc-2021-SITC2021.203>

KSQ-004: UNBIASED PAIR-WISE DISCOVERY OF SOCS1 AND REGNASE-1 AS THE TOP CRISPR/CAS9 DUAL-EDIT COMBINATION ENHANCING IN VIVO TIL POTENCY AGAINST SOLID TUMORS

<http://dx.doi.org/10.1136/jitc-2021-SITC2021.204>

Karrie Wong, Christopher Wrocklage, Sharon Lin, Isabelle Le Mercier, Caroline Bullock, Louise Cadzow, Anja Hohmann, Sol Shenker, Katri Sofjan, Leila Williams, Gregory Kryukov, Conor Calnan, Frank Stegmeier, Micah Benson*, Michael Schlabach. *KSQ Therapeutics, Cambridge, MA, USA*

Background The application of CRISPR/Cas9-gene-editing to enhance the anti-tumor activity of T cell Adoptive Cell Therapies (ACT) is a promising approach in the treatment of patients with solid tumors. We developed an in vivo CRISPR² screening approach and interrogated the top dual-edit combinations enhancing T cell anti-tumor function. We discovered that across all possible dual-edit combinations of T cell targets, inactivation of Regnase-1 and SOCS1 led to the greatest enhancement in anti-tumor T cell potency in vivo. We applied these findings to discover KSQ-004, a Regnase-1/SOCS1 dual-edited human CRISPR/Cas9-engineered TIL (eTIL) therapy currently under development for therapeutic use.

Methods We generated randomly paired CRISPR guide libraries (CRISPR2) targeting top hits from previous single-gene Immune CRISPRomics[®] screens. CRISPR² libraries with over 1200 gene pairs were screened in primary mouse OT1 and PMEL-TCR-Tg-T cells in the relevant syngeneic tumor models. Top dual-edit combinations were then evaluated in the immunotherapy-refractory B16F10 metastatic lung tumor model. The efficacy of the top combo was further evaluated in a mouse TIL model wherein TIL from B16-Ova tumors were expanded and engineered ex vivo and adoptively transferred into tumor bearing hosts for efficacy assessment.

Results Of the 1200+ combinations tested in the CRISPR² screens, the Regnase-1/SOCS1 combination ranked amongst the top dual-edits, with this combination enhancing T cell infiltration into tumors >3500-fold in comparison to controls. Studies conducted in the checkpoint therapy refractory B16F10 lung metastasis model revealed that Regnase-1/SOCS1 dual-edited PMEL-TCR-Tg-T cells conferred remarkable survival benefit relative to controls, significantly extending median survival of animals from 21 days to 53 days. Furthermore, Regnase-1+SOCS1-edited mouse TIL isolated and expanded from B16-Ova tumors exerted complete control of tumors upon re-infusion into hosts, suggesting rejuvenation of tumor-experienced TILs by this edit combination. To apply these insights for therapeutic use, we discovered KSQ-004, a human Regnase-1/SOCS1 dual-edited CRISPR/Cas9-engineered TIL (eTIL). Methods were developed to manufacture KSQ-004 from melanoma and NSCLC tumor samples, with eTIL demonstrating robust expansion and viability comparable to unedited control TIL with over 90% knockout of both targets. Importantly, KSQ-004 produced elevated IFN γ upon autologous tumor stimulation and exerted greater control of tumor spheroids in vitro.

Conclusions We used a novel CRISPR² screen approach to identify Regnase-1/SOCS1 as the top dual edit combination enhancing T cell function in the tumor microenvironment. We translated these findings to therapeutic use with the discovery of KSQ-004, a dual-edited eTIL therapy engineered that possesses enhanced anti-tumor potency and persistence against solid tumors.

AGENT-797, A NATIVE ALLOGENEIC 'OFF-THE-SHELF' INKT CELL THERAPY PRODUCT SHOWS ANTI-TUMOR ACTIVITY IN PRECLINICAL XENOGRAFT MODELS

¹Burcu Yigit*, ¹Darrian Moskowitz, ¹Xavier Michelet, ²Antoine Tanne, ¹Marc Van Dijk. ¹Mink Therapeutics, Lexington, MA, USA; ²Agenus, Lexington, MA, USA

10.1136/jitc-2021-SITC2021.1

Background agenT-797 is an allogeneic, native invariant natural killer T (iNKT) cell therapy product currently in phase I clinical trials for cancer (heme and solid). iNKT cells are a distinct population of T cells that can recognize tumors via direct recognition of CD1d (an MHC-I like molecule presenting glycolipids) through the TCR or recognition of NK cell receptor ligands via various NK receptors. We developed agenT-797 from isolated and ex-vivo expanded peripheral blood iNKT cells. Here we describe in vivo xenograft models to demonstrate the overall tissue distribution, tumor infiltration and efficacy of agenT-797 in liquid as well as solid tumors.

Methods We utilized NOG-hIL15 (human IL-15) transgenic mice to ensure persistence/maintenance of ex-vivo expanded human iNKT cells throughout the studies. For studying efficacy in liquid tumors, we used NALM6, an acute lymphoblastic leukemia (ALL) cell line and for solid tumors selected A375, a melanoma cell line. Both cell lines were engineered to overexpress CD1d. Upon injection of iNKT cells, tumor growth and iNKT cell tissue/tumor infiltration as well as phenotype were studied.

Results Injection of iNKT cells in NALM6- engrafted NOG-hIL15 mice resulted in an overall reduction in leukemic burden as measured by luminescence-based imaging. Flow cytometric analysis revealed infiltration of iNKT cells at the site of leukemic expansion, namely blood, spleen, bone marrow and liver. Cells were activated when reaching the site of the tumor. In addition, iNKT cells produced IFN γ and TNF α and low levels of IL-13/IL-4, consistent with a Th1 response. When iNKT cells were injected into A375 engrafted mice we observed infiltration of iNKT cells into the tumor, where they become activated and proliferate overtime. We observed an overall reduction in tumor size when iNKT cells were injected compared to control group, demonstrating the impact of iNKT cells on tumor growth.

Conclusions We established xenograft mouse models to address various biological questions around human iNKT cells as a cell therapy product. We have demonstrated homing and infiltration of iNKT cells at the site of tumor and relative proliferation and expansion. These models provide a suitable platform for in-vivo preclinical studies on agenT -797 in cancer.

Ethics Approval All procedures performed in studies involving human participants were in accordance with the ethical standards of the institutional and/or national research committee and with the 1964 Helsinki declaration and its later amendments or comparable ethical standards.

<http://dx.doi.org/10.1136/jitc-2021-SITC2021.205>

206

THE DEVELOPMENT OF 'CHIMERIC CD3E FUSION PROTEIN' AND 'ANTI-CD3-BASED BISPECIFIC T CELL ACTIVATING ELEMENT' ENGINEERED T (CAB-T) CELLS FOR THE TREATMENT OF SOLID MALIGNANCIES

¹Andy Tsun*, ²Zhiyuan Li, ²Zhenqing Zhang, ²Weifeng Huang, ³Shaogang Peng, ²Jitian Chai. ¹Biotheus Inc., Zhuhai, China; ²Biotheus (Suzhou) Co., Ltd., Zhuhai, China; ³Biotheus (Suzhou) Co., Ltd., Suzhou, China

Background Cancer immunotherapy has achieved unprecedented success in the complete remission of hematological tumors. However, serious or even fatal clinical side-effects have been associated with CAR-T therapies to solid tumors, which mainly include cytokine release syndrome (CRS), immune effector cell-associated neurotoxicity syndrome (ICANS), macrophage activation syndrome, etc. Furthermore, CAR-T therapies have not yet demonstrated significant clinical efficacy for the treatment of solid tumors. Here, we present a novel T cell therapeutic platform: a Chimeric CD3e fusion protein and anti-CD3-based bispecific T cell activating element (BiTA) engineered T (CAB-T) cells, which target tumor antigens via the secretion of BiTAs that act independently of MHC interactions. Upon BiTA secretion, CAB-T cells can simultaneously achieve anti-tumor cytotoxic effects from the CAB-T cells and simultaneously activate bystander T cells.

Methods CAB-T cells were generated by co-expressing a chimeric CD3e fusion protein and an anti-CD3-based bispecific T cell activating element. The chimeric CD3e contains the extracellular domain of CD3e, a CD8 transmembrane domain, 4-1BB costimulatory domain, CD3z T cell activation domain and a FLAG tag, while the BiTA element includes a tumor antigen targeting domain fused with an anti-CD3 scFv domain and a 6x His-tag. CAR-T cells were generated as a control. Cytokine release activity, T cell activation and exhaustion markers, T cell killing activity and T cell differentiation stages were analysed. We also tested their tumor growth inhibition activity, peripheral and tumor tissue distribution, and their safety-profiles in humanized mouse models.

Results CAB-T cells have similar or better in vitro killing activity compared with their CAR-T counterparts, with lower levels of cytokine release (IL-2 and IFN γ). CAB-T cells also showed lower levels of exhaustion markers (PD-1, LAG-3 and TIM-3), and higher ratios of naive/Tscm and Tcm T cell populations, after co-culture with their target tumor cells (48h). In in vivo studies, CAIX CAB-T and HER2 CAB-T showed superior anti-tumor efficacy and tumor tissue infiltration activity over their corresponding CAR-T cells. For CLDN18.2 CAB-T cells, similar in vivo anti-tumor efficacy was observed compared to CAR-T after T cell infusion, but blood glucose reduction and animal mortality was observed in the mice administered with CAR-T cells.

Conclusions The advantages of CAB-T in in vitro and in vivo studies may result from TCR signal activation of both the engineered CAB-T cells and the non-engineered bystander T cells via cross-bridging by the secreted BiTA molecules, thus offering superior anti-tumor efficacy with a potential better safety-profile compared to conventional CAR-T platforms.

<http://dx.doi.org/10.1136/jitc-2021-SITC2021.206>

ENHANCED ANTIGEN CAPTURE, ANTIGEN-PRESENTING CELL (APC)-LIKE FUNCTION, AND CYTOTOXIC RESPONSES WITH CHIMERIC ENGULFMENT RECEPTOR (CER) T CELLS

¹Daniel Corey*, ¹Sunil Thomas, ¹Brandon Cieniewicz, ¹Linh Nguyen, ¹Jared Clever, ¹Josephine Brysting, ¹Remus Veza, ¹John Rossi, ²Kurt Diem, ²Lei Jin, ²Lawrence Corey. ¹CERO Therapeutics, South San Francisco, CA, USA; ²Fred Hutchinson Cancer Research Center, Seattle, WA, USA

Background Activated T cells have limited antigen presenting capability due to inefficient capture.¹ This process can be enhanced through novel chimeric engulfment receptors (CERs) expressing a human Tim-4 phagocyte receptor that recognizes phosphatidylserine (Ptd-Ser)² fused to T cell and macrophage/dendritic cell-derived signaling domains. CERs can facilitate antigen capture, processing, and presentation, and impart target-dependent cytotoxic function when expressed in T cells. This combined function is hypothesized to improve tumor clearance and durability of response, making CER T cell products ideal clinical candidates.

Methods We generated Tim-4 receptors fused to toll-like receptor (TLR)-2 or -8, CD28 or CD3 zeta and tested phagocytic, antigen presentation and cytotoxic function in healthy donor T cells. To assess phagocytosis, target cells treated with a small molecule to induce Ptd-Ser externalization were labeled with pH-Rodo followed by co-culture with CER T cells. Activated CER T cells were evaluated by transmission electron microscopy (TEM) or flow cytometry (FC) for lysosomal uptake of cell fragments. Antigen capture and presentation were characterized by FC for the capacity of human papilloma virus 16 (HPV 16) E7 peptide-pulsed CER T cells to activate and induce proliferation of autologous HPV 16 E7-TCR transduced T cells. Cytotoxic function was evaluated in co-culture assays of CER T cells in the presence of subtherapeutic doses of BTKi (ibrutinib)-treated JeKo-1 lymphoma cells.

Results TEM imaging demonstrated that CER T cells engulfed target cell fragments, illustrated by multi-vesicular bodies containing tumor fragments (some measuring >0.5 μM) and pseudo-pod like formations around apoptotic target cell blebs. RNA analysis revealed upregulation of TLR, myeloid differentiation, and antigen presentation pathways. In the HPV 16 E7 co-culture model, T-cell surface activation markers CD25 and CD69 were upregulated 41% and 23%, respectively, on E7-TCR-T cells relative to controls. In addition, the percentage of dividing E7-TCR-T cells was increased (44% vs 8%) after 6 days in co-culture. Addition of CER T cells to JeKo-1 target cells in the presence of BTKi at low effector: target ratios enhanced cytotoxicity by over 99%, demonstrating synergy with a targeted small molecule to fully eliminate lymphoma cells.

Conclusions Novel Tim-4/TLR containing CERs can capture tumor cell fragments and present soluble antigen, a function previously demonstrated to be a barrier to effective antigen presentation in T cells. Enhanced T-cell antigen capture and presentation capability alongside inducible and target-specific cytotoxic function in single T cells represents a significant advancement in the potential for chimeric receptor-based therapies.

REFERENCES

1. Lanzavecchia A, Roosnek E, Gregory T, Berman P, Abrignani S. T cells can present antigens such as HIV gp120 targeted to their own surface molecules. *Nature* 1988 Aug 11; **334**(6182):530–2.

2. Caronni N, Piperno GM, Simoncello F, Romano O, Vodret S, Yanagihashi Y, et al. TIM4 expression by dendritic cells mediates uptake of tumor-associated antigens and anti-tumor responses. *Nat Commun* 2021 Apr 14; **12**(1):2237.

<http://dx.doi.org/10.1136/jitc-2021-SITC2021.207>

208

RTX-224, AN ENGINEERED ALLOGENEIC RED CELL THERAPEUTIC EXPRESSING 4-1BBL AND IL-12, ACTIVATES IMMUNE CELLS IN BLOOD AND SPLEEN TO PROMOTE TUMOR GROWTH INHIBITION IN MICE

Anne-Sophie Dugast*, Shannon McArdel, Zafira Castano, Maegan Hoover, Arjun Reddy Bollampalli, Enping Hong, Shannon Leonard, Ryan Pepi, Alex Nanna, Laurence Turka, Sivan Elloul. *Rubius Therapeutics, Cambridge, MA, USA*

Background Agonist antibodies and recombinant cytokines have had limited success in the clinic due to three factors: severe toxicity leading to a narrow therapeutic index, the diminished activity of an agonistic antibody compared with natural ligand, and the lack of multiple signals needed to effectively activate most cell types. To address these limitations, Rubius Therapeutics has developed RTX-224, an allogeneic red cell therapeutic genetically engineered to express hundreds of thousands of copies of 4-1BBL and IL-12 in their natural conformation on the cell surface. RTX-224 is designed to activate four key target cell types: CD4+ and CD8+ T cells, antigen presenting cells and NK cells for a broad and effective anti-tumor response while providing improved safety due to the restricted biodistribution of red blood cells to the vasculature and spleen. Here we investigated the potential efficacy and mechanism of action of RTX-224 using the mouse surrogate mRBC-224.

Methods mRBC-224 was administered intravenously (i.v.) to normal or tumor-bearing mice (B16F10 tumor models). Blood, spleen and tumors were harvested and the pharmacodynamic effects of mRBC-224 on immune cells were evaluated.

Results mRBC-224 administered to mice inoculated i.v. with B16F10 melanoma reduced the number of metastases ($p < 0.0001$ and 76.8% tumor growth inhibition on Day 14). This was accompanied by increased proliferation (Ki67+) and cytotoxicity (GzmB+) of tumor-infiltrating CD8+ T cells and NK cells, and an increased CD8+ effector memory (TEM) phenotype. Similarly, mRBC-224 reduced tumor growth in the B16F10 s.c. model ($p < 0.0001$ and 56.2% tumor growth inhibition on Day 9), and this was associated with increased frequency of activated (MHC-II+) tumor-infiltrating macrophages. Consistent with the known biodistribution of red cells, mRBC-224 did not distribute to the tumor but was predominantly localized in the blood and spleen raising the question about mRBC-224 mechanism of action in mediating antitumor responses. In normal and B16F10 s.c. tumor-bearing mice, mRBC-224 induced the activation of CD8+ T cells, NK cells and monocytes/macrophages in blood and spleen in a dose-dependent manner. PD studies in the tumor suggest that these activated immune cells are capable of trafficking from blood/spleen to the tumor. These results align with published data suggesting that activated T cells in the spleen or blood can replenish exhausted tumor-infiltrating cells.

Conclusions Taken together, these data unveil the mechanism of action of mRBC-224 and suggest that mRBC-224 activate immune cells in the spleen and blood, leading to their trafficking into the tumor microenvironment to promote efficacy.

<http://dx.doi.org/10.1136/jitc-2021-SITC2021.208>

**GENETICALLY ENGINEERED MYELOID CELLS (GEMYS)
AS A PLATFORM TO ENHANCE ANTITUMOR IMMUNITY**

Sabina Kaczanowska*, Daniel Beury, Haiying Qin, Rosandra Kaplan. *National Cancer Institute, Bethesda, MD, USA*

Background Immune suppression is a major hurdle in cancer immunotherapy for solid tumors. Innate myeloid cells are key regulators of the immune system and can dampen the antitumor response against cancer. We have identified that bone marrow-derived myeloid cells play an immunosuppressive role in the metastatic microenvironment, limiting immune surveillance and facilitating the growth of tumor cells. We hypothesized that targeting the myeloid-mediated immune suppression program in the metastatic and primary tumor microenvironment could facilitate antitumor immune activation and be a successful immunotherapeutic approach.

Methods To take advantage of the unique capability of myeloid cells to home to and infiltrate tumor and metastatic sites, we designed an immunotherapeutic approach in which we generate genetically engineered myeloid cells (GEMys) as a platform to locally deliver modulatory factors into the tumor and metastatic microenvironment.

Results Mice treated with IL-12-secreting GEMys (IL12-GEMys) exhibited a robust IFN γ response associated with increased expression of antigen processing and presentation machinery as well as numbers of T and NK cells expressing markers associated with activation and cytotoxicity. These microenvironmental changes were associated with reduced metastasis, delayed tumor growth, and increased survival. When combined with chemotherapy pre-conditioning, IL12-GEMys cured mice of established tumors and generated long-lived T cell memory, as these mice were immune to subsequent tumor challenge. We are currently working on translating these exciting findings into the human setting.

Conclusions This work demonstrates that IL12-GEMys can functionally modulate the core program of immune suppression in the pre-metastatic niche to successfully rebalance the dysregulated metastatic microenvironment in cancer. This approach holds promise to limit metastatic progression in patients with high risk and advanced cancers.

REFERENCES

1. Kaczanowska S, Beury DW, Gopalan V, Tycko AK, Qin H, Clements ME, Drake J, Nwanze C, Murgai M, Rae Z, Ju W, Alexander KA, Kline J, Contreras CF, Wessel KM, Patel S, Hannenhalli S, Kelly M, Kaplan RN. Genetically engineered myeloid cells rebalance the core immune suppression program in metastasis. *Cell* 2021;**184**:1–20.

<http://dx.doi.org/10.1136/jitc-2021-SITC2021.209>

210

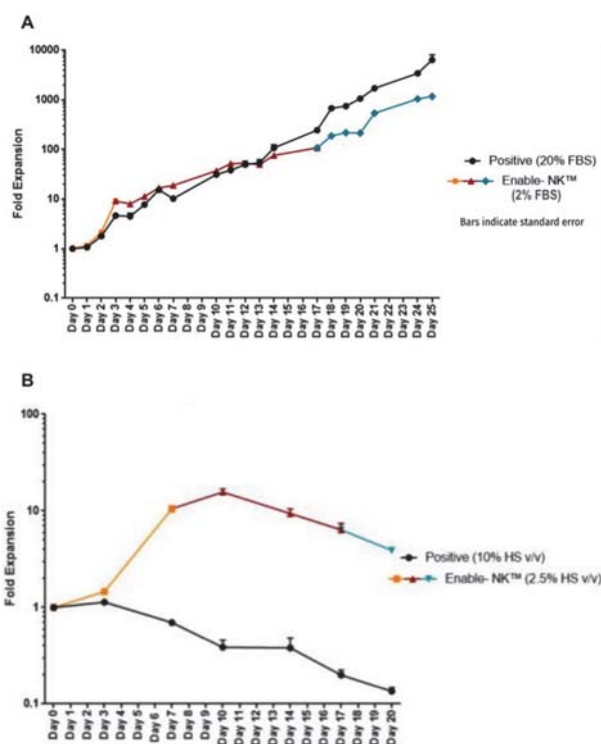
A NOVEL MEDIUM FOR INCREASED CYTOTOXICITY AND SERUM-MINIMAL EX VIVO EXPANSION OF NATURAL KILLER (NK) CELLULAR IMMUNOTHERAPIES

¹Marc Gillig, ¹Graeme Lambert, ²Matthew Forsberg, ¹Donna Sonntag, ¹Jason Cahoon, ¹Rafet Amoor, ¹Borom Chean, ³Lea Picard, ³Sabine Wingert, ⁴Caroline Hull, ⁵Jacki Kombluth, ³Carsten Watzl, ²Christian Capitini, ¹Rachit Ohri*. ¹Enable Life Sciences LLC, Worcester MA; ²University of Wisconsin, Madison, Madison, WI USA; ³Leibniz Research Centre, Germany; ⁴Leucid Bio Ltd, London; ⁵St. Louis University

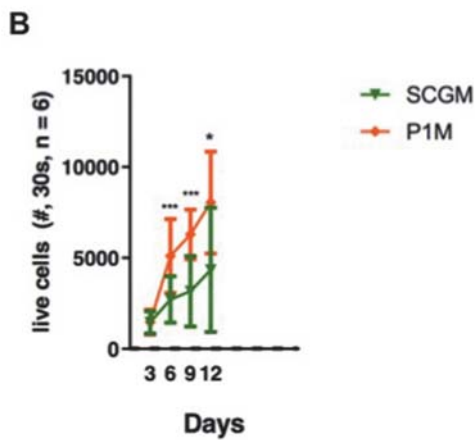
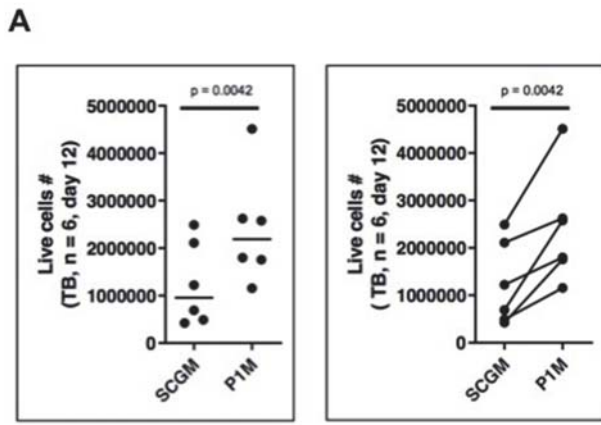
Background Despite significant clinical breakthroughs,^{1, 2} cellular immunotherapy remains unacceptably variable in performance³ and impractically expensive for mainstream adoption.⁴ These hurdles are particularly true for new cancer immunotherapies with natural killer (NK) cells. Culturing NK cells ex vivo is challenging due to short half-lives, reduced functionality, and increased exhaustion.⁵ Also, the use of serum introduces inconsistency and increases cost.⁶ Here we introduce a novel prototype medium specifically formulated for NK cells, which uses a unique combination of plant extracts and molecular ingredients to increase cytotoxic performance while allowing the reduction of serum by up to 90 percent.

Methods KHYG-1 NK cell line, or primary NK cells, were brought to 2% or 2.5% serum, respectively, in the prototype media. DMEM/F12 with 20% serum (for KHYG-1) or 10% serum (for primary cells) was the control. All media was supplemented with 100 U/mL IL-2. Cell numbers were periodically assessed, using a cell counter or flow cytometry. For cytotoxicity assays, K562 target cells were cocultured with KHYG-1 cells (effector:target ratio 20:1) for 5h, or with primary NK cells (4:1) for 18h. Cells were stained with annexin V and propidium iodide to determine the levels of apoptosis and necrosis by flow cytometry. Levels of secreted proteins were determined using Luminex. Expression of CD56 was determined by flow cytometry.

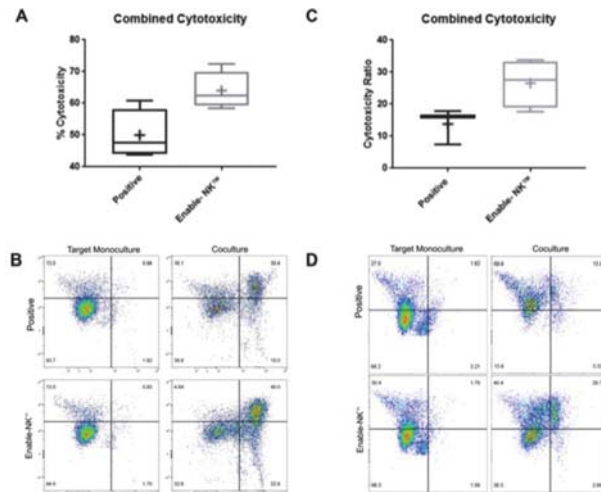
Results Following adaptation to 2% serum, growth of KHYG-1 cells in the prototype media stayed nearly on pace with the control for over 3 weeks. Human primary NK cells grew 10-fold over 10 days in the prototype media with 2.5% serum, without feeder cells; in contrast, primary cells did not proliferate in control medium (figure 1). Beta testing confirmed that the prototype media improved the proliferation of primary NK cells over a 12-day period, relative to a gold standard medium (figure 2). After culture in prototype media, both KHYG-1 cells and primary NK cells exhibited higher cytotoxic activity toward K562 cells, compared with the activity of the same cells cultured in control medium (figure 3). Secretion of interferon-gamma, perforin, and granzyme A was increased in KHYG-1 cells cultured in prototype media (figure 4). Additionally, culture in this media pushes NK cells toward a more CD56-dim phenotype (figure 5), which is associated with increased cytotoxic activity.



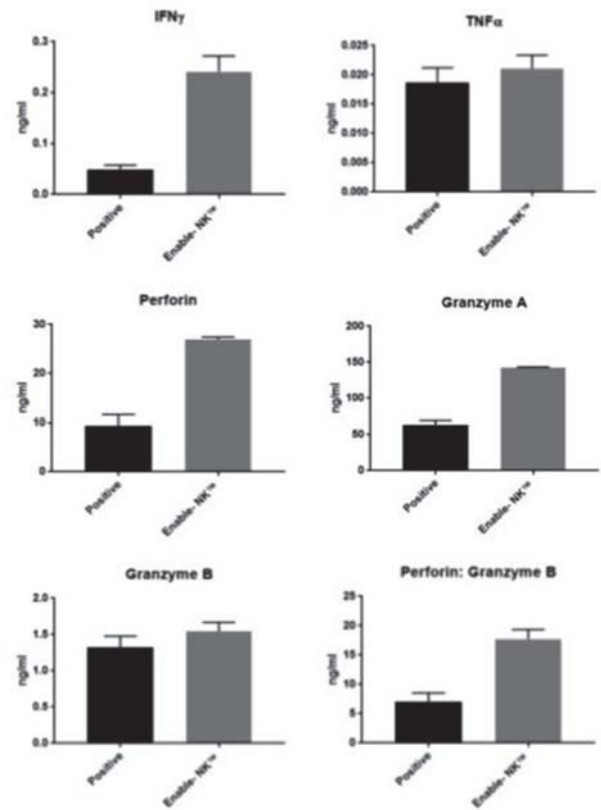
Abstract 210 Figure 1 Growth of NK cell line and human primary NK cells. (A) Growth of the KHYG-1 cell line, cultured in prototype media, kept pace with cells cultured in control medium. Orange indicates gradual adaptation to lower serum content; red indicates culturing in the formulation optimized for cell proliferation; blue indicates culturing in the formulation developed for NK cell activation. (B) Growth of primary NK cells was achieved in prototype media, but these cells did not grow in control medium.



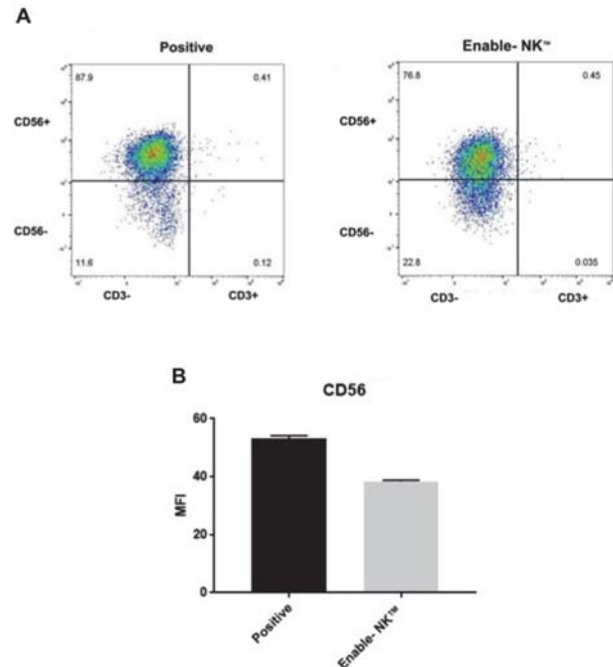
Abstract 210 Figure 2 Primary NK cells grow better in prototype media



Abstract 210 Figure 3 NK cytotoxicity is enhanced by prototype media. (A and B) KHYG-1 cell line cocultured with K562 target cells. (C and D) Primary human NK cells cocultured with K562 target cells



Abstract 210 Figure 4 Secretion of interferon, perforin, and granzyme A



Abstract 210 Figure 5 Shift to CD56-dim phenotype

Conclusions The prototype media increases the cytotoxic activity of NK cells against cancer cells. Also, it supports proliferation of NK cell lines and primary NK cells, even at reduced serum content.

REFERENCES

1. Hirayama AV, Gauthier J, Hay KA, Voutsinas JM, Wu Q, Pender BS, Hawkins RM, Vakil A, Steinmetz RN, Riddell SR, Maloney DG. High rate of durable complete remission in follicular lymphoma after CD19 CAR-T cell immunotherapy. *Blood* 2019;**134**(7):636–640.
2. Martinez VG, Park D, Acton SE. Immunotherapy: breaching the barriers for cancer treatment. *Philos Trans R Soc B Biol Sci* [Internet] Royal Society, 2019 August 19;**374**(1779):20180214. Available from: <https://doi.org/10.1098/rstb.2018.0214>
3. Burke C, Zylberberg C. Sources of variability in manufacturing of cell therapeutics. *Regen Eng Transl Med* 2019;**5**:332–40.
4. Leech AA, Neumann PJ, Cohen JT, Jagasia M, Dusetzina SB. Balancing value with affordability: cell immunotherapy for cancer treatment in the U.S. oncologist [Internet]. John Wiley & Sons, Ltd, 2020 July 1;**25**(7):e1117–9. Available from: <https://doi.org/10.1634/theoncologist.2020-0025>
5. Fang F, Xiao W, Tian Z. Challenges of NK cell-based immunotherapy in the new era. *Front Med* [Internet], 2018;**12**(4):440–50. Available from: <https://doi.org/10.1007/s11684-018-0653-9>
6. Aijaz A, Li M, Smith D, Khong D, LeBlon C, Fenton OS, *et al.* Biomanufacturing for clinically advanced cell therapies. *Nat Biomed Eng* [Internet] 2018;**2**(6):362–76. Available from: <https://doi.org/10.1038/s41551-018-0246-6>

<http://dx.doi.org/10.1136/jitc-2021-SITC2021.210>

SQZ™ EAPCS GENERATED FROM PBMCs BY DELIVERY OF MULTIPLE MRNAs ENCODING FOR ANTIGENS, COSTIMULATORY PROTEINS, AND ENGINEERED CYTOKINES

¹Michael Maloney*, ¹Emrah Ilker Ozay, ¹Amy Merino, ¹Andrea Silva, ¹Amber Martin, ¹Sanjana Manja, ¹Madhav Upadhyay, ²Christine Trumpfheller, ²Pablo Umana, ¹Armon Sharei, ¹Howard Bernstein, ¹Scott Loughhead. ¹SQZ Biotechnologies, Watertown, MA, USA; ²Roche Glycart AG, Schlieren, Switzerland

Background Antigen-specific CD8+ T cells are critical components of mounting an effective immune response against tumors. Generation of antigen-specific T cells require interactions with multiple signals produced by antigen presenting cells (APCs). These signals are comprised of three components: (signal 1) the peptide-MHC complex binding to the T cell receptor, (signal 2) costimulatory molecules on the surface of APCs, and (signal 3) inflammatory cytokines binding to cognate receptors on T cells.

Methods To engineer all major cell subsets of human peripheral blood mononuclear cells (PBMCs) to become enhanced APCs (eAPCs), we used Cell Squeeze® technology to deliver multiple mRNA encoding for non-self-antigens (signal 1), CD86 (signal 2), and/or membrane-bound cytokines (signal 3). The signal 3 molecules, membrane-bound IL-12 (mbIL-12) and membrane-bound IL-2 (mbIL-2), are chimeric proteins designed to increase the localized concentration of the cytokines and limit off-target effects. Flow cytometry and western blots were used to confirm the translation of each of the delivered mRNA. The increased capabilities of these enhanced APCs were assessed in vitro by culturing the APCs with antigen-specific T cells for multiple days before measuring the functionality of antigen-specific T cells via intracellular cytokine staining or ELISA.

Results We demonstrate that Cell Squeeze® processing of PBMCs with mRNA encoding for signals 1, 2, and 3 results in highly effective enhanced APCs in vitro. In a single squeeze process, efficient delivery and translation of up to five mRNA is observed in all major PBMC cell subsets including T cells, B cells, NK cells, and monocytes. Once translated, the chimeric mbIL-2 and mbIL-12 can bind to their cognate receptors and exhibit minimal shedding from the surface. We show that enhanced APCs can present antigenic peptides derived from mRNA encoding for a foreign antigen on MHC complexes in an HLA agnostic manner, which drives antigen-specific T cell responses. The addition of CD86, mbIL-2, and mbIL-12 further enhance the activation and potency of antigen-specific T cells, as measured by an increase in the secretion of inflammatory cytokines upon restimulation (i.e. IFN γ).

Conclusions Cell squeezing of human PBMCs with mRNA encoding for signals 1, 2, and 3 has the potential to generate enhanced APCs that drive robust CD8+ T cell response against multiple targets across several disease areas. The versatility of the Cell Squeeze® technology potentially enables rapid exchange of mRNA to other antigens or T cell activation signals.

<http://dx.doi.org/10.1136/jitc-2021-SITC2021.211>

TUMOR ADJACENT CYTOKINE FACTORIES FOR ERADICATION OF OVARIAN CANCER TUMOR BURDEN IN MICE THROUGH CYTOTOXIC T-CELL ACTIVATION WITH SAFE AND PREDICTABLE DOSING IN NON-HUMAN PRIMATES

¹Amanda Nash*, ¹Maria Jarvis, ¹Samira Aghlara-Fotovat, ¹Sudip Mukherjee, ¹Andrea Hernandez, ¹Andrew Hecht, ²Peter Rios, ²Sofia Ghani, ²Ira Joshi, ²Douglas Isa, ¹Yufei Cui, ¹Shirin Nouraein, ¹Jared Lee, ³Chunyu Xu, ¹David Zhang, ⁴Rahul Sheth, ³Weiji Peng, ²Jose Oberholzer, ¹Oleg Igoshin, ⁴Amir Jazaeri, ¹Omid Veisheh. ¹Rice University, Houston, TX, USA; ²CellTrans Inc, Chicago, IL, USA; ³University of Houston, Houston, TX, USA; ⁴MD Anderson Cancer Center, Houston, TX, USA

Background Pro-inflammatory cytokines have been approved by the FDA for the treatment of metastatic melanoma and renal carcinoma.^{1, 2} However, effective cytokine therapy is limited by its short half-life in circulation and the severe adverse effects associated with high systemic exposure.³ To overcome these limitations, we developed a clinically translatable localized cytokine delivery platform composed of polymer encapsulated epithelial cells that produce localized natural cytokines (IL2, IL7, IL10, or IL12) with temporal regulation.

Methods

Cytokine PK Studies Supernatant from individual capsules were assayed at 1-, 2-, 4-, or 24-hours using ELISA (n=6). **Mouse Studies:** For IP tumor models of ID8-Fluc; 10x10⁶ cells suspended in HBSS were injected in the IP space of female albino C57BL/6 or NU/NU Nude mice (n=4–6). Cytokine factories were implanted 7 days post tumor injection. **Primate Studies:** Increasing doses of cytokine factories were administered to cynomolgus macaques (n=3). Complete blood count and blood chemistry analysis were performed 28 days after administration. **IVIS Imaging:** Mice were injected in the IP space with D-luciferin (300 µg/mL, PerkinElmer). Photographs and luminescent images were acquired 10 minutes after injection. **Flow Cytometry:** All antibodies were commercially obtained and prepared the day of staining. Intracellular staining was performed using the FOXP3/Transcription Factor Staining Buffer Set (Cat. 00-5523-00, eBioscience) and the BD Cytofix/cytoperm fixation/permeabilization solution kit (Cat. 554714, BD Bioscience).

Results Tumor-adjacent local administration of these cytokine factories demonstrated predictable dose modulation with spatial and temporal control and provided ovarian cancer immunotherapy without systemic toxicities. Interestingly, the murine IL2 local concentration (IP space) was greater than 100x higher than the systemic concentration (blood) demonstrating the ability of the platform to deliver native cytokines in vivo and create a high local concentration of cytokines with limited peripheral exposure. A similar concentration differential was seen with IL7, IL10 and IL12. Treatment of peritoneal tumors using IL2 producing cytokine factories provided sustained eradication of peritoneal tumors in an ovarian cancer mouse model. Our data confirmed local increases in the activation (CD25+CD8+) and proliferation (Ki67+CD8+) of cytotoxic T cells within the IP space of cytokine factory treated mice. Significantly, this platform produced local and systemic T cell biomarker profiles that predict efficacy without toxicity in non-human primates.

Conclusions Our findings demonstrate the safety and efficacy of IL2 cytokine factories in preclinical animal models and provide rationale for future clinical testing for the treatment of metastatic peritoneal cancers in humans.

REFERENCES

- 1.. Choudhry H, Helmi N, Abdulaal WH, Zeyadi M, Zamzami MA, Wu W, Mahmoud MM, Warsi MK, Rasool M, Jamal MS. Prospects of IL-2 in cancer immunotherapy. *Biomed Res Int* 2018;(2018): 9056173.
- 2.. McDermott DF, Atkins MB. Interleukin-2 therapy of metastatic renal cell carcinoma—predictors of response. *Semin Oncol* **33**(2006):583–587.
- 3.. Muhlradt PF, Opitz HG. Clearance of interleukin 2 from the blood of normal and T cell-depleted mice. *Eur J Immunol* **12**(1982):983–985.

Ethics Approval All mouse experiments were approved by Rice University's Institution Animal Care and Use Committee (IACUC). All cynomolgus macaque procedures and post-operative care were performed in accordance with the Guidelines for Care and Use of Laboratory Animals of the University of Illinois-Chicago (UIC) and approved by the Institutional Use and Animal Care Committee (IACUC) of UIC.

<http://dx.doi.org/10.1136/jitc-2021-SITC2021.212>

213 AB-X INTEGRATED CIRCUIT T CELLS DEMONSTRATE IMPROVED POTENCY, EXPANSION, AND SPECIFICITY COMPARED TO MSLN CAR T CELLS

Stephen Santoro*, Aaron Cooper, Natalie Bezman, Jun Feng, Kanika Chawla, Jaspal Williams, John Gagnon, Jason Hall, Dina Polyak, Angela Borroughs, Michelle Nguyen, Suchismita Mohanty, Adam Litterman, Jeff Granja, David DeTomaso, Grace Zheng, Jenessa Smith, Drake LeFace, Tarjei Mikkelsen, Susie Jun. *Arsenal Biosciences, South San Francisco, CA, USA*

Background In solid tumors, CAR T cell efficacy is limited by off-tumor toxicity and suppression by the tumor microenvironment (TME). AB-X is an integrated circuit T cell (ICT cell) intended for the treatment of ovarian cancer. AB-X includes a transgene cassette with two functional modules: 1) an "AND" logic gate designed to limit off-tumor toxicity through dual tumor antigen recognition; 2) a dual shRNA-miR to resist TME suppression and improve ICT cell function. The AB-X logic gate consists of a priming receptor that induces expression of an anti-mesothelin (MSLN) CAR upon engagement of a ALPG/P (alkaline phosphatase germ-line/placental). The dual shRNA-miR mediates downregulation of FAS and PTPN2. The AB-X DNA cassette is inserted into the T cell genome at a defined novel genomic site via CRISPR-based gene editing.

Methods Dual-antigen specificity of the logic gate was assessed in mice harboring MSLN+ and ALPG/P+MSLN+ K562 tumors established on contralateral flanks. Potency was measured in a subcutaneous MSTO xenograft model. Logic-gated ICT cells were compared with MSLN CAR T cells in both models. In vitro, expansion of ICT cells with the FAS/PTPN2 shRNA-miR was evaluated in a 14 day repetitive stimulation assay (RSA). In vivo, expansion and potency were measured in the MSTO xenograft model. An in vitro FAS cross-linking assay was conducted to assess the impact of FAS knockdown on FAS-mediated apoptosis.

Results Logic-gated ICT cells demonstrated specific activity against ALPG/P+MSLN+ tumors, but had no effect against MSLN+ tumors in the K562 in vivo specificity model. In addition, logic-gated ICT cells demonstrated greater in vivo potency than MSLN CAR T cells in the MSTO xenograft model. In our RSA, ICT cells containing the FAS/PTPN2 shRNA-miR had 8-fold greater expansion than the MSLN CAR T cells. Enhanced expansion was confirmed in vivo with ICT cells demonstrating >10-fold expansion in tumors and peripheral blood, enabling comparable growth inhibition in MSTO xenografts at less than one quarter the dose of the MSLN CAR T cells. Importantly, PTPN2 knockdown resulted in balanced expansion of all T cell subsets, including CD45RA+, CCR7+ memory cells. Lastly, ICT cells containing the FAS/PTPN2 shRNA-miR were resistant to FAS-mediated apoptosis.

Conclusions AB-X ICT cells specifically recognize ALPG/P+MSLN+ tumors, demonstrate superior potency, expansion, and persistence compared with MSLN CAR T cells, and are resistant to ovarian TME suppression. AB-X will be evaluated in clinical trials for treatment of platinum resistant/refractory ovarian cancer.

Acknowledgements We would like to acknowledge all of our colleagues at Arsenal Biosciences, without whom this work would not have been possible.

<http://dx.doi.org/10.1136/jitc-2021-SITC2021.213>

SIRP α -DEFICIENT MACROPHAGES ACTIVATE POLYCLONAL TISSUE-RESIDENT CYTOTOXIC CD8 T CELLS TO ELIMINATE IRRADIATION-REFRACTORY NON-SMALL CELL LUNG CARCINOMA

Zhen Bian*, Lei Shi, Koby Kidder, Yuan Liu. *Georgia State University, Atlanta, GA, USA*

Background Radiotherapy (RT) is a mainstay treatment for cancer and may not only eliminate irradiated tumors but also induce cytotoxic CD8 T cell immunity to regress abscopal metastases. However, even when combining RT with immunomodulatory agents, adequate immune-mediated tumor elimination is limited, especially when tumors are advanced and highly immunosuppressive. Thus, revealing the mechanisms by which tumors resist RT and resolving methods to enhance RT-induced immunity are needed. SIRP α is a myeloid-expressed receptor that inhibits macrophages from phagocytosing self-cells by interacting with its ligand CD47. Cancers often increase their CD47 to suppress macrophages. Although merely depleting SIRP α -mediated inhibition (SIRP α -deficient) does not elicit phagocytosis, activating SIRP α -deficient macrophages with certain proinflammatory cytokines or TLR agonists enables them to phagocytose cancer cells. Given that macrophages are abundant in solid tumors and often contribute to RT-resistance, we postulated that RT-induced damage in the tumor microenvironment (TME) would stimulate TLRs on SIRP α -deficient macrophages to then phagocytose cancer cells and better control RT-resistant tumors.

Methods Tumors were established by engrafting syngeneic non-small cell lung carcinoma (LLC) into wild-type (WT) or SIRP α -deficient C57BL6 mice. Tumors were allowed to progress to various stages, then mice were treated with tumor-directed RT (4–15Gy). In some cases, RT was combined with intravenous or intratumoral adoptive transfer of macrophages. To compare the therapeutic efficacy of RT plus macrophage transfer, head-to-head studies were conducted using anti-CD47 antibodies or SIRP α -Fc fusion-proteins with cancer-specific antibodies and RT. Flow cytometry, Nanostring RNA sequencing, and several cell function assays were used to analyze responses to treatments.

Results Global knockout of SIRP α in mice sensitizes their otherwise RT-resistant tumors to low-dose RT and achieves up to 100% complete response and 100% overall survival. SIRP α -deficient macrophages are essential to the therapeutic response, as depleting them abrogated efficacy while transferring them recapitulated this efficacy in WT mice. SIRP α -deficient macrophages not only eliminate tumors by phagocytosing cancer cells but more so by conducting in situ antigen presentation to CD8 T cells that are highly cancer-specific and cytotoxic. In addition, RT synergizes with activated SIRP α -deficient macrophages to reprogram the TME into a pro-inflammatory niche infiltrated by cytotoxic NK cells and neutrophils but comprising few CD4 T regulatory cells (Tregs) and myeloid-derived suppressor cells (MDSCs).

Conclusions The results demonstrate that SIRP α predominantly underlies tumor resistance to RT and provide proof-of-principle for SIRP α -deficient macrophage-based therapies to cure lung cancer, including those at advanced stages with poor immunogenicity and metastases.

Acknowledgements The authors thank the Georgia State University Animal Resources Program for assisting many experiments; This work was supported, in part, by grants from National Institutes of Health (CA241271 and AI106839), a Georgia Research Alliance (GRA) Venture Development grant,

a Bioclicity Innovation & Commercialization grant, a Careers in Immunology fellowship from American Association of Immunologist (Z.B.), a Molecular Basis of Disease fellowship from Georgia State University (K.K.) and an Ahmed T. Abde-lal Molecular Genetics and Biotechnology fellowship from Georgia State University (K.K.).

Ethics Approval All experiments using animals and procedures of animal care and handling were carried out following protocols approved by the Institutional Animal Care and Use Committee (IACUC) of Georgia State University.

<http://dx.doi.org/10.1136/jitc-2021-SITC2021.214>

215

TISSUE-RESIDENT NATURAL KILLER CELLS RESEMBLING INTRAEPITHELIAL ILC1 HAVE POTENT ANTI-TUMOR ACTIVITY IN HUMAN HEAD AND NECK CANCER AND REPRESENT A NOVEL CLASS OF EFFECTOR CELLS FOR IMMUNOTHERAPY

June Shin*, Nina Horowitz, Quan Tran, Chen Chen, Uriel Moreno-Nieves, Joshua Tay, Saumyaa Saumyaa, John Sunwoo*. *Stanford University, Stanford, CA, USA*

Background Natural killer (NK) cells comprise a subset of the innate lymphoid cell (ILC) family. Although NK cells have been observed to be present in most solid tumors, their role in the protection against tumor formation in humans has been unclear. Studies have been hampered by the heterogeneity of NK cells within the tumor microenvironment (TME) and lack of information about the broader ILC subsets found in tumors. Further, there is an increasing recognition of plasticity between NK cells and other ILC family members in various disease contexts, calling for a broader examination of ILCs within solid tumors. We previously analyzed the ILC population in primary samples from human head and neck squamous cell carcinoma (HNSCC) and matched blood by single-cell RNA sequencing (scRNA-seq).¹ Those studies revealed that peripheral NK cells differentiate along two divergent trajectories in the TME, resulting in different end-states: one with a hyporesponsive phenotype and another possessing potent anti-tumor activity and resembling intraepithelial ILC1s (ieILC1s).

Methods In vitro co-culture approaches and in vivo mouse models were used to investigate the ability of peripheral NK cells to differentiate into alternate ILC states with heterogeneous functions. Cytotoxicity assays were used to assess functional activity of in vitro derived ieILC1-like cells. Adoptive cell transfer of ieILC1-like cells into tumor-bearing mice was also used to assess anti-tumor function.

Results Peripheral human NK cells could be efficiently differentiated into ieILC1-like cells using an in vitro co-culture system. These ieILC1-like cells had enhanced natural cytotoxicity against target cells compared to conventional IL-15-activated and K562-expanded NK cells. In addition, they infiltrated the TME efficiently and were a more effective means of adoptive cell therapy against HNSCC solid tumor xenografts in vivo compared to conventional NK cells.

Conclusions Our data indicate that peripheral NK cells change cell states within the TME of HNSCC. The heterogeneity in the relative proportion of the cell states may influence host response to tumors. We identified the ieILC1-like cell state to be the phenotype with the most potent anti-tumor activity within the TME. Importantly, this cell state can be induced from peripheral donor NK cells ex vivo for differentiation into and expansion of highly active ieILC1-like cells, providing a platform for a novel class of effector cells for adoptive cell immunotherapy.

Acknowledgements These studies were supported by the Lokey Stem Cell Research Building (SIM1) Flow Cytometry core facility for cell sorting and flow cytometric analysis and the Stanford Cancer Institute Tissue Bank for procurement of tumor samples and blood. This work was supported by funding from the National Institutes of Health (R01CA158516; R35DE030054; U54CA209971) to J.B.S.

REFERENCE

1. Moreno-Nieves UY, Tay JK, Saumyaa S, Shin JH, Horowitz NB, Mohammad IA, Luca B, Mundy DC, Gulati GS, Bedi N, Chang S, Chen C, Kaplan MJ, Rosenthal EL, Holsinger FC, Divi V, Baik FM, Sirjani DB, Gentles AJ, Newman AM, Freud AG, Sunwoo JB. Landscape of ILCs in human head and neck cancer reveals

divergent NK cell states in the tumor microenvironment. *Proc Natl Acad Sci U S A* 2021;118(28):e2101169118.

Ethics Approval The studies reported here were approved by the Stanford Institutional Review Board (IRB 11402) and the Stanford Administrative Panel on Laboratory Animal Care (APLAC 20547).

<http://dx.doi.org/10.1136/jitc-2021-SITC2021.215>

**MULTIPLEX BASE EDITING OF NK CELL TO ENHANCE
CANCER IMMUNOTHERAPY**

Minjing Wang*, Mitchell Kluesner, Patricia Claudio Vázquez, Beau Webber, Branden Moriarity. *University of Minnesota, Minneapolis, MN, USA*

Background Natural killer (NK) cells have many unique features that have gained attention in cancer immunotherapy. NK cells can kill in antigen independent and dependent fashion, can be used as an allogeneic product, and perform antibody-dependent cell-mediated cytotoxicity (ADCC). However, NK cell function is regulated by many activating and inhibitory receptors, which cancer cells take advantage of to avoid being killed by NK cells. NK cells are also known for their technical and biological challenges which result in low editing efficiencies, compared to T cells and other immune cells.

Methods Base editing (BE) is a CRISPR-Cas9 based genome editing technology that allows precise single base transitions. Previously, we reported a high efficiency method for multiplex engineering of T cells using BE and thus reasoned that applying similar concepts in NK cells may offer an opportunity to alter many genes simultaneously at higher efficiency through multiplex base editing. We thus selected a panel of genes bearing critical roles in NK cell function for immunotherapy, including inhibitory intracellular regulator AHR and CISH, inhibitory checkpoint receptor KLRG1, TIGIT, KLRC1, and PDCD1, and Fc receptor CD16A. CD16A is responsible for NK cell ADCC and is regulated via cleavage upon NK activation. Non-cleavable CD16A improves ADCC killing and can be achieved through single-base substitution with BE.

Results Using the adenosine BE (ABE8e), we achieved multiplex editing (6 genes) rates up to 99% and 95% editing/knockout at DNA and protein levels, respectively. Notably, we assessed for reduction in editing efficiency when additional genes were targeted and found no significant reduction in editing efficiencies when targeting up to 6 genes simultaneously. Moreover, functional evaluation of non-cleavable CD16A NK cells revealed up to 35% increase of cytotoxicity against Raji cells.

Conclusions We were able to achieve high multiplex editing efficiency in primary human NK cells using ABE8e and there was no significant decrease of editing efficiency as the number of gene of interest increases, up to 6 genes in total. Functional assay confirmed increased NK cell cytotoxicity against tumor cells. Our end goal is to achieve high efficiency multiplex editing in CAR-expressing NK cells to further improve NK cell activity and toxicity for cancer immunotherapy.

REFERENCE

1. Webber B, Lonetree C, Kluesner M, *et al.* Highly efficient multiplex human T cell engineering without double-strand breaks using Cas9 base editors. *Nat Commun* 2019;**10**:5222.

<http://dx.doi.org/10.1136/jitc-2021-SITC2021.216>

CYTOTOXICITY OF NICOTINAMIDE ENHANCED NATURAL KILLER CELLS GDA201 IS BASED ON METABOLIC MODULATION AS DEMONSTRATED BY ARTIFICIAL INTELLIGENCE ASSISTED ANALYSIS OF NK CELL TRANSCRIPTOME AND METABOLOME

¹Dima Yackoubov*, ¹Aviad Pato, ¹Julia Rifman, ¹Sherri Cohen, ¹Astar Hailu, ¹Nurit Brycman, ¹Orit Berhani-Zipori, ¹Avishay Edri, ²Boaz Buhandler, ²Moshe Shahor, ²Nathan Dinowitz, ²Amram Ben David, ²Avi Izraeli, ³Vered Chalifa-Caspi, ³Liron Levin, ⁴Joshua Rabinowitz, ⁴Wenyun Lu, ¹Tracey Lodie, ¹Julian Adams, ¹Yona Geffen. ¹*Gamida-Cell, Jerusalem, Israel*; ²*Pomicell, Jerusalem, Israel*; ³*NIBN, Beer Sheva, Israel*; ⁴*Princeton, Princeton, NJ, USA*

Background Nicotinamide (NAM), an allosteric inhibitor of NAD-dependent enzymes, has been shown to preserve cell function and prevent differentiation in ex vivo cell culture. GDA-201 is an investigational natural killer (NK) cell immunotherapy derived from allogeneic donors and expanded using IL-15 and NAM. In previous preclinical studies, NAM led to increased homing and cytotoxicity, preserved proliferation, and enhanced tumor reduction of NK cells. In a phase I clinical trial, treatment with GDA-201 showed tolerability and clinical responses in patients with refractory non-Hodgkin lymphoma (NHL) (Bachanova, et. al., *Blood* 134:777, 2019). While NAM is known to affect cellular metabolism and participate in 510 enzymatic reactions –in 66 as an inhibitor or activator– its mechanism of action and role in GDA-201 cytotoxicity is unknown.

Methods In order to define the network of intracellular interactions that leads to the GDA-201 phenotype, flow-cytometry, next generation sequencing (NGS), and liquid chromatography–mass spectrometry (LC-MS)-based metabolite quantification were performed on NK cells cultured for 14 days with IL-15 and human serum in the presence or absence of NAM (7 mM). Artificial Intelligence (AI) machine learning analysis was applied by Pomicell in order to analyze the data using the Pomicell databases supporting data extracted from multiple origins including scientific articles organized using natural language processing tools. AI training was done using a combined algorithm designed to blindly explain and predict the transcriptomic and metabolomic (omics) profile.

Results Omics analyses defined 1,204 differentially expressed genes, and 100 significantly modified metabolites in the presence of NAM. An in silico model was created that successfully predicted the experimental data in 83% of the cases. Upregulation of TIM-3 expression in GDA-201 was predicted to be mediated by inhibition of IL-10 and SIRT3, via CREB1/HLA-G signaling and adrenoceptor beta 2 (ADRB2) upregulation. Adenosine metabolite reduction supports this and suggests dopaminergic activation of NK cytotoxicity. Upregulation of CD62L in the presence of NAM was predicted to be mediated by transcription factor Dp-1 (TFDP1) via dihydrofolate reductase (DHFR) activation and intracellular folic acid reduction. Interferon-gamma and CASP3 modulation (via JUN and MCL1, respectively), via PPARa inhibition, support that finding.

Conclusions In conclusion, AI machine learning of transcriptome and metabolome data revealed multiple pleiotropic metabolic pathways modulated by NAM. These data serve to further elucidate the mechanism by which NAM enhances cell function, leading to the observed cytotoxicity and potency of GDA-201.

Ethics Approval We hereby declare that the collection of the Apheresis units in the three participating institutes (sites) has been done under an approved clinical study that meets the

following requirements:1. Ethics approval has been obtained from the local EC at each of the sites, prior to any study related activities.2. The working procedures of the EC at the sites for conduct of clinical studies are in due compliance with local regulations (Israeli Ministry of Health) and provisions of Harmonized International Guidelines for Good Clinical Practice, namely: ICH-GCP3. Sites follow EC conditions & requirements in terms of submissions, notifications, and approval renewals. 4. Participants gave Informed Consent (approved by the EC) before taking part in the study.5. Informed Consent has been approved by the ECs. The Israeli template of Informed Consent is in used and it includes study specific information (e.g. study goal, design, method, duration, risks, etc.). Name of the Institute Name of the EC/IRB EC Study No.Hadassah Medical Center Helsinki Committee 0483-16-HMORambam Health Care Campus Helsinki Committee 0641-18-RMBIChilov Sourasky Medical Center Tel-Aviv Helsinki Committee 0025-17-TLV

<http://dx.doi.org/10.1136/jitc-2021-SITC2021.217>

AUTOLOGOUS GLIOBLASTOMA TUMOR CELLS AND AN ANTISENSE OLIGONUCLEOTIDE AGAINST INSULIN-LIKE GROWTH FACTOR TYPE 1 RECEPTOR PROTECT AGAINST TUMOR CHALLENGE AND GENERATE T CELL ANTI-TUMOR RESPONSES

¹Jenny Zilberberg, ¹Amelia Zellander, ¹Kenneth Kirby, ¹Christopher Uhl, ¹Christopher Cultrara, ²Charles Scott, ¹David Andrews, ¹Mark Exley*. ¹Imvax, Philadelphia, PA, USA; ²CBS squared Inc., Philadelphia, PA, USA

Background IGV-001 is a novel immunotherapy that combines irradiated, patient-derived glioblastoma tumor cells and an antisense oligonucleotide against insulin-like growth factor type 1 receptor (IMV-001) in biodiffusion chambers (0.1-micron pore size). We recently evaluated IGV-001 in patients with newly diagnosed glioblastoma.¹ In a subgroup of IGV-001-treated, Stupp-eligible patients² with methylated O6-methylguanine–DNA methyl-transferase (MGMT) promoter, median progression free survival was 38.4 months¹ compared with 8.3 months in historical standard-of-care-treated patients ($p=0.0008$).² We utilized the GL261-Luciferase (-Luc) glioblastoma orthotopic murine model and conducted in vitro immunological assays using patient-derived GBM tumor cells and matched peripheral blood mononuclear cells (PBMC) to unravel the potential mechanisms associated with the activity of IGV-001.

Methods Biodiffusion chambers containing phosphate-buffered saline (PBS) alone or IGV-001 prepared with 1×10^6 GL261-Luc cells were implanted in the flanks of C57BL/6 albino mice and explanted 48 hours later, as per the clinical protocol. GL261-Luc intracranial tumor challenge was conducted 28 days after chamber implantation. Mice were monitored for survival and tumor growth, as determined by bioluminescence intensity (BLI). For in vitro experiments, IGV-001 prepared with patient tumor cells were co-cultured with patient-derived PBMC to evaluate activated and memory T cell subsets and responses. To elucidate the immunostimulatory underpinnings of IGV-001, ATP release assay was conducted as a surrogate measure of immunogenic cell death.

Results 59% of IGV-001 treated mice were alive and continued to gain weight at the termination of the study, 58 days post-intracranial tumor challenge. In comparison, there were no survivors in the PBS group by day 24 ($p<0.001$). Fluorospot assays demonstrated enhanced T cell IFN-gamma responses to tumor cell antigens. In IGV-001 treated mice, serum IL-6 was positively correlated with BLI, meaning that treated mice with lower BLI signal had less circulating IL-6 ($p<0.01$). Fluorospot assays demonstrated enhanced T cell IFN-gamma responses to tumor cell antigens. Tumor co-culture studies showed elevated percentage of activated CD4 and CD8 T cells as well as increased central and effector memory phenotypes in both T cell subsets compared to IMV-001-treated PBMC controls. Lastly, tumor cells treated with IMV-001 released significantly more ($p<0.01$) ATP than untreated or sense oligonucleotide-treated controls.

Conclusions These data support the antitumor activity of IGV-001 in newly diagnosed glioblastoma, as evidenced in the phase 1 study. Th1 anti-tumor T cell activity was demonstrated. The ATP results suggest a possible immunogenic conversion by which IGV-001 stimulates the immune system and suppresses tumor growth, which can be quantified via circulating IL-6.

REFERENCES

- Andrews DW, Judy KD, Scott CB, Garcia S, Harshyne LA, Kenyon L, Talekar K, Flanders A, Atsina KB, Kim L, Martinez N, Shi W, Werner-Wasik M, Liu H, Prosniak M, Curtis M, Kean R, Ye DY, Bongiorno E, Sauma S, Exley MA, Pigott K, Hooper DC. Phase Ib clinical trial of IGV-001 for patients with newly diagnosed glioblastoma. *Clin Cancer Res* 2021 April 1;**27**(7):1912–1922. doi: 10.1158/1078-0432.CCR-20-3805. Epub 2021 Jan 26. PMID: 33500356.
- Stupp R, Mason WP, van den Bent MJ, Weller M, Fisher B, Taphoorn MJ, Belanger K, Brandes AA, Marosi C, Bogdahn U, Curschmann J, Janzer RC, Ludwin SK, Gorlia T, Allgeier A, Lacombe D, Cairncross JG, Eisenhauer E, Mirimanoff RO, European Organisation for Research and Treatment of Cancer Brain Tumor and Radiotherapy Groups, National Cancer Institute of Canada Clinical Trials Group. Radiotherapy plus concomitant and adjuvant temozolomide for glioblastoma. *N Engl J Med* 2005 March 10;**352**(10):987–96. doi: 10.1056/NEJMoa043330. PMID: 15758009.

Ethics Approval Ethical consent was obtained for all human biospecimens with the appropriate IRB approval.

Consent Informed consent was obtained for all human biospecimens with the appropriate IRB approval.

<http://dx.doi.org/10.1136/jitc-2021-SITC2021.218>

CD47 AND PHOSPHATIDYLSERINE CONTRIBUTE TO THE INTERACTION BETWEEN ANTIGEN PRESENTING CELLS AND THE ALLOGENEIC CELL-BASED RELAPSE VACCINE DCP-001

¹Haoxiao Zuo, ¹Satwinder Kaur Singh*, ¹Marie-José Van Lierop, ¹Jorn Kaspers, ¹Remco Bos, ²Alwin Kamerlings, ²Helga E de Vries, ²Tanja de Gruijl, ¹Ada Kruisbeek, ¹Erik Manting, ¹Satwinder Kaur Singh. ¹Immunicum AB, Leiden, Netherlands; ²Amsterdam University Medical Center, Amsterdam, Netherlands

Background DCP-001 is a cancer relapse vaccine derived from the DCOne[®] human leukemic cell line. During manufacturing, DCOne[®] cells are shifted towards a mature dendritic cell (mDC) phenotype, combining an endogenous tumor antigen repertoire (e.g. WT-1, RHAMM and PRAME) with a mDC costimulatory profile and providing the basis for the highly immunogenic vaccine DCP-001. In a phase I clinical study in acute myeloid leukemia (AML), DCP-001 demonstrated to be safe and to induce multifunctional antitumor immune responses.¹ It has also been reported that DCP-001 induces antitumor immunity against multiple myeloma cells in peripheral blood mononuclear cells (PBMC) from multiple myeloma patients and that DCP-001 antigenic material is transferred to host antigen presenting cells (APC), possibly via extracellular vesicles.² However, the possibility of direct interactions between DCP-001 and host APC has not yet been investigated.

Methods To further elucidate the mode of action of DCP-001, we studied the interactions of DCP-001 with human PBMC and isolated immature monocyte-derived DCs (iMoDC) in in vitro co-culture studies. A human skin explant model was used to determine uptake of DCP-001 by migrating skin DCs after intradermal injection.

Results We found that DCP-001 stimulates the secretion of various proinflammatory cytokines (IL-1 β , GM-CSF, IFN- γ , IL-2, TNF- α , and IL-6) and chemokines (IL-8 and RANTES) in PBMC. In addition, we demonstrate that DCP-001 is efficiently taken up by iMoDC via direct cell-cell interactions and that this phagocytic process is influenced by "eat-me" and "don't eat me" signaling pathways. Blocking of the "eat-me" signals calreticulin and phosphatidylserine inhibited the uptake of DCP-001, whereas blockade of the "don't eat me" signal CD47 enhanced DCP-001 uptake. After intradermal injection of DCP-001 in an ex-vivo human skin model, its uptake by skin-emigrating DCs was demonstrated as well as simultaneous activation of these DCs.

Conclusions Our data suggest a key role for host antigen presenting cells in the triggering of immune responses upon DCP-001 vaccination. In addition, the data provide rationale for potential combination therapies based on DCP-001 and inhibitors of the CD47 pathway.

REFERENCES

1. van de Loosdrecht AA, et al. A novel allogeneic off-the-shelf dendritic cell vaccine for post-remission treatment of elderly patients with acute myeloid leukemia. *Cancer Immunol Immunother* 2018;**67**(10):1505–1518.
2. Leaf RK, et al. DCOne as an allogeneic cell-based vaccine for multiple myeloma. *J Immunother* 2017;**40**(9):315–322.

<http://dx.doi.org/10.1136/jitc-2021-SITC2021.219>

TRANSFECTION OF HUMAN ADIPOSE-DERIVED MAST CELLS: A CHARACTERISTIC STUDY USING DIFFERENT CHEMICAL REAGENTS

¹Mona Motaghd*, ²Christopher Kepley, ¹Kristen Dellinger, ²Mohammad Fereydouni, ¹Elnaz Ahani. ¹North Carolina AandT State University, Greensboro, NC, USA; ²The University of North Carolina at Greensboro (UNCG), Greensboro, NC, USA

Background Mast cells are essential initiators and regulators in both innate and adaptive immunity in addition to being mediators of Type I hypersensitivity. Their role in cancer pathogenesis has been challenging to assess, given they contain both pro- and anti-tumorigenic mediators. Thus, to elucidate the functions of mast cell-derived gene products in cancer pathogenesis and mast cell differentiation, it is critical to study them by comparing their functional responses between those with selected gene knockdown and those without. However, primary human mast cells are known as hard-to-transfect cells and a fast and efficient method for transient transfection of primary human adipose mast cells has not been reported.

Methods We investigated different approaches to transfect primary human adipose-derived mast cells from 10 donors (24 - 55 yrs.). Three cationic lipid nanoparticles (Metafectene and Metafectene-Pro, Biontex Laboratories, and Lipofectamine 3000, Thermo Fisher), one lipid/histone-based nanoparticle (Turbofectin 8.0, OriGene), and two non-liposomal polymeric reagents (TransIT-LT1 and TransIT-2020, MirusBio) were evaluated in conjunction with green fluorescent protein (GFP)-tagged genes (e.g., tryptase) at different ratios of DNA plasmid to the reagent. The functional and phenotypic responses of the mast cells were compared to non-transfected mast cells.

Results We found that transfection of primary human adipose mast cells is highly donor-dependent. Parameters that affect transfection efficiency include donor age, stem cell isolation procedure, in vitro age of mast cells at the time of transfection, the type and dosage of the transfection reagent, incubation time, presence of antibiotics, and serum content. The transfection rate efficiencies of human mast cells using lipid synthetic nanoparticles was higher than the lipid/histone-based and non-liposomal polymeric reagents. The maximum Median Fluorescence Intensity (MFI) fold change compared to the non-transfected mast cells was about 17 for the youngest donor that was transfected 7 to 10 weeks after isolation using Metafectene-Pro.

Conclusions In general, older donor mast cells and mast cell progenitors were less susceptible to transfection. Also, a higher transfection rate is accompanied by increased cytotoxicity, so the analysis of various transfection conditions limiting cell death was the primary goal. Metafectene-Pro significantly increased GFP reporter gene expression compared to the other reagents. The transfected mast cells were phenotypically and functionally similar to non-transfected cells and were viable compared to control mast cells from the same donors. These studies will aid in determining if mast cell mediators have pro- or anti-tumor cell effects to help define the role these cells have in cancer pathogenesis.

Ethics Approval This study was approved by UNCG IRB, approval number 12-099, and under the NIH-defined "exempt" status for human subjects research.

<http://dx.doi.org/10.1136/jitc-2021-SITC2021.220>

CRISPR SCREEN IDENTIFIES LOSS OF IFN γ R SIGNALING AND DOWNSTREAM ADHESION AS A RESISTANCE MECHANISM TO CAR T-CELL CYTOTOXICITY IN SOLID BUT NOT LIQUID TUMORS

¹Rebecca Larson*, ²Michael Kann, ²Stefanie Bailey, ³Nicholas Haradhvala, ³Kai Stewart, ²Amanda Bouffard, ²Irene Scarfo, ²Mark Leick, ²Trisha Berger, ²Max Jan, ³Julia Joung, ³Tamara Ouspenskaia, ³Travis Law, ³Aviv Regev, ¹Gad Getz, ¹Marcela Maus. ¹Harvard University, Cambridge, MA, USA; ²Massachusetts General Hospital, Boston, MA, USA; ³Massachusetts General Hospital, Boston, MA, USA; ³Broad Institute of MIT and Harvard, Cambridge, MA, USA

Background Chimeric Antigen Receptor (CAR) therapy has had a transformative impact on the treatment of hematologic malignancies^{1–6} but success in solid tumors remains elusive. We hypothesized solid tumors have cell-intrinsic resistance mechanisms to CAR T-cell cytotoxicity.

Methods To systematically identify resistance pathways, we conducted a genome-wide CRISPR knockout screen in glioblastoma cells, a disease where CAR T-cells have had limited efficacy.^{7–8} We utilized the glioblastoma cell line U87 and targeted endogenously expressed EGFR with CAR T-cells generated from 6 normal donors for the screen. We validated findings in vitro and in vivo across a variety of human tumors and CAR T-cell antigens.

Results Loss of genes in the interferon gamma receptor (IFN γ R) signaling pathway (IFN γ R1, JAK1, JAK2) rendered U87 cells resistant to CAR T-cell killing in vitro. IFN γ R1 knockout tumors also showed resistance to CAR T cell treatment in vivo in a second glioblastoma line U251 in an orthotopic model. This phenomenon was irrespective of CAR target as we also observed resistance with IL13R α 2 CAR T-cells. In addition, resistance to CAR T-cell cytotoxicity through loss of IFN γ R1 applied more broadly to solid tumors as pancreatic cell lines targeted with either Mesothelin or EGFR CAR T-cells also showed resistance. However, loss of IFN γ R signaling did not impact sensitivity of liquid tumor lines (leukemia, lymphoma or multiple myeloma) to CAR T-cells in vitro or in an orthotopic model of leukemia treated with CD19 CAR. We isolated the effects of decreased cytotoxicity of IFN γ R1 knockout glioblastoma tumors to be cancer-cell intrinsic because CAR T-cells had no observable differences in proliferation, activation (CD69 and LFA-1), or degranulation (CD107a) when exposed to wildtype versus knockout tumors. Using transcriptional profiling, we determined that glioblastoma cells lacking IFN γ R1 had lower upregulation of cell adhesion pathways compared to wildtype glioblastoma cells after exposure to CAR T-cells. We found that loss of IFN γ R1 reduced CAR T-cell binding avidity to glioblastoma.

Conclusions The critical role of IFN γ R signaling for susceptibility of solid tumors to CAR T-cells is surprising given that CAR T-cells do not require traditional antigen-presentation pathways. Instead, in glioblastoma tumors, IFN γ R signaling was required for sufficient adhesion of CAR T-cells to mediate productive cytotoxicity. Our work demonstrates that liquid and solid tumors differ in their interactions with CAR T-cells and suggests that enhancing T-cell/tumor interactions may yield improved responses in solid tumors.

Acknowledgements RCL was supported by T32 GM007306, T32 AI007529, and the Richard N. Cross Fund. ML was supported by T32 2T32CA071345-21A1. SRB was supported by T32CA009216-38. NJH was supported by the Landry Cancer Biology Fellowship. JJ is supported by a NIH F31 fellowship (1F31-MH117886). GG was partially funded by the Paul C. Zamecnik Chair in Oncology at the Massachusetts General

Hospital Cancer Center and NIH R01CA 252940. MVM and this work is supported by the Damon Runyon Cancer Research Foundation, Stand Up to Cancer, NIH R01CA 252940, R01CA238268, and R01CA249062.

REFERENCES

- Maude SL, et al. Tisagenlecleucel in children and young adults with B-cell lymphoblastic leukemia. *N Engl J Med* 2018;**378**:439–448.
- Neelapu SS, et al. Axicabtagene ciloleucel CAR T-cell therapy in refractory large B-cell lymphoma. *N Engl J Med* 2017;**377**:2531–2544.
- Locke FL, et al. Long-term safety and activity of axicabtagene ciloleucel in refractory large B-cell lymphoma (ZUMA-1): a single-arm, multicentre, phase 1–2 trial. *The Lancet Oncology* 2019;**20**:31–42.
- Schuster SJ, et al. Chimeric antigen receptor T cells in refractory B-cell lymphomas. *N Engl J Med* 2017;**377**:2545–2554.
- Wang M, et al. KTE-X19 CAR T-cell therapy in relapsed or refractory mantle-cell lymphoma. *N Engl J Med* 2020;**382**:1331–1342.
- Cohen AD, et al. B cell maturation antigen-specific CAR T cells are clinically active in multiple myeloma. *J Clin Invest* 2019;**129**:2210–2221.
- Bagley SJ, et al. CAR T-cell therapy for glioblastoma: recent clinical advances and future challenges. *Neuro-oncology* 2018;**20**:1429–1438.
- Choi BD, et al. Engineering chimeric antigen receptor T cells to treat glioblastoma. *J Target Ther Cancer* 2017;**6**:22–25.

Ethics Approval All human samples were obtained with informed consent and following institutional guidelines under protocols approved by the Institutional Review Boards (IRBs) at the Massachusetts General Hospital (2016P001219). Animal work was performed according to protocols approved by the Institutional Animal Care and Use Committee (IACUC) (2015N000218 and 2020N000114).

<http://dx.doi.org/10.1136/jitc-2021-SITC2021.221>

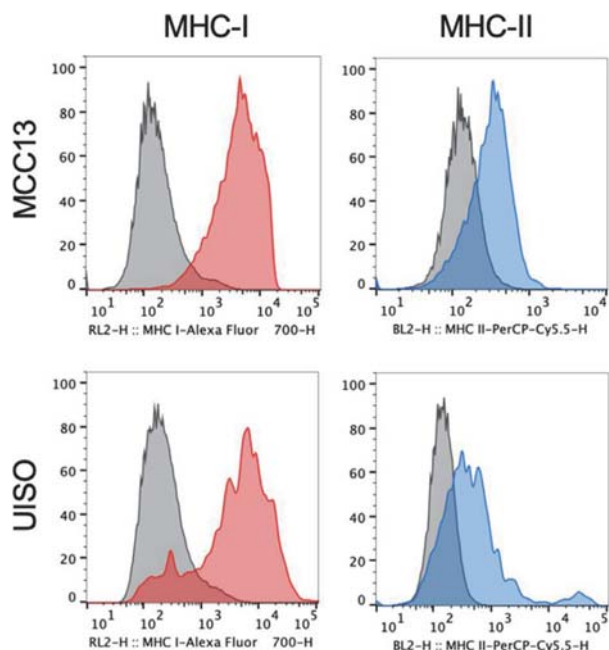
222

GENETIC REPROGRAMMING OF MERKEL CELL CARCINOMA AND MELANOMA LEADS TO INCREASED MHC-I EXPRESSION AND ANTITUMOR IMMUNE ACTIVATION IN VITRO AND IN VIVO

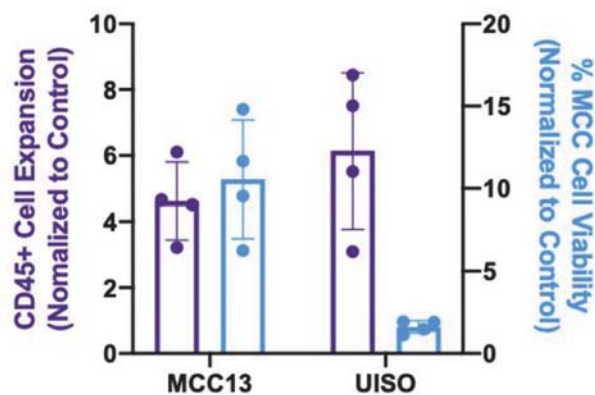
Kathryn Luly*, Jordan Green, Stephany Tzeng, Joel Sunshine. *Johns Hopkins University, Baltimore, MD, USA*

Background Merkel cell carcinoma (MCC) is a rare skin cancer with 46% disease-associated mortality and half of patients unresponsive to immune checkpoint inhibitors.^{1 2} MCC and melanomas often display decreased MHC class I (MHC-I) expression on the surface of cells, which prevents antigen recognition by T cells ("signal 1") and hampers immune activation. We therefore sought to genetically reprogram cells to express their own costimulatory molecules ("signal 2") and immunostimulatory cytokines ("signal 3") to increase MHC-I expression and drive a targeted immune response.

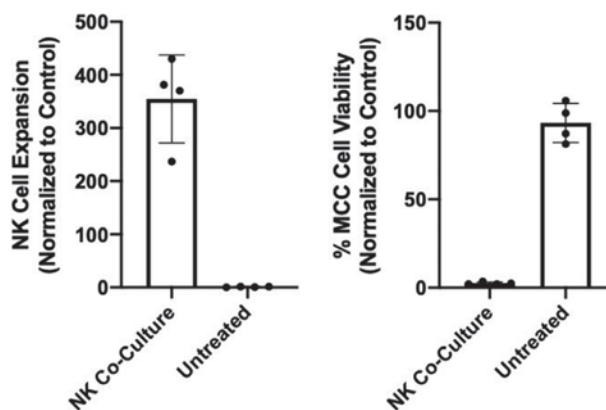
Methods We used biodegradable poly(beta-amino ester) nanoparticles (NPs) to co-deliver plasmids encoding a signal 2 molecule (4-1BBL) and two signal 3 molecules (IL-12 and IFN γ) to cancer cells. For in vitro evaluation of NPs we used two patient-derived MCC cell lines with low baseline MHC-I expression; MCC13 and UI50. Co-culture experiments were performed with human PBMCs or primary human natural killer (NK) cells. All in vitro analysis was performed 7 days following PBMC or NK cell addition. For in vivo evaluation, subcutaneous B16F10 mouse melanoma tumors were implanted in C57BL/6J mice and NPs were administered by direct injection into the tumor with and without intraperitoneal injection of α PD1. Tumors were harvested for analysis on day 16.



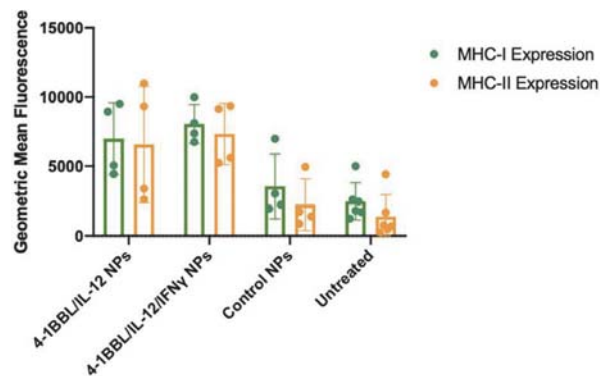
Abstract 222 Figure 1 Administration of signal 2/3 NPs to MCC13 and UI50 cells led to increases in MHC-I and MHC-II expression after 7 days. MHC-I expression in transfected cells (red) and MHC-II expression in transfected cells (blue) compared to untreated control (black)



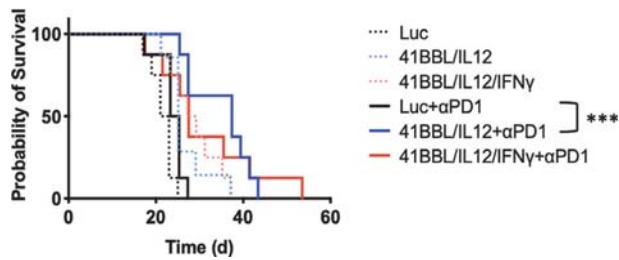
Abstract 222 Figure 2 Co-culture of transfected MCC cells with human PBMCs led to increases in CD45+ cells and reduced MCC cell viability after 7 days



Abstract 222 Figure 3 Co-culture of 4-1BBL/IL-12 transfected MCC13 cells with isolated CD56+ NK cells demonstrated robust NK-cell expansion and low MCC cell viability after 7 days



Abstract 222 Figure 4 Direct intratumoral injection with signal 2 and 3 NPs led to increases in MHC-I and MHC-II in cancer cells in vivo.



Abstract 222 Figure 5 NPs were administered intratumorally \pm intraperitoneal α PD1 on day 9, 11, and 13 following B16F10 melanoma tumor implantation. 4-1BBL/IL12 particles in combination with α PD1 demonstrated a significant improvement in survival compared to control particles (Luc) with α PD1 ($p=0.0010$)

Results Transfection with particles delivering the three plasmids to MCC13 and UI50 increased MHC-I expression (mean fluorescence intensity) 1.6- and 5.0-fold, respectively, and MHC-II expression increased 1.6- and 6.3-fold, respectively (figure 1). In co-culture with human PBMCs, signal 2/3 particles resulted in increased leukocyte proliferation (4.6- and 6.1-fold increase, respectively) and led to significantly reduced MCC viability (10.6 and 1.6% vs control particles)(figure 2). When MCC13 cells were co-cultured with primary human NK cells, NK cell expansion increased 355-fold with 4-1BBL/IL-12 particles compared to control particles and was accompanied by 2.5% MCC13 cell viability, indicating a potent innate immune response with signal 2/3 NP administration in vitro (figure 3). Following evaluation of NPs in vivo, assessment of MHC-I and MHC-II expression in the melanoma tumors found increased expression with signal 2/3 NPs compared to control NPs (figure 4). When signal 2/3 NPs were administered in combination with α PD1 treatment, 4-1BBL/IL-12 NPs with α PD1 demonstrated improved survival compared to α PD1 treatment with control NPs ($p=0.0010$) (figure 5).

Conclusions Together, these results show the ability of signal 2/3 NPs to reprogram MCC and melanoma cells, leading to increased MHC-I expression in vitro and in vivo, eliciting a productive immune response against cancer cells.

REFERENCES

- 1.. Hughes MP, Hardee ME, Cornelius LA, Hutchins LF, Becker JC, Gao L. Merkel cell carcinoma: epidemiology, target, and therapy. *Curr Dermatol* 2014;46–53.
- 2.. Nghiem PT, Bhatia S, Lipson EJ, Kudchadkar RR, Miller NJ, Annamalai L, Berry S, Chertash EK, Daud A, Fling SP, Friedlander PA, Kluger HM, Kohrt HE, Lundgren L, Margolin K, Mitchell A, Olencki T, Pardoll DM, Reddy SA, Shantha EM, Sharfman WH, Sharon E, Shemanski LR, Shinohara MM, Sunshine JC, Taube JM, Thompson JA, Townson SM, Yearley JH, Topalian SL, Cheever MA. PD-1 blockade with pembrolizumab in advanced merkel-cell carcinoma. *N Engl J Med* 2016;**374**:2542–2552.

<http://dx.doi.org/10.1136/jitc-2021-SITC2021.222>

223

POTENT INHIBITION OF PI3K δ PROMOTES ENHANCED T CELL STEMNESS AND MITOCHONDRIAL FITNESS

¹Guillermo Rangel Rivera*, ¹Connor Dwyer, ¹Hannah Knochelmann, ¹Aubrey Smith, ²Anna Cole, ²Megan Wyatt, ²Brandon Ware, ²Chrystal Paulos. ¹Medical University of South Carolina, Atlanta, GA, USA; ²Emory University, Atlanta, GA, USA

Background Durable responses have been observed with adoptive T cell therapy (ACT) in chemotherapy and immunotherapy refractory patients. However, current T cell products do not always lead to therapeutic responses. Therapy failure has been attributed to terminally-differentiated T cell profiles, diminished host engraftment and poor mitochondrial metabolism. T cell activation and a switch towards glycolysis is regulated by signals downstream of the PI3K signaling pathway. We hypothesized that by inhibiting the T cell specific PI3K δ subunit, that we would prevent overt T cell differentiation, enhance mitochondrial metabolism and improve anti-tumor immunity of adoptively transferred T cells.

Methods To test this, we primed melanoma-specific CD8+ pmel-1 T cells in the presence of increasing concentrations of CAL-101, a PI3K δ specific inhibitor, and infused them into B16F10 tumor-bearing mice, following non-myeloablative total body irradiation. In vitro we tested how PI3K δ inhibition altered T cell stemness features by flow cytometry and RNA sequencing. Further, we tested the ability of PI3K δ inhibited T cells to survive against antigen rechallenge, and assessed how mitochondrial phenotypes changed using dyes indicating mass, membrane potential and reactive oxygen species. Moreover, we tested how real time mitochondrial respiration was changed with PI3K δ inhibition via Seahorse.

Results Potent inhibition of PI3K δ in vitro enhanced tumor immunity and survival in a dose dependent manner. High doses of CAL-101 enriched T cells with phenotypic and transcriptional signatures of stemness. We found that CAL-101 decreased glucose uptake and increased mitochondrial mass and membrane potential while reducing mitochondrial reactive oxygen species. Potent inhibition of PI3K δ enhanced mitochondrial respiration, however gene expression of fatty acid oxidation was not enriched, suggesting an alternative pathway involved in the enhanced spare respiratory capacity of CAL-101 treated T cells.

Conclusions These findings indicate that blocking PI3K δ is sufficient to mediate lasting tumor immunity of adoptively transferred T cells by preserving stemness features and improving mitochondrial fitness. Our data suggest that addition of CAL-101 to ACT expansion protocols could greatly improve responses to solid tumors by rewiring T cell stemness and promoting mitochondrial fitness.

Acknowledgements We would like to thank all the researchers and clinicians leading the way in translating immunological principles into effective therapies, as well as the patients whose support is integral for the furthering of medicine.

Ethics Approval All animal procedures performed at the Medical University of South Carolina or Emory University were approved by each university's Institutional Animal Care & Use Committee, protocol number 0488 or 201900225, respectively

<http://dx.doi.org/10.1136/jitc-2021-SITC2021.223>

M2 MACROPHAGE-MEDIATED IMMUNE SUPPRESSION OF CHIMERIC ANTIGEN RECEPTOR T CELLS VIA PD-L1 SIGNALING IN PROSTATE CANCER

Yukiko Yamaguchi*, Jackson Gibson, Kevin Ou, Saul Priceman. *City of Hope National Medical Center, Duarte, CA, USA*

Background The immune suppressive tumor microenvironment (TME) that inhibits T cell infiltration, survival, and anti-tumor activity has posed a major challenge for developing effective immunotherapies for solid tumors. Chimeric antigen receptor T cell therapy has shown unprecedented clinical response in treating patients with hematological malignancies, and intense investigation is underway to achieve similar responses with solid tumors. Immunologically cold tumors, including prostate cancers, are often infiltrated with abundant macrophages, and infiltration of M2 macrophages correlates with metastasis and poor prognosis.

Methods To model this in vitro, we utilized a novel co-culture system with tumor cells, prostate stem cell antigen (PSCA)-directed CAR T cells, and polarized macrophages. To investigate the TME in vivo, we took advantage of "humanized" MISTRG mice, which are immunocompromised mice with knocked-in human genes that support human hematopoiesis and efficient tumor-infiltration of myeloid cell populations. Humanized MISTRG mice were intratibially engrafted with LAPC9 tumor cells to model bone metastatic disease.

Results We observed significant hampering of PSCA-CAR T cell activity in vitro with the presence of M2 macrophages, but not M1 macrophages, coinciding with a robust induction of PD-L1 in both tumor cells and macrophages. We also observed PD-L1 expression in tumor-associated macrophages infiltrating tumors following PSCA-CAR T cell therapy in the humanized mice. Anti-PD-L1 monoclonal antibodies in combination with CAR-T cell therapy altered phenotype and survival of M2 macrophages, resulting in improved anti-tumor activity of PSCA-CAR T cells in the presence of M2 macrophages.

Conclusions Recently, immune checkpoint (IC) blockade (ICB) has been utilized in combination with chimeric antigen receptor (CAR) T cell therapy, with the notion that induction of immune responses with CAR T cells may instigate checkpoint pathways in immunologically cold tumors that would otherwise not respond to ICB. This study gives insights to a mechanism by which CAR T cells and ICB work in synergy to modulate immune landscape of immunologically cold tumors, and our ongoing studies will continue to elucidate the TME-mediated immunosuppression of CAR T cell therapy.

<http://dx.doi.org/10.1136/jitc-2021-SITC2021.224>

225

OPTIMAL-AFFINITY MAGE-A1-SPECIFIC T CELL RECEPTORS (TCRS) GENERATED USING THE HUMANIZED TCR-TRANSGENIC MOUSE PLATFORM HUTCR ARE SUPERIOR TO HUMAN DONOR-DERIVED TCRS

¹Ioannis Gavvovidis*, ²Matthias Leisegang, ¹Vivian Scheuplein, ²Matthias Obenaus, ³Thomas Blankenstein, ¹Elisa Kieback. ¹T-knife GmbH, Berlin, Germany; ²Charité – Universitätsmedizin Berlin, Berlin, Germany; ³Max Delbrück Center for Molecular Medicine, Berlin, Germany

Background As cancer-testis antigens are self-antigens, T cells expressing high-affinity TCRs against such antigens are eliminated via negative selection. Therefore, human-derived TCRs are typically of low affinity and exhibit reduced anti-tumor activity. Affinity maturation by mutagenesis is a common tool to increase affinity but may result in reduced specificity and off-target toxicity. Using our proprietary HuTCR mouse platform, which consists of mouse lines carrying the full human TCR- α/β loci and human HLA alleles, we have isolated naturally optimized high-affinity TCRs specific for the cancer-testis antigen MAGE-A1 and compared them in vitro and in vivo to human-derived MAGE-A1-specific TCRs that are currently reported to be in clinical development.

Methods MAGE-A1-specific TCRs were isolated from HuTCR mice immunized with the MAGE-1 antigen using scRNAseq or were synthesized based on publicly available databases of human donor-derived MAGE-A1-specific TCRs. All TCRs were re-expressed in primary human T cells as verified using peptide-MHC-multimer staining. Functional activity of the TCRs was analyzed by coculture with T2 target cells loaded with titrated amounts of epitope and measuring cytokine concentration by ELISA. Reactivity of TCRs to endogenously processed MAGE-A1 protein was assessed by coculture with tumor cell lines with variable MAGE-A1 and/or MHC-class-I expression. Tumor rejection potential of TCRs was evaluated in vivo using a syngeneic mouse model (TNA2 mice) expressing MAGE-A1 and HLA-A*02 on syngeneic tumor cells.

Results Immunization of HuTCR mice with the MAGE-A1 antigen resulted in robust CD8+ T cell responses and several TCR clonotypes were identified by scRNAseq, with the majority of clonotypes being specific to the MAGE-A1-derived peptide KVLEYVIKV and TCR functional avidities ranging from 0.3nM to 3nM. In sharp contrast, human-derived TCRs of the same epitope specificity exhibited lower functional avidity with EC50 from 3nM to 60nM. In addition, HuTCR-mouse-derived TCRs were more sensitive in recognition of tumor cells expressing low MAGE-A1 and/or MHC-class-I. Adoptive T-cell transfer to TNA2-mice with established tumors resulted in complete rejection without relapse of tumors only in mice treated with HuTCR-mouse-derived TCR but not with human-derived or control TCRs.

Conclusions The HuTCR mouse platform allows for the generation of high-affinity MAGE-A1-specific human TCRs with increased anti-tumor efficacy as compared to human-derived TCRs against the same cancer antigen. The in vitro and in vivo comparative data presented herein highlight the HuTCR-derived MAGE-A1-specific TCR as the most favorable candidate for clinical translation and a clinical trial evaluating its safety and efficacy in a variety of solid malignancies will be initiated November 2021.

Ethics Approval All animal experiments were performed according to institutional and national guidelines, after approval by the responsible authority (Landesamt für Gesundheit und Soziales, Berlin). Blood collection from healthy human

donors was done after prior informed consent and experiments were conducted in accordance with the ethical standards of Declaration of Helsinki.

<http://dx.doi.org/10.1136/jitc-2021-SITC2021.225>

NEOANTIGEN-SPECIFIC TCR-T CELLS TARGETING SHARED HOTSPOT MUTATIONS FOR ADOPTIVE CELL THERAPY IN COMMON EPITHELIAL CANCERS

Ana Korngold, Lin-Kin Yong*, Ugochi Ibekwe, Julissa Simmons, Phillip Eckels, Elizabeth Figueroa, Michelle Hotard, Frances Adeyemi, Thomas Hunt, Tegan Markus, Lenka Hurton, Yaoyao Shi, Matthew Collinson-Pautz, Priya Balasubramanian, Cathy Wang, Jourdan Andersson, Lauren Heese, Mariam Khalil, David Torres, Emarco Olivares, Geraldine Bardelli, Kelly O'Brien, Haroon Hashmi, Alena Chekmasova, Raffaele Baffa, Tom Spencer, Eleanor De Groot, Drew Deniger. *Ziopharm Oncology, Inc., Boston, MA, USA*

Background *EGFR*, *KRAS* and *TP53* have frequent somatic hotspot mutations giving rise to biologically relevant amino acid substitutions in *EGFR*, *KRAS* and *p53* proteins, respectively, that can be processed and presented on the cell surface by human leukocyte antigen (HLA) molecules as neoantigens to T cells through their T-cell receptor (TCR). These mutations are critical for the cancer cell and are absent in normal tissue; thus, these shared neoantigens are attractive and likely safe targets. Given the complexity of different neoantigen/HLA combinations needed to effectively target a large patient population, a TCR library approach is warranted and can be used "off-the-shelf" for any patient with matching somatic hotspot mutation and HLA restriction. *Sleeping Beauty* transposition is the most advanced non-viral gene transfer technology for TCR-T cells and is appealing for TCR libraries given its low cost, speed, and flexibility.

Methods In this study, *Sleeping Beauty* transposons were constructed with TCRs targeting *EGFR*, *KRAS* and *p53* neoantigens restricted by either or both HLA Class-I and HLA Class-II molecules. Donor T cells from peripheral blood were co-electroporated with TCR transposon and *Sleeping Beauty* transposase and grown *in vitro* to clinical scale quantities ($>10^9$ TCR-T cells) with high expression ($>60\%$) of the introduced neoantigen-specific TCRs.

Results The specificity of TCRs to neoantigens was confirmed in TCR-T cell co-cultures with antigen-presenting cells pulsed with peptides, which demonstrated interferon- γ secretion and/or up-regulation of 41BB on the TCR-T cell surface in response to the neoantigen with high avidity (<1 ng/mL for some TCRs) and negligible recognition of wild type peptides. Furthermore, TCR-T cells lysed tumor cells with endogenous expression of the somatic mutation and HLA restriction element but did not recognize tumor cells lacking either somatic mutation or HLA restriction element, indicating that the targeted neoantigens are normally displayed on the tumor cell at sufficient levels for elimination by TCR-T cells. Ziopharm has a cleared corporate-sponsored IND for a Phase 1/2 clinical trial, being conducted in collaboration with MD Anderson Cancer Center, in which patients with matching somatic hotspot mutation and HLA restriction will be identified, genes encoding suitable neoantigen-specific TCR will be inserted into their autologous T cells from peripheral blood by *Sleeping Beauty* transposition, and TCR-T cells will be adoptively transferred for the treatment of bile duct, colon, lung, pancreas and gynecological cancers.

Conclusions Ziopharm's library TCR-T cell program has the potential to result in safe, durable, objective clinical regressions of cancer at a commercial scale.

<http://dx.doi.org/10.1136/jitc-2021-SITC2021.226>

Checkpoint Blockade Therapy

227

A COMPUTATIONAL SEMI-MECHANISTIC PHARMACOLOGY MODEL OF ATG101, A PD-L1/4-1BB BISPECIFIC ANTIBODY FOR TREATMENT OF SOLID TUMORS AND NHL

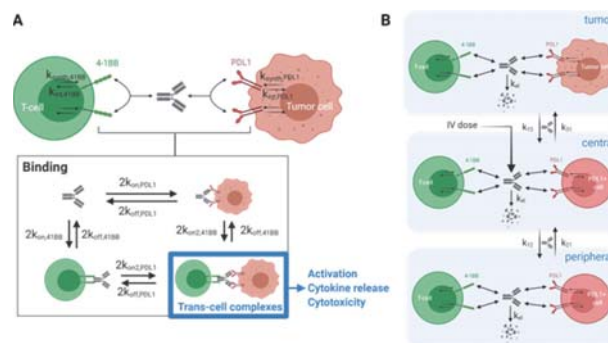
¹David Flowers*, ¹Marc Presler, ¹Kas Subramanian, ¹Theresa Yuraszek, ²Hui Yuwen, ³Bing Hou, ⁴Dirk Hoenemann. ¹Applied BioMath, LLC, Concord, MA, USA; ²Shanghai Antengene Corporation Limited, Shanghai, China; ³Antengene Corporation Co., Ltd, Shanghai, China; ⁴Antengene Pty Ltd, Melbourne, Australia

Background Bispecific antibodies have shown significant promise as therapies for various cancers.¹ ATG101 is a bispecific antibody that crosslinks tumor-expressed PD-L1 to T-cell-expressed 4-1BB, thereby selectively activating tumor-infiltrating T-cells while inhibiting immune checkpoints. The pharmacologically active complex, which is a trimer consisting of drug bound to both PD-L1 and 4-1BB and is difficult to measure directly, was predicted using a semi-mechanistic pharmacological model by integrating and calibrating against data from multiple in vitro assays. The model was then used to predict both (1) the number of PD-L1:ATG101:4-1BB trimers formed per T-cell and (2) PD-L1 occupancy, allowing it to quantify 4-1BB-driven activation as well as checkpoint blockade along the PD-1:PD-L1 axis in vivo.

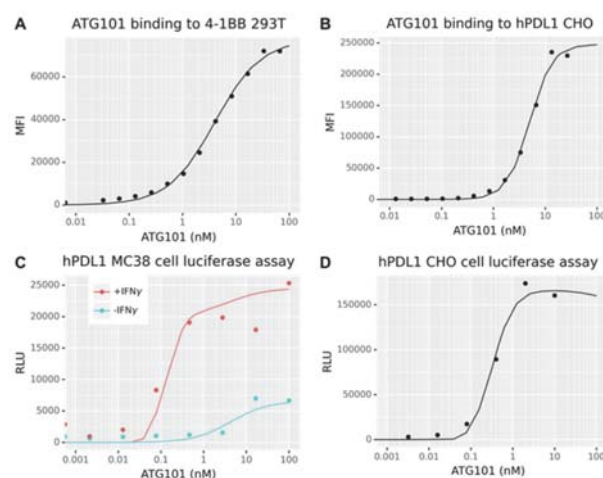
Methods

Model structure A single-compartment in vitro model and a three-compartment in vivo model were built (figure 1). The bispecific molecules could first bind to either 4-1BB or PD-L1 and then crosslink the other receptor to form a trimer. Parameter estimation: The model's binding parameters were calibrated to experimental in vitro data (figure 2). Two crosslinking rates were carried forward to model predictions to capture uncertainty in its value. Other model parameters were estimated from the literature. Model validation: The model was validated by comparing model simulations to data from two in vitro assays (figure 3). In vivo predictions: Simulations of ATG101 in human solid tumor patients were performed using the calibrated binding parameters and standard antibody pharmacokinetic parameters. Simulations varied the crosslinking rate and number of PD-L1 receptors per tumor cell to capture important sources of uncertainty and variability. Single IV bolus doses ranging from 0.001 to 30 mg/kg were simulated.

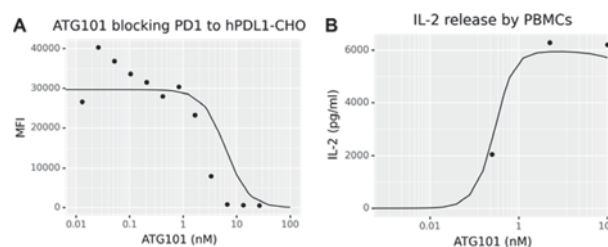
Results The model predicts trimer formation exhibits a non-monotonic dose response and that doses between 0.3 and 3 mg/kg maximize trimer formation. Simulations predict that ATG101 can sustain greater than 80% and 70% trimer formation and 90% and 95% PD-L1 occupancy in the tumor at a dose of 2 mg/kg and 3 mg/kg, respectively, once every three weeks (figure 4).



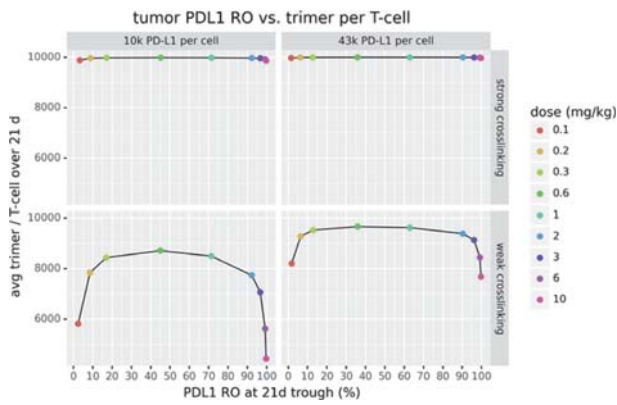
Abstract 227 Figure 1 Model structure diagram for (A) the one-compartment in vitro model and (B) the three-compartment in vivo model



Abstract 227 Figure 2 Comparison of in vitro model simulations to data used for calibration. The 4-1BB and PD-L1 monovalent binding affinities were calibrated to (A) 4-1BB expressing 293T cell binding data and (B) PD-L1-expressing CHO cell data. The crosslinking rate was calibrated to luciferase assays measuring NFκB signaling via 4-1BB crosslinking. In these assays, 4-1BB-expressing 293T cells were incubated with ATG101 and either (C) unstimulated or IFNγ-stimulated PD-L1-expressing MC38 cells or (D) PD-L1-expressing CHO cells



Abstract 227 Figure 3 Comparison of in vitro model simulations to data used for model validation. Lines show simulations, and points show data. (A) PD-1:PD-L1 blockade assay. Reduction in PD-1 binding to PD-L1 at various concentrations of ATG101 was measured on hPD-L1-expressing CHO cells via flow cytometry. (B) IL-2 release assay. PBMCs were activated with staphylococcal enterotoxin A and incubated with ATG101.



Abstract 227 Figure 4 Trimer formation versus PD-L1 RO at day 21 following a single dose, predicted for different PD-L1 expression levels and crosslinking strengths. Each point represents a dose, with the color indicating the dose level. Panels show predictions for different numbers of PD-L1 receptors per tumor cell (columns) and crosslinking strengths (rows). The x axis indicates the PD-L1 RO at day 21, and the y axis indicates the average number of trimers per T-cell over the 21-day interval following the dose.

Conclusions For bispecific antibodies acting via both receptor crosslinking and checkpoint blockade, reductions in trimer at large doses may complicate dose selection. By predicting PD-L1 RO and trimer formation, the model provides a rational basis for clinical dose selection. ATG101 is predicted to be capable of maintaining near-maximal trimer levels across a range of concentrations, allowing it to be dosed at levels high enough to attain greater than 90% PD-L1 receptor occupancy.

REFERENCES

1.. Huehls AM, Coupet TA, Sentman CL. Bispecific T-cell engagers for cancer immunotherapy. *Immunol Cell Biol* 2015;**93**:290–296

<http://dx.doi.org/10.1136/jitc-2021-SITC2021.227>

228

ANTAGONISTIC PH-SELECTIVE VISTA ANTIBODY SNS-101 POTENTIATES ANTI-PD-1/PD-L1-INDUCED ANTI-TUMOR IMMUNITY

¹Thomas Thisted, ¹Arbab Mukherjee, ¹Kanam Malhotra, ¹Zuzana Biesova, ¹Yuliya Kleschenko, ¹Zhi-Gang Jiang, ¹Anokhi Cifuentes, ²Nadthakarn Boland, ²Nels Nielson, ¹Edward van der Horst*. ¹*Sensei Biotherapeutics Inc., Rockville, MD, USA;* ²*Adimab LLC., Lebanon, NH, USA*

Background Immunotherapies, especially immune checkpoint inhibitors, have become a cornerstone of cancer treatment. Remarkable clinical responses have been observed blocking the programmed cell death protein 1 (PD-1)/programmed death-ligand 1 (PD-L1) axis across a spectrum of indications. However, innate and/or acquired resistance to anti-PD-1 blockade remains a major challenge. V-domain Ig suppressor of T-cell activation (VISTA) is a B7-family member, which promotes T-cell and myeloid quiescence and represents a promising target, particularly in combination with anti-PD-1/PD-L1 treatment. Recently, the interaction of VISTA with its receptor PSGL-1 was demonstrated to be significantly enhanced by the acidic tumor microenvironment (TME). As VISTA is highly expressed on myeloid cells, including those in the blood, antibodies binding VISTA at physiological pH 7.4 could result in rapid elimination from circulation through targeted-mediated drug disposition, making efficacious drug occupancy levels difficult to reach and potentially narrowing the therapeutic window. An antibody engineered to selectively bind and block VISTA at low pH in the TME may therefore be an ideal drug candidate.

Methods In this study, fully human anti-VISTA antibodies were generated through pH-selective enrichment strategies of a yeast-based display library comprising highly diverse synthetic immune repertoires. The 'parental' antibodies have been extensively characterized using in vitro flow-cytometry, surface-plasmon resonance (SPR) and PSGL-1/VISTA inhibition assays in primary human CD4 and CD8 T-cells at pH 6.0 and pH 7.4. Eight parental antibodies were identified and tested for combinatorial efficacy with anti-PD-1 in vivo in human VISTA knock-in mice inoculated with syngeneic MC-38 tumors. These antibodies underwent further optimization for enhanced binding affinity at pH 6.0 and decreased binding at pH 7.4. 'Progeny' antibody ranking was based on the same in vitro and in vivo characterization as parental antibodies.

Results Eighty four parental antibodies were initially discovered. Flow-cytometry and SPR analysis revealed candidates displaying pH-dependent binding to endogenously expressed native VISTA on cells, and a PSGL-1/VISTA inhibition assay at pH 6.0 was run to identify and rank potent interface blockers. Eight candidate antibodies were tested in an in vivo intervention study in combination with anti-murine PD-1 demonstrating varied combinatorial efficacy with a subset leading to superior tumor rejection. Characterization of optimized progeny antibodies led to identification of anti-VISTA antibody SNS-101.

Conclusions Enrichment of highly diverse antibody libraries led to the identification of a pH-selective inhibitory anti-VISTA antibody SNS-101, which exerts excellent combinability with anti-PD-1 leading to superior anti-tumor activity in a mouse model.

<http://dx.doi.org/10.1136/jitc-2021-SITC2021.228>

229 CX3CR1 IN EXHAUSTED CD8 T CELL STATES

¹Apoorvi Chaudhri*, ²Yunfei Wang, ³Shao-Hsi Hung, ³Gregory Lizee, ⁴Ulrich Von Andrian, ²Patrick Hwu, ⁵Gordon Freeman. ¹Dana-Farber Cancer Institute, Boston, MA, USA; ²MD Anderson Cancer Center, Houston, TX, USA; ²Moffitt Cancer Center, Tampa, FL, USA; ³MD Anderson Cancer Center, Houston, TX, USA; ⁴Harvard Medical School, Boston, MA, USA; ⁵Dana-Farber Cancer Institute, Boston, MA, USA

Background Cancer has chronic antigen exposure that results in a suppressed CD8 T cell state termed exhaustion. An outcome of anti PD-1 blockade therapy is the expansion of early exhausted CD8+ T cells into a terminally differentiated exhausted state. The reversal of this transcriptionally plastic yet epigenetically fixed state of CD8 T cell exhaustion has the potential to increase responses to anti PD-1 therapy.

Methods CX3CR1 is a marker of CD8 T cell activation, effector function however less is known about the contribution of CX3CR1 in CD8 T cell exhaustion. We identified three distinct subsets of CD8+ tumor infiltrating lymphocytes (TILs) based on high, mid, and negative CX3CR1 expression in a mouse model of colon carcinoma.

Results The CX3CR1 high CD8+ T cells are more exhausted with higher PD1+TIM3+ expression compared to CX3CR1 mid and CX3CR1 negative cells thereby representing the terminal state of CD8 T cell exhaustion. Moreover, CX3CR1 high CD8 T cells increase following anti PD-1 blockade, and their abundance is associated with a positive response to anti PD-1.

Conclusions We identify a consequence of CX3CR1 in terminal T cell exhaustion, and our work can offer strategies to increase responses to anti PD-1.

Ethics Approval Animal experiments were performed as per the IACUC regulations at the Dana Farber cancer Institute, and the MD Anderson Cancer Center

<http://dx.doi.org/10.1136/jitc-2021-SITC2021.229>

230

PRECLINICAL EFFICACY OF CLEC-1 ANTAGONIST AS NOVEL MYELOID IMMUNE CHECKPOINT THERAPY FOR ONCOLOGY

¹Vanessa Gauttier*, ¹Marion Drouin, ¹Sabrina Pengam, ²Javier Saenz, ²Bérangère Evrard, ¹Stéphanie Neyton, ¹caroline Mary, ¹Géraldine Teppaz, ¹Ariane Desselle, ¹Virginie Thépénier, ¹Emmanuelle Wilhelm, ¹Nicolas Poirier, ²Elise Chiffolleau. ¹OSE Immunotherapeutics, Nantes, France; ²CRTI – UMR1064, Nantes, France

Background C-type lectin receptors (CLRs) are powerful pattern recognition receptors shaping immune cell-mediated tissue damage by positively or negatively regulating myeloid cell functions and hence tumor elimination or evasion. We previously reported that the orphan CLR CLEC-1 expressed by dendritic cells (DCs) tempers T cell's responses in vivo by limiting antigen cross-presentation by cDC1. Furthermore, we observed that CLEC-1 is highly expressed by myeloid cells purified from human tumor microenvironment, in particular tumor-associated macrophages.

Methods Macrophages were generated from monocytes of healthy volunteers for phagocytosis assays. MC38 and Hepa 1.6 murine tumor cells were implanted in Clec1a KO or KI mice for immunotherapeutic treatment evaluation.

Results Using newly developed anti-human CLEC-1 monoclonal antibodies (mAbs), we found that antagonist anti-CLEC-1 mAbs with the capacity to block CLEC-1/CLEC-1Ligand interaction, as opposed to non-antagonist CLEC-1 mAbs, increase the phagocytosis of CLEC-1Ligand-positive human tumor cells by human macrophages, in particular when opsonized by tumor-associated antigen mAbs (Rituximab, Cetuximab, Trastuzumab) or with anti-CD47 mAb (Magrolimab). In-vivo, CLEC-1 knock-out (KO) mice (n=19) display significant prolonged survival in monotherapy as compared to wild-type littermates (n=12) in an orthotopic hepatocellular carcinoma (HCC) model and anti-tumor memory responses was demonstrated by tumor rechallenge in cured mice. CLEC1 KO mice also illustrate significant eradication of MC38 colorectal tumors in combination with chemotherapy promoting CLEC-1Ligand expression by tumor cells (n=16 with Gemcitabine or n=11 with Cyclophosphamide). HCC tumor microenvironment analysis after 2 weeks of tumor implantation shows significantly higher number of CD8+ and memory CD8+ T cells with reduced PD1 expression in CLEC1 KO animals (n=16 versus n=12 for KO vs WT mice respectively). Finally, we recently generated human CLEC-1 knock-in mice expressing the extracellular human CLEC1 domain fused to the intracellular mouse CLEC1 tail and confirmed preclinical efficacy in vivo with anti-human CLEC1 antagonist mAb in monotherapy in the orthotopic HCC model.

Conclusions These data illustrate that CLEC-1 inhibition represents a novel therapeutic target for immuno-oncology modifying T cell immune responses and tumor cell phagocytosis by macrophages.

<http://dx.doi.org/10.1136/jitc-2021-SITC2021.230>

MOLECULAR INSIGHTS ON SAFETY AND ANTI-TUMOR ACTIVITY OF A NON-IRAE-INDUCING ANTI-CTLA-4 MONOCLONAL ANTIBODY ONC-392

¹Yang Liu*, ²Yan Zhang, ³Xuexiang Du, ³Mingyue Liu, ⁴Xianfeng Fang, ⁴Libing Mu, ¹Vadim Tevetnitsky, ¹Martin Devenport, ¹Pan Zheng, ¹OncoC4, Inc., Rockville, MD, United States; ²Shanghai Institute of Immunology, Shanghai, China; ³University of Maryland Baltimore, Jinan, China; ⁴Acrolmmune, Ltd, Guangzhou, China

Background Anti-CTLA-4 antibodies have brought about limited clinical benefit because severe toxicity limits dosing levels and/or duration. We used CTLA-4 knockin mice to screen for antibodies with higher anti-tumor activity but lower autoimmunity. We have revealed that the key for better safety and preclinical efficacy is preservation of CTLA-4 for immune tolerance and intratumoral Treg depletion. Our work established that, independent of blocking activities, mAbs that preserve CTLA-4 recycling maintain the physiological immune tolerance checkpoint function while allowing more efficient and selective elimination of tumor-infiltrating regulatory T cells, resulting in highest efficacy and lowest toxicity and was thus developed for clinical testing of all antibodies tested.^{1–6} The antibody with best safety and efficacy profile, ONC-392 was developed for clinical testing. The first-in human studies showed that ONC-392 is safe and well tolerated. Remarkably, no irAE has been reported among patients who has received repeated dosing of 3.0 mg/kg and 10.0 mg/kg of ONC-392. The molecular and cellular characterization of ONC-392 will be presented.

Methods In vitro binding and disassociation assay were determined between pH 4.0–7.0. The intracellular traffic of both antibodies and CTLA-4 molecules were visualized by confocal microscopy. The binding to human and mouse FcγRI, IIA, IIB, and III (A), FcRn as well as mouse FcγRIV were evaluated by surface plasmon resonance (SPR). Depletion of regulatory T cells in tumor and lymphoid tissues were determined by flow cytometry.

Results ONC-392 is a pH-sensitive antibody that preserves CTLA-4 recycling. By preserving cell surface CTLA-4, Onco-392 preserves immune tolerance. Preserving CTLA-4 on tumor-infiltrating Treg contribute to more effective immunotherapy. In addition to its unique feature of pH sensitive binding, OncoC4 also have several important features in Fc. ONC-392 shown comparable binding to human FcγRI and IIIA as wild-type IgG1s. As expected from the mutations introduced, ONC-392 show about 6 fold higher affinity for FcRn than wild-type IgG1. Interestingly, ONC-392 has shown 7–10-fold reduction to FcγRIIB, which is generally considered to be a negative signaling FcR. ONC-392 binding to mouse FcγRI-IV was lower than WT IgG1.

Conclusions Unlike other clinical anti-CTLA-4 antibodies, ONC-392 preserves CTLA-4 recycling and thus Treg function in the peripheral tissues. The higher cell surface CTLA-4 allows more efficient Treg depletion in the tumor microenvironment. In addition, despite reduced binding to mouse activating FcγRI, III/IV, ONC-392 was more effective in intratumor Treg depletion in the mice. Therefore, lacking negative signaling from FcγRIIB may also contribute to its anti-tumor activity.

Trial Registration NCT04140526

REFERENCES

1. Du X, *et al.* Uncoupling therapeutic from immunotherapy-related adverse effects for safer and effective anti-CTLA-4 antibodies in CTLA4 humanized mice. *Cell Res* 2018;**28**:433–447.

2. Du X, *et al.* A reappraisal of CTLA-4 checkpoint blockade in cancer immunotherapy. *Cell Res* 2018;**28**:416–432.
3. Liu Y, Zheng P. How does an anti-CTLA-4 antibody promote cancer immunity? *Trends Immunol* 2018;**39**:953–956.
4. Zhang Y, *et al.* Hijacking antibody-induced CTLA-4 lysosomal degradation for safer and more effective cancer immunotherapy. *Cell Res* 2019;**29**:609–627.
5. Liu Y, Zheng P. Preserving the CTLA-4 checkpoint for safer and more effective cancer immunotherapy. *Trends Pharmacol Sci* 2020;**41**(1):4–12.
6. Zhang P, *et al.* Mechanism- and immune landscape-based ranking of therapeutic responsiveness of 22 major human cancers to next generation anti-CTLA-4 antibodies. *Cancers* 2020;**12**:284.

<http://dx.doi.org/10.1136/jitc-2021-SITC2021.231>

232

INCB090244, A POTENT SMALL MOLECULE THAT INHIBITS THE PD-L1/PD-1 AXIS AND FUNCTIONS SIMILARLY TO PD-L1 ANTIBODIES

¹Jonathan Rios-Doria*, ¹Alla Volgina, ²Prafulla Gokhale, ¹Hao Liu, ¹Christina Stevens, ¹Nina Zolotarjova, ¹Darlise DiMatteo, ¹Kanishk Kapilashrami, ¹Elham Behshad, ¹Pramod Thekkat, ¹Gengjie Yang, ¹Leslie Hall, ¹Chrysi Kanellopoulou, ¹Mark Rupar, ¹Christopher Maddage, ¹April Horsey, ¹Krista Burke, ¹Yan-ou Yang, ¹Maryanne Covington, ¹Steve Wang, ¹Phillip Liu, ¹Richard Wynn, ²David Reardon, ¹Holly Koblisch. ¹Incyte Corporation, Wilmington, USA; ²Harvard, Boston, MA, USA

Background Blocking the PD-L1 immune checkpoint axis with therapeutic antibodies against either the ligand or PD-1 has proven to be an effective treatment modality for multiple cancer histologies. Small molecules targeting the PD-L1/PD-1 axis represent an alternate modality of blocking this pathway. INCB090244 is a small molecule that blocks the PD-L1/PD-1 interaction and restores T cell function similar to the clinical stage PD-L1 inhibitor INCB086550.

Methods MDA-MB-231 or CHO cells overexpressing PD-L1 were used to investigate effects of INCB090244 on PD-L1 dimerization, and intracellular trafficking. In vivo, CD34+ humanized mice harboring MDA-MB-231 tumors or C57Bl/6 mice bearing GL261 subcutaneous or orthotopic tumors were used to investigate the efficacy, biodistribution, and pharmacodynamic effects of INCB090244. Human specific gene expression changes in tumors from MDA-MB-231 bearing humanized mice were analyzed by RNA sequencing.

Results In vitro, INCB090244 potently disrupted the PD-L1:PD-1 interaction, induced PD-L1 dimerization, and inhibited PD-1-mediated negative signaling, resulting in enhanced IFN gamma and IL-2 production in primary human immune cells. Following dimerization, INCB090244 induced internalization of PD-L1 resulting in co-localization with the Golgi apparatus and partial localization in the nucleus. After cell treatment and washing, full restoration of PD-L1 at the cell surface was observed after 5 days of culture in vitro. In vivo, INCB090244 reduced tumor growth in CD34+ humanized mice bearing MDA-MB-231 tumors, to similar levels as atezolizumab. Antitumor activity was completely abrogated in immunodeficient mice, confirming the pharmacologic dependency on a competent immune system. RNA sequencing analysis on tumors from these mice demonstrated similar T cell activation gene signatures as clinical checkpoint blockade antibodies. Biodistribution studies in mice bearing both subcutaneous and orthotopically implanted GL261 glioma tumors demonstrated higher accumulation of INCB090244 in tumor tissue compared to PD-L1 antibodies.

Conclusions INCB090244 effectively disrupted the PD-L1/PD-1 interaction, induced dimerization and internalization of PD-L1, restored immunity in in vitro and in vivo tumor models, and is a suitable surrogate for the clinical candidate INCB086550. RNA sequencing demonstrated T cell activation signatures similar to those observed in patients receiving checkpoint blockade antibodies. Biodistribution studies demonstrated higher subcutaneous and brain tumor penetration by INCB090244 compared to PD-L1 antibodies, suggesting a potential advantage of small molecule PD-L1 inhibitors in accessing intratumoral regions. These data further support the clinical evaluation of small molecule PD-L1 inhibitors as an alternative approach to immune therapy.

<http://dx.doi.org/10.1136/jitc-2021-SITC2021.232>

HUMAN PD-L2 TRIGGERS A UNIQUE T CELL INHIBITORY PROGRAM THROUGH PD-1 ENGAGEMENT DISTINCT FROM THAT OF PD-L1

¹Anupallavi Srinivasamani*, ¹Michael Curran, ²Qinying Liu, ¹Shwetha Hegde, ¹Chao-Hsien Chen, ³Kimal Rajapakshe, ³Cristian Coarfa. ¹University of Texas MD Anderson Cancer Center, Houston, TX, USA; ²Fudan University, Shanghai, China; ³Baylor College of Medicine, Houston, TX, USA

Background PD-1/PD-L1 blockade is responsible for the majority of the success of cancer immunotherapy.¹ However, only 14% of patients eligible to receive checkpoint blockade achieve objected clinical responses.^{2 3} The reason for the failure of PD-L1 blockade may be attributed to the recently appreciated widespread expression of PD-L2 across human cancers and its immunosuppressive stromal cells.⁴ PD-L2 expression was shown to be as or more predictive of response to PD-1 blockade than PD-L1. PD-L2 traditionally was dismissed as functionally redundant to PD-L1 varying only in pattern of expression. We hypothesize that PD-L2 engages PD-1 to generate a distinct inhibitory signal from that of PD-L1, and antibody mediated blockade and depletion of PD-L2 + cells may promote anti-tumor immunity that is superior to PD-L1 blockade alone.

Methods Cell based bioluminescent assay demonstrated the nature of regulation mediated by human PD-L2 through the PD-1 co-receptor. RNA-sequencing identified key differences in the signaling pathways generated in Jurkat T cells by PD-1 binding to PD-L1 or PD-L2. Multidimensional flow cytometry determined the differential effects of PD-L1 and PD-L2 on human T cell proliferation and effector function. Western blot elucidated the temporal kinetics of inhibition mediated by PD-L1 and PD-L2. Survival studies in murine syngeneic lymphoma model evaluated the efficacy of antibody mediated blockade and depletion of PD-L2+ cells.

Results We validated that human PD-L2, unlike murine PD-L2, generates a purely co-inhibitory signal in human T cells, albeit with a reduced inhibitory potential relative to PD-L1. We discovered significant differences in downstream T cell signaling pathways generated by PD-L1 versus PD-L2 through PD-1 engagement. Human PD-L1 and PD-L2 differentially modulated T cell effector function and proliferation with PD-L2 preferentially arresting T cells in S-phase of cell cycle. PD-L1 and PD-L2 also differed in the temporal kinetics of dephosphorylation of the membrane proximal proteins in the TCR-CD3 signaling complex. We observed that combination blockade of PD-L1 and PD-L2 improves on blockade of PD-L1 alone resulting in increased production of IL-2 and IFN γ in primary human mixed lymphocyte reactions. Our data in a syngeneic murine model of EL4 showed that effector-function capable PD-L2 blocking antibodies are therapeutically superior to PD-L1 or PD-L2 blockade alone.

Conclusions We are the first to report on T cell immunoregulatory functions of PD-L2 which are distinct from those of PD-L1, and demonstrate that the more tumor-selective expression pattern of PD-L2 relative to PD-L1 provides a therapeutic advantage to effector-function capable PD-L2 antibodies.

Acknowledgements AS was supported by the CPRIT Research Training Grant(RP170067)

REFERENCES

- 1.. Ribas A, Wolchok JD (2018). Cancer immunotherapy using checkpoint blockade. *Science* **359**:1350–1355.
- 2.. Cristescu R, Mogg R, Ayers M, Albright A, Murphy E, Yearley J, Sher X, Liu XQ, Lu H, Nebozhyn M, Zhang C, Luceford JK, Joe A, Cheng J, Webber AL, Ibrahim N, Plimack ER, Ott PA, Seiwert TY, Ribas A, McClanahan TK, Tomassini JE,

Loboda A, Kaufman D (2018). Pan-tumor genomic biomarkers for PD-1 checkpoint blockade-based immunotherapy. *Science* **362**.

- 3.. Haslam A, Prasad V (2019). Estimation of the percentage of US patients with cancer who are eligible for and respond to checkpoint inhibitor immunotherapy drugs. *JAMA Netw Open* **2**:e192535.
- 4.. Yearley JH, Gibson C, Yu N, Moon C, Murphy E, Juco J, Luceford J, Cheng J, Chow LQM, Seiwert TY, Handa M, Tomassini JE, McClanahan T (2017). PD-L2 expression in human tumors: relevance to anti-PD-1 therapy in cancer. *Clin Cancer Res* **23**:3158–3167.

<http://dx.doi.org/10.1136/jitc-2021-SITC2021.233>

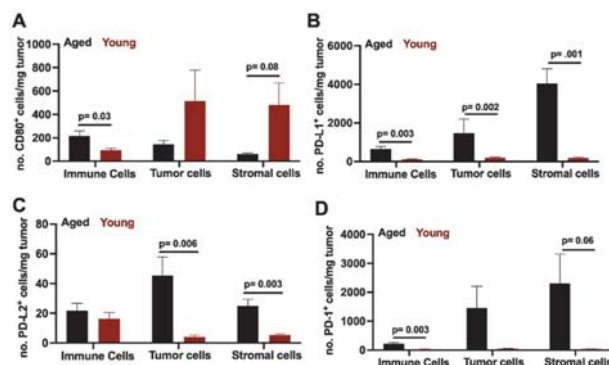
234 **DISTINCT EFFICACY AND IMMUNOLOGICAL RESPONSES TO α PD-1, α PD-L1 AND α PD-L2 IMMUNOTHERAPY IN AGED VERSUS YOUNG HOSTS**

Yilun Deng, Harshita Gupta, Myrna Garcia*, Aravind Kancharla, Ryan Reyes, Alvaro Padron, Tyler Curiel. *University of Texas Health San Antonio, San Antonio, TX, USA*

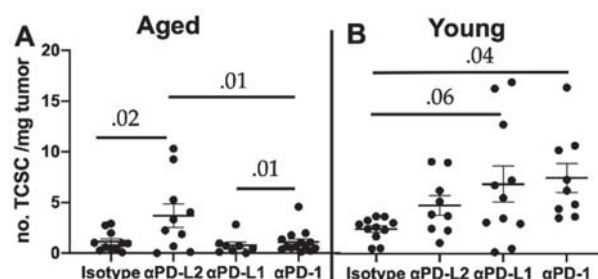
Background Aging is the biggest risk factor for cancer, yet there are limited pre-clinical/clinical data regarding aging effects on immune checkpoint (IC) inhibition (ICI) outcomes. α PD-1 can potentially block PD-L1 and PD-L2 while α PD-L1 can block PD-1 and CD80. Melanoma response to α PD-1/ α PD-L1 correlates with CD8+TCF1+ T cell stem cell (TCSC) generation.¹ Lack of host IL-17 can lead to increased IFN- γ production.^{2 3}

Methods We tested α PD-1 (200 μ g/mouse), α PD-L1 (100 μ g/mouse) or α PD-L2 (200 μ g/mouse) in aged (18–33 months) and young (3–8 months) mice challenged orthotopically with B16 (WT or PD-L1ko) or TPN61R melanoma (NRAS mutation melanoma model)⁴ (α PD-L2 only) (SQ). Tumors were analyzed by flow. We tested α PD-L2 (20 μ g/ml) effects by co-culturing young or aged T cells \pm young or aged myeloid cells.

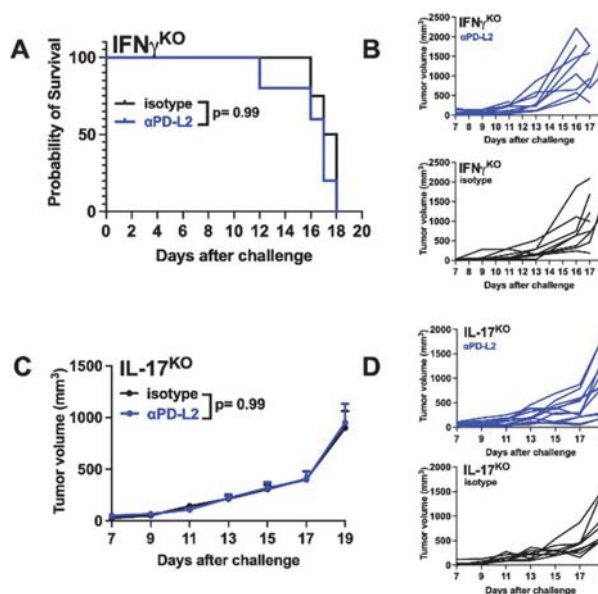
Results We reported that α PD-1 treats young and aged with B16 whereas α PD-L1 treats young not aged.⁵ α PD-L2 treated B16 and TPN61R melanoma in aged but, remarkably, not young, the first single agent anti-cancer immunotherapy exhibiting this property (figure 1). B16 tumors from aged had differential IC content (PD-1, PD-L1, CD80, PD-L2) versus tumors from young (e.g., more PD-L2+ tumor and stroma cells in aged mice; figure 2). Efficacy in young (α PD-1, α PD-L1) and aged (α PD-L2) correlated with increased tumor TCSC content (figure 3). α PD-L2 efficacy against B16 in aged mice required host IFN- γ and IL-17 (figure 4). α PD-1 efficacy against B16 in aged appeared to be host and tumor PD-L1 independent (figure 5). PD-L1KO B16 response to α PD-1 in aged also correlated with increased tumor TCSC content. Myeloid cell PD-L2 signaling inhibited aged but not young CD8+ T cell IL-2 production in vitro (figure 6).



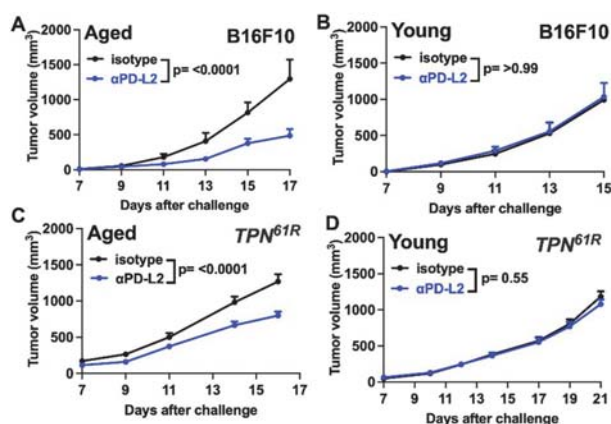
Abstract 234 Figure 2



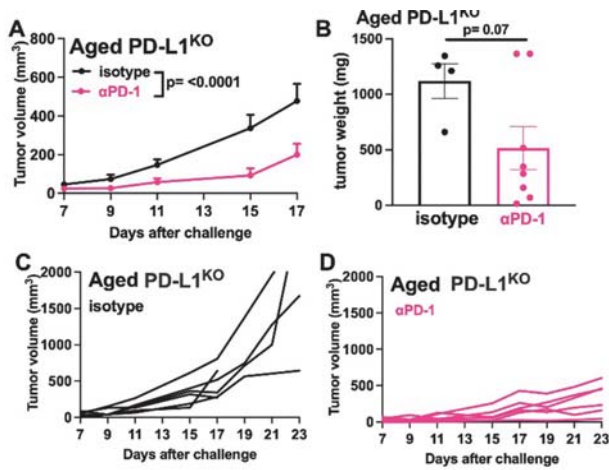
Abstract 234 Figure 3



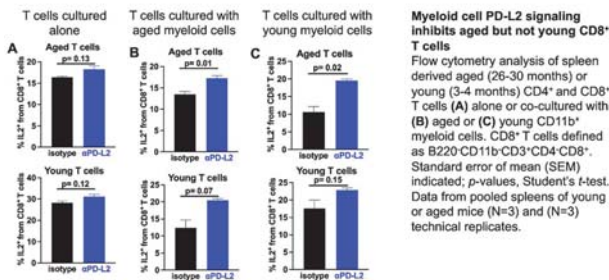
Abstract 234 Figure 4



Abstract 234 Figure 1



Abstract 234 Figure 5



Abstract 234 Figure 6

Conclusions Treatment differences in aged versus young could depend on IC, TCSC and/or host cytokine differences (IL-17/IFN- γ). α PD-1 efficacy in aged PD-L1KO mice challenged with PD-L1KO B16 suggests that PD-L2 block is sufficient for α PD-1 efficacy in aged. PD-L2 expression differences in the tumor microenvironment could also contribute to treatment efficacy differences. PD-L2 inhibitory signaling on aged but not young CD8+ T cells is a likely mechanism for α PD-L2 efficacy in aged but not young. We are now testing the role of IL-17 in α PD-L2 efficacy as it could be upstream of IFN- γ effects, and TCSC effects in aged versus young. Our work can improve cancer immunotherapy in aged hosts and provides insights into treatment failure, including in young hosts.

Acknowledgements South Texas MSTP training grant (NIH T32GM113896), TL1TR002647, NIH T32AI138944, R01 CA231325, Waxman Grant, UL1 TR001120

REFERENCES

- 1.. Miller BC, Sen DR, Al Aboosy R, Bi K, Virkud YV, LaFleur MW, Yates KB, Lako A, Felt K, Naik GS, *et al.* Subsets of exhausted CD8(+) T cells differentially mediate tumor control and respond to checkpoint blockade. *Nat Immunol* 2019;**20**(3):326–336.
- 2.. Moroda M, Takamoto M, Iwakura Y, Nakayama J, Aosai F. Interleukin-17A-deficient mice are highly susceptible to toxoplasma gondii infection due to excessively induced T. gondii HSP70 and interferon gamma production. *Infection and immunity* 2017;**85**(12):e00399–00317.
- 3.. Yi T, Zhao D, Lin C-L, Zhang C, Chen Y, Todorov I, LeBon T, Kandeel F, Forman S, Zeng D. Absence of donor Th17 leads to augmented Th1 differentiation and exacerbated acute graft-versus-host disease. *Blood, The Journal of the American Society of Hematology* 2008;**112**(5):2101–2110.

- 4.. Burd CE, Liu W, Huynh MV, Waqas MA, Gillahan JE, Clark KS, Fu K, Martin BL, Jeck WR, Souroullas GP. Mutation-specific RAS oncogenicity explains NRAS codon 61 selection in melanoma. *Cancer discovery* 2014;**4**(12):1418–1429.
- 5.. Padron A, Hurez V, Gupta HB, Clark CA, Pandeswara SL, Yuan B, Svatek RS, Turk MJ, Drerup JM, Li R, *et al.* Age effects of distinct immune checkpoint blockade treatments in a mouse melanoma model. *Exp Gerontol* 2018;**105**:146–154.

Ethics Approval All animal studies are approved by UTHSA IACUC.

<http://dx.doi.org/10.1136/jitc-2021-SITC2021.234>

235

NOVEL BIPARATOPIC TIM-3 ANTIBODY EFFECTIVELY BLOCKS MULTIPLE INHERENT LIGANDS AND ACTIVATES ANTI-TUMOR IMMUNITY

Yuji Mishima*, Kanto Nakajima, Mamoru Shiraishi, Haruka Matsumura, Takahiko Aramaki, Noriko Matsumoto, Norihiro Nakamura. *Brightpath Biotherapeutics, Kawasaki, Japan*

Background T cell immunoglobulin and mucin domain-containing protein 3 (TIM-3) is a part of modules expressed on dysfunctional or exhausted T cells as well as dendritic cells and has emerged as a target for several therapeutic antibodies that are under clinical development. Co-blockade of TIM-3 and PD-1 results in tumor regression in preclinical models and improves anticancer T cell responses in patients with advanced cancers. TIM-3 has been reported to have multiple ligands including galectin-9, phosphatidylserine, CEACAM-1 and HMGB1, which bind to different regions on the extracellular domain of TIM-3. Most of the TIM-3 antibodies developed to date are intended to inhibit phosphatidylserine that binds to the pocket in TIM-3 immunoglobulin V domain. Galectin-9 binds to carbohydrate motifs on the opposite side of phosphatidylserine-binding site in immunoglobulin V domain and thereby induces cell death in TIM-3+ T cells. We report herein novel antibodies that block TIM-3 binding to multiple ligands including these two important ligands simultaneously.

Methods Anti-TIM-3 antibodies were generated by immunizing mice with a purified recombinant TIM-3 protein and TIM-3-expressing mammalian cell line. Phage display libraries were constructed using cDNAs of splenocytes and lymph node cells of the immunized mice, then subjected to the biopanning using recombinant TIM-3 proteins. After analyzing specificities and affinities to the TIM-3 protein, scFvs obtained were classified by epitope bin and inhibitory effects on TIM-3 binding to the multiple ligands. The scFvs were converted to scFv-Fc to generate biparatopic (bispecific) antibodies.

Results At least five classes of TIM-3 antibodies were obtained, and each class was grouped into different epitope bins and has unique inhibitory profiles for multiple ligands of TIM-3. Their biparatopic (bispecific) forms were produced from the scFv clones and subjected to the analyses of TIM-3 binding, inhibition of ligand binding, and immune activation. As expected, the biparatopic antibodies that recognize two different epitopes showed higher affinity and specificity to TIM-3 than monospecific forms. A lead biparatopic antibody that block the binding of TIM-3 to galectin-9 and phosphatidylserine showed remarkable potency on T cell activation, protection from exhaustion and apoptotic cell death of T cells as well as more potent anti-tumor efficacy.

Conclusions This study demonstrates the successful development of a novel biparatopic antibody that blocks the binding of TIM-3 to phosphatidylserine and galectin-9 simultaneously. The antibody shows the advantages over conventional TIM-3 antibodies in reducing T cell exhaustion and potentially manipulated for the development of human monoclonal antibodies for therapeutic treatment of cancer.

<http://dx.doi.org/10.1136/jitc-2021-SITC2021.235>

236 PREDICTORS OF ICI RENAL TOXICITY: A PATHOLOGICAL APPROACH

¹Ala Abudayyeh*, ²Liye Suo, ¹Heather Lin, ¹Omar Mamlouk, ¹Cassian Yee, ¹Amanda Tchakarov, ¹Jamie Lin. ¹The University of Texas MD Anderson Cancer Center, Houston, TX, USA; ²State University of New York Upstate Medical University, New York, NY, USA

Background Inflammatory response in unintended tissues and organs associated with the use of immune checkpoint inhibitors also known as immune related adverse events (irAEs) is a management challenge, and renal irAEs are associated with increased patient morbidity and mortality. The most common renal toxicity is acute interstitial nephritis (AIN), characterized by infiltration of renal tissue with immune cells, and may be analogous to kidney transplant rejection. Using both clinical variables and tissue findings we evaluated a large cohort of ICI cases to determine predictors of renal response and overall survival.

Methods We retrospectively reviewed all patients treated with ICI (August 2007 to August 2020) at MD Anderson Cancer Center. A total of 38 patients with biopsy confirmed AIN and available tissue were identified. All slides were reviewed by two board certified renal pathologists and the severity of inflammation and chronicity was graded using transplant rejection BANFF criteria. Patients were categorized as renal responders if creatinine improved or returned to baseline after treatment and non-responders if it did not. Fisher's exact tests for categorical variables and t-test/ANOVA or the counterparts of the non-parametric approaches (Wilcoxon rank-sum or Kruskal-Wallis) for continuous variables were used to compare patient's characteristics between groups. The distribution of overall survival (OS) was estimated by the Kaplan-Meier method. Log-rank test was performed to test the difference in survival between groups.

Results Based on the detailed pathological findings, patients with increased interstitial fibrosis were less likely to have renal response with treatment compared to patients with less fibrosis, ($p < 0.05$). Inflammation, tubulitis, number of eosinophils and neutrophils had no impact on renal response. Patients with response within 3 months of AKI treatment had a superior OS in comparison to patients who responded late (12-month OS rate: 77% vs 27%, $p < 0.05$). Notably, patients who received concurrent ICI and achieved renal response within 3 months had the best OS while those who did not receive concurrent ICI nor achieved renal response had worst OS (12-month OS rate: 100% (renal response and concurrent ICI) vs 72% (renal response with no concurrent ICI), vs 27% (no renal response and nonconcurrent ICI) ($p < 0.05$).

Conclusions This is the first analysis of ICI induced nephritis where a detailed pathological and clinical evaluation was performed to predict renal response. Our findings highlight the importance of early diagnosis and treatment of ICI-AIN while continuing concurrent ICI therapy.

Ethics Approval This retrospective study was approved by the institutional review board at The University of Texas MD Anderson Cancer Center, and the procedures followed were in accordance with the principles of the Declaration of Helsinki.

<http://dx.doi.org/10.1136/jitc-2021-SITC2021.236>

INFECTIOUS COMPLICATIONS IN PATIENTS WITH NON-SMALL CELL LUNG CANCER TREATED WITH ANTI-PD(L)1 IMMUNE CHECKPOINT INHIBITORS

¹Matthew Guo*, ¹Aanika Balaji, ¹Joseph Murray, ²Joshua Reuss, ³Seema Mehta Steinke, ⁴Jarushka Naidoo. ¹Johns Hopkins School of Medicine, Baltimore, MD, USA; ²Georgetown University, Washington, DC, USA; ³Johns Hopkins School of Medicine; University of Pittsburgh School of Medicine, Pittsburgh, PA, USA; ⁴Johns Hopkins School of Medicine; Beaumont Hospital, Baltimore, MD, USA; Royal College of Surgeons in Ireland University of Health Sciences, Dublin, Ireland

Background Immune checkpoint inhibitors (ICI) are standard treatment for stage III/IV non-small cell lung cancer (NSCLC). ICIs may cause immune-related adverse events (irAEs) often requiring corticosteroids or other immunosuppressive therapy and are associated with increased risk of opportunistic infections.^{1 2} The burden of infectious complications in NSCLC patients (pts) treated with ICIs is poorly described.

Methods We retrospectively reviewed NSCLC pts treated with ICIs between 2016–2020 at a large tertiary academic center. An infectious complication related to ICIs was defined as a pathogen-confirmed or clinically diagnosed infection requiring antimicrobials during or within 3 months of ICI discontinuation. High-grade infections were defined as those requiring IV antibiotics (grade 3), life-threatening or requiring ICU stay (grade 4), or resulting in death (grade 5). irAEs were defined by the treating provider and treated according to standard guidelines. Patient demographics, treatment data, cancer outcomes, infectious complications, and irAE details were annotated in an IRB-approved database. An AE treated as both an infection and/or irAE with antibiotics and immunosuppression was coded as a concomitant irAE/infection event. The association between patient features and infectious complications was examined using logistic regression. Treatment and disease characteristics for concomitant irAE with infection were also described.

Results 302 ICI-treated NSCLC pts were included. 211 pts received PD-1 monotherapy and 91 received PD-1 therapy with CTLA-4 therapy, chemotherapy, or other investigational therapy. The majority (175/302, 57.9%) had a documented infection (bacterial=138, viral=17, fungal=19, mycobacterial=1) during or within 3 months of ICI discontinuation. Grade ≥ 3 infections occurred in 33.4% of pts (101/302). Pulmonary infections were most common (35.4%), followed by gastrointestinal, urinary, and skin (<10%, each). A subset of pts were treated as having concomitant irAE/infection events (63/302, 20.9%). Among 63 pts who experienced irAEs, pneumonia occurred most commonly (47/63, 74.6%) followed by colitis (7/63, 11.1%); other irAEs (hepatitis, myocarditis, thyroiditis) occurred in <3 patients each. A concomitant event was associated with a trend toward higher odds of hospitalization (OR 3.91, CI 0.5–30.76) when adjusted for grade ≥ 3 infection. Similarly, steroid use within one month prior to infection, was also associated with a trend toward higher odds of hospitalization (OR 8.88, CI 0.81–97.15), adjusted for grade ≥ 3 infection.

Conclusions In this retrospective study of NSCLC pts treated with ICIs, the majority experienced infections during or within 3 months of ICI discontinuation. The most common infections were bacterial pulmonary in origin. Concomitant irAE/infection was associated with trend toward higher odds of hospitalization.

REFERENCES

- 1.. Hamashima R, Uchino J, Morimoto Y, *et al.* Association of immune checkpoint inhibitors with respiratory infections: a review. *Cancer Treatment Reviews* 2020;**90**:102109. doi:10.1016/j.ctrv.2020.102109
- 2.. Lu M, Zhang L, Li Y, *et al.* Recommendation for the diagnosis and management of immune checkpoint inhibitor related infections. *Thorac Cancer* 2020;**11**(3):805–809. doi:10.1111/1759-7714.13313

Ethics Approval This retrospective chart review study has obtained ethics approval from the Institutional Review Board at the Johns Hopkins School of Medicine (number: IRB00129424).

<http://dx.doi.org/10.1136/jitc-2021-SITC2021.237>

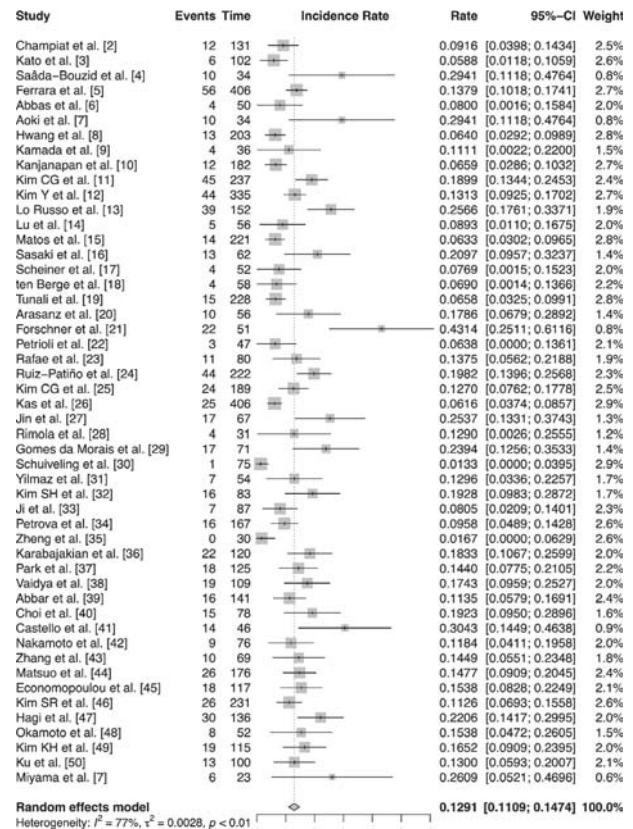
META-ANALYSIS ON THE INCIDENCE OF HYPERPROGRESSIVE DISEASE DURING IMMUNE CHECKPOINT INHIBITOR THERAPY

¹Seung Pyo Hong*, ¹Min Jeong Kim, ²Allison Belette, ¹Youjin Oh, ³Sukjoo Cho, ¹Young Kwang Chae. ¹Northwestern University Feinberg School of Medicine, Chicago, IL, USA; ²University of Texas, Houston, TX, USA; ³University of South Florida Morsani College of Medicine, Tampa, FL, USA

Background Hyperprogressive disease (HPD) is a distinct pattern of rapid tumor progression observed in patients with cancer who are undergoing immune checkpoint inhibitor therapy. Despite the growing evidence, a universal definition of HPD remains to be established, and incidence rates vary based on the defining criteria. Therefore, a refinement of currently existing criteria is warranted to better characterize this phenomenon and evaluate its incidence.

Methods Two independent investigators performed a systematic literature search in EMBASE and MEDLINE using keywords selected in Park et al.¹: checkpoint, immunotherapy, pd1, pdl1, ctla4, ipilimumab, nivolumab, pembrolizumab, atezolizumab, avelumab, durvalumab and hyperprogress. Studies published from March 3, 2020 to April 20, 2020 that included the incidence and definition of HPD in patients receiving immunotherapy were included for analysis. Selected studies were then combined with those included in the meta-analysis by Park et al.¹ Duplicates were removed, and the study with a larger cohort was selected in instances of overlap between two cohorts. In total, 50 studies were included for meta-analysis.²⁻⁵¹ Pooled incidence rates of HPD and prespecified subgroup analyses based on four categories defining HPD (tumor growth rate ratio, tumor growth kinetics ratio, early tumor burden increase, and combination) were obtained with 95% confidence intervals (CI) using a random effects model performed on R.

Results A total of 6009 patients from 50 studies were included in the meta-analysis. Incidences varied from 0.0% to 43.1% (figure 1), and the overall pooled incidence of HPD was 12.9% (95%CI, 11.1%–14.7%). Significant heterogeneity was observed (I²= 77%; p<0.01). Studies were also grouped into one of 4 categories (table 1) based on the definition of HPD used to calculate the tumor growth acceleration: tumor growth rate ratio (pooled incidence of HPD 10.5%; 95% CI, 7.9%–13.0%), tumor growth kinetics ratio (pooled incidence, 14.8%; 95% CI, 12.0%–17.5%), early tumor burden increase (pooled incidence, 17.2%; 95% CI, 9.7%–24.7%), and combinations of the above (pooled incidence, 12.2%; 95% CI, 9.2%–15.2%).



Abstract 238 Figure 1 Overall pooled incidence of HPD. The overall pooled incidence of HPD was 12.9% (95% CI, 11.1%–14.7%). Significant heterogeneity was observed (I² = 77%; p<0.01).

Conclusions The overall incidence of HPD from 50 studies was 12.9% (95%CI, 11.1%–14.7%). HPD incidence varied from 0% to 43.1% depending on the definition each investigator chose. There is a growing need for a more uniform definition of HPD that does not underestimate or overestimate its incidence.

REFERENCES

1. Park HJ, Kim KW, Won SE, et al. Definition, incidence, and challenges for assessment of hyperprogressive disease during cancer treatment with immune checkpoint inhibitors: a systematic review and meta-analysis. *JAMA Netw Open* 2021;4(3):1–16. doi:10.1001/jamanetworkopen.2021.1136
2. Champiat S, Derle L, Ammari S, et al. Hyperprogressive disease is a new pattern of progression in cancer patients treated by anti-PD-1/PD-L1. *Clin Cancer Res* 2017;23(8):1920–1928. doi:10.1158/1078-0432.CCR-16-1741
3. Kato S, Goodman A, Walavalkar V, Barkauskas DA, Sharabi A, Kurzrock R. Hyperprogressors after immunotherapy: analysis of genomic alterations associated with accelerated growth rate. *Clin Cancer Res* 2017;23(15):4242–4250. doi:10.1158/1078-0432.CCR-16-3133
4. Saàda-Bouzd E, Defauchoux C, Karabajakian A, et al. Hyperprogression during anti-PD-1/PD-L1 therapy in patients with recurrent and/or metastatic head and neck squamous cell carcinoma. *Ann Oncol* 2017;28(7):1605–1611. doi:10.1093/annonc/mdx178
5. Ferrara R, Mezquita L, Texier M, et al. Comparison of fast-progression, hyperprogressive disease, and early deaths in advanced non-small-cell lung cancer treated with PD-1/PD-L1 inhibitors or chemotherapy. *JCO Precis Oncol* 2020;4(4):829–840. doi:10.1200/PO.20.00021
6. Abbas W, Rao RR, Popli S. Hyperprogression after immunotherapy. *South Asian J Cancer* 2019;08(04):244–246. doi:10.4103/sajc.sajc_389_18
7. Aoki M, Shoji H, Nagashima K, et al. Hyperprogressive disease during nivolumab or irinotecan treatment in patients with advanced gastric cancer. *ESMO Open* 2019;4(3):1–10. doi:10.1136/esmoopen-2019-000488

Abstract 238 Table 1 Subgroup analyses based on definitions of HPD

Factor	Pooled incidence of HPD (%)	P value			
		vs Category 1	vs Category 2	vs Category 3	vs Category 4
HPD definition					
Category 1 (TGR ratio)	10.5 (7.9–13.0)	-	0.025	0.097	0.385
Category 2 (TGK ratio)	14.8 (12.0–17.5)	0.025	-	0.552	0.223
Category 3 (early tumor burden increase)	17.2 (9.7–24.7)	0.097	0.552	-	0.229
Category 4 (combination)	12.2 (9.2–15.2)	0.385	0.223	0.229	-

Abbreviation: TGR, tumor growth rate; TGK, tumor growth kinetics.

- 8.. Hwang I, Park I, Yoon S kyo, Lee JL. Hyperprogressive disease in patients with urothelial carcinoma or renal cell carcinoma treated with PD-1/PD-L1 inhibitors. *Clin Genitourin Cancer* 2020;**18**(2):e122-e133. doi:10.1016/j.clgc.2019.09.009
- 9.. Kamada T, Togashi Y, Tay C, et al. PD-1+ regulatory T cells amplified by PD-1 blockade promote hyperprogression of cancer. *Proc Natl Acad Sci U S A* 2019;**116**(20):9999–10008. doi:10.1073/pnas.1822001116
- 10.. Kanjanapan Y, Day D, Wang L, et al. Hyperprogressive disease in early-phase immunotherapy trials: clinical predictors and association with immune-related toxicities. *Cancer* 2019;**125**(8):1341–1349. doi:10.1002/cncr.31999
- 11.. Kim CG, Kim KH, Pyo KH, et al. Hyperprogressive disease during PD-1/PD-L1 blockade in patients with non-small-cell lung cancer. *Ann Oncol* 2019;**30**(7):1104–1113. doi:10.1093/annonc/mdz123
- 12.. Kim Y, Kim CH, Lee HY, et al. Comprehensive clinical and genetic characterization of hyperprogression based on volumetry in advanced non-small cell lung cancer treated with immune checkpoint inhibitor. *J Thorac Oncol* 2019;**14**(9):1608–1618. doi:10.1016/j.jtho.2019.05.033
- 13.. Russo G Lo, Moro M, Sommariva M, et al. Antibody-Fc/FcR interaction on macrophages as a mechanism for hyperprogressive disease in non-small cell lung cancer subsequent to PD-1/PD-L1 blockade. *Clin Cancer Res* 2019;**25**(3):989–999. doi:10.1158/1078-0432.CCR-18-1390
- 14.. Lu Z, Zou J, Hu Y, et al. Serological markers associated with response to immune checkpoint blockade in metastatic gastrointestinal tract cancer. *JAMA Netw Open* 2019;**2**(7):1–15. doi:10.1001/jamanetworkopen.2019.7621
- 15.. Matos I, Martin-Liberal J, Garcia-Ruiz A, et al. Capturing hyperprogressive disease with immune-checkpoint inhibitors using RECIST 1.1 criteria. *Clin Cancer Res* 2020;**26**(8):1846–1855. doi:10.1158/1078-0432.CCR-19-2226
- 16.. Sasaki A, Nakamura Y, Mishima S, et al. Predictive factors for hyperprogressive disease during nivolumab as anti-PD1 treatment in patients with advanced gastric cancer. *Gastric Cancer* 2019;**22**(4):793–802. doi:10.1007/s10120-018-00922-8
- 17.. Scheiner B, Kirstein MM, Hucke F, et al. Programmed cell death protein-1 (PD-1)-targeted immunotherapy in advanced hepatocellular carcinoma: efficacy and safety data from an international multicentre real-world cohort. *Aliment Pharmacol Ther* 2019;**49**(10):1323–1333. doi:10.1111/apt.15245
- 18.. Ten Berge DMHJ, Hurkmans DP, den Besten I, et al. Tumour growth rate as a tool for response evaluation during PD-1 treatment for non-small cell lung cancer: a retrospective analysis. *ERJ Open Res* 2019;**5**(4):00179–02019. doi:10.1183/23120541.00179-2019
- 19.. Tunali I, Gray JE, Qi J, et al. Novel clinical and radiomic predictors of rapid disease progression phenotypes among lung cancer patients treated with immunotherapy: an early report. *Lung Cancer* 2019;**129**:75–79. doi:10.1016/j.lungcan.2019.01.010
- 20.. Arasanz H, Zuazo M, Bocanegra A, et al. Early detection of hyperprogressive disease in non-small cell lung cancer by monitoring of systemic T cell dynamics. *Cancers (Basel)* 2020;**12**(2):1–14. doi:10.3390/cancers12020344
- 21.. Forschner A, Hilke FJ, Bonzheim I, et al. MDM2, MDM4 and EGFR amplifications and hyperprogression in metastatic acral and mucosal melanoma. *Cancers (Basel)* 2020;**12**(3). doi:10.3390/cancers12030540
- 22.. Petrioli R, Mazzei MA, Giorgi S, et al. Hyperprogressive disease in advanced cancer patients treated with nivolumab: a case series study. *Anticancer Drugs*. Published online 2020:190–195. doi:10.1097/CAD.0000000000000864
- 23.. Refae S, Gal J, Brest P, et al. Author correction: hyperprogression under immune checkpoint inhibitor: a potential role for germinal immunogenetics (Scientific Reports, (2020), 10, 1, (3565), 10.1038/s41598-020-60437-0). *Sci Rep* 2020;**10**(1):1–8. doi:10.1038/s41598-020-66841-w
- 24.. Ruiz-Patiño A, Arrieta O, Cardona AF, et al. Immunotherapy at any line of treatment improves survival in patients with advanced metastatic non-small cell lung cancer (NSCLC) compared with chemotherapy (Quijote-CLiCaP). *Thorac Cancer* 2020;**11**(2):353–361. doi:10.1111/1759-7714.13272
- 25.. Kim CG, Kim C, Yoon SE, et al. Hyperprogressive disease during PD-1 blockade in patients with advanced hepatocellular carcinoma. *J Hepatol* 2021;**74**(2):350–359. doi:10.1016/j.jhep.2020.08.010
- 26.. Kas B, Talbot H, Ferrara R, et al. Clarification of definitions of hyperprogressive disease during immunotherapy for non-small cell lung cancer. *JAMA Oncol* 2020;**6**(7):1039–1046. doi:10.1001/jamaoncol.2020.1634
- 27.. Jin T, Zhang Q, Jin QF, Hua YH, Chen XZ. Anti-PD1 checkpoint inhibitor with or without chemotherapy for patients with recurrent and metastatic nasopharyngeal carcinoma. *Transl Oncol* 2021;**14**(2):100989. doi:10.1016/j.tranon.2020.100989
- 28.. Rimola J, Da Fonseca LG, Sapena V, et al. Radiological response to nivolumab in patients with hepatocellular carcinoma: a multicenter analysis of real-life practice. *Eur J Radiol* 2021;**135**(December 2020). doi:10.1016/j.ejrad.2020.109484
- 29.. Gomes da Moraes AL, de Miguel M, Cardenas JM, Calvo E. Comparison of radiological criteria for hyperprogressive disease in response to immunotherapy. *Cancer Treat Rev* 2020;**91**(September). doi:10.1016/j.ctrv.2020.102116
- 30.. Schuiveling M, Tonk EHI, Verheijden RJ, Suijkerbuijk KPM. Hyperprogressive disease rarely occurs during checkpoint inhibitor treatment for advanced melanoma. *Cancer Immunol Immunother* 2021;**70**:1491–1496. doi:10.1007/s00262-020-02716-3
- 31.. Yilmaz M. Atypical response patterns in metastatic melanoma and renal cell carcinoma patients treated with nivolumab: a single center experience. *J Oncol Pharm Pract* 2021;**27**(5):1106–1111. doi:10.1177/1078155220949642
- 32.. Kim SH, Choi CM, Lee DH, et al. Clinical outcomes of nivolumab in patients with advanced non-small cell lung cancer in real-world practice, with an emphasis on hyper-progressive disease. *J Cancer Res Clin Oncol* 2020;**146**(11):3025–3036. doi:10.1007/s00432-020-03293-9
- 33.. Ji Z, Cui Y, Peng Z, et al. Use of radiomics to predict response to immunotherapy of malignant tumors of the digestive system. *Med Sci Monit* 2020;**26**:1–9. doi:10.12659/MSM.924671
- 34.. Petrova MP, Donev IS, Radanova MA, et al. Sarcopenia and high NLR are associated with the development of hyperprogressive disease after second-line pembrolizumab in patients with non-small-cell lung cancer. *Clin Exp Immunol* 2020;**202**(3):353–362. doi:10.1111/cei.13505
- 35.. Zheng B, Shin JH, Li H, Chen Y, Guo Y, Wang M. Comparison of radiological tumor response based on iRECIST and RECIST 1.1 in metastatic clear-cell renal cell carcinoma patients treated with programmed cell death-1 inhibitor therapy. *Korean J Radiol* 2021;**22**(3):366–375. doi:10.3348/kjr.2020.0404
- 36.. Karabajakian A, Garrivier T, Crozes C, et al. Hyperprogression and impact of tumor growth kinetics after PD1/PDL1 inhibition in head and neck squamous cell carcinoma. *Oncotarget* 2020;**11**(18):1618–1628. doi:10.18632/oncotarget.27563
- 37.. Park JH, Chun SH, Lee YG, et al. Hyperprogressive disease and its clinical impact in patients with recurrent and/or metastatic head and neck squamous cell carcinoma treated with immune-checkpoint inhibitors: Korean cancer study group HN 18–12. *J Cancer Res Clin Oncol* 2020;(0123456789). doi:10.1007/s00432-020-03316-5
- 38.. Vaidya P, Bera K, Patil PD, et al. Novel, non-invasive imaging approach to identify patients with advanced non-small cell lung cancer at risk of hyperprogressive disease with immune checkpoint blockade. *J Immunother Cancer* 2020;**8**(2). doi:10.1136/jitc-2020-001343
- 39.. Abbar B, De Castelbajac V, Gougis P, et al. Definitions, outcomes, and management of hyperprogression in patients with non-small-cell lung cancer treated with immune checkpoint inhibitors. *Lung Cancer* 2021;**152**(December 2020):109–118. doi:10.1016/j.lungcan.2020.12.026
- 40.. Choi YJ, Kim T, Kim EY, Lee SH, Kwon DS, Chang YS. Prediction model for hyperprogressive disease in non-small cell lung cancer treated with immune checkpoint inhibitors. *Thorac Cancer* 2020;**11**(10):2793–2803. doi:10.1111/1759-7714.13594
- 41.. Castello A, Rossi S, Mazziotti E, Toschi L, Lopci E. Hyperprogressive disease in patients with non-small cell lung cancer treated with checkpoint inhibitors: the role of 18F-FDG PET/CT. *J Nucl Med* 2020;**61**(6):821–826. doi:10.2967/jnumed.119.237768
- 42.. Nakamoto R, C Zaba L, Rosenberg J, et al. Imaging characteristics and diagnostic performance of 2-deoxy-2-[18F]fluoro-d-Glucose PET/CT for melanoma patients who demonstrate hyperprogressive disease when treated with immunotherapy. *Mol Imaging Biol* 2021;**23**(1):139–147. doi:10.1007/s11307-020-01526-4
- 43.. Zhang L, Wu L, Chen Q, et al. Predicting hyperprogressive disease in patients with advanced hepatocellular carcinoma treated with anti-programmed cell death 1 therapy. *EClinicalMedicine* 2021;**31**:100673. doi:10.1016/j.eclinm.2020.100673
- 44.. Matsuo N, Azuma K, Kojima T, et al. Comparative incidence of immune-related adverse events and hyperprogressive disease in patients with non-small cell lung cancer receiving immune checkpoint inhibitors with and without chemotherapy. *Invest New Drugs* Published online 2021. doi:10.1007/s10637-021-01069-7
- 45.. Economopoulou P, Anastasiou M, Papaxoinis G, et al. Patterns of response to immune checkpoint inhibitors in association with genomic and clinical features in patients with head and neck squamous cell carcinoma (HNSCC). *Cancers (Basel)* 2021;**13**(2):1–15. doi:10.3390/cancers13020286
- 46.. Kim SR, Chun SH, Kim JR, et al. The implications of clinical risk factors, CAR index, and compositional changes of immune cells on hyperprogressive disease in non-small cell lung cancer patients receiving immunotherapy. *BMC Cancer* 2021;**21**(1):1–11. doi:10.1186/s12885-020-07727-y
- 47.. Hagi T, Kurokawa Y, Kawabata R, et al. Multicentre biomarker cohort study on the efficacy of nivolumab treatment for gastric cancer. *Br J Cancer* 2020;**123**(6):965–972. doi:10.1038/s41416-020-0975-7
- 48.. Okamoto I, Sato H, Tsukahara K. Overall survival and PD-L1 expression in patients with recurrent or metastatic head and neck cancer treated with nivolumab. *Auris Nasus Larynx* 2020;**47**(4):676–686. doi:10.1016/j.anl.2020.04.001
- 49.. Kim KH, Hur JY, Koh J, et al. Immunological characteristics of hyperprogressive disease in patients with non-small cell lung cancer treated with anti-pd-1/pd-l1 abs. *Immune Netw* 2020;**20**(6):1–11. doi:10.4110/in.2020.20.e48
- 50.. Ku BM, Kim Y, Lee KY, et al. Tumor infiltrated immune cell types support distinct immune checkpoint inhibitor outcomes in patients with advanced non-small cell

lung cancer. *Eur J Immunol* Published online 2021:1–9. doi:10.1002/eji.202048966

- 51.. Miyama Y, Morikawa T, Miyakawa J, *et al.* Squamous differentiation is a potential biomarker predicting tumor progression in patients treated with pembrolizumab for urothelial carcinoma. *Pathol Res Pract* 2021;**219**(February):153364. doi:10.1016/j.prp.2021.153364

<http://dx.doi.org/10.1136/jitc-2021-SITC2021.238>

EFFICACY AND TOXICITY OF SINGLE AGENT IMMUNE CHECKPOINT INHIBITORS AMONG ADULTS WITH CANCER AGED ≥ 80 YEARS: A MULTICENTER INTERNATIONAL COHORT STUDY

¹Caroline Nebhan*, ²Alessio Cortellini, ³Weijie Ma, ⁴Teja Ganta, ¹Haocan Song, ¹Fei Ye, ¹Rebecca Irlmeier, ⁴Neha Debnath, ⁵Anwaar Saeed, ³Maluki Radford, ⁶Asrar Alahmadi, ⁶Akiva Diamond, ⁷Christopher Hoimes, ⁶Nikhil Ramaiya, ⁸Carolyn Presley, ⁸Dwight Owen, ⁹Sarah Abou Alaiwi, ⁹Amin Nassar, ⁹Biagio Ricciuti, ¹⁰Giuseppe Lamberti, ¹¹Melissa Bersanelli, ¹¹Chiara Casartelli, ¹¹Sebastiano Buti, ¹²Paolo Marchetti, ¹²Raffaele Giusti, ¹Marco Filetti, ¹³Vito Vanella, ¹³Domenico Mallardo, ¹⁴Shravanti Macherla, ¹⁵Tamara Sussman, ¹⁶Andrea Botticelli, ¹⁷Domenico Galetta, ¹⁷Annamaria Catino, ¹⁷Pamela Pizzutilo, ¹⁸Carlo Genova, ¹⁹Maria Giovanna Dal Bello, ²⁰Foteini Kalofonou, ²⁰Ella Daniels, ¹³Paolo Ascierto, ²⁰David Pinato, ⁹Toni Choueiri, ¹Douglas Johnson, ⁴Thomas Marron, ³Yinghong Wang, ²¹Abdul Rafeh Naqash. ¹Vanderbilt University Medical Center, Nashville, TN, USA; ²University of L'Aquila, L'Aquila, Italy; ³MD Anderson Cancer, Houston, TX, USA; ⁴Icahn School of Medicine at Mount Sinai, New York, USA; ⁵University of Kansas Cancer Center, Kansas City, KS, USA; ⁶Case Western Reserve University, Cleveland, USA; ⁷Duke Cancer Institute, Durham, OH, USA; ⁸The Ohio State University Comprehensive, Columbus, OH, USA; ⁹Dana-Farber Cancer Center, Boston, MA, USA; ¹⁰University of Bologna, Bologna, Italy; ¹¹University of Parma, Parma, Italy; ¹²Universitaria Sant'Andrea, Rome, Italy; ¹³Istituto Nazionale Tumori IRCCS, Napoli, Italy; ¹⁴East Carolina University Brody School of, Greenville, USA; ¹⁵Cleveland Clinic Foundation, Cleveland, OH, USA; ¹⁶Sapienza University of Rome, Rome, Italy; ¹⁷IRCCS Istituto Tumori Giovanni Paolo II, Bari, Italy; ¹⁸Università degli Studi di Genova, Genova, Italy; ¹⁹IRCCS Ospedale Policlinico San Martino, Genova, Italy; ²⁰Imperial College London, London, UK; ²¹National Cancer Institute, Silver Spring, MD, USA

Background Immune checkpoint inhibitors (ICIs) are approved by the U.S. Food&Drug Administration in over 17 tumor types. Older adult patients make up about a quarter of all cancer patients but are historically understudied in cancer clinical trials. ICIs are associated with immune-related adverse events (irAEs), which may be particularly morbid for older adult patients with underlying comorbidities and impaired functional status. In this study, we provide insight into the real-world safety and efficacy of ICIs among older adult patients (≥ 80 years) with cancer.

Methods This is a multicenter, international retrospective study of tumor-agnostic older adult patients with cancer treated with single-agent ICIs between 2010–2019 from 18 academic centers in the U.S. and Europe. A cohort of 928 patients aged ≥ 80 years during treatment with ICI was assembled and analyzed to evaluate clinical outcomes and irAE patterns in older adult patients treated with single-agent ICIs.

Results Median age at ICI initiation was 83.0 years (range 75.8–97.0). Most patients (86.9%) were treated with anti-PD-1 therapy. Among the full cohort, the three most common tumors were non-small cell lung cancer (NSCLC, 37.2%, n=345), melanoma (35.5%, n=329), and genitourinary (GU) tumors (16.5%, n=153). Objective response rates for patients with NSCLC, melanoma, and GU tumors were 32.2%, 39.3%, and 26.2%, respectively. Median progression-free survival (PFS) was 6.7 months (95%CI, 5.2–8.6) for patients with NSCLC, 11.1 months (95%CI, 8.9–16.0) for patients with melanoma, and 6.0 months (95% CI, 5.0–10.7) for patients with GU malignancy. Median overall survival (OS) was 10.9 months (95%CI, 8.6–13.1) for patients with NSCLC, 30.0 months (95%CI, 23.6–46.4) for patients with melanoma, and 15.0 months (95%CI 9.1–25.4) for GU patients (Figure 1A-C). Within histology-specific cohorts (NSCLC, melanoma and GU), clinical outcomes were similar across age subgroups (<85, 85–89, >90). Among all patients (N=928), 41.3% experienced ≥ 1 irAE(s), including 12.2% reported to be grade (G)3–4. No irAE-related deaths occurred. The median time to irAE onset was 9.8 weeks; 57% occurred

within the first 3 months after ICI initiation. ICI was discontinued due to irAEs in 16.1% patients. There was no significant difference in the rate of irAEs among patients age <85, 85–89, and ≥ 90 years (p=0.15). Despite similar rates of G3+ irAEs, ICIs were discontinued due to irAE more than twice as often among patients ≥ 90 years compared to patients <90 years (30.9% vs. 15.1%, p=0.008) (table 1).

Conclusions ICIs are effective and generally well-tolerated among older patients with cancer. However, ICI discontinuation due to irAE is more frequent with increasing age.

<http://dx.doi.org/10.1136/jitc-2021-SITC2021.239>

DISCOVERY OF BIOMARKERS OF RESISTANCE TO IMMUNE CHECKPOINT BLOCKADE IN NON-SMALL-CELL LUNG CANCER (NSCLC) USING HIGH-PLEX DIGITAL SPATIAL PROFILING

¹Myrto Moutafi*, ¹Sandra Martinez-Morilla, ²Prajan Divakar, ¹Ioannis Vathiotis, ¹Niki Gavrielatou, ¹Thazin Aung, ¹Vesal Yaghoobi, ¹Aileen Fernandez, ³Jon Zugazagoitia Fraile, ¹Kurt Schalper, ¹David Rimm. ¹Yale, New Haven, CT, USA; ²Nanostring, Seattle, USA; ³12 de Octubre Hospital, Madrid, Spain

Background Despite the clinical effectiveness of Immune Checkpoint Inhibitors (ICI) in lung cancer, only around 20% remain disease free at 5 years. Predictive biomarkers for ICIs are neither sensitive nor specific. Here, we used the GeoMx Digital Spatial Profiler (DSP) (NanoString, Inc.) to analyze high-plex protein in a quantitative and spatially resolved manner from single formalin-fixed paraffin embedded tissue sections toward the goal of identification of new biomarkers with better predictive value.

Methods Pre-treatment samples from 56 patients with NSCLC treated with ICI were collected, represented in Yale tissue microarray 471 (YTMA471), and analyzed. A panel of 71 photocleavable oligonucleotide-labeled primary antibodies (NanoString Human IO panel) was used for protein detection. Protein expression was measured in 4 molecularly defined tissue compartments, defined by fluorescence co-localization (tumor [panCK+], leukocytes [CD45+/CD68-], macrophages [CD68+] and an aggregate stromal immune cell compartment, defined as the sum of leukocyte and macrophage expression [panCK-/CD45+/CD68+]) generating 284 variables representing potential predictive biomarkers. Promising candidates were orthogonally validated with Quantitative Immunofluorescence (QIF). Pre-treatment samples from 40 patients with NSCLC (YTMA404) that received ICI, and 174 non-ICI treated operable NSCLC patients (YTMA423) were analyzed to provide independent cohort validation. All statistical testing was performed using a two-sided significance level of $\alpha=0.05$ and multiple testing correction (Benjamini-Hochberg method, FDR < 0.1).

Results Initial biomarker discovery on 284 protein variables were generated by univariate analysis using continuous log-scaled data. High PD-L1 expression in tumor cells predicted longer survival (PFS; HR 0.67, $p=0.017$) and validated the training cohort. We found 4 markers associated with PFS, and 3 with OS in the stromal compartment. Of these, expression of CD66b in stromal immune cells predicted significantly shorter OS (HR 1.31, $p=0.016$) and shorter PFS (HR 1.24, $p=0.04$). Tertile analysis using QIF on all three tissue cohorts for CD66b expression, assessed by QIF, showed that CD66b was indicative but not prognostic for survival [discovery cohort, YTMA471 (OS; HR 3.02, $p=0.013$, PFS; HR 2.38, $p=0.023$), validation cohort; YTMA404 (OS; HR 2.97, $p=0.018$, PFS; HR 1.85, $p=0.1$), non-ICI treated cohort YTMA423 (OS; HR 1.02, $p>0.9$, PFS; HR 0.72, $p=0.4$)].

Conclusions Using the DSP technique, we have discovered that CD66b expressed in the stromal immune [panCK-/CD45+/CD68+] molecular compartment is associated with resistance to ICI therapy in NSCLC. This observation was validated by an orthogonal approach in an independent ICI treated NSCLC cohort. Since CD66b identifies neutrophils, further studies are warranted to characterize the role of neutrophils in ICI resistance.

Acknowledgements Dr Moutafi is supported by a scholarship from the Hellenic Society of Medical Oncologists (HESMO)

Ethics Approval All tissue samples were collected and used under the approval from the Yale Human Investigation Committee protocol #9505008219 with an assurance filed with and approved by the U.S. Department of Health and Human Services

<http://dx.doi.org/10.1136/jitc-2021-SITC2021.240>

241

IMMUNE CHECKPOINT BLOCKADE (ICB) IN BRAIN METASTASES (BM) FROM ADVANCED SMALL CELL UROTHELIAL CANCER (ASCUC)

¹Nathaniel Wilson*, ²Omar Alhalabi, ²Elshad Hasanov, ²Lianchun Xiao, ²John Papadopoulos, ²Matthew Campbell, ²Amishi Shah, ²Jianjun Gao, ²Paul Corn, ²Ana Aparicio, ²Jennifer Wang, ²Bogdan Czerniak, ²Charles Guo, ²Christopher Logothetis, ²Jing Li, ²Seungtaek Choi, ²Chad Tang, ²Nizar Tannir, ²Arlene Siefker-Radtke. ¹University of Texas Health Science Center-Houston, Houston, TX, USA; ²University of Texas MD Anderson Cancer Center, Houston, TX, USA

Background The risk of BMs in patients with aSCUC, having bulky tumors or non-cerebral metastasis at presentation, is high. We aimed to investigate the impact of ICB on the clinical outcomes of patients with aSCUC and BMs.

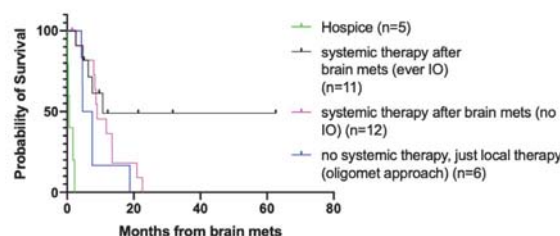
Methods Patients with aSCUC treated at MD Anderson Cancer Center between April 1992 and July 2019 were included if they had brain imaging and developed BMs during their disease course. Median overall survival (mOS) was calculated from diagnosis of BMs until death and if alive was censored at last contact. Hazard ratios (HR) and 95% confidence intervals (95% CI) were calculated using logrank test.

Results Among 216 patients with aSCUC, 111 underwent computed tomography or magnetic resonance imaging of the brain, and 34 (31%) were diagnosed with BMs. Baseline characteristics are included (table 1). At initial diagnosis of SCUC, clinical stage was cT1/x,cT2,≥cT3/4 or N+ (15%,44%,41%, respectively). Twenty-three (67.6%) underwent prior cystectomy, 16 (47%) had received neoadjuvant chemotherapy (NACT). Pathologic response at cystectomy after NACT was pT0/Tis,pT1,pT2,≥pT3b/4 or N+ (31%,6%,13%,50%, respectively). Those who did not undergo cystectomy (11, 32%) were either due to progression, declining surgery, or had de novo metastatic disease (27%,18%,55%, respectively). Regarding localized BM management, 9 (26%) patients received whole brain radiation therapy, 7 (21%) received stereotactic radiosurgery (SRS) and 7 (21%) received both. Median follow-up from BM diagnosis was 31.7 months. Five patients elected to pursue comfort care only, with mOS 0.7 months. Twenty-three patients received systemic therapy, including 11 (48%) who received ICB during any line of therapy. Majority of patients received ICB as single agent anti-PD(L)1; one patient received a doublet of anti-PD1+anti-CTLA4. Patients who were treated with ICB had numerically longer mOS as compared to those who solely received chemotherapy (10.7 months vs. 9.0 months, HR=0.47,95%CI=0.18–1.25,P=0.15), (figure 1). mOS decreased in patients with 1 vs 2 vs 3 vs ≥5 BMs (18.8,8.7,7.5 and 4.7 months, respectively, P=0.02), (figure 2). Furthermore, mOS improved with combination of ICB +SRS vs chemotherapy+SRS vs ICB without SRS vs chemotherapy without SRS (unreached,20.9,7.5,8.4, respectively, P=0.03) (figure 3).

Abstract 241 Table 1 Baseline characteristics of patients

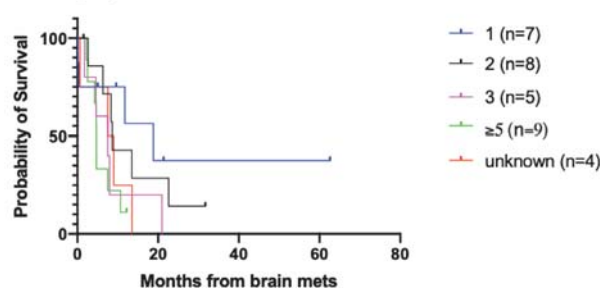
Characteristics	All patients (n=34)	Received systemic therapy not IO (n=12)	Received IO* (n=11)	P value
Age at brain mets diagnosis				
Median	65	62	63	0.804
Range	26-81	26-69	35-80	
Interquartile range	57-70	55-69	56-67	
Sex - no. (%)				
Male	26 (76)	9 (75)	10 (91)	0.590
Female	8 (24)	3 (25)	1 (9)	
Primary site - no. (%)				
Bladder	33 (97)	11 (92)	11 (100)	1
Urethra	1 (3)	1 (8)	0 (0)	
Histology - no. (%)				
Pure or Predominant small cell	27 (79)	10 (83)	8 (73)	0.640
Focal small cell	7 (21)	2 (17)	3 (27)	
Localized disease management - no. (%)				
Underwent cystectomy	23 (68)	6 (50)	10 (91)	
Received neoadjuvant chemo	19 (56)	3 (25)	10 (91)	
pCR	5 (15)	0 (0)	3 (27)	0.338
≥pT1 or N+	18 (53)	6 (50)	6 (55)	
Progressed prior to surgery	2 (6)	1 (7)	1 (9)	
Number of brain mets**				
1	8	1	4	0.383
2-4	13	7	4	
≥5	9	2	3	
Brain metastases local therapy				
Craniotomy + RT	6	2	2	
Craniotomy+SRS	3	0	1	1
Craniotomy+WBRT+SRS	2	1	1	
Craniotomy+WBRT	1	1	0	
RT alone	17	5	8	
WBRT***	8	2	3	1
SRS	4	1	3	
WBRT+SRS	5	2	2	
Sites of concomitant metastases				
Liver	10	5	2	0.710
Bone	8	5	2	
Lung	12	4	3	
Distal nodes	14	5	6	

Survival proportions: Survival of Brain mets systemic therapy



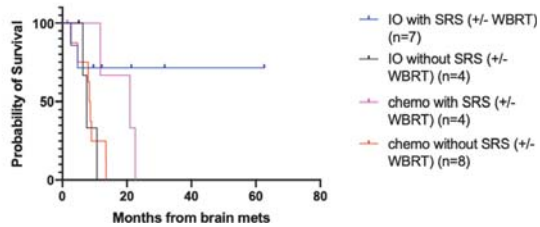
Abstract 241 Figure 1 Survival based on systemic therapy approach among all SCUC patients with brain metastases (n=34)

Survival proportions: Survival of Brain mets #mets



Abstract 241 Figure 2 Survival based on number of brain metastases among all 34 patients

Survival proportions: Survival of Brain mets systemic+local therapy



Abstract 241 Figure 3 Survival based on systemic + local therapy approach among SCUC patients with brain metastases with brain metastases who received both (n=23)

Conclusions In this first analysis to describe outcomes of patients with aSCUC and BMs with the inclusion of ICB treatment and despite the small sample size, we see a trend toward increased survival with fewer BMs, especially with combined ICB and SRS. Although challenging due to its rarity, future prospective trials evaluating the synergy between ICB and SRS in SCUC should be considered.

Ethics Approval This retrospective study received approval from the MD Anderson Cancer Center institutional review board

<http://dx.doi.org/10.1136/jitc-2021-SITC2021.241>

242

PHARMACOLOGIC TUMOR PD-L1 DEPLETION WITH CHLORAMBUCIL TREATS OVARIAN CANCER AND MELANOMAS IN A TUMOR PD-L1-DEPENDENT MANNER AND RENDERS α PD-L1-RESISTANT TUMORS α PD-L1-SENSITIVE

Haiyan Bai*, Álvaro Padrón, Yilun Deng, Anand Kornepati, Srikanth Polusani, Suresh Kari, Clare Murray, Myrna García, Ryan Reyes, Niannian Ji, Harshita Gupta, Matthew Hart, Tyler Curiel. *University of Texas Health San Antonio, San Antonio, TX, USA*

Background Programmed cell death ligand-1 (PD-L1) overexpression in tumor cells inhibits T cells activity and delivers pathologic intracellular signals that can reduce cancer treatment responses in pre-clinical models.^{1 2}

Methods To reduce tumor intracellular PD-L1-mediated pathology, we performed a drug screen that identified chlorambucil as a tumor cell PD-L1 depletion drug.

Results Chlorambucil depletes basal tumor PD-L1 expression through the ubiquitination proteasome pathway. In the tumor microenvironment, high chlorambucil doses treated orthotopic B16 melanoma and ID8agg ovarian cancer. Chlorambucil treatment efficacy was lost or reduced in PD-L1^{lo} ID8agg and PD-L1KO B16 tumors, corroborated with in vitro data. These data suggest that chlorambucil anti-tumor activity of CAMB requires tumor PD-L1 expression, confirmed in PD-L1KO host challenge with CTRL tumor, which chlorambucil treated effectively. Chlorambucil rendered α PD-L1 resistant CTRL ID8agg and PD-L1^{lo} B16 tumors α PD-L1 sensitive, preliminarily possibly due to tumor STING activation, and associated with enhanced tumor NK cell infiltration and central memory T cell generation. Chlorambucil also phenocopied genetic PD-L1KO by reducing tumor cell mTORC1 signals and stem cell content,³ suggesting additional treatment potential.

Conclusions Chlorambucil could be a useful strategy to reprogram tumor PD-L1 signals and boost immune-based therapies especially for anti-PD-L1-resistant tumors.

REFERENCES

- 1.. Clark CA *et al.* Tumor-intrinsic PD-L1 signals regulate cell growth, pathogenesis, and autophagy in ovarian cancer and melanoma. *Cancer Res* 2016;**76**:6964–6974.
- 2.. Juneja VR *et al.* PD-L1 on tumor cells is sufficient for immune evasion in immunogenic tumors and inhibits CD8 T cell cytotoxicity. *J Exp Med* 2017;**214**:895–904.
- 3.. Gupta HB *et al.* Tumor cell-intrinsic PD-L1 promotes tumor-initiating cell generation and functions in melanoma and ovarian cancer. *Signal Transduct Target Ther* 2016;**1**:2095–9907.

Ethics Approval We received approval from the UT Health San Antonio Institutional Animal Care and Use Committee (IACUC) for each procedure that used mice. We conducted each experiment per the standards required by the UT Health San Antonio Department of Laboratory Animal Resources.

<http://dx.doi.org/10.1136/jitc-2021-SITC2021.242>

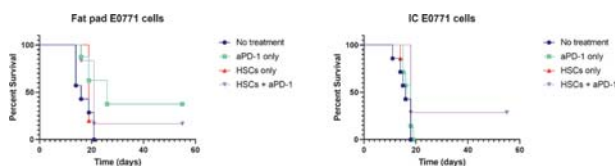
UNDERSTANDING AND OVERCOMING THE MECHANISM OF RESISTANCE TO ANTI-PD-1 MONOTHERAPY IN BRAIN METASTASIS

Laura Falceto Font*, Catherine Flores, Jack Figg, Bayli DiVita Dean, Connor Francis, Carmelle Kuizon, Ginger Moore. *University of Florida, Gainesville, FL, USA*

Background The average overall survival for patients with brain tumors is only 8 to 12 months. For example, the 5-year survival rate for adults over 40 years old living with Glioblastoma multiforme, a type of brain tumor, is only 6%. The brain is also a common organ for metastasis deriving from tumors such as breast cancer. The field of cancer immunotherapy has been making efforts to develop strategies that can target these brain metastases more efficiently than the standard of care in the clinic. Immune checkpoint inhibitors such as anti-PD-1 (anti-programmed cell death-1) therapy are under investigation to treat brain metastases. However, several studies have shown brain metastases to be resistant to anti-PD-1 monotherapy. Our findings have shown that a hematopoietic stem cell (HSC) transfer can overcome this resistance in brain metastasis. Our goal is to elucidate and overcome the mechanism of resistance to anti-PD-1 therapy in brain metastasis.

Methods We performed both orthotopic mammary fat pad and intracranial (IC) tumor implantations in C57/BL6J mice using a murine breast cancer cell line (E0771). Three days after tumor implantation, we administered the first of four doses of anti-PD-1 therapy delivered five days apart from each other. We measured survival and chemokine (from blood samples) differences between treatments.

Results We have observed that orthotopic mammary fat pad tumors are responsive to anti-PD-1 alone. Interestingly, when tumors derived from the same breast cancer cell line are implanted into the brain, they become non-responsive to anti-PD-1 monotherapy. We have also discovered that performing a hematopoietic stem cell transfer overcomes resistance to anti-PD-1 therapy in brain metastases (figure 1). Furthermore, in our preliminary studies we have found that both CD8+ and CD4+ T cells are required for the protective effects of anti-PD-1 against E0771 tumors.



Abstract 243 Figure 1 A hematopoietic stem cell transfer overcomes resistance to anti-PD-1 in brain metastasis

Conclusions Brain metastasis are resistant to anti-PD-1 monotherapy. We have found that a hematopoietic stem cell transfer overcomes resistance to anti-PD-1 in brain metastasis. We hypothesize that, while peripheral T cells successfully remove breast tumors, they fail to mount anti-tumor responses in breast metastatic brain tumors. Therefore, the next step is to understand the mechanism of resistance to anti-PD-1 monotherapy in brain metastasis and to further elucidate the type of T cell immune responses required to overcome this resistance in brain metastasis.

Ethics Approval IACUC Protocol #201910777

<http://dx.doi.org/10.1136/jitc-2021-SITC2021.243>

GENOMIC DETERMINANTS OF RESPONSE TO CHEMORADIATION AND DURVALUMAB CONSOLIDATION FOR STAGE III NON-SMALL CELL LUNG CANCER

Matthew Guo*, Joseph Murray, Paola Ghanem, Kinh Ranh Voong, Russell Hales, Josephine Feliciano, Kristen Marrone. *Johns Hopkins School of Medicine, Baltimore, MD, USA*

Background Durvalumab consolidation after chemoradiation for unresectable stage III non-small cell lung cancer (NSCLC) improves overall survival. However, up to 25% of patients progress within 18 months following durvalumab consolidation. Little is known regarding the genomic determinants of response to therapy.^{1 2}

Methods We retrospectively reviewed medical records of 76 patients with stage III NSCLC who received definitive chemoradiation and durvalumab consolidation between 2015–2020 at a large tertiary academic center. Tumor characteristics, molecular profiling, and clinical outcomes including response, progression-free survival (PFS), and overall survival (OS) were documented in an IRB-approved database. Outcomes were assessed by molecular alterations identified from diagnostic biopsy samples using Kaplan-Meier analysis.

Results Of 76 patients with stage III NSCLC treated with definitive chemoradiation and durvalumab consolidation, 74 were evaluable for PFS and OS. Median age at diagnosis was 66.5 years and 43% were women (n=32). Histology included adenocarcinoma (55%, n=41) and squamous cell carcinoma (32%, n=24). Median follow-up time was 23.0 months from start of durvalumab. The cohort's median PFS was 15.9 months with 36 patients having documented radiographic progression. Overall survival for the cohort was 32.0 months with 28 deaths. Molecular profiling was performed at time of diagnosis in 35 patients (47%), of which 30 had adenocarcinoma histology. 18 patients had *KRAS* mutations including *KRAS* p.G12C (n=8), which were mutually exclusive with 8 patients who had other clinically targetable alterations (*EGFR* mutations n=1, *ALK* fusion n=1, *RET* fusion n=1, *MET* exon 14 skipping mutation n=1, or *ERBB2* mutation n=4). Three patients had non-targetable mutations (*BRAF* non-p.V600E, *STK11*, *KEAP1*) and the remaining six patients lacked an identifiable alteration. There was no significant difference in PFS (p=0.92 by log-rank) or OS (p=0.36 by log-rank) between patients with *KRAS* mutations, other targetable alterations, non-targetable mutations, or those without molecular profiling. Within patients with *KRAS* mutations, there was no significant difference in PFS (p=0.33 by log-rank) or OS (p=0.69 by log-rank) when comparing *KRAS* p.G12C to non-p.G12C mutations.

Conclusions Our study of real-world cohort of patients with stage III NSCLC examined genomic determinants of response to treatment with definitive chemoradiation and durvalumab. Results from this retrospective study suggest that patients with *KRAS*-mutated tumors derive similar benefit from therapy than patients with other targetable, non-targetable or no identifiable genomic alterations. Future directions for this cohort include analysis of post-progression therapy, subgroup analysis comparing genomic alterations to patterns of progression, and examination of molecular signatures of patients with progression.

REFERENCES

1. . Antonia SJ, Villegas A, Daniel D, *et al.* Durvalumab after chemoradiotherapy in stage III non-small-cell lung cancer. *N Engl J Med* 2017;**377**(20):1919–1929. doi:10.1056/NEJMoa1709937

2. . Faivre-Finn C, Vicente D, Kurata T, *et al.* Four-year survival with durvalumab after chemoradiotherapy in stage III NSCLC—an update from the PACIFIC trial. *Journal of Thoracic Oncology* 2021;**16**(5):860–867. doi:10.1016/j.jtho.2020.12.015

Ethics Approval This retrospective chart review study has obtained ethics approval from the Institutional Review Board at the Johns Hopkins School of Medicine (number: IRB00232313).

<http://dx.doi.org/10.1136/jitc-2021-SITC2021.244>

HOST MYELOID RESPONSE TO TUMOR AND IMMUNOTHERAPY IS ASSOCIATED WITH HETEROGENEITY IN OUTCOMES TO ANTI-PDL1<http://dx.doi.org/10.1136/jitc-2021-SITC2021.245>

¹Ann Hanna*, ²Xiaopeng Sun, ¹Paula Gonzalez-Ericsson, ¹Violeta Sanchez, ¹Melinda Sanders, ¹Justin Balko. ¹Vanderbilt University Medical Center, Nashville, TN, USA; ²Vanderbilt University, Nashville, TN, USA

Background Immune checkpoint inhibitors (ICI) improve patient survival in some cancer types but yield limited success in breast cancer. Phase-III clinical trials in triple-negative breast cancer (TNBC) patients, who harbor extensive tumor-infiltrating lymphocytes, demonstrate increased progression-free survival (IMpassion130) and pathologic complete response (KEYNOTE-522). Consequently, combinations of ICI and chemotherapy have been FDA-approved for metastatic TNBC patients. However, the therapeutic benefit of ICI alone and the most efficacious chemotherapy combinations are poorly characterized. We sought to model ICI response *in vivo* to elucidate the mechanisms of immunotherapy efficacy in breast cancer and ascertain the therapeutic benefits of different chemotherapeutic combinations with ICI.

Methods Using an immunocompetent EMT6 orthotopic mammary tumor model, we investigated the efficacy of single-agent immunotherapy and in combination with standard-of-care chemotherapy (paclitaxel [PAC] or doxorubicin [DOX]). We used single-cell RNA sequencing and bulk RNA and T-cell receptor (TCR) sequencing to assess the cellular landscape of the primary tumor in response to combinatorial therapeutic strategies and identify systemic genetic alterations and T-cell expansion, respectively.

Results Single-agent anti-PD-L1 robustly suppressed primary tumor growth ($p = 0.0046$) and extended survival ($p < 0.0001$) beyond the isotype control. Chemotherapy demonstrated moderate therapeutic efficacy without potentiating the benefit of single-agent anti-PD-L1. Interestingly, despite using a genetically identical murine tumor model/host, anti-PD-L1 induced heterogeneous responses, from complete response to intrinsic resistance. Longitudinal analysis of peripheral blood from heterogeneously responding mice uncovered myeloid cell recruitment signatures corresponding to transient responses ultimately converting to resistance. We identified specific clonal T cell expansion present only in responders. Single-cell transcriptomic profiling of the tumor microenvironment revealed increased T cells and natural killer cells and reduced regulatory T cells in the combination groups versus chemotherapy alone, although this did not translate into improved benefit. Gene-set enrichment analysis on infiltrating T cells identified a robust signature of cytotoxic T cell activation characterized by a significant enrichment in inflammatory pathways in both single-agent anti-PD-L1 and in combination with chemotherapy.

Conclusions We identify a heterogeneously ICI-responsive *in vivo* model that emulates TNBC patient response to combinatorial ICI approaches. We describe single-agent ICI efficacy in upregulating cytotoxic immune cell infiltration and expansion within the primary tumor that diminishes tumor growth and enhances survival. Moreover, this study describes differential responses in a genetically similar host, which reflects heterogeneous patient response to ICI. Further characterization may identify systemic biomarkers and tumor antigen-specific T cell clones to accurately predict immunotherapy response in patients and uncover mechanisms for sensitizing refractory tumors to ICI

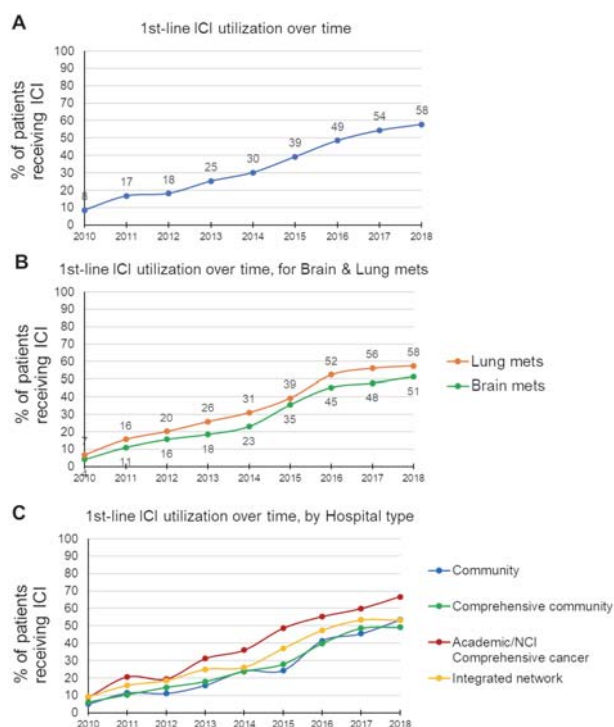
EFFECTIVENESS AND UTILIZATION OF FIRST-LINE IMMUNE CHECKPOINT INHIBITORS FOR PATIENTS WITH EXTRACRANIAL & INTRACRANIAL METASTATIC MELANOMA

¹Nayan Lamba, ²Bryan Iorgulescu*. ¹Harvard Medical School, Boston, MA, USA; ²Dana-Farber Cancer Institute, Boston, MA, USA

Background We previously demonstrated the effectiveness of 2nd-line immune checkpoint inhibitors (ICI) for stage 4 melanoma patients.¹ ²In late 2015, ICI was FDA-approved and NCCN-recommended in the 1st-line setting.³ ⁴ Here we assess the real-world effectiveness and utilization of 1st-line ICI among advanced melanoma patients following 2015.

Methods Patients newly-diagnosed with stage 4 melanoma during 2010–2018 were identified using the U.S. National Cancer Database (comprises >70% of newly-diagnosed cancers).⁵ Post-approval 1st-line ICI's overall survival (OS, estimated by Kaplan-Meier techniques) and utilization were assessed for patients diagnosed in 2016–2018, using multivariable Cox and logistic regression, respectively. To account for immortal time bias in receiving ICI, we only included those patients in regression analyses who survived at least until the landmark timepoint, defined as the median time from diagnosis to ICI initiation (49 days).¹ ² The more conservative 75th percentile diagnosis-to-ICI-initiation landmark timepoint (80 days) was also evaluated. Analyses were adjusted for patient, tumor, treatment, socioeconomic, and care setting characteristics.

Results Among 14,912 stage 4 melanoma patients, 1st-line immunotherapy utilization increased from 8.4% in 2010 to 39.2% in 2015, and 57.9% in 2018.(Figure 1) Altogether, median OS improved from 8.0 mos (95%CI=7.3–8.8) in 2010 to 16.1 mos (95%CI=14.0–18.5) in 2017. For patients diagnosed in 2016+ who survived at least until the landmark timepoints, OS improved with 1st-line ICI (median OS=33.1 mos, 95%CI=29.4–40.5; vs just 13.6 mos for no ICI, 95% CI=12.1–16.1; HR=0.58, 99%CI=0.50–0.68; padj<0.001) (figure 2A-B)—even after adjusting for patient, disease, and treatment factors, and using either landmark.(Table 1) This included patients with either brain metastases (ICI median OS=16.7 mos, 95%CI=13.1–19.9; vs no ICI=7.8 mos, 95% CI=6.8–9.0; padj<0.001) or lung metastases (ICI median OS=26.0 mos, 95%CI=20.0–33.0; vs no ICI=9.3 mos, 95% CI=8.0–10.5; padj<0.001).(Figure 2C-F)We then used multivariable logistic regression (with landmark timepoints to reduce bias from early mortality) to identify putative barriers to receiving 1st-line ICI in 2016+. Advanced melanoma patients who had more comorbidities or brain metastases, or who were older, uninsured/Medicaid-insured, from the poorest quartile of households, or managed at community hospitals were less likely to receive ICI.(all p<0.05, table 2)



Abstract 246 Figure 1 (A) The percent of stage 4 melanoma patients diagnosed each year who received 1st-line immune checkpoint inhibitor (ICI), with stratification by (B) brain or lung metastatic involvement, and (C) treating hospital type.

Abstract 246 Table 1 Multivariable Cox regression analysis of overall survival among stage 4 melanoma patients in 2016+. To account for immortal time bias, landmark timepoints were utilized, defined by the median (i.e. 49d; panels A, C, E) and 75th percentile (i.e. 80d; panels B, D, F) time from diagnosis to ICI initiation. Patients had to survive at least as long as the landmark timepoint to be included in the analysis. Results are shown for all stage 4 patients, as well as those with brain or lung metastases. p values are only displayed for the primary association of interest.

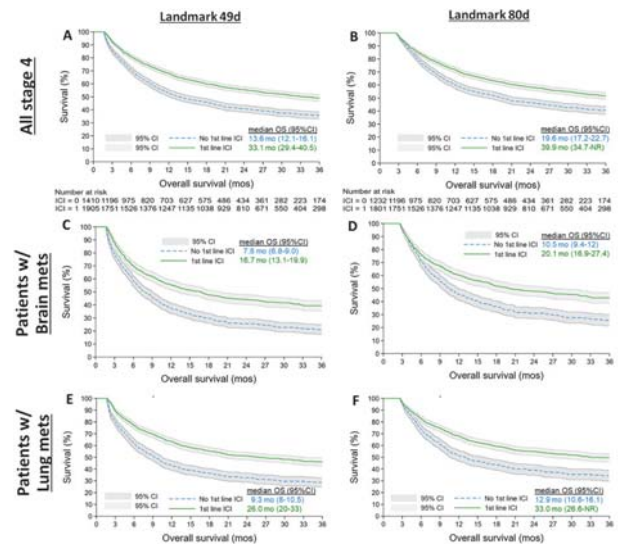
	Overall				Brain mets				Lung mets			
	Landmark 49d n=2,873	Landmark 80d n=2,750	Landmark 49d n=1,143	Landmark 80d n=993	Landmark 49d n=1,495	Landmark 80d n=1,251	Landmark 49d n=1,495	Landmark 80d n=1,251				
1st-line ICI	Ref	Ref	Ref	Ref	Ref	Ref	Ref	Ref				
No	0.58 (0.54-0.63)	<0.001 (0.61-0.87)	<0.001 (0.48-0.39-0.6)	<0.001 (0.45-0.73)	<0.001 (0.36-0.55)	<0.001 (0.43-0.71)	<0.001 (0.35-0.60)	<0.001 (0.43-0.71)				
Age at diagnosis (yr)												
<50	0.80 (0.65-1)	0.80 (0.64-1)	0.75 (0.54-0.99)	0.69 (0.54-0.91)	0.74 (0.55-1)	0.74 (0.55-1.03)	0.74 (0.55-1.03)	0.74 (0.55-1.03)				
50-59	0.80 (0.74-1.11)	0.80 (0.72-1.1)	0.99 (0.75-1.3)	0.94 (0.68-1.25)	0.87 (0.66-1.15)	0.88 (0.65-1.2)	0.88 (0.65-1.2)	0.88 (0.65-1.2)				
60-69	Ref	Ref	Ref	Ref	Ref	Ref	Ref	Ref				
70-79	1.43 (1.18-1.72)	1.36 (1.11-1.67)	1.47 (1.11-1.93)	1.33 (0.99-1.8)	1.31 (1.01-1.68)	1.31 (0.98-1.7)	1.28 (0.96-1.7)	1.28 (0.96-1.7)				
≥80	1.48 (1.16-2.07)	1.77 (1.41-2.22)	1.77 (1.26-2.5)	1.88 (1.28-2.76)	1.45 (1.08-1.94)	1.57 (1.13-2.17)	1.57 (1.13-2.17)	1.57 (1.13-2.17)				
Charlson-Deyo comorbidity index												
0	Ref	Ref	Ref	Ref	Ref	Ref	Ref	Ref				
1	1.13 (0.91-1.36)	1.10 (0.89-1.37)	1.09 (0.82-1.45)	1.06 (0.77-1.46)	1.01 (0.77-1.32)	1.01 (0.75-1.35)	1.01 (0.75-1.35)	1.01 (0.75-1.35)				
≥2	1.33 (1.07-1.65)	1.25 (0.99-1.59)	1.28 (0.91-1.76)	1.29 (0.91-1.83)	1.39 (1.02-1.9)	1.36 (0.98-1.9)	1.36 (0.98-1.9)	1.36 (0.98-1.9)				
Chemotherapy												
None	Ref	Ref	Ref	Ref	Ref	Ref	Ref	Ref				
Single-agent	0.99 (0.68-1.2)	1.00 (0.82-1.21)	0.82 (0.56-1.19)	0.94 (0.62-1.43)	0.67 (0.45-0.99)	0.76 (0.51-1.21)	0.76 (0.51-1.21)	0.76 (0.51-1.21)				
Multi-agent	0.77 (0.62-0.95)	none	0.66 (0.40-0.88)	0.63 (0.4-1.15)	0.55 (0.41-0.74)	0.76 (0.55-1.04)	0.76 (0.55-1.04)	0.76 (0.55-1.04)				
Radiotherapy (ref no)	1.29 (1.14-1.51)	1.35 (1.15-1.6)	1.34 (1.06-1.68)	1.49 (1.14-1.94)	1.54 (1.23-1.93)	1.62 (1.26-2.09)	1.62 (1.26-2.09)	1.62 (1.26-2.09)				
Year of diagnosis	0.97 (0.84-1.1)	0.99 (0.86-1.17)	0.99 (0.82-1.2)	1.03 (0.84-1.26)	0.99 (0.84-1.19)	1.01 (0.82-1.24)	1.01 (0.82-1.24)	1.01 (0.82-1.24)				
Metastases (ref no)	0.76 (0.68-0.9)	0.75 (0.67-0.87)	0.82 (0.67-1.01)	0.76 (0.6-0.96)	0.72 (0.6-0.88)	0.89 (0.76-1.04)	0.89 (0.76-1.04)	0.89 (0.76-1.04)				
Brain mets (ref no)	1.94 (1.65-2.28)	1.83 (1.54-2.18)	1.84 (1.38-2.5)	1.81 (1.3-2.5)	1.75 (1.4-2.2)	1.71 (1.34-2.2)	1.71 (1.34-2.2)	1.71 (1.34-2.2)				
Lung mets (ref no)	1.25 (1.08-1.43)	1.17 (1.05-1.36)	1.24 (1.08-1.43)	1.31 (1.05-1.63)	1.15 (1.01-1.3)	1.15 (1.01-1.3)	1.15 (1.01-1.3)	1.15 (1.01-1.3)				
Liver mets (ref no)	1.75 (1.49-2.05)	1.58 (1.32-1.88)	1.46 (1.13-1.88)	1.35 (1.09-1.67)	1.51 (1.22-1.87)	1.34 (1.05-1.71)	1.34 (1.05-1.71)	1.34 (1.05-1.71)				
Brain LN mets (ref no)	1.62 (1.39-1.89)	1.60 (1.35-1.9)	1.42 (1.11-1.81)	1.41 (1.07-1.86)	1.70 (1.37-2.1)	1.62 (1.26-2.05)	1.62 (1.26-2.05)	1.62 (1.26-2.05)				
Distast LN mets (ref no)	1.12 (0.96-1.29)	1.10 (0.94-1.29)	1.13 (0.94-1.4)	1.11 (0.91-1.46)	1.05 (0.87-1.29)	0.99 (0.78-1.25)	0.99 (0.78-1.25)	0.99 (0.78-1.25)				
Other organ mets (ref no)	1.01 (0.92-1.12)	1.03 (0.88-1.19)	1.06 (0.84-1.33)	1.03 (0.8-1.33)	1.08 (0.88-1.32)	1.08 (0.88-1.34)	1.08 (0.88-1.34)	1.08 (0.88-1.34)				

ICI = immune checkpoint inhibitor. HR = hazard ratio. CI = confidence interval. LN = lymph node.

Abstract 246 Table 2 Multivariable logistic regression analysis of 1st-line immune checkpoint inhibitor (ICI) receipt among stage 4 melanoma patients in 2016+. To account for bias due to early mortality, landmark timepoints were utilized, defined by the median (i.e. 49d) and 75th percentile (i.e. 80d) time from diagnosis to ICI initiation. Patients had to survive at least as long as the landmark timepoint to be included in the analysis. Results are shown for all stage 4 patients, as well as those with brain or lung metastases. Variables that demonstrate a significant association with ICI receipt are highlighted in yellow.

	Landmark 48d n=3,678			Landmark 80d n=3,459		
	OR	95% CI	p val	OR	95% CI	p val
Age at diagnosis (yr)						
<50	1.33	(0.91-1.94)	0.05	1.34	(0.91-1.97)	0.06
50-59	0.99	(0.74-1.33)	0.958	0.99	(0.74-1.34)	0.96
60-69	Ref			Ref		
70-79	0.78	(0.59-1.03)	0.02	0.84	(0.63-1.13)	0.13
≥80	0.44	(0.32-0.61)	<0.001	0.45	(0.32-0.63)	<0.001
Sex						
Male	Ref			Ref		
Female	0.91	(0.74-1.12)	0.253	0.90	(0.72-1.11)	0.19
Race/Ethnicity						
White, non-Hispanic	Ref			Ref		
Black, non-Hispanic	1.45	(0.65-3.26)	0.235	1.47	(0.64-3.37)	0.23
Asian/Pacific Islander	0.93	(0.29-2.96)	0.874	0.88	(0.27-2.82)	0.77
Hispanic	0.78	(0.43-1.43)	0.292	0.77	(0.41-1.46)	0.3
Other	1.29	(0.47-3.56)	0.51	1.27	(0.41-3.89)	0.58
n/a	0.77	(0.2-2.99)	0.616	0.72	(0.18-2.82)	0.54
Charlson-Deyo comorbidity index						
0	Ref			Ref		
1	0.91	(0.69-1.19)	0.356	0.91	(0.69-1.21)	0.42
≥2	0.72	(0.53-0.98)	0.007	0.75	(0.54-1.05)	0.03
Year of diagnosis	1.10	(0.98-1.24)	0.039	1.02	(0.9-1.15)	0.72
Primary skin site						
Lip	0.71	(0.05-10.6)	0.741	0.63	(0.04-9.61)	0.66
Eyelid	0.20	(0.02-2.05)	0.074	0.18	(0.02-1.88)	0.06
External ear	1.74	(0.52-5.78)	0.235	2.29	(0.6-8.82)	0.11
Face	0.89	(0.47-1.69)	0.651	0.85	(0.44-1.64)	0.54
Scalp & neck	1.16	(0.73-1.85)	0.406	1.18	(0.73-1.91)	0.38
Trunk	Ref			Ref		
Upper limb & shoulder	0.96	(0.62-1.49)	0.813	0.92	(0.58-1.44)	0.62
Lower limb & hip	1.53	(0.97-2.43)	0.017	1.56	(0.97-2.52)	0.02
Overlapping	2.00	(0.32-12.54)	0.329	3.04	(0.37-25.09)	0.18
Skin, NOS	0.91	(0.64-1.3)	0.498	0.88	(0.61-1.28)	0.37
Liver mets (ref no)	1.03	(0.81-1.31)	0.777	1.08	(0.83-1.4)	0.44
Lung mets (ref no)	1.56	(1.29-1.91)	<0.001	1.59	(1.3-1.96)	<0.001
Bone mets (ref no)	1.05	(0.83-1.34)	0.584	1.12	(0.87-1.45)	0.25
Brain mets (ref no)	0.55	(0.43-0.7)	<0.001	0.57	(0.44-0.74)	<0.001
Distant LN mets (ref no)	1.51	(1.21-1.89)	<0.001	1.59	(1.26-2.01)	<0.001
Other organ mets (ref no)	0.99	(0.81-1.22)	0.945	0.98	(0.8-1.21)	0.82
Primary site surgery						
None	0.96	(0.68-1.35)	0.733	1.00	(0.7-1.43)	0.99
Excisional biopsy	1.02	(0.7-1.48)	0.884	1.07	(0.72-1.57)	0.67
Gross or wide excision	Ref			Ref		
Radiotherapy (ref no)	1.91	(1.5-2.44)	<0.001	1.92	(1.49-2.49)	<0.001
Chemotherapy						
None	Ref			Ref		
Single-agent	0.19	(0.12-0.32)	<0.001	0.18	(0.11-0.3)	<0.001
Multi-agent	0.11	(0.07-0.15)	<0.001	0.10	(0.07-0.14)	<0.001
Metastectomy (ref no)	1.03	(0.81-1.31)	0.731	1.06	(0.83-1.36)	0.56
Insurance status						
Not insured	0.60	(0.36-1.01)	0.01	0.63	(0.37-1.09)	0.03
Private insurance	Ref			Ref		
Medicaid	0.57	(0.39-0.84)	<0.001	0.56	(0.37-0.84)	<0.001
Medicare	0.78	(0.6-1.03)	0.02	0.79	(0.59-1.04)	0.03
Other Government	0.37	(0.18-0.77)	<0.001	0.35	(0.17-0.74)	<0.001
Unknown	0.62	(0.24-1.6)	0.194	0.70	(0.24-1.99)	0.36
Median household income of patient's ZIP code						
<\$8,227	Ref			Ref		
\$8,227-50,353	1.29	(0.94-1.77)	0.035	1.36	(0.98-1.88)	0.02
\$50,354-63,332	1.14	(0.84-1.57)	0.269	1.15	(0.83-1.59)	0.27
>=\$63,333	1.40	(1.03-1.9)	0.005	1.52	(1.1-2.09)	<0.001
Hospital program type						
Community	0.65	(0.43-0.98)	0.007	0.68	(0.44-1.06)	0.02
Comprehensive community	0.58	(0.46-0.72)	<0.001	0.57	(0.45-0.72)	<0.001
Academic/NCI comprehensive	Ref			Ref		
Integrated Network	0.70	(0.53-0.92)	<0.001	0.69	(0.51-0.91)	<0.001
Hospital location						
New England	1.46	(0.87-2.43)	0.058	1.47	(0.86-2.5)	0.06
Middle Atlantic	1.20	(0.85-1.71)	0.169	1.25	(0.86-1.79)	0.12
South Atlantic	1.07	(0.79-1.46)	0.56	1.09	(0.79-1.51)	0.47
East North Central	Ref			Ref		
East South Central	1.08	(0.72-1.62)	0.632	1.18	(0.77-1.81)	0.31
West North Central	1.59	(1.03-2.45)	0.006	1.71	(1.08-2.71)	<0.001
West South Central	1.20	(0.8-1.81)	0.242	1.19	(0.78-1.82)	0.29
Mountain	1.51	(0.94-2.42)	0.024	1.58	(0.97-2.57)	0.02
Pacific	1.17	(0.82-1.66)	0.259	1.14	(0.79-1.65)	0.36

ICI = immune checkpoint inhibitor. OR = odds ratio. CI = confidence interval. LN = lymph node.



Abstract 246 Figure 2 Overall survival associated with 1st-line immune checkpoint inhibitors (ICI) for stage 4 melanoma patients diagnosed after 2015 (A-B), including patients with brain (C-D) and lung metastases (E-F). To account for immortal time bias, landmark timepoints were utilized, defined by the median (i.e. 49d; panels A, C, E) and 75th percentile (i.e. 80d; panels B, D, F) time from diagnosis to ICI initiation. Patients had to survive at least as long as the landmark timepoint to be included in the analysis.

Conclusions Following FDA-approval in 2015, 1st-line ICI was associated with dramatic improvements in OS for stage 4 melanoma patients—including those with brain or lung metastases. As of 2018, 42% of patients still weren't receiving 1st-line ICI in the U.S.—particularly patients who were underinsured, from the poorest quartile of households, or managed at community hospitals—suggesting that disparities exist in guideline-recommended 1st-line ICI utilization for advanced melanoma patients.

REFERENCES

- Doby A, Zogg C, Hodi F, Smith T, Ott P, Iorgulescu JB. Management of metastatic melanoma: improved survival in a national cohort following the approvals of checkpoint blockade immunotherapies and targeted therapies. *Cancer Immunol Immunother* 2018 December;67(12):1833–1844.
- Iorgulescu JB, Harary M, Zogg C, Ligon K, Reardon D, Hodi F, Aizer A, Smith T. Improved risk-adjusted survival for melanoma brain metastases in the era of checkpoint blockade immunotherapies: results from a national cohort. *Cancer Immunol Res* 2018 September;6(9):1039–1045.
- Beaver JA, Theoret MR, Mushti S, He K, Libeg M, Goldberg K, Sridhara R, McKee AE, Keegan P, Pazdur R. FDA approval of nivolumab for the first-line treatment of patients with BRAFV600 wild-type unresectable or metastatic melanoma. *Clin Cancer Res* 2017 July 15;23(14):3479–3483
- National Comprehensive Cancer Network Clinical Practice Guidelines in Oncology. Melanoma, Version 1.2016.
- Boffa DJ, Rosen JE, Mallin K, Loomis A, Gay G, Palis B, Thoburn K, Gress D, McKellar DP, Shulman LN, Facktor MA, Winchester DP. Using the national cancer database for outcomes research: a review. *JAMA Oncol* 2017 December 1;3(12):1722–1728.

<http://dx.doi.org/10.1136/jitc-2021-SITC2021.246>

247 THE FULLY HUMAN ANTIBODY SRF617 IS A POTENT INHIBITOR OF ECTO-ENZYME CD39 IN VIVO

¹Stephan Matissek*, ¹Marisella Panduro Sicheva, ¹Secil Koseoglu, ¹Ricard Masia, ¹Michael Warren, ¹Matthew Rausch, ¹Benjamin Lee, ²Sandra Pommey, ²Isabelle Cousineau, ²John Stagg, ¹Vito Palombella, ¹Andrew Lake. ¹*Surface Oncology, Inc., Cambridge, MA, USA*; ²*Université de Montréal, Montreal, Canada*

Background The purine nucleotide adenosine plays an important role in dampening both the innate and adaptive arms of the immune system. In contrast, extracellular adenosine triphosphate (ATP), which can be generated at high levels due to cell stress, initiates proinflammatory responses. Extracellular ATP can be produced in cancerous tumors, and its conversion to adenosine monophosphate by CD39 (ENTPD1) and subsequent degradation to free adenosine by CD73 (NT5E) in the tumor microenvironment (TME) is a major contributor to tumor immune evasion. Accordingly, CD39 serves as an important immune regulator. CD39 is highly expressed in the TME of various tumor types, including lung, prostate, colon, ovarian, and pancreatic cancers, making CD39 an attractive target for immune-based anticancer therapy. SRF617 is a fully human anti-CD39 antibody designed to target human CD39 and inhibit its enzymatic activity. SRF617 provides a dual mechanism of immune activation by increasing inflammatory responses through accumulation of free ATP and alleviating immune suppression by reducing adenosine production. In this way, SRF617 shifts the TME to a proinflammatory state leading to reactivation of the immune system and antitumor function.

Methods A pharmacokinetic/pharmacodynamic profile was determined in CT26 tumor-bearing human CD39 knock-in (hCD39 KI) mice by measuring plasma SRF617 concentration, peripheral blood target occupancy (TO), and ATP hydrolysis activity in frozen tissue sections. Wild-type mice bearing subcutaneous (s.c.) KPC1245 tumors were treated with anti-murine CD39 antibody, alone or in combination with gemcitabine.

Results Circulating SRF617 was observed in the plasma after intravenous injection of CT26 tumor-bearing hCD39 KI mice, which correlated with CD39-bound SRF617 on B cells. The presence of SRF617 correlated with a decrease in ATPase activity and CD39 expression in tissues. In the KPC tumor model, a combination effect was observed for anti-CD39 treatment with gemcitabine. Treatment with anti-CD39 antibody resulted in an increase in CD8+ T cells in the TME as measured by flow cytometry.

Conclusions SRF617 treatment of hCD39 KI mice led to reduction of ATPase activity in the TME that correlated with peripheral TO and plasma concentration. Anti-CD39 treatment alone or in combination with gemcitabine led to tumor growth inhibition and increased tumor-infiltrating lymphocytes as measured by flow cytometry in s.c. KPC tumors. These studies demonstrate the therapeutic potential of targeting CD39 for the treatment of cancer. SRF617 is currently being evaluated in a Phase 1 clinical trial in patients with advanced solid tumors (NCT04336098) and in combination with chemotherapy in patients with pancreatic cancer.

<http://dx.doi.org/10.1136/jitc-2021-SITC2021.247>

EMPIRIC PROFILING OF PERIPHERAL T CELL RECALL RESPONSES TO TUMOR MUTANOMES VERSUS IN SILICO PREDICTIONS IN NSCLC PATIENTS UNDERGOING PEMBROLIZUMAB TREATMENT ± CHEMOTHERAPY

¹Madison Milaszewski*, ¹James Loizeaux, ¹Emily Tjon, ¹Crystal Cabral, ¹Tulin Dadali, ¹Justin Strickland, ¹Jamie Foti, ¹Kevin Mancini, ²Kesi Michael, ¹Louisa Dowal, ¹Vijetha Vemulapalli, ¹Alberto Visintin, ¹Thomas Davis, ¹Jessica Flechtner, ²Mark Awad. ¹Genocea Biosciences, Cambridge, MA, USA; ²Dana-Farber Cancer Institute, Boston, MA, USA

Background Effective immune checkpoint blockade (ICB) treatment is dependent on T-cell recognition of patient-specific mutations (neoantigens). Empirical identification of neoantigens ex vivo has revealed shortcomings of in silico predictions.¹ To better understand the impact of ICB treatment on T cell responses and differences between in silico and in vitro methods, neoantigen-specific T cell responses were evaluated in patients with non-small cell lung cancer undergoing first-line therapy with pembrolizumab ± chemotherapy.

Methods Tumor and whole blood samples were collected from 14 patients prior to and after immunotherapy; seven each in monotherapy and combination therapy cohorts. The ex vivo ATLAS™ platform was used to profile neoantigen-specific T-cell responses. Patient-specific tumor mutations identified by next-generation sequencing (NGS) were expressed individually as ATLAS clones, processed patient-specific autologous antigen presenting cells, and presented to their T cells in vitro. ATLAS-verified antigens were compared with epitope predictions made using algorithms.

Results On average, 150 (range 37–339) non-synonymous mutations were identified. Pre-treatment, ATLAS identified T cell responses to a median of 15% (9–25%) of mutations, with nearly equal proportions of neoantigens (8%, 5–15%) and Inhibigens™, targets of suppressive T cell responses (8%, 3–13%). The combination therapy cohort had more confirmed neoantigens (46, 20–103) than the monotherapy cohort (7, 6–79). After treatment, the median ratio of CD4:CD8 T cells doubled in the monotherapy but not combination cohort (1.2 to 2.4 v. 1.6 to 1.3). Upon non-specific stimulation, T cells from patients on combination therapy expanded poorly relative to monotherapy (24 v. 65-fold, $p = 0.014$); no significant differences were observed pre-treatment (22 v. 18-fold, $p = 0.1578$). Post-treatment, the median number of CD8 neoantigens increased in the combination therapy cohort (11 to 15) but in monotherapy were mostly unchanged (6 to 7). Across timepoints, 36% of ATLAS-identified responses overlapped. In silico analysis resulted in 1,895 predicted epitopes among 961 total mutations; among those, 30% were confirmed with ATLAS, although nearly half were Inhibigens, which could not be predicted. Moreover, 50% of confirmed neoantigens were missed by in silico prediction.

Conclusions Monotherapy and combination therapy had differential effects on CD4:CD8 T cell ratios and their non-specific expansion. A greater proportion of neoantigens was identified than previously reported in studies employing in silico predictions prior to empirical verification.² Overlap between confirmed antigens and in silico prediction was observed, but in silico prediction continued to have a large false negative rate and could not characterize Inhibigens.

Acknowledgements We would like to acknowledge and thank the patients and their families for participating in this study.

REFERENCES

- 1.. Lam H, McNeil LK, Starobinets H, DeVault VL, Cohen RB, Twardowski P, Johnson ML, Gillison ML, Stein MN, Vaishampayan UN, DeCillis AP, Foti JJ, Vemulapalli V, Tjon E, Ferber K, DeOliveira DB, Broom W, Agnihotri P, Jaffee EM, Wong KK, Drake CG, Carroll PM, Davis TA, Flechtner JB. An empirical antigen selection method identifies neoantigens that either elicit broad antitumor T-cell responses or drive tumor growth. *Cancer Discov* 2021;**11**(3):696–713. doi: 10.1158/2159-8290.CD-20-0377. Epub 2021 January 27. PMID: 33504579.
- 2.. Rosenberg SA. Immersion in the search for effective cancer immunotherapies. *Mol Med* 27,**63**(2021). <https://doi.org/10.1186/s10020-021-00321-3>

<http://dx.doi.org/10.1136/jitc-2021-SITC2021.248>

CHARACTERIZATION OF UNRESECTABLE AND/OR METASTATIC SOLID TUMORS PATIENTS TREATED WITH SYSTEMIC ANTICANCER THERAPY IN FIRST-LINE SETTINGS: A PAN-TUMOR COMMUNITY-ONCOLOGY BASED STUDY

¹Elise Wu, ²Sneha Sura*, ³Alexander Spira. ¹Merck and Co., Inc., Kenilworth, NJ, USA; ²McKesson Life Sciences, The Woodlands, TX, USA; ³Texas Oncology, Fairfax, VA, USA

Background Since the introduction of immunotherapy (I/O) in 2014, increasing number of patients with solid tumor are treated with I/O. This study aimed to describe demographic and clinical characteristics of patients initiating I/O versus non-I/O-based systemic anticancer therapy (SACT) in the first-line (1L) settings among patients diagnosed with unresectable and/or metastatic solid tumors in a real-world US community oncology setting from pan-tumor perspective.

Methods This retrospective observational study used the US Oncology Network's iKnowMed electronic health record database and included adults diagnosed with unresectable and/or metastatic solid tumors who initiated SACT. We selected 11 solid tumors in the cohort because I/O has been approved as 1L treatment for unresectable and/or metastatic tumors prior to August 2019. We included I/O indicated patients who initiated either 1L I/O or non-I/O-based SACT between 01/01/2014 and 08/31/2019. All analysis was performed based on pan-tumor perspective with no stratification by tumor types. Descriptive statistic was conducted to characterize demographic and clinical characteristics among those who used I/O versus non-I/O-based SACT.

Results A total of 20,057 patients were included in the study cohort. 5,119 (25.5%) used I/O and 14,938 (74.5%) used non-I/O-based SACT. The use of I/O increased from 4.0% in 2014 to 66.3% in 2019 with a corresponding decline in non-I/O use during the same period. Patients who initiated I/O were older (69.4 vs. 67.8 years, $p < 0.0001$), and a greater proportion were male (57.8% vs. 53.0%, $p < 0.0001$) and had Medicare insurance (57.0% vs. 55.2%, $p = 0.025$) compared to those who initiated non-I/O-based SACT. Race distribution and smoking status were significantly different between I/O users and non-users ($p < 0.0001$ for both). The mean duration of time from unresectable and/or metastatic solid tumors diagnosis to SACT initiation was higher in I/O users compared to non-I/O-based SACT users (10.1 weeks vs. 6.1 weeks, $p < 0.0001$). Among clinical characteristics, a greater proportion of I/O users had ECOG performance status of 3+ (2.1% vs. 1.6%, $p < 0.0001$), lung as a site of metastases (13.9% vs. 10.1%, $p < 0.0001$), and had 1+ Charlson comorbidities (19.2% vs. 15.6%, $p = 0.002$).

Conclusions This real-world study provides insight into characteristics of patients with unresectable and/or metastatic solid tumors who initiated SACT in real-world oncology settings. Patients who received I/O appeared to be older, and sicker and takes a longer time to receive treatment since diagnosis compared to those who received non-I/O-based SACT. Future research should carefully adjust patients' characteristics while evaluating the effect of I/O therapy on clinical and economic outcomes.

Trial Registration The authors would like to acknowledge Lisa Kaspin-Powell, PhD, ELS, an employee of Ontada, for editorial assistance, which was funded by Merck & Co., Inc.

<http://dx.doi.org/10.1136/jitc-2021-SITC2021.249>

SPATIAL-TRANSCRIPTOMIC ANALYSIS OF TUMOR-IMMUNE MICROENVIRONMENT IN AML PATIENTS RECEIVING PEMBROLIZUMAB AND DECITABINE

¹Chen Zhao*, ¹Abigail Wong-Rolle, ²Prajan Divakar, ³Katherine Calvo, ⁴Christopher Hourigan. ¹National Cancer Institute, North Bethesda, MD, USA; ²NanoString, Seattle, WA, USA; ³National Institutes of Health Clinical Center, Bethesda, MD, USA; ⁴National Heart, Lung, and Blood Institute, Bethesda, MD, USA

Background Relapsed or refractory Acute Myeloid Leukemia (R-AML) is a deadly disease with an inadequate response rate to current treatments. Recent advances in immunotherapy shed light on R-AML, and several clinical trials have shown promising potential for combining immune checkpoint inhibitors (ICIs) with hypomethylating agents. A deeper understanding of the tumor-immune microenvironment in R-AML during combination ICI treatment is urgently needed for developing better therapeutics and stratifying treatment strategies.

Methods To dissect the tumor-immune interactions in the bone marrow microenvironment, we employed nanoString GeoMx Digital Spatial Profiler (DSP) and performed a spatial-transcriptomic analysis of patients with R-AML who received pembrolizumab and decitabine. We compared the transcriptomic profiles and TCR clonalities of tumor-interacting T cells, bystander T cells, and other cells at baseline, post-pembrolizumab treatment, and post-decitabine, which enable us to identify R-AMLs suppressive immune microenvironment and immune cells' responses to ICI and hypomethylating agent.

Results We obtained the spatial-transcriptomic profiles of T cells, stromal cells, and leukemia cells in patients with R-AML at different treatment points. Our TCR-specific probes were able to track T cell clonal changes during treatments.

Conclusions R-AML harbored a complex tumor immune microenvironment and diverse T cell clonality.

Acknowledgements This research was supported in part by the Intramural Research Program of the NCI (the Center for Cancer Research), NHLBI, and NIH Clinical Center.

Ethics Approval This study is approved by NHLBI IRB.

<http://dx.doi.org/10.1136/jitc-2021-SITC2021.250>

251

THE USE OF SMALL MOLECULE INHIBITORS TO TARGET NOVEL PATHWAYS IN EXHAUSTED T CELLS FOR IMMUNO-ONCOLOGY THERAPEUTIC INTERVENTION

Francis Acklam, Joanne Hay, Darryl Turner, Mark Barbour, Preeti Singh, Courtney Grant, Hayley Gooding, Justyna Rzepecka, Rhoanne McPherson*. *Concept Life Sciences, Edinburgh, UK*

Background The ability to reverse exhaustion in CD8+ T cells holds great promise for therapeutic intervention in oncology. Indeed, treatment with therapeutics targeted at checkpoint inhibitors, such as Nivolumab (anti-PD-1), have shown great promise in the treatment of a subset of individuals and tumour types. However, pre-clinical success does not always translate to success in clinical trials and resistance to these approaches is prevalent. As such, there is a pressing need to develop novel approaches that target alternative pathways for use alone or potentially in combination with checkpoint inhibitor modulation. A secondary need is the requirement for advanced assays that accurately recapitulate the pathways and cell phenotypes prevalent in the tumour environment.

Methods Here we describe the characteristics of an *in vitro* human T cell exhaustion assay whereby *in vitro* stimulated T cells phenotypically and functionally recapitulate the exhausted T cells found within the tumour microenvironment. We also demonstrate the effect of checkpoint blockade as well as small molecule inhibition of a novel target on the exhausted T cell phenotype.

Results In this assay, exhaustion can be partially but not fully reversed by treatment with anti-PD-1 alone. In addition, we demonstrate the effect of a small molecule inhibitor targeting IKZF3, a transcription factor shown to be upregulated in T cell exhaustion, on reversing T cell exhaustion alone and in combination with checkpoint inhibitor blockade.

Conclusions These assays and approaches enable investigation into the ability of compounds to influence reversal of T cell exhaustion where anti-PD-1 treatment does not fully reverse the exhausted phenotype and offers the ability to test combination therapy approaches.

Acknowledgements This work was aided by the valuable input and insight of Professor Stephen Anderton.

Ethics Approval The study obtained ethics approval from West Midlands – Black Country Research Ethics Committee under IRAS project ID 270936. All donors gave informed consent before taking part.

<http://dx.doi.org/10.1136/jitc-2021-SITC2021.251>

NOVEL DNAM-1 AXIS MEMBER, PVRIG, IS POTENTIALLY A DOMINANT CHECKPOINT INVOLVED IN STEM-LIKE MEMORY T CELLS – DENDRITIC CELL INTERACTION

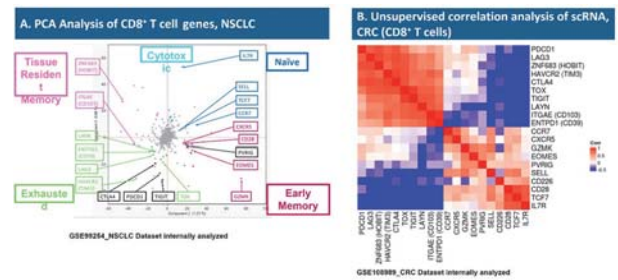
Zoya Alteber, Gady Cojocar, Masha Frenkel, Emmanuel Weyl, Niv Sabath, Assaf Wool, Amit Novik, Yossef Kliger, Zurit Levine, Eran Ophir*. *Compugen Ltd., Holon, Israel*

Background T-cell accumulation in tumors is a prerequisite for response to cancer immunotherapy. Recent studies highlighted the importance of an early-memory (stem-like) T-cell sub-population, that can self-renew and differentiate into effector cells, and of dendritic cells (DCs), which are essential for T-cell priming and expansion following checkpoint blockade.^{1 2} PVRIG is a novel inhibitory receptor that competes with the co-activating receptor DNAM-1, for the binding of a shared ligand, PVRL2. PVRIG expression is induced on T and NK tumor infiltrating cells, whereas PVRL2 is expressed on tumor, endothelial and myeloid cells in the tumor micro-environment (TME).³ We investigated the expression of PVRIG and PVRL2 across TME immune subpopulations.

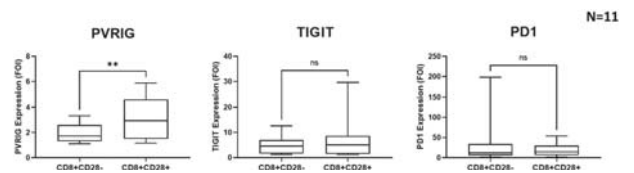
Methods Publicly available TME scRNA sequencing datasets were analyzed for the expression of PVRIG and PVRL2 across immune subsets. Unsupervised principal-component-analysis and hierarchical co-expression pattern among genes known to be expressed on naïve, memory, and exhausted CD8+ T-cells was performed. Observations were validated by flow-cytometry and immunohistochemistry analysis across a variety of tumor indications. Proximity Extension Assay (PEA, Olink) was conducted using serums collected at several time-points from COM701 (anti-PVRIG antibody) and nivolumab treated patients in a Phase-1 study (NCT03667716).

Results Across scRNA datasets, PVRIG, like TIGIT and PD-1, was expressed by both stem-like (TCF1+PD1+) and exhausted (TIM3+CD39+) CD8+ T-cells. High resolution unsupervised scRNA gene co-expression analysis revealed that while TIGIT is strongly correlated with PD-1, CTLA-4, and other markers of exhausted T-cells, PVRIG uniquely clusters with markers of early memory T-cells (figure 1). Accordingly, PVRIG protein expression was increased on CD28+ early-memory T-cells across indications (figure 2). RNA expression data also revealed that PVRL2 is more abundantly expressed across DC-subtypes compared to PD-L1 and PVR (ligand of TIGIT, figure 3). Flow cytometry confirmed dominant PVRL2 expression on DC subtypes across tumor indications. Immunohistochemistry analysis identified PVRL2 expression in Tertiary Lymphoid Structures (figure 4). Finally, preliminary analysis of serum from COM701+nivolumab treated patients revealed elevated induction of activated-DC markers in two patients that responded clinically (RECIST criteria), compared to non-responders (figure 5).

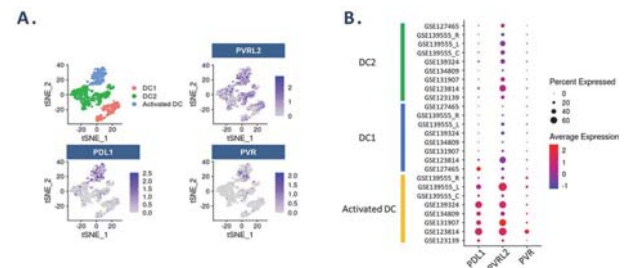
Conclusions PVRIG is co-expressed with PD-1 and TIGIT on stem-like and exhausted T cells but has a unique dominant expression on early memory cells, while PVRL2 is abundantly expressed across DC-types. PVRIG blockade could therefore enhance memory T-cells activation by DCs, resulting in their increased expansion and differentiation. Accordingly, early data shows increased induction of activated DC markers, potentially following efficient T-DC interaction, in serum of two patients responding to COM701+nivolumab.



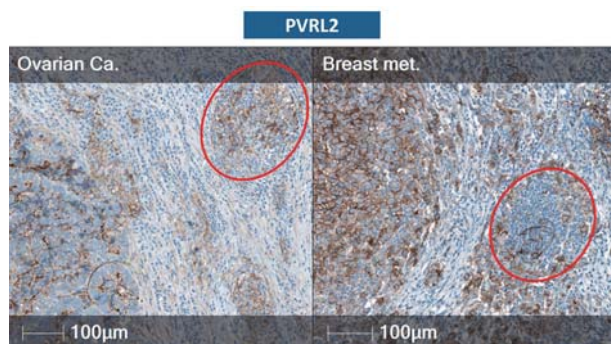
Abstract 252 Figure 1 PVRIG clusters with early differentiation/memory genes, unlike other immune checkpoints that cluster with exhausted genes, in CD8+ T cells. (A) Unsupervised PCA analysis was performed on a scRNA expression matrix of TME CD8+ T cells, which includes all variable genes. Using cells as features and genes as entries, hierarchical co-expression pattern among genes known to be expressed on naïve, memory, and exhausted CD8+ T-cells was performed. (B) scRNA-Seq datasets were analyzed for co-expression pattern among 19 genes, including genes known to be expressed on naïve (TCF7, IL7R, SELL), memory (GZMK, EOMES), and exhausted (PDCD1, LAG3, HAVCR2) CD8 T cells. Average gene-gene correlation over all datasets was calculated. Representative dataset of n=13 (CRC, NSCLC, HNSCC, Melanoma, Liver cancer) is presented.



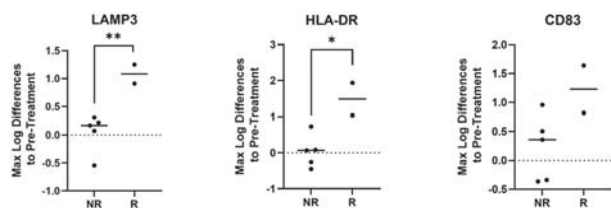
Abstract 252 Figure 2 PVRIG is expressed by early memory CD8+ T cells in the TME. Samples (n=11) of CRC, ovarian and bladder cancer were dissociated to single cell suspensions and analyzed for gene expression by flow-cytometry. Paired T-test was used to compare between PVRIG expression among cell populations



Abstract 252 Figure 3 PVRL2 is dominantly expressed on dendritic cells. (A) tSNE map depicting the expression profile of PVR/PVRL2/PDL1 in major dendritic cell subsets in Basal Cell Carcinoma patients. (B) Dot plots showing the percent of cells and average level of expression of PVR/PVRL2/PDL1 in major dendritic cell subsets across multiple scRNA cancer studies.



Abstract 252 Figure 4 PVRL2 is expressed in tertiary lymphoid structures in the tumor bed. Tertiary Lymphoid Structures (TLSs) were identified in subsets of samples across all tumors tested (NSCLC, CRC primary and metastasis, ovarian cancer, endometrial cancer, breast primary TNBC and breast metastasis) and for most cases TLSs were positive for PVRL2. Staining was performed using a proprietary rabbit mAb raised against the ECD of PVRL2 on a Dako Autostainer



Abstract 252 Figure 5 Elevated induction of activated-DCs markers in patients that clinically responded to COM701+nivolumab, compared to non-responders. Serum of 7 patients from the nivolumab+COM701 dose escalation arm, were analyzed using Olink Explore 1536. For each patient, the difference between all on-treatment time points to pre-treatment were calculated. Group difference based on response, RECIST criteria (responders (R): CR+PR vs. non responders (NR): SD+PD) were compared by student t-test for all available time points grouped

REFERENCES

- 1.. Jansen CS, Prokhnevskaya N, Master VA, *et al.* An intra-tumoral niche maintains and differentiates stem-like CD8 T cells. *Nature* 2019;**576**:465–470.
- 2.. Held W, *et al.* Intratumoral CD8+ T cells with stem cell-like properties: implications for cancer immunotherapy. *Sci Transl Med* 2019;**11**(515):eaay6863
- 3.. Whelan S, Ophir E, Kotturi MF, Levy O, Ganguly S, Leung L, *et al.* PVRIG and PVRL2 are induced in cancer and inhibit CD8+ T-cell function. *Cancer Immunol Res* 2019;**7**:257–68.

Ethics Approval

Clinical trial identification NCT03667716The study was approved by each site's ethics board.

Consent

Clinical trial identification NCT03667716Written informed consent was obtained from the patient for publication of this abstract and any accompanying images. A copy of the written consent is available for review by the Editor of this journal.

<http://dx.doi.org/10.1136/jitc-2021-SITC2021.252>

**PD1 AND LAG3 CONVERGE TO LIMIT
POLYFUNCTIONALITY AND SYSTEMIC IMMUNITY**

¹Lawrence Andrews*, ²Sasikanth Manne, ²E John Wherry, ¹Creg Workman, ¹Dario Vignali.
¹University of Pittsburgh, Pittsburgh, USA; ²University of Pennsylvania, Philadelphia, PA, USA

Background Targeting PD1 with monoclonal antibodies has yielded clinical success across a variety of tumor types, yet overcoming inhibitory receptor (IR)-mediated tolerance is essential to improve immunotherapeutic responses. LAG3 co-expresses with PD1 on CD8+ tumor-infiltrating T cells (TIL), signifying a highly exhausted phenotype, and dual PD1/LAG3 blockade in C57BL/6 mice enhances antitumor immunity. As CD8+ TIL is the dominant LAG3-expressing TIL population, it is hypothesized that PD1 and LAG3 synergizes to limit CD8+ TIL function controlling antitumor immunity.

Methods To understand the cellular and mechanistic basis for PD1/LAG3 synergy, conditional knock-in mice "surgically dissect" *Pdcd1* and/or *Lag3* floxed alleles restricted to CD8+ T cells expressing E81Cre.GFP. These mice were crossed with the *Pmel* transgene to assess PD1 and/or LAG3-sufficient or deficient gp100-specific CD8+ T cell populations. CD8+ *Pmel* cells were isolated and adoptively transferred into C57BL/6 mice harboring a B16-gp100-overexpressing tumor to observe therapeutic benefit, or to assess T cell functionality within the tumor.

Results While little therapeutic benefit was observed with a prophylactic adoptive transfer of wild-type CD8+ *Pmel* cells into mice which then received B16-gp100 tumor, there was reduced tumor growth in mice receiving PD1-deficient CD8+ *Pmel* cells, which was further enhanced in mice receiving PD1/LAG3-deficient CD8+ *Pmel* cells with long-term tumor-free survival. Likewise, a therapeutic administration of PD1/LAG3-deficient CD8+ *Pmel* cells into mice once the tumor has been established showed an initial therapeutic benefit, with enhanced survival, that was not demonstrated with adoptive transfer of PD1 or LAG3-deficient, or wild-type, counterparts. Each PD1 and/or LAG3-sufficient or deficient CD8+ *Pmel* mice were differentially congenically marked to assess each of the four genotypes that can be adoptively transferred into the same host as a "quad transfer" system. Recovery of these populations within the tumor show that the PD1/LAG3-deficient CD8+ *Pmel* cells out-compete PD1 or LAG3-deficient, or wild-type, counterparts due to enhanced proliferation (Ki67/BrdU). Furthermore, PD1/LAG3-deficient CD8+ T cells were more functional with increased IFN γ and GzmB release observed by flow cytometry.

Conclusions Overall PD1 and LAG3 limit anti-tumor immune effects as removal of both IRs on a gp100 antigen-specific CD8+ T cell population results in reduced B16-gp100 tumor growth and enhanced survival in an adoptive transfer model, as a result of enhanced CD8+ TIL functionality and proliferation. These results provide striking evidence that the development of anti-LAG3 agents in the clinic would yield improved responses with anti-PD1.

<http://dx.doi.org/10.1136/jitc-2021-SITC2021.253>

NTX-1088, A POTENT ANTI-PVR MAB INDUCES DNAM1-MEDIATED ANTITUMOR IMMUNITY

¹Anas Atieh, ¹Akram Obiedat, ¹Guy Cinamon, ²Tihana Lenac Rovis, ²Paola Kucan Brlic, ²Lea Hirs, ³Ofer Mandelboim, ²Stipan Jonjic, ¹Keren Paz, ¹Pini Tsukerman*. ¹*Nectin Therapeutics, Jerusalem, Israel*; ²*University of Rijeka, Rijeka, Croatia*; ³*Hebrew University, Jerusalem, Israel*

Background Poliovirus receptor (PVR, CD155) represents a resistance mechanism to approved immune checkpoint inhibitors (ICIs). It is a key regulator of immune activation, that modifies function through multiple mechanisms. Increased PVR expression levels on tumor cells have been associated with resistance to anti-PD-(L)1 therapy, while loss of PVR led to reduced tumor growth. Targeting PVR using mAbs offers an attractive therapeutic approach for patients with advanced cancer, who are not responding to other ICIs. NTX-1088 is a first-in-class, anti-PVR mAb developed for the treatment of solid tumors and will enter clinical trials early 2022. The antibody binds PVR with high affinity, blocks its interactions with TIGIT and CD96, preventing their inhibitory signaling. Moreover, NTX-1088 forte is manifested through its ability to block the critical interaction between PVR and DNAM1 (CD226). This blockade prevents internalization of DNAM1, restores its expression on the surface of immune cells and results in a robust antitumor activity.

Methods NTX-1088 was rigorously tested in vitro and in-vivo. Various cancer cell lines were incubated with immune effector cells from healthy human donors, in the presence of NTX-1088, alone and in combination with anti-PD-1 mAb (pembrolizumab).

Results NTX-1088 significantly increased immune cell activation, as measured by IFN γ release from activated polyclonal CD8+ T cells, induction of CD137 and killing of tumor cells. When tested in combination with pembrolizumab, NTX-1088 further increased all measured activation parameters, suggesting a potential synergistic effect. A synergistic effect was obtained when NTX-1088 was combined with the anti-CD112R mAb, NTX-2R13, superior to TIGIT-CD112R combinations. When compared to anti-TIGIT mAb (tiragolumab), NTX-1088 demonstrated clear superiority in activating T and NK cells as stand-alone agent. Furthermore NTX-1088 in combination with pembrolizumab, was superior to the combination of pembrolizumab with anti-TIGIT. Importantly, NTX-1088 was the only intervention that significantly restored DNAM1 levels, whereas DNAM1 blockade reduced the activity of NTX-1088 to levels comparable to that of anti-TIGIT mAb. Humanized murine models confirmed the above observations; NTX-1088 exhibited a robust tumor growth inhibition, accompanied by significantly higher prevalence of CD137+, DNAM1+, CD8+ T cells, compared to mice treated by other ICIs.

Conclusions This is the first report of drug-induced DNAM1 restoration and immune activation. NTX-1088 shows, for the first time, exclusive triple mechanism of action, whereby simultaneous and effective blockade of TIGIT and CD96 is complemented by the efficient restoration of DNAM1. This is a step change in antitumor immune activation, which will be validated in the clinic starting early 2022.

<http://dx.doi.org/10.1136/jitc-2021-SITC2021.254>

255 INVESTIGATING VISTA'S ROLE INTRINSIC TO T CELLS IN THE TUMOR MICROENVIRONMENT

Cassandra Gilmour*, Li Wang, Juan Dong, Sarah Stone, Keman Zhang, Hieu Ta. *Cleveland Clinic Foundation, Cleveland, OH, USA*

Background Cancer immunotherapies, specifically checkpoint blockade therapies, have demonstrated clinical importance for long term patient survival. One of the major limitations to checkpoint blockade therapies, is the low response rate: ~30% with anti-CTLA4 and anti-PD1 treatment. This may be due to heterogeneity of the patients' immune system and the tumor microenvironment including T cell inhibitions. There is a clear need to study this phenomenon and develop additional therapies for long term survival to include a broad range of patients. V-domain Immunoglobulin Suppressor of T-cell Activation (VISTA) is a suppressive protein expressed on many cell types in the tumor microenvironment including cytotoxic T cells. VISTA's role on T cells has been described as maintaining quiescence and peripheral tolerance in a graft vs host disease model, but is not fully understood in context of the tumor microenvironment.

Methods We use a series of in vivo experiments, including T cell specific VISTA knock outs, to understand the role of VISTA on T cells in the tumor microenvironment.

Results Here we show a series of in vivo experiments that suggest VISTA has a potent intrinsic role on T cells and therefore anti-tumor immunity. Using a T cell specific VISTA knock out, our results suggest that the absence of VISTA on T cells in combination with anti-CTLA4 and vaccine is a very powerful tumor suppressor compared to vaccine and anti-CTLA4 treatment alone. These results also indicate that the absence of VISTA alters the phenotype of cytotoxic T cells in several ways including the production of inflammatory cytokines.

Conclusions Our preliminary data provides foundation to study VISTA's role intrinsic to T cells in the tumor microenvironment and how disrupting VISTA's influence intrinsic to T cells may be advantageous for anti-tumor immunity and long term patient survival.

Ethics Approval All in vivo studies were reviewed and approved by Institutional Animal Care and Use Committee (Approval number 2019–2142).

<http://dx.doi.org/10.1136/jitc-2021-SITC2021.255>

256

THE TIGIT/CD226/CD155 AXIS AND THE EFFECTS OF COMBINING PD-1/PD-L1 BLOCKADE WITH TIGIT-TARGETING ANTIBODY THERAPY IN SYNGENEIC MURINE GLIOBLASTOMA MODELS

¹Prafulla Gokhale, ¹Bryan Iorgulescu*, ²Max Klapholz, ¹Michael Poiras, ¹Benjamin Eschle, ¹Gordon Freeman, ³Ana Anderson, ¹David Reardon. ¹Dana-Farber Cancer Institute, Boston, MA, USA; ²University of Pennsylvania, Philadelphia, PA, USA; ³Brigham and Women's Hospital, Boston, MA, USA

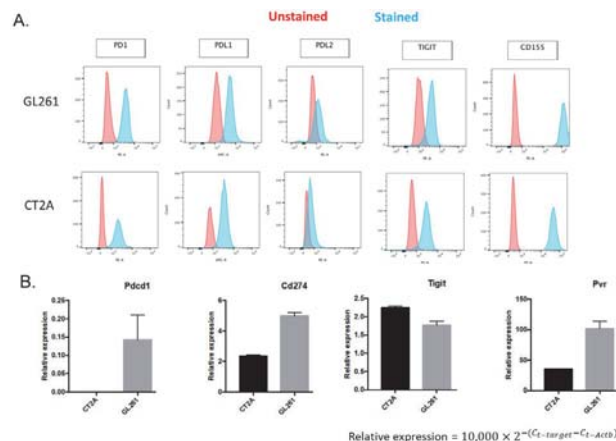
Background Recently, TIGIT+PD1 blockade was shown to confer additive survival benefits in orthotopic glioblastoma and colon cancer mouse models^{1, 2}—notably, this included experiments³ that used the 1G9 TIGIT monoclonal antibody (mAb) that has potentially agonistic effects.¹ Herein we investigated the TIGIT/CD226/CD155 axis and effects of combining clinically analogous PD-1/PD-L1 mAbs with TIGIT-targeting 1G9 mAb in murine glioblastoma models.

Methods The overall survival (OS) associated with TIGIT (non-depleting 1G9; 200µg every 3days for 4 doses),¹ PD-1 (8H3; initial 500µg followed by 250µg every 3days for 7 doses), PD-L1 (6A2; initial 500µg followed by 250µg every 3days for 7 doses), and/or IgG mAbs was assessed in immunocompetent C57BL/6 albino mice intracranially implanted with syngeneic GL261-luc2 or CT2A-luc.^{4, 5} The roles of T cells and NK cells were examined using depletion with CD8a, CD4, or NK1.1 mAbs. Expression of TIGIT/CD226/CD155 and PD-1/PD-L1/PD-L2 by tumor and tumor-infiltrating immune cells was evaluated using flow cytometry and RT-qPCR.

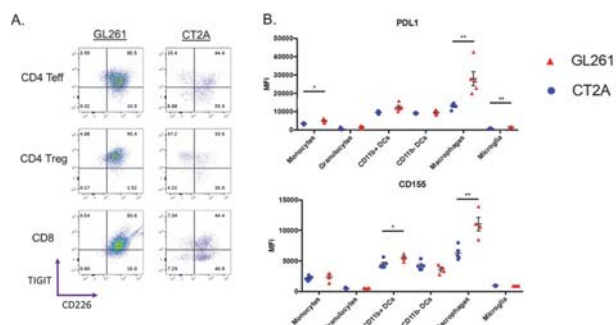
Results In vitro, GL261-luc2 and CT2A-luc tumor cells moderately expressed PD-L1, PD-1, and TIGIT; but strongly expressed TIGIT's inhibitory ligand CD155.(Figure 1A-B) Ex vivo, >83% of CD8+ and CD4+TILs in GL261-luc2 co-expressed TIGIT+/CD226+: ≥2x the proportions in CT2A-luc.(Figure 2A) CD155 and PD-L1 were highly co-expressed on tumor-infiltrating macrophages: greater in GL261-luc2 than CT2A-luc tumors.(Figure 2B)In GL261-luc2 mice, anti-TIGIT monotherapy displayed minimal OS improvement; whereas anti-PD-1 and anti-PD-L1 monotherapies demonstrated robust OS responses.(Figure 3A) Adding anti-TIGIT to PD-1/PD-L1 blockade demonstrated synergism with anti-PD-1. Anti-TIGIT plus anti-PD-1 displayed nominally improved OS in CT2A-luc compared to anti-PD-1 monotherapy (p=0.11).(Figure 3B). Given robust T-cell expression of TIGIT and PD-1, we examined how CD4+ or CD8+ depletion affected responses in GL261-luc2 mice: depletion completely abrogated anti-PD-1's benefits.(Figure 4) Although CD4/CD8 depletion also reduced anti-TIGIT+anti-PD1's efficacy, the resulting OS matched that of non-depleted anti-PD-1 monotherapy. Additionally, NK cell depletion had no effect on anti-TIGIT+anti-PD1's efficacy.

Conclusions Our results recapitulate published findings regarding the synergistic benefits of combining TIGIT 1G9 mAb with anti-PD-1 using the clinically-relevant 8H3 mAb in syngeneic mouse glioblastoma, and extend those findings to anti-TIGIT+anti-PDL1 combinations. TIGIT/CD226 was highly co-expressed by immuno-responsive GL261-luc2's tumor-infiltrating lymphocytes (TILs); whereas CD155/PD-L1 expression predominated in tumor-infiltrating myeloid cells. Depletion of CD8+ or CD4+ TILs modestly reduced anti-TIGIT+anti-PD1's efficacy—suggesting a mechanism that is at least

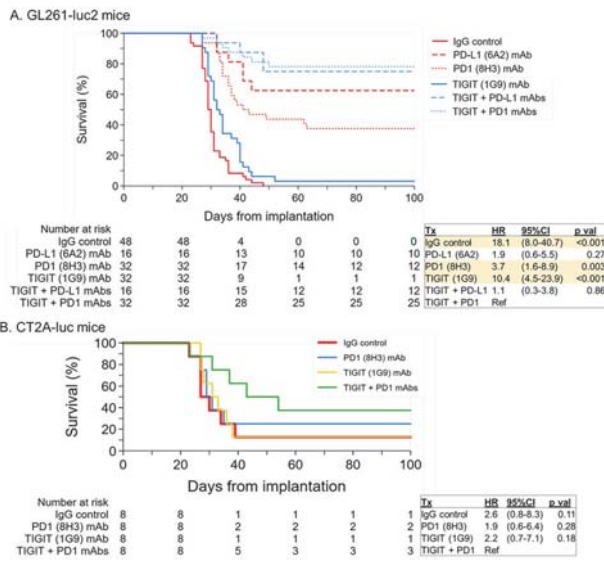
partially independent of T (and NK) cells. Our preliminary results suggest a complex interplay between TIGIT/CD226/CD155 and PD-1/PD-L1/PD-L2 axes in tumors and their microenvironmental constituents that warrants further investigation; plus, careful consideration of antibody clones' functionality is necessary for designing immunotherapy combinations.



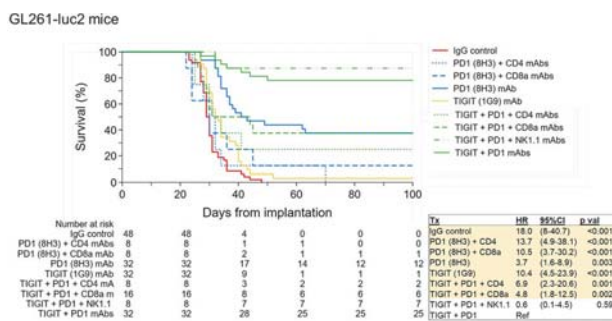
Abstract 256 Figure 1 TIGIT/CD155 axis and PD-1/PD-L1/PD-L2 axis expression in murine glioblastoma model tumor cells. Protein and RNA expression of the TIGIT and PD-1 immune checkpoints — and their ligands CD155 and PDL-1/PD-L2 respectively — on GL261-luc2 and CT2A-luc tumor cells using (A) flow cytometry (blue=samples, red=unstained controls) and (B) RT-qPCR (grey=GL261-luc2, black=CT2A-luc). Pdc1 encodes PD-1, Cd274 encodes PD-L1, Pvr encodes CD155



Abstract 256 Figure 2 TIGIT/CD155 axis and PD-1/PD-L1/PD-L2 axis expression in murine glioblastoma model tumor-infiltrating immune cells. (A) Flow cytometry analysis of protein expression for TIGIT (y-axis) and CD226 (x-axis; a competitor of TIGIT) on CD8+, CD4+/FOXP3+ Treg, and CD4+/FOXP3- Teff tumor-infiltrating lymphocytes (TILs) from GL261-luc2 and CT2A-luc tumor-bearing mice. (B) Flow cytometry analysis of protein expression for CD155 (TIGIT's ligand; bottom) and PD-L1 (PD-1's ligand; top) on tumor-infiltrating myeloid populations from GL261-luc2 and CT2A-luc tumor-bearing mice. Mean fluorescent intensity (MFI) was compared between cell lines, *indicates statistical significance. Myeloid populations included CD45+/CD11b+/CD11c+/F4-80+ macrophages, CD11b+/CD11c+ and CD11b-/CD11c+ dendritic cells (DCs), CD11b+/CD11c-/Ly6C+/Ly6G- monocytes, CD11b+/CD11c-/Ly6Cmid/Ly6G+ granulocytes, and CD45dim/CX3CR1+ microglia. Tumors were dissociated and leukocytes were enriched for using Percoll gradient. n=5 mice per group.



Abstract 256 Figure 3 The survival associated with TIGIT-targeting mAb therapy with/without clinically-analogous PD-1/PD-L1 blockade. (A) Kaplan-Meier estimated overall survival (measured from day of intracranial tumor implantation) of GL261-luc2 mice treated with TIGIT (1G9), PD-1 (8H3), PD-L1 (6A2), TIGIT + PD-1, TIGIT + PD-L1 mAbs, or IgG control. (B) Kaplan-Meier estimated overall survival (measured from day of intracranial tumor implantation) of CT2A-luc mice treated with TIGIT (1G9), PD-1 (8H3), TIGIT + PD-1 mAbs, or IgG control. For both experiments, all treatments were started on day 6 following implantation, with the following dosing: anti-TIGIT was given as 200µg every 3days for 4 doses. Both anti-PD-1 and anti-PD-L1 were given as an initial 500µg dose followed by 250µg every 3days for 7 doses.⁴ The n per group and number at risk table is included underneath each graph, along with the corresponding Cox regression analysis. Treatment groups with significantly different OS from the combination TIGIT + PD-1 combination-treated reference group were highlighted in yellow. HR = hazard ratio, CI = confidence interval.



Abstract 256 Figure 4 How depletion of CD8+ T cells, CD4+ T cells, or NK cells affects survival associated with TIGIT-targeting mAb therapy with/without clinically-analogous PD-1 blockade. Kaplan-Meier estimated overall survival (measured from day of intracranial tumor implantation) of GL261-luc2 mice treated with TIGIT (1G9), PD-1 (8H3), TIGIT + PD-1 mAbs, or IgG control; and compared to groups that additionally had CD8+, CD4+, or NK1.1+ antibody-based depletion. The treatment and dosing characteristics were the same as Figure 3. The n per group and number at risk table is included underneath the graph, along with the corresponding Cox regression analysis. Treatment groups with significantly different OS from the combination TIGIT + PD-1 combination-treated reference group were highlighted in yellow. HR = hazard ratio, CI = confidence interval.

Acknowledgements We gratefully acknowledge the support of the The Jennifer Oppenheimer Cancer Research Initiative; The Ben and Catherine Ivy Foundation; Hope It's A Beach Thing; and the Pan Mass Challenge (Erica's Entourage and CRUS11-TOUR), and the NCI (P01CA236749; K12CA090354).

REFERENCES

- Dixon KO, Schorer M, Nevin J, Etminan Y, Amoozgar Z, Kondo T, Kurtulus S, Kasam N, Sobel RA, Fukumura D, Jain RK, Anderson AC, Kuchroo VK, Joller N. Functional anti-TIGIT antibodies regulate development of autoimmunity and anti-tumor immunity. *J Immunol* 2018 April 15; **200**(8):3000–3007.
- Hung AL, Maxwell R, Theodoros D, Belcaid Z, Mathios D, Luksik AS, Kim E, Wu A, Xia Y, Garzon-Muvdi T, Jackson C, Ye X, Tyler B, Selby M, Korman A, Barnhart B, Park SM, Youn JI, Chowdhury T, Park CK, Brem H, Pardoll DM, Lim M. TIGIT and PD-1 dual checkpoint blockade enhances antitumor immunity and survival in GBM. *Oncoimmunology* 2018 May 24; **7**(8):e1466769.
- Raphael I, Kumar R, McCarl LH, Shoger K, Wang L, Sandlesh P, Sneiderman CT, Allen J, Zhai S, Campagna ML, Foster A, Bruno TC, Agnihotri S, Hu B, Castro BA, Lieberman FS, Broniscer A, Diaz AA, Amankulor NM, Rajasundaram D, Pollock IF, Kohanbash G. TIGIT and PD-1 immune checkpoint pathways are associated with patient outcome and anti-tumor immunity in glioblastoma. *Front Immunol* 2021 May 7; **12**:637146.
- Reardon DA, Gokhale PC, Klein SR, Ligon KL, Rodig SJ, Ramkissoon SH, Jones KL, Conway AS, Liao X, Zhou J, Wen PY, Van Den Abbeele AD, Hodi FS, Qin L, Kohl NE, Sharpe AH, Dranoff G, Freeman GJ. Glioblastoma eradication following immune checkpoint blockade in an orthotopic, immunocompetent model. *Cancer Immunol Res* 2016 February; **4**(2):124–35.
- Iorgulescu JB, Gokhale PC, Speranza MC, Eschle BK, Poitras MJ, Wilkens MK, Soroko KM, Chhoeu C, Knott A, Gao Y, Lim-Fat MJ, Baker GJ, Bonal DM, Nguyen QD, Grant GRL, Ligon KL, Sorger PK, Chiocca EA, Anderson AC, Kirschmeier PT, Sharpe AH, Freeman GJ, Reardon DA. Concurrent dexamethasone limits the clinical benefit of immune checkpoint blockade in glioblastoma. *Clin Cancer Res* 2021 January 1; **27**(1):276–287.

<http://dx.doi.org/10.1136/jitc-2021-SITC2021.256>

257

COMBINATION OF ADENOSINE ANTAGONISTS A2AR (TT-10) AND A2BR (TT-4) WITH CHECKPOINT INHIBITORS DEMONSTRATE ANTI-TUMOR ACTIVITY IN CT-26 MURINE COLON TUMOR ALLOGRAFT MODEL

Desa Rae Pastore*, Sushant Kumar, Brian Schwartz, Kasim Mookhtiar, Vijay Reddy. *Tarus Therapeutics, Batavia, NY, USA*

Background TT-10 and TT-4 are potent and selective antagonists of adenosine A2A receptor (A2AR) and A2B receptor (A2BR) respectively. Both agents are being developed for the treatment of advanced cancers initially as monotherapy, using high levels of adenosine receptor expression in tumor tissue as biomarker.

Methods Balb/c mice were implanted with CT-26 cells and randomly assigned to 8 groups per study; (1) vehicle control, (2) adenosine antagonist - 1 mg/kg A2AR (TT-10) 1 mg/kg or 3 mg/kg A2BR (TT-4), (3) 10 mg/kg Anti-mPD-1, (4) 5 mg/kg Anti-mCTLA-4, (5) 100 mg/kg Irinotecan, (6) adenosine antagonist + Anti-mPD-1, (7) adenosine antagonist + Anti-mCTLA-4, (8) adenosine antagonist+ Irinotecan. Adenosine antagonists and control were given daily by oral gavage, Anti-mPD-1, Anti-mCTLA-4 and Irinotecan were administered Intraperitoneal. Treatment was started on day 1 post implant and mice were followed until individual tumor volume reached 2,000 or 3000 mm³ (as defined by protocol) or moribund. Tumor measurements and weights were taken every 2 to 3 days. In addition, a subset of mice were investigated for changes in peripheral whole blood and intra-tumor analysis on days 3 and 10 via flow cytometry. The populations of interest included CD223+, CD3+, CD4+, CD8+, CD25+FoxP3+, CD25-CD69+ and CD44+CD62L.

Results All implanted mice developed measurable tumors. Mean suppression of tumor growth was observed to be greater in single agent adenosine antagonists TT-10 and TT-4 when compared to the vehicle control and was observed to show overall greater suppression of tumor growth when combined with anti-mPD-1 or anti-m-CTLA-4. Tumor infiltrating lymphocyte analysis by flow cytometry, showed higher amounts of CD25+FoxP3+ present in control mice at day 3, than was observed in mice that were treated with A2AR alone, A2AR + anti-mPD-1 and A2AR + anti-m-CTLA-4.

Conclusions TT-10 and TT-4 alone was superior to vehicle control in slowing tumor growth. However, the combination of TT-10 + Anti-mPD-1 and TT-4 + Anti-mCTLA-4 showed the greatest tumor response and growth suppression. Furthermore, a striking reduction of CD25+FoxP3+ within the tumor was observed at day 3 in mice treated with A2AR alone, A2AR + anti-mPD-1 and A2AR + anti-m-CTLA-4 when compared to the vehicle control.

<http://dx.doi.org/10.1136/jitc-2021-SITC2021.257>

AB308 IS AN ANTI-TIGIT ANTIBODY THAT ENHANCES IMMUNE ACTIVATION AND ANTI-TUMOR IMMUNITY ALONE AND IN COMBINATION WITH OTHER I-O THERAPEUTIC AGENTS

Dana Piovesan*, Alejandra Lopez, Patrick Schweickert, Ferdie Soriano, Soonweng Cho, Ada Chen, Hema Singh, Xiaoning Zhao, Stephen Young, Nigel Walker, Matthew Walters, Kelsey Sivick Gauthier. *Arcus Biosciences, Hayward, CA, USA*

Background TIGIT (T-cell immunoreceptor with Ig and ITIM domains) is an inhibitory receptor expressed on natural killer (NK) cells, CD8⁺ T cells, CD4⁺ T cells and regulatory T cells (T_{regs}). On the surface of these cells, TIGIT competes with another receptor, CD226, for shared receptor ligands (mainly CD155) that are expressed by cancer and antigen-presenting cells. Binding of CD155 to TIGIT results in immune suppression through multiple mechanisms. When TIGIT is blocked, binding of CD155 to CD226 promotes immune activation and anti-tumor immunity. We describe the preclinical characterization of AB308, a humanized wild-type IgG1 anti-TIGIT antibody that is currently undergoing clinical evaluation.

Methods Binding of AB308 to TIGIT and inhibition of the TIGIT/CD155 interaction were evaluated *in vitro*. Functional assays were used to evaluate the immunomodulatory activity of AB308 alone or in combination with zimberelelimab (anti-PD-1) or etrumadenant (a small molecule A_{2A} adenosine receptor antagonist). Surrogate Fc-silent and Fc-enabled antibodies that recognize mouse TIGIT or PD-1 were leveraged to interrogate TIGIT biology in syngeneic mouse tumor models.

Results Human tumor-infiltrating lymphocytes from a variety of cancer types expressed appreciable levels of TIGIT on relevant immune populations, including tumor reactive CD39⁺ CD103⁺ CD8⁺ T cells and T_{regs}. AB308 has a high binding affinity for human TIGIT, potently blocks the TIGIT-CD155 interaction, and induces Fcγ receptor (FcγR)-mediated signaling. In line with FcγRIII binding, AB308 also demonstrated the ability to induce NK cell-driven antibody-dependent cell-mediated cytotoxicity against TIGIT-expressing target cells. AB308 significantly increased IL-2 secretion by peripheral blood mononuclear cells activated with superantigen A, an activity that was further enhanced with zimberelimab. Blocking TIGIT with AB308 potently activated CD226 signaling in Jurkat T cells co-cultured with CD155-expressing cells, and combination of AB308 with etrumadenant in this system abrogated adenosine-mediated T cell suppression that occurred even in the presence of checkpoint inhibition. In mice, while combining Fc-silent or Fc-enabled anti-mouse TIGIT antibody with anti-PD-1 resulted in greater tumor growth inhibition than with anti-PD-1 alone, the activity of Fc-enabled anti-TIGIT was associated with intratumoral T_{regs} depletion.

Conclusions AB308 is a potent and highly effective anti-TIGIT antibody. Concurrent blockade of multiple immune checkpoints has the potential to confer effective and durable responses in the treatment of cancer. The data presented here support the clinical use of AB308 and provides a rationale for combination with zimberelimab and adenosine pathway blocking agents such as etrumadenant and CD73 small molecule inhibitor, AB680.

Ethics Approval Animal experiments were performed at Arcus Biosciences, Inc. in accordance with federal, state and

Institutional guidelines and were approved by Arcus' Institutional Animal Care and Use Committee.

<http://dx.doi.org/10.1136/jitc-2021-SITC2021.258>

259

INJECTABLE CHITOSAN HYDROGEL FOR LOCALIZED DELIVERY OF IMMUNE CHECKPOINT INHIBITORS

Siena Mantooth*, David Zaharoff, Siena Mantooth. North Carolina State University, Cary, NC, USA

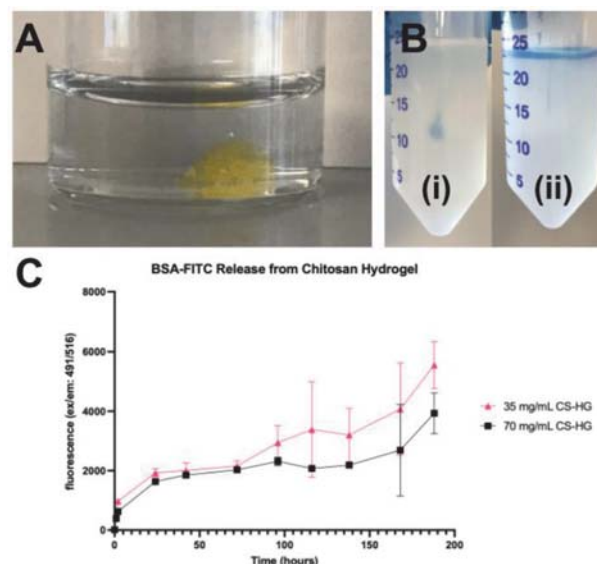
Background Systemic delivery of checkpoint inhibitors risks the development of immune-related adverse events (irAEs) in up to 85% of patients.¹ Localized delivery methods with slow-release kinetics have the potential to avoid systemic exposure and reduce irAEs. Direct tumor injection is extremely difficult, as saline-based solutions are rapidly excluded from the high-pressure tumor environment. Utilizing hydrogels as a delivery medium and local depot can address this shortcoming. To this end, we developed an injectable chitosan-based hydrogel for intratumoral delivery of checkpoint antibodies.

Methods

Hydrogel Low-viscosity, 80% deacetylated chitosan (Heppe Medical Chitosan; Halle, Germany) was reacted with 1-ethyl-3-(3-dimethylaminopropyl) carbodiimide hydrochloride (EDC) and N-hydroxysuccinimide (NHS) in the presence of β -glycerophosphate at room temperature for 48 hours. The mixture was then washed with ethanol and dried at 60°C. The resulting solid was dissolved in phosphate buffered saline (PBS) at concentrations from 35–70 mg/mL. *In vitro* release. 300 μ g/mL bovine serum albumin (BSA) labeled with fluorescein-5-isothiocyanate (FITC) as a model protein drug was loaded into the hydrogel. The hydrogel was injected through a 28g needle and incubated with PBS. Samples were taken over a week period. Release kinetics were analyzed by fitting fluorescence data to zero-order, first-order, and Korsmeyer-Peppas models. To visualize retention after injection, dye-loaded hydrogels or dye in PBS alone were injected into a 0.6 wt% agar tissue phantom. *In vivo* imaging and tumor treatment. Flank MC38 tumors will be established in C57BL/6 mice. At tumor volumes of 50–100 mm³, 200 μ g of fluorescently labeled aCTLA-4 and aPD-L1 included in the chitosan hydrogel will be delivered intratumorally. Images will be captured using an *In Vivo* Imaging System (IVIS). Antitumor activity will be assessed in a separate cohort using unlabeled antibodies.

Results The chitosan hydrogel was found to be injectable in needles as thin as 28g. After exiting the needle, the hydrogel reformed (figure 1A). Upon injection into the tissue phantom, dyed PBS immediately leaked out, primarily through the needle track, while the dyed hydrogel was retained (figure 1B). *In vitro* release studies demonstrated long-term, nearly zero-order, week-long sustained release (figure 1C). *In vivo* retention and tumor treatment studies are ongoing.

Conclusions A novel injectable chitosan hydrogel was found to provide sustained release of a large model protein over a 1–2 week period with favorable *in vitro* kinetics. Importantly, this hydrogel can be engineered to provide faster or slower release as needed. Ongoing studies *in vivo* will quantify intratumoral retention, systemic dissemination, and antitumor activity.



Abstract 259 Figure 1 Injectable chitosan hydrogel. (A) Re-formed BSA-FITC hydrogel in 1x PBS; (B) (i) Retained hydrogel in agar tissue phantom, (ii) Excluded 1x PBS in agar tissue phantom; (C) Release kinetics in 1x PBS.

Acknowledgements This work is supported by the National Science Foundation Graduate Research Fellowship.

REFERENCE

- Hommes J, Verheijden R, Suijkerbuijk K, Hamann D. Biomarkers of checkpoint inhibitor induced immune-related adverse events—a comprehensive review. *Front Oncol* 2021;10:1–16.

Ethics Approval Animal use was in compliance with the Public Health Service Policy on Human Care and Use of Laboratory Animals. All experiments involving laboratory animals were approved by the Institutional Animal Care and Use Committee at North Carolina State University (Protocol #19–795).

<http://dx.doi.org/10.1136/jitc-2021-SITC2021.259>

260

CD47 ANTIBODY, AO-176 DEMONSTRATES POTENT ANTI-TUMOR ACTIVITY IN PRE-CLINICAL SOLID TUMOR XENOGRAFTS AS A SINGLE AGENT AND IN COMBINATION WITH MULTIPLE CLASSES OF THERAPEUTICS

Gabriela Andrejeva*, Benjamin Capoccia, Rachel Delston, Michael Donio, Ronald Hiebsch, Robyn Puro, Casey Wilson, Arun Kashyap, Daniel Pereira. *Arch Oncology, St. Louis, MO, USA*

Background CD47 is a cell surface protein expressed on tumors that binds SIRP α on macrophages and dendritic cells resulting in a "don't eat me" signal that allows tumors to evade phagocytosis. The highly differentiated monoclonal antibody, AO-176 directly targets CD47 and blocks this signal. AO-176 is currently being tested in phase 1 clinical trials in solid tumors and multiple myeloma. The purpose of this study was to assess in vivo efficacy of AO-176 in solid tumor models as a single agent and in combination with multiple classes of therapeutics including chemotherapeutics, monoclonal antibodies and T-cell checkpoint inhibitors.

Methods CD47 expression levels on solid tumor types were assessed by immunohistochemistry using a tumor tissue microarray. Cell-based binding was performed using flow cytometry under acidic and physiologic pH conditions to characterize the functional activity of AO-176 in the two pH environments representing tumor and normal physiologic environments. In vivo studies were performed using models of solid cancers.

Results All 12 solid tumor indications assessed were positive for cell membrane localized CD47 (3.3–98.6 H-scores). Cell-based binding of AO-176 to solid cancer cell lines was significantly greater (1.6–25-fold decrease in EC₅₀, 11–39% increase in B_{max}) in acidic conditions as compared to a neutral pH environment, demonstrating improved binding in the lower pH environments associated with solid tumors. AO-176 treatment in solid tumor xenograft models resulted in potent anti-tumor activity as a monotherapy (40–58% TGI) and in combination with paclitaxel in an ovarian model (99% TGI), cisplatin in an ovarian model (84% TGI), cisplatin in a gastric model (76% TGI), and an anti-VEGFR-2 in a gastric model (86% TGI). In vivo efficacy of CD47 blockade alone (~33% TGI) and in combination with anti-PD-1 (74% TGI) and anti-PD-L1 (80% TGI) T-cell checkpoint inhibitors was observed in a syngeneic model of colon cancer using a surrogate anti-CD47 blocking antibody.

Conclusions AO-176 is a differentiated anti-CD47 agent that in addition to blocking the don't eat me signal, directly kills cancer cells, shows lower binding to normal cells such as RBCs and demonstrates increased binding activity in acidic conditions as found in the microenvironment of solid tumors. AO-176 also elicits potent anti-tumor activity in xenograft and syngeneic models as a single agent and in combination with chemotherapies, monoclonal antibodies and T-cell checkpoint inhibitors. AO-176 is currently in clinical trials as a single agent and in combination in patients with select solid cancers (NCT03834948) and in multiple myeloma (NCT04445701).

<http://dx.doi.org/10.1136/jitc-2021-SITC2021.260>

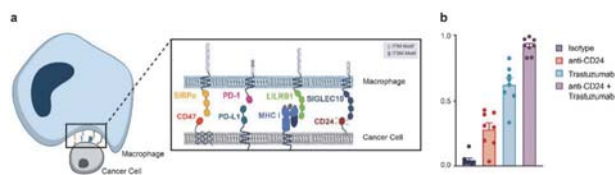
261 **A FUNCTIONAL GENETIC SCREEN UNCOVERS REGULATORS OF INTRATUMORAL MACROPHAGE FUNCTION AND REVEALS CD24 AS A NOVEL TARGET FOR CANCER IMMUNOTHERAPY BY MACROPHAGES**

¹Amira Barkal*, ²Rachel Brewer, ²Irving Weissman. ¹Brigham and Women's Hospital, Boston, MA, USA; ²Stanford University School of Medicine, Stanford, CA, USA

Background Cancer cells are capable of evading clearance by macrophages through the overexpression of anti-phagocytic, innate immune checkpoint molecules called 'don't eat me' signals, including CD47,¹ PD-L1,² and MHC class I.³ Monoclonal antibodies that antagonize the interaction of 'don't eat me' signals with their macrophage-expressed receptors have demonstrated therapeutic potential in several cancers. However, variability in the magnitude and durability of the responses to these agents has suggested the presence of additional, as yet unknown innate immune checkpoints. Here, we present a functional screening platform which identifies tumor-specific regulators of intratumoral macrophage function. We show that CD24 is a dominant innate immune checkpoint in many solid tumors, including ovarian cancer and breast cancer.⁴

Methods By applying our screening method, we uncovered the novel innate immune checkpoint molecule, CD24. To characterize the role of CD24 as a macrophage checkpoint, we leveraged the MCF-7 human xenograft tumor model and the ID8 syngeneic ovarian cancer tumor model. We evaluated the anti-tumor effect of CD24 antagonism through genetic ablation experiments in addition to therapeutic CD24 monoclonal antibody (mAb) blockade. We also utilized primary human immune cells and tumor specimens to assess the effect of CD24 blockade either alone or in combination with additional tumor-targeting antibodies.

Results We demonstrate that CD24 promotes immune evasion through its interaction with the inhibitory macrophage receptor Siglec-10. Genetic ablation of either CD24 or Siglec-10, as well as blockade of the CD24-Siglec-10 interaction using monoclonal antibodies, robustly augmented the phagocytosis of all CD24-expressing human tumors that we tested. Therapeutic blockade of CD24 resulted in a macrophage-dependent reduction of tumor growth in vivo and an increase in survival time. The therapeutic efficacy of anti-CD24 mAbs was enhanced when combined with a second anti-tumor antibody. In particular, dual treatment of HER2-positive breast cancers with anti-CD24 mAb and trastuzumab, augmented phagocytosis relative to either treatment alone, even among cancers with inherent trastuzumab resistance (figure 1).



Abstract 261 Figure 1 Macrophage checkpoints are therapeutic targets. (A) There are four defined innate immune checkpoint signaling axes which exist between macrophages and cancer cells, which all rely on ITIM or ITSM signaling on the cytoplasmic side of the macrophage. (B) Phagocytosis of BT-474 (n = 8 donors) in the presence of anti-CD24 mAb, anti-HER2 mAb or dual treatment, compared with IgG control.

Conclusions These data reveal CD24 as a highly expressed, anti-phagocytic signal in several cancers, and demonstrate the therapeutic potential for CD24 blockade in cancer immunotherapy, either alone or in combination with existing anti-cancer treatments. Collectively, this work suggests a new paradigm that innate immune checkpoints are redundant and employed in a tissue-specific and even tumor-specific manner, and makes clear the need to measure the collective expression of these 'don't eat me' signals in order to optimize patient responses to both innate and adaptive immunotherapies.

REFERENCES

- 1.. Majeti R, *et al.* CD47 is an adverse prognostic factor and therapeutic antibody target on human acute myeloid leukemia stem cells. *Cell* 2009;**138**: 286–299.
- 2.. Gordon SR, *et al.* PD-1 expression by tumour-associated macrophages inhibits phagocytosis and tumour immunity. *Nature* 2017;**545**:495–499.
- 3.. Barkal AA, *et al.* Engagement of MHC class I by the inhibitory receptor LILRB1 suppresses macrophages and is a target of cancer immunotherapy. *Nat Immunol* 2018;**19**:76–84.
- 4.. Barkal AA, Brewer RE, Markovic M, Kowarsky MA, Barkal SA, Zaro BW, Krishnan V, Hatakeyama J, Dorigo O, Barkal LJ, Weissman IL. CD24 signaling through macrophage siglec-10 is a new target for cancer immunotherapy. *Nature* 2019;**572**:392–396.

Ethics Approval The Human Immune Monitoring Center Biobank and the Stanford Tissue Bank all received IRB approval from the Stanford University Administrative Panels on Human Subjects Research and complied with all ethical guidelines for human subjects research to obtain samples from patients with ovarian cancer and breast cancer, and received informed consent from all patients.

<http://dx.doi.org/10.1136/jitc-2021-SITC2021.261>

PRECLINICAL CHARACTERIZATION OF HUMANIZED ANTI-SIGLEC-15 ANTIBODIES THAT RESCUE T CELLS FROM MACROPHAGE-MEDIATED IMMUNE SUPPRESSION

Huyen Dinh, Sam Lam, Valerie Wall, Francisco Zapata, Darbie Whitman, Ramya Chandrasekaran, Lauren Loh, Texia Loh, Tom Graddis, Peter Probst*, Myriam Bouchlaka. *OncResponse Inc., Seattle, WA, USA*

Background Siglec-15 is an immunosuppressive sialic acid-binding Ig-like lectin expressed by myeloid cells, tumor associated macrophages (TAMs), and some human tumors. Interactions between Siglec-15 on TAMs and sialoglycans found on cancer cells contribute to the immunosuppressive tumor microenvironment. Furthermore, Siglec-15 expressed by TAMs inhibits anti-tumor immune responses by engaging unknown immune checkpoint(s) on T cells. Notably, the mutually exclusive expression of Siglec-15 and the checkpoint ligand PD-L1 in the tumor tissue emphasizes Siglec-15 as an attractive target for combination immunotherapy. Anti-Siglec-15 antibody is currently being evaluated in clinical trials for the treatment of cancer.

Methods Anti-Siglec-15 antibodies were cloned from B cells derived from rabbits immunized with human Siglec-15 protein. The antibodies were evaluated for binding to human and cynomolgus Siglec-15 by enzyme-linked immunosorbent assay (ELISA). Top clones were selected based on activity in a panel of functional and phenotypic assays using primary human macrophages and T cells and were subsequently fully humanized. The humanized anti-Siglec-15 IgG1 antibodies were screened for binding to human and cynomolgus Siglec-15 by ELISA, binding to cells expressing Siglec-15, and ability to rescue T cell functional activity (proliferation and IFN- γ) from M2c-mediated immune suppression *in vitro*. The pharmacokinetics of lead humanized Siglec-15 IgG1 antibodies and their anti-tumor activity were evaluated in humanized mouse models.

Results We have identified a panel of fully humanized anti-Siglec-15 antibodies that bind to recombinant human and cynomolgus Siglec-15 proteins, to Siglec-15-expressing cell lines and immunosuppressive M2c macrophages without appreciable binding to other Siglec family members. Lead antibodies were identified using functional screens modeling Siglec-15-mediated immune suppression by M2c macrophages. These antibodies restored T cell immune responses in two different M2c/CD8 T cell coculture assays. In the first model, lead antibodies rescued the proliferative and IFN- γ responses of anti-CD3-activated human T cells from the inhibitory activity of M2c macrophages. In the second model, these antibodies restored the ability of exhausted CD8 T cells to secrete IFN- γ in the presence of M2c macrophages. Lead antibodies demonstrated a half-life of 6–11 days in humanized FcRn mice, and tumor growth inhibition in humanized NSG-SGM3 mice.

Conclusions We have identified novel humanized anti-Siglec-15 antibodies that restore effector function of activated and exhausted T cells from M2c-mediated immune suppression, with excellent half-life and anti-tumor activity in humanized mouse models. These data provide a strong rationale for further development of these antibodies for anti-cancer immunotherapy.

<http://dx.doi.org/10.1136/jitc-2021-SITC2021.262>

ASD141, AN INNATE CHECKPOINT INHIBITOR, MODULATES TUMOR ASSOCIATED MYELOID CELLS THROUGH CD11B AND ENHANCES CURRENT IMMUNE CHECKPOINT BLOCKADE IN PRECLINICAL MODEL

Chia-Ming Chang, Jason (Ping-Yen) Huang*, I-Fang Tsai, Yen-Ta Lu. *ASCENDO Biotechnology, Inc., Taipei, Taiwan, Province of China*

Background Tumor-associated myeloid cells (TAMCs) are a heterogeneous population of myeloid cells present in the tumor microenvironment (TME). They contribute to immunosuppression and growth of solid tumor. These myeloid cells are highly expressed with CD11b, the alpha-chain of integrin receptor alphaMbeta2 (also known as CD11b/CD18, Mac-1, CR3). It has been suggested that activation of CD11b could facilitate the development of peripheral tolerance by inhibiting T helper 17 differentiation. Antigen-presenting cells (dendritic cells and macrophages) have been shown to enhance T cell proliferation with the treatment of anti-CD11b antibody. Furthermore, CD11b plays a critical role in inflammation by modulating Toll-Like receptor (TLR) responses. High avidity activated form of CD11b leads to a rapid inhibition of TLR signaling by promoting degradation of MyD88 and TRIFs. Therefore, CD11b may serve as an innate checkpoint that function as a negative immune regulator.

Methods In order to investigate the impact of CD11b in modulating the TME and tumor growth, ASCENDO Biotechnology generated a surrogate chimeric mouse IgG1 antibody, mouse ASD141 (Xi2396), which targets mouse CD11b. These antibodies were then tested in murine MC38 colon cancer.

Results Mouse ASD141 as monotherapy results in statistically significant growth inhibition in murine colon cancer models. Xi2396 remodels the TME by decreasing infiltration of TAMCs, and increased infiltration of dendritic cells (cDCs, NKDCs, and pDCs). Furthermore, Xi2396 also enhanced the antigen presentation ability, which is accompanied by an increased expression of MHCII, CD80 and CD86. These results indicate that the anti-CD11b monoclonal antibody, ASD141, designed to modulate TAMCs of the TME represents a novel approach of cancer immunotherapy. Xi2396 treatment also induced high levels of PD-L1 expression in the TME. Since PD-L1 expression in the TME was associated with response to current immune checkpoint blockades, we sought to determine whether Xi2396 treatment is capable of enhancing anti-tumor response to anti-PD1 therapy. Our results showed that combination of Xi2396 and anti-PD1 synergistically suppressed tumor growth.

Conclusions Altogether, our results provide support for clinical efforts to evaluate ASD141 as an innate immune checkpoint drug, especially in combination with commercial immune checkpoint inhibitors.

Ethics Approval This study was approved by National Laboratory Animal Center's Institutional Animal Care and Use Committee; approval number NLAC-110-D-006-R2.

<http://dx.doi.org/10.1136/jitc-2021-SITC2021.263>

SIRP α BLOCKADE SYNERGIZES WITH RADIATION THERAPY IN MURINE BREAST CANCER MODELS

¹Maud Charpentier*, ¹Claire Lhuillier, ¹Ines Mota, ²Sergio Trombetta, ¹Sandra Demaria. ¹Weill Cornell Medicine, New York, NY, USA; ²Boehringer Ingelheim, Ridgefield, CT, USA

Background Focal tumor radiation-therapy (RT) induces an immunogenic cell-death associated with endogenous adjuvants that promote uptake of cancer antigens by conventional dendritic cells (cDCs). The expression of CD47 is markedly increased in a high proportion of breast cancers (BC) and correlates with poor-prognosis molecular subtypes. CD47 interaction with SIRP α on cDCs and macrophages provides a negative signal that inhibits phagocytosis of dying cancer cells, hindering cross-presentation of tumor-derived antigens and activation of anti-tumor T cells. Thus, we hypothesized that the "don't-eat-me" signal mediated by CD47/SIRP α acts as a barrier to RT-induced anti-tumor immunity. Using two mouse BC models refractory to immune-checkpoint blockade, we investigated the effects of RT combined with SIRP α blockade on the development of anti-tumor immunity.

Methods BALB/c or C57BL/6 mice were inoculated subcutaneously in one or both flanks with respectively TSA and AT-3 BC cells. RT was delivered to one tumor, 8Gy on 3 consecutive days once tumor volume reached 60–80mm³. SIRP α -blockade (MY1,1) or isotype antibodies were given one day prior to RT and every 3 days thereafter. Some mice received PD-L1-blocking Abs (BioXcell) every 3 days starting one day after RT completion. cDC depletion experiments were performed on AT-3 bearing C57BL/6 mice using the inducible diphtheria toxin-dependent CD11c-DTR model.²

Results SIRP α -blockade alone did not inhibit TSA tumor growth, but significantly improved tumor response to RT ($p < 0.05$), leading to complete regression of the irradiated tumor in 50–60% of the mice. In addition, SIRP α -blockade + RT combination significantly inhibited the growth ($p < 0.05$) of contralateral non-irradiated tumors (abscopal response), suggesting that it induced a systemic anti-tumor immune response. Consistent with systemic immune activation, the percentage of PD1+CD4 T cells was increased in the spleen of mice treated with anti-SIRP α compared to control Abs ($p < 0.01$), regardless of RT. In the myeloid compartment, cDC1 and macrophages showed increased PD-L1 expression. However, addition of anti-PD-L1 to RT + anti-SIRP α did not further improve abscopal responses. In the AT-3 model, SIRP α blockade significantly improved tumor control induced by RT ($p < 0.01$) but no complete regression was observed. Depletion of cDC in AT-3 bearing mice abrogated the benefit of the combination of SIRP α blockade to RT.

Conclusions Overall, our results support the hypothesis that SIRP α -blockade potentiates the ability of RT to induce anti-tumor T cell responses and improve local and systemic tumor control. We are currently investigating the mechanisms of RT interaction with SIRP α blockade to provide the rationale for translating these findings to the clinic

REFERENCES

- 1.. Noel Verjan Garcia, *et al.* SIRP α /CD172a regulates eosinophil homeostasis. *The Journal of Immunology* September 1, 2011;**187**(5):2268–2277.
- 2.. Jung S, *et al.* In vivo depletion of CD11c+ dendritic cells abrogates priming of CD8+ T cells by exogenous cell-associated antigens. *Immunity* 2002;**17**(2):211–20.

<http://dx.doi.org/10.1136/jitc-2021-SITC2021.264>

¹Xavier Chauchet*, ¹Elise Pernarrieta, ¹Nicolas Bosson, ¹Sébastien Calloud, ¹Louis Hellequin, ¹Margaux Legrand, ¹Alizée Viandier, ¹Françoise Richard, ¹Laura Cons, ¹Pauline Malinge, ¹Tereza Bautzova, ¹Jérémie Bourguignon, ¹Guillemette Pontini, ²Mengzhu Sun, ¹Ulla Ravn, ¹Valéry Moine, ¹Yves Poitevin, ²Stéphanie Hugues, ¹Nicolas Fischer, ¹Limin Shang, ¹Walter Ferlin, ¹Krzysztof Masternak. *Light Chain Bioscience/Novimmune, Plan les Ouates, Switzerland; ²University Medical Center (CMU), Geneva, Switzerland*

Background PD-1/PD-L1 blockade can significantly improve survival across many types of cancer, but only in a minority of patients. To broaden its therapeutic efficacy, several combination partners are now being evaluated together with PD-1/PD-L1 blockade. Agents blocking CD47/SIRP α innate immune checkpoint are one such example, and co-targeting PD-1/PD-L1 and CD47 with monoclonal antibody (mAb) combinations showed increased antitumor responses in preclinical studies. However, CD47 mAbs are hindered by ubiquitous CD47 expression leading to rapid target-mediated clearance and safety concerns. Consequently, dual-targeting CD47xPD-L1 bispecific antibodies (bsAbs) enabling preferential inhibition of CD47 on PD-L1-positive cells are being tested as an alternative approach. We compare here two distinct bsAbs, based on a common PD-L1 antibody arm, with differing Fc γ R-enabling effector functions and CD47-binding arm affinities.

Methods An array of fully human bsAbs associating a high affinity PD-L1 arm to CD47 arms with varying affinities were generated using the $\kappa\lambda$ -body platform.¹ CD47xPD-L1 bsAbs of human IgG1 isotype (CD47 low affinities) or IgG4 isotype (CD47 high affinities) were screened in various binding assays (including to red blood cells (RBC)) and in receptor-blocking assays, and then tested for their Fc-mediated killing and T-cell activation activity (SEA-stimulated PBMC assay). Selected molecules were evaluated in vivo.

Results Both bsAb approaches demonstrated strong blockade of PD-1/PD-L1 interaction and significantly enhanced T-cell activation in vitro. CD47lowxPD-L1 IgG1 bsAbs did not bind to RBC and showed PD-L1-guided inhibition of CD47. ADCP and ADCC experiments with a panel of tumor cell lines expressing various target levels showed superior killing activity with CD47lowxPD-L1 IgG1 bsAbs as compared to the anti-PD-L1 IgG1 mAb, avelumab. On the other hand, CD47highxPD-L1 IgG4 bsAbs showed residual RBC binding and PD-L1-independent blocking of CD47/SIRP α . These CD47high IgG4 bsAbs were able to enhance the anti-tumor activity of anti-tumor-associated antigen (TAA) mAbs in vitro (phagocytosis), and in vivo (Raji lymphoma xenograft model). In addition, anti-tumor activity of mouse CD47xPD-L1 bsAbs in a syngeneic MC38 colon carcinoma model was demonstrated.

Conclusions With the objective of finding the optimal CD47xPD-L1 bsAb design, two approaches targeting CD47 and PD-L1 inhibition were tested. Both the CD47lowxPD-L1 IgG1 bsAbs and CD47highxPD-L1 IgG4 bsAbs were able to mediate enhanced antitumor responses, the former as a stand-alone treatment, the latter in conjunction with an anti-TAA mAb. To further characterize the CD47lowxPD-L1 and CD47highxPD-L1 bsAbs, lead candidates will be tested in PK and tolerability studies in non-human primates.

REFERENCES

1. Fischer N, Elson G, Magistrelli G, Dheilly E, Fouque N, Laurendon A, *et al.* Exploiting light chains for the scalable generation and platform purification of native human bispecific IgG. *Nat Commun* 2015 May;6(1):6113.

<http://dx.doi.org/10.1136/jitc-2021-SITC2021.265>

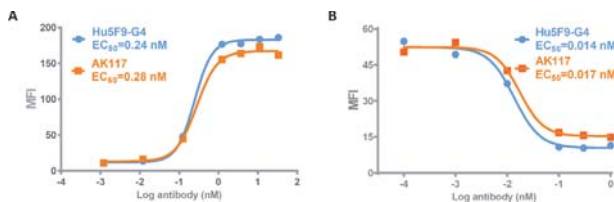
AK117, A CD47 BLOCKING ANTIBODY WITH ROBUST MACROPHAGE ACTIVATION WITHOUT RED BLOOD CELL HEMAGGLUTINATION

¹Zhaoliang Huang, ¹Xinghua Pang, ¹Tingting Zhong, ¹Tailong Qu, ¹Chunshan Jin, ¹NA Chen*, ¹Xinrong He, ¹Dennis Xia, ²Xiaoping Jin, ¹Zhongmin Wang, ¹Xu Xia, ¹Baiyong Li. ¹Akeso Biopharma Inc., Zhongshan, China; ²Akeso Biopharma Inc, Potomac, USA

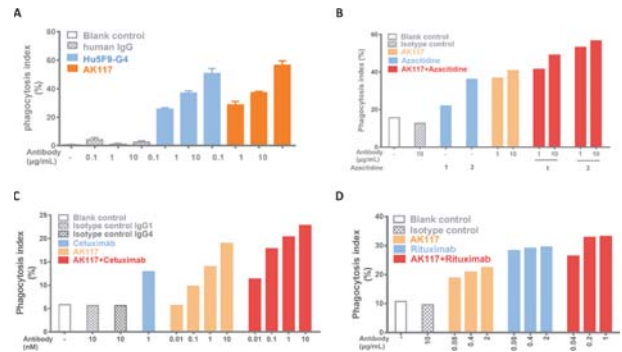
Background AK117 is a humanized monoclonal antibody targeting CD47 which widely expresses on innate immune cells, such as macrophages, and functions as a regulator of phagocytosis. CD47 serves as the ligand for a receptor on these innate immune cells, SIRP α , which in turn delivers an inhibitory signal for phagocytosis. Hematology toxicity is the major concern of an anti-CD47 antibody. As an agent targeting CD47 being investigated as an anti-tumor therapeutic, AK117 is engineered on a human IgG4 scaffold to minimize recruitment of Fc-dependent effector functions, as well as identified with favorable hematology safety profile and robust pro-phagocytosis activity.

Methods Activity of AK117 binding to CD47 to block the interaction between CD47 and SIRP α were determined by FACS, and binding of AK117 to human RBC was also evaluated. Raji cells, HT-29 cells, and HL-60 cells which highly express CD47 were used as target cells to evaluate a pro-phagocytic activity of AK117 as a monotherapy or in combination with anti-EGFR antibody, anti-CD20 antibody or azacitidine. In in-vivo pharmacology studies, anti-tumor activity of AK117 was investigated in SCID/beige mouse Raji tumor model. Effects of AK117 on hemagglutination of human RBC at was tested. Hemoglobin (HGB) and hematocrit (HCT) was evaluated after single dose of 10 mg/kg AK117 or Hu-5F9 in male and female cynomolgus monkeys (n=1/gender).

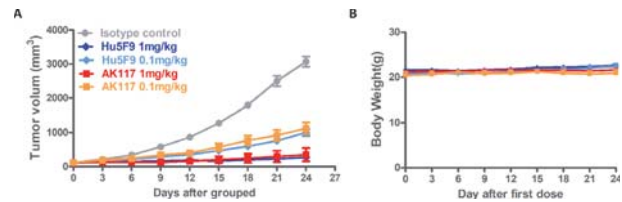
Results AK117 could effectively binds to CD47, and competes with SIRP α for binding to the antigen on Raji cells (figure 1). AK117 alone or combines with anti-EGFR antibody, anti-CD20 antibody and azacitidine shows potent phagocytosis of tumor cells in a dose-dependent manner (figure 2). AK117 significantly inhibited tumor growth in these tumor models (figure 3). Favorable hematology safety profile of AK117 was observed. A significant weaker binding to human RBC of AK117 was identified (figure 4), and AK117 does not induce hemagglutination of human RBC up to a concentration of 1050 μ g/mL, while Hu-5F9 triggers hemagglutination even at a low concentration of 1.44 μ g/mL (figure 5). AK117 has minimal anemia effect in monkey studies compared to hu5F9-G4 after single dose in cynomolgus monkeys (figure 6). AK117 showed a rather superior safety profile to Hu5F9-G4 as a shorter duration of anemia.



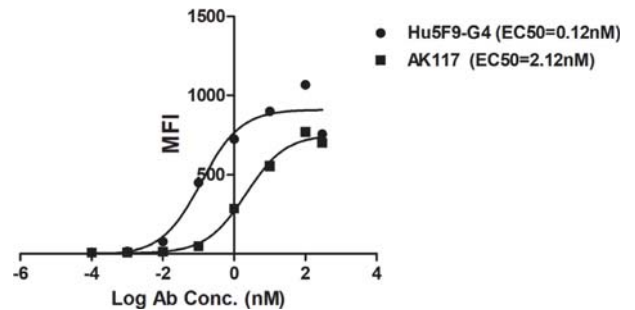
Abstract 266 Figure 1 Binding and Competition activity of AK117 to CD47. (A) FACS binding curves of AK117 and Hu5F9-G4 to CD47 on Raji cells. (B) FACS competitive binding curve of AK117 and Hu5F9-G4 with SIRP α ECD-mFc to CD47 on Raji cells.



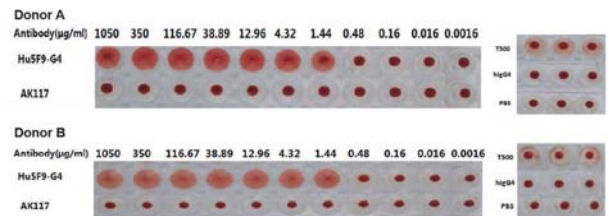
Abstract 266 Figure 2 The pro-phagocytic activity against tumor cells. (A) The phagocytic index of Raji cells by macrophages with AK117. (B) The phagocytic index of HL-60 cells by macrophages with AK117 and azacitidine. (C) The phagocytic index of HT-29 cells by macrophages with AK117 and cetuximab. (D) The phagocytic index of Raji cells by macrophages with AK117 and rituximab.



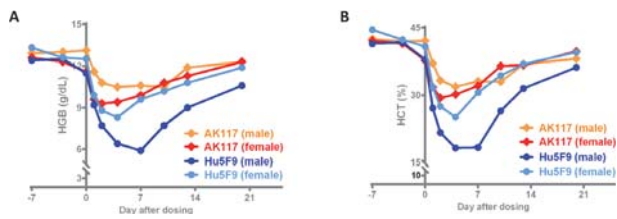
Abstract 266 Figure 3 Anti-tumor activity in Raji tumor mouse model. The (A) Tumor growth curves and (B) Body weight curves of different groups in SCID/Beige mice with subcutaneous Raji tumor.



Abstract 266 Figure 4 Binding activity of AK117 to human RBCs. Binding Curves of Hu5F9-G4 and AK117 to CD47 on human RBCs



Abstract 266 Figure 5 Hemagglutination effect on human erythrocytes. Hemagglutination effect of AK117 on human erythrocytes



Abstract 266 Figure 6 HGB and HCT in cynomolgus monkeys. The curves of (A) hemoglobin and (B) Hematocrit at different times in cynomolgus monkeys.

Conclusions With pre-clinical pharmacology activities comparable to Hu5F9-G4 as well as superior safety properties demonstrated in non-clinical pharmacodynamics studies, AK117 has emerged as a promising new treatment for solid tumor.

<http://dx.doi.org/10.1136/jitc-2021-SITC2021.266>

267

DUAL CHECKPOINT BLOCKADE OF CD47 AND PD-L1 USING AN AFFINITY-TUNED BISPECIFIC ANTIBODY MAXIMIZES ANTI-TUMOR IMMUNITY AND IMPROVES THERAPEUTIC WINDOW

Shih-Hsun Chen, Pawel Dominik, Jessica Stanfield, Sheng Ding, Wenjing Yang, Nadia Kurd*, Ryan Llewellyn, Jonathan Heyen, Carole Wang, Zea Melton, Kevin Lindquist, Thomas Van Blarcom, Javier Chaparro-riggers, Shahram Salek-Ardakani. *Pfizer, San Diego, CA, USA*

Background T cell checkpoint immunotherapies have shown promising results in the clinic, but most patients remain non-responsive. CD47-SIRP α myeloid checkpoint blockade has shown early clinical activity in hematologic malignancies. However, CD47 expression on peripheral blood limits α CD47 antibody selectivity and thus efficacy in solid tumors.

Methods To improve the antibody selectivity and therapeutic window, we developed a novel affinity-tuned bispecific antibody targeting CD47 and PD-L1 to antagonize both innate and adaptive immune checkpoint pathways. This PD-L1-targeted CD47 bispecific antibody was designed with potent affinity for PD-L1 and moderate affinity for CD47 to achieve preferential binding on tumor and myeloid cells expressing PD-L1 in the tumor microenvironment (TME).

Results The antibody design reduced binding on red blood cells and enhanced selectivity to the TME, improving the therapeutic window compared to α CD47 and its combination with α PD-L1 in syngeneic tumor models. Mechanistically, both myeloid and T cells were activated and contributed to anti-tumor activity of α CD47/PD-L1 bispecific antibody. Distinct from α CD47 and α PD-L1 mono- or combination therapies, single-cell RNA sequencing (scRNA-seq) and gene expression analysis revealed that the bispecific treatment resulted in unique innate activation, including Pattern Recognition Receptor (PRR)-mediated induction of type I IFN pathways and antigen presentation in DCs and macrophage populations. Furthermore, treatment increased the Tcf7+ stem-like CD8 T cell population in the TME and promoted its differentiation to an effector-like state. Consistent with mouse data, the compounds were well tolerated and demonstrated robust myeloid and T cell activation in non-human primates (NHPs). Notably, RNA-seq analysis in NHPs provided evidence that the innate immune activation was mainly contributed by CD47-SIRP α but not PD-L1-PD-1 blockade from the bispecific antibody.

Conclusions These findings provide novel mechanistic insights into how myeloid and T cells can be uniquely modulated by the dual innate and adaptive checkpoint antibody and demonstrate its potential in clinical development (NCT04881045) to improve patient outcomes over current PD-(L)1 and CD47-targeted therapies.

<http://dx.doi.org/10.1136/jitc-2021-SITC2021.267>

**KVA 12.1 A NOVEL FULLY HUMAN ANTI-VISTA
ANTIBODY: CLINICAL TRIAL DESIGN IN MONOTHERAPY
AND IN COMBINATION WITH AN ANTI-PD1 ANTIBODY**

Thierry Guillaudeau*, Shawn Iadonato, Eric Tarcha, Craig Phillips. *Kineta Inc., Seattle, WA, USA*

Background V-domain Ig Suppressor of T cell Activation (VISTA) is an immune-suppressive checkpoint inhibitor of T cell response. VISTA is expressed in the immuno-suppressive tumor microenvironment, mostly by cells of the myeloid lineage, and its blockade can restore an efficient antitumor immune response especially in hard-to-treat tumors.¹ In addition, an increase in VISTA expression has been described after treatment by the current immune checkpoint inhibitors, anti-CTLA-4 or anti-PD1-(L),¹ especially in patients refractory to these treatments.^{2 3} Therefore, VISTA may be involved in a compensatory resistance mechanism to checkpoint inhibitors.

Methods Kineta has selected a lead candidate anti-VISTA monoclonal antibody, KVA12.1, after a deep screen of 107 fully human and highly diverse antibodies directed against the extracellular domain of VISTA.

Results KVA12.1 exhibits high potency and binds to a unique epitope. It restores T cell activation and induces a pro-inflammatory response in in vitro assays. In vivo, in human VISTA knock-in mice, KVA12.1 treatment mediates strong single-agent antitumor activity in multiple syngeneic tumor models and shows enhanced efficacy in combination with either anti-PD-(L)1 or anti-CTLA-4 treatment. Finally, our anti-VISTA antibody was well-tolerated in exploratory toxicology studies in cynomolgus monkey, where hematology and clinical chemistry evaluations as well as clinical observations including monitoring of body weight revealed no indicators of toxicity. Safety endpoints, including the monitoring of cytokine levels related to cytokine release syndrome (CRS), clinical pathology and immunogenicity were evaluated. Cytokine levels associated with CRS (e.g., TNF-alpha, IL-6, IL-1 β) were assessed, and none were elevated to levels associated with CRS. These studies provided drug exposures (AUC) well over the expected exposures required for clinical efficacy, and KVA12.1 exhibits a good half-life consistent with other monoclonal check-point inhibitors. We are currently engaged in pre-IND studies and manufacturing of KVA12.1.

Conclusions Here we are presenting the design of a phase 1/2 multicenter, open label, dose escalation and dose expansion study of intravenous infusion of KVA12.1 as a monotherapy and in combination with a fixed dose of an anti-PD1 antibody in patients with advanced refractory or metastatic solid tumors.

REFERENCES

1. ElTanbouly MA, Schaafsma E, Noelle RJ, Lines JL. VISTA: Coming of age as a multi-lineage immune checkpoint. *Clin Exp Immunol* 2020;**200**(2):120–130.
2. Kuklinski LF, Yan S, Li Z, Fisher JL, Cheng C, Noelle RJ, Angeles CV, Turk MJ, Ernstoff MS. VISTA expression on tumor-infiltrating inflammatory cells in primary cutaneous melanoma correlates with poor disease-specific survival. *Cancer Immunol Immunother* 2018 July;**67**(7):1113–1121.
3. Kakavand H, Jackett LA, Menzies AM, Gide TN, Carlino MS, Saw RPM, Thompson JF, Wilmott JS, Long GV, Scolyer RA. Negative immune checkpoint regulation by VISTA: a mechanism of acquired resistance to anti-PD-1 therapy in metastatic melanoma patients. *Mod Pathol* 2017 December;**30**(12):1666–1676.

<http://dx.doi.org/10.1136/jitc-2021-SITC2021.268>

269

UTILIZING SERUM PROTEOME TO UNDERSTAND RESPONSE AND RESISTANCE TO IMMUNE CHECKPOINT INHIBITORS IN ADVANCED NON-SMALL CELL LUNG CANCER

¹Leeseul Kim*, ²Young Kwang Chae, ²Dong-Uk Lee. ¹AMITA Health Saint Francis Hospital Evanston, Chicago, IL, USA; ²Developmental Therapeutics Northwestern Medicine, Chicago, IL, USA

Background Predictive biomarkers are more in need considering that responses and resistance to immune checkpoint inhibition (ICI) are poorly understood. We used a validated serum-based proteomic test, Primary Immune Response (PIR), to predict response and Protein Set Enrichment Analysis (PSEA) scores to elucidate mechanisms of early resistance to ICI in patients with advanced non-small cell lung cancer (NSCLC). (Muller et al., 2020)

Methods Serum of 43 consented NSCLC patients was collected prospectively at 2 timepoints: baseline (prior to ICI initiation) and 3 weeks after ICI initiation (median 22 days). Blinded samples were classified by the PIR test. Clinical response was evaluated using RECIST. Outcomes, including progression-free survival (PFS) and overall survival (OS), were analyzed by PIR classifications as intermediate/sensitive (not resistant) vs. resistant at baseline and 3 weeks. Multivariable regression was performed. PSEA scores indicating activity of 10 processes of interest (e.g., Type 1 immunity (Th1), complement, interferon-gamma (IFN γ)) were compared between PIR groups.

Results Of the 43 patients, 28 received chemotherapy with ICI (chemo+ICI) and 15 received ICI alone. 31 of 43 patients (72%) were treatment naïve at baseline blood draw. PIR-resistant patients had worse survival compared to patients classified as not resistant (HR, 10.4; 95%CI, 1.3–81 ; P = 0.025). OS was also significantly lower for patients with PIR resistant result at 3 weeks (HR, 9.1; 95%CI, 1.2–72 ; P = 0.036). The difference in survival between PIR classification groups was consistently observed in the treatment naïve patients treated with chemo+ICI (log rank P = 0.02). No significant differences were observed in PFS. Clinical and pathologic characteristics, including PD-L1 expression, were not significantly associated with PIR result. In multivariable analysis including performance status, line of therapy, and PD-L1 status, PIR resistant remained a significant negative prognostic factor (HR, 8.2; 95%CI, 1.01–67; P = 0.049). PSEA scores at baseline and 3 weeks after ICI initiation showed significantly higher levels of complement, IFN γ , Th1, immune tolerance, and a lower level of wound healing (all P<0.0001) in PIR-resistant vs. PIR-intermediate/sensitive.

Conclusions These data further validate the utility of the PIR test in predicting patient survival on ICI. Processes associated with PIR resistant result included activation of complement, IFN γ , Th1, and immune tolerance, elucidating early mechanisms of resistance to ICI in a clinical cohort.

<http://dx.doi.org/10.1136/jitc-2021-SITC2021.269>

ANTI-CD47 IMMUNOTHERAPY AS A THERAPEUTIC STRATEGY FOR THE TREATMENT OF BREAST CANCER BRAIN METASTASIS

¹Jessica Mackert*, ¹Elizabeth Stirling, ¹Mitra Kooshki, ²Dawen Zhao, ²Alexandra Thomas, ²Glenn Lesser, ²Pierre Triozzi, ¹David Soto-Pantoja. ¹Wake Forest University, Winston-Salem, NC, USA; ²Wake Forest Baptist Health, Winston-Salem, NC, USA

Background Triple-negative breast cancer (TNBC) is a highly aggressive subtype of breast cancer characterized by a lack of specific targets and a 35% incidence of brain metastasis. There is no targeted treatment for managing brain metastasis associated with TNBC; therefore, new strategies are urgently needed to overcome disease mortality. The presence of cell surface protein CD47 allows cancer cells to evade innate and adaptive immune surveillance resulting in metastatic spread. CD47 binds to and activates SIRP α on the surface of myeloid cells, inhibiting their phagocytic activity. On the other hand, CD47 binds the matricellular protein Thrombospondin-1 limiting T cell activation. Thus, blocking the CD47 is a potential therapeutic strategy for the prevention of brain metastasis.

Methods Breast cancer patient biopsies were stained with antibodies against CD47. An anti-CD47 antibody was used in a syngeneic model of orthotopic triple-negative breast cancer. CD47 null mice were used in a breast cancer brain metastasis model by intracardiac injection of the E0071-Br-Luc cell line. Brain metastatic burden was measured by the in vivo imaging system (IVIS) and quantified by luciferase luminescence. Immunohistochemical analysis was performed to quantify tumor-infiltrating macrophages. Gene expression analysis of tumors was carried out by RNA-sequencing.

Results Immunohistochemical staining of patient biopsies revealed an 89% increase in CD47 expression in metastatic brain tumors compared to primary lesions ($p \leq 0.05$). Anti-CD47 treatment in mice bearing brain metastatic 4T1br3 orthotopic tumors reduced tumor volume and tumor weight by over 50% compared to control mice ($p \leq 0.05$) and increased F4/80 macrophage marker 5-fold tumors compared to control ($p \leq 0.05$). CD47 null mice had a 60% increase in survival ($p \leq 0.05$) and an 89% decrease in metastatic brain lesions ($p \leq 0.05$) compared to control mice in a brain metastasis model. Additionally, RNA sequencing revealed 318 uniquely expressed genes and a significant reduction of genes related to extracellular matrix organization in tumors treated with an anti-CD47 antibody.

Conclusions CD47 was increased in metastatic brain tumors compared to primary lesions in breast cancer patients. CD47 blockade reduced orthotopic brain-metastatic tumor burden associated with increased macrophage infiltration and reduced extracellular matrix-associated gene expression. Additionally, CD47 null mice had improved overall survival and reduced brain metastatic lesions. Thus, CD47 blockade may be an effective therapeutic for triple-negative breast cancer brain metastasis.

Acknowledgements This work is supported by a NCI R21 CA249349 and the American Cancer Society Research Scholar Grant (133727-RSG-19-150-01-LIB).

Ethics Approval Animal studies were approved by the Wake Forest School of Medicine Animal Care and Use Committee (ACAUC). Human subject studies were approved by the institutional review board (IRB).

<http://dx.doi.org/10.1136/jitc-2021-SITC2021.270>

271 **DEVELOPMENT OF OR2805, AN ANTI-CD163 ANTIBODY DERIVED FROM AN ELITE RESPONDER TO CHECKPOINT INHIBITOR THERAPY THAT RELIEVES IMMUNOSUPPRESSION CAUSED BY M2C MACROPHAGES**

Peter Probst, Randi Simmons, Huyen Dinh, Meghan Zuck, Valerie Wall, Myriam Bouchlaka, Sam Lam, Ray Fox, Darbie Whitman, Tom Graddis, Kamal Puri*. *OncResponse Inc., Seattle, WA, USA*

Background OR2805 antibody was discovered using B cells derived from an elite responder to checkpoint inhibitor (CPI) therapy. It is a fully human IgG1 antibody that binds to CD163, an immune-suppressive receptor highly expressed on tumor associated macrophages (TAMs). High numbers of CD163-expressing TAMs generally predict an unfavorable prognosis in solid tumors. These CD163-expressing TAMs contribute to an immune-suppressive tumor microenvironment and inhibit an anti-tumor T-cell response by engaging immune checkpoints and secreting immune-suppressive cytokines. Relieving the immune suppression of CD163-expressing TAMs to improve anti-tumor T-cell responses is a rational therapeutic strategy as monotherapy and in combination with CPI therapy. **Methods** Cocultures of immunosuppressive primary human polarized M2c macrophages with autologous CD8+ T cells or phytohemagglutinin (PHA)-T cell blasts (exhausted T cells) were used to interrogate OR2805-dependent immunomodulatory responses as single agent and in combination with pembrolizumab, an anti-PD1 antibody. The anti-tumor activity of OR2805 was evaluated in humanized mouse models. Safety and pharmacokinetics (PK) profile of OR2805 was evaluated in cynomolgus monkeys and human whole blood for cytokine release assessment.

Results In coculture assays, OR2805-treatment relieved the suppressive effect of M2c macrophages as demonstrated by increased T-cell proliferation and the release of IFN- γ and perforin. OR2805 restored the IFN- γ production of exhausted T cells and showed a synergistic effect on cocultures treated in combination with pembrolizumab. OR2805-treatment demonstrated significant anti-tumor activity in lung cancer xenograft models in humanized NSG-SGM3 mice. In cynomolgus monkeys, OR2805 demonstrated a typical IgG1 PK profile and good serum exposure. Furthermore, OR2805 did not trigger the release of IL-1 β , IL-2, IL-4, IL-6, IL-10, IFN- γ , or TNF- α cytokines in whole blood from either healthy donors or NSCLC patients.

Conclusions OR2805 reduced M2c-mediated immunosuppression and enhanced T cell effector functions. OR2805-treatment resulted in significant anti-tumor activity in lung cancer xenograft models in humanized mice. The pharmacology, PK, and toxicokinetic data support further development of OR2805 as an anti-cancer therapy, both as a monotherapy and in combination with CPI therapy.

<http://dx.doi.org/10.1136/jitc-2021-SITC2021.271>

272

A NOVEL BISPECIFIC MACROPHAGE ENGAGER ANTIBODY (BiME) DESIGNED FOR CANCER IMMUNOTHERAPY

Hongtao Lu*, Dawei Sun, Xiaofeng Niu, Yanan Geng, Jing Wang, Haixia Jiang, Rui Gao, Zhihao Wu, Yangsheng Qiu. *Elpiscience Biopharmaceuticals, Shanghai, China*

Background Anti-CD3-based bispecific T cell engagers (BiTE) showed limited clinical efficacy in solid tumors. This is partly due to the difficulty and scarcity of T cells infiltrating into tumor microenvironment (TME). Macrophages are major component of immune cell infiltrate in the TME and can constitute up to 50% of a solid tumor mass. Signal regulatory protein- α (SIRP α) is a major myeloid cell inhibitory receptor that engages the "don't eat me" signal from CD47 expressed on tumors. Similar to BiTE where T cells are activated by the CD3 antibody, we constructed a novel bispecific macrophage engager (BiME) where macrophage is activated by a SIRP α inhibitory antibody that is directed to a particular tumor via the tumor associated antigen (TAA) antibody, resulting in phagocytosis of the tumor. Previously, we have developed a human SIRP α monoclonal antibody called ES004-B4, that blocks CD47 binding. ES004 greatly augments antibody dependent cellular phagocytosis killing of cancer cell lines. We utilize ES004 to make a BiME called ES028 where the SIRP α antibody is linked to a Claudin18.2 antibody, targeting claudin18.2-expressing cancers like gastric cancer.

Methods Through Elpiscience BiME platform, we have generated a panel of anti-Claudin18.2/SIRP α bispecific antibodies, including different anti-Claudin18.2 arm and anti-SIRP α arm positions, ratios and IgG isotypes. The binding and blocking ability of these bispecific antibodies were evaluated by ELISA and FACS. In vitro function activity was determined by phagocytosis assay using human monocyte derived macrophage and mouse bone marrow derived macrophage. In vivo anti-tumor efficacy was investigated in a syngeneic tumor model with hSIRP α knock-in mice.

Results We demonstrate that an anti-Claudin18.2/SIRP α bispecific antibody ES028 exhibited super anti-cancer effects, with improved phagocytosis of cancer in vitro and extended survival of claudin18.2-expressing tumor burden mice. In the syngeneic model, ES028 showed almost 100% tumor growth inhibition in the SIRP α knock-in models without causing cytokine storm. ES028 could not induce phagocytosis of Claudin18.2 negative cells, proving its specificity and selectivity.

Conclusions We have developed a bispecific macrophage engager (BiME) platform that is capable of activating phagocytosis to kill cancer cells. A number of preclinical programs are ongoing to design specific BiME for particular tumor indication. Our SIRP α -based macrophage engager ES028 is the first to have reached the pre-clinical stage with a demonstrated favorable safety profile and promising therapeutic efficacy. Taken together, these results indicate that the bi-specific macrophage engager platform is feasible and could be a powerful weapon in the battle towards the elimination of cancers.

<http://dx.doi.org/10.1136/jitc-2021-SITC2021.272>

**APPLICATION OF PHARMACOKINETIC-
PHARMACODYNAMIC MODELING TO SELECT THE
OPTIMAL DOSE OF ALX148, A CD47 BLOCKER**

Oleg Demin*, Elena Vasileva. *ISyBio, Moscow, Russian Federation*

Background ALX148 is a fusion protein comprised of a high-affinity CD47 blocker linked to an inactive immunoglobulin Fc region. Optimal doses selection is increasingly important in clinical setup and can be guided by an assessment of target receptor occupancy (RO) and pharmacodynamics (PD) effect in the site of action. However, direct measurement of RO and PD effect in the tumor tissue is challenging. A mechanistic pharmacokinetic (PK)-PD model was developed to predict CD47 occupancy and PD effect in tumor tissues for ALX148.

Methods The developed semi-mechanistic PK/RO/PD model describes the PK of ALX148 and its distribution to non-Hodgkin lymphoma tumor tissues (lymph nodes, spleen, and bone marrow). The model includes non-linear clearance of ALX148 due to target CD47 receptor binding and further internalization of the complex. CD47 RO was described on red blood cells and tumor cells taking into account the number of cells and CD47 expression (molecules per cell). Parameters were fitted against clinical PK and in vitro data. In vitro data on stimulation of phagocytosis by ALX148 in the presence of antibodies inducing antibody-dependent cellular phagocytosis (ADCP) was used to estimate the RO-PD relationship. Clinical data on RO in the periphery was used for model validation.

Results The model successfully described dose-dependence ALX148 clinical PK and RO data. Predicted trough median CD47 occupancy in the spleen, lymph nodes, and bone marrow during the treatment with 10 mg/kg QW ALX148 was 98% (95% confidence bands: 95%–99%), whereas 30 mg/kg Q2W resulted in 99% CD47 occupancy (95% confidence bands: 98%–99%). ADCP of cancer cells was predicted to be increased by ~1.8 times during the treatment with both regimens of ALX148: 10 mg/kg QW and 30 mg/kg Q2W. Dose 3 mg/kg resulted in the lower induction of ADCP than 10 mg/kg: 1.6 vs 1.8 (p-value < 0.001).

Conclusions The model was successfully calibrated and validated against both in vitro and clinical data on ALX148. It was predicted that 10 mg/kg QW is an optimal dose of ALX148 to occupy more than 90% of CD47 in the tumor tissues to achieve maximal induction of phagocytosis caused by ADCP stimulating antibodies such as rituximab. This approach can be applied for the optimal dose selection of other anti-CD47 agents taking into account their specific features as binding properties, size, etc.

<http://dx.doi.org/10.1136/jitc-2021-SITC2021.273>

274

CD47 X EPCAM BISPECIFIC ANTIBODY REPRESENTS A NOVEL APPROACH FOR TREATING EPCAM OVEREXPRESSION SOLID TUMORS

Xinhua Wang*, Oi Kwan Wong, Lei Shi, Qi Fei, Leonard Post, Xiaocheng Chen. *Virtuoso Therapeutics, San Mateo, CA, USA*

Background CD47 conveys a "don't eat me" signal through the interaction with its ligand signal regulatory protein- α (SIRP α) on myeloid cells and blocks macrophage mediated phagocytosis. Tumor cells, which express high level of CD47, exploit this mechanism to evade from immune surveillance. CD47/SIRP α axis is an important checkpoint of innate immune system and CD47 is considered a prominent target for cancer treatment.¹ However, the wide expression of CD47 on normal cells could cause antigen sink and lead to safety issues, such as anemia and thrombocytopenia. EpCAM is highly expressed in many epithelial cancers, particularly in colorectal, gastric, endometrial and lung cancers. Here we describe a novel CD47 x EpCAM bispecific antibody, which specifically targets CD47+/EpCAM+ tumors in preclinical studies.

Methods The CD47 x EpCAM bispecific antibody was generated using novel anti-CD47 antibody and anti-EpCAM antibody. A series of in vitro assays including FACS binding, FACS-based SIRP α blocking, ADCP, RBC binding and hemagglutination were performed to characterize the CD47 x EpCAM bispecific antibody. In vivo efficacies of this bispecific antibody were evaluated in xenograft tumor models with high EpCAM and CD47 expression.

Results Compared to monoclonal CD47 antibody, the CD47 x EpCAM bispecific antibody selectively binds to tumor cells overexpressing EpCAM. The bispecific antibody exhibited potent SIRP α blocking and antibody-dependent cellular phagocytosis (ADCP) activity on CD47+/EpCAM+ tumor cells, but not on cells lacking EpCAM expression. Compared to its parental CD47 monoclonal antibody, the EC₅₀ of SIRP α blocking activity were improved 30–80 folds with the treatment of the CD47 x EpCAM bispecific antibody in tumor cell lines with high EpCAM expression. No significant RBC binding and RBC phagocytosis were observed upon treatment with the CD47 x EpCAM bispecific antibody. The bispecific antibody did not cause any appreciable hemagglutination with up to 1 μ M antibody treatment. Most importantly, the bispecific antibody demonstrated potent anti-tumor activities in in vivo solid tumor cell line-derived xenograft (CDX) models that overexpress both CD47 and EpCAM.

Conclusions Our findings suggest that the novel CD47 x EpCAM bispecific antibody selectively binds to CD47 and blocks CD47/SIRP α binding on EpCAM overexpressing tumor cells. The bispecific antibody has minimum RBC binding compared to the bivalent CD47 monoclonal antibodies. The bispecific antibody shows potent in vivo efficacy and specificity toward EpCAM positive tumor cells and represents a novel approach for treating EpCAM+ tumors.

REFERENCES

- 1.. Chao M, Weissman I, Majeti R. The CD47-SIRP α pathway in cancer immune evasion and potential therapeutic implications. *Curr Opin Immunol* 2012;**24**(2):225–232.

Ethics Approval The protocol and any amendment(s) or procedures involving the care and use of animals in these animal studies were reviewed and approved by the Institutional Animal Care and Use Committee (IACUC) of WuXi AppTec prior

to conduct. During the studies, the care and use of animals were conducted in accordance with the regulations of the Association for Assessment and Accreditation of Laboratory Animal Care (AAALAC)

<http://dx.doi.org/10.1136/jitc-2021-SITC2021.274>

FLOW CYTOMETRY AND NANOSTRING PROVIDE A COMPREHENSIVE CELL- AND GENE-BASED TUMOR PROFILE FOLLOWING CHECKPOINT INHIBITION IN A MURINE BLADDER CANCER MODEL

David Draper*, Philip Lapinski, Scott Wise. *Labcorp Drug Development, Ann Arbor, MI, USA*

Background Bladder cancer (BC) is the thirteenth leading cause of cancer-related deaths.¹ Five checkpoint immunotherapies that target the PD-1/PD-L1 axis are FDA approved, and gene- and protein-based approaches are helping to identify new combination treatment strategies for therapeutic intervention.² Using the murine MB49 model for BC, we demonstrate how non-targeted immune gene expression profiling can combine with flow cytometry to provide a gene and cell-specific signature for the tumor microenvironment and help identify potential targets for novel treatment approaches.

Methods Animals with established MB49 tumors were treated with anti-mPD-1 or isotype control antibodies. Tumors were collected 7 days after the last treatment. Flow cytometry examined anti-mPD-1 treatment-induced immunophenotypic modulation for eleven tumor-infiltrating immune subsets. The mouse PanCancer IO 360™ panel (NanoString) provided transcriptomic analysis of 770 immuno-oncology-related genes. The ROSALIND™ platform (OnRamp BioInformatics) was used to identify differentially regulated genes between treatment groups (± 1.5 fold-change; $p < 0.05$).

Results Anti-mPD-1 had moderate anti-tumor activity, with a 58% tumor growth inhibition at day 18 post-implant in treated compared to control animals. Flow cytometry revealed anti-mPD-1 triggered an increase in tumor-infiltrating CD8+ T cells (45%) compared to control animals. Furthermore, the CD8+ T cell phenotype was altered by anti-mPD-1 treatment. The percentage of CD8+ T cells that expressed ICOS and LAG-3 was increased in tumors from anti-mPD-1 treated animals (22% and 35% respectively). A reduction in PD-1 expression was also observed (33%). In myeloid cells, iNOS expression increased in tumor-associated macrophages from treated animals compared to controls. NanoString analysis revealed 62 genes were differentially regulated in tumors from anti-mPD-1 treated animals compared to controls. ROSALIND analysis classified 30 of the genes as regulators of interferon, cytotoxicity, antigen presentation, and cytokine/chemokine signaling. Also, among the genes upregulated by anti-mPD-1 were IDO, HAVCR2 (TIM-3), and CSFR1, which can promote tumor growth and are clinical targets actively being investigated for new immunotherapies.

Conclusions NanoString analysis complemented flow cytometry to provide a comprehensive profile of the MB49 tumor. Together, these data demonstrate that anti-mPD1 increases T cell recruitment into the tumor and upregulates the expression of genes known to enhance T cell recruitment and anti-tumor activity. iNOS protein upregulation indicates that anti-mPD-1 treatment may also exert effects by reprogramming M2 macrophages towards an M1 phenotype. Upregulation of IDO, HAVCR2, and CSFR1 genes may effectively counteract anti-mPD-1 treatment. Further investigation may elucidate clinical implications for inhibitors of these gene products as combination treatment partners with anti-mPD-1.

REFERENCES

1. Saginala K, Barsouk A, Aluru JS, Rawla P, Padala SA, Barsouk A. Epidemiology of bladder cancer. *Med Sci* 2020;1:15–26.

2. Lopez-Beltran A, Cimadamore A, Blanca A, Massari F, Vau N, Scarpelli M, Cheng L, Montironi R. Immune checkpoint inhibitors for the treatment of bladder cancer. *Cancers* 2021;1:131–146.

Ethics Approval N/A

<http://dx.doi.org/10.1136/jitc-2021-SITC2021.275>

276

DISCOVERY AND PRECLINICAL CHARACTERIZATION OF ANTI-LILRB2 ANTIBODIES THAT RESCUE T CELLS FROM MACROPHAGE-MEDIATED IMMUNE SUPPRESSION

Meghan Zuck*, Huyen Dinh, Valerie Wall, Sam Lam, Ramya Chandrasekaran, Francisco Zapata, Texia Loh, Lauren Loh, Myriam Bouchlaka, Tom Graddis, Meghan Zuck, Kamal Puri, Peter Probst. *OncResponse, Seattle, WA, USA*

Background The inhibitory receptor leukocyte immunoglobulin-like receptor subfamily B member 2 (LILRB2, ILT4), is expressed on immunosuppressive myeloid cells, and has emerged as a key immune checkpoint in the tumor microenvironment (TME). Interaction of LILRB2 with the HLA class I ligands (e.g., HLA-G, HLA-A, etc.) mediates immune suppression by myeloid cells and promotes tumor immune evasion. Targeting this pathway in the TME may enhance efficacy of T cell checkpoint inhibitors. Antibodies targeting LILRB2 are currently being evaluated in clinical trials for the treatment of cancer.

Methods Anti-LILRB2 antibodies were cloned from B cells derived from rabbits immunized with human LILRB2 recombinant protein. Cells were cultured at clonal density, and IgG antibodies in supernatants were evaluated for binding to human and cynomolgus LILRB2. Variable-regions from positive hits were sequenced, cloned, and expressed as recombinant rabbit-human chimeras. Anti-LILRB2 chimeric antibodies were evaluated in a panel of functional and phenotypic assays using primary human macrophages and T cells, and then prioritized for evaluation in a humanized NSG-SGM3 tumor model.

Results Twenty-seven rabbit anti-LILRB2 clones were selected and expressed as rabbit-human IgG4 chimeras based on binding to recombinant human LILRB2 protein and blocking of HLA-G binding to LILRB2. A subset of chimeric clones demonstrated binding to stably expressing LILRB2 cells, and lack of binding to other LILRB or LILRA family members by enzyme-linked immunosorbent assay and by flow cytometry of transiently transfected HEK cells. Lead clones were identified based on their ability to block interaction of LILRB2 to HLA-G expressed on tumor cells, and activity in functional cell-based assays modeling LILRB2-mediated immune suppression. These clones enhanced LPS-induced IFN- γ production by PBMCs and increased the release of TNF- α by CD40L-activated macrophages. Selected clones also relieved M2c-macrophage-mediated immune suppression in a M2c/CD8+ T cell coculture assay by restoring T-cell proliferation and secretion of pro-inflammatory cytokines. Importantly, lead chimeric LILRB2 clones demonstrated in vivo efficacy with significant tumor growth inhibition and tumor regression in an SK-MEL-5 tumor model in humanized NSG-SGM3 mice.

Conclusions We identified novel anti-LILRB2 antibodies that restore innate and adaptive immune responses by modulating immunosuppressive macrophages. These data provide a strong rationale for further development of these antibodies as an anti-cancer immunotherapy.

<http://dx.doi.org/10.1136/jitc-2021-SITC2021.276>

SAFETY AND EFFICACY OF INTRATUMORAL IPILIMUMAB WITH IV NIVOLUMAB IN METASTATIC MELANOMA. THE NIVIPIT TRIAL

¹Lambros Tselikas*, ¹Caroline Robert, ²Stephane Dalle, ³Nicolas Meyer, ⁴Celeste Lebbe, ¹Samy Ammari, ¹François-Xavier Danlos, ¹Severine Roy, ¹Camille Jannin, ¹Siham Farhane, ¹Severine Mourad, ¹Guillaume Escriou, ¹Thibault Raoult, ¹Jean-Yves Scoazec, ¹Matthieu Texier, ¹Nathalie Chaput-Gras, ¹Laurence Zitvogel, ¹Thierry De Baere, ²Aurélien Marabelle. ¹Gustave Roussy, Villejuif, France; ²HCL, Claude Bernard University, Lyon, France; ³IUCT-O, CHU Toulouse, Toulouse, France; ⁴APHP, Paris, France; ⁵Gustave Roussy, Villejuif, France

Background Intratumoral (IT) administration of Ipilimumab (Ipi), could maximize its dose/efficacy ratio while preventing its on-target/off-tumor systemic adverse events. We report the results of a randomized multicenter Phase 1b study comparing IT vs IV Ipi with intravenous nivolumab (nivo) in patients with metastatic melanoma.

Methods Previously untreated metastatic melanoma patients were randomly assigned 1:2, to receive IV Nivo (1mg/kg) in combination with either IV Ipi (3mg/kg) or 10x lower dose IT Ipi (0.3mg/kg) Q3W for 4 doses, followed by Nivo 3mg/kg Q2W for up to 2 years. The primary objective was to compare \geq grade 3 irAE rates at 6 months. Secondary objectives were to assess anti-tumor efficacy and related predictive immune biomarkers. Fresh tumor biopsies pre & on-treatment on both injected and non-injected tumors were analyzed by flow-cytometry, and soluble factors from their supernatant were titrated with Meso-Scale-Discovery® multiplex. Fresh sequential whole blood samples were collected for flow-cytometry phenotyping of immune cells, and for measuring systemic exposure to Ipi using ELISA

Results 40 patients were treated in the IT-arm and 21 in the IV-arm. The study met its primary endpoint with lower toxicity rate at 6 months in the IT-arm, with 30% [18.1;45.4] vs 57.1% [36.5;75.5] of patients presenting \geq grade 3 treatment related AEs, and no procedure-related \geq grade 3 AEs in the IT-arm out of 162 IT injections performed (including deep seated lesions). ORR per RECIST 1.1 were observed in 50% [32.9;67.1] in the IT-arm vs 65.0% [0.41;0.85] in the IV-arm. In the IT-arm, 65.7% of the injected tumors showed a CR or PR. Serum Ipi concentrations were much lower in the IT arm (:10). At C2, patients in both arms had significant decreased circulating naïve Tregs independently from tumor responses. Presence of intratumoral CD25hi CD39hi activated Tregs that decreased significantly upon IT (but not IV) injection only in responders, was predictive of the overall tumor response in the IT-arm. Moreover, granzyme B concentrations in tumor secretome at baseline were higher in responders than non-responders in both arms.

Conclusions 0.3mg/kg IT Ipi in combination with IV Nivo is not only safe but could reduce \geq grade 3 toxicity of the ICB combination. The high response rate in injected lesions was associated with the reduction of local Treg -not observed with systemic Ipi- and prompts a use in the oligometastatic and neoadjuvant setting. Direct assessment of cytolytic and regulatory pathways on fresh biopsies represents a novel, simple and rapid strategy to predict treatment efficacy.

Acknowledgements Authors would like to thank the patients taking part to the Nivipit trial, and all the medical and paramedical staff that contributed to this trial.

Trial Registration NCT02857569 EudraCT 2015-005429-37

Ethics Approval This study was approved by the national ethics committee (CPP, ANSM). Written informed consent was obtained from all patients.

Consent

N/A

<http://dx.doi.org/10.1136/jitc-2021-SITC2021.277>

**SYSTEMATIC REVIEW AND META-ANALYSIS
EVALUATING THE IMPACT OF ANTIBIOTIC USE ON
CLINICAL OUTCOMES OF NON-SMALL-CELL LUNG
CANCER PATIENTS TREATED WITH IMMUNE
CHECKPOINT INHIBITORS**

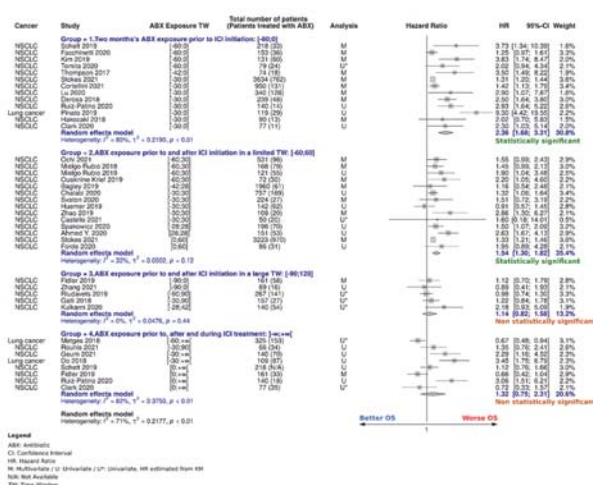
¹Athéna Crespin*, ¹Pierre-Alain Bandinelli, ¹Clément Le Bescop, ¹Renaud Buffet, ¹Jean De Gunzburg, ¹Fabien Vity, ²Gérard Zalcman, ¹Julie Cervesi. ¹Da Volterra, Paris, France; ²Hôpital Bichat-Claude Bernard, Assistance Publique Hôpitaux de Paris, Université de Paris. U830 INSERM "Genetics and Biology of Cancers, ART Group", Curie Institute, Paris, France, Paris, France

Background In recent years, the gut microbiome has increasingly emerged as influencing the response to immune checkpoint inhibitors (ICIs).¹⁻³ Antibiotic (ABX) exposure, that leads to microbiome dysbiosis, was further shown in numerous studies to adversely influence the clinical outcomes of cancer patients treated with ICIs, especially in non-small-cell lung cancer (NSCLC).⁴⁻⁶ We published in 2020 a meta-analysis confirming that ABX use could hamper survival of NSCLC patients treated with ICIs.⁷ The present study aims at updating this prior work by incorporating studies published until July 2021 and by studying new clinical outcomes.

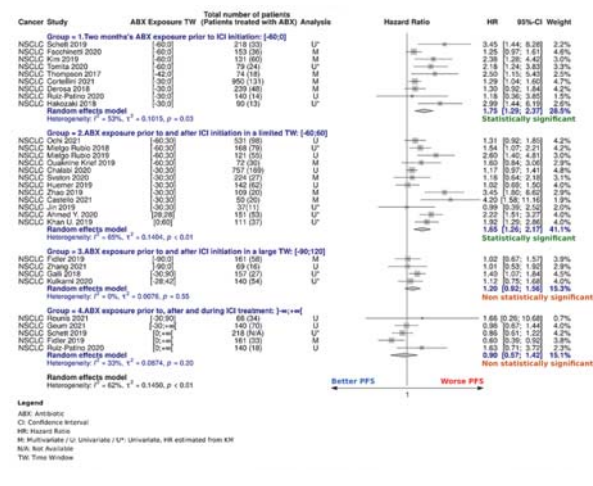
Methods PubMed and major oncology conferences' proceedings were systematically searched to identify studies assessing the impact of ABX on the clinical outcomes of NSCLC patients treated with ICIs. Studies were included when reporting a hazard ratio (HR) or Kaplan–Meier curves for Overall Survival (OS) or Progression-Free Survival (PFS) based on antibiotic exposure, and/or data on treatment response such as Overall Response Rate (ORR) and Progressive Disease Rate (PD) according to antibiotic exposure. Pooled HRs for OS and PFS and Odds Ratios (OR) for ORR and PD were calculated, as well as HRs for OS and PFS according to different time windows of ABX exposure.

Results Overall, 35 independent cohorts were included for a total of 12,235 patients. The pooled HRs for OS (12,235 patients) and PFS (5,356 patients) were 1.63 [95% Confidence Interval (CI) 1.37–1.94] and 1.49 [95% CI 1.26–1.76], respectively, confirming a significantly reduced survival in patients exposed to ABX. The subgroup analyses of OS and PFS based on the time window of ABX exposure (figures 1 and 2) suggest a harmful effect of ABX when taken around ICI initiation. The pooled OR for ORR (1,992 patients) and PD (1,272 patients) were 0.66 [95% CI 0.44–0.99] and 1.98 [95% CI 1.39–2.8], respectively, reflecting both a decreased odd of treatment response and an almost two-fold increased odd of cancer progression among ABX users (figures 3 and 4). These findings confirm the previously reported deleterious effect of ABX on all clinical outcomes (table 1).

Conclusions Antibiotics were shown to impair clinical outcomes of NSCLC patients treated with ICIs in this study. Two (non mutually exclusive) mechanisms are increasingly discussed in the literature to explain the role of microbiome on immunotherapy response: the immunomodulatory effects of bacterial molecules,⁸ and antigenic mimicry between commensal bacteria and tumor antigens cross reactive for the same antigen specific T cells.^{9, 10}



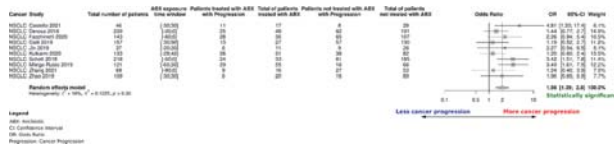
Abstract 278 Figure 1 Forest plot of hazard ratios for overall survival of patients diagnosed with NSCLC and exposed to antibiotics versus not exposed to antibiotics, according to the time window of antibiotic exposure



Abstract 278 Figure 2 Forest plot of hazard ratios for progression-free survival of patients diagnosed with NSCLC and exposed to antibiotics versus not exposed to antibiotics, according to the time window of antibiotic exposure



Abstract 278 Figure 3 Forest plot of odds ratios for overall response rate of patients diagnosed with NSCLC and exposed to antibiotics versus not exposed to antibiotics



Abstract 278 Figure 4 Forest plot of odds ratios for progressive disease rate of patients diagnosed with NSCLC and exposed to antibiotics versus not exposed to antibiotics

Abstract 278 Table 1 Summary of the impact of antibiotic use on all clinical outcomes

TW of ABX Exposure in Relation to ICI Start (Days)	Number of Patients for OS (ABX users)	Pooled HR OS [95% CI]	Number of Patients for PFS (ABX users)	Pooled HR PFS [95% CI]	Number of Patients for ORR (ABX users)	Pooled OR ORR [95% CI]	Number of Patients for PD (ABX users)	Pooled OR PD [95% CI]
All Time Windows Confounded	12,235 (2,939)	1.63 [1.37-1.94]	5,356 (1,346)	1.49 [1.26-1.76]	1,992 (382)	0.66 [0.44-0.99]	1,272 (314)	1.98 [1.39-2.8]
[-60;0]	6,244 (1,307)	2.36 [1.68-3.31]	2,074 (577)	1.75 [1.29-2.37]				
[-60;60]	7,990 (1,745)	1.54 [1.30-1.82]	2,473 (661)	1.65 [1.26-2.17]				
[-90;120]	794 (296)	1.14 [0.82-1.58]	527 (155)	1.20 [0.92-1.56]				
[>120]	1,236 (> 430)	1.32 [0.75-2.31]	725 (> 155)	0.90 [0.57-1.42]				

Statistically significant. Non statistically significant

REFERENCES

- 1.. Gopalakrishnan V, Spencer CN, Nezi L, Reuben A, Andrews MC, Karpinets TV, *et al.* Gut microbiome modulates response to anti-PD-1 immunotherapy in melanoma patients. *Science* 5 January 2018;**359**(6371):97–103.
- 2.. Routy B, Le Chatelier E, Derosa L, Duong CPM, Alou MT, Daillère R, *et al.* Gut microbiome influences efficacy of PD-1-based immunotherapy against epithelial tumors. *Science* 5 January 2018;**359**(6371):91–7.
- 3.. Matson V, Fessler J, Bao R, Chongsuwat T, Zha Y, Alegre M-L, *et al.* The commensal microbiome is associated with anti-PD-1 efficacy in metastatic melanoma patients. *Science* 5 January 2018;**359**(6371):104–8.
- 4.. Derosa L, Hellmann MD, Spaziano M, Halpenny D, Fidelle M, Rizvi H, *et al.* Negative association of antibiotics on clinical activity of immune checkpoint inhibitors in patients with advanced renal cell and non-small-cell lung cancer. *Ann Oncol Off J Eur Soc Med Oncol* 1 June 2018;**29**(6):1437–44.
- 5.. Pinato DJ, Howlett S, Ottaviani D, Urus H, Patel A, Mineo T, *et al.* Association of prior antibiotic treatment with survival and response to immune checkpoint inhibitor therapy in patients with cancer. *JAMA Oncol* 1 December 2019;**5**(12):1774–8.
- 6.. Rounis K, Makrakis D, Papadaki C, Monastirioti A, Vamvakas L, Kalbakis K, *et al.* Prediction of outcome in patients with non-small cell lung cancer treated with second line PD-1/PDL-1 inhibitors based on clinical parameters: results from a prospective, single institution study. *PLoS One* 2021;**16**(6):e0252537.
- 7.. Lurienne L, Cervesi J, Duhalde L, de Gunzburg J, Andremont A, Zalcman G, *et al.* NSCLC immunotherapy efficacy and antibiotic use: a systematic review and meta-analysis. *J Thorac Oncol Off Publ Int Assoc Study Lung Cancer* July 2020;**15**(7):1147–59.
- 8.. Sepich-Poore GD, Zitvogel L, Straussman R, Hasty J, Wargo JA, Knight R. The microbiome and human cancer. *Science* 26 March 2021;**371**(6536):eabc4552.
- 9.. Fluckiger A, Daillère R, Sassi M, Sixt BS, Liu P, Loos F, *et al.* Cross-reactivity between tumor MHC class I-restricted antigens and an enterococcal bacteriophage. *Science* 21 août 2020;**369**(6506):936–42.
- 10.. Bessell CA, Isser A, Havel JJ, Lee S, Bell DR, Hickey JW, *et al.* Commensal bacteria stimulate antitumor responses via T cell cross-reactivity. *JCI Insight* 23 avr 2020;**5**(8):135597.

<http://dx.doi.org/10.1136/jitc-2021-SITC2021.278>

279

ILT3 BLOCKADE REDUCES TUMOR BLAST CELLS IN ACUTE MYELOID LEUKEMIA PBMC AND INHIBITS TUMOR CELL GROWTH IN A HUMANIZED AML TUMOR MODEL

¹Alan Byford*, ¹Yujie Qu, ¹Haiyan Xu, ¹Gain Robinson, ¹Latika Singh, ¹Eric Muise, ¹Elaine Pinheiro, ²Mei Chen, ¹Lily Moy, ¹Stephen Alves, ¹Jie Zhang-Hoover. ¹Merck, Boston, MA, USA; ²Merck, Kenilworth, NJ, USA

Background Immunoglobulin-like transcript 3 (ILT3), an immune-inhibitory receptor expressed on myeloid cells, is highly expressed in acute myeloid leukemia (AML) with monocytic differentiation (M4 and M5 subtypes) and clinically is negatively correlated with overall survival. We examined the effects of a highly selective and potent chimeric anti-ILT3 mAb (c52B8) on tumor cell survival/growth and human immune cell modulation in AML PBMC and AML tumor cell lines in pre-clinical in vitro and in vivo models.

Methods ILT3 mRNA and cell surface expression levels were measured by RNAseq and FACS, respectively. PBMC from AML patients with different levels of ILT3 cell surface expression were treated with c52B8 in vitro. A systemic AML model was generated by IV inoculation of NSG mice with luciferase-transfected MV-4-11 human AML cells, with or without human PBMC engraftment. Tumor bearing mice were treated weekly with c52B8, modified to contain the human Fc of either the IgG1 or IgG4 subclass. MV-4-11 growth in vivo was measured by bioluminescence imaging (BLI). CyTOF was performed to phenotype AML PBMC in in vitro culture and bone marrow samples from the systemic MV-4-11 model after the treatment. THP-1 cells/human T cell co-cultures stimulated with anti-CD3/CD28 antibodies were treated with c52B8. Human T cell activity was assessed by levels of IFN γ production in the culture using MSD ELISA.

Results In ILT3 high AML patient PBMC, c52B8 treatment in vitro decreased the frequency of tumor blasts, modulated Tregs, and increased monocytic myeloid cells. In the MV-4-11 model, weekly treatment with c52B8 significantly reduced tumor burden in vivo, regardless of the IgG subclass. Importantly, tumor cell growth inhibition by c52B8 occurred in the absence of human PBMC. Additional post-mortem CyTOF analysis of bone marrow cells from MV-4-11/human PBMC inoculated mice confirmed a reduction in MV-4-11 cells, identified by CD3-CD19- human myeloid cells following c52B8 treatment. In THP-1/human T cell co-cultures, c52B8 treatment reversed THP-1 induced T cell suppression, as measured by enhanced IFN γ production.

Conclusions Anti-ILT3 mAb (c52B8) is efficacious in blocking progression of AML with monocytic differentiation by directly influencing tumor cell growth and enhancing human T cell activity in pre-clinical models. These studies support a potential role for this compound in humans.

Ethics Approval All animal work was reviewed and approved by Merck IACUC before experiments were conducted.

<http://dx.doi.org/10.1136/jitc-2021-SITC2021.279>

CLINICAL OUTCOMES OF IMMUNOTHERAPY CONTINUED BEYOND RADIOGRAPHIC PROGRESSION IN OLDER ADULTS WITH ADVANCED NON-SMALL CELL LUNG CANCER

¹Eric Singhi*, ¹Frank Mott, ²Michelle Worst, ¹Cheuk Hong Leung, ¹Jack Lee, ¹Brett Carter, ³Carolyn Presley, ¹Jeff Lewis, ¹Waree Rinsurongkawong, ¹Vadeerat Rinsurongkawong, ¹Jianjun Zhang, ¹Don Gibbons, ¹Ara Vaporciyan, ¹John Heymach, ¹Mehmet Altan. ¹University of Texas MD Anderson Cancer Center, Houston, TX, USA; ²Medscape Oncology, New York, NY, USA; ³The Ohio State University Comprehensive Cancer Center, Columbus, OH, USA

Background While the clinical outcomes of immune checkpoint inhibitor (ICI) use in older adults with advanced-stage non-small cell lung cancer (NSCLC) have been described, the role of ICI use continued beyond disease progression (BDP) remains to be well defined for this population. This retrospective single-center study explored the clinical outcomes of continuing ICIs BDP among older adult patients with advanced NSCLC.

Methods Using MD Anderson's Gemini Lung Cancer database, we retrospectively reviewed the clinical outcomes of older adults (≥ 70 years) diagnosed with advanced-stage NSCLC treated with anti-PD-(L)1 monotherapy from March 2015 through April 2019 to correlate clinicopathologic features with clinical outcomes. Clinical therapy responses were evaluated by Response Evaluation Criteria in Solid Tumors, version 1.1 (RECIST v1.1). Toxicities were assessed using Common Terminology Criteria for Adverse Events (CTCAE), version 5. Patients treated BDP were defined as individuals receiving ICIs for ≥ 8 weeks prior to documentation of progression who subsequently remained on ICIs for ≥ 6 weeks.

Results Of the 159 older adults meeting the inclusion criteria, 33 (21%) received ICIs BDP (64% male, median age 74.9 years (70.1–82.0) at the start of ICI treatment, 3 received first-line ICI therapy). Most patients were former (85%) or current (6%) smokers. 79% had adenocarcinoma histology. The median duration of immunotherapy continued BDP was 7.1 months (95% CI: 3.0–8.2). After a follow-up of 30.1 months, the median overall survival (mOS) was 31.5 months (95% CI: 16.5–not reached). Eight (24%) received local consolidative radiotherapy with a median duration of ICI BDP of 8.2 months (95% CI: 1.9–13.3). Twenty-five (76%) did not receive local consolidative therapy and achieved a median duration of ICI BDP of 4.1 months (95% CI: 2.3–7.8). Six (18%) exhibited pseudo-progression (i.e. delayed response to immunotherapy with decreased tumor burden on subsequent radiologic studies), with 4 achieving "stable disease" as best response and 2 achieving a partial response. The median duration of immunotherapy continued beyond pseudo-progression was 11.7 months (95% CI: 7.1–35.7), and the mOS was 26.2 months (95% CI: 16.5–40.0). Patients treated with ICI BDP most commonly experienced fatigue (18%), pneumonitis (12%), rash (9%), and hypothyroidism (9%). Three patients (9%) experienced grade 3 or higher toxicities (one grade 3 arthralgias and two grade 3 pneumonitis).

Conclusions ICI-use BDP in older adults with advanced NSCLC may benefit a subset of patients. Additionally, local consolidative therapy with radiation may offer prolonged duration of ICI treatment.

Acknowledgements Supported by the generous philanthropic contributions to The University of Texas MD Anderson Lung Moon Shot Program and the MD Anderson Cancer Center Support Grant P30 CA01667. Special acknowledgment to the GEMINI team.

Ethics Approval This study was approved and conducted in accordance with the institutional review board at the University of Texas MD Anderson Cancer Center; approval number (PA13-0589).

<http://dx.doi.org/10.1136/jitc-2021-SITC2021.280>

MEASURING IMMUNE CHECKPOINT INHIBITOR EFFICACY USING PRIMARY PATIENT-DERIVED 3D SPHEROIDS

Kathryn Appleton*, Katy Lassahn, Ashley Elrod, Tessa DesRochers. *KIYATEC, Inc., Greenville, SC, USA*

Background Cancerous cells can utilize immune checkpoints to escape T-cell-mediated cytotoxicity. Agents that target PD-1, PD-L1 and CTLA4 are collectively deemed immune checkpoint inhibitors (ICIs), and many have been approved for treatment of non-small cell lung cancer (NSCLC) and melanoma. Unfortunately, many patients do not respond to these therapies and often experience disease progression. Immunohistochemistry assays to predict response to ICIs have been inconsistent in their readouts and often patients with low expression levels respond to ICIs. Understanding the determinants of ICI response in individual patients is critical for improving the clinical success of this drug class. Using patient-derived spheroids from NSCLC and melanoma primary tissue, we developed a multi-plexed assay for detecting ICI efficacy.

Methods Nine NSCLC and 11 melanoma primary tumor samples were dissociated to single cells, classified for immune checkpoint expression and cell content by flow cytometry, and seeded for spheroid formation. Spheroids were treated with pembrolizumab, nivolumab, atezolizumab, ipilimumab or durvalumab across a range of concentrations and monitored for cytotoxicity at 24-hours and viability at 72-hours by multiplexing CellTox™ Green Cytotoxicity Assay and CellTiter-Glo® 3D Cell Viability Assay. IFN γ and granzyme B secretion was assessed using Luminex technology. ICI response was evaluated by determining the concentration-response relationship for all three read-outs.

Results Increased IFN γ and granzyme B were detected for every ICI in one or more patient samples. ICI-induced IFN γ secretion inversely correlated with PD-1+ immune cells. Durvalumab was significantly more cytotoxic for both NSCLC and melanoma spheroids compared to the other ICIs and significantly reduced spheroid viability with mean spheroid survival decreasing to 19.5% for NSCLC and 58.2% for melanoma. We evaluated if there was an association between durvalumab response and cell composition and found that percent spheroid survival significantly correlated with CD8+ T-cells for both NSCLC ($r=-0.7920$, $p=0.0191$) and melanoma ($r=-0.6918$, $p=0.0390$). Furthermore, CD8+ T-cells correlated with durvalumab-induced granzyme B secretion for NSCLC ($r=-0.7645$, $p=0.0271$) and melanoma ($r=-0.7419$, $p=0.0221$).

Conclusions In this study we show ICI-specific increases in immune-related analytes in a concentration-dependent manner for NSCLC and melanoma patient-derived spheroids. We detected spheroid cytotoxicity following short term ICI treatment which closely mirrored decreased spheroid viability at a later timepoint. Finally, we can decipher response mechanisms as exemplified by durvalumab-induced granzyme B secretion correlating with the presence of CD8+ T-cells which results in reduced spheroid viability for both tested cancer indications.

<http://dx.doi.org/10.1136/jitc-2021-SITC2021.281>

BISPECIFIC ANTIBODIES (BSABS) TARGETING ABCB1/PGP AND CD47 PROVIDE A MULTI-MODAL, TUMOR SPECIFIC APPROACH TO COMBAT DRUG RESISTANT CANCERS

¹Robert Arathoon*, ¹Raffaella Briante, ¹Alissa O'Connor, ¹Cindy Tan, ²Pamela Klein, ¹Jessica Morgan, ¹Paul Ponath, ³Leonard Presta, ⁴Qianting Zhai, ⁵Suchismita Mohanty, ¹Pinping Zhang. ¹Kenjockey Biotechnology Inc., South San Francisco, CA, USA; ²PMK BioResearch, San Francisco, CA, USA; ³Consultant, San Francisco, CA, USA; ⁴Abiosciences Inc., South San Francisco, CA, USA; ⁵ArsenalBio, South San Francisco, CA, USA

Background Bispecific antibodies (BsAbs) are gaining momentum in several immunotherapeutic^{1 2 3} and immuno-oncology settings.⁴ Certain designs of BsAbs enable tumor-specific targeting when two targets are concurrently expressed on tumor but not normal tissue. Judicious choice of bispecific immunotherapeutic targeting enables separate effects that are simultaneously beneficial and specific against tumor cells. This provides a multi-modal approach to the previously intractable problem of counteracting Efflux Pump (EP) mediated drug resistance in tumors. EP mediated drug resistance (EPMDR) adversely impacts a broad range of therapeutics including anti-neoplastics, TKIs, ADC-toxins and others. Elevated EP activity can also promote cancer cell growth by expelling catabolites and inhibitory substances from tumor cells. Prior efforts to combat EPMDR have focused on small molecule antagonists to EP intracellular domains; although some showed early promise^{5 6} these ultimately failed mainly for lack of tumor specificity and off-target toxicity. In contrast, BsAbs targeting extracellular domains of efflux pumps together with other tumor associated antigens (TAA) provide for: a) Tumor specific targeting b) Specific masking or antagonizing of the TAA target c) Concurrent counteraction of tumor cell efflux mechanismsd) Invoking an Fc-mediated immune attack on tumor cells Use of the Kenjockey BASE Platform™ (Bispecific Antibodies Specific to Efflux Pumps) has yielded BsAbs that have successfully targeted four different EPs together with several TAAs.

Methods Monoclonal antibodies to EPs have been raised and engineered into BsAbs with a common light chain^{7 8} in IgG frameworks. These concurrently target an EP and a TAA. By design, each arm of the antibody binds with relatively weak affinity to its target on normal tissue. However, when both targets are displayed together on tumor cells, their concurrent engagement results in stronger, efficacious binding.

Results A prototype BsAb that concurrently targets CD47 and the EP, P-glycoprotein, provided compelling, dose-dependent proofs of concept in various in vitro studies and in drug-resistant hematologic and solid tumor xenograft models. Efficacy was shown with and without additional therapeutics. In cynomolgus studies the BsAb also demonstrated a lack of off-tumor toxicities typically associated with each target.

Conclusions BsAbs concurrently targeting EPs and TAAs (including immuno-oncology targets) provide promising new tumor-specific therapies for treatment of patients with drug resistant cancers.

REFERENCES

1. Sheridan C. 2021. Despite slow progress, bispecifics generate buzz. *Nat Biotechnol* 2016; **34**:1215–1217.
2. Huang S, van Duijnhoven A, Sijts A, van Elsas A. Bispecific antibodies targeting dual tumor-associated antigens in cancer therapy. *J Cancer Res Clin Oncol* 2020;**146**:3111–3122.
3. Ma J, Mo Y, Tang M, et al. Bispecific antibodies: from research to clinical application. *Front Immunol* 2021;**12**:626–616.

4. Dheilly E, Moine V, Broyer L et al. Selective blockade of the ubiquitous checkpoint receptor CD47 is enabled by dual-targeting bispecific antibodies. *Mol Ther* 2017;**25**:523–533.
5. Amiri-Kordestani L, Basseville A, Kurdziel K, et al. Targeting MDR in breast and lung cancer: discriminating its potential importance from the failure of drug resistance reversal studies. *Drug Resist Update* 2012;**15**:50–61.
6. Robey R, Pluchino M, Hall M, et al. Revisiting the role of ABC transporters in multidrug-resistant cancer. *Nat Rev Cancer* 2018;**18**:452–464.
7. Speiss C, Zhai Q, Carter P. Alternative molecular formats and therapeutic applications for bispecific antibodies. *Mol Immunol* 2015;**67**:95–106.
8. Labrijn A, Janmaat M, Reichert J et al. Bispecific antibodies: a mechanistic review of the pipeline. *Nat Rev Drug Discov* 2019;**18**:585–608.

<http://dx.doi.org/10.1136/jitc-2021-SITC2021.282>

TIM-3 BLOCKADE MODULATES THE TUMOR MICROENVIRONMENT IMPROVING THE OUTCOME OF PRECLINICAL PEDIATRIC DIFFUSE MIDLINE GLIOMA MODELS

¹Iker Ausejo-Mauleon*, ¹Sara Labiano, ¹Virginia Laspidea, ¹Marc Garcia-Moure, ¹Daniel de la Nava, ²Oren Becher, ³Mariella Filbin, ⁴Fernando Pastor, ¹Marta Alonso. ¹*Clinica Universidad de Navarra, Pamplona, Spain*; ²*Ann and Robert H. Lurie Children's Hospital, Chicago, IL, USA*; ³*Dana-Farber Boston Children's Cancer and, Boston, MA, USA*; ⁴*Center for Applied Medical Research, Pamplona, Spain*

Background Diffuse Midline Gliomas (DMGs), encompassing Diffuse Intrinsic Pontine Gliomas (DIPGs), are the most aggressive pediatric brain tumors. Their meager survival has not changed despite the combination of radiotherapy with targeted therapies emphasizing the urgent need for effective treatments. Recent research suggested that the DIPG tumor microenvironment is neither highly immunosuppressive nor inflammatory.¹ These analyses showed the lack of infiltrating lymphocytes and the abundance of CD11b+ cells. TIM-3 is a member of the T-cell immunoglobulin and mucin domain protein family expressed on multiple immune cell types, including T cells, Treg, NK cells, monocytes, dendritic cells, and microglia, where it potently regulates not only adaptive immunity but also innate immunity.²⁻³ Therefore, TIM-3 inhibitors could challenge several components in the tumor microenvironment, thereby providing potentially effective treatment for DMGs.

Methods NP53 and XFM murine DIPG cell lines were used for animal experiments in immunocompetent orthotopic models. The tumors were processed by mechanical and enzymatic digestion and immune populations were analyzed by a flow cytometry panel. Antibodies against NK cells (NK1.1), CD4 (GK1.5), CD8 (CD8 β) were used for animal depletion experiments alone or in combination.

Results In silico assessment of TIM-3 expression in DIPG datasets showed a robust expression of this gene. Moreover, single-cell sequencing analyses of DIPG biopsies uncover its expression in the myeloid compartment (especially in microglia). In vivo efficacy studies showed that treatment with anti-TIM-3 antibody significantly increased the overall survival in two DIPG immunocompetent orthotopic animal models (doubling the median), lead to long-term survivors free of disease (50%) and showed immune memory. Analyses of CD45+ populations in the tumor microenvironment showed a significant increase in microglia, granulocytes, NK and CD8+ cells corresponding with a NK and T-cell activate phenotypes in treated-mice. In addition, we have a substantial decrease in the Treg population, which causes an increase in the CD8/Treg ratio. CD4 and CD8 T-cell depletion led to a significant but not total loss of treatment efficacy. NK cells depletion also reduced the effectiveness of this therapy, albeit to a lesser extent than CD4-CD8 depletion. We are currently investigating the role of microglia in the outcome of the treatment.

Conclusions Our data uncovered TIM-3 as a potential target for the treatment of DIPG tumors. Inhibition of this molecule led to a potent antitumor effect mediated by a profound tumor microenvironment remodelling.

REFERENCES

- 1.. Lieberman NAP, DeGolier K, Kovar HM, *et al.* Characterization of the immune microenvironment of diffuse intrinsic pontine glioma: implications for development of immunotherapy. *Neuro Oncol* 2019;**21**(1):83–94. doi:10.1093/neuonc/ny145.
- 2.. Acharya N, Sabatos-Peyton C, Anderson AC. Tim-3 finds its place in the cancer immunotherapy landscape. *J Immunother Cancer* 2020;**8**(1):e000911. doi:10.1136/jitc-2020-000911.

- 3.. Wolf Y, Anderson AC, Kuchroo VK. TIM3 comes of age as an inhibitory receptor. *Nat Rev Immunol* 2020;**20**(3):173–185. doi:10.1038/s41577-019-0224-6

<http://dx.doi.org/10.1136/jitc-2021-SITC2021.283>

INTEGRATED MOLECULAR CHARACTERIZATION OF PRIMARY RESISTANCE MECHANISMS TO IMMUNE CHECKPOINT BLOCKADE IN ADVANCED NON-SMALL CELL LUNG CARCINOMA (A-NSCLC)

¹Benjamin Besse, ²DIB Colette, ²Eladio Marquez*, ²Joon Sang Lee, ²Shu Yan, ²Marielle Chiron, ²Cecile Combeau, ²Angelique Biancotto, ¹Félix Blanc-Durand, ¹Mihaela Aldea, ¹David Planchard, ¹Jean-Yves Scoazec, ¹Ludovic Lacroix, ¹Etienne Rouleau, ¹Nathalie Chaput-Gras, ¹Saloomeh Rafie, ¹Aurélien Marabelle, ¹Eric Angevin, ²Jack Pollard. ¹IGR, Villejuif, France; ²Sanofi, VITRY SUR SEINE, France

Background Reinvigoration of anti-tumor immunity via immune checkpoint blockade (ICB) has transformed outcomes in a-NSCLC. However, a majority of patients are innately resistant to ICB, and a better understanding of the resistance mechanisms may guide the development of new treatment strategies and therapies for patients.

Methods Biopsies performed immediately before treatment with single agent ICB in patients with a-NSCLC (MATCH-R trial [NCT02517892]) were analyzed. The stromal microenvironment and immune context were characterized via an integrated analysis of whole transcriptome (RNA-seq), whole exome sequencing (WES), and immunohistochemistry (IHC) of CD3, CD8, FOXP3 and PDL1. Specifically, the immune context and the relative abundance of 10 immune and stromal cell types were assessed with integrated IHC and Cell Populations-counter (MCP-counter) [1] analysis of the RNA-seq. Somatic mutations and Tumor Mutation Burden (TMB) were evaluated. The transcriptional state of the tumor and its microenvironment were assessed by GSEA analysis [2] of the MSigDB collection [3]. Patient's outcome was associated to molecular data. Primary resistance to ICB was defined as PD (progressive disease) in the first radiological examination, or a median PFS inferior to 3 months.

Results Fifty-two patients with NSCLC were enrolled (43 adeno, 6 squamous, and 3 other carcinoma); Median age was 61 (34–93), 18 were female, 46 were smokers, 22 were responders, and 30 were non-responders. Median tumor cellularity was 60% (30%–90%). Patients may be divided into two groups (HIGH and LOW) at baseline based on their degree of immune infiltration as assessed by RNAseq or IHC. A hallmark of the HIGH infiltration group is an increase in Interferon Gamma (IFN- γ) pathway signature [4]. In contrast, patients in the LOW infiltration group (relative to the HIGH infiltration group) exhibit a decrease in IFN- γ pathway signaling and concomitantly an increase in hypoxia and gluconeogenic pathway signatures. Response rates to ICB were not associated to immune infiltration groups at baseline, but an analysis within each infiltration group revealed that high TMB is only associated to response in the HIGH infiltration group. Furthermore, only in the LOW infiltration group was increased the transforming growth factor (TGF- β) pathway signature associated to ICB response.

Conclusions This study suggests that the tumor and its micro-environment influence baseline immune infiltration. Tumors with LOW baseline infiltration show altered metabolism such as gluconeogenic activation and hypoxia activation. In contrast, factors such as TMB are not associated with baseline infiltration

<http://dx.doi.org/10.1136/jitc-2021-SITC2021.284>

BREAKING THROUGH THE RESISTANCE OF BREAST CANCER TO IMMUNE CHECKPOINT BLOCKERS IN A UNIQUE MOUSE MODEL OF HR+ DISEASE

¹Norma Bloy*, ²Aitziber Buqué Martínez, ²Bhavneet Binder, ²Giulia Petroni, ²Takahiro Yamazaki, ²Ai Sato, ²Olivier Elemento, ²Silvia Formenti, ²Lorenzo Galluzzi. ¹Weill Cornell Medical College, New York, NY, USA; ²Weill Cornell Medicine, New York, NY, USA

Background Hormone receptor (HR)+ breast cancer (BC) causes most BC-related deaths in the US.¹ Standard treatment for non-metastatic disease involves surgery plus adjuvant hormone therapy. However, approximately 50% of patients ultimately relapse and require additional lines of treatment including chemotherapy, which is unfortunately associated with limited clinical benefits and severe toxicity. In HR+ BC patients, the efficacy of immunotherapy has also been disappointing so far. Indeed, objective responses to PD-1 blockade with pembrolizumab in women with HR+ BC have been in the range of 5–10%, with no clear advantage on survival. Thus, resistance to PD-1 blockers constitutes a major obstacle towards the implementation of immunotherapy in HR+ BC patients.

Methods To obtain insights into the immunological alterations accompanying disease relapse in HR+ BC exposed to PD-1 blockade, we harnessed a unique endogenous model of BC driven in immunocompetent mice by progesterone and a carcinogen. This model recapitulates key aspects of human luminal B BC, including a relatively ‘cold’ microenvironment, hence limited sensitivity to PD-1 blockade.² We undertook an in-depth characterization of the tumors (by DNAseq and RNAseq) and systemic (by flow cytometry on the splenic compartment) immune microenvironment of C57BL/6 female mice bearing tumors that recovered normal growth after PD-1 treatment.

Results There was no clear difference after PD-1 blockade at the systemic level in the myeloid, or lymphoid compartments; or in the activation of T cells, nor their capacity to degranulate upon ex vivo stimulation. Whole exome sequencing showed a higher mutational burden in PD-1 treated tumors after relapse. At the gene expression level, unsupervised analysis showed a clustering independent of the treatment groups, probably due to the heterogeneity of the model. Targeted pathway analysis with supervised clustering showed however differences in immune pathways that are currently further investigated, and results will be available shortly.

Conclusions Breaking through resistance of HR+ tumors to PD-1 blockers can direct strategies to overcome resistance in HR+ BC patients, the majority of BC patients. If successful, this can inform therapeutic approaches to enable superior therapeutic responses in patients with HR+ BC, hence significantly reducing BC-related deaths.

REFERENCES

1. Siegel RL, Miller KD, Jemal A. Cancer statistics, 2020. *CA Cancer J Clin* 2020;**70**:7–30.
2. Buque A, Bloy N, Perez-Lanzon M, Iribarren K, Humeau J, Pol JG, Levesque S, Mondragon L, Yamazaki T, Sato A, Aranda F, Durand S, Boissonnas A, Fucikova J, Senovilla L, Enot D, Hensler M, Kremer M, Stoll G, Hu Y, Massa C, Formenti SC, Seliger B, Elemento O, Spisek R, Andre F, Zitvogel L, Delalogue S, Kroemer G, Galluzzi L. Immunoprophylactic and immunotherapeutic control of hormone receptor-positive breast cancer. *Nat Commun* 2020;**11**:3819.

Ethics Approval This study was approved by Weill Cornell Medical College’s Ethics Board; approval number 2018–0053.

<http://dx.doi.org/10.1136/jitc-2021-SITC2021.285>

SEX DIFFERENCES IN THE TRANSCRIPTIONAL PROFILES OF MUCOSAL-ASSOCIATED INVARIANT T CELLS IN NEOADJUVANT ANTI-PD-1 TREATED NON-SMALL CELL LUNG CANCER (NSCLC)

¹Poromendro Burman*, ¹Boyang Zhang, ²Zhicheng Ji, ¹Justina Caushi, ¹Frank Housseau, ¹Andrew Pardoll, ¹Zhang Jijia, ¹Hongkai Ji, ¹Kellie Smith. ¹Johns Hopkins School of Medicine, Baltimore, MD, USA; ²Duke University, Durham, NC, USA

Background Mucosal Associated Invariant T Cells (MAIT cells) are unconventional T cells that recognize vitamin B metabolites derived from bacteria and are mainly present in mucosal tissues and peripheral blood.¹ Their activation by T Cell Receptor (TCR)-dependent and -independent pathways can result in effector function that can either promote or inhibit cytotoxic effects.² MAIT cells are known to be involved in the pathogenesis of multiple diseases that involve mucosal tissues, such as non-small cell lung cancer (NSCLC).² Recently, studies have shown that disparate outcomes to SARS-CoV-2-infection between males and females may involve a differential activation of MAIT cells in the lung mucosa.³ It is therefore conceivable to hypothesize that sex differences of MAIT cells in NSCLC may also impact outcome, however their involvement in progression and subsequent treatment response of NSCLC has never been explored.

Methods To study the transcriptional program of MAIT cells in NSCLC as a function of sex, peripheral blood and tissue biospecimens were obtained from the first-in-human clinical trial of neoadjuvant anti-PD-1 (nivolumab) in resectable non-small cell lung cancer; NCT02259621.⁴ Coupled single-cell RNAseq/TCRseq was performed on tumor infiltrating lymphocytes (TIL), paired adjacent normal lung, and tumor-draining lymph nodes (TDLN). MAIT cells were identified by expression of SLC4A10 and the invariant TRAV1-2 and TRAJ33/12/20 TCR. Computational analysis revealed 4 distinct MAIT cell clusters and differentially expressed genes in the tumors and healthy normal lung of males as compared to females.

Results In MAIT cells from females, we found upregulation of CD8A, GNLY, and NKG7 genes. These genes are involved with T cell activation and cytolytic function, suggesting that the activation of these genes in MAIT cells could be contributing towards their cytolytic activity in females. In MAIT cells from males, we found upregulation of PDE3B and PCBP2 genes, which are known to be involved with immunosuppression and downregulation of cytotoxic T lymphocyte (CTL) responses. These findings were consistent in the healthy normal lung, suggesting these transcriptional programs may be due to the normal lung biology and not necessarily a byproduct of carcinogenesis.

Conclusions These results highlight the potential for dual characteristics of MAIT cells in neoadjuvant anti-PD-1-treated NSCLCs and provide an important foundation in our study of the often dichotomous responses between males and females to immunotherapy. Future analyses will focus on the interplay of MAIT cells with other cells in the tumor microenvironment (TME) as a function of immunotherapy treatment and clinical response.

REFERENCES

- Chen Z, Wang H, D'Souza C, et al. Mucosal-associated invariant T-cell activation and accumulation after in vivo infection depends on microbial riboflavin synthesis and co-stimulatory signals. *Mucosal Immunol* 2017;**10**:58–68.
- Wen X, Zhang X, et al. Title of article: mucosal-associated invariant T cells in lung cancers. *Elsevier* 2021;**94**.
- Yu C, Littleton S, et al. Mucosal-associated invariant T cell responses differ by sex in COVID-19. *CellPress* 2021;**2**:755–772.

- Caushi JX, Zhang J, Ji Z, et al. Transcriptional programs of neoantigen-specific TIL in anti-PD-1-treated lung cancers. *Nature* 2021.

Ethics Approval This study was approved by the Institutional Review Boards (IRB) at Johns Hopkins University (JHU) and Memorial Sloan Kettering Cancer Center and was conducted in accordance with the Declaration of Helsinki and the International Conference on Harmonization Good Clinical Practice guidelines. The patients described in this study provided written informed consent.

<http://dx.doi.org/10.1136/jitc-2021-SITC2021.286>

COMBINED COX-2 INHIBITION WITH FISH OIL AND ASPIRIN AS ADJUNCTS TO ANTI-PD-1 IMMUNOTHERAPY IN METASTATIC MELANOMA

Alexander Chacon*, Alexa Melucci, Shuyang Qin, Paul Burchard, Katherine Jackson, Rachel Jewell, Peter Prieto. *University of Rochester Medical Center, Rochester, NY, USA*

Background Only 30–40% of metastatic melanoma patients experience objective responses to first line anti-PD-1 immune checkpoint inhibition (α PD-1 ICI). Cyclooxygenase (COX-1/2) inhibition with aspirin (ASA) and other non-steroidal anti-inflammatory drugs has been associated with prolonged time to recurrence and improved responsiveness to ICI in human melanoma,¹ with inhibition of myeloid-induced immunosuppression in the tumor microenvironment (TME) a purported mechanism.² Similarly, dietary omega-3 fatty acids metabolized by COX-2 elicit downstream effects on T-cell differentiation akin to ASA administration, abrogating murine melanoma and human breast cancer progression. Mechanisms of ICI resistance remain unclear, and adjunct therapies look to bridge the gap from current response rates to cure.

Methods YUMM 1.7 melanoma cells were injected into flanks of C57-BL6/J mice. Mice were fed control diets or supplemented with omega-3 rich fish oil (FO) chow (10% weight/weight, 30%kcal/kcal), ASA in drinking water (ASA, LO – 300, MED – 600, HI - 1000 ug/mL), or the combination of these agents (COMBO, with ASA-MED) starting at day 7 post tumor implantation. Intraperitoneal α PD1 was administered every 3–4 days starting at day 12. Tumors were assessed for growth, harvested at day 32 (day 26 for ASA LO/HI), and characterized with flow cytometry. All significant results ($p < 0.05$) assessed by 2-way ANOVA or t-test as appropriate.

Results FO resulted in lesser tumor volume at day 32 in α PD-1 treated mice, while ASA-HI resulted in lesser tumor volume in mice not treated with α PD-1 but did not synergize with α PD-1. ASA-MED and COMBO groups trended towards decreased tumor size ($p = 0.07$ and 0.07 respectively) by day 32 in α PD-1 treated mice. FO and COMBO increased total CD3+ T-cells and monocytes (CD45+, CD19-, CD11b+, Ly6C+, Ly6G -) in the TME. FO increased PD-L1 + CD4+ T-cells, while COMBO increased total CD8+ T-cells and PD1 + CD8+ T-cells. ASA-HI increased monocytes and the proportion of PD-1+, CD8+ T-cells in the TME.

Conclusions Myeloid-induced suppression of T-cell function in tumors may contribute to immune checkpoint inhibition resistance. In the present study, both fish oil and aspirin altered melanoma tumor growth, with only fish oil synergizing with anti-PD-1 at the doses assessed. Both fish oil and aspirin augmented monocyte populations in the tumor microenvironment, with differential effects on T-cell populations. The partially synergistic mechanism between substrate-limited (FO) and pharmacologic (ASA) inhibition of cyclooxygenase-2 may provide a cost-effective avenue to combat immune escape in melanoma patients treated with anti-PD-1 immune checkpoint inhibition, requiring further investigation in humans.

REFERENCES

- 1.. Wang SJ, et al. Effect of cyclo-oxygenase inhibitor use during checkpoint blockade immunotherapy in patients with metastatic melanoma and non-small cell lung cancer. *J Immunother Cancer* 2020;**8**(2).
- 2.. Zelenay S, et al. Cyclooxygenase-dependent tumor growth through evasion of immunity. *Cell* 2015;**162**(6):1257–70.

<http://dx.doi.org/10.1136/jitc-2021-SITC2021.287>

THE COX-2 PATHWAY AS A MEDIATOR OF RESISTANCE TO ANTI-PD-1 THERAPY

Shuming Chen*, Tracee McMiller, Preethi Sankaran, Kyle Kampta, Suzanne Topalian. *Johns Hopkins University School of Medicine, Baltimore, MD, USA*

Background We previously found upregulation of the cyclooxygenase-2/prostaglandin E2 (COX-2/PGE2) pathway in the tumor microenvironment (TME) of cancers that respond poorly to anti-PD-1 therapy.¹⁻² The potential functional role of this pathway in anti-PD-1 resistance is unknown. We therefore studied modulation of COX-2 expression in cultured human tumor and immune cells, PGE2-mediated effects on myeloid cells and their reversal with prostaglandin (EP) receptor inhibitors.

Methods Nineteen tumor lines representing 6 histologies were treated with cytokines reported to induce COX-2 (IL-1B, IL-17A, TNF- α). Peripheral blood monocytes (Monos) were treated with toll-like receptor (TLR) agonists or TME-resident cytokines associated with high PD-L1 expression (IL-1A, IL-10, IL-27, IL-32g, IFN-g).³⁻⁴ COX-2 protein was detected by Western blotting and flow cytometry. In some experiments, Monos were pre-incubated with EP2i (PF-04418948) and/or EP4i (ONO-AE3-208), then treated with PGE2 \pm TLR4 (LPS) or TLR7 (imiquimod) agonists. IL-6, IL-10, TNF- α , and VEGF secretion were detected by ELISA. Monocytic DCs generated with GM-CSF+IL-4 were matured with CD40L, \pm PGE2, then phenotyped.

Results Among 19 tumor cell lines, 6 expressed COX-2 constitutively, and 13 were induced to express COX-2 by 1-day exposure to IL-1B, IL-17A, or TNF- α . In Monos, COX-2 was induced by IL-1A and IL-1B, but not IFN-g or IL-27. TLR 1-9 agonists induced COX-2, with TLR2/4/5 agonists being the strongest inducers. COX-2 induction by these factors was non-overlapping with PD-L1 induction in tumor cells and Monos, suggesting non-redundant pathways of immune resistance. PGE2 had context-dependent effects in Monos, depending on the cytokines, TLR agonists, and donors assayed: PGE2 increased VEGF secretion by resting Monos from 4/4 donors tested, but increased IL-6, IL-10 and TNF- α secretion in only 1/4 donors; PGE2 increased imiquimod-induced TNF- α secretion, but decreased LPS-induced TNF- α secretion. EP2 and EP4 inhibitors counteracted PGE2-mediated cytokine modulation, and showed synergistic effects when combined in the context of high dose of PGE2 (500nM). Additionally, PGE2 suppressed the in vitro generation of mature DCs, reducing CD80 and CD83 expression and increasing CD16.

Conclusions Understanding and preventing anti-PD-1 treatment resistance is a critical goal. Our results suggest that the COX-2/PGE2 pathway is expressed in tumor and immune cells, and modulates myeloid cell functions in a context-dependent manner. COX-2 expression is non-redundant with PD-L1 expression, providing a rationale to test COX-2 pathway inhibition in conjunction with anti-PD-1. Available drugs targeting this pathway, including IL-1R and IL-1B inhibitors, NSAIDs, and EP2 and EP4 inhibitors, will enable the clinical development of combination treatment regimens.

Acknowledgements We gratefully acknowledge support from NCI R01-CA142779, Bristol Myers Squibb, and the Johns Hopkins Bloomberg-Kimmel Institute for Cancer Immunotherapy.

REFERENCES

- 1.. Duffield AS, Ascierto ML, Anders RA, *et al.* The immunosuppressive tumor microenvironment (TME) in nasopharyngeal carcinoma: implications for immunotherapy. *AACR* 2018;Abstract 4750.
- 2.. Besharati S, McMiller T, Yarchoan M, *et al.* The immunosuppressive tumor microenvironment (TME) in Epstein-Barr virus (EBV)-positive and EBV-negative gastric cancers: implications for immunotherapy. *SITC* 2018;P541 (abstr).
- 3.. Taube JM, Young GD, McMiller TL, *et al.* Differential expression of immune-regulatory genes associated with PD-L1 display in melanoma: implications for PD-1 pathway blockade. *Clin Cancer Res* 2015;**21**:3969–76.
- 4.. Duffield AS, Ascierto ML, Anders RA, *et al.* Th17 immune microenvironment in Epstein-Barr virus negative Hodgkin lymphoma: implications for immunotherapy. *Blood Advances* 2017;**1**:1324–34.

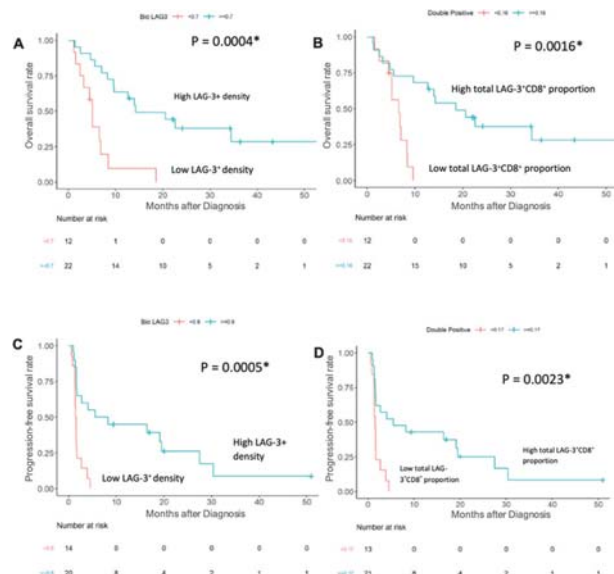
<http://dx.doi.org/10.1136/jitc-2021-SITC2021.288>

289 CADONILIMAB, AN ANTI-PD1/CTLA4 BI-SPECIFIC ANTIBODY WITH FC EFFECTOR NULL BACKBONE

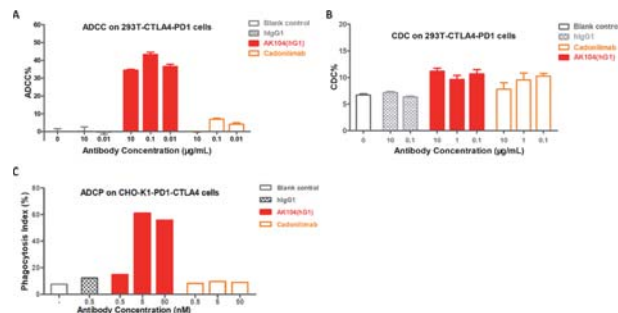
¹Zhaoliang Huang, ¹Xinghua Pang, ¹Tingting Zhong, ¹Na Chen*, ¹Xinrong He, ¹Dennis Xia, ²Xiaoping Jin, ²Zhongmin Wang, ¹Xu Xia, ¹Baiyong Li. ¹Akeso Biopharma Inc., Zhongshan, China; ²Akeso Biopharma Inc, Potomac, USA

Background Tumor infiltrating lymphocytes co-express PD-1 and CTLA-4 at much higher levels compared to normal tissues and peripheral blood cells, thus anti-PD1/CTLA4 bi-specific antibody with a preferential tumor tissue enrichment over normal tissue would contribute to enhanced efficacy and safety. Currently available anti-PD1 and anti-CTLA4 antibodies used in combination therapy are of residual bindings to FcγRs, which mediate antibody-dependent cell-mediated cytotoxicity (ADCC), antibody-dependent cellular phagocytosis (ADCP), leading to compromise on efficacy and safety. Moreover, activated macrophage in tumor microenvironment plays key role in mediating immune suppression by secreting proinflammatory cytokines, such as IL-6. Cadonilimab, also known as AK104, is an IgG1 scaffold Fc-engineered antibody, which is designed to eliminate binding to FcγRs and C1q, and subsequently minimize lymphocyte loss, and antibody dependent cytokine release from macrophage, which associate with irAEs and poor prognosis in immunotherapy.¹

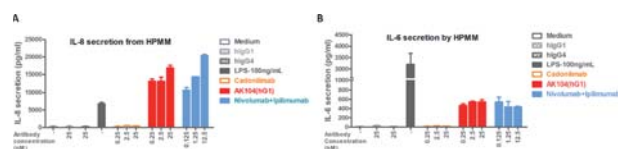
Methods PD-1 and CTLA4 antigen co-binding activity of Cadonilimab was determined by Fortebio and assay of co-culture Cadonilimab with Hoechst33342-labelled Jurkat cells expressing PD-1 and CHO-K1-CTLA4 cells. Binding kinetics of Cadonilimab to C1q, FcγRIa, FcγRIIa_H131, FcγRIIa_R131, FcγRIIIa_V158 and FcγRIIIa_F158 were measured by Fortebio. ADCC, ADCP and CDC activities were determined in cellular assays. IL-6 and IL-8 from macrophage were detected in a assay of human macrophage and CHO-K1-PD1-CTLA4 cells co-culture.



Abstract 289 Figure 1 AK104 crosslinks cells expressing CTLA-4 and PD-1. AK104 can crosslink cells expressing CTLA-4 with cells expressing PD-1. CTLA-4-expressing CHO-K1 cells were plated into the plates. Then the mixture of AK104 or control antibodies with Hoechst 33342 labelled PD-1-expressing Jurkat cells were added into the plates and incubated for 20min. After the incubation, suspended Jurkat cells were removed, and the crosslinking between PD-1 and CTLA-4 expressing cells was analyzed microscopically.



Abstract 289 Figure 2 ADCC, CDC and ADCP activities of AK104. (A) Antibody-dependent cell-mediated cytotoxicity (ADCC) activities of AK104 (hG1), a version of Cadonilimab with wildtype IgG1 scaffold and Cadonilimab were determined by measuring lactase dehydrogenase (LDH) release from 293T-CTLA4-PD1 cells. (B) Complementary-dependent cell-mediated cytotoxicity (CDC) activities of AK104 (hG1) and Cadonilimab were determined by measuring LDH release from 293T-CTLA4-PD1 cells. (C) Antibody-dependent cellular phagocytosis (ADCP) activities of AK104 (hG1) and Cadonilimab were studied by examining phagocytosis of CHO-K1-PD1-CTLA4 cells by murine bone marrow derived macrophages. Data are expressed as mean±SEM of two independent experiments.



Abstract 289 Figure 3 IL-8 and IL-6 secretion induced by AK104. Effects of Fc engineering of cadonilimab on the release of inflammatory cytokines. (A) IL-8 and (B) IL-6 by HPMMs in the presence of IFN-γ. Data are expressed as mean ±SEM of two independent experiments.

Abstract 289 Table 1 Affinity of AK104 to FcγRs and C1q. Affinity of cadonilimab to FcγRIa, FcγRIIa_H131, FcγRIIa_R131, FcγRIIIa_V158, FcγRIIIa_F158 and C1q.

FcγR/C1q	Antibody	KD (M)	kon (1/Ms)	SE (kon)	kdis (1/s)	SE (kdis)	Rmax (nm)
FcγRIa	Cadonilimab	N.D.	N.D.	N.D.	N.D.	N.D.	N.D.
	AK104(hG1)	5.92E-09	3.06E+05	8.35E+03	1.81E-03	5.75E-05	0.53-0.62
FcγRIIa_H131	Cadonilimab	N.D.	N.D.	N.D.	N.D.	N.D.	N.D.
	AK104(hG1)	2.22E-08	3.83E+05	4.03E+04	8.49E-03	7.44E-04	0.96-1.63
FcγRIIa_R131	Cadonilimab	4.20E-08	3.72E+05	4.19E+04	1.56E-02	8.99E-04	0.16-0.36
	AK104(hG1)	1.43E-08	3.58E+05	3.13E+04	5.10E-03	5.87E-04	0.66-1.34
FcγRIIIa_V158	Cadonilimab	N.D.	N.D.	N.D.	N.D.	N.D.	N.D.
	AK104(hG1)	1.77E-07	1.21E+05	1.64E+04	2.14E-02	3.71E-03	1.56-1.61
FcγRIIIa_F158	Cadonilimab	N.D.	N.D.	N.D.	N.D.	N.D.	N.D.
	AK104(hG1)	2.21E-07	1.12E+05	1.39E+04	2.47E-02	3.43E-03	0.39-0.64
C1q	Cadonilimab	N.D.	N.D.	N.D.	N.D.	N.D.	N.D.
	AK104(hG1)	2.53E-09	2.05E+06	2.10E+05	5.17E-03	5.81E-04	0.05-0.18

Results Cadonilimab binds to the antigens PD-1 and CTLA-4 simultaneously, and as shown in figure.1, Cadonilimab crosslinks cells expressing CTLA-4 with those expressing PD-1 (figure 1). Cadonilimab exhibited no binding to FcγRIa, FcγRIIa_H131, FcγRIIIa_V158, FcγRIIIa_F158 or C1q (table 1), eliciting no apparent ADCC, ADCP or CDC (figure 2).

Cadonilimab induced no remarkable IL-6 or IL-8 release by human macrophage compared with combination of nivolumab and ipilimumab (figure 3). Clinical trials of Cadonilimab as monotherapy, in combination with chemotherapy or tyrosine kinase inhibitor, such as Lenvatinib and Anlotinib, to treat metastatic cervical cancer (NCT04380805), gastric adenocarcinoma/gastroesophageal junction adenocarcinoma (NCT04728321), non-small cell lung cancer (NCT04647344) and hepatocellular carcinoma (NCT04444167) are ongoing, and a promising efficacy and acceptable safety profile were observed.

Conclusions Cadonilimab, an IgG1 antibody with Fc-engineering, exhibits neither Fc effector functions including ADCC, ADCP, CDC, nor activating macrophage to secrete IL-6 or IL-8. Possible tumor tissue preferential retention of Cadonilimab over conventional anti-PD-1 and anti-CTLA-4 antibodies noted above could potentially lead to better safety profile.

REFERENCE

1. Yang F, He Z, Duan H, Zhang D, Li J, Yang H, Dorsey JF, Zou W, Ali Nabavizadeh S, Bagley SJ, Abdullah K, Brem S, Zhang L, Xu X, Byrne KT, Vonderheide RH, Gong Y, Fan Y. Synergistic immunotherapy of glioblastoma by dual targeting of IL-6 and CD40. *Nat Commun* 2021 June 8;12(1):3424.

<http://dx.doi.org/10.1136/jitc-2021-SITC2021.289>

291 **DUAL-SPECIFIC ANTIBODIES BLOCKING BOTH PD-L1 AND PD-L2 ENGAGEMENT OF PD-1 RESTORE ANTI-TUMOR IMMUNITY**

¹Coline Couillault*, ¹Anupallavi Srinivasamani, ¹Shweta Hedge, ²Qinying Liu, ³Ashwin Jaiswal, ¹Dongxing Zha, ¹Michael Curran. ¹MD Anderson Cancer Center, Houston, TX, USA; ²Fudan University, Shanghai, China; ³Astrazeneca, Gaithersburg, MD, USA

Background Inhibition of T cell activation and effector function via engagement of the co-inhibitory receptor PD-1 is a critical mechanism enabling tumors to evade host immunity. The two ligands for PD-1, PD-L1 and PD-L2, can be expressed by a variety of immunosuppressive stromal cells, particularly of the myeloid lineage, endothelial cells, and by tumors themselves. In addition to PD-1, PD-L1 engages B7-1 in an additional co-inhibitory interaction. Blocking only PD-1 or only PD-L1 thus does not relieve all inhibitory components of this pathway. We hypothesized that bispecific antibodies blocking both PD-L1 and PD-L2 could more fully restore tumor-specific T cell activation and potentiate anti-cancer immunotherapy. Furthermore, we speculated that enhancing the cytotoxic effector function of these antibodies might further enhance their efficacy through the depletion of tumor cells and supportive stroma.

Methods We investigated the capacity of monoclonal antibodies capable of bivalent binding to both PD-L1 and PD-L2 to restore the function of PD-1-suppressed T cells in vitro. To assess the in vivo therapeutic efficiency of bispecific PD-Ligand antibodies with ADCC capacities, mouse IgG2a and modified human IgG1 versions were generated. We assessed their ADCC activity in vitro using a bioluminescent reporter assay, and their therapeutic efficiency in vivo in syngeneic or human-cell derived tumors.

Results The bispecific antibodies we generated restore the function of PD-1-suppressed T cells in vitro with equivalent efficiency to the FDA approved PD-1 antibody Pembrolizumab. Moreover, our modified human bispecific antibodies lead to significantly higher FcγRIIIa activation than FDA-approved clinical human IgG1 PD-L1 antibodies in vitro. In vivo, ADCC-capable PD-Ligand bispecific antibodies suppress the growth of U2940 lymphoma in immunodeficient mice more efficiently than Rituximab, and in a syngeneic model of PD-L1/PD-L2 double positive colon carcinoma, these antibodies demonstrate superiority to PD-1 blocking antibodies to limit tumor growth and increase survival. Furthermore, treatment with our bispecific antibodies increases T cell proliferation and cytotoxicity and reduces density of immunosuppressive myeloid stroma in vivo.

Conclusions ADCC-capable PD-Ligand bispecific antibodies display higher therapeutic potential than existing anti-PD-1 antibodies and represent a new class of PD-1 pathway therapeutics with significant potential for the treatment of a variety of human cancers.

Acknowledgements I would like to thank Anupallavi Srinivasamani, PhD student in Michael Curran's lab, who performed a considerable amount of the work on this project before I joined.

<http://dx.doi.org/10.1136/jitc-2021-SITC2021.291>

EX VIVO PROFILING OF PD-1 BLOCKADE USING AN ORGANOTYPIC TISSUE SLICE MODEL IN SOLID TUMORS

Lina Ding*, Kristin Sullivan, Chensheng Zhou, Jimena Trillo-Tinoco, Anne Lewin, Catherine King, David Nelson, Benjamin Chen, Michaela Bowden. *Bristol Myers Squibb, Cambridge, MA, USA*

Background Tumor explant models provide a powerful ex vivo tool to evaluate complex biological mechanisms in a controlled environment. Ex vivo models retain much of the original tumor biology, heterogeneity, and tumor microenvironment, and therefore provide a useful preclinical platform and functional approach to assess drug responses rapidly and directly.

Methods To explore mechanisms of resistance to cancer immunotherapy, we established an organotypic tissue slice Air-Liquid Interface (ALI) ex vivo system utilizing surgical tumor specimens from patients to assess the impact of the clinically utilized anti-PD-1 antibody nivolumab (OPDIVO). In the present study, we built a real-world patient cohort comprised of six tumor types: non-small cell lung cancer, melanoma, pancreatic ductal adenocarcinoma, breast cancer, prostate cancer, and colorectal cancer. We assessed tissue morphology, histology, PD-L1 IHC (CPS and TPS), CD8 T cell topology, proliferation in the tumor and stromal compartments, and secretome profiling.

Results Our tumor slice model highly recapitulated features of the original tumor, including tumor architecture, immune phenotypes, and the prognostic markers. To identify responses to aPD-1 treatment, we compared baseline values for the cultured tumor slices with values at different timepoints post treatment. Secretome profiling of tissue explant supernatants using a panel of 94 analytes, revealed alterations to cytokines produced in the tumor microenvironment in response to aPD-1 treatment. We found that soluble expression patterns were associated with T-cell patterns (inflamed, excluded and desert) and PD-L1 score (CPS and TPS) in tumor tissues. These cytokines mediate critical functions across the immune cell cycle. Ongoing efforts to characterize T cell activation, exhaustion, tumor intrinsic responses and microenvironment composition using Imaging Mass Cytometry will be presented.

Conclusions In this study, we demonstrated the feasibility of using fresh, surgically resected human tumors to test aPD-1 responses in an ex vivo system. Further, this model system has the potential to drive discovery and translational efforts by evaluating mechanisms of resistance to cancer immunotherapy and evaluate new single agent or combination therapies in the ex vivo setting.

<http://dx.doi.org/10.1136/jitc-2021-SITC2021.292>

DISTINCT TUMOR INFILTRATING TREG LINEAGES ARE ASSOCIATED WITH RESPONSE TO ANTI-PD1 CHECKPOINT BLOCKADE IN NON-SMALL CELL LUNG CANCER

¹Arbor Dykema*, ¹Boyang Zhang, ¹Jiajia Zhang, ²Zhicheng Ji, ¹Taibo Li, ¹Poromendro Burman, ¹Justina Caushi, ¹Hongkai Ji, ¹Andrew Pardoll, ¹Kellie Smith. ¹Johns Hopkins University, Baltimore, MD, USA; ²Duke University, Durham, NC, USA

Background Immune-checkpoint blockade (ICB) has proved a major success, especially in highly mutated tumors such as lung cancer. Nevertheless, not all patients respond to ICB.¹ It is possible that regulatory T cells (Tregs) play a role in this lack of response by suppressing tumor-reactive cytotoxic T cells,² however the specific mechanisms that lead to this suppression remain elusive. Additionally, Tregs are necessary for protection against autoimmune disease³ and broadly depleting them could induce severe immune adverse events. It is therefore necessary to understand the functional programming and suppressive nature of Treg subsets in the tumor microenvironment to define targetable molecules for future biomarker-driven therapeutics.

Methods In this study we performed single cell RNA-sequencing on T cells isolated from resected tissue and peripheral blood from 15 neoadjuvant nivolumab (anti-PD1)-treated and 10 untreated non-small cell lung cancer (NSCLC) patients. We identified and analyzed 71,251 CD4+ FoxP3+ Tregs. Refined clustering was performed, and we used pseudotime and differential gene analyses to understand the transcriptional relationship between clusters and patient groups. We plan to relate our Treg subcluster compositions and enriched gene sets with previously defined mouse models of ICB response as well as human head and neck squamous cell carcinoma (HNSCC).

Results With our highly refined clustering approach, we identified 7 distinct Treg clusters that could reflect differing functionalities within the tumor microenvironment. We demonstrate two separate Treg subsets that diverge towards either an activated state, expressing members of the tumor necrosis factor receptor (TNFR) superfamily: OX40, 41BB, GITR, or a resting state. These lineages separate ICB responders from non-responders, whose tumors are enriched in activated Tregs. We plan to stimulate receptors associated with non-response using agonist ligands or antibodies and hypothesize that their induced signaling will result in transcriptional program changes leading to highly suppressive Tregs.

Conclusions Together, this study provides an in-depth look at the Treg-derived suppressive mechanisms governing their function in the TME of anti-PD-1-treated vs. untreated tumors. Using biospecimens obtained from the neoadjuvant setting, we were also able to study the impact of PD-1 blockade on Treg intra-tumoral function. This in-depth analysis of tumor Tregs has identified specific targetable biomarkers which could be used to improve ICB response while mitigating off-target immune adverse events by specifically inhibiting a small subset of Tregs without disturbing systemic immune homeostasis.

REFERENCES

1. Forde PM, Chaft JE, Smith KN, Anagnostou V, Cottrell TR, Hellmann MD, *et al.* Neoadjuvant PD-1 blockade in resectable lung cancer. *N Engl J Med* [Internet] 2018 April 16; **378**(21):1976–86. Available from: <https://doi.org/10.1056/NEJMoa1716078>
2. Bonertz A, Weitz J, Pietsch DK, Rahbari NN, Schlude C, Ge Y, *et al.* Antigen-specific tregs control T cell responses against a limited repertoire of tumor antigens in patients with colorectal carcinoma. *J Clin Invest* 2009; **119**(11).
3. Montane J, Bischoff L, Soukhatcheva G, Dai DL, Hardenberg G, Levings MK, *et al.* Prevention of murine autoimmune diabetes by CCL22-mediated treg recruitment to the pancreatic islets. *J Clin Invest* [Internet] 2011/07/01. 2011 August

1;121(8):3024–8. Available from: <https://www.ncbi.nlm.nih.gov/pubmed/21737880>

Ethics Approval This study was approved by the Institutional Review Boards (IRB) at Johns Hopkins University (JHU) and Memorial Sloan Kettering Cancer Center (NA_00092076; NCT02259621) and was conducted in accordance with the Declaration of Helsinki and the International Conference on Harmonization Good Clinical Practice guidelines. The patients described in this study provided written informed consent.

<http://dx.doi.org/10.1136/jitc-2021-SITC2021.293>

294

EVALUATION OF RADIOGRAPHIC RESPONSE IN THE INTACT RENAL MASS (INTACT-RMASS) TO IMMUNE CHECKPOINT INHIBITOR (ICI) COMBINATION REGIMENS IN PATIENTS WITH METASTATIC RENAL CELL CARCINOMA (MRCC)

¹Hamid Eramekhoo*, ¹Danubia Hester, ²Saqib Abbasi, ¹Jens Eickhoff, ³Tristan Bice, ⁴Luna Archaya, ⁵Ellen Jeager, ⁶Moshe Ornstein, ¹Ali Pirasteh, ⁵Pedro Barata, ⁴Yousef Zakharia, ³Deepak Kilari, ⁷Elizabeth Wulff-Burchfield, ¹Christos Kyriakopoulos. ¹University of Wisconsin – Madison, Madison, WI, USA; ²University of Kansas Medical Center, Kansas City, KS, USA; ³Medical College of Wisconsin, Milwaukee, WI, USA; ⁴University of Iowa, Iowa City, IA, USA; ⁵Tulane Cancer Center, New Orleans, LA, USA; ⁶Cleveland Clinic, Cleveland, OH, USA; ⁷Kansas University Medical Center, Kansas City, KS, USA

Background As most of the patients previously enrolled in trials had nephrectomy before starting systemic treatment (syst-Rx), the response of the intact-Rmass to novel ICI and tyrosine kinase inhibitor (TKI) combination regimens is not well described.

Methods A retrospective review of 227 patients with mRCC who were treated with ICI (single agent or combinations) in the 1st- or 2nd-line was conducted. Following the appropriate regulatory process, collaborators from 6 US sites collected clinical, pathological, and outcome data via chart review. Overall response was investigator-assessed for all patients with at least one post-treatment scan or evidence of clinical progression after treatment initiation. Overall radiographic response (ORR) represents any radiographic response in the metastatic disease per investigator's assessment. To accurately assess response in intact-Rmass, 3-dimensional measurement of the intact-Rmass was performed and Rmass volume was calculated at baseline and at the time of best overall response for 1st- and 2nd-line therapy. Radiographic response in intact-Rmass is defined as >30% decrease in the Rmass volume.

Results Median age at diagnosis was 62 years, 69% were male, 82% had clear cell histology. 15% and 12% had sarcomatoid and rhabdoid features, respectively. Overall, 82 patients (36%) had a measurable intact-Rmass while receiving syst-Rx. 63 (28%) patients never had a nephrectomy, and 10 (4%) patients had delayed nephrectomy after a good overall response to syst-Rx. 108 (48%) received ICI in 1st-line (88/108 received ipilimumab/nivolumab combination). 91 (40%), and 18 (8%) patients received TKI, or ICI+TKI in 1st-line. 161 (71%) and 86 (38%) of the patients received 2nd-line and 3rd-line therapy, respectively. 104 (46%) received ICI in 2nd-line (75/104 treated with single-agent ICI). 48 (21%), and 4 (2%) patients received TKI, or ICI+TKI in 2nd-line. Radiographic response in intact-Rmass for evaluable patients is summarized in table 1. The highest response rates in intact-Rmass were seen with ICI+TKI combinations. Higher rates of radiographic response in intact-Rmass were seen in patients treated with ICI in 1st-line compared to 2nd-line, possibly related to higher usage of ICI combinations (ipilimumab/nivolumab) in 1st-line. Overall metastatic disease response to different regimens in the 1st-line or 2nd-line was not different based on the history of nephrectomy prior to syst-Rx (table 2).

Abstract 294 Table 2 Overall radiographic response (ORR) per investigator assessment

	No previous nephrectomy	Had previous nephrectomy	p-value
ICI - 1 st line	10/37 (27%)	25/71 (35%)	0.39
ICI - 2 nd line	6/20 (30%)	11/84 (13%)	0.09
TKI - 1 st line	6/15 (40%)	23/76 (30%)	0.55
TKI - 2 nd line	3/19 (16%)	10/29 (34%)	0.15
ICI+TKI - 1 st line	6/10 (60%)	3/8 (38%)	0.64
ICI+TKI - 2 nd line	1/3 (33%)	0/1 (0%)	0.99

Conclusions Higher radiographic response rates in the intact-Rmass were seen in patients treated with ICI+TKI and ICI in the 1st-line. There was no significant difference in overall metastatic disease response to 1st- or 2nd-line treatment based on the history of nephrectomy prior to syst-Rx.

Ethics Approval Each of the 6 participating centers had their IRB approved protocol for retrospective study and data collection. Data Use Agreements were obtained for each center to share limited data set data with University of Wisconsin - Madison (IRB protocol UW17148 # 2018-0213). Final analysis was performed at University of Wisconsin.

Consent not applicable to retrospective studies.

<http://dx.doi.org/10.1136/jitc-2021-SITC2021.294>

Abstract 294 Table 1 Radiographic response ($\geq 30\%$ decrease in volume) in the intact renal mass

	ICI	TKI	ICI+TKI
1 st Line systemic treatment	32/108 (30%)	23/91 (25%)	10/18 (56%)
2 nd Line systemic treatment	10/104 (10%)	18/48 (48%)	2/4 (50%)

295

TUMOR CELL- INTRINSIC EXPRESSION OF FGFR3 DRIVES ANTI-PDL-1 IMMUNOTHERAPY RESISTANCE IN A MURINE BLADDER CANCER MODEL

Erica Fleming-Trujillo*, Jeffrey Bloodworth, Anthony Fernald, Aubrianna Ramsland, Thomas Gajewski, Randy Sweis. *University of Chicago, Chicago, IL, USA*

Background Immune checkpoint blockade therapy has recently shown efficacy in treating advanced urothelial bladder cancer and anti-PD-1/PD-L1 therapy is currently the standard of care. However, most patients do not respond to these drugs and resistance mechanisms remain elusive. The non-T cell-inflamed tumor microenvironment phenotype correlates with poor prognosis and immunotherapy resistance. We previously found that activating mutations in Fibroblast Growth Factor Receptor 3 (FGFR3) were exclusive to non-T cell-inflamed bladder cancers. We investigated the impact of tumor cell-intrinsic FGFR3 activation on T cell infiltration and tumor responsiveness to anti-PD-1/PD-L1 in a murine model.

Methods We developed a syngeneic transplantable murine bladder cancer model using the MB49 cell line engineered to express FGFR3 with either the activating G370C mutation (FGFR3-G370C), a kinase-dead mutation K508M (FGFR3-K508M), a truncating mutation resulting in a secreted receptor (FGFR3-sec), or control. Mice were injected subcutaneously into flank and size was measured every 3 days along with PD-L1 therapy (BioXcell clone 10F.9G2). Tumors, draining lymph nodes, and spleens were harvested at endpoint for flow cytometry.

Results Tumors from mice inoculated with MB49-FGFR3-G370C cells showed diminished CD8+ T cell accumulation within the tumor and were resistant to anti-PD-L1 checkpoint blockade compared to MB49 controls. To determine if FGFR3-mediated immune resistance was dependent on FGFR3 kinase activity, MB49-FGFR3-K508M tumors were evaluated and unexpectedly found to be resistant to anti-PD-L1 treatment. Tumors with a secreted FGFR3 receptor (FGFR3-sec) retained responsiveness to anti-PD-L1 therapy.

Conclusions In a murine bladder cancer model, FGFR3 activation led to relative T cell exclusion and resistance to immune checkpoint blockade. The mechanism of resistance was not dependent on receptor kinase activity. Further studies are ongoing to determine the biochemical mechanisms of FGFR3-mediated immunotherapy resistance in bladder cancer.

<http://dx.doi.org/10.1136/jitc-2021-SITC2021.295>

A COMPREHENSIVE CLINICAL AND GENOMIC CHARACTERIZATION OF LONG-TERM RESPONDERS RECEIVING IMMUNE CHECKPOINT BLOCKADE FOR METASTATIC NON-SMALL CELL LUNG CANCER

¹Paola Ghanem*, ¹Joseph Murray, ²Melinda Hsu, ¹David Ettinger, ¹Josephine Feliciano, ¹Patrick Forde, ¹Christine Hann, ¹Vincent Lam, ¹Benjamin Levy, ¹Julie Brahmer, ¹Kristen Marrone. ¹Johns Hopkins University, Baltimore, MD, USA; ²University Hospital Case Western Reserve, Cleveland, OH, USA

Background Five-year survival analyses of patients receiving immune checkpoint inhibitors (ICIs) for metastatic non-small cell lung cancer (NSCLC) have demonstrated continued clinical benefit compared to chemotherapy.^{1 2} Our study aims at understanding and defining the unique clinical and genomic underpinnings of a durable response to ICI in advanced NSCLC.

Methods We conducted a retrospective case-control study using information abstracted from a Johns Hopkins IRB-approved database of NSCLC patients treated with an ICI-containing regimen. We defined long-term responders (LR) as patients who have achieved an overall survival (OS) of at least 3 years. We identified a comparison arm (C) of patients whose OS was less than a year. Univariate and multivariate analyses of the clinical and molecular characteristics were conducted between the LR and C groups using IBM Statistical Package for Social Sciences version 25.

Results A cohort of 89 patients were included; 41 patients as LR and 48 as C. Mean duration of ICI was 21.6 months and 3.5 months for LR and C, respectively. On univariate analysis, there was no statistically significant difference in age, sex, race, histology or treatment characteristics between arms. However, ECOG performance status (PS) of 2 ($p=0.011$) and evidence of liver metastases were independently associated with a shorter response to ICI ($p=0.012$). Increased PD-L1 expression was significantly associated with likelihood of LR status (OR= 1.018, $p=0.027$). 65.9% ($n=27$) of LR patients developed an immune-related adverse event (irAE), of which 20 patients required discontinuation of therapy. In the C arm, 16.7% ($n=8$) of patients developed an irAE of which 4 patients required discontinuation. On multivariate analysis, including age, sex, race, ethnicity, smoking status, BMI, PS, liver and brain metastases as well as the presence of common oncogenic molecular alterations, PS of < 2 was statistically significantly associated with an OS ≥ 3 years (OR=16.7, $p=0.017$). Molecular profiling was completed in 53 patients (LR=29, C=24). Common molecular alterations were identified in 28 out of 53 patients (LR=16, C=12). KRAS mutation was assessed in 34 patients (LR=16, C=18) and was associated with LR status versus C (Fisher's exact test value $p=0.0386$).

Conclusions Our retrospective study assessing multiple clinical and molecular determinants of patients with long-term response to immune checkpoint blockade, identified PS at diagnosis and KRAS mutation status to be associated with long-term response. Current efforts are ongoing to interrogate more deeply molecular features of LR, as well as their relationship to clinical aspects of a sustained benefit from ICI in NSCLC.

REFERENCES

1. . Borghaei H, et al. Five-year outcomes from the randomized, phase III trials check-Mate 017 and 057: nivolumab versus docetaxel in previously treated non-small-cell lung cancer. *Journal of Clinical Oncology* 0, JCO.20.01605, doi:10.1200/jco.20.01605 (2021)

- 2.. Reck M, et al. Five-year outcomes with pembrolizumab versus chemotherapy for metastatic non-small-cell lung cancer with PD-L1 tumor proportion score ≥ 50 . *J Clin Oncol* 39:2339–2349, doi:10.1200/jco.21.00174 (2021)

Ethics Approval The retrospective case-control study has obtained ethics approval from the Institutional Review Board at the Johns Hopkins School of Medicine.

<http://dx.doi.org/10.1136/jitc-2021-SITC2021.296>

TUMOR CELL-INTRINSIC MTORC1 SIGNALING THROUGH RAPTOR MAKES MELANOMA AND OVARIAN CANCER IMMUNOTHERAPY RESISTANT BY REGULATING INTERFERON-GAMMA RESPONSIVENESS AND PROMOTING TUMOR-INITIATING CELLS

¹Harshita Gupta*, ²Suresh Kari, ²Emily Salinas, ²Haiyan Bai, ²Erica Osta, ²Anand Kornepati, ²Juan Wang, ²Xinyue Zhang, ²Yidong Chen, ²Ratna Vadlamudi, ²Tyler Curiel. ¹UTHSCSA, San Antonio, TX, USA; ²UTHSA, San Antonio, TX, USA

Background Although immunotherapy can induce durable anti-tumor response in multiple cancers, immune checkpoint blockade (ICB) therapy resistance in ovarian cancer and melanoma remains problematic. Here, we report that tumor cell-intrinsic mTORC1 regulates ICB response through mTORC1 defining subunit Raptor (Rptor) by modulating interferon-gamma (IFN γ) resistance and tumor-initiating cell (TIC) virulence.

Methods We knocked down two distinct mTORC1 signaling components: Rptor (Rptorlo, aids in mTORC1 assembly) and Lamtor1 (Ltor1lo, docks mTORC1 on lysosomes) in murine ovarian cancer ID8agg and melanoma B16 cells. PD-L1 was CRISPR knocked out in B16 and human ovarian cancer line ES2. Mice with tumors were treated with a-PD-L1 \pm a-CD8 antibody. TICs were estimated by flow-cytometry.¹

Results Rptorlo B16 and ID8agg, but not Ltor1lo B16 tumors grew slower and were a-PD-L1 responsive unlike control (ctrl) in WT mice. We noted that ctrl and Rptorlo B16 and ID8agg cells expressed similar surface PD-L1 in vitro. Thus, Rptor suppresses a-PD-L1 response in ICB-resistant tumors. Tumor immune analysis revealed increased CD8+ T cell% and a trend to increased IFN γ +CD8+ T cells in a-PD-L1 treated Rptorlo, but not ctrl B16. Rptorlo a-PD-L1 efficacy was lost with a-CD8 and in IFN γ knockout mice. In vitro, IFN γ suppressed Rptorlo ID8agg proliferation, unlike ctrl. These data suggested that lack of Rptor makes tumors ICB responsive, possibly by making tumors IFN γ -sensitive and increasing IFN γ +CD8+ T cells. Further, tumor and draining lymph node (DLN) TCF1+PD-1+ T cell stem cells (critical for aPD-L1/PD-1 success²⁻³) were significantly higher in a-PD-L1 treated Rptorlo tumors. Thus, tumor Rptor status could regulate tumor microenvironment and distal DLN immune landscape on a-PD-L1 treatment. We previously published that mTORC1 promotes PD-L1-dependent tumor proliferation, TIC virulence¹⁻⁴ PD-L1KO B16 and ES2 cells expressed similar total Rptor protein. However, lower levels of Rptor were loaded in mTOR complex in absence of PD-L1, as assessed by a-mTOR immunoprecipitation, suggesting that pro-tumorigenic Rptor functions were downstream of, and dependent on PD-L1. Successful Rptorlo aPD-L1 treatment reduced TIC in vivo, an effect reversed in absence of CD8+ T cells or host IFN γ . Inhibiting ID8agg mTORC1 with rapamycin reduced stemness genes oct4, nanog expression by QPCR. Further, ID8agg Rptorlo TIC formed significantly smaller tumors versus ctrl TIC in immune-compromised NSG mice, confirming their reduced virulence. Rptor, but not Ltor1, expression inversely correlated with tumor CD8+ infiltrate in IMvigor210 trial, and strongly with TIC gene signature in ovarian cancer patients.⁵⁻⁶

Conclusions Tumor-cell intrinsic Rptor modulates ICB resistance, IFN γ responsiveness, immune microenvironment, and TIC virulence.

Acknowledgements N/A

Trial Registration N/A

REFERENCES

1. Gupta HB, et al. Tumor cell-intrinsic PD-L1 promotes tumor-initiating cell generation and functions in melanoma and ovarian cancer. *Signal Transduct Target Ther* 2016;**1**, Article number:16030.
2. Im SJ, et al. Defining CD8+ T cells that provide the proliferative burst after PD-1 therapy. *Nature* 2016;**537**:417–421.
3. Dammeijer F, et al. The PD-1/PD-L1-checkpoint restrains T cell immunity in tumor-draining lymph nodes. *Cancer Cell* 2020;**38**:685–700.
4. Clark CA, et al. Tumor-intrinsic PD-L1 signals regulate cell growth, pathogenesis, and autophagy in ovarian cancer and melanoma. *Cancer Res* 2016;**76**:6964–6974.
5. Smith BA, et al. A human adult stem cell signature marks aggressive variants across epithelial cancers. *Cell Rep* 2018;**24**:3353–3366.
6. Hoffman-Censits JH, et al. IMvigor 210, a phase II trial of atezolizumab (MPDL3280A) in platinum-treated locally advanced or metastatic urothelial carcinoma (mUC). *J Clin Oncol* 2016;**34**, no.2_suppl:355–355.

<http://dx.doi.org/10.1136/jitc-2021-SITC2021.298>

BROAD T ANTIGEN-SPECIFIC CD8+ T CELL REPERTOIRE IS ASSOCIATED WITH RESPONSE TO PD-1 BLOCKADE IN VIRUS POSITIVE MERKEL CELL CARCINOMA

¹Ulla Hansen*, ²Candice Church, ¹Amalie Bentzen, ³Steven Fling, ³Nirasha Ramchurren, ⁴Suzanne Topalian, ²Paul Nghiem, ¹Sine Hadrup. ¹Technical University of Denmark, Kgs. Lyngby, Denmark; ²University of Washington, Seattle, USA; ³Fred Hutchinson Cancer Research Center, Seattle, WA, USA; ⁴Johns Hopkins University School of Med., Baltimore, MD, USA

Background Merkel cell carcinoma (MCC) is an aggressive human skin cancer primarily induced by Merkel Cell Polyomavirus (MCPyV) driven by expression of the oncogenic T antigens (T-Ags): Large T and Small T antigen. Checkpoint inhibition therapy blocking the programmed cell death protein-1 (PD-1) pathway has proven effective with a clinical response rate up to 58%,¹ highlighting the critical role of immune surveillance for tumor control. Yet, evidence for the impact of T-Ag-specific T cells following immunotherapy is still limited.

Methods Potential CD8+ T cell epitopes derived from the T-Ags and the Viral capsid protein 1 (VP1) were predicted with netMHCpan 4.0 as 9- and 10-mer peptides with a rank score <2 for binding to 33 different HLA class I types. Peripheral blood mononuclear cells (PBMC) were obtained from 24 MCPyV+ MCC patients prior and post anti-PD-1 therapy initiation (CITN-09/Keynote-017). T cell recognition of the MCPyV-derived peptides during therapy was evaluated using the high-throughput technology of DNA barcode labeled pMHC multimers. Phenotypic characteristics of multimer-binding T cells were evaluated for selected patients.

Results Across all patients, 40 T-Ag-specific CD8+ T-cell populations were detected recognizing 31 epitopes restriction to 14 different HLA class I types. T-Ag-specific CD8+ T cells were detected in responders (complete and partial response, n=17) during therapy with a trend of increased number of responses observed after therapy initiation. Whereas only a single T-Ag-specific population was detectable in non-responders (stable and progressive disease, n=7). Moreover, the T cell repertoire after therapy initiation was significantly increased in the responder group compared to non-responder with the T-Ag-specific T cells showing an activated effector memory phenotype.

Conclusions The current study indicates that the T-Ag-specific T cells are associated with clinical benefit to checkpoint inhibitor therapy. Furthermore, the broad identification of novel T-Ag-derived T cell epitopes could potentially facilitate the use of targeted T cell therapy to enhance T cell recognition and clearance of MCC in combination with checkpoint inhibition.

Acknowledgements Supported by the Cancer Immunotherapy Trials Network (CITN)

REFERENCE

1. Nghiem P, Bhatia S, Lipson E. Three-year survival, correlates and salvage therapies in patients receiving first-line pembrolizumab for advanced Merkel cell carcinoma. *J Immunother cancer* 2021;9:e002478.

<http://dx.doi.org/10.1136/jitc-2021-SITC2021.299>

LONGITUDINAL PLASMA PROTEOMIC PROFILING OF NON-SMALL CELL LUNG CANCER PATIENTS UNDERGOING IMMUNE CHECKPOINT BLOCKADE-BASED THERAPY

¹Michal Harel*, ¹Coren Lahav, ¹Eyal Jacob, ¹Itamar Sela, ¹Yehonatan Elon, ¹Galit Yahalom, ²Iris Kamer, ¹Ofer Sharon, ³Yuval Shaked, ⁴Adam Dicker, ⁵David Carbone, ²Jair Bar. ¹Oncohost LTD, Binyamina, Israel; ²Chaim Sheba Medical Center, Ramat Gan, Israel; ³Technion-Israel Institute of Technology, Haifa, Israel; ⁴Thomas Jefferson University, Philadelphia, PA, USA; ⁵The Ohio State University, Columbus, OH, USA

Background Immune checkpoint inhibitors (ICIs) have revolutionized cancer treatment by shifting the focus from the tumor to the immune system of the host. Despite durable response to ICIs, only a small proportion of non-small lung cancer (NSCLC) patients respond to this treatment. Thus, great effort is currently focused on uncovering mechanisms of resistance and identifying predictive biomarkers for outcome.

Methods Blood plasma was obtained from 143 NSCLC patients treated with ICI-based therapy at baseline and early on-treatment (following the first treatment), and the levels of approximately 800 proteins were determined using ELISA-based arrays. Bioinformatic analysis was performed in order to detect novel patterns of resistance to ICI-based therapy. To identify a signature that predicts clinical outcome, a machine learning algorithm was applied.

Results Unsupervised bioinformatic analysis of the plasma proteomic profiles classified the patients into 3 clusters with distinct clinical and biological features. Patients in cluster #1 exhibited resistance to therapy, bone metastasis and high TNM (tumors, nodes and metastasis) staging; this cluster displayed high levels of proteins related to glycan and pyrimidine metabolism and cell-adhesion. Cluster #2 was enriched with responders, males, and patients with low TNM staging; this cluster displayed a strong representation of desmoglein proteins. Cluster #3 was enriched with female patients while the proteome of these patients displayed high levels of MAPK signaling related proteins. Patient clusters were largely unchanged when comparing baseline and on-treatment data, suggesting pre-existing rather than acquired resistance to therapy. A further comparison between responders and non-responders identified six significantly differentially expressed proteins comprised of both host- and tumor-related proteins, with non-responders displaying a significant enrichment of neutrophil proteins at baseline and early-on-treatment. Notably, there was no significant difference in the neutrophil count between responders and non-responders, suggesting a functional shift in neutrophils upon treatment in non-responders. Lastly, we identified a predictive signature for response comprised of two proteins and two clinical features. The performance of the predictive signature reached an area under the curve (AUC) of the receiver operating characteristics (ROC) plot of 0.8 in an independent validation subset of the cohort, indicating a high predictive power.

Conclusions Here we performed a deep bioinformatic analysis of plasma proteome profiles of 143 NSCLC patients undergoing ICI-based therapy. Our study sheds light on underlying mechanisms of resistance to ICI-based therapy and reveals a predictive signature for response in NSCLC patients.

Ethics Approval Data and study specimens were purchased from Indivumed and Sheba medical center, approval number 0226-13-SMC (institutional review board). Participants gave informed consent before taking part.

<http://dx.doi.org/10.1136/jitc-2021-SITC2021.300>

301 **OMX-0407, A HIGHLY POTENT SIK3 INHIBITOR, SENSITIZES TUMOR CELLS TO APOPTOSIS AND ERADICATES TUMORS IN COMBINATION WITH PD-1 INHIBITION**

¹Christina Hartl, ¹Tillmann Michels, ¹Ronny Milde, ¹Vanessa Klein, ²Philipp Beckhove, ¹Hannes Loferer, ¹Stefan Bissinger*. ¹*iOmx Therapeutics AG, Martinsried/Munich, Germany;* ²*RCI Center for Interventional Immunology, Regensburg, Germany*

Background Interference with post-translational modifications such as methylation and acetylation of DNA and histones may enhance the intrinsic anti-tumor capacity of the immune system. Using the iOTarg genetic screening platform, salt-inducible kinase 3 (SIK3) was recently identified as a novel immune checkpoint that controls T cell-mediated apoptosis in tumor cells. SIK3, a serine/threonine kinase of the AMPK family, regulates pro-survival gene expression in tumor cells through epigenetic modulation of the NF- κ B-driven gene landscape via histone deacetylase 4 (HDAC4), causing the tumor to evade T cell-mediated killing.

Methods In turn, SIK3 knockout or knockdown abates downstream pro-survival signaling and sensitizes a panel of murine and human tumor cells to death receptor-mediated apoptosis. OMX-0407, an orally available, single-digit nanomolar inhibitor of SIK3 was shown to effectively reduce TNF-induced HDAC4 phosphorylation and downstream NF- κ B activity in a dose-dependent manner, thereby enhancing caspase-mediated apoptosis in murine and human tumor cell lines. Decreased intratumoral NF- κ B activity was demonstrated in vivo with an MC38 NF- κ B-luc reporter cell line.

Results Inhibition of the pro-tumorigenic NF- κ B pathway using OMX-0407 monotherapy translated into significant tumor growth inhibition (TGI) as well as prolonged survival in the highly infiltrated syngeneic murine colorectal carcinoma model MC38 (76% TGI). Moreover, OMX-0407 repolarized the tumor microenvironment (TME) by strongly reducing the number of regulatory T cells (T-regs) and M2-polarized macrophages in the tumor bed, while not affecting the peripheral T cell compartment. Thereby, exposure to OMX-0407 achieved a pronounced pro-inflammatory TME, characterized by a rise in activated cytotoxic T lymphocytes (CTL) and an increased CTL-to-T-reg ratio. Using the breast cancer mouse model EMT6, which represents an immune-excluded, cold tumor phenotype, we demonstrated that despite the minimal anti-tumor efficacy of OMX-0407 and anti-PD-1 monotherapy, respectively, upon combination treatment, both therapies synergize by combining apoptosis sensitization with a reduction in immunosuppressive TME and an increase in cytotoxic T cell activity. Combination treatment resulted in partial and complete tumor remissions in 60% of the animals, along with a significant prolongation of overall survival.

Conclusions In summary, OMX-0407, a first-in-class oral SIK3 inhibitor, demonstrates potent monotherapy efficacy in a pro-inflammatory tumor setting by reshaping the immune compartment and sensitizing tumor cells to death receptor-mediated apoptosis. The ability of OMX-0407 to remodel an immunosuppressed TME in a generally cold tumor setting, harbors great clinical potential for OMX-0407 combination therapy with anti-PD-1/PD-L1 immune checkpoint blockade, specifically in patients with high unmet medical need who are resistant to current immune checkpoint inhibitor monotherapy.

<http://dx.doi.org/10.1136/jitc-2021-SITC2021.301>

302

CHARACTERIZATION OF TIGIT AND PVR EXPRESSION IN COLORECTAL LIVER METASTASES

¹Antoine Bernard*, ¹David Henault, ¹Sandy Pelletier, ¹Pamela Thebault, ¹Benoit Barrette, ²Simon Turcotte. ¹CHUM, Montreal, Canada; ²Centre hospitalier de l'Université de Montréal, Montreal, Canada

Background Metastatic colorectal cancer (CRC) is common and lethal and generally not responsive to current immunotherapies. We hypothesize that efficacious T cell-based immunotherapy can be developed for this malignancy, provided that immune checkpoints relevant to liver metastasis, the first site of disease progression, are targeted. Here, we characterized CRC liver metastases by RNAseq, FACS and in vitro functional assays to identify candidate immune checkpoints.

Methods We performed deep RNAseq clustering and differential gene expression analysis on bulk RNA extracted from 52 mismatch repair gene proficient CRC liver metastases. By multiparameter FACS, we analyzed the expression of candidate immune checkpoints in cell suspensions derived from 18 liver metastases, matched non-tumoral livers, and pre-operative PBMCs. We evaluated IFN- γ (ELISA) secretion and tumor lysis (Incucyte) of tumor-infiltrating T lymphocytes (TILs) expanded from liver metastases stimulated by autologous cancer cells with or without monoclonal antibodies blocking candidate immune checkpoints.

Results Out of 52 metastases, 21 (40.3%) clustered as immune reactive (IR) defined by concurrent high expression of transcripts related to antigen processing, immune cell lineage, immune checkpoints, interferon-gamma response, cytokines, and chemokines, whereas 25 (48.1%) were classified as non-IR. Of all inhibitory ligands assessed, PVR and PVRL2 had the highest expression, both in IR and non-IR metastases, and higher than PD-L1 and PD-L2 expression. The expression of corresponding receptors TIGIT and CD226 was significantly higher in IR compared to non-IR metastases, at absolute levels higher than PD-1. By FACS analysis, PVR and PVRL2 expression by tumor-infiltrating myeloid and tumor cells was higher than PD-L1 and PD-L2 expression. High PVR expression was also found in hepatocytes, liver macrophages and circulating monocytes in the same patients. In TILs, TIGIT was significantly overexpressed in activated CD4+CD25+ (74.8 \pm 3.0%) and CD8+CD25+ (68.7 \pm 8.4%) compared to resting CD25neg T cells, an expression pattern that was not seen for PD-1 or in T cells infiltrating the liver or circulating in the blood. The majority of cancer cell lines derived from liver metastases expressed PVR, but low levels of PD-L1. TIL clones expanded from liver metastases expressed TIGIT at various levels inducible by TCR stimulation. Upon co-culture with autologous cancer cell lines, TIL clones were more lytic and secreted more IFN- γ in presence of anti-TIGIT blocking antibody.

Conclusions By expression and functional data, the TIGIT/PVR immune suppressive axis appears as a biologically promising target for the development of immunotherapy in patients with CRC metastatic to the liver.

Acknowledgements This work is supported by Bristol Myers Squibb and by the Quebec Cancer Consortium. A.B. holds a postdoctoral scholarship award from the Institut du cancer de Montréal. S.T. holds a Junior 2 clinical-scientist salary award from the Fond de recherche Santé-Québec. The University of Montreal Roger des Groseillers Research Chair in hepatopancreatobiliary surgical oncology supports the biobanking and clinicopathological database associated with this project.

Ethics Approval Institutional review board approvals were obtained to conduct this project (16.262) and all patients provided informed consent to contribute to this project with biospecimens and clinicopathological data (09.237).

<http://dx.doi.org/10.1136/jitc-2021-SITC2021.302>

303 NON-FUNCTIONAL T CELL RESPONSES IN NON-SMALL CELL LUNG CANCER ARE INDUCED DURING TUMOR ANTIGEN-SPECIFIC T CELL PRIMING IN THE MEDIASTINAL LYMPH NODE

Brendan Horton*, Duncan Morgan, Elen Torres-Mejia, Maria Zagorulya, Vidit Bhandarkar, Noor Momin, K Wittrup, J Love, Stefani Spranger. *Massachusetts Institute of Technology, Cambridge, MA, USA*

Background In non-small cell lung cancer (NSCLC), response to checkpoint blockade therapy (CBT) is associated with tumor-infiltrating CD8+ T cells, but not all T cell-infiltrated tumors respond to CBT. The subgroup of T cell-infiltrated but CBT-resistant tumors has been clinically described as containing "non-functional" T cell responses. Mechanisms governing the generation of non-functional T cell responses remain poorly understood, and treatment options for this subgroup are limited.

Methods We utilized a transplantable, syngeneic murine NSCLC cell line derived from an autochthonous NSCLC driven by Kras^{G12D} expression and p53 deletion (KP cell line) to model non-functional T cell responses. To study antigen-specific responses, we engineered KP cells to express the model CD8+ T cell antigen SIY for certain experiments. CBT consisted of combined anti-CTLA-4 and anti-PD-L1 therapy.

Results Orthotopic KP lung tumors failed to respond to CBT, but KP flank tumors were controlled by CBT. Lung and flank tumors contained activated CD8+ T cells, providing a platform to compare functional and non-functional CD8+ T cell responses in NSCLC. Single-cell RNA sequencing revealed that lung tumor-infiltrating CD8+ T cells lacked effector and exhaustion molecules despite clonal expansion. Analysis of antigen-specific CD8+ T cells revealed that this lung cancer-specific T cell dysfunction was established during priming in lung-draining mediastinal lymph nodes (mLN) despite robust T cell proliferation. RNA sequencing and flow cytometry of antigen-specific CD8+ T cells found that T cells primed in the mLN underwent blunted effector differentiation characterized by a lack of effector molecules CD25, Granzyme B, and TIM-3, but retention of TCF-1. This phenotype persisted in lung tumors, consistent with our initial observations of absent effector and exhaustion molecule expression. Many CD8+ T cells from NSCLC patients expressed an analogous gene expression program distinct from T cell exhaustion. TCF-1+ CD8+ T cells in lung tumors did not mediate tumor control and failed to differentiate into effector cells after CBT. To investigate alternative therapeutic strategies of reinvigorating lung tumor-reactive T cells, we focused on IL-2 and IL-12, as expression of their receptors was reduced in mLN-primed T cells. Administering recombinant IL-2 and IL-12 was sufficient to restore effector T cell differentiation, induce lung tumor control, and significantly extend survival of lung tumor-bearing mice.

Conclusions Our results suggest that non-functional CD8+ T cell responses in NSCLC arise from failed effector T cell differentiation during priming. Transient combination therapy with IL-2 and IL-12 overcomes this dysfunctional state to induce protective T cell responses in CBT-resistant tumors.

Ethics Approval All mouse experiments were approved by MIT's Committee on Animal Care (CAC) - DHHS Animal Welfare Assurance # D16-00078

<http://dx.doi.org/10.1136/jitc-2021-SITC2021.303>

ANTAGONISTIC ANTIBODIES TARGETING LAIR1 ENHANCE T LYMPHOCYTE ACTIVATION AND PROMOTE INFLAMMATORY PHENOTYPES IN MYELOID CELLS

¹Tao Huang*, ¹Caroline Bonnans, ¹Maria Jose Costa, ¹Azita Tabrizi, ¹Jing-Tyan Ma, ²Jingjing Xie, ²Heyu Chen, ¹Kyu Hong, ¹Krista McCutcheon, ¹Ryan Stafford, ¹Hongyu Tian, ²Cheng Cheng Zhang, ³Xun Gui, ³Ningyan Zhang, ³Zhiqiang An, ¹X Charlene Liao, ¹An Song. ¹*Immune-Onc Therapeutics, Inc., Palo Alto, CA, USA*; ²*UT Southwestern Medical Center, Dallas, TX, USA*; ³*UT Health Science Center, Houston, TX, USA*

Background The Leukocyte Associated Immunoglobulin-like Receptor 1 (LAIR1) is an immune inhibitory transmembrane glycoprotein expressed on lymphocytes and myeloid cells. The known ligands for LAIR1 are proteins containing collagen-like domains including collagen, complement component 1q (C1q), and stromal protein Colec12.^{1 2 3} Myeloid-derived suppressor cells (MDSC), tumor associated macrophages (TAMs), as well as collagens, are important contributors of the immune-suppressive tumor microenvironment, and LAIR1 expression is negatively correlated with patient survival in many solid tumors.⁴ These findings prompt us to investigate LAIR1 as a novel immuno-oncology target in collagen-rich tumors. Utilizing LAIR1 antagonist antibodies, we aim to mobilize anti-tumor immunity by changing the collagen-induced tolerogenic state of the immune cells into proinflammatory.

Methods The mRNA expression levels of LAIR1, collagen, and C1q in diverse human cancers were analyzed using the TCGA database. LAIR1 protein expression on tumor infiltrated immune cells were measured by flow cytometry. Human tumor samples were obtained from Cooperative Human Tissue Network (CHTN) by the National Cancer Institute (NCI). Purified human T cells from healthy donors were stimulated with immobilized anti-CD3 in the presence of plate-coated human collagen I. Human monocyte-derived macrophages and dendritic cells (DC) were differentiated with M-CSF+IL-4 or GM-CSF+IL-4, respectively. Immune cell phenotypes were assessed by flow cytometry and cytokine secretion by Luminex.

Results Analysis of the TCGA database using signature genes specific to macrophages, T cells, DCs, and natural killer (NK) cells demonstrate that LAIR1 is highly expressed in most macrophage-infiltrated tumors and certain T cell-enriched tumors. LAIR1 and collagen are co-expressed at high levels in multiple macrophage-enriched tumors. Flow cytometry analysis of infiltrated immune cells from fresh tumor tissues showed that the highest level of LAIR1 protein expression was detected on TAMs, followed by monocytes, monocytic MDSCs, DCs, and lymphocytes. In vitro, LAIR1 antagonizing antibodies enhanced T-cell activation, proliferation, and IFN γ and TNF α production in comparison to isotype controls in the presence of collagen. Blocking LAIR1 interaction with collagen also decreased the expression of M2 markers such as PD-L1 and CD209 on monocyte-derived M2 macrophages. Additionally, treatment of monocyte-derived DCs by these antibodies increased the expression of the co-stimulatory protein CD86 and promoted the release of IL-12, a crucial cytokine for lymphocyte activation.

Conclusions These in vitro data suggest that LAIR1 blockade could potentially reverse T-cell and myeloid immunosuppression mediated by collagen, demonstrating the therapeutic potential of anti-LAIR1 antagonistic antibodies.

REFERENCES

1.. Meyaard L. The inhibitory collagen receptor LAIR-1 (CD305). *J Leukoc Biol* 2008;**83**:799–803.

2. . Son M, *et al.* C1q limits dendritic cell differentiation and activation by engaging LAIR-1. *PNAS* 2012;**109**:3160–3167.
- 3.. Keerthivasan S, *et al.* Homeostatic functions of monocytes and interstitial lung macrophages are regulated via collagen domain-binding receptor LAIR1. *Immunity* 2021;**54**:1511–1526.
- 4.. Xu L, *et al.* Cancer immunotherapy based on blocking immune suppression mediated by an immune modulator LAIR-1. *Oncol Immunology* 2020;**9**:e17404771–e17404779.

<http://dx.doi.org/10.1136/jitc-2021-SITC2021.304>

305

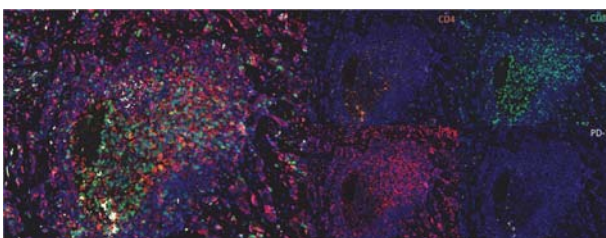
UNRAVELLING THE ROLE OF CD4+ AND CD8+ T CELLS IN PEMBROLIZUMAB INDUCED MYCOBACTERIUM TUBERCULOSIS GRANULOMA FORMATION IN NASOPHARYNGEAL CARCINOMA

Tae Yang Desmond Hung*, Ngar Woon Kam, Victor Ho Fun Lee. *The University of Hong Kong, Hong Kong, Hong Kong*

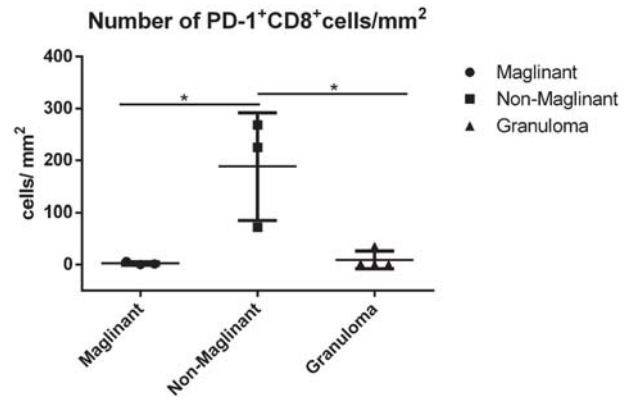
Background Nasopharyngeal carcinoma (NPC), an endemic disease in Southeast Asia, is characterized by high immune cell infiltration. Pembrolizumab, an immune checkpoint inhibitor that blocks the programmed death-1 (PD-1) surface protein on CD4+ and CD8+ T cells and reactivate tumor autoimmunity,¹ has shown promising results in early NPC trials.² Despite the encouraging results, pembrolizumab induced mycobacterium tuberculosis (MTB) activation/reactivation cases have been reported.³ CD4+ T cells play a crucial role initiating MTB granuloma formation through releasing interferon gamma (IFN γ), and the CD4+PD1+ subtype is known to be crucial for controlling MTB infection.³ ⁴ Indeed, CD8+ T cells are believed to play a less important role in MTB immunity. However, the mechanism of pembrolizumab induced MTB granuloma formation remains poorly understood, and the current study objective is to decipher the enigma through investigating the PD-1 and IFN γ expression of CD4+ and CD8+ T cells.

Methods We encountered two NPC patients who suffered from pembrolizumab induced MTB granuloma formation, and their biopsy samples were collected and separated into three groups, malignant, non-malignant and granuloma. The samples were stained with the Opal multiplex immunohistochemistry kit (figure1).

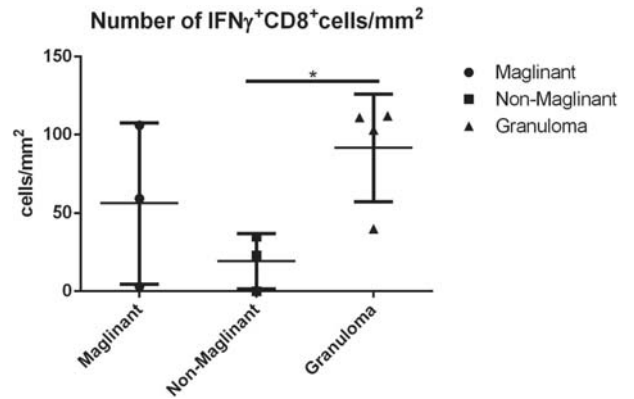
Results The non-malignant group had the highest of amount of PD-1+CD8+ (188.3 cells/mm²), and the cell density was significantly higher than the malignant group (2.3 cells/mm², p= 0.035) and the granuloma group (9 cells/mm², p=0.017) (figure 2). Meanwhile, the IFN γ +CD8+ cell density of the granuloma group was the highest (91.5 cells/mm²), which was higher than the non-malignant group (19.3 cells/mm², p=0.020) and the malignant group (56 cells/mm²/ p= 0.320) (figure 3). The cell density of PD-1+CD4+ was the highest in the non-malignant group (245 cells/mm²), which was also higher than the malignant group (10.7 cells/mm², p=0.174) and the granuloma group (35.5 cells/mm², p=0.155) (figure 4). Similarly, the cell density of IFN γ +CD4+ (96.5 cells/mm²) was the highest in granuloma group, which was higher than the malignant group (26.7 cells/mm², p=0.550) and non-malignant group (15.22 cells/mm², p=0.124) (figure 5).



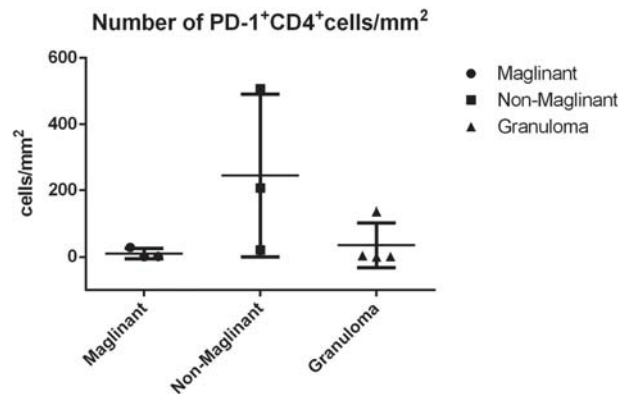
Abstract 305 Figure 1 Multiplex Staining. Staining were performed using Opal multiplex immunohistochemistry staining kit



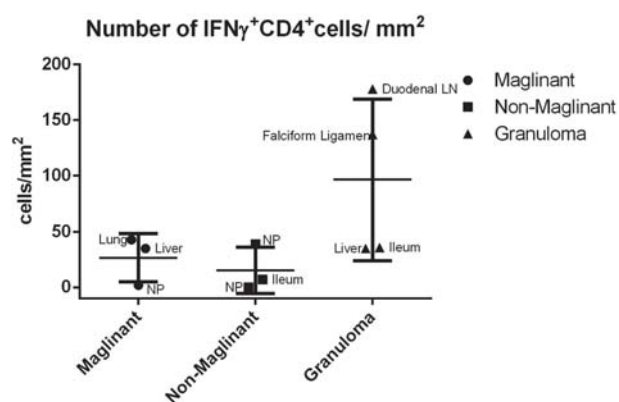
Abstract 305 Figure 2



Abstract 305 Figure 3



Abstract 305 Figure 4



Abstract 305 Figure 5

Conclusions CD8⁺ cells displayed more significant PD-1 downregulation and IFN γ upregulation in the granuloma group than CD4⁺ cells. The significant phenotypical and functionality changes in CD8⁺ cells might suggest that pembrolizumab could diminish CD4⁺ cells' role in MTB immunity, which was different from the conventional mechanism in MTB infection. Since IFN γ is important for inducing granuloma formation, the increase in IFN γ from CD8⁺ cells might provide a logical reason for pembrolizumab induced MTB granuloma formation in NPC patients.

REFERENCES

- Graves M, *et al.* Monitoring patient response to pembrolizumab with peripheral blood exhaustion marker profiles. *Front Med (Lausanne)* 2019;**6**:113.
- Jain A, Chia WK, Toh HC. Immunotherapy for nasopharyngeal cancer-a review. *Chin Clin Oncol* 2016;**5**(2):22.
- Barber DL, *et al.* Tuberculosis following PD-1 blockade for cancer immunotherapy. *Sci Transl Med* 2019;**11**(475).
- Green AM, Difazio R, Flynn JL. IFN-gamma from CD4 T cells is essential for host survival and enhances CD8 T cell function during mycobacterium tuberculosis infection. *J Immunol* 2013;**190**(1):270–7.

<http://dx.doi.org/10.1136/jitc-2021-SITC2021.305>

DECR2 REGULATES TUMOR CELL FERROPTOSIS AND IS REQUIRED FOR IMMUNOTHERAPY EFFICACY

Shuyin Li*, Thomas Gajewski, Shuyin Li, Emily Higgs. *University of Chicago, Chicago, IL, USA*

Background Checkpoint blockade therapies have transformed the landscape of cancer care. Durable clinical responses have been observed in a subset of patients. However, many patients do not respond, and understanding the mechanisms underlying tumor resistance to checkpoint blockade drugs could potentially expand clinical benefit. We therefore performed an unbiased CRISPR library screen to identify novel gene alterations sufficient to mediate resistance to T cell-mediated killing. **Methods** B16.SIY cells were transduced with a genome-scale gRNA lentivirus to generate loss of function mutants. In vitro-primed CD8+ T cells isolated from 2C/Rag2^{-/-} TCR transgenic mice specific for the SIY antigen were co-cultured with transduced B16.SIY tumor cells. Resistant cells were collected and targeted genes were identified by sequencing the gRNAs. The gene encoding *Decr2*, a peroxisomal 2,4-dienoyl-CoA reductase, was identified. To investigate the role of *Decr2* in tumor growth and immune responses in vivo, the *Decr2* knock-down or *Decr2* overexpressed tumors were transplanted into C57BL/6 mice for studies of anti-PD-L1 efficacy and immune response analysis. Based on a hypothesized role in ferroptosis, RNA-seq was performed and lipid reactive oxygen species were quantified.

Results *Decr2* mutants were relatively resistant to CD8+ T cell killing in vitro. In vivo, *Decr2* knock-down tumors showed almost complete loss of anti-PD-L1 efficacy, without affecting early T cell priming or immune cell infiltration. However, tumor-infiltrating T cells failed to expand following anti-PD-L1 therapy in *Decr2* knock-down tumors. RNA-seq analysis revealed upregulation of ferroptosis-related genes in *Decr2*-deficient tumor cells, and these tumor cells were relatively resistant to ferroptosis-inducers in vitro. *Decr2* knock-down cells also showed defective induction of lipid ROS in response to CD8+ T cells in vitro, or when analyzed following anti-PD-L1 treatment ex vivo. Analysis of tumor RNA-seq data from human melanoma patients treated with checkpoint blockade revealed decreased *Decr2* levels in non-responding patients.

Conclusions Our results identify tumor cell-expressed *Decr2* as novel regulator of ferroptosis and implicate the process of ferroptosis as a major mechanism of immune-mediated tumor cell killing in vivo. Pharmacologic strategies to facilitate tumor cell ferroptosis could have therapeutic utility.

<http://dx.doi.org/10.1136/jitc-2021-SITC2021.306>

307

INTERACTION OF ANTI-PD-1/PD-1 IMMUNOCOMPLEXES WITH HUMAN FCγRS: BINDING PROPERTIES AND FUNCTIONAL IMPLICATION

¹Elena Daveri*, ¹Elena Luison, ¹Viviana Vallacchi, ²Barbara Vergani, ¹Veronica Huber, ¹Agata Cova, ²Biagio Eugenio Leone, ¹Marina Garassino, ¹Mariangela Figini, ¹Licia Rivoltini. ¹Fondazione IRCCS Istituto Nazionale Dei Tumori, Milan, Milano, Italy; ²University of Milano Bicocca, Monza, Italy

Background Rescue of exhausted T cell immunity through the inhibition of PD-1/PD-L1 interaction is a pillar of immunotherapeutic anti-PD-1 monoclonal antibodies (mAbs), as Nivolumab and Pembrolizumab. Despite the IgG4 subclass, anti-PD-1 mAbs can bind different FcγRs and trigger immunosuppressive activity in FcR-expressing myeloid cells. This effect is evident when anti-PD-1 mAbs engage soluble PD-1 (sPD-1) forming a stable sPD-1-antiPD-1mAb immune complex (PD-1 IC). In the present study we dissect the process by investigating which of the FcγRs displays the highest affinity for monomeric or complexed Nivolumab. In addition, methods for detecting and quantifying PD-1 ICs in plasma of patients treated with PD-1 blockers mAbs are under development for clinical application.

Methods By surface plasmon resonance (SRP) (Biacore™ T200, Cytiva), the interaction of FcγRI/CD64, FcγRIIa/CD32a, FcγRIIb/CD32b, FcγRIIIa/CD16a and FcγRIIIb/CD16b with anti-PD1 Nivolumab and the corresponding PD-1-IC has been evaluated, and their cellular localization has been assessed by confocal microscopy. Further, sPD-1 and PD-1 IC has been determined by customized ELISAs and western blot approaches in plasma of anti-PD-1 mAb-treated patients.

Results The binding of anti-PD1 and PD-1-IC occurred with all the FcγRs tested, albeit sensorgrams revealed diverse degrees of affinity. No major difference in the overall affinity of the monomeric anti-PD-1 versus PD-1 IC is observed for FcγRI/CD64, FcγRIIa/CD32a, FcγRIIb/CD32b. Instead, the dissociation phase was clearly slowest for PD-1 IC with respect to the monomeric mAb in FcγRIIIa/CD16a and FcγRIIIb/CD16b binding studies. Nevertheless, only PD-1 IC undergoes internalization when interacting with human FcγR+ myeloid cells in vitro, through pathways that does not appear to lead to lysosomal co-localization. Customized ELISA for PD-1 IC quantification has been developed to detect the complex after enrichment of plasma IgG4 by specific matrix. Data concerning the evaluation of PD-1 IC concentration in plasma of cancer patients treated with Nivolumab, will be presented.

Conclusions Despite the IgG4 subclass is expected to display the lowest binding affinity to Fcγs, we report here that anti-PD-1 therapeutic antibodies bind significantly to CD16, CD32 and CD64, particularly if stabilized in the IC form by engaging soluble PD-1. This evidence, if occurring in vivo, could introduce novel functional properties to these therapeutic agents, with potential detrimental effects on their clinical efficacy. Our findings imply that tools to antagonize PD-1-related exhaustion by Fc-null mAbs or non-mAb-based strategies could be preferred to engage full-fledged antitumor immune responses without unwanted effects related to FcR triggering.

<http://dx.doi.org/10.1136/jitc-2021-SITC2021.307>

TRANSCRIPTOMIC ANALYSIS OF MELANOMA PATIENTS IN ADJUVANT SETTING TREATED WITH ANTI PD1 THERAPY: REAL LIFE STUDY

¹Domenico Mallardo*, ¹Claudia Trojaniello, ¹Maria Grazia Vitale, ¹grazia d'angelo, ²Andrew White, ¹Mariaelena Capone, ¹Antonio Sorrentino, ¹Gabriele Madonna, ¹Marilena Tuffanelli, ¹Vito Vanella, ¹Lucia Festino, ¹Ester Simeone, ¹Corrado Caracò, ¹Nicola Normanno, ²Sarah Warren, ¹Paolo Ascierto. ¹Istituto Nazionale Tumori IRCCS Pascale, Naples, Italy; ²NanoString Technologies, Seattle, WA, USA

Background Adjuvant treatment of melanoma patients with immune-checkpoint inhibition (ICI) significantly improved relapse-free survival (RFS).¹ In the phase 3 keynote-054 trial showed that pembrolizumab (anti-PD1) administration in adjuvant setting provided a longer RFS (59,8%) than the placebo group (41,4%) at a 3.5-year median follow-up.² Moreover, 4 years RFS results from the phase 3 checkmate 238 trial, showed a superior efficacy of nivolumab versus ipilimumab in patients with resected AJCC-7 stage III or IV melanoma. RFS rate was of 58% in the nivolumab arm and 45% in the ipilimumab arm.³ Although treatment with ICIs has improved the RFS of melanoma patients in adjuvant setting, there is still a large proportion of patients who do not respond to the treatment and then relapse. The aim of this study was to investigate the molecular mechanisms underlying resistance to anti-PD1 treatment in the adjuvant setting.

Methods From December 2018 to July 2020, n. 121 melanoma patients in stage III or IV NED were treated with anti-PD1s as adjuvant (minimum follow up of 12 months, range 12–30 months). These patients received nivolumab (n=95) or pembrolizumab (n=26). Distant and local metastases was observed in 33 (27%) and 7 (6%) patients, respectively (patients baseline characteristics are listed in table1). Gene expression profiles, using NanoString IO 360 panel, were performed from peripheral blood mononuclear cell (PBMCs), collected retrospectively, from n.73 patients (of which n.26 had relapse). All patients have appropriately signed informed consent. Statistical analysis was performed via Bonferroni correction, P< 0.05 was considered statistically significant for median stratification.

Results At a minimum follow-up of 12 months, the 12-month rate of Relapse-free survival was 72%, confirming the data reported by checkmate 238 trial. In the transcriptomic analysis we observed that in patients with local-regional metastases there was a higher expression of ITGA2 (p<0.05), a gene that promotes malignant tumor aggression by up-regulating PD-L1 expression through STAT3 pathway and the downregulation of DUSP1 (p<0.05) that is linked in promotion of angiogenesis, invasion and metastasis. Moreover, in male group we found a higher expression of HLA-DQB1 and HLA-DQA1 which belonged to HLA class II beta chains.

Abstract 308 Table 1

patients' clinical parameters.	
Patients Characteristic	N = 121
Median age	54 (range 17-85)
Gender: female/male, n (%)	48 (40)/73(60)
BRAF Status	
Wilde type, n (%)	56 (46)
Mutation, n (%)	45 (37)
NA, n (%)	20 (17)
BMI	
Normal weight (18.5>BMI≤24.9), n (%)	33 (27)
Overweight (25>BMI≤29.9), n (%)	23 (20)
Obese (BMI ≥30), n (%)	32 (26)
NA, n (%)	33 (27)
RFS, n (%)	80 (66)
Relapse in the 1° Year, n (%)	34 (28)
Local MTX¹, n (%)	7 (6)
Distant MTX¹, n (%)	33 (27)
Median OS² in months	25.5
Median DFS³ in months	20

¹Metastases, ² Overall survival, ³ Disease Free Survival

Conclusions In this preliminary report we found that RFS 1-yr rate is similar to checkmate 238 study, and that patients with local metastasis have a higher expression of genes related to promote PDL1 levels. Further investigations are needed to get additional information.

Acknowledgements The study was supported by the Institutional Project "Ricerca Corrente" of Istituto Nazionale Tumori IRCCS Fondazione "G. Pascale" of Napoli, Italy.

REFERENCES

1. Weber J, Mandala M, Del Vecchio M, et al, CheckMate 238 Collaborators. Adjuvant nivolumab versus ipilimumab in resected stage III or IV melanoma. *N Engl J Med* 2017 November 9;377(19):1824–1835.

2. . Eggermont AMM, Blank CU, Mandalà M, *et al.* EORTC melanoma group. Adjuvant pembrolizumab versus placebo in resected stage III melanoma (EORTC 1325-MG/KEYNOTE-054): distant metastasis-free survival results from a double-blind, randomised, controlled, phase 3 trial. *Lancet Oncol* 2021 May;**22**(5):643–654.
3. . Ascierto PA, Del Vecchio M, Mandalà M, *et al.* Adjuvant nivolumab versus ipilimumab in resected stage IIIB-C and stage IV melanoma (CheckMate 238): 4-year results from a multicentre, double-blind, randomised, controlled, phase 3 trial. *Lancet Oncol* 2020 November;**21**(11):1465–1477.

Ethics Approval The study was approved by internal ethics board of the Istituto Nazionale Tumori IRCCS Fondazione "G. Pascale" of Napoli Italy, approval number of registry 33/17 OSS.

Consent Written informed consent was obtained from the patient for publication of this abstract and any accompanying images. A copy of the written consent is available for review by the Editor of this journal.

<http://dx.doi.org/10.1136/jitc-2021-SITC2021.308>

VISUALIZING THE IMMUNOTHERAPY-INDUCED SPATIAL REORGANIZATION OF THE TUMOR-IMMUNE MICROENVIRONMENT BY CODEX MULTIPLEX IMAGING

¹Ruan Medrano*, ¹Fei Han, ²Bassem Ben Cheikh, ³Patrick Leinert, ³Wm Pat Leinert, ²Oliver Braubach, ¹Robert Schreiber. ¹Washington University School of Medicine, St Louis, MO, USA; ²Akoya Biosciences, Marlborough, MA, USA; ³Leinco Technologies, St. Louis, MO, USA

Background Tumors contain spatially organized microenvironments in which the location and composition of the cellular components ultimately determine tumor fate. We previously characterized CD45+ cells infiltrating T3 sarcomas using complementary forms of high-dimensional profiling (scRNAseq and CyTOF) and identified key immune cell populations that became associated either with growing tumors in mice treated with control antibody (cmAb) or rejecting tumors in mice treated with immune-checkpoint therapy (ICT) i.e., anti-PD-1 and/or anti-CTLA-4. To better understand the effects of the intratumoral immune cell populations on one another and on the tumor itself, we used CODEX multiplex imaging to simultaneously characterize expression of 35 distinct immune cell markers on tumor tissue sections thereby maintaining the spatial relationships between effector cells and their cognate tumor cell targets

Methods T3 tumor bearing syngeneic mice were treated with cmAb or a-PD-1/a-CTLA-4 on days 6,9 and 12, harvested on different days, fresh frozen, cut in 8µM sections, transferred to coverslips, and stained with a panel of commercially available and custom-made CODEX antibodies following optimized staining conditions using the manufacturer's protocol. Whole tumor tissue raw TIFF images were subjected to an image processing pipeline developed by Akoya Biosciences, Inc, where dapi+ cells used for cell segmentation by the Startdist method. Unsupervised clustering using Scanpy toolkit based on normalized marker expression profiles identified and validated 12 unique cell clusters

Results When compared to the cmAb group, a-PD-1/a-CTLA-4 tumors harvested on day 10 displayed a marked increase in percentage as well as density of CD4+ and CD8+ T cells, Ly6G neutrophils, MHC-II+cd11c+cd24+DCs and a decrease of CD140a+ tumor cells. Spatial analysis indicated statistically significant differences in the organization of these cell types upon treatment with a-PD-1/a-CTLA-4 compared to cmAb treatment. Specifically, immune cells were found at the border of the tumor in cmAb treated mice and heavily infiltrated tumors following ICT. Neighborhood identification analysis revealed changes in the composition of the main neighborhood clusters, of which the top three clusters present in cmAb treated tumors (macrophage, tumor, and other immune cells) were substituted by clusters of CD4+ and CD8+ T cells, neutrophils, and macrophages.

Conclusions These results not only confirm the remodeling of both the lymphoid and myeloid compartments previously observed with scRNAseq and CyTOF but also suggest that changes in the spatial organization of immune cells are drivers of the tumor rejection process upon treatment with ICT.

<http://dx.doi.org/10.1136/jitc-2021-SITC2021.309>

T CELL INTRINSIC DNA DAMAGE AND REPAIR RESPONSE AS A NOVEL MARKER ASSOCIATED WITH CLINICAL RESPONSE TO PD-1 BLOCKADE<http://dx.doi.org/10.1136/jitc-2021-SITC2021.310>

¹Yuki Muroyama*, ¹Sasikanth Manne, ¹Allison Greenplate, ¹Divij Mathew, ²Derek Oldridge, ³Lakshmi Chilukuri, ⁴Caiyue Xu, ⁵Ramin Herati, ¹Alexander Huang, ⁶Dimitriy Zamarin, ⁶Claire Friedman, ¹E John Wherry. ¹University of Pennsylvania, Perelman School of Medicine, Philadelphia, PA, USA; ²Children's Hospital of Philadelphia, Philadelphia, PA, USA; ³University of Pennsylvania, Perelman School of Medicine, Philadelphia, PA, USA; ⁴University of Pennsylvania, Philadelphia, PA, USA; ⁵New York University, New York, NY, USA; ⁶Memorial Sloan Kettering Cancer Center, New York, NY, USA

Background Despite the success of immune checkpoint blockade (ICB), many patients still fail to achieve durable clinical benefit. Previous studies have shown that CD8 T cells are reinvigorated by ICB. However, not all patients with this immunological response experience an effective clinical response, suggesting additional parameters may be relevant. DNA damage and repair (DDR) has been extensively studied in the context of inducing cell death of highly-proliferating tumor cells. However, whether T cell-intrinsic DDR impacts T cell differentiation and function, and how the coordination of DDR affects immunological and clinical response to proliferation-inducing ICBs have been largely unexplored. We hypothesized that the T cell-intrinsic DDR responses to proliferative and genotoxic stress might contribute to the disparity between immunological and clinical response.

Methods To understand the impact of cell-intrinsic DDR on T cell differentiation and responses to cancer therapies, we developed a novel high-dimensional cytometry platform. This DDR-Immune platform enables simultaneous analysis of T cell differentiation state and multiple DDR pathways at single cell resolution. We then investigated immune reinvigoration and its association with DDR, in a cohort of chemotherapy-resistant hypermutated or microsatellite instability-high (MSI-H) uterine cancer patients treated with nivolumab. Peripheral blood samples were examined every 2–4 weeks after initiating anti-PD-1 treatment (N = 21).

Results The DDR-Immune platform revealed consistent T cell subset specific patterns of DDR, as well as specific DDR pathways induced by different types of DNA damage, such as γ -irradiation (IR), UV irradiation (UV) or proliferative stress (i.e. anti-CD3/CD28 stimulation). For example, terminally differentiated effector cells had higher DNA damage accumulation and cell death. In contrast, stem cell memory (TSCM) and regulatory T cells (Treg) displayed high DDR with less cell death, suggesting better cell-intrinsic DDR against genotoxic stress for survival advantage. In hypermutated MSI-H uterine cancer patients, CD8 T cells underwent rapid pharmacodynamic proliferation 2–4 weeks after starting PD-1 blockade, which did not correlate with clinical response. Application of the DDR-Immune platform to this cohort revealed, however, that in clinical responders but not clinical non-responders, Ki67+ CD8 T cells responding to PD-1 blockade had rapid induction of DDR represented as a spike increase of phosphorylated-ATM, presumably adapting T cell 'fitness' in response to proliferative stress induced by PD-1 blockade.

Conclusions Collectively, the new platform reveals previously unrecognized roles for T cell-intrinsic DDR as a novel determinant of immune responsiveness and clinical outcome to ICB and have potential application to other cancer therapies including chemotherapy and radiotherapy.

Ethics Approval The study was approved by MSKCC Ethics Board, approval number 17–180 (NCT03241745).

312

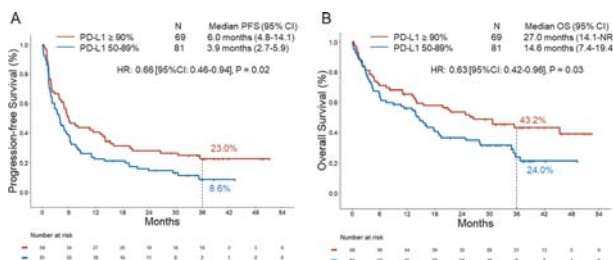
THREE-YEAR OUTCOMES WITH FIRST-LINE PEMBROLIZUMAB FOR METASTATIC NON-SMALL-CELL LUNG CANCER (NSCLC) WITH A VERY HIGH PD-L1 TUMOR PROPORTION SCORE (TPS) $\geq 90\%$

¹Biagio Ricciuti*, ¹Joao Victor Alessi, ¹Stephanie Alden, ¹Giuseppe Lamberti, ¹Victor Vaz, ¹Adriana Barricello, ²Lynette Sholl, ¹Mark Awad. ¹Dana-Farber Cancer Institute, Boston, MA, USA; ²Brigham and Women's Hospital, Boston, MA, USA

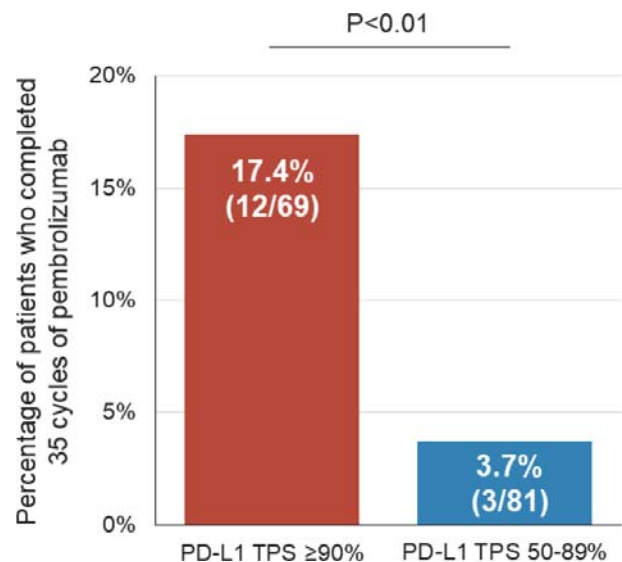
Background Although 1st-line PD-1 monotherapy has improved survival in patients with advanced NSCLC and a PD-L1 TPS $\geq 50\%$, responses occur in $\sim 45\%$ of patients. We have previously shown that among patients with NSCLC and PD-L1 expression of $\geq 50\%$ treated with 1st-line pembrolizumab, clinical outcomes are significantly improved in those with a PD-L1 TPS of $\geq 90\%$.¹ Here, we report the 3-year follow-up outcomes to 1st-line pembrolizumab in patients with a PD-L1 TPS $\geq 90\%$ vs $< 50-89\%$, and genomic differences between these groups.

Methods Patients with stage IV EGFR/ALK wild type NSCLC and PD-L1 TPS $\geq 50\%$ who received 1st-line pembrolizumab monotherapy at Dana-Farber Cancer Institute were included. Comprehensive tumor genomic profiling was performed to examine genomic correlates of a very high PD-L1 expression on an expanded cohort of NSCLC samples.

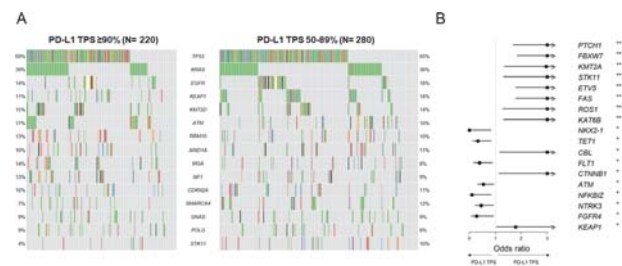
Results Among 150 patients included, median age was 69 (range: 46–92), 55.3% were women, 91.9% were current smokers, and 34.0% had a KRAS mutation. At a median follow-up of 38.5 months, median progression-free (mPFS) and overall survival (mOS) in the entire cohort were 4.8 months, and 20.0 months, respectively. When compared to patients with a PD-L1 expression of 50–89% (N=81), those with PD-L1 TPS $\geq 90\%$ (N=69) had a significantly longer mPFS (6.0 vs 3.9 months, HR 0.66, P=0.02), and longer mOS (27.0 vs 14.6 months, HR 0.63, P=0.03; figure 1). Kaplan-Meier estimates of the 3-year PFS and OS were 23.0% and 43.2% in the PD-L1 TPS $\geq 90\%$ groups, and 8.6% and 24.0% in the PD-L1 TPS 50–89% group, respectively. A PD-L1 TPS $\geq 90\%$ was confirmed to be an independent predictor of improved PFS (HR 0.58, P=0.02) and OS (HR 0.57, P=0.01) at multivariable analysis. Patients whose tumors had a PD-L1 TPS $\geq 90\%$ were also significantly more likely to complete 35 cycles of therapy compared to those with PD-L1 TPS of 50–89% (17.4% vs 3.7%, P<0.01, figure 2). Tumor genomic profiling from 500 NSCLC samples revealed that mutations in STK11, KEAP1, FBXW7, and CTNNB1, which have been previously correlated with immunotherapy resistance, were significantly enriched tumors with a PD-L1 TPS of 50–89% compared to those with a PD-L1 TPS $\geq 90\%$ (figure 3).



Abstract 312 Figure 1 (A) Progression-free and (B) overall survival to 1st line pembrolizumab among patients with PD-L1 TPS $\geq 90\%$ vs 50–89%, at a 3-year follow-up.



Abstract 312 Figure 2 Barplot showing the percentage of patients who completed 35 cycles of pembrolizumab monotherapy in the PD-L1 TPS $\geq 90\%$ and 50–89% groups



Abstract 312 Figure 3 (A) Oncoprint plot showing the top 15 genes mutated in NSCLC with PD-L1 TPS $\geq 90\%$ and 50–89%. (B) Gene mutation enrichment analysis showing differentially mutated genes between NSCLCs with PD-L1 TPS $\geq 90\%$ and 50–89%. ** Adjusted P value <0.01; * Adjusted P value <0.05.

Conclusions Pembrolizumab monotherapy continues to demonstrate a meaningful long-term survival benefit at a 3-year follow-up in patients with advanced NSCLC and a PD-L1 TPS $\geq 90\%$ vs 50–89%. NSCLCs with very high PD-L1 TPS have a more favorable genomic profile. These findings have implications for treatment selection and for clinical trial interpretation and design.

REFERENCE

1. Aguilar EJ, Ricciuti B, Gainor JF, et al. Outcomes to first-line pembrolizumab in patients with non-small-cell lung cancer and very high PD-L1 expression. *Ann Oncol* 2019 October 1;30(10):1653–1659

<http://dx.doi.org/10.1136/jitc-2021-SITC2021.312>

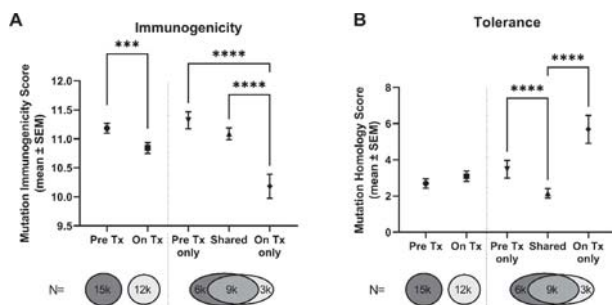
313 STEALTHIER MUTANOMES ARE INDUCED AFTER NIVOLUMAB IMMUNOTHERAPY

¹Guilhem Richard*, ¹Michael Princiotta, ²Gary Steinberg, ³William Martin, ³Anne de Groot. ¹EpiVax Therapeutics, Inc., Providence, RI, USA; ²NYU Langone Health, Chicago, NY, USA; ³EpiVax, Inc., Providence, RI, USA

Background As tumor genomes are shaped by their interaction with the immune system, a phenomenon known as immunoeediting, it is critical to understand how immunotherapies impact this process. Checkpoint inhibitors directly influence T cells responding to neoantigens, as such, these therapies drastically affect the genomes of surviving tumor clones. Similar to the concept of immune camouflage, observed in infectious diseases, where genomes of pathogens evolve in a way to avoid immune detection, we hypothesized that tumor clones surviving checkpoint inhibition therapy harbor mutations more prone to immune avoidance.

Methods We analyzed a cohort of nivolumab-treated melanoma patients (n=41) for which tumor samples were collected from the same site prior ("Pre" samples) and during ("On" samples) nivolumab therapy.¹ The immunogenic and tolerance potential of mutations from the Pre and On samples were evaluated with the Ancer neoantigen screening platform,² which includes the EpiMatrix algorithm to identify HLA-I and HLA-II neoepitopes and the JanusMatrix algorithm to evaluate neoepitopes homology with self. Prior work with JanusMatrix showed epitopes highly homologous to self can be inhibitory.³ Matching Pre and On therapy samples were compared to identify mutations deleted (unique to the Pre samples), maintained (found in both the Pre and On samples), and induced while on therapy (unique to the On samples).

Results Mutations from the On therapy samples had a lower immunogenic potential than mutations found in the Pre therapy samples (figure 1A, Mann-Whitney test, p=0.0001). After further distinguishing mutations deleted, maintained, and induced while on therapy, we observed that newly induced mutations had a significantly lower immunogenic potential compared to other mutations (Kruskal-Wallis test, p<0.0001). In addition, newly induced mutations were more homologous to self than other mutations (figure 1B, Kruskal-Wallis test, p<0.0001), indicating a greater likelihood for these new mutations to be tolerated by the immune system. In summary, we showed that mutations generated after nivolumab therapy are less immunogenic and more tolerated than mutations found prior to therapy.



Abstract 313 Figure 1 Immunogenicity (A) and tolerance (B) potentials of mutations found in matching melanoma tumor samples collected before (Pre) and during (On) nivolumab therapy.

Conclusions Our Ancer analysis suggests that nivolumab therapy affects the immunogenicity and tolerance profiles of newly generated mutations in a manner that is consistent with the concepts of immunoeediting and immune camouflaging. Mutations induced after therapy appear less immunogenic and more self-like, illustrating a potential mechanism tumors employ to avoid immune surveillance. Furthermore, our approach highlights in silico tools can distinguish effector from tolerance inducing neoepitopes, a critical feature for designing novel neoantigen-based precision immunotherapies.

REFERENCES

- 1.. Riaz N, Havel JJ, Makarov V, *et al.* Tumor and microenvironment evolution during immunotherapy with nivolumab. *Cell* 2017 November 2;**171**(4):934–949.
- 2.. Richard G, De Groot AS, Steinberg GD, *et al.* Multi-step screening of neoantigens' HLA- and TCR-interfaces improves prediction of survival. *Sci Rep* 2021 May 11;**11**(1):9983.
- 3.. De Groot AS, Rosenberg AS, Miah SMS, *et al.* Identification of a potent regulatory T cell epitope in factor V that modulates CD4+ and CD8+ memory T cell responses. *Clin Immunol* 2021 Mar;**224**:108661

<http://dx.doi.org/10.1136/jitc-2021-SITC2021.313>

NKG2A AND HLA-E DEFINE A NOVEL ALTERNATIVE IMMUNE CHECKPOINT AXIS IN BLADDER CANCER

¹Berengere Salome*, ¹John Sfakianos, ¹Andrew Charap, ¹Adam Farkas, ¹Daniel Geanon, ¹Geoffrey Kelly, ¹Ronaldo de Real, ¹Brian Lee, ¹Kristin Beaumont, ¹Sanjana Shroff, ¹Ying-Chih Wang, ¹Yuan-Shuo Wang, ¹Li Wang, ¹Robert Sebra, ¹Alice Kamphorst, ²Karl-Johan Malmberg, ³Emanuela Marcenaro, ⁴Pedro Romero, ¹Rachel Brody, ⁵Yuko Yuki, ⁵Maureen Martin, ⁵Mary Carrington, ¹Reza Mehrazin, ¹Peter Wiklund, ¹Jun Zhu, ¹Matthew Galsky, ¹Nina Bhardwaj, ¹Amir Horowitz. ¹Icahn School of Medicine at Mount Sinai, New York, NY, USA; ²University of Oslo, Oslo, Norway; ³Department of Experimental Medicine, Geno, Italy; ⁴Department of Oncology UNIL CHUV, Epalinges, Switzerland; ⁵Frederick National Laboratory for Cancer Research, Frederick, MD, USA

Background Bladder cancer is characterized by a poor prognosis, with muscle-invasive cases harboring a 34–76% 10-year recurrence-free survival rate.¹ Neoadjuvant PD-1/PD-L1 blockade strategies have recently been approved by the US Food and Drug Administration for bladder cancer treatment, yet only achieving a complete response rate of 31–37%, thereby suggesting additional mechanisms of resistance.² HLA-E is a known inhibitor of NKG2A+ CD8 T cells and NK cell responses. A monoclonal antibody binding to the NKG2A receptor has been developed and proven to restore CD8 T cell and NK cell responses in head and neck cancer, with ongoing clinical trials across multiple tumor indications.^{3–4} We evaluated the potential role of the HLA-E/NKG2A inhibitory pathway in modulating T cell immunity in bladder cancer.

Methods CyTOF was performed on CD8+ T cells from fresh bladder tumors (n=6), as well as on expanded CD8+ T cells from bladder-draining lymph nodes (n=11) and tumors (n=8). Flow cytometry (n=25) and single-cell RNA-sequencing (scRNAseq) (n=13) were performed on cells from fresh bladder tumors.

Results Mechanisms of tumor escape from CD8+ T cell recognition include impairment of antigen presentation. Accordingly, we found a significant reduction of HLA class I expression on tumors. However, expression of DNAM-1-activating ligands (e.g. CD112, CD155) on bladder tumors was retained, indicating a possible role for TCR-independent activation pathways traditionally ascribed to natural killer (NK) cells. Using mass cytometry and scRNAseq, we observed that acquisition of NKG2A on tumor-derived PD-1+ CD8+ T cells promotes tissue-resident memory features alongside diminished CD28 expression and significantly weaker sensitivity to CD3/CD28-signaling. However, NKG2A+ CD8 T cells possess a proliferative advantage with enhanced expression of DNAM-1 and cytolytic machinery. Strikingly, we found that NKG2A+ PD-1+ CD8 T cells are strongly activated in response to HLA class I-deficient tumors compared to their NKG2A- PD-1+ CD8 T cell counterparts. TCR-independent NK-like function by NKG2A+ CD8 T cell is partly mediated by the DNAM-1 pathway and inhibited by HLA-E. NKG2A+ CD8 T cell functions are restored upon NKG2A blockade, where efficiency positively correlates with HLA-E expression on bladder tumors.

Conclusions Collectively, our data indicate that NKG2A+ CD8 T cells display a strong capacity for TCR-independent activation that enables them to circumvent bladder tumor evasion mechanisms. NKG2A+ CD8 T cells lack expression of CD28 suggesting a lower susceptibility to PD-1-mediated inhibition. Our data suggest a need for thorough reappraisal of current protocols that assess CD8 T cell exhaustion and for strategies to restore their antitumor functions.

REFERENCES

- 1.. Sanli O, Dobruch J, Knowles MA, Burger M, Alemezaffar M, Nielsen ME, Lotan Y. Bladder cancer. *Nat Rev Dis Primers* 2017 April 13;**3**:17022. doi: 10.1038/nrdp.2017.22. PMID: 28406148.
- 2.. Rouanne M, Bajorin DF, Hannan R, Galsky MD, Williams SB, Necchi A, Sharma P, Powles T. Rationale and outcomes for neoadjuvant immunotherapy in urothelial carcinoma of the bladder. *Eur Urol Oncol* 2020 December;**3**(6):728–738. doi: 10.1016/j.euo.2020.06.009. Epub 2020 Nov 8. PMID: 33177001.
- 3.. André P, Denis C, Soulas C, Bourbon-Caillet C, Lopez J, Arnoux T, Bléry M, Bonnafous C, Gauthier L, Morel A, Rossi B, Remark R, Bresó V, Bonnet E, Habif G, Guia S, Lalanne AI, Hoffmann C, Lantz O, Fayette J, Boyer-Chammard A, Zerbib R, Dodion P, Ghadially H, Jure-Kunkel M, Morel Y, Herbst R, Narni-Mancinelli E, Cohen RB, Vivier E. Anti-NKG2A mAb is a checkpoint inhibitor that promotes anti-tumor immunity by unleashing both T and NK Cells. *Cell* 2018 December 13;**175**(7):1731–1743.e13. doi: 10.1016/j.cell.2018.10.014. Epub 2018 Nov 29. PMID: 30503213; PMCID: PMC6292840.
- 4.. van Hall T, André P, Horowitz A, Ruan DF, Borst L, Zerbib R, Narni-Mancinelli E, van der Burg SH, Vivier E. Monalizumab: inhibiting the novel immune checkpoint NKG2A. *J Immunother Cancer* 2019 October 17;**7**(1):263. doi: 10.1186/s40425-019-0761-3. PMID: 31623687; PMCID: PMC6798508.

<http://dx.doi.org/10.1136/jitc-2021-SITC2021.314>

315

APPLICATION OF THE SITC IMMUNOTHERAPY RESISTANCE TASKFORCE DEFINITIONS OF ANTI-PD-1 RESISTANCE TO STUDIES EVALUATING PATIENTS WITH ADVANCED MELANOMA

¹Irene Shui*, ¹Emilie Scherrer, ²Andrew Frederickson, ³Eric Druyts, ⁴Hussein Tawbi. ¹Merck and Co., Inc., Kenilworth, NJ, USA; ²PRECISIONheor, New York, NY, USA; ³Pharmalytics Group, Vancouver, Canada; ⁴MD Anderson Cancer Center, Houston, TX, USA

Background Until the recent 2020 publication by the Society for Immunotherapy of Cancer (SITC) Immunotherapy Resistance Taskforce, there was little consensus on defining primary and secondary resistance to anti-programmed cell death protein 1 monotherapy. Our objective was to characterize the clinical outcomes reported in peer-reviewed literature when categorized according to the SITC definitions.

Methods A systematic literature review (SLR) was conducted in Medical Literature Analysis and Retrieval System Online, Excerpta Medica database, and Cochrane Central Register of Controlled Trials (September 2015 - September 2020). Data were extracted on the proportion of patients with progressive disease (PD), and SITC criteria were applied to define resistance (table 1).

Results Thirty six studies were included, yielding 55 patient cohorts with data on PD; 42 cohorts reported PD specifically by best overall response, while 13 cohorts provided another definition of response. Response evaluation criteria in solid tumors (RECIST) 1.1 was most commonly used (37 cohorts), followed by immune-RECIST (7 cohorts). Twenty four cohorts reporting PD also had data on length of drug exposure, 13 on duration of response, 22 on utilization of a confirmatory scan, and 1 on whether progression occurred within 12 weeks of the last dose of therapy; no studies reported on all 4 criteria. We were able to partially apply SITC criteria for primary resistance to 42 of 55 cohorts and the proportion of patients with primary resistance ranged from 25% to 81%. Only a few studies had data on secondary resistance, but none provided enough granularity to fully categorize secondary resistance by SITC.

Abstract 315 Table 1 SITC definitions of primary and secondary resistance in advanced disease

Resistance Type	Drug exposure	Best response*	Confirmatory scan**	Progressed on treatment or ≤12 weeks of last dose
Primary	≥6 weeks	PD; SD for <6 m***	Y	Yes
Secondary	≥6 months	CR, PR, SD for >6 m	Y	Yes

*By RECIST1.1

**≥4 weeks after disease progression unless rapid clinical deterioration

***CR/PR for <6 months also considered primary resistance

Conclusions The majority of studies in this SLR did not report complete criteria to apply the SITC definitions; however, partial categorization of primary resistance was possible. The patient characteristics and outcomes reported varied, thus the data assessed were heterogeneous. Future studies should consider utilizing the SITC consensus definitions to harmonize how resistance is classified and facilitate meaningful context for clinical activity.

<http://dx.doi.org/10.1136/jitc-2021-SITC2021.315>

LEUCINE-RICH REPEATS AND IMMUNOGLOBULIN-LIKE DOMAINS PROTEIN 1 IS HIGHLY EXPRESSED ON TUMOR-INFILTRATING T CELLS AND MAY PLAY A ROLE IN MODULATING T CELL ACTIVATION

Li Wang, Timothy Chan, Cassandra Gilmour, Keman Zhang, Tyler Alban, Hieu Ta*, Hieu Ta.
Cleveland Clinic, Cleveland, OH, USA

Background Immune checkpoint receptors (ICRs) regulate T cell-mediated immune responses to self - and neo-antigens, thereby play an important role in the development of autoimmunity and immune responses to infections. In cancer, ICRs such as PD-1 and CTLA4 impair immuno-surveillance against neoplastic cells, while other costimulatory molecules like ICOS, OX40 could augment the immune responses. Immunotherapy that targets either inhibitory or costimulatory immune checkpoint have become the breakthrough therapy for cancer treatment. However, the efficacy of this class of therapy is limited to a fraction of patients, pointing the need to overcome non-redundant immuno-inhibitory pathways or discover new immuno-costimulatory pathways.

Methods Examining surface proteins that are highly expressed in various mouse tumors by flow cytometry and immunohistochemistry

Results This study identified the expression of Leucine-rich repeats and immunoglobulin-like domains protein 1 (LRIG1) in activated CD4+ and CD8+ T cells. LRIG1 is a type-I transmembrane protein with 1092 amino acids (120 kD) and ubiquitous tissue expression patterns. We show that LRIG1 expression is not detectable on naïve CD4+ and CD8+ murine T cells but is induced upon T cell receptor (TCR) stimulation in vitro, and in tumor-infiltrating lymphocytes (TILs) from multiple murine models. We also detected LRIG1 expression on CD4+ and CD8+ TILs in several types of cancer patients such as non-small-cell lung cancer, breast cancer, melanoma, B cell lymphoma.

Conclusions LRIG1 was originally identified as a tumor suppressor gene in a variety of tissues, but its expression and function have not been explored in immune cells. Our data suggest that LRIG1 is highly expressed in TILs in multiple cancer types and might play a role in regulating the anti-tumor immune response

Ethics Approval Our studies have been approved by the ethics committee of the Cleveland Clinic.

Consent Written informed consent was obtained from the patient for publication of this abstract and any accompanying images. A copy of the written consent is available for review by the Editor of this journal.

<http://dx.doi.org/10.1136/jitc-2021-SITC2021.316>

317

AN IMMUNOSUPPRESSIVE TUMOR POPULATION DRIVES GLOBAL AND REGIONAL PATTERNS OF IMMUNE INFILTRATION IN HETEROGENEOUS TUMORS

Miho Tanaka*, Lotus Lum, Kenneth Ng, Zoe Adams, Daphne Superville, Melissa Reeves.
University of California, San Francisco, San Francisco, CA, USA

Background Intratumoral heterogeneity (ITH) is cellular and molecular diversity within a tumor. ITH is linked to failure of immunotherapy in multiple cancer types. One of the suggested mechanisms of this failure is the absence of a productive immune response, which can be driven by the dominance of a tumor population that creates immunosuppressive microenvironment. However, the molecular mechanisms that mediate such dominant immunosuppressive effects and how a dominant immunosuppressive tumor population affects the efficacy of immune checkpoint blockade (ICB) therapy are poorly understood.

Methods We generated a library of squamous skin cell carcinoma cell lines derived from DMBA+TPA carcinogen-treated mice. Upon transplantation into immunocompetent mice, two cell lines (CF6 and CF9) gave rise to highly and poorly immune-infiltrated tumors, respectively. These two cell lines were tagged with YFP and RFP, respectively, mixed at a 1:1 ratio and injected subcutaneously. The resulting mixed tumors contained a patchwork of distinct regions that are predominantly occupied with YFP (CF6) cells, occupied with RFP (CF9) cells, or are a mixture of YFP and RFP cells. These mixed tumors were microdissected into YFP, RFP, and mixed regions, and the immune infiltrate in each region was analyzed by flow cytometry.

Results We found mixed tumors were "cold" on a whole-tumor level. However, regional analysis showed a higher frequency of total and CD4 T cells in YFP regions compared to RFP regions. In contrast, macrophages exhibited a preferential localization to RFP regions. This suggests that local factors unique to each region drive the immune infiltration patterns of CD4 T cells and macrophages. Interestingly, although CD8 T cells showed a low frequency in all regions, a majority of CD8 T cells from YFP regions produced IFN γ in response to PMA/Ionomycin stimulation while IFN γ +CD8 T cells from RFP regions made up a small fraction. This suggests that the presence of CF9-RFP regions inhibits infiltration of CD8 T cells throughout the tumor, but may not affect the anti-tumoral potential of CD8 T cells that succeed in infiltrating CF6-YFP regions.

Conclusions An immunosuppressive tumor population rendered our model heterogeneous tumors "cold" on the whole. Nonetheless, we observed regional patterns in the quantity and quality of immune infiltrates, with local immune infiltration being shaped by the tumor cells present in that region. Understanding how these immune infiltration patterns impact the response of each region to ICB therapy will provide insights into the mechanism by which ITH poses barriers to immunotherapy.

<http://dx.doi.org/10.1136/jitc-2021-SITC2021.317>

318 ENFORCED TUMOR SPECIFIC MHC-I HETEROGENEITY IN TRIPLE NEGATIVE BREAST CANCER DRIVES IMMUNOTHERAPY RESISTANCE

¹Brandie Taylor*, ²Justin Balko, ²Melinda Sanders, ²Paula Gonzalez-Ericsson, ²Violeta Sanchez. ¹Vanderbilt University, Nashville, TN, USA; ²Vanderbilt University Medical Center, Nashville, TN, USA

Background Despite the broad success of immune checkpoint inhibition (ICI e.g. anti-Programmed Death Ligand-1 [PD-L1]) in cancer treatment, tumor-intrinsic factors leading to intrinsic and acquired resistance are poorly understood. Tumor specific MHC-I expression is indispensable for anti-PD-1/L1 response as complete loss of MHC-I via B2M deletion results in inability of CD8+ T cells to recognize tumor-associated antigens. However, MHC-I is heterogeneously downregulated or lost in many tumor types. Tumor cell destruction can also occur through non-synaptic mechanisms, in a so-called 'field effect'. Therefore, we modeled heterogeneous loss of MHC-I expression in breast cancer and experimentally evaluated how heterogeneous MHC-I loss affects response to anti-PD-L1 therapy.

Methods We performed quantitative immunofluorescence for MHC-I and Pan-CK on breast cancer tumors (n=410). To determine the functional effect of MHC-I heterogeneity on anti-PD-L1 response, we used an immunocompetent EMT6 orthotopic mammary tumor model which ubiquitously expresses MHC-I at baseline. Using CRISPR/Cas9, we engineered EMT6 cells with B2m loci excision resulting in complete knockout of MHC-I on the cell surface. We then orthotopically implanted B2m-comtetent and B2m-KO cells at varying inoculum ratios (100:0, 90:10, 50:50, 10:90, 0:100) into syngeneic Balb/C mice and assessed immune responsiveness and efficacy of checkpoint inhibition. Additionally, to look at how loss of MHC-I affects the tumor microenvironment we will use the PanCancer Immune NanoString panel (n=770 genes) to evaluate gene expression patterns in tumor cells and infiltrating immune cells.

Results In patient samples, we identified high diversity in MHC-I expression across all clinical subtypes, with triple negative breast cancer (TNBC) having the highest MHC-I expression. Chemotherapy-treated tumors had higher MHC-I levels than untreated tumors. In mice when 10% of cells were B2m-KO, we observed a 50% reduction in complete eradication of EMT6 tumors with aPD-L1 treatment and reduced disease-stabilization and no complete responses when a 50% mixture of MHC-I deficient cells. An increasing percentage of B2m KO leads to worse outcomes overall and a decrease in infiltrating T cells.

Conclusions Our work suggests that there is an ICI-responsive phenotype that is driven by heterogeneity in MHC-I expression levels. As little as 10% of tumor specific MHC-I loss can lead to therapeutic resistance and a decrease in complete responders. This represents that early TNBC may be less responsive to single-agent PD-L1 due to specific percentages of MHC-I loss. MHC-I expression can influence therapy outcomes and potentially lead to novel observations of how to overcome lack of, or limited, MHC-I expression.

<http://dx.doi.org/10.1136/jitc-2021-SITC2021.318>

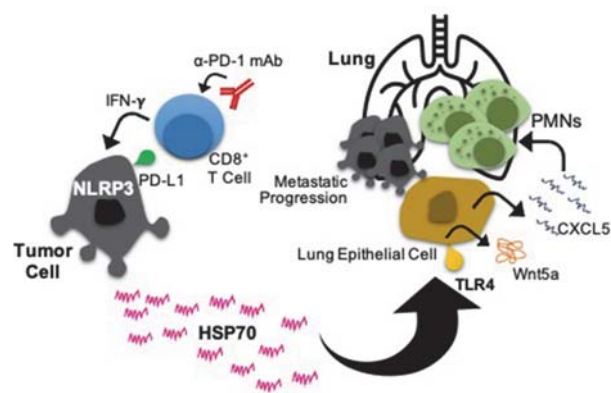
319 THE TUMOR-INTRINSIC NLRP3 INFLAMMASOME ESTABLISHES A PULMONARY METASTATIC NICHE VIA TYPE II EPITHELIAL HSP70/TLR4 SIGNALING AND FACILITATES DISEASE HYPERPROGRESSION IN RESPONSE TO IMMUNOTHERAPY

Balamayooran Theivanthiran*, Fang Liu, Nicholas DeVito, Michael Plebanek, Brent Hanks. Duke University, Durham, NC, USA

Background Our understanding of those underlying mechanisms that contribute to metastatic progression in melanoma remains limited. While uncommon, melanoma hyperprogression in response to immunotherapy is likely to be an extreme form of acquired resistance. Therefore, studies that define the underlying mechanisms of these processes are expected to provide insight into the discovery of novel therapeutic targets and predictive biomarkers. We previously demonstrated that tumor-intrinsic NLRP3 drives adaptive resistance to anti-PD-1 immunotherapy (anti-PD-1) by inducing the recruitment of polymorphonuclear myeloid-derived suppressor cells (PMN-MDSCs) via the upregulation of CXCL5. Gain-of-function polymorphisms in the TLR4 gene have been associated with pulmonary metastases in melanoma patients. We have shown HSP70 to promote PMN-MDSC chemotaxis via the stimulation of TLR4 signaling. As a result, we hypothesized that the tumor NLRP3 inflammasome may also contribute to distant metastatic progression and disease hyperprogression during immunotherapy by establishing a long-distance signaling axis mediated by HSP70-TLR4 signaling in the lung.

Methods We pharmacologically and genetically inhibited the NLRP3 inflammasome and HSP70 in a transgenic BRAFV600E mouse model to examine their role in distant metastatic progression before and during anti-PD-1. An inducible type II pulmonary epithelial cell-specific TLR4 knock-out mouse model was engineered to examine the role of distant HSP70-TLR4 signaling in the recruitment of PMN-MDSCs and subsequent metastatic progression to the lung. Plasma HSP70 levels were monitored in melanoma patients undergoing anti-PD-1

Results Anti-PD-1 significantly increases CXCL2/CXCL5 expression and PMN-MDSC accumulation in the lungs of the transgenic BRAFV600E model. This effect is reversed by 1) tumor-targeted ablation and pharmacologic inhibition of NLRP3 but not systemic host knock-out of NLRP3, 2) Pharmacologic Wnt5a ligand inhibition, 3) tumor-specific ablation and inhibition of HSP70. Inducible knock-out of TLR4 in type II epithelial cells suppressed Wnt5a and CXCL5 expression and inhibited the recruitment of PMN-MDSCs to the lung in response to anti-PD-1. Tumor-specific inhibition of NLRP3/HSP70 and lung-specific ablation of TLR4 suppressed metastatic progression following anti-PD-1 in the BRAFV600E melanoma model. Combination anti-PD-1 and NLRP3 inhibition suppressed primary melanoma progression and distant melanoma metastases versus anti-PD-1 monotherapy. Elevated plasma levels of HSP70 were associated with disease hyperprogression in metastatic melanoma patients undergoing anti-PD-1



Abstract 319 Figure 1 Tumor-intrinsic NLRP3 inflammasome and metastasis

Conclusions Together, these results describe a novel cross-talk mechanism between the primary tumor and the lung that mediates distant metastatic progression that is accentuated following anti-PD-1 (figure 1). Future clinical studies are needed to evaluate the pharmacologic inhibition of this tumor-lung NLRP3/HSP70/TLR4/Wnt5a/CXCL5 axis on melanoma metastasis and disease hyperprogression during checkpoint inhibitor immunotherapy

<http://dx.doi.org/10.1136/jitc-2021-SITC2021.319>

320

TUMOR CELL-INTRINSIC SIGNALING MEDIATES T CELL EXCLUSION AND PROMOTES RESISTANCE TO CHECKPOINT BLOCKADE THERAPY IN NON-SMALL CELL LUNG CANCER

Elen Torres-Mejia*, Kim Nguyen, Ellen Duong, Stefani Spranger. *MIT, Cambridge, MA, USA*

Background Lung cancer is the leading cause of cancer-related death worldwide.¹ Immunotherapies such as checkpoint blockade therapy (CBT) can be an effective approach to treat patients with metastatic tumors. However, only a fraction of patients is responsive to CBT treatments.² Patients with a non-T cell-infiltrated tumor microenvironment correlate with a poor response to CBT and T cell infiltration can be influenced by tumor cell-intrinsic signaling pathways.^{3 4} Therefore, understanding the tumor cell-intrinsic mechanisms affecting anti-tumor immune response will aid us to design better treatments for lung cancer patients. Preliminary work in our group showed that patients with non-small cell lung cancer (NSCLC) can be segregated according to the expression of a T cell gene signature into T cell-infiltrated and non-T cell-infiltrated cohorts. Using an unbiased pathway analysis, we identified that upregulation of specific gene modules significantly correlate with low expression of the T cell gene signature gene (non-T cell-infiltration). In this project, we aim to investigate how the overexpression of one specific pathway in NSCLC cells impacts the anti-tumor immune responses.

Methods We used a lung cancer cell line derived from a KrasG12D/+ and Tp53-/- mouse (KP) to overexpressed our gene of interest (KP-A). Tumors were induced by subcutaneous or orthotopic implantation and were treated with anti-PD-L1 and anti-CTLA-4 blocking antibodies and analyzed for tumor burden. Infiltration of cytotoxic T cells and regulatory T cells were evaluated by fluorescence microscopy. Additionally, we engineered the KP-A and KP cell lines to express the model antigen SIY which allowed us to characterize tumor-specific T cell responses and utilize SIY-reactive TCR-transgenic T cells.

Results We identified that the overexpression of our gene of interest in KP cells impairs the response to CBT mediated by T cell exclusion from the tumor. Analyses of tumor-reactive T cells indicated that T cell activation and differentiation into effector T cells was not affected, however, effector T cells failed to infiltrate KP-A tumors. We are currently investigating the molecular mechanism whereby our gene of interest mediates T cell exclusion.

Conclusions Our results strongly suggest that tumor cell-intrinsic activation of specific pathways in NSCLC promote immune evasion and contribute to immunotherapy resistance. Understanding the molecular and immunological mechanisms mediating T cell exclusion from the lung tumor microenvironment will facilitate the development of novel combination treatment strategies for NSCLC patients.

Acknowledgements This work was supported by a postdoctoral fellowship from the Ludwig Center at MIT's Koch Institute for Integrative Cancer Research

REFERENCES

- 1.. Chen Z, Fillmore CM, Hammerman PS, Kim CF, Wong KK. Non-small-cell lung cancers: a heterogeneous set of diseases. *Nat Rev Cancer* 2014;**14**:535–546.
- 2.. Hellmann MD, Paz-Ares L, Bernabe Caro R, Zurawski B, Kim SW, Carcereny Costa E, Park K, Alexandru A, Lupinacci L, de la Mora Jimenez E, Sakai H, Albert I, Vergnenegre A, Peters S, Syrigos K, Barlesi F, Reck M, Borghaei H, Brahmer JR, O'Byrne KJ, Geese WJ, Bhagavatheswaran P, Rabindran SK, Kasinathan RS, Nathan FE, Ramalingam SS. Nivolumab plus ipilimumab in advanced non-small-cell lung cancer. *N Engl J Med* 2019;**381**:2020–2031.

- 3.. Chen DS, Mellman I. Elements of cancer immunity and the cancer-immune set point. *Nature* 2017;**541**:321–330.
- 4.. Nguyen KB, Spranger S. Modulation of the immune microenvironment by tumor-intrinsic oncogenic signaling. *J Cell Biol* 2020;**219**.

Ethics Approval All mouse experiments in this study were approved by MIT's Committee on Animal Care (CAC) - DHHS Animal Welfare Assurance # D16-00078

<http://dx.doi.org/10.1136/jitc-2021-SITC2021.320>

321 PD-L1 CHECKPOINT BLOCKADE ERADICATES RESIDUAL LEUKEMIA IN A MOUSE MODEL OF ACUTE LYMPHOBLASTIC LEUKEMIA BY COUNTERING EXHAUSTION OF CYTOTOXIC AND EFFECTOR CD4+ T-CELLS

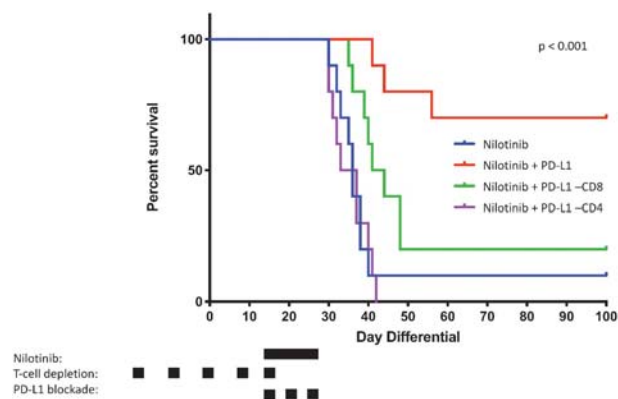
¹Sean Tracy*, ¹Hrishi Venkatesh, ¹Lynn Heltemes-Harris, ¹Gregory Hubbard, ²Can Hekim, ¹Michael Farrar. ¹University of Minnesota, Minneapolis, MN, USA; ²Orion Pharma, Espoo, Finland

Background Phenotypic exhaustion of CD4+ T-cells is a strong negative prognostic factor in acute lymphoblastic leukemia (ALL).¹⁻³ Despite this, PD1/PD-L1 immune checkpoint therapy has shown little activity in this disease setting to date. Factors influencing the responsiveness of the T-cell compartment to checkpoint blockade are unknown.

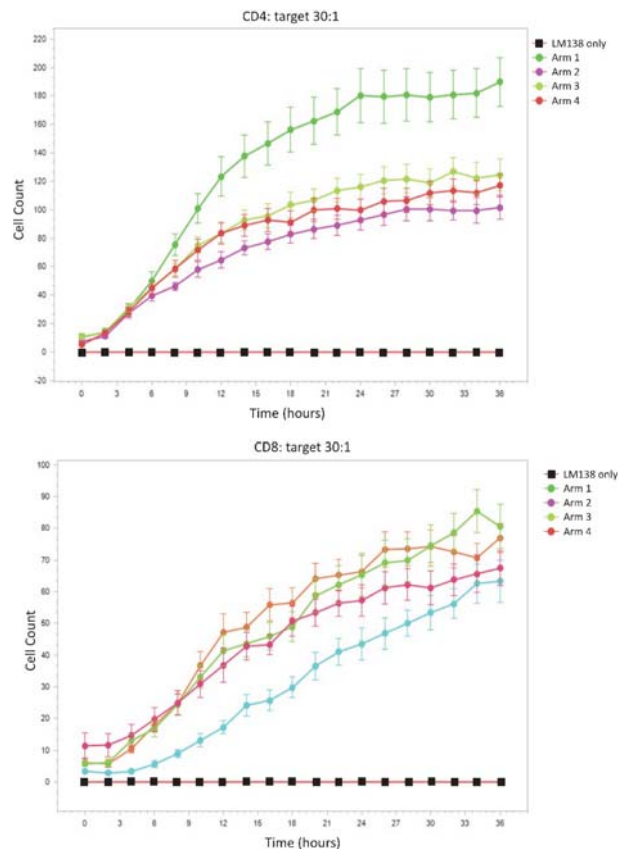
Methods An established murine model of BCR-ABL+ ALL was used. Leukemia was established by tail vein injection, and mice were treated with the BCR-ABL tyrosine kinase inhibitor nilotinib with or without PD-L1 mAb therapy. scRNAseq/TCRseq was performed using multiple treatment groups.

Results Treatment of leukemia-bearing mice with a combination of the BCR-ABL tyrosine kinase inhibitor nilotinib and PD-L1 immune checkpoint blockade led to eradication of leukemia in 70% of treated mice (figure 1). Efficacy was dependent on the presence of CD4+ T-cells, while CD8+ T-cells appeared to play a lesser role. Direct cytotoxicity by CD4+ T-cells was confirmed in live cell-killing assays (figure 2). Mice that were treated with PD-L1 blockade and survived to day 100 were found to have no detectable residual leukemia. They were also protected from leukemia rechallenge, suggesting the elicitation of a memory response. scRNAseq analysis revealed that CD44^{hi} CD4+ T-cells were highly heterogeneous, with regulatory, effector, and stem-like TCF7+ precursor subsets present (figures 3-4). A unique population of CD4+ T-cells was elicited by live leukemia challenge (clusters 6 and 7 in figure 3) but not by vaccination with heat-killed leukemia cells. This subset was characterized by relatively low levels of expression of TCF7, but high levels of expression of Granzyme B, TOX, the effector cytokines IFN γ and TNF α , the inhibitory receptors PD1, TIM3, and LAG3, and the chemokine CCL5 (figure 5). PD-L1 checkpoint blockade was associated with early narrowing of the clonality of this population (figure 6), decreased markers of exhaustion, and more robust synthesis of TNF α .

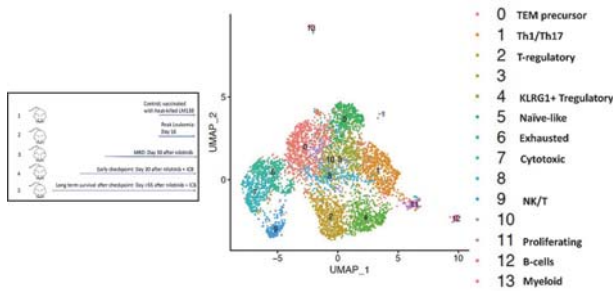
Conclusions PDL1 immune checkpoint blockade is effective at eradicating residual disease in preclinical models of BCR-ABL + ALL. ALL elicits a unique CD4+ memory/effector subset characterized by the potential for both chemotactic and cytotoxic functions. Leukemia induces early exhaustion of this subset, which is countered by PDL1 blockade. Efforts to extend these observations to human specimens are underway and will be reported.



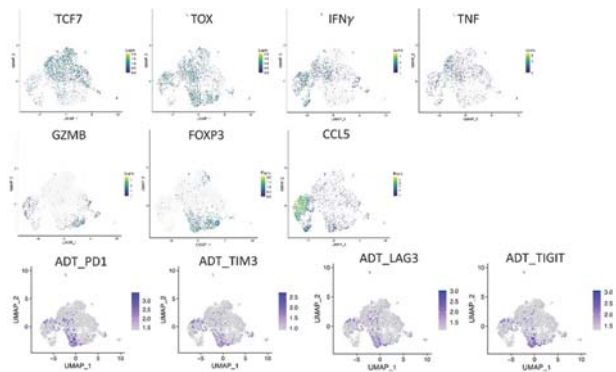
Abstract 321 Figure 1 Survival analysis. BCR-ABL+ ALL was established by tail vein injection on day 0. Nilotinib (75 mg/kg) was administered via oral gavage. mAbs targeting PD-L1 with or without depleting antibodies towards CD4 or CD8 were administered via intraperitoneal injection. p-value derived by log-rank analysis



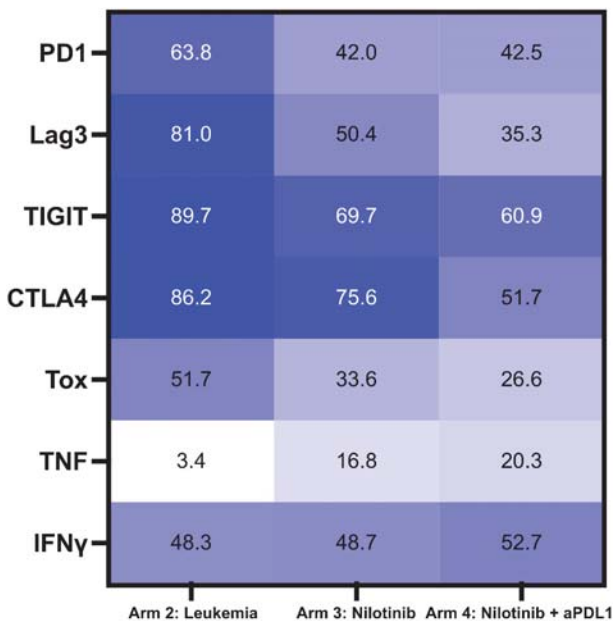
Abstract 321 Figure 2 Analysis of the increase in the number of dead cells (y-axis) over time (x-axis) from a live killing assay (Incucyte) using splenic CD4+ or CD8+ T-cells from experimental arms as treated in figure 3. Control traces from separate wells with LM138 target cells only are included. Experiments were done using Cytotox NIR



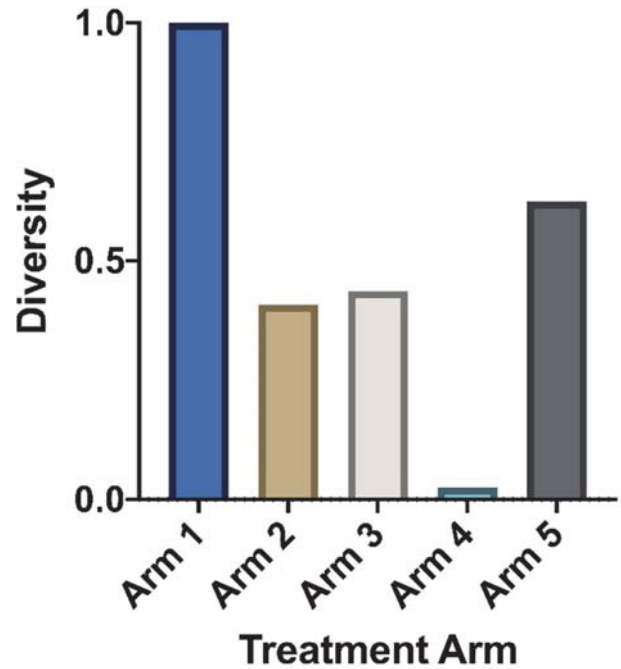
Abstract 321 Figure 3 (Left) Experimental approach. 5 groups (n=4 mice/group) were treated in parallel with the indicated conditions. CD44^{hi} CD4⁺ T-cells from the spleen and bone marrow of mice in each group were labelled with oligo-conjugated hashtag antibodies (Biolegend) and CITE-SEQ antibodies towards PD1, TIM3, LAG3, CD25, and TIGIT, prior to FACS-sorting. scRNAseq/TCRseq analysis (10x Genomics) was performed on 5,349 individual cells after multiplet removal. (Right) UMAP plots of all cells combined. Clusters were identified by differential expression of canonical gene products



Abstract 321 Figure 4 Feature plots demonstrating expression of canonical gene products projected onto the UMAP plot in figure 3. Antibody derived tags (ADTs; bottom row) indicate expression level of surface proteins profiled using CITESEQ antibodies



Abstract 321 Figure 5 Heatmap of select gene product expression levels in exhausted (cluster 6) CD4⁺ T-cells across treatment conditions



Abstract 321 Figure 6 Simpsons diversity index of the TCR repertoire across treatment arms. Lower values indicate relatively decreased clonality

REFERENCES

- 1.. Hohtari H, Brück O, Blom S, *et al.* Immune cell constitution in bone marrow microenvironment predicts outcome in adult ALL. *Leukemia* 2019;**33**(7):1570–1582.
- 2.. Blaeschke F, Willier S, Stenger D, *et al.* Leukemia-induced dysfunctional TIM-3. *Leukemia* 2020;**34**(10):2607–2620.
- 3.. Liu L, Chang YJ, Xu LP, *et al.* T cell exhaustion characterized by compromised MHC class I and II restricted cytotoxic activity associates with acute B lymphoblastic leukemia relapse after allogeneic hematopoietic stem cell transplantation. *Clin Immunol* 2018;**190**:32–40.

<http://dx.doi.org/10.1136/jitc-2021-SITC2021.321>

322

MELANOMA-INTRINSIC HYPOXIA-INDUCIBLE FACTOR-1 α RESULTS IN DIMINISHED T CELL ACCUMULATION WITHIN THE TUMOR MICROENVIRONMENTEmily Higgs, Thomas Gajewski, Jonathan Trujillo*. *University of Chicago, Chicago, IL, USA*

Background The hypoxia-inducible factor (HIF) system, consisting of the transcription factors HIF-1 α and HIF-2 α , mediates cellular adaptation to hypoxia, and can promote cancer progression, invasion, and metastasis. HIF pathway activation in the tumor microenvironment has been implicated in cancer immune evasion; however, a direct causal role for tumor cell-intrinsic HIF-1 α and HIF-2 α activation in mediating T cell exclusion and cancer cell resistance to immune checkpoint inhibitor therapy has not been demonstrated.

Methods We performed gene expression analysis of melanoma tumors in the Cancer Genome Atlas (TCGA) data set to determine whether increased HIF-1 α pathway activation correlated with reduced T cell-based inflammation. The magnitude of HIF-1 α pathway activation across melanoma samples was determined by applying a quantitative scoring system on the expression of a melanocyte-specific hypoxia-induced, HIF-1 α -target gene signature consisting of 81 genes. The Pearson correlation test was used to compare the HIF-1 α activation score and our 160-gene T-cell-inflamed gene signature. To determine the impact of cancer cell-intrinsic HIF-1 α or HIF-2 α activation on the endogenous anti-tumor T cell response, we developed an inducible autochthonous mouse melanoma model driven by BRAFV600E expression and PTEN-deletion, with or without inducible expression of either a stabilized variant of HIF-1 α or HIF-2 α . These murine tumor models are being used to determine the impact of cancer cell-intrinsic HIF-1 α or HIF-2 α activation on tumor sensitivity to anti-PD-1/PD-L1 and anti-CTLA-4 treatment.

Results Gene expression analysis of human melanomas in the TCGA demonstrated a statistically significant inverse correlation between the HIF-1 α activation score and T cell-inflammation score. Braf/PTEN murine melanomas with and without stabilized HIF-1 α expression developed with comparable tumor onset and growth kinetics. Multiparameter immunofluorescence staining of melanoma tissue revealed a significant decrease in tumor-infiltrating T cells within Braf/PTEN melanoma tumors expressing stabilized HIF-1 α compared to control Braf/PTEN melanomas.

Conclusions Our data demonstrate that tumor-cell intrinsic HIF-1 α activation leads to diminished T cell accumulation within the tumor microenvironment, which has implications for cancer immunotherapy. The mechanism of this effect is being elucidated. These novel murine models will help elucidate the roles of cancer cell-intrinsic HIF-1 α and HIF-2 α activation in modulating the anti-tumor T cell response, providing mechanistic insight that will inform the evaluation of novel selective HIF inhibitors, which are showing promising anti-tumor activity in clinical trials in patients with advanced solid tumors.

<http://dx.doi.org/10.1136/jitc-2021-SITC2021.322>

323 IMMUNOGENIC SYNGENEIC MODEL MC38-OVA FOR THE PRECLINICAL EVALUATION OF IMMUNE EVASION AND CHECKPOINT BLOCKADE

Jessie Wang*, Kaixia Lian, Jia Zheng, Chenpan Nie, Annie An, Henry Li. *Crown Bioscience Inc., Taicang, Suzhou, China*

Background The development of immuno-oncology (I/O) therapeutics has revolutionized the cancer treatment landscape. Despite this achievement, the mechanism behind limited responses is poorly understood. Tumor immune evasion has been reported to arise through the loss of tumor necrosis factor (TNF) signaling, interferon- γ (IFN- γ) signaling, and antigen presentation pathways, which are crucial to CD8+ T cell-mediated killing. Syngeneic mouse models have been widely used as they have an intact immune system, are easily accessible, and have a vast array of historical data for comparison. However, limited syngeneic models respond to immune checkpoint inhibitors, possibly due to low intrinsic immunogenicity. The expression of ovalbumin (OVA) has previously shown to sufficiently alter the susceptibility of syngeneic tumors to host T cell-mediated responses. In this study, the newly developed OVA-expressing MC38 syngeneic line was characterized for tumor immunity, checkpoint blockade response and response durability.

Methods Murine colon cancer MC38 cells were transduced by lentiviral vector with chicken OVA coding cDNA. A single clone was selected, and OVA expression was confirmed by western blot. The MC38-OVA cells were subcutaneously implanted into immunocompetent mice to evaluate the tumorigenicity and in vivo response to anti-PD-1 antibody treatment. Blood was collected 2 days post final dose of anti-PD-1 treatment for phenotypic analysis by FACS. Spleen and tumor draining lymph nodes were collected at termination for FACS analysis of IFN- γ + T cells and OVA specific CD8+ T cells. Adoptive transfer was evaluated by challenge studies in both MC38-OVA and MC38 tumor-bearing mice with T cells derived from MC38-OVA mice, anti-PD-1 cured mice and OT-I mice. In vitro killing assays were performed to evaluate the function of adoptive CD3+ T cells transfer.

Results OVA-expressing MC38 presented complete regression under anti-PD-1 treatment in vivo. T cell expansion was observed after anti-PD-1 treatment in peripheral blood with increased IFN- γ + T cells in both tumor-draining lymph nodes and spleen. Additionally, anti-PD-1 cured mice generated robust tumor specific memory T cell, which successfully inhibited MC38-OVA and MC38 tumor growth following adoptive transfer. CD3+ T cells from MC38-OVA-bearing mice and OT-I mice showed anti-tumor immunity in vivo. In vitro killing assay demonstrated increased immunity.

Conclusions Syngeneic mouse tumor models are preferred pre-clinical models for I/O research, despite limited intrinsic immunogenicity. OVA expression in syngeneic tumors largely increased T cell-mediated immunity to enhance antigen-specific T cell responses during tumorigenesis, providing novel immunogenic models for preclinical immunotherapy evaluation.

<http://dx.doi.org/10.1136/jitc-2021-SITC2021.323>

PRECLINICAL EVALUATION OF ANTI-VISTA ANTIBODY CI-8993 IN A SYNGENEIC HUVISTA-KI MODEL

¹Fiona Scott, ¹Christian Wichmann, ¹Ingrid Burvenich, ¹Alexander McDonald, ¹Nancy Guo, ¹Angela Rigopoulos, ²Raul Soikes, ²Steven Angelides, ²Reinhard von Roemeling, ¹Andrew Scott*. ¹Olivia Newton-John Cancer Research Institute, Melbourne, Australia; ²Curis Inc., Lexington, MA, USA

Background VISTA (V-domain Ig suppressor of T-cell activation) inhibits anti-tumour immune responses. The Investigational product CI-8993 is a fully human IgG1k monoclonal antibody that binds specifically to this immune checkpoint molecule. Phase I safety has been established in prior trials in patients with advanced cancer (NCT02671955). To assist determining the pharmacokinetics and biodistribution of CI-8993 in patients we aimed to develop a Zirconium-89 (89Zr)-labelled CI-8993 for PET imaging and quantitation, and validate in preclinical models prior to a planned human trial.

Methods Conjugation conditions of CI-8993 to the metal ion chelator desferrioxamine B (Df-) were established by optimisation of Df:mAb ratio, reaction temperature, time and purification method. Conjugates were assessed by SE-HPLC, SDS-PAGE, and ELISA. Radiolabelling was performed with 89Zr and the radioconjugate was tested for specific activity, radiochemical purity and binding affinity for huVISTA. The in-vivo biodistribution and properties of 89Zr-Df-CI-8993 and IgG1 isotype control radioconjugates were assessed in huVISTA knock-in female (C57BL/6N-Vsir< sup >tm1.1(VSIR)Geno</ sup >) or control C57BL/6 mice bearing syngeneic MB49 bladder cancer tumours. Whole body animal PET/CT imaging was performed on day of radioconjugate synthesis and injection and day 1 and day 3 p.i. Biodistribution was assessed by image analyses, and tissue counting, with IHC analyses performed to verify VISTA antigen expression.

Results Conjugation of Df- to CI-8993 for 60 minutes at room temperature followed by purification via gel filtration resulted in stable constructs with an average chelator-to-antibody ratio of 1.81. SDS-PAGE showed integrity of CI-8993 was maintained after conjugation, and ELISA indicated no impact of conjugation on binding to human VISTA. Radiochemical purity (iTLC) and protein integrity (SE-HPLC) at EOS were > 99% and 93%. PET imaging and biodistribution in MB49 tumour-bearing huVISTA knock-in female mice showed specific localisation of 89Zr-Df-CI-8993 to VISTA expressing organs (liver: 14.98 ± 0.50 %ID/g; spleen: 292.00 ± 14.51 %ID/g; n = 3) compared to 89Zr-Df-IgG1 control (liver: 4.615 ± 0.15 %ID/g; spleen: 6.37 ± 0.22 %ID/g; n = 4) or in the presence of competing unlabelled CI-8993 (liver: 8.14 ± 0.50 %ID/g; spleen: 41.14 ± 3.00 %ID/g; n = 5). Tumour-to-blood ratios indicated specific tumour targeting of 89Zr-Df-CI-8993 in the presence of unlabelled CI-8993 (20.47 ± 3.09) compared to trace dose 89Zr-Df-CI-8993 (0.97 ± 0.12 ; P = 0.0001) or 89Zr-Df-IgG1 control (1.75 ± 0.11 ; P < 0.0001).

Conclusions We have validated 89Zr-Df-CI-8993 for specific binding to huVISTA in-vivo. A clinical trial of 89Zr-Df-CI-8993 is planned in solid tumour patients.

Ethics Approval All animal studies were approved by the Austin Health Animal Ethics Committee and were conducted in compliance with the Australian Code for the care and use of animals for scientific purposes.

<http://dx.doi.org/10.1136/jitc-2021-SITC2021.324>

¹Michelle Winkler*, ²Michael Curran. ¹MD Anderson Cancer Center UTHealth in Houston, Houston, TX, USA; ²MD Anderson Cancer Center, Houston, TX, USA

Background Anti-checkpoint antibodies blocking T cell co-inhibitory molecules (e.g. α PD-1, α CTLA-4) allow immune effector cells to persist, expand, and maintain cytotoxic function in the tumor microenvironment (TME). Despite being effective in immune "hot" tumors that are infiltrated by effector anti-tumor cells, immune "cold" tumors fail to respond to checkpoint blockade. "Cold" tumors are populated with immune suppressive cells including regulatory T cells, M2 macrophages, and myeloid derived suppressor cells, which inhibit immune effector infiltration and function. These suppressive populations, along with tumor cells, express co-inhibitory checkpoints already targeted with current immunotherapeutics, but also some checkpoints in need of further investigation. We hypothesized that by targeting these checkpoints with cytoreductive antibodies which selectively deplete suppressive populations and tumor cells via ADCC/ADCP, we will compromise "cold" immune privilege and restore an efficient anti-tumor immune response.

Methods To identify novel targets to produce checkpoint cytoreductive antibodies we conducted in silico analysis that prioritized immune-inhibitory targets with tumor-specific or tumor-selective expression on cell surface. We cross-referenced a previously published list of transmembrane proteins against publicly sourced datasets including TCGA, HPA, GTEx, BioGPS, and SAGE.¹ We then characterized the expression profile of each selected target on tumor cells in vitro and on cell populations in the TME ex vivo via multiparameter flow cytometry. Finally, we assessed the impact of existing checkpoint-targeting cytoreductive antibodies on survival and tumor growth in murine "hot" and "cold" tumors.

Results VISTA and DLL3 were identified via in silico analysis as co-inhibitory surface proteins specifically and selectively in the TME and not in healthy tissues. DLL3 is mainly expressed on tumor cells while VISTA was described mostly on immunosuppressive myeloid cells. An anti-DLL3 antibody was produced by a previous laboratory as an IgG1 antibody, and we engineered a version in the depletive (IgG2a) isotype, which will enable us to target this checkpoint with either a blocking or a depleting antibody. Flow cytometry analysis identified VISTA on multiple myeloid cell populations in "cold" 4T1 murine mammary tumors while its expression was low in spleen. To start assessing the efficiency of depleting versus non-depleting antibodies, "hot" CT26 murine tumors and 4T1 tumors were treated with an α CTLA-4-IgG2a or α CTLA-4-IgG1. Groups treated with depleting antibodies showed increased survival compared to groups treated with non-depleting antibodies.

Conclusions Novel immune-inhibitory checkpoints can be identified and targeting them with cytoreductive antibodies leads to a higher anti-tumor immune response. This investigation opens the door to more efficient combination therapies.

Acknowledgements Supported by a training fellowship from The University of Texas Health Science Center at Houston Center for Clinical and Translational Sciences TL1 Program (Grant No. TL1 TR003169).

REFERENCES

1. Wang J, et al. Siglec-15 as an immune suppressor and potential target for normalization cancer immunotherapy. *Nat Med* **25**,(2019).

326

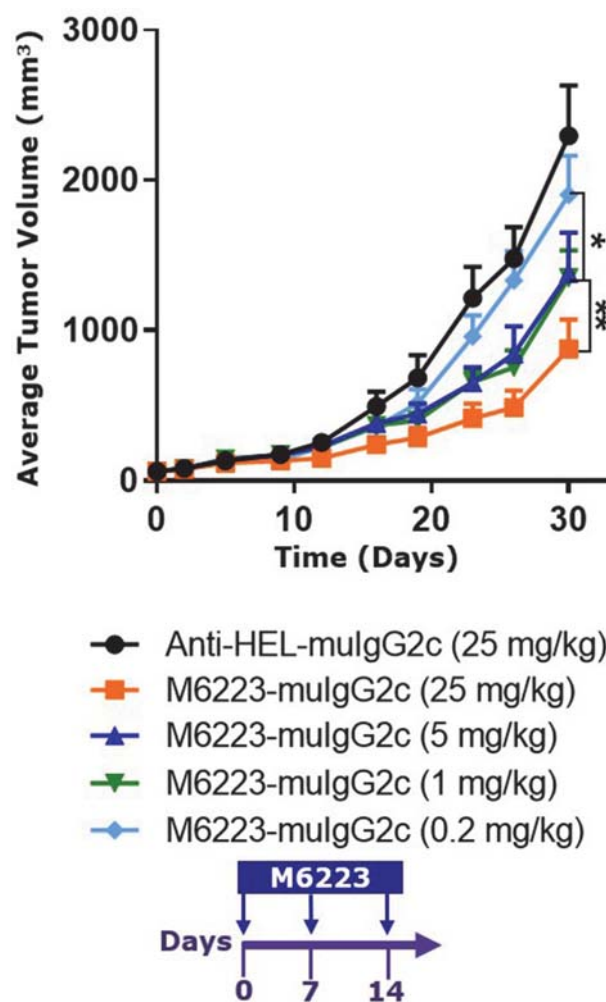
THE ANTI-TIGIT ANTIBODY M6223 INDUCES SIGNIFICANT ANTI-TUMOR EFFICACY AND IMMUNE RESPONSE VIA MULTIPLE MECHANISMS OF ACTION

¹Chunxiao Xu*, ²Feng Jiang, ²Hui Huang, ²Lindsay Webb, ²Sireesha Yalavarthi, ²Clotilde Bourin, ²Hong Wang, ²Natalya Belousova, ²Zhouxiang Chen, ²Christie Kelton, ²Dong Zhang, ²Joern-Peter Halle, ²Andree Blaukat, ¹Jacques Moisan. ¹Merck KGaA, Belmont, MA, USA; ²EMD Serono, Billerica, MA, USA

Background M6223 is a fully human antagonistic anti-T cell immunoreceptor with immunoglobulin and ITIM domains (TIGIT) antibody in IgG1 format with Fc-mediated effector function.

Methods The ability of M6223 to block the interaction of TIGIT with its ligands, CD155 and CD112, and the interaction of TIGIT with CD226 was determined by a flow cytometry-based binding assay. The anti-tumor efficacy, immune profile, and effector function of M6223 were investigated in syngeneic tumor models in huTIGIT knock-in mice. M6223 was either formatted with an effector competent mouse IgG2c constant region (M6223-mulgG2c) or formatted with effector null mouse IgG1-D256A constant region (M6223-mulG1) as two versions of chimeric antibodies for the in vivo studies.

Results M6223 dose-dependently blocked the binding of TIGIT to its ligands, including CD155 and CD112, thereby inhibiting a TIGIT-mediated immunosuppressive pathway. In addition, M6223 interrupted the interaction of TIGIT with the costimulatory receptor CD226. By blocking the interactions, the chimeric protein M6223-mulgG2c showed anti-tumor efficacy in multiple tumor models, including an MC38 tumor model (figure 1), and generated tumor antigen-specific long-term protective immunity in immunocompetent huTIGIT knock-in mice. M6223 monotherapy dose-dependently elevated the ratio of CD8+ cytotoxic T cells to regulatory T cells and the ratio of CD226 to TIGIT expression in immune cells in the tumor microenvironment. We also found that M6223 selectively depleted suppressive and exhausted TIGIT+ immune cell subsets and the anti-tumor activity of effector null M6223-mulG1 was significantly lost ($p < 0.0001$), suggesting that Fc-mediated effector function contributes to M6223 anti-tumor activity. Antibody depletion studies demonstrated that CD8+ T cells and natural killer cells contributed to the anti-tumor activity of M6223 in a complementary manner.



* $p < 0.05$; ** $p < 0.01$.

Abstract 326 Figure 1 M6223-mulgG2c displayed dose-dependent anti-tumor efficacy. M6223-mulgG2c displayed dose-dependent anti-tumor efficacy in an MC38 tumor model in huTIGIT knock-in mice.

Conclusions Given that TIGIT blockade can inhibit an immunosuppressive pathway as well as remove the suppression on a costimulatory pathway, M6223 has the potential to induce an anti-tumor immune response by three complementary mechanisms: direct blockade of the TIGIT pathway, stimulation of CD226 dimerization/activation, and depletion of TIGIT+ immune subsets by Fc-mediated effector function. Our data demonstrate that these complementary mechanisms orchestrate

the anti-tumor activity of M6223. A Phase I, first-in-human clinical trial (NCT04457778) is underway to determine the safety, tolerability, maximum tolerated dose and recommended dose for expansion of M6223 as a single agent (Part 1A) and in combination with bintrafusp alfa (Part 1B) in patients with metastatic or locally advanced solid unresectable tumors.

Ethics Approval All animal experiments were performed in accordance with EMD Serono Research & Development Institute, Inc., Billerica, MA, USA, an affiliate of Merck KGaA (protocol 17-008, 20-005) and Wuxi AppTec Animal Care and Use Committee (IACUC) guidelines.

<http://dx.doi.org/10.1136/jitc-2021-SITC2021.326>

327

DEVELOPMENT AND VALIDATION OF A NEOANTIGEN-SPECIFIC T CELL GENE SIGNATURE TO IDENTIFY ANTITUMOR T CELLS IN LUNG CANCER AND MELANOMA

¹Jijia Zhang*, ¹Justina Caushi, ²Giacomo Oliveira, ¹Boyang Zhang, ¹Zhicheng Ji, ³Jarushka Naidoo, ¹Kristen Marrone, ¹Janis Taube, ⁴Matthew Hellmann, ¹Julie Brahmer, ⁴Taha Merghoub, ¹Patrick Forde, ¹Srinivasan Yegnasubramanian, ²Catherine Wu, ¹Hongkai Ji, ¹Andrew Pardoll, ¹Kellie Smith. ¹*Johns Hopkins University, Baltimore, MD, USA*; ²*Dana-Farber Cancer Institute, Boston, USA*; ³*Beaumont Hospital, Baltimore, MD, USA*; ⁴*Memorial Sloan Kettering Cancer Center, New York, NY, USA*

Background Mutation-associated neoantigen (MANA)-specific T cells play a key role in tumor control and response to immune checkpoint inhibition (ICI).¹⁻² However, the majority of tumor-infiltrating lymphocytes (TIL) are not specific for the tumor.³ Herein, we developed and validated MANAscore, a bioinformatic scoring algorithm based on the transcriptional programs of MANA-specific T cells to isolate antitumor T cells from bystander T cells in lung cancer and melanoma.

Methods Combined single-cell (sc) RNA-seq/TCR-seq was performed on TIL obtained from 15 resectable non-small cell lung cancer (NSCLC) patients receiving neoadjuvant anti-PD-1 (NCT02259621). MANA-specific clonotypes were identified by coculturing autologous T cells with predicted MANA, and were validated by cloning the full TCR alpha and beta chain as previously described.¹ Using the TCRβ CDR3 as a barcode, antigen-specific T cells were linked with their intratumoral sc expression profile. Using the first two patients enrolled in the clinical trial as a discovery cohort, MANAscore was developed to identify gene programs that best distinguish MANA-specific vs viral-specific T cells from NSCLC. Prediction performance was assessed in independent patients from the NSCLC and melanoma cohort.² Seven MANAscore^{hi} TCRs were cloned and queried for reactivity to peptide libraries of putative MANA derived from whole-exome sequencing of the respective tumor. Association of MANAscore^{hi} clones with response to ICIs among all patients was assessed.

Results A total of 890 MANA- and 542 viral-specific T cells were identified in sc TIL from six NSCLC patients. MANA- and viral-specific TIL presented with unique transcriptional profiles. Particularly, MANA-specific CD8 TIL expressed a partially activated cytolytic program with co-expression of multiple immune checkpoints and upregulated transcriptional regulators of T cell dysfunction. MANAscore showed high prediction accuracy and outperformed CD39 in identifying tumor-reactive T cells in independent NSCLC patients, as well as in an external validation cohort of melanoma patients (3936 MANA-specific T cells and 626 viral-specific T cells from 4 patients). Of seven MANAscore^{hi} clones tested for reactivity, three were confirmed as MANA-specific. The pseudobulk expression profile of MANAscore^{hi} clones showed a significant correlation with response to ICI, which is not observed in total CD8+ TIL.

Conclusions MANA-specific TIL demonstrated a distinct gene signature that enabled us to identify de novo antitumor TIL in NSCLC and melanoma. MANAscore may serve as a useful tool in facilitating mechanistic studies of ICI response and resistance.

Trial Registration NCT01970358, NCT02259621

REFERENCES

1. Simoni, Yannick, *et al.* "Bystander CD8+ T cells are abundant and phenotypically distinct in human tumour infiltrates." *Nature* 557.7706 (2018):575–579.
2. Caushi, Justina X, *et al.* "Transcriptional programs of neoantigen-specific TIL in anti-PD-1-treated lung cancers." *Nature* (2021):1–7.
3. Oliveira, Giacomo, *et al.* "Phenotype, specificity and avidity of antitumour CD8+ T cells in melanoma." *Nature* (2021):1–7.

Ethics Approval The melanoma clinical trial was approved by the Dana-Farber/Harvard Cancer Center Institutional Review Board (IRB) (NCT01970358). The NSCLC clinical trial was approved by the Institutional Review Boards (IRB) at Johns Hopkins University (JHU) and Memorial Sloan Kettering Cancer Center (NCT02259621)

Consent Written informed consent was obtained from the patient for publication of this abstract and any accompanying images. A copy of the written consent is available for review by the Editor of this journal

<http://dx.doi.org/10.1136/jitc-2021-SITC2021.327>

328

BATF3 DENDRITIC CELLS AND 4-1BB/4-1BB LIGAND AXIS ARE REQUIRED AT THE EFFECTOR PHASE WITHIN THE TUMOR MICROENVIRONMENT FOR ANTI-PD-L1 EFFICACY

¹Andrea Ziblat*, ²Brendan Horton, ¹Emily Higgs, ¹Ken Hatogai, ¹Thomas Gajewski.
¹University of Chicago, Chicago, IL, USA; ²MIT, Cambridge, MA, USA

Background PD-1/PD-L1 blockade has shown clinical benefit across many cancer types. However, a large fraction of patients are resistant to immune checkpoint blockade therapy and others eventually relapse. Understanding the mechanisms involved in α PD1/PD-L1 immunotherapy efficacy may enable new strategies for improving clinical outcomes. Given that Batf3-lineage dendritic cells (DCs) are needed for spontaneous T cell priming in the tumor-draining lymph node and for recruitment of effector CD8⁺ T cells to the tumor, in the current work we examined whether Batf3⁺ DCs are also required during the effector phase of the anti-tumor immune response at the time of anti-PD-L1 administration for therapeutic efficacy.

Methods We utilized the B16-SIY melanoma model, CD11c-DTR-GFP, and CD11c-DTR-GFP/Batf3 KO bone marrow chimeras to study the role Batf3⁺ DCs play during anti-PD-L1 immunotherapy. To focus on the effector phase of the immune response, we depleted CD11c⁺ cells with diphtheria toxin from day seven of tumor injection while simultaneously blocking new T cell entry with FTY720. As flow cytometry revealed high 4-1BBL expression on intratumoral Batf3-DCs, 4-1BB KO mice and anti-4-1BBL blocking antibodies were used. Tumor growth and phenotypic analysis of the tumor infiltrate were evaluated.

Results Strikingly, we observed that CD11c⁺ cells, and specifically Batf3⁺ DCs, were required in the tumor prior to α PD-L1 treatment for immunotherapy efficacy. The normal intratumoral expansion of antigen (Ag)-specific CD8⁺ tumor-infiltrating T cells (TILs) and increased ratio between Ag-specific CD8⁺ TILs and regulatory T cells following anti-PD-L1 therapy was eliminated with Batf3⁺ DC depletion. Batf3⁺ DCs expressed high levels of 4-1BBL, and increased expression of 4-1BB on antigen-specific CD8⁺ TILs upon α PD-L1 treatment required Batf3⁺ DCs. Mechanistic experiments confirmed a requirement for 4-1BB expression on immune cells for α PD-L1 efficacy, and blocking antibodies against 4-1BBL eliminated anti-PD-L1 efficacy as well. Using appropriate bone marrow chimeras, agonistic 4-1BB antibodies were sufficient to bypass the need for CD11c⁺ DCs at the effector phase for tumor control. In human melanoma samples, co-localization of Batf3⁺ DCs and CD8⁺ T cells was observed in T cell-inflamed tumors, which correlated with anti-PD-1 efficacy in metastatic melanoma.

Conclusions Our results indicate that Batf3⁺ DCs are necessary during the effector phase of the anti-tumor immune response for anti-PD-L1 efficacy to occur, at least in part through 4-1BB/4-1BBL-mediated reinvasion of Ag-specific CD8⁺ TILs.

Ethics Approval The study obtained ethics approval, IRB protocol 15-0837.

<http://dx.doi.org/10.1136/jitc-2021-SITC2021.328>

Clinical Trials Completed

329

EARLY BLOOD CELL COUNT TEST (BCT) FOR SURVIVAL PREDICTION FOR NON-SMALL CELL LUNG CANCER PATIENTS TREATED WITH ATEZOLIZUMAB: INTEGRATED ANALYSIS OF 4 MULTICENTER CLINICAL TRIALS

¹Jian-Guo Zhou*, ²Ada Hang-Heng Wong, ³Haitao Wang, ⁴Su-Han Jin, ⁵Fangya Tan, ⁶Yu-Zhong Chen, ⁷Si-si He, ⁷Gang Shen, ⁸Benjamin Frey, ⁸Rainer Fietkau, ⁸Markus Hecht, ⁶Bo Shen, ⁴Hu Ma, ⁸Udo Gaipl. ¹The Second Affiliated Hospital of Zunyi Medical University, Zunyi, China; ²University of Macau, Macau SAR, China; ³National Cancer Institute, Bethesda, MD, USA; ⁴Zunyi Medical University, Zunyi, China; ⁵University at Buffalo, Buffalo, NY, USA; ⁶Jiangsu Cancer Hospital, Nanjing, China; ⁷2nd affili Hosp of Zunyi Med Uni, zunyi, China; ⁸Universitätsklinikum Erlangen, Erlangen, Germany

Background Immune checkpoint inhibitor (ICI) therapy is a major breakthrough for non-small cell lung cancer (NSCLC) treatment given its high efficacy and tolerable toxicity. Although pre-treatment PD-L1 expression levels and tumor mutation burden (TMB) may serve as prognostic biomarkers for patient stratification, effective predictive biomarkers are lacking. Blood cell count test (BCT) is a routine, regular blood test conducted before and during treatment to provide a direct overview of the immune landscape based on the counts of various types of immune cells (ICs). For instance, previous studies showed that neutrophil-to-lymphocyte ratio (NLR) and platelet-to-lymphocyte ratio (PLR) both indicate poor treatment outcomes of ICI therapy of NSCLC patients.

Methods This study analyzed relevant combinations of IC counts from four international, multi-center clinical trials of OAK, BIRCH, POPLAR and FIR to conduct post-hoc analysis of NSCLC patients undergoing atezolizumab (anti-PD-L1) single-agent treatment (n = 1,479), while docetaxel single-agent treatment (n = 707) was used as control. BCT was conducted at three timepoints, T1 to T3, during pre-treatment and on the first day of treatment cycles 3 and 5, which correspond to baseline, 6, and 12 weeks on-treatment, respectively. Univariate and multivariate Cox regression analysis was conducted to identify NLR_T3, PLR_T3 and neutrophil-to-monocyte (NMR) at T2 as early BCT biomarkers that may predict ICI efficacy. Next, univariate and multivariate Cox proportional hazards regression analysis were used to identify any effective combination of BCT biomarkers and their absolute cutoff values that may serve as predictive biomarkers to predict atezolizumab treatment outcomes. Lastly, combinations of these BCT biomarkers were tested to optimize BCTscore model for clinical evaluation.

Results The final BCT biomarker combination, comprising of the BCT biomarkers of NLR and PLR at 12 weeks on-treatment (T3) and NMR at 6 weeks on-treatment (T2), was identified to be a strong predictive biomarker for atezolizumab (Ate)-treated NSCLC patients in comparison to docetaxel (Dtx)-treated patients regarding overall survival (OS) (BCTscore low-risk: HR Ate vs Dtx = 1.54 (95% CI: 1.04–2.27), P = 0.036; high-risk: HR Ate vs Dtx = 0.84 (95% CI: 0.62–1.12), P = 0.236). Our BCTscore model consistently exhibited better OS AUC in the OAK (AUC_{12month}=0.696), BIRCH (AUC_{12month}=0.672) and POPLAR+FIR studies (AUC_{12month}=0.727) than that of each of the three BCT biomarkers in these three studies.

Conclusions The BCTscore of NLR at 12 weeks, PLR at 12 weeks and NMR at 6 weeks is a strong efficacy predictive biomarker for atezolizumab-treated NSCLC patients.

Acknowledgements The authors declare no conflict of interest. This publication is based on research using data from Genentech, Inc. (one of subsidiaries of Roche Group) that has been made available through Vivli, Inc (Data Request ID: 5935; Lead Investigator: Dr. Jian-Guo Zhou). Vivli has not contributed to or approved, and is not in any way responsible for, the contents of this publication.

Trial Registration Deidentified individual participant data from the single-arm phase II studies of FIR study (NCT01846416; as of January 7, 2015) [Spigel2018] and BIRCH (NCT02031458; as of May 28, 2015) [Peters2017], and the two-arm randomized controlled trials (RCT) of the POPLAR phase II study (NCT01903993; as of May 8, 2015) [Fehrenbacher2016] and the OAK phase III study (NCT02008227; as of July 7, 2016) [Rittmeyer2017] were made available by Genentech Inc. and accessed through the secure Vivli online platform.

Ethics Approval Both studies were approved by the respective national ethics committees and institutional review boards and written informed consent was obtained from all patients.

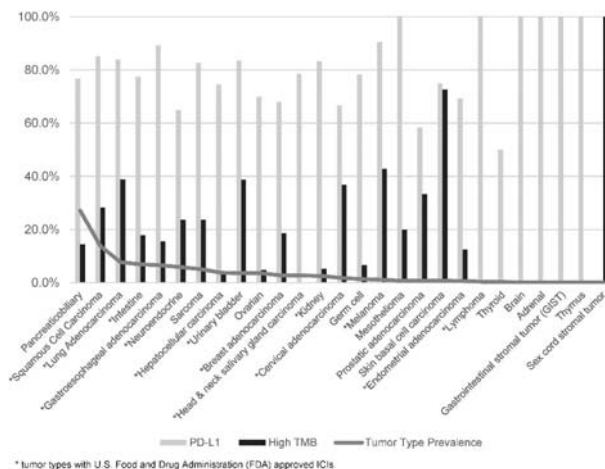
<http://dx.doi.org/10.1136/jitc-2021-SITC2021.329>

330

INTEGRATION OF MOLECULAR CANCER CLASSIFICATION AND NEXT-GENERATION SEQUENCING TO IDENTIFY METASTATIC PATIENTS ELIGIBLE FOR IMMUNE CHECKPOINT INHIBITORS

¹Daruka Mahadevan*, ²Li Ma, ²Kai Treuner, ²Jenna Wong, ²Catherine Schnabel. ¹Mays Cancer Center, University of Texas Health San Antonio, San Antonio, TX, USA; ²Biotheranostics, Inc., San Diego, CA, USA

Background Immune checkpoint inhibitors (ICIs) have improved patient outcomes and are a new standard of care for treating a variety of cancers. Eligibility for ICIs is established through determination of tumor type and use of predictive biomarkers. PD-L1, microsatellite instability (MSI), and tumor mutation burden (TMB) are FDA-approved predictive biomarkers for ICI therapies. However, the validity of these biomarkers remains controversial, as studies have shown a failure to predict ICI response in many cancer types.^{1 2} The 92-gene assay (CancerTYPE ID) is a validated gene expression classifier of 50 tumor types and subtypes for metastatic patients with ambiguous diagnoses. CancerTYPE ID provides critical cancer type identification to guide ICI treatment eligibility and selection. In the current study, analyses integrating tumor type with multimodal biomarker testing for PD-L1 and TMB were evaluated to identify patients for ICI eligibility. **Methods** MOSAIC (Molecular Synergy to Advance Individualized Cancer Care) is an IRB-approved, de-identified database of CancerTYPE ID results from 2572 patients with tumor-specific multimodal biomarker testing by next-generation sequencing for TMB and immunohistochemistry for PD-L1. The Cochran-Mantel-Haenszel test was used to evaluate the relationship between PD-L1 and TMB across tumor types.



Abstract 330 Figure 1 Prevalence of PD-L1 expression and high TMB in the 27 identified tumor types

Results Tumor type was determined in 2377 of 2572 cases (92.4%), comprising 27 different tumor types including 14 tumor types with FDA-approved ICI therapies. Among the top 20 tumor types, PD-L1 was present in a larger proportion of tumors (weighted mean=78.9%, range=58.3%–100%) versus TMB (20.9%, 0%–72.7%) (figure 1). Varying expression levels of PD-L1 and TMB were noted across tumor types (Figure 1), and no relationship between PD-L1 and TMB ($P=0.15$) was observed. Prevalence of high TMB in melanoma (42.9%) and lung adenocarcinoma (38.9%), which are more likely to

respond to ICI treatment, are consistent with published data; however, prevalence of high TMB in mesothelioma (20.0%), sarcoma (23.6%) and prostatic adenocarcinoma (33.3%), which are not likely to respond to ICI treatment, are higher than previously reported.³

Conclusions Tumor type classification and cellular context are critical for ICI eligibility. CancerTYPE ID successfully differentiated 14 ICI-eligible tumor types from 13 non-ICI-eligible tumor types. Further, since there is no relationship between PD-L1 and TMB for different tumor types, accurate tumor type identification is necessary to select the most appropriate biomarker. This highlights the clinical utility of CancerTYPE ID combined with multimodal biomarker testing to guide ICI treatment and predict response based on tumor type identification, which may improve outcomes in patients with metastatic cancer.

REFERENCES

- McGrail DJ, Pilié PG, Rashid NU, *et al.* High tumor mutation burden fails to predict immune checkpoint blockade response across all cancer types. *Ann Oncol* 2021;**32**(5):661–672.
- Gjoerup O, Brown CA, Ross JS, *et al.* Identification and utilization of biomarkers to predict response to immune checkpoint inhibitors. *AAPS J* 2020;**22**(6):132.
- Yarchoan M, Albacker LA, Hopkins AC, *et al.* PD-L1 expression and tumor mutational burden are independent biomarkers in most cancers. *JCI Insight* 2019;**4**(6): e126908.

<http://dx.doi.org/10.1136/jitc-2021-SITC2021.330>

331

TUMOR MARKERS ASSOCIATED WITH INCREASED SURVIVAL IN A PHASE II TRIAL OF DENDRITIC CELL/TUMOR-INITIATING-CELL VACCINE AV-GBM-1 IN PATIENTS WITH NEWLY DIAGNOSED GLIOBLASTOMA

¹Daniela Bota*, ²David Piccioni, ³Christopher Duma, ⁴Renato LaRocca, ⁵Santosh Kesari, ⁶Jose Carrillo, ⁷Frank Hsu, ⁸Xiao-Tang Kong, ⁹Mehrdad Abedi, ¹⁰Robert Aiken, ¹¹Thomas Taylor, ¹²Candace Hsieh, ¹³Gabriel Nistor, ¹⁴Robert Dillman. ¹University of California Irvine, Orange, CA, USA; ²University of California San Diego, San Diego, CA, USA; ³Hoag NeuroSciences Institute, Newport Beach, CA, USA; ⁴Norton Cancer Institute, Louisville, KY, USA; ⁵John Wayne Cancer Institute, Santa Monica, CA, USA; ⁶University of California Davis, Sacramento, CA, USA; ⁷Rutgers Cancer Center, New Brunswick, NJ, USA; ⁸AVITA Biomedical Inc., Irvine, CA, USA

Background Standard aggressive therapy of glioblastoma (GBM), which includes maximum safe resection, concurrent radiation therapy and temozolomide chemotherapy (RT/TMZ) followed by maintenance TMZ, is associated with a 25% 2-year overall survival (OS). Adding treatment with AV-GBM-1, a vaccine consisting of autologous dendritic cells (DC) pulsed with autologous tumor antigens (ATA) may improve OS by inducing and/or enhancing the host anti-GBM immune response. Methylation of the O-6-methylguanine-DNA methyltransferase (MGMT) gene promoter, and mutation of the gene for isocitrate dehydrogenase (IDH) are favorable prognostic markers in newly diagnosed GBM. An objective of a multicenter phase II clinical trial was to determine whether these markers were still prognostic for OS in patients treated with adjunctive AV-GBM-1.

Methods Key eligibility criteria for intent-to-treat (ITT) enrollment were: (1) confirmation of primary GBM, (2) successful GBM cell culture, (3) collection of sufficient numbers of monocytes (MC) by leukapheresis, (4) Karnofsky Performance Status 70 or greater after recovery from surgery, and (5) plan to treat with concurrent RT/TMZ. AV-GBM-1 was manufactured while patients were being treated with RT/TMZ. Interleukin-4 and granulocyte-macrophage colony stimulating factor (GM-CSF) were used to differentiate DC from MC. Each vaccine consisted of autologous DC incubated with ATA from the lysate of irradiated cultured GBM cells grown in serum-free media with factors that favor survival and proliferation of stem cells and early progenitor cells (tumor-initiating cells). After recovery from RT/TMZ, intent was to vaccinate for up to six months with cryopreserved AV-GBM-1 admixed with 500 mg GM-CSF. All patients had testing for MGMT-methylation and IDH-mutation. OS was calculated from date of ITT enrollment.

Results 60 patients were enrolled during August 2018 to January 2020. MGMT promoter methylation was detected in 21 (35%), mutated IDH in 7 (12%), and one or both in 25 (42%). At a minimum follow-up of 15 months, median OS had not been reached for patients with a methylated MGMT promoter, IDH mutation, or one or both, compared to 14.6 months for 38 with unmethylated MGMT promoter ($p=0.026$), 14.7 months for 53 with IDH wild-type ($p=0.044$), and 14.6 months for 35 who had neither ($p=0.017$). 18-month OS rates were 59% vs 35% for MGMT promoter methylation, 71% vs 40% for IDH mutation and 58% vs 32% for either.

Conclusions Both MGMT promoter methylation and IDH mutation were associated with a substantial and similar survival benefit in primary GBM patients treated with AV-GBM-1 in addition to standard aggressive therapy.

Trial Registration ClinicalTrials.gov NCT03400917

Ethics Approval This study was approved by the Western IRB, approval number 20182582; all participants gave written informed consent before taking part

<http://dx.doi.org/10.1136/jitc-2021-SITC2021.331>

TUMOR COLLECTION AND ESTABLISHMENT OF TUMOR-INITIATING CELL CULTURES AS ANTIGEN SOURCE FOR AV-GBM-1 DENDRITIC CELL VACCINES FOR A PHASE II TRIAL IN PATIENTS WITH NEWLY DIAGNOSED GLIOBLASTOMA

<http://dx.doi.org/10.1136/jitc-2021-SITC2021.332>

¹Christopher Duma, ²Daniela Bota*, ²Frank Hsu, ³David Piccioni, ⁴Renato LaRocca, ⁵Santosh Kesari, ⁶Mehrdad Abedi, ³Jose Carrillo, ⁷Robert Aiken, ²Xiao-Tang Kong, ²Thomas Taylor, ⁸Candace Hsieh, ⁸Gabriel Nistor, ⁸Robert Dillman. ¹NeuroScience Institute, Newport Beach, CA, USA; ²University of California Irvine, Orange, CA, USA; ³University of California San Diego, San Diego, CA, USA; ⁴Norton Cancer Institute, Louisville, KY, USA; ⁵John Wayne Cancer Institute, Santa Monica, CA, USA; ⁶University of California Davis, Sacramento, CA, USA; ⁷Rutgers Cancer Center, New Brunswick, NJ, USA; ⁸AIVITA Biomedical Inc., Irvine, CA, USA

Background Despite standard aggressive therapy (maximum safe surgical resection, concurrent radiation therapy and temozolomide chemotherapy (RT/TMZ), then maintenance TMZ), 2-year survival is only about 25% for patients with newly diagnosed primary glioblastoma (GBM). Adding AV-GBM-1, a vaccine consisting of autologous dendritic cells (DC) pulsed with autologous tumor antigens (ATA) may improve survival. One objective of a multi-center phase II clinical trial was to determine the feasibility of collecting fresh GBM and establishing short-term cell cultures of GBM tumor-initiating cells (TIC) to serve as ATA source.

Methods Key eligibility criteria for tumor collection were (1) clinical suspicion of new primary GBM, (2) age 18 to 70 years (3) tentative agreement to undergo a leukapheresis procedure after recovery from surgery, and (4) tentative plans for RT/TMZ. Fresh tumor was placed in media and shipped in a transport kit by overnight courier to AIVITA where a cell suspension was placed in culture and incubated in serum-free medium with factors that favor survival and proliferation of TICS (stem cells and early progenitor cells). The intent was to produce a patient-specific DC-ATA vaccine by incubating a lysate of irradiated TICs with autologous DC for subsequent subcutaneous injection.

Results Patients were enrolled from five sites in California, one in Kentucky and one in New Jersey. Tumors were collected between August 2018 and January 2020. 106 patients consented for tumor collection, but 15 were not GBM, 4 had insufficient tissue to send, 2 patients withdrew consent, 4 were ineligible because of age, and 1 was ineligible because of autoimmune disease. Of the 80 GBM tumors that were placed into culture, 7 were discontinued because of patient withdrawal. 71/73 (97%) resulted in a successful cell culture; two were unsuccessful because of contamination. 60/71 subsequently consented for intent-to-treat ; 46/60 (77%) had cells in culture for 28 days or less, 11 were in culture for 30 to 35 days, and the remaining 3 were cultured 46, 54, and 55 days. The average number of cells per culture at the time of irradiation was 14.0 million (range 0.78 to 63.3 million). 58/60 (97%) yielded more than 1 million TICs for irradiation for the tumor cell lysate; 36/60 (60%) had more than 10 million cells irradiated. 57 patients were subsequently treated with AV-GBM-1 after recovery from RT/TMZ.

Conclusions Self-renewing GBM TIC cultures can be reliably and rapidly established for use as the antigen source for personal DC-ATA vaccines.

Trial Registration ClinicalTrials.gov NCT03400917

Ethics Approval This study was approved by the Western IRB, approval number 20182582; all participants gave written informed consent before taking part

333

CHANGES IN PROTEOMIC MARKERS AFTER INJECTIONS OF PERSONAL AV-GBM-1 DENDRITIC CELL/TUMOR INITIATING CELL VACCINES IN A PHASE II TRIAL IN PATIENTS WITH NEWLY DIAGNOSED GLIOBLASTOMA

¹Santosh Kesari, ²Daniela Bota*, ³David Piccioni, ⁴Christopher Duma, ⁵Renato LaRocca, ²Xiao-Tang Kong, ²Frank Hsu, ¹Jose Carrillo, ⁶Mehrdad Abedi, ⁷Robert Aiken, ²Thomas Taylor, ⁸Aleksandra Poole, ⁸Candace Hsieh, ⁸Gabriel Nistor, ⁸Robert Dillman. ¹John Wayne Cancer Institute, Santa Monica, CA, USA; ²University of California Irvine, Orange, CA, USA; ³University of California San Diego, San Diego, CA, USA; ⁴Hoag NeuroSciences Institute, Newport Beach, CA, USA; ⁵Norton Cancer Institute, Louisville, KY, USA; ⁶University of California Davis, Sacramento, CA, USA; ⁷Rutgers Cancer Center, New Brunswick, NJ, USA; ⁸AVITA Biomedical, Inc., Irvine, CA, USA

Background Despite standard aggressive therapy, including maximum safe surgical resection, concurrent radiation therapy and temozolomide chemotherapy (RT/TMZ) followed by maintenance TMZ, survival is still extremely poor for patients with newly diagnosed primary glioblastoma (GBM). Adding treatment with AV-GBM-1, a personal vaccine consisting of autologous dendritic cells (DC) pulsed with autologous tumor antigens (ATA) may improve survival. One objective of a multi-center phase II clinical trial was to determine changes in blood proteomics before and after injections of AV-GBM-1.

Methods AV-GBM-1 consists of autologous DC incubated with ATA from a lysate of irradiated autologous GBM cells that had been placed in culture and incubated in serum-free medium with factors that favor the survival and proliferation of stem cells and early progenitor cells. After recovery from RT/TMZ, GBM patients were injected subcutaneously with AV-GBM-1 admixed in granulocyte-macrophage colony-stimulating factor (GM-CSF) at weeks 1, 2, 3, 8, 12, 16, 20, and 24. Blood samples obtained at baseline (week-0), just prior to the third injection (week-2) and just prior to the fourth injection (week-8), were cryopreserved and subsequently analyzed for 448 proteomic markers using quantitative, multiplex enzyme-linked immunosorbent assays (Raybiotech, Inc., Norcross, GA.). In this preliminary analysis the averages of paired samples for each time point were determined and compared using the student T-Test with a focus on differences of $p < 0.01$.

Results Patients were enrolled from five sites in California, and one each in Kentucky and New Jersey. 57 patients were treated during November 2018 to October 2020. Paired samples from all three time points were available for 49 patients. After two weekly injections there were increases in thymus- and activation-regulated chemokine (TARC, CCL17), the chemotactic protein chemerin, lipocalin-2, (expressed by macrophages and epithelium in response to inflammation) and angiotensin-1 (suppressor of vascular inflammation), and decreases in thrombospondin-5 (possibly involved in synaptogenesis in brain repair), angiotensinogen (a precursor of all angiotensin peptides), and beta-fibroblast growth factor (important in tissue repair). The increase in TARC ($p < 0.0000001$) was attributed to GM-CSF; TARC had declined almost to baseline levels by week-8. The other six markers had p values between 0.0011 and 0.0087. The only marker that was still changed at week-8 was thrombospondin-5 ($p = 0.023$).

Conclusions If there were humoral changes in proteins associated with Th1 and Th2 responses, these were no longer present after two weekly vaccinations. More sophisticated analyses of this data set, such as principal component analysis, may be needed to understand the effects of AV-GBM-1.

Trial Registration ClinicalTrials.gov NCT03400917

Ethics Approval This study was approved by the Western IRB, approval number 20182582; all participants gave written informed consent before taking part

<http://dx.doi.org/10.1136/jitc-2021-SITC2021.333>

334

PHASE I STUDY OF SAFETY AND ACTIVITY OF PERSONALIZED NEOANTIGEN-BASED VACCINES IN COMBINATION WITH TUMOR TREATING FIELDS FOR NEWLY DIAGNOSED GLIOBLASTOMA PATIENTS

Adilia Hormigo*, Julia Kodysh, Cansu Cimen Bozkus, Mansi Saxena, Marcia Meseck, Alexander Rubinsteyn, O Timothy, Tin Htwe Thin, Rachel Brody, John Mandeli, Nina Bhardwaj. *Icahn School of Medicine at Mount Sinai, New York, NY, USA*

Background Glioblastoma (GBM) is one of the most aggressive and lethal cancers (median survival 15 months) characterized by a highly heterogeneous and immunosuppressive tumor microenvironment (TME). New treatments need to include innovative strategies that impact the TME, such as immunomodulation using neoantigen vaccines combined with other modalities like Tumor Treating Fields (TTFields) shown to significantly increase progression-free and overall survival. TTFields disrupt metaphase by delivering 200 kHz low-intensity, alternating electric fields via arrays applied to the scalp. Pre-clinical TTFields studies reveal a role for tumor-infiltrating CD8+ cytotoxic lymphocytes in controlling local disease and decreasing metastases. Therefore, combining the standard care for GBM with a vaccine platform and TTFields may enhance efficacy and improve outcomes.

Methods Adult patients diagnosed with GBM that underwent a maximum debulking surgery, yielding sufficient specimen for sequencing, and treated with standard care (radiotherapy with concurrent and adjuvant Temozolomide chemotherapy) were enrolled to receive personalized neoantigen vaccines with or without TTFields (NCT03223103). Neoantigens were identified using the OpenVax computational pipeline. PBMCs were collected at baseline and weeks 3, 5, 11, 19, 27, 35, 39, 43, 47, 52 and 104. The primary objectives were the safety and toxicity of the vaccines alone and in combination with TTFields. The secondary objectives were patient survival, evaluation of TME using multiplexed immunohistochemistry analysis, and ex vivo and in vitro immunogenicity assays to characterize vaccine-induced epitope-specific T cell responses.

Results We completed the enrollment of 12 patients (median age 60, range 32–84) between December 2017 and July 2020. The median tumor mutational burden found in the tumors was 3 coding mutations/MB, with a median of 18 predicted neoantigens (range 7 - 155). Each patient was vaccinated with a median of 10 (range 6 -10) synthetic long peptides (each up to 25 amino acids). Patients received up to 14 peptide vaccines, with poly-ICLC as an adjuvant, every other week for two months and once a month thereafter. Some patients elected to receive additional vaccines after the planned 14 injections. The most common adverse events were injection site reactions and flu-like symptoms. Combination with TTFields did not increase toxicity. Nine patients who have a median follow-up of 25 months are alive, with eight remaining disease-free.

Conclusions The combined treatment is well tolerated with minimal addition of adverse events related to vaccination. Preliminary analysis demonstrated induction of robust epitope-specific T cell responses. More immune monitoring data, TME evaluation, and mature survival analysis are anticipated in November.

Acknowledgements Thank you to all the patients and families who have been so eager to participate in the study.

Ethics Approval This study was approved by the Institutional Review Board of the Icahn School of Medicine at Mount

Sinai, number 17-00204. All the patients gave informed consent.

<http://dx.doi.org/10.1136/jitc-2021-SITC2021.334>

335

LEUKAPHERESIS TO OBTAIN MONOCYTES TO PRODUCE DENDRITIC CELLS IN MANUFACTURING OF PERSONAL AUTOLOGOUS AV-GBM-1 VACCINES IN A PHASE II TRIAL IN PATIENTS WITH NEWLY DIAGNOSED GLIOBLASTOMA

¹Renato LaRocca, ²Daniela Bota*, ³David Piccione, ⁴Christopher Duma, ⁵Santosh Kesari, ⁵Jose Carrillo, ²Xiang-Tang Kong, ²Frank Hsu, ⁶Robert Aiken, ⁷Mehrdad Abedi, ²Thomas Taylor, ⁸Candace Hsieh, ⁸Gabriel Nistor, ⁸Robert Dillman. ¹Norton Cancer Institute, Louisville, KY, USA; ²University of California Irvine, Orange, CA, USA; ³University of California San Diego, San Diego, CA, USA; ⁴Hoag NeuroSciences institute, Newport Beach, CA, USA; ⁵John Wayne Cancer Institute, Santa Monica, CA, USA; ⁶Rutgers Cancer Center, New Brunswick, NJ, USA; ⁷University of California Davis, Sacramento, CA, USA; ⁸AIVITA Biomedical Inc., Irvine, CA, USA

Background For patients with newly diagnosed primary glioblastoma (GBM), maximum safe surgical resection, concurrent radiation therapy and temozolomide chemotherapy (RT/TMZ) followed by maintenance TMZ results in a 2-year survival of only 25%. Adding treatment with AV-GBM-1, a personal vaccine consisting of autologous dendritic cells (DC) pulsed with autologous tumor antigens (ATA), may improve survival. One objective of a multi-center phase II clinical trial was to determine the feasibility of collecting sufficient monocytes (MC) from which to generate DC for pulsing with ATA from GBM tumor-initiating cells (TIC).

Methods Peripheral blood mononuclear cells were collected by leukapheresis per local standard operating procedures, then shipped by overnight courier to the AIVITA laboratory in Irvine, CA. The product was enriched for MC using the Elutra[®] Cell Separation System (Terumo, Lakewood, CO.). If fewer than 450 million MC were collected, an additional leukapheresis was allowed. MC were cryopreserved in liquid nitrogen and subsequently thawed and incubated in media containing granulocyte-macrophage colony-stimulating factor and interleukin-4 to differentiate MC into DC. Batches of patient-specific AV-GBM-1 were produced by incubating autologous DC with a lysate of irradiated TICs and aliquoted into individual doses.

Results Patients enrolled from five sites in California, one in Kentucky and one in New Jersey. 65 patients underwent 77 leukapheresis procedures between September 2018 and February 2020; 54 underwent a single pheresis, 10 two phereses, and 1 three (all unsuccessful). The average time from surgical resection to first pheresis was 26 days (range 6 to 90; 64/65 within 51 days). 63/65 (97%) had sufficient MC collected, 53/65 (82%) from a single leukapheresis; 10 required a second procedure. The interval from surgery to first pheresis was the same for those for whom MC collections were satisfactory after one pheresis compared to those who required more than one. The success rate for MC collection for East-coast sites was 14/15 versus 52/62 for West-coast sites ($p=0.68$); so, longer shipping distance was not an issue. 60 patients who enrolled with intent-to-treat had an average of 1.7 billion monocytes cryopreserved, which were subsequently thawed and differentiated into DC. An average of 750 million DC were incubated with ATA for the final DC-ATA product.

Conclusions Leukapheresis procedures reliably resulted in collection of sufficient numbers of monocytes to generate DC and large batches of personal AV-GBM-1 vaccines. Success after a single leukapheresis was not related to the interval from surgery to pheresis procedure, or distance from the processing site.

Trial Registration ClinicalTrials.gov NCT03400917

Ethics Approval This study was approved by the Western IRB, approval number 20182582; all participants gave written informed consent before taking part

<http://dx.doi.org/10.1136/jitc-2021-SITC2021.335>

336

ADVERSE EVENTS IN A PHASE II TRIAL OF AV-GBM-1: DENDRITIC CELL VACCINE PULSED WITH LYSATE ENRICHED FOR AUTOLOGOUS TUMOR-INITIATING CELL ANTIGENS FOR PATIENTS WITH NEWLY DIAGNOSED GLIOBLASTOMA

¹David Piccioni, ¹David Piccioni*, ²Daniela Bota, ³Renato LaRocca, ⁴Santosh Kesari, ⁴Jose Carillo, ²Xiao-Tang Kong, ⁵Christopher Duma, ⁶Mehrdad Abedi, ⁷Robert Aiken, ²Thomas Taylor, ⁸Candace Hsieh, ⁸Gabriel Nistor, ⁸Robert Dillman. ¹University of California San Diego, San Diego, CA, USA; ²University of California Irvine, Orange, CA, USA; ³Norton Cancer Institute, Louisville, KY, USA; ⁴John Wayne Cancer Institute, Santa Monica, CA, USA; ⁵Hoag Neuro Sciences Institute, Newport Beach, CA, USA; ⁶University of California Davis, Sacramento, CA, USA; ⁷Rutgers University, New Brunswick, NJ, USA; ⁸AIVITA Biomedical Inc., Irvine, CA, USA

Background Standard glioblastoma (GBM) therapy includes maximum safe resection, concurrent radiation therapy and temozolomide chemotherapy (RT/TMZ), and maintenance TMZ, but it is associated with a 2-year survival of only about 25%. Adding treatment with AV-GBM-1, a vaccine consisting of autologous dendritic cells (DC) pulsed with autologous tumor antigens (ATA) may improve survival, but it may be associated with additional toxicity. One objective of a multi-center phase II clinical trial was to identify, characterize, and enumerate treatment-emergent adverse events (TEAE) and serious AE (SAE) that occurred during AV-GBM-1 treatment.

Methods Key eligibility criteria for enrollment prior to starting RT/TMZ, were: (1) confirmation of primary GBM, (2) successful GBM cell culture, (3) collection of sufficient numbers of monocytes (MC) from leukapheresis, (4) Karnofsky Performance Status 70 or higher, and (5) planning to treat with concurrent RT/TMZ. Interleukin-4 and granulocyte-macrophage colony stimulating factor (GM-CSF) were used to differentiate DC from MC. AV-GBM-1 was manufactured while patients were being treated with RT/TMZ. Each vaccine consisted of autologous DC incubated with ATA from the lysate of irradiated GBM cells grown in serum-free media with factors that favor survival and proliferation of tumor initiating cells, i.e., tumor stem cells and early progenitor cells. Following RT/TMZ, patients were injected subcutaneously with cryopreserved AV-GBM-1 admixed with 500 µg GM-CSF at weeks 1, 2, 3, 8, 12, 16, 20 and 24. Adverse events (AE) were identified and classified per Common Terminology Criteria for Adverse Events (CTCAE v 4.03).

Results 57 patients received at least one injection of AV-GBM-1 during November 2018 to October 2020. Patients received an average of 6.9 injections; 39 (68.4%) received all 8 injections. Injections generally were well-tolerated. Only 26 AE were attributed to AV-GBM-1, 24 grade-1 and 2 grade-2, including injection site reactions (16%), flu-like symptoms (10%), and bone discomfort (7%). The most frequent TEAE were fatigue (54%), headache (37%), seizures (33%), nausea (30%), and focal weakness (28%). The frequency of seizures is higher than reported in other GBM trials; one patient discontinued AV-GBM-1 because of seizures. There were 55 SAE reported for 29 patients, including hospitalizations for 16 episodes of seizures in 13 patients, 7 falls in 6 patients, 6 episodes of focal weakness in 4 patients, and 3 for cerebral edema.

Conclusions AV-GBM-1 was well-tolerated, but it was associated with a high frequency of TEAE and SAE. The high frequency of focal neurologic events may be secondary to local inflammation induced by AV-GBM-1.

Trial Registration ClinicalTrials.gov NCT03400917

Ethics Approval This study was approved by the Western IRB, approval number 20182582; all participants gave written informed consent before taking part

<http://dx.doi.org/10.1136/jitc-2021-SITC2021.336>

337

INTRATUMORAL IMMUNE THERAPY FOR RECURRENT BREAST CANCER WITH POLYICLC, AND TREMELIMUMAB COMBINED WITH SYSTEMIC DURVALUMAB

¹Craig Slingluff*, ¹Ileana Mauldin, ¹Elizabeth Gaughan, ¹Patrick Dillon, ²Mateusz Opyrchal, ²Igor Puzanov, ³Megan Kruse, ³Brian Gastman, ⁴Philip Friedlander, ⁴Thomas Marron, ⁵Kristen Aufero, ⁵Mary Macri, ⁵Paul Schwarzenberger, ⁶Toni Ricciardi, ⁵Aileen Ryan, ⁵Ralph Venhaus, ⁴Mansi Saxena, ¹Nicole Edmonds, ⁴Nina Bhardwaj. ¹University of Virginia, Charlottesville, VA, USA; ²Roswell Park Cancer Institute, Buffalo, NY, USA; ³Cleveland Clinic, Cleveland, OH, USA; ⁴Mount Sinai School of Medicine, New York, NY, USA; ⁵Ludwig Institute for Cancer Research, New York, NY, USA; ⁶Ludwig Institution for Cancer Research, New York, NY, USA

Background Intratumoral (IT) cancer therapies may enhance T cell activation and tumor infiltration when combined with systemic checkpoint blockade. This approach may improve treatment of advanced breast cancer, which is commonly resistant to immune therapy.

Methods A multicenter basket-style trial (NCT02643303) was performed in patients with advanced solid tumors, who received polyICLC IT 1mg x 6, then intramuscular (IM) x 3, combined with intravenous (IV) durvalumab 1500 mg q4W. Most were assigned to cohorts also receiving tremelimumab: 10 mg IT or 75 mg IV. Goals were to assess tolerability and clinical activity. Treated tumors were evaluated for immune infiltrates on days (d) 0, 15, and 29 by multiparameter immunofluorescence histology. A strong signal for clinical response was in breast cancer patients; thus, an expansion cohort was enrolled. We report analysis of that breast cancer subgroup.

Results Nineteen participants with treatment-refractory recurrent breast cancer with median 4 prior lines of therapy were enrolled and treated with IV durvalumab and IT/IM polyICLC. Seventeen also received tremelimumab (15 IT, 2 IV). Common treatment-related AEs were fatigue, injection site pain, and chills. There was one dose-limiting toxicity in a participant who received tremelimumab IV, and died with severe hyponatremia (DLT) and progressive disease. Objective clinical responses (1 complete; 4 partial (1 unconfirmed)) were observed in 5 (26%), including 2/9 patients with triple-negative breast cancer (TNBC) and 3/10 with non-TNBC. Median OS was longer for those with CR, PR, or SD (not reached) vs. those with PD or not evaluable (5 months): two responders remain alive at 34+ and 40+ months. In injected tumors, there were significant increases from d0 to d29 in numbers/mm² of CD8+ T cells, CD20+ B cells, mature dendritic cells (DC), macrophages, and CD56+ NK cells, and in CD8+ cells with antigen-experience (CD45RO), cytotoxic function (granzyme B), activation (ICOS1), or proliferation (Ki67). CD8+ cells expressing LAG3 and TIM3 increased, as did PDL1+ tumor cells and stromal cells. There were no differences in cells expressing IDO, ARG1, CD39, or CD73. Among patients with objective response, vs. all others, proportions of intratumoral CD8+ cells expressing Ki67 increased ($p < 0.04$).

Conclusions IT tremelimumab and polyICLC plus systemic durvalumab is safe and has clinical activity in patients with advanced TNBC and non-TNBC. The therapy enhances intratumoral immune effectors and markers of T cell function in hypothesis-generating data that warrant confirmatory studies. Clinical response was associated with longer survival and increased CD8 T cell proliferation.

Trial Registration NCT02643303

Ethics Approval The study has been performed with approval of the institutional review boards of each participating institution (Roswell Park Cancer Institute: STUDY 00000121/1291016; Mount Sinai School of Medicine: IRB-17-01692;

University of Virginia: IRB # 19276; Cleveland Clinic: 18-694; Toledo: 300176; Dartmouth: STUDY00031630; Emory: IRB00099445). All participants give informed consent before enrolling and participating. The study was also performed with approval from the FDA

<http://dx.doi.org/10.1136/jitc-2021-SITC2021.337>

338

EFFECTS OF PEMBROLIZUMAB ON THE TUMOR MICROENVIRONMENT (TME) AFTER ONE PRESURGERY TREATMENT CYCLE IN PATIENTS WITH TRIPLE-NEGATIVE BREAST CANCER (TNBC): PHASE 1B KEYNOTE-173 STUDY

¹Peter Schmid*, ²Yeon Hee Park, ³Eva Muñoz-Couselo, ⁴Sung-Bae Kim, ⁵Joohyuk Sohn, ⁶Seock-Ah Im, ⁷Esther Holgado, ⁸Theodoros Foukakis, ⁹Sherko Kümmel, ¹⁰Rebecca Dent, ¹¹Yuan Sun, ¹¹Lingfang Huang, ¹¹Jennifer Yearley, ¹¹Petar Jelinic, ¹¹Vassiliki Karantz, ³Javier Cortés. ¹Centre for Experimental Cancer Medicine, London, UK; ²Samsung Medical Center, Seoul, Korea, Republic of; ³Vall d'Hebron Institute of Oncology (VHIO), Barcelona, Spain; ⁴Asan Medical Center, University of Ulsan College of Medicine, Seoul, Korea, Republic of; ⁵Yonsei Cancer Center, Yonsei University College of Medicine, Seoul, Korea, Republic of; ⁶Seoul National University Hospital, Cancer Research Institute, Seoul National University College of Medicine, Seoul, Korea, Republic of; ⁷Ramón y Cajal University, Madrid, Spain; ⁸Karolinska Institutet and Breast Cancer Center, Theme Cancer, Karolinska University Hospital, Solna, Sweden; ⁹Kliniken Essen-Mitte, Essen, Germany; ¹⁰International Breast Cancer Center Quironsalud Group, Singapore, Singapore; ¹¹Merck and Co., Inc., Kenilworth, NJ, USA

Background In the phase 3 KEYNOTE-522 trial, neoadjuvant pembrolizumab+chemotherapy followed by adjuvant pembrolizumab monotherapy resulted in a statistically significant improvement in pathologic complete response (pCR) and event-free survival, compared with neoadjuvant chemotherapy alone, in patients with early-stage TNBC. In the phase 1b KEYNOTE-173 (NCT02622074) trial—another neoadjuvant pembrolizumab+chemotherapy trial—we evaluated TNBC biopsy samples at baseline and collected after one cycle of neoadjuvant pembrolizumab, before the initiation of chemotherapy, to explore the features within the TME at both time-points that might be potentially predictive of clinical response and the effects of a single cycle of pembrolizumab on cell populations within the TME.

Methods Twenty paired samples (baseline and obtained following one cycle of pembrolizumab before the initiation of chemotherapy) were included. Multiplex immunohistochemistry analyzed deconvoluted cell fractions by spatial localization (tumor compartment, stromal compartment, or total tumor) using three 6-plex panels: T cell (CD3/CD8/FoxP3/Ki67/granzyme B/PD-1), myeloid cell (CD68/CD163/MHCII/arginase/CD33/CD11c), and natural killer cell (CD16/CD56/CD11b/CD20/CD3/CD45). Area under the receiver operating characteristic (AUROC) was used to assess associations between immune subsets and pCR. Analyses were descriptive, with top-ranked findings reported, and were deemed hypothesis generating; no claims of statistical significance are made.

Results At baseline, 6 of 75 evaluated immune subsets (counting different compartments) showed 95% CIs of AUROC not crossing 0.5 with pCR. These include some myeloid cell populations within the tumor compartment (AUROC, 95% CI), specifically CD11c⁺ (macrophage and dendritic cell [DC]: 0.85, 0.63–1.00), CD11c⁺/MHCII⁺/CD163⁻/CD68⁻ (DC: 0.76, 0.53–0.99), CD11c⁺/MHCII⁻/CD163⁻/CD68⁻ (nonactivated/immature DC: 0.8, 0.54–1.00), and CD11c⁺/CD163⁺ (M2 macrophage: 0.77, 0.55–0.99). Other associations with pCR included baseline CD11c⁺/MHCII⁻/CD163⁻/CD68⁻ (nonactivated/immature DC) within the total tumor (AUROC, 0.76; 95% CI, 0.51–1.00) and the baseline ratio of CD11c/CD3 within the tumor compartment (AUROC, 0.75; 95% CI, 0.52–0.98). Although T-cell associations were relatively weak, specific CD8 subsets, especially CD8⁺/granzyme B⁺/Ki67⁺, showed a trend toward association. Negative correlations between change from baseline and baseline values were observed; therefore, baseline detrending was applied to change

from baseline values. One immune subset showed a negative association trend between change from baseline and pCR after baseline detrending: CD163⁺/MHCII⁺ (DC3) within the stroma (AUROC, 0.2; 95% CI, 0.0–0.42).

Conclusions Although the sample size in this exploratory analysis was small (n=20), myeloid cell populations within the tumor compartment at baseline show a promising association trend, as evaluated by AUROC, with pCR after neoadjuvant pembrolizumab+chemotherapy in early-stage TNBC. Changes in immune subsets following one cycle of pembrolizumab were not strongly associated with pCR.

Trial Registration ClinicalTrials.gov, NCT02622074

Ethics Approval The study protocol and all amendments were approved by the relevant institutional review board or ethics committee at each study site.

Consent All patients provided written informed consent to participate in the clinical trial.

<http://dx.doi.org/10.1136/jitc-2021-SITC2021.338>

IMMUNE PROFILING TO INVESTIGATE IMPROVED SURVIVAL IN PATIENTS WITH METASTATIC TRIPLE-NEGATIVE BREAST CANCER RECEIVING TRILACICLIB PRIOR TO CHEMOTHERAPY

¹Aaron Stevens*, ²Joyce O'Shaughnessy, ¹Subing Cao, ¹Jessica Sorrentino, ¹Janet Horton, ¹John Yi, ³Antoinette Tan. ¹G1 Therapeutics, Inc., Research Triangle Park, NC, USA; ²Baylor University Medical Center, Texas Oncology Dallas, US Oncology Research, Dallas, TX, USA; ³Levine Cancer Institute, Atrium Health, Charlotte, NC, USA

Background Trilaciclib is an intravenous cyclin-dependent kinase 4/6 inhibitor approved to reduce the incidence of chemotherapy-induced myelosuppression in patients with extensive-stage small cell lung cancer (myeloprotection). In a randomized, open-label phase 2 trial in patients with metastatic triple-negative breast cancer (mTNBC), adding trilaciclib prior to gemcitabine/carboplatin (GCb) increased overall survival in both PD-L1-positive and -negative populations versus GCb alone.^{1 2} We investigated potential immune mechanisms of anti-tumor efficacy among patients who received trilaciclib plus GCb.

Methods Peripheral blood was collected prior to and on treatment for flow cytometric analysis, and total RNA isolated from diagnostic tumor biopsies for sequencing. Differential gene expression analysis between responders and non-responders was based on negative binomial distribution and related pathways identified by Kyoto Encyclopedia of Genes and Genomes pathway analysis. Tumor inflammation signatures and deconvolution-based approaches were used to assess the tumor immune microenvironment. PD-L1 expression was considered positive if $\geq 1\%$ of the total tumor area contained PD-L1-labelled immune cells (Ventana SP142 assay). Patients were defined as responders (confirmed complete or partial response) or non-responders (stable or progressive disease) according to RECIST criteria.

Results Of 68 patients who received trilaciclib prior to GCb, tumor response status and RNA sequencing data were available for 51 patients, comprising 24 responders and 27 non-responders. Tumors from responders had 253 differentially expressed genes compared with non-responders. Analysis of immune gene signatures revealed a higher T-cell exhaustion score at baseline among responders versus non-responders ($P=0.044$). Among patients with PD-L1-positive tumors, responders had a greater peripheral immune response at baseline compared with non-responders, including more T cells ($P=0.037$; particularly memory CD8 T cells [$P=0.042$]), and a trend toward fewer myeloid-derived suppressor cells (MDSCs). Additionally, tumors from responders had more dendritic cells ($P=0.044$) and a trend toward enriched tumor inflammation signatures compared with non-responders. By contrast, among patients with PD-L1-negative tumors, responders had similar peripheral immune populations at baseline compared with PD-L1-negative non-responders, but fewer MDSCs ($P=0.016$), and a trend toward increased T-cell numbers after two cycles of trilaciclib plus GCb. Responders with both PD-L1-positive and -negative tumors had increased numbers of naïve CD8 T cells after two treatment cycles compared with non-responders.

Conclusions The data suggest that adding trilaciclib prior to GCb enhances antitumor efficacy by modulating the composition of immune cell subsets. The impact of trilaciclib on changes to the tumor-infiltrating immune response is being further investigated in a phase 3 trial in patients with mTNBC (NCT04799249).

Acknowledgements Flow cytometry and RNA sequencing analyses were performed by Covance, Inc., and Q2 Laboratory Solutions, respectively.

Trial Registration www.clinicaltrials.gov/NCT02978716

REFERENCES

1. Tan AR, Wright GS, Thummala AR, Danso MA, Popovic L, Pluard TJ, Han HS, Vojnović Ž, Vasev N, Ma L, Richards DA, Wilks ST, Milenković D, Yang Z, Antal JM, Morris SR, O'Shaughnessy J. Trilaciclib plus chemotherapy versus chemotherapy alone in patients with metastatic triple-negative breast cancer: a multicentre, randomised, open-label, phase 2 trial. *Lancet Oncol* 2019;**20**(11):1587–1601.
2. O'Shaughnessy J, Wright GS, Thummala AR, Danso MA, Popovic L, Pluard TJ, Han HS, Vojnović Ž, Vasev N, Ma L, Richards DA, Wilks ST, Milenković D, Xiao J, Sorrentino JA, Horton J, Tan AR. Abstract PD1-06: trilaciclib improves overall survival when given with gemcitabine/carboplatin in patients with metastatic triple-negative breast cancer: final analysis of a randomized phase 2 trial. *Cancer Res* 2021;**81**(4 Supplement):PD1-06.

Ethics Approval The study protocol and all associated amendments and study-related materials were approved by the institutional review board or independent ethics committee of each investigational site.

<http://dx.doi.org/10.1136/jitc-2021-SITC2021.339>

A PHASE IB STUDY OF THE SAFETY AND TOLERABILITY OF PIXATIMOD PLUS NIVOLUMAB IN SUBJECTS WITH ADVANCED SOLID TUMORS WITH AN EXPANSION COHORT IN METASTATIC PANCREATIC ADENOCARCINOMA (MPDAC)

¹Charlotte Lemech*, ²Keith Dredge, ²Darryn Bampton, ²Edward Hammond, ³Amanda Stanley, ³Lucie Leveque-ElMouttie, ³Grace Chojnowski, ⁴Andrew Haydon, ⁵Nick Pavlakis, ⁶Matthew Burge, ⁷Michael Brown, ⁸David Goldstein. ¹Scientia Clinical Research Pty Ltd, Randwick, Australia; ²Zucero Therapeutics Ltd, Brisbane, Australia; ³QIMR Berghofer, Brisbane, Australia; ⁴The Alfred Hospital, Melbourne, Australia; ⁵Royal North Shore Hospital, Sydney, Australia; ⁶Royal Brisbane and Women's Hospital, Brisbane, Australia; ⁷Royal Adelaide Hospital, Adelaide, Australia; ⁸Prince of Wales Hospital, Sydney, Australia

Background Pixatimod is a novel immunomodulatory agent which stimulates dendritic cells (DC) via Toll-Like Receptor (TLR9) pathway to activate natural killer (NK) cells.¹ In combination with PD1 inhibitors, it also enhances T cell infiltration in vivo.² We report on safety, pharmacokinetics (PK) and pharmacodynamics (PD), and antitumor activity of pixatimod plus nivolumab in advanced cancer patients (stage 1) and in an expansion cohort of mPDAC (stage 2).

Methods In the dose escalation stage (3+3 design), eligible patients (ECOG≤1) with advanced solid malignancies who failed standard therapies received pixatimod once weekly as a 1-hour i.v. infusion plus nivolumab (240 mg, every other week) until disease progression or discontinuation due to intolerance. The primary objective was determination of the maximum tolerated dose (MTD). Secondary objectives evaluated safety, antitumor activity per RECIST v1.1, PK of pixatimod, and PD (PBMC, plasma cytokines and chemokines). Stage 2 comprised mPDAC subjects who had received no more than one prior line of chemotherapy in the metastatic setting.

Results The dose-escalation stage recruited 16 subjects across two cohorts (25 & 50 mg pixatimod). Two dose limiting toxicities (DLTs) in 50 mg cohort were pulmonary edema and multi-organ failure. Of note, the subject with multi-organ failure had substantially higher CA19.9, Pan-immune-Inflammatory Value (PIV = Neutrophils x Platelets x Monocytes/Lymphocytes) and interleukins (IL) IL-1 α and IL-23 at baseline compared with the cohort. One DLT occurred in the 25 mg cohort, pneumonitis, which was identified as the MTD. A further 14 mPDAC subjects were recruited to the expansion stage (25 mg). Seven SAEs were reported to be possibly or likely related to the combination. No objective responses were reported in the mPDAC stage, the best response was SD (n = 3). In another submitted abstract by Lemech et al, we report two subjects in the dose escalation stage with MSS mCRC were confirmed PR, and data from the amended study to include an MSS mCRC expansion cohort will also be presented. Time versus concentration data for pixatimod in advanced cancer patients was similar to that previously reported in monotherapy setting. In mPDAC subjects, there was minimal immune activation as evidenced by a lack of change in effector memory T cells or NK cells in PBMC, plasma cytokines and chemokines.

Conclusions Pixatimod is well tolerated at 25 mg in combination with nivolumab but did not provide clear clinical benefit or evidence of immune activation in the mPDAC cohort.

Acknowledgements Research funding was provided by Zucero Therapeutics Ltd and Bristol Myers Squibb (BMS), Australia.

Trial Registration Clinical trial information: ACTRN12617001573347.

REFERENCES

- 1.. Brennan TV, Lin L, Brandstadter JD, Rendell VR, Dredge K, Huang X, et al. Heparan sulfate mimetic PG545-mediated antilymphoma effects require TLR9-dependent NK cell activation. *J Clin Invest* 2016;**126**(1):207–19.
- 2.. Hammond E, Haynes NM, Cullinane C, Brennan TV, Bampton D, Handley P, et al. Immunomodulatory activities of pixatimod: emerging nonclinical and clinical data, and its potential utility in combination with PD-1 inhibitors. *J Immunother Cancer* 2018;**6**(1):54.

Ethics Approval The clinical trial entitled “An open-label, multi-centre Phase Ib study of the safety and tolerability of IV infused PG545 in combination with nivolumab in patients with advanced solid tumours with an expansion cohort in patients with metastatic pancreatic cancer. Protocol ZU545102” obtained ethics approval from the Royal Adelaide Hospital (HREC Reference number, HREC/17/RAH/195 and the CALHN Reference number, R20170515) and Bellberry Limited (Application No: 2018-08-695). All participants in the study gave informed consent before taking part in ZU545102.

<http://dx.doi.org/10.1136/jitc-2021-SITC2021.340>

A PHASE IB EXPANSION COHORT OF PIXATIMOD PLUS NIVOLUMAB IN PREVIOUSLY TREATED, MICROSATELLITE STABLE METASTATIC COLORECTAL CANCER (MSS MCRC)

¹Charlotte Lemech*, ²Keith Dredge, ²Darryn Bampton, ²Edward Hammond, ³Andrew Clouston, ⁴Nigel Waterhouse, ⁴Amanda Stanley, ⁴Lucie Leveque-ElMouttie, ⁴Grace Chojnowski, ⁵Andrew Haydon, ⁶Nick Pavlakis, ³Matthew Burge, ⁷Michael Brown, ⁸David Goldstein. ¹Scientia Clinical Research Pty Ltd, Randwick, Australia; ²Zucero Therapeutics Ltd, Brisbane, Australia; ³Royal Brisbane and Women's Hospital, Brisbane, Australia; ⁴QIMR Berghofer, Brisbane, Australia; ⁵The Alfred Hospital, Melbourne, Australia; ⁶Royal North Shore Hospital, Sydney, Australia; ⁷Royal Adelaide Hospital, North Ice, Adelaide, SA, Australia; ⁸Prince of Wales Hospital, Sydney, Australia

Background Pixatimod is a novel immunomodulatory agent which stimulates dendritic cells (DC) via Toll-Like Receptor 9 (TLR9) pathway to activate natural killer (NK) cells.¹ It also enhances T cell infiltration into tumors when combined with PD1 inhibitors in vivo.² We report on safety, pharmacodynamics (PD), and antitumor activity of pixatimod plus nivolumab in a cohort of previously treated MSS mCRC subjects.

Methods Eligible MSS mCRC patients (ECOG≤1) with a median of 3 lines of previous treatment received 25 mg pixatimod once weekly as a 1-hour i.v. infusion plus nivolumab (240 mg, every other week) until disease progression or discontinuation due to intolerability. Primary and secondary objectives included the assessment of safety and antitumor activity per RECIST v1.1 at the recommended dose, and evidence of immune activation in peripheral blood mononuclear cells (PBMC), plasma cytokines/chemokines, and paired tumor tissue biopsies, where available.

Results Thirty-three subjects with MSS mCRC (42% male) started treatment. Median age was 58 (range 35–80), median number of previous lines of chemotherapy was 3 (range 1–6), ECOG PS 0/1 was 67%/33%, 64% had target liver metastases, and primary tumor site was right-sided/transverse colon in 21% and left-sided colon/rectum 79%. Median number of cycles completed was 2 (range 0–13). Treatment-related AEs led to treatment discontinuation in 2 patients (autoimmune hepatitis and pneumonitis). Ten Grade 3 treatment-related AEs were reported in 4 subjects (12%). Thirty subjects received at least one cycle of treatment (1-month), with 25 subjects having initial post-baseline assessment scans > 6 weeks (as per RECIST v1.1). Of these, 3 subjects had confirmed partial responses and 8 had stable disease. Lower Pan-immune-Inflammatory Value (PIV = Neutrophils x Platelets x Monocytes/Lymphocytes) at screening were associated with clinical benefit (PR/SD). Post-treatment increases in plasma IP-10 and IP-10/IL-8 ratio, effector memory (CD45RA-CCR7-) CD4+ and CD8+ T cells, and Ki-67 expression in CD4+ and CD8+ T cells from PBMC were also detected in the clinical benefit cohort compared to subjects with progressive disease. Conversely, plasma levels of IL-6 were significantly lower in patients with clinical benefit. Analyses of pre- & on-treatment biopsies from the only PR patient with available paired biopsies demonstrated an increase in T cell infiltration.

Conclusions Pixatimod is well tolerated at 25 mg in combination with a standard dose of nivolumab. The efficacy signal and pharmacodynamic changes in MSS mCRC warrants further investigation of pixatimod plus nivolumab for this patient population.

Acknowledgements Research Funding provided by Zucero Therapeutics Ltd and Bristol Myers Squibb (BMS), Australia.

Trial Registration

Clinical trial information ACTRN12617001573347

REFERENCES

- 1.. Brennan TV, Lin L, Brandstadter JD, Rendell VR, Dredge K, Huang X, *et al.* Heparan sulfate mimetic PG545-mediated antilymphoma effects require TLR9-dependent NK cell activation. *J Clin Invest* 2016;**126**(1):207–19.
- 2.. Hammond E, Haynes NM, Cullinane C, Brennan TV, Bampton D, Handley P, *et al.* Immunomodulatory activities of pixatimod: emerging nonclinical and clinical data, and its potential utility in combination with PD-1 inhibitors. *J Immunother Cancer* 2018;**6**(1):54.

Ethics Approval The clinical trial entitled “An open-label, multi-centre Phase Ib study of the safety and tolerability of IV infused PG545 in combination with nivolumab in patients with advanced solid tumours with an expansion cohort in patients with metastatic pancreatic cancer. Protocol ZU545102” obtained ethics approval from the Royal Adelaide Hospital (HREC Reference number, HREC/17/RAH/195 and the CALHN Reference number, R20170515) and Bellberry Limited (Application No: 2018-08-695). All participants in the study gave informed consent before taking part in ZU545102.

<http://dx.doi.org/10.1136/jitc-2021-SITC2021.341>

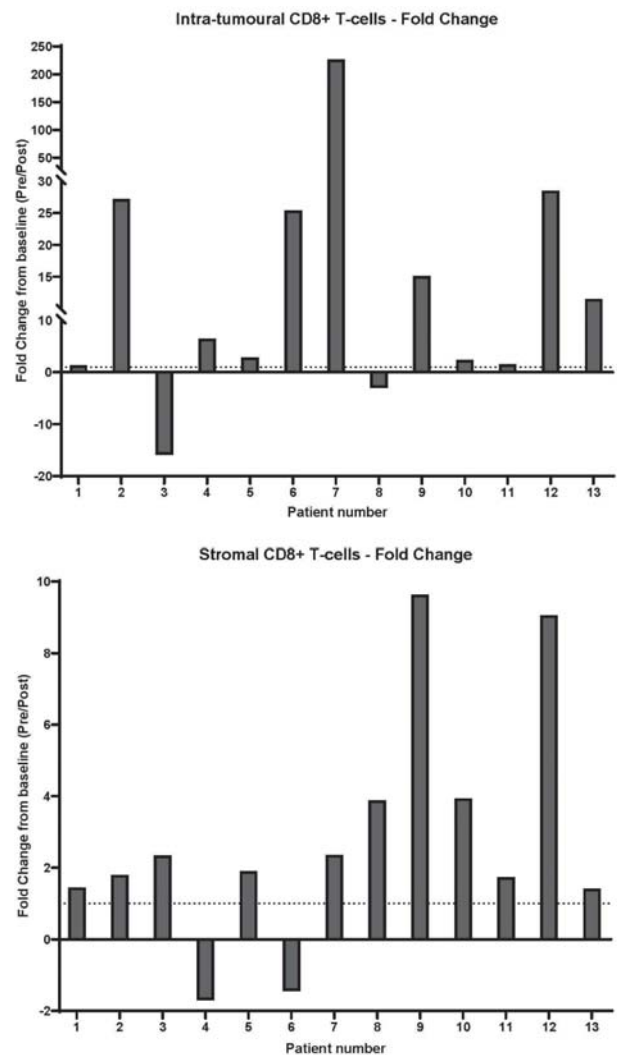
COMBINING ENADENOTUCIREV AND NIVOLUMAB INCREASED TUMOUR IMMUNE CELL INFILTRATION/ACTIVATION IN PATIENTS WITH MICROSATELLITE-STABLE/INSTABILITY-LOW METASTATIC COLORECTAL CANCER IN A PHASE 1 STUDY

¹David Krige*, ²Marwan Fakhri, ³Lee Rosen, ⁴Ding Wang, ⁵Wael Harb, ⁶Hani Babiker, ⁷Jordan Berlin, ¹Gianfranco Di Genova, ¹David Miles, ¹Mark Powell, ¹Minesh Patel, ¹Jo Carter, ¹Richard Brown, ¹Tom Lillie. ¹PsiOxus Therapeutics Ltd, Abingdon, UK; ²City Of Hope Cancer Centre, Duarte, CA, USA; ³UCLA Medical Center, Los Angeles, CA, USA; ⁴Henry Ford Hospital, Detroit, MI, USA; ⁵Horizon Oncology Research Inc, Lafayette, IN, USA; ⁶Mayo Clinic Cancer Center, Jacksonville, FL, USA; ⁷Vanderbilt Ingram Cancer Center, Nashville, TN, USA

Background Microsatellite-stable (MSS) and instability-low (MSI-L) metastatic colorectal cancer (mCRC) are typically characterised as "immune-excluded/desert" tumour microenvironments lacking T-cell infiltration. Anti-PD-1 monotherapy has little clinical benefit in MSS/MSI-L mCRC¹ and knowledge of the effects of PD-1 inhibition on T-cell activation/infiltration in this population is limited. Novel combination therapies to overcome anti-PD-1 resistance are required. SPICE is a multi-centre, open-label, phase 1 study of the tumour-selective chimeric Ad11/Ad3 group B oncolytic adenovirus enadenotucirev plus nivolumab in patients with metastatic/advanced epithelial tumours refractory to standard therapy. Preliminary data from patients with MSS/MSI-L mCRC demonstrated a median overall survival of 14 months, manageable tolerability and intratumoural T-cell infiltration.² Here we characterise the immunological effects of tumour re-engineering with enadenotucirev in combination with nivolumab in patients with MSS/MSI-L mCRC.

Methods Patients received increasing doses and/or cycles of intravenous enadenotucirev followed by up to 8 cycles of nivolumab as previously described.² Wherever possible, pre- and post-treatment (~5 weeks post-first enadenotucirev) biopsies were collected; samples were analysed using immunohistochemistry and automated image analysis. Peripheral blood mononuclear cell immunophenotyping (multiparameter flow cytometry) and serum cytokines were assessed at multiple times.

Results 43 patients with mCRC were treated (86% MSS/MSI-L; 14% unknown). Among the 13 patients (12/13 MSS/MSI-L; 1/13 unknown) with matched biopsies, 11 had increased intratumoural and stromal CD8+ T-cell infiltration in post-treatment biopsies (median [Q1-Q3] fold changes 6.5× [1.5–25.4] and 1.9× [1.5–3.9], respectively; figure 1). CD4+ T-cell density increased in 10/13 patients and 8/13 patients had increased proportions of PD-L1+ immune cells. Increases in CD8 T-cell proliferation (Ki67; 7/9 patients) and cytolytic activity (Granzyme B; 7/13 patients) markers were seen. 4/13 patients converted from a "desert" to an "inflamed" immune phenotype (pathologist scored CD8/pan-cytokeratin staining). Immunophenotyping showed trends towards increased T-cell activation (CD38+ and HLA-DR+ CD8+ T cell populations) post-treatment (9/10 patients), including in one patient who had only received enadenotucirev prior to sampling. Persistent increases in inflammatory cytokines (IFN γ , IL-12p70, IL-17a) were seen in two patients from ~Day 15, including one who achieved a sustained objective response.



Abstract 342 Figure 1 Tumour immune cell infiltration following treatment with enadenotucirev plus nivolumab

Conclusions These data show that intravenous enadenotucirev plus nivolumab can induce immune infiltration/activation within MSS/MSI-L mCRC. These encouraging findings suggest that immune activation can be achieved even in "immune-excluded/desert" tumours. SPICE has been closed following completion of dose-escalation. Efforts are now focused on the development of next-generation variants of enadenotucirev designed to further re-programme the tumour microenvironment by expressing immune-enhancer transgenes (T-SIGN vectors); these studies are ongoing (NCT04830592, NCT04053283, NCT03852511).

Acknowledgements This study was funded by PsiOxus Therapeutics Limited and Bristol Myers Squibb. Medical writing support: Lola Parfitt, MRes, of PsiOxus Therapeutics Limited. **Trial Registration** EudraCT number: 2017-001231-39NCT number: NCT02636036

REFERENCES

- 1.. Kawazoe A, Kuboki Y, Shinozaki E, *et al.* Multicenter phase I/II trial of napabucicin and pembrolizumab in patients with metastatic colorectal cancer (EPOC1503/SCOOP trial). *Clin Cancer Res* 2020;**26**:5887–5894.
2. . Fakhri M, Wang D, Harb W, *et al.* SPICE: a phase I multicenter study of enadenotucirev in combination with nivolumab in tumors of epithelial origin: an analysis of the metastatic colorectal cancer patients in the dose escalation phase. *Ann Oncol* 2019;**30**(suppl_5):v252.

Ethics Approval The study was approved by the WCG Institutional Review Board (study approval number 20152656), UCLA Institutional Review Board (study approval number IRB#15-002010), Vanderbilt Institutional Review Board (study approval number IRB #171453) and Henry Ford Institutional Review Board (study approval number IRB #10349).

<http://dx.doi.org/10.1136/jitc-2021-SITC2021.342>

MULTIOMIC BIOMARKER SIGNATURES IDENTIFY SUBSETS OF PATIENTS WHO MAY BENEFIT FROM EITHER NIVOLUMAB OR SOTIGALIMAB IN COMBINATION WITH CHEMOTHERAPY IN METASTATIC PANCREATIC CANCER

¹Deena Maurer*, ¹Jia Xin Yu, ²Kamil Sklodowski, ²Marco Tognetti, ²Lukas Reiter, ²Roland Bruderer, ²Jakob Vowinkel, ¹Shannon Pfeiffer, ³Mark O'Hara, ⁴Eileen O'Reilly, ⁵Robert Wolff, ⁶Zev Wainberg, ⁷Andrew Ko, ⁸Osama Rahm, ⁹George Fisher, ¹Jadlyn Lyman, ¹Christopher Cabanski, ¹Pier Federico Gherardini, ¹⁰Jill O'Donnell-Tormey, ¹Theresa LaVallee, ³Robert Vonderheide, ¹Lacey Kitch. ¹Parker Institute for Cancer Immunotherapy, San Francisco, CA, USA; ²Biognosys, Schlieren, Switzerland; ³Abramson Cancer Center at University of Pennsylvania, Philadelphia, PA, USA; ⁴Memorial Sloan Kettering Cancer Center, New York, NY, USA; ⁵University of Texas MD Anderson Cancer, Houston, TX, USA; ⁶University of California, Los Angeles, Santa Monica, CA, USA; ⁷University of California, San Francisco, San Francisco, CA, USA; ⁸Dana-Farber Cancer Institute, Boston, MA, USA; ⁹Stanford University School of Medicine, Stanford, CA, USA; ¹⁰Cancer Research Institute, New York, NY, USA

Background Gemcitabine/nab-Paclitaxel (GnP) is a standard of care regimen for first-line metastatic pancreatic ductal adenocarcinoma (PDAC) and has a 1-year overall survival (OS) rate of approximately 35%. There is an urgent need for novel therapeutics and precision medicine approaches in PDAC. PRINCE, a randomized phase 2 trial, reported an increased 1-year OS relative to historical data, for patients treated with nivolumab (nivo)/GnP (57.3%, $p = 0.007$, $n=34$) and sotigalimab (sotiga) (APX005M; CD40 agonist)/GnP (48.1%, $p = 0.062$, $n= 36$).

Methods To investigate immune modulatory and pharmacodynamic (PD) effects of nivo or sotiga in combination with GnP we used several orthogonal minimally invasive, blood-based biomarker technologies. Immune population profiles were evaluated by CyTOF and features of T cell phenotype and function by multicolor flow cytometry. Soluble proteins were evaluated with predefined panels using the Olink platform (Immuno-oncology (IO) and Immune Response) along with an unbiased mass spectrometry proteomic approach (Biognosys) that identified circulating soluble proteins of significance.

Results Relative to baseline, patients who received nivo/GnP had numerically increased frequencies of proliferating, activated CD8+ and CD4+ effector memory T cells in circulation across multiple timepoints. These patients also had significantly increased levels of soluble proteins associated with type II interferon responses and immune cell migration and T cell activation, as well as significantly decreased levels of immunomodulatory proteins. Patients who received sotiga/GnP had increased expression of the co-stimulatory molecule CD86 on conventional dendritic cells. These patients also had significantly increased concentrations of soluble proteins associated with mature antigen presenting cells, and the activation of helper CD4+ T cells, B cells, and monocytes. Significant increases in soluble proteins associated with type-1 cell-mediated effector immunity and decreases in immunosuppressive factors were observed in both arms. Significant proteins were defined as $p \leq 0.05$, \log_2 expression fold change ≥ 0.5 (Olink) and Sparse PLS discriminant analysis was used with zero as a threshold (Biognosys).

Conclusions This study is a first to use multiomic minimally invasive biomarker approaches in PDAC to demonstrate PD effects and immune modulation with immunotherapy/chemotherapy combinations. Orthogonal assays demonstrate that nivo/GnP and sotiga/GnP elicit unique immune responses and the observed effects are consistent with their distinct mechanisms of action. These data suggest that multiomic biomarker

signatures may identify subsets of patients who may benefit from an immunotherapy/chemo approach in PDAC. Moreover, results from these analyses will support early phase clinical study development decisions.

Acknowledgements We extend our gratitude to the patients, their families, the clinical investigators, and their site staff members who are making this trial possible. We would also like to thank Sultan Nawabi at Parker Institute for Cancer Immunotherapy (PICI) for operations leadership of the trial. We thank Bristol Myers Squibb (BMS) and Apexigen for collaboration and study drugs. The study was funded by Cancer Research Institute, BMS and PICI.

Trial Registration NCT03214250

Ethics Approval This study was approved by University of Pennsylvania Institutional Review Board; Federalwide assurance #00004028.

<http://dx.doi.org/10.1136/jitc-2021-SITC2021.343>

344

AVELUMAB + BINIMETINIB IN METASTATIC PANCREATIC DUCTAL ADENOCARCINOMA (MPDAC): DOSE-ESCALATION RESULTS FROM THE PHASE 1B/2 JAVELIN PARP MEKI TRIAL

¹Jordi Rodon*, ²Daniel Weng Tan, ³Ignacio Garrido Laguna, ⁴Wael Harb, ⁵J Thaddeus Beck, ⁶Nathan Bahary, ⁷Sylvie Rottey, ⁸Zhou Zhu, ⁸Shibing Deng, ⁹Karen Kowalski, ⁹Grainne O'Neill, ¹⁰Caimiao Wei, ⁸Nuzhat Pathan, ¹¹Wells Messersmith. ¹The University of Texas MD Anderson Cancer Center, Houston, Texas, USA, Houston, TX, USA; ²National Cancer Centre Singapore, Singapore; ³University of Utah Huntsman Cancer Institute, Salt Lake City, Utah, USA, Salt Lake City, UT, USA; ⁴Horizon Oncology Research, Inc, Lafayette, Indiana, USA, Lafayette, IN, USA; ⁵Highlands Oncology Group, Fayetteville, Arkansas, USA, Fayetteville, AR, USA; ⁶UPMC Cancer Pavilion, Pittsburgh, Pennsylvania, USA, Pittsburgh, PA, USA; ⁷UZ Gent, Gent, Belgium, GENT, Belgium; ⁸Pfizer, San Diego, California, USA, San Diego, CA, USA; ⁹Pfizer, Walton Oaks, Surrey, UK, Walton Oaks, UK; ¹⁰Pfizer, Groton, Connecticut, USA, Groton, CT, USA; ¹¹University of Colorado Cancer Center, Aurora, Colorado, USA, aurora, CO, USA

Background Preclinical studies of avelumab (anti-PD-L1) + binimetinib (MEK inhibitor [MEKi]) showed encouraging anti-tumor activity. We report results from the phase 1b JAVELIN PARP MEKi trial (NCT03637491) evaluating avelumab + binimetinib in patients with mPDAC.

Methods Eligible patients had mPDAC and disease progression during or following 1–2 prior lines for advanced or metastatic disease. Patients received avelumab 800 mg intravenously every 2 weeks and binimetinib 30 or 45 mg orally twice daily. The primary endpoint for phase 1b was dose-limiting toxicity (DLT). Secondary endpoints included safety, confirmed objective response per investigator (RECIST 1.1), pharmacokinetics, immunogenicity, and biomarker analyses. PD-L1 expression (SP263 assay) and CD8+ tumor-infiltrating lymphocytes (TILs) in baseline tumor samples were assessed using immunohistochemistry. Molecular alterations were assessed via plasma ctDNA analyses. Blood samples were collected to assess trough concentrations for avelumab, binimetinib, and AR00426032 (binimetinib metabolite) and end-of-infusion concentration for avelumab.

Results 22 patients received avelumab + binimetinib 30 mg (n=10) or 45 mg (n=12); all discontinued treatment. Among 21 DLT-evaluable patients, DLTs occurred in 3/10 (30.0%) in the 30-mg group (mucosal inflammation, dermatitis acneiform, blood creatine phosphokinase increased [n=1 each]) and 5/11 (45.5%) in the 45-mg group (detachment of retinal pigment epithelium, abdominal pain, diarrhea, nausea, vomiting, rash pustular, hypertension, blood creatine phosphokinase increased [n=1 each]). Any-grade treatment-related adverse events (TRAEs) occurred in all 22 patients; grade =3 TRAEs occurred in 8 (80.0%) and 4 (33.3%) in the 30- and 45-mg groups, respectively, most commonly blood creatine phosphokinase increased (n=3 [30.0%], n=2 [16.7%], respectively). No treatment-related deaths occurred. Objective response rates (95% CI) in the 30- and 45-mg groups were 0% (0.0–30.8) and 8.3% (0.2–38.5; 1 partial response), respectively; 1 (10.0%) and 6 (50.0%) had a best overall response of stable disease. Tumor shrinkage was associated with higher baseline PD-L1 expression, higher number of CD8+ TILs, and *MEK1/2*, *PIK3CA*, and *RNF43* alterations, whereas *ERBB4* alterations correlated inversely with tumor size change. Available data indicate that avelumab, binimetinib, and AR00426032 exposures were within range of previous monotherapy studies.

Conclusions This study was terminated before a recommended phase 2 dose was established. In patients with mPDAC who received avelumab + binimetinib, DLTs occurred in both dose groups, although TRAEs were generally consistent with single

agent safety profiles. The 45-mg binimetinib dose had a higher number of patients with stable disease and one confirmed partial response. Biomarker findings provide insights into potential mechanisms of treatment resistance and response.

Trial Registration NCT03637491

Ethics Approval The trial was approved by each site's independent ethics committee.

<http://dx.doi.org/10.1136/jitc-2021-SITC2021.344>

PHASE I/II TRIAL OF CABOZANTINIB PLUS DURVALUMAB IN ADVANCED GASTROESOPHAGEAL CANCER AND OTHER GASTROINTESTINAL MALIGNANCIES (CAMILLA): PHASE IB SAFETY AND EFFICACY RESULTS

¹Anwaar Saeed*, ²Robin Park, ³Junqiang Dai, ¹Raed Al-Rajabi, ¹Anup Kasi, ¹Joaquina Baranda, ¹Stephen Williamson, ¹Zachary Collins, ¹Jacob Ripp, ⁴Azhar Saeed, ³Kelly Mulvaney, ³Vanna Manirad, ³Rashna Madan, ³Dharmalingam Subramaniam, ³Shrikant Anant, ³Milind Phadnis, ³Weijing Sun. ¹Kansas University Cancer Center, Fairway, KS, USA; ²MetroWest Medical Center, Framingham, MA, USA; ³Kansas University Medical Center, Kansas City, KS, USA; ⁴University of Minnesota Medical Center, Minneapolis, MN, USA

Background Cabozantinib is a multi-tyrosine kinase inhibitor primarily targeting VEGFR, MET, and AXL. These targets promote a tumor immune permissive microenvironment. Cabozantinib has demonstrated immunomodulatory properties & clinical synergy when paired with PD-L1 inhibitors such as durvalumab. Here, we present final results of phase Ib of the Camilla trial assessing cabozantinib plus durvalumab in advanced GE adenocarcinoma (GEA), colorectal cancer (CRC), and hepatocellular carcinoma (HCC). This is an investigator-initiated trial funded by Exelixis & AstraZeneca.

Methods Patients were administered cabozantinib + durvalumab in a dose escalation (3+3) then expansion to find the Dose Limiting Toxicities (DLTs), Recommended Phase 2 Dose (RP2D), ORR, PFS, and OS. Subgroup analysis was conducted to assess efficacy in patients with PD-L1 Combined Positive Score (CPS) \geq 5. Dosing of cabozantinib was 20mg QD, 40mg QD, and 60mg QD PO in the 1st, 2nd, and 3rd cohorts. Dosing of durvalumab was 1500mg IV Q4W in all cohorts. DLT window was 28 days. Treatment beyond progression was allowed following modified RECIST v1.1 criteria.

Results 35 patients (14F, 21M), median age 53 years (range 27–79) were enrolled. 10 patients had GEA, 20 had CRC, and 5 had HCC; none had MMR deficiency. Median number of prior systemic therapies was 3 (range 0–3). No DLTs were observed during dose escalation. Per mature tolerability data, 11/14 patients receiving cabozantinib 60mg required dose-reduction post cycle 2 to 40mg. RP2D was determined to be cabozantinib 40mg QD plus durvalumab 1500mg Q4W. Of the 247 observed Treatment-Related Adverse Events (TRAEs), 10% (24) were grade \geq 3. Most common TRAEs were grade 1–2 fatigue (57%), nausea (43%), anorexia (40%), diarrhea (37%), transaminitis (34%), hand-foot syndrome (23%), & weight loss (23%). 2 patients each developed grade \geq 3 fatigue, weight loss, & abdominal pain. Overall, 30 pts were evaluable for efficacy. ORR 26.7%; DCR 83.3%; median PFS 4.5 months; 6-month PFS 36.7%; and median OS 9.1 months. 12 patients had PD-L1 CPS \geq 5. In this subgroup, ORR 33.33%; DCR 91.67%; median PFS 6.13 months; 6-month PFS 50%; and median OS was not reached.

Conclusions Cabozantinib plus durvalumab demonstrated promising efficacy and was fairly tolerated without new safety signals. High PD-L1 expression defined as CPS \geq 5 was associated with improved efficacy & survival. The phase II multi-cohort part of the trial is currently ongoing.

Trial Registration NCT03539822

Ethics Approval The study was approved by the participating site's local IRB.

Consent All study participants granted a written informed consent prior to treatment initiation.

<http://dx.doi.org/10.1136/jitc-2021-SITC2021.345>

**TRANSLATIONAL PROGRAM OF THE PHASE II
MEDITREME TRIAL: IDENTIFICATION OF PROGNOSTIC
FACTORS FOR RESPONSE TO DURVALUMAB AND
TREMELIMUMAB IN COMBINATION WITH FOLFOX IN
METASTATIC COLORECTAL CANCER**<http://dx.doi.org/10.1136/jitc-2021-SITC2021.346>

¹Marion Thibaudin*, ¹Elise Ballot, ¹Emeric Limagne, ²Caroline Laheurte, ¹Jean-David Fumet, ¹Caroline Truntzer, ²Olivier Adotevi, ¹François Ghiringhelli. ¹*Anticancer Center Georges François Lederç, Dijon, France;* ²*INSERM UMR 1098, Besançon, France*

Background Single agent PD-1/PD-L1 inhibition are not effective in metastatic colorectal cancer with microsatellite stable tumors. However, signal of efficacy was shown using combination of anti-PD-L1 and anti-CTLA-4 in multitreated patients and the combination with FOLFOX regimen could lead to a potential positive effect on antitumor immune response. We report here the immune response observed following immunomonitoring of patients before and during MEDITREME trial.

Methods MEDITREME was a single arm phase II trial which aimed at evaluating efficacy and safety of mFOLFOX in combination with durvalumab and tremelimumab. We studied the phenotypic and functional immune response at inclusion and after 15 days (C2), 5 (C5) and 12 (C12) weeks of treatment by flow cytometry and the specific T response by ELISPOT. These immune parameters could be linked to survival data (RECIST criteria, progression free-survival) to highlight factors that may be prognostic of treatment response. One patient with a complete response allowed further a more detailed analysis of antitumoral immune response by single cell (sc) RNA- and TCR-sequencing, ELISPOT and flow cytometry analyses of the blood and tumor infiltrated immune cells.

Results Computational cytometry analyses showed that high baseline levels of Th2, Tc2 and PDL1+ MDSC were associated with non-responder patients. Conversely, a high baseline level of activated T cells secreting IFN γ and TNF α and a high level of activated T cells expressing ICOS and high level of CD45RA+ Treg after a treatment cycle were associated with responder patients. Concerning specific T cells response, TERT response at C2 and C5 was associated with responder patients and with high PFS. ScRNA sequencing performed on CD8 cells isolated from blood and tumor samples from the patient with a complete response showed an accumulation of polyfunctional CD8 T cells in tumor with high level of expression of effector cytokine and cytotoxic molecules. TCR sequencing analysis underlined the expansion of multiple clonotypes in TILS with some similarity between clone found in TILS and blood at the time of surgery. Moreover, we showed that only in TILS and blood at surgery charged multiple TCR clones predicted to recognize similar antigen. Finally, we generated the 14 predicted CD8 neoantigen peptides thanks to tumor exome sequencing and found that blood T cells and TILs response against neoantigens.

Conclusions Immunomonitoring has allowed us to associate peripheral immune parameters with treatment efficacy. ScRNA sequencing underlines the ability of the treatment to induce a specific immune response against neoantigens in a complete responder patient.

Acknowledgements Thanks to AstraZeneca for their financial support.

Trial Registration ClinicalTrials.gov Identifier: NCT03202758

Ethics Approval

Eudra-CT registration number 2016-005006-19

KEYNOTE-365 COHORT C: PEMBROLIZUMAB + ENZALUTAMIDE IN PATIENTS WITH ABIRATERONE ACETATE-PRETREATED METASTATIC CASTRATION-RESISTANT PROSTATE CANCER (mCRPC)—DATA AFTER MINIMUM OF 22 MONTHS OF FOLLOW-UP

¹Leonard Appleman*, ²Tilman Todenhoefer, ³William Berry, ⁴Howard Gurney, ⁵Margitta Retz, ⁶Henry Conter, ⁷Brigitte Laguerre, ⁸Peter Fong, ⁹Cristiano Ferrario, ¹⁰Gwenaëlle Gravis, ¹¹Josep Piulats, ¹²Urban Emmenegger, ¹³Neal Shore, ¹⁴Emanuela Romano, ¹⁵Loïc Mourey, ¹⁶Xin Tong Li, ¹⁶Christian Poehlein, ¹⁶Charles Schloss, ¹⁷Johann De Bono, ¹⁸Evan Yu. ¹UPMC, Pittsburgh, PA, USA; ²Studienpraxis Urologie, Nürtingen, Germany; ³Duke Cancer Center Cary, Cary, NC, USA; ⁴Westmead Hospital and Macquarie University Hospital, Sydney, Australia; ⁵Klinikum rechts der Isar, Technische Universität München, Munich, Germany; ⁶University of Western Ontario, Brampton, Canada; ⁷Center Eugène Marquis, Rennes, France; ⁸Auckland City Hospital, Auckland, New Zealand; ⁹Jewish General Hospital, Montreal, Canada; ¹⁰Institut Paoli Calmettes, Marseille, France; ¹¹Catalan Institute of Oncology, Barcelona, Spain; ¹²Odette Cancer Centre, Toronto, Canada; ¹³Carolina Urologic Research Center, Myrtle Beach, SC, USA; ¹⁴Center for Cancer Immunotherapy, Institut Curie, Paris, France; ¹⁵Insitut Universitaire du Cancer-Oncopole, Toulouse, France; ¹⁶Merck and Co., Inc., Kenilworth, NJ, USA; ¹⁷The Royal Marsden NHS Foundation Trust, London, UK; ¹⁸University of Washington, Seattle, WA, USA

Background Previous data from cohort C of phase 1b/2 study KEYNOTE-365 (NCT02861573) showed that PD-1 inhibitor pembrolizumab + enzalutamide was well tolerated and showed antitumor activity in patients with abiraterone acetate-pretreated mCRPC. Updated data after a minimum of 22 months of follow-up are presented.

Methods Patients in the prechemotherapy mCRPC state who were intolerant to ≥ 4 weeks' treatment with abiraterone acetate or for whom this treatment failed, had progressive disease ≤ 6 months before screening, and had ECOG PS 0-2 were enrolled. Patients received pembrolizumab 200 mg IV Q3W + enzalutamide 160 mg orally QD. Primary end points were PSA response rate (decrease $\geq 50\%$ from baseline), confirmed ORR per RECIST v1.1 by blinded independent central review (BICR), and safety. Secondary end points were time to PSA progression; DCR (CR or PR of any duration + SD or non-CR/non-PD ≥ 6 months) and DOR per RECIST v1.1 by BICR; rPFS per PCWG3-modified RECIST v1.1 by BICR; and OS.

Results Of 103 enrolled patients, 102 were treated. Median age was 70.0 years (range, 43–87); 29.4% of patients were PD-L1+; 37.3% had RECIST-measurable disease. Median follow-up (time from enrollment to data cutoff) was 40.2 months (range, 22.3–49.9). Confirmed PSA response rate in patients with baseline PSA measurement (N = 101) was 23.8%. Median time to PSA progression was 4.0 months (95% CI, 3.5–4.4). In 38 patients with measurable disease, ORR was 10.5% (2 CR; 2 PR). Median DOR was 11.8 months (4.3 to 38.3+ months); 1 patient had a response ≥ 12 months. DCR for the total population was 33.3%. Median (95% CI) rPFS was 6.0 months (4.1–6.3); rPFS at 12 months was 30.1%. Median (95% CI) OS was 20.1 months (16.9–25.2); OS at 12 months was 76.2%. Treatment-related AEs (TRAEs) occurred in 92.2% of patients; most common ($\geq 20\%$) were fatigue (39.2%), nausea (21.6%), and rash (21.6%). Grade 3–5 TRAEs occurred in 42.2%, most commonly rash (7.8%) and fatigue (5.9%). Four patients died of AEs: 1 death was treatment-related (unknown cause).

Conclusions After a minimum follow-up of 22 months, pembrolizumab + enzalutamide continued to show antitumor activity in abiraterone acetate-pretreated mCRPC. The safety profile of pembrolizumab + enzalutamide was generally consistent with individual profiles of each agent. There was a higher incidence than typically reported for the individual

agents of all-grade (21.6%) and grade 3 (7.8%) rash, which resolved with standard-of-care treatment. The combination is being further evaluated in the phase 3 study KEYNOTE-641.

Acknowledgements Medical writing and/or editorial assistance was provided by Matthew Grzywacz, PhD, of ApotheCom (Yardley, PA, USA). This assistance was funded by Merck Sharp & Dohme Corp., a subsidiary of Merck & Co., Inc., Kenilworth, NJ, USA. Funding for this research was provided by Merck Sharp & Dohme Corp., a subsidiary of Merck & Co., Inc., Kenilworth, NJ, USA.

Trial Registration ClinicalTrials.gov, identifier: NCT02861573

Ethics Approval The study and the protocol were approved by the Institutional Review Board or ethics committee at each site.

<http://dx.doi.org/10.1136/jitc-2021-SITC2021.347>

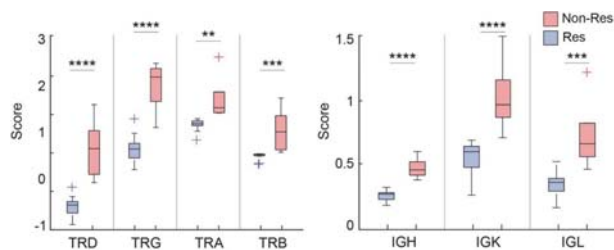
348 INTERLEUKIN 2(IL-2) SYSTEMS IMMUNOLOGY
MODELING: MACHINE LEARNING FOR CANCER
IMMUNOTHERAPY

¹Jennifer Bone*, ¹Newell Washburn, ²Jian Han, ²Miranda Steele, ³Pranav Murthy, ⁴Michael Lotze. ¹Carnegie Mellon University, Pittsburgh, PA, USA; ³Repertoire, Hunstville, AL, USA; ⁴UPMC, Pittsburgh, PA, USA; ⁵Nurix, PITTSBURGH, PA, USA

Background Clinical outcomes are correlated with aggregate B (BCR) and T cell receptor (TCR) diversity (the adaptome) in several infectious diseases and cancers. Advances in dimer avoidance multiplexed PCR (DAM-PCR) followed by next-generation sequencing (NGS) enable measurements of immune repertoire diversity and clonality, allowing prediction of cancer states and response to treatment. Clonotype-mediated predictions collapse a space of up to 1025 possible CDR3 variable region sequences into descriptors such as whole-sequence diversity. Broad descriptors, however, mask cancer-specific information embedded within clonotype sequences. Deep learning algorithms typically need large patient cohorts to make accurate predictions. We present a statistical model predicting response to IL-2 immunotherapy for small cohorts based on natural language processing (NLP) of CDR3 TCR and BCR clonotypes.

Methods In a completed Phase 2 trial (NCT01550367), the adaptome of 29 patients with metastatic clear cell renal carcinoma (RCC) treated with high dose (HD) IL-2 and the autophagy inhibitor, hydroxychloroquine (HCQ) were measured from peripheral blood samples by DAM-PCR. All seven TCR and BCR chains were measured at three treatment points (pre-treatment, 14D after HCQ initiation, and following recovery from the first cycle of IL-2 on D15). Outcomes were assessed by assigning two states (responder or non-responder) one year following treatment based on radiographic changes in tumor size. Cancer-specific amino acid motifs from TCR and BCR CDR3 sequences on D15 were mined by counting amino acid pairs and calculating a 400-feature transition probability matrix, scoring the likelihood of a motif belonging to the responder or non-responder cohort.

Results Seven-chain NLP analysis of CDR3 amino acid motifs at > 90% accuracy for each chain independently predicted patient response to IL-2 by D15 (figure 1). Furthermore, longitudinal monitoring of patient CDR3s across the three time-points revealed a dichotomy in repertoire orchestration. Responding patients, convincingly, were more likely to demonstrate either a TCR-driven ($p < 0.01$) or a BCR-driven ($p < 0.001$) entropy bias while non-responding patients unanimously showed no significant bias.



Abstract 348 Figure 1 Classification of nonresponding (Non-Res) and responding (Res) patients based on scoring from Feature Selection Filter and Analysis. ****, $p < 0.0001$; ***, $p < 0.001$; **, $p < 0.01$

Conclusions NLP of both TCR and BCR repertoires can provide early predictions of cancer response to treatment. Furthermore, seven-chain longitudinal monitoring across treatment revealed a surprisingly robust repertoire orchestration in responders that was not observed in non-responders, suggesting that the methodology proposed here can be used to gain new mechanistic insight into the role of repertoire evaluation in cancer immunotherapy.

<http://dx.doi.org/10.1136/jitc-2021-SITC2021.348>

349

TOLERABILITY OF TIVOZANIB VS. SORAFENIB IN ELDERLY AND/OR IMMUNOTHERAPY-PRETREATED PATIENTS WITH METASTATIC RENAL CELL CANCER (MRCC) IN TIVO-3

¹Vijay Kasturi, ²Bernard Escudier, ³Brian Rini, ⁴Sumanta Pal*, ⁵David McDermott, ⁶Camillo Porta, ⁷Elena Verzoni. ¹Aveo Oncology, Boston, MA, USA; ²Institute Gustave Roussy, Villejuif, France; ³Vanderbilt-Ingram Cancer Center, Nashville, TN, USA; ⁴City of Hope Comprehensive Cancer Center, Duarte, CA, USA; ⁵Beth Israel Deaconess Medical Center, Boston, MA, USA; ⁶Aldo Moro University of Bari, Bari, Italy; ⁷IRCCS Istituto Nazionale dei Tumori, Milan, Italy

Background The TIVO-3 trial demonstrated improved progression-free survival (PFS) with TIVO when compared to sorafenib (SOR; 5.6 mo. vs 3.9 mo., respectively; HR 0.73) and better tolerability with reduced need for dose interruptions (p = 0.0164), dose reductions (p = 0.0147), and discontinuations ¹. As the majority of patients diagnosed with mRCC in the US are >65 years, with the largest recent increase in incidence among those ≥75, and front-line treatment now standardly includes immunotherapy (IO), tolerability of new therapies for relapsed or refractory (R/R) mRCC must be acceptable in the elderly and/or IO pretreated population

Methods Data was analyzed to identify relationships between tolerability and advanced age or IO pretreatment. In addition to measures of drug exposure, any grade ≥3 treatment related adverse events (TRAEs) and VEGFR TKI class effect grade ≥3 TRAEs are reported by age (<65, 65–74, ≥75) and prior IO (yes, no)

Results Of the 343 patients treated on study, 120 (35%) were between age 65 and 75 and 34 (10%) were over 75. Patients received 1.5-2x more cycles of TIVO compared to SOR and fewer overall grade ≥3 TRAEs in all age groups and irrespective of prior IO. Differences in VEGFR TKI class effect TRAEs seen in the total population were retained across most subgroups (table 1). Among patients 75 and over, there were almost half the rate of the dose reductions or discontinuations with TIVO compared to SOR. Prior IO was associated with less asthenia overall, more HTN with TIVO, and more rash but less diarrhea with SOR

REFERENCE

- Rini B, Pal S, Escudier B, Atkins M, Hutson T, et al. Tivozanib versus sorafenib in patients with advanced renal cell carcinoma (TIVO-3): a phase 3, multicentre, randomised, controlled, open-label study. *Lancet Oncol* 2020;21:95–104

Ethics Approval This trial was approved by the institutional review board or ethics committee at every centre and complied with Good Clinical Practice guidelines, the Declaration of Helsinki, and local laws. All patients provided written informed consent before any trial procedure. The trial protocol including the relevant centres is provided in the appendix of the reference 1

<http://dx.doi.org/10.1136/jitc-2021-SITC2021.349>

Abstract 349 Table 1 Drug exposure, dose modifications, and TRAEs in TIVO-3 by age and prior IO

	All		Age <65		Age 65-74		Age ≥75		Prior IO		No prior IO	
	TIVO (n=173)	SOR (n=170)	TIVO (n=97)	SOR (n=92)	TIVO (n=61)	SOR (n=59)	TIVO (n=15)	SOR (n=19)	TIVO (n=88)	SOR (n=43)	TIVO (n=125)	SOR (n=127)
Drug exposure (mean cycles)	11.9	6.7	10.1	6.7	15	6.6	11.2	7.3	12.3	5.5	11.7	7.2
Dose interruption (%)	48	64	41	51	59	80	73	74	69	81	43	57
Dose reduction (%)	24	39	20	26	33	51	33	63	33	35	22	40
Dose discontinuation (%)	21	30	26	25	15	36	20	37	25	40	20	27
TRAE Gr ≥3 (%)												
Any	46	55	38	46	56	68	53	63	58	67	41	51
HTN	21	14	23	12	23	20	7	0	35	12	16	14
Diarrhea	2	9	1	5	3	13	0	11	2	5	2	11
Fatigue	3	5	3	2	3	8	7	5	4	7	3	4
Asthenia	5	4	3	0	8	5	7	16	2	2	6	4
Nausea	0	2	-	-	0	5	0	5	0	2	0	2
Vomiting	<1	2	-	-	2	3	0	5	-	-	<1	2
Rash	0	8	0	5	0	12	0	5	0	23	0	2
PEP	<1	10	0	9	2	12	0	11	0	12	<1	9

Conclusions Tolerability benefits with TIVO compared to SOR in mRCC are retained in elderly patients and those previously treated with IO. This finding, paired with consistently improved PFS in these subpopulations (age >65: HR 0.59, prior IO: HR 0.55), suggests TIVO is a safe and effective option in the context of the current R/R mRCC treatment paradigm

Trial Registration ClinicalTrials.gov Identifier: NCT02627963

**PHASE 2 TRIAL OF A DNA VACCINE WITH
PEMBROLIZUMAB IN PATIENTS WITH METASTATIC,
CASTRATION-RESISTANT PROSTATE CANCER (MCRPC)**

<http://dx.doi.org/10.1136/jitc-2021-SITC2021.350>

¹Douglas McNeel*, ²Jens Eickhoff, ²Ellen Wargowski, ²Laura Johnson, ²Christos Kyriakopoulos, ²Hamid Emamekhoo, ²Joshua Lang, ²Mary Jane Brennan, ²Glenn Liu. ¹Carbone Cancer Center, University of Wis, Madison, WI, USA; ²University of Wisconsin, Madison, WI, USA

Background We previously reported a pilot clinical trial using a DNA vaccine encoding prostatic acid phosphatase (pTVG-HP), given over 12 weeks either concurrently or in sequence with pembrolizumab, in patients with mCRPC. We report here the final analysis of this trial following two additional treatment arms in which patients with mCRPC were treated beyond 12 weeks until progression.

Methods Patients with mCRPC were treated with pTVG-HP and pembrolizumab every 3 weeks (Arm 3, n=20), or pTVG-HP every 2 weeks and pembrolizumab every 4 weeks (Arm 4, n=20). The primary objectives were safety, 6-month PFS, median time to radiographic progression, and objective response rates. Secondary objectives included immunological evaluations.

Results Treatment was without unexpected toxicity, and only 1 grade 4 event (hyperglycemia) was observed. Immune related adverse events (irAE) > grade 1 included adrenal insufficiency, hepatitis, colitis, thyroid dysfunction, pancreatitis, pneumonitis, and rash, occurring in 42% of patients overall. 10/25 patients with measurable disease experienced any decrease in tumor volume from baseline, with 1 confirmed PR and no CR. 23/66 (35%) experienced any PSA decline from baseline. Overall median TTP was 5.4 months (95% CI; 5.3–8.1 months); median TTP for Arm 3 was 5.3 months compared to 8.0 months for Arm 4. Overall, 41.7% of patients had no radiographic progression at 6 months (29.9% Arm 3, 57.9% Arm 4). Median overall survival was 22.9 months. IFN γ and/or granzyme B immune response to PAP was detected in 2/20 patients in Arm 3 and 6/20 patients in Arm 4. Cytokines associated with immune activation and CD8+ T cell recruitment were augmented in the plasma of patients at weeks 6 and 12. Increased IFN γ in the sera at week 6 trended with prolonged TTP (p=0.010) and overall survival (p=0.025). The development of irAE was associated with a prolonged TTP (HR=0.25, p=0.003).

Conclusions PD-1 pathway inhibitors have demonstrated little clinical activity to date as monotherapies for mCRPC. Our findings demonstrate that combining PD-1 blockade with tumor-targeted T-cell activation using pTVG-HP is safe, can augment tumor-specific T cells, and result in objective changes with longer time to progression than what has been observed in previous trials. The association of progression or survival with increased IFN γ , irAE, and vaccine schedule suggests T cell activation by vaccination is critical to the mechanism of action of this combination. This study suggests this approach should be further evaluated in randomized clinical trials for patients with advanced mCRPC.

Acknowledgements Funding for this trial was from a 2014 Movember Prostate Cancer Foundation Challenge Award and Madison Vaccines, Inc.

Trial Registration NCT02499835

Ethics Approval This trial was reviewed and approved by the University of Wisconsin Human Subjects' Review Committee (IRB), protocol 2015-0453. All participants provided IRB-approved written informed consent before taking part.

KEYNOTE-365 COHORT D: PEMBROLIZUMAB PLUS ABIRATERONE ACETATE AND PREDNISONE IN PATIENTS WITH CHEMOTHERAPY-NAIVE METASTATIC CASTRATION-RESISTANT PROSTATE CANCER (mCRPC)

¹Josep Piulats*, ²Cristiano Ferrario, ³Mark Linch, ⁴Michael Stoeckle, ⁵Brigitte Laguerre, ⁶Jose Arranz, ⁷Tilman Todenhofer, ⁸Peter Fong, ⁹William Berry, ¹⁰Urban Emmenegger, ¹¹Loic Mourey, ¹²Nataliya Mar, ¹³Leonard Appleman, ¹⁴Anthony Joshua, ¹⁵Henry Conter, ¹⁶Xin Tong Li, ¹⁶Charles Schloss, ¹⁶Christian Pehlein, ¹⁷Johann De Bono, ¹⁸Evan Yu. ¹Catalan Institute of Oncology, Barcelona, Spain; ²Jewish General Hospital, Montreal, Canada; ³University College London Hospital, London, UK; ⁴Saarland University Hospital, Homburg, Germany; ⁵Center Eugène Marquis, Rennes, France; ⁶Hospital Universitario Gregorio Marañon, Madrid, Spain; ⁷Studienpraxis Urologie, Nürtingen, Germany; ⁸Auckland City Hospital, Auckland, New Zealand; ⁹Duke Cancer Center Cary, Cary, NC, USA; ¹⁰Odette Cancer Centre, Toronto, Canada; ¹¹Insitut Universitaire du Cancer–Oncopole, Toulouse, France; ¹²UCI Medical Center, Orange, CA, USA; ¹³UPMC, Pittsburgh, PA, USA; ¹⁴Saint Vincent's Hospital Sydney, Sydney, Australia; ¹⁵University of Western Ontario, Brampton, Canada; ¹⁶Merck and Co., Inc., Kenilworth, NJ, USA; ¹⁷The Royal Marsden NHS Foundation Trust, London, UK; ¹⁸University of Washington, Seattle, WA, USA

Background Treatment with abiraterone acetate + prednisone can improve outcomes in mCRPC patients with or without prior chemotherapy. Cohort D of phase 1b/2 study KEYNOTE-365 (NCT02861573) evaluated safety and efficacy of PD-1 inhibitor pembrolizumab + abiraterone acetate and prednisone in patients who had not received chemotherapy for mCRPC.

Methods Patients were enrolled who had not received second-generation hormonal manipulation for mCRPC or failed/were intolerant to enzalutamide for mCRPC; had progressive disease ≤ 6 months before screening; and had ECOG PS 0/1. Patients received pembrolizumab 200 mg IV Q3W + abiraterone acetate 1000 mg orally QD and prednisone 5 mg orally BID. Primary end points: safety, PSA response rate (PSA decrease $\geq 50\%$ from baseline), and confirmed ORR per RECIST v1.1 by blinded independent central review (BICR). Secondary end points: rPFS per PCWG3-modified RECIST v1.1, DCR, DOR, and OS.

Results One hundred three patients were treated. Median (range) age was 70.0 (46–89) years, 30.1% were PD-L1+, 35.9% had RECIST-measurable disease, 18.4% had visceral disease, and 26.2% had previously received enzalutamide only. Median (range) time from enrollment to data cutoff was 17.6 (9.7–27.0) months. Confirmed PSA response rate in patients with PSA measurement at baseline (n=103) was 56.3%. For 37 patients with RECIST-measurable disease, ORR was 16.2% (1 CR; 5 PRs); 2 patients with RECIST-nonmeasurable disease had CR. In total population, 5 patients had a response ≥ 6 months; DCR was 44.7%. ORR for RECIST-measurable patients was 7.7% for those who previously received enzalutamide only (n=13) and 21.7% for those who had not previously received NHAs (n=23); DCR was 11.1% in all patients who previously received enzalutamide (n=27) and 57.3% in all patients who had not received NHAs (n=75). Median (95% CI) rPFS was 15.1 (9.2–NR) months; rPFS at 12 months was 54.9%. Median (95% CI) OS was NR (23.3 months–NR); OS at 12 months was 82.9%. Sixty-nine patients (67.0%) discontinued treatment, mostly because of progressive disease (37.9%). Treatment-related AEs (TRAEs) were experienced by 90.3% of patients and most common ($\geq 15\%$) were ALT increase (22.3%), AST increase (17.5%), asthenia (16.5%), and diarrhea (16.5%); 36.9% experienced grade 3–5 TRAEs. There were 18.4%/12.5% grade 3 or 4 ALT/AST laboratory elevations. Five patients died of AEs; 1 was treatment related (myasthenic syndrome).

Conclusions Pembrolizumab + abiraterone acetate and prednisone demonstrated antitumor activity in patients with chemotherapy-naive mCRPC. Safety was generally consistent with individual profiles of each agent. There was an increased incidence of grade 3–4 ALT/AST laboratory elevations.

Acknowledgements Medical writing and/or editorial assistance was provided by Matthew Grzywacz, PhD, of ApotheCom (Yardley, PA, USA). This assistance was funded by Merck Sharp & Dohme Corp., a subsidiary of Merck & Co., Inc., Kenilworth, NJ, USA. Funding for this research was provided by Merck Sharp & Dohme Corp., a subsidiary of Merck & Co., Inc., Kenilworth, NJ, USA.

Trial Registration ClinicalTrials.gov, identifier: NCT02861573

Ethics Approval The study and the protocol were approved by the Institutional Review Board or ethics committee at each site.

<http://dx.doi.org/10.1136/jitc-2021-SITC2021.351>

TARGET MODULATION WITHIN THE TUMOR MICROENVIRONMENT (TME) BY DARATUMUMAB (ANTI-CD38) BUT NOT EDICOTINIB (CSF-1R INHIBITOR) IN MEN WITH HIGH-RISK LOCALIZED PROSTATE CANCER<http://dx.doi.org/10.1136/jitc-2021-SITC2021.352>

Bilal Siddiqui*, Brian Chapin, Sonali Jindal, Fei Duan, Shalini Singh, Curtis Pettaway, John Ward, Rebecca Tidwell, Paul Corn, Christopher Logothetis, James Allison, Padmanee Sharma, Sumit Subudhi. *MD Anderson Cancer Center, Houston, TX, USA*

Background Prostate cancer is "immunologically cold," with enrichment of myeloid populations, immunosuppressive cytokines, and few T cells within the tumor microenvironment (TME). CD38 is expressed on myeloid cells, T cells, plasma B cells, and NK cells. Macrophage colony-stimulating factor-1 receptor (CSF-1R) controls macrophage differentiation and function. We hypothesized that either anti-CD38 (daratumumab) or CSF-1R inhibitor (edicotinib) would be safe and well-tolerated for primary prostate cancer, with successful target modulation on immune populations within the TME.

Methods In this single-center, open-label, presurgical study, patients were enrolled into Arm A (daratumumab, four weekly doses pre-surgery) or Arm B (edicotinib, orally daily for four weeks pre-surgery). Patients had high-risk localized or locally advanced prostate cancer (at least 1 core Gleason ≥ 8) appropriate for radical prostatectomy (RP), ≥ 3 biopsies involved with cancer, and no radiographic evidence of metastatic disease. Treated and untreated (Gleason-matched) fresh and formalin-fixed paraffin-embedded prostatectomy specimens and paired blood (PBMCs), bone marrow biopsies (BMBx) and aspirates (BMA) were evaluated for target modulation using IHC (prostate, BMBx) and flow cytometry (prostate, BMA, PBMCs). The primary endpoint was incidence of adverse events (AEs). The secondary endpoint was pathologic complete remission (pCR) rate.

Results Twenty-five patients were treated (Arm A, n=15; Arm B, n=10) and completed four doses of daratumumab or four weeks of edicotinib prior to RP. The most common AEs were Arm A: daratumumab infusion reaction (33%, 5/15); Arm B: increased aspartate aminotransferase (40%, 4/10). Grade 3 related AEs in Arm A occurred in 3 patients (12%; infusion reaction, n=2; urticaria, n=1), with no Grade 4/5 related events. No \geq Grade 3 related AEs occurred in Arm B. All patients completed surgery, however no patients achieved pCR. IHC revealed lower density of CD38+ cells in daratumumab-treated vs. untreated prostate tumors and in patient-matched post-treatment vs. pre-treatment BMBx. Similarly, flow cytometry showed decreased frequency of CD38+ T cells and macrophages in daratumumab-treated vs. untreated prostate tumors and patient-matched post-treatment vs. pre-treatment PBMCs and BMAs. Edicotinib did not demonstrate an impact on CSF-1R+ immune cells in prostate, bone marrow, or PBMCs.

Conclusions Daratumumab and edicotinib were safe and well-tolerated as presurgical therapy for high-risk localized prostate cancer, with no pCRs. Evidence of target modulation was consistently observed in prostate tumors, bone marrow, and PBMCs for daratumumab, but not edicotinib. Myeloid-targeted agents such as daratumumab alone are insufficient to generate anti-tumor responses in prostate cancer.

Trial Registration NCT03177460

Ethics Approval This study was approved by MD Anderson Cancer Center Institutional Review Board; protocol numbers 2017-0103 and PA13-0291.

IDENTIFICATION OF POTENTIAL RESPONSE PREDICTORS TO MAVEROPEPIMUT-S (DPX-SURVIVAC), A NOVEL T CELL ACTIVATING IMMUNOTHERAPY, IN PATIENTS WITH ADVANCED RECURRENT OVARIAN CANCER

¹Oliver Dorigo*, ²Walead Ebrahimzadeh, ²Barry Kennedy, ²Lisa MacDonald, ²Stephan Fiset, ³Jeannine Villella, ⁴OZA Amit, ⁵Tanja Pejovic, ⁶Prafull Ghatage, ⁷Sharad Ghamande, ⁸Diane Provencher, ²Yogesh Bramhecha. ¹Stanford Women's Cancer Center, Stanford, Stanford, CA, USA; ²IMV inc., Dartmouth, Canada; ³Lenox Hill Hospital, New York, NY, USA; ⁴Princess Margaret Cancer Centre, UHN, Toronto, Canada; ⁵Oregon Health and Science University, Portland, OR, USA; ⁶Alberta Health Services, Calgary, Canada; ⁷Georgia Cancer Center, Augusta, GA, USA; ⁸Institut du cancer de Montréal, Montreal, Canada

Background Epithelial ovarian cancer (OvCa) is the most lethal of gynecological malignancies. The high mortality is related to a late diagnosis with over 75% being at an advanced stage, high recurrence rates, and ultimately resistance to chemotherapy. Previous studies have consistently demonstrated a strong association between higher tumor T cell infiltration and improved survival in OvCa patients supporting the potential clinical utility of T cell activating immunotherapy approaches. Maveropepimut-S (MVP-S, formerly named DPX-Survivac) is a T cell activating immunotherapy which is a formulation of the proprietary drug delivery platform DPX™ with immunogenic T-cell epitopes derived from the tumor-associated antigen survivin. MVP-S in combination with intermittent low-dose cyclophosphamide has been shown to induce robust and durable antigen-specific T cell responses and anti-tumor clinical activity in recurrent OvCa patients. The current study presents translational data aimed at identifying tumor tissue-based predictive biomarkers for response to treatment with MVP-S.

Methods Baseline and on-treatment tumor biopsies were collected from patients treated with MVP-S primed with immune-modulating low dose cyclophosphamide. Multiplex-immunohistochemistry (mIHC, Akoya Biosciences) and RNA-seq analyses (Personalis Inc.) were used to analyze the tumor immune environment and identify potential response predictors to MVP-S.

Results Twenty-two patients with advanced, recurrent OvCa were enrolled in this study. mIHC analysis demonstrated that higher baseline CD3+CD8+ T cell infiltration in tumor tissue was significantly associated with anti-tumor clinical activity of MVP-S defined as >10% on-treatment tumor regression. Pathway enrichment analyses using the differentially expressed genes associated with anti-tumor clinical activity confirmed these findings. In addition, we identified B cell pathway genes to be significantly upregulated in patients with >10% on-treatment tumor regression. mIHC analyses of paired biopsies available for one subject with clinical response (PR) demonstrated that MVP-S treatment induced increased T and B cell infiltration in the on-treatment biopsy compared to the baseline biopsy. These findings suggest that immunogenic tumors are more susceptible to the MVP-S treatment, in line with its mechanism of action. Pathway enrichment analyses further revealed that upregulation of genes or pathways related to immune-suppression (e.g. WNT pathway) or immune evasion/exclusion (CD276, Arg2) were significantly associated with lack of anti-tumor activity indicative of potential mechanism of primary resistance.

Conclusions Collectively, these results provide insight for possible response predictors to MVP-S based therapy

Trial Registration NCT02785250

Ethics Approval The protocol and patient-informed consent form received approval by Institutional Review Boards. Written informed consent was obtained from all patients. REBs:

Comite d'éthique de la recherche du CHUM (Montreal, Canada); Western Institutional Review Board 20161075 (Augusta, GA, USA); FWA #00002505 (NEW YORK, NY, USA); FWA00000161, IRB00000471 (Portland, Oregon, USA); University Health Network REB (Toronto, Canada); FWA00000935, FWA00000934 (Stanford, CA, USA); Health Research Ethics Board of Alberta, (Edmonton, Canada)

<http://dx.doi.org/10.1136/jitc-2021-SITC2021.353>

LENVATINIB AND PEMBROLIZUMAB IN ADVANCED ENDOMETRIAL CARCINOMA (EC): LONG-TERM EFFICACY AND SAFETY UPDATE FROM A PHASE 1B/2 STUDY

¹Vicky Makker*, ²Carol Aghajanian, ³Allen Cohn, ⁴Margarita Romeo, ⁵Raquel Bratos, ⁶Marcia Brose, ⁷Mark Messing, ⁸Lea Dutta, ⁸Corina Dutcus, ⁸Jie Huang, ⁹Emmett Schmidt, ⁹Robert Orlowski, ¹⁰Matthew Taylor. ¹Memorial Sloan Kettering Cancer Center, Weill Cornell Medical Center, New York, NY, USA; ²Memorial Sloan Kettering Cancer Center, New York, NY, USA; ³Rocky Mountain Cancer Center, Denver, CO, USA; ⁴Catalan Institute of Oncology, Badalona, Spain; ⁵MD Anderson Cancer Center España, Madrid, Spain; ⁶Abramson Cancer Center, University of Pennsylvania, Philadelphia, PA, USA; ⁷Texas Oncology, Bedford, TX, USA; ⁸Eisai Inc., Woodcliff Lake, NJ, USA; ⁹Merck and Co. Inc., Kenilworth, NJ, USA; ¹⁰Earle A. Chiles Research Institute, Providence Cancer Institute, Portland, OR, USA

Background Lenvatinib is a multikinase inhibitor of VEGFR 1–3, FGFR 1–4, PDGFR α , RET, and KIT. Pembrolizumab is an anti-programmed death-1 monoclonal antibody. We previously reported results from a cohort of 108 patients with metastatic EC (data cutoff date, January 10, 2019) who received lenvatinib + pembrolizumab as part of an ongoing multicenter, open-label, phase 1b/2 study evaluating the combination treatment in patients with selected solid tumors (NCT02501096). Lenvatinib + pembrolizumab showed a tolerable safety profile and promising antitumor activity per immune-related (ir) Response Evaluation Criteria In Solid Tumors (RECIST) by investigator assessment, including an objective response rate (ORR) of 38.9% (95% confidence interval [CI], 29.7–48.7), median progression-free survival (PFS) of 7.4 months (95% CI, 5.3–8.7), and median overall survival (OS) of 16.7 months (95% CI, 15.0–not estimable).¹ Here we present updated efficacy and safety data (data cutoff date: August 18, 2020).

Methods Patients included in the EC cohort had histologically confirmed, measurable metastatic EC and had received ≤ 2 prior chemotherapies (unless discussed with the sponsor). Patients received lenvatinib (20 mg orally once daily) and pembrolizumab (200 mg intravenously once every 3 weeks). The phase 2 efficacy endpoints included ORR, PFS, OS, and duration of response. Tumor assessments for primary and secondary endpoints were evaluated by investigators per irRECIST.

Results The 108 patients from the key efficacy analysis set for the previously reported results were all included in these updated analyses. Median follow-up duration for the study was 34.7 months. Efficacy outcomes are summarized in table 1. Treatment-related adverse events (TRAEs) occurred in 104 (96%) patients (94 [87%] grade ≤ 3 , 10 [9%] grade ≥ 4). TRAEs led to study-drug interruption of 1 or both drugs in 80 (74.1%) patients and dose reductions of lenvatinib in 73 (67.6%) patients; 23 (21.3%) patients discontinued 1 or both drugs due to a TRAE. The most common grade ≥ 3 TRAEs were hypertension (33.3%), lipase increased (9.3%), fatigue (8.3%), and diarrhea (7.4%).

Abstract 354 Table 1

	Previously Treated Endometrial Carcinoma	
	Updated data cutoff date (Aug 18, 2020) ^a (N=108)	Previous data cutoff date (Jan 10, 2019) (N=108)
Investigator assessment per irRECIST		
Objective response rate, n (%)	43 (39.8)	42 (38.9)
95% CI	30.5–49.7	29.7–48.7
Complete response, n (%)	9 (8.3)	8 (7.4)
Partial response, n (%)	34 (31.5)	34 (31.5)
Median duration of response, months (95% CI)	22.9 (10.2–NE)	21.2 (7.6–NE)
Kaplan-Meier estimate of duration of response ≥ 6 months, ^b n	36	32
Probability (95% CI)	0.88 (0.73–0.95)	0.87 (0.72–0.95)
Median progression-free survival, months (95% CI)	7.4 (5.2–8.7)	7.4 (5.3–8.7)
Median overall survival, months (95% CI)	17.7 (15.5–25.8)	16.7 (15.0–NE)
Time to response (months), mean (SD)	3.2 (3.41)	2.6 (1.6)
Median study follow-up time (months) (95% CI)	34.7 (30.9–41.2)	18.7 (13.1–20.3)

^a2 Patients remained on treatment at data cutoff date; ^bprobabilities of patients achieving a duration of response ≥ 6 months were calculated using the Kaplan-Meier product-limit method and Greenwood formula.

CI, confidence interval; irRECIST, Immune-related Response Evaluation Criteria In Solid Tumors; NE, not estimable.

Conclusions With extended follow-up, our updated efficacy analysis continued to show clinical benefit in patients with metastatic EC who received lenvatinib + pembrolizumab. Moreover, the combination had a manageable safety profile that was generally consistent with the established safety profiles of the individual monotherapies. No new safety signals were detected. A phase 3 study of lenvatinib + pembrolizumab versus treatment of physician's choice in advanced endometrial cancer further supports the lasting clinical benefits observed in our study.²

Trial Registration www.clinicaltrials.gov NCT02501096

REFERENCES

1. Makker V, Taylor MH, Aghajanian C, et al. Lenvatinib plus pembrolizumab in patients with advanced endometrial cancer. *J Clin Oncol* 2020;**38**(26):2981–2992.
2. Makker V, Colombo N, Casado Herráez A, et al. A multicenter, open-label, randomized, phase 3 study to compare

Ethics Approval This study was approved by the following ethics committees/institutional review boards (IRBs): Oregon Health & Sciences University IRB, IntegReview IRB, Memorial Sloan Kettering Cancer Center IRB, University of Pennsylvania Office of Regulatory Affairs IRB, Dana-Farber Cancer Institute IRB, The University of Chicago Biological Sciences Division IRB, University of Texas MD Anderson Cancer Center IRB, Western IRB, Quorum Review IRB, US Oncology, Inc. IRB, CEIm - Comité de Ética de la Investigación con Medicamentos, Regional Komite for Medisinsk og Helsefaglig Forskningsetikk, and REC - Regional Committees for Medical and Health Research Ethics. All participants gave informed consent before taking part in this study.

Consent No identifying information is contained in this abstract so no permission from participants is considered necessary.

<http://dx.doi.org/10.1136/jitc-2021-SITC2021.354>

355 PEMBROLIZUMAB AND BEVACIZUMAB IN PLATINUM RESISTANT EPITHELIAL OVARIAN CANCER PATIENTS

¹Judith Michels*, ²Jean-Sebastien Frenel, ³Catherine Genestie, ⁴François Ghiringhelli, ³Caroline Brard, ⁵Benoit You, ⁶Anne Floquet, ⁷Lauriane Eberst, ¹Rastilav Bahleda, ¹Corinne Balleyguier, ¹Angelo Paci, ⁸Joseph Ciccolini, ¹Emeline Colomba, ¹Fanny Pommeret, ³Christophe Massard, ¹Patricia Pautier, ¹Aurelien Marabelle, ¹Alexandra Leary. ¹Gustave Roussy Institute, Paris, France; ²Institut de Cancérologie de l'Ouest, Saint-Herblain, France; ³Gustave Roussy, Villejuif, France; ⁴Centre Georges François Leclerc, Dijon, France; ⁵Institut de Cancérologie des Hospices Ci, Lyon, France; ⁶Institut Bergonié, Bordeaux, France; ⁷Institut de Cancérologie de Strasbourg, Strasbourg, France; ⁸La Timone University Hospital, Marseille, France

Background There is a medical need in platinum resistant ovarian cancer patients. Median progression-free survival (PFS) is 3.4 months with chemotherapy and 6.7 months with chemotherapy-bevacizumab combination regimens.¹ RECIST overall response rate (ORR) is 11.8% and 27.3%, respectively. The ORR is 15.9% for bevacizumab as a monotherapy with a median PFS of 4.4 months.²

Methods NCT03596281 An open-label phase 1b trial with a modified toxicity probability interval design to evaluate the combination of a flat dose of 400mg bevacizumab for 6 cycles and 200mg pembrolizumab until disease progression, unacceptable toxicity or completed 24 months of treatment in patients with platinum resistant ovarian cancer. The primary evaluation criteria is safety, the secondary endpoint is the efficacy.

Results 19 patients have been enrolled between January 2019 and February 2021 in 6 French centers. Patients' characteristics are reported (table 1). No dose limiting toxicities were observed. Grade 3 treatment related adverse events occurred in 3 patients (i.e. arterial thromboembolism, bowel perforation, proteinuria and sepsis). No grade 4/5 toxicities were induced. A median of 7 cycles (range 3–14) were administered. Median follow-up of patients was 4.1 months (1.8–23). The RECIST ORR was 26.3% (1 complete response and 4 partial responses) (table 2). The disease control rate was 78.9%. The time to progression was not yet reached in 6 patients. The ORR was equivalent whether patients have been pretreated or not with bevacizumab (27.3 and 25% respectively) (table 3). The ORR according to the combined positive score (CPS) for the evaluation of PD-L1 was 50.0% for CPS \geq 10% (n=4), 30.0% for a CPS \geq 1% (n=10) and 25.0% for CPS $<$ 1 (n=8) (table 4).

Conclusions A chemotherapy-free regimen combining pembrolizumab and bevacizumab was well tolerated and showed encouraging results in heavily pretreated platinum resistant ovarian cancer patients independent of their previous challenge with antiangiogenic agents.

Acknowledgements Funding for this research was provided by Fondation Cancer du Luxembourg and Merck Sharp & Dohme Corp., a subsidiary of Merck & Co., Inc., Kenilworth, NJ, USA.

Trial Registration NCT03596281

REFERENCES

- 1.. Pujade-Lauraine E, et al. Bevacizumab combined with chemotherapy for platinum-resistant recurrent ovarian cancer: The AURELIA open-label randomized phase III trial. *J Clin Oncol Off J Am Soc Clin Oncol* 32,1302–1308 (2014).
2. Cannistra SA, et al. Phase II study of bevacizumab in patients with platinum-resistant ovarian cancer or peritoneal serous cancer. *J Clin Oncol Off J Am Soc Clin Oncol* 33,5180–5186 (2007).

Ethics Approval This study was approved by CPP Sud Méditerranée V institution's Ethics Board; approval number 18.020 (EudraCT number 2017-004197-34).

Consent Written informed consent was obtained from the patient for publication of this abstract and any accompanying images. A copy of the written consent is available for review by the Editor of this journal.

<http://dx.doi.org/10.1136/jitc-2021-SITC2021.355>

356

PERSONALIZED IMMUNOTHERAPY BY ADOPTIVE T CELL TRANSFER DURING CHEMOTHERAPY WITH OR WITHOUT INTERFERON-ALPHA IN PATIENTS WITH RECURRENT PLATINUM-SENSITIVE EPITHELIAL OVARIAN CANCER

¹Els Verdegaal*, ¹Marten Visser, ¹Lien van der Minne, ¹Linda de Bruin, ²Inge Roozen, ²Pauline Meij, ¹Sjoerd van der Burg, ²Judith Kroep. ¹Leiden University Medical Center and Oncode Institute, Leiden, Netherlands; ²Leiden University Medical Center, Leiden, Netherlands

Background Epithelial ovarian cancer (EOC) is considered an immunogenic tumor, as illustrated by the clear correlation between T-cell infiltration and overall survival. This suggests that patients with EOC may be eligible for immunotherapy including adoptive cell therapy with autologous Tumor Infiltrating Lymphocytes (TIL). However, immunosuppressive cells including myeloid derived suppressor cells and regulatory T cells are also abundant in EOC and may need to be targeted simultaneously to achieve the full potential of the infused TIL. Carboplatin-paclitaxel chemotherapy (CPC) reduces the number of immunosuppressive cells in cervical cancer patients,¹ creating a window-of-opportunity for TIL to exert their full effector function. Interferon-alpha further supports infused TIL. A phase I/II trial (NCT04072263) was initiated to study the feasibility and safety of TIL during CPC with or without additional interferon-alpha in patients with recurrent platinum-sensitive EOC.

Methods Fifteen patients with recurrent platinum-sensitive EOC received 6 cycles of CPC intravenously every 3 weeks and TIL intravenously 2 weeks after the 2nd, 3rd and 4th CPC cycle. Pegylated-interferon-alpha was added in the second cohort for 12 weeks, starting one week before the first TIL infusion. Patients who received 3 TIL infusions were evaluable. The primary endpoint was feasibility and safety of TIL administration during CPC with or without interferon-alpha. As secondary endpoints signs of activity, underlying mechanisms, immunomodulation, and T-cell reactivity were studied.

Results Thirteen patients were available for analysis. Median age 63 years (range, 29–77). TIL could be successfully expanded for all patients. Treatment with TIL during CPC was safe and did not add toxicity. Addition of IFN α resulted in grade 3 leucopenia and grade 3 thrombocytopenia in the first 2 patients and was therefore omitted in subsequent patients. CPC alleviated the immunosuppressive status, reflected by reduced plasma IL-6 levels and circulating myeloid-cell numbers, while lymphocytes numbers are not affected. This was most prominently at 1–2 weeks after the 2nd CPC and is suggested to reflect improved conditions promoting intra-tumoral T-cell reactivity. Objective responses were observed in 10/13 (77%) patients and 3 patients had stable disease. Interestingly, in at least one patient the ongoing platinum-free interval of 25 months far exceeds the first platinum-free interval of 8 months after similar CPC. In depth studies on immune modulation by chemotherapy and by TIL/Interferon-alpha, and correlations between TIL phenotype and clinical outcome are ongoing and will be presented.

Conclusions Combined treatment with CP chemotherapy and properly timed TIL may result in clinical benefit for patients with EOC.

Acknowledgements The unrestricted funding of the trial by Ovacure is greatly acknowledged.

Trial Registration The trial is registered at www.clinicaltrials.gov under number NCT04072263.

REFERENCE

1. . Welters MJ, van der Sluis TC, van Meir H, Loof NM, van Ham VJ, van Duikeren S, Santegoets SJ, Arens R, de Kam ML, Cohen AF, van Poelgeest MI, Kenter GG, Kroep JR, Burggraaf J, Melief CJ, van der Burg SH. Vaccination during myeloid cell depletion by cancer chemotherapy fosters robust T cell responses. *Sci Transl Med* 2016;**8**(334):334ra52. doi: 10.1126/scitranslmed.aad8307

Ethics Approval This study was approved by Leiden University Medical Center's Ethics Board; approval number L18-012 and the Central Committee on Research Involving Human Subjects; approval number NL63434.000.17.

<http://dx.doi.org/10.1136/jitc-2021-SITC2021.356>

TORIPALIMAB PLUS CHEMORADIOTHERAPY IN PATIENTS WITH RECURRENT OR METASTATIC CERVICAL CANCER: A MULTICENTER, OPEN-LABEL, SINGLE-ARM, PHASE II TRIAL

¹Xiaoting Xu*, ²Jian Huan, ³Hui Miao, ⁴Hao Wang, ¹Yue Wang, ²Hongyu Zhu, ⁴Jun Jiang, ⁵Juying Zhou. ¹The First Affiliated Hospital of Soochow, Suzhou, China; ²The Affiliated Suzhou Science and Technology, Suzhou, China; ³Xuzhou Cancer Hospital, Suzhou, China; ⁴The First Affiliated Hospital of Anhui, Hefei, China; ⁵The First Affiliated Hospital of Soochow University, Su Zhou, China

Background Recurrent or metastatic cervical cancer patients who progressed after standard therapy have limited treatment options and poor prognosis with a 1-year survival rate ranging between 15% and 20%. This study evaluates the efficacy and safety of toripalimab plus chemoradiotherapy in patients with recurrent or metastatic cervical cancer (Clinical trial ID: ChiCTR2000029068)

Methods In this open-label, single-arm, phase 2 study conducted at four radiotherapy centers in East China, eligible patients were confirmed by pathology and/or imaging for recurrent or metastatic cervical cancer. According to the first-line therapies for cervical cancer recommended by NCCN guidelines, all patients were received paclitaxel plus cisplatin regimen, with or without bevacizumab, combined with radiotherapy. After seven fractions radiotherapy at the recurrent or metastatic regions, 240 mg toripalimab every three weeks for six cycles or more were given in combination.

Results Between Jan 14th, 2020, and May 1st, 2021, 24 patients were enrolled. All patients were staged at the first visit, as seven patients were with FIGO (2018) stage I, 10 with stage II, 2 with stage III, 1 with stage IV, and 2 with unclear stage. Of 24 included patients, 22 (91.67%) had squamous cervical cancer. The median age was 55 (range, 33–72) years. As of May 31, 2021, median follow-up time was 8.5 months [95% CI: 2.3–10.1]. 14 (58.3%) of 24 patients who achieved an objective response, including 10 (41.7%) complete response (CR) and 4 (16.7%) partial response (PR). The median duration of response was not reached and 7 (29.1%) patients continued toripalimab treatment after the previous 6-cycle immunotherapy. The disease control rate was 75% (18/24). Median progression-free survival (PFS) was 8.61 months (95% CI: 4.14–not reached). For subgroup analysis, the median PFS was significantly prolonged in the CR/PR group compared with that in the SD/PD group [not reached (95% CI: 6.21–not reached) versus 5.5 months (95% CI: 2.69–6.870), $P = 0.023$]. There was no significant difference in the median PFS between patients who previously received radiotherapy (8.61 months) and those who didn't (6.87 months) ($P = 0.641$). 8 (33.3%) patients had grade 3–4 treatment-related adverse events (TRAEs). The most common grade 3–4 TRAEs were myelosuppression (29.2%), hypertriglyceridemia (8.3%), hypoalbuminemia (4.2%), pneumonia (4.2%), and hypercholesterolemia (4.2%).

Conclusions Toripalimab plus chemoradiotherapy showed promising antitumor activity and tolerable toxicities in patients with recurrent or metastatic cervical cancer.

<http://dx.doi.org/10.1136/jitc-2021-SITC2021.357>

358

RAMUCIRUMAB IN COMBINATION WITH PEMBROLIZUMAB AS FIRST-LINE TREATMENT FOR RECURRENT OR METASTATIC HEAD AND NECK SQUAMOUS-CELL CARCINOMA: A PHASE 1–2 TRIAL

Douglas Adkins*, Jessica Ley, Kevin Palka, Miriam Jacobs, Jingxia Liu, Peter Oppelt. Washington University School of Medicine, St. Louis, MO, USA

Background VEGF, a key mediator of angiogenesis and resistance to immunotherapy, is overexpressed in head and neck squamous-cell carcinoma (HNSCC). The primary aims of this trial were to determine the recommended phase 2 dose (RP2D) of ramucirumab, a potent inhibitor of VEGF receptor-2, given with pembrolizumab, and the objective response rate (ORR) of this combination as first-line treatment for recurrent or metastatic (RM)-HNSCC.

Methods Study participants provided written informed consent. Eligible patients had incurable HNSCC originating in the oral cavity, oropharynx, larynx, or hypopharynx. RM disease within 6 months of curative-intent systemic therapy and programmed death ligand (PD-L1) negative disease were permitted. In a dose de-escalation phase 1 design, patients received ramucirumab (level one: 10 mg/kg; then 8 and 6 mg/kg) and pembrolizumab (200 mg) on day 1 of each 21-day cycle until discontinuation criteria were met. Each dose level included three patients. The RP2D of ramucirumab was defined as the highest dose level at which one or fewer patients experienced a dose-limiting toxicity (DLT) during cycle one. In a Simon two-stage phase 2 design, patients with measurable, previously untreated RM-HNSCC received ramucirumab at the RP2D with pembrolizumab. Tumor response was assessed by RECIST1.1. When the trial was developed, the ORR of pembrolizumab given as first-line treatment wasn't known; however, the ORR for platinum pre-treated disease was 13–18%. Therefore, an ORR of <13% was deemed unacceptable and an ORR of >32% was of clinical interest. In stage one, two or more responses among ten patients were required to enroll to stage two. Eight or more responses among 33 evaluable patients (those with at least one response assessment) was evidence for efficacy (80% power; one-sided $\alpha = 0.05$).

Results Three patients were treated in phase 1 and 37 in phase 2. Eleven patients (28%) had recurrent disease within 6 months of curative-intent systemic therapy. In phase 1, no DLT occurred at the starting dose of ramucirumab. Tumor response occurred in 2 of these 3 patients. In phase 2, tumor response occurred in 19 of 33 evaluable patients (ORR 57.6%, 95%CI: 39.2–74.5). Tumor response by PD-L1 CPS is shown in the table below (table 1). No unexpected safety concerns were identified.

pembrolizumab monotherapy when given as first-line treatment for RM-HNSCC.

Trial Registration This trial is registered with ClinicalTrials.gov (NCT03650764).

Ethics Approval This study was approved by Washington University's Ethics Board; approval number 201809094.

<http://dx.doi.org/10.1136/jitc-2021-SITC2021.358>

Abstract 358 Table 1

Best Response (RECIST 1.1)	# Evaluable Patients*	# Patients with PD-L1 CPS Status**		
		≥20 (n=15)	1-19 (n=12)	0 (n=5)
CR + PR	19	9	7	2
Stable	7	2	2	3
Progression	7	4	3	0

CPS, combined positive score; CR, complete response; PR, partial response

* Underwent at least one tumor response assessment.

**PD-L1 status pending for one patient.

Conclusions The RP2D of ramucirumab given with pembrolizumab was 10 mg/kg on day 1 of each 21-day cycle. The primary hypothesis was accepted: the ORR with ramucirumab and pembrolizumab was higher than expected with

RESULTS FROM A PHASE II STUDY OF EFTILAGIMOD ALPHA (SOLUBLE LAG-3 PROTEIN) AND PEMBROLIZUMAB IN PATIENTS WITH PD-L1 UNSELECTED METASTATIC 2ND LINE HEAD AND NECK SQUAMOUS CELL CARCINOMA (HNSCC)

¹Antonio López Pousa*, ²Enriqueta Felip, ³Martin Forster, ⁴Bernard Doger, ⁵Patricia Roxburgh, ⁶Pawan Bajaj, ⁷Julio Peguero, ⁸Enric Carcereny, ⁹Matthew Krebs, ¹⁰Christian Mueller, ¹¹Frederic Triebel. ¹Hospital Sant Pau, Barcelona, Spain; ²Vall d'Hebron University Hospital, Barcelona, Spain; ³UCL Cancer Institute/NHS Foundation, London, UK; ⁴START Madrid- Fundación Jiménez Díaz, Madrid, Spain; ⁵Beatson West of Scotland Cancer Center, Glasgow, UK; ⁶Tasman Oncology, Queensland, Australia; ⁷Oncology Consultants, P. A., Houston, TX, USA; ⁸Catalan Institute of Oncology Badalona, Badalona, Spain; ⁹Christie NHS Foundation Trust, Manchester, UK; ¹⁰Clinical Development, Immuteq GmbH, Berlin, Germany; ¹¹Research and Development, Immuteq S.A.S., Chateaufort, France

Background Eftilagimod alpha (efti) is a soluble LAG-3 protein targeting a subset of MHC class II, thus mediating antigen presenting cell (APC) and CD8 T-cell activation. Such stimulation of the dendritic cell network and resulting T cell recruitment by efti may lead to stronger anti-tumor responses than observed with pembrolizumab alone. We hereby report results of the 2nd line metastatic head and neck squamous cell carcinoma (HNSCC) cohort (part C) of the TACTI-002 phase II trial (NCT03625323).

Methods Eligible patients (pts) with HNSCC, unselected for PD-L1 expression with disease progression on or after 1st line platinum-based therapy, received 30 mg subcutaneous efti Q2W for 24 weeks and 200 mg pembrolizumab Q3W for up to 2 years or until disease progression. The study used a Simon's 2-stage design with objective response rate (ORR) as the primary endpoint (EP). Secondary EPs included tolerability, progression free survival (PFS), overall survival (OS), pharmacokinetics, pharmacodynamics, and immunogenicity. Tumor response was assessed Q9W. PD-L1 was assessed centrally (22C3 clone). The study was approved by ethic committees and institutional review boards.

Results Between Mar 2019 and Jan 2021, 39 pts were enrolled (cut-off Apr 2021). The median age was 62 yrs (range 37–84) with 90% male pts. ECOG was 0 and 1 in 33% and 67%, respectively. Primary tumor location at diagnosis was oropharynx (36%), oral cavity (31%), hypopharynx (18%) and larynx (15%) with all PD-L1 subgroups (CPS < 1, ≥1 to ≤19; ≥20) being represented. All pts were pre-treated with platinum-based chemotherapy. Thirty-seven (37) pts were evaluated for response with ORR (iRECIST) of 30% (95% CI 16–47%) with 5 (14%) CRs; 6 (16%) PRs; 3 (8%) SDs; 17 (46%) PDs and 6 (16%) pts not evaluable. Median PFS was 2.1 months and 30+% were progression-free at 6 months. One patient (3%) discontinued due to pembro-related adverse event. The most common (>10%) treatment emergent adverse events were hypothyroidism (21%), cough (18%), asthenia (15%), fatigue (13%), anemia (13%), diarrhea (13%) and weight decreased (13%).

Conclusions Efti in combination with pembrolizumab is safe, showing encouraging antitumor activity in platinum pre-treated, 2nd line HNSCC patients. For further investigation of this combination, a 1st line HNSCC trial (NCT04811027) has been initiated.

Trial Registration NCT03625323

Ethics Approval The study was approved by relevant ethic committees and institutional review boards

<http://dx.doi.org/10.1136/jitc-2021-SITC2021.359>

360

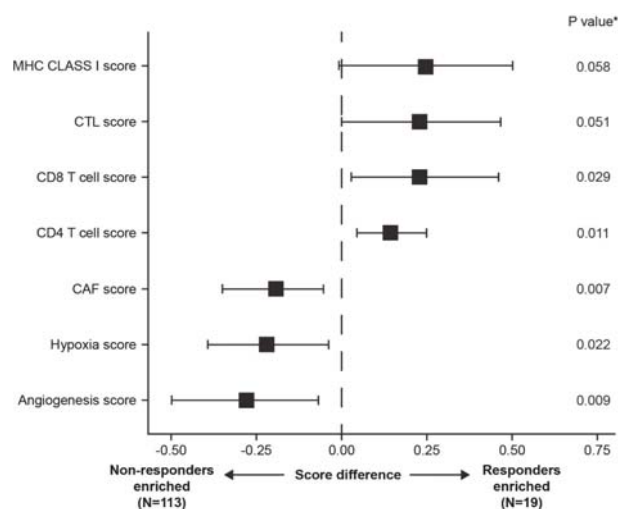
TUMOR-IMMUNE SIGNATURES ASSOCIATED WITH RESPONSE OR RESISTANCE TO TISLELIZUMAB IN PATIENTS WITH PREVIOUSLY TREATED ADVANCED HEPATOCELLULAR CARCINOMA (HCC)

¹Chiun Hsu*, ²Julien Edeline, ³Gianluca Masi, ⁴Yuk Ting Ma, ⁵Weilin Wang, ⁶Henning Wege, ⁷Cong Fei, ⁷Chen Ling, ⁸Xiaopeng Ma, ⁸Pei Zhang, ⁷Ruiqi Huang, ⁷Xikun Wu, ⁸Zhirong Shen, ⁸Bai Li, ⁹Sandra Chica Duque, ¹⁰Zhiqiang Meng. ¹National Taiwan University College of Medicine, Taipei City, Taiwan; ²Centre Eugène Marquis, Rennes, France; ³University of Pisa, Pisa, Italy; ⁴University of Birmingham, Birmingham, UK; ⁵First Affiliated Hospital, Zhejiang University School of Medicine, Hangzhou, China; ⁶Gastroenterology and Hepatology, University Medical Center Hamburg-Eppendorf, Hamburg, Germany; ⁷BeiGene (Shanghai) Co., Ltd., Shanghai, China; ⁸BeiGene (Beijing) Co., Ltd., Beijing, China; ⁹BeiGene (San Mateo) Co., Ltd., San Mateo, CA, USA; ¹⁰Fudan University Shanghai Cancer Center, Shanghai, China

Background Tislelizumab, an anti-programmed cell death protein-1 monoclonal antibody, demonstrated clinical activity and was well tolerated in patients with previously treated advanced HCC in the open-label, multicenter, Phase 2 RATIONALE-208 study (NCT03419897). We report exploratory analysis of the association of gene expression profiles (GEPs) with response to tislelizumab in patients with previously treated advanced HCC.

Methods Eligible patients who had received ≥ 1 prior line of systemic therapy for advanced HCC received tislelizumab (200 mg) intravenously once every 3 weeks and tumor response was evaluated per RECIST v.1.1. Baseline tumor sampling was optional and GEP analysis was performed using HTG EdgeSeq Precision Immuno-Oncology panel in 138 tumor samples (fresh tumor, n=6; archival tumor, n=132). Signature scores were calculated using Gene Set Variation Analysis package with publicly available gene signatures (GS). GS or genes differentially expressed between responders and non-responders (NRs) were determined using Wilcoxon rank-sum test and modified t-test with limma. Distributions of overall survival (OS) and progression-free survival (PFS) for GS subgroups (high vs low) were estimated by Kaplan-Meier method. Hierarchical clustering of NRs was achieved using 1-Pearson's correlation and average linkage. All statistical analysis results are post-hoc exploratory and thereby p values are descriptive.

Results 249 patients were enrolled and received ≥ 1 dose of tislelizumab; 138 patients had evaluable GEP data, of which 132 patients had evaluable GEP and tumor response data. GEP analysis demonstrated that CD4 T cell, CD8 T cell, cytotoxic T lymphocyte and major histocompatibility complex class I signatures were enriched in responders, and cancer-associated fibroblasts, angiogenesis and hypoxia signatures were enriched in NRs (figure 1). CD8B_PDCD1_9, a novel GS identified, comprises 9 genes highly expressed in responders: CD8B, CXCL13, KLRD1, NKG7, HLA-A, HLA-G, LAG3, PDCD1 and KREMEN1. Higher objective response rate (ORR; $p < 0.0001$, by Fisher's exact test) and longer PFS ($p = 0.005$, by log rank test) were observed in patients with high vs low CD8B_PDCD1_9 score (ORR: 26% vs 3%; median PFS: 2.8 months vs 1.8 months). To explore the heterogeneity of molecular features in NRs, NRs were clustered into 3 subgroups using a series of tumor-immune GS. OS and PFS for the 3 NR subgroups with distinct GS are summarized in table 1.



Abstract 360 Figure 1 Correlation between GS and ORR in patients with previously treated advanced HCC treated with tislelizumab monotherapy

Abstract 360 Table 1 OS and PFS of NR subgroups

NR subgroups	N	Highly enriched GS	Median OS months, (95% CI)	Median PFS months, (95% CI)
NR1	36	DNA repair	14.0	1.4
		Cell cycle	(9.7, NE)	(1.4, 2.7)
NR2	10	Pembro 18 genes	14.3	5.8
		Treg genes	(3.1, NE)	(2.6, 14.4)
		Immune inhibition		
NR3	67	Angiogenesis	8.6	1.4
		Hypoxia	(6.8, 12.4)	(1.4, 2.7)

CI, confidence interval; NE, not evaluable; GS, gene signature; NR, non-responder; OS, overall survival; PFS, progression-free survival

Conclusions This exploratory analysis identified distinct GS associated with tumor response and resistance to tislelizumab monotherapy in patients with previously treated advanced HCC and increases our understanding of the tumor microenvironment. Further GEP analyses will be undertaken in an ongoing Phase 3 study (NCT03412773).

Acknowledgements This study is sponsored by BeiGene Ltd. Medical writing support for the development of this abstract, under direction of the authors, was provided by Claire White, PhD, of Ashfield MedComms, an Ashfield Health company, and was funded by BeiGene Ltd.

Trial Registration NCT03419897

Ethics Approval This study was conducted according to the ethical principles of the Declaration of Helsinki, Good Clinical Practice guidelines, the principles of informed consent and the requirements of the public registration of clinical trials. Written informed consent was obtained from each patient prior to screening. The protocol was approved by the institutional ethics committee and was monitored by a safety monitoring committee.

<http://dx.doi.org/10.1136/jitc-2021-SITC2021.360>

361 HETEROGENEITY OF PD-1HI T CELLS ASSOCIATES WITH RESPONSE TO PD-1 BLOCKADE IN HEPATOCELLULAR CARCINOMA

Assaf Magen*, Assaf Magen, Pauline Hamon, Myron Schwartz, Thomas Marron, Alice Kamphorst, Miriam Merad. *MSSM, New York, NY, USA*

Background Blockade of the PD-1 pathway is a therapeutic strategy to reinvigorate T cell responses against tumors, and when combined with other biologic therapies in the first line setting this achieves significant clinical response in about 25% of hepatocellular carcinoma (HCC) patients. We hypothesize that phenotypic diversity of tumor infiltrating T cells can explain, at least partially, the disparate clinical responses to immunotherapy.

Methods Here, we analyze the molecular diversity of T cells in tumor, adjacent tissue and tumor-draining lymph node (dLN) by single-cell RNA sequencing of tissue from 23 patients with early stage HCC treated by neoadjuvant PD-1 blockade (NCT03916627).

Results We identify distinct subsets of PD-1hi T cells with varying degrees of exhaustion and effector gene programs. Compared to parallel analysis of untreated HCC tumors, we observed that PD-1 blockade resulted in expansion of PD-1hi T cells in the tumor, regardless of clinical response. PD-1hi T cells subsets were highly clonal and enriched in the tumor compared to adjacent tissue, suggesting specificity to tumor antigens. Remarkably, within the PD-1hi T cell population we find an association between specific transcriptomic phenotype that correlates with response to PD-1 blockade. Using T cell receptor (TCR) sequencing to study the differentiation patterns between T cell states, we found that clonotypes present among expanded PD-1hi T cells were also found in CD8 effector cells; these data identify characteristic clonally related T cell populations that are enriched in clinical responders. Furthermore, we find that dLN harbor clonotypes of PD-1hi T cells expanded in tumor. In the dLN, these potentially tumor-specific T cells have features of activation and exhaustion suggesting a continuous role of dLN in anti-tumor responses. This study suggests a link between particular PD-1hi T cell subsets and responsiveness to PD-1 blockade.

Conclusions These results will be corroborated with 8 additional patient samples in which we will further analyze the role of tumor-specific T cells in dLN. Furthermore, our ongoing sequencing of pre-treatment lesions will enable monitoring of T cell clonal expansion, and additionally transcriptomic characterization of these samples will be correlated with post-treatment T cell programs to test predictive potential of baseline lymphoid phenotype. Correlations of these phenotypes with response to PD-1 blockade will allow for validation of predictive biomarkers, and characterizing these T cell programs in the dLN and the tumor microenvironment will enable superior and personalized therapeutic interventions.

Ethics Approval Samples of tumor and non-involved liver were obtained from surgical specimens of patients undergoing resection at Mount Sinai Hospital (New York, NY) after obtaining informed consent in accordance with a protocol reviewed and approved by the Institutional Review Board at the Icahn School of Medicine at Mount Sinai (RUTH Human Subjects Electronic Submission System 18-00407 and 20-04150) and in collaboration with the Biorepository and Department of Pathology.

<http://dx.doi.org/10.1136/jitc-2021-SITC2021.361>

ASSOCIATION OF NEUTROPHIL-TO-LYMPHOCYTE RATIO AND PLATELET-TO-LYMPHOCYTE RATIO WITH CLINICAL OUTCOMES TO TISLELIZUMAB MONOTHERAPY IN PATIENTS WITH PREVIOUSLY TREATED ADVANCED HEPATOCELLULAR CARCINOMA

¹Philippe Merle*, ²Helena Verdaguer Mata, ³Congying Xie, ⁴Richard Hubner, ⁵Yong Liu, ⁶Jane Margetts, ⁷Ying Cheng, ⁸Yee Chao, ⁹Cong Fei, ⁹Chen Ling, ⁹Ruiqi Huang, ⁹Xikun Wu, ¹⁰Zhirong Shen, ¹⁰Bai Li, ¹¹Sandra Chica Duque, ¹²Zhenggang Ren. ¹Hospital La Croix-Rousse, Lyon, France; ²Vall d'Hebron Institute of Oncology, Barcelona, Spain; ³Second Affiliated Hospital of Wenzhou Me, Wenzhou, China; ⁴The Christie NHS Foundation Trust, Manchester, UK; ⁵Xuzhou Central Hospital, School of Medicine, Southeast University, Xuzhou, China; ⁶Northern Centre for Cancer Care, Newcastle-upon-Tyne Hospitals NHS Foundation Trust, Newcastle upon Tyne, UK; ⁷Jilin Cancer Hospital, Changchun, China; ⁸Taipei Veterans General Hospital, Taipei, Taiwan, Province of China; ⁹BeiGene (Shanghai) Co., Ltd., Shanghai, China; ¹⁰BeiGene (Beijing) Co., Ltd., Beijing, China; ¹¹BeiGene (San Mateo) Co., Ltd., San Mateo, CA, USA; ¹²Liver Cancer Institute, Zhongshan Hospital, Fudan University, Shanghai, China

Background Tislelizumab, an anti-PD-1 monoclonal antibody, demonstrated clinical activity and was well-tolerated in patients with previously treated advanced hepatocellular carcinoma (HCC) in the Phase 2 RATIONALE-208 study (NCT03419897). We explored whether baseline neutrophil-to-lymphocyte ratio (NLR) and platelet-to-lymphocyte ratio (PLR) or their post-treatment change correlated with clinical efficacy of tislelizumab treatment.

Methods Eligible patients (>18 years) who had received ≥ 1 prior line of systemic therapy for advanced HCC were administered open-label tislelizumab (200 mg) intravenously every 3 weeks until no further clinical benefit was observed. NLR and PLR were assessed using peripheral blood samples collected at baseline, Cycle 2 Day 1 (C2D1), C3D1, and C4D1. Survival analysis (progression free survival [PFS] and overall survival [OS]) was conducted by Kaplan-Meier method and survival rate at risk was compared by log rank test. Logistic regression was used to analyze association of post-treatment change of NLR or PLR with objective response rate (ORR). In the baseline analysis, median NLR or PLR in this study was used as a cut-off. All statistical analysis results are post-hoc exploratory and thereby p values are descriptive.

Results Overall, 249 patients were enrolled, of which 249, 234, 203, and 186 patients had evaluable NLR and PLR data at baseline, C2D1, C3D1, and C4D1, respectively. Analysis of NLR at baseline, using median NLR (3.2) as cut-off, demonstrated higher OS ($p=0.0024$) and PFS ($p=0.071$) in NLR-low versus NLR-high groups (median OS [mOS]:17.4 versus 9.9 months; median PFS [mPFS]: 2.8 versus 1.5 months). Analysis of PLR at baseline, using median PLR (141.4) as cut-off, showed higher OS ($p=0.0085$) and PFS ($p<0.0001$) in PLR-low versus PLR-high groups (mOS: 16.2 versus 10.8 months; mPFS: 2.8 versus 1.4 months). In post-treatment analysis, patients with decreased NLR or PLR at C2D1, C3D1 or C4D1 had higher ORR (table 1) and longer OS (figure 1) compared with patients with increased NLR or PLR at each timepoint.

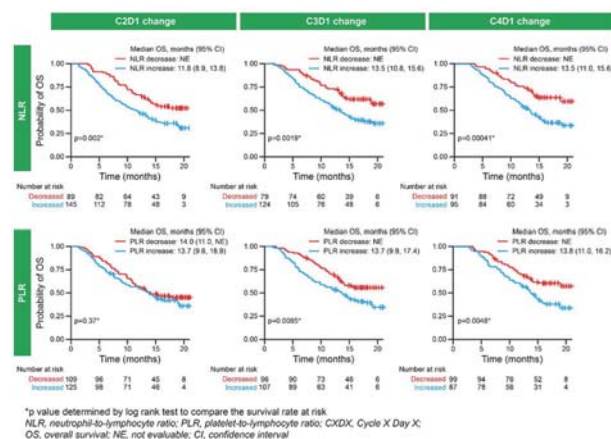
Abstract 362 Table 1 Post-treatment decreases in NLR or PLR were associated with response to tislelizumab monotherapy

NLR	C2D1 change		C3D1 change		C4D1 change	
	Decreased (N=89)	Increased (N=145)	Decreased (N=79)	Increased (N=124)	Decreased (N=91)	Increased (N=95)
ORR	22%	8%	27%	9%	26%	7%
OR (95% CI), p value*	0.31 (0.14, 0.67) 0.0031		0.28 (0.12, 0.61) 0.0015		0.22 (0.09, 0.55) 0.0011	
PLR	C2D1 change		C3D1 change		C4D1 change	
	Decreased (N=109)	Increased (N=125)	Decreased (N=96)	Increased (N=107)	Decreased (N=99)	Increased (N=87)
ORR	19%	10%	25%	8%	27%	5%
OR (95% CI), p value*	0.47 (0.22, 1.02) 0.0556		0.24 (0.10, 0.57) 0.0012		0.13 (0.04, 0.38) 0.0002	

*Determined by logistic regression

NLR, neutrophil-to-lymphocyte ratio; PLR, platelet-to-lymphocyte ratio; CXDX, Cycle X Day X;

ORR, objective response rate; OR, odds ratio; CI, confidence interval



Abstract 362 Figure 1 Post-treatment decreases in NLR or PLR were associated with improved OS following tislelizumab monotherapy

Conclusions In patients with previously treated advanced HCC that received tislelizumab monotherapy, lower baseline NLR or PLR was associated with longer OS and PFS, and post-treatment decreases of NLR or PLR were associated with higher ORR and longer OS. These observations support NLR and PLR as potential prognostic biomarkers in patients with advanced HCC treated with tislelizumab and will be further investigated in an on-going Phase 3 study (NCT03412773).

Acknowledgements This study is sponsored by BeiGene Ltd. Medical writing support for the development of this abstract, under direction of the authors, was provided by Claire White, PhD, and Kirsty Millar, MSc, of Ashfield MedComms, an Ashfield Health company, and was funded by BeiGene Ltd.

Trial Registration NCT03419897

Ethics Approval This study was conducted according to the ethical principles of the Declaration of Helsinki, Good Clinical Practice guidelines, the principles of informed consent and the requirements of the public registration of clinical trials. Written informed consent was obtained from each patient prior to screening. The protocol was approved by the institutional ethics committee and was monitored by the investigators and study sponsor.

<http://dx.doi.org/10.1136/jitc-2021-SITC2021.362>

KEYNOTE-042 5-YEAR SURVIVAL UPDATE: PEMBROLIZUMAB VERSUS CHEMOTHERAPY IN PATIENTS WITH PREVIOUSLY UNTREATED, PD-L1-POSITIVE, LOCALLY ADVANCED OR METASTATIC NON-SMALL-CELL LUNG CANCER

¹Gilberto de Castro*, ²Iveta Kudaba, ³Yi-Long Wu, ⁴Gilberto Lopes, ⁵Dariusz M Kowalski, ⁶Hande Z Turna, ⁷Christian Caglevic, ⁸Li Zhang, ⁹Boguslawa Karaszewska, ¹⁰Konstantin K Laktionov, ¹¹Vichien Srimuninnimit, ¹²Igor Bondarenko, ¹³Kaoru Kubota, ¹⁴Rinee Mukherjee, ¹⁴Jianxin Lin, ¹⁴Fabricio Souza, ¹⁵Tony SK Mok, ¹⁶Byoung Chul Cho. ¹Instituto do Câncer do Estado de São Paulo, São Paulo, Brazil; ²Latvian Oncology Center, Riga East Clinical University, Riga, Latvia; ³Guangdong Lung Cancer Institute, Guangdong Provincial People's Hospital and Guangdong Academy of Medical Sciences, Guangdong, China; ⁴Department of Medical Oncology, Sylvester Comprehensive Cancer Center at the University of Miami, Miami, FL, USA; ⁵Department of Lung Cancer and Chest Tumours, Maria Skłodowska-Curie National Research Institute of Oncology, Warsaw, Poland; ⁶Department of Internal Medicine, Istanbul University Cerrahpasa Medical Faculty, Istanbul, Turkey; ⁷Cancer Research Department, Instituto Oncologico Fundación Arturo Lopez Perez, Santiago, Chile; ⁸Peking Union Medical College Hospital, Beijing, China; ⁹Przychodnia Lekarska KOMED, Konin, Poland; ¹⁰Federal State Budgetary Institution "N.N. Blokhin National Medical Research Center of Oncology" of the Ministry of Health of the Russian Federation (N.N. Blokhin NMRCO), Moscow, Russian Federation; ¹¹Department of Medicine, Siriraj Hospital, Bangkok, Thailand; ¹²Oncology and Medical Radiology Department, Dnipro State Medical University, Dnipro, Ukraine; ¹³Department of Pulmonary Medicine and Oncology, Nippon Medical School Hospital, Tokyo, Japan; ¹⁴Merck and Co., Inc., Kenilworth, NJ, USA; ¹⁵Clinical Oncology, State Key Laboratory of Translational Oncology, Chinese University of Hong Kong, Shatin, Hong Kong, China; ¹⁶Division of Medical Oncology, Yonsei Cancer Center, Seoul, Korea, Republic of

Background Primary analysis of KEYNOTE-042 (NCT02220894), a global, randomized, phase 3 trial, showed that pembrolizumab significantly improved OS versus platinum-based chemotherapy in patients with locally advanced or metastatic non-small-cell lung cancer (NSCLC) without sensitizing *EGFR/ALK* alterations and with PD-L1 tumor proportion score (TPS) $\geq 50\%$, $\geq 20\%$, and $\geq 1\%$ with fewer treatment-related AEs than chemotherapy. We report an updated analysis with ~5 years of follow-up.

Methods Eligible adults were randomized 1:1 to receive pembrolizumab 200 mg Q3W for 35 cycles or investigator's choice of chemotherapy (carboplatin + paclitaxel or pemetrexed) Q3W for 4–6 cycles with optional maintenance pemetrexed (nonsquamous only). Primary endpoints were OS in patients with PD-L1 TPS $\geq 50\%$, $\geq 20\%$, and $\geq 1\%$; secondary endpoints included PFS and ORR per RECIST v1.1 by central review, and safety (secondary). Eligible patients randomized to pembrolizumab who completed 35 cycles with SD or better or stopped treatment after confirmed CR could begin a second course of pembrolizumab at the time of progression.

Results 1274 patients were randomized to pembrolizumab or chemotherapy (n = 637 each). Median (range) time from randomization to data cutoff (Apr 28, 2021) was 61.1 (50.0–76.3) months. OS outcomes favored the pembrolizumab group (vs chemotherapy alone) regardless of PD-L1 TPS (HR [95% CI] for TPS $\geq 50\%$, 0.68 [0.57–0.81]; TPS $\geq 20\%$, 0.75 [0.64–0.87]; TPS $\geq 1\%$, 0.79 [0.70–0.89]), with estimated 5-year OS rates (95% CI) of 21.9% (17.3%–26.9%), 19.4% (15.6%–23.4%) and 16.6% (13.7%–19.6%), respectively, in the pembrolizumab group (table 1). Median duration of response (DOR) was 28.1 vs 10.8 months in PD-L1 TPS $\geq 50\%$ group, 27.7 vs 10.8 months in PD-L1 TPS $\geq 20\%$ group and, 26.5 vs 8.4 months in PD-L1 TPS $\geq 1\%$ for pembrolizumab group vs chemotherapy. Treatment-related grade 3–5 AEs occurred in 120 patients (18.9%) in the pembrolizumab group and 257 (41.8%) in the chemotherapy group. Among 102 patients who completed 35 cycles of pembrolizumab:

ORR was 84.3%; estimated 4-year OS rate after completion of 35 cycles of pembrolizumab (ie, approximately 6 years after randomization) was 61.8%. Among 33 patients who received second-course pembrolizumab, ORR was 15.2%.

Abstract 363 Table 1 Key efficacy outcomes in the KEYNOTE-042 ITT population

ITT Population	PD-L1 TPS $\geq 50\%$		PD-L1 TPS $\geq 20\%$		PD-L1 TPS $\geq 1\%$	
	Pembrolizumab n = 299	Chemo n = 300	Pembrolizumab n = 413	Chemo n = 405	Pembrolizumab n = 637	Chemo n = 637
OS, median (95% CI), mo	20.0 (15.9–24.2)	12.2 (10.4–14.6)	18.0 (15.5–21.5)	13.0 (11.6–15.3)	16.4 (14.0–19.6)	12.1 (11.3–13.3)
OS, HR (95% CI)	0.68 (0.57–0.81)		0.75 (0.64–0.87)		0.79 (0.70–0.89)	
OS, 5 y rate (95% CI), %	21.9 (17.3–26.9)	9.8 (6.6–13.7)	19.4 (15.6–23.4)	10.1 (7.2–13.5)	16.6 (13.7–19.6)	8.5 (6.4–11.0)
PFS, median (95% CI), mo	6.5 (5.9–8.6)	6.5 (6.2–7.6)	6.2 (5.4–7.8)	6.9 (6.3–8.2)	5.6 (4.3–6.2)	6.8 (6.4–7.9)
PFS, HR (95% CI)	0.88 (0.72–1.02)		0.84 (0.81–1.09)		1.03 (0.91–1.16)	
PFS, 5 y rate (95% CI), %	9.2 (5.9–13.4)	2.1 (0.7–5.0)	7.8 (5.2–11.1)	1.6 (0.5–3.9)	6.9 (4.9–9.4)	1.2 (0.5–2.7)
PFS2*, median (95% CI), mo	15.0 (11.6–19.2)	10.1 (8.9–11.2)	12.9 (10.9–15.5)	10.2 (9.1–11.3)	11.3 (10.1–12.9)	9.4 (8.8–10.3)
PFS2*, HR (95% CI)	0.64 (0.54–0.76)		0.67 (0.58–0.78)		0.74 (0.65–0.83)	
ORR (95% CI), %	39.1 (33.6–44.9)	32.3 (27.1–37.9)	33.2 (28.6–37.9)	29.1 (24.8–33.8)	27.3 (23.9–31.0)	26.7 (23.3–30.3)
DOR, median (range), mo	28.1 (2.1+ to 70.0+)	10.8 (1.8+ to 63.5+)	27.7 (2.1+ to 70.0+)	10.8 (1.8+ to 63.5+)	26.5 (2.1+ to 70.0+)	8.4 (1.8+ to 63.5+)

Chemo, chemotherapy; DOR, duration of response.
 +, indicates no PD by the time of last assessment.
 *PFS2: time from randomization to second/subsequent PD on next-line treatment or death.

Conclusions With 5 years of follow-up, first-line pembrolizumab monotherapy continued to show substantial clinical benefit with higher 5-year OS rates, and durable response over chemotherapy in patients with PD-L1-positive, locally advanced/metastatic NSCLC without *EGFR/ALK* alterations. First-line pembrolizumab remains a standard of care in patients with PD-L1 TPS $\geq 1\%$, as underscored by these long-term results.

Acknowledgements Medical writing assistance was provided by Kathleen Estes, PhD, of ICON plc (North Wales, PA, USA). This assistance was funded by Merck Sharp & Dohme Corp., a subsidiary of Merck & Co., Inc., Kenilworth, NJ, USA.

Trial Registration ClinicalTrials.gov, NCT02220894

Ethics Approval The protocol and all amendments were approved by the appropriate ethics committee at each center, the study was conducted in accordance with the standards of Good Clinical Practice and in compliance with the Declaration of Helsinki. Patients provided written informed consent before enrollment.

<http://dx.doi.org/10.1136/jitc-2021-SITC2021.363>

KRAS MUTATIONS IN PATIENTS WITH NONSQUAMOUS NON–SMALL-CELL LUNG CANCER: PREVALENCE AND RELATIONSHIP WITH PD-L1 EXPRESSION, TUMOR MUTATION BURDEN AND SMOKING STATUS

¹Marina Chiara Garassino*, ²Delvys Rodriguez-Abreu, ³Shirish M Gadgeel, ⁴Dariusz M Kowalski, ⁵Kazuo Kasahara, ⁶Enriqueta Felip, ⁷Yi-Long Wu, ⁸Gilberto de Castro, ⁹Byoung Chul Cho, ¹⁰Hande Z Turna, ¹¹Hidehito Horinouchi, ¹²Martin Reck, ¹³Rina Hui, ¹⁴Edward B Garon, ¹⁵Michael Boyer, ¹⁶Tony SK Mok, ¹⁷Gilberto Lopes, ¹⁸Julie Kobie, ¹⁸Yongjin Li, ¹⁸Mark A Ayers, ¹⁸Razvan Cristescu, ¹⁸Bin Zhao, ¹⁸M Catherine Pietanza, ¹⁹Roy S Herbst. ¹University of Chicago Medicine and Biological Sciences, Chicago, IL, USA; ²Complejo Hospitalario Universitario Insular Materno-Infantil de Gran Canaria, Universidad de Las Palmas de Gran Canaria, Las Palmas de Gran Canaria, Spain; ³Henry Ford Cancer Institute/Henry Ford Health System, Detroit, MI, USA; ⁴Maria Sklodowska-Curie National Research Institute of Oncology, Warsaw, Poland; ⁵Kanazawa University Hospital, Kanazawa, Japan; ⁶Vall d'Hebron University, Vall d'Hebron Institute of Oncology (VHIO), Barcelona, Spain; ⁷Guangdong Lung Cancer Institute, Guangdong Provincial People's Hospital and Guangdong Academy of Medical Sciences, Guangdong, China; ⁸Instituto do Câncer do Estado de São Paulo, São Paulo, Brazil; ⁹Yonsei Cancer Center, Seoul, Korea, Republic of; ¹⁰Istanbul University Cerrahpasa Medical Faculty, Istanbul, Turkey; ¹¹National Cancer Center Hospital, Tokyo, Japan; ¹²LungenClinic, Airway Research Center North, German Center for Lung Research, Grosshansdorf, Germany; ¹³Westmead Hospital and University of Sydney, Sydney, NSW, Australia; ¹⁴David Geffen School of Medicine at UCLA, Los Angeles, CA, USA; ¹⁵Chris O'Brien Lifehouse, Camperdown, Australia; ¹⁶State Key Laboratory of Translational Oncology, Chinese University of Hong Kong, Hong Kong Special Administrative Region, China; ¹⁷Sylvester Comprehensive Cancer Center at the University of Miami and the Miller School of Medicine, Miami, FL, USA; ¹⁸Merck and Co., Inc., Kenilworth, NJ, USA; ¹⁹Yale University School of Medicine, Yale Comprehensive Cancer Center, New Haven, CT, USA

Background Pembrolizumab is a standard-of-care first-line treatment for advanced/metastatic NSCLC, either as monotherapy (for patients with PD-L1 tumor proportion score [TPS] $\geq 1\%$) or combined with platinum chemotherapy. An improved OS benefit has been demonstrated for both pembrolizumab monotherapy and pembrolizumab plus chemotherapy in patients with higher tumor PD-L1 expression, and for pembrolizumab monotherapy in patients with higher tissue tumor mutation burden (tTMB). Mutations in *KRAS* occur relatively frequently in patients with nonsquamous NSCLC but infrequently in those with squamous NSCLC; most mutations are in codon 12. Notably, the pembrolizumab OS treatment effect was not diminished in patients with *KRAS* G12C mutations in phase 3 studies evaluating pembrolizumab monotherapy and pembrolizumab in combination with chemotherapy.^{1, 2} Herein we describe prevalence of *KRAS* mutations among patients with advanced nonsquamous NSCLC from two phase 3 clinical studies evaluating first-line pembrolizumab (KEYNOTE-042 and KEYNOTE-189) and the relationship of such mutations with select patient characteristics.

Methods KEYNOTE-042 (NCT02220894) evaluated pembrolizumab versus platinum-based chemotherapy for advanced PD-L1-positive NSCLC (any histology) without *EGFR/ALK* alterations. KEYNOTE-189 (NCT02578680) evaluated pembrolizumab plus platinum-based chemotherapy versus platinum-based chemotherapy alone for metastatic nonsquamous NSCLC without *EGFR/ALK* alterations irrespective of tumor PD-L1 expression. Whole-exome sequencing of tumor tissue and matched normal DNA (blood) was performed for patients with nonsquamous histology. PD-L1 TPS was evaluated using the PD-L1 IHC 22C3 pharmDx assay (Agilent Technologies, Carpinteria, CA, USA). Prevalence of *KRAS* mutations and their relationships with TMB, PD-L1 TPS, and smoking status were analyzed descriptively.

Results 590 patients with nonsquamous NSCLC were included in these analyses (KEYNOTE-042, n=301; KEYNOTE-189, n=289). Overall, 42.9% of patients had tTMB ≥ 175 mut/exome,

81.4% were current/former smokers and, 40.3%, 42.7%, and 16.9% had PD-L1 TPS $\geq 50\%$, 1–49% and $< 1\%$ respectively. *KRAS* G12C, G12D, and G12V mutations occurred in 11.0%, 4.1%, and 5.4% of patients, respectively. Prevalence of *KRAS* mutations by patient characteristics is summarized in the table (table 1). *KRAS* G12C mutations occurred almost exclusively in current/former smokers. *KRAS* G12C was enriched in tumors with tTMB ≥ 175 mut/exome and tumors with PD-L1 TPS $\geq 50\%$. Prevalence was highest in tumors with both tTMB ≥ 175 mut/exome and PD-L1 TPS $\geq 50\%$.

Abstract 364 Table 1 *KRAS* Mutation Prevalence

<i>KRAS</i> Mutation Prevalence, n (%)	N	<i>KRAS</i> G12C	<i>KRAS</i> G12D	<i>KRAS</i> G12V
Smoking status				
Current/former	480	64 (13.3)	22 (4.6)	29 (6.0)
Never	110	1 (0.9)	2 (1.8)	3 (2.7)
tTMB				
≥ 175 mutations/exome	253	44 (17.4)	7 (2.8)	16 (6.3)
< 175 mut/exome	337	21 (6.2)	17 (5.0)	16 (4.7)
PD-L1 expression^a				
TPS $\geq 50\%$	236	39 (16.5)	11 (4.7)	12 (5.1)
TPS 1%–49%	250	21 (8.4)	9 (3.6)	12 (4.8)
TPS $< 1\%$	99	5 (5.1)	4 (4.0)	8 (8.1)
tTMB and PD-L1 expression				
≥ 175 mut/exome and PD-L1 TPS $\geq 50\%$	109	31 (28.4)	3 (2.8)	7 (6.4)
≥ 175 mut/exome and PD-L1 TPS 1%–49%	94	11 (11.7)	4 (4.3)	5 (5.3)
≥ 175 mut/exome and PD-L1 TPS $< 1\%$	50	2 (4.0)	0	4 (8.0)
< 175 mut/exome and PD-L1 TPS $\geq 50\%$	127	8 (6.3)	8 (6.3)	5 (3.9)
< 175 mut/exome and TPS 1%–49%	156	10 (6.4)	5 (3.2)	7 (4.5)
< 175 mut/exome and TPS $< 1\%$	49	3 (6.1)	4 (8.2)	4 (8.2)

^a5 patients were unevaluable for PD-L1 TPS.

Conclusions *KRAS* G12C mutations occurred with moderate frequency in patients with nonsquamous NSCLC, with most occurring in current/former smokers. *KRAS* G12C mutations occurred at higher frequency in patient subgroups defined by higher tTMB and PD-L1 TPS.

Acknowledgements Medical writing assistance was provided by Christabel Wilson, MSc, of ICON plc (North Wales, PA, USA), funded by Merck Sharp & Dohme Corp., a subsidiary of Merck & Co., Inc., Kenilworth, NJ, USA.

Trial Registration KEYNOTE-042, ClinicalTrials.gov, NCT02220894; KEYNOTE-189, ClinicalTrials.gov, NCT02578680

REFERENCES

- Gadgeel S, Rodriguez-Abreu D, Felip E, et al. *KRAS* mutational status and efficacy in KEYNOTE-189: pembrolizumab (pembro) plus chemotherapy (chemo) vs placebo plus chemo as first-line therapy for metastatic non-squamous NSCLC. *Ann Oncol* 2019;**30**(suppl 11):xi64-xi5.
- Herbst RS, Lopes G, Kowalski DM, et al. Association of *KRAS* mutational status with response to pembrolizumab monotherapy given as first-line therapy for PD-L1-positive advanced non-squamous NSCLC in KEYNOTE-042. *Ann Oncol* 2019;**30**(suppl 11):xi63-xi4.

Ethics Approval For both trials, the protocol and all amendments were approved by the appropriate ethics committee at each center, the study was conducted in accordance with the standards of Good Clinical Practice. Patients provided written informed consent before enrollment.

<http://dx.doi.org/10.1136/jitc-2021-SITC2021.364>

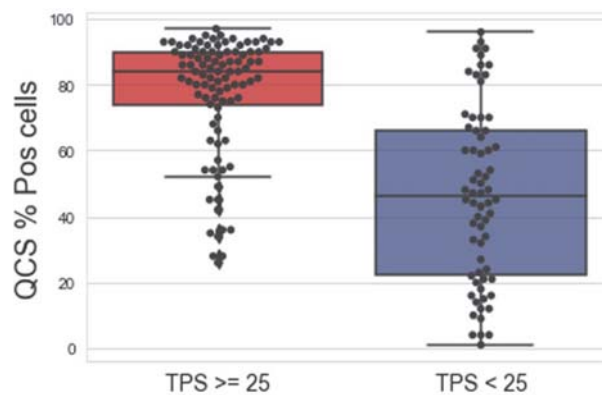
365

COMPUTATIONAL PATHOLOGY DELIVERS OBJECTIVE AND QUANTITATIVE PD-L1 EXPRESSION ANALYSIS FOR ENRICHMENT OF RESPONDERS TO DURVALUMAB IN NON-SMALL CELL LUNG CANCER (NSCLC)

Guenter Schmidt*, Ansh Kapil, Lina Meinecke, Farzad Sekhavati, Jan Lesniak, Anatoliy Shumilov, Thomas Padel. *AstrZeneca Computational Pathology GmbH, Munich, Germany*

Background The pathologist’s visual assessment of tumor proportion score (TPS) with 25% cutoff on PD-L1 stained tissue samples is an established method to select metastatic NSCLC patients that are likely to respond to an anti-PD-L1 monotherapy.¹ However, manual scoring is often subject to subjectivity in human perception² and there remains a critical need for more objective and quantitative methods to assess PD-L1 expression in immuno-oncology.

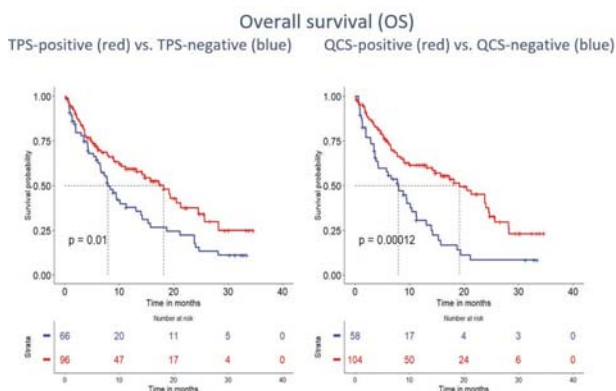
Methods We used deep learning (DL) based image analysis (IA) to generate a novel PD-L1 Quantitative Continuous Score (QCS)³ in tumor cells. PD-L1 QCS consists of two DL models to first segment epithelial regions and second detect membranes, cytoplasm and nuclei of each tumor cell in PD-L1 immunohistochemically (IHC) stained tissue slides. The PD-L1 expression of each tumor cell compartment was estimated by the respective optical density (OD) of DAB, and tumor cells with a membrane OD greater than ODmin are considered as PD-L1-positive. A slide comprising at greater percentage of PD-L1-positive tumor cells than a cutoff value (CoV) is considered QCS-positive. The ODmin and CoV parameters were linked to patient overall survival (OS), by minimizing the Kaplan Meier log-rank p-values and keeping at least 50% prevalence in the QCS-positive subgroup. Fully supervised QCS-IA models were extensively trained using pathologists’ annotations and the performance was validated on unseen data to ensure its generalization and robustness.^{3 4} The QCS IA was locked and blindly applied on clinical trial data (NCT01693562, durvalumab-treated late-stage NSCLC cohort) without further refinement.



Abstract 365 Figure 2 QCS scores within TPS positive and negative groups. Box plot indicating percent positive cells (OD≥8) as measured by PD-L1 QCS within the PD-L1 high (red) and low (blue) groups as per pathologist assessment by TPS.

Results Data analytics techniques were used to determine optimal PD-L1 QCS parameters for the clinical trial cohort of N=162 late-stage NSCLC patients. A PD-L1 QCS algorithm (ODmin=8, CoV=57%) is able to stratify durvalumab-treated NSCLC patients at a higher prevalence and more significant log rank p-value (64%, p=0.0001) for OS (figure 1) compared to pathologist TPS (59%, p=0.01). Median OS times of (19.2 months vs 7.9 months) was observed in the QCS-positive vs negative subgroups, respectively. The box plots (figure 2) indicate an overall good agreement (72% concordance) of the fully automated QCS with the pathologists TPS, which quantitatively supports the positive visual assessment of the cell segmentation accuracy.

Conclusions The novel Quantitative Continuous Scoring (QCS) provides an objective way of correlating a quantitative estimate of PD-L1 IHC expression on tumor cells with survival of durvalumab-treated NSCLC patients. This data establishes a first proof-of-concept demonstrating the potential utility of PD-L1 QCS towards precision medicine in immuno-oncology.



Abstract 365 Figure 1 Kaplan Meier (KM) curves for OS stratification. KM curves for Overall Survival (OS) stratification with (left) manual PD-L1 TPS score (25% cutoff), and (right) automated QCS (57% cutoff).

REFERENCES

1. Rebelatto M, et al. Development of a programmed cell death ligand-1 immunohistochemical assay validated for analysis of non-small cell lung cancer and head and neck squamous cell carcinoma. *Diagnostic Pathology* 2016.
2. Tsao M S, et al. PD-L1 immunohistochemistry comparability study in real-life clinical samples: results of blueprint phase 2 project. *Journal of Thoracic Oncology* 2018.
3. Gustavson M, et al. Novel approach to HER2 quantification: digital pathology coupled with AI-based image and data analysis delivers objective and quantitative HER2 expression analysis for enrichment of responders to trastuzumab deruxtecan (T-DXd; DS-8201), specifically in HER2-low patients. (2021) DOI: 10.1158/1538-7445.SABCS20-PD6-01
4. Kapil A, et al. Domain adaptation-based deep learning for automated tumor cell (TC) scoring and survival analysis on PD-L1 stained tissue images. *IEEE Transactions on Medical Imaging* DOI: 10.1109/TMI.2021.3081396

Ethics Approval Clinical study NCT01693562, from which data in this report were obtained, was carried out in accordance with the Declaration of Helsinki and Good Clinical Practice guidelines. The study protocol, amendments, and participant informed consent document were approved by the appropriate institutional review boards.

<http://dx.doi.org/10.1136/jitc-2021-SITC2021.365>

COMBINED EXPLORATORY IMMUNOPHENOTYPING AND TRANSCRIPTOMIC TUMOR ANALYSIS IN PATIENTS TREATED WITH OSE2101 VACCINE IN HLA-A2+ ADVANCED NON-SMALL CELL LUNG CANCER (NSCLC) FROM THE ATALANTE-1 TRIAL

¹Santiago Viteri*, ²Werner Hilgers, ³Fabrice Denis, ⁴Elisabeth Quoix, ⁵Gilles Robinet, ⁶Enriqueta Felip, ⁷Rafal Dziadziuszko, ⁸Nicolas Poirier, ⁸Claudia Fromond, ⁸Isabelle Girault, ⁸Thomas Vandewalle, ⁸Dominique Costantini, ⁸Bérangère Vasseur, ⁹Federico Cappuzzo, ¹⁰Giuseppe Giaccone, ¹¹Benjamin Besse. ¹Instituto Universitario Dexeus and UOMI cancer center, Clinica Mi NovAliança, Barcelona, Spain; ²Institut Ste Catherine, Avignon, France; ³Institut Inter-régional de Cancérologie Jean Bernard Elsan, Le Mans, France; ⁴Hôpitaux Universitaires de Strasbourg, Nouvel Hôpital Civil, Strasbourg, France; ⁵C.H.U. Brest – Hôpital Morvan, Brest, France; ⁶Vall d’Hebron University Hospital, Barcelona, Spain; ⁷Medical University of Gdansk, Gdansk, Poland; ⁸OSE IMMUNOTHERAPEUTICS, Nantes, France; ⁹Instituto Nazionale Tumori IRCCS, Rome, Italy; ¹⁰Weill-Cornell Medicine, New York City, NY, USA; ¹¹Institut Gustave Roussy, Villejuif, France

Background OSE2101 (Tedopi[®]) is an anticancer vaccine with HLA-A2+ restricted modified epitopes targeting five tumor-associated antigens (TAAs) frequently expressed in lung cancer (CEA, HER2, MAGE2, MAGE3, P53). Step-1 results of the phase III, randomized, open-label ATALANTE-1 study comparing Tedopi[®] vs standard treatment (SoC) showed a favorable benefit/risk of Tedopi[®] over SoC (HR 0.71 for overall survival OS) in HLA-A2+ NSCLC patients in 2nd or 3rd line treatment after progression on immune checkpoint blockers (ICB).¹ We analyze available tumor biopsies at initial diagnosis from some patients treated with Tedopi[®] to determine the expression of the 5 TAAs and to identify other tumor factors associated with long-term survival.

Methods Tumor biopsies were available for 8 HLA-A2+ (blood test) stage IV NSCLC patients included in the trial. Primary (<12 weeks) and secondary (≥ 12 weeks) resistance to ICB were observed in 3 (38%) and 5 (62%) of patients. Best response to Tedopi[®] and OS were: 1 partial response (PR) (OS of 33 months), 3 stable disease (SD) (OS of 22, 26 and 41 mo.) and 4 disease progression (PD) (OS of 3, 4, 30 and 31 mo.). HLA-class I, PD-L1, CD8 T-cells, HER2, CEA and P53 tumor expression were evaluated by immunohistochemistry (IHC). NanoString gene expression profiling was performed using the Pan Cancer Immune gene set.

Results HLA-class I was expressed in all tumor samples. IHC analysis revealed that P53, CEA and HER2 were expressed in 6/7, 5/7 and 0/7 patients, respectively. P53, CEA, HER2, MAGE2, and MAGE3 were detected at RNA level in 5/5 tested patients (table 1). IMMUNOSCORE[®] IC CD8/PDL1 analysis showed High/High, High/Low and Low/Low scores for 1/7, 1/7 and 5/7 patients, respectively. The High/High IMMUNOSCORE[®] with a pronounced CD8+ T-cell tumor infiltration was observed in the patient with PR. High percentage of tumor cells expressing P53 (69%–97%) and over-expression of genes associated with activated macrophages (TREM2, MARCO, SLC11A1, CHIT1, SERPINB2) were observed in the PR and SD patients. High IFN-gamma and Expanded Immune Gene Signature scores were observed in long-term survivor patients with secondary resistance to ICB, even after progressive disease.

Abstract 366 Table 1 Summary of clinical and translational data

Patient ID	Secondary Resistance ICB	Best Response Tedopi	PFS Tedopi	OS Tedopi	Tumor HLA-class I	%CEA positive cells	CEA mRNA	HER2 IHC Score	HER2 mRNA	%P53 positive cells	P53 mRNA	Number of CD8+ T-cells/mm ²	IMMUNOSCORE [®] IC CD8/PDL1	Effy Signature (ssGSEA)	Expanded Immune Gene Signature
1709005	No	SD	18.8	41.0	Yes	ND	ND	ND	ND	ND	ND	285	High / Low	ND	ND
1308015	Yes	PR	4.2	33.2	Yes	10%	437	Negative	408	90%	364	425	High / High	371	348
1315018	Yes	SD	4.1	13.6	Yes	0%	ND	Negative	ND	69%	ND	ND	ND	ND	ND
1318013	Yes	SD	2.8	22.2	Yes	20%	395	Negative	1251	97%	873	46	Low / Low	74	107
1318008	Yes	PD	1.4	30.3	Yes	20%	281	Negative	1355	16%	739	107	Low / Low	136	55
1322013	No	PD	1.4	3.9	Yes	3%	ND	Negative	ND	3%	ND	142	Low / Low	ND	ND
1315019	No	PD	1.4	4.2	Yes	30%	135	Negative	2219	18%	1542	1	Low / Low	29	10
1709007	Yes	PD	1.2	30.3	Yes	0%	144	Negative	2248	0%	971	89	Low / Low	118	52

CEA Carcinoembryonic antigen; HER2: Human Epidermal Growth Factor Receptor-2; ICB: Immune checkpoint blocker; IHC: Immunohistochemistry; ND: Not determined; OS: Overall Survival; Patient ID: Patient identification; PDL1: Programmed death-ligand 1; PFS: Progression-free survival; ssGSEA: Single-sample Gene Set Enrichment Analysis. Blue bars = Length of overall survival; Green bars = Gene Signature upregulation; Red bars = Gene Signature downregulation

Conclusions This study shows that all HLA-A2+ patients (blood test), expressed HLA class I in the tumors at initial diagnosis. Transcriptomic data in the patients that benefited from Tedopi[®] showed activated macrophage pathway, high IFN-gamma and Expanded Immune Gene Signatures scores. These data will be validated on larger number of patients treated with Tedopi[®] after the step 2 analysis.

Acknowledgements We thank Julie Le Boulicaut, François Montestruc and Constant Josse (eXYSTAT, Malakoff, France) for the statistical analysis, and HaliDx for the IHC and NanoString analysis.

Trial Registration EudraCT number: 2015-003183-36; NCT number: NCT02654587

REFERENCE

- Giaccone, et al. Activity of OSE-2101 in HLA-A2+ non-small cell lung cancer (NSCLC) patients after failure to immune checkpoint inhibitors (ICI): step 1 results of phase III ATALANTE-1 randomised trial. *ESMO meeting 2020*, abstract #1260MO.

Ethics Approval The study protocol and its related documents (including the patient information and informed consent form) received approval from the Institutional Review Board (IRB), and the Competent Authority prior to study initiation.

Consent Each patient gave his/her written informed consent prior to study enrolment.

<http://dx.doi.org/10.1136/jitc-2021-SITC2021.366>

367

PHARMACOKINETIC AND IMMUNOLOGIC DATA FROM A PHASE I STUDY OF THE CLICK CHEMISTRY-BASED THERAPY SQ3370 IN ADVANCED SOLID TUMORS AND SOFT-TISSUE SARCOMA PROVIDES PROOF-OF-CONCEPT FOR THE CAPAC PLATFORM

¹Vivek Bhadri*, ²Vivek Subbiah, ³James Strauss, ⁴Sant Chawla, ⁵Nam Bui, ⁶Vineet Kwatra, ⁷Mia Weiss, ⁸Kathleen Batty, ⁹Michael Zakharian, ⁹Jose Mejia Oneto, ⁹Sangeetha Srinivasan, ⁹Nathan Yee, ⁹Rosalind Wilson, ⁹M Wayne Saville, ⁸Alexander Guminski. ¹Chris O'Brien Lifehouse, Camperdown, Australia; ²MD Anderson Cancer Center, Houston, TX, USA; ³Mary Crowley, Dallas, TX, USA; ⁴Sarcoma Oncology Santa Monica, Santa Monica, CA, USA; ⁵Stanford Cancer Institute, Palo Alto, CA, USA; ⁶Cancer Research South Australia, Adelaide, Australia; ⁷Washington University, St. Louis, St. Louis, MO, USA; ⁸Royal North Shore Hospital, St Leonards, Australia; ⁹Shasqi, Inc., San Francisco, CA, USA

Background Conventional chemotherapeutics lack specificity for tumor tissue and usually have a narrow therapeutic index. SQ3370, a novel therapy that activates doxorubicin (Dox) at the tumor site while minimizing systemic exposure, is based on intratumoral injection of a prodrug-activating hyaluronic acid-based biopolymer (SQL70) followed by five daily intravenous (IV) doses of an attenuated prodrug of Dox (SQP33). SQ3370 utilizes Shasqi's proprietary Click Activated Prodrugs Against Cancer (CAPAC) platform where mutually-reactive click chemistry groups in the two components allow release of active Dox specifically at the tumor site. In animals, SQ3370 allowed for an 8.95-fold increase in dosing with minimal systemic adverse events and no cardiotoxicity. SQ3370 treatment of mouse tumor models showed improved overall survival, enhanced T-cell infiltration, and a robust anti-tumor response against both biopolymer-injected and non-injected lesions,¹ suggesting that SQ3370 promotes activation of the native immune system against the tumor.

Methods SQ3370-001 (NCT04106492) is a phase 1 trial open to patients with relapsed/refractory soft-tissue sarcoma or other advanced, potentially anthracycline-responsive solid tumors with an injectable local or metastatic lesion and =300 mg/m² prior exposure to Dox (or equivalent). Primary objectives include safety, tolerability, and recommended Phase 2 dose. Additional objectives include preliminary efficacy, plasma and tumor biopsy pharmacokinetics (PK), and immune response by peripheral blood mass cytometry/tumor IHC.

Results To date, ten patients have been enrolled. SQ3370 treatment has been well-tolerated with no dose-limiting toxicities observed. Plasma PK appeared consistent with preclinical data; rapid conversion of SQP33 prodrug to active Dox occurred but slowed as the residence time of the injected biopolymer lengthened. Systemic exposure to active Dox peaked on days 1–2 post biopolymer injection, followed by a decline on days 3–5. Preliminary tumor analysis shows that substantial local exposure to Dox continues 2 weeks after the last SQP33 dose. Immune response analysis of early patient samples suggests increased tumor immune cell infiltration that dynamically changes with each cycle of treatment.

Conclusions SQ3370 appears to be well-tolerated and demonstrates proof-of-concept for the first click-chemistry-based therapy in the clinic. Preclinical and clinical PK are consistent; high tumor exposure can be achieved, so far without the typical clinical adverse events seen with IV Dox and potentially improving the therapeutic index of a frequently-used chemotherapeutic agent.

Trial Registration NCT04106492

REFERENCE

1. Srinivasan S, Yee NA, Wu K, et al. SQ3370 activates cytotoxic drug via click chemistry at tumor and elicits sustained responses in injected and non-injected lesions. *Advanced Therapeutics* 2021;4(3):2000243.

<http://dx.doi.org/10.1136/jitc-2021-SITC2021.367>

**CONSISTENT PATTERN OF IMMUNE ACTIVATION
INDUCED BY ONCOLYTIC ADENOVIRUS ONCOS-102
ACROSS DIVERSE TYPES OF SOLID TUMORS**

¹Lukasz Kuryk, ¹Anne-Sophie Moller, ¹Sandeep Kumar, ²Alexander Shoushtari, ³Luis Paz Ares, ¹Magnus Jaderberg, ¹Erik Digman Wiklund, ¹Victor Levitsky*, ¹Targovax ASA, Oslo, Norway; ²Memorial Sloan Kettering Cancer Center, New York, NY, USA; ³Hospital Universitario 12 Octubre, Madrid, Spain

Background Solid tumors exhibit highly variable compositions of immune infiltrates. Therapeutic compounds driving uniform remodeling of tumor microenvironment (TME) across tumor types may improve the efficacy of cancer immunotherapy. ONCOS-102, a granulocyte-macrophage colony stimulating factor (GM-CSF)-expressing oncolytic adenovirus (Ad5/3-D24-GMCSF), was tested for its safety, therapeutic efficacy and capacity to remodel TME in recently completed phase I/II clinical studies in anti-PD-1 refractory melanoma (NCT03003676) and malignant pleural mesothelioma (MPM) (NCT02879669).

Methods Biopsies were obtained from tumor lesions of patients treated with intra-tumoral injections of ONCOS-102 in combination with chemotherapy or pembrolizumab for MPM and melanoma, respectively. Tumor immune infiltrates were analyzed by immunohistology using several antibody panels. On-treatment biopsies were compared to paired baseline samples as well as to samples from control patients treated with chemotherapy alone in the case of MPM. Gene expression data obtained by next generation RNA sequencing were used to complement the immunohistology analysis and all results were correlated to clinical outcomes.

Results Comparative TME analysis of anti-PD-1 refractory melanoma and MPM tumors revealed noticeably lower baseline T-cell infiltration in mesothelioma. Thus, fractions of CD8+ T-cells were significantly below 10% in 80% of MPM biopsies while approaching or exceeding this level in 60% of melanoma baseline samples. Comparison of tumor biopsies obtained at baseline or on-treatment, demonstrated increased infiltration by both CD4+ and CD8+ T-cells in large proportions of melanoma (CD4+: 13/20 (65%); CD8+: 16/19 (84%) and MPM (CD4+: 10/15 (67%); CD8+: 9/15 (60%) tumor lesions in response to ONCOS-102. Frequencies of cytotoxic T-cells with high granzyme-B expression also increased in response to the treatment in both tumor types, in particular when assessed as percentage of total CD8+ T-cells. Other observed changes induced by ONCOS-102 in samples taken from CR, PR and SD patients with MPM or melanoma included increased CD8/Treg ratio and modulation of PD-L1 expression. Biological and clinical importance of these findings was further supported by correlation between modulation of several subsets of genes related to the process of T-cell activation, such as cytotoxic granule components and co-stimulatory molecules, and clinical response to ONCOS-102 in melanoma and both tumor response and overall survival in MPM patients.

Conclusions ONCOS-102 drives pro-inflammatory modulation of immune TME across tumor types of different origins, anatomical locations and immunological baseline characteristics. Our data support potential of ONCOS-102 to serve as a potent immune sensitizing agent in combination therapies with various classes of immunomodulatory compounds and chemotherapy.

<http://dx.doi.org/10.1136/jitc-2021-SITC2021.368>

369

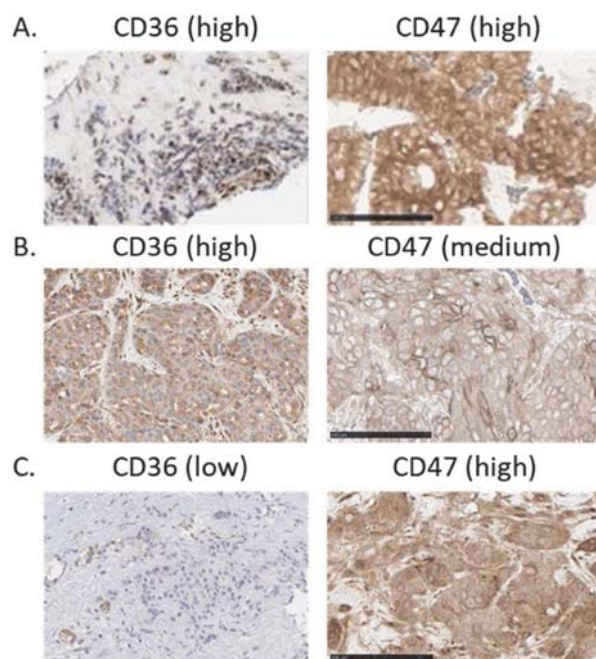
CLINICAL UPDATE OF VT1021, A FIRST-IN-CLASS CD36 AND CD47 TARGETING IMMUNOMODULATING AGENT, IN SUBJECTS WITH PANCREATIC CANCER AND OTHER SOLID TUMORS STRATIFIED BY NOVEL BIOMARKERS

¹Devalingam Mahalingam, ¹Mary Mulcahy, ²Dejan Juric, ³Manish Patel, ⁴Shubham Pant, ⁵Susanna Ulahannan, ⁶Afshin Dowlati, ⁷Andrea Bullock, ⁸Lou Vaickus, ⁹Susanne Fyfe, ⁹Melanie Vincent, ⁹Suming Wang, ⁹Jian Chen, ⁹Marsha Crochiere*, ¹⁰Randolph Watnick, ⁹Michael Cieslewicz, ⁹Jing Watnick. ¹Northwestern University Medical School, Chicago, IL, USA; ²Massachusetts General Hospital, Boston, MA, USA; ³Florida Cancer Specialists/Sarah Cannon, Sarasota, FL, USA; ⁴MD Anderson, Houston, TX, USA; ⁵University of Oklahoma Health Sciences C, OKC, OK, USA; ⁶Case Western, Cleveland, OH, USA; ⁷Beth Israel Deaconess Hospital, Boston, MA, USA; ⁸akta Pharmaceutical Development, Boston, MA, USA; ⁹Vigeo Therapeutics, Cambridge, MA, USA; ¹⁰Boston Children's Hospital, Boston, MA, USA

Background One barrier to treating pancreatic cancer is the immunosuppressive tumor microenvironment (TME). VT1021 is a cyclic peptide derived from prosaposin and stimulates thrombospondin-1 (Tsp-1) production in myeloid derived suppressor cells. Tsp-1 binds to CD36 on macrophages to convert M2 macrophages to anti-tumorigenic M1 macrophages; on tumor cells to induce apoptosis; and increases the CD8+/Treg ratio. Tsp-1 also binds to CD47 on tumor cells to block the "do not eat me signal". In a recently completed phase I/II clinical study (NCT03364400), VT1021 had no major adverse events and a predictable pharmacokinetic profile.

Methods To evaluate potential predictive biomarkers of VT1021, CD36/CD47 levels were analyzed on pre-treatment biopsy samples and on-study tumor biopsies collected during the treatment using immunohistochemistry (IHC). Samples were stained and scored by software-based image analysis and manual review (figure 1). Induction of Tsp-1 in circulating peripheral blood mononuclear cells (PBMCs) by ELISA was correlated with Tsp-1 induction in on-study biopsy samples via IHC, and with clinical responses. To be considered "evaluable", subjects completed ≥ 1 cycle of VT1021 treatment and tumor imaging during cycle 2.

Results In the pancreatic cancer expansion study, 21 of 32 enrolled subjects (66%) had dual high (DH) expression of CD36/CD47. There were 5 subjects with stable diseases among 15 evaluable subjects with disease control rate of 33%. Of the 13 subjects with measurable disease, all 5 subjects with reduction of tumor burden were DH CD36/CD47 and remained on study for an average of 105 days. Moreover, paired tumor biopsies revealed increased Tsp-1 expression, CTL infiltration and M1:M2 ratio among subjects that obtained disease control with DH baseline CD36/CD47 expression. To identify other solid tumor indications that could benefit from VT1021 treatment based on CD36/CD47 expression, commercially available tumor tissue microarrays from 16 different indications were evaluated. Several indications demonstrated high percentage of DH CD36/CD47, including gastric (59%), head and neck (57%), and pancreatic cancers (56%).



Abstract 369 Figure 1 Expression intensities of CD36/CD47 in subjects with pancreatic cancer

Conclusions Pancreatic cancer subjects who were DH for CD36/CD47 were more likely to have a reduction in tumor burden and stay on study longer than non-DH subjects. Increased Tsp-1 induction in circulating PBMCs and in the TME was confirmed. Remodeling of the TME by VT1021 to be more immune sensitive via CTL and M1 accumulation was demonstrated. Based on these findings, the DH expression of CD36/CD47 could be a useful predictive biomarker to stratify subjects for inclusion in future trials in pancreatic cancer, and in other solid tumor indications.

Trial Registration Trial Registration: NCT03364400

<http://dx.doi.org/10.1136/jitc-2021-SITC2021.369>

TIME COURSE OF TREATMENT-RELATED ADVERSE EVENTS (TRAEs) DURING DOSTARLIMAB THERAPY IN THE GARNET TRIAL

¹Bhavana Pothuri*, ²Dominique Berton, ³Victor Moreno, ⁴Ana Oaknin, ⁵Jose Manuel Trigo Perez, ⁶Giuseppe Curigliano, ⁷Susan Ellard, ⁸Joanna Pikiel, ⁹Susana Banerjee, ¹⁰Maria-Pilar Barretina-Ginesta, ¹¹Rowan Miller, ¹²Anna Tinker, ¹³Andrea Jewell, ¹⁴Ruth Plummer, ¹⁵Florence Joly, ¹⁶Jennifer Veneris, ¹⁶Tao Duan, ¹⁷Thierry Andre. ¹Gynecologic Oncology Group (GOG) and Department of Obstetrics/Gynecology, Perlmutter Cancer Center, NYU Langone Health, New York, NY, USA; ²GINECO and Institut de Cancerologie de l'Ouest, Centre René Gauducheau, Saint-Herblain, France; ³START Madrid-FJD, Fundación Jiménez Díaz Hospital, Madrid, Spain; ⁴Vall d'Hebron University Hospital, Vall d'Hebron Institute of Oncology (VHIO), Barcelona, Spain; ⁵Medical Oncology Department, Hospital Virgen de la Victoria IBIMA, Málaga, Spain; ⁶Division of Early Drug Development for Innovative Therapies, IEO, European Institute of Oncology IRCCS, and University of Milano, Milan, Italy; ⁷BC Cancer-Kelowna, British Columbia, Canada; ⁸Regional Center of Oncology, Gdansk, Poland; ⁹The Royal Marsden NHS Foundation Trust and Institute of Cancer Research, London, UK; ¹⁰Institut Català d'Oncologia, Hospital Universitari Dr. J. Trueta, Girona, Spain; ¹¹University College London, St. Bartholomew's Hospital London, London, UK; ¹²BC Cancer, Vancouver, British Columbia, Canada; ¹³University of Kansas Medical Center, Kansas City, KS, USA; ¹⁴Northern Institute for Cancer Research Medical School, University of Newcastle upon Tyne, London, UK; ¹⁵Medical Oncology Department, Centre Francois Baclesse, Caen, France; ¹⁶GlaxoSmithKline, London, UK; ¹⁷Sorbonne University and Saint-Antoine Hospital, Paris, France

Background Dostarlimab is a humanized programmed death 1 (PD-1) receptor monoclonal antibody that blocks interaction with the ligands PD-L1 and PD-L2. Dostarlimab is approved as a monotherapy in adult patients (pts) with mismatch repair deficient (dMMR; US) or dMMR/microsatellite-instability high (EU) recurrent or advanced endometrial cancer that has progressed progressing on or following prior treatment with a platinum-containing regimen. GARNET is a phase 1 study assessing antitumor activity and safety of dostarlimab monotherapy in pts with solid tumors.

Methods Pts with dMMR solid tumors, mismatch repair proficient endometrial cancer, and non-small cell lung cancer that progressed on or after prior therapy received 500 mg of dostarlimab IV every 3 weeks (Q3W) for 4 cycles, then 1000 mg IV every 6 weeks (Q6W) for up to 2 years or until disease progression or discontinuation. Here, we report TRAEs by cycle.

Results A total of 515 pts were included. Of these pts, 60 (11.7%) experienced TRAEs leading to treatment interruption, and 25 (4.9%) experienced TRAEs leading to discontinuation. TRAEs of any grade with overall incidence of $\geq 10\%$ of pts are shown (table 1). The majority of TRAEs occurred during cycles 1–3, with highest incidence during cycle 1. Grade 3 or 4 TRAEs were rare; those seen in $\geq 1\%$ of pts are shown. Immune-related (ir) TRAEs of any grade with overall incidence of $\geq 2\%$ of pts are shown. Most cases (96.9%) of irTRAEs occurred during cycles 1–8. The peak incidence of hypothyroidism occurred during cycle 4; in addition, frequency was increased during cycles 5–8, compared with cycles 1–4. No deaths were attributed to dostarlimab.

Abstract 370 Table 1 Time course of adverse events in the GARNET trial

Preferred term, n (%)	Overall N=515	500 mg Q3W				1000 mg Q6W			
		C1 N=915	C2 N=468	C3 N=421	C4 N=382	C5 N=322	C6 N=250	C7 N=214	C8 N=195
Any-grade TRAEs occurring in $\geq 10\%$ of pts									
Fatigue	77 (15.0)	34 (6.6)	11 (2.4)	7 (1.7)	4 (1.0)	3 (0.9)	5 (2.0)	2 (0.9)	0
Dizziness	66 (12.8)	27 (5.2)	15 (3.2)	9 (2.1)	4 (1.0)	2 (0.6)	3 (1.2)	3 (1.4)	0
Asthenia	69 (11.5)	27 (5.2)	12 (2.6)	7 (1.7)	6 (1.6)	2 (0.6)	2 (0.8)	1 (0.5)	1 (0.5)
Nausea	56 (10.9)	23 (4.5)	12 (2.6)	8 (1.9)	5 (1.3)	3 (0.9)	2 (0.8)	1 (0.5)	1 (0.5)
Grade ≥ 3 TRAEs occurring in $\geq 1\%$ of pts									
Anemia	9 (1.7)	2 (0.4)	3 (0.6)	1 (0.2)	1 (0.3)	0	1 (0.4)	0	0
Fatigue	8 (1.6)	2 (0.4)	1 (0.2)	1 (0.2)	0	3 (0.9)	0	0	0
Lipase increased	7 (1.4)	0	2 (0.4)	2 (0.5)	0	1 (0.3)	0	0	0
Alanine aminotransferase increased	5 (1.0)	2 (0.4)	0	0	1 (0.3)	1 (0.3)	0	0	1 (0.5)
Diarrhea	5 (1.0)	0	1 (0.2)	2 (0.5)	1 (0.3)	0	1 (0.4)	0	0
Any-grade irTRAEs occurring in $\geq 2\%$ of pts									
Hypothyroidism	34 (6.6)	0	2 (0.4)	3 (0.7)	13 (3.4)	2 (0.6)	5 (2.0)	5 (2.3)	3 (1.6)
Diarrhea	19 (3.7)	3 (0.6)	8 (1.7)	2 (0.5)	3 (0.8)	0	2 (0.8)	0	0
Alanine aminotransferase increased	11 (2.1)	4 (0.8)	0	0	3 (0.8)	2 (0.6)	1 (0.4)	0	1 (0.5)

Conclusions No new safety signals were detected with dostarlimab compared to other anti-PD-1 inhibitors. Most TRAEs were low grade. The majority of TRAEs and grade ≥ 3 TRAEs occurred in the first 3 cycles (first 12 weeks), but some cases occurred later, suggesting a need for ongoing monitoring. Few increases in the incidence of TRAEs were seen during cycle 5 following the transition to the 1000-mg Q6W dosing schedule; the TRAEs with increased incidence after the transition were fatigue and lipase increased. An increase in the frequency of the irTRAE hypothyroidism was seen after transitioning to the 1000-mg Q6W schedule.

<http://dx.doi.org/10.1136/jitc-2021-SITC2021.370>

371 ANALYSIS OF CHANGES IN PLASMA CYTOKINE LEVELS IN RESPONSE TO IL-12 THERAPY IN THREE CLINICAL TRIALS

Emily Schwarz*, Brooke Benner, Lianbo Yu, William Carson. *The Ohio State University, Columbus, OH, USA*

Background The ability of IL-12 to stimulate NK and T cell anti-tumor activity has made it an attractive candidate for overcoming immunosuppressive tumor microenvironments. Our group has demonstrated in pre-clinical models that IL-12 will enhance IgG receptor-mediated NK cell responses to antibody-coated tumor cells and conducted three studies where IL-12 was used in combination with an anti-tumor monoclonal antibody. These were OSU-9968, Phase 1 study of IL-12 + trastuzumab; OSU-1067, Phase 1 study of IL-12 + trastuzumab + paclitaxel in HER2-positive cancers and OSU-11010, Phase I/II study of IL-12 + cextuximab in head and neck cancer.¹⁻³ Cytokine levels were measured in patients with varying responses in an effort to better characterize IL-12-induced immunity.

Methods Plasma cytokine levels in 21 patients across 3 studies were measured at baseline and at 4 time points after IL-12 administration. 2 patients had complete responses, 1 had a partial response, 9 patients had stable disease > 60 days and 9 had progressive disease. A combination of 7 U-PLEX, V-PLEX, and R-PLEX Human Biomarker Assays (Meso Scale Discovery) were performed to monitor levels of 23 cytokines: GM-CSF, IFN-gamma, IL-10, IL-8, IP-10, MCP-1, MDC, MIP-1alpha, MIP-1β, TNF-alpha, IL-15, IL-18, MCP-2, MIG, IL-13, IL-17, IL-1β, IL-4, IL-5, IL-6, IL-1alpha, TGFβ, VEGF. Student's t-test on GraphPad Prism 9.0.0 was used for statistical analyses.

Results Nine cytokines were significantly upregulated following IL-12 therapy. IFN-gamma levels increased from a mean of 27.42 pg/mL at baseline to 1764 pg/mL after IL-12 treatment ($p=0.0246$). GM-CSF, TNF-alpha and IL-10 also increased following IL-12 therapy ($p=0.0199$, 0.0004 , 0.0003). Several chemotactic factors including MCP-1, MDC, MIP-1alpha, and MIP-1β increased from means of 483.1 pg/mL to 695.7 pg/mL, 3112 pg/mL to 4305 pg/mL, 62.44 pg/mL to 130.3 pg/mL and 263.1 to 487.4 pg/mL, respectively (p -values all < 0.013). Levels of IL-18 increased from a baseline mean of 2059 pg/mL to 3952 pg/mL ($p=0.0003$). Several cytokines were also differentially induced across response groups with MCP-1 and GM-CSF increased in responding patients ($p=0.02$, $p=0.04$) and IL-10, MIP-1β and IL-6 increased in progressive disease patients ($p=0.02$, $p=0.01$, $p=0.03$).

Conclusions The ability to detect significant changes in cytokines as a result of IL-12 therapy across three separate clinical trials supports the broad effects of IL-12 on NK cells and other immune compartments. The additional differential effect in responders vs. progressive disease patients indicates that these cytokines likely affect patient outcome and will be further evaluated as possible markers of response.

REFERENCES

1. Parihar R, *et al.* A phase I study of interleukin 12 with trastuzumab in patients with human epidermal growth factor receptor-2-overexpressing malignancies. *Clin Cancer Res* 2004;**10**:5027 LP-5037.
2. Bekaii-Saab TS, *et al.* A phase I trial of paclitaxel and trastuzumab in combination with interleukin-12 in patients with HER2/neu-expressing malignancies. *Mol Cancer Ther* 2009;**8**:2983-2991.
3. McMichael EL, *et al.* A phase I/II trial of cetuximab in combination with interleukin-12 administered to patients with unresectable primary or recurrent head and neck squamous cell carcinoma. *Clin Cancer Res* 2019;**25**:4955 LP-4965.

Ethics Approval These studies were approved by the Human Institutional Review Board at The Ohio State University Medical Center; approval numbers 99H0185, 1999C0326 and 2011c0019, respectively.

<http://dx.doi.org/10.1136/jitc-2021-SITC2021.371>

ASSOCIATION OF TUMOR MUTATION BURDEN (TMB) AND GENOMIC ALTERATIONS (GA) WITH CLINICAL OUTCOMES IN CHINESE PATIENTS WITH ADVANCED SOLID TUMORS TREATED WITH TISLELIZUMAB

¹Lin Shen*, ²Qingyuan Zhang, ³Tianshu Liu, ⁴Hongming Pan, ²Yuxian Bai, ⁵Ying Yuan, ⁶Xuerui Luo, ⁷Yang Shi, ⁷Yun Zhang, ⁶Ruiqi Huang, ⁷Juan Zhang, ⁷Zhirong Shen. ¹Peking University Cancer Hospital and Institute, Beijing, China; ²Harbin Medical University Cancer Hospital, Harbin, China; ³Zhongshan Hospital Fudan University, Shanghai, China; ⁴Sir Run Run Shaw Hospital, Zhejiang University, School of Medicine, Hangzhou, China; ⁵The Second Affiliated Hospital of Zhejiang University School of Medicine, Hangzhou, China; ⁶BeiGene (Shanghai) Co., Ltd., Shanghai, China; ⁷BeiGene (Beijing) Co., Ltd., Beijing, China

Background Studies have demonstrated correlation of GA and TMB with clinical efficacy of an anti-programmed cell death protein-1 (PD-1) therapy, but this correlation has not yet been demonstrated in Chinese patients treated with tislelizumab (anti-PD-1 antibody). We report the association between TMB, GA, and the clinical efficacy of tislelizumab in Chinese patients with different tumor types from a Phase 1/2 study (NCT04068519).

Methods Chinese patients with advanced solid tumors who received tislelizumab monotherapy and had available tissues for genomic testing (BurningRock OncoScreen Plus 520 NGS panel) were eligible. Patients were classified as having hyperamplification (HA) if their genome harbored ≥ 1 amplified gene with a copy number >5 . Logistic regression was used to analyze the association of TMB with objective response rate (ORR) and Cox proportional hazard was used to determine the association of TMB with progression-free survival (PFS) and overall survival (OS).

Results A total of 156 patients were evaluable. TMB was higher in responders (R) versus non-responders (NR) (median [m] TMB: 9.3 vs 6.2 mut/Mb, $p=0.003$). TMB-H was defined as ≥ 8 mut/Mb according to the receiver operating characteristic curve. Patients in the TMB-H group showed superior clinical benefit compared with the TMB-L group (table 1). Further GA analysis showed a trend toward a higher frequency of HA in NR (40.00%; 16/40) compared with R (28.78%; 5/18), in the TMB-H group. A total of 33.33% (10/30) of these amplified genes in NR belonged to the RTK-RAS-PI3K signaling pathway. When TMB-H patients with HA in this pathway were excluded, ORR reached 37.78%.

resistance mechanisms to anti-PD-1 therapy, even in patients with TMB-H tumors.

Acknowledgements Editorial writing support for the development of this abstract, under direction of the authors, was provided by Louise Oakes, PhD, of Ashfield MedComms, an Ashfield Health company, and was funded by BeiGene Ltd.

Trial Registration NCT04068519

Ethics Approval This study was conducted according to the ethical principles of the Declaration of Helsinki, Good Clinical Practice guidelines, the principles of informed consent and the requirements of the public registration of clinical trials. Written informed consent was obtained from each patient prior to screening. The protocol was approved by the institutional ethics committee and was monitored by the investigators and study sponsor.

<http://dx.doi.org/10.1136/jitc-2021-SITC2021.372>

Abstract 372 Table 1 Median study follow-up and clinical efficacy data

	Overall (N=156)	TMB-H (n=58)	TMB-L (n=98)
ORR, % (95% CI)	16.03 (10.65–22.74)	31.03 (19.54–44.54)	7.14 (2.92–14.17)
ORR odds ratio (95% CI)	–	–	5.85 (2.27–15.11)
Median PFS, mo (95% CI)	2.30 (2.17–2.92)	6.11 (2.20–10.45)	2.20 (2.10–2.30)
PFS hazard ratio (95% CI)	–	–	0.54 (0.38–0.78)
Median OS, mo (95% CI)	12.48 (8.51–17.58)	21.74 (12.88–NE)	8.94 (5.88–13.44)
OS hazard ratio (95% CI)	–	–	0.55 (0.36–0.83)
Median follow-up, mo (95% CI)	28.55 (26.68–32.46)	29.37 (26.78–33.05)	27.56 (24.48–32.46)

NE, non-estimable

Conclusions TMB-H status was associated with improved clinical efficacy of tislelizumab in Chinese patients with advanced solid tumors, consistent with other PD-1 inhibitors. These observations support TMB-H as a potential predictive biomarker for response to tislelizumab in this patient population. HA in the RTK-RAS-PI3K pathway may be associated with

373

ENHANCEMENT OF TCR-ENGINEERED T-CELLS TARGETING MAGE-A4 ANTIGEN BY CO-EXPRESSION OF CD8 α AND INHIBITION OF AKT SIGNALING DURING EX VIVO T-CELL EXPANSION

Emily Schmidt, Katerina Mardilovich, Natalie Bath, Gareth Betts, William Spinner, Kathryn Sun, Ian Donaldson, Cheryl McAlpine, Raymond Luke, Jean-Marc Navenot, Joseph Sanderson, Phil Bassett, Chris Evans, Karen Miller, Quan Lin, Mark Dudley, Alex Tipping*. *Adaptimmune, Abingdon, UK*

Background Autologous Specific Peptide Enhanced Affinity Receptor (SPEAR) T-cells targeting MAGE-A4 can be effective treatment for solid tumors.¹⁻³ To improve efficacy, we developed a next-generation SPEAR-T cell targeting MAGE-A4 co-expressing CD8 α (ADP-A2M4CD8). ADP-A2M4CD8 is under investigation in the Phase 1 SURPASS trial (NCT04044859). Enhancements have also been made to the manufacturing process with an AKT inhibitor (AKTi) during ex vivo expansion to provide a greater proliferative potential and enhanced memory phenotype.⁴

Methods SPEAR-T cells were manufactured using a Lentiviral vector with CD8 α and MAGE-A4 targeted TCR genes. AKTi was added during ex vivo expansion. T-cell attributes were evaluated, including markers of differentiation (flow cytometry), capacity for in vitro tumor lysis (Incucyte) and changes to gene expression (scRNASeq) initially assessed with the first-gen product. Post-infusion, the presence of transduced T-cells in the peripheral circulation (PCR) and levels of inflammatory cytokines in serum (MesoScale Discovery Assay [MSD]) were evaluated.

Results As of May 24, 2021, 18 patients with 9 different primary tumor types were evaluable. Twelve pts received product that had AKTi during manufacture. Five patients had objective responses (RECIST), and 10 had stable disease. Responses occurred at lower MAGE-A4 expression levels and lower transduced T-cell doses relative to the first-gen product targeting MAGE-A4.¹ CD4⁺ T-cells from manufactured ADP-A2M4CD8 demonstrated direct in vitro tumor cell killing similar to CD8⁺ T-cells (Incucyte). scRNASeq gene expression profiles of first-gen ADP-A2M4 product manufactured with AKTi revealed the AKTi-expanded T-cells had a greater proliferation or an enhanced memory phenotype; scRNASeq analyses are ongoing for the ADP-A2M4CD8 product. An increase in IL-12 levels (MSD) in serum post-infusion suggests that endogenous immune cells are being activated, further resulting in increased levels of IFN gamma (MSD) secretion relative to patients who received first-gen product. Manufacturing with AKTi resulted in T-cells with a less differentiated phenotype (flow cytometry), and post-infusion was associated with enhanced antigen-specific serum cytokine responses, increased proliferative state (i.e., elevated levels of IL-2), and higher persistence of T-cells in peripheral blood by PCR.

Conclusions SPEAR T-cells targeting MAGE-A4 expressing cancers have been enhanced by co-expressing CD8 α and adding AKTi during manufacture. These enhanced products improve CD4⁺ T-cell killing, release more inflammatory cytokines, proliferate more robustly with an early memory phenotype, and better engage the patient's endogenous immune system when compared to first-gen products or next-gen manufactured without AKTi.

Trial Registration NCT04044859

REFERENCES

- 1.. Hong, *et al. ASCO* 2020.
- 2.. D'Angelo, *et al. ASCO* 2021.
- 3.. Hong, *et al. SITC* 2020.
- 4.. Mardilovich, *et al. SITC* 2020.

<http://dx.doi.org/10.1136/jitc-2021-SITC2021.373>

374

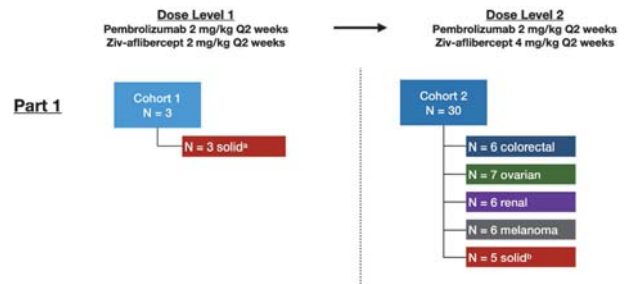
A PHASE IB TRIAL OF ZIV-AFLIBERCEPT PLUS PEMBROLIZUMAB IN PATIENTS WITH ADVANCED SOLID TUMORS

¹Kevin Tyan*, ²Osama Rahma, ³Anita Giobbie-Hurder, ⁴Andrew Brohl, ⁵Philippe Bedard, ⁶Daniel Renouf, ⁷Elad Sharon, ⁷Howard Streicher, ³Emma Hathaway, ³Rachel Cunningham, ³Michael Manos, ³Mariano Severgnini, ⁸Scott Rodig, ³F Stephen Hodi. ¹Harvard Medical School, Boston, MA, USA; ²Dana Farber Cancer Institute, Boston, MA, USA; ³Dana-Farber Cancer Institute, Boston, MA, USA; ⁴Moffitt Cancer Center, Tampa, FL, USA; ⁵Princess Margaret Cancer Centre, Toronto, Canada; ⁶BC Cancer and Department of Medicine, British Columbia, Canada; ⁷Cancer Therapy Evaluation Program, NCI, Bethesda, MD, USA; ⁸Brigham and Women's Hospital, Boston, MA, USA

Background Angiogenic factors play a role in regulating immune suppression in the tumor microenvironment and driving resistance to immune checkpoint inhibitor therapy.¹ Ziv-aflibercept is a soluble decoy receptor that "traps" endogenous vascular endothelial growth factor (VEGF) with 100-fold increased binding affinity compared to Bevacizumab.² The combination of ziv-aflibercept with either cytotoxic T-lymphocyte-associated protein 4 (CTLA-4) or programmed cell death protein 1 (PD-1) blockade has shown promising antitumor efficacy in mouse models.³⁻⁴ We hypothesized that a novel combination of ziv-aflibercept and anti-PD-1 would be tolerable and lead to clinical benefits in tumors that traditionally do not respond to checkpoint blockade.

Methods This is a multicenter phase 1B dose escalation study (NCT02298959) of the combination of ziv-aflibercept (at 2–4 mg/kg) plus pembrolizumab (at 2 mg/kg) administered intravenously every 2 weeks with expansion cohorts in PD-1/PD-L1 naïve melanoma, renal cell carcinoma (RCC), microsatellite stable colorectal cancer (MSS CRC), and ovarian cancer (figure 1). The primary objective was to determine the maximum tolerated dose (MTD) and recommended dose of the combination. Secondary endpoints included overall response rate (ORR) and overall survival (OS). Exploratory objectives included correlation of clinical efficacy and immune population densities in the tissue and periphery.

Results Overall, 33 patients were enrolled during dose escalation (n=3) and dose expansion (n=30). No dose-limiting toxicities (DLTs) were reported in the initial dose level. Ziv-aflibercept 4 mg/kg plus pembrolizumab 2 mg/kg every 2 weeks was established as the MTD. Grade ≥3 treatment-related adverse events occurred in 19/33 patients (58%), the most common being hypertension (36%) and proteinuria (18%). ORR in the dose expansion cohort was 16.7% (5/30; 95% CI, 7–32%). Complete responses occurred in melanoma (n=2), partial responses occurred in RCC (n=1), mesothelioma (n=1), and melanoma (n=1). Efficacy outcomes by tumor type are shown in table 1 and figure 2. Median OS was as follows: melanoma, not reached; RCC, 15.7 months (90% CI, 2.5–15.7); CRC, 3.3 months (90% CI, 0.6–3.4), ovarian, 12.5 months (90% CI, 3.8–13.6), other solid tumors, not reached (figure 3). Activated tumor infiltrating CD8 T cells at baseline (CD8+PD1+), high CD40L expression (figure 4), and increased memory CD8 T cells in the periphery (figure 5) correlated with clinical response to the combination therapy.

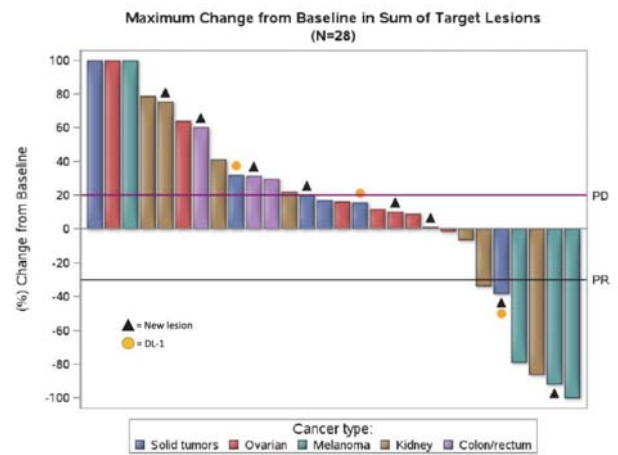


Abstract 374 Figure 1 Study Schema of dose escalation and dose expansion. (A) Cohort 1 included the following tumors: clear cell sarcoma, triple negative breast cancer (TNBC), and mesothelioma. (B) Other solid tumors in Cohort 2 were: epithelioid mesothelioma (2) and TNBC (1).

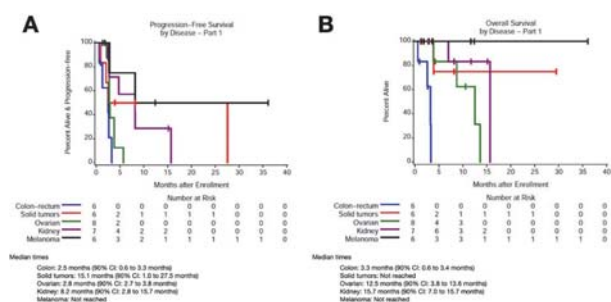
Abstract 374 Table 1 Efficacy outcomes by dose level and tumor type

Best response	Overall (n = 33)	Dose level 1 (n = 3)	Dose level 2 (n = 30)	CRC (n = 6)	Solid Tumor* (n = 6)	Ovarian (n = 8)	RCC (n = 7)	Melanoma (n = 6)
Complete Response (CR)	2 (6%)	0	2 (7%)	0	0	0	0	2 (33%) [†]
Partial Response (PR)	3 (9%)	0	3 (10%)	0	1 (16.7%)	0	1 (14%)	1 (17%)
Stable Disease (SD)	8 (24%)	1 (33%)	7 (23%)	0	2 (33%)	2 (25%)	4 (57%)	0
Progressive Disease (PD)	15 (45%)	2 (67%)	13 (43%)	3 (50%)	3 (50%)	6 (75%)	2 (29%)	1 (17%)
Unknown	5 (15%)	0	5 (17%)	3 (50%)	0	0	0	2 (33%)

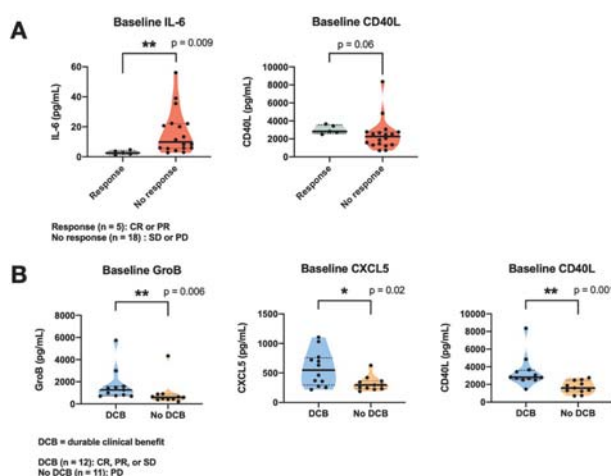
* Solid tumors include clear cell sarcoma (1), breast cancer (2), mesothelioma (3).



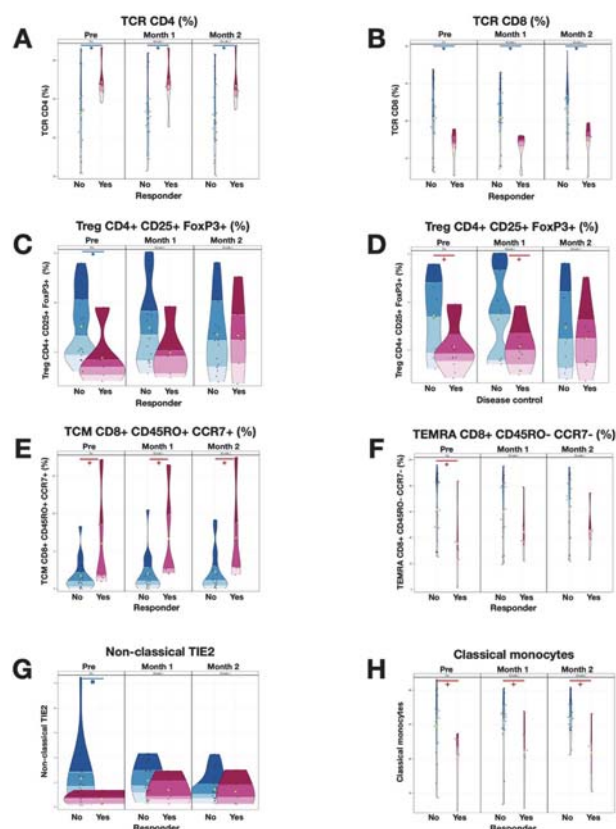
Abstract 374 Figure 2 Waterfall plot of best RECIST response. Waterfall plot of maximum change from baseline in sum of target lesions for 28 patients with tumor measurements over time. Plot is color-coded by tumor type. Triangles indicate patients who developed new lesions, yellow circles indicate the 3 patients who received DL1.



Abstract 374 Figure 3 Progression and overall survival by tumor type. Kaplan-Meier curves for (A) progression-free survival and (B) overall survival based on tumor type.



Abstract 374 Figure 4 Luminex assay analysis of clinical response. Luminex analysis of baseline biomarkers. Patients were analyzed by clinical response (complete response [CR] and partial response [PR]) and durable clinical benefit (DCB) which includes patients with CR, PR, and stable disease (SD). (A) Baseline levels of IL-6 were lower in responders vs. non-responders (median 2.605 vs. 9.847 pg/mL, $p = 0.009$). Baseline CD40L was increased in responders (median 2,840 vs. 2,267 pg/mL, $p = 0.06$). (B) Baseline levels of GroB (median 1,272 vs. 592 pg/mL, $p = 0.006$), CXCL5 (median 547.5 vs. 296.2 pg/mL, $p = 0.02$), and CD40L (median 2,807 vs. 1,595 pg/mL, $p = 0.001$) were higher in patients with DCB vs. no DCB. P-values for baseline comparisons were obtained through Wilcoxon rank-sum test. The solid black line indicates median. Violins show range and kernel density estimate distributions of each group. (*) $p < 0.05$, (**) $p < 0.01$.



Abstract 374 Figure 5 Flow cytometry analysis. Flow cytometry analysis comparing T cell populations and monocytes between patients with clinical response (CR or PR, $n = 5$) and non-responders ($n = 18$) and patients with disease control (CR, PR, or SD, $n = 12$) and no disease control ($n = 11$). (A) CD4+ populations were increased in responders vs. non-responders at all time points. (B) CD8+ populations were decreased in responders vs. non-responders at all time points. (C) Treg CD4+/CD25+/FoxP3+ was decreased at baseline in responders. (D) Treg CD4+/CD25+/FoxP3+ were decreased at baseline and 1-month in patients with disease control vs. no disease control. (E) TCM CD8+/CD45RO+/CCR7+ was increased at all time points in responders vs. non-responders. (F) TEMRA CD8+/CD45RO-/CCR7- was decreased in responders at baseline. (G) Non-classical TIE2 was increased at baseline in non-responders. (H) Classical monocytes were increased at all time points in non-responders.

Conclusions The combination of ziv-aflibercept and pembrolizumab demonstrated an acceptable safety profile with antitumor activity in solid tumors. The combination is currently being studied in sarcoma and anti-PD-1 resistant melanoma.

Acknowledgements This trial was supported by the National Cancer Institute (NCI) and by Merck, Sharpe, and Dohme and Sanofi via Cooperative Research and Development Agreements with the NCI. PLB was supported by NCI UM1 Grant CA186644.

Trial Registration NCT02298959

REFERENCES

- 1.. Rahma OE, Hodi FS. The intersection between tumor angiogenesis and immune suppression. *Clin Cancer Res* September 15 2019;**25**(18):5449–5457. doi:10.1158/1078-0432.CCR-18-1543
- 2.. Holash J, Davis S, Papadopoulos N, *et al.* VEGF-trap: a VEGF blocker with potent antitumor effects. *Proceedings of the National Academy of Sciences* 2002;**99**(17):11393–11398. doi:10.1073/pnas.172398299
- 3.. Burova E, Ioffe E, Taduriyasas C, *et al.* Abstract 5035: blockade of VEGF with ziv-aflibercept (VEGF Trap) enhances anti-tumor efficacy of CTLA-4 blocking antibody in an Fc dependent manner. *Cancer Research* 2014;**74**(19 Supplement):5035–5035. doi:10.1158/1538-7445.am2014-5035
- 4.. Di Tacchio M, Macas J, Weissenberger J, *et al.* Tumor vessel normalization, immunostimulatory reprogramming, and improved survival in glioblastoma with combined inhibition of PD-1, angiopoietin-2, and VEGF. *Cancer Immunology Research* 2019;**7**(12):1910–1927. doi:10.1158/2326-6066.cir-18-0865

Ethics Approval This trial (NCT02298959) was approved by all participating IRBs.

<http://dx.doi.org/10.1136/jitc-2021-SITC2021.374>

375

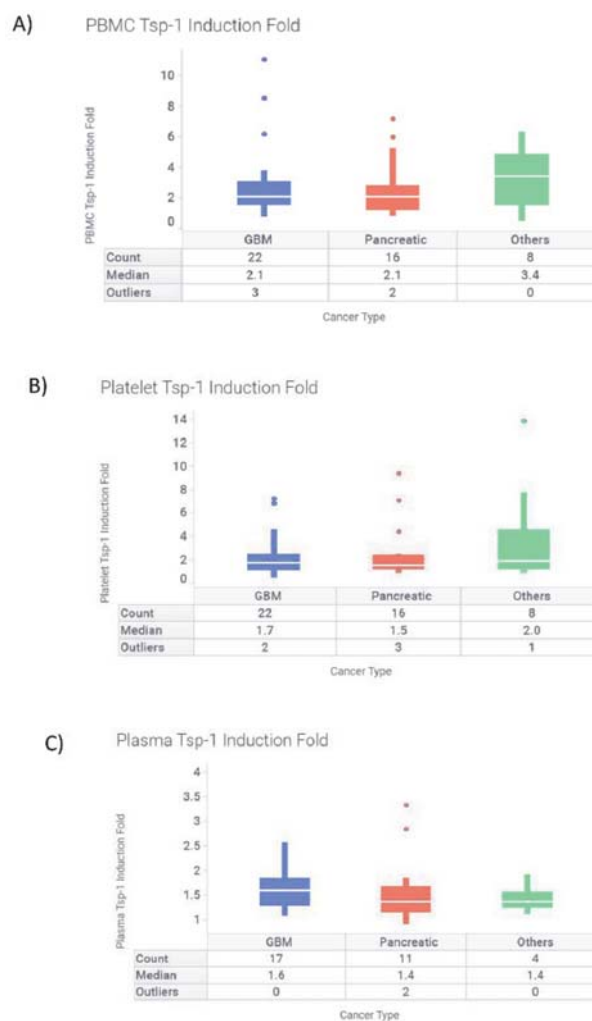
DEVELOPMENT OF THROMBOSPONDIN-1 AS A CLINICAL PHARMACODYNAMIC BIOMARKER FOR VT1021, A FIRST-IN-CLASS THERAPEUTIC AGENT THAT REPROGRAMS THE TUMOR MICROENVIRONMENT

¹Jian Chen*, ¹Marsha Crochiere, ¹Melanie Vincent, ¹Suming Wang, ¹Susanne Fyfe, ¹Wendy Li, ¹Simai Deng, ²Randolph Watnick, ¹Jing Watnick, ¹Michael Cieslewicz. ¹Vigeo Therapeutics, Cambridge, MA, USA; ²Boston Children's Hospital, Boston, MA, USA

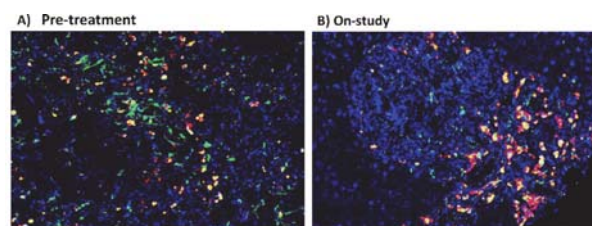
Background VT1021 is a first-in-class therapeutic agent in Phase I clinical studies in solid tumors. In vivo preclinical studies demonstrated that VT1021 inhibited tumor growth via stimulation of p53 and Thrombospondin-1 (Tsp-1) in MDSCs. Moreover, induction of Tsp-1 reprogrammed the tumor microenvironment and induced apoptosis in tumor cells via its cell surface receptors CD36 and CD47. Here we report on the utility of Tsp-1 as a pharmacodynamic biomarker and its correlation with clinical response.

Methods Tsp-1 protein levels in PBMCs, platelets and plasma were assessed by ELISA following SepMate-based fractionation of subject blood samples. Tsp-1 mRNA levels in peripheral blood cells were analyzed by quantitative RT-PCR following extraction of total RNA from subject whole blood samples via PAXgene Blood RNA kit. Tsp-1 levels in subject biopsy samples were analyzed by immunohistochemistry as described previously.

Results Up-regulation of Tsp-1 protein was observed in PBMCs, platelets and plasma in all evaluable subjects following treatment with VT1021 across multiple indications in a phase 1 clinical study, indicating that Tsp-1 induction is a pharmacodynamic biomarker for VT1021 (figure 1). Induction of Tsp-1 by VT1021 was also shown at the transcriptional level via RT-PCR measurement of whole blood samples. Strikingly, maximum PBMC Tsp-1 levels induced by VT1021 were higher in subjects with glioblastoma (GBM) that had objective responses (complete or partial response) compared to subjects with stable disease (SD) or progressive disease (PD). Of note, pre-dose levels of Tsp-1 were predictive of response, as subjects with objective responses had higher basal levels of Tsp-1 than those that had stable or progressive disease. For subjects with pancreatic cancer, Tsp-1 induction was higher in SD subjects compared to PD subjects, suggesting that Tsp-1 induction in PBMCs can be a potential prognostic biomarker. In tumor biopsy samples from subjects with pancreatic cancer, increased colocalization of Tsp-1 and CD11b was observed in on-study samples, supporting a role of Tsp-1 in reprogramming the tumor microenvironment (figure 2).



Abstract 375 Figure 1 Up-regulation of Tsp-1 protein levels have been observed in PBMCs(A), platelets (B) and plasma (C) in all evaluable subjects post-dosing with VT1021 across multiple inductions in a phase 1 clinical study.



Abstract 375 Figure 2 Increased colocalization of Tsp-1 and CD11b was observed in tumor microenvironment in tumor biopsy samples from a subject with pancreatic cancer post-dosing with VT1021

Conclusions Based on both protein and mRNA levels, Tsp-1 induction has the potential to be a useful prognostic pharmacodynamic biomarker for VT1021 in various tumor types. In subjects with GBM, both basal and induced Tsp-1 levels in PBMCs are potential predictive and prognostic biomarkers, respectively. For subjects with pancreatic cancer, Tsp-1 protein induction in PBMCs is a potential prognostic biomarker. The predictive/prognostic utility coupled with the ability to measure levels in peripheral blood makes Tsp-1 a powerful biomarker to assess and predict clinical response to VT1021.

<http://dx.doi.org/10.1136/jitc-2021-SITC2021.375>

376

RADIATION SUB-STUDY TO CHARACTERIZE SAFETY AND TOLERABILITY OF LOW-DOSE RADIATION IN COMBINATION WITH AFAMI-CEL IN PATIENTS WITH ADVANCED CANCERS (NCT03132922)

¹James Welsh*, ¹Danxia Ke, ¹Nahum Puebla Osorio, ¹Hampartsoum Barsoumian, ²Bryan Jackson, ²Jane Bai, ²Marisa Rosenberg, ²Cheryl McAlpine, ²Robyn Broad, ²Ashley Liddle, ²Jean-Marc Navenot, ²Stavros Rafail, ²Ruoxi Wang, ²Amy Sauer, ²Quan Lin, ²Hassan Danesi, ¹David Hong. ¹The University of Texas MD Anderson Cancer Center, Houston, TX, USA; ²Adaptimmune, Philadelphia, PA, USA

Background Autologous cell therapies with an engineered T-cell receptor targeting MAGE-A4 have shown responses in patients with synovial sarcoma¹ with additional responses in myxoid/round cell liposarcoma (MRCLS), head and neck, lung, esophagogastric junction, and melanoma cancers.^{2 3} Low-dose radiation may control tumor growth locally and modulate stroma of solid tumors,⁴ potentially facilitating T-cell infiltration into tumors and antitumor activity.

Methods Sub-study designed to assess safety, tolerability, and efficacy in up to 10 patients with low-dose radiation in combination with lymphodepleting chemotherapy, followed by afami-cel (an autologous TCR cell T-cell therapy targeting MAGE-A4). Eligible patients are HLA-A*02⁺ with MAGE-A4 expressing tumors including urothelial, melanoma, head and neck, ovarian, non-small cell lung, esophageal, gastric, synovial sarcoma, and MRCLS cancers. Patients receive afami-cel by infusion following low-dose radiation and lymphodepleting chemotherapy. Radiation was 4.2–7 Gy per lesion or isocenter (maximum of 5). Lymphodepleting regimen was IV fludarabine 30 mg/m²/day for 4 days (–7 to –4) and cyclophosphamide 600 mg/m²/day for 3 days (–7 to –5). Afami-cel doses ranged from 1.2 × 10⁹ to 10 × 10⁹ transduced cells. Pts receive afami-cel infusion on Day 1.

Results As of Dec 27, 2020, a total of 8 patients, including 4 patients (1 male) with melanoma (2), HNSCC (1), or ovarian (1) cancers received low-dose radiation and afami-cel. Most frequently reported AEs (4/4 pts) were leukopenia/decreased white blood cell count, lymphopenia/decreased lymphocyte count, and neutropenia/decreased neutrophil count; all of which were related to the lymphodepletion regimen. The most commonly (>1 patient) reported AEs considered related to T-cell infusion were cytokine release syndrome (2/4 pts) and fatigue (2/4 pts). Two patients had a total of 5 SAEs: adrenal insufficiency, hyperglycemia, neurotoxicity, pneumonia aspiration, and pneumothorax. The only SAE considered to be related to treatment was Grade 3 neurotoxicity. Best overall responses per RECIST 1.1: 1 partial response (melanoma, –42% in target lesions), 2 stable diseases (ovarian cancer, –23%; HNSCC, no change), and 1 patient did not have post-baseline scans yet. Translational analyses showed peripheral persistence and serum cytokine response profiles consistent with that of afami-cel monotherapy, whilst a relatively greater T cell infiltration in tumor biopsies was evident.

Conclusions Afami-cel with low-dose radiation has had an acceptable safety profile. Most AEs were consistent with those typically experienced by cancer patients undergoing lymphodepletion cytotoxic chemotherapy and cellular therapy. Infused T-cells were observed in tumor biopsies at high frequency, and one patient exhibited a clinical partial response.

Trial Registration NCT03132922

REFERENCES

1. Van Tine BA, et al. *CTOS* 2020.
2. Hong DS, et al. *ASCO* 2020.
3. Hong DS, et al. *SITC* 2020.
4. De Selm C, et al. *Mol Ther* 2018;**26**(11):2542–2552.

<http://dx.doi.org/10.1136/jitc-2021-SITC2021.376>

377

CHARACTERIZATION OF PERIPHERAL BIOMARKERS OF GS-1423, A FIRST IN CLASS BIFUNCTIONAL ANTI-CD73-TGF β RECEPTOR II- TRAP MOLECULE, IN A PHASE 1 DOSE ESCALATION STUDY IN PATIENTS WITH ADVANCED SOLID TUMORS

¹Marianna Zavodovskaya*, ²Anthony Tolcher, ³Michael Gordon, ⁴James Strauss, ⁵Kathleen Mahoney, ¹Ping Cheng Yi, ¹Rick Sorensen, ⁶Xiaoyun Yang, ¹Kai-Wen Lin, ¹Biao Li, ¹Anna Seto, ¹Matthew Peach, ¹Audrey Goddard, ¹Tianling Chen, ¹Juliane Jürgensmeier. ¹Gilead Sciences, Woodside, CA, USA; ²NEXT Oncology, San Antonio, TX, USA; ³HonorHealth Research Institute, Scottsdale, AZ, USA; ⁴Mary Crowley Research Center, Dallas, TX, USA; ⁵Beth Israel Deaconess Medical Center, Boston, MA, USA; ⁶Roche, South San Francisco, CA, USA

Background GS-1423 is a first-in-class bifunctional molecule comprised of an anti-CD73 antibody fused to the extracellular domain of TGF β receptor II (TGF β RII). GS-1423 is designed to inhibit CD73-mediated adenosine production and neutralize active TGF β within the tumor microenvironment. Dual antagonism of these 2 broadly immunosuppressive barriers is anticipated to facilitate productive anti-tumor immunity.

Methods This open label Phase 1a study (NCT03954704) evaluated the safety, tolerability, and pharmacokinetics of GS-1423. Exploratory biomarkers included the evaluation of the inhibition of GS-1423 targets, i.e. CD73 and TGF β , in the periphery. Biomarker assessments were performed in serial blood samples from patients receiving GS-1423 every two weeks (Q2W). Biomarker assays, unless otherwise stated, were custom built and qualified to measure the following: 1) TGF-beta 1/2/3 (Luminex, Bio-Rad) in platelet poor plasma, 2) CD73 target occupancy (TO) on B and CD8 T cells in whole blood, 3) free soluble CD73 (sCD73) not bound to GS-1423, and 4) sCD73 activity in platelet poor plasma. Biomarker values were plotted longitudinally by patient and by dose.

Results A dose dependent decrease in TGF-beta 1/2/3 in plasma of patients was observed on treatment. There was no detectable TGF β at the 20 mg/kg dose level and above at 2 hours post first dose and for the duration of the Q2W dosing interval. A dose dependent increase in CD73 TO on B and CD8 T cells was also observed with treatment, and complete TO was achieved at 20 mg/kg and above at 2 hours post first dose for the duration of the Q2W dosing interval. Free sCD73 decreased at 2 hours post first dose, while remaining above the lower limit of quantitation, and then increased above baseline after 24 hours post-dose at the 3 mg/kg dose level and above. The sCD73 activity in blood correlated with changes in free sCD73 levels.

Conclusions Blood biomarker analyses of GS-1423 in patients with advanced solid tumors demonstrated undetectable soluble TGF β 1/2/3 and complete TO of CD73 on B and T cells at the 20 mg/kg dose level and above. The mechanism underlying the increase in sCD73 following GS-1423 treatment remains to be elucidated.

Ethics Approval The study obtained ethics approval from the IRB/IEC and all participants gave informed consent before taking part in the study.

<http://dx.doi.org/10.1136/jitc-2021-SITC2021.377>

378

EFFICACY, SAFETY AND ANCILLARY ANALYSES OF PEMBROLIZUMAB IN COMBINATION WITH NINTEDANIB FOR THE TREATMENT OF PATIENTS WITH RELAPSED ADVANCED MESOTHELIOMA

¹Francois-Xavier Danlos*, ¹Capucine Baldini, ¹Matthieu Texier, ¹Andreea Varga, ²Severine Mouraud, ¹Bastien Job, ³Diane Letourneur, ¹Lydie Cassard, ²Delphine Bredel, ¹Salim Laghouati, ⁴Julien Adam, ¹Nathalie Droin, ¹Aurelien Parpaleix, ⁵Nathalie Chaput-Gras, ⁶Audrey Rabeau, ⁷Gerard Zalcman, ¹David Planchard, ¹Christophe Massard, ¹Jean-Charles Soria, ¹Aurelien Marabelle. ¹Gustave Roussy, VILLEJUIF, France; ²Gustave Roussy, INSERM, CLAMART, France; ³Gustave Roussy, ENS Lyon, Villejuif, France; ⁴Hopital Paris Saint-Joseph, Villejuif, France; ⁵Gustave Roussy, Université Paris Saclay, Villejuif, France; ⁶Institut Universitaire Oncologie, Toulouse, France; ⁷CHU Bichat, APHP, Paris, France

Background We report the results from the advanced malignant mesothelioma (aMM) expansion cohort of the PEMBIB Phase Ib trial (NCT02856425) evaluating the safety, efficacy & biomarkers of an antiangiogenic tyrosine kinase inhibitor (nintedanib) with an anti-PD1 immunotherapy (pembrolizumab).

Methods Patients with aMM relapsing after at least one line of platinum doublet chemotherapy and not previously pre-exposed to IO were treated with a combination of oral nintedanib (150mg BID) & IV pembrolizumab (200mg Q3W) with a 7 days nintedanib lead-in preceding pembrolizumab initiation. Baseline and on-treatment (cycle D2, day 1 [C2D1]) fresh tumor & blood samples were prospectively phenotyped by flow cytometry (FC). RNAseq was run on tumor samples. Immune factors were titrated on tumor secretome and plasma.

Results 30 aMM patients were treated and 29 evaluable for response. Median age was 68 years old (38–85) and 86% of aMM were epithelioid. The most frequent adverse events (AE) (grades 1–3) related to the combination were liver enzymes increase, fatigue, nausea, and diarrhea. 4 (13.3%) patients developed grade 3–5 immune-related AE. Patients died of cancer progression (n=14, 46.7%), myocarditis with thromboembolic event (n=1, 3.3%) and COVID-19 (n=1, 3.3%). Median follow-up was 14.8 months (95%CI [9.70–18.2]). Best Overall Response Rates (BORR) per RECISTv1.1 were Partial Response (PR, n=7/29; 24.1%), Stable Disease (SD, n=17/29; 58.6%) and Progressive Disease (n=5/29; 17.2%). Disease Control Rate (DCR) (defined as PR + SD) was 46.6% at 6 months. Patients with DCR at 6 months had significantly higher percentage of PDL1 expression on tumor cells (by Immuno-Histo-Chemistry, antibody clone SP263) and higher CD8+ T cells infiltrate in tumor biopsies (by FC) at screening. Upon treatment, soluble plasma rate of CXCL9 and CXCL13 increased in all patients, as well as tumor immune infiltrates estimated by deconvolution of tumor biopsies RNA-seq. But deconvoluted estimates of NK cells, T cells and myeloid dendritic cells infiltrates on baseline tumors and C2D1 biopsies were higher in patients with DCR at 6 months. Pre & on-treatment IL6 and IL8 rates in tumor secretome & plasma were higher in patients without DCR. Gene Set Enrichment Analyses on RNA-seq from screening biopsies highlighted an enrichment in E2F, MYC and KRAS gene pathways and lower expression of type 1 interferon signature in patients without DCR than those with DCR at 6 months.

Conclusions With a BORR of 24% and a DCR of 47% at 6 months, pembrolizumab and nintedanib combination provided valuable therapeutic benefits for patients with aMM.

Trial Registration ClinicalTrials.gov, NCT02856425. Registered August 4, 2016 — Prospectively registered, [https://clinicaltrials.gov/ct2/show/NCT02856425?](https://clinicaltrials.gov/ct2/show/NCT02856425?term=PEMBIB&draw=2&rank=1)

[term=PEMBIB&draw=2&rank=1](https://clinicaltrials.gov/ct2/show/NCT02856425?term=PEMBIB&draw=2&rank=1).

Ethics Approval The protocol was first approved by the Agence Nationale de Sécurité du Médicament (ANSM) on June 24th 2016 (Ref #160371A-12). The protocol was also approved by the Ethical Committee (Comité de Protection des Personnes Ile de France 1) on Jul 12th 2016 (Ref #2016-mai-14236ND).

<http://dx.doi.org/10.1136/jitc-2021-SITC2021.378>

379

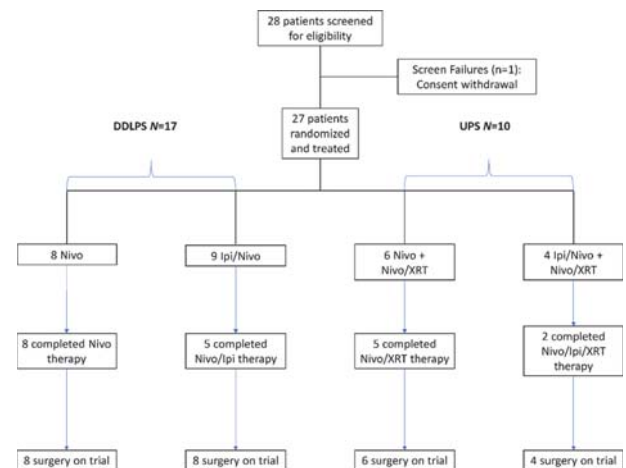
IMMUNE INFILTRATES ARE ASSOCIATED WITH CLINICAL OUTCOMES IN PATIENTS WITH RESECTABLE SOFT TISSUE SARCOMA (STS) TREATED WITH NEOADJUVANT IMMUNE CHECKPOINT BLOCKADE (ICB)

Emily Keung*, Elise Nassif, Heather Lin, Alexander Lazar, Wei-Lien Wang, Edwin Parra, Cibelle Lima, Ignacio Wistuba, Ashleigh Guadagnolo, Andrew Bishop, Valerae Lewis, Keila Torres, Kelly Hunt, Barry Feig, Christopher Scally, Ahmed Al Rawi, Shadara Crosby, Grace Mathew, Davis Ingram, Khalida Wani, Jennifer Wargo, Neeta Somaiah, Christina Roland. *The University of Texas MD Anderson Cancer Center, Houston, TX, USA*

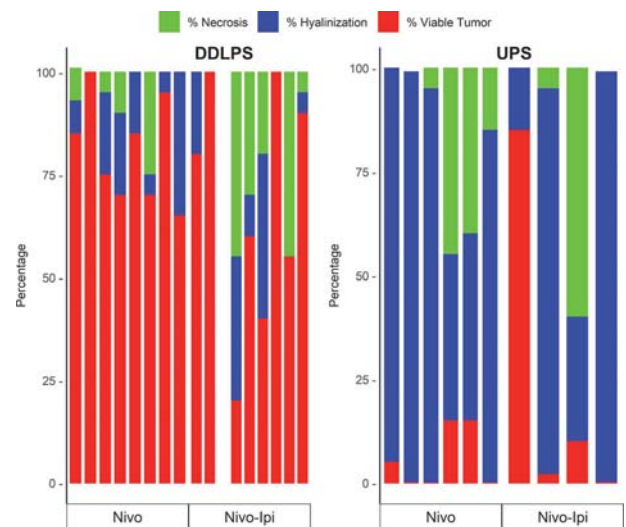
Background Recurrences are common after surgery for localized STS.^{1,2} ICB has shown activity in metastatic undifferentiated pleomorphic sarcoma (UPS) and dedifferentiated liposarcoma (DDLPS)³ with intratumoral B-cells associated with improved outcomes.⁴ We assessed biomarkers of response in a novel phase II trial of neoadjuvant ICB for resectable UPS and DDLPS.

Methods DDLPS (n=17) and UPS (n=10) patients were randomized to neoadjuvant nivolumab or ipilimumab+nivolumab, with UPS patients receiving concurrent radiotherapy⁵ (figure 1). Baseline and on-treatment tumor biopsies were obtained; primary endpoint was pathologic response defined as >30% hyalinization at surgery after optimal cutoff determination.⁶ We examined association of tumor-infiltrating immune cells, assessed by immunohistochemistry and multiplex immunofluorescence (mIF), with pathologic response, survival and resistance as defined by Society for Immunotherapy of Cancer Criteria.⁷ Statistical analysis included Kruskal-Wallis, Wilcoxon and McNemar tests. Log-rank tests were performed to compare relapse-free survival (RFS) and overall survival (OS).

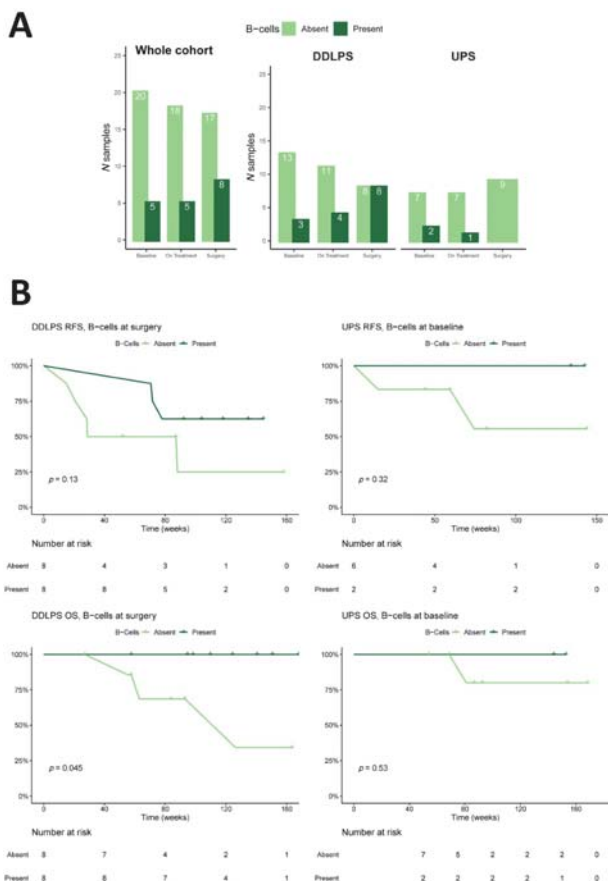
Results Pathologic response was seen in 18% DDLPS (N=3/17) and 90% UPS (N=9/10) patients (figure 2). At a median follow-up of 23 months from treatment initiation, 12 (44%) patients (9 DDLPS, 3 UPS) relapsed and 4 (14%) died due to recurrence (3 DDLPS, 1 UPS). The percentage of DDLPS tumors with CD20+/CD21+ B-cell infiltration increased with ICB (baseline: 19%, surgery: 50%; p=0.056; figure 3) and presence of B-cells at surgery for DDLPS displayed a trend toward longer median RFS (Not Reached [NR], 95% CI 15–NR months versus 13.4 months, 95% CI 3.5–NR; p=0.13). All DDLPS patients with B-cells at surgery are alive whereas median OS in absence of B-cells was 28 months (p=0.045). Two UPS patients had baseline intratumoral B-cells but none were found at surgery, presumably because B-cells are radio-sensitive; neither have relapsed (follow-up: 33 and 31 months). By mIF (figure 4), tumors with baseline infiltration of CD3+CD8+/CD3+ >17% had longer RFS (p=0.0038; figure 5). Pathologic non-responders had higher density of baseline CD3+FoxP3+CD8- and on-treatment CD3+CD45RO+FoxP3+CD8- lymphocytes (p=0.037 and p=0.012, respectively; figure 6). Furthermore, primary resistant STS had higher baseline CD3+FoxP3+CD8- cell density (p=0.068); STS with secondary resistance had higher density of CD3+FoxP3+CD8- cell density at surgery (p=0.036; figure 6).



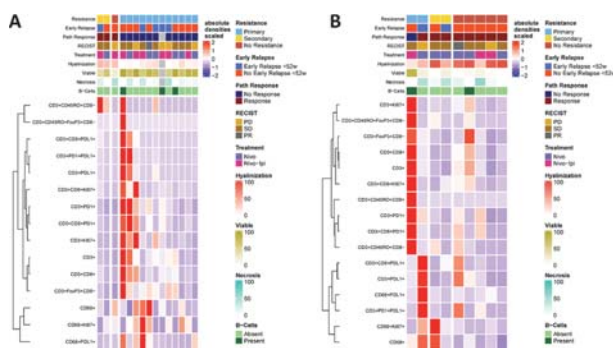
Abstract 379 Figure 1 Trial schema. Patients with DDLPS were randomized to receive either three cycles of nivolumab monotherapy (3mg/kg every 2 weeks) or one cycle of combination nivolumab/ipilimumab (nivolumab 3mg/kg and ipilimumab 1mg/kg) followed by two cycles of nivolumab monotherapy (3mg/kg every 2 weeks). Patients with UPS were randomized to receive either one cycle of nivolumab followed by concurrent radiation therapy (50Gy) with three cycles of nivolumab (3mg/kg every 2 weeks) or one cycle of combination nivolumab/ipilimumab (Nivolumab 3mg/kg and Ipilimumab 1mg/kg) followed by concurrent radiation therapy (50Gy) with three cycles of Nivolumab (3mg/kg every 2 weeks).



Abstract 379 Figure 2 Pathologic response to preoperative immune checkpoint blockade by treatment arm. The primary endpoint of this study was pathologic response as measured by percent tumor hyalinization. In the intention-to-treat population of all 27 randomized patients, median percent hyalinization was 8% (95% CI 0%–20%) in the DDLPS cohort and 89% (95% CI 30%–99%) in the UPS cohort. There were no differences in percent hyalinization between nivolumab monotherapy and combination nivolumab/ipilimumab treatment arms in either cohort. Median residual viable tumor in DDLPS was 77.5% (95% CI 60%–95%) and 3.5% (95% CI 0–15%) in UPS cohorts and was similar between nivolumab monotherapy and combination ipilimumab/nivolumab treatment arms.

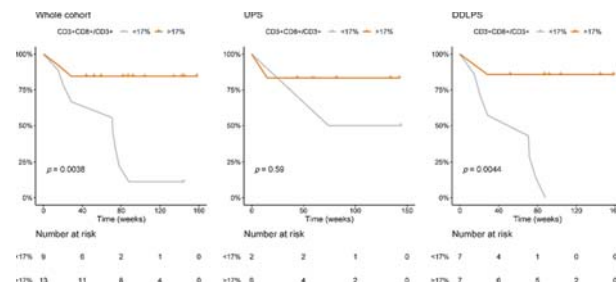


Abstract 379 Figure 3 Intratumoral B-cells kinetics and association with survival. (A) Number of samples positive and negative for B-cell staining at each clinical time point in the whole cohort (left panel) and histotype-specific (right panel) as assessed and verified by CD20 and CD21 immunohistochemistry, respectively. Increase in the number of B-cell positive samples in DDLPS with immune checkpoint blockers. Decrease in the UPS group due to radiosensitivity. (B) Association between presence of B-cells and relapse-free survival (RFS, top panels) and overall survival (OS, bottom panels). DDLPS patients with intratumoral B-cells at surgery experienced longer RFS and OS. UPS patients with intratumoral B-cells at baseline experienced longer RFS and OS. *p-values are Log-rank

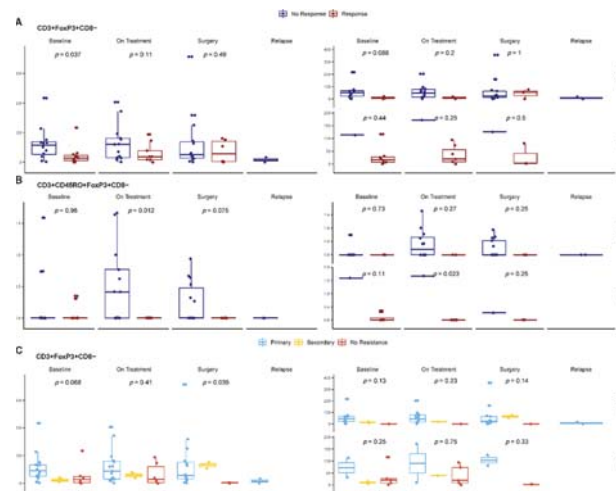


Abstract 379 Figure 4 Association of baseline tumor immune infiltrate with clinical outcomes. Baseline tumor infiltrating immune cells were assessed and quantified by multiplexed immunofluorescence. Densities have been scaled and patients were classified by resistance according to Society for Immunotherapy of Cancer (SITC) criteria. Immune cells are grouped by hierarchical clustering correlation using Spearman's coefficient. (A) Heatmap of absolute densities of immune

infiltrating cells at baseline in DDLPS. Three patients had pathologic response, and only one of these patients did not relapse and was considered non-resistant. (B) Heatmap of absolute densities of immune infiltrating cells at baseline in UPS. One patient did not have pathologic response, two patients displayed early relapse and one patient had relapse after one year.



Abstract 379 Figure 5 Cytotoxic lymphocytes at baseline are associated with longer relapse-free survival. Kaplan Meier curves of relapse-free survival according to relative density of CD3+CD8+/CD3+ > 17% at baseline. *p-values are Log-rank.



Abstract 379 Figure 6 T-regulatory cells are associated with poorer pathologic response and resistance to immune checkpoint blockade. (A) Absolute densities of regulatory T cells CD3+FoxP3+CD8- lymphocytes by pathological response at each clinical time point (entire cohort, left panel; by histotype, right panel). *p-values are Wilcoxon. (B) Absolute densities of memory/regulatory T-cells CD3+CD45RO+FoxP3+CD8- lymphocytes by pathological response at each clinical time point (entire cohort, left panel; by histotype, right panel). *p-values are Wilcoxon. (C) Absolute densities of regulatory T cells CD3+FoxP3+CD8- lymphocytes by resistance as defined by SITC criteria at each clinical time point (entire cohort, left panel; by histotype, right panel). *p-values are Kruskal Wallis.

Conclusions B-cells at baseline in UPS and at surgery in DDLPS and cytotoxic T cells CD3+CD8+ at baseline are associated with better survival outcomes. T-regulatory cells are associated with poorer pathologic response and resistance to neoadjuvant ICB for DDLPS and UPS.

Acknowledgements This study was supported by Bristol Myers Squibb. EZK received support from the QuadW Foundation. EFN received support from Fondation pour la Recherche

Medicale and Fondazione Nuovo-Soldati. CLR received support from American College of Surgeons.

Trial Registration clinicaltrials.gov unique identifier: NCT03307616

REFERENCES

- 1.. Blay JY, Honore C, Stoeckle E, *et al.* Surgery in reference centers improves survival of sarcoma patients: a nationwide study. *Ann Oncol* 2019;**30**:1407.
2. . Gronchi A, Palmerini E, Quagliuolo V, *et al.* Neoadjuvant chemotherapy in high-risk soft tissue sarcomas: final results of a randomized trial from Italian (ISG), Spanish (GEIS), French (FSG), and Polish (PSG) sarcoma groups. *Journal of Clinical Oncology* 2020;**38**:2178–2186.
- 3.. Tawbi HA, Burgess M, Bolejack V, *et al.* Pembrolizumab in advanced soft-tissue sarcoma and bone sarcoma (SARC028): a multicentre, two-cohort, single-arm, open-label, phase 2 trial. *The Lancet Oncology* 2017;**18**:1493–1501.
- 4.. Petitprez F, de Reynies A, Keung EZ, *et al.* B cells are associated with survival and immunotherapy response in sarcoma. *Nature* 2020;**577**:556–560.
- 5.. Keung EZ, Lazar AJ, Torres KE, *et al.* Phase II study of neoadjuvant checkpoint blockade in patients with surgically resectable undifferentiated pleomorphic sarcoma and dedifferentiated liposarcoma. *BMC Cancer* 2018;**18**.
- 6.. Schaefer I-M, Hornick JL, Barysaukas CM, *et al.* Histologic appearance after pre-operative radiation therapy for soft tissue sarcoma: assessment of the European organization for research and treatment of cancer–soft tissue and bone sarcoma group response score. *International Journal of Radiation Oncology*Biophysics* 2017;**98**:375–383.
7. . Kluger HM, Tawbi HA, Ascierto ML, *et al.* Defining tumor resistance to PD-1 pathway blockade: recommendations from the first meeting of the SITC immunotherapy resistance taskforce. *J Immunother Cancer* 2020;**8**.

Ethics Approval This study was approved by MD Anderson Cancer Center Institutional Review Board; approval number 2017–0143.

<http://dx.doi.org/10.1136/jitc-2021-SITC2021.379>

380

GS-3583, A NOVEL FLT3 AGONIST FC FUSION PROTEIN, EXPANDS CONVENTIONAL DENDRITIC CELLS IN HEALTHY VOLUNTEERS

¹Nishanthan Rajakumaraswamy*, ¹Anees Dauki, ¹Michelle Kuhne, ¹Torsten Trowe, ¹Winnie Weng, ¹Kai-Wen Lin, ¹Emon Elboudjwarej, ¹Brian Carr, ¹Angela Worth, ¹Anshu Vashishtha, ²Christian Schwabe, ¹Ahmed Othman. ¹Gilead Sciences, Inc., Foster City, CA, Foster City, CA, USA; ²New Zealand Clinical Research, Auckland, New Zealand, Auckland, New Zealand

Background Conventional dendritic cells subtype 1 (cDC1) play a vital role in the priming and expansion of tumor specific CD8+ T cells and their recruitment to tumor microenvironment (TME). However, cDC1s are often underrepresented in the TME. Systemic administration of Fms-like tyrosine kinase 3 ligand (FLT3L), a hematopoietic growth factor that binds to FLT3 on myeloid and lymphoid progenitor cells, leads to expansion of cDC1s in the periphery which can then be recruited into the TME. FLT3 pathway stimulation using GS-3583, a novel FLT3 agonistic Fc fusion protein, has the potential to promote T cell mediated anti-tumor activity. We sought to evaluate the pharmacodynamic (PD) effect of a single dose of GS-3583 in healthy volunteers alongside its safety. Herein, we present the updated results of the study.

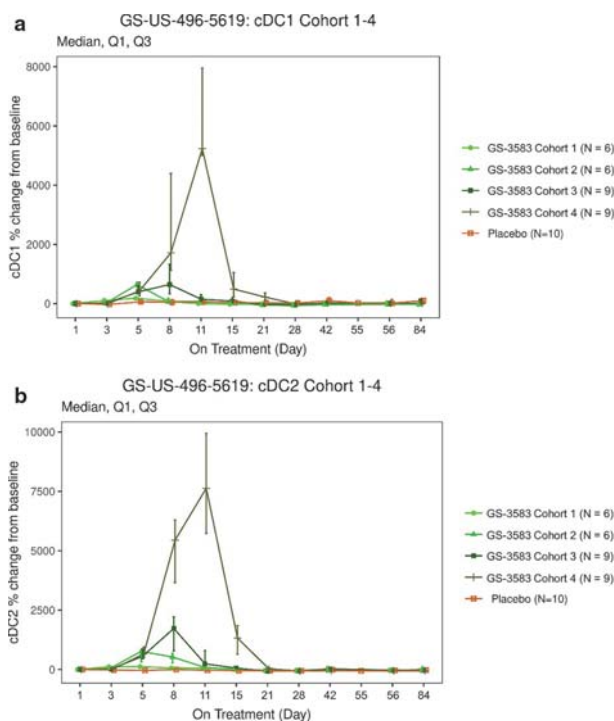
Methods This was a first-in-human, placebo-controlled study of GS-3583 in healthy volunteers to evaluate the safety, pharmacokinetics (PK), and PD of escalating single doses (ranging from 75 micrograms to 2000 micrograms) of GS-3583. The study was blinded to the subjects and the investigator. Each dose cohort enrolled 8–12 healthy subjects who received GS-3583 or placebo as single IV infusion at 3:1 ratio. Subjects were observed in the phase 1 unit for 15 days and then for 12 weeks as outpatients. As part of the PD evaluation, we investigated the changes in the number of cDC1 and cDC2 cells.

Results As of 2nd July 2021, selected safety, PK and PD data from all 4 cohorts were available. GS-3583 was well tolerated and all subjects had been discharged. To date, there have been no serious or grade 3 or higher adverse events. Preliminary PK analysis suggested dose-dependent increase in GS-3583 exposure (AUC and Cmax). Preliminary PD analysis shows that administration of GS-3583 resulted in temporary, dose-dependent increases in cDC1/cDC2 cells that peaked between days 5–11 (higher doses resulted in later peaks) and returned to baseline within 3 weeks of drug administration (table 1, figure 1).

Abstract 380 Table 1 Selected subject characteristics and pharmacodynamic results

Cohort	1	2	3	4
Subjects treated (A=active; P=placebo)	8 (6A; 2P)	8 (6A; 2P)	12 (9A; 3P)	12 (9A; 3P)
Age, years median (range)	32 (20, 38)	27 (23, 45)	22 (18, 45)	31.5 (18, 42)
Male n (%)	5 (62.5%)	5 (62.5%)	8 (66.7%)	9 (75.0%)
cDC1 peak cell count*	Day 5	Day 5	Day 8	Day 11
median (Q1, Q3)	69.6 (62.9, 89.2)	169.0 (121.1, 215.1)	147.2 (130.1, 258.6)	922.2 (528.6, 1355.2)
cDC1, fold change from baseline*	Day 5	Day 5	Day 8	Day 11
median (Q1, Q3)	1.85 (1.38, 2.4)	6.42 (5.62, 7.17)	6.47 (3.29, 13.31)	52.33 (50.01, 79.53)
cDC2 peak cell count*	Day 5	Day 5	Day 8	Day 11
median (Q1, Q3)	1346.0 (1124.8, 1395.1)	2937.0 (1679.8, 3731.9)	10677.6 (7565.6, 13702.6)	36741.8 (29835.8, 55246.2)
cDC2, fold change from baseline*	Day 5	Day 5	Day 8	Day 11
median (Q1, Q3)	1.20 (0.71, 1.85)	7.61 (3.21, 8.03)	17.30 (7.86, 22.13)	76.33 (57.33, 99.42)

* Data shown only from the subjects who received GS-3583; placebo data are excluded



Abstract 380 Figure 1 A) Comparison of cDC1 cell quantitative changes in cohorts 1–4; B) Comparison of cDC2 cell quantitative changes in cohorts 1–4

Conclusions GS-3583 infusion was well tolerated and induced dose dependent expansion of dendritic cells in the periphery in healthy volunteers. In patients with cancer, this increase in dendritic cells can be utilized to enhance anti-tumor therapeutic effects of immuno-oncology therapies.

Acknowledgements Funding provided by Gilead Sciences, Inc.

Ethics Approval The study received study site IRB/Ethics Committee approval prior to enrollment of subjects.

<http://dx.doi.org/10.1136/jitc-2021-SITC2021.380>

381

INTRATUMORAL ONCOLYTIC VIRUS V937 PLUS IPILIMUMAB IN PATIENTS WITH ADVANCED MELANOMA: THE PHASE 1B MITCI STUDY

¹Brendan Curti*, ²Jon Richards, ³John Hyingstrom, ⁴Gregory Daniels, ⁵Mark Faries, ⁶Lynn Feun, ⁷Kim Margolin, ²Sigrun Hallmeyer, ⁸Mark Grose, ⁹Yiwei Zhang, ⁹Anlong Li, ¹⁰Robert HI Andtbacka. ¹Providence Cancer Institute, Earle A. Chiles Research Institute, Portland, OR, USA; ²AdvocateAurora Health, Park Ridge, IL, USA; ³Huntsman Cancer Institute, Salt Lake City, UT, USA; ⁴Moore's Cancer Center, UCSD, La Jolla, CA, USA; ⁵Cedars-Sinai Medical Center, Angeles Clinic and Research Institute, Santa Monica, CA, USA; ⁶Sylvester Comprehensive Cancer Center, University of Miami, Miami, FL, USA; ⁷City of Hope, Duarte, CA, USA; ⁸Vivalytics, Vivalytics Limited, Sydney, Australia; ⁹Merck and Co., Inc., Kenilworth, NJ, USA; ¹⁰Huntsman Cancer Institute, University of Utah, Salt Lake City, UT, USA

Background Intratumoral administration of V937, a bioselected genetically unmodified Coxsackievirus A21, has shown antitumor activity both as a monotherapy and in combination with the anti-PD-1 antibody pembrolizumab.¹⁻³ V937 induces lytic tumor cell infection and upregulation of members of immune checkpoint pathways.² We present the results from the phase 1b MITCI study that evaluated V937 plus ipilimumab for advanced melanoma.

Methods Eligible patients had unresectable or metastatic stage IIIB/C or IV melanoma amenable to intratumoral injection. Patients received intratumoral V937 3×10⁸ TCID₅₀ on days 1, 3, 5, 8, and 22, then Q3W for 14 more injections plus intravenous ipilimumab 3 mg/kg Q3W administered 4 times starting on day 22. Imaging was done Q6W beginning at day 106; response was assessed per immune-related response criteria (irRC). The primary endpoints were safety and ORR in the overall population and in patients whose disease progressed on prior anti-PD-1 therapy.

Results 50 patients were enrolled and received ≥1 dose of study treatment. At data cutoff (February 21, 2020), all had discontinued the study and study therapy. Median (range) age was 64.5 (28–88) years. Fourteen patients (28%) had stage III disease. Forty patients (80%) had received prior systemic treatment, 33 of whom had received anti-PD-1 therapy. The median number of cycles of ipilimumab was 4 (range, 1–4), and the number of intratumoral injections of V937 was 9 (range, 5–19). Among the 94% of patients who had ≥1 treatment-related AE, 14% had grade 3/4 treatment-related AEs, none of which were considered related to V937. The most common grade 3/4 treatment-related AEs were dehydration, diarrhea, and hepatotoxicity (4% each). No grade 5 treatment-related AEs occurred. The most common treatment-related AEs were pruritus (50%), fatigue (44%), diarrhea (32%), and nausea (22%). Efficacy outcomes for the overall population and by prior anti-PD-1 therapy use are presented in table 1. Tumor regression was observed in injected and noninjected lesions.

Conclusions V937 plus ipilimumab was safe and the toxicities were manageable and consistent with that anticipated for the individual treatment components. ORR was robust and significantly higher than anticipated with ipilimumab monotherapy, including in patients who had received prior anti-PD-1 therapy. Most responses were durable (≥26 weeks), and responses seen in noninjected metastases provided evidence of probable systemic immune activation. The combination of V937 plus ipilimumab warrants further investigation in a larger trial in patients with advanced melanoma.

Abstract 381 Table 1

	All patients N = 50	Prior anti-PD-1 therapy n = 33	No prior anti-PD-1 therapy n = 17
ORR (95% CI), %	30 (18–45)	21 (9–39)	47 (23–72)
DOR, median (95% CI), mo	8.8 (5.9–8.8)	8.8 (5.9–8.8)	NR (4.9–NR)
PFS, median (95% CI), mo	6.2 (3.5–9.0)	3.5 (3.5–10.6)	8.3 (3.4–NR)
OS, median (95% CI), mo	45.1 (28.3–NR)	29.7 (14.5–NR)	45.1 (22.4–NR)
DOR, duration of response; NR, not reached.			

Acknowledgements Medical writing assistance was provided by Kathleen Estes, PhD, of ICON plc (North Wales, PA, USA), funded by Merck Sharp & Dohme Corp., a subsidiary of Merck & Co., Inc., Kenilworth, NJ, USA.

Trial Registration NCT02307149

REFERENCES

- 1.. Pandha H, Harrington K, Ralph C, Melcher A, Gupta S, Akerley W, *et al*. Abstract CT115: phase 1b KEYNOTE 200 (STORM study): a study of an intravenously delivered oncolytic virus, coxsackievirus A21 in combination with pembrolizumab in advanced cancer patients. *Cancer Res* 2017;**77**(13 suppl):CT115.
- 2.. Andtbacka RHI, Curti BD, Kaufman H, Nemunaitis JJ, Daniels GA, Hallmeyer S, *et al*. Dynamics of tumor response in advanced melanoma patients treated with coxsackievirus A21. *J Clin Oncol* 2016;**34**(15 suppl):9553.
- 3.. Silk AW, Kaufman H, Gabrail N, Mehnert J, Bryan J, Norrell J, *et al*. Phase 1b study of intratumoral coxsackievirus A21 (CVA21) and systemic pembrolizumab in advanced melanoma patients: interim results of the CAPRA clinical trial. *Cancer Res* 2017;**77**(13 suppl):CT026.

Ethics Approval An independent institutional review board or ethics committee approved the protocol at each study site, and the trial was conducted in compliance with Good Clinical Practice guidelines and the Declaration of Helsinki. All patients provided informed consent.

<http://dx.doi.org/10.1136/jitc-2021-SITC2021.381>

382 THE SYNTHETIC LONG PEPTIDE CANCER VACCINE UV1 IN COMBINATION WITH IPILIMUMAB INDUCES A CD4+ TH1 ANTI-hTERT IMMUNE RESPONSE AND AN INFLAMMATORY TUMOR MICROENVIRONMENT IN PATIENTS WITH MELANOMA

¹Espen Ellingsen*, ²Ilana Kerzeli, ³Irantzu Anzar, ⁴Nadia Mensali, ³Trevor Clancy, ²Sara Mangsbo, ¹Steinar Aamdal, ⁴Elin Aamdal, ⁴Tormod Guren, ⁴Else-Marit Inderberg-Suso, ⁴Eivind Hovig, ¹Gustav Gaudernack. ¹Ultimovacs ASA, Oslo, Norway; ²Uppsala University, Uppsala, Sweden; ³NEC Oncoimmunity, Oslo, Norway; ⁴Oslo University Hospital, Oslo, Norway

Background Checkpoint inhibitors (CPIs) have revolutionized the treatment of malignant melanoma. Although melanoma patients may experience deep and durable clinical responses to CPI treatment, the majority develop disease progression requiring additional therapy. Combining CPIs with therapeutic cancer vaccines may augment the anti-tumor immune response and thus improve clinical outcomes. UV1 is a therapeutic cancer vaccine based on synthetic antigens derived from the tumor-associated antigen telomerase reverse transcriptase (hTERT). hTERT is activated in 85–90% of all cancers and leads to replication of telomeric DNA, an essential mechanism for increased proliferation, immortality, and invasiveness of cancer cells. In this phase I/IIa study combining UV1 with ipilimumab in patients with melanoma (NCT02275416), we hypothesized that UV1 and ipilimumab might provide synergy in the expansion of vaccine-induced T cells. Furthermore, an augmented CD4+ Th1 immune response targeting a shared tumor antigen may increase T cell infiltration in the tumor microenvironment, promoting immune-mediated cancer cell death.

Methods The immune response dynamics were assessed by longitudinal immunomonitoring for up to 5 years using a standard proliferation assay. The phenotype and functionality of vaccine-induced T cells were assessed by patient-derived T cell cloning and subsequent in vitro characterization by flow cytometry, peptide stimulation, and cytokine release assays. On available biopsies harvested at baseline and 12 weeks after treatment initiation, the tumor microenvironment was assessed based on whole-exome sequencing, RNA sequencing, and immunohistochemistry.

Results Twelve patients with metastatic melanoma were enrolled in the study and received up to 9 vaccine doses over a 20-week period. A persistent (up to 5 years) vaccine-induced immune responses were demonstrated in 91% of evaluable patients (10/11). Vaccine-specific T cell clones were polyfunctional CD4+ Th1 cells, producing both IFN- γ and TNF- α upon in vitro peptide stimulation. Differential gene expression analysis and immunohistochemical characterization of biopsies at baseline and 12 weeks showed induction of an inflammatory "hot" tumor microenvironment in clinical responders with available paired biopsies.

Conclusions UV1 in combination with ipilimumab leads to robust and long-lasting CD4+ Th1 anti-hTERT immune responses sculpting the local tumor microenvironment.

Trial Registration NCT02275416

Ethics Approval The study was approved by Regional Ethical Committee South East (ID number 25 165). The patients provided their written informed consent to participate in the study.

<http://dx.doi.org/10.1136/jitc-2021-SITC2021.382>

383

DURABLE RESPONSES WITH INTRATUMORAL ELECTROPORATION OF PLASMID INTERLEUKIN 12 PLUS PEMBROLIZUMAB IN PATIENTS WITH ADVANCED MELANOMA PROGRESSING ON AN ANTI-PD-1 ANTIBODY: UPDATED DATA FROM KEYNOTE 695

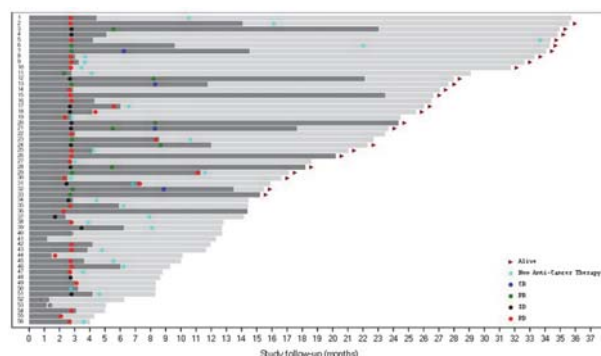
¹Pablo Fernandez-Penas, ²Matteo Carlino, ³Katy Tsai, ⁴Victoria Atkinson, ⁵Monaster Shaheen, ⁶Sajeve Thomas, ⁷Catalin Mihalciou, ⁸Tom Van Hagen, ⁹Rachel Roberts-Thomson, ¹⁰Andrew Haydon, ¹¹Andrew Mant, ¹²Marcus Butler, ³Gregory Daniels, ¹³Elizabeth Bunchbinder, ¹⁴John Hyngstrom, ¹⁵Mecker Moller, ¹⁶Igor Puzanov, ¹⁷C Lance Cowey, ¹⁸Eric Whitman, ¹⁹Carmen Ballesteros-Merino, ¹⁹Shawn Jensen, ¹⁹Bernard Fox, ²⁰Emmett Schmidt, ²⁰Scott Diede, ²¹Rebecca Setta, ²¹Jendy Sell, ²¹David Canton, ²¹Sandra Aung, ²¹Christopher Twitty, ²¹Sunny Xie, ²¹Ying Lu, ²¹Bridget O'Keefe, ³Alain Algazi, ³Adil Daud*. ¹Westmead Hospital, University of Sydney, Westmead, Australia; ²Melanoma Institute Australia, Sydney, Australia; ³University of California, San Francisco, CA, USA; ⁴Princess Alexandra Hospital, University of Queensland, Woolloongabba, Australia; ⁵University of Arizona, Tucson, AZ, USA; ⁶UF Health Cancer Center at Orlando Health, Orlando, FL, USA; ⁷McGill University Health Centre, Montreal, Canada; ⁸St. John of God Hospital, Subiaco, Australia; ⁹Adelaide Oncology and Haematology, Adelaide, Australia; ¹⁰The Alfred Hospital, Melbourne, Australia; ¹¹Box Hill Hospital, Box Hill, Australia; ¹²Princess Margaret Cancer Centre, Toronto, Canada; ¹³Dana Faber Cancer Institute, Boston, MA, USA; ¹⁴University of Utah Healthcare Huntsman Cancer Institute, Salt Lake City, UT, USA; ¹⁵University of Miami Sylvester Cancer Center, Miami, FL, USA; ¹⁶Roswell Park Comprehensive Cancer Center, Buffalo, NY, USA; ¹⁷Baylor University Medical Center, Dallas, TX, USA; ¹⁸Atlantic Health System, Morristown, NJ, USA; ¹⁹Earle A. Chiles Research Institute, Portland, OR, USA; ²⁰Merck and Co., Inc, Kenilworth, NJ, USA; ²¹Oncosec Medical Incorporated, San Diego, CA, USA

Background Electroporated plasmid interleukin-12 (pIL-12-EP; tavokinogene telseplasmid; TAVO) induces sustained intratumoral expression of IL-12, a cytokine that is integral for response to anti-PD-1 antibodies. Here, we present updated safety and response duration data from KEYNOTE 695, a Phase 2, multicenter, open-label trial of pIL-12-EP in combination with pembrolizumab in patients with stage III/IV melanoma immediately following confirmed progression on an anti-PD-1 antibody.

Methods Patients with confirmed disease progression after ≥ 12 weeks' treatment with an anti-PD-1 antibody alone or in combination were eligible. Patients received intratumoral pIL-12-EP on days 1, 5 and 8 every 6 weeks and pembrolizumab 200 mg every 3 weeks. Responses were assessed by the investigator at 12-week intervals using RECIST v1.1; overall survival (OS) and duration of response (DoR) assessments were conducted using the Kaplan-Meier method.

Results Of the first 56 patients treated, 50% had visceral disease (M1b-d), 80% had received 1–2 and 20% ≥ 3 prior lines of therapy, 27% had prior ipilimumab and 21% prior BRAF/MEK inhibitors. 61% of patients were primary refractory to anti-PD-1. 54 patients were efficacy evaluable, defined as patients who had at least one post-treatment scan. The investigator-assessed objective response rate (ORR) per RECIST was 27.8% (4 CR, 11 PR); ORR per iRECIST was 29.6%. In patients with M1b-d staging, ORR was 33.3% (n=9/27), and in those receiving prior ipilimumab, ORR was 33.3% (n=5/15). Seven patients had 100% reduction in target lesions, and regression was observed in non-injected lesions. The median DoR had not been reached. With a median follow up of 19.3 months, the median OS (95% CI) was 24.5 (14.4, NR) months (figure 1). The study is now fully enrolled. In 105 patients with safety data, there were no Grade 4/5 treatment-related adverse events (TRAEs) reported. Grade 3 TRAEs occurred in 5.7% and comprised cellulitis in two patients and arthralgia, pneumonitis, enteritis, keratoacanthoma, lichen planus and musculoskeletal chest pain in one patient each. The Grade 1/2 TRAEs in $\geq 10\%$ patients were fatigue (27.6%),

procedural pain (20.0%), diarrhea (17.1%), nausea (10.5%) and pruritus (10.5%). ORR by blinded independent central review has commenced and a global phase 3 trial is planned.



Abstract 383 Figure 1 Overall survival in patients treated with pIL-12-EP in combination with pembrolizumab. Dark grey bars: time on study treatment, light grey bars: end of treatment to death or censoring

Conclusions Patients with anti-PD-1 therapy refractory advanced melanoma can achieve deep, durable responses in both injected and non-injected lesions with pIL-12-EP plus pembrolizumab. Intratumoral pIL-12-EP in combination with pembrolizumab was generally well tolerated, with minimal Grade 3 and no Grade 4/5 TRAEs.

Trial Registration NCT03132675

Ethics Approval The study was approved by a central IRB and/or local institutional IRB/Ethics Committee as required for each participating institution.

Consent Written informed consent was obtained from the patients participating in the trial; the current abstract does not include information requiring additional consent

<http://dx.doi.org/10.1136/jitc-2021-SITC2021.383>

AN INVESTIGATION INTO THE ROLE OF CD4+ TUMOR-INFILTRATING LYMPHOCYTES (TIL) IN METASTATIC MELANOMA PATIENTS WITH A COMPLETE RESPONSE TO ADOPTIVE CELL THERAPY

¹MacLean Hall*, ¹Holly Branthoover, ¹Patrick Innamarato, ¹Amy Hall, ¹Alex Alfaro, ¹Allison Richards, ¹Jeani Rich, ¹Jonathan Hensel, ²Jim Bender, ²Jake Ceccarelli, ²TJ Langer, ¹Matthew Beatty, ¹John Mullinax, ¹Jamie Teer, ¹Amod Sarnaik, ¹Shari Pilon-Thomas. ¹Moffitt Cancer Center, Tampa, FL, USA; ²Turnstone Biologics, New York, NY, USA

Background Immunotherapy for cancer has long been focused on the generation of CD8+ cytotoxic T lymphocyte responses, independent of their dynamic CD4+ T cell counterpart. One promising approach, adoptive cell transfer (ACT) of tumor-infiltrating lymphocytes (TIL), has yielded response rates ranging from 28–55%.^{1–2} Investigation into the role of CD4+ TIL in this setting remains critically underexplored as an opportunity to improve upon these successes.

Methods Two metastatic melanoma patients (PT1 and PT2) were treated with TIL on a completed clinical trial at Moffitt Cancer Center (NCT01005745). Tumor recognition by TIL was assessed via co-culture with tumor. Whole exome (WES) and RNA Sequencing were performed on cryopreserved tumor sections and mutant peptide-MHC binding was predicted. TIL were stimulated with antigen presenting cells (APCs) loaded with neoantigen-derived 25mer peptides and sorted based on 41BB/OX40 upregulation, followed by functional immunologic assays. TCR sequencing was conducted on patient peripheral blood as well as isolated neoantigen-specific TIL clones to determine persistence in vivo and cognate peptide-MHC targets were determined empirically.

Results PT1, infused with predominantly CD4+ TIL (88%), achieved a complete response (CR) despite lack of IFN γ detection with conventional in vitro tumor co-culture methods. Infusion product TIL were sorted by upregulation of OX40 and 41BB upon stimulation with APCs loaded with the mutant peptide pool. Neoantigen reactivity arose from a single peptide sequence, which conferred recognition by a CD4+ TIL clone, which comprised 17% of the infusion product and enriched to greater than 80% after sorting via FACS. These CD4+ TIL produced IFN γ , TNF α , and granzyme B in response to peptide-loaded APCs in an HLA-DR dependent manner. TCR β overlap revealed this CD4+ clone peaked at two weeks post-infusion (40%) and persisted after infusion for at least six weeks. PT2 was infused with highly reactive, primarily CD8+ (88%) TIL and also achieved a CR. Isolated CD4+ TIL were also responsive to tumor antigens in the context of MHC Class II in vitro. Tumor-reactive CD4+ TIL were enriched by IFN γ capture and delayed xenograft growth in vivo ($p < 0.01$). Neoantigen peptides stimulated predominantly CD4+ TIL to upregulate OX40/41BB and produce IFN γ , TNF α , and granzyme B.

Conclusions Investigation of these case studies demonstrated evidence of CD4+ TIL involvement in complete clinical responses after ACT. Ongoing studies will define the precise role of tumor-reactive CD4+ T cells in the anti-tumor immune response and provide the framework for future investigation into their function and therapeutic efficacy.

Trial Registration NCT01005745

REFERENCES

1.. Bailey SR, *et al.* Human CD26high T cells elicit tumor immunity against multiple malignancies via enhanced migration and persistence. *Nat Commun* 2017;**8** (1):1961.

2.. Tran E, *et al.* Cancer immunotherapy based on mutation-specific CD4+ T cells in a patient with epithelial cancer. *Science* 2014;**344**(6184):641–5.

Ethics Approval Approved by USF IRB approval number Ame5_107905. All participants gave informed consent before taking part.

<http://dx.doi.org/10.1136/jitc-2021-SITC2021.384>

385

IDENTIFICATION AND ENRICHMENT OF NEOANTIGEN-REACTIVE T CELLS TO OPTIMIZE ADOPTIVE CELL TRANSFER WITH TUMOR-INFILTRATING LYMPHOCYTES (TIL)

¹MacLean Hall*, ¹Holly Branthoover, ¹Matthew Beatty, ²Kwame Twumasi-Boateng, ²Jim Bender, ²Jake Ceccarelli, ²TJ Langer, ¹Jamie Teer, ¹Amod Sarnaik, ¹Shari Pilon-Thomas. ¹Moffitt Cancer Center, Tampa, FL, USA; ²Turnstone Biologics, New York, NY, USA

Background Adoptive cell transfer (ACT) using tumor-infiltrating lymphocytes (TIL) has achieved an overall response rate of 39% in metastatic melanoma patients at Moffitt Cancer Center. In these trials, a substantial fraction of patients were non-responders by RECIST, but demonstrated a mixed response to therapy. These results suggest that the infused TIL product contained tumor-reactive T cells with therapeutic potential, which could be further optimized to improve ACT with TIL. We hypothesized that outcomes might be improved by identifying and enriching neoantigen-reactive TIL within bulk products. The purpose of this study is to define approaches to optimize ACT with TIL, by identifying, enriching, and analyzing neoantigen reactive TIL from the ACT infusion product of previously treated metastatic melanoma patients.

Methods Patient-derived cryopreserved tumor tissue, PBMC, and TIL from completed metastatic melanoma TIL trials were used for this study. Whole exome and RNA sequencing were performed on DNA and RNA extracted from tumor tissue and compared to DNA from autologous PBMC. Genetic sequencing and gene expression data were utilized to determine protein-modifying somatic mutations. Peptides were then predicted for their ability to be presented on MHC molecules, prioritized, and up to 192 custom 25-mers were synthesized per patient sample. Neoantigen peptides were loaded onto patient-derived dendritic cells (DC) and co-cultured with autologous TIL. These TIL were then sorted by FACS on their ability to upregulate 41BB and OX40 and expanded through the rapid expansion protocol (REP). Enriched TIL were subsequently screened for neoantigen reactivity by 41BB/OX40 upregulation, cytokine release, and degranulation.

Results Protein-altering somatic mutations from metastatic melanoma tissues ranged from 49 to 1631 mutations (median = 389). On average, 16.2% of TIL were sorted for upregulation of 41BB/OX40 upon co-culture with DC pulsed with the neoantigen peptide pool (range: 2.7–31.1%). CD4⁺ TIL displayed a 3.75-fold upregulation of 41BB/OX40, while CD8⁺ TIL saw a 1.88-fold increase (n=6). This coincided with substantial production of IFN γ , TNF α , and granzyme B (n=6). Neoantigen-reactive (41BB+/OX40+) and non-reactive (41BB-/OX40-) TIL expanded to similar degrees in REP (average of 639-fold vs. 611-fold; n=6). Restimulation of enriched neoantigen-specific TIL resulted in superior pro-inflammatory functionality (granzyme B, IFN γ , and TNF α) when compared to non-reactive TIL.

Conclusions TIL from metastatic melanoma patient samples were successfully enriched for neoantigen-reactive TIL, which maintained increased reactivity against these predicted peptides upon restimulation when compared non-reactive TIL. These data support further investigation into the use of neoantigen-enriched TIL products to enhance efficacy of ACT.

Trial Registration NCT01005745, NCT01659151, NCT01701674

Ethics Approval NCT01005745 was approved by USF IRB approval number Ame5_107905. NCT01659151 was approved

by Advarra IRB approval number 14.03.0083. NCT01701674 was approved by USF IRB approval number Ame13_Pro00009061. All participants gave informed consent before taking part.

<http://dx.doi.org/10.1136/jitc-2021-SITC2021.385>

387

THE UTILITY OF AI-POWERED SPATIAL CLASSIFICATION OF INTRATUMORAL CD8+ IMMUNE-CELL DISTRIBUTION IN PREDICTING OVERALL SURVIVAL IN PATIENTS WITH MELANOMA AS PART OF THE CHECKMATE 067 CLINICAL TRIAL

George Lee*, Keyur Desai, Hao Tang, Daniel Cohen, Scott Ely, John Wojcik, Jimena Trillo-Tinoco, Benjamin Chen, Akshita Gupta, Daniel Tenney, Vipul Baxi, Robin Edwards, Megan Wind-Rotolo. *Bristol Myers Squibb, Princeton, NJ, USA*

Background Spatial patterns of CD8+ T cells in the tumor microenvironment are associated with clinical outcomes in patients with advanced solid tumors. However, attempts to quantify spatial topology are hindered by challenges in manual scoring, heterogeneous immune-cell infiltrates, and interpathologist variability. Artificial intelligence (AI)-powered analysis can quantify CD8 topology in a biologically meaningful, reproducible, and scalable way. Using an AI-driven algorithm, we retrospectively assessed CD8 topology as a biomarker of response to immunotherapy in patients with advanced melanoma.

Methods We trained a random forest classifier to predict CD8 topology using parenchymal and stromal CD8+ immune-cell measurements derived from a deep-learning platform (PathAI, Boston, MA). For model validation, pathologists manually classified CD8 immunohistochemistry (C8/144B, Agilent, Santa Clara, CA) in melanoma samples into inflamed (CD8+ cells in tumor parenchyma), excluded (CD8+ cells restricted to stroma), and desert (deficient in CD8+ cells) patterns. We explored the association with overall survival (OS) in a subset of patients with previously untreated metastatic melanoma who received nivolumab + ipilimumab (NIVO+IPI, n=102) or NIVO alone (n=107) in the CheckMate 067 phase 3 trial. Retrospective analysis of baseline AI-defined CD8 topology was performed alone and combined with manually scored programmed death ligand 1 (PD-L1) expression on tumor cells.

Results Classifier model predictions were concordant with manual scoring (determined by a consensus of pathologists) and non-inferior to the agreement between 2 pathologists, via Cohen's kappa coefficient $k=0.79$ and $k=0.65$, respectively. No statistically meaningful differences in outcomes were observed between CD8-excluded and CD8-inflamed phenotypes within the PD-L1 $\geq 1\%$ population. However, patients with PD-L1 $<1\%$ /CD8-excluded tumors exhibited longer median OS compared with those with PD-L1 $<1\%$ /CD8-inflamed (table 1). 38% (40/104) of PD-L1 $<1\%$ tumors were CD8-excluded. Within PD-L1 $<1\%$, patients with an excluded phenotype also exhibited lower frequency of severe adverse events (grade ≥ 3) than patients with inflamed phenotype following treatment: NIVO+IPI, 75% (n=20) vs 91% (n=11); NIVO, 61% (n=18) vs 80% (n=15). Compared with PD-L1 status, the composite biomarker (AI-classified CD8-excluded plus PD-L1 $\geq 1\%$) identified a larger group of patients who had greater survival benefit with NIVO+IPI or NIVO alone (table 2).

Abstract 387 Table 1 Immunotherapy outcomes by CD8+ topology in PD-L1 $<1\%$ melanoma

Treatment arm	NIVO+IPI		NIVO	
	PD-L1 $<1\%$, CD8-excluded (20)	PD-L1 $<1\%$, CD8-inflamed (12)	PD-L1 $<1\%$, CD8-excluded (20)	PD-L1 $<1\%$, CD8-inflamed (15)
Median OS (months)	>50	10.1	>50	25.8
OS HR (95% CI)	0.23 (0.09–0.61), $P<0.01$		0.68 (0.27–1.70), $P=0.41$	

In a subset of patients with melanoma and tumor cell PD-L1 expression $<1\%$ in the CheckMate 067 clinical trial, those with a CD8-excluded phenotype demonstrated longer overall survival compared with those with a CD8-inflamed phenotype when treated with NIVO \pm IPI.

Abstract 387 Table 2 Composite biomarker outcomes in Checkmate 067

Treatment arm (n)	PD-L1 $\geq 1\%$		Composite biomarker (PD-L1 $\geq 1\%$ plus CD8-excluded)	
	n (%)	OS HR (95% CI)	n (%)	OS HR (95% CI)
NIVO+IPI (102)	52 (51%)	0.50 (0.29–0.89), $P=0.017$	72 (71%)	0.35 (0.20–0.61), $P<0.001$
NIVO (107)	53 (50%)	0.46 (0.27–0.79), $P=0.005$	73 (68%)	0.37 (0.22–0.62), $P<0.001$

In patients with melanoma in the CheckMate 067 clinical trial, the composite biomarker (AI-classified CD8-excluded phenotype plus PD-L1 expression $\geq 1\%$) identified more biomarker-positive patients and demonstrated increased overall survival benefit vs PD-L1 status alone for patients treated with NIVO \pm IPI. Hazard ratios represent patients with a PD-L1 expression of $\geq 1\%$ compared with PD-L1 $<1\%$ or patients with a PD-L1 expression of $\geq 1\%$ and CD8-excluded phenotype compared with PD-L1 expression $<1\%$ and not CD8-excluded.

Conclusions This study explores the utility of combining AI-powered CD8 topology classifications with PD-L1 expression as a composite biomarker associated with immunotherapy response. In patients with PD-L1 $<1\%$ melanoma, median OS with NIVO+IPI was significantly longer in patients with CD8-excluded tumors than with an inflamed phenotype. Further studies are underway to identify mechanisms underlying responses to NIVO+IPI.

Acknowledgements We would like to thank the team at PathAI for development of the AI classifier, and Dako, an Agilent Technologies, Inc. company, for collaborative development of the PD-L1 IHC 28-8 pharmDx assay. Editorial support was provided by Emily Motola, PharmD, and Matthew Weddig of Spark Medica Inc.

Trial Registration ClinicalTrials.gov number NCT01844505

Ethics Approval The study protocol and all amendments were approved by local institutional review boards, and the protocol was conducted in accordance with the Declaration of Helsinki and Good Clinical Practice Guidelines, as defined by the International Conference on Harmonisation of Technical Requirements for Pharmaceuticals for Human Use. All patients provided written informed consent before enrollment.

<http://dx.doi.org/10.1136/jitc-2021-SITC2021.387>

388

A TRIAL TO EVALUATE THE SAFETY, IMMUNOGENICITY, AND CLINICAL ACTIVITY OF A HELPER PEPTIDE VACCINE PLUS PD-1 BLOCKADE (MEL64, PATHVACS: PD-1 ANTIBODY AND T-HELPER VACCINE AND CORRELATIVE STUDIES)

Craig Slingluff*, Kimberly Chianese-Bullock, Ileana Mauldin, Walter Olson, Kelly Smith, Lynn Dengel, Kathleen Haden, Elizabeth Gaughan, Varinder Kaur, William Grosh. *University of Virginia, Charlottesville, VA, USA*

Background A multipeptide vaccine containing 6 melanoma-associated peptides to stimulate helper T cells (6MHP) is safe and immunogenic and has clinical activity. A phase I/II trial was designed to evaluate safety and immunogenicity of 6MHP vaccines plus PD1 blockade.

Methods Participants with measurable advanced melanoma, age ≥ 18 years, and ECOG performance status 0–1 were administered 6MHP vaccine intradermally and subcutaneously in an incomplete Freund's adjuvant on days (D) 1, 8, 15, 43, 64, and 85. Pembrolizumab 200 mg was administered intravenously every 3 weeks for up to two years. Biopsies of accessible tumors at baseline and D22 were analyzed by multiparameter immunofluorescence histology. Primary endpoints were safety (CTCAE 4.03) and immunogenicity (ex vivo IFN γ ELISpot assay). Secondary and exploratory endpoints included changes in the tumor microenvironment (TME), and clinical outcomes.

Results Twenty-two eligible participants were enrolled and treated, including 6 naïve to PD-1 Ab and 16 anti-PD-1 Ab-experienced. Median follow-up was 20 months. Treatment-related adverse events (any grade) experienced by $>20\%$ were injection site reactions, fatigue, anemia, nausea, fever, bruising, and rash. Treatment-related dose limiting toxicities (grade 3 elevated AST, skin ulcer, or uveitis) were observed in 3 (14%), which did not cross the study safety bound. Objective clinical responses were observed in 23% (1 CR, 4 PR), including 4/6 anti-PD-1 Ab-naïve (67%) and one 1/16 anti-PD1 Ab-experienced (6%). Four participants (18%) had SD as best radiographic response (18%), all in the Ab-experienced cohort. T cell responses to 6MHP were detected in seven participants (32%) by week 13 and were associated with clinical response (CR/PR 80% vs. SD/PD 18%; $p = 0.01$). Overall survival was prolonged for anti-PD-1 Ab naïve vs experienced ($p = 0.0048$), for those with T cell response ($p = 0.045$, landmark analysis after week 13), and for those with objective response ($p = 0.0148$). TME evaluation in 12 participants revealed significant increases by D22 in the densities (per mm²) of CD8 + T cells ($p = 0.0186$), CD20+ B cells ($P = 0.002$), and Tbet+ cells ($p = 0.034$).

Conclusions In patients with advanced melanoma, combined treatment with the 6MHP vaccine plus pembrolizumab was safe, increased intratumoral T and B cells, as well as Th1 (Tbet+) cells, and induced T cell responses that were associated with objective response and with overall survival. The promising objective response rate and overall survival in patients naïve to PD1 blockade supports consideration of a larger study to assess definitive benefit in that clinical setting.

Acknowledgements We acknowledge the support of Merck for providing pembrolizumab at no charge, and the University of Virginia Cancer Center Support grant P30 CA044579 for support of shared resource facilities.

Trial Registration The clinical trial Mel64 (PATHVACS) is registered with Clinicaltrials.gov (NCT02515227).

Ethics Approval The clinical trial Mel64 (PATHVACS) was performed with IRB (#18174) and FDA approval (IND #10825) and is registered with Clinicaltrials.gov (NCT02515227). Written informed consent was obtained from each participant prior to participation in the study.

<http://dx.doi.org/10.1136/jitc-2021-SITC2021.388>

PHASE II OF CD40 AGONISTIC ANTIBODY SOTIGALIMAB (APX005M) IN COMBINATION WITH NIVOLUMAB IN SUBJECTS WITH METASTATIC MELANOMA WITH CONFIRMED DISEASE PROGRESSION ON ANTI-PD-1 THERAPY

¹Sarah Weiss, ¹Mario Sznol, ²Montaser Shaheen, ³Miguel-Ángel Berciano-Guerrero, ⁴Enriqueta Felip, ⁵Delys Rodríguez-Abreu, ⁶Ana María Arance, ⁷Valentina Boni, ⁸Gerald Linette, ⁸Lynn Schuchter, ⁹Maria Gonzalez-Cao, ¹⁰Nicholas Iannotti, ¹¹Apar Kishor Ganti, ¹²Ralph Hauke, ¹³Alfonso Berrocal, ¹⁴Erin Filbert, ¹Harriet Kluger*. ¹Yale University School of Medicine, New Haven, CT, USA; ²University of Arizona Cancer Center, Tucson, AZ, USA; ³Victoria University Hospital, Málaga, Spain; ⁴Vall d'Hebron University Hospital, Barcelona, Spain; ⁵Universidad de Las Palmas de Gran Canaria, Las Palmas, Spain; ⁶Hospital Clinic Barcelona, Barcelona, Spain; ⁷Hospital Universitario HM Sanchinarro, Madrid, Spain; ⁸University of Pennsylvania, Philadelphia, PA, USA; ⁹Dexeus University Hospital, Barcelona, Spain; ¹⁰Hem-Onc Associates of the Treasure Coast, Port Saint Lucie, FL, USA; ¹¹University of Nebraska Medical Center, Omaha, NE, USA; ¹²Nebraska Cancer Specialists, Omaha, NE, USA; ¹³University General Hospital of Valencia, Valencia, Spain; ¹⁴Apexigen, Inc., San Carlos, CA, USA

Background A significant number of melanoma patients treated with anti-PD-1 alone or in combination with anti-CTLA-4 have transient or no response to treatment. Sotigalimab is a CD40 agonist antibody with unique epitope specificity and Fc receptor binding profile for optimal therapeutic application. Preclinical studies suggest that sotigalimab can be combined with PD-1 blockade to trigger effective anti-tumor immunity. We conducted a multi-center, open label, Phase Ib-parallel arm phase II trial (NCT03123783) to evaluate the combination of sotigalimab with nivolumab in subjects with anti-PD-1/PD-L1 refractory metastatic melanoma.

Methods The study objective was to evaluate the efficacy and safety of sotigalimab in combination with nivolumab in anti-PD-1/PD-L1 refractory advanced melanoma patients. Subjects received sotigalimab (0.3mg/kg) combined with nivolumab (360mg) every 3 weeks. Thirty-eight subjects with unresectable or metastatic melanoma who had confirmed progressive disease during treatment with anti-PD-1 therapy (documented by 2 consecutive tumor assessments) were enrolled (evaluable for safety) and 33 subjects were evaluable for efficacy.

Results Six subjects had PR (including one unconfirmed PR) for an ORR of 18%. The mDOR was 18.7 months. Two subjects with PR received treatment for >2 years. Three of the six responding subjects remain off all therapy for ≥ 26 months, and one patient required stereotactic radiosurgery to a single brain lesion ten months after stopping therapy and has not required additional local or systemic therapy since. Three additional subjects had prolonged SD (12.6, 7.6, 6.2 months). The DCR was 48% and 33% of subjects experienced reduction in target lesions. Efficacy was observed in patients regardless of their tumor PD-L1 expression. The overall safety profile of the combination is consistent with the profiles of individual agents. The majority of AEs observed were of mild to moderate intensity (CTCAE Grade ≤ 2). The most commonly observed AEs were: pyrexia, chills, nausea, fatigue, pruritus, transaminitis, headache, asthenia, myalgia, rash, vomiting and arthralgia. There were no Grade 4 or 5 AEs related to study drugs. There were no treatment discontinuations due to AEs.

Conclusions The combination of sotigalimab and nivolumab demonstrated treatment benefit (tumor response or prolonged disease control) in anti-PD-1/PD-L1 refractory melanoma patients with an overall favorable safety and tolerability profile. Notably, a subset of patients remain in response off

treatment for ≥ 26 months. These results warrant further study of this combination in advanced, refractory melanoma.

Acknowledgements We extend our gratitude to the patients and their families who made this trial possible and the clinical study teams involved in this trial. We thank BMS for providing the nivolumab for this study.

Trial Registration NCT03123783

Ethics Approval This study was approved by the Institutional Review Boards at Yale University (#20170300), University of Nebraska Medical Center (#543-18-CB) and The Hospital Regional de Málaga (#19.03.1341E1-GHM).

<http://dx.doi.org/10.1136/jitc-2021-SITC2021.389>

Clinical Trials In Progress

390

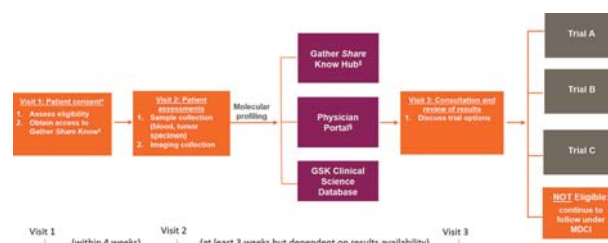
A GLOBAL, MOLECULAR DISEASE CHARACTERIZATION INITIATIVE (MDCI) IN ONCOLOGY CLINICAL TRIALS

¹Melissa Johnson*, ²Adrian Sacher, ²Marcus Butler, ³Hassane Zarour, ⁴Jeffrey Weber, ⁵Edward Garon, ⁶David Carbone, ⁷Arindam Dhar, ⁷Cristina Messina, ⁷Roma Patel, ⁷Kristin Blouch, ⁸Axel Hoos, ⁷Anne-Marie Martin. ¹*Sarah Cannon Research Institute LLC, Nashville, TN, USA;* ²*Princess Margaret Cancer Centre, Toronto, Canada;* ³*University of Pittsburgh Medical Center, Pittsburgh, PA, USA;* ⁴*NYU Grossman School of Medicine, New York, NY, USA;* ⁵*David Geffen School of Medicine, University of California, Los Angeles, Santa Monica, USA;* ⁶*The Ohio State University, Columbus, OH, USA;* ⁷*GlaxoSmithKline, Collegetown, PA, USA;* ⁸*GlaxoSmithKline (at the time of publication), Collegetown, PA, USA*

Background To address the heterogeneity of response to therapies, the oncology field is moving toward precision medicine (PM), with therapy tailored to a patient's disease. Biomarker assessment is now critical when screening for enrollment into clinical studies, such as for T-cell receptor therapies and combination studies, and determining status of a single analyte does not always correlate to clinical benefit.¹ This shift may increase enrollment screen-failure rates due to restrictive eligibility criteria (e.g., biomarker prevalence). For oncology patients, the need for timely treatment does not allow for a sequential, complex, and time-consuming screening process for each individual clinical trial. The design and data from studies such as Lung MAP have emphasized a need to change clinical trial screening. As we begin to target less common genomic and immunotherapy subtypes, comprehensive molecular characterization may lead to rapid delivery of therapies to patients while maximizing the quality of data.² The Molecular Disease Characterization Initiative (MDCI; GlaxoSmithKline Study 213299 [NCT04772053]) screens for multiple studies at once by collecting a baseline assessment of disease prior to treatment with different therapeutic modalities, and evaluating the patient's tumor and blood genetics. The MDCI creates a platform to accelerate the availability of new therapeutic options for patients through matched investigative and PM clinical trials, while building a scientific database to facilitate the investigation of biological mechanisms underpinning clinical outcomes.

Methods This multicenter study enrolls patients (N= 400) with advanced/metastatic malignancies, initially non-small cell lung cancer, to collect biospecimens for broad molecular profiling and examining the expression of specific antigens (e.g. NY-ESO-1, LAGE-1a), immune markers (e.g. ICOS, PD-L1), tumor-infiltrating immune cells, differentially expressed genes, and human leukocyte antigen (HLA). In this single-arm, non-interventional, molecular analysis study there is no administration of investigational product. MDCI interrogates patient tumor specimens using CLIA-validated immunohistochemistry assays coupled with next-generation sequencing of DNA and RNA. Blood is also collected for assessment (e.g. HLA typing, ctDNA). Based on this molecular profiling and previous medical history, potential clinical trial options are returned to both physicians and patients with the aim to reduce time-to-treatment (figure 1). Participants may be subsequently matched to ongoing clinical trials of novel immunotherapeutics or adoptive cell therapy. Patients who do not match to a clinical trial but continue with standard of care may choose longitudinal follow-up and re-analyses of disease at progression.

Acknowledgements Study 213299 (NCT04772053) is funded by GlaxoSmithKline.



Abstract 390 Figure 1 MDCI study design schema. *MDCI will be an optional protocol under select GSK oncology protocols. [†]Gather Share Know is an optional patient-facing portal where patients can view subsets of their results. [‡]Subset of data to be shared on Gather Share Know. §Patient's molecular profile and medical history will be compared against the eligibility criteria of select GSK oncology protocols to identify potential trial options. MDCI, Molecular Disease Characterization Initiative.

REFERENCES

- Blons H, Garinet S, Laurent-Puig P, Oudart JB. Molecular markers and prediction of response to immunotherapy in non-small cell lung cancer, an update. *J Thorac Dis* 2019;**11**(Suppl 1):S25–S36.
- Lam, Vincent K, Papadimitrakopoulou V. Master protocols in lung cancer: experience from lung master protocol. *Curr Opin Oncol* 2018;**30**:p92–97.

Ethics Approval The study was approved by Advarra Central IRB, approval date 4 January 2021.

<http://dx.doi.org/10.1136/jitc-2021-SITC2021.390>

BIOMARKER CORRELATES OF RESPONSE IN PATIENTS WITH ADVANCED MYXOID/ROUND CELL LIPOSARCOMA (MRCLS) TREATED WITH NY-ESO-1 TCR T CELLS (LETETRESGENE AUTOLEUCEL)

¹Gurpreet Kapoor*, ¹Stefan Zajic, ¹Sunil Suchindran, ¹Jaegil Kim, ¹Ioanna Eleftheriadou, ¹Anne Huff, ¹Michael Nathenson, ²Mihaela Druta, ³Brian Van Tine, ⁴Neeta Somaiah, ⁵David Liebner, ⁶Scott Schuetze, ⁷Sandra D'Angelo. ¹GlaxoSmithKline, Collegeville, USA; ²H. Lee Moffitt Cancer Center, Tampa, FL, USA; ³Washington University in St. Louis, St Louis, USA; ⁴University of Texas/MD Anderson Cancer Center, Houston, USA; ⁵The Ohio State University, Columbus, OH, USA; ⁶University of Michigan, Ann Arbor, USA; ⁷Memorial Sloan Kettering Cancer Center, New York, USA

Background This is an open label pilot study (NCT02992743) on letetresgene autoleucel (lete-cel; GSK3377794), an NY-ESO-1-specific autologous CD4+ and CD8+ T cells expressing a high affinity T-cell receptor which recognizes the NY-ESO-1 antigen epitope in complex with specific HLA- alleles A*02, which exhibited anti-tumor activity and manageable safety profiles in patients with advanced MRCLS based on interim analysis (IA) data.¹ Lymphodepletion has been shown to enhance the expansion, persistence, and homing of therapeutically infused T-cells, thereby potentiating therapeutic efficacy against malignant diseases.² Initial T-cell kinetics data from this study demonstrated that lymphodepletion regimen (LDR)-B robustly depleted lymphocytes at infusion and was trended with higher peak cell expansion (Cmax) vs. LDR-A. The peak expansion was significantly associated with weight-normalized transduced cell dose and trended with response.¹ Here, we will be discussing additional cell kinetics data and other exploratory biomarker correlates of response.

Methods Patients with advanced MRCLS were enrolled to 2 cohorts and received either planned A (N=10) or B (N=10) LDRs prior to letete-cel infusion (table 1). Response was assessed per RECIST v1.1. Transduced cell kinetics were measured by quantitative PCR of transgene vector copies in DNA from peripheral blood mononuclear cells (PBMCs). Serum cytokines (Meso Scale Discovery immunoassay) as pharmacodynamic (PD) markers of response and their association with T cell kinetics will be discussed. Phenotypic characterization of the cell product (pre- and post- infusion) via Flow cytometry using Cytek Aurora (23 color panel), to help understand correlation of response with engineered cell product attributes, will be presented. Potential biomarker correlates of clinical response were tested using generalized linear models.

Results Five out of 6 responders with available lab data exhibited robust lymphocyte depletion at infusion (0–25 cell/ μ L) and high Cmax (>50,000 vector copies/ μ g gDNA) with LDR. Only 6/14 non-responders exhibited low lymphocytes counts at infusion and high Cmax. LDR-B also induced strong depletion of monocytes at infusion (p=0.03) vs. LDR-A, but depletion of monocytes did not show association with response. Higher Cmax was correlated with exposure (AUC_{0–28d}) (Adj. R²=0.606). AUC_{0–28d} was a better predictor of response in patients receiving LDR-B (p=0.0182), with AUC_{0–28d} trending towards predicting response in the LDR-A cohort. AUC_{0–28d} was associated with tumor volume reduction (p=0.0569).

Abstract 391 Table 1

Cohort	NY-ESO-1 Expression	Planned Lymphodepletion Regimen	Response Rate (%)	Mean Transduced Cell Dose in Billions (Min, Max)	Mean (SD) Peak Persistence (vector copies/ μ g DNA)
Cohort 1 N=10	High • IHC score 2+ or 3+ in =50% of tumor cells	LDR-A: • Fludarabine: 30 mg/m ² IV on Days -7 to -5 • Cyclophosphamide: 600 mg/m ² IV on Days -7 to -5	2/10 (20%)	3.58 (1.01, 5.7)	94,097.62 (73,670.816)
Cohort 2 N=10	High • IHC score 2+ or 3+ in =50% of tumor cells	LDR-B: • Fludarabine: 30 mg/m ² IV Days -8 to -5 • Cyclophosphamide: 900 mg/m ² IV on Days -7 and -5	4/10 (40%)	4.42 (2.8, 6.3)	121,956 (66,302.35)

IHC, immunohistochemistry; IV, intravenous; LDR, lymphodepletion regimen; SD, standard deviation.

Conclusions Exposure–response analysis of this study reveals that efficacy appears to be driven by weight-normalized transduced cell dose and LDR via AUC_{0–28d}. Higher AUC_{0–28d} was correlated with Cmax and maximum tumor volume reduction. **Acknowledgements** This study (208469; NCT02992743) was funded by GlaxoSmithKline.

Trial Registration NCT02992743

REFERENCES

1. D'Angelo SP, et al. *J Clin Oncol* 2021;39:15_suppl:11521.
2. Bechman, Maher. *Expert Opin Biol Ther* 2021;21(5):627–637.

Ethics Approval This study was approved by institutional review boards (IRB) at the six participating sites.

<http://dx.doi.org/10.1136/jitc-2021-SITC2021.391>

392

A PHASE 1A/B STUDY OF IK-175, AN ORAL AHR INHIBITOR, ALONE AND IN COMBINATION WITH NIVOLUMAB IN PATIENTS WITH LOCALLY DVANCED OR METASTATIC SOLID TUMORS AND UROTHELIAL CARCINOMA

¹Meredith McKean, ²Jason Luke*, ³Nehal Lakhani, ⁴Babar Bashir, ⁵David Aggen, ⁶Alan Tan, ⁷Katherine Kacena, ⁸Lei Wang, ⁹Marissa Timothy, ⁸Sergio Santillana. ¹Tennessee Oncology, Nashville, TN, USA; ²UPMC Hillman Cancer Center, Pittsburgh, PA, USA; ³START Midwest, Grand Rapids, MI, USA; ⁴Thomas Jefferson University, Philadelphia, PA, USA; ⁵Memorial Sloan Kettering Cancer Center, New York, NY, USA; ⁶Rush University, Chicago, IL, USA; ⁷Katherine Kacena Consulting, Natick, MA, USA; ⁸Ikena Oncology, Boston, MA, USA

Background Aryl Hydrocarbon Receptor (AHR) is a transcription factor that regulates the activity of multiple innate and adaptive immune cells after binding to several endogenous and exogenous ligands, including kynurenine, generated from tryptophan by IDO1 and TDO2. Binding of kynurenine to AHR leads to a net immunosuppressive tumor microenvironment, making AHR an attractive therapeutic target in multiple cancer types. IK-175 is a selective, small molecule AHR inhibitor being developed as an oral (PO) agent. In human T-cells, IK-175 induces an activated T-cell state, interleukin (IL)-22 gene expression, and leads to an increase in proinflammatory cytokines, such as IL-2 and IL-9. IK-175 demonstrates antitumor activity as a single agent or in combination with checkpoint inhibitors in multiple mouse tumor models.¹ AHR immunohistochemistry (IHC) tumor microarray analysis across 15 different tumor types revealed that bladder cancer has the highest level of AHR protein expression and AHR nuclear localization, an indicator of active AHR signaling. Therefore, nuclear AHR in urothelial carcinoma tumors is being investigated for potential predictive clinical benefit with IK-175.

Methods This is a first-in-human, phase 1a/b, open-label, multicenter, dose-escalation and expansion study to evaluate the safety, tolerability, pharmacokinetics (PK), pharmacodynamics (PD), and preliminary antitumor activity of IK-175 administered PO daily in 21 or 28 day-cycle as a single agent, and in combination with nivolumab, 480 mg q4w on Day 1 of every cycle, in 93 adult patients with advanced solid tumors (dose escalation) and urothelial carcinoma (dose expansion) in both treatment arms. Key eligibility criteria include patients with histologically confirmed solid tumors (including urothelial carcinoma) who have locally recurrent or metastatic disease that have progressed on or following all standard of care therapies deemed appropriate by the treating physician. Primary endpoints include dose-limiting toxicities and treatment-emergent adverse events. Key secondary endpoints include IK-175 PK profile on both treatment arms, PD of IK-175, and preliminary efficacy. The study will explore tumor AHR nuclear localization by IHC as a predictive biomarker in patients with urothelial carcinoma in both treatment arms. A minimum of 10 patients having a positive AHR nuclear localization test (cutoff for positive AHR is 65% tumor cells positive for 2+/3 + nuclear AHR by a validated IHC assay) will be enrolled in the combination arm. Exploratory biomarkers of IK-175 mediated PD effects, PK-PD correlations, and correlative analyses of predictive and PD measurements with response and resistance will be performed. The study started in January 2020 and is ongoing

Acknowledgements Ikena Oncology would like to recognize and express gratitude to Dr. Jason Sager for his contributions to the implementation of this trial.

Trial Registration ClinicalTrials.gov registration: NCT04200963

REFERENCE

1. McGovern K, Castro A, Cavanaugh J, Discovery of clinical candidate IK-175, a selective orally active AHR antagonist. *SITC* 2020, poster presentation.

<http://dx.doi.org/10.1136/jitc-2021-SITC2021.392>

A PHASE 1/2 STUDY OF SBT6050 COMBINED WITH TRASTUZUMAB DERUXTECAN (T-DXd) OR TRASTUZUMAB AND TUCATINIB WITH OR WITHOUT CAPECITABINE IN PATIENTS WITH HER2-EXPRESSING OR HER2-AMPLIFIED CANCERS

<http://dx.doi.org/10.1136/jitc-2021-SITC2021.393>

¹Samuel Klemperer*, ²John Strickler, ³Lindsey Gourley, ³Celine Jacquemont, ³Vinona Bhatia, ³Naomi Hunder, ³Valerie Odegard, ⁴Sarina Piha-Paul. ¹Massachusetts General Hospital, Boston, MA, USA; ²Duke University Health System, Durham, NC, USA; ³Silverback Therapeutics, Inc., Seattle, WA, USA; ⁴University of Texas, MD Anderson, Houston, TX, USA

Background SBT6050 is a novel therapeutic comprising a selective small molecule toll-like receptor 8 (TLR8) agonist linked to the HER2-directed monoclonal antibody pertuzumab, allowing for combination with trastuzumab-based agents and regimens. SBT6050 is designed to activate myeloid cells in tumors expressing moderate to high levels of HER2. TLR8 agonism directly activates myeloid cells, including macrophages and dendritic cells (DCs), and secondarily activates NK and T cells, inducing a broad spectrum of anti-tumor immune mechanisms. SBT6050 is currently being tested as a single agent and in combination with checkpoint inhibitors (NCT04460456). Initial results show early evidence of anti-tumor effects, activation of myeloid and NK/T cells, and a safety profile consistent with an immune activator that is generally non-overlapping with that of T-DXd or tucatinib-based regimens. A strong scientific rationale supports the combination of SBT6050 with T-DXd and SBT6050 with trastuzumab and tucatinib ± capecitabine. Both treatment regimens drive tumor cell death and release of tumor neoantigens. SBT6050 can enhance tumor neoantigen presentation and subsequent activation of T cell responses through its direct activation of DCs. SBT6050 combined with T-DXd or trastuzumab and tucatinib ± capecitabine is postulated to drive increased anti-tumor T cell responses. In addition, T-DXd and trastuzumab support antibody-dependent cell mediated cytotoxicity (ADCC) and antibody-dependent cellular phagocytosis (ADCP) and SBT6050 can enhance both functions. SBT6050 activates myeloid cells to secrete cytokines that amplify ADCC by NK cells. Additionally, SBT6050 activation downmodulates SIRPα on the surface of myeloid cells which can increase ADCP through attenuation of the CD47-SIRPα interaction. Consistent with this mechanism of action, in preclinical studies in mice, the combination of trastuzumab and a mouse surrogate of SBT6050 led to enhanced activity in the HER2-positive NCI-N87 human tumor xenograft model compared to either agent alone.

Methods Protocol SBT6050-201 is a phase 1/2, open-label, dose-escalation and expansion study evaluating SBT6050 in combination with either T-DXd (Part 1) or tucatinib and trastuzumab +/- capecitabine (Part 2). Eligible patients are at least 18 years old, have HER2-positive metastatic breast cancer, gastric/GEJ cancer, colorectal cancer, or HER2-expressing or amplified NSCLC, and have received at least one prior therapy for metastatic disease. Patients will receive SBT6050 subcutaneously q3wk starting at a dose with demonstrated pharmacodynamic activity in phase 1. Pharmacodynamic markers of myeloid and NK/T cell activation will be assessed in peripheral blood and on-treatment tumor biopsies. Circulating tumor DNA will be evaluated as an exploratory assessment.

Ethics Approval This clinical study has not yet obtained ethics approval or started enrollment. All participants will be required to give informed consent before taking part.

DETECTION OF VIRAL ANTIGEN AND IMMUNE ACTIVATION AFTER INTRA-TUMOR INJECTION OF CAN-3110 (ICP-34.5 EXPRESSING HSV-1 ONCOLYTIC VIRUS) IN PATIENTS WITH RECURRENT HIGH-GRADE GLIOMA

¹Francesca Barone*, ²Sean Lawler, ¹Laura Aguilar, ¹Jessica Dwyer, ¹Brian Guzik, ³Isaac Soloman, ²Hiroshi Nakashima, ³Daniel Triggs, ²Abigail Tianai Zhang, ⁴Yu Zeng, ⁴Jared Woods, ³James Grant, ⁴David Reardon, ⁴Patrick Wen, ³Eudocia Quant Lee, ⁴Keith Ligon, ⁴William Pisano, ²Scott Rodig, ⁵Mario Suva, ⁴Kai Wucherpfennig, ⁴Sascha Marx, ⁶Simon Gritsch, ⁴Nathan Mathewson, ⁴Mariano Severgnini, ⁴Anita Giobbie-Hurder, ¹David Krisky, ¹Estuardo Aguilar-Cordova, ¹Paul Tak, ³E Antonio Chiocca. ¹*Candel Therapeutics, Inc., Needham, MA, USA*; ²*Brigham and Women's Hospital, Boston, MA, USA*; ³*Brigham and Women's Hospital, Boston, MA, USA*; ⁴*Dana-Farber Cancer Institute, Boston, MA, USA*; ⁵*Massachusetts General Hospital, Boston, MA, USA*; ⁶*Massachusetts General Hospital, Boston, MA, USA*

Background Recurrent high-grade glioma (HGG) represents a significant clinical unmet need with expected survival between 6 to 9 months. Oncolytic viruses are a new therapeutic approach for solid tumors that deploy oncolytic activity combined with local and systemic immune activation. CAN-3110 (rQNestin34.5v2) is an oncolytic herpes simplex virus (HSV), modified to encode the HSV1 ICP34.5 protein under control of the nestin promoter. Selective expression of nestin in brain tumors confers tumor-restricted replication of CAN-3110. We conducted an open-label dose-escalation phase 1 clinical trial in patients with recurrent HGG to evaluate safety, tolerability, and immunological changes after CAN-3110 treatment.

Methods Thirty patients with biopsy-confirmed recurrent HGG were enrolled from September 2017 to February 2020. CAN-3110 was injected intratumorally starting at 1x10⁶ plaque forming units (pfu) and dose-escalated by half log to 1x10¹⁰ pfu. Patients also received standard of care. Peripheral blood mononuclear cells (PBMCs), plasma and tumor samples were collected for analysis at different time-points post treatment. We evaluated HSV antigen expression in tumor tissue. RNA sequencing and T cell receptor (TCR) rearrangement analysis was performed in matched tissue and PBMCs. Cytokine profiling was completed in 29 patients at baseline, day 2, and day 28 post treatment.

Results Eighteen patients were recruited at their first recurrence and 12 at the second recurrence. Three patients presented with multifocal disease. Tumor volume ranged from 357.4 to 54,036.1mm³ (median 7,733.9mm³, SDV 15,610.2). CAN-3110 was well-tolerated with no dose-limiting toxicity. Median overall survival was 11.7 months. We demonstrated persistence of HSV antigen and CD8+ T cell infiltrates at the site of injected tumor. Preliminary analysis revealed expansion of shared TCR clonotypes and upregulation of pro-inflammatory genes in post-treatment tumors and peripheral blood samples. Longitudinal modeling of cytokine profiling demonstrated increased levels of IL-6, VEGF alpha, CCL2 and IL1-RA and a decrease in GCP-2 levels at day 2 post-treatment ($p < 0.05$). Significant correlations were observed between CXCL2 and CXCL6 ($r=0.89$ and $r=0.95$, respectively, at day 2 and day 28 post treatment; $p < 0.05$), CCL2 and CXCL6 ($r=0.73$ and $r=0.61$ at days 2 and 28 post treatment; $p < 0.05$) and between CCL2 and CXCL2 ($r=0.68$, $p < 0.05$ at day 2 post treatment) in patients surviving more than 12 months.

Conclusions Intratumoral administration of CAN-3110 appears well-tolerated in recurrent HGG. Histologic, molecular, and cytokine analyses demonstrate persistence of viral antigen as well as local and systemic immune activation after treatment.

Ethics Approval The study was approved by the Office for Human Research Studies at Dana-Farber Cancer Institute, Protocol Number 16-557.

<http://dx.doi.org/10.1136/jitc-2021-SITC2021.395>

NT-17, A LONG-ACTING INTERLEUKIN-7, PROMOTES EXPANSION OF CD8 T CELLS AND NK CELLS AND IMMUNE ACTIVATION IN PATIENTS WITH NEWLY DIAGNOSED HIGH-GRADE GLIOMAS AFTER CHEMORADIATION

¹Alice Zhou*, ¹Michael Rettig, ¹Jennifer Foltz, ¹Jingqin Luo, ¹Omar Butt, ¹Chai Avvaru, ¹Ruth Katumba, ¹Albert Kim, ¹Gavin Dunn, ¹Christopher Abraham, ²Se Hwan Yang, ²Jean Fan, ²Byung Ha Lee, ²NgocDiep Le, ¹George Ansstas, ¹Tanner Johanns, ¹Jiayi Huang, ¹Milan Chheda, ¹Todd Fehniger, ¹Jian Campian. ¹Washington University in Saint Louis, St. Louis, MO, USA; ²NealImmuneTech, Inc., Rockville, MD, USA

Background Lymphopenia is common after chemoradiation for treatment of high-grade gliomas (HGG) and is associated with reduced survival.¹ Interleukin-7 (IL-7) promotes T-cell maturation and proliferation and is inappropriately low in lymphopenic patients with HGG.² We previously demonstrated that first-in-class long-acting IL-7, NT-17 (efineptakin alfa), reverses lymphopenia and improves survival in murine glioma models.³ This study reports the correlative immune changes after NT-17 treatment in patients with newly diagnosed HGG in a Phase I/II clinical trial.

Methods Enrolled patients had newly diagnosed HGG treated with concurrent radiotherapy (RT) and temozolomide (TMZ) plus adjuvant TMZ every 4 weeks. NT-17 was administered intramuscularly 1 week after completion of RT/TMZ and then every 12 weeks, for up to 4 total doses. Phase I utilized the 3+3 design to identify the maximum tolerated dose (MTD). Phase II is a double-blinded, placebo-controlled study with 10 patients in each arm. Immune profiling of patients from the Phase I study was performed with multiparametric flow cytometry and multiplex cytokine analysis.

Results Phase I was completed with 19 patients. The most common adverse events were grade 1 or 2 injection site reactions (42%). Two patients had dose-limiting toxicities at 960 µg/kg (grade 3 elevated alanine aminotransferase and grade 3 back pain), prompting the selection of MTD as 720 µg/kg. Preliminary analysis of Phase I subjects demonstrated dose-dependent increases in absolute lymphocyte count (ALC; 1.3X-4.1X fold increase from pre-therapy measurements) that peaked at week 4, before adjuvant TMZ. Flow cytometry analysis of peripheral blood showed a significant increase in the frequency of CD8+ T-cells, CD4+ T-cells, and CD56bright natural killer (NK) cells after NT-17 administration. There was no change in B cell counts. Expression of the IL-7 receptor (CD127) was downregulated on most immune subsets within 1 week after NT-17 administration and recovered to baseline by week 4. Serum cytokine analysis showed a rapid and significant increase in tumor necrosis factor (TNF), chemokine ligand 9 (CXCL9), and a trend to higher interferon-gamma (IFNγ), 1 week after NT-17 administration.

Conclusions NT-17 is well tolerated when administered after RT/TMZ for HGG patients. NT-17 administration prompted an increase in ALC, especially cytotoxic T-cells and NK cells. We also observed rapid increases in key cytokines and chemokines, suggesting immune activation. These findings provide insight into the mechanism of action for NT-17. Phase II enrollment and additional immune profiling correlates are ongoing.

Trial Registration NCT03687957

REFERENCES

1.. Mendez JS, Govindan A, Leong J, Gao F, Huang J, Campian JL. Association between treatment-related lymphopenia and overall survival in elderly patients with newly diagnosed glioblastoma. *J Neurooncol* 2016;**127**:329.

- 2.. Campian JL, Ye X, Gladstone DE, Ambady P, Nirschl TR, Borrello I, Golightly M, King KE, Holdhoff M, Karp J, Drake CG, Grossman SA. Pre-radiation lymphocyte harvesting and post-radiation reinfusion in patients with newly diagnosed high grade gliomas. *J Neuro-Oncology* 2015 1242. 2015;**124**:307–316.
- 3.. Ghosh S, Yan R, Thotala S, Jash A, Mahadevan A, Hu T, Lee B, Yang SH, Hallahan D, Chheda M, Thotala D, Campian J. 565 a novel long-acting interleukin-7 agonist, NT-17, increases cytotoxic CD8+ T cells and enhances survival in mouse glioma models. *J Immunother Cancer* 2020;**8**(Suppl 3):A599–A599.

Ethics Approval This study was approved by Washington University's ethics board (the Human Research Protection Office); approval number 201810185. Study participants provided written informed consent.

<http://dx.doi.org/10.1136/jitc-2021-SITC2021.396>

397

**A PHASE I/II TRIAL OF INTRACEREBROVENTRICULAR
177LU DTPA OMBURTAMAB RADIOIMMUNOTHERAPY
FOR LEPTOMENINGEAL METASTASIS FROM SOLID
TUMORS**

¹Elena Pentsova*, ²Maria Düring, ²Charlotte Lybek Lind, ²John Rømer Nielsen. ¹Memorial Sloan Kettering Cancer Center, New York, NY, USA; ²Y-mAbs Therapeutics, Inc., Hørsholm, Denmark

Background Leptomeningeal metastasis (LM) from solid tumors may be diagnosed in approximately 10% of patients with metastatic cancer and can occur with virtually all malignant tumors. Median overall survival (OS) is poor and limited to a few months with LM-directed treatment, including available targeted therapy, immunotherapy and radiation therapy. Omburtamab specifically binds to B7-H3 (CD276), a transmembrane glycoprotein of the immunoglobulin superfamily. The limited expression of B7-H3 on normal cells, including normal brain, combined with the broad expression in various types of solid tumors, makes B7-H3 a target for radioimmunotherapy of LM from solid tumors. In this first-in-human trial the safety and efficacy of intracerebroventricular administration of radiolabeled omburtamab, ¹⁷⁷Lu-DTPA-omburtamab, will be evaluated in patients with LM from ductal or lobular breast cancer, non-small cell lung cancer, or melanoma.

Methods This is an open-label phase I/II study. Part 1 is a dose-escalation phase to be conducted at ~4 sites (US/Europe) with a primary objective of identifying the maximum tolerated dose and/or recommended phase II dose for Part 2 (RP2D). It will follow a 3+3 design with pts receiving up to five 5-week cycles of ¹⁷⁷Lu-DTPA-omburtamab. Part 2 is a cohort-expansion phase at ~9 sites (US/Europe) in which a maximum of 48 patients in 3 cohorts (ductal or lobular breast cancer [cohort A], non-small cell lung cancer [cohort B], and melanoma [cohort C]) with up to 16 patients in each will receive up to five 5 week cycles of treatment with intracerebroventricular ¹⁷⁷Lu DTPA omburtamab at the RP2D determined in Part 1. The primary objective of Part 2 is to establish the safety of repeat doses of ¹⁷⁷Lu-omburtamab. Additional objectives of Parts 1/2 include the evaluation of absorbed radiation doses, PK profile, investigator-assessed response, duration of response, progression-free survival, and OS. Key inclusion criteria include diagnosis of either ductal or lobular breast cancer, non-small cell lung cancer, or malignant melanoma and diagnosis of recurrent or refractory LM; prior standard of care treatment of leptomeningeal disease; acceptable hematological, liver and kidney status; and a life expectancy of >2 months. The study has been approved by each institution's ethics board, and patients provided informed consent before taking part.

Trial Registration NCT04315246

Ethics Approval The study has been approved by each institution's ethics board, and patients provided informed consent before taking part.

<http://dx.doi.org/10.1136/jitc-2021-SITC2021.397>

NEOIRX: A PHASE II TRIAL OF LOCOREGIONAL CYTOKINE THERAPY TO PROMOTE IMMUNOLOGIC PRIMING AND CLINICAL RESPONSE TO NEOADJUVANT PEMBROLIZUMAB PLUS CHEMOTHERAPY IN TRIPLE NEGATIVE BREAST CANCER (TNBC)

<http://dx.doi.org/10.1136/jitc-2021-SITC2021.398>

¹Katherine Sanchez*, ²Alison Conlin, ³Parvin Peddi, ²Sasha Stanton, ⁴Janet Ruzich, ²Kelly Perlewitz, ²Yaping Wu, ²Nicole Moxon, ²Staci Mellinger, ²Zhaoyu Sun, ²William Redmond, ²David Page. ¹Baylor College of Medicine, Houston, TX, USA; ²Providence Cancer Institute, Portland, OR, USA; ³St John Cancer Institute, Santa Monica, CA, USA; ⁴Providence Cancer Institute Newberg, Clackamas, OR, USA

Background Background: The FDA has approved pembrolizumab in combination with neoadjuvant chemotherapy (doxorubicin, cyclophosphamide, paclitaxel [ACT], and carboplatin) for stage II/III TNBC, on the basis of improved event free survival (EFS) and pathologic complete response (pCR) rate in the Keynote-522 study.¹ Novel combination immunotherapy strategies may further improve outcomes and allow the opportunity to de-escalate the chemotherapy backbone, potentially mitigating grade III/IV toxicities which occurred in 81% of recipients. We have previously reported safety and feasibility of pre-operative IRX-2, a novel cytokine biotherapeutic, that is administered locoregionally in the peri-areolar tissue to enhance the immune microenvironment within the sentinel lymph nodes, the putative site of antigen presentation.² In this phase Ib study, pre-operative IRX-2 was safe and was associated with increased tumor infiltrating lymphocytes (sTILs, by H&E and multispectral immunofluorescence [mIF]), PD-L1 expression (Ventana SP142 assay, mIF), and lymphocyte activation (by RNA sequencing). Similar effects were observed in a pre-operative head and neck carcinoma trial. These findings support further study of IRX-2 in combination with anti-PD-1 in early stage TNBC.

Methods

Methods neoIRX is an open-label, phase II trial to evaluate the clinical and immunological activity of induction IRX-2 plus pembrolizumab, followed by de-escalated chemotherapy (ACT) and pembrolizumab as neoadjuvant therapy in TNBC. Patients are randomized to receive pembrolizumab induction (single dose 200mg IV, n=15), versus pembrolizumab + IRX-2 induction (1mL SQ x 2 daily, x 10 days, n=15), followed by research biopsy. All patients will then receive neoadjuvant pembrolizumab plus ACT every three 3 weeks. Eligible subjects will have previously untreated, resectable stage II/III TNBC. The primary endpoint is pCR. The secondary endpoint is safety. On-treatment biopsies will permit a prospective, randomized validation of previously reported immunomodulatory effects of IRX-2 (sTILs, PD-L1, lymphocyte RNA signatures). As of 7/28/2021, n=7/30 subjects are enrolled (Providence Cancer Institute, Portland, OR, Providence St. John's Cancer Institute, Santa Monica, CA, Baylor Medicine, Houston, TX).

Trial Registration NCT04373031

REFERENCES

1. Schmid PN. *Engl J Med* 2020; **382**:810–821.
2. Page DB. *Clinical Cancer Research* 26.7(2020):1595–1605.

Ethics Approval The study protocol was approved by the Providence Portland Medical Center IRB committee and was conducted in accordance with the ethical standards established by the Declaration of Helsinki, PH&S IRB# 2019000486. Written informed consent was obtained for all trial participants.

A PHASE II STUDY OF NIVOLUMAB, IPILIMUMAB, PLUS ANDROGEN RECEPTOR BLOCKADE WITH BICALUTAMIDE TO ENHANCE THYMIC T-CELL PRODUCTION AND IMMUNOTHERAPY RESPONSE IN METASTATIC BREAST CANCER

¹David Page, ²Krystle Collins, ¹Brie Chun*, ¹Zhaoyu Sun, ¹Yoshinobu Koguchi, ¹William Redmond, ¹Maritza Martel, ³Yaping Wu, ¹Nicole Moxon, ¹Staci Mellinger, ¹Walter Urba, ⁴Ayca Gucalp, ⁵Tiffany Traina. ¹Earle A. Chiles Research Institute, Providence Cancer Institute, Portland, OR, USA; ²Providence Cancer Institute, Portland, OR, USA; ³Earle A. Chiles Research Institute, Prov, Portland, OR, USA; ⁴Memorial Sloan Cancer Center, New York, NY, USA; ⁵Memorial Sloan Kettering Cancer Center, New York, NY, USA

Background It has previously been shown that immune checkpoint blockade (ICB) with anti-programmed death 1/ligand 1 (anti-PD-1/L1) improves survival when combined with chemotherapy in PD-L1-positive first-line triple-negative metastatic breast cancer (MBC). Given the lower efficacy of ICB in hormone receptor positive (HR+) or PD-L1-negative disease, and in later lines of therapy, novel combinations are necessary. Dual ICB with nivolumab (anti-PD-1) and ipilimumab (anti-CTLA-4) has shown success in other solid tumors but has not been extensively studied in MBC. Furthermore, MBCs often express the androgen receptor (AR), which can be targeted to modulate immune response. AR blockade may stimulate thymic production of naïve T-cell clones by modulating the Notch pathway,¹ whereas ICB can amplify the immune activity of recent thymic emigrants by blocking PD-1-mediated peripheral tolerance.²

Methods This is an open-label, Simon 2-stage phase II trial investigating the dual ICB (nivolumab 240mg IV q2w; ipilimumab 1mg/kg IV q6w) and AR blockade (bicalutamide, 150mg PO daily) in MBC. Two cohorts will be studied: AR-positive TNBC [> 1% by IHC, constituting ~50% of TNBCs]; and HR+ MBC (of which the great majority are AR-positive). Eligible patients must have RECIST1.1 measurable disease, Eastern Cooperative Oncology Group performance score 0 or 1, adequate hematological/hepatic function, and received no more than 1 prior course of non-curative chemotherapy. Target accrual is n=15 per arm (stage I), with a maximum of 46 patients per cohort. Current cohort accrual n=15 HR+ and n=5 TNBC. The primary endpoint is week 24 clinical benefit by iRECIST criteria, with success defined as >20% improvement over historical control (30% per EMBRACE clinical trial).³ Safety will be evaluated by CTCAE v4.0. Biomarkers of recent thymic activation will be evaluated via quantitative deep sequencing of T-cell receptors (TcR, ImmunoSEQ assay), TcR excision circles (TRECs), and flow cytometry using markers for recent thymic emigration (CD3+CD45RA+CD45RO-CD31+)

Trial Registration NCT03650894. The trial is open at Providence Cancer Institute (Portland, OR) and Memorial Sloan Kettering Cancer Center (New York, NY).

REFERENCES

1. Velardi E, Tsai JJ, Holland AM, et al. Sex steroid blockade enhances thymopoiesis modulating notch signaling. *J Exp Med* 2014;**211**(12):2341–49.
2. Thangavelu G, Parkman JC, Even CL, et al. Programmed death-1 is required for systemic self-tolerance in newly generated T cells during the establishment of immune homeostasis. *Journal of autoimmunity* 2011;**36**(3–4):301–12.
3. Kaufman PA, Awada A, Tweles C, et al. Phase III open-label randomized study of eribulin mesylate versus capecitabine in patients with locally advanced or metastatic breast cancer previously treated with an anthracycline and a taxane. *J Clin Oncol* 2015;**33**(6):594–601.

Ethics Approval This study was approved by the IRB department and Providence Portland Medical Center, Clinical Trials Department for study NCT03650894.

Consent Written, informed consent is obtained from each participant.

<http://dx.doi.org/10.1136/jitc-2021-SITC2021.399>

PERSISTENCE AND TISSUE DISTRIBUTION OF AGENT-797 – A NATIVE ALLOGENEIC iNKT CELL-THERAPY DRUG PRODUCT

¹Marco Purbhoo*, ¹Burcu Yigit*, ¹Darrian Moskowitz, ²Min Lim, ²Irina Shapiro, ²Ayat Alsaraby, ¹Xavier Michelet, ¹Marc Van Dijk. ¹*Mink Therapeutics, Abingdon, UK*; ²*Agenus, Lexington, MA, USA*

Background Invariant Natural Killer T (iNKT) cells are key effectors and regulators of immune responses, making them an ideal immunotherapy. There is a paucity of evidence describing the persistence and trafficking of these cells in humans to inform the optimal clinical application. Here, we describe the development of a murine Xenograft model for the study of an unmodified human iNKT cell therapy (Agent-797) and present data on the persistence and tissue distribution of human iNKT cells in this model. We further describe the development and validation of a digital PCR-based methodology to track unmodified allogeneic human iNKT cells in blood and tissue and present exploratory clinical data on iNKT cell persistence in patients with cancer and viral ARDS treated with Agent-797.

Methods Persistence and tissue distribution of ex-vivo expanded human iNKT cells was investigated in immune compromised mice (NOG), as well as in NOG mice expressing human IL15 (NOG-hIL15), a key cytokine promoting iNKT cell survival. Persistence of iNKT cells was determined over a 35-day period, with takedowns on day 1, 7, 14, 21 and 35. iNKT cells were phenotyped for activation markers by flow cytometry. An assay based on Imegen Quimera digital PCR technology was developed and validated to quantify human iNKT in an allogeneic setting. We employed this assay to measure persistence of Agent-797 drug product in patients participating in clinical trials using iNKT cell-based immunotherapy in viral ARDS (NCT04582201) or multiple myeloma (NCT04754100).

Results Human IL15 was essential for the engraftment and persistence of human iNKT cells in NOG mice. Following injection, iNKT cells located to the blood, lung, liver, spleen, and bone marrow. iNKT cells persisted most prominently in bone marrow, where they demonstrated an activated phenotype. In mice challenged with hematological tumor cells (ALL cell line NALM6 expressing CD1d) persistence of iNKT cells in blood was prolonged. Initial data from human trials confirmed rapid translocation from peripheral blood of this tissue resident immune cell population following infusion of Agent-797.

Conclusions We established a murine xenograft model and digital PCR-based methodology to characterize the persistence, trafficking, and efficacy of native allogeneic human iNKT cell-based products. Our models recapitulated the human iNKT distribution and demonstrated iNKTs induced preclinical efficacy in a tumor model. We further successfully developed a validated methodology to track unmodified allogeneic iNKT cells in humans.

Trial Registration NCT04582201 and NCT04754100

Ethics Approval All procedures performed in studies involving human participants were in accordance with the ethical standards of the institutional and/or national research committee and with the 1964 Helsinki declaration and its later amendments or comparable ethical standards

<http://dx.doi.org/10.1136/jitc-2021-SITC2021.400>

402

PEGASUS GI, A PLATFORM STUDY OF SAR444245 (THOR-707, A PEGYLATED RECOMBINANT NON-ALPHA IL2) WITH ANTI-CANCER AGENTS OF PARTICIPANTS WITH ADVANCED AND METASTATIC GASTROINTESTINAL CANCER

¹William Harris, ²Adyb Baakili*, ³Yoon-Koo Kang, ²Brigitte Demers, ²Fatima-Zohra Menas, ²Alice Gosselin, ⁴Giovanni Abbadessa, ⁵Eric Van Cutsem. ¹University of Washington School of Medic, Seattle, WA, USA; ²Sanofi-Aventis, Vitry-sur-Seine, France; ³University of Ulsan College of Medicine, Seoul, Korea, Republic of; ⁴Sanofi, Cambridge, MA, USA; ⁵University of Leuven, Leuven, Belgium

Background SAR444245 (THOR-707) is a recombinant human IL-2 molecule that includes a PEG moiety irreversibly bound to a novel amino acid via click chemistry to block the alpha-binding domain while retaining near-native affinity for the beta/gamma subunits. In animal models, SAR444245 showed anti-tumor benefits, but with no severe side effects, both as single agent and when combined with anti-PD1 comparing with historical data from aldesleukin. Preclinical study demonstrated SAR444245 enhances ADCC function of cetuximab. The HAMMER trial, which is the FIH study, shows preliminary encouraging clinical results: initial efficacy and safety profile with SAR444245 monotherapy and in combination with pembrolizumab or with cetuximab support a non-alpha preferential activity, validating preclinical models. The Pegasus GI Ph 2 study will evaluate the clinical benefit of SAR444245 in combination with pembrolizumab or cetuximab for the treatment of participants with advanced or metastatic gastrointestinal cancer [esophageal squamous cell carcinoma (ESCC), gastric cancer (GC) or gastro-esophageal junction adenocarcinoma (GEJ), Hepatocellular carcinoma (HCC) or colorectal cancer (CRC)]

Methods Pegasus GI will enroll approximately 280 patients in 7 separate cohorts concurrently (4 cohorts) or sequentially (3 cohorts). In cohort A, 2–3 line (L) ESCC participants who have progressed after checkpoint inhibitor (CPI)-based therapy will receive SAR444245 + pembrolizumab. In cohorts B1, B2 & B3 participants with GC and GEJ cancers will receive SAR444245 + pembrolizumab. Cohort B1 & B2 will enroll 1–3L CPI-naïve patients. Cohort B3 will enroll 2–4L patients post CPI-based therapy). In cohort C, 2–3L HCC participants who have progressed after CPI-based therapy will receive SAR444245 + pembrolizumab. In cohorts D1 and D2, 3–6L CRC participants will receive SAR444245 + pembrolizumab (any RAS) or SAR444245 + cetuximab (RAS-wild type) SAR444245 is administered IV at a dose of 24 ug/kg Q3W until disease progression or completion of 35 cycles. Pembrolizumab is administered as per label, Q3W for up to 35 cycles. Cetuximab is administered per label, QW until PD. The study primary objective is to determine the antitumor activity of SAR444245 in combination with other anticancer therapies. Secondary objectives are to assess safety profile, other indicators of antitumor activity, the pharmacokinetic profile and immunogenicity of SAR444245. The study will be conducted in the US, France, Germany, Spain, Italy, Belgium, Netherlands, Poland, Russia, South Korea and China

Acknowledgements The Pegasus GI study is sponsored by Sanofi

Ethics Approval All applicable ECs are obtained

Consent All participant consents are obtained

<http://dx.doi.org/10.1136/jitc-2021-SITC2021.402>

403

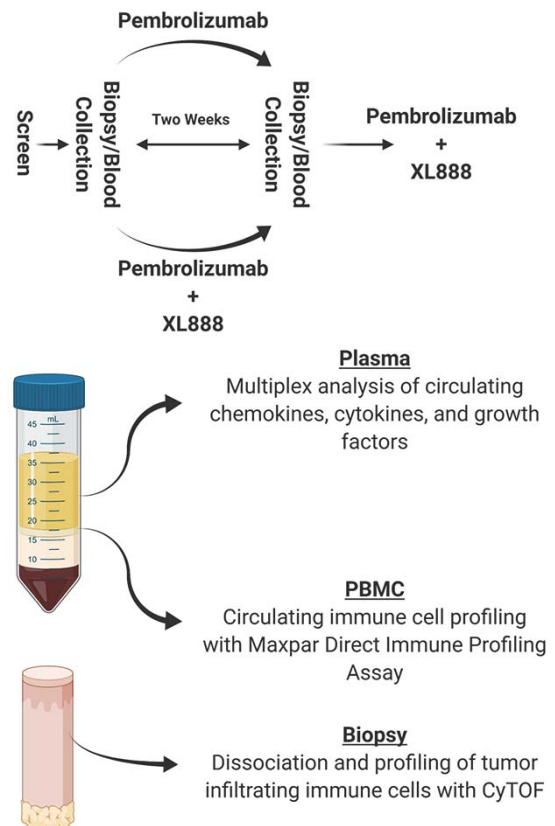
CORRELATIVE ANALYSIS OF BLOOD AND BIOPSY SAMPLES FROM A CLINICAL TRIAL OF HSP90 INHIBITION IN COMBINATION WITH PEMBROLIZUMAB REVEALS INCREASED INTRATUMORAL MYELOID CELL ACCUMULATION AFTER TREATMENT

¹Cameron Herting*, ²Yuchen Zhang, ¹Deon Doxie, ¹Michael Ware, ¹Olatunji Alese, ¹Christina Wu, ¹Mehmet Akce, ¹Mohammad Zaidi, ¹Amanda Ruggieri, ¹Madhav Dhodapkar, ¹Kavita Dhodapkar, ¹Juan Sarmiento, ¹Rafi Ahmed, ¹Shishir Maitheh, ¹Bassel El-Rayes, ¹Gregory Lesinski. ¹Emory University, Decatur, GA, USA; ²Xi'an Jiaotong University, Shaanxi, China

Background Pancreatic ductal adenocarcinoma (PDAC) has yet to widely benefit from T cell-targeted immunotherapy and displays universally poor prognosis. Thus, enhancing the activity of immunotherapy is a high priority. Our laboratory recently reported that heat shock protein-90 (Hsp90) inhibition enhances the efficacy of PD-1 blockade in murine models of PDAC (Zhang Y. et al., *Mol Cancer Ther*, 2020). Hsp90 inhibitors can limit activation of cancer associated fibroblasts (CAF) and promote infiltration of T cells when combined with PD-1 blockade in preclinical systems.

Methods Based on these data, we are conducting a Phase Ib/II clinical trial to evaluate the combination of XL888 (Hsp90 inhibitor) and pembrolizumab in patients with metastatic pancreatic cancer. We hypothesize that this combination will be safe and elicit pronounced microenvironmental changes, leading to enhanced efficacy of checkpoint blockade in a tumor type that is otherwise refractory to this approach. During the phase II portion patients were randomized to receive a three week lead in with either pembrolizumab or pembrolizumab and XL888. Paired biopsies and blood samples were obtained at baseline and at week two on treatment and CyTOF was used to assess changes in circulating and tumor infiltrating immune populations. Further, CyTOF profiling of circulating immune cells was performed to assess impacts of XL888 on over thirty phenotypically defined immune populations (figure 1).

Results As of June 2021, paired liver biopsy specimens from sites of metastasis have been successfully obtained from a total of 8 patients and paired peripheral blood mononuclear cell samples have been analyzed in 24 patients. Our CyTOF analysis illustrated a surprising increase in myeloid cell populations within the tumor following treatment. Analysis of circulating immune cells illustrated a decrease in natural killer cells and Th17 populations following treatment while naïve B cells were increased. These data will be validated by immunohistochemical analysis of FFPE biopsy specimens obtained in parallel at the time of CyTOF analysis. The impact of XL888 on systemic cytokines and chemokines (n=48 total) in the peripheral blood from patients enrolled in the clinical trial is therefore being assessed as a potential mechanism to explain this observation.



Abstract 403 Figure 1 Clinical trial and correlative analysis schema. Patients were randomized to receive either pembrolizumab alone or in combination with the HSP90 inhibitor XL888 for a two week cycle prior to crossover to the combination arm. Plasma, peripheral blood mononuclear cells (PBMC), and biopsies were assayed to evaluate immunomodulatory effects of the therapies.

Conclusions Clinical data from this trial indicates that this combination is safe in patients. As clinical data matures, changes in soluble and cellular biomarkers will be correlated with response to elucidate mechanisms of response or resistance to this combination therapy.

Trial Registration This clinical trial is underway and registered with the ID NCT03095781

Ethics Approval The study was approved by Emory University's Ethics Board, approval IRB00087397.

Consent Written informed consent was obtained from the patient for publication of this abstract and any accompanying images. A copy of the written consent is available for review by the Editor of this journal.

<http://dx.doi.org/10.1136/jitc-2021-SITC2021.403>

INITIAL BIOMARKER AND CLINICAL DATA OF A PHASE 2A STUDY OF NT-17, A LONG-ACTING INTERLEUKIN-7, PLUS PEMBROLIZUMAB: COHORT OF SUBJECTS WITH CHECKPOINT INHIBITOR-NAÏVE ADVANCED MSS-COLORECTAL CANCER

¹Richard Kim*, ²Minal Barve, ³Hirva Mamdani, ⁴Melissa Johnson, ⁵Byung Ha Lee, ⁵Sara Ferrando-Martinez, ⁶Marya Chaney, ⁵Jean Fan, ⁵NgocDiep Le, ⁷Aung Naing. ¹Moffitt Cancer Center, Tampa, FL, USA; ²Mary Crowley Cancer Research, Dallas, TX, USA; ³Karmanos Cancer Institute, Detroit, USA; ⁴Sarah Cannon/Tennessee Oncology, PLLC, Nashville, TN, USA; ⁵NeImmuneTech, Inc, Rockville, MD, USA; ⁶Merck and Co, Inc, Kenilworth, NJ, USA; ⁷MD Anderson Cancer Center, Houston, TX, USA

Background Checkpoint inhibitor (CPI) monotherapy is ineffective for microsatellite stable colorectal cancer (MSS-CRC). NT-17 (efineptakin alfa) is the first-in-class long-acting IL-7 that can increase T-cell infiltration in the tumor microenvironment (TME). We hypothesize that NT-17 may create a favorable immune-reactive TME to enhance the efficacy of CPI when combined with pembrolizumab (pembro).

Methods This is an open-label, phase 2a study in subjects with relapsed/refractory (R/R) tumors, including CPI-naïve R/R MSS-CRC. Subjects received the recommended-phase-2-dose of NT-17 intramuscularly at 1200 µg/kg every 6 weeks (Q6W) plus pembro 200 mg intravenously Q3W. Preliminary anti-tumor activity based on Overall Response Rate (ORR) was assessed by Response Evaluation Criteria in Solid Tumors (RECIST) v1.1 as a primary objective and by iRECIST as an exploratory objective. Biomarker analyses in peripheral blood and tumor biopsies were performed.

Results As of 15-July-2021, 19 subjects were enrolled in the CPI-naïve R/R MSS-CRC cohort. Six subjects are ongoing. Median age 58 years [37–81], ECOG PS 0 (26%), 1 (74%). Sixteen (84%) subjects received ≥ 2 prior therapies. All subjects had metastatic or locally advanced disease at enrollment. The median duration of follow-up was 4.64 months. Among 15 evaluable subjects, disease-control rate (DCR) based on RECIST1.1 was 47% and 1 subject achieved partial response per iRECIST (iPR) with 33% tumor reduction. Treatment-related adverse events (AEs) occurred in 14 (73.7%) subjects, 9 (47.4%) G1–2 events and 5 (26.3%) G3 events; no G4 or G5 AEs were reported. No subjects discontinued from the study due to AE. NT-17 + pembro elicited a significant increase in the absolute lymphocyte count that peaked at week 3 (>3X from baseline, p<0.0001) and was sustained at least until week 18. CD4+/CD8+ T-cell subsets followed the same response pattern. Importantly, Stem-Cell Memory CD8+ T-cells (TSCM), the potential target for CPIs that differentiate into effectors, were remarkably increased post-study treatment (>25X from baseline, p<0.01). Plasmatic chemokines (CXCL9, CXCL10, CXCL11 and CCL9) were significantly increased after the first dose. The iPR subject had an enhanced T-cell infiltration in the TME at week 5. Subject's follow-up continues and more updated data will be presented.

Conclusions The chemo-free combination of NT-17 + pembro was well tolerated and showed encouraging anti-tumor activity in subjects with CPI-naïve R/R MSS-CRC. Increased TSCM and CD8+ T-cell infiltration in TME may be the underlying mechanisms of action for the observed efficacy. These results support continued evaluation of NT-17 + pembro in CPI-naïve subjects with R/R MSS-CRC.

Acknowledgements The authors thank ICON for their partnership in conducting this trial.

Trial Registration NCT04332653

Ethics Approval The trial was approved by MD Anderson IRB (#2020–0008_MOD001), Mary Crowley IRB (#20–13) and Advarra IRB (#Pro00042639) All participant gave informed consent prior to study enrollment.

<http://dx.doi.org/10.1136/jitc-2021-SITC2021.404>

405

CAMRELIZUMAB COMBINED WITH PACLITAXEL AND NEDAPLATIN AS NEOADJUVANT THERAPY FOR LOCALLY ADVANCED ESOPHAGEAL SQUAMOUS CELL CARCINOMA (ESPRIT): A PHASE II, SINGLE-ARM, EXPLORATORY RESEARCH

Trial Registration ChiCTR2000033761

<http://dx.doi.org/10.1136/jitc-2021-SITC2021.405>

Jianqun Ma*, Jinfeng Zhang, Yingnan Yang, Dayong Zheng, Xiaoyuan Wang, Hao Liang, Luquan Zhang, Yanzhong Xin, Xiaodong Ling, Chengyuan Fang, Hao Jiang, Hongxue Meng, Wei Zheng. *Affiliated Cancer Hospital of Harbin Medical University, Harbin, China*

Background Camrelizumab has been approved as a standard therapy in the second-line treatment of esophageal squamous cell carcinoma (ESCC). This study aimed to explore the efficacy and safety of camrelizumab combined with commonly used chemotherapy (paclitaxel and platinum) in neoadjuvant treatment of ESCC.

Methods In this single-arm, phase II study, patients with advanced ESCC who were expected to receive neoadjuvant therapy followed by radical surgery were recruited. The patients received 2–4 cycles of camrelizumab (200mg, iv, q3w) in combination with paclitaxel (155mg/m², iv, q3w) and nedaplatin (80mg/m², iv, q3w) as neoadjuvant therapy, and the therapeutic effects were determined every 2 cycles. The radical surgery was performed on patients whose tumors were evaluated as resectable. The primary endpoint was pathological complete remission (pCR) rate, and the secondary endpoints were objective response rate (ORR), disease control rate (DCR), disease-free survival (DFS), overall survival (OS) and safety.

Results From June 2020 to July 2021, 42 patients with a median age of 63 years (range 48–73 years) were enrolled. The median treatment duration was 67 days. Among all patients, 23 patients were available for efficacy analysis, of which 1 patient achieved complete response, 12 patients achieved partial response, and 10 patients had stable disease. The ORR was 56.52% and DCR was 100%. The tumor in 1 patient shrank significantly after neoadjuvant therapy and the patient preferred radiotherapy instead of surgery as the radical therapeutic method. 2 patients abandoned surgery because of personal reasons. 23 patients were in the process of neoadjuvant therapy and had not undergone surgery yet. The remaining 16 patients underwent radical surgery and 6 patients (37.5%) achieved pCR (pT0N0M0). The adverse reactions in this study includes reduction of red blood cell (21.4%), anemia (21.4%), hypomagnesemia (19.1%), fatigue (16.7%), thrombocytopenia (16.7%), proteinuria (14.3%), hand-foot skin reaction (14.3%), hyponatremia (11.9%), neutropenia (7.1%) and reactive cutaneous capillary endothelial proliferation (7.1%). The main treatment-related grade 3/4 adverse event (AE) was neutropenia (2.3%). All the AEs were manageable. The average intraoperative blood loss was 206 ml and the average hospitalization time after operation was 11 days (range 7–19 days). No anastomotic leakage and treatment-related death occurred.

Conclusions The ESPRIT study suggested that camrelizumab in combination with paclitaxel and nedaplatin as a neoadjuvant therapy was well tolerated. 37.5% of the patients can achieved pCR, which was of great significance for improving the prognosis and prolonging the survival time. This encouraging result promoted us to continue this phase II study.

Acknowledgements The authors thank the patients and their families and caregivers for participating in this trial as well as all investigators and site personnel who participated in this study.

CAMRELIZUMAB COMBINED WITH PACLITAXEL AND NEDAPLATIN IN THE FIRST-LINE TREATMENT OF LOCALLY ADVANCED/ADVANCED ESOPHAGEAL SQUAMOUS CELL CARCINOMA: A PHASE II, SINGLE-ARM, EXPLORATORY RESEARCH

<http://dx.doi.org/10.1136/jitc-2021-SITC2021.406>

Jianqun Ma*, Jinfeng Zhang, Yingnan Yang, Dayong Zheng, Xiaoyuan Wang, Hao Liang, Luquan Zhang, Yanzhong Xin, Xiaodong Ling, Chengyuan Fang, Hao Jiang, Wei Zheng. *Affiliated Cancer Hospital of Harbin Medical University, Harbin, China*

Background Treatment options for patients with locally advanced/advanced esophageal squamous cell carcinoma (ESCC) are limited. Current guidelines for first-line treatment of advanced ESCC recommend chemotherapy containing a platinum and a paclitaxel agent. Camrelizumab demonstrated antitumor activity in the first-line treatment of advanced ESCC. This study aimed to explore the efficacy and safety of camrelizumab combined with paclitaxel and platinum in the first-line treatment of ESCC.

Methods In this single-arm, phase II study, patients were eligible for enrollment if they had a histologically or cytologically confirmed diagnosis of locally advanced/advanced unresectable ESCC. The patients received camrelizumab (200mg, iv, q3w) in combination with chemotherapy. The chemotherapy regimen consists of paclitaxel (155mg/m², iv, q3w) and nedaplatin (80mg/m², iv, q3w) for 6 cycles, and the therapeutic effects were determined every 2 cycles (6 weeks). The primary endpoint was the rate of 12-month overall survival, and the secondary endpoints were objective response rate (ORR), disease control rate (DCR), progression-free survival (PFS).

Results From May 2020 to July 2021, 83 patients with a median age of 58 years (range 44–75 years) were enrolled. The median treatment duration was 87 days. Among them, 50 patients were available for efficacy analysis, of which 31 patients achieved partial response (PR), and 18 had stable disease (SD). The ORR was 62% and DCR was 98%. 33 patients were in the process of therapy and had not completed 2 cycles, and the efficacy evaluation cannot be performed yet. The adverse reactions in this study include reduction of red blood cell (20.1%), anemia (17.7%), hypomagnesemia (15.10%), fatigue (14%), thrombocytopenia (10.1%), hand-foot skin reaction (8.9%), proteinuria (7.6%), hyponatremia (6.3%), neutropenia (2.5%), reactive cutaneous capillary endothelial proliferation (10.1%) and immune pneumonia (1.2%). During the course of therapy, all adverse events (AEs) were grade 1/2, and no patient experienced grade 3/4 AEs. No patient was hospitalized because of treatment-related complications. The treatment was well tolerated and no toxic death occurred. All the AEs can be controlled and alleviated after symptomatic treatment.

Conclusions Camrelizumab in combination with paclitaxel and platinum displayed controllable security and similar therapeutic effect to other immune checkpoint inhibitors. This encouraging result promoted us to continue this phase II study.

Acknowledgements The authors thank the patients and their families and caregivers for participating in this trial as well as all investigators and site personnel who participated in this study.

Trial Registration ChiCTR2100046355

Ethics Approval The study has obtained ethics approval. The name of the ethics committee: Chinese Ethics Committee of Registering Clinical Trials. Registration number: ChiCTR2100046355. The authors stated that the participants gave informed consent before taking part.

407

A PHASE 1B KEYNOTE-B79 TRIAL EVALUATING NON-GENE EDITED ALLOGENEIC CAR T-CELLS, CYAD-101, POST FOLFOX PRECONDITIONING, FOLLOWED BY PEMBROLIZUMAB, IN REFRACTORY METASTATIC COLORECTAL CANCER PATIENTS

Anne Flament*, Frédéric Lehmann, Erik Alcantar-Orozco, Emilie Cerf, Caroline Lonez, David Gilham, Charles Morris. *Celyad Oncology, Mont-Saint-Guibert, Belgium*

Background The peptide-based allogeneic chimeric antigen receptor (CAR) T-cell treatment CYAD-101 utilizes an NKG2D receptor that targets eight ligands expressed on tumor cells and non-malignant stromal cells of many cancer types. CYAD-101 also co-expresses a peptide intended to eliminate the potential of graft versus host disease (GvHD). In the phase 1 alloSHRINK study (NCT03692429), CYAD-101 was administered with FOLFOX preconditioning chemotherapy to 15 patients with metastatic colorectal cancer (mCRC). The treatment was well tolerated with no evidence of GvHD, no treatment-related adverse events \geq Grade 3 and only two patients who presented a cytokine release syndrome grade 1. By contrast, encouraging clinical activity was observed including two partial responses. Evidence of changes in the TCR repertoire and modulation of the cytokine profile four months post-treatment with CYAD-101 were also observed implying that the NKG2D CAR T may also be modulating the immune suppressive environment in patients reflecting that seen in pre-clinical models (ASCO GI 2021 abstract #74). Given the expansion of the T cell repertoire after CYAD-101 therapy, we considered that employing a checkpoint inhibitor to release this expanded T cell population may drive more durable clinical responses beyond that currently seen with the CAR T alone.

Methods The KEYNOTE-B79 trial evaluates the safety and clinical activity of multiple infusions of CYAD-101, administered post FOLFOX preconditioning chemotherapy, then followed three weeks after CYAD-101 by a pembrolizumab consolidation treatment (200 mg every three weeks for a maximum two years total treatment duration) in microsatellite stable/mismatch-repair proficient mCRC patients with recurrent/progressing disease after at least one metastatic line of therapy which must include FOLFOX chemotherapy. The schedule of administration of three CYAD-101 infusions at the dose 1×10^9 cells/infusion Q2W post-FOLFOX preconditioning chemotherapy are based on the alloSHRINK study. This sequencing of checkpoint inhibitor at a timepoint after CYAD-101 therapy ensures that the modulated endogenous immune response is enabled by pembrolizumab. This study is not focused on impacting the CAR T cell itself largely since CYAD-101 cells at the time of manufacture show negligible expression of PD-1 and that this sequencing ensures no overlap of potential toxicities that could arise from the CAR T or checkpoint inhibitor therapies. The KEYNOTE-B79 study is planned to be initiated in Q4-2021.

Ethics Approval The study was approved by all relevant authorities and submitted to Institution's Ethics Boards for their approval before study initiation.

<http://dx.doi.org/10.1136/jitc-2021-SITC2021.407>

PRELIMINARY BIOMARKER AND CLINICAL ATA OF A PHASE 2A STUDY OF NT-I7, A LONG-ACTING INTERLEUKIN-7, PLUS PEMBROLIZUMAB: COHORT OF SUBJECTS WITH CHECKPOINT INHIBITOR-NAÏVE ADVANCED PANCREATIC CANCER

Aung Naing*, ²Richard Kim, ³Minal Barve, ⁴Melissa Johnson, ⁵Byung Ha Lee, ⁶Sara Ferrando-Martinez, ¹Shubham Pant, ¹Robert Wolff, ¹Cara Haymaker, ⁷Marya Chaney, ²Dae Won Kim, ⁶Jean Fan, ⁶NgocDiep Le, ⁸Hiiva Mamdani. ¹MD Anderson Cancer Center, Houston, TX, USA; ²Moffitt Cancer Center, Tampa, FL, USA; ³Mary Crowley Cancer Research, Dallas, TX, USA; ⁴Sarah Cannon/Tennessee Oncology, PLLC, Nashville, TN, USA; ⁵NeolImmuneTech, Inc, Rockville, MD, USA; ⁶NeolImmuneTech, Inc., Rockville, MD, USA; ⁷Merck and Co, Inc., Kenilworth, NJ, USA; ⁸Karmanos Cancer Institute, Detroit, USA

Background Pancreatic cancer (PaC) is immune-quiescent and resistant to single-agent checkpoint inhibitor (CPI). NT-17 (efineptakin alfa) is the first-in-class long-acting IL-7 that can increase T-cell infiltration in the tumor microenvironment (TME) and may enhance tumor responsiveness to CPI therapy. We hypothesize that the combination of NT-17 and pembrolizumab may result in enhanced efficacy in CPI-naïve advanced PaC.

Methods This is an open-label, phase 2a, study in subjects with relapsed/refractory (R/R) tumors, including CPI-naïve R/R PaC. Subjects received NT-17 intramuscularly at 1200 µg/kg every 6 weeks (Q6W) plus pembro 200 mg intravenously Q3W. Antitumor activity based on Overall Response Rate (ORR) was assessed by Response Evaluation Criteria in Solid Tumors (RECIST) v1.1. Biomarker analyses of peripheral blood and tumor biopsies were performed.

Results As of 15-July-2021, 26 subjects were enrolled in the CPI naïve R/R PaC cohort. Median age 69 years [31–81], ECOG PS 0 (35%), 1 (65%). Twenty-one (81%) subjects had ≥ 2 prior therapies All subjects had metastatic or locally advanced disease at enrollment. The median duration of follow-up was 3.3 months. Among 10 subjects with at least 1 post-treatment tumor assessment, the RECIST1.1-based ORR and disease-control rate (DCR) were 10% and 50%, respectively. One subject with MSS and TMB of 1, achieved a confirmed partial response (cPR) with 65% tumor reduction and drastically improving CA19-9. Treatment-related adverse events (AEs) occurred in 14 (53.8%) subjects, 9 (34.6%) G1–2, 3 (11.5%) G3; 2 (7.7%) G4; no G5 AEs were reported. No subjects discontinued from treatment due to AE. NT-17 + pembro elicited a significant increase in the peripheral absolute lymphocyte count that peaked at week 3 (>3X from baseline, $p < 0.0001$) and was sustained at least until week 18. CD4+/CD8+ T-cells subsets followed the same response pattern. Importantly, Stem-Cell Memory CD8+ T-cells (TSCM), the potential target for CPI, were markedly increased (>15X, $p < 0.05$) post-study treatment. The CD8+ Effector-to-Treg ratio and plasmatic chemokines (CXCL9, CXCL10, CXCL11 and CCL9) were also significantly increased. The cPR subject had enhanced T-cell infiltration in the TME at week 5. Subject's follow-up continues and updated data will be presented.

Conclusions The chemo-free combination of NT-17 + pembro was well tolerated and showed promising anti-tumor activity in subjects with CPI-naïve R/R PaC. Increased TSCM and CD8+ T-cell infiltration within TME may be the underlying mechanisms of action for the observed efficacy. These results support continued evaluation of NT-17 + pembro in subjects with CPI-naïve R/R PaC.

Acknowledgements The authors thank ICON for their partnership in conducting this trial.

Trial Registration NCT04332653

Ethics Approval The trial was approved by MD Anderson IRB (#2020-0008_MOD001), Mary Crowley IRB (#20-13) and Advarra IRB (#Pro00042639) All participant gave informed consent prior to study enrollment.

<http://dx.doi.org/10.1136/jitc-2021-SITC2021.408>

TRIAL IN PROGRESS: A PHASE 2 STUDY TO ASSESS THE SAFETY, EFFICACY OF FLX475 COMBINED WITH PEMBROLIZUMAB IN PATIENTS WITH ADVANCED OR METASTATIC GASTRIC CANCER

¹Do-Youn Oh*, ²Min Hee Ryu, ³Jun-Eul Hwang, ⁴Jaeyong Cho, ⁵Dae Young Zang, ⁶Sang Cheul Oh, ⁷Jeeyun Lee, ⁸Keun-Wook Lee, ⁹Hyun Cheol Chung, ¹⁰Byoung Yong Shim, ¹¹Michael Chisamore, ¹²William Ho, ¹³Paul Rhee, ¹⁴Ji Yeong Won, ¹⁵Taewan Kim, ¹⁶Eunhye Baek, ¹⁷Seungjae Baek. ¹Seoul National University College of Medicine, Seoul, Korea, Republic of; ²University of Ulsan College of Medicine, Seoul, Korea, Republic of; ³Chonnam National University Medical School, Gwangju, Korea, Republic of; ⁴Yonsei University College of Medicine, Seoul, Korea, Republic of; ⁵Hallym University College of Medicine, Anyang, Korea, Republic of; ⁶Korea University Guro Hospital, Seoul, Korea, Republic of; ⁷Sungkyunkwan University School of Medicine, Seoul, Korea, Republic of; ⁸The Catholic University of Korea, Suwon, Korea, Republic of; ⁹Merck and Co., Inc., Wheaton, IL, USA; ¹⁰RAPT Therapeutics, South San Francisco, CA, USA; ¹¹Hanmi Pharmaceutical Co., Ltd., Seoul, Korea, Republic of

Background Regulatory T-cells (Treg) are essential in maintaining self tolerance, but they can also suppress anti-tumor immunity in the tumor microenvironment (TME). Treg are recruited into tumors by C-C motif chemokine ligand 17 (CCL17), and 22 (CCL22), which are produced by tumor cells and other cells in the TME. These chemokines serve as a "homing signal" to Treg by binding to their cognate receptor, C-C chemokine receptor type 4 (CCR4), the predominant chemokine receptor on human Treg.^{1 2 3} FLX475, is an orally available and selective small-molecule antagonist of CCR4. In preclinical studies it has demonstrated potent inhibition of CCL17- and CCL22-induced CCR4-mediated chemotaxis, an increase in the intratumoral Teff/Treg ratio, and anti-tumor efficacy as a single agent and in combination with checkpoint inhibitors. In a first-in-human healthy volunteer study, the orally-available CCR4 antagonist was well tolerated, with solid safety profile. A receptor occupancy (RO) pharmacodynamic (PD) assay using peripheral blood Treg demonstrated the ability to safely achieve exposure levels predicted to maximally inhibit Treg recruitment into tumors.⁴ The proposed mechanism of action, pharmacokinetics (PK), PD, and safety profile of FLX475 have enabled the optimized design of an ongoing Phase 2 study to assess the safety, efficacy of FLX475 in combination with pembrolizumab in patients with advanced or metastatic gastric cancer.

Methods This clinical trial is a Phase 2, open-label study to assess the safety and efficacy of FLX475 in combination with pembrolizumab in patients with advanced or metastatic gastric cancer (NCT04768686). Approximately 90 subjects may be enrolled across 2 cohorts to examine the safety and efficacy when administered 100mg PO QD of FLX475 with 200mg IV Q3W of pembrolizumab. In cohort 1, checkpoint inhibitor naïve Epstein-Barr Virus (EBV)-negative gastric cancer subjects who have progressed on at least 2 prior systemic treatments for advanced or metastatic gastric cancer will be enrolled, and in cohort 2, checkpoint inhibitor naïve EBV-positive gastric cancer subjects who had at least 1 prior systemic treatment for advanced or metastatic gastric cancer will be enrolled. Both EBV negative and positive gastric cancer are predicted to express high levels of CCR4 ligands and enriched in Treg (i.e. 'charged tumor'). The study is planned initially as a 2-stage design for each cohort, and an interim analysis reviewing efficacy and safety results as well as available PK and PD data for both cohorts will be performed prior to stage 2.

Acknowledgements Thanks to the patients, and to their families and caregivers for allowing us to be part of the journey. RAPT Therapeutics, Inc., South San Francisco, CA, USA is

providing FLX475 for the study. Merck Sharp & Dohme Corp., a subsidiary of Merck & Co., Inc., Kenilworth, NJ, USA is providing pembrolizumab for the study. Trial Registration NCT04768686

REFERENCES

- 1.. Talay O, et al. Potent and selective C-C chemokine receptor (CCR4) antagonists potentiate anti-tumor immune responses by inhibiting regulatory T cells (Treg). *J Immunother Cancer* 2017;**5**(Suppl 2):P467 (SITC 2017).
- 2.. Curiel, Tyler J, et al. Specific recruitment of regulatory T cells in ovarian carcinoma fosters immune privilege and predicts reduced survival. *Nature medicine* 10.9 (2004):942–949.
- 3.. Nakayama et al. Selective induction of Th2-attracting chemokines CCL17 and CCL22 in human B cells by latent membrane protein 1 of Epstein-Barr virus. *J Virol* 2004 February; **78**(4):1665–74.
- 4.. van Marle S, et al. Pharmacokinetics, pharmacodynamics, and safety of FLX475, an orally-available, potent, and selective small-molecule antagonist of CCR4, in healthy volunteers. *J Immunother Cancer* 2018;**6**(Suppl 1):P484 (SITC 2018).

<http://dx.doi.org/10.1136/jitc-2021-SITC2021.409>

PHASE I INTERIM STUDY RESULTS OF NOUS-209, AN OFF-THE-SHELF IMMUNOTHERAPY, WITH PEMBROLIZUMAB, FOR THE TREATMENT OF TUMORS WITH A DEFICIENCY IN MISMATCH REPAIR/ MICROSATELLITE INSTABILITY (dMMR/MSI)

¹Michael Overman*, ²Marwan Fakhri, ³Dung Le, ⁴Anthony Shields, ⁵Katrina Pedersen, ⁶Manish Shah, ⁷Sarbajit Mukherjee, ⁸Thea Faivre, ⁹Guido Leoni, ⁹Anna Morena D'Alise, ⁹Gabriella Cotugno, ⁹Francesca Langone, ¹⁰Stefania Capone, ¹⁰Maria Rosaria Del Sorbo, ⁹Elisa Scarselli, ⁸Patricia Delaite. ¹MD Anderson Cancer Center, Houston, TX, USA; ²City of Hope Comprehensive Cancer Center, Duarte, CA, USA; ³Johns Hopkins University, Baltimore, MD, USA; ⁴Barbara Ann Karmanos Cancer Institute, Detroit, MI, USA; ⁵Washington University School of Medicine, Saint Louis, MO, USA; ⁶Weill Cornell Medicine, New York, NY, USA; ⁷Roswell Park Comprehensive Cancer Center, Buffalo, NY, USA; ⁸Nouscom AG, Basel, Switzerland; ⁹Nouscom Srl, Rome, Italy; ¹⁰Reitheria Srl, Rome, Italy

Background Defective DNA mismatch repair (dMMR) leads to high levels of microsatellite-instability (MSI-H) and insertions or deletions in coding regions, resulting in the generation of tumor-specific frameshift peptides (FSPs). We selected 209 shared FSPs among subjects with first- or second-line metastatic dMMR/MSI-H colorectal (CRC), gastric, and gastroesophageal junction (GEJ) cancers, to develop an off-the-shelf vaccine for the treatment of dMMR/MSI-H tumors. Selected FSPs were cloned into four proprietary Great Apes Adenoviral (GAd) and four Modified Vaccinia Ankara (MVA) vectors to generate a polyvalent viral vectored vaccine called Nous-209 [Leoni G., et al., *Cancer Res.* 2020]

Methods This phase 1 first in human (FIH) study (NCT04041310) was designed to evaluate safety and tolerability of two dose levels (one log difference for both GAd and MVA) of Nous-209 genetic polyvalent vaccine in combination with the programmed death receptor-1 (PD-1)-blocking antibody pembrolizumab, to assess immunogenicity of the combination and to detect preliminary evidence of anti-tumor activity. Nous-209 is administered intramuscularly, concomitantly with pembrolizumab (doses and schedule per approved label): one prime (GAd-209-FSP) at the 2nd pembrolizumab infusion and three booster (MVA-209-FSP) injections at subsequent infusions each 3 weeks apart. The study is composed of two sequential cohorts: dose escalation and dose expansion

Results Twelve evaluable subjects with first- or second-line metastatic dMMR/MSI-H cancers were evaluated as of May 28, 2021. Three subjects enrolled in dose level 1 (2 CRC and 1 GEJ cancer) demonstrated durable confirmed partial responses (PRs). In dose level 2 (6 CRC and 3 gastric cancers), 4 subjects had PRs, 2 had stable disease (SD) and 3 had progressive disease (PD). The median follow-up for subjects in dose level 1 is 17.9 months (range 15.3–20 months), and 8 months (range 3.8–12.5 months) for subjects in dose level 2 as of the above cut-off date. No dose limiting toxicities (DLTs) were observed, and the treatment combination was determined to be safe and tolerable. Vaccine immunogenicity was demonstrated by ex-vivo interferon-gamma ELISpot assay in 67% of subjects in dose level 1, and 100% of patients with evaluable samples in dose level 2

Conclusions The combination of the Nous-209 genetic polyvalent cancer vaccine and pembrolizumab has been demonstrated to be safe, immunogenic, and continues to show early signs of clinical efficacy, which may be attributed to the vaccine contribution

REFERENCE

- 1.. Leoni G, et al. A genetic vaccine encoding shared cancer neoantigens to treat tumors with microsatellite instability. *Cancer Res* 2020 July 20;**80**(18):3972–3982.

Ethics Approval The study was approved by The University of Texas MD Anderson Cancer Center, IRB number 2019–0651_MOD001. The study was approved by Feinstein Institute for Medical Research Northwell Health, IRB number 19–1086. The study was approved by WCG The Trusted Partner in Ethical Review, IRB number 20200155. The study was approved by Johns Hopkins Medicine, IRB number IRB00220323/CIR00053809. The study was approved by City of Hope, IRB number 19277/176947. The study was approved by Advarra Advancing Better Research. The study was approved by Dana-Faber Cancer Institute. The study was approved by Weill Cornell IRB. The study was approved by Roswell Park IRB.

<http://dx.doi.org/10.1136/jitc-2021-SITC2021.410>

411

INNATE: IMMUNOTHERAPY DURING NEOADJUVANT THERAPY FOR RECTAL CANCER TO ELUCIDATE LOCAL AND SYSTEMIC THERAPEUTIC RESPONSES

¹Nina Sanford, ¹Eslam Elghonaimy, ²Adel Kardosh, ¹Syed Kazmi, ¹Javier Salgado Pogacnik, ³Xiaodong Yang, ¹Robert Timmerman, ¹Todd Aguilera*. ¹UT Southwestern, Dallas, TX, USA; ²OHSU, Portland, OR, USA; ³Apexigen Inc, Redwood Shores, CA, USA

Background The relative risk of developing rectal cancer has quadrupled in young adults over the last 40 years and approximately 50% of patients develop recurrence within 3 years. Thus, there is a critical need for new approaches to improve survival but cancer Immunotherapy has had little impact on colorectal cancer. The anti-CD40 agonist immunotherapy is emerging and APX005M has shown promise in phase I and ongoing phase II trials. Anti-CD40 can stimulate both innate and adaptive immune responses and a greater response can be achieved combining anti-CD40 with radiation therapy (RT) in animal models. We developed the INNATE trial, a phase II randomized trial of neoadjuvant short course RT followed by chemotherapy with or without the addition of APX005M for rectal cancer (NCT04130854).

Methods The INNATE trial is a multi-center, 58 patient, 3:2 randomization clinical trial, that adds APX005M to short course RT (SCRT) and subsequent FOLFOX chemotherapy prior to definitive radiation. Eligibility includes stage III and high risk stage II rectal cancer and candidates for standard neoadjuvant therapy and no contraindications for immunotherapy or radiation. Patients receive 5Gy x 5 fractions over five days and if randomized to experimental arm will receive APX005M on day 3 of radiation. After a two week break patients receive an optional endoscopy and biopsy followed by standard FOLFOX chemotherapy with APX005M infusion after disconnection of 5-FU chemotherapy pump. Study arm receives APX005M with 5 of 6 cycles of FOLFOX. After treatment patients undergo restating, endoscopy, and trans abdominal resection. The primary endpoint is pathologic complete response with the null estimated to be 20% and alternative 50% for a power of 0.8 and type 1 error of 0.1. Secondary endpoints include overall survival, toxicity analysis, and disease free survival. For correlative analysis, tissue is collected pre-treatment, two weeks after RT, and at surgery, then blood collected during treatment and at follow up.

Results To date 16 patients have been randomized and initiated treatment. The treatment is well tolerated. Fifteen patients received pre- and post-SCRT biopsies. The study team plans correlative analysis including single cell RNA sequencing, multiplex immunohistochemistry, and bulk sequencing. Preliminary data shows changes in the immune tumor microenvironment from patients treated as their own control and between SCRT versus SCRT + APX00M.

Conclusions The INNATE trial shows feasibility of incorporating novel immunotherapies with an emerging standard of care incorporating short course RT. It serves as an important platform for scientific and clinical investigation.

Trial Registration ClinicalTrials.gov: NCT04130854

Ethics Approval The clinical trial has institutional review board approval at the University of Texas Southwestern, Oregon Health and Sciences University, Wake Forest, and Moffitt. All patients have provided informed consent.

<http://dx.doi.org/10.1136/jitc-2021-SITC2021.411>

CAMRELIZUMAB AND APATINIB COMBINED WITH CHEMOTHERAPY (MFOLFOX6) AS NEOADJUVANT THERAPY FOR LOCALLY ADVANCED RIGHT-SIDED COLON CANCER (AMBITION)

Zhou Tong*, Sen Lu, Xiaomeng Dai, Xiaobin Cheng, Xuanwen Bao, Xudong Zhu, Xiaofei Cheng, Qihan Fu, Danyang Wang, Hangyu Zhang, Qinsong Sheng, Lulu Liu, Guoliang Zhang, Yi Zheng, Fanlong Liu, Peng Zhao, Wenbin Chen, Weijia Fang, Xiangmin Xu. *The First Affiliated Hospital, Zhejiang University School of Medicine, Hangzhou, China*

Background Colorectal cancer is a heterogeneous disease with complicated genetic alterations. Right colon and left colon have different features while right colon cancer displays an even worse prognosis. The randomized phase III FOxTROT trial demonstrated better downstaging effect with neoadjuvant plus adjuvant chemotherapy compared with adjuvant chemotherapy alone ($P=0.04$).¹ Moreover, 2-year relapse rate was improved with neoadjuvant therapy, though the difference was not statistically significant. The NICHE study of neoadjuvant immunotherapy (maximum 6 weeks) showed that the pathological response was observed in 20/20 mismatch repair-deficient (dMMR) resectable colon cancers, with 19 major pathological responses and 12 pathological complete responses (pCRs).² Recently, KEYNOTE-177 study showed improved progression-free survival with PD-1 inhibitor over chemotherapy (16.5 months vs. 8.2 months) in untreated microsatellite instability-high (MSI-H)/dMMR colon cancer patients, including 68% of right colon cancers.³ In addition, camrelizumab (PD-1 inhibitor) plus apatinib (vascular endothelial growth factor receptor-2 tyrosine kinase inhibitor) demonstrated favorable antitumor effects and a manageable safety profile in advanced hepatocellular carcinoma and gastric cancer.^{4 5} This phase II trial aims to explore whether the combination of camrelizumab, apatinib and chemotherapy (mFOLFOX6) could significantly improve the pathological regression rate in locally advanced right colon cancer so as to bring considerable survival benefit for patients.

Methods Eligible patients are aged 18–75 years, with locally advanced (T4 or T3 with extramural depth ≥ 5 mm, N0-2, M0, AJCC 8th) adenocarcinoma of right colon (including ileocecal area, ascending colon, and transverse colon to splenic flexion), and without prior systemic chemotherapy or immunotherapy. All patients will receive 5 cycles of camrelizumab (200 mg once every 2 weeks) plus mFOLFOX6 and 2 months of apatinib (250 mg orally once a day), followed by surgery and 7 cycles of adjuvant camrelizumab plus mFOLFOX6. The primary endpoint is the proportion of patients with tumor regression grade (TRG) 2–4 according to the Dworak criteria (TRG2: dominantly fibrotic changes with few tumor cells or groups; TRG3: very few tumor cells in fibrotic tissue; TRG4: no tumor cells). Secondary endpoints include downstaging rate, pCR rate, R0 resection rate, 2-year disease-free survival rate, 2-year event-free survival, overall survival, quality of life, and safety.

Results To date, three of planned 64 patients have been enrolled. Two patients have completed surgery. According to Dworak criteria, TRG ranked 4 (pathologic complete response) for the first patient and 3 (very few tumor cells in fibrotic tissue) for the second patient. No severe adverse events have been observed for all patients.

Trial Registration This trial has been registered at ClinicalTrials.gov (NCT04625803).

REFERENCES

1. G. Foxtrot Collaborative. Feasibility of preoperative chemotherapy for locally advanced, operable colon cancer: the pilot phase of a randomised controlled trial. *Lancet Oncol* **13**(11) (2012):1152–60.
2. Chalabi M, Fanchi LF, Dijkstra KK, Van den Berg JG, Aalbers AG, Sikorska K, Lopez-Yurda M, Grootsholten C, Beets GL, Snaebjornsson P, Maas M, Mertz M, Veninga V, Bounova G, Broeks A, Beets-Tan RG, de Wijkerslooth TR, van Lent AU, Marsman HA, Nuijten E, Kok NF, Kuiper M, Verbeek WH, Kok M, Van Leerdam ME, Schumacher TN, Voest EE, Haanen JB. Neoadjuvant immunotherapy leads to pathological responses in MMR-proficient and MMR-deficient early-stage colon cancers. *Nat Med* **26**(4) (2020):566–576.
3. André T, Shiu KK, Kim TW, Jensen BV, Jensen LH, Punt C, Smith D, Garcia-Carbonero R, Benavides M, Gibbs P, de la Fouchardiere C, Rivera F, Elez E, Bendell J, Le DT, Yoshino T, Van Cutsem E, Yang P, Farooqui MZH, Marinello P, Diaz Jr LA. Pembrolizumab in microsatellite-instability-high advanced colorectal cancer. *N Engl J Med* **383**(23) (2020):2207–2218.
4. Xu J, Shen J, Gu S, Zhang Y, Wu L, Wu J, Shao G, Zhang Y, Xu L, Yin T, Liu J, Ren Z, Xiong J, Mao X, Zhang L, Yang J, Li L, Chen X, Wang Z, Gu K, Chen X, Pan Z, Ma K, Zhou X, Yu Z, Li E, Yin G, Zhang X, Wang S, Wang Q. Camrelizumab in combination with apatinib in patients with advanced hepatocellular carcinoma (RESCUE): a nonrandomized, open-label, phase II trial. *Clin Cancer Res* **27**(4) (2021):1003–1011.
5. Xu J, Shen J, Gu S, Zhang Y, Wu L, Wu J, Shao G, Zhang Y, Xu L, Yin T, Liu J, Ren Z, Xiong J, Mao X, Zhang L, Yang J, Li L, Chen X, Wang Z, Gu K, Chen X, Pan Z, Ma K, Zhou X, Yu Z, Li E, Yin G, Zhang X, Wang S, Wang Q, Xu J, Zhang Y, Jia R, Yue C, Chang L, Liu R, Zhang G, Zhao C, Zhang Y, Chen C, Wang Y, Yi X, Hu Z, Zou J, Wang Q. Camrelizumab in combination with apatinib in patients with advanced hepatocellular carcinoma (RESCUE): a nonrandomized, open-label, phase II trial anti-PD-1 antibody SHR-1210 combined with apatinib for advanced hepatocellular carcinoma, gastric, or esophagogastric junction cancer: an open-label, dose escalation and expansion study. *Clin Cancer Res* **27**(4) (2021):1003–1011.

Ethics Approval Study protocol was approved by the Clinical Research Ethics Committee of the First Affiliated Hospital, College of Medicine, Zhejiang University (2020–119)

Consent Written informed consent was obtained from the patient for publication of this abstract and any accompanying images. A copy of the written consent is available for review by the Editor of this journal.

<http://dx.doi.org/10.1136/jitc-2021-SITC2021.412>

413 TORIPALIMAB IN COMBINATION WITH CONCURRENT CHEMORADIATION IN PATIENTS WITH ADVANCED/METASTATIC ESOPHAGEAL CARCINOMA: PROTOCOL FOR A SINGLE-ARM, PROSPECTIVE, OPEN-LABEL, PHASE II CLINICAL TRIAL

Lei Wu*, Yi Wang, Gang Wan, Jiahua Lv, Qifeng Wang, Jinyi Lang, Tao Li. *Sichuan Cancer Hospital and Institute, Chengdu, China*

Background Esophageal carcinoma is a disease with high morbidity and mortality in China and, recently, Immune checkpoint inhibitors(ICIs) combined with chemotherapy have shown good efficacy and safety for treatment; however, some patients still suffer from tumor progression or metastasis after treatment. Clinical studies have confirmed that immunotherapy combined with chemoradiotherapy can significantly improve the prognosis of patients with advanced esophageal cancer, but the efficacy and safety of adding radiotherapy to immunotherapy and chemotherapy have been less reported.

Methods This is an open-label, single-arm, and single-center phase II trial. Patients with unresectable stage IV esophageal squamous cell carcinoma(ESCC) who had not received prior systemic therapy were enrolled. The patients were treated with two cycles of toripalimab (240 mg d1, Q3W) combined with induction chemotherapy (paclitaxel 135–175 mg/m², d1 +carboplatin AUC=4–6, d1, Q3W), sequentially combined with concurrent chemoradiotherapy (30–50 Gy in 15–25 fractions, paclitaxel 135–175 mg/m², d1+carboplatin AUC=4–6 d1, Q3W), followed by maintenance treatment with toripalimab (240 mg d1, Q3W) for 1 year. The primary objective of this trial is to evaluate the progression-free survival (PFS) of this combination therapy; and the secondary objective is related to the assessment of objective response rate (ORR), the disease control rate (DCR), the duration of remission (DOR), the 1- and 2-year overall survival(OS) rates, the safety and tolerability of patients to treatment, and the identification of the changes in the health-related quality of life (HRQoL) of patients. Furthermore, we aimed to identify predictive biomarkers (such as the expression of PD-L1 ctDNA and cytokines) and to explore the relationship between these biomarkers and tumor response to the study treatment.

Acknowledgements We thank all the participants and their advisors involving in this study. We owe thanks to the patients in our study and their family members.

Trial Registration ChiCTR(ChiCTR2100046715). Registered on the 27th of May 2021.

Ethics Approval The study protocol is approved by Ethics Committee of Sichuan Cancer Hospital (SCCHEC-02-2021-021). Changes to the protocol will be communicated via protocol amendment by the study principal investigators. Written informed consent will be obtained from all participants.

<http://dx.doi.org/10.1136/jitc-2021-SITC2021.413>

414

A RANDOMIZED PHASE II STUDY OF SYSTEMIC THERAPY PLUS WEILESHU (WLS) VERSUS SYSTEMIC THERAPY ALONE IN PATIENTS WITH METASTATIC COLORECTAL CANCER (mCRC)

¹Ruyi Zhang, ¹Xiaoxuan Tu*, ¹Zhou Tong, ¹Hangyu Zhang, ¹Xudong Zhu, ¹Weijia Fang, ²Lanfang Yu, ²Haibo Mou. ¹The First Affiliated Hospital, College of Medicine, Zhejiang University, Hangzhou, China; ²Shulan Hospital, Hangzhou, China

Background In recent years, the role of inflammatory microenvironment induced by gut microbiome in the occurrence and development of CRC has received increased attention across a number of disciplines. WLS is a probiotics product consisted of with 6 billion live probiotics, mainly *Lactobacillus helveticus* and *Bifidobacterium longum*. To further explore the influence of gut microbiome in the anti-tumor efficacy of patients with mCRC, we conducted a randomized controlled trial (NCT04021589).

Methods Patients receiving corresponding systemic therapy were randomly included into the WLS-intervention and the control arms. Fecal samples were collected at baseline and about two months after treatment initiation. Gut microbiota composition was assessed using shotgun metagenomic sequencing. Best clinical response was dichotomized as partial remission (clinical benefit, CB) versus stable disease or disease progression (non-clinical benefit, NCB). Metagenomic analysis across patients with CB and NCB was conducted and random forest model training was employed to predict the efficacy of treatment.

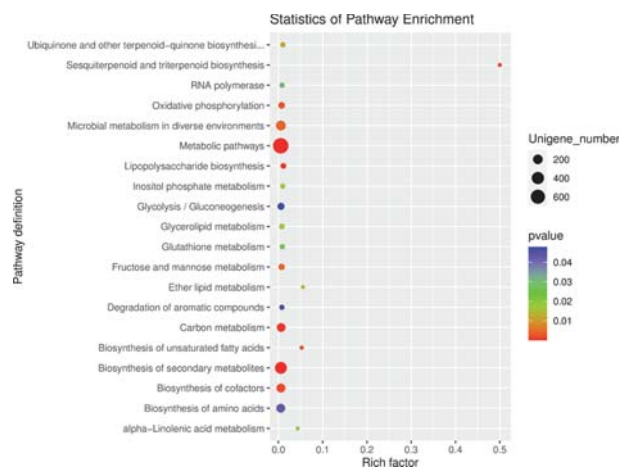
while WLS intervention down-regulated genes related to its synthesis pathway, which may slow the development of CRC. Random forest model showed abundance of *Desulfovibrio_vulgaris* and *Parvimonas_sp_oral_taxon_393* predominantly discriminated between CB and NCB. They were then used to construct a classifier, which achieved an AUC of 0.95 for efficacy prediction.

Conclusions This prospective randomized pilot study provided insights for influence of the gut microbiome with probiotics in mCRC. WLS could maintain intestinal microecological balance of patients with mCRC by decreasing the degree of abundance of gut microbiome fall after chemotherapy and down-regulating lipopolysaccharide metabolism-related pathway. We established a novel classifier that accurately distinguished between patients with CB and NCB on systemic therapy.

Trial Registration NCT04021589

Ethics Approval This study has been approved by Clinical Research Ethics Committee of the First Affiliated Hospital, College of Medicine, Zhejiang University. Acceptance number: IIT20200348A-R1

<http://dx.doi.org/10.1136/jitc-2021-SITC2021.414>



Abstract 414 Figure 1 Metabolic pathways for differential enrichment. Metabolic pathways for differential enrichment of the gut microbiome genome in microbiota preparation group through KEGG analysis

Results A total of 40 patients with mCRC in two tertiary hospitals were enrolled. Dynamic metagenomic analysis indicated that during systemic treatment, the diversity of the gut microbiome were all decreased in both arms. It has been reported that higher a diversity is associated with a better prognosis, while the degree of decline in WLS-intervention group was a relatively minor change. GO enrichment analysis of differential genes indicated a strong enrichment for genes related to lipid metabolism after WLS intervention (figure 1; $p < 0.01$). Lipopolysaccharide (LPS) could regulate the accumulation of monocyte-like macrophages and promote the inflammatory microenvironment in a chemokine-dependent manner,

416

AN OPEN-LABEL PHASE 2 STUDY OF 2 DOSES OF THE HYPOXIA-INDUCIBLE FACTOR (HIF)-2 α INHIBITOR BELZUTIFAN FOR THE TREATMENT OF ADVANCED CLEAR CELL RENAL CELL CARCINOMA AFTER PROGRESSION ON SYSTEMIC THERAPY<http://dx.doi.org/10.1136/jitc-2021-SITC2021.416>

¹Michael Atkins*, ²Yanfang Liu, ²Rodolfo Perini, ²Ananya Roy, ³John Haanen. ¹Georgetown Lombardi Comprehensive Cancer, Washington, DC, USA; ²Merck and Co., Inc., Kenilworth, NJ, USA; ³Netherlands Cancer Institute, Amsterdam, Netherlands

Background Accumulation and aberrant stabilization of transcription factor HIF-2 α drives the expression of genes associated with progression of clear cell renal cell carcinoma (ccRCC). Belzutifan, a first-in-class HIF-2 α inhibitor, has demonstrated promising antitumor activity with a favorable safety profile in patients with heavily pretreated ccRCC. The efficacy and safety of 2 doses of belzutifan in patients with advanced ccRCC who experienced progression after systemic therapy will be evaluated in this randomized, open-label, multicenter, phase 2 trial (NCT04489771).

Methods Approximately 150 adults will be randomly assigned 1:1 to receive oral belzutifan 120 mg once daily or 200 mg once daily. Patients with locally advanced or metastatic ccRCC (per RECIST v1.1) who experienced progression on or after 1 line of anti-PD-1/PD-L1 therapy as monotherapy or combined with other agents, with the immediately preceding line of treatment an anti-PD-1/PD-L1 therapy, will be enrolled. Progression is defined as received ≥ 2 doses of an anti-PD-1/PD-L1 agent and having demonstrated radiographic disease progression (per investigator). Other key eligibility criteria: ≤ 3 prior systemic regimens and a Karnofsky Performance Status Scale score $\geq 70\%$. Patients who previously received belzutifan or another HIF-2 α inhibitor; require supplemental oxygen; have a baseline hemoglobin level < 10 g/dL; have a history of HIV, hepatitis B, or hepatitis C infection; or have active central nervous system metastases are excluded. Patients will be stratified by International mRCC Database Consortium prognostic scores (0, 1 or 2, or 3–6) and by number of prior tyrosine kinase inhibitor-containing therapies (0, 1, or 2 or 3). Treatment will continue until progression, unacceptable toxicity, or withdrawal of consent. Computed tomography or magnetic resonance imaging will be performed at baseline, every 8 weeks through week 49, and every 12 weeks thereafter. Adverse events will be monitored throughout the study and for 30 days after treatment (90 days for serious adverse events). The primary end point is objective response rate per RECIST v1.1 by blinded independent central review (BICR). Secondary end points are progression-free survival, duration of response, and clinical benefit rate per RECIST v1.1 by BICR, overall survival, pharmacokinetics, and safety. The study will enroll patients in at least 9 countries (Australia, Belgium, Greece, Ireland, Israel, Netherlands, Russia, the United Kingdom, and the United States) and is recruiting.

Acknowledgements Medical writing and/or editorial assistance was provided by Matthew Grzywacz, PhD of ApotheCom (Yardley, PA, USA). This assistance was funded by Merck Sharp & Dohme Corp., a subsidiary of Merck & Co., Inc., Kenilworth, NJ, USA. Funding for this research was provided by Merck Sharp & Dohme Corp., a subsidiary of Merck & Co., Inc., Kenilworth, NJ, USA.

Trial Registration ClinicalTrials.gov, NCT04489771

Ethics Approval The study and the protocol were approved by the Institutional Review Board or ethics committee at each site.

PHASE 3 STUDY OF PEMBROLIZUMAB + BELZUTIFAN + LENVATINIB OR PEMBROLIZUMAB/QUAVONLIMAB + LENVATINIB VERSUS PEMBROLIZUMAB + LENVATINIB AS FIRST-LINE TREATMENT FOR ADVANCED RENAL CELL CARCINOMA

¹Toni Choueiri*, ²Elizabeth Plimack, ³Thomas Powles, ⁴Martin Voss, ⁴Howard Gurney, ⁵Rachel Silverman, ⁵Rodolfo Perini, ⁵Karla Rodriguez-Lopez, ⁶Brian Rini. ¹Dana-Farber Cancer Institute and Harvard Medical School, Boston, MA, USA; ²Fox Chase Cancer Center, Philadelphia, PA, USA; ³Barts Health NHS Trust and the Royal Free NHS Foundation Trust, London, UK; ⁴Memorial Sloan Kettering Cancer Center, New York, NY, USA; ⁵Merck and Co., Inc., Kenilworth, NJ, USA; ⁶Vanderbilt-Ingram Cancer Center, Nashville, TN, USA; ⁷Westmead Hospital and Macquarie University Hospital, Sydney, Australia

Background Pembrolizumab + vascular endothelial growth factor (VEGF) inhibitor lenvatinib demonstrated antitumor activity as first-line treatment for advanced clear cell renal cell carcinoma (ccRCC) in phase 3 trial KEYNOTE-581/CLEAR (NCT02811861). Hypoxia-inducible factor 2 α (HIF-2 α) inhibitor belzutifan (MK-6482) showed antitumor activity in ccRCC, and a coformulation of pembrolizumab and CTLA-4 inhibitor quavonlimab (MK-1308A) showed antitumor activity in non-small cell lung cancer. HIF-2 α or CTLA-4 inhibition with PD-1 and VEGF inhibition backbone combination may provide additional benefit as first-line treatment in ccRCC. This open-label, randomized, phase 3 study (NCT04736706) will be conducted to compare novel combination therapies pembrolizumab + belzutifan + lenvatinib (arm A) and MK-1308A + lenvatinib (arm B) with pembrolizumab + lenvatinib (arm C).

Methods Approximately 1431 adults with metastatic ccRCC, measurable disease per RECIST v1.1, and Karnofsky Performance Status Scale score $\geq 70\%$ who had not previously undergone systemic therapy for advanced ccRCC will be enrolled. Patients will be randomly assigned 1:1:1 to arm A (belzutifan 120 mg + lenvatinib 20 mg oral once daily + pembrolizumab 400 mg IV every 6 weeks), arm B (MK-1308A [quavonlimab 25 mg + pembrolizumab 400 mg] IV every 6 weeks and lenvatinib 20 mg oral once daily), or arm C (pembrolizumab 400 mg IV every 6 weeks + lenvatinib 20 mg oral once daily). Treatment will continue until documented disease progression, withdrawal of consent, or other discontinuation event; patients will receive pembrolizumab and MK-1308A for up to 18 cycles (approximately 2 years). Patients will be stratified by International mRCC Database Consortium (IMDC) score (favorable vs intermediate vs poor), region of the world (North America vs Western Europe vs rest of the world), and sarcomatoid features (yes vs no). Response will be assessed by CT or MRI per RECIST v1.1 by blinded independent central review (BICR) at week 12 from randomization, every 6 weeks through week 78, and every 12 weeks thereafter. Adverse events and serious adverse events will be monitored throughout the study and for 90 days after treatment. Dual primary end points are progression-free survival per RECIST v1.1 by BICR and overall survival. Primary end points will be assessed in arm A compared with arm C and in arm B compared with arm C for patients with IMDC intermediate/poor status and in all patients regardless of IMDC status. Secondary end points are objective response rate and duration of response per RECIST v1.1 by BICR, patient-reported outcomes, and safety.

Acknowledgements Medical writing and/or editorial assistance was provided by Matthew Grzywacz, PhD, of ApotheCom (Yardley, PA, USA). This assistance was funded by Merck Sharp & Dohme Corp., a subsidiary of Merck & Co., Inc., Kenilworth, NJ, USA, and Eisai Inc., Woodcliff Lake, NJ,

USA. Funding for this research was provided by Merck Sharp & Dohme Corp., a subsidiary of Merck & Co., Inc., Kenilworth, NJ, USA, Eisai Inc., Woodcliff Lake, NJ, USA.

Trial Registration ClinicalTrials.gov, NCT04736706

Ethics Approval The study and the protocol were approved by the Institutional Review Board or ethics committee at each site.

<http://dx.doi.org/10.1136/jitc-2021-SITC2021.417>

PHASE 1B/2 KEYNOTE-365 COHORT I: PLATINUM-CONTAINING CHEMOTHERAPY ALONE OR IN COMBINATION WITH PEMBROLIZUMAB FOR TREATMENT-EMERGENT NEUROENDOCRINE PROSTATE CARCINOMA<http://dx.doi.org/10.1136/jitc-2021-SITC2021.418>

¹Johann De Bono*, ²Neal Shore, ³Gero Kramer, ⁴Anthony Joshua, ⁵Xin Tong Li, ⁵Christian Poehlein, ⁵Charles Schloss, ⁶Evan Yu. ¹The Royal Marsden NHS Foundation Trust, London, UK; ²Carolina Urologic Research Center, Myrtle Beach, SC, USA; ³Medical University of Vienna, Vienna, Austria; ⁴Saint Vincent's Hospital Sydney, Sydney, Australia; ⁵Merck and Co., Inc., Kenilworth, NJ, USA; ⁶University of Washington, Seattle, WA, USA

Background Treatment-emergent neuroendocrine prostate carcinoma (t-NE) can occur de novo or after diagnosis of prostate adenocarcinoma. Treatment often includes platinum-containing chemotherapy because of t-NE's histologic similarity to small cell lung cancer. The PD-1 inhibitor pembrolizumab has shown promising efficacy and acceptable safety when combined with olaparib, docetaxel, or enzalutamide for treatment of metastatic castration-resistant prostate cancer (mCRPC) in the multicohort phase 1b/2 KEYNOTE-365 study (NCT02861573). Cohort I will be used to compare platinum-containing chemotherapy alone with chemotherapy + pembrolizumab as treatment for t-NE.

Methods Patients who have t-NE ($\geq 1\%$ neuroendocrine cells in a recent biopsy specimen confirmed by central histology review); experienced progression within 6 months of starting a next-generation hormonal agent (NHA) for mCRPC or hormone-sensitive prostate cancer and experienced progression within 6 cycles of docetaxel treatment for mCRPC; and have an Eastern Cooperative Oncology Group (ECOG) performance status score of 0 or 1 are eligible. Prior therapy with ≤ 2 NHAs and 1 other chemotherapy for mCRPC is permitted. Patients will be randomly assigned 1:1 to receive pembrolizumab 200 mg IV on day 1 of each cycle every 3 weeks + carboplatin AUC of 5 IV on day 1 + etoposide 100 mg/m² IV on days 1, 2, and 3 of each 21-day cycle for 4 cycles (arm 1) or the same chemotherapy regimen without pembrolizumab (arm 2); in each arm 40–100 patients will be enrolled. Pembrolizumab treatment will continue up to 2 years until disease progression, unacceptable toxicity, or withdrawal of consent. Patients will be stratified by ECOG performance status score (0 or 1). Computed tomography or magnetic resonance imaging will be performed every 9 weeks through week 54 and every 12 weeks thereafter. Primary end points are safety and tolerability, prostate-specific antigen (PSA) response rate, and objective response rate (ORR) per RECIST v1.1 by blinded independent central review (BICR). Secondary end points are time to PSA progression; ORR and radiographic progression-free survival (PFS) per PCWG3-modified RECIST v1.1 by BICR; duration of response and disease control rate per RECIST v1.1 by BICR and PCWG3-modified RECIST v1.1 by BICR; and overall survival. End points will be summarized for each arm without formal hypothesis testing.

Acknowledgements Medical writing and/or editorial assistance was provided by Matthew Grzywacz, PhD, of ApotheCom (Yardley, PA, USA). This assistance was funded by Merck Sharp & Dohme Corp., a subsidiary of Merck & Co., Inc., Kenilworth, NJ, USA. Funding for this research was provided by Merck Sharp & Dohme Corp., a subsidiary of Merck & Co., Inc., Kenilworth, NJ, USA.

Trial Registration ClinicalTrials.gov, NCT02861573

Ethics Approval The study and the protocol were approved by the Institutional Review Board or ethics committee at each site.

419

**PEMBROLIZUMAB + LENVATINIB IN PATIENTS WITH
ADENOCARCINOMA METASTATIC CASTRATION-
RESISTANT PROSTATE CANCER (mCRPC) OR
TREATMENT-EMERGENT NEUROENDOCRINE mCRPC:
PHASE 1B/2 KEYNOTE-365 COHORTS E/F**

¹Gero Kramer*, ²Neal Shore, ³Anthony Joshua, ⁴Xin Tong Li, ⁴Christian Poehlein, ⁴Charles Schloss, ⁵Johann De Bono, ⁶Evan Yu. ¹Medical University of Vienna, Vienna, Austria; ²Carolina Urologic Research Center, Myrtle Beach, SC, USA; ³Saint Vincent's Hospital Sydney, Sydney, Australia; ⁴Merck and Co., Inc., Kenilworth, NJ, USA; ⁵The Royal Marsden NHS Foundation Trust, London, UK; ⁶University of Washington, Seattle, WA, USA

Background Treatment of adenocarcinoma mCRPC includes abiraterone, enzalutamide, or docetaxel but is not curative, and ~20% of patients develop treatment-emergent neuroendocrine mCRPC (t-NE) after diagnosis of adenocarcinoma. Monotherapy with the PD-1 inhibitor pembrolizumab showed promising antitumor activity in the phase 2 KEYNOTE-199 trial in adenocarcinoma mCRPC. The vascular endothelial growth factor (VEGF)/fibroblast growth factor receptor (FGFR) inhibitor lenvatinib inhibits proliferation and angiogenesis in mice models. Combined PD-1 and VEGF/FGFR inhibition may have enhanced benefit in adenocarcinoma mCRPC or t-NE.

Methods The nonrandomized, open-label, multicohort, phase 1b/2 KEYNOTE-365 study (NCT02861573) will be conducted to evaluate several pembrolizumab combination therapies in patient populations with adenocarcinoma mCRPC or t-NE. In cohorts E and F each, 40–100 adults with Eastern Cooperative Oncology Group performance status score of 0/1 who received docetaxel for mCRPC will be enrolled. Prior therapy with ≤2 next-generation hormonal agents (NHAs) and 1 other chemotherapy for mCRPC is permitted. Patients in cohort E must have confirmed adenocarcinoma of the prostate without small cell histology at study entry. Patients in cohort F must have t-NE (≥1% neuroendocrine cells in a recent biopsy specimen confirmed by central histology review) that progressed within 6 months of starting an NHA for mCRPC or hormone-sensitive metastatic prostate cancer and progressed within 6 cycles of docetaxel for mCRPC. Both cohorts will receive pembrolizumab 200 mg intravenously every 3 weeks + oral lenvatinib 20 mg daily until disease progression, consent withdrawal, or other discontinuation event. Computed tomography or magnetic resonance imaging will be performed at screening, every 9 weeks through week 54, and every 12 weeks thereafter. Adverse events will be monitored through 30 days after discontinuation (90 days if serious) and graded per CTCAE v4.0. Primary end points are safety and tolerability, prostate-specific antigen (PSA) response rate, and objective response rate (ORR) per RECIST v1.1 by blinded independent central review (BICR). Secondary end points are time to PSA progression; ORR and radiographic progression-free survival (rPFS) per Prostate Cancer Working Group 3 (PCWG3)-modified RECIST v1.1 by BICR; duration of response and disease control rate per RECIST v1.1 and PCWG3-modified RECIST v1.1 by BICR; and overall survival.

Acknowledgements Medical writing and/or editorial assistance was provided by Matthew Grzywacz, PhD, of ApotheCom (Yardley, PA, USA). This assistance was funded by Merck Sharp & Dohme Corp., a subsidiary of Merck & Co., Inc., Kenilworth, NJ, USA. Funding for this research was provided by Merck Sharp & Dohme Corp., a subsidiary of Merck & Co., Inc., Kenilworth, NJ, USA.

Trial Registration ClinicalTrials.gov, NCT02861573

Ethics Approval The study and the protocol were approved by the Institutional Review Board or ethics committee at each site.

<http://dx.doi.org/10.1136/jitc-2021-SITC2021.419>

PROSTVAC IN COMBINATION WITH NIVOLUMAB ENHANCED IMMUNE CELL INFILTRATION IN PROSTATE CANCER

¹Shania Bailey*, ²Wiem Lassoued, ¹Antonios Papanicolau-Sengos, ¹Jennifer Marte, ¹Nikki Williams, ¹Amy Hankin, ¹Michell Manu, ¹William Dahut, ¹Peter Pinto, ¹Fatima Karzai, ¹Ravi Madan, ¹Houssein Abdul Sater, ¹James Gulley. ¹NIH, Bethesda, MD, USA; ²NCI, Frederick, MD, USA

Background Prostate cancer (PC) is the most common non-cutaneous diagnosed cancer among men in USA.¹ Although clinical outcomes are favorable for patients with localized disease, 20–30% of patients will develop metastatic prostate cancer (mPC) and have poor prognosis. Immunotherapy, as a single agent, provides benefit to a small subset of PC patients, which is thought to be partially due to its known cold tumor immune microenvironment (TIME). Combination studies are needed to enhance benefit.² Prostavac is a therapeutic cancer vaccine engineered to activate an immune response against prostate-specific Antigen (PSA).³ Prostavac alone could induce systemic immune response by increasing immune-cell infiltrates in and around the tumor.⁴ In this study, we are exploring the effect of Prostavac in combination with nivolumab in TIME in prostate cancer.

Methods We treated locally advanced prostate cancer patients (n=6) undergoing radical prostatectomy (RP) with neoadjuvant Prostavac in combination with nivolumab, an immune checkpoint PD-1 inhibitor. Dynamic changes in TIME before and after treatment were studied using multiplex immunofluorescence (Opal Method). Formalin fixed paraffin-embedded sections from matched pre-treated prostate biopsies and post-treated RP samples were stained with a validated T cell panel (DAPI, CD4, CD8, FOXP3, Ki67, Pan CK and PD-L1). To analyze the data, TIME was segmented into 3 compartments: intratumoral, invasive margin and benign.

Results Combination immunotherapy significantly increased CD4+ T cell density in the invasive margin (mean 211.5 cells/mm² vs 592.2 cells/mm², p<0.05), with similar trend in the intratumoral and the benign compartments. CD8+ T cell density increased after treatment in the invasive margin (mean 47.25 cells/mm² vs 157cells/mm²) and the benign compartment. 5/6 and 4/6 patients showed more than 2-fold increase of CD4 and CD8 T cells in the TIME, respectively, in at least one of the three compartments. Increased proliferative indices in CD4+ and CD8+ T cells were also seen after treatment. Tregs were present in low frequencies in TIME (maximum of 12 cells/mm²) with no significant changes. Moreover, a significant drop in tumor cell Ki67 after treatment (mean 252.8 cells/mm² vs 100.5 cells/332, p<0.05) suggests that the combination may control tumor growth.

Conclusions The combination of Neoadjuvant Prostavac and nivolumab was associated with increased immune cell infiltration in a cohort of early prostate cancer patients. A broader examination of the TIME and the role immune cells undertake to control tumor growth is on-going.

Trial Registration NCT02933255

REFERENCES

1. Siegel RL, Miller KD, Jemal A. Cancer statistics, 2020. *CA Cancer J Clin (Internet)* 2020;**70**:7–3
2. Zhao SG, Lehrer J, Chang SL, et al. The immune landscape of prostate cancer and nomination of PD-L2 as a potential therapeutic target. *J Natl Cancer Inst* 2018;**111**:301–10.
3. Madan RA, Arlen PM, Mohebtash M, et al. Prostavac-VF: a vectorbased vaccine targeting PSA in prostate cancer. *Expert Opin Investig Drugs* 2009;**18**:1001–11

4. Abdul Sater H, Marté JL, Donahue RN, et al. Neoadjuvant PROSTVAC prior to radical prostatectomy enhances T-cell infiltration into the tumor immune microenvironment in men with prostate cancer. *J Immunother Cancer* 2020;**8**(1):655–64

Ethics Approval This study was performed in compliance with ethical standard and was approved by the NIH IRB, 17C-0007. All patients participating in this study gave an informed consent before taking part.

<http://dx.doi.org/10.1136/jitc-2021-SITC2021.420>

A FIRST-IN-HUMAN (FIH) PHASE I/IIA CLINICAL TRIAL ASSESSING A RIBONUCLEIC ACID LIPOPLEX (RNA-LPX) ENCODING SHARED TUMOR ANTIGENS FOR IMMUNOTHERAPY OF PROSTATE CANCER; PRELIMINARY ANALYSIS OF PRO-MERIT

¹Mark Linch*, ²Zsuzsanna Papai, ³Istvan Takacs, ⁴Esteban Rodrigo Imedio, ⁴Marie-Cristine Kühnle, ⁴Evelyna Derhovanessian, ⁴Isabel Vogler, ⁴Stephanie Renken, ⁴Phillippa Graham, ⁴Ugur Sahin, ⁴Özlem Türeci. ¹University College London Hospitals NHS Foundation Trust, London, UK; ²Magyar Honvédség EK, Onkológiai Osztály, Budapest, Hungary; ³Semmelweis Egyetem, Belgyógyászati Klinika, Farmakológiai Részleg, Budapest, Hungary; ⁴BioNTech SE, Mainz, Germany

Background PRO-MERIT is a FIH, open-label, multicenter, Phase I/IIa trial investigating a liposomal RNA vaccine (BNT112) targeting the prostate cancer tumor-associated antigens (TAAs) kallikrein-2, kallikrein-3, acid phosphatase prostate, homeobox B13 (HOXB13), and NK3 homeobox 1. BNT112 is being investigated as monotherapy and in combination with cemiplimab in patients with metastatic castration-resistant prostate cancer (mCRPC) and newly diagnosed high risk localized prostate cancer (LPC).

Methods The trial involves dose titration in mCRPC patients (who have progressed after at least 2 but no more than 3 lines of systemic therapy) with BNT112 monotherapy (Part 1, fully recruited), followed by expansion cohorts (Part 2, recruiting) in both mCRPC and LPC with either BNT112 as monotherapy or in combination with cemiplimab. Primary trial endpoints investigate safety, tolerability, and preliminary anti-tumor activity (by Prostate Cancer Working Group 3 criteria). Secondary endpoints include determination of systemic induction or expansion of vaccine antigen-specific T cells. Vaccine-induced immune responses are analyzed *ex vivo* using an interferon- γ enzyme-linked immune absorbent spot (ELISpot) assay and following short-term *in vitro* stimulation.

Results As of 17 May 2021, 11 patients have received BNT112 monotherapy (9 Part 1; 2 in Part 2) and 3 patients have received BNT112 in combination with cemiplimab (at least one cycle completed). In Part 1, all 9 patients were stage IV at diagnosis and were receiving androgen deprivation therapy. Median age was 68 years. Two out of 9 patients experienced Grade 3 hypertension, leading to one dose reduction, that was initially reported as dose-limiting toxicity (DLT). All recovered within 24 h with no sequelae and the Safety Review Committee eventually concluded the events did not meet the DLT definition. Most common related adverse events (AEs) were pyrexia and hypertension. Eight serious AEs were reported in 5 patients, all unrelated to BNT112. In the 5 patients in Part 2, no additional safety signals or concerns were identified to date, either with BNT112 as monotherapy or in combination with cemiplimab. ELISpot data showed vaccine-induced immune responses were present in 7/7 ELISpot-evaluable patients. All 5 BNT112 TAAs were found to be immunogenic. Responses to each antigen were observed in at least 2 subjects. Initial responses with decreased prostate-specific antigen (PSA) levels have been observed in 2 patients in the BNT112 monotherapy arm.

Conclusions These data suggest that BNT112 has an acceptable safety profile. Additionally, BNT112 induces robust immune and PSA responses in patients with advanced prostate cancer.

Acknowledgements The authors would like to acknowledge Camilla West (BioNTech SE) for medical writing support.

Trial Registration ClinicalTrials.gov: NCT04382898.

Ethics Approval Ethics & Institutional Review Board approvals were obtained from the respective participating countries prior to initiation of the trial.

<http://dx.doi.org/10.1136/jitc-2021-SITC2021.421>

SAFETY AND EFFICACY OF NEOADJUVANT INTRAVESICAL ONCOLYTIC MV-NIS IN PATIENTS WITH UROTHELIAL CARCINOMA

¹Tanner Miest, ²Bradley Leibovich, ³Stephen Bardot, ²Paul Young, ²Stephen Boorjian, ⁴Mark Gonzalgo, ²Loren Herrera-Hernandez, ²Matthew Tollefson, ²Jeffrey Karnes, ²Paige Nichols, ²Tessa Kroeninger, ³Rachel Graham, ⁴Carole Lahana, ⁵Monica Reckner, ²Alysha Newsom, ⁶Nandakumar Packiriswamy, ⁷Janice Anoka, ²Kah Whye Peng, ⁷Erol Wiegert, ⁷Alice Bexon, ⁶Shruthi Naik*. ¹University of Texas and Mayo Clinic, Houston, TX, USA; ²Mayo Clinic, Rochester, MN, USA; ³Ochsner Clinic, New Orleans, LA, USA; ⁴University of Miami, Miami, FL, USA; ⁵Vyriad, Inc., Rochester, MN, USA; ⁶Mayo Clinic and Vyriad Inc., Rochester, MN, USA; ⁷Vyriad Inc., Rochester, MN, USA

Background Bladder cancer is a leading cause of cancer death in the United States.¹ The histology in > 90% of cases is urothelial carcinoma (UC). Tumors may present either as non-muscle-invasive (NMIBC) or muscle-invasive disease (MIBC). Current standard of care for patients with high risk NMIBC includes transurethral resection of bladder tumor (TURBT) followed by intravesical immunotherapy with Bacillus Calmette-Guérin (BCG).² Meanwhile, patients with BCG unresponsive NMIBC or MIBC are recommended to undergo radical cystectomy (RC), which adversely impacts quality of life and is associated with significant morbidity.³ MV-NIS is an investigational oncolytic measles virus with an excellent clinical safety profile.⁴ This ongoing phase I clinical study is designed to test the safety, efficacy and identify the recommended phase 2 dose (RP2D) of intravesical MV-NIS in patients with NMIBC or MIBC who are scheduled for RC and not eligible for neoadjuvant chemotherapy.

Methods Bladder UC patients were evaluated for eligibility and provided informed consent prior to enrolling. To date 8 patients have been enrolled: 4 to the single dose safety cohort, and 4 to the multi-dose expansion cohort. Patients were administered intravesical $\sim 1 \times 10^9$ TCID₅₀ MV-NIS once at least 1 week prior to RC (safety cohort), or twice at 4 and 2 weeks prior to RC (expansion cohort). Patients were closely monitored during the 2-hour instillation period. Tumor specimens from the pre-treatment TURBT and post-treatment RC were analyzed to determine pre- and post-treatment pathological stage and evaluate tumor killing and immune cell infiltrate.

Results Intravesical MV-NIS treatment was well tolerated in all patients. Only a single Adverse Event (AE) attributable to MV-NIS treatment (Grade 1 hematuria). AEs Grade > 2 were related to post-surgical complications. Tumor pathology findings are summarized in table 1. Tumor downstaging was observed in 4 of 8 patients. Among 4 patients in the expansion cohort, 2 had no residual disease (pT0). Central assessment of RC tissues showed significant inflammatory infiltrate in all treated bladder specimens. Detailed analyses are ongoing to characterize MV infection and immune infiltrate in bladder tissue

Conclusions The higher-than-expected rate of tumor downstaging and pT0 pathology, paired with the significant immune infiltrate observed in post-treatment bladder tissue, provide compelling evidence that intravesical MV-NIS has clinical activity against UC. These results support the use of two doses of $\sim 1 \times 10^9$ TCID₅₀ as the RP2D in future clinical studies for BCG unresponsive NMIBC or MIBC patients. MV-NIS induced inflammation may act synergistically with checkpoint blockade therapies.

Abstract 422 Table 1 Pre-treatment (TURBT) and post-treatment (RC) pathology

	PID	TURBT pathology (local)	RC pathology (central)
SINGLE DOSE COHORT	201-001	MIBC: High grade pT3	High grade pT3: Significant inflammatory infiltrate (lamina propria): eosinophils, monocytes/macrophages, T-cells. Necrosis present in normal and tumor tissue.
	201-002	NMIBC: High grade pTis	pT0 – No residual disease. Significant inflammatory infiltrate (lamina propria): neutrophils, eosinophils, monocytes/macrophages, T-cells, plasma cells.
	208-003	MIBC: High grade pT2 with <25% glandular diff.	High grade pT3 with glandular differentiation. Significant inflammatory infiltrate including neutrophils, eosinophils, T-cells and plasma cells.
	201-004	MIBC: High grade pT2	High grade pTis – Disease downstaging. Significant inflammatory infiltrate including neutrophils, eosinophils, T-cells, plasma cells. Necrosis present.
TWO DOSE	201-005	NMIBC: High grade pT1	pT0 – No residual disease. Significant inflammatory infiltrate (lamina propria): T-cells.
	201-006	MIBC: High grade pT2	pT0 – No residual disease. Significant inflammatory infiltrate (predominantly T-cell lymphocytes and plasma cells).
	201-007	NMIBC: High grade pTis	pTis – significant inflammatory infiltrate (predominantly T-cells). Necrosis is absent.
	201-008	MIBC: High grade pT3	Persistent pT3 disease with squamous differentiation. Significant inflammatory infiltrate (predominantly lymphocytes) – neutrophils, eosinophils, B- and T-cells, monocytes/macrophages.

Trial Registration NCT03171493

REFERENCES

1. Siegel RL, Miller KD, Jemal A. Cancer statistics, 2019. *CA Cancer J Clin* 2019;**69**(1):7–34.
2. Knowles MA, Hurst CD. Molecular biology of bladder cancer: new insights into pathogenesis and clinical diversity. *Nat Rev Cancer* 2015;**15**(1):25–41.
3. Zakaria AS, Santos F, Dragomir A, Tanguay S, Kassouf W, Aprikian AG. Postoperative mortality and complications after radical cystectomy for bladder cancer in Quebec: A population-based analysis during the years 2000–2009. *Can Urol Assoc J* 2014;**8**(7–8):259–267.
4. Galanis E, Atherton PJ, Maurer MJ, Knutson KL, Dowdy SC, Cliby WA, Haluska P Jr, Long HJ, Oberg A, Aderca I, Block MS, Bakkum-Gamez J, Federspiel MJ, Russell SJ, Kalli KR, Keeney G, Peng KW, Hartmann LC. Oncolytic measles virus expressing the sodium iodide symporter to treat drug-resistant ovarian cancer. *Cancer Res* 2015;**75**(1):22–30.

Ethics Approval Approval was received from the Institutional Review boards (IRBs) at all clinical sites including Mayo Clinic (#17–004167); Ochsner Health (#2020 060); and University of Miami (#20200174). All study participants are required to review and sign an IRB approved informed consent before taking part in the clinical trial.

<http://dx.doi.org/10.1136/jitc-2021-SITC2021.422>

423

A PHASE 2 STUDY OF IBRUTINIB AS NEOADJUVANT THERAPY IN PATIENTS WITH LOCALIZED PROSTATE CANCER

¹Russell Pachynski*, ¹Melissa Reimers, ¹Cody Weimholt, ¹Katie Slane, ¹Peter Oppelt, ¹Jason Frankel, ¹Robert Figenshau, ¹Eric Kim, ¹Gerald Andriole, ²Lawrence Fong. ¹Washington University School of Medicine, St Louis, MO, USA; ²UCSF, San Francisco, CA, USA

Background Treatment of localized prostate cancer with surgery or radiotherapy remains suboptimal with failure rates of 35–40%.¹ Neoadjuvant androgen deprivation therapy improved pathologic outcomes, but did not significantly impact progression-free or overall survival.² Prostate cancer with higher density of B cells correlates with higher stage disease and higher risk of recurrence or progression.³ Elevated levels of BTK (Bruton's tyrosine kinase) – an enzyme known to have critical roles in B cell function – have also been noted in prostate cancer compared to normal prostate tissue, correlate with cancer grade, and may play a role in prostate tumorigenesis. Preclinical modeling shows pharmacologic suppression of BTK inhibits growth of prostate cancer.⁴ Ibrutinib, a potent BTK inhibitor, can target B-cell signaling pathways and has an established safety profile. Ibrutinib may act to reduce immunosuppression by intratumoral B cells, which can secrete anti-inflammatory IL-10 and inhibit Th1 and cytotoxic CD8 T cell activity.⁵ Therefore, we hypothesized that ibrutinib will augment anti-tumor immune responses in localized prostate cancer.

Methods Accrual began in July 2016 for this ongoing trial (NCT02643667). 23 of 24 planned patients have been enrolled to date. Eligible patients have received no prior treatment for their histologically confirmed prostatic adenocarcinoma and have no evidence of metastatic disease. Patients must have decided upon surgery and been deemed suitable candidates to undergo a radical prostatectomy. Following completion of an initial three patient safety cohort of 840 mg, qd ibrutinib dosing for 14 days, all remaining patients receive treatment with 840 mg/day oral ibrutinib for 28 days. Radical prostatectomy will occur 7–12 days after the last dose of ibrutinib. Patients are assessed 4 weeks after surgery. The primary objectives are to assess safety of ibrutinib and characterize B and T cell infiltration within prostate tissue in the ibrutinib treated patients compared to a reference population. Correlative tissue samples will be obtained to characterize the B and T cell infiltration within prostate tissue treated with ibrutinib compared to an untreated reference population. Correlative blood samples will be used to investigate circulating B and T cells induced by ibrutinib. BTK and PD-L1 expression in tumor and immune-infiltrating immune cells will also be examined. This is the first clinical trial of ibrutinib in prostate cancer, lays the foundation for larger future studies.

Trial Registration NCT02643667

REFERENCES

1. Kuban DA, Thames HD, Levy LB, et al. Long-term multi-institutional analysis of stage T1-T2 prostate cancer treated with radiotherapy in the PSA era. *Int J Radiat Oncol Biol Phys* 2003 Nov 15;**57**(4):915–28. PubMed PMID: 14575822.
2. Scolieri MJ, Altman A, Resnick MI. Neoadjuvant hormonal ablative therapy before radical prostatectomy: a review. Is it indicated? *J Urol* 2000 Nov;**164**(5):1465–72. PubMed PMID: 11025684.
3. Woo JR, Liss MA, Muldong MT, et al. Tumor infiltrating B-cells are increased in prostate cancer tissue. *J Transl Med* 2014 Jan 30;**12**–30. Pubmed PMID: 24475900.
4. Guo W, Liu R, Bhardwaj G, et al. Targeting Btk/Etk of prostate cancer cells by a novel dual inhibitor. *Cell Death Dis* 2014 Sep 4;**5**:e1409. PubMed PMID: 25188519.

5. Gunderson AJ, Coussens LM. B cells and their mediators as targets for therapy in solid tumors. *Exp Cell Res* 2013 Jul 1;**319**(11):1644–9. PubMed PMID: 23499742.

Ethics Approval This study obtained ethics approval from the Washington University School of Medicine IRB (#201808057), and participating individuals gave informed consent before taking part.

<http://dx.doi.org/10.1136/jitc-2021-SITC2021.423>

424

A PHASE 1B/2 RANDOMIZED STUDY OF AVB-S6-500 IN COMBINATION WITH CABOZANTINIB VERSUS CABOZANTINIB ALONE IN PATIENTS WITH ADVANCED CLEAR CELL RENAL CELL CARCINOMA WHO HAVE RECEIVED FRONT-LINE TREATMENT

¹Kathryn Beckermann*, ²Nicholas Vogelzang, ³Mao Shifeng, ⁴Moshe Ornstein, ⁵Neil Shah, ⁶Hans Hammers, ⁷Matthew Campbell, ⁸Xin Gao, ⁹David McDermott, ¹⁰Randy Anderson, Vanessa Esquibel, ¹⁰Eduardo Pennella, ¹⁰Reshma Rangwala, ¹¹Eric Jonasch. ¹Vanderbilt-Ingram Cancer Center, Nashville, TN, USA; ²Comprehensive Cancer Centers of Nevada, Las Vegas, NV, USA; ³Allegheny Health Network, Pittsburgh, PA, USA; ⁴Cleveland Clinic, Cleveland, OH, USA; ⁵Memorial Sloan Kettering Cancer Center, New York, USA; ⁶University of Texas, Southwestern, Dallas, USA; ⁷University of Texas MD Anderson Ca Ctr, Houston, TX, USA; ⁸Massachusetts General Hospital, Boston, MA, USA; ⁹Beth Israel Deaconess Medical Center, Boston, MA, USA; ¹⁰Aravive, Inc., Houston, TX, USA; ¹¹University of Texas, MD Anderson Ca Ctr, Houston, TX, USA

Background In clear cell renal cell carcinoma (ccRCC) the constitutive expression of hypoxia induced factor 1- α leads to increased expression of AXL. AXL overexpression has been associated with the development of resistance to VEGF inhibitors and suppression of the innate immune response through inhibition of macrophage-driven inflammation. AVB-S6-500 (AVB-500) is recombinant fusion protein dimer containing an extracellular region of human AXL combined with the human immunoglobulin G1 heavy chain (Fc), which demonstrates highly potent, specific AXL inhibition. In mouse ccRCC xenograft models, AVB-500 showed significantly more tumor reduction in combination with pazopanib versus pazopanib alone. In a Ph1b study of AVB-500 plus chemotherapy in platinum-resistant ovarian cancer (NCT03639246), no dose limiting toxicity (DLT) or treatment discontinuation due to adverse events was observed. The recommended phase 2 dose (RP2D) of 15 mg/kg was established by a model-informed drug development (MIDD) approach.

eligibility criteria include clear cell histology RCC and at least one prior line of therapy administered in the advanced or metastatic setting.

Results As of July 21, 2021, seven patients have received at least one dose of AVB-500 15 mg/kg and cabozantinib, with six patients ongoing treatment. No DLTs were observed. Trough levels at C1D15 were above the minimally efficacious concentration (MEC) identified from MIDD and GAS6 (AXL ligand) levels were suppressed prior to C2D1. Partial responses were observed in 3 of 5 patients (table 1); all patients demonstrated tumor decrease from baseline.

Conclusions AVB-500 in combination with cabozantinib demonstrates promising preliminary clinical activity and tolerability in patients with ccRCC. AVB-500 15 mg/kg is the presumptive RP2D with C1D15 AVB-500 troughs consistently above MECs observed. Safety, PK/PD and clinical activity will be updated at the time of presentation. (NCT04300140)

Ethics Approval This study has obtained ethics approval from WIRB Institutional Review Board®, Protocol ID #20200159, and all subjects provided informed consent prior to taking part in this study.

<http://dx.doi.org/10.1136/jitc-2021-SITC2021.424>

Abstract 424 Table 1 Preliminary clinical activity in NCT04300140

	Prior lines of therapy in the advanced/metastatic setting	# Cycles completed	Best overall response
102-001	1) Nivolumab/ipilimumab 2) Axitinib 3)	1.5, discontinued study	SD
102-002	1) Pazopanib 2) Pembrolizumab/axitinib	3, ongoing	SD
103-001	1) Nivolumab/ipilimumab	4, ongoing	PR, unconfirmed
105-002	1) Sunitinib 2) Nivolumab	2, ongoing	PR, unconfirmed
107-002	1) Pazopanib 2) Everolimus 3) Axitinib 4) Nivolumab/ipilimumab 5) Pembrolizumab/axitinib (Best response to therapy PD)	2, ongoing	PR, unconfirmed

Methods The P1b portion of this trial is a 3+3 dose escalation study to evaluate safety, pharmacokinetics, and pharmacodynamics of AVB 500 in combination with cabozantinib 60 mg daily. Dose levels of AVB-500 may include 15, 20, and 25 mg/kg every two weeks. The primary objective is to evaluate safety and tolerability. Secondary objectives include identification of the RP2D of AVB-500 and clinical activity. Key

425

PEMBROLIZUMAB + VIBOSTOLIMAB IN PATIENTS WITH ADENOCARCINOMA METASTATIC CASTRATION-RESISTANT PROSTATE CANCER (MCRPC) OR TREATMENT-EMERGENT NEUROENDOCRINE MCRPC: PHASE 1B/2 KEYNOTE-365 COHORTS G/H

¹Neal Shore*, ²Johann De Bono, ³Gero Kramer, ⁴Anthony Joshua, ⁵Xin Tong Li, ⁵Christian Poehlein, ⁵Charles Schloss, ⁶Evan Yu. ¹Carolina Urologic Research Center, Myrtle Beach, SC, USA; ²The Royal Marsden NHS Foundation Trust, London, UK; ³Medical University of Vienna, Vienna, Austria; ⁴Saint Vincent's Hospital Sydney, Sydney, Australia; ⁵Merck and Co., Inc., Kenilworth, NJ, USA; ⁶University of Washington, Seattle, WA, USA

Background Frontline treatment for patients with adenocarcinoma mCRPC includes docetaxel, radium 223, or the next-generation hormonal agents (NHAs) abiraterone or enzalutamide. For patients with disease progression on these therapies, approximately 20% will develop treatment-emergent neuroendocrine mCRPC (t-NE) after diagnosis of prostate adenocarcinoma. The PD-1 inhibitor pembrolizumab showed antitumor activity when combined with olaparib in cohort A of the phase 1b/2 KEYNOTE-365 trial, and the TIGIT inhibitor vibostolimab showed antitumor activity in preclinical models. Combining PD-1 and TIGIT inhibition may have enhanced benefit in adenocarcinoma mCRPC or t-NE.

Methods KEYNOTE-365 is a nonrandomized, open-label, multicohort study (NCT02861573) to assess several pembrolizumab combination therapies in patient populations with adenocarcinoma mCRPC or t-NE. In each of cohorts G and H, 40–100 adults with Eastern Cooperative Oncology Group performance status (ECOG PS) 0/1 who received docetaxel for mCRPC will be enrolled. Prior therapy with ≤ 2 NHAs and 1 other chemotherapy for adenocarcinoma mCRPC is permitted. Patients in cohort G must have adenocarcinoma of the prostate without small cell histology at study entry. Patients in cohort H must have t-NE ($\geq 1\%$ neuroendocrine cells in a recent biopsy specimen confirmed by central histology review) that progressed within 6 months of starting an NHA for mCRPC or hormone-sensitive prostate cancer and progressed within 6 cycles of docetaxel for mCRPC. All patients will receive MK-7684A, a coformulation of pembrolizumab 200 mg and vibostolimab 200 mg intravenously every 3 weeks until disease progression, consent withdrawal, or other discontinuation event. Adverse events will be monitored through 30 days after discontinuation (90 days if serious) and graded per CTCAE v4.0. Computed tomography or magnetic resonance imaging will be performed at screening, every 9 weeks through week 54, and every 12 weeks thereafter. Primary end points are safety and tolerability, prostate-specific antigen (PSA) response rate, and objective response rate (ORR) per RECIST v1.1 by blinded independent central review (BICR). Secondary end points are time to PSA progression, ORR and radiographic progression-free survival per Prostate Cancer Working Group 3 (PCWG3)-modified RECIST v1.1 by BICR; duration of response and disease control rate per RECIST v1.1 and PCWG3-modified RECIST v1.1 by BICR; and overall survival.

Acknowledgements Medical writing and/or editorial assistance was provided by Matthew Grzywacz, PhD, of ApotheCom (Yardley, PA, USA). This assistance was funded by Merck Sharp & Dohme Corp., a subsidiary of Merck & Co., Inc., Kenilworth, NJ, USA. Funding for this research was provided by Merck Sharp & Dohme Corp., a subsidiary of Merck & Co., Inc., Kenilworth, NJ, USA.

Trial Registration ClinicalTrials.gov, NCT02861573

Ethics Approval The study and the protocol were approved by the Institutional Review Board or ethics committee at each site.

<http://dx.doi.org/10.1136/jitc-2021-SITC2021.425>

426

A PHASE 3, SINGLE-ARM STUDY OF CG0070 IN SUBJECTS WITH NON-MUSCLE INVASIVE BLADDER CANCER (NMIBC) UNRESPONSIVE TO BACILLUS CALMETTE-GUERIN (BCG)

¹Ed Uchio, ²Donald Lamm, ³Neal Shore, ⁴Paul Anderson, ⁵Tran Ben, ⁶Ashish Kamat, ⁷John McAdory, ⁷Melody Keel, ⁷Paola Grandi, ⁷James Burke*. ¹UCI Health, Irvine, CA, USA; ²BCG Oncology, Phoenix, AZ, USA; ³Carolina Urologic Research Center, Myrtle Beach, SC, USA; ⁴Royal Melbourne Hospital, Melbourne, Australia; ⁵Peter MacCallum Cancer Centre, Melbourne, Australia; ⁶MD Anderson Cancer Center, Houston, TX, USA; ⁷CG Oncology, Irvine, CA, USA

Background CG0070 is a serotype 5 adenovirus engineered to express GM-CSF and replicate in cells with mutated or deficient RB, with response rates (RR) of approximately 45% observed in patients with recurrent NMIBC after BCG.^{1 2} This single arm phase 3 study (NCT04452591) was launched to confirm the clinical activity of CG0070 in patients with BCG Unresponsive NMIBC.

Methods 110 patients with BCG-unresponsive CIS with or without concurrent Ta or T1 disease will be treated with intravesical (IVe) CG0070 at a dose of 1x10¹² vp. CG0070 will be administered as follows: induction weekly x 6 followed by weekly x 3 maintenance instillations at months 3, 6, 9, 12, and 18. Patients with persistent CIS or HG Ta at 3 m may receive re-induction with weekly x 6 CG0070. Assessment of response will include q 3 m cystoscopy with biopsy of areas suspicious for disease, urine cytology, CTU/MRU, and mandatory bladder mapping at 12 m. Detection of high grade disease within the bladder will be enumerated as recurrence or non-response. The primary endpoint of the study is CR at any time on study as assessed by biopsy (directed to cystoscopic abnormalities and mandatory mapping at 12 m), urine cytology, and radiography, as above. Secondary endpoints include CR at 12 m, duration of response, progression free survival, cystectomy free survival and safety. Correlative assessments include changes in the tumor immune microenvironment, systemic immune induction as reflected in the peripheral blood and urine, as well as viral replication and transgene expression. Baseline expression of coxsackie adenovirus receptor, E2F transcription factor as well as anti-adenovirus antibody titer will be correlated with tumor response. Study enrollment globally is ongoing.

Trial Registration NCT04452591

REFERENCE

1. Packiam VT, Lamm DL, Barocas DA, Trainer A, Fand B, Davis RL 3rd, Clark W, Kroeger M, Dumbadze I, Chamie K, Kader AK, Curran D, Gutheil J, Kuan A, Yeung AW, Steinberg GD. An open label, single-arm, phase II multicenter study of the safety and efficacy of CG0070 oncolytic vector regimen in patients with BCG-unresponsive non-muscle-invasive bladder cancer: Interim results. *Urol Oncol* 2018;**36**:440–447.

Ethics Approval CASTLE IRB: BOND-003 (CG3002S)

<http://dx.doi.org/10.1136/jitc-2021-SITC2021.426>

427

EFFICACY AND SAFETY OF AK112, AN ANTI-PD-1/VEGF-A BISPECIFIC ANTIBODY, IN PATIENTS WITH PLATINUM-RESISTANT/REFRACTORY EPITHELIAL OVARIAN CANCER IN A PHASE 1 STUDY

¹Jermaine Coward*, ²Sophia Frentzas, ¹Anna Mislang, ³Bo Gao, ⁴Charlotte Lemech, Xiaoping Jin, ⁵Baiyong Li, ⁵Max Wang, ⁵Kon Yew Kwek, ⁵Yiting Zhou, ⁵Yu Xia. ¹Icon Cancer Centre, South Brisbane, Australia; ²Monash Health, Melbourne, Australia; ³Blacktown Hospital, Blacktown, Australia; ⁴Scientia Clinical Research, Randwick, Australia; ⁵Akeso Biopharma Inc, Potomac, USA

Background Platinum-resistant/refractory epithelial ovarian cancer (PROC) is a high unmet medical need with limited treatment options and a median survival of 12–15 months.¹ Single agent PD-(L)1 inhibitors have objective response rates (ORR) of less than 10%.^{2–3} However, combination of nivolumab plus bevacizumab yields a higher ORR of 16.7% in platinum-resistant patients (pts), indicating synergistic activity between PD-1 inhibition and anti-angiogenic therapy in this disease.⁴ Here, we present initial efficacy and safety data for AK112, a bispecific antibody targeting PD-1 and VEGF-A, in pts with PROC. **Methods** Pts with PROC were enrolled in an ongoing Phase 1a/1b study of AK112 (NCT04047290). Tumor assessments based on RECIST v1.1 were performed once every 8 weeks/2 cycles for the first 12 months, and every 12 weeks thereafter. **Results** As of 16 July 2021, 19 PROC pts, of which 6 had platinum-refractory disease, have received AK112 at doses ranging from 3 mg/kg to 30 mg/kg Q2W. Seventeen pts (89.5%) had ≥2 lines of prior therapy in the recurrent/metastatic setting and 7 pts (36.8%) had prior bevacizumab. Seventeen pts had at least 1 post-baseline tumor assessment. Median duration of follow-up was 4.5 months. ORR was 29.4% (5/17; 2 clear cell, 3 high-grade serous). Among the 5 responders, 3 pts received 20mg/kg Q2W AK112 and 1 pt each had 3mg/kg and 10mg/kg Q2W AK112. Median duration of response was not reached. One pt, who had clear cell PROC and received prior immune checkpoint inhibitor (ICI) therapy, had tumor shrinkage of 70% and continued treatment for more than 17 months. Another pt, who had high-grade serous ovarian cancer and prior treatment with bevacizumab, had tumour shrinkage of 65% and continued treatment for more than 4 months. Disease control rate (DCR) was 76.5% (13/17), with tumor shrinkage observed in 11 pts (64.7%). Twelve out of 19 (63.2%) pts experienced treatment-related adverse events (TRAEs). Three pts (15.8%) experienced Grade 3 TRAEs (hypertension and transaminitis in 1 pt; and hypertension and colitis). There were no Grade 4–5 TRAEs. Commonly reported TRAEs were hypertension (15.8%), arthralgia (15.8%), fatigue (15.8%), hypothyroidism (10.5%) and rash (10.5%).

Conclusions The initial results from Study AK112-101 demonstrate that AK112 garners an encouraging anti-tumor activity and a favorable safety profile in patients with platinum-resistant/refractory epithelial ovarian cancer. AK112 will be further evaluated for the treatment of platinum-resistant/refractory epithelial ovarian cancer in a Phase 2 study.

Acknowledgements Akeso Biopharma, Inc would like to thank the patients, investigators and site staff for their participation in this study.

Trial Registration ClinicalTrials.gov Identifier: NCT04047290

REFERENCES

1. Pujade-Lauraine E, Banerjee S, Pignata S. Management of platinum-resistant, relapsed epithelial ovarian cancer and new drug perspectives. *J Clin Oncol* 2019; **37**:2437–2448.

2. Disis ML, Taylor MH, Kelly K, et al. Efficacy and Safety of Avelumab for Patients With Recurrent or Refractory Ovarian Cancer: Phase 1b Results From the JAVELIN Solid Tumor Trial. *JAMA Oncol* 2019; **5**:393–401.
3. Matulonis UA, Shapira-Frommer RS, Santin A, et al. Antitumor activity and safety of pembrolizumab in patients with advanced recurrent ovarian cancer: Interim results from the phase 2 KEYNOTE-100 study. *J Clin Oncol* 2018; **36**: suppl abstr 5511.
4. Liu JF, Herold C, Gray KP, et al. Assessment of Combined Nivolumab and Bevacizumab in Relapsed Ovarian Cancer: A Phase 2 Clinical Trial. *JAMA Oncol* 2019; **5**:1731–1738.

Ethics Approval This study received ethics approval from Bellberry Human Research Ethics Committee (HREC) on 05 Nov 2019 (Application number 2019-05-459-AB). In accordance with ICH Good Clinical Practice Guidelines and the Declaration of Helsinki, study participants gave informed consent voluntarily before participating in this study.

<http://dx.doi.org/10.1136/jitc-2021-SITC2021.427>

428

PRELIMINARY CLINICAL RESULTS OF TORIPALIMAB MONOTHERAPY OR COMBINATION THERAPY FOR RECURRENT OR REFRACTORY GYNECOLOGIC CANCER

Peng Diao*, Qian Peng, Xingbo Luo, Qing Huang, Gaoshu Yan, Yan Tan. *Sichuan cancer hospital, Chengdu, China*

Background PD-1 inhibitor have demonstrated significant efficacy in the treatment of recurrent or refractory gynecologic cancer. However, the clinical data among Chinese patients is still limited. In this study, the efficacy and safety of toripalimab in the treatment of recurrent or refractory gynecologic cancer was evaluated.

Methods A retrospective analysis of patients with recurrent or refractory gynecologic cancer who were treated with toripalimab in Sichuan Cancer Hospital from September 2019 to December 2020 was performed. The treatment regimens included toripalimab monotherapy or toripalimab in combination with other therapies (eg, radiotherapy, chemotherapy, targeted therapy). Statistical analysis of the objective response rate(ORR), progression-free survival(PFS), and toxicity after the treatment was carried out.

Results In total 18 recurrent or refractory gynecologic cancer patients who received toripalimab were reviewed in this study, including 12 patients with cervical cancer, 3 patients with vulvar cancer, 2 patients with uterine tumor, and 1 patient with pelvic wall squamous cell carcinoma. The patients previously received ≤ 1 line of treatment for advanced or recurrent cancer. The median follow-up period was 8 months [3.17–19.27 months]. The overall ORR was 33.3% (6/18), DCR was 77.8% (14/18), and median PFS was 8 months [95% CI: 6.53-NA]. For patients who received toripalimab as monotherapy, the ORR was 22.2% (2/9), DCR was 66.7% (6/9), and median PFS was 11.8 months (95% CI: 6.53-NA). For patients treated with toripalimab combination therapy, the ORR was 44.4% (4/9), DCR was 88.9% (8/9), and median PFS was 8 months (95% CI: 6.23-NA). Select treatment related AEs (TRAEs) of any grade were observed in 46.7% (7/18) patients. Grade 3 hepatotoxicity was recorded in 1 case. There was no treatment-related deaths.

Conclusions Toripalimab as monotherapy or Toripalimab combining with traditional anti-cancer therapy shows promising efficacy and acceptable toxicity in Chinese recurrent or refractory gynecologic cancer

<http://dx.doi.org/10.1136/jitc-2021-SITC2021.428>

429

PHASE 1 DOSE ESCALATION STUDY OF THE AGONIST REDIRECTED CHECKPOINT, SL-172154 (SIRP α -FC-CD40L) IN SUBJECTS WITH PLATINUM-RESISTANT OVARIAN CANCER

¹Nehal Lakhani* ²Debra Richardson, ³Timothy Kristedja, ⁴Fatima Rangwala, ⁴Hannah McKay, ⁴Louis Gonzalez, ⁴Bo Ma, ⁴Lini Pandite, ⁵Erika Hamilton. ¹Start Midwest, Grand Rapids, MI, USA; ²Stephenson Cancer Center OUHSC/SCRI, Oklahoma City, OK, USA; ³John Wayne Cancer Center, Santa Monica, CA, USA; ⁴Shattuck Labs, Durham, NC, USA; ⁵Sarah Cannon Research Institute, Nashville, TN, USA

Background SIRP α -Fc-CD40L is a hexameric, bi-functional fusion protein consisting of SIRP α (binding affinity to CD47 is 0.628 nM) linked to CD40L (binding affinity to CD40 is 4.74 nM) through an Fc linker protein.¹ By augmenting antigen processing and promoting antigen presenting cell (APC) maturation, this molecule is designed to bridge innate and adaptive immunity, enhancing tumor cell phagocytosis and antigen cross-presentation to CD8 T cells.

Methods The first-in-human, Phase 1 dose escalation study is evaluating SL-172154 as monotherapy in patients (pts) with platinum resistant ovarian, fallopian tube and primary peritoneal cancers. Objectives include evaluation of safety, dose-limiting toxicity (DLT) and recommended phase 2 dose (RP2D), pharmacokinetic (PK) parameters, pharmacodynamic (PD) effects and antitumor activity based on RECIST.

Results As of 6 July 2021, 14 heavily pretreated pts (median age, 67 years) were enrolled and treated with intravenous (IV) administration of SL-172154 across 4 dose levels on 2 schedules: schedule 1 (day 1, 8, 15, 29, Q2 weeks) at 0.1, 0.3 mg/kg and schedule 2 (weekly) at 0.3, 1.0, 3.0 mg/kg. The most common treatment-related (>20%) adverse events (AEs) of any grade (G) were fatigue (n=7, 50%), infusion-related reactions (IRR) (n=6, 43%), nausea (n=4, 29%), and decreased appetite (n=3, 21%). Treatment-related IRRs (G1/G2) generally occurred near the end of infusion or immediately post-infusion; the full dose was able to be delivered in each IRR event, and subsequent infusions in patients having IRRs were managed with pre-medications. No treatment related \geq G3 AEs or DLTs have occurred. CD47 receptor occupancy (RO) on leukocytes approached 90% at 1.0 and 3.0 mg/kg. Minimal binding to CD47+ red blood cells was observed at all dose levels. CD40 RO on B cells was >60% at doses \geq 0.1 mg/kg and 75%–100% at 1.0 and 3.0 mg/kg. Rapid, transient B cell and monocyte margination was observed following infusion of SL-172154 and was consistent with dose-dependent increases in IL-12, MCP-1, MIP-1 β , MIP-1 α , and MDC. No appreciable increases in IL-6 or TNF α were noted and there was no correlation between IRRs and cytokine increases. Among 12 evaluable pts, the best response was stable disease in 3 pts.

Conclusions SL-172154 has been well tolerated with no evidence of anemia, thrombocytopenia, liver dysfunction or cytokine release syndrome. A unique serum cytokine signature consistent with CD40 RO and activation has been observed and this signature is maintained following repeat dosing. Dose escalation is ongoing.

Acknowledgements Thanks are extended to study participants; Cathrine Leonowens, PhD, Nuventra Pharma Sciences, Durham, NC, United States and Cadence Communications and Research, Thousand Oaks, CA, United States. This study is funded by Shattuck Labs, Inc. Austin, TX and Durham, NC, United States.

Trial Registration NCT04406623

REFERENCES

1. de Silva S, Fromm G, Shuptrine CW, Johannes K, Patel A, Yoo KJ, et al. CD40 enhances type I interferon responses downstream of CD47 blockade, bridging innate and adaptive immunity. *Cancer Immunol Res* 2020; **8**: 230–245.

Ethics Approval This study is being conducted in full conformity with the Declaration of Helsinki and was approved by all IRBs/ethics committees from each clinical site participating in the study. Specific approval numbers can be provided upon request.

<http://dx.doi.org/10.1136/jitc-2021-SITC2021.429>

A PHASE 1B/II CLINICAL STUDY OF AK112, A PD-1/VEGF BISPECIFIC ANTIBODY, IN COMBINATION WITH OLAPARIB IN BRCA GERMLINE WILD-TYPE PLATINUM SENSITIVE RECURRENT OVARIAN CANCER

¹Lingying Wu*, ²Gailing Li, ³Bairong Xia, ⁴Rong Li, ⁵Jing Wang, ⁶Ruifang An, ⁷Li Wang, ⁸Yunxia Li, ⁹Kun Song, ¹⁰Hongying Yang, ¹¹Yaqing Chen, ¹²Yuzhi Li, ¹³Huilin Huang, ¹³Xiaoping Jin, ¹³Baiyong Li, ¹³Yu Xia. ¹Chinese Academy of Medical Sciences and Peking Union Medical College, Beijing, China; ²Wuhan Union Hospital, Wuhan, China; ³Cancer Hospital of Anhui Province, Hefei, Hefei, China; ⁴Chongqing Cancer Hospital, Chongqing, China, Chongqing, China; ⁵Cancer Hospital of Hunan Province, Changsha, China; ⁶First Affiliated Hospital of Xi'an Jiaotong University, Xi'an, China, Xi'an, China; ⁷Cancer Hospital of Henan Province, Zhengzhou, China; ⁸General Hospital of Ningxia Medical University, Yinchuan, China; ⁹Qilu Hospital of Shandong University, Jinan, China; ¹⁰Cancer Hospital of Yunnan Province, Kunming, China; ¹¹Cancer Hospital of Zhejiang Province, Hangzhou, China; ¹²The First Affiliated Hospital of Bengbu, Bengbu, China; ¹³Akeso Biopharma, Inc., Zhongshan, China, Zhongshan, China

Background Ovarian cancer is the most lethal gynecologic malignancy. Most patients will experience disease recurrence after initial platinum-based chemotherapy. Although PRAP inhibitors showed clinical benefit in terms of progression free survival (PFS) as recurrence therapy in platinum-sensitive ovarian cancer with BRCA mutation, there is limited treatment options for patients who are BRCA wild-type. MEDIOLA study showed that the combination of PD-L1 inhibitor (durvalumab) plus PARP inhibitor (olaparib) and bevacizumab demonstrated higher ORR and PFS than reported for PD-1 and PARP inhibitor doublet or single-agent PARP or VEGF inhibitors in non-gBRCAm platinum-sensitive relapsed ovarian cancer.¹ Therefore, AK112, a bispecific antibody against PD-1 and VEGF, combined with PARP inhibitor may achieve a better anti-tumor effect in recurrent ovarian cancer.

Methods This multicenter, open-label, phase Ib/II study will evaluate the safety and efficacy of AK112 in combination with PARP inhibitor in BRCA1/2 germline wild-type (gBRAC1/2 WT) platinum-sensitive recurrent ovarian cancer patients. The dose-escalation phase will evaluate three dose levels of AK112 (10mg/kg, 20mg/kg, and 30mg/kg Q2W) in combination with fixed dose of olaparib (300 mg, BID) using a 3+3 study design to determine the recommended Phase 2 dose (RP2D). Phase II study will evaluate the efficacy and safety of AK112 at RP2D in combination with olaparib in subjects with BRCA1/2 germline wild-type (gBRAC1/2 WT) platinum-sensitive recurrent ovarian cancer. The primary efficacy endpoint is objective response rate (ORR) based on RECIST v1.1. Secondary endpoints include disease control rate (DCR), duration of response (DoR), time to response (TTR), progression free survival (PFS), overall survival (OS), pharmacokinetics, immunogenicity, the correlation between the antitumor activity and PD-L1 expression or the gBRCA1/2 mutation status in peripheral blood. Exploratory endpoints are the correlations between clinical activity and homologous recombination deficiency (HRD) as well as tumor infiltrating lymphocytes in tumor tissues. Subjects with gBRAC1/2 WT platinum-sensitive ovarian cancer who had received ≥ 2 lines of platinum-based chemotherapy will be enrolled. Subjects with active or prior autoimmune disease that may relapse, significant cardiovascular disease, prior exposure to PARP inhibitor, antiangiogenic therapy or immunotherapy will not be eligible.

Acknowledgements Akeso Biopharma, Inc would like to thank the patients, investigators and site staff for their participation in this study.

Trial Registration Clinical registration number: CTR20210713

REFERENCES

1. Annals of Oncology (2020) 31 (suppl_4): S551-S589. 10.1016/annonc/annonc276.

Ethics Approval This study received ethics approval from Ethics Committee of National Cancer Center/Cancer Hospital, Chinese Academy of medical sciences and Peking Union Medical College on 11 Mar 2021 (Approval number: 21/125-2796). In accordance with ICH Good Clinical Practice Guidelines and the Declaration of Helsinki, study participants gave informed consent voluntarily before participating in this study.

<http://dx.doi.org/10.1136/jitc-2021-SITC2021.430>

431

FIRST-IN-HUMAN PHASE I CLINICAL TRIAL EVALUATING INTRAPERITONEAL ADMINISTRATION OF MOV19-BBZ CAR T CELLS IN PATIENTS WITH ALPHA FOLATE RECEPTOR-EXPRESSING RECURRENT HIGH GRADE SEROUS OVARIAN CANCER

¹Payal Shah*, ¹Richard Shlanksy-Goldberg, ¹Lainie Martin, ¹Gregory Nadolski, ¹Elizabeth Hexner, ¹Susan Shamimi-Noori, ¹Wei-Ting Hwang, ¹Tina Matlawski, ¹Amanda Cervini, ¹Joanne Shea, ¹Lauren Nelson, ¹Simon Lacey, ¹Gabriela Plesa, ¹Lester Lledo, ¹Karen Dengel, ¹Amy Marshall, ¹Rachel Leskowitz, ²Lana Kandalaft, ³Mariangela Figini, ³Silvana Canevari, ²George Coukos, ¹Daniel Powell. ¹University of Pennsylvania, Philadelphia, PA, USA; ²University Hospitals of Canton Vaud, Lausanne, Switzerland; ³Fondazione IRCCS Istituto Nazionale dei, Milano, Italy

Background Most women with epithelial ovarian cancer develop uniformly incurable disease recurrence. Chimeric antigen receptor (CAR) T cells pair the MHC-independent tumor-recognition capabilities of monoclonal antibodies with the cytotoxicity of effector T cells. The success of CAR T cell therapy in solid tumors has been hindered by (1) difficulty identifying highly expressed, tumor-specific, cell surface target antigens; (2) limited trafficking and infiltration; and (3) suboptimal cytotoxic activity. Alpha folate receptor (FR α) is a transmembrane protein involved in cellular folate transport; expression has been reported in 80% of ovarian cancer, with limited physiologic expression on epithelial cells including bronchial, renal, and intestinal tissue. We hypothesize that intraperitoneal administration of alpha folate receptor (FR α) directed CAR T cells with dual 4-1BB and TCRzeta signaling domains will circumvent the above challenges and be safe, feasible, and elicit anti-tumor responses.

Methods We initiated a first-in-human phase I clinical trial to evaluate the feasibility, safety and preliminary efficacy of intraperitoneal administration of FR α directed CAR T cells with and without antecedent lymphodepleting chemotherapy (LDC) in women with recurrent high grade serous ovarian cancer. The lentivirally-transduced CAR is composed of a MOv19 anti-FR α -specific single chain variable fragment fused to 4-1BB and TCRzeta signaling domains. Eligible patients have persistent or recurrent high grade serous epithelial ovarian, fallopian tube, or primary peritoneal carcinoma that is not platinum refractory and expresses $\geq 2+$ FR α staining in $\geq 70\%$ of tumor cells. Subjects must have an ECOG performance status 0–1, measurable disease, adequate hematologic and organ function, and must have progressed on at least two prior chemotherapy regimens for advanced disease. Patients undergo biopsy pre-infusion and Day +14 after infusion. After same-day placement of an intraperitoneal catheter by Interventional Radiology, CAR T cells are administered via a single infusion on three dose cohorts: Cohort 1 (starting cohort), $1-3 \times 10^7/m^2$ cells without LDC; Cohort 2, $1-3 \times 10^7/m^2$ CAR T cells after LDC; Cohort 3, $1-3 \times 10^8/m^2$ cells after LDC. Catheter is removed after infusion. A 3+3 dose escalation design to determine maximum tolerated dose (MTD) yields approximately 9 to 18 subjects. The primary objective is safety and feasibility, and secondary objectives are anti-tumor response (endpoints: overall response rate based on RECIST v 1.1 and irRECIST when feasible, progression-free survival and overall survival). Correlative endpoints include CAR T cell engraftment and persistence in peripheral blood and body fluids examined via quantitative PCR of CAR T DNA, and bioactivity of CAR T cells. Enrollment is ongoing.

Trial Registration This trial is registered at ClinicalTrials.gov (NCT03585764).

Ethics Approval This study was approved by the Institutional Review Board at the University of Pennsylvania (IRB 830111). All subjects provided written informed consent prior to any study-related procedures.

<http://dx.doi.org/10.1136/jitc-2021-SITC2021.431>

NEMVALEUKIN ALFA, A NOVEL ENGINEERED IL-2 CYTOKINE, IN COMBINATION WITH THE ANTI-PD-1 ANTIBODY PEMBROLIZUMAB IN PATIENTS WITH RECURRENT/METASTATIC HEAD AND NECK SQUAMOUS CELL CARCINOMA (ION-01 STUDY)

¹Brian Gastman*, ²Mac Cheever, ²Steven Fling, ³Cesar Perez, ⁴Manish Patel, ⁵Jessica Geiger, ⁶Zujun Li, ⁷Marshall Posner, ⁸Conor Steuer, ²Leonard D'Amico, ²Angela Shaulov Kask, ⁹Yangchun Du, ⁹Derek Matthies, ⁹Sung Jin Huh, ⁹Yan Wang, ⁹Julie Graham, ¹⁰Laura Chow. ¹Cleveland Clinic, Cleveland, OH, USA; ²Fred Hutchinson Cancer Research Center, Seattle, WA, USA; ³Sylvester Comprehensive Cancer Center, Miami, FL, USA; ⁴Masonic Cancer Center, Rochester, MN, USA; ⁵Cleveland Clinic Main Campus, Cleveland, OH, USA; ⁶Perlmutter Cancer Center at NYU, New York, NY, USA; ⁷Icahn School of Medicine at Mt Sinai, New York, NY, USA; ⁸Winship Cancer Institute, Atlanta, GA, USA; ⁹Alkermes, Inc., Waltham, MA, USA; ¹⁰University of Texas Austin, Austin, TX, USA

Background Nemvaleukin alfa (nemvaleukin, ALKS 4230) is a novel engineered cytokine that selectively binds to the intermediate-affinity IL-2R to preferentially activate and expand anti-tumor CD8+ T and NK cells with minimal expansion of regulatory T cells (Treg), thereby leveraging antitumor effects of the IL-2 pathway while mitigating potential toxicity that limits use.¹ Nemvaleukin single-agent activity has been demonstrated in checkpoint inhibitor-experienced patients, and deep and durable responses have been achieved in combination with pembrolizumab in multiple tumor types (eg, breast, head and neck, gastrointestinal, genitourinary, gynecological).²

Methods ION-01 (NCT04144517) is a nonrandomized trial in adult patients with histologically/cytopathologically confirmed diagnosis of metastatic/recurrent head and neck squamous cell carcinoma. Eligible patients have progressive disease after ≥ 8 weeks on anti-PD-(L)1 therapy. The primary endpoint is the rate of new or improved antitumor response after the addition of nemvaleukin. Secondary objectives include characterization of the antitumor response and evaluation of safety and tolerability of the combination regimen. Patients receive intravenous nemvaleukin (3 $\mu\text{g}/\text{kg}$) once daily for the first 5 days and pembrolizumab (200 mg) on day 1 of each 21-day cycle. Tumor imaging and biopsies were performed at baseline and at pre-specified times. We present preliminary safety and antitumor activity (RECIST v1.1) data as of June 2021.

Results Fourteen patients with progressive disease received combination therapy with nemvaleukin and pembrolizumab; 8 had no prior response to pembrolizumab, 6 had previous best response of stable disease or partial response. Mean (\pm SD) age was 62 ± 12 years, 86% were male, and all were Caucasian. Prior anti-cancer therapy included radiotherapy (93%) and surgery (50%). ECOG performance status was 0 (14%) and 1 (86%) at baseline. Treatment-related adverse events of any grade in $\geq 30\%$ of patients were chills (64.3%), pyrexia (57.1%), fatigue (42.9%), and nausea (35.7%). Five patients had stable disease as best response. One patient achieved a partial response (complete response in the target lesion) and remains on treatment (8+ cycles). Expansion of CD8+ T and NK cells with minimal Treg expansion was observed.

Conclusions Nemvaleukin and pembrolizumab combination therapy was generally well tolerated; adverse events were consistent with those observed with intravenous nemvaleukin in ARTISTRY studies [2]. Peripheral immune cell expansion profiles are comparable to that observed with the same regimen in the ARTISTRY 1 phase 1 study. Emerging data from pre-treatment and on-treatment paired biopsies will further characterize specific antitumor effects of nemvaleukin and pembrolizumab in this patient population.

Acknowledgements The authors would like to thank all the patients who are participating in this study and their families. The study is sponsored by Alkermes, Inc. Medical writing and editorial support was provided by Parexel, and funded by Alkermes, Inc.

Trial Registration ClinicalTrials.gov NCT04144517

REFERENCES

1. Lopes JE, Fisher JL, Flick HL, et al. ALKS 4230: a novel engineered IL-2 fusion protein with an improved cellular selectivity profile for cancer immunotherapy. *J Immunother Cancer* 2020;**8**:e000673. doi: 10.1136/jitc-2020-000673.
2. Boni V, Winer IS, Gilbert L, et al. ARTISTRY-1: Nemvaleukin alfa monotherapy and in combination with pembrolizumab in patients (pts) with advanced solid tumors. *J Clin Oncol* 2021;**39**(Suppl 15):abstr 2513.

Ethics Approval This study was approved by Quorum Review IRB (now Advarra IRB), approval number QR 33752.

<http://dx.doi.org/10.1136/jitc-2021-SITC2021.432>

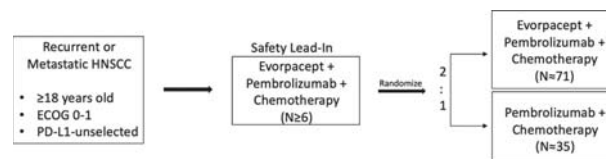
433

A PHASE 2 STUDY OF EVORPACEPT (ALX148) IN COMBINATION WITH PEMBROLIZUMAB AND CHEMOTHERAPY IN PATIENTS WITH ADVANCED HEAD AND NECK SQUAMOUS CELL CARCINOMA (HNSCC); ASPEN-04

¹Beatriz Cirauqui*, ²Ezra Cohen, ³Bhumsuk Keam, ⁴Jean-Pascal Machiels, ⁵Sjoukje Oosting, ⁶Tim Welliver, ⁶Shanhong Guan, ⁶Feng Jin, ⁶Allison Forgie, ⁶Philip Fanning, ⁶Katherine Ruffner, ⁶Jaume Pons, ⁶Sophia Randolph, ⁷Kevin Harrington. ¹*Institut Catala d'Oncologia, Barcelona, Spain*; ²*University of California San Diego, La Jolla, CA, USA*; ³*Seoul National University Hospital, Seoul, Korea, Republic of*; ⁴*Cliniques Universitaires Saint-Luc, Brussels, Belgium*; ⁵*University of Groningen, Groningen, Netherlands*; ⁶*ALX Oncology, Inc, Burlingame, CA, USA*; ⁷*The Royal Marsden Hospital, London, UK*

Background Anticancer immunity relies on the release of tumor antigens and subsequent activation of the innate and adaptive immune systems. After cytotoxic chemotherapy induces neoantigen release, myeloid checkpoint inhibitors can help potentiate innate immune cell activity including antigen presentation. CD47 is a marker of self that interacts with SIRP α on myeloid immune cells and is upregulated by tumors to evade immune responses. Evorpcept is a high affinity CD47-blocking fusion protein with an inactive Fc region designed to safely enhance standard anticancer therapeutics. Pembrolizumab, a T cell checkpoint inhibitor that activates cytotoxic lymphocytes, is a standard option for patients with previously untreated recurrent/metastatic (R/M) HNSCC, both as a monotherapy and in combination with 5FU + platinum. Through increased activation of the immune system, a combination of evorpcept + pembrolizumab + 5FU/platinum might have more anti-tumor activity in R/M HNSCC than current standard therapeutic approaches. This combination approach could be particularly beneficial to R/M HNSCC patients with low PD-L1 expression, where anti-PD-(L)1 therapy historically has diminished efficacy. The combination of evorpcept + pembrolizumab + 5FU/platinum has undergone preliminary testing in the ongoing Phase 1 ASPEN-01 study,¹ demonstrating initial clinical response and tolerability. In previously untreated, PD-L1-unselected R/M HNSCC patients treated with evorpcept + pembrolizumab + 5FU/platinum, patients experienced objective responses, including complete response. The ASPEN-04 study will assess the efficacy and safety of evorpcept in combination with pembrolizumab and chemotherapy in previously untreated patients with PD-L1-unselected R/M HNSCC.

Methods ASPEN-04 (figure 1) is an ongoing non-comparative, open-label, randomized Phase 2 global study of evorpcept + pembrolizumab + chemotherapy (5FU + either carboplatin or cisplatin) or pembrolizumab + chemotherapy in patients with PD-L1-unselected metastatic or unresectable recurrent HNSCC who have not yet been treated for their advanced disease. After an initial safety lead-in cohort, ~106 patients will be randomized to receive evorpcept + pembrolizumab + chemotherapy or pembrolizumab + chemotherapy. Minimization factors used to randomize patients include geography, PD-L1 combined positive score, and HPV (p16) status. Patients in the evorpcept treatment arm will receive evorpcept 45 mg/kg IV Q3W. All patients will receive pembrolizumab 200 mg IV Q3W (maximum of 35 cycles) and standard administration of 5FU and platinum agents. The primary endpoint in this Simon two-stage trial design is objective response rate using RECIST v1.1. Key secondary endpoints include duration of response, progression-free survival, overall survival, and safety. Exploratory endpoints will characterize pharmacodynamic properties.



Abstract 433 Figure 1 ASPEN-04 Study Schema

Acknowledgements We would like to thank all the participating patients, their families, and site research teams.

Trial Registration ClinicalTrials.gov identifier, NCT04675333

REFERENCES

- Keun-Wook Lee, Hyun Cheol Chung, Won Seog Kim, et al. ALX148, a CD47 blocker, in combination with standard chemotherapy and antibody regimens in patients with gastric/gastroesophageal junction (GC) cancer and head and neck squamous cell carcinoma (HNSCC); ASPEN-01. Poster presented at: Society for Immunotherapy of Cancer Annual Meeting; November 2020.

Ethics Approval The study was approved by all participating institutions' Ethics and/or Review Boards.

<http://dx.doi.org/10.1136/jitc-2021-SITC2021.433>

434

PHASE 1/2 STUDY TO EVALUATE PEPINEMAB IN COMBINATION WITH PEMBROLIZUMAB IN ADVANCED, RECURRENT OR METASTATIC HEAD AND NECK CANCER (KEYNOTE B84)

¹Elizabeth Evans*, ¹Terrence Fisher, ¹Crystal Mallow, ¹Amber Foster, ¹Ernest Smith, ¹John Leonard, ²Marya Chaney, ¹Maurice Zauderer. ¹Vaccinex, Rochester, NY, USA; ²Merck and Co, Kenilworth, NJ, USA

Background Immunosuppressive myeloid cells in the tumor microenvironment (TME) are a critical limitation to the efficacy of immune checkpoint inhibitors (ICIs) in patients with head and neck squamous cell carcinoma (HNSCC). Both semaphorin 4D (SEMA4D, CD100) and MDSCs are reported to play important roles in the growth and progression of HNSCC. Preclinical and clinical data demonstrated that antibody blockade of SEMA4D promotes tumor infiltration and activation of dendritic cells and CD8+ T cell, reverses immunosuppression, including attenuation of MDSC recruitment and function, and leading to enhanced efficacy of ICIs.^{1 2} In a study evaluating pepinemb, a humanized SEMA4D blocking antibody, in combination with avelumab in patients with non-small cell lung cancer, the combination appeared to provide clinical benefit in patients with difficult to treat ICI-resistant and PD-L1-low tumors.³ Pembrolizumab is approved as first line therapy as monotherapy or in combination with chemotherapy in recurrent or metastatic (R/M) HNSCC, however not all patients respond to ICIs and require more effective treatments.

Methods KEYNOTE B84 (NCT04815720) is a multicenter, single-arm open-label study to evaluate the safety, efficacy, PK/PD of pepinemb in combination with pembrolizumab in subjects with locally advanced, R/M HNSCC. Subjects with measurable disease per RECIST1.1 will be enrolled, including oropharynx, oral cavity, hypopharynx and larynx, and ECOG PS of 0 or 1. Subjects who have received prior ICIs are excluded. This study will include a Safety Run-in phase (n=3–18) and a Dose Expansion (maximum n=62) phase. Pepinemb, which is well-tolerated in combination with other ICIs, will be evaluated starting with the highest intended dose of 20 mg/kg, in combination with 200 mg pembrolizumab, both administered intravenously every 3 weeks. The Dose Expansion phase will include an even distribution of subjects who have combined positive scores of <20 and ≥20. The primary efficacy endpoint is ORR, and secondary endpoints include DOR, OS, PFS, as well as exploratory biomarker analysis. Pre- and on-treatment biopsies will be collected for evaluation of immune contexture in TME.

Results Screening has been initiated at several of a planned total of 18 sites. Multiplex immunohistochemistry (IHC) panels have been established to phenotype cells in the TME, including CD8+ T cells, DCs, MDSCs, Tregs, monocytes, macrophages.

Conclusions There remains a clear unmet need for more effective immunomodulatory treatment options to overcome immunosuppressive factors in the TME. The KEYNOTE B84 study will evaluate pepinemb as a potential treatment option to overcome resistance to and enhance activity of pembrolizumab in HNSCC.

Trial Registration NCT04815720

REFERENCES

1. Clavijo PE, Friedman J, Robbins Y, Moore EC, Smith E, Zauderer M, Evans EE, Allen CT. Semaphorin4D Inhibition Improves Response to Immune-Checkpoint

Blockade via Attenuation of MDSC Recruitment and Function. *Cancer Immunol Res* 2019 Feb;7(2):282–291.

2. Evans EE, Jonason AS Jr, Bussler H, Torno S, Veeraraghavan J, Reilly C, Doherty MA, Seils J, Winter LA, Mallow C, Kirk R, Howell A, Giralico S, Scrivens M, Klimatcheva K, Fisher TL, Bowers WJ, Paris M, Smith ES, Zauderer M. Antibody Blockade of Semaphorin 4D Promotes Immune Infiltration into Tumor and Enhances Response to Other Immunomodulatory Therapies. *Cancer Immunol Res* 2015 Jun;3(6):689–701.
3. Shafique MR, Fisher TL, Evans EE, Leonard JE, Pastore DRE, Mallow CL, Smith E, Mishra V, Schröder A, Chin KM, Beck JT, Baumgart MA, Govindan R, Gabrail NY, Spira AI, Seetharamu N, Lou Y, Mansfield AS, Sanborn RE, Goldman JW, Zauderer M. A Phase Ib/II Study of Pepinemb in Combination with Avelumab in Advanced Non-Small Cell Lung Cancer. *Clin Cancer Res* 2021 Jul 1;27(13):3630–3640.

Ethics Approval This study was approved by WIRB Copernicus Group's Ethics Board on 11Feb2021; approval number 20210250.

<http://dx.doi.org/10.1136/jitc-2021-SITC2021.434>

435

PEGASUS HNSCC, A PLATFORM STUDY OF SAR444245 (THOR-707, A PEGYLATED RECOMBINANT NON-ALPHA IL-2) WITH ANTI-CANCER AGENTS IN PATIENTS WITH RECURRENT/METASTATIC HEAD AND NECK SQUAMOUS CELL CARCINOMA

¹Robin Meng*, ²Caroline Even, ³Lisa Licitra, ⁴Chia-Jui Yen, ⁵Myung Ju Ahn, ¹Giovanni Abbadessa, ¹Fatima-Zohra Menas, ¹Miao Zang, ⁶George Blumenschein. ¹Sanofi, Cambridge, USA; ²Institut de Cancerologie Gustave-Roussy, Villejuif, France; ³Fondazione IRCCS, Istituto Nazionale dei, Milan, Italy; ⁴National Cheng Kung University Hospital, Tainan City, Taiwan, Province of China; ⁵Samsung Medical Center, Seoul, Korea, Republic of; ⁶MD Anderson Cancer Center, Houston, TX, USA

Background SAR444245 (THOR-707) is a recombinant human IL-2 molecule that includes a PEG moiety irreversibly bound to a novel amino acid via click chemistry to block the alpha-binding domain while retaining near-native affinity for the beta/gamma subunits. In animal models, SAR444245 showed anti-tumor benefits, but with no severe side effects, both as single agent and when combined with anti-PD1 comparing with historical data from aldeslakin. Preclinical study demonstrated SAR444245 enhances ADCC function of cetuximab. The HAMMER trial, which is the FIH study shows preliminary encouraging clinical results: initial efficacy and safety profile with SAR444245 monotherapy and in combination with pembrolizumab or with cetuximab support a non-alpha preferential activity, validating preclinical models. The Pegasus Head and Neck Ph 2 study will evaluate the clinical benefit of SAR444245 in combination with other anticancer therapies for the treatment of patients with R/M HNSCC.

Methods The Pegasus Head and Neck will enroll approximately 272 patients in 4 separate cohorts concurrently. In cohorts A1 & A2, 1L R/M HNSCC patients will receive SAR444245 + pembrolizumab, or SAR444245 + pembrolizumab + cetuximab respectively. In cohort B1 & B2 patients with 2/3L R/M HNSCC failed a checkpoint based regimen & a platinum containing regimen will receive SAR444245 + pembrolizumab, or SAR444245 + cetuximab. Patients to be enrolled in cohort B2 need to be cetuximab-naïve in R/M setting. SAR444245 is administered intravenously IV at a dose of 24 ug/kg Q3W until disease progression (PD) or completion of 35 cycles. Pembrolizumab is administered at a dose of 200 mg Q3W until PD or completion of 35 cycles. Cetuximab is administered at a dose of 400/250 mg/m² QW until PD. The study primary objective is to determine the antitumor activity of SAR444245 in combination with other anticancer therapies. Secondary objectives include confirmation of dose and safety profile, assess other indicators of antitumor activity, and assess the pharmacokinetic profile and immunogenicity of SAR444245. The study will be conducted in the US, Canada, France, Germany, Italy, Netherlands, Poland, South Korea, Spain and Taiwan.

Acknowledgements The Pegasus Head and Neck study is sponsored by Sanofi.

<http://dx.doi.org/10.1136/jitc-2021-SITC2021.435>

A PHASE II STUDY OF AK104, A BISPECIFIC ANTIBODY TARGETING PD-1 AND CTLA-4, IN PATIENTS WITH METASTATIC NASOPHARYNGEAL CARCINOMA (NPC) WHO HAD PROGRESSED AFTER TWO OR MORE LINES OF CHEMOTHERAPY

¹Haiqiang Mai*, ²Shaojun Lin, ³Dongping Chen, ⁴Xiaozhong Chen, ⁵Song Qu, ⁶Qin Lin, ⁷Ying Luo, ⁸Chunhong Hu, ⁹Dehua Wu, ¹⁰Tianxin Qin, ¹¹Feng Jin, ¹²Nianyong Chen, ¹³Yunxiu Luo, ¹⁴Zhifang Yao, ¹⁴Xiaoping Jin, ¹⁴Baiyong Li, ¹⁴Yu Xia, ¹Rui-Hua Xu. ¹Sun Yat-Sen University Cancer Center, Guangzhou, China; ²Fujian Provincial Cancer Hospital, Fuzhou, China; ³The Affiliated Cancer Hospital of Guangzhou Medical University, Guangzhou, China; ⁴Cancer Hospital of Zhejiang Province, Hangzhou, China; ⁵Affiliated Tumor Hospital of Guangxi Medical University, Nanning, China; ⁶The First Affiliated Hospital of Xiamen University, Xiamen, China; ⁷Cancer Hospital of Hunan Province, Changsha, China; ⁸Second Xiangya Hospital of Central South University, Changsha, China; ⁹NanFang Hospital of Southern Medical University, Guangzhou, China; ¹⁰The First Affiliated Hospital of Guangdong Pharmaceutical University, Guangzhou, China; ¹¹Cancer Hospital of Guizhou Province, Guiyang, China; ¹²West China Hospital of Sichuan University, Chengdu, China; ¹³Cancer Hospital of Hainan Province, Haikou, China; ¹⁴Akeso Biopharma, Inc., Zhongshan, China., Zhongshan, China

Background Nasopharyngeal cancer (NPC) is common in Southeast Asia, especially in Southern China. Combination of CTLA-4 and PD-1 blockade has consistently demonstrated the increase of the response rates and survival rates of the patients (pts) compared to monotherapy in various tumors.¹ Dual CTLA-4/PD-1 blockade with ipilimumab plus nivolumab provided durable responses in patients with recurrent or metastatic NPC,² suggesting the combination of CTLA-4 and PD-1 blockers have synergistic effect in NPC. Here, this Phase II study present initial safety and efficacy data for AK104, a PD-1/CTLA-4 bispecific antibody, in metastatic NPC pts.

Methods AK104-204 (NCT04220307) is a multicenter, single-arm, open-label study of AK104 in patients (pts) with metastatic NPC who have failed at least two lines of chemotherapy and didn't receive any anti-PD-1/PD-L1 antibodies previously. All patients received AK104 6 mg/kg every 2 weeks until progression or unacceptable toxicity. The primary endpoint was objective response rate (ORR) based on Response Evaluation Criteria in Solid Tumors version 1.1 (RECIST v1.1). Tumor proportion score (TPS)=50% was regarded as PD-L1 positive.

Results As of 6 June 2021, 23 pts were enrolled. Median age was 43[range:19–64] years old, 87.0% was male, 73.9% ECOG performance status was 1. Of 20 efficacy-evaluable pts, the confirmed ORR was 30% (6/20); the disease control rate (DCR) was 70% (14/20). Among them, the ORR was 57.1% (4/7) in pts with PD-L1 positive and the 18.2% (2/11) in pts with PD-L1 negative. Grade 3 treatment-related adverse events (TRAEs) occurred in 21.7% (5/23) of pts. No Grade 4 or 5 TRAEs occurred. Most frequent TRAEs (incidence = 20%) were anaemia (30.4%), white blood cell count decreased (26.1%), hypothyroidism (26.1%), neutrophil count decreased (21.7%), and rash (21.7%).

Conclusions AK104 demonstrated encouraging anti-tumor activity and favorable safety profile in pts with NPC who had disease progression after =2 prior lines of therapy. NPC pts with PD-L1–positive tumors receiving AK104 showed more benefits than those with PD-L1-negative tumors. AK104 for the treatment of NPC should be further evaluated.

Acknowledgements Akeso Biopharma, Inc would like to thank the patients, investigators and site staff for their participation in this study.

Trial Registration Clinical registration number: NCT04220307

REFERENCES

1. Rotte A. Combination of CTLA-4 and PD-1 blockers for treatment of cancer. *Journal of Experimental & Clinical Cancer Research* 2019, **38**(1): 1–12.
2. *Annals of Oncology* 2020;**3**(suppl_6): S1347-S1354. 10.1016/annonc/annonc360.

Ethics Approval This study received ethics approval from Ethics Committee of Sun Yat-Sen University Cancer Center on 04 Dec 2019 (Approval number: A2019-085-01). In accordance with ICH Good Clinical Practice Guidelines and the Declaration of Helsinki, study participants gave informed consent voluntarily before participating in this study.

Consent Written informed consent was obtained from the patient for publication of this abstract and any accompanying images. A copy of the written consent is available for review by the Editor of this journal.

<http://dx.doi.org/10.1136/jitc-2021-SITC2021.436>

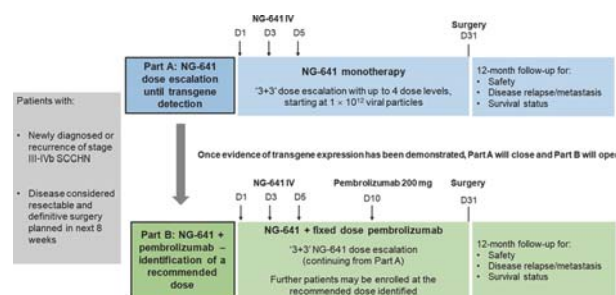
437

A MULTICENTRE PHASE 1B STUDY OF NG-641, A NOVEL TRANSGENE-ARMED AND TUMOUR-SELECTIVE ADENOVIRAL VECTOR, AND PEMBROLIZUMAB AS NEOADJUVANT TREATMENT FOR SQUAMOUS CELL CARCINOMA OF THE HEAD AND NECK

¹Christian Ottensmeier, ²Mererid Evans, ³Emma King, ⁴Ioannis Karydis, ⁵Tom Lillie*, ⁵David Krige, ⁵Jenny Lee, ⁵Matthew Thomas, ⁶Kevin Harrington. ¹University of Liverpool and Clatterbridge Cancer Centre NHS Foundation Trust, Liverpool, UK; ²Velindre University NHS Trust, Cardiff, UK; ³University of Southampton Faculty of Medicine and University Hospitals Dorset, Poole, UK; ⁴University of Southampton and Southampton University Hospitals NHS Foundation Trust, Southampton, UK; ⁵PsiOxus Therapeutics Ltd, Abingdon, UK; ⁶The Institute of Cancer Research and Royal Marsden Hospital NHS Trust, London, UK

Background Despite multimodal management strategies, outcomes for patients with locally advanced squamous cell carcinoma of the head and neck (SCCHN) remain poor. Immune checkpoint inhibitors have demonstrated promise as a neoadjuvant strategy to reduce relapse rates¹; however, the immunosuppressive SCCHN tumour microenvironment (TME) has limited the efficacy of immunotherapy to date. This 'cold' TME is characterised by an absence of T-cell activation/inflammation² and high levels of stromal fibroblast activating protein (FAP),³ indicative of immunosuppressive cancer-associated fibroblasts (CAFs). Novel approaches to ameliorate this immunosuppressive TME are required to realise the full benefit of immunotherapy in SCCHN. NG-641 is a next-generation blood-stable and transgene-armed Tumour-Specific Immuno Gene Therapy (T-SiGn) adenoviral vector that selectively replicates in epithelial tumour cells. NG-641 encodes four immunostimulatory transgenes: a FAP-directed bi-specific T-cell activator antibody to target CAFs, interferon alpha 2 to promote innate and adaptive immune responses, and C-X-C motif chemokine ligands 9 and 10 to induce T cell infiltration.⁴ Together, these transgenes are designed to locally re-programme the immunosuppressive TME and promote functional anti-cancer immune responses while minimising systemic immune-related toxicities. This mechanism of action is particularly suited to SCCHN and should complement anti-PD-1 inhibitors. We, therefore, designed a study to assess neoadjuvant treatment with NG-641 and pembrolizumab in locally advanced SCCHN.

Methods The mode-of-action transgene (MOAT) study is a multicentre, open-label, dose-escalating, phase 1b study of NG-641 as monotherapy or with pembrolizumab. Patients are eligible if they have newly diagnosed or recurrent locally advanced SCCHN and have definitive surgery planned within 8 weeks of screening. In Part A, patients will receive three doses of intravenous NG-641 monotherapy prior to surgery (figure 1). Once NG-641 transgene expression is confirmed in excised tumour tissues, Part A will close and NG-641 dose-escalation can continue in Part B. Patients will then also receive a single dose of pembrolizumab given ~5 days after NG-641 to minimize toxicity and take advantage of the mechanism of NG-641 prior to PD-1 blockade. The primary objective is to characterise the safety and tolerability of NG-641 ± pembrolizumab in SCCHN; secondary objectives are to identify a recommended dose of NG-641 plus pembrolizumab and to assess treatment outcomes, including pathological tumour responses and overall survival. Pharmacodynamic outcomes will be assessed following NG-641 ± pembrolizumab, including characterising immune/inflammatory biomarkers in both tumour and blood. The study is to be conducted at 4 sites in the UK; up to 36 patients will be enrolled.



Abstract 437 Figure 1 MOAT study schematic

Acknowledgements This study was funded by PsiOxus Therapeutics Ltd.

Trial Registration This trial is registered as NCT04830592 on clinicaltrials.gov.

REFERENCES

- Uppaluri R, Campbell KM, Egloff AM, et al. Neoadjuvant and Adjuvant Pembrolizumab in Resectable Locally Advanced, Human Papillomavirus-Unrelated Head and Neck Cancer: A Multicenter, Phase II Trial. *Clin Cancer Res* 2020;**26**:5140–52.
- Cristescu R, Mogg R, Ayers M, et al. Pan-tumor genomic biomarkers for PD-1 checkpoint blockade-based immunotherapy. *Science* 2018;**362**:eaar3593.
- Dolznic H, Schweifer N, Puri C, et al. Characterization of cancer stroma markers: In silico analysis of an mRNA expression database for fibroblast activation protein and endosialin. *Cancer Immun* 2005;**5**:10.
- Champion BR, Besneux M, Patsalidou M, et al. NG-641: An oncolytic T-SiGn virus targeting cancer-associated fibroblasts in the stromal microenvironment of human carcinomas. *Cancer Res* 2019;**79**:5013.

Ethics Approval This study was approved by a central United Kingdom Research Ethics Committee (South Central - Oxford A Research Ethics Committee); approval reference 20/SC/0425, Integrated Research Application System ID 290504. All participants must provide informed consent prior to enrolment.

<http://dx.doi.org/10.1136/jitc-2021-SITC2021.437>

A PHASE 1 TRIAL OF CUE-101, A NOVEL HPV16 E7-PHLA-IL2-FC FUSION PROTEIN, ALONE AND IN COMBINATION WITH PEMBROLIZUMAB IN PATIENTS WITH RECURRENT/METASTATIC HPV16+ HEAD AND NECK CANCER

¹Christine Chung, ²A Dimitrios Colevas, ³Michael Gibson, ⁴Douglas Adkins, ⁵Ammar Sukari, ⁶Lori Wirth, ⁷Barbara Burtress, ⁸Julie Bauman, ⁹Cristina Rodriguez, ¹⁰Francis Worden, ¹¹Nabil Saba, ¹²Bonnie Glisson, ¹³Lara Dunn, ¹⁴Tanguy Seiwert, ¹⁵Laura Agensky, ¹⁵Matteo Levisetti, ¹⁵Reena Lynam, ¹⁵Steven Margossian, ¹⁵Raymond Moniz, ¹⁵Steve Quayle, ¹⁵Kenneth Pienta, ⁶Sara Pai*. ¹H. Lee Moffitt Cancer Center, Tampa, FL, USA; ²Stanford University School of Medicine, Stanford, CA, USA; ³Vanderbilt University Medical Center, Nashville, TN, USA; ⁴Washington University School of Medicine, St. Louis, MO, USA; ⁵Karmanos Cancer Center, Detroit, MI, USA; ⁶Massachusetts General Hospital, Boston, MA, USA; ⁷Yale School of Medicine, New Haven, CT, USA; ⁸University of Arizona Cancer Center, Tucson, AZ, USA; ⁹University of Washington, Seattle, WA, USA; ¹⁰University of Michigan, Ann Arbor, MI, USA; ¹¹Emory University, Atlanta, GA, USA; ¹²The University of Texas MD Anderson, Houston, TX, USA; ¹³Memorial Sloan Kettering Cancer Center, New York, NY, USA; ¹⁴Johns Hopkins University School of Medicine, Baltimore, MD, USA; ¹⁵Cue Biopharma Inc, Cambridge, MA, USA

Background Immuno-STATsTM are novel, modular fusion proteins designed to selectively activate tumor-antigen-specific CD8+ T cells. CUE-101 is comprised of a human leukocyte antigen (HLA) complex, HLA-A*0201, a peptide epitope derived from the HPV16 E7 protein, and 4 molecules of a reduced affinity human interleukin-2 (IL-2) and is designed to bind and activate HPV16-specific T cells for treatment of HPV16-driven cancers. In preclinical studies CUE-101 demonstrated selective binding, activation, and expansion of HPV16 E7-specific CD8+ T cells, and a murine surrogate activated anti-tumor immunity.¹

Methods CUE-101-01 is a first-in-human study in HLA-A*0201 positive patients with HPV16+ recurrent/metastatic head and neck squamous cell carcinoma (R/M HNSCC). Safety of escalating monotherapy and combination doses was evaluated to establish the recommended phase 2 dose (RP2D) for expanded enrollment. Patients with R/M HNSCC refractory to 1 or more prior platinum or pembrolizumab based systemic treatments received CUE-101 monotherapy, and patients with R/M HNSCC and PD-L1 tumor expression received combination CUE-101 and 200 mg pembrolizumab as first line treatment. Study treatment was administered intravenously every 3 weeks until progression or toxicity. Objectives included evaluation of safety, pharmacokinetics (PK), pharmacodynamics (PD), and antitumor activity.

Results As of June 30, 2021, 39 patients have received CUE-101 monotherapy ranging from 0.06 to 8 mg/kg. The maximum tolerated dose (MTD) was not identified. Based on PK, PD and clinical data, a monotherapy RP2D of 4 mg/kg was selected. The combination cohort of 1 mg/kg CUE-101 and pembrolizumab has been tested and dose escalation is ongoing. Adverse events have included CTCAE grade 2 or less fatigue (41%), anemia (31%), lymphopenia (24%), chills (21%), decreased appetite (19%) and dyspnea (17%). CUE-101 PK data demonstrate dose-dependent increases in drug exposure that are sustained upon repeat dosing. PD data demonstrate dose-dependent expansion of HPV-16 E711-20-specific CD8+ T cells, sustained increase in natural killer cells and transient increase in Treg cells. An increase in CD3+ GZMB+ tumor infiltrating T cells was observed in tissue following treatment with CUE-101 in one patient with available pre- and post-treatment biopsies. One patient at the CUE-101 monotherapy RP2D has an ongoing partial response and 8 of 33 patients have experienced stable disease \geq 12 weeks based on RECIST 1.1 criteria.

Conclusions CUE-101 is a novel immunotherapeutic demonstrating acceptable safety and tolerability with encouraging PD signals, supporting selective activation of tumor-specific T cells, and promising antitumor activity. Enrollment continues in both monotherapy and combination cohorts.

Acknowledgements The authors would like to thank all the patients who are participating in this study. The study is sponsored by Cue Biopharma.

Trial Registration ClinicalTrials.gov NCT03978689

REFERENCES

1. Quayle SN, Girgis N, Thapa DR, et al. CUE-101, a Novel HPV16 E7-pHLA-IL-2-Fc fusion protein, enhances tumor antigen specific T cell activation for the treatment of HPV16-driven malignancies. *Clin Cancer Res* 2020;**26**:1953–64.

Ethics Approval This study was approved by Ethics and Institutional Review Boards (IRBs) at all study sites. IRB reference numbers: Advarra Pro00037736 (Moffitt Cancer Center), IRB 52744 (Stanford University School of Medicine), IRB 191714 (Vanderbilt University Medical Center Vanderbilt-Ingram Cancer Center), HRPO# 201905108 (Washington University School of Medicine), 2019–087 Karmanos Cancer Institute, DF/HCC IRB# 19-374 (Massachusetts General Hospital), WIRB 2000026098 (Yale Cancer Center), WIRB 1908869642 (University of Arizona Cancer Center), WIRB STUDY00008948 (University of Washington, Seattle), IRB (IRBMED) HUM00165746 (University of Michigan Comprehensive Cancer Center), WIRB IRB00112341 (Winship Cancer Institute/Emory University), 2019–0578 (The University of Texas MD Anderson Cancer Center), IRB 20-073 (Memorial Sloan Kettering Cancer Center), IRB00255391 (Johns Hopkins University School of Medicine).

<http://dx.doi.org/10.1136/jitc-2021-SITC2021.438>

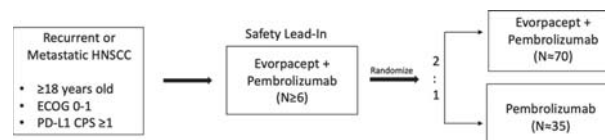
439

A PHASE 2 STUDY OF EVORPACEPT (ALX148) IN COMBINATION WITH PEMBROLIZUMAB IN PATIENTS WITH ADVANCED HEAD AND NECK SQUAMOUS CELL CARCINOMA (HNSCC); ASPEN-03

¹Jong Chul Park*, ²Kevin Harrington, ³Bhumsuk Keam, ⁴Jean-Pascal Machiels, ⁵Sjoukje Oosting, ⁶Tim Welliver, ⁶Shanhong Guan, ⁶Feng Jin, ⁶Alison Forgie, ⁶Phillip Fanning, ⁶Katherine Ruffner, ⁶Jaume Pons, ⁶Sophia Randolph, ⁷Ezra Cohen. ¹Massachusetts General Hospital, Boston, MA, USA; ²The Royal Marsden Hospital, London, UK; ³Seoul National University Hospital, Seoul, Korea, Republic of; ⁴Cliniques Universitaires Saint-Luc, Brussels, Belgium; ⁵University of Groningen, Groningen, Netherlands; ⁶ALX Oncology, Inc, Burlingame, CA, USA; ⁷University of California San Diego, La Jolla, CA, USA

Background Both innate and adaptive immune responses are important components of anticancer immunity. CD47 is a marker of self that interacts with SIRP α on myeloid immune cells, inhibiting their function. CD47 is upregulated by tumors to evade immune responses and its expression is associated with poor prognosis. Evorpaccept is a high affinity CD47-blocking fusion protein with an inactive Fc region designed to be safely combined with and to enhance the efficacy of standard anticancer therapeutics. Evorpaccept used in combination with pembrolizumab has the potential to augment both innate and adaptive anti-tumor immune responses. As an antibody inhibiting PD-1/PD-L1 signaling in the T cell immune checkpoint, pembrolizumab has demonstrated anti-tumor efficacy through activation of tumor-infiltrating lymphocytes. Pembrolizumab as a single agent is a standard treatment option for patients with previously untreated recurrent or metastatic (R/M) HNSCC with PD-L1-positive (combined positive score [CPS] ≥ 1) tumors. The combination of evorpaccept + pembrolizumab has shown preliminary efficacy and acceptable tolerability in initial results available from the cohort of patients with ≥ 2 nd line advanced HNSCC in the ongoing Phase 1 ASPEN-01 study.¹ PD-L1-unselected patients who had not received prior checkpoint inhibitor treatment were treated with evorpaccept + pembrolizumab and experienced a 40% ORR and 4.6 months median PFS, comparing favorably with historical controls. Based on these encouraging results, the ASPEN-03 study will assess the efficacy and safety of evorpaccept in combination with pembrolizumab in previously untreated patients with metastatic or unresectable recurrent PD-L1 positive HNSCC.

Methods ASPEN-03 (figure 1) is an ongoing non-comparative, open-label, randomized Phase 2 global study of evorpaccept + pembrolizumab or pembrolizumab alone in patients with metastatic or unresectable recurrent, PD-L1-positive (CPS ≥ 1) HNSCC who have not yet been treated for their advanced disease. After an initial safety lead-in cohort, ~ 105 patients will be randomized 2:1 to receive evorpaccept + pembrolizumab or pembrolizumab alone. Minimization factors used to randomize patients include geography, CPS, and HPV (p16) status. Patients in the evorpaccept + pembrolizumab treatment arm will receive evorpaccept 45 mg/kg IV Q3W. All patients will receive pembrolizumab 200 mg IV Q3W (maximum of 35 cycles). The primary endpoint in this Simon two-stage trial design is objective response rate using RECIST v1.1. Key secondary endpoints include duration of response, progression-free survival, overall survival, and safety. Exploratory endpoints will characterize pharmacodynamic properties.



Abstract 439 Figure 1 ASPEN-03 study schema

Acknowledgements We would like to thank all the participating patients, their families, and site research teams.

Trial Registration ClinicalTrials.gov identifier, NCT04675294

REFERENCES

1. Keun-Wook Lee, Hyun Cheol Chung, Won Seog Kim, et al. ALX148, a CD47 blocker, in combination with standard chemotherapy and antibody regimens in patients with gastric/gastroesophageal junction (GC) cancer and head and neck squamous cell carcinoma (HNSCC); ASPEN-01. Poster presented at: Society for Immunotherapy of Cancer Annual Meeting; November 2020.

Ethics Approval The study was approved by all participating institutions' Ethics and/or Review Boards.

<http://dx.doi.org/10.1136/jitc-2021-SITC2021.439>

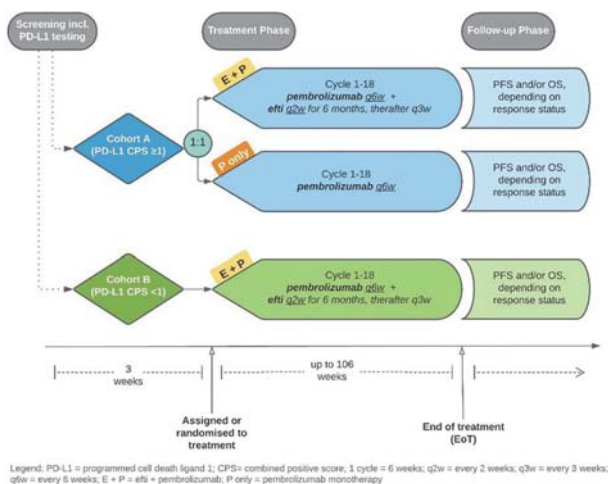
440

A PHASE II STUDY OF EFTILAGIMOD ALPHA (SOLUBLE LAG-3 PROTEIN) AND PEMBROLIZUMAB IN PATIENTS UNSELECTED FOR PD-L1 EXPRESSION IN FIRST LINE METASTATIC HEAD AND NECK SQUAMOUS CELL CARCINOMA (HNSCC)

¹Julio Peguero*, ²Frederic Triebel. ¹Oncology Consultants, P.A., Houston, TX, USA; ²Research and Development, Immutep S.A.S., Chatenay Malabry, France

Background Eftilagimod alpha (efti) is a soluble LAG-3 protein targeting a subset of MHC class II molecules, effectively mediating antigen presenting cell (APC) and CD8 T-cell activation. Interim data from a phase II trial of efti plus pembrolizumab (TACTI-002) showed encouraging antitumor activity and manageable safety in patients treated for second line metastatic head and neck squamous cell carcinoma (HNSCC). TACTI-003 (NCT04811027) is the multicenter, open label, randomized phase II trial to investigate efti plus pembrolizumab in the first line setting for HNSCC patients.

Methods A planned total of 154 patients (pts), unselected for PD-L1 expression, will be recruited into two cohorts (figure 1). In cohort A, CPS \geq 1 pts will be randomly assigned 1:1 to receive either efti (30 mg subcutaneously Q2W for initial 6 months, thereafter Q3W for up to 2 years) plus pembrolizumab (400 mg intravenously Q6W for up to two years) or pembrolizumab alone. CPS will be stratified (1–19 vs. \geq 20 and ECOG 0 vs. 1). Cohort B will include pts with CPS<1 who will receive efti plus pembrolizumab without randomization. Imaging will be performed every 9 weeks. The primary end point (EP) is objective response rate (ORR) by RECIST1.1. Secondary EPs include overall survival, ORR according to iRECIST, time to and duration of response, disease control rate, progression free survival, occurrence of anti-efti -specific antibodies, safety, and quality of life. Exploratory endpoints comprise biomarkers. The study has been approved by relevant competent authorities, ethic committees and IRBs.



Abstract 440 Figure 1 Trial design

Trial Registration NCT04811027

Ethics Approval The study was approved by relevant ethic committees and institutional review boards.

<http://dx.doi.org/10.1136/jitc-2021-SITC2021.440>

441 **POPULATION PHARMACOKINETICS OF AN ANTI-PD-1 ANTIBODY, PENPULIMAB IN PATIENTS WITH ADVANCED MALIGNANCIES**

Benchao Chen, Xiaoping Jin, Yongcheng Dong, Max Wang, Dennis Xia, Michelle Xia, Baiyong Li*. *Akeso Biopharma Co., Ltd., zhongshan, China*

Background Penpulimab is a humanized IgG1 monoclonal antibody targeting PD-1 and is being evaluated in a variety of malignancies. The objective of the present study was to develop a population pharmacokinetic (PopPK) model of penpulimab in patients with hematologic malignancies and solid tumors, and to characterize the impact of demographic and disease factors on the pharmacokinetics.

Methods Pharmacokinetic data in patients with advanced malignancies were analyzed from six clinical studies with doses of 1, 3, 10 mg/kg, 200 mg every 2 weeks (Q2W), or 200 mg every 3 weeks (Q3W) of penpulimab (N=332). Noncompartmental analyses were performed on PK data from a subset of participants and the pharmacokinetic characteristics of penpulimab were summarized.

Results The PopPK of penpulimab was adequately described with a two-compartment model with first-order elimination using a non-linear mixed effects model (NONMEM). Typical values for these PK parameters were estimated at 0.232 L/day for Clearance (CL), 3.42 L for the volume of distribution of central compartment (V1). There was no clinical correlation between penpulimab pharmacokinetics and baseline covariates, such as age, race, immunogenicity, hepatic function, creatinine clearance, tumor type, and ECOG score. Several indicators, including the impact of albumin, lactic dehydrogenase, and gender on CL, and the impact of weight and gender on V1, were found to be statistically significant, but the geometric mean ratios for the PK parameters ranged between 0.7 and 1.3, with a difference of less than 30% and no clinically significant relevance. Drug exposure increased proportionally with dose from 1.0 mg/kg to 10.0 mg/kg, and at 1mg/kg or more, the PD-1 receptor occupancy reached 80% to 100% two days after penpulimab infusion. PopPK simulation showed that concentration ranges of penpulimab following administration at a fixed dose (200 mg Q2W) or by body weight (3.0 mg/kg Q2W) were basically consistent. More than 97.5% of the patients, at either dosing regimen (200 mg Q2W or Q3W), had steady-state trough concentrations >10 µg/mL, which is much higher than the concentration (0.5 µg/mL) needed for reaching 90% to 100% PD-1 receptor occupancy.

Conclusions The PopPK model adequately assessed the pharmacokinetic characteristics and impact factors of penpulimab in the hematologic malignancies as well as solid tumors. This simulation indicates that both weight-based dose and fixed dose (200mg Q2W or Q3W) are appropriate for penpulimab.

Ethics Approval These studies were conducted in accordance with the protocol, good clinical practice standards and the Declaration of Helsinki. The protocols and subsequent amendments were approved by the appropriate institutional review board (IRB) or ethics committee at each participating institution. All patients provided voluntary written informed consent.

Consent Written informed consent was obtained from the patient for publication of this abstract and any accompanying images. A copy of the written consent is available for review by the Editor of this journal.

<http://dx.doi.org/10.1136/jitc-2021-SITC2021.441>

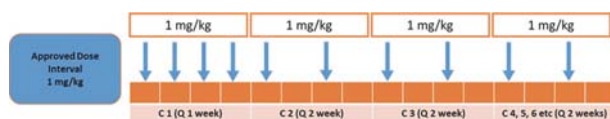
443

OPEN-LABEL, PHASE 2 STUDY TO ASSESS THE SAFETY OF MOGAMULIZUMAB AT 2 MG/KG Q4W MAINTENANCE DOSING IN PATIENTS WITH RELAPSED/REFRACTORY MF/SS SUBTYPES OF CTCL

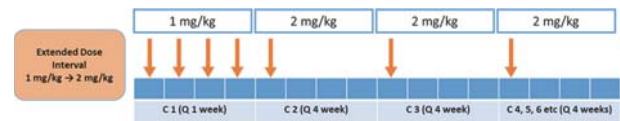
Karen Dwyer, Roland Meier, Matthew Hruska, Floyd Fox, Takahiro Ito. *Kyowa Kirin, Inc., Princeton, NJ, USA*

Background Mogamulizumab is approved in the United States, Japan, and the European Union for patients with relapsed/refractory mycosis fungoides (MF)/Sézary syndrome (SS) who have received at least one prior systemic therapy. The approved dose and schedule of mogamulizumab induction therapy are 1 mg/kg administered intravenously (IV) on Days 1, 8, 15, and 22 of the first 28-day cycle (figure 1). After induction, patients continue with 1 mg/kg IV on Days 1 and 15 of subsequent cycles. Patients must return to a clinic for administration, which can be inconvenient for patients with inadequate support systems or lack of accessibility. Additional clinic visits can also impact patient care when unforeseen circumstances, such as the COVID-19 pandemic, limit access to treatment. Limiting the number of clinic visits needed for infusion should also decrease the risk of possible exposure to nosocomial infections. This study's purpose is to evaluate the safety, tolerability, and pharmacokinetics of mogamulizumab in patients receiving standard induction treatment followed by 2 mg/kg every 4 weeks in subsequent cycles. Data from this study will be combined with data from previous studies using modeling and simulation methods to understand how every-4-week dosing compares to every-2-week dosing in terms of exposure, safety, and activity profiles. By extending the treatment interval of mogamulizumab, patients with MF/SS will have fewer clinic visits and reduced risk of exposure to nosocomial infections.

Methods This is a phase 2, open-label, multicenter, international study of mogamulizumab in adult patients with relapsed/refractory MF/SS who have failed at least one prior course of systemic therapy. All patients will receive mogamulizumab induction therapy. Therapy will then be administered as a 2 mg/kg IV infusion on day 1 of each subsequent 28-day cycle (figure 2). The primary objective is to evaluate the safety and tolerability of mogamulizumab 2 mg/kg administered every 4 weeks by observing the percentage of patients experiencing treatment-emergent adverse events. Secondary objectives include characterization and evaluation of mogamulizumab's pharmacokinetic profile, immunogenicity, anti-tumor activity (global composite response and response by compartment), and pharmacodynamic profile. A maximum of 33 patients will be enrolled in this clinical trial. The study consists of a 28-day screening period followed by a treatment period of up to 2 years from Cycle 1. No dose adjustment or modification is planned or permitted. Patients will be treated until disease progression or unacceptable toxicity or upon reaching 2 years from first dose.



Abstract 443 Figure 1 Approved mogamulizumab dosing: 1 mg/kg every 2 weeks following induction



Abstract 443 Figure 2 Study mogamulizumab dosing: 2 mg/kg every 4 weeks following induction

Acknowledgements The study was sponsored by Kyowa Kirin. Medical writing assistance was provided by Jonathan Mitchell, PharmD, of MedVal Scientific Information Services (Princeton, NJ, USA) and funded by Kyowa Kirin, Inc. (Princeton, NJ, USA).

Trial Registration ClinicalTrials.gov identifier: NCT04745234

Ethics Approval This study has been approved by the Advarra Institutional Review Board (Approval MOD00923851). Participants will be informed that their participation is voluntary and will be required to sign a statement of informed consent that meets the requirements of 21 CFR 50, local regulations, ICH guidelines, requirements of the Health Insurance Portability and Accountability Act of 1996, where applicable, and the IRB/EC or study center.

<http://dx.doi.org/10.1136/jitc-2021-SITC2021.443>

444

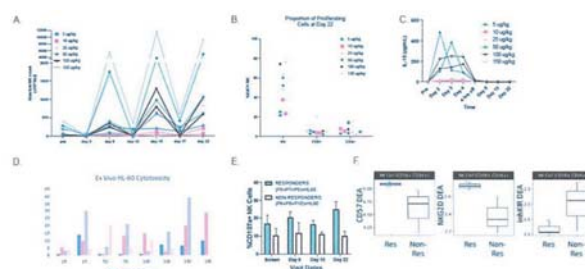
GTB-3550 TRI-SPECIFIC KILLER ENGAGER TRIKE™ DRIVES NK CELLS EXPANSION AND CYTOTOXICITY IN ACUTE MYELOID LEUKEMIA (AML) AND MYELODYSPLASTIC SYNDROMES (MDS) PATIENTS

¹Martin Felices, ¹Erica Warlick, ¹Mark Juckett, ¹Daniel Weisdorf, ¹Daniel Vallera, ¹Sarah Miller, ¹Rose Wangen, ¹Dixie Lewis, ¹JoAnne Knox, ²Martin Schroeder, ¹Jeffrey Miller*. ¹University of Minnesota, Minneapolis, MN, USA; ²GT Biopharma, Beverly Hills, CA, USA

Background Treatment for relapsed/refractory [r/r] AML and high risk MDS is dismal and NK cell infusions (with IL-2 or IL-15) after lymphodepleting chemotherapy can result in 30–40% remission. However, NK cells lack antigen specificity and require cytokine for expansion. We have developed a novel tri-specific molecule,¹ termed GTB-3550 TriKE, comprised of IL-15 surrounded by two single chain variable fragments (scFvs), one against CD16 on NK cells and one against CD33 on blasts.

Methods Supported by pre-clinical data, adults with CD33+ malignancies (r/r AML or MDS) are eligible (NCT03214666). Correlative objectives include the number, phenotype (Flow and CyTOF), and function of NK cells before and after therapy.

Results Twelve patients have completed therapy at doses of 5–150 mcg/kg/day without dose limiting toxicity. Out of the 11 with post treatment disease assessment, 3 patients had blasts decreases of 33, 61 and 63% at cohorts 25, 50, and 100 mcg/Kg/day, respectively. One patient (150 mcg/Kg/day) was found to have a multilineage leukemia with a significant population of CD19+/CD33- blasts not affected but demonstrated a 50% decrease of on-target CD19-/CD33+ blasts. Correlative studies show dose-dependent NK cell activity across cohorts, primarily by a robust expansion of NK cells without CD16 loss (figure 1A). Expansion is NK cell specific with preferential Ki-67 expression on NK cells at day 22 on study (figure 1B). Using IL-15 detection as a measure of GTB-3550 in serum, we find a short half-life as predicted with no evidence of drug accumulation (figure 1C). Despite rapid clearance, patient mononuclear cells without further activation demonstrate dose-dependent enhanced cytotoxicity against CD33+ HL-60 targets at days 8, 15, and 22 post initial treatment, 3 days after last drug (figure 1D). To better predict factors in responsiveness, responder and non-responder patient blood (d22) was incubated with IL-15 and HL-60 cells (no GTB-3550 added) and NK cell degranulation (CD107a) was measured (figure 1E). Results indicate that responders have higher degranulating than non-responders. To explore further, we carried out 42-antigen CyTOF analysis. Differential expression analysis (DEA) on mature NK cells (CD56+CD16+) at day 22 showed increased expression of the maturation marker CD57 and activation receptor NKG2D, while showing decreased expression of inhibitory KIR (figure 1F).



Abstract 444 Figure 1 Correlative studies outline potent, NK specific, activity of GTB-3550

Conclusions Our Phase I study demonstrates GTB-3550 TriKE safety, robust expansion of endogenous NK cells and a clinical signal of activity. Immune monitoring suggests that a schedule to maximize function in vivo with repeat courses will further enhance activity.

Trial Registration NCT03214666

REFERENCES

- Vallera DA, Felices M, McElmurry R, McCullar V, Zhou X, Schmohl JU, et al. IL15 Trispecific Killer Engagers (TriKE) Make Natural Killer Cells Specific to CD33+ Targets While Also Inducing Persistence, In Vivo Expansion, and Enhanced Function. *Clinical cancer research: an official journal of the American Association for Cancer Research* 2016;**22**(14):3440–50.

Ethics Approval The protocol and consent procedures were approved by the University of Minnesota Institutional Review Board (HSC # STUDY00000881). The study was approved by the FDA under BB-IND 136205. All patients and donors gave informed consent for treatment and prospective data collection in accordance with the Declaration of Helsinki.

<http://dx.doi.org/10.1136/jitc-2021-SITC2021.444>

445

TRIAL IN PROGRESS: A PHASE 1B/2 STUDY OF ALRIZOMADLIN (APG-115), ALONE OR COMBINED WITH 5-AZACITIDINE, IN PATIENTS WITH RELAPSED/REFRACTORY ACUTE MYELOID LEUKEMIA (R/R AML)

¹Yifan Zhai, ²Tapan Kadia*. ¹Ascentage Pharma, Rockville, MD, USA; ²MD Anderson Cancer Center, Houston, TX, USA

Background Acute myeloid leukemia (AML) is the most common form of acute leukemia in adults, with an incidence that increases with age and a generally poor prognosis. This aggressive blood and bone-marrow malignancy is characterized by rapid and uncontrolled clonal proliferation of abnormal myeloid progenitor cells. Patients with R/R AML have very few approved effective treatment options, especially in the absence of a targetable mutation. Alrizomadlin is a novel, orally active, potent, small-molecule selective inhibitor that destabilizes the p53-MDM2 complex and activates p53-mediated apoptosis in tumor cells with wild-type TP53 and/or MDM2 amplification. In acute leukemia human wild-type TP53 AML cell lines and xenograft models, alrizomadlin potently inhibited tumor cell growth when administered alone or with concomitant chemotherapy.

Methods This US open-label study is evaluating the safety and tolerability of alrizomadlin, with or without 5-azacitidine, in adults with histologically confirmed R/R AML and adequate organ function. Eligible candidates will have AML with no known available therapies that are either indicated or expected to confer a durable response. In Part 1 of this trial, the safety and tolerability of alrizomadlin monotherapy are being assessed by evaluating the dose-limiting toxicity rate during the first 4 weeks of treatment, using a standard 3+3 design. The starting once-daily oral dose of alrizomadlin administered on Day 1 to 5 of every 28-day cycle is 100 mg, increasing to 150, 200, and 250 mg in each subsequent cohort. The severity of adverse events is being assessed using NCI CTCAE v5.0. Once the recommended phase 2 dose (RP2D) has been determined, 3 to 6 additional patients will be enrolled in the dose-expansion phase. In Part 2, alrizomadlin will be administered in combination with 5-azacitidine 75 mg/m²/day on Days 1–7 of a 28-day cycles. Alternatively, a 5-days-on, 2-days-off, 2-days-on schedule is allowed if consecutive day infusion is not available. A standard 3+3 design will also be implemented to determine the maximum tolerated dose/RP2D in the dose-escalation phase. Once the RP2D has been determined, there will be an expansion cohort of up to 15 patients. As of July 13, 2021, 2 patients have been enrolled in the alrizomadlin monotherapy dose-escalation phase. The overall estimated enrollment will be 69 study participants. Internal study identifier APG115AU101. ClinicalTrials.gov identifier: NCT04358393.

Trial Registration ClinicalTrials.gov identifier: NCT04358393

<http://dx.doi.org/10.1136/jitc-2021-SITC2021.445>

447

INTERIM RESULTS OF A PHASE 1 STUDY OF THE NOVEL ENGINEERED TOXIN BODY TAK-169 IN PATIENTS WITH RELAPSED OR REFRACTORY MULTIPLE MYELOMA

¹Shaji Kumar*, ²Admasu Mamuye, ²Kristina Dabovic, ²Jingyuan Wang, ²Banmeet Anand, ²Amy Yuet, ³Bhagirathbhai Dholaria, ¹Vivek Roy. ¹Mayo Clinic, Rochester, MN, USA; ²Molecular Templates, Inc., New York, NY, USA; ³Vanderbilt University Medical Center, Tampa, FL, USA

Background Engineered toxin bodies (ETBs) are comprised of a proprietary engineered and de-immunized Shiga-like Toxin-I A1 subunit genetically fused to an antibody-like binding domain. ETBs can force receptor internalization, induce potent cell-kill via enzymatic and permanent inactivation of ribosomes, and may not be subject to resistance mechanisms of other therapeutics. TAK-169 is a second-generation ETB targeting CD38 in hematologic malignancies including multiple myeloma (MM).

Methods This multicenter, open-label, phase 1 study is designed to evaluate the safety, tolerability, preliminary efficacy, pharmacokinetics, and pharmacodynamics of TAK-169 monotherapy in patients with relapsed or refractory MM (RRMM). The primary objective of the expansion phase (Part 2) is to provide a preliminary evaluation of the clinical activity of TAK-169 monotherapy in patients with RRMM. The starting dose of TAK-169 in Part 1 is 50 µg/kg IV once weekly. Subsequent planned dose levels are 100, 200, 335, 500, and 665 µg/kg (NCT04017130).

Results At the data cut-off in June 2021, 4 patients with a median age of 70 years were enrolled at the initial TAK-169 dose level of 50 µg/kg. All 4 patients were heavily pretreated with at least 5 previous lines of therapy. All patients have discontinued the study, 3 due to progressive disease and 1 due to a treatment-emergent adverse event (TEAE). The TEAE was asymptomatic grade 2 reversible myocarditis diagnosed by cardiac magnetic resonance imaging (MRI) and grade 3 hs-troponin elevation in the absence of ischemia, ECG, or echocardiographic abnormalities. Comparative baselines were not available for either the cardiac MRI or hs-troponin levels. No other cardiac TEAEs have been observed with any other patient. All other related TEAEs were either grade 1 or 2 events. All patients had quantifiable drug concentrations on Cycle 1 Day 1, with the mean elimination half-life calculated as 1 hour. The geometric mean of C_{max} in the 4 patients was 1.73 nM, which is lower than the EC₅₀ of 5 nM observed in MM cell-killing assays using patient bone marrow aspirates. Number of natural killer (NK) cells in peripheral blood for the 4 patients was reduced by a maximum of 56%, 85%, 88%, and 92% after the first dose. The patient with 56% reduction in NK cells had the lowest NK cell count at baseline, along with a low percentage of CD38+ NK cells.

Conclusions These data demonstrate that, at 50 mcg/kg, TAK-169 was engaging its target CD38, leading to robust NK-cell reductions. Dose escalation is ongoing.

Trial Registration ClinicalTrials.gov identifier: NCT04017130

Ethics Approval Vanderbilt University Institutional Review Board (1313 21st Ave S, Suite 505. Nashville, TN 37232-4315) gave approval on 6/25/2021 (IRB #191752). Participants gave informed consent before taking part in the study.

<http://dx.doi.org/10.1136/jitc-2021-SITC2021.447>

448

LEMZOPARLIMAB (TJ011133), AN ANTI-CD47 ANTIBODY, WITH/WITHOUT DEXAMETHASONE PLUS ANTI-MYELOMA REGIMENS FOR RELAPSED/REFRACTORY MULTIPLE MYELOMA: A PHASE 1B DOSE ESCALATION AND EXPANSION STUDY

¹Edward Stadtmauer, ²Lionel Karlin, ³Katja Weisel, ⁴Moshe Etzion Gatt, ⁵Ankit Kansagra, ⁶Gregory Monohan, ⁷Andrew Yee, ⁸Shayna Rockow-Magnone, ⁸Jose Cordero, ⁸David Hoffman, ⁸Orlando Bueno, ⁸Kevin Wu, ⁹Cristina Gasparetto*. ¹University of Pennsylvania, Philadelphia, PA, USA; ²Centre Hospitalier Lyon Sud, Lyon, France; ³University Medical Center Hamburg-Eppend, Hamburg, Germany; ⁴Hadassah Medical Center-Hebrew University, Jerusalem, Israel; ⁵University of Texas Southwestern Medical, Dallas, TX, USA; ⁶University of Kentucky, Lexington, KY, USA; ⁷Massachusetts General Hospital, Boston, MA, USA; ⁸AbbVie Inc., North Chicago, IL, USA; ⁹Duke University Hospital, NC, USA

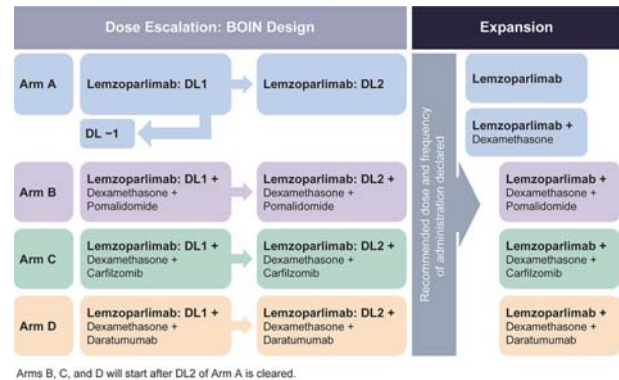
Background Despite therapeutic advancements for multiple myeloma (MM), most patients with MM develop relapsed/refractory (R/R) disease, which is associated with high mortality and highlights an unmet need for novel treatments. A key characteristic of MM cells is the overexpression of CD47, which downregulates phagocytosis, thereby allowing malignant plasma cells to evade destruction by the immune system. Blocking CD47 with lempzoparlimab, an anti-CD47 monoclonal antibody, may enhance macrophage-mediated anti-tumor activity. This study will characterize the safety, dose-limiting toxicity, and recommended dosing of lempzoparlimab (TJ011133) with or without dexamethasone and combined with other anti-myeloma regimens in patients with R/R MM.

Methods This phase 1b, open-label, dose-escalation and expansion study (NCT04895410) will enroll adults with R/R MM, an Eastern Cooperative Oncology Group Performance Status ≤ 2 , prior treatment history (varies based on treatment arm; Figure 1), and measurable disease (serum monoclonal paraprotein [M-protein] ≥ 0.5 g/dL, urine M-protein ≥ 200 mg/24 hours, or serum-free light chain ≥ 100 mg/L). Patients will be enrolled in 2 phases (escalation and expansion), divided into 4 arms to receive treatment in 28-day cycles (figure 1): (A) lempzoparlimab \pm dexamethasone; (B) lempzoparlimab + dexamethasone + pomalidomide (4 mg orally daily [Days 1–21]); (C) lempzoparlimab + dexamethasone + carfilzomib (56 mg/m² intravenously, 6 doses/cycle [first 2 doses in Cycle 1: 20 mg/m²]); and (D) lempzoparlimab + dexamethasone + daratumumab (1800 mg subcutaneously [Cycle 1, start on Day 2; Cycles 1–2, once weekly; Cycles 3–6, every 2 weeks; Cycles ≥ 7 , Day 1]). Dexamethasone will be administered orally twice weekly at 20 mg for Arm C, and orally or intravenously weekly at 40 mg for other arms. Dose escalation will follow Bayesian optimal interval design. Once maximum tolerated dose/recommended phase 2 dose (RP2D) is determined, patients will be enrolled in the expansion. Treatment discontinuation criteria are: unacceptable toxicity, disease progression, consent withdrawal, or investigator's discretion. The primary endpoint is determination of the RP2D. Secondary endpoints include safety and efficacy measures. Time-to-event endpoints will be analyzed using the Kaplan–Meier method.

Acknowledgements AbbVie is funding this study and participating in the study design, research, analysis, data collection, interpretation of data, reviewing, and approval of the publication. All authors had access to relevant data and participated in the drafting, review, and approval of this publication. No honoraria or payments were made for authorship. Medical writing support was provided by Marta Rossi, PhD, of Fishawack Communications Ltd, and funded by AbbVie.

Trial Registration ClinicalTrials.gov: NCT04895410

Ethics Approval The protocol, informed consent form(s), recruitment materials, and all patient materials will be submitted to the Independent Ethics Committee/Institutional Review Board for review and approval.



Abstract 448 Figure 1 Study schematic

The dose escalation phase will follow BOIN; it will start with lempzoparlimab (TJ011133) monotherapy at DL1 in Arm A. If DL1 is not tolerated as monotherapy or as combination therapy, DL -1 will be evaluated. Investigation of combination arms will start after evaluation of monotherapy.

Arms A, B, C and D will include patients with R/R MM after progressing on defined therapies and number of prior lines of therapy.

BOIN, Bayesian optimal interval; DL, dose level; MM, multiple myeloma; R/R, relapsed/refractory.

<http://dx.doi.org/10.1136/jitc-2021-SITC2021.448>

CONCURRENT IBRUTINIB ENHANCES T CELL FUNCTION IN PATIENTS WITH CHRONIC LYMPHOCYTIC LEUKEMIA (CLL) TREATED WITH LISOCABTAGENE MARALEUCEL (LISO-CEL), A CHIMERIC ANTIGEN RECEPTOR (CAR) T CELL THERAPY

Jerill Thorpe*, Julie Rytlewski, Heidi Gillenwater, Ken Ogasawara, Yeonhee Kim, Diana Shepektor, Eniko Papp, Leanne Peiser. *Bristol Myers Squibb, Seattle, WA, USA*

Background CLL is an incurable hematologic malignancy characterized by progressive accumulation of clonally derived CD19+ B-cell lymphocytes. CAR T cell therapies are promising treatments but inherent T cell dysfunction has limited their development in CLL. Preclinical studies suggest ibrutinib may modulate CAR T cells directly to improve their function independently of antitumor effects. Liso-cel is an autologous, CD19-directed, defined composition, 4-1BB CAR T cell product administered at equal target doses of CD8+ and CD4+ CAR+ T cells. The ongoing TRANSCEND CLL 004 study evaluates the efficacy and safety of liso-cel alone (monotherapy) or with concurrent ibrutinib (combination) in relapsed/refractory (R/R) CLL.¹ We investigated the effect of ibrutinib on post-infusion CAR+ and endogenous T cells relative to monotherapy using a novel cell-sorting, low-input RNA-seq method for analysis of patient cells beyond peak expansion, including 1 and 2 months after liso-cel infusion.

Methods CAR+ and endogenous T cells from patients in TRANSCEND CLL 004 (NCT03331198; monotherapy, n=16; combination, n=19) were isolated from peripheral blood mononuclear cells by fluorescence-activated cell sorting. RNA-seq was performed using cell lysate as input material. CAR+ T cell pharmacokinetics were assessed by flow cytometry. Serum interleukin-6 was measured by electrochemiluminescent multiplex immunoassay. Minimal residual disease (<10⁻⁴) was evaluated by flow cytometry in peripheral blood and next-generation sequencing in bone marrow.

Results Gene set enrichment analyses revealed positive enrichment of cell proliferation-associated gene sets and negative enrichment of inflammation-associated gene sets at peak expansion in CAR+ T cells from combination relative to monotherapy patients. Similar, but less marked, proliferation- and inflammation-associated gene expression changes were also observed in endogenous T cells. Accordingly, increased CAR+ T cell expansion and reduced serum interleukin-6 were observed in combination patients. In addition, an independently derived CLL ibrutinib gene expression score² was increased and sustained in CAR+ and endogenous T cells from combination but not monotherapy patients over time. A higher ibrutinib score trended with a higher rate of undetectable minimal residual disease, longer progression-free survival (PFS), and longer duration of response. Lastly, a T cell exhaustion-related gene signature was significantly reduced in CAR+ but not endogenous T cells with combination treatment, and this reduction was associated with improved PFS.

Conclusions Concurrent ibrutinib treatment in patients with R/R CLL resulted in measurable effects in CAR+ and endogenous T cells, including changes in gene signatures related to proliferation, inflammation, and T cell exhaustion. These changes were associated with enhanced CAR T cell function and efficacy.

Acknowledgements We would like to thank the patients, caregivers, investigators, and study personnel. This study was funded by Juno Therapeutics, a Bristol-Myers Squibb Company. All authors contributed to and approved the abstract;

writing and editorial assistance were provided by Allison Green, PhD, of The Lockwood Group (Stamford, CT, USA), funded by Bristol Myers Squibb.
Trial Registration NCT03331198

REFERENCES

1. Wierda WG, Dorritle KA, Munoz J, et al. TRANSCEND CLL 004: phase 1 cohort of lisocabtagene maraleucel (liso-cel) combined with ibrutinib (IBR) for patients (pts) with R/R CLL/SLL. *Hematol Oncol* 2021;**39**(S2):141–143.
2. Rendeiro AF, Krausgruber T, Fortelny N, et al. Chromatin mapping and single-cell immune profiling define the temporal dynamics of ibrutinib response in CLL. *Nat Commun* 2020;**11**:577.

Ethics Approval This study used patient cells obtained from a clinical trial that was done in accordance with with the Declaration of Helsinki, International Conference on Harmonization Good Clinical Practice guidelines, institutional review boards at participating institutions approved the study protocol and amendments, and all patients provided written informed consent.

<http://dx.doi.org/10.1136/jitc-2021-SITC2021.449>

450

TRIAL IN PROGRESS: A PHASE 1B STUDY OF ALRIZOMADLIN, ALONE OR PLUS 5-AZACITIDINE OR CYTARABINE, IN PTS WITH RELAPSED/REFRACTORY ACUTE MYELOID LEUKEMIA AND RELAPSED HIGHER-RISK MYELODYSPLASTIC SYNDROME

¹Yifan Zhai, ²Jianxiang Wang*. ¹Ascentage Pharma, Rockville, MD, USA; ²Blood Diseases Hospital Chinese Academy, Tianjin, China

Background Patients with relapsed/refractory acute myeloid leukemia (R/R AML) and higher-risk myelodysplastic syndrome (MDS) have fewer approved effective treatment options, especially in the absence of a targetable mutation. Certain treatment-resistant cancers overexpress mouse double minute 2 homolog (MDM2) which is a negative regulator of tumor suppressor p53. Alrizomadlin (APG-115) is a novel, orally active, potent, small-molecule selective inhibitor that destabilizes the p53-MDM2 complex and activates p53-mediated apoptosis in tumor cells with wild-type TP53 and/or MDM2 amplification. Alrizomadlin can also augment MDM2-modulated signal transducer and activator of transcription 5 (STAT5) stability, which in turn can increase survival and function of tumor-infiltrating CD8⁺ T cells. There is preclinical evidence of antitumor synergy when alrizomadlin is combined with immune checkpoint inhibitors. Through these pathways, alrizomadlin functions as an immunomodulator and may be complementary to other therapies in restoring antitumor activity.

Methods This open-label trial in Chinese patients is evaluating the safety and tolerability of oral alrizomadlin in adults with histologically confirmed R/R AML (according to WHO classification); relapsed/progressed, high- (or very high-) risk MDS according to IPSS-R stratification; an ECOG performance status of 0 to 1; and leukocytes < 50 × 10⁹/L. Excluded are patients with acute promyelocytic leukemia, a recent history of hematopoietic stem cell transplantation, uncontrolled cardiovascular diseases and certain active infections, and/or recent anticancer therapies. Alrizomadlin is administered orally once daily (QD) from Days 1 to 7 every 28 days. Part 1 is a standard 3 + 3 dose-escalation to determine the dose-limiting toxicity (DLT), maximum tolerated dose (MTD), and recommended phase 2 dose (RP2D) of alrizomadlin. Part 2 will determine DLT, MTD, and RP2D of alrizomadlin combined with either 5-azacitidine (Arm A; 75 mg/m² subcutaneously QD on Days 1–7 of a 28-day cycle) or cytarabine (Arm B; 1 g/m² IV QD on Days 3–7 of a 28-day cycle). Part 3 is a dose-expansion of the alrizomadlin combination regimens at RP2D. The primary outcome measure comprises DLTs, which are defined as clinically significant drug-related adverse events during Cycle 1 (graded by NCI CTCAE v5). Secondary endpoints include (1) overall response rate (complete response [CR] + CR with incomplete hematologic recovery + partial response) measured up to 6 cycles for 1 month after the last dose and (2) overall survival measured up to 6 months after the last treatment dose. As of July 16, 2021, 7 patients have been enrolled. Internal study identifier APG115AC101. Clinical trial registration: NCT04275518.

Trial Registration Clinical trial registration: NCT04275518

<http://dx.doi.org/10.1136/jitc-2021-SITC2021.450>

PRELIMINARY ANALYSIS OF A REAL-WORLD STUDY (RWS) OF CAMRELIZUMAB TREATMENT IN PRIMARY LIVER CANCER (PLC)

¹Zhendong Chen, ¹Nianfei Wang*, ²Dayong Luo, ¹Bo Jiang, ³Mu Yuan, ⁴Xinzhong Li, ⁵Chunmei Yao, ⁶Hong Qian, ⁷Qingsheng Kan, ⁸Erxuan Wang. ¹The second Hospital of Anhui Medical University, Hefei, China; ²The second people's Hospital of Fuyang City, Fuyang, China; ³The first affiliated Hospital of Bengbu Medical College, Bengbu, China; ⁴Huaibei people's Hospital, Huaibei, China; ⁵Huaibei miners General Hospital Group, Huaibei, China; ⁶The people's Liberation Army Navy Anqing Hospital, Anqing, China; ⁷Suzhou Municipal Hospital of Anhui Province, Suzhou, China; ⁸Wangjiang County people's Hospital, Anqing, China

Background Immune checkpoint inhibitors (ICIs) have revolutionized the landscape of PLC management at all evolutionary stages.¹ As an anti-programmed cell death-1 (PD-1) antibody, camrelizumab monotherapy and in combination with apatinib, an anti-angiogenic tyrosine kinase inhibitor of vascular endothelial growth factor receptor (VEGFR)-2, chemotherapy or locoregional therapy, have demonstrated their efficacy in advanced hepatocellular carcinoma (HCC).^{2 3 4 5}

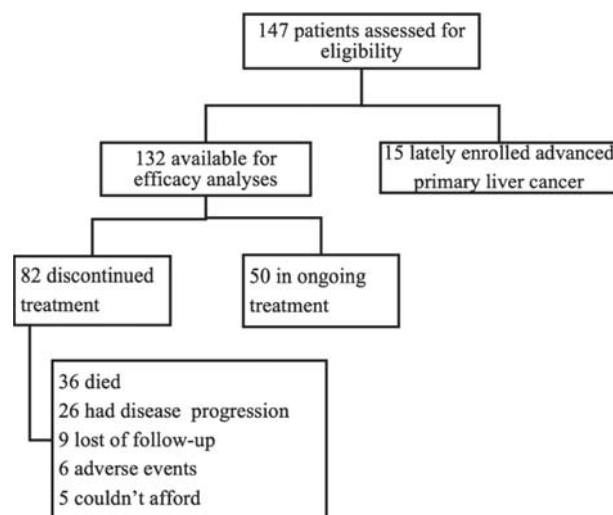
Methods This prospective, open-label, multi-center, observational RWS was conducted to evaluate efficacy and safety of camrelizumab in treatment of PLC in clinical practice. Eligible patients were histopathologically or cytologically identified HCC or intrahepatic cholangiocarcinoma, who were going to receive camrelizumab treatment, with age ≥ 18 ages, Eastern Cooperative Oncology Group performance status (ECOG PS) score of 0–2 and Child-Pugh score ≤ 9 . Patients were treated at clinician discretion. Three hundred patients were planned to enroll, including advanced or peri-operative PLC. The primary endpoint was progress-free survival for advanced PLC, whose efficacy was available to analysis. Efficacy was assessed per Response Evaluation Criteria in Solid Tumors version 1.1.

Results From March 29, 2020 to June 10, 2021, a total of 147 eligible patients of advanced PLC were enrolled and included in this interim analysis, with 128 (87.1%) men, 130 (94.9%) ECOG PS of 0–1, 139 (94.6%) HCC, 74 (50.4%) Barcelona Clinic Liver Cancer stage C, 98 (66.7%) Child-Pugh B, and 72 (49.0%) with extrahepatic metastases, shown in table 1. Of the 147 patients, 45 (30.1%) patients were treated with camrelizumab monotherapy, 79 (53.8%) patients with combination with angiogenesis inhibitors, of which 55 (37.4%) in combination with apatinib, 21 (14.3%) patients with camrelizumab and chemotherapy. Patients, who had at least one efficacy assessment, were included in the efficacy analyses. Up to July 19, 2021, with a median follow time of 6.2 months, 132 patients were available for efficacy analyses. Patient disposition was shown in figure 1. Objective response rate (ORR) and disease control rate (DCR) were 10%/30.8%/35.3% and 75.0%/86.5%/70.6% in camrelizumab monotherapy/combined with apatinib/combined with chemotherapy, respectively. (table 2) The most common camrelizumab-treatment related adverse events (AEs) included reactive cutaneous capillary endothelial proliferation (RCCEP) (12, 8.2%), ICI-induced pneumonia (2, 1.4%), enterocolitis (2, 1.4%), and nephritis (1, 0.7%), of which all these AEs recovered. Other AEs included increase of transaminase (5, 3.4%) and hypertension (4, 2.7%). All AEs were 1–2 grade and no treatment-related death occurred.

Abstract 452 Table 1 Baseline characteristics

Baseline characteristics (N=147)		
Average age		57.79±13.06
Sex	Male	128(87.1%)
	Female	19(12.9%)
ECOG PS score	0	60 (40.8%)
	1	73 (49.7%)
	2	14 (9.5%)
Histopathological features	HCC	139 (94.6%)
	ICC	8 (5.4%)
BCLC stage	UK	24 (16.3%)
	B	49 (33.3%)
	C	74 (50.4%)
Child-Pugh	A	49 (33.3%)
	B	98 (66.7%)

Data are n (%). ECOG-PS, Eastern Cooperative Oncology Group Performance Status; HCC, hepatocellular carcinoma; ICC, intrahepatic cholangiocarcinoma; BCLC, Barcelona Clinic Liver Cancer; UK, unknown.



Abstract 452 Figure 1 Patient disposition

Abstract 452 Table 2 Confirmed tumor response assessed by investigators per RECIST v1.1

Confirmed tumor response assessed by investigators per RECIST v1.1						
Camrelizumab treatment regimen (N=132)	CR, n (%)	PR, n (%)	SD, n (%)	PD, n (%)	ORR (%)	DCR (%)
Monotherapy (N=40)	0	4(10.0%)	26(65.0%)	10(25.0%)	10.0%	75.0%
Combined with anti-angiogenic agents (N=73)	1(1.4%)	21(28.7%)	40(54.8%)	11(15.1%)	30.1%	84.9%
Combined with apatinib (N=52)	1(1.9%)	15(28.8%)	29(55.8%)	7 (13.5%)	30.8%	86.5%
Combined with chemotherapy (N=17)	1(5.9%)	5(29.4%)	6(35.3%)	5 (29.4%)	35.3%	70.6%
Combined TACE or radiotherapy (N=2)	0	1(50.0%)	1(50.0%)	0	50%	100%

RECIST v1.1: Response Evaluation Criteria in Solid Tumors version 1.1; CR, complete response; PR, partial responses; SD, steady disease; PD, progressive disease; ORR, objective response rate; DCR, disease control rate; TACE, transarterial chemoembolization; NA, not available.

Conclusions Camrelizumab, combined with anti-angiogenic agents or chemotherapy, or monotherapy, demonstrated good efficacy and safety in treatment of PLC.

Trial Registration ChiCTR2000034264

REFERENCES

- Llovet JM, Kelley RK, Villanueva A, et al. Hepatocellular carcinoma. *Nat Rev Dis Primers* 2021;**7**(1):6–28.
- Qin S, Ren Z, Meng Z, et al. Camrelizumab in patients with previously treated advanced hepatocellular carcinoma: a multicentre, open-label, parallel-group, randomised, phase 2 trial. *Lancet Oncol* 2020;**21**(4):571–580.
- Xu J, Shen J, Gu S, et al. Camrelizumab in Combination with Apatinib in Patients with Advanced Hepatocellular Carcinoma (RESCUE): A Nonrandomized, Open-label, Phase II Trial. *Clin Cancer Res* 2021;**27**(4):1003–1011.
- Mei K, Qin S, Chen Z, et al. Camrelizumab in combination with apatinib in second-line or above therapy for advanced primary liver cancer: cohort A report in a multicenter phase Ib/II trial. *J Immunother Cancer* 2021;**9**(3).
- Qin S, Bai Y, Lim HY, et al. Randomized, multicenter, open-label study of oxaliplatin plus fluorouracil/leucovorin versus doxorubicin as palliative chemotherapy in patients with advanced hepatocellular carcinoma from Asia. *J Clin Oncol* 2013;**31**(28):3501–3508.

Ethics Approval This study was approved by China registered clinical trial ethics review committee with No. ChiECRCT20200042.

<http://dx.doi.org/10.1136/jitc-2021-SITC2021.452>

PERSONALIZED DNA NEOANTIGEN VACCINE (GNOS-PV02) IN COMBINATION WITH PLASMID IL-12 AND PEMBROLIZUMAB FOR THE TREATMENT OF PATIENTS WITH ADVANCED HEPATOCELLULAR CARCINOMA

<http://dx.doi.org/10.1136/jitc-2021-SITC2021.453>

¹Mark Yarchoan*, ²Edward Gane, ³Thomas Marron, ⁴Sarah Rochestie, ⁴Neil Cooch, ⁴Joann Peters, ³Ildiko Csiki, ⁴Alfredo Perales-Puchalt, ⁴Niranjan Sardesai. ¹*Johns Hopkins Sidney Kimmel CCC, Baltimore, MD, USA;* ²*New Zealand Clinical Research, Auckland, New Zealand;* ³*Icahn School of Medicine at Mount Sinai, New York, NY, USA;* ⁴*GENEOS THERAPEUTICS, Philadelphia, PA, USA;* ⁵*City of Hope, Duarte, CA, USA*

Background Hepatocellular carcinoma (HCC) is the fourth most common cause of cancer-related death. Immune checkpoint inhibitors targeting PD-1 have limited activity in HCC as monotherapy, with response rates ranging from 14–17%. Tumor neoantigens derived from tumor-specific mutations can be incorporated into personalized therapeutic cancer vaccines to generate tumor-specific T cell immunity, potentially priming the immune system for anti-PD1 therapy. DNA vaccines have been shown to elicit strong CD8 and CD4 T cell responses in preclinical and clinical trials. GNOS-PV02 is a personalized DNA vaccine, encoding up to 40 patient-specific neoantigens. In the GT-30 trial, it is used in combination with INO-9012 (plasmid-encoded IL-12) and pembrolizumab for the treatment of advanced HCC.

Methods GT-30 is a single-arm phase I/II clinical trial to assess the safety, immunogenicity, and preliminary efficacy of GNOS-PV02 in combination with INO-9012 and pembrolizumab in patients with advanced HCC. Twenty-four patients are anticipated to be enrolled. Patients are recruited upon diagnosis or during first-line treatment with tyrosine kinase inhibitors (TKI). Tumors are biopsied for exome and transcriptome sequencing, and peripheral blood collected for germline sequencing and histogenetics. The tumor specific vaccine is designed, optimized and manufactured during first-line therapy. Each vaccine encodes up to 40 neoantigens. After progression or intolerance with first-line therapy, patients commence concurrent personalized vaccine and pembrolizumab. GNOS-PV02 + INO-9012 are administered Q3w for the first 4 doses and Q9w thereafter. Pembrolizumab is delivered Q3w.

Results We performed a data cut-off on the first 12 patients. The median age was 66 years (range 55–75 years). GNOS-PV02 + INO-9012 with pembrolizumab has had no reported DLTs or drug related SAEs. The most common treatment-related AE were grade 1 fatigue (25%) and grade 1 injection site reactions (17%). By including up to 40 epitopes in the vaccine we were able to target all neoantigens present in 83% of the patients. The objective response rate was 25% (3/12 partial response, 5/12 stable disease, 4/12 progressive disease). Analysis of the TCR repertoire in peripheral blood and tumor tissue identified novel and significantly expanded T cell clones post-vaccination in all patients analyzed. Many of the novel peripheral T cell clones were also identified to have trafficked to the TME at week 9, potentially mediating the observed tumor regressions.

Conclusions These data demonstrate the potential of GNOS-PV02 + INO-9012 with pembrolizumab to target multiple neoepitopes, and provide initial support for the safety and efficacy of this regimen in patients with advanced HCC.

Trial Registration NCT04251117

Ethics Approval The study obtained IRB approval (IRB) and all patients signed informed consent prior to taking part in the clinical trial. NZCR EC: 20/NTA/6; JHU: IRB00227771; Mount Sinai: HS#: 20-00076

ANALYSIS OF NY-ESO-1 EXPRESSION IN SPECIMENS FROM A PHASE I/II NY-ESO-1 T-CELL THERAPY CLINICAL TRIAL IN NON-SMALL CELL LUNG CANCER AND FROM EXPLORATORY STUDIES IN MULTIPLE TUMOR TYPES

¹Bryan Barnes*, ¹Ming Shan, ¹Kristin Blouch, ²Mehmet Altan*, ¹Jaegil Kim, ¹Natalia Ramos-Hernandez, ¹Ellie Corigliano. ¹GlaxoSmithKline, Collegeville, PA, USA; ²MD Anderson Cancer Center, Houston, TX, USA

Background This analysis evaluates an NY-ESO-1 immunohistochemistry (IHC) clinical trial assay in multiple tumor types for the identification of patients who may be eligible for NY-ESO-1 TCR T-cell targeted therapy. We provide an analysis of NY-ESO-1 expression and prevalence in non-small cell lung carcinoma (NSCLC) tumor samples from a patient cohort of an early Phase I/II clinical trial assessing NY-ESO-1 TCR T-cell therapy. Furthermore, we describe exploratory analyses of NY-ESO-1 prevalence and expression in a preliminary set of multiple tumor types to identify new indications for NY-ESO-1 TCR T-cell therapy.

Methods An IHC assay was developed to detect NY-ESO-1 expression in formalin-fixed paraffin-embedded (FFPE) specimens utilizing an anti-NY-ESO-1 monoclonal antibody, clone E978. NY-ESO-1 protein expression levels and diagnostic status were determined by pathological evaluation under light microscopy to capture the percentage of tumor cell staining across all tumor cells in specimens at staining intensities 0, 1+, 2+ and 3+. NY-ESO-1 expression data were assessed for: prevalence using a $\geq 10\%$ cutoff at $\geq 1+$ intensity to assign positivity, and prevalence across classification (primary and metastatic) and subtype (adenocarcinoma and squamous cell carcinoma) for the NSCLC specimens.

Results The overall prevalence for NSCLC specimens from the Phase I/II trial was 15% (49/325) for NY-ESO-1. A prevalence of 15% (29/191) for primary and 14% (19/132) for metastatic samples, 13% (20/159) for adenocarcinoma, and 14% (5/35) for squamous cell carcinoma was observed. No significant difference was observed between subtype or %Tumor at each intensity. The preliminary set of indications used in exploratory studies had an observed prevalence as follows: gastric adenocarcinoma, 14 (4/28)%; esophageal adenocarcinoma & gastric esophageal junction, 9% (3/35); urothelial, 19% (6/31); head and neck squamous cell carcinoma, 10% (3/30); triple negative breast, 10% (3/30); hepatocellular carcinoma, 3%(1/30); and melanoma, 11% (3/27). NY-ESO-1 protein expression was localized in the cells' nuclei and surrounding cytoplasm.

Conclusions Multiple indications assessed by the IHC clinical trial assay demonstrated similar NY-ESO-1 expression across the range of staining intensities and percentage of positive tumor observed as that in NSCLC, therefore warranting further development and validation of an IHC assay for NY-ESO-1 detection in these additional tumor types for use in clinical trials. These data support the use of IHC as a tool for the identification of patients whose tumors upregulate NY-ESO-1 in NSCLC and further encourage the investigation of multiple tumor types that may upregulate NY-ESO-1 as potential targets for NY-ESO-1 TCR T-cell therapies.

Acknowledgements This study (NCT03709706) was funded by GlaxoSmithKline.

Trial Registration NCT03709706

REFERENCES

1. Thomas R, et al. *Front Immunol* 2018;9:947

Ethics Approval This study was approved by the appropriate institutional review boards and independent ethics committees.

<http://dx.doi.org/10.1136/jitc-2021-SITC2021.454>

455

PEGASUS LUNG, A PLATFORM STUDY OF SAR444245 (THOR-707, A PEGYLATED RECOMBINANT NON-ALPHA IL-2) WITH ANTI-CANCER AGENTS IN PATIENTS WITH NON-SMALL CELL LUNG CANCER (NSCLC) AND MESOTHELIOMA

¹Robin Meng*, ²Benjamin Besse, ³Melissa Johnson, ⁴Jaafar Bennouna, ⁵Luca Toschi, ¹Giovanni Abbadessa, ¹Amele Amrate, ¹Miao Zang, ⁶Luis Paz Ares. ¹Sanofi, Cambridge, USA; ²Institut de Cancerologie Gustave-Roussy, Villejuif, France; ³Tennessee Oncology, Nashville, TN, USA; ⁴Centre Hospitalier Universitaire de Nant, Nantes, France; ⁵IRCCS Humanitas Research Hospital, Rozzano, Italy; ⁶Hospital Universitario 12 de Octubre, Madrid, Spain

Background SAR444245 (THOR-707) is a recombinant human IL-2 molecule that includes a PEG moiety irreversibly bound to a novel amino acid via click chemistry to block the alpha-binding domain while retaining near-native affinity for the beta/gamma subunits. In animal models, SAR444245 showed anti-tumor benefits, but with no severe side effects, both as single agent and when combined with anti-PD1 comparing with historical data from aldesleukin. The HAMMER trial, which is the FIH study shows preliminary encouraging clinical results: initial efficacy and safety profile with SAR444245 monotherapy and in combination with pembrolizumab support a non-alpha preferential activity, validating preclinical models. The Pegasus Lung Ph2 study will evaluate the clinical benefit of SAR444245 in combination with other anticancer therapies for the treatment of patients with lung cancer or pleural mesothelioma

Methods The Pegasus Lung (NCT04914897) will enroll approximately 354 patients in 6 separate cohorts concurrently or sequentially. In cohorts A1 & A2, patients with first line (L) NSCLC will receive SAR444245 + pembrolizumab. In cohort A3, patients with 1L non-squamous NSCLC will receive SAR444245 + pembrolizumab + pemetrexed + carboplatin/cisplatin. In cohort B1 & B2 patients with 2/3L NSCLC who have progressed on a checkpoint inhibitor (CPI)-based therapy will receive SAR444245 + pembrolizumab, or SAR444245 + pembrolizumab + nab-paclitaxel. In cohort C patients with 2/3L CPI naïve mesothelioma will receive SAR444245 + pembrolizumab. SAR444245 is administered IV at a dose of 24 ug/kg Q3W in an outpatient setting until disease progression or completion of 35 cycles. Pembrolizumab is administered at a dose of 200 mg Q3W until PD or completion of 35 cycles. The study primary objective is to determine the antitumor activity of SAR444245 in combination with other anticancer therapies. Secondary objectives include confirmation of dose and safety profile, assess other indicators of antitumor activity, and assess the pharmacokinetic profile and immunogenicity of SAR444245. The study will be conducted in the US, Australia, France, Italy, Japan, Poland, South Korea, Spain, and Taiwan.

Acknowledgements The Pegasus Lung study is sponsored by Sanofi.

Trial Registration NCT04914897

Ethics Approval This study has been approved by applicable ethics committees or institutional review boards. All participants gave informed consent before taking part.

Consent Written informed consent was obtained from the patient for publication of this abstract and any accompanying images. A copy of the written consent is available for review by the Editor of this journal.

<http://dx.doi.org/10.1136/jitc-2021-SITC2021.455>

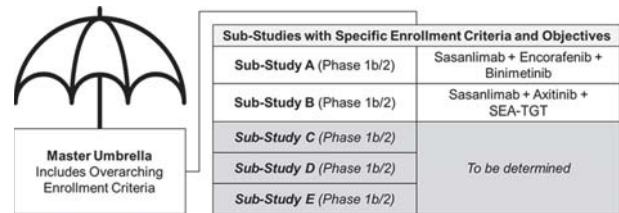
A PHASE 1B/2 UMBRELLA STUDY OF ANTI-PD-1 SASANLIMAB IN COMBINATION WITH OTHER THERAPIES FOR PATIENTS WITH STAGE IIIB/IV NON-SMALL CELL LUNG CANCER (NSCLC): THE LANDSCAPE 1011 TRIAL IN PROGRESS

¹Michael Boyer*, ²Sandip Patel, ³Thomas Marron, ⁴Nick Pavlakis, ⁵Sagun Parakh, ⁶Shirish Gadgeel, ⁷Michael Shafique, ⁸Robert Hoyer, ⁹D Ross Camidge, ¹⁰Charles Farber, ¹¹Ranee Mehra, ¹²Tarek Mekhail, ¹³Prunella Blinman, ¹⁴Karey Kowalski, ¹⁴Craig Davis, ¹⁴Dmitri Pavlov, ¹⁴Nayra Gad, ¹⁵Erminia Massarelli. ¹Chris O'Brien Lifehouse, Camperdown, Australia; ²UC San Diego Health, La Jolla, CA, USA; ³Icahn School of Medicine at Mount Sinai, New York, NY, USA; ⁴The University of Sydney, Sydney, Australia; ⁵ONJ Cancer Research Institute, Heidelberg, Australia; ⁶Henry Ford Cancer Institute, Detroit, MI, USA; ⁷Moffitt Cancer Center, Tampa, FL, USA; ⁸UCHealth Memorial Hospital Central, Colorado Spring, CO, USA; ⁹University of Colorado, Aurora, CO, USA; ¹⁰Morristown Medical Center, Morristown, NJ, USA; ¹¹University of Maryland, Baltimore, MD, USA; ¹²Advent Health Cancer Institute, Orlando, FL, USA; ¹³Concord Repatriation General Hospital, Sydney, Australia; ¹⁴Pfizer, La Jolla, CA, USA; ¹⁵City of Hope Comprehensive Cancer Center, Duarte, CA, USA

Background Programmed cell death protein 1 (PD-1) inhibitors as monotherapy or in combination with chemotherapy have become a standard of care first-line therapy for Stage IIIB/IV non-small cell lung cancer (NSCLC). However, many patients experience disease progression and require subsequent therapy within the first year of treatment.¹ For patients requiring salvage chemotherapy, prognosis is poor, with a median progression-free survival (PFS) and overall survival (OS) of 4.0 and 8.5 months, respectively.² Combinations of PD-1 blockade using sasanlimab (PF-06801591) and other immune and/or targeted therapies may be able to achieve clinical response in patients who have progressed on standard chemoimmunotherapy.

Methods LANDSCAPE 1011 (NCT04585815) is a prospective, open-label, multi-center, parallel group, phase 1b/2 umbrella study evaluating the safety, efficacy, pharmacokinetics, and pharmacodynamics of sasanlimab in combination with other therapies, in patients with Stage IIIB/IV NSCLC. The study is expected to enrol ~375 patients age 18 years or older diagnosed with stage IIIB/IV NSCLC. During phase 1b, the safety of each sub-study combination with subcutaneous sasanlimab will be assessed and the recommended phase 2 dose determined for each combination. Phase 2 will further evaluate safety and anti-tumor activity of each combination using the respective recommended phase 2 dose (figure 1). Up to 5 parallel sub-studies are planned. Currently, 2 sub-studies are ongoing. Sub-Study A will investigate sasanlimab, encorafenib (a BRAF inhibitor), and binimetinib (a MEK inhibitor) in patients with BRAF^{V600E} mutations (only including treatment-naïve patients in phase 2). Sub-Study B will investigate sasanlimab, axitinib (a vascular endothelial growth factor receptor inhibitor), and SEA-TGT (an anti-TIGIT antibody). In phase 2, this will involve treatment-naïve patients without oncogene drivers who have PD ligand 1-positive tumors or whose disease has progressed on prior immune checkpoint inhibitor-containing regimens. The primary phase 1b endpoint is the dose-limiting toxicity during the first cycle (28 days). The primary phase 2 endpoint in Sub-Study A is durable objective response (OR) defined as confirmed complete response or partial response lasting 10 or more months; and in Sub-Study B, OR defined as confirmed complete response or partial response, according to Response Evaluation Criteria in Solid Tumors (RECIST) v1.1. Secondary endpoints include adverse events and laboratory abnormalities, duration of response, time to tumor response, PFS, OS, OR by PD-L1

expression at baseline, pharmacokinetic parameters, incidence of anti-drug antibodies and neutralizing antibodies, and health-related quality of life. The first patient was enrolled in November 2020.



Abstract 456 Figure 1 LANDSCAPE 1011 study overview

Acknowledgements This study was sponsored by Pfizer. Medical writing and editorial support was provided by Simon Stones at Engage Scientific Solutions, and funded by Pfizer. The authors would like to acknowledge the late Aron Thall, who was highly devoted to the execution and success of this study.

Trial Registration ClinicalTrials.gov NCT04585815

REFERENCES

- Gandhi L, Rodriguez-Abreu D, Gadgeel S, et al. Pembrolizumab plus Chemotherapy in Metastatic Non-Small-Cell Lung Cancer. *N Engl J Med* 2018;**378**:2078–92.
- Herbst RS, Baas P, Kim DW, et al. Pembrolizumab versus docetaxel for previously treated, PD-L1-positive, advanced non-small-cell lung cancer (KEYNOTE-010): a randomised controlled trial. *Lancet* 2016;**387**:1540–50.

Ethics Approval The study is approved at each study site according to local regulations.

<http://dx.doi.org/10.1136/jitc-2021-SITC2021.456>

KEYNOTE-495/KEYIMPACT: INTERIM ANALYSIS OF A RANDOMIZED, BIOMARKER-DIRECTED, PHASE 2 TRIAL OF PEMBROLIZUMAB-BASED COMBINATION THERAPY FOR NON-SMALL CELL LUNG CANCER (NSCLC)

¹Martin Gutierrez*, ²Wei-Sen Lam, ³Matthew Hellmann, ⁴Matthew Gubens, ⁵Charu Aggarwal, ⁶Daniel Shao Weng Tan, ⁷Enriqueta Felip, ⁸Joanne WY Chiu, ⁹Jong-Seok Lee, ¹⁰James Chih-Hsin Yang, ¹¹Edward Garon, ¹²Giovanna Finocchiaro, ¹³Myung-Ju Ahn, ¹⁴Alexander Luft, ¹⁵Gregory Landers, ¹⁶Andrea Basso, ¹⁶Hua Ma, ¹⁶Julie Kobie, ¹⁶John Palcza, ¹⁶Razvan Cristescu, ¹⁷Lawrence Fong, ¹⁶Alexandra Snyder, ¹⁶Jianda Yuan, ¹⁸Roy Herbst. ¹Hackensack University Medical Center, Hackensack, NJ, USA; ²Fiona Stanley Hospital and Western Australia Country Health Service, Perth, Australia; ³Memorial Sloan Kettering Cancer Center, New York, NY, USA; ⁴University of California, San Francisco, San Francisco, CA, USA; ⁵Perelman School of Medicine at the University of Pennsylvania, Philadelphia, PA, USA; ⁶SingHealth Duke NUS Academic Medical, Singapore, Singapore; ⁷Vall d'Hebron University Hospital, Vall d'Hebron Institute of Oncology, Barcelona, Spain; ⁸University of Hong Kong, Queen Mary Hospital, Hong Kong, Hong Kong; ⁹Seoul National University, Bundang Hospital, Seongnam, Korea, Republic of; ¹⁰National Taiwan University Hospital and National Taiwan University Cancer Center, Taipei City, Taiwan, Province of China; ¹¹David Geffen School of Medicine at UCLA, Santa Monica, USA; ¹²IRCCS Humanitas Research Hospital, Milan, Italy; ¹³Samsung Medical Center, Sungkyunkwan University of Medicine, Seoul, Korea, Republic of; ¹⁴Leningrad Regional Clinical Hospital, St. Petersburg, Russian Federation; ¹⁵The Oncology Centre, KwaZulu-Natal, South Africa; ¹⁶Merck and Co., Inc., Kenilworth, NJ, USA; ¹⁷Helen Diller Family Comprehensive Cancer Center, University of California San Francisco, San Francisco, CA, USA; ¹⁸Comprehensive Cancer Center Yale School, New Haven, CT, USA

Background T-cell-inflamed gene expression profile (Tcell_{inf}GEP) and tumor mutational burden (TMB) are clinically validated biomarkers that independently predict pembrolizumab response. This study investigated prospective Tcell_{inf}GEP and TMB assessment in evaluating first-line pembrolizumab-based combination therapies; the different treatment combinations evaluated may provide insight into the unique biology of each biomarker subgroup.

Methods KEYNOTE-495/KeyImPaCT is a group-sequential, adaptively randomized, multisite, open-label, phase 2 study investigating first-line pembrolizumab plus the VEGF/FGFR inhibitor lenvatinib, CTLA-4 inhibitor quavonlimab (MK-1308), or LAG-3 inhibitor favezelimab (MK-4280) in patients with advanced NSCLC. DNA and RNA were extracted from tumor tissue to determine Tcell_{inf}GEP and TMB; patients were assigned to one of four biomarker-defined subgroups (Tcell_{inf}GEP^{low}TMB^{low}, Tcell_{inf}GEP^{low}TMB^{high}, Tcell_{inf}GEP^{high}TMB^{low}, Tcell_{inf}GEP^{high}TMB^{high}) and randomly assigned 1:1:1 to receive pembrolizumab (200mg IV Q3W)+lenvatinib (20mg oral QD), pembrolizumab+quavonlimab (75mg IV Q6W), or pembrolizumab+favezelimab (200mg [n=30] or 800mg [n=34] Q3W; the initial prespecified dose was 200mg but changed to 800mg based on emerging data). The primary end point was investigator-assessed ORR per RECIST v1.1. Multiple interim analyses will be performed until the prespecified clinical signal is observed. The first interim analysis for each combination therapy occurred after ≥10 patients had ≥12 weeks of follow-up.

Results At the data cutoff (January 11, 2021), 208 patients were treated (pembrolizumab+lenvatinib, n=72; pembrolizumab+quavonlimab, n=72; pembrolizumab+favezelimab 200mg, n=30; pembrolizumab+favezelimab 800mg, n=34). The overall assay success rate for testing and determining Tcell_{inf}GEP and TMB was 94%. In patients treated with pembrolizumab+lenvatinib, pembrolizumab+quavonlimab, or pembrolizumab+favezelimab, ORRs were generally highest in the Tcell_{inf}GEP^{high}TMB^{high} subgroup (table 1); response rates were similar across combinations within this subgroup. ORR was low across combinations within the Tcell_{inf}GEP^{low}TMB^{low}

subgroup. Treatment-related adverse events (TRAEs) occurred in 88%, 65%, 57%, and 59% of patients in the pembrolizumab+lenvatinib, pembrolizumab+quavonlimab, pembrolizumab+favezelimab 200mg and pembrolizumab+favezelimab 800mg arms, respectively. Consistent with the known TRAEs of these agents, most TRAEs were grade 1 or 2 in severity except in the pembrolizumab+lenvatinib arm (grade 3–5, 63%). Three deaths from TRAEs occurred (pembrolizumab+lenvatinib [n=2], brain hemorrhage and myocardial infarction; pembrolizumab+favezelimab 800 mg [n=1], pneumonitis).

Abstract 457 Table 1 Confirmed ORR by Therapy and Biomarker Status

Arm, % (95% CI) [n/N]	Tcell _{inf} GEP ^{low} TMB ^{low}	Tcell _{inf} GEP ^{low} TMB ^{high}	Tcell _{inf} GEP ^{high} TMB ^{low}	Tcell _{inf} GEP ^{high} TMB ^{high}	Total
Pembro + lenvatinib	12 (3-31) [3/25]	22 (3-60) [2/9]	30 (12-54) [6/20]	39 (17-64) [7/16]	25 (16-37) [18/72]
Pembro + quavonlimab	12 (2-30) [3/26]	33 (8-70) [3/9]	9 (1-29) [2/22]	40 (16-68) [6/15]	19 (11-30) [14/72]
Pembro + favezelimab 200 mg	0 (0-28) [0/11]	33 (4-78) [2/6]	25 (3-65) [2/8]	60 (15-95) [3/5]	23 (10-42) [7/30]
Pembro + favezelimab 800 mg	N/A*	50 (7-93) [2/4]	11 (1-35) [2/18]	42 (15-72) [5/12]	26 (13-44) [9/34]

*Not applicable; this group did not proceed because of the lack of clinical activity in this subgroup observed at the 200 mg dose of favezelimab.

Conclusions These data demonstrate the feasibility and clinical usefulness of prospective Tcell_{inf}GEP and TMB assessment to study the clinical activity of three first-line pembrolizumab-based combination therapies in patients with advanced NSCLC. Although sample sizes were small, the Tcell_{inf}GEP^{high}TMB^{high} subgroup demonstrated the best response among the biomarker subgroups for all three combination therapies; further validation is needed to determine additional signals and may be addressed as more mature data become available.

Acknowledgements Jeanne Fahey, PhD, of Merck & Co., Inc., Kenilworth, New Jersey, USA, provided critical review of the abstract. Elisha Dettman PhD, Mark Ayers MS, and Andrey Loboda PhD of Merck & Co., Inc., Kenilworth, New Jersey, USA, provided critical review of study translational data. Medical writing and/or editorial assistance was provided by Shane Walton, PhD, and Lei Bai, PhD, of ApotheCom (Yardley, PA, USA). This assistance was funded by Merck Sharp & Dohme Corp., a subsidiary of Merck & Co., Inc., Kenilworth, NJ, USA.

Trial Registration ClinicalTrials.gov, NCT03516981

Ethics Approval The study protocol and all amendments were approved by the relevant institutional review board or ethics committee at each study site. All patients provided written informed consent to participate in the clinical trial.

<http://dx.doi.org/10.1136/jitc-2021-SITC2021.457>

FIRST PHASE 2 RESULTS OF AUTOLOGOUS TUMOR-INFILTRATING LYMPHOCYTE (TIL; LN-145) MONOTHERAPY IN PATIENTS WITH ADVANCED, IMMUNE CHECKPOINT INHIBITOR-TREATED, NON-SMALL CELL LUNG CANCER (NSCLC)

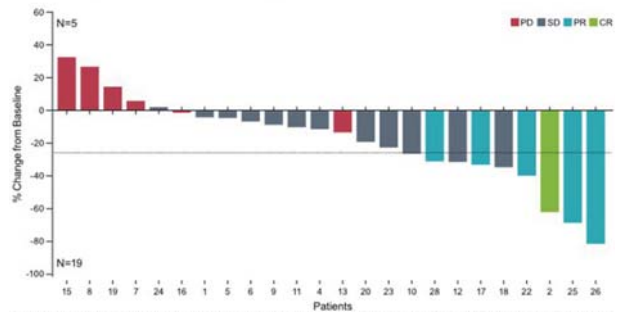
¹Adam Schoenfeld*, ²Sylvia Lee, ³Luis Paz-Ares, ⁴Bernard Doger, ⁵Scott Gettinger, ⁶Simon Haefliger, ⁷Angela Orcurto, ⁸Ammar Sukari, ⁹Sophie Papa, ¹⁰Juan Francisco Rodriguez Moreno, ¹¹Friedrich Graf Finckenstein, ¹¹Madan Jagasia, ¹¹Rana Fiaz, ¹¹Giri Sulur, ¹¹Guang Chen, ¹¹Viktoria Gontcharova, ¹²Kai He. ¹Memorial Sloan Kettering Cancer Center, New York, NY, USA; ²Fred Hutchinson Cancer Research Center, Seattle, WA, USA; ³Hospital Universitario 12 de Octubre, Madrid, Spain; ⁴Hospital Universitario Fundación Jimenez Diaz, Madrid, Spain; ⁵Yale Cancer Center, New Haven, CT, USA; ⁶Universitätsspital Bern, Bern, Switzerland; ⁷Centre Hospitalier Universitaire Vaudois, Lausanne, Switzerland; ⁸Karmanos Cancer Institute, Detroit, MI, USA; ⁹Guy's and St Thomas' NHS Foundation Trust, London, UK; ¹⁰Hospital Universitario HM Sanchinarro, Madrid, Spain; ¹¹Iovance Biotherapeutics, Inc., San Carlos, CA, USA; ¹²Ohio State University, Columbus, OH, USA

Background A majority of patients with advanced NSCLC develop disease progression with first-line immune-checkpoint inhibitors (ICI) ± chemotherapy. In the setting of ICI resistance, effective strategies to provide deep and durable responses are urgently needed. Lifileucel (LN-144) and LN-145 are centrally manufactured (cryopreserved drug-product, 22-day manufacturing process) autologous TIL products that have demonstrated activity in advanced melanoma, cervical cancer, and head and neck carcinoma.¹⁻⁴ Here, we report the first safety and efficacy data for LN-145 as monotherapy in patients with advanced NSCLC.

Methods IOV-COM-202 (NCT03645928) is a phase 2 multicenter, multicohort, open-label study evaluating autologous TIL cell therapy in patients with solid tumors. We report data from Cohort 3B, investigating LN-145 monotherapy in patients with advanced or metastatic NSCLC. Eligibility required 1–3 prior lines of systemic therapy, including either ICI or oncogene-directed therapy. Treatment included nonmyeloablative lymphodepletion, TIL infusion, and ≤6 interleukin-2 doses. Primary endpoints were safety (incidence of Grade ≥3 treatment-emergent adverse events [TEAEs]) and objective response rate (ORR, investigator-assessed using RECIST v1.1). Exploratory biomarker analyses, including T-cell receptor (TCR) repertoire, were performed.

Results As of 24 June 2021, 28 patients received LN-145 (full-analysis set [FAS]; table 1) and 24 were efficacy-evaluable; all had received prior ICI. TIL were most commonly harvested from lung metastases (57.1%). Safety was consistent with the underlying disease and known TEAE profiles of nonmyeloablative lymphodepletion and interleukin-2. Grade ≥3 TEAEs in ≥30% of patients were thrombocytopenia and anemia. The ORR in the FAS and efficacy-evaluable set was 21.4% (6/28) and 25.0% (6/24; figure 1), respectively. Median duration of response was not reached and 83% (5/6) of responses were ongoing at last follow-up (median study follow-up, 8.2 months). One patient had a complete metabolic response, ongoing at 20.7 months; 2 responses occurred in patients who were PD-L1-negative. All responders received ≥2 prior lines of systemic therapy. Twenty-six patients had TIL available from the final drug-product for TCR repertoire analysis; mean (min-max) number of unique TCR clones was 13,142 (3093–35,734) and Shannon Entropy index was 7.34 (3.7–12). Updated data will be presented.

Best Percentage Change from Baseline in Target Lesion Sum of Diameters for Efficacy-Evaluable Set



For patient 2 the overall response of CR was based on investigator assessment of a complete metabolic response via negative FDG-PET scan.

CR, complete response; FDG-PET, fluorodeoxyglucose-positron emission tomography; PD, progressive disease; PR, partial response; SD, stable disease.

Abstract 458 Figure 1 Best percentage change from baseline in target lesion sum of diameters for efficacy-evaluable set

Abstract 458 Table 1 Baseline patient demographic and clinical characteristics; efficacy parameters

Baseline Patient Demographic and Clinical Characteristics; Efficacy Parameters	
COM-202 Cohort 3B (N=28)	
Sex, n (%)	
Male	14 (50.0)
Female	14 (50.0)
Median (min, max) age, y	61.0 (40, 74)
Histologic cell type, n (%)	
Nonsquamous cell carcinoma	23 (82.1)
Adenocarcinoma	22 (78.6)
Large-cell carcinoma	1 (3.6)
Squamous cell carcinoma	5 (17.9)
Tumor PD-L1 expression, n (%) ^a	
TPS <1%	4 (14.3)
TPS ≥1%	18 (64.3)
Median (min, max) number of target and non-target lesions	4.5 (2, 11)
Target lesion sum of diameters, mm	
Median	79.0
Min, max	(22, 179)
Median (min, max) number of prior systemic therapies	2.0 (1, 5)
Prior systemic therapies, n (%)	
Anti-PD-1 and/or anti-PD-L1	28 (100)
Chemotherapy	27 (96.4)
Other monoclonal antibody	9 (32.1)
Anti-CTLA-4	6 (21.4)
EGFR inhibitor	1 (3.6)
Median (min, max) study follow-up, mo	8.2 (0.1+, 22.1)
Efficacy, n/N (%)	
ORR (FAS)	6/28 (21.4)
ORR (efficacy-evaluable set)	6/24 (25.0)
CR	1/28 (3.6)
PR	5/28 (17.9)
SD	12/28 (42.9)
DCR (FAS)	18/28 (64.3)
DCR (efficacy-evaluable set)	18/24 (75.0)
NE ^b	4/28 (14.3)
Median (min, max) DOR, mo	NR (1.2+, 20.7+)

^aPer central laboratory; tumor PD-L1 expression data were missing for 6 patients.

^bExcluded from efficacy-evaluable set due to death prior to first assessment.

CR, complete response; CTLA-4, cytotoxic T-lymphocyte-associated protein 4; DCR, disease control rate; DOR, duration of response; EGFR, epidermal growth factor receptor; FAS, full-analysis set; NR, not reached; ORR, objective response rate; PD-1, programmed cell death protein-1; PD-L1, programmed death-ligand 1; PR, partial response; SD, stable disease; TPS, tumor proportion score.

Conclusions LN-145 was successfully manufactured and one-time treatment produced an expected safety profile and durable responses in heavily pretreated patients with NSCLC, regardless of PD-L1 expression. The activity of LN-145 monotherapy is encouraging and warrants further investigation of LN-145 as a single-agent and in combination in patients with NSCLC in ongoing studies IOV-LUN-202 (NCT04614103) and IOV-COM-202 Cohorts 3A and 3C (3B closed to enrollment).

Acknowledgements This study and analysis were funded by Iovance Biotherapeutics, Inc. (San Carlos, CA, USA). Writing support was provided by Amanda Kelly (Iovance); graphics support was provided by Cognition Studio (Seattle, WA, USA).
Trial Registration NCT03645928

REFERENCES

1. Sarnaik AA, et al. *J Clin Oncol* 2021; doi: 10.1200/JCO.21.00612.
2. Thomas SS, et al. *J Clin Oncol* 2021;**39**: (suppl; abstract 9537).
3. Jazaeri A, et al. *J Clin Oncol* 2019;**37**: (suppl; abstract 2538).
4. Jimeno A, et al. *J Immunother Cancer* 2020;**8**: (suppl; abstract A378).

Ethics Approval The study was approved by Advarra Institutional Review Board, approval number Pro00035064 and all study participants provided written consent via signature of the IRB-approved Informed Consent form.

<http://dx.doi.org/10.1136/jitc-2021-SITC2021.458>

PHASE 3 STUDY OF FIRST-LINE PEMBROLIZUMAB WITH AND WITHOUT VIBOSTOLIMAB (ANTI-TIGIT) IN PATIENTS WITH PD-L1-POSITIVE METASTATIC NSCLC

¹Matthew Hellmann*, ²Byoung Cho, ³Rosalyn Juergens, ⁴Ying Cheng, ⁵Gilberto de Castro, ⁶Mustafa Erman, ⁷Jessica Bauman, ⁸Toshiaki Takahashi, ⁹Paul Schwarzenberger, ⁹Pingye Zhang, ⁹M Catherine Pietanza, ¹⁰James Chih-Hsin Yang. ¹Memorial Sloan Kettering Cancer Center, New York, NY, USA; ²Yonsei Cancer Center, Yonsei University College of Medicine, Seoul, South Korea; ³McMaster University, Juravinski Cancer Centre, Hamilton, ON, Canada; ⁴Jilin Cancer Hospital, Changchun, China; ⁵Instituto do Câncer do Estado de São Paulo, São Paulo, Brazil; ⁶Department of Medical Oncology, Hacettepe University Cancer Institute, Ankara, Turkey; ⁷Fox Chase Cancer Center, Philadelphia, PA, USA; ⁸Shizuoka Cancer Center, Sunto-gun, Japan; ⁹Merck and Co., Inc., Kenilworth, NJ, USA; ¹⁰National Taiwan University Hospital and National Taiwan University Cancer Center, Taipei City, Taiwan, Province of China

Background Vibostolimab (MK-7684) is a humanized monoclonal antibody (mAb) that binds to the T-cell immunoreceptor with immunoglobulin and ITIM domains (TIGIT), blocking the interaction between TIGIT and its ligands, CD112 and CD155. Pembrolizumab, an anti-PD-1 mAb, significantly improves OS versus chemotherapy in patients with PD-L1-positive advanced non-small-cell lung cancer (NSCLC). In the first-in-human study (NCT02964013), the combination of vibostolimab plus pembrolizumab had a manageable safety profile and showed promising antitumor activity in patients with advanced NSCLC naive to anti-PD-(L)1 therapy; ORR was 31% and 25% in patients with PD-L1 tumor proportion score (TPS) $\geq 1\%$ and $< 1\%$, respectively. The current phase 3 study (NCT04738487) is comparing first-line treatment with MK-7684A, a co-formulation of vibostolimab plus pembrolizumab, versus pembrolizumab monotherapy in patients with PD-L1-positive metastatic NSCLC.

Methods This randomized, multicenter, double-blind study is enrolling adults with pathologically confirmed, previously untreated, metastatic NSCLC with PD-L1 TPS $\geq 1\%$ (centrally confirmed). Patients must have measurable disease per RECIST v1.1, an ECOG PS of 0–1, have no *EGFR* mutations or *ALK* or *ROS1* gene rearrangements, and have no active or untreated CNS metastases. Patients are randomized 1:1 to receive intravenous treatment with vibostolimab 200 mg plus pembrolizumab 200 mg Q3W or pembrolizumab 200 mg Q3W for up to 35 cycles (approximately 2 years) or until PD, unacceptable AEs, intercurrent illness, or investigator decision. Patients who stop treatment after a CR or after completing 35 cycles and subsequently have PD can receive up to 17 additional cycles (approximately 1 year) of their randomized therapy. Randomization is stratified by ECOG PS (0 vs 1), PD-L1 TPS (1%–49% vs $\geq 50\%$), and region of enrollment (East Asia vs non-East Asia). The dual primary endpoints are PFS, per RECIST v1.1 by blinded independent central review (BICR), and OS. Secondary endpoints include ORR and DOR per RECIST v1.1 by BICR, patient-reported outcomes, and safety. Radiographic imaging occurs at baseline, Q9W from randomization through week 54, and then Q12W until PD, the start of new anticancer treatment, withdrawal of consent, or death. Health-related quality of life is assessed using validated patient-reported outcome instruments including the European Organisation for Research and Treatment of Cancer Quality of Life Questionnaire-Core 30. AEs are graded according to National Cancer Institute Common Terminology Criteria for Adverse Events v5.0. Approximately 598 patients will be randomized. Enrollment began in April of 2021, and is ongoing at 42 sites in 11 countries.

Acknowledgements Medical writing assistance was provided by Rozena Varghese, PharmD, CMPP, of ICON plc (North Wales, PA, USA), funded by Merck Sharp & Dohme Corp., a subsidiary of Merck & Co., Inc., Kenilworth, NJ, USA.

Trial Registration ClinicalTrials.gov, NCT04738487

Ethics Approval An independent institutional review board or ethics committee approved the protocol at each study site, and the trial is being conducted in compliance with Good Clinical Practice guidelines and the Declaration of Helsinki. All patients are required to provide informed consent prior to participation in the study.

<http://dx.doi.org/10.1136/jitc-2021-SITC2021.459>

SPATIAL DISTRIBUTION OF INFILTRATING T LYMPHOCYTES WITH IMMUNOSCORE® CR T CELLS EXHAUSTION TEST HELPS STRATIFICATION OF NSCLC PATIENTS TREATED WITH PD1/PDL1 INHIBITORS IN THE PIONEER PROJECT

¹Vanina Leca, ¹Alboukadel Kassambara, ¹Lamia Ghezali, ¹Pernelle Outters, ¹Christelle Cotteaux-Lautard, ¹Fanny Arnoux, ¹Thomas Sbarrato, ¹Florence Monville, ¹Florence Monville*, ²Maryannick Le Ray, ²Marie Roumieux, ³Stephane Garcia, ⁴Richard Malkoun, ³Noémie Resseguier, ⁵Arnaud Boyer, ⁶Louisiane Lebas, ⁷Hervé Pegliasco, ⁸Patricia Barré, ⁹Clarisse Audigier-valette, ¹⁰Sarah Zahi, ¹¹Luc Odier, ¹²Stéphane Hominal, ¹³Maurice Perol, ¹⁴Julien Mazieres, ¹⁵Laurent Greillier, ²Fabrice Barlesi, ¹Jacques Fieschi-Meric. ¹HaliDx, Marseille, France; ²Aix Marseille Université, Marseille, France; ³Aix Marseille Université, APHM, Marseille, France; ⁴APHM, Marseille, France; ⁵Hôpital St-Joseph Centre médical Clairval, Marseille, France; ⁶CHIVA, Foix, France; ⁷Hôpital Européen, Marseille, France; ⁸Centre Hospitalier Jean Rougier, Cahors, France; ⁹Centre Hospitalier Sainte-Musse, Toulon, France; ¹⁰Centre Hospitalier, Montauban, France; ¹¹Hôpital Nord-Ouest, Villefranche Sur Saône, France; ¹²Centre Hospitalier Annecy Genevois, Pringy, France; ¹³Centre Léon Bérard, Lyon, France; ¹⁴Toulouse University Hospital, Toulouse, France; ¹⁵APHM, Aix Marseille Université, Marseille, France

Background PD1/L1 Immune Checkpoint Inhibitors (ICI) have significantly improved long-term outcome in about 20% of advanced Non Small Cells Lung Cancer (NSCLC) patients (pts), but 80% present primary or secondary resistance. The PIONeeR project (NCT03493581) aims to predict the response/resistance to PD1/L1 ICIs in advanced NSCLC pts through a comprehensive agnostic multiparametric and longitudinal biomarkers assessment. Data presented here are a focus on the quantification of tumor infiltration by lymphocytes, their activation as potential markers of the resistance to treatment by ICI.

Methods Advanced NSCLC pts with available archived tumor tissue at screening visit (VS), treated with standard PD1/L1 ICIs (nivolumab, pembrolizumab or atezolizumab), alone (2nd line or more) or combined with chemotherapy (1st line), were re-biopsied at 6 weeks (V2) of treatment. PD1/L1 ICIs overall response rate (ORR) was assessed by RECIST 1.1 every 6 weeks. The multiplex IHC test "Immunoscore® CR T Cells Exhaustion" (IS TCE) quantifies cytotoxic lymphocytes expressing three checkpoints: PD1, LAG3, TIM3, extrapolating their exhaustion status, both in the stroma and parenchyma. The unsupervised neural-network-based machine learning algorithm SOM (Self-Organizing Maps) was used to classify samples based on the 27 IS TCE variables. Statistical significance of survival differences between groups was evaluated using the log-rank test.

Results Among the first 100 pts, (male (64%), smokers (91,8%), <70yrs (69%), with an ECOG PS0/1 (97%), treated in 2nd line setting (86%)), 79 VS + 30 V2 biopsies were tested with IS TCE. SOM clustering highlighted four distinct clusters: a group with moderate T-cells infiltration (group 1), hot tumors with high T cells infiltration in both stroma and parenchyma (group 2), cold tumors with very low T cells infiltration (group 3), and finally, a highly distinguishable group with important T-cells density in stroma only (group 4). None of the 11 responders was present in the Group 3, "Cold" cluster. The four groups presented different Progression Free Survival (PFS) rates ($p=5,2e-4$) with better relapse-free survival Groups 1 and 2. Additionally, V2/VS ratios showed lymphocytes recruitment induced by the treatment in parenchyma only: no significant lymphocytes recruitment was observed in the stromal compartment. Interestingly, the most recruited lymphocyte populations expressed PD1.

Conclusions IS TCE test may help stratifying and predicting responders to anti PD1/L1 therapy through checkpoint

expressing lymphocytes quantification and spatial distribution. Additional tests performed on the PIONeeR cohort to explore other aspects of the immune response to cancer should complete these results.

Acknowledgements This work is supported by French National Research Agency (ANR-17-RHUS-0007), a partnership of AMU, APHM, AstraZeneca, Centre Léon Bérard, CNRS, HaliDx, ImCheck Therapeutics, Innate Pharma, Inserm, Institut Paoli Calmettes and sponsored by AP HM. Drug supply is funded by AstraZeneca. Special thanks to patients and families.

Trial Registration NCT03493581

Ethics Approval The study is conducted in accordance with Good Clinical Practice and the French applicable regulatory requirements (Public Health Code, article L.1121-1/La loi n° 2012-300 du 5 mars 2012 relative aux recherches impliquant la personne humaine (dite loi Jardé), the applicable subject privacy requirements, and the ethical principles that are outlined in the Declaration of Helsinki. The study was approved by the French Ethic Committee, CPP Ouest II - Angers, ref. CPP: 2028/08, Ref ANSM (French competent authority) 2018020500208, 2018072600120, 2019083000148. Freely given written informed consent was signed and obtained from each individual participating in the study, before any study specific procedure was undertaken and after the provision of information about the study by the investigator during a physician-patient consultation and sufficient time for reflection.

<http://dx.doi.org/10.1136/jitc-2021-SITC2021.460>

461 **UPDATED PFS ANALYSIS OF TORIPALIMAB WITH ANLOTINIB AND CHEMOTHERAPY AS FIRST-LINE THERAPY IN PATIENTS WITH EXTENSIVE-STAGE SMALL-CELL LUNG CANCER (ES-SCLC)**

Hao Luo*, Dan Jian, Yan Feng, Li Zhong, Qian Chen, Wei Guan, Shiheng Zhang, Jiamin Luo, Xueqin Yang, Kan Gong, Yanli Xiong, Mengxia Li, Mingfang Xu, Yu Pu, Liang Zhao, Chengyuan Qian, Nan Dai, Dong Wang. *Cancer Center of Daping Hospital, Army Medical Center, Chongqing, China*

Background This trial is an open-label, single-arm, phase II study that aims to observe the efficacy and safety of toripalimab combined with anlotinib and platinum-etoposide (EP) chemotherapy as first-line treatment in ES-SCLC (Clinical trial information: NCT04731909). The preliminary results of the study have been presented in 2020 ASCO abstract e20570, which demonstrated 100% objective response rate (ORR) and tolerable safety. Here we report PFS analysis results of the study.

Methods The study enrolled treatment-naïve ES-SCLC patients (18–75 years, ECOG PS ≤ 2) who have measurable target lesion evaluated by RECIST v1.1. All enrolled patients received toripalimab (240 mg, d1) combined with etoposide (100 mg/m², d1–3) plus carboplatin (AUC=5, d1)/cisplatin (75 mg/m², d1) and anlotinib (12 mg QD, d1–14) of a 21-day cycle. After 4–6 cycles of the treatment, patients who achieved complete response (CR), partial response (PR) or stable disease (SD) could continue to receive maintenance therapy with toripalimab and anlotinib until disease progression. The primary endpoint was overall survival (OS). ORR, disease control rate (DCR), progression-free survival (PFS) and safety were set as secondary endpoints.

Results As of July 16, 2021, the median follow-up was 13.7 months. 9 disease progression events occurred of the enrolled 16 treatment-naïve ES-SCLC patients (14 males, 2 females, median age 63). The investigator-assessed median PFS was 13.3 months (95%CI: 5.0–21.6). The PFS rate at 6 months was 81.3% and the PFS rate at 12 months was 31.3%. 15 patients were still alive and the study treatments for 7 patients were still ongoing. At the data cutoff, there was only 1 patient dead with 37.6 months OS and the median OS was not reached. No new unexpected adverse events were observed.

Conclusions Combined with preliminary data at 2020 ASCO, toripalimab combined with anlotinib and EP chemotherapy showed excellent ORR and PFS as well as tolerable safety in treatment-naïve ES-SCLC. The combination therapy is expected to provide clinically meaningful OS benefit and become a promising treatment option.

Trial Registration This study is registered with ClinicalTrials.gov (National Institutes of Health), number NCT04731909.

Ethics Approval The program was approved by the ethics committee of Army Medical Center (Daping Hospital).

<http://dx.doi.org/10.1136/jitc-2021-SITC2021.461>

462

A RANDOMISED OPEN-LABEL PHASE I/II STUDY ADDING ONCOS-102 TO PEMETREXED/CISPLATIN IN PATIENTS WITH UNRESECTABLE MALIGNANT PLEURAL MESOTHELIOMA – 24 MONTH SURVIVAL DATA

¹Magnus Jaderberg, ²Luis Paz-Ares*, ³Susana Cedres, ⁴Charles Ricordel, ⁵Nicolas Isambert, ²Santiago Ponce Aix, ¹Victor Levitsky, ¹Lukasz Kuryk, ¹Anne-Sophie Moller, ¹Sylvia Vetthus. ¹Targovax ASA, Lysaker, Norway; ²Hospital Universitario 12 Octubre, Madrid, Spain; ³University Hospital Vall d'Hebron, Barcelona, Spain; ⁴Centre Hospital Universitaire de Rennes, Rennes, France; ⁵Centre Hospitalier Universitaire de Poitiers, Poitiers, France

Background Malignant pleural mesothelioma (MPM) is an aggressive malignancy without curative treatment. Standard of care (SOC) include pemetrexed/cisplatin and nivolumab/ipilimumab with median overall survival in unresectable disease of 12.1 months and 18.1 months respectively.^{1 2} ONCOS-102 is a granulocyte-macrophage colony stimulating factor (GM-CSF) expressing oncolytic adenovirus (Ad5/3-D24-GMCSF) with a unique ability to both prime and boost immune responses. The aim of the study was to assess efficacy and safety of ONCOS-102 in combination with SOC chemotherapy in 1st and 2nd line unresectable MPM.

Methods Twenty patients (experimental arm) were allocated to receive ONCOS-102 given intratumorally under CT or US guidance at a dose of 3 x 10¹¹ VP on Day 1, 4, 8, 36, 78 and 120 plus six cycles of SOC starting on Day 22. Eleven patients (control group) received SOC. Imaging was done at baseline, Day 43–64 and 127–148 with regular monitoring of blood and biopsy based immune markers. Primary objective was safety and tolerability. Secondary objectives were ORR, PFS and OS as well as immunological activation. An analysis of 24 month survival data compared randomised only patients excluding six patients in the single-arm safety lead-in.

Results 24-month survival rate for 1st line pts was 50% in the experimental group and 0% in the control group with mOS of 25.0 months and 13.5 months respectively (N.S). Based on censoring, mOS in the experimental group will be within 21.9 – 25.0 months range. mOS across both 1st and 2nd line was 19.3 and 18.3 months for experimental and control patients (N.S). mPFS was 9.8 months in the experimental group and 7.6 in the control group (N.S.).

Conclusions The survival rate of patients receiving ONCOS-102 in combination with SOC was seen to be numerically higher than previously reported for SOC or nivolumab/ipilimumab. Improved survival was associated with ONCOS-102 induced immune activation with a favourable TME modulation providing scientific rationale for combination with checkpoint inhibition.

Trial Registration ClinicalTrials.gov NCT02879669

REFERENCES

1. Vogelzang, et al, Phase III study of pemetrexed in combination with cisplatin versus cisplatin alone in patients with malignant pleural mesothelioma. *J Clin Oncol* 2003;**21**: 2636–44.
2. Baas P, et al, First-line nivolumab plus ipilimumab in unresectable pleural mesothelioma (CheckMate 743): a multicentre, randomised, open-label, phase 3 trial. *The Lancet* 2021; **397**: 375–386.

Ethics Approval This study was approved by the IRBs of all the participating sites in Madrid, Barcelona, Rennes and Poitiers.

<http://dx.doi.org/10.1136/jitc-2021-SITC2021.462>

463

VIBOSTOLIMAB PLUS PEMBROLIZUMAB WITH/WITHOUT DOCETAXEL VS DOCETAXEL IN NSCLC AFTER PLATINUM CHEMOTHERAPY AND IMMUNOTHERAPY

¹Solange Peters*, ²Dae Ho Lee, ³Rodryg Ramlau, ⁴Balazs Halmos, ⁵Christian Schumann, ⁶David Planchard, ⁷Niyati Bhagwati, ⁷Diana (Qiusheng) Chen, ⁷Debra Kush, ⁸Silvia Novello. ¹University of Lausanne, Centre Hospitalier Universitaire Vaudois, Lausanne, Switzerland; ²Asan Medical Center, Seoul, Korea, Republic of; ³Poznan University of Medical Sciences, Poznan, Poland; ⁴Department of Oncology, Montefiore Einstein Center for Cancer Care, New York, NY, USA; ⁵Klinik für Pneumologie, Thoraxonkologie, Schlaf- und Beatmungsmedizin, Klinikverbund Allgäu, Kempten, Germany; ⁶Gustave Roussy, Department of Medical Oncology, Thoracic Group, Villejuif, France; ⁷Merck and Co., Inc., Kenilworth, NJ, USA; ⁸Department of Oncology, Azienda Ospedaliero-Universitaria San Luigi Gonzaga University of Turin, Orbassano, Italy

Background Agents blocking interactions between the T-cell immunoreceptor with immunoglobulin and ITIM domains (TIGIT) and its ligands (CD112, CD155) have demonstrated preclinical antitumor activity. Anti-TIGIT humanized monoclonal antibody vibostolimab (MK-7684) showed promising antitumor activity and manageable toxicity in heavily pretreated patients across multiple tumor types, particularly when combined with the PD-1 inhibitor pembrolizumab (NCT02964013). Pembrolizumab has significantly improved OS versus chemotherapy in PD-L1–positive advanced non–small-cell lung cancer (NSCLC). However, many patients present with primary or acquired resistance to immunotherapy. This phase 2 study (NCT04725188) evaluates efficacy and safety of MK-7684A, a co-formulation of vibostolimab plus pembrolizumab, administered with/without docetaxel versus docetaxel alone in patients with previously treated metastatic NSCLC.

Methods This randomized, placebo- and active-controlled, multicenter, partial-blind study is enrolling adults with histologically/cytologically confirmed metastatic NSCLC with PD after platinum-doublet chemotherapy and 1 prior anti-PD-(L)1 therapy. Patients must have measurable disease per RECIST v1.1, ECOG PS of 0–1, and no known active CNS metastases (previously treated brain metastases allowed if radiologically/clinically stable). Tumor tissue from archival or newly-obtained core or excisional biopsies are evaluated centrally for PD-L1 expression before randomization, and local documentation of the absence of *EGFR* mutations or *ALK/ROS1* gene rearrangements must be provided. Patients are randomized 1:1:1 to receive intravenous vibostolimab (200 mg) plus pembrolizumab (200 mg) Q3W (open-label), vibostolimab plus pembrolizumab plus docetaxel (standard-of-care dose) Q3W (blinded), or docetaxel plus placebo Q3W (blinded). Randomization is stratified by ECOG PS (0/1), prior anti-PD-(L)1 therapy (immediate/no immediate prior therapy), and PD-L1 tumor proportion score (<50%/≥50%). Treatment continues for up to 35 cycles (approximately 2 years) of vibostolimab plus pembrolizumab, and per locally approved label for docetaxel, or until PD, unacceptable AEs, intercurrent illness, or investigator decision. Patients with SD/PR/CR may be eligible for up to 17 additional rechallenge cycles of vibostolimab plus pembrolizumab following BICR-verified radiographic PD by RECIST v1.1 after initial treatment or first course is completed or stopped for confirmed CR. Primary endpoint is PFS per RECIST v1.1 by BICR. Secondary endpoints are OS, ORR and DOR per RECIST v1.1 by BICR, and safety. Radiographic imaging occurs at baseline, Q6W through week 36, Q9W through week 54, and then Q12W until PD, start of new anticancer treatment, withdrawal of consent, or death. AEs are assessed by NCI CTCAE v5.0. Approximately 240

patients will be randomized. Enrollment began in April of 2021, and is ongoing at 42 sites in 10 countries.

Acknowledgements Medical writing assistance was provided by Rozena Varghese, PharmD, CMPP, of ICON plc (North Wales, PA, USA), funded by Merck Sharp & Dohme Corp., a subsidiary of Merck & Co., Inc., Kenilworth, NJ, USA.

Trial Registration ClinicalTrials.gov, NCT04725188

Ethics Approval An independent institutional review board or ethics committee approved the protocol at each study site, and the trial is being conducted in compliance with Good Clinical Practice guidelines and the Declaration of Helsinki. All patients are required to provide informed consent prior to participation in the study.

<http://dx.doi.org/10.1136/jitc-2021-SITC2021.463>

464

2SMALL (NCT04253145) PHASE I PART: LURBINECTIDINE (LUR) IN COMBINATION WITH ATEZOLIZUMAB (ATZ) FOR SECOND LINE EXTENSIVE STAGE SMALL CELL LUNG CANCER (ES-SCLC) PATIENTS (PTS)

¹Santiago Ponce Aix*, ²Alejandro Navarro, ³Reyes Bernabe, ⁴Maria Eugenia Olmedo, ⁵Trigo Jose Manuel, ¹Jon Zugazagoitia Fraile, ¹Luis Paz-Ares. ¹Hospital Universitario 12 de Octubre, Madrid, Spain; ²Hospital Univeristari Vall d'Hebron, Barcelona, Spain; ³Hospital Universitario Virgen del Rocío, Seville, Spain; ⁴Hospital Universitario Ramon y Cajal, Madrid, Spain; ⁵Hospital U. Virgen de la Victoria, Malaga, Spain

Background Current front-line treatment for ES-SCLC includes chemotherapy plus a PD-L1 inhibitor. FDA has recently approved LUR for pretreated patients with SCLC. 2SMALL is a two-part phase 1/2 study assessing the safety, tolerability and efficacy of LUR in combination with ATZ as second line treatment for ES-SCLC. Here we report data from phase I part of the 2SMALL trial (data cut off 14-07-2021)

Methods 2SMALL phase I was an open-label, single arm, dose exploration trial. Eligible patients had confirmed ES-SCLC, who progressed to first line platinum based treatment, ECOG performance status score 0-1 and adequate organ function; prior exposure to immunotherapy was not allowed. During dose finding phase pts received increasing doses of LUR (2.5 mg/m² - 3.2 mg/m²) on day (D) 1 plus a fixed dose of ATZ (1200 mg) every 3 weeks following a standard 3+3 dose escalation design. Study endpoints included the definition of the safety profile and the recommended dose. Additional objectives included efficacy (ORR and PFS).

Results 26 patients were treated, including male 14 pts (53,84%), with median age 60.6 years. Five pts received LUR 2.5 mg/m² + ATZ 1200 mg, and 3 pts were evaluable without DLT. Out of the 21 pts who received LUR 3.2 mg/m²+ ATZ 1200 mg (6 pts with primary G-CSF), 5 pts (20.83%) developed DTLs: 2 pts G3 febrile neutropenia (9.52%) (1 pt with G4 thrombocytopenia), 2 pts G4 neutropenia lasting more than 72h (9.52%), 1 pt G4 thrombocytopenia (4.76%). Most frequent haematological adverse events ≥ grade 2 (21 pts) were neutropenia (42.86%), thrombocytopenia (28.57%), anaemia (19.05%); lymphopenia (4.76%) and febrile neutropenia (4.76%). The most common non-haematological TAEs ≥ grade 2 was asthenia 30,76%. No deaths treatment-related were reported. Objective responses were observed in 15 pts (ORR: 57.69%), including complete responses in 2 pts (7.69%), partial response in 13 pts (50%). 6 pts had stable disease (26.92%) and 3 pts progressive disease (11.54%). Disease control rate was 84.61%. With 8 pts censored for progression, median PFS was 4.93 months (range 3.37 - 7.67 months).

Conclusions The combination of LUR plus ATZ was well tolerated, without unexpected toxicities. Transient haematological toxicity was dose limiting. The RD for further studies is LUR 3.2 mg/m² on D1 + ATZ 1200 mg D1 with G-CSF. Preliminary anti-tumor activity is remarkable. 2SMALL trial part II is ongoing, and will provide further data regarding efficacy and safety of the regimen for second line SCLC.

Trial Registration NCT04253145

REFERENCES

1. Subbiah V, Paz-Ares L, Besse B, et al. Antitumor activity of lurbinectedin in second-line small cell lung cancer patients who are candidates for re-challenge with the first-line treatment. *Lung Cancer* 2020; **150**:90–96.
2. Trigo J, Subbiah V, Besse B, et al. Lurbinectedin as second-line treatment for patients with small-cell lung cancer: a single-arm, open-label, phase 2 basket trial. *Lancet Oncol* 2020; **21**(5):645–654.

Ethics Approval Ethics committee Hospital Universitario 12 de Octubre

<http://dx.doi.org/10.1136/jitc-2021-SITC2021.464>

BINTRAFUSP ALFA IN COMBINATION WITH CHEMOTHERAPY IN PATIENTS WITH STAGE IV NSCLC: SAFETY AND PHARMACOKINETIC RESULTS OF THE INTR@PID LUNG 024 STUDY

¹Christian Rolfo*, ²Laurent Greillier, ³Remi Veillon, ⁴Firas Badin, ⁵Francois Ghiringhelli, ⁶Nicolas Isambert, ⁷Astrid Paulus, ⁸Marc Lambrechts, ⁹Surendra Chaudhary, ⁹Xiaoli You, ⁹Yulia Vugmeyster, ¹⁰Christoph Helwig, ¹¹Sandrine Huret. ¹Mount Sinai Health System, New York, NY, USA, New York, NY, USA; ²Aix Marseille University, Assistance Publique-Hôpitaux de Marseille, Marseille, France, Marseille, France; ³Centre Hospitalier Universitaire de Bordeaux, Bordeaux, France, Bordeaux, France; ⁴Baptist Health Lexington, Lexington, KY, USA, Lexington, KY, USA; ⁵Centre Georges François Leclerc, Dijon, France, Dijon, France; ⁶CHU de Poitiers, Poitiers, France, Dijon Cedex, France; ⁷CHU Sart Tilman, Liege, Belgium, Liege, Belgium; ⁸Algemeen Ziekenhuis Sint-Maarten, Mechelen, Belgium, Mechelen, Belgium; ⁹EMD Serono, Billerica, MA USA, Billerica, MA, USA; ¹⁰The healthcare business of Merck KGaA, Darmstadt, Germany, Darmstadt, Germany; ¹¹Institut de Cancérologie de l'Ouest, Saint-Herblain, France, Saint Herblain, France

Background Bintrafusp alfa is a first-in-class bifunctional fusion protein composed of the extracellular domain of the TGF- β RII receptor (a TGF- β "trap") fused to a human IgG1 mAb blocking PD-L1. Here we report cumulative safety and pharmacokinetic (PK) results from the global, phase 1b/2 INTR@PID LUNG 024 study (NCT03840915), which evaluated bintrafusp alfa in combination with chemotherapy (CT) in patients with stage IV NSCLC.

Methods Adult patients with stage IV nonsquamous or squamous NSCLC and an ECOG PS \leq 1 were included. Cohorts A, B, and C included patients with no prior systemic therapy; patients in cohort D had disease that progressed with previous anti-PD-(L)1 therapy. Cohorts received bintrafusp alfa 2400 mg every 3 weeks intravenously in combination with CT for 4 cycles (A [nonsquamous only]: cisplatin or carboplatin + pemetrexed; B: carboplatin + nab-paclitaxel or paclitaxel; C: cisplatin or carboplatin + gemcitabine; D: docetaxel) followed by bintrafusp alfa maintenance (monotherapy or in combination with pemetrexed in cohort A) for up to 31 cycles. The primary objective of this study was to evaluate the safety of bintrafusp alfa in combination with CT. Dose-limiting toxicities (DLTs) were assessed during a 3-week observation period. Serial samples were drawn to assess serum concentration and calculate PK parameters by noncompartmental analysis.

Results As of the May 5, 2021, data cutoff, 70 patients received bintrafusp alfa in combination with CT. Of 35 patients included in the DLT analysis, 4 experienced 1 DLT according to a safety monitoring committee (data cutoff May 5, 2021; A: n=1/8; B: n=1/8; C: n=0/8; D: n=2/11). Cumulative safety data are reported in table 1. PK data were available for 67 patients (A: n=38; B: n=9; C: n=8; D: n=12). PK profiles were similar across cohorts and between patients who did and did not experience a DLT. Observed bintrafusp alfa first-cycle exposures (C_{max}, AUC, and C_{trough}) were consistent with the published population PK (popPK) model.¹

Abstract 465 Table 1 Safety results from the INTR@PID LUNG 024 study

	Cohort A (n=40)	Cohort B (n=9)	Cohort C (n=8)	Cohort D (n=12)
DLTs, n/N* (%)	1/8 (12.5)	1/8 (12.5)	0/8 (0)	2/11 (18.2)
TEAEs, n (%)				
Any	40 (100.0)	9 (100.0)	9 (100.0)	12 (100.0)
Grade \geq 3	32 (80.0)	8 (88.9)	7 (77.8)	12 (100.0)
Grade \geq 4	16 (40.0)	3 (33.3)	5 (55.6)	6 (50.0)
Leading to dose reduction of CT	14 (35.0)	3 (33.3)	5 (55.6)	4 (33.3)
Leading to permanent discontinuation of bintrafusp alfa	16 (40.0)	1 (11.1)	5 (55.6)	4 (33.3)
Leading to permanent discontinuation of CT	16 (40.0)	1 (11.1)	4 (44.4)	3 (25.0)
Treatment-related AEs, n (%)				
Any bintrafusp alfa-related AEs	35 (87.5)	9 (100.0)	9 (100.0)	12 (100.0)
Bintrafusp alfa-related serious AEs	12 (30.0)	1 (11.1)	1 (11.1)	3 (25.0)
Bintrafusp alfa-related AEs leading to death	0	0	0	0
AEs of special interest, n (%)				
Any skin lesions [†]	6 (15.0)	1 (11.1)	4 (44.4)	1 (8.3)
Any immune-related AEs	19 (47.5)	3 (33.3)	5 (55.6)	6 (50.0)
Any infusion-related reactions	5 (12.5)	1 (11.1)	1 (11.1)	1 (8.3)
Anemia	20 (50.0)	6 (66.7)	9 (100.0)	9 (75.0)
Any bleeding events	19 (47.5)	5 (55.6)	8 (88.9)	8 (66.7)

AE, adverse event; CT, chemotherapy; DLT, dose-limiting toxicity; TEAE, treatment-emergent adverse event.
^{*}Assessed in patients in the safety part of the study.
[†]Defined as actinic keratosis, basal cell carcinoma, Bowen's disease, hyperkeratosis, keratoacanthoma, lip squamous cell carcinoma, and squamous cell carcinoma of skin. Actinic keratosis, hyperkeratosis, and keratoacanthoma were reported in this study.

Conclusions The safety profile of bintrafusp alfa in combination with CT was manageable and similar to that reported for ICIs in combination with CT, with the exception of TGF- β -related skin lesions known to occur with TGF- β inhibition. No new safety signals were identified and there were no treatment-related deaths. The PK profile was consistent with the predicted monotherapy popPK model, suggesting no victim DDI potential for bintrafusp alfa with CT.

Acknowledgements The authors thank the patients and their families, investigators, co-investigators, and the study teams at each of the participating centers, at the healthcare business of Merck KGaA, Darmstadt, Germany, and at EMD Serono, Billerica, Massachusetts, USA.

Trial Registration NCT03840915

REFERENCE

- Wilkins JJ, Vugmeyster Y, Dussault I. Population pharmacokinetic analysis of bintrafusp alfa in different cancer types. *Adv Ther* 2019;**36**:2414–2433.

Ethics Approval The trial was approved by each site's independent ethics committee.

<http://dx.doi.org/10.1136/jitc-2021-SITC2021.465>

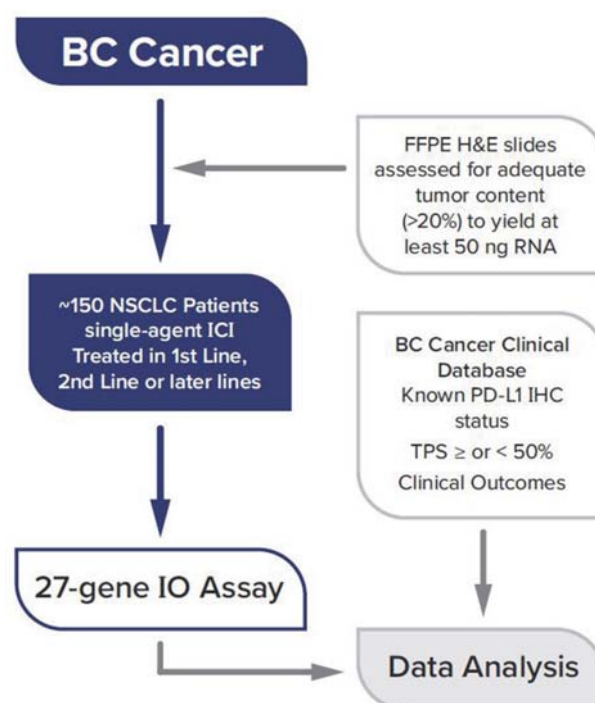
466

USE OF A 27-GENE IMMUNO-ONCOLOGY (IO) ASSAY TO ASSOCIATE RESPONSE TO SINGLE-AGENT IMMUNE CHECKPOINT INHIBITOR (ICI) THERAPY IN ADVANCED-STAGE NSCLC PATIENTS FROM A LARGE CANADIAN COHORT

¹David Saltman*, ²Nicole Croteau, ¹Heather Lockyer, ³Rob Seitz, ³Frank McMahon, ³Jeremy Spille, ³Andrea Dickey, ³Matthew Varga, ³Kim McGregor, ³Tyler Nielsen, ³David Hout, ³Brock Schweitzer, ³Douglas Ross, ⁴David Gandara. ¹BC Cancer, Victoria, Canada; ²The University of British Columbia, Victoria, Canada; ³Oncocyte Corporation, Nashville, TN, USA; ⁴UC Davis, Sacramento, CA, USA

Background Lung cancer is the leading cause of cancer-related deaths worldwide. The advent of ICIs specifically targeting programmed cell death protein-1 (PD-1), or its ligand (PD-L1) represents a major therapeutic advance that is now included in standard of care regimens for non-small-cell-lung cancer (NSCLC). PD-L1 expression measured by immunohistochemistry (IHC) staining is the current gold standard predictive biomarker for immune checkpoint inhibitor (ICI) therapy in NSCLC, however many factors beyond PD-L1 expression alone affect the outcome of ICI therapy. Evaluation of other factors to better inform clinical practice will reduce both the potential for adverse immune-related toxicities and expenditure on ineffective costly therapies while potentially identifying patients otherwise missed by PD-L1 staining. The 27-gene IO assay is a RT-qPCR based gene expression panel¹ that was developed to classify the tumor immune microenvironment (TIME). It has been shown to be associated with response to ICI therapy in multiple tumor types including triple negative breast cancer, metastatic urothelial carcinoma, and NSCLC where the association was independent of PD-L1 status in patients treated either with monotherapy or combination therapy.² Currently, BC Cancer measures PD-L1 status by IHC using the PD-L1 22C3 PharmDx assay and reports the tumor proportional score (TPS) to inform clinical decision. Patients with a TPS \geq 50% may be eligible for first-line treatment with ICI monotherapy and those with $<$ 50% TPS are eligible for second line or later ICI monotherapy. We established this retrospective study of ICI monotherapy treated NSCLC patients to assess the 27-gene IO assay as an informative biomarker for NSCLC ICI treatment decisions.

Methods This retrospective study is utilizing the BC Cancer Study Database to select approximately 150 patients with stage IIIB or IV NSCLC treated with single-agent ICI therapy across four BC Cancer centers from 2017 forward (figure 1). Patients are selected based on availability of adequate biopsy specimens (FFPE with at least 20% tumor content), availability of PD-L1 IHC results or sufficient tissue to conduct staining, and for whom outcome data is available via chart review. RNA from patient samples is isolated from FFPE biopsies (either primary or metastatic sites) and those that yield \geq 50ng RNA will be analyzed by the 27-gene IO assay¹ to derive IO scores (IO positive or IO negative) based on previously defined thresholds.³ The association between patient outcomes on ICI monotherapy and IO scores and PD-L1 IHC will be reported and compared.



Abstract 466 Figure 1 Schematic representation of patient workflow for

REFERENCES

1. Saltman, A, et al. Prostate cancer biomarkers and multiparametric MRI: is there a role for both in prostate cancer management? *Ther Adv Urol* 2021;**13**: 1756287221997186.
2. Ranganath HJA, Smith JR, et al. One-year progression-free survival in lung cancer patients treated with immune checkpoint inhibitors is significantly associated with a novel immunomodulatory signature but not PD-L1 staining. in SITC. *Journal Immunotherapy Cancer*. 2019.
3. Nielsen, TJ, et al. A novel immuno-oncology algorithm measuring tumor microenvironment to predict response to immunotherapies. *Heliyon* 2021;**7**(3):e06438.

Ethics Approval The University of British Columbia BC Cancer Research Ethics Board Chair, Vice-Chair or second Vice-Chair, has reviewed the above described research project, including associated documentation, and finds the research project acceptable on ethical grounds for research involving human subjects. All participants have provided informed consent before taking part in the study. REB Number H20-02635.

<http://dx.doi.org/10.1136/jitc-2021-SITC2021.466>

PHASE II CLINICAL STUDY OF TORIPALIMAB IN COMBINATION WITH STEREOTACTIC RADIOTHERAPY AS A NEOADJUVANT THERAPY FOR THE TREATMENT OF RESECTABLE (N1-N2) NON-SMALL CELL LUNG CANCER

Zhen Wang*, Xi-xu Zhu, Yong Song. *Nanjing Jinling Hospital, Nanjing, China*

Background Background: Early stage non-small cell lung cancer (NSCLC) possessed highly local and distant recurrence rates after surgery. Recent studies showed neoadjuvant therapy can improve pathological response and postoperative survival.^{1–3} Using immune checkpoint inhibitors as a neoadjuvant treatment could release neoantigens from dying tumour cells and stimulate the priming and expansion of neoantigen-specific T cells in the tumour before surgical resection.⁴ Previous study indicated radiotherapy combined with chemotherapy as neoadjuvant didn't improve event-free or overall survival in stage III/N2 NSCLC.⁵ Subsequently, the study of neoadjuvant chemoradiation plus pembrolizumab have demonstrated that radiotherapy can enhance the effect of immunotherapy, achieving better complete pathological response.⁶ Stereotactic body radiation therapy (SBRT) is a precise radiotherapy model that has shown good efficacy in treating early lung cancer, combining with immunotherapy as neoadjuvant therapy for NSCLC may improve pathological response and postoperative survival.

Methods This is a prospective, single-center, two-part, phase II study assessing the safety, tolerability and efficacy of SBRT combined with toripalimab as neoadjuvant in patients with stage IIB–IIIA NSCLC without driver mutations (Clinical trial information: ChiCTR2000029277). Eligibility criteria include IIB–IIIA NSCLC (AJCC v8), adequate organ function, and ECOG PS 0 or 1. The primary endpoints were the safety and pathologic response, while the secondary endpoint was the radiographic response, recurrence-free survival and overall survival. The trial also aimed at exploring prognosis biomarkers (included Tumor infiltrates lymphocytes, CD8+Tcell, PD-L1 protein expression, tTMB and the correlation with pathologic response rate). 30 patients will receive SBRT (50 Gy/5 fractions over 5 days) on the first week. Afterwards, all patients will receive 2 cycles of intravenous toripalimab starting on Day15 (240 mg, q3w). Preoperative assessment will be performed two weeks (week 8) before surgery (week 10). In part 1 of the study, 6 patients will be enrolled to determine the safety and feasibility of the combination therapy. Subjects will be followed up for 90 days to observe perioperative adverse events. If the rate of delayed surgery (delay time >37 days) is >90% or the rate of grade 3/4 adverse effects is >70%, the study will be terminated. If not, 24 patients will be enrolled in part 2 of the study. This study is currently open and accruing patients.

REFERENCES

1. Cascone T, William WN Jr, Weissferdt A, et al. Neoadjuvant nivolumab or nivolumab plus ipilimumab in operable non-small cell lung cancer: the phase 2 randomized NEOSTAR trial. *Nat Med* 2021;**27**(3):504–514.
2. Provencio M, Nadal E, Insa A, et al. Neoadjuvant chemotherapy and nivolumab in resectable non-small-cell lung cancer (NADIM): an open-label, multicentre, single-arm, phase 2 trial. *Lancet Oncol* 2020 Nov;**21**(11):1413–1422.
3. Forde PM, Chaft JE, Smith KN, et al. Neoadjuvant PD-1 Blockade in Resectable Lung Cancer. *N Engl J Med* 2018 May 24;**378**(21):1976–1986.
4. Liu J, Blake SJ, Yong MC, et al. Improved efficacy of neoadjuvant compared to adjuvant immunotherapy to eradicate metastatic disease. *Cancer Discov* 2016;**6**:1382–99.
5. Pless M, Stupp R, Ris HB, et al. Induction chemoradiation in stage IIIA/N2 non-small-cell lung cancer: a phase 3 randomised trial. *Lancet* 2015 12;**386**(9998):1049–56.
6. Lemmon C, Videtic GM. M, Murthy SC, et al. A phase I safety and feasibility study of neoadjuvant chemoradiation plus pembrolizumab followed by

consolidation pembrolizumab in resectable stage IIIA non-small cell lung cancer. *J Clin Oncol* 2020; **38** (suppl; abstr 9009).

<http://dx.doi.org/10.1136/jitc-2021-SITC2021.467>

A PHASE 2 STUDY OF TORIPALIMAB PLUS ANLOTINIB AS MAINTENANCE THERAPY IN EXTENSIVE-STAGE SMALL CELL LUNG CANCER

Dongqing Lv, Guixian Wu*. Taizhou Hospital of Zhejiang Province, Taizhou, China

Background Maintenance therapy is a promising therapeutic approach for extensive-stage small cell lung cancer (ES-SCLC), especially in light of IMpower 133.¹ The results of E3501, SALUTE and CALGB 30306 trials showed that in the first-line treatment of ES-SCLC, bevacizumab combined with chemotherapy improved only progression-free survival (PFS) but not overall survival (OS).^{2–4} Recent studies supported that combination of PD-1/PD-L1 immune checkpoint inhibitors (ICIs) and anti-angiogenic agents could be a promising therapeutic strategy for normalization of the immunosuppressive microenvironment and overcoming the low efficacy of ICIs.^{5–6} Toripalimab is a novel PD-1 inhibitor, combining with anlotinib as maintenance therapy for ES-SCLC may improve disease control.

Methods The eligible ES-SCLC patients with measurable target lesion (RECIST v1.1), ECOG performance status 0 or 1 and required to have complete response, partial response or stable disease per RECIST 1.1 following 4 to 6 cycles of platinum-based chemotherapy. 20 participants will be enrolled to receive maintenance therapy with toripalimab (240mg, IV, Q3W) and anlotinib (12mg, QD, Q3W) until disease progression, unacceptable toxicity or up to 2 years. Prophylactic cranial irradiation (PCI) was permitted at the investigator's discretion. The primary endpoints are the progression-free survival (PFS) and overall survival(OS). Secondary endpoints include safety, objective response rate (ORR), disease control rate (DCR) and time to response (TTR).

Results Between April, 2020, and June, 2021, 11 extensive-stage small cell lung cancer (ES-SCLC) patients (10 males, 1 females) were enrolled in the study: both of them completed four to six cycles chemotherapy, 11 (100%) achieved a best response of disease control (partial response or stable disease). The median age was 66 (range, 53–78) years. As of June 30, 2021 (data cutoff date), the median follow-up was 4.6 months. The median PFS had not been reached (range, 1.4+ to 14.5+ month). One (1/11) patients had disease progression after 7 months of maintenance treatment. All patients were still alive, and the median OS had not been reached. 90.9% (10/11) patients were still receiving treatment. The most common adverse events (AEs) were grade 1–2 rash (17.2%), decreased appetite (13.8%), leucopenia (6.9%), and Myalgia (6.9%). Two patients had herpes zoster, treatment with ICIs may result in varicella-zoster reactivation. Four patients had Grade 3 AEs (1 pneumonitis 2 hypothyroidism; 1 rash, and 1 myalgia). No grade 4/5 AEs occurred.

Conclusions In this phase 2 study, patients with ES-SCLC who continued toripalimab with anlotinib as maintenance therapy after induction therapy with etoposide-platinum chemotherapy showed promising anti-tumor activity and tolerable toxicities.

Trial Registration Clinical trial information: NCT04363255.

REFERENCES

- Horn L, Mansfield AS, Szczesna A, et al. IMpower133 Study Group. First-line atezolizumab plus chemotherapy in extensive-stage small-cell lung cancer. *N Engl J Med* 2018; **379**(23): 2220–2229.
- Horn L, Dahlberg SE, Sandler AB, et al. Phase II study of cisplatin plus etoposide and bevacizumab for previously untreated, extensive-stage small-cell lung cancer: Eastern Cooperative Oncology Group Study E3501. *J Clin Oncol* 2009;**27**(35): 6006–11.

- Spigel DR, Townley PM, Waterhouse DM, et al. Randomized phase II study of bevacizumab in combination with chemotherapy in previously untreated extensive-stage small-cell lung cancer: results from the SALUTE trial. *J Clin Oncol* 2011;**29**(16): 2215–22.
- Ready NE, Dudek AZ, Pang HH, et al. Cisplatin, irinotecan, and bevacizumab for untreated extensive-stage small-cell lung cancer: CALGB 30306, a phase II study. *J Clin Oncol* 2011; **29**(33): 4436–41.
- Chen DS, Mellman I. Elements of cancer immunity and the cancer-immune set point. *Nature* 2017;**541**: 321–30.
- Ellis LM, Hicklin DJ. VEGF-targeted therapy: mechanisms of anti-tumour activity. *Nat Rev Cancer* 2008;**8**(8):579–91.

Ethics Approval Ethics approval was granted by Committee of Enze Hospital of Taizhou Enze Medical (Center NO. K20200402)

Consent Informed written consent for publication was obtained from the patient prior to collecting information. The patient gave written consent for personal or clinical details along with any identifying images to be published in this study.

<http://dx.doi.org/10.1136/jitc-2021-SITC2021.468>

469

A PHASE 1 FIRST IN HUMAN STUDY OF HMBD-002, AN IGG4 MONOCLONAL ANTIBODY TARGETING VISTA, AS A MONOTHERAPY AND COMBINED WITH PEMBROLIZUMAB IN PATIENTS WITH ADVANCED SOLID MALIGNANCIES

¹Leah DiMascio*, ¹Dipti Thakkar, ¹Siyu Guan, ¹Eric Rowinsky, ²Jordi Rodon, ³Joshua Gruber, ⁴Benjamin Musher, ⁵Joseph Kim, ⁶Alain Mita, ⁷Monica Mita, ¹Piers Ingram, ¹Jerome Boyd-Kirkup. ¹Hummingbird Bioscience, Houston, TX, USA; ²The University of Texas, MD Anderson Cancer Center, Houston, TX, USA; ³The University of Texas Southwestern, Dallas, TX, USA; ⁴Baylor College of Medicine, Houston, TX, USA; ⁵Yale School of Medicine, New Haven, CT, USA; ⁶Cedars Sinai Medical Center, Los Angeles, CA, USA; ⁷Cedars-Sinai Medical Center, Los Angeles, CA, USA

Background V-domain Ig suppressor of T cell Activation (VISTA), an immune checkpoint regulator predominantly expressed on myeloid cells, represents a promising therapeutic target due to its role in suppressing pro-inflammatory, anti-tumor responses within the tumor microenvironment (TME). Based on VISTA's broad expression across immune cell subtypes, HMBD-002 has been designed as a non-depleting, IgG4 monoclonal antibody with high affinity and specificity to VISTA across species (human, cynomolgus monkey, and rodent) that has the ability to block a predicted counter-structure binding site. In preclinical studies, HMBD-002 significantly inhibited tumor growth, both as a monotherapy and in combination with pembrolizumab, while decreasing infiltration of suppressive myeloid cells within the TME and increasing T cell activity. While rapid serum clearance and immune toxicities (e.g. cytokine release syndrome) have been reported for IgG1 antibodies, these were not observed preclinically with HMBD-002. In addition to VISTA expression on pro-inflammatory immune cells, examination of VISTA expression across cancer types has revealed that several malignancies, particularly human samples of triple negative breast cancer (TNBC) and non-small cell lung cancer (NSCLC), express high levels of VISTA, thereby providing a rationale for exploring these indications in clinical studies.

Methods This Phase 1, first in human study is being conducted in two parts and will evaluate multiple doses and schedules of intravenously (IV) administered HMBD-002, with or without pembrolizumab, in patients with advanced solid tumors. Part 1 (dose escalation) seeks to identify the maximum tolerated dose (MTD), or the maximum tested dose, of HMBD-002 as a monotherapy, and separately, in combination with pembrolizumab to define the recommend doses for subsequent disease directed studies (i.e., recommended phase 2 dose [RP2D]). Part 2 (dose expansion) will assess the anti-cancer activity of HMBD-002 as a monotherapy at the RP2D in previously treated patients with TNBC, and NSCLC, and in combination with pembrolizumab in patients with TNBC, NSCLC, and other VISTA-expressing malignancies. The size of the disease-directed cohorts will be determined based on an interim futility analysis conducted upon enrollment of 15 patients. Safety, efficacy, pharmacokinetic, and pharmacodynamic endpoints will be monitored and reported. Correlative studies will assess pre- and post-treatment markers of immune activity in the periphery and the tumor microenvironment.

Acknowledgements This work was funded in part by the Cancer Prevention and Research Institute of Texas (CPRIT).

Ethics Approval The study was approved by each participating Institution's Institutional Review Board.

<http://dx.doi.org/10.1136/jitc-2021-SITC2021.469>

470 **A PHASE 1/2, OPEN-LABEL, DOSE ESCALATION AND EXPANSION STUDY OF GI-101 AS A SINGLE AGENT AND IN COMBINATION WITH A PEMBROLIZUMAB, LENVATINIB OR LOCAL RT IN ADVANCED SOLID TUMORS (KEYNOTE-B59)**

¹Byoung Chul Cho*, ¹Sang Joon Shin, ²Jae-Lyun Lee, ³Byoung Yong Shim, ³Hyung Soon Park, ⁴Nari Yun, ⁴Mina Ham, ⁴Young Jun Koh, ⁴Myoung Ho Jang. ¹Yonsei University College of Medicine, Seoul, Korea, Republic of; ²University of Ulsan College of Medicine, Seoul, Korea, Republic of; ³The Catholic University of Korea, Suwon, Korea, Republic of; ⁴GI Innovation, Inc, Seoul, Kosovo, Republic of

Background GI-101 is a novel bispecific fusion protein containing CD80 and interleukin-2 (IL-2) variant, designed to exhibit high affinity to cytotoxic T-lymphocyte-associated protein 4 (CTLA4) and preferential binding to IL-2R β subunit. In various animal models, GI-101 exerted strong anti-tumor efficacy, accompanied by robust stimulation of CD8+ T and NK cell proliferation without a significant increase in regulatory T cells. GI-101 also elicited synergistic anti-tumor efficacy when used in combination with pembrolizumab (anti-PD1 agents), lenvatinib (tyrosine kinase inhibitor) and radiation in vivo.¹ Given the complementary mechanisms of action of GI-101 via blocking CTLA4 with IL-2 activity to enhance the proliferation and activation of effector T and NK cells, it was hypothesized that GI-101 as a single agent or in combination with other immunotherapies, VEGF inhibitors or RT may exert anti-tumor activity in cancers with high unmet needs.

Methods KEYNOTE-B59 (NCT04977453) is an ongoing phase 1/2 study composed of 4 parts. This study is planned to enroll approximately 374 patients across the indications. Patients assigned to Part A and B receive either GI-101 monotherapy (Part A) or GI-101 + 200 mg of pembrolizumab (Part B) via IV infusion on every 3 weeks (q3w). In Part C, patients will receive GI-101 q3w in combination with lenvatinib (oral, once daily). In Part D, patients will be given GI-101 q3w in combination with local tumor irradiation. Each part is initiated with dose-escalation/optimization phases which will enroll patients with advanced solid tumors, except Part D that enrolls advanced melanoma and sarcoma only. This phase utilizes conventional 3+3 design to determine the maximum tolerated dose and recommended phase 2 dose (RP2D) of GI-101 as a monotherapy and in combination. Once RP2D is determined, patients will be enrolled in dose-expansion phases of each part that includes specific tumor types, such as solid cancers failed on standard of care, treatment-naïve unselected or CPI-treated solid tumors. Patients with advanced solid tumors and recovered from prior therapy will be enrolled. This study will assess safety, tolerability, dose-limiting toxicities, MTD, RP2D, preliminary anti-tumor activity, and pharmacokinetics/pharmacodynamics of GI-101 as a single agent and in combination.

Results This study is currently enrolling patients with advanced or metastatic solid tumors.

Acknowledgements The authors would like to thank all the patients who are participating in this study. The study is sponsored by GI Innovation, Inc.

Trial Registration NCT04977453

REFERENCE

1. Pyo KH, Synn CB, Koh YJ, et al. Comprehensive preclinical study on GI-101, a novel CD80-IgG4-IL2 variant protein, as a therapeutic antibody candidate with bispecific immuno-oncology target. *Cancer Res* 2021;**81**(13_Suppl).

Ethics Approval This study was approved by Severance hospital institutions' Ethics Review Board (IRB); approval number 4-2021-0185, Asan Medical center's IRB; approval number 2021-0669.

<http://dx.doi.org/10.1136/jitc-2021-SITC2021.470>

471

PHARMACOKINETICS OF FIRST AND REPEATED DOSING OF NON-IRAE-INDUCING ANTI-CTLA-4 MONOCLONAL ANTIBODY ONC-392 IN ADVANCED CANCER PATIENTS

¹Hung-Yen Chou*, ²Tianhong Li, ²Karen Kelly, ²Anthony Martinez, ²Stacy Joo, ³Mei Tang, ¹Martin Devenport, ¹Yang Liu, ¹Pan Zheng. ¹OncoC4, Inc., Rockville, MD, USA; ²UC Davis Comprehensive Cancer Center, Sacramento, CA, USA; ³Greater Baltimore Medical Center, Baltimore, MD, USA

Background ONC-392 preserves CTLA-4 recycling and thereby maintains its physiological immune tolerance checkpoint function while allowing more efficient and selective elimination of tumor-infiltrating regulatory T cells. The safety data in the first-in-human trial showed that ONC-392 is safe and well tolerated with no observed immunotherapy-related adverse events (irAE). Serum samples were used to determine pharmacokinetic parameters of ONC-392 to establish systemic drug exposure.

Methods Samples from the first and third dosing cycles were collected at predose and 0.5, 6, 24, 48, 192, 360, and 504 hours postdose. For other dosing cycles, predose and 0.5 hour postdose samples were collected. Serum ONC-392 concentrations were measured by ELISA and the PK parameters were analyzed under noncompartmental condition using linear trapezoidal method.

Results Systemic exposure of ONC-392 is positively correlated to dosing concentration and number of doses. Mean C_{max} and AUC 0–504hr values increase proportionately to dosing concentrations from 0.1mg/kg to 10mg/kg. Dose ratio in cycle 1 is 1:3:30:100. The mean cycle 1 C_{max} and AUC 0–504hr ratios are 1:3.34:31.32:106.28 and 1:3.13:28.46:100.63 respectively. The C_{max} in patients receiving one or more doses of ONC-392 at 3mg/kg is 89±16µg/mL. The C_{max} in patients receiving one or more doses of ONC-392 at 10mg/kg is 259±55µg/mL. Inclusive of all dosing concentrations (0.1, 0.3, 1, 3, 10mg/kg) and cycles, T_{max} is between 1.5–6 hours with one outlier observed at 24-hour postdose. The t_{1/2} range from 201 to 478 hours (8 - 20 days). The cycle 1 mean of t_{1/2} for 0.1, 0.3, 3, 10mg/kg dosing concentrations are 411.02, 359.25, 246.22, 355.01 hours respectively. A direct comparison between first and third cycle in the 3mg/kg dosing group confirms ONC-392 accumulation in repeated dosing. The trough levels (C_{min}) in patients receiving one or multiple doses of ONC-392 at 3mg/kg and 10mg/kg are between 12–51µg/mL and 49–71µg/mL respectively. Lastly, inclusive of all dosing concentrations (0.1, 0.3, 1, 3, 10mg/kg) and cycles, MRT range from 307.91–655.04 hours, V_z range from 0.0305–0.0726 mg/(µg/mL), and Cl range from 0.000052–0.00019 mg/(µg/mL)/h.

Conclusions Intravenous infusion of ONC-392 provide adequate and dose-dependent exposure over extended period. Overall exposure is comparable or higher than those reported by others using different anti-CTLA-4 antibodies. The apparent lack of irAE in ONC-392 recipients despite the high exposure indicates intrinsic safety and tolerability of ONC-392.

<http://dx.doi.org/10.1136/jitc-2021-SITC2021.471>

472

BDB001, A TOLL-LIKE RECEPTOR 7 AND 8 (TLR7/8) AGONIST, CAN BE SAFELY ADMINISTERED INTRAVENOUSLY IN COMBINATION WITH ATEZOLIZUMAB AND SHOWS CLINICAL RESPONSES IN ADVANCED SOLID TUMORS<http://dx.doi.org/10.1136/jitc-2021-SITC2021.472>

¹Manish Patel*, ²Drew Rasco, ³Melissa Johnson, ⁴Anthony Tolcher, ⁴David Sommerhalder, ⁵Omid Hamid, ⁶Alexander Chung, ⁶Lixin Li, ⁶Robert Andtbacka. ¹Florida Cancer Specialists/Sarah Cannon Research Institute, Sarasota, FL, USA; ²South Texas Accelerated Research Therapeutics, San Antonio, TX, USA; ³Sarah Cannon Research Institute, Nashville, TN, USA; ⁴NEXT Oncology, San Antonio, TX, USA; ⁵The Angeles Clinic and Research Institute, A Cedars-Sinai Affiliate, Los Angeles, CA, USA; ⁶Seven and Eight Biopharmaceuticals Inc, Edison, NJ, USA

Background BDB001 is an intravenously administered TLR 7/8 dual agonist immune modulator capable of reprogramming dendritic cells to produce antitumor activities. BDB001 monotherapy has demonstrated favorable tolerability and robust systemic immune activation leading to durable clinical responses in a Phase I trial. Here, we report on the safety and efficacy of BDB001 in combination with atezolizumab in a Phase I dose escalation/expansion trial in advanced solid tumors (NCT04196530).

Methods BDB001-102 is a Phase 1, open label, dose escalation/expansion trial of BDB001 (IV, Q1W) in combination with an anti-PD-L1 antibody, atezolizumab (IV, Q3W), in patients with advanced solid tumors. The primary endpoint was safety and tolerability. Secondary endpoints included efficacy, pharmacokinetics and pharmacodynamic profiling of immune activation.

Results Forty-one subjects with 17 different tumor types were enrolled across 4 dose levels. Fifty-nine percent were female, median age was 67 years (range, 32–80), median number of prior therapies was 3 (range, 0–8), and 63% of tumors had progressed on prior anti-PD-(L)1 therapy. Overall, BDB001 in combination with atezolizumab was well tolerated and 13 (31.7%) subjects did not experience any treatment related adverse events (TRAEs). No dose-limiting toxicities were observed. Common TRAEs were transient Grade 1 or 2 fatigue (31.7%), fever (26.8%) and chills/rigor (26.8%). Only 3 (7.3%) subjects experienced Grade 3 TRAEs of fatigue and nausea. There were no Grade 4 or 5 TRAEs and no new safety concerns. Pharmacodynamic evaluation of plasma cytokine levels showed robust increases in interferon gamma and interferon inducible protein-10 (IP-10) at BDB001 Dose Level 4. IP-10 induction was associated with clinical responses. Preliminary efficacy evaluation of the 19 subjects at Dose Level 4 showed durable and deep clinical responses in 3 (16%) subjects, 2 with urothelial carcinoma and 1 with anti-PD-1 mAb refractory NSCLC. All responders remain on treatment, with a duration of response ranging from 7.1+ to 34.1+ weeks. Ten (53%) subjects had stable disease (DCR 68%), 3 of whom had a reduction in tumor burden and were on treatment for over 18 weeks (up to 56 weeks).

Conclusions Intravenous BDB001 in combination with atezolizumab is well tolerated. Deep and durable clinical responses were observed in PD-1 refractory and naive patients, supported by robust systemic immune activation. BDB001 in combination with atezolizumab is a promising therapeutic option for patients with advanced solid tumors. A phase 2 trial (NCT03915678) of BDB001 in combination with atezolizumab and radiotherapy is currently enrolling patients.

Ethics Approval This study was approved by the institutional review boards at the five participating institutions. All subjects signed informed consent before enrolling in the clinical trial.

IMMUNE PROFILING OF PATIENTS WITH ADVANCED SOLID TUMORS TREATED WITH INTRATUMORALLY ADMINISTERED CV8102 AS A SINGLE-AGENT OR IN COMBINATION WITH ANTI-PD-1 ANTIBODIES IN PHASE I CLINICAL TRIAL

¹Paula Codó*, ²Thomas Eigentler, ³Lucie Heinzerling, ⁴Juergen Krauss, ⁵Carsten Weishaupt, ⁶Sebastian Ochsenreither, ⁷Celeste Lebbe, ⁸Peter Mohr, ⁹Marc Oliva, ¹⁰Honey Oberoi, ¹¹Patrick Terheyden, ¹²José Trigo Pérez, ¹³Franz-Georg Bauernfeind, ¹⁴Michael Fluck, ¹⁵Erika Richtig, ¹⁶Ainara Soria, ¹Marina Gonzalez, ¹Fatma Funkner, ¹Peter Wengenmayer, ¹Dominik Vahrenhorst, ¹Tobias Seibel, ¹Gianluca Quintini, ¹Beate Schmitt-Bormann, ¹Birgit Scheel, ¹Martin Falk, ¹Ulrike Gnad-Vogt. ¹CureVac AG, Frankfurt, Germany; ²University Medical Center Tübingen, Tübingen, Germany; ³University of Erlangen, Erlangen, Germany; ⁴National Center for Tumor diseases (NCT), Heidelberg, Germany; ⁵University of Münster, Münster, Germany; ⁶Charité Comprehensive Cancer Center, Berlin, Germany; ⁷Hôpital Saint Louis, Paris, France; ⁸Elbe Medical Center, Buxtehude, Germany; ⁹Institut Catala d'Oncologia (ICO), Barcelona, Spain; ¹⁰Vall d'Hebron University Hospital, Barcelona, Spain; ¹¹University of Lübeck, Lübeck, Germany; ¹²Hospital Clínico V de la Victoria, Málaga, Spain; ¹³University Clinic Bonn, Bonn, Germany; ¹⁴Fachklinik Hornheide, Münster, Germany; ¹⁵Medical University of Graz, Graz, Austria; ¹⁶Hospital Ramon y Cajal, Madrid, Spain

Background CV8102 is a non-coding, non-capped RNA complexed with a carrier peptide activating the innate (via TLR7/8, RIG-I) and adaptive immune system.^{1 2} An ongoing phase I trial is investigating the intratumoral (i.t.) administration of CV8102 in patients with advanced cutaneous melanoma (cMEL), squamous cell carcinoma of the skin (cSCC) or head and neck (hnSCC) and adenoid cystic carcinoma (ACC), either as a single agent or in combination with systemic anti-PD-1 antibodies. Preliminary immune profiling results will be reported.

Methods An open-label, cohort-based, dose escalation and expansion study in patients with advanced cMEL, cSCC, hnSCC or ACC is ongoing investigating CV8102 i.t. as single agent and in combination with anti-PD-1 antibodies. Eight i.t. injections of CV8102 were administered over a 12 week period with optional continuing treatment in case of clinical benefit. In the initial dose escalation part, the recommended phase II dose for subsequent cohort expansion was defined. Blood samples for immune cell phenotyping, RNA sequencing (RNAseq) and serum cytokine/chemokine analysis were collected at baseline and multiple time points during the treatment period. For characterization of the tumor microenvironment (TME), optional core needle biopsies of injected and/or non-injected lesions were taken before, during and after treatment. Changes on various tumor-infiltrating immune cells were assessed by multiplex immunofluorescence (MultiOmyx < sup >TM</sup >) and immune-related gene expression profiling using nCounter® Pan Cancer IO360 < sup >TM</sup > panel (NanoString).

Results During the dose escalation part, 33 patients received CV8102 (dose range of 25–900 µg) as single agent and 25 patients received CV8102 in combination with an anti-PD-1 antibody. A dose of 600 µg was selected as recommended phase II dose. Serum cytokine/chemokine and blood RNAseq analysis showed transient increases in several markers like interferons alpha and gamma after the first dose. First analyses of paired biopsies showed changes in the TME of injected and non-injected lesions. Complete results of cytokine and chemokine analysis in serum and blood RNAseq for the dose escalation cohorts will be presented. Multiplex immunofluorescence and gene expression profiling from paired biopsies from individual patients will be also included.

Conclusions Intratumoral injection of CV8102 activated several cytokine/chemokine pathways in the peripheral blood and

showed immunological changes in the tumor microenvironment of injected and non-injected lesions.

Trial Registration NCT03291002

REFERENCES

1. Ziegler A, Soldner C, Lienenklaus S, Spanier J, Trittel S, Riese P, Kramps T, Weiss S, Heidenreich R, Jasny E, Guzmán CA, Kallen KJ, Fotin-Mleczek M, Kalinke U. A New RNA-Based Adjuvant Enhances Virus-Specific Vaccine Responses by Locally Triggering TLR- and RLH-Dependent Effects. *J Immunol* 2017;**198**(4):1595–1605. doi: 10.4049/jimmunol.1601129.
2. Heidenreich R, Jasny E, Kowalczyk A, Lutz J, Probst J, Baumhof P, Scheel B, Voss S, Kallen KJ, Fotin-Mleczek M. A novel RNA-based adjuvant combines strong immunostimulatory capacities with a favorable safety profile. *Int J Cancer* 2015 Jul 15;**137**(2):372–84. doi: 10.1002/ijc.29402.

Ethics Approval The study was approved by the Central Ethics Committees in Tuebingen, Germany under 785/2016AMG1, in France by the COMITE DE PROTECTION DES PERSONNES SUD-EST I under 2019–49, approval dated 17-May-2019, in Barcelona, Spain by the CEC COMITÉ DE ÉTICA DE INVESTIGACIÓN CLÍNICA CON MEDICAMENTOS del Hospital Universitari Vall d'Hebron, approval date 28-Nov-2019 under the EUdraCT number, in Austria by the Central Ethics Committee in Graz under 31–426 ex 18/19 approved on 19-Sep-2019.

Consent Written informed consent from the patient was obtained for publication of this abstract and any accompanying images. A copy of the written consent is available for review by the Editor of this journal.

<http://dx.doi.org/10.1136/jitc-2021-SITC2021.473>

PHASE 1 STUDY OF SEA-TGT, A HUMAN, NONFUOSYLATED ANTI-TIGIT MONOCLONAL ANTIBODY WITH ENHANCED IMMUNE-EFFECTOR FUNCTION, IN PATIENTS WITH ADVANCED MALIGNANCIES (SGNTGT-001, TRIAL IN PROGRESS)

¹Diwakar Davar*, ²Vincent Ribrag, ²Clementine Sarkozy, ³Elena Garralda, ³Honey Kumar Oberoi, ⁴Amitkumar Mehta, ⁵Giuseppe Curigliano, ⁶Carmen Belli, ⁷Jasmine Zain, ⁷Alex Herrera, ⁸Rachel Sanborn, ⁹Ecaterina Dumbrava, ¹⁰Andres Forero-Torres, ¹¹Stephen Ansell. ¹UPMC Hillman Cancer Center, Pittsburgh, PA, USA; ²Gustave-Roussy Institute, Villejuif, France; ³Vall d'Hebron University Hospital, Barcelona, Spain; ⁴Birmingham Comprehensive Cancer Center, Birmingham, AL, USA; ⁵University of Milano and European Institute of Oncology, IRCCS, Milan, Italy; ⁶European Institute of Oncology, IRCCS, Milan, Italy; ⁷City of Hope Medical Center, Duarte, CA, USA; ⁸Providence Cancer Institute, Portland, OR, USA; ⁹MD Anderson Cancer Center, Houston, TX, USA; ¹⁰Seagen Inc, Seattle, WA, USA; ¹¹Mayo Clinic, Rochester, MN, USA

Background T-cell immunoreceptor with immunoglobulin and immunoreceptor tyrosine-based inhibitory domains (TIGIT), and costimulatory receptor CD226 competitively bind 2 ligands, CD155 and CD112, which are expressed by tumor cells and antigen-presenting cells in the tumor microenvironment.^{1 2} Dual TIGIT/programmed cell death protein-1 (PD-1) blockade increased tumor antigen-specific CD8+ T-cell expansion and function in vitro and promoted potent antitumor response in vivo.^{3 4} TIGIT/PD-1 dual blockade using a TIGIT monoclonal antibody (mAb) with intact Fc produced clinical responses in advanced cancer.⁵ SEA-TGT is an investigational, human, nonfucosylated mAb directed against TIGIT. SEA-TGT binds to TIGIT, blocking inhibitory checkpoint signals directed at T cells. SEA-TGT enhances binding to activating FcγRIIIa and decreases binding to inhibitory FcγRIIb; this depletes immunosuppressive regulatory T cells and amplifies naive and memory T cells, potentially augmenting PD-1 inhibition effects. Preclinically, at suboptimal doses, SEA-TGT plus anti-PD-1 mAbs had superior antitumor activity than either agent alone.⁶

Methods Safety and antitumor activity of SEA TGT in ~377 adults (≥18 years) will be evaluated in this phase 1, multicenter, open-label, dose-escalation/expansion study. Part A will assess the safety/tolerability of SEA TGT to determine maximum tolerated and recommended doses. Part B will assess the safety and antitumor activity of the recommended dose in disease-specific expansion cohorts. Part C will assess SEA-TGT plus sasanlimab in dose-expansion cohorts after an initial safety run-in. Patients with histologically/cytologically confirmed relapsed/refractory/progressive metastatic solid tumors including non-small cell lung cancer (NSCLC), head and neck squamous cell carcinoma (HNSCC), gastric/gastroesophageal junction carcinoma, cutaneous melanoma, bladder, cervical, ovarian or triple-negative breast cancer, or selected lymphomas will be eligible for Parts A and B. Part C will enroll patients with histologically confirmed advanced NSCLC (high [tumor proportion score (TPS) ≥50%] and low [TPS=1–49%] PD ligand 1 [PD-L1] expression), cutaneous melanoma, and HNSCC without previous anti-PD-1/PD-L1 therapy exposure. SEA TGT will be administered on Day 1 of 21-day cycles. Laboratory abnormalities, adverse events, dose-limiting toxicities, and dose-level safety and activity are primary endpoints. Secondary endpoints are objective response (OR) and complete response (CR) rates, duration of OR/CR, progression-free survival, overall survival, pharmacokinetics (PK), and antidrug antibodies. Exploratory analysis will include pharmacodynamics (PD), PK/PD relationships, biomarkers, and resistance to SEA-TGT. This trial is recruiting in Europe and North America.

Trial Registration NCT04254107

REFERENCES

1. Blake SJ, Dougall WC, Miles JJ, et al. Molecular pathways: Targeting CD96 and TIGIT for cancer immunotherapy. *Clin Cancer Res* 2016;**22**(21):5183–5188.
2. Chauvin JM, Zarour HM. TIGIT in cancer immunotherapy. *J ImmunoTher Cancer* 2020;**8**:e000957.
3. Johnston RJ, Comps-Agrar L, Hackney J, et al. The immunoreceptor TIGIT regulates antitumor and antiviral CD8+ T cell effector function. *Cancer Cell* 2014;**26**(6):923–937.
4. Chauvin JM, Pagliano O, Fourcade J, et al. TIGIT and PD-1 impair tumor antigen-specific CD8+ T cells in melanoma patients. *J Clin Invest* 2015;**125**(5):2046–2058.
5. Rodriguez-Abreu D, Johnson ML, Hussein MA, et al. Primary analysis of a randomized, double-blind, phase 2 study of the anti-TIGIT antibody tiragolumab (tira) plus atezolizumab (atezo) versus placebo plus atezo as first-line (1L) treatment in patients with PD-L1-selected NSCLC (CITYSCAPE). *J Clin Oncol* 2020;**38**(15 suppl):9503.
6. Smith A, Zeng W, Lucas S, et al. Poster 1583. SEA-TGT is an empowered anti-TIGIT antibody that displays superior combinatorial activity with several therapeutic agents. Presented at: American Association for Cancer Research Annual Meeting; April 9–14, 2021; Virtual Meeting.

Ethics Approval Institutional review boards or independent ethics committees of participating sites approved the trial, which will be conducted in compliance with the Declaration of Helsinki and International Conference on Harmonisation Guidelines for Good Clinical Practice. All patients will provide written informed consent.

<http://dx.doi.org/10.1136/jitc-2021-SITC2021.474>

475

GEN-011–101 (THE TITAN-1 TRIAL): PHASE 1 STUDY TO EVALUATE THE SAFETY, PROLIFERATION AND PERSISTENCE OF GEN-011, AN AUTOLOGOUS NEOANTIGEN-TARGETED PERIPHERAL T CELL THERAPY IN SOLID TUMORS

Thomas Davis*, Arthur DeCillis, Richard Hernandez, Jessica Price, Craig Carey, Kevin Mancini. *Genocea, Centreville, MD, USA*

Background GEN-011 is a personalized neoantigen-targeted peripheral blood T cell therapy (NPT) developed for the treatment of adult patients (pts) with solid tumors. The proprietary ATLAS™ (Antigen Lead Acquisition System) will be used to identify true immunogenic neoantigens from each patient's tumor mutanome that are recognized by their own CD4+ and/or CD8+ T cells. ATLAS will also identify Inhibigens™, antigen targets of T cells that promote tumor growth.¹ Autologous peripheral T cells will be specifically stimulated by up to 30 ATLAS-identified neoantigens, avoiding Inhibigens, to generate an adoptive T cell product. Preliminary data show yields of billions of highly active T cells with 96% neoantigen targeting across 89% of ATLAS selected neoantigens.

Methods TITAN-1 is a multicenter Phase 1 study of GEN-011 NPTs in patients with refractory melanoma, non-small cell lung cancer (NSCLC), squamous cell carcinoma of the head and neck (SCCHN), urothelial carcinoma (UC), renal cell carcinoma (RCC), small cell lung cancer (SCLC), cutaneous squamous cell carcinoma (CSCC), and anal squamous cell carcinoma (ASCC). Patients may enter into one of 2 cohorts of 6 DLT-evaluable patients, either a multiple lower dose (MLD) regimen of GEN-011 as an IV infusion at 4-week intervals, up to 5 doses maximum without lymphodepletion, or a single high dose (SHD) regimen of GEN-011 after flu/cy lymphodepletion. Each dose of GEN-011 will be followed by a course of interleukin-2 (IL-2). Patients will be followed for safety, immunogenicity, and anti-tumor activity over approximately a 5-month treatment period. A long-term follow-up will continue through 2 years after the initial dose of GEN-011.

Trial Registration ClinicalTrials.gov identifier: NCT04596033

REFERENCES

1. Lam H, et al. An empirical antigen selection method identifies neoantigens that either elicit broad anti-tumor response or drive tumor growth. *Cancer Discovery* 2021 March; **11**(3):696–713.

Ethics Approval This study was approved by Western Institutional Review Board, approval number 1-1078861-1

<http://dx.doi.org/10.1136/jitc-2021-SITC2021.475>

FIRST-IN-HUMAN PHASE 1/2 STUDY OF THE FIRST-IN-CLASS SUMO-ACTIVATING ENZYME INHIBITOR TAK-981 IN PATIENTS WITH ADVANCED OR METASTATIC SOLID TUMORS OR RELAPSED/REFRACTORY LYMPHOMA: PHASE 1 RESULTS

¹Arkadiusz Dudek*, ²Dejan Juric, ³Afshin Dowlati, ⁴Ulka Vaishampayan, ⁴Hadeel Assad, ⁵Jordi Rodón, ⁶Bo Chao, ⁶Bingxia Wang, ⁶John Gibbs, ⁶Vaishali Shinde, ⁶Sharon Friedlander, ⁶Allison Berger, ⁶Christine Ward, ⁶Alonzo Martinez, ⁶Robert Gharavi, ⁶Alejandro Gomez-Pinillos, ⁶Igor Proscurshim, ⁷Anthony Olszanski. ¹University of Minnesota and HealthPartners, St. Paul, MN, USA; ²Massachusetts General Hospital Cancer Center and Harvard Medical School, Boston, MA, USA; ³University Hospitals Seidman Cancer Center and Case Western Reserve University, Cleveland, OH, USA; ⁴Wayne State University/University of Michigan, Ann Arbor, MI, USA; ⁵The University of Texas MD Anderson Cancer Center, Houston, TX, USA; ⁶Takeda Development Center Americas, Inc., Cambridge, MA, USA; ⁷Fox Chase Cancer Center, Philadelphia, PA, USA

Background SUMOylation is a post-translational modification that serves as an important modulator of immune responses via its role in constraining the type I interferon (IFN-1) response. TAK-981 is a small molecule that inhibits SUMOylation and increases IFN-1-dependent innate immune responses with the potential to enhance adaptive immunity. Here, we report dose-escalation data from a TAK-981 Phase 1/2 clinical study (NCT03648372), the first clinical data for a SUMOylation inhibitor.

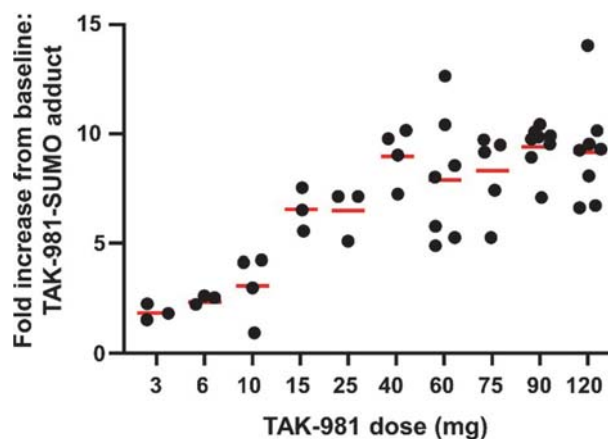
Methods Adults with advanced/metastatic solid tumors or relapsed/refractory lymphomas received TAK-981 IV twice-weekly (BIW; days 1, 4, 8, 11) or once-weekly (QW; days 1, 8) in 21-day cycles. Dose escalation was guided by a Bayesian Logistic Regression Model (BLRM) with overdose control, plus available pharmacokinetic/pharmacodynamic (PK/PD) data. Phase 1 objectives were to determine TAK-981 safety/tolerability and establish the recommended phase 2 dose (RP2D).

Results Seventy-six patients received TAK-981 at 10 dose levels (3–40 mg BIW; 60–120 mg QW/BIW). Median age was 61 years (range, 38–79); 42 (55.3%) patients were female. Four dose-limiting toxicities were seen in 62 evaluable patients (transient grade 3 ALT/AST elevation, 60 mg BIW; grade 3 pneumonitis, 90 mg BIW; grade 3 stomatitis and grade 3 cognitive disturbance, 120 mg BIW). Per BLRM, 120 mg BIW was determined to be the maximum tolerated dose. At data cut-off, median treatment duration was 2 cycles (range, 1–12); 13 (17.1%) patients were ongoing. Table 1 summarizes TAK-981 safety. The most common ($\geq 20\%$) treatment-emergent adverse events (TEAEs) were fatigue (42.1%), nausea (39.5%), headache (31.6%), diarrhea (28.9%), pyrexia (27.6%), vomiting (23.7%), decreased appetite (22.4%). Common ($\geq 5\%$) grade ≥ 3 TEAEs were hypokalemia (9.2%), anemia (7.9%), lymphocyte count decreased (6.6%), abdominal pain (5.3%). Grade 2 cytokine release syndrome was reported in 4 (5.2%) patients; symptoms resolved within 12–24 hours with supportive oxygen and/or IV fluids. One partial response was observed at 40 mg TAK-981 BIW in a patient with relapsed/refractory HER2-negative, hormone receptor-positive breast cancer. TAK-981 exhibited linear PK, with approximately dose-proportional exposure and a mean terminal half-life of 3.8–10.8 hours at ≥ 60 mg. Evidence of dose-dependent target engagement (Figure 1), and PD (Figures 2–4) in blood were observed. The single-agent TAK-981 RP2D was 90 mg BIW.

Abstract 476 Table 1 Summary of TAK-981 safety profile

Patients with ≥1 event, n (%)	TAK-981 dose escalation					Total (n=76)
	375 mg BIW or QW* (n=48)	90 mg QW (n=7)	90 mg BIW (n=8)	120 mg QW (n=5)	120 mg BIW (n=8)	
Any TEAE	44 (91.6)	7 (100.0)	8 (100.0)	4 (80.0)	8 (100.0)	71 (93.4)
Drug-related TEAE	31 (64.6)	7 (100.0)	7 (87.5)	4 (80.0)	8 (100.0)	57 (75.0)
Grade ≥3 TEAE	21 (43.8)	5 (71.4)	6 (75.0)	3 (60.0)	6 (75.0)	41 (53.9)
Drug-related grade ≥3 TEAE	5 (10.4)	3 (42.9)	2 (25.0)	1 (20.0)	4 (50.0)	15 (19.7)
SAE	19 (39.6)	2 (28.6)	5 (62.5)	2 (40.0)	5 (62.5)	33 (43.4)
Drug-related SAE	3 (6.3)	0	1 (12.5)	1 (20.0)	2 (25.0)	7 (9.2)
TEAE resulting in discontinuation of TAK-981	2 (4.2)	0	4 (50.0)	1 (20.0)	2 (25.0)	9 (11.8)
Drug-related TEAE resulting in discontinuation of TAK-981	0	0	2 (25.0)	1 (20.0)	1 (12.5)	4 (5.3)
On-study deaths	4 (8.3)	0	2 (25.0)	0	0	6 (7.8)
On-study deaths related to TAK-981	0	0	0	0	0	0
DLT†	1 (2.1)	0	1	2	0	4

AE, adverse event; BIW, twice weekly; DL, dose-limiting toxicity; QW, once weekly; SAE, serious adverse event; TEAE, treatment-emergent adverse event.
 *3 mg BIW (n=1), 6 mg BIW (n=1), 10 mg BIW (n=4), 15 mg BIW (n=3), 25 mg BIW (n=4), 40 mg BIW (n=4), 60 mg QW (n=5), 60 mg QW (n=5), 75 mg QW (n=5), and 90 mg QW (n=5).
 †DLTs were based on the DLT evaluation population: 40 DLT evaluations patients on the BIW schedule and 37 on the QW schedule.

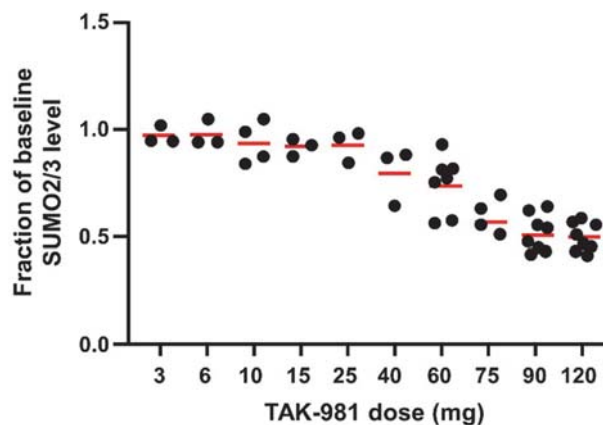


Red lines represent mean fold-change at each dose.

Abstract 476 Figure 1

PD in patients receiving TAK-981 on the BIW schedule: target engagement.

Blood samples were collected on Cycle 1 Day 1 pre-dose and at multiple timepoints after TAK-981 administration. Target engagement in T cells was detected by flow cytometry with an antibody recognizing the TAK-981-SUMO adduct formed during the inhibition of the SUMO-activating enzyme by TAK-981; Cycle 1 Day 1 signal increased at 1 hour post-end-of-infusion compared to the background level observed pre-dose.



Red lines represent mean fold-change at each dose.

Abstract 476 Figure 2

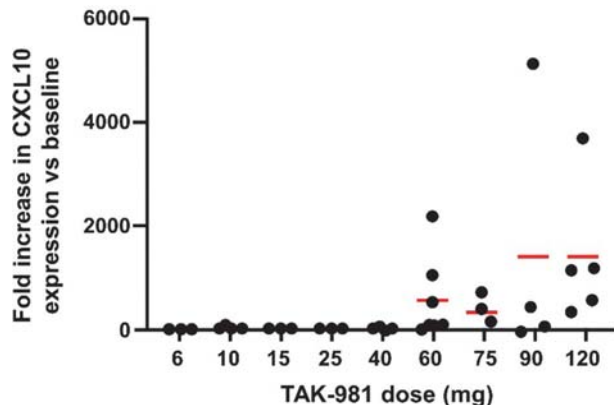
PD in patients receiving TAK-981 on the BIW schedule: SUMOylation.

SUMOylation in T cells, detected by flow cytometry with an antibody recognizing SUMO2/3, decreased at 1 hour post-end-of-infusion on Cycle 1 Day 1 compared to pre-dose, indicating that fewer SUMO2/3 chains are formed when the SUMO-activating enzyme is inhibited.

Trial Registration Clinical Trial identification: ClinicalTrials.gov. Identifier: NCT03648372

Ethics Approval The study was approved by the Institutional Review Board or Institutional Ethics Committee of all participating institutions

<http://dx.doi.org/10.1136/jitc-2021-SITC2021.476>

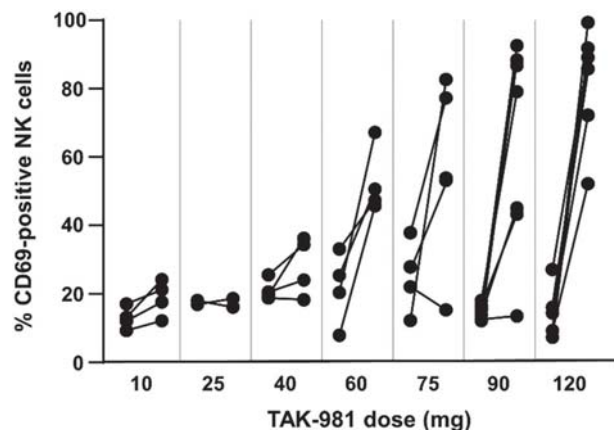


Red lines represent mean fold-change at each dose.

Abstract 476 Figure 3

PD in patients receiving TAK-981 on the BIW schedule: upregulation of CXCL10 expression.

Upregulation of mRNA levels of *CXCL10*, an IFN-I-regulated gene, in peripheral blood. Gene expression was measured using Nanostring nCounter at Cycle 1 Day 1 pre-dose and at several timepoints post-dose. Data for maximum increase at 8 or 24 hours, relative to pre-dose, is shown.



Abstract 476 Figure 4

PD in patients receiving TAK-981 on the BIW schedule: NK cell activation.

NK cell activation in peripheral blood measured by flow cytometry. Percentage of CD69-positive NK cells at Cycle 1 Day 1 pre-dose and at 24 hours post-end-of-infusion is shown by patient for each dose.

Conclusions The data generated in this study support continued TAK-981 development for treatment of solid tumors and lymphoma. The Phase 2 study expansion is ongoing in patients with advanced/metastatic non-small-cell lung, cervical, and colorectal cancer, and in relapsed/refractory non-Hodgkin lymphoma.

477

**COM902 (ANTI-TIGIT ANTIBODY) MONOTHERAPY –
PRELIMINARY EVALUATION OF SAFETY, TOLERABILITY,
PHARMACOKINETICS AND RECEPTOR OCCUPANCY IN
PATIENTS WITH ADVANCED SOLID TUMORS
(NCT04354246)**

¹Ecaterina Dumbrava*, ²Drew Rasco, ²Amita Patnaik, ³Daniel Vaena, ²Kyriakos Papadopoulos, ³Adam ElNaggar, ⁴Adeboye Adewoye, ⁴Robina Smith, ⁴Pierre Ferré, ⁴Ilan Vaknin, ⁵Srinivas Devarakonda, ⁶Manish Sharma. ¹MDACC, Houston, TX, USA; ²START – San Antonio, San Antonio, TX, USA; ³West Cancer Center and Rsch Institute, Memphis, TN, USA; ⁴Compugen USA Inc., San Francisco, USA; ⁵Ohio State University, Columbus, OH, USA; ⁶START – Midwest, Grand Rapids, MI, USA

Background COM902 is an IgG4 fully human high-affinity monoclonal antibody, inhibitor of TIGIT (T cell Ig and immunoreceptor tyrosine-based inhibitory motif [ITIM] domain) binding to poliovirus receptor (PVR). TIGIT blockade by COM902 was shown to enhance anti-tumor immunity in pre-clinical models. We hypothesized that COM902 as monotherapy will have an acceptable safety and tolerability profile in subjects with advanced solid tumors.

Methods Utilizing an accelerated titration and 3+3 study design we enrolled 18 patients (pts) at the following COM902 doses 0.01, 0.03, 0.1, 0.3, 1, 3 and 10 mg/kg IV Q3 wks. Key primary objectives were to evaluate the safety, tolerability (CTCAE v5.0), to characterize the pharmacokinetics (PK) and to select a recommended dose for expansion (RDFE). An exploratory objective was evaluation of peripheral receptor occupancy (RO). Key inclusion criteria: Age \geq 18 yrs, histologically/cytologically confirmed advanced malignancy who have exhausted all available standard therapy or not a candidate for standard therapy. Patients with performance status ECOG 0-1, prior ICI permissible. Dose-limiting toxicities (DLTs) were evaluated within a 21-day window in the 1st cycle of dose escalation.

Results In the safety population [N=18], 12 pts reported treatment emergent adverse events (TEAEs). The most frequent TEAEs [\geq 2pts] were fatigue 7 pts (39%) all G1/2, diarrhea 3 pts (17%) all G1/2. Two pts reported DLTs deemed related to study drug, a pt with G2 nausea (single pt cohort, 0.01 mg/kg) and a pt with G3 atrial fibrillation (1 mg/kg). Serious adverse events were reported in 2 pts, 1 pt with atrial fibrillation (deemed by the investigator as possibly related to COM902) and 1 pt with spinal cord compression (deemed by the investigator as unrelated to COM902, related to disease). Preliminary PK profiles were generally dose proportional and peripheral RO above 90% was reported from 0.1 mg/kg dose. **Conclusions** COM902 has an acceptable safety, tolerability and PK profiles. A COM902 3 mg/kg IV Q3 wks is the RDFE. Enrollment into combination cohort (COM902 + COM701), for evaluation of safety/tolerability at the RDFE of both study drugs, combination dose expansion (COM902 + COM701) in pts with HNSCC, NSCLC and CRC-MSS and COM902 monotherapy dose expansion (pts with multiple myeloma) all at the RDFE of study drug(s) are planned. Data cut June 28, 2021.

Trial Registration NCT04354246

Ethics Approval The study obtained approval from IRBs of the participating clinical trial sites. The study participants gave informed consent before taking part. o 0002: MOD01006350 (START) o 0003: 20202320 (West Cancer Center) o 0012: 2020-0195 (MDACC) o 0013: MOD01006350 (START mid-west) o 0014: 20202320 (OSU)

<http://dx.doi.org/10.1136/jitc-2021-SITC2021.477>

COM701 IN COMBINATION WITH BMS-986207 (ANTI-TIGIT ANTIBODY) AND NIVOLUMAB – PRELIMINARY RESULTS OF SAFETY, TOLERABILITY AND PHARMACOKINETICS IN PATIENTS WITH ADVANCED SOLID TUMORS (NCT04570839)

¹Ecaterina Dumbrava*, ²Manish Sharma, ³Gini Fleming, ⁴Kyriakos Papadopoulos, ⁵Ryan Sullivan, ⁶Daniel Vaena, ⁴Amita Patnaik, ⁶Adam ElNaggar, ⁷Adeboye Adewoye, ⁷Robina Smith, ⁷Pierre Ferré, ⁷Inbal Barbiro, ⁸Emerson Lim, ⁴Drew Rasco. ¹MDACC., Houston, TX, USA; ²START – Midwest., Grand Rapids, MI, USA; ³University of Chicago., Chicago, IL, USA; ⁴START – San Antonio., San Antonio, TX, USA; ⁵Massachusetts General Hospital., Boston, MA, USA; ⁶West Cancer Center and Rsrch Institute., Memphis, TN, USA; ⁷Compugen USA Inc., San Francisco, USA; ⁸Columbia University Cancer Center., New York City, NY, USA

Background COM701, a novel first-in-class immune checkpoint inhibitor (ICI) binds to poliovirus receptor related immunoglobulin domain containing (PVRIG) leading to enhanced activation of T and NK-cells. COM701 in combination with nivolumab has a favorable safety profile, is well tolerated and demonstrates antitumor activity.¹ We hypothesized that the addition of BMS-986207 as a triplet thereby inhibiting the DNAM axis will have an acceptable safety/tolerability profile. We present preliminary results on safety/tolerability and pharmacokinetics (PK) parameters.

Methods Using an accelerated titration and 3+3 study design we enrolled 14 patients (pts) with advanced solid tumors. Doses of COM701 were 0.3, 1, 3, 10 or 20 [mg/kg IV Q4 wks]; in combination with nivolumab and BMS-986207 (both 480 mg IV Q4 wks). Key objectives were to evaluate the safety and tolerability, to determine the recommended dose for expansion (RDFE) and to characterize preliminary pharmacokinetic parameters. Key inclusion criteria: Age \geq 18 yrs, histologically confirmed locally advanced or metastatic solid malignancy and has exhausted all available standard treatments. Key exclusion criteria: history of immune-related toxicities on prior immunotherapy treatment leading to discontinuation.

Results In the safety population [N=14], 12 pts reported treatment emergent adverse events (TEAEs). The most frequent TEAEs [\geq 3 pts] were fatigue 5 pts (36%), pyrexia 3 pts (21%), vomiting 3 pts (21%). No DLTs were reported in any of the dose levels. The most frequent tumor types enrolled: CRC (n=3), and prostate, melanoma and OVCA/primary peritoneal cancer (n=2 each). Median number of prior therapies was 10 (range 1–19). Four pts had received prior immunotherapy. Serious adverse events [\geq 2 pts] were 2 pts (14%) with G3 abdominal pain, 2 pts (14%) with vomiting (1pt with G1/2 vomiting, 1 pt with G3 vomiting) all assessed by the investigator as unrelated to study drug. Preliminary PK profiles of COM701 were generally dose proportional.

Conclusions COM701 in combination with BMS-986207 and nivolumab demonstrates a favorable safety, tolerability and PK profiles. COM701 20 mg/kg has been selected as the RDFE in combination with BMS-986207 and nivolumab (both 480 mg) all administered IV Q4 wks. The expansion cohorts are enrolling pts with platinum resistant ovarian cancer and endometrial cancer. Data cutoff 28 Jun 2021.

Acknowledgements This study is in collaboration with Bristol Myers Squibb.

Trial Registration NCT04570839

REFERENCES

1. Vaena, DA, Fleming GF et al. COM701 with or without nivolumab: Results of an ongoing phase 1 study of safety, tolerability and preliminary antitumor activity in

patients with advanced solid malignancies (NCT03667716). *J Clin Oncol* 2021;39: (suppl 15; abstr 2504).

Ethics Approval The study obtained ethics approval from all the participating sites. All study participants gave informed consent before taking part.- 0002: START2020.15- 0003: 20210109- 0005: IRB20-1549- 0006: 21-060- 0007: IRB-AAAT4904- 0012: 2020-0755- 0013: STMW2020.16- 0015: 20210109

<http://dx.doi.org/10.1136/jitc-2021-SITC2021.478>

479

AGEN1181, AN FC-ENHANCED ANTI-CTLA-4 ANTIBODY, ALONE AND IN COMBINATION WITH BALSTILIMAB (ANTI-PD-1) IN PATIENTS WITH ADVANCED SOLID TUMORS: INITIAL PHASE I RESULTS

¹Anthony El-Khoueiry*, ²Andrea Bullock, ³Apostolia Tsimberidou, ⁴Daruka Mahadevan, ⁵Breelyn Wilky, ⁶Przemyslaw Twardowski, ²Bruno Bockorny, ⁷Justin Moser, ⁸Waldo Ortuzar Feliu, ⁸Joseph Grossman, ⁸Katherine Rosenthal, ⁸Steven O'Day, ⁷Michael Gordon. ¹USC Norris Comprehensive Cancer Center, Los Angeles, CA, USA; ²Beth Israel Deaconess Medical Center, Boston, MA, USA; ³MD Anderson Cancer Center, Houston, TX, USA; ⁴UT Health Science Center at San Antonio, San Antonio, TX, USA; ⁵University of Colorado Cancer Center, Aurora, CO, USA; ⁶St John's Cancer Institute, Santa Monica, CA, USA; ⁷HonorHealth Research Institute, Scottsdale, AZ, USA; ⁸Agenus Inc, Lexington, USA

Background AGEN1181 is a novel anti-CTLA-4 antibody with enhanced FcγR-dependent functionality, engineered to bind high and low binding alleles of FcγRIIIA, promoting superior T cell priming, memory responses, and depletion of intratumoral T regulatory cells. Further, AGEN1181 avoids complement recruitment, predictive of better tolerability. Here we report initial safety and efficacy findings from a phase I/Ib study of AGEN1181 as monotherapy and in combination with balstilimab (BAL; anti-PD-1).

Methods Eligible patients (pts) had advanced solid tumors refractory to standard therapies. AGEN1181 was dosed Q3W (0.1–3 mg/kg) or Q6W (1–2 mg/kg) as monotherapy, or Q6W (0.1–2 mg/kg) in combination with BAL Q2W (3 mg/kg).

Results As of July 16th 2021, 102 pts received AGEN1181 (43 monotherapy, 59 combination). Median age, 63 years (29–83); 50.5% with ≥3 prior lines of therapy. MTD not yet reached with AGEN1181 dosing up to 3 mg/kg Q3W as monotherapy and 2 mg/kg in combination with BAL. The most common treatment-related adverse events (TRAEs) of any grade were fatigue (34.3%), diarrhea (32.4%), and nausea (19.6%) with grade ≥3 events in 21.6% (diarrhea/colitis, 11.8%, fatigue, 2.9%). Notably, no immune-related hypophysitis or pneumonitis has been observed. Discontinuation from AGEN1181 due to TRAEs occurred in 15% of pts. Grade 5 TRAEs occurred in two pts (colitis [chronic], intestinal perforation). The disease control rate in evaluable pts (completed ≥1 on-treatment scan) defined as best overall response of CR, PR, or SD ≥6 weeks was 48.1% for AGEN1181 monotherapy ≥1 mg/kg (1 CR, 3 PR, 9 SD) and 70% for combination (3 PR, 6 unconfirmed PR [uPR], 19 SD). Monotherapy responders include individual pts with MSS endometrial cancer (CR), PD-1-relapsed/refractory cervical cancer (PR), PD-1-relapsed/refractory melanoma (PR), and pancreatic cancer (PR). Enrollment is continuing in several disease expansion cohorts with combination therapy. For MSS CRC, 2 PR, 2 uPR, and 7 SD have been seen in 17 evaluable ≥1 mg/kg patients to date. In the ovarian cohort (n=6), 2 PRs and 3 SD are noted. Additional combination responders include one PR and uPR in MSS endometrial cancer, two uPRs in visceral angiosarcoma (uPRs) and one uPR in PD-1-relapsed/refractory NSCLC (uPR); the majority of the responses are recent and ongoing.

Conclusions AGEN1181 alone and in combination with BAL demonstrates favorable tolerability and compelling clinical activity, notably in poorly immunogenic tumor types and PD-1-refractory pts. These results underscore the significant potential of AGEN1181 to expand benefit of anti-CTLA-4 therapy to a broader patient population.

Trial Registration NCT03860272

Ethics Approval The study obtained ethics approval at each participating center (UT Health Sciences Center at San Antonio, University of Colorado Cancer Center, St John's Cancer

Institute, and HonorHealth under WIRB Study number 1256391; USC Norris Comprehensive Cancer Center, Beth Israel Deaconess Medical Center, and MD Anderson Cancer Center, approval numbers HS19-00277, 19-132, and 140346, respectively). All patients provided written informed consent in accordance with federal, local, and institutional guidelines.

<http://dx.doi.org/10.1136/jitc-2021-SITC2021.479>

A FIRST-IN-HUMAN PHASE I DOSE-ESCALATION TRIAL OF THE B7-H6/CD3 T-CELL ENGAGER BI 765049 ± EZABENLIMAB (BI 754091) IN PATIENTS WITH ADVANCED SOLID TUMORS EXPRESSING B7-H6

¹Gerald Falchook*, ²David Spigel, ³Manish Patel, ⁴Babar Bashir, ⁵Susanna Ulahannan, ⁶Christine Duffy, ⁷Daniela Maier, ⁸Hisaya Azuma. ¹*Sarah Cannon Research Institute at HealthONE, Denver, CO, USA;* ²*Sarah Cannon Research Institute/Tennessee Oncology, PLLC, Nashville, TN, USA;* ³*Florida Cancer Specialists and Sarah Cannon Research Institute, Sarasota, FL, USA;* ⁴*Sidney Kimmel Cancer Center at Thomas Jefferson University, Philadelphia, PA and Sarah Cannon Research Institute, Philadelphia, PA, USA;* ⁵*The University of Oklahoma Health Sciences Center/Sarah Cannon Research Institute, OKC, OK, USA;* ⁶*Boehringer Ingelheim Pharmaceuticals Inc., Ridgefield, CT, USA;* ⁷*Boehringer Ingelheim Pharma GmbH and Co. KG, Biberach/Riss, Germany;* ⁸*Boehringer Ingelheim International GmbH, Ingelheim am Rhein, Germany*

Background B7-H6 is a member of the B7 family of immune receptors, which is expressed in several solid tumor types but very little expression can be detected in normal tissues.^{1 2} BI 765049 is a novel IgG-like bispecific T-cell engager designed to bind simultaneously to B7-H6 on tumor cells and CD3 on T cells, resulting in cytolytic synapse formation and tumor lysis. Preclinical studies have demonstrated that BI 765049 monotherapy induced dose-dependent anti-tumor activity in humanized in vivo CRC tumor models. Consistent with the mode of action, the treatment with BI 765049 led to target cell apoptosis, local T-cell activation/proliferation and cytokine production in the tumor tissue, with PD-(L)1 upregulation.³ Activation of the PD-(L)1 provides the rationale for combining BI 765049 with a PD1 inhibitor.

Methods NCT04752215 is a first-in-human, open-label, dose-escalation trial of BI 765049 ± the PD-1 inhibitor, ezablenlimab. Adults with advanced, unresectable and/or metastatic CRC, NSCLC, HNSCC, hepatocellular, gastric or pancreatic carcinoma are eligible. Patients must have failed on, or be ineligible, for standard therapies. B7-H6 positivity must be confirmed at screening by central review (immunohistochemistry assay) in archived tissues/in-study fresh biopsies (except CRC). Patients must have ≥1 evaluable lesion (modified RECIST 1.1) outside of the central nervous system and adequate organ function. The primary objective is to determine the maximum tolerated dose (MTD) or recommended dose for expansion of BI 765049 ± ezablenlimab, based on dose-limiting toxicities during the MTD evaluation period. Further objectives are to evaluate safety, tolerability, PK/PD and preliminary efficacy of BI 765049 ± ezablenlimab. The trial may assess up to 4 dosing regimens: A (BI 765049 once every 3 weeks [q3w]); B1 (BI 765049 qw); B2 (BI 765049 qw with step-in doses); C (BI 765049 + ezablenlimab [q3w]). Dose escalation will be guided by a Bayesian Logistic Regression Model with overdose control that will be fitted to binary toxicity outcomes using a hierarchical modelling approach to jointly model all dosing regimens. Treatment will be allowed to continue until confirmed progressive disease, unacceptable toxicity, other withdrawal criteria or for a maximum duration of 36 months, whichever occurs first. Approximately 150–175 patients will be screened and ~120 patients enrolled. As of July 2021, patients are being recruited in early dose-escalation cohorts.

Acknowledgements Medical writing support for the development of this abstract, under the direction of the authors, was provided by Becky O'Connor, of Ashfield MedComms, an Ashfield Health company, and funded by Boehringer Ingelheim.

Trial Registration NCT04752215

REFERENCES

1. Brandt et al. *J Exp Med* 2009;**206**:1495–503.
2. Boehringer Ingelheim. Data on file.
3. Hipp et al. AACR Annual Meeting 2021.

Ethics Approval The trial will be carried out in compliance with the protocol, the ethical principles laid down in the Declaration of Helsinki, in accordance with the ICH Harmonized Guideline for Good Clinical Practice (GCP) and the EU directive 2001/20/EC/EU regulation 536/2014.

<http://dx.doi.org/10.1136/jitc-2021-SITC2021.480>

481 **PHASE 1/2 STUDY OF THOR-707 (SAR444245), A PEGYLATED RECOMBINANT NON-ALPHA IL-2, AS MONOTHERAPY AND IN COMBINATION WITH PEMBROLIZUMAB OR CETUXIMAB IN PATIENTS (PTS) WITH ADVANCED SOLID TUMORS**

¹Gerald Falchook*, ²Hui Gan, ³Siqing Fu, ¹Meredith McKean, ⁴Arun Azad, ⁵David Sommerhalder, ⁶Judy Wang, ⁷Tira Tan, ⁸Chen Chee, ⁹Minal Barve, ¹⁰Charlotte Lemeque, ¹¹Nicole Acuff, ¹¹Helene Pham, ¹¹Jill Mooney, ¹²Rui Wang, ¹²Neysa Marina, ¹²Giovanni Abbadessa, ¹³Tarek Meniawy. ¹Sarah Cannon Research Institute, Denver, CO, USA; ²Olivia Newton-John Cancer Wellness, Melbourne, Australia; ³MD Anderson Cancer Center, Houston, TX, USA; ⁴Peter MacCallum Cancer Center, Melbourne, Victoria, Australia; ⁵NEXT Oncology, Texas Oncology, San Antonio, TX, USA; ⁶Florid Cancer Specialists and Research, Sarasota, FL, USA; ⁷National Cancer Center Singapore, Singapore, Singapore; ⁸National Cancer University Centre, Singapore, Singapore; ⁹Mary Crowley Cancer Research, Dallas, TX, USA; ¹⁰Scientia Clinical Research, Randwick, Australia; ¹¹Synthorx, A Sanofi Company, San Diego, CA, USA; ¹²Sanofi, Cambridge, MA, USA; ¹³Linear Clinical Research, Nedlands, WA, Australia

Background THOR-707 (SAR444245) is a recombinant human IL-2 molecule irreversibly bound to a PEG chain to block alpha-binding while retaining near-native affinity for beta/gamma IL-2 receptor subunits. We report updated results from the ongoing HAMMER phase 1/2 trial.

Methods SAR444245 was given via IV infusion as monotherapy Q2W [A] or Q3W [B], with pembrolizumab 200mg IV Q3W [C], or Q3W with cetuximab 400mg/m² IV on D1 then 250mg/m² IV QW [D] after pre-medication and peri-infusion hydration. A 3+3 design was used to identify the MTD/RP2D in pts with advanced solid tumors. Key objectives included assessments of safety, efficacy, pharmacokinetics (PK) and pharmacodynamics (PD).

Results 68 pts, median age 61.5 (37–78) yrs with median 3 (1–10) prior therapies enrolled. Most common tumors: melanoma (n=10), colorectal (n=11). Doses tested by cohort: [A]: 8–16 µg/kg (n=9); [B]: 8–40 µg/kg (n=29); [C]: 8–32 µg/kg (n=20); [D]: 16–24 µg/kg (n=10). The most common (>30%) AEs included pyrexia (52.5%), nausea (50.0%), flu-like symptoms (44.1%), vomiting (36.8%), chills (32.4%), fatigue (32.4%), AST elevation (30.9%). AEs generally resolved promptly with supportive care. Grade(G) 3/4 (>5%) related AEs included ALT/AST elevation (5.9%), and decreased lymphocyte count (26.5% within first 24 hrs, recovering by 48–72 hrs, this lymphocyte migration is mechanistically consistent with immune cell migration). G3/4 CRS was observed in 2 pts. Two DLTs occurred: G3 infusion reaction (32 µg/kg [B]) and G3 AST/ALT/G2 bilirubin elevation with G2 CRS (24 µg/kg [C]). No vascular leak syndrome, QTc prolongation, cardiac, or end organ toxicity was observed. Half-life was ~10 h. Sustained increases in CD8 T and NK cells were observed (fold relative to baseline): monotherapy (1–9.4x and 2–43.3x); with pembrolizumab (0.5–5.78x and 1.5–26.9x); with cetuximab (1.3–7.57x and 3.6–45.4x). Max CD4 and eosinophils increased to 136 cell/µL and 1078 cell/µL. No IL-5 elevation or ADAs were observed. Transient IL-6 increases in 4 pts (500, 627, 1000, 1100 pg/mL) were not associated with AEs. Four pts had confirmed PRs (1 PD1-treated SCC, unknown primary [B]; 2 PD1-naïve BCC and 1 PD1-treated HNSCC [C]); 3 pts had minor responses – prostate (-24%) and PD1-treated melanoma (-17%) [B]; PD1-treated NSCLC (-29%) [C] – after ≥2 scans. 23 pts completed ≥5 cycles.

Conclusions SAR444245 was well tolerated and demonstrated antitumor activity in heavily pretreated patients, including prior checkpoint inhibitor therapy. Clinical safety, efficacy and PD suggest a wide therapeutic window. Combination with

pembrolizumab and cetuximab leveraged SAR444245's effects on CD8 T and NK cells.

Trial Registration NCT04009681

Ethics Approval The clinical trial was approved by each institutions ethics' and review board prior to beginning study enrollment.

<http://dx.doi.org/10.1136/jitc-2021-SITC2021.481>

PHASE 1/2 STUDY OF AN ANTI-GALECTIN-9 ANTIBODY, LYT-200, IN PATIENTS WITH METASTATIC SOLID TUMORS

¹Aleksandra Filipovic, ²Zev Wainber*, ³Judy Wang, ⁴Johanna Bendell, ⁵Filip Janku, ⁶Manish Sharma, ⁷Amit Mahipal, ¹Joseph Bolen, ¹Eric Elenko, ¹Christopher Korth, ⁸George Dranitsaris. ¹Puretech Health, Boston, MA, USA; ²UCLA School of Medicine, Los Angeles, CA, USA; ³Florida Cancer Specialists/SCRI, Sarasota, FL, USA; ⁴Sarah Cannon Research Institute, Nashville, TN, USA; ⁵MD Anderson Cancer Center, Houston, TX, USA; ⁶START Midwest, Grand Rapids, MI, USA; ⁷Mayo Clinic, Rochester, MN, USA; ⁸Falk College, Syracuse University, Syracuse, NY, USA

Background Galectin-9 (gal-9) acts as a pivotal immuno-suppressor that disables immune mediated activity through modulation of T cells, macrophages and other immune functions. As such it has emerged as a powerful biological target for cancer immunotherapy and a potential biomarker of response and/or prognosis. Patients exhibiting high gal-9 expression in tumors and blood often have poor prognosis and tumors with aggressive and immunosuppressed molecular features (Chen L. et al, AACR 2020-LB-350). LYT-200 is a fully human IgG4 monoclonal antibody targeting gal-9. LYT-200 has high affinity, high specificity, stability, and blocks galectin-9 interactions with its binding partners in biochemical and human cell-based assays. In murine models of melanoma and pancreatic cancer, LYT-200 significantly reduced tumor growth, extended survival and modulated the intra-tumoral immune microenvironment. LYT-200 treated patient derived tumor organoids showed an increase in T cell activation (Chen L. et al, SITC 2019-P765).

Methods LYT-200 is now being evaluated in the USA, in the first part of an adaptive Phase 1/2 trial (NCT04666688) in relapsed/refractory solid tumors. Patients with solid tumor malignancy that is metastatic or unresectable and refractory to prior therapy are included. Patients are treated with LYT-200 by IV infusion, every 2 weeks (Q2W), until disease progression or toxicity. Phase 1 of the study uses the continuous reassessment design (CRM), and entails recruiting two patients per dosing level. Starting dose level was 0.2mg/kg Q2W. Additionally, the protocol stipulates six patients must be treated at the dose level intended to be declared recommended phase 2 dose (RP2D), for more robust assessment of safety/tolerability. RP2D may be the maximum tolerated dose or the optimal biological dose. The primary objective of the ongoing Phase 1 is to assess the safety and tolerability of LYT-200 and to identify the RP2D. The Phase 1 is also assessing LYT-200's pharmacokinetics, immunogenicity and pharmacodynamics (measuring circulating gal-9 and cytokine levels, immunophenotyping peripheral blood mononuclear cells and tumor tissue). Preliminary efficacy is captured as an exploratory endpoint in Phase 1. Phase 2 expansion cohorts would implement the Simon's two-stage design to further assess LYT-200 as a single agent and/or in combination with chemotherapy and tislelizumab. Phase 2 is currently planned in pancreatic cancer and other/different tumor types for Phase 2 may be guided by results of the Phase 1.

Acknowledgements All clinical trial sites participating in the LYT-200 study. Shohei Koide, Linxiao Chen and George Miller and their teams at New York University Langone Health & New York University School of Medicine, NY for all the preclinical work on LYT-200.

Trial Registration NCT04666688

<http://dx.doi.org/10.1136/jitc-2021-SITC2021.482>

483

INITIAL SAFETY RESULTS AND IMMUNE RESPONSES INDUCED BY A NOVEL HUMAN PAPILLOMAVIRUS (HPV)-SPECIFIC GORILLA ADENOVIRUS IMMUNOTHERAPY VACCINE, PRGN-2009, IN PATIENTS WITH ADVANCED HPV-ASSOCIATED CANCERS

¹Charalampos Floudas*, ¹Julius Strauss, ²Clint Allen, ¹Renee Donahue, ¹Caroline Jochems, ¹Seth Steinberg, ¹Lisa Cordes, ³Douglas Brough, ³Amy Lankford, ¹Sheri McMahon, ¹Jenn Marte, ¹Jason Redman, ¹Fatima Karzai, ¹Ravi Madan, ¹Jeffrey Schlom, ¹James Gully. ¹NCI, NIH, Bethesda, MD, USA; ²NIDCD, NIH, Bethesda, USA; ³Precigen, Inc., Germantown, MD, USA

Background PRGN-2009 is a novel gorilla adenovirus vaccine containing 35 non-HLA-restricted epitopes of HPV 16 and 18 which is being tested in an open-label, NCI-sponsored, single-center Phase I/II study alone and combined with the bifunctional TGF- β "trap"/anti-PD-L1 fusion protein bintrafusp alfa (BA) (NCT04432597).

Methods For the Phase I of the trial, eligible patients are adults with previously treated (checkpoint blockade allowed) recurrent/metastatic HPV-associated cancers. Objectives are to assess the safety and determine the recommended phase 2 dose (RP2D) of PRGN-2009 alone and combined with BA. Treatment followed a single-agent 3+3 dose escalation at two dose levels of PRGN-2009 (dose level 1: 1x10¹¹ viral particle units (VPU), dose level 2: 5x10¹¹ VPU) subcutaneously Q2W for 3 times, then Q4W for up to one year in total. After determination of RP2D, a combination cohort of 10 patients treated with PRGN-2009 at the RP2D combined with BA (1200 mg IV Q2W for 52 weeks) opened. Peripheral blood mononuclear cells collected from patients before and after vaccination with PRGN-2009 were stimulated with overlapping peptide pools and assessed by intracellular cytokine staining to identify HPV-16 and HPV-18 specific T-cells, as well as T-cells targeting cascade antigens not encoded by the vaccine.

Results Six patients were enrolled in the single-agent PRGN-2009 dose-escalation phase (3 with cervical cancer, 2 with anal cancer, 1 with vaginal cancer). Observed adverse events were Grade 1-2 flu-like syndrome (headache, body aches), injection site reactions (erythema, pruritus, soreness, localized edema), fatigue, and rash. There were no dose limiting toxicities, and 5x10¹¹ VPU was selected as RP2D. Four patients had stable disease as best response, (one ongoing, 10 months on treatment). T-cells targeting HPV-16 and/or HPV-18 were increased after vaccination in 100% of patients, with 3/6 (50%) developing HPV-16 T cells and 5/6 (83%) developing HPV-18 T cells. In some patients, the magnitude and breadth of HPV-16 and HPV-18 specific T cells were notably increased after repeated vaccination. T cells that target the cascade antigens brachyury and MUC1 were also increased in all patients evaluated. Multifunctional T-cell responses against all these antigens were also developed after vaccination in the majority of patients. No differences in immunogenicity were noted between the two dose levels. Enrollment is underway in combination with BA. Updated data will be presented.

Conclusions The Phase 1 results demonstrate the safety of single-agent PRGN-2009 and induction of anti-HPV T-cell immune responses, supporting the hypothesis that PRGN-2009 could potentially induce anti-tumor effects in HPV-associated cancers.

Acknowledgements This research was supported in part by the Intramural Research Program of the NIH, NCI.

Trial Registration NCT04432597

Ethics Approval Approved by the NIH IRB (Ref No 543876). All participants have given informed consent before taking part in the study.

<http://dx.doi.org/10.1136/jitc-2021-SITC2021.483>

484

PRELIMINARY EFFICACY OF THE IL-15 SUPERAGONIST SO-C101 IN COMBINATION WITH PEMBROLIZUMAB IN PATIENTS WITH ADVANCED/METASTATIC SOLID TUMORS

¹Elena Garralda*, ¹Vladimir Galvao, ²Stephane Champiat, ³Patricia LoRusso, ⁴Peter Grell, ⁵Aung Naing, ⁵Filip Janku, ⁶Richard Sachse, ⁷David Bechard, ⁶Joachim Kiemle-Kallee, ²Aurelien Marabelle, ¹Elena Garralda. ¹Hospital Universitari Vall d'Hebron, Vall d'Hebron Institute of Oncology (VHIO), Barcelona, Spain, Barcelona, Spain; ²Institute de Cancerologie, Gustave Roussy, Villejuif, France, Villejuif, France; ³Yale University School of Medicine, New Haven, New Haven, USA; ⁴Masaryk Memorial Cancer Institute (MMCI), Brno, CZE, Brno, Czech Republic; ⁵Department of Investigational Cancer Therapeutics, MD Anderson Cancer Center, Houston, TX, Houston, TX, USA; ⁶SOTIO Biotech AG, Basel, Switzerland, Basel, Switzerland; ⁷Cytune Pharma, Nantes, France, Nantes, France

Background SO-C101 (IL 15/IL-15R α sushi + domain fusion protein) was investigated in a multicenter, open-label, dose escalation study as monotherapy and in combination with pembrolizumab in patients with selected advanced/metastatic tumors (NCT04234113). Synergistic effects of SO-C101 and an anti-programmed cell death protein 1 (PD-1) antibody have been validated in various tumor mouse models inducing a protective memory response.

Methods The combination part of the study follows a classical 3+3 dose escalation design. Study objectives are to determine the maximum tolerated dose (MTD) and the recommended phase 2 dose (RP2D). The evaluation period for dose-limiting toxicities in each dose step is 21 days. The RP2D is defined as MTD or a dose below, taking into consideration pharmacokinetic and pharmacodynamic parameters. The study is ongoing (data cut-off 21 June 2021).

Results A total of 12 patients with a median of 2 (range 1–6) lines of previous systemic therapies were treated at SO-C101 dose levels 1.5 μ g/kg (3 patients), 3.0 μ g/kg (3 patients), and 6.0 μ g/kg (6 patients) together with 200 mg of pembrolizumab. One dose-limiting toxicity of grade (G) 3 cytokine release syndrome (CRS) was observed in one patient at 6.0 μ g/kg. The MTD has not yet been reached. Of the treated patients, 2 had long-term stable disease (anal squamous cell carcinoma patient at 1.5 μ g/kg, duration 25 weeks; gastric carcinoma patient at 3.0 μ g/kg, duration 14 weeks) and 3 achieved a partial response (thyroid gland cancer patient at 3.0 μ g/kg, target lesion decrease by 36%; skin squamous cell carcinoma patient at 6.0 μ g/kg, target lesion decrease by 40%; and melanoma patient at 6.0 μ g/kg, target lesion decrease by 58%). The patients with skin squamous cell carcinoma and melanoma had previously progressed on anti-PD-1 therapy, while the patient with thyroid cancer was anti-PD-1 naïve. The most common study drug-related adverse events were lymphopenia, local injection site reactions, transaminase increase, fever, chills as well as CRS-related symptoms (all mainly G1 or G2 and resolved). The only study drug-related adverse event >G2 that occurred in more than one patient was lymphopenia. No treatment-related death was reported.

Conclusions Although the MTD of SO-C101 in combination with pembrolizumab has not been reached yet, clinical efficacy signals were already observed in 5 patients. Available safety data indicate good tolerability. SO-C101 in combination with pembrolizumab has already shown the potential to provide an additional clinical benefit to patients with solid tumors.

Trial Registration NCT04234113

Ethics Approval This study was approved by the FDA (IND 140011) and by the Ethics Boards of participating institutions

<http://dx.doi.org/10.1136/jitc-2021-SITC2021.484>

LONG TERM RESULTS FROM A PHASE 1 TRIAL OF GEN-009, A PERSONALIZED NEOANTIGEN VACCINE, COMBINED WITH PD-1 INHIBITION IN ADVANCED SOLID TUMORS

¹Maura Gillison*, ²Mark Awad, ³Przemyslaw Twardowski, ⁴Ammar Sukari, ⁵Melissa Johnson, ⁶Rudy Lackner, ⁷Mark Stein, ⁸Arthur DeCillis, ⁹Richard Hernandez, ⁸Jessica Price, ⁸Kevin Mancini, ⁸Mara Shainheit, ⁸Gabriella Santone, ⁸Syukri Shukor, ⁸Ece Bicak, ⁸Vijetha Vemulapalli, ⁸Emily Tjon, ⁸Jessica Flechtner, ⁸Thomas Davis, ⁹Roger Cohen. ¹MD Anderson Cancer Center, Houston, TX, USA; ²Dana-Farber Cancer Institute, Boston, MA, USA; ³John Wayne Cancer Institute, Duarte, CA, USA; ⁴Karmanos Cancer Institute, Detroit, MI, USA; ⁵Sarah Cannon Research Institute, Nashville, TN, USA; ⁶University of Nebraska Medical Center, Omaha, NE, USA; ⁷Columbia University Medical Center, New York City, NY, USA; ⁸Genoea, Madison, CT, USA; ⁹University of Pennsylvania, Philadelphia, PA, USA

Background GEN-009 adjuvanted personalized cancer vaccine contains up to 20 neoantigens selected by ATLAS™, an ex vivo bioassay screening autologous T-cells for immune responses against both neoantigens and Inhibigens™. Inhibigen-specific T-cells suppress immunity, have been shown to accelerate tumor progression in mice, and are excluded from GEN-009. In cohort A, all patients immunized in the adjuvant setting with GEN-009 monotherapy developed immune responses. Ninety-nine percent of selected peptides were immunogenic: ex vivo CD4+ and CD8+ fluorospot responses specific for 51% and 41% of immunized peptides, respectively.¹ Six of 8 patients continue without progression with a median follow up >2 years.

Methods GEN-009 was administered to patients with advanced cancer who received standard-of-care (SOC) PD-1 inhibitor as monotherapy or in combination therapy during vaccine manufacturing. Five vaccine doses were administered over 24 weeks in combination with single agent anti-PD-1. Patients who progressed prior to vaccination received salvage therapy followed by GEN-009 in combination. Peripheral T-cell responses were measured by ex vivo and in vitro stimulated fluorospot assays. Circulating tumor (ct) DNA levels were evaluated in a subset of patients pre- and post-GEN-009 administration.

Results 15 patients received GEN-009 in combination with PD-1 inhibitor; 1 patient received GEN-009 monotherapy. Median number of neoantigens per vaccine was 14 (range 5–18). GEN-009-related adverse events were limited to vaccine injection site reactions, mild myalgias or fatigue. Sequential vaccination with GEN-009 had an additive effect on the magnitude of ex vivo T-cell responses, that persisted in some patients for 12+ months post first vaccine dose. An association between proportion of peptides eliciting significant cytokine responses and RECIST response is apparent. Epitope spread was detected in CD8+ T-cells from CPI-sensitive patients, but not refractory patients. Four patients who responded to PD-1 inhibition followed by disease stabilization then demonstrated further tumor reduction after GEN-009 vaccination. Seven of 9 CPI responsive patients are progression-free 7 to 18 months after first vaccine dose. Three of 7 CPI-refractory patients have experienced unexpected prolonged stable disease, with 2 PR and 1 SD after vaccination lasting up to 10 months. Plasma ctDNA kinetics mirrored RECIST responses in each tested patient; in some responders, all evidence of ctDNA disappeared, including non-targeted antigens.

Conclusions Vaccination with GEN-009 alone or in combination with anti-PD-1 was well tolerated. Preliminary data demonstrate induction of robust, durable neoantigen-specific immune responses and epitope spreading in the presence of

PD-1 CPI. Broad immunity against tumor specific targets and encouraging patient outcomes support further study. Trial Registration ClinicalTrials.gov identifier: NCT03633110

REFERENCES

1. Lam H, et al. An empirical antigen selection method identifies neoantigens that either elicit broad anti-tumor response or drive tumor growth. *Cancer Discovery* 2021 March;11(3):696–713.

Ethics Approval This study was approved by Western Institutional Review Board, approval number 1-1078861-1

<http://dx.doi.org/10.1136/jitc-2021-SITC2021.485>

487

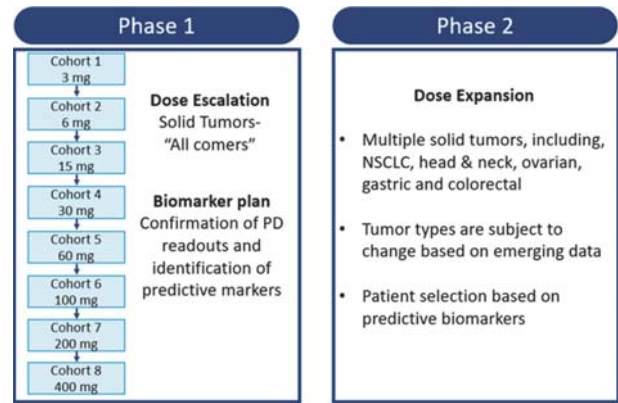
NC410, A FUSION PROTEIN OF LAIR-2 (LEUKOCYTE ASSOCIATED IMMUNOGLOBULIN-LIKE RECEPTOR) WITH HUMAN IGG1 FC, IS SAFE & TOLERABLE WITH EVIDENCE OF IMMUNE MODULATION IN SUBJECTS WITH ADVANCED SOLID TUMORS

¹Han Myint*, ¹Linjie Tian, ¹Jahangheer Shaik, ¹Emilia Barbu, ¹Qinjie Zhou, ¹Aaron Morawski, ¹Hasan Abukharma, ¹Linda Liu, ²John Shin, ¹Dallas Flies, ¹Ron Copeland, ¹Megan Nelson, ¹Stephanie Zeidan, ²Marijo Bilusic, ²Danielle Pastor, ²Ravi Madan, ³Siqing Fu, ⁴Martin Gutierrez, ¹Solomon Langermann. ¹NextCure LLC, Beltsville, MD, USA; ²National Cancer Institute, Bethesda, MD, USA; ³MD Anderson Cancer Center, Houston, TX, USA; ⁴Hackensack Cancer Center, Hackensack, NJ, USA

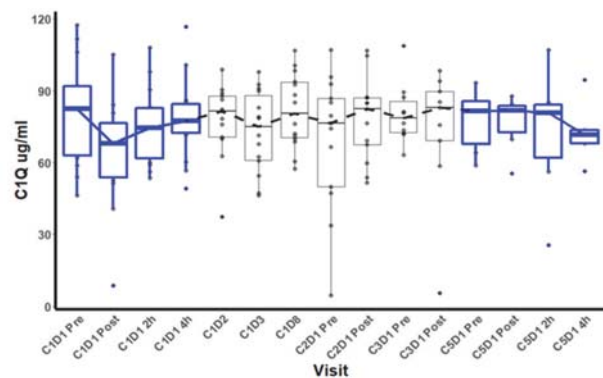
Background Collagen and C1q in the extracellular matrix (ECM), are the predominant ligands for LAIR-1, an inhibitory receptor expressed on the cell surface of several immune cell subsets that inhibits immune activation and migration. LAIR-2, a soluble homolog of LAIR-1, competes for binding to collagen and C1q and serves as a natural decoy to promote immune function under normal conditions. Dysregulation of the ECM and increased expression of collagen and C1q within the tumor microenvironment (TME) plays a critical role in promoting tumor progression. NC410 was engineered to overcome this highly immunosuppressive environment by blocking LAIR-1 function, reversing immune suppression, and inducing ECM remodeling to promote immune cell infiltration within the TME.

Methods This is a first in human, phase 1/2, open-label, single-armed dose-escalation study to determine the safety, tolerability, dose-limiting toxicity (DLT), maximum tolerated dose (MTD), recommended phase 2 dose, preliminary efficacy and to explore pharmacodynamic biomarkers of NC410 (figure 1). Key eligibility criteria include subjects with advanced or metastatic solid tumors with measurable disease based on RECIST v1.1.

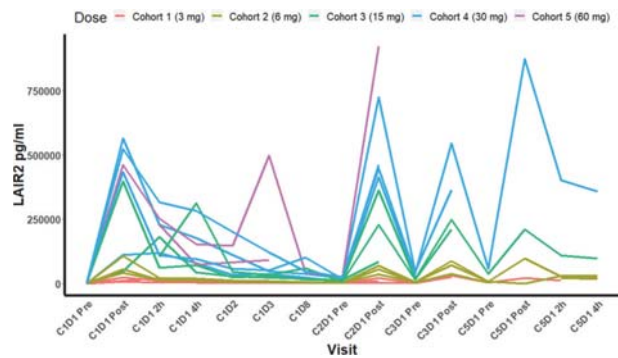
Results As of 07/22/2021, a total of 16 patients have been enrolled, treated, and completed the DLT period. NC410 (up to 60 mg), was well tolerated, with no safety concerns, infusion-related toxicities, or DLT reported. No anti-drug antibody (ADA) was detected post-NC410 up to 60 mg treatment. As expected, the C1Q level decreased immediately after the NC410 infusion and was replenished after two hours. Evaluation from samples to date available up to cycle 5 suggests that there was no reduction in the baseline C1Q level with subsequent dosing (figure 2). LAIR-2 levels continued to increase in a dose-dependent fashion post-NC410 dosing and marginal increase pre-dose (figure 3). Interestingly, we observed an increase in soluble LAIR-1 over time in a similar pattern to LAIR-2 (figure 4). Furthermore, immunophenotyping of patient whole blood suggests a trend towards an increase in CD4+ and CD8+ T cells including LAIR-1+ T cells in cohort 4, although overall expression levels of LAIR-1 did not appear to increase (ongoing analysis). Cytokines, chemokines, and collagen degradation products (CDP) will be evaluated as potential pharmacodynamic biomarkers as we continue through higher dose cohorts.



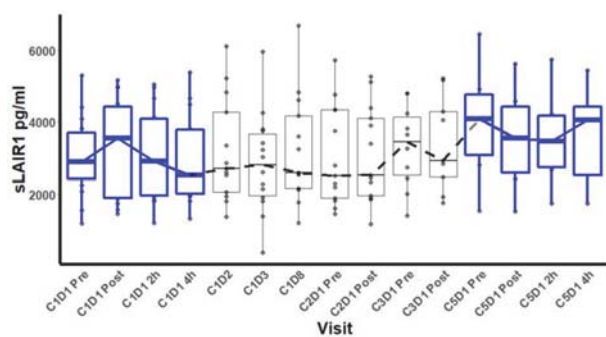
Abstract 487 Figure 1 NC410: study schema



Abstract 487 Figure 2 C1Q levels show immediate reduction after NC410 dosing with no accumulated depletion



Abstract 487 Figure 3 LAIR-2 levels show an increase in dose-dependent fashion after NC410 dosing with marginal increase pre-dose



Abstract 487 Figure 4 Soluble LAIR-1 levels show a similar pattern to LAIR-2 levels

Conclusions Preliminary evaluation of NC410 in subjects with advanced or metastatic solid tumors appears to be safe and well-tolerated with evidence of immune modulation consistent with predictive PK/PD modeling in a Phase 1/2 open-label study. Further evaluation will be done with increasing doses to confirm these initial findings.

Trial Registration NCT04408599

Ethics Approval This study has been approved by the IRB of all the participating institutions, and all participants have given informed consent before taking part in the study.

Consent Written informed consent was obtained from the patient for publication of this abstract and any accompanying images. A copy of the written consent is available for review by the Editor of this journal.

<http://dx.doi.org/10.1136/jitc-2021-SITC2021.487>

PHASE 1 TRIAL OF FIRST-IN-CLASS ANTI-CD96 MONOCLONAL ANTIBODY INHIBITOR, GSK6097608, MONOTHERAPY AND COMBINATION WITH ANTI-PD-1 MONOCLONAL ANTIBODY, DOSTARLIMAB, IN ADVANCED SOLID TUMORS

¹Omid Hamid*, ²Dawn Baxter, ²Rachael Easton, ³Lilian Siu. ¹The Angeles Clinic and Research Institute, Los Angeles, CA, USA; ²GlaxoSmithKline, Philadelphia, PA, USA; ³Princess Margaret Cancer Centre, Toronto, Canada

Background The CD226 axis plays an important role in natural killer (NK)- and T-cell biology and cancer immune surveillance.¹⁻⁴ CD226 is an immune costimulatory molecule expressed on T and NK cells, which binds to its ligands, CD155 and CD112, on tumors and antigen-presenting cells to stimulate an immune response. The immune checkpoints TIGIT, CD96, and PVRIG compete with CD226 binding to CD155 and CD112 to suppress immune activation. Combinations of agents that target these checkpoints and PD(L)1 could augment CD226-mediated antitumor activity. Inhibition or deletion of CD96 resulted in antitumor activity in syngeneic mouse tumor models alone and in combination with PD-1 inhibition.⁵⁻⁶ GSK6097608 is a monoclonal antibody that blocks CD96, enhancing CD155-CD226 NK/T-cell activation.⁷ Based on these results, GSK6097608 is being explored alone and in combination with the anti-PD-1 monoclonal antibody, dostarlimab, in a phase 1, dose-escalation trial.⁸

Methods Adults (≥18 years of age) with histological or cytological documentation of locally advanced, recurrent, or metastatic solid malignancy that has progressed after standard therapy for the specific tumor type are eligible. Prior anti-PD-1 therapy is allowed. Other key inclusion criteria include Eastern Cooperative Oncology Group performance status 0-1, adequate organ function, and life expectancy of ≥12 weeks. Patients with prior bone marrow or solid organ transplant, uncontrolled central nervous system metastases, or active autoimmune disease are ineligible. In this open label, nonrandomized, sequential assignment trial (N≈100; NCT04446351), patients will receive intravenous infusion GSK6097608 every 3 weeks as monotherapy alone or in combination with intravenous dostarlimab (every 3 weeks for 4 doses and every 6 weeks thereafter). Based on the safety, pharmacokinetics, and pharmacodynamics of monotherapy, the combination arm will be opened. The primary endpoints are dose-limiting toxicities and adverse events. Secondary endpoints include abnormal laboratory values, cardiac parameters, and vital signs; dose reduction, dose delay, or withdrawal due to adverse events; overall response rate per Response Evaluation Criteria in Solid Tumors version 1.1; and antidrug antibodies against and pharmacokinetic parameters of GSK6097608 and dostarlimab. The trial is actively recruiting patients.

Acknowledgements The authors thank the participating patients, families, investigators, site staff, and colleagues at GlaxoSmithKline (GSK) and 23andMe. Funding for the study was provided by GSK (study 212214). Writing and editorial support, funded by GSK (Waltham, MA, USA) and coordinated by Hasan H. Jamal, of GSK, was provided by MediTech Media.

Trial Registration www.ClinicalTrials.gov, NCT04446351

REFERENCES

- Georgiev H, Ravens I, Papadogianni G, Bernhardt G. Coming of age: CD96 emerges as modulator of immune responses. *Front Immunol* 2018;**9**:1072.
- Torphy RJ, Schulick RD, Zhu Y. Newly emerging immune checkpoints: promises for future cancer therapy. *Int J Mol Sci* 2017;**18**:2642.

- Sanchez-Correa B, Valhondo I, Hassouneh F, et al. DNAM-1 and the TIGIT/PVRIG/TACTILE axis: novel immune checkpoints for natural killer cell-based cancer immunotherapy. *Cancers (Basel)* 2019;**11**:877.
- Qin S, Xu L, Yi M, et al. Novel immune checkpoint targets: moving beyond PD-1 and CTLA-4. *Mol Cancer* 2019;**18**:155.
- Blake SJ, Stannard K, Liu J, et al. Suppression of metastases using a new lymphocyte checkpoint target for cancer immunotherapy. *Cancer Discov* 2016;**6**:446-459.
- Harjunpää H, Blake SJ, Ahern E, et al. Deficiency of host CD96 and PD-1 or TIGIT enhances tumor immunity without significantly compromising immune homeostasis. *Oncoimmunology* 2018;**7**:e1445949.
- Sun H. Update on the next generation of immune-oncology treatments: discovery of an anti-CD96 mAb as a novel check point inhibitor in solid tumors. Oral presentation at: 17th Annual PEGS Boston Virtual Conference & Expo; May 11-13, 2021.
- Study of the safety and effectiveness of GSK6097608 in participants with advanced solid tumors. National Institutes of Health. ClinicalTrials.gov. Accessed May 20, 2021. <https://clinicaltrials.gov/ct2/show/NCT04446351>

Ethics Approval The study was reviewed and approved by the institutional review board and independent ethics committee before the study sites were initiated.

<http://dx.doi.org/10.1136/jitc-2021-SITC2021.488>

TWT-101: A PHASE 1 STUDY OF THE NOVEL HPK1 INHIBITOR CFI-402411 IN PATIENTS WITH ADVANCED CANCER

¹Omid Hamid*, ²Johanna Bendell, ³Siqing Fu, ⁴Kyriakos Papadopoulos, ⁵Judy Wang, ⁶Brigitte Ma, ⁷Anna Spreafico, ⁸Alexander Spira, ⁹Mark Bray, ⁹Graham Fletcher, ⁹Glenn Michelson, ⁹Emily Roberts-Thomson. ¹The Angeles Clinic and Research Inst., Los Angeles, CA, USA; ²Hoffmann La Roche, Basel, Switzerland; ³MD Anderson, Houston, TX, USA; ⁴START San Antonio, San Antonio, TX, USA; ⁵Florida Cancer Specialists/SCRI, Sarasota, FL, USA; ⁶The Chinese University of Hong Kong, Sha Tin, Hong Kong; ⁷Princess Margaret Cancer Centre, Toronto, Canada; ⁸Virginia Cancer Specialists, Fairfax, VA, USA; ⁹Treadwell Therapeutics, Toronto, Canada

Background CFI-402411 is an orally available small molecule potent inhibitor of HPK1 (Hematopoietic progenitor kinase 1). T-cells are negatively-regulated at different junctures of cancer-immunity cycle by this regulatory kinase. HPK1, (also mitogen activated protein kinase kinase kinase 1 (MAP4K1)) is a protein serine/threonine kinase predominantly expressed in hematopoietic cells. In T-cells, following T-cell receptor activation, HPK1 is recruited to the plasma membrane where it phosphorylates the adapter protein SH2 domain-containing leukocyte protein of 76 kDa (SLP-76), down-regulating signaling events required for T cell activation and proliferation. Selected for development based on its pharmacologic properties and preclinical activity in a variety of syngeneic cancer models and assays, with an IC₅₀ = 4.0±1.3 nM, CFI-402411 is expected to relieve HPK1-mediated inhibition of T and B cells, facilitating an anti-tumor immune response.

Methods Phase 1, 3 + 3 design in patients. Patients have acceptable laboratory, other parameters for study entry. Single agent dose daily oral escalation cohort (A1) in advanced tumors, then dose expansion (A3) with biomarker backfill (A2) in select advanced tumors; combination with PD-1 Inhibitor (pembrolizumab) (B1, pembrolizumab eligible tumors with no prior grade ≥3 related to CPI) and expansion (B2, PD-1/PD-L1 naïve pembrolizumab eligible tumors). DLT defined as any grade ≥3 toxicity in first cycle of therapy (21d cycles). Standard assessments for response per RECIST v1.1 or iRECIST. The starting dose level was 80mg.

Results At 10 June 2021 data is available for 12 patients from A1. Median age 61.5 years (range 33–73), 8 patients female, and 10 white. Diagnoses were pancreatic cancer, colorectal (3 pts), ovarian, basal cell, cholangiocarcinoma, sigmoid, salivary and breast cancer (1 pt). Six patients (50%) had 4 prior therapies, 1 patient (basal cell) had prior treatment with immune checkpoint inhibitor, pembrolizumab. Four doses studied: 80, 120, 180 and 270mg. TEAEs across all CTCAE grades, (in >2 patients) were diarrhea (6 patients), nausea (4 patients), dyspepsia (3 patients), fatigue (3 patients). No related grade 3–5 events, one immune related event (grade 1, weight loss). 3 grade 3 events all unrelated to study drug - pleural effusion, rash, thromboembolic event. Discontinuation due to disease progression was main reason (7 patients). PK and PD assessments will be updated at time of presentation.

Conclusions CFI-402411 is a potent inhibitor of HPK1 that is well tolerated with a manageable adverse event profile and dose escalations continue. Further safety and efficacy results will be presented at the meeting including additional cohorts if available.

Acknowledgements Treadwell Therapeutics thanks all sites, importantly their patients and their families.

Trial Registration ClinicalTrials.gov Identifier: NCT04521413

Ethics Approval This study obtained has obtained ethics approvals at multiple institutions globally including;USAWCG IRB - Western Institutional Review Board - MOD00002618 (Submission ID)IntegReview Institutional Review Board - N/AAdvarra Central IRB - SSU00130103IntegReview Institutional Review Board N/AAdvarra Central IRB - SSU00137751Advarra Central IRB - SSU00143275The University of Texas MD Anderson Cancer Center Institutional Review Board - 2020-0678 (IRB ID Number)Hong KongJoint Chinese University of Hong Kong - New Territories East Cluster Clinical Research Ethics Committee - 2020.367 (Ref Number)CanadaOntario Cancer Research Ethics Board - 3320 (Project ID)Health Research Ethics Board of Alberta, HREBA Cancer Committee - HREBA.CC-20-0504 (Ethics ID Number)South KoreaimCORE - Seoul National University Hospital Institutional Review Board - H-2012-094-1182 (IRB Number)National Cancer Institute Review Board - 2020-0525-0001 (Receipt Number) All participants gave informed consent before taking part in this clinical trial.

<http://dx.doi.org/10.1136/jitc-2021-SITC2021.489>

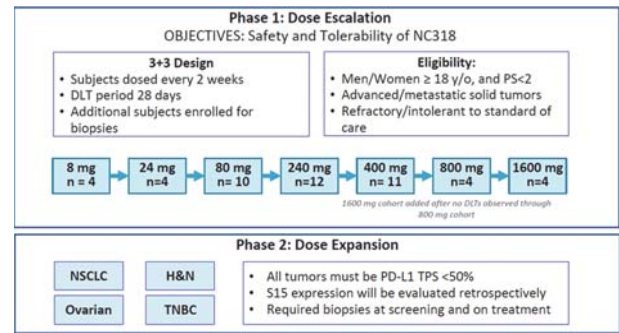
490

CLINICAL BENEFIT THROUGH SIGLEC-15 TARGETING WITH NC318 ANTIBODY IN SUBJECTS WITH SIGLEC-15 POSITIVE ADVANCED SOLID TUMORS

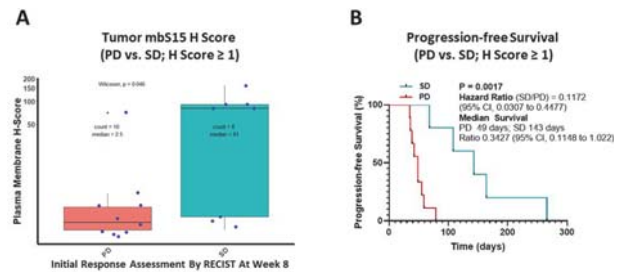
¹Elaine Shum*, ²Han Myint, ²Jahangheer Shaik, ²Qinjie Zhou, ²Emilia Barbu, ²Aaron Morawski, ²Hasan Abukharma, ²Linda Liu, ²Megan Nelson, ²Stephanie Zeidan, ²Zachary Cusumano, ³Anthony Tolcher, ²Solomon Langermann, ⁴Martin Gutierrez, ⁵Omid Hamid. ¹NYU Langone Health, New York, NY, USA; ²NextCure LLC, Beltsville, MD, USA; ³NEXT Oncology, San Antonio, TX, USA; ⁴Hackensack Cancer Center, Hackensack, NJ, USA; ⁵Angeles Clinic, Los Angeles, CA, USA

Background Siglec-15 (S15) is a member of the Siglec family of immunoglobulin superfamily proteins involved in immune regulation. NC318 is a first-in-class humanized IgG1κ monoclonal antibody that blocks S15-mediated immune suppression. **Methods** The Phase 1 dose-escalation study was a classical 3 +3 design in 15 tumor types (n=49). Phase 2 (n=47) was conducted at 400 mg q2w in 4 tumor types. Inclusion criteria included subjects with advanced/metastatic solid tumors refractory or resistant to currently available therapies with a TPS PD-L1 score <50%. The median number of previous therapies was ≥3, including checkpoint inhibitors (figure 1).

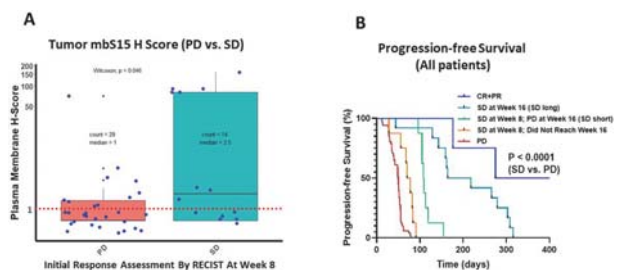
Results NC318 was well tolerated with no novel immunologic or safety signals observed. Disease control rate amongst evaluable population (n=83) is 38% {1 CR, 3 PR and 28 SD (stable disease)}. Median duration of disease control is 24 weeks (16–48 weeks) amongst 20 subjects achieving a minimal 16-week duration of stable disease. Two NSCLC subjects (1CR and 1PR) are still on therapy over 2 years. We observed an increase in a soluble form of Siglec-15 (sS15) in all patients receiving NC318 treatment that was dose-dependent. sS15 serves as a pharmacodynamic marker for NC318 activity. PK/PD modeling of NC318 from this Phase1/2 study using sS15 as a PD marker suggested increasing the dose of NC318 to 800 mg q1w to enhance overall exposure of NC318. Development of an S15 specific IHC assay allowed us to do post-hoc analysis by immuno-histochemistry (IHC) from screening biopsies amongst subjects who showed disease control (CR, PR and SD) compared to subjects with progressive disease. S15 expression on tumor cell membrane was a predictor for stable disease, longer duration on therapy when compared to progressive disease {H score ≥ 1 (p=0.046), including NSCLC subjects}, as well as for progression-free survival (PFS) (figures 2 and 3). There was no correlation with the outcome whether PD-L1 was positive or negative. Together, development of a predictive indicator of S15 staining coupled with the NC318 PK/PD data, resulted in a protocol amendment to prospectively enroll subjects with Siglec-15+ adenocarcinoma lung, squamous H&N, and breast cancers at 800 mg q1w. Soluble S15, immunophenotyping, cytokine and chemokine levels and neutrophil-lymphocyte ratio will be presented at the meeting.



Abstract 490 Figure 1 NC318: study schema



Abstract 490 Figure 2 Tumor membrane S15 H score ≥ 1 and progression-free survival. **A)** All Individuals with available H-Scores ≥ 1 were stratified into two groups (Progressive disease (PD) and Stable disease (SD)) based on the RECIST criteria and their plasma membrane H-scores were compared using Wilcoxon test. Significant differences among H-scores were observed between the groups with a p-value of 0.046; **B)** Survival analysis was performed by stratifying individuals with H-Scores ≥ 1 into two groups (PD or SD). Statistical analysis was performed by Log-rank (Mantel-Cox) and Hazard Ratio (Mantel-Haenszel) test.



Abstract 490 Figure 3 Tumor membrane S15 H score and PFS (SD vs. PD). **A)** All Individuals with available H-Scores were stratified into two groups (Progressive disease (PD) and Stable disease (SD)) based on the RECIST criteria and their plasma membrane H-scores were compared using Wilcoxon test. Significant differences among H-scores were observed between the groups with a p-value of 0.046. All individuals with H-score ≥ 1 are above the dashed red horizontal line; **B)** Survival analysis was performed by stratifying as CR or PR, SD at week 16, SD at week 8 and PD at week 16, SD at week 8 and did not reach week 16, and PD by RECIST criteria. P value is generated by Log-rank (Mantel-Cox) test between groups of SD (all three subsets combined) vs. PD. Analysis indicates differences in median survival rates with better survival attributed to individuals with response in the above specified order

Conclusions NC318 shows promising early evidence of disease control in subjects with Siglec-15 positive advanced or metastatic solid tumors in phase 1 & 2 studies, prompting evaluation of S15 expression as a predictive biomarker in the prospective study at 800mg q1w dosing.

Trial Registration NCT03665285

Ethics Approval This study has been approved by the IRB of all the participating institutions, and all participants have given informed consent before taking part in the study.

Consent Written informed consent was obtained from the patient for publication of this abstract and any accompanying images. A copy of the written consent is available for review by the Editor of this journal.

<http://dx.doi.org/10.1136/jitc-2021-SITC2021.490>

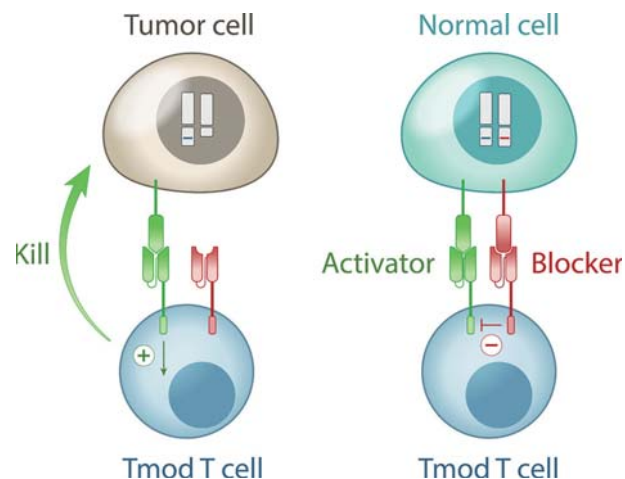
491

BASECAMP-1: AN OBSERVATIONAL STUDY TO IDENTIFY RELAPSED SOLID TUMOR PATIENTS WITH HUMAN LEUKOCYTE ANTIGEN (HLA) LOSS OF HETEROZYGOSITY (LOH) AND LEUKAPHERESIS FOR FUTURE CAR T-CELL THERAPY

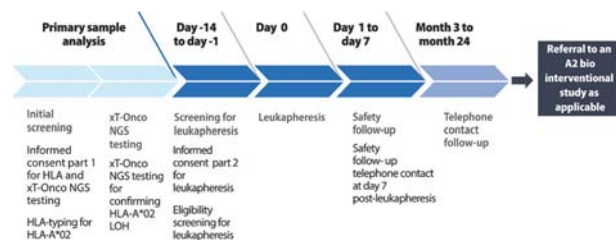
¹Julian Molina*, ²William Go, ³Scott Kopetz, ⁴Diane Simeone, ⁵Sandip Patel, ¹Yi Lin, ²Kirstin Liechty, ²Michelle Fan-Port, ⁶Jason Perera, ²Armen Mardiros, ⁷Karl Beutner, ⁷Ariane Lozac'hmeur, ²Eric Ng, ⁸David Maloney, ⁹J Randolph Hecht. ¹Mayo Clinic, Rochester, MN, USA; ²A2 Biotherapeutics, Inc., Agoura Hills, CA, USA; ³University of Texas MD Anderson Cancer, Houston, TX, USA; ⁴New York University Langone Health, New York, NY, USA; ⁵University of California San Diego, La Jolla, CA, USA; ⁶former Tempus, Chicago, IL, USA; ⁷Tempus, Chicago, IL, USA; ⁸Fred Hutchinson Cancer Research Center, Seattle, WA, USA; ⁹David Geffen School of Medicine at UCLA, Los Angeles, USA

Background Solid tumors comprise >90% of cancers. Metastatic colorectal cancer, non-small cell lung cancer, and pancreatic cancer are among the leading causes of cancer-related mortality (5-year overall survival: 14%, 6%, and 3%, respectively).¹ Chimeric antigen receptor (CAR) T-cell therapy demonstrated clinical outcomes in hematologic malignancies.²⁻³ However, translating engineered T-cell therapies to solid tumors proves difficult due to a lack of tumor-specific targets that discriminate cancer cells from normal cells. In previous studies, the use of a carcinoembryonic antigen T-cell receptors and mesothelin CARs both resulted in dose-limiting on-target, off-tumor toxicities.⁴⁻⁵ TmodTM CAR T-cell therapy addresses these challenges by leveraging dual receptors to create a robust AND NOT signal integrator capable of killing tumor cells, while leaving healthy cells intact (figure 1).⁶ Tmod platform technology is a versatile system that may be applied to T cells and natural killer cells in autologous and allogeneic settings. HLA LOH offers a definitive tumor versus normal discriminator target for CAR T-cell therapy.⁶⁻⁷ The 2 receptors comprise an activator that recognizes an antigen present on the surface of normal and tumor cells and a blocker that recognizes a second surface antigen from an allele lost only in tumor cells. HLA LOH has been observed in ~13% across all solid tumors and up to 33% of pancreatic cancers.⁸ New technologies have shown higher HLA LOH rates; however, it is unclear whether patients with HLA LOH in their primary tumor tissues are at higher risk for recurrence. BASECAMP-1 is an observational study with key objectives: 1) To determine and identify patients with somatic HLA LOH eligible for Tmod CAR T-cell therapy, and 2) Subsequent leukapheresis and manufacturing feasibility for future Tmod CAR T-cell trials.

Methods BASECAMP-1 (NCT04981119) patient eligibility has 2 parts (figure 2): 1) Patients will be initially screened to identify germline HLA-A*02 heterozygosity by central next-generation sequencing (NGS). If HLA-A*02 heterozygosity is confirmed, primary archival tumor tissue will be analyzed by xT-Onco NGS testing⁹ to determine if somatic tumor HLA-A*02 LOH is present; 2) If the tumor demonstrates HLA-A*02 LOH and the patient screens eligible, the patient will undergo leukapheresis. Patients enrolled in the study who undergo leukapheresis will be evaluated for safety 7 days post-leukapheresis and followed for relapsed status. Banked T cells will be available for subsequent autologous Tmod CAR T-cell therapy at the time of relapse.



Abstract 491 Figure 1 Illustration of the Tmod T cell engaging with tumor cells with somatic loss of HLA-A*02 and with normal cells



Abstract 491 Figure 2 Study schema. HLA, human leukocyte antigen; LOH, loss of heterozygosity; NGS, next generation sequencing

Trial Registration NCT04981119

REFERENCES

- American Cancer Society. Cancer Facts & Figures 2021. Atlanta: American Cancer Society; 2021.
- Neelapu S, Locke F, Bartlett N, et al. Axicabtagene ciloleucel CAR T-cell therapy in refractory large B-cell lymphoma. *N Engl J Med* 2017;**377**(26):2531–2544.
- Maude S, Laetsch T, Buechner J, et al. Tisagenlecleucel in children and young adults with B-cell lymphoblastic leukemia. *N Engl J Med* 2018;**378**(5):439–448.
- Parkhurst M, Yang J, Langan R, et al. T cells targeting carcinoembryonic antigen can mediate regression of metastatic colorectal cancer but induce severe transient colitis. *Mol Ther* 2011;**19**(3):620–626.
- Haas AR, Tanyi JL, O'Hara MH, et al. Phase I study of lentiviral-transduced chimeric antigen receptor-modified T cells recognizing mesothelin in advanced solid cancers. *Mol Ther*. 2019;**27**(11):1919–1929.
- Hamburger A, DiAndreth B, Cui J, et al. Engineered T cells directed at tumors with defined allelic loss. *Mol Immunol* 2020;**128**:298–310.
- Hwang M, Mog B, Douglass J, et al. Targeting loss of heterozygosity for cancer-specific immunotherapy. *Proc Natl Acad Sci U S A* 2021;**118**(12):e2022410118.
- The Cancer Genome Atlas (TCGA) Research Network. <https://www.cancer.gov/tcga>. Accessed June 2021.
- Perera J, Mapes B, Lau D, et al. Detection of human leukocyte antigen class I loss of heterozygosity in solid tumor types by next-generation DNA sequencing. *J Immunother Cancer* 2019;**7**(suppl 1):103.

<http://dx.doi.org/10.1136/jitc-2021-SITC2021.491>

PHASE 2 EFFICACY AND SAFETY OF AUTOLOGOUS TUMOR-INFILTRATING LYMPHOCYTE (TIL) CELL THERAPY IN COMBINATION WITH PEMBROLIZUMAB IN IMMUNE CHECKPOINT INHIBITOR-NAÏVE PATIENTS WITH ADVANCED CANCERS

¹David O'Malley*, ²Sylvia Lee, ³Amanda Psyrry, ⁴Ammar Sukari, ⁵Sajeve Thomas, ⁶Robert Wenham, ⁷Helen Gogas, ⁸Amir Jazaeri, ⁹Bradley Monk, ¹⁰Peter Rose, ¹¹Antonio Reuda, ¹²Friedrich Graf Finckenstein, ¹²Madan Jagasia, ¹²Rana Fiaz, ¹²Brigid Garelik, ¹²Wen Shi, ¹²Anjali Desai, ¹²Giri Sulur, ¹²Guang Chen, ¹²Xiao Wu, ¹³Antonio Jimeno. ¹Ohio State University, Columbus, OH, USA; ²Fred Hutchinson Cancer Center, Seattle, WA, USA; ³Attikon University General Hospital, Athens, Greece; ⁴Karmanos Cancer Institute, Detroit, MI, USA; ⁵Orlando Health Cancer Institute, Orlando, FL, USA; ⁶Moffitt Cancer Center, Tampa, FL, USA; ⁷Natl. and Kapodistrian University of Athens, Athens, Greece; ⁸MD Anderson Cancer Center, HOUSTON, TX, USA; ⁹Arizona Oncology (US Oncology Network), Phoenix, AZ, USA; ¹⁰Cleveland Clinic, Columbus, OH, USA; ¹¹Hospital Regional Universitario de Malag, Malaga, Spain; ¹²Iovance Biotherapeutics, Inc., San Carlos, CA, USA; ¹³Univ. of Colorado School of Medicine, Aurora, CO, USA

Background Immune checkpoint inhibitors (ICI) are standard-of-care in the treatment of several types of cancer; however, an unmet medical need exists for early-line combination therapies that are able to provide higher response rates, more durable responses, and manageable long-term safety. Lifileucel (LN-144) and LN-145, adoptive cell therapies using tumor-infiltrating lymphocytes (TIL), have demonstrated encouraging efficacy with acceptable safety in patients with advanced cancer that has failed ICI.¹⁻² To improve efficacy and safety of early-line treatment options, we explored a combination of TIL and pembrolizumab in patients with ICI-naïve melanoma, head and neck squamous cell carcinoma (HNSCC), and cervical cancer.

Methods IOV-COM-202 (NCT03645928) and C-145-04 (NCT03108495) are ongoing Phase 2 multicenter, multicohort, prospective, open-label studies evaluating TIL cell therapy in ICI-naïve patients with solid tumors. We report efficacy and safety from IOV-COM-202 (Cohort 1A: lifileucel and pembrolizumab in patients with unresectable or metastatic melanoma; Cohort 2A: LN-145 and pembrolizumab in patients with advanced, recurrent, or metastatic HNSCC) and C-145-04 (Cohort 3: LN-145 and pembrolizumab in patients with stage 4b, persistent or recurrent cervical cancer who have not received prior systemic therapy). Eligibility across cohorts included ECOG PS ≤1, ≥1 resectable lesion (diameter ≥1.5 cm post-resection) for TIL manufacturing, and ≥1 measurable lesion for response assessment (by investigator per RECIST v1.1). Lifileucel and LN-145 are cryopreserved TIL infusion products generated at central GMP facilities in a 22-day process. Treatment included tumor resection for TIL manufacturing, followed by 1 dose of pembrolizumab, nonmyeloablative lymphodepletion (cyclophosphamide and fludarabine), TIL infusion, ≤6 interleukin-2 doses (600,000 IU/kg IV), and continued pembrolizumab for ≤24 months.

Results As of 09July2021, 32 patients received TIL and pembrolizumab (full-analysis set [FAS]; table 1). Across all cohorts, the objective response rate (ORR) in the FAS was 56.3% (Cohort 1A [melanoma], 87.5%; Cohort 2A [HNSCC], 42.9%; Cohort 3 [cervical], 50.0%; figure 1). Among confirmed responders (n=17), 10 responses (58.8%) were ongoing at data cutoff, with a median study follow-up of 9.7 months. The treatment-emergent adverse-event (TEAE) profile was consistent with the underlying diseases and known profiles of pembrolizumab, nonmyeloablative lymphodepletion, and interleukin-2. The most common (≥30%) Grade ≥3 TEAEs were thrombocytopenia (53.1%), anemia (50.0%), neutropenia (46.9%), and febrile neutropenia (43.8%).

Abstract 492 Table 1 Baseline demographic and clinical characteristics and efficacy

Baseline Demographic and Clinical Characteristics and Efficacy			
	COM-202 Cohort 1A Melanoma (N=8)	COM-202 Cohort 2A HNSCC (N=14)	C-145-04 Cohort 3 Cervical (N=10)
Sex, n (%)			
Male	7 (87.5)	12 (85.7)	0
Female	1 (12.5)	2 (14.3)	10 (100)
Median (min, max) age, y	52.0 (34, 59)	59.5 (24, 66)	52.0 (37, 73)
Tumor PD-L1 expression, n (%)			
TPS <5%	2 (25.0)	CPS <20% 2 (14.3)	CPS <1% 1 (10.0)
TPS ≥5%	4 (50.0)	CPS ≥20% 9 (64.3)	CPS ≥1% 7 (70.0)
Missing	2 (25.0)	Missing 3 (21.4)	Missing 2 (20.0)
Median (min, max) number of target and non-target lesions	4.5 (3, 7)	4.0 (1, 8)	7.0 (2, 10)
Target lesion sum of diameters, mm			
Mean	113.9	64.3	76.9
Min, max	(32, 355)	(21, 134)	(17, 143)
Median (min, max) number of pembrolizumab doses	7.0 (2, 15)	6.5 (1, 26)	5.0 (2, 12)
Median study follow-up, mo*	9.8	9.8	8.7
Efficacy, n/N (%)			
ORR (FAS)	7/8 (87.5)	6/14 (42.9)*	5/10 (50.0)
ORR (efficacy-evaluable set)	7/8 (87.5)	6/13 (46.2)	5/10 (50.0)
CR	3/8 (37.5)	1/14 (7.1)	1/10 (10.0)
uCR [†]	0	1/14 (7.1)	0
PR	3/8 (37.5)	4/14 (28.6)	4/10 (40.0)
uPR [‡]	1/8 (12.5)	0	0
SD	1/8 (12.5)	7/14 (50.0)	4/10 (40.0)
DCR	8/8 (100)	13/14 (92.9)	9/10 (90.0)
NE [§]	0	1/14 (7.1)	0

*Based on overall survival data using the reverse Kaplan-Meier method.

[†]ORR in SITC 2020 dataset (16October2020 data cutoff; n=9, ORR=44.4%)[3].

[‡]At the time of the datacut, patient had not yet had confirmatory assessment after initial CR, but was a confirmed PR.

[§]At the time of the datacut, patient had a first PR assessment, but had not yet reached the confirmatory assessment.

[¶]Excluded from efficacy-evaluable set due to death prior to first assessment.

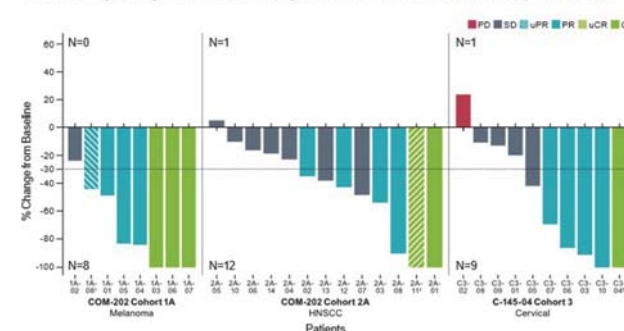
CPS, combined positive score; CR, complete response; DCR, disease control rate; FAS, full-analysis set;

HNSCC, head and neck squamous cell carcinoma; NE, not evaluable; ORR, objective response rate; PD-

L1, programmed death-ligand 1; PR, partial response; SD, stable disease; TPS, tumor proportion score;

uCR, unconfirmed complete response; uPR, unconfirmed partial response.

Best Percentage Change from Baseline in Target Lesion Sum of Diameters for Efficacy-Evaluable Set*



*One patient in COM-202 Cohort 2A who did not have post-dose tumor response assessment was excluded.

[†]Patient 1A-08 had a first PR assessment, but had not reached the confirmatory assessment at the time of the datacut.

[‡]At the time of the datacut, patient 2A-11 had not yet had confirmatory assessment after initial CR.

[§]For patient C3-04, -100% change from baseline includes lymph node lesions that resolved to <10 mm.

CR, complete response; HNSCC, head and neck squamous cell carcinoma; PD, progressive disease; PR,

partial response; SD, stable disease; uCR, unconfirmed complete response; uPR, unconfirmed partial

response.

Abstract 492 Figure 1 Best percentage change from baseline in target lesion sum of diameters for efficacy-evaluable set*

Conclusions The observed efficacy, including ORR and CR rate, and acceptable safety profile are encouraging and warrant continued investigation of the combination of TIL and pembrolizumab in early-line treatment of patients with advanced cancer. Enrollment is ongoing; updated data will be presented.

Acknowledgements This study and analysis were funded by Iovance Biotherapeutics, Inc. (San Carlos, CA, USA). Writing support was provided by Amanda Kelly (Iovance); graphics support was provided by Cognition Studio (Seattle, WA, USA).

Trial Registration NCT03645928 and NCT03108495

REFERENCES

- Sarnaik AA, et al. *J Clin Oncol* 2021; doi: 10.1200/JCO.21.00612.
- Jazaeri AA, et al. *J Clin Oncol* 2019;37 (suppl; abstract 182).
- Jimeno A, et al. *J Immunother Cancer* 2020;8 (suppl; abstract 353).

Ethics Approval The IOV-COM-202 study was approved by Advarra Institutional Review Board, approval number Pro00035064; the C-145-04 was approved by WIRB Copernicus Group, approval number 7-1425772-1. All study participants provided written consent via signature of the IRB-approved informed consent form.

<http://dx.doi.org/10.1136/jitc-2021-SITC2021.492>

FIRST-IN-HUMAN PHASE 1/2 TRIAL TO EVALUATE THE SAFETY AND INITIAL CLINICAL ACTIVITY OF DUOBODY®-CD40×4-1BB (GEN1042) IN PATIENTS WITH ADVANCED SOLID TUMORS

¹Melissa Johnson*²Juanita Lopez, ³Patricia LoRusso, ⁴Jessica Bauman, ⁵Daniel Haggstrom, ⁶Eleni Lagkadinou, ⁷Gaurav Bajaj, ⁸Özlem Türeci, ⁹Homer Adams III, ¹⁰Uğur Şahin, ¹¹Yali Fu, ¹²Tahamtan Ahmadi, ¹³Kristoffer Rohrberg. ¹*Sarah Cannon Research Institute, Nashville, TN, USA;* ²*Royal Marsden NHS Foundation Trust, Sutton, UK;* ³*Yale Cancer Center, New Haven, USA;* ⁴*Fox Chase Cancer Center, Philadelphia, PA, USA;* ⁵*Levine Cancer Institute, Charlotte, NC, USA;* ⁶*BioNTech SE, Mainz, Germany;* ⁷*Genmab, Princeton, NJ, USA;* ⁸*Rigshospitalet, University Hospital of Copenhagen, Copenhagen, Denmark*

Background Despite the preclinical promise of CD40 and 4-1BB as immuno-oncologic targets, clinical efforts evaluating these agonists as monotherapy have had limited success due to minimal efficacy and/or severe toxicity. DuoBody-CD40×4-1BB (GEN1042) is a first-in-class, bispecific, agonistic antibody that combines targeting and conditional activation of CD40 and 4-1BB on immune cells, resulting in enhanced priming and (re-)activation of tumor-specific immunity. Furthermore, preclinical data suggest that combination with anti-PD-1 can enhance antitumor activity. We present preliminary data from the ongoing, first-in-human, open-label, phase 1/2 trial of DuoBody-CD40×4-1BB in advanced solid tumors (NCT04083599).

Methods During dose escalation, patients with metastatic/unresectable non-CNS solid tumors who had exhausted standard therapies received flat-dose DuoBody-CD40×4-1BB (0.1–400 mg) intravenously every 3 weeks until disease progression or unacceptable toxicity. Primary endpoint was dose-limiting toxicity (DLT). Secondary endpoints included adverse events (AEs), pharmacokinetic parameters, and preliminary antitumor activity (RECIST v1.1). Pharmacodynamic biomarkers were assessed as exploratory endpoints.

Results As of June 11, 2021, 50 patients were enrolled (median age, 57 years). The most common cancer types were colorectal (22%), melanoma (20%), and non-small-cell lung cancer (8%). Patients received a median (range) of 2.5 (1–21) treatment cycles; C_{max} was observed shortly after end of infusion. Treatment-related AEs occurring in ≥10% of patients (all grades; grade ≥3) were fatigue (22%; 0%), pyrexia (16%; 0%), nausea (10%; 0%), and transaminase elevation (10%; 6%). Maximum tolerated dose was not reached. One DLT of elevated transaminases (grade 4) was observed at the 200-mg dose that resolved upon corticosteroid administration. No drug-related grade ≥3 thrombocytopenia events were reported. Disease control, defined as best overall response of complete/partial response and stable disease, was achieved in 51% of patients (25/49), including 2 confirmed partial responses per RECIST v1.1 in melanoma and neuroendocrine lung cancer. Modulation of pharmacodynamic endpoints was observed across dose levels, with more pronounced effects near the 100-mg dose. Increases in peripheral IFN-γ, TARC (monocyte/DC chemokine), and proliferating CD8+ total and effector memory T cells were observed during cycle 1. Using physiologically based pharmacokinetic/pharmacodynamic modeling and available safety, efficacy, and pharmacodynamic data, 100 mg every 3 weeks was identified as the expansion dose for further evaluation.

Conclusions DuoBody-CD40×4-1BB demonstrated biologic and early antitumor activity with a favorable safety profile in patients with advanced solid tumors. Expansion cohorts, including combination therapy with PD-1 inhibitors, are currently enrolling.

Acknowledgements This trial was funded by Genmab A/S and BioNTech SE.

Trial Registration NCT04083599

Ethics Approval This trial is undertaken following full approval of the final protocol, amendments, informed consent form, applicable recruiting materials, and subject compensation programs by the Independent Ethics Committee/Institutional Review Board.

<http://dx.doi.org/10.1136/jitc-2021-SITC2021.493>

PHASE 1 DOSE ESCALATION AND DOSE EXPANSION STUDY OF AN AGONIST REDIRECTED CHECKPOINT (ARC) FUSION PROTEIN, SL-279252 (PD1-FC-OX40L), IN SUBJECTS WITH ADVANCED SOLID TUMORS OR LYMPHOMAS

¹Melissa Johnson*, ²Lilian Siu, ³David Hong, ⁴Patrick Schoffski, ⁵Vladimir Galvao, ⁶Fatima Rangwala, ⁶Robert Hernandez, ⁶Louis Gonzalez, ⁶Bo Ma, ⁶Lini Pandite, ⁵Irene Brana. ¹Sarah Cannon Research Institute, Nashville, TN, USA; ²Princess Margaret Cancer Center, Toronto, Canada; ³MD Anderson Cancer Center, Houston, TX, USA; ⁴Univ. Hospitals, Leuven Cancer Institute, Leuven, Belgium; ⁵Vall d'Hebron Institute of Oncology, Barcelona, Spain; ⁶Shattuck Labs, Durham, NC, USA

Background PD1-Fc-OX40L, is a hexameric, bi-functional fusion protein with an extracellular domain (ECD) of PD-1 (70 pM affinity to PD-L1) linked to the ECD of OX40L (324 pM affinity to OX40) through an Fc linker. The therapeutic activity of mPD1-Fc-OX40L in murine tumors was superior to PD1 blocking, OX40 agonist or combination antibody therapy.¹

Methods The first-in-human, Phase 1 dose escalation study is evaluating SL-279252 as monotherapy in patients (pts) with advanced solid tumors or lymphomas. Objectives include evaluation of safety, dose-limiting toxicity (DLT), recommended phase 2 dose (RP2D), pharmacokinetic (PK) parameters, pharmacodynamic (PD) effects, and anti-tumor activity per iRECIST.

Results As of 11 June 2021, 43 pts were enrolled and dosed intravenously with SL-279252 (median age 64 years; 56% male; median [range] of 3 [0–5] prior systemic therapies for metastatic disease): 30 pts were treated on schedule 1 (day 1, 8, 15, 29, then every 2 weeks) from dose level 0.0001–6 mg/kg, and 13 pts treated on schedule 2 (weekly) from dose level 0.3–3 mg/kg. 58% of pts were PD-1/L1 inhibitor experienced, and most tumors lacked PD-L1 expression. Common (>15%) treatment emergent adverse events (AEs) of any grade (G) were constipation in 11 (26%) pts, back pain 8 (19%) pts, anemia 7 (16%) pts and decreased appetite 7 (16%) pts. Infusion-related reactions (G1/2) were noted in 3 (7%) pts. G3 treatment-related AEs (TRAEs) were neutropenia (2%) and hypercalcemia (2%); no G4/5 TRAEs or DLTs occurred. SL-279252 C_{max} and AUC increased linearly up to 3mg/kg, and greater than proportional increase in AUC was observed at 6 mg/kg. The preliminary T_{1/2} was ~23 hours. Dose-dependent receptor occupancy on CD4+OX40+ T cells persisted for >7 days and these cells rapidly margined from the peripheral blood post infusion. Increases in the number of proliferating central and/or effector memory T cells were seen in some pts at doses of ≥1mg/kg. Analysis of paired tumor biopsies is ongoing. Best response was 1 durable confirmed iPR (ocular melanoma, 4 prior systemic regimens) in a pt who remained on treatment for >1 yr, and iSD in 12 pts (1 unconfirmed iPR). iSD for > 24 wks occurred in 6/12 pts.

Conclusions SL-279252 is well-tolerated in pts with refractory solid tumors with no maximum tolerated dose (MTD) reached. OX40-dependent PD effects and durable anti-tumor activity was observed. Trends for PK/PD effects at ≥1 mg/kg suggests dose exploration in PD-L1 expressing cancers is warranted beyond 6 mg/kg.

Acknowledgements Thanks are extended to study participants; Takeda Pharmaceutical Company, Boston, MA, United States; Cathrine Leonowens, PhD, Nuventra Pharma Sciences, Durham, NC, United States and Cadence Communications and Research, Thousand Oaks, CA, United States. This study is

funded by Shattuck Labs, Inc. Austin, TX and Durham, NC, United States.

Trial Registration NCT03894618

REFERENCES

1. Fromm G, de Silva S, Johannes K, Patel A, Hornblower JC, Schreiber TH. Agonist redirected checkpoint, PD1-Fc-OX40L, for cancer immunotherapy. *J Immunother Cancer* 2018;**6**: 1–16.

Ethics Approval This study is being conducted in full conformity with the Declaration of Helsinki and was approved by all IRBs/ethics committees from each clinical site participating in the study. Specific approval numbers can be provided upon request.

<http://dx.doi.org/10.1136/jitc-2021-SITC2021.494>

495

TRIAL OF SNX281, A SYSTEMICALLY DELIVERED SMALL MOLECULE STING AGONIST, IN SOLID TUMORS AND LYMPHOMAS

¹Judy Wang*, ²Gerald Falchook, ³Salah Nabhan, ³Meghana Kulkarni, ³Peter Sandy, ⁴Ololade Dosunmu, ³Humphrey Gardner, ²Johanna Bendell, ²Melissa Johnson. ¹Florida Cancer Specialists, Sarasota, FL, USA; ²Sarah Cannon Research Institute, Denver, CO, USA; ³Stingthera, Boston, MA, USA; ⁴Sarah Cannon Development Innovations, Nashville, TN, USA

Background Innate immune activation is a desirable goal in anticancer therapy. Stimulator of Interferon Genes (STING) agonists represent one approach to this goal; to date most studies have utilized intra-tumoral administration. SNX281 is a novel small molecule agonist of human and mammalian STING with favorable pharmacokinetic properties that enable systemic intravenous administration. The molecule dimerizes in the binding site of STING to induce activation. In preclinical studies using THP-1 cells or human PBMCs, SNX281 caused both pathway activation and the induction of signature cytokines, IFN- β , TNF- α and IL-6 in a STING dependent manner. Intravenously delivered SNX281 caused complete and durable tumor regression in mice bearing CT26 colon carcinomas with induction of immune memory. Mice that were cured of their primary CT26 tumors were completely resistant to re-challenge. Increased T cell responses were observed against the endogenous CT26 rejection antigen AH1. Maximal tumor control depended on CD8+ T cells, confirming the involvement of an adaptive immune component in SNX281 mediated anti-tumor activity, although some tumor control was observed even in the absence of T cells. In addition, combining STING-dependent T cell priming induced by SNX281 with anti-PD-1 resulted in robust antitumor activity and significant survival benefit in multiple tumor models (CT26, MC38 and B16- F10) that are resistant to checkpoint therapy alone.

Methods This is a multicenter, open-label, phase I dose-escalation followed by dose expansion study of SNX281 as monotherapy and in combination with pembrolizumab. SNX281 is administered as a 30-minute intravenous infusion QW for 3 weeks followed by Q3W for six cycles. Eligible patients for the dose escalation phase will have, among other criteria, histologically confirmed advanced solid tumors or lymphomas which have failed prior therapy and/or are not eligible for therapies, as well as adequate organ function, life expectancy of at least 12 weeks, and measurable disease. Monotherapy dose escalation accrued initially with single patient cohorts advancing to a 3+3 design. The dose expansion phases of each treatment arm will begin following the determination of an MTD or alternative dose of SNX281 in each respective treatment arm. The single-agent treatment arm of SNX281 is planned to evaluate at least 2 expansion cohorts in ovarian cancer and colorectal carcinoma while the combination treatment arm of SNX281 and pembrolizumab is planned to enroll subjects with advanced cancer who have relapsed on or have become refractory to prior immune checkpoint therapy given in an indicated setting. Clinical Trial Information: NCT04609579

Trial Registration NCT04609579

Ethics Approval IRB approval from IntegReview IORG0000689.

<http://dx.doi.org/10.1136/jitc-2021-SITC2021.495>

496

TOXICITY OF AN FC ENGINEERED ANTI-CD40 ANTIBODY IS ABROGATED BY INTRATUMORAL INJECTION AND RESULTS IN DURABLE ANTI-TUMOR IMMUNITY IN PATIENTS

¹David Knorr*, ¹Jeffrey Ravetch, ²Gabriela D'Andrea, ²Linda Vahdat, ²Christopher Klebanoff, ²Mark Robson. ¹Rockefeller University, New York, USA; ²MSKCC, New York, NY, USA

Background Currently approved immune-based therapeutics primarily block inhibitory T cell checkpoints. Alternative approaches involve activation of immune pathways by agonism of stimulatory receptors, such as CD40. CD40 provides a central mechanism for the activation dendritic cells and is well established in pre-clinical models. Despite its promise, multiple clinical trials with agonistic anti-CD40 antibodies have reported minimal clinical responses and systemic toxicity. Efficient CD40 agonism requires receptor multimerization which we achieved by engineering the human anti-CD40 antibody CP-870,893 with 5 point-mutations in the Fc domain selectively increasing its binding to human FcγRIIB (herein "2141-V11"). The re-engineered antibody demonstrated significantly enhanced anti-tumor activity as compared to its parental IgG2 version using a mouse model carrying human Fcγ receptors (FcγR) and human CD40 (hFcγR/hCD40) in place of their mouse homologues.¹ When given systemically, enhanced in vivo activity was accompanied by thrombocytopenia and transaminitis, similar toxicities seen with current clinical anti-CD40 antibodies, resulting from the expression of CD40 on platelets and Kupffer cell activation. As a prelude to clinical studies of 2141-V11 an optimized a dosing and delivery regimen resulting in minimal toxicity with optimal anti-tumor activity was developed, demonstrating that direct intratumoral injection led to potent local and systemic anti-tumor immunity.²

Methods We performed pre-clinical toxicology testing in macaques and found no toxicity up to 100 mg/kg subcutaneously, in contrast to the toxicity observed in hCD40/hFcγR mice. CD40 agonistic antibodies require engagement by their Fc to FcγRIIB to achieve receptor multimerization and agonistic signaling. This lack of toxicity in macaques resulted from the observation that while 2141-V11 can engage the macaque CD40 molecule it does not engage the macaque inhibitory FcγRIIB, highlighting the importance of matching antibodies with their species specific Fc receptors. Full toxicology results will be reported at the annual meeting. We are now testing intratumoral 2141-V11 in a phase I clinical study using a 3+3 design in patients with solid tumors with injectable cutaneous, subcutaneous, or nodal lesions.

Results We have completed the first two cohorts without DLTs. In 5/6 patients with breast cancer the best overall response was stable disease. In one patient with melanoma in-transit disease we saw a complete response in the second dose group. The third dose group is currently enrolling and updated results will be reported at the meeting.



Abstract 496 Figure 1 Intratumoral 2141-V11 leads to both local and distant anti-tumor responses (melanoma)

Conclusions Intratumoral therapy with the Fc-enhanced CD40 agonist 2141-V11 has been demonstrated to be safe, with promising signs of early activity in both injected and distant non-injected lesions (figure 1).

Trial Registration NCT04059588

REFERENCES

1. Dahan R, Barnhart BC, Li F, Yamniuk AP, Korman AJ, Ravetch JV. Therapeutic Activity of Agonistic, Human Anti-CD40 Monoclonal Antibodies Requires Selective FcγR Engagement. *Cancer Cell* 2016;**0**(0):3755–66.
2. Knorr DA, Dahan R, Ravetch JV. Toxicity of an Fc-engineered anti-CD40 antibody is abrogated by intratumoral injection and results in durable antitumor immunity. *Proceedings of the National Academy of Sciences* 2018. Oct 23;**115**(43):11048–11053.

Ethics Approval This study was approved by the Rockefeller University IRB.

<http://dx.doi.org/10.1136/jitc-2021-SITC2021.496>

497

A STUDY OF ALPN-202, A PD-L1-DEPENDENT CD28 COSTIMULATOR AND DUAL CHECKPOINT INHIBITOR, IN COMBINATION WITH PEMBROLIZUMAB IN PATIENTS WITH ADVANCED MALIGNANCIES

¹Nehal Lakhani*, ²Meredith McKean, ³Amita Patnaik, ⁴Kristi Manjarrez, ⁴Hany Zayed, ⁵Michael Chisamore, ⁶Stanford Peng, ⁴Zelanna Goldberg. ¹START Midwest, Grand Rapids, MI, USA; ²Tennessee Oncology, Nashville, TN, USA; ³START San Antonio, San Antonio, TX, USA; ⁴Alpine Immune Sciences, Seattle, WA, USA; ⁵Merck and Co., Wheaton, IL, USA

Background Despite successes with checkpoint inhibition (CPI) in a wide range of tumors, most patients demonstrate primary or acquired resistance, thus driving the need for better IO therapy. Research has suggested that CPI therapy exerts much of its benefit via releasing the inhibition of CD28 signaling, which would only be expected to show clinical benefit in the presence of intra-tumoral engagement of CD28 by its ligands CD80/86. ALPN-202, a variant CD80 vIgD-Fc fusion protein, was engineered to provide tumor localizing PD-L1-dependent CD28 agonism, while inhibiting the PD-L1 and CTLA-4 checkpoints. It has demonstrated superiority to CPI-only therapies in vitro and in in vivo tumor models, while also demonstrating additional benefit in combination with targeted PD-1 axis blockade.¹ The benefit appeared to be at least additive in tumor models of poorly immunogenic tumors, suggesting the possibility of meaningful clinical benefit where CPI therapeutic efficacy is limited, i.e., "non-inflamed or cold" tumors. Single agent safety and tolerability of ALPN-202 has been demonstrated along with pharmacodynamic evidence of CD28 engagement with immune checkpoint inhibition.²

Methods An open-label dose escalation and expansion study of ALPN-202 in combination with pembrolizumab in adults with advanced solid tumors or lymphoma was initiated in June 2021 (NCT04920383). Eligibility includes those tumors where single agent PD-(L)1 antagonists are SOC or patients refractory or resistant to standard therapies (including approved CPIs), or those without available standard or curative therapy. The study is a standard 3+3 dose escalation design with two schedules of ALPN-202 in parallel, Q1W and Q3W. Pembrolizumab is given per label at 400 mg IV Q6W. Objectives include evaluation of safety and tolerability, identification of the recommended phase 2 dose, PK, PD, exploratory predictive biomarker analysis (i.e., PD-L1, CD28, CD80 and CD86, as well as immunophenotyping of immune cell populations on treatment) and preliminary anticancer activity of ALPN-202 in combination with pembrolizumab. Disease assessments are evaluated by RECIST v1.1 for solid tumors or by Lugano Classification for lymphoma. Efficacy endpoints include ORR, duration of response and disease control rate. Once the recommended phase 2 dose combination is identified, dose expansion cohorts will be initiated. Approximately 30–35 patients will be enrolled in each tumor type-specific expansion cohort, including histologies that have not been demonstrated to be CPI responsive, as well as those where CPIs are approved SOC. This study is being conducted in collaboration with Merck & Co., Inc., Kenilworth, NJ, USA.

Acknowledgements We thank the patients and their families for their clinical trial participation and the site staff for their work on this trial.

Trial Registration NCT04920383

REFERENCES

1. Lewis, Katherine, et al. ALPN-202, a Conditional CD28 Costimulator and Dual Checkpoint Inhibitor, Enhances the Activity of Multiple Standard of Care Modalities. *Journal for ImmunoTherapy of Cancer* 2019;**7**.

2. Moser, Justin C, et al. First-in-human dose escalation of ALPN-202, a conditional CD28 costimulator and dual checkpoint inhibitor, in advanced malignancies. 2021; 2547–2547.

Ethics Approval All required ethics committees have reviewed and approved the protocol. The first was WCG IRB, Approval number 20211877. All participants provided informed consent before study participation.

<http://dx.doi.org/10.1136/jitc-2021-SITC2021.497>

EVORPACEPT (ALX148), A CD47 MYELOID CHECKPOINT INHIBITOR, IN PATIENTS WITH HEAD AND NECK SQUAMOUS CELL CARCINOMA (HNSCC) AND WITH GASTRIC/GASTROESOPHAGEAL CANCER (GC); ASPEN-01

¹Keun-Wook Lee*, ²Hyun Chung, ³Tae Min Kim, ⁴Nehal Lakhani, ⁵Wells Messersmith, ⁶Rafael Santana-Davila, ⁷Won Seog Kim, ⁸Patricia LoRusso, ⁹Yung-Jue Bang, ¹⁰Laura Chow, ¹⁰Philip Fanning, ¹¹Pierre Squifflet, ¹⁰Feng Jin, ¹⁰Alison Forgie, ¹⁰Hong Wan, ¹⁰Jaume Pons, ¹⁰Sophia Randolph, ¹²Justin Gainor. ¹Seoul National University Bundang Hosp, Seoul, Korea, Republic of; ²Yonsei Cancer Center, Seoul, Korea, Republic of; ³Seoul National University College of Med, Seoul, Korea, Republic of; ⁴START Midwest, Grand Rapids, MI, United States; ⁵University of Colorado Cancer Center, aurora, CO, United States; ⁶University of Washington, Seattle, WA, United States; ⁷Samsung Medical Center, Seoul, Korea, Republic of; ⁸Yale Cancer Center, New Haven, United States; ⁹Seoul National University Hospital, Seoul, Korea, Republic of; ¹⁰ALX Oncology Inc., Burlingame, CA, United States; ¹¹International Drug Development Institute, Brussels, Belgium; ¹²Massachusetts General Hosp, Cancer Ctr., Boston, MA, United States

Background Evorpcept is a high affinity, CD47-blocking, myeloid checkpoint inhibitor (CPI) with an inactive Fc region designed to safely enhance anticancer therapeutics.¹⁻³ In combination with standard chemotherapy and antibody regimens, evorpcept was evaluated in patients with advanced HNSCC or HER2-positive GC.

Methods Patients with untreated advanced HNSCC or previously treated HER2-positive GC received evorpcept (E) 10 mg/kg QW or 15 mg/kg QW in combination with pembrolizumab (P) + 5FU (F) + cisplatin or carboplatin (C) as 1st line therapy, or in combination with trastuzumab (T) + ramucirumab (R) + paclitaxel (P) as ≥2nd line treatment. The primary endpoint was first-cycle dose limiting toxicity (DLT). Tumor response, pharmacokinetic, and pharmacodynamic markers were assessed in all patients. Data from fully-enrolled HNSCC and GC cohorts, and follow-up data from patients with HNSCC administered EP are reported as of 15Jun2021.

Results Forty-one patients fully enrolled the following study cohorts: Thirteen patients with 1L HNSCC received EPFC. No DLTs were reported and the evorpcept maximum administered dose (MAD) was 15 mg/kg QW. Thirteen patients experienced an AE, 2 patients experienced treatment-related AEs (TRAE) of pneumonitis, anemia, fatigue, neutropenia, and hypersensitivity reaction (each n=1, 7.7%). Of 13 evaluable patients, 1CR/4PR/6SD (ORR 38.5%), mPFS 5.6 mo [3.6, NR], mOS not reached, and estimated 12-month OS of 83.3% were reported. Survival follow-up of 10 patients with CPI naïve HNSCC administered EP (2nd or later-line; ORR 40%) demonstrated a mPFS 4.6 mo [0.5,7.5], mOS 24.5 mo [3.1,NR] and estimated 12-month OS of 80%. Eighteen patients with ≥2L GC received ETRP. No DLTs were reported and the evorpcept MAD was 15 mg/kg QW. All patients experienced an AE, 8 patients experienced TRAEs, where the most common were urticaria, rash, and diarrhea (each n=3, 17%), fatigue and pruritus (each n=2, 11%). Of 18 evaluable patients, there were 1CR/12PR/3SD (ORR 72.2%; mDOR unreached) with a mPFS 9.8 mo [5.4,NR], mOS not reached, and estimated 12-month OS of 77.7%.

Conclusions Initial data suggest evorpcept is well tolerated with no DLTs in combination with the antibody/cytotoxic chemotherapy regimens evaluated above and a MAD of 15 mg/kg QW. Consistent with standard CPI therapeutic agents, the initial response benefit seen with evorpcept in combination is notably magnified in longer term PFS and OS endpoints in both the HNSCC and GC populations. Evorpcept's preliminary positive impact on critical survival endpoints compares

favorably with historical standards and warrants further evaluation in patients with HNSCC and GC.

Acknowledgements We would like to thank all of the participating patients, their families and site research teams.

Trial Registration ClinicalTrials.gov identifier NCT03013218.

REFERENCES

1. Kauder S, et al. ALX148 blocks CD47 and enhances innate and adaptive antitumor immunity with a favorable safety profile. *PLoS ONE* 2018;**13**(8).
2. Chow L, et al. A phase I study of ALX148, a CD47 blocker, in combination with standard anticancer antibodies and chemotherapy regimens in patients with advanced malignancy. *Journal of Clinical Oncology* 2020;**38**:15_suppl, 3056–3056.
3. Chung H et al, ASPEN-01: A Phase 1 study of ALX148, a CD47 blocker, in combination with trastuzumab, ramucirumab and paclitaxel in patients with 2nd line HER2-positive advanced gastric or gastroesophageal junction (G/GJ) cancer. *ESMO-GI* 2021; #S0-31.

Ethics Approval The study was approved by all participating institutions' Ethics and/or Review Boards

<http://dx.doi.org/10.1136/jitc-2021-SITC2021.498>

499

A FIRST-IN-HUMAN, PHASE 1/2 CLINICAL TRIAL OF TK-8001, A MAGE-A1 DIRECTED T CELL RECEPTOR IN PATIENTS WITH ADVANCED-STAGE SOLID TUMORS (THE "IMAG1NE"-TRIAL)

¹Fiona Thistlethwaite*, ²Antonia Busse, ³Emiliano Calvo, ⁴Marie-Luise Goebeler, ⁵Martin Wernke, ⁶Sylvie Rottey, ⁷Nuria Kotecki, ⁸Matthias Obenaus, ⁹Vivian Scheuplein, ⁹Ralf Wolter, ⁹Carolina Perdomo-Ortiz, ⁹Ioannis Gavovodis, ⁹Elisa Kieback, ¹⁰Thomas Blankenstein, ⁹Eugen Leo. ¹Christie NHS/Univ of Manchester, Manchester, UK; ²Charité Universitätsmedizin, Berlin, Germany; ³START Madrid-CIOCC, Madrid, Spain; ⁴Universitätsklinik Würzburg, Würzburg, Germany; ⁵Universitätsklinikum Dresden, Dresden, Germany; ⁶Ghent University Hospital, GENT, Belgium; ⁷Institut Jules Bordet, Brussels, Belgium; ⁸Charité Universitätsmedizin, Berlin, Germany; ⁹T-knife Therapeutics Inc., Berlin, Germany; ¹⁰Max Delbrueck Center, Berlin, Germany

Background Melanoma-associated antigen 1 (MAGE-A1) is a cancer-testis antigen with highly selective expression in testis (which is an immune privileged site) and in multiple high unmet medical need cancers. Therefore, it represents an attractive target for T cell receptor (TCR)-based therapies. TK-8001 is a MAGE-A1 directed TCR with optimized affinity and specificity, derived from the huTCR mouse platform,¹ introduced by retroviral transduction into autologous patient-derived CD8 + T cells. The anticipated mode of action of TK-8001 is to bind to MAGE-A1-epitope presenting tumor cells and eliminate them via CD8+ cytotoxic activity and interferon- γ release. Preclinical exploration of the TK-8001 TCR has demonstrated potent antitumor activity, even in low-expressing MAGE-1 positive tumor cells, and favorable benchmarking vs. existing MAGE-A1 directed TCRs derived from human donors. This abstract describes the currently launched phase 1/2 trial for TK-8001.

Methods The IMAG1NE trial (Immunotherapeutic MAGE-A1 directed Neoplasm Elimination) is a phase 1/2, first-in-human, open-label, accelerated titration, two-part clinical trial of TK-8001 (MAGE-A1-directed TCR-transduced autologous CD8+ T cells) in subjects with HLA-A*02:01 genotype and advanced-stage/metastatic, MAGE-A1+ solid tumors that either have no approved therapeutic alternative(s) or are in non-curable state and have received a minimum of two lines of systemic therapy. Major endpoints for the IMAG1NE trial will be safety, pharmacokinetics, pharmacodynamics (e.g. cytokine profiles) as well as preliminary clinical efficacy (degree of tumor mass reduction and duration of response). In Part 1 of the trial, three different doses of TK-8001 will be explored for safety and preliminary clinical efficacy in an accelerated titration design. The starting dose is set at 1×10^8 MAGE-A1 TCR transduced CD8+ T cells followed by two escalation steps. Part 2 of the trial will enroll up to 30 subjects with advanced-stage, MAGE-A1 positive cancer to confirm safety and efficacy. The study is expected to open for enrolment in Q4/2021. For further information please contact T-knife GmbH at info@t-knife.com.

REFERENCES

1. Li, Liang-Ping, J Christoph Lampert, Xiaojing Chen, Catarina Leitao, Jelena Popović, Werner Müller, and Thomas Blankenstein. Transgenic mice with a diverse human T cell antigen receptor repertoire. *Nature Medicine* 2010;**16**: 1029–34.

Ethics Approval In progress, expected 11/2021

<http://dx.doi.org/10.1136/jitc-2021-SITC2021.499>

SYNB1891, A BACTERIUM ENGINEERED TO PRODUCE A STING AGONIST, DEMONSTRATES TARGET ENGAGEMENT IN HUMANS FOLLOWING INTRATUMORAL INJECTION

¹Richard Riese, ²Jason Luke*, ³Karl Lewis, ⁴Filip Janku, ⁴Sarina Piha-Paul, ⁵Claire Verschraegen, ¹Aoife Brennan, ⁶Michael Armstrong, ⁷Mary Varterasian, ¹Anna Sokolovska, ⁸James Strauss. ¹Synlogic Inc, Cambridge, MA, USA; ²UPMC Hillman Cancer Center, Pittsburgh, PA, USA; ³University of Colorado, Aurora, CO, USA; ⁴University of Texas, Houston, TX, USA; ⁵Ohio State University, Columbus, OH, USA; ⁶QVIA Biotech, Durham, NC, USA; ⁷Ann Arbor Drug Safety, LLC, Ann Arbor, MI, USA; ⁸Mary Crowley Cancer Research, Dallas, TX, USA

Background SYNB1891 is a live, modified strain of probiotic *E. coli* Nissle engineered to produce cyclic dinucleotides under hypoxia leading to stimulator of interferon genes (STING)-activation in phagocytic antigen-presenting cells in tumors and activating complementary innate immune pathways.

Methods This first-in-human study (NCT04167137) enrolled patients with refractory advanced solid tumors to receive intratumoral (IT) injections of SYNB1891 monotherapy or in combination atezolizumab. Patients enrolled in the monotherapy arms received doses of 1×10^6 - 3×10^8 live cells on Days 1, 8 and 15 of the first 21-day cycle and then on Day 1 of each subsequent cycle. Patients enrolled in the 2 combination cohorts received doses of 1×10^7 - 3×10^7 live cells in combination with atezolizumab administered on a 21-day cycle. The primary objective of the study was to evaluate safety and tolerability of SYNB1891 alone and in combination with atezolizumab. Other objectives include SYNB1891 kinetics in blood and injected tumor, STING-target engagement as assessed by IT gene expression and serum cytokines, and tumor responses.

Results This interim analysis includes 23 patients across 6 monotherapy cohorts dosed at 1×10^6 , 3×10^6 , 1×10^7 , or 3×10^7 , 1×10^8 and 3×10^8 live cells, and 7 patients dosed in 2 combination therapy cohorts (1×10^7 and 3×10^7 live cells). The mean (range) age was 61 (25–82); 19 patients were female. There were 4 cytokine release syndrome events in monotherapy cohorts, including one grade 3 event which met the criterion for dose limiting toxicity at 3×10^8 live cells; there were no other SYNB1891-related serious adverse events. There were no SYNB1891-related infections. SYNB1891 was not detected in the blood at 6 or 24 hours after the first dose or intratumorally 7 days following the first dose. Treatment with SYNB1891 demonstrated activation of the STING pathway and target engagement as assessed by upregulation of interferon-stimulated genes (ISG15, IFIT1, IFI2), chemokines/cytokines (CXCL9, CXCL10, TNFRS18, TNFSF10) and T-cell response genes (GZMA, CD4, PD-L2) in core biopsies obtained pre-dose and 7 days following the third weekly dose. In addition, there was a dose-response increase in serum cytokines. Durable, stable disease was observed in two patients treated with SYNB1891 monotherapy refractory to prior PD-1/L1 antibodies with vulvar melanoma (1×10^6 live cells; RECIST -28%) and small cell lung cancer (1×10^7 live cells; RECIST -12%).

Conclusions Repeat IT injection of SYNB1891 as monotherapy and in combination atezolizumab in this ongoing study is safe and well-tolerated up to at least 1×10^8 live cells, and shows evidence of STING pathway target engagement.

Acknowledgements We thank Inessa Vulfova for her clinical support in conduct of this study.

Trial Registration clinicaltrials.gov (NCT04167137)

Ethics Approval The study protocol, the informed consent form (ICF), and printed subject information materials were

reviewed and approved by the institutional review board (IRB) at the investigational site before any study procedures were performed. Written informed consent to participate in the study was obtained from each subject before any study-specific procedures were performed. The Ohio State University Cancer Institutional Review Board; Approval ID: 2020C0194MD Anderson Cancer Center Institutional Review Board; Approval ID: 2019-0576Mary Crowley Medical Research Center Institutional Review Board; Approval ID: 19-31 SYNB1891-CP-001North Texas Institutional Review Board; Approval ID: 2019.040WIRB Approval ID: 20192779University of Pittsburgh Institutional Review Board Approval ID: STUDY20010116

<http://dx.doi.org/10.1136/jitc-2021-SITC2021.500>

SURVIVAL AND IMMUNE RESPONSE DATA FROM INTRATUMORAL INT230-6 ALONE (IT-01) AND WITH PEMBROLIZUMAB [KEYNOTE-A10] IN SUBJECTS WITH LOCALLY ADVANCED, UNRESECTABLE AND METASTATIC SOLID TUMORS

¹Jacob Thomas*, ¹Anthony El-Khoueiry, ²Anthony Olszanski, ³Nilofar Azad, ⁴Giles Whalen, ¹Diana Hanna, ⁵Matthew Ingham, ⁶Syed Mahmood, ⁶Lewis Bender, ⁶Ian Walters, ⁷Lillian Siu. ¹Keck School of Medicine of USC, Los Angeles, CA, USA; ²Fox Chase Cancer Center, Philadelphia, PA, USA; ³Johns Hopkins University School of Med, Chevy Chase, MD, USA; ⁴UMASS Memorial Med Ctr, Worcester, MA, USA; ⁵Columbia University Med Ctr, New York, NY, USA; ⁶Intensity Therapeutics, Inc., Westport, CT, USA; ⁷Princess Margaret Cancer Center, Toronto, Canada

Background Background: Study IT-01 (KEYNOTE-A10) evaluates INT230-6, a novel formulation of cisplatin (CIS) and vinblastine (VIN) with an amphiphilic cell penetration enhancer designed for intratumoral (IT) administration, as monotherapy and in combination with pembrolizumab (PEM). In preclinical studies, INT230-6 increases drug dispersion throughout the tumor, allows drug diffusion into cancer cells and recruits dendritic, CD4 and CD8 T cells. The addition of PEM improves these responses in mouse models.

Methods IT-01 is an open-label phase 1/2 study, currently enrolling adult subjects with solid tumors in phase 2. The study assesses the safety and efficacy of INT230-6 IT Q2W up to 5 doses as monotherapy or with PEM 200mg Q3W. Biopsies from injected tumor are taken pretreatment and Day 28 for immunohistochemistry (IHC) analysis.

Results Fifty-seven INT230-6, two INT230-6 then PEM combination, and thirteen INT230-6 + PEM combination subjects were enrolled having a median of 4 prior therapies (0, 10). Median age was 62. 20+ cancer types were accrued; breast cancer and sarcoma were the most frequent. Over 500 image guided INT230-6 IT injections were given (253 to deep tumors) at doses of 0.3 to 172mL (86 mg CIS, 17.2 mg VIN) in a single session (contains higher amounts than typical IV chemo doses). PK shows that 95% of INT230-6 active agents remain in the tumor.¹ The most common (>25%) related adverse events (AEs) for INT230-6 alone were localized pain (59%), nausea (37%), and fatigue (29%). Safety profile of the PEM combination was similar. There were no related grade 4 or 5 AEs in either arm. The median overall survival (mOS) estimated with removal of <2cm³ and >700cm³ tumor burdens was 433 days for monotherapy (n=51) and 513 days for PEM combination (n=12), which compares favorably to results seen in basket studies of patients having similar prognostic factors (ECOG, LDH, # of metastatic sites).² IHC results indicate influx of CD4 and CD8 T-cells in injected lesions. No meaningful changes were observed in circulating inflammatory cytokines. Abscopal effects in the monotherapy arm were observed in 15 visceral/deep lesions in 11 patients, primarily who received an INT230-6 dose >50% of their total tumor burden (TTB).

Conclusions INT230-6 is well tolerated when administered IT as monotherapy and combined with PEM. Data suggests that INT230-6 prolongs survival compared to published basket studies in patients with similar prognostic factors. IHC and abscopal results indicate dosing INT230-6 may also activate a T-cell mediated immune response.

Acknowledgements N/A

Trial Registration NCT# 03058289

REFERENCES

1. Owelien. Historical PK data from IV administration. *J Cancer Res* 1977; **8**.

2. Abstract. Wagner M, et al. Validation of the Royal Marsden Hospital (RMH) prognostic score in 100 patients with advanced sarcoma enrolled in early phase clinical trials at a major cancer center. *JCO* 2015. https://ascopubs.org/doi/abs/10.1200/jco.2015.33.15_suppl.10558

Ethics Approval The protocol was approved by an institutional review board, independent ethics committee, or research ethics board at each institution. All subjects or their legally acceptable representative provided written informed consent before screening. The study was designed, undertaken, and reported in accordance with the Declaration of Helsinki, and is registered with clinicaltrials.gov with registration no NCT03058289.

<http://dx.doi.org/10.1136/jitc-2021-SITC2021.501>

RECOMMENDED PHASE 2 DOSE, PHARMACOKINETICS, PHARMACODYNAMICS, AND PRELIMINARY EFFICACY OF THE IL-15 SUPERAGONIST SO-C101 AS MONOTHERAPY IN PATIENTS WITH ADVANCED/METASTATIC SOLID TUMORS

¹Aurelien Marabelle*, ¹Stéphane Champiat, ²Vladimir Galvao, ³Aung Naing, ³Filip Janku, ⁴Patricia LoRusso, ⁵Peter Grell, ⁶Richard Sachse, ⁷David Bechard, ⁶Joachim Kiemle-Kallee, ²Ellena Garralda. ¹Institute de Cancerologie, Gustave Roussy, Villejuif, France; ²Hospital Universitari Vall d'Hebron, Vall d'Hebron Institute of Oncology (VHIO), Barcelona, Spain; ³Department of Investigational Cancer Therapeutics, MD Anderson Cancer Center, Houston, TX, USA; ⁴Yale University School of Medicine, New Haven, USA; ⁵Masaryk Memorial Cancer Institute (MMCI), Brno, Czech Republic; ⁶SOTIO Biotech AG, Basel, Switzerland; ⁷Cytune Pharma, Nantes, France

Background SO-C101 is a superagonist fusion protein of IL-15 and the IL-15 receptor α sushi+ domain. SO-C101 was investigated in a multicenter, open-label, dose escalation study as monotherapy and in combination with pembrolizumab in patients with selected advanced/metastatic tumors (NCT04234113).

Methods The SO-C101 monotherapy part of the study followed a classical 3+3 dose escalation design. Study objectives were to determine the maximum tolerated dose (MTD) and the recommended phase 2 dose (RP2D). The evaluation period for dose-limiting toxicities in each dose step was 21 days. The RP2D was defined as MTD or below, also considering pharmacokinetic and pharmacodynamic parameters. The study is ongoing (data cut-off 21 June 2021).

Results Thirty patients with a median of 3 (range 1–9) lines of previous systemic therapies were treated at doses 0.25, 0.75, 1.5, 3.0, 6.0, 9.0, 12.0, and 15 μ g/kg. At 15 μ g/kg, 2 of 3 patients had a dose-limiting toxicity (hyperbilirubinaemia grade [G] 4 and transaminase increase G3). The MTD was reached at 12 μ g/kg. This dose was determined as the RP2D, supported by a dose-dependent increase in NK- and CD8+ T cell activation, the latter reaching a plateau at 12 μ g/kg. SO-C101 plasma concentration increased dose-proportionally (T_{max} was 5.5 hours and T_{1/2} was 4 hours). The most common adverse events (AEs) were G1 or G2 lymphopenia, local injection site reactions, transaminase increase, flu-like syndrome, and CRS-related symptoms such as fever and chills. Study drug-related AEs >G2 that occurred more than once were lymphopenia and transaminase increase. No treatment-related death was reported. One patient with cutaneous squamous cell carcinoma, who had previously progressed on cemiplimab, showed a partial response at 6.0 μ g/kg (duration >4 months, target lesion decrease of 58%). After progression, the patient was put on combination treatment (SO-C101 and pembrolizumab) and again achieved a significant partial response. Two other patients treated with doses below the RP2D had confirmed stable disease for 6 and 15 weeks. At the RP2D, one patient out of 6 discontinued due to progression, while 5 are stable and receiving treatment (range 4–11 weeks).

Conclusions The RP2D was defined at 12 μ g/kg. SO-C101 administration induced a strong activation of peripheral NK and CD8+ T cells reproducible after each dosing. Related AEs were manageable and resolved quickly. Preliminary clinical efficacy signals including stable disease and partial response were observed in this heavily pretreated patient population. SO-C101 monotherapy has the potential to provide additional clinical benefit to patients with solid tumors.

Trial Registration NCT04234113

Ethics Approval This study was approved by the FDA (IND 140011) and by the Ethics Boards of participating institutions.

<http://dx.doi.org/10.1136/jitc-2021-SITC2021.502>

CLINICAL ACTIVITY OF ICT01, AN ANTI-BTN3A-TARGETED, γ 9 δ 2-ACTIVATING MAB, ALONE AND IN COMBINATION WITH PEMBROLIZUMAB IN PATIENTS WITH ADVANCED/REFRACTORY SOLID TUMORS: EVICTION TRIAL

¹Martin Wermke*, ²Aurelien Marabelle, ³Christiane Jungels, ⁴Johann De Bono, ⁵Norbert Vey, ⁵Cécile Vicier, ⁶Elena Garralda, ⁷Steven Le Gouill, ⁸Patricia LoRusso, ²Stephane Champiat, ¹Catrin List, ⁶Vladimir Galvão de Aguiar, ¹Katrin Wetzko, ¹Leo Rhunke, ⁹Aude de Gassart, ⁹Patrick Brune, ⁹Emmanuel Valentin, ¹⁰Marina Iche, Daniel Olive, ¹¹, ⁹Paul Frohna. ¹Medical Faculty Carl Gustav Carus, Technical University, Dresden, Germany, Dresden, Germany; ²Gustave Roussy, Paris, France, Villejuif, France; ³Institut Jules Bordet, Brussels, Belgium; ⁴The Institute for Cancer Research and Royal Marsden, London, UK, London, UK; ⁵Institut Paoli-Calmettes, Marseille, France; ⁶Vall d'Hebron Institute of Oncology, Barcelona, Spain; ⁷CHU de Nantes, Nantes, France; ⁸Yale University Cancer Center, New Haven, USA; ⁹Imcheck Therapeutics, Marseille, France; ¹⁰Life consulting, Argenteuil, France; ¹¹CRCM, INSERM U1068, Marseille, France

Background We presented EVICTION Trial data from patients with solid tumors that showed microgram doses of ICT01 rapidly activate γ 9 δ 2 T cells that release inflammatory cytokines (e.g., IFN γ) and traffic from the circulation (Abstract #316, SITC 2020). Confirming tumor infiltration of activated γ 9 δ 2 T cells and the subsequent clinical benefit are the next steps in characterizing the therapeutic potential of ICT01.

Methods EVICTION is an ongoing Phase 1/2a, EU and US trial assessing ICT01 monotherapy (IV Q3W) in advanced/refractory solid and hematologic cancers, and ICT01 in combination with pembrolizumab (200mg IV Q3W) in solid tumor patients who failed ≥ 1 CPI. Pharmacodynamic activity was monitored by immunophenotyping and cytokine level analysis. Tumor biopsies (baseline, Day 28) were used for immunohistochemistry of BTN3A and tumor-infiltrating lymphocytes, and gene expression profiling. Efficacy evaluations were conducted every 8 weeks.

Results ICT01 monotherapy dose escalation (20 μ g to 200mg IV ICT01 Q3W) in solid tumor patients (Group A, n=32) has been completed, and 3 dose cohorts of ICT01 (700 μ g, 2 and 7 mg) plus Pembro (Group C, n=12) were completed; both without any DLTs. First-dose fever and chills (Grade 1/2) were the most common AEs that increased in frequency but not severity with dose and did not recur. ICT01 induced trafficking of $>95\%$ of circulating γ 9 δ 2 T cells within 30 min post ICT01 (≥ 2 mg), which was sustained for 21 days at doses ≥ 75 mg. Transient, dose-dependent increases in serum cytokines at 30 min (TNF α) or 4h (IFN γ) post-dose were correlated with baseline γ 9 δ 2 T cell counts and with activation and migration of NK and CD8 T cells out of the blood at doses ≥ 7 mg. Higher baseline circulating γ 9 δ 2 T cells and lower TILs were associated with more robust intra-tumoral increases in total γ 8(3–34x increase), CD3 (3–55x increase) and CD8 T cells (1.3–66x increase), which demonstrated the potential to transform an immune desert tumor phenotype. Disease control by ITT analysis of RECIST1.1 data was observed in 6/32 (SD) and 4/7 patients (3 SD (bladder, melanoma, NSCLC), 1 PR (bladder)) in Groups A and C, respectively, with 5/6 patients at 7mg in Group C not yet evaluable.

Conclusions These results show a broad antitumor immune response in the blood and tumors comprising γ 9 δ 2, CD8 T cell, and NK cell activation and tumor-infiltration following ICT01 alone and in combination with pembrolizumab. Preliminary efficacy data suggest low-dose ICT01 plus pembrolizumab may be more effective than ICT01 monotherapy for advanced/refractory solid tumors, which requires confirmation.

Acknowledgements Lena Daher for her medical/scientific writing support.

Trial Registration www.clinicaltrials.gov NCT04243499; EudraCT Number: 2019-003847-31

Ethics Approval This study was approved by the following Ethics Committees: COMITE DE PROTECTION DES PERSONNES, Sud-Méditerranée V (Gustave Roussy, IPC, Nantes), Comité d'Ethique Institut Jules Bordet, COMITÉ DE ÉTICA DE INVESTIGACIÓN CLÍNICA CON MEDICAMENTOS del Hospital Universitari Vall d'Hebron, Ethikkommission an der TU Dresden, HRA London-Surrey Borders Research Ethics Committee.

Consent Written informed consent was obtained from the patient for publication of this abstract and any accompanying images. A copy of the written consent is available for review by the Editor of this journal.

<http://dx.doi.org/10.1136/jitc-2021-SITC2021.503>

A PHASE I, FIRST-IN-HUMAN CLINICAL TRIAL OF THE GDF-15 NEUTRALIZING ANTIBODY CTL-002 IN SUBJECTS WITH ADVANCED STAGE SOLID TUMORS (ACRONYM: GDFATHER)

¹Ignacio Melero*, ²Emiliano Calvo, ³Maria-Elisabeth Goebeler, ⁴Elena Garralda, ⁵Reinhard Dummer, ⁶Maria Rodríguez-Ruiz, ²Maria de Miguel, ³Cyrus Michael Sayehli, ⁷Guzman Alonso Casal, ⁸Egle Ramelyte, ⁹Martin Schuler, ⁹Tanja Gromke, ⁶Miguel Sanmamed, ²Irene Moreno, ³Ralf Bargou, ⁷Maria Lostes, ¹⁰Julia-Tatjana Maul, ⁵Corinne Eggenschwiler, ⁹Heike Richly, ¹¹Petra Fettes, ¹¹Kathrin Klar, ¹¹Christine Schuberth-Wagner, ¹¹Markus Haake, ¹²Jörg Wischhusen, ¹¹Eugen Leo. ¹Universidad de Navarra, Navarra, Spain; ²START Madrid-Centro Integral Oncológico Clara Campal, Madrid, Spain; ³University Hospital Würzburg, Würzburg, Germany; ⁴Hospital Universitari Vall d'Hebron, Barcelona, Spain; ⁵University Hospital Zürich, Zurich, Switzerland; ⁶Clinica Universidad de Navarra, Pamplona, Spain; ⁷Hospital Universitari Vall d'Hebron, Barcelona, Spain; ⁸University Hospital Zurich, Zürich, Switzerland; ⁹University Hospital Essen, Essen, Germany; ¹⁰University Hospital Zürich, Zürich, Switzerland; ¹¹CatalYm GmbH, Planegg, Germany; ¹²University of Würzburg, Wuerzburg, Germany

Background Growth and differentiation factor 15 (GDF-15) is a TGF- β superfamily member physiologically expressed mainly in placenta and linked to feto-maternal tolerance. Under pathophysiologic conditions, prevention of excessive immune cell infiltration during tissue damage and cachexia induction have been ascribed to GDF-15. Recent research has though indicated a prominent role in modulation of the tumor microenvironment and the immune synapse, too^{1 2} indicating that GDF-15 may be a major tumor-derived immunosuppressant. Importantly, several cancer entities secrete high levels of GDF-15, correlating with poor prognosis and reduced overall survival [Front Immunol 2020 May 19;11:951]. To block this effect the GDF-15 neutralizing antibody CTL-002 was generated. In preclinical models CTL-002 demonstrated potent effector T cell shifting into tumor tissue by neutralizing GDF-15.

Methods This is a phase 1, first-in-human (FIH), two-part, open-label clinical trial of intravenous (IV) administration of CTL-002 given as monotherapy and in combination with an anti-PD-1 antibody in subjects with advanced-stage, relapsed/refractory solid tumors who relapsed or were refractory to a prior anti-PD-1/PD-L1 therapy. Eligible subjects have exhausted all available approved standard treatments, including prior anti-PD1/PD-L1 treatment, and present with a biopsy-accessible tumor for serial biopsy taking. The trial is termed GDFATHER, for "GDF-15 Antibody-mediaTed Effector cell Relocation". Main endpoints are safety of CTL-002 monotherapy and CTL-002 combination with an anti-PD-1 antibody, pharmacokinetics, pharmacodynamics (e.g. degree of GDF-15 neutralization achieved and change in immune-cell number and composition in the tumor tissue) as well as preliminary clinical efficacy (tumor mass reduction; anticachexia effect). In part A of the trial (dose escalation) up to 24 subjects will receive escalating doses of CTL-002 IV (0.3 – 20 mg/kg) in a "mono-followed-by-combination"-design with CTL-002 given as monotherapy and followed by combination with an anti-PD-1 checkpoint inhibitor. In part B (expansion) up to 5 cohorts with up to 25 subjects per cohort with defined tumor entities expected to be GDF-15 dependent will be treated to determine the recommended phase 2 dose (RP2D) and further evaluate safety and preliminary efficacy of CTL-002 monotherapy and the combination. The study was initiated in December 2020 and enrolled the first patient on Dec 09, 2020. Cohort 4 is ongoing at time of submission (07/2021) and so far no DLT has occurred. Updated safety, biomarker and response assessments will be reported at the meeting. The ClinicalTrials.

gov Identifier is NCT04725474. For more information please contact info@catalym.com.

Trial Registration NCT04725474

REFERENCES

1. Wischhusen J, Wistuba-Hamprecht K, Harter PN, Cheng P, Martens A, Gogolla F, Nonomura Y, Romer P, Koch SD, Haake M, Schuberth-Wagner C, Rudiger M, Leo E, Mittelbronn M, Levesque MP, Hackl H, Dummer R, Weide B. Identifying GDF-15 as potential novel immunotherapeutic target linked to immune cell exclusion in tumors and resistance to anti-PD-1 treatment [abstract]. In: Proceedings of the Annual Meeting of the American Association for Cancer Research 2020; 2020 Apr 27–28 and Jun 22–24. Philadelphia (PA): AACR; *Cancer Res* 2020;**80**(16 Suppl): Abstract nr 2161.
2. Hurt E, Thomas S, Mulgrew K, Blackmore S, Moynihan J, Cusdin F, Dodd R, Cariuk P, Sigurdardottir A, Brannigan E, Dobson C, Kumar R, Cobbold M. AZD8853: A novel antibody targeting GDF15 for immunotherapy refractory tumors [abstract]. In: Proceedings of the American Association for Cancer Research Annual Meeting 2021; 2021 Apr 10–15 and May 17–21. Philadelphia (PA): AACR; *Cancer Res* 2021;**81**(13_Suppl): Abstract nr 1828.

Ethics Approval All participants gave informed consent prior to participation. EC approval by Gobierno de Navarra, Departamento de Salud, EC_2020/30, Dated: Oct 13, 2020 in Pamplona, Spain. Respective additional national lead EC approvals for Germany (Ethikkommission der Universität Würzburg, 203–20ff of Oct 26, 2020) and Switzerland (Kantonale Ethikkommission Zürich, 2020–02308 of Nov 24, 2020).

<http://dx.doi.org/10.1136/jitc-2021-SITC2021.504>

505

RELATIONSHIP OF INFUSION DURATION AND DOSE TO SAFETY, EFFICACY AND PHARMACODYNAMICS: SECOND PART OF A PHASE 1–2 STUDY USING VSV-IFN β -NIS (VV1) ONCOLYTIC VIRUS IN PATIENTS WITH REFRACTORY SOLID TUMORS

¹Manish Patel*, ²Steven Powell, ³James Strauss, ⁴Melissa Johnson, ⁵Timothy Cripe, ⁶Kah-Whye Peng, ⁶Stephen Russell, ⁷Luke Russell, ⁸Monica Reckner, ⁸Erol Wiegert, ⁸Alice Bexon, ⁹Jaime Merchan. ¹University of Minnesota, Rochester, MN, USA; ²Sanford Health, Sioux Falls, SD, USA; ³Texas Oncology, Dallas, TX, USA; ⁴Sarah Cannon Research Institute, Nashville, TN, USA; ⁵Nationwide Children's Hospital, Columbus, OH, USA; ⁶Vyriad Inc. and Mayo Clinic, Rochester, MN, USA; ⁷Vyriad Inc., Rochestersre, MN, USA; ⁸Bexon Clinical Consulting LLC, Rochester, MN, USA; ⁹University of Miami, Miami, FL, USA

Background Oncolytic viruses (OVs) show significant potential for treating tumors alongside immunotherapies.¹ VV1 is an OV derived from the innocuous vesicular stomatitis virus (VSV). VV1 has been engineered to express human interferon (IFN) β and thyroidal sodium iodide symporter (NIS).² VV1-infected cells produce IFN β , which protects non-cancer cells from VV1 and allows VV1 to spread more efficiently in cancerous tissue.³ ⁴ NIS expression on cells imports ^{99m}Tc pertechnetate, which facilitates in vivo imaging of virus infection.² This three-part, phase 1–2 study was designed to determine the safety and tolerability of VV1 in patients with advanced unresectable and metastatic solid tumors. Here we report on the second part of this study: selection of recommended phase 2 regimen (RP2D), comprising further assessment of both duration and dose.

Methods Patients (n=29) were enrolled to receive a single IV infusion of VV1 monotherapy. 23 patients received IV VV1 1.7×10^{10} TCID₅₀ over 15, 30, 60 or 180 min. Six patients received 1.0×10^{11} TCID₅₀ over 30 min with aggressive pre-medication and fluid support overnight. Patients were monitored for dose limiting toxicities over 21 days with efficacy assessments after 6 weeks and then every 3 months for survival. The primary objective was to establish the safety and tolerability of IV VV1. Secondary objectives included preliminary efficacy, pharmacokinetics and pharmacodynamics.

Results In this study VV1, demonstrated an acceptable safety profile. No deaths or Grade 4 infusion-related reactions (IRR) were reported. VV1 shedding by buccal swabs was negative at all study visits. Peak IFN β serum levels and preliminary efficacy signals (2 PRs) were associated with 30 min infusion duration and higher dose, with RECIST data pending for 1×10^{11} (table 1).

Abstract 505 Table 1

Infusion duration (min)	Dose	N	DLT (N)	IRR G1 (N)	IRR G2 (N)	Shedding (N)	CRS max Grade 1 (N/%)	CRS max Grade 2 (N/%)	IRR/CRS max Grade 3 (N/%)	IFN β > 150 pg/mL (N)	RECIST PR/SD (N)
15	1.7×10^{10}	5	2*	1	3 (+1G3)	0	1 (20)	3 (60)	1 (20)	0	2
30	1.7×10^{10}	7	0	4	3	0	4 (57)	3 (43)	0	4	4
60	1.7×10^{10}	5	0	4	1	0	3 (60)	1 (20)	0	0	2
180	1.7×10^{10}	6	1	2	3	0	2 (33)	3 (50)	0	0	1
30	1.0×10^{11}	6	1	1	4	0	1 (17)	4 (67)	0	2	1

*CRS & Hyperbilirubinemia with AST G3

Conclusions In this study, the absence of viral shedding demonstrates that VV1 is safe for patient and caregiver with little/no environmental impact. There was no difference in safety between the lower and the higher dose infusions. In this patient population acceptable tolerability was observed at the higher dose with 30 min duration, thus the RP2D is 1×10^{11} over 30 mins.

Trial Registration NCT02923466

REFERENCES

- Hemminki O, Dos Santos JM, Hemminki A. Oncolytic viruses for cancer immunotherapy. *J Hematol Oncol* 2020;**13**(1):84.
- Naik S, Nace R, Federspiel MJ, Barber GN, Peng KW, Russell SJ. Curative one-shot systemic virotherapy in murine myeloma. *Leukemia* 2012;**26**(8):1870–1878.
- Barber GN. Vesicular stomatitis virus as an oncolytic vector. *Viral Immunol* 2004;**17**(4):516–527.
- Lichty BD, Power AT, Stojdl DF, Bell JC. Vesicular stomatitis virus: re-inventing the bullet. *Trends Mol Med* 2004;**10**(5):210–216.

Ethics Approval Ethics approval was granted by WCG IRB. IRB tracking number: 20163005. Voluntary written informed consent was obtained from every patient prior to participation.

<http://dx.doi.org/10.1136/jitc-2021-SITC2021.505>

IGNYTE: AN OPEN-LABEL, MULTICENTER, PHASE 1/2 (PH 1/2) CLINICAL TRIAL OF RP1 ± NIVOLUMAB IN PATIENTS WITH ADVANCED SOLID TUMORS

¹Mark Middleton*, ²Mohammed Milhem, ³Francesca Aroldi, ⁴Joseph Sacco, ⁵Ari VanderWalde, ⁶Scott Baum, ⁶Adel Samson, ⁷Jason Chesney, ⁸Jiaxin Niu, ⁹Terence Rhodes, ⁹Tawnya Bowles, ¹⁰Hamid Emamekhoo, ¹¹Katy Tsai, ¹²Gino In, ¹³Georgia Beasley, ¹⁴Bartosz Chmielowski, ¹⁵Sophie Dalac-Rat, ¹⁶Katharina Kahler, ¹⁷Eva Muñoz, ⁴Anna Olsson-Brown, ¹⁸Praveen Bommareddy, ¹⁸Lavita Menezes, ¹⁸Andrea Pirzkall, ¹⁸Robert Coffin, ¹⁹Kevin Harrington. ¹Churchill Hospital, Oxford, UK; ²Holden Comprehensive Cancer Center, Iowa City, IA, USA; ³University of Oxford, Oxford, UK; ⁴Clatterbridge Cancer Centre, Wirral, UK; ⁵West Cancer Center and Research Institute, Germantown, TN, USA; ⁶University of Leeds, Leeds, UK; ⁷James Graham Brown Cancer Center, Louisville, KY, USA; ⁸Banner MD Anderson Cancer Center, Gilbert, AZ, USA; ⁹Intermountain Med Ctr, St. George, UT, USA; ¹⁰Carbone Cancer Center, Madison, WI, USA; ¹¹Helen Diller Family Comprehensive Cancer, San Francisco, CA, USA; ¹²Norris Comprehensive Cancer Center, Los Angeles, CA, USA; ¹³Duke Cancer Institute, DURHAM, NC, USA; ¹⁴University of California Los Angeles, Los Angeles, CA, USA; ¹⁵CHU Dijon Bourgogne, Bourgogne, France; ¹⁶University of Kiel, Kiel, Germany; ¹⁷Vall d'Hebron Hospital, Vall D'hebron, Spain; ¹⁸Replimune, Woburn, MA, USA; ¹⁹The Institute of Cancer Research, London, UK

Background RP1 is an enhanced potency oncolytic HSV-1 which expresses a fusogenic glycoprotein (GALV-GP R-) and granulocyte macrophage colony stimulating factor (GM-CSF).¹ In pre-clinical studies, RP1 demonstrated potent GALV-GP R-enhanced anti-tumor activity and immunogenic cell death. This Phase 1/2 (Ph 1/2) study was designed to evaluate the safety and efficacy of RP1 ± nivolumab (nivo) in patients (pts) with advanced solid tumors, including pts whose disease failed prior anti-PD-1/PD-L1 therapy and has reported promising interim data in a number of tumor types including cutaneous squamous cell carcinoma (CSCC) and anti-PD1 failed melanoma to date.²

Methods This is a multi-center, first-in-human, open label, multi-cohort, non-randomized Ph1 study of RP1 alone and combined with nivo followed by Ph2 in combination with nivo in pts with recurrent advanced solid tumors including those that progressed after prior anti-PD-1/PD-L1 therapy. The Ph 1 monotherapy dose escalation (n=14) and RP-1 combination expansion (n=22) cohorts are fully enrolled. Approximately 260 pts are expected to be enrolled in the ongoing Ph 2 portion across five cohorts; melanoma (n=30, enrollment complete), non-melanoma skin cancer (n=45, to include 15 pts with anti-PD-1/PD-L1 failed disease), anti-PD-1 failed MSI-H/dMMR tumors (n=30), anti-PD-1/PD-L1-failed non-small-cell lung cancer (n=30) and a registration-directed cohort in anti-PD-1 failed cutaneous melanoma (n=125). Pts in the Ph 2 portion receive up to 10 mL of RP1 intratumorally into one or more superficial or deep seated/visceral lesions at the recommended Ph 2 dose (1×10^6 PFU/mL \times 1 followed by 1×10^7 PFU/mL \times 7, Q2W). Following the first dose of RP1, nivo (240 mg IV Q2W for 4 months then 480 mg IV Q4W for up to 2 years) is subsequently administered in combination. Pts may receive up to 8 additional doses of RP1 if they meet protocol-specified criteria. Tumor assessments are performed Q8W. The primary objectives of the Ph 2 part of the study are to assess the safety, tolerability, and overall response rate (ORR) of RP1 in combination with nivo, by independent review for the anti-PD1 failed melanoma cohort. Secondary objectives include duration of response, complete response rate, disease control rate, PFS, 1-year and 2-year survival rates. Exploratory objectives include biodistribution and shedding analysis of RP1 and biomarker studies, including analyses of tumor biopsies and blood samples. Enrollment is currently ongoing in the UK and US, with

additional sites in the EU (including France and Spain) are expected to open in 2021.

Trial Registration NCT03767348

REFERENCES

1. Thomas S, Kuncheria L, Roulstone V, Kyula JN, Mansfield D, Bommareddy PK, Smith H, Kaufman HL, Harrington KJ, Coffin RS. Development of a new fusion-enhanced oncolytic immunotherapy platform based on herpes simplex virus type 1. *J Immunother Cancer* 2019;**7**(1):214.
2. Coffin R, Astley-Sparke P, and Middleton M (2021, June 3rd). Retrieved from <https://ir.replimune.com/static-files/f4fe3349-e082-4d41-94a1-106ce7e78a23>

Ethics Approval The study was approved by institutional review board or the local ethics committee at each site. Informed consent was obtained from patients prior to enrollment.

<http://dx.doi.org/10.1136/jitc-2021-SITC2021.506>

507

A PHASE 1 CLINICAL TRIAL OF RP2, AN ENHANCED POTENCY ONCOLYTIC HSV EXPRESSING AN ANTI-CTLA-4 ANTIBODY, AS A SINGLE AGENT AND COMBINED WITH NIVOLUMAB IN PATIENTS WITH ADVANCED SOLID TUMORS

¹Mark Middleton*, ²Joseph Sacco, ³Kevin Harrington, ²Anna Olsson-Brown, ⁴Tze Chan, ³Pablo Nenclares, ³Isla Leslie, ¹Francesca Aroldi, ⁵Praveen Bommareddy, ⁵Imran Saleem, ⁵Henry Castro, ⁵Andrea Pirzkall, ⁵Robert Coffin. ¹University of Oxford, Oxford, UK; ²Clatterbridge Cancer Centre, Wirral, UK; ³Institute of Cancer Research, London, UK; ⁴Royal Liverpool University Hospital, Liverpool, UK; ⁵Replimune, Woburn, MA, USA

Background RP2 is a first-in-class, enhanced potency oncolytic herpes simplex virus (HSV) -1 expressing GM-CSF, a fusogenic protein (GALV-GP R-), and an anti-CTLA-4 antibody-like molecule that is being tested in an open-label, multicenter, phase 1 study alone and combined with nivolumab (nivo). Preliminary data with RP2 as monotherapy has been presented previously [1–2]. We present updated safety, tolerability, and clinical activity data of RP2 alone and initial data in combination with nivolumab.

Methods Using a 3+3 dose escalation, patients (pts) received intratumoral injections of up to 10 mL RP2 to superficial and/or visceral tumors Q2W up to 5 times at two dose levels (Dose level 1: 10^5 PFU/mL then 4 doses of 10^6 PFU/mL; dose level 2: 10^6 PFU/mL then 4 doses of 10^7 PFU/mL). Following determination of the RP2D (10^6 PFU/mL, followed by subsequent doses of 10^7 PFU/mL, Q2W X 7), a combination cohort of 30 pts were dosed with RP2 up to 8 times combined with nivo (240 mg Q2W for 4 mos from the second RP2 dose, then 480 mg Q4W for 20 mos). Re-initiation of up to 8 additional RP2 doses is permitted in prespecified circumstances.

Results Nine pts were enrolled into the RP2 monotherapy phase (6 seropositive and 3 seronegative for HSV). Objective responses were observed in 3 pts, 1 ongoing CR for ≥ 15 months in mucoepidermoid carcinoma, 1 ongoing PR for ≥ 18 months in esophageal cancer with liver metastases, 1 PR in uveal melanoma with liver metastases that progressed at 15 months. As of June 3rd 2021, 27 patients had been enrolled and ongoing partial responses had been observed in 4/9 anti-PD-1 failed cutaneous melanoma, 1/3 uveal melanoma and 1/3 SCCHN pts. A further 8 patients remained on study with the opportunity for response. Biomarker analyses indicate T cell infiltration, increase in tumor inflammation signature, expansion of existing T cell clones and emergence of new T cell clones, together indicative of local and systemic anti-tumor activity. The combination was well tolerated and no new safety signals were identified.

Conclusions RP2 \pm nivo demonstrated good tolerability and durable systemic responses in pts with difficult-to-treat, heavily pretreated and anti-PD-1 failed advanced cancers. These data continue to support the hypothesis that oncolytic delivery of anti-CTLA-4 into tumors, with accompanying antigen release, presentation and immune activation, can provide potent systemic anti-tumor effects. Updated data from the full 30 patient cohort will be presented.

Trial Registration NCT04336241

REFERENCES

1. Aroldi F, Sacco J, Harrington K, Olsson-Brown A, Nenclares P, Menezes L, Bommareddy P, Thomas S, Kaufman H, Samakoglu S, Coffin R and Middleton M. 421, Initial results of a phase 1 trial of RP2, a first in class, enhanced potency, anti-CTLA-4 antibody expressing, oncolytic HSV as single agent and combined with nivolumab in patients with solid tumors *Journal for Immuno Therapy of Cancer* 2020;**8**.

2. Harrington KJ, Aroldi F, Sacco JJ, Milhem MM, Curti B, Vanderwalde A, et al. LB180-Clinical biomarker studies with two fusion-enhanced versions of oncolytic HSV (RP1 and RP2) alone and in combination with nivolumab in cancer patients indicate potent immune activation. *Cancer Res* 2021. LB-180

Ethics Approval The study was approved by institutional review board or the local ethics committee at each site. Informed consent was obtained from patients prior to enrollment.

<http://dx.doi.org/10.1136/jitc-2021-SITC2021.507>

A FIRST-IN-HUMAN PHASE 1 STUDY OF NL-201 IN PATIENTS WITH RELAPSED OR REFRACTORY CANCER

¹Aung Naing, ²Margaret Callahan, ³Brian Costello, ⁴Brendan Curti, ⁵Evan Hall, ⁶Aaron Hansen, ⁷Georgina Long, ⁸Anthony Joshua, ⁹Brooke Shankles, ⁹Umut Ulge*, ⁹Umut Ulge, ¹⁰Andrew Weickhardt. ¹MD Anderson Cancer Center, Houston, TX, USA; ²Memorial Sloan Kettering Cancer Center, New York, NY, USA; ³Mayo Clinic, Rochester, MN, USA; ⁴Providence Portland Medical Center, Portland, OR, USA; ⁵Seattle Cancer Care Alliance, Seattle, WA, USA; ⁶Princess Margaret Hospital, Toronto, Canada; ⁷University of Sydney and Royal North Shore and Mater Hospitals, Sydney, Australia; ⁸St Vincent's Hospital Sydney, Sydney, Australia; ⁹Neoleukin Therapeutics, Inc., Seattle, WA, USA; ¹⁰Olivia Newton-John Cancer Wellness and Res, Heidelberg, VT, Australia

Background NL-201 is a selective and long-acting computationally designed alpha-independent agonist of the IL-2 and IL-15 receptors, which share beta and gamma signaling subunits. NL-201 is being developed as a potent activator of CD8 + T cells and NK cells for cancer immunotherapy. Binding to the beta and gamma subunits selectively stimulates dose-dependent expansion and tumor infiltration of cytotoxic CD8 + T cells and NK cells, thereby enhancing the immune response in the tumor. The absence of binding to the IL-2 alpha subunit reduces the undesirable effects of traditional IL-2 therapies, such as vascular leak syndrome and expansion of immunosuppressive regulatory T cells. As such, NL-201 is designed to promote the desired immunomodulatory antitumor effects of IL-2 with an improved safety profile.

Methods NL201-101 is a Phase 1 first-in-human, open-label, dose-escalation, and cohort expansion study consisting of two parts. Part 1 is an adaptive monotherapy dose escalation study in up to 60 adult patients with advanced and/or refractory solid tumors to determine the safety profile and the recommended phase 2 dose (RP2D) and schedule of NL-201. During dose escalation, two different schedules will be evaluated: dosing every 21 days or on days 1 and 8 of each 21-day cycle. Tumor response to treatment will be assessed by Response Evaluation Criteria in Solid Tumours (RECIST) 1.1 and/or RECIST for use in cancer immunotherapy trials (iRECIST). In Part 2, patients with pathologically proven diagnosis of indication-specific cohorts (up to N=30/cohort), who have advanced and/or refractory measurable disease and have failed at least one line of treatment, which may include checkpoint inhibitors, will be enrolled. Key exclusion criteria include history of brain cancer, carcinomatous meningitis, neurologic autoimmune disease, or active central nervous system metastases; patients previously receiving CAR-T or IL-2-based therapies are not eligible. Recruitment of Part 1 began in April 2021, and the trial is actively enrolling. Clinicaltrials.gov identifier: NCT04659629.

Trial Registration ClinicalTrials.gov identifier: NCT04659629.

Ethics Approval All relevant documents have been or will be submitted to an Institutional Review Board (IRB)/Independent Ethics Committee (IEC) by the investigator and reviewed and approved by the IRB/IEC before the study is initiated. Site 1001: Belberry HREC, application number 2020-09-925 (Belberry does not provide an approval number); Site 1003: Austin Health HREC, approval number HREC/69340/Austin-2020; Site 2003: MDACC Office of Human Subjects Protection, approval number 2020-0383.

<http://dx.doi.org/10.1136/jitc-2021-SITC2021.509>

510 **SO-C101, A HIGH-AFFINITY IL-15RBG AGONIST, INDUCES SAFE AND POTENT ANTI-TUMOR IMMUNE ACTIVITIES IN PATIENTS WITH SOLID TUMORS AND SUPPORTS FURTHER CLINICAL INVESTIGATIONS**

Lenka Palová*. *SOTIO Biotech, Praha, Czech Republic*

Background SO-C101 is a high affinity superagonist fusion protein of interleukin (IL)-15 and the IL-15 receptor α (IL-15R α) sushi domain, representing a promising clinical candidate for the treatment of cancer. SO-C101 specifically stimulates natural killer (NK) cells and memory CD8⁺ T cells with no significant expansion and activation of regulatory T cell compartment.

Methods Blood and tumor samples from patients with advanced/metastatic solid tumors included in Phase clinical I study (NCT04234113) were analysed by flow cytometry, immunohistochemistry and NanoString analyses for the activation of immune cells induced by SO-C101 monotherapy or in combination with pembrolizumab.

Results SO-C101 showed a dose-dependent activity in blood of all patients with no clear correlation between the increase of immune cell proliferation and counts in blood and recruitment of immune cells into the tumor tissue. SO-C101 (RLI-15) as a monotherapy or in combination with pembrolizumab increases immune cell infiltration in tumors in clinically responsive patients in Phase clinical I study (NCT04234113) which is accompanied by NK and CD8⁺ T cell activation and cytotoxicity, increased proinflammatory chemokines and IFN-gamma signaling genes signatures.

Conclusions All patients showed dose-dependent pharmacodynamic responses in blood, however SO-C101 activity in the tumor microenvironment might be pivotal for the therapeutic success. Favorable safety profile and potent anti-tumor immune activities in patients with solid tumors support further clinical investigations.

Trial Registration NCT04234113

Ethics Approval This study was approved by the FDA (IND 140011) and by the Ethics Boards of participating institutions. The participants provided written informed consent.

<http://dx.doi.org/10.1136/jitc-2021-SITC2021.510>

INITIAL RESULTS OF A PHASE 1 STUDY OF INTRATUMORAL ONCR-177, AN ONCOLYTIC HERPES-SIMPLEX VIRUS-1 EXPRESSING FIVE IMMUNOMODULATORY TRANSGENES, IN SUBJECTS WITH ADVANCED INJECTABLE TUMORS

¹Jong Chul Park*, ²Hatem Soliman, ³Gerald Falchook, ⁴Taofeek Owonikoko, ⁵Anna Spreafico, ⁶Erminia Massarelli, ⁷Meredith McKean, ⁸Laura Chow, ⁹Patrick Ott, ¹⁰Robert Wesolowski, ¹¹Christos Fountzilas, ¹²Corey Whalen, ¹²Adrienne Yanez, ¹²Christopher Dupont, ¹²Julia Auer, ¹²Tooba Cheema, ¹²John Goldberg, ¹²Ted Ashburn, ¹¹Igor Puzanov. ¹Massachusetts General Hospital, Boston, MA, USA; ²Moffitt Cancer Center, Tampa, FL, USA; ³Sarah Cannon Research Institute at HealthONE, Denver, CO, USA; ⁴Emory University, Atlanta, GA, USA; ⁵Princess Margaret Cancer Centre, Toronto, Canada; ⁶City of Hope, Duarte, CA, USA; ⁷Sarah Cannon Research Institute-Tennessee, Nashville, TN, USA; ⁸Dell Seton Medical Center at the U. of Texas, Austin, TX, USA; ⁹Dana Farber Cancer Institute, Boston, MA, USA; ¹⁰Ohio State University, Columbus, OH, USA; ¹¹Roswell Park Comprehensive Cancer Center, Buffalo, NY, USA; ¹²Oncorus, Inc, Cambridge, MA, USA

Background ONCR-177 is a recombinant oncolytic herpes simplex virus (oHSV) that retains γ 34.5 and is engineered to express five immunomodulatory transgenes (IL-12, FLT3LG ECD, CCL4 and anti-PD-1 and anti-CTLA-4 antibodies) for the intratumoral treatment of solid tumors. Attenuation by miRNA leads to selective replication in tumor cells, and mutations in UL37 act as an orthogonal safety strategy. Transgenes elicit potent systemic stimulation of anti-tumor immunity.¹ ONCR-177 is being tested in an open-label, multicenter, phase 1 study alone and in combination with pembrolizumab (NCT04348916), for surface lesion injection and intrahepatic injection. Here we present the surface lesion escalation data.

Methods The objectives were determination of safety and recommended phase 2 dose (RP2D) of ONCR-177 monotherapy in subjects with advanced and/or refractory injectable surface lesions using a modified toxicity probability interval-2 (mTPI-2) escalation design at four dose levels: (Cohort 1: 1×10^6 PFU in 1 mL, Cohort 2: 1×10^7 PFU in 1 mL, Cohort 3: 1×10^8 PFU in 1 mL and Cohort 4: 4×10^8 PFU in 4 mL). Subjects received ONCR-177 by intratumoral injection once every 2 weeks (up to 10 times) until disease progression or unacceptable toxicity. There was no inpatient dose escalation.

Results As of June 28, 2021, 14 subjects with injectable tumors were enrolled in the dose escalation phase (3 in cohort 1, 4 in cohort 2, 3 in cohort 3 and 4 in cohort 4). Enrolled tumor types included: melanoma (3), breast (3), anal squamous cell (1), lung (1), duodenal (1), basal cell (1), chondrosarcoma (1), thyroid (1), oropharyngeal (1) and papillary renal cell (1). Subject median age was 67 years. Median number of prior lines of therapy was 4 (range 2–11), including 11 of 14 subjects with prior immunotherapy. Nine subjects were HSV-1 seropositive at baseline, 4 were negative, one was unknown. Treatment-related Adverse Events were all Grade 1–2. Most commonly reported were: cytokine release syndrome (2 occurrences in Cohort 4), fatigue, nausea, chills, headache, decreased appetite, hypotension, and injection site pain. There were no dose-limiting toxicities. The RP2D was selected as 4×10^8 PFU in 4 mL every 2 weeks up to 10 doses. Clinical data, including safety, viral shedding and exploratory biomarker data including peripheral payloads, peripheral cytokines and immune infiltration and PD-L1 expression in the tumor microenvironment will be presented.

Conclusions ONCR-177 monotherapy in heavily pretreated subjects with advanced, injectable, solid tumors at the RP2D was safe and tolerable. Enrollment at the RP2D is underway in monotherapy expansion.

Trial Registration NCT04348916

REFERENCES

1. Haines BB, Denslow A, Grzesik P, Lee JS, Farkaly T, Hewett J, Wambua D, Kong L, Behera P, Jacques J, et al. ONCR-177, an Oncolytic HSV-1 Designed to Potently Activate Systemic Antitumor Immunity. *Cancer Immunol Res* 2021;**9**: 291–308

Ethics Approval This study was approved by the following institutional Ethics Boards:-University Health Network Research Ethics Board (ID Number: 20-5069)-Integreview IRB (ID Number RM 694) -WCG IRB (ID Number: 20200150)-Advarra (ID Number: 00000971)-Roswell Park IRB (ID Number: STUDY00001189/P-553719)-The Ohio State University Cancer IRB (ID Number: 2020C0139) -Dana Farber Cancer Institute IRB (ID Number 354020)All participants gave informed consent before taking part in this clinical trial.

<http://dx.doi.org/10.1136/jitc-2021-SITC2021.511>

512 PHASE I DOSE ESCALATION OF KD033, A PDL1-IL15 BISPECIFIC MOLECULE, IN METASTATIC AND ADVANCED SOLID TUMORS

¹Jason Luke*, ²Anthony Olszanski, ³Igor Puzanov, ³Christos Fountzilas, ⁴Lee Rosen, ⁵Dan Lu, ⁵Adrian Hackett, ⁵Stella Martomo, ⁵Olivier Schueller, ⁵David Eiznhamer, ⁵Alessandro Mora, ⁵Miranda Ross, ⁵Jeegar Patel. ¹UPMC, Pittsburgh, PA, USA; ²Fox Chase Cancer Center, Philadelphia, PA, USA; ³Roswell Park Cancer Center, Buffalo, NY, USA; ⁴UCLA Division of Hematology-Oncology, Los Angeles, CA, USA; ⁵Kadmon Corporation, NEW YORK, NY, USA

Background While IL-2 and IL-15 signal through the shared IL-2/15 $\beta\gamma$ receptor, IL-15 does not directly expand regulatory T cells (Tregs) or mediate activation-induced cell death and may have an improved therapeutic index. KD033 is a fusion antibody combining a fully human, high affinity anti-human Programmed Death Ligand 1 (PD-L1) IgG1 antibody with the human IL-15 receptor alpha (IL15R α) sushi domain and human IL-15 (IL-15). KD033 and its mouse cross-reactive surrogate molecule, srKD033, have been extensively characterized in multiple in vitro and in vivo nonclinical studies and have demonstrated robust efficacy and therapeutic benefits compared to IL-15 alone.

Methods This is a phase 1, open-label, multiple ascending dose, multi-center clinical trial being conducted in patients with metastatic or locally advanced solid tumors (NCT04242147). The primary objective is to determine the safety, tolerability, and MTD of KD033. Secondary objectives include characterization of PK and immunogenicity, evaluation of CD8+ T and NK cell activation, and assessment of best overall response and duration of response. KD033 is administered by IV infusion over 30 minutes every 14 days. The study design follows 3+3 escalation investigating dose ranges from 3 μ g/kg to 600 μ g/kg.

Results A total of 12 patients have received treatment. Three patients were dosed in Cohort 1 (C1), four patients were dosed in Cohort 2 (C2), and three patients were dosed in Cohort 3 (C3). Two patients in Cohort 4 (C4) have been dosed. Through three dose escalation cohorts (3 μ g/kg – 50 μ g/kg), no dose-limiting toxicities have been reported. Grade 1–2 treatment-related toxicities resolved within 24 hours with supportive management. Grade 4 decreases in lymphocytes were noted the day after dosing in C3 and C4, which resolved on day 3 and were expected. One patient (adenoid cystic carcinoma) in C1 was shown to have stable disease for more than 6 months and one patient (metastatic gastric adenocarcinoma) in C3 was shown to have stable disease for more than 4 months.

Conclusions To date, KD033 has been well tolerated in all subjects with on-mechanism pharmacodynamics consistent with IL-15 agonism.

Ethics Approval This study obtained ethics approval from WIRB.

<http://dx.doi.org/10.1136/jitc-2021-SITC2021.512>

TRIAL IN PROGRESS: PHASE 1 FIRST-IN-HUMAN STUDY OF XL092 ADMINISTERED ALONE OR IN COMBINATION WITH IMMUNE CHECKPOINT INHIBITORS IN PATIENTS WITH INOPERABLE LOCALLY ADVANCED OR METASTATIC SOLID TUMORS

¹Amita Patnaik*, ²Vivek Subbiah, ³Geoffrey Shapiro, ⁴Sumanta Pal, ⁵Neeraj Agarwal, ⁶Kristopher Wentzel, ⁷Jing Li, ⁷Elizabeth McIlvaine, ⁷Jana Waldes, ⁸Edward Cha, ⁹Keywan Tadjalli-Mehr, ¹⁰Manish Sharma. ¹START, San Antonio, TX, USA; ²MD Anderson Cancer Center, Houston, TX, USA; ³Dana-Farber Cancer Institute, Boston, MA, USA; ⁴City of Hope Comprehensive Cancer Center, Duarte, CA, USA; ⁵University of Utah, Salt Lake City, UT, USA; ⁶The Angeles Clinic and Research Institute, Los Angeles, CA, USA; ⁷Exelixis, Inc., Alameda, CA, USA; ⁸Genentech Inc., Singapore, CA, USA; ⁹the healthcare business of Merck KGaA, Darmstadt, Germany; ¹⁰START Midwest, Grand Rapids, MI, USA

Background XL092 is a novel oral multi-targeted inhibitor of receptor tyrosine kinases. In preclinical studies, oral dosing with XL092 resulted in pharmacodynamic inhibition of MET, TAM kinases (AXL, MER), and VEGFR2 phosphorylation and was associated with significant anti-tumor activity in xenograft tumor models. Drugs targeting TAM kinases may promote an immune-permissive environment, which may enhance response to immune checkpoint inhibitors (ICIs). The combination of XL092 and anti-PD-1 ICI exhibited greater anti-tumor activity in a syngeneic tumor model than either agent alone.[1] Preliminary XL092 pharmacokinetic data indicate a median terminal half-life of 21 hours, suitable for daily dosing.

Methods This multi-center, phase 1, open-label study aims to enroll approximately 800 patients total in dose-escalation and cohort-expansion stages (NCT03845166). The dose-escalation stage will enroll patients with inoperable locally advanced or metastatic solid tumors in a 3+3 design (monotherapy cohorts) or rolling 6 design (combination cohorts). Patients will receive escalating doses of XL092 alone or in combination with ICIs (atezolizumab 1200mg Q3W or avelumab 800mg Q2W). Following identification of the maximum tolerated dose (MTD) and/or recommended dose (RD) of XL092 monotherapy, the expansion stage will enroll XL092 monotherapy cohorts in 3 tumor-specific indications (renal cell carcinoma [RCC], metastatic castration-resistant prostate carcinoma [mCRPC], and hormone-receptor positive breast carcinoma [HR+ BC]) using a Simon's optimal 2-stage design. Once the MTDs/RDs are identified for XL092 in combination with each ICI, the expansion stage will also enroll patients in tumor-specific cohorts for XL092+atezolizumab (RCC, mCRPC, HR+ BC, and colorectal carcinoma) and XL092 +avelumab (urothelial carcinoma) using Simon's optimal 2-stage design or a Precision-Based design. A limited number of patients will be enrolled in dedicated biomarker cohorts, with tumor and blood samples collected, to evaluate the pharmacodynamic effects of XL092 alone and in combination with ICIs. Key eligibility criteria include unresectable or metastatic solid tumors; measurable disease per RECIST 1.1 (expansion cohorts only); available tumor tissue (archival or fresh biopsy); and ECOG 0-1. The primary objective of the dose-escalation stage is to determine MTDs/RDs of XL092 when administered alone or in combination with ICIs, and the primary objective of the expansion stage is to evaluate objective response rate and progression-free survival rate by investigator per RECIST 1.1 of XL092 as monotherapy or in combination with ICIs. Secondary objectives include evaluation of the safety of XL092 alone and in combination with ICIs and evaluation of plasma pharmacokinetics of XL092 and its potential metabolites. The study is open for enrollment.

Acknowledgements Medical writing support provided by Griselda Zuccarino-Catania, PhD (Exelixis, Inc.)
Trial Registration NCT03845166

REFERENCES

1. Hsu J, Chong C, Goon L, et al. XL092, a Multi-targeted Inhibitor of MET, VEGFR2, AXL and MER with an Optimized Pharmacokinetic Profile. *European Journal of Cancer [abstract 33]* 2020;**138** Suppl 2:S16.

Ethics Approval Study approved by institutional Review Boards at each investigational site.

<http://dx.doi.org/10.1136/jitc-2021-SITC2021.513>

A PHASE 1 STUDY OF MYELOID MODULATING AGENT MTL-CEBPA IN COMBINATION WITH PEMBROLIZUMAB IN ADULT PATIENTS WITH ADVANCED SOLID TUMOURS

¹Ruth Plummer, ²Mikael Sodergren*, ²David Pinato, ³Debashis Sarker, ²Vikash Reebye, ²Duncan Spalding, ⁴Nina Raulf, ⁴Laura Sinigaglia, ²Thomas Talbot, ²Alessio Cortellini, ²Antonio D'Alessio, ⁴Ilian Tchakov, ⁴Robert Habib, ⁵John Rossi, ⁴Nagy Habib. ¹Newcastle University, London, UK; ²Imperial College London, London, UK; ³King's College London, London, UK; ⁴MINA Therapeutics, London, UK; ⁵City of Hope, Duarte, CA, USA

Background MTL-CEBPA is a novel immunotherapy targeting the myeloid cell lineage which has shown promising clinical activity as monotherapy and combination therapy with tyrosine kinase inhibitors in hepatocellular carcinoma (HCC). Immunosuppressive myeloid cells are associated with worse outcomes to checkpoint inhibitors. Pre-clinical data have shown that MTL-CEBPA potentiates the oncological effect of PD-1 inhibitors.

Methods This phase 1A/B, first-in-human, open-label, multicenter study evaluates the safety, tolerability, PK, and efficacy of MTL-CEBPA in combination with a pembrolizumab in adult patients with advanced solid tumours across 3 dose cohorts (70mg/98mg/130mg/m² MTL-CEBPA once weekly for 3 consecutive weeks with final week break per cycle, with 200mg pembrolizumab every 3 weeks). The primary endpoint is safety and ORR; key secondary endpoints include PK, CR rate & DCR. Key inclusion criteria: Patients with advanced solid tumours who have progressed on standard of care therapy or for whom no standard therapy is available, measurable disease, ECOG PS <2, life expectancy >3 months. A dose exploration will determine the maximum tolerated dose (MTD) or recommended phase 2 dose (RP2D).

Results 10 pts (3 men, 7 women; median age 50.5yrs), all with different tumor types (1 each of triple negative breast, methothelioma, squamous thymic, cholangiocarcinoma, eccrine, fibrolamellar hepatocellular, colorectal, pancreatic and 2 platinum resistant high-grade serous ovarian). 4 pts had ≥4 prior lines of treatment. All pts reported treatment-related AEs, 7 pts reported AEs considered related to MTL-CEBPA only and all were grade 1 or 2. The most common was nausea (n=3) followed by anaemia, headache, insomnia, neutropenia, pyrexia, transaminase increase and ventricular extrasystole (all n=1). Five pts reported AEs considered related to pembrolizumab only, 2 AEs in 1 pt only were grade 3 (ALT and AST increases) There were no DLTs, SAEs or AEs leading to discontinuation or to death in the study. Tumor response was evaluated in 9 pts. 2 pts had a PR (epithelioid mesothelioma at 2 months with 83% tumour reduction, pt ongoing at 9 months & serous ovarian cancer at 2 months with 69% reduction in tumour, pt progressed at 6 months). Three pts had SD, 4 pts had PD as BOR, and 4 pts are continuing to receive treatment.

Conclusions MTL-CEBPA in combination with pembrolizumab demonstrated manageable toxicity at the dose levels tested and has shown antitumor activity. MTD was not reached and RP2D was determined at 130mg/m² on day 1, 8 and 15 of a 28 day cycle. Enrolment into the dose expansion is ongoing.

Trial Registration This study was registered with ClinicalTrials.gov, number NCT04105335.

Ethics Approval The study was approved by the North East - Newcastle & North Tyneside 2 Research Ethics Committee, approval number 19/NE/0312.

<http://dx.doi.org/10.1136/jitc-2021-SITC2021.515>

PERIPHERAL AND TUMORAL IMMUNE ACTIVITY IN THE EXPANSION PART OF THE FIRST-IN-HUMAN DUOBODY®-PD-L1×4-1BB (GEN1046) TRIAL

¹Santiago Ponce Aix*, ²Emiliano Calvo, ³Victor Moreno, ⁴Elena Garralda, ⁵Andrés Cervantes, ⁶Suresh Ramalingam, ⁷José Trigo Pérez, ⁸Patricia LoRusso, ⁹Muhammad Furqan, ¹⁰Daniel Cho, ¹¹Alexander Muik, ¹¹Eleni Lagkadinou, ¹¹Özlem Türeci, ¹²Suzana Couto, ¹²Nora Pencheva, ¹²Ulf Forssmann, ¹¹Uğur Şahin, ¹²Tahamtan Ahmadi, ¹²Brandon Higgs, ¹²Maria Jure-Kunkel, ¹³Ignacio Meler. ¹Hospital Universitario 12 de Octubre, Madrid, Spain; ²START Madrid-CIOCC, Madrid, Spain; ³START Madrid-FJD, Hospital Fundación Jiménez Díaz, Madrid, Spain; ⁴Vall d'Hebron Institute of Oncology, Barcelona, Spain; ⁵University Hospital of Valencia, Valencia, Spain; ⁶Winship Cancer Institute of Emory Univer, Atlanta, USA; ⁷Hospital Universitario Virgen de la Victoria, Málaga, Spain; ⁸Yale Cancer Center, New Haven, USA; ⁹University of Iowa, Iowa City, USA; ¹⁰NYU Langone Health Tisch Hospital, New York, NY, USA; ¹¹BioNTech SE, Mainz, Germany; ¹²Genmab, Princeton, USA; ¹³Clínica Universidad de Navarra, Navarra, Spain

Background DuoBody-PD-L1×4-1BB (GEN1046) is a class-defining, bispecific immunotherapy designed to induce an anti-tumor immune response by simultaneous and complementary PD-L1 blockade and conditional 4-1BB stimulation. Encouraging clinical activity and manageable safety were observed during dose escalation in the ongoing phase 1/2a trial in patients with advanced solid tumors (NCT03917381). We report exploratory pharmacodynamic analyses and potential biomarkers of response in an expansion cohort of patients with PD-(L)1-R/R NSCLC.

Methods Patients with metastatic/unresectable NSCLC who had multiple lines of prior systemic therapy, including a checkpoint inhibitor, received flat-dose DuoBody-PD-L1×4-1BB (100 mg) intravenously every 3 weeks. Immunophenotyping of peripheral blood and measurements of soluble immune mediators were evaluated in serial blood samples in cycles 1–2. Tumor PD-L1 and 4-1BB expression and additional immune markers were evaluated by immunohistochemistry in core needle tumor biopsy specimens collected before treatment and at cycle 2.

Results As of May 2021, 40 patients with PD-(L)1-R/R NSCLC were enrolled (median age, 63 years). Treatment with DuoBody-PD-L1×4-1BB elicited pharmacodynamic modulation of immune endpoints within the first 2 cycles. Induction of peripheral IFN- γ , CXCL9/10, and expansion of peripheral CD8+ effector memory T cells and activated NK cells were observed starting at cycle 1 (>2-fold from baseline) and maintained or increased through cycle 2. Based on 9 paired tumor biopsy samples, increased PD-L1 and 4-1BB expression and cytotoxic CD8+/GZMB+ cell density were detected following treatment. In a subset of patients with clinical response (n=5 confirmed PRs), a trend of greater induction of IFN- γ , CXCL9/10, and activated NK cells was observed vs nonresponders. Disease control rates were higher in patients who had progressed on prior anti-PD-1 therapy within 8 months (64% [16/25]) from the first dose of DuoBody-PD-L1×4-1BB. As expected, among patients with evaluable baseline tumors (n=26), most with any degree of tumor reduction (best change, <0%) harbored PD-L1+ tumors (\geq 1% tumor positive score; 7/10) and showed close spatial proximity between PD-L1+ and 4-1BB+ cells. Conversely, most patients without any degree of tumor reduction presented with PD-L1– tumors (12/16).

Conclusions In patients with NSCLC who progressed on PD-(L)1 therapy, DuoBody-PD-L1×4-1BB elicited pharmacodynamic effects consistent with its proposed mechanism of action. Relationships between disease control and PD-L1 tumoral expression, as well as time from last prior anti-PD-1

therapy, were observed. These findings support that patient selection and/or anti-PD-1 combination therapy may lead to improved clinical efficacy. Further analyses are ongoing and updated results will be presented.

Acknowledgements The authors thank Hrefna Kristin Johannsdottir, Lei Pang, and Kate Sasser at Genmab A/S and Friederike Gieseke at BioNTech SE for their valuable contributions. This trial was funded by Genmab A/S and BioNTech SE.

Trial Registration NCT03917381

Ethics Approval This trial is undertaken following full approval of the final protocol, amendments, informed consent form, applicable recruiting materials, and subject compensation programs by the Independent Ethics Committee/Institutional Review Board.

Consent Written informed consent, in accordance with principles that originated in the Declaration of Helsinki 2013, current ICH guidelines including ICH-GCP E6(R2), applicable regulatory requirements, and sponsor policy, was provided by the patients.

<http://dx.doi.org/10.1136/jitc-2021-SITC2021.516>

517

LUMINOS-103: A BASKET TRIAL EVALUATING THE SAFETY AND EFFICACY OF PVSRIPO AND PVSRIPO IN COMBINATION WITH ANTI-PD-1/L1 CHECKPOINT INHIBITORS IN PATIENTS WITH ADVANCED SOLID TUMORS

¹Brant Inman, ²Matthew Milowsky, ³Raj Pruthi, ⁴Marshall Posner, ⁵Melissa Polasek, ⁵Shannon Morris*, ⁵Lori Mixson, ⁵Kristin Orr, ⁵Elizabeth Woodson, ⁵Andrea Kelly, ⁵Garrett Nichols, ⁶Arjun Balar. ¹Duke University Medical Center, Durham, NC, USA; ²University of North Carolina Lineberger, Chapel Hill, USA; ³University of California San Francisco, San Francisco, CA, USA; ⁴Icahn School of Medicine at Mount Sinai, New York, NY, USA; ⁵Istari Oncology, Morrisville, NC, USA; ⁶New York University Langone Health, New York, NY, USA

Background PVSRIPO, a novel intratumoral viral immunotherapy, infects cells via CD155, which is widely expressed on solid tumors and antigen-presenting cells (APC). Infection is lethal in malignant cells, but a unique, activating, nonlethal infection of local APCs yields type-I/III interferon (IFN)-dominant inflammation with subsequent anti-tumor T-cell priming and activation resulting in anti-tumor efficacy. In preclinical models, PVSRIPO-dependent inflammation upregulated the PD-1/L1 pathway, and greater anti-tumor response was observed with PVSRIPO + anti-PD-1/L1 (α PD-1/L1). Promising clinical activity with PVSRIPO monotherapy was observed in patients with recurrent glioblastoma and advanced α PD-1-refractory melanoma.^{1 2} Collectively, these results warrant further clinical investigation of PVSRIPO \pm α PD-1/L1.

Methods LUMINOS-103 (NCT04690699) is a phase (Ph) 1/2, open-label, multi-center, single-arm basket trial evaluating repeat administration of PVSRIPO \pm α PD-1/L1 in adults with solid tumors. Trial objectives are to assess the safety and tolerability of PVSRIPO monotherapy in each cohort in Ph 1 and the safety, tolerability, and antitumor efficacy of PVSRIPO + α PD-1/L1 in each cohort in Ph 2. The first two study cohorts include patients with muscle-invasive bladder cancer being treated in the neoadjuvant setting (A) and patients with metastatic bladder cancer being treated in the 1st/2nd line setting (B); these cohorts have been described previously.³ Cohort C includes patients with resectable, locally advanced head and neck squamous cell carcinoma (HNSCC) being treated in the neoadjuvant setting; Cohort D includes patients with recurrent/metastatic HNSCC with a PD-L1 Combined Positive Score ≥ 1 being treated in the 1st line setting. Eligibility: HNSCC patients must have histologically or cytologically-proven SCC of the oral cavity, oropharynx, hypopharynx, or larynx. All patients must have prior and boosted PV immunization and tumors amenable to injection and biopsy. Key exclusion criteria: Requirement for oxygen supplementation, systemic or intratumoral therapy ≤ 6 months prior to the first dose of study drug, CNS metastases requiring immediate treatment, systemic immunosuppressive medications ≤ 4 weeks prior to the first dose of study drug, and severe active comorbidities. Patients who are HIV+, HBV+ or HCV+ are eligible provided they meet certain criteria. Primary endpoints include safety (all cohorts), tolerability (all cohorts), surgical complication rate (A, C), pathologic treatment effect/response (A, C), and objective response rate (B, D). Secondary endpoints include overall survival (all cohorts), pathologic downstaging and relapse-free survival (A, C), duration of response and progression-free survival (B, D), and assessment of tumor/blood biomarkers (all cohorts).

Trial Registration ClinicalTrials.gov: NCT04690699

REFERENCES

1. Desjardins A, et al. Recurrent glioblastoma treated with recombinant poliovirus. *N Engl J Med* 2018;**379**(2):150–161.
2. Beasley GM, et al. Phase I trial of intratumoral PVSRIPO in patients with unresectable, treatment-refractory melanoma. *J Immunother Cancer* 2021;**9**(4):e002203.
3. Inman BA, et al. LUMINOS-103: A basket trial evaluating the safety and efficacy of PVSRIPO in patients with advanced solid tumors. *Cancer Res* 2021;**81**(13_Suppl):Abstract nr CT242.

Ethics Approval The study has been approved by the central Institutional Review Board (IRB), WCG (Study# 1310534) and will be approved by all local IRBs and other required committees, as applicable. The study will be conducted in accordance with the provisions of the Declaration of Helsinki and the Good Clinical Practice guidelines of the International Conference on Harmonization. All patients will provide written informed consent.

<http://dx.doi.org/10.1136/jitc-2021-SITC2021.517>

FIRST-IN-HUMAN RESULTS WITH THE NOVEL TUMOR-TARGETING ANTIBODY ATRC-101: PHASE 1B STUDY IN PATIENTS WITH SOLID TUMORS

¹John Powderly*, ²Jeremy Jones, ²Tanios Bekaii-Saab, ³Yan Xing, ²S John Weroha, ⁴Susanna Ulahannan, ⁵Deborah Doroshow, ⁶Frances Valdes-Albini, ⁷Carl Millward, ⁷Kimberly Walter, ⁷Andrew Wrong, ⁷Paul Del Castillo, ⁷Lixia Wang, ⁷Ngan Nguyen, ⁷Mark Whidden, ⁷Jonathan Benjamin, ⁸Steven Isakoff. ¹*Carolina BioOncology Institute, Huntersville, NC, USA;* ²*Mayo Clinic, Jacksonville, FL, USA;* ³*City of Hope Comprehensive Cancer Center, Duarte, CA, USA;* ⁴*University of Oklahoma Health Stephenson Cancer Center, OKC, OK, USA;* ⁵*Mount Sinai, New York, NY, USA;* ⁶*University of Miami Sylvester Comprehensive Cancer Center, Miami, FL, USA;* ⁷*Atreca, Inc, San Carlos, CA, USA;* ⁸*Massachusetts General Hospital, Boston, MA, USA*

Background ATRC-101 is an engineered version of an immunoglobulin G1 antibody that was discovered in a patient with non-small cell lung cancer (NSCLC) experiencing stable disease while being treated with anti-programmed death-1 therapy. ATRC-101 targets a tumor-specific ribonucleoprotein complex containing polyadenylate binding protein-1, which has been found to be present in the majority of NSCLC, acral melanoma, breast, colorectal, and ovarian cancer samples tested. Target immunoreactivity and single-agent activity have been observed in mouse models. Preclinical data suggest that ATRC-101 stimulates both innate and adaptive immune activity against tumors.

Methods ATRC-101-A01 is a phase 1b trial (3+3 dose escalation with expansion cohorts) in patients with solid tumors treated with ATRC-101 monotherapy every 2 or 3 weeks (Q2W or Q3W), or ATRC-101 in combination with pembrolizumab, until unacceptable toxicity or disease progression at doses of 0.3–30 mg/kg, pending dose-limiting toxicities. The primary objective is safety and secondary objectives are to characterize the pharmacokinetic profile, immunogenicity, and anti-tumor activity of ATRC-101, and to determine the recommended dose for expansion. Pharmacodynamic studies will also be performed to evaluate changes from baseline in specific immune cell populations and cytokine levels in blood and tumors. Results from the ATRC-101 0.3–30 mg/kg monotherapy Q3W cohorts are presented in this abstract (data cutoff: July 16, 2021).

Results Twenty-four participants with solid tumors (13 colorectal, 5 ovarian, 3 breast, 2 NSCLC, 1 acral melanoma) aged 27–75 years with a median 5 lines of prior therapy were treated Q3W in five dose cohorts. No dose-limiting toxicities were observed. Eight participants (33%) experienced grade ≥ 3 treatment-emergent adverse events. The maximum serum concentration of ATRC-101 and treatment exposure appeared to be dose proportional. Stable disease was observed in eight patients and best response per RECIST v1.1 was associated with expression of the ATRC-101 target. Multiple biomarkers, such as treatment-associated changes in the composition of CD3+, CD4+, and CD8+ T cells in the blood, and serum cytokines/chemokines, including those predicted to activate antigen-presentation pathways, support the proposed mechanism of action of ATRC-101 and will be presented.

Conclusions These first-in-human data suggest a manageable safety profile for ATRC-101 Q3W, with no dose-limiting toxicities observed. Pharmacokinetics appear to be dose proportional. Enrollment in the Q2W monotherapy dose-escalation cohort and at the 30 mg/kg dose level Q3W is continuing. Trial sites have been activated to test ATRC-101 in combination with pembrolizumab, and combination with chemotherapy is also planned.

Trial Registration Trial Registration: NCT04244552

Ethics Approval This study was approved by the institutional review board or ethics committee as required for each participating site.

<http://dx.doi.org/10.1136/jitc-2021-SITC2021.518>

519 **A FIRST-IN-HUMAN, MULTICENTER, PHASE 1/2, OPEN-LABEL STUDY OF XTX101 IN PATIENTS WITH ADVANCED SOLID TUMORS**

¹John Powderly*, ²Teleen Norman, ²Meghan Duncan, ²Martin Huber, ²Jennifer O'Neil, ²Ekta Patel, ³Andrae Vandross. ¹Carolina BioOncology Institute, Huntersville, NC, USA; ²Xilio Therapeutics, Waltham, MA, USA; ³Next Oncology, Austin, TX, USA

Background Anti-CTLA-4 agents have demonstrated clinical benefit in a range of tumors; however, the safety risks limit the dose and their use in certain settings.¹⁻⁴ XTX101 is a fully humanized mAb with an engineered Fc region for enhanced FcγR binding and with covalently linked peptides that mask each CTLA-4 antigen-binding region of the antibody. The masking peptides are designed to be selectively cleaved and released by proteases that are more active in the tumor microenvironment compared to healthy tissue. XTX101 is intended to have minimal peripheral CTLA-4 binding and inhibition. Upon proteolytic cleavage of the masking peptides within the tumor microenvironment, the cleaved and active form of XTX101 is intended to bind to CTLA-4, inhibit its function, and induce antibody-dependent cellular cytotoxicity (ADCC). Here we describe the first-in-human study that is currently enrolling subjects with locally advanced or metastatic disease who have failed standard therapy, or standard therapy is not curative or available.

Methods The objectives of this study are to determine a dose or doses of XTX101 administered every 21 days that are well-tolerated, biologically active, and suitable for advancing into further studies. The initial portion of the study consists of three parts. Part 1A will evaluate ascending fixed doses of XTX101 monotherapy using an accelerated, single-subject, dose-level design for the first three dose cohorts followed by a standard 3+3 design. Part 1B will examine XTX101 monotherapy in patients with any histologically or cytologically confirmed solid tumor malignancy for which anti-PD-1 or anti-PD-L1 treatment is approved and has progressed on or after prior anti-PD-1 or anti-PD-L1 therapy. Currently approved tumor types for anti-PD-1 or anti-PD-L1 treatment include melanoma, squamous cell skin cancer, non-small cell lung cancer, head and neck carcinoma, esophageal carcinoma, renal cell cancer, urothelial carcinoma, or microsatellite instability-high/mismatch deficient colorectal cancer. Part 1B will require mandatory fresh tumor biopsies pre-dose and post-dose to fully characterize the pharmacodynamic profile of XTX101. Part 1C will examine escalating doses of XTX101 in combination with pembrolizumab. Subjects may receive XTX101 for up to 24 months in the absence of disease progression, toxicity, a complete response, or termination of the study. Disease responses will be determined by iRECIST methods every third treatment cycle for the first year and then every four treatment cycles thereafter until progressive disease.

Trial Registration NCT04896697

REFERENCES

1. Hamid O, Schmidt H, Nissan A, et al. A prospective phase II trial exploring the association between tumor microenvironment biomarkers and clinical activity of ipilimumab in advanced melanoma. *J Transl Med* 2011;**9**:204–19.
2. Lebbé C, Meyer N, Mortier L, et al. Evaluation of two dosing regimens for nivolumab in combination with ipilimumab in patients with advanced melanoma: results from the phase IIIb/IV CheckMate 511 trial. *J Clin Oncol* 2019;**37**:867–875.
3. Wolchok JD, Hodi FS, Weber JS, et al. Development of ipilimumab: a novel immunotherapeutic approach for the treatment of advanced melanoma. *Ann N Y Acad Sci* 2013; **1291**:1-13.
4. Wolchok JD, Neyns B, Linette G, et al. Ipilimumab monotherapy in patients with pretreated advanced melanoma: a randomised, double-blind, multicentre, phase 2, dose-ranging study. *Lancet Oncol* 2010;**11**:155–64.

Ethics Approval This study was approved by an Institutional Review Board for each participating site.

<http://dx.doi.org/10.1136/jitc-2021-SITC2021.519>

PRELIMINARY BIOMARKER AND PHARMACODYNAMIC (PD) ACTIVITY OF THE TGF β INHIBITOR SAR439459, ALONE OR IN COMBINATION WITH CEMPLIMAB, IN A PHASE 1 CLINICAL STUDY IN PATIENTS WITH ADVANCED SOLID TUMORS

¹Debbie Robbrecht, ²Grob Jean-Jacques, ³Oliver Bechter, ⁴Armando Santoro, ⁵Bernard Doger, ⁶Ivan Borbath, ⁷Butler Marcus, ⁸Cheng Tina, ⁹Patricia Martin, ¹⁰Bennouna Jaafar, ¹¹Massimo Di Nicola, ¹²Giuseppe Curigliano, ¹³Min-Hee Ryu, ¹⁴Alejo Rodriguez-Vida, ¹⁵Dirk Schadendorf, ¹⁶Elena Garralda, ¹⁷Giovanni Abbadessa, ¹⁷Brigitte Demers, ¹⁷Amele Amrate, ¹⁷Tun Tun Lin, ¹⁷Manisha Brahmachary, ¹⁷Joon Sange Lee, ¹⁷Joachim Theilhaber, ¹⁷Rob Pomponio*, ¹⁷Rui Wang. ¹Erasmus Medical Centre, Rotterdam, Netherlands; ²APHM – Hopital de la Timone, Marseille, France; ³UZ Leuven, NA, Belgium; ⁴Istituto Clinico Humanitas, NA, Italy; ⁵Instituto de Investigación Sanitaria Fundación Jiménez Díaz, Madrid, Spain; ⁶UCL Saint Luc, NA, Belgium; ⁷Princess Margaret Hospital, NA, Canada; ⁸Tom Baker Cancer Centre, NA, Canada; ⁹Institut Gustave Roussy, NA, France; ¹⁰CHU de Nantes – Hotel Dieu, NA, France; ¹¹Istituto Nazionale dei Tumori, NA, Italy; ¹²Istituto Europeo Di Oncologia, Milan, Italy; ¹³Asan Medical Center, NA, Korea, Republic of; ¹⁴Hospital Del Mar, NA, Spain; ¹⁵Universitätsklinikum Essen, NA, Germany; ¹⁶Hospital Universitari de la Vall d'Hebron, Barcelona, Spain; ¹⁷Sanofi, Cambridge, MA, USA

Background Transforming growth factor beta (TGF β) is a bifunctional regulator of tumor growth playing a role in tumor immune evasion and resistance to checkpoint blockade. Increased activation of TGF β pathway correlated with reduced overall survival in patients with PD-1 resistance/refractory tumors. Therefore, the combination of a TGF β inhibitor with an anti-PD-1 agent may benefit patients who are resistant to checkpoint blockade. SAR439459 is a "second generation" human anti-TGF β IgG4 monoclonal antibody. Here we report the preliminary PD results and patient selection strategy (mesenchymal CRC) of SAR439459 \pm anti-PD-1 cemiplimab in patients with advanced tumors from an on-going phase 1 study (NCT03192345).

Methods Peripheral blood, serum and tumor biopsies from patients were collected for the assessment of both predictive and PD biomarkers. A consensus molecular subtyping 4 (CMS4) gene classifier was developed and used to identify mesenchymal CRC tumors based on an in-silico experiment followed by a validation using ~200 procured CRC tumor biopsy samples with customized NanoString assay. TGF β level in plasma and tumor was measured by ELISA to assess target engagement of SAR439459. Well-known immune modulation events as the PD readout were measured: 1) immunophenotyping of circulating immune cells ; 2) cytokine/chemokine production by MSD assay; 3) PD-L1, CD8+ T cells and FoxP3+ Tregs in tumor micro-environment (TME) by immunohistochemistry; 4) TGF β pathway activation gene signature in TME by RNAseq.

Results SAR439459 \pm cemiplimab, induced inhibition of plasma TGF β level \geq 90% at doses \geq 0.25mg/kg Q2W, together with a clear trend of decrease in intra-tumoral TGF β . RNAseq data from paired biopsies revealed concomitant down-regulation of TGF β pathway. In periphery, SAR439459 \pm cemiplimab increased proliferating T and NK cells. Concomitantly, enhanced production of pro-inflammatory cytokines/chemokines confirmed peripheral immune activation. In TME, a trend of increased CD8+ T cell infiltration and conversion from "immune-excluded" to "immune-inflamed" phenotype was observed following the combination treatment in several cases. No significant modulation of PD-L1 or FoxP3 was observed from the available paired biopsies. Out of 137 pre-screened CRC patients, 58 (42%) were identified as carrying the CMS4 phenotype based on the gene classifier.

Conclusions Clinical modulation of TGF β level and the related pathway demonstrated SAR439459's target engagement.

Further analysis confirmed the peripheral immune activation in patients treated with SAR439459 \pm cemiplimab. Coupled with CD8+ T cell modulation in TME, these findings suggest the identification of early PD biomarkers impacted by SAR439459 which is consistent with the mechanism of action and biological activity of TGF β blockade therapy.

Trial Registration NCT03192345

Ethics Approval The study protocols were approved by the institutional review board or independent ethics committee of each participating institution. All patients provided written informed consent prior to enrollment.

Consent Written informed consent was obtained from the patient for publication of this abstract and any accompanying images. A copy of the written consent is available for review by the Editor of this journal.

<http://dx.doi.org/10.1136/jitc-2021-SITC2021.520>

521

GEN-009, A PERSONALIZED NEOANTIGEN VACCINE CANDIDATE, ELICITS DIVERSE AND DURABLE IMMUNE RESPONSES ASSOCIATED WITH CLINICAL EFFICACY OUTCOMES

Mara Shainheit*, Ece Bicak, Masoud Golshadi, Gabriella Santone, Syukri Shukor, Emily Tjon, Li Xue, Thomas Davis, Jessica Flechtner. *Genocea Biosciences, Cambridge, MA, USA*

Background GEN-009, a personalized vaccine candidate comprised of ATLAS™-prioritized neoantigens combined with Hil-tonol®, is currently being evaluated in a Phase 1/2a clinical trial (NCT03633110). ATLAS™ is a cell-based recall assay that, without predictions, screens each patient's mutanome to identify neoantigens for vaccine inclusion and deleterious Inhibigens™ for exclusion. In the Part A monotherapy cohort, vaccine-specific immune responses were generated in all subjects, against 99% of administered peptides.¹ Here we characterize immune responses and their association with reduction in tumors in Part B of the study, in which patients were treated with GEN-009 combined with anti-PD-1-based checkpoint inhibitors (CPI).

Methods Fourteen adults with solid tumors were enrolled in the study. During the screening and manufacturing period, patients received standard of care anti-PD-1 CPI. Subsequently, patients were immunized with GEN-009 in combination with anti-PD-1. CPI refractory patients received salvage therapy prior to GEN-009. Peripheral blood mononuclear cells were collected at baseline, pre-vaccination (D1), as well as multiple days post first dose. The magnitude and durability of vaccine-induced immune responses were assessed by quantifying neo-antigen-specific responses in fluorospot assays. Proliferation of neoantigen-specific T cells and T cell phenotypes were evaluated by flow cytometry. Circulating tumor DNA (ctDNA) levels were monitored pre- and post-GEN-009 dosing to assess its potential as a predictive biomarker.

Results GEN-009 immunization induced neoantigen-specific T cell responses in all evaluable patients, with ex vivo responses emerging as early as 1 month and persisting up to 366 days in some subjects. Comparing RECIST responders (PR, CR) to non-responders (SD, PD), the median breadth of statistically positive responses to vaccine antigens at day 50 was greater in non-responders ex vivo (29 vs. 75%, respectively), however, by IVS assay the proportions inverted (83% vs. 38%). Longitudinal evaluation of neoantigen-specific responses revealed an association between the magnitude and kinetics of cytokine secretion and increased activated and proliferating Ki-67+ T cells and TEM cells in both T cell subsets. Quantification of ctDNA in a subset of patients supported the RECIST readouts in association with the enhanced neoantigen-specific T cell responses.

Conclusions Vaccination with GEN-009 combined with anti-PD-1-based therapy induced early, durable, and neoantigen-specific CD4+ and CD8+ T cell responses with pronounced Ki-67+ and TEM cell populations. Overall, a greater breadth of response to vaccine neoantigens was associated with improved clinical benefit, which was further supported by ctDNA levels. These data support that GEN-009, in combination with checkpoint blockade, represents a unique approach to treat solid tumors.

REFERENCES

1. Lam H, et al. An empirical antigen selection method identifies neoantigens that either elicit broad anti-tumor response or drive tumor growth. *Cancer Discovery* 2021 March; **11**(3):696–713.

Ethics Approval ETHICS STATEMENT: This study was approved by Western Institutional Review Board, approval number 1-1078861-1

<http://dx.doi.org/10.1136/jitc-2021-SITC2021.521>

522

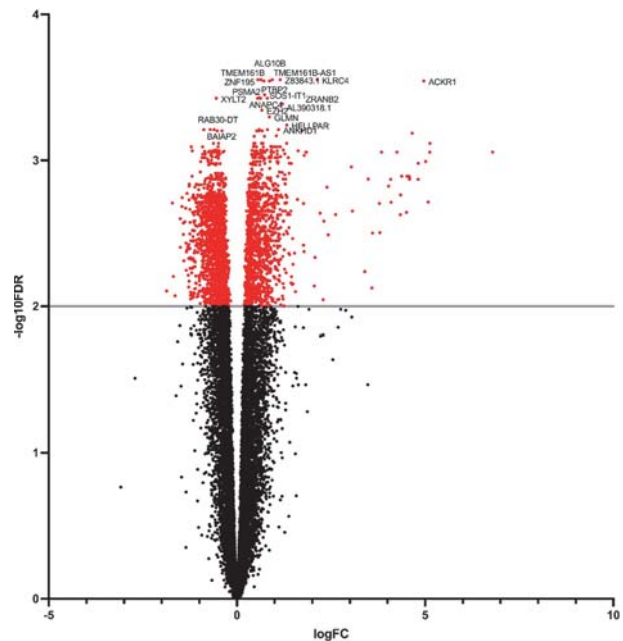
TRANSCRIPTOMIC CHANGES IN CANCER PATIENTS TREATED WITH IMMUNE-CHECKPOINT INHIBITORS

¹Dmitrii Shek*, ²Bo Gao, ³Joey Lai, ²Won-Hee Yoon, ⁴Tania Moujaber, ⁴Adnan Nagrial, ⁵Matteo Carlino, ³Scott Read, ¹Golo Ahlenstiel. ¹Western Sydney University, Sydney, New South Wales, Australia; ²Blacktown Hospital, Blacktown, Australia; ³Westmead Institute for Medical Research, Sydney, Australia; ⁴Westmead Hospital, Sydney, Australia; ⁵The University of Sydney, Sydney, Australia

Background Immune-checkpoint inhibitors (ICIs) are monoclonal antibodies that block inhibitory CTLA-4/PD-1 signalling pathways and thus boost cytotoxic T cell antitumor activity. ICIs have been proven effective in various malignancies, but there is a lack of knowledge regarding factors associated with ICI efficacy and safety. This study aims to examine transcriptomic changes in cancer patients treated with ICIs and their potential association with related clinical outcomes.

Methods This is a prospective multicentre cohort study (NCT04631731) recruiting cancer patients treated with (1) ICI monotherapy; (2) ICI dual therapy; (3) ICI + kinase inhibitor; (4) ICI + platinum-doublet chemotherapy. Peripheral blood is collected at baseline and 6–8 weeks after first ICI treatment as well as after the development of immune-related adverse events (irAEs, grade 2 and higher). Whole transcriptome sequencing (Novaseq S4 300 cycle lane, Illumina) was performed and followed by functional annotation using the ConsensusPath-DB platform.

Results 22 patients were recruited to the study and had paired blood taken. Two patients had developed grade 3–4 irAEs. RNA sequencing analysis identified 3,000 genes that were significantly dysregulated at week 6–8 after ICI commencement as compared to pre-treatment in n=20 recruited patients without irAEs (figure 1). Functional annotation established that 132 pathways were associated with the identified set of dysregulated genes. Among them: (1) pre-NOTCH processing in Golgi, (2) Interleukin-15 signalling; (3) STAT5 activation, and (4) RORA activation of gene expression possessed a gene set enrichment of at least 80% and $p < 0.01$. In 2 patients with grade 3 immune-mediated hepatitis, both treated with combination of CTLA-4/PD-1 inhibitors, analysis revealed that 360 and 325 were 2-fold up- and downregulated respectively upon onset of toxicity as compared to both pre-treatment and 1-week post-steroid treatment. Interestingly, this gene set possessed minimal overlap when compared to genes dysregulated in patients without irAEs. Moreover, functional annotation established different pathways that were associated with toxicity. The highest enrichment scores belonged to pathways regulating cell cycle and apoptotic pathways driven by CDC25A, p53 and BCL-2, among others.



Abstract 522 Figure 1 Volcano plot representing the differentially expressed genes

The figure representing differentially expressed genes elucidated in this pilot study. N=3000 genes were significantly dysregulated between pre- and week 6–8 post-IO commencement.

Conclusions The preliminary analysis of the first 22 patients recruited to NCT04631731 confirms that ICI treatment interferes with expression of coding and non-coding RNAs. Importantly, patients with and without irAEs show different patterns of transcriptomic changes as well as variability among activated cellular pathways. This data emphasises the need for further exploration and validation of transcriptomic changes in a larger cohort. In the near future, RNA signatures may be utilised as biomarkers to rapidly and accurately diagnose irAEs.

Acknowledgements N/A

Trial Registration ClinicalTrials.gov identification number: NCT04631731

REFERENCES

N/A

Ethics Approval This study has been approved by the Western Sydney Local Health District (WSLHD) Human Research Ethics Committee on the November 9th, 2020 to be conducted at Blacktown and Westmead Public Hospitals of the WSLHD, Sydney, NSW, Australia.

Consent Each participant recruited to this translational study has provided written consent approved on the November 6th, 2020 (MASTER version) by the WSLHD HREC.

<http://dx.doi.org/10.1136/jitc-2021-SITC2021.522>

PRELIMINARY CLINICAL EXPERIENCE WITH XmAB20717, A PD-1 X CTLA-4 BISPECIFIC ANTIBODY, IN PATIENTS WITH ADVANCED SOLID TUMORS

¹Elaine Shum*, ²Matthew Reilley, ³Yana Najjar, ⁴Adil Daud, ⁵John Thompson, ⁶Joaquina Baranda, ⁷R Donald Harvey, ⁸Anthony Shields, ⁹Ezra Cohen, ¹⁰Shubham Pant, ¹¹Rom Leidner, ¹²Alain Mita, ¹³Roger Cohen, ¹⁴Bartosz Chmielowski, ¹⁵Mark Stein, ¹⁶Siwon Hu-Lieskovan, ¹⁷Catherine Fleener, ¹⁷Ying Ding, ¹⁷Lei Bao, ¹⁷Sowmya Chollate, ¹⁷Jolene Shorr, ¹⁷Raphael Clynes, ¹⁷Barbara Hickingbottom. ¹New York University, New York, NY, USA; ²University of Virginia, Charlottesville, VA, USA; ³University of Pittsburgh, Pittsburgh, PA, USA; ⁴University of California, San Francisco, San Francisco, CA, USA; ⁵University of Washington, Seattle, WA, USA; ⁶University of Kansas Cancer Center, Kansas City, KS, USA; ⁷Emory University School of Medicine, Atlanta, GA, USA; ⁸Karmanos Cancer Center, Detroit, MI, USA; ⁹University of California San Diego, La Jolla, CA, USA; ¹⁰MD Anderson Cancer Center, Houston, TX, USA; ¹¹Providence Cancer Institute, Portland, OR, USA; ¹²Cedars-Sinai Medical Center, Los Angeles, CA, USA; ¹³Perelman School of Medicine at UPenn, Philadelphia, PA, USA; ¹⁴UCLA, Los Angeles, CA, USA; ¹⁵Columbia University, New York City, NY, USA; ¹⁶Huntsman Cancer Institute, Salt Lake City, UT, USA; ¹⁷Xencor, Inc., San Diego, CA, USA

Background XmAb20717 is a humanized bispecific monoclonal antibody that simultaneously targets PD-1 and CTLA-4. We report updated data on patients treated at the recommended expansion dose from an ongoing, multicenter, Phase 1, dose-escalation and -expansion study of intravenous XmAb20717 in patients with selected advanced solid tumors that progressed after treatment with all standard therapies or with no standard therapeutic options.

Methods A maximum tolerated dose was not reached in dose escalation. XmAb20717 10 mg/kg every 2 weeks (Q2W) was selected as the expansion dose, based on consistent T-cell proliferation in peripheral blood indicative of dual PD-1/CTLA-4 checkpoint blockade, and response to treatment (RECIST [1.1]).¹ Parallel expansion cohorts included ~20 patients each with melanoma, renal cell carcinoma (RCC), non-small cell lung cancer (NSCLC), castration-resistant prostate cancer (CRPC), and a basket of tumor types without an FDA-approved checkpoint inhibitor (CI). Patients treated with 10 mg/kg in dose escalation were pooled with expansion cohorts for analysis of clinical activity and safety.

Results As of 9 June 2021, 110 patients, ranging in age from 39 to 89 years and 66.4% male, were treated, and 5 were continuing treatment. Patients had received a median of 4 prior systemic treatment regimens, including CI therapy for 64.5%. The objective response rate was 13.0% (10/77 patients evaluable for efficacy), including 1 complete response (melanoma [confirmed]) and 9 partial responses (confirmed: 1 melanoma, 2 RCC, 2 CRPC, 1 ovarian cancer; unconfirmed: 1 melanoma, 2 NSCLC). The CRPC responders (2/7 with RECIST-measurable disease) had confirmed PSA decreases \geq 50% from baseline (to 0.02 and 0.3 ng/mL); neither had progression on bone scans. All responders had prior CI exposure, except those with CRPC. Robust CD4 and CD8 T-cell activation was seen. Low baseline tumoral expression of myeloid recruitment genes, including *IL-8*, was associated with clinical benefit. Grade \geq 3 immunotherapy-related adverse events in \geq 3 patients included rash (16.4%), transaminase elevations (9.1%), hyperglycemia (4.5%), acute kidney injury (3.6%), amylase and lipase increased (2.7%), and lipase increased (2.7%).

Conclusions Preliminary data indicate 10 mg/kg XmAb20717 Q2W was associated with complete and partial responses in multiple tumor types and was generally well-tolerated in these heavily pretreated patients with advanced cancer. Changes in T-cell populations in the periphery and tumor are consistent with robust dual checkpoint blockade. These findings support

further development of XmAb20717 in advanced solid tumors, including metastatic prostate cancer.

Trial Registration NCT03517488

REFERENCES

1. Shum E, Daud A, Reilley M, et al. Preliminary safety, pharmacokinetics/pharmacodynamics, and antitumor activity of XmAb20717, a PD-1 x CTLA-4 bispecific antibody, in patients with advanced solid tumors. *JITC* 2020;**8**(3):A247-8.

Ethics Approval The study was approved by each institution's IRB.

<http://dx.doi.org/10.1136/jitc-2021-SITC2021.523>

A PHASE 2, MULTI-ARM STUDY OF ANTI-CD47 ANTIBODY, MAGROLIMAB, IN COMBINATION WITH DOCETAXEL IN PATIENTS WITH LOCALLY ADVANCED OR METASTATIC SOLID TUMORS

¹Vivek Subbiah*, ²Ulka Vaishampayan, ³Sonam Puri, ⁴Lanjia Lin, ⁴Mark Chao, ⁴Giri Ramsingh, ⁵Shivaani Kумmar, ⁶James Strauss, ⁷Sandip Patel. ¹The University of Texas MD Anderson Cancer Center, Houston, TX, USA, Houston, TX, USA; ²Rogel Cancer Center, University of Michigan, Ann Arbor, MI, USA, Ann Arbor, MI, USA; ³Huntsman Cancer Center at the University of Utah, Salt Lake City, UT, USA, Salt Lake City, UT, USA; ⁴Gilead Sciences, Inc., Foster City, CA, USA, Foster City, CA, USA; ⁵Oregon Health and Science University, Portland, OR, USA, Portland, OR, USA; ⁶Mary Crowley Cancer Research, Dallas, TX, USA, Dallas, TX, USA; ⁷University of California, San Diego, San Diego, CA, USA, La Jolla, CA, USA

Background Patients with solid tumors who progress on standard chemotherapy and/or immune checkpoint inhibitors, have limited efficacy with existing standard of care chemotherapy options (objective response rates [ORR] ~10%). These patients have a significant unmet medical need. Novel agents that can safely enhance treatment efficacy are urgently needed. Magrolimab is a first-in-class monoclonal antibody that blocks the macrophage inhibitory immune checkpoint CD47, a "do not eat me" signal overexpressed on tumor cells. Pre-clinical studies provide compelling evidence that magrolimab triggers phagocytosis and eliminates cancer cells from human solid tumors and hematologic malignancies. Magrolimab has demonstrated clinical activity in both hematologic and solid tumor malignancies. Chemotherapeutic agents, including taxanes, enhance phagocytic signals on tumor cells, leading to synergistic antitumor activity when combined with magrolimab. This study (NCT04827576) is evaluating the safety, tolerability, and efficacy of magrolimab with docetaxel in relapsed/refractory (R/R) metastatic non-small cell lung cancer (mNSCLC), urothelial cancer (mUC), and small cell lung cancer (mSCLC).

Methods This phase 2, open-label, multi-arm study consists of a safety run-in cohort and a phase 2 cohort. Eligible patients are ≥18 years old with chemotherapy and/or immunotherapy refractory mNSCLC, mSCLC, or mUC. Magrolimab is administered intravenously (IV) with an initial 1 mg/kg priming dose to mitigate on target anemia, followed by 30 mg/kg dose during cycle 1 (cycles are 21 days) in the safety run-in to identify any dose-limiting toxicities (DLTs) and determine a recommended phase 2 dose (RP2D). De-escalation may occur for DLTs per protocol. In phase 2, following the priming dose on day 1, magrolimab RP2D will be administered on days 8 and 15 of cycle 1; days 1, 8, 15 of cycle 2; and day 1 for cycles 3 and beyond. Docetaxel 75 mg/m² (IV) is administered on day 1 of each cycle for all study participants. Patients may continue treatment until unacceptable toxicity, progressive disease by RECIST 1.1, or patient/investigator choice to discontinue. The primary endpoints are incidence of adverse events (safety and phase 2 cohorts) and ORR (phase 2). Secondary endpoints (phase 2) are progression-free survival, duration of response, and overall survival. Exploratory endpoints are to evaluate the pharmacodynamic, mechanism of action, and/or therapeutic response of biomarkers in blood and tumor biopsy samples and to explore biomarkers that may predict response to therapy. Planned enrollment is approximately 116 patients, and recruitment is ongoing.

Acknowledgements Funding provided by Gilead Sciences, Inc.

Trial Registration NCT04827576

Ethics Approval The study protocol was approved by an institutional review board before enrollment of patients.

Consent Patients provided written informed consent based on Declaration of Helsinki principles.

<http://dx.doi.org/10.1136/jitc-2021-SITC2021.524>

525

PRELIMINARY SAFETY, PK/PD AND EFFICACY RESULTS FROM A FIRST-IN-HUMAN PHASE I/IIA CLINICAL TRIAL OF BNT411, A SYSTEMIC TOLL-LIKE RECEPTOR 7 AGONIST IN PATIENTS WITH SOLID TUMORS

¹Stefan Symeonides*, ²Devalingam Mahalingam, ²Young Kwang Chae, ³Emiliano Calvo, ³Maria Miguel, ⁴Hendrik-Tobias Arkenau, ⁵Elena Garralda, ⁵Vladimir Galvao, ⁶Alain Mita, ⁷Hariz Hassan, ⁷Annette Baumhauer, ⁷Timo Völker, ⁷Marie-Cristine Kühnle, ⁷Roman Rösemann, ⁷Stefan Strobl, ⁷Oezlem Tuerci, ⁷Ugur Sahin. ¹Edinburgh Cancer Research Centre, University of Edinburgh, and Edinburgh Cancer Centre, NHS Lothian, Edinburgh, UK; ²Robert H. Lurie Comprehensive Cancer Center, Northwestern University, Chicago, IL, USA; ³START Madrid-CIOCC, Centro Integral Oncológico Clara Campal, Madrid, Spain; ⁴Sarah Cannon Research Institute, London, UK; ⁵HUVH – Hospital Universitari Vall d'Hebron/VHIO – Vall d'Hebron Institute of Oncology, Barcelona, Spain; ⁶Cedars-Sinai Medical Center, Los Angeles, CA, USA; ⁷BioNTech SE, Mainz, Germany

Background The intravenously administered small-molecule Toll-like receptor 7 (TLR7) agonist BNT411 was developed to systemically activate plasmacytoid dendritic cells, characterized by a Type 1 interferon-dominated release of cytokines. The activation of cytotoxic CD8+ T cells and broad modulation of the innate immune system is intended to enhance pre-existing anti-tumor responses and induce de novo responses, especially in combination with cytotoxic therapies and immune checkpoint inhibitors.

Methods This first-in-human, open label, multi-center trial (BNT411-01) involves dose titration in patients (ECOG 0 or 1) with solid tumors with BNT411 administered weekly (q1w) for a month, then q3w thereafter until disease progression, unacceptable toxicity, or death. Part 1A is a single-agent dose escalation (accelerated titration) of BNT411 in patients with metastatic or unresectable solid tumors that have exhausted available treatment options, with bifurcation to Part 1B, a dose escalation of BNT411 in combination with atezolizumab, carboplatin and etoposide in patients with chemotherapy-naïve extensive-stage small cell lung cancer (ES-SCLC), followed by expansion cohorts (Part 2). Endpoints of Part 1A and 1B are safety, determination of maximum-tolerated dose (MTD)/recommended phase 2 dose (RP2D), pharmacokinetics, pharmacodynamic (PD) profiling of immune activation, and preliminary efficacy of BNT411 (RECIST 1.1).

Results As of 1st July 2021, 11 patients have received BNT411 in Part 1A and 5 of 8 dose levels have been cleared. Patients (median age 62 years) had previously received a median of 3 (range 2–5) prior systemic cancer therapies. The only drug-related adverse events (AEs) reported in two or more patients were pyrexia (n=2 patients [18.2%], Grades 1 and 3 [non-serious]) and anaemia (n=2 patients, [18.2%], Grades 1 and 2). There were no dose limiting toxicities, grade 4–5 AEs, or related SAEs reported. Plasma cytokine levels showed the strongest response at BNT411 Dose Level (DL) 5 (2.4 µg/kg), with an increase (2.7–9.2 fold) of interferon-γ induced protein IP10 in 3/4 patients. The best response seen was 5 months of stable disease in one patient with squamous cell carcinoma of the lung at DL4 after 13 doses. Three dose levels remain to be tested in Part 1A (up to 16 µg/kg), with recruitment to Part 1B initiated.

Conclusions BNT411 has an acceptable safety profile at all doses tested as monotherapy, with encouraging PD signals that warrants study continuation. Updated data will be presented, including combination treatment in the first-line setting of ES-SCLC.

Acknowledgements BNT411-01 is funded by BioNTech SE. The authors would like to acknowledge Andrew Finlayson (BioNTech SE) for medical writing support.

Trial Registration ClinicalTrials.gov: NCT04101357

Ethics Approval Ethics & Institutional Review Board approvals were obtained from the respective participating countries prior to initiation of the trial.

<http://dx.doi.org/10.1136/jitc-2021-SITC2021.525>

REMOVAL OF SOLUBLE TUMOR NECROSIS FACTORS RECEPTORS 1/2 IN PATIENTS WITH METASTATIC SOLID TUMORS USING IMMUNE APHERESIS

¹Ayala Tamir, ²Hagit Harati, ²Nethanel Asher, ²Ronen Stoff, ²Shirly Grynberg, ³Robert Segal, ³Adam Ostrowski, ³Lawrence Florin, ²Ronnie Shapira-Frommer*, ⁴Gal Markel. ¹Sheba Medical Center, Israel, Ramat Gan, Israel; ²Sheba Medical Center, Ramat Gan, Israel; ³Immunicom Inc., San Diego, CA, USA; ⁴Rabin Medical Center, Petach Tikva, Israel

Background TNF α is a cytokine produced by immune cells and by tumor cells. The soluble forms of membrane TNF receptors 1/2 (sTNF-R1/2) act as decoy to neutralize TNF α , and are highly abundant in cancer patients. Elimination of sTNF-R1/2 may therefore unmask endogenous TNF α , to presumably exert anti-neoplastic effects and reverse resistance to immune checkpoint inhibitors. Immune Apheresis (IA) is a procedure designed to specifically capture sTNF-R1/2 from plasma by passing it over an affinity column. Here we employed Immunicom's LW-02 Immunopheresis[®] device for removal of sTNF-R1/2 from plasma of cancer patients.

Methods In cohort A, patients with melanoma, RCC, NSCLC or TNBC refractory to standard therapy were treated with IA only. IA treatment of 2 plasma volumes was done x3/week, for three treatment cycles (4 weeks each) up to a total of 36 treatments. Cohort B patients currently receive concurrent IA and Nivolumab therapy (240mg q2 weeks starting on week 5). sTNF-Rs removal and circulating inflammatory biomarkers were measured by immuno-assays, such as multiplex cytokine detection and mass cytometry. Pre- and post-treatment tumor biopsies were analyzed for tumor markers and TILs by immunohistochemistry.

Results Cohort A included six patients (3 Melanoma and 3 TNBC): three patients completed full study regimen, and three others were withdrawn due to clinical progression. AEs included chills (4/6), fever (2/6), anemia (6/6), central line thrombosis (1/6) and pulmonary embolism (1/6) All were Grade 2 except G3 anemia (1/6). There were no treatment related SAE's. sTNF-Rs levels were significantly reduced, followed by enhanced detection of TNF α , and IFN γ in some cases. In two patients, CD8 counts and PD-1 and PD-L1 expression were increased. Congruently, blood mass cytometry showed reduction in Treg subsets and differential increase of CD8 subsets following treatment.

Conclusions The use of Immunicom's LW-02 Immunopheresis[®] device in combination with Terumo BCT Spectra Optia Apheresis System is safe and efficient in the removal of sTNF-Rs from blood plasma. Subsequent immuno-assay analyses indicated formation of inflammatory response which may facilitate effects of immunotherapy, yet to be investigated in cohort B.

Trial Registration NCT04142931

Ethics Approval Sheba Medical Center Ethics Committee, 6136-19

Consent Written informed consent was obtained from the patient for publication of this abstract and any accompanying images. A copy of the written consent is available for review by the Editor of this journal

<http://dx.doi.org/10.1136/jitc-2021-SITC2021.526>

DIGITAL SPATIAL PROFILING OF PAIRED TUMOR BIOPSIES REVEALS INDOLEAMINE 2,3-DIOXYGENASE (IDO)1 AS A POTENTIAL RESISTANCE MECHANISM FOR A TUMOR-TARGETED 4-1BB AGONIST IN PATIENTS WITH SOLID TUMORS

<http://dx.doi.org/10.1136/jitc-2021-SITC2021.527>

¹Tamara Tanos, ¹Christian Heichinger, ¹Sabine Wilson, ²Marta Canamero, ¹Mariana Bustamante, ¹Chiahuey Ooi, ¹Irina Klamann, ¹Bruno Gomes, ¹Maurizio Ceppi*, ¹Maurizio Ceppi. ¹Roche Innovation Center Basel, Basel, Switzerland; ²Roche Innovation Center Munich, Penzberg, Germany

Background We previously described the capacity of RO7122290 (RO) - a FAP-targeted 4-1BB bispecific antibody - to induce CD8+ T cell infiltration and activation in the tumor (Moreno V. et al, SITC 2020). Aiming to compare pharmacodynamic (PD) changes in tumor nests and stroma, paired tumor biopsies from patients treated with RO (Part A) and RO + atezolizumab (Part B) were analysed by digital spatial profiling (DSP, Nanostring).

Methods Seven paired (baseline and on-treatment) FFPE tumor tissue biopsies (three from Part A, four from Part B) obtained from an ongoing Phase 1/1b trial (EUDRACT 2017-003961-83) were assessed for mRNA and protein expression. Biopsies were taken from six different tumor types at different RO doses. Up to twelve Regions of Interest (ROIs) were collected per slide and the morphology markers PanCK, CD8, CD3 and DAPI were applied. The ROIs were further annotated in tumor nests and stroma segments based on PanCK staining. The immune-oncology 58-plex protein and 78-plex mRNA expression panels (Nanostring) were used to profile all samples. Data were normalized according to Nanostring guidelines and filtered based on relevance (absolute log₂ fold change > 1) and significance (FDR < 0.05, p-value).

Results The level of CD8+ T cell infiltration measured by spatial profiling correlated with the level measured by IHC, in both tumor nests and stroma. The activation markers 4-1BB and PD-1 were upregulated, confirming the PD effect already measured by mRNA sequencing. We also identified novel protein markers - CD40, PD-L1 and IDO1 - being upregulated after treatment. Spatial regulation differed among the markers with 4-1BB, PD-1 and CD40 upregulated only in the stroma, PD-L1 and IDO1 upregulated in the tumor nests and in the stroma. IDO1 induction is particularly relevant, since this protein is known to attenuate 4-1BB-mediated effector responses. Conventional IHC analysis performed on 14 paired biopsies confirmed IDO1 being upregulated in 11 out of 14 cases and revealed dendritic cells, macrophages and stromal cells to express IDO1. Importantly, IDO1 upregulation was observed in both Part A (3 out of 3) and Part B (8 out of 11).

Conclusions Spatial profiling allowed us to identify key markers that are spatially regulated after treatment and to gain new insights on the MoA of RO. The induction of IDO1 by RO confirms the dual immunoregulatory nature of 4-1BB signaling and highlights IDO1 as a potential resistance mechanism for RO in the clinical setting, both as single agent and in combination with atezolizumab.

Trial Registration EUDRACT Number: 2017-003961-83; Protocol Number: BP40087

REFERENCES

1. Moreno V. et al, Pharmacodynamic assessment of a novel FAP-targeted 4-1BB agonist, administered as single agent and in combination with atezolizumab to patients with advanced solid tumors, Nov 1 2020, Journal for Immunotherapy of Cancer, presented at SITC 2020

528

CORRELATION OF BASELINE CIRCULATING VG9VD2 T CELL COUNTS AND PHARMACODYNAMIC ACTIVITY OF ICT01 IN CANCER PATIENTS: PRELIMINARY RESULTS FROM EVICTION AND A NOVEL PATIENT ENRICHMENT STRATEGY

¹Emmanuel Valentin*, ¹Aude de Gassart, ¹Patrick Brune, ¹Clément Ghigo, ¹Sophie Agaugué, ²Daniel Olive, ¹Paul Frohna. ¹Imcheck Therapeutics, Marseille, France; ²CRCM, INSERM U1068, Marseille, France

Background ICT01, a novel, anti-BTN3A immunotherapeutic mAb for activating g9d2T cells, is currently evaluated in a Phase 1/2a clinical trial in patients with advanced-stage, relapsed/refractory cancer (NCT04243499, EVICTION). ICT01 indirectly activates g9d2 T cells that secrete inflammatory cytokines and migrate into tumors to coordinate antitumor immune responses. Therefore, the baseline number of g9d2 T effector cells constitutes a biomarker of interest and a potential selection criterion for target patients.

Methods Full immunophenotyping (cell counts and activation state) was performed by flow cytometry on fresh blood collected pre- and on-treatment. Serum cytokines were monitored at baseline and post-treatment. Tumor biopsies were harvested at baseline and on Day 28, and multiplex IHC coupled with digital pathology was used to quantify g9d2T cell, CD8 T cell, NK cell, and T reg infiltration and activation state

Results Baseline circulating g9d2 T cell count was highly variable in solid tumor patients enrolled in the monotherapy arm of EVICTION (median 6918 cell/mL, n=26). Melanoma and colorectal patients displayed respectively the highest (median 42277 cell/mL, n=3) and the lowest (median 3040 cell/mL, n=9) baseline number. During the dose escalation phase, g9d2 T cell activation (CD69+) and migration from the blood was observed 30 min post-ICT01 administration. Serum cytokine levels showed variability within ICT01 dose cohorts. IFN γ , TNF α , IL-6 and IL-8 levels post-ICT01 dosing were ICT01 dose dependent and clearly related to baseline number of circulating g9d2 T cells. Activation of peripheral blood NK cells, granulocytes and CD8 T cells was observed post-dosing at ICT01 doses \geq 7 mg, which was significantly correlated with baseline g9d2 T cell counts, but not with other immune subsets (Spearman $r=0.51$, 0.47 and 0.65 for CD69+NK, CD69+CD8 and PD-L1+granulocytes respectively, $p<0.05$, $n=19$). Baseline circulating g9d2 T cell count was positively correlated with gdTCR+ T cell density in baseline tumor biopsies (Spearman $r=0.76$, $p=0.0086$, $n=11$). Finally, a trend was observed between baseline g9d2 T cell counts and overall tumor immune cell infiltration and activation post-ICT01 treatment, with 4 patients (out of 13 with available biopsy pairs) with g9d2 T cell counts above the median displaying the highest tumor immune cell infiltration and activation.

Conclusions These results suggest the utility of measuring baseline g9d2 T cells as part of the patient selection process for ICT01 clinical trials. Patient enrichment based on this biomarker will be tested in EVICTION expansion arms where a minimum baseline threshold of g9d2 T cells counts will be one of the eligibility criteria.

Trial Registration NCT04243499

Ethics Approval The study has obtained Competent Authority and Ethics Committee approvals. Informed consent forms were obtained from all enrolled patients.

<http://dx.doi.org/10.1136/jitc-2021-SITC2021.528>

529

PHASE 1 STUDY OF INCB086550, AN ORAL PD-L1 INHIBITOR, IN IMMUNE-CHECKPOINT NAIVE PATIENTS WITH ADVANCED SOLID TUMORS

¹Eric Van Cutsem*, ²Hans Prenen, ³Brant Delafontaine, ⁴Kristen Spencer, ⁵Tara Mitchell, ⁶Howard Burris, ⁷Nuria Kotecki, ⁸Rebecca Kristeleit, ⁹David Pinato, ¹⁰Solmaz Sahebjam, ¹¹Donna Graham, ¹²Thomas Karasic, ¹³Jeannie Daniel, ¹⁴Kevin O'Hayer, ¹⁵Ryan Geschwindt, ¹⁶Sarina Piha-Paul. ¹University of Leuven, Leuven, Belgium; ²University Hospital Antwerp, Antwerp, Belgium; ³Ghent University Hospital, Ghent, Belgium; ⁴Rutgers Cancer Institute of New Jersey, New Brunswick, NJ, USA; ⁵University of Pennsylvania, Philadelphia, PA, USA; ⁶Sarah Cannon, Nashville, TN, USA; ⁷Jules Bordet Institute, Brussels, Belgium; ⁸Guy's and St Thomas' Hospital, London, UK; ⁹Imperial College London, London, UK; ¹⁰Moffitt Cancer Center, Tampa, FL, USA; ¹¹The Christie NHS Foundation Trust, Manchester, UK; ¹²Incyte Corporation, Wilmington, DE, USA; ¹³University of Texas, MD Anderson Cancer, Houston, TX, USA

Background INCB086550 is an orally administered small molecule that binds PD-L1 and inhibits PD-1/PD-L1 interaction. Translational data demonstrating markers of immune activation in patients following INCB086550 were previously reported.¹ Preliminary clinical data from this phase 1 study are presented below.

Methods Adult patients (≥18 years) with advanced solid tumors were enrolled into this open-label study. Patients had disease progression after standard available therapy or were intolerant of or ineligible for standard treatment. Measurable disease was required. A modified 3+3 dose-escalation design was employed, followed by dose expansions. The primary endpoints were safety and tolerability of INCB086550, identification of a pharmacologically active dose and/or MTD, and confirmation of the RP2D. Secondary endpoints included PK, pharmacodynamics, and efficacy as assessed by investigator-determined ORR and DCR (CR, PR, or SD ≥12 weeks).

Results As of 9Apr2021, 79 patients received treatment (Table 1); 57.0% were female, 62.0% had ≥2 prior lines of therapy, and 16% received prior IO treatment. Forty-six (58.2%) patients had treatment-related TEAEs; those occurring in ≥5% of patients are presented in Table 2. Ten patients (12.7%) had grade ≥3 treatment-related TEAEs. Immune-related TEAEs occurred in 15 patients (19.0%); the most common (>1 patient) included peripheral sensory neuropathy (n=5), pruritus (n=3), immune-mediated neuropathy (n=2), and peripheral motor neuropathy (n=2). In total, 10 (12.7%) patients had TEAEs of peripheral neuropathy; all were grade ≤3. All grade 2 or 3 TEAEs of peripheral neuropathy resolved or improved with either study drug continuation without dose modification, dose reduction, or drug interruption/discontinuation. Patients with TEAEs leading to treatment interruption were 21 (26.6%), dose reduction 5 (6.3%), and discontinuation 13 (16.5%). Five patients (6.3%) died of a TEAE (cerebrovascular accident, dyspnea, general physical health deterioration, intestinal obstruction, intracranial hemorrhage [each n=1]); all fatal TEAEs were considered unrelated to study drug. The efficacy-evaluable population included 68 patients; ORR was 11.8% (95%CI, 5.2%–21.9%; CR, 1.5%; PR, 10.3%), and DCR was 19.1% (95%CI, 10.6%–30.5%; Table 3). Eight objective responses were observed at doses ≥400 mg BID (Table 4); 3 of these were noted among the 5 IO treatment-naive patients with MSI-H tumors who received 400 mg BID.

Conclusions Immune-related AEs observed in this ongoing phase 1 study are consistent with those seen with antibody immune checkpoint inhibitors, with the exception of peripheral neuropathy. Preliminary efficacy of INCB086550 in tumor types known to be responsive to anti-PD-(L)1 therapy is encouraging and warrants further investigation.

Abstract 529 Table 1 Number of patients per dose level

Dose Level	Number of Patients
100 mg QD	6
200 mg QD	3
200 mg BID	24
400 mg QD	4
400 mg BID	32
800 mg QD	1
800 mg BID	6
400 mg BID 1 week; 100 mg QD 1 week; repeat	1
400 mg BID 2 weeks; 100 mg QD 2 weeks; repeat	2
Total	79

BID, twice daily; QD, once daily.

The tumor types in the study included breast, cervical, colorectal, endometrial, esophageal, gastric, hepatocellular, melanoma, mesothelioma, ovarian, small cell lung cancer, squamous cell carcinoma of the head and neck, renal cell, urothelial, adrenal, anal, cholangiocarcinoma, gall bladder, pancreatic, penile, salivary gland, sarcoma, vaginal, prostate, basal cell, pleomorphic sarcoma, fallopian, carcinoma of parotid gland, well-differentiated liposarcoma, myoepithelial, castrate-resistant prostate cancer, cancer of unknown primary, neuroendocrine, prostate adenocarcinoma with neuroendocrine differentiation, glioblastoma, anal canal, angiosarcoma, and gastroesophageal junction.

Abstract 529 Table 2 Treatment-related TEAEs reported by ≥5% of patients (N=79)

Preferred Term, n (%)	Any Related TEAE	Grade ≥3 Related TEAE
Nausea	13 (16.5)	0
Fatigue	8 (10.1)	1 (1.3)
Decreased appetite	7 (8.9)	0
Vomiting	7 (8.9)	1 (1.3)
Diarrhea	6 (7.6)	0
Lipase increased	6 (7.6)	0
Headache	5 (6.3)	0
Peripheral sensory neuropathy	5 (6.3)	2 (2.5)
Pruritus	5 (6.3)	1 (1.3)
Rash	5 (6.3)	1 (1.3)

TEAE, treatment-emergent adverse event.

TEAE, treatment-emergent adverse event.

Abstract 529 Table 3 Summary of best overall response by RECIST v1.1 or RANO*

Response, n (%)	Efficacy-Evaluable Population† (N=68)
ORR (CR+PR)	8 (11.8)
CR	1 (1.5)
PR	7 (10.3)
DCR (CR+PR+SD ≥12 weeks)	13 (19.1)
SD (SD ≥12 weeks)	5 (7.4)
Progressive disease	39 (57.4)
Not evaluable‡	8 (11.8)
Not assessed§	8 (11.8)

CR, complete response; DCR, disease control rate; GBM, glioblastoma; ORR, objective response rate; PR, partial response; RANO, Response Assessment of Neuro-Oncology;

* RECIST, Response Evaluation Criteria in Solid Tumors; SD, stable disease.
† 1 patient with GBM was assessed by RANO and had best overall response of progressive disease.

‡ The efficacy-evaluable population included all solid tumor participants enrolled in the study who received at least 1 dose of INCB086550, completed a baseline scan, and met at least 1 of the following criteria: ≥1 postbaseline scan, participant had been on the study for a minimum of 63 days of follow-up, or participant had discontinued from treatment.

§ "Not evaluable" indicates participants in the efficacy-evaluable population that did not have valid postbaseline overall response assessments by RECIST or RANO.

§ "Not assessed" indicates participants in the efficacy-evaluable population that did not have any postbaseline overall response assessments by RECIST or RANO.

Abstract 529 Table 4 Tumor types with investigator-assessed objective response per RECIST v1.1 (n=8)

Tumor Type	IO Treatment -Naive	Dose	Best Overall Response	Duration of Response (Months)
Squamous cell anal cancer	Yes	800 mg BID	Partial Response	4.17
Squamous cell anal cancer	Yes	400 mg BID	Complete Response	5.78
MSI-H colon adenocarcinoma	No	400 mg BID	Partial Response	5.78+
Clear cell ovarian cancer	Yes	400 mg BID	Partial Response	3.35+
MSI-H colon adenocarcinoma	Yes	400 mg BID	Partial Response	3.71+
dMMR gastric cancer	Yes	400 mg BID	Partial Response	1.87+
MSI-H neuroendocrine colon cancer	Yes	400 mg BID	Partial Response	1.87
Squamous cell vaginal cancer	Yes	400 mg BID	Partial Response	0.03+

BID, twice daily; dMMR, deficient mismatch repair; IO, immuno-oncology; MSI-H, high microsatellite instability; RECIST, Response Evaluation Criteria in Solid Tumors.

+Ongoing response.
BID, twice daily; dMMR, deficient mismatch repair; IO, immuno-oncology; MSI-H, high microsatellite instability; RECIST, Response Evaluation Criteria in Solid Tumors.

+Ongoing response.

Trial Registration ClinicalTrials.gov identifier NCT03762447

REFERENCES

1. Piha-Paul S, et al. *J Immunother Cancer*. 2020;8(suppl 3):A255.

Ethics Approval The study protocol was approved by institutional review boards (IRB) or independent ethics committees at participating centers. All study participants gave informed consent before taking part. The approval numbers were: Integ Review IRB (Austin, TX), RM 598; MD Anderson Cancer Center Office of Human Subject Protection (Houston, TX), IRB ID 2018-0765; ADVARRA (Columbia, MD), IRB# 00000971; Ethisch Comité/Comité d' Ethique Hospital (Brussels, Belgium), A2021/085; Hôpital Saint-Louis (Paris, France), Prof Le Tourneau – 2020-118/Ref. of the Promoter 0.09.22.72214; NHS Health Research Authority London - City & East Research Ethics Committee (Bristol, UK), IRAS project ID:282291/REC reference: 20/LO/1001; Comitato Etico IRCCS Pascale (Milan, Italy), ISS Validation Protocol Number 29111(2020)-PRE21-1835; Comitato Etico Della Fondazione IRCCS "Istituto Nazionale Dei Tumori"- Milano CE150053 (Milan, Italy), INT 230/20; Comitato Etico Regione Toscana - Area Vasta Sud Est CE150047, 18064; Comitato Etico Indipendente Istituto Clinico Humanitas CE150081, 940/20; Regulatory Pharma Net (Pisa, Italy), IEC 1393.

<http://dx.doi.org/10.1136/jitc-2021-SITC2021.529>

530

A FIRST-IN-HUMAN PHASE I STUDY OF M6223 (TIGIT INHIBITOR) AS MONOTHERAPY OR IN COMBINATION WITH BINTRAFUSP ALFA IN PATIENTS WITH METASTATIC OR LOCALLY ADVANCED SOLID UNRESECTABLE TUMORS

¹Geoffrey Watson, ²Meredith McKean, ³Anthony Tolcher, ⁴Anja Victor, ⁵Sen Zhang, ⁵Vadryn Pierre, ⁴Emilia Richter, ⁶Aung Naing, ⁶Aung Naing*. ¹Princess Margaret Cancer Center, Toronto, Canada; ²Sarah Cannon Research Institute, Nashville, TN, USA; ³South Texas Accelerated Research Ther, San Antonio, TX, USA; ⁴Merck KGaA, Darmstadt, Germany; ⁵EMD Serono, Billerica, MA, USA; ⁶University of Texas MD Anderson Cancer Center, Houston, TX, USA

Background T cell immunoreceptor with immunoglobulin and immunoreceptor tyrosine-based inhibitory motif domains (TIGIT) is an inhibitory receptor expressed on T cells, including regulatory T cells (Tregs) and natural killer (NK) cells. In the tumor microenvironment, TIGIT is often overexpressed and directly inhibits both T cell and NK cell effector function and proliferation. TIGIT is also involved in regulating Treg function. Therefore, inhibiting the TIGIT-related immunosuppressive pathway may result in antitumor activity. M6223 is an intravenously (IV) administered, human, antagonistic, immunoglobulin G1 (IgG1) anti-TIGIT antibody with an Fc mediated effector region. Bintrafusp alfa is a first-in-class bifunctional fusion protein composed of the extracellular domain of the human transforming growth factor β receptor II (a TGF β "trap") fused to a human IgG1 monoclonal antibody blocking programmed death ligand 1 (PD-L1). As TIGIT and programmed death receptor 1 (PD-1) are co-expressed on T cells, dual inhibition of both immune checkpoints may enhance antitumor activity. This phase Ia study (NCT04457778) aims to determine the safety, tolerability, maximum tolerated dose and recommended dose for expansion of M6223 monotherapy and M6223 (both the once every 2 weeks [Q2W] and once every 3 weeks [Q3W] regimens) in combination with bintrafusp alfa. Secondary objectives include the evaluation of pharmacokinetics and clinical activity of M6223 with and without bintrafusp alfa.

Methods Eligible patients include those aged ≥ 18 years with: an Eastern Cooperative Oncology Group performance status ≤ 1 ; adequate baseline hematological, renal and hepatic function; and histologically or cytologically proven locally advanced or advanced solid tumors, for which no effective standard therapy is available. Patients previously treated with a TIGIT targeting agent or bintrafusp alfa are excluded. Patients with brain metastases are also excluded, except those without neurological symptoms ≥ 4 weeks before start of treatment and those receiving either a stable or decreasing dose of steroids < 10 mg/day or no steroid treatment. In the monotherapy dose escalation phase, approximately 17–26 patients will receive M6223 IV at one of the six dose levels planned (10–1600 mg Q2W). In the combination dose escalation phase, 18–21 patients will receive M6223 IV at one of four dose levels planned (300, 900, 1600 mg Q2W and 2400 mg Q3W) in combination with bintrafusp alfa IV (1200 mg Q2W or 2400 mg Q3W). Dose escalation is determined by the safety monitoring committee and supported by a Bayesian 2-parameter logistic regression model. The study is currently ongoing in the United States and Canada.

Acknowledgements The authors would like to thank Daniel Holland of the healthcare business of Merck KGaA, Darmstadt, Germany for his involvement and contribution to the design and conduct of this study. Medical writing assistance was provided by David Lester of Bioscript Stirling Ltd,

Macclesfield, UK, and funded by the healthcare business of Merck KGaA, Darmstadt, Germany [CrossRef Funder ID: 10.13039/100009945]. Funding: The healthcare business of Merck KGaA, Darmstadt, Germany (CrossRef Funder ID: 10.13039/100009945).

Trial Registration NCT04457778

Ethics Approval The study and the protocol were approved by the Institutional Review Board or ethics committee at each site. All patients provided written informed consent before any study procedures were performed.

<http://dx.doi.org/10.1136/jitc-2021-SITC2021.530>

531

A PHASE 1B MULTI-TUMOR COHORT STUDY OF CABOZANTINIB PLUS ATEZOLIZUMAB IN ADVANCED SOLID TUMORS: RESULTS OF THE TRIPLE-NEGATIVE BREAST CANCER, OVARIAN CANCER, AND ENDOMETRIAL CANCER COHORTS

¹Ira Winer*, ²Akhila Wimalasingham, ³Joaquina Baranda, ⁴Armando Santoro, ⁵Kristen Spencer, ⁶Capucine Baldini, ⁷Linda Duska, ⁸Vivek Subbiah, ⁹Sandip Patel, ¹⁰Polina Khrizman, ¹¹Griet Van Lancker, ¹²Lana Andrianova, ¹²Sumandeep Atwal, ¹²Keerti Sharma, ¹³Luis Manso. ¹Karmanos Cancer Institute, Detroit, MI, USA; ²Queen Mary University of London, London, UK; ³University of Kansas Cancer Center, Kansas City, KS, USA; ⁴Humanitas University, IRCCS, Rozzano-Milan, Italy; ⁵Rutgers Cancer Institute of New Jersey, New Brunswick, NJ, USA; ⁶DITEP, Gustave Roussy, Villejuif, France; ⁷University of Virginia, Charlottesville, VA, USA; ⁸The University of Texas MD Anderson Cancer Center, Houston, TX, USA; ⁹University of California San Diego, La Jolla, CA, USA; ¹⁰MD Anderson Cancer Center at Cooper, Camden, NJ, USA; ¹¹Ghent University, Ghent, Belgium; ¹²Exelixis, Inc., Alameda, CA, USA; ¹³Hospital Universitario 12 de Octubre, Madrid, Spain

Background Cabozantinib, a multiple receptor tyrosine kinase inhibitor, promotes an immune-permissive environment which might enhance the activity of immune checkpoint inhibitors. COSMIC-021 (NCT03170960), a multicenter phase 1b study, is evaluating the combination of cabozantinib with atezolizumab in advanced solid tumors; here we present efficacy and safety results in patients with triple negative breast cancer (TNBC), ovarian cancer (OC), and endometrial cancer (EC).

Methods Eligible patients had locally advanced or metastatic TNBC, OC, or EC and had radiographically progressed on prior systemic anticancer therapy. One or two lines of prior therapy were permitted. Patients with OC were platinum resistant or refractory. Prior treatment with anti-PD-1 or anti-PD-L1 agents was allowed for patients with TNBC. Patients received cabozantinib, 40 mg PO QD, plus atezolizumab, 1200 mg IV Q3W. The primary endpoint was objective response rate (ORR) per RECIST 1.1 as assessed by investigator. Other endpoints included safety, duration of response (DOR), progression free survival (PFS), and overall survival (OS). CT/MRI scans were performed Q6W for the first year and Q12W thereafter.

Results As of February 19, 2021, 30–32 patients were enrolled in each of the cohorts. 47% of patients with TNBC, 47% with OC, and 40% with EC had received 2 lines of prior therapy. Median follow-up was 18.7 months, 20.8 months, and 19.0 months for the TNBC, OC, and EC cohorts, respectively. Grade 3/4 treatment-related adverse events occurred in 33% of patients with TNBC, 56% with OC, and 37% with EC. One Grade 5 treatment-related adverse event of pulmonary hemorrhage occurred in the TNBC cohort and one of encephalitis occurred in the OC cohort. Cabozantinib plus atezolizumab demonstrated clinical activity in all three tumor cohorts (table 1).

Abstract 531 Table 1

Endpoint	Cohort		
	TNBC (N=30)	OC (N=32)	EC (N=30)
ORR, % (95% CI)*	17 (5.6, 34.7)	19 (7.2, 36.4)	7 (0.8, 22.1)
†Disease Control Rate, %	67	63	53
Median DOR, months (95% CI)	9.2 (1.9, NE)	8.3 (5.6, NE)	NR‡
Median PFS, months (95% CI)	4.0 (1.4, 5.8)	3.9 (1.5, 6.1)	2.7 (1.4, 8.4)
Median OS, months (95% CI)	14.8 (9.9, NE)	9.3 (5.1, 23.6)	15.5 (8.3, NE)

*complete response+partial response+stable disease per RECIST 1.1 six months following treatment

†For TNBC, 2 confirmed complete responses and 3 confirmed partial responses; for OC, 6 confirmed partial responses; for EC, 2 confirmed partial responses

‡Median not reached

Conclusions Cabozantinib in combination with atezolizumab demonstrated encouraging clinical activity in patients with previously treated advanced cancers.

Acknowledgements Medical writing support provided by Suva-jit Sen, PhD (Exelixis, Inc.)

Trial Registration NCT03170960

Ethics Approval Yes

Consent Yes

<http://dx.doi.org/10.1136/jitc-2021-SITC2021.531>

FIRST-IN-HUMAN PHASE 1 TRIAL OF SRK-181: A LATENT TGF β 1 INHIBITOR, ALONE OR IN COMBINATION WITH ANTI-PD-(L)1 TREATMENT IN PATIENTS WITH ADVANCED SOLID TUMORS (DRAGON TRIAL)

¹Timothy Yap*, ²Minal Barve, ³Justin Gainor, ⁴Bruno Bockorny, ⁵Yawen Ju, ⁵Shaun Cote, ⁵Sanela Bilic, ⁵Lan Liu, ⁵Yung Chyung, ⁵Michelle Legler, ⁵Lu Gan, ⁶Meredith McKean. ¹University of Texas MD Anderson Cancer Center, Houston, TX, USA; ²Mary Crowley Cancer Research, Dallas, TX, USA; ³Massachusetts General Hospital; Harvard Medical School, Boston, MA, USA; ⁴Beth Israel Deaconess Medical Center, Boston, MA, USA; ⁵Scholar Rock, Inc., Cambridge, MA, USA; ⁶Sarah Cannon Research Institute; Tennessee Oncology, Nashville, TN, USA

Background Transforming growth factor-beta 1 (TGF β 1) plays an important role in mediating the primary resistance to PD-1/PD-L1 [PD-(L)1] blockade. SRK-181 is a fully human monoclonal antibody that selectively inhibits latent TGF β 1 activation. Mouse tumor models (bladder, melanoma, and breast cancer) demonstrated that treatment with SRK-181+anti-PD-1 overcame primary anti-PD-1 resistance. Four-week GLP non-clinical toxicology studies showed that SRK-181 has improved safety profile (no cardiotoxicities) compared to broad TGF β pathway inhibition.

Methods The DRAGON trial (NCT04291079) is an ongoing open-label, phase 1 study. Part A of the study follows a standard 3+3 dose escalation design to determine the dose for Part B. Part B (expansion phase) evaluates combination treatment in patients with non-small cell lung cancer (NSCLC), urothelial carcinoma, melanoma, or other advanced solid tumors. SRK-181 is administered IV every 3 or 2 weeks (Q3W/Q2W) alone in patients with advanced solid tumors (Part A1), or in combination with anti-PD-(L)1 in patients who did not respond to prior anti-PD-(L)1 therapy (Part A2/B).

Results As of 7 June 2021, 25 patients have enrolled to Part A; median 4 prior lines of therapies (range 1–9). Cancer types: colorectal, ovarian, prostate, and unknown primary (Part A1); liver, melanoma, NSCLC, oropharynx, renal cell carcinoma (RCC) and uterine (Part A2). In Part A1, 15 patients were treated with SRK-181 monotherapy at doses of 80, 240, 800, 1600, 2400, 3000mg Q3W, with no dose limiting toxicity (DLT) observed. The last cohort (2000mg Q2W) remains under evaluation. The most common treatment-related AEs (TRAE, >10%) of any grade were decreased appetite and fatigue (each: 13.3%, n=2). Six patients had stable disease (SD) as best response (2/colorectal cancer, 1/prostate cancer, and 3/ovarian cancer). Three ovarian cancer patients were stable \geq 153 days with tumor regressions. In Part A2, 10 patients were treated with SRK-181 at doses of 240, 800 and 1600mg Q3W+pembrolizumab. No DLT was observed up to 800mg. 1600mg Q3W is under evaluation. No TRAE (>10%) of any grade were observed. One confirmed RECIST1.1 partial response (PR) was observed (800mg) in a patient with anti-PD-1 resistant RCC and 2 patients had best response of SD (1/oropharynx cancer, 1/liver cancer). The half-life of SRK-181 ranged from 3.9 to 19.3 days across the doses tested.

Conclusions As of 7 June 2021, SRK-181 has been well tolerated as monotherapy and in combination with anti-PD-(L)1. One RECIST1.1 PR (800mg) was observed in a patient with anti-PD-1 resistant RCC. Next planned dose in Part A2 will be 2400mg Q3W.

Trial Registration DRAGON trial (NCT04291079)

Ethics Approval The human study was approved by the Massachusetts General Hospital and Beth Israel Deaconess Medical Center (20–286), Sarah Cannon Research Institute (1276118), Mary Crowley Cancer Research (20–06), MD Anderson

Cancer Center (2020–0110) Institutional Review Boards with written informed consent obtained from each participant and/or their legal representative, as appropriate.

<http://dx.doi.org/10.1136/jitc-2021-SITC2021.532>

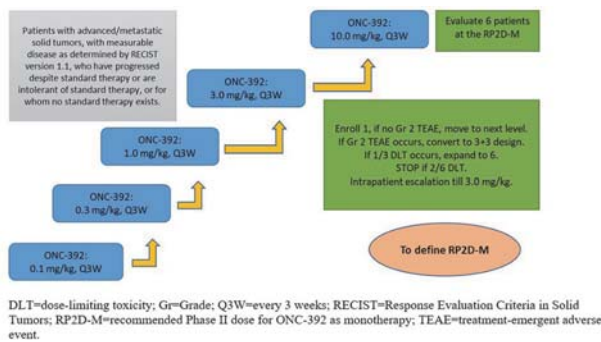
533

AN OPEN LABEL PHASE IA/IB STUDY FOR SAFETY, PHARMACOKINETICS (PK), AND EFFICACY OF ONC 392 AS A SINGLE AGENT AND IN COMBINATION WITH PEMBROLIZUMAB IN ADVANCED SOLID TUMORS

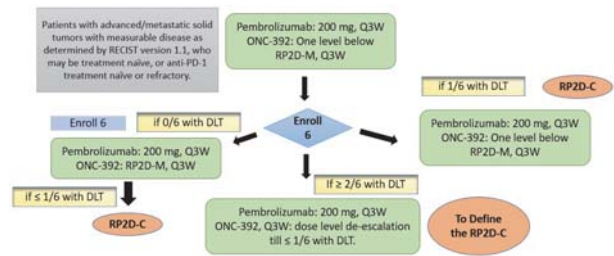
¹Pan Zheng*, ²Kun He, ¹Yang Liu. ¹OncoC4, Inc., Rockville, MD, USA; ²R and G Pharma US, Inc., Rockville, MD, USA

Background ONC-392 is a highly selective, humanized monoclonal IgG1 antibody against CTLA-4. The parental clone was identified through in vivo screening in a humanized CTLA-4 mouse model for high anti-tumor efficacy and low autoimmune toxicity. By preserving CTLA-4 on the cell surface, ONC 392 leaves a higher ligand density for better antibody-dependent cellular cytotoxicity (ADCC), resulting in more efficient in Treg depletion in the tumor microenvironment (TME) and more potent tumor rejection in pre-clinical models. Based on encouraging Phase I dose escalation study, a major revision of the protocol has been performed to expand clinical indications among patients with advanced solid tumors.

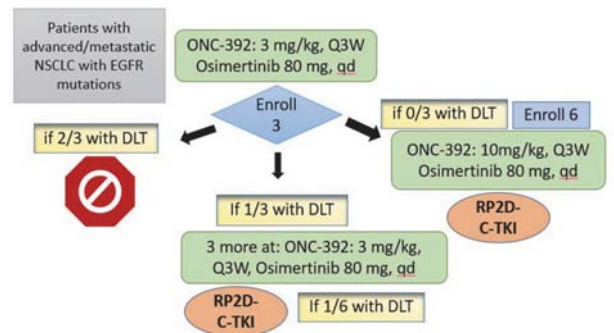
Methods This is a Phase IA/IB, open label, dose-escalation, and dose-expansion study of intravenous (IV) ONC 392 as a single agent and in combination with Pembrolizumab (anti PD-1, marketed as KEYTRUDA® by Merck) in patients with advanced/metastatic solid tumors. The study consists of three parts: (1) Part A (Figure 1) is a dose-finding rapid titration study of ONC-392 as a single agent in patients with advanced solid tumors of various histology to define the recommended Phase II dose for ONC-392 monotherapy (RP2D-M). (2) Part B (Figure 2 and 3) has Part B1 and Part B2 as dose-finding for combination therapy with either pembrolizumab or Osimertinib 80 mg orally once daily to define the recommended Phase II dose for ONC-392 in combination with either drug (3) Part C (Figure 4) Phase IB expansion cohorts of ONC-392 in monotherapy and in combination therapy with Pembrolizumab to determine safety and initial efficacy. A total of 8 cohorts encompassing monotherapy for pancreatic cancer and triple negative breast cancer and combination therapy of non-small cell lung carcinoma, melanoma and Merkel cell carcinoma. The primary endpoints for Part A and B are safety and tolerability to observe maximal tolerable dose and recommended doses for Phase II, while that for part C is efficacy as measured by overall response rates. The planned enrollment is 300 patients and the study duration is 18 months.



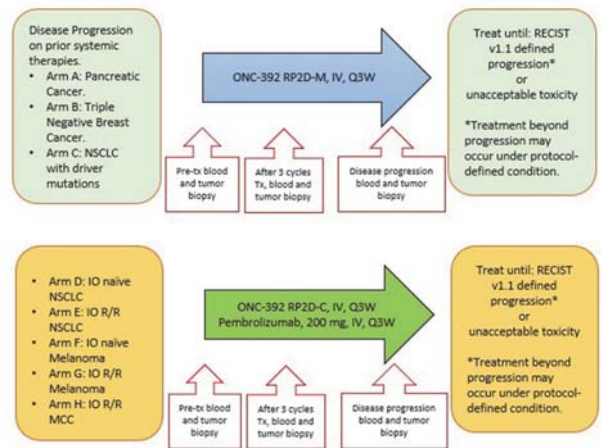
Abstract 533 Figure 1 Diagram of ONC-392-001 study Part A



Abstract 533 Figure 2 Diagram of ONC-392-001 study Part B1



Abstract 533 Figure 3 Diagram of ONC-392-001 study Part B2



Abstract 533 Figure 4 Diagram of ONC-392-001 study Part C

Acknowledgements The study is partially supported by an NIH grant R44CA250824 to OncoC4, Inc. Trial Registration NCT04140526

Ethics Approval The study obtained ethics approval from WIRB, study number 20193108. The participants gave informed consent before the enrollment and treatment.

<http://dx.doi.org/10.1136/jitc-2021-SITC2021.533>

535

A PHASE I/II STUDY OF REGN7075 (EGFRxCD28 COSTIMULATORY BISPECIFIC ANTIBODY) IN COMBINATION WITH CEMIPIMAB (ANTI-PD-1) IN PATIENTS WITH ADVANCED SOLID TUMORS

¹Nehal Lakhani*, ²Melissa Johnson, ³Roman Groisberg, ⁴Hyunsil Han, ⁴Kerry Casey, ⁴Siyu Li, ⁴Dimitris Skokos, ⁴Frank Seebach, ⁴Israel Lowy, ⁴Matthew Fury, ⁴Melissa Mathias.

¹START Midwest, Grand Rapids, MI, USA; ²Sarah Cannon Research Institute, Nashville, TN, USA; ³Rutgers Cancer Institute of New Jersey, New Brunswick, NJ, USA; ⁴Regeneron Pharmaceuticals, Inc., Tarrytown, NY, USA

Background T-cell redirecting bispecific antibodies (bsAbs) are therapeutics that recognize two distinct antigens: a tumor-associated antigen on tumor cells to promote recruitment of T-cells to the tumor, and a receptor on T-cells to potentiate anti-tumor activity. REGN7075 is a human immunoglobulin G4-based costimulatory bsAb designed to bridge epidermal growth factor receptor (EGFR) positive tumor cells with CD28 positive T-cells and to provide amplified T-cell receptor-CD3 complex-mediated T-cell activation within the tumor, through the activation of CD28 co-stimulation. In genetically humanized immunocompetent mouse models, REGN7075 in combination with anti-PD-1 (antibody directed against programmed cell death-1 receptor) improved anti-tumor activity compared with either single agent alone.¹

Methods This is an open label, Phase I/II, first-in-human study evaluating the safety, tolerability, pharmacokinetics, and preliminary anti-tumor activity of REGN7075 (EGFRxCD28) alone and in combination with cemiplimab in patients with advanced solid tumors (NCT04626635). Patients must have a protocol-defined advanced solid tumor, be ≥ 18 years of age (≥ 20 years in Japan), have an Eastern Cooperative Oncology Group performance status of 0 or 1, and be naïve to anti-PD-1/anti-PD-ligand(L)1. This study includes dose escalation (a 4+3 design modified from 3+3; Part 1) and expansion phases (Part 2). In Part 1, patients will receive a lead-in of REGN7075 monotherapy for 3 weeks followed by combination therapy with cemiplimab 350 mg every 3 weeks. Study therapies are administered until disease progression, intolerable adverse events, withdrawal of consent, or other stopping criterion is met. Once a recommended Phase 2 dose is determined in Part 1, four tumor-specific expansion cohorts will be opened: non-small cell lung cancer (PD-L1 $\geq 50\%$), triple-negative breast cancer, colorectal cancer (microsatellite stable), and cutaneous squamous cell carcinoma. Primary endpoints are safety and tolerability of REGN7075 alone or in combination with cemiplimab for Part 1, and objective response rate per Response Evaluation Criteria in Solid Tumors version 1.1 for Part 2. This study is currently open to enrollment.

Trial Registration ClinicalTrials.gov identifier NCT04626635.

REFERENCES

1. Waite JC, Wang B, Haber L, et al. Tumor-targeted CD28 bispecific antibodies enhance the antitumor efficacy of PD-1 immunotherapy. *Sci Transl Med* 2020;**12**:2325.

Ethics Approval This study was conducted in accordance with the principles of the Declaration of Helsinki and the International Conference on Harmonization Good Clinical Practice guidelines. The study protocol and all amendments were approved by the institutional review board/ethics committee at each participating study site.

Consent All patients provided written informed consent.

<http://dx.doi.org/10.1136/jitc-2021-SITC2021.535>

INTRATUMORAL INT230-6 SHOWS A FAVORABLE SAFETY PROFILE AND EARLY SIGNS OF EFFICACY IN ADVANCED SOFT TISSUE SARCOMA WITH MONOTHERAPY AND IN COMBINATION WITH IPI-LIMUMAB [INTENSITY IT-01; BMS#CA184-592]

¹Matthew Ingham*, ²James Hu, ³Giles Whalen, ²Jacob Thomas, ²Anthony El-Khoueiry, ²Diana Hanna, ⁴Anthony Olszanski, ⁵Christian Meyer, ⁵Nilofer Azad, ⁶Syed Mahmood, ⁶Lewis Bender, ⁶Ian Walters, ⁷Lilian Siu, ⁷Albiruni Razak. ¹New York Presbyterian Hospital/Columbia, New York, NY, USA; ²Keck School of Medicine of USC, Los Angeles, CA, USA; ³UMass Memorial Medical Center, Worcester, MA, USA; ⁴Fox Chase Cancer Center, Philadelphia, PA, USA; ⁵Johns Hopkins, Baltimore, MD, USA; ⁶Intensity Therapeutics, Inc., Westport, CT, USA; ⁷Princess Margaret Cancer Centre, Toronto, Canada

Background Study IT-01 evaluates INT230-6, a novel formulation of cisplatin (CIS) and vinblastine (VIN) with an amphiphilic cell penetration enhancer designed for intratumoral (IT) administration, as monotherapy or in combination with ipilimumab (IPI). In preclinical studies, INT230-6 increases drug dispersion throughout the tumor, allows drug diffusion into cancer cells and recruits dendritic, CD4 and CD8 T-cells. Further, the addition of IPI has shown to improve INT230-6 responses in preclinical models.¹

Methods IT-01 is an open-label phase 1/2 study, currently enrolling adult subjects with locally advanced, unresectable or metastatic solid tumors, including soft tissue sarcoma (STS). The study assesses the safety and efficacy of INT230-6 administered IT Q2W up to 5 treatment sessions as monotherapy or with IPI 3mg/kg IV Q3W for 4 doses. Biopsies from injected tumor are taken pretreatment and Day 28 for immunohistochemistry (IHC) analysis.

Results 22 subjects with STS (14 INT230-6 monotherapy, 8 IPI combination) have been enrolled with a median age was 65, having a median of 4 (2,10) prior therapies. INT230-6 doses of up to 175 mL (87.5 mg of CIS, 17.5 mg VIN) were injected in one or more tumors at a single dosing session, which contains doses exceeding the typical IV doses of the cytotoxic drugs.² PK analysis estimates that 95% of INT230-6 active agents remain in the tumor. The most common (>25%) related adverse events (AEs) in evaluable monotherapy subjects (n=13) were localized pain (77%), fatigue (39%), decreased appetite (31%), and nausea (31%). The most common (>25%) related AEs in evaluable IPI subjects (n=4) were anemia (50%), fatigue (50%), pruritus (50%), and rash maculo-papular (50%). There were no related grade 4 or 5 AEs in either cohort. The median overall survival (OS) estimate for the monotherapy population (n=14) has not been reached with a median follow-up of 425 days, which compares favorably to results seen in basket studies of patients with similar prognostic factors (ECOG, LDH, # of metastatic sites).^{3 4} IHC results indicate influx of CD4 and CD8 T-cells without meaningful changes in circulating inflammatory cytokines. Abscopal effects in the monotherapy arm were observed in multiple lesions in 4 subjects. OS data for the 8 IPI combination subjects is immature.

Conclusions IT INT230-6 is well tolerated when administered as monotherapy and combined with IPI in STS subjects. INT230-6 monotherapy survival compares favorably to published basket studies in STS with similar prognostic factors. IHC and abscopal effects indicate dosing may activate a T-cell mediated immune response.

Trial Registration NCT # 03058289

REFERENCES

1. Bloom AC, et al. Intratumorally delivered formulation, INT230-6, containing potent anticancer agents induces protective T cell immunity and memory. *Oncoimmunology* 2019.
2. Owelien. Historical PK data from IV administration. *J Cancer Res* 1977; **8**.
3. Livingston J, et al. Validation of prognostic scoring and assessment of clinical benefit for patients with bone sarcomas enrolled in phase I clinical trials. *Oncotarget* 2016;**7**: 64421–64430. <https://www.oncotarget.com/article/10910/>
4. Abstract M, et al. Validation of the Royal Marsden Hospital (RMH) prognostic score in 100 patients with advanced sarcoma enrolled in early phase clinical trials at a major cancer center. *JCO* 2015. https://ascopubs.org/doi/abs/10.1200/jco.2015.33.15_suppl.10558Wagner

Ethics Approval The protocol was approved by an institutional review board, independent ethics committee, or research ethics board at each institution. All subjects or their legally acceptable representative provided written informed consent before screening. The study was designed, undertaken, and reported in accordance with the Declaration of Helsinki, and is registered with clinicaltrials.gov with registration no NCT03058289.

<http://dx.doi.org/10.1136/jitc-2021-SITC2021.536>

537

OPTIMIZE-1, AN OPEN-LABEL PHASE 1B/2 STUDY ASSESSING THE SAFETY AND EFFICACY OF MITAZALIMAB IN COMBINATION WITH CHEMOTHERAPY IN PATIENTS WITH METASTATIC PANCREATIC DUCTAL ADENOCARCINOMA

¹Yago Pico de Coaña*, ¹Karin Enell Smith, ¹Anette Fält, ¹Maria Flärdh, ²Peter Ellmark, ³Philippe Cassier, ⁴Jean-Luc van Laethem, ¹Malin Carlsson. ¹Alligator Bioscience, Lund, Sweden; ²Alligator Bioscience AB, Lund, Sweden; ³Centre Léon Bérard, Lyon, France; ⁴Hôpital Erasme, Bruxelles, Belgium

Background Mitazalimab is a human CD40 agonistic antibody (IgG1) developed for cancer immunotherapy. Targeting CD40 provides an opportunity to kickstart the cancer-immunity cycle by priming and activating tumor-specific T cells.^{1 2} Furthermore, the effects of CD40 agonists on myeloid cells promote degradation of the tumor stroma, improving the influx of T cells and chemotherapeutic agents into the tumor.¹ Targeting CD40 with mitazalimab in pancreatic ductal adenocarcinoma (PDAC), which is defined by a desmoplastic tumor stroma that hosts immune-suppressive macrophages, has the potential to augment responses to chemotherapy, initiating an effective anti-tumor immune response. Data from a phase 1 study (NCT02829099) demonstrated early signs of clinical activity in solid tumors with one partial response and SD in 37% of the patients.³ Mitazalimab was safe and tolerable at intravenous doses up to 1200 µg/kg and most drug-related adverse events were grade 1 or 2.³ Biomarker data from this study demonstrated proof of mechanism, validating mitazalimab's ability to activate CD40 in cancer patients. In preclinical hCD40tg mouse models, repeated administration of mitazalimab in combination with FOLFIRINOX induced a long-term survival when compared to chemotherapy alone.⁴

Methods OPTIMIZE-1 is a phase 1b/2, open-label, multicenter study designed to evaluate safety, tolerability, and efficacy of mitazalimab in combination with chemotherapy (mFOLFIRINOX) in adults diagnosed with previously untreated metastatic PDAC. Mitazalimab and mFOLFIRINOX will be administered by intravenous infusions following a 14-day cycle schedule where mitazalimab will be administered 2 days after mFOLFIRINOX, except for the first cycle of 21 days where mitazalimab will be administered on Day 1 and 10 and infusion of mFOLFIRINOX will start Day 8. In Part 1 (Phase 1b) of the study, the dose of mitazalimab will be escalated from 450 µg/kg to 900 µg/kg (2 dose levels to be evaluated) to obtain the recommended phase 2 dose (RP2D). Part 1 follows a Bayesian optimal interval design (BOIN) with at least 3 patients enrolled at each dose level. A minimum of 6 patients will be evaluated at the RP2D. In Part 2 of the study, the RP2D of mitazalimab will be administered in combination with mFOLFIRINOX to all patients. The study expansion will evaluate the clinical efficacy of mitazalimab in combination with mFOLFIRINOX assessing objective response rate (ORR) (primary endpoint), Progression-free survival (PFS) and Overall survival (OS) (secondary endpoints). The study expansion includes a Simon's two-stage design with an interim analysis to allow stopping for futility or efficacy based on ORR.

Trial Registration NCT04888312

REFERENCES

1. Enell Smith K, Deric A, Hägerbrand K, Norlén P & Ellmark P. Rationale and clinical development of CD40 agonistic antibodies for cancer immunotherapy. *Expert Opinion on Biological Therapy* 2021 Jun 17, 1–12.
2. Ellmark P, Mangsbo SM, Furebring C, Totterman TH & Norlen P. Kick-starting the cancer-immunity cycle by targeting CD40. *Oncoimmunology* 2015;4:e1011484.

3. Calvo E, et al. A phase I study to assess safety, pharmacokinetics (PK), and pharmacodynamics (PD) of JNJ-64457107, a CD40 agonistic monoclonal antibody, in patients (pts) with advanced solid tumors. *Journal of Clinical Oncology* 2019;37:2527–2527.
4. Adnan Deric MT, Anneli Nilsson, Peter Ellmark, Anette Fält, Karin Enell Smith. Mitazalimab, a potent CD40 agonist with potential for combination with chemotherapy. *AACR Annual meeting Abstract* 2021;1593.

Ethics Approval The study was approved 19 July 2021 by CHU UCL Namur, site Godinne Comité d'éthique Avenue Docteur G. Thérasse 1 5530 YVOIR, Belgium, approval number 32/2021and2 July 2021 by Comite de Protection des Personnes EST I, France, approval number SI2G 21.00648.677157

<http://dx.doi.org/10.1136/jitc-2021-SITC2021.537>

538

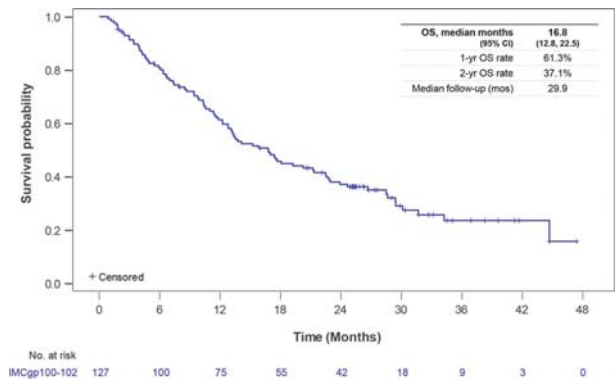
UPDATED SURVIVAL OF PATIENTS WITH PREVIOUSLY TREATED METASTATIC UVEAL MELANOMA WHO RECEIVED TEBENTAFUSP

¹Joseph Sacco*, ²Richard Carvajal, ³Marcus Butler, ⁴Alexander Shoushtari, ⁵Jessica Hassel, ⁶Alexandra Ikeguchi, ⁷Leonel Hernandez-Aya, ⁸Paul Nathan, ⁹Omid Hamid, ¹⁰Josep Piulats, ¹¹Matthew Rieth, ¹²Douglas Johnson, ¹³Jason Luke, ¹⁴Enrique Espinosa, ¹⁵Serge Leyvraz, ¹⁶Chris Holland, ¹⁶Michelle McCully, ¹⁶Shaad Abdullah, ¹⁷Takami Sato. ¹The Clatterbridge Cancer Centre, Wirral, UK; ²Columbia University Medical Center, New York, USA; ³Princess Margaret Cancer Centre, Toronto, Canada; ⁴Memorial Sloan-Kettering Hospital, New York, NY, USA; ⁵University Hospital Heidelberg, Heidelberg, Germany; ⁶Stephenson Cancer Center, University of Oklahoma, Oklahoma City, USA; ⁷Washington University School of Medicine, St. Louis, USA; ⁸Mount Vernon Hospital, Northwood, UK; ⁹The Angeles Clinic and Research Institute, Los Angeles, CA, USA; ¹⁰Institut Català d'Oncologia, Barcelona, Spain; ¹¹University of Colorado Cancer Center, Colorado, USA; ¹²Vanderbilt-Ingram Cancer Center, Nashville, TN, USA; ¹³UPMC Hillman Cancer Center, Pittsburgh, PA, USA; ¹⁴Hospital Universitario La Paz, Madrid, Spain; ¹⁵Charité Comprehensive Cancer Center, Berlin, Germany; ¹⁶Immunocore, Rockville, USA; ¹⁷Sidney Kimmel Cancer Center, Philadelphia, PA, USA

Background Tebentafusp, a bispecific fusion protein consisting of an affinity-enhanced T cell receptor fused to an anti-CD3 effector that can redirect T cells to target gp100+ cells, has shown an overall survival benefit for patients with untreated metastatic uveal melanoma (mUM) in a Ph3 trial (NCT03070392). Metastatic uveal melanoma (mUM) is a historically treatment-refractory tumor with 1-year (yr), 2-yr and 3-yr OS rates of 37%, 15% and 9%, respectively, and median OS of 7.8 months in 2L+ patients.¹ In the primary analysis of the phase 2 IMCgp100–102 study (NCT02570308) enrolling patients with previously treated mUM, the 1-year overall survival (OS) rate was 62% with median OS of 16.8 months.² We present updated OS and safety after 2-year follow-up.

Methods 127 HLA-A*02:01+ 2L+ mUM patients were dosed weekly with tebentafusp following intra-patient dose escalation: 20mcg dose 1, 30mcg dose 2 and 68mcg dose 3+. Primary objective was ORR and secondary objectives included safety, OS and PFS. Here we present the updated OS and safety (data cut-off 31 Mar 2021).

Results Median follow-up was 29.9 mos (range 1.8 – 59.9 mos). With extended follow-up, the 1-yr, 2-yr and 3-yr OS rates were 61%, 37% and 24%, respectively (figure 1). Median OS remained unchanged at 16.8 mos (95% CI, 12.8 – 22.5 mos). Mean and median duration of treatment were 9.5 mos and 5.6 mos (0 – 47.4 mos), respectively. As previously reported, most treatment-related AEs (TRAEs) occurred early on treatment. Beyond 6 months, no TRAE led to treatment discontinuation. No new safety signals, changes in the type or treatment-related deaths were reported. Beyond 12 months, there were a total of 7 Grade (G) 3 or 4 events in 3 (7%) patients, all were temporally related to tumor progression and majority included lab abnormalities. Episodes of rash, a common tebentafusp-related AE early on-treatment, were infrequent after 6 months, with no Grade 3 or 4 events.



Abstract 538 Figure 1 Kaplan-Meier estimate of overall survival at 2-yr follow-up of IMCgp100-102

Conclusions This study provides the longest follow-up of OS and safety of a soluble TCR therapeutic to date. Tebentafusp continued to show promising survival for 2L+ mUM patients with estimated 2-yr OS rate of 37%. Tebentafusp's safety profile was as expected and consistent with primary analysis showing that most adverse events occur early on treatment with incidence and severity decreasing with prolonged exposure.

Trial Registration NCT02570308

REFERENCES

1. Rantala ES, Hernberg M, Kivela TT. Overall survival after treatment for metastatic uveal melanoma: a systematic review and meta-analysis. *Melanoma Res* 2019;**29**:561–568.
2. Sacco JJ, Carvajal R, Butler MO, et al. A phase (ph) II, multi-center study of the safety and efficacy of tebentafusp (tebe) (IMCgp100) in patients (pts) with metastatic uveal melanoma (mUM). *Ann Oncol* 2020;**31**: S1442–S1143.

Ethics Approval The institutional review board or independent ethics committee at each center approved the trial. The trial was conducted in accordance with the Declaration of Helsinki and the International Conference on Harmonization Good Clinical Practice guidelines.

<http://dx.doi.org/10.1136/jitc-2021-SITC2021.538>

PHASE 1 STUDY OF MRNA-2752, A LIPID NANOPARTICLE ENCAPSULATING MRNAS ENCODING HUMAN OX40L/IL-23/IL-36 γ , FOR INTRATUMORAL (ITU) INJECTION +/- DURVALUMAB IN ADVANCED SOLID TUMORS AND LYMPHOMA

¹Manish Patel, ²Antonio Jimeno, ³Ding Wang, ⁴Salomon Stemmer, ⁵Todd Bauer, ⁶Randy Sweis, ⁷Ravit Geva, ⁸Shivaani Kummur, ⁹Patrick Reagan, ¹⁰Ruth Perets, ¹¹Patricia LoRusso, ¹²Shilpa Gupta, ¹³Sima Zacharek, ¹³Andressa Laino, ¹³Oleg Milberg, ¹³Josh Frederick, ¹³Sheryl Chen, ¹³Stephanie Pascarella, ¹³William Randolph, ¹³Praveen Aanur, ¹³Lisa Johansen, ¹³Khanh Do, ¹³Robert Meehan, ¹⁴Ryan Sullivan*. ¹SCRI/ Florida Cancer Specialists, Sarasota, FL, USA; ²University of Colorado Cancer Center, Aurora, CO, USA; ³Henry Ford Hospital, Detroit, MI, USA; ⁴Rabin Medical Center, Tel Aviv, Israel; ⁵Sarah Cannon Research Institute, Franklin, TN, USA; ⁶The University of Chicago, Chicago, IL, USA; ⁷Sourasky Medical Center, Tel-Aviv, Israel; ⁸Oregon Health and Science University, Portland, OR, USA; ⁹University of Rochester, Rochester, NY, USA; ¹⁰Rambam Medical Center and Technion, Haifa, Israel; ¹¹Yale School of Medicine, New Haven, USA; ¹²The Cleveland Clinic Foundation, Cleveland, OH, USA; ¹³Moderna Therapeutics, Cambridge, MA, USA; ¹⁴Massachusetts General Hospital, Boston, MA, USA

Background mRNA-2752 is a novel mRNA-based therapeutic agent encoding OX40L T cell co-stimulator, IL-23 and IL-36 γ pro-inflammatory cytokines. Preclinical data demonstrate synergy in combination with PD-L1 blockade.

Methods This study evaluated the safety and efficacy of ITu mRNA-2752 administered Q2W up to 7 doses as monotherapy (Arm A) or in combination with the PD-L1 inhibitor durvalumab (Arm B) in patients (pts) with palpable tumors or tumors accessible with image guidance. Biomarker analyses included IHC of immune markers, whole transcriptome assessments, and protein evaluations of IL-23, IL-36 γ and pro-inflammatory cytokines in pre- and post-treatment tumor biopsies and plasma. A PK/PD model was built to capture the IL-23 serum concentrations at the Q2W regimen to predict the exposure at the QW regimen to support an exploratory cohort.

Results As of 08April 2021, 49 pts were treated: Arm A (n=19) and Arm B (n=30) at doses ranging from 0.25 to 8mg Q2W. Treatment emergent adverse events (TEAEs) occurring in $\geq 10\%$ of pts included Gr 1/2 injection site erythema/pain/swelling, fever, chills, fatigue, AST/ALT increase, lumbar myalgia, and maculopapular rash. One DLT of cytokine release syndrome was seen at the 8mg dose in Arm B. A squamous-cell bladder cancer and DLBCL have achieved confirmed PRs on Arm B, ongoing for 23 and 16 cycles, respectively. Biomarker analyses show increased IL-23 and IL-36 γ protein expression, and their respective downstream cytokines IL-22 and IL-6, in tumor and plasma 6–24h after dosing; most cytokines assessed were elevated after treatment. Increased IFN γ and TNF α in tumor and plasma, sustained increases in interferon response genes including PD-L1 and markers of T cell infiltration, and activation in the TME (particularly in pts achieving a PR) indicate pro-inflammatory treatment effects with mRNA-2752 +/- durvalumab. PK/PD modeling showed the C_{max} of IL-23 serum concentration of mRNA-2752 at 8mg approached a plateau, and simulations showed increasing the dosing frequency from Q2W to QW vs. dose increase may have a greater effect on increasing drug exposure.

Conclusions ITu mRNA-2752 is safe and tolerable when combined with durvalumab. The recommended dose for expansion is 8mg mRNA-2752. Analyses of tumor and plasma biomarkers suggest a sustained treatment effect that includes elevated IFN γ , TNF α , and PD-L1 levels, providing rationale for combination therapy. Enrollment is ongoing in expansion cohorts of TNBC, urothelial cancer, lymphoma, immune-

checkpoint refractory melanoma and NSCLC. PK/PD modeling supports QW dosing which is being explored in cutaneous melanoma in the neoadjuvant setting.

Trial Registration NCT03739931

REFERENCES

- Hewitt SL, Bai A, Bailey D et al. Durable anticancer immunity from intratumoral administration of IL-23, IL-36 γ , and OX40L mRNAs. *Sci Transl Med.* 2019;11(477):1–15.

Ethics Approval The study was approved by the respective participating Institution's Ethics Board and conducted in accordance with the International Council for Harmonisation harmonised tripartite guideline E6(R1): Good Clinical Practice and all applicable government regulations.

Consent Written informed consent was obtained from the patient for publication of this abstract and any accompanying images. A copy of the written consent is available for review by the Editor of this journal.

<http://dx.doi.org/10.1136/jitc-2021-SITC2021.539>

540

BASELINE MTOR TRANSCRIPTIONAL SIGNATURES IN CD8 T CELLS ARE ASSOCIATED WITH IMMUNE-RELATED ADVERSE EVENTS BUT NOT ANTI-TUMOR RESPONSES IN PATIENTS RECEIVING IMMUNE CHECKPOINT INHIBITORS

¹Chen Zhao*, ³Matthew Mule, ³Andrew Martins, ⁴Iago Pinal Fernandez, ²Renee Donahue, ³Jinguo Chen, ²Jeffrey Schlom, ²James Gulley, ⁴Andrew Mammen, ³John Tsang, ²Arun Rajan. ¹NIH, North Bethesda, USA; ²NCI, North Bethesda, USA; ³NIAID, North Bethesda, USA; ⁴NIAMS, North Bethesda, USA

Background Immune checkpoint inhibitors (ICIs) have changed the cancer treatment landscape, but immune-related adverse events (irAEs) can affect a wide range of tissues in patients receiving ICIs. Severe irAEs can be life-threatening or fatal and prohibit patients from receiving further ICI treatment. While the clinical features of irAEs are well documented, the pathological mechanisms and predictive biomarkers are largely unknown. In addition, there is a critical need to preserve ICI-induced anti-tumor immunity while controlling for irAEs, which requires deciphering molecular and cellular signatures associated specifically with irAEs beyond those more generally linked to anti-tumor immunity.

Methods To unbiasedly identify immune cells and states associated with irAEs, we applied CITE-seq to measure transcripts and surface proteins (83 protein markers) from PBMCs collected from patients with thymic epithelial tumors before and after treatment with an anti-PD-L1 antibody (avelumab, NCT01772004, NCT03076554).

Results Samples from 9 patients were analyzed. No patient had a history of pre-existing paraneoplastic autoimmune disease. Anti-tumor activity was observed in all cases, and 5 patients had clinical and/or biochemical evidence of immune-related muscle inflammation (myositis with or without myocarditis). Multilevel models applied within highly resolved cell clusters revealed transcriptional states associated with ICI response and more uniquely with irAEs. A total of 190,000 cells were included in the analysis after quality control. Most notably, CD45RA+ effector memory CD8 T cells with an mTOR transcriptional signature were highly enriched at baseline and post treatment in patients with irAEs.

Conclusions Our findings suggest the potential therapeutic avenues by using mTOR inhibitors to dampen autoimmune responses while potentially sparing anti-tumor activity, to prevent treatment discontinuation and improve clinical outcomes for cancer patients treated with ICIs.

Acknowledgements This research was supported in part by the Intramural Research Program of the NCI (the Center for Cancer Research), NIAID and NIAMS, and through a Cooperative Research and Development Agreement between the National Cancer Institute and EMD Serono.

Trial Registration NCT01772004, NCT03076554

Ethics Approval This study is approved by NCI institutional review board.

<http://dx.doi.org/10.1136/jitc-2021-SITC2021.540>

542

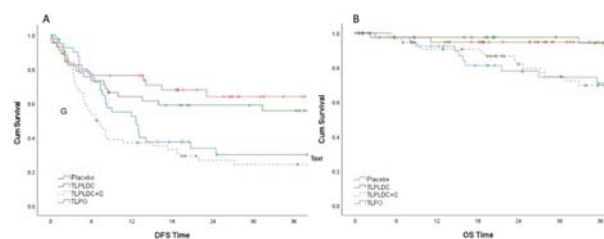
RANDOMIZED TRIAL OF TUMOR LYSATE PARTICLE ONLY VACCINE VS. TUMOR LYSATE PARTICLE-LOADED, DENDRITIC CELL VACCINE TO PREVENT RECURRENCE OF RESECTED STAGE III/IV MELANOMA: 36-MONTH ANALYSIS

¹Elizabeth Carpenter*, ¹Lexy Adams, ¹Robert Chick, ¹Guy Clifton, ¹Timothy Vreeland, ¹Franklin Valdera, ¹Patrick McCarthy, ¹Anne O'Shea, ¹Diane Hale, ¹Phillip Kemp Bohan, ¹Annelies Hickeron, ¹John Myers, ¹Jessica Cindass, ²John Hyngstrom, ³Adam Berger, ⁴Jeffrey Sussman, ⁵James Jakob, ⁶Montaser Shaheen, ⁷Xianzhong Yu, ⁸Thomas Wagner, ⁹Mark Faries, ¹⁰George Peoples. ¹Brooke Army Medical Center, San Antonio, TX, USA; ²Huntsman Cancer Institute, Salt Lake City, UT, USA; ³Rutgers Cancer Institute of New Jersey, New Brunswick, NJ, USA; ⁴University of Cincinnati, Cincinnati, OH, USA; ⁵Mayo Clinic, Rochester, MN, USA; ⁶University of Arizona, Tucson, AZ, USA; ⁷Clemson University, Clemson, SC, USA; ⁸Orbis Health Solutions, Greenville, SC, USA; ⁹The Angeles Clinic, Santa Monica, CA, USA; ¹⁰Cancer Vaccine Development Program, San Antonio, TX, USA

Background The tumor lysate, particle-loaded, dendritic cell (TLPLDC) vaccine is an autologous tumor vaccine that decreased recurrence in stage III/IV melanoma when granulocyte-colony stimulating factor (G-CSF) was not used to harvest the dendritic cells in a randomized phase 2B adjuvant trial.¹The tumor lysate (TL) particle only (TLPO) vaccine utilizes a similar mechanism, but with autologous TL-loaded yeast cell wall particles; this eliminates the need for dendritic cell (DC) collection and ex-vivo loading and reduces production costs and time. The TLPO vaccine was compared to TLPLDC in an embedded bridging portion of the trial. Here, we examine 36-month outcomes of the ongoing randomized, double-blind phase 2 trial in patients (pts) with resected stage III/IV melanoma.

Methods Pts were randomized 2:1 to receive TLPO or TLPLDC as a continuation of a previously established clinical trial comparing TLPLDC versus placebo. The TLPLDC group was analyzed separately based on use (or not) of G-CSF for collection of DC. Safety was measured by the Common Terminology Criteria for Adverse Events (CTCAE). Kaplan-Meier and log-rank analysis was used to compare 36-month disease-free survival (DFS) and overall survival (OS) in the intention-to-treat (ITT) main arms as well as pre-specified subgroups.

Results A total of 187 pts were randomized with 41, 47, 56, and 43 pts enrolled in the placebo, TLPLDC without G-CSF (TLPLDC), TLPLDC with G-CSF (TLPLDC+G), and TLPO arm, respectively. Pts randomized to the TLPO arm were more likely to have stage IV melanoma (22.0% for placebo, 20.4% for TLPLDC and TLPLDC+G, and 44.2% for TLPO; $p = 0.002$) and to receive prior immunotherapy (36.6% for placebo, 39.8% for both TLPLDC and TLPLDC+G, and 83.7% for TLPO; $p < 0.001$). Grade 3+ adverse events were not significantly different between arms. In the ITT analysis, 36-month DFS was 30.0% for placebo, 55.8% for TLPLDC, 24.4% for TLPLDC+G, and 64.0% for TLPO ($p < 0.001$). OS at 36 months was 70.9% for placebo, 94.2% for TLPLDC, 69.8% for TLPLDC+G, and 94.8% for TLPO ($p = 0.011$) (figure 1).



Abstract 542 Figure 1 Kaplan-Meier curves demonstrating DFS (A) and OS (B) between Placebo (n=41), TLPLDC (n=47), TLPLDC+G (n=56), and TLPO (n=43)

Conclusions The TLPO and TLPLDC (without G-CSF) vaccines improved 36-month DFS and OS in this randomized phase 2 trial. The efficacy of the TLPO and TLPLDC vaccines will be confirmed in a phase III trial in resected Stage III/IV melanoma pts.

Trial Registration NIH, clinicaltrials.gov, NCT02301611

REFERENCES

- O'Shea AE, Chick RC, Clifton GT, et al. The effect of pretreatment with G-CSF prior to dendritic cell collection during the phase IIb trial of an autologous DC-based vaccine for advanced, resectable melanoma. Presented at: Society for Immunotherapy of Cancer 35th Anniversary Annual Meeting & Preconference Programs (SITC 2020); November 11–14, 2020. Abstract 310. *J Immunother Cancer*. 2020;8(Suppl 3):A656–A959.

Ethics Approval The clinical trial protocol was approved by the Western Institutional Review Board (2014–1932). All participants provided informed consent prior to enrollment in the trial.

<http://dx.doi.org/10.1136/jitc-2021-SITC2021.542>

SENSITIVE QUANTIFICATION AND TRACKING OF THE ACTIVE COMPONENTS OF A CLONAL NEOANTIGEN T CELL (CNET) THERAPY: FROM MANUFACTURE TO PERIPHERAL CIRCULATION

¹Samra Turajlic*, ²Mariam Jamal-Hanjani, ³Andrew Furness, ⁴Ruth Plummer, ⁵Judith Cave, ⁶Fiona Thistlethwaite, ⁷Emma Leire, ⁷Jen Middleton, ⁷Eloise Williams, ⁷Amy Baker, ⁷Chloe Maine, ⁷Michael Epstein, ⁷Monica Sassi, ⁷Katy Newton, ⁷Michael Grant, ⁷Matilde Saggese, ⁷Sergio Quezada, ²Martin Forster. ¹Royal Marsden NHS Foundation Trust, London, UK; ²UCL Cancer Institute, London, UK; ³Royal Marsden NHS Trust, London, UK; ⁴Newcastle Hospitals NHS Foundation Trust, London, UK; ⁵University Hospital Southampton, Southampton, UK; ⁶The Christie NHS Foundation Trust, Manchester, UK; ⁷Achilles Therapeutics UK Ltd, London, UK

Background Ex-vivo expanded tumour infiltrating lymphocytes (TIL) show promise in delivering durable responses among several solid tumour indications. However, characterising, quantifying and tracking the active component of TIL therapy remains challenging as the expansion process does not distinguish between tumour reactive and bystander T-cells. Achilles Therapeutics has developed ATL001, a patient-specific TIL-based product, manufactured using the VELOS™ process that specifically targets clonal neoantigens present in all tumour cells within a patient. Two Phase I/IIa clinical trials of ATL001 are ongoing in patients with advanced Non-Small Cell Lung Cancer, CHIRON (NCT04032847), and metastatic or recurrent melanoma, THETIS (NCT03997474). Extensive product characterisation and immune-monitoring are performed through Achilles' manufacturing and translational science programme. This enables precise quantification and characterisation of the active component of this therapy – Clonal Neoantigen T cells (cNeT) – during manufacture and following patient administration, offering unique insight into the mechanism of action of ATL001 and aiding the development of next generation processes.

Methods ATL001 was manufactured using procured tumour and matched whole blood from 8 patients enrolled in the THETIS (n=5) and CHIRON (n=3) clinical trials. Following administration of ATL001, peripheral blood samples were collected up to week 6. The active component of the product was detected via re-stimulation with clonal neoantigen peptide pools and evaluation of IFN- γ and/or TNF- α production. Deconvolution of individual reactivities was achieved via ELISPOT assays. Immune reconstitution was evaluated by flow cytometry. cNeT expansion was evaluated by restimulation of isolated PBMCs with peptide pools and individual peptide reactivities (ELISPOT).

Results The median age was 57 (range 30 – 71) and 6/8 patients were male. The median number of previous lines of systemic anti-cancer treatment at the time of ATL001 dosing was 2.5 (range 1 – 5). Proportion of cNeT in manufactured products ranged from 0.20% - 77.43% (mean 26.78%) and unique single peptide reactivities were observed in 7 of 8 products (range 0 – 28, mean 8.6). Post-dosing, cNeTs were detected in 5/8 patients and cNeT expansion was observed in 3/5 patients.

Conclusions These data underscore our ability to sensitively detect, quantify and track the patient-specific cNeT component of ATL001 – during manufacture and post dosing. As the dataset matures, these metrics of detection and expansion will be correlated with product, clinical and genomic characteristics to determine variables associated with peripheral cNeT dynamics and clinical response.

Trial Registration NCT04032847, NCT03997474

REFERENCES

Ethics Approval The first 8 patients described have all been located within the UK and both trials (CHIRON and THETIS) have been approved by the UK MHRA (among other international bodies, e.g FDA). Additionally, these trials have been approved by local ethics boards at active sites within the UK. Patient's are fully informed by provided materials and investigators prior to consenting to enrol into either ATL001 trial.

<http://dx.doi.org/10.1136/jitc-2021-SITC2021.543>

DELTA-1: A GLOBAL, MULTICENTER PHASE 2 STUDY OF ITIL-168, AN UNRESTRICTED AUTOLOGOUS TUMOR-INFILTRATING LYMPHOCYTE (TIL) CELL THERAPY, IN ADULT PATIENTS WITH ADVANCED CUTANEOUS MELANOMA

¹Brian Gastman*, ²Omid Hamid, ³Pippa Corrie, ⁴Geoffrey Gibney, ⁵Gregory Daniels, ⁶Bartosz Chmielowski, ⁷Sajeve Thomas, ⁸Evidio Domingo-Musibay, ⁹Donald Lawrence, ¹⁰Yizhou Jiang, ¹¹Audrey Kennedy, ¹⁰Jeff Aycok, ¹⁰Ruben Alvarez-Rodriguez, ¹⁰Paul Robbins, ¹⁰John Le Gall, ¹⁰Zachary Roberts, ¹⁰Robert Hawkins, ¹²Amod Sarnaik. ¹Cleveland Clinic, Cleveland, OH, USA; ²The Angeles Clinic and Research Institute, Los Angeles, CA, USA; ³Cambridge University Hospitals, Cambridge, UK; ⁴Georgetown Lombardi Comprehensive Cancer, Washington, DC, USA; ⁵University of California San Diego, La Jolla, CA, USA; ⁶University of California Los Angeles, Los Angeles, CA, USA; ⁷University of Florida, Orlando, FL, USA; ⁸University of Minnesota Medical Center, Minneapolis, MN, USA; ⁹Massachusetts General Hospital, Boston, MA, USA; ¹⁰Instil Bio, Inc., Dallas, TX, USA; ¹¹Instil Bio, Inc, Dallas, TX, USA; ¹²Moffitt Cancer Center, Tampa, FL, USA

Background Patients with advanced cutaneous melanoma and persistent disease after checkpoint inhibitor therapy have poor outcomes and limited treatment options, highlighting a significant unmet medical need.¹ Autologous TIL cell therapies have shown promise in this population attributable, in part, to their intrinsic and patient-specific antitumor activity²; however, no such therapies are approved. Made from each patient's digested and cryopreserved tumor, ITIL-168 is an autologous TIL cell therapy manufactured to offer an unrestricted T-cell receptor repertoire. A single-center compassionate use clinical series demonstrated the feasibility and clinical utility of an earlier version of ITIL-168.³ DELTA-1 is a global, multicenter phase 2 study to evaluate efficacy and safety of ITIL-168. DELTA-1 will enroll patients with melanoma relapsed after or refractory to PD-1 inhibitors (PD-1i), patients intolerant to PD-1i, and patients whose best response to PD-1i was stable disease.

Methods Patients aged ≥ 18 years with histologically confirmed advanced cutaneous melanoma, ECOG performance status 0–1, and adequate organ function will be enrolled in 1 of 3 cohorts. Cohort 1 (n=80) will include patients who relapsed after or were refractory to ≥ 1 prior line of systemic therapy, including a PD-1i and, if BRAF-mutated, a BRAFi \pm MEKi. Cohorts 2 and 3 (n=25 each) will include patients intolerant to PD-1i and those with stable disease after ≥ 4 doses of PD-1i, respectively. After tumor resection for TIL harvest, patients must have ≥ 1 remaining measurable lesion per Response Evaluation Criteria in Solid Tumors (RECIST) 1.1. Patients with uveal, acral, or mucosal melanoma, prior allogeneic transplant or cell therapy, and with central nervous system (CNS) disorder or symptomatic and/or untreated CNS metastases are ineligible. Patients will receive 5 days of lymphodepleting chemotherapy (cyclophosphamide $\times 2$ days overlapping with fludarabine $\times 5$ days) followed by a single ITIL-168 infusion ($\geq 5 \times 10^9$ cells) and supportive short course high-dose IL-2. The primary endpoint is objective response rate (ORR) per central review. Key secondary endpoints include duration of response, progression-free survival, overall survival, disease control rate, TIL persistence, and safety. Hypothesis testing of ORR will be performed for cohort 1. Two interim analyses will occur after 20 patients in cohort 1 have been followed for ≥ 28 days (safety) and evaluated for response ≥ 3 months after ITIL-168 infusion (futility). The primary analysis will occur when all patients in the cohort 1 modified intent-to-treat population have been followed for ≥ 6 months after the first posttreatment disease assessment.

Acknowledgements Medical writing support was provided by Christopher Waldapfel, PharmD, of Instil Bio, Inc, and Phyllicia Aaron, PhD, of Nexus GG Science, with funding from Instil Bio, Inc.

REFERENCES

- Schadendorf D, van Akkoi ACJ, Berking C, et al. Melanoma. *Lancet* 2018;**392**(10151):971–984.
- Borch TH, Anderson R, Ellebaek E, et al. Future role for adoptive T-cell therapy in checkpoint inhibitor-resistant metastatic melanoma. *J Immunother Cancer* 2020;**8**(2):e000668.
- Hawkins RE, Jiang Y, Lorigan PC, et al. Clinical feasibility and treatment outcomes with unselected autologous tumor infiltrating lymphocyte therapy in patients with advanced cutaneous melanoma. *Cancer Res* 2021;**81**(13):LB150.

Ethics Approval All patients will provide written informed consent. The study will be approved by the Institutional Review Board/Independent Ethics Committee at each site and conducted in accordance with the Good Clinical Practice Guidelines of the International Conference on Harmonisation. **Consent** N/A; the abstract does not contain sensitive or identifiable patient information.

<http://dx.doi.org/10.1136/jitc-2021-SITC2021.544>

A PHASE 2 STUDY OF RETIFANLIMAB IN PATIENTS WITH ADVANCED OR METASTATIC MERKEL CELL CARCINOMA (MCC) (POD1UM-201)

¹Giovanni Grignani, ²Piotr Rutkowski, ³Celeste Lebbe, ⁴Natalie Prinzi, ⁵Jean-Jaques Grob, ⁶Enrica Teresa Tanda, ⁷Michele Guida, ⁸Melissa Burgess, ⁹Jennifer Pulini, ⁹Sadhna Shankar, ⁹Chuan Tian, ¹⁰Shailender Bhatia*. ¹Candiolo Cancer Institute, FPO-IRCCS, Candiolo, Italy; ²Maria Sklodowska-Curie National Research Institute of Oncology, Warsaw, Poland; ³Université de Paris, Department of Dermatology and CIC, AP-HP Hôpital Saint-Louis, Paris, France; ⁴Fondazione IRCCS Istituto Nazionale dei Tumori, Milan, Italy; ⁵Aix-Marseille University, AP-HM Timone, Marseille, France; ⁶IRCCS Ospedale Policlinico San Martino, Skin Cancer Unit, Genoa, Italy; ⁷Unit Melanoma and Rare Tumors, IRCCS Istituto Tumori Giovanni Paolo II, Bari, Italy; ⁸UPMC Cancer Center, Pittsburgh, PA, USA; ⁹Incyte Corporation, Ambler, USA; ¹⁰University of Washington, Seattle, WA, USA

Background Retifanlimab (INCMGA00012) is a humanized, hinge-stabilized immunoglobulin G4 kappa (IgG4κ), anti-programmed cell death protein (PD)-1 monoclonal antibody with safety and clinical pharmacology that are characteristic for the class. Evaluation of retifanlimab in solid tumors is under investigation in phase 2 and 3 studies. POD1UM-201 is an open-label, single-arm, multicenter, phase 2 study evaluating the efficacy and safety of retifanlimab in patients with chemotherapy-naïve or chemotherapy-refractory advanced/metastatic Merkel cell carcinoma (MCC). Updated results from the chemotherapy-naïve cohort are reported here.

Methods Eligible patients were ≥18 years of age, had metastatic or recurrent unresectable loco-regional MCC, Eastern Cooperative Oncology Group performance status ≤1, measurable disease per Response Evaluation Criteria in Solid Tumors (RECIST) v1.1, and had not received prior systemic treatment for MCC. Retifanlimab 500 mg IV every 4 weeks (Q4W) was administered for up to 2 years. The primary endpoint was overall response rate (ORR) assessed by independent central review per RECIST v1.1. Secondary endpoints included duration of response, disease control rate (DCR; defined as proportion of patients with either an objective response or stable disease lasting at least 6 months), progression-free survival, overall survival, safety, and pharmacokinetics.

Results As of April 16, 2021, 87 patients with chemotherapy-naïve advanced/metastatic MCC had received retifanlimab. Per protocol, the primary efficacy analyses are based on the first 65 patients assessed. At the data cutoff, 34 of these 65 patients (52.3%) were on treatment; 4 (6.2%) had completed treatment; and 27 (41.5%) had discontinued treatment for reasons including disease progression (18 [27.7%]), adverse event (AE; 7 [10.8%]), death (1 [1.5%]), and physician decision (1 [1.5%]). The ORR in these patients was 46.2% (n=30: complete response, 8 [12.3%]; partial response, 22 [33.8%]). The DCR was 53.8% (n=35). Other secondary efficacy results are not yet mature. Among all treated patients (n=87), 66 (75.9%) had a treatment-emergent AE (TEAE), 25 (28.7%) had a grade ≥3 TEAE, and 12 (13.8%) had a grade ≥3 treatment-related AE. Twenty-three patients (26.4%) had an immune-related AE (irAE), and 8 (9.2%) had a grade ≥3 irAE. Four patients (4.6%) discontinued treatment due to irAEs (peripheral sensorimotor neuropathy, pancreatitis, eosinophilic fasciitis, and polyarthritis [each n=1]). One patient (1.1%) had a grade 3 infusion reaction.

Conclusions These data from the POD1UM-201 trial show that retifanlimab monotherapy at 500 mg Q4W continues to demonstrate promising clinical activity and safety in patients

with advanced/metastatic chemotherapy-naïve MCC. Updated results will be presented at the meeting.

Acknowledgements The study is sponsored by Incyte Corporation (Wilmington, DE). Statistical support was provided by Xiaohan Xu of Incyte Corporation. Editorial assistance was provided by Matthew Bidgood of Envision Pharma Group (Philadelphia, PA, USA).

Trial Registration ClinicalTrials.gov NCT03599713; EudraCT 2018-001627-39

Ethics Approval The study was approved by institutional review boards or independent ethics committees in Canada (McGill University Health Center-Research Ethics Board [MP-37-2019-5103, MEO-37-2019-1616]; Ontario Cancer Research Ethics Board [1728]; Health Research Ethics Board of Alberta – Cancer Committee [HREBA.CC-19-0004, HREBA.CC-19-0020]); Czech Republic (Eticka komise Fakultni nemocnice Kralovske Vinohrady, Eticka komise IKEM a FTNsP; Eticka komise Nemocnice Na Bulovce, Statni ustav pro kontrolu lecv, Eticka komise FN a LF UP Olomouc [169/18MEK24, LEK/04/07/2018, (L-18-85) 8522/23.3.2021, 22.3.2021/9965/EK-Z]); France (Comité de Protection des Personnes Ile de France X [CNRIIPH : 18.11.19.49212/Id. 2043]; Agence Nationale de Sécurité du Médicament et des Produits de Santé); Germany (Ethik-Kommission der Medizinischen Fakultät der Universitaet Duisburg-Essen [18-8371-AF]; Bundesamt fuer Strahlenschutz; Paul-Ehrlich Institute); Hungary (Egeszsegugyi Tudomanyos Tanacs Klinikai Farmakologiai Etikai Bizottsaga [IV/2407-0/2021-EKL, OGYÉI/11697-2/2021]; Orszagos Gyogyszereszeti es Elelmezes-egeszsegugyi Intezet); Italy (Comitato Etico IRCCS Pascale Napoli [116/21 E - 87/18]; Comitato Etico IRCCS di Candiolo [232/2021]; Istituto Tumori Giovanni Paolo II IRCCS Ospedale Oncologico Bari [736/CE]; Comitato Etico Locale per la Sperim. Clin. dei Medicinali dell'Az. Osp.ra Univ.ria Senese di Siena [14107]; Comitato Etico dell'IRCCS Istituto Nazionale per la Ricerca sul Cancro di Genova [389/2018 - 24/05/2021]; Comitato etico degli IRCCS Istituto Europeo di Oncologia e Centro Cardiologico Monzino [IEO 948 - RE3065/IB Edition 7 dated 10Nov2020 (SA7)]; Comitato Etico, Fondazione IRCCS Istituto Nazionale dei Tumori, .c. Medicina Oncologica 1 – Fondazio [INT 01/19]; Comitato Etico IRCCS Istituto Oncologico Veneto di Padova [EM 109/2021]; Comitato Etico dell'IRCCS Istituto Dermatologico dell'Immacolata Ospedale Generale S. Carlo di Roma [550/7]; AIFA – Agenzia Italiana del Farmaco [0040152-01/04/2021-AIFA-AIFA_USC-P]; Comitato Etico Policlinico di Modena [1017/2018/FARM/AOUMO - EMENDAMENTO SOSTANZIALE IB EDIZIONE 7 DEL 10/11/20 (201800162739-010) (p. 9869/21)]; Poland (Komisja Bioetyczna przy Centrum Onkologii [no. 55/2019]; Office for Registration of Medicinal Products, Medical Devices and Biocidal Products [UR/DBL/D/328/2019]); Spain (CEIC Hospital General Universitario Gregorio Marañon [280/18]; Agencia Española del Medicamento y Productos Sanitarios); Switzerland (Kantonale Ethikkommission Zürich (KEK-Zürich) [2019-00200]; Swissmedic [2019DR2035]); United Kingdom (North East – York Research Ethics Committee [248465]; Medicines and Healthcare products Regulatory Agency; Health Research Authority); United States (Copernicus Group IRB; Western Institutional Review Board [20181738, Work order number – IQV1-18-309];

Roswell Park Cancer Institute IRB [STUDY00000802/P 75918]; Inova Institutional Review Board, Human Research Protection Program; Stanford IRB Research Compliance Office [48198]; Rush University Medical Center [18072304-IRB01]; University of Miami IRB; Mayo Clinic IRB – Rochester).

<http://dx.doi.org/10.1136/jitc-2021-SITC2021.545>

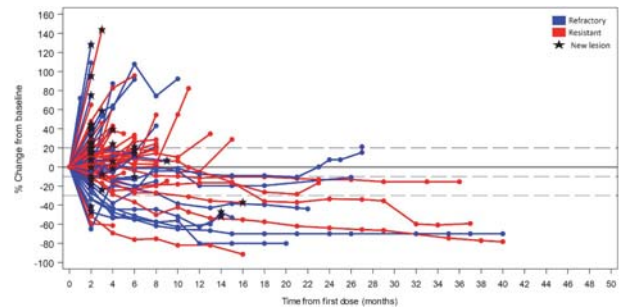
RESULTS FROM PHASE IB STUDY OF TEBENTAFUSP (TEBE) IN COMBINATION WITH DURVALUMAB (DURVA) AND/OR TREMELIMUMAB (TREME) IN METASTATIC CUTANEOUS MELANOMA (MCM)

¹Omid Hamid*, ²Jessica Hassel, ³Alexander Shoushtari, ⁴Friedegund Meier, ⁵Todd Bauer, ⁶April Salama, ⁷John Kirkwood, ⁸Paolo Ascierto, ⁹Paul Lorigan, ¹⁰Cornelia Mauch, ¹¹Marlana Orloff, ¹²Jeff Evans, ¹³Ramakrishna Edukulla, ¹³Chris Holland, ¹³Shaad Abdullah, ¹³Renee Mundy, ¹⁴Mark Middleton. ¹The Angeles Clinic and Research Institute, Los Angeles, CA, USA; ²University Hospital Heidelberg, Heidelberg, Germany; ³Memorial Sloan-Kettering Hospital, New York, NY, USA; ⁴University Hospital Carl Gustav Carus, Dresden, Germany; ⁵Tennessee Oncology, Franklin, TN, USA; ⁶Duke University Health System, Durham, NC, USA; ⁷University of Pittsburgh Medical Center, Pittsburgh, PA, USA; ⁸Fondazione IRCCS Istituto Nazionale dei Tumori, Napoli, Italy; ⁹The Christie NHS Foundation Trust, Manchester, UK; ¹⁰University Hospital Cologne, Cologne, Germany; ¹¹Sidney Kimmel Cancer Center, Philadelphia, PA, USA; ¹²Beatson West of Scotland Cancer Centre, Glasgow, UK; ¹³Immunocore, Rockville, USA; ¹⁴University of Oxford, Oxford, UK

Background Tebe, a T cell receptor fused to an anti-CD3 effector, can redirect T cells to target gp100+ cells and in Ph3, demonstrated overall survival (OS) benefit as monotherapy in metastatic uveal melanoma. In Ph2, any tumor shrinkage (44% of patients) was a better predictor of OS than response rate. In Ph1, Tebe had monotherapy activity in mCM, also a gp100+ tumor, with 1-year OS ~74% in PD-1 naïve mCM. A Ph1 dose escalation of tebe with durva (anti-PD-L1) and/or treme (anti-CTLA4) was conducted in pre-treated mCM [NCT02535078], with nearly all patients having prior PD1-treatment, and where recently reported therapies have 1-yr OS of ~55%.

Methods Heavily pre-treated HLA-A2+ mCM patients received weekly IV tebe alone (Arm 4) or with increasing doses of durva and/or treme (Arm 1–3) administered IV monthly starting day 15 of each cycle. Primary objective was to identify RP2D of combination therapy. Secondary objectives included adverse events (AE) and efficacy.

Results 112 pts received ≥ 1 tebe dose. Median age was 59, 77% were ECOG 0, and 37% were BRAFm (of which 71% received prior BRAFi/MEKi). 91% of pts were 2L+, while 74% were 3L+. 103 (92%) received prior PD-1 inhibitor, of which 87% also received prior ipilimumab. 43 pts received tebe + durva (Arm 1), 13 received tebe + treme (Arm 2), 29 received triplet therapy (Arm 3), and 27 received tebe alone (Arm 4). Maximum target doses of tebe (68 mcg) + durva (20 mg/kg) and treme (1 mg/kg) were tolerated. MTD was not formally identified for any arm. Two DLTs occurred: prolonged grade 3 rash (Arm 1) and grade 2 diarrhea leading to treatment delay (Arm 2). Related AEs that were Grade ≥ 3 or led to discontinuations were: 44%/0% (Arm 1), 23%/0% (Arm2), 38%/7% (Arm3), 26%/4% (Arm 4). There were no treatment-related deaths. In prior PD-1 pts, tumor shrinkage occurred in 36% and 1-yr OS was 68%. Of 51 evaluable PD-1 resistant pts (best response CR/PR/SD to prior PD1), tumor shrinkage occurred in 28% and 1-yr OS was 73% (figure 1). In 35 evaluable PD-1 refractory pts (prior best response PD), tumor shrinkage occurred in 49% and 1-yr OS was 61%. For 38 prior PD-1 pts who received ≥ 10 mg/kg durva, 1-yr OS was 81%.



Abstract 546 Figure 1 % tumor change from baseline in evaluable patients with known response to prior PD1 exposure

Conclusions Tebe with anti-PD-L1 and/or anti-CTLA4 had an acceptable safety profile. Tebe + durva demonstrated durable tumor shrinkage and promising 1-yr OS rates in prior-PD1 treated mCM relative to recent reports.

Trial Registration NCT02535078

Ethics Approval The institutional review board or independent ethics committee at each center approved the trial. The trial was conducted in accordance with the Declaration of Helsinki and the International Conference on Harmonization Good Clinical Practice guidelines.

<http://dx.doi.org/10.1136/jitc-2021-SITC2021.546>

CERPASS: A RANDOMIZED, CONTROLLED, OPEN-LABEL, PHASE 2 STUDY OF CEMIPIMAB ± RP1 IN PATIENTS WITH ADVANCED CUTANEOUS SQUAMOUS CELL CARCINOMA

¹Andrew Haydon*, ²Muhammad Alamgeer, ³Daniel Brungs, ⁴Frances Collichio, ⁵Nikhil Khushalani, ⁶Dimitrios Colevas, ⁷Danny Rischin, ⁸Ragini Kudchadkar, ⁹Wanxing Chai-Ho, ¹⁰Gregory Daniels, ¹¹Jose Lutzky, ¹²Jenny Lee, ¹³Samantha Bowyer, ¹⁴Michael Migden, ¹⁵Ann Silk, ¹⁶Celeste Lebbe, ¹⁷Jean-Jaques Grob, ¹⁸Ignacio Melero, ¹⁹Piyush Sheladia, ¹⁹Praveen Bommareddy, ¹⁹Shui He, ¹⁹Claudia Andreu-Vieyra, ²⁰Matthew Fury, ²¹Andrew Hill. ¹Alfred Hospital, Melbourne, Australia; ²Monash Medical Centre, Clayton, Australia; ³Southern Medical Day Care Centre, Wollongong, Australia; ⁴Lineberger Comprehensive Cancer Center, Chapel Hill, NC, USA; ⁵Moffitt Cancer Center, Tampa, FL, USA; ⁶Stanford University School of Medicine, Stanford, CA, USA; ⁷Peter MacCallum Cancer Center, East Melbourne, Australia; ⁸Emory University, Atlanta, GA, USA; ⁹University of California, Los Angeles, Los Angeles, USA; ¹⁰UC San Diego, La Jolla, CA, USA; ¹¹University of Miami, Miami, FL, USA; ¹²Chris O'Brien Lifehouse, Camperdown, Australia; ¹³Sir Charles Gairdner Hospital, Nedlands, Australia; ¹⁴MD Anderson Cancer Center, Houston, TX, USA; ¹⁵Harvard Medical School, Boston, MA, USA; ¹⁶Université de Paris, Paris, France; ¹⁷Hôpital de la Timone Service de Dermatol, Marseille, France; ¹⁸Universidad de Navarra, Navarra, Spain; ¹⁹Replimune, Woburn, USA; ²⁰Regeneron, Tarrytown, NY, USA; ²¹Tasman Health Care, Southport, Australia

Background The prognosis for advanced and metastatic cutaneous squamous cell carcinoma (CSCC) remains poor for many patients with the disease despite approval of the anti-PD1 antibodies cemiplimab and pembrolizumab.^{1 2} RP1 is an oncolytic virus (HSV-1) that expresses a fusogenic glycoprotein (GALV-GP R-) and granulocyte macrophage colony stimulating factor (GM-CSF). In preclinical studies, RP1 induced immunogenic tumor cell death and provided potent systemic anti-tumor activity, which is further improved by combining anti-PD-1 therapy.³ Preliminary results from IGRYTE, a phase I/II clinical study of RP1 in combination with nivolumab showed a high rate of deep and durable responses in patients (pts) with CSCC.⁴ The objective of this trial is to evaluate the safety and efficacy of cemiplimab + RP1 versus cemiplimab alone in advanced CSCC.

Methods This global, multicenter, randomized phase 2 study is enrolling pts with metastatic or unresectable, locally advanced CSCC who are not candidates for/refuse surgery and/or radiotherapy. Key eligibility criteria include no prior treatment with anti-PD1/PD-L1 antibodies or oncolytic viruses. The clinical trial will enroll approximately 180 pts from centers in the EU, Australia, Canada and USA. Pts will be randomized in a 2:1 ratio favoring the RP1 + cemiplimab arm. Pts will receive 350 mg of cemiplimab intravenously (IV) Q3W for up to 108 weeks. In the RP1 + cemiplimab arm, RP1 will be injected intratumorally at a starting RP1 dose of 1×10^6 plaque forming units (PFU)/mL alone, followed by up to 7 doses of RP1 at 1×10^7 PFU/mL Q3W together with cemiplimab. Pts in the combination arm may receive up to 8 additional RP1 doses. No crossover will be allowed. Pts will be stratified by disease status and prior systemic therapy. Tumor assessments will be performed every 9 weeks. Primary endpoints are overall response rate and complete response rate by blinded independent review. Secondary endpoints include safety, progression free survival, duration of response and overall survival. Exploratory endpoints include viral shedding and biodistribution, and immune biomarker analyses. This trial is currently enrolling pts.

Trial Registration NCT04050436

REFERENCES

1. Migden MR, Rischin D, Schmults CD, Guminski A, Hauschild A, Lewis KD, Chung CH, Hernandez-Aya L, Lim AM, Chang ALS, Rabinowits G, Thai AA, Dunn LA, Hughes BGM, Khushalani NI, Modi B, Schadendorf D, Gao B, Seebach F, Li S, Li

- J, Mathias M, Booth J, Mohan K, Stankevich E, Babiker HM, Brana I, Gil-Martin M, Homs J, Johnson ML, Moreno V, Niu J, Owonikoko TK, Papadopoulos KP, Yancopoulos GD, Lowy I, Fury MG. PD-1 blockade with cemiplimab in advanced cutaneous squamous-cell carcinoma. *N Engl J Med* 2018;**379**(4):341–351.
2. Grob JJ, Gonzalez R, Basset-Seguín N, Vornicova O, Schachter J, Joshi A, Meyer N, Grange F, Piulats JM, Bauman JR, Zhang P, Gumuscu B, Swaby RF, Hughes BGM. Pembrolizumab monotherapy for recurrent or metastatic cutaneous squamous cell carcinoma: a single-arm phase II trial (KEYNOTE-629). *J Clin Oncol* 2020;**38**(25):2916–2925.
3. Thomas S, Kuncheria L, Roulstone V, Kyula JN, Mansfield D, Bommareddy PK, Smith H, Kaufman HL, Harrington KJ, Coffin RS. Development of a new fusion-enhanced oncolytic immunotherapy platform based on herpes simplex virus type 1. *J Immunother Cancer* 2019;**7**(1):214.
4. Middleton M, Aroldi F, Sacco J, Milhem M, Curti B, VanderWalde A, Baum S, Samson A, Pavlick A, Chesney J, Niu J, Rhodes T, Bowles T, Conry R, Olsson-Brown A, Earl Laux D, Kaufman H, Bommareddy P, Deterding A, Samakoglu S, Coffin R, Harrington K. 422 An open-label, multicenter, phase 1/2 clinical trial of RP1, an enhanced potency oncolytic HSV, combined with nivolumab: updated results from the skin cancer cohorts. *J Immunother Cancer* 2020; 8 (3).

Ethics Approval The study was approved by institutional review board or the local ethics committee at each site. Informed consent was obtained from patients before participating into the trial.

<http://dx.doi.org/10.1136/jitc-2021-SITC2021.547>

PHASE 2 STUDY OF FLX475 IN COMBINATION WITH IPIILIMUMAB IN ADVANCED MELANOMA

Rakesh Goyal*, Nicole Nasrah, Dan Johnson, William Ho. *RAPT Therapeutics, South San Francisco, CA, USA*

Background Regulatory T cells (Treg) can dampen antitumor immune responses in the tumor microenvironment (TME) and have been shown to correlate with poor clinical outcome. Translational studies have demonstrated an accumulation of Treg in tumors after treatment with immunotherapies including CAR-T cells and anti-CTLA-4, which could potentially reflect a mechanism of adaptive immune resistance.^{1–2} CCR4, the receptor for the chemokines CCL17 and CCL22, is the predominant chemokine receptor on human Treg and is responsible for the migration and accumulation of Treg in the TME. Preclinical studies with orally available CCR4 antagonists have demonstrated potent inhibition of Treg migration into tumors, an increase in the intratumoral Teff/Treg ratio, and antitumor efficacy as a single agent and in combination with checkpoint inhibitors, including anti-CTLA-4.³ In a first-in-human trial conducted in healthy volunteers, the oral CCR4 antagonist FLX475 was demonstrated to be well tolerated with outstanding pharmacokinetic and pharmacodynamic properties.⁴ An ongoing Phase 1/2 clinical trial of FLX475 is examining the safety and preliminary antitumor activity of FLX475 as monotherapy and in combination with pembrolizumab in subjects with several types of advanced cancer.⁵ Given the preclinical data demonstrating a significant enhancement of the antitumor activity of anti-CTLA-4 when combined with FLX475, a Phase 2 study investigating the combination of FLX475 and ipilimumab is now being conducted in subjects with advanced melanoma.

Methods This clinical trial is a Phase 2, multicenter, open-label, single-arm study to determine the antitumor activity of FLX475 in combination with ipilimumab in subjects with advanced melanoma previously treated with an anti-PD-1 or anti-PD-L1 agent. The primary objectives of the study are to evaluate objective response rate, and the safety and tolerability of this combination. The study will first examine the safety of the combination of the 100 mg PO QD recommended Phase 2 dose of FLX475 and the approved 3 mg/kg IV Q3W dose of ipilimumab as part of a safety run-in phase, prior to examining the degree of antitumor activity in approximately 20 subjects. Evidence of an overall response rate (ORR) notably greater than the expected ORR of ipilimumab monotherapy alone in such subjects, which has been shown to be approximately 14%,⁶ would provide preliminary clinical evidence in support of the clinical hypothesis that CCR4 blockade by FLX475 can significantly enhance the antitumor activity of an anti-CTLA-4 checkpoint inhibitor.

Trial Registration ClinicalTrials.gov Identifier: NCT04894994

REFERENCES

- O'Rourke D, Nasrallah M, Desai A, Melenhorst J, Mansfield K, Morrisette J, Martinez-Lage M, Brem S, Maloney E, Shen A, Isaacs R, Mohan S, Plesa G, Lacey S, Navenot J, Zheng Z, Levine B, Okada H, June C, Brogdon J, Maus M. A single dose of peripherally infused EGFRvIII-directed CAR T cells mediates antigen loss and induces adaptive resistance in patients with recurrent glioblastoma. *Sci Transl Med* 2017;**9**:eaaa0984. doi: 10.1126/scitranslmed.aaa0984.
- Sharma A, Subudhi S, Blando J, Vence L, Wargo J, Allison JP, Ribas A, Sharma P. Anti-CTLA-4 immunotherapy does not deplete FOXP3+ regulatory T cells (Tregs) in human cancers-Response. *Clin Cancer Res* 2019;**25**:1233–1238.
- Marshall L, Marubayashi S, Jorapur A, Jacobson S, Zibinsky M, Robles O, Hu D, Jackson J, Pookot D, Sanchez J, Brovarney M, Wadsworth A, Chian D, Wustrow D, Kassner P, Cutler G, Wong B, Brockstedt D, Talay O. Tumors establish resistance to immunotherapy by regulating Treg recruitment via CCR4. *J Immunother Cancer* 2020;**8**:e000764.
- van Marle S, van Hoogdalem E, Johnson D, Okal A, Kassner P, Wustrow D, Ho W, Smith S. Pharmacokinetics, pharmacodynamics, and safety of FLX475, an orally-available, potent, and selective small-molecule antagonist of CCR4, in healthy volunteers. *J Immunother Cancer* 2018; **6**(Suppl 1):P484(SITC 2018).
- Powderly J, Chmielowski B, Brahmer J, Piha-Paul S, Bowyer S, LoRusso P, Catenacci D, Wu C, Barve M, Chisamore M, Nasrah N, Johnson D, Ho W. Phase I/II dose-escalation and expansion study of FLX475 alone and in combination with pembrolizumab in advanced cancer. *Journal of Clinical Oncology* 2020;**38** (15_suppl): TPS3163 (ASCO 2020).
- Long G, Mortier L, Schachter J, Middleton M, Neyns B, Sznol M, Zhou H, Ebbinghaus S, Ibrahim N, Arance A, Ribas A, Blank C and Robert C. Society for Melanoma Research 2016 Congress. *Pigment Cell & Melanoma Research* 2017;**30**:76–156.

Ethics Approval This study has been approved by the Institutional Review Board at each investigational site.

<http://dx.doi.org/10.1136/jitc-2021-SITC2021.548>

AN RNA-LIPOPLEX (RNA-LPX) VACCINE DEMONSTRATES STRONG IMMUNOGENICITY AND PROMISING CLINICAL ACTIVITY IN A PHASE I TRIAL IN CUTANEOUS MELANOMA PATIENTS WITH NO EVIDENCE OF DISEASE AT TRIAL INCLUSION

¹Carmen Loquai*, ²Jessica Hassel, ³Patrick Brück, ³Evelyna Derhovanessian, ³Katarina Cuk, ³Verena Lörks, ³Julian Sikorski, ³Maïke Gold, ³Daniel Maurus, ³Doreen Schwarck-Kokarakis, ³Marion Kästner, ³Thomas Weisenburger, ³Ann-Kathrin Eller, ⁴Sebastian Attig, ⁴Silvana Hempel, ³Petra Oehm, ³Tana Omokoko, ³Lena Kranz, ³Juliane Quinkhardt, ³Isabel Vogler, ³Inga Liebig, ³Stephanie Renken, ²Melanie Leierer, ⁵Verena Müller, ¹Heidrun Mitzel-Rink, ¹Matthias Miederer, ¹Stephan Grabbe, ⁶Jochen Utikal, ⁷Roland Kaufmann, ³Ugur Sahin, ³Özlem Türeci. ¹University Medical Center of the Johannes Gutenberg University, Mainz, Germany; ²Heidelberg University Hospital, Mainz, Germany; ³BioNTech, Mainz, Germany; ⁴Translational Oncology Mainz (TRON), Mainz, Germany; ⁵University of Heidelberg, Mainz, Germany; ⁶German Cancer Research Center, Heidelberg, Germany; ⁷University Hospital Frankfurt am Main, Frankfurt am Main, Germany

Background Lipo-MERIT is an ongoing, first-in-human, open-label, dose-escalation Phase I trial investigating safety, tolerability and immunogenicity of BNT111 in patients with advanced melanoma. BNT111 is an RNA-LPX vaccine targeting the melanoma tumor-associated antigens (TAAs) New York esophageal squamous cell carcinoma 1 (NY-ESO-1), tyrosinase, melanoma-associated antigen 3 (MAGE-A3), and transmembrane phosphatase with tensin homology (TPTE). A previous exploratory interim analysis showed that BNT111, alone or combined with immune checkpoint inhibition (CPI), has a favorable adverse event (AE) profile, gives rise to antigen-specific T-cell responses and induces durable objective responses in CPI-experienced patients with unresectable melanoma.¹ Here, we present preliminary data in patients with no evidence of disease (NED) at trial inclusion in the BNT111 monotherapy subgroup.

Methods Patients with stage IIIB/C and IV pre-treated cutaneous melanoma were intravenously administered with BNT111 using a prime/boost protocol. Patients were treated in seven dose escalation cohorts (7.2 to 400 µg total RNA) and three expansion cohorts to further explore dose levels of 14.4, 50 and 100 µg. In this analysis, patients receiving BNT111 monotherapy were grouped as having evidence of disease (ED) or NED, and immunogenicity, efficacy and safety were evaluated. Vaccine-induced immune responses were analyzed using an interferon-γ enzyme-linked immune absorbent spot (ELISpot) assay directly *ex vivo*.

Results As of May 24, 2021, 115 patients have received BNT111 within the Lipo MERIT trial. Of 71 patients treated with BNT111 monotherapy, 38 patients had ED and 33 patients had NED after prior therapies. Baseline characteristics were similar between the two groups. ELISpot data revealed comparable BNT111-induced T-cell responses against at least one TAA in ED vs. NED patients (14/22 [64%] and 19/28 [68%] patients with available ELISpot-evaluable samples, respectively), suggesting that BNT111 has the ability to induce T-cell immunity irrespective of the presence of a detectable tumor. As previously reported for ED patients, vaccine-induced CD4⁺ as well as CD8⁺ T-cell responses were also observed in NED patients, with a substantial fraction of *de novo* induced responses undetectable prior to vaccination. In NED patients, clinical efficacy was promising; median disease-free survival was 34.8 months (95% confidence interval: 7.0–not reached). The safety profile was similar in ED vs. NED patients; 38/38 (100%) and 32/33 (97%) patients experienced related treatment-emergent AEs, respectively, of which the majority were mild-to-moderate flu-like symptoms.

Conclusions Immunogenicity and safety profiles of BNT111 monotherapy were comparable in ED and NED patients. Promising signs of clinical activity were observed in NED patients.

Acknowledgements The authors would like to acknowledge Camilla West (BioNTech SE) for medical writing support.

Trial Registration ClinicalTrials.gov: NCT02410733; EudraCT No. 2013-001646-33.

REFERENCES

1. Sahin U, Oehm P, Derhovanessian E, et al. An RNA vaccine drives immunity in checkpoint-inhibitor-treated melanoma. *Nature* 2020;**585**(7823):107–112.

Ethics Approval Ethics & Institutional Review Board approval was obtained prior to initiation of the trial (2018-13393_21-AMG federführend).

<http://dx.doi.org/10.1136/jitc-2021-SITC2021.549>

ARTACUS: AN OPEN-LABEL, MULTICENTER, PHASE 1B/2 STUDY OF RP1 IN SOLID ORGAN TRANSPLANT RECIPIENTS WITH ADVANCED CUTANEOUS MALIGNANCIES

¹Jason Luke*, ²Michael Migden, ³Wanxing Chai-Ho, ⁴Diana Bolotin, ⁵Trisha Wise-Draper, ⁶Andrew Poklepovic, ⁷Douglas Laux, ⁸Meenal Kheterpal, ⁹Claire Verschraegen, ¹⁰Frances Collichio, ¹¹Jose Lutzky, ¹²Gregory Daniels, ¹³Katy Tsai, ¹⁴Susan Navia, ¹⁴Henry Castro, ¹⁴Praveen Bommareddy, ¹⁴Andrea Pirzkall, ¹⁴Robert Coffin. ¹UPMC Hillman Cancer Center, Pittsburgh, PA, USA; ²University of Texas MD Anderson Cancer C, Houston, TX, USA; ³UCLA David Geffen School of Medicine, Los Angeles, USA; ⁴University of Chicago, Chicago, IL, USA; ⁵UC Vontz Center for Molecular Studies, Cincinnati, OH, USA; ⁶Virginia Commonwealth University, Richmond, MA, USA; ⁷University of Iowa Hospitals and Clinics, Iowa City, IA, USA; ⁸Duke University, Durham, NC, USA; ⁹Ohio State University Comprehensive Ctr, Columbus, OH, USA; ¹⁰UNC, Chapel Hill, Chapel Hill, NC, USA; ¹¹Sylvester Comprehensive Cancer Center, Miami, FL, USA; ¹²UC San Diego, La Jolla, CA, USA; ¹³University of California San Francisco, San Francisco, CA, USA; ¹⁴Replimune, Woburn, MA, USA

Background Solid organ transplantation (SOT) has emerged as an important lifesaving procedure for patients with a wide range of end-organ diseases characterized by dysfunction or specific organ function failure. SOT rejection is a major complication requiring patients (pts) to undergo lifelong immunosuppression to prevent allograft rejection.¹ Skin cancers (SCs) including cutaneous squamous cell carcinoma (CSCC) are common post transplant malignancies.² SC in SOT pts is generally managed with surgical resection, radiation therapy and chemotherapy or targeted therapy. Use of immune checkpoint inhibitors in SOT recipients has improved outcomes but are associated with the high risk of allograft rejection.^{3–5} Thus, there is a high unmet need for a safe and effective treatment that also protects pts from allograft rejection. RP1 is an oncolytic virus (HSV-1) that expresses a fusogenic glycoprotein (GALV-GP R-) and granulocyte macrophage colony stimulating factor (GM-CSF). In preclinical studies, RP1 induced immunogenic tumor cell death and provided potent systemic anti-tumor activity⁶ and clinical data in combination with nivolumab has demonstrated a high rate of deep and durable response in patients with advanced SCs.⁷ The objective of this study is to assess the safety and efficacy of single agent RP1 in kidney and liver transplant recipients with SCs, with focus on CSCC. After determining the safety and tolerability in the initial cohort with kidney and liver transplants the study may also enroll heart and lung transplant recipients.

Methods This study will enroll up to 65 evaluable allograft transplantation pts with locally advanced or metastatic SCs. Key inclusion criteria are pts with confirmed recurrent, locally advanced or metastatic CSCC and up to 10 pts with non-CSCC SC, stable allograft function and ECOG performance status of ≤ 1 . Pts with prior systemic anti-cancer treatment are allowed. Key exclusion criteria are prior treatment with an oncolytic therapy, active herpetic infections or prior complications of HSV-1 infection and a history of organ graft rejection within 12 months. Pts will receive an initial dose of 1×10^6 plaque-forming units (PFU) of RP1. Two weeks later they will receive 1×10^7 PFU of RP1 and continue every two weeks until pre-specified study endpoints are met. RP1 will be administered by intra-tumoral injection including through imaging guidance as clinically appropriate. The primary objective of the trial is to assess efficacy determined by ORR and safety of single agent RP1. Additional secondary endpoints include DOR, CR, DCR, PFS and OS.

Trial Registration NCT04349436

REFERENCES

1. Frohn C, Fricke L, Puchta JC, Kirchner H. The effect of HLA-C matching on acute renal transplant rejection. *Nephrol Dial Transplant* 2001;**16**(2):355–60.
2. Madeleine MM, Patel NS, Plasmeijer EI, Engels EA, Bouwes Bavinck JN, Toland AE, Green AC; the Keratinocyte Carcinoma Consortium (KeraCon) Immunosuppression Working Group. Epidemiology of keratinocyte carcinomas after organ transplantation. *Br J Dermatol* 2017;**177**(5):1208–1216.
3. Spain L, Higgins R, Gopalakrishnan K, Turajlic S, Gore M, Larkin J. Acute renal allograft rejection after immune checkpoint inhibitor therapy for metastatic melanoma. *Ann Oncol* 2016;**27**(6):1135–1137.
4. Herz S, Höfer T, Papapanagiotou M, Leyh JC, Meyenburg S, Schadendorf D, Ugurel S, Roesch A, Livingstone E, Schilling B, Franklin C. Checkpoint inhibitors in chronic kidney failure and an organ transplant recipient. *Eur J Cancer* 2016;**67**:66–72.
5. Kittai AS, Oldham H, Cetnar J, Taylor M. Immune checkpoint inhibitors in organ transplant pts. *J Immunother* 2017;**40**(7):277–281.
6. Thomas S, Kuncheria L, Roulstone V, Kyula JN, Mansfield D, Bommareddy PK, Smith H, Kaufman HL, Harrington KJ, Coffin RS. Development of a new fusion-enhanced oncolytic immunotherapy platform based on herpes simplex virus type 1. *J Immunother Cancer* 2019 **10**;7(1):214.
7. Middleton M, Aroldi F, Sacco J, Milhem M, Curti B, Vanderwalde A, Baum S, Samson A, Pavlick A, Chesney J, Niu J, Rhodes T, Bowles T, Conry R, Olsson-Brown A, Earl-Laux D, Kaufman H, Bommareddy P, Deterding A, Samakoglu S, Coffin R, Harrington K. 422 An open-label, multicenter, phase 1/2 clinical trial of RP1, an enhanced potency oncolytic HSV, combined with nivolumab: updated results from the skin cancer cohorts. *J Immunother Cancer* 2020;**8**(3): doi: 10.1136/jitc-2020-SITC2020.0422

Ethics Approval The study was approved by institutional review board or the local ethics committee at each participating site. Informed consent was obtained from patients before participating in the trial.

<http://dx.doi.org/10.1136/jitc-2021-SITC2021.550>

551

PEGASUS SKIN, A STUDY OF SAR444245 (THOR-707, A PEGYLATED RECOMBINANT NON-ALPHA IL2) WITH CEMIPIMAB FOR THE TREATMENT OF PARTICIPANTS WITH ADVANCED UNRESECTABLE OR METASTATIC SKIN CANCERS

¹PARK John, ²Adyb Baakili*, ²Brigitte Demers, ³Rao Saleem, ²Alice Gosselin, ³Giovanni Abbadessa, ⁴Paolo A Ascierto. ¹Macquarie University, Macquarie, Australia; ²Sanofi-Aventis, Vitry-sur-Seine, France; ³Sanofi, Cambridge, MA, USA; ⁴Instituto Nazionale Tumori IRCCS, Naples, Italy

Background SAR444245 (THOR-707) is a recombinant human IL-2 molecule that includes a PEG moiety irreversibly bound to a novel amino acid via click chemistry to block the alpha-binding domain while retaining near-native affinity for the beta/gamma subunits. In animal models, SAR444245 showed anti-tumor benefits, but with no severe side effects, both as single agent and when combined with anti-PD1 comparing with historical data from aldesleukin. The HAMMER trial, which is the FIH study, shows preliminary encouraging clinical results: initial efficacy and safety profile with SAR444245 monotherapy and in combination with pembrolizumab supporting non-alpha preferential activity, validating preclinical models. The Pegasus Skin Phase 1/2 study will evaluate the clinical benefit of SAR444245 in combination with cemiplimab (anti-PD1) for the treatment of participants with cutaneous squamous cell carcinoma (CSCC) or melanoma

Methods Pegasus Skin (NCT04913220) will enroll approximately 80 participants in 2 separate cohorts. In cohort A, participants with a locally advanced, unresectable or metastatic melanoma will receive SAR444245 + cemiplimab as first line (1L) therapy. In cohort B, participants with locally advanced or metastatic CSCC who have not received more than 2 prior lines of systemic therapy and are not candidates for curative surgery or radiation will receive SAR444245 + cemiplimab. The study will start with a dose escalation to determine the recommended phase 2 dose (RP2D) of SAR444245 when combined with cemiplimab. The starting dose will be 16 µg/kg Q3W (DL1) with a possibility to de-escalate to 8 µg/kg Q3W (DL -1) or escalate to 24 µg/kg Q3W (DL2) based on the occurrence of DLT and overall assessment of safety. Participants enrolled in the Dose Escalation and treated at the RP2D selected for Dose Expansion will be included in the total number of participants for efficacy and safety evaluation. Participants will receive study treatment until disease progression, unacceptable toxicity, or completion of 35 cycles. Cemiplimab will be administered 350 mg per label, Q3W

Acknowledgements The Pegasus Skin study is sponsored by Sanofi

Trial Registration NCT04913220

Ethics Approval All applicable ECs are obtained

Consent All participant consents are obtained

<http://dx.doi.org/10.1136/jitc-2021-SITC2021.551>

Combination Immunotherapies

552

AMPHIPHILE-PEPTIDE BOOSTING WITH FMC63-BINDING SURROGATE PEPTIDE MIMOTOPES INDUCES ACTIVATION AND POTENT EFFECTOR FUNCTION IN CAR-T CELLS TARGETING CD19

Peter DeMuth, Amy Tavares, Ana Castano*. *Elicio Therapeutics, Cambridge, MA, USA*

Background Genetic engineering of T cells to express anti-CD19 Chimeric Antigen Receptors (CAR-T cells) has been FDA approved for the treatment of refractory/relapsing acute lymphocytic leukemia and diffuse large B cell lymphoma. With more patients receiving treatment with CAR-T cells it has been observed that approximately 10–20% of patients fail to enter remission after therapy,¹ and 30–50% of patients who achieve remission with anti-CD19 CAR T cells have disease relapse.² In prior studies, CAR-binding amphiphile (AMP)-peptides were shown to effectively localize in lymph nodes (LN), where they decorate endogenous antigen-presenting cells (APC) and stimulate CAR signaling to promote potent CAR-T responses against solid tumors.³ In this study, we describe how CD19 mimotope peptides specific for FMC63-based CARs can be modified with AMP technology to enhance peptide accumulation in LNs, enable presentation on APCs to CAR-Ts, and promote activation and effector functionality of CAR-T cells.

Methods We performed phage-screening and enrichment for CD19 surrogate peptides recognized by FMC-63-scFv. Surface Plasmon Resonance (SPR) was utilized to evaluate the affinity of the peptides to immobilized FMC-63. AMP versions of peptides were generated. In vitro, human dendritic cells (DCs) were preconditioned with AMP-CD19 or soluble peptides and cocultured with autologous T cells engineered to express CD19 CARs (FMC63-28z and FMC63-41BBz). Markers for activation, proliferation, cytotoxicity, and effector functions were evaluated. In vivo experiments were performed to evaluate the biodistribution of peptides. Luciferase-expressing murine CAR-T cells were engineered to evaluate the expansion and biodistribution of CAR-T cells in combination with AMP or soluble regimens.

Results We found surrogate CD19 peptide mimotopes that bind to FMC-63 with different affinities evaluated by ELISA and SPR. Assessment in human autologous DC/CAR-T cell cocultures demonstrated that AMP-CD19 peptides can decorate DCs effectively and promote potent activation (OX40, 41BB, CD69), proliferation, cytokine production (IFN γ , TNF α , and IL2), cytotoxicity (CD107a), and phenotypic enhancement of CD19-specific CAR-T cells. Assessment in vivo showed that AMPs are effectively delivered to LN where endogenous APCs are decorated to promote the activity of murine CAR-T cells.

Conclusions In vitro, AMP modification of CAR-binding peptide mimotopes induces activation, cytotoxicity, and effector functions of CAR-T cells. These AMP-peptides effectively accumulate in LN and boost CAR-T activation and expansion in vivo. This platform can potentially be utilized as a mechanism to expand and functionally enhance CAR-T cells in vivo for blood and solid tumors.

REFERENCES

1. Maude SL et al. Tisagenlecleucel in children and young adults with B-cell lymphoblastic leukemia. *N Engl J Med* 2018;**378**:439–448.
2. Park JH et al. Long-term follow-up of CD19 CAR therapy in acute lymphoblastic leukemia. *N Engl J Med* 2018;**378**:449–459.

3. Ma L et al. Enhanced CAR-T cell activity against solid tumors by vaccine boosting through the chimeric receptor. *Science* 2019;**365**(6449):162–168.

Ethics Approval All animal experiments in this study were performed in accordance with the approval of IACUC Protocol CR-0039.

<http://dx.doi.org/10.1136/jitc-2021-SITC2021.552>

FIRST-IN-CLASS INHIBITORS OF ERAP1 ALTER THE IMMUNOPEPTIDOME OF CANCER, DRIVING A DIFFERENTIATED T CELL RESPONSE LEADING TO TUMOR GROWTH INHIBITION

¹Peter Joyce*, ²Martin Quibell, ³Jason Shiers, ³Carmen Tong, ³Kristopher Clark, ⁴Nicola Ternette, ²Kate Anderton, ²Jessica Sette, ⁴Wayne Paes, ²Andrew Leishman. ¹Grey Wolf Therapeutics Ltd, Oxford, UK; ²Grey Wolf Therapeutics, Oxford, UK; ³Sygnature Discovery, Nottingham, UK; ⁴University of Oxford, Oxford, UK

Background Clinical data demonstrates increased antigen presentation diversity is an important factor in determining response rates to checkpoint inhibitors.¹ In addition to tumor mutational burden, increased HLA heterozygosity and HLA evolutionary diversity are non-overlapping factors which further diversify the immunopeptidome and improve clinical response to checkpoint therapies.^{2–3} Endoplasmic reticulum aminopeptidase 1 (ERAP1) is an enzyme that trims peptides loaded into classical and nonclassical MHC Class I molecules.⁴ ⁵ Ablation of mouse ERAAP modifies the immunopeptidome, resulting in improved immunogenicity, generation of CD8+ T cell responses and tumor growth inhibition.^{6–7} We report the characterisation of ERAP1 inhibitors in syngeneic tumor models and development of biomarkers to enable translation of this mechanism into the clinic.

Methods Human and mouse cancer cell lines treated with ERAP1 inhibitors were assessed by immunopeptidomics⁸ to profile peptide repertoire changes. ERAP1 inhibitor with and without checkpoint inhibition were used to treat syngeneic mouse tumor models, followed by analysing effects on the T cell receptor (TCR) repertoire, RNA sequencing profile, immune cell infiltration and tumor growth inhibition.

Results Extensive analysis of the immunopeptidomes of diverse cancer cell lines robustly show that ERAP1 inhibition modulates the cancer-related antigen repertoire across diverse ERAP1 and HLA genotypes and cancer-type backgrounds. ERAP1 inhibition drives changes in T cell activation and response, leading to increased T cell infiltration into CT26 syngeneic tumors and alteration of the TCR repertoire at early and late timepoints in tumor growth. Consistent peptide length changes in the immunopeptidome, caused by ERAP1 inhibition, is a proof of mechanism biomarker, whilst tumor immunohistochemistry, TCR repertoire analysis and RNA sequencing are potential proof of principle biomarkers that can all be translated into the clinic. Importantly, the antigen and T cell changes we see following ERAP1 inhibition lead to robust tumor growth inhibition in different syngeneic mouse models when combined with anti-PD-1. We are also exploring the potential of ERAP1 inhibitors to enhance tumour immune responses in combination with additional therapies (e.g. chemotherapy and radiotherapy), across different tumor microenvironments.

Conclusions Grey Wolf Therapeutics ERAP1 inhibitors significantly modify the immunopeptidome and combination with anti PD-1 leads to significant TCR repertoire change, T cell infiltration and tumor growth inhibition in syngeneic mouse tumor models. These data provide the foundation from which we will explore the potential of our first-in-class ERAP1 inhibitor development candidate in the clinic, as well as identifying useful biomarkers to demonstrate desired biological activity.

REFERENCES

1. Rizvi N, Hellmann MD, Snyder A, et al. Mutational landscape determines sensitivity to PD-1 blockade in non-small cell lung cancer. *Science* 2015;**348** (6230):124–128.

- Chowell D, et al. Patient HLA class I genotype influences cancer response to checkpoint blockade immunotherapy. *Science* 2018;**359** (6375):582–587.
- Chowell D, Chirag Krishna, Federica Pierini, et al. Evolutionary divergence of HLA class I genotype impacts efficacy of cancer immunotherapy. *Nature Medicine* 2019;**25**(11):1715–1720.
- Shastri N, Nagarajan N, Lind KC, et al. Monitoring peptide processing for MHC class I molecules in the endoplasmic reticulum. *Curr Opin Immunol* 2014;**26**:123–127.
- Mpakali A, Maben Z, Stern LJ, et al. Molecular pathways for antigenic peptide generation by ER aminopeptidase 1. *Mol Immunol* 2018;**13**:50–57.
- James E, Bailey I, Sugiyarto G, et al. Induction of protective antitumor immunity through attenuation of ERAAP function. *J Immunol* 2013;**190**(11):5839–5846.
- Manguso RT, Pope, HW, MD Zimmer, et al. In vivo CRISPR screening identifies Ptpn2 as a cancer immunotherapy target. *Nature* 2017;**547**(7664):413–418.
- Purcell AW, Ramarathinam SH, Ternette N. Mass spectrometry-based identification of MHC-bound peptides for immunopeptidomics. *Nat Protoc* 2019;**14** (6):1687–1707.

<http://dx.doi.org/10.1136/jitc-2021-SITC2021.553>

THE PANORAMA OF TUMOR INTRINSIC IMMUNE REGULATORS EXHIBITED BY GENOME-WIDE CRIPSR IMMUNE SCREEN INTEGRATED WITH COMPREHENSIVE CLINICAL DATASET ANALYSIS

¹Jiakai Hou*, ²Yunfei Wang, ³Leilei Shi, ³Yuan Chen, ¹Chunyu Xu, ¹Arash Saeedi, ³Ke Pan, ¹Ritu Bohat, ¹Nicholas Egan, ³Jodi McKenzie, ³Rina Mbofung, ³Leila Williams, ³Zhenhuang Yang, ³Ming Sun, ¹Xiaofang Liang, ³Jordi Rodon Ahnert, ¹Navin Varadarajan, ³Cassian Yee, ³Yiwen Chen, ²Patrick Hwu, ¹Weiyi Peng. ¹University of Houston, Houston, TX, USA; ²H. Lee Moffitt Cancer Center, Tampa, FL, USA; ³MD Anderson Cancer Center, Houston, TX, USA

Background Despite approval of immunotherapy for wide ranges of cancers, the majority of patients fail to respond to immunotherapy or relapse following initial response which is partially attributed to immunosuppression co-opted by tumor cells. However, it is challenging to utilize conventional methods to systematically evaluate the potential of tumor intrinsic factors to act as immune regulators in cancer patients.

Methods In this study, an unbiased integrative strategy were designed to leverage the complementary strength of in vitro functional genomic screens and multi-omics clinical dataset to assess roles of individual tumor-intrinsic factors in regulating T cell tumor infiltration and T cell-mediated tumor killing, the two most important rate-limiting steps of cancer immunotherapy. Initially, a genome-wide CRISPR-Cas9 screening system using paired murine tumors and tumor-reactive T cells was employed to globally screen tumor intrinsic factors modulating the tumor sensitivity to T cell-mediated killing. Then, findings from the screening were integrated with the bioinformatics analysis of clinical datasets to further evaluate roles of each tumor intrinsic factor in governing antitumor immunity.

Results The integrative analysis successfully identified several novel tumor intrinsic factors as effectors of immune resistance, but also demonstrated distinct roles of these factors in controlling immune cell trafficking and tumor sensitivity to T cell-mediated killing. Among these factors, candidates controlling both rate-limiting steps of T cell tumor infiltration and T cell-mediated tumor killing were termed as "Dual immune resistance regulators" and the remaining factors whose expression levels were not associated with tumor immune infiltration were termed as "Cytotoxicity resistance regulators". By selecting PRMT1 and RIPK1 as the representatives of these two groups respectively, we confirmed that genetically depletion of PRMT1 and RIPK1 sensitized tumors to T-cell mediated killing via two independent experimental approaches. Furthermore, inhibiting Prmt1 or Ripk1 sensitizes tumors to cancer immunotherapy, such as anti-PD-1 and anti-OX40 treatments (Tumor size (mm²) on day 21 after tumor inoculation: for anti-PD-1 treatment, Ctrl 84.05±23.10, PRMT1 KO 7.30±7.81, RIPK1 KO 2.03±4.96; for anti-OX40 treatment, Ctrl 81.04±7.72, PRMT1 KO 55.80±15.74, RIPK1 KO 38.78±14.06) and extended the survival of tumor-bearing mice. Moreover, by using a RIPK1-specific inhibitor, GSK2982772, we demonstrated that targeting cytotoxicity resistance regulators could enhance the antitumor activity of T cell-based cancer immunotherapy, despite limited impact on T cell tumor infiltration.

Conclusions Collectively, our data not only demonstrate distinct immunoregulatory roles and therapeutic potentials of PRMT1 and RIPK1 in T cell-mediated antitumor activity, but also provide a rich resource of novel targets for rational immuno-oncology combinations.

<http://dx.doi.org/10.1136/jitc-2021-SITC2021.554>

555

A HIGH-THROUGHPUT IN SITU SCREEN TO IDENTIFY SYNERGISTIC COMBINATIONS OF IMMUNE-ONCOLOGY DRUGS WITH TARGETED AND CYTOTOXIC AGENTS IN A PATIENT-DERIVED HUMANIZED MOUSE MODEL OF RENAL CANCER

¹Oliver Jonas, ²Eva Oswald, ²Kanstantsin Lashuk, ¹Sebastian Ahn, ³Julia Schuler*. ¹Harvard Medical School, Boston, MA, USA; ²Charles River Research Services Germany, Freiburg, Germany; ³Charles River Discovery, Freiburg, Germany

Background Identifying how to optimally combine immunotherapies with other available anti-cancer therapies is a major challenge in oncology. A systematic method to screen many potential combination therapies ideally in vivo has remained elusive. We have utilized an implantable microdevice (IMD) performing cassette microdosing that measures intratumor drug responses and anti-tumor immunity for 20 agents in parallel. For each of the agents, local tumor response is measured by cyclical immunofluorescence for deep cellular response phenotyping. This approach is combined with systemic administration of checkpoint inhibitors to examine whether local immunogenic cell death (ICD) induced by a given drug microdose potentiates the immunotherapy's anti-tumor effect.

Methods The measurements were performed in a humanized mouse model of renal cancer, patient derived xenograft (PDX) RXF488. The PDX is derived from a 68 year old male patient suffering from clear cell renal carcinoma. RXF488 was implanted subcutaneously in 30 NSG mice. Animals were stratified into 6 groups with n= 4–6. Humanization was performed by the intravenous injection of 5x10e6 human peripheral blood mononuclear cells (PBMC) prior to the first treatment. Systemic anti-PD1 treatment was applied in the presence and absence of the microdevice loaded with eleven different drugs. Control groups received the microdevice in the presence or absence of PBMC. Beside the histological examination of the tumor tissue, flow cytometry (FC) was performed on bone marrow, spleen and tumor tissue to determine infiltration of human immune cells.

Results FC analyses revealed no influence of the treatment on the human immune cells in bone marrow and spleen. The anti-PD1 treatment induced an increase in huCD45+ cells specifically in the tumor tissue and a decrease of the CD4/CD8 ratio in these cells only 48h after treatment. Our combination screen identified LXH254, Sorafenib and Doxorubicin exhibiting the highest increase in apoptosis induction when combined with checkpoint inhibitors. The increased efficacy from immunotherapy administration coincided with increased induction of ICD. We were able to verify the results of the screening experiment in a conventional setting with systemic combination treatment in the same PDX model.

Conclusions Our results demonstrate that local tumor response signatures of ICD can be used to systemically identify synergistic combinations of a range of drugs with immunotherapy on a tumor specific basis. The approach may represent a new paradigm for efficient in vivo screening of novel combinations, particularly with combinations involving immunotherapies.

<http://dx.doi.org/10.1136/jitc-2021-SITC2021.555>

Shreya Kumar*, Marxa Figueiredo. *Purdue University, West Lafayette, IN, USA*

Background Prostate cancer is the second most common cancer and is one of the leading causes of cancer-related death among American men.¹ Prostate cancer exhibits significant tropism for the bone and once metastasis occurs, survival rates fall rapidly compared to primary tumors.² Bone metastasis can lead to bone loss and fractures which can severely compromise the patient's quality of life. Current treatment options are limited and focused on symptom management. Immune-based treatments are rapidly emerging as a possible therapeutic option for a variety of cancers including prostate cancer, however, patient sensitivity remains a concern. Chemotherapies such as cabozantinib have been shown to have immune-priming effects which can sensitize tumors to immunotherapies.³ Additionally, lower doses of chemotherapy can be used in this context which can reduce side effects. For this project, we hypothesized that a combination of chemotherapy (cabozantinib) and immunotherapy (Interleukin-27) could be effective in treating bone-metastatic prostate cancer and can help reverse some of the bone damage caused by the tumor. IL-27 is a multi-functional cytokine, which recruits immune cells to the tumor site, and promotes bone repair.⁴

Methods To test our hypothesis, we performed an in vivo experiment where syngeneic C57BL/6J mice were implanted with intratibial (cortical bone) TRAMP-C2ras tumors (TRAMP-C2 cells were infected with Lv-HrasG12V to make them more aggressive and gain the ability to grow in bone, and marked with Lv-Luc to follow tumor growth). Immunotherapy was administered in the form of sonoporation-assisted intramuscular gene delivery,⁴ with control (empty) vectors or vectors expressing mouse IL-27. Following immunotherapy, the animals received either cabozantinib (60 mg/kg) or vehicle control by oral gavage daily for two weeks. Bioluminescence imaging (BLI) was used to monitor Luc-expressing tumor size twice a week. Upon reaching a humane endpoint, the animals were euthanized, and tumor samples were harvested.

Results BLI showed that mice treated with a combination of IL-27 and cabozantinib had smaller tumor sizes compared to mice treated with individual treatments. The combination group had a significantly lower tumor burden compared to the control group. RNA sequencing was used to characterize changes in gene expression relating to the impact of therapeutics in signaling and cellular composition in the tumor microenvironment.

Conclusions We envision that chemo-immunotherapy approaches will emerge as a novel therapeutic strategy for treating bone-metastatic prostate cancer while reducing chemotherapy-associated toxicity, improving sensitivity to immunotherapy, and promoting healthy musculoskeletal tissue repair.

Acknowledgements Source of research support: R01CA196947

REFERENCES

1. Prostate Cancer Statistics | CDC 2021. [https://www.cdc.gov/cancer/prostate/statistics/index.htm.]
2. Survival Rates for Prostate Cancer. [https://www.cancer.org/cancer/prostate-cancer/detection-diagnosis-staging/survival-rates.html.]
3. Kwilas AR, Ardiani A, Donahue RN, Aftab DT, Hodge JW. Dual effects of a targeted small-molecule inhibitor (cabozantinib) on immune-mediated killing of tumor cells and immune tumor microenvironment permissiveness when combined with a cancer vaccine. *J Transl Med* 2014;**12**(1):1–15.
4. Figueiredo ML, Neto MF, Salameh JW, Decker RE, Letteri R, Chan-Seng D, Emrick T. Ligand-Mediated Targeting of Cytokine Interleukin-27 Enhances Its Bioactivity In Vivo. *Mol Ther Methods Clin Dev* 2020;**17**:739–751.

557

NEOADJUVANT CAMRELIZUMAB IN COMBINATION WITH ALBUMIN PACLITAXEL AND CISPLATIN FOR PATIENTS WITH LOCALLY ADVANCED ESOPHAGEAL SQUAMOUS CELL CARCINOMA (ESCC)

Huilai Lv*, Yang Tian, Zhenhua Li, Chao Huang, Yanzhao Xu, Ziqiang Tian. *The Fourth Hospital of Hebei Medical University, shijiazhuang, China*

Background The pathologic complete response (pCR) rate occurs less than 10% of patients(pts) with neoadjuvant chemotherapy agents in locally advanced ESCC, Programmed death-1 (PD-1) blockade may induce tumor regression in pts with advanced ESCC. Camrelizumab (anti-PD-1) is standard of care as second-line therapy for advanced ESCC in China. With the potential benefit of combining Camrelizumab with neoadjuvant chemotherapy, we intended to assess the efficacy and safety of Camrelizumab combined with albumin paclitaxel and cisplatin in neoadjuvant therapy of locally advanced ESCC.

Methods 28 pts with histologically confirmed stage II-IVA ESCC were enrolled. Eligible pts were aged 18~75 years with no prior any therapy. Pts received 2~4 cycles of Camrelizumab (200mg IV q3w) plus albumin paclitaxel (260 mg/m² IV q3w) and cisplatin (75 mg/m² IV q3w) followed by surgery within 4~6 weeks after completion of neoadjuvant therapy. The primary endpoint was pCR, the secondary endpoints included major pathologic response (MPR), R0 resection rate, objective response rate (ORR), disease-free survival (DFS) and safety.

Results From Jul 27 2019 to Jan 29 2021, 28 eligible pts were enrolled, neoadjuvant treatment was completed in 28 pts. 12 pts (42.9%) had clinical complete response (cCR), and the ORR was 78.6% (22/28). All pts underwent surgery and surgical treatment was not delayed. The pCR was 32.1% (9/28), MPR was 53.6% (15/28). Notably, R0 resection rate was 100% (28/28). None of 28 pts progressed, the DFS was not yet achieved. The average intraoperative blood loss was 139ml (100~300ml) and the average hospitalization time after operation was 17 days (11~35 days). No patient developed anastomotic leak and other surgical treatment-related toxicity. The grade 1~2 treatment-related AEs were reactive cutaneous capillary endothelial proliferation (RCCEP) (35.7%), hepatotoxicity (21.4%), weakness (10.7%), thyroid dysfunction (10.7%). No serious AEs resulted in termination of treatment.

Conclusions Camrelizumab in combination with albumin paclitaxel and cisplatin followed by surgery for locally advanced ESCC showed promising downstaging effect and pCR with good tolerance, and further study is needed.

<http://dx.doi.org/10.1136/jitc-2021-SITC2021.557>

PRECLINICAL EVALUATION OF PEGYLATED LIPOSOMAL DOXORUBICIN OR DOXORUBICIN WITH MATRC-101 IN THE EMT6 SYNGENEIC MOUSE MODEL

Danhui Zhang, Nikhil Vad*, Erin Wechsler*. *Atreca, Inc., San Carlos, CA, USA*

Background We previously described ATRC-101, a fully human, engineered IgG1 antibody which is currently under evaluation in the clinic as a monotherapy for solid tumors. A chimeric version of this antibody expressed on a mouse IgG2a (mATRC-101) has shown robust anti-tumor activity as a monotherapy in the EMT6 syngeneic tumor model. In order to assess the potential utility of ATRC-101 in combination with chemotherapeutic agents, non-clinical studies were performed to assess the efficacy of mATRC-101 in combination with chemotherapeutic agents, including Doxorubicin and pegylated liposomal Doxorubicin (PLD), and the impact of these anti-tumor small molecules on mATRC-101 immunoreactivity in mouse tumor and normal tissues.

Methods Female BALB/c mice with established EMT6 tumors were dosed with mATRC-101 (1 or 3 mg/kg) or vehicle intraperitoneally (IP) twice weekly plus Doxorubicin (2 or 5 mg/Kg) or vehicle (saline) IV once weekly following randomization on Day 6. Statistical analyses of tumor volumes were performed using the normalized area above the curve and the normalized growth rate metrics developed at Atreca. One-sided log-rank (Mantel-Cox) test was used to assess survival advantage relative to the indicated reference group. P-values ≤ 0.05 were considered significant. In monotherapy studies with Doxorubicin and PLD, EMT6 tumor and non-tumor bearing mice were dosed with vehicle or Doxorubicin (2, 10 mg/kg) or PLD (1, 2, 5, 10 mg/kg). Normal mouse tissues were collected at 24 hours and 2 weeks after the last dose. Reactivity for mATRC-101 in EMT6 tumor and normal mouse tissues was evaluated by immunohistochemistry

Results The combination of 3 mg/kg mATRC-101 and 5 mg/kg Doxorubicin demonstrated significant tumor growth inhibition compared to either monotherapy, or vehicle ($p < 0.05$) through Day 22. Moreover, the combination resulted in a significant survival benefit compared to vehicle and 5 mg/kg Doxorubicin monotherapy ($p < 0.0005$). Immunohistochemical analyses of mATRC-101 reactivity in EMT6 tumors from mice treated with chemotherapy alone showed apparent dose-dependent increase in immunofluorescence intensity with increasing concentrations of Doxorubicin or PLD. Furthermore, tissue cross-reactivity studies in selected normal organs from mice treated with Doxorubicin or PLD demonstrated no reactivity above vehicle.

Conclusions This study provides non-clinical evidence that administration of mATRC-101 in combination with Doxorubicin increases anti-tumor activity in the EMT6 model. Exposure to Doxorubicin or PLD in EMT6 tumor-bearing mice increased mATRC-101 immunoreactivity in the tumor, in a dose-dependent manner. Moreover, mATRC-101 immunoreactivity in normal tissues was not influenced by Doxorubicin or PLD. Taken together, these findings support clinical evaluation of the combination of ATRC-101 and doxorubicin.

<http://dx.doi.org/10.1136/jitc-2021-SITC2021.559>

IMMUNOTHERAPEUTIC AND ANTIMETASTATIC ACTIVITY OF LTX-315 IN PRECLINICAL MODELS OF ICI-RESISTANT BREAST CANCER

¹Takahiro Yamazaki*, ¹Erik Wennerberg, ²Michal Hensler, ¹Aitziber Buqué Martínez, ¹Jeffrey Kraynak, ²Jitka Fucikova, ¹Xi Zhou, ³Baldur Sveinbjornsson, ³Oystein Rekdal, ¹Sandra Demaria, ¹Lorenzo Galluzzi. ¹Weill Cornell Medical College, New York, NY, USA; ²Sotio, Prague, Czech Republic; ³Lytix Biopharma, Tromsø, Norway

Background Oncolytic peptides are attractive tools for the development of novel anticancer regimens [1]. LTX-315 is a synthetic peptide with a marked capacity to elicit tumor-targeting immunity in preclinical cancer models [2]. Indeed, LTX-315 has been shown to elicit immunogenic cell death (ICD) in malignant cells [3, 4] and to deplete immunosuppressive cells such as CD4+CD25+FOXP3+ TREG cells and myeloid-derived suppressor cells (MDSCs) from the tumor microenvironment (TME) [5]. Accordingly, LTX-315 synergized with immunogenic chemotherapeutics or immune checkpoint inhibitors (ICIs) in preclinical tumor models [5, 6]. Moreover, recent findings from a Phase I clinical trial in patients with advanced solid tumors (NCT01986426) indicate that intratumoral LTX-315 is safe, clinically active, and elicits alterations in the TME that support the initiation of anticancer immunity [7, 8]. However, the dependency of LTX-315 therapeutic effects on the immune system in preclinical models of breast cancer has not been mechanistically investigated.

Methods We harnessed three distinct mouse models of ICI-resistant breast cancer, namely hormone receptor (HR)-positive TS/A established and triple-negative breast cancer (TNBC) 4T1 cells established in immunocompetent syngeneic BALB/c mice, as well as medroxyprogesterone acetate (MPA, M)-initiated, 7,12-dimethylbenz[a]anthracene (DMBA, D)-driven mammary carcinomas evolving in C57BL/6 mice to assess the immunotherapeutic effects of LTX-315 optionally combined with radiation therapy (RT), based on the primary tumor growth, metastatic dissemination and overall survival (depending on model). Multilesion models, rechallenge assays, antibody-mediated depletion experiments as well as experiments in Rag1^{-/-} mice were employed to elucidate the mechanistic involvement of the immune system.

Results In the multilesion TS/A models, intratumoral LTX-315 to one lesion combined with hypofractionated RT to another lesion resulted in superior systemic disease control as manifested by eradication of a 3rd untreated lesion in up to 50% of mice, which were protected from a subsequent rechallenge with living TS/A cells. In the single lesion 4T1 model, LTX-315 mediated enable robust local and metastatic disease control, which could be enhanced (only locally) with RT and dependent on natural killer (NK) cells, but less so on T lymphocytes (as determined with anti-asialo GM1 antibodies and Rag1^{-/-} hosts). In the M/D-driven model, LTX-315 considerably controlled the growth of primary tumors and delayed relapse, an effect that depended on NK cells (as demonstrated with anti-NK1.1 antibodies).

Conclusions LTX-315, alone and combined with RT, mediates robust immunotherapeutic effects in multiple models of ICI-resistant breast cancer. Intriguingly, NK cells appear to be required for such effects, potentially linked to the emergence of immunological memory.

Acknowledgements We are indebted to Dr. Fred Miller (Karmanos Cancer Center, Detroit, MI) for the kind gift of 4T1 cells, as well as to Dr. Karsten A. Pilonis (Weill Cornell Medicine, New York, NY) and Maria E. Rodriguez-Ruiz (University of Navarra, Pamplona, Spain) for help with clonogenic assays.

This work has been sponsored by a research grant by Lytix Biopharma (Oslo, Norway) to S.D. and L.G.

REFERENCES

1. Kepp, O. et al. (2020) Oncolysis without viruses - inducing systemic anticancer immune responses with local therapies. *Nat Rev Clin Oncol* 17 (1), 49–64.
2. Vitale, I. et al. (2021) Targeting Cancer Heterogeneity with Immune Responses Driven by Oncolytic Peptides. *Trends Cancer* 7 (6), 557–572.
3. Eike, L.M. et al. (2015) The oncolytic peptide LTX-315 induces cell death and DAMP release by mitochondria distortion in human melanoma cells. *Oncotarget* 6 (33), 34910–23.
4. Zhou, H. et al. (2016) The oncolytic peptide LTX-315 triggers immunogenic cell death. *Cell Death Dis* 7 (3), e2134.
5. Yamazaki, T. et al. (2016) The oncolytic peptide LTX-315 overcomes resistance of cancers to immunotherapy with CTLA4 checkpoint blockade. *Cell Death Differ* 23 (6), 1004–15.
6. Camilio, K.A. et al. (2019) Combining the oncolytic peptide LTX-315 with doxorubicin demonstrates therapeutic potential in a triple-negative breast cancer model. *Breast Cancer Res* 21 (1), 9.
7. Jebsen, N.L. et al. (2019) Enhanced T-lymphocyte infiltration in a desmoid tumor of the thoracic wall in a young woman treated with intratumoral injections of the oncolytic peptide LTX-315: a case report. *J Med Case Rep* 13 (1), 177.
8. Spicer, J. et al. (2021) Safety, Antitumor Activity, and T-cell Responses in a Dose-Ranging Phase I Trial of the Oncolytic Peptide LTX-315 in Patients with Solid Tumors. *Clin Cancer Res* 27 (10), 2755–2763.

Ethics Approval This study was approved by Weill Cornell Medical College's Ethics Board; approval number 2015-0028, 2018-0002.

<http://dx.doi.org/10.1136/jitc-2021-SITC2021.560>

561 **TRIPLE CHECKPOINT BLOCKADE, BUT NOT ANTI-PD1 ALONE, ENHANCES THE EFFICACY OF ENGINEERED ADOPTIVE T CELL THERAPY IN ADVANCED OVARIAN CANCER**

Kristin Anderson*, Yapeng Su, Madison Burnett, Breanna Bates, Magdalia Rodgers Suarez, Susan Ruskin, Aesha Vakil, Valentin Voillet, Raphael Gottardo, Philip Greenberg. *Fred Hutchinson Cancer Research Center, Seattle, WA, USA*

Background Over 20,000 women are diagnosed with ovarian cancer annually, and more than half will die within 5 years. This rate has changed little in the last 20 years, highlighting the need for therapy innovation. A promising new strategy with the potential to control tumor growth without toxicity to healthy tissues employs immune T cells engineered to target proteins uniquely overexpressed in tumors. Mesothelin (Msln) contributes to the malignant and invasive phenotype in ovarian cancer, and has limited expression in healthy cells, making it a candidate immunotherapy target in these tumors.

Methods The ID8_{VEGF} mouse cell line was used to evaluate if T cells engineered to express a mouse Msln-specific high-affinity T cell receptor (TCRMsln) can kill murine ovarian tumor cells in vitro and in vivo. Tumor-bearing mice were treated with TCR_{Msln} T cells plus anti-PD-1, anti-Tim-3 or anti-Lag-3 checkpoint-blocking antibodies administered alone or in combination, ultimately allowing targeting up to three inhibitory receptors simultaneously. Single cell RNA sequencing was used to profile the impact of combination checkpoint blockade on both the engineered T cells and the tumor microenvironment.

Results In a disseminated ID8 tumor model, adoptively transferred TCR_{Msln} T cells preferentially accumulated within established tumors, delayed ovarian tumor growth, and significantly prolonged mouse survival. However, our data also revealed that elements in the tumor microenvironment (TME) limited engineered T cell persistence and ability to kill cancer cells. Triple checkpoint blockade, but not single- or double-agent treatment, dramatically increased anti-tumor function by intratumoral TCR_{Msln} T cells. Single cell RNA-sequencing revealed distinct transcriptome changes in engineered T cells and the TME following triple blockade compared to single- and double-agent treatment. Moreover, combining adoptive immunotherapy with triple checkpoint blockade prolonged survival in the cohort of treated tumor-bearing mice, relative to TCR_{Msln} with or without anti-PD1, or double-agent treatments.

Conclusions Inhibitory receptor/ligand interactions within the tumor microenvironment can dramatically reduce T cell function, suggesting tumor cells may evade T cell responses by upregulating the ligands for PD-1, Tim-3 and Lag-3. In a model of advanced ovarian cancer, triple checkpoint blockade significantly improved the function of transferred engineered T cells and improved outcomes in mice in a setting in which single checkpoint blockade had no significant activity. The results suggest that T cell therapy with triple blockade, which can ultimately be more safely pursued in a cell intrinsic form through T cell genetic engineering, may overcome barriers to achieving therapeutic efficacy in patients.

Ethics Approval The Institutional Animal Care and Use Committees of the University of Washington and the Fred Hutchinson Cancer Research Center approved all animal studies.

<http://dx.doi.org/10.1136/jitc-2021-SITC2021.561>

REAL-WORLD ASSESSMENT OF CURRENT TREATMENT PATTERNS AND CLINICAL OUTCOMES AMONG PATIENTS WITH EGFR AND ALK WILD TYPE NON-SMALL CELL LUNG CANCER (NSCLC) IN THE US

¹Lyudmila Bazhenova, ²Jonathan Kish, ³Beilei Cai*, ³Nydia Caro, ²Bruce Feinberg. ¹University of California San Diego Moores Cancer Center, San Diego, CA, USA; ²Cardinal Health Specialty Solutions, Miami, OH, USA; ³Novartis Pharmaceuticals Corporation, East Hanover, NJ, USA

Background Treatment for advanced non-small cell lung cancer (NSCLC) has dramatically advanced in the past 5 years with the advent of immunotherapy (IO). This study sought to describe treatment patterns and clinical outcomes in a representative sample of NSCLC patients.

Methods Patients were identified by physicians from a voluntary sample of community practices across the US. Stage IIIB/IV NSCLC patients with EGFR/ALK wild-type initiating any first-line (1L) systemic therapy between 01/01/2016 and 12/31/2019 with at least 2 months of follow-up (unless deceased) were included, and were followed until November 2020. Sampling quotas included 250 patients who initiated 1L in 2016/2017 and 250 patients who did so in 2018/2019. Best tumor response was collected from patient charts during each line of therapy (LOT). Progression-free survival (PFS) and overall survival (OS) were calculated from initiation of 1L by Kaplan-Meier method. Baseline characteristics and clinical outcomes are described and presented by treatment regimen received.

Results Of 500 submitted patients, 497 were included post QA/QC. Across all patients, mean age at 1L initiation was 65 years, 57.3% were male, 92.9% had stage IV disease, and 68.6% were ECOG-OS 0/1 (Table 1). Overall, 60.2% (n=299), 33.2% (n=165), and 6.6% (n=33) received 1, 2, or =3 LOTs during the study period. Most common 1L regimens (%) were platinum-doublet chemotherapy plus IO (PDC+IO) (40.6%), PDC (29.4%), IO monotherapy (20.7%), PDC+bevacizumab (6.2%); while most common 2L regimens were IO monotherapy (42.4%), single-agent chemotherapy (SAC) (18.2%), SAC+VEGF inhibitor (15.7%), PDC (8.1%), and PDC+bevacizumab (5.6%). Over 90% of pts who received IO monotherapy had PD-L1 >50%. Moving from 2016/2017 to 2018/2019, utilization of 1L PDC declined from 45.0% to 13.7% while utilization of 1L PDC+IO increased from 27.3% to 54.0%. Among those who received only one LOT (n=299), 44.5% were still on 1L, 14.0% stopped receiving 1L, and 41.5% were deceased. Overall response rates were 67.3%, 35.6%, 60.2%, and 61.3% for 1L PDC+IO, PDC, IO monotherapy, and PDC+bevacizumab, respectively (Table 1). First-line median PFS/OS (months) was 15.6/26.5, 5.3/13.7, 17.8/NR, and 10.8/18.6, respectively for PDC+IO, PDC, IO monotherapy, and PDC+bevacizumab (table 1).

Conclusions Data from 2016 to 2020 was used provide a contemporary assessment of treatment patterns among EGFR/ALK wild-type NSCLC patients. Although 1L treatment utilization shifted to IO-based regimens in recent years, 41.5% of patients did not survive to receive second-line therapy, 1L PFS did not exceed 1.5 years, and median OS remained limited across all 1L treatment groups.

Abstract 562 Table 1

	All Patients (n=497)		PDC+IO (n=202)		PDC (n=146)		IO monotherapy (n=103)		PDC+ bevacizumab (n=31)			
Years of 1L initiation (n, row %)	2016/2017	249 50.1%	68 27.3%	112 45.0%	41 16.5%	22 8.8%	2018/2019	248 49.9%	134 54.0%	34 13.7%	62 25.0%	9 3.6%
Age at 1L initiation, years (mean, SD)	65	9.5	63.0	9.2	64.7	8.4	69.1	10.6	65.5	7.4		
Male (n, %)	285	57.3%	120	59.4%	85	58.2%	53	51.5%	21	67.7%		
Non-squamous*	349	70.2%	146	72.3%	73	50.0%	86	83.5%	31	100%		
Stage IVA/B at diagnosis (n, %)	462	92.9%	185	91.6%	135	92.5%	98	95.1%	30	96.8%		
ECOG-PS 0/1 (n, %)	339	68.6%	156	77.2%	80	55.9%	66	64.1%	29	93.5%		
PD-L1 (n, %)	<1%	99 19.9%	37 18.3%	47 32.2%	0 0.0%	10 32.3%	1-49%	219 44.1%	133 65.8%	59 40.4%	10 9.7%	9 29.0%
	≥ 50%	127 25.6%	29 14.4%	4 2.7%	93 90.3%	0 0.0%	Unknown	52 10.5%	3 1.5%	36 24.7%	0 0.0%	12 38.7%
1L response (PR or CR) (n, %)	275	55.3%	136	67.3%	52	35.6%	62	60.2%	19	61.3%		
1L PFS (median, 95% CI)	11.6 (10.4-12.7)	15.6 (13.4-17.1)	5.3 (4.0-6.0)	17.8 (15.7-32.5)	10.8 (8.4-12.2)							
1L OS (median, 95% CI)	21.2 (18.6-23.0)	26.5 (21.0-NR)	13.7 (9.4-17.3)	NR (24.0-NR)	18.6 (16.9-30.1)							

* All remaining patients with either squamous or mixed histology.

Keys: 1L – first-line; CI – confidence interval; CR – complete response; ECOG-PS – Eastern Cooperative Oncology Group performance status; IO – immunotherapy; NR – not reached; OS – overall survival; PDC – platinum doublet chemotherapy; PDC+IO – platinum doublet chemotherapy plus immunotherapy; PD-L1 – programmed death-ligand 1; PFS – progression-free survival; PR – partial response; SD – standard deviation.

Ethics Approval On August 20, 2020, Western Institutional Review Board (WIRB) approved a request for a waiver of authorization for use and disclosure of protected health information (PHI) for this research. The study is exempt under 45 CFR § 46.104(d)(4).

<http://dx.doi.org/10.1136/jitc-2021-SITC2021.562>

ICT01, AN ANTI-BTN3A MAB, AND NL-201, AN ALPHA-INDEPENDENT IL-2/IL-15 AGONIST, COMBINE TO ELICIT A POTENT ANTI-TUMOR RESPONSE BY SYNERGISTICALLY STIMULATING VG9VD2 T CELL ACTIVATION AND PROLIFERATION

¹Aude De Gassart*, ¹Patrick Brune, ¹Maelle Mairesse, ¹Sophie Agaugué, ²Ryan Swanson, ¹Loui Madakamutil, ²Carl Walkey, ¹Paul Frohna. ¹*ImCheck Therapeutics, Marseille, France;* ²*Neoleukin Therapeutics Inc, Seattle, WA, USA*

Background γ 9 δ 2 T-cells are attractive mediators of cancer immunotherapy due to their strong cytolytic and pro-inflammatory activities and the positive correlation between tumor infiltration and good prognosis [1,2]. ICT01, a novel anti-BTN3A mAb activating γ 9 δ 2 T-cells, is being evaluated in a Phase 1/2a clinical study (NCT04243499)[3,4]. Previous studies have shown that IL-2 (Proleukin[®]) promotes γ 9 δ 2 T-cells expansion following ICT01 stimulation, which may be clinically useful given that γ 9 δ 2 T-cells are normally <5% of total T-cells [5]. However, the severe toxicity of IL-2 has limited its widespread use. NL-201 is a de novo alpha-independent IL-2/IL-15 agonist that preferentially stimulates CD8 T and NK cell proliferation at low concentrations, enabling a potentially wider therapeutic index than IL-2, and is being evaluated in a Phase 1 clinical study (NCT04659629)[6,7]. Here, we explore the potential of ICT01 and NL-201 to synergistically stimulate the activation and proliferation of γ 9 δ 2 T-cells.

Methods Flow cytometry was used to assess IL-2R signaling (pSTAT5), and γ 9 δ 2 T-cell activation and expansion after in vitro culture of huPBMCs with ICT01, NL201 or the combination. Tumor cell killing activity was monitored upon co-culture of huPBMCs with tumor cell lines (Incucyte). In vivo pharmacology was performed in NCG mice engrafted with 20x10⁶ huPBMCs and treated with ICT01 (1 mg/kg IV)±NL-201 (1, 3 or 10 μ g/kg IV). Immune cells were phenotyped by flow cytometry in blood and organs collected at sacrifice (Day 16).

Results NL-201 is ~100X more potent than IL-2 in triggering IL-2R signaling in γ 9 δ 2 T-cells, without preferential activity on Tregs. NL-201 plus ICT01 induces synergistic expansion of γ 9 δ 2 T-cells, approaching ~50% of T-cells after 8 days versus ~10% with single agents. In addition, the combination of NL-201 and ICT01 promotes γ 9 δ 2 T-cell effector memory differentiation, in contrast to IL-2, which induces primarily central memory phenotype. Importantly, NL-201 enhances ICT01-mediated killing of cancer cells by γ 9 δ 2 T-cells. In mice, a dose-dependent expansion of peripheral γ 9 δ 2 T-cells from ~1–2% at baseline to up to 40% of T-cells was observed in the ICT01+NL-201 combination groups. Consistently, γ 9 δ 2 T-cell number and frequency increase in spleen and lungs of the ICT01+NL-201 treated animals as compared to controls. Expanded γ 9 δ 2 T-cells in the combination groups display an effector memory phenotype, confirming our in vitro results.

Conclusions These results demonstrate the ability of the ICT01+NL-201 combination to synergistically trigger γ 9 δ 2 T-cell activation, expansion and anti-tumor activity and support clinical evaluation of this combination as a novel therapeutic approach for cancer patients.

REFERENCES

- Gentles, A. J. et al. The prognostic landscape of genes and infiltrating immune cells across human cancers. *Nat Med* 21, 938–945, doi:10.1038/nm.3909 (2015).
- Tosolini, M. et al. Assessment of tumor-infiltrating TCRVgamma9Vdelta2 gamma-delta lymphocyte abundance by deconvolution of human cancers microarrays. *Oncoimmunology* 6, e1284723, doi:10.1080/2162402X.2017.1284723 (2017).

- Gassart, A. d. et al. 687 Enhancement of anti-tumor immunity by ICT01: a novel γ 9 δ 2 T cell-activating antibody targeting butyrophilin-3A (BTN3A). *Journal for Immunotherapy of Cancer* 8, A412-A413, doi:10.1136/jitc-2020-SITC2020.0687 (2020).
- Marabelle, A. et al. 316 EVICTION Study: Preliminary results in solid tumor patients with ICT01, a first-in-class, gamma9 delta2 T cell activating antibody targeting butyrophilin-3A. *Journal for Immunotherapy of Cancer* 8, A194-A195, doi:10.1136/jitc-2020-SITC2020.0316 (2020).
- Gassart, A. d. et al. 442 ICT01, an anti-BTN3A mAb that activates Vg9Vd2 T cells, plus interleukin-2: a potent and promising combination for cancer immunotherapy. *Journal for Immunotherapy of Cancer* 8, A268-A269, doi:10.1136/jitc-2020-SITC2020.0442 (2020).
- Walkey, C., Swanson, R., Ulge, U., Silva Manzano, D. A. & Drachman, J. 576 NL-201, a de novo IL-2 and IL-15 agonist, demonstrates enhanced in vivo antitumor activity in combination with multiple cancer immunotherapies. *Journal for Immunotherapy of Cancer* 8, A346-A346, doi:10.1136/jitc-2020-SITC2020.0576 (2020).
- Walkey, C. D. et al. Abstract 4518: Pre-clinical development of NL-201: A *de novo* α -independent IL-2/IL-15 agonist. *Cancer Research* 80, 4518–4518, doi:10.1158/1538-7445.Am2020-4518 (2020).

Ethics Approval All procedures involving animals described in this study have been reviewed and approved by the local ethic committee (CELEAG) and the French Ministry of Research.

<http://dx.doi.org/10.1136/jitc-2021-SITC2021.563>

564

SINGLE-CELL TRANSCRIPTOMIC ANALYSIS OF IMMUNE COMPARTMENTS FOLLOWING COMBINATION IMMUNOTHERAPY TREATMENT IN POORLY IMMUNOGENIC TUMORS

¹Ang Cui*, ²Kelly Moynihan, ¹Shuqiang Li, ²Chensu Wang, ³Jackson Southard, ¹Nir Hacohen, ²Darrell Irvine. ¹Broad Institute of MIT and Harvard, Cambridge, MA, USA; ²MIT, Cambridge, MA, USA; ³Dana-Farber Cancer Institute, Boston, MA, USA

Background A major goal in cancer immunology is to rationally design combination therapies that lead to a higher response rate, especially for poorly immunogenic tumors that do not respond to immune checkpoint blockade therapy alone. We previously developed a combination therapeutic strategy, termed AIPV, consisting of a tumor-targeting antibody, a recombinant interleukin-2 with an extended half-life, an anti-PD-1 antibody, and a T cell vaccine [1]. The full AIPV therapy can eradicate large, aggressive, poorly immunogenic tumors in multiple mouse tumor models. However, the exact cellular and molecular pathways involved in such an effective response remain poorly understood.

Methods In this study, we used single-cell RNA-sequencing to define the detailed cellular and molecular changes in tumors and tumor-draining lymph nodes following the full AIPV therapy or a less effective sub-combination therapy in mice with poorly immunogenic B16F10 tumors.

Results Using our approach, we were able to uncover T cells, NK cells, neutrophils, macrophages/monocytes, classical dendritic cells, and plasmacytoid dendritic cells in tumors. We observed profound remodeling of every immune cell type following the effective therapeutic treatment. In particular, we found that classical dendritic cells take up tumor antigens, become activated, and migrate to draining lymph nodes following the AIPV therapy, but not following the less effective IPV therapy. We characterized the transcriptomic changes of these dendritic cells and found that they over-express molecules involved in antigen uptake.

Conclusions Our study comprehensively characterized a system that can overcome resistance to immune checkpoint blockade therapy, paving a cellular and molecular roadmap for immune-based therapeutic strategies that offer clinical benefits for poorly immunogenic tumors.

REFERENCES

1. Moynihan KD, Opel CF, Szeto GL, Tzeng A, Zhu EF, Engreitz JM, et al. Eradication of large established tumors in mice by combination immunotherapy that engages innate and adaptive immune responses. *Nat Med.* 2016;22: 1402–1410.

Ethics Approval All mouse experiments were reviewed and approved by the Koch Institute and Broad Institute Animal Care and Use Committee (IACUC) (ID 0222-08-18).

<http://dx.doi.org/10.1136/jitc-2021-SITC2021.564>

565 **COMBINATORIAL HSCS AND ANTI-PD-1 THERAPY IN
MICROSATELLITE STABLE COLORECTAL CANCER**

Bayli DiVita Dean*, John Figg, Laura Falceto Font, Connor Francis, Duane Mitchell, Catherine Flores. *University of Florida, Gainesville, FL, USA*

Background Colon cancer (CRC) is the second leading cause of cancer-related deaths in the US. CRC incidence is on the rise and there is an alarming increase in young onset CRC cases. Immune checkpoint inhibitors (ICIs) have yielded promising anti-tumor results in microsatellite instable high (MSI-high) patients, which represent only 15% of tumors. The remaining 85% are denoted as microsatellite stable (MSS) and are unresponsive to ICI. Using a murine glioma model, our group has previously found the combination of anti-PD-1 and a transfer of hematopoietic stem cells (HSCs) can sensitize mice that are resistant to anti-PD-1 alone. We evaluated survival after treatment with this combinatorial platform 3 or 5 days post-implantation in subcutaneous CRC-bearing mice and also phenotyped the splenic compartment of mice at endpoint. **Methods** 1×10^6 MSS CRC cells, CT26, were subcutaneously injected into the right flank of BALB/cJ mice. 3 or 5 days later, HSCs were isolated from naïve BALB/cJ mice and injected through the tail vein into CT26-bearing mice and were also given 10 mg/kg anti-PD-1. Mice were given 3 additional doses of anti-PD-1 for a total of doses either every 3 or 5 days. Mice were sacrificed when tumors reached 1.5 cm at its widest point and spleens were excised and stained for flow cytometry.

Results When mice were treated with HSC/anti-PD-1 3 days post-tumor implantation, we observed a statistically significant increase in survival in mice that received combinatorial HSCs and anti-PD-1 relative to no treatment control mice ($p=0.0034$, Mantel-Cox long-rank test) as well as mice that received HSCs alone ($p=0.0462$, Mantel-Cox log-rank test). In the same 3 day cohort, no differences in the frequency of T cell populations were observed. However, we found mice that received this combination therapy had a significant increase in the frequency of splenic CD11c+ MHC II+ dendritic cells (DCs) relative to no treatment control mice ($p=0.0364$, Mann-Whitney t test). When mice were treated with HSC/anti-PD-1 5 days post-tumor implantation, we found a statistically significant increase in survival of mice treated with combinatorial HSCs and anti-PD-1 compared to no treatment control mice ($p=0.0024$, Mantel-Cox log-rank test) and relative to mice that received HSC monotherapy ($p=0.0462$, Mantel-Cox log-rank test).

Conclusions These results suggest combinatorial HSCs and anti-PD-1 represents a promising therapeutic axis in a murine model of MSS CRC. In addition, the increase in splenic DCs suggests the mechanism behind this anti-tumor response may be expansion of DCs within the periphery.

Ethics Approval All animal work approved through University of Florida IACUC # 201910777

<http://dx.doi.org/10.1136/jitc-2021-SITC2021.565>

ATOR-1017, A SECOND GENERATION 4-1BB ANTIBODY WITH POTENTIAL TO ENHANCE EFFICACY OF PD-1 THERAPIES

¹Karin Enell Smith*, ¹Anneli Nilsson, ²Peter Ellmark. ¹Alligator Bioscience, Lund, Sweden; ²Alligator Bioscience AB, Lund, Sweden

Background ATOR-1017 is a Fc γ -receptor (Fc γ R) crosslinking dependent agonistic IgG4 antibody targeting the costimulatory receptor 4-1BB, designed for improved tolerability and efficacy. 4-1BB is highly expressed on tumor infiltrating CD8+ T effector cells (T effs) in several cancer indications. By binding to 4-1BB, ATOR-1017 enhances the activity of tumor reactive T effs and NK cells within the tumor and induces a potent anti-tumor response. 4-1BB is a promising candidate for immunotherapy and holds great potential for combination with other immunomodulatory antibodies, targeting e.g. the PD-1 pathway.

Methods Human 4-1BB knock-in transgenic mice with established murine colon carcinoma MC38 tumors were used to demonstrate anti-tumor efficacy after systemic treatment with ATOR-1017 in combination with anti-PD-1. Further, the effect of combining ATOR-1017 with anti-PD-1 on T cell activation (measured as production of IFN γ) was evaluated in a mixed lymphocyte reaction (MLR) assay with human primary CD4+ T cells and mature monocyte-derived DCs (mDC) expressing endogenous levels of both 4-1BB and PD-1.

Results ATOR-1017 in combination with anti-PD-1 improved survival and reduced tumor growth significantly in human 4-1BB knock-in transgenic mice with established tumors compared with each monotherapy alone. The potential for combining ATOR-1017 and PD-1 was further supported by data from a MLR assay demonstrating that the combination of ATOR-1017 with anti-PD-1 induced a more potent CD4+ T cells activation than each monotherapy alone. The functional activation profile of ATOR-1017 is expected to minimize the risk of systemic immune activation and toxicity, by directing a potent immune response to immune cells in tumor tissue and tumor draining lymph nodes. This is supported by early data from the ongoing first-in-human phase I study where ATOR-1017 has been shown to be safe and tolerable.

Conclusions In summary, these results support further clinical development of ATOR-1017 in combination with PD-1 antibodies. By combining ATOR-1017 with anti-PD-1, tumor infiltrating T cells can be more effectively activated and potentially increase the response rate in multiple indications.

Ethics Approval All animal procedures were in accordance to IACUC guidance

<http://dx.doi.org/10.1136/jitc-2021-SITC2021.566>

ISOFORM SPECIFIC ANTI-TGF β THERAPY ENHANCES ANTITUMOR EFFICACY IN MOUSE MODELS OF STROMA POOR CANCERS

¹Sadna Budhu*, ²Aditi Gupta, ²Kelly Fitzgerald, ²Rachel Giese, ²Adam Michel, ²Aliya Holland, ²Luis Felipe Campesato, ³Jacques Van Snick, ³Catherine Uyttenhove, ³Gerd Ritter, ²Jedd Wolchok, ²Taha Merghoub. ¹Memorial Sloan-Kettering Cancer Center, New York, NY, USA; ²Memorial Sloan Kettering Cancer Center, New York, NY, USA; ³Ludwig Institute for Cancer Research, Brussels, Belgium

Background TGF β is a potential target in cancer treatment due to its dual role in tumorigenesis and homeostasis. There are three isoforms of TGF β (TGF β 1, TGF β 2 and TGF β 3), which are secreted by immune and non-immune cells as an inactive latent complex. Depending on the local context and players, TGF β can adopt opposing roles in carcinogenesis and in modulating the immune system. However, the expression of TGF β and its inhibition within the tumor microenvironment has mainly been investigated in stroma-rich tumors.

Methods We examined expression of TGF β 1 and TGF β 3 isoforms on immune cells in two stroma-poor mouse tumor models (B16 melanoma and CT26 colon carcinoma) and investigated the anti-tumor efficacy of antibodies that block TGF β 1 and TGF β 3 in these two models.

Results Depending on local expression of TGF β isoforms, specific inhibition of either TGF β 1 or TGF β 3 may be effective. The "TGF β signature" of CT26 colon carcinoma is defined by TGF β 1 expression on immune cells and TGF β 1 inhibition results in tumor delay; B16 melanoma has equal expression of both TGF β 1 or TGF β 3 isoforms and inhibition of either TGF β 1 or TGF β 3 controls tumor growth. We show that the mechanism of tumor growth delay is enhanced CD8+ T cell activation and effector function. In addition, we found that combining TGF β inhibition with immune checkpoint blockade results in improved tumor control and survival.

Conclusions Our findings suggests that expression of TGF β isoforms in the TME is variable in different tumor types and their expression may be used to predict anti-tumor responses to TGF β inhibition. Isoform specific TGF β inhibition in stroma poor tumors shifts the local immune environment to favor tumor regression alone or in combination with immune checkpoint blockade.

<http://dx.doi.org/10.1136/jitc-2021-SITC2021.567>

TUMOR-DERIVED GDF-15 PREVENTS THERAPY SUCCESS OF CHECKPOINT INHIBITORS BY BLOCKING T-LYMPHOCYTE RECRUITMENT

¹Markus Haake, ²Tina Schäfer, ²Beatrice Haack, ¹Neha Vashist, ³Sabrina Genßler, ⁴Patrick Harter, ⁵Alexander Martens, ⁶Kilian Wistuba-Hamprecht, ²Florian Wedekink, ²Birgitt Fischer, ⁷Michel Mittelbronn, ⁸Mitchell Levesque, ⁸Phil Cheng, ⁸Reinhard Dummer, ⁶Benjamin Weide, ¹Kathrin Klar, ¹Eugen Leo, ⁹Falk Nimmerjahn, ¹Christine Schubert-Wagner, ²Jörg Wischhusen*. ¹CatalYm GmbH, Planegg, Germany; ²Würzburg University Hospital, Würzburg, Germany; ³CatalYm GmbH, Planegg, Germany; ⁴German Cancer Consortium, Frankfurt, Germany; ⁵University of Tuebingen, Tuebingen, Germany; ⁶University of Tubingen, Tuebingen, Germany; ⁷University of Luxembourg, Luxembourg, Luxembourg; ⁸University of Zurich Hospital, Zurich, Switzerland; ⁹University of Erlangen, Erlangen, Germany

Background Immune checkpoint blockade (ICB) can achieve durable responses in a subgroup of patients with metastatic cancer, only. Poor immune effector cell infiltration into the tumor microenvironment is a major obstacle to successful therapy. Growth and differentiation factor 15 (GDF-15) is a divergent member of the TGF- β superfamily and has been linked to feto-maternal tolerance, anorexia but recently also to potent local immunosuppression under physiologic and pathophysiologic conditions. GDF-15 is overexpressed in a wide variety of tumors and may be key factor produced by tumors to prevent effective immune cell infiltration into the tumor and to potentially block checkpoint inhibitor activity.

Methods Effects of recombinant GDF-15 and a proprietary GDF-15 neutralizing antibody (CTL-002) on immune cell trafficking and activation were analyzed by adhesion and interaction assays and in melanoma-bearing humanized mouse models. The impact of GDF-15 overexpression was tested in subcutaneously implanted, GDF-15-transgenic MC38 cells. Additionally, patient GDF-15 serum levels were correlated with immune infiltration and OS in cutaneous melanoma. Associations between GDF-15 serum levels, response to PD-1-based ICB and corresponding OS were assessed in two independent cohorts of melanoma patients.

Results GDF-15 impairs adhesion of T and NK cells on activated endothelia. In HV18-MK bearing humanized mice, inhibition of GDF-15 strongly enhances infiltration of activated myeloid and lymphoid cells. In MC38 tumors, GDF-15 overexpression can abrogate tumor rejection upon anti-PD-1 therapy. 50% of the mice with GDF-15 overexpressing tumors were, however, rescued when anti-PD-1 was combined with anti-GDF-15 (CTL-002). Likewise, anti-GDF-15 improved responses to anti-CD40 + poly(I:C) in the same tumor model. Clinically, inverse correlations of GDF-15 levels with CD8+ T cell infiltration were shown for melanoma brain metastases. In two independent melanoma patient cohorts, low baseline serum GDF-15 levels predicted clinical response to anti-PD1 treatment and superior OS. Bivariate analysis including LDH indicates that GDF-15 is an independently predictor for poor survival in anti-PD-1 treated melanoma patients.

Conclusions Tumor-derived GDF-15 blocks the infiltration of immune effector cells into tumor tissues. Neutralizing GDF-15 with CTL-002 restores the ability of immune cells to extravasate blood vessels and enter the tumor microenvironment in vivo. GDF-15 thus represents a promising target for cancer immunotherapy. Antibodies against GDF-15 may support treatments with anti-PD-1 and other immunotherapeutic agents. A clinical trial combining anti-GDF-15 (CTL002) with anti-PD-1 (NCT04725474, submitted Abstract ID 15073) is ongoing.

Ethics Approval Use of patient samples for this study had been approved by the institutional ethics committee Tübingen

(ethic vote 125/2015BO2). Use of surplus sera collected in the University of Zurich Hospital (USZ) Biobank during routine blood draws from consenting metastatic melanoma patients was performed according to IRB approval (KEK.Zh- 647/800) and followed the Declaration of Helsinki on Human Rights.

Consent All patients had given written informed consent to have clinical data recorded by the Central Malignant Melanoma Registry (CMMR) database.

<http://dx.doi.org/10.1136/jitc-2021-SITC2021.568>

569 A NOVEL MICROBIOME-DERIVED PEPTIDE REVERSES RESISTANCE TO ANTI-PD-1 THERAPY

Dhwani Haria*, Jayamary Divya Ravichandar, Jill Desnoyer, Sabina Lau, Jina Lee, Erica Rutherford, Preeti Lal, Karim Dabbagh, Helena Kiefel. *Second Genome, Inc, Brisbane, CA, USA*

Background Despite the unprecedented clinical success of immune checkpoint therapy (ICI) in many cancers there is still a large unmet need since many patients have an inadequate response. Fecal Matter Transplant from anti-PD-1 responding subjects into non-responders improves response in many subjects, providing a strong rationale that the gut microbiome has a critical role in modulating effects of ICI therapies. However, the causative mechanisms and host targets that mediate these beneficial therapeutic effects are still poorly understood. The objective of the present study was to demonstrate that peptides derived from the microbiome of ICI responders, have the potential to bring a similar therapeutic benefit to ICI non-responders via direct immunomodulatory effects through a host target.

Methods Using Second Genome's proprietary algorithms, we derived a microbial signature that was enriched in responding subjects across multiple cohorts. The peptides identified from these strains were screened in a classical drug discovery pipeline to discover peptides that modulate the human immune system by secreting proinflammatory cytokines and chemokines such as CXCL10 and TNF- α by human dendritic cells (DCs), and mediate anti-tumor immunity and improve response to anti-PD-1 therapy in mouse tumor models.

Results We found several peptides which bind primary human cells, exert immune function, and exert anti-tumor effects. Particularly, peptide SG-3-00802 showed improved anti-tumor responses in combination with anti-PD-1 in the anti-PD-1 insensitive RENCA model. Treatment with SG-3-00802, alone or in combination with anti-PD-1 significantly improved overall survival with many animals showing complete tumor regression. Surviving animals with fully regressed tumors rejected newly implanted tumors when rechallenged with RENCA cells, indicating that combination treatment of SG-3-00802 + anti-PD-1 generates long lasting anti-tumor memory responses.

Conclusions Microbiome interacts with the human immune system to impact anti-tumor immunity. Microbiome-derived peptides identified by Second Genome's discovery platform sg4sight modulate innate immune cells e.g. dendritic cells to promote anti-tumor immunity. SG-3-00802 peptide has the greatest potential to impact subjects who are potentially going to be non-responders to anti-PD-1 or have derived inadequate response to ICI therapies.

<http://dx.doi.org/10.1136/jitc-2021-SITC2021.569>

570

BLOCKADE OF THE INHIBITORY COLLAGEN RECEPTOR LAIR-1, PD-L1, AND TGF- β PROMOTES ANTI-TUMOR ACTIVITY THROUGH T CELL ACTIVATION AND MYELOID CELL POLARIZATION

¹Lucas Horn*, ¹Haiyan Qin, ¹Kristen Fousek, ¹Masafumi Iida, ²Dallas Flies, ²Ronald Copeland, ²Zachary Cusumano, ²Han Myint, ²Solomon Langermann, ¹Jeffrey Schlom, ¹Claudia Palena. ¹National Cancer Institute, Bethesda, MD, USA; ²NextCure, Beltsville, MD, USA

Background Leukocyte-associated immunoglobulin-like receptor 1 (LAIR-1) is an immune inhibitory receptor that binds collagen-like domains commonly found in extracellular matrix (ECM) collagens and complement component C1q. LAIR-1 is expressed on several immune cell types including activated T cells, B cells, NK cells, dendritic cells, and macrophages. Numerous cancer types including gastric, colon, ovarian, bladder, and others, upregulate collagens which enhances tumor growth, metastases, and invasion while actively suppressing antitumor immunity. While a soluble decoy, LAIR-2, is expressed in humans and competes with LAIR-1 for binding of collagen domains, excess LAIR ligands in the tumor often result in an immune suppressive environment.

Methods Here, we report on a novel immunotherapy approach combining NC410, a novel fusion protein consisting of two LAIR-2 molecules grafted on to an IgG1 antibody backbone, capable of targeting the tumor ECM and blocking LAIR-1 signaling; and bintrafusp alfa, a first-in-class bifunctional fusion protein composed of the extracellular domain of the human transforming growth factor β receptor II (TGF- β RII or TGF- β "trap") fused via a flexible linker to the C-terminus of each heavy chain of an IgG1 antibody blocking programmed death ligand 1 (anti-PD-L1).

Results We have demonstrated that the combination of NC410 and bintrafusp alfa more effectively controls in vivo tumor growth of the collagen rich MC38 colon and EMT6 mammary carcinomas compared to either monotherapy. We demonstrate that this potent anti-tumor immune response is propagated through the synergy of activated tumor infiltrating lymphocytes and a repolarization of myeloid cells in the tumor microenvironment. MC38 tumors treated with the combination of NC410 plus bintrafusp alfa contained higher numbers of infiltrating T cells, NK cells, and M1 polarized macrophages.

Conclusions This study highlights the synergy of reshaping the large suppressive myeloid cell populations often present in tumors with activation of adaptive T-cell immune responses dampened by checkpoint inhibition. The results also provide the rationale for the future evaluation of this combination therapy in the clinic.

<http://dx.doi.org/10.1136/jitc-2021-SITC2021.570>

571

IL-2 COMBINATION WITH IMM-TAC OVERCOMES CD163 + TAM-LIKE M2 MACROPHAGE INHIBITION OF IMM-TAC-MEDIATED T CELL KILLING OF TUMOR CELLS

Rahul Khanolkar*, Revashnee Naidoo, Esra Güç, Emma Leach, Sarah Stanhope, Duncan Gascoyne, Laura Collins, Koustubh Ranade, Adel Benlahrech. *Immunocore, Abingdon, UK*

Background ImmTAC molecules are bispecific fusion proteins consisting of an affinity-enhanced T cell receptor fused to an anti-CD3 effector that can redirect T cells to target cells. Tebentafusp, a gp100-directed ImmTAC, has demonstrated survival benefit in metastatic uveal melanoma [1]. We previously reported that a tumor microenvironment with a high immunosuppressive CD163+ tumor-associated macrophage (TAM): CD3 T cell ratio was associated with reduced benefit from tebentafusp [2]. Here, we explored whether IL-2 could potentiate T cells to overcome inhibition of ImmTAC-mediated killing by TAM-like M2 macrophages.

Methods Tumor biopsies from a Phase 2 trial of metastatic uveal melanoma HLA-A*02:01+ patients treated with tebentafusp (NCT02570308) were used to quantify CD163+ TAMs and CD3+ T cells by immunohistochemistry (N=107) and to measure gene expression by bulk RNAseq (N=70). Pro-inflammatory M1 and TAM-like M2 macrophages were generated in vitro from healthy donors (N=5) and their effect on ImmTAC-mediated T cell activation and tumor killing was assessed against THP-1 tumor cells. T cells were untreated or pre-treated for 4 days with commercially sourced IL-2 or IL-15.

Results In vitro, ImmTAC-mediated T cell killing of tumor cells was reduced by 85±5% in the presence of TAM-like M2 but not M1 macrophages. Consistent with this finding, below median CD163:CD3 ratio was associated with greater tumor shrinkage (TS) (odds ratio OR=2.9, p=0.014) and longer overall survival (OS) (hazard ratio HR=0.4, p=0.001) in tebentafusp-treated patients. We next explored in vitro whether the T cell activating cytokines IL-2 and IL-15 could overcome TAM-mediated inhibition of T cell redirection by ImmTAC. At clinically relevant doses, IL-2 but not IL-15 treatment resulted in dose dependent restoration of ImmTAC-mediated T cell killing of tumor cells in the presence of TAM-like M2 macrophages—60% and 83% restoration of killing at 50 and 150 U/ml of IL-2, respectively. Consistent with this observation, increased expression of IL2RB (HR 0.3, p<0.001) and IL2RG (HR 0.4, p=0.002), but not IL2RA (HR 0.8, p=0.5) in tumors was associated with longer OS on tebentafusp.

Conclusions Low CD163+ TAM to CD3 T cell ratio and high IL2RB/G expression in tumors at baseline were associated with longer OS and greater TS in tebentafusp-treated metastatic uveal melanoma patients in a Phase 2 trial. In vitro, TAM-like M2 macrophages suppressed ImmTAC-mediated T cell killing of tumor cells, an effect abrogated by IL-2. These observations provide strong rationale for combining IL-2 biased to IL2RB/G with ImmTAC molecules to enhance benefit in tumors with high levels of TAMs.

Trial Registration NCT02570308

REFERENCES

1. Piperno-Neumann S, Hassel JC, Rutkowski P et al. Abstract CT002: Phase 3 randomized trial comparing tebentafusp with investigator's choice in first line metastatic uveal melanoma. *Cancer Res.* 2021; 81 (13 Supplement) CT002.
2. Hassel JC, Benlahrech A, Stanhope S, et al. Abstract 1673: Uveal melanoma study patients with low CD163:CD3 ratio in tumor biopsy and low serum IL-6

showed enhanced tumor shrinkage (TS) and overall survival (OS) on tebentafusp. *Cancer Res.* 2021; 81 (13 Supplement) 1673.

Ethics Approval The Oxford A REC approved protocol 13/SC/0226 was used to obtain written consent for all blood donations and was fully approved by the National Research Ethics Committee South Central.

<http://dx.doi.org/10.1136/jitc-2021-SITC2021.571>

572 COMBINATION THERAPY OF EXOSTING, EXOIL-12 ACTIVATES SYSTEMIC ANTI-TUMOR IMMUNITY

Katherine Kirwin*, Su Chul Jang, Christine Sia, Kevin Dooley, Tong Zi, Kelvin Zhang, Yanyan Liu, Kyriakos Economides, Shil Patel, Sriram Sathyanarayanan. *Codiak BioSciences, Cambridge, MA, USA*

Background Engineered exosomes are emerging as a novel therapeutic modality for cancer immunotherapy. Leveraging cell type specific delivery, tumor restricted pharmacology and compartmental dosing, exosome-based immunotherapy can elicit a tumor specific immune response that may not be achievable with other traditional drugging modalities. Pre-clinical studies have shown that exosomes loaded with a STING agonist (exoSTINGTM) or engineered to express the cytokine interleukin-12 (exoIL-12TM) can substantially improve potency and selectivity resulting in improved therapeutic window [1,2]. Both exoSTING and exoIL-12 are currently in clinical trials in cancer patients. Utilizing a combination strategy involving exoSTING and exoIL-12, we demonstrate the development of potent systemic anti-tumor responses in both injected and non-injected tumors.

Methods exoSTING exosomes are engineered to overexpress PTGFRN, an abundant exosome surface protein, and loaded *ex vivo* with a proprietary STING agonist. exoIL-12 exosomes are engineered to overexpress functional IL-12 attached via fusion to PTGFRN. In these studies, exoSTING and exoIL-12 were dosed intratumorally into one flank tumor into mice bearing dual flank subcutaneous MC38 or B16F10 tumors, or B16F10 single flank subcutaneous tumors with B16F10 lung metastases. T-cell infiltration in the non-injected tumor was monitored by histopathology.

Results In the checkpoint therapy refractory B16F10 melanoma dual flank tumor model, exoSTING/exoIL-12 combination provided 93% and 78% tumor growth inhibition (TGI) in both the injected and non-injected tumors, respectively, whereas monotherapy of exoSTING or exoIL-12 provided modest anti-tumor activity (44% and 48% TGI) in the non-injected tumors, respectively. In a MC38 subcutaneous CRC model, the addition of anti-PD-1 checkpoint inhibitor further enhanced anti-tumor activity with 100% TGI (7/7 CR) in injected and non-injected tumors. The tumor free animals were refractory to tumor re-challenge demonstrating immunological memory. A dosing schedule optimization experiment showed that same day dosing of exoSTING and exoIL-12 significantly inhibited the tumor growth in the non-injected tumors. In a lung metastasis model, the triple combination also showed potent anti-tumor effect in decreasing distal lung metastases when dosed intratumorally into the subcutaneous tumors. Subsequent imaging and histology studies demonstrated enhanced T cell infiltration in the non-injected subcutaneous tumor with the combination therapy.

Conclusions By combining both exosome immunotherapies with a checkpoint blockade, we are able to elicit systemic anti-tumor immune immunity in both injected and non-injected tumors.

REFERENCES

1. Jang SC, Economides KD, Moniz RJ, et al. ExoSTING, an extracellular vesicle loaded with STING agonists, promotes tumor immune surveillance. *Commun Biol.* 2021;4(1):497.
2. Lewis ND, Sia CL, Kirwin K, et al. Exosome surface display of IL12 results in tumor-retained pharmacology with superior potency and limited systemic exposure compared with recombinant IL12. *Mol Cancer Ther.* 2020;20(3):523-534.

Ethics Approval All animals were maintained and treated at the animal care facility of Codiak Biosciences in accordance with the regulations and guidelines of the Institutional Animal Care and Use Committee (CB2020-001).

<http://dx.doi.org/10.1136/jitc-2021-SITC2021.572>

573

FS120, AN OX40/CD137 TETRAVALENT BISPECIFIC DUAL AGONIST ANTIBODY, SYNERGISTICALLY INCREASES THE ANTITUMOR ACTIVITY OF ANTI-PD-1 IN PRECLINICAL STUDIES

Matthew Lakins*, Wenjia Liao, Emma McConnell, Quincy Kaka, Jennifer Ofoedu, Cristian Gradinaru, Raffaella Giambalvo, Miguel Gaspar, Edmund Poon, Michelle Morrow, Neil Brewis. *F-star Therapeutics Inc, Cambridge, UK*

Background Immune checkpoint inhibitors have demonstrated durable clinical responses and an increase in overall survival for some patients with cancer. Next generation cancer immunotherapies, such as tumor necrosis factor receptor superfamily (TNFRSF) agonists, have potential to further improve on this success. FS120 is a tetravalent bispecific antibody targeting OX40 and CD137 (4-1BB), currently being evaluated in a Phase I clinical trial (NCT04648202). FS120 activates CD4⁺ and CD8⁺ T cells by concurrent binding to both targets via an FcγR-independent mechanism [1]. In preclinical tumor models, FS120 induced T cell proliferation and cytokine production associated with significant tumor regression, better than that observed with a monoclonal antibody combination. Here, we demonstrate the ability of FS120 to improve anti-PD-1 induced T cell activity, increasing tumor growth inhibition and survival, in syngeneic mouse tumor models, compared to monotherapy.

Methods FS120 *in vitro* activity in combination with anti-PD-1 was assessed by utilizing staphylococcal enterotoxin A (SEA) superantigen assays and mixed leukocyte reaction (MLR) assays. An anti-mouse OX40/CD137 bispecific antibody (FS120 surrogate) was tested in CT26 syngeneic mouse tumor models in combination with an anti-mouse PD-1 antibody to assess efficacy and pharmacodynamic endpoints, including T cell proliferation by *ex vivo* flow cytometry and serum cytokine levels.

Results FS120 in combination with anti-PD-1 enhanced primary human T cell activity, when compared to either monotherapy, in both SEA and MLR assays. FS120 surrogate significantly improved survival of CT26 tumor-bearing mice treated with anti-mPD-1 antibody. FS120 surrogate and anti-PD-1 combination significantly enhanced serum interferon-gamma levels and increased proliferating granzyme B⁺ CD8⁺ T cells in the blood of tumor-bearing mice, when compared to either monotherapy treatments.

Conclusions FS120 combination with anti-PD-1 enhances T cell activity in multiple human primary immune assays. In combination with anti-PD-1, FS120 surrogate increased the antitumor efficacy with pharmacodynamic changes related specifically to T cell activation, when compared to monotherapies. These data support the development of FS120 in combination with anti-PD-1 in patients with hard-to-treat cancers who may not benefit fully from either treatment as a monotherapy.

REFERENCES

1. Gaspar M, Pravin J, Rodrigues L, Uhlenbroich S, Everett K L, Wollerton F, Morrow M, Tuna M, Brewis N. CD137/OX40 Bispecific Antibody Induces Potent Antitumor Activity that Is Dependent on Target Coengagement. *Cancer Immunol Res.* 2020; (8) (6) 781–793

Ethics Approval Murine studies were conducted under a U.K. Home Office License in accordance with the U.K. Animal (Scientific Procedures) Act 1986 and EU Directive EU 2010/63.

<http://dx.doi.org/10.1136/jitc-2021-SITC2021.573>

574

MULTIPLEX MICROSCOPY REVEALS UNIQUE SPATIOTEMPORAL EFFECTS OF CANCER IMMUNOTHERAPIES

¹Vivien Maltez*, ²Katelyn Byrne, ¹Ronald Germain. ¹National Institutes of Health, Bethesda, MD, USA; ²University of Pennsylvania, Philadelphia, PA, USA

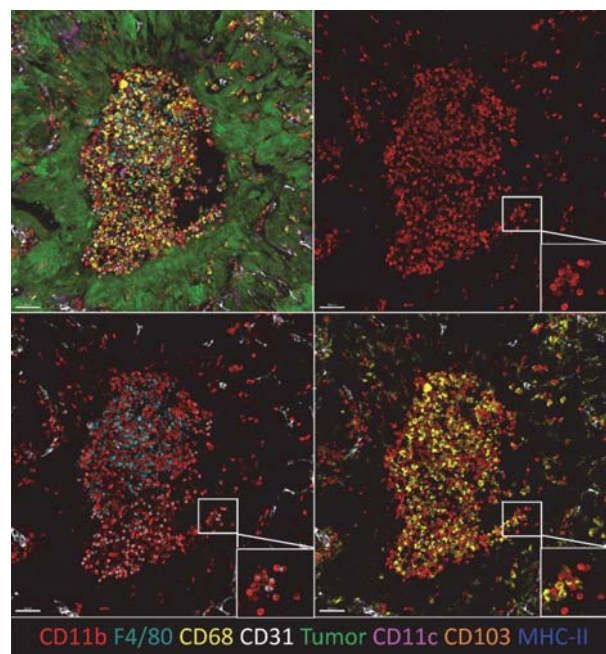
Background Pancreatic ductal adenocarcinoma (PDA) is an aggressive and insidious cancer because it often remains undetectable until later stages and is typically refractory to current treatments. Additionally, the tumor microenvironment (TME) of PDA tumors is immunologically heterogeneous, which complicates therapies like checkpoint blockade. Many mouse models fail to recapitulate the tumor heterogeneity seen in human cancer, something that has severely constrained our understanding of the mechanistic response to therapy. To address this issue, we are using a library of tumor clones derived from the mouse model of PDA that elicit a spectrum of reproducibly unique immune cell infiltration profiles upon implantation into C57Bl/6 mice. Clones with high numbers of infiltrating T cells (T cell high-TCH) are responsive to a combination of checkpoint blockade and CD40 therapies, while clones with low numbers of infiltrating T cells (T cell low-TCL) are not [1]. However, the analysis of the TME in these divergent tumors is quite limited, and emerging high content imaging methods able to reveal the phenotype, activity, and spatial organization of the many cellular populations within these tumors remain to be employed.

Methods 1) Histocytometry: quantitative analysis of microscopy images that combines the spatial information of microscopy with the quantitative immune cell information of flow cytometry. (2) IBEX: iterative staining that facilitates high content tissue imaging (HCT) of immunofluorescent antibody (IF)-stained tissues [2]. (3) Two-photon intravital microscopy (2P-IVM): dynamically image tissues in real time

Results My initial goal was to utilize multiplex imaging methods to profile the immune landscapes of representative TCH and TCL clones at early days post tumor implantation; this would provide me with a ground truth for comparison to therapeutic intervention. As early as day 5 post tumor injection, I found striking differences between the TCH and TCL tumors: T cells are predominantly excluded to the outer rim of the TCL tumors, and there are well-defined myeloid cell clusters scattered throughout the TME (Figure 1). In contrast, TCH tumors have substantial T cell infiltration throughout the tumor proper and lack these distinctive myeloid cell clusters. Therapy also uniquely alters regulatory T cells in the TCH TME, severely depleting, reprogramming, and restricting the remaining cells to the tumor periphery.

IBEX was used to illustrate the complexity of myeloid cells within the tumor microenvironment

Conclusions These data raise important questions regarding the spatial positioning of cellular subsets, and the implications of these positions on therapeutic efficacy. This work was supported in part by the Intramural program of NIAID, NIH.



Abstract 574 Figure 1 Cold tumor myeloid cluster

REFERENCES

1. Li, J. and Byrne, K., et al. Tumor Cell-Intrinsic Factors Underlie Heterogeneity of Immune Cell Infiltration and Response to Immunotherapy. *Immunity* 2018; 49, 178–193.
2. Radtke, A. J. et al. IBEX: A versatile multiplex optical imaging approach for deep phenotyping and spatial analysis of cells in complex tissues. *Proc National Acad Sci.* 2020; 117, 33455–33465

Ethics Approval This study involved the use of mice. This study (LISB 4E) obtained ethics approval via NIAID ACUC (Animal Care and Use Committee) and AAALAC.

<http://dx.doi.org/10.1136/jitc-2021-SITC2021.574>

575

DUAL BLOCKADE OF LAG3 AND TIGIT IMPROVES THE TREATMENT EFFICACY OF A NANOPARTICLE-MEDIATED IMMUNORADIATION IN ANTI-PD1 RESISTANT LUNG CANCER IN MICE

¹Yun Hu*, ¹James Welsh, ²Sebastien Paris, ¹Genevieve Bertolet, ¹Hampartsoum Barsoumian, ¹Lily Schuda, ¹Kewen He, ¹Duygu Sezen, ¹Mark Wasley, ¹Joylise Mitchell, ¹Tiffany Voss, ¹Fatemeh Masrourpour, ²SILVA Jordan, ¹Claudia Kettlun Leyton, ¹Liangpeng Yang, ¹Nahum Puebla-Osorio, ¹Saamil Gandhi, ¹Quynh-Nhu Nguyen, ¹Angelica Cortez. ¹MD Anderson Cancer Center, Houston, TX, USA; ²Nanobiotix, Paris, France

Background TIGIT and LAG3 are inhibitory receptors expressed on cytotoxic CD8+ T cells and NK cells and directly inhibit the activation and proliferation of these cells. We proposed that blockade of TIGIT and LAG3 could improve antitumor immune response in a mouse model of anti-PD1 (aPD1)-resistant mice.

Methods 129Sv/Ev mice were inoculated with 50,000 aPD1-resistant 344SQR cells in the right leg on day 0 (primary tumor) and with 50,000 cells in the left leg on day 4 (secondary tumor). Primary tumors were injected with NBTXR3 radioenhancer nanoparticles on day 7 and irradiated with 12 Gy on days 8, 9, and 10. Anti-PD1, aLAG3, and aTIGIT were given to mice by intraperitoneal injections on days 5, 8, 11, 14, 21, 28, 35, and 42. On day 21, primary tumors, secondary tumors, and blood samples were harvested and analyzed with flow cytometry to evaluate changes in immune cell populations. The RNA extracted from the tumors were also analyzed by Nanostring. Mice in which tumors were completely eradicated were re-challenged with another 50,000 344SQR cells in the right flank at least two months post radiation; no further treatment was given to these mice, and tumor growth was monitored.

Results The addition of aTIGIT, aLAG3, or aTIGIT+aLAG3 to NBTXR3+XRT+aPD1 therapy significantly improved control of tumors, and the addition of aTIGIT+aLAG3 also led to fewer spontaneous lung metastases. The addition of either aTIGIT or aLAG3 to NBTXR3+XRT+aPD1 extended mouse survival time relative to NBTXR3+XRT+aPD1. None of the 8 mice in either the NBTXR3+XRT+aPD1+aTIGIT group or the NBTXR3+XRT+aPD1+aLAG3 group survived more than 32 days; in contrast, 3 of the 8 mice that received NBTXR3+XRT+aPD1+aTIGIT+aLAG3 survived until the end of the experiment. These surviving mice were found to have developed memory against 344SQR cells, and no further tumor growth was observed after re-challenge. Flow cytometry analysis showed that adding aTIGIT+aLAG3 to NBTXR3+XRT+aPD1 increased the percentages of proliferating CD8+ T cells in primary tumors, secondary tumors, and blood. Furthermore, Nanostring transcriptomic analysis of cells isolated from the tumors of mice thus treated showed evidence of classical two-step immunological priming, with an elevation of innate immune genes at the primary tumor and full-blown activation of the immune system within the secondary tumor.

Conclusions Blockade of TIGIT and LAG3 with NBTXR3+XRT+aPD1 improved CD8+ T-cell proliferation, augmented the antitumor response at both irradiated and unirradiated (abscopal) tumors, and induced potent long-term antitumor memory in mice.

Acknowledgements This work was supported by Cancer Center Support (Core) Grant CA016672 to The University of Texas MD Anderson Cancer Center; the Goodwin family research fund; the family of M. Adnan Hamed and the Orr Family Foundation to MD Anderson Cancer Center's Thoracic

Radiation Oncology program; an MD Anderson Knowledge Gap award; Nanobiotix.

<http://dx.doi.org/10.1136/jitc-2021-SITC2021.575>

**TUMOR TARGETED SUPERANTIGEN (TTS),
NAPTUMOMAB ESTAFENATOX (NAP), ENHANCES CAR-T
CELLS POTENCY AND CAN BOOST CAR-T EFFICACY
AGAINST SOLID TUMORS**

<http://dx.doi.org/10.1136/jitc-2021-SITC2021.576>

Yael Sagi*, Michal Shahar, Marina Pinsker. *NeTX, Rehovot, Israel*

Background CAR-T therapy has limited efficacy against solid tumors due to low trafficking to the tumor, limited cell expansion in patients, tumor antigen heterogeneity, and an immunosuppressive microenvironment. TTS are fusion proteins that consist of genetically engineered Superantigens (Sag) linked to Fragment antigen binding (Fab) moieties directed to tumor associated antigens. It was previously shown that TTS selectively activates a subset of T cells [1], turns "cold tumors hot" [2] and, in preclinical models, can lead to long-term memory responses [3]. Here we present preclinical data demonstrating that the lead TTS compound, NAP (5T4 targeted Sag), enhanced the efficacy of CAR-T treatment against tumor cells in vitro, suggesting that NAP may overcome current CAR T limitations.

Methods Her2-CAR-T cells were produced in the presence of NAP or CD3&CD28, and their potency was evaluated against the FaDu cell line and by measurement of T cell activation markers (CD25, CD137, IFN-gamma, CD107a). The expression of memory markers (CCR7, CD45RA/CD45RO, CD95) and Th1 polarization (transcription factors) of the resulted CAR-T cells were analyzed by staining with specific antibodies. The combined potency of NAP with CAR-T was also tested in vitro against the FaDu cell line (which expresses both Her2 and 5T4 antigens). The chemotactic activity of T cells was assessed using a chemotactic chamber.

Results PBMCs grown in the presence of NAP, in comparison with PBMCs grown in the presence of CD3&CD28 antibodies, resulted in the production of more potent CAR-T cells as measured both by killing assay using the FaDu cell line and by INF γ production, activation markers and T cell degranulation. Central memory (CM) percentages were increased and Th1 polarization was significantly more prominent after NAP stimulation. Following incubation with NAP, the chemotaxis towards the tumor cells was significantly enhanced. Finally, combination of CAR-T and NAP resulted in a synergistic killing effect of the tumor cell line.

Conclusions Our studies show that NAP generates more potent CAR-T cells and acts synergistically with CAR-T against tumor cell lines in vitro. The ability of NAP administration to activate T cells outside of the immunosuppressive microenvironment (in the lymphoid organs), promote T cell infiltration into the tumor and induce long-term memory responses, strongly suggests that combination of CAR-T cells with NAP may overcome the limited effect of CAR-T therapy against solid tumors. NAP is currently being evaluated in clinical studies in combination with durvalumab [NCT03983954] and docetaxel [NCT04880863].

REFERENCES

- Hedlund G, Eriksson H, Sundstedt A, et al. The Tumor Targeted Superantigen ABR-217620 Selectively Engages TRBV7-9 and Exploits TCR-pMHC Affinity Mimicry in Mediating T Cell Cytotoxicity. *PLoS One*. 2013; 8(10): e79082.
- Azulay M, Lifshits S, Friedmann A, et al. Naptumomab Estafenatox induces T cell recognition, turning anti-PD-1 unresponsive "cold" tumors into "hot" responsive tumors. *Cancer Research*. Jul 2018, 78 (13 Supplement) abstract # 2712 AACR Annual Meeting 2018; Chicago, IL; DOI: 10.1158/1538-7445.AM2018-2712.
- Azulay M, Lifshits S, Shany E, et al. Selective T cell Redirection Proteins (STR) Enhance the Anti-Tumor Activity of Checkpoint Inhibitors (CPIs) and can Lead to Long-Lasting Immunity Against the Tumor. Abstract # P657. SITC 34th Annual Meeting, 2019. National Harbor, Maryland, USA.

NON-CLINICAL EFFICACY, PHARMACOKINETICS, AND PHARMACODYNAMICS OF A NOVEL BI-FUNCTIONAL ANTI-CD73-TGF β RII-TRAP MOLECULE IN COMBINATION WITH IMMUNE CHECKPOINT THERAPY<http://dx.doi.org/10.1136/jitc-2021-SITC2021.577>

Susanna Stinson*, Jianhua He, Kyung-Hoon Kim, Becky Yang, Marianna Zavodovskaya, Ping Yi, Federico Campigotto, Monika Sobczyk, Rutwij Dave, Brian Carr, In Kyoung Mah, Shiva Zabolji, Jens Brodbeck, Scott Turner, Vivian Barry, Kelli Boyd, Valeria Fantin. *Gilead Sciences, Foster City, CA, USA*

Background A novel murine bi-functional molecule, G04-trap, comprised of an anti-CD73 antibody fused to the extracellular domain of TGF β receptor II, is designed to potently antagonize two prominent immunosuppressive and pro-tumorigenic pathways present across a variety of cancer types. Inhibition of both CD73-adenosine and TGF β pathways is expected to create favorable conditions within the tumor microenvironment and restore antitumor immune responses.

Methods G04-trap was evaluated in Detroit562, MC38, and Hepa1-6 efficacy tumor models. Tumor growth inhibition (TGI) was determined when ≥ 9 animals were alive in each group. Tumor-bearing mice received isotype control (200 microgram), G04-trap (246 microgram), anti-PD-(L)1 (200 microgram) or G04-trap + anti-PD-(L)1 twice per week for 3 weeks. Pharmacokinetic (PK) and pharmacodynamic (PD) assessment was performed on MC38 tumor-bearing mice dosed with 3 mg/kg, 10 mg/kg, or 30 mg/kg G04-trap. Plasma and tumor PK, CD73 target occupancy on T cells, plasma TGF β , plasma free-sCD73, and tumor CD73 activity were measured after a single dose administration of G04-trap

Results Administration of G04-trap to mice harboring TGF β -dependent human pharyngeal Detroit562 xenograft tumors led to a dose-dependent anti-tumor response (83% TGI, at 246 microgram vs. isotype control on day 21). In addition, treatment with G04-trap in combination with immune checkpoint inhibition showed anti-tumor activity in MC38 and Hepa1-6 syngeneic mouse models. In MC38 on day 18, there was a statistically significant TGI with G04-trap + anti-PD-L1 (99% TGI vs. isotype control or 98% TGI vs. anti-PD-L1 alone). A more modest effect was observed in Hepa1-6, with 47% TGI in mice receiving G04-trap + anti-PD-1 vs. isotype control on day 27. To further interpret the efficacy observed in the MC38 tumor model, we performed in-depth PK/PD analysis. Intravenous administration of G04-trap at 3-30 mg/kg resulted in 10% tumor-to-plasma exposure ratio. Full TGF β target coverage and full CD73 target occupancy on blood T cells was sustained for >3 days, supporting a BIW dosing schedule in non-clinical studies. Treatment also resulted in a dose-dependent inhibition of CD73 activity in tumors. In contrast to cellular CD73, a dose-dependent increase in free sCD73 concentration above baseline was measured in the plasma, consistent with previous reports evaluating anti-CD73 antibodies [1].

Conclusions Dual inhibition of CD73 and TGF β in combination with immune checkpoint blockade resulted in enhanced anti-tumor activity in xenograft and syngeneic tumor models. These results suggest that further exploration of this approach is warranted.

REFERENCES

1. Zhao Y, Gu H, Postelnek J, DeMichele M, Yuan L, Zhang YJ, et al. Fit-for-purpose protein biomarker assay validation strategies using hybrid immunocapture-liquid chromatography-tandem-mass spectrometry platform: Quantitative analysis of total soluble cluster of differentiation 73. *Anal Chim Acta*. 2020;1126:144–53.

578

CD8-TARGETED IL-2 DRIVES POTENT ANTI-TUMOR EFFICACY AND PROMOTES ACTION OF TUMOR SPECIFIC VACCINES

¹Hussein Sultan, ²Kelly Moynihan, ¹Yuang Song, ¹Samuel Ameh, ³Ton Schumacher, ²Yik Andy Yeung, ²Ivana Djuretic, ¹Robert Schreiber*. ¹Washington University School of Medicine, St. Louis, MO, USA; ²Asher Biotherapeutics, South San Francisco, CA, USA; ³Netherlands Cancer Institute, Amsterdam, Netherlands

Background IL-2 and currently available engineered variants are of interest for solid tumor treatment, but their efficacy and toxicity profiles remain suboptimal. These results reflect the pleiotropic signaling via IL-2 receptors on different cell types that may simultaneously drive desired and undesired responses. We hypothesized that restricting IL-2's activity to CD8+ T cells would improve efficacy while also lowering its toxicity profile.

Methods We developed a cis-targeted IL-2 that selectively acts on CD8+ T cells (CD8-IL2) and assessed its activity using the T3 progressor MCA sarcoma model, which was selected because (a) it is sensitive to anti-PD-1 therapy when tumors are small but develops insensitivity as tumor size increase, (b) rejection requires both CD4+ and CD8+ T cells and (c) rejection is dependent on tumor expression of two neoantigens: mIlgb1 (MHC-II) and mLama4 (MHC-I).

Results Whereas mice bearing 8-day T3 tumors had become insensitive to anti-PD-1 mediated tumor rejection, 90% of mice treated with single dose CD8-IL2 monotherapy rejected their tumors, while high dose IL-2 produced minimal efficacy. Efficacy occurred without body weight loss. These results suggest that CD8-IL2 can induce therapeutic effects at a time when tumors became insensitive to anti-PD-1. To assess this possibility in a more controlled manner, we used a tumor neoantigen vaccine model that depends on CD4+ T cell help for development of functional CD8+ T cells at both the priming stage in the lymph node as well as the effector stage at the tumor site. Mice bearing T3 tumors were vaccinated with a synthetic long peptide (SLP) containing the mLama4 neoepitope and either a high or low dose of an SLP containing the mIlgb1 neoepitope. Whereas 85% of tumor bearing mice that received the vaccine containing mLama4 plus low dose mIlgb1 SLP rejected their tumors, surprisingly none of the mice receiving high dose mIlgb1 underwent tumor rejection. This high dose inhibition was reversed when CD8-IL2 was administered after high dose vaccination and at concentrations that had only modest activity in tumor bearing, non-vaccinated mice. With CD8-IL2 treatment, antigen specific T cells were expanded and displayed increased expression of activation-associated markers and reduced expression of exhaustion-associated markers.

Conclusions CD8-IL2 outperformed other forms of engineered IL-2 in anti-tumor efficacy, showed a significantly improved toxicity profile, and rescued deficient CD8 T cell responses resulting from poor CD4 help. In sum, we demonstrate high level antitumor efficacy and tolerability with a new form of targeted IL-2.

Ethics Approval Mice used in this study were between 8 and 12 weeks of age and were maintained in accordance with procedures approved by the Association for Assessment and Accreditation of Laboratory Animal Care and Accredited Animal Studies Committee of Washington University in St. Louis

<http://dx.doi.org/10.1136/jitc-2021-SITC2021.578>

EXPLOITING TUMOR NEOANTIGEN-TARGETED IMMUNOTHERAPY IN IMMUNOLOGICALLY HOT VERSUS COLD MURINE LUNG CANCER MODELS

¹Changbo Sun*, ¹Koji Nagaoka, ²Yukari Kobayashi, ¹Jun Nakajima, ¹Kazuhiro Kakimi. ¹University of Tokyo Hospital, Tokyo, Japan; ²University of Tokyo, Bunkyo-ku, Japan

Background The treatment of non-small cell lung cancer has been altered by immune-checkpoint therapy in the last 10 years. However, many patients still do not respond to it or, eventually, the disease progresses. One of the factors leading to primary resistance to ICI is the "cold" tumor, characterized by the absence of T cell infiltration and not sufficiently primed for immune recognition. Here, we compared the neoantigen-based immunotherapy in two lung cancer cell lines: T cell-inflamed ASB-XIV and non-T cell-inflamed LLC1.

Methods Whole-exome and RNA sequencing were performed to identify neoantigens. First, MHC binding scores of expressed mutated peptides (FPKM>1) were estimated to select candidate neoantigens. Next, the immunogenicity of predicted mutated peptides was investigated. Then, the anti-tumor effect of immunogenic mutated peptides was accessed. Finally, immunosuppressive molecules in the non-T cell inflamed tumor microenvironment were investigated and targeted for effective treatment.

Results Inflamed ASB-XIV tumors were sensitive to ICI, while non-inflamed LLC1 tumors were resistant to ICI. Using ASB-XIV-specific CTLs, we screened the panel of candidate neoantigen peptides and identified Phf3 N1867K mutated peptide as neopeptide. Mutated Phf3 peptide-pulsed DCs induced peptide-specific CD8+ T cells and inhibited the ASB-XIV tumor growth in the prophylactic and therapeutic setting. Furthermore, adoptive transfer of mPhf3-specific CTLs also eradicated the ASB-XIV tumors. In the case of LLC1, twenty-five out of 132 short mutated peptides induced peptide-specific CD8+ T cell response, but they could not inhibit the LLC1 tumor growth. DC vaccines pulsed with long peptides (LP) induced both CD4+ and CD8+ T cell responses ex vivo. Of them, DC pulsed with LP82 partly delayed the LLC1 growth in vivo. By RNA-Seq, CD38 was highly expressed in LLC1. Thereby, an anti-CD38 antibody was administered in LLC1-bearing mice immunized with DC pulsed with LP82. The tumor growth was suppressed in the combination treatment, partly because CD38 blockade decreased regulatory T cells in the tumor.

Conclusions Responses to neoantigen-targeted immunotherapy preferentially observed in T cell-inflamed tumors. Regulation of immunosuppressive tumor microenvironment is required to make neoantigen-targeted immunotherapy effective in non-inflamed tumors.

<http://dx.doi.org/10.1136/jitc-2021-SITC2021.579>

580

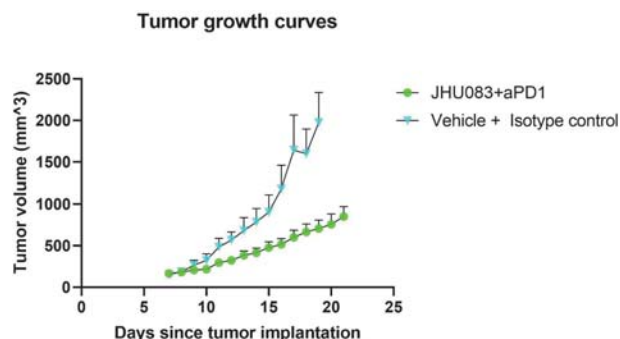
GLUTAMINE BLOCKADE IN COMBINATION WITH IMMUNE CHECKPOINT BLOCKADE REMODELS THE MYELOID LANDSCAPE IN MOUSE MODELS OF SOFT TISSUE SARCOMAS

¹Aditya Suru*, ²Marwa Islam, ¹Ada Tam, ¹John Gross, ¹Nicolas Llosa. ¹Johns Hopkins University, Baltimore, MD, USA; ²Macaulay Honors College, New York City, USA

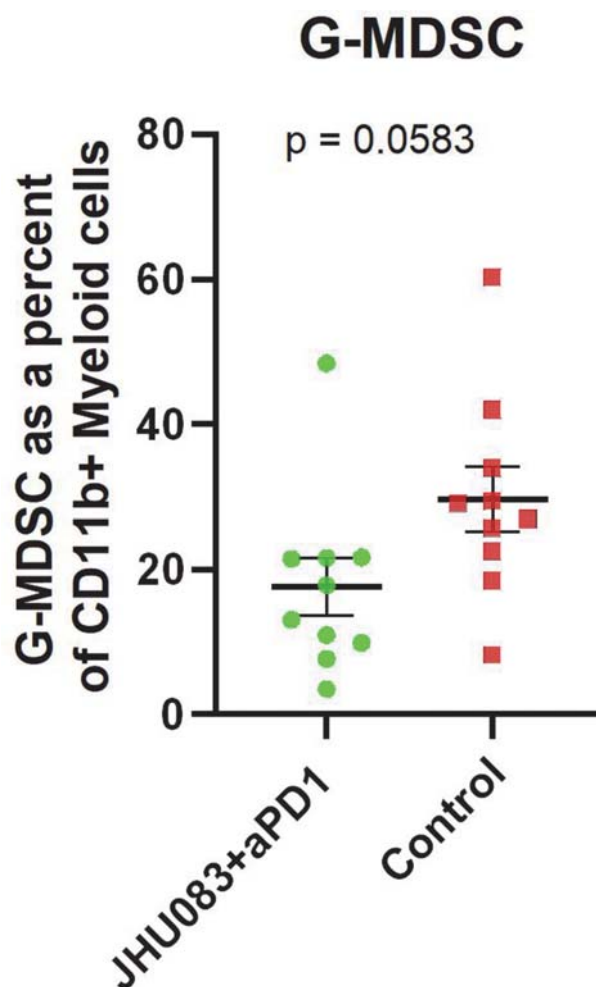
Background Immunotherapy holds great potential to treat cancers such as sarcomas for which the clinical outcomes using conventional therapies haven't changed much in decades. A major impediment for immune mediated tumor killing in sarcomas is a strong presence of immunosuppressive cell types such as Myeloid Derived Suppressor Cells (MDSC) dominating the Tumor Immune Micro-Environment (TIME) and a dearth of effector cell types such as T Cells [1]. Cellular metabolism has emerged as a novel immune-checkpoint to modulate the immune responses by targeting various metabolic pathways. Glutamine is a key metabolite participating in the TCA cycle and is implicated in sarcoma-genesis [2] and its blockade has shown to skew immune cell function and phenotype [3]. We used JHU083, a novel prodrug of a glutamine antagonist (6-Diazo-5-oxo-L-norleucine) to rid the TME of glutamine and interrogate its downstream effects on the TIME.

Methods We employed a transplantable mouse model of soft tissue sarcomas [4]: Cells derived from primary tumors from LSL-Kras^{G12D/+} p53^{fllox/fllox} mice (KP Cells). Wild-type C57BL/6J mice were subcutaneously injected with 200,000 KP cells. They were treated with JHU083 (1mg/kg on days 7–11 and 0.3mg/kg till end) and anti-PD1 monoclonal antibody (100ug on days 7, 9, 11 and 13) or vehicle control and isotype control. On Day 22, the mice were sacrificed, and the tumors were harvested and interrogated using flow cytometry and Immuno-histochemistry (IHC) to reveal the effects of different treatment groups on the immune landscape.

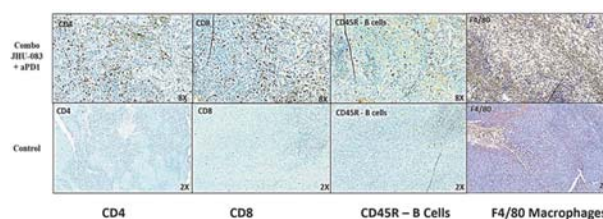
Results The combination treated group had significantly less tumor burden at the end of Day 21 than the control group (Figure 1). Although the myeloid cells outnumbered the lymphocytes across both the groups, the percentage of G-MDSCs reduced significantly in the combination treated group (17% in the combination, vs 29% in the control, $p=0.058$, Figure 2). The density of T cells and B cells infiltrating the tumors was also higher for the combination treated group than other groups as measured by IHC (Figure 3).



Abstract 580 Figure 1 The mice treated with a combination of JHU083 and anti-PD1 therapy had significantly less tumor burden than the mice treated with vehicle control and isotype control



Abstract 580 Figure 2 Combination of JHU083 and anti-PD1 therapy led to a decrease in the number of G-MDSCs (defined as CD11b⁺Lineage⁺Ly6C^{low}Ly6G⁺MHC2⁺) as a proportion of the myeloid cells (CD11b⁺Lineage⁺)



Abstract 580 Figure 3 The photomicrographs of the single chromogenic IHC stains for CD4, CD8, CD45R, F4/80 show that the combination treated tumors had higher density of the CD8 T Cells and the B Cells as measured by Immunohistochemistry

Conclusions Our data suggests that blocking glutamine with anti-PD1 therapy leads to a change in the proportion of myeloid cells in the TIME. The combination treatment increased the influx of T and B cells while reducing the density of the

immunosuppressive G-MDSCs. For cancers with immune excluded/desert phenotypes this therapy has the potential to make the tumors amenable to immunotherapy leading to better clinical outcomes. Further transcriptomic and metabolomic studies will reveal the mechanistic pathways by which glutamine blockade is able to remodel the myeloid landscape.

Acknowledgements The authors would like to thank Prof. Jonathan Powell and his lab for providing us with the JHU083 drug and valuable inputs. The Immunohistochemistry work was performed by the Oncology Tissue Services Core at the Johns Hopkins University. We would also like to thank the BKI Flow cytometry core for providing support for the flow cytometry experiments.

REFERENCES

1. L Chen et al, The Immunosuppressive Niche of Soft-Tissue Sarcomas is Sustained by Tumor-Associated Macrophages and Characterized by Intratumoral Tertiary Lymphoid Structures. *Clinical Cancer Research*. 2020; 26: 4018–4030.
2. Lee, P., Malik, D., Perkons, N. et al. Targeting glutamine metabolism slows soft tissue sarcoma growth. *Nat Commun* 11, 498 (2020).
3. Min-Hee Oh et al, Targeting glutamine metabolism enhances tumor-specific immunity by modulating suppressive myeloid cells, *J Clin Invest*. 2020;130(7):3865–3884.
4. D Kirsch et al, A spatially and temporally restricted mouse model of soft tissue sarcoma. *Nat Med*. 2007 Aug;13(8):992–7

Ethics Approval All animal procedures performed were approved by the Johns Hopkins University Animal Care Committee.

<http://dx.doi.org/10.1136/jitc-2021-SITC2021.580>

581 **MULTI-DIMENSIONAL SYNERGY OF COMBINATIONS (MUSYC) ALGORITHM OPTIMIZES COMBINATORIAL STING AND TLR ADJUVANT CANCER VACCINES**

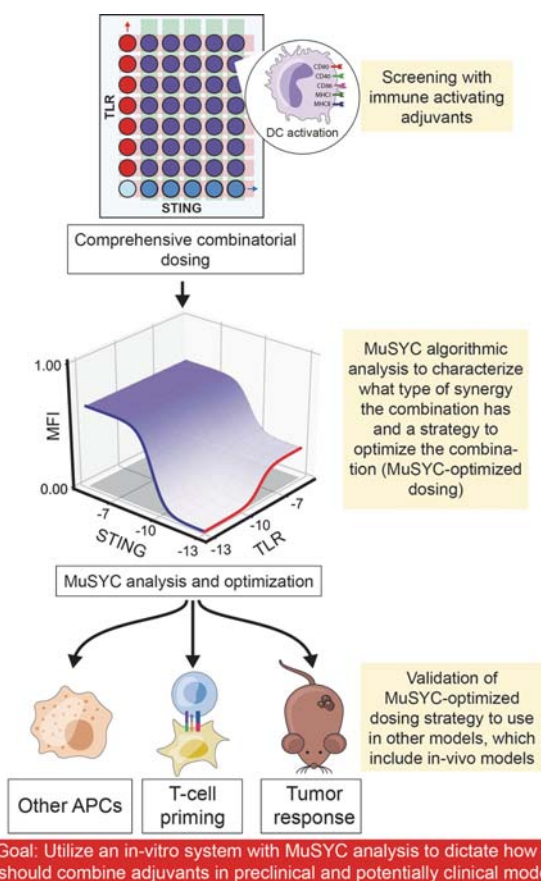
<http://dx.doi.org/10.1136/jitc-2021-SITC2021.581>

David Taylor*, Michael Korrer. *Vanderbilt University, Nashville, TN, USA*

Background Optimized cancer vaccine's T cell priming potential can promote their translation in the current clinical climate of immune checkpoint inhibitor approval for many cancers.

Methods To rigorously optimize adjuvant combinations that would effectuate an improved in vivo anti-tumor response, we utilized a novel algorithm, the multi-dimensional synergy of combinations (MuSYC), to maximize efficacy and minimize dosing for various classes of adjuvant combinations (Figure 1).

Results In-vitro, the MuSYC algorithm characterized the combination of R848 (TLR7/8 adjuvant) and STING agonist as synergistically efficacious and potent in activating murine bone marrow-derived dendritic cells (mBMDs) and human monocytic cell line THP-1. These two selected adjuvants were then used to generate a MuSYC-derived optimized combination strategy for optimal in vivo priming. Finally, using B16 melanoma and MOC1 head and neck models, MuSYC-optimized cancer vaccines had the best anti-tumor response associated with increased tumor-infiltrating lymphocytes and changes in myeloid infiltration.



Abstract 581 Figure 1

Conclusions Cumulatively, we believe our MuSYC-centered approach will optimize translatable adjuvant combinations to improve cancer immunotherapy.

IMMUNE CORRELATES FROM QUEST1 IN MEN WITH CASTRATION-RESISTANT PROSTATE CANCER

¹Nicole Toney*, ¹Yo-Ting Tsai, ²Jason Redman, ²James Gulley, ²Jeffrey Schlom, ²Renee Donahue. ¹National Institutes of Health, Bethesda, MD, USA; ²National Institutes of Health, Bethesda, MD, USA

Background Immune checkpoint inhibitors have limited efficacy in unselected metastatic castration-resistant prostate cancer (mCRPC) patients. Combination immunotherapy approaches to generate a tumor-directed immune response (vaccine) and facilitate the resulting anti-tumor immune activity (checkpoint inhibitors, cytokines) have shown synergy pre-clinically. In the phase I/II Quick Efficacy Seeking Trial (QuEST1, NCT03493945), combination of a brachyury-targeting vaccine (BN-brachyury), TGF- β /anti-PD-L1 blocking bifunctional fusion protein (bintrafusp alfa), and IL-15 superagonist (N-803) have produced preliminary evidence of efficacy in CRPC, with 5/12 patients having a sustained prostate-specific antigen (PSA) response that included 2 radiographic partial responses, compared to 1/13 patients who received BN-brachyury plus bintrafusp alfa. Here, we present immune correlates from patients enrolled in Arm 2.1A (BN-brachyury + bintrafusp alfa) and Arm 2.2A (BN-brachyury + bintrafusp alfa + N-803).

Methods Peripheral blood mononuclear cells (PBMC) and serum were obtained from 25 patients pre and multiple time points post treatment. PBMCs were assessed for antigen specific T cells targeting brachyury and MUC-1 by intracellular cytokine staining, 158 peripheral immune cell subsets by multicolor flow cytometry, and TCRV β sequencing. Patients were also evaluated for complete blood counts, and serum cytokines/soluble factors using ELISA assays and OLINK's immuno-oncology panel. Immune parameters were compared between Arm 2.1A and Arm 2.2A and evaluated for associations with clinical response in Arm 2.2A.

Results Brachyury and MUC-1 specific T cells were increased in most patients post treatment in both arms. A greater increase in total NK cells, refined NK subsets expressing markers of activation/adhesion, and TCR diversity was observed after 2 weeks of therapy in Arm 2.2A than Arm 2.1A. Absolute lymphocyte counts and serum levels of granzyme B, sCD27, and sCD40L were also increased after 2 weeks in Arm 2.2A compared to Arm 2.1A. Serum proteomic analyses revealed a greater increase in analytes related to NK cell signaling in Arm 2.2A than Arm 2.1A. Specific immune parameters at baseline associated with development of clinical response in patients treated in Arm 2.2A; responders had trends of higher frequencies of CD4+ and CD8+ T cells, lower frequencies of MDSCs and monocytes, and lower levels of serum IL-6 and sCD40 than non-responders.

Conclusions These findings demonstrate enhanced immune activation of both NK and T cells with the addition of N-803 in Arm 2.2A, where more clinical activity was observed than in Arm 2.1A. These findings support the continued evaluation of the combination of BN-brachyury, bintrafusp alfa, and N-803 in patients with mCRPC.

Acknowledgements This research was supported in part by the Intramural Research Program of the Center for Cancer Research, National Cancer Institute (NCI), National Institutes of Health, and via Cooperative Research and Development Agreements (CRADAs) between the NCI and EMD Serono, the NCI and Bavarian Nordic, and the NCI and ImmunityBio.

Trial Registration NCT03493945

Ethics Approval The trial was approved by the Institutional Review Board of the Center for Cancer Research, National Cancer Institute (ClinicalTrials.gov identifier: NCT03493945).

<http://dx.doi.org/10.1136/jitc-2021-SITC2021.582>

583

EXPLORING THE POTENTIAL OF T CELL ACUTE LYMPHOBLASTIC LEUKEMIA (T-ALL) FOR GENERATING LEUKEMIA-SPECIFIC T CELL RESPONSES THAT CAN BE THERAPEUTICALLY HARNESSSED WITH IMMUNOTHERAPY

¹Todd Triplett*, ²Joshua Rios, ¹Alexander Somma, ³Sarah Church, ³Khrystyna North, ³Andrew White, ⁴Nisha Holay, ⁵Andrew Weinberg. ¹University of Texas at Austin Dell Med, Austin, TX, USA; ²Aganox, austin, TX, USA; ³NanoString, Seattle, WA, USA; ⁴University of Texas at Austin, Austin, TX, USA; ⁵Earle A Chiles Research Institute, Portland, OR, USA

Background T cell Acute Lymphoblastic Leukemia (T-ALL) is a devastating malignancy found primarily in pediatric populations. Unfortunately, standard of care for T-ALL has not progressed from highly toxic, intensive regimens of chemotherapy, which fails to cure all patients. Immunotherapies designed to activate patients' leukemia-specific T cells may provide a new therapeutic avenue to increase complete response rates, reduce toxicity without the need to engineer (e.g. CAR) cells. However, it is unknown whether T-ALL is capable of being recognized by T cells due given its relatively low mutation-rate. These studies therefore sought to investigate whether signs of leukemia-specific T cell responses are generated by T-ALL. Because T-ALL results in systemic disease and infiltrates multiple lymphoid and non-lymphoid tissues, these studies also determined how the divergent immune contextures of these TMEs impacts T cell responses to T-ALL. From this, we aim to identify immunotherapeutic targets capable of activating T cells across tissues to eradicate leukemia systemically.

Methods Primary leukemia cells isolated from a spontaneous murine model (LN3 mice) into immune-competent, congenic (CD45.1) recipient mice. Tissues were harvested at distinct stages of disease for analysis by flow cytometry or utilizing NanoString Technologies' GeoMX Digital Spatial Profiling (DSP) platform.

Results Flow cytometric analysis of T cells revealed extensive changes in response to T-ALL that included multiple features of exhaustion typically associated with anti-tumor responses as determined by upregulation of co-inhibitory receptors and TOX. This included a surprisingly high-frequency of PD1+ T cells, which was accompanied by PDL1- and PDL2-expressing myeloid cells that likely are restraining these subsets. Importantly, combination immunotherapy with OX40 agonists while inhibiting PD1 resulted in drastically reduced tumor burden and concomitant expansion of proliferating granzyme-expressing CD8 T cells. To gain better insight into T cell responses within distinct organs, we analyzed tissue sections using DSP. This technique enabled us to evaluate T cells in direct contact with leukemia infiltrates compared to T cells in regions without T-ALL, which further revealed an enrichment of activated subsets. Importantly, these studies have provided critical insight needed to better understand how T cells responding to T-ALL diverge between distinct types of tissues.

Conclusions The results from these studies collectively suggest that T cells are activated by T-ALL and that they can be therapeutically harnessed despite relatively low mutation-rates. Future studies will continue analysis of individual organs and use these results to rationally design combinations of immunotherapies by tailoring to activate T cells in all tissue types.

Acknowledgements Special thanks to all the support and analysis from everyone at NanoString, along with financial support provided by a SITC-NanoString DSP Fellowship awarded to Dr. Todd Triplett used for DSP analysis of all frozen tissues in these studies. Salary support for Dr. Triplett and pilot funding was provided by departmental funds via a Cancer Prevention

and Research Institute of Texas (CPRIT) Scholar Award (Grant #RR160093; awarded to Dr. Gail Eckhardt).

<http://dx.doi.org/10.1136/jitc-2021-SITC2021.583>

POWERFUL SYNERGISTIC EFFECTS OF A STING AGONIST AND THE IL-2 SUPERKINE, H9, IN ELICITING NK AND T CELL RESPONSES AGAINST MHC I- AND MHC I+ TUMORS

¹Natalie Wolf*, ¹Cristina Blaj, ²Lora Picton, ¹Gail Snyder, ¹Li Zhang, ¹Christopher Nicolai, ³Chudi Ndubaku, ⁴Kelsey Sivick Gauthier, ³Sarah McWhirter, ²K Christopher Garcia, ¹David Raulet. ¹University of California Berkeley, Berkeley, CA, USA; ²Stanford University, Palo Alto, CA, USA; ³Aduro Biotech, Berkeley, CA, USA; ⁴Arcus Biosciences, Hayward, CA, USA

Background Most current cancer immunotherapies are based on mobilizing CD8 T cell responses. However, many types of tumors evade CD8 T cell recognition by displaying few or no antigens, or losing expression of MHC I. These considerations underlie the need for complementary therapies that mobilize other antitumor effector cells, such as NK cells, which preferentially kill MHC I-deficient cells. Cyclic dinucleotides (CDNs) activate the cGAS-STING pathway of the innate immune system and are candidates as immunotherapy agents. Intratumoral CDN injections induce type I IFNs and other mediators that amplify the CD8 T cell response and induce tumor regression [1]. CDN therapy also induces long-term tumor regressions in some MHC I-deficient tumor models, mediated primarily by NK cells [2].

Methods To extend the efficacy of CDN therapy, we combined the IL-2 superkine, H9, or half-life extended H9, with CDNs to target and activate NK cells in the tumor microenvironment and prevent or delay the onset of NK cell desensitization [3,4]. In these studies, we utilized B16-F10 and MC38 tumor cells lacking B2m to examine effects of the combination therapy on MHC I-deficient tumor growth as well as to examine the activation of NK cells by flow cytometry and cytotoxicity assays. We also utilized B16-F10 WT and the spontaneous tumor model, MCA, to assess the effect of the combination therapy on MHC I+ tumors.

Results Here we show that H9 synergized with CDN therapy to mobilize much more powerful antitumor responses against MHC I-deficient tumors than CDN alone. The responses were mediated by NK cells and in some cases CD4 T cells, and were accompanied by increased recruitment to and sustained activation of NK cells in the tumor. This combination therapy regimen activated NK cells systemically, as shown by antitumor effects distant from the site of CDN injection and enhanced cytolytic activity of splenic NK cells against tumor cell targets ex vivo. Finally, the same combination therapy regimen synergistically mobilized powerful CD8 T cell responses in the case of MHC I+ tumor cells, suggesting the generality of the approach. The approach was effective against primary sarcomas, as well, especially when combined with checkpoint therapy, leading to tumor regressions and long-term survival of many mice with MCA-induced sarcoma.

Conclusions Overall, our work demonstrates the impact of a novel combination therapy in mobilizing powerful NK and T cell-mediated antitumor activity, providing important justification for evaluating this approach for treating cancers that are refractory to available treatment options.

REFERENCES

- Corrales, L., Glickman, L.H., McWhirter, S.M., Kanne, D.B., Sivick, K.E., Katibah, G.E., Woo, S.R., Lemmens, E., Banda, T., Leong, J.J., et al. (2015). Direct Activation of STING in the Tumor Microenvironment Leads to Potent and Systemic Tumor Regression and Immunity. *Cell Rep* 11, 1018–1030.
- Nicolai, C.J., Wolf, N., Chang, I.C., Kim, G., Marcus, A., Ndubaku, C.O., McWhirter, S.M., and Raulet, D.H. (2020). NK cells mediate clearance of CD8(+)

T cell-resistant tumors in response to STING agonists. *Science immunology* 5, eaaz2738.

- Levin, A.M., Bates, D.L., Ring, A.M., Krieg, C., Lin, J.T., Su, L., Moraga, I., Raeber, M.E., Bowman, G.R., Novick, P., et al. (2012). Exploiting a natural conformational switch to engineer an interleukin-2 'superkine'. *Nature* 484, 529–533.
- Ardolino, M., Azimi, C.S., Iannello, A., Trevino, T.N., Horan, L., Zhang, L., Deng, W., Ring, A.M., Fischer, S., Garcia, K.C., and Raulet, D.H. (2014). Cytokine therapy reverses NK cell anergy in MHC-deficient tumors. *J Clin Invest* 124, 4781–4794.

<http://dx.doi.org/10.1136/jitc-2021-SITC2021.584>

585

**LIGHT (TNFSF14) CO-STIMULATION ENHANCES
MYELOID CELL ACTIVATION AND ANTI-TUMOR
IMMUNITY IN THE SETTING OF PD-1 AND TIGIT
CHECKPOINT BLOCKADE**

¹George Fromm*, ²Kyung Jin Yoo, ²Kelsey Johannes, ²Casey Shuptrine, ²Zach Opheim, ²Arpita Patel, ²Haley Andreasen, ²Jaya Miriyala, ²Suresh De Silva, ²Taylor Schreiber. ¹Shattuck Labs, Inc, APEX, NC, USA; ²Shattuck Labs, Inc., Durham, NC, USA

Background Co-inhibition of TIGIT and PD-1/L1 improves response rates compared to monotherapy PD-1/L1 blockade in checkpoint naïve NSCLC with PD-L1 expression >50%. TIGIT mAbs with an effector competent Fc can induce myeloid cell activation, and some have also demonstrated effector T cell depletion, which carries a clinical liability of unknown significance. TIGIT antibody blockade translates to anti-tumor activity by enabling PVR signaling through CD226 (DNAM-1), which can be directly inhibited by PD-1. Further, DNAM-1 is downregulated on TIL in advanced and CPI resistant cancers. Therefore, broadening clinical responses from TIGIT blockade into PD-L1low or CPI resistant tumors, may be enhanced by immune co-stimulation that independently operates from PD-1/L1 inhibition.

Methods Mouse and human TIGIT-Fc-LIGHT molecules were generated and assessed using Octet, MSD, and cell binding assays, and function was evaluated using in vitro/in vivo activation and anti-tumor efficacy experiments; including a pre-clinical model engineered to mimic human CPI acquired resistance.

Results TIGIT-Fc-LIGHT was nominated using in vitro and genomic screening assays designed to identify TNF costimulatory receptors widely expressed on TIL, T stem cell memory (Tscm), and NK cells; relative to DNAM-1 expression. HVEM was prioritized, and its ligand TNFSF14 (LIGHT) also directly activates myeloid cells through binding to a second receptor, LTβR. TIGIT-Fc-LIGHT simultaneously engaged TIGIT and LIGHT receptors at low nanomolar affinities (~3.5–6.5 nM), without the requirement for an effector competent Fc. HVEM signaling overlaps with DNAM-1, and TIGIT-Fc-LIGHT activated canonical and non-canonical NFκB pathways, leading to increased tumor infiltration of antigen-specific CD8+ T and NK cells. Importantly, anti-tumor efficacy induced by monotherapy TIGIT-Fc-LIGHT was maintained in aggressive anti-PD-1 acquired resistant tumors, a model where combined PD-1 and TIGIT antibody blockade was inactive. Because HVEM lacks cytoplasmic domain homology to DNAM-1, HVEM signaling is unlikely to be regulated by PD-1. Indeed, while anti-tumor activity of TIGIT-Fc-LIGHT was enhanced by PD-1/L1 blockade, it was not dependent upon combination. TIGIT-Fc-LIGHT also directly activated myeloid cells and increased the expression of CXCL10 and CXCL11, and stimulated proinflammatory cytokines, including CCL2, CCL4, and CXCL13.

Conclusions TIGIT-Fc-LIGHT was designed to overcome the limitations of TIGIT blocking antibodies through: 1) preserved costimulation in advanced tumors, 2) direct myeloid cell activation, 3) blockade of all known TIGIT ligands, and with 4) no risk of depleting effector lymphocytes since TIGIT-Fc-LIGHT activity does not require Fc function. Pre-clinical data indicate that these goals were achieved, and further development is warranted.

<http://dx.doi.org/10.1136/jitc-2021-SITC2021.585>

586

MONITORING THE IMPACT OF MDSC TARGETING DRUGS IN COMBINATION WITH NIVOLUMAB ON ACTIVATION AND PROLIFERATION OF TUMOR RESIDENT EFFECTOR IMMUNE CELLS IN PATIENT-DERIVED 3D-EXPLORE PLATFORM

Jared Ehrhart*, Brittany Bunch, Kelly Sussman, Kelly Guzman, Soner Altioik. *Nilogen Oncosystems, Tampa, FL, USA*

Background Myeloid-derived suppressor cells (MDSCs) represent a diverse population of immature myeloid cells with a strong capacity to suppress the functions of NK cells and CD4+ and CD8+ T-cells in tumor immune microenvironment, thereby reducing the efficacy of immunotherapeutic drugs. MDSC depletion strategies are being investigated to determine if the immunosuppressive effects of MDSCs in the tumor microenvironment can be reduced to improve the efficacy of cancer immunotherapy. Here we employed the 3D-Explore ex vivo platform to test the efficacy of MDSC targeting agents alone and in combination with nivolumab using patient derived 3D-tumoroids which retain the tumors' original stroma and suppressive immune landscape.

Methods 3D-tumoroids approximately 150 μm in size were generated from fresh patient renal cell carcinoma tumor samples, which were obtained with informed consent and relevant IRB approval. Tumoroids were treated ex vivo with a Phosphodiesterase-5 inhibitor Tadalafil, an HDAC inhibitor entinostat, a potent steroidal liver X receptor (LXR) ligand DMHCA or a selective CK2 (casein kinase II) inhibitor TBCA alone and in combination with nivolumab. Flow cytometry, high content confocal analysis and cytokine release assays were performed to monitor treatment-mediated changes in tumor immune landscape and tumor cell killing.

Results Multi-parameter flow cytometry (14 color) analysis demonstrated the heterogeneity of tumor immune cell populations including polymorphonuclear (PMN-MDSC) and monocytic (M-MDSC) MDSCs in different patient tumor samples. Furthermore, we performed flow cytometry analysis to assess treatment-induced changes in NK and effector T-cells activation and proliferation profiles that were further correlated with drug impacts on MDSC, Tregs and myeloid cell populations in the ex vivo treatment groups. Additionally, immune cell functions were assessed by multiplex cytokine analysis and treatment-induced tumor cell killing was quantified by high content confocal imaging.

Conclusions Our data demonstrated that the ex vivo 3D-Explore is a clinically relevant platform to identify combination of immunotherapy agents capable of overcoming the unique suppressive environment developed by an individual tumor. Furthermore, the 3D-EXplore platform provides unique insight into the intact tumor immune microenvironment to develop therapeutic strategies to overcome immunosuppressive effects of MDSCs to improve the efficacy of immunotherapeutic agents in cancer.

<http://dx.doi.org/10.1136/jitc-2021-SITC2021.586>

587

INDUCING MISMATCH REPAIR DEFICIENCY IN COMBINATION WITH ANTI-CTLA4 THERAPY IS HIGHLY EFFECTIVE AGAINST NON-IMMUNOGENIC NEUROBLASTOMA TUMORS

Mikal El-Hajjar, Lara Gerhardt*, Mithunah Krishnamoorthy, Rene Figueredo, Xiufen Zheng, James Koropatnick, Saman Maleki. *Western University, Montreal, Canada*

Background Despite rigorous multimodal therapy, recurrence is common among high-risk neuroblastoma patients. Neuroblastoma is a poorly immunogenic tumor with low tumor mutational burden (TMB). Currently, immunotherapy with immune checkpoint inhibitors (ICIs) are not approved for neuroblastoma. Novel strategies to sensitize neuroblastoma to ICIs are urgently needed. We have induced mismatch repair (MMR) deficiency in mouse neuro-2a tumors and show that these tumors become highly immunogenic and responsive to anti-CTLA4 but not anti-PD1 therapy.

Methods The MMR gene *Mlh1* was knocked out of neuro-2a and B16F10 cells, and clones were selected. MMR-deficient (dMMR) and -proficient (pMMR) neuroblastoma tumors were grown in immunocompetent and immunodeficient animals. Tumors were harvested, and tumor-infiltrating lymphocytes (TILs) were analyzed by flow cytometry. Neuro-2a tumor-bearing mice were treated with anti-PD1, anti-CTLA4, or a combination of both antibodies. NK cells were depleted in mice treated with anti-CTLA4 using the anti-asialo GM1 antibody to examine their role in the efficacy of anti-CTLA4 treatment. dMMR B16F10 melanoma tumor-bearing mice were treated with anti-PD1 followed by the analysis of TILs. Publicly available TARGET and TCGA databases were mined to examine the effect of T-cell infiltration on neuroblastoma and melanoma patient's survival, respectively.

Results We show that high-risk neuroblastoma and melanoma patients with tumors containing high levels of T-cell and memory T-cell-related genes have improved survival. Additionally, inducing MMR deficiency in neuro-2a cells renders these tumors immunogenic, with high T-cell infiltration, and inhibits tumor growth in mice in an immune-dependent manner. We also show that dMMR neuroblastoma tumors are highly sensitive to anti-CTLA4 but not anti-PD1 treatment. Anti-CTLA4 therapy cured most tumor-bearing mice, inducing immune memory, epitope spreading, and increased tumor-specific T-cells in cured animals. Notably, the effect of anti-CTLA4 therapy was independent of NK cells. In neuroblastoma tumors with induced MMR deficiency, anti-PD1 treatment antagonized anti-CTLA4 by upregulating inhibitory molecules on T-cells and increasing the level of dysfunctional TILs. Interestingly, anti-PD1 therapy was effective against high TMB-background melanoma tumors with induced MMR deficiency. Our data suggests that this effect relied on lowering T-cell inhibitory molecules rather than increasing T-cell infiltration into tumors.

Conclusions Inducing MMR deficiency in low and high TMB-background tumors leads to distinct responses to anti-PD1 therapy, with low levels of T-cell exhaustion being a positive indicator of response. Anti-CTLA4 therapy in combination with induced MMR deficiency is a novel strategy for treating low TMB-background high-risk neuroblastoma.

Ethics Approval This study was approved by the Animal Care Committee at Western University; approval number 2017-030.

<http://dx.doi.org/10.1136/jitc-2021-SITC2021.587>

CALORIC RESTRICTION SENSITIZES MELANOMA TO ANTI-PD-1 IMMUNE CHECKPOINT INHIBITION

Alexa Melucci*, Shuyang Qin, Alexander Chacon, Rachel Jewell, Peter Prieto. *University of Rochester Medical Center, Rochester, NY, USA*

Background Individual response to immune checkpoint inhibition (ICI) in patients with metastatic melanoma varies from 10–40% for monotherapy and 50–60% with combination therapy [1]. Identification of adjuncts to ICI to further bridge treatment response to cure is imperative. We focus on caloric restriction (CR) as an adjunct to anti-PD-1 ICI given its inexpensive nature, relative ease of application, and increased tolerability as compared to fasting.

Methods 12-week C57BL/6J mice were inoculated with Yale University Mouse Melanoma (YUMM 1.7), randomized into diet groups and further randomized into α PD-1 and control (IgG) groups on day 12 (D12). Full diet mice ad lib fed while CR mice were 40% calorically restricted based on average daily food intake. Tumors were measured every 3 days with digital calipers (q3d). α PD-1 or control was intraperitoneally injected starting D12 continuing q3d for 7 injections. Mice were sacrificed and tumors harvested on D31. RNA sequencing was performed on CD45+ CD3+ T cells.

Results Under CR conditions, mice treated with α PD-1 had significantly smaller tumor volumes compared to the full diet cohort treated with α PD-1 (D22, 271.15 m³ vs. 336.72 m³, $p=0.031$) and persisted to harvest (D31, 600.96 m³ vs. 1039.84 m³, $p=0.034$). A significant difference in tumor volumes between CR α PD-1 and CR control treated cohorts was observed starting at D28 (439.34 m³ vs. 667.63 m³, $p=0.005$) and persisted to harvest (D31, 600.96 m³ vs. 884.08 m³, $p=0.009$). However, no significant difference in tumor growth under full diet conditions in murine cohorts treated with α PD-1 or control or separately between CR and full diet cohorts treated with control was observed. On pathway enrichment analysis inflammatory response, cytokine-mediated, response to interferon-gamma, and cell proliferation pathways were downregulated in the CR + α PD-1 cohort. Notable genes found in these pathways include B-cell linker protein (BLNK), tyrosine-protein kinase Lyn (LYN), SYK (spleen tyrosine kinase), toll-like receptor (TLR) TLR4, TLR7, and TLR8.

Conclusions Caloric restriction significantly sensitizes YUMM 1.7 murine melanoma to anti-PD-1 therapy resulting in decreased tumor growth. We show significant modulation of tumor growth in a murine tumor cell line, which has previously demonstrated limited response to α PD-1. In the present study, caloric restriction may decrease inflammation via downregulation of cytokine and toll-like receptor mediated pathways. Furthermore, caloric restriction may reverse the immunosuppressive tumor microenvironment and provide an inexpensive means to increase treatment response to anti-PD-1 therapy.

REFERENCES

1. Ward WH, Farma JM. *Cutaneous Melanoma: Etiology and Therapy*. Brisbane (AU): Codon Publications. 2017; Chapter 8.

Ethics Approval This study was approved by the University Committee on Animal Resources (UCAR), UCAR-2018-014.

<http://dx.doi.org/10.1136/jitc-2021-SITC2021.588>

ENHANCEMENT OF THE ANTI-TUMOR EFFECTS OF CD47 BLOCKADE IN SOLID TUMORS BY COMBINATION WITH TARGETED RADIOIMMUNOTHERAPY

Sagarika Pachhal, Emily Greer, Jesse Hwang, Qing Liang, Mary Chen, Eileen Geoghegan, Helen Kotanides, Dale Ludwig, Denis Beckford*. *Actinium Pharmaceuticals, New York, NY, USA*

Background One mechanism that tumors use to escape immunosurveillance is the overexpression of CD47, which inhibits the macrophage mediated phagocytosis pathway. Although blockade of the CD47-SIRP α axis is a promising approach to enhance tumor targeted phagocytosis, anti-CD47 monotherapies have not shown meaningful responses in clinical studies of solid tumors. Combination cancer therapies aim to increase the probability of response in settings of resistance by combining drugs with different mechanisms of action. Antibody radioconjugates (ARCs) specifically target and deliver therapeutic radiation directly to cancer cells. We rationalized that the immunogenic and cytotoxic properties of ARCs will upregulate calreticulin (CRT), a pro-phagocytic signal, thereby synergizing with CD47 blocking therapies to enhance phagocytosis and antitumor activity. Here for the first time, we demonstrate the combination benefit of a HER2 specific targeting ARC and a CD47 blocking antibody to enhance therapeutic efficacy in preclinical solid tumor models.

Methods The anti-HER2 antibody trastuzumab was conjugated with p-SCN-DOTA and radiolabeled with Ac-225 or Lu-177. The biological activity of both radioconjugates was evaluated using human recombinant HER2 and receptor positive tumor cell lines. The cytotoxic effect of radioconjugates and the ability to upregulate CRT was evaluated using XTT assay and flow cytometry, respectively, in a panel of HER2 expressing cells. To evaluate the synergy of anti-HER2 ARC and CD47 antibody combination in vitro, a flow cytometry macrophage phagocytosis assay was developed. We further evaluated the antitumor synergy in vivo between anti-HER2 ARC and CD47 antibody in human HER2 positive tumor xenograft mouse model.

Results The anti-HER2 ARCs have similar binding properties to native antibody and demonstrate specific cytotoxicity. Importantly, we observe ARC-mediated CRT upregulation in HER2 expressing cells. Furthermore, the combination of HER2 targeting ARC and CD47 blocking antibody enhances in vitro macrophage mediated tumor cell phagocytosis compared to each agent alone. Remarkably, the in vivo anti-HER2 ARC and CD47 antibody combination shows enhanced therapeutic effect with reduced toxicity and improved survival benefit in a human preclinical solid tumor model.

Conclusions Here for the first time, we demonstrate enhanced therapeutic efficacy between an anti-HER2 ARC and CD47 blocking antibody combination in a preclinical solid tumor model. The finding suggests that ARC mediated upregulation of CRT potentiates the pro-phagocytic signal and synergizes with the anti-CD47 mode of action thereby enhancing antitumor immune response. This combination mechanism provides a very promising strategy to improve therapeutic responses in patients harboring solid tumors and warrants further preclinical evaluation.

Ethics Approval All animal experiments were approved by IACUC.

<http://dx.doi.org/10.1136/jitc-2021-SITC2021.589>

590

**ANTI-CD33 ACTINIUM-225 TARGETED
RADIOIMMUNOTHERAPY ENHANCES THE BIOLOGIC
ACTIVITY OF ANTI-CD47 ANTIBODY IMMUNOTHERAPY
IN PRECLINICAL MODELS OF ACUTE MYELOID
LEUKEMIA**

Sagarika Pachhal, Emily Greer, Jesse Hwang, Qing Liang, Mary Chen, Eileen Geoghegan, Helen Kotanides, Dale Ludwig, Denis Beckford*. *Actinium Pharmaceuticals, New York, NY, USA*

Background Actimab-A, the anti-CD33 antibody lintuzumab armed with the radioisotope Actinium-225 (Ac-225), has demonstrated single agent antileukemic effects in patients with relapsed or refractory acute myeloid leukemia (AML). Up-regulation of CD47, a macrophage checkpoint that suppresses phagocytosis, is one mechanism by which myeloid malignancies such as AML can evade targeting by the innate immune response. Therapeutic blocking antibodies against this pathway have shown early clinical promise. We hypothesized that Actimab-A will enhance phagocytosis in AML cells by specifically upregulating calreticulin (CRT), a pro-phagocytic signal. Moreover, we hypothesized that combination of the anti-CD33 antibody radioconjugate (ARC) and CD47 blocking antibody could act in synergy to enhance therapeutic outcomes in AML compared to single agent. In this study, we examined, for the first time, the potential mechanistic benefit of combining the anti-CD33 ARC armed with Ac-225 or Lutetium-177 (Lu-177) and a CD47 blocking antibody, using in vitro and in vivo human AML preclinical models.

Methods Lintuzumab was conjugated with p-SCN-DOTA and radiolabeled with Ac-225 or Lu-177. The biological activity of both radioconjugates was examined using human recombinant CD33 and receptor positive AML cells. The cytotoxic effect of radioconjugates and the ability to upregulate CRT was evaluated using XTT assay and flow cytometry, respectively, in a panel of CD33 expressing cells. To assess the therapeutic combination of anti-CD33 ARC and CD47 antibody in vitro, a flow cytometry macrophage phagocytosis assay was used. We further evaluated the therapeutic efficacy in vivo of anti-CD33 ARC and CD47 antibody combination in human AML mouse model.

Results The anti-CD33 ARCs have similar binding properties to native antibody and demonstrate specific cell cytotoxicity. We show ARC-mediated upregulation of cell surface CRT in a panel of CD33 expressing AML cells. Furthermore, the in vitro combination of CD33 targeting ARC and CD47 blocking antibody enhances macrophage mediated phagocytosis of AML cells compared to each monotherapy. Interestingly, the in vivo anti-CD33 ARC and CD47 antibody combination demonstrates a significant increase in survival and reduces toxicity in a human AML preclinical model.

Conclusions Our findings suggest a novel synergistic mechanism whereby the CD33 ARC targeted radiation induces upregulation of CRT, thereby potentiating a pro-phagocytic innate immune response in combination with anti-CD47 blocking antibody. More importantly, clinical translation of this approach could enhance therapeutic efficacy in AML and warrants further preclinical exploration.

Ethics Approval All animal studies were approved by IACUC.

<http://dx.doi.org/10.1136/jitc-2021-SITC2021.590>

591 **SURVIVAL RATES IN STAGE IV MELANOMA PATIENTS
TREATED WITH RADIATION AND IMMUNOTHERAPY
DIFFER DEPENDING ON AGE AND RADIATION
TREATMENT SITE**

Catherine Colonna*, Nasreen Vohra, Aiden Burke, Matthew Peach, Andrew Ju. *ECU Brody School of Medicine, Greenville, NC, USA*

Background Melanoma is difficult to treat due to its propensity of evading the immune system. Radiation can be combined with immune checkpoint inhibitors to potentially prolong survival. Radiation has been shown to reduce tumor sizes both at the site of radiation and at non-irradiated lesions, also known as the abscopal effect. However, the interaction of immunotherapy and radiation treatment in melanoma cancer is not well-defined. This study seeks to better characterize factors influencing survival in Stage IV melanoma patients treated with both radiation and immunotherapy.

Methods Retrospective data was collected from melanoma patients receiving both radiation and immunotherapy within 6 months of each other between 2008–2021 at our institution. Patient and treatment characteristics were examined for their influence on overall survival and progression-free survival using the log-rank test on Kaplan Meier survival curves. Radiographic response was assessed according to PERCIST/RECIST criteria and analyzed against patient/treatment characteristics using the Mann-Whitney U Test. For the abscopal effect, the percent changes both before and after radiation treatment were subtracted in non-irradiated lesions to produce a "delta-delta" percent change to reflect the rate of change in tumor response to radiation treatment.

Results Younger patients trended towards worse overall ($p=0.141$) and progression free ($p=0.06$) survival as well as less favorable PERCIST/RECIST response to radiation ($p=.0562$) compared to older patients. Combination CTLA-4 and PD-1 inhibition therapy tended to produce better PERCIST/RECIST tumor response ($p=0.09$), but it did not significantly affect survival times. In addition, there was lower overall ($p=0.22$) and significantly lower progression free ($p=0.012$) survival among patients with intracranial irradiated lesions. However, no difference was found in PERCIST/RECIST response in the irradiated lesions between the intra- or extracranial groups. Non-irradiated lesions in patients with extracranial irradiated lesions had a pattern of less favorable rate of change in tumor size ($p=0.16$).

Conclusions Lower survival times in younger patients is unexpected and may reflect differences in immunotherapy response in patients receiving both radiotherapy and immunotherapy, which requires further investigation. Combination CTLA-4 and PD-1 inhibition therapy correlating with better tumor response confirms the effect is still present in this cohort receiving radiotherapy. The lower survival times among intracranial lesion patients is most likely due to lower expectancy of brain metastasized patients; however, it could also be the brain is less responsive to immunotherapy. Further research in a larger cohort is needed for deeper analysis, but this series is still comparable in size to other published series.

Ethics Approval This retrospective review was approved by the University IRB, UMCIRB 15-001726. Consent of participants was waived due to the retrospective nature of this review.

<http://dx.doi.org/10.1136/jitc-2021-SITC2021.591>

ATR-MEDIATED CD47 AND PD-L1 UPREGULATION RESTRICTS RADIOTHERAPY-INDUCED IMMUNE PRIMING AND ABCOPAL RESPONSES IN COLORECTAL CANCER

¹Rodney Cheng-En Hsieh*, ²Sunil Krishnan, ³Ren-Chin Wu, ¹Akash Boda, ¹Arthur Liu, ¹Michelle Winkler, ¹Wen-Hao Hsu, ¹Steven Lin, ⁴Mien-Chie Hung, ¹Li-Chuan Chan, ¹Krithikaa Bhanu, ¹Anupallavi Srinivasamani, ¹Ricardo De Azevedo, ³Yung-Chih Chou, ¹Ronald Depinho, ¹Matthew Gubin, ¹Eduardo Vilar-Sanchez, ¹Chao-Hsien Chen, ¹Ravaen Slay, ¹Priyamvada Jayaprakash, ¹Shweta Hegde, ¹Genevieve Hartley, ¹Spencer Lea, ¹Rishika Prasad, ¹Brittany Morrow, ¹Coline Couillaud, ¹Madeline Steiner, ³Chun-Chieh Wang, ⁵Bhanu Venkatesulu, ¹Cullen Taniguchi, ¹Betty Kim, ¹Junjie Chen, ¹Nils-Petter Rudqvist, ¹Michael Curran. ¹The University of Texas MD Anderson Cancer Center, Houston, TX, USA; ²Mayo Clinic, Jacksonville, FL, USA; ³Chang Gung Memorial Hospital, Taoyuan City, Taiwan, Province of China; ⁴China Medical University, Taichung, Taiwan, Province of China; ⁵Loyola University, Chicago, USA

Background Background: Radiotherapy of colorectal cancer (CRC) can prime adaptive immunity against tumor-associated antigen (TAA)-expressing CRC cells systemically; however, incidences of abscopal tumor remission are extremely rare. We sought to unravel the post-irradiation immune escape mechanisms in CRC.

Methods

Methods Flow cytometry, gene knockdown, RNA and T cell receptor sequencing, and multiple murine syngeneic CRC models were used to interrogate mechanisms of CRC immune evasion following radiotherapy. Comparison of immunohistochemistry staining between pretreatment biopsy and post-irradiation surgical specimens was performed in rectal patients who underwent neoadjuvant radiotherapy with 5 Gy for 5 fractions.

Results

Results We find that CRC cells utilize a common DNA repair signaling pathway — ATR/Chk1/STAT3 — to upregulate both CD47 and PD-L1 in response to radiotherapy, which through engagement of SIRP α and PD-1 suppresses the capacity of antigen-presenting cells (APCs) to phagocytose them thereby preventing TAA cross-presentation. This post-irradiation CD47 and PD-L1 upregulation can be observed in CRC cells treated with either photon or proton radiotherapy and across a wide variety of human solid tumor cells. Concordantly, rectal cancer patients who responded poorly (tumor regression grade 4–5, n = 10) to neoadjuvant radiotherapy exhibited significantly elevated post-irradiation CD47 levels (P = 0.005). In murine CRC models, the combination of radiotherapy, α SIRP α and α PD-1 (RSP) profoundly enhances TAA uptake, activation of innate immune sensors, and TAA cross-priming across various antigen-presenting myeloid populations in the irradiated tumor microenvironment and facilitates TAA-presenting APC migration to secondary lymphoid organs. Furthermore, we observed robust production of TAA-specific CD8 T cells, functional activation of effector T cells, and increased tumor-infiltrating T cell clonality and clonal diversity in mice treated with RSP. Importantly, radiotherapy coupled with phagocytosis checkpoint blockade significantly improves complete response rates in both irradiated and abscopal tumors and prolongs survival in three distinct murine CRC models, including a cecal orthotopic model. In addition, α SIRP α exerts superior tumoricidal efficacy than α CD47 in combination with RT and α PD-1. We find RSP efficacy to be STING dependent as knockout animals lose most benefit of phagocytosis checkpoint blockade.

Conclusion ATR-mediated CD47 and PD-L1 upregulation restrains radiation-induced immune priming in CRC. Blockade of the phagocytosis checkpoints SIRP α and PD-1 during

radiotherapy promotes vigorous anti-CRC immune priming leading to systemic tumor regression.

Acknowledgements This study is supported in part by NIH grant P30 CA16672, the MD Anderson Andrew Sabin Family Fellowship, and Chang Gung Memorial Hospital grant CMRPG3K1751. RCH was supported by the CPRIT Research Training Grant (RP170067) and Ralph B. Arlinghaus Ph.D. Scholarship. The authors are grateful to the members of the Advanced Cytometry & Sorting Facility at South Campus, Tissue Bank of Chang Gung Memorial Hospital at Linkou, and MHC Tetramer Core Facility at Baylor College of Medicine for their invaluable help.

Ethics Approval This study was approved by the Institutional Review Board of Chang Gung Memorial Hospital, Taiwan; approval number: 202001191B0C601.

<http://dx.doi.org/10.1136/jitc-2021-SITC2021.592>

593

**PI3K γ δ INHIBITOR COMBINED WITH RADIATION
ENHANCES THE ANTITUMOR IMMUNE EFFECT OF PD-1
BLOCKADE IN SYNGENIC MURINE BREAST CANCER
MODEL AND HUMANIZED PATIENT-DERIVED
XENOGRAFT MODEL**

¹MIn Guk Han*, ¹Bum Sup Jang, ¹Mi Hyun Kang, ²Deukchae Na, ¹In Ah Kim. ¹Seoul National University, Seoul, Korea, Republic of; ²Ewha Woman 's University, Seoul, Korea, Republic of

Background Breast cancer is viewed as immunologically cold, imposing an immune-suppressive tumor microenvironment and responding poorly to lone immune checkpoint blockade. As an adjunct to ICB, radiation therapy holds promise in terms of in situ tumor vaccination effect, although it is known to promote immune suppression, increasing regulatory T cells, myeloid-derived suppressor cell, and M2 tumor-associated macrophages. It was our contention that combined use of RT and a PI3K γ δ inhibitor to combat immune suppression might enhance the efficacy of ICB.

Methods Murine breast cancer cells (4T1) were grown in both immune-competent and -deficient BALB/c mice, and tumors were irradiated by 3 fractions of 24 Gy. A PD-1 blockade and a PI3K γ δ inhibitor were then administered every other day for 2 weeks. Tumors from humanized patient-derived breast cancer xenograft model was sequenced to identify immune-related pathways and to profile infiltrated immune cells. Transcriptomic and clinical data were acquired from The Cancer Genome Atlas pan-cancer cohort, and the deconvolution algorithm was used to profile immune cell repertoire.

Results In the immune-competent syngenic 4T1 murine tumor model, PD-1 blockade alone led to tumor hyperprogression, whereas a three-pronged strategy of PI3K γ δ inhibitor, RT, and PD-1 blockade significantly delayed primary tumor growth, boosted abscopal effect, and improved animal survival by comparison. The immune-deficient syngenic 4T1 murine tumor model failed to show this synergism in delaying tumor growth and the abscopal effect. According to FACS analysis, RT significantly increased not only CD8+cytotoxic T-cell fractions but also immune-suppressive Treg cells, MDSCs, and M2 TAMs. However, PI3K γ δ inhibitor significantly lowered proportions of Treg, MDSCs, and M2 TAMs, achieving dramatic gains in splenic, nodal, and tumor CD8+ T-cell populations after triple combination therapy. There were significantly decreased tumor expressions of p-AKT, PD-L1, and HIF1 α by PI3K γ δ inhibition. Triple combination therapy significantly delayed primary tumor growth in humanized PDX model as well and analyses of RNA sequencing data of humanized PDX samples showed decreased immune suppressive pathways with decreased and M2 macrophage and increased CD8+ T-cell by triple combination therapy. In the TCGA pan-cancer cohort, high Treg/CD8+T-cell and M2/M1 TAM ratios and poor overall patient survival was associated with high PIK3CG (PI3K γ) or PIK3CD (PI3K δ) gene expression.

Conclusions These findings collectively indicate that PI3K γ and PI3K δ are clinically relevant targets in an immunosuppressive TME. Combining PI3K γ δ inhibitor, RT, and PD-1 blockade may thus be a viable approach, helping to overcome the therapeutic resistance of immunologically cold tumors such as breast cancer.

<http://dx.doi.org/10.1136/jitc-2021-SITC2021.593>

COMBINATION OF ANTIGEN-SPECIFIC VACCINATION AND TARGETED RADIONUCLIDE THERAPY IMPROVES ANTI-TUMOR EFFICACY IN A MURINE PROSTATE MODEL

Hemanth Potluri*, Carolina Ferreira, Joseph Grudzinski, Christopher Massey, Reinier Hernandez, Jamey Weichert, Douglas McNeel. *UW-Madison, Madison, WI, United States*

Background While checkpoint blockade has been unsuccessful in prostate cancer trials, the approval of Sipuleucel-T demonstrates the value of antigen-specific vaccination approaches for this disease. We have studied a DNA vaccine specific for the ligand-binding domain of the androgen receptor (pTVG-AR) as a more scalable vaccination approach, though its efficacy is likely limited by the immunosuppressive prostate microenvironment. External beam radiotherapy has been shown to sensitize poorly responsive tumors to immunotherapy, but is infeasible for patients with widely metastatic disease. Our group has developed a compound called NM600 that can deliver radiation to all cancer sites simultaneously, similar to other targeted radionuclide therapy (TRT) approaches. In this study, we used TRT in combination with pTVG-AR to improve anti-tumor efficacy in a murine prostate cancer model.

Methods 6-week old male C57BL/6 mice were implanted subcutaneously with TRAMP-C1 cells. pTVG-AR or the empty vector were administered weekly from the day after tumor implantation. An intravenous injection was administered of 50 ("low-dose") or 250 μ Ci ("high dose") of 90Y-NM600, estimated to deliver a dose of 3.1 Gy or 15.5 Gy to 300 mm³ tumors, respectively. In one study, this TRT treatment was repeated once after three weeks. Groups of mice (n=5) were euthanized at several time points for flow cytometry analysis of the tumors. Separate cohorts (n=7) were followed for survival.

Results Low-dose TRT administered once in combination with pTVG-AR (median survival 91 days) significantly improved survival more than low-dose TRT alone (median survival 59 days; p=.049) or pTVG-AR alone (median survival 59 days; p=0.01). Low-dose TRT plus pTVG-AR was also superior to high-dose TRT plus pTVG-AR (median survival 67 days; p=0.05). We next examined the effect of giving high-dose TRT twice in combination pTVG-AR. We found that the combination of fractionated TRT and pTVG-AR greatly slowed tumor growth unlike fractionated TRT alone (p=0.03). High-dose TRT + pTVG-AR caused a two-fold increase in CD86 expression on dendritic cells (p=0.0009) on Day 3 and a 10% increase in effector memory CD8+ T cells (p=0.002) on Day 1 compared to TRT alone. This combination also resulted in T cells with 3-fold lower PD-1 expression (p=4e-7) and 2-fold lower TIGIT expression (p=0.01).

Conclusions These data suggest that the combination of antigen-specific vaccination and TRT can be an effective treatment for cancers that are refractory to immunotherapy. This combination may act through increasing co-stimulation by dendritic cells, leading to a more active cytolytic CD8+ T cell population.

<http://dx.doi.org/10.1136/jitc-2021-SITC2021.594>

595

INHIBITION OF INTEGRIN α V β 8 IN COMBINATION WITH LOW DOSE RADIATION INDUCES ANTITUMOR EFFECT IN ADVANCED IMMUNE CHECKPOINT BLOCKADE REFRACTORY TUMOR MODEL

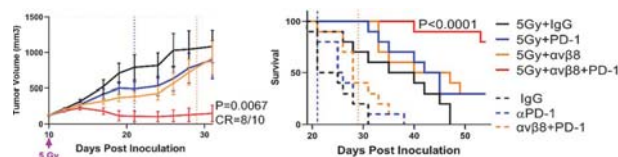
¹Natalia Reszka-Blanco*, ¹Megan Krumpoch, ¹Michaela Mentzer, ¹Vinod Yadav Yadav, ¹Brianna Bannister, ¹Dan Cui, ¹Elizabeth Konopka, ¹Dooyoung Lee, ¹Fu-Yang Lin, ¹Terence Moy, ¹Eugene Nebelitsky, ¹Qi Qiao, ¹Inese Smutske, ²Charlotte Root, ²Patrick Allison, ²Sarah Krueger, ¹Dawn Troast, ¹Blaise Lippa, ¹Bruce Rogers, ¹Adrian Ray. ¹Morphic Therapeutic, Inc., Waltham, MA, WALTHAM, MA, USA; ²Labcorp Drug Development, Ann Arbor, MI, Ann Arbor, MI, USA

Background Integrin α V β 8 activates TGF β in immune cells. α V β 8 inhibitors have been shown to potentiate immune checkpoint blockade (ICB) in preclinical models [1]. Radioimmunotherapy (RIT) induces immunogenic cell death and antigen presentation, however it concurrently activates immunosuppressive pathways. Interestingly, α V β 8 immunosuppressive activity was implicated in radiotherapy resistance [2]. We have explored whether antagonizing α V β 8 overcomes the suppressive effect of TGF β and restores anti-tumor immunity in advanced ICB and RIT resistant tumors.

Methods Efficacy was evaluated after combination treatment with low dose radiation, α V β 8 (clone C6D4) and PD-1 (clone J43) mAb in an advanced CT26 colon cancer syngeneic mouse model. Mice were treated at tumor volume of >120 mm³ and euthanized at 2,000 mm³. Flow cytometry and transcriptomic analysis were used to assess the mechanism of action. Tumor volumes are presented as mean \pm SEM. Statistics were performed by one-way ANOVA, or log-rank test. Bone marrow derived dendritic cell (BMdDC) cultures were isolated from C57BL/6 mice.

Results Cell death, including radiation-induced apoptosis, induced immunoregulatory and maturation program in a population of ex vivo cultured BMdDC, recently described as mregDC/DC3 [3,4]. mregDC/DC3 signature was associated with increased α V β 8 expression, suggesting a role of this integrin in inducing an immunosuppressive phenotype. A CT26 model was established to mimic the progression of late-stage tumors and was unresponsive to radiation, ICB and RIT. In CT26 implanted mice, α V β 8 is expressed on tumor stroma, and is not detectable on cancer cells. Addition of α V β 8 mAb to RIT markedly increased tumor regression (P=0.0067) and survival (P<0.0001). There were 8/10 complete responders with addition of α V β 8 mAb relative to 3/10 in RIT alone. Improved efficacy correlated with enhanced T cell activation and improved DC functionality. Consistent with a recent report in a less advanced CT26 model [5], α V β 8 mAb + radiation resulted in similar efficacy as conventional RIT although the effect was modest in more advanced tumors (Figure 1, A, B).

Conclusions Inhibition of α V β 8 in combination with RIT eradicated an advanced tumor, unresponsive to the respective monotherapies or conventional RIT. The anti-tumor effect was driven by enhancement of adaptive immunity, improvement of DC function and reduced tumor tolerance. These data provide evidence that α V β 8 inhibition enhances RIT and may be effective against ICB refractory tumors.



Abstract 595 Figure 1 Complete response (CR) with improved survival when α V β 8 inhibition is added to RIT in CT26 syngeneic model of colorectal cancer in an advanced, ICB and RIT unresponsive stage. (A) Effect of combination therapy with low dose radiation (small animal radiation research platform (SARRP) at 5 Gray (Gy) on the day of staging (day 10)), PD-1 mAb (10 mg/kg twice weekly for 2 weeks) and α V β 8 mAb (7 mg/kg three times weekly for 3 weeks) measured by tumor burden. 5Gy+PD-1 and 5Gy+ α V β 8 has a minimal effect on tumor growth inhibition showing slight improvement relative to radiation alone (5Gy+IgG). Addition of α V β 8 antagonist (5Gy+ α V β 8 +PD-1) improves anti-tumor responses leading to CR in 8 of 10 mice. (B) Kaplan-Meier Curve presenting time to progression. 5Gy+IgG improved survival over monotherapy with either α V β 8 or PD-1 mAb. 5Gy+ α V β 8+PD-1 resulted in a profound improvement of the survival over all other treatment conditions

REFERENCES

- Reszka-Blanco NJ, Yadav V, Krumpoch M, Cappellucci L, Cui D, Dowling JE, et al., Inhibition of integrin α V β 8 enhances immune checkpoint induced anti-tumor immunity by acting across immunologic synapse in syngeneic models of breast cancer. AACR; Cancer Res 2021;81(13_Suppl):Abstract nr 1559.
- Jin S, Lee WC, Aust D, Pilarsky C, Cordes N, β 8 integrin mediates pancreatic cancer cell radiochemoresistance. Mol Cancer Res. 2019; 17(10): 2126–2138.
- Maier B, Leader AM, Chen ST, Tung N, Chang C, LeBerichel J, et al., A conserved dendritic-cell regulatory program limits antitumor immunity. Nature. 2020; 580(7802): 257–262.
- Garris CS, Arlauckas SP, Kohler RH, Trefny MP, Garren S, Piot C, Engblom C, et al., Successful anti-PD-1 cancer immunotherapy requires T cell-dendritic cell cross-talk involving the cytokines IFN- γ and IL-12. Immunity. 2018; 49(6): 1148–1161.
- Dodagatta-Marri E, Ma H-Y, Liang B, Li J, Meyer DS, Chen S-Y, et al., Integrin α V β 8 on T cells suppresses anti-tumor immunity in multiple models and is a promising target for tumor immunotherapy. Cell Report. 2021; 36(1): 109309

Ethics Approval All animal work was approved by the site Institutional Animal Care and Use Committee and was performed in conformance with the Guide for the Care and Use of Laboratory Animals within an AAALAC-accredited program. Humane euthanasia criteria were predetermined on the basis of body weight and defined clinical observations.

<http://dx.doi.org/10.1136/jitc-2021-SITC2021.595>

596

COMBINING BEMPEGALDESLEUKIN (CD122-PREFERENTIAL IL-2 PATHWAY AGONIST) AND NKTR-262 (TLR7/8 AGONIST) PAIRS LOCAL INNATE ACTIVATION WITH SYSTEMIC CD8+ T CELL EXPANSION TO ENHANCE ANTI-TUMOR IMMUNITY

¹Annah Rolig*, ¹Daniel Rose, ¹Grace Helen McGee, ²Saul Kivimae, ²Werner Rubas, ¹William Redmond. ¹Earle A. Chiles Research Institute, Portland, OR, USA; ²Nektar Therapeutics, San Francisco, CA, USA

Background Tumor cell death caused by radiation therapy (RT) can trigger anti-tumor immune responses in part because dying cells release adjuvant factors that amplify and sustain DC and T cell responses. We previously demonstrated that bempegaldesleukin (BEMPEG;NKTR-214, a first-in-class CD122-preferential IL-2 pathway agonist), significantly enhanced the anti-tumor efficacy of RT through a T cell-dependent mechanism. Because RT can induce either immunogenic or tolerogenic cell death, depending on a multitude of factors (radiation dose, cell cycle phase, and tumor microenvironment), we hypothesized that providing a specific immunogenic adjuvant, like intratumoral NKTR-262, a novel toll-like receptor (TLR) 7/8 agonist, to the tumor site would further improve systemic tumor-specific immunity by promoting synergistic activation of local immunostimulatory innate immune responses. Therefore, we evaluated whether intratumoral NKTR-262, combined with systemic BEMPEG treatment would result in improved tumor-specific immunity and survival compared to BEMPEG combined with RT.

Methods Tumor-bearing mice (CT26; EMT6) received BEMPEG (0.8 mg/kg; iv), RT (16 Gy x 1), and/or intratumoral NKTR-262 (0.5 mg/kg). Flow cytometry was used to evaluate CD4+ and CD8+ T cell activation status in the blood and tumor (7 days post-treatment). The contribution of specific immune subsets was determined by depletion of CD4+, CD8+, or NK cells. CD8+ T cell cytolytic activity was determined in vitro with an Incucyte assay. Data are representative of 1–2 independent experiments (n=5–14/group) and statistical significance was determined by 1-way ANOVA (p-value cut-off of 0.05).

Results BEMPEG/NKTR-262 resulted in significantly improved survival compared to BEMPEG/RT. Both combination therapies were CD8+ T cell dependent. However, response to BEMPEG/NKTR-262 was characterized by a significant expansion of activated CD8+ T cells (GzmA+; Ki-67+; ICOS+; PD-1+) in the blood, which correlated with reduced tumor size (p<0.05). In the tumor, BEMPEG/NKTR-262 induced higher frequencies of GzmA+ CD8+ T cells exhibiting reduced expression of suppressive molecules (PD-1+, TIM-3+), compared to BEMPEG/RT. Additionally, CD8+ T cells isolated from BEMPEG/NKTR-262-treated tumors had greater cytolytic capacity than those from BEMPEG/RT-treated mice.

Conclusions Combining BEMPEG with NKTR-262 lead to a more robust expansion of activated CD8+ T cells compared to the BEMPEG/RT combination. Enhancement of the activated CD8+ T cell response in mice treated with NKTR-262 in combination with BEMPEG suggests that intratumoral TLR stimulation provides superior antigen presentation and costimulatory activity compared to RT. A clinical trial of BEMPEG/NKTR-262 for patients with metastatic solid tumors is in progress (NCT03435640).

<http://dx.doi.org/10.1136/jitc-2021-SITC2021.596>

THE ROLE OF CCL20 IN MEDIATING REGULATORY T CELL INFILTRATION AND RESISTANCE TO RADIOTHERAPY IN HEAD AND NECK SQUAMOUS CELL CARCINOMA

Cleopatra Ruthinda, Leanié Moreau, Safia Chelighem, Ayman Oweida*. *Université de Sherbrooke, Sherbrooke, Canada*

Background Radiotherapy (RT) is commonly used to treat solid tumors but its efficacy varies widely. In non-virally driven head and neck cancer (HNC), radioresistance is responsible for most cases of tumor progression and tumor recurrence. The combination of RT and immunotherapy (IT), in the form of anti-PD-1/PD-L1, improved survival for a minority of patients with tumors that have pre-existing immunity or which are susceptible to RT-induced tumor immunity. In contrast, tumors with an immunosuppressive microenvironment show resistance to RT and/or IT. Regulatory T cells (Tregs) have been shown to be prevalent in HNC tumors and can promote treatment resistance. We identified the chemokine, CCL20 as a factor that can promote infiltration of Tregs into HNC tumors. CCL20 is secreted by the cancer cell and binds to its sole receptor, CCR6, expressed on Tregs. We therefore hypothesized that radiation induces CCL20 secretion resulting in infiltration of Tregs and radioresistance. We further hypothesized that blocking CCL20 in HNCs where CCL20 is induced in response to RT can decrease tumor growth.

Methods Human and murine HNC cell lines (SCC9, Cal27, MOC1, MOC2) were irradiated at doses of 2Gy or 10Gy. Conditioned media (CM), RNA and protein were obtained 24h and 72h after radiation. The concentration of CCL20 was analyzed using a chemokine array. Gene expression was determined using qPCR. For in vivo studies, the MOC2 cell line was used. Mice were inoculated in the buccal cavity. Neutralizing CCL20 antibody was administered alone and in combination with RT. Blood samples were collected before and after RT for analysis of serum levels of CCL20.

Results Gene expression analysis showed that Cal27 and MOC2 tumors had a gene signature associated with immune-suppression and Treg cell infiltration. In contrast, SCC9 and MOC1 tumors displayed a gene signature associated with an inflamed microenvironment. In vitro, radiation induced a significant increase in CCL20 gene expression and secreted CCL20 in Cal27 and MOC2 cells relative to control. In contrast, MOC1 and SCC9 did not show a significant increase in CCL20 after radiation. In vivo, inhibition of CCL20 decreased tumor growth compared to control in MOC2 tumors. The combination of RT and anti-CCL20 showed a significant decrease in tumor growth compared to RT alone.

Conclusions Collectively, our data suggest that radiation promotes the induction of CCL20 in tumors with immune-suppressive mechanisms and inhibition of CCL20 can enhance the response to RT.

Ethics Approval All animal studies were conducted in accordance with the animal protection and ethics committee of the faculty of medicine at Université de Sherbrooke (Le Comité facultaire de protection des animaux). Protocol #: 2019-2333.

<http://dx.doi.org/10.1136/jitc-2021-SITC2021.597>

598 LOCAL RADIATION IN COMBINATION WITH CPG AND ANTI-OX40 INDUCES ENHANCED T CELL ACTIVATION AND PROLIFERATION

¹Dan Spiegelman*, ¹Alexander Pieper, ¹Luke Zangl, ¹Arika Feils, ¹Anna Hoefges, ¹Mildred Felder, ¹Sritha Moram, ¹Alexander Rakhmievich, ¹Amy Erbe, ¹Jacquelyn Hank, ²Ravi Patel, ¹Zachary Morris, ¹Paul Sondel. ¹University of Wisconsin-Madison, Madison, WI, USA; ²University of Pittsburgh, Pittsburgh, PA, USA

Background We, and others, have previously shown that the in-situ vaccine of hypomethylated CG-enriched oligodeoxynucleotide (CpG) with agonist anti-OX40 antibody (OX40) is effective at curing mice in the A20 lymphoma model [1–4]. In separate preclinical models where CpG+OX40 fails to cause tumor regression, radiation therapy (RT) prior to the in-situ vaccine enhances the anti-tumor effect of CpG+OX40 [4]. We investigated the immune response, and specifically the activity of T cells, following treatment with RT+CpG+OX40 in the B78 melanoma model where CpG+OX40 typically fails to cause tumor regression.

Methods C57BL/6 mice were inoculated with 2x10⁶ B78 melanoma cells on the right flank and allowed to grow until the average tumor size was ~150mm³. In two independent experiments, mice were randomized (n=4–5 per group per experiment) and treated with one of the following: 1) PBS, 2) CpG+OX40, 3) RT, 4) RT+CpG+OX40. 12 Gy external beam RT was dosed to the flank tumor on day 0 and intratumoral CpG (50µg)+OX40 (20 µg) were given on days 5, 7, and 9 after RT. Spleens and tumor draining lymph nodes (TDLNs) were harvested on day 12. T cell activation and proliferation were assessed via flow cytometry.

Results Compared to all other groups in the study, mice treated with RT+CpG+OX40 demonstrated significantly elevated levels of CD4+ and CD8+ T cell activation in the TDLNs, as measured by interferon gamma expression. Similar trends of CD4+ and CD8+ T cell activation were measured in the spleens. Splenic CD8+ T cells from RT+CpG+OX40 treated mice demonstrated significantly elevated levels of proliferation over PBS and RT, as measured by Ki67.

Conclusions In B78 melanoma, a weakly immunologic tumor model, combining RT with the in-situ vaccine CpG+OX40 enhances the activity of T cells, evidenced by significantly increased CD4+ and CD8+ T cell activation in the TDLN and spleen and elevated CD8+ T cell proliferation in the spleen.

REFERENCES

- Houot, R. and Levy, R. T-cell modulation combined with intratumoral CpG cures lymphoma in a mouse model without the need for chemotherapy. *Blood*, 2009. 113(15):3546–52.
- Marabelle, A., et al. Depleting tumor-specific Tregs at a single site eradicates disseminated tumors. *J Clin Invest*, 2013. 123(6):2447–63.
- Sagiv-Barfi, I., et al. Eradication of spontaneous malignancy by local immunotherapy. *Sci Transl Med*, 2018. 10(426).
- Zangl, LM. Et al. External Beam Radiotherapy Required for Tumor Regression When Using CpG-Oligodeoxynucleotide and Anti-OX40 in an Immunologically Cold Tumor Model. *Red Journal*. 2019. 105:588.

<http://dx.doi.org/10.1136/jitc-2021-SITC2021.598>

599

CYCLOPHOSPHAMIDE AUGMENTS THE EFFICACY OF AN IN SITU VACCINE IN A MOUSE MELANOMA MODEL

Noah Tsarovsky*, Mildred Felder, Mackenzie Heck, Jacob Slowinski, Kayla Rasmussen, Sabrina VandenHeuvel, Zachary Morris, Amy Erbe, Paul Sondel, Alexander Rakhmievich. *University of Wisconsin-Madison, Madison, WI, USA*

Background We have previously shown that a direct intratumoral (IT) injection of the hu14.18-IL2 immunocytokine (IC), an anti-GD2 antibody linked to interleukin 2, can serve as an in situ vaccine and synergize with local radiotherapy (RT) to induce T cell-mediated antitumor effects. We hypothesized that cyclophosphamide (CY), a chemotherapeutic agent capable of depleting T regulatory cells (Tregs), would augment in situ vaccination.

Methods GD2+ B78 mouse melanoma cells were injected intradermally in syngeneic C57BL/6 mice. Treatments with RT (12Gy) and/or CY (100 mg/kg i.p.) started when tumors reached the size of 100–200 mm³ (day 0) followed by five daily injections of IT-IC (25 mcg) on days 5–9. In some experiments, CY was given prior or after RT. Tumor growth and survival were followed. In addition, tumors were analyzed by flow cytometry.

Results A single injection of CY led to an enhanced antitumor effect of IC comparable to that of RT. The strongest antitumor effect was achieved when CY, RT and IC were combined, as compared to combinations of CY+RT, CY+IC or RT+IC. This augmented effect of the triple combination was seen when CY was given on the same day as RT. Flow cytometric analyses showed that CY treatment decreased Tregs and increased the ratio of CD8+ cytotoxic cells to Tregs within the tumors. Moreover, the combination of RT, CY and IT-IC led to a systemic antitumor effect against the untreated tumor in a two-tumor model. Cured mice developed immunological memory as they were able to reject B78 tumor rechallenge.

Conclusions CY can augment the antitumor efficacy of IT- IC given alone or in combination with local RT in tumor-bearing mice. These preclinical results suggest the value of initiating clinical testing of the combination of CY, RT and IT-IC as an in situ vaccine.

<http://dx.doi.org/10.1136/jitc-2021-SITC2021.599>

600

BR101801 STIMULATES ANTI-TUMOR IMMUNITY AND ENHANCES THE EFFICACY OF RADIATION IN A SYNGENEIC MODEL

¹Seungho Wang*, ²Yi Na Yoon, ¹Mi kwon Son, ¹Soo Jung Kim, ¹Bo Ram Lee, ¹Eun hee Yang, ¹Byeongwook Jeon, ¹Seung Hyun Lee, ²Tae-Jin Kim, ²Jae-Sung Kim, ¹Joo Han Lee. ¹Boryung Pharmaceutical, Gyeonggi-do, Ansan-si, Korea, Republic of; ²Korea Institute of Radiological and Medical Sciences, Seoul, Korea, Republic of

Background BR101801 is an inhibitor of PI3K γ/δ and DNA-PK. It has received clinical approval from the U.S. FDA as an anticancer drug candidate, and phase 1a/1b is ongoing in the U.S. and South Korea. According to the prior studies PI3K γ/δ inhibition exhibits anticancer immune effects by changing the tumor microenvironment [1]. In addition, ionizing radiation (IR) activates the immune response by causing the destroyed cells to act as antigens [2]. Therefore, the combination of BR101801 and IR can induce cancer cell death and amplify anticancer immune effects. This study aims to demonstrate efficacy of the BR101801 as a potent cancer immunotherapy.

Methods The enzymatic potency of PI3K isotype and DNA-PK was analyzed by Eurofins. The effects of BR101801 on cell viability were evaluated in 4T1 (breast cancer) and CT-26 (colon cancer) cells for 72 h using WST-8 assay. For in vivo studies, the tumor (4T1 or CT-26)-bearing syngeneic mice were treated with BR101801. To evaluate the synergistic effect, CT-26 tumor-bearing syngeneic mice were treated with vehicle, BR101801, IR (2 Gy or 7.5 Gy), and BR101801 + IR. Immune cells from the spleen or tumor were quantified by flow cytometry.

suppressor cells (MDSC) were decreased and CD8+ T cells were increased in the spleens isolated from the tumor-bearing mice. Compared with other PI3K inhibitors, BR101801 had the highest efficacy, confirming that it changes the immune microenvironment. Moreover, BR101801 was synergistic in combination with 2 Gy or 7.5 Gy of IR in the syngeneic model. Notably, Tregs & Macrophage2 were decreased and CD8+ T cells were increased in the tumor tissue, confirming that the anticancer efficacy.

The combination of BR101801 and ionizing radiation showed synergistic effects in the CT-26 Syngeneic model. BR101801 increases anti-cancer immune cells, CD8 + T cells, and decreases immune suppressor cells Tregs and macrophages through a combination of radiation, resulting in immuno-cancer effects.

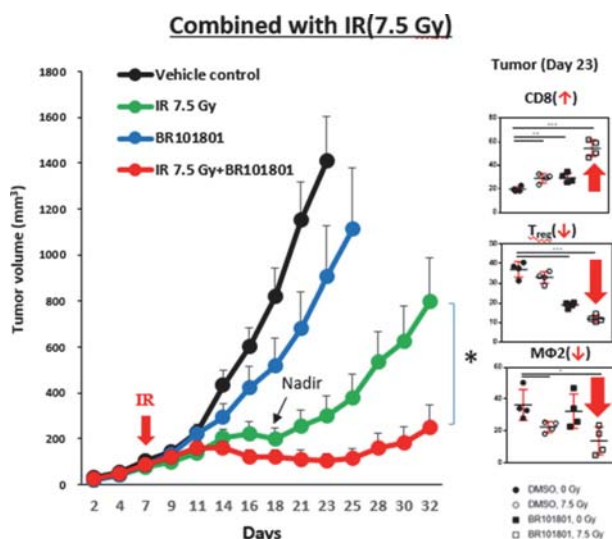
Conclusions BR101801 demonstrated an anticancer immune effect by changing the tumor microenvironment and showed synergistic effects with radiation combination therapy. We will confirm the anticancer immunity effect in ongoing clinical trials.

REFERENCES

- Okkenhaug K, Graupera M, Vanhaesebroeck B. Targeting PI3K in Cancer: Impact on Tumor Cells, Their Protective Stroma, Angiogenesis, and Immunotherapy. *Cancer Discov.* 2016; 10: 1090–1105.
- McKelvey K, Hudson A, Back M, Eade T, Diakos C. Radiation, inflammation and the immune response in cancer. *Mammalian Genome.* 2018;9:843–865

Ethics Approval The protocol and any amendment(s) or procedures involving the care and use of animals in this study were reviewed and approved by the Institutional animal Care and Use Committee (IACUC) of BoRyung Pharm. prior to conduct.[Approval number:BR18130]

<http://dx.doi.org/10.1136/jitc-2021-SITC2021.600>



Abstract 600 Figure 1 Synergistic effect with ionizing radiation In Vivo

Results In vitro selectivity and target potency of BR101801 on different PI3K isotypes and DNA-PK were studied in a cell-free system. The biochemical IC₅₀ values of BR101801 for PI3K γ , δ , and DNA-PK were 15 nM, 2 nM, and 6 nM, respectively. In vitro 50% of maximal inhibition of cell proliferation (GI₅₀) in 4T1 and CT26 cell lines were both above 10 μ M. In 4T1 and CT-26 syngeneic models, BR101801 showed the highest tumor inhibitor efficacy (Figure 1). In particular, regulatory T cells (Tregs) & Myeloid derived

601

SEQUENCING IMMUNOTHERAPY BEFORE LYMPHATIC ABLATION UNLEASHES CDC1-DEPENDENT ANTITUMOR IMMUNITY IN HNSCC

¹Robert Saddawi-Konefka*, ²Aoife O'Farrell, ¹Farhoud Faraji, ¹Michael Allevato, ¹Zhiyong Wang, ¹Victoria Wu, ¹Bryan Yung, ¹Nana-Ama Anang, ¹Ida Franiak-Pietryga, ³Aaron Simon, ⁴Shawn Jensen, ⁴Bernard Fox, ¹Andrew Sharabi, ¹Ezra Cohen, ¹Joseph Califano, ¹J Silvio Gutkind. ¹UC San Diego School of Medicine, La Jolla, CA, USA; ²University of Pennsylvania, Philadelphia, PA, USA; ³San Diego School of Medicine, San Diego, CA, USA; ⁴Providence Cancer Institute, Portland, OR, USA

Background Despite the proven efficacy of immune checkpoint inhibitor (ICI) therapy in the recurrent/metastatic setting for head and neck squamous cell carcinoma (HNSCC), clinical trials of ICI combined with curative-intent therapies have yielded equivocal results [1–4]. Collectively, this highlights gaps in our understanding of rational immune oncology (IO) treatment sequencing and suggests that the efficacy ICI may be disrupted by standard therapies, which necessarily compromise regional lymphatics.

Methods We employ a preclinical model of tobacco-signature HNSCC to identify sequences of therapy that maximize durable response. By mapping the cervical lymphatic basins in the mouse, we define patterns of active antitumor immunosurveillance. Additionally, we establish tumors with distinct patterns of regional lymphatic drainage and develop a murine neck dissection (ND) model.

Results We find that cervical lymphatic ablation, with ND or stereotactic body radiation therapy, in tumor bearing animals abolishes the response to ICI therapy, significantly impacting overall survival. Examination of the tumor immune microenvironment following ND reveals dramatic changes with a ten-fold increase in CD45 cells and exclusion of cytotoxic and antigen-specific lymphocytes. By examining the lymphatics removed at the time of ND, we find that conventional type I dendritic cells (cDC1s) and type I interferon (IFN-I) signaling are significantly increased, suggesting that these effectors are lost after curative-intent therapy. Depleting IFN-I or cDC1s blocks the response to ICI similar to lymphatic ablation. We find that successful primary response to ICI leads to durable immunity, conferred by systemically distributed memory T cells, not impaired by delayed ND. Lastly, we discover a rational IO treatment sequence by delivering neoadjuvant ICI followed by ND. Neoadjuvant ICI leads to complete tumor response, accumulation of nodal cDC1, and durable immunity. Surprisingly, the incidence of nodal metastasis at early timepoints reveals a similar burden of nodal disease between control and ICI-treated animals that decreases at late timepoints only with ICI treatment (44% vs 15%, $n=25$, $p=0.033$). This suggests that ICI also drives active immunosurveillance in regional, tumor-draining lymphatics, challenging the landmark findings from the definitive clinical trial demonstrating the benefit of elective versus therapeutic neck dissection for oral SCC patients with clinically negative necks.

Conclusions This work demonstrates the necessity of preserving tumor-draining lymphatics during the tumor response to ICI therapy in HNSCC. Overall, we define rational IO treatment sequences to achieve optimal primary tumor response, durable antitumor immunity and immunosurveillance of regional metastatic disease. These findings can inform future clinical trials investigating combination IO therapy and treatment sequencing.

REFERENCES

- Harrington, K. J. et al. Nivolumab versus standard, single-agent therapy of investigator's choice in recurrent or metastatic squamous cell carcinoma of the head and neck (CheckMate 141): health-related quality-of-life results from a randomised, phase 3 trial. *Lancet Oncology* 18, 1104–1115 (2017).
- Burtneß, B. et al. Pembrolizumab alone or with chemotherapy versus cetuximab with chemotherapy for recurrent or metastatic squamous cell carcinoma of the head and neck (KEYNOTE-048): a randomised, open-label, phase 3 study. *Lancet* (London, England) 394, 1915–1928 (2019).
- Lee, N. Y. et al. Avelumab plus standard-of-care chemoradiotherapy versus chemoradiotherapy alone in patients with locally advanced squamous cell carcinoma of the head and neck: a randomised, double-blind, placebo-controlled, multicentre, phase 3 trial. *Lancet Oncol* 22, 450–462 (2021).
- D'Cruz, A. K. et al. Elective versus Therapeutic Neck Dissection in Node-Negative Oral Cancer. *New England Journal of Medicine* 373, 521–529 (2015).

<http://dx.doi.org/10.1136/jitc-2021-SITC2021.601>

AXL TARGETING WITH BEMCENTINIB RESTORES PD-1 BLOCKADE SENSITIVITY OF STK11/LKB1 MUTANT NSCLC THROUGH INNATE IMMUNE CELL MEDIATED EXPANSION OF TCF1+ CD8 T CELLS

¹Huiyu Li*, ²Zhida Liu, ¹Longchao Liu, ¹Hongyi Zhang, ¹Chuanhui Han, ¹Luc Girard, ¹Hyunsil Park, ¹Anli Zhang, ¹Chunbo Dong, ¹Jianfeng Ye, ³Austin Rayford, ¹Michael Peyton, ¹Xiaoguang Li, ¹Kim Avila, ¹Xuezhi Cao, ¹Shuiqing Hu, ¹Esra Akbay, ⁴Luisa Solis, ⁴Carmen Behrens, ⁴Sharia Hernandez-Ruiz, ⁴Lu Wei, ⁴Ignacio Wistuba, ⁴John Heymach, ⁵Michael Chisamore, ³David Micklem, ³Hani Gabra, ³Gro Gausdal, ⁶James Lorens, ¹Bo Li, ¹Yang-Xin Fu, ¹John Minna, ¹Rolf Brekken. ¹UT Southwestern Medical Center, Dallas, TX, USA; ²SAARI, Taiyuan, China; ³BergenBio ASA, Bergen, Norway; ⁴The University of Texas MD Anderson Cancer Center, Houston, TX, USA; ⁵Merck and Co., Inc., Wheaton, IL, USA; ⁶University of Bergen, Bergen, Norway

Background Mutations in tumor suppressor STK11/LKB1 are associated with negative predictive and prognostic impact in NSCLC patients receiving immune checkpoint inhibitors (CPI) in several published cohorts, although there have been some conflicting reports on the association of such mutations with patient outcomes in this setting [1–9]. STK11/LKB1 tumors are characterized by a suppressive tumor micro-environment devoid of cytotoxic T cells, and we hypothesized that targeting the receptor tyrosine kinase AXL, a known driver of an innate immune suppressive microenvironment, would restore sensitivity to PD-1 in syngeneic pre-clinical models as well as in patients harboring STK11/LKB1 mutated NSCLC.

Methods Stk11/Lkb1 (L) mutation was introduced by CRISPR technology into murine lung adenocarcinomas driven by mutant Kras and Trp53 loss (KP). Sensitivity towards anti-PD-1 was evaluated in the absence and presence of the small molecule AXL inhibitor bemcentinib in the KPL model and in a human NSCLC xenograft model carrying a STK11/LKB1 mutation. The immune tumor landscape was mapped following introduction of the Stk11/Lkb1 mutation and therapeutic intervention with anti-PD-1/pembrolizumab and bemcentinib. FFPE fine-needle aspirate biopsies of target lesions were acquired from patients at screening immediately prior to enrollment in BGBC008, a PhII single-arm, 2-stage study with bemcentinib (200mg/d) and pembrolizumab (200 mg/q3wk) for previously-treated stage IV lung adenocarcinoma patients who were CPI naïve or CPI refractory. Patients were assessed for response according to RECIST1.1 criteria at scheduled scan intervals.

Results Introduction of a STK11/LKB1 mutation into murine lung adenocarcinomas driven by mutant Kras and Trp53 loss resulted in a PD-1 refractory syngeneic KPL tumor. Mechanistically this occurred because KPL mutant NSCLCs lacked TCF1-expressing CD8 T cells, a phenotype that was recapitulated in human STK11/LKB1 mutant NSCLCs. Systemic inhibition of AXL with bemcentinib resulted in increased type I interferon secretion from dendritic cells resulting in expansion of tumor-associated TCF1+PD-1+CD8 T cells and restored therapeutic response to PD-1. This effect was observed in a syngeneic immunocompetent mouse model and in humanized mice bearing STK11/LKB1 mutant NSCLC human tumor xenografts. In an ongoing clinical trial (NCT03184571), 3 evaluable NSCLC patients with identified STK11/LKB1 mutations demonstrated objective clinical response/clinical benefit to the combination of AXL inhibitor bemcentinib and pembrolizumab.

Conclusions In these models, AXL is a critical targetable driver of immune suppression in STK11/LKB1 mutant NSCLC contributing to CPI resistance. Our results show that inhibition of AXL rescues this deficit and represents a new clinical

strategy in combination with anti-PD-1 therapy in NSCLC patients carrying a STK11/LKB1 mutation

Acknowledgements The authors would like to thank all patients and their caretakers for participating in this trial.

Trial Registration Patients treated with bemcentinib and pembrolizumab combination therapy were enrolled in the BGBC008 clinical trial (BerGenBio ASA and Merck & Co., Inc., Kenilworth NJ, USA, NCT03184571)

REFERENCES

1. Gu M, Xu T, Chang P. KRAS/LKB1 and KRAS/TP53 co-mutations create divergent immune signatures in lung adenocarcinomas. *Ther Adv Med Oncol.* 2021;13:17588359211006950.
2. Cho BC, Lopes G, Kowalski DM. Relationship between STK11 and KEAP1 mutational status and efficacy in KEYNOTE-042: pembrolizumab monotherapy as first-line therapy for PD-L1 positive advanced NSCLC. *Cancer Res.* 2020;80(16 Supplement):CT084.
3. Aredo JV, Padda SK, Kunder CA. Impact of KRAS mutation subtype and concurrent pathogenic mutations on non-small cell lung cancer outcomes. *Lung Cancer.* 2019;133:144–150.
4. Kwack WG, Shin SY, Lee SH. Primary Resistance to Immune Checkpoint Blockade in an STK11/TP53/KRAS-Mutant Lung Adenocarcinoma with High PD-L1 Expression. *Oncol Targets Ther.* 2020;13:8901–8905.
5. Shire NJ, Klein AB, Golozar A. STK11 (LKB1) mutations in metastatic NSCLC: Prognostic value in the real world. *PLoS One.* 2020;15(9):e0238358.
6. Skoulidis F, Goldberg ME, Greenawald DM. STK11/LKB1 Mutations and PD-1 Inhibitor Resistance in KRAS-Mutant Lung Adenocarcinoma. *Cancer Discov.* 2018;8(7):822–835.
7. Wang H, Guo J, Shang X. Less immune cell infiltration and worse prognosis after immunotherapy for patients with lung adenocarcinoma who harbored STK11 mutation. *Int. Immunopharmacol.* 2020;84:106574.
8. Kitajima S, Ivanova E, Gou S. Suppression of STING Associated with LKB1 Loss in KRAS-Driven Lung Cancer. *Cancer Discov.* 2019;9(1):34–45.
9. Mograbi B, Heeke S, Hofman P. The Importance of STK11/LKB1 Assessment in Non-Small Cell Lung Carcinomas. *Diagnostics (Basel).* 2021;11(2):196.

Ethics Approval This study was approved by the following ethical committees: Use of human cord blood: UT Southwestern (UTSW) Parkland Hospital, STU 112010-047 Animal studies: UTSW Medical Center, Institutional Animal Care and Use Committee, APN 2015-100921 Clinical study: London Bridge Research Ethics Committee (UK): 17/LO/0418; REC-South East (Norway): 2017/473; Drug Research Ethics Committee of the University Hospital Clinic of Barcelona (Spain): BGBC008/MK-3475_PN-531; Medical College of Wisconsin Institutional Review Board #4 (USA): PRO00029453

<http://dx.doi.org/10.1136/jitc-2021-SITC2021.602>

603 **TARGETED STAT3 DEGRADATION LEADS TO
REMODELING OF AN IMMUNOSUPPRESSIVE TUMOR
MICROENVIRONMENT AND SUBSEQUENT
SENSITIZATION TO IMMUNE CHECKPOINT THERAPY**

Joyoti Dey*, Phillip Liu, Michele Mayo, Rahul Karnik, Bin Yang, Vaishali Dixit, Jieun Jeong, Jared Gollub, Chris De Savi. *Kymera Therapeutics, Watertown, MA, USA*

Background Signal Transducer and Activator of Transcription 3 (STAT3), a multifaceted transcription factor, is aberrantly activated across a variety of malignancies; however, its selective targeting has to-date remained a therapeutic challenge. STAT3 plays a pivotal role in shaping the tumor immune landscape through cancer cell-intrinsic mechanisms, direct regulation of immune cell function and via cancer cell- tumor microenvironment (TME) crosstalk, that collectively result in an immunosuppressive TME. Targeted protein degradation represents a novel therapeutic modality enabling direct targeting of previously undruggable oncoproteins. We have developed potent and selective STAT3 heterobifunctional degraders demonstrating activity across diverse tumor and immune cell types.

Methods We investigated the immunomodulatory impact of STAT3 degradation on tumorigenesis in syngeneic mouse models representing cancers with heterogeneous immune milieus. Methods included in vivo pharmacological approaches, immunophenotyping and gene expression profiling.

Results Treatment of CT-26 (colorectal cancer) and A20 (B-cell lymphoma) tumor-bearing mice with a STAT3 degrader resulted in significant tumor growth inhibition compared to controls, with loss of STAT3 protein in both tumor cells and TME. This was accompanied by a decrease in M2 polarized macrophages and concomitant increases in M1 polarized macrophages and tumor infiltrating lymphocytes. The anti-tumor responses were abrogated by antibody mediated CD8+ T cell depletion or by using immunodeficient host-strains implicating the observed efficacy to be predominantly driven by immune-directed mechanisms. Gene expression profiling of STAT3 degrader-treated CT-26 tumors showed marked increases in proinflammatory genes including T cell and M1 macrophage activation markers, compared to controls. Notably, induction of an *Ifn γ* -responsive gene signature (*Ifn γ* , *Stat1*, *Cxcl9*, *Cxcl10*, *Ido1*) suggested that STAT3 degradation results in a T-cell inflamed phenotype associated with responsiveness to immune checkpoint therapy (ICT). Furthermore, on-treatment tumors showed an upregulation of genes such as *Pd11*, *Ctla4*, *Lag3* which reflect T cell activation as well as counterregulatory mechanisms. Therefore, we evaluated STAT3 degradation in combination with anti-PD1 in these models which are poorly responsive to anti-PD1 monotherapy. Robust synergy was observed in the CT-26 model with 60% complete responses and development of immunological memory as confirmed by tumor re-challenge studies. Studies are underway to ascertain the applicability of this combination therapy in different tumor-immune contextures and indications, and to elucidate the mechanistic basis of synergy.

Conclusions STAT3 degradation remodels an immunosuppressed TME activating anti-tumor immunity as monotherapy and effectively combines with anti-PD1. These data provide a rationale for selectively degrading STAT3 as a strategy to sensitize cancers with relevant immune contextures to ICT in the clinic.

<http://dx.doi.org/10.1136/jitc-2021-SITC2021.603>

604 **COMBINING A NOVEL DUAL RAF/MEK INHIBITOR WITH IMMUNOMODULATION TO PROMOTE AN ANTI-TUMOR RESPONSE**

Lauren Dong*, Hyejin Choi, Sadna Budhu, Isabell Schulze, Nezar Mehanna, Neal Rosen, Taha Merghoub, Jedd Wolchok. *Memorial Sloan Kettering Cancer Center, New York, NY, USA*

Background The therapeutic scope of MEK inhibitors (MEKis) is currently limited to use in BRAF mutant melanoma. Therefore, we aim to develop new strategies to extend their usage to MEKi resistant RAS mutant cancers, which represent an unmet clinical need. In Ras mutant murine lung cancers, CH5126766 (CKI27) is novel due to its ability to inhibit both RAF and MEK, preventing the rebound of p-ERK that normally results from the relief of negative feedback in the MAPK/ERK pathway. However, CKI27 is also capable of inhibiting T cell functions because the MAPK/ERK pathway is activated downstream of T cell receptor signaling. We aim to balance the positive and negative immunomodulatory effects of MEKis for optimal combination with immunotherapy.

Methods To evaluate the effects of CKI27 on tumor cells and T cells in vitro, we performed flow cytometry, cytokine analysis, and functional co-culture assays. Lewis lung carcinoma (LLC) tumor bearing mice were treated either with CKI27 combined with co-stimulatory agonist antibody targeting GITR and checkpoint blockade antibody targeting CTLA-4 or the appropriate controls to determine efficacy and changes in the tumor microenvironment.

Results We observed that CKI27 increased MHC expression on tumor cells and T cell mediated killing. Yet, CKI27 also decreased T cell proliferation, activation, and cytolytic activity. Implementing a break for T cells to recover with intermittent dosing of CKI27 partially relieved these inhibitory effects. Further combination with agonist antibodies anti-OX40 and GITR completely alleviated these T cell toxicities and increased combination efficacy with checkpoint blockade antibody anti-CTLA-4.

Conclusions Understanding the immunomodulatory effects of combining CKI27 with immunotherapy will elucidate the mechanism behind their increased efficacy. This will allow us to make more informed decisions in dosing regimens, overcoming resistance, and generating long-term immune responses in current and future clinical trials treating patients with RAS mutant cancers.

<http://dx.doi.org/10.1136/jitc-2021-SITC2021.604>

605

NHS-IL12 PLUS ENTINOSTAT COMBINATION EFFECTIVELY TARGETS ANTI-PD-1/PD-L1 CHECKPOINT RESISTANT MURINE TUMORS HARBORING MHC CLASS I AND ANTIGEN PROCESSING MACHINERY DEFICIENCY

Christine Minnar*, Paul Chariou, Kristin Hicks, Jeffrey Schlom, Sofia Gameiro. *National Cancer Institute, Bethesda, MD, USA*

Background Immune checkpoint blockade (ICB) has achieved unprecedented success in treating multiple cancer types. However, clinical benefit remains modest for most patients with solid malignancies with the majority having primary resistance to these therapies. Additionally, many patients that initially respond often acquire resistance. Tumor-intrinsic loss of MHC class I and aberrations in the interferon gamma (IFN γ) pathway have been shown to play an important role in ICB resistance. Entinostat, a class I HDAC inhibitor, has previously been shown to upregulate MHC class I molecules and antigen processing machinery (APM). NHS-IL12 (M9140), an IL12 fusion protein targeting necrotic tissue, increases anti-tumor effector functions through an influx of interferon gamma into the tumor microenvironment (TME). Here, we investigated the combination of Entinostat and NHS-IL12 in three different murine ICB-refractory tumor models (TC-1/a9, CMT.64, or RVP3) harboring varying MHC-class I and APM deficiencies.

Methods Entinostat and murine NHS-IL12 were administered to mice bearing lung TC-1/a9 (HPV16 E6/E7+), CMT.64 (lung), or RVP3 (sarcoma) tumors. Anti-tumor efficacy and survival were monitored. Comprehensive tumor and spleen immune profile analyses were carried out using flow cytometry. Tumor supernatants and sera were analyzed for cytokine and chemokine profiles. Additionally, whole transcriptomic analysis was carried out on TC-1/a9 tumors. TCGA datasets were analyzed for translational relevance.

Results We demonstrated that combination therapy elicits potent anti-tumor activity in ICB-resistant MHC-I deficient tumors through prolonged activation of cytotoxic CD8+ T cells. TC-1/a9 tumor-bearing athymic nude mice and depletion studies confirmed CD8 T cells were required for tumor growth control and survival. Importantly, we show for the first time that combination therapy synergizes to promote antigen presentation, MHC-I and APM upregulation and enrichment of IFN γ and antigen processing pathways increasingly described as hallmarks of ICB resistance. Moreover, combination therapy promoted M1-macrophages and activated antigen presenting cells while suppressing M2-macrophages and Tregs in a tumor-dependent manner. Combination therapy induced high levels of IFN γ , IL-12, CXCL9 and CXCL13 in the TME, resulting in significant anti-tumor activity including in the IFN γ signaling-impaired RVP3 tumor model. A biomarker signature of the mechanism involved in these studies is associated with patients' overall survival across multiple tumor types.

Conclusions Our findings provide a rationale for combining NHS-IL12 with Entinostat in the clinical setting for patients unresponsive to ICB.

Acknowledgements The authors thank Curtis Randolph for his excellent technical assistance.

<http://dx.doi.org/10.1136/jitc-2021-SITC2021.605>

SAR444245 (THOR-707), AN ENGINEERED NON-ALPHA IL-2, ENHANCES NK MEDIATED ANTIBODY-DEPENDENT CELLULAR CYTOTOXICITY

Julie-Ann Gavigan, Nicole Acuff, Christen Buetz, Michael Lampa, Chaomei Shi, Yulan Zhang, Liqing Chen, Kelly Balko, Virna Cortez-Retamozo, Jill Mooney, Carolina Caffaro, Marcos Milla, Joachim Theilhaber, Donald Jackson, Timothy Wagenaar, Giovanni Abbadessa, Donald Shaffer, Xiangming Li*. *Sanofi, Cambridge, MA, USA*

Background SAR444245 is a non-alpha IL-2 Synthorin™ molecule designed with a site-specific non-natural amino acid serving as a bioconjugation site for a single PEG. The non-natural amino acid is positioned to enable the PEG bioconjugation to obscure block binding to the IL-2 alpha receptor, while retaining near-native affinity with the intermediate affinity $\beta\gamma$ IL-2 receptor. The non-alpha features of SAR444245 minimize activation of immune suppressive regulatory CD4+ T cells, while retaining activity on CD8+ T cells and NK cells expressing the IL-2 $\beta\gamma$ receptors. NK cells exert anti-tumor activity through antibody dependent cellular cytotoxicity (ADCC) of IgG antibodies as well as antibody independent mechanisms.

Methods Here, we utilized a panel of human primary PBMC based immunoassays and transcriptomic analysis to evaluate whether SAR444245 may improve ADCC function of IgG1 anti-tumor target antibodies.

Results We characterized the ability of SAR444245 to enhance the cytolytic function of NK cells towards the prototypic NK target cell K562 as well as to modulate NK cell ADCC in combination with EGFR or CD20-targeting antibodies. In vitro assays demonstrated that SAR444245 can activate NK cells, promote NK cell proliferation and improve cytotoxicity of NK cells against K562 cells and across a panel of human EGFR and CD20 positive cell lines. In PBMC based ADCC assays with 1 μ g/ml of antibody, SAR444245 improved ADCC function maximally by 9-fold for an anti-EGFR antibody and at 5-fold for an anti-CD20 antibody. SAR444245 exhibited dose-dependent enhancement of NK cell ADCC function. Notably, this activity was observed in cell lines expressing varying levels of EGFR and CD20. SAR444245 treatment was associated with dose dependent increases in NK cell degranulation and IFN- γ production. Transcriptomic profiling revealed that SAR444245 had broad effects on NK cell biology leading to changes in inhibitory and activating receptors.

Conclusions In summary, these results indicate that SAR444245 can enhance the cytolytic activity of NK cells and enhance the ADCC effect of tumor-directed antibodies by activating NK cells.

<http://dx.doi.org/10.1136/jitc-2021-SITC2021.606>

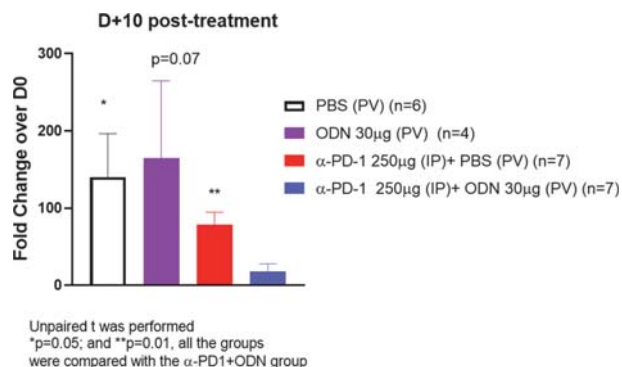
607 REGIONAL DELIVERY OF A TLR9 AGONIST TO BOOST CHECKPOINT INHIBITOR RESPONSIVENESS IN LIVER METASTASES

¹Chandra Ghosh*, ¹Kyle O'Connell, ¹Kara Heatherton, ¹Jason Laporte, ¹Prajna Guha, ²Bryan Cox, ¹Steven Katz, ²Steven Katz. ¹Roger Williams Medical Center, Providence, RI, USA; ²Trisalus Life Sciences, Westminster, CO, USA

Background Class C TLR9 agonists, CpG oligodeoxynucleotides (ODNs) enhance responsiveness to anti-PD1 therapy in solid tumors through favorable modulation of the tumor microenvironment (TME) [1]. Recently, we reported that regional delivery of a TLR9 agonist eliminated myeloid derived suppressor cells (MDSC) and promoted pro-inflammatory/anti-tumorigenic M1 macrophage programming in the TME of liver metastases (LM) [2]. Further, we found enhanced TLR9 activation in LM following regional TLR9 agonist infusion compared to the systemic treatment. We hypothesize that regional delivery of a TLR9A into LM will enhance the responsiveness to systemically infused anti-PD1 therapy.

Methods In this study, we treated mice with established MC38-CEA-Luc LM with ODN-2395 (30µg/mouse) regionally with or without anti PD-1 antibody (250µg/mouse) intraperitoneally.

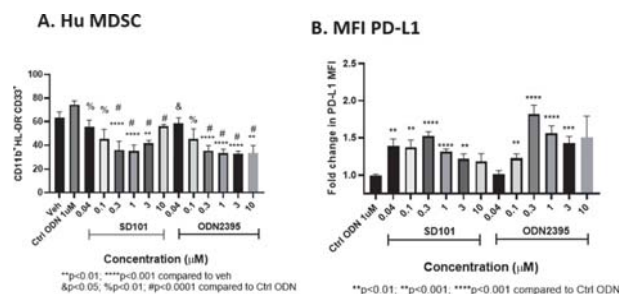
Results Control of LM growth (Figure 1) was significantly higher with combinatorial treatment as compared to anti-PD1 (p<0.01) or PBS treatments (p<0.05). To study the impact of TLR9 activation on human MDSC, we treated healthy donor PBMCs with ODN-2395 or SD101. We found that both reduced the hu-MDSC (CD11b+CD33+HLADR-) population in a dose-dependent manner with an increase in PD-L1 expression as determined by flow cytometry (FC) analysis (Figure 2). Moreover, by using Luminex, demonstrated that ODN-2395 and SD101 enhanced expression of IL 29, IFNα, and NFκB, along with downstream cytokines IL 6 and IL 10. To investigate the effect of SD101 in modulating the differentiation of huMDSC from huPBMC, we treated huPBMC with IL6+GM-CSF in the presence or absence of SD101. By FC analysis, we found that SD-101 blocked huMDSC development induced by IL6+GM-CSF, preferentially limited the more immunosuppressive monocytic MDSC subtype, and drove M1 macrophage polarization. Treatment of SD101 only once for 48hrs was sufficient to inhibit huMDSC differentiation for two weeks.



Abstract 607 Figure 1 Combinatorial treatment of CPI and ODN's reduces t
PV = portal vein; IP = intraperitoneal.

Eight to twelve weeks old male C57/BL6 mice were challenged intra-splenic with 0.5e6 MC38-CEA-Luc cells for a

week. Bioluminescence value was determined by IVIS on D0, and mice were randomized accordingly and treated with 30 µg/mouse ODN2395 via PV with or without 250 µg/mouse anti-PD1 antibody via IP on D0, D+3 and D+6. PBS served as the vehicle (Veh) control and administered via PV. Fold change of the tumor burden was calculated based on D0 baseline bioluminescence. Tumor progression was analyzed unpaired t test among groups. (*p <0.05).



Abstract 607 Figure 2 Human PBMC treated with ODN2395 and SD101 reduces

Ctrl = control; MDSC = ODN = oligodeoxynucleotide' PBMC = peripheral blood monocytes.

Human PBMC were isolated from the Leukoreduction system chamber. 1e6/ml PBMCs were treated with increasing concentrations (0.04–10 µM) SD101, ODN2395 along with ctrl ODN5328 (1µM) for 48 hours. Panels A and B: MDSC population and their corresponding PD-L1 expression were evaluated (n=12). Four donors with three replicates were used. Data represented as mean ± SEM.

Conclusions Both the in vitro and in vivo findings suggest that regional TLR9 stimulation in a model of LM improves responsiveness to systemic anti-PD-1 therapy through elimination of MDSC, and the effect on huMDSC was confirmed in vitro. Increased PDL-1 expression in response to TLR9 stimulation among MDSC may further enhance the anti-PD-1 effect. Therefore, combing regional infusions of a TLR9 agonist with systemic anti-PD-1 agents may be a promising approach for liver tumor treatment.

REFERENCES

- Wang, S., et al., Intratumoral injection of a CpG oligonucleotide reverts resistance to PD-1 blockade by expanding multifunctional CD8+ T cells. *Proc Natl Acad Sci U S A*, 2016. 113(46): p. E7240-E7249.
- Ghosh CC, H.K., O'Connell K, Laporte J, Guha P, Cox B, Jaroch D, Katz SC, Regional administration of class C CpG Oligodeoxynucleotides results in superior intrahepatic TLR9 activation and immunomodulation compared to systemic infusion, Abstract: AACR Annual Meeting, 2021.

<http://dx.doi.org/10.1136/jitc-2021-SITC2021.607>

608

SYNERGISTIC EFFECT OF THE COMBINATION OF ATG-017, AN ERK1/2 INHIBITOR, AND IMMUNE CHECKPOINT INHIBITOR IN PRECLINICAL CANCER MODELS

²Peng Chen, ²Yun Liu, ²Min Deng, ²Jian Wang, ³Dirk Hoenemann, ³Kevin Lynch, ¹Jay Mei, ¹Bo Shan, ¹Bing Hou*. ¹Antengene Corporation Co., Ltd, Shanghai, China; ²Shanghai Antengene Corporation Limited, Shang Hai, China; ³Antengene Pty Ltd, Melbourne, Australia

Background The RAS/MAPK pathway has emerged as a critical pathway for therapeutic targeting in a spectrum of solid tumor and hematological malignances. Inhibitors targeting MAPK pathway targets, such as RAS, BRAF, or MEK have been approved for the treatment of cancer either as monotherapy or in combination. However, there has been no approved drug targeting ERK1/2, the terminal kinases in the Ras-Raf-MEK-ERK signal transduction cascade. The combination of ERK1/2 inhibitor and checkpoint inhibitors as therapeutic strategy has not been explored in clinic. ATG-017 is an oral, potent, and highly selective inhibitor of ERK1/2, which is under Phase 1 clinical investigation. ATG-012 is a novel inhibitor of KRAS G12C. In this study, we tested the anti-tumor effect induced by the combination of ATG-017, or ATG-012, and an anti-PDL1 antibody in preclinical cancer models.

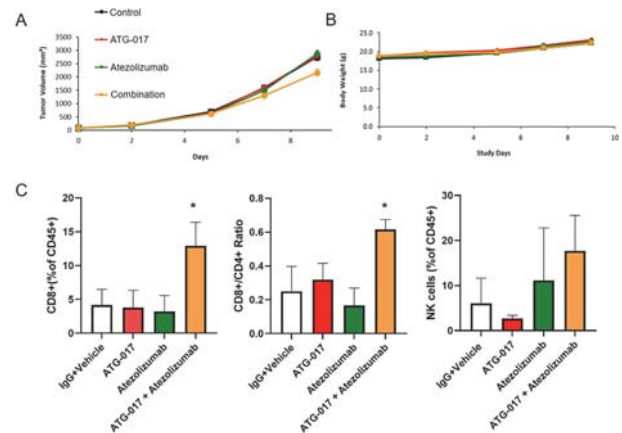
Methods We assessed the anti-cancer effects of ERK1/2, KRAS G12C and PD1/PDL1 inhibition as monotherapy, and as combinations. Anti-PDL1 antibody (atezolizumab), the combination of ATG-012 or ATG-017 and atezolizumab, and the triple combination of atezolizumab, ATG-012 and ATG-017 were tested in a PD(L)1 blockade insensitive syngeneic lung cancer model, LL/2. The ATG-017-atezolizumab combination was also evaluated in a KRAS G13C-mutant, PD(L)1 blockade insensitive lymphoma model, EL4. To further investigate if ERK1/2 inhibition could enhance the efficacy of atezolizumab in a MAPK aberration-independent manner, the ATG-017-atezolizumab combination was tested in a MAPK wild type lymphoma model, A20. As well as assessment of impact on tumor growth, the impact of the drugs on tumor infiltrating leukocytes were analyzed by flow cytometry.

Results The combination of ERK1/2 inhibition and an anti-PDL1 antibody showed enhanced efficacy in mouse syngeneic tumor models. In the EL4 model, neither ATG-017 nor atezolizumab showed single agent activity, while the combination showed significant tumor growth inhibition (TGI=22%) on day 9. No body weight loss was observed. The percentage of infiltrating CD8+ T cells, NK cells and CD8:CD4 ratio were found increased in the combination group. The mean percentage of CD8+T cells among CD45+ cells increased from 4.17% (IgG +Vehicle control), 3.81% (ATG-017), 3.23% (atezolizumab), to 12.92% in the combination group. The CD8:CD4 ratio were 0.25 (IgG+Vehicle), 0.32(ATG-017), 0.17 (atezolizumab) and 0.67 (combination), respectively (Figure 1). More data from LL/2 and A20 model are being generated.

Conclusions Synergism has been observed for the combination of checkpoint inhibition and ERK1/2 inhibition in vivo, suggesting promising therapeutic strategies for cancer patients that warrants further clinical investigation.

Ethics Approval The protocol and any amendment(s) or procedures involving the care and use of animals in this study were reviewed and approved by the Institutional Animal Care and Use Committee (IACUC) of CrownBio prior to execution. During the study, the care and use of animals were conducted in accordance with the regulations of the Association for Assessment and Accreditation of Laboratory Animal Care

(AAALAC). All studies were conducted following an approved IACUC protocol. AUP NO.: AN-2004-09-309



Abstract 608 Figure 1 ATG-017-Atezolizumab combination showed in vivo synergism

(A) Tumor growth curve and (B) mean body weight of EL4 syngeneic model; N=8 for each treatment group. (C) ATG-017-Atezolizumab combination increased tumor infiltrating CD8+T cells (left), CD8+/CD4+ ratio (middle), and tumor infiltrating NK cells (right). The TILs were isolated from tumor samples shown in (A). N=3 for each group.

<http://dx.doi.org/10.1136/jitc-2021-SITC2021.608>

609

COMBINING BINTRAFUSP ALFA WITH ABITUZUMAB ENHANCES SUPPRESSION OF THE TGF- β SIGNALING PATHWAY

Feng Jiang*, Hong Wang, Tsz-Lun Yeung, Guozhong Qin, Bo Marelli, Hui Huang, Kin-Ming Lo, Yan Lan. *EMD Serono, Billerica, MA USA, Billerica, MA, USA*

Background Bintrafusp alfa is a first-in-class bifunctional fusion protein composed of the extracellular domain of the TGF- β RII receptor fused to a human IgG1 antibody blocking PD-L1. The TGF- β RII moiety of bintrafusp alfa functions as a "trap" to sequester active TGF- β but does not block TGF- β release from its latent form. Multiple mechanisms lead to the release of active TGF- β . Integrins control local activation of latent TGF- β stored in the extracellular matrix and cell-surface reservoirs in the tumor microenvironment (TME). Alpha v integrin mRNA expression is correlated with multiple TGF- β gene signatures. It has been shown that $\alpha v\beta 8$ integrin mediates TGF- β activation without releasing it from the latent TGF- β complex, suggesting that the TGF- β RII moiety of bintrafusp alfa may be unable to sequester TGF- β activated by $\alpha v\beta 8$ integrin. Therefore, we hypothesize that combining abituzumab, a pan- αv integrin antibody, with bintrafusp alfa may lead to enhanced suppression of TGF- β signaling.

Methods The expression of αv and $\beta 6$ integrin mRNA was determined by RNA sequencing of triple-negative breast cancer (TNBC) tumor samples from a phase 1 clinical trial of bintrafusp alfa and correlated with patient response to bintrafusp alfa. The combination of bintrafusp alfa and abituzumab was investigated in vitro and in vivo in a TGF- β -dependent human tumor model, Detroit 562. In this study, CellTiter-Glo 2.0 Assay measured cell proliferation in vitro and enzyme-linked immunosorbent assay measured the level of latency-associated protein (LAP). A TGF- β reporter cell line MDA-MB-231 measured the level of active TGF- β . Antitumor activity in vivo was evaluated via tumor growth of Detroit 562 xenograft model in SCID mice.

Results In TNBC, increased expression of αv and $\beta 6$ integrin mRNA was associated with poor response to bintrafusp alfa, suggesting that TGF- β activated by αv integrin may not be blocked by bintrafusp alfa. In Detroit 562 cells, abituzumab increased LAP levels in the cell culture medium, confirming modulation of the TGF- β pathway. As a result, the amount of active TGF- β released into culture medium was reduced by abituzumab. In vitro, both abituzumab and bintrafusp alfa suppressed Detroit 562 cell proliferation, and the combination suppressed cell proliferation further. In vivo, the combination led to increased tumor growth inhibition of Detroit 562 xenograft tumors relative to either monotherapy, further supporting the potential of this combination.

Conclusions Collectively, these preclinical findings support clinical development of bintrafusp alfa and abituzumab combination therapy to maximally suppress TGF- β signaling in the TME.

Acknowledgements We thank George Locke for his analysis of the RNAseq data.

Ethics Approval This study was approved by the Institutional Animal Care and Use Committee at EMD Serono, Inc.; approval number [17-008].

<http://dx.doi.org/10.1136/jitc-2021-SITC2021.609>

SUSTAINABLE REGRESSION OF DISSEMINATED SOLID TUMORS MEDIATED BY IN SITU COMBINATIONAL TREATMENT WITH ADOPTIVE T CELL THERAPY AND ONCOLYTIC ADENOVIRUS DELTA-24-RGDOX<http://dx.doi.org/10.1136/jitc-2021-SITC2021.610>

Hong Jiang*, Dong Ho Shin, Sagar Sohoni, Teresa Nguyen, Yanhua Yi, Xuejun Fan, Joy Gumin, Sanjay Singh, Frederick Lang, Candelaria Gomez-Manzano, Juan Fueyo. *MD Anderson Cancer Center, Houston, TX, USA*

Background Unlike its remarkable success in treating hematological malignancies, adoptive T cell therapy (ACT), such as CAR T therapy, targeting limited tumor-associated antigens (TAAs) is far less effective in patients with heterogeneous solid tumors. Oncolytic viruses, including oncolytic adenovirus Delta-24-RGDOX from our group [1, 2], are emerging as promising immunotherapy drugs. To take advantage of instant antitumor activity of T cells and oncolytic adenovirus mediated in situ autovaccination against heterogeneous cancer cells, we hypothesize that intratumorally injected Delta-24-RGDOX complements with ACT to overcome antigen escape, leading to more sustainable anti-cancer effect.

Methods We used B16-OVA-C57BL/6 subcutaneous (s.c.)/s.c. melanoma model [2] to assess the systemic therapeutic effect in disseminated tumors. OVA (or gp100)-specific CD8+ T cells were injected into the first tumor, followed by three injections of Delta-24-RGDOX into the same tumor. T cells from the mice were profiled for surface markers with flow cytometry. Activity of splenocytes against tumor cells and specific TAAs was measured with ELISA. Tumor growth was monitored through measuring tumor size three times a week. The animal survival curves were plotted according to the Kaplan–Meier method.

Results TAA-specific T cells injected into the first s.c. tumor showed tropism for disseminated s.c. and intracranial tumors, tumor draining lymph nodes, compared to normal tissue, spleen and peripheral blood. Delta-24-RGDOX increased total T cell presence within the tumors, and the activity of the T cells against the tumor cells and targeting other antigens than the one targeted by the transferred T cells. Consequentially, the combination of OVA-specific T cells and Delta-24-RGDOX was more potent to inhibit the injected first tumor and untreated disseminated second tumor growth and resulted in improved survival rate than either of the agent alone ($p < 0.05$). Interestingly, we observed relapse of the regressed tumors in the group treated by T cells alone. But the relapse was not observed in most of the mice in the combination group. The survivors from the combination therapy were protected from rechallenging with B16-OVA cells but not lung carcinoma cells, suggesting the development of immune memory.

Conclusions Delta-24-RGDOX collaborates with ACT to induce more potent systemic immunity against the tumors, leading to sustainable tumor regression and improved survival rate. Our study indicates the virus induces antigen spread, resulting in expansion of T cell repertoire to prevent cancer relapse in ACT.

REFERENCES

1. Jiang, H., et al., Localized Treatment with Oncolytic Adenovirus Delta-24-RGDOX Induces Systemic Immunity against Disseminated Subcutaneous and Intracranial Melanomas. *Clin Cancer Res*, 2019. 25(22): p. 6801–6814. <https://cancerres.aacr-journals.org/content/25/22/6801.long>.
2. Jiang, H., et al., Oncolytic Adenovirus and Tumor-Targeting Immune Modulatory Therapy Improve Autologous Cancer Vaccination. *Cancer Res*, 2017. 77(14): p. 3894–3907. <https://clincancerres.aacrjournals.org/content/25/22/6801.full-text.pdf>

611 EXPLOITING T CELLS AS VEHICLES OF LIPOSOMAL SHP2I TO ENHANCE ADOPTIVE CELL THERAPY

Xin Li*, Hólmiðridur Halldórsdóttir, Sven Weller, Anna Colliander, Ditte Jæhger, Martin Bak, Gael Clergeaud, Thomas Andresen. *Technical University of Denmark, Kgs. Lyngby, Denmark*

2020-15-0201-00482. The participants gave informed consent before taking part.

<http://dx.doi.org/10.1136/jitc-2021-SITC2021.611>

Background Adoptive T cell therapy (ACT) is often accompanied by supporting immunomodulatory drugs to protect T cells from the suppressive tumor microenvironment (TME) [1]. However, systemic administration of these immunomodulators can cause serious side effects and fail to distribute optimally to exert sufficient lymphocyte stimulation within the tumor and lymphoid compartments. Loading T cells with adjuvant drugs or cytokines prior to cell transfer provides a solution to this issue, showing the potential to use T cells as vehicles to carry immunomodulatory molecules to target sites [2]. SHP2 is an important hub connecting several intracellular oncogenic signaling pathways including PD-1/PD-L1, representing a notable target for cancer immunotherapy. SHP2 inhibition has been shown to elicit tumor regression by improving CD8+ T cells activity [3]. Herein we present a lipid nanoparticle system encapsulating an SHP2 inhibitor (SHP2i) that allows high T cell loading capacity and enhances their therapeutic activity.

Methods Remote-loading gradients were used to achieve high encapsulation efficiency of SHP2i into the lipid nanoparticle platform. Mouse cytotoxic T cells were loaded with SHP2i, and loading efficiency and release rates from the T cells were evaluated *in vitro*. Flow cytometry was used to assess T cell viability, proliferation, and phenotype. *In vivo* biodistribution of loaded T cells was evaluated by labeling lipid nanoparticles with gadolinium and T cells with Cell-trace-marker, which were measured with ICP-MS and Flow respectively. The therapeutic anti-tumor efficacy of the loaded T cells was demonstrated on EG.7-OVA tumor-bearing mice.

Results The developed formulation allowed high T cell loading efficiency of SHPi and extended-release over 5 days. Loading T cells with lipid formulated SHP2i did not compromise cell viability and proliferation and resulted in T cells retaining a central memory phenotype than unloaded counterparts. Adoptively transferred T cells loaded with lipid nanoparticles showed the same distribution and proliferation behavior as the unloaded T cells *in vivo*, accumulating into tumor tissue three days post cell infusion. Loaded OT.I T cells significantly improved tumor growth inhibition and overall survival than OT.I T cells alone, with 5 out of 6 mice completely tumor-free, resulting in durable long-term responders.

Conclusions Loading T cells with liposomal SHP2i before ACT allowed specific and controlled delivery of immunomodulatory drugs by T cells. The loaded T cells showed improved anti-tumor efficacy. The developed lipid formulation allows the loading of a variety of immunomodulatory drugs to T cells, which serve both as a drug delivery vehicle and enhance the tumor efficacy of the transferred cells.

REFERENCES

1. Waldman AD, Fritz JM, Lenardo MJ. A guide to cancer immunotherapy: from T cell basic science to clinical practice. *Nat. Rev. Immunol.* 2020. p. 651–68.
2. Combes F, Meyer E, Sanders NN. Immune cells as tumor drug delivery vehicles. *J Control Release.* Elsevier; 2020;327:70–87.
3. Yuan X, Bu H, Zhou J, Yang CY, Zhang H. Recent Advances of SHP2 Inhibitors in Cancer Therapy: Current Development and Clinical Application. *J Med Chem.* 2020;63:11368–96.

Ethics Approval The study has been approved by the Danish Animal Experiments Inspectorate with the permit number

612 HUMAN RIBONUCLEASES ACT AS POTENTIAL PLASMA BIOMARKERS FOR TARGETED THERAPY AND IMMUNOTHERAPY IN HEPATOCELLULAR CARCINOMA

¹Zhengyu Zha, ¹Chen hao Zhou, ¹Dihua Yu, ²Mien-Chie Hung, ¹Chunxiao Liu*, ³Ning Ren. ¹MD Anderson Cancer Center, Houston, TX, USA; ²China Medical University, Taichung, Taiwan, Province of China; ³Fudan University, Shanghai, China

Background Ribonucleases, known as RNases, are secreted in the circulatory system that are recognized as part of the host defense system against pathogens. Although RNases are involved in multiple physiologically and pathologically-relevant cell events, including cancer cell growth, stem cell self-renewal and regenerative capabilities, the regulation and function of RNases in cancer therapy remained unclear. Herein, we examined whether RNases could serve as plasma biomarkers to stratify hepatocellular carcinoma (HCC) patients for combination of targeted therapy and immunotherapy.

Methods Two independent HCC patient cohorts were analyzed to evaluate the pathological relevance of RNases. The association between RNases and receptor tyrosine kinases were validated by immunoprecipitation, duolink and immunofluorescence assays. Tumor specimens from HCC patients, who were categorized according to clinical response to nivolumab, were subjected for whole-transcriptome sequencing to identify critical biomarker for combination therapy. The therapeutic efficacy of targeted therapy and immunotherapy was evaluated in HCC orthotopic models.

Results We discovered that RNase7, belongs to RNases superfamily proteins, acts as ROS1 ligand and triggers oncogenic transformation independent of its catalytic activities via activation of ROS1 signaling. In addition, clinical data analysis revealed that ROS1 and RNase7 co-expression occurs in approximately 30% of HCC patients and is highly correlated with poorer survival. Moreover, high plasma levels of RNase7 are positively correlated with ROS1 phosphorylation in approximately 45% of tumor tissues from HCC patients. Treatment with crizotinib, which was approved by the FDA for NSCLC patients with ROS1 rearrangement, induces significant anti-tumor effect in mouse models of HCC harboring activation of RNase7/WT ROS1 axis. We also found that RNases family proteins are upregulated in non-responders to nivolumab treatment of HCC patients, and enhances anti-PD1 resistance through regulating macrophage polarization. Blocking RNase-induced pathway activation dramatically enhanced immunotherapy efficacy in HCC orthotopic model.

Conclusions Our findings identified the oncogenic role for human RNase7 in HCC suggesting that RNase7 exhibits a potential to serve as a plasma biomarker to stratify HCC patients for anti-ROS1 targeted therapy. Furthermore, inhibiting RNase function leads to substantial changes to the tumor immune profile in patients with HCC, which may convert immunologically "cold" tumor into "hot" tumor and be effectively combined with immunotherapeutic agents. Clinical research and more patient tissue samples are under evaluation to validate these findings.

<http://dx.doi.org/10.1136/jitc-2021-SITC2021.612>

613

9-ING-41, A SELECTIVE SMALL MOLECULE INHIBITOR OF GLYCOGEN SYNTHASE KINASE-3 BETA (GSK-3BETA), MAY ENHANCE NEUROBLASTOMA IMMUNOGENICITY

¹Angela Markovska, ²Ludimila Cavalcante*, ²Francis Giles, ³Marianne Boes. ¹University Medical Center Utrecht, Utrecht, Netherlands; ²Actuate Therapeutics Inc., Fort Worth, TX, USA; ³UMC Utrecht, Utrecht, Netherlands

Background Neuroblastoma (NBL) is an embryonic tumor originating from neural crest precursor cells. It is one of the most prevalent pediatric solid tumors, with an estimated five-year progression free survival of less than 50% in stage-4 patients. While T-cell mediated therapies, including immune checkpoint inhibition, have marked activity against many cancers in adults, NBL is relative refractory to these approaches. One reason for the limited success of the existing immune therapies is the extremely low peptide/MHC-I complex expression of NBL cells. There is an unmet need to improve immunogenicity of NBL, and thus to enhance the cytotoxic T lymphocyte (CTL)-mediated anti-tumor response. The serine/threonine kinase GSK-3beta is overexpressed by NBL and has been proposed as a therapeutic target. This kinase is broadly involved in energy metabolism pathways and thus may regulate peptide/MHC-I complex display at the tumor cell surface. 9-ING-41 has broad spectrum pre-clinical anti-cancer activity, including against NBL. It has established efficacy and a favourable safety profile in adult patients with refractory cancers – studies in children are underway. IFN- γ upregulates MHC-I expression by inducing the expression of multiple genes related to MHC-I antigen processing and presentation.

Methods We assessed the potential of 9-ING-41 to increase immunogenicity, using four distinct NBL cell lines which we cultured for 24 or 72 hours in the continuous presence of IFN- γ and/or 9-ING-41. We measured cell surface expression of MHC-I and PD-L1 using flow cytometry analyses.

Results In GIMEN, SH-SY5Y, SK-N-BE, and IMR32 NBL lines, we found that 9-ING-41 significantly increased IFN- γ -mediated MHC-I surface expression on all 4 cell lines, markedly so in the cell lines without MYCN amplification. PD-L1 expression was also upregulated in two of the cell lines, suggesting that 9-ING-41 combined with PD-1/PD-L1 immune checkpoint blockade is worthy of further investigation.

Conclusions These data indicate that 9-ING-41 may facilitate recognition and killing of NBL by CTL and support the further development of 9-ING-41 as a potential treatment for NBL.

<http://dx.doi.org/10.1136/jitc-2021-SITC2021.613>

614 **INVESTIGATING IMMUNE MEDIATED MECHANISMS OF PARPI RESISTANCE IN BRCA1-ASSOCIATED TRIPLE NEGATIVE BREAST CANCER (TNBC)**

¹Anita Mehta, ¹Madeline Townsend, ¹Madisson Oliwa, ²Patrice Lee, ²Nicholas Saccomano, ³Filipa Lynce, ³Geoffrey Shapiro, ¹Elizabeth Mittendorf, ¹Jennifer Guerrero*. ¹Brigham and Women's Hospital, Boston, MA, USA; ²Pfizer, Boulder, CO, USA; ³Dana-Farber Cancer Institute, Boston, MA, USA

Background Poly(ADP-ribose) polymerase inhibitors (PARPi) have improved the outcomes of BRCA-associated breast cancer; however, treatment responses are often not durable. Our preclinical studies demonstrated that PARPi activates the cGAS/STING pathway and recruitment of anti-tumor CD8+ T-cells that are required for tumor clearance [1]. These studies contributed to development of clinical trials testing PARPi plus immune checkpoint blockade (ICB). Unfortunately, early phase trials of PARPi + ICB have not yet suggested efficacy will be superior to PARPi monotherapy. Lack of demonstrated clinical synergy between PARPi + ICB underscores the need to study the tumor microenvironment (TME) during PARPi therapy to identify optimal strategies to enhance T-cell activation. We recently showed that PARPi induces CSF-1R+ suppressive tumor associated macrophages (TAMs) that restrict antitumor immune responses, contributing to PARPi resistance [2]. Removing TAMs with anti-CSF-1R therapy in combination with PARPi significantly enhanced overall survival (OS) compared to PARPi monotherapy in preclinical models [2]. Here, we investigate how modulating TAMs can enhance PARPi + ICB.

Methods Mice bearing BRCA1-deficient TNBC (K14-Cre; Brca1f/f;p53f/f) tumors were treated for 98 days with PARPi (Talazoparib) ± small molecule inhibitor of CSF-1R (ARRAY-382; CSF-1Ri) ± anti-PD-1 and then followed for survival. Flow cytometry was employed to elucidate changes in the TME after treatment.

Results PARPi conferred a significant survival advantage over vehicle treated mice (median OS 33 v. 14 days; p=0.0034) and 2/8 PARPi-treated mice experienced complete tumor clearance at day 98. PARPi + CSF-1Ri treated mice (median OS 140 days) remarkably cleared 7/10 tumors by day 98. The addition of anti-PD-1 to PARPi did not enhance OS compared to PARPi monotherapy. The triple combination of anti-PD-1 + PARPi + CSF-1Ri has not yet significantly enhanced the median OS compared to PARPi + CSF-1Ri (ongoing; 168 v. 140 days); nor did it increase clearance of tumor by day 98 (7/10). However, the triple combination led to superior long term tumor clearance. At day 161 the triple combination exhibited 5/10 tumor free mice compared to 2/10 treated with PARPi + CSF-1Ri. To elucidate how CSF-1Ri enhanced PARPi + ICB responses, flow cytometry was performed and revealed increased expression of the co-stimulatory molecule CD80, reduced tissue resident macrophages (CX3CR1+) and lower CSF-1R expression compared to PARPi + ICB.

Conclusions These data suggest that targeting immunosuppressive macrophages may induce a favorable anti-tumor immune response and enhance responses to PARPi plus ICB. We are currently evaluating the adaptive immune response in this context.

REFERENCES

1. Pantelidou, C., et al., PARP inhibitor efficacy depends on CD8+ T cell recruitment via intratumoral STING pathway activation in BRCA-deficient models of triple-negative breast cancer. *Cancer Discovery*, 2019; p. CD-18-1218.

2. Mehta, A.K., et al., Targeting immunosuppressive macrophages overcomes PARP inhibitor resistance in BRCA1-associated triple-negative breast cancer. *Nat Cancer*, 2021. 2(1): p. 66–82.

<http://dx.doi.org/10.1136/jitc-2021-SITC2021.614>

615 REACTIVATING ANTITUMOR IMMUNITY IN GLIOMAS WITH OSTEOPONTIN/INTEGRIN BLOCKING PEPTIDE

¹Paulina Pilanc-Kudlek*, ¹Katarzyna Poleszak, ¹Aleksandra Ellert-Miklaszewska, ¹Adria-Jaume Roura Canalda, ²Salwador Cyranowski, ¹Julian Swatler, ¹Bartłomiej Gielniewski, ¹Bożena Kamińska. ¹Nencki Institute of Experimental Biology, Polish Academy of Sciences, Warsaw, Poland, Warsaw, Poland; ²Postgraduate School of Molecular Medicine, Medical University of Warsaw, Warsaw, Poland, Warsaw, Poland

Background Glioblastoma (GBM) is the most common and aggressive primary brain tumor in adults. Despite improvements in imaging, surgical techniques, radiotherapy and chemotherapy, the prognosis of patients with GBM remains poor with a median overall survival of 15 months [1,2]. GBM is immunologically a "cold" tumor with low infiltration of functional T and NK cells, which imposes poor responsiveness of GBM patients to immunotherapies. The immunosuppressive microenvironment in GBM is created by the malignant cells and tumor-associated macrophages (TAMs), such as resident brain microglia and recruited peripheral myeloid cells [3]. Osteopontin/Spp1 is one of glioma-derived factors that is responsible for the protumorigenic reprogramming of TAMs [4]. SPP1 expression is highly elevated in tumor tissues and sera from GBM patients, and inversely correlates with patient survival [5]. Cross-talk between malignant cells and TAMs relays on osteopontin binding to integrin receptors (mainly $\alpha v \beta 3$ and $\alpha v \beta 5$) via its RGD motif [6]. Thus, with the use of a RGD peptide (our in-house designed competitor of binding to integrins) we interfered with glioma-microglia interaction in vitro and evaluated the in vivo antitumor efficacy of integrin blockade as a monotherapy and in combination with an immune check-point inhibitor.

Methods The efficacy of the RGD peptide to block microglia-dependent glioma invasion was determined in a Matrigel invasion assay. Antitumor activity of the peptide was assessed in a murine syngeneic orthotopic GL261 glioma model. RGD peptide was administrated intratumorally via osmotic pumps. For combination therapy, the animals received anti-PD-1 or isotype IgG antibody (4 inj. x 10 mg/kg i.p.). Tumor volume was measured using MRI. Heterogeneity of the immune cells compartment of glioma microenvironment was analysed by flow cytometry. The transcriptomes of CD11b+ cells immunosorted from tumor-bearing mouse brains were evaluated using RNA-seq. Cytokine levels in the blood and the brain homogenates were measured using Luminex bead-based assays.

Results The microglia-stimulated invasion of GL261 glioma cells was reduced significantly in the presence of the RGD peptide in the in vitro co-culture system. The RGD peptide administrated to tumor-bearing mice induced proinflammatory reprogramming of TAMs. Combination of the RGD peptide with anti-PD-1 therapy increased the production of proinflammatory cytokines and the percentage of effector CD8+(CD44+CD62L-) cells in the tumors.

Conclusions These results demonstrate that blockade of osteopontin/integrin signaling using the RGD peptide can mitigate the immunosuppressive microenvironment, reactivate the antitumor immunity and lay ground for improved response to immunotherapy in GBM.

REFERENCES

1. Jemal A, Murray T, Ward E, Samuels A, Tiwari RC, Ghafoor A, Feuer EJ, Thun MJ: Cancer statistics, 2005. *CA Cancer J Clin* 2005, 55(1):10–30.
2. Stupp R, Hegi ME, Mason WP, van den Bent MJ, Taphoorn MJ, Janzer RC, Ludwin SK, Allgeier A, Fisher B, Belanger K et al: Effects of radiotherapy with concomitant and adjuvant temozolomide versus radiotherapy alone on survival in

glioblastoma in a randomised phase III study: 5-year analysis of the EORTC-NCIC trial. *Lancet Oncol* 2009, 10(5):459–466.

3. Woroniecka KI, Rhodin KE, Chongsathidkiet P, Keith KA, Fecci PE: T-cell Dysfunction in Glioblastoma: Applying a New Framework. *Clin Cancer Res* 2018, 24(16):3792–3802
4. Denhardt, D.T., M. Noda, A.W. O'Regan, D. Pavlin, and J.S. Berman. 2001. Osteopontin as a means to cope with environmental insults: regulation of inflammation, tissue remodeling, and cell survival. *J Clin Invest* 107:1055–1061.
5. Grassinger, J., D.N. Haylock, M.J. Storan, G.O. Haines, B. Williams, G.A. Whitty, et al. 2009. Thrombin-cleaved osteopontin regulates hemopoietic stem and progenitor cell functions through interactions with $\alpha 9 \beta 1$ and $\alpha 4 \beta 1$ integrins. *Blood* 114:49–59.
6. Anborgh, P.H., J.C. Mutrie, A.B. Tuck, and A.F. Chambers. 2010. Role of the metastasis-promoting protein osteopontin in the tumour microenvironment. *Journal of cellular and molecular medicine* 14:2037–2044

Ethics Approval All research protocols conformed to the Guidelines for the Care and Use of Laboratory Animals (European and national regulations 2010/63/UE September 22, 2010 and Dz. Urz. UE L276/20.10.2010, respectively). Animals were decapitated by a qualified researcher. The First Warsaw Local Ethics Committee for Animal Experimentation approved the study (approval no. 812/2019).

<http://dx.doi.org/10.1136/jitc-2021-SITC2021.615>

616

CD47 BLOCKADE MODULATES IMMUNOSUPPRESSIVE CHECKPOINT MOLECULES AND CELLULAR METABOLISM TO SENSITIZE TRIPLE-NEGATIVE BREAST CANCER TUMORS TO IMMUNE CHECKPOINT BLOCKADE THERAPY

Elizabeth Stirling*, Adam Wilson, Katherine Cook, Alexandra Thomas, Pierre Triozzi, David Soto-Pantoja. *Wake Forest School of Medicine, Winston-Salem, NC, USA*

Background Triple-negative breast cancer (TNBC) lacks drugable targets and has high metastatic incidence. Immune checkpoint blockades (ICB) are FDA approved for TNBC treatment, but therapeutic response and biomarkers are limited. CD47 is an integral membrane protein overexpressed on cancer cells that alters anti-tumor immunosurveillance, resulting in tumor progression. CD47 is involved in metabolic reprogramming but whether CD47 is a marker of progression and its role in ICB response for TNBC remains unknown.

Methods Human TNBC biopsies were subjected to immunohistochemical analysis to determine CD47 role in TNBC progression. To determine CD47 impact on tumor burden, a carcinogen-induced TNBC model was performed in female wild type (WT) and *cd47* null (*cd47*^{-/-}) C57Bl/6 mice. To evaluate immune infiltrate signaling, tumors underwent spatial tissue proteomics by multiplexing photo-cleavable antibodies in Formalin-Fixed Paraffin-Embedded samples. An orthotopic EMT-6 murine TNBC model was performed to investigate tumor burden for CD47 monotherapy or in combination with anti-PD-L1 therapy.

Results Human matched primary, and metastatic TNBC biopsies increased immunoreactivity to CD47, signifying a potential therapeutic target (n=24). CD47 deficiency in the carcinogen-induced DMBA model decreased tumor incidence, weight, and area compared to WT (n=8/group, *p<0.003). Since CD47 can regulate metabolism, tumors underwent metabolomic analysis. Principal component analysis displayed differentially regulated metabolites between WT and *cd47*^{-/-} tumors. Decreased carnitine conjugated fatty acids and ketone bodies were observed in *cd47*^{-/-} tumors compared to WT, suggesting decreased fatty acid availability and/or metabolism (n=9/group, *p<0.05). TNBC cell respiratory measurements validated that targeting CD47 shifted metabolic dependency from fatty acid oxidation to glycolysis (n=3, *p<0.05). Kynurenine/tryptophan pathway metabolites, which catabolize Indoleamine-2,3-dioxygenase (IDO1) and involved in anti-PD-1/PD-L1 resistance, were decreased in *cd47*^{-/-} tumors compared to WT (n=9/group, *p<0.05). Spatial proteomic analysis determined that *cd47*^{-/-} tumors had elevated immune cell infiltration (CD45+, CD3+), suggesting CD47 absence enhances tumor immunogenicity and immune-mediated tumor ablation. Multiplexing of photo-cleavable antibodies increased protein expression of immune checkpoint molecules (PD-L1, VISTA, B7-H3, BatF3) and immunosuppressive cell types (CD11b+, Ly6c+) in WT tumors compared to *cd47*^{-/-}, suggesting CD47 absence limits immunosuppressive signaling (n=16/group, *p<0.05). Since anti-PD-L1 therapies are approved to treat TNBC and WT tumors have PD-L1 upregulation, we examined how targeting CD47 would impact tumor burden of mice receiving anti-PD-L1 therapy. Targeting CD47 or PD-L1 as monotherapy decreased tumor burden; however, in combination it further reduced tumor burden compared to anti-PD-L1 treatment due to increased intratumoral granzyme B secreting cytotoxic T cells (n=4-8/group, *p<0.05).

Conclusions Our data indicates that CD47 may serve as a marker of anti-PD-L1 response, and targeting CD47 enhances immunogenicity and decreases immunosuppressive molecules, sensitizing TNBC tumors to anti-PD-L1 therapy to reduce tumor burden.

Acknowledgements DSP is supported by the NCI R21 (CA249349) and the American Cancer Society Research Scholar Grant (133727-RSG-19-150-01-LIB). ERS is supported by the NIAID Immunology and Pathogenesis T32 Training Grant (T32AI007401).

Ethics Approval Animal studies were approved by the Institutional Care and Use Committee, Wake Forest Health Sciences.

<http://dx.doi.org/10.1136/jitc-2021-SITC2021.616>

617 **TRASTUZUMAB AND PERTUZUMAB COMBINATION THERAPY ACTIVATES COMPLEMENT-DEPENDENT CYTOTOXICITY AND PHAGOCYTOSIS AGAINST HER2+ BREAST CANCER**

Li-Chung Tsao*, Zachary Hartman. *Duke University, Durham, NC, USA*

Background Standard-of-care frontline treatment for HER2+ breast cancers (BC) is comprised of two HER2-specific monoclonal antibodies (mAb), Trastuzumab and Pertuzumab with chemotherapy. This combination (T+P) has proven highly effective, however its synergistic mechanism of action is largely unknown. Initial studies demonstrated that Pertuzumab suppressed HER2 hetero-dimerization, thus the T+P mechanism of action (MOA) has been widely reported as due to Pertuzumab-mediated signaling suppression in combination with Trastuzumab-mediated induction of immunity. However, the therapeutic MOA for Pertuzumab remains unclear, especially combination with Trastuzumab. As the only solid cancer effectively treated by a mAb combination, unraveling this MOA may be critical in extending this strategy to other cancers, as well as to improving this treatment modality.

Methods In this study, we used multiple mouse models of human HER2 expressing breast cancer, and an endogenous transgenic HER2+ BC model that is tolerant to human HER2, and by using both novel murine and human versions of Pertuzumab and Trastuzumab, we elucidated the synergistic antitumor immune mechanism of the two antibodies when used in combination.

Results First, we demonstrated that Pertuzumab, just like Trastuzumab [1], can engage with Fc receptors and activate Antibody-Dependent-Cellular-Phagocytosis (ADCP) to elicit antitumor efficacy, as well as inhibit oncogenic signaling of HER2. More importantly, we identified that the combination of Pertuzumab with Trastuzumab synergistically and strongly induced classical pathway complement activation, enabling both direct complement-dependent cytotoxicity (CDC) of tumor cells, as well as anti-tumor complement-dependent cellular phagocytosis (CDCP) by macrophages. Furthermore, tumor expression of C1q was positively associated with survival outcome in HER2+ BC patients, whereas expression of complement regulators CD55 and CD59 were inversely correlated. Accordingly, depletion of C1q in mice abolished the synergistic antitumor effect of T+P therapy, whereas knock-down of CD55 and CD59 expression enhanced T+P therapeutic efficacy.

Conclusions Our study identifies complement activation as a potentially significant antitumor MOA for T+P therapies that may be clinically enabled by complement regulatory blockade to augment therapeutic efficacy.

REFERENCES

1. Tsao L, et al. CD47 blockade augmentation of trastuzumab antitumor efficacy dependent on antibody-dependent cellular phagocytosis. *JCI Insight*. 2019; 4(24): e131882.

<http://dx.doi.org/10.1136/jitc-2021-SITC2021.617>

618 EXPANDING CANCER IMMUNOTHERAPY BY EXPLOITING RECALL IMMUNITY – A NEW CO-THERAPY OPTION FOR CHECKPOINT INHIBITORS

Kathlynn Brown, Michael McGuire, Anuja Pande, Indu Venugopal*. *SRI International, Rockingham, VA, USA*

Background Immune checkpoint inhibitors (CIs) have emerged as a revolutionary treatment for several cancer types. Despite significant improvement in prognosis for some patients, there are associated challenges. CIs do not work well on immune-cold tumors, thereby eliciting an insufficient immune response. They are also not as effective in tumors with low mutational burden due to dependence on tumor self-antigens for immune recognition. Therefore, there is a need for a solution to improve the efficacy of CIs to make them applicable to the entire cancer patient population.

Methods To address this challenge, we have developed a novel immunotherapy capable of delivering previously encountered antigenic peptides specifically to cancer cells and facilitating their presentation through the MHC class I pathway. Our therapy utilizes a synthetic nanoparticle delivery system comprising of three components: a neutral stealth liposome, an encapsulated synthetic immunogenic HLA class I restricted peptide derived from measles virus (MV), and a tumor-targeting peptide on the external surface of the liposome. The targeting peptide results in accumulation of the liposomes specifically inside cancer cells, and facilitates presentation of the MV-derived immunogenic peptides in HLA class I molecules. We refer to this system as TALL (Targeted Antigen Loaded Liposomes). As a result, TALL can generate a strong secondary immune response specifically against the targeted tumor cells in a patient who has been previously vaccinated against or infected by MV. In short, we are attempting to trick the immune system into responding as though the cancer cell is infected with MV without the use of a viral particle. Advantageously, as TALL can provide a potent synthetic antigen specifically to tumor cells, it can convert immune-cold tumors into immune-hot, resulting in a robust cytotoxic T lymphocyte response. Therefore, we conducted pilot studies to determine the efficacy of combining TALL with the anti-PD1 checkpoint inhibitor.

Results Treatment with TALL alone substantially reduces growth of lung, triple-negative breast, and pancreatic tumors in mice. Treatment with TALL and CI combination therapy showed at least a 10-fold reduction in tumor burden in mice bearing orthotopic breast and pancreatic tumors when compared to using CI treatment alone. The combination treatment also successfully prevented metastasis from occurring.

Conclusions TALL can successfully be used in combination with existing immunotherapies like checkpoint inhibitors, to generate a robust cytotoxic T lymphocyte response directed specifically against the tumor, resulting in a drastic reduction of tumor burden.

<http://dx.doi.org/10.1136/jitc-2021-SITC2021.618>

619

PHARMACOLOGIC MODULATION OF TUMOR GLYCOLYSIS TO IMPROVE RESPONSES TO IMMUNE CHECKPOINT BLOCKADE THERAPY

¹Svena Verma*, ¹Rachana Maniyar, ¹Myat Ko, ¹Sadna Budhu, ²Inna Serganova, ²Roberta Zappasodi, ¹Ronald Blasberg, ¹Taha Merghoub, ¹Jedd Wolchok, ¹Levi Mangarin. ¹Memorial Sloan Kettering, New York, NY, USA; ²Weill Cornell Medicine, New York, NY, USA

Background Immune checkpoint blockade (ICB) has revolutionized the treatment of many cancer types; however, many patients do not benefit from these therapies due to inherent or acquired resistance. Preferential engagement in glycolysis is a hallmark of cancer cells and contributes to the progression and metastasis of many tumor types, including melanoma and triple-negative breast cancer (TNBC). Tumor reliance on glycolysis is emerging as a mechanism of resistance to immunotherapy, due in part to lactate-mediated acidification and competition for glucose in the tumor microenvironment. We recently found that knocking down the glycolytic enzyme lactate dehydrogenase A (LDHA) in 4T1 TNBC results in improved and long-lasting anti-tumor responses to CTLA-4 blockade in mice. These LDHA-defective tumors consume less glucose than wild-type tumors, leaving more glucose available in the TME for effector T cells to exert their tumoricidal function directly and via lineage destabilization of regulatory T cells. However, it remains to be determined whether systemic pharmacologic targeting of LDH can improve the efficacy of immunotherapy.

Methods Lactate production and glucose consumption was quantified by YSI enzymatic analysis of metabolites. LDHA was detected by immunoblot in tumor and T cells. A clonogenic killing assay was used to assess T-cell killing. B16-F10-bearing mice were treated daily with LDH inhibitor GNE-140 and/or biweekly with anti-CTLA-4.

Results Since activated T cells rely on glycolysis, we first determined that glycolytic cancers overexpress LDH compared to immune cells by analyzing single-cell transcripts from patient melanoma biopsies. LDHA gene expression is significantly higher in malignant cells than infiltrating CD8+ T cells, and we replicated these findings at the protein level in whole cell lysate from B16-F10 melanoma and 4T1 TNBC tumor cells vs. activated tumor-antigen specific T cells *in vitro*. We showed that the LDH inhibitor GNE-140 reduces tumor lactate production and glucose consumption without inhibiting anti-tumor T-cell killing *in vitro*. Daily treatment with GNE-140 results in reduced growth in immunocompetent but not immune deficient mice. Additionally, our preliminary findings indicate that targeting LDHA in combination with CTLA-4 blockade is more effective in slowing B16-F10 growth compared with CTLA-4 blockade alone.

Conclusions These results suggest that targeting LDH with GNE-140 is a safe, efficacious method for relieving tumor glycolysis-mediated immunosuppression within the TME, without adversely affecting immune cell function within the tumor. Our long-term goal is to determine optimal combinations of metabolic inhibitors with ICB to alleviate the metabolic competition between tumor and infiltrating immune cells and better potentiate anti-tumor immune responses.

<http://dx.doi.org/10.1136/jitc-2021-SITC2021.619>

620 ONCO-IMMUNOLOGICAL MECHANISMS OF FOCAL ABLATION AND LOCALIZED IL-12 IMMUNOTHERAPY

Maura Vrabel*, David Zaharoff, Siena Mantooth. *NC State University, Raleigh, NC, USA*

Background Unresectable solid malignancies are responsible for a major proportion of total cancer-related mortalities, making focal ablation an attractive alternative. Nevertheless, there are high rates of recurrence after ablation [1,2]. The addition of an immune agonist to ablation has the potential to prevent this recurrence and improve treatment outcomes. The goal of this study is to determine if localized interleukin-12 (IL-12) can prevent primary tumor recurrence after cryoablation in both minimal ablation and metastasis models.

Methods LLC (LL/2) (ATCC) and MC38 (NCI) were implanted in 6–9 week old C57BL/6 mice. All tumors were treated at volumes of 200–500 mm³. LLC tumors with treated with three cycles of freeze/thaw and then monitored for tumor recurrence and lung metastasis 22–25 days after implantation. MC38 tumors were treated with a minimal cryoablation protocol where the tumor undergoes one cycle of freezing at 100% intensity up to the tumor margin by visual inspection, followed by one cycle of active thaw until the cryo probe can be removed. Ablation was performed using the Argon-Helium Visual-ICETM Cryoablation System (Boston Scientific). Interleukin-12 (IL-12) in 1.5% (w/v) chitosan acetate (CS) dissolved in dPBS was injected intratumorally within an hour after cryoablation, or as indicated. The dose of IL-12 was 1 ug unless otherwise indicated.

Results We established a model of 100% recurrence using the minimal cryoablation protocol. Using this protocol, we demonstrated that a single intratumoral injection of CS/IL-12 within an hour after cryoablation prevents recurrence in 7/8 mice while only 3/8 mice remained tumor-free without CS/IL-12 (Figure 1). Studies evaluating the impact of CS/IL-12 on tumor-specific T cell responses following cryoablation are ongoing. In the spontaneously metastatic LLC model, delivering CS/IL-12 two days before treatment, either resection or cryoablation, reduced the number of metastatic lung nodules and furthermore prevented the recurrence of the primary tumor after resection (Figure 2).

Conclusions Due to the high percentage of solid malignancies that are unresectable at diagnosis, focal ablation is an attractive alternative, yet has a high rate of recurrence. We demonstrated that intratumoral neoadjuvant CS/IL-12 protects not only against primary recurrence after cryoablation, but also protects against lung metastasis and recurrence after resection. Further studies are necessary to explore the immune populations responsible for this therapeutic effect.

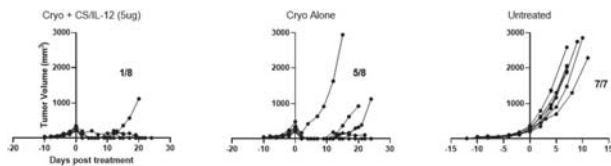
Acknowledgements This work is supported by Boston Scientific, the NC State University Provost’s Fellowship, the NSF Graduate Research Fellowship and startup funds provided by the College of Engineering at NC State University.

REFERENCES

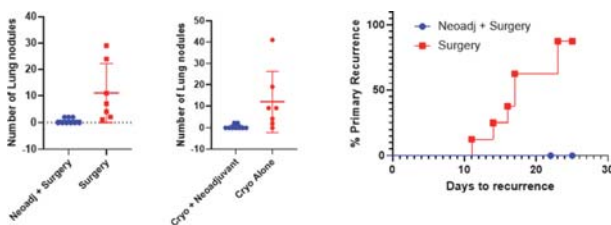
1. Weld KJ, Landman J. Comparison of cryoablation, radiofrequency ablation and high-intensity focused ultrasound for treating small renal tumours. *BJU Int.* 2005;96(9):1224–1229. doi:10.1111/j.1464–410X.2005.05848.x.
2. Guenther E, Klein N, Zapf S, et al. Prostate cancer treatment with Irreversible Electroporation (IRE): Safety, efficacy and clinical experience in 471 treatments. *PLoS One.* 2019;14(4):e0215093. doi:10.1371/journal.pone.0215093

Ethics Approval The Institutional Animal Care and Use Committee at North Carolina State University approved of all animal protocols (#19–795) in compliance with The Guide for Care and Use of Laboratory Animals (National Research Council).

<http://dx.doi.org/10.1136/jitc-2021-SITC2021.620>



Abstract 620 Figure 1 CS/IL-12 prevents tumor recurrence after minimal cryo



Abstract 620 Figure 2 CS/IL-12 before cryo or surgery prevents metastasis

NKG2A AND HLA-E DEFINE A NOVEL MECHANISM OF RESISTANCE TO IMMUNOTHERAPY WITH M. BOVIS BCG IN NON-MUSCLE-INVASIVE BLADDER CANCER PATIENTS

¹Amir Horowitz*, ¹Jorge Daza, ¹Y Alice Wang, ¹Daniel Ranti, ¹Berengere Salome, ¹Elliot Merritt, ¹Julie-Ann Cavallo-Fleming, ²Everado Hegewisch-Solloa, ²Emily Mace, ¹Adam Farkas, ¹Sanjana Shroff, ¹Michelle Tran, ¹Jingjing Qi, ¹Manishkumar Patel, ¹Daniel Geanon, ¹Geoffrey Kelly, ¹Ronaldo de Real, ¹Brian Lee, ¹Seunghye Kim-Schulze, ¹Tin Htwe Thin, ¹Monica Garcia-Barros, ¹Kristin Beaumont, ¹Ying-Chih Wang, ¹Li Wang, ³Dominic LaRoche, ³Yong Lee, ¹Robert Sebra, ¹Rachel Brody, ¹Reza Mehrazin, ¹Jun Zhu, ¹Anna Tocheva, ¹Benjamin Hopkins, ¹Peter Wiklund, ¹Matthew Galsky, ¹Nina Bhardwaj, ¹John Sfakianos. ¹Icahn School of Medicine at Mount Sinai, New York City, NY, USA; ²Columbia University, New York, NY, USA; ³HTG Molecular Diagnostics, Tucson, AZ, USA

Background 75% of diagnosed bladder tumors are non-muscle-invasive (NMIBC)[1, 2]. Most require intravesical instillation of M.bovis Bacillus Calmette-Guérin (BCG). Recurrence after immunotherapy occurs in ~50% patients. Development of treatments for BCG-resistant disease has lagged partly because few studies have attempted to understand the relationship between timing of tumor recurrence, reasoning for the recurrence, and the state of immune system at the time of recurrence. Immune exhaustion is observed following microbial infections, cancers and chronic inflammation [3–5]. Natural Killer (NK) cells are among the earliest responders[6–8] and undergo a similar program of exhaustion as T cells[9]. HLA-E strongly inhibits NKG2A-expressing NK and CD8+T cells and is commonly upregulated on tumors[10]. We evaluated the potential restorative capacity of NKG2A and PD-L1-blockade for reinvigorating NK and CD8+T cell antitumor functions in BCG-resistant bladder cancer.

Methods mRNA analysis of 2,892 genes was performed on tumor tissue of NMIBC patients before and after BCG therapy (n=35). Immunostaining (serial-IHC, immunofluorescence, imaging-mass cytometry) was performed on consecutive tissue sections. Single-cell-RNA-sequencing (scRNAseq) was performed on fresh bladder tumors (NMIBC, n=4; MIBC, n=9). OLink Proteomics (“Inflammation” panel) was performed longitudinally on plasma/urine from a prospective cohort of NMIBC patients. Patient tumors (n=3) were expanded as organoids and co-cultured with autologous tumor-derived NK and CD8+T cells in presence/absence of anti-PD-L1/NKG2A antibodies.

Results We demonstrate a robust local TME and systemic response to BCG that correlates with chronic inflammation and adaptive resistance rather than with preventing tumor recurrence. This resistance is mediated through IFN- γ -production by tumor-infiltrating NKG2A+NK and NKG2A+PD-1+CD8+T cells and results in increased HLA-E and PD-L1 on recurring tumors. Co-culture of treatment-naïve NMIBC tumors with recombinant IFN-gamma directly enhanced expression of PD-L1 and HLA-E. Longitudinal analysis of plasma before and during BCG immunotherapy revealed an inflammatory signature, including but not limited to IFN-gamma, that is maintained throughout treatment. Immunostaining and scRNAseq of NMIBC specimens revealed highly enriched infiltration by NKG2A+NK and NKG2A+CD8+T cells in HLA-EbrightPD-L1+ tumors and were spatially organized relative to tumors in a manner suggesting direct inhibition. Tumor-derived NK and CD8+T cells from BCG-resistant patients were co-cultured with autologous tumor organoids. Preliminary analyses demonstrated an improved anti-tumor response in presence of NKG2A/PD-L1-blockade.

Conclusions Our data support a model of BCG-resistance that points to a novel checkpoint axis that contributes to BCG-

resistance: HLA-E/NKG2A. New insights into this axis in NMIBC and how it is altered with repeated BCG exposure will enable us to explore combination therapies (PD-L1/NKG2A-blockade) that may reduce BCG-resistance and provide durable response.

REFERENCES

- Eidinger D, Morales A: Discussion paper: treatment of superficial bladder cancer in man. *Ann N Y Acad Sci* 1976, 277:239–240.
- Morales A, Eidinger D, Bruce AW: Intracavitary Bacillus Calmette-Guerin in the treatment of superficial bladder tumors. *J Urol* 1976, 116:180–183.
- Blank CU, Haining WN, Held W, Hogan PG, Kallies A, Lugli E, Lynn RC, Philip M, Rao A, Restifo NP et al: Defining ‘T cell exhaustion’. *Nat Rev Immunol* 2019, 19:665–674.
- Hashimoto M, Kamphorst AO, Im SJ, Kissick HT, Pillai RN, Ramalingam SS, Araki K, Ahmed R: CD8 T Cell Exhaustion in Chronic Infection and Cancer: Opportunities for Interventions. *Annu Rev Med* 2018, 69:301–318.
- McLane LM, Abdel-Hakeem MS, Wherry EJ: CD8 T Cell Exhaustion During Chronic Viral Infection and Cancer. *Annu Rev Immunol* 2019, 37:457–495.
- Lanier LL: NK cell receptors. *Annu Rev Immunol* 1998, 16:359–393.
- Biron CA, Gazzinelli RT: Effects of IL-12 on immune responses to microbial infections: a key mediator in regulating disease outcome. *Curr Opin Immunol* 1995, 7:485–496.
- Welsh RM, Jr.: Cytotoxic cells induced during lymphocytic choriomeningitis virus infection of mice. I. Characterization of natural killer cell induction. *J Exp Med* 1978, 148:163–181.
- da Silva IP, Gallois A, Jimenez-Baranda S, Khan S, Anderson AC, Kuchroo VK, Osman I, Bhardwaj N: Reversal of NK-cell exhaustion in advanced melanoma by Tim-3 blockade. *Cancer Immunol Res* 2014, 2:410–422.
- van Hall T, Andre P, Horowitz A, Ruan DF, Borst L, Zerbib R, Narni-Mancinelli E, van der Burg SH, Vivier E: Monalizumab: inhibiting the novel immune checkpoint NKG2A. *J Immunother Cancer* 2019, 7:263.

Ethics Approval Primary urothelial bladder cancer tumor tissue was obtained after obtaining informed consent in the context of an Institutional Review Board (IRB)-approved genitourinary cancer clinical database and specimen collection protocol (IRB #10-1180) at the Tisch Cancer Institute, Icahn School of Medicine at Mount Sinai (New York, NY).

<http://dx.doi.org/10.1136/jitc-2021-SITC2021.621>

DISRUPTED OXYGEN SUPPLY AND TUMOR HYPER-OXYGEN CONSUMPTION CONTRIBUTE INDEPENDENTLY TO PROSTATE CANCER IMMUNE PRIVILEGE

¹Priyamvada Jayaprakash*, ¹Meghan Rice, ¹Krithikaa Rajkumar Bhanu, ¹Brittany Morrow, ¹Joseph Marszalek, ¹Jason Gay, ¹Christopher Vellano, ²Benjamin Cowen, ²Dean Welsch, ¹Michael Curran. ¹The University of Texas MD Anderson Cancer Center, Houston, TX, USA; ²Immunomet Therapeutics Inc., Houston, USA

Background Despite the success of immunotherapy in immune-infiltrated "hot" tumors like melanoma, "cold" tumors like prostate cancer remain unresponsive [1,2,3]. We find that these tumors harbor regions of hypoxia that act as islands of immune privilege that exclude T cells, while retaining immunosuppressive myeloid cells. Targeting hypoxia using the hypoxia-activated prodrug, TH-302 (Evoxofosamide) reduced hypoxic regions and co-operated with immune checkpoint blockade (anti-CTLA-4+anti PD-1) to drive tumor regression in transplantable and spontaneous murine prostate tumors [4]. In a Phase I clinical trial, the combination of Evoxofosamide and anti CTLA-4 (Ipilimumab) elicited both objective responses and prolonged disease stabilization in late-stage "cold" tumor patients. However, Evoxofosamide reduces but does not eliminate hypoxia and patient tumors resistant to treatment with Evoxofosamide and Ipilimumab were hyper-metabolic [5]. Heightened tumor oxidative metabolism has been shown to generate hypoxic zones that resist PD-1 blockade therapy [6] and treatment with Metformin, a mitochondrial complex I inhibitor may reduce hypoxia and improve responses [7]. We hypothesized that targeting tumor oxidative metabolism using mitochondrial complex I inhibitors might diminish tumor hypoxia and, in conjunction with Evoxofosamide, sensitize unresponsive tumors to immunotherapy.

Methods We investigated the capacity of two mitochondrial complex I inhibitors to reduce tumor oxidative metabolism, diminish myeloid suppressive capacity and improve anti-tumor T cell immunity, alone and in combination with Evoxofosamide and checkpoint blockade. We assessed tumor burden and immune composition and characterized metabolic profiles using Seahorse XFe96 analyzer (Agilent).

Results While Evoxofosamide or inhibition of oxidative metabolism alone did not significantly impact tumor regression, dual combination and triple combination with checkpoint blockade led to a significant reduction in tumor burden. Assessment of the tumor immune microenvironment identified improvements in CD8 and CD4 effector T cell proliferation. In vitro metabolic and functional profiling of TRAMP-C2 prostate tumors, pre-activated T cells and myeloid derived suppressor cells revealed differential effects of complex I inhibition, with inhibition resulting in reduced tumor proliferation and myeloid suppressive function but increases in proliferation and cytotoxic function of pre-activated T cells.

Conclusions Our findings indicate that tumor hypoxia and associated immune suppressive programming can be reduced through both local tissue remodeling and limitation of tumor oxygen metabolism. Complex I inhibition selectively inhibits tumor and myeloid cell function, while sparing T cells. This provides opportunities to craft synergistic immuno-metabolic therapies with the potential to treat "cold" tumor patients refractory to current FDA approved immunotherapeutics.

REFERENCES

1. Curran MA, Montalvo W, Yagita H, and Allison JP. PD-1 and CTLA-4 combination blockade expands infiltrating T cells and reduces regulatory T and myeloid cells

within B16 melanoma tumors. *Proc Natl Acad Sci U S A*. 2010; 107(9): 4275–80.

2. Wolchok JD, Kluger H, Callahan MK, Postow MA, Rizvi NA, Lesokhin AM, et al. Nivolumab plus ipilimumab in advanced melanoma. *N Engl J Med*. 2013; 369(2): 122–33.
3. Kwon ED, Drake CG, Scher HI, Fizazi K, Bossi A, van den Eertwegh AJ, et al. Ipilimumab versus placebo after radiotherapy in patients with metastatic castration-resistant prostate cancer that had progressed after docetaxel chemotherapy (CA184-043): a multicentre, randomised, doubleblind, phase 3 trial. *Lancet Oncol*. 2014;15(7):700–12.
4. Jayaprakash P, Ai M, Liu A, Budhani P, Bartkowiak T, Sheng J, et al. Targeted hypoxia reduction restores T cell infiltration and sensitizes prostate cancer to immunotherapy. *J Clin Invest*. 2018; 128 (11): 5137–5149.
5. Hegde A, Jayaprakash P, Couillault CA, Piha-Paul S, Karp D, Rodon J, et al. A Phase I Dose-Escalation Study to Evaluate the Safety and Tolerability of Evoxofosamide in Combination with Ipilimumab in Advanced Solid Malignancies. *Clin Cancer Res*. 2021; 27(11): 3050–3060.
6. Najjar YG, Menk AV, Sander C, Rao U, Karunamurthy A, Bhatia R, et al. Tumor cell oxidative metabolism as a barrier to PD-1 blockade immunotherapy in melanoma. *JCI Insight*. 2019 4(5): e124989. A.
7. Scharping NE, Menk AV, Whetstone RD, Zeng X, Delgoffe GM. Efficacy of PD-1 Blockade Is Potentiated by Metformin-Induced Reduction of Tumor Hypoxia. *Cancer Immunol Res*. 2017; 5(1):9–16.

<http://dx.doi.org/10.1136/jitc-2021-SITC2021.622>

623

NOTCH ORCHESTRATES A MULTIFACETED IMMUNE EVASION PROGRAM IN HEPATOCELLULAR CARCINOMA

Katherine Lindblad*, Marina Ruiz de Galarreta, Romain Donne, Marina Bárcena-Varela, Ian Liebling, David Repáraz, Melissa Yao, Maxime Dhainaut, Brian Brown, Alice Kamphorst, Amaia Lujambio. *Icahn School of Medicine at Mount Sinai, New York, NY, USA*

Background Hepatocellular carcinoma (HCC) is a major global health concern, causing over 700,000 deaths annually [1]. For decades, treatment for advanced HCC was restricted to broad-acting tyrosine kinase inhibitors that conferred limited survival benefits [2]. Recently, immunotherapies have revolutionized treatment of advanced HCC with objective response rates of around 30% [3]. However, with 70% of patients remaining insensitive, there is an urgent need to identify biomarkers of resistance and response and to design novel combination therapies that restore sensitivity in the resistant patients.

Methods To understand mechanisms of HCC immune evasion, we performed transcriptomic analysis on a collection of immune-escaped murine tumors harboring MYC overexpression and loss of p53 (MYC;p53^{-/-}) [4]. The immune-escaped tumors could be categorized into "immune-inflamed" and "immune-desert" through single sample gene set enrichment analysis. We further identified an enrichment signature of Notch signaling in immune-inflamed tumors that was associated with a specific deficit of CD8⁺ T cells – a result validated in HCC patient samples. To test the role of Notch in immune escape, we generated a novel murine model of HCC based on MYC overexpression, activated Notch1 Intracellular Domain (MYC;NICD1), and customized expression of tumor antigens.

Results Expression of tumor antigens in MYC;p53^{-/-} mice led to enhanced survival and active immune surveillance/tumor clearance by antigen-specific CD8⁺ T cells compared to control MYC;p53^{-/-} mice without tumor antigens. However, this survival advantage conferred by tumor antigen expression was abrogated in MYC;NICD1 mice, demonstrating that Notch activation drives immune evasion in HCC in the presence of antigen expression. Mechanistically, Notch activation in the liver led to a reduced number of tumor antigen-specific CD8⁺ T cells within the tumor microenvironment compared to the MYC;p53^{-/-} mice while the presence of dendritic cells was similar. Adoptive transfer experiments have revealed a potential impairment of CD8⁺ T cell priming and activation. Further, Notch1-driven tumors were resistant to anti-PD1 monotherapy as well as anti-PDL1/anti-VEGFR2 and anti-PDL1/anti-TGFB1 combination therapies, indicating a multifaceted immune resistance mechanism mediated in part by VEGF and TGFB1. Resistance to anti-PDL1/anti-VEGF combination therapy has been confirmed in HCC patients.

Conclusions Together, Notch activation promotes a multifaceted immune escape program in HCC. Additionally, it promotes resistance to currently approved immunotherapies, establishing the Notch pathway as a putative biomarker for HCC patient stratification.

Acknowledgements This study was funded by Damon Runyon-Rachleff Innovator Award and NCI-NIH R37 Award. KEL was supported by 5T32AI078892-12.

REFERENCES

1. Bray F, Ferlay J, Soerjomataram I, Siegel RL, Torre LA, Jemal A. Global cancer statistics 2018: GLOBOCAN estimates of incidence and mortality worldwide for 36 cancers in 185 countries. *CA Cancer J Clin.* 2018 Nov;68(6):394–424.
2. Llovet JM, Ricci S, Mazzaferro V, Hilgard P, Gane E, Blanc JF, de Oliveira AC, Santoro A, Raoul JL, Forner A, Schwartz M, Porta C, Zeuzem S, Bolondi L, Greten TF, Galle PR, Seitz JF, Borbath I, Häussinger D, Giannaris T, Shan M, Moscovici

M, Voliotis D, Bruix J; SHARP Investigators Study Group. Sorafenib in advanced hepatocellular carcinoma. *N Engl J Med.* 2008 Jul 24;359(4):378–90.

3. Finn RS, Qin S, Ikeda M, Galle PR, Ducreux M, Kim TY, Kudo M, Breder V, Merle P, Kaseb AO, Li D, Verret W, Xu DZ, Hernandez S, Liu J, Huang C, Mulla S, Wang Y, Lim HY, Zhu AX, Cheng AL; IMbrave150 Investigators. Atezolizumab plus Bevacizumab in Unresectable Hepatocellular Carcinoma. *N Engl J Med.* 2020 May 14;382(20):1894–1905.
4. Ruiz de Galarreta M, Bresnahan E, Molina-Sánchez P, Lindblad KE, Maier B, Sia D, Puigvehi M, Miguela V, Casanova-Acebes M, Dhainaut M, Villacorta-Martin C, Singhi AD, Moghe A, von Felden J, Tal Grinspan L, Wang S, Kamphorst AO, Monga SP, Brown BD, Villanueva A, Llovet JM, Merad M, Lujambio A. β -Catenin Activation Promotes Immune Escape and Resistance to Anti-PD-1 Therapy in Hepatocellular Carcinoma. *Cancer Discov.* 2019 Aug;9(8):1124–1141.

Ethics Approval All mouse experiments were approved by the ISMMS Animal Care and Use Committee (protocol number IACUC-2014–0229).

<http://dx.doi.org/10.1136/jitc-2021-SITC2021.623>

TARGETING TYPE I ARGININE METHYLTRANSFERASES PROMOTES T CELL MEDIATED ANTITUMOR IMMUNE RESPONSES

¹Leilei Shi*, ²Andrew Fedoriv, ²Shane O'Brien, ²Kimberly Smitheman, ³Yunfei Wang, ⁴Jiakai Hou, ²Christian Sherk, ²Satyajit Rajapurkar, ²Jenny Laraio, ¹Leila Williams, ⁴Chunyu Xu, ¹Guangchun Han, ⁴Qin Feng, ¹Mark Bedford, ¹Linghua Wang, ²Olena Barbash, ²Ryan Kruger, ³Patrick Hwu, ²Helai Mohammad, ¹Weiyei Peng. ¹MD Anderson Cancer Center, Houston, TX, USA; ²GlaxoSmithKline, Collegeville, USA; ³Moffitt Cancer Center, Tampa, FL, USA; ⁴University of Houston, Houston, TX, USA

Background Although immunotherapy produced dramatic clinical responses in a certain population of cancer patients, tumor cells can employ a variety of immunosuppressive measures to limit the immunotherapeutic efficacy. This highlights a great need to develop novel strategies to expand the clinical benefits of immunotherapy to a broader population of cancer patients. PRMTs have been described as vital regulators of immune responsive pathways in several cell types, but the immunoregulatory role of Type I PRMTs in the tumor microenvironment remains poorly understood.

Methods In this study, we analyzed the correlation between Type I PRMT expression levels with the clinical outcome or immune signature. Gene expression changes were evaluated in a panel of immunogenic and non-immunogenic cancer cell lines with Type I PRMT inhibitor treatment. The antitumor and immunological effects of Type I PRMT inhibitor were evaluated in combination with checkpoint blockade in a panel of syngeneic tumor models.

Results Using TCGA dataset analysis, increased mRNA expression levels of several Type I PRMTs were associated with poor clinical response and decreased immune infiltration in melanoma patients. Particularly, tumors with high expression of PRMT1, the major Type I PRMTs, displayed significantly reduced relapse-free survival (HR=1.891, p=0.038), and were associated with lower cytolytic score (logFC=-0.875, p=1.49e-08) and lower lymphocyte infiltration score (logFC=-0.783, p=0.00077). RNA-seq results showed that interferon signaling was significantly altered after Type I PRMT inhibitor treatment in 10 of 15 cell lines analyzed, with most related genes showing increased expression. In addition, VEGFA was down-regulated by 25% or more in 7/8 human and 3/5 mouse cancer cell lines, and a moderate decrease in chromatin accessibility at the Vegfa promoter was observed in ATAC-seq data. Furthermore, Type I PRMT inhibitor combined with anti-PD1 treatment significantly extended the survival of tumor-bearing mice and delayed tumor growth in a panel of immunocompetent mouse models. Mechanistically, Type I PRMT inhibitor significantly increased the apoptotic sensitivity of tumor cells to autologous tumor-reactive T cells in vitro and the infiltration of total T cells (CD3+) in 3 of 4 tested tumor models and cytotoxic T cells (CD8+) in two tested tumor models in vivo.

Conclusions Taken together, these data indicated that Type I PRMT inhibition exhibits immunomodulatory properties and synergizes with immune checkpoint blockade to induce durable antitumor responses in a T cell dependent manner. This study provides a rationale to combine Type I PRMT inhibitor with immune checkpoint blockade to maximize clinical benefits in cancer patients.

Acknowledgements The authors would like to thank past and present members of the MDACC TIL lab for tumor/TIL processing and banking.

<http://dx.doi.org/10.1136/jitc-2021-SITC2021.624>

COVID and Immunotherapy

625 COVID-19 VACCINATION IN PATIENTS WITH RENAL CANCER OR MELANOMA RECEIVING IMMUNE CHECKPOINT INHIBITORS

Joyce Hwang, Hannah Dzimitrowicz*, Riddhishkumar Shah, Kathleen Ashcraft, Daniel George, April Salama, Tian Zhang. *Duke University, Durham, United States*

Background Patients with cancer are at high risk for severe COVID-19 disease and mortality¹; however, patients on active cancer treatment, including immune checkpoint inhibitors (ICI), were excluded from COVID-19 vaccine trials.²⁻³ Thus, safety and efficacy of COVID-19 vaccination in patients receiving ICIs is not well described.

Methods We identified patients with renal cell carcinoma (RCC) or melanoma who received at least one dose of an FDA-authorized COVID-19 vaccine (vax+), with or without being on ICI, between the dates of December 1, 2020 and April 1, 2021, and had at least 3 months of documented follow up at Duke Cancer Center. Retrospective chart abstraction of patient encounters during three months following vaccination was performed. Patient characteristics included demographics and oncologic treatments. Primary outcome was adverse events attributed to vaccination; other outcomes included immune related adverse events (IRAE) following vaccination and subsequent COVID-19 infection.

patients (4%) and 0 patients developed COVID-19 infection after one and two vaccine doses, respectively.

Conclusions Amongst a heterogeneous population of patients receiving ICI therapy, COVID-19 vaccination appears to be well tolerated and safe. The higher rate of symptoms reported post-vaccination in patients receiving ICI therapy is likely related to more frequent follow up intervals versus control. The rate of new or worsening IRAEs post-vaccination is no higher than historically reported.⁴⁻⁵ An update of this data with a larger cohort will be presented. Larger cohort studies of patients receiving ICIs are needed to fully assess the safety and efficacy of COVID-19 vaccination in this population; however, these data support the safety of vaccination in patients receiving ICIs.

REFERENCES

1. Kuderer NM, Choueiri TK, Shah DP, Shyr Y, Rubinstein SM, Rivera DR et al. Clinical impact of COVID-19 on patients with cancer (CCC19): a cohort study. *The Lancet* 2020;**395**:1907–1918.
2. Polack FP, Thomas SJ, Kitchin N, Absalon J, Gurtman A, Lockhart S, et al. Safety and efficacy of the BNT162b2 mRNA Covid-19 Vaccine. *N Engl J Med* 2020;**383**(27):2603–15.
3. Baden LR, El Sahly HM, Essink B, Kotloff K, Frey S, Novak R, et al. Efficacy and safety of the mRNA-1273 SARS-CoV-2 Vaccine. *N Engl J Med* 2020.
4. Xing P, Zhang F, Wang G, Xu Y, Li C, Wang S, et al. Incidence rates of immune-related adverse events and their correlation with response in advanced solid tumors treated with NIVO or NIVO+IPI: a systematic review and meta-analysis. *J Immunotherapy Cancer* 2019;341.
5. Osta B, Hu F, Sadek R, Chintalapally R, Tang S. A meta-analysis of immune-related adverse events of immune checkpoint inhibitors from cancer clinical trials. *Submitted Abstracts Immunotherapy of Cancer* 2016;27.

Abstract 625 Table 1 Baseline characteristics of ICI and control populations

Characteristic	Vax+ with ICI	Vax+ not on active treatment
Age, years		
Median (range)	70 (33-93)	72 (35-88)
Primary Cancer (N, %)		
Renal Cell Carcinoma	25, 49%	12, 52%
Melanoma	26, 51%	11, 48%
Gender (N, %)		
Male	38, 75%	8, 35%
Female	13, 25%	15, 65%
Treatment Regimen (N, %)		
Ipilimumab + Nivolumab	13, 25%	NA
Nivolumab	19, 37%	NA
Nivolumab + Cabozantinib	6, 12%	NA
Pembrolizumab	9, 18%	NA
Pembrolizumab + Axitinib	3, 9%	NA
Pembrolizumab + Lenvatinib	1, 2%	NA
COVID-19 Vaccine (N, %)		
Pfizer	34, 67%	18, 78%
Moderna	16, 31%	4, 17%
Johnson and Johnson	1, 2.0%	1, 4.3%

Results 51 study patients (vax+ with ICI) and 23 control patients (vax+ not on active treatment) were initially identified. Baseline characteristics are in table 1. 27.5% of ICI patients (N = 14/51) reported symptoms attributed to vaccination. Common symptoms reported by the ICI group were fever (9.8%; N = 5), chills (7.8%; N = 4), arm pain (7.8%; N = 4), myalgias (7.8%; N = 4), lymphadenopathy (7.8%; N = 4), headache (5.9%; N = 3), and diarrhea (3.9%; N = 2). None of these were reported in the control group. One patient in the ICI group developed a rash at the injection site, and one developed porokeratoses following the second dose. From the control group, one patient developed a stye and one patient developed PVCs. Five ICI patients (9.8%) developed a new or worsening IRAE requiring systemic steroids and/or treatment hold. These IRAEs included: colitis (N = 2), hepatitis, rash, and concurrent pancreatitis/colitis. Two ICI

<http://dx.doi.org/10.1136/jitc-2021-SITC2021.625>

626

DISSECTING THE SPATIAL HETEROGENEITY OF SARS-COV-2-INFECTED TUMOUR MICROENVIRONMENT REVEALS A LYMPHOCYTE-DOMINANT IMMUNE RESPONSE IN A HBV-ASSOCIATED HCC PATIENT WITH COVID-19 HISTORY

¹Benedict Tan*, ²Yi Yang, ²Chun Chau Lawrence Cheung, ¹Denise Goh, ¹Mai Chan Lau, ¹Xinru Lim, ¹Jeffrey Lim, ¹Li Wen Justina Nadia Lee, ¹Tracy Tien, ²Shirin Kalimuddin, ³Wai Meng David Tai, ²Jenny Low, ³Cedric Chuan Young Ng, ⁴Wei Qiang Leow, ⁴Thuan Tong Tan, ⁴Tony Lim, ³Jin Liu, ¹Joe Yeong. ¹IMCB, A*STAR, Singapore, Singapore; ²Duke-NUS Medical School, Singapore, Singapore; ³National Cancer Centre Singapore, Singapore, Singapore; ⁴Singapore General Hospital, Singapore, Singapore; ⁵Duke-NUS, Singapore, Singapore

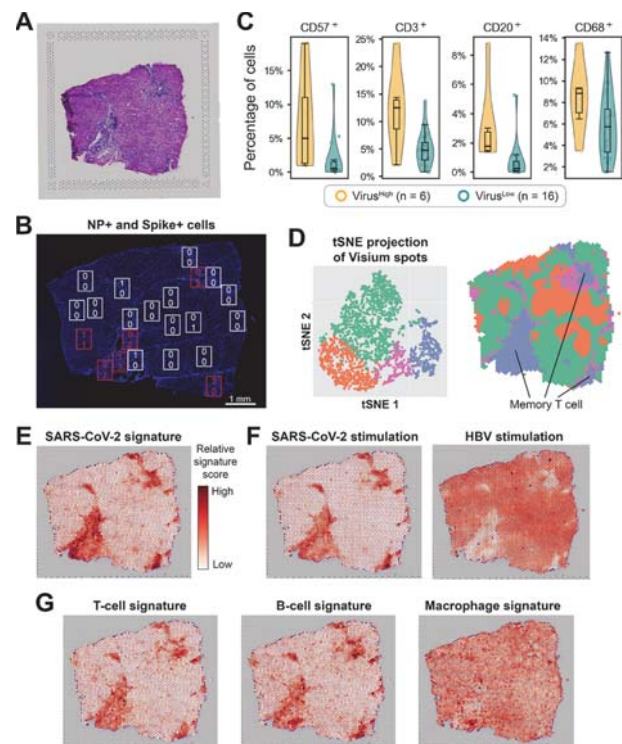
Background We previously reported the presence of SARS-CoV-2 RNA in the hepatic tissues of recovered patients¹ but the spatial immune profile of SARS-CoV-2 infection remains poorly understood. To address this, here we performed deep spatial profiling in tumour-adjacent normal hepatic tissue from a HBV-associated hepatocellular carcinoma (HCC) patient with history of COVID-19.

Methods We obtained tissue from curative resection of a HCC patient 85 days post-recovery from COVID-19. Spatial immune profiling was performed by multiplex immunohistochemistry (mIHC)² and more deeply using the Visium spatial transcriptomics platform complemented with signatures derived from single-cell RNA sequencing (scRNA-seq) and published signatures.

Results SARS-CoV-2 nucleocapsid and spike proteins were detected in a tumour-adjacent normal hepatic section in a spatially-restricted pattern (figure 1A and B) and higher abundance of lymphocytes but not macrophages were observed in regions with virus detection (figure 1C). We employed spatial transcriptomics and scRNA-seq to further characterize the immune microenvironment of SARS-CoV-2 post-infection. Unsupervised clustering and automatic annotation³ of Visium spots revealed that the distribution of SARS-CoV-2 viral proteins partially coincided with a memory T-cell signature (figure 1D). Quantification of Visium transcriptomic spots using an independent transcriptomic signature based on genes differentially upregulated in immune cells in SARS-CoV-2 infection⁴ (figure 1E) resulted in an enrichment pattern similar to the SARS-CoV-2 protein distribution. Additionally, a signature derived from scRNA-seq of hepatic tumour-infiltrating lymphocytes after *ex vivo* peptide stimulation using a pool of SARS-CoV-2 peptides showed a strongly associated distribution, in line with a SARS-CoV-2-specific immune response⁵ whereas that from using a pool of HBV peptides resulted in an anti-correlated distribution (figure 1F). These illustrate the ability of spatial transcriptomics to quantify with microenvironment-level resolution the SARS-CoV-2-specific immune response. Recapitulating the mIHC protein data, deconvolution of immune populations⁶ revealed marked spatial associations between SARS-CoV-2 viral presence and the distributions of lymphocytes but not of macrophages (figure 1G).

Conclusions We believe this is the first deep profiling report of non-post-mortem samples which adopts a multi-modal approach combining mIHC, spatial transcriptomics, and transcriptomic signatures derived from scRNA-seq to interrogate the *in situ* immune response to viral infection. Applying this to SARS-CoV-2 infection, we detected tissue spatial heterogeneity in viral presence and an associated lymphocyte-dominant immune response in the COVID-19-recovered patient, in contrast to post-mortem observations of scarce lymphocytes in cases of severe COVID-19.⁷ Ongoing work including further

validation of the findings in local and overseas cohorts and their correlation with patient clinical outcomes.



Abstract 626 Figure 1 Spatial heterogeneity of SARS-CoV-2 infection uncovers an association with a dominant lymphocytic response

REFERENCES

- Cheung CCL, et al. Residual SARS-CoV-2 viral antigens detected in GI and hepatic tissues from five recovered patients with COVID-19. *Gut*, p. gutjnl-2021-324280, 2021. doi: 10.1136/gutjnl-2021-324280.
- Lim JCT, et al. An automated staining protocol for seven-colour immunofluorescence of human tissue sections for diagnostic and prognostic use. *Pathology (Phila.)* 2018;**50**(3):333–341. doi: 10.1016/j.pathol.2017.11.087.
- Shao X, Liao J, Lu X, Xue R, Ai N, Fan X. scCATCH: automatic annotation on cell types of Clusters from Single-Cell RNA Sequencing Data. *iScience* 2020;**23**(3):100882, doi: 10.1016/j.isci.2020.100882.
- Lee JS, et al. Immunophenotyping of COVID-19 and influenza highlights the role of type I interferons in development of severe COVID-19. *Sci Immunol* 2020;**5**(49):p.eabd1554. doi: 10.1126/sciimmunol.abd1554.
- Schub D, et al. High levels of SARS-CoV-2-specific T cells with restricted functionality in severe courses of COVID-19. *JCI Insight* 2020;**5**(20):p.e142167. doi: 10.1172/jci.insight.142167.
- Newman AM, et al. Robust enumeration of cell subsets from tissue expression profiles. *Nat Methods* 2015;**12**(5):453–457. doi: 10.1038/nmeth.3337.
- Wang Y, et al. SARS-CoV-2 infection of the liver directly contributes to hepatic impairment in patients with COVID-19. *J Hepatol* 2020;**73**(4):807–816. doi: 10.1016/j.jhep.2020.05.002.

Ethics Approval This study was approved by the SingHealth Centralised Institutional Review Board (reference number: 2019/2653)

<http://dx.doi.org/10.1136/jitc-2021-SITC2021.626>

Data Sharing, Handling, and Access

627

IMMUNOATLAS: AN ONLINE PUBLIC PORTAL FOR SHARING, VISUALIZING, AND REFERENCING MULTIPLEX IMMUNOHISTOCHEMISTRY/IMMUNOFLUORESCENCE (MIHC/IF) IMAGES AND RESULTS FOR IMMUNO-ONCOLOGY

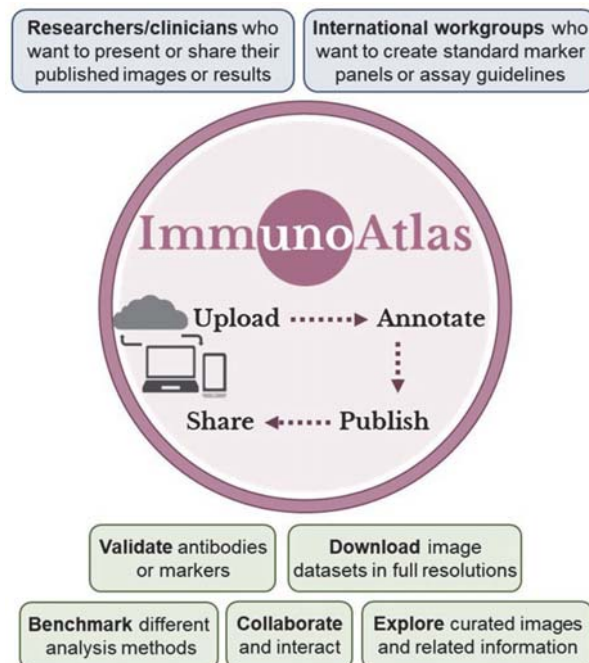
Jia Ying Joey Lee¹, Joe Yeong², Li Wen Justina Nadia Lee¹, Lit-Hsin Loo^{1*}, Jiahui Dong¹.
¹Agency for Science, Technology and Research (A*STAR), Singapore, Singapore; ²Singapore General Hospital, Singapore, Singapore

Background Recent advances in multiplex immunohistochemistry/immunofluorescence (mIHC/IF) technologies have enabled simultaneous measurements of large numbers of markers on the same tissue sections, and more comprehensive views of the cellular compositions and immune responses of the tumor microenvironment. However, the reproducibility and interpretation of the complex staining patterns and analysis results obtained from these markers remain major barriers to more general adoptions of these technologies. Here, we report the availability of an online public portal, “ImmunoAtlas”, which would enable researchers/clinicians to present or share their published mIHC/IF images or results; international workgroups to create and share standard marker panels or assay guidelines; end users to validate antibodies or protocols; or computational scientists to benchmark different analysis methods on standard reference images (figure 1).

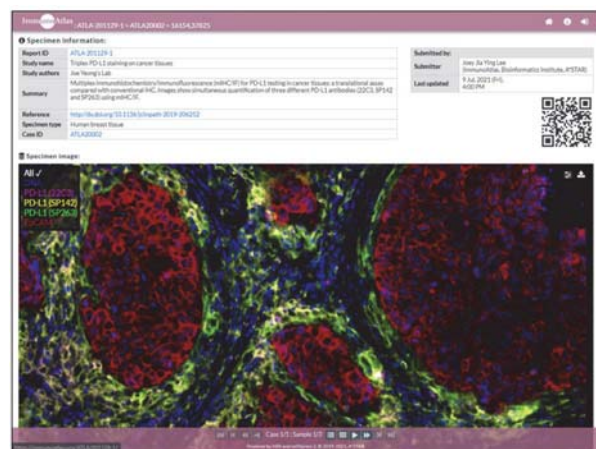
Methods ImmunoAtlas is based on a HistoPathological image management and Analysis (HPA) software platform developed by us, and hosted in the data center of Bioinformatics Institute. The platform uses the cellXpress software,¹ which is written in C++ and supports parallel processing, to efficiently process and manage large numbers of huge mIHC/IF or brightfield images. The web interface of ImmunoAtlas is also completely developed by us in PHP and JavaScript to address the specific needs and requirements in managing these images.

Results ImmunoAtlas is a user-friendly online portal for sharing, visualizing, and referencing original tissue images and analysis results (<https://ImmunoAtlas.org>). We have completed the first phase of development of the portal. Users can now perform image uploading, annotation, publishing, sharing, and viewing with standard web browsers on desktop computers or mobile devices/phones (figure 2). The portal supports image files from common microscopes and slide scanners, and can process mIHC/IF or brightfield images from selected areas, tissues microarrays, or whole slides. It can handle up to 1000 multiplexed markers, and whole-slide images that are >20GB/image. Several internal and external immuno-oncology studies have deposited and shared their images via ImmunoAtlas. They include a study of multiplexed PD-L1 markers in breast cancers²; the development of a panel of 56 highly-multiplexed markers for cutaneous T cell lymphoma³; and a study of CD38 scoring in hepatocellular carcinoma.⁴

Conclusions ImmunoAtlas promotes open science and collaborations that can accelerate the adoptions of mIHC/IF technologies in immuno-oncology. The next phase of development will focus on adding image searching and comparison functions to the portal. The community is welcome to use and share their images and analysis results via the portal.



Abstract 627 Figure 1 Key target users and applications of ImmunoAtlas



Abstract 627 Figure 2 ImmunoAtlas' web interface for sharing and visualizing mIHC

REFERENCES

- Laksameethanasan D, Tan RZ, Toh GW-L, et al. cellXpress: a fast and user-friendly software platform for profiling cellular phenotypes. *BMC Bioinformatics* 2013;**14**:S4. doi:10.1186/1471-2105-14-S16-S4.
- Yeong J, Tan T, Chow ZL, et al. Multiplex immunohistochemistry/immunofluorescence (mIHC/IF) for PD-L1 testing in triple-negative breast cancer: a translational assay compared with conventional IHC. *J Clin Pathol* 2020;**73**:557–62. doi:10.1136/jclinpath-2019-206252.
- Phillips D, Schürch CM, Khodadoust MS, et al. Highly multiplexed phenotyping of immunoregulatory proteins in the tumor microenvironment by CODEX tissue imaging. *Front Immunol* 2021;0. doi:10.3389/fimmu.2021.687673.
- Ng HHM, Lee RY, Goh S, et al. Immunohistochemical scoring of CD38 in the tumor microenvironment predicts responsiveness to anti-PD-1/PD-L1 immunotherapy in hepatocellular carcinoma. *J Immunother Cancer* 2020;**8**:e000987. doi:10.1136/jitc-2020-000987

<http://dx.doi.org/10.1136/jitc-2021-SITC2021.627>

Education and Treatment Management

628

REAL-WORLD CLINICAL OUTCOMES AMONG PATIENTS WITH ADVANCED MERKEL CELL CARCINOMA TREATED WITH AVELUMAB IN ACADEMIC MEDICAL CENTERS IN THE UNITED STATES

¹Shailender Bhatia, ²Paul Nghiem, ³S Phani Veeranki, ⁴Alejandro Vanegas, ⁵Kristina Lachance, ⁶Lisa Tachiki, ³Kevin Chiu, ³Emily Boller, ⁷Murtuza Bharmal*. ¹University of Washington, Seattle, WA, USA, Seattle, WA, United States; ²UW Medical Center at Lake Union, Seattle, WA, USA, Seattle, WA, United States; ³PRECISIONheor, Los Angeles, CA, USA, Los Angeles, CA, United States; ⁴RTI Health Solutions, Parsippany, NJ, USA, Parsippany, NJ, United States; ⁵University of Washington, Seattle, WA, Seattle, WA, United States; ⁶Fred Hutchinson Cancer Research Center, University of Washington, Seattle, WA, USA, Seattle, WA, United States; ⁷EMD Serono, Billerica, MA, USA, Billerica, MA, United States

Background Merkel cell carcinoma (MCC) is a rare, aggressive cutaneous neuroendocrine neoplasm with annual incidence rates ranging from 0.13 to 1.6 cases per 100,000 per year.¹ Chemotherapy for metastatic MCC (mMCC) has high objective response rates (ORRs), but responses are not durable and overall survival (OS) is poor. In March 2017, avelumab (anti-PD-L1) was approved for the treatment of mMCC and has demonstrated meaningful survival benefit and durable response.² This study sought to investigate real-world clinical outcomes of avelumab-treated patients with advanced (stage IIIB/IV) MCC in academic medical centers in the United States (US).

Methods A retrospective chart review study of patients with advanced MCC who initiated avelumab between March 1, 2017, and July 31, 2019 was conducted at 6 US academic medical centers across the 4 US census regions. Eligible patients were followed through December 30, 2020. Descriptive analyses were conducted to assess demographics, clinical characteristics, and outcomes. Kaplan-Meier curves were constructed to illustrate real-world duration of response (rwDOR), real-world progression free survival (rwPFS), OS, and time-to-treatment discontinuation.

Results Ninety patients with advanced MCC were treated with avelumab, with a median follow-up of 15.0 months (95% CI, 13.1–17.8). Median age was 68 years; the majority were male (58%) and White (93%). During the time of avelumab initiation, 74 patients had stage IV MCC and 16 patients had stage IIIB MCC. Primary tumor was located most commonly on the lower limb (38%), with metastasis primarily to lymph nodes (67%) and lung (52%); 52% of patients had visceral metastases. Approximately 42% and 26% of patients had an Eastern Cooperative Oncology Group (ECOG) performance status of 2 and 3, respectively. Seventy-three patients (81%) received avelumab as first-line treatment of advanced MCC, whereas 17 (19%) received avelumab as second-line or later. Median duration of avelumab treatment was 13.5 months (95% CI, 6.4–30.6); 58% discontinued by the end of follow-up. Patients with avelumab treatment (n=90) had a rwORR of 73% (95% CI, 64–83), median rwPFS of 24.4 months (95% CI, 8.3-not reached [NR]), and median OS of 30.7 months (95% CI, 11.2-NR). Other clinical outcomes by line of avelumab treatment and stage at avelumab initiation are reported in table 1.

Conclusions This real-world study of patients with advanced MCC treated with avelumab demonstrates high response rate with durable responses and prolonged survival. The study findings are consistent with the efficacy results demonstrated

in pivotal clinical trials² and other recent observational studies.^{3, 4}

Abstract 628 Table 1 Clinical outcomes among avelumab-treated patients with advanced MCC by line-of-treatment and stage at avelumab initiation

Outcomes	Avelumab 1L (n=73)	Avelumab 2L+ (n=17)	Stage IIIB (n=16)	Stage IV (n=74)
Physician assessed rwORR (95% CI), %	75.3 (65.2-85.4)	64.7 (39.4-90.0)	100	67.6 (56.6-78.5)
Median rwDOR (95% CI), months	NR (NR-NR)	4.6 (1.1-NR)	NR (NR-NR)	NR (7.0-NR)
Median rwPFS (95% CI), months	36.1 (9.3-NR)	6.4 (4.5-NR)	NR (NR-NR)	10.3 (4.9-NR)
Median OS (95% CI), months	41.7 (10.2-NR)	15.9 (4.3-NR)	NR (NR-NR)	15.9 (8.4-41.7)

1L, first line; 2L+, second line or later; NR, not reached; OS, overall survival; rwDOR, real-world duration of response; rwORR, real-world objective response rate; rwPFS, real-world progression-free survival; CI, confidence interval.

Acknowledgements The authors would like to acknowledge all physicians at the respective sites who participated in the data collection process for the study.

REFERENCES

- Müller-Richter UDA, Gesierich A, Kübler AC, Hartmann S, Brands RC. Merkel cell carcinoma of the head and neck: recommendations for diagnostics and treatment. *Ann Surg Oncol* 2017;**24**:3430–3437.
- D'Angelo SP, Bhatia S, Brohl AS, et al. Avelumab in patients with previously treated metastatic Merkel cell carcinoma: long-term data and biomarker analyses from the single-arm phase 2 JAVELIN Merkel 200 trial. *J Immunother Cancer* 2020;**8**:e000674.
- Cowey CL, Liu FX, Kim R, et al. Real-world clinical outcomes with first-line avelumab in locally advanced/metastatic Merkel cell carcinoma in the USA: SPEAR-Merkel. *Future Oncol* 2021;**17**:2339–2350.
- Levy S, Aarts MJB, Eskens FALM, et al. Avelumab for advanced Merkel cell carcinoma in the Netherlands: a real-world cohort. *J Immunother Cancer* 2020;**8**:e001076.

Ethics Approval The study was approved by New England Institutional Review Board.

<http://dx.doi.org/10.1136/jitc-2021-SITC2021.628>

629

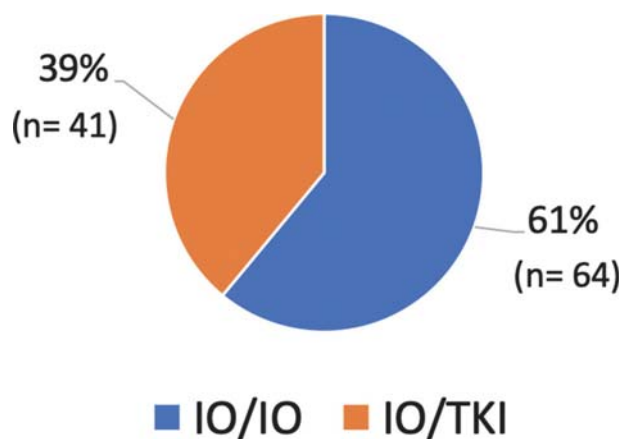
EVALUATION OF PROVIDER PREFERENCES IN FIRST-LINE METASTATIC RENAL CELL CARCINOMA: COMPARISON BETWEEN DUAL IMMUNOTHERAPY VS. IMMUNOTHERAPY/TYROSINE KINASE INHIBITORS

Priyanka Chablani*, Theodore Karrison, Walter Stadler. *University of Chicago Medical Center, Chicago, IL, United States*

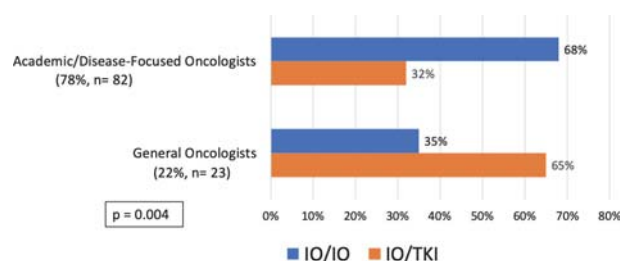
Background Dual immunotherapy (ipilimumab/nivolumab, IO/IO) and immunotherapy/tyrosine kinase inhibitor (IO/TKI) combinations (e.g. pembrolizumab/axitinib) are approved for first-line therapy of intermediate/poor risk metastatic renal cell carcinoma (RCC),¹⁻⁴ but there is limited comparative data between these two options. We sought to understand how physicians decide between IO/IO vs. IO/TKI for this indication.

Methods We sent a 10-question survey focused on a patient scenario of intermediate/poor risk metastatic RCC to 294 general and academic/disease-focused oncologists throughout the country using RedCAP software to solicit treatment preferences and rationale.

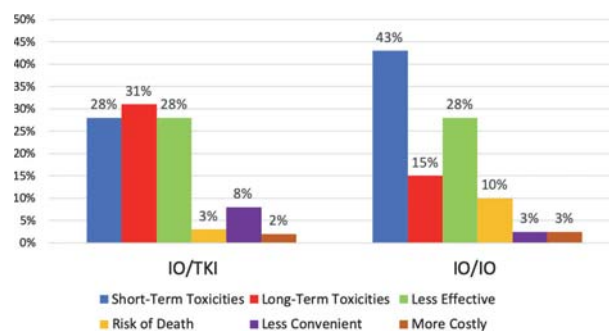
Results We received 105 responses (36% response rate): 61% (64) of providers chose IO/IO, 39% (41) chose IO/TKI (figure 1). 78% (82) of oncologists were academic or disease-focused, 22% (23) were general. Academic/disease-focused oncologists were significantly more likely to choose IO/IO (56/82, 68%) than general oncologists (8/23, 35%), $p = 0.004$ (figure 2). Among those who chose IO/IO, the perceived main issue with IO/TKI was: long-term toxicities - 31% (20), short-term toxicities - 28% (18), less effective - 28% (18), less convenient - 8% (5). Among those who chose IO/TKI, the perceived main issue with IO/IO was: short-term toxicities - 43% (17), less effective - 28% (11), long-term toxicities - 15% (6), and risk of death - 10% (4) (figure 3). 88% (92) of all providers would be comfortable enrolling patients into a phase III trial comparing IO/IO vs. IO/TKI. We found no associations between therapy chosen by a provider and participation as PI in a trial of IO/IO or IO/TKI, or receipt of outside funding from an IO/IO or IO/TKI company.



Abstract 629 Figure 1 Choice of therapy for patient scenario: IO/IO vs. IO/TKI



Abstract 629 Figure 2 Association between type of practice and choice of therapy



Abstract 629 Figure 3 Perceived main issue with IO/TKI or IO/IO as per oncologists who chose the alternate treatment

Conclusions In response to a representative patient scenario of intermediate-risk RCC, 61% of providers chose IO/IO, 39% chose IO/TKI. There was a significant association between type of practice and choice of therapy, with academic/disease-focused oncologists being more likely to choose IO/IO. The vast majority of oncologists would be comfortable enrolling patients into a phase III trial comparing IO/IO vs. IO/TKI, demonstrating equipoise in the community regarding this question and providing support for such a trial.

REFERENCES

- Motzer RJ, Tannir NM, McDermott DF. Nivolumab plus Ipilimumab versus Sunitinib in Advanced Renal-Cell Carcinoma. *N Engl J Med* 2018;**378**(14):1277–1290.
- Rini BI, Plimack ER, Stus V. Pembrolizumab plus Axitinib versus Sunitinib for advanced Renal-Cell Carcinoma. *N Engl J Med* 2019;**380**(12):1116–1127.
- Choueiri TK, Powles T, Burotto M. Nivolumab plus Cabozantinib versus Sunitinib for advanced Renal-Cell Carcinoma. *N Engl J Med* 2021;**384**(9):829–841.
- Motzer R, Alekseev B, Rha SY. Lenvatinib plus Pembrolizumab or Everolimus for advanced renal cell Carcinoma. *N Engl J Med* 2021;**384**(14):1289–1300.

Ethics Approval This study was approved by the IRB at The University of Chicago Biological Sciences Division/University of Chicago Medical Center. The study ID is: IRB20-1570.

<http://dx.doi.org/10.1136/jitc-2021-SITC2021.629>

630

ONCOLOGISTS' PERSPECTIVES ON EVOLUTION OF FIRST-LINE IMMUNE CHECKPOINT INHIBITOR MAINTENANCE THERAPY IN MANAGEMENT OF ADVANCED UROTHELIAL CARCINOMA IN THE US

¹Petros Grivas, ²Phani Veeranki, ³Kevin Chiu, ⁴Vivek Pawar, ⁵Jane Chang, ⁶Murtuza Bharmal*. ¹Department of Medicine, Division of Oncology, University of Washington, Seattle, WA, USA; ²Clinical Research Division, Fred Hutchinson Cancer Research Center, Seattle Cancer Care Alliance, Seattle, WA, Seattle, United States; ³PRECISIONheor, Los Angeles, CA, USA (At the time of the study), Los Angeles, CA, United States; ⁴PRECISIONheor, Los Angeles, CA, USA, Los Angeles, CA, United States; ⁵EMD Serono, Billerica, MA, USA, Billerica, MA, United States; ⁶Pfizer, New York, NY, USA, New York, NY, United States

Background Avelumab, a PD-L1 immune checkpoint inhibitor (ICI), was recently approved as first-line (1L) maintenance therapy for locally advanced/unresectable or metastatic urothelial carcinoma (aUC) after disease control with platinum-based chemotherapy.¹ Given the evolving treatment landscape, the study aim was to gain real-world insights into clinical decision-making among oncologists for patients with aUC.

Methods In March 2021, a cross-sectional web-based survey was administered to a sample of US oncologists treating patients with aUC. Oncologists' demographics, practice characteristics, and treatment patterns were obtained; descriptive statistics were used.

would consider 1L ICI maintenance therapy after disease control with platinum-based chemotherapy for over 40% of their patients. Future studies are warranted to evaluate real-world treatment patterns, barriers, and utilization of ICI maintenance therapy as the new 1L standard of care.

Acknowledgements The authors would like to acknowledge all physicians at who participated and completed the survey for the study.

REFERENCE

1. Powles T, et al. *N Engl J Med* 2020;**383**(13):1218–1230.

Ethics Approval The study was reviewed and determined to be exempt by Advarra IRB.

Consent All survey participated signed a consent form.

<http://dx.doi.org/10.1136/jitc-2021-SITC2021.630>

Abstract 630 Table 1 Oncologists characteristics and considerations for 1L ICI maintenance therapy

	High consideration (1L ICI maintenance for ≥40% of their patients) (N=118)	Low consideration (1L ICI maintenance for <40% of their patients) (N=33)
Age, mean (SD), years	49.8 (10.1)	49.9 (10.5)
Male, %	69.5	81.8
Practice location, %*		
Solo	8.5	12.1
Group/partnership	49.1	60.5
University	30.5	15.2
Hospital	10.2	12.1
Years of practice, %		
<10	18.6	18.2
11-20	51.7	57.6
>20	28.0	24.2
Cisplatin-eligible regimen, mean % of patients in practice (SD)	54.4 (21.0)	53.6 (23.5)
Carboplatin-eligible regimen, mean % of patients in practice (SD)	30.1 (16.3)	32.0 (21.5)
Number of cycles of chemotherapy before initiating 1L ICI maintenance, %*		
2	5.9	15.2
3	19.5	24.2
4	64.4	42.4
5	16.1	12.1
6	28.0	36.4

*Responses not mutually exclusive.

Results The study included 151 medical oncologists, who reported that 54% and 31% of their patients, on average, would be classified as cisplatin or carboplatin eligible for their 1L treatment, respectively. Approximately 78% of oncologists (n=118) considered using ICI maintenance in ≥40% of their patients following disease control with platinum chemotherapy and were categorized as the “high-consideration” group, for further exploratory analysis; the rest (22%) were in the low-consideration group (See table 1). Approximately, 31% and 27% of oncologists in the high- and low-consideration groups reported administering ICI maintenance with a 2–3-week gap after chemotherapy, while 45% and 46% reported administering it with a 4–6-week gap after chemotherapy, respectively.

Conclusions Surveyed oncologists reported that 85% of patients with aUC in US may be eligible for platinum-based chemotherapy. Further, 78% of the surveyed oncologists

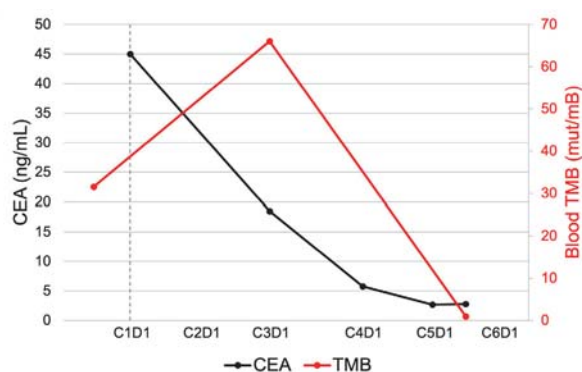
631 **DEEP, DURABLE RESPONSE TO PD-1 INHIBITOR MONOTHERAPY IN MICROSATELLITE-STABLE, TUMOR MUTATIONAL BURDEN-HIGH COLORECTAL CANCER**

¹Samuel Schellenberg*, ²Leeseul Kim, ¹Young Kwang Chae. ¹Northwestern University Feinberg School of Medicine, Chicago, IL, United States; ²AMITA Health Saint Francis Hospital, Chicago, IL, United States

Background Immune checkpoint inhibitors have revolutionized care for a number of different cancer types. For colorectal cancer (CRC), a leading cause of cancer-related death in the United States, programmed cell death protein 1 (PD-1) inhibition is a treatment option for certain subsets of patients. High microsatellite instability (MSI-H) tumors are immunogenic, and thus PD-1 inhibition is first-line treatment. Anti-PD-1 therapy is generally not utilized for microsatellite stable (MSS) patients. Tumor mutational burden (TMB) is another predictive biomarker for immunotherapy response in all solid tumors. Here we present the case of a patient with MSS, TMB-H CRC resistant to multiple lines of chemotherapy, who responded to anti-PD-1 monotherapy.

Methods Case presentation.

Results A 64-year-old man with a family history significant for colon cancer was diagnosed with colorectal cancer, revealed to be moderately differentiated mucinous adenocarcinoma (stage IIIC) on biopsy. A tissue-based comprehensive genomic profiling of the cancer showed KRASG12D and ERBB2 amplification, microsatellite-stable, and TMB of 11mut/mB (FoundationOne). The patient progressed on multiple lines of therapy with multiple metastatic sites, and was briefly put under home hospice with diffuse abdominal pain and weight loss. The patient was started on pembrolizumab monotherapy, around 3.5 years after initial presentation. After five months on pembrolizumab, imaging showed significant improvement in pulmonary, hepatic, adrenal, and retroperitoneal metastases and the patient demonstrated partial response to treatment according to RECIST 1.1 criteria. The patient's carcinoembryonic antigen (CEA) levels had decreased from 45 ng/mL at treatment initiation to 2.8 ng/mL, and ctDNA analysis showed a blood TMB decrease from 31.58 mut/mB at treatment initiation to .96 mut/mB (figure 1), accompanied by decreases in the variant allele frequencies of the five most prevalent variants at the time of treatment initiation (Guardant 360). The patient's pain had nearly resolved by this point and pain medications were tapered off.



Abstract 631 Figure 1 Carcinoembryonic antigen (CEA) and blood tumor mutational burden (TMB) levels through six cycles of treatment with pembrolizumab

Conclusions This case demonstrates the existence of a subset of CRC patients who are MSS but TMB-H and may respond to immune checkpoint blockade. Comprehensive genomic profiling must be utilized in order to not miss this subset of patients. The mechanism of response in this subset of patients is unknown but warrants further exploration. Further studies should clarify the mechanism and likelihood of response to immunotherapy in MSS, TMB-H CRC patients, as this is critical to providing effective treatment for this subset.

Consent Written informed consent was obtained from the patient for publication of this abstract and any accompanying images. A copy of the written consent is available for review by the Editor of this journal.

<http://dx.doi.org/10.1136/jitc-2021-SITC2021.631>

632

TORIPALIMAB COMBINED WITH PLATINUM-BASED CHEMOTHERAPY AS A SECOND-LINE TREATMENT FOR SMALL CELL LUNG CANCER (SCLC) WITH BRAIN METASTASES: A CASE REPORT

Jieqiong Fan*, Yao Zhang, Xiaofei Mo, Jing Guo. *Chongqing University Three Gorges Hospital, Chongqing, China*

Background Immunotherapy targeting PD-L1 together with platinum-based chemotherapy has demonstrated clinical activity in extensive-stage small cell lung cancer (ES-SCLC). However, brain metastasis seems to be an adverse prognostic factor. Here we report a case of a pretreated ES-SCLC patient with brain metastases who obtained marked clinical benefit from a combination of the anti-PD-1 antibody (toripalimab) together with platinum-based chemotherapy.

Methods A 56-year-old male smoker first presented at our hospital on March 17, 2018, with a dull pain in the right chest wall, without obvious cause. The patient underwent a biopsy of the right lung, revealing small cell carcinoma. Between April 20, 2018 and June 27, 2018, the patient received four cycles of platinum-based chemotherapy (irinotecan with carboplatin) and achieved a partial response (PR) (RECIST 1.1). However, at the end of 2019, his condition began to deteriorate. He had left upper abdominal pain without obvious cause, followed by dizziness, headache, unsteady walking, dull pain in the middle and upper abdomen, accompanied by acid regurgitation and belching. CT and MRI showed secondary malignant tumors in the liver, intracranially and in the pancreas with lymph node metastasis. Because the patient refused radiotherapy, from June 2020 he was treated with etoposide (160 mg, every 3 weeks on day 1–3) plus cisplatin (40 mg, every 3 weeks on day 1–3) combined with toripalimab (240 mg, every 3 weeks on day 1).

Results Following two cycles of treatment, MRI showed significant shrinkage of the patient's intracranial tumor. After the next sequential 4 cycles of therapy, MRI showed that the intracranial tumor had almost disappeared, CT images showed similar shrinkage of the liver and pancreas tumors. The overall efficacy assessment was PR. The patient tolerated the treatment with no side effects and is experiencing a durable clinical benefit. He now maintains immunotherapy and leads a normal life with no progression at the latest follow up on June 2021.

Conclusions Immunotherapy targeting PD-L1 added to platinum-based chemotherapy has been shown to prolong overall survival in ES-SCLC patients. Even in pretreated patients with brain metastases, PD-1 inhibitors plus platinum-based chemotherapy may also play a potential role. This is worthy of further investigation in formal clinical trials.

<http://dx.doi.org/10.1136/jitc-2021-SITC2021.632>

633

**INCORPORATING CHECKPOINT INHIBITORS INTO
CANCER CARE: A STUDY OF THE IMPACT OF DIGITAL
EDUCATION ON CLINICAL COMPETENCE AND PRACTICE
PATTERNS**

¹Tariqa Ackbarali*, ¹Elizabeth del Nido, ²Brian Rini, ³Michael Overman, ³Ignacio Witsuba.
¹PlatformQ Health Education, Lake Worth, FL, United States; ²Vanderbilt-Ingram Cancer
Center, Nashville, TN, United States; ³MD Anderson Cancer Center, Houston, TX, United
States

Background Immune checkpoint inhibitors have transformed the treatment landscape for a variety of tumors and have significantly improved patient prognosis and longevity. Evolving practice standards for diagnostic testing and extensive emerging clinical trial data have left clinicians challenged to apply newer treatments in practice and manage associated side effects. Additionally, improved patient prognosis has created a greater need for survivorship care plans; clinicians must be able to tailor plans to the needs of patients treated with these agents. Education pertaining to biomarker testing, applications of checkpoint inhibitors, adverse event management, and survivorship care is critical to ability to improve patient experience and quality of life.

Methods A 4-hour CME activity was broadcast live-online in June, July, and August 2020 and remained on-demand through February 2021 at OMedLive.com. The program was provided in partnership with the Society for Immunotherapy in Cancer (SITC). The initiative was divided into themes including biomarker usage for checkpoint inhibitor selection, adverse event management, survivorship care, and use of checkpoint inhibitors and combination therapies in the metastatic setting. Knowledge and competence questions were administered pre-, immediate post-, and 2 mos. post-activity. Behavioral impact questions were also asked at follow-up. Data from these questions were analyzed to determine engagement and clinical impact.

Results Final program results from 1,909 learners showed that post-activity engagement resulted in 61% reporting a positive impact on patient experience, and 74% reporting a positive impact on clinical practice, with 179 qualitative write-in examples detailing improvements in diagnosis, use of newer therapies, ability to manage adverse events, and patients' tolerance of treatments. All 14 CME test questions reflected statistically significant improvements on biomarker utility, checkpoint inhibitors, combination therapy applications, adverse event management, and survivorship care, with an average of 15% pre to 2-month follow-up improvement. The overall average effect size from pre- to post-test was $d = 1.27$, and $d = 0.429$ for pre- to 2-month follow-up point. Practice pattern questions elucidated preferences for biomarker testing, challenges of integrating immunotherapy, areas of difficulty in survivorship care, and challenges enrolling in clinical trials.

Conclusions The activity was successful in improving clinician understanding of the use of biomarker testing to determine treatment plans, applications of checkpoint inhibitors and combination therapies, adverse event management, and survivorship care planning. Open-ended responses to behavioral impact questions illustrated clear improvements in clinician-reported patient impacts, including improved psychological tolerance of treatment, quality of life, and overall wellness.

<http://dx.doi.org/10.1136/jitc-2021-SITC2021.633>

635

ONLINE CME IMPROVES THE INTERPROFESSIONAL TEAM'S ABILITY TO MANAGE PATIENTS WITH MALIGNANT PLEURAL MESOTHELIOMA

¹Michelle Worst*, ¹Emily Van Laar, ¹Megan Whitney, ²Anne Tsao, ³Hossein Borghaei. ¹*Medscape Oncology, New York, NY, United States*; ²*University of Texas MD Anderson Cancer Center, Houston, TX, United States*; ³*Fox Chase Cancer Center, Philadelphia, PA, United States*

Background Malignant pleural mesothelioma (MPM) is a rare and aggressive inflammatory cancer commonly associated with prior exposure to asbestos. Until recently, approved systemic treatments for MPM have been limited to chemotherapy regimens that have had limited survival benefit with overall poor outcomes. Both immune checkpoint inhibitors (ICIs) and tumor treating fields (TTF) have been associated with improved survival in this population. As a result of these advancements and changing of the treatment landscape, many members of the interprofessional team are challenged to stay current with emerging data and knowing how best to integrate these regimens into MPM treatment paradigms. The objective of this study was to determine if an online continuing medical education (CME) intervention could improve oncologists' and pharmacists' ability in managing patients with MPM.

Methods The activity consisted of a 30-minute video discussion between two expert faculty.¹ Educational effect was assessed with a repeated pairs pre-/post-assessment study including a 3-item, multiple choice, knowledge/competence questionnaire and one confidence assessment question, with each participant serving as his/her own control. Pre- and post-assessment scores were compared to determine relative changes in the proportion of correct responses to knowledge/competence questions. A paired samples t-test assessed overall number correct and confidence change statistical significance. The activity launched 5 January 2021; data were collected until 3 May 2021.

Results Overall, statistically significant improvements in knowledge/competence were seen after education consumption for oncologists (N = 44, P < .001) and pharmacists (N = 223, P < .001). Relative improvement in correct answers was 79% for oncologists and 123% for pharmacists (total correct responses pre-/post-assessment were 33%/59% and 22%/49%, respectively). Following the activity, 41% of oncologists and 57% of pharmacists had a measurable increase in confidence regarding their ability to collaborate as part of the interprofessional team in the management of patients with MPM.

Conclusions Participation in an online, video discussion-based CME-certified activity resulted in statistically significant improvements in knowledge/competence, and measurable increases in confidence of oncologists and pharmacists regarding the management of patients MPM. These results have the ability to translate to improvements in clinical care. The need for additional educational activities was also identified to address residual gaps and further increase clinicians' ability in this clinical setting.

Acknowledgements Sources of support: Developed through an independent educational grant from Bristol Myers Squibb Company and Novocure.

REFERENCE

1. Tsao A, Borghaei H. Moving the Needle in Mesothelioma: advances in treatment. *Medscape* 2021. <https://www.medscape.org/viewarticle/943353>.

<http://dx.doi.org/10.1136/jitc-2021-SITC2021.635>

636

PATIENT-REPORTED DISTRESS WITH IMMUNOTHERAPY-BASED FIRST-LINE TREATMENT FOR MNSCLC: A REAL-WORLD EVIDENCE STUDY

¹Monica Bodd*, ²Susan Locke, ²Scott Antonia, ²Jeffrey Crawford, ³John Hartman, ²Kris Herring, ²Neal Ready, ²Thomas Stinchcombe, ¹Jesse Troy, ³Chakita Williams, ¹Steven Wolf, ²Jeffrey Clarke, ²Thomas LeBlanc. ¹Duke University School of Medicine, Durham, NC, United States; ²Duke Cancer Institute, Durham, NC, United States; ³Bristol Myers Squibb, Lawrenceville, NJ, United States

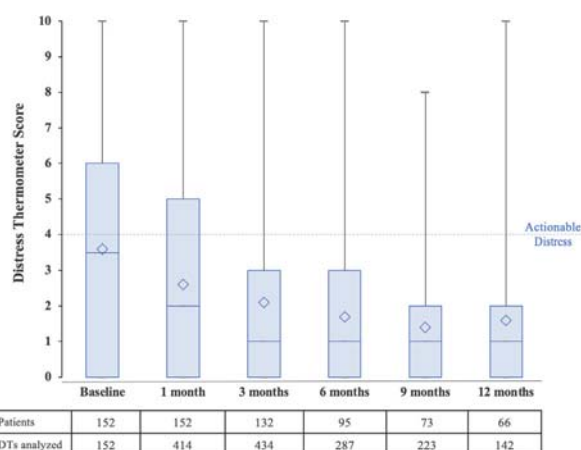
Background There are limited published real-world data about patient-reported outcomes with immunotherapies (IO) in metastatic non-small cell lung cancer (mNSCLC). We describe the patient experience with first-line IO-based treatments vs. chemotherapy in this setting.

Methods We conducted a retrospective chart review of adult patients with mNSCLC treated at Duke University from March 2015-June 2020. At each visit, patients self-reported their distress level and sources of distress using the NCCN Distress Thermometer (DT) tool, consisting of an 11-point ordinal scale reporting overall distress and a 39-item Problem List (PL). We abstracted demographic, clinical, distress, response data (by investigator assessment), then analyzed these data using descriptive statistics and generalized estimating equations accounting for clustering of clinic visits within participants and generalized linear models accounting for study exposure time.

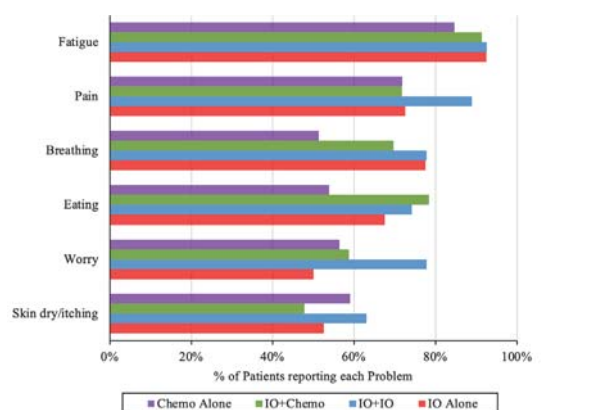
Results 152 patients were analyzed in four groups: single agent immunotherapy (IO alone, n=40), dual immunotherapy (IO+IO, n=27), chemo-immunotherapy (IO+Chemo, n=46), and chemotherapy alone (n=39). Patients were followed for up to 1 year or earliest of: death, last contact, or 2nd line therapy start. Participants' mean age was 65.7 years. In all patients, overall distress was worst before treatment start (figure 1), and the odds of actionable distress (DT score >4) decreased over time by 10% per month (OR=0.901, 95% CI:0.813, 0.998, p=0.045). There were no significant differences in actionable distress across treatment groups. Symptom distress remained high over time, while other sources of distress (practical, family, and emotional) decreased. The most frequent sources of symptom distress were fatigue (90% of patients ever reported, 40% of all DTs), pain (75% of patients, 30% of DTs), and breathing (68% of patients, 22% of DTs) (figure 2). Treatment with chemotherapy alone yielded the fewest tumor responses (50%) and lowest clinical benefit rate (74.4%) compared to any IO therapy. Unplanned healthcare utilization was significantly different across treatment groups; IO+IO resulted in the lowest utilization rate (0.57, 95% CI:0.36, 0.90), while chemotherapy yielded the highest (1.46, 95% CI:1.00,2.12). Palliative care was utilized in 40% of patients; among those with actionable distress at any time (n=113; 74%), 53% (n=60) had a palliative care visit.

Conclusions This single-center, real-world evidence study demonstrates that patients with mNSCLC experience significant distress prior to starting first-line treatment, with persistent symptom distress over time. Furthermore, IO treatment is associated with reduced healthcare utilization compared to chemotherapy. Increased utilization of integrated palliative care services may improve the patient experience of mNSCLC treatment, especially for management of symptom distress.

Ethics Approval This clinical study involves retrospective analyses of data extracted from medical charts and was approved by Duke University School of Medicine Institutional Review Board (IRB#106013).



Abstract 636 Figure 1 Overall distress thermometer scores over time



Abstract 636 Figure 2 Most frequently reported problems by treatment type

Consent As there was no prospective enrollment of subjects, consent was obtained through a Waiver or Alteration of Consent and Authorization and Decedent Research Notification of the Health Insurance Portability and Accountability Act (HIPAA) 1996.

<http://dx.doi.org/10.1136/jitc-2021-SITC2021.636>

¹Helen Nichols, ¹Cynthia Schwartz*, ²Elise Wu. ¹*Cancer Support Community, Philadelphia, PA, United States*; ²*Merck & Co., Kenilworth, NJ, United States*

Background Background: Immunotherapy (IO) have demonstrated the superior clinical benefits compared to previous anticancer treatments. A better understanding of the IO patient experience in real world will allow healthcare professionals to develop effective supportive resources, help improve clinical practice and assist patients in managing anticancer journey. However, little information of informational and supportive needs to IO patients are available. This study aims to describe IO cancer patient experiences from multiple perspectives.

Methods This cross-sectional qualitative study consisted of cancer patients, who reported receiving IO targeting PD1/L-1 receptors irrespective of cancer types. The study included three independent focus groups, participants were assigned to a group based on how long they received treatment prior to enrolling in the study: Focus Group 1 (0–6 months), Focus Group 2 (6–12 months), and Focus Group 3 (12+ months), with 4–8 participants each. Thematic analyses followed a deductive approach. Codes and themes were generated based on the European Organization for Research and Treatment of Cancer Quality of Life Questionnaire (EORTC QLQ-C30).¹ This study was approved by Ethical & Independent Review Services.

Results: This study included 18 total participants, across three focus groups, diagnosed with cancer from 2006–2020. Fifteen out of 18 were Caucasian; average age was 57.3 years. Participants in all groups reported fatigue as the most common side effect, less ability to do daily tasks due to fatigue, that other patients with the same diagnosis provided the greatest emotional support, concerns regarding finances/careers, and most reported they had adjusted to their “new normal” and were satisfied with the coordination between members of their healthcare team and communication with their oncologist. Participants in Group 1 were more concerned with recurrence and trying to figure out their new roles at home and at work. Participants in Focus Groups 2 and 3 were mostly unable to work due to diagnosis/treatment and reported this was a difficult adjustment that affected their identity. Focus Group 3 participants were particularly concerned about non-medical expenses and reported receiving insufficient information about IO.

Conclusion: By understanding the IO cancer patient experience at different time points in treatment, healthcare providers can more accurately address unmet needs from patients' perspective, increase healthcare professionals' awareness of IO patients' challenges, and support good communication practices. This will aid healthcare professionals working towards the goal of improving patient well-being, ultimately contributing to treatment adherence in this population.

REFERENCE

1. Giesinger JM, Kuijpers W, Young T, Tomaszewski KA, Friend E, Zabernigg A, Holzner B, Aaronson NK. Thresholds for clinical importance for four key domains of the EORTC QLQ-C30: physical functioning, emotional functioning, fatigue and pain. *Health and Qual Life Outcomes* 2016;**14**:1–8.

Ethics Approval: IRB approval received from Ethical & Independent Review Services.

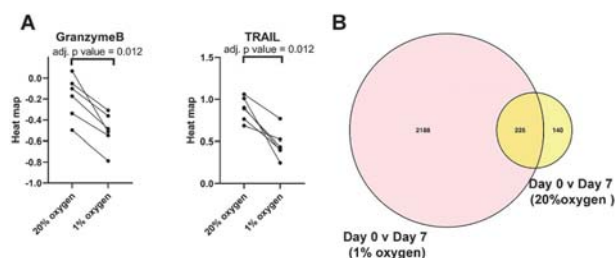
Immune Cell Biology

638 HYPOXIA REPROGRAMS NATURAL KILLER CELLS AND IMPAIRS THEIR THERAPEUTIC POTENTIAL

¹Philippa Kennedy*, ¹Upasana Sunil Arvindam, ¹Brianna Ettestad, ¹Shee Kwan Phung, ¹Quinlan Kile, ¹Peter Hinderlie, ²Yunmin Li, ²James Lim, ¹Jeffrey Miller, ¹Martin Felices. ¹University of Minnesota, Minneapolis, MN, United States; ²Xcell Biosciences, Minneapolis, MN, United States

Background Natural killer (NK) cell-based immunotherapies, from biologics to cell products, are being studied in the clinic across many cancer settings. These treatments have had therapeutic success for hematological malignancies but their impact on solid tumors remains limited. To succeed in the solid tumor setting, NK cells must enter the tumor microenvironment, with its low oxygen concentration (hypoxia), and retain functionality. Hypoxia is known to impair NK cell function, but a greater understanding of the mechanisms driving this impairment could lead to improvements in NK cell immunotherapy for solid tumors.

Methods We used an advanced incubator system: AVATARTM (Xcell biosciences), to finely tune the oxygen conditions in vitro to mimic the physiologic (5–12% oxygen) and hypoxic (1% oxygen) conditions found in vivo. Human NK cells were isolated from healthy donor blood and cultured with a low dose of interleukin 15 for up to 7 days, at 20% oxygen (standard incubator) or at 12%, 5% or 1% oxygen, to replicate the physiological conditions found in blood, bone marrow or hypoxic tumor, respectively. Phenotypes were analyzed by mass cytometry. Confocal and live cell imaging examined the cytotoxic process. Metabolic processes were assessed by flow cytometry and Seahorse assay. RNAseq and ATACseq were performed.



Abstract 638 Figure 1 NK cells are altered by exposure to hypoxia. Human NK cells from healthy donor blood were cultured in standard incubators (20% oxygen) or hypoxia (1% oxygen) for 7 days. (A) The relative abundance of granzyme B and TRAIL were compared on these NK cells at day 7 by time of flight mass cytometry. Analyzed by differential expression analysis through Astrolabe Diagnostics. Each line represents a donor. (B) Venn diagram of overlap between ATACseq differential expression analysis peaks. 2,413 regions were open at day 7 compared to day 0, when cultured under hypoxia (red circle); 365 regions were open at day 7 compared to day 0, when cultured in standard incubators (yellow circle).

Results NK cells were capable of natural cytotoxicity and antibody-dependent cellular cytotoxicity at physiological oxygen concentrations (5–20% oxygen), but killing was impaired under hypoxia (1% oxygen). Examination of the cytotoxic process revealed conjugate formation, polarization of granules to the synapse and granule release were not impaired by hypoxia. However, granzyme B (a component of cytotoxic

granules) and the death receptor TRAIL were decreased in NK cells exposed to hypoxia (figure 1A). RNAseq revealed upregulation of histone demethylases under hypoxia, with a shift in metabolism and decrease in the cell cycle. Glycolysis was upregulated under hypoxia and there was a concomitant increase in reactive oxygen species. ATACseq revealed profound epigenetic regulation of NK cells exposed to hypoxia, with limited changes occurring in NK cells cultured in 20% oxygen (figure 1B). Activation, adhesion, killing, proliferation and cytokine secretion were all pathways differentially regulated under hypoxia compared to 20% oxygen.

Conclusions NK cells exposed to hypoxia fail to kill tumor cells. Mechanistically, a lack of granzyme B and death receptors contribute to this deficit. ATACseq reveals epigenetic signatures associated with NK cell function that may allow interventions crucial to overcome barriers to solid tumor immunotherapy.

Acknowledgements We would like to acknowledge the services of the Minnesota Supercomputing Institute, the University Imaging Centers and the University Flow Cytometry Resource, all University of Minnesota.

<http://dx.doi.org/10.1136/jitc-2021-SITC2021.638>

PIK3IP1/TRIP IMMUNE REGULATION ON CD8+ T CELLS RESTRICTS ANTI-TUMOR IMMUNITY

Benjamin Murter*, Hridesh Banerjee, Andrea Szymczak-Workman, Lawrence Kane.
University of Pittsburgh, Pittsburgh, PA, United States

Background The signaling pathways involving phosphoinositide-3-kinases (PI3Ks) are highly conserved and tightly regulated to influence the activation, proliferation, and survival of all cell types. PI3K signaling plays a major role in T cell responses to antigen due to its position directly downstream of T cell receptor (TCR)/CD28 ligation.^{1 2} Our lab has recently shown that the cell surface protein TrIP (Transmembrane Inhibitor of PI3K, gene name: *Pik3ip1*) has a distinctly high expression on T cells and is capable of downregulating PI3K signaling in CD4+ T cells, acting as a negative regulator of T cell immune responses.^{3 4} These studies revealed that CD4+ T cells lacking TrIP expression exhibit a more Th1 inflammatory phenotype compared to WT T cells, both in vivo and in vitro.³ These data have led us to propose that TrIP restricts the inflammatory activity of T cells more generally, including CD8+ T cells, and that targeting/knockout of this negative regulator may promote anti-tumor immunity.

Methods Using a conditional TrIP knockout mouse model developed in our lab, we have performed syngeneic tumor challenges in CD8+ T cell-specific TrIP knockout mice (*TrIPfl/fIE8icre*). We have also characterized the tumor immune infiltrate of these mice to understand the impact of T cell-specific TrIP deficiency on the immune landscape.

Results Our data thus far show that CD8+ T cell-specific TrIP knockout mice (*TrIPfl/fIE8icre*) are resistant to growth of syngeneic tumors. In addition to increased tumor resistance, we have also found that tumors harvested from our *TrIPfl/fIE8icre* knockout mice contain twice as many infiltrating T cells compared to their WT counterparts. We also found that CD8+ T cells appeared to be the main drivers of this increased T cell infiltration, as their frequency was double that of the CD4+ population in tumors transplanted into TrIP KO mice.

Conclusions We describe data demonstrating that TrIP, a relatively novel PI3K inhibitor, plays a significant role in the anti-tumor immune activity of CD8+ T cells. Our that CD8+ T cell-specific TrIP knockout mice are resistant to tumor challenge and show more robust tumor CD8+ T cell infiltrate. With these data, we are excited to propose TrIP as a potential future immunotherapeutic target worthy of continued investigation.

REFERENCES

1. Okkenhaug K, Turner M, Gold MR. PI3K signaling in B cell and T cell biology. *Front Immunol* 2014;**5**:557. doi:10.3389/fimmu.2014.00557
2. Kane LP, Weiss A. The PI-3 kinase/Akt pathway and T cell activation: pleiotropic pathways downstream of PIP3. *Immunol Rev* 2003;**192**:7–20. doi:10.1034/j.1600-065X.2003.00008.x
3. Uche UU, Piccirillo AR, Kataoka S, et al. PIK3IP1/TrIP restricts activation of T cells through inhibition of PI3K/Akt. *J Exp Med* 2018;**215**:3165–3179. doi:10.1084/jem.20172018
4. DeFrances MC, Debelius DR, Cheng J, Kane LP. Inhibition of T-cell activation by PIK3IP1. *Eur J Immunol* 2012;**42**:2754–2759. doi:10.1002/eji.201141653

<http://dx.doi.org/10.1136/jitc-2021-SITC2021.639>

640 STEM-LIKE CD4 T CELLS IN CANCER

Maria Cardenas*, Nataliya Prokhnevskaya, Caroline Jansen, Viraj Master, Haydn Kissick.
Emory University, Atlanta, GA, United States

Background CD4 T cells can differentiate into multiple effector subsets that can mediate variable functions. In this work we aim to understand how CD4 T cells differentiate in response to tumor antigens and their respective function in the anti-tumor response.

Methods Tumor tissue was collected from patients undergoing surgery at Emory University Hospital. Activated PD1+ CD45RA- tumor infiltrating CD4 T cells were sent for 10X single cell RNA-seq. Tumor samples were also processed for flow cytometry and ex vivo functional analyses. For in vivo studies, prostate cancer mouse model expressing the LCMV glycoprotein (TRAMPC1-GP) was used, as well as LCMV Armstrong infection.

Results To characterize the heterogeneity of CD4 T cells infiltrating kidney tumors, we performed single cell RNAseq. We found three distinct activated (PD1+ CD45RA-) CD4 T cell populations. Two effector clusters consisting of Th1-like (EOMES+) and Treg (FOXP3+) cells, and a third cluster expressing TCF1, and genes associated with stemness and survival that did not fit defined CD4 effector lineages. We further confirmed these data by flow cytometry and found the same tumor infiltrating CD4 subsets in 100 kidney cancer patients. When placed in culture under different polarization conditions, tumor TCF1+ CD4 T cells proliferated and differentiated into the Th1-like and Treg effector populations found in the tumor, in addition to other effector lineages (Th1, Tfh) given the appropriate conditions, while the Th1-like and Treg cells underwent no proliferation or phenotype changes. These data suggests that the TCF1+ CD4s act as activated unpolarized precursors to the effector subsets in the tumor. To further test this hypothesis in vivo, we adoptively transferred tumor specific (SMARTA) CD4 T cells into mice followed by TRAMPC1-GP tumor inoculation. Transferred SMARTAs activated and first acquired a TCF1+ phenotype in the TDLN prior to predominantly differentiating into Tregs in the tumor. Given their plasticity in vitro, we asked whether TCF1+ SMARTAs primed in tumors were destined to differentiate into Tregs. To test this, we transferred 4-week activated TCF1 + SMARTAs from TDLNs of TRAMPC1-GP mice into naïve mice that were immediately infected with LCMV Armstrong. We found that the transferred SMARTAs differentiated into Th1 and Tfh cells in response to the virus, similar to the endogenous virus specific CD4 T cells.

Conclusions Overall, this work shows that CD4 T cells remain in an activated phenotype in the tumor with the capacity to differentiate into non-suppressive effector lineages given the appropriate conditions that may benefit the anti-tumor response.

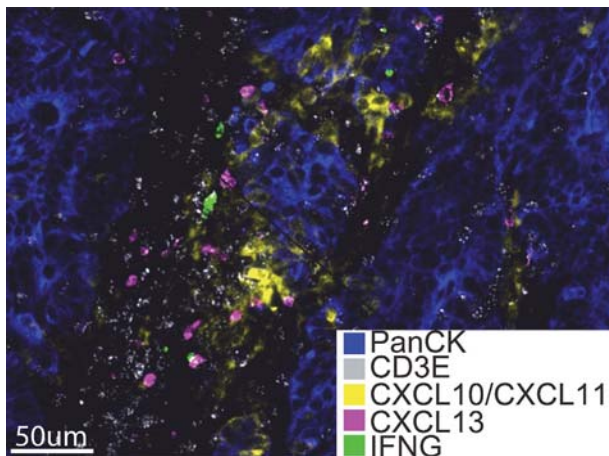
<http://dx.doi.org/10.1136/jitc-2021-SITC2021.640>

641 SPATIALLY ORGANIZED MULTICELLULAR IMMUNE HUBS IN MMRD AND MMRP COLORECTAL CANCER

¹Jonathan Chen*, ²Karin Pelka, ²Matan Hofree, ³Marios Giannakis, ¹Genevieve Boland, ³Andrew Aguirre, ⁴Ana Anderson, ²Orit Rozenblatt-Rosen, ²Aviv Regev, ¹Nir Hacohen. ¹Massachusetts General Hospital, Cambridge, MA, United States; ²Broad Institute, Cambridge, MA, United States; ³Dana-Farber Cancer Institute, Boston, MA, United States; ⁴Harvard Medical School, Boston, MA, United States

Background Immune responses to cancer are highly variable, with DNA mismatch repair-deficient (MMRd) tumors exhibiting more anti-tumor immunity than mismatch repair-proficient (MMRp) tumors. Almost all tumors are infiltrated with immune cells, but the types of immune responses and their effects on tumor growth, metastasis and death, vary greatly between different cancers and individual tumors. Which of the numerous cell subsets in a tumor contribute to the response, how their interactions are regulated, and how they are spatially organized within tumors remains poorly understood.

Methods To understand the rules governing these varied responses, we transcriptionally profiled 371,223 single cells from colorectal tumors and adjacent normal tissues of 28 MMRp and 34 MMRd treatment-naive patients. We developed a systematic approach to discover cell types, their underlying gene programs, and cellular communities based on single cell RNA-seq (scRNAseq) profiles and applied it to study the distinguishing features of human MMRd and MMRp colorectal cancer. Cellular communities discovered from this analysis were spatially mapped in tissue sections using multiplex RNA in situ hybridization microscopy.



Abstract 641 Figure 1 A coordinated network of CXCL13+ T cells with myeloid and malignant cells expressing ISGs. Image shows a portion of formalin-fixed paraffin-embedded tissue from an MMRd CRC specimen stained with multiplex RNA ISH / IF for PanCK-IF, CD3E-ISH, CXCL10/CXCL11-ISH, CXCL13-ISH, and IFNG-ISH. Note IFNG+ and CXCL13+ cells in proximity to cells expressing the chemokines CXCL10/CXCL11

Results To understand the basis for differential immune responses in CRC, we first determined and compared the immune cell composition of MMRd and MMRp CRC and normal colon tissue, finding dramatic remodeling between tumor and normal tissue and between MMRd and MMRp tumors, particularly within the myeloid, T cell, and stromal compartments. Among the clusters enriched in MMRd tumors were activated CXCL13+ CD8 T cells. Importantly, gene

program co-variation analysis revealed multicellular networks. We discovered a myeloid cell-attracting hub at the tumor-luminal interface associated with tissue damage, and an MMRd-enriched immune hub within the tumor, with activated IFNG + and CXCL13+ T cells together with malignant and myeloid cells expressing T-cell-attracting chemokines (figure 1).

Conclusions Our study provides a rich dataset of cellular states, gene programs and their transformations in tumors across a relatively large cohort of patients with colorectal cancer. Our predictions of several multicellular hubs based on co-variation of gene expression programs, and subsequent spatial localization of two major immune-malignant hubs, organizes a large set of cell states and programs into a smaller number of coordinated networks of cells and processes. Understanding the molecular mechanisms underlying these hubs, and studying their temporal and spatial regulation upon treatment will be critical for advancing cancer therapy.

Ethics Approval This study was approved by the DF-HCC institutional review board (protocols 03-189 and 02-240).

<http://dx.doi.org/10.1136/jitc-2021-SITC2021.641>

642

DECREASED HOST PKC-DELTA IS ASSOCIATED WITH THE T CELL-INFLAMED TUMOR MICROENVIRONMENT AND IMPROVES ANTI-TUMOR IMMUNITY

Kyle Cron*, Ayelet Sivan, Keston Aquino-Michaels, Emily Higgs, Jessica Fessler, Seoho Lee, Randy Sweis, Thomas Gajewski. *University of Chicago, Chicago, IL, United States*

Background Favorable clinical responses to immunotherapy have been correlated with a T cell-inflamed tumor microenvironment. The degree of spontaneous immune infiltration in tumors varies widely between individual patients. We hypothesized that germline polymorphisms in immune regulatory genes may affect the host immune response to solid tumors, similar to their influence on autoimmune susceptibility.

Methods Melanoma TCGA RNAseq and germline SNP data were utilized to identify germline polymorphisms associated with the magnitude of an immune gene signature score. The top GWAS hit associated with increased immune gene expression in melanoma was SNP rs1483185 ($p = 8.812e-08$, Bonferroni corrected <0.05), within the PKC-delta gene. Using a lymphoblastic cell line GTEx database, this SNP was associated with lower expression PKC-delta, implying a loss of function phenotype. Germline mutations in PKC-delta had previously been associated with familial lupus. To study the role of PKC-delta in anti-tumor immunity, knockout hematopoietic cells and conditional knockout mice were utilized, and implanted tumors were monitored along with detailed immune response analysis.

Results B16.SIY tumors grew more slowly in chimeras reconstituted with PKC-delta^{-/-} bone marrow compared to WT bone marrow, and this effect was dependent on CD8⁺ cells. T cell priming in the tumor-draining lymph node was comparable in WT and KO hosts. However, tumors in PKC-delta^{-/-} bone marrow chimeras had increased numbers of CD8⁺ T cells in the tumor at endpoint, and also responded better to anti-PD-L1 therapy. Single cell RNAseq of the tumor microenvironment revealed that PKC-delta loss primarily altered gene expression in myeloid cell subsets, leading to increased expression of M1 associated genes and decreased expression of M2 associated genes in PKC-delta^{-/-} chimeras. To follow up further, a conditional PKC-delta KO mouse was developed and crossed to the hematopoietic Vav1-iCre and also to LysM-Cre transgenic mice. In both instances, immune-mediated tumor control was improved, demonstrating that loss of PKC-delta in the myeloid compartment is sufficient to recapitulate the phenotype.

Conclusions Our results demonstrate that germline variants in immune regulatory genes can profoundly affect anti-tumor immunity and the efficacy of PD-1/PD-L1 blockade. In particular, the myeloid-expressed molecule PKC-delta plays an important regulatory role such that decreased expression/activity mediates improved anti-tumor immunity by altering the M1/M2 ratio. The development of pharmacologic approaches to phenocopy this loss of function phenotype may be attractive to pursue as a novel therapeutic strategy.

Ethics Approval University of Chicago IRB Protocol 15-0837

<http://dx.doi.org/10.1136/jitc-2021-SITC2021.642>

VASOACTIVE INTESTINAL PEPTIDE AS A NOVEL IMMUNE CHECKPOINT MOLECULE IN ACTIVATED T CELLS

Sruthi Ravindranathan, Tenzin Passang Fnu*, Edmund Waller. *Emory University, Atlanta, GA, United States*

Background Only a fraction of cancer patients responds to current antibody-based immune checkpoint inhibitors.¹ Our lab has identified vasoactive intestinal peptide-receptor (VIP-R) signaling as a targetable immune checkpoint pathway in cancer. VIP is a small neuropeptide with known immunosuppressive effects on T cells, in particular, CD4+ T cells.²⁻⁵ However, little is known about VIP-R signaling in CD8+ T cells. To define mechanisms by which VIP limits T cell activation and function, we studied the regulation of VIP and VIP receptors (VIP-R) in T cells following their activation in vitro and in mouse models of cancer.

Methods T cells from healthy human donors and murine splenocytes were activated using anti-CD3 coated plates. Western blots measured intracellular pre-pro-VIP, along with its cognate receptors; VPAC1 and VPAC2. Purified cultures of CD4+ and CD8+ T cells were used to interrogate the protein expression on specific T cell subsets. Activation and chemokine receptor expression was assessed by flow cytometry to evaluate T cell response to VIP-R antagonists in vitro and in tumor-bearing mice engrafted with pancreatic cancer cell lines.

Results Both murine and human T cells upregulate pre-pro-VIP following TCR stimulation with similar kinetics of VIP receptors between species. VIP expression is upregulated in vivo following treatment of tumor-bearing mice with anti-PD1 MoAb. VIP expression is temporally correlated with the upregulation of other co-inhibitory molecules. VPAC1 expression modestly increased in activated T cells while VPAC2 expression decreased. A non-canonical high molecular weight (HMW) form of VPAC2-related protein robustly and transiently increase in activated T cells. Expression of HMW form of VPAC2 is only detected in activated CD4+ T cells. Of note, activated CD4+ but not CD8+ T cells upregulate pre-pro-VIP. Pharmacological inhibition of VIP-R signaling significantly increased CD69+, OX40+, Lag3+, and PD1+ expression in CD4+ subsets compared to activated T cells without VIP-R antagonists ($p < 0.05$). In contrast, CD8+ T cells upregulate VPAC1 but not VPAC2 receptor following activation. VIP-R antagonist treatment of activated CD8+ T cells significantly decreased CXCR4+ expression ($p < 0.05$). CXCR3 and CXCR5 expression were not affected by VIP-R antagonist treatment.

Conclusions VIP-R signaling is a novel immune autocrine and paracrine checkpoint pathway in activated CD4+ T cells. Activated CD4+ and CD8+ T cells demonstrate different kinetics of VPAC1 and VPAC2 expression, suggesting different immune-regulatory responses to VIP-R antagonists. Understanding VIP-R signaling induced during T cell activation can lead to specific drugs that target VIP-R pathways to enhance cancer immunotherapy.

Acknowledgements We thank healthy volunteers for blood samples. The authors also thank the shared resources at Emory University, namely, Emory Flow Cytometry Core (EFCC) and Integrated Cellular Imaging Core (ICI) and Yerkes Nonhuman Primate Genomics Core that provided services or instruments at subsidized cost to conduct some of the reported experiments. This work was supported in part by Katz Foundation funding, Georgia Research Alliance, and

Emory School of Medicine Dean's Imagine, Innovate and Impact (I3) venture award to Edmund K. Waller.

REFERENCES

1. Darvin P, Toor SM, Sasidharan Nair V, Elkord E. Immune checkpoint inhibitors: recent progress and potential biomarkers. *Experimental and Molecular Medicine* 2018.
2. Wang HY, Jiang XM, Ganea D. The Neuropeptides VIP and PACAP Inhibit IL-2 Transcription by Decreasing c-Jun and Increasing JunB Expression in T Cells. *J Neuroimmunol* 2000;**104**(1):68–78.
3. Delgado M. Vasoactive intestinal peptide generates CD4+CD25+ regulatory T Cells in Vivo. *J Leukoc Biol* 2005.
4. Anderson P, Gonzalez-Rey E. Vasoactive intestinal peptide induces cell cycle arrest and regulatory functions in human T cells at multiple levels. *Mol Cell Biol* 2010.
5. Delgado M, Ganea D. Vasoactive intestinal peptide: a neuropeptide with pleiotropic immune functions. *Amino Acids*. NIH Public Access July 2013, 25–39.

Ethics Approval De-identified blood samples from consented healthy volunteers (IRB 00046063) were obtained with approval from Institutional Review Boards.

<http://dx.doi.org/10.1136/jitc-2021-SITC2021.643>

644

TUMOR-MEDIATED SUPPRESSIVE SIGNALING AND HYPOXIA SUPPORTS ALTERED CHROMATIN LANDSCAPES THAT LIMIT THE TRANSCRIPTIONAL AND FUNCTIONAL POTENTIAL OF TERMINAL T CELL EXHAUSTION

Rhodes Ford*, Natalie Rittenhouse, Nicole Scharping, Paolo Vignali, Greg Delgoffe, Amanda Poholek. *University of Pittsburgh, Pittsburgh, PA, United States*

Background CD8+ T cells are a fundamental component of the anti-tumor response; however, tumor-infiltrating CD8+ T cells (TIL) are rendered dysfunctional by the tumor microenvironment. CD8+ TIL display an exhausted phenotype with decreased cytokine expression and increased expression of co-inhibitory receptors (IRs), such as PD-1 and Tim-3. The acquisition of IRs mark the progression of dysfunctional TIL from progenitors (PD-1^{Low}) to terminally exhausted (PD-1⁺Tim-3⁺). How the chromatin landscape changes during this progression has not been described.

Methods Using a low-input ChIP-based assay called Cleavage Under Targets and Release Using Nuclease (CUT&RUN), we have profiled the histone modifications at the chromatin of tumor-infiltrating CD8+ T cell subsets to better understand the relationship between the epigenome and the transcriptome as TIL progress towards terminal exhaustion.

Results We have identified two epigenetic characteristics unique to terminally exhausted cells. First, we have identified a unique set of genes, characterized by active histone modifications that do not have correlated gene expression. These regions are enriched for AP-1 transcription factor motifs, yet most AP-1 family factors are actively downregulated in terminally exhausted cells, suggesting signals that promote downregulation of AP-1 expression negatively impacts gene expression. We have shown that inducing expression of AP-1 factors with a 41BB agonist correlates with increased expression of these anticorrelated genes. We have also found a substantial increase in the number of genes that exhibit bivalent chromatin marks, defined by the presence of both active (H3K4me3) and repressive (H3K27me3) chromatin modifications that inhibit gene expression. These bivalent genes in terminally exhausted T cells are not associated with plasticity and represent aberrant hypermethylation in response to tumor hypoxia, which is necessary and sufficient to promote downregulation of bivalent genes.

Conclusions Our study defines for the first time the roles of costimulation and the tumor microenvironment in driving epigenetic features of terminally exhausted tumor-infiltrating T cells. These results suggest that terminally exhausted T cells have genes that are primed for expression, given the right signals and are the basis for future work that will elucidate that factors that drive progression towards terminal T cell exhaustion at the epigenetic level and identify novel therapeutic targets to restore effector function of tumor T cells and mediate tumor clearance.

<http://dx.doi.org/10.1136/jitc-2021-SITC2021.644>

SINGLE-CELL TRANSCRIPTIONAL AND CLONAL CHARACTERIZATION OF CD4+ T CELLS ACROSS TISSUES IN LONG-TERM MELANOMA SURVIVORS

<http://dx.doi.org/10.1136/jitc-2021-SITC2021.645>

¹Jichang Han*, ²Yanding Zhao, ³Keisuke Shirai, ¹Tyler Searles, ¹Nikhil Khatwani, ¹Jennifer Vella, ¹Fatima Haidar, ¹Fred Kolling, ¹Jiang Gui, ⁴Chao Cheng, ¹Mary Turk, ⁵Christina Angeles. ¹Geisel School of Medicine at Dartmouth, Lebanon, NH, United States; ²Baylor College of Medicine, Houston, TX, United States; ³Dartmouth-Hitchcock Medical Center, Lebanon, NH, United States; ⁴Baylor School of Medicine, Houston, NH, United States; ⁵University of Michigan, Ann Arbor, MI, United States

Background Melanoma patients who develop immunotherapy-related adverse events often have durable responses to treatment. We previously identified that long-term melanoma survivors presenting with the autoimmune adverse event, vitiligo, developed long lived CD8+ resident memory T cell (TRM) responses in skin and tumor with circulating memory T cell (TCIRC) clonal counterparts in blood.¹ Despite the focus on CD8+ T cells in prior studies, CD4+ T cell features remain largely in the background.

Methods Using the same patient cohort, we performed parallel single-cell RNA sequencing (scRNAseq) and single-cell TCR sequencing (scTCRseq) on CD4+ T cells sorted from matched skin, tumor, and blood using the 10X Genomics platform. The UMI counts-based gene expression matrix was processed using the R package Seurat (v.3.0).

Results Eleven distinct CD4+ T cell clusters were identified. The FOXP3 expressing regulatory T cell (Treg) cluster was comprised of cells from skin, tumor, and blood, and could be further sub-clustered into 3 distinct populations with one having transcripts associated with Treg activation. Of the T helper-like clusters, we identified subsets with transcripts associated with cytotoxicity (GZMA, GNLY, CX3CR1; TCYTO), exhaustion (PDCD1, HAVCR2, TOX; TEX), and three clusters that were excluded from blood with clear resident memory characteristics (high CD69, low KLF2, S1PR1). These three clusters were differentiated by expression of IL2 (TRM-IL2); ID2 and CD40LG (TRM-ACTIVATED) and CD28 (TRM-CD28). Paired scTCRseq revealed a high level of clonal overlap between the TCYTO and the TRM-ACTIVATED clusters, with RNA velocity analysis supporting a potential differentiation trajectory from TRM-ACTIVATED to TCYTO. Integrating our previously published CD8+ TRM and TCIRC profiles, we identified a core TRM signature and core TCIRC signature from both the CD4+ and CD8+ TRM and TCIRC cells, respectively, in melanoma patients. The core TRM signature predicted better overall survival of advanced melanoma patients in TCGA, while the core TCIRC signature did not.

Conclusions This study supports the crucial anti-tumor role of TRM in cancer patients and extends this important observation to CD4+ T cells.

REFERENCE

1. Han JC, Zhao YD, Shirai K, Molodtsov A, Kolling FW, Fisher JL, Zhang PS, Yan SF, Searles TG, Bader JM, Gui J, Cheng C, Ernstoff MS, Turk MJ, Angeles CV. Resident and circulating memory T cells persist for years in melanoma patients with durable responses to immunotherapy. *Nature Cancer* 2021;**2**(3).

Ethics Approval IRB-approved written informed consent was obtained from patients with advanced melanoma, to perform skin and tumor biopsies, draw blood, and to access historical banked tissue and blood samples for analysis. All human studies were performed in accordance with ethical regulation, and pre-approved by the Committee for the Protection of Human Subjects at Dartmouth-Hitchcock Medical Center IRB (#00029821).

646

TRANSCRIPTOME ANALYSIS OF TUMOR AND MATCHED INFILTRATING LYMPHOCYTES IDENTIFIES POTENTIAL NEW TARGETS FOR AUGMENTING INTRA-TUMORAL NK FUNCTION IN SOFT TISSUE SARCOMAS

Sean Judge*, Joshua Bloomstein, Sylvia Cruz, Anyana Razmara, Cyrus Sholevar, Robert Canter. *University of California, Davis, Sacramento, CA, United States*

Background The success of current immunotherapies in soft tissue sarcomas (STS) has been limited, although pre-clinical studies have shown evidence of natural killer (NK) cell activity. We set out to evaluate the gene expression profile of tumor-infiltrating NK cells, tumor-infiltrating T cells, and tumor-intrinsic genes with the goal of identifying potential novel therapeutic targets and potential drivers of immune infiltration.

Methods Matched peripheral blood and freshly excised STS tissue were collected and processed for FACS isolation of purified peripheral and tumor-infiltrating NK and T cells and tumor cells from STS patients undergoing surgery. Sorted CD45+CD3-CD56+ and CD45+CD3+CD56- immune populations and viable CD45- tumor cells were then evaluated by RNA sequencing analysis. To allow for analysis of survival differences and differential gene expression based on gene expression, we also queried the publicly available TCGA database to compare outcomes in high and low gene expression.

Results Comparing differential gene expression (DGE) of intra-tumoral NK cells to circulating NK cells revealed upregulation of genes involved in mitogen signaling inhibition (DUSP4) and metabolic function (SMPD3, SLC7A5) ($P < 0.05$), but not of genes associated with cytotoxic function (e.g. IFNG, GZMB). In contrast, intra-tumoral T cells showed significant upregulation of established activating (CD137) and inhibitory genes (TIM-3) compared to circulating T cells. Tumors with higher immune infiltration exhibited significantly increased expression of the pro-inflammatory receptor TLR4. TCGA analysis demonstrated that patients with high TLR4 expression had significantly improved survival compared to low expression ($P = 0.03$).

Conclusions Unlike T cells, which demonstrated significant DGE in activating and inhibiting receptors between circulating and tumor-infiltrating subsets, NK cells appear to have a more similar gene expression pattern between blood and tumor, with alterations in metabolic pathways. Tumor expression of TLR4 is associated with increased immune infiltration and warrants evaluation as a potential prognostic and predictive factor in STS.

Ethics Approval The collection of matched whole blood and tumor specimens was approved by the IRB at the University of California, Davis (Protocol # 218204-9).

<http://dx.doi.org/10.1136/jitc-2021-SITC2021.646>

647

POSSIBILITY OF IMMUNOTHERAPY FOR THE GLIOBLASTOMA PATIENTS WITH O6-METHYL-GUANINE DNA METHYLTRANSFERASE (MGMT) EXPRESSION OR PROMOTER UNMETHYLATED

¹Yoshihiro Kushiara*, ²Yukari Kobayashi, ²Koji Nagaoka, ²Kazuhiro Kakimi. ¹The University of Tokyo, Bunkyo-ku, Japan; ²The University of Tokyo Hospital, Bunkyo-ku, Japan

Background It has been widely accepted that O6-methyl-guanine DNA methyltransferase (MGMT) promoter methylation in glioblastoma is associated with a benefit from temozolomide (TMZ) treatment. MGMT is a DNA repair protein that removes the cytotoxic O6-methylguanine (O6MG) DNA lesions generated by TMZ; thereby, MGMT expression is mechanistically linked to TMZ resistance. However, thus far, there is no effective treatment for these patients with MGMT promoter unmethylated. Therefore, a new treatment for GBM patients with MGMT expression is urgently needed.^{1 2} To this end, we examined the tumor microenvironment in GBM with or without MGMT expression.

Methods Based on The Cancer Genome Atlas (TCGA) primary GBM cohort, the tumor-infiltrating lymphocyte expression level was calculated using the CIBERSORTx algorithms and the single-sample Gene Set Enrichment Analysis (ssGSEA) method. Furthermore, the differential expression gene analysis was conducted and pathway analysis was performed using Ingenuity Pathway Analysis (IPA). The results were validated using the GBM cohort from the Chinese Glioma Genome Atlas (CGGA) database. In addition, tumor-infiltrating lymphocytes (TILs) were isolated from 13 surgically removed primary GBM tumors in our institution. Their responses to autologous tumors were evaluated by IFN γ ELISA.

Results T cells CD8 score by CIBERSORTx was significantly higher in the MGMT-high tumor. Similarly, ssGSEA scores for activated CD8 T cell, Macrophage, activated B cell, and Type 1 T helper cell were significantly higher in the MGMT-high tumor. Conversely, T cells CD4 naive was significantly higher in the MGMT-low tumor. These results indicate that more immune cell infiltration is associated with MGMT-high tumors. Consistently, tumor-reactive TILs were detected in the MGMT-high tumor. Pathway analysis showed that oxidative phosphorylation (OXPHOS) was highly enriched in the MGMT-high tumor. There were many CD8 T cells and tumor-reactive T cells in the MGMT-high tumors. However, it has been reported that anti-PD-1/PD-L1 monotherapy was not effective in glioblastoma. In this study, we demonstrated that OXPHOS was highly activated in the MGMT-high tumors. Thus, metabolic therapy can be combined with immunotherapy in these MGMT-high tumors to enhance anti-tumor immune responses.

Conclusions Although MGMT-high tumors are resistant to TMZ, the existence of immune cell infiltration in the tumor microenvironment of MGMT-high tumors suggest the potential of immunotherapy in these patients.

REFERENCES

1. Stupp R, Hegi ME, Mason WP, van den Bent MJ, Taphoorn MJB, Janzer RC, Ludwin SK, Allgeier A, Fisher B, Belanger K, Hau P, Brandes AA, Gijtenbeek J, Marosi C, Vecht CJ, Mokhtari K, Wesseling P, Villa S, Eisenhauer E, Gorlia T, Weller M, Lacombe D, Cairncross Jy, Mirimanoff R-O, European Organisation for Research and Treatment of Cancer Brain Tumour and Radiation Oncology Groups; National Cancer Institute of Canada Clinical Trials Group. *Lancet Oncol* 2009;**10**(5):459–66.
2. Wick W, Weller M, van den Bent M, Sanson M, Weiler M, von Deimling A, Plass C, Hegi M, Platten M, Reifenberger G. *Nat Rev Neurol* 2014;**10**(7):372–85.

Ethics Approval G3545-(26)

Consent Written informed consent was obtained from the patient for publication of this abstract and any accompanying images. A copy of the written consent is available for review by the Editor of this journal.

<http://dx.doi.org/10.1136/jitc-2021-SITC2021.647>

648 T CELL INTRINSIC CASPASE 1 SIGNALING NEGATIVELY REGULATES T CELL ANTI-TUMOR RESPONSE

Young Kim, Michael Korner, Cara Lang*. *Vanderbilt University, Antioch, TN, United States*

Background The inflammasome is a multi-protein signaling pathway in immune and epithelial cells that is important for activation of the innate immune system and protection from pathogens. This pathway is well characterized in myeloid cell populations, however the T cell intrinsic effects of the inflammasome are not well understood.

Methods In this study we utilize an inflammasome null mouse model to investigate the functional and phenotypic differences in inflammasome null and wildtype T cells. We utilize a whole cell vaccine against B16 mouse tumors to generate B16 tumor antigen specific T cells. In addition, we utilize clinically relevant PD-1 inhibitory antibodies to model checkpoint inhibition with inflammasome null T cells.

Results Here we show that the inflammasome is expressed and activated in tumor infiltrating T cells in both humans and mice. We find that inflammasome null T cells have an altered phenotype causing them to become more proliferative and increase killing capacity. In addition, caspase 1 null T cells are present in the TME at a greater frequency than wildtype T cells. We also show that caspase 1 knockout T cells have higher checkpoint expression, most notably an increase in PD-1 expression, and combination caspase 1 and PD-1 blockade results in a significant reduction in tumor burden.

Conclusions Therefore, we propose that T cell intrinsic inflammasome signaling acts as a negative regulator to inhibit T cell activation and cytotoxicity. Together our findings reveal the inflammasome as an attractive pathway that can be targeted in combination with checkpoint blockade therapies to improve anti-tumor T cell responses.

<http://dx.doi.org/10.1136/jitc-2021-SITC2021.648>

EFFEROCYTOSIS DRIVES MYELOID INFLAMMASOME SIGNALING AND GASDERMIN D INDEPENDENT SECRETION OF IL-1 β TO PROMOTE TUMOR GROWTH

¹Sohini Roy*, ²Cara Lang, ³Yu Wang, ²Diana Graves, ²Xu Yaomin, ²Young Kim. ¹VUMC, Nashville, TN, United States; ²Vanderbilt University, Antioch, TN, United States; ³Vanderbilt University, Nashville, TN, United States

Background Inflammation has long been associated with different stages of tumorigenesis as well as response to therapy. A key signaling pathway in this context is the casp-1 inflammasome. However, to date, its role in cancer has been contradictory and context dependent. We previously reported myeloid casp-1 can promote tumor growth in T cell independent manner. However, the regulatory mechanism that drives the myeloid intrinsic inflammasome signaling in the context of tumor growth remains largely unknown.

Methods In order to gain finer details about the inflammasome pathway components in the different myeloid clusters, we analyzed tumor and blood samples from head and neck cancer patients using bulk as well as 10X single cell sequencing platforms. For in vivo tumor studies, genetically engineered preclinical mice models were used. For in vitro functional studies, cells were isolated from mice or human tumors/blood and differentiated to either MDSC or macrophages and subjected to various assays.

Results Our bulk sequencing of myeloid cells isolated from treatment naïve head and neck tumors revealed an enrichment for inflammasome genes. Unbiased pathway analysis of tumor infiltrating myeloid cells compared to matched peripheral blood monocytes revealed IL-1 β signaling to be significantly altered in the tumor myeloids. In our single cell transcriptomic sequencing dataset on human head & neck carcinoma with matched peripheral blood monocytes, we observed similar elevated inflammasome transcriptomic activity within specific clusters of tumor-infiltrating macrophages and myeloid derived suppressor cells. Interestingly, distinct inflammasome sensor genes, specifically NLRP3, had distinct co-expressions with IL-1 β in specific myeloid subsets within the TME. Our data also indicates that myeloid-intrinsic caspase-1 signaling paradoxically increased tumor infiltrating myeloid cell survival without significant intratumoral trafficking into the tumor. When we explored the TME regulatory factors that regulate intratumoral myeloid inflammasome signaling, we found that NLRP3 dependent inflammasome signaling and IL-1 β production promotes tumor growth in a Gasdermin D independent mechanism. Mechanistically, we show that efferocytosis of dying tumor cells by myeloid cells in the TME directly activates NLRP3 dependent inflammasome signaling and IL-1 β production in myeloid cells to promote tumor growth rate.

Conclusions To our knowledge, we are the first to attribute the tumor supporting role of myeloid inflammasome signaling to efferocytic clearance of apoptotic debris in the tumor microenvironment. Our study thus opens an enticing option of novel therapeutic modality for treatment of solid tumors in future.

Ethics Approval All experimental procedures were approved by the Institutional Review Board of Vanderbilt University Medical Center (IRB: 170172).

<http://dx.doi.org/10.1136/jitc-2021-SITC2021.649>

650 TARGET THE ACTIVIN RECEPTOR 1C ON CD4+ T CELLS TO ACHIEVE ANTI-TUMOR THERAPEUTIC EFFECTS

¹Ying Zheng*, ²Andriana Lebid, ²Andrew Pardoll, ²Juan Fu, ²Chirag Patel, ²Xiaoxu Wang. ¹Johns Hopkins University, School of Medicine, Baltimore, MD, United States; ²Johns Hopkins Univ, School of Medicine, Baltimore, MD, United States

Background Activins, members of the transforming growth factor- β (TGF- β) superfamily, were isolated and identified in endocrine system, and have been widely studied in endocrine-related cancers,^{1, 2} but not substantially in the context of immune system and endocrine-unrelated cancers.³⁻⁵ It has been reported that upon binding to the receptors, activins cause the intracellular recruitment and phosphorylation of smad proteins, which mediate the expression of Foxp3.⁶⁻⁹ Therefore, we hypothesized that the blockade of the interaction of activins and their receptors will inhibit the activin-mediated Foxp3 induction in CD4+ T cells, thus modify the immune suppressive tumor microenvironment and achieve the goal of cancer immunotherapy.

Methods ELISA (enzyme-linked immunosorbent assay) has been performed to determine the plasma level of Activin A in tumor-bearing mice and cancer patients. In vitro iTreg (induced regulatory T cells) differentiation has been done to naïve CD4+ cells isolated from wild type mice in the presence or absence of Activin A, and the percentage of Foxp3+ cells was demonstrated by flow cytometric analysis. qRT-PCR analysis has been conducted to determine the mRNA level of activin receptor isoforms in the immune subpopulations sorted from Foxp3-YFP mice. In the end, in vivo subcutaneous transplanted tumor studies have been done to evaluate the anti-tumor therapeutic effects of activin-receptor 1c blockade.

Results We show here that tumor-bearing mice had elevated Activin A levels, which correlated directly with tumor burden. Likewise, cancer patients had elevated plasma Activin A compared to healthy controls. Importantly, our in vitro studies suggested that Activin A promoted differentiation of conventional CD4+ cells into Foxp3-expressing induced Tregs, especially when TGF- β was limited. Database and qRT-PCR analysis of sorted major immune cell subsets in mice revealed that activin receptor 1C (Acvr1c) was uniquely expressed on Tregs and was highly upregulated during iTreg differentiation. Mice deficient in Acvr1c were more resistant to cancer progression compared to wild type mice. This phenotype correlated with reduced expression of the FoxP3 transcription factor in CD4+ cells. Similar phenomena were observed when we treated the mice with anti-Acvr1c antibody after tumor inoculation. This anti-tumor therapeutic effect was more significant when anti-Acvr1c antibody was administered in combination with anti-PD-1 antibody.

Conclusions Blocking Activin A signaling through its receptor 1c is a promising and disease-specific strategy for preventing the accumulation of immunosuppressive iTregs in cancer. Hence it represents a potential candidate for cancer immunotherapy.

Acknowledgements This research is supported by the Bloomberg-Kimmel Institute (Immunometabolism Program & Immune Modulation Program), the Melanoma Research Alliance, the NIH (RO1AI099300, RO1AI089830, and RO1AI137046), and The DoD (PC130767).

REFERENCES

1. Risbridger GP, Schmitt JF, Robertson DM. Activins and inhibins in endocrine and other tumors. *Endocr Rev* 2001;**22**(6):836–858.

2. Cui X, et al. Perspectives of small molecule inhibitors of activin receptor-like kinase in anti-tumor treatment and stem cell differentiation (Review). *Mol Med Rep* 2019;**19**(6):5053–5062.
3. Michael IP, et al. ALK7 signaling manifests a homeostatic tissue barrier that is abrogated during tumorigenesis and metastasis. *Dev Cell* 2019;**49**(3):409–424.
4. Wu B, et al. The TGF- β superfamily cytokine Activin-A is induced during autoimmune neuroinflammation and drives pathogenic Th17 cell differentiation. *Immunity* 2021;**54**(2):308–323.
5. Antsiferova M, et al. Activin promotes skin carcinogenesis by attraction and reprogramming of macrophages. *MBO Mol Med* 2017;**9**(1):27–45.
6. Tsuchida K, et al. Activin isoforms signal through type I receptor serine/threonine kinase ALK7. *Mol Cell Endocrinol* 2004;**220**(1–2):59–65.
7. Khalil AM, et al. Differential binding activity of TGF- β family proteins to select TGF- β receptors. *J Pharmacol Exp Ther* 2016;**358**(3):423–430.
8. Huber S, et al. Activin a promotes the TGF-beta-induced conversion of CD4+CD25- T cells into Foxp3+ induced regulatory T cells. *J Immunol* 2009;**182**(8):4633–4640.
9. Iizuka-Koga M, et al. Induction and maintenance of regulatory T cells by transcription factors and epigenetic modifications. *J Autoimmun* 2017;**83**:113–121.

Ethics Approval All animal experiments were performed under protocols approved by the Johns Hopkins University Institutional Animal Care and Use Committee (IACUC).

<http://dx.doi.org/10.1136/jitc-2021-SITC2021.650>

MOLECULAR SIGNATURE OF NEOANTIGEN-REACTIVE CD4+ AND CD8+ T CELLS FROM METASTATIC HUMAN CANCERS ENABLES PROSPECTIVE ANTITUMOR TCR PREDICTION

Frank Lowery*, Sri Krishna, Rami Yoseph, Neilesh Parikh, Praveen Chatani, Yong-Chen William Lu, Nikolaos Zacharakis, Paul Robbins, Maria Parkhurst, Steven Rosenberg. *NCI, Bethesda, MD, United States*

Background Autologous patient T cells engineered to express antitumor T cell receptors (TCRs) and chimeric antigen receptors (CARs) have been effective for the treatment of certain cancer types,¹⁻⁴ and tumor neoantigens encoded by cancer-specific mutations have emerged as major targets of CD4+ and CD8+ T cells in immune checkpoint blockade (ICB) and in adoptive cell therapy (ACT).⁵⁻⁹ However, only a minority of intratumoral T cells are reactive to cancer antigens while the majority represent bystander cells.¹⁰⁻¹² Conventional approaches to isolate tumor-reactive T cells and identify their TCRs from tumors rely on T cell function and can be impaired due to T cell exhaustion and dysfunction.^{13 14}

Methods We performed single-cell RNA and T cell receptor (TCR) sequencing (scRNA/TCR-seq) on over 46,000 T cells isolated from eleven archival metastatic tumor samples whose primary cancer types included colon, rectal, breast, anal, and melanoma. From these samples, 15 CD8+ and 17 CD4+ neoantigen-reactive TCR clonotypes (NeoTCRs) were known. We then performed transcriptomic clustering of these cells and mapped known NeoTCR clonotypes onto the transcriptomic map. Subsequently we predicted NeoTCRs from prospective metastatic colon cancer samples based on their presence within clusters sharing gene expression with NeoTCR+ clusters in the archival samples.

Results Projecting known NeoTCRs onto the TIL transcriptomic map, we observed 325 total T cells bearing these NeoTCRs, and the majority (>80%) of NeoTCRs were expressed by T cells within 2 clusters, one CD4+ and one CD8+, that included by expression of CXCL13, ENTPD1 (CD39), TOX, TIGIT, LAG3, and PDCD1 (PD-1), indicating a dysfunctional state. Reasoning that T cells sharing phenotypes with those within the NeoTCR clusters could be novel NeoTCRs, we developed gene signatures (NeoTCR4 and NeoTCR8) of CD4 and CD8 NeoTCR+ cells, respectively, and four prospective patients' TIL were analyzed by scRNA/TCR-seq and scored according to NeoTCR signatures. We expressed predicted NeoTCRs in healthy donor PBL and screened them with antigen presenting cells (APCs) expressing candidate neoantigens. 33/73 predicted NeoTCRs (including both CD4 and CD8) were reactive against patients' tumors or candidate neoantigens.

Conclusions This study enabled successful detection of tumor-specific NeoTCRs in the sequenced TIL of 14/14 patients for whom reactivity was studied. Deconvolution of NeoTCRs from bystander TCRs within the tumor-immune microenvironment represents an important step in the development of personalized immunotherapeutics, and prospective NeoTCR isolation based on TIL transcriptional phenotypes will allow for rapid development of personalized immunotherapy in the form of lymphocytes expressing these tumor-specific TCRs.

Acknowledgements We thank the Surgery Branch TIL Laboratory and clinical team for generating TIL, and patients enrolled in our clinical protocols. Support from CCR Single Cell Analysis Facility was funded by FNLCR Contract HHSN261200800001E. This work utilized the computational

resources of the NIH HPC Biowulf cluster (<http://hpc.nih.gov>). We also thank NIDAP for providing additional computational support and the CCR Genomics Core for next-generation sequencing support

REFERENCES

1. Robbins PF, Morgan RA, Feldman SA, Yang JC, Sherry RM, Dudley ME, Wunderlich JR, Nahvi AV, Helman LJ, Mackall CL, Kammula US, Hughes MS, Restifo NP, Raffeld M, Lee CCR, Levy CL, Li YF, El-Gamil M, Schwarz SL, Laurencot C, Rosenberg SA. Tumor regression in patients with metastatic synovial cell sarcoma and melanoma using genetically engineered lymphocytes reactive with NY-ESO-1. *J Clin Oncol* 2011;**29**:917-924.
2. Morgan RA, Dudley ME, Wunderlich JR, Hughes MS, Yang JC, Sherry RM, Royal RE, Topalian SL, Kammula US, Restifo NP, Zheng Z, Nahvi A, de Vries CR, Rogers-Freezer LJ, Mavroukakis SA, Rosenberg SA. Cancer regression in patients after transfer of genetically engineered lymphocytes. *Science* 2006;**314**:126-129.
3. June CH, Sadelain M. Chimeric Antigen Receptor Therapy. *N Engl J Med* 2018;**379**:64-73.
4. Kochenderfer JN, Yu Z, Frasher D, Restifo NP, Rosenberg SA. Adoptive transfer of syngeneic T cells transduced with a chimeric antigen receptor that recognizes murine CD19 can eradicate lymphoma and normal B cells. *Blood* 2010;**116**:3875-3886.
5. Tran E, Robbins PF, Rosenberg SA. "Final common pathway" of human cancer immunotherapy: targeting random somatic mutations. *Nat Immunol* 2017;**18**:255-262.
6. Robbins PF, Lu YC, El-Gamil M, Li YF, Gross C, Gartner J, Lin JC, Teer JK, Cliften P, Tycksen E, Samuels Y, Rosenberg SA. Mining exomic sequencing data to identify mutated antigens recognized by adoptively transferred tumor-reactive T cells. *Nat Med* 2013;**19**:747-752.
7. Parkhurst MR, Robbins PF, Tran E, Prickett TD, Gartner JJ, Jia L, Ivey G, Li YF, El-Gamil M, Lalani A, Crystal JS, Sachs A, Groh E, Ray S, Ngo LT, Kivitz S, Pasetto A, Yossef R, Lowery FJ, Goff SL, Lo W, Cafri G, Deniger DC, Malekzadeh P, Ahmadzadeh M, Wunderlich JR, Somerville RPT, Rosenberg SA. Unique Neoantigens Arise from Somatic Mutations in Patients with Gastrointestinal Cancers. *Cancer Discov* 2019;**9**:1022-1035.
8. Gubin MM, Zhang X, Schuster H, Caron E, Ward JP, Noguchi T, Ivanova Y, Hundal J, Arthur CD, Krebber WJ, Mulder GE, Toebes M, Vesely MD, Lam SSK, Korman AJ, Allison JP, Freeman GJ, Sharpe AH, Pearce EL, Schumacher TN, Aebersold R, Rammensee HG, Melief CJM, Mardis ER, Gillanders WE, Artyomov MN, Schreiber RD. Checkpoint blockade cancer immunotherapy targets tumour-specific mutant antigens. *Nature* 2014;**515**:577-581.
9. van Rooij N, van Buuren MM, Philips D, Velds A, Toebes M, Heemskerk B, van Dijk LJA, Behjati S, Hilkman H, el Atmioui D, Nieuwland M, Stratton MR, Kerkhoven RM, Keşmir C, Haanen JB, Kvistborg P, Schumacher TN. Tumor Exome Analysis Reveals Neoantigen-Specific T-Cell Reactivity in an Ipilimumab-Responsive Melanoma. *Journal of Clinical Oncology* 2013;**31**:e439-e442.
10. Duhon T, Duhon R, Montler R, Moses J, Moudgil T, de Miranda NF, Goodall CP, Blair TC, Fox BA, McDermott JE, Chang SC, Grunkemeier G, Leidner R, Bell RB, Weinberg AD. Co-expression of CD39 and CD103 identifies tumor-reactive CD8 T cells in human solid tumors. *Nat Commun* 2018;**9**:2724.
11. Simoni Y, Becht E, Fehlings M, Loh CY, Koo SL, Teng KWW, Yeong JPS, Nahar R, Zhang T, Kared H, Duan K, Ang N, Poidinger M, Lee YY, Larbi A, Khng AJ, Tan E, Fu C, Mathew R, Teo M, Lim WT, Toh CK, Ong BH, Koh T, Hillmer AM, Takano A, Lim TKH, Tan EH, Zhai W, Tan DSW, Tan IB, Newell EW. Bystander CD8 T cells are abundant and phenotypically distinct in human tumour infiltrates. *Nature* 2018;**557**:575-579.
12. Scheper W, Kelderman S, Fanchi LF, Linnemann C, Bendle G, de Rooij MAJ, Hirt C, Mezzadra R, Slagter M, Dijkstra K, Kluijn RJC, Snaebjornsson P, Milne K, Nelson BH, Zijlmans H, Kenter G, Voest EE, Haanen JBAG, Schumacher TN. Low and variable tumor reactivity of the intratumoral TCR repertoire in human cancers. *Nat Med* 2019;**25**:89-94.
13. Blank CU, Haining WN, Held W, Hogan PG, Kallies A, Lugli E, Lynn RC, Philip M, Rao A, Restifo NP, Schietinger A, Schumacher TN, Schwartzberg PL, Sharpe AH, Speiser DE, Wherry EJ, Youngblood BA, Zehn D. Defining "T cell exhaustion." *Nat Rev Immunol* 2019;**19**:665-674.
14. van der Leun AM, Thommen DS, Schumacher TN. CD8 T cell states in human cancer: insights from single-cell analysis. *Nat Rev Cancer* 2020;**20**:218-232.

<http://dx.doi.org/10.1136/jitc-2021-SITC2021.651>

652

ANTI-PD-L1/IL-15 KD033 ACTIVATED MACROPHAGES AND INDUCED ANTI-TUMOR IMMUNITY IN THE TUMOR-MICROENVIRONMENT

Stella Martomo*, George Wang, Zhanna Polonskaya, Xenia Luna, Dan Lu, Jeegar Patel.
Kadmon Corporation, New York, NY, United States

Background KD033 is a clinical-stage bispecific fusion molecule consisting of a high-affinity anti-human-PD-L1 antibody and human IL-15. Previous studies with KD033 in mice expressing functional human PD-1 and PD-L1 showed that KD033 was efficacious in reducing the growth of both PD-L1 positive and negative tumors.¹ In the microenvironment of PD-L1 negative tumors, PD-L1 would still be expressed by some immune cells such as macrophages. The goal of the current study is to evaluate direct effect of KD033 on macrophages through in vitro studies and assess its contribution to anti-tumor immunity.

Methods Monocyte-derived human macrophages were treated with either KD033, the non-targeting IL15 fusion counterpart (ntKD033) or anti-PD-L1 antibody in vitro, and the supernatants were analyzed for cytokine/chemokine secretion. Human PD-1/PD-L1 transgenic C57BL/6 mice subcutaneously transplanted with the human-PD-L1 positive or negative MC38 colon carcinoma were treated with KD033 intravenously when tumors reached 100 mm³. Tumor infiltrating cell populations were evaluated with Immunohistochemistry (IHC).

Results In vitro cultures with KD033 induced macrophages to secrete inflammatory cytokines such as IFN γ to a much higher level compared to ntKD033 cultures at the same concentrations. The anti-PD-L1 antibody alone did not induce macrophages to secrete IFN γ . IHC on KD033-treated human PD-1/PD-L1 transgenic mice showed that PD-L1 negative and positive MC38 tumors have similar levels of CD8 T cell tumor infiltrations. IHC with the macrophage marker CD68 showed higher level of CD68/IFN γ double positive cell infiltrations on PD-L1 negative tumors that was correlated with increased tumor growth inhibitions.

Conclusions Increased in vitro IFN γ secretion from KD033-treated macrophages correlated with increased CD68/IFN γ double positive cell infiltrations in PD-L1 negative MC38 tumors from KD033-treated human PD-1/PD-L1 transgenic mice as evaluated by IHC. We hypothesized that our anti-PD-L1/IL15 KD033 induces anti-tumor immunity in PD-L1 negative tumors by activating PD-L1-expressing immune cells such as macrophages in the tumor microenvironment.

REFERENCE

1. Martomo S, et al. Single-Dose anti-PD-L1/IL-15 fusion protein KD033 generates synergistic antitumor immunity with robust tumor-immune gene signatures and memory responses. *Mol Cancer Ther* 2021;**20**(2):347–356.

Ethics Approval Mouse studies were conducted for Kadmon by Wuxi AppTec Inc. All the procedures related to animal handling, care and the treatment in the study were performed according to the guidelines approved by the Institutional Animal Care and Use Committee (IACUC) of WuXi AppTec following the guidance of the Association for Assessment and Accreditation of Laboratory Animal Care (AAALAC).

<http://dx.doi.org/10.1136/jitc-2021-SITC2021.652>

THE IMMUNE LANDSCAPE OF PRIMARY AND RECURRENT ADOLESCENT AND YOUNG ADULT BONE SARCOMAS<http://dx.doi.org/10.1136/jitc-2021-SITC2021.653>

¹Anthony Cillo*, ¹Elina Mukherjee, ²Jessica Daley, ¹Sayali Onkar, ¹Xiang Li, ¹Dongyan Liu, ¹Dario Vignali, ¹Tullia Bruno, ¹Kelly Bailey. ¹University of Pittsburgh, Pittsburgh, PA, United States; ²UPMC Children's Hospital, Pittsburgh, PA, United States

Background Pediatric patients with metastatic or recurrent bone sarcomas have poor survival, necessitating new therapies. Studies of immunobiology in pediatric bone sarcomas have focused on analysis of samples from surgical local control, when patients are receiving immunosuppressive chemotherapy, with little data available from relapse. Here, we sought to leverage transcriptomic and imaging approaches in tandem to characterize the immune landscape of primary and recurrent Ewing sarcoma and osteosarcoma and to identify new therapeutic avenues for these patient populations.

Methods Single-cell RNAseq (scRNAseq; 10X Genomics) was performed on sorted CD45+ cells from paired peripheral mononuclear cells (PBMC) and tumor infiltrating leukocytes (TIL) from freshly resected bone tumor specimens in the setting of pre-treatment or >6 months post-chemotherapy in the setting of disease relapse. Multiplexed immunofluorescence (mIF) analysis for CD45, DAPI, CD4, CD8, CD68, CD20, and FOXP3 was also performed on FFPE tissue from the same tumors. CIBERSORTx was used in conjunction with TARGET-OS bulk RNAseq from osteosarcoma tumors to infer cell type frequencies. Expression of ligands and receptors in primary versus relapsed disease was assessed from scRNAseq using CellTalker.

Results We analyzed a total of 29,993 cells from 20 donors (4 paired PBMC/TIL from osteosarcoma, 4 paired samples from Ewing sarcoma, 4 healthy donor PBMC) by scRNAseq. A total of 5 TIL samples were from primary disease sites and 3 were from metastatic sites. We identified major immune populations by canonical expression profiles and used transcriptional profiles from TIL to derive a signature matrix for CIBERSORTx. In 88 osteosarcoma samples from TARGET-OS, we found that higher frequencies of CD14+CD16+ macrophages were associated with better survival (HR:0.28, $p = 0.01$). scRNAseq from our cohort revealed expression of CXCL12, CCL7, and CCL3L1 by CD14+CD16+ macrophages, suggesting this macrophage population may drive tumor immune infiltration. In both Ewing sarcoma and osteosarcoma, mIF revealed greater numbers of tumor-infiltrating immune cells in the setting of relapse versus primary tumors. scRNAseq analysis revealed higher levels of interferon-gamma expressing CD8+ T cells and CD4+ regulatory T cells in relapsed versus primary disease, suggesting that recurrent tumors may be more immunogenic.

Conclusions Although pediatric bone sarcomas are typically considered “immunologically cold”, our transcriptomic and imaging approaches revealed a role for a myeloid cell subset in overall survival and increased immune infiltration and T cell activation in recurrent disease. These data suggest specific immunotherapeutic avenues should be tailored to both primary and recurrent disease to improve outcomes in pediatric bone sarcoma.

Ethics Approval Human specimens were collected with written informed consent under the IRB approved STUDY19030108 and the IRB approved Musculoskeletal Oncology Biobank and Tumor Registry.

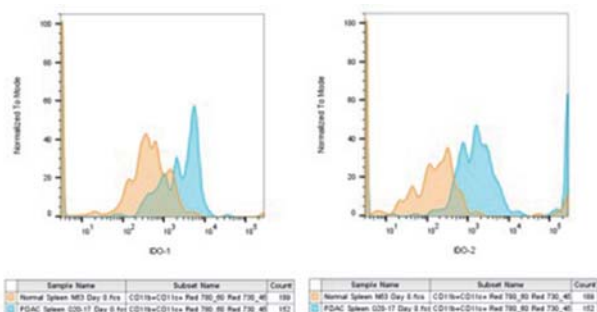
654

ANALYSIS OF IDO-1 EXPRESSION ON DENDRITIC CELLS AND FACTORS INFLUENCING ITS UP- AND DOWNREGULATION IN PANCREATIC CANCER

Michael Hollingsworth, Kamiya Mehla, Kirsten Eberle, Ying Huang, Aleata Triplett, Paul Grandgenett, Clara Mundry*, Thomas Caffrey. *University of Nebraska Medical Center, Omaha, NE, United States*

Background Pancreatic Ductal Adenocarcinoma (PDAC) is bad. An immunosuppressive tumor microenvironment (TME) with an excess of immunosuppressive immune cells and cytokine/chemokine factors contribute to local and systemic immunosuppression in PDAC.¹ Our laboratory has generated single-cell RNA-Sequencing (scRNA-Seq.) data from spleens derived from PDAC patients and healthy counterparts. This data demonstrates the existence of dendritic cell (DC) subsets with a tolerogenic phenotype. These DCs display increased expression of several markers, including Indoleamine 2,3-dioxygenases (IDO-1 and IDO-2), widely accepted as markers for a specific population of DCs: tolerogenic DCs. These cells evoke an immunosuppressive signal leading to activation of regulatory T cells and MDSCs as well as apoptosis of CD8+ and CD4+ effector T cells.²⁻³

Methods To validate our scRNA-Seq. data, we performed pilot investigations harvesting DCs from the spleen of PDAC patients and healthy subjects. Besides examining human specimens, we also investigated the IDO-1 expression on splenic DCs from tumor-bearing mice, orthotopically implanted with LSL-KrasG12D; LSL-Trp53R172H/+; Pdx1-Cre (KPC)-derived cell lines. It is known that tumor-derived exosomes can impact DC-differentiation to a tolerogenic phenotype.⁴ Exosome purification using differential ultracentrifugation is a well-established method in our lab and optimized for our autopsy samples. We analyzed tumor-derived exosomes for their potential in modulating IDO-1 expression on DCs in in vitro assays. Briefly, we incubated DCs with different exosome concentrations and harvested the cells for RNA-sequencing and flow cytometry.

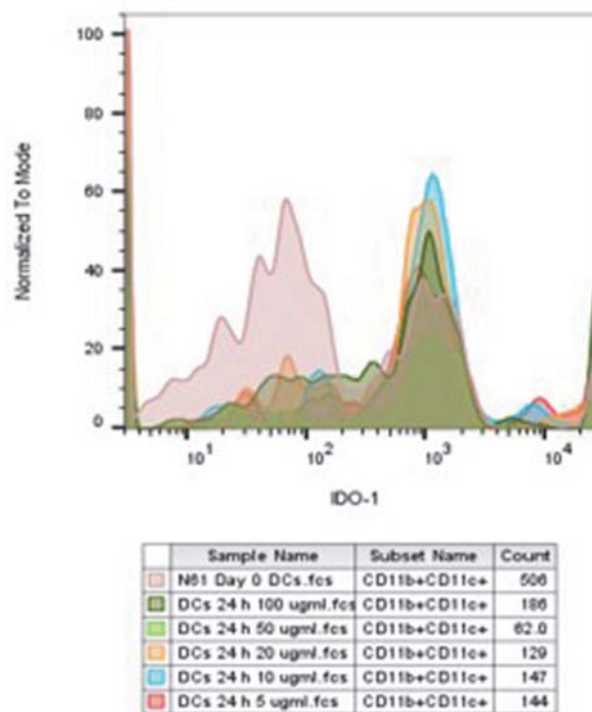


Abstract 654 Figure 1 Expression of IDO-1 and IDO-2 on DCs from PDAC spleen (blue) and normal spleen (orange)

Results Compared to normal spleens, DCs from PDAC spleens displayed higher expression of IDO-1 (figure 1). Additionally, KPC-tumor-bearing mice showed higher expression of IDO-1 on DCs from the spleen and blood compared to wild-type mice. Further investigating the influence of PDAC-derived exosomes on marker expression on DCs have shown an apparent increase in expression of IDO-1 when culturing splenic-derived DCs with tumor-derived exosomes (figure 2).

Conclusions While tolerogenic DCs are essential in regulating the homeostasis between immune response and immune

tolerance,⁵ several studies have shown IDO-1 overexpression in cancer. Investigating tolerogenic DCs is an essential part of our lab's efforts to understand the nature of the immune response in PDAC. Future directions for this project include determining molecular pathways that regulate the expression of IDO-1. Additionally, we will investigate downstream mechanisms through which exosomes modulate the switch to a tolerogenic phenotype. We also plan to further characterize different splenic DC populations by evaluating their interplay with other immune cells in the context of antigen-specificity and other factors influencing these cells' properties.



Abstract 654 Figure 2 Change in expression of IDO-1 through treatment of DCs with different concentrations of tumor-derived exosomes

REFERENCES

- Mundry CS, Eberle KC, Singh PK, Hollingsworth MA, Mehla K. Local and systemic immunosuppression in pancreatic cancer: targeting the stalwarts in tumor's arsenal. *BBA - Reviews on Cancer* 2020;**1874**(1):188387.
- Liu M, Wang X, Wang L, Ma X, Gong Z, Zhang S, Li Y. Targeting the IDO1 pathway in cancer: from bench to bedside. *Journal of Hematology & Oncology* 2018;**11**(1):100.
- Hornýák L, Dobos N, Koncz G, Karányi Z, Páll D, Szabó Z, Halmos G, Székelyólyi L. The role of Indoleamine-2,3-Dioxygenase in cancer development, diagnostics, and therapy. *Frontiers in Immunology* 2018;**9**:1.
- Bronte V, Pittet MJ. The spleen in local and systemic regulation of immunity. *Immunity* 2013;**39**(5):806–818.
- Domogalla MP, Rostan PV, Raker VK, Steinbrink K. Tolerance through education: how tolerogenic dendritic cells shape immunity. *Frontiers in Immunology* 2017;**8**:1764.

Ethics Approval This study was approved by the University of Nebraska Medical Center Ethics Board; approval numbers IRB#: 440-16-EP and IRB#: 091-01.

<http://dx.doi.org/10.1136/jitc-2021-SITC2021.654>

655 LANDSCAPE OF HELPER AND REGULATORY CD4+ T CELLS IN MELANOMA

¹Giacomo Oliveira*, ¹Kari Stromhaug, ²Susan Klaeger, ¹Nicoletta Cieri, ¹Bryan Iorgulescu, ¹Shuqiang Li, ¹David Braun, ¹Donna Neuberger, ²Steven Carr, ¹Kenneth Livak, ³Dennie Tompers, ¹Edward Fritsch, ⁴Megan Wind-Rotolo, ²Nir Hacohen, ³Moshe Sade-Feldman, ¹Derin Keskin, ¹Patrick Ott, ⁵Scott Rodig, ³Genevive Boland, ¹Catherine Wu. ¹Dana-Farber Cancer Institute, Boston, United States; ²Broad Institute of MIT and Harvard, Cambridge, United States; ³Massachusetts General Hospital, Boston, United States; ⁴Bristol-Myers Squibb, Princeton, NJ, United States; ⁵Brigham and Women's Hospital, Boston, MA, United States

Background Within the tumor microenvironment, distinct CD4+ T cell subsets can play different and even opposite roles either promoting or suppressing anti-tumor responses through the recognition of antigens presented by human leukocyte antigen (HLA) class II molecules. However, how cancers co-opt these processes to shape the intratumoral CD4+ landscape and achieve immune evasion remains incompletely understood.

Methods We performed single-cell characterization of CD4+ tumor infiltrating lymphocytes (TILs) collected from four human melanoma with low or high HLA-class II expression and we utilized TCR reconstruction and antigen specificity screening to unambiguously discover the tumor reactivity of CD4+ TILs. By testing TCR-transduced T cells against autologous patient-derived melanoma cell lines or against autologous antigen presenting cells (APCs) loaded with tumor lysates, we assessed the capacity of CD4+ TCRs to directly or indirectly recognize tumor cells. We defined the antigen-specificity of antitumor CD4+ TCRs by assessing their reactivity towards personal neoantigens (NeoAg) or public melanoma associated antigens (MAAs). Finally, we correlated NeoAg burden and HLA-class II expression in a series of 116 melanoma specimens from 4 independent cohorts of patients.

Results Analysis of single-cell data showed that the cluster distribution of cells within each CD4+ TCR clonotype family was highly homogeneous and appeared to follow 3 distinct major phenotypes, corresponding to non-exhausted memory cells, exhausted cells and regulatory cells (T_{Regs}). Strikingly, clonally expanded CD4+ T_{Reg}-TILs were highly abundant within the tumor microenvironment of HLA class II^{Pos} melanomas. We found that TCRs from exhausted cytotoxic CD4+ T cells could be directly triggered by melanoma cells not only through recognition of HLA class II restricted antigens, but also through presentation of HLA class I restricted MAAs. T_{Reg}-TCRs could be indirectly elicited through presentation of tumor antigens via APCs. Notably, numerous tumor-reactive CD4+ T_{Reg}-TCRs were directly stimulated by HLA class II^{Pos} melanoma and demonstrated specificity for melanoma NeoAgs. In HLA class II^{Pos} melanomas, the clonal expansion of numerous tumor-reactive and NeoAg-specific T_{Regs}-clones appeared to be favored by a dramatically high tumor NeoAg load. Analysis of 116 melanoma specimens confirmed the association of elevated HLA-class II expression with extremely high NeoAg burden.

Conclusions Our data elucidate the landscape of infiltrating CD4+ T cells in melanoma and point to presentation of HLA-class II restricted NeoAgs and direct engagement of immunosuppressive CD4+ T_{Regs} as a novel mechanism of immune evasion favored in HLA class II^{Pos} melanoma.

<http://dx.doi.org/10.1136/jitc-2021-SITC2021.655>

CHARACTERIZATION AND THERAPEUTIC TARGETING OF A TUMOR-ASSOCIATED TOLEROGENTIC DC SUBPOPULATION DRIVEN BY SREBP2 AND THE MEVALONATE METABOLIC PATHWAY

Michael Plebanek*, Nicholas DeVito, Fang Liu, Balamayooran Theivanthiran, Georgia Beasley, Brent Hanks. *Duke University, Durham, NC, United States*

Background Conventional dendritic cells (DCs) are essential mediators of anti-tumor immunity and the efficacy of anti-PD-1 checkpoint immunotherapies.¹ Recent studies suggest that tumor-mediated development of a sub-population of tolerogenic DCs plays an important role in immune evasion.²⁻³ Metabolic reprogramming regulates tolerogenic DCs in the tumor microenvironment (TME).⁴⁻⁵ Activation of DCs leads to rewiring of cDC metabolism towards glycolysis to support T cell activation while tolerogenic DCs display enhanced fatty acid oxidation.⁶ Related to DC metabolic alterations, tumor-associated DCs (TADCs) are enriched in lipids and have a reduced capacity to present antigen to T cells. Lipid homeostasis is maintained through a complex network of transcription factors including sterol regulatory element-binding protein-2 (SREBP2) which drives the expression of mevalonate pathway genes.⁷ The identification of those tumor-controlled pathways that regulate tolerogenic DCs in the TME is expected to lead to the discovery of a novel family of immunotherapeutic targets.

Methods We use transgenic mouse models of melanoma, sentinel lymph node (LN) tissue specimens derived from melanoma patients, single-cell RNA sequencing (scRNAseq), and flow cytometry-based metabolic assays to identify novel tumor-associated regulatory programs amongst different sub-populations of conventional DCs in the TME.

Results scRNAseq of DCs isolated from the tumor-draining LN (TDLN) of a BRAFV600EPTEN^{-/-} transgenic melanoma model revealed critical genetic differences in distinct DC sub-populations. We observed a migratory DC subset enriched in the expression of numerous immunoregulatory genes and identified CD63 as a surface marker to distinguish this DC subset from other conventional cDC1s and cDC2s. Further studies demonstrated CD63⁺ DCs to suppress T cell activation and promote CD4⁺FOXP3⁺ regulatory T cell (Treg) differentiation. Relative to other cDC subsets, CD63⁺ DCs overexpress genes of the mevalonate pathway leading to increased lipid content. Treatment of melanoma-bearing mice with a pharmacologic inhibitor of SREBP2 leads to a significant reduction in CD63⁺ DCs in the TDLN and reduced Tregs, resulting in suppressed tumor growth. Importantly, scRNAseq of DCs isolated from sentinel LNs of melanoma patients reveal that this population is conserved in humans.

Conclusions Lipid homeostasis in TADCs is a major determinant of their metabolic state, but despite significant advances, the molecular pathways regulating tolerogenic DCs have remained poorly understood. Collectively, this data demonstrates an important role of the mevalonate pathway in driving a tolerogenic DC program and highlights the therapeutic targeting of SREBP2 and DC lipid metabolism as a promising approach to overcoming immune tolerance in the TME and boosting immunotherapy responses.

REFERENCES

1. Gardner A, Ruffell B. Dendritic cells and cancer immunity. *Trends Immunol* 2016;**37**:855–865. doi:10.1016/j.it.2016.09.006

- DeVito NC, Plebanek MP, Theivanthiran B, Hanks BA. Role of tumor-mediated dendritic cell tolerization in immune evasion. *Front Immunol* 2019;**10**:2876. doi:10.3389/fimmu.2019.02876
- Gerhard GM, Bill R, Messemaker M, Klein AM, Pittet MJ. Tumor-infiltrating dendritic cell states are conserved across solid human cancers. *J Exp Med* 2021;**218**. doi:10.1084/jem.20200264
- Plebanek MP, Sturdivant M, DeVito NC, Hanks BA. Role of dendritic cell metabolic reprogramming in tumor immune evasion. *Int Immunol* 2020;**32**:485–491. doi:10.1093/intimm/dxaa036
- Wculek SK, Khouili SC, Priego E, Heras-Murillo I, Sancho D. Metabolic control of dendritic cell functions: digesting information. *Front Immunol* 2019;**10**:775. doi:10.3389/fimmu.2019.00775
- Zhao F. et al. Paracrine Wnt5a-beta-Catenin signaling triggers a metabolic program that drives dendritic cell tolerization. *Immunity* 2018;**48**:147–+, doi:10.1016/j.immuni.2017.12.004
- Xue L. et al. Targeting SREBP-2-Regulated mevalonate metabolism for cancer therapy. *Front Oncol* 2020;**10**:1510, doi:10.3389/fonc.2020.01510

Ethics Approval Collection of human tissue specimens was approved by the Duke Institutional Review Board under the title Immune Markers of Sentinel Nodes in Melanoma and the protocol number Pro00090678. All patients gave informed consent prior to participating in the study. All experiments involving animals were approved by the Duke University Institutional Animal Care and Use Committee (IACUC) under protocol number A174-18-07

<http://dx.doi.org/10.1136/jitc-2021-SITC2021.657>

658 CD8 T CELL ACTIVATION IN CANCER IS COMPRISED OF TWO DISTINCT PHASES

Nataliya Prokhnevska*, Maria Cardenas, Rajesh Valanparambil, Ewelina Sobierajska, Caroline Jansen, Viraj Master, Martin Sanda, Haydn Kissick. *Emory University, Atlanta, GA, United States*

Background CD8 T cells are a crucial part of the immune response to tumors, with CD8 infiltration predicting disease progression in numerous cancer types. Recently two subsets of CD8 T cells that respond to tumors have been described, a stem-like (TCF1+) CD8 T cell that can give rise to a more cytotoxic terminally differentiated (TD) (TCF1-Tim3+) CD8 T cell. In this study we aimed to understand the origin of stem-like TCF1+ CD8 T cells within tumors.

Methods Human patient TDLN and tumor samples from kidney and prostate cancer were processed after resection and used for flow cytometry, RNA-seq, TCR-seq and whole genome DNA methylation analysis. We also used a prostate cancer mouse model that expresses the LCMV GP protein (TRAMP1-LCMV-GP) to track tumor-specific CD8 T cells in both TDLNs and tumors.

Results We studied human prostate and kidney cancer tumor-draining lymph nodes (TDLN) and found that CD8 T cells are activated but fail to acquire an effector phenotype within the TDLN. Instead, they share functional, transcriptional, and epigenetic traits with stem-like cells in the tumor. We also found that activated CD8 T cells from TDLNs shared TCR overlap with both CD8 subsets within tumors. This suggests that these activated cells are a precursor to the stem-like CD8 T cells in tumors. To further test this hypothesis, we used our TRAMP1-LCMV-GP tumor model to study tumor-specific CD8 T cell activation. We found that CD8 T cells are activated in TDLNs but fail to acquire an effector program. These cells then establish the stem-like CD8s within tumor where they require additional co-stimulation from antigen presenting cells to differentiate into TCF1- TD CD8 T cells. This is strikingly different from canonical CD8 T cell activation to acute viruses, where the effector program is acquired immediately. We also showed that human stem-like CD8 T cells require co-stimulation and TCR stimulation to divide and differentiate into terminally differentiated CD8s in-vitro, and DCs from autologous tumors can also induce this differentiation.

Conclusions Overall this work shows a model of CD8 T cell activation in response to tumors that has two distinct phases. The first occurs in the TDLN where CD8 T cells are initially activated, the second occurs in the tumor where CD8 T cells acquire an effector function after additional co-stimulation. This model of T cell differentiation adds to our understanding of basic CD8 T cell biology and has important implications to improve our current immunotherapies.

<http://dx.doi.org/10.1136/jitc-2021-SITC2021.658>

659

T CELL RECEPTOR EXCHANGE BY ZYGOTE ENGINEERING RESULTS IN PHYSIOLOGICAL T CELL RESPONSES FOR THERAPEUTIC USE IN PANCREATIC DUCTAL ADENOCARCINOMA

Meagan Rollins*, Jackson Raynor, Ebony Miller, Ellen Spartz, Walker Lahr, Adam Burrack, Yun You, Branden Morarity, Beau Webber, Ingunn Stromnes. *University of Minnesota, Minneapolis, MN, United States*

Background Pancreatic ductal adenocarcinoma (PDA) is a lethal malignancy characterized by a highly suppressive tumor microenvironment. Despite this, engineered T cell therapy has promise for effectively targeting PDA. To identify the underlying mechanisms of antigen-specific engineered T cell immunosuppression in PDA, we create novel TCR knock-in mouse models for a robust and standardized source of naïve mesothelin (Msln)-specific T cells.

Methods Specifically, we integrate two murine mesothelin-specific TCRs into the physiologic Trac locus in primary murine T cells and zygotes using CRISPR/Cas9 and rAAV expressing the TCR DNA. Simultaneously using CRISPR/Cas9, Msln was disrupted to circumvent T cell tolerance.

Results This strategy resulted in the rapid generation of homozygous TCR Trac knock-in mice and with homozygous null mutations in Msln. In these TCR-exchanged (TRex) mice, most T cells expressed the 1045 (high affinity) or 7431 (low affinity) as determined by tetramer staining. TRex T cells exhibit a naïve phenotype and rapidly differentiate into effector T cells upon antigenic stimulation. While the high affinity 1045 TCR elicits function in CD4 T cells, the lower affinity 7431 T cells exhibit a higher functional avidity and less TCR downregulation when antigen is limiting. Historical TCR transgenic T cells, in which the TCR is randomly integrated into the genome, exhibit increased PD1, CD25, and CD69, decreased functionality, and a bias to CD25-Foxp3+ Treg as compared to T cells from TRex mice. Further, TCR Trac integration in primary T cells retain superior function following repetitive antigenic stimulations retrovirally transduced T cells. Adoptive transfer of 1045 TRex T cells significantly prolongs survival of mice bearing autochthonous PDA. When combined with a vaccine, 1045 TRex T cells cause involution of the fibroinflammatory tumor stroma.

Conclusions In sum, we rapidly generate mice that physiologically express the desired TCR, circumventing the shortcomings of standard T cell engineering strategies and TCR transgenic models.

Ethics Approval University of Minnesota Institutional Animal Care and Use Committee approved all animal studies to Dr. Ingunn Stromnes (2005-38115A.) Generation of TCR knockin (KI) animals was performed in the Mouse Genetic Laboratory at the University of Minnesota.

<http://dx.doi.org/10.1136/jitc-2021-SITC2021.659>

660

TARGETING T CELL FATES: CONVERTING EXHAUSTION TO MEMORY TO IMPROVE IMMUNOTHERAPEUTIC RESPONSES TO CANCER

Nicole Scharping*, Allison Cafferata, Maximilian Heeg, Quynhanh Nguyen, Ananda Goldrath. *University of California San Diego, La Jolla, CA, United States*

Background In cancer, CD8+ T cells have the power to target and kill tumor cells with precision, but often fail due to chronic activation from the immunosuppressive tumor microenvironment (TME). T cells that experience prolonged activation in the TME differentiate into a severely dysfunctional cell state known as exhaustion. In healthy tissues, T cells differentiate into tissue-resident memory cells (TRM) in response to infection, which remain lodged in tissues to provide protection from reinfection. When TRM-like cells are found in patient tumors, they are correlated with improved outcomes and responses to immunotherapy. Understanding how to manipulate T cell fates in an effort to prevent exhaustion and favor TRM-characteristics could benefit cancer immunotherapy.

Methods To explore differences between these cell states, we screened the core TRM gene-expression signatures for genes downregulated as T cells undergo terminal exhaustion. Targets were then overexpressed in antigen-specific T cells and adoptively transferred into tumor-bearing mice for analysis.

Results Interestingly, many genes related to protein regulation and processing were identified, including a novel gene called Neuralized E3 Ubiquitin Protein Ligase 3 (Neurl3). Neurl3's function is not well described, however, experimentally mutating the RING domain suggests Neurl3 transfers ubiquitin to target proteins for degradation. When Neurl3 was overexpressed in tumor-specific T cells, we found tumor infiltrating lymphocytes still upregulated inhibitory receptors PD1 and Tim3, but showed enhanced anti-tumor function. Neurl3-overexpressing T cells had increased accumulation in the TME, upregulated canonical TRM markers CD69 and CD103, produced more cytokines, controlled tumor growth, and increased mouse survival in B16 melanoma.

Conclusions These results highlight the understudied field of negative regulation of T cell function by protein degradation in T cell differentiation fate and uncover a potential gene target for immunocellular therapies to favor functional T cell fates in cancer.

Ethics Approval The study was approved by UCSD's Institutional Animal Care and Use Committee, protocol number S04105.

<http://dx.doi.org/10.1136/jitc-2021-SITC2021.660>

661

NEOANTIGEN-SPECIFIC CD4+ T CELLS IN HUMAN MELANOMA HAVE DIVERSE DIFFERENTIATION STATES AND CORRELATE WITH CD8+ T CELL, MACROPHAGE, AND B CELL FUNCTION

¹Naina Singhi, ¹Carolyn Shasha, ¹Sylvia Lee, ¹Julia Szeto, ¹Ata Moshiri, ¹Teresa Kim, ²John Thompson, ¹Scott Tykodi, ¹Venu Pillarisetty, ¹David Byrd, ¹Kimberly Smythe, ¹Shailender Bhatia, ¹Evan Hall, ¹Evan Newell, ¹Raphael Gottardo, ¹Stanley Riddell, ¹Joshua Veatch*. ¹Fred Hutchinson Cancer Research Center, Seattle, WA, United States; ²University of Washington, Seattle, WA, United States

Background Tumor-antigen specific CD4+ T cells are crucial for the efficacy of antibodies that block immune checkpoint proteins in mouse tumor models, but their activities in human tumor immunity are less clear. CD8+ T cells infiltrating human tumors, including those specific for tumor antigens, have been studied using single cell profiling techniques and exist in a variety of dysfunctional states. The transcriptional states of tumor-specific CD4+ T cells present in tumors and their potential contributions to the tumor microenvironment are less well understood.

Methods We used targeted single cell RNA sequencing and matching of T cell receptor (TCR) sequences to identify phenotypic signatures that discriminated tumor antigen- and viral antigen-specific CD4+ T cells infiltrating human melanoma tumors in four patients. The presence of CD4+ T cells with these signatures was correlated with the number and phenotype of other immune cells in the tumor microenvironment in an extended cohort of 20 patients.

Results We identified 259 CD4+ T cells representing 40 different TCR clonotypes specific for 13 neoantigens and 108 cells representing 14 TCR clonotypes specific for self-antigens in four melanoma patients. High expression of CXCL13 defined conventional CD4+ T cells that recognize tumor associated neoantigens and self-antigens from bystander and viral antigen-specific CD4+ T cells. Tumor-reactive CD4+ T cells could be subdivided into clusters expressing memory and T follicular helper markers, and those expressing cytolytic markers and IFN- γ . In an extended cohort of 20 patients with melanoma, the frequency of CXCL13+ CD4+ T cells in the tumor microenvironment correlated with the presence and proliferation of CD8+ T cells, the presence and maturation of B cells, the activation of interferon responsive genes in tumor associated macrophages, and patient survival. CD4+ T cells with similar transcriptional signatures were identified in data sets from breast and non-small cell lung cancer, suggesting these markers may enrich for tumor-reactive CD4+ T cells in many cancers.

Conclusions These results identify a subset of tumor infiltrating conventional CD4+ T cells in melanoma that are enriched for reactivity to tumor antigens and exist in multiple phenotypic states. Correlations of the presence of these cells with the frequency and phenotype of other immune cells suggest roles for these tumor antigen-specific CD4+ T cells in providing CD8+ T cell help, driving recruitment and maturation of B cells, and activating macrophages. Isolating such cells based on their unique phenotype and utilizing them for adoptive therapy could alter the tumor microenvironment for therapeutic benefit.

Ethics Approval All Patient samples in this study were obtained from patients who signed informed consent in a study approved by the institutional review board of the Fred Hutchinson Cancer Research Center (protocol #2643).

<http://dx.doi.org/10.1136/jitc-2021-SITC2021.661>

DISSECTING THE CD226 IMMUNE AXIS IN THE TUMOR MICROENVIRONMENT USING CYTOF-BASED HIGH-DIMENSIONAL IMMUNOPHENOTYPING

Katie Vowell*, Michael Conner, Florence Perrin, Paul Bojczuk, Kenneth Hance, Iris Roth, Christine Donahue, James Smothers, Jeremy Waight. *GlaxoSmithKline, Collegeville, PA, United States*

Background In recent years, a regulatory network involving nectin/nectin-like immune receptors has emerged as a potential point of manipulation for cancer immunotherapy. Central to this axis, CD226 (DNAM-1) is a T and NK cell co-stimulatory receptor that competes for ligand (CD155 and CD112) binding with multiple inhibitory receptors (TIGIT, CD96, and PVRIG [CD112R]). Despite a large body of literature for TIGIT, detailed cellular characterization of the entire axis is still lacking. Therefore, we used mass cytometry (CyTOF) to systematically evaluate expression of the CD226 axis in tumors from a range of indications.

Methods To thoroughly characterize the CD226 axis in the tumor microenvironment, we immunophenotyped approximately 100 tumor samples derived from a variety of cancer types using a bespoke 46-parameter CyTOF panel. Human biological samples were sourced ethically and their research use was in accord with the terms of the informed consents under an IRB/EC approved protocol. Using a suite of high-dimensional analytical tools, including FlowSOM, UMAP, and tSNE, we revealed distinct expression profiles for each receptor; a finding that was previously obscured due to a lack of sufficient resolution.

Results We observed a notable divergence in expression profiles between the CD226 axis members across tumor indications. For example, TIGIT expression was found to be highest on activated CD4+ regulatory T (Treg) cells, where its expression correlated strongly with ICOS, FoxP3, CD25, and CCR8. By contrast, CD96 and PVRIG exhibited broad expression across intratumoral T and NK cell populations. Other receptors (e.g., CD226) demonstrated variegated expression profiles across T and NK cell subsets. Finally, despite relatively consistent expression profiles of certain CD226 axis (i.e., TIGIT on Treg cells) across tumors, we also found several cell subsets/clusters unique to specific indications.

Conclusions Using high-parameter CyTOF analysis, we were able to thoroughly characterize the CD226 axis (CD226, TIGIT, CD96, PVRIG) and related immune receptors across a range of tumor indications. These analyses revealed divergent expression profiles for each CD226 axis member, suggesting distinct/contextual biological role(s) for each receptor. However, future studies will need to dissect the importance of the distinct cellular representation for each CD226 axis member.

Ethics Approval All samples were purchased from Discovery Life Sciences (DLS). DLS represents and warrants that it has ownership of all Products available for sale and has properly obtained, where required under HHS/OHRP 45 CFR 46.102 (d) (f), IRB approval (or appropriate research approval for institutions outside the U.S.) for study protocols and informed consent documents for all human subject derived biological materials.

<http://dx.doi.org/10.1136/jitc-2021-SITC2021.662>

663

MEDIA BASED ON THE METABOLIC COMPOSITION OF TUMOR INTERSTITIAL FLUID REVEALS PERSISTENT T CELL DYSFUNCTION INDUCED THROUGH ARGININE DEPRIVATION AND EXPOSURE TO THE ONCOMETABOLITE PHOSPHOETHANOLAMINE

¹Yupeng Wang*, ²Chufan Cai, ¹Dayana Rivadeneira, ²Alexander Muir, ¹Greg Delgoffe.
¹University of Pittsburgh, Pittsburgh, PA, United States; ²University of Chicago, Chicago, United States

Background While CD8 T cells are crucial for anti-tumor immunity, tumor infiltrating CD8 T cells encounter stressors which deviate their differentiation to a dysfunctional, exhausted phenotype. T cell functions are closely regulated by T cell metabolism, and the dysfunctional vasculature in tumor tissues and the deregulated metabolism of tumor cells lead to depletion of nutrients and accumulation of metabolic wastes in the tumor microenvironment (TME). Thus, the unbalanced levels of the nutrients and the metabolic wastes might skew the metabolism of T cells thus contributing to T cell dysfunction.

Methods Ovalbumin-specific OT-I cells were activated with SIINFEKL/IL2 and cultured with IL2. The tumor interstitial fluid media (TIFM) was formulated based on the concentrations of the metabolites measured in the tumor interstitial fluid of pancreatic ductal adenocarcinoma.¹ Purified arginine and phosphoethanolamine (PEtn) were used to change their levels in TIFM/RPMI1640 culture. Expression level of cytokines and PD-1 was measured by flow cytometry.

Results We sought to determine how T cells would differentiate, in vitro, if they were exposed only to the metabolites present in the TME. Using media formulated to model the metabolic composition of tumor interstitial fluid (TIFM),¹ we show that CD8 T cells develop features of exhausted T cells in the TIFM culture: reduced proliferation, increased expression of PD-1 and decreased cytokine production. Using 'drop-out' and 'add-back' approaches, we found arginine levels as a major contributor to the proliferation defect observed in TIFM-cultured T cells. Arginine was sufficient to restore proliferative capacity to T cells cultured in TIFM, but had no effect on the inhibited cytokine production. We then asked which metabolites were enriched in the TIFM, finding that PEtn, an intermediate in the ethanolamine branch of the Kennedy pathway and an oncometabolite enriched in the interstitial of many solid tumors, up-regulates PD-1 expression and compromises the cytokine production of the cells in culture. Depletion of Pcyt2, the metabolizing enzyme of PEtn and the rate limiting enzyme in the Kennedy pathway, makes CD8 T cells resistant to the effects of PEtn.

Conclusions Our data shows that the metabolic environment in the TME can be recapitulated in vitro and is sufficient to drive T cell dysfunction. Arginine depletion acts as a major inhibitor of T cell proliferation in the TME, but the oncometabolite PEtn drives a hypofunctional effector fate of T cells. Targeting PEtn metabolism via Pcyt2 depletion or inhibition is a potential target to reinvigorate T cells and enhance anti-tumor immunity.

REFERENCE

1. Sullivan MR, Danai LV, Lewis CA, Chan SH, Gui DY, Kunchok T, Dennstedt EA, Vander Heiden MG, Muir A. Quantification of microenvironmental metabolites in murine cancers reveals determinants of tumor nutrient availability. *Elife* 2019;**8**: e44235. doi: 10.7554/eLife.44235. PMID: 30990168; PMCID: PMC6510537.

<http://dx.doi.org/10.1136/jitc-2021-SITC2021.663>

664 **PULMONARY PRIMING OF TUMOR-REACTIVE CD8⁺ T CELLS BY DC1 IS IMPAIRED BY REGULATORY T CELLS**

Maria Zagorulya*, Duncan Morgan, Leon Yim, Brendan Horton, Elen Torres-Mejia, Stefani Spranger. MIT, Cambridge, MA, United States

Background Although failure to respond to checkpoint blockade immunotherapies (CBT) is frequently associated with a lack of T cell infiltration into the tumor, emerging clinical data suggests that specifically in patients with lung cancer, T cell-inflamed tumors can also be resistant to therapy.¹ Recent work by our group identified that immunotherapy resistance in a T cell-inflamed pre-clinical mouse model of lung cancer is driven by a lung cancer-specific CD8⁺ T cell dysfunctional program (T_{Ldys}), characterized by blunted production of IFN γ and reduced cytolytic capacity. Intriguingly, this T_{Ldys} program is established during priming in the tumor-draining mediastinal lymph nodes (mLN). Understanding the lung-specific mechanisms blunting the activation of anti-tumor T cell responses could enable development of novel therapies needed to improve outcomes of patients with CBT-resistant T cell-inflamed lung cancer.

Methods To study anti-tumor immune responses against lung tumors, a syngeneic lung cancer cell line (KP) was implanted orthotopically or subcutaneously into C57BL/6 mice. KP cells were engineered to express SIINFEKL and ZsGreen to enable studies of tumor-reactive T cells and antigen uptake by dendritic cells (DC).

Results Lung KP tumors led to the induction of tumor-reactive T_{Ldys} CD8⁺ T cells lacking CD25 and GzmB in the mLN, in contrast to subcutaneous KP tumors, which induced CD25^{high} GzmB^{high} tumor-reactive CD8⁺ T cells in the inguinal LN (iLN). Mouse models lacking DC1 revealed that DC1 are necessary to prime tumor-reactive CD8⁺ T cells in both LNs. Flow cytometry characterization of DC1 from LNs revealed equivalent levels of antigen load, but reduced levels of costimulatory molecules CD80, CD86 and the cytokine IL-12 in the mLN compared to iLN, suggesting a blunted stimulatory capacity in the lung setting. Regulatory T cell (Treg) depletion using FoxP3^{DTR} mice rescued expression of effector T cell priming in tumor-draining mLN, suggesting that T_{Ldys} induction requires the presence of local Treg. Ex vivo co-cultures of antigen-specific CD8⁺ T cells with DC1 and Treg sorted from the mLN fully recapitulated the in vivo observation, suggesting that both DC1 and Treg are required and sufficient for T_{Ldys} induction. Blockade of the MHCII-dependent DC1:Treg interaction restored an effector-like profile of tumor-reactive CD8⁺ T cells.

Conclusions Treg restrain DC1 stimulatory function in the tumor-draining mLN, leading to the induction of lung cancer-specific dysfunction in tumor-reactive CD8⁺ T cells and thus rendering the T cell response refractory to CBT-mediated reinvigoration. Blockade of Treg:DC1 interactions can restore priming of lung cancer-reactive effector T cell responses.

Acknowledgements Pew-Stewart Scholarship, Training grant

REFERENCE

- Herbst RS, et al. Predictive correlates of response to the anti-PD-L1 antibody MPDL3280A in cancer patients. *Nature* 2014;**515**:563–567.

Ethics Approval All mouse experiments in this study were approved by MIT's Committee on Animal Care (CAC) - DHHS Animal Welfare Assurance # D16-00078

<http://dx.doi.org/10.1136/jitc-2021-SITC2021.664>

665

TRANSCRIPTIONAL LANDSCAPE OF TUMOR-REACTIVE TIL IN LUNG CANCER AND MELANOMA

Jiajia Zhang*, Justina Caushi, Boyang Zhang, Zhicheng Ji, Taibo Li, Hongkai Ji, Andrew Pardoll, Kellie Smith. *Johns Hopkins University, Baltimore, MD, United States*

Background Melanoma and lung cancers have two of the highest response rates to immune checkpoint inhibitors (ICIs).¹ However, patients may respond unpredictably, partly due to heterogeneity in the quantity and quality of tumor-specific T cells. In this study, we performed an integrated transcriptomic analysis of anti-tumor CD8+ TIL from non-small cell lung cancer (NSCLC) and melanoma. Our goal was to study the global transcriptomic landscape of tumor-specific T cells and to compare their functional programming in lung cancer vs. melanoma.

Methods TIL from 19 patients (15 NSCLC and 3 melanoma) were sequenced using combined single-cell (sc) RNA-seq/TCR-seq. All NSCLC patients received neoadjuvant anti-PD-1 (nivolumab, NCT02259621) whereas melanoma patients received a personal neoantigen vaccine (NCT01970358). Neoantigen-, tumor-associated antigen-, and viral-specific CD8+ T cell clonotypes were identified using functional assays and were validated by TCR cloning as previously described.^{2 3} Transcriptional profiles of antigen-specific T cells were identified using the TCRβ CDR3 as a barcode to link with the antigen specificity output from the functional assays. The prevalence, phenotype, and differentiation trajectory of tumor-specific T cells were compared between the two cancer types.

Results A total of 175,826 CD8+ TIL were analyzed, of which 30,174 single cells were from the melanoma cohort and 145,652 were from the NSCLC cohort. Tumor-specific T cells were detected at variable frequencies among CD8+ TIL (median=1.2%, range 0.01%–35.8%) across nine patients, with melanoma having more clonal tumor-specific T cells as compared to NSCLC. CD8+ TIL from melanoma were more enriched in an activated tissue resident T cell (TRM) cluster characterized by upregulated expression of CXCL13, CRTAM, 4-1BB, XCL1/2, and FABP5, whereas those from NSCLC have a greater representation of a cytotoxic TRM cluster with an exhaustion signature (coexpression of GZMB, GZMH, PDCD1, and CTLA4). Distinct from EBV-specific T cells and flu-specific T cells, tumor-specific T cells primarily resided in TRM clusters in both cancers. More MANA-specific TIL from melanoma presented with an effector phenotype and were more proliferative as compared to those from NSCLC. To reveal the differentiation trajectory and regulatory programs of tumor-specific T cells upon tumor recognition and association with response to ICIs, pseudotime/velocity analysis of tumor-specific TIL is underway.

Conclusions This is the first analysis to inform on the global transcriptomic landscape of tumor-specific CD8+ TIL in lung cancer and melanoma at single cell resolution. This provides a useful framework to study the underlying mechanisms of T cell exhaustion and dysfunction in human cancer.

Trial Registration NCT02259621, NCT01970358

REFERENCES

1. Yarchoan M, Hopkins A, Jaffee EM. Tumor mutational burden and response rate to PD-1 inhibition. *The New England Journal of Medicine* 2017;**377**(25):2500.
2. Caushi JX, et al. Transcriptional programs of neoantigen-specific TIL in anti-PD-1-treated lung cancers. *Nature* 2021;1–7.
3. Oliveira G, et al. Phenotype, specificity and avidity of antitumour CD8+ T cells in melanoma. *Nature* 2021;1–7.

Ethics Approval The melanoma clinical trial was approved by the Dana-Farber/Harvard Cancer Center Institutional Review Board (IRB) (NCT01970358). The NSCLC clinical trial was approved by the Institutional Review Boards (IRB) at Johns Hopkins University (JHU) and Memorial Sloan Kettering Cancer Center (NCT02259621). All participants gave informed consent before taking part.

Consent Written informed consent was obtained from the patient for publication of this abstract and any accompanying images. A copy of the written consent is available for review by the Editor of this journal.

<http://dx.doi.org/10.1136/jitc-2021-SITC2021.665>

666 DELETION OF DRP1 IN T CELLS INCREASES OXPHOS AND CD8+ MEMORY T CELL POPULATION

Timothy Bullock, Marissa Gonzales*. *University of Virginia, Charlottesville, VA, United States*

Background Memory CD8 T cells are able to more rapidly respond to a secondary exposure to viruses or tumor antigens than naïve T cells. These memory cells have been shown in vitro to exhibit more elongated mitochondria, more mitochondrial mass, and high spare respiratory capacity, allowing for a rapid response time.^{1 2} During the activation and differentiation of T cells, the metabolic demands fluctuate between the necessity for glycolysis or oxidative phosphorylation (OXPHOS), which is supported by shifting of the mitochondrial network state.

Methods Mice are given aCD40, PolyI:C, and OVA protein IP. Cells stimulated in vitro are treated with 5 mg/mL aCD3, 2 µg/mL aCD28, and 10 IU IL2.

Results We hypothesized that manipulating T cells to elongate mitochondria would provide a metabolic benefit to effector functions and could ultimately increase the function of tumor infiltrating lymphocytes. Using mice lacking Drp1, a mitochondrial fission protein, in T cells as a model of elongated mitochondria, we see increased spare respiratory capacity and OXPHOS as compared to WT T cells with fission capability. Interestingly, we find that these mice are more likely to generate memory precursor CD8 T cells as represented by KLRG1lo and CD127hi during a primary response to aCD40, PolyI:C, and ovalbumin protein. As indicated by the increase in memory precursors, we find that Drp1^{-/-} T cells form more CD8+ memory than WT animals after a 28 day rest period. Mice were then challenged with an adenovirus expressing ovalbumin to elicit a recall response. This recall response of CD8 T cells is greater in animals lacking Drp1 in the T cells. Additionally, T cells treated with pharmacological reagents M1 and Mdivi to inhibit mitochondrial fission and induce fusion show increased spare respiratory capacity. We are currently testing if this pharmacological method and others can increase spare respiratory capacity in tumor infiltrating lymphocytes. Further studies of differentiation and contraction are still required to determine how the memory CD8 T cell population is increased. In addition to the increase in T cell numbers seen, we anticipate an increase in metabolic function. The mouse model here has Drp1^{-/-} CD4 T cells and we are determining if the CD8 T cell effects are intrinsic by adoptively transferring memory CD8 T cells to WT mice as well as creating mixed chimera mice. We ultimately aim to exploit control of mitochondria to increase memory T cell development and metabolism as well as control of solid tumors.

Conclusions N/A

REFERENCES

1. van der Windt GJ, Everts B, Chang CH, Curtis JD, Freitas TC, Amiel E, Pearce EJ, Pearce EL. Mitochondrial respiratory capacity is a critical regulator of CD8+ T cell memory development. *Immunity* 2012;**36**(1):68–78.
2. van der Windt GJ, O'Sullivan D, Everts B, Huang SC, Buck MD, Curtis JD, Chang CH, Smith AM, Ai T, Faubert B, Jones RG, Pearce EJ, Pearce EL. CD8 memory T cells have a bioenergetic advantage that underlies their rapid recall ability. *Proc Natl Acad Sci U S A*. 2013;**110**(35):14336–41.

<http://dx.doi.org/10.1136/jitc-2021-SITC2021.666>

TUMOR-DERIVED ALPHA-FETOPROTEIN REQUIRES POLYUNSATURATED FATTY ACIDS FOR IMMUNOMETABOLIC DYSREGULATION

Paul Munson*, Juraj Adamik, Lisa Butterfield. *Parker Institute for Cancer Immunotherapy, San Francisco, CA, United States*

Background Hepatocellular carcinoma (HCC) is the fourth leading cause of cancer deaths worldwide.¹ The immuno-regulatory environment of the liver, coupled with tumor-specific immuno-suppressive mechanisms, has negatively impacted the development of clinically effective immunotherapies. Most HCC tumors secrete alpha-fetoprotein (AFP), which we previously demonstrated inhibited monocyte to dendritic cell (DC) differentiation and metabolism.²⁻³ These immunoregulatory effects depended upon a previously unidentified low molar mass ligand bound to tumor-derived (tAFP) but not cord-blood-derived 'normal' AFP (nAFP). To delineate the mechanism, we identified and tested fatty acids (FA) unique to tAFP necessary for immunosuppression.

Methods Fatty acids bound to samples of ovalbumin (OVA), nAFP, and tAFP (n=3 each), were quantified by mass spectrometry and gas chromatography by the UCSD Lipidomics Core. Analysis of the single-cell metabolism was measured using the SCENITH assay⁴ via spectral-flow cytometry. Bulk measurement of metabolism was measured by microarray and glucose/lactate quantification of supernatants during monocyte to DC differentiation in vitro. Lastly, several fatty acids (FAs) were co-incubated with ligand-free preparations of OVA, nAFP, and tAFP to determine which FAs contribute to limiting DC differentiation in vitro.

Results SCENITH analysis revealed a stark increase in lactate secretion and a marked switch from oxidative-phosphorylation (OXPHOS) to glycolysis in tAFP-treated DCs, which correlated with reduced co-stimulatory marker expression and increased PD-L1. g:Profiler analysis of microarray data confirmed dysregulation of FA metabolism. We identified three polyunsaturated fatty acids (PUFAs) that were enriched on tAFP by mass-spectrometry and gas chromatography. Screening of FAs on ligand-free preparations revealed two PUFAs on tAFP were uniquely able to decrease differentiation of iDC and mDCs in vitro.

Conclusions We have identified unique FA ligands of tAFP and determined specific FAs that restore its immunoregulatory activities. To our knowledge, these are the first data demonstrating a role of a novel PUFA in inhibiting DC formation and are consistent with previous reports showing arachidonic (20:4) inhibits DC formation in vitro.⁵ Furthermore, we have identified key metabolic pathways of the immuno-metabolic dysregulation of DCs in HCC. These findings identify targets for strategies to reverse the tAFP induced immuno-metabolic dysfunction in vivo could be a strategy to potentiate robust anti-tumor immunity and improve survival in HCC patients.

Acknowledgements We wish to acknowledge the Parker Institute for Cancer Immunotherapy, Dr. Oswald Quehenberger and Milda Simonaitis of the UCSD Lipid omics Core for their consultation on the lipid panel, as well as Vin Nguyen of the UCSF Flow Cytometry Core for his assistance with the flow cytometry panels.

REFERENCES

1. Sung H, Ferlay J, Siegel RL, Laversanne M, Soerjomataram I, Jemal A, et al. Global Cancer Statistics 2020: GLOBOCAN estimates of incidence and mortality worldwide for 36 cancers in 185 Countries. *CA Cancer J Clin* 2021;**71**:209–49. <https://doi.org/10.3322/caac.21660>.

2. Pardee AD, Shi J, Butterfield LH. Tumor-Derived α -Fetoprotein Impairs the differentiation and T Cell stimulatory activity of human dendritic cells. *J Immunol* 2014;**193**:5723–32. <https://doi.org/10.4049/jimmunol.1400725>.
3. Santos PM, Menk AV, Shi J, Tsung A, Delgoffe GM, Butterfield LH. Tumor-Derived α -Fetoprotein suppresses fatty acid metabolism and oxidative phosphorylation in dendritic cells. *Cancer Immunol Res* 2019;**7**:1001–12. <https://doi.org/10.1158/2326-6066.cir-18-0513>.
4. Argüello RJ, Combes AJ, Char R, Gigan J-P, Baaziz AI, Bousiquot E, et al. SCENITH: a flow cytometry-based method to functionally profile energy metabolism with single-cell resolution. *Cell Metab* 2020;**32**:1063–1075.e7. <https://doi.org/10.1016/j.cmet.2020.11.007>.
5. Zeyda M, Säemann MD, Stuhlmeier KM, Mascher DG, Nowotny PN, Zlabinger GJ, et al. Polyunsaturated fatty acids block dendritic cell activation and function independently of NF- κ B activation. *J Biol Chem* 2005;**280**:14293–301. <https://doi.org/10.1074/jbc.m410000200>.

Ethics Approval The Cancer Immunotherapeutics Tissue Use Committee approved samples from healthy donors at UCSF.

<http://dx.doi.org/10.1136/jitc-2021-SITC2021.667>

**LIPID-INSTRUCTED METABOLIC REWIRING UNLEASH
THE ANTI-TUMOR POTENTIAL OF CD8+ T CELLS**

¹Teresa Manzo*, ¹Carina Nava Lauveson, ¹Teresa Maria Frasconi, ¹Silvia Tiberti, ²Ignazio Caruana, ¹Luigi Nezi, ³Philip Greenberg. ¹European Institute of Oncology- IEO, Milan, Italy; ²University Children Hospital of Würzburg, Würzburg, Germany; ³Fred Hutchinson Cancer Research Center, Seattle, WA, United States

Background Adoptive cell therapy (ACT) harnesses the immune system to recognise tumor cells and carry out an anti-tumor function. However, metabolic constraints imposed by the tumour microenvironment (TME) suppress anti-tumor responses of CTL by reshaping their metabolism and epigenetic landscape. We have recently demonstrated that progressive accumulation of specific long-chain fatty acids (LCFAs) impair mitochondrial function and drives CD8+ T cell dysfunction. In this scenario, maintaining T cells in a less-differentiated state and with high metabolic plasticity during ex vivo T cell production and after infusion may have a strong therapeutic impact. Here, we propose a novel strategy to boost ACT efficacy by implementing T cell long-term functionality, metabolic fitness and preventing exhaustion through lipid-induced mitochondrial rewiring.

Methods We screen different LCFAs and assess their ability to shape CD8+ T cell differentiation using multi-parametric flow cytometry, proliferation and cytotoxic assays, together with a complete transcriptomic and epigenomic profiling. Metabolic reprogramming of lipid-treated CD8+ T cell was examined by bioenergetic flux measurements paired with metabolomic and lipidomic analysis. Finally, the anti-tumor responses of lipid-instructed CD8 T cells was evaluated in a melanoma mouse model, known to poorly respond to immunotherapy.

Results LCFAs-treated CD8+ T cells are endowed with highly effector and cytotoxic features but still retaining a memory-like phenotype with decreased PD1 protein levels. Consistently, analysis of the bioenergetic profile and mitochondrial activity has shown that LCFA-instructed CD8+ T cells display a greater mitochondrial fitness. Thus, in vitro LCFA-instructed CD8+ T cells are characterized by higher mitochondrial fitness, potent functionality, memory-like phenotype and PD-1 down-regulation, overall evoking the ideal T cell population associated with a productive anti-tumor response. The therapeutic potential of CD8 T cells lipid-induced metabolic rewiring was further confirmed in vivo. ACT performed with LCFA-reprogrammed CD8 T cells induces higher frequency of memory T cells, which show high polyfunctionality and mitochondrial function, decreased PD1 expression, ultimately resulting in improved tumor control. In addition, LCFA-induced metabolic rewiring during manufacturing of human CAR-redirectioned T cells, generated a CD8+ T cell memory-like population with higher mitochondrial fitness coupled with a much potent cytotoxic activity.

Conclusions These results suggest that LCFAs dictate the fate of CD8+ T cell differentiation and could be considered as a molecular switch to fine-tune memory T cell formation and metabolic fitness maintenance, linking lipid metabolism to anti-tumor surveillance. This will be of fundamental importance for a new generation of adoptive T cell-based therapies.

Ethics Approval The experiments described were performed in accordance with the European Union Guideline on Animal Experiments and mouse protocols were approved by Italian Ministry of Health and the IEO Committee.

<http://dx.doi.org/10.1136/jitc-2021-SITC2021.668>

669

LACTATE UPTAKE THROUGH MCT11, A NOVEL MONOCARBOXYLATE TRANSPORTER, ENFORCES DYSFUNCTION IN TERMINALLY EXHAUSTED T CELLSRonald Peralta*, Greg Delgoffe. *University of Pittsburgh, Pittsburgh, PA, United States*

Background Upon infiltration into tumors, T cells experiencing persistent antigen stimulation progressively differentiate into a state of dysfunction, known as exhaustion. Exhausted T cells are characterized by the sustained upregulation of co-inhibitory molecules and reduced effector cytokine production. Additionally, exhausted T cells exist in a state of metabolic dysfunction in the tumor microenvironment (TME), due to disrupted mitochondrial biogenesis, hypoxia and lack of metabolites. Highly glycolytic tumor and stromal cells outcompete T cells for glucose, and secrete lactate into the TME, acidifying the extracellular space. Recent studies have shown lactate can be metabolized by tumor infiltrating Tregs and macrophages. We hypothesized that CD8+ tumor-infiltrating lymphocytes (TIL) may also take up lactate as an alternative carbon source to meet their metabolic demands.

Methods For lactate uptake experiments, B16 melanoma single cell suspensions from B6 mice were loaded with the pH sensitive dye pHrodo, then pulsed with 5 μ M lactic acid. MCT11 KO OT-I T cells were generated via transfection of Slc16a11 sgRNA-Cas9 ribonucleoprotein complexes, and adoptively transferred into B16-OVA bearing mice.

Results RNA sequencing and flow cytometry data from CD8+ T cell subsets in the TME revealed MCT11 (encoded by Slc16a11), a monocarboxylate transporter (MCT) only recently discovered, to be highly and uniquely expressed in terminally exhausted T cells (Tex). As lactate is an abundant monocarboxylate in tumors, we asked whether MCT11 supports lactate uptake into Tex cells. Antibody blockade of MCT11 resulted in reduced lactic acid uptake, but whether lactic acid promoted or inhibited effector function. Intriguingly, overexpression of MCT11 in OT-I T cells adoptively transferred into B16-OVA bearing mice resulted in accelerated exhaustion: increased co-inhibitory marker expression and decreased TNF α and IFN production. Conversely, knockdown of MCT11 in the same model resulted in decreased co-inhibitory marker expression and increased TNF α and IFN production. Further, MCT11 KO OT-I T cells used therapeutically had decreased tumor burden over mice treated with control OT-I T cells. As MCT11's uptake function was blocked with an antibody, we also used the antibody therapeutically, revealing that single-agent MCT11 antibody treatment reduced tumor burden and increased survival in B16 melanoma bearing mice.

Conclusions Our data support a model where exhausted CD8+ T cells upregulate MCT11, which renders them sensitive to toxic lactic acid in the TME. Our data suggest MCT11 could be deleted on therapeutic T cells or blocked using an antibody on endogenous T cells to render exhausted T cells impervious to lactic acid such and promote tumor eradication.

<http://dx.doi.org/10.1136/jitc-2021-SITC2021.669>

OXIDATIVE STRESS ORIGINATING IN THE MITOCHONDRIA DAMAGES TELOMERES SUFFICIENT TO DRIVE CERTAIN FEATURES OF T CELL DYSFUNCTION

<http://dx.doi.org/10.1136/jitc-2021-SITC2021.670>

¹Dayana Rivadeneira*, ¹Jess Yana, ¹Sanjana Thosar, ²Marcel Bruchez, ¹Patricia Lynn, ¹Greg Delgoffe. ¹University of Pittsburgh, Pittsburgh, PA, United States; ²Carnegie Mellon University, Pittsburgh, PA, United States

Background The functional state of infiltrating lymphocytes is a critical determinant of antitumor immunity and immunotherapy response. Key factors responsible for driving T cell dysfunction are metabolic barriers such as nutrient competition, low oxygen tension and damaging byproducts, like reactive oxygen species (ROS). ROS are critical contributors to T cell dysfunction observed during aging as well as in the tumor microenvironment. While we have shown ROS accumulation drives T cell exhaustion in part by altering signaling, ROS can affect other cellular functions further contributing to T cell dysfunction. One of the main downstream consequences observed with ROS accumulation is DNA damage, in particular telomeric DNA. However, little is known on whether telomeric shortening vs damage and the associated response affects T cell fate and function.

Methods We performed telomeric analyses of endogenous tumor-infiltrating T cells. In vitro, direct induction of oxidative stress in mitochondria or telomeres was performed using a photosensitizer approach employing fluorogen-activating peptide (FAP)¹ targeted to the mitochondria (COXVIII-FAP) or to the telomeric shelterin protein TRF1, which produces singlet oxygen and 8-oxoguanine specifically in the mitochondria or at the telomeres.² Our lab generated mouse models to express this telomeric-FAP (Rosa26-LSL-TRF1-FAP) or mitochondrial-FAP (Rosa26-LSL-COXVIII-FAP) specifically in T cells (Cd4Cre).

Results Telomere analysis of tumor-infiltrating exhausted (PD1hiTim3+) vs non-exhausted (PD1int) cells revealed exhausted T cells do not have shorter telomeres (like senescent T cells), but rather damaged telomeres. Using a photosensitizer strategy to specifically induce oxidative damage to the mitochondria, we recapitulated our previous work in vitro, resulting in ROS cascades, severe T cell dysfunction, and damage to telomeres. We next directly assessed the role of telomere oxidative damage using a telomeric-targeted photosensitizer, showing oxidative damage to telomeres promotes a persistent T cell dysfunction, resulting in sustained Tim3 and PD1 expression and severely decreased functions. However, oxidative damage to telomeric DNA alone does not induce all of the features of T cell exhaustion, suggesting that telomere damage is a crucial piece, but not fully sufficient to drive T cell dysfunction.

Conclusions Our data support a model where oxidative stress originating in the mitochondria alters cellular biology in part by damaging telomeric DNA. While this activity does not shorten telomeres, it induces stress responses sufficient to deviate differentiation into a dysfunctional phenotype. While telomeric damage alone does not fully recapitulate exhaustion, it nevertheless remains a crucial part of the dysfunctional phenotype in tumor infiltrating lymphocytes.

REFERENCES

1. He J, Wang Y, Missinato MA, Onuoha E, Perkins LA, Watkins SC, St Croix CM, Tsang M, Bruchez MP. A genetically targetable near-infrared photosensitizer *Nat Methods* 2016;**13**:263–268.
2. Fouquerel E, Barnes RP, Uttam S, Watkins SC, Bruchez MP, Opreko PL. Targeted and persistent 8-Oxoguanine base damage at telomeres promotes telomere loss and crisis. *Mol Cell* 2019;**75**(1):117–130.e6.

671

**BIOLOGICAL IMPACTS OF STANDARD OF CARE
CHEMOTHERAPIES ON IMMUNE EFFECTOR CELLS FROM
AML PATIENTS**

¹Dmitry Zhigarev*, ¹Alexander MacFarlane, ²Christina Drenberg, ¹Reza Nejati, ¹Asya Varshavsky, ¹Kerry Campbell. ¹Fox Chase Cancer Center, Philadelphia, PA, United States; ²Janssen R&D, Spring House, PA, United States

Background Acute myeloid leukemia (AML) is a heterogeneous group of malignant bone marrow diseases, characterized by massive and uncontrolled proliferation of myeloid precursor cells, which alters normal blood cell ratios. This disease is common to older adults and collectively displays one of the lowest 5-year overall survival rates (<25%) among all cancers, currently representing the deadliest form of leukemia. Improved treatments are clearly needed, and immunotherapies are attractive candidate therapies to explore. There are currently several standard chemotherapeutic treatment schemes for AML, which could be divided into two major groups: (1) cytotoxic chemotherapy (“7+3” or daunorubicin-cytarabine) and (2) hypomethylating agents (HMAs). HMAs include both 5-azacytidine and decitabine, which are cytidine analogs that inhibit DNA methyltransferase, resulting in the hypomethylation of DNA and inducing expression of silenced gene loci. Currently, HMAs are routinely delivered in combination with the Bcl-2 inhibitor venetoclax. The goals of this study are to determine how these standard first line therapies can affect the frequency and functional integrity of effector immune cells in patients' blood and establish when the phenotype and function of immune cells are restored to identify time windows when second line immunotherapies could be most effective.

Methods More than 100 blood samples were obtained from 33 previously untreated AML patients. More than 50 measurable biomarkers were analyzed using 14-color flow cytometry to assess immune phenotypes of T and NK cells in peripheral blood of AML patients prior to treatment and at up to four timepoints after initiation of treatment with HMA or chemotherapy.

Results We found several significant changes in immune cell phenotype and function that occur in response to these therapies. Treatment with HMAs was strikingly less impactful on immune cells in patients compared to previously published in vitro studies. Nevertheless, HMA treatment increased perforin levels in T and NK cells, inhibited IFN-gamma secretion by CD8+ T cells, and changed expression of several checkpoint molecules. While chemotherapy caused fewer phenotypic changes it dramatically decreased the total number of immune cells. We also determined viable, functional and phenotypical recovery periods for immune effector cells after the treatments.

Conclusions Our results are important for introducing new second line immunotherapies to these chemotherapeutic regimens for treating AML and to improve overall understanding of immune cell behavior under conditions of anti-tumor treatment.

Acknowledgements Supported by grants from Janssen and the U.S./Israel Binational Science Foundation.

Ethics Approval The study was approved by the Fox Chase Cancer Center Institutional Review Board, approval number 17-8010, and all patients provided informed consent before taking part in the study.

<http://dx.doi.org/10.1136/jitc-2021-SITC2021.671>

THE EFFECT OF CHEMORADIOTHERAPY AND TUMOR HISTOLOGY ON THE IMMUNE CONTEXTURE OF TUMOR-DRAINING LYMPH NODES IN NSCLC

¹Marieke Fransen*, ¹Famke Schneiders, ¹Vinitha Kandiah, ²Teodora Radonic, ²Idris Bahce, ²Chris Dickhoff, ¹Tanja de Gruij. ¹Cancer Center Amsterdam, Amsterdam UMC, Amsterdam, Netherlands; ²Amsterdam UMC, Amsterdam, Netherlands

Background Recently, the concept of locally delivered immune modulatory agents (re-)invigorating sub-optimally primed tumor-specific T cells and lifting suppression in the tumor microenvironment (TME) and tumor-draining lymph nodes (TDLN) has gained attention. TDLN play an important role in the induction of tumor-specific effector T cells. It is here that specialized dendritic cell (DC) subsets present tumor-derived antigens to naïve T cells and start effective adaptive immune responses to cancer. Unfortunately, TDLN are also rapidly targeted by tumors for immune suppression, which may impair the efficacy of immunotherapy. Currently, there is limited knowledge on the immune contexture of TDLN in non-small cell lung cancer (NSCLC), differences between types of tumor histology, and the influence of standard treatment.

Methods In an exploratory study, we collected and analyzed viable cells from TDLN from patients with NSCLC, scheduled for surgical resection. To date, we have analyzed 43 TDLN from a total of 10 patients with multiparameter flowcytometry panels, either untreated or after neoadjuvant chemoradiotherapy (nCRT).

Results Our analyses reveal differences between squamous cell carcinoma (SCC) and adenocarcinoma (AC), discernable even within this small cohort. In AC, higher levels of PD-L1 on CD11c+CD1c- LN-resident macrophages and CD1a+ migratory DC were accompanied by a lower activation state of CD8+ T cells by PD-1, CTLA-4 and CD69 expression levels. Furthermore, we found decreased activation of LN-resident DCs (by PD-L1 and CD83 levels) and a striking decrease in PD-1 and CD69 on CD8+ T cells, a decrease in effector and central memory CD8+ T cells, and an increase in naïve CD8+ T cells and Treg subsets after nCRT treatment, the current standard treatment of stage III NSCLC patients.

Conclusions These AC/SCC -related differences and nCRT-induced alterations in the immune status of hold clues for future patient stratification and combinatorial design of CRT with immunotherapy.

Ethics Approval This study was approved by the Medical Ethics Committee; 2017.545

<http://dx.doi.org/10.1136/jitc-2021-SITC2021.672>

673 (RE-) SOLVING THE BIOLOGY OF COLORECTAL CANCER ONSET AND PROGRESSION TO IMPROVE TREATMENT AND PREVENTION

Jessica Roelands*, Manon van der Ploeg, Hao Dang, Lukas Hawinkels, Hans Morreau, Noel de Miranda. *Leiden University Medical Center, Leiden, Netherlands*

Background Colorectal cancer (CRC) development is accompanied by the gradual accumulation of genetic alterations in epithelial cells of the colon and rectum.^{1,2} The paradigm of the adenoma-carcinoma sequence was originally centered around cancer cells; however, it is now clear that the tumor microenvironment plays a substantial role in cancer progression and patient outcome.³ In recent years, technologies have evolved rapidly, allowing the multiplexed quantification of gene expression while preserving spatial context.⁴ Furthermore, some spatial transcriptomic technologies also allow the parallel interrogation of different cell populations in the tumor microenvironment. Here, we performed digital spatial profiling on early-stage CRC samples to elucidate the biological processes that are at the basis of malignant transformation and to identify novel therapeutic targets and (immune) biomarkers.

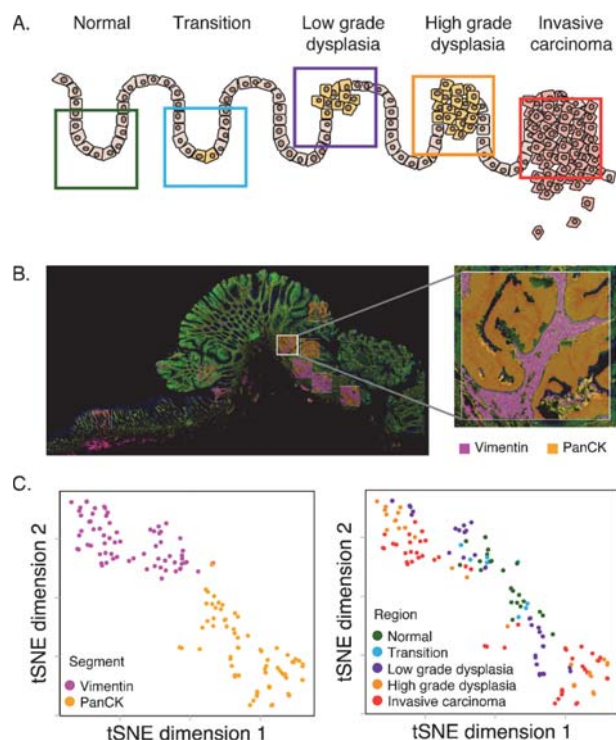
Methods Endoscopically resected early-stage CRC samples were obtained at Leiden University Medical Center. In total, 144 areas of illumination were interrogated with GeoMx digital spatial profiling using the Cancer Transcriptome Atlas (>1,800 genes). In each of eight samples, nine regions of interest with different levels of cancer progression were selected, including normal epithelium, transition areas, low-, and high-grade dysplasia, and invasive carcinoma (figure 1A). We segmented each region based on cytokeratin and vimentin protein expression (figure 1B). Immunohistochemical detection was performed on these samples and 26 additional samples to validate targets associated with disease progression.

Results Digital spatial profiling allowed us to dissect transcriptional alterations in epithelial and stromal fractions between different regions from healthy tissue, different degrees of dysplasia, and cancer. Gene expression data revealed a clear separation of profiled areas by histologic category. Interestingly, gene expression features in the stromal compartment provided a better data-driven separation of histologic categories than the epithelial fraction (figure 1C). Substantial changes in immune-related pathways were identified, including differential expression of specific immunomodulators. We validated the expression of several candidate biomarkers/targets that demonstrated consistent alterations from normal tissue to cancer by immunohistochemistry. Several proteins were identified that could clearly discriminate benign from malignant tissue.

Conclusions We here demonstrated the unique biological insights that are provided by spatial examination of early-stage CRC by digital spatial profiling. We identified specific genes that were altered during CRC tumorigenesis, in epithelial and stromal/immune fractions. Furthermore, our results indicate an essential role for innate immunity in colorectal cancer onset and progression. The genes identified by this approach could potentially serve as novel biomarkers and targets for early interception or prevention of CRC development.

Acknowledgements This work was supported by the European Research Council (ERC) Starting grant awarded to Dr. Noel F. de Miranda and the Stichting Management Apothekers en de Gezondheidszorg (STIMAG) Research grant awarded to Jessica Roelands.

Trial Registration N/A



Abstract 673 Figure 1 Transcriptional alterations in early-stage colorectal cancer. Digital spatial profiling defines transcriptional alterations in early-stage colorectal cancer. (A) Schematic representation of an early-stage CRC sample containing regions with different levels of cancer progression, including normal epithelium, transition areas, low-, and high-grade dysplasia, and invasive carcinoma. (B) Segmentation based immunofluorescent labelling with antibodies directed against PanCK and Vimentin in one of the early-stage CRC samples. Artificial overlay of implemented segmentation is indicated for each ROI, visualizing Vimentin+ (pink) and PanCK+ (orange) segments. Inset: higher magnification of an individual ROI. (C) Dimension reduction of expression of all quantified genes by t-Distributed Stochastic Neighbor Embedding (tSNE). tSNE plots are annotated by segment (left), and histological region (right).

REFERENCES

1. Fearon ER, Vogelstein B. A genetic model for colorectal tumorigenesis. *Cell* 1990;**61**(5):759–767. doi: 10.1016/0092-8674(90)90186-l.
2. Nowell PC. The clonal evolution of tumor cell populations. *Science* 1976;**194**(4260):23–28. doi: 10.1126/science.959840.
3. Hanahan D, Weinberg RA. Hallmarks of cancer: the next generation. *Cell* 2011;**144**(5):646–674. doi: 10.1016/j.cell.2011.02.013.
4. Merritt CR, et al. Multiplex digital spatial profiling of proteins and RNA in fixed tissue. *Nat Biotechnol* 2020;**38**(5):586–599. doi: 10.1038/s41587-020-0472-9.

Ethics Approval This study was approved by the METC Leiden-Den Haag-Delft (protocol B20.039). Patient samples were anonymised and handled according to the medical ethical guidelines described in the Code of Conduct for Proper Secondary Use of Human Tissue of the Dutch Federation of Biomedical Scientific Societies.

<http://dx.doi.org/10.1136/jitc-2021-SITC2021.673>

674

IL-27 SIGNALING DRIVES A TYPE 1 INTERFERON-LIKE GENE EXPRESSION PROGRAM OF IMMUNOREGULATORY PATHWAYS ASSOCIATED WITH CANCER PROGRESSION

Jonathan Hill*, Devapregasan Moodley, Jing Hua, Kerry White, Christine Miller, Secil Koseoglu, Ricard Masia, Benjamin Lee, Vito Palombella. *Surface Oncology, Inc., Cambridge, MA, United States*

Background Interleukin (IL)-27 is a heterodimeric immunoregulatory cytokine that signals through the JAK/STAT pathway to increase the expression of coinhibitory receptors on immune cells (e.g. PD-L1, TIM-3, LAG-3) and dampen inflammatory cytokine production. Blockade of IL-27 leads to antitumor activity in preclinical mouse models of lung metastases. A Phase 1 trial of SRF388 (NCT04374877), a first-in-class anti-IL-27 antibody, has demonstrated monotherapy antitumor activity in a patient with non-small cell lung cancer (NSCLC).¹ The current study aimed to characterize the immunoregulatory impact of IL-27 signaling by gene expression profiling.

Methods Gene expression changes induced by IL-27 were examined in activated human CD4+ T cells, human peripheral blood mononuclear cells (PBMCs), and the IL-27RA-expressing lung cancer cell line NCI-H2228 by microarray or single cell RNA-sequencing. The resulting IL-27 signature genes were interrogated by Gene Set Enrichment Analysis (GSEA) using publicly available datasets, including single cell RNA-seq analysis of the tumor microenvironment, from patients with NSCLC.²

Results IL-27 induced a robust gene expression program in human immune cells that included several inhibitory receptors and canonical interferon regulated genes such as guanylate-binding proteins and interferon regulatory factors. GSEA and interferon signature analysis showed a striking overlap with those genes regulated by interferon-beta, a cytokine known to drive immune suppression associated with chronic viral infection and that is used therapeutically for controlling inflammation associated with the autoimmune disease multiple sclerosis. Moreover, interferon regulated pathways have recently emerged as a mechanism of resistance to immune checkpoint blockade in cancer. Exploration of the IL-27 gene signature in published datasets showed enrichment in macrophage populations associated with progressive disease in patients with NSCLC. While many of the properties of IL-27-mediated immune regulation have focused on hematopoietic cells, IL-27RA is also expressed on tumor cells from NSCLC patients with progressive disease as well as lung cancer cell lines in which IL-27 can upregulate PD-L1, IDO1, and other canonical interferon regulated genes.

Conclusions These studies elucidate the transcriptional networks that are engaged after IL-27 signaling in immune and cancer cells and highlight the parallels with interferon-associated immune regulation. Blockade of IL-27 provides a novel therapeutic strategy to alleviate a gene transcriptional program implicated in immune suppression and checkpoint resistance.

REFERENCES

1. Patnaik A, Morgensztern D, Mantia C, et al. Results of a phase 1 study of SRF388, a first-in-human, first-in-class, high-affinity anti-IL-27 antibody in advanced solid tumors. *J Clin Oncol* 2021;**39**:2551–2551.
2. Maynard A, McCoach CE, Rotow JK, et al. Therapy-induced evolution of human lung cancer revealed by single-cell RNA sequencing. *Cell* 2020;**182**:1232–1251.

<http://dx.doi.org/10.1136/jitc-2021-SITC2021.674>

675 GENOMIC DRIVERS OF LARGE B-CELL LYMPHOMA RESISTANCE TO CD19 CAR-T THERAPY

¹Michael Jain, ²Bachisio Ziccheddu, ²Caroline Coughlin*, ¹Rawan Faramand, ²Anthony Griswold, ¹Kayla Reid, ²Ola Landgren, ¹Frederick Locke, ²Francesco Maura, ¹Marco Davila, ²Jonathan Schatz. ¹Moffitt Cancer Center, Tampa, FL, United States; ²University of Miami Miller School of Medicine, Miami, FL, United States

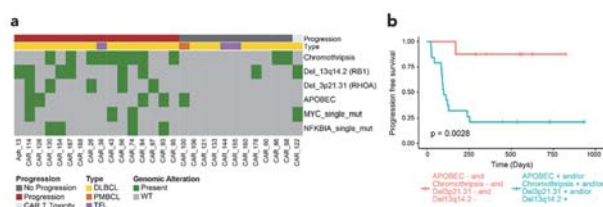
Background CD19-directed chimeric antigen receptor-reprogrammed autologous T cells are breakthrough immunotherapies for heavily pretreated patients with diffuse large B-cell lymphoma (DLBCL), but across CAR-19 products, ~60% of patients fail to respond or relapse. Inflammatory markers and clinical factors associate with impaired responses, but tumor-intrinsic resistance drivers are largely undefined.

Methods To characterize the genomic mechanisms involved in resistance to CAR-19, we interrogated whole genome sequencing (WGS) from 28 relapsed/refractory (r/r) aggressive lymphoma patients uniformly treated with axicabtagene ciloleucel (axi-cel).

Results Because prognostic factors defined in the frontline treatment setting are largely inapplicable to CAR-19, we leveraged the WGS data, including comparative analyses with untreated DLBCL cases in the Pan-Cancer Analysis of Whole Genomes (PCAWG) (figure 1). In analyses of individual mutated genes, TP53 was significantly enriched ($p=0.002$) in CAR-19 patients, but did not predict outcome. However, mutations in either NFKBIA or MYC associated with worse PFS after CAR-19 ($p=0.04$, $p=0.025$ respectively). We next identified 12 single base substitution (SBS) mutational signatures in our cohort and found presence of APOBEC (SBS2 and SBS13) signatures associated with worse PFS, with 4/5 patients progressing ($p=0.03$). Copy number analysis by GISTIC2.0 revealed focal deletions of RHOA and RB1 to be significantly enriched in our cohort and independently predicted poor outcome ($p=0.0007$, $p=0.05$ respectively). WGS identifies structural variants and complex events. We found chromothripsis, a catastrophic shattering and reassembly of chromosomes, in 39.3% of r/r DLBCL, which was strongly associated with poor CAR-19 outcome, with 9/11 affected cases progressing ($p=0.041$). Finally, reduced expression ($n=3$) or genomic alteration ($n=3$) of CD19 did not associate with poor outcome. One case with durable response contained a sub-clonal CD19 mutation (L174V) previously reported as associated with CAR-19 resistance. These findings demonstrate predominance of CD19-independent resistance and indicate antigen-mediated tumor killing is not the only mechanism of tumor eradication. Genomic complexity appears to promote an immunosuppressive tumor microenvironment (TME), limiting CAR-19 efficacy.

Conclusions Leveraging the resolution of WGS, we observed that markers of genomic complexity (chromothripsis and APOBEC) and specific genomic alterations (RHOA and RB1 deletions) associate with resistance to CAR-19 immunotherapy for aggressive B-cell lymphomas (figure 1). 93.8% of CAR-19 relapsed patients contained at least one or these genomic alterations. Recent patient data demonstrate that an immunosuppressed TME leads to CAR-19 failure. Combining these findings with our genomics findings, successful CAR-19 therapy must overcome the immune-exhausted TME to mobilize the host immune system and eliminate the tumor.

<http://dx.doi.org/10.1136/jitc-2021-SITC2021.675>



Abstract 675 Figure 1 Genomic alterations associated with disease progression. (a) The heatmap shows the significant genomic alteration present in at least 4 patients associated with progression after CD19 CAR-T cell therapy. (b) Kaplan-Meier curve of progression free survival with the combination of statistically significant genomic anomalies

676 ALTERED CIRCULATING MYELOID STATES ASSOCIATED WITH ANTI-PD-1 RESISTANCE INDUCE T CELL PARALYSIS IN HUMAN BILIARY CANCER

Bridget Keenan*, Elizabeth McCarthy, Arielle Ilano, Hai Yang, Li Zhang, Kathryn Allaire, Zenghua Fan, Tony Li, David Lee, Yang Sun, Alexander Cheung, Hewitt Chang, Brenna Sheldon, Robin Kelley, Chun Jimmie Ye, Lawrence Fong. *University of California San Francisco, San Francisco, CA, United States*

Background Advanced biliary cancers (ABC) have a poor prognosis and low rates of response to immune checkpoint inhibition (CPI), with overall response rates ranging from 3–13%.^{1–3} Although suppressive myeloid cells have been proposed as a mechanism of resistance to immunotherapy in general, their relationship to response to CPI is unknown.

Methods We used multiplexed simultaneous single cell RNA sequencing and cell surface proteomics (CITE-seq) to profile circulating immune cells in ABC patients receiving anti-PD-1 at longitudinal timepoints pre-immunotherapy and on treatment, as well as from healthy donors. We also performed single cell RNA sequencing on resected biliary tumors.

Results We identified a novel population of circulating cancer-enriched myeloid cells (CEM) characterized by chemokines and extracellular matrix digestion-related gene expression, which were present pre-treatment. Anti-PD-1 treatment drove the CEMs into two diverging states that were associated with response or resistance to treatment. CEM induced in non-responders constituted over 40% of the circulating myeloid cells and expressed immunosuppressive programs, including the upregulation of suppressive cytokines and chemokines. The frequency of these myeloid cells were correlated with the abundance of SOCS3-expressing CD4⁺ T cells. These SOCS3⁺CD4⁺ T cells also colocalized with tumor-infiltrating myeloid cells that share CEM gene expression signatures in the biliary cancer microenvironment. Moreover, CEM can directly induce SOCS3-expressing T cells, which despite their naïve phenotype are functionally unresponsive. Finally, expression signatures of CEM and of SOCS3⁺CD4⁺ T cells are associated with worse survival in a larger cohort of ABC patients.

Conclusions These results demonstrate the capacity of CEM to induce T cell paralysis as an alternate mode of tumor-mediated immunosuppression. A deeper understanding of immune cell biology in ABC provides insights for developing novel therapeutics that can overcome immunotherapy resistance in biliary cancer as well as other tumor types.

Trial Registration NCT02703714

REFERENCES

1. Ueno M, et al. Nivolumab alone or in combination with cisplatin plus gemcitabine in Japanese patients with unresectable or recurrent biliary tract cancer: a non-randomised, multicentre, open-label, phase 1 study. *Lancet Gastroenterol Hepatol* 2019;**4**:611–621.
2. Piha-Paul SA, et al. Efficacy and safety of pembrolizumab for the treatment of advanced biliary cancer: results from the KEYNOTE-158 and KEYNOTE-028 studies. *Int J Cancer* 2020.
3. Kim RD, et al. A Phase 2 Multi-institutional study of nivolumab for patients with advanced refractory biliary tract cancer. *JAMA Oncol* 2020;**6**:888–894.

Ethics Approval Informed consent was obtained from all patients for participation in the listed trial and for use of blood and tumor samples in research studies.

<http://dx.doi.org/10.1136/jitc-2021-SITC2021.676>

677

REVERSE ABSCOPAL EFFECT: INTERTUMORAL HETEROGENEITY SUPPRESSES SYSTEMIC CD8 T CELL-MEDIATED ANTITUMOR IMMUNITY AND CONFERS PD-1 INHIBITOR RESISTANCE IN SYNCHRONOUS MELANOMA

¹Shuyang Qin*, ¹Booyeon Han, ²Alexander Chacon, ²Alexa Melucci, ²Alyssa Williams, ²Rachel Jewell, ¹Minsoo Kim, ²David Linehan, ²Scott Gerber, ²Peter Prieto. ¹University of Rochester School of Medicine and Dentistry, Rochester, NY, United States; ²University of Rochester Medical Center, Rochester, NY, United States

Background Despite recent advancements in systemic therapy, only a minority of metastatic patients develop meaningful clinical responses to immune checkpoint inhibitors. Inherent genetic instability of melanoma generates genomically and microenvironmentally distinct metastases. These different tumor microenvironments (TMEs) contain numerous T cell suppression mechanisms, such as upregulation of the PD-1/PD-L1 exhaustion pathway. However, as synchronous metastases share one host immune system, intertumoral heterogeneity may result in increasing cross-talk between metastases that impairs systemic antitumor immunity and promotes PD-1 immunotherapy resistance.

Methods YUMM 1.7 (less immunogenic) and YUMMER 1.7 (more immunogenic cell line derived from YUMM following UVB irradiation) melanoma cell lines were simultaneously injected into opposite flanks of the same mice as a model of synchronous melanoma. We assessed tumor growth in wild-type, interferon-gamma (IFN- γ) knockout, and CD8-depleted mice as well as in response to PD-1 inhibitor. We characterized the TME with flow cytometry and performed TCR sequencing on tumor-infiltrating CD8 T cells.

Results Distinct TMEs were observed for YUMM and YUMMER tumors simultaneously grown in the same mouse. The presence of the less immunogenic YUMM tumor allows the more immunogenic YUMMER tumors to escape IFN- γ and CD8 T cell-mediated rejection, despite abundant tumor-infiltrating, clonally expanded CD8 T cells. Identical immunodominant CD8 T cell clones were found in both YUMM and YUMMER tumors within the same mouse. Synchronous YUMMER-infiltrating CD8 T cells exhibit suppressed phenotypes, including increased persistence of surface PD-1 and decreased surface CD107a expressions. Simultaneously, these synchronous YUMMER tumors additionally upregulate macrophage surface PD-L1 expression, which potentially contributes to tumor immune escape. Lastly, synchronous YUMMER tumors become resistant to PD-1 inhibition, in direct contrast to control YUMMER tumors.

Conclusions In a host with multiple melanoma lesions, immunogenicity of all tumors contribute to the systemic antitumor immune response. We show that two synchronous tumors with synonymous mutations (<40%), as is the case with metastatic patients, lead to skewed CD8 T cell expansion of the same clones in both tumors. The presence of a less immunogenic tumor prevents CD8 and IFN- γ mediated rejection of the more immunogenic tumor. Furthermore, CD8 T cells in the more immunogenic tumor exhibit decreased effector function and increased resistance to PD-1 blockade, as tumor-infiltrating macrophages concurrently become more immunosuppressive. These results are highly suggestive of a “reverse abscopal effect,” by which immunologically “cold” tumors generate systemic immunosuppression that facilitate PD-1 immunotherapy resistance and immune escape of all other tumors in synchronous metastatic melanoma patients.

Acknowledgements We would like to thank Dr. Marcus Bosenberg from the Department of Dermatology at Yale University

for kindly gifting us with the YUMMER 1.7 murine melanoma cell line.

Ethics Approval Animal experiments were approved by the University Committee on Animal Resources and performed in accordance with University of Rochester approved guidelines.

<http://dx.doi.org/10.1136/jitc-2021-SITC2021.677>

678

THE NEONATAL FC RECEPTOR IS ELEVATED IN MONOCYTE-DERIVED IMMUNE CELLS IN PANCREATIC CANCER

Justin Thomas*, Molly Torok, Kriti Agrawal, Trang Vu, Alyssa Castillo, Min Chen, Bryan Remaily, Kyeongmin Kim, Zhiliang Xie, Samuel Kulp, Dwight Owen, Mitch Phelps, Christopher Coss, Thomas Mace. *The Ohio State University, Columbus, OH, United States*

Background Pancreatic ductal adenocarcinoma (PDAC) is the third leading cause of cancer-related death in the United States with 5-year survival rates below 10%. PDAC is commonly diagnosed after metastasis has occurred and treatment options are limited. Immune checkpoint inhibitor (ICI) monoclonal antibody (mAb) therapy has shown great promise in other cancers, however little efficacy has been observed in patients with PDAC. The protein responsible for recycling IgG based mAb therapeutics like ICIs in the bloodstream, as well as processing peptides for antigen presentation, is the neonatal Fc receptor (FcRn). Little is known about FcRn in cancer, and to our knowledge no characterization of host FcRn, or FcRn extrinsic to tumor cells exists in PDAC patients. We hypothesized that PDAC patients and tumor-bearing animals would have altered FcRn expression by their immune populations compared to their healthy counterparts.

Methods C57BL/6 mice were orthotopically injected with KPC-luc (KrasLSL-G12D, Trp53LSL-R270H, Pdx1-cre) pancreatic tumor cells, and FcRn expression in myeloid-derived splenocytes were analyzed by fluorescence cytometry. Time-of-flight mass cytometry (CyTOF) was utilized to immunophenotype peripheral blood mononuclear cells (PBMCs) of PDAC or non-cancer patients for expression levels of FcRn within these immune populations.

Results PDAC tumor-bearing mice exhibit altered FcRn expression among myeloid immune cell populations. Mice with pancreatic tumors had elevated expression of FcRn on migratory cDC2 (CD8-CD11b+CD103+CD24⁺⁺; $p = 0.017$), monocytic MDSC (CD11b+Ly6G-Ly6C⁺; $p = 0.0023$), granulocytic MDSC (CD11b+Ly6G+Ly6C[±]; $p = 0.0542$), and cDC2 (CD8-CD11b+CD103-CD24[±]; $p=0.036$) cells. PBMCs from non-cancer obese patients (healthy control samples; $n=8$) and PDAC patients prior to surgical resection ($n=13$) were subjected to CyTOF analyses. The majority of FcRn expression was concentrated to monocyte ($p=0.017$), DCs ($p=0.017$) and MDSC ($p=0.012$) immune populations. Overall, we observed increased expression of FcRn on myeloid-derived immune populations from patients with PDAC. FcRn expression was elevated in both monocytes and DC populations in PDAC relative to non-cancer PBMCs. Monocytic and granulocytic MDSC from patients with PDAC had significantly elevated FcRn positivity compared to healthy controls ($p = 0.034$, $p = 0.026$, respectively).

Conclusions FcRn is upregulated in monocytes, dendritic cells and MDSC immune populations in patients and mice with pancreatic tumors. Future investigations into FcRn function in preclinical models and PDAC patients will hopefully elucidate new mechanisms of ICI resistance and possible alternative approaches for improving immunotherapy efficacy in these patients.

Ethics Approval All patients provided voluntary written informed consent (Institutional Review Board protocol: 2010C0051) to participate. The protocols and subsequent amendments were approved by The Ohio State University Institutional Review Board. All animal protocols were approved by the Ohio State University Institutional Animal

Care and Use Committee (IACUC) at The Ohio State University (Approved IACUC protocols 2009A0178-R4 and 2017A00000117-R1) and mice were treated in accordance with institutional guidelines for animal care. The Ohio State University Laboratory Animal Shared Resource is an Association for Assessment and Accreditation of Laboratory Animal Care International accredited program that follows Public Health Service policy and guidelines. All other experiments were completed under the research protocols (2014R00000086; 2013R00000056) approved by the Ohio State University Institutional Biosafety Committee.

<http://dx.doi.org/10.1136/jitc-2021-SITC2021.678>

TUMOR HYPOXIA DRIVES SUPPRESSOR FUNCTION IN EXHAUSTED T CELLS LIMITING ANTITUMOR IMMUNITY

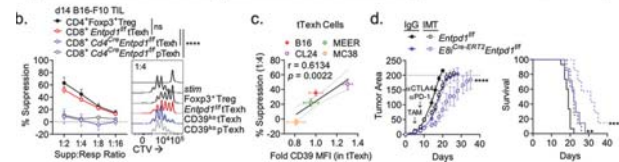
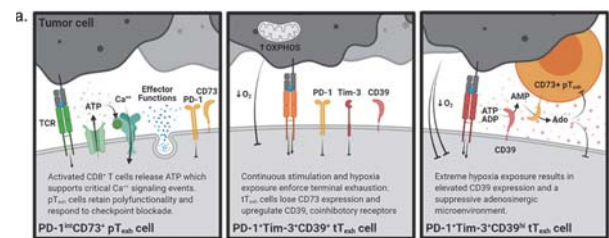
¹Paolo Vignali*, ¹Kristin DePeaux, ¹McLane Watson, ²Nicole Scharping, ¹Ashley Menk, ¹Greg Delgoffe. ¹University of Pittsburgh, Pittsburgh, PA, United States; ²University of California San Diego, La Jolla, CA, United States

Background While CD8+ cytotoxic T cells are clearly critical for identification and elimination of cancer cells, factors concentrated within the tumor microenvironment drive altered differentiation of these cells to a hypofunctional, short-lived state termed T cell exhaustion¹ (figure 1a). Exhaustion is a progressive lineage, and it is now clear that terminally exhausted T (tTexh) cells are not the targets of checkpoint blockade immunotherapy but may serve as factors that limit immunotherapeutic efficacy.²⁻⁶ Compared directly, tumor-infiltrating CD8+ tTexh cells bear notable phenotypic similarity to CD4+Foxp3+ regulatory T (Treg) cells in expression of immunosuppressive molecules suggesting beyond loss of effector function, tTexh cells may be directly anti-functional and constrain tumor-specific immunity. Thus, we hypothesize that tTexh cells potentiate the suppressive microenvironment of solid tumor and that strategies to limit their generation or reprogram their immunosuppressive nature will improve control of tumor progression.

Methods T cell populations were isolated from murine tumor lines, B16-F10 melanoma, Ptenflox/floxBrafLSL.V600EYr2Cre. ERT2-derived Clone 24 melanoma, MEER head and neck carcinoma, and MC38 adenocarcinoma. T cell-specific CD39 (Entpd1) deletion was accomplished by crossing Entpd1flox/flox mice to Cd4Cre or E8iGFP-Cre-ERT2. Enforced expression of CD39 in effector T cells was attained by murine retroviral vector delivery. Tumor hypoxia was alleviated by CRISPR-Cas9-directed deletion of mitochondrial genes in B16-F10 or by treatment with axitinib or metformin.

Results When sorted directly from tumor, CD8+PD-1hiTim-3+ tTexh cells, but not progenitor PD-1intTim-3- pTexh cells, induce marked suppression of T cell effector responses, comparable to CD4+Foxp3+ Treg cells from the same environment (figure 1b-c). The ectonucleotidase, CD39, increases as cells progressively differentiate and is associated with terminal exhaustion.^{7,8} CD8+ T cell-restricted deletion of CD39 restricts regulatory functions of tTexh cells (figure 1b), improving tumor control and augmenting response to checkpoint blockade (figure 1d). CD39 expression correlates with hypoxia exposure and tTexh cells sorted from tumors engineered to be less hypoxic or treated with hypoxia-mitigating agents displayed a significant loss of suppressive capacity. Our data suggest that tumor hypoxia enforces Hif1a-dependent expression of CD39 which depletes extracellular ATP, supports adenosine generation, and limits therapeutic efficacy.

Conclusions Our data support a model that as CD8+ T cells progress to terminal exhaustion, hypoxia exposure enforces the upregulation of CD39, providing tTexh cells a mechanism to suppress proinflammatory processes and promote tumor progression. These findings suggest tTexh cells are not solely dysfunctional but rather are deleterious to antitumor immunity and may need to be drastically reprogrammed or depleted to improve patient outcomes.



Abstract 679 Figure 1 (a) Schematic depicting differentiation of CD8+ T cells to terminal exhaustion in cancer and subsequent suppression of local immune responses by expression of ectonucleosidase, CD39; (b) When assayed directly ex vivo, CD8+ terminally exhausted T (tTexh) cells, but not progenitor exhausted T (pTexh) cells, suppress effector functions as effectively as CD4+Foxp3+ Treg isolated from the same environment. Deletion of CD39 alleviates tTexh-mediated suppression; (c) CD8+ T cell suppression correlates with expression of CD39 on tTexh from various tumor models. (d) CD8+ T cell-specific deletion of CD39 slows tumor growth and improves immune response to checkpoint blockade-resistant tumors. Data are pooled from ≥ 3 experiments. Statistics are two-way ANOVA with multiple comparisons or Pearson correlation. * $p < 0.05$, ** $p < 0.01$, *** $p < 0.001$, **** $p < 0.0001$.

REFERENCES

- Blank CU, et al. Defining "T cell exhaustion". *Nat Rev Immunol* 2019;**19**:665–674.
- Miller BC, et al. Subsets of exhausted CD8+ T cells differentially mediate tumor control and respond to checkpoint blockade. *Nat Immunol* 2019;**20**:326–336.
- Blackburn SD, et al. Selective expansion of a subset of exhausted CD8 T cells by alphaPD-1 blockade. *Proc Natl Acad Sci USA* 2008;**105**:15016–15021.
- Sade-Feldman M, et al. Defining T Cell states associated with response to checkpoint immunotherapy in Melanoma. *Cell* 2018;**175**:998–1013.e20.
- Im SJ, et al. Defining CD8+ T cells that provide the proliferative burst after PD-1 therapy. *Nature* 2016;**537**:417–421.
- Siddiqui I, et al. Intratumoral Tc1+PD-1+CD8+ T Cells with stem-like properties promote tumor control in response to vaccination and checkpoint blockade immunotherapy. *Immunity* 2019;**50**:195–211.e10.
- Canale FP, et al. CD39 expression defines cell exhaustion in tumor-infiltrating CD8+ T Cells. *Cancer Res* 2018;**78**:115–128.
- Gupta PK, et al. CD39 expression identifies terminally exhausted CD8+ T cells. *PLoS Pathog* 2015;**11**:e1005177.

<http://dx.doi.org/10.1136/jitc-2021-SITC2021.679>

ISOFORMS OF NEUROPILIN-2 REGULATE DISTINCT MACROPHAGE FUNCTIONS AND ARE ASSOCIATED WITH UNIQUE TUMOR-ASSOCIATED MACROPHAGES IN MURINE AND HUMAN BREAST CANCER

¹Rajeev Dhupar, ¹Katherine Jones, ¹Amy Powers, ¹Seth Eisenberg, ²Kai Ding, ²Fangyuan Chen, ³Cecile Nasarre, ³Amanda LaRue, ⁴Elizabeth Yeh, ¹James Luketich, ²Adrian Lee, ²Steffi Oesterreich, ¹Michael Lotze, ³Robert Gemmill, ¹Adam Soloff*. ¹University of Pittsburgh School of Medicine, Pittsburgh, PA, United States; ²Womens Cancer Research Center, Pittsburgh, PA, United States; ³Medical University of South Carolina, Charleston, SC, United States; ⁴Indiana University School of Medicine, Indianapolis, IN, United States

Background Tumor-associated macrophages (TAMs) exert profound influence over breast cancer progression, promoting immunosuppression, angiogenesis, and metastasis.¹ Neuropilin-2 (NRP2), consisting of NRP2a and NRP2b isoforms, is a co-receptor for heparin-binding growth factors including VEGF-C and Class 3 Semaphorins. Selective upregulation in response to environmental stimuli and independent signaling pathways endow the NRP2 isoforms with unique functionality.^{2, 3} We have shown that the two isoforms of NRP2 endow opposing functionality to tumor cells due to distinct signaling pathways, with NRP2b promoting metastatic behavior.³ Although NRPs have been shown to regulate macrophage/TAM biology, the role of NRP2 isoforms in TAM functionality has yet to be evaluated.

Methods To assess the contribution of NRP2 isoforms to macrophage biology, conditional NRP2a and NRP2b knockout mice and stable shRNA knockdown of NRP2a or NRP2b in Raw264.7 macrophages were generated. Phagocytosis, lysosomal processing of phagocytosed cargo, cytokine production, and influence on tumor cell migration were assessed in vitro using NRP2 isoform knockdown macrophages. NRP2 isoform expression was evaluated on TAMs from murine 4T1 and EO771 mammary carcinoma models using spectral cytometry and single-cell qPCR. NRP2 isoforms and approximated immune composition were evaluated in paired primary tumors and distant metastasis using RNAseq in a cohort of 99 breast cancer patients. High-dimensional myeloid phenotyping was performed on malignant pleural effusions (MPEs) from breast cancer patients or effusions of benign origin using 33-color spectral cytometry and unbiased computational analysis.

Results NRP2 isoform expression was significantly increased in TAMs from murine tumors compared to macrophages from healthy mammary glands. NRP2 isoforms in human primary and metastatic breast cancer were strongly correlated with one another and positively correlated with increased TAMs. Distinct phenotypes of NRP2 isoform-expressing TAMs in were present in 4T1 and EO771 mouse breast cancers and within MPEs from breast cancer patients which were associated with high levels of activation and potential response to a hypoxic tumor niche. Genetic depletion of either NRP2 isoform resulted in dramatic reduction of LPS-induced IL-10 production, defects in phagosomal processing of apoptotic breast cancer cells, and increase in cancer cell migration following coculture. By contrast, inhibition of IL-6 production was specific in NRP2b knockdown cells while phagocytic uptake of labeled particulates was inhibited only by NRP2a knockdown.

Conclusions These results demonstrate that NRP2 isoforms regulate both shared and distinct functionality in macrophages and that NRP2 isoform expression identifies unique TAM subsets in breast cancer.

Acknowledgements This work was supported by awards from the Susan G. Komen Foundation (CCR15329745), U.S.

Department of Defense (W81XWH1910650), and American Lung Association/Thoracic Surgery Foundation to ACS. RD was supported by funding from a Department of Veteran's Affairs Career Development Award (CX001771-01A2) and the University of Pittsburgh's Dean Faculty Advancement Award. ESY was supported by the NCI of the NIH under R03 CA245774. MTL was supported by the NCI of the NIH under awards R01CA181450 and R01CA206012 as well as ITTC/UPMCE. RD and ACS were further supported by funding from the Department of Cardiothoracic Surgery.

REFERENCES

1. Williams CB, Yeh ES, Soloff AC. Tumor-associated macrophages: unwitting accomplices in breast cancer malignancy. *Npj Breast Cancer [Internet]*. Breast Cancer Research Foundation/Macmillan Publishers Limited; 2016;**2**:15025. Available from: <http://dx.doi.org/10.1038/npjbcancer.2015.252>.
2. Nasarre P, Gemmill RM, Potiron VA, Roche J, Lu X, Barón AE, et al. Neuropilin-2 is upregulated in lung cancer cells during TGF- β 1-Induced epithelial-mesenchymal transition. *Cancer Res [Internet]* 2013;**73**:7111 LP-7121. Available from: <http://cancerres.aacrjournals.org/content/73/23/7111.abstract3>.
3. Gemmill RM, Nasarre P, Nair-Menon J, Cappuzzo F, Landi L, D'Incecco A, et al. The neuropilin 2 isoform NRP2b uniquely supports TGF β -mediated progression in lung cancer. *Sci Signal [Internet]* 2017;**10**. Available from: <http://stke.sciencemag.org/content/10/462/eaag0528.abstract>

Ethics Approval The study was approved by the University of Pittsburgh's Institutional Review Board approval number CR19120172-005.

<http://dx.doi.org/10.1136/jitc-2021-SITC2021.680>

681 **AN EX VIVO 3D TUMOROID MODEL OF FRESH PATIENT TISSUE (3D-EXPLORE) TO ASSESS THE PHAGOCYtic ACTIVITY OF TUMOR RESIDENT INNATE IMMUNE CELLS**

Kelly Guzman*, Olivia McIntosh, Brittany Bunch, Jacob Yarinsky, Jared Ehrhart, Soner Altioik. Nilogen Oncosystems, Tampa, FL, United States

Background CD47 is an innate immune checkpoint receptor that is overexpressed on tumor cells and contributes to immune evasion through engagement of a myeloid-lineage inhibitory protein SIRP α . Blockade of the CD47-SIRP α interaction is proved to enhance the phagocytosis of cancer cells and to induce effective antitumor immune response. Here we developed a novel ex vivo platform using fresh patient tumor samples with intact stromal components and tumor immune microenvironment to assess the therapeutic activity of immunotherapeutic drugs targeting CD47-SIRP α signaling axis in combination with the human IgG1 α PD-L1 antibody avelumab.

Methods All tumor samples were obtained with patient consent and relevant IRB approval. Unpropagated 3D tumoroids with intact TME measuring 150 μ m in size were prepared from fresh tumor samples of renal cell carcinoma using proprietary technology developed at Nilogen Oncosystems. Tumoroids prepared from each patient's tumor sample were pooled to represent the tumor heterogeneity and treated ex vivo with phrodo-labeled avelumab alone or in combination with anti-CD47 or anti-SIRP α therapeutics.

Results Multiparameter flow analysis demonstrated tumor binding of avelumab confirming drug penetration into the intact tumor stroma that is further corroborated by high content confocal analysis. Using our confocal-based tumor cell killing assay we were able to quantify drug-induced tumor cell killing ex vivo. We further documented the impact of anti-CD47 and anti-SIRP α therapeutics on phagocytosis of dead tumor cells by tumor resident macrophages and activation of innate and adaptive effector cells by flow cytometry and confocal imaging. Additionally, pHrodo-labeled bioparticles were used to corroborate treatment-mediated changes in the phagocytic activity of tumor resident macrophages.

Conclusions In this comprehensive study we demonstrate that the 3D-EXplore ex vivo platform can be used to assess the efficacy of therapeutic blockade of CD47/SIRP α axis on stimulation of phagocytic process within an intact tumor immune microenvironment.

<http://dx.doi.org/10.1136/jitc-2021-SITC2021.681>

Immune Cell Types

682 PKC AGONISM RESTRICTS INNATE IMMUNE SUPPRESSION, PROMOTES ANTIGEN CROSS-PRESENTATION AND SYNERGIZES WITH AGONISTIC CD40 THERAPY IN BREAST CANCER

Mehdi Chaib*, Liza Makowski, John Yarbro, Laura Sipe, Deidre Daria. *Uthsc, Memphis, TN, United States*

Background Immunotherapies that reinvigorate T cell responses have transformed the treatment of many cancers showing unprecedented durable antitumor responses. However, most patients do not respond to immunotherapy due in part to immunosuppression. Immunotherapy non-responders have high levels of circulating myeloid-derived suppressor cells (MDSCs)-an innate cell population that expands in pathological conditions such as cancer and suppresses T cells via production of immunosuppressive factors. In contrast, immunotherapy success is dependent on the ability of antigen-presenting cells (APCs) to cross-present tumor antigens to cytotoxic T cells. Immunogenic cross-presentation by APCs requires a specific subtype of dendritic cells (DCs) called conventional DC1 (cDC1) which are dysfunctional in cancer. Novel ways to increase cDC1 function are promising and under active investigation. One of these ways is ligation of CD40 which is primarily expressed by myeloid cells and its agonism leads to myeloid cell activation. Thus, targeting MDSCs while simultaneously expanding cross-presenting DCs represents a promising strategy that, when combined with agonistic CD40, will likely result in long-lasting protective immunity.

Methods Using in vitro, ex vivo, in vivo and adoptive transfer systems, we investigated the effect of PKC agonists PEP005 and prostratin on MDSC expansion, differentiation to APC-like cells and recruitment to the TME. MDSC suppressive capacity was investigated using functional coculture assays with CD8+ T cells. Furthermore, we assessed the effect of PKC agonists on MDSC cross-priming capacity using in vitro coculture assay with OT-I CD8+ T cells as well as adoptive transfer experiments. We also investigated the effect of PKC agonists on cDC1 expansion from the BM in vitro and in vivo. Finally, we tested the efficacy of PKC agonism in combination with agonistic CD40 using the E0771 murine breast cancer orthotopic mouse model.

Results Herein, we show that PKC agonists decreased MDSC expansion from hematopoietic progenitors in the BM and induced M-MDSC differentiation to an APC-like phenotype that expresses cDC1-related markers and the transcription factor Irf8. Simultaneously, PKC agonists favored cDC1 expansion at the expense of cDC2 and plasmacytoid DCs (pDC). Functionally, PKC agonists blunted MDSC suppressive function of T cells and promoted MDSC cross-priming capacity. Finally, combination of PKC agonism with agonistic CD40 mAb resulted in a marked reduction in tumor growth while synergistically increased intratumoral activated CD8+ T cells and tissue-resident memory CD8+ T cells.

Conclusions In sum, we propose a novel promising strategy to simultaneously target MDSCs and promote APC function that may have potential clinical relevance in cancer patients.

<http://dx.doi.org/10.1136/jitc-2021-SITC2021.682>

683

TYPE-I-INTERFERON ACTIVATES CROSS-DRESSED CD11b⁺CONVENTIONAL DENDRITIC CELLS TO ENHANCE ANTI-TUMOR IMMUNITY

Ellen Duong*, Timothy Fessenden, Emi Lutz, Teresa Dinter, Leon Yim, Sarah Blatt, Arjun Bhutkar, K. Wittrup, Stefani Spranger. *Koch Institute, Cambridge, MA, United States*

Background Conventional dendritic cells (cDC) are critical mediators of protective anti-tumor CD8⁺ T-cell responses.¹ Batf3-driven DC1 are the predominant cDC subset driving anti-tumor immunity due to their specialized ability to cross-present antigens for T-cell activation.²⁻⁴ However, the contribution of other tumor-infiltrating DC subsets such as CD11b⁺ DC2 to anti-tumor immunity remains poorly characterized. Recent studies suggest that under inflammation, DC subsets can exist in various functional states with differential impacts on their stimulatory potential.⁵⁻⁷ In this study, we sought to dissect the contributions of distinct DC states during a productive or dysfunctional anti-tumor immune response. A nuanced understanding of DC activation states in tumors and the signals that drive them carries therapeutic potential to modulate anti-tumor immunity and enhance immunotherapy responses.

Methods We compared the DC infiltrate of a regressing tumor and a progressing tumor to study DC states. Flow immunophenotyping and RNA-sequencing was performed to profile the intratumoral DC compartment. Sorted DC subsets were co-cultured with T-cells *ex vivo* to evaluate their stimulatory capacity. Cross-dressing (*in vivo/ex vivo*) was assayed by staining for transfer of tumor-derived H-2^b MHC complexes to MHC-mismatched or β 2M-deficient DC.

Results Anti-tumor CD8⁺ T-cell responses in Batf3^{-/-} mice lacking DC1 were maintained in regressor tumors but not progressor tumors, suggesting DC1-independent anti-tumor immunity. Functional assays and RNA-sequencing of the intratumoral DC compartment of regressor tumors revealed a Zbtb46-dependent CD11b⁺ cDC activation state expressing an interferon-stimulated gene signature (ISG⁺ DC) that was critical for driving optimal anti-tumor CD8⁺ T-cell responses. Sorted ISG⁺ DC could activate CD8⁺ T-cells similar to DC1. Unlike cross-presenting DC1, however, ISG⁺ DC acquired antigens by cross-dressing with tumor-derived peptide-MHC, thereby bypassing the requirement for cross-presentation to initiate CD8⁺ T-cell-immunity. Interestingly, ISG⁺ DC were enriched in regressor tumors compared to progressor tumors, and this was attributable to constitutive tumor cell-intrinsic type-I-interferon (IFN-I) production in regressor tumors. Ablation of tumor cell-derived IFN-I in regressor tumors led to complete loss of anti-tumor T-cell responses in Batf3^{-/-} mice. Conversely, addition of IFN β to progressor tumors induced ISG⁺ DC and rescued anti-tumor T-cell responses in Batf3^{-/-} mice.

Conclusions We identified a novel IFN-I-induced activation state of CD11b⁺ cDC, called ISG⁺ DC, that was capable of driving anti-tumor CD8⁺ T cell immunity by cross-dressing with tumor-derived pMHC complexes in the absence of DC1. Engaging additional functional states of DC, such as ISG⁺ DC, will strengthen anti-tumor immunity and may improve immunotherapy responses.

REFERENCES

1. Merad M, et al. The dendritic cell lineage: ontogeny and function of dendritic cells and their subsets in the steady state and the inflamed setting. *Annu Rev Immunol* 2013;**31**:563–604

2. Hildner K, et al. Batf3 deficiency reveals a critical role for CD8 α ⁺ dendritic cells in cytotoxic T cell immunity. *Science* 2008;**322**(5904):1097–100.
3. Broz ML, et al. Dissecting the tumor myeloid compartment reveals rare activating antigen-presenting cells critical for T cell immunity. *Cancer Cell* 2014;**26**(5):638–52.
4. Roberts EW, et al. Critical role for CD103(+)/CD141(+) dendritic cells bearing CCR7 for tumor antigen trafficking and priming of T cell immunity in Melanoma. *Cancer Cell* 2016;**30**(2):324–336.
5. Maier B, et al. A conserved dendritic-cell regulatory program limits antitumour immunity. *Nature* 2020;**580**(7802):257–262.
6. Bosteels C, et al. Inflammatory Type 2 cDCs acquire features of cDC1s and macrophages to orchestrate immunity to respiratory virus infection. *Immunity* 2020;**52**(6):1039–1056.e9.
7. Zilionis R, et al. Single-cell transcriptomics of human and mouse lung cancers reveals conserved myeloid populations across individuals and species. *Immunity* 2019;**50**(5):1317–1334.e10.

<http://dx.doi.org/10.1136/jitc-2021-SITC2021.683>

THE *IN VITRO* EFFECTS OF 5-AZACITIDINE ON THE IMMUNOPHENOTYPE OF MONOCYTE-DERIVED DENDRITIC CELLS FROM PATIENTS WITH HIGHER-RISK MYELODYSPLASTIC SYNDROMES

¹Randy Tsai*, ²Hannah Fields, ¹Xinlian Zhang, ³Valentina Ferrari, ¹Soo Park, ¹Rafael Bejar, ⁴Tiffany Tanaka. ¹UC San Diego, San Diego, CA, United States; ²ImmunoScape, San Diego, CA, United States; ³Humanitas University, Milan, Italy; ⁴UC San Diego Moores Cancer Center, San Diego, United States

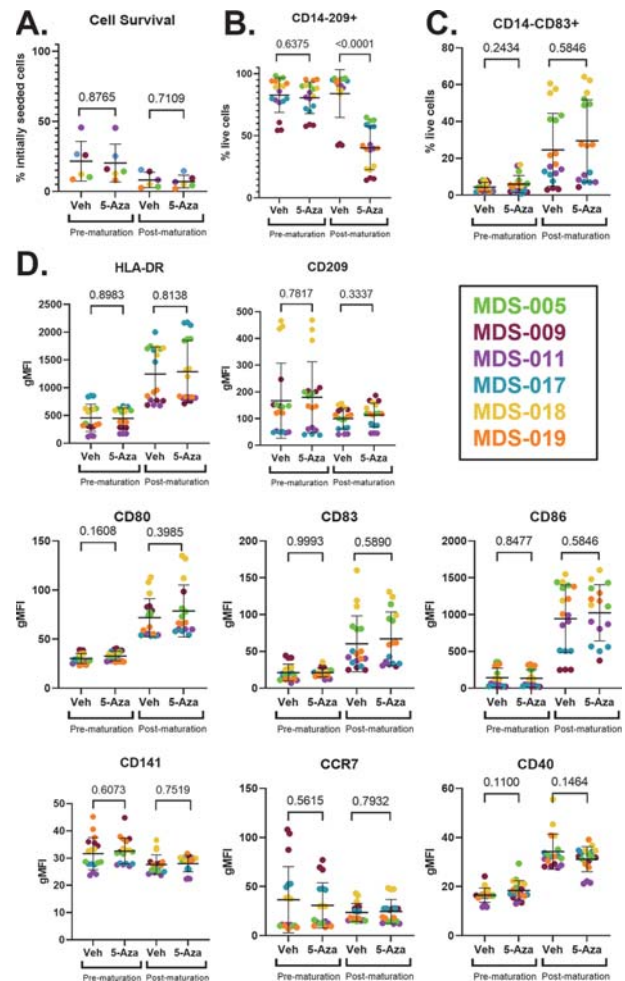
Background Myelodysplastic syndromes (MDS) are the most common acquired cause of bone marrow failure. Though DNA hypomethylating agents (HMAs) such as 5-Azacytidine (5-Aza) may increase survival of patients with higher-risk MDS, their mechanistic effects on hematopoiesis and immune cell function remain unclear. Using whole exome sequencing analysis, we previously identified MDS-related mutations within monocyte-derived dendritic cells (moDCs) from patients with higher-risk MDS. Here we examine the effect of 5-Aza on the phenotype of moDCs from the same cohort of patients with higher-risk MDS.

Methods Purified CD14⁺ cells were magnetically isolated from peripheral blood mononuclear cells from 6 patients with IPSS-R Intermediate/High/Very High-risk MDS (herein collectively referred to as higher-risk MDS). Cells were cultured in complete medium with IL-4 (800 U/mL) and GM-CSF (1200 U/mL) for 5 days. Freshly prepared 5-Aza or dimethylsulfoxide (DMSO) vehicle was added to cultures every 24 hours for a total of three 1 μ M doses starting on Day 1. Immature moDCs were then stimulated with poly(I:C) (20 ng/mL), IL-1 β (25 ng/mL), IFN- α (3000 U/mL), IFN- γ (1000 U/mL), and TNF- α (50 ng/mL) for 48 hours to generate moDCs. Flow cytometry analyses were performed with Guava easyCyte 8HT before and after addition of maturation cocktail.

Results Based on trypan blue staining, *in vitro* addition of 5-Aza to CD14⁺ cells from 6 patients with higher-risk MDS did not result in a significant reduction in the percentage of cell survival on Day 5 and Day 7 in culture (figure 1a, $p=0.8765$ and $p=0.7109$, respectively). Treatment with 5-Aza significantly reduced the percentage of CD14-CD209⁺ moDCs on Day 7 following the addition of maturation cocktail (figure 1b, $p<0.0001$). Flow cytometry assessment showed comparable expression of common maturation and co-stimulatory markers such as CD80, CD83, CD86, HLA-DR, CD209, CD141, CD40, and CCR7 between 5-Aza and DMSO-treated immature moDCs on Day 5 (figure 1c). Similarly, 5-Aza treatment had no significant effect on marker expression on mature moDCs generated with maturation cocktail on Day 7.

Conclusions There was no significant difference in maturation and co-stimulatory marker expression of immature and mature moDCs from patients with higher-risk MDS following *in vitro* treatment with 5-Aza. Though recent studies have identified important immunoregulatory effects of 5-Aza, functional changes that may occur within the dendritic cell population are not fully understood. Further studies are planned, including cytokine analyses and transcriptome sequencing of mature moDCs, and may help elucidate the immunological mechanisms underlying the therapeutic effects of 5-Aza in patients with higher-risk MDS.

Ethics Approval The study is being conducted as per the Declaration of Helsinki and was approved by the University of California San Diego Institutional Review Board (#161345) and registered with ClinicalTrials.gov (NCT02667093). All patients were provided written informed consent.



Abstract 684 Figure 1 5-Aza and DMSO vehicle-treated moDCs from patients with higher-risk MDS were evaluated for phenotypic markers before and after stimulation with maturation cocktail. Purified CD14⁺ cells were magnetically isolated from PBMC from 6 higher-risk MDS patients and cultured with IL-4 and GM-CSF for 5 days followed by addition of poly(I:C), IL-1 β , IFN- α , IFN- γ , and TNF- α for 48 hours at 37°C in a 5% CO₂ incubator. Freshly prepared 5-Aza or DMSO vehicle was added to cultures every 24 hours for a total of three 1 μ M doses starting on Day 1. (A) Cultured cells were stained with trypan blue to determine the percentage of cell survival on Day 5 and Day 7 in culture. (B) Treatment with 5-Aza significantly reduced the percentage of CD14-CD209⁺ moDCs on Day 7 following addition of maturation cocktail ($p<0.0001$). (C) The percentage of CD14-CD83⁺ cells is comparable between 5-Aza and vehicle-treated immature moDCs on Day 5 and mature moDCs on Day 7 ($p=0.2434$ and $p=0.5846$, respectively). (D) Cultured cells were stained with fluorochrome-conjugated antibodies to determine the expression of common maturation and co-stimulatory markers using flow cytometry. Cells were gated on CD14-CD11c⁺ to distinguish moDCs, and scatterplots represent the geometric mean fluorescence intensity (gMFI) of marker expression pre- and post-maturation. Individual dots represent one of three experimental replicates performed for the 6 higher-risk MDS patient samples. Each dot is labeled by MDS patient sample. Statistical analysis was performed by Welch's t-test using GraphPad Prism.

<http://dx.doi.org/10.1136/jitc-2021-SITC2021.684>

CHARACTERIZATION OF MOLECULAR AND SPATIAL DIVERSITY OF MACROPHAGES IN HEPATOCELLULAR CARCINOMA

¹Pauline Hamon*, ¹Assaf Magen, ¹Joel Kim, ¹Mark Buckup, ¹Leanna Troncoso, ¹Steven Hamel, ¹Jessica Le Berichel, ²Oren Barboy, ²Eyal David, ¹Alexandra Tabachnikova, ¹Christie Chang, ¹Zhen Zhao, ²Merav Cohen, ²Amir Giladi, ¹Nausicaa Malissen, ¹Fiona Desland, ²Ido Amit, ¹Ephraim Kenigsberg, ¹Myron Schwartz, ¹Thomas Marron, ¹Miriam Merad. ¹*Icahn School of Medicine at Mount Sinai, New York, NY, United States;* ²*Weizmann Institute of Science, Rehovot, Israel*

Background Hepatocellular carcinoma (HCC) has a dismal prognosis, and though checkpoint blocking antibodies have significantly improved patient outcome, many patients remain left out, highlighting the need to identify additional immune target to enhance therapeutic immunity. Macrophages (MF) are an abundant and heterogeneous population in the tumor microenvironment (TME), and are associated with a poor prognosis in multiple tumor types, including HCC, however, their molecular and functional diversity is still poorly understood.

Methods We analyzed the molecular and spatial organization patterns of immune cells within the TME and adjacent tissue of 26 resected HCC lesions using single-cell RNA sequencing and multiplex immunohistochemistry (IHC).

Results We found that Kupffer cells, the self-renewing tissue-resident macrophages in liver tissue, are lacking from the TME, which is dominated by monocyte-derived macrophages. ScRNAseq followed by high-resolution clustering identified distinct MF molecular programs within the monocyte-derived macrophage compartment. One MF subset expressed a shared signature with monocytes including FCN1, S100A8 and T cell activation genes like CXCL9 and IL32. Conversely, one subset of MF expressed FOLR2, SEPP1 and genes of the complement (C1Qs), a program shared with KC in the adjacent tissue, and include another intratumoral subset enriched for the expression of TREM2 and GPNMB. Guided by these results, we are developing an IHC antibody panel that allows to visualize distinct MF localization in the TME. Intratumoral MF interface with, and potentially regulate, the T cell compartment within the TME. We are analyzing HCC tumor lesions in our treatment-naïve cohort and in patients treated with neoadjuvant anti-PD-1 therapy (NCT03916627) to study colocalization and direct interaction of MF and T cells using physically-interacting cell sequencing (PICseq). This analysis enables us to identify MF with direct cell-cell contact with T cells, and our preliminary analysis demonstrates an enrichment in MF with an immunosuppressive phenotype. We are also using spatial transcriptomic to map molecular programs of MF in the TME, that we will corroborated with additional patients.

Conclusions Taken together, our data provide a new understanding of intratumoral MF diversity and highlight the presence of specific immunoregulatory MF programs unique to tumor lesions, with subsets of these MF found to be directly interacting with T cells, potentially modulating anti-tumor responsiveness. Our analysis of resected tumor from anti-PD-1 treated patients, will allow us to correlate MF programs, and direct T cell interaction, with clinical response, and will inform therapeutic trials targeting specific MF populations so as to improve clinical efficacy of cancer immunotherapy.

Trial Registration NCT03916627

Ethics Approval Samples of tumor and non-involved liver were obtained from surgical specimens of patients undergoing resection at Mount Sinai Hospital (New York, NY) after obtaining

informed consent in accordance with a protocol reviewed and approved by the Institutional Review Board at the Icahn School of Medicine at Mount Sinai (RUTH Human Subjects Electronic Submission System 18-00407 and 20-04150) and in collaboration with the Biorepository and Department of Pathology.

<http://dx.doi.org/10.1136/jitc-2021-SITC2021.685>

686

CHARACTERIZATION OF A NOVEL COMPOUND THAT INHIBITS PEROXYNITRITE GENERATION BY MYELOID DERIVED SUPPRESSOR CELLS

^{1,2}Gabriella Lapurga*, ²Steven Sun, ²Erick Carlson, ²Himanshu Savardekar, ²Kari Kendra, ²Blake Peterson, ²William Carson. ¹The Ohio State University Comprehensive Cancer Center, Chillicothe, OH, United States; ²The Ohio State University, Chillicothe, OH, United States

Background Myeloid-derived suppressor cells (MDSC) are immature immune cells that suppress immunity and mediate resistance to immune-based cancer therapies. MDSC exert their immunosuppressive effects partly through the production of reactive nitrogen and oxygen species, which combine to form peroxynitrite (PNT). PNT reacts with the tyrosine residues of key immune cell signaling proteins and inactivates them via nitration. Targeting MDSC via PNT inhibitors is an attractive avenue to improve the response to immunotherapy. The Peterson and Carson Labs have collaborated to develop a novel inhibitor of PNT and have explored its use in murine tumor models and human patients with cancer.

Methods Splenocytes (comprised of 12% MDSC) were isolated from mice bearing tumors derived from the EMT6 breast cancer cell line and cultured with 10 μ m beads labelled with polyclonal antibodies (immunoglobulin-G or IgG). Fluorescence emitted upon MDSC recognition and reaction with IgG was detected with a previously reported fluorescent sensor compound termed PS3. Cells were mixed with PS3 and IgG beads (or controls: IgG without beads and beads without IgG) and treated for 4 hours with the following agents: (1) BRP0112233, a novel biaryl furan discovered via high-throughput screening using PNT depletion as the readout (6 or 12 μ M); (2) Ibrutinib, an FDA-approved Bruton's tyrosine kinase inhibitor shown by the Carson Lab to inhibit the activity of nitric oxide synthase in MDSC, (2, 10 μ M); and (3) PBS control. Fluorescence produced by reaction of PS3 with PNT was measured in triplicate wells using a Clariostar plate reader.

Results Splenocytes from tumor-bearing mice produced significantly greater levels of PNT than normal splenocytes (24-fold vs 8-fold increase over plain beads, $p < 0.0001$). Differences in fluorescence were confirmed via confocal microscopy. BRP0112233 inhibited PNT levels by 40% and 85% for the 6 and 12 μ M doses, respectively. Ibrutinib inhibited PNT output by 90% and 100% at 2 and 10 μ M. Cell viability was $>90\%$ except for the higher BRP dose (60% viability). In humans, peripheral blood mononuclear cells (PBMC) isolated from patients with cancer produced more PNT than healthy donor PBMC.

Conclusions PNT output could be reproducibly quantified via this assay and BRP0112233 and ibrutinib greatly inhibited MDSC PNT production. Using the EMT6 model, these compounds are being tested in combination with anti-PD-1 antibodies approved for patients with cancer. This assay has shown similar results in human peripheral blood mononuclear cells isolated from patients with cancer.

Acknowledgements We thank the NIH (NCI UM1 CA186712, R01CA211720), a OSUCCC Translational Therapeutics Seed Grant, and the Pelotonia Fellowship Program for financial support.

<http://dx.doi.org/10.1136/jitc-2021-SITC2021.686>

MDSC GENE EXPRESSION ANALYSIS IN PATIENTS WITH CANCER AND THE RESPONSE TO INHIBITION OF BRUTON'S TYROSINE KINASE

<http://dx.doi.org/10.1136/jitc-2021-SITC2021.687>

Himanshu Savardekar*, Carter Allen, Dionisia Quiroga, Donjun Chung, Emily Schwarz, Gabriella Lapurga, Jami Shaffer, Bradley Blaser, Matthew Old, Robert Wesolowski, Kari Kendra, William Carson. *The Ohio State University, Dublin, OH, United States*

Background Myeloid-derived suppressor cells (MDSC) are an immunosuppressive immature population of myeloid cells that are elevated in cancer patients. Increased levels of MDSC has been linked to dysregulated anti-tumor responses and reduced efficacy of immune checkpoint therapies thus making them an attractive target. MDSC express Bruton's tyrosine kinase (BTK) and can be depleted using ibrutinib, an FDA-approved irreversible inhibitor of BTK. BTK inhibition leads to reduced MDSC expansion/function in murine models and significantly improved activity of anti-PD-1 antibodies. In this study, single cell RNA-seq (scRNA-seq) was used to characterize the gene expression of MDSC from different cancer types and the effect of ibrutinib on MDSC gene expression.

Methods Peripheral blood mononuclear cells were isolated from patients with melanoma (n=2), head & neck (n=1), and breast cancer (n=1). MDSC were isolated via fluorescence activated cell sorting. MDSC isolated from melanoma patients (n=2) were treated in vitro for 4h with 1 uM ibrutinib or DMSO and scRNA-seq was performed using the Chromium 10x Genomics platform. ScRNA-seq samples were analyzed using the standard integrative workflow of Seurat v3, which addresses the sample heterogeneity. Cell clusters were identified using Seurat and annotated using SingleRversion3.12. Identification of gene markers for each cell cluster and cell-cluster-specific differential expression analyses were conducted using Seurat.

Results Baseline gene expression of MDSC from patients with breast and head & neck cancer revealed similarities among the top expressed genes (S100A8, VCAN, and LYZ). In vitro ibrutinib treatment of MDSC from patients with melanoma resulted in significant changes in gene expression within the MDSC cluster compared to DMSO treatment. GBP1(-1.72 log fold change), IL 1 β (-1.27 log fold change), and CXCL8(-0.63 log fold change) were among the top downregulated genes (p<0.001) and RGS2 (0.68 log fold change) and ABHD5(0.52 log fold change) were among the top upregulated genes (p<0.001). MDSC subset (PMN-MDSC, M-MDSC, early-MDSC, and CD14+/CD15+ double positive) gene expression changes mirrored total MDSC gene changes. Ingenuity pathway analysis revealed significant downregulated pathways including TREM1 (p<0.001), nitric oxide signaling (p<0.003), and IL-6 signaling (p<0.004). Multiple genes associated with cellular movement (CXCL8, CXCL10) and activation of macrophages (CXCL10, CCL3) were downregulated (p<0.001). PCR analysis on isolated melanoma MDSC (n=2) treated in vitro with ibrutinib verified downregulation of CXCL8 (0.42 fold decrease, p<0.05) and CXCL10 (0.40 fold decrease, p<0.001).

Conclusions Analysis via scRNA-seq revealed similar gene expression patterns for MDSC from different cancer patients. There was downregulation of multiple genes and pathways important to MDSC function and migration after BTK inhibition.

Ethics Approval The study obtained ethics approval.

IRB# 1999C0348

KNOCKOUT OF THE INHIBITORY RECEPTOR TIGIT ENHANCES ANTI-TUMOR RESPONSE OF EX VIVO EXPANDED NK CELLS

Taylor Croom-Perez*, Md Faqru Hasan, Thomas Dieffenthaler, Liza Robles-Carrillo, Jonathan Eloriaga, Alicja Copik. *University of Central Florida, Orlando, FL, United States*

Background Natural Killer (NK) cells are an important immune cell population crucial for the success of many immunotherapies due to their critical role in both the innate response and in priming an adaptive immune response. Recently, much focus has been on generating highly cytotoxic NK cells for use in adoptive cell therapy and combinatorial immune-oncology therapies. The robust cytotoxicity against cancer cells and NK cell activation relies on fine tuning of activating and inhibitory signals. NK cell inhibitory receptors are often upregulated upon stimulation and activation and can be a marker for exhaustion. One of the major NK inhibitory receptors, T-cell immunoglobulin and ITIM domain (TIGIT), is highly expressed in ex vivo expanded NK cells. In this study, we will investigate if knockout of TIGIT in ex vivo expanded NK cells will enhance their anti-tumor activity.

Methods CRISPR was used to make a targeted TIGIT knockout (KO) in ex vivo expanded NK cells. TIGIT KO NK cells were then compared to wild type NK cells to determine any changes in phenotypic markers. IFN γ , TNF α , and the degranulation marker CD107a expression were analyzed after co-culture with cancer cells. Cytotoxicity of TIGIT KO NK cells was compared to wild type NK cells against multiple different cancer cell spheroids using a kinetic live-cell imaging assay. Multiple NK cell:target cell ratios were analyzed over time to determine killing half-time and maximum killing. Data were fit to dose-response curves to determine cytotoxicity EC50 values.

Results CRISPR was used to efficiently knockout TIGIT in ex vivo expanded NK cells and decreased expression levels to less than 5%. After co-culture with Raji cells expressing the TIGIT ligand PVR (CD155), TIGIT KO NK cells showed increased expression of IFN γ , TNF α and CD107a. TIGIT KO NK cells showed improved killing compared to wild type NK cells. TIGIT KO cells killed more target cells faster with significant decreases in half-killing time and more than a 2-fold decrease in EC50 cytotoxicity values in 3D spheroid cytotoxicity models against six different cancer cell lines. When NK cell:target cell ratios were low, the maximum cytotoxicity was also significantly higher in TIGIT KO cells.

Conclusions Knockout of the TIGIT gene in ex vivo expanded NK cells resulted in higher functioning NK cells with increased cytokine expression, degranulation, and cytotoxicity against multiple cancer cell lines. These TIGIT knockout NK cells with improved antitumor activity provide a promising universal effector population with the potential for enhanced therapeutic efficacy.

Acknowledgements We thank FL DOH Grant #9JK04 for funding and MaxCyte for providing instrument for testing.

<http://dx.doi.org/10.1136/jitc-2021-SITC2021.688>

Zerick Dunbar*, Anil Shanker. *Meharry Medical College, Nashville, TN, United States*

Background Natural killer (NK) cells play significant roles in cancer immunity largely due to their direct cytolytic and indirect immune regulatory functions. Clinical studies have demonstrated the role of NK cells in controlling cancer. The number of infiltrating NK cells in tumor tissues has also been shown to be a significant relation to cancer prognosis. However, NK cells have yet to be fully harnessed in immunotherapy partially due to the extensive heterogeneity and plasticity seen among them. For example, the origin, phenotype, and functions of tissue-resident vs circulating NK cells remains controversial. The objective of this study is to elucidate NK cell activation and effector function diversity in solid lung and breast tumor microenvironments. We hypothesize that NK cells from different tissue locations display unique genetic and functional profiles that can predict NK effectiveness in these solid tumor microenvironments. Here, we show the biological diversity that exists among NK cells from distinct locations plus and minus interaction with solid lung and breast murine tumors.

Methods We include the heterogeneity of NK cell specific cluster of differentiation markers and gene expression perspectives based on flow cytometry, qPCR, cytotoxicity, and bioinformatics analyses in conjunction with C57BL/6 \pm LL/2 and BALB/c \pm 4T1.2-HA mouse tumor models, respectively.

Results Thus far we see significant varied expression of the activating and costimulatory NKG2D receptor both across tissue locations and in response to these solid tumors in vivo and ex vivo. We also see varied cytotoxicity and tumor infiltration of NK cells from different tissue locations.

Conclusions Understanding NK cells in solid tumor microenvironments will help answer critical NK cell research questions and lead to advancements in NK-based cancer immunotherapy applications, ultimately helping to mitigate discrepancies between resources applied towards cancer treatment and patient outcomes.

Acknowledgements This work was supported by the NIH RISE grant R25 GM059994.

<http://dx.doi.org/10.1136/jitc-2021-SITC2021.689>

**690 TIGIT BLOCKADE IMPROVES ANTI-TUMOR ACTIVITY OF
EX VIVO EXPANDED NK CELLS**

Md Faqrul Hasan*, Alicja Copik. *University of Central Florida, Orlando, FL, United States*

Background Natural killer (NK) cells are innate immune cells that directly kill and coordinate responses against cancer prompting interest in using *ex vivo* expanded NK cells as an adoptive cell therapy for treatment of cancer. NK cells express a set of activating and inhibitory receptors that regulate their activity. Inhibitory receptor TIGIT (T cell Immunoreceptor with Ig and ITIM domain) is upregulated on intratumoral NK cells in some cancers, inhibits NK cell activity and promotes NK cell exhaustion. In this study, the effect of TIGIT blockade on the anti-tumor activities of *ex vivo* expanded NK cells was evaluated.

Methods NK cells were activated overnight with cytokines or *ex vivo* expanded with PM21-particles. Their TIGIT expression was determined with qRT-PCR and flow cytometry. Cytotoxicity was assessed by kinetic, imaging-based assay (Incucyte S3) against A549 and NCI-H1299 cells cultured in 3D. Cytotoxicity was calculated based on untreated controls at different time-points. Results from multiple donors were normalized to cytotoxicity of NK cells with isotype for individual donors and was compared to the cytotoxicity of NK cells with anti-TIGIT. Unpaired t test was used to determine statistical significance. K562 cells stably expressing Polio Virus Receptor (PVR), were used to restimulate A549 spheroid-exposed NK cells to measure IFN γ , TNF α and degranulation. Furthermore, phenotypic changes of NK cells upon TIGIT blockade were examined by analyzing a set of activating and inhibitory receptors by flow cytometry.

Results The effect of NK cell expansion/activation on TIGIT expression was assessed. TIGIT was upregulated on expanded and cytokine-activated NK cells both on mRNA and protein level. The effect of TIGIT blockade on NK cell cytotoxicity was examined by co-culturing PM21-NK cells with cancer cells in the presence of anti-TIGIT antibodies or respective isotypes. TIGIT blockade significantly increased cytotoxicity of PM21-NK cells against A549 (1.3 fold, $P < 0.0001$) and NCI-H1299 (1.3 fold, $P = 0.0003$) spheroids after 48 h. To assess exhaustion, NK cells exposed to A549 spheroids for 7 days were restimulated with PVR⁺ K562 cells. TIGIT blockade prevented NK cell exhaustion resulting in increased expression of IFN γ , TNF α and surface CD107a on restimulated NK cells. TIGIT blockade did not result in changes to the surface phenotype of NK cells.

Conclusions TIGIT was highly expressed on expanded and cytokine-activated NK cells. TIGIT blockade improved anti-tumor activities of PM21-NK cells. Thus, PM21-NK cells and TIGIT antibodies have translational potential as a combination therapy to improve anti-tumor response.

<http://dx.doi.org/10.1136/jitc-2021-SITC2021.690>

691

IDENTIFICATION OF SHARED TUMOR EPITOPES FROM ENDOGENOUS RETROVIRUSES INDUCING HIGH AVIDITY CYTOTOXIC T CELLS FOR CANCER IMMUNOTHERAPY

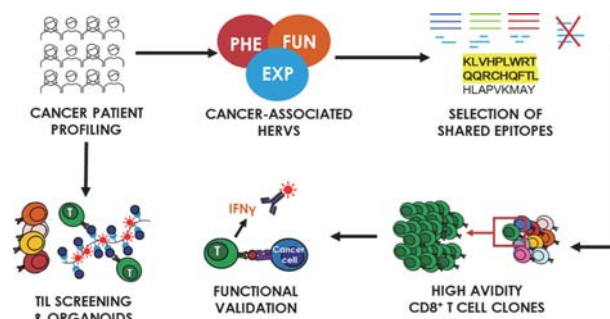
¹Paola Bonaventura*, ²Vincent Alcazer, ¹Virginie Mutez, ³Laurie Tonon, ⁴Juliette Martin, ¹Nicolas Chuvin, ¹Rasha Boulos, ¹Yann Estornes, ²Jenny Valladeau-Guilemond, ³Alain Viari, ²Christophe Caux, ¹Stephane Depil. ¹*ErVaccine technologies, Lyon, France*; ²*Centre de Recherche en Cancerologie Lyon, Lyon, France*; ³*Synergie Lyon Cancer, Lyon, France*; ⁴*CNRS, Lyon, France*

Background Human endogenous retroviruses (HERVs) are aberrantly expressed by tumor cells and may represent a source of T cell epitopes

Methods Using TCGA pancancer RNAseq data (n=8,893 samples), we developed a bioinformatics-based method to select cancer-specific HERVs associated with a cytotoxic T cell response (“cyt-HERVs”) and identify shared T cell epitope candidates. T cells were primed with selected short and long peptide candidates from HLA-A2+ healthy donors. Peptide-specific dextramers were used to sort and expand specific CD8+ T cell clones and determine their TCR sequences and avidity. Cytotoxicity was assessed against HERV-expressing tumor cell lines and patient-derived organoids using Incucyte and Nanolive technologies (Flowchart, figure 1).

Results In a pancancer analysis, we identified 57 HML-2/HERV-K HLA-A*0201 epitope candidates from 27 distinct open reading frames. Six shared HLA-A2 strong binders 9-mer peptides, present on multiple HERVs located on different chromosomes, and with translational evidence found in mass spectrometry public datasets, were selected and synthesized. In vitro HLA binding assay confirmed peptide-HLA affinity. Priming assays showed the presence of specific CD8+ T cells leading to polyfunctional IFN- γ + TNF- α + T cell responses with upregulation of the degranulation marker CD107A upon co-culture with peptide-pulsed T2 cells. Synthetic long peptides containing the epitopes were used to confirm the correct processing by antigen-presenting cells. The functionality of the sorted T cell clones was confirmed using an Elispot assay (GrzB+ IFN- γ +). Their sequenced TCRs were predicted to stably interact with their respective MHC-peptide complexes in a 3D model. This was confirmed by measurement of the functional avidity, which was in the same order as CMV-specific T cell clones. HERV-specific CD8+ T cells induced specific cell death of HLA-A2+ cancer cell lines, associated with IFN- γ production, in a HLA-A2 restricted manner. Finally, pre-existing HERV-specific CD8+ T cells were identified using dextramers among tumor infiltrating lymphocytes (TILs) from cancer patients. HERV-specific T cells co-cultured with patient derived organoids showed signs of activation with lysis of the organoid.

Conclusions Our bioinformatics-based approach allowed us to identify shared HERV-derived CD8+ T cell epitopes specifically expressed by tumor cells and inducing high avidity T cell clones able to kill tumor cells in a class I-restricted manner. The detection of TILs recognizing HERV peptides suggests natural presentation of these epitopes in the tumors. These HERV-derived epitopes may thus represent relevant targets for the development of new cancer vaccines or T cell-based therapies, especially in tumors with low mutational burden.



Abstract 691 Figure 1 Graphical flowchart of HERV antigen validation. Graphical representation of the flowchart used to identify and validate specific CD8+ T cells for shared tumor epitopes from endogenous retroviruses <http://dx.doi.org/10.1136/jitc-2021-SITC2021.691>

<http://dx.doi.org/10.1136/jitc-2021-SITC2021.691>

692

TIM-3 EXPRESSION DRIVES PHENOTYPIC AND FUNCTIONAL CHANGES IN TREG IN SECONDARY LYMPHOID ORGANS AND THE TUMOR MICROENVIRONMENT, EFFECTING TUMOR BURDEN

¹Hridesh Banerjee*, ²Hector Nieves-Rosado, ¹Benjamin Murter, ¹Lawrence Kane. ¹University of Pittsburgh, Pittsburgh, PA, United States; ²UPMC, Pittsburgh, PA, United States

Background Regulatory T cells (T reg) are critical mediators of self-tolerance but can also limit effective anti-tumor immunity. We and others previously reported that 40–60% percent of T reg-infiltrating head and neck cancer (HNC) and other tumors highly express Tim-3, compared with about 5% in lymphoid organs, it therefore gets imperative to characterize if Tim-3 is driving any T reg specific function in tumor microenvironment and under homeostasis.

Methods Using a conditional TIM-3 inducible and knockout mouse model developed in our lab, we have performed syngeneic tumor challenges in T reg-specific Tim-3 transgenic and knockout mice (FoxP3ERT2CreSFS-Tim-3 and FoxP3ERT2Cre-FLEX4). We have also characterized the tumor immune infiltrate of these mice to understand the impact of T reg specific Tim-3 induction and deficiency on the immune landscape.

Results Tim-3 induction on T reg leads to rapid growth associated with higher progression of CD8 compartment towards exhaustion, while Tim-3 knockout in T reg specific manner leads to overall decline in T reg compartment in tumors associated with lower exhaustion in the CD8 compartment and decrease in tumor burden,

Conclusions Tumor-infiltrating Tim-3+ Treg have enhanced suppressive function and display a more effector-like phenotype. Using a novel mouse model with cell type-specific Tim-3 expression, we show here that expression of Tim-3 by Treg is sufficient to drive Treg to a more effector-like phenotype, and increases suppressive activity, effector T cell exhaustion and tumor growth. We also show that inducible deletion of Tim-3 specifically from Treg enhances anti-tumor immunity and decrease in tumor burden along with a decrease in tumor associated Treg compartment. These findings may help to reconcile previous reports that some Tim-3 antibodies enhance T cell responses in vivo, while expression of Tim-3 has a cell-intrinsic ability to enhance TCR signaling and T cell activation. A major role of Tim-3 was found to be mediated through IL-10 and IL-10 R pathway in both Treg and CD8 compartment. Thus, we propose that Tim-3 regulates anti-tumor immunity at least in part through enhancement of Treg function. To our knowledge, this is the first example in which expression of a single co-stimulatory molecule is sufficient to drive differentiation of Treg in this manner.

Acknowledgements We acknowledge Dr. Robert L. Ferris and Dr. Greg M. Delgoffe for their inputs and guidance with human and metabolism associated experiments.

<http://dx.doi.org/10.1136/jitc-2021-SITC2021.692>

693

MUCOSAL-ASSOCIATED INVARIANT T (MAIT) CELL REGULATION NETWORKS IN ANTI-TUMOR IMMUNITY

¹Benjamin Ruf*, ²Vanessa Catania, ²Noemi Kedei, ²Simon Wabitsch, ²Chi Ma, ²Laurence Diggs, ²Qianfei Zhang, ²Bernd Heinrich, ²Varun Subramanyam, ²Linda Cui, ²Shunsuke Sakai, ²Sangmi Oh, ³Merrill Stovroff, ²Clifton Barry III, ²Daniel Barber, ³Alexander Kroemer, ²Firouzeh Korangy, ²Tim Greten. ¹National Institutes of Health (NIH), Bethesda, MD, United States; ²NIH, Bethesda, MD, United States; ³Georgetown University Medical Center, Washington, DC, United States

Background MAIT cells are MR1-restricted innate-like T cells that recognize non-peptide antigens including riboflavin derivatives. They account for up to 10 % of circulating T cells, but they are further enriched at mucosal sites and the liver. On one hand, altered MAIT number and function have been reported in liver cancer with MAITs correlating with poor clinical outcome. On the other hand, we recently demonstrated that MAIT cells can potentially have anti-tumor activity suggesting them as a novel target for cancer immunotherapy. Yet, the cellular and humoral factors that determine MAIT cell fate in the context of malignancies remain largely unknown.

Methods Highly multiplexed immunofluorescence-based CODEX imaging and high-dimensional flow cytometry was used to analyze MAIT cell infiltration and phenotype in human HCC samples. We recently developed an experimental framework to manipulate MAIT cells in vivo using VitaminB2 synthesis pathway-derived antigen 5-(2-oxopropylideneamino)-6-D-ribitylaminouracil (5-OP-RU) in combination with Toll-like receptor 9 agonist CpG. Next, we used murine models of orthotopic primary liver cancer and liver metastasis across two different mouse strains, to assess anti-tumor activity of MAIT cells. A series of pharmacological depletion experiments and genomic knockout mouse strains were used to identify additional effector immune cells and humoral factors mediating the anti-tumor effect.

Results Using flow cytometry and spatially resolved analysis of multiplexed CODEX microscopy images, we found impaired infiltration and altered phenotype of MAIT cells in human HCC tumors compared to unaffected liver tissue. Thus, we sought out to experimentally increase MAIT cell infiltration into liver cancers using murine models. Co-administration of 5-OP-RU + CpG induced a strong systemic in vivo expansion and activation of MAIT cells with Th1/NK-like polarization. We found MAIT cells to be potent orchestrators of anti-tumor function in vivo when activated by a combination of 5-OP-RU + CpG. MAIT-directed 5-OP-RU/CpG showed pronounced and consistent anti-tumor activity against different models of liver cancer and prolonged mouse survival. Importantly, such tumor inhibition was absent in MAIT-deficient MR1 k.o. mice but nor dependent on MR1 expression on tumor cells. Additional pharmacological depletion studies/genomic k.o. models helped to identify antigen presenting cells, downstream effector cells as well as co-stimulatory cytokines as critical components needed for MAIT-induced tumor suppression.

Conclusions MAIT cells are important players in cancer immunology and represent an attractive novel target for cancer immunotherapy. Fine-tuned, context-dependent mechanisms determine MAIT-cell fate in vivo as they undergo a phenotypic switch upon 5-OP-RU and CpG treatment enabling them to exert potent anti-tumor function.

<http://dx.doi.org/10.1136/jitc-2021-SITC2021.693>

Immune-Stimulants and Immune Modulators

694

POSSIBLE IMMUNE-MODULATION OF CDK4/6 INHIBITORS AND CLINICAL TRIAL DEVELOPMENT IN BETEL-NUTS RELATED HEAD AND NECK SQUAMOUS CELL CARCINOMA IN TAIWAN

¹Jo-Pai Chen*, ²Jui-Ying Chang, ³Hsiang-Fong Kao, ³Ruey-Long Hong. ¹National Taiwan University Hospital, Yun-lin Branch, Yun-lin, Taiwan, Province of China; ²National Taiwan University Hospital, Yun-lin, Taiwan, Province of China; ³National Taiwan University Hospital, Taipei, Taiwan, Province of China

Background Betel nuts in Taiwan might contribute to strong angiogenesis & invasion with resistance to traditional therapies. In our research, betel-nuts exposed HNSCC cell line, TW2.6, had high PDL1, defective p53 mutation, p16 loss, and BCL2 overexpression. PI3K/AKT/mTOR inhibitors, anti-angiogenesis therapies, CDK4/6 inhibitors, DDR interventions, and immunotherapy-containing regimens will be future backbones and reverse treatment refractoriness(AACR-AHNS2017). The genomic signature of TW2.6 has been figured out (AACR2020) mainly with PIK3CA H1047R mutation, high TMB(8.42 muts /Mb)/MSS, p53/MYC/HRAS/DDR2/PDGFRbeta/ EPHB1/ATM mutations, FAT1 loss, amplification of VEGF-A/TERT/ FGF10/CCND3/SOX9/IL-7R/SDHA/RIC-TOR/FLCN, CDK12 loss of function, and deletions of STK11/ARID1B/MITF/TNFAIP3. CDK4/6 inhibitor was effective in HPV-negative and pRB-positive HNSCC and had strong immuno-modulation(suppress Treg, increase CTLs, enhance MHC I/II upregulation and antigen presentation). Palbociclib was effective on TW2.6 and could resensitize TW2.6 to docetaxel, afatinib, & radiation & enhance further response to BYL719& foretinib(VEGFR2/c-MET/Axl triple inhibitor). Western blotting showed (1) Slug, Snail, N-cadherin, Twist, Vimentin, Claudin-1, Axl, p-Akt and p70S6K decrease; (2) BMI-1, pRB, and PDL1 drop(ASCO218).

Methods SCC4, SCC9, SCC15, SCC25, FaDu, KB, Cal27, SAS, and TW2.6 for (1)in vitro sensitivity to palbociclib, ribociclib, abemaciclib; (2)synergistic effects with other therapies by MTT assay, colony formation assay, and western blotting. NGS studies were used to study molecular biomarkers of CDK4/6 inhibitors efficacy.

Results Palbociclib had greatest efficacy over SCC15(classical HPV-negative type with EGFR overexpression) followed by SCC25, SAS, TW2.6(HPV-negative EMT type), & CAL27; but little efficacy over KB. In HPV-positive cell lines, palbociclib had (1) promising response on SCC25(classical HPV+ type); (2) little response on FaDu(HPV+ mesenchymal type) & KB (basal type in TCGA). In other HNSCC cell lines with basal types, however, SAS & CAL27 responded well to palbociclib. Palbociclib response seemed to correlate to CCND1 gain and CDKN2A deletion; but FaDu had not so good palbociclib response with these two changes and TW2.6 had good response even without these two. TW2.6 was most sensitive to palbociclib, moderately sensitive to ribociclib, and mildly sensitive to abemaciclib.

Conclusions TW2.6 is responsive to CDK4/6 inhibitor(palbociclib>ribociclib>abemaciclib). FAT1 loss, CCND1/3 overt amplification, PI3K/AKT/mTOR derangements, and FGFR amplification might confer CDK4/6 inhibitor resistance in our genomic study. Based on immuno-modulatory effects of CDK4/6 inhibitor, we have initiated a study using ribociclib with spartalizumab in R/M HNSCC(RISE-HN: NCT04213404). We might develop a ctDNA-driven(intact

PTEN & FAT1, CDKN2A deletion, high CDK4/6 copy numbers, no CCND1/3 overt amplification or FGFR amplification or other PI3K/AKT/mTOR derangements) clinical trial with palbociclib and avelumab in betel-nuts related R/M HNSCC in Taiwan. Abemaciclib may have better immune-modulation.

<http://dx.doi.org/10.1136/jitc-2021-SITC2021.694>

695

COMBINATION OF CLICK CHEMISTRY-BASED SQ3370 WITH IMMUNOTHERAPIES ENHANCES ANTITUMOR EFFECT IN MURINE TUMORS WITH MINIMIZED SYSTEMIC TOXICITY

Amir Mahmoodi*, Sangeetha Srinivasan, Michael Zakharian, Nathan Yee, Jesse McFarland, Jose Mejia Oneto. *Shasqi, Inc., San Francisco, CA, United States*

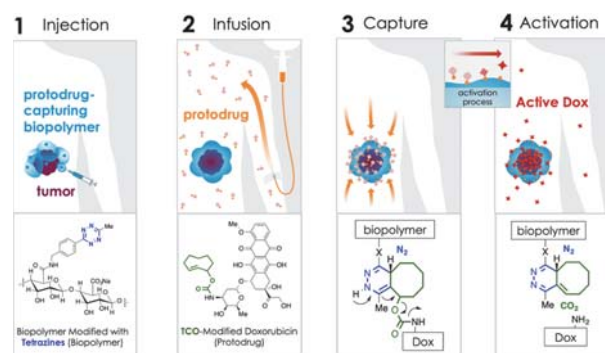
Background Immunotherapies have enabled unprecedented durable responses in solid tumors. However, they benefit only a subset of patients and have varying response rates across tumor types. Conversely, conventional chemotherapies are effective in a larger patient population, but lack specificity and result in severe dose-limiting systemic toxicities. While anthracyclines such as doxorubicin (Dox) may provide added benefit by inducing anti-tumor immune activation,¹ their overall effect is limited by cumulative dose cardiotoxicity.² Here, we present the Click Activated Protodrugs Against Cancer (CAPAC) platform that activates cytotoxic protodrugs at the tumor using click chemistry. The CAPAC platform is agnostic to tumor characteristics such as biomarker expression and can be applied in a variety of tumor types. SQ3370 (lead candidate of CAPAC) consists of an intratumorally-injected biopolymer that can activate multiple doses of a systemic protodrug to release active Dox at the tumor. SQ3370 enables a 19-fold increase over the conventional Dox dose in mice with minimal systemic toxicity.³ In tumor-bearing mice, SQ3370 improved overall survival, T-cell infiltration, and induced a robust anti-tumor response against both biopolymer-injected and non-injected lesions,⁴ suggesting that SQ3370 promotes anti-tumor immune activation. This makes SQ3370 an ideal candidate for combination approaches with immunotherapies.

Methods SQ3370 treatment is described in figure 1. Immunocompetent mice were inoculated with MC38 tumors. SQL70 was given intratumorally; SQP33 was given intravenously as five daily doses. Immune adjuvants such as toll-like receptor (TLR) agonists or STING agonist were coadministered with SQ3370. Saline and conventional Dox served as controls.

Results Combining SQ3370 with endosomal TLR agonists such as poly I:C (TLR3a), imiquimod (TLR7a) or CpG ODN (TLR9a) resulted in improved tumor growth inhibition and survival in MC38 tumor-bearing mice compared with monotherapy. Combination with STING agonist, ADU-S100, also enhanced antitumor efficacy. Body weight data suggests minimal impact of the monotherapy or combination therapy on systemic toxicity.

Conclusions CAPAC represents a new therapeutic modality to treat solid tumors by expanding the pharmacological capabilities of cancer drugs with known efficacy and experimental drugs. SQ3370, CAPAC's lead candidate, improves safety and efficacy as compared to conventional Dox, and combination of SQ3370 with immunotherapy shows enhanced benefit. SQ3370 is being evaluated in a Phase I study in advanced solid tumors (NCT04106492).

Acknowledgements This work was supported by Shasqi and the National Institutes of Health.



Abstract 695 Figure 1 Illustration and Molecular Description of SQ3370. SQ3370 consists of 2 components and utilizes Shasqi's proprietary click chemistry-based CAPAC platform. First, SQL70, a tetrazine-modified sodium hyaluronate biopolymer, is injected at the tumor site. Then, SQP33, a trans-cyclooctene (TCO)-modified protodrug of doxorubicin (Dox), is given systemically as 5 daily doses. SQP33 protodrug has attenuated toxicity and is converted to active Dox by SQL70 biopolymer through an efficient covalent reaction between tetrazine and TCO moieties

REFERENCES

- Mattarollo SR, Loi S, Duret H, Ma Y, Zitvogel L, Smyth MJ. Pivotal role of innate and adaptive immunity in anthracycline chemotherapy of established tumors. *Cancer Res* 2011;**71**:4809–20.
- Quintana RA, Banchs J, Gupta R, Lin HY, Raj SD, Conley A, Ravi V, Araujo D, Benjamin RS, Patel S, Vadhan-Raj S. Early evidence of cardiotoxicity and tumor response in patients with sarcomas after high cumulative dose doxorubicin given as a continuous infusion. *Sarcoma* 2017;7495914.
- Wu K, Yee NA, Srinivasan S, Mahmoodi A, Zakharian M, Oneto JM, Royzen M. Click activated protodrugs against cancer increase the therapeutic potential of chemotherapy through local capture and activation. *Chem Sci* 2021;**12**:1259–71.
- Srinivasan S, Yee NA, Wu K, Zakharian M, Mahmoodi A, Royzen M, Mejia Oneto JM. SQ3370 activates cytotoxic drug via click chemistry at tumor and elicits sustained responses in injected and non-injected lesions. *Adv Ther* 2021;**4**:2000243.

Ethics Approval This study, project number: SSQ-FFS-ON-20210225-01V3_1, was approved by the Institutional Animal Care and Use Committee (IACUC) of the vendor, following the guidance of Association for Assessment and Accreditation of Laboratory Animal Care (AAALAC), accreditation number 001516.

<http://dx.doi.org/10.1136/jitc-2021-SITC2021.695>

SINGLE-CELL RNA-SEQ REVEALS THE CRITICAL ROLES OF THE STING- AND MDA5-MEDIATED CYTOSOLIC NUCLEIC ACID-SENSING PATHWAYS AS WELL AS IFNAR/STAT2 SIGNALING IN RECOMBINANT MVA-INDUCED ANTITUMOR IMMUNITY

¹Shuaitong Liu*, ¹Gregory Mazo, ²Tuo Zhang, ¹Ning Yang, ¹Yi Wang, ²Adrian Tan, ³Jiahui Wang, ⁴John Choi, ²Jenny Zhaoying Xiang, ¹Taha Merghoub, ¹Jedd Wolchok, ¹Liang Deng. ¹Memorial Sloan Kettering Cancer Center, New York, NY, United States; ²Weill Cornell Medical College, New York, NY, United States; ³Genvira Biosciences, Ottawa, Canada; ⁴IMVAQ Therapeutics, New York, NY, United States

Background Oncolytic viruses are promising therapeutic agents for advanced cancers because of their ability to induce antitumor innate and adaptive immunity. Modified vaccinia virus Ankara (MVA) is an attenuated, replication-deficient poxvirus safe for human use, making it a favorable platform for cancer immunotherapy. Previously we discovered the E5R gene in MVA encodes an inhibitor of the cGAS/STING-mediated cytosolic DNA-sensing pathway. The engineered MVA deleting the E5R gene and expressing a dendritic cell (DC) growth factor Flt3L together with a T cell co-stimulator OX40L generates strong antitumor immunity when delivered intratumorally. We also demonstrated that intratumoral (IT) injection of 1st generation rMVA promotes CD8+ activation in a cGAS/STING- and STAT1/STAT2-dependent manner and depletes the OX40hi regulatory T cells (Tregs) via OX40L/OX40 interaction and IFNAR signaling. The E3L gene from MVA encodes an inhibitor of the cytosolic dsRNA-sensing pathways. The purpose of this study is to investigate whether rMVAΔE3L, with the deletion of E3L from rMVA (MVAΔE5R-hFlt3L-mOX40L), further improves its antitumor effects. We also focused on utilizing single-cell RNA-seq (scRNA-seq) to investigate the alteration of the immunosuppressive tumor microenvironment by IT delivery of rMVAΔE3L.

Methods We engineered rMVAΔE3L by deleting the E3L gene from rMVA. We investigated the innate immune responses of bone marrow-derived DCs (BMDCs) and tumor cell lines to rMVAΔE3L and rMVA. We also compared the antitumor efficacy of the two viruses in murine B16-F10 melanoma and MC38 colon cancer models. In addition, we performed scRNA-seq of sorted tumor-infiltrating CD45+ immune cells from tumors harvested two days after IT injection with rMVAΔE3L or PBS in wild-type, MDA5/STING-, STAT2-, or IFNAR1-deficient mice.

Results Compared with rMVA, rMVAΔE3L more potently activates both the cGAS/STING- and MDA5/MAVS-mediated nucleic acid-sensing pathways in DCs and tumor cell lines. IT rMVAΔE3L generates stronger antitumor effects than rMVA. Our results showed that after rMVAΔE3L treatment, there was an influx of inflammatory monocytes into the tumors in WT mice, absent in STAT2 or IFNAR knockout mice. Evaluation of viral transcriptomes at a single-cell level revealed that macrophages and monocytes were more susceptible to rMVAΔE3L than other cell types. The transcriptomic changes on DC subsets are largely dependent on IFNAR/STAT2 signaling. By contrast, MDA5/STING-mediated pathway determines the transcriptome profile of inflammatory monocytes in response to rMVAΔE3L.

Conclusions Taken together, our results demonstrate that scRNA-seq is a powerful approach to interrogate the host immune responses to immunogenic viruses, which would guide future designs of more effective viral-based cancer immunotherapy.

Acknowledgements This work was supported that the Society of Memorial Sloan Kettering (MSK) research grant (L.D.), MSK Technology Development Fund (L.D.), Parker Institute for Cancer Immunotherapy Career Development Award (L.D.), sponsored research award from IMVAQ Therapeutics. This work was supported in part by the Swim across America (J.D. W., T.M.), Ludwig Institute for Cancer Research (J.D.W., T. M.), National Cancer Institute grants R01 CA56821 (J.D.W.). This research was also funded in part through the NIH/NCI Cancer Center Support Grant P30 CA008748.

<http://dx.doi.org/10.1136/jitc-2021-SITC2021.696>

697

TELOMERASE-DRIVEN TELOMERIC DNA MODIFICATION IN CANCER CELLS LEADS TO EFFICIENT INDUCTION OF CGAS-MEDIATED INNATE AND ADOPTIVE IMMUNE RESPONSES

¹Mihail Obrocea, ²Jerry Shay, ³Sergei Gryaznov*, ²Ilgen Mender, ⁴Silvia Siteni, ³Vlad Vitoc. ¹MAIA Biotechnology, Chicago, IL, United States; ²UT Southwestern Medical Center, Dallas, TX, United States; ³MAIA Biotechnology, Inc, Chicago, IL, United States; ⁴UT Southwestern Medical Center, Dallas, TX, United States

Background Telomeres and telomerase in cancer cells are highly attractive targets for specific anti-tumor therapy, since telomerase is almost universally expressed in cancer cells, but not in the majority of normal counterparts.

Methods In this presentation we summarize an unexpected, yet promising functional property of a modified nucleoside - 6-thio-2'-deoxyguanosine (6-thio-dG; THIO), as a potential anticancer agent with a unique mechanism of action. In vitro and in vivo, THIO is readily converted into the corresponding 5'-triphosphate, which is a substrate for mammalian telomerase. Incorporation of THIO into de novo synthesized cancer cell telomeres by telomerase leads to a fast induction of DNA damage responses and cancer cell senescence and apoptosis. Importantly, cancer cell death occurs in a telomere length-independent manner. THIO treatment leads to the generation of chromosomal bridges and, eventually, to the formation of cytosolic micronuclei structures, containing de novo modified telomeric DNA fragments. In addition to activation of innate immunity (i.e., cGAS pathway and NK cells), these in situ produced neo-adjuvants are exported extracellularly and then sensed by host-derived naïve dendritic cells, resulting in an enhanced cross-priming and tumor-specific T- cell (both CD4+ and CD8+) activation.

Results Treatment with THIO overcomes resistance to checkpoint blockade (by aPD-1 or aPD-L1 agents) in advanced in vivo cancer models, leading to profound and persistent tumor regression with induction of cancer type specific long-term immune memory. Thus, in vivo cancer curative activity was observed in murine syngeneic models of colorectal (MC-38) and lung (LLC) cancers, when THIO administration was followed sequentially by atezolizumab. Combinations with other immune checkpoint inhibitors (cemiplimab; pembrolizumab) were also highly effective

Conclusions In summary, our findings demonstrate the importance of cancer cell telomeric DNA structural and functional integrity, as well as a therapeutically attractive opportunity to induce telomerase-mediated telomere replication stress. THIO modified telomeres increase innate sensing and adaptive antitumor immunity via “cancer cell self-produced” chemical modification of telomeres.

Acknowledgements Supported in part by CA070907 to JWS

<http://dx.doi.org/10.1136/jitc-2021-SITC2021.697>

698 PD-L1 TARGETED CD28 COSTIMULATORY BISPECIFIC ANTIBODIES ENHANCE T CELL ACTIVATION IN SOLID TUMORS

¹Veronica Zeng*, ²Gregory Moore, ¹Juan Diaz, ¹Christine Bonzon, ¹Kendra Avery, ¹Ruschelle Love, ¹Matthew Dragovich, ¹Rumana Rashid, ¹Irene Leung, ¹Michael Hackett, ¹Jing Qi, ¹Charles Bakhit, ¹Umesh Muchhal, ¹Norman Barlow, ¹John Desjarlais, ¹Michael Hedvat. ¹Xencor, Inc., Monrovia, CA, United States; ²Xencor, Inc, Monrovia, CA, United States

Background T cells in the tumor microenvironment require T cell receptor (TCR) /major histocompatibility complex engagement and costimulatory receptor engagement to achieve complete activation. Tumor cells lack expression of CD28 ligands, so we hypothesized that activation of CD28 signaling at the T cell /tumor cell interface could enhance anti-tumor activity. We designed PD-L1 x CD28 bispecific antibodies that conditionally costimulate CD28 only in the presence of PD-L1 and TCR engagement. As PD-1/PD-L1 signaling has been shown to directly inhibit CD28 costimulation, this novel bispecific antibody can promote CD28 costimulation while simultaneously preventing the suppression of the same signal.

Methods We designed a set of stability-optimized anti-CD28 antibodies that can be paired with anti-PD-L1 antibodies to engage both PD-L1 and CD28 monovalently using Xencor's XmAb[®] 1+1 bispecific antibody platform. In vitro T cell activation with these bispecifics was measured by T cell proliferation, cytokine production, and cytotoxicity, in co-cultures of human cancer cell lines mixed with primary human CD3-stimulated T cells. In vitro activity was validated in a Cytomegalovirus (CMV) recall assay measuring CMV+ T cell proliferation of CMV+ peripheral blood mononuclear cells (PBMC) co-cultured with cancer cell lines ectopically treated with CMV-pp65-derived peptide. In vivo activity was determined with hCD28 humanized mice inoculated with MC38 tumors stably expressing hPD-L1-antigen. Finally, safety, tolerability, and pharmacodynamics of PD-L1 x CD28 were determined in cynomolgus monkeys.

Results PD-L1 x CD28 bispecifics were generated by incorporating an anti-PD-L1 mAb capable of blocking PD-1/PD-L1 interaction and anti-CD28 single-chain fragment variable covering a range of affinities. PD-L1 x CD28 antibodies enhanced T cell degranulation, cytokine secretion, and cancer cell cytotoxicity in concert with CD3 stimulation only in the presence of PD-L1. PD-L1 x CD28 enhanced proliferation of CMV+ T cells recognizing cancer cells loaded CMV-pp65-derived peptide. In hCD28 mice inoculated with MC38 tumors expressing hPD-L1, PD-L1 x CD28 inhibited tumor growth significantly greater than an anti-PD-L1 antibody alone. PD-L1 x CD28 was well tolerated in cynomolgus monkeys.

Conclusions PDL1 x CD28 bispecific antibodies show promising anti-tumor activity and warrant further development.

<http://dx.doi.org/10.1136/jitc-2021-SITC2021.698>

ATYR2810 AN ANTI-NRP2 MONOCLONAL ANTIBODY TARGETS TUMOR-ASSOCIATED MACROPHAGES

Samantha Tyler*, Michaela Ferrer, Erik Escobedo, Kaitlyn Rauch, Sofia Klopp-Savino, Justin Rahman, Zhiwen Xu, Esther Chong, Suzanne Paz, Leslie Nangle. *aTyr Pharma, San Diego, CA, United States*

Background Neuropilin-2 (NRP2) is a single transmembrane pleiotropic receptor that utilizes co-receptors for signal transduction and is known to impact tumor progression and metastasis.¹ Deletion of NRP2 in murine tumor-associated macrophages (TAMs) downregulated several immunosuppressive and tumor-promoting genes and upregulated immune-stimulatory genes in the myeloid compartment.² However, little is known about the role of NRP2 in human TAMs. We previously reported significant expression of NRP2 on TAMs derived from triple negative breast cancer (TNBC),³ and demonstrated the ability of ATYR2810, a monoclonal anti-NRP2 antibody, to regulate epithelial-mesenchymal transition (EMT) genes, such as the transcription factor ZEB1, and to enhance chemotherapeutic efficacy for aggressive breast cancer.⁴ Knowing TAMs play an important role in EMT transition and therapy resistance of cancer, and also rely on ZEB1 for their cancer promoting roles such as immune regulation,⁵ we sought to investigate the effects of ATYR2810 on TAMs.

Methods MDA-MB-231 TAMs were generated from monocytes in the presence or absence of ATYR2810. TAM phenotypes, gene expression and ability to secrete cytokines were assessed by flow cytometry, qRT-PCR and MSD respectively. TAM suppressive-ness was measured in co-culture experiments. T cell proliferation and activation markers were monitored by flow cytometry and cytokine production by MSD.

Results NRP2 is highly expressed on TAMs, which suppress T cell proliferation, activation and cytokine release. When differentiated in the presence of ATYR2810, a significant decrease in their suppressive capabilities against T cells was observed. Briefly, T cells were more proliferative, active and altered cytokine production when co-cultured with TAMs exposed to ATYR2810 compared to TAMs differentiated in its absence. Interestingly, we observed a significant decrease in ZEB1 gene and protein expression in ATYR2810 treated TAMs compared to non-treated TAMs. ATYR2810 also decreased the suppressive ability of TAMs when present in co-culture experiments.

Conclusions We show here for the first time that ATYR2810, known to bind NRP2 tumor cells, can also bind and exert effects on human TAMs. Given the intricate relationship between TAMs and tumors, we believe that this novel finding provides additional insight into the mechanism of action of ATYR2810 as a potential immune regulator. We show for the first time that NRP2 has the ability to regulate ZEB1 expression in TAMs; reducing their suppressive nature, pointing to a novel role of NRP2 in TAMs. These findings indicate ATYR2810s potential to be an effective anti-cancer agent through regulation of ZEB1 in both TAMs and tumors.

REFERENCES

1. Caunt M, Mak J, Liang W-C, Stawicki S, Pan Q, Tong RK, Kowalski J, Ho C, Reslan HB, Ross J, Berry L, Kasman I, Zlot C, Cheng Z, Le Couter J, Filvaroff EH, Plowman G, Peale F, French D, Carano R, Koch AW, Wu Y, Watts RJ, Tessier-Lavigne M, Bagri A. Blocking Neuropilin-2 function inhibits tumor cell metastasis. *2008*; **13**(4):331–342. <https://doi.org/10.1016/j.ccr.2008.01.029>.
2. Roy S, Bag AK, Dutta S, Polavaram NS, Islam R, Schellenburg S, Banwait J, Guda C, Ran S, Hollingsworth MA, Singh RK, Talmage JE, Muders MH, Batra SK, Datta K. Macrophage-derived neuropilin-2 exhibits novel tumor-promoting functions. *Cancer Res* 2018; **78**(19):5600–5617. doi: 10.1158/0008–5472.CAN-18-0562.
3. Tyler S, Ferrer M, Polizzi C, Da Silva R, Eide L, Walwick K, Seikkula M, Burkart C, Paz S, Nangle L. Neuropilin-2 is expressed on immune cells present in the tumor

microenvironment, and may contribute to the suppression of immune regulation leading to progression and metastasis of cancer. *Keystone Symposia: Tumor Metabolism and the Microenvironment*. 2021. https://www.atyrpharma.com/wp-content/uploads/2021/01/Jan-2021-Keystone-Poster_ST_FINAL.pdf.

4. Xu Z, Burkart C, Goel HL, Rahman J, Polizzi C, Seikkula M, Burman L, Mercurio AM, Nangle LA. A domain-specific antibody to NRP2 down-regulated epithelial-mesenchymal transition genes and enhanced efficacy of standard-of-care therapeutics for aggressive breast cancer. *American Society for Cancer Research*, 2021. https://www.atyrpharma.com/wp-content/uploads/2021/04/2021Mar_AACR-poster_ZX_Final_v2.pdf.
5. Cortés M, Sanchez-Moral L, de Barrios O, Fernández-Aceñero MJ, Martínez-Campanario MC, Esteve-Codina A, Darling DS, Györfy B, Lawrence T, Dean, DC, Postigo A. Tumor-associated macrophages (TAMs) depend on ZEB1 for their cancer-promoting roles. *EMBO* 2017; **36**(22):3336–3355. doi: 10.15252/emj.201797345. Epub 2017 Oct 16.

<http://dx.doi.org/10.1136/jitc-2021-SITC2021.699>

INCREASING MHC-I EXPRESSION TO POTENTIATE IMMUNE CHECKPOINT BLOCKADE THERAPY

¹Shengqing Gu*, ¹Wubing Zhang, ¹Xiaoqing Wang, ²Peng Jiang, ³Nicole Traugh, ¹Ziyi Li, ¹Clifford Meyer, ⁴Blair Stewig, ¹Yingtian Xie, ¹Xia Bu, ¹Michael Manos, ¹Alba Font-Tello, ¹Evisa Gjini, ¹Ana Lako, ¹Klothilda Lim, ¹Jake Conway, ¹Alok Tewari, ¹Zexian Zeng, ¹Avinash Das Sahu, ¹Collin Tokheim, ¹Jason Weirather, ¹Jingxin Fu, ¹Yi Zhang, ¹Benjamin Kroger, ⁵Jin Hua Liang, ¹Paloma Cejas, ¹Gordon Freeman, ⁶Scott Rodig, ¹Henry Long, ⁶Benjamin Gewurz, ¹F. Stephen Hodi, ¹Myles Brown, ¹X Shirley Liu. ¹Dana-Farber Cancer Institute, Boston, MA, United States; ²National Cancer Institute, Bethesda, MD, United States; ³Tufts University, Boston, MA, United States; ⁴Boston Children's Hospital, Boston, MA, United States; ⁵Brigham and Women's Hospital, Boston, MA, United States; ⁶Brigham and Women's Hospital, Boston, MA, United States

Background Cancer immunotherapy, especially immune checkpoint blockade (ICB) therapy, is leading to a paradigm shift in cancer treatment, as a small percentage of cancer patients have obtained durable remission following ICB treatment. Successful ICB responses rely on cancer cells presenting antigens to the cell surface via the major histocompatibility complex (MHC), which activates antigen-specific T-lymphocytes to kill cancer cells. Type-I MHC (MHC-I) is widely expressed in all cell types and mediates the interaction with cytotoxic CD8 T cells. However, over 65% of cancer patients are estimated to show defects in MHC-I-mediated antigen presentation, including downregulation of its expression that can lead to primary or acquired resistance to ICB therapy, and therapeutic strategies to effectively restore or boost MHC-I are limited.

Methods Here, we employed a CRISPR screening approach with dual-marker FACS sorting to identify factors that decouple the regulation of MHC-I and PD-L1. The experimentally validated target was used to generate a KO differential expression signature. Using this signature, we analyzed transcriptome data from drug perturbation studies to identify drugs that regulate MHC-I but not PD-L1. Finally, we validated the effect of the identified drug to enhance ICB response in a T-cell-dependent manner in vivo.

Results CRISPR screens identified TRAF3, a suppressor of the NF- κ B pathway, as a negative regulator of MHC-I but not PD-L1. The Traf3-knockout (Traf3-KO) gene expression signature is associated with better survival in ICB-naive cancer patients and better ICB response. We then screened for drugs with similar transcriptional effects as this signature and identified SMAC mimetics. We experimentally validated that the SMAC mimetic birinapant upregulates MHC-I, sensitizes cancer cells to T-cell-dependent killing, and adds to ICB efficacy. However, in cancer cells with high NF- κ B activity, the effect of birinapant on MHC-I is weak, indicating context-dependent MHC-I regulation.

Conclusions In summary, Traf3 deletion specifically upregulates MHC-I without inducing PD-L1 in response to various cytokines and sensitizes cancer cells to T-cell-driven cytotoxicity. The SMAC mimetic birinapant phenocopies Traf3-knockout and sensitizes MHC-I-low melanoma to ICB therapy. Further studies are needed to elucidate the context-dependencies of MHC-I regulation. Our findings provide preclinical rationale for treating some tumors expressing low MHC-I with SMAC mimetics to enhance sensitivity to immunotherapy. The approach used in this study can be generalized to identify other drugs that enhance immunotherapy efficacy.

Acknowledgements This study was supported by grants from the NIH (R01CA234018 to XSL, R01AI137337 to BEG, P50CA101942-12 and P50CA206963 to GJF), Breast Cancer Research Foundation (BCRF-19-100 to XSL), Burroughs Wellcome Career Award in Medical Sciences (to BEG), and Sara

Elizabeth O'Brien Trust Fellowship (to SG). We thank Drs. Kai Wucherpfennig and Deng Pan for their insightful suggestions on this study.

Ethics Approval All mice were housed in standard cage in Dana-Farber Cancer Institute Animal Resources Facility (ARF). All animal procedures were carried out under the ARF Institutional Animal Care and Use Committee (IACUC) protocol and were in accordance with the IACUC standards for the welfare of animals.

<http://dx.doi.org/10.1136/jitc-2021-SITC2021.700>

ACTIVATING CD73 ON B CELLS AS A TARGET FOR IMMUNOTHERAPY OF COVID-19 AND VIRAL ASSOCIATED CANCERS: CLINICAL ACTIVITY IN HUMAN PAPILLOMA VIRUS POSITIVE (HPV) HEAD AND NECK SQUAMOUS CELL CANCERS (HNSCC)

¹Jason Luke*, ²Jaime Merchan, ³Brett Hughes, ⁴Jeffrey Sosman, ⁵Abhishek Tripathi, ⁶Igor Puzanov, ⁷Thomas Marron, ⁸Kristen Marrone, ⁹Craig Hill, ⁹James Janc, ⁹Jenny Rudnick, ⁹Shenshen Hu, ⁹Mehrdad Mobasher, ⁹Suresh Mahabhashyam, ⁹Richard Miller. ¹UPMC Hillman Cancer Center, Pittsburgh, PA, United States; ²University of Miami, Miami, FL, United States; ³Royal Brisbane and Women's Hospital and University of Queensland, Herston, Australia; ⁴Northwestern University, Chicago, IL, United States; ⁵University of Oklahoma Stephenson Cancer Center, Oklahoma City, OK, United States; ⁶Roswell Park Cancer Institute, Buffalo, NY, United States; ⁷Mount Sinai Hospital, New York, NY, United States; ⁸Johns Hopkins University, Baltimore, MD, United States; ⁹Corvus Pharmaceuticals Inc, Burlingame, CA, United States

Background Mupadolimab (mupa) is a humanized FcγR binding-deficient IgG1 anti-CD73 antibody that has agonistic properties.¹ CD73 is involved in production of adenosine and in cellular trafficking. Mupa reacts with the majority of circulating B cells leading to activation and expression of differentiation markers CD69, CD138 and CD38, and transformation into plasmablasts with secretion of IgM and IgG. B cell activation provided the rationale to develop mupa for immunotherapy of cancer and Covid-19. Intratumor HPV specific B cells have been reported in HNSCC.² This report describes properties of mupa and the early signs of clinical activity in HPV+ HNSCC.

Methods ELISA and flow cytometry were used to measure binding of anti-CD73. Humanized NSG-SGM3 mice were used to evaluate effects of Mupa on human anti-SARS CoV2 spike protein (SP) response. CD73 expression in biopsies was measured by immunohistochemistry. Mupa (IV q 3 weeks) with or without pembrolizumab is being evaluated in an ongoing phase 1 trial in patients with refractory cancers.

Results Mupa binding to CD73 was blocked by APCP, an analog of adenosine diphosphate that locks CD73 in the closed conformation, indicating mupa binding to the open conformation. Cross blocking and cellular internalization studies showed that mupa is distinct from other anti-CD73 antibodies such as MEDI9447 and AD2. NSG-SGM3 mice were immunized with 50 μg SP subcutaneously and treated with mupa 10mg/kg or control IgG IP. Mupa treated animals mounted an antigen specific human anti-SP response; no antibody responses were seen in controls (P=0.02). In the dose-escalation portion of the phase 1 trial, mupa doses of ≥12 mg/kg saturated CD73 sites on circulating B cells. High stromal CD73 expression was observed in HPV+ HNSCC biopsies from 5 evaluable patients with chemotherapy and anti-PD1 refractory disease, and tumor regression was seen in 2 of these patients receiving 7 and 16 cycles of ≥12 mg/kg mupa without pembrolizumab. Safety of mupa+pembrolizumab was evaluated in 16 patients with no MTD reached and no changes in serum immunoglobulins. Transient reductions in circulating CD73 B cells were observed consistent with redistribution to lymphoid tissues.

Conclusions CD73 plays a role in B cell activation and differentiation. Mupa is an antibody with agonistic activity that stimulates B cells and enhances antigen specific antibody production. This activity supports a strategy to combine mupa with pembrolizumab to enhance both humoral and cellular immunity in the treatment of viral associated cancers such as HPV+HNSCC, and viral infections.

Trial Registration NCT03454451

REFERENCES

1. Willingham S, Criner G, Hill C, Hu S, Rudnick J, Daine-Matsuoka B, Hsieh J, Mashhedi H, Hotson A, Brody J, Marron T, Piccione E, Buggy J, Mahabhashyam S, Jones W, Mobasher M, Miller R. Characterization and Phase 1 trial of a B cell activating anti-CD73 antibody for the immunotherapy of COVID-19. *medRxiv*, 2020; <https://doi.org/10.1101/2020.09.10.20191486>.
2. Wieland A, Patel M, Cardenas M, Eberhardt C, Hudson W, Obeng R, Griffith C, Wang X, Chen Z, Kissick H, Saba N, Ahmed R. Defining HPV-specific B cell responses in patients with head and neck cancer. *Nature* 2020; <https://doi.org/10.1038/s41586-020-2931-3>.

Ethics Approval The study was approved by Western IRB, approval number 1-1066703-1. Participants gave informed consent before taking part.

<http://dx.doi.org/10.1136/jitc-2021-SITC2021.701>

702 TJ-CD4B (ABL111), A CLAUDIN18.2-TARGETED 4-1BB TUMOR ENGAGER INDUCES POTENT TUMOR-DEPENDENT IMMUNE RESPONSE WITHOUT DOSE-LIMITING TOXICITY IN PRECLINICAL STUDIES

¹Wenqing Jiang*, ¹Zhengyi Wang, ¹Zhen Sheng, ²Jaeho Jung, ¹Taylor Guo. ¹I-MAB Biopharma, Shanghai, China; ²ABL Bio, Seongnam, Korea, Republic of

Background 4-1BB (CD137) is a co-stimulatory receptor that stimulates the function of multiple immune cells. Its ability to induce potent anti-tumor activity makes 4-1BB an attractive target for immuno-oncology. However, clinical development of a monospecific 4-1BB agonistic antibody has been hampered by dose-limiting hepatic toxicities. To minimize systemic toxicities, we have developed a novel Claudin18.2 (CLDN18.2) x 4-1BB bispecific antibody, TJ-CD4B (ABL111) that stimulates 4-1BB pathway only when it engages with Claudin 18.2, a tumor-associated antigen specifically expressed in gastrointestinal cancers. TJ-CD4B (ABL111) is now being evaluated in patients with advanced solid tumors in a first-in-human trial (NCT04900818).

Methods TJ-CD4B (ABL111) was evaluated in vivo using the human 4-1BB knock-in mice bearing CLDN18.2 expressing MC38 tumor cells. Pharmacodynamic effects upon treatment were characterized in tumor tissue and blood. Immunophenotyping of the tumor microenvironment (TME) and peripheral blood was performed by flow cytometry. Soluble biomarkers were measured using Luminex-based multiplex assay. In-depth gene expression analysis was performed on primary human CD8+ T cells that were co-cultured with CLDN18.2 expressing cells in the presence of anti-CD3 using NanoString nCounter[®]. Pharmacokinetic (PK) and toxicity study were performed in cynomolgus monkeys.

Results TJ-CD4B (ABL111) elicited complete tumor regression in 13 out of 18 MC38 tumor bearing mice given at a dose above 2 mg/kg. Dose-dependent anti-tumor activity was associated with enhanced T cell activation in TME and expansion of memory T cells in the peripheral blood. Increased CD8+ T cells number and proliferation were observed in both tumor nest and surrounding stroma while the level of soluble 4-1BB in the serum was also elevated in response to the treatment. In vitro gene expression analysis by Nanostring revealed TJ-CD4B(ABL111) effectively activated immune pathways characterized by IFN γ -signaling and T cell inflammation. Preclinically, TJ-CD4B was well tolerated at the repeated doses up to 100 mg/kg/wk in cynomolgus monkeys without the adverse influence on the liver function which is generally affected by 4-1BB activation. Besides, no cytokine release or immune activation was observed in the periphery.

Conclusions TJ-CD4B (ABL111) is a novel CLDN18.2 dependent 4-1BB bispecific agonist antibody that induced T cell activation and memory response in tumor with CLDN18.2 expression, leading to a strong anti-tumor activity in vivo. TJ-CD4B did not induce systemic immune response nor hepatic toxicity due to the CLDN18.2 dependent 4-1BB stimulation. These data warrant the current clinical development in phase I trial to validate the safety properties and tumor specific responses.

<http://dx.doi.org/10.1136/jitc-2021-SITC2021.702>

703

FAVORABLE PRE-CLINICAL SAFETY PROFILE OF THE NOVEL NOT-ALPHA IL-2 AGONIST ANV419 SUPPORTS FIRST IN HUMAN CLINICAL DEVELOPMENT

¹Christoph Huber*, ²Guzman Alonso, ²Elena Gerralda, ¹Christoph Bucher, ³Philippe Jacqmin, ¹Andreas Katopodis, ⁴Jennifer Sims. ¹Anaveon AG, Basel, Switzerland; ²Vall d' Hebron Institute of Oncology, Barcelona, Spain; ³MnS, Dinant, Belgium; ⁴Integrated Biologix, Basel, Switzerland

Background ANV419 is a novel interleukin-2 (IL-2)/anti-IL-2 fusion protein with preferential signaling through the IL-2 beta/gamma receptor that induces selective proliferation of CD8 T cells and NK cells in vivo for the treatment of cancer. The safety and pharmacodynamic effects of ANV419 were studied in a 4-week cynomolgus monkey GLP study to support the ongoing PhI dose escalation clinical trial.

Methods ANV419 was administered by i.v. injection over 1 min at doses of 0.03, 0.1, 0.3 mg/kg, or vehicle control on days 1 and 15 of the 29-day study. Assessments included body weight, blood pressure, hematology, clinical pathology, serum cytokines, immunophenotyping, histopathology, and pharmacokinetics.

Results The pharmacokinetics of ANV419 were characterized by target mediated disposition, with a half-life of approximately 24h at concentrations not affected by target mediated clearance. Dose-dependent increases in WBC were observed after each injection, driven by preferential expansion of CD8 T cells and NK cells over Tregs. NK cells were more sensitive to ANV419 than CD8 T cells reaching maximal proliferation in blood at 0.03 mg/kg vs. 0.3 mg/kg for CD8 T cells. Hematological changes included: transient dose-dependent increase in basophils; elevation in eosinophils, up to 2.2-fold above control animals at > 0.03 mg/kg, remaining within the normal range for cynomolgus monkeys (<1.94 G/L); minor decrease in platelets at day 4 after each injection. There were no relevant treatment-related changes in inflammatory serum cytokines (IL-1b, IL-5, IL-6, IL-8, IFNg, TNFa, GM-CSF). A mild systemic inflammatory response was observed at 0.3 mg/kg evidenced by a transient increase of CRP on days 4 and 19, preceded after the first injection by a slight dose dependent increase in IL-1RA at 4h post injection, and an increase in IL-10 at 24h post treatment at 0.3mg/kg. No significant changes in body weights or blood pressure and no signs of capillary leak were observed during the entire study. A multi-part PhI dose-escalation study of ANV419 has been initiated in cancer patients. In the part A single patient escalation cohort, two patients have been dosed Q2W multiple times with 0.003mg/kg and 0.006mg/kg respectively with the expected PD profile and no DLT observed.

Conclusions Consistent findings, relating to expected effects of ANV419 as a not-alpha IL-2 agonist, demonstrated a favorable tolerability and safety profile at pharmacodynamically relevant doses that strongly support its translational development in cancer patients to identify clinical benefits.

<http://dx.doi.org/10.1136/jitc-2021-SITC2021.703>

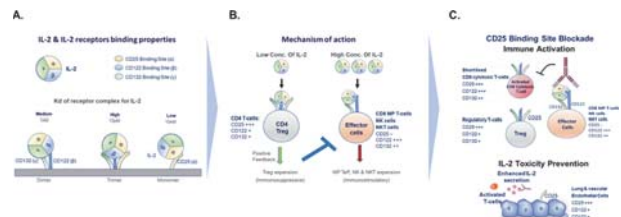
THE COMPUTATIONALLY DESIGNED HUMAN ANTIBODY, AU-007, MEDIATES HUMAN IMMUNE ACTIVATION BY ENDOGENOUS IL-2, WHILE UNIQUELY BREAKING THE IL-2 AUTO-INHIBITORY LOOP AND PREVENTING TREG EXPANSION

¹Inbar Amit, ¹Itay Levin, ²Timothy Wyant, ¹Natalie Levitin, ¹Reut Barak, ¹May Ben-Mayor, ¹Olga Bluvshtein, ¹Noam Grossman, ¹Yehezkel Sasson, ¹Guy Nimrod, ¹Michael Zehnin, ¹Sharon Fischman, ¹Marek Štrajbl, ¹Liron Danielpur, ³Aron Knickerbocker, ³James Vasselli, ^{4,5}Yanay Ofran*. ¹Biologic Design, Rehovot, Israel; ²Biologic Design and Aulos Bioscience, Boston, MA, United States; ³Aulos Bioscience, LARKSPUR, CA, United States; ⁴Aulos Bioscience & Biologic Design, Rehovot, Israel; ⁵Biologic design & Aulos Bioscience, Rehovot, Israel

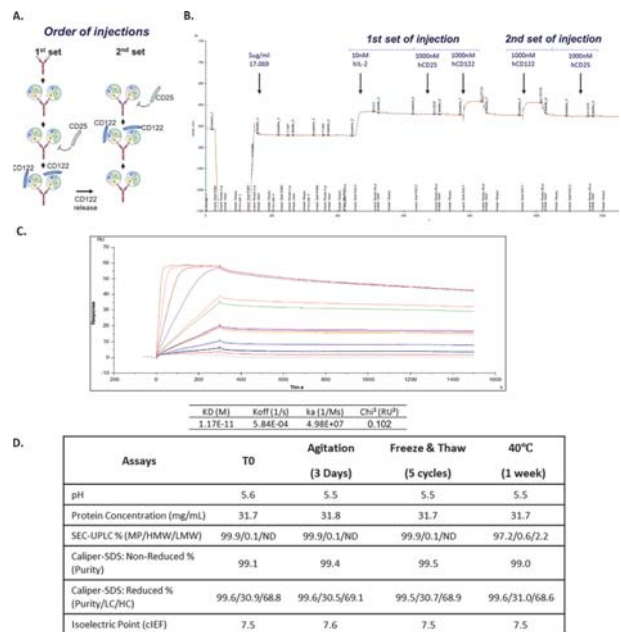
Background IL-2 binds two forms of IL-2 receptor: a high affinity trimeric receptor composed of CD25, CD122, and CD132, and a low affinity dimeric receptor composed of CD122 and CD132. Binding to the dimeric receptors, expressed on effector cells, causes expansion of the effector arm of the immune system including CD8 T-cells, NK-cells and NKT-cells. Binding to the trimeric receptor, expressed on Tregs as well as on pulmonary and vascular epithelium, results in expansion of Treg cells and Vascular Leak Syndrome, both are undesired outcomes of high-dose recombinant IL-2 (Aldesleukin), approved for treatment of Melanoma and Renal-Cell-Carcinoma.

Methods Flow-cytometry analysis of immune-cell populations of C57BL/6 mice and hPBMCs. Tumor-Growth-Index of murine cancer models.

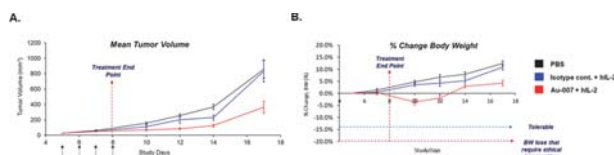
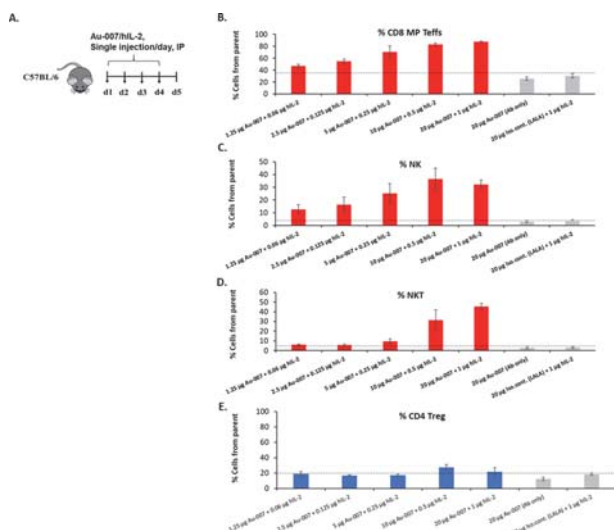
Results AU-007, is a computationally designed human antibody that bind the CD25-binding portion on IL-2, preventing binding of IL-2 to the trimeric receptor, but not the dimeric receptor. This leads to immune effector activation while also preventing the Treg expansion via the autoinhibitory loop caused by endogenous IL-2 secreted from activated T effector cells (figure 1). AU-007 binds human IL-2 with picomolar affinity and has excellent biophysical properties with low potential for anti-drug immunogenicity (figure 2). Administration of an AU-007/low dose hIL-2 complex to non-tumor bearing C57BL/6 mice promoted proliferation of effector cells with no effect on Tregs (figure 3). Additionally, an AU-007/low dose hIL-2 complex was highly effective in inhibiting tumor progression in a syngeneic B16F10 melanoma model (figure 4). pSTAT5 analysis of hPBMCs incubated with AU-007 and hIL-2 demonstrated activation of the effector cells and inhibition of Tregs expansion (figure 5). hPBMCs activated with anti-CD3/anti-CD28 and treated with either AU-007 or an isotype control antibody but without exogenous IL-2, showed expansion of effector cells. However, while the isotype control antibody expanded also Tregs, AU-007 inhibited Tregs proliferation, indicating that AU-007 captures endogenous IL-2 and prevents the Treg expansion autoinhibitory loop caused by endogenous IL-2 secreted from activated T effector cells (figure 6). Additionally, following establishment of the IL-2 auto-secretion feedback loop in mice genetically engineered to express hIL-2 instead of murine IL-2, AU-007 treatment significantly inhibited MC38 colorectal-tumor growth for twelve days, in a manner comparable to treatment with anti-PD1 (figure 7).



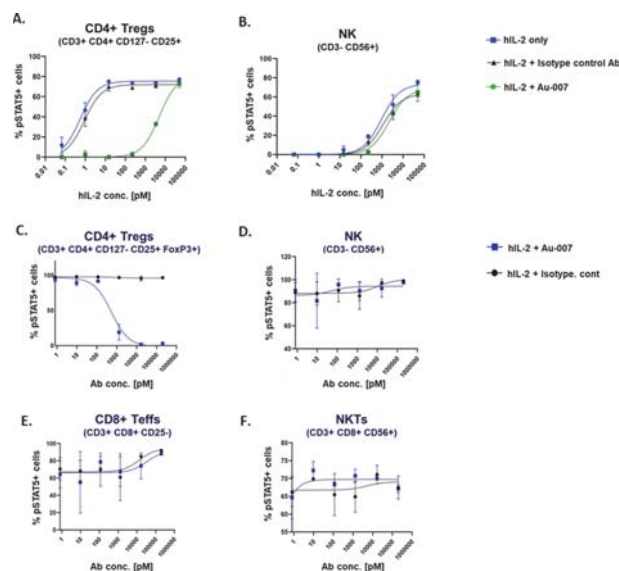
Abstract 704 Figure 1 Schematic representation of IL-2 mechanism of action and its dual role in controlling immune response. IL-2 structure consists of three binding epitope sites that interact with different forms of IL-2-R complexes with different affinities (Left Panel). IL-2R complexes expressed on different cell populations and their different affinities to IL-2 allow immunosuppression under conditions of low local concentrations of IL-2 and immune stimulation when IL-2 local concentration rises (middle panel). Au-007 utilize autocrine human IL-2 MOA to promote immune stimulation. Targeting IL-2 to different cell populations can be used to modulate the immune response towards immune activation. An anti-human IL-2 antibody tumor clearance while reducing IL-2's undesired interactions with endothelial CD25 expressing cells preventing IL-2 induced pulmonary edema and vascular leaking.



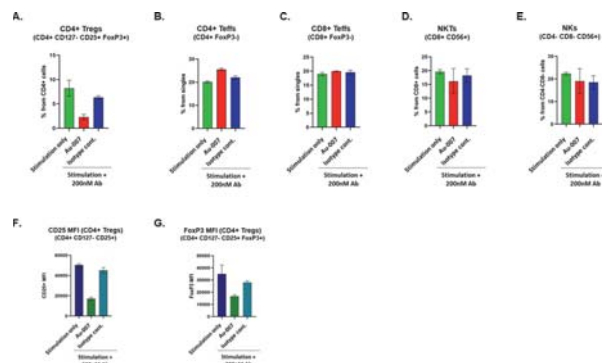
Abstract 704 Figure 2 Au-007 bind human IL-2 with high affinity and inhibits the binding to CD25 while preserving the binding to CD122. Affinity and binding site are demonstrated using Surface Plasmon Resonance. Au-007 was captured on CM5 chip and soluble hIL-2 was injected, forming a complex. Subsequently, soluble CD25 was injected followed by injection of soluble CD122 (A). SPR trace of complex formation of Ab/IL-2/IL-2R arrows indicate where Au-007 (17.069), hIL-2, CD25 and CD122 were injected (B). SPR trace and calculated binding kinetics of chip bound Au-007 with hIL-2 serving as analyte (C). Biophysical profile of Au-007. Au-007 was subjected to five freeze thaw cycles, agitation for 3 days and incubation at 40°C for 1 week. Post treatment Au-007 integrity and indicated biophysical properties were measured (D).



Abstract 704 Figure 4 Au-007 inhibits tumor growth in an I/O resistant tumor model with a tolerable profile. C57BL/6 healthy mice were inoculated with B16F10 melanoma tumor cells (day 0), at day 5 mice were randomized to experimental groups (n=10 per group) and administered daily, with single injection per day of Ab/hIL-2 mix (20 ug/1 ug respectively) or with PBS for four days. From the end of schedule administration at day 8 until experiment endpoint, mice were monitored daily for tumor volume (A) and for mean percent of body weight change for each experimental group (B).

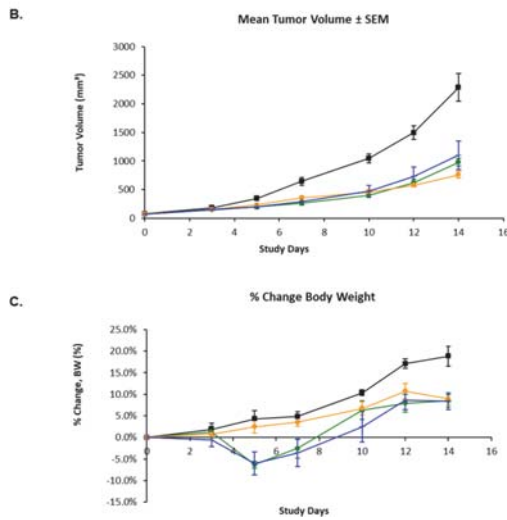
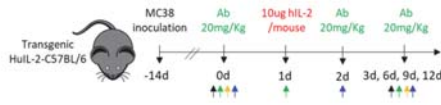


Abstract 704 Figure 5 AU-007 inhibits the effect of IL-2 on Tregs while preserving its effect on Teffs and NKs. (A and B) Phosphorylated STAT5 levels of human immune cell subsets responding to various concentrations of hIL-2 with and without 200 nM AU-007. Total naïve hPBMC culture were incubated with increasing doses of hIL-2 or with increasing doses of hIL-2 + 200nM AU-007 for 15 min. Immune cells subpopulations were analyzed by flow cytometry, gating was defined based on FMOs. (C–F) Phosphorylated STAT5 levels of human immune cell subsets responding to titrated AU-007 or isotype control. Total naïve hPBMC culture were incubated with hIL-2 and with increasing doses of indicated antibody for 15 min. Data presented is an average of 3 biological repeats from 3 human PBMC donors.



Abstract 704 Figure 6 Au-007 can rely on endogenous IL-2 to break auto-inhibitory loop in human PBMCs. Total hPBMCs were stimulated for 24h with anti-CD3/anti-CD28 (stimulation only, green) or stimulated with anti-CD3/anti-CD28 in the presence of: 200 nM of Au-007 mAb (red) or with 200 nM of isotype control mAb (blue). No exogenous IL-2 was added. Immune cells subpopulations were analyzed by flow cytometry. Percentage of immune cell sub-populations demonstrate exclusive inhibition of Tregs (A–E). Au-007 downregulate the suppressive markers of CD4+ regulatory Tregs from panel A, as defined by significant reduction in MFI of CD25 and FoxP3 (F and G). Gating was defined based on FMOs. Data presented is an average of 3 biological repeats from 3 human PBMC donors.

- A. ■ PBS
 ■ Au-007 only (20mg/Kg), every 3 days (D0, D3, etc.) + single boost of hIL-2 (10ug/mouse) at day 1
 ■ Anti-mPD-1 (200ug/mouse), every 3 days (D0, D3, etc.)
 ■ Complex (25ug Au-007 / 1.25ug hIL-2), 4 daily injections followed with every 3 days (D0, D1, D2, D3, D6 etc.)



Abstract 704 Figure 7 Au-007 captures endogenous hIL-2 and inhibits tumor growth in colorectal cancer model (MC38). Genetically modified C57BL/6 mice, engineered to express human IL-2 in the background of complete knock-out of mouse IL-2, were inoculated with MC38 colorectal tumor cells. All animals treated with Au-007 showed significant inhibition in tumor growth with no observed significant adverse effects. (A) Administration outline: PBS (black), anti-mouse-PD-1 antibody (yellow), Au-007 pre-complexed with low dose IL-2 (blue) and Au-007 alone every three days followed with a single immune kick start with IL-2 (green, IL-2 single dose is marked in red). (B) Tumor growth progression of the four groups treated. (C) Percent of body weight changes per treatment.

Conclusions AU-007 is a human antibody that blocks the CD25-binding epitope on IL-2. It redirects endogenous IL-2 to promote effector cell expansion while simultaneously blocking the Treg expansion autoinhibitory loop, indicating its unique therapeutic profile and high potential as a novel cancer treatment. AU-007 is expected to enter clinical testing in 2021.

<http://dx.doi.org/10.1136/jitc-2021-SITC2021.704>

706

CONDITIONAL CYTOKINE THERAPEUTICS FOR TUMOR-SELECTIVE BIOLOGICAL ACTIVITY: PRECLINICAL CHARACTERIZATION OF A DUAL-MASKED IFN-A2B

Alexey Berezhnoy*, Hsin Wang, Na Cai, Hikmat Assi, Nicole Lapuyade, Madan Paidhungat, Kenneth Wong, Michael Krimm, Robert Dunn, Dylan Daniel, Marcia Belvin, Erwan Le Scolan. *CytomX Therapeutics, South San Francisco, CA, United States*

Background Cytokines have been shown to elicit broad anti-tumor activity in preclinical models. These results have translated into the approval for clinical use of IFN-alpha and IL-2 before the checkpoint therapy era. However, to date, the clinical success of cytokines has been limited by systemic toxicity and poor exposure. CytomX Therapeutics has developed a new class of antibodies called Probody® therapeutics (Pb-Tx), designed to widen the therapeutic window by minimizing binding to targets in healthy tissue while being preferentially activated in the tumor microenvironment (TME) by tumor-associated proteases. CytomX has applied the Pb-Tx platform across multiple modalities including traditional antibodies, antibody-drug conjugates and T-cell engaging bispecifics and has advanced multiple programs into clinical studies. Here we have expanded the Pb-Tx platform with a conditionally activated cytokine version of IFN- α 2b that has the potential to improve the therapeutic index of IFN-alpha therapy and allow systemic delivery.

Methods We engineered an IFN- α 2b with a dual masking strategy using a cleavable Fc domain at one end of IFN-a2b, and a cleavable affinity peptide mask at the other end. The construct was optimized to both maximize cleavability and minimize IFN-a2b toxicity. All animal experiments were reviewed and approved by CytomX's Institutional Animal Care and Use Committee (IACUC Protocol AP303).

Results The optimized IFN-a2b conditionally activated cytokine strongly reduced IFN-a2b activity in vitro (5,000X) in its dual-masked form. Its activity was fully restored upon protease activation. Transcriptional profiling of in vitro treated PBMC confirmed reduction of interferon-mediated activities of the masked molecule. In vitro studies with dissociated tumors indicated its ability to activate tumor immune infiltrate, that could be further enhanced by concomitant PD-L1 blockade. In mouse xenograft studies, conditionally activated IFN-a2b cytokines induced complete regression at doses as low as 0.1mpk (activity comparable to peginterferon). Surrogate conditionally activated IFN-a2b molecules were also highly potent in syngeneic mice in vivo efficacy studies. Finally, we established an in vivo safety model in hamster which has been shown to be sensitive to IFN-a-mediated toxicity in the liver and bone marrow. In hamster, we showed that conditionally activated IFN-a2b cytokines are well tolerated up to 15mpk and have reduced systemic IFN-a2b mediated toxicity as compared to the unmasked cytokine.

Conclusions Taken together these preclinical data further support the development of conditionally activated IFN-a2b with the potential to improve the therapeutic index of IFN-a therapy and to enable single agent and combination treatment in multiple clinical settings.

Ethics Approval All animal experiments were reviewed and approved by CytomX's Institutional Animal Care and Use Committee (IACUC Protocol AP303).

<http://dx.doi.org/10.1136/jitc-2021-SITC2021.706>

IL12 FC-FUSIONS ENGINEERED FOR REDUCED POTENCY AND EXTENDED HALF-LIFE EXHIBIT STRONG ANTI-TUMOR ACTIVITY AND IMPROVED THERAPEUTIC INDEX COMPARED TO WILD-TYPE IL12 AGENTS

¹Matthew Burnett*, ¹Ke Liu, ¹Christine Bonzon, ¹Michael Hackett, ¹Katrina Bykova, ¹Rumana Rashid, ¹Nicole Rodriguez, ¹Nargess Hassanzadeh-Kiabi, ¹Connie Ardila, ¹Norman Barlow, ¹Irene Leung, ¹Hanh Nguyen, ¹Araz Eivazi, ¹Kendra Avery, ²Rajat Varma, ¹Umesh Muchhal, ¹John Desjarlais. ¹Xencor, Inc., MONROVIA, CA, United States; ²Independent Consultant, Monrovia, CA, United States

Background Interleukin-12 (IL12) is a proinflammatory cytokine that induces differentiation of Th1 cells and increased cytotoxicity of T and NK cells. Stimulation by IL12 leads to production of IFN γ and an inflammatory tumor microenvironment critical for anti-tumor responses. Studies in mice revealed IL12 can dramatically shrink syngeneic tumors, however human clinical studies resulted in severe toxicity and a small therapeutic window, limiting response rates. Prior work at Xencor demonstrated that reduced-potency IL15/IL15R α -Fc fusion proteins exhibited superior therapeutic index (TI) in non-human primates (NHP) by reducing receptor-mediated clearance. Applying similar principles to IL12, we created IL12 heterodimeric Fc-fusions (IL12-Fc) with reduced potency to improve TI.

Methods IL12 is a heterodimer of two subunits, so we engineered IL12-Fc fusions by fusing the IL12p35 subunit to one side of a heterodimeric (and inactive) Fc domain, and IL12p40 to the other side. These Fc-fusions were tuned for optimal activity by introducing amino acid substitutions at putative receptor-interface positions and screening for reductions of in vitro potency. In vitro activity was assessed on human PBMCs by measuring signaling in a STAT4 phosphorylation assay and IFN γ production in a mixed-lymphocyte reaction (MLR). In vivo anti-tumor activity of human IL12-Fc was assessed in huPBMC-NSG-DKO and huCD34+ MCF7 xenograft models. Surrogate mouse potency-reduced IL12-Fc were evaluated in syngeneic tumor models. Tolerability and pharmacodynamic activity were assessed in NHP.

Results An IL12-Fc potency series was created, and variants had up to a 10,000-fold reduction in STAT4 signaling and IFN γ production in an MLR assay compared to wild-type IL12-Fc. Anti-tumor activity was achieved with potency-reduced IL12-Fc as single-agents and in combination with anti-PD1, with weaker variants maintaining anti-tumor activity at higher dose levels. Analysis of peripheral lymphocytes indicated increased numbers of T and NK cells as well as activation of CD8+ T cells. Increased expression of immune checkpoints including PD1 was also observed. Analysis of serum indicated up to 200-fold increases in IFN γ levels. Surrogate potency-reduced IL12-Fc had improved tolerability and greater selectivity of IFN γ production in tumors compared to spleen and less production of IL10 compared to wild-type IL12-Fc. In NHP, potency-reduced IL12-Fc had superior exposure with slower, more sustained accumulation of IFN γ and IP10, and a more gradual dose-dependent peak response, as well as more sustained margination of T and NK cells compared to wild-type IL12-Fc.

Conclusions Potency-reduced IL12-Fc retain strong anti-tumor activity, while potentially overcoming safety and tolerability issues related to narrow TI associated with wild-type IL12 or IL12-Fc agents.

<http://dx.doi.org/10.1136/jitc-2021-SITC2021.707>

**NOVEL WAYS TO EXPLOIT IL-21 TO AUGMENT
ADOPTIVE T CELL TRANSFER THERAPY AGAINST
TUMORS**

¹Anna Cole*, ¹Guillermo Rangel Rivera, ¹Aubrey Smith, ¹Megan Wyatt, ¹Brandon Ware, ²Hannah Knochelmann, ¹Chrystal Paulos. ¹Emory University, Atlanta, GA, United States; ²Medical University of South Carolina, Charleston, SC, United States

Background IL-21 enhances the anti-tumor capacity of adoptively transferred CD8+ T cells, while IL-2 and IL-15 impair T cell immunity by driving their expansion to a more differentiated status. Yet, these cytokines can act on many different immune cells. Given the potency of IL-21, we tested if this cytokine directly augments T cells or rather if it enhances other immune cells in the culture that indirectly improves T cell therapy.

Methods To test this question, splenocytes from pmel-1 transgenic mice were used, as all CD8+ T cells express a transgenic TCR specific for tumor-antigen gp100₂₅₋₃₃ overexpressed on melanoma. We then peptide activated naïve CD8+ T cells enriched or not from the spleen of pmel-1 mice and expanded them in the presence of IL-21 or IL-2 (10 ng/mL) for four days. Expanded pmel-1 from these various cultures were then restimulated with irradiated splenocytes pulsed with gp100₂₅₋₃₃ and grown an additional seven days with IL-2 (10 ng/mL), irrespective of their initial cytokine condition. The *in vitro* memory phenotype, exhaustion profile, and cytokine secretion of these cultures were then assayed. Furthermore, mice bearing B16KVP melanoma tumors were infused with pmel-1 T cells expanded via these various approaches and compared for their relative capacity to engraft, persist, and regress tumor *in vivo*.

Results Interestingly, we discovered that IL-21-treated T cells generated from bulk splenocytes are phenotypically and functionally distinct from IL-21-treated isolated T cells. Upon restimulation, IL-21-treated T cells from bulk splenocytes exhibited an exhausted phenotype that was like anergic IL-2-treated T cells. Moreover, few cells expressed CD62L but expressed heightened markers of suppression, including TIM3, PD-1, and EOMES. Moreover, they produced more effector molecules, including granzyme B and IFN-gamma. *In vivo* IL-21-treated T cells expanded from bulk splenocytes engrafted and persisted poorly, in turn mediating suboptimal regression of melanoma. Conversely, IL-21 dramatically bolstered the engraftment and antitumor activity of T cells only if they were first isolated from the spleen prior to their expansion and infusion into the animal.

Conclusions Collectively, our data shows that IL-21 may improve ACT therapy best when used directly on antitumor CD8+ T cells. Further studies will illuminate the mechanism behind this striking difference and determine whether other cell subsets reactive to IL-21 cause T cell dysfunction and/or reduced bioavailability. These findings are important for defining the best culture conditions in which to use IL-21 for ACT.

Acknowledgements We would like to acknowledge Emory University, The Winship Cancer Institute, and the Pediatrics/Winship Flow Cytometry Core.

Ethics Approval All animal procedures were approved by the Institutional Animal Care and Use Committee of Emory University, protocol number 201900225.

<http://dx.doi.org/10.1136/jitc-2021-SITC2021.708>

709

PEPTIDYL IL-2/15R β γ C-RESTRICTED AGONISTS, HIGHLY-ATTENUATED AND LINKED TO ANTI-PD-1 ANTIBODIES TO ACHIEVE SELECTIVITY AND AMPLIFIED POTENCY IN STIMULATING PD-1-HIGH LYMPHOCYTES

¹William Dower*, ¹Alice Bakker, ¹Steven Cwirla, ¹Blake Williams, ¹Prarthana Joshi, ¹Praechompoo Pongtornpipat, ²Michael Needels, ²Ronald Barrett. ¹Medikine, Menlo Park, CA, United States; ²Medikines, Menlo Park, CA, United States

Background Recent reports demonstrate that directing a “non-alpha” IL-2 mutant to a PD-1high CD8+ stem-like population induces proliferation, and differentiation into a highly functional cytotoxic phenotype. We previously reported small synthetic peptides, unrelated to IL-2 or IL-15, that bind IL-2/15R β γ c to induce receptor signaling. These peptides do not bind IL-2R α and are therefore IL-2/15R β γ c-restricted agonists. We now describe fusion of potency-attenuated peptide agonists to an anti-PD-1 antibody (α -PD-1) to achieve selective targeting to PD-1high lymphocytes, and enhanced potency of IL-2R agonists acting in Cis with α -PD-1 binding.

Methods Peptidyl IL-2/15R β γ c agonists with attenuated potency due to weakened binding to either IL-2/15R β or γ c were fused to the C-termini of both heavy chains of an α -PD-1 IgG and expressed in CHO cells. The fusion proteins retained PD-1 binding affinity comparable to the α -PD-1; and were evaluated for potency of IL-2R β γ c-dependent STAT5 phosphorylation in TF-1 β cells (with undetectable PD-1 expression), and in TF-1 β -derived lines expressing varying levels of PD-1. The fusion proteins were also assessed for R β γ c stimulation of CD8+ cells treated with anti-CD3 and anti-CD28 to induce elevated PD-1 expression.

Results An analysis of pembrolizumab (Pem) fused to MDK1169, a potent IL-2R β γ c agonist, showed a 15-fold increase in potency in TF-1 β /PD-1+ cells. This served as an initial demonstration of the PD-1-directed, cis-acting mechanism; but the potency of MDK1169 in this construct (~500pM, EC50 pSTAT5 induction) is too high (relative to the affinity of Pem for PD-1) to achieve a more substantial selectivity for PD-1+ cells. To improve selectivity, fusions of α -PD-1 to peptide agonists with potencies as weak as 1 μ M on TF-1 β cells were constructed. Some of these fusion proteins exhibited up to 100-fold increase in potency when tested on TF-1 β /PD-1high compared to parental TF-1 β cells; and addition of an excess of α -PD-1 blocked this gain in potency in the PD-1high cells. When tested on CD8+ cells activated to express elevated PD-1 levels, potency of the PD-1-directed agonists correlated with PD-1 expression.

Conclusions The malleability of peptidyl agonists makes them useful for optimizing antibody-targeted cis-acting agonists designed to produce minimal activity on non-targeted cells and high potency at targeted cells. IL-2/15R β γ c agonists directed by PD-1 binding to a stem-like highly cytotoxic tumor infiltrating CD8+ population may have useful anti-tumor applications.

<http://dx.doi.org/10.1136/jitc-2021-SITC2021.709>

710

DIFFERENCES IN THE SUSCEPTIBILITY OF HUMAN SMALL CELL LUNG CANCER VARIANTS TO NK CELL-MEDIATED LYSIS CAN BE OVERCOME WITH THE ADDITION OF N803 (IL-15 SUPERAGONIST)

¹Kristen Fousek*, ¹Lucas Horn, ¹Haiyan Qin, ²Bobby Reddy, ²Lennie Sender, ²Patrick Soon Shiong, ¹Jeffrey Schlom, ¹Claudia Palena. ¹National Institutes of Health, Bethesda, MD, United States; ²ImmunityBio, Inc., Culver City, CA, United States

Background Small cell lung cancer (SCLC) is a highly aggressive tumor with a 5-year survival rate of less than 5%. Traditionally characterized as a neuroendocrine (NE) cancer, several subtypes have now been identified which vary in their phenotypic and transcriptional profiles. Classical NE tumors are molecularly defined as ASCL1+ or NEUROD1+ and exhibit an epithelial phenotype, expressing cytokeratin and E-cadherin (E-Cad). In contrast, non-classical variants express POU2F3 or YAP1 and are enriched in mesenchymal features, such as high levels of vimentin (Vim). Prior studies describe that non-NE variants of SCLC are less susceptible to chemotherapy and may arise via therapeutic selection. With the addition of immune checkpoint blockade to first-line chemotherapy for the treatment of advanced SCLC, understanding whether SCLC variants respond differently to immunotherapy is crucial.

Methods We utilized a range of pre-clinical models to investigate whether molecular and phenotypic variants of SCLC differ in their susceptibility to immune-mediated lysis. Following extensive characterization at the RNA and protein levels for expression of ASCL1, NEUROD1, POU2F3, YAP1, epithelial E-Cad, mesenchymal Vim, and other markers of cell phenotype, a panel of cells including each variant subtype were selected for further study.

Results Upon exposure to healthy donor effector NK cells, the more epithelial cells were highly susceptible to NK-mediated cytotoxicity while all mesenchymal SCLC cells remained highly refractory to NK-mediated lysis. This prompted us to investigate immunotherapy approaches such as the addition of N803, a mutant IL-15 superagonist, to improve the activation and proliferation of NK cells. In a xenograft model utilizing the mesenchymal YAP1+ H841 cell line subcutaneously implanted into nude mice devoid of all immune cells except for NK cells, we observed that the weekly administration of N803 resulted in a significant increase in the number of activated NK cells within the spleens of treated mice. Additionally, NK cells from treated mice produced significantly higher levels of IFN-gamma and granzyme B, resulting in a significant decrease in overall tumor burden.

Conclusions Our data indicates that N803-activated NK cells effectively mediate lysis of SCLC across all variant types, including those previously completely refractory to traditional NK cell lysis. These results highlight the potential of N803 as a novel immune-based intervention for the treatment of all variants of SCLC.

Ethics Approval PBMCs were obtained from healthy donors at the NIH Clinical Center Blood Bank (NCT00001846). All animal studies were approved and conducted in accordance with an IACUC-approved animal protocol (LTIB-57) with the approval of the NIH/NCI Institutional Animal Care and Use Committee.

<http://dx.doi.org/10.1136/jitc-2021-SITC2021.710>

711

IGM-7354 IS AN ANTI-PD-L1 IGM ANTIBODY AND IL-15 CYTOKINE FUSION THAT ENHANCES NK AND CD8+ T CELL PROLIFERATION AND TUMOR CYTOTOXICITY PLUS POTENTLY REVERSES T CELL EXHAUSTION

Thierry Giffon*, Melanie Desbois, Dean Ng, Poonam Yakkundi, Marigold Manlusoc, Miho Oyasu, Rodnie Rosete, Daniel Machado, Susan Calhoun, Tasnim Kothambawala, Avneesh Saini, Beatrice Wang, Maya Kotturi, Bruce Keyt, Angus Sinclair. *IGM Biosciences Inc, Mountain View, CA, United States*

Background While approved PD-1/PD-L1 inhibitory antibodies have demonstrated clinical efficacy in certain cancer patients, relapse following a primary response is often observed. Enhancing anti-tumor immune responses with an immunostimulatory cytokine, IL-15 is an attractive combination strategy to enhance anti-tumor NK and memory CD8+ T cell expansion and survival. We have developed IGM-7354, a high affinity, high avidity anti-PD-L1 pentameric IgM antibody with an IL-15R α chain and IL-15 fused to the joining (J) chain, designed to deliver IL-15 to PD-L1 expressing tumors for enhancing anti-tumor immune responses.

Methods IGM-7354 was generated by grafting heavy chain variable regions of a high affinity humanized anti-PD-L1 IgG onto the IgM heavy chain framework, co-expressed with the light chain and the J chain which included a single IL-15R α and IL-15 fusion. Binding ELISAs were performed using recombinant antigens. Human and cynomolgus monkey PBMCs were used for potency testing. Reversal of T cell exhaustion was tested using in vitro MLR. In vitro cytotoxicity assays were performed with luciferase-tagged MDA-MB-231 cells and PBMCs. In vivo pharmacodynamic studies were conducted in mice and cynomolgus monkeys.

Results IGM-7354 bound human and cynomolgus monkey PD-L1 with the same affinity but did not bind to rat or mouse PD-L1. In addition, the IL-15 component of IGM-7354 bound to human and cynomolgus β chain of the trimeric IL-15 receptor with similar affinities, but with weaker binding affinity to rodent IL-15R β . Using in vitro assays with PBMCs, IGM-7354 dose dependently enhanced the proliferation of human and cynomolgus monkey NK and CD8+ T cells. Furthermore, IGM-7354 was able to reverse T cell exhaustion in an in vitro MLR beyond that of an IL-15/IL15R α complex or anti-PD-L1 IgM or IgG alone, as demonstrated by an increase in activation and effector cytokine secretion. IGM-7354 also enhanced in vitro killing of PD-L1-expressing MDA-MB-231 breast cancer cells by human PBMCs. Pharmacodynamic studies in an MDA-MB-231 xenograft mouse model showed dose-dependent increases in circulating NK and CD8+ T cells and tumor infiltrating lymphocytes, which correlated with tumor regression. In cynomolgus monkeys, intravenous administration of IGM-7354 was well tolerated and dose dependently induced the proliferation of NK and CD8+ T cells.

Conclusions IGM-7354 stimulates NK and CD8+ T cell expansion in vitro and in vivo plus induces tumor regressions in mouse tumor models. This approach may enhance tumor localization of the immunostimulatory cytokine IL-15 through high affinity and high avidity binding to PD-L1 thereby improving anti-tumor responses and minimizing toxicity.

Ethics Approval All animal studies were conducted according to approved Institutional Animal Care and Use Committee (IACUC) protocols of the testing facilities.

<http://dx.doi.org/10.1136/jitc-2021-SITC2021.711>

712

PRECLINICAL CHARACTERIZATION OF GT-00A X IL15: A NOVEL IL-15-BASED IMMUNOCYTOKINE WITH UNIQUE TUMOR TARGETING PROPERTIES

Anika Jaekel*, Patrik Kehler, Timo Lischke, Christoph Goletz, Anke Flechner, Antje Danielczyk, Johanna Gellert. *Glycotope GmbH, Berlin, Germany*

Background IL-15 is a potent pro-inflammatory cytokine that enhances the differentiation, proliferation and cytolytic activity of NK cells and T cells. Due to the huge potential of IL-15 to activate both innate and adaptive anti-tumor immunity, several IL-15-based immunocytokines are currently in clinical development. However, all of them preferentially act in the periphery and not locally within the tumor. To further increase the efficacy and safety of IL-15-based immunocytokines, we developed GT-00A x IL15, an immunocytokine targeting a tumor-associated, glycosylated epitope of MUC-1 (TA-MUC1). GT-00A x IL15 was designed to induce anti-tumor responses directly within the tumor microenvironment for the treatment of solid tumors.

Methods GT-00A x IL15 was extensively studied in vitro and in vivo to adequately characterize its complex mechanisms of action and to analyze its anti-tumor efficacy. The relevance of TA-MUC1 binding as differentiation criteria against untargeted IL-15 (super)agonists was investigated in detail. In vitro cytotoxicity and 3D tumor spheroid immune cell infiltration mediated by GT-00A x IL15 was compared to the parental antibody GT-00A and an untargeted IL-15 control. In vivo, several pharmacokinetic, pharmacodynamic, biodistribution and efficacy studies were performed in tumor-free or tumor-bearing mice.

Results We could show in vitro that GT-00A x IL15 increased the cytotoxic activity of PBMC against TA-MUC1-positive tumor cell lines compared to parental GT-00A and an untargeted IL-15 control construct. Additionally, dose-dependent infiltration of NK and T cells into MCF-7 tumor spheroids is mediated by GT-00A x IL15 but not the untargeted IL15 control construct or parental GT-00A. In vivo single agent efficacy of GT-00A x IL15 was shown in different tumor models by means of tumor growth inhibition and increased survival. Subsequent flow cytometric analysis of tumor samples confirmed activation and expansion of tumor-infiltrating NK and CD8+ T cells. Furthermore, in a biodistribution study using radioactively labelled GT-00A x IL15 we observed significantly increased enrichment in the tumor compared to the untargeted IL-15 control construct.

Conclusions Our results confirm the relevance of TA-MUC1-mediated tumor cell binding for the mechanisms of action of our immunocytokine. GT-00A x IL15 shows increased accumulation in the tumor and mediates enhanced cytotoxicity and immune cell infiltration compared to an untargeted IL-15 control construct highlighting the potential to increase the efficacy and safety of IL-15-based immunocytokines by tumor targeting. GT-00A x IL15 shows great promise for the treatment of TA-MUC1-positive solid tumors either as monotherapeutic agent or as valuable combination partner.

<http://dx.doi.org/10.1136/jitc-2021-SITC2021.712>

713

NOVEL PROTEASE ACTIVATABLE LINKER WITH TUMOR TARGETING MOTIFS ENHANCES THE RETENTION OF CYTOKINE PRODRUG AND ACTIVE CYTOKINE AT DISEASE SITE AND DEMONSTRATES IMPROVED EFFICACY IN PRECLINICAL MODEL

¹Emma Langley*, ²Chen Li, ²Jessica Zaid, ²Tani-Ann Lee, ²Deepak Yadav, ²Brian Grot, ²Jay Singh, ²Johnvan Kim. ¹Trutino Biosciences Inc, San Diego, CA, United States; ²Trutino Biosciences, San Diego, CA, United States

Background An emerging class of new protease-activatable prodrugs designed to enhance on-target activity and reduce off-target toxicity are being actively developed. Cytokines are complex immune mediators which display potent anti-tumor activity in preclinical models and have delivered clinical responses in several advanced tumor types. However, clinical development of cytokine therapies has been hampered by high systemic toxicity, a narrow therapeutic index and short circulatory half-life. To address these shortcomings, we have developed next-generation cytokine therapies, On Demand Cytokines or ODCs.

Methods ODCs are protease-activatable cytokine prodrugs in which the cytokine is linked to an inhibitory moiety via a short proprietary peptide motif. These recombinant proteins are designed to exploit the protease activity present within the tumor microenvironment (TME) and enable the local release of active cytokine to trigger an anti-tumor immune response. ODCs contain tumor stroma targeting elements to further enhance their retention and activation within the malignant tissue. We have developed an array of stromaphilic ODCs, including a panel of IL-2 prodrugs containing single or dual tumor stroma binding motifs and report their preclinical in vitro and in vivo characterization.

Results All IL-2 prodrugs were successfully manufactured and activated in vitro by Matrix Metalloprotease cleavage which triggered the release of functional cytokine. Binding of prodrugs to tumor stroma components was confirmed in vitro. The ODC-IL2 panel was tested in vivo as single agent in the subcutaneous syngeneic B16F10 melanoma model. The uncleaved drugs were retained in the tumor at 5 to 20-fold higher levels than a control cytokine prodrug lacking any tumor targeting elements. Furthermore, intratumoral levels of IL-2 and IFN γ were increased 8 to 80-fold and 10 to 40-fold respectively compared to cytokine levels measured in the control non-targeted ODC treated arm. Finally, stromaphilic ODCs displayed substantially enhanced levels in circulation over non-targeted ODC. Superior anti-tumor efficacy was observed for all stroma targeting pro-cytokines with near complete tumor growth inhibition achieved with the dual targeting site construct.

Conclusions We have demonstrated that the On Demand Cytokine platform can generate protease-activatable cytokine prodrugs with enhanced tumor retention and on-target activity, to ultimately deliver safer and more effective immunotherapies.

<http://dx.doi.org/10.1136/jitc-2021-SITC2021.713>

714

SELECTIVE EXPANSION OF ANTIGEN-SPECIFIC CD8 T CELLS WITH ENGINEERED ANTIGEN PRESENTING EXOSOME

¹Tomoyoshi Yamano*, ²Xiabing Lyu, ¹Rikinari Hanayama. ¹Kanazawa University, Kanazawa, Ishikawa, Japan; ²Kanawaza University, Kanazawa, Japan

Background Exosomes are vesicular granules of about 100 nm and are secreted by many types of cells. Exosomes contain various proteins, lipids, and RNAs that are transported to target cells which induce functional and physiological changes. Exosomes are promising nano-vesicles for clinical application, owing to their high biocompatibility, low immunogenicity, and high drug delivery efficacy. Recent studies have demonstrated that exosomes from tumor cells or antigen presenting cells (APCs) regulate immune responses. Tumor derived exosomes express PD-L1 on their surface and suppress tumor immunity systemically. On the other hand, mature dendritic cells derived exosomes exert immune activation, and tumor immunotherapy using DCs exosome has been developed. However, few studies have been found to exert a significant effect on cancer treatment, may be because of low expression of costimulatory molecules and lack of cytokines on DCs derived exosomes.

Methods It has been demonstrated that GFP can be conveyed into exosomes by conjugating GFP with tetraspanins, exosome-specific surface proteins. First, we generated a tetraspanin fusion protein with a single-chain MHCI trimer (scMHCI). IL-2 is inserted on the second extracellular loop of CD81, allowing robust and functional expression of IL-2 on the exosome. We collected exosomes from HEK293 cells culture, which stably express scMHCI-CD81-IL2 and CD80-MFGE8, and used as Antigen-presenting exosome(AP-Exo).

Results AP-Exo expresses high expression of MHCI-peptide complex, costimulatory molecule, and cytokine, activating cognate CD8 T cells as dendritic cells do. AP-Exo selectively delivered co-stimulation and IL-2 to antigen-specific CD8 T cells, resulting in a massive expansion of antigen-specific CD8 T cells without severe adverse effects in mice. AP-Exo can expand endogenous tumor-specific CD8 T cells and induce the potent anti-tumor effect.

Conclusions Our strategy for building engineered exosomes that work like APCs might develop novel methods for cancer immunotherapy.

Ethics Approval All mice were housed in a specific pathogen-free facility, and all animal experiments were performed according to a protocol approved by Kanazawa University, Kanazawa, Japan.

<http://dx.doi.org/10.1136/jitc-2021-SITC2021.714>

715

WTX-330 IS AN IL-12 PRO-DRUG THAT IS CONDITIONALLY ACTIVATED WITHIN THE TUMOR MICROENVIRONMENT AND INDUCES REGRESSIONS IN MOUSE TUMOR MODELS

¹Kristin Morris*, ¹Heather Brodtkin, ¹Daniel Hicklin, ¹Nesreen Ismail, ¹Christopher Nirschl, ¹Andres Salmeron, ¹Philipp Steiner, ¹Zoe Steuert, ²Jenna Sullivan, ¹William Winston. ¹Werewolf Therapeutics, Cambridge, MA, United States; ²Werewolfx.com, Cambridge, MA, United States

Background Systemic administration of proinflammatory cytokines is a promising approach to treat cancer. However, poor pharmacokinetic properties and dose-limiting toxicities after systemic administration of cytokines such as interleukin 12 (IL-12) renders this strategy impractical. WTX-330 is a novel therapy identified using the Predator™ discovery platform that is designed to selectively deliver active wild-type IL-12 to the tumor microenvironment.

Methods WTX-330 is an inducible polypeptide (INDUKINE™ molecule) that consists of wild-type IL-12 tethered to a high affinity antibody blockade domain and a half-life extension (HLE) domain via tumor protease-sensitive linkers.

Results WTX-330 shows favorable inducible activity in vitro. WTX-330 incubated ex vivo with various primary human tumors led to the release of active IL-12, while WTX-330 was stable in human serum and normal tissues. Intraperitoneal (i. p.) administration of mouse WTX-330 led to complete tumor regression in multiple syngeneic tumor models. Importantly, equimolar amounts of wild-type IL-12, while active, was not tolerated by the mice compared to the IL-12 INDUKINE™ molecule. Mouse surrogate WTX-330 led to increased activation and frequencies of cross-presenting dendritic cells, NK cells and tumor specific CD8 T cells in B16F10 tumors. Moreover, mouse WTX-330, but not wild type IL-12, led to increased T cell activation specifically within B16F10 tumors as compared to the periphery. WTX-330 was well tolerated in non-human primates at different dose levels and schedules with exposure levels which exceeded the levels needed for anti-tumor activity in mice. In addition, there was low systemic exposure of IL-12 in the plasma after dosing with WTX-330 as compared to levels observed after treatment with wild-type IL-12.

Conclusions Pharmacological and translational data obtained so far clearly support continued preclinical development with the goal of moving this innovative and differentiated engineered IL-12 therapy into human clinical testing.

<http://dx.doi.org/10.1136/jitc-2021-SITC2021.715>

716

NL-201 INDUCES INFLAMMATION IN A 'COLD' TUMOR MICROENVIRONMENT THROUGH UPREGULATION OF MHC-I, EXPANSION OF THE TCR REPERTOIRE, AND POTENT ANTITUMOR ACTIVITY WHEN COMBINED WITH PD-1 INHIBITION

Christie Mortales*, Benjamin Dutzar, Jerry Chen, Alex Chen, Justin Huard, Luis Blancas-Mejia, Carl Walkey, Ryan Swanson. *Neoleukin Therapeutics, Inc., Seattle, WA, United States*

Background NL-201 is a potent, selective, and long-acting computationally designed alpha-independent agonist of the IL-2 and IL-15 receptors that is being developed as an immunotherapy for cancer. Downregulation of MHC class I (MHC-I) expression by tumors is a well-known mechanism of immune escape, and IFN γ is known to upregulate MHC-I. Here, we investigated whether NL-201 monotherapy can convert a 'cold' tumor microenvironment (TME) to an immunologically 'hot' TME through IFN γ -mediated MHC-I expression. This effect could expand the TCR repertoire for increased antitumor response and improve anti-PD-1 combination therapy.

Methods For *in vitro* assays, mouse splenocytes were cultured with Neo-2/15 to assess effector cell function, as well as cocultured with B16F10 cells to assess IFN γ -induced MHC-I and PD-L1 expression. B16F10 tumors were established in C57BL/6 mice and dosed with NL-201, anti-PD-1, or both to assess *in vivo* efficacy. B16F10 tumors were excised and dissociated for phenotyping of tumor-infiltrating lymphocytes (TILs) using flow cytometry. For gene expression analysis, RNA and genomic DNA were extracted from tumors and submitted for NanoString Pancancer Immune Profiling and Adaptive ImmunoSEQ analysis, respectively.

Results *In vitro*, Neo-2/15 induced greater CD8+ T cell and NK cell proliferation, as well as granzyme B production and IFN γ -dependent MHC-I upregulation on B16F10 tumor cells, compared to IL-2 or IL-15. In 'cold' B16F10 syngeneic tumors, NL-201 monotherapy reduced tumor growth and induced MHC-I, IFN γ , and granzyme B upregulation. Gene expression analysis of NL-201-treated tumors demonstrated increased TCR repertoire diversity and inflammatory signature at the tumor. In addition, PD-L1 was significantly upregulated on B16F10 cells. While the B16F10 tumors exhibited resistance to anti-PD-1 monotherapy, combination treatment with NL-201 significantly improved anti-PD-1 activity. This may explain the potent anti-tumor activity of NL-201 with anti-PD-1 combination therapy.

Conclusions NL-201 induces potent inflammatory effects on effector cells and is able to turn 'cold' TMEs 'hot'. We demonstrate that NL-201 strongly upregulated MHC-I expression *in vitro* and *in vivo* via an IFN γ -dependent pathway. Increased antigen presentation drives TCR diversity while augmenting the inflammatory signature at the tumor. This adaptive response also upregulates PD-L1 expression and results in impressive antitumor activity when NL-201 and PD-1 inhibitors are co-administered. The demonstration that NL-201 can convert 'cold' tumors to immunologically 'hot' tumors may provide a novel therapeutic option for patients unresponsive to current standard of care checkpoint inhibitors. A Phase 1 study of NL-201 in patients with advanced solid tumors is currently underway (NCT04659629).

Ethics Approval All experiments were approved by the Institutional Animal Care and Use Committee of Bloodworks Northwest and performed under protocol 5360-03.

<http://dx.doi.org/10.1136/jitc-2021-SITC2021.716>

SELECTIVE ACTIVATION OF CD8+ T CELLS BY A CD8-TARGETED IL-2 RESULTS IN ENHANCED ANTI-TUMOR EFFICACY AND SAFETY

¹Kelly Moynihan, ¹Danielle Pappas, ¹Terrence Park, ¹Wei Chen, ¹Irene Ni, ¹Paul Bessette, ¹Mike Chin, ²Ton Schumacher, ¹Andy Yeung, ¹Ivana Djuretic*, ¹Asher Biotherapeutics, South San Francisco, CA, United States; ²The Netherlands Cancer Institute, Amsterdam, Netherlands

Background High-dose IL-2 induces complete responses in a subset of cancer patients, but severe toxicity, including vascular leak syndrome (VLS), limits its clinical potential. Insights into IL2R α 's role in the development of VLS sparked a wave of second-generation IL-2 molecules referred to as “not- α ” IL-2s. Emerging clinical data suggests that although not- α IL-2s avoid VLS, they induce suboptimal monotherapy activity in patients. Given the observation that CD8+ T cells are the dominant effector cells with IL-2-based therapies,^{1 2} we hypothesized that maximizing the activity of IL-2 on CD8+ T-cells and limiting its activity on immunosuppressive Tregs and highly IL-2-sensitive innate populations would improve IL-2's efficacy and tolerability. We developed cis-targeted IL-2 (CD8-IL2) fusion proteins that selectively activate CD8+ T cells and have minimal activity on CD8-negative cells.

Methods In vitro selectivity of CD8-IL2 molecules was tested on primary immune cells including mouse splenocytes and human PBMCs. In vivo activity was evaluated in syngeneic tumor models and non-human primates.

Results Due to the 10–20x higher expression of IL2R β on NK cells over other lymphocytes, not- α IL-2 induced preferential NK cell expansion in mice. Toxicity-induced body weight loss with not- α IL-2 treatment was dependent on cells expressing NK1.1 but not CD8. To avoid overt activation of IL2R β high NK cells, IL-2R α -associated toxicity, and Treg activation, we generated cis-targeted fusion proteins consisting of anti-CD8 antibodies and IL-2 muteins with attenuated binding to IL2R α and IL2R β . We demonstrated that CD8-IL2 fusions preferentially activated CD8+ T cells within mouse, human, and cynomolgus immune populations, with 100–1000 fold selectivity over NK cells and Tregs for all three species. Selective expansion of CD8+ T cells over NK cells and Tregs was demonstrated in tumor and peripheral blood compartments in mice. Selective CD8+ T cell expansion was also demonstrated in cynomolgus monkeys. Furthermore, a single dose of CD8-IL2 in mice elicited strong monotherapy efficacy in MC38 tumors, with a majority of mice demonstrating complete responses without detectable body weight loss at doses that were well tolerated in cynomolgus monkeys. In contrast, not alpha IL-2 induced >10% body weight loss prior to reaching efficacious doses in mice and did not drive any complete anti-tumor responses.

Conclusions CD8-targeted IL-2 has superior efficacy and lower toxicity compared to second-generation not- α IL-2. Development of AB248, a novel CD8-targeted IL-2 molecule is underway.

REFERENCES

1. Rakhmilevich A, North R. Elimination of CD4+ T cells in mice bearing an advanced sarcoma augments the antitumor action of interleukin-2. *Cancer Immunol Immunother* 1994;**38**(2):107–12.
2. Sun Z, Ren Z. A next-generation tumor-targeting IL-2 preferentially promotes tumor-infiltrating CD8+ T-cell response and effective tumor control. *Nat Commun* 2019;**3874**:1–12.

<http://dx.doi.org/10.1136/jitc-2021-SITC2021.717>

WTX-124 IS A NOVEL IL-2 PRO-DRUG THAT IS CONDITIONALLY ACTIVATED IN TUMORS AND DRIVES ANTITUMOR IMMUNITY IN MURINE SYNGENEIC CANCER MODELS

Christopher Nirschl*, Heather Brodtkin, Daniel Hicklin, Nesreen Ismail, Kristin Morris, Andres Salmeron, Cindy Seidel-Dugan, Philipp Steiner, Zoe Steuert, Jenna Sullivan, William Winston. *Werewolf Therapeutics, Cambridge, MA, United States*

Background Cancer immunotherapy has established itself as the fourth pillar of cancer treatment thanks to the clinical success of checkpoint inhibitors. However, durable anti-tumor responses following immunotherapy are still limited to certain cancer types, and only a fraction of patients respond to the treatment, demonstrating the need for additional immunotherapeutic agents. Preclinical and clinical studies have demonstrated the promise of cytokine therapy to increase antitumor immunity. One of these key cytokines, interleukin-2 (IL-2), is approved for clinical use in metastatic melanoma and renal cell carcinoma. Unfortunately, this treatment requires dosing every 8 hours due to its poor pharmacokinetic profile and is linked to serious toxicities which limits its utility.

Methods To address these limitations, we designed WTX-124, an IL-2 pro-drug (IL-2 INDUKINE™ protein) that takes advantage of dysregulated protease activity in the tumor microenvironment (TME) to selectively deliver active IL-2 to the tumor after systemic administration. Peripheral inactivation is achieved by linking the cytokine to an inactivation domain using a tumor protease-sensitive linker. The INDUKINE™ molecule is also engineered with a half-life extension element to improve the pharmacokinetic profile and maintain longer exposure in the tumor. Once the IL-2 INDUKINE™ protein reaches the tumor, tumor-associated proteases cleave the linker and release the fully active cytokine.

Results Treatment with WTX-124 resulted in the complete rejection of MC38 tumors in a manner dependent on proteolytic processing of the INDUKINE™ protein, as a non-cleavable version of WTX 124 lacked anti-tumor activity. Furthermore, the INDUKINE™ format greatly enhanced the PK profile of WTX 124 over free IL-2, resulting in greater exposure with less overall dosing, and demonstrating a favorable accumulation of free IL-2 in tumors compared to plasma. Mechanistically, WTX 124 treatment drove the expansion and activation of tumor infiltrating CD8+ T cells and NK cells which increased the production of effector cytokines in the tumor. This resulted in tumor rejection that translated into durable immune memory, as animals that rejected the tumors upon IL-2 INDUKINE™ protein treatment were protected against a subsequent re-challenge with the same tumor cells. WTX 124 also demonstrated favorable pharmacokinetic and tolerability characteristics in cynomolgus monkeys resulting in minimal release of IL-2 in the periphery.

Conclusions The combination of tumor-selective activation of WTX-124 with reduced peripheral toxicities and its favorable pharmacokinetic profile supports moving this compound into clinical development.

Ethics Approval All animal in vivo work was performed in accordance with current regulations and standards of the U.S. Department of Agriculture and the NIH.

<http://dx.doi.org/10.1136/jitc-2021-SITC2021.718>

719

XTX301, A PROTEIN-ENGINEERED IL-12, EXHIBITS TUMOR-SELECTIVE ACTIVITY IN MICE WITHOUT PERIPHERAL TOXICITIES AND IS WELL TOLERATED IN NON-HUMAN PRIMATES

Ekta Patel*, Natalia Malkova, Sallyann Vu, Rebekah O'Donnell, Manoussa Fanny, Wilson Guzman, Parker Johnson, Megan McLaughlin, Oleg Yerov, Kurt Jenkins, Hanumantha Rao Madala, Caitlin O'Toole, Magali Pederzoli-Ribeil, Jia Chen, Benjamin Nicholson, Bill Avery, Huawei Qiu, Ronan O'Hagan, Jennifer O'Neil. *Xilio Therapeutics, Waltham, MA, United States*

Background Interleukin-12 (IL-12) is a proinflammatory cytokine which bridges innate and adaptive immunity via induction of T helper 1 differentiation and promoting cytolytic activity of natural killer and T cells. IL-12 has demonstrated potent antitumor activity in syngeneic mouse models and promising anti-tumor efficacy in humans. However, development of IL-12 has been limited by severe systemic toxicities. To overcome toxicity and improve the therapeutic index of IL-12, we employed protein engineering to generate XTX301, a highly potent, half-life extended and masked IL-12. The masking domain of XTX301 is designed to pharmacologically inactivate IL-12 systemically and render an active IL-12 moiety upon cleavage by proteases that are enriched in the tumor microenvironment.

Methods We conducted experiments to assess the binding, bioactivity, safety, and anti-tumor efficacy of XTX301. Binding interactions were measured via SPR, bioactivity was measured using STAT-4 phosphorylation in a reporter cell line, and IFN-g production was assessed in human PBMCs via ELISA. Anti-tumor efficacy and pharmacodynamics were assessed in MC38 and B16F10 syngeneic tumor mouse models using a XTX301 murine surrogate, mXTX301. Safety and pharmacokinetics of XTX301 were evaluated in non-human primates (NHP).

Results XTX301 showed no detectable binding to the high affinity IL12RB2 demonstrating that the masking domain indeed prevents interaction with the receptor. Upon cleavage of the masking domain by relevant proteases, binding was observed and was comparable to XTX300 unmasked control. Likewise, restoration of activity upon proteolytic cleavage was observed in an IL-12-dependent reporter gene assay and in primary human PBMCs. Human IL-12 does not cross react with mouse IL-12 receptors; hence a murine surrogate (mXTX301) was created for in vivo anti-tumor efficacy evaluation. A single dose of mXTX301 demonstrated up to 90% tumor growth inhibition in an inflamed MC38 and non-inflamed B16F10 syngeneic mouse models. mXTX301 induced a ~3 fold increase in IFN-g in tumors compared to vehicle control and ~150 fold less peripheral IFN-g compared to mXTX300. XTX301 exhibits minimal elevation in liver enzymes and a 50-fold improvement in tolerability compared to XTX300, in a repeat dose NHP safety study.

Conclusions Our data demonstrates that both XTX301 and mXTX301 are inactive when in masked form and become activated upon proteolytic cleavage to exert bioactivity comparable to recombinant IL-12. For efficacy, mXTX301 demonstrated tumor selective activity in syngeneic mouse models. XTX301 was well tolerated in repeat dose NHP safety study. In conclusion, XTX301 has potential for exerting potent anti-tumor activity with a favorable tolerability profile.

<http://dx.doi.org/10.1136/jitc-2021-SITC2021.719>

720

CUE-102 SELECTIVELY ACTIVATES AND EXPANDS WT1-SPECIFIC T CELLS FOR THE TREATMENT OF PATIENTS WITH WT1+ MALIGNANCIES

¹Christie Zhang*, ¹Natasha Girgis, ¹Zohra Merazga, ¹Steven Hatfield, ¹Alex Histed, ¹Fan Zhao, ¹Raymond Moniz, ¹Kristin Yeung, ¹Fulvio Diaz, ¹Jason Brown, ¹Mark Haydock, ¹Luke Witt, ¹Wynona Bautista, ¹John Ross, ¹Saso Cemerski, ¹Anish Suri, ²Kenneth Pienta, ¹Matteo Levisetti, ¹Steve Quayle. ¹Cue Biopharma, Cambridge, MA, United States; ²Johns Hopkins School of Medicine, Cambridge, MA, United States

Background Wilms' Tumor 1 (WT1) was ranked as the highest priority antigen for therapeutic targeting in an effort by the National Cancer Institute. Development of novel modalities targeting WT1 provide a significant opportunity to address high unmet medical need in WT1-positive malignancies, including AML, ovarian, endometrial, breast, lung, colorectal and pancreatic cancer. Leveraging the Immuno-STAT platform of targeted IL-2 therapies, and the ongoing development of CUE-101, CUE-102 is being developed as a novel therapeutic fusion protein to selectively activate tumor antigen-specific T cells to treat WT1-expressing cancers. CUE-102 consists of two human leukocyte antigen (HLA) molecules presenting a WT1 peptide, four affinity-attenuated human interleukin-2 (IL-2) molecules, and an effector attenuated human immunoglobulin G (IgG1) Fc domain.

Methods Human PBMCs were tested to demonstrate cellular activity and specificity of CUE-102, while in vivo activity of CUE-102 was assessed in HLA-A2 transgenic mice. HLA-A2/WT1-specific TCRs were validated and expressed in primary human CD8 T cells. Tetramer staining and flow cytometry identified cell populations and activation markers.

Results Multiple in vitro assessments demonstrate that CUE-102 selectively activates and expands WT1-specific CD8+ T cells from PBMC of healthy and cancer bearing donors. These CUE-102-expanded CD8+ T cells exhibit polyfunctional and cytotoxic responses upon challenge with WT1-presenting target cells. In addition, significant functional attenuation of the IL-2 components of CUE-102 was shown, similar to preclinical results obtained with CUE-101. In vivo studies in HLA-A2 transgenic mice confirm that CUE-102 elicits and expands polyfunctional WT1-specific CD8+ T cells from naïve and previously immunized mice without significantly altering the frequencies of other immune lineages. The WT1-specific CD8+ T cells expanded in vivo exhibit polyfunctionality in response to peptide-loaded target cells, and selectively kill WT1-presenting target cells in vivo.

Conclusions CUE-102 elicits selective expansion of a WT1-specific population of cytotoxic CD8+ T cells both in vitro and in vivo. These results, together with its similarity to CUE-101, support its anticipated tolerability profile and potential for clinical efficacy in a Phase 1 trial planned to initiate in 2022.

Ethics Approval All animal studies followed guidance from the SmartLabs Institutional Animal Care and Use Committee protocol MIL-100 and were performed in compliance with federal guidelines.

<http://dx.doi.org/10.1136/jitc-2021-SITC2021.720>

721 **INTRATUMORAL IMMUNOTHERAPY WITH ALUMINUM HYDROXIDE-TETHERED IL-12 INDUCES POTENT LOCAL AND SYSTEMIC IMMUNITY WITH MINIMAL TOXICITY**

¹Michael Schmidt*, ¹Gregory Papastoitsis, ¹Howard Kaufman, ²Darrell Irvine, ²K Wittrup. ¹Ankyra Therapeutics, Boston, MA, United States; ²Massachusetts Institute of Technology, Cambridge, MA, United States

Background Interleukin-12 (IL-12) is a potent pro-inflammatory cytokine that promotes Th1 skewing, IFN γ expression, T- and NK-cell activation, and antigen presentation. In animal models, IL-12 can elicit robust anti-tumor responses through activation of both innate and adaptive immunity. However, clinical translation of IL-12 has been hindered by significant immune-related toxicity when delivered systemically, necessitating low doses that are often insufficient for efficacy. Intratumoral (IT) administration can expand the therapeutic window of IL-12 by increasing the local tumor concentration relative to systemic exposure but is in turn limited by rapid vascular and lymphatic clearance of injected drug from the tumor and corresponding systemic accumulation. Here we describe an approach to locally retain intratumorally administered IL-12 by complexing it to the common vaccine adjuvant aluminum hydroxide (alum) through a novel phosphopeptide linkage.

Methods Single-chain murine IL-12 (mIL12) was genetically fused at its c-terminus to a short alum-binding peptide (ABP) that is specifically phosphorylated on multiple serines when co-expressed with the kinase Fam20C. Phosphorylated mIL12-ABP proteins were complexed with a 10x mass excess of aluminum hydroxide through a naturally occurring ligand exchange reaction between the phosphoserines in the ABP and surface hydroxyl groups on alum. mIL12-ABP/alum complexes were characterized for in vitro potency and in vivo efficacy in multiple syngeneic tumor models including MC38, CT26, A20, 4T1, and B16F10 following IT administration. Immune analyses and re-challenge experiments are in progress.

Results mIL12-ABP is phosphorylated on multiple sites when co-expressed with Fam20C and is stably retained on aluminum hydroxide in vitro under elution conditions containing phosphate and serum. Alum-bound mIL12-ABP remains active in cellular assays with a 3–4 fold increase in EC₅₀ compared to free protein. Following intratumoral administration, the mIL12-ABP/alum complexes have significantly extended tumor retention compared to unmodified mIL12, leading to potent local immune activation for >1 week. One or two doses of IT administered mIL12-ABP/alum is sufficient to induce robust monotherapy efficacy in diverse syngeneic tumor models including cold tumors resistant to checkpoint blockade and other immunotherapies. Locally administered mIL12-ABP/alum is further able to prime a systemic immune response leading to efficacy against non-injected tumors and spontaneous metastases. Doses required for optimal efficacy are well tolerated in mice with no significant weight loss or other evidence of systemic toxicity.

Conclusions Ankyra's platform is a differentiated approach to expand the therapeutic window of IL-12 and other cytokine drugs by enhancing tumor retention following IT administration.

<http://dx.doi.org/10.1136/jitc-2021-SITC2021.721>

722

INBRX-121 IS AN NKP46-TARGETED DETUNED IL-2 WITH ANTITUMOR ACTIVITY AS A MONOTHERAPY OR IN COMBINATION WITH MULTIPLE CANCER IMMUNOTHERAPY MODALITIES

Florian Sulzmaier*, Heather Kinkead, Anya Polovina, Nadja Kern, Angelica Sanabria, Chelsie Macedo, Abraham Hussain, Sae Jeong Ahn, Rajay Pandit, William Crago, John Timmer, Analeah Heidt, Brendan Eckelman. *Inhibrx Inc., La Jolla, CA, United States*

Background Natural Killer (NK) cells play a pivotal role in cancer immunosurveillance due to their potent cytolytic activity and NK cell-centric therapies have emerged as safer alternatives to targeting T cells.¹⁻² Interleukin 2 (IL-2) drives NK cell expansion and activity, but its therapeutic utility is limited by rapid clearance, expansion of immunosuppressive regulatory T cells, and by severe dose-limiting toxicities.³ INBRX-121 overcomes these liabilities through specific targeting of an affinity-detuned IL-2 variant to cells expressing Nkp46.

Methods An IL-2 variant was engineered to eliminate binding to CD25 and to have attenuated affinity for CD122. This detuned cytokine was fused to a high-affinity single-domain antibody targeting Nkp46 to generate INBRX-121. The ability of INBRX-121 to target IL-2-like signaling specifically to Nkp46-expressing cells was evaluated in vitro using human lymphocytes by measuring STAT5 signaling and cytotoxic activity in tumor cell co-cultures. Characterization of the pharmacokinetic/pharmacodynamic relationship of INBRX-121 was completed in non-human primates across escalating dose levels, while anti-tumor activity as a monotherapy and in combination with Rituximab or PD-1 checkpoint blockade was tested in Raji xenografts and syngeneic CT-26 mouse models, respectively.

Results INBRX-121 induces a STAT5 signal equal to that of wild-type IL-2 in human lymphocytes but shows an NK cell-centric activity profile. Cells targeted by INBRX-121 have increased proliferative capacity and improved cytotoxicity in antibody-dependent and -independent tumor cell killing assays. INBRX-121 shows prolonged pharmacokinetic exposure in vivo and is well-tolerated in mice and cynomolgus monkeys. The Nkp46-specific IL-2 stimulus in these models results in a robust, dose-dependent NK cell expansion. As predicted by its in vitro activity, INBRX-121 also enhances the cytotoxic capacity of NK cells in vivo measured via elevated intracellular levels of Granzyme B. In a Raji xenograft model, INBRX-121 slows tumor growth as a single agent and synergizes with Rituximab to induce complete tumor regression. Similarly, co-treatment with INBRX-121 improves the incomplete suppression of CT-26 tumor growth by a PD-1 blocking antibody to yield complete responses that show immunological memory upon re-challenge.

Conclusions INBRX-121 offers a unique approach to overcoming the limitations of current IL-2 therapeutics. Nkp46-targeting of a detuned IL-2 variant helps to avoid IL-2-mediated toxicity while enhancing the antitumor activities of NK cells. Through its novel therapeutic concept INBRX-121 provides a promising treatment option for multiple cancer indications both as a monotherapy and in combination with a variety of frontline agents.

REFERENCES

1. Shimasaki N, Jain A, Campana D. NK cells for cancer immunotherapy. *Nat Rev Drug Discov* 2020;**19**:200–218.
2. Liu S, Galat V, Galat Y, Lee Y, Wainwright D, Wu J. NK cell-based cancer immunotherapy: from basic biology to clinical development. *J Hematol Oncol* 2021;**14**:7.

3. Overwijk W, Tagliaferri M, Zalevsky J. Engineering IL-2 to give new life to T Cell immunotherapy. *Annu Rev Med* 2021;**72**:281–311.

Ethics Approval All animal studies were conducted in accordance with AAALAC regulations and were approved by the IACUC for Explora BioLabs (#SP17-010-013) and BTS Research (20-015 Enrollment 05).

<http://dx.doi.org/10.1136/jitc-2021-SITC2021.722>

723

WTX-613, A CONDITIONALLY ACTIVATED IFN α INDUKINE™ MOLECULE, INDUCES ANTI-TUMOR IMMUNE RESPONSES RESULTING IN STRONG TUMOR GROWTH CONTROL IN SYNGENEIC MOUSE TUMOR MODELS

Ethika Tyagi*, Heather Brodtkin, Josue Canales, Dan Hicklin, Nesreen Ismail, Kristin Morris, Christopher Nirschl, Andres Salmeron, Cindy Seidel-Dugan, Philipp Steiner, Zoe Steuert, Jenna Sullivan, William Winston. *Werewolf Therapeutics, Cambridge, MA, United States*

Background Interferon α (IFN α) was the first cytokine clinically tested as a cancer therapy. IFN α is a member of the type-I IFN family and activates immune responses either directly by engaging IFN α receptors (IFNAR) ubiquitously expressed on immune cells or indirectly by inducing chemokines that attract myeloid and lymphoid cells to the tumor site. High dose IFN α therapy was approved for melanoma, lymphoma, and leukemia but its use is limited by systemic toxicity and modest efficacy.

Methods WTX-613 is a novel systemically delivered IFN α 2b pro-drug identified using the Predator™ discovery platform. The inducible WTX-613 INDUKINE™ molecule is designed to deliver wild-type IFN α 2b in the tumor microenvironment to reduce systemic toxicity. WTX-613 has two identical half-life extension (HLE) domains tethered to IFN α 2b via a tumor protease-sensitive linker. The HLE domain supports less frequent systemic administration but importantly also prevents binding of WTX-613 to IFNAR due to steric hindrance until removal of the HLE domains by tumor proteases.

Results WTX-613 was selected as a lead molecule due to its improved in vitro profile. Since human IFN α is not functional in the mouse, a surrogate WTX-613 molecule was created consisting of mouse IFN α 1 to explore anti-tumor responses in mouse syngeneic tumor models. Intraperitoneal (i.p.) administration of the WTX-613 surrogate resulted in anti-tumor responses in the more immunogenic MC38 colon model which was well tolerated by the mice. Furthermore, less immunogenic tumor models such as B16F10 melanoma and EMT6 breast carcinoma, which are generally less responsive to I/O therapy, also responded with similar anti-tumor activity. Importantly, wild-type mouse IFN α 1 was only active in mouse models during the dosing period, and tumors grew back once treatment was stopped. However, the WTX-613 surrogate INDUKINE™ molecule had long lasting anti-tumor activity when dosed at equimolar amounts compared to the native IFN α during the dosing period. The WTX-613 surrogate strongly activated NK and CD8+ cell responses and induced APC and effector cell markers in MC38 tumors. Specifically, the WTX-613 surrogate was better than native IFN α 1 in inducing CD8+, NK, and DC cells.

Conclusions Preclinical data obtained so far support the continued development of this innovative and differentiated engineered IFN α therapy and progression into clinical trials.

Ethics Approval All mouse in vivo work was performed in accordance with current regulations and standards of the U.S. Department of Agriculture and the NIH at Charles River Laboratories (Morrisville, NC and Worcester, MA).

<http://dx.doi.org/10.1136/jitc-2021-SITC2021.723>

EVALUATION OF AN ANTI-HUMAN IL-1 β ANTIBODY IN MONOSODIUM URATE CRYSTALS-INDUCED PERITONITIS MODEL IN hIL-1 β HUGEMM™ MICE

¹Xiaoyu An, ¹Kaixia Lian, ¹Jia Zheng, ²Fei Jian, ¹Henry Li, ¹Tao Yang*. ¹*Crown Biosciences, Taicang, China;* ²*Shanghai Model Organisms, Shanghai, China*

Background Gout is a chronic inflammatory disease featuring the deposition of monosodium urate (MSU) crystals in the synovial fluid of patients, followed by NLRP3 (NOD-, LRR- and pyrin domain-containing protein 3) inflammasome activation and bioactive IL-1 β release, which recruits neutrophils to the local inflammation sites. Blocking IL-1 β function is becoming a potent therapeutic approach for gout and gouty arthritis. Conventional MSU-induced peritonitis in C57BL/6 mice provides a simple and rapid evaluation of therapeutics targeting inflammasome activation. However, this murine model has limitations when it comes to the evaluation of human-specific antibodies, for example, anti-human IL-1 β (anti-hIL-1 β) monoclonal antibodies (mAb). Thus, a murine model to assess the efficacy of anti-hIL-1 β mAb is needed. We have developed a hIL-1 β knock-in mouse model (hIL-1 β HuGEMM™), which is able to facilitate the pre-clinical evaluation of drugs targeting specific human biological molecules especially when mouse ortholog is not available. Therefore, an MSU crystals induced peritonitis model using hIL-1 β HuGEMM™ mice provides a robust model to evaluate therapies targeting hIL-1 β .

Methods MSU crystals were injected intraperitoneally into human IL-1 β (hIL-1 β) knock-in mice, where the coding sequence of mouse IL-1 β was replaced by hIL-1 β . Prior to MSU crystal administration, mice received treatment of either vehicle or anti-hIL-1 β antibody. Six hours facilitate post MSU crystal injection, serum and lavage flushed with PBS were collected. Subsequently, cytokine protein levels in the serum were determined by MSD, and the population of polymorphonuclear leukocytes (PMNs) (live CD11b+ Ly-6G^{Hi} cells) in the lavage was analysed by flow cytometry.

Results The vehicle treatment group showed a dramatic increase in hIL-1 β secretion and PMN leukocytes, in comparison to the group that did not receive MSU, which suggests a successful induction of acute inflammatory response in the peritoneal cavity. In contrast, mice that received a single administration of anti-hIL-1 β antibody 24 hours prior to MSU injection exhibited a significantly lower level of hIL-1 β when compared to the vehicle treatment group, which implies that the anti-hIL-1 β mAb efficaciously neutralized hIL-1 β secretion. In addition, TNF- α and IL-6, two further cytokines downstream of IL-1 β , were significantly reduced in the anti-hIL-1 β mAb treatment group. However, the PMN leukocyte infiltration in the anti-hIL-1 β mAb treatment group did not change in comparison to the vehicle group.

Conclusions In this study, an MSU crystals-induced peritonitis model was successfully established in hIL-1 β HuGEMM mice, which has the potential to evaluate immune therapeutics with anti-hIL-1 β blockades.

<http://dx.doi.org/10.1136/jitc-2021-SITC2021.724>

725

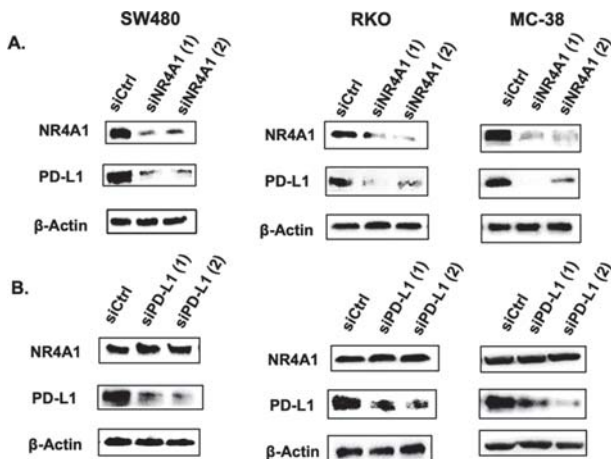
IMMUNOMODULATION BY TARGETING PDL-1 IN COLON CANCER USING NUCLEAR RECEPTOR 4A1 (NR4A1) ANTAGONISTS

¹Maen Abdelrahim*, ²Kumaravel Mohankumar, ²Keshav Karki, ²Stephen Safe. ¹Houston Methodist Cancer Center, Houston, TX, United States; ²Texas A&M University, College Station, TX, United States

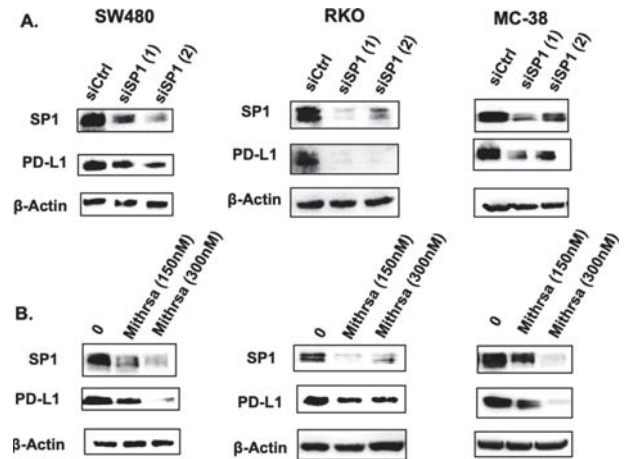
Background The nuclear orphan receptor 4A1 (NR4A1, Nur77, TR3) is overexpressed in multiple solid tumors including colorectal tumors and is a negative prognostic factor for patient survival.¹⁻³ NR4A1 is expressed in colon cancer cells and exhibit pro-oncogenic activity⁴ and results of examination of several colon cancer cell lines show that PD-L1 expression is limited and NR4A1 and PD-L1 are co-expressed in SW480 and RKO colon cancer cell lines. Previous studies showed that PD-L1 was regulated by NR4A1 which activates transcription factor Sp1 bound to the PD-L1 gene promoter.⁵⁻⁷ Knockdown of NR4A1 or Sp1 by RNA interference or treatment with mithramycin an inhibitor of Sp-mediated transcription decreased expression of PD-L1 in RKO and SW480 colon cancer cell lines.

Methods SW480, RKO and MC-38 cells were used in this study. Cells were treated for 24 hrs with DIM series of compounds.

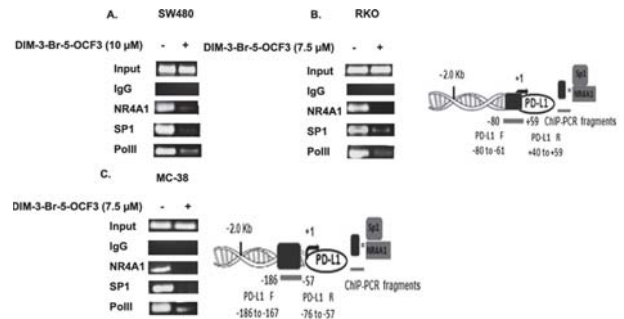
Results Current data coupled with ongoing gene expression and PD-L1 promoter studies demonstrate that PD-L1 expression is regulated by NR4A1/Sp1 in colon cancer cells (figures 1-3). Bis-indole derived NR4A1 ligand that act as receptor antagonists have been developed in this laboratory and these compounds block pro-oncogenic NR4A1-regulated genes/pathways. Treatment of RKO and SW480 colon cancer cell lines with a series of potent 1,1-bis(3[]-indolyl)-1-(3,5-disubstituted-phenyl) analogs decreased expression of PD-L1. These results show that bis-indole derived NR4A1 antagonists act as small molecule mimics of immunotherapeutics that target PD-L1. In vivo applications of NR4A1 ligands that target PD-L1 and their effects on tumor growth and immune surveillance are currently being investigated.



Abstract 725 Figure 1 NR4A1 inactivation inhibits PD-L1 expression. SW480, RKO and MC-38 cells were transfected with siCtrl (non-specific oligonucleotide) and two oligonucleotides targeting NR4A1 (siNR4A1(1) and siNR4A1(2)) or PD-L1 (siPD-L1(1) and siPD-L1(2)) for 72 hrs. Protein expression from whole cell lysates were analyzed by western blots and effects on PD-L1 expression were determined



Abstract 725 Figure 2 Sp1 inactivation inhibits PD-L1 expression. SW480, RKO and MC-38 cells were transfected with siCtrl and oligonucleotides targeting Sp1 (siSp1(1) and siSp1(2)) for 72 hrs as well as treated with Mithramycin (150 and 300 nM) for 24 hrs. Protein expression from was analyzed by western blots and effects on PD-L1 levels were determined.



Abstract 725 Figure 3 Role of NR4A1/Sp in regulation of PD-L1. SW480, RKO and MC-38 cells were treated with DIM-3-Br-5-OCF3 for 24 hrs and protein interactions with the GC-rich PD-L1 promoter region were analyzed by ChIP using primers encompassing GC-rich region of the promoter

Conclusions Bis-indole derived NR4A1 antagonists inhibit PD-L1 expression. NR4A1/SP1 regulates PD-L1 and is inhibited by NR4A1 antagonist. NR4A1 ligands such as DIM-3-Br-5-OCF3 were among the most potent of the substituted DIM compounds and ongoing in vivo studies show that this DIM compound also inhibits tumor growth in a syngenic mouse model (data not shown). Data from this study demonstrate the pro-oncogenic activity of NR4A1 and show that the synthetic buttressed analog DIM-3-Br-5-OCF3 acts as an NR4A1 antagonist and inhibits PD-L1 expression. These drugs can be developed for future clinical applications.

REFERENCES

- www.cancer.org/cancer/colon-rectal-cancer/about/key-statistics.html.
- Garcia-Villatoro et al., Effects of high-fat diet and intestinal aryl hydrocarbon receptor deletion on colon carcinogenesis. *Am J Physiol Gastrointest Liver Physiol* 2020;**318**(3):G451-G463.
- Safe S, Jin UH, Hedrick E, et al. Minireview: role of orphan nuclear receptors in cancer and potential as drug targets. *Mol Endocrinol* 2014;**28**(2):157-72.

4. Maxwell MA, Muscat GE. The NR4A subgroup: immediate early response genes with pleiotropic physiological roles. *Nucl Recept Signal* 2006;**4**:e002.
5. Lee SO, Li X, Hedrick E, et al. Diindolylmethane analogs bind NR4A1 and are NR4A1 antagonists in colon cancer cells. *Mol Endocrinol* 2014;**28**(10):1729–39.
6. Safe S, Kim K. Non-classical genomic estrogen receptor (ER)/specificity protein and ER/activating protein-1 signaling pathways. *J Mol Endocrinol* 2008;**41**(5):263–75.
7. Tao LH, Zhou XR, Li FC, Chen Q, Meng FY, Mao Y, et al. A polymorphism in the promoter region of PD-L1 serves as a binding-site for SP1 and is associated with PD-L1 overexpression and increased occurrence of gastric cancer. *Cancer Immunol Immunother* 2017;**66**(3):309–18.

<http://dx.doi.org/10.1136/jitc-2021-SITC2021.725>

TUMOR TREATING FIELDS (TTFIELDS) INDUCE AN ALTERED POLARIZATION PROGRAM IN M1/M2 MACROPHAGES

Yiftah Barsheshet*, Boris Brant, Tali Voloshin, Alexandra Volodin, Lilach Koren, Anat Klein-Goldberg, Efrat Zemer-Tov, Rom Paz, Moshe Giladi, Uri Weinberg, Yoram Palti. *Novocure, Afula, Israel*

Background Tumor Treating Fields (TTFields) are low intensity (1–3 V/cm), intermediate frequency (100–500 kHz), alternating electric fields, with demonstrated anti-mitotic effects on cancerous cells. TTFields are clinically approved for treatment of patients with glioblastoma and mesothelioma in the US and Europe. The current study aimed to examine the potential of TTFields to polarize unstimulated M0 macrophages and to regulate the phenotypes of M1 and M2 macrophages.

Methods Bone marrow-derived macrophages (BMDMs) were generated from bone marrow cells flushed from the femurs and tibias of 5–8-week-old Balb/C mice. Unstimulated (M0 phenotype) BMDMs and BMDMs stimulated with LPS+IFN- γ (M1 polarization) or IL-4 (M2 polarization) were treated with TTFields (150 kHz) for 24 or 48 hours. Surface expression of the macrophage biomarker F4/80 and the activation markers CD80, major histocompatibility complex class II (MHC II), and inducible nitric oxide synthase (iNOS) were examined by flow cytometry. The heterogeneity of the stimulated macrophages was examined by a multiplexed secretion assay, capturing 13 different proteins: CXCL1 (KC), IL-18, IL-23, IL-12p70, IL6, TNF- α , IL-12p40, free active TGF- β 1, CCL22 (MDC), IL-10, IL-6, G-CSF, CCL17 (TARC) and IL-1 β .

Results Application of TTFields to polarized (M1 or M2) or unpolarized BMDMs significantly increase in the percentage of CD80+/MHC IIhigh cells. M1 polarized BMDMs treated with TTFields also displayed elevation of intracellular iNOS levels. Cell supernatants of M1 and M2 stimulated BMDMs, as well as of unstimulated M0 BMDMs, displayed a pro-inflammatory secretion pattern following delivery of TTFields, with increased levels of CXCL1, IL-18, IL-23, IL-12p70, TNF- α , IL-12p40, CCL22, G-CSF, CCL17 and IL-1 β .

Conclusions This research showed that TTFields polarized unstimulated BMDMs to the M1 phenotype, elevated the pro-inflammatory phenotype of M1 polarized BMDMs, and induced phenotype skewing of M2 polarized BMDMs to the M1 phenotype. These results elucidate a novel immunoregulatory role of TTFields on macrophage polarization. Future studies will aim to focus on the mechanism governing this phenotypic skewing.

<http://dx.doi.org/10.1136/jitc-2021-SITC2021.726>

RESISTANCE TO ENZALUTAMIDE AND ABIRATERONE DRIVES TUMOR PHENOTYPIC PLASTICITY AND RESISTANCE TO IMMUNE-MEDIATED CYTOTOXICITY<http://dx.doi.org/10.1136/jitc-2021-SITC2021.727>

Madeline Dahut*, Kristen Fousek, Lucas Horn, Haiyan Qin, Jeffrey Schlom, Claudia Palena. NIH, Bethesda, MD, United States

Background Background: Treatment of patients with castration-resistant prostate cancer (CRPC) includes the use of next-generation hormonal therapies such as abiraterone or enzalutamide. Although these agents extend survival, a significant proportion of patients exhibit primary or acquired resistance to treatment. In recent years, immune checkpoint blockade has led to remarkable responses in patients with several tumor types, however, CRPC has remained resistant to immunotherapy. Previous studies have demonstrated that different tumor variants could emerge along the progression of prostate cancer, including tumors undergoing phenotypic plasticity in the context of an epithelial-mesenchymal transition. Our laboratory and others have shown that phenotypic plasticity is a driver of resistance to immunotherapy. Based on this knowledge, we investigated whether changes in tumor phenotype could affect the response of CRPC to immune-based therapies, and ways this can be mitigated.

Methods The androgen sensitive LNCAP prostate cancer cell line was used to derive LNCAP cells resistant to enzalutamide (LNCAP-EnzaR) or abiraterone (LNCAP-AbiR). Resistant cell lines and parental LNCAP cells were comparatively evaluated for features of EMT and neuroendocrine phenotype via RT-PCR, ELISA, western blot, immunofluorescence, and RNAseq. Changes in the susceptibility to NK-cell mediated cytotoxicity were evaluated with NK cells isolated from peripheral blood from healthy donors. LNCAP-EnzaR cells were also grown in vivo in NSG MHC-deficient mice, and tumors were characterized for phenotypic markers and potential therapeutic targets.

Results Acquisition of resistance to both enzalutamide and abiraterone was associated with a significant increase in mesenchymal tumor features, including high levels of vimentin and fibronectin, and the loss of epithelial features and cell-to-cell attachments. LNCAP-EnzaR and LNCAP-AbiR cells showed a significant reduction (up to 90%) in susceptibility to NK-cell mediated cytotoxicity and antibody-dependent cell cytotoxicity (ADCC), compared with parental cells. These results prompted us to investigate approaches to improve immune-mediated lysis, including inhibition of estrogen receptor 1 (ESR1), which was identified as highly upregulated in LNCAP-EnzaR cells via RNAseq analysis. In a xenograft model of LNCAP-EnzaR cells, we corroborated the maintenance of tumor phenotypic plasticity and the expression of actionable targets.

Conclusions Our data indicates that acquisition of resistance to androgen receptor inhibition is associated with marked reduction of susceptibility to immune attack, and the acquisition of tumor phenotypic plasticity. Future studies will investigate approaches that revert tumor plasticity, including blockade of ESR1, TGF-beta or IL-8, for potential improvement of tumor susceptibility to immune attack in CRPC.

Ethics Approval PBMCs were obtained from healthy donors at the NIH Clinical Center Blood Bank (NCT00001846). All animal studies were approved and conducted in accordance with an IACUC-approved animal protocol (LTIB-57) with the approval the NIH/NCI Institutional Animal Care and Use Committee.

IMMUNOLOGIC TUMOR CELL INTRINSIC EFFECTS OF STANDARD OF CARE THERAPIES FOR OVARIAN CANCER

¹Nicole James*, ²Melih Ozsoy, ²Payton De La Cruz, ¹Morgan Woodman, ¹Jennifer Ribeiro. ¹Women and Infants Hospital, Providence, RI, United States; ²Brown University, Providence, RI, United States

Background Outcomes for high grade serous ovarian cancer (HGSOC) patients have remained dismal due to the inevitable development of chemotherapy resistance with recurrent disease.¹ In order to better tailor treatment approaches and uncover opportunities for novel treatments, we need to better understand factors contributing to chemotherapy resistance. Recent studies have shown that immune-related gene expression profiles may serve as prognostic indicators of response to chemotherapy and clinical outcomes in solid tumors, including ovarian cancer.²⁻⁷ Moreover, immunologic factors have been shown to mediate chemotherapy resistance.⁸ Reports in the literature show that common ovarian cancer therapeutics, including chemotherapy, PARP inhibitors, and bevacizumab, modulate tumor cell expressed PD-L1 levels through immunologic signaling pathways.⁹⁻¹² However, very little research has addressed the effect of these treatments on other immune ligands or the differences in immunologic responses between platinum-sensitive and platinum-resistant HGSOC cell lines.

Methods The HGSOC cell lines OVCAR4 (naturally platinum-resistant), PEO1 and PEO4 (matched platinum-sensitive and -resistant lines from the same patient), were treated with common ovarian cancer therapeutics (carboplatin/paclitaxel, olaparib, and bevacizumab), in the presence or absence of peripheral blood mononuclear cells. Western blot was employed to identify levels of immune ligands of interest and a proteome profiler was used to detect broad immunologic changes in response to standard of care therapeutics.

Results Olaparib and bevacizumab treatment strikingly upregulated levels of tumor cell expressed immune ligands ICOSL and PVRL2. Platinum status or presence of an immune component had no bearing on the effect. Moreover, blockade of PVRL2 using siRNA or monoclonal antibodies suppressed STAT3 signaling. When examining the effect of these therapeutics on cytokine levels in HGSOC cell lines treated in immune cell co-culture, OVCAR4 cells displayed marked changes in cytokine levels, particularly CXCL10, CXCL12, SERPINE1, IL1A, and IL1RA. While PEO1 and PEO4 cells displayed more subtle cytokine changes compared to OVCAR4 cells, differences in basal levels and treatment responses were observed between the platinum-sensitive and -resistant lines, most strikingly higher basal levels of SERPINE1 and CCL5/RANTES in PEO4 cells, and a robust increase in IL8 levels in response to chemotherapy in only PEO1 cells and not PEO4.

Conclusions In conclusion, common ovarian cancer chemotherapeutics and targeted agents induce tumor cell intrinsic immunologic effects that could potentially be exploited as combinatorial therapeutic targets. Differences in immunologic responses may help define platinum-sensitive and -resistant disease. These results will require further exploration in immune-competent mouse models and human HGSOC tissue.

REFERENCES

1. Cortez AJ, Tudrej P, Kujawa KA, Lisowska KM. Advances in ovarian cancer therapy. *Cancer Chemother Pharmacol* 2018;**81**(1):17–38.
2. James NE, Miller K, LaFranzo N, Lips E, Woodman M, Ou J, Ribeiro JR. Immune modeling analysis reveals immunologic signatures associated with improved outcomes in high grade serous ovarian cancer. *Front Oncol* 2021;**11**:622182.
3. Liu R, Hu R, Zeng Y, Zhang W, Zhou H-H. Tumour immune cell infiltration and survival after platinum-based chemotherapy in high-grade serous ovarian cancer

- subtypes: a gene expression-based computational study. *EBioMedicine* 2020;**51**:102602.
4. Liu J, Meng H, Nie S, Sun Y, Jiang P, Li S, et al. Identification of a prognostic signature of epithelial ovarian cancer based on tumor immune microenvironment exploration. *Genomics*. 2020.
5. Ding J, Zhang Q, Chen S, Huang H, He L. Construction of a new tumor immunity-related signature to assess and classify the prognostic risk of ovarian cancer. *Aging (Albany, NY)*. 2020;**12**.
6. Wu Y, Xia L, Zhao P, Deng Y, Guo Q, Zhu J, et al. Immune profiling reveals prognostic genes in high-grade serous ovarian cancer. *Aging (Albany, NY)*. 2020;**12**(12):11398–11415.
7. Montfort A, Owen S, Piskorz AM, Supernat A, Moore L, Al-Khalidi S, et al. Combining measures of immune infiltration shows additive effect on survival prediction in high-grade serous ovarian carcinoma. *Br J Cancer* 2020;**122**(12):1803–1810.
8. Liu W, Wang Y, Xie Y, Dai T, Fan M, Lu C, Zou Y. Cisplatin remodels the tumor immune microenvironment via the transcription factor EB in ovarian cancer. *Cell Death Discov*. 2021;**7**(1):136.
9. Peng J, Hamanishi J, Matsumura N, Abiko K, Murat K, Baba T, Yamaguchi K, Horikawa N, Hosoe Y, Murphy SK, Konishi I, Mandai M. Chemotherapy induces programmed cell death-Ligand 1 overexpression via the nuclear factor- κ B to foster an immunosuppressive tumor microenvironment in Ovarian cancer. *Cancer Res* 2015;**75**(23):5034–45.
10. Jiao S, Xia W, Yamaguchi H, Wei Y, Chen M-K, Hsu J-M, et al. PARP inhibitor upregulates PD-L1 expression and enhances cancer-associated immunosuppression. *Clin Cancer Res* 2017;**23**(14):3711–3720.
11. Xue C, Xu Y, Ye W, Xie Q, Gao H, Xu B, et al. Expression of PD-L1 in ovarian cancer and its synergistic antitumor effect with PARP inhibitor. *Gynecol Oncol* 2020;**157**(1):222–233.
12. Zhang L, Chen Y, Li F, Bao L, Liu W. Atezolizumab and bevacizumab attenuate cisplatin resistant Ovarian cancer cells progression synergistically via suppressing epithelial-Mesenchymal transition. *Front Immunol* 2019;**10**:867.

<http://dx.doi.org/10.1136/jitc-2021-SITC2021.729>

730

HYPOXIA REDUCTION IN TANDEM WITH ANTI-ANGIOGENIC THERAPY REMODELS THE PDAC MICROENVIRONMENT AND POTENTIATES CD40 AGONIST THERAPY

Arthur Liu*, Michael Curran. *The University of Texas MD Anderson Cancer Center, Houston, TX, United States*

Background The majority of patients with pancreatic ductal adenocarcinoma (PDAC) fail to derive any durable responses from single agent immune checkpoint blockade therapy. This refractory state originates from PDAC's unique tumor microenvironment that is densely populated by immunosuppressive myeloid cells while excluding most antitumor CD8 T cells.¹ In addition, PDAC is highly hypoxic and exhibits poor vascularity, both qualities which further limit antitumor immunity.^{2, 3} We showed that the hypoxia-activated prodrug TH-302 (Evoxofosfamide) potentiates immunotherapy responses.⁴ Mechanistically, TH-302 decreases intratumoral hypoxia and initiates normalization of the tumor vasculature. While TH-302 facilitates a cellular remodeling process that diminishes tumor hypoxia, the nature of the vascular remodeling involved remains unknown, as do the downstream consequences for the composition of the tumor microenvironment and responsiveness to immunotherapy. We hypothesized that anti-angiogenic therapy and Evoxofosfamide might cooperate to normalize tumor vasculature and diminish hypoxia.

Methods TH-302 and a vascular endothelial growth factor receptor-2 (VEGFR-2) blocking antibody were used to treat several syngeneic murine models, including orthotopic pancreatic cancer and a transplantable model of prostate cancer. Immunofluorescence and flow cytometry were used to assess intratumoral hypoxia, vessel normalization, and tumor immune infiltrate.

Results We find that anti-VEGFR-2 (DC101) in combination with TH-302 demonstrates a cooperative benefit to combat both orthotopically implanted pancreatic cancer and transplantable prostate cancer. Combination therapy reduces intratumoral hypoxia, leads to pruning of the tumor vasculature, and increases the infiltration of endothelial cells into hypoxic regions. Across models, the combination of DC101 and TH-302 significantly enhance CD8 T cell function and limits their exhausted state. At the same time, tumor associated macrophages exhibit decreased expression of M2-like features. Similar to other anti-angiogenic therapies, combination DC101 and TH-302 leads to an increased frequency of PD-L1 expressing cells. Concurrent anti-PD-1 failed to provide any additional therapeutic benefit, which in part may be due poor CD8 T cell infiltration. Instead, we find that CD40 agonist therapy is improved when combined with TH-302 and DC101.

Conclusions TH-302 and DC101 utilize unique yet complementary mechanisms to improve the survival of mice challenged with pancreatic or prostate tumors. This combination relieves hypoxia and simultaneously reinvigorates T cell function and reduces macrophage mediated immunosuppression. In this setting, CD40 agonist therapy provides an additive benefit in prolonging mouse survival. Put together, these data indicate that targeted hypoxia reduction with anti-angiogenic therapy remodels the tumor microenvironment and enhances immunotherapy responses in PDAC.

REFERENCES

1. Bear AS, Vonderheide RH, O'Hara MH. Challenges and opportunities for pancreatic cancer immunotherapy. *Cancer Cell*. 2020;**38**(6):788–802. doi: 10.1016/j.cell.2020.08.004. Epub 2020 Sep 17. PMID: 32946773; PMCID: PMC7738380.

2. Koong AC, Mehta VK, Le QT, Fisher GA, Terris DJ, Brown JM, Bastidas AJ, Vierra M. Pancreatic tumors show high levels of hypoxia. *Int J Radiat Oncol Biol Phys* 2000;**48**(4):919–22. doi: 10.1016/s0360-3016(00)00803-8. PMID: 11072146.
3. Olive KP, Jacobetz MA, Davidson CJ, Gopinathan A, McIntyre D, Honess D, Madhu B, Goldgraben MA, Caldwell ME, Allard D, Frese KK, Denicola G, Feig C, Combs C, Winter SP, Ireland-Zecchini H, Reichelt S, Howat WJ, Chang A, Dhara M, Wang L, Rückert F, Grützmann R, Pilarsky C, Izeradjene K, Hingorani SR, Huang P, Davies SE, Plunkett W, Egorin M, Hruban RH, Whitebread N, McGovern K, Adams J, Iacobuzio-Donahue C, Griffiths J, Tuveson DA. Inhibition of Hedgehog signaling enhances delivery of chemotherapy in a mouse model of pancreatic cancer. *Science* 2009;**324**(5933):1457–61. doi: 10.1126/science.1171362. Epub 2009 May 21. PMID: 19460966; PMCID: PMC2998180.
4. Jayaprakash P, Ai M, Liu A, Budhani P, Bartkowiak T, Sheng J, Ager C, Nicholas C, Jaiswal AR, Sun Y, Shah K, Balasubramanyam S, Li N, Wang G, Ning J, Zal A, Zal T, Curran MA. Targeted hypoxia reduction restores T cell infiltration and sensitizes prostate cancer to immunotherapy. *J Clin Invest* 2018;**128**(11):5137–5149. doi: 10.1172/JCI96268. Epub 2018 Oct 15. PMID: 30188869; PMCID: PMC6205399.

<http://dx.doi.org/10.1136/jitc-2021-SITC2021.730>

731

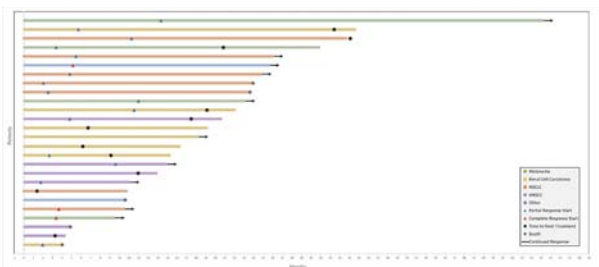
CONCURRENT IMMUNOTHERAPY AND DIPEPTIDYL PEPTIDASE-4 INHIBITION AMONG PATIENTS WITH SOLID TUMORS

¹Kayla Miranda*, ²Matthew Tucker, ²Yu-Wei Chen, ²Kathryn Beckermann, ²Brian Rini. ¹Vanderbilt University Medical Center, Nashville, TN, United States; ²Vanderbilt-Ingram Cancer Center, Nashville, TN, United States

Background Durable remissions are possible for patients with solid tumors treated with immune checkpoint inhibitors (IO); however, response rates remain relatively low. Recent preclinical data with dipeptidyl peptidase-4 inhibitors (DPP4i), widely used for diabetes management, have shown synergistic anti-tumor activity with IO in mouse models.^{1 2} However, there are no currently available data on concurrent use of DPP4i among patients treated with IO.

Methods We performed a retrospective, IRB-approved, review of all patients with solid tumors treated with IO at Vanderbilt-Ingram Cancer Center and concurrent DPP4i treatment for diabetes mellitus through review of the electronic medical record. Inclusion criteria required patients were to be on DPP4i at the start of IO treatment. The cutoff date was June 22, 2021. Outcomes measured were objective response rate (ORR), time on treatment, time to next treatment (TTNT), immune-related adverse events (iRAE), and overall survival (OS). All patients were included in the toxicity analysis; however, patients treated in the adjuvant setting, those without measurable radiographic disease, and those without available post-treatment scan were excluded from the response analysis.

Results In total, 34 patients were identified on concurrent IO plus DPP4i. The most common tumor types were melanoma (29%), renal cell carcinoma (21%), and non-small cell lung cancer (21%). Pembrolizumab was the most common IO agent (47%), followed by nivolumab (41%), ipilimumab (15%), atezolizumab (6%), and durvalumab (3%). Sitagliptin (74%) was the most common DPP4i, followed by linagliptin (18%), saxagliptin (6%), and alogliptin (3%). 14/34 patients (41%) developed any grade iRAE while on treatment with 6/34 (18%) requiring discontinuation of IO. Of the 26 patients who met inclusion criteria for the response analysis, 18 (69%) had PR or CR, 4 (15%) had stable disease, and 4 (15%) had PD as best response (figure 1). The median follow-up time was 19.0 months (IQR: 11–25.2) and the median time on treatment was 10.1 months (95% CI: 4.9–14.5). The median TTNT was 23.9 months (95% CI: 10.7–34.5) and median OS was 31.4 months (95% CI: 21.0–NE).



Abstract 731 Figure 1 Swimmers plot. An illustration of clinical events for 26 patients treated with concurrent checkpoint inhibitor (IO) and dipeptidyl peptidase-4 inhibitors (DPP4i). The timeline begins on the date of IO initiation. Each subject is represented along the y axis, with various symbols noting events such as Partial Response (PR), Complete Response (CR), start date of next line of therapy, continued response, or death. Duration of follow up ended with either patient death or study completion (6/22/21)

Conclusions This analysis represents the first data on concurrent DPP4i with IO in the treatment of solid tumors. While the cohort for response analysis was small, the ORR was high. Prospective evaluation of IO plus DPP4-i is needed to determine potential clinical efficacy of this combination.

REFERENCES

1. Barreira da Silva R, Laird ME, Yatim N, Fiette L, Ingersoll MA, Albert ML. Dipeptidylpeptidase 4 inhibition enhances lymphocyte trafficking, improving both naturally occurring tumor immunity and immunotherapy. *Nat Immunol* 2015;**16**(8):850–858. doi:10.1038/ni.3201.
2. Hollande C, Boussier J, Ziai J, et al. Inhibition of the dipeptidyl peptidase DPP4 (CD26) reveals IL-33-dependent eosinophil-mediated control of tumor growth. *Nat Immunol*. 2019;**20**(3):257–264. doi:10.1038/s41590-019-0321-5

Ethics Approval Vanderbilt University Institutional Review Board approved this study under “exempt” status (IRB# 202314). All patient information was de-identified and secured.

<http://dx.doi.org/10.1136/jitc-2021-SITC2021.731>

732

A NOVEL NUCLEAR RECEPTOR 4A1 (NR4A1) ANTAGONISTS ATTENUATES T-CELL EXHAUSTION IN COLORECTAL CANCER

¹Kumaravel Mohankumar*, ¹Gus Wright, ¹Subhashree Kumaravel, ¹Rupesh Shrestha, ²Maen Abdelrahim, ¹Robert Chapkin, ¹Stephen Safe. ¹Texas A&M University, College Station, TX, United States; ²Houston Methodist Cancer Center, Houston, TX, United States

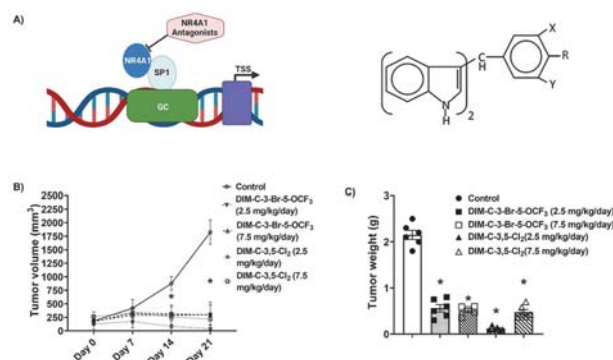
Background Colorectal cancer (CRC) is a highly complex disease with multiple risk factors and both genetic and environmental components contribute to disease incidence.¹⁻² Cancer immunotherapy using immune-checkpoint blockades represents a major advance in treatment strategy.³⁻⁴ The orphan nuclear receptor 4A1 (NR4A1) is overexpressed in lung, colon, liver and breast cancers and in Rhabdomyosarcoma and is a negative prognostic factor for cancer patient survival.⁵⁻⁸ Previous studies in breast cancer cells showed that PD-L1 was regulated by NR4A1 which activates transcription factor Sp1 bound to the PD-L1 gene promoter. Genome-wide studies have identified NR4A1 as a key mediator of T-cell dysfunction and NR4A1 also plays an important role in regulating genes which are involved in tumor-induced T-cell exhaustion.⁹ Bis-indole derived NR4A1 ligand that act as receptor antagonists have been developed in this laboratory and these compounds block pro-oncogenic NR4A1-regulated genes/pathways.

Methods Immune competent C57BL/6 mice and mouse MC-38 colon cancer cells were used and tumor Infiltrating Lymphocytes (TILs) were isolated from mice either untreated or treated with CDIM/NR4A1 antagonists. FACS analysis and Real-Time PCR were performed to determine expression of exhaustion markers in these tumor T-cell population.

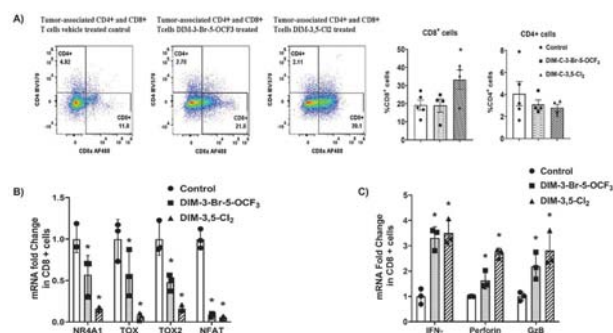
Results

Two compounds: 1,1-bis(3-indolyl)-1-(3-bromo-5-trifluoromethoxyphenyl)methane (DIM-3-Br-5-OCF₃) and 3,5-dichlorophenyl analog (DIM-3,5-Cl₂) inhibited tumor growth and weight at doses of 2.5 and 7.5 mg/kg/day (figure 1). Tumor CD8+ T-cells isolated from mice treated with DIM-3,5-Cl₂ and DIM-3-Br-5-OCF₃ exhibited decreased mRNA expression of NR4A1 and high mobility group – box transcription factors NFAT, TOX and TOX2 and increased mRNA levels of Interferon- γ (IFN γ), granzyme β (GzB) and perforin compared to control animals (figure 2). As TOX and TOX2 cooperate with NR4A1 to modulate CD8+ T-cell exhaustion, we investigated the expression of several inhibitory receptors of T-cell exhaustion in CD8+ TILs, including PD-1, 2B4, TIGIT and TIM3. Following treatment with DIM-3,5-Cl₂ or DIM-3-Br-5-OCF₃, there was a significant decrease in the percentage of PD1 and 2B4 cells and a decrease in TIGIT and TIM3 (figure 3). These results indicate that NR4A1 antagonists reverses T-cell exhaustion.

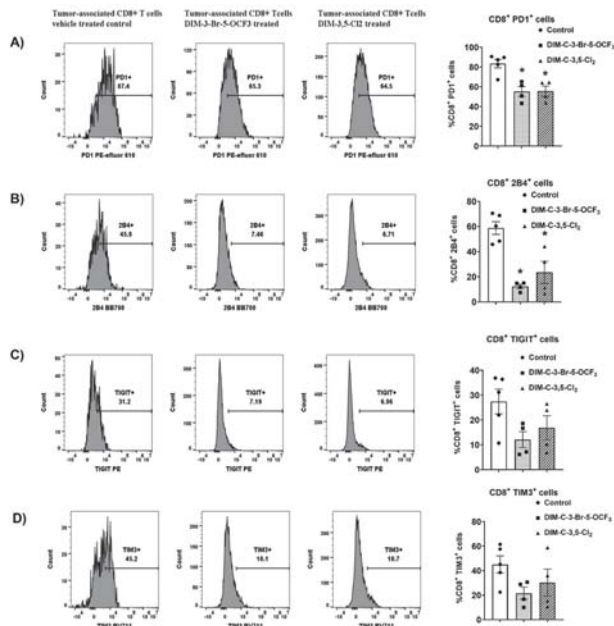
Conclusions NR4A1 plays a critical role in T-cell dysfunction, and this includes T-cell exhaustion.¹⁰⁻¹¹ Our results demonstrate that the NR4A1 antagonists reverse many markers of T-cell exhaustion including activation of cytokines. The combined effects of NR4A1 antagonists in both tumors and T-cells result in inhibition of colon tumorigenesis by targeting pathways/genes in tumor cells and by enhancing immune surveillance via reversal of T-cell exhaustion.



Abstract 732 Figure 1 CDIM/NR4A1 antagonists inhibit colon tumor growth. Model for regulation of genes with GC-rich promoters by NR4A1/SP1 (A). C57BL/6 mice bearing MC-38 cells as xenografts were treated for 21 days with corn oil (control), DIM-3-Br-5-OCF₃ (2.5 and 7.5 mg/kg/d), DIM-3,5-Cl₂ (2.5 and 7.5 mg/kg/d) and effects on tumor volume (B), and tumor weights (C) were determined.



Abstract 732 Figure 2 CDIM analogs alter transcription factors expression. FACS analysis and CD4 and CD8 – specific antibodies were used to determine T-cell population in tumors of mice treated with corn oil (control), DIM-3-Br-5-OCF₃ (2.5 and 7.5 mg/kg/d) and DIM-3,5-Cl₂ (2.5 and 7.5 mg/kg/d) (A). Real time PCR was used to determine expression of nuclear factors (B) and cytokine (C) mRNA levels in CD8+ T-cells isolated from tumors. Results are expressed as means \pm SD replicates from each treatment group and significant ($p < 0.05$) induction or inhibition is indicated (*)



Abstract 732 Figure 3 NR4A1 ligands decreases T-cell exhaustion markers. FACS analysis in tumors derived from mice treated with corn oil (control), DIM-3-Br-5-OCF3 (2.5 and 7.5 mg/kg/d) and DIM-3,5-Cl2 (2.5 and 7.5 mg/kg/d) using specific antibodies was carried out to determine percentage of CD8+ T-cells expressing T-cell exhaustion markers - PD1 (A), 2B4 (B), TIGIT (C) and TIM3 (D). Significant ($p < 0.05$) induction or inhibition is indicated (*) and results are expressed as means \pm SD for at least 4 separate mice per treatment group.

REFERENCES

- Ahmed M. Colon cancer: a Clinician's perspective in 2019. *Gastroenterology Res* 2020;**13**(1):1–10. Epub 2020/02/26. doi: 10.14740/gr1239.
- Keum N, Giovannucci E. Global burden of colorectal cancer: emerging trends, risk factors and prevention strategies. *Nat Rev Gastroenterol Hepatol* 2019;**16**(12):713–32. Epub 2019/08/29. doi: 10.1038/s41575-019-0189-8.
- Pardoll DM. The blockade of immune checkpoints in cancer immunotherapy. *Nat Rev Cancer* 2012;**12**(4):252–64. Epub 2012/03/23. doi: 10.1038/nrc3239.
- Ribas A, Wolchok JD. Cancer immunotherapy using checkpoint blockade. *Science* 2018;**359**(6382):1350–1355.
- Yang et al. Distinct epigenetic features of tumor-reactive CD8+ T cells in colorectal cancer patients revealed by genome-wide DNA methylation analysis. *Genome Biol* 2019;**21**(1):2. doi: 10.1186/s13059-019-1921-y.
- Safe S, Karki K. The paradoxical roles of orphan nuclear receptor 4A (NR4A) in cancer. *Mol Can Res* 2020. Epub 2020/10/28. doi: 10.1158/1541-7786.MCR-20-0707.
- Lee SO, et al. Diindolylmethane analogs bind NR4A1 and are NR4A1 antagonists in colon cancer cells. *Molecular Endocrinology*. 2014;**28**(10):1729–39. doi: 10.1210/me.2014-1102.
- Hedrick E, et al. The nuclear orphan receptor NR4A1 regulates β 1-integrin expression in pancreatic and colon cancer cells and can be targeted by NR4A1 antagonists. *Mol Carcinog* 2017;**56**(9):2066–2075.
- Liu X, et al. Genome-wide analysis identifies NR4A1 as a key mediator of T cell dysfunction. *Nature* 2019;**567**(7749):525–9. Epub 2019/03/01. doi: 10.1038/s41586-019-0979-8.
- Chen J et al. NR4A transcription factors limit CAR T cell function in solid tumours. *Nature*. 2019;**567**(7749):530–4. Epub 2019/03/01. doi: 10.1038/s41586-019-0985-x. PubMed PMID: 30814732; PMCID: PMC6546093.
- Seo H, et al. TOX and TOX2 transcription factors cooperate with NR4A transcription factors to impose CD8(+) T cell exhaustion. *Proc Natl Acad Sci USA* 2019;**116**(25):12410–5.

Ethics Approval All animal studies were carried out according to the ethical procedures approved by the Texas A&M University Institutional Animal Care and Use Committee. Approval number is 2020-0138.

<http://dx.doi.org/10.1136/jitc-2021-SITC2021.732>

733

IMMUNOLOGICAL MECHANISMS OF RESISTANCE TO CDK4/CDK6 INHIBITORS IN BREAST CANCER

¹Giulia Petroni, ²Kenneth Gouin, ¹Aitziber Buqué Martínez, ²Simon Knott, ¹Silvia Formenti, ¹Lorenzo Galluzzi*. ¹Weill Cornell Medical College, Brooklyn, United States; ²Cedars Sinai, Los Angeles, United States; ³Weill Cornell Medicine, New York, NY, United States

Background Hormone receptor+ (HR+) breast cancer (BC) is the most frequent cause of BC-related deaths. CDK4/6 inhibitors (CDK4/6i) combined with endocrine therapy (ET) emerged as an effective approach for metastatic HR+ BC. However, >60% women with HR+ BC receiving CDK4/6i +ET ultimately relapse, potentially due to activation of poorly characterized immunosuppressive pathways in the tumor microenvironment (TME).¹ Thus, strategies breaking resistance to CDK4/6i+ET in women with HR+ BC are urgently awaited. Radiation therapy (RT) mediates immunostimulatory effects that only partially overlap with those of CDK4/6i+ET,² standing out as a promising therapeutic partner. Consistent with this notion, we recently demonstrated that RT followed by the CDK4/6i palbociclib + ET (RT-P+ET) enables superior tumor control in various immunocompetent mouse models of HR+ BC.³ These findings have inspired the design of a randomized phase II clinical trial testing P+ET vs. RT-P+ET in patients with oligometastatic HR+ BC (CIMER, NCT04563507). In this context, we set out to dissect the immunological mechanisms underlying sensitivity vs. resistance to treatment in HR+ BC exposed to P+ET vs. RT-P+ET.

Methods To dissect the impact of these treatments on immune contexture in HR+ BC, we performed single-cell RNAseq on CD45+ cells infiltrating MPA/DMBA (M/D)-driven carcinomas established in immunocompetent mice (a unique model of luminal B BC), coupled to bulk RNAseq, bioinformatic analysis on public patient datasets, functional studies on ex vivo immune cells and efficacy studies.

Results We observed that (1) RT and P+ET alone mediate partial efficacy correlating with accumulation of immunosuppressive TREG and IL17A-producing $\gamma\delta$ T cells, respectively, (2) $\gamma\delta$ T cell depletion improves the efficacy of P+ET, (3) RT-P+ET mediates superior (but incomplete) tumor control, which is partially offset by CD4+/CD8+ T cell co-depletion and correlates with limited infiltration by $\gamma\delta$ T cells and TREGs, but accumulation of PD-L1 expressing myeloid cells and M2-polarized TREM2+ macrophages, which have been ascribed robust immunosuppressive effects in multiple settings⁴; and (4) that PD-1 blockage does not ameliorate the therapeutic effects of RT-P+ET (not shown), pointing to TREM2+ macrophages as to the main culprits for resistance in this setting.

Conclusions Our observations suggest that $\gamma\delta$ T cells and TREM2+ macrophages support the resistance of HR+ BC to CDK4/6i and RT-CDK4/6i, and hence constitute potential targets to delay disease progression.

REFERENCES

- Pandey et al. Molecular mechanisms of resistance to CDK4/6 inhibitors in breast cancer: a review. *Int J Cancer* 2019;**145**(5):1179–1188.
- Rodriguez-Ruiz et al. Immunological impact of cell death signaling driven by radiation on the tumor microenvironment. *Nat Immunol* 2020;**21**(2):120–134.
- Petroni et al. Radiotherapy delivered before CDK4/6 inhibitors mediates superior therapeutic effects in ER + Breast cancer. *Clin Cancer Res* 2021;**27**(7):1855–1863.
- Xiong et al. A gene expression signature of TREM2 hi macrophages and $\gamma\delta$ T cells predicts immunotherapy response. *Nat Commun* 2020;**11**(1):5084.

Ethics Approval Animal experiments were approved by the Institutional Animal Care and Use Committee (IACUC) of Weill Cornell Medical College (n° 2019–2022).

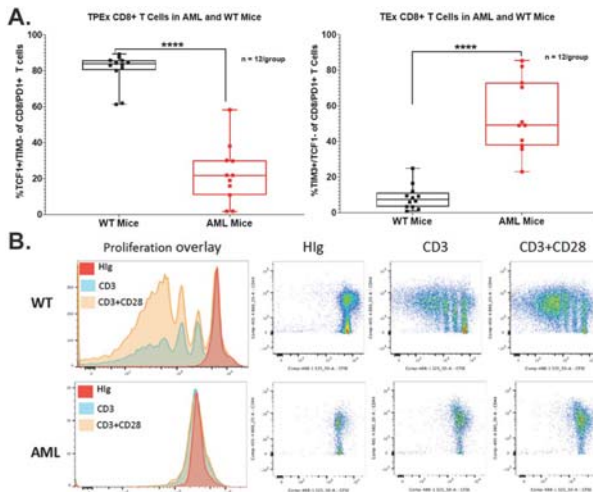
<http://dx.doi.org/10.1136/jitc-2021-SITC2021.733>

734

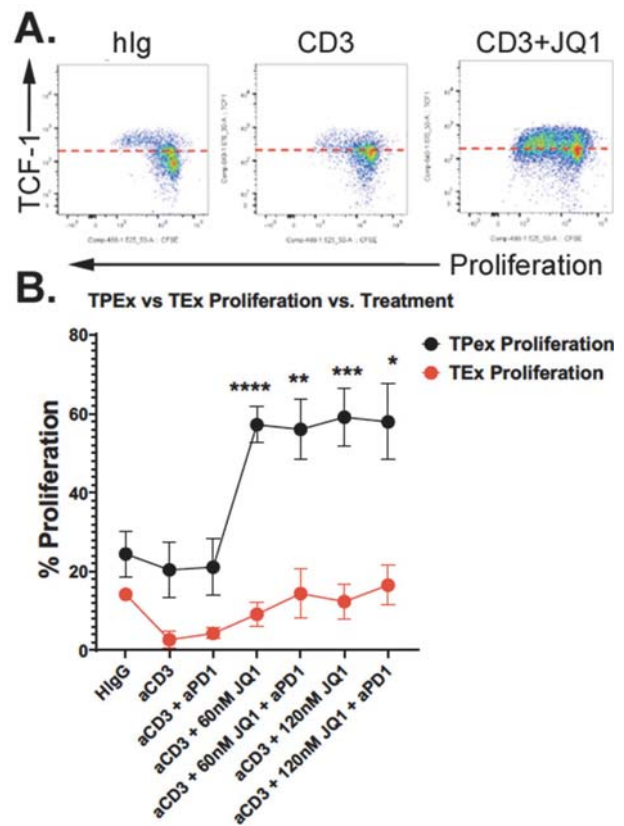
BET INHIBITORS SYNERGIZE WITH ANTI-PD1 BY RESCUING TCF1+ PROGENITOR EXHAUSTED T CELLS IN ACUTE MYELOID LEUKEMIA

¹Kyle Romine, ¹Hyun-Jun Cho, ¹Yoko Kosaka, ²Kaelan Byrd, ¹Jesse Coy, ¹Patrick Flynn, ³Matthew Newman, ¹Christopher Loo, ¹Evan Lind*. ¹Oregon Health & Science University, Portland, OR, United States; ²Oregon Health and Science University, Portland, OR, United States; ³Oregon Health & Science University, Portland, OR, United States; ⁴OHSU, Portland, United States

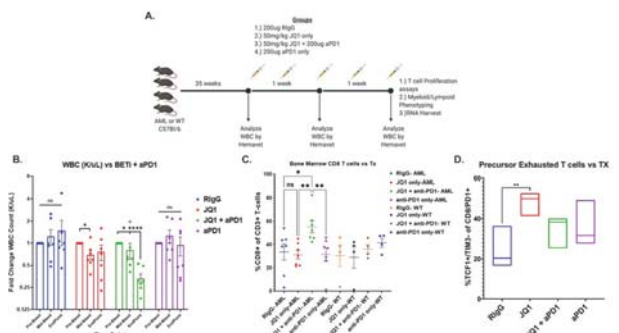
Background Acute Myeloid Leukemia (AML) is the most common adult leukemia and has a very poor prognosis. With a 5-year survival of under 30% (seer.cancer.gov), most people diagnosed with AML will die from the disease. AML is caused by an uncontrolled proliferation of poorly differentiated myeloid precursor cells which results from a combination of three classes of mutations that affect proliferation, differentiation and epigenetic state. For this reason, drugs targeting epigenetic modifications are being actively studied in AML. AML has been shown to avoid immune recognition through inhibiting the function of multiple cell types, especially T cells¹⁻² and therefore immune checkpoint blockade presents a promising therapy for any immune-targeted strategy; however, clinical trials to date have shown very modest efficacy.³⁻⁵ T cell exhaustion in cancer has been shown to be a regulated process involving transcriptional and epigenetic changes.⁶⁻⁹ BRD4 has been shown to be important for maintaining this exhaustion state.¹⁰⁻¹¹ It stands to reason that drugs designed to target epigenetic pathways in tumors will have effects on T cell populations present in the tumor microenvironment. In these studies, we investigated the effects of the BET inhibitor (BETi) JQ1 on T cell exhaustion and checkpoint responsiveness in a murine model of AML.



Abstract 734 Figure 1 T cell exhaustion in the AML mouse model. (A) Cytotoxic T cells show an exhausted phenotype in mice with AML. Spleen cultures from mice with AML or WT controls were stained with antibodies to CD3, CD8, TIM3, PD1, and TCF1. Left shows percent of TPEX CD8 T cells. Right panel shows TEX CD8 T cells. N = 12 animals per group. (B) Proliferative defect in T cells in mice with AML. Splenocytes were labeled with the proliferation dye CFSE. Whole spleen suspensions were stimulated with anti-CD3 or anti-CD3 and anti-CD28 for 3 days. FACs plots show proliferation of T cells in each condition



Abstract 734 Figure 2 Treatment with JQ1 results in expansion of T cells with TPEX. (A) Example of proliferation (CFSE dilution) vs TCF-1 expression showing unstimulated, CD3 or CD3+JQ1 120 nM in vitro 3-day culture. Results gated on CD8 T cells. (B) Summary of T cell proliferation from 4 independent experiments showing the percent proliferation of CD8 T cells with TPEX (PD1+ Tim3- TCF1+) (black line) or TEx (PD1+Tim3+TCF1-) phenotype (red line). Statistics are unpaired T-Test for each treatment condition.



Abstract 734 Figure 3 In vivo treatment of FTL mice with the BETi JQ1. (A) Schematic overview of treatment protocol. (B) White blood cell counts at pre-treatment, 1 week and 2 weeks after JQ1, PD1 blockade or both. (C) Percent of CD8+ T cells of all CD3-gated T cells in the BM of treated animals. (D) A-C Percent of precursor-exhausted CD8+ T cells as a percent of all T cells in the spleen of treated animals. Results combined from 2 separate experiments n=7. D One experiment n=3.

Methods The AML mouse model bears FLT3-ITD and deletion of TET2 restricted to the myeloid lineage. For in vitro studies, splenocytes were stimulated with anti-CD3 and either JQ1, anti-PD1 or both and proliferation and differentiation status were assessed by flow cytometry. For in vivo studies, treatment consisted of 2 weeks with JQ1, anti-PD1 or both.

Results This mouse model of AML exhibits an expansion of terminally exhausted T cells and impaired proliferative capacity after stimulation through the TCR (figure 1). Ex vivo treatment with BETi and anti-PD1 reverses CD8+ T cell exhaustion via rescue of proliferative dysfunction and expansion of more functional precursor exhausted T cells (TPEX-CD8, PD1+, TCF1+, TIM3-) (figure 2). Finally, we show that BETi synergizes with anti-PD1 in vivo leading to a reduction of tumor cells in multiple organ sites, and enrichment of CD8+ T cells in the bone marrow (figure 3).

Conclusions Using an AML mouse model that exhibits leukemia-induced immune exhaustion, we demonstrate the pre-clinical efficacy of combining BETi and anti-PD1 therapy in the treatment of AML.

REFERENCES

1. Lamble AJ, Lind EF. Targeting the immune microenvironment in acute myeloid leukemia: a focus on T Cell immunity. *Front Oncol* 2018;**8**:213.
2. Lamble AJ, Kosaka Y, Laderas T, Maffit A, Kaempf A, Brady LK, et al. Reversible suppression of T cell function in the bone marrow microenvironment of acute myeloid leukemia. *Proc Natl Acad Sci U S A*. 2020;**117**(25):14331–41.
3. Boddu P, Kantarjian H, Garcia-Manero G, Allison J, Sharma P, Daver N. The emerging role of immune checkpoint based approaches in AML and MDS. *Leuk Lymphoma* 2018;**59**(4):790–802.
4. Bewersdorf JP, Shallis RM, Zeidan AM. Immune checkpoint inhibition in myeloid malignancies: moving beyond the PD-1/PD-L1 and CTLA-4 pathways. *Blood Rev* 2020:100709.
5. Daver N, Garcia-Manero G, Basu S, Boddu PC, Alfayez M, Cortes JE, et al. Efficacy, safety, and biomarkers of response to azacitidine and nivolumab in relapsed/refractory acute myeloid leukemia: a nonrandomized, Open-Label, Phase II Study. *Cancer Discov* 2019;**9**(3):370–83.
6. Beltra JC, Manne S, Abdel-Hakeem MS, Kurachi M, Giles JR, Chen Z, et al. Developmental Relationships of Four Exhausted CD8(+) T Cell subsets reveals underlying transcriptional and epigenetic landscape control mechanisms. *Immunity* 2020;**52**(5):825–41 e8.
7. Khan O, Giles JR, McDonald S, Manne S, Ngiow SF, Patel KP, et al. TOX transcriptionally and epigenetically programs CD8(+) T cell exhaustion. *Nature* 2019;**571**(7764):211–8.
8. Pauken KE, Sammons MA, Odorizzi PM, Manne S, Godec J, Khan O, et al. Epigenetic stability of exhausted T cells limits durability of reinvigoration by PD-1 blockade. *Science* 2016;**354**(6316):1160–5.
9. Abdel-Hakeem MS, Manne S, Beltra JC, Stelekati E, Chen Z, Nzingha K, et al. Epigenetic scarring of exhausted T cells hinders memory differentiation upon eliminating chronic antigenic stimulation. *Nat Immunol* 2021;**22**(8):1008–19.
10. Milner JJ, Toma C, Quon S, Omilusik K, Scharping NE, Dey A, et al. Bromodomain protein BRD4 directs and sustains CD8 T cell differentiation during infection. *J Exp Med* 2021;**218**(8).
11. Kagoya Y, Nakatsugawa M, Yamashita Y, Ochi T, Guo T, Anczurowski M, et al. BET bromodomain inhibition enhances T cell persistence and function in adoptive immunotherapy models. *J Clin Invest* 2016;**126**(9):3479–94.

Ethics Approval This study has been approved by the OHSU IACUC committee protocol IP00000907 “Immune-based therapeutic approaches for acute myeloid leukemia” Evan Lind PI.

<http://dx.doi.org/10.1136/jitc-2021-SITC2021.734>

735

IDENTIFICATION OF A SMALL MOLECULE THAT PREVENTS T CELL EXHAUSTION USING MACHINE LEARNING ALGORITHMS PAIRED WITH HIGH-RESOLUTION SINGLE CELL RNA-SEQ

Isabelle Le Mercier*, Sunny Sun, Dongmei Xiao, Laura Isacco, Daniel Treacy, Emilie Artru, Scott Steelman, John Bradley, Alex Wolf, Morag Stewart, Effie Tozzo. *Cellarity, Cambridge, MA, United States*

Background T cell responses are tightly regulated and require a constant balance of signals during the different stages of their activation, expansion, and differentiation. As a result of chronic antigen exposure, T cells become exhausted in solid tumors, preventing them from controlling tumor growth.

Methods We identified a transcriptional signature associated with T cell exhaustion in patients with melanoma and used our proprietary machine learning algorithms to predict molecules that would prevent T cell exhaustion and improve T cell function. Among the predictions, an orally available small molecule, Compound A, was highly predicted.

Results Compound A was tested in an in vitro T cell Exhaustion assay and shown to prevent loss of proliferation and expression of immune checkpoint receptors. Transcriptionally, Compound A-treated cells looked indistinguishable from conventionally expanded, non-exhausted T cells. However, when assessed in a classical T cell activation assay, Compound A demonstrated dose dependent activity. At low dose, Compound A was immuno-stimulatory, allowing cells to divide further by preventing activation induced cell death. At higher doses, Compound A demonstrated immuno-suppressive activity preventing early CD69 upregulation and T cell proliferation. All together, these observations suggest that Compound A prevented exhaustion with a mechanism of action involving TCR signaling inhibition. While cessation of TCR signaling or rest has been recently associated with improved CAR-T efficacy by preventing or reversing exhaustion during the in vitro manufacturing phase, it is unclear if that mechanism would translate in vivo. Compound A was evaluated in the CT26 and MC38 syngeneic mouse models alongside anti-PD1. At low dose Compound A closely recapitulated anti-PD1 mediated cell behavior changes by scRNA-seq and flow cytometry in CT26 mice. At high dose, Compound A led to the accumulation of naive cells in the tumor microenvironment (TME) confirming the proposed mechanism of action. Low dose treatment was ineffective in MC38 mouse model but a pulsed treatment at high dose also recapitulated anti-PD1 activity in most animals. Importantly, we identified a new T cell population responding to anti-PD1 that was particularly increased in the MC38 mouse model; Compound A treatment also impacted this population.

Conclusions These data confirm that mild TCR inhibition either suboptimal or fractionated can prevent exhaustion in vivo. However, this approach has a very limited window of activity between immuno-modulatory and immuno-suppressive effects, thereby limiting potential clinical benefit. Finally, these results demonstrate that our approach and platform was able to predict molecules that would prevent T cell exhaustion in vivo.

<http://dx.doi.org/10.1136/jitc-2021-SITC2021.735>

736

TREATMENT WITH DECITABINE (DAC) INDUCES THE EXPRESSION OF STEMNESS MARKERS, PD-L1 AND NY-ESO-1 IN COLORECTAL CANCER

¹Nassiba Taib*, ¹Maysaloun Merhi, ¹Varghese Inchakalody, ¹Sarra Mestiri, ¹Afsheen Raza, ¹Shahab Uddin, ²Cristina Maccalli, ¹Mohammed Ussama AlHoms, ¹Said Dermime. ¹Hamad Medical Corporation, DOHA, Qatar; ²Sidra Medicine, DOHA, Qatar

Background Colorectal cancer (CRC) is a leading cause of cancer related deaths. Epigenetic silencing of numerous tumor suppressor genes by promoter region hypermethylation has been found in a variety of cancers including CRC. The chemotherapeutic drug decitabine (DAC) is a strong inducer of DNA demethylation. Primary cancer cells are known to express stemness markers as an escape pathway of treatment. Moreover, immunoregulatory genes can be inactivated in these cells by methylation of promoter CpG islands. Both mechanisms are known to play crucial roles in tumor progression. In this study, we investigated the effect of DAC on the expression of stemness markers, Programmed cell death ligand (PD-L1) and New York esophageal squamous cell carcinoma 1 (NY-ESO-1) in a metastatic (1872 Col) and a primary (1076 Col) colorectal cancer cell lines isolated from patients' tumor tissues.

Methods The 1076 Col and 1872 Col cell lines were treated with 5 μ M of DAC for 48 hours. Differential expression of a panel of stemness and immunoregulatory markers before and after treatment was analyzed by Flow cytometry (FACS), Western Blotting (WB) and quantitative real time PCR (qRT-PCR).

Results

The following stemness markers: CD44, Nanog, KLF-4, CD133 and MSI1 were up-regulated in both 1076 Col and 1872 Col cell lines after treatment. However, significant up-regulation of the immunoinhibitory PD-L1 marker was recorded after treatment only in the metastatic 1872 Col. Interestingly, the NY-ESO-1 tumor antigen was significantly upregulated in both 1076 Col and 1872 Col cell lines after treatment.

Conclusions Treatment of colon cancer cells with DAC induces chemotherapeutic resistance as evidenced by the induction/upregulation of the stemness markers; and immune escape mechanism through the induction/upregulation of PD-L1. However, such treatment resulted in the induction/expression of the most immunogenic NY-ESO-1 tumor antigen. Our data suggest the importance use of a combined treatment strategy utilizing chemotherapy (DAC) with anti-PD-L-1/PD-1treatment in colon cancer patients.

Ethics Approval The study obtained ethical approval from Hamad Medical Corporation, Medical Research Center Ethic Board: Grant ID : IRGC-04-SI-17-142.

<http://dx.doi.org/10.1136/jitc-2021-SITC2021.736>

737

INHIBITION OF P21-ACTIVATED KINASE 4 (PAK4) REVERTS IMMUNE EXCLUSION AND RESTORES ANTI- TUMOR IMMUNITY IN THE TUMOR MICROENVIRONMENT

Yu 'Jerry' Zhou*, Gina Chu, Eleanore Hendrickson, Johnni Gullo-Brown, Brandy Chavez, Indrawan McAlpine, Eugene Rui, Shawn Doran, Sergei Timofeevski, Jonathan Heyen, Jennifer Kinong, Szu-Yu Tang, Jon Oyer, Vinayak Rayannavar, Andrew Nager, Keith Ching, Stephanie Shi, Rajarshi Bhadra, Christopher Dillon, Murali Gururajan. *Pfizer, San Diego, CA, United States*

Background P21-activated kinase 4 (PAK4) is a serine/threonine protein kinase that is mostly expressed in tumor and stroma cells. PAK4 activates tumor WNT/ β -catenin pathway and regulates cellular morphology, motility, EMT, cell proliferation and survival. Recent studies also showed that PAK4 can actively exclude T cells from tumors, suggesting that therapeutic inhibition of PAK4 can increase T cell infiltration in tumor microenvironment and overcome resistance to checkpoint inhibitor immunotherapy.¹

Methods We generated PAK4 knockout (KO) clones in human and mouse tumor cells to validate its biology in vitro and in vivo. We also performed pharmacological evaluation of PAK4 inhibition using Pfizer compounds (referred to as 'PAK4i compounds' below) for their potential tumor-intrinsic and immune-regulatory roles.

Results Nanostring, qPCR and RNASeq analysis showed that PAK4 depletion led to increase of cytokine expression in tumor, including conventional dendritic cell (cDC)- recruiting chemokine CCL4, and type I IFN / ISG pathway genes that are associated with MHC upregulation such as CXCL10. In addition, PAK4 KO sensitizes B16F10 tumors to anti-PD-1 treatment and increases infiltration of cDC and T cells in the tumor microenvironment. We also showed that small molecule PAK4i compounds induced more potent cancer cell growth inhibition over treated normal PBMCs. PAK4i compounds also increased immune-activating and decreased immune exclusion genes in B16F10 cells and tumor explants in vitro. Although PAK4 target engagement is demonstrated by CETSA assay, the compound potency on modulating PAK4 downstream Wnt/ β -catenin pathway is low, suggesting that the aforementioned phenotypic changes induced by PAK4i compounds may be partially attributed to other off-target effects.

Conclusions Collectively, our data suggests that genetic depletion or pharmacological inhibition of PAK4 may induce immune-activating cytokine production in tumor cells, revert immune cell exclusion in tumor microenvironment, and synergize with checkpoint blockade therapies. However, further optimization on these PAK4i compounds is needed to improve its specificity on modulating PAK4 enzyme activities.

REFERENCE

1. Abril-Rodriguez G, Torrejon DY, Liu W, Zaretsky JM, Nowicki TS, Tsoi J, Puig-Saus C, Baselga-Carretero I, Medina E, Quist MJ, Garcia AJ, Senapedis W, Baloglu E, Kalbasi A, Cheung-Lau G, Berent-Maoz B, Comin-Anduix B, Hu-Lieskovan S, CWang CY, Grasso CS & Ribas A. PAK4 inhibition improves PD-1 blockade immunotherapy. *Nat Cancer* 2020;1:46–58.

Ethics Approval All animal studies were conducted in accordance with protocols approved by the Institutional Animal Care and Use Committee of Pfizer. Approved protocol # LAJ-2019-01347

<http://dx.doi.org/10.1136/jitc-2021-SITC2021.737>

INTRATUMORAL ADMINISTRATION OF ALUM-TETHERED ENGINEERED INFLAMMATORY CYTOKINES SAFELY ELICITS POTENT LOCAL AND SYSTEMIC IMMUNITY

Yash Agarwal*, K. Wittrup, Darrell Irvine. *Massachusetts Institute of Technology, Cambridge, MA, United States*

Background While immune checkpoint blockade therapy has improved progression-free survival in patients suffering from cancer over other treatments,^{1–4} these typically elicit durable responses in only minority of patients, in part because of the highly immunosuppressive tumor microenvironment (TME).^{5–6} Rational combinations with inflammatory cytokines can relieve some immunosuppression,^{7–8} but systemic dosing of these proteins is impeded by severe immune-related adverse events (irAE).^{9–14} One approach to focus the activity of immunostimulatory agents in tumors while lowering systemic toxicity is to administer these drugs intratumorally. However, intratumoral injection alone generally achieves limited persistence in the TME, as drugs quickly clear from the tumor via lymphatics and the tumor vasculature, rapidly leading to harmful accumulation in the circulation.^{15–16} Thus, approaches to promote in vivo retention of intratumorally administered drugs are necessary to maximize local stimulation.

Methods We engineered Interleukin-12 (IL-12) with a peptide tag containing multiple phosphoserine (pSer) residues, through in-cell phosphorylation during recombinant expression in mammalian cells. We then inoculated mice with B16F10, or Ag104A tumors, treated established tumors intratumorally with a single dose of IL-12 mixed with alum, and monitored the tumor size and weights over time. Immunophenotyping of tumors and draining lymph nodes (dLNs) was conducted at several timepoints after treatment. Tumors and serum were also collected to perform bead-based Luminex analysis of many cytokines (including IL-12 and IFN- γ).

Results Cytokines with pSer tags bind tightly to the common vaccine adjuvant aluminum hydroxide (alum) via ligand exchange (72% pSer-IL-12 vs 3.5% IL-12, $P < 0.0001$). Alum particles form a physical depot at injection sites that is persistent over weeks. So, intratumoral injection of pSer-IL-12-loaded alum led to >400-fold greater retention of protein relative to unanchored pSer-IL-12 with 2-fold lower serum ALT (a biomarker for IL-12 systemic toxicity). Further, a single dose of alum-tethered pSer-IL-12 induced 5-fold greater IFN- γ secretion ($P = 0.0031$) at the tumor primarily by CD8+ T cells and doubled ($P < 0.0001$) the proportion of tumor antigen-carrying, CD86-expressing CD103+ DCs in dLN relative to free IL-12. Further, intratumoral alum/pSer-IL-12 therapy enhanced responses to checkpoint blockade (anti-PD1), leading to a cure rate of 52% in poorly immunogenic B16F10 tumors compared to 0% for free IL-12. Local intratumoral treatment of ipsilateral tumors in mice also led to clearance of large, untreated contralateral tumors in 9/15 animals for alum/pSer-IL-12 vs. 5/17 animals for unanchored IL-12 ($P = 0.04$).

Conclusions Thus, intratumoral treatment with alum-anchored cytokines presents a safe, tumor-agnostic approach to improve local and systemic anti-cancer immunity.

REFERENCES

1. Wolchok JD, Chiarion-Sileni V, Gonzalez R, Rutkowski P, Grob JJ, Cowey CL, et al. Overall survival with combined nivolumab and ipilimumab in advanced melanoma. *New England Journal of Medicine* 2017;**377**(14):1345–56.
2. Ansell SM, Lesokhin AM, Borrello I, Halwani A, Scott EC, Gutierrez M, et al. PD-1 Blockade with nivolumab in relapsed or refractory Hodgkin's lymphoma. *New England Journal of Medicine [Internet]*. 2015;**372**(4):311–9. Available from: <http://www.nejm.org/doi/10.1056/NEJMoa1411087>.

3. Brahmer J, Reckamp KL, Baas P, Crinò L, Eberhardt WEE, Poddubskaya E, et al. Nivolumab versus docetaxel in advanced squamous-cell non-small-cell lung cancer. *New England Journal of Medicine [Internet]*. 2015;**373**(2):123–35. Available from: <http://www.nejm.org/doi/10.1056/NEJMoa1504627>.
4. Bellmunt J, de Wit R, Vaughn DJ, Fradet Y, Lee J-L, Fong L, et al. Pembrolizumab as second-line therapy for advanced urothelial carcinoma. *New England Journal of Medicine [Internet]*. 2017;**376**(11):1015–26. Available from: <http://www.nejm.org/doi/10.1056/NEJMoa1613683>.
5. Yi M, Jiao D, Xu H, Liu Q, Zhao W, Han X, et al. Biomarkers for predicting efficacy of PD-1/PD-L1 inhibitors [Internet]. Vol. 17, *Molecular Cancer*. BioMed Central Ltd.; 2018 [cited 2021 May 2]. p. 1–14. Available from: <https://doi.org/10.1186/s12943-018-0864-3>.
6. Anderson KG, Stromnes IM, Greenberg PD. Obstacles posed by the tumor microenvironment to T cell activity: a case for synergistic therapies [Internet]. Vol. 31, *Cancer Cell*. Cell Press; 2017 [cited 2021 May 2]. p. 311–25. Available from: <https://pubmed.ncbi.nlm.nih.gov/28292435/>.
7. Smyth MJ, Ngiew SF, Ribas A, Teng MWL. Combination cancer immunotherapies tailored to the tumour microenvironment [Internet]. Vol. 13, *Nature Reviews Clinical Oncology*. Nature Publishing Group; 2016;143–58. Available from: <https://pubmed.ncbi.nlm.nih.gov/26598942/>.
8. Moynihan KD, Opel CF, Szeto GL, Tzeng A, Zhu EF, Engreitz JM, et al. Eradication of large established tumors in mice by combination immunotherapy that engages innate and adaptive immune responses. *Nature Medicine* 2016;**22**(12):1402–10.
9. Milling L, Zhang Y, Irvine DJ. Delivering safer immunotherapies for cancer. *Advanced Drug Delivery Reviews [Internet]*. 2017;**114**:79–101. Available from: <http://dx.doi.org/10.1016/j.addr.2017.05.011>.
10. Lasek W, Zagożdżon R, Jakobisiak M. Interleukin 12: still a promising candidate for tumor immunotherapy? *Cancer Immunology, Immunotherapy* 2014;**63**(5):419–35.
11. Kirchner G, Franzke A, Buer J, Beil W, Probst-Kepper M, Wittke F, et al. Pharmacokinetics of recombinant human interleukin-2 in advanced renal cell carcinoma patients following subcutaneous application. *British Journal of Clinical Pharmacology [Internet]* 1998;**46**(1):5–10. Available from: <http://pmc/articles/PMC1873983/>.
12. June CH, Warshauer JT, Bluestone JA. Is autoimmunity the Achilles' heel of cancer immunotherapy? *Nature Medicine [Internet]* 2017;**23**(5):540–7. Available from: <http://www.nature.com/articles/nm.4321>.
13. Leonard JP, Sherman ML, Fisher GL, Buchanan LJ, Larsen G, Atkins MB, Sosman JA, Dutcher JP, Vogelzang JLR. Effects of single-dose interleukin-12 exposure on interleukin-12–Associated toxicity and interferon- γ Production. *Blood* 1997;**2541**–8.
14. Atkins MB, Robertson MJ, Gordon M, Lotze MT, DeCoste M, DuBois JS, et al. Phase I evaluation of intravenous recombinant human interleukin 12 in patients with advanced malignancies. *Clinical Cancer Research* 1997;**3**(3).
15. van Herpen CML, van der Voort R, van der Laak JAWM, Klases IS, de Graaf AO, van Kempen LCL, et al. Intratumoral rhIL-12 administration in head and neck squamous cell carcinoma patients induces B cell activation. *International Journal of Cancer [Internet]* 2008;**123**(10):2354–61. Available from: <https://pubmed.ncbi.nlm.nih.gov/18729197/>.
16. Pfreundschuh MG, Tillman Steinmetz H, Tüschen R, Schenk V, Diehl V, Schaadt M. Phase I study of intratumoral application of recombinant human tumor necrosis factor. *European Journal of Cancer and Clinical Oncology [Internet]* 1989;**25**(2). Available from: <https://pubmed.ncbi.nlm.nih.gov/2702990/>

Ethics Approval All animal studies and procedures were carried out following federal, state and local guidelines under an institutional animal care and use committee-approved animal protocol (Protocol no. 0720-070-23) by the Committee of Animal Care at MIT.

<http://dx.doi.org/10.1136/jitc-2021-SITC2021.738>

INTRATUMOR CHILDHOOD VACCINE-SPECIFIC CD4+ T CELL RECALL HELPS ANTITUMOR CD8 T CELLS

Michael Brown*, Zachary McKay, Yuanfan Yang, Darell Bigner, Smita Nair, Matthias Gromeier. *Duke University, Durham, United States*

Background PVSRIPO, a recombinant poliovirus derived from the live-attenuated Sabin oral polio vaccine strain, is being tested in multi-institutional phase II clinical trials for recurrent glioblastoma (NCT04479241) and unresectable, PD-1 refractory melanoma (NCT04577807) in combination with PD1 blockade. PVSRIPO capsid is identical to the Sabin vaccine strain and >99% identical to the inactivated Polio vaccine (IPOL, Salk), against which public health mandated childhood vaccination is near universal. In non-vaccinated mice, PVSRIPO mediates antitumor efficacy in a replication-dependent manner via engaging innate inflammation and antitumor T cells. Accordingly, it is anticipated that pre-existing immunity to PVSRIPO impedes antitumor therapy. However, recent evidence indicates that immunological 'recall', or reactivation of memory T cells, may mediate anti-tumor effects.

Methods The impact of prior polio vs control (KLH) vaccination on intratumor viral replication, tumor inflammation, and overall tumor growth after intratumor PVSRIPO therapy was assessed in murine tumor models. The role of polio capsid and tetanus recall antigens in mediating intratumor inflammation and antitumor efficacy was similarly studied in mice non-permissive to PVSRIPO infection. To mechanistically define antitumor effects of polio recall, B cell and CD8 T cell knock-out mice were used, in addition to adoptive transfer of CD4 + T cells from vaccinated mice. Intratumor polio or tetanus recall antigen therapy was performed after OT-I transfer (OVA-specific T cells) in the B16-OVA melanoma model to gauge antitumor T cell activity. Lastly, the inflammatory effects of polio and tetanus antigens was tested in human peripheral blood mononuclear cells (PBMCs).

Results Despite curtailing intratumor viral replication, prior polio vaccination in mice potentiated subsequent antitumor efficacy of PVSRIPO. Intratumor recall responses induced by polio and tetanus antigens also delayed tumor growth. Recall antigen therapy was associated with marked intratumor influx of eosinophils, conventional CD4+ T cells, and increased expression of IFN- γ , TNF, and Granzyme B in tumor infiltrating T cells. The antitumor efficacy of polio recall antigen was mediated by CD4+ T cells, partially depended upon CD8+ T cells, and was impaired by B cells. Both polio and tetanus recall antigen therapy bolstered the antitumor function of tumor-specific OT-I CD8+ T cells. Polio and tetanus antigens induced CXCL10 and type I/II/III IFNs in PBMCs in vitro.

Conclusions Childhood vaccine-specific CD4+ T cells hold cancer immunotherapy potential. In the context of PVSRIPO therapy, antitumor and inflammatory effects of polio vaccine-specific CD4+ T cell recall supersedes inhibitory effects of attenuated intratumor viral replication, and represents a novel mechanism of action.

Ethics Approval The animal work described in this study was approved by the Duke University IACUC.

<http://dx.doi.org/10.1136/jitc-2021-SITC2021.739>

740

RADIOTHERAPY-ACTIVATED NBTXR3 NANOPARTICLES INCREASE CD8+ T CELL INFILTRATION AND DIVERSITY IN TUMORS, AND MODULATE THE IMMUNOPEPTIDOME OF CANCER CELLSAudrey Darmon, Ping Zhang, Jordan Da silva*, Sebastien Paris. *Nanobiotix, Paris, France*

Background When exposed to radiotherapy (RT), NBTXR3 nanoparticles increase radiation dose deposition from within the cancer cells. NBTXR3 is intended for a single intratumor injection. Results from a phase II/III clinical trial in patients with locally advanced Soft Tissue Sarcoma demonstrated significant superiority and clinical benefits of NBTXR3 activated by RT compared to RT alone, and was well tolerated. NBTXR3 is currently being evaluated in several other tumors including head and neck, liver, and pancreatic cancer as a single agent or in combination with anti-PD1. Moreover, preclinical studies have demonstrated that NBTXR3 can produce a significant abscopal effect, whereas RT alone cannot. Here, we explored the impact of NBTXR3 activated by RT on CD8+ infiltrates and TcR repertoire diversity change, and the effect on the immunopeptidome of cancer cells.

Methods CT26 (murine colorectal cancer cells) were subcutaneously injected in BALB/c mice in one flank. Then, tumors were intratumorally injected with NBTXR3 (or vehicle) and irradiated 24 hours later with 4Gy per fraction for 3 consecutive days. Tumors were collected 3 days after the last RT fraction and immune cell infiltrates were measured using immunohistochemistry (IHC) and digital pathology. For TcR repertoire sequencing, the same workflow was followed, except cells were injected in both flanks. Only right tumors received treatment, while left tumors remained untreated. For immunopeptidome analysis, in vitro cells were irradiated by 4Gy. After one day, cells were collected for isolation and sequencing of MHC I-loaded peptides.

Results IHC analyses showed a significant increase of CD8+ T cell infiltrates in tumors of mice treated with NBTXR3+RT, while RT alone had no significant effect. In addition, NBTXR3+RT treatment was able to increase TcR repertoire diversity, both in treated and untreated tumors, compared to RT alone. Finally, analysis of immunopeptidome showed that NBTXR3+RT changed the profile of MHC-I-loaded peptides.

Conclusions Our in vivo data indicate that NBTXR3+RT can modulate the microenvironment of treated tumors, leading to enhanced CD8+ T cell infiltration as well as modification of the TcR repertoire, both in treated and distant untreated tumors. These NBTXR3+RT-induced responses may be related to changes in the immunopeptidome of cancer cells triggered by this treatment.

<http://dx.doi.org/10.1136/jitc-2021-SITC2021.740>

EXPRESSION OF GALECTIN-3 INHIBITORS FROM A SELF-REPLICATING RNA VECTOR AS TREATMENT FOR PEDIATRIC OSTEOSARCOMA

Guillermo Herrador Cañete*, Marta Zalacain, Sara Labiano, Javier Martinez, Cristian Smerdou, Marta Alonso. *Cima Universidad de Navarra, Pamplona, Spain*

Background Osteosarcoma is an aggressive bone tumor, primarily arising in the pediatric age. Despite years of intensive research, outcome for metastatic and non-responder patients is very poor and has not improved in the last 30 years. These tumors harbor a highly immunosuppressive environment, making the existing immunotherapies ineffective. Inhibition of galectin-3 (Gal3), a protein involved in immunosuppression,¹⁻³ adhesion of tumor cells,⁴⁻⁵ and metastases,⁶⁻⁹ has been demonstrated to reduce tumor progression in different tumor models, including osteosarcoma.¹⁰⁻¹² On the other hand, virotherapy based on recombinant Semliki Forest Virus (SFV), a self-replicating RNA virus, has shown therapeutic effect in orthotopic osteosarcoma mouse models.¹³

Methods We generated SFV vectors expressing truncated forms of Gal3, including its carboxy-terminal domain (SFV-Gal3-C) and its amino-terminal domain alone (SFV-Gal3-N) or fused to the Gal3 inhibitor peptide C12 (SFV-Gal3-N-C12). An additional construct expressed the C12 peptide¹⁴⁻¹⁵ (SFV-C12). We analyzed Gal3 expression in different murine and human osteosarcoma cell lines. Orthotopic osteosarcoma tumors, induced by intratibial injection of K7M2 murine cells, which showed high expression of Gal3, were treated with SFV vectors expressing Gal3 inhibitors or luciferase or with PBS (control). Animals were maintained under standard conditions, and all procedures were approved by the Institutional Ethical Committee (CEEA) in accordance with the guidelines of the University of Navarra, approval number 044-21.

Results Treatment with the SFV-Gal3-N-C12 vector showed the highest antitumor activity, significantly reducing tumor growth compared to control mice that received PBS. In fact, this vector prolonged animal survival, leading to 47% of complete regressions. Among the other vectors, SFV-Gal3-N and SFV-C12 were also able to transiently decrease tumor growth, although they had no impact on animal survival. Moreover, the number of spontaneous lung metastasis were reduced in mice treated with SFV vectors expressing Gal3 inhibitors. Preliminary mechanistic studies showed an increase of CD3 cells infiltration in tumors treated with SFV-Gal3-N-C12 and SFV-Gal3-N vectors. Despite the antitumor effect observed with SFV-Gal3-N-C12, no protection against tumor rechallenge was observed in cured mice, indicating the lack or insufficient memory immune response generation. These data suggested that this therapeutic approach might benefit from combination with other immunomodulatory strategies. We are currently characterizing the underpinnings of the mechanisms underlying this strategy.

Conclusions In summary, we believe that inhibition of Gal3 using SFV vectors could constitute a potential approach to explore as therapy for pediatric osteosarcoma.

REFERENCES

1. Farhad M, Rolig AS, Redmond WL. The role of Galectin-3 in modulating tumor growth and immunosuppression within the tumor microenvironment. *Oncoimmunology* 2018;**7**(6):p.e1434467.
2. Ruvolo PP. Galectin 3 as a guardian of the tumor microenvironment. *Biochim Biophys Acta* 2016;**1863**(3):427-437.
3. Guo Y, et al. Roles of galectin3 in the tumor microenvironment and tumor metabolism (Review). *Oncol Rep* 2020;**44**(5):1799-1809.

4. Cao Z, et al. Endogenous and exogenous galectin-3 promote the adhesion of tumor cells with low expression of MUC1 to HUVECs through upregulation of N-cadherin and CD44. *Lab Invest* 2018;**98**(12):1642-1656.
5. Kim SJ, Chun KH. Non-classical role of Galectin-3 in cancer progression: translocation to nucleus by carbohydrate-recognition independent manner. *BMB Rep* 2020;**53**(4):173-180.
6. Pereira JX, et al. Galectin-3 regulates the expression of tumor glycosaminoglycans and increases the metastatic potential of breast cancer. *J Oncol* 2019;**2019**:9827147.
7. Song M, et al. Galectin-3 favours tumour metastasis via the activation of beta-catenin signalling in hepatocellular carcinoma. *Br J Cancer* 2020;**123**(10):1521-1534.
8. Fortuna-Costa A, et al. Extracellular galectin-3 in tumor progression and metastasis. *Front Oncol* 2014;**4**:138.
9. Nakajima K, et al. Galectin-3 in bone tumor microenvironment: a beacon for individual skeletal metastasis management. *Cancer Metastasis Rev* 2016;**35**(2):333-46.
10. Nakajima K, Balan V, Raz A. Galectin-3: an immune checkpoint target for musculoskeletal tumor patients. *Cancer Metastasis Rev* 2021;**40**(1):297-302.
11. Lei P, et al. Small interfering RNA-induced silencing of galectin-3 inhibits the malignant phenotypes of osteosarcoma in vitro. *Mol Med Rep* 2015;**12**(4):6316-22.
12. Park GB, et al. Silencing of galectin-3 represses osteosarcoma cell migration and invasion through inhibition of FAK/Src/Lyn activation and beta-catenin expression and increases susceptibility to chemotherapeutic agents. *Int J Oncol* 2015;**46**(1):185-94.
13. Ketola A, et al. Oncolytic Semliki forest virus vector as a novel candidate against unresectable osteosarcoma. *Cancer Res* 2008;**68**(20):8342-50.
14. Sun W, et al. G3-C12 peptide reverses galectin-3 from foe to friend for active targeting cancer treatment. *Mol Pharm* 2015;**12**(11):4124-36.
15. Sun W, et al. Two birds, one stone: dual targeting of the cancer cell surface and subcellular mitochondria by the galectin-3-binding peptide G3-C12. *Acta Pharmacol Sin* 2017;**38**(6):806-822.

Ethics Approval Animals were maintained under standard conditions, and all procedures were approved by the Institutional Ethical Committee (CEEA) in accordance with the guidelines of the University of Navarra, approval number 044-21.

<http://dx.doi.org/10.1136/jitc-2021-SITC2021.741>

MULTI-ARMED MYXOMA VIRUS INDUCES POTENT ANTI-TUMOR RESPONSES IN VITRO AND IN VIVO

Wazir Abdullahi, Lina Franco, Christopher Fraser, Heather Hrach, Nicole Grigaitis, Mario Abrantes, Zachary Tacner, Ana de Matos, Leslie Sharp*. *OncoMyx Therapeutics, Phoenix, AZ, United States*

Background Myxoma virus (MYXV) has been shown to selectively infect cancer cells in humans in vitro and inhibit tumor growth in mice. The genome of MYXV is large and amenable to engineering for expression of multiple transgenes. We armed MYXV with mouse or human IL-12 and human decorin. IL-12 is an immune modulator. Cellular responses to decorin include tumor cell intrinsic signaling effects, tumor matrix remodeling, and inhibition of the TGF-beta pathway. We hypothesized that MYXV armed with decorin and IL-12 would be an effective anti-tumor therapy. The current work describes the oncolytic activity and transgene expression, following exposure to armed MYXV in human cancer cell lines in vitro and efficacy in in vivo in murine models, as single agents and in combination with immune checkpoint inhibition. **Methods** Cytotoxicity was measured by a cell viability assay. ELISAs were used to detect transgene expression, Caspase-3 activation, and TGF-beta induced SMAD phosphorylation. Mouse tumor models were treated with vehicle control or the indicated virus.

Results MYXV carrying payloads of decorin and mouse IL-12 (vMYX-mIL-12/Dec) or human IL-12 (vMYX-hIL-12/Dec) were tested. Human tumor cell lines infected with vMYX-hIL-12/Dec in vitro showed independent effects when levels of transgene expression and cytotoxicity were compared, suggesting that oncolytic activity and transgene expression differentially contribute to MYXV activity. Virus-free supernatants derived from infected cells suggested a decorin specific response in caspase-3 activation, and inhibition of TGF-beta signaling. Human IL-12 is not active on mouse immune cells giving the opportunity to evaluate the role of decorin in tumor regression. B16-F10 murine melanoma mice treated with vMYX-mIL-12/Dec showed a robust response while vMYX-hIL-12/Dec showed an intermediate anti-tumor response suggesting decorin has cancer inhibitory activity and synergized with IL-12. We tested anti-PD-1 and vMYX-mIL-12/Dec in the colon adenocarcinoma model MC38. We observed that the combination for multi-armed MYXV with an immune checkpoint inhibitor showed dramatically reduced tumor growth and improved survival.

Conclusions Our data demonstrates that MYXV with IL-12 and decorin payloads have cytotoxic activity in vitro and inhibit tumor growth in vivo. Cellular responses to decorin in vitro included inhibition of processes intrinsic to tumor progression. In mouse tumor models decorin played a role in inhibiting tumor progression and synergized with IL-12 implying the combination has immune-modulatory activity. Interestingly, MYXV with IL-12 and decorin payloads significantly synergized with anti-PD-1 in preventing tumor growth, suggesting a potentially new approach towards anti-cancer therapy.

Ethics Approval All studies and procedures involving animals were carried out under the institutional guidelines of Translational Drug Development Institutional Animal Care and Use Committee

<http://dx.doi.org/10.1136/jitc-2021-SITC2021.742>

743

RESISTANCE TO ONCOLYTIC VACCINIA CAN BE REVERSED BY TARGETING REGULATORY T CELLS WITH VACCINIA-DIRECTED DELIVERY OF A TGFβ INHIBITOR

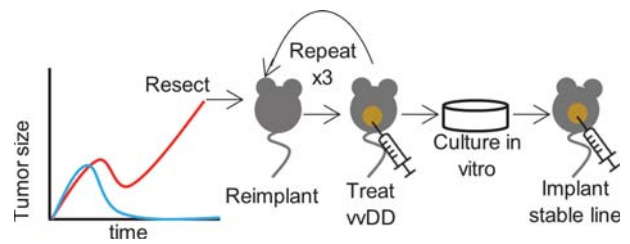
¹Kristin DePeaux*, ¹Dayana Rivadeneira, ¹McLane Watson, ¹Andrew Hinck, ²Stephen Thorne, ¹Greg Delgoffe. ¹University of Pittsburgh, Pittsburgh, PA, United States; ²Kalivir Immunotherapeutics, Pittsburgh, PA, United States

Background Oncolytic viruses are an underappreciated immunotherapy capable of inflaming the tumor microenvironment (TME), vaccinating a patient against their own tumor, and delivering gene therapy to the TME. However, apart from the oncolytic HSV T-vec, these therapies have not seen widespread use, due in part to incomplete understanding of their immunologic mechanisms of action. We sought to determine features of oncolytic vaccinia virus (VV) response and resistance using subclones of the HPV+ head and neck cancer model MEER rendered sensitive or resistant to VV.

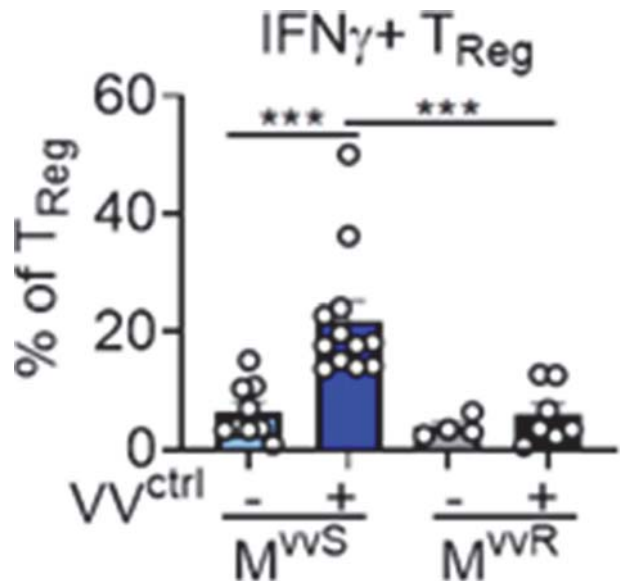
Methods A VV sensitive MEER tumor resisting treatment was serially passaged in mice and treated with VV until a stably resistant line was generated (Fig1). Sensitive or resistant MEER tumors were implanted, treated with a single intratumoral dose of VV, and harvested 4–7 days later for cytometric analysis. A genetically encoded TGFβ inhibitor was recombined into oncolytic VV (VV-TGFβi).

Results We used serial in vivo passaging to generate a VV-resistant MEER line (MEERvvR) from one sensitive to VV (MEERvvS, figure 1) and compared their immune infiltrate. While VV promoted acute cytokine production and cytotoxicity in conventional T cells, the major determining factor between sensitivity and resistance was the phenotype of Treg cells. At baseline, Treg cells in MEERvvS had lower Nrp1 expression and higher IFNγ-STAT1 signaling compared to MEERvvR, indicative of Treg 'fragility'. VV treatment induced MEERvvS Treg cells to become immunostimulatory and produce IFNγ (figure 2). RNAseq revealed MEERvvR produced more TGFβ than MEERvvS cells, suggesting these tumors directly stabilize Treg cells. To determine if MEERvvR could be sensitized to VV, we engineered oncolytic vaccinia to produce a genetically-encoded TGFβ inhibitor which binds TGFβRII, preventing TGFβ1-3 binding (VV-TGFβi). When MEERvvR were treated with VV-TGFβi, elite responses were restored, with commensurate increase in survival (figure 3) associated with increased STAT1 signaling in Treg cells.

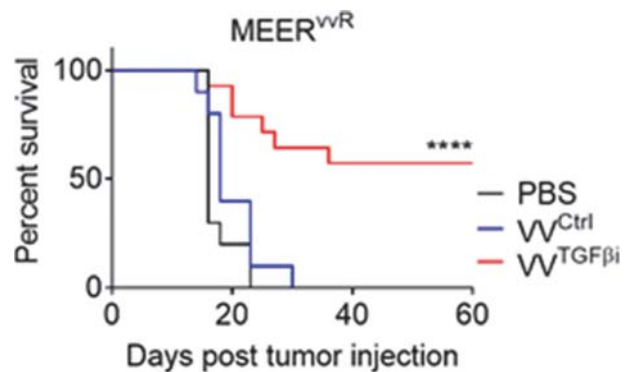
Conclusions Resistance to oncolytic vaccinia is controlled by Treg cell phenotype; tumors harboring more fragile Treg cells respond exquisitely to VV. An oncolytic vaccinia engineered to produce a novel TGFβi could remodel the TME to be less supportive of Tregs, rendering resistant tumors sensitive to VV. Our data highlight the importance of Treg cell status in resistance to oncolytic virus therapy and suggest TGFβ can be effectively targeted through an inhibitor encoded within the virus. Importantly, this TME directed production of the TGFβi carries no toxicity previously associated with systemic TGFβ inhibition, suggesting a viral approach to TGFβ inhibition can be an effective strategy support broader immunotherapy response.



Abstract 743 Figure 1 Strategy used to generate a vaccinia resistant MEER (MEERvvR) from vaccinia sensitive MEER (MEERvvS)



Abstract 743 Figure 2 IFNγ production in Treg cells in MEERvvS and MEERvvR after treatment with PBS or control vaccinia (VV-Ctrl)



Abstract 743 Figure 3 Survival of VV-resistant MEER treated with PBS, control vaccinia (VV-Ctrl), or vaccinia engineered to deliver a potent inhibitor of TGFβ (VV-TGFβi)

<http://dx.doi.org/10.1136/jitc-2021-SITC2021.743>

744

MULTI-ARMED MYXOMA VIRUS HAS THERAPEUTIC POTENTIAL FOR TREATMENT OF MULTIPLE MYELOMA

Lina Franco, Christopher Fraser, Lino Torres-Dominguez, Nicole Grigaitis, Jack St. Peter, Mario Abrantes, Zachary Tacner, Heather Hrach, Ana de Matos, Leslie Sharp*. *OncoMyx Therapeutics, Phoenix, AZ, United States*

Background Despite improvements with new therapeutics, multiple myeloma (MM) patients still relapse and become refractory. Myxoma virus (MYXV) selectively replicates in human tumor cells and stimulates the immune system. MYXV selectively kills human patient MM cells and spares normal progenitors. MYXV also eradicates growth of a disseminated mouse MM in vivo. MYXV is a large, double stranded DNA poxvirus, and has a genome size amenable to insertion of multiple transgenes. We generated MYXV carrying IL-12 and decorin. IL-12 is an immune modulator that activates T- and NK-cells. Cellular responses to decorin include tumor cell intrinsic signaling effects, tumor matrix modulation, and inhibition of the TGF-beta pathway. This represents a promising therapeutic option for MM patients that do not respond well to immunotherapy. The current work suggests MYXV armed with IL-12 and decorin could be an effective anti-MM therapy.

Methods Cytotoxicity assays were performed using a cell viability assay. Transgene expression levels were analyzed by microscopy, flow cytometry, and ELISA.

Results Human MM cell line U266 infected with MYXV (vMYX-hIL-12/Dec) carrying human IL-12, decorin, and green fluorescent protein (GFP) produced transgenes in a dose and time responsive manner. A panel of human MM cell lines was infected with vMYX-hIL-12/Dec and transgene expression in supernatant, cell killing EC50, and GFP levels were evaluated. Sensitive and resistant human MM cell lines were identified. The comparison of replication, cell killing capacity, and transgene expression highlighted the independent importance of these mechanisms in overall activity.

Conclusions The current work describes the oncolytic activity and transgene expression following exposure to vMYX-hIL-12/Dec in human MM cell lines in vitro. Our initial studies suggest there is significant value in pursuing vMYX-hIL-12/Dec and other armed MYXV as a new approach towards MM therapy.

<http://dx.doi.org/10.1136/jitc-2021-SITC2021.744>

ONCOLYTIC ADENOVIRUS EXPRESSING 4-1BBL DEMONSTRATES A SIGNIFICANT INCREASE OF SURVIVAL IN DIFFUSE MIDLINE GLIOMA MODELS

¹Virginia Laspidea*, ¹Sara Labiano, ¹Iker Ausejo-Mauleon, ¹Daniel de la Nava, ¹Marc García-Moure, ¹Javier Marco-Sanz, ²Juan Fueyo, ²Candelaria Gomez-Manzano, ¹Ana Patiño-García, ¹Marta Alonso. ¹Clinica Universidad de Navarra, Pamplona, Spain; ²MD Anderson Cancer Center, Houston, TX, United States

Background Diffuse Midline Gliomas (DMG) are aggressive pediatric brain tumors that arise in the brainstem of children between 5–10 years old. DMGs are the leading cause of pediatric death caused by a brain tumor, with a median survival of only 9 months.^{1,2} We have previously shown that the administration of the oncolytic adenovirus Delta-24-RGD is safe and lead to an increase in long-term survivors in murine models.^{3,4} In order to further increase the antitumor effect of Delta-24-RGD by boosting the immune response, we have constructed a new adenovirus, Delta-24-ACT, which incorporates the 4-1BBL (CD137L) into its backbone. 4-1BBL is a costimulatory receptor that promotes the survival and expansion of activated T cells and NK cells and the generation and maintenance of memory CD8+ T cells, among other functions.^{5,6}

Methods Murine and human DMG cell lines were used. 4-1BBL expression was assessed in infected cells by flow cytometry and immunofluorescence. Viral protein expression was measured by western blot, viral replication was analyzed using a method based on hexon detection and the oncolytic effect by MTS assay. For in vivo experiments, cells were injected in the pons of mice using a screw-guided system.⁷ A single administration of the adenovirus was injected intratumorally using the same procedure. The tumor immune populations were analyzed by flow cytometry.

Results We first confirmed by flow cytometry that DMG cells infected with Delta-24-ACT expressed 4-1BBL in their membrane in a dose-dependent manner. Afterwards, we analyzed the oncolytic effect of Delta-24-ACT in vitro. Delta-24-ACT was able to express viral early and late proteins in murine and human DMG cell lines and to replicate efficiently in human cells. In addition, the virus caused cell death in a dose-dependent manner. In vivo, Delta-24-ACT administration demonstrated to be safe and to produce a significant survival benefit in murine DMG models, obtaining 30–50% of long-term survivors depending on the model. More importantly, Delta-24-ACT generated immune memory, as long-term survivors were disease-free after cell rechallenge. On the other hand, we analyzed immune infiltration 7 or 10 days after the viral administration into the tumor and observed a significant increase of tumor infiltration in treated mice, which showed an activated state.

Conclusions Delta-24-ACT administration into DMG murine tumor models significantly increases the recruitment and activation of immune cells, which leads to long term survivors and immunological memory.

REFERENCES

- Cooney T, Lane A, Bartels U, Bouffet E, Goldman S, Leary S, Foreman NK, Packer RJ, Broniscer A, Minturn JE, Shih C, Chintagumpala M, Hassall T, Gottardo NG, Dholaria H, Hoffman L, Chaney B, Baugh J, Doughman R, Leach JL, Jones BV, Fouladi M, Warren KE, Monje M. Contemporary survival endpoints: an International Diffuse Intrinsic pontine glioma registry study. *Neuro Oncol* 2017;19(9):1279–1280.
- Grasso CS, Tang Y, Truffaux N, Berlow NE, Liu L, Debily MA, Quist MJ, Davis LE, Huang EC, Woo PJ, Ponnuswami A, Chen S, Johung TB, Sun W, Kogiso M, Du Y, Qi L, Huang Y, Hütt-Cabezas M, Warren KE, Le Dret L, Meltzer PS, Mao H, Quezado M, van Vuurden DG, Abraham J, Fouladi M, Svalina MN, Wang N,

Hawkins C, Nazarian J, Alonso MM, Raabe EH, Hulleman E, Spellman PT, Li XN, Keller C, Pal R, Grill J, Monje M. Functionally defined therapeutic targets in diffuse intrinsic pontine glioma. *Nat Med* 2015;21(6):555–9.

- Martínez-Vélez N, García-Moure M, Marigil M, González-Huarriz M, Puigdelloses M, Gallego Pérez-Larraya J, Zalacain M, Marrodán L, Varela-Guruceaga M, Laspidea V, Aristu JJ, Ramos LI, Tejada-Solis S, Díez-Valle R, Jones C, Mackay A, Martínez-Climent JA, García-Barchino MJ, Raabe E, Monje M, Becher OJ, Junier MP, El-Habr EA, Chneiweiss H, Aldave G, Jiang H, Fueyo J, Patiño-García A, Gomez-Manzano C, Alonso MM. The oncolytic virus Delta-24-RGD elicits an antitumor effect in pediatric glioma and DIPG mouse models. *Nat Commun* 2019;10(1):2235.
- García-Moure M, Gonzalez-Huarriz M, Labiano S, Guruceaga E, Bandres E, Zalacain M, Marrodán L, de Andrea C, Villalba M, Martínez-Velez N, Laspidea V, Puigdelloses M, Gallego Perez-Larraya J, Iñigo-Marco I, Strippecke R, Chan JA, Raabe EH, Kool M, Gomez-Manzano C, Fueyo J, Patiño-García A, Alonso MM. Delta-24-RGD, an oncolytic adenovirus, increases survival and promotes proinflammatory immune landscape remodeling in models of AT/RT and CNS-PNET. *Clin Cancer Res* 2021;27(6):1807–1820.
- Chester C, Sanmamed MF, Wang J, Melero I. Immunotherapy targeting 4-1BB: mechanistic rationale, clinical results, and future strategies. *Blood* 2018;131(1):49–57.
- Yonezawa A, Dutt S, Chester C, Kim J, Kohrt HE. Boosting cancer immunotherapy with anti-CD137 antibody therapy. *Clin Cancer Res* 2015;21(14):3113–20.
- Marigil M, Martínez-Velez N, Domínguez PD, Idoate MA, Xipell E, Patiño-García A, Gonzalez-Huarriz M, García-Moure M, Junier MP, Chneiweiss H, El-Habr E, Díez-Valle R, Tejada-Solis S, Alonso MM. Development of a DIPG orthotopic model in mice using an implantable guide-screw system. *PLoS One* 2017;12(1):e0170501.

<http://dx.doi.org/10.1136/jitc-2021-SITC2021.745>

VECTORIZED TREG-DEPLETING ANTI-CTLA-4 ELICITS ANTIGEN CROSS-PRESENTATION AND CD8+ T CELL IMMUNITY TO REJECT "COLD" TUMORS

¹Monika Semmrich*, ²Jean-Baptiste Marchand, ¹Matilda Rehn, ²Laetitia Fend, ²Christelle Remy-Ziller, ¹Petra Holmkvist, ²Nathalie Silvestre, ¹Carolin Svensson, ²Patricia Kleinpeter, ²Jules Deforges, ¹Fred Junghus, ¹Linda Martensson, ²Johann Foloppe, ¹Ingrid Teige, ²Eric Quemeneur, ¹Bjorn Frendeus. ¹BioInvent International AB, Lund, Sweden; ²Transgene SA, Illkirch-Graffenstaden, France

Background Immune checkpoint blockade (ICB) is a clinically proven concept to treat cancer. Still, a majority of cancer patients including those with poorly immune infiltrated "cold" tumors are resistant to currently available ICB therapies. CTLA-4 is one of few clinically validated targets for ICB, but toxicities linked to efficacy in approved anti-CTLA-4 regimens have restricted their use and precluded full therapeutic dosing. At a mechanistic level, accumulating preclinical and clinical data indicate dual mechanisms for anti-CTLA-4; immune checkpoint blockade and Treg depletion are both thought to contribute efficacy and toxicity in available, systemic, anti-CTLA-4 regimens. Accordingly, strategies to deliver highly effective, yet safe, anti-CTLA-4 therapies have been lacking. Here, BioInvent and Transgene present and preclinically characterize a highly efficacious and potentially safe strategy to target CTLA-4 in the context of oncolytic virotherapy.

Methods A novel human IgG1 CTLA-4 antibody (4-E03) was identified using function-first screening for mAbs and targets associated with superior Treg depleting activity. A tumor-selective oncolytic Vaccinia vector was then engineered to encode this novel, strongly Treg-depleting, checkpoint-blocking, anti-CTLA-4 antibody and GM-CSF (VV_{GM}-ahCTLA4, BT-001). Viruses encoding a matching Treg-depleting mouse surrogate antibody were additionally generated, enabling proof-of-concept studies in syngeneic immune competent mouse tumor models.

Results Our studies demonstrate that intratumoral (i.t.) administration of VV_{GM}-aCTLA4 achieved tumor-restricted CTLA-4 receptor saturation and Treg-depletion, which elicited antigen cross-presentation and stronger systemic expansion of tumor-specific CD8+ T cells and antitumor immunity compared with systemic anti-CTLA-4 antibody therapy. Efficacy correlated with FcγR-mediated intratumoral Treg-depletion and the reduction of exhausted CD8+ T cells. Remarkably, in a clinically relevant mouse model resistant to systemic immune checkpoint blockade, i.t. VV_{GM}-aCTLA4 synergized with anti-PD-1 to reject "cold" tumors.

Conclusions Our findings demonstrate in vivo proof-of-concept for spatial restriction of strongly Treg-depleting, immune checkpoint blocking, vectorized anti-CTLA-4 as a highly effective and safe strategy to target CTLA-4 which is able to overcome current limitations of approved anti-CTLA-4 regimens. A clinical trial evaluating i.t. VV_{GM}-ahCTLA4 (BT-001) alone and in combination with anti-PD-1 in metastatic or advanced solid tumors has commenced.

Ethics Approval All mouse experiments were approved by the local ethical committee for experimental animals (Malmö/Lunds djurförsöksetiska nämnd); at BioInvent under permit numbers 17196/2018 or 2934/2020; or at Transgene APAFIS Nr21622 project 2019072414343465 and performed in accordance with local ethical guidelines.

<http://dx.doi.org/10.1136/jitc-2021-SITC2021.746>

747

CODALYTIC™, A NOVEL CODON-PAIR DEOPTIMIZED INFLUENZA VIRUS CREATES AN IMMUNE-STIMULATORY TUMOR MICROENVIRONMENT LEADING TO MONOTHERAPY EFFICACY IN A PRECLINICAL MODEL OF BREAST CANCER<http://dx.doi.org/10.1136/jitc-2021-SITC2021.747>

Marcin Stawowczyk, Katie Pfeffer, Juliana Tafrova, Charles Stauff, Anna Kushnir, Sybil Tasker, Steffen Mueller, J Robert Coleman, Johanna Kaufmann*. *Codagenix Inc., Farmingdale, NY, United States*

Background Oncolytic viruses (OVs) of multiple species have been demonstrated to induce beneficial changes in the tumor microenvironment (TME), increasing immune cell infiltration and activating stimulatory immune responses, which ultimately support induction of an anti-tumor immune response. The majority of OVs are attenuated by either gene deletion or mutations and then armed with immunomodulatory transgenes to promote anti-tumor immune responses. Here, we describe a next-generation OV that is rationally attenuated via codon-pair deoptimization and capable of activating anti-tumor immune responses in a mouse model of triple-negative breast cancer without the need of transgenes.

Methods Hemagglutinin and neuraminidase genes of influenza virus strain A/California/07/2009 were codon-pair deoptimized using an algorithm to design synthetic viral genomes, yielding CodaLytic, a genetically stable OV with over 600 silent mutations across the two genes. For in vivo studies, EMT6 cells were implanted into inguinal mammary fat pads and treated intratumorally with CodaLytic three times a week for up to 4 weeks for efficacy studies or for up to 5 doses for pharmacodynamic readouts. Tumor infiltrating immune cells were characterized by flow cytometry or RNA was isolated for transcriptomic analysis. Anti-tumor memory was assessed by intravenous EMT6 rechallenge and interferon- γ ELISpot in splenocytes of long-term survivors.

Results CodaLytic treatment of orthotopic EMT6 tumors led to dose-dependent tumor growth retardation and increased survival with significant tumor growth inhibition of 60% and 40–60% complete regressions at 108 pfu/dose across repeat experiments. Intravenous rechallenge of long-term survivors led to a 27-fold reduction in lung nodule formation (colony mean 0.75 vs 19.92 in naïve control animals, $p = 0.005$). Anti-tumor efficacy after CodaLytic treatment was accompanied by a change in the composition of the tumor immune infiltrate with significant increases in CD4+ T, B and NK cells and increased gene expression of interferon- γ , MHC-II and CCL-5. Further evidence of induction of anti-tumor immunity was an EMT6-specific interferon- γ recall response in splenocytes from long-term survivors.

Conclusions These data demonstrate the induction of innate and adaptive changes in the TME and anti-tumor efficacy after intratumoral treatment of EMT6 tumors with CodaLytic. Additional holistic gene expression analysis is ongoing to further characterize the mechanisms of immune activation. Taken together with preclinical safety data and demonstrated clinical safety and immunogenicity of this attenuated influenza virus after intranasal administration in healthy individuals, CodaLytic is a promising immunotherapeutic to be further developed as monotherapy and in combination with immune checkpoint inhibitors or other modalities.

Ethics Approval All animal studies were conducted in compliance with protocol 2019-01-17-COD-1, approved by the Mispro Biotech Services Institutional Animal Care and Use Committee.

TARGETING VASOACTIVE INTESTINAL PEPTIDE RECEPTOR SIGNALING IN PANCREATIC DUCTAL ADENOCARCINOMA FOR ENHANCED ANTI-TUMOR RESPONSE TO CHECKPOINT BLOCKADE

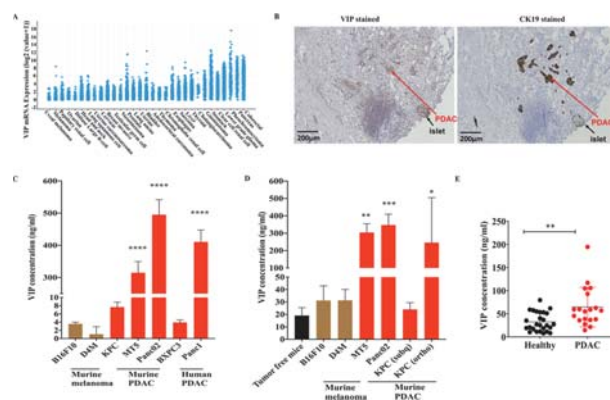
¹Sruthi Ravindranathan*, ¹Tenzin Passang Fnu, ¹Jian Ming Li, ¹Rohan Dhamsania, ¹Michael Ware, ¹Mohammad Zaidi, ¹Shuhua Wang, ¹Jingru Zhu, ¹Maria Cardenas, ¹Yuan Liu, ¹Sanjeev Gumber, ¹Brian Robinson, ²Anish Majumdar, ¹Shanmuganathan Chandrakasan, ¹Haydn Kissick, ²Alan Frey, ³Susan Thomas, ¹Bassel El-Rayes, ¹Gregory Lesinski, ¹Edmund Waller. ¹Emory University, Atlanta, GA, United States; ²Cambium oncology, Atlanta, GA, United States; ³Georgia Institute of Technology, Atlanta, GA, United States

Background Paucity of T cells in the immune privileged tumor microenvironment (TME) of pancreatic ductal adenocarcinoma (PDAC) is a major reason that PDAC is refractory to immune checkpoint blockade.¹ In this study, we show that human PDAC tumors over-express vasoactive intestinal peptide (VIP), an immunosuppressive neuropeptide, that inhibits effector T cell responses and regulates chemokine receptor expression on activated T cells.^{2, 3} We thus hypothesized that pharmacological inhibition of VIP receptor signaling could enhance anti-tumor responses in PDAC.

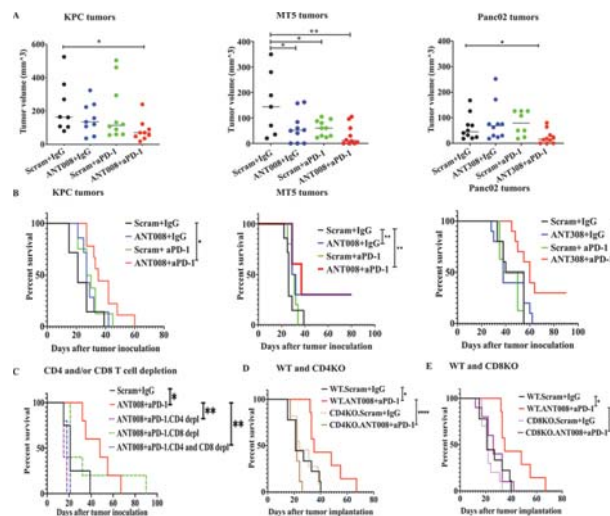
Methods VIP levels in plasma were determined via VIP-specific enzyme immunoassay and confirmed with immunohistochemistry (IHC) of tissue sections. VIP receptor (VIP-R) signaling in C57BL/6 immunocompetent murine models of KPC, MT5 or Panc02 pancreatic cancer was inhibited by daily sub-cutaneous treatment with ANT008 or ANT308, two novel VIP-R antagonists with predicted high binding affinities to VIP receptors.⁴⁻⁷ Multiplex IHC or flow cytometry detected frequencies and phenotypes of intra-tumoral T cells across treatment groups.

Results Human PDAC tumors expressed VIP by immunohistochemistry, and PDAC patients had significantly elevated plasma VIP levels when compared to healthy volunteers ($p < 0.01$, figure 1). Inhibiting VIP-R signaling in combination with anti-PD-1 monoclonal antibody (MoAb) synergistically enhanced T-cell dependent anti-tumor responses in murine PDAC resulting in elimination of tumors in up to 30% of the animals and increased intratumoral CD4+ or CD8+ T cell density in orthotopic murine PDAC (figure 2). VIP-R antagonist+anti-PD-1 combination therapy significantly increased intratumoral T cell activation and the proportion of tumor specific CD8+ T cells when compared to control ($p < 0.01$, figure 3-5). Furthermore, tumor-free mice that had been treated with VIP-R antagonist and anti-PD-1 MoAb remained tumor-free upon tumor rechallenge, indicating that combination treatment induced robust immunological memory. Interestingly, anti-PD-1 monotherapy increased expression of CXCR4 on T cells in tumor draining lymph nodes, a chemokine receptor that has been shown to trap T cells in the extracellular tumor matrix. On the other hand, combination therapy with VIP-R antagonists and anti-PD1 MoAb significantly decreased CXCR4 expression and promoted homing of adoptively-transferred GFP+ T cells into the tumors.

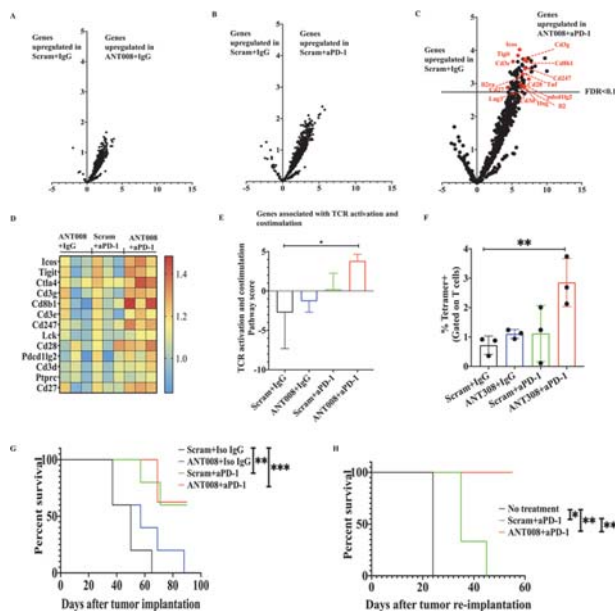
Conclusions VIP-R antagonists represent a novel approach to treat PDAC. VIP and VIP-R sequences are highly conserved between humans and mice,⁸ and human T cells are activated in vitro following treatment with VIP-R antagonists. Thus, we predict comparable anti-tumor activity of the combination of VIP-R antagonist and anti-PD-1 MoAb in human PDAC patients. Further clinical development of this novel concept will require appropriate pre-clinical pharmacokinetic and toxicology studies.



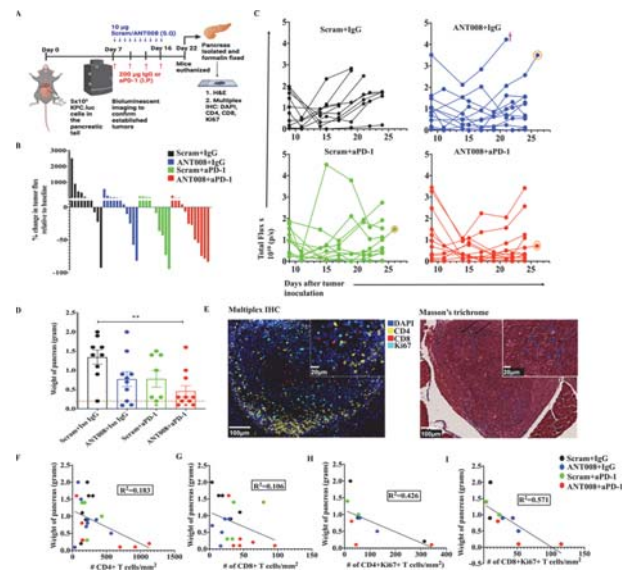
Abstract 748 Figure 1 VIP is over-expressed by PDAC. (A) VIP mRNA expression levels in various solid malignancies, as obtained from TCGA. (B) Representative images of human PDAC tumor stained with antibodies to VIP or CK19, showing VIP co-expression in islets (black arrow) and cancer epithelial cells (red arrow). Levels of VIP in (C) culture supernatants collected from murine and human PDAC cell lines cultured for 24 hours ($n=3$ per cell line) were compared to culture supernatants from B16F10 and D4M melanoma cells; (D) plasma of mice bearing melanoma or PDAC tumors ($n=5$) compared to plasma of non-tumor-bearing mice; (E) plasma of PDAC patients ($n=19$) compared to that from healthy volunteers ($n=26$). Statistical differences in C and D were performed by ANOVA followed by Dunnett's post-test and in E were performed by student's t-test. Error bars show mean \pm SEM. * $p < 0.05$, ** $p < 0.01$, *** $p < 0.001$ and **** $p < 0.0001$.



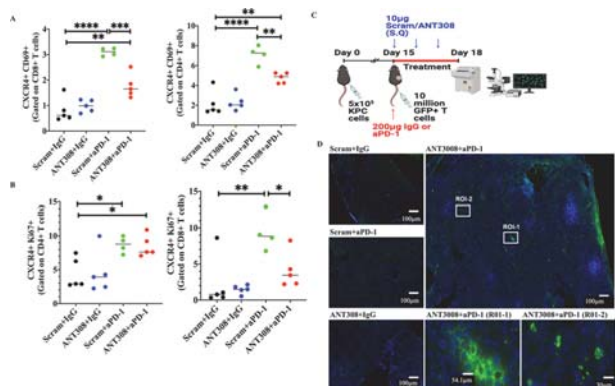
Abstract 748 Figure 2 VIP-R antagonists improve responses to anti-PD-1. KPC.Luc, MT5 or Panc02 cells were subcutaneously implanted in immunocompetent C57BL/6 mice. About one week after tumor implantation, when the tumors were palpable, mice were randomized into treatment groups and treated with VIP-R antagonist and/or anti-PD-1 as described in methods. (A) KPC.Luc, MT5 and Panc02 tumor volumes as measured by Vernier calipers on day 22 after subcutaneous tumor implantation. (B) Kaplan-Meier survival plots of C57BL/6 mice with subcutaneously implanted KPC.Luc, MT5 or Panc02 tumors stratified by treatment. Kaplan-Meier survival plots of (C) C57BL/6 mice receiving monoclonal CD4 and/or CD8 monoclonal antibodies (D) CD4KO or (E) CD8KO mice compared to wild-type C57BL/6 mice with subcutaneously implanted KPC.Luc tumors, stratified by treatment. Statistical differences in A were calculated by ANOVA followed by Dunnett's post-test. Solid line shows mean with in each treatment group. Statistical differences in B-E are calculated via Log-rank test. * $p < 0.05$, ** $p < 0.01$ and *** $p < 0.001$, **** $p < 0.0001$.



Abstract 748 Figure 3 Enhanced T cell response with combination therapy. mRNA expression in T cells isolated from subcutaneous KPC. Luc tumors in C57BL/6 mice treated with ANT008 and/or anti-PD-1 (n=3 per treatment group), were analyzed via Nanostring metabolism panel. Volcano plot showing differential expression of genes in T cells from (A) ANT008+ isotype IgG (IgG) vs scrambled peptide (Scram) + isotype IgG, (B) scrambled peptide +anti-PD-1 vs scrambled peptide + isotype IgG and (C) ANT008+anti-PD-1 vs scrambled peptide + isotype IgG (n=3 mice per treatment group). Genes that are associated with TCR activation and co-stimulation and are at levels significantly higher when compared to Scram+ isotype IgG (FDR<0.1) are labeled in red. (D) Heat map showing gene expression changes in genes associated with TCR activation and co-stimulation. (E) TCR activation and co-stimulation pathway score between the T cells in tumors of mice from the different treatment groups. (F) CD8+ T cells in subcutaneous KPC. Luc tumors were stained with MuLV p15E-H2Kb tetramer after 10 days of treatment with ANT308 and/or anti-PD-1 (n=3 per treatment group) and analyzed via flow cytometry for percentage of tetramer+ CD8+ T cells. (G) Kaplan-Meier survival curves of subcutaneous KPC. Luc bearing mice treated with ANT008 and/or anti-PD-1 from day 3–12 after tumor implantation (n=3 per scrambled peptide + isotype IgG, ANT008+ isotype IgG and scrambled peptide + anti-PD-1 treatment groups; n=8 in ANT008 + anti-PD-1 treatment group). (H) Kaplan-Meier survival curves of tumor free mice from G that were re-challenged with KPC. Luc tumors on the opposite flank (n=3 per scrambled peptide + isotype IgG and scrambled peptide + anti-PD-1 treatment group; n=5 in ANT008 +anti-PD-1 treatment group). Statistical differences in E and F were calculated via ANOVA followed by Dunnett's post-test and in G and H were calculated using Log-rank test. Error bars show mean ± SEM *p<0.05, **p<0.001, ***p<0.0001.



Abstract 748 Figure 4 Increased T cell density with combination therapy. KPC. Luc cells were orthotopically implanted in the tail of the pancreas of C57BL/6 mice and treated with ANT008 and/or anti-PD-1 with n=9, 10, 8 and 11 in scrambled+IgG, ANT008+IgG, scrambled +anti-PD-1 and ANT008+anti-PD-1, respectively. (A) Schematic showing orthotopic implantation of KPC. Luc cells and treatment strategy with ANT008 and/or anti-PD-1. (B) Waterfall plot showing % change in tumor flux on day 22 relative to day 7 prior to start of treatment. (C) Total flux as measured by IVIS bioluminescent imaging in the different treatment groups. Cross symbol represents mice that were euthanized before day 25 due to ulceration of the tumor and circle symbol represent mouse that were imaged on day 26 via MRI imaging shown in supplementary figure S5. (D) Bar graph showing weight of pancreas on day 25 when the mice were euthanized. 'Star' shaped data points indicate tumor free mice and dotted horizontal line represents the average weight of healthy pancreas from naïve mice. (E) Representative multiplex IHC images (right) showing pancreatic tumors stained for DAPI (blue), CD4 (yellow), CD8 (red) and Ki67 (cyan) and trichrome staining (left) with black arrows showing blue collagen stain in the tissue. XY plot showing the correlation between number of (F) CD4+ or (G) CD8+ T cells/mm²; and (H) Ki67+ CD4+ or (I) Ki67+ CD8+ T cells/mm² with weight of the pancreas with n=4 to 6 mice per group. P values in panel D were calculated using student ANOVA followed by Dunnett's post hoc test (comparing each treatment group with Scram +IgG). Error bars show mean ± SEM. *p<0.05, **p<0.01.



Abstract 748 Figure 5 Increased T cell homing with combination therapy. KPC.Luc tumors were subcutaneously implanted in C57BL/6 mice and treated with VIP-R antagonist and/or anti-PD-1 checkpoint therapy for 10 days after the tumors were palpable. Tumor draining lymph nodes were then analyzed for percentage of (A) CXCR4+CD69+ and (B) CXCR4+Ki67+ cells in CD4+ (left) and CD8+ (right) subsets of T cells. In a separate experiment, on day 15 after subcutaneous implantation of KPC.Luc tumors, GFP+ T cells from enhanced GFP transgenic mice (C57BL/6 background) were adoptively transferred (via tail vein injections) and treated with ANT308± aPD-1 for 3 days. (C) Schematic showing GFP+ T cell transfer and treatment strategy in mice with subcutaneous KPC.Luc tumors. (D) Representative Hoescht (blue for nucleus) stained tumor tissues from tumors of each treatment group. Two regions of interest (ROI) in ANT308+aPD-1 treated tumors are shown at higher magnification. Statistical differences in A and B were determined via repeated measures ANOVA and Dunnett's post-test with $n=4-5$ mice per group. * $p<0.05$, ** $p<0.01$, *** $p<0.001$, **** $p<0.0001$.

Acknowledgements The authors thank healthy volunteers and patients for blood and/or tissue samples. The authors also thank the shared resources at Emory University, namely the Emory Integrated Genomics Core (EIGC), Emory Flow Cytometry Core (EFCC), Cancer Animal Models Shared Resource (CAMS), Cancer Tissue Pathology Core (CTP), Biostatistics Shared Resource (BSR) and Integrated Cellular Imaging Core (ICI), that provided services or instruments at subsidized cost to conduct some of the reported experiments. BioRender was used to make figure 4A and 5C. This work was supported in part by Katz Foundation funding and Emory School of Medicine Dean's Imagine, Innovate and Impact (I3) venture award to Edmund K. Waller and NIH R01 CA207619 awarded to Susan N. Thomas. Part of the cost for the immunohistochemistry staining of tissues was covered by Winship Cancer Institute Development Discovery and Therapeutic Program Pilot funding to Sruthi Ravindranathan.

REFERENCES

1. Sahin IH, et al. Immunotherapy in pancreatic ductal adenocarcinoma: an emerging entity? *Ann Oncol* 2017;**28**(12):2950–2961.
2. Gonzalez-Rey E, Anderson P, Delgado M. Emerging roles of vasoactive intestinal peptide: a new approach for autoimmune therapy. *Ann Rheum Dis* 2007;**66**(Suppl 3):p. iii70–6.
3. Anderson P, Gonzalez-Rey E. Vasoactive intestinal peptide induces cell cycle arrest and regulatory functions in human T cells at multiple levels. *Mol Cell Biol* 2010;**30**(10):2537–51.
4. Li JM, et al. VIPhyb, an antagonist of vasoactive intestinal peptide receptor, enhances cellular antiviral immunity in murine cytomegalovirus infected mice. *PLoS One* 2013;**8**(5):e63381.
5. Moody TW, et al. VIP receptor antagonists and chemotherapeutic drugs inhibit the growth of breast cancer cells. *Breast Cancer Res Treat* 2001;**68**(1):55–64.
6. Moody TW, et al. A vasoactive-Intestinal-Peptide antagonist inhibits nonsmall cell lung-cancer growth. *Proceedings of the National Academy of Sciences of the United States of America* 1993;**90**(10):4345–4349.

7. Zia H, et al. Breast cancer growth is inhibited by vasoactive intestinal peptide (VIP) hybrid, a synthetic VIP receptor antagonist. *Cancer Res* 1996;**56**(15):3486–9.
8. Sena M, et al. High conservation of upstream regulatory sequences on the human and mouse vasoactive intestinal peptide (VIP) genes. *DNA Seq* 1994;**5**(1):25–9.

Ethics Approval All experimental procedures involving mice were approved by the Institutional Animal Care and Use Committee (IACUC) at Emory University. De-identified blood samples from consented patients with PDAC (IRB 00087397) or healthy volunteers (IRB 00046063) were obtained with approval from Institutional Review Boards.

<http://dx.doi.org/10.1136/jitc-2021-SITC2021.748>

A NOVEL TRANSLATIONAL MOUSE MODEL FOR ASSESSMENT OF HUMAN STING-TARGETING THERAPIES

Fabiane Sônego*, Gaëlle Martin, Audrey Beringer, Chloé Beuraud, Angela Pappalardo, Yacine Cherifi, Patricia Isnard-Petit, Kader Thiam. ¹genOway, Lyon, France; ²IGM Biosciences, Mountain View, CA, United States; ³Antinéo, Lyon, France; ⁴Crown Bioscience, Paris, France

Background Although Immune checkpoint inhibitors (ICI)-targeting therapies have revolutionized the treatment of cancer, several tumors do not respond to those therapies. Preclinical and clinical evidences suggest that STING is a promising target to improve the immunogenicity of tumors, turning them responsive to ICI, and enhancing anti-tumor response. DMXAA failed to show efficacy in clinical trials, despite its encouraging anti-tumor response in preclinical phase, highlighting the need of accurate translational preclinical models. On top of the specificity barrier reported for STING-targeting agents, the heterogeneity of STING variants and their variability in the response to STING-targeting therapies, brings another level of complexity in preclinical evaluation of anti-STING therapies. Here, we report the generation of STING humanized (hSTING) mouse models enabling the *in vivo* assessment of STING-targeting agents.

Methods Human STING variants show a high heterogeneity and population stratification. Different variants, and isoforms, respond differently to STING agonists. We developed mouse models expressing the main human STING variants and isoforms found in the population to recapitulate this complexity. Human STING was inserted by knock-in at the endogenous locus to enable a physiological expression pattern of STING while invalidating the mouse gene. Herein, we will focus on the human STING full length H323 model.

Results T and B lymphocytes, NK, DCs and monocytes frequency in the spleen, bone marrow and blood were found to be similar in hSTING and WT mice, suggesting that the humanization of STING did not alter the immune cell distribution in these compartments. These cells express human STING, while no expression of mouse STING was observed. Splenocytes isolated from hSTING and WT mice produced IL-6 and IFN- γ upon activation with 2'3'-cGAMP, a cyclic dinucleotide with activity towards both mouse and human STING. Similarly, a mouse and human STING agonist induced the activation of DCs in both hSTING and WT mice, as observed by the increased expression of CD80/CD86 on DCs *ex vivo* and *in vivo*. Moreover, systemic production of IL-6, IFN- γ and TNF- α in response to this STING agonist was observed and suggest that human STING is functional in hSTING mice. As expected, hSTING mice did not respond to activation with DMXAA *in vivo*, whereas this agonist induced the systemic production of cytokines and activation of DCs in WT mice.

Conclusions The novel hSTING model described here supports the assessment of human STING-targeting agents in immunoncology and inflammation. Intercrosses of this model with ICI humanized models could support the assessment of combination therapies

<http://dx.doi.org/10.1136/jitc-2021-SITC2021.749>

750

AK119, A CD73 TARGETING ANTIBODY WITH DUAL MECHANISM OF ACTION

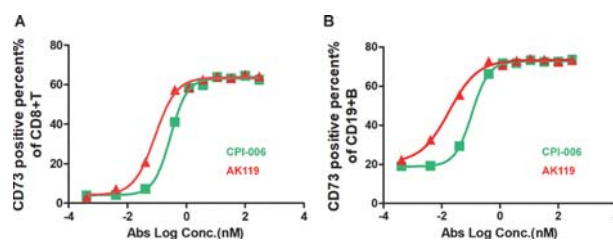
¹Zhaoliang Huang, ²Xinghua Pang, ²Tingting Zhong, ²Chunshan Jin, ²Na Chen*, ²Xinrong He, ²Dennis Xia, ³Xiaoping Jin, ²Zhongmin Wang, ²Xu Xia, ²Baiyong Li. ¹Akeso Biopharma Inc., Zhongshan, China; ²Akeso Biopharma Inc., Zhongshan, China; ³Akeso Biopharma Inc, Potomac, United States

Background AK119 is an Fc-engineered humanized IgG1 monoclonal antibody targeting human CD73. CD73-extracellular adenosine pathway regulates conversion of pro-inflammatory and immuno-stimulatory extracellular adenosine ATP into immunosuppressive adenosine. CD73 expresses on cancer cells, endothelial cells, fibroblasts, lymphocytes and myeloid cells. CD73 upregulated can be a result of tissue hypoxia,¹ epithelial-to-mesenchymal transition,² inflammation³ and/or cytotoxic stress.⁴ Also, increasing immune response may lead to faster viral clearance, shorter recovery time, less complications, longer immunity and protection from re-infection. Inhibiting CD73 was reported to evoke B cells activation and shows anti-fibrotic effects. The ability of enhancing immune response provides a potential opportunity to treat COVID-19. Thus, we investigated pharmacological activity of AK119 as an agent treating cancers, COVID-19 and fibrosis.

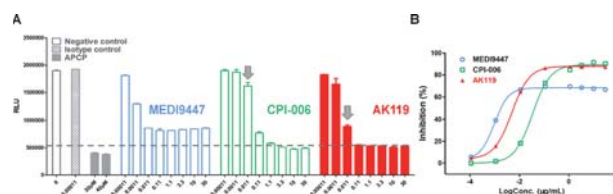
Methods AK119 inhibition of CD73 enzymatic activity was tested in human PBMCs based assay. The ability of AK119 to enhance B cells immune response was detected by cell-based assay. PBMCs were incubated overnight with APCP (inhibitor of CD73 enzyme activity) or AK119, CPI006 or MEDI9447. Flow cytometry analysis was performed with gating on B cells (CD19+CD3-) and MFI and positive percent were reported for antibody staining of CD69 or CD83, as well as HLA-DR and IgM. Enhancement of anti-SARS-CoV-2 antibody production was studied using human CD73 transgenic mouse immunized with SARS-CoV-2 spike protein. The in-vivo activity of AK119 was further studied in bleomycin-induced pulmonary fibrosis model in human CD73 transgenic mouse.

Results AK119 shows a more potent antigen binding (figure 1) and completely CD73 enzyme inhibition activity (figure 2). AK119 promotes B cell proliferation, and upregulating CD69, CD83, HLA-DR and IgM that are markers of B cell activation (figure 3). B cell activation induced by AK119 is independent of adenosine. AK119 show significantly higher bioactivity to induce B cells activation in comparison with MEDI9447 or CPI006 (figure 4). In human CD73 transgenic mice, AK119 increased secretion of anti-S protein IgG (figure 5). In pulmonary fibrosis mouse model, number of inflammatory cell in bronchoalveolar lavage fluid of AK119 was significantly decreased, and decreased HYP representing collagen content in lung tissue homogenate of mice was found in both AK119 50 mg/kg and 10 mg/kg group (figure 6).

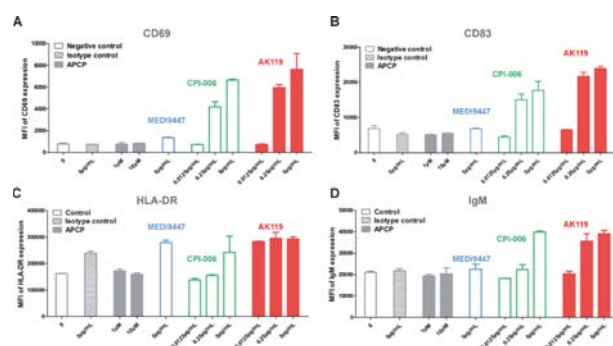
Conclusions AK119 selectively binds to and inhibits the ectonucleotidase activity of CD73 thus reducing adenosine accumulation. Results from non-clinical pharmacology studies reveal potent bioactivities as well as favorable safety properties of AK119. AK119 is intended for advanced solid tumors, pulmonary fibrosis and therapy of COVID-19.



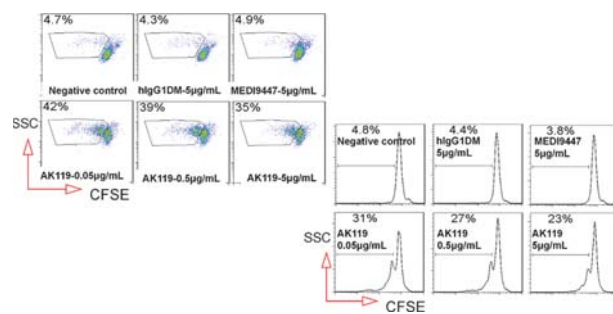
Abstract 750 Figure 1 Binding activity of AK119 to human PBMCs. Binding Curve of AK119 to CD73 expressed on (A) CD8+ T cells and (B) CD19+ B cells in human PBMCs



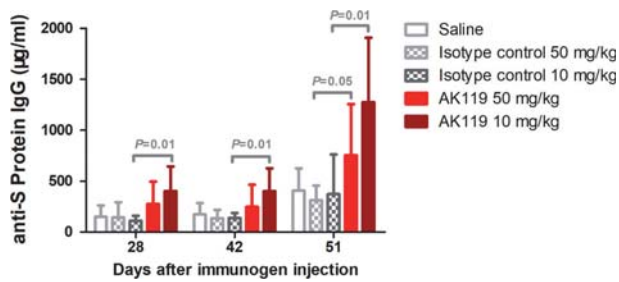
Abstract 750 Figure 2 Inhibition activity of CD73 on human PBMCs. AK119 Inhibits Enzymatic Activity of CD73 Expressed on human PBMCs



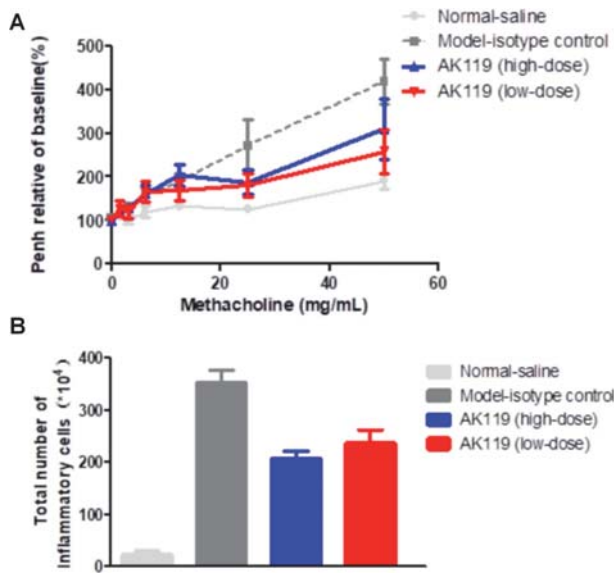
Abstract 750 Figure 3 Effect of upregulating B cell markers by AK119. AK119 Upregulates (A) CD69, (B) CD83, (C) HLA-DR and (D) IgM Expression on B cells



Abstract 750 Figure 4 Stimulation of B cell Proliferation by AK119



Abstract 750 Figure 5 Therapeutic activity in the COVID-19 mouse model. Serum Concentration of S protein-specific IgG in Mouse Model of COVID-19



Abstract 750 Figure 6 Therapeutic activity in the asthma mouse model. (A) AK119 relieves the increased airway resistance and restore the lung function. (B) Reduction of the inflammatory cells in BALF by AK119

REFERENCES

1. Bullen JW, Tchernyshyov I, Holewinski RJ, DeVine L, Wu F, Venkatraman V, Kass DL, Cole RN, Van Eyk J, Semenza GL, Protein kinase A-dependent phosphorylation stimulates the transcriptional activity of hypoxia-inducible factor 1. *Sci Signal* 2016;**9**(430):ra56.
2. Lupia M, Angiolini F, Bertalot G, Freddi S, Sachsenmeier KF, Chisci E, Kutryb-Zajac B, Confalonieri S, Smolenski RT, Giovannoni R, Colombo N, Bianchi F, Cavallaro U. CD73 regulates stemness and epithelial-Mesenchymal transition in ovarian cancer-initiating cells, *Stem Cell Rep* 2018;**10**(4):1412–1425.
3. Reinhardt J, Landsberg J, Schmid-Burgk JL, Ramis BB, Bald T, Glodde N, Lopez-Ramos D, Young A, Ngiow SF, Nettersheim D, Schorle H, Quast T, Kolanus W, Schadendorf D, Long GV, Madore J, Scolyer RA, Ribas A, Smyth MJ, Tumeah PC, Tuting T, Holzner M. MAPK signaling and inflammation link melanoma phenotype switching to induction of CD73 during immunotherapy. *Cancer Res* 2017;**77**(17):4697–4709.
4. Samanta D, Park Y, Ni X, Li H, Zahnow CA, Gabrielson E, Pan F, Semenza GL. Chemotherapy induces enrichment of CD47(+)/CD73(+)/PDL1(+) immune evasive triple-negative breast cancer cells, *Proc Natl Acad Sci USA*. 2018;**115**(6):E1239–E1248.

<http://dx.doi.org/10.1136/jitc-2021-SITC2021.750>

751

NEO-X-PRIME BISPECIFIC ANTIBODIES TARGETING CD40 AND TUMOR ANTIGENS PROMOTE CROSS-PRESENTATION OF TUMOR EXOSOME-DERIVED NEOANTIGEN AND INDUCE SUPERIOR ANTI-TUMOR RESPONSES COMPARED TO CD40 MAB

¹Karin Hagerbrand*, ¹Mattias Levin, ¹Laura Von Schantz, ¹Laura Varas, ¹Anna Säll, ¹Adnan Deric, ¹Anette Sundstedt, ¹Lill Ljung, ¹Karin Barchan, ¹Doreen Werchau, ¹Anna Rosén, ¹Barnabas Nyesiga, ¹Eva Lindqvist, ¹Mia Thagesson, ²Peter Ellmark. ¹Alligator Bioscience, Lund, Sweden; ²Alligator Bioscience AB, Lund, Sweden

Background Alligator's Neo-X-Prime platform aims to enable antigen presenting cells to efficiently enhance priming of tumor neoantigen-specific T cells with the goal of overcoming PD-1 resistance in certain tumor types. We hypothesize that binding of a CD40 x TAA bispecific antibody (bsAb) to CD40 on dendritic cells (DCs) and a tumor-associated antigen (TAA) on tumor exosomes or tumor debris leads to (i) activation of the DC, (ii) uptake of the tumor material, (iii) cross-presentation of tumor-derived neoantigen (present in exosomes or debris) and, iv) priming of tumor neoantigen-specific T cells, resulting in an increased quantity and/or quality of the tumor-targeting T cell pool.

Methods Functionality was evaluated in vitro using CD40 reporter cells and monocyte-derived DCs, co-cultured with cells expressing TAA. Further, co-localization of TAA-expressing cellular debris with a CD40-expressing human B cell line in the presence of bsAbs was assessed using live cell imaging. In vivo, anti-tumor efficacy and immunological memory were assessed in human CD40 transgenic (hCD40tg) mice bearing MB49 bladder carcinoma tumors transfected with human TAA or controls. T cells isolated from OVA-specific TCR-transgenic mice were used to evaluate the effect of Neo-X-Prime bsAbs on antigen-specific T cell expansion in the presence of hCD40tg DCs and exosomes from MB49 tumors transfected with both human TAA and OVA using flow cytometry.

Results Using CEA as a highly expressed TAA, we have developed lead Neo-X-Prime CD40-CEA bsAbs engineered to achieve an optimal profile. Further, using Neo-X-Prime concept molecules targeting EpCAM, we have demonstrated the ability to mediate co-localization of tumor debris and CD40 expressing antigen presenting cells that is dependent on the receptor density of the TAA. We have further shown that addition of Neo-X-Prime bsAbs to a co-culture of murine DCs, T cells and tumor-derived exosomes induces increased expansion of model neoantigen-specific T cells. In vivo, Neo-X-Prime bsAbs display a potent, TAA-dependent anti-tumor effect that is superior to CD40 mAbs. Cured mice develop a broad immunological memory that is not dependent on expression of the TAA. The tumor-localizing property of Neo-X-Prime bsAbs also shows potential for improved safety compared to CD40 monospecific antibodies.

Conclusions Neo-X-Prime bsAbs have the potential to tumor-selectively target CD40-expressing antigen-presenting cells to mediate an expansion of the tumor-specific T cell repertoire, resulting in increased T cell infiltration and potent anti-tumor effects.

Ethics Approval All experiments were performed after approval from the Malmö/Lund Animal Ethics Committee.

<http://dx.doi.org/10.1136/jitc-2021-SITC2021.751>

**NOVEL, ORALLY ADMINISTERED HPK1 INHIBITORS
DEMONSTRATE ANTI-TUMOR EFFICACY AND
ENHANCED IMMUNE RESPONSE**

Stefan Chmielewski*, Maciej Kujawa, Eliza Zimolag, Michal Galezowski, Andrzej Gondela, Pawel Guzik, Agata Dudek, Joanna Szeremeta-Spisak, Marta Bugaj, Iana Levenets, Marcin Nowogrodzki, Marianna Girardi, Anna Zagorska, Przemyslaw Wyrebek, Magdalena Zastawna, Agnieszka Gibas, Sylwia Sudol, Oleksandr Levenets, Mateusz Swirski, Sujit Sasmal, Adam Radzimierski, Marta Sowinska, Paulina Niedziejko, Karol Zuchowicz, Martin Swarbrick, Karolina Gluza, Patryk Kret, Mateusz Ogorek, Dominika Stanko, Kinga Michalik, Agnieszka Piatek, Katarzyna Banaszak, Adrian Podkowa, Aniela Golas, Peter Littlewood, Krzysztof Brzozka, Stefan Chmielewski. *Ryvu Therapeutics, Kraków, Poland*

Background Hematopoietic progenitor kinase 1 (HPK1, MAP4K1) is emerging as a well-renowned, druggable target for T cell-based immunotherapies. HPK1 is a member of the serine/threonine MAP4K family, predominantly expressed in hematopoietic cell lineages and shown to be a negative regulator of the T cell receptor (TCR) signaling pathway. Upon TCR activation, HPK1 is recruited to the proximity of the cell membrane and phosphorylates an adaptor protein SLP-76 at the Ser376 residue which, in turn, abrogates TCR signaling. Other studies point to a potential role of HPK1 in T cell exhaustion as well as in functional re-programming of regulatory T cells. Moreover, mounting evidence suggest that HPK1 kinase activity suppresses the immune functions of a wide range of other immune cell subsets like B cells and dendritic cells. Taken together, these observations support small-molecule HPK1 inhibitors as an attractive modality in cancer immunotherapy either as single agents or in combination with immune checkpoint inhibitors.

Methods Activity of compounds against HPK1 and selected off- and anti-targets was assessed in biochemical assays. Phosphorylation of SLP-76 was measured either by flow cytometry or TR-FRET. Jurkat and primary T cells were activated and cultured in the presence of tested compounds and immunosuppressive agents. Impact on TCR selectivity and T cell function was measured by AlphaLISA and flow cytometry. Target engagement was measured in splenocytes of mice administered orally with tested compounds followed by IP injection of aCD3 antibody. Anti-tumor efficacy of HPK1 inhibitors was assessed in a syngeneic tumor model.

Results Ryvu's proprietary small molecule HPK1 inhibitors exhibit sub-nanomolar activity against human and mouse HPK1 proteins and good selectivity against other TCR pathway kinases. Tested compounds efficiently block phosphorylation of SLP-76 upon TCR engagement. TCR selectivity of Ryvu's inhibitors, measured as a ratio between CD69 and pSer376 SLP-76 inhibition, is on par or superior to reference molecules. Tested compounds are not only able to overcome PGE-2 induced resistance following TCR activation in human PBMCs, inducing elevated IL-2 release but also affect T cell function in co-culture assay. Developed molecules have favorable PK profiles, allowing for sustained target coverage in proposed dosing regimens and demonstrate efficacy in a mammary carcinoma syngeneic model.

Conclusions Ryvu has developed potent and selective HPK1 inhibitors with favorable PK and PD profiles, whose activity in vitro translates to in vivo efficacy. Further preclinical work is warranted to select a lead candidate for IND-enabling studies and subsequently clinical studies across a variety of solid tumors.

<http://dx.doi.org/10.1136/jitc-2021-SITC2021.752>

753

INHIBIGEN™ ADMINISTRATION PROMOTES ABERRANT T CELL RESPONSES IN CANCER BUT MAY BE BENEFICIAL FOR AMELIORATION OF AUTOIMMUNE DISEASE

Victoria DeVault*, Hanna Starobinets, Julie Arnold, Stephanie Rinaldi, Charley Hubbard, Osaruese Odeh, Cindy Nguyen, Laura Apolloni, Dmitry Lineker, Jessica Flechtner, Hubert Lam. *Genocea Biosciences, Cambridge, MA, United States*

Background Selecting neoantigens that generate robust anti-tumor T cell responses remains a challenge for cancer immunotherapy design. The ATLAS™ platform, a functional recall assay using patient autologous cells, identifies both stimulatory and inhibitory (Inhibigen) neoantigens via up- or downregulation of T cell cytokine secretion.¹ We propose that stimulatory neoantigens are ideal targets for cancer vaccines and T cell therapies. In contrast, data suggest that Inhibigens be excluded, due to their association with accelerated tumor growth and dampened immunity in a murine melanoma model.² While detrimental to cancer immunotherapy, the Inhibigen-associated downregulation of cytokine production may be beneficial in the context of autoimmunity.

Methods ATLAS screens were performed as previously described.^{1, 2} Peptide vaccines containing tumor-specific neoantigens ± Inhibigens were evaluated in prophylactic and therapeutic B16F10 melanoma tumor models for immunogenicity and efficacy. RNAseq analysis was performed on T cells sorted from draining lymph nodes of vaccinated tumor-bearing mice. For experimental autoimmune encephalomyelitis (EAE) studies, mice were administered a vaccine containing MOG peptide ± the melanoma MMP9_{F5} Inhibigen. Immune responses and phenotypic analyses for both models were measured by flow cytometry, ELISPOT, and immunohistochemistry.

Results In the melanoma model, inclusion of the Inhibigen MMP9_{F5} accelerated tumor growth in a non-dose dependent manner and abrogated immune responses. RNAseq of T cells from tumor-bearing mice vaccinated with MMP9_{F5} showed a higher level of differentially expressed genes (adjusted P value of <0.05) in TCR-signaling regulation and suppressor GO pathways (>5 distinct pathways/gene) as compared to stimulatory controls, indicating Inhibigen-specific effects on T cells. In the EAE model of autoimmunity, animals treated with MOG peptide + MMP9_{F5} exhibited dampened anti-MOG immune responses, delayed disease onset, reduced disease incidence and scoring (average 1 vs. 3) and decreased spinal cord immune infiltration as compared to control vaccination. These data indicate that Inhibigen administration has the potential to ameliorate autoimmune sequelae, independent of cognate antigen expression.

Conclusions Functional identification and exclusion of Inhibigens from cancer immunotherapies may be critical to protective immunity since their inclusion can result in quelling of otherwise beneficial immune responses. Conversely, Inhibigen-specific responses can dampen destructive autoimmune sequelae. Mechanistic studies show altered T cell signaling pathways in the context of therapeutic Inhibigen vaccination. These data suggest that Inhibigen-specific responses, while detrimental for the treatment of cancer, may have a therapeutic benefit in other disease contexts.

REFERENCES

1. Nogueira C, Kaufmann JK, Lam H, Flechtner JB. Improving cancer immunotherapies through empirical neoantigen selection. *Trends in Cancer* 2018;**4**(2):97–100.
2. Lam H, et al. An empirical antigen selection method identifies neoantigens that either elicit broad anti-tumor response or drive tumor growth. *Cancer Discovery* 2021;**11**(3):696–713.

Ethics Approval All animal studies were undertaken in conformity with the Cambridge, MA Ordinance 1086 of the city's Municipal Code and in accordance with the policies and protocols approved by Genocea's Institutional Animal Care and Use Committee (IACUC).

<http://dx.doi.org/10.1136/jitc-2021-SITC2021.753>

TIGIT-PVR IS A KEY IMMUNE CHECKPOINT AND THERAPEUTIC TARGET IN HPV-POSITIVE HEAD AND NECK SQUAMOUS CELL CARCINOMAS

¹Xiuning Le*, ¹Minghao Dang, ¹Venkatesh Hegde, ¹Bo Jiang, ¹Ravaen Slay, ¹Weihong Xiao, ¹Keiko Akagi, ¹Joseph Fresquez, ¹Kathrina Marcelo, ¹Qianyun Luo, ¹Pragya Sinha, ¹Ananta Yanamandra, ¹Diana Bell, ¹Michelle Williams, ¹Edwin Parra Cuentas, ¹Ryan Goepfert, ¹Stephen Lai, ¹Neil Gross, ²Amit Agrawal, ¹Alexandre Reuben, ¹Jeffrey Myers, ¹Michael Curran, ¹Jagannadha Sastry, ¹Linghua Wang, ¹Maura Gillison. ¹MD Anderson Cancer Center, Houston, TX, United States; ²The Ohio State University Medical Center, Columbus, United States

Background Human papillomavirus (HPV)-positive head and neck squamous cell carcinoma (HPV+ HNSCC) is a disease that has moderate response to anti-PD-1/L1 immune checkpoint blockade, with the response rates less than 20% and median progression-free survival less than 3 months. A greater understanding of tumor intrinsic and extrinsic factors that restrict anti-tumor immunity in the tumor immune microenvironment (TIME) is needed to identify other immune checkpoints to enhance therapeutic efficacy.

Methods Two cohorts (TCGA n=72 and a separate cohort n=84) of surgically resected, treatment-naïve HPV+ HNSCC with RNA-seq were analyzed to understand the immune features. In addition, single-cell RNA-seq and TCR-seq were performed on 18 cases to further delineate the immune molecules' interactions. An immune-competent murine HPV+ HNSCC model was used to preliminarily evaluate the therapeutic efficacy.

Results In two bulk-sequenced HPV+ HNSCC cohorts, TIGIT ligands PVR and NECTIN2 were found to associate with an epithelial-to-mesenchymal gene expression signature, suppression of IFN α and IFN γ signaling, a stromal-enriched or immune-excluded TIME, and poor survival. Single-cell RNA-seq of over 72,000 cells of HPV+ HNSCC revealed that the PVR/NECTIN ligand TIGIT was highly prevalent in T-cells (34%), significantly higher than PD1- (20%, p<0.01). There is an enrichment of cell-cell interactions mediated by TIGIT-PVR/NECTIN2 in the TIME of HPV+HNSCC versus normal tonsil. TIGIT was the most differentially upregulated immune checkpoint on clonally expanded CD8+T-cells and was abundant on antigen-experienced, tissue-resident memory CD8+T-cell and T-regulatory subsets. TIGIT ligands PVR, NECTIN1, and NECTIN2 were abundant on mature regulatory dendritic cells (DCs), immunosuppressive plasmacytoid (p)DCs, and macrophages, respectively. TIGIT and PD-1 co-blockade in the mEER syngeneic murine model significantly reduced tumor growth, improved survival, restored effector function of HPV16E7-specific CD8+T cells, natural killer cells, and DCs, and conferred tumor re-challenge protection.

Conclusions TIGIT-PVR/NECTIN receptors/ligands are more abundant than PD-1/L1 in the TIME of HPV+ HNSCC. Co-blockade of TIGIT and PD-1 immune checkpoints enhanced anti-tumor efficacy in a CD8+ T-cell-dependent manner and conferred long-term immune protection in a murine model. Our study nominates TIGIT as a therapeutic target for HPV+ HNSCC.

<http://dx.doi.org/10.1136/jitc-2021-SITC2021.754>

755

PHARMACOLOGIC TUMOR PD-L1 DEPLETION REDUCES CHK2 CONTENT AND SENSITIZES TUMORS TO SMALL MOLECULE CHK1 DNA DAMAGE REPAIR INHIBITORS

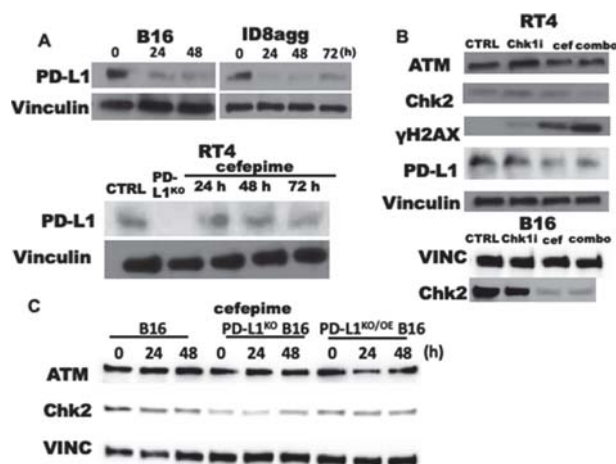
Clare Murray*, Anand Kornepati, Alvaro Padron, Myrna Garcia, Haiyan Bai, Yilun Deng, Tyler Curiel. *UT Health San Antonio, San Antonio, TX, United States*

Background Tumor PD-L1 canonically signals to PD-1 on immune cells to evade immune destruction.¹ We reported that tumor PD-L1 also mediates diverse pathologic intracellular signals,²⁻³ including promoting the ATM/Chk2 DNA damage response, and that genetically PD-L1 deficient tumors are sensitized to Chk1 inhibitor therapy.⁴ DNA damage increases cytosolic DNA, which induces immunogenic STING signals through inflammatory type I interferon and cytokine production.⁵

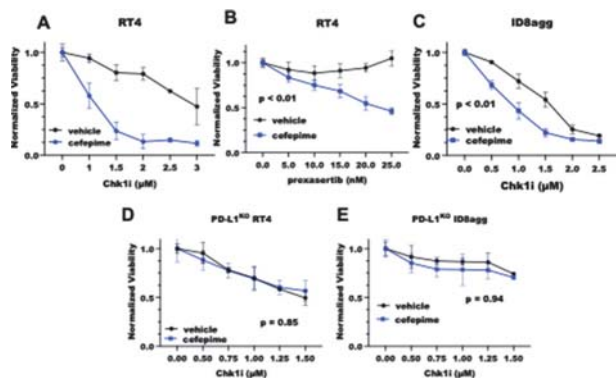
Methods We conducted a high-throughput drug screen that identified the β-lactam cephalosporin antibiotic cefepime as a pharmacologic tumor PD-L1 depleting agent. In vitro tests of β-lactam antibiotics used 80 μM and the Chk1 inhibitors rabusertib and prexasertib were used at indicated concentrations. Cell lines were RT4 human bladder cancer, ID8agg murine ovarian cancer, and B16 mouse melanoma. Viability was by MTT and proteins by immunoblot. We challenged NSG mice (n = 5 per group) with RT4 (SQ) and treated with cefepime (200 mg/kg), rabusertib (2.5 mg/kg), vehicle, or combination daily.

Results Cefepime at pharmacologically relevant concentrations depletes tumor PD-L1 and phenocopies genetic tumor PD-L1 depletion by decreasing Chk2 protein and increasing DNA damage (γH2AX) (figure 1). Chk2 is depleted by cefepime in CTRL cells, but not in PD-L1KO or PD-L1 overexpressing cells, and sensitizes PD-L1+ tumor cells to Chk1 inhibitors in vitro in a PD-L1-dependent manner (figures 1 and 2). Combining cefepime with rabusertib in vivo significantly prolonged severely immunodeficient NSG mice survival in RT4 challenge versus cefepime alone while rabusertib alone was not effective (figure 3). Antimicrobial mechanisms, reported to influence tumor treatment responses,⁶ are unlikely in NSG mice. To test β-lactam contributions to cefepime efficacy, we found that ceftazidime, a structurally related cephalosporin, also depletes tumor PD-L1 and Chk2 protein and sensitizes tumors to rabusertib in a PD-L1 dependent manner (figures 4 and 5). Structurally-unrelated β-lactam antibiotics did not sensitize tumors to rabusertib. Both cefepime and ceftazidime activate tumor STING, suggesting they could augment immunotherapies by increasing tumor immunogenicity (figure 6).

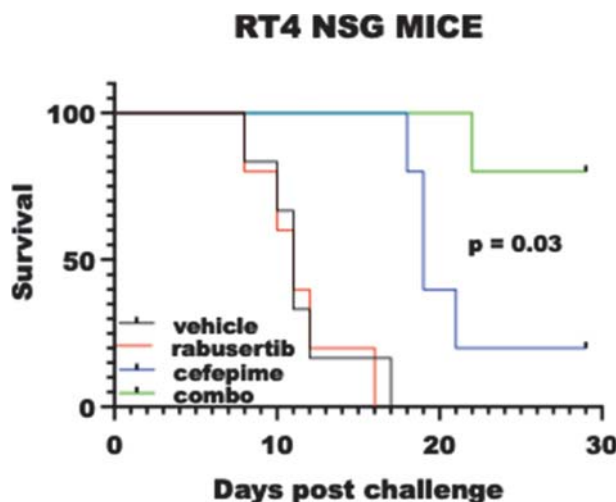
Conclusions As genetic PD-L1 depletion is not yet clinically feasible, we provide pharmacologic means to deplete tumor PD-L1 to improve clinical treatment efficacy as a rapidly translated approach. Cefepime is the prototype agent, but ceftazidime is structurally similar with significant activity, suggesting important structure activity relationships to explore. Pharmacologic tumor PD-L1 depletion could augment other standard of care approaches, including immunotherapy, and deserves further investigation.



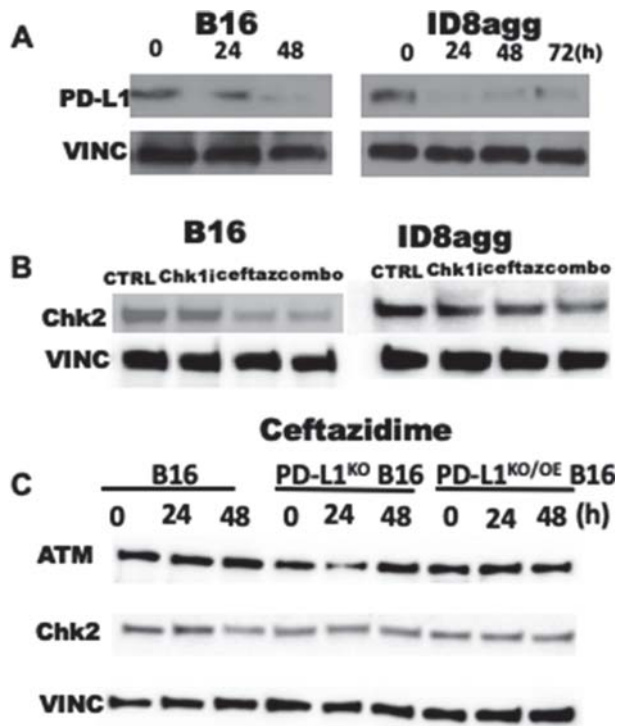
Abstract 755 Figure 1 Cefepime depletes tumor PD-L1 and Chk2 and induces γH2AX



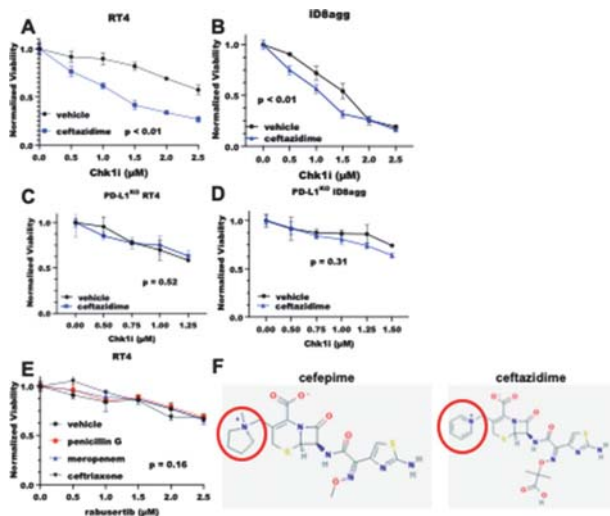
Abstract 755 Figure 2 Cefepime sensitizes tumors to Chk1 inhibitors in a PD-L1 dependent manner



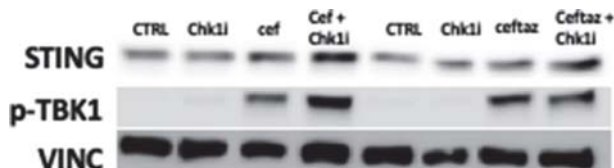
Abstract 755 Figure 3 Cefepime combined with Chk1 inhibitors in vivo prolongs NSG mouse survival



Abstract 755 Figure 4 Ceftazidime depletes tumor PD-L1 and Chk2



Abstract 755 Figure 5 Ceftazidime, but not other B-lactam antibiotics, sensitizes RT4 to Chk1 inhibitors in a PD-L1 dependent manner



Abstract 755 Figure 6 Cefepime and ceftazidime induce STING and p-TBK1

REFERENCES

1. Dong H, Strome SE, Salomao DR, Tamura H, Fumiya H, Flies DB, et al. Tumor-associated B7-H1 promotes T-cell apoptosis: a potential mechanism of immune evasion. *Nat Med* 2002;**8**:793–800.
2. Clark CA, Gupta HB, Gangadhara S, Pandeswara S, Lao S, Yuan B, et al. Tumor-Intrinsic PD-L1 signals regulate cell growth, pathogenesis, and autophagy in Ovarian Cancer and Melanoma. *Cancer Res* 2016;**76**(23):6964–6974.
3. Gupta HB, Clark CA, Yuan B, Sareddy G, Pandeswara S, Padron AS, et al. Tumor cell-intrinsic PD-L1 promotes tumor-initiating cell generation and functions in melanoma and ovarian cancer. *Signal Transduct Target Ther* 2016;1.
4. Kornepati AV, Zhang D, Hambright HG, Kari SC, Deng Y, Clark CA, et al. Cell-intrinsic programmed death ligand-1 (PD-L1) inhibits cytotoxic chemo, promotes DNA damage repair, and enhances ATM/ATR signaling following exposure to DNA damaging agents in bladder, melanoma, and ovarian cancer cells. *J Immunol* 2019;**202**(1):195.17.
5. Gehrke N, Mertens C, Zillinger T, Wenzel J, Bald T, Zahn S, et al. Oxidative damage of DNA confers resistance to cytosolic nuclease TREX1 degradation and potentiates STING-dependent immune sensing. *Immunity* 2013;**39**(3):482–495.
6. Gopalakrishnan V, Spencer CN, Nezi L, Reuben A, Andrews MC, Karpnits TV, et al. Gut microbiome modulates response to anti-PD-1 immunotherapy in melanoma patients. *Science* 2018;**359**(6371):97–103.

Ethics Approval This protocol was approved by the UTHSCSA IACUC.

<http://dx.doi.org/10.1136/jitc-2021-SITC2021.755>

756

IDENTIFYING THE ROLE OF B7-H4 AS A SUPPRESSOR OF TUMOR INFILTRATING LYMPHOCYTES AND A TARGET FOR IMMUNOTHERAPY IN BREAST CANCER

Elizabeth Wescott*, Paula Gonzalez-Ericsson, Violeta Sanchez, Melinda Sanders, Justin Balko. *Vanderbilt University, Nashville, TN, United States*

Background Immune checkpoint inhibitors (ICI) have improved patient survival in some cancer types but yielded limited success in breast cancer. Combinations of ICI (α PD-L1/PD-1) and chemotherapy have been FDA-approved for metastatic TNBC patients, and potentially in the early breast cancer setting, but many patients remain non-responsive to ICI. B7-H4 is a B7 family ligand with proposed immunosuppressive functions being explored as a cancer immunotherapy target and may be associated with resistance to α PD-L1. We confirmed an inverse expression pattern between B7-H4 and PD-L1 in breast tumor cells, which has previously been noted by others. B7-H4 was expressed in immune-excluded tumors, while PD-L1 was expressed in immune-infiltrated tumors. Based on these findings, we hypothesized ectopic B7-H4 expression would induce α PD-L1 resistance through immune cell suppression in vivo.

Methods Using an immunocompetent and α PD-L1-sensitive EMT6 orthotopic mammary cancer model, we induced ectopic expression of B7-H4 and performed animal survival studies to assess therapy response, and RNA analysis to assess changes to cell signaling among tumor infiltrating immune cells. Finally, we performed transcriptomic correlation analyses from the cancer cell line encyclopedia dataset to identify potential regulators of B7-H4 in breast cancer.

Results In the α PD-L1-sensitive EMT6 mammary cancer model, tumors with cell-surface B7-H4 expression were more resistant to immunotherapy. Additionally, tumor infiltrating immune cells had reduced immune activation signaling based on transcriptomic analysis. We also observed strong correlation with B7-H4 mRNA and epithelial cell markers, in contrast to gene expression markers of mesenchymal cells.

Conclusions Our data support the hypothesis that B7-H4 induces tumor resistance to α PD-L1 ICI through an immunosuppressive function. Additionally, the strong correlation of B7-H4 to epithelial cell markers suggests a potential regulatory mechanism of B7-H4 expression independent of PD-L1 regulation.

<http://dx.doi.org/10.1136/jitc-2021-SITC2021.756>

757

M9657, A NOVEL TUMOR-TARGETED CONDITIONAL ANTI-CD137 AGONIST DISPLAYS MSLN-DEPENDENT ANTI-TUMOR IMMUNITY

¹Chunxiao Xu*, ¹Brain Rabinovich, ¹Amit Deshpande, ¹Xueyuan Zhou, ²Frederic Christian Pipp, ³Rene Schweickhardt, ¹Lindsay Webb, ¹Sireesha Yalavarthi, ¹Clotilde Bourin, ³Payel Ghatak, ¹Barroq Safi, ⁴Francisca Wollerton, ⁴Neil Brewis, ⁴Jose Munoz-Olaya, ¹Natalya Belousova, ¹Marat Alimzhanov, ²Martina Hubensack, ²Joern-Peter Halle, ²Andree Blaukat, ¹Jacques Moisan. ¹EMD Serono Research and Development Institute, Belmont, MA, United States; ²The Healthcare Business of Merck KGaA, Billerica, MA, United States; ³EMD Serono Research and Development Inst, Billerica, MA, United States; ⁴F-star Therapeutics, Cambridge, United Kingdom

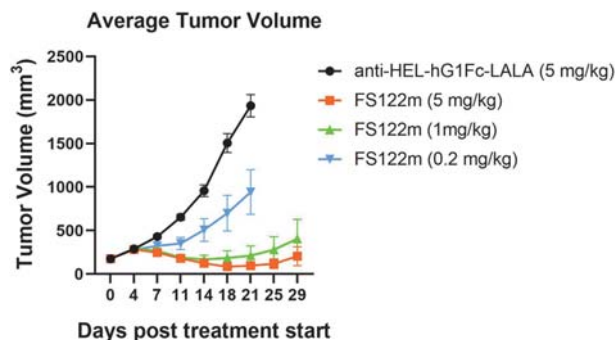
Background The costimulatory receptor CD137 (also known as 4-1BB and TNFRSF9) plays an important role in sustaining effective cytotoxic T cell immune responses and its agonism has been investigated as a cancer immunotherapy. In clinical trials, the systemic administration of the 1st generation CD137 agonist monotherapies, utomilumab and urelumab, were suspended due to either low anti-tumor efficacy or hepatotoxicity mediated by recognized epitope on CD137 and FcγR ligand-dependent clustering.

Methods M9657, a bispecific antibody was engineered a tetra-valent bispecific antibody (mAb2) format with the Fab portion binding to the tumor antigen Mesothelin (MSLN) and a modified CH2-CH3 domain as Fc antigen binding (Fcab) portion binding to CD137. M9657 has a human IgG1 backbone with LALA mutations to abrogate the binding to Fcγ receptor. The biological characteristics and activities of M9657 were investigated in a series of in vitro assays and the in vivo efficacy was investigated in syngeneic tumor models with FS122m, a murine-reactive surrogate with the same protein structure of M9657.

Results M9657 binds efficiently to both human and Cynomolgus CD137 as well as MSLN. In the cellular functional assay, M9657 displayed MSLN- and TCR/CD3 interaction (signal 1)-dependent cytokine release and tumor cell cytotoxicity associated with Bcl-XL activation and immune memory formation. FS122m demonstrated potent MSLN- and dose- dependent in vivo anti-tumor efficacy (figure 1). Comparing with 3H3, a Urelumab surrogate Ab, FS122m displayed an improved therapeutic window with significantly lower for on-target /off-tumor toxicity.

Ethics Approval All animal experiments were performed in accordance with EMD Serono Research & Development Institute (protocol 17-008, 20-005) and Wuxi AppTec Animal Care and Use Committee (IACUC) guidelines.

<http://dx.doi.org/10.1136/jitc-2021-SITC2021.757>



Abstract 757 Figure 1 FS122m displayed dose-dependent anti-tumor efficacy

Conclusions Taken together, M9657 exhibits a promising developability profile as a tumor-targeted immune agonist with potent anti-cancer activity, but without systemic immune activation.

HIGH-POTENCY SYNTHETIC STING AGONISTS REWIRE THE MYELOID STROMA IN THE TUMOUR MICROENVIRONMENT TO AMPLIFY IMMUNE CHECKPOINT BLOCKADE EFFICACY IN REFRACTORY PANCREATIC DUCTAL ADENOCARCINOMA

¹Akash Boda*, ²Casey Ager, ³Kimal Rajapakse, ¹Spencer Lea, ⁴Maria Emilia Di Francesco, ⁴Philip Jones, ⁴Michael Curran. ¹University of Texas MD Anderson UTHealth Graduate School of Biomedical Sciences, Houston, TX, United States; ²Columbia University Irving Medical Center, New York, NY, United States; ³Baylor College of Medicine, Houston, TX, United States; ⁴UT MD Anderson Cancer Center, Houston, TX, United States

Background Pancreatic ductal adenocarcinoma (PDAC) is one of the most lethal malignancies and is clinically unresponsive to immune checkpoint blockade (ICB) immunotherapy.^{1–2} High densities of immunosuppressive myeloid cells,³ a paucity of antigen-presenting cells^{4–6} and T cell exclusion from tumour microenvironment⁷ all contribute to the refractory nature of PDAC to immune-based therapies. We and others have shown that innate immune activation of myeloid stroma via engagement of the STING (Stimulator of Interferon Genes) pathway can mediate proinflammatory remodeling and trigger a flood of T cell infiltration into otherwise 'cold' tumours.^{8–11} To that end, intratumoral injection of cyclic dinucleotide (CDN) agonists of the STING pathway has been shown to foster local and abscopal tumor immunity.^{8–10} Despite proven therapeutic efficacy in preclinical models, the mechanistic basis at a cellular level of how CDNs reprogram the suppressive myeloid stroma to sensitise tumours to ICB is poorly understood.

Methods Using RNA sequencing and protein arrays we profiled myeloid-derived suppressor cell (MDSC) and M2 macrophage function following stimulation with CDNs of ascending potency. We describe the effects of CDN STING agonists on cell cycle dynamics, metabolic reprogramming and c-Myc expression in MDSCs. Next, in an orthotopic Kras+/G12DTP53+/R172HPdx1-Cre (KPC)-derived model of PDAC, we determined the ability of intratumorally-administered CDNs to sensitise PDAC to checkpoint blockade using bioluminescent in vivo imaging and multi-parameter flow cytometry of tumor stroma post-therapy.

Results Multi-omics profiling of MDSCs and M2 Macrophages of human and murine origin show that high-potency synthetic STING agonists rewire these populations from immunosuppressive to immune-permissive phenotypes in part through inhibition of c-Myc signaling, energy metabolic modulation, and antagonism of cell cycle. Intratumoral injection of the STING agonist, IACS-8803 resulted in an amplified therapeutic response to checkpoint blockade that was dependent on T/NK cell infiltration into the tumour. Furthermore, dimensionality reduction analyses of multiparameter flow cytometry data show proinflammatory remodeling of the myeloid stroma and enhanced T cell function as salient features of synthetic agonists versus natural CDNs in orchestrating the in vivo therapeutic benefit.

Conclusions This study uncovers molecular and cellular mechanisms by which STING agonists drive proinflammatory conversion of tumour myeloid stroma. We are the first to report that synthetic CDN STING agonists affect MDSC and M2 macrophage repolarization through altering energy metabolism and c-Myc signalling. Lastly, we demonstrate the potential for high-potency STING agonists to overcome resistance to checkpoint blockade in an aggressive orthotopic tumour model of PDAC.

REFERENCES

- Royal RE, Levy C, et al. Phase 2 trial of single agent Ipilimumab (anti-CTLA-4) for locally advanced or metastatic pancreatic adenocarcinoma. *J Immunother* 2010;**33**(8):828–33.
- Brahmer JR, Tykodi SS, et al. Safety and activity of anti-PD-L1 antibody in patients with advanced cancer. *N Engl J Med* 2012;**366**(26):2455–65.
- Karakhnova S, Link J. Characterization of myeloid leukocytes and soluble mediators in pancreatic cancer: importance of myeloid-derived suppressor cells. *Oncimmunology* 2015;**4**:e998519.
- Dallal RM, Christakos P, et al. Paucity of dendritic cells in pancreatic cancer. *Surgery* 2002;**131**:135–138.
- Yamamoto T, Yanagimoto H, et al. Circulating myeloid dendritic cells as prognostic factors in patients with pancreatic cancer who have undergone surgical resection. *J Surg Res* 2012;**173**:299–308.
- Hegde S, Krisnawan V, et al. Dendritic cell paucity leads to dysfunctional immune surveillance in pancreatic cancer. *Cancer Cell* 2020;**37**(3):289–307.
- Beatty GL, Winograd R, et al. Exclusion of T cells from pancreatic carcinomas in mice is regulated by Ly6Clow F4/80+ extratumoral macrophages. *Gastroenterology* 2015;**149**(1):201–210.
- Baird JR, Friedman D, et al. Radiotherapy combined with novel STING-Targeting oligonucleotides results in regression of established tumors. *Cancer Res* 2016;**76**(1):50–61.
- Ager CR, Reilley MJ, et al. Intratumoral STING activation with T-cell checkpoint modulation generates systemic antitumor immunity. *Cancer Immunol Res* 2017;**5**(8):676–84.
- Smith TT, Moffett HF, et al. Biopolymers codelivering engineered T cells and STING agonists can eliminate heterogeneous tumors. *J Clin Invest* 2017;**127**(6):2176–91.
- Jing W, McAllister D, et al. STING agonist inflames the pancreatic cancer immune microenvironment and reduces tumor burden in mouse models. *J Immunother Cancer* 2019;**7**(1):115.

<http://dx.doi.org/10.1136/jitc-2021-SITC2021.758>

759

SINGLE-CELL PROTEOGENOMICS (CITE-SEQ) ANALYSIS OF CGAS-STING PATHWAY ACTIVATION ALONE AND IN COMBINATION WITH NIVOLUMAB USING A PATIENT-DERIVED 3D EX VIVO TUMOROID PLATFORM

Brittany Bunch*, Autumn Joerger, Nino Mtchedlidze, Olivia Hoff, Kelly Guzman, Jared Ehrhart, Soner Altioik. *Nilogen Oncosystems, TAMPA, FL, United States*

Background The tumor immune microenvironment comprises a heterogeneous collection of adaptive and innate immune cells that play a critical role in immune evasion and response to immunotherapeutic agents. cyclic GMP-AMP synthase-stimulator of interferon genes (cGAS-STING) pathway results in activation of various immune cells promoting innate immunity in addition to senescence of cancer cells. However, the mechanisms involved in response and resistance to cGAS-STING pathway activation is not well understood. Using Cellular Indexing of Transcriptomes and Epitopes by sequencing (CITE-seq), we explored immunological heterogeneity of tumor microenvironment in colorectal cancer and analyzed transcriptional and compositional changes of the immune landscape in response to cGAS-STING pathway activation alone and in combination with a PD-1 inhibitor nivolumab.

Methods All human tumor samples were obtained with proper patient consent and IRB approval. Fresh patient tumor tissue was processed to generate uniform sized live 3D tumoroids measuring 150 μm in size. Treatment groups included a STING agonist, ADU-S100, alone or in combination with nivolumab. Here, we applied multi-modal CITE-seq profiling using the 10X Genomics platform to interrogate cellular responses to ex vivo treatment. Culture supernatants were collected for multiplex analysis of cytokine release in media. Additionally, flow cytometry was used to assess the activation profile of resident immune cells.

Results Multimodal analysis of transcriptomes or proteomics at the single-cell level provided an unprecedented view of cellular diversity and enabled better understanding of how activation of STING pathway alone and in combination with nivolumab affects the TME in colorectal cancer. Flow cytometric analysis of immune cell populations isolated from 3D tumoroids demonstrated treatment mediated activation of tumor resident T-cells and changes in the innate immune cells, which coincided with marked changes in pro-and anti-inflammatory cytokine profiles determined by multiplex analysis.

Conclusions These results demonstrate that the 3D-EXplore ex vivo tumoroid model provides a unique platform to assess the efficacy of immunotherapeutic agents and to develop novel therapeutic combinations. Furthermore, implementation of this platform in the clinical studies may also allow identifying clinically relevant biomarkers to enable the most effective treatment strategies for individual patients.

<http://dx.doi.org/10.1136/jitc-2021-SITC2021.759>

760

IN VIVO DEMETHYLATION-MEDIATED REVERSAL OF TUMOR CELL-INTRINSIC CGAS SILENCING IMPROVES THE EFFICACY OF STING AGONIST THERAPY

¹Rana Falahat*, ¹Patricio Perez-Villarroel, ¹Anders Berglund, ¹Shari Pilon-Thomas, ²Glen Barber, ¹James Mule. ¹Moffitt Cancer Center, Tampa, FL, United States; ²University of Miami, Miami, FL, United States

Background While STING-activating agents have shown limited efficacy in early phase clinical trials, multiple lines of evidence suggest the importance of the so far unappreciated tumor cell-intrinsic STING function in antitumor immune responses. Accordingly, we have shown that although there is a widespread impairment of STING signaling among human melanomas, its restoration through epigenetic reprogramming can augment antigenicity and T cell recognition of melanoma cells.^{1,2} In this study, we determined if rescue of tumor cell-intrinsic STING signaling using a DNA methyltransferase inhibitor can improve the therapeutic efficacy of a STING agonist in mouse models of melanoma.

Methods We subjected three distinct murine melanoma cell lines (B16-F10, B16-ISG and Yumm1.7) to treatment with 5-aza-2'-deoxycytidine (5AZADC) and evaluated their activation of STING following stimulation with the STING agonist ADU-S100. Using a B16-F10 subcutaneous model, we assessed the effect of 5AZADC treatment on the efficacy of intratumorally administered ADU-S100 in STING^{gt/gt} mice. Additionally, we performed mechanistic studies using T-cell depletion experiments as well as phenotypic and gene expression profiling.

Results We observed reconstitution of cGAS in all three 5AZADC-pretreated cell lines as well as up to a 46-fold increase in induction of IFN-beta ($p < 0.001$) and a 4.5-fold increase in MHC class I surface expression ($p < 0.01$) compared to untreated controls following stimulation with ADU-S100. In B16-F10 tumor-bearing mice, while treatment with a combination of 5AZADC plus ADU-S100 resulted in a marked increase in *Irf1* transcripts within tumors ($p < 0.001$), it significantly delayed tumor growth compared to treatment with ADU-S100 alone ($p = 0.0244$ on day 22). Antibody-mediated depletion studies in mice receiving the combination therapy further indicated that this antitumor activity depends on the generation of functional tumor antigen-specific CD8⁺ T cells ($p = 0.0111$ on day 22); however, tumor growth remained unaltered by the depletion of CD4⁺ T cells.

Conclusions We show that reversal of methylation silencing of cGAS in murine melanoma cell lines using a clinically available DNA methylation inhibitor can improve agonist-induced STING activation and type I IFN induction, which in tumor-bearing mice is capable of inducing tumor regression through a CD8⁺ T cell-dependent immune response. These findings not only provide mechanistic insight into how STING signaling dysfunction in tumor cells can contribute to impaired responses to STING agonist therapy, but also suggest, depending on tumor cell-intrinsic STING signaling status, its pharmacologic restoration should be considered for improving therapeutic efficacy of STING agonists in future clinical studies.

Acknowledgements

Funding: NCI P50 CA168536, Cindy and Jon Gruden Fund, Chris Sullivan Fund, V Foundation, Dr. Miriam and Sheldon G. Adelson Medical Research Foundation.

REFERENCES

1. Falahat R, Perez-Villarroel P, Mailloux AW, Zhu G, Pilon-Thomas S, Barber GN, Mulé JJ. STING signaling in melanoma cells shapes antigenicity and can promote antitumor T-cell activity. *Cancer Immunol Res* 2019;**7**(11):1837–48.
2. Falahat R, Berglund A, Putney RM, Perez-Villarroel P, Aoyama S, Pilon-Thomas S, Barber GN, Mulé JJ. Epigenetic reprogramming of tumor cell-intrinsic STING function sculpt antigenicity and T cell recognition of melanoma. *PNAS* 2021;**118**(15).

<http://dx.doi.org/10.1136/jitc-2021-SITC2021.760>

761 **EXOSTING DEMONSTRATES POTENT ANTI-TUMOR ACTIVITY IN A MOUSE MODEL OF LEPTOMENINGEAL DISEASE**

Xudong Feng*, John Lin*, Su Chul Jang, Seveda Lule, Paloma Sanchez-Jauregui, Katherine Kirwin, Tong Zi, Samuel Kaserer, Silvia Siso, Kelvin Zhang, Shil Patel, Sriram Sathyanarayanan, Kyriakos Economides, Wendy Broom. *Codiak BioSciences, Cambridge, MA, United States*

Background Leptomeningeal disease (LMD) occurs when cells from primary tumors metastasize to the cerebrospinal fluid (CSF) space leading to multifocal neurological deficits. LMD has an overall prevalence of ~5% in cancer patients, but is most commonly observed in breast, lung and melanoma patients. With improved therapies emerging for several primary tumor types, the incidence of LMD is rising, and with treatment options limited to radiotherapy and chemotherapy, the median survival of LMD patients remains poor at 3–6 months. Thus, there is high unmet medical need for development of effective therapeutic strategies for LMD. The STING (Stimulator of Interferon Genes) pathway has been shown to play a critical role in activating anti-tumor immunity through initiation of a tumor antigen-specific T cell response. exoSTING is an engineered extracellular vesicle exogenously loaded with a CDN (cyclic dinucleotide) STING agonist. We have previously demonstrated that it enhances the potency of the CDN, preferentially activates antigen presenting cells in the tumor microenvironment and increases CNS retention of the drug without systemic inflammatory cytokine stimulation. Histological data in LMD is scarce, however high levels of inhibitory macrophages and low T cell infiltration have recently been described, providing support for the therapeutic potential of exoSTING in LMD.

Methods A mouse model of LMD was generated by intracerebral inoculation of B16F10-Luc melanoma cells and was used to assess the efficacy of intracranial administration of exoSTING.

Results Tumor growth was monitored by bioluminescence imaging during course of each study, with rapid loss of signal post treatment observed in exoSTING treated groups compared to steady tumor growth in vehicle treated groups. Animals within vehicle treated groups demonstrated survival less than 30 days, whereas exoSTING treated mice survived 50+ days with a high complete response rate (over 85%), confirmed by ex vivo histopathological analysis. Peripheral immunological responses were demonstrated by lack of tumor growth following flank rechallenge in exoSTING treated mice. Strong anti-tumor response and tumor-specific immune activation in the absence of systemic inflammation was demonstrated. The presentation will summarize the immunological changes in the tumor microenvironment following exoSTING administration.

Conclusions exoSTING, which previously showed strong efficacy against primary melanoma in mouse models, has been demonstrated in this study to also suppress tumor growth and improve survival in the LMD context. Our study supports the therapeutic rationale for using exoSTING for the treatment of LMD.

<http://dx.doi.org/10.1136/jitc-2021-SITC2021.761>

762

STING AGONISM COMBINED WITH ARGINASE, NOS2, AND PTGES/COX2 INHIBITORS FOR IMPROVED ANTI-TUMOR IMMUNOTHERAPEUTIC BENEFIT

¹Jessica Filderman*, ²Manoj Chelvanambi, ¹Walter Storkus. ¹University of Pittsburgh, Pittsburgh, United States; ²MD Anderson Cancer Center, Pittsburgh, PA, United States

Background Tertiary lymphoid structures (TLS) are non-encapsulated immune cell aggregates that form at sites of chronic inflammation. Recent studies have shown that the presence of TLS in human tumors predicts extended survival and superior response to interventional immunotherapy. Our lab has recently demonstrated that treating mice bearing established tumors with agonists of STING, a cytosolic dsDNA sensor, leads to an inhibition in tumor growth in association with tumor vascular normalization, immune cell recruitment, and local formation of non-classical TLS within the tumor micro-environment. However, STING agonism also results in the upregulated expression of compensatory immune regulatory molecules, including ARG2 and enzymes involved in the production of immunosuppressive prostaglandins (i.e. PTGES and PTGS2/COX2), yielding an overall sub-optimal therapeutic paradigm. We are currently determining if combined treatment with STING agonists along with pharmacologic inhibitors of ARG2, NOS2 and/or PTGES/COX2 results in improved control of tumor growth, increased formation of TLS, and more robust anti-tumor immune responses in vivo in murine melanoma models.

Methods Melanoma tumor-bearing C57Bl/6 were treated with pharmacologic inhibitors of ARG2 or PTGES/COX2 i.p. in combination with STING agonist treatment i.t. Mice were monitored for tumor survival and growth. Tumors were also collected from mice at various timepoints post-treatment to evaluate the immune cell infiltration by flow cytometry and immunofluorescence microscopy (IFM). Tumor sections were also evaluated for TLS formation by IFM.

Results Treatment of mice systemically with inhibitors of ARG2, NOS2, and COX2/PTGES leads to changes in the immune composition of the tumor, including increases in effector immune cells and decreases in suppressive/regulatory immune cells. Combined treatment of melanoma-bearing mice with STING agonist ADU-S100 along with immune regulatory inhibitors (ARGi, NOSi, Celecoxib) slows tumor growth vs. individual monotherapies and is expected to extend overall survival.

Conclusions Combination of STING agonism with inhibitors of various immune regulatory molecules (ARG2, COX2) has the potential to improve the anti-tumor benefits of STING agonism alone.

<http://dx.doi.org/10.1136/jitc-2021-SITC2021.762>

763

INTRATUMORAL DELIVERY OF HIGH POTENCY STING AGONISTS MODULATES THE IMMUNOSUPPRESSIVE MYELOID COMPARTMENT AND INDUCES CURATIVE RESPONSES IN CHECKPOINT-REFRACTORY GLIOBLASTOMA MODELS

¹Spencer Lea*, ²Chao-Hsien Chen, ²Genevieve Hartley, ¹Rodney Cheng-En Hsieh, ²Michael Curran. ¹The University of Texas MD Anderson Cancer Center UTHHealth Graduate School of Biomedical Sciences, Houston, TX, United States; ²The University of Texas MD Anderson Cancer Center, Houston, TX, United States

Background Glioblastoma is an aggressive primary brain malignancy that is characterized by a highly suppressive tumor microenvironment, including myeloid-derived suppressor cells, tumor-associated macrophages, and brain-resident microglia, but lacking significant T cell infiltration.^{1, 2} This phenotype is reflected in the recently developed QKi^{-/-} Pten^{-/-} P53^{-/-} (QPP) tumor model,³ which we show is resistant to PD1 or CTLA-4 blockade, but sensitive to agonists of the innate immune sensor Stimulator of Interferon Genes (STING). We have previously shown that agonists of the innate dsDNA-sensing cGAS-STING pathway are capable of proinflammatory repolarization in in vitro models of suppressive myeloid cells, although their function in the context of the Glioblastoma myeloid compartment in vivo remains poorly understood.⁴

Methods We utilized the synthetic cyclic di-nucleotide STING agonists IACS-8803 (8803) and ML-RR-S2-CDA (MLRR) to assess survival and tumor immune infiltrate functional reprogramming in two orthotopic transplantable human and murine Glioblastoma tumor models, U87 and the recently developed QPP8 (QKi^{-/-} Pten^{-/-} P53^{-/-}). Using in vitro models of M2-polarized microglia, we investigated the ability of natural (2'3'-cGAMP) and synthetic (MLRR and 8803) STING agonists to reverse immunosuppressive microglial polarization.

Results We found that intratumoral delivery of STING agonists significantly prolonged survival in the murine QPP8 orthotopic Glioblastoma tumor model, in contrast to checkpoint blockade which had no benefit on survival. In huNOG-EXL mice engrafted with human hematopoietic stem cells implanted with orthotopic U87 Glioblastoma, intratumoral delivery of STING agonists significantly prolonged survival and reduced expression of CD163 and CD206 on human tumor-infiltrating myeloid populations. Preliminary data suggests that in vitro suppressively-polarized microglia reduce expression of M2 functional markers, and increase expression of iNOS, PD-L1, CD80, and CD86 in a STING agonist potency-dependent manner.

Conclusions We found that STING agonists can induce curative responses in checkpoint-refractory murine Glioblastoma models and mediate significant extension of survival in a humanized mouse U87 xenograft setting. This prolonged survival is associated with a decrease in immunosuppressive M2 functional markers in human tumor infiltrating myeloid populations. Additionally, M2-polarized microglia demonstrated a reduction in M2 functional markers and upregulation of proinflammatory M1 markers following treatment with STING agonists. Together these results indicate that delivery of STING agonists can induce proinflammatory repolarization of the Glioblastoma myeloid stroma, including both infiltrating myeloid populations and brain-resident microglia, to drive prolonged survival in refractory models of Glioblastoma.

REFERENCES

1. Gabrusiewicz K, Rodriguez B, Wei J, et al. Glioblastoma-infiltrated innate immune cells resemble M0 macrophage phenotype. *JCI Insight* 2016;**1**(2).

2. Quail DF, Joyce JA. The microenvironmental landscape of brain tumors. *Cancer Cell* 2017;**31**(3):326–41.
3. Shingu T, Ho AL, Yuan L, et al. Qki deficiency maintains stemness of glioma stem cells in suboptimal environment by downregulating endolysosomal degradation. *Nat Genet* 2017;**49**(1):75–86.
4. Ager C, Boda A, Rajapakshe K, et al. (2021) "High potency STING agonists engage unique myeloid pathways to reverse pancreatic cancer immune privilege. *JITC* (in press)

Ethics Approval All experiments were conducted according to protocols approved by the University of Texas MD Anderson Cancer Center Institutional Animal Care and Use Committee.

<http://dx.doi.org/10.1136/jitc-2021-SITC2021.763>

764

CHARACTERIZATION OF RVU-27065 A NOVEL SMALL-MOLECULE STING AGONIST SUITABLE FOR SYSTEMIC ADMINISTRATION

Maciej Rogacki*, Stefan Chmielewski, Magdalena Zawadzka, Aniela Golas, Aleksandra Poczka, Katarzyna Dziedzic, Kamil Kuś, Magnus Widegren, Jolanta Mazurek, Mirosława Gładysz, Justyna Jabłońska, Izabela Strojny, Grzegorz Cwiertnia, Łukasz Dudek, Marcin Leś, Urszula Głowniak-Kwitek, Nilesh Gaud, Arkadiusz Białas, Kinga Michalik, Raghuram Tangirala, Peter Littlewood, Krzysztof Brzózka. *Ryvu Therapeutics, Kraków, Poland*

Background Stimulator of Interferon Genes (STING) is a key signaling protein involved in activation of the immune system in response to self-DNA. In recent years, STING signaling has been demonstrated to play a major role in activating the anti-tumor immune response and therefore is considered an attractive drug target in immuno-oncology. The first wave of STING agonists, cyclic-dinucleotide analogues of the internal ligand cGAMP, were developed for local, intratumoral administration. Herein we present the most recent profiling results of our frontrunner molecule RVU-27065, a potent and selective systemic STING agonist with a favorable drug profile.

Methods Binding to recombinant STING protein was examined using Fluorescence Thermal Shift and Fluorescence Polarisation. Primary activity screen was performed in THP-1 Dual reporter cells. Selectivity was confirmed in THP-1 reporter cells with knocked out STING or expressing STING variants. T cell viability and proliferation was assessed by flow cytometry using activated human T cells. PBMCs were isolated by density gradient from whole blood of healthy donors. Downstream STING pathway activation in cells treated with RVU-27065 was confirmed using Western blot analysis. BALB/c mice were inoculated with EMT6 tumor cells and the compound was administered intravenously followed by regular monitoring of tumor growth. Cured animals were rechallenged by repeated inoculation of EMT6 cells.

Results RVU-27065 binds and strongly thermostabilizes recombinant STING proteins of all tested species. Binding to the protein results in activation of downstream signalling pathway, confirmed by western blot analysis. The agonist is characterized by selectivity and excellent potency in THP-1 dual reporter cells as well as in human PBMCs and dendritic cells. Short term incubation of RVU-27065 has no impact on T cell viability, activation or proliferation. Furthermore, STING activation with RVU-27065 leads to repolarization of immunosuppressive M2 macrophages into pro-inflammatory M1-like phenotype. In vivo efficacy of RVU-27065 was confirmed, leading to significant tumor growth inhibition and complete tumor regressions in an EMT6 mouse breast cancer syngeneic tumor model.

Conclusions RVU-27065 is a novel representative of a 3rd generation of Ryvu STING agonists – small-molecule, non-macrocyclic molecules built around a unique chemotype. The compound is characterized by high in vitro potency which translates to efficacy in vivo in preclinical animal models. Drug-like properties, excellent selectivity and a good safety profile make RVU-27065 an attractive candidate for further development for standalone as well as targeted delivery, which holds high potential for improved immunotherapy in cancer patients.

<http://dx.doi.org/10.1136/jitc-2021-SITC2021.764>

765

THE FIRST-IN-CLASS SMALL MOLECULE TREX1 INHIBITOR CPI-381 DEMONSTRATES TYPE I IFN INDUCTION AND SENSITIZATION OF TUMORS TO IMMUNE CHECKPOINT BLOCKADE<http://dx.doi.org/10.1136/jitc-2021-SITC2021.765>

Costa Salojin*, Anna Gardberg, Valerie Vivat, Lei Cui, Jeffrey Lauer, Nico Cantone, Jacob Stuckey, Florence Poy, Ingrid Almeciga, Richard Cummings, Jonathan Wilson, Julian Levell, Jennifer Rocnik, Patrick Trojer. *Constellation Pharmaceuticals, Cambridge, MA, United States*

Background TREX1 is an exonuclease that functions as a negative regulator of innate immunity. TREX1 controls dsDNA sensing in tumor and immune cells by preventing aberrant dsDNA buildup that triggers STING-mediated Type 1 Interferon (IFN) induction leading to priming of the adaptive immune system. Loss of function mutations in TREX1 and genetic ablation of *trex1* in mice lead to induction of IFN-beta-driven autoimmunity. Thus, TREX1 is a promising target to elicit IFN-mediated anti-tumor immunity.

Methods To characterize TREX1 inhibitors we developed cell-based assays utilizing human HCT116 carcinoma and THP-1 monocytic Dual reporter cell lines to monitor IRF activity. Activation of cGAS was assessed by measuring cGAMP levels in B16F10 melanoma cells. The potency of TREX1 inhibitors in primary human dendritic cells (DC)s was analyzed by measuring IFNbeta induction by exogenous dsDNA. Analysis of tumor growth inhibition following TREX1 inhibitor treatment was conducted in mouse syngeneic tumor models. TREX1 activity was assessed by measuring degradation of a custom dsDNA substrate.

Results We report here the development of a small molecule TREX1 inhibitor, CPI-381, with nanomolar cellular potency, which translated into a robust induction of IRF reporter activity. We observed a significant increase in cGAMP production in B16F10 cells transfected with DNA in the presence of CPI-381, suggesting that CPI-381-mediated inhibition of TREX1 leads to the activation of dsDNA sensors, such as cGAS. Treatment of THP-1 cells with CPI-381 induced the expression of several key ISG involved in innate immunity. Moreover, inhibition of TREX1 with CPI-381 phenocopied the effect of TREX1 genetic deletion in primary human DCs by upregulating IFNbeta. To evaluate whether TREX1 negatively regulates IFNbeta production in syngeneic tumor models, we knocked down *trex1* in B16F10, MB49, MC38, and CT26 murine cells. Accumulation of cytosolic dsDNA resulted in a substantial increase in IFNbeta secretion by all four TREX1-KO cell lines. In vivo efficacy studies with CPI-381 demonstrated reduced tumor growth in the MC38 syngeneic tumor model either alone or in combination with anti-PD1. We observed a reduction of TREX1 activity in CPI-381 treated tumors, confirming an inverse relationship between TREX1 intra-tumor activity and tumor growth, and efficient target engagement after systemic (oral) delivery.

Conclusions We have developed a first-in-class, potent TREX1 inhibitor demonstrating excellent in vitro and in vivo potency via enhancement of cytosolic dsDNA sensing and induction of IFNbeta in cancer and immune cells. CPI-381-induced tumor-intrinsic TREX1 inhibition elicits antitumor immunity as a single agent and increases response to immune checkpoint blockade via mechanisms downstream of TREX1 that activate type I IFN signaling.

Ethics Approval All animal work was approved and conducted under the oversight of the Charles River Accelerator and Development Lab (CRADL, Cambridge, MA) Institutional Animal Care and Use Committee (protocol # 2021-1258).

766 TOWARD SAFE, SYSTEMIC DELIVERY OF SYNTHETIC
TLR7/8 AGONISTS USING BOTTLEBRUSH PRODRUGS
(BPDs)

Sachin Bhagchandani*, Lauren Milling, Bin Liu, Timothy Fessenden, Stefani Spranger, Jeremiah Johnson, Darrell Irvine. *Massachusetts Institute of Technology, Cambridge, MA, United States*

Background Although toll-like receptor (TLR) agonists such as imidazoquinoline derivatives (IMDs) have been well researched and are FDA approved as topical solutions for treatment of skin cancer, their systemic delivery for treatment of metastatic disease has not been successful due to toxicity issues. Therefore, to lessen the degree of the adverse effects of intravenous delivery of IMDs such as resiquimod (R848), a bottlebrush prodrug (BPD) system enabling controlled release of R848 at tunable rates was designed and synthesized. We hypothesized that this approach would allow for minimizing the release of the free drug in serum, allowing for a higher concentration to accumulate in the tumor while minimizing systemic side effects.

Methods R848 was conjugated to a bottlebrush polymer with different linkers designed to precisely tune the R848 release rate. The release rates of the drug delivered through this system were first tested in PBS. These prodrug formulations were validated for drug activity in vitro in mouse and human TLR reporter cells. The maximum tolerable dose was defined by monitoring weight loss and serum cytokine levels upon intravenous administration at multiple concentrations. Finally, anti-tumor efficacy of the BPD system was tested in vivo using the MC38 colon cancer model as a monotherapy and in combination with anti-PD-1 antibody treatment.

Results The in-vitro half-lives of the conjugated drugs varied from a few days to over a month when tested in PBS. The different BPDs demonstrated linker dependent TLR activation upon culturing with TLR reporter cells validating the immunomodulatory activity of R848. It was found that the R848-BPDs, which accumulated at the tumor site over time, significantly delayed tumor growth and improved survival rates, which was further enhanced when used in combination with anti-PD-1.

Conclusions Overall, our research suggests that our R848-BPD platform allows for safe, systemic delivery of TLR agonists to activate the immune system in treatment of cancer.

<http://dx.doi.org/10.1136/jitc-2021-SITC2021.766>

ACTIVATION OF CD8+ T CELLS IN THE PRESENCE OF MULTIPLE TLR AGONISTS AFFECTS THE EXPRESSION OF T-CELL CHECKPOINT RECEPTORS VIA IL-12 AND TYPE-1 INTERFERON<http://dx.doi.org/10.1136/jitc-2021-SITC2021.767>

Donghwan Jeon*, Douglas McNeel. *University of Wisconsin-Madison, Madison, WI, United States*

Background T-cell checkpoint receptors are expressed when T-cell are activated, and activation of these receptors can impair the function of T-cells and their anti-tumor efficacy.¹ We previously found that T-cells activated with cognate antigen increase the expression of PD-1, while this can be attenuated by the presence of specific Toll-like receptor (TLR) agonists.²³ This effect was mediated by IL-12 secretion from professional antigen presenting cells and resulted in CD8+ T cells with greater anti-tumor activity. In the current report, we sought to determine whether combination of TLR agonists can further affect the expression of T-cell checkpoint receptors and improve T-cell anti-tumor immunity.

Methods OT-1 CD8+ T cells were stimulated with peptide (SIINFEKL) and dendritic cells (DC) in the presence of two different TLR agonists. The cells were collected and evaluated for the expression of T-cell checkpoint receptors (PD-1, CTLA-4, CD160, CD244, LAG-3, TIM-3, TIGIT and VISTA) by flow cytometry, and for transcriptional changes by RNA-seq. Purified DC were stimulated with TLR combinations and evaluated for cytokine release by ELISA. The anti-tumor efficacy of vaccination using peptide and TLR agonist combinations was evaluated in EG7-OVA tumor-bearing mice.

Results Activation of CD8+ T cells in the presence of specific TLR ligands resulted in decreases in expression of PD-1 and/or CD160. These changes in T-cell checkpoint receptor expression were modestly affected when TLR ligands were used in combination, and notably with combinations of TLR1/2, TLR3, and TLR9 agonists. Immunization of tumor-bearing mice, co-administered with combinations of these agonists, showed greater anti-tumor effects. However, while the effect of TLR1/2 and/or TLR9 was abrogated in IL12KO mice, TLR3 demonstrated anti-tumor activity when co-administered with peptide vaccine. RNA sequencing of TLR-conditioned CD8+ T-cells revealed IL-12 pathway activation, and IFN β pathway activation following TLR3 stimulation. Stimulation of DC with TLR3 agonist, alone or in combination with other TLR agonists, resulted in increased IL-12 and IFN β secretion. Co-incubation of OT-1 splenocytes with rIL12 and/or rIFN β during peptide activation led to reduced expression of PD-1, and this could be reversed with antibodies blocking IL12R or IFNAR-1.

Conclusions Multiple TLR agonists can modulate the expression of T-cell checkpoint receptors, notably PD-1, by upregulating the secretion of IL-12 and IFN β . These data provide the mechanistic rationale for choosing optimal combinations of TLR ligands to use as adjuvants to improve the efficacy of anti-tumor vaccines.

REFERENCES

1. Jin H-T, et al. Cooperation of Tim-3 and PD-1 in CD8 T-cell exhaustion during chronic viral infection. *Proceedings of the National Academy of Sciences* 2010;**107**(33):14733–14738.
2. Zahm CD, Colluru VT, McNeel DG. Vaccination with high-affinity epitopes impairs antitumor efficacy by increasing PD-1 expression on CD8+ T cells. *Cancer Immunology Research* 2017;**5**(8):630–641.
3. Zahm CD, et al. TLR stimulation during T-cell activation lowers PD-1 expression on CD8+ T Cells. *Cancer Immunology Research* 2018;**6**(11):1364–1374.

768

SYSTEMIC DELIVERY OF A TUMOR-TARGETED TLR9 AGONIST CONJUGATE TRANSFORMS THE TUMOR IMMUNE LANDSCAPE AND INDUCES TUMOR REGRESSION IN MICE

Caitlyn Miller Candidate*, Idit Sagiv-Barfi, Patrick Neuhofer, Debra Czerwinski, Steven Artandi, Carolyn Bertozzi, Ronald Levy, Jennifer Cochran. *Stanford University, Stanford, CA, United States*

Background Tumor-localized delivery of Toll-like receptor (TLR) agonists is a promising strategy to promote immune activation within the tumor microenvironment (TME) to overcome tumor immunosuppression and induce anti-tumor immune responses. To enable localization to multiple tumor sites following systemic administration, we developed a fully-synthetic tumor-targeting TLR9 agonist and demonstrate its potential to transform the tumor immune microenvironment for effective tumor regression in mice.

Methods An engineered synthetic peptide (PIP) that binds to multiple integrin receptors overexpressed in many solid tumors was chemically conjugated to a synthetic CpG oligonucleotide (TLR9 agonist), thereby generating a tumor-targeting immunostimulant referred to as PIP-CpG. To facilitate clinical translation, PIP-CpG is cross-reactive between mouse, non-human primate, and human. Therapeutic studies were conducted in immune-competent mice bearing breast or pancreatic tumors to evaluate the efficacy of intravenously (IV)-injected PIP-CpG compared to IV-injected unmodified CpG or vehicle (PBS). We then performed mechanistic studies to evaluate the immune response elicited by PIP-CpG therapy.

Results Intravenous dosing of PIP-CpG led to tumor regression and prolonged survival, and in some cases cures, relative to vehicle or unmodified CpG therapy in both murine breast (4T1) and pancreatic cancer (KPC-G2) models. This tumor regression was dependent on T cells as T cell depletion resulted in loss of therapeutic response. To study the effect of systemic therapy on the cellular landscape in the TME, we analyzed 4T1 breast tumors by flow cytometry. We found that vehicle and CpG IV-dosed mice had immunosuppressive TMEs comprised mostly of myeloid-derived suppressor cells (MDSCs; 43–68% of live cells) with minimal infiltrating T cells and B cells (5–16% of live cells). In contrast, the TME of PIP-CpG treated mice was transformed into a lymphocyte-rich “hot” tumor phenotype with massive infiltration by T cells and B cells (92–95% of live cells) and plummeting levels of MDSCs (down to ~1%). In addition, tumor-specific effector CD8+ T cells were generated in response to PIP-CpG therapy, but not CpG dosed IV, indicating that PIP-CpG therapy transforms the TME and elicits a T cell-mediated tumor-specific immune response. Furthermore, PIP-CpG was effective for treating MMTV-PyMT transgenic mice, which spontaneously develop multiple breast tumors. Murine toxicity studies indicated that effects of PIP-CpG were similar to CpG dosed IV or intratumorally, which have been well-tolerated in human clinical trials.

Conclusions Tumor-directed systemic delivery of a TLR9 agonist transforms the TME via activated B and T cells and is promising for further development in patients with solid tumors.

Ethics Approval All mouse experiments were performed in accordance with protocols approved by the Stanford Administrative Panel on Laboratory Animal Care.

<http://dx.doi.org/10.1136/jitc-2021-SITC2021.768>

769

A SINGLE DOSE OF INTRATUMORAL TRANSCON™ TLR7/8 AGONIST MONOTHERAPY PROMOTED SUSTAINED ACTIVATION OF ANTIGEN PRESENTING CELLS RESULTING IN CD4+ AND CD8+ T CELL ACTIVATION AND TUMOR GROWTH INHIBITION<http://dx.doi.org/10.1136/jitc-2021-SITC2021.769>

Luis Zuniga*, Karan Uppal, Kathy Bang, Enping Hong, Simran Sabharwal, Yuchi Lee, Solomon Martinez, David Rosen, Amer Mirza, Juha Punnonen. *Ascendis Pharma, Inc., Redwood City, CA, United States*

Background The use of pattern recognition receptor agonists (PRRAs) such as Toll-like receptor (TLR) agonists is an attractive approach for cancer immunotherapy. TLR agonism elicits anti-tumor activity by activating antigen presenting cells (APCs) to promote a proinflammatory microenvironment and anti-tumor immunity. Local delivery of TLR agonists has shown encouraging preclinical and clinical anti-tumor benefit. However, intratumoral (IT) delivery of naked PRRAs may lead to rapid effusion from the tumor microenvironment, potentially impacting their effectiveness in inducing local inflammation and may promote systemic cytokine release, increasing the risk of adverse effects.

Methods TransCon™ TLR7/8 Agonist was designed to address the current limitations of PRRA therapies and IT delivery through sustained and controlled release of resiquimod, a potent TLR7/8 agonist, following IT administration of a hydrogel depot.

Results A single IT injection of TransCon TLR7/8 Agonist induced potent tumor growth inhibition in a dose-dependent manner in syngeneic mouse CT26 tumors. Following IT TransCon TLR7/8 Agonist treatment, acute and sustained upregulation of cell surface markers indicative of activation of APCs, such as CD54, CD69, and CD86, in the tumor was observed by fluorescence activated flow cytometry (FACs). Additionally, TransCon TLR7/8 Agonist treatment was associated with an increase in the frequency of APCs with an activated phenotype in tumor draining lymph nodes (LNs). Further, a concomitant potentiation in the frequency of activated CD4 and CD8 T cells in tumor draining LNs following IT TransCon TLR7/8 Agonist treatment was observed, as demonstrated by increased expression of Ki67, ICOS, or granzyme B.

Conclusions These data support that a single IT dose of TransCon TLR7/8 Agonist can mediate robust anti-tumor activity as a monotherapy in the CT26 syngeneic mouse tumor model while promoting local activation of intratumoral APCs. Such activation may promote tumor antigen uptake and migration to tumor-associated lymphoid tissue, as evidenced by an increase in APCs with an activated phenotype in tumor draining LNs following TransCon TLR7/8 Agonist treatment. Activated tumor antigen-bearing APCs can promote the priming and activation of tumor-specific T cells in the tumor-draining LNs. Consistently, a dose-dependent increase in the frequency of T cells with an activated effector phenotype in tumor draining LNs following administration of TransCon TLR7/8 Agonist was observed. These preclinical data further support TransCon TLR7/8 Agonist as a novel and potentially efficacious PRRA therapy. A clinical trial to evaluate safety and efficacy of TransCon TLR7/8 Agonist as monotherapy, and in combination with pembrolizumab, in cancer patients has been initiated (transcendIT-101; NCT04799054).

Ethics Approval The animal studies performed described were performed in accordance with the "Guide for the Care and Use of Laboratory Animals: Eighth Edition" and approved by the institutional animal care and use committee (IACUC).

770

PERSONALIZED SYNTHETIC POLYPEPTIDE DNA CANCER VACCINES ENCODING A NOVEL PYROPTIC ADJUVANT TO GENERATE EFFECTIVE ANTI-TUMOR T CELL IMMUNITY

¹Jeroen Van Bergen*, ²Tsolere Arakelian, ¹Kedar Moharana, ¹Bram Teunisse, ³Iris Zoutendijk, ²Marcel Camps, ²Ramon Arens, ²Fery Ossendorp, ¹Gerben Zondag. ¹Immunetune, Leiden, Netherlands; ²LUMC, Leiden, Netherlands; ³Synvolux, Leiden, Netherlands

Background As every tumor carries its unique set of neoantigens distinguishing it from healthy tissue, cancer vaccines need to be produced quickly and on an individual basis to swiftly induce a broad immune response targeting multiple antigens. DNA provides an ideal platform to achieve this, as a single polypeptide vaccine can encode multiple (>20) antigens. However, standard plasmid DNA vaccines take months to produce and tend to be poorly immunogenic in humans.

Methods To address the first issue, a GMP-compatible method (AmpliVax) was developed that allows the simultaneous production of milligram amounts of multiple DNA vaccines in single vessel reactions within two days. This method relies on a primer-free, isothermal, rolling-circle amplification using high fidelity DNA polymerase and RNA polymerase to amplify circular DNA templates into linear double-stranded concatemers. Concatemers are digested into single linear expression cassettes which are subsequently protected by nuclease-resistant caps. To improve DNA vaccine immunogenicity, two avenues were explored. First, neoantigen DNA vaccines were tested in a therapeutic setting together with a checkpoint inhibitor drug. Second, DNA vaccines were combined with a novel caspase-1-based genetic adjuvant (PyroVant) that induces pyroptosis by exploiting the inflammasome pathway.

Results Upon intradermal injection in mice, synthetic AmpliVax DNA vaccines matched plasmid DNA vaccines in terms of in vivo expression, immunogenicity and tumor protection. While treatment of mice carrying an MC38 colorectal tumor with either a polypeptide neoantigen DNA vaccine or anti-PD-1 did not significantly delay tumor outgrowth compared to untreated mice (0% survival), the combination of the neoantigen vaccine and anti-PD1 resulted in up to 70% tumor-free survival. PyroVant DNA accelerated and amplified antigen-specific CD8 T cell responses when administered simultaneously with a polypeptide DNA vaccine. What's more, subsequent challenge with melanoma cells revealed that PyroVant also significantly improved tumor-free survival.

Conclusions In conclusion, we have created a novel synthetic DNA vaccine platform suitable for the production of effective personalized cancer vaccines. Current efforts are aimed at testing combinations of therapeutic synthetic DNA vaccines, PyroVant and checkpoint inhibitors in multiple pre-clinical tumor models.

<http://dx.doi.org/10.1136/jitc-2021-SITC2021.770>

NOVEL LIPID NANOPARTICLE VACCINE PLATFORM FOR EFFICIENT DELIVERY OF HIGH- AND LOW-AFFINITY EPITOPES

¹Unnur Jóna Björgvinsdóttir*, ²Laura Stentoft Carstensen*, ¹Anna Colliander, ¹Ditte Elisabeth Jæhger, ¹Gael Clergeaud Veiga, ¹Hólmfríður Rósa Halldórsdóttir, ¹Matilde Smærup Jørgensen, ¹Esben Christensen, ¹Sara Vangsgaard, ¹Aristeidis Koukos, ¹Martin Bak, ¹Paul Kempen, ¹Thomas Lars Andresen. ¹Technical University of Denmark, Lyngby, Denmark; ²Technical University of Denmark, Lyngby, Denmark

Background Therapeutic cancer vaccines represent an intriguing approach to cancer immunotherapy and they have been widely explored for the last decade. As opposed to standard modalities, such as surgery and chemotherapy, an effective vaccine-based immune response may provide protection against metastatic disease. Peptide based vaccines can elicit a highly targeted immune response and include a simple, fast and cost-effective production due to recent developments in solid phase peptide synthesis. Recent development within the field of COVID-19 vaccines has highlighted the use of lipid nanoparticles as an effective drug delivery system for vaccination. Incorporation of peptide antigens into engineered micro- and nanoparticles enables induction of a potent T cell response, partly attributed to prolonged and improved antigen presentation by dendritic cells after particle internalization. Peptide-based vaccines are often based on delivery of high-affinity T cell model epitopes. However, the therapeutic relevance of vaccination with low-affinity epitopes is gaining increasing support following the observation that high-affinity epitopes can promote T cell exhaustion resulting from excessive T cell receptor stimulation. Here, we characterize and evaluate a novel lipid nanoparticle (LNP) vaccine platform that is suited for delivery of both high- and low-affinity epitopes in the setting of therapeutic cancer vaccination.

Methods LNPs were formulated to carry high- or low-affinity peptide epitopes from Ovalbumin (OVA) in conjunction with the TLR7 agonist 1V270. The peptides were anchored to the surface of the LNPs via a reducible DSPE-PEG2000 linker system. The therapeutic vaccine platform was evaluated in vivo both as a monotherapy and in combination with adoptive transfer of OT-I T cells in the syngeneic B16-OVA murine melanoma model.

Results The LNP vaccine promotes efficient antigen-release and ensures high, continuous antigen-presentation by antigen-presenting cells. While the LNPs can be administered via multiple routes, intratumoral vaccination favors enhanced particle uptake in dendritic cells in the tumor. Formulated with either high- or low-affinity epitopes, intratumorally delivered vaccine particles promote superior tumor-infiltration of adoptively transferred T cells, which translates into potent anti-tumor efficacy in vivo. Finally, we show that vaccination with both CD8+ and CD4+ epitopes can delay tumor growth and prolong survival in an antigen-dependent manner.

Conclusions This study presents a versatile and multi-purpose LNP vaccine platform that ensures effective delivery of high- and low-affinity epitopes. Intratumoral administration promotes vaccine particle uptake by intratumoral dendritic cells, which is followed by T cell infiltration and anti-tumor efficacy in vivo.

Ethics Approval All animal procedures were approved by the Danish National Animal Experiments Inspectorate.

<http://dx.doi.org/10.1136/jitc-2021-SITC2021.771>

MHC-I SKEWING IN MUTANT CALRETICULIN-POSITIVE MYELOPROLIFERATIVE NEOPLASMS IS COUNTERED BY HETEROCLITIC PEPTIDE CANCER VACCINATION

¹Mathieu Gigoux*, ¹Roberta Zappasodi, ¹Joseph Park, ²Cansu Cimen Bozkus, ¹Levi Mangarin, ¹David Redmond, ¹Svena Verma, ¹Sara Schad, ¹Mariam George, ¹Divya Venkatesh, ¹Arnab Ghosh, ¹Zaki Molvi, ³Baransel Kamaz, ³Anna Marneth, ³William Duke, ⁴Matthew Leventhal, ³Max Jan, ³Vincent Ho, ³Gabriela Hobbs, ⁵Trine Knudsen, ⁵Vibe Skov, ⁵Lasse Kj r, ⁶Thomas Larsen, ⁶Dennis Hansen, ³R. Lindsley, ⁵Hans Hasselbalch, ⁷Jacob Grauslund, ⁷Mads Andersen, ⁷Morten Holmstrom, ¹Timothy Chan, ¹Raajit Rampal, ¹Omar Abdel-Wahab, ²Nina Bhardwaj, ³Ann Mullally, ¹Jedd Wolchok, ¹Taha Merghoub. ¹Memorial Sloan Kettering Cancer Center, New York, NY, United States; ²Icahn School of Medicine at Mount Sinai, New York, United States; ³Harvard Medical School, Boston, United States; ⁴Broad Institute, Cambridge, MA, United States; ⁵Zealand University Hospital, Roskilde, Denmark; ⁶Odense University Hospital, Odense, Denmark; ⁷University of Copenhagen, Copenhagen, Denmark

Background The majority of JAK2V617F-negative myeloproliferative neoplasms (MPN) have disease-initiating frameshift mutations in calreticulin (CALR) resulting in a common novel C-terminal mutant fragment (CALRMUT), representing an attractive source of neoantigens for cancer vaccines. However, studies have shown that CALRMUT-specific T cells are rare in CALRMUT MPN patients, but the underlying reasons for this phenomenon are unknown. We speculate that this is due to an increased chance of immune-mediated tumor rejection by individuals expressing one of these MHC-I alleles such that the disease never clinically manifests. As a consequence of this MHC-I allele restriction, we reasoned that CALRMUT MPN patients would not efficiently respond to cancer vaccines composed of the CALRMUT neoantigen, but could do so when immunized with a properly epitope-optimized CALRMUT heteroclitic peptide vaccine approach.

Methods We examined MHC-I allele frequency in CALRMUT MPN patients from two independent cohorts to identify under-represented MHC-I alleles. These MHC-I alleles were assessed for their ability to bind to CALRMUT-derived peptides using NetMHC and were subsequently validated experimentally in healthy donors and in CALRMUT MPN patients having received a CALRMUT cancer vaccine (clinical trial NCT03566446) to determine if these MHC-I were potentiating immunogenicity against the CALRMUT antigen. Epitope-optimized heteroclitic variants of the CALRMUT neoantigen were identified and tested experimentally in vitro in human PBMCs and in vivo in mice for their ability to mount an immune response against the non-modified CALRMUT neoantigen.

Results We observed that MHC-I alleles that present CALRMUT neoepitopes with high affinity are under-represented in CALRMUT MPN patients. Heteroclitic CALRMUT peptides specifically designed for CALRMUT MPN patient MHC-I alleles efficiently elicited a cross-reactive CD8⁺ T cell response in human PBMC samples otherwise unable to respond to the matched weakly immunogenic CALRMUT native peptides. We also modeled this effect in mice and observed that C57BL/6J mice, which are unable to mount an immune response to the human CALRMUT fragment, can mount a cross-reactive CD8⁺ T cell response against a CALRMUT-derived peptide upon heteroclitic peptide immunization and this was further amplified by combining the heteroclitic peptide vaccine with blockade of the immune checkpoint molecule PD-1.

Conclusions Our study shows that MHC-I alleles able to present CALRMUT neoepitopes are under-represented in CALRMUT MPN patients, demonstrating that MHC-I haplotype is a major mechanism of passive immune-evasion in

CALRMUT MPN. However, we show that a cancer vaccine composed of heteroclitic variants of the CALRMUT antigen could overcome this limitation.

Ethics Approval Approval was obtained for the use of patient-derived specimens and access to clinical data extracted from patient charts by the Institutional Review Boards at Memorial Sloan Kettering Cancer Center, the Dana-Farber Cancer Institute and the Massachusetts General Hospital, as well as by the Danish Regional Science Ethics Committee.

<http://dx.doi.org/10.1136/jitc-2021-SITC2021.772>

773 A NOVEL CANCER IMMUNOTHERAPY; VACCINATION AGAINST TUMOR VASCULAR EXTRACELLULAR VIMENTIN

Elisabeth Huijbers*, Judy van Beijnum, Karlijn van Loon, Arjan Griffioen. *Amsterdam UMC, Cancer Center Amsterdam, Amsterdam, Netherlands*

Background Angiogenesis, the development of neovasculature, is required to sustain tumor growth and metastasis of solid tumors. The tumor neovasculature expresses specific markers, which are selectively overexpressed in tumor endothelial cells compared to normal healthy adult endothelium and are therefore ideal targets for vaccination.

Methods One of these tumor vascular markers is the extracellular cytoskeletal protein vimentin. This marker is externalized from tumor endothelial cells, while expression in all other cells in the body is exclusively intracellular. Extracellular vimentin (eVim) is pro-angiogenic and functionally mimics vascular endothelial growth factor (VEGF) action, while concomitantly acting as inhibitor of leukocyte-endothelial interactions, thereby hampering leukocyte infiltration into the tumor. eVim is overexpressed in the vasculature of different solid tumors, but not present in normal healthy tissue.

Results Using iBoost, our proprietary conjugate vaccine technology for induction of efficient antibody responses against self-antigens, we were able to generate strong eVim specific humoral immune responses, resulting in inhibition of tumor growth in preclinical models without affecting the normal healthy vasculature. Furthermore, in an ongoing clinical study in client owned dogs with spontaneous bladder cancer our eVim vaccine shows effective and safe inhibition of angiogenesis and tumor growth.

Conclusions Targeting of extracellular vimentin by vaccination therefore presents a promising antiangiogenic immunotherapy strategy that is currently translated into clinical testing.

<http://dx.doi.org/10.1136/jitc-2021-SITC2021.773>

AN INDUCED PLURIPOTENT STEM CELL (iPSC) VACCINE IS HIGHLY IMMUNOGENIC AND REDUCES LUNG METASTASES IN A MOUSE MODEL OF MELANOMA

<http://dx.doi.org/10.1136/jitc-2021-SITC2021.774>

Matthias Hundt*, Peter Bove, Ivan Hernandez, Michelle Li, Lucia Beviglia, Pratima Kundu, Babacar Ndoye, Nigel Kooreman, Stephen Wolpe, Lynne Bui. *Khloris Biosciences, Mountain View, CA, United States*

Background Extensive data on gene expression, metabolic state and glycosylation of cancer cells suggest that cancer represents a reversion of adult cells to an embryonic state and that induced pluripotent stem cells (iPSC) model this state. In contrast to cancer cells, iPSC have never undergone immunoediting and therefore present hundreds of oncofetal antigens in their native conformations. In this study, we administered a vaccine comprising syngeneic iPSC together with the Toll-like receptor (TLR) 9 agonist CpG1826 as an adjuvant and assessed its immunogenicity and preclinical efficacy in a mouse model of melanoma lung metastases with and without checkpoint inhibition.

Methods C57BL/6 mice were immunized with 2×10^6 irradiated (60Gy) iPSC admixed with 500pmol CpG, or with PBS or CpG alone as controls. Four immunizations were administered subcutaneously one week apart. Mice were challenged with 1×10^5 B16F10 murine melanoma cells intravenously one week after the second immunization. After tumor cell injection some groups were also treated with anti-PD-L1 (200µg, 2X/week, i.p.). All mice were euthanized 19 days after intravenously B16F10 injection and lung metastases were counted in a blinded fashion. Cellular and humoral immune responses were measured by IFN-gamma ELISpot, serum IgG binding to iPSC and B16F10 and flow cytometric analysis of splenocytes.

Results Treatment of mice with anti-PD-L1+CpG, iPSC+CpG and iPSC+CpG+anti-PD-L1 significantly reduced the number of lung metastases in comparison to CpG (One-way ANOVA with Dunnett's multiple comparisons test) (table 1). Immunization with iPSC+CpG was as effective as treatment with anti-PD-L1+CpG. No synergism of iPSC+CpG with anti-PD-L1 was detectable. Only immunization with iPSC+CpG induced a significant increase in IFN-gamma spots after in vitro challenge with iPSC and B16F10 lysates in comparison to CpG. Comparable results were obtained for serum IgG binding to iPSC and B16F10. Percentage of regulatory T cells in the spleen was significantly reduced in iPSC+CpG and iPSC+CpG+anti-PD-L1 in comparison to CpG. Similar results were obtained in a second independent study.

Abstract 774 Table 1 Number of lung metastases

Treatment	PBS	CpG	αPD-L1	CpG+αPD-L1	iPSC+CpG	iPSC+CpG+αPD-L1
Median	66.0	69.5	49.0	24.0	21.5	26.0
Mean	62.4	64.3	43.8	33.7	28.4	31.9
SEM	8.5	7.7	11.6	7.7	5.6	6.4
N	5	12	4	9	10	10

Conclusions Irradiated syngeneic iPSC admixed with TLR9 agonist CpG1826 in combination with or without checkpoint blockade induced T cell and antibody responses to iPSC and B16F10 thereby reduced the number of melanoma lung metastases in mice. These results warrant further investigation of autologous iPSC vaccines in clinical trials.

Ethics Approval The studies were approved by Explora BioLabs' Animal Care and Use Committee; approval number EB17-010-118.

AN INDUCED PLURIPOTENT STEM CELL (iPSC) VACCINE DECREASES TUMOR GROWTH AND IMPROVES SURVIVAL IN A THERAPEUTIC MOUSE MODEL OF COLON CANCER

<http://dx.doi.org/10.1136/jitc-2021-SITC2021.775>

Matthias Hundt*, Michelle Li, Hui Huang, Carlos Obejero-Paz, Peter Bove, Ivan Hernandez, Pratima Kundu, Nigel Kooreman, Stephen Wolpe, Lynne Bui. *Khlolis Biosciences, Mountain View, CA, United States*

Background Extensive data on gene expression, metabolic state and glycosylation of cancer cells suggest that cancer represents a reversion of adult cells to an embryonic state and that induced pluripotent stem cells (iPSC) are good surrogates for this state. In contrast to cancer cells, iPSC have never undergone immunoediting and therefore present hundreds of oncofetal antigens in their native conformations. In this study, we administered syngeneic iPSC together with the Toll-like receptor (TLR) 9 agonist CpG1826 in a therapeutic mouse model of colon cancer with and without checkpoint inhibition.

Methods C57BL/6 mice (n=10) were injected with 5×10^5 MC-38 murine colon adenocarcinoma cells s.c. One week later, mice received a course of 4 weekly injections with 10×10^6 irradiated (60Gy) iPSC admixed with 1nmol CpG1826, or PBS or CpG alone as controls. Some groups also received anti-PD-1 (200µg, 2X/week, i.p.) for 4 weeks. Tumor growth and survival were monitored for 108 days post tumor injection. Mice were euthanized when tumor volume reached 2000 mm³. Serum IgG binding to iPSC and MC-38 was measured by flow cytometry 1 week after the last immunization in all 60 mice and IFN-gamma ELISPOTs were determined after in vitro challenge of splenocytes with iPSC and MC-38 lysates in 10 surviving mice at the end of the study.

Results Treatment of mice with anti-PD-1, anti-PD-1+CpG, iPSC+CpG and iPSC+CpG+anti-PD-1 significantly increased median survival in comparison to CpG alone (Gehan-Breslow-Wilcoxon test) by ~50% (table 1). Therapeutic vaccination with iPSC+CpG was as effective as treatment with anti-PD-1, and anti-PD-1+CpG. Similar data were obtained for tumor growth; iPSC+CpG vaccination was as effective in reducing tumor growth as anti-PD-1. Only immunization with iPSC +CpG and iPSC+CpG+anti-PD-1 induced a significant increase in serum IgG binding to iPSC and MC-38; IFN-gamma spots after in vitro challenge with iPSC and MC-38 lysates were only detectable in mice that had been injected with iPSC.

Abstract 775 Table 1 Median survival in days post tumor injection

Treatment	PBS	CpG	αPD-1	CpG+αPD-1	iPSC+CpG	iPSC+CpG+αPD-1
Median survival [days]	58	52	82.5	74.5	73.5	75.5
P value for CpG vs ...	0.9697	NA	0.0332	0.0107	0.0269	0.0156

Conclusions Irradiated syngeneic iPSC admixed with TLR9 agonist CpG1826 with or without combination with checkpoint inhibition induced T cell and antibody responses to iPSC that cross-reacted with MC-38. The iPSC vaccine was effective in delaying and decreasing tumor growth and in increasing median survival in a therapeutic model of colon cancer comparable to checkpoint inhibition.

Ethics Approval The study was approved by Valley Bio Services' Institutional Animal Care and Use Committee; approval number VBS1002.

THE ANTI-TUMOR ACTIVITY OF HER-2/NEU ICD THERAPEUTIC CANCER VACCINE (AST-301, PNGVL3-HICD) IN HER2-EXPRESSED GASTRIC CANCER XENOGRFT MODEL

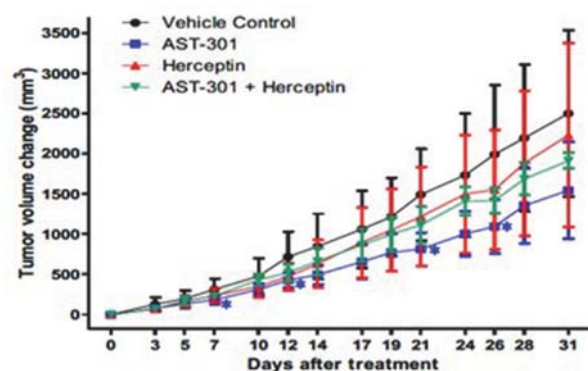
¹Gyeong Seok Jo, ²Eunkyo Joung*, ¹Jung Hyu Shin, ¹Hye Lim Lee, ²Jinback Lim, ²Yoonyi Kim, ²Hyo-Hyun Park, ²Hunwoo Shin, ²Hun Jung. ¹Osong Medical Innovation Foundation, Chungcheong-do, Korea, Republic of; ²Aston Sci. Inc., Seoul, Korea, Republic of

Background The HER-2/neu, potent oncogenic protein, has several characteristics that make it a good antigen to serve as the model for developing pDNA-based tumor vaccine strategies.¹⁻³ The observation that immunity co-exists with antigen-positive cancer cells indicates that HER-2 is immunogenic. AST-301 (pNGVL3-hICD) is a plasmid DNA-based therapeutic cancer vaccine encoding HER2 ICD sequence. The clinical efficacy and safety of AST-301 were already proven in HER2-positive breast cancer population, and long-term immunogenicity and survival were demonstrated well via phase 1 study (PN 109, NCT00436254) In this in-vivo study, AST-301 was investigated to evaluate the efficacy in HER2/neu-expressed gastric cancer xenograft model.

Methods A HER2-expressed gastric cancer xenograft model was established with NCI-N87 cell line inoculation in athymic-nude mice. Treatment groups were assigned as AST-301 alone (AST-301, 0.1 mg/head, i.d.), Trastuzumab (TZM, 20 mg/kg, i.p.) or AST-301 combining with Trastuzumab (AST-301+TZM) respectively. To evaluate tumor protective effect of drugs, mice were immunized 3 times in every week. Immunization of AST-301 or AST-301+TZM was completed, followed by tumor cell line inoculation. In another study to verify the anti-tumor effect of them, the administration of drugs was started when the tumor volumes reached approximately 150 mm³. AST-301 was immunized 3 times in every week to post-implantation 32nd day and TZM was injected 5 times per week. The tumor volumes were estimated and the percentage of tumor growth inhibition was calculated.

Results In our two in vivo efficacy studies, there was no significant specific safety issue in all groups. Tumor protective effect was observed in AST-301 group (1506.7±1603.0 mm³) compared with control group (GM-CSF, 1266.3±862.5 mm³) as an immune adjuvant (figure 1). However, AST-301+TZM group (1533.0±1186.3 mm³) did not show the tumor protective effect. The groups of AST-301 and AST-301+TZM were significantly higher to the anti-tumor activity than control group, and AST-301 was more effective than AST-301+TZM or TZM alone. On day 33 (32 days after starting treatment), tumor growth inhibition rate were 38.3 % (2503.4±1034.6 mm³), 10.9 % (1545.0±599.9 mm³) and 23.6 % (1912.9±97.1 mm³) in groups of AST-301, TZM and AST-301+TZM compared with control group, respectively.

Conclusions Tumor protective and tumor therapeutic effect of AST-301 were demonstrated well in various doses and regimens on HER2/neu positive gastric cancer xenograft model. These data would be supporting a proof of concept (PoC) clinical study of HER-2/neu ICD therapeutic cancer vaccine in certain type of HER2/neu-expressed gastric cancer patient.



Abstract 776 Figure 1 Tumor protective and tumor therapeutic effect of AST-301 on HER2/neu positive gastric cancer xenograft model

REFERENCES

- Disis ML. Enhancing cancer vaccine efficacy via modulation of the tumor microenvironment. *Clin Cancer Res* 2009;**15**:6476–6478.
- Disis ML, Wallace DR, Gooley TA, et al. Concurrent trastuzumab and HER2/neu-specific vaccination in patients with metastatic breast cancer. *J Clin Oncol* 2009;**27**:4685–4692.
- Disis ML, Schiffman K, Guthrie K, et al. Effect of dose on immune response in patients vaccinated with an her-2/neu intracellular domain protein-based vaccine. *J Clin Oncol* 2004;**22**:1916–1925.

Ethics Approval This experiment was conducted ethically with the approval of the Institutional Animal Care and Use Committee (KBIO-IACUC-2021-038) in the Osong Medical Innovation Foundation Experimental Animal Center.

Consent N/A

<http://dx.doi.org/10.1136/jitc-2021-SITC2021.776>

777

PERSONALIZED DNA VACCINE IN COMBINATION WITH PLASMID ENCODED IL-12 FOR THE TREATMENT OF A PATIENT WITH ANAPLASTIC ASTROCYTOMA

¹Tanner Johanns, ²Alfredo Perales-Puchalt*, ²Sarah Rochestie, ²Neil Cooch, ²Joann Peters, ¹Gavin Dunn, ²Niranjan Sardesai. ¹Washington University School of Medicine, St. Louis, MO, United States; ²Geneos Therapeutics, Plymouth Meeting, PA, United States

Background Tumor neoantigens are epitopes derived from tumor-specific mutations. Such mutations can be incorporated in personalized vaccines to prime T cell responses against tumor specific antigens. DNA vaccines delivered with electroporation have recently shown strong CD8 and CD4 T cell responses in clinical trials. In preclinical studies, DNA-encoded neoantigen vaccines have shown induction of CD8 T cells against 50% of predicted high affinity epitopes with the ability to impact tumor growth.

Methods Two resection samples from a patient with IDH+MGMT-methylated anaplastic astrocytoma were subject to whole exome and transcriptome sequencing. Epitopes derived from 27 neoantigens and 3 shared tumor-associated antigens were prioritized and included in a personalized vaccine. The patient was treated with surgery, radiotherapy and temozolomide starting June 2018 and received the first dose of the personalized vaccine in June 2019 under a compassionate use single patient IND application with the FDA.

Results As of July 23rd, 2021, the patient has received 11 doses of the DNA personalized vaccine. No serious adverse events have been reported. Related adverse events are limited to grade 1 injection site reactions. The patient remains progression-free 37 months after surgery and 25 months after starting vaccination. Three weeks following the 3rd dose, a hyperintense image on the tumor bed was identified, which disappeared on the following MRI, 2 weeks following dose 5, being catalogued as pseudo progression. Ex vivo ELISpot have identified T cell responses to 28/30 epitopes (93.3%), including 25/27 (92.6%) neoantigens and 3/3 (100%) shared antigens. Flow cytometry analysis has determined that T cell responses are 92.3% CD8 and 69.2% CD4 (30.8% CD8 only; 61.5% both CD8 and CD4; and 7.7% CD4 only).

Conclusions This compassionate use treatment in an adjuvant setting demonstrates manufacturing feasibility, safety, tolerability, immunogenicity, and suggests potential for persistent clinical response of DNA encoded personalized vaccines. The data supports further investigation of DNA-encoded personalized vaccines into newly diagnosed high-grade gliomas.

Ethics Approval The study was approved by Washington University's IRB. The participant gave informed consent before taking part in the study.

<http://dx.doi.org/10.1136/jitc-2021-SITC2021.777>

MODULATING TUMOR MICROENVIRONMENT WITH ARGINASE-1 SPECIFIC T CELLS

¹Evelina Martinenaite*, ²Mia Aaboe Jørgensen, ²Rasmus Erik Johansson Mortensen, ²Shamaila Munir Ahmad, ²Stine Emilie Weis-Banke, ²Morten Orebo Holmström, ¹Ayako Wakatsuki Pedersen, ²Özcan Met, ²Inge Svane, ²Mads Hald Andersen. ¹IO Biotech, Copenhagen, Denmark; ²National Center for Cancer ImmuneTherapy, Herlev, Denmark

Background IO112 is an immune modulatory cancer therapy under preclinical development to target arginase-1-expressing tumor cells and immune inhibitory myeloid cells, such as myeloid derived suppressor cells (MDSCs), and tumor associated macrophages (TAMs). Arginase-1 acts as a metabolic immune regulator at the tumor site by reducing availability of L-arginine to the infiltrating immune cells thus reducing T cell functionality and proliferation. Previously, we demonstrated that IO112 triggers activation of spontaneous CD4+ and CD8+ T-cell responses against arginase-1, found in both cancer patients and healthy individuals.¹ These T cells are present in the memory T cell compartment, and are activated in arginase-1 inducing conditions, such as presence of TH2 cytokines IL-4 or IL-13 in vitro.^{2 3} In this study we aimed to explore the role of arginase-1-specific T cells as immune modulators in immune homeostasis and tumor microenvironment for the development of IO112 immunomodulatory therapy.

Methods Human arginase-1-specific T cells were isolated and expanded for functional characterization of reactivity against arginase-1 expressing target cells as well as subsequent phenotyping of the targeted arginase-1 positive cells. Syngeneic C57BL/6 mouse tumor models were used to assess the therapeutic efficacy of IO112.

Results We show that arginase-1-specific memory T cells specifically recognize arginase-1 expressing cells, such as mRNA transfected autologous dendritic cells (DCs) and B cells as well as M2 polarized macrophages in vitro. In addition, activated arginase-1-specific T cells produce pro-inflammatory cytokines IFN γ and TNF α . Secretion of TH1 cytokines by these T cells suggests that they may act as potent immune modulators in the tumor microenvironment, since many arginase-1 expressing myeloid cells are not terminally differentiated and they can be re-polarized to an immunostimulatory, M1-like phenotype. We also observed that targeting of M2-polarized arginase-1 expressing monocytic leukemia cell line THP-1 with arginase-1-specific CD4+ T cells induces upregulation of PD-L1 on the THP-1 cells. Furthermore, we demonstrate anti-tumor activity of IO112 in syngeneic mouse tumor models (B16 and MC38), both as monotherapy and in combination with anti-PD-1 treatment. The therapeutic effect was associated with increased immune infiltration in the IO112-treated mice compared to the control.

Conclusions We demonstrate that arginase-1 specific T cells can influence the polarization of arginase-1-expressing immune cells. Our study provides evidence that IO112 immune therapy against arginase-1 is an attractive way of modulating the immune suppressive tumor microenvironment for therapeutic benefit. With this rationale, we are currently undertaking Investigational New Drug (IND) application enabling studies to explore this approach in a clinical setting.

REFERENCES

1. Martinenaite E, Mortensen REJ, Hansen M, Holmström MO, Ahmad SM, Jørgensen NGD, Met Ö, Donia M, Svane IM, Andersen MH. Frequent adaptive immune responses against arginase-1. *Oncoimmunology* 2018;7(3):e1404215.
2. Martinenaite E, Ahmad SM, Svane IM, Andersen MH. Peripheral memory T cells specific for Arginase-1. *Cell Mol Immunol* 2019;16(8):718–719.

3. Martinenaite E, Ahmad SM, Bendtsen SK, Jørgensen MA, Weis-Banke SE, Svane IM, Andersen MH. Arginase-1-based vaccination against the tumor microenvironment: the identification of an optimal T-cell epitope. *Cancer Immunol Immunother* 2019;68(11):1901–1907.

Ethics Approval This study was approved by the Scientific Ethics Committee for The Capital Region of Denmark and Danish Ethics Committee on experimental animal welfare.

<http://dx.doi.org/10.1136/jitc-2021-SITC2021.778>

779

INHIBITING TYPE-I INTERFERON SIGNALING PROMOTES MEMORY T-CELL FORMATION FOLLOWING IMMUNIZATION WITH LISTERIA ANTI-CANCER VACCINES

Zachary Morrow*, John-Demian Sauer. *The University of Wisconsin-Madison, Madison, WI, United States*

Background The aspiration of cancer immunotherapy is to generate large numbers of highly functional anti-tumor CD8+ T-cells. We and others have optimized *Listeria monocytogenes* as a powerful anti-cancer vaccine platform to drive such T-cell responses. Early clinical trial data suggest the number of T-cells generated correlates with efficacy, demanding an understanding of the factors that dictate vaccine-induced T-cell responses. The CD8+ T-cell response is intimately linked to magnitude and quality of the innate immune response triggered by vaccines. *Listeria*-based vaccines activate numerous innate pathways and can be engineered to hyper- or hypo-induce these pathways. We sought to understand how modulating innate immunity would impact vaccine efficacy.

Methods To dissect the impact of type I interferon signaling and the inflammasomes on *L. monocytogenes* induced T-cell responses, we immunized IFNAR^{-/-}, Caspase1/11^{-/-}, and novel IFNAR^{-/-}-Caspase1/11^{-/-} double knockouts mice we generated for this study. CD8+ T-cell responses were assessed at the peak T-cell response, after contraction and memory formation, and after rechallenge. The phenotype and magnitude of CD8 + T-cells was assessed at each stage, and functional outcomes were assessed by measuring protection from reinfection by wild-type *Listeria*.

Results IFNAR^{-/-} mice developed the largest number of CD8+ T-cells during the peak primary response contradicting the dogma that Type-I Interferon promotes robust CD8+ T-cell responses. Caspase1/11^{-/-} mice were not significantly different from wild-type mice. The frequency of short-lived effector cells (assessed by expression of CD127 and KLRG1) was no different between wild-type and IFNAR^{-/-} mice, however we observed more than twice as many memory precursor cells at the peak CD8+ T-cell response. These findings extend to the memory and recall stage with more antigen-specific T-cells observed after contraction and upon rechallenge. Finally, IFNAR^{-/-} mice are remarkably more protected from wild-type *Listeria* rechallenge than their counterparts after immunization demonstrating the efficacy of the increased memory T-cell pool. Data are representative of at least two independent replicates with at least 5 mice per group and significance was assessed by one-way ANOVA with * $p < 0.05$.

Conclusions We demonstrated that type-I interferon signaling deficiency leads to enhanced prophylactic vaccine efficacy through increased memory T-cell formation. Ultimately, for patients with slow growing tumors or with high-risk mutations, prophylactic tumor vaccines could elicit life-long protection from disease. Importantly, increased memory precursor T-cell abundance did not come at the expense of short-lived effectors leaving open the possibility that blocking Type-I IFN could potentiate lasting immunological memory in both the therapeutic and prophylactic setting.

<http://dx.doi.org/10.1136/jitc-2021-SITC2021.779>

Immuno-Conjugates and Chimeric Molecules

780

ALTA-002, A SIRP α -DIRECTED TLR9 AGONIST ANTIBODY CONJUGATE ACTIVATES MYELOID CELLS AND PROMOTES ANTI-TUMOR IMMUNITY

¹Ons Harrabi*, ¹Amy Chen, ¹Emma Sangalang, ¹Danielle Fontaine, ¹Min Li, ²Jaume Pons, ¹Hong Wan, ¹Janet Sim, ¹Tracy Kuo. ¹Tallac Therapeutics, Burlingame, CA, United States; ²ALX Oncology Holdings Inc, Burlingame, CA, United States

Background Novel therapies engaging both innate and adaptive immune responses may engender durable anti-tumor immunity. Activation of toll-like receptor 9 (TLR9) by unmethylated CpG oligonucleotides promotes innate inflammatory responses and induces adaptive immunity. Immune cells expressing TLR9 encompass B cells and myeloid cells (including dendritic cells and plasmacytoid dendritic cells). Recently, several TLR9 agonists have demonstrated clinical benefit in patients with melanoma when administered intra-tumorally.¹ Specifically designed for systemic administration, we developed a novel Toll-like Receptor Agonist Antibody Conjugate (TRAAC) molecule comprised of a differentiated TLR-9 agonist (T-CpG) conjugated to an antibody against SIRP α (ALTA-002). Signal regulatory protein α (SIRP α) is a myeloid inhibitory receptor that suppresses immune activation following binding of its ligand CD47. Blockade of CD47-SIRP α myeloid checkpoint pathway has been shown to promote myeloid-mediated anti-tumor functions leading to the induction of adaptive immunity.² Additionally, SIRP α is highly expressed in various tumor types including renal cell carcinoma and melanoma.³ Here we present preclinical data demonstrating that ALTA-002 delivers T-CpG to SIRP α expressing myeloid cells, triggering TLR9 signaling, cell activation and immune modulation resulting in robust anti-tumor efficacy.

Methods In vitro activity of ALTA-002 was evaluated using human PBMCs co-cultured in the presence of SIRP α positive and negative tumor cells. Anti-tumor efficacy of mouse ALTA-002 surrogate was evaluated in multiple syngeneic tumor models with varying immunogenicity profiles.

Results In vitro co-culture of human PBMC and SIRP α positive or negative tumor cells with ALTA-002 stimulates myeloid cells, leading to increased IRF7 induction, expression of co-stimulatory molecules, and cytokine secretion. In vitro treatment with ALTA-002 led to enhanced phagocytic engulfment by human monocyte-derived macrophages across multiple SIRP α positive and negative tumor cell lines. Following systemic delivery of a mouse ALTA-002 surrogate, durable anti-tumor activity was observed in both SIRP α positive and negative expressing tumors. ALTA-002 treated mice with eradicated tumors suppressed tumor growth upon tumor re-challenge, indicating tumor-specific immune memory.

Conclusions These results demonstrate the unique properties of systemically administered ALTA-002, which integrates TLR9 activation and blockade of CD47-SIRP α interaction on myeloid cells to engender both innate and adaptive anti-tumor immune responses. These data support the development of ALTA-002 as an anti-cancer therapeutic for a variety of tumor malignancies.

REFERENCES

1. Hamid O, Ismail R, Puzanov I. Intratumoral Immunotherapy-Update 2019. *Oncologist* 2020;**25**(3):e423-e4382.
2. Kuo T, Chen A, Harrabi O. Targeting the myeloid checkpoint receptor SIRP α potentiates innate and adaptive immune responses to promote anti-tumor activity. *J Hematol Oncol* 2020;**13**:160-1783.

3. Yanagita T, Murata Y, Tanaka D. Anti-SIRP α antibodies as a potential new tool for cancer immunotherapy. *JCI Insight* 2017;**2**(1):e89140.

Ethics Approval In vivo studies were approved by the Institutional Animal Care and Use Committee of Tallac Therapeutics.

<http://dx.doi.org/10.1136/jitc-2021-SITC2021.780>

GT-001 - ANTI-LEWIS Y ANTIBODY WITH SUPERIOR FINE-SPECIFICITY AND REDUCED OFF-TARGET BINDING

Anika Jaekel, Patrik Kehler*, Timo Lischke, Lisa Weiß, Christoph Goletz, Evelyn Hartung, Anke Flechner, Sven Bahrke, Johanna Gellert, Antje Danielczyk. *Glycotope GmbH, Berlin, Germany*

Background The Lewis Y (CD174) carbohydrate antigen is widely expressed in primary and metastatic epithelial tumors like colon, lung, ovarian, and breast. Targeting Lewis Y for cancer therapy was pursued before, however, other anti-Lewis Y antibodies tested in clinical trials showed cross-reactivity to related carbohydrate structures expressed on blood cells and mostly failed for efficacy and/or safety reasons.¹⁻⁴ We have developed a humanized antibody (GT-001) that shows superior fine-specificity and higher affinity compared to clinically tested anti-Lewis Y antibodies BR96 and h3S193.

Methods The specificity and cross-reactivity of GT-001, BR96 and h3S193 were compared. Cross-reactivity binding to related carbohydrate PAA-conjugates was tested via ELISA and affinity towards Lewis Y-PAA was measured using switch-SENSE[®] technology (DRX2, Dynamic Biosensors). Functional binding to several tumor cell lines and healthy human leukocytes was analyzed via flow cytometry. Binding of GT-001 to different cancer indications was analyzed by immunohistochemistry. Inhibition of tumor cell proliferation was tested using GT-001 coupled to ProtG-MMAE.

Results GT-001 is strictly specific for Lewis Y and does not cross-react with >90 related carbohydrate structures tested. Our lead candidate shows superior fine-specificity compared to BR96, for which we could confirm the reported cross-reactivity towards Lewis X,⁵ and stronger binding of Lewis Y compared to h3S193 as shown by affinity measurement. Further, GT-001 shows no/weak binding to blood cells whereas BR96 and h3S193 significantly bind to different leukocyte subsets. IHC studies reveal that GT-001 stains tumor tissue of different cancer indications (breast cancer, colorectal cancer, head and neck cancer, (non) small cell lung cancer and ovarian cancer) at a high percentage of cases. In ADC surrogate assays, GT-001 potently inhibits the proliferation of several tumor cell lines indicating effective internalization.

Conclusions Lewis Y is expressed on many epithelial tumor indications of high medical need. However, several approaches of targeting Lewis Y have failed in the past for efficacy and/or safety reasons. We have developed a humanized antibody that shows superior fine-specificity and higher affinity compared to clinically tested anti-Lewis Y antibodies BR96 and h3S193. Due to the superior fine-specificity, GT-001 shows no/reduced binding of healthy leukocytes potentially reducing side effects as observed for BR96 in the clinic. Its strong target binding and internalization properties make GT-001 an ideal candidate for ADC development.

REFERENCES

1. Ajani JA, Kelsen DP, Haller D, Hargraves K, Healey D. A multi-institutional phase II study of BMS-182248-01 (BR96-doxorubicin conjugate) administered every 21 days in patients with advanced gastric adenocarcinoma. *Cancer J* 2000;**6**(2):78-81.
2. Saleh MN, Sugarman S, Murray J, Ostroff JB, Healey D, Jones D, Daniel CR, LeBerz D, Brewer H, Onetto N, LoBuglio AF. Phase I trial of the anti-Lewis Y drug immunoconjugate BR96-doxorubicin in patients with lewis Y-expressing epithelial tumors. *J Clin Oncol* 2000;**18**(11):2282-92.
3. Scott AM, Tebbutt N, Lee FT, Cavicchiolo T, Liu Z, Gill S, Poon AM, Hopkins W, Smyth FE, Murone C, MacGregor D, Papenfuss AT, Chappell B, Saunder TH, Brechbiel MW, Davis ID, Murphy R, Chong G, Hoffman EW, Old LJ. A phase I biodistribution and pharmacokinetic trial of humanized monoclonal antibody

Hu3s193 in patients with advanced epithelial cancers that express the Lewis-Y antigen. *Clin Cancer Res* 2007;**13**(11):3286-92.

4. Smaletz O, Diz MD, do Carmo CC, Sabbaga J, Cunha-Junior GF, Azevedo SJ, Maluf FC, Barrios CH, Costa RL, Fontana AG, Madrigal V, Wainstein AJ, Yeda FP, Alves VA, Moro AM, Blasbalg R, Scott AM, Hoffman EW. A phase II trial with anti-Lewis-Y monoclonal antibody (hu3S193) for the treatment of platinum resistant/refractory ovarian, fallopian tube and primary peritoneal carcinoma. *Gynecol Oncol* 2015;**138**(2):272-7.
5. Zhang S, Zhang HS, Cordon-Cardo C, Reuter VE, Singhal AK, Lloyd KO, Livingston PO. Selection of tumor antigens as targets for immune attack using immunohistochemistry: II. Blood group-related antigens. *Int J Cancer* 1997;**73**(1):50-6.

<http://dx.doi.org/10.1136/jitc-2021-SITC2021.781>

782

PD-L1-TARGETED ISAC COMBINES MYELOID CELL ACTIVATION, IMMUNE-CHECKPOINT INHIBITION AND ADCP TO IMPROVE ANTI-TUMOR EFFICACY OVER ANTI-PD-L1 ANTIBODIES IN PRECLINICAL MODELS

Justin Kenkel, Rishali Gadkari, Karla Henning, Romas Kudirka, William Mallet, Po Ho, Ganapathy Sarma, Steven Chapin, Liz Bogaert, Jennifer Melrose, Matthew Zhou, Suprit Deol, Cindy Kreder, Yuyi Shen, Puneet Anand, Arthur Lee, Hai Li, Shelley Ackerman, Brian Safina, David Dornan, Michael Alonso, Marcin Kowanetz*. *Bolt Biotherapeutics, Redwood City, CA, United States*

Background PD-L1 is an immune checkpoint that regulates anti-tumor T cell responses and is expressed on tumor cells as well as tumor-infiltrating immune cells across many tumor types. Immune-stimulating antibody conjugates (ISACs) consist of tumor-targeting antibodies conjugated to immune stimulants and are designed to activate the innate and adaptive immune systems against tumor cells following systemic administration. Here we show that PD-L1-targeted TLR7/8 ISACs elicit robust myeloid cell activation which leads to improved anti-tumor responses compared to anti-PD-L1 treatment in pre-clinical tumor models.

Methods A panel of proprietary anti-PD-L1 antibodies was identified through a phage display screen and subsequently tested for PD-L1 binding affinity and specificity, PD-L1/PD-1 blocking, antibody-dependent cellular phagocytosis (ADCP) by myeloid cells, and anti-tumor efficacy. Lead antibodies were conjugated to proprietary TLR7/8 agonists, and the resulting PD-L1 ISACs were evaluated for in vitro myeloid cell activation and in vivo efficacy against syngeneic and xenograft tumors.

Results Anti-PD-L1 antibodies induced robust ADCP by myeloid effector cells and medium to strong PD-L1/PD-1 blockade in vitro. Selected antibodies inhibited the growth of syngeneic MC38-hPD-L1 tumors in vivo, confirming efficient immune-checkpoint blockade. The conjugated PD-L1 ISACs induced robust, target-dependent activation of myeloid cells when co-cultured with PD-L1-expressing tumor cells, as measured by increased secretion of such cytokines as IL-12p70, IFN-alpha, and TNF-alpha. Importantly, myeloid activation was observed following co-culture with tumor cells having various levels of endogenous PD-L1 expression that was within the range of PD-L1 expression observed in human tumors. Systemically administered surrogate PD-L1 ISACs were well tolerated in mice and showed improved anti-tumor efficacy over anti-PD-L1 antibodies, with significant tumor growth delay or complete responses frequently observed in syngeneic (e.g. MB49, MC38-hPD-L1) as well as xenograft (e.g. HCC1954-hPD-L1) tumor models.

Conclusions These data demonstrate the potential of a PD-L1-targeted ISAC as a multifunctional therapeutic that may improve efficacy of PD-L1/PD-1 inhibition by combining three mechanisms of action into a single molecule: TLR-mediated myeloid cell activation, T cell activation through immune-checkpoint inhibition as well as ADCP.

Ethics Approval All animal studies were performed in accordance with Institutional Animal Care and Use Committee (IACUC)-approved protocols.

<http://dx.doi.org/10.1136/jitc-2021-SITC2021.782>

SGN-PDL1V, A NOVEL, INVESTIGATIONAL PD-L1-DIRECTED ANTIBODY-DRUG CONJUGATE FOR THE TREATMENT OF SOLID TUMORS

Byron Kwan*, Megan Ramirez, Steven Jin, Changpu Yu, Serena Wo, Priyanka Gupta, Sean Allred, Jessica Simmons, Kelly Hensley, Christina Zuch de Zafra, Haley Neff-LaFord, Shawna Hengel, Andres Forero-Torres, Heather Van Epps. *Seagen, Bothell, WA, United States*

Background PD-1/PD-L1 immune checkpoint inhibitors have transformed oncology, but a significant unmet need persists for patients with relapsed/refractory tumors following PD-1/PD-L1 treatment. PD-L1 is expressed in patients across a broad spectrum of tumor types and displays limited normal tissue expression, highlighting the potential of PD-L1 as a target for antibody-drug conjugates (ADCs) in addition to its role as an immune checkpoint. SGN-PDL1V is a PD-L1-directed ADC currently under preclinical investigation, which is comprised of an anti-PD-L1 antibody conjugated to the vedotin drug-linker. The vedotin drug-linker, consists of the microtubule disrupting agent, monomethyl auristatin E (MMAE), and a protease-cleavable peptide linker, which has been clinically validated in multiple ADC programs including brentuximab vedotin, enfortumab vedotin and polatuzumab vedotin.¹⁻³ The proposed SGN-PDL1V primary mechanism of action is direct cytotoxicity against PD-L1-expressing malignant cells through delivery of the MMAE payload. Additionally, MMAE induces immunogenic cell death, leading to subsequent immune activation in the tumor microenvironment.⁴ Here, we characterize the preclinical activity and tolerability of SGN-PDL1V.

Methods SGN-PDL1V cytotoxicity was evaluated using PD-L1 expressing tumor cell lines in vitro and xenograft tumor models in vivo. Inhibition of the PD-1/PD-L1 immune checkpoint was assessed in a luminescent reporter system in vitro and a syngeneic tumor model in vivo. The tolerability and safety profile of SGN-PDL1V was determined in a non-human primate study.

Results In vitro, SGN-PDL1V demonstrated internalization and potent cytotoxic activity against PD-L1 expressing tumor cells. In vivo, SGN-PDL1V achieved tumor regressions in multiple tumor xenograft models at doses as low as 1 mg/kg when dosed weekly for a total of three doses. This activity was observed in immunocompromised mice, which lack responses to PD-1/PD-L1 inhibition. Notably, activity was observed even in xenograft models with low, heterogeneous PD-L1 expression, supporting the possibility to treat patients across a wide range of PD-L1 expression levels. Additionally, SGN-PDL1V exhibited potential to inhibit the PD-1/PD-L1 checkpoint in vitro and in vivo. The tolerability and safety profile of SGN-PDL1V were assessed in a non-human primate study and found to be comparable to other FDA-approved vedotin ADCs.

Conclusions SGN-PDL1V is a promising PD-L1 directed ADC with a unique cytotoxic mechanism of action among other PD-L1-targeted therapeutics. SGN-PDL1V demonstrated robust activity in multiple preclinical models and comparable tolerability and safety profile to other vedotin ADCs in non-human primates. Collectively, these data support further evaluation of SGN-PDL1V in a planned, first-in-human Phase 1 study.

Acknowledgements We would like to thank Kerry Klussman for assay support and Jamie Mitchell for conjugation support.

Trial Registration N/A

REFERENCES

1. Senter PD, Sievers EL. The discovery and development of brentuximab vedotin for use in relapsed Hodgkin lymphoma and systemic anaplastic large cell lymphoma. *Nat Biotechnol* 2012;**30**(7):631–7. Epub 2012/07/12. doi: 10.1038/nbt.2289. PubMed PMID: 22781692.
2. Rosenberg JE, O'Donnell PH, Balar AV, McGregor BA, Heath EI, Yu EY, et al. Pivotal trial of enfortumab vedotin in urothelial carcinoma after platinum and anti-programmed death 1/Programmed death ligand 1 therapy. *J Clin Oncol* 2019;**37**(29):2592–600. Epub 2019/07/30. doi: 10.1200/JCO.19.01140. PubMed PMID: 31356140; PubMed Central PMCID: PMC6784850.
3. Tilly H, Morschhauser F, Bartlett NL, Mehta A, Salles G, Haioun C, et al. Polatuzumab vedotin in combination with immunochemotherapy in patients with previously untreated diffuse large B-cell lymphoma: an open-label, non-randomised, phase 1b-2 study. *Lancet Oncol* 2019;**20**(7):998–1010. Epub 2019/05/19. doi: 10.1016/S1470-2045(19)30091-9. PubMed PMID: 31101489.
4. Klussman K, Tenn E, Higgins S, Mazahreh R, Snead K, Hamilton J, Grogan B, Sigurjonsson J, Cao A, Gardai S, Liu B. 618 Vedotin ADCs induce ER stress and elicit hallmarks of ICD across multiple cancer indications. *J Immunother Cancer* 2020;**8**(Suppl 3):A372. DOI:10.1136/jitc-2020-SITC2020.0618.

Ethics Approval All animal studies were conducted in accordance with protocols reviewed and approved by the Institutional Animal Care and Use Committee at Seagen or the external testing facility that conducted the studies.

<http://dx.doi.org/10.1136/jitc-2021-SITC2021.783>

784

BDC-2034: DISCOVERY OF A CEA-TARGETING IMMUNE-STIMULATING ANTIBODY CONJUGATE (ISAC) FOR SOLID TUMORS

^{1,2}William Mallet*, ²Rishali Gadkari, ²Cecelia Pearson, ²Laughing Bear Torrez Dulgeroff, ²Angela Luo, ²Angela Luondrew Luo, ²Jennifer Melrose, ²Jess Nolin, ²Arthur Lee, ²Matthew Zhou, ²Puneet Anand, ²Ganapathy Sarma, ²Karla Henning, ²Lisa Blum, ²Steven Chapin, ²Liz Bogaert, ²Shelley Ackerman, ²Romas Kudirka, ²Yuyi Shen, Amreen Husain², ²Edith Perez, ²Marcin Kowanetz, ²Michael Alonso, ²Brian Safina, ²David Dornan. ¹BOLT BIOTHERAPEUTICS INC, Redwood City, CA, United States; ²Bolt Biotherapeutics, Redwood City, CA, United States

Background CEA (CEACAM5) is a well-validated cell-surface antigen that is highly expressed in multiple solid tumors. Bolt's immune-stimulating antibody conjugates (ISACs) direct a TLR7/8 agonist into tumors to activate tumor-infiltrating myeloid cells and initiate a broad innate and adaptive anti-tumor immune response.¹ The favorable properties of CEA, including robust cell surface expression, low internalization rate, and limited normal tissue expression, suggest that the antigen may be a suitable ISAC target. We are evaluating an anti-CEA ISAC, BDC-2034, as a multi-functional approach to treat CEA-expressing cancers.

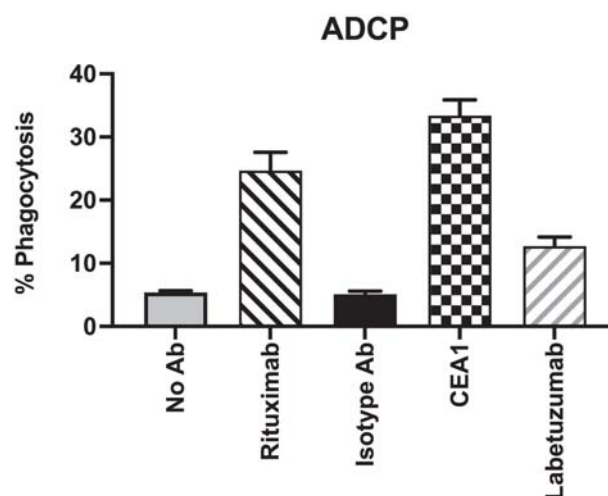
Methods Anti-CEA antibodies were tested for binding affinity and specificity, CEA-targeted antibody-dependent cellular phagocytosis (ADCP), and myeloid-mediated tumor cell killing. Selected antibodies were conjugated to proprietary TLR7/8 agonists, and the resulting CEA ISACs were evaluated for in vitro myeloid activation and in vivo efficacy against xenograft tumors.

Results Antibody CEA1 binds to the CEA protein with high affinity ($EC_{50} = 0.25$ nM), binds selectively to CEA-positive tumor cell lines, and mediates ADCP more efficiently than a reference anti-CEA antibody, labetuzumab (figure 1). We generated BDC-2034 by conjugating a potent TLR7/8 agonist to CEA1. BDC-2034 tumor cell binding drives myeloid effector cell ADCP, agonist delivery to TLR7 and TLR8 in endosomes, and secretion of cytokines critical for innate and adaptive immunity (including IL-12p70, CXCL10, and TNF α). In the HPAF II + cDC co-culture model, IL-12p70 is induced with $EC_{50} = 1.2$ nM, and the level of induction is at least ten-fold higher than with ISACs using labetuzumab (figure 2). Potent cellular activity is strictly dependent on tumor cell CEA expression; in whole blood, in the absence of CEA-expressing tumor cells, cytokine induction was only observed at approximately 100-fold higher concentrations. BDC-2034 inhibits the growth of HPAF II xenograft tumors in SCID/beige mice with a minimal efficacious dose (MED) of 1 mg/kg, demonstrating anti-tumor activity solely through innate immune activation (figure 3). The TLR7/8 agonist in BDC-2034 has relatively poor activity in mice; a surrogate CEA1 ISAC with a mouse TLR7-activating agonist achieved MED = 0.5 mg/kg in the HPAF II model, with eradication of all tumors at the 5 mg/kg dose.

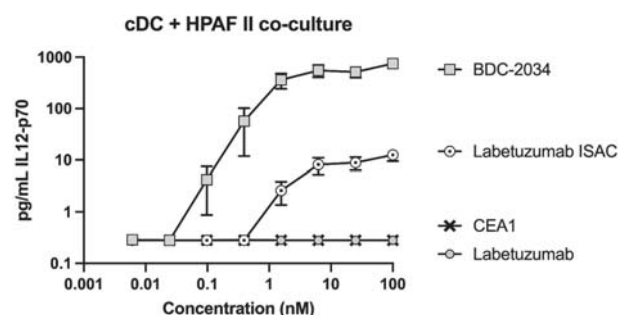
Conclusions These pre-clinical data demonstrate the potential of BDC-2034 to treat CEA-expressing human cancers. Most importantly, the antigen-dependent induction of immune-stimulating cytokines promises a robust immune response that combines the activation of innate and adaptive arms.

REFERENCE

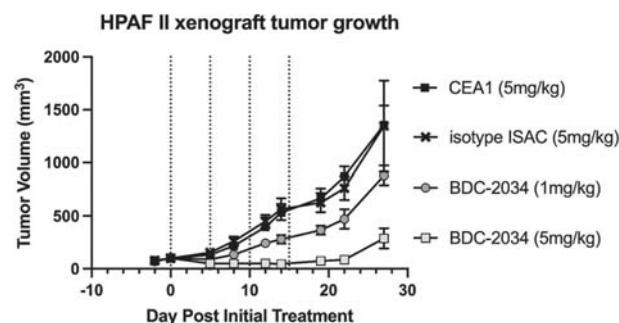
- Ackerman S, Pearson C, Gregorio J. Immune-stimulating antibody conjugates elicit robust myeloid activation and durable antitumor immunity. *Nature Cancer* 2021;2:18–33. <https://doi.org/10.1038/s43018-020-00136-x>



Abstract 784 Figure 1 ADCP. Anti-CEA antibody CEA1 is an efficient inducer of ADCP of Raji/CEA cells by M-CSF differentiated monocyte-derived macrophages



Abstract 784 Figure 2 Tumor-dependent dendritic cell activation. BDC-2034 induces IL-12p70 secretion from primary dendritic cells (cDC); native CEA1 antibody and reference anti-CEA ISAC are ineffective



Abstract 784 Figure 3 Efficacy against xenograft tumors. BDC-2034 inhibits the growth of HPAF II tumors in SCID/beige mice; native CEA1 antibody and isotype ISAC are ineffective

<http://dx.doi.org/10.1136/jitc-2021-SITC2021.784>

STING-AGONIST ADCS TARGETING TUMOR-ASSOCIATED ANTIGENS COORDINATE IMMUNE-MEDIATED KILLING OF ANTIGEN-NEGATIVE CANCER CELLS

Phonphimon Wongthida*, Kalli Catcott, Kelly Lancaster, Keith Bentley, Anouk Dirksen, Bingfan Du, Timothy Eitas, Eugene Kelleher, Naniye Malli, Rebecca Mosher, Marina Protopopova, Pamela Shaw, Cheri Stevenson, Joshua Thomas, Alex Uttard, Jeremy Duvall, Dorin Toader, Marc Damelin, Raghida Bukhalid, Timothy Lowinger. *Mersana Therapeutics, Cambridge, MA, United States*

Background The tumor microenvironment is a complex, multi-cellular system, composed not only of malignant cancer cells but also of a diversity of stromal cells including vascular cells, immune cells, and fibroblasts that support tumorigenesis. Antigens expressed on these cells tend to be widely expressed across a range of malignancies, presenting unique opportunities for development of anti-cancer therapies.

Methods We have previously demonstrated that STING-agonist antibody-drug conjugates (Immunosynthen ADCs) targeting tumor cell antigens induce target-dependent anti-tumor immune responses in vitro and in vivo. To that effect, we hypothesized that Immunosynthen ADCs targeting tumor-associated antigens would coordinate immune-mediated killing of cancer cells not expressing the tumor-associated antigens (antigen-negative cancer cells) and induce anti-tumor activity.

Results Herein, we demonstrate that targeting tumor-associated antigens with STING-agonist ADCs activate the STING pathway in immune cells via Fcγ receptor-mediated uptake. In addition, due to the intrinsic ability of certain tumor-associated cells to activate the STING pathway, STING-agonist ADCs targeting those cells can induce STING signaling in both the targeted cells and the immune cells, which constitutes a therapeutic advantage of ADCs that activate the STING pathway. In triple co-cultures of antigen-positive tumor-associated cells, antigen-negative cancer cells, and immune cells, the STING-agonist ADC specifically induced potent cell killing of the antigen-negative cancer cells with minimal impact on the immune and tumor-associated cells, thus representing a non-traditional, yet highly effective mechanism of ADC targeting. In vivo efficacy studies showed that STING-agonist ADCs developed for two tumor-associated antigens induced complete, sustained tumor regressions in syngeneic tumor models and exhibited immunological memory after rechallenge. CD8⁺ T cells contributed to the anti-tumor activity of the STING-agonist ADCs.

Conclusions In summary, Immunosynthen STING-agonist ADCs targeting tumor-associated antigens represent a novel approach for ADC-mediated cancer immunotherapy and enable the multifaceted activation of the STING pathway in a tumor-targeted manner beyond tumor antigens.

<http://dx.doi.org/10.1136/jitc-2021-SITC2021.785>

DOSE SELECTION FOR DUOBODY®-PD-L1×4-1BB (GEN1046) USING A SEMIMECHANISTIC PHARMACOKINETICS/PHARMACODYNAMICS MODEL THAT LEVERAGES PRECLINICAL AND CLINICAL DATA

¹Gaurav Bajaj*, ²Fereshteh Nazari, ²Marc Presler, ¹Craig Thalhauser, ³Ulf Forssmann, ¹Maria Jure-Kunkel, ⁴Alexander Muik, ⁴Eleni Lagkadinou, ⁴Özlem Tureci, ⁴Ugur Sahin, ¹Tahamtan Ahmadi, ¹Manish Gupta. ¹Genmab US, Princeton, NJ, United States; ²Applied Biomath LLC, Concord, MA, United States; ³Genmab A/S, Copenhagen, Denmark; ⁴BioNTech SE, Mainz, Germany

Background DuoBody-PD-L1×4-1BB (GEN1046) is a class-defining bispecific antibody, designed to elicit an anti-tumor immune response by simultaneous and complementary blockade of PD-L1 on tumor cells and conditional stimulation of 4-1BB on T-cells and NK cells. Optimizing target engagement for a bispecific antibody is challenging, as it involves binding with two targets, and predicting trimer levels in tumors based on affinity of individual arms and target expression. Here we describe a semimechanistic, physiologically based pharmacokinetic/pharmacodynamic (PK/PD) model that predicts a dosing regimen for DuoBody-PD-L1×4-1BB, which results in the formation of maximum levels of a therapeutically active 4-1BB-bispecific antibody-PD-L1 trimolecular complex (trimer), and optimal PD-L1 receptor occupancy (RO).

Methods An integrated semimechanistic PK/PD model that describes the distribution of DuoBody-PD-L1×4-1BB into central and peripheral compartments and partitioning into tumor/lymph nodes was developed. The model used PK/PD data and physiological parameters from the literature for parameterizations of PD-L1 and 4-1BB expression levels and T-cell trafficking. The model incorporates dynamic binding of DuoBody-PD-L1×4-1BB to its targets to predict trimer formation and RO for PD-L1 in tumors. Model parameters were calibrated to match in vitro PD studies, such as analyses of T-cell proliferation and cytokine release, as well as clinical PK data. Sensitivity to model assumptions were assessed by varying PK/PD parameters, and assessing their impact on trimer formation and PD-L1 RO. The model was subsequently used to explore in vivo trimer levels and PD-L1 RO in tumors at various dosing regimens.

Results The model was able to adequately describe the PK of DuoBody-PD-L1×4-1BB in the central compartment. Simulations showed a bell-shaped response for average trimer levels in tumors that peaked at 100 mg every 3 weeks (Q3W), with doses >100 mg resulting in reduced trimer formation. Average PD-L1 receptor occupancy at the 100 mg dose was predicted to be approximately 70% over 21 days and increased at higher doses. Based on these model predictions, and available safety, anti-tumor activity, and PD data from the ongoing GCT1046-01 trial (NCT03917381), 100 mg Q3W was chosen as the expansion dose for further evaluation in Part 2 of the study.

Conclusions This semimechanistic PK/PD model provides a novel approach for dose selection of bispecific antibodies such as DuoBody-PD-L1×4-1BB, by using preclinical and clinical PK/PD data to predict formation of optimal trimer levels and PD-L1 receptor occupancy.

Acknowledgements The authors thank Friederike Gieseke and Zuzana Jirakova at BioNTech SE; Kalyanasundaram Subramanian at Applied Biomath LLC for their valuable contributions.

Trial Registration Written informed consent, in accordance with principles that originated in the Declaration of Helsinki 2013, current ICH guidelines including ICH-GCP E6(R2),

applicable regulatory requirements, and sponsor policy, was provided by the patients.

<http://dx.doi.org/10.1136/jitc-2021-SITC2021.786>

787

NATURAL KILLER CELL ENGAGERS ACTIVATE INNATE AND ADAPTIVE IMMUNITY AND SHOW SYNERGY WITH PROINFLAMMATORY CYTOKINES

Katrina Bykova*, Matthew Faber, Ke Liu, Noor Siddiqi, Matthew Bernett, Christine Bonzon, Juan Diaz, Dong Hyun Nam, Kendra Avery, Jing Qi, Rumana Rashid, Rena Bahjat, John Desjarlais. *Xencor, Monrovia, CA, United States*

Background Natural Killer cell Engagers (NKEs) are multifunctional molecules that target activating receptors on the surface of NK cells, bind to tumor associated antigens and engage Fc gamma receptors expressed on effector cells of the immune system. NKEs promote tumor cell lysis by redirecting NK cells to their targets, and drive activation and proliferation of NK cells. Engagement of NK cells, an effector cell population of the innate immune system, provides an opportunity to target cancers with reduced expression of MHC molecules that are less responsive to therapies targeting the adaptive immune system. Therefore, NKEs have a potential to provide an additional treatment option to patients who respond poorly to T cell tailored immunotherapies.

Methods Expanding on Xencor's XmAb bispecific Fc platform, we developed NKE molecules targeting NKG2D, an activating receptor expressed on cytotoxic immune cells, B7H3, a pan tumor antigen, while simultaneously engaging Fc gamma receptors. Functional activity of NKEs was evaluated via assessing anti-tumor cytotoxicity and activation of NK and T cells in co-culture studies with human cancer cell lines.

Results NKEs were engineered for synergistic effects on NK cells by the simultaneous engagement of NKG2D and Fc gamma receptors. Additionally, the NKG2D variable domains were selected for their ability to provide a co-stimulatory signal to T cells in the presence of TCR-mediated signaling. Developed NKEs showed cytotoxic activity and immune cell activation in co-culture studies of human cancer cell lines with either PBMCs, T cells or NK cells. Combination of NKEs with proinflammatory cytokines, such as IL15, showed enhancement of the cytotoxic activity against tumor cells and augmented NK cell activation.

Conclusions XmAb bispecific NKEs engineered to engage innate and adaptive immunity show encouraging tumor cell killing activity and synergistic cytotoxicity in combination with proinflammatory cytokines. These data have identified several promising candidate NKEs for future in vivo efficacy studies in mouse tumor models expressing B7H3.

<http://dx.doi.org/10.1136/jitc-2021-SITC2021.787>

788

A NOVEL T- LYMPHOCYTE BINDING APTAMER ASSEMBLED INTO A BISPECIFIC COMPOUND FOR THE TREATMENT OF SOLID TUMORS

Irit Carmi Levy*, Erez Lavi, Neta Zilony Hanin, Zohar Pode, Karin Mizrahi, Ronit Farhi, Anastasia Paz, Neria Reiss, Chen Shimoni, Vitaliy Buravenkov, Liron Levy-Efrati, Rotem Haimovich, Ohad Glaiach, Itay Liron, Hadas Aharoni Zazrin, Ido Bachelet, Raanan Berger, Guy Neev. *Aummunne, Tel Aviv, Israel*

Background T-cell engagers are bispecific molecules directed against the CD3 complex on one end and a tumor specific antigen on the other end, allowing a physical link of T cell to a tumor cell, resulting in tumor killing and immune activation. Bispecific molecules harnessing and redirecting T-cells towards tumor cells are a promising therapeutic agents. Aptamers are single stranded oligonucleotides with binding and recognition propensities similar to those of antibodies. Aptamers have a number of advantages over bispecific antibodies including shorter generation time and low immunogenicity. Thus, aptamers capable of targeting T cells would have great potential for use as anti-cancer therapeutics

Methods Systematic evolution of ligands by exponential enrichment (SELEX) methodology was employed in order to identify a novel CD3e binding aptamer. CD3 binding aptamer was subsequently linked into a bispecific T cell engager structure with a tumor-targeting aptameric arm. The tumor-targeting aptamer is developed by Aummunne's proprietary tailored therapeutic platform.¹ based on identifying functional aptamer sequences capable of specifically killing targeted tumor cells and sparing healthy tissue. Exemplary bispecific aptamers were tested for T cell stimulation by flow cytometry. In vivo antitumor activity was investigated in syngeneic and in xenograft tumor models.

Results We have successfully identified a novel CD3e –targeting aptamer with a Kd of 31nM. A bispecific T cell engager comprised of this aptamer and a tumor-targeting aptamer induced a potent stimulation of T cells in vitro, resulting in CD69 upregulation and IFN γ secretion. Next, the CD3e targeting aptamer was hybridized to tumoricidal aptamers identified by Aummunne's platform (VS12) to target either the human colon carcinoma HCT116 cells or (VS32) the murine triple negative breast cancer 4T1 cells. Both bispecific entities (CS6-VS12 and CS6-VS32) effectively lead to inhibition of tumor growth in vivo and increased survival in the corresponding models.

Conclusions Our data above provide a proof-of-concept for Aummunne's Bispecific Aptamer efficacy and provide a framework for the clinical development of this novel tailored immune therapeutic agents. Indeed, we are currently in the process of developing a first-in-human clinical study in subjects with solid tumors.

REFERENCE

1. Mamet N, et al, *Commun Biol* 2020.

<http://dx.doi.org/10.1136/jitc-2021-SITC2021.788>

GENERATION OF A BICYCLE NK-TICA™, A NOVEL NK CELL ENGAGING MOLECULE TO ENHANCE TARGETED TUMOR CYTOTOXICITY

Fay Dufort*, Christopher Leitheiser, Gemma Mudd, Julia Kristensson, Alexandra Rezvaya, Elizabeth Repash, Eric Haines, Katie Gaynor, Sandra Uhlenbroich, Liudvikas Urbonas, Heather Allen, Helen Harrison, Lihong Chen, Philip Brandish, Kevin McDonnell, Nicholas Keen. *Bicycle Therapeutics, Lexington, MA, United States*

Background Natural killer (NK) cells are immune cells that can detect and eliminate tumor cells and bridge innate to adaptive immune responses. Tumor specific activation of NK cells is thus an area of active investigation in immune oncology, but to date has relied on complex biologic modalities (e. g., antibodies, fusion proteins, or cell therapies), each of which has inherent disadvantages in this application. Thus, alternative approaches are warranted. Bicycle® are small (ca. 1.5 kDa), chemically synthetic, structurally constrained peptides discovered via phage display and optimized using structure-driven design and medicinal chemistry approaches. We have now applied this technology to identify Bicycles that bind specifically to the key activating receptors, NKp46 and CD16a. When chemically coupled to tumor antigen binding Bicycles this results in highly potent, antigen-dependent receptor activation and NK cell activation. We term this new class of fully synthetic molecules Bicycle® natural killer- tumor-targeted immune cell agonists (NK-TICAs™) and we will describe their discovery and evaluation in this presentation.

Methods Using our unique phage display screening platform, we have identified high affinity, selective binders to NKp46 and CD16a. By conjugating the Bicycle® NK cell-engaging binders to a model tumor antigen EphA2-binding Bicycle®, we have developed a bifunctional Bicycle NK-TICA™ molecule. In *in vitro* functional assays, we evaluated the ability of the Bicycle NK-TICAs™ to induce NK cell activation as well as cell-mediated cytotoxicity and cytokine production in NK-tumor co-culture assays.

Results We have developed a novel modular compound with high affinity and selectivity to NK cell receptors with specific tumor targeting capability. We demonstrate potent, selective binding of our Bicycles to receptor-expressing cells and the capability of the bifunctional molecule to induce NK cell function. With Bicycle's novel NK-TICA™ compound, we demonstrate engagement of NK cells, specific activation and function of NK cells, and enhanced EphA2-expressing tumor cytotoxicity, in a dose dependent manner.

Conclusions Bicycle NK-TICAs™ are novel therapeutic agents capable of enhancing the landscape of immune oncology. We hypothesize that utilization of Bicycle NK-TICA™ as a multifunctional immune cell engager will promote modulation of NK cells, and infiltration and anti-tumor activity of NK cells in solid tumors. The data presented here provide initial proof of concept for application of the Bicycle technology to drive NK cell-mediated tumor immunity.

<http://dx.doi.org/10.1136/jitc-2021-SITC2021.789>

790

DSP502 — A NOVEL APPROACH FOR TARGETING TIGIT AND PD1 PATHWAYS FOR CANCER IMMUNOTHERAPY

¹Ayelet Chajut*, ¹Shirley Greenwald, ²Matthew Weber, ¹Ami Tamir, ¹Iris Pecker, ¹Rinat Tabakman, ¹Lucy Ganthous, ¹Liat Tamir, ¹Roy Kahn, ¹Jasmine Avichzer, ¹Alexandra Aronin, ³Elina Zorde-Khvaleyevsky, ³Amnon Peled, ⁴Michal Michal Elhalel Dranitzki, ¹Adam Foley-Comer, ²Mark Tykocinski. ¹Kahr Medical Ltd., Jerusalem, Israel; ²Thomas Jefferson University, Philadelphia, PA, United States; ³Hebrew University Hospital, Jerusalem, AZ, Israel; ⁴Hadassah Medical Center, Jerusalem, Israel

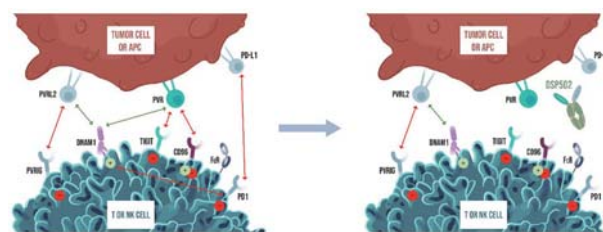
Background TIGIT, an inhibitory immune checkpoint, is a target of interest for immuno-oncology combination therapies. TIGIT is part of a complex molecular network containing four receptors (DNAM1, TIGIT, PVRIG and CD96) and two ligands (PVR and PVRL2). Here we describe Dual Signaling Protein 502 (DSP502), a novel, multi-functional IgG1-Fc-fusion protein targeting this molecular pathway in a unique way. DSP502, comprising the extracellular domains of TIGIT and PD1, is designed to simultaneously bind its two respective ligands, PVR and PD-L1, overexpressed on cancer and myeloid cells in the tumor microenvironment. DSP502 binds PVR preventing inhibitory signaling through TIGIT and CD96 and promoting DNAM1 costimulatory signaling on activated T- and NK-cells. DSP502's PD1 arm binds PD-L1 to unleash effector T-cells through checkpoint inhibition. In parallel, DSP502's IgG1-Fc delivers an immune-activating signal via Fc receptors. The net effect is enhanced anti-tumor immunity (figure 1).

Methods DSP502 heterodimer was successfully produced in a mammalian expression system. DSP502 was evaluated for binding to its cognate ligands on cells and in ELISA-based assays, with and without competing antibodies. NK and PBMC killing activity were evaluated against human K562 CML cells overexpressing PVR. Simultaneous binding of DSP502 to fluorescently-labeled tumor and NK-cells was evaluated by FACS. In vivo activity of DSP502 was evaluated in a humanized NSG A549 NSCLC xenograft mouse model.

Results Both DSP502 arms were shown to bind their cognate ligands in ELISA and on cell surface. DSP502 binding was dependent on the presence of both ligands on cells and was abolished by competing antibodies to the respective targets, demonstrating binding specificity and the 'AND-gate' phenomenon. Overexpression of PVR reduced the sensitivity of K562 cells to NK-cell mediated killing, while DSP502 treatment restored it as measured by target cell killing and granzyme-B secretion. Increased, dose-dependent, complexation of NK- and tumor cells was observed following DSP502 treatment and was abolished by both PVR and FcR antibodies. Treatment with DSP502 markedly inhibited tumor growth of A549-NSCLC xenograft in a humanized NSG mouse model, with all mice being tumor-free at the end of the experiment, compared to control PBMC-injected mice.

Conclusions Here we report the design and function of a novel immunotherapeutic fusion protein, DSP502, that offers multiple functionalities that can coordinately and synergistically drive anti-tumor immunity. Beyond targeting PVR and PDL1, DSP502 has the potential to additionally impact the TIGIT pathway through its effects on CD96 and DNAM1. DSP502 is currently in IND-enabling studies and CMC development.

Ethics Approval The study was conducted at the Authority of Biological and Preclinical Models, the Hebrew University of Jerusalem, Ein Kerem, Sharet Specific Pathogen-Free (SPF) Unit under the Hebrew university ethic committee board approval (number MD-19-15815-5).



Abstract 790 Figure 1

<http://dx.doi.org/10.1136/jitc-2021-SITC2021.790>

**MULTI-SPECIFIC GUIDANCE AND NAVIGATION
CONTROL (GNC) T CELL ENGAGERS CONVERT PDL1
ADAPTIVE RESISTANCE TO DRUG SENSITIVITY**

Jahan Khalili*, Mark Gilchrist, Sarah Rickli, Daphne Toglia, Yi Zhu. *SystImmune Inc, Redmond, WA, United States*

Background Major challenges to T cell engager drugs are antigen loss and adaptive resistance, often in the form of PDL1 upregulation on cancer cells or the tumor microenvironment. Engaged T cells are dependent on cancer cell co-stimulation, and synaptic engagements that may deteriorate the function of the effector T cell compartment.

Methods Guidance and Navigation Control (GNC) drugs are multi-specific cell engagers. This platform of GNC T cell engagers is designed to mediate direct cytolysis of cancer cells by T cells, and influence the outcome of synaptic engagement, overcome PDL1 resistance, and respond to biological signals in the tumor microenvironment to increase functional potency. GNC that bind tumor antigens, CD3, 4-1BB and PDL1 are designed to redirect T cells toward tumor antigens and engage PDL1 as a target antigen.

Results T cell activation resulting from tumor associated antigen and CD3/41BB binding, results in IFN-gamma release. The local IFN-gamma upregulates PDL1 on cancer cells, increasing the antigen density and converting a major mechanism of adaptive resistance into local drug sensitivity. This novel design and first-in-class mechanism of action may reduce resistance mediated by both antigen loss, and immune suppression through cytolysis of PDL1 expressing cells within the tumor microenvironment.

Conclusions Knowledge of PDL1 regulation and its role as a universal target in the solid tumor microenvironment provides one path forward for multi-modal T cell engagers with potential for broad clinical efficacy. Multi-specific GNC demonstrated preclinical functionality, and developability. GNC T cell engagers targeting tumor associated and tumor specific antigens are currently in Phase I trials for solid and liquid cancer indications.^{1 2}

REFERENCES

1. A Study of GNC-038, a Tetra-specific Antibody, in Participants With R/R Non-Hodgkin Lymphoma. ClinicalTrials.gov Identifier: NCT04606433.
2. A Study of GNC-039, a Tetra-specific Antibody, in Participants With Relapsed/Refractory or Metastatic Solid Tumors. ClinicalTrials.gov Identifier: NCT04794972.

<http://dx.doi.org/10.1136/jitc-2021-SITC2021.791>

792

CREATING AN IMMUNE-FAVORABLE TUMOR MICROENVIRONMENT BY A NOVEL ANTI-CD39/TGF β -TRAP BISPECIFIC ANTIBODY

Hongtao Lu, Dawei Sun*, Jun Sun, Yanan Geng, Jinhui Zhang, Rui Gao, Lei Li, Zhihao Wu, Lily Tang, Yangsheng Qiu. *Elpiscience Biopharmaceuticals, Shanghai, China*

Background Adenosine and TGF β are two key immune suppressors in tumor microenvironment (“TME”) that cause broad immune suppression resulting in resistance to current CPI immunotherapies. Cancers frequently express transforming growth factor- β (TGF β), which drives immune dysfunction in the tumor microenvironment by inducing regulatory T cells (Tregs), inhibiting CD8+ activation and infiltration into TME, and promoting epithelial–mesenchymal transition (EMT). We observed that TGF β induces the expression of CD39, a critical enzyme that regulates adenosine generation. CD39 is highly expressed in Tregs within TME, it drives the production of adenosine, an immunoinhibitory molecule that partly mediates Treg inhibitory function. To inhibit CD39-Adenosine and TGF β simultaneously to create an immune favorable tumor microenvironment, we designed a bi-specific antibody targeting both CD39 and TGF β (ES014), which aims to inhibit the generation of adenosine and iTreg in TME. The immuno-stimulating effect of ES014 was demonstrated in a PD-1-unresponsive mouse model where tumor growth was significantly inhibited after the treatment of the bi-specific antibody.

Methods The bifunctional antibody–ligand trap ES014 was created by fusing the TGF β receptor II ectodomain to an antibody targeting CD39. ES014 molecule could simultaneously inhibit CD39 enzymatic function to prevent extracellular ATP from degradation and neutralize autocrine/paracrine TGF β in the target cell microenvironment. The immunological function of ES014 was studied in an in vitro Elpiscience proprietary ImmunoShine platform which includes T cell activation and apoptosis assay, iTreg differentiation and suppression assay, NK cell activation assay and DC maturation activity. The in vivo efficacy of ES014 was investigated in a human PBMC engrafted cancer model.

Results We demonstrated that ES014 bispecific antibody can inhibit CD39 enzymatic activity and neutralizes TGF β -induced effect, resulting in greater T cell activation and suppression of Treg differentiation. Interestingly, we found ES014 molecule demonstrated a unique mechanism by significantly protecting effector T cell from anti-Fas induced apoptosis or activation induced cell death (AICD) that is not observed in monotherapy or combo treatment. The ES014 molecule is more effective in inhibiting tumor growth as compared with anti-CD39 antibody or TGF β -trap in a human PBMC engrafted in vivo model.

Conclusions We find that by simultaneously targeting CD39 and TGF β by a novel bi-specific molecule ES014, a more immune-favorable TME and synergistic anti-tumor effects can be achieved. Our pre-clinical data demonstrate that ES014 counteracts TGF β -mediated inhibitory effect and adenosine induced immune tolerance and has a unique ability to protect T cell from apoptosis. ES014 demonstrated strong efficacy in in vivo tumor growth inhibition.

<http://dx.doi.org/10.1136/jitc-2021-SITC2021.792>

TARGETING ENGINEERED INTERLEUKIN-2 (IL-2) TO ANTIGEN SPECIFIC T CELLS VIA NOVEL BIOLOGIC PLATFORMS

Raymond Moniz*, Ahmet Vakkasoglu, Zohra Merazga, Tina Daigneault, Steve Quayle, Natasha Girgis, Ronald Seidel, John Ross, Simon Low, Anish Suri. *Cue BioPharma, Cambridge, MA, United States*

Background A key challenge with IL-2 immunotherapy for cancers is lack of selectivity for anti-tumor immune cells and safety liabilities related to indiscriminate activation of immune cells. The CUE-100 series of Immuno-STATs (ISTs) are designed to selectively activate tumor-specific T cells while avoiding IL-2 toxicities due to systemic activation. CUE-100 series ISTs are rationally engineered Fc fusion proteins comprised of bivalent tumor-peptide-HLA (pHLA) complexes and four affinity-attenuated IL-2 molecules to preferentially engage and activate tumor-specific T cells directly in the patient. Emerging clinical data from our lead candidate CUE-101, which targets HPV-specific T cells in 2L+ R/M HNSCCC, provides PoC for the approach and builds confidence for broad applications in numerous cancers. Building on the CUE-100 series framework, our Neo-STAT (NST) platform contains HLA molecules manufactured with an “empty” peptide-binding pocket, into which diverse tumor-peptides can be chemically conjugated, hence addressing tumor heterogeneity in a cost- and time-efficient manner. Our RDI-STAT (Re-Directed Immuno-STAT) platform further expands the CUE-100 series by redirecting the pre-existing protective viral-specific T cell repertoire to target tumor cells via scFv moieties. RDI-STATs are designed to circumvent potential tumor escape mechanisms linked to HLA loss or defects in antigen-presenting pathways. We present here preclinical data supporting the mechanism of action of these platforms to enhance anti-tumor immune responses.

Methods NSTs were engineered with “empty” HLA-A*0201, into which relevant antigenic peptides were conjugated, and assessed for capacity to expand T cells. RDI-STATs were engineered with TAA-specific scFv and viral-specific pHLA complexes, and assessed for their capacity to induce redirected killing of tumor cells while avoiding systemic activation of all T cells.

Results The NST platform demonstrated that different T cell epitopes can be efficiently conjugated into the HLA-binding pocket, and that these molecules activate and expand antigen specific T cells in vitro. RDI-STATs were able to expand anti-viral T cell repertoires and drive anti-viral T cell redirected killing of TAA-expressing cells. In contrast to pan anti-CD3 bispecific molecules, RDI-STATs demonstrated significantly lower induction of pro-inflammatory cytokines.

Conclusions The IST, NST, and RDI-STAT platforms provide novel opportunities for selective targeting of IL-2 to tumor-relevant T cells while avoiding global immune activation and cytokine release. The scalability and versatility of NSTs highlight the potential to target multiple TAA T cell responses, while RDI-STATs highlight a novel means to harness antiviral immunity against cancer, especially in cases where the tumor may escape immune detection due to loss of HLA.

<http://dx.doi.org/10.1136/jitc-2021-SITC2021.793>

794

LONG-TERM ANTI-TUMOR PRECLINICAL EFFICACY OF AN OPTIMIZED ANTI PD-1/IL-7 BIFUNCTIONAL ANTIBODY SUSTAINING ACTIVATION OF PROGENITOR STEM-LIKE CD8 TILS AND DISARMING TREG SUPPRESSIVE ACTIVITY

Aurore morello*, Margaux Seite, Justine Durand, Geraldine Teppaz, Virginie Thepenier, caroline Mary, Isabelle Girault, Emmanuelle Wilhem, Nicolas Poirier. *OSE Immunotherapeutics, Nantes, France*

Background Despite the PD-(L)1 therapy success, a majority of patients remain resistant. PD-1+IL7R+ progenitors CD8 TILs is a key T-cell subset associated with durable PD-(L)1 therapy response. However, this subset may rapidly undergo apoptosis and/or being fully exhausted after PD-(L)1 blockade. Some cytokines have the potential to strengthen PD-(L)1 therapy by promoting T cell survival, however, their clinical developments are limited by a shortened half-life and systemic toxicity. To redirect immunotherapy to tumor-specific T cells, expressing PD1, we propose to selectively deliver the pro-survival IL-7 to PD-1+ T cells using a bifunctional anti-PD1/IL-7 mutein antibody. We previously described that the anti-PD1/IL-7v abrogated suppressive activity of human Treg. Here we evaluated its preclinical anti-tumor efficacy and how it promotes the response of PD1+IL7R+ tumor-specific T cells.

Methods Proliferation, IFN- γ , IL-7R signaling, and NFAT assays were tested to determine the mechanism of this antibody. For the suppressive assay, CD4 Treg and autologous CD8 Teff were co-cultured. In vivo experiments were performed in hPD-1 KI immunocompetent or humanized immunodeficient mice.

Results The anti-PD1/IL-7v antibody design has been optimized with a monovalent approach to enhance its biological activity: (1) preserved PD-1 antagonist activity, (2) improved pSTAT5 IL7R signaling, and (3) enhanced in vivo drug exposure and antitumor efficacy. An IL7 mutein has been designed to improve activity on PD1+ T cells while sparing PD1neg T cells. Using a chronic antigen stimulation model, anti-PD1/IL-7v restores the proliferation & survival of both early and fully exhausted CD8+ or CD4+ T cells. Similarly, anti-PD1/IL-7v, but not anti-PD1 alone, reactivates exhausted TILs isolated from human resected tumors. Gene expression analysis by Nanostring showed increase cytotoxicity, antigen presentation, and chemokines signatures. In vivo, anti-PD1/IL-7v demonstrated high monotherapy efficacy (90%) in a PD-1 sensitive orthotopic immunocompetent mouse tumor model as well as in a PD-1 refractory tumor model with 70% of CR vs 15% for anti-PD-1 alone. A selective higher expansion of stem-like/progenitors CD8 TILs was observed after therapy with anti-PD1/IL-7v compared to anti-PD1. Memory immune response was demonstrated in 100% of cured mice after tumor rechallenge in the absence of new treatment in 3 different tumor models. Finally, using two different humanized mouse models implanted with human tumors (A549 or MDA-MB231), we confirmed significant preclinical monotherapy efficacy of the anti-PD-1/IL7v.

Conclusions These data highlight the potential of anti-PD1/IL-7 bifunctional drug to overcome immunotherapy resistance and to promote durable anti-tumor efficacy by preferentially reinvigorating PD-1+IL7R+ stem-like progenitors CD8 T cells.

<http://dx.doi.org/10.1136/jitc-2021-SITC2021.794>

795

APVO603: A DUAL 4-1BB AND OX40 BISPECIFIC APPROACH UTILIZING ADAPTIRTM TECHNOLOGY DESIGNED TO DELIVER A CONDITIONAL T CELL/NK RESPONSE AGAINST SOLID TUMORS

Michelle Nelson*, Ashly Lucas, Rebecca Gottschalk, Catherine McMahan, Jane Gross, Hilario Ramos. *Aptevo Therapeutics, Seattle, WA, United States*

Background APVO603 is a dual targeting bispecific antibody for 4-1BB (CD137) and OX40 (CD134), engineered with Aptevo's ADAPTIRTM technology. We have previously shown that the distinct characteristics of APVO603 may enable conditional agonism of 4-1BB and OX40 only when cross-linked through engagement of the other receptor via cis and/or trans cellular interactions. Thus, APVO603 is designed with the potential to overcome both the on-target toxicity and limited efficacy observed with 4-1BB and OX40 monoclonal antibody treatment in the clinic.

Methods Geneinvestigator Software was used to analyze curated transcriptomic data for the expression profiles of OX40 and 4-1BB across select human heme and solid cancer patient sample data sets, as well as, non diseased tissue. Primary inducible Treg (iTreg) cells were sub-optimally stimulated with an anti-CD3/CD28 antibody and cell proliferation was assessed using CFSE-labelled. Cytokines were measured using intracellular flow-based methods. For in vitro tumor lysis studies, activated T cells were co-cultured with Nuclight-labelled tumor cells expressing a tumor-associated antigen (TAA) and activated with TAA x CD3 bispecific protein. Live tumor cells were continually assessed using the Incucyte Live-Cell Analysis System and Cell-By-Cell Software Module.

Results OX40 and 4-1BB displayed distinct tumor expression profiles, however, several tumor indications were identified with high co-expression and may aid in identifying indications for the clinical development of APVO603. In vitro, APVO603 favored activation of effector T cell subsets and had minimal impact in augmenting iTreg cells proliferation, cytokine production or expression of effector-related molecules, despite the fact that a portion of the iTreg cells expressed OX40 and 4-1BB. The mechanistic activity of APVO603 resulted in dose-dependent control of in vitro tumor growth when paired with a T-cell activating TAA x CD3 bispecific under standard conditions or those leading to T cell exhaustion. In preclinical assays using PBMCs sub-optimally stimulated with TAA x CD3, APVO603 enhanced TAA-expressing tumor cell lysis when compared to TAA x CD3 alone.

Conclusions APVO603 is a dual-agonistic bispecific antibody that augments the effector function of activated CD4+ and CD8+ T cells and NK cells, but not iTreg cells, in a dose-dependent manner and reduces growth of tumors in vitro and in vivo. Further, mechanistic evaluation supports the ability of APVO603 to pair with T-cell modulating IO approaches to support a more fit T cell response and favorable TME. This preclinical data supports further development of APVO603, a promising immuno-oncology therapeutic with potential for benefit in hematologic and solid tumors.

<http://dx.doi.org/10.1136/jitc-2021-SITC2021.795>

796

ALG.APV-527: A 5T4 TUMOR DIRECTED BISPECIFIC APPROACH UTILIZING ADAPTIRTM TECHNOLOGY DESIGNED FOR CONDITIONAL 4-1BB T CELL/NK AGONISM AGAINST SOLID TUMORS

¹Michelle Nelson*, ²Anette Sundstedt, ²Yago Pico de Coaña, ¹Ashly Lucas, ²Anneli Nilsson, ²Lill Ljung, ¹Allison Chunya, ²Lena Schultz, ¹Catherine McMahan, ¹Jane Gross, ²Sara Frizell, ¹Hilario Ramos, ²Peter Ellmark. ¹Aptevo Therapeutics, Seattle, WA, United States; ²Alligator Bioscience, Lund, Sweden

Background 4-1BB (CD137) is an activation-induced co-stimulatory receptor that regulates immune responses of activated CD8+ T cells and NK cells. Leveraging the therapeutic benefit of 1st generation 4-1BB monospecifics has been challenging due to dose limiting hepatotoxicity. To minimize systemic immune toxicities and enhance activity at the tumor site, we have developed a novel 4-1BB x 5T4 bispecific antibody that stimulates 4-1BB function only when co-engaged with 5T4, a highly selective tumor-associated antigen. The combined pre-clinical dataset presented here provides an overview of the potential indication landscape, mechanism of action and the efficacy and safety profile of ALG.APV-527, supporting its advancement into the clinic.

Methods Genevestigator Software was used to analyze curated transcriptomic data from bulk tumor mRNA-sequencing data libraries and from single cell RNA-seq libraries for the expression profiles of CD8, 4-1BB and 5T4 across selected human solid tumor datasets. ADCC and ADCP reporter bioassays were utilized to assess Fc engagement by ALG.APV-527. For in vitro tumor lysis studies, human T cells were co-cultured with labelled tumor cells and sub-optimally activated with anti-CD3. Cytotoxicity of tumor cells were continually assessed using a Live-Cell Analysis System.

Results Dual expression of CD8 and 5T4 occurred in many tumor types and correlated well with indications that are pursued in the clinical development of ALG.APV-527. 4-1BB expression was observed in tumor-derived lymphoid subpopulations, especially in those with an exhausted phenotype. Since ALG.APV-527 is designed with a non-Fcγ receptor binding Fc, minimal ADCC & ADCP was induced in vitro. Additionally, ALG.APV-527 enhanced primary immune cell-mediated killing of 5T4-expressing tumor cells when compared to anti-CD3 alone, demonstrating the potential benefit of 4-1BB agonism for enhancing cytotoxic anti-tumor responses in the clinic.

Conclusions

ALG. APV-527 is designed to elicit safe and efficacious 4-1BB-mediated antitumor activity in a range of 5T4-expressing tumor indications. Transcriptional profiling of patient tumor samples demonstrates 4-1BB expression in multiple tumor-infiltrating lymphocyte subsets and identifies potential indications with 5T4 expression and CD8+ T cell infiltration. The unique design of the molecule minimizes systemic immune activation and hepatotoxicity, allowing for highly efficacious tumor-specific responses as demonstrated by potent activity in in vitro models. Based on these preclinical data, ALG.APV-527 is a promising anti-cancer therapeutic for the treatment of a variety of 5T4-expressing solid tumors and is progressing towards a phase I clinical trial in 2021.

<http://dx.doi.org/10.1136/jitc-2021-SITC2021.796>

A NOVEL ANTI-PD-1/IL15 BI-FUNCTIONAL ANTIBODY WITH ROBUST ANTI-TUMOR ACTIVITY IN MULTIPLE SOLID TUMORS

Dan Lu, Tzu-Pei Chang*, Zhanna Polonskaya, Stella Martomo, Xenia Luna, Zhikai Zhang, Stanley Ng, Jeegar Patel. *Kadmon Pharmaceuticals, LLC, New York, NY, United States*

Background Immune checkpoint inhibitors (ICI) such as PD-1/PD-L1 have revolutionized cancer therapy, but only a fraction of patients responded to approved ICIs; the majority are either resistant or quickly become refractory. IL-15 is a key cytokine promoting CD8+ T, NK, and NKT cell proliferation and has demonstrated clinical activity. Kadmon has established a cytokine fusion protein platform to extend the IL-15 serum half-life and direct its action to tumors and/or T cells in tumor microenvironment (TME).¹⁻³ An important asset of this platform is KD050, an anti-PD1/IL15 bi-functional antibody with a novel mutation on the IL15 to lower the systemic toxicity of IL-15. Previous studies showed that KD050¹ and its mouse surrogate² were cis-presented to PD-1 and IL2/15R β ? co-expressed TILs. The simultaneous binding to both PD-1 and IL2R β potentially maximized KD050 bi-functionality of PD-1 blockade and IL-15 stimulation, resulting in robust anti-tumor activity in a PD-1/PD-L1 resistant human PD-1/PD-L1 transgenic colon carcinoma model (hPD-1/PD-L1 CT26) and murine lung cancer model (LL/2), respectively. Here, we continue to evaluate KD050 surrogate anti-tumor activity in multiple murine solid tumor models.

Methods KD050 mouse surrogate, mPD-1 antibody m3A7 and anti-PD-1/ non-mutated IL15 fusion (wtKD050) were generated and characterized in vitro as done previously.^{1 2} Single-dose efficacy of KD050 mouse surrogate was evaluated in 12 syngeneic murine models (MC38, CT26, H22, LL/2, Pan02, A20, B16-F10, B16-BL6, Renca, Hepa1-6, RM-1 and EMT6), and anti-tumor efficacy was further evaluated in Pan02 model in different dose levels and frequencies. Briefly, tumor cells were subcutaneously transplanted to the mice and the treatment was started when tumors reached 100 mm³.

Results KD050 surrogate showed similar potencies as the mPD-1 antibody m3A7 in binding to the soluble and cell expressed human PD-1 and blocking of the PD-L1 binding to PD-1. Comparing to wtKD050 (anti-PD-1/ non-mutated IL15 fusion), mutated IL15 fusion KD050 surrogate showed lower CD8 T cell stimulation in the CTLL2 and mouse spleen cell proliferation. In vivo, different levels of tumor regression were observed in all 12 models with no significant systemic toxicity. Furthermore, tumor rejection in some mice was achieved in the MC38, CT26, A20, H22, Pan02 and EMT6 models, and dose response anti-tumor efficacy was observed in Pan02 model.

Conclusions We demonstrated that KD050 surrogate had very robust anti-tumor activity and low systemic toxicity in mice bearing multiple solid tumors. These findings suggest that the bi-functional antibody KD050 has encouraging therapeutic potential.

REFERENCES

1. Martomo S. etc. *Mol Cancer Ther* February 1 2021;**20**(2):347–356; DOI: 10.1158/1535-7163.MCT-20-0457.
2. Polonskaya Z. etc. *AACR 2020* #2263.
3. Polonskaya Z. etc. *SITC 2020* #573

Ethics Approval All studies were conducted following an approved IACUC protocol. Although this study was not conducted in accordance with the FDA Good Laboratory Practice

regulations, 21 CFR Part 58, all experimental data management and reporting procedures were in strict accordance with applicable Crown Bioscience, Inc. Guidelines and Standard Operating Procedures. The methods and results in the Final Study Report accurately reflect the raw data generated during the execution of the study.

<http://dx.doi.org/10.1136/jitc-2021-SITC2021.797>

798

CDX-585, A BISPECIFIC ANTIBODY WITH DUAL TARGETING OF ILT4 AND PD-1 CHECKPOINT PATHWAYS

¹Laura Vitale, ²Michael Murphy*, ³Collin Xia, ³Zeyu Peng, ²Thomas O'Neill, ²Ed Natoli, ²Jay Lillquist, ²Linda Crew, ²Anna Wasiuk, ²Jeff Weidlick, ²Jenifer Widger, ²Laura Mills-Chen, ²Andrea Crocker, ²Colleen Patterson, ²James Boyer, ²April Baronas, ²Russell Hammond, ³Hugh Davis, ³Mark Ma, ²Joel Goldstein, ²Lawrence Thomas, ²Diego Alvarado, ²Henry Marsh, ²Tibor Keler. ¹Celldex Therapeutics, Hampton, NJ, United States; ²Celldex Therapeutics, New Haven, CT, United States; ³Biosion, Inc., Nanjing, China

Background Activation of the ITIM-bearing ILT4/LILRB2 receptor by its cognate ligands (HLA-G and HLA Class I) has been postulated as a resistance mechanism for checkpoint blockade of PD-1 and CTLA-4. Dual inhibition of receptors that suppress myeloid and T cell compartments through the generation of bispecific antibodies (bsAbs) is a promising strategy to improve outcomes for patients whose tumors are resistant to checkpoint inhibition.

Methods We describe the discovery and characterization of CDX-585 a bsAb developed from novel ILT4 and PD-1 antagonist mAbs that revert myeloid cell suppression by antagonizing ILT4 and activating T-cell responses through PD-1 inhibition. The bsAb was engineered as a tetravalent molecule using the PD-1 IgG1 mAb linked to scFv of the ILT4 mAb at the C-terminus of the heavy chain. A series of mutations were introduced in the Fc domain to eliminate Fcγ receptor binding and increase affinity to the neonatal Fc receptor. CDX-585 has good biophysical characteristics and retains functional properties similar to, or better, than the parental mAbs.

Results CDX-585 has sub-nanomolar affinity binding to ILT4 and PD-1 and is a potent competitor of their respective ligands. Primary cultures of human macrophages and dendritic cells treated with CDX-585 enhanced production of inflammatory cytokines/chemokines, which was further potentiated in the presence of toll like receptor activation with lipopolysaccharide (LPS). CDX-585 was particularly effective in promoting T cell activation as measured by mixed lymphocyte reactions, and in polarizing macrophages towards M1 based on their cytokine profile. Pilot studies in mice and cynomolgus macaques confirmed a favorable pharmacokinetic profile without adverse effects of treatment noted in clinical observations or clinical chemistry.

Conclusions CDX-585 effectively combines ILT4 and PD-1 blockade into one molecule with favorable biophysical and functional characteristics supporting the initiation of development activities including manufacturing and IND-enabling studies.

<http://dx.doi.org/10.1136/jitc-2021-SITC2021.798>

NEOANTIGEN-CYTOKINE-CHEMOKINE MULTIFUNCTIONAL NATURAL KILLER CELL ENGAGER FOR IMMUNOTHERAPY OF SOLID TUMORS

Xue Yao*, Sandro Matosevic. *Purdue University, Lafayette, IN, United States*

Background The effectiveness of natural killer (NK) cell-based immunotherapy against solid tumors is limited by the lack of specific antigens and the immunosuppressive tumor microenvironment (TME). Glioblastoma multiforme (GBM) is one such heavily immunosuppressive tumor that has been particularly hard to target and remains without a viable treatment. The development of novel approaches to enhance the efficacy of NK cells against GBM is urgently needed. NK cell engagers (NKCE) have been developed to enhance the efficacy of NK cell therapy.

Methods To improve the clinical efficacy of NK cell therapy, we are developing a new generation of multi-specific killer engagers, which consists of a neoantigen-targeting moiety, together with cytokine and chemokine-producing domains. Neoantigens are new antigens formed specifically in tumor cells due to genome mutations, making them highly specific tools to target tumor cells. Our engager has been designed to target Wilms' tumor-1 (WT-1), a highly specific antigen overexpressed in GBM among other solid tumors. This is done through the generation of an scFv specific targeting the complex of WT-1126-134/HLA-A*02:01 on the surface of GBM. On the NK cell side, the engager is designed to target the activating receptor Nkp46. Incorporation of the cytokine IL-15 within the engager supports the maturation, persistence, and expansion of NK cells *in vivo* while favoring their proliferation and survival in the tumor microenvironment. Additionally, our data indicated that the chemokine CXCL10 plays an important role in the infiltration of NK cells into GBM, however, GBM tumors produce low levels of this chemokine. Incorporation of a CXCL10-producing function into our engager supports intratumoral NK cell trafficking by promoting, through their synthetic production, increased levels of CXCL10 locally in the tumor microenvironment.

Results Collectively, this has resulted in a novel multifunctional NK cell engager, combining neoantigen-cytokine-chemokine elements fused to an activating domain-specific to NK cells, and we have investigated its ability to support and enhance NK cell-mediated cytotoxicity against solid tumors *in vitro* and *in vivo* against patient-derived GBM models. The multi-specific engager shows both high tumor specificity, as well as the ability to overcome NK cell dysfunction encountered in the GBM TME.

Conclusions We hypothesize that taking advantage of our multi-functional engager, NK cells will exhibit superior *in vivo* expansion, infiltration, and antitumor activity in the treatment of GBM and other solid tumors.

<http://dx.doi.org/10.1136/jitc-2021-SITC2021.799>

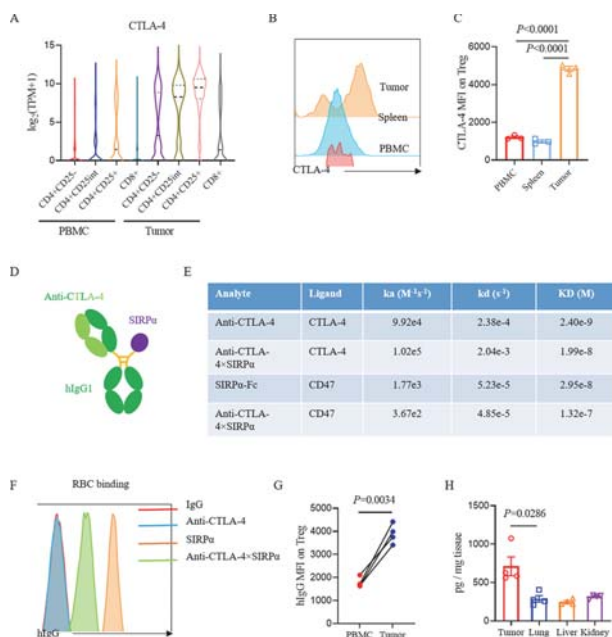
800

DUAL TARGETING OF CTLA-4 AND CD47 ON TREG CELLS REJUVENATES IMMUNITY AGAINST SOLID TUMORS

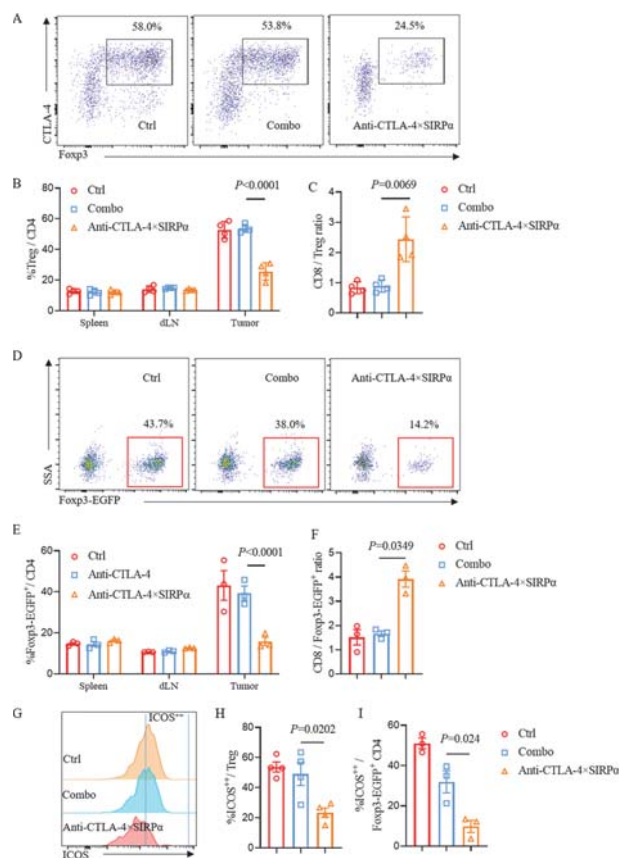
¹Anli Zhang*, ¹Zhenhua Ren, ²Kuo-fu Tseng, ³Xiajuan Liu, ¹Huiyu Li, ¹Changzheng Lu, ³Yueqi Cai, ¹John Minna, ¹Yang-Xin Fu. ¹UTSW, Dallas, TX, United States; ²Aetio Biotherapy, Dallas, TX, United States; ³Institute of Biophysics, Beijing, China

Background Although approved by FDA, anti-CTLA-4 treatment has severe side effect that limits its clinical usage. Blockade of CD47, the “don't eat me” signal, has limited effects in solid tumors despite its potent anti-tumor effects in hematopoietic malignancies. Targeted delivery of immune blockers into tumor tissues are desirable.

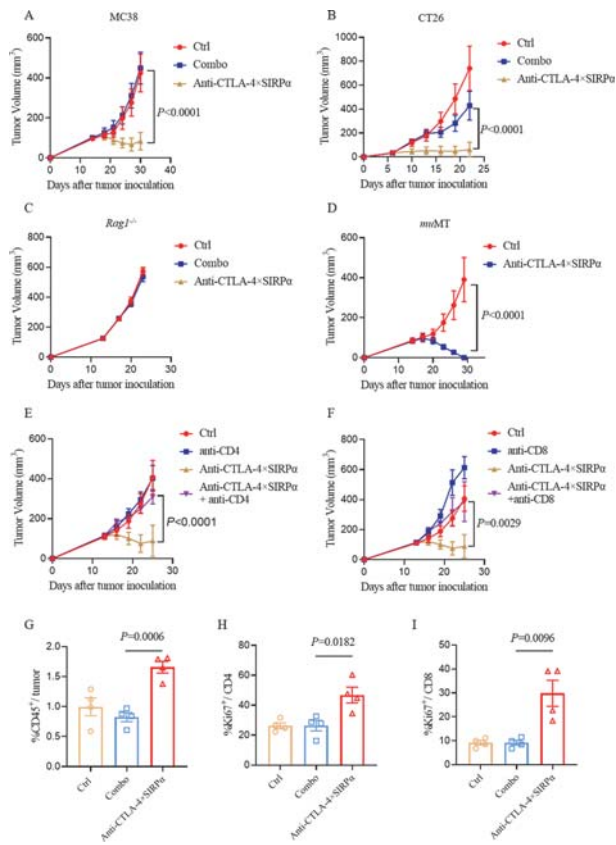
Methods Taking advantage of the high expression of CTLA-4 on Treg cells and abundant Fc receptor+ active phagocytes inside the tumor microenvironment (TME), we design and test an anti-CTLA-4×SIRPα (CD47 ligand)-Fc heterodimer that selectively blocks CD47 on intratumoral Treg cells and increases antibody-dependent cellular phagocytosis (the “eat me” signal).



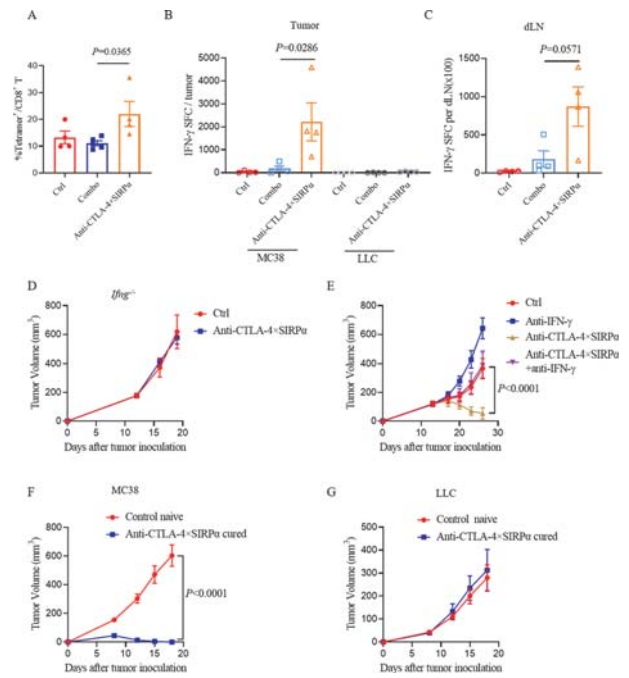
Abstract 800 Figure 1 Anti-CTLA-4×SIRPα selectively targets intratumoral Treg. (A) Expression of CTLA-4 transcripts in colorectal cancer patient tissues based on single cell sequencing online database (29). (B and C) CTLA-4 expression on Treg cells from PBMC, spleen and tumor cells in MC38 tumor-bearing mice on day 14. (D) Schematic diagram of anti-CTLA-4×SIRPα heterodimer. (E) Kinetic association (k_a), dissociation (k_d), and calculated affinity (KD) for binding of the indicated analyte to mouse CTLA-4 or CD47 antigen were measured by surface plasmon resonance using OpenSPR instrument. (F) Binding of SIRPα, CTLA-4 and anti-CTLA-4×SIRPα to RBC from C57BL/6 mice, $n=4$. (G) Anti-CTLA-4×SIRPα binding on Treg of PBMC and tumor cells from MC38 tumor-bearing mice. (H) C57BL/6 mice were inoculated with 5×10^5 MC38 tumor cells. After 13 days, $20 \mu g$ anti-CTLA-4×SIRPα was injected intraperitoneally. Five days later, mice were perfused with PBS, and tumor and other tissues were harvested and homogenized. Anti-CTLA-4×SIRPα protein abundance was determined with ELISA, $n=4$.



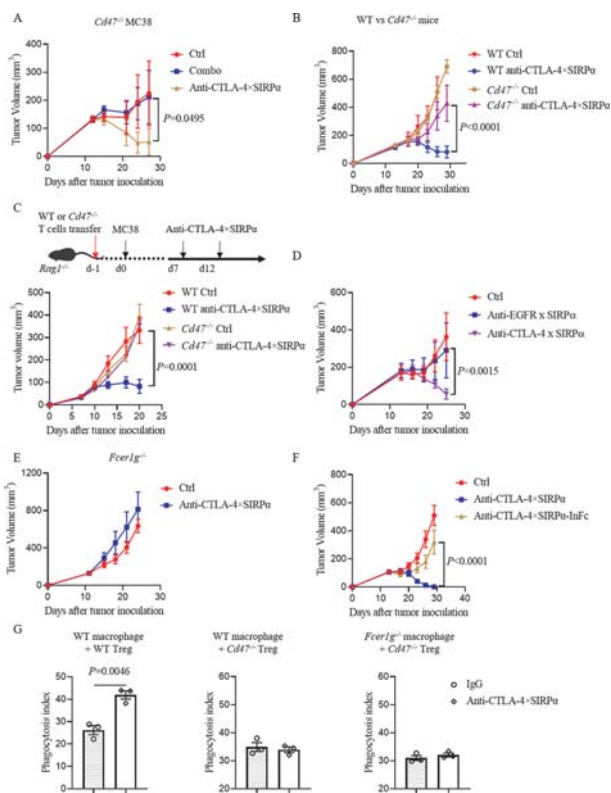
Abstract 800 Figure 2 Anti-CTLA-4×SIRPα preferentially depletes ICOS^{hi} Treg. (A–C) C57BL/6 mice ($n=4$) were inoculated with 5×10^5 MC38 tumor cells and treated with Combo or anti-CTLA-4×SIRPα on day 13. Five days later, Treg cells from tumor, spleen and draining lymph node (dLN) were analyzed. The representative flow cytometric gating was shown in (A). Treg cells frequency from different groups was shown in (B). The ratio of CD8+ T cells to Treg was shown in (C). (D–F) Foxp3-EGFP reporter mice ($n=3$) were inoculated with 5×10^5 MC38 tumor cells and treated with Combo or anti-CTLA-4×SIRPα on day 13. Five days later, Foxp3-EGFP+ cells from tumor, spleen and dLN were analyzed. The representative flow cytometric gating was shown in (D). Foxp3-EGFP+ cell frequency from different groups was shown in (E). The ratio of CD8+ T cells to Foxp3-EGFP+ cells was shown in (F). (G–I) Same experiment scheme as (A–F). Representative ICOS expression on Treg cells was shown in (G). (H) ICOS⁺⁺ frequency among Treg cells (H) and ICOS⁺⁺ frequency among YFP+ cells (I) were shown.



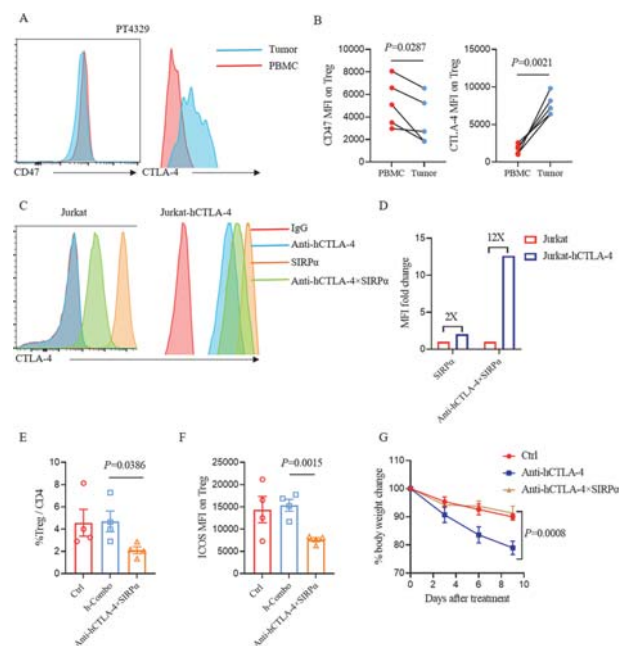
Abstract 800 Figure 3 Anti-CTLA-4×SIRP α reduces tumor in T cell dependent way. (A) C57BL/6 mice were inoculated with 5×10^5 MC38 tumor cells and treated with equal moles of anti-CTLA-4 plus SIRP α (Combo, 12 μ g + 8 μ g) or anti-CTLA-4×SIRP α (20 μ g) on day 14. Tumor growth was measured every 3 days, n=5. (B) BALB/c mice were inoculated with 5×10^5 CT26 tumor cells and treated with Combo (30 μ g+ 20 μ g) or anti-CTLA-4×SIRP α (50 μ g) on day 6. Tumor growth was measured every 3 days, n=5. (C) Rag1^{-/-} mice were inoculated with 1×10^5 MC38 tumor cells and treated with Combo (12 μ g+ 8 μ g) or anti-CTLA-4×SIRP α (20 μ g) on day 13. Tumor growth was measured every 3 days, n=5. (D) MuMT mice were inoculated with 1.5×10^6 MC38 tumor cells and treated with anti-CTLA-4×SIRP α (20 μ g) on day 14. Tumor growth was measured every 3 days, n=4. (E and F) C57BL/6 mice were inoculated with 5×10^5 MC38 tumor cells and treated with anti-CTLA-4×SIRP α on day 13. 200 μ g of anti-CD4 (E) or anti-CD8 (F) was administrated one day before treatment initiation and then twice a week for 2 weeks. Tumor growth was measured every 3 days, n=5. (G-I) C57BL/6 mice (n=4) were inoculated with 5×10^5 MC38 tumor cells and treated with Combo or anti-CTLA-4×SIRP α on day 14. Five days later, tumor-infiltrating lymphocytes (TILs) were analyzed for total CD45 in tumor (E), Ki67 expression on CD4 and CD8 T cells from different groups (F and G) after treatment.



Abstract 800 Figure 4 Anti-CTLA-4×SIRP α enhances tumor-specific T cell IFN-gamma. (A) C57BL/6 mice (n=4) were inoculated with 5×10^5 MC38 tumor cells and treated with Combo or anti-CTLA-4×SIRP α on day 13. Five days later, TILs were analyzed for tumor specific T cells. (B and C) C57BL/6 mice (n=4) were inoculated with 5×10^5 MC38 tumor cells and treated with Combo or anti-CTLA-4×SIRP α on day 13. Five days later, TILs were purified with CD45⁺ positive selection magnetic beads. TILs (A) and dLN (B) were re-stimulated with irradiated MC38 tumor cells or irrelevant control Lewis lung cancer (LLC) cells for 48 h. IFN- γ producing cells were determined by ELISPOT assay. (D) WT or *Irfng*^{-/-} C57BL/6 mice were inoculated with 5×10^5 MC38 tumor cells and treated with anti-CTLA-4×SIRP α on day 13. Tumor growth was measured every 3 days, n=4. (E) C57BL/6 mice were inoculated with 5×10^5 MC38 tumor cells and treated with anti-CTLA-4×SIRP α on day 13. 150 μ g of anti-IFN- γ was administrated one day before treatment initiation and then twice a week for 2 weeks. Tumor growth was measured every 3 days, n=5. (F and G) C57BL/6 mice were inoculated with 5×10^5 MC38 tumor cells and treated with anti-CTLA-4×SIRP α on day 14. Six weeks later, anti-CTLA-4×SIRP α cured mice and control naive mice were re-challenged with 5×10^6 MC38 tumor cells on the left flank (opposite to the original injection flank) (F), and 5×10^5 LLC tumor cells were injected on the right flank (G). Tumor growth was measured every 3 days, n=5.



Abstract 800 Figure 5 CD47 expression on Treg cells is essential. (A) *Cd47*^{-/-} tumor bearing C57BL/6 mice were treated with Combo or anti-CTLA-4×SIRP α on day 13. Tumor growth was measured every 3 days, n=5. (B) WT or *Cd47*^{-/-} C57BL/6 mice were inoculated with 5×10^5 MC38 tumor cells and treated with anti-CTLA-4×SIRP α on day 14. Tumor growth was measured every 3 days, n=5. (C) WT or *Cd47*^{-/-} T cells were purified by negative selection magnetic beads and intravenously transferred to *Rag1*^{-/-} mice. 2×10^5 MC38 tumor cells were inoculated into the recipient mice the next day. Mice were treated with 40 μ g anti-CTLA-4×SIRP α on day 7 and day 12. Experiment scheme was shown in upper panel and tumor growth was shown in lower panel, n=5. (D) C57BL/6 mice were inoculated with 5×10^5 MC38-cEGFR tumor cells and treated with 30 μ g anti-EGFR×SIRP α or anti-CTLA-4×SIRP α on day 14. Tumor growth was measured every 3 days, n=3–4. (E) WT or *Fcer1g*^{-/-} C57BL/6 mice were inoculated with 1×10^5 MC38 tumor cells and treated with anti-CTLA-4×SIRP α on day 13. Tumor growth was measured every 3 days, n=5. (F) WT C57BL/6 mice were inoculated with 5×10^5 MC38 tumor cells and treated with anti-CTLA-4×SIRP α or anti-CTLA-4×SIRP α with mutant Fc (Anti-CTLA-4×SIRP α -InfC) on day 14. Tumor growth was measured every 3 days, n=5. (G) Bone marrow derived macrophages from WT or *Fcer1g*^{-/-} mice were mixed with CFSE labelled in vitro differentiated Treg cells from WT or *Cd47*^{-/-} mice for 3 h. Phagocytosis was determined with flow cytometry. Phagocytosis index was defined as the percentage of CFSE+ macrophages among total macrophages.



Abstract 800 Figure 6 A human version anti-CTLA-4×SIRP α heterodimer depletes Treg. (A and B) CD47 and CTLA-4 expression level on Treg cells of PBMC and tumor from NSCLC patients. The representative flow cytometric gating was shown in (A), pooled data from different patients was shown in (B). (C) Anti-hCTLA-4, SIRP α and anti-hCTLA-4×SIRP α binding on Jurkat and Jurkat-hCTLA-4 expressing cells. (D) Comparison of anti-hCTLA-4×SIRP α binding on Jurkat and Jurkat-hCTLA-4 cells based on (C). (E and F) PBMC-humanized NSG mice were inoculated with 2.5×10^6 A549 tumor cells and treated with anti-hCTLA-4 plus SIRP α (h-Combo, 18 μ g +12 μ g) or anti-hCTLA-4×SIRP α (30 μ g) on day 12. Two days later, the frequency of tumor-infiltrating Treg cells (G) and ICOS expression level on Treg cells (F) were analyzed, n=4. (G) PBMC-humanized NSG mice were treated with 200 μ g anti-hCTLA-4 or anti-hCTLA-4×SIRP α twice a week for 4 times. Mouse body weight was monitored every 3 days, n=5. Data are shown as mean \pm SEM from two independent experiments. P value was determined by paired t test (B), unpaired t test (E and F) and two-way ANOVA with Geisser-Greenhouse's correction (G). The normality of data was confirmed by Shapiro-Wilk test.

Results Anti-CTLA-4×SIRP α preferentially depletes ICOS^{high} immunosuppressive Treg cells in the TME (figure 1–3) and enhances immunity against solid tumors. Mechanistically, we discovered that CD47 expression on Treg cells limits anti-CTLA-4 mediated depletion while Fc on the heterodimer enhances the depletion. Furthermore, anti-human CTLA-4×SIRP α depletes tumor Treg cells (figure 4–6) and exhibits less toxicity than anti-human CTLA-4 in a humanized mouse model.

Conclusions Collectively, these results highlight coordinately modulating “eat me” and “don't eat me” signals for depleting Treg cells inside the TME as a unique strategy for solid tumor treatment.

<http://dx.doi.org/10.1136/jitc-2021-SITC2021.800>

Immunotherapy Toxicities

802 AN ELECTRONIC HEALTH RECORD-BASED APPROACH TO IDENTIFY AND CHARACTERIZE PATIENTS WITH IMMUNE CHECKPOINT INHIBITOR-ASSOCIATED ARTHRITIS

Steven Tran*, Luke Rasmussen, Jennifer Pacheco, Carlos Galvez, Kyle Tegtmeier, Yuan Luo, Jeffrey Sosman, Abel Kho, Theresa Walunas. *Northwestern University Feinberg School of Medicine, Chicago, IL, United States*

Background Immune checkpoint inhibitors (ICIs) are a pillar of cancer therapy with demonstrated efficacy in a variety of malignancies. However, they are associated with immune-related adverse events (irAEs) that affect many organ systems with varying severity, inhibiting patient quality of life and in some cases the ability to continue immunotherapy. Research into irAEs is nascent, and identifying patients with adverse events poses a critical challenge for future research efforts and patient care. This study's objective was to develop an electronic health record (EHR)-based model to identify and characterize patients with ICI-associated arthritis (checkpoint arthritis).

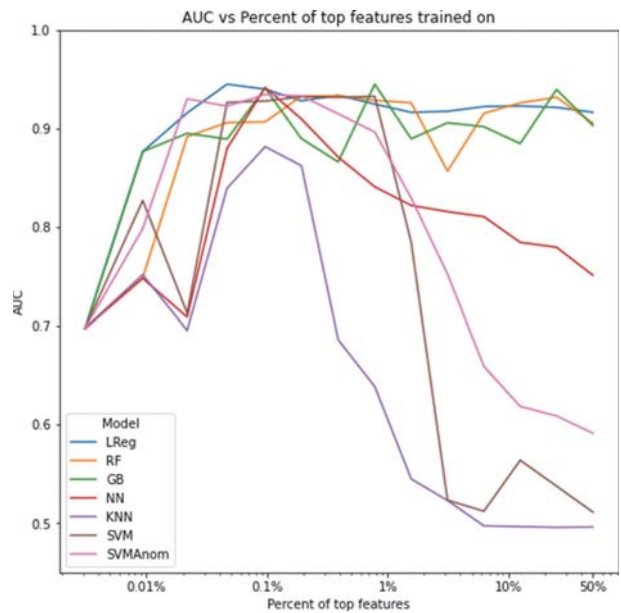
Methods Forty-two patients with checkpoint arthritis were chart abstracted from a cohort of all patients who received checkpoint therapy for cancer (n=2,612) in a single-center retrospective study. All EHR clinical codes (N=32,198) were extracted including International Classification of Diseases (ICD)-9 and ICD-10, Logical Observation Identifiers Names and Codes (LOINC), RxNorm, and Current Procedural Terminology (CPT). Logistic regression, random forest, gradient boosting, support vector machine, K-nearest neighbors, and neural network machine learning models were trained to identify checkpoint arthritis patients using these clinical codes. Models were evaluated using receiver operating characteristic area under the curve (ROC-AUC), and the most important variables were determined from the logistic regression model. Models were retrained on smaller fractions of the important variables to determine the minimum variable set necessary to achieve accurate identification of checkpoint arthritis.

Results Logistic regression and random forest were the highest performing models on the full variable set of 32,198 clinical codes (AUCs: 0.911, 0.894, respectively) (table 1). Retraining the models on smaller fractions of the most important variables demonstrated peak performance using the top 31 clinical codes, or 0.1% of the total variables (figure 1). The most important features included presence of ESR, CRP, rheumatoid factor lab, prednisone, joint pain, creatine kinase lab, thyroid labs, and immunization, all positively associated with checkpoint arthritis (figure 2).

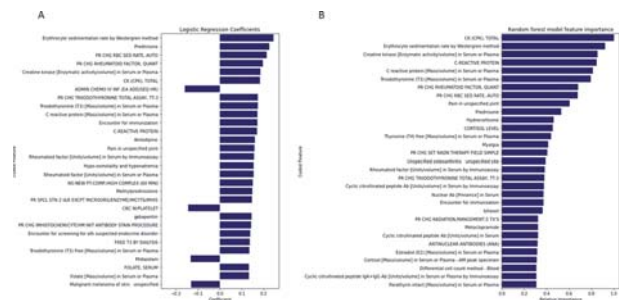
Abstract 802 Table 1 Model performance metrics

Model	AUC	Sensitivity	Specificity	PPV	NPV
Logistic Regression	0.911	0.238	0.999	0.833	0.988
Random Forest	0.894	0.286	0.999	0.857	0.988
Gradient Boosting	0.826	0.571	0.982	0.343	0.993
Support Vector Machine	0.566	1.000	0.132	0.018	1.000
K-Nearest Neighbor	0.497	0.000	0.995	0.000	0.984
Neural Network	0.763	0.000	0.999	0.000	0.984
SVM Anomaly Detection	0.589	0.000	0.953	0.000	0.983

AUC was calculated from the ROC curve. Sensitivity, specificity, PPV, and NPV were determined at the threshold maximizing the F1-score. AUC = area under the curve, ROC = receiver operating characteristic, PPV = positive predictive value, NPV = negative predictive value



Abstract 802 Figure 1 Model AUC trained on decreasing fractions of the most important variables, determined by the random forest model. 100% = 32,198 clinical codes. LReg = logistic regression, RF = random forest, GB = gradient boosting, NN = neural network, KNN = K-nearest neighbor, SVM = support vector machine, SVMAnom = SVM anomaly detection



Abstract 802 Figure 2 The 31 most important variables determined by the logistic regression (A, coefficients) and random forest (B, relative importance) models

Conclusions Our study demonstrates that a data-driven, EHR based approach can robustly identify checkpoint arthritis patients. The high performance of the models using only the 0.1% most important variables suggests that only a small number of clinical attributes are needed to identify these patients. The variables most important for identifying checkpoint arthritis included several unexpected clinical features, such as thyroid labs and immunization, indicating potential underlying irAE associations that warrant further exploration. Finally, the flexibility of this approach and its demonstrated effectiveness could be applied to identify and characterize other irAEs.

Ethics Approval This study was approved by the Northwestern University Institutional Review Board, ID STU00210502, with a granted waiver of consent

<http://dx.doi.org/10.1136/jitc-2021-SITC2021.802>

803

IMMUNE-RELATED ADVERSE EVENTS CORRELATE WITH IMPROVED OUTCOMES IN PATIENTS WITH ADVANCED NON-SMALL CELL LUNG CANCER TREATED WITH COMBINATIONS OF IMMUNE-CHECKPOINT INHIBITORS AND CHEMOTHERAPY

¹Lindsey Shantzer*, ¹Sean Dougherty*, ¹Wendy Novicoff, ²John Melson, ³Daniel Reed, ¹Alia Lynch, ¹Ryan Gentzler, ¹Richard Hall. ¹University of Virginia Health System, Charlottesville, VA, United States; ²Tufts Medical Center, Boston, MA, United States; ³Wake Forest Baptist Health, Winston-Salem, NC, United States

Background Immune checkpoint inhibitors (ICIs) have become the backbone of treatment for most driver-mutation negative, advanced non-small cell lung cancers. ICIs have been approved both as monotherapy and in combination with chemotherapy for front line management. While ICIs are generally regarded as well-tolerated, an unintended activation of the immune system can result in a variety of immune-related adverse events (irAEs), which can limit their use in severe cases. In patients with NSCLC treated with ICI monotherapy, the occurrence of an irAE and the development of multisystem irAEs have been associated with improved clinical outcomes, suggesting irAE occurrence could have prognostic implications.^{1–4} However, in patients treated with combination immunotherapy plus chemotherapy, the correlation between irAEs and survival has not been completely elucidated.

Methods We conducted a retrospective chart review of 94 patients with advanced NSCLC treated with a combination of ICI plus chemotherapy between 2015 and 2021 to evaluate for a correlation between irAE occurrence and overall survival (OS). Patients were divided into two groups: those who experienced at least one irAE and those who did not experience an irAE. To account for immortal time bias, we conducted landmark analyses at 12 and 24 weeks. We additionally investigated the impact of multisystem irAEs on clinical outcomes and described the profile of irAEs observed at our institution.

Results Among the 94 evaluable patients identified in our population, 43.6% experienced at least one irAE. Of those patients who experienced an irAE, 26 (63.4%) experienced a single irAE, 9 (22.0%) experienced 2 irAEs, and 6 (14.6%) experienced 3 or more irAEs. The most commonly observed irAEs were dermatitis followed by pneumonitis and colitis. In our cohort, patients with at least one irAE had significantly longer median OS (16.8 mos vs 9.8 mos) compared to those who did not experience an irAE (HR 0.51, 95% CI 0.43–0.76, p=0.011) (figure 1). Landmark survival analyses at 12 and 24 weeks continued to support significant differences in median OS based on presence or absence of an irAE (HR 0.49, 95% CI 0.24–0.46, and HR 0.45, 95% CI 0.21–0.60 respectively). Among patients with at least one irAE, the subset of patients who experienced multiple irAEs had further improved median OS compared to those with a single irAE.

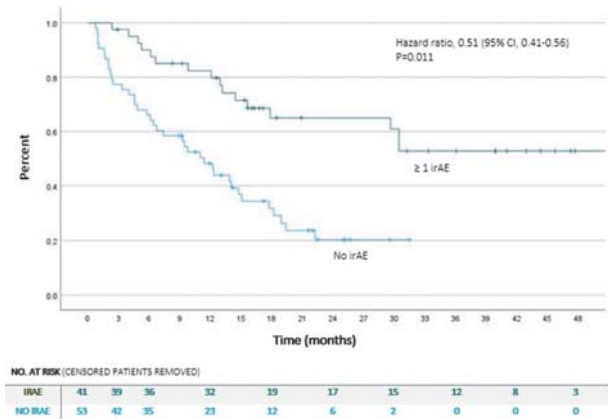
Conclusions In patients with advanced NSCLC treated with combination ICI plus chemotherapy, the occurrence of an irAE is associated with improved overall survival.

REFERENCES

1. Teraoka S, Fujimoto D, Morimoto T, et al. Early Immune-related adverse events and association with outcome in advanced non-small cell lung cancer patients treated with Nivolumab: a prospective cohort study. *Journal of Thoracic Oncology : Official Publication of the International Association for the Study of Lung Cancer* 2017;**12**(12):1798–1805. doi:10.1016/j.jtho.2017.08.022.
2. Ricciuti B, Genova C, De Giglio A, et al. Impact of immune-related adverse events on survival in patients with advanced non-small cell lung cancer treated with nivolumab: long-term outcomes from a multi-institutional analysis. *Journal of Cancer Research and Clinical Oncology* 2019;**145**(2):479–485. doi:10.1007/s00432-018-2805-3.

3. Toi Y, Sugawara S, Kawashima Y, et al. Association of immune-related adverse events with clinical benefit in patients with advanced non-small-cell lung cancer treated with nivolumab. *The Oncologist*. 2018;**23**(11):1358–1365. doi:10.1634/theoncologist.2017-0384.
4. Shankar B, Zhang J, Naqash AR, et al. Multisystem immune-related adverse events associated with immune checkpoint inhibitors for treatment of non-small cell lung cancer. *JAMA Oncol* 2020;**6**(12):1952–1956. doi:10.1001/jamaoncol.2020.5012

Ethics Approval This research study obtained ethics approval by the institutional review board at the University of Virginia, IRB# 19083.



Abstract 803 Figure 1 Overall Survival by presence or absence of an irAE in patients with advanced lung cancer treated with immune checkpoint inhibitors plus chemotherapy

<http://dx.doi.org/10.1136/jitc-2021-SITC2021.803>

REAL-WORLD INCIDENCE AND IMPACT OF PNEUMONITIS IN LUNG CANCER PATIENTS TREATED WITH IMMUNE CHECKPOINT INHIBITORS

¹Bruce Tiu*, ²Leyre Zubiri, ³James Iheke, ²Vartan Pahalyants, ²Nicholas Theodosakis, ²Pearl Ugwu-Dike, ²Jayhyun Seo, ²Kimberly Tang, ²Ryan Sullivan, ²Meghan Mooradian, ²Yevgeniy Semenov, ²Kerry Reynolds. ¹Harvard Medical School, Boston, MA, United States; ²Massachusetts General Hospital, Boston, MA, United States; ³University of Alabama at Birmingham SoM, Birmingham, AL, United States

Background Immune checkpoint inhibitors (ICI) generate T-cell mediated anti-tumor responses that are effective across numerous malignancies, but their use is frequently complicated by immune-related adverse events (irAEs). irAEs may lead to treatment delays, need for immunosuppression, morbidity, and even mortality.^{1–3} Checkpoint inhibitor pneumonitis (CIP) is the most common cause of fatality related to anti-programmed cell death receptor/ligand 1 (PD-1/PD-L1) agents, and can be difficult to diagnose.³ We aimed to characterize the real-world incidence and management of CIP, as well as its impact on clinical course and healthcare utilization, in a large cohort of ICI patients using a multi-institutional database.

Methods Propensity score-matched cohorts of 14,461 lung cancer patients who did or did not receive PD-1/PD-L1 inhibitors between 2014 to 2021 were identified from TriNetX Dataworks, a database of health records and claims data from over 40 institutions. Incidence of pneumonia/pneumonitis was estimated using billing codes. A subgroup of 158 patients was selected by the most specific code group and confirmed to have features consistent with suspected CIP, permitting analysis of management practices and outcomes. To describe differences in healthcare utilization and survival, a second propensity score-matched cohort was generated for the subgroup.

Results The attributable risk of pneumonitis to PD-1/PD-L1 inhibitors in lung cancer at 1 year after ICI initiation was 6.88% (95% CI 6.01–7.75%). Median time to onset of drug-induced pneumonitis in the subgroup was 4.4 months (IQR 2.1–7.8 months). Of 158 patients, 21 (13.3%) underwent bronchoscopy within 30 days after diagnosis. Prednisone (130/158, 82.3%), methylprednisolone (80/158, 50.6%), and antibiotics (135/158, 85.4%) were frequently prescribed. ICI was discontinued in 69.5% of patients within 90 days of drug-induced pneumonitis. Within the first year of PD-1/PD-L1 therapy, patients with pneumonitis had more hospitalizations (83.5% vs 49.4%, RR 1.69, $p < 0.0001$) and ICU requirements than controls (28.5% vs 8.9%, RR 3.21, $p < 0.0001$). Landmark analysis at 6 months demonstrated that CIP associated with reduced overall survival, with a mortality HR of 1.43 (95% CI 1.03–1.97, $p = 0.03$).

Conclusions To our knowledge, this is the largest study of CIP to date. Importantly, the study found that the incidence of PD-1/PD-L1-induced pneumonitis, 6.88%, is higher than clinical trial estimates (2–5%), but lower than reported in uncontrolled real-world studies (17–19%).^{4–8} CIP had significant negative impacts on therapy continuation, healthcare utilization, and overall survival in lung cancer. This work demonstrates proof of concept that studies of irAE incidences and patient outcomes are feasible using large claims and electronic health record databases.

REFERENCES

1. Brahmer JR, Lacchetti C, Schneider BJ, et al. Management of immune-related adverse events in patients treated with immune checkpoint inhibitor therapy: American society of clinical oncology clinical practice guideline. *Journal of Clinical Oncology* 2018;**36**(17):1714–1768. doi:10.1200/JCO.2017.77.6385.

2. Puzanov I, Diab A, Abdallah K, et al. Managing toxicities associated with immune checkpoint inhibitors: consensus recommendations from the Society for Immunotherapy of Cancer (SITC) Toxicity Management Working Group. *Journal for Immunotherapy of Cancer* 2017;**5**(1):95. doi:10.1186/s40425-017-0300-z.
3. Wang DY, Salem JE, Cohen JV, et al. Fatal toxic effects associated with immune checkpoint inhibitors: a systematic review and meta-analysis. *JAMA Oncology* 2018;**4**(12):1721–1728. doi:10.1001/jamaoncol.2018.3923.
4. Nishino M, Giobbie-Hurder A, Hatabu H, Ramaiya NH, Hodi FS. Incidence of programmed cell death 1 inhibitor-related pneumonitis in patients with advanced cancer: a systematic review and meta-analysis. *JAMA Oncology* 2016;**2**(12):1607–1616. doi:10.1001/jamaoncol.2016.2453.
5. Naidoo J, Wang X, Woo KM, et al. Pneumonitis in patients treated with anti-programmed death-1/programmed death ligand 1 therapy. *Journal of Clinical Oncology* 2017;**35**(7):709–717. doi:10.1200/JCO.2016.68.2005.
6. Delaunay M, Cadranet J, Lusque A, et al. Immune-checkpoint inhibitors associated with interstitial lung disease in cancer patients. *European Respiratory Journal* 2017;**50**(2). doi:10.1183/13993003.00050-2017.
7. Suresh K, Voong KR, Shankar B, et al. Pneumonitis in non-small cell lung cancer patients receiving immune checkpoint immunotherapy: incidence and risk factors. *Journal of Thoracic Oncology* 2018;**13**(12):1930–1939. doi:10.1016/j.jtho.2018.08.2035.
8. Cathcart-Rake EJ, Sangaralingham LR, Henk HJ, Shah ND, Riaz I bin, Mansfield AS. A population-based study of immunotherapy-related toxicities in lung cancer. *Clinical Lung Cancer* 2020;**21**(5):421–427.e2. doi:10.1016/j.clc.2020.04.003

Ethics Approval As described on TriNetX's website (<https://trinetx.com/trinetx-publication-guidelines/>), all data available on the network is de-identified and in-line with HIPAA Privacy Rule standards.

<http://dx.doi.org/10.1136/jitc-2021-SITC2021.804>

CLONAL, ACTIVATED CD8+ T CELLS RECOGNIZING CARDIAC ALPHA-MYOSIN DRIVE IMMUNE CHECKPOINT INHIBITOR ASSOCIATED MYOCARDITIS IN MICE

¹Margaret Axelrod*, ¹Wouter Meijers, ¹Elie Tannous, ¹Xiaopeng Sun, ¹Juan Qin, ¹Ayaka Sugiura, ¹Elizabeth Wescott, ¹Elles Screever, ²Spencer Wei, ¹Susan Opalenik, ¹Yueli Zhang, ¹Douglas Johnson, ²James Allison, ¹Javid Moslehi, ¹Justin Balko. ¹Vanderbilt University, Nashville, TN, United States; ²MD Anderson Cancer Center, Hayward, CA, United States

Background Nearly half of all U.S. oncology patients meet FDA eligibility criteria to receive treatment with an immune checkpoint inhibitor (ICI). With increasing use of ICIs, preventing, diagnosing and treating immune-related adverse events (irAEs) are urgent clinical challenges. Myocarditis is an uncommon irAE, affecting < 1% of ICI-treated patients, but is highly fatal, with a mortality rate of nearly 50%. Genetically altered *Pdcd1*^{-/-}*Ctla4*[±] mice die prematurely and specifically due to myocarditis. This model recapitulates the clinical and pathological features of ICI-myocarditis, including abundant cardiac infiltrating CD8+ T cells. The potential autoantigen(s) involved in ICI-myocarditis are unknown for both human disease and our murine model.

Methods We used *Pdcd1*^{-/-}*Ctla4*[±] mice on the C57BL/6 background as a model of ICI-myocarditis. Single cell RNA and T cell receptor (TCR) sequencing was performed on sorted CD45+ cardiac immune cells from four affected *Pdcd1*^{-/-}*Ctla4*[±] mice compared to six healthy wild type mice. The most three clonal TCRs (TCR-A, B, C), derived from two independent *Pdcd1*^{-/-}*Ctla4*[±] mice, were reconstructed using *stiTChR* and transduced into reporter T cell lines for antigen discovery. Alpha-myosin was selected as a candidate autoantigen due to lack of presentation in the thymus. Reporter TCR-A, B, and C cells were screened using a library of overlapping 20 amino acid peptides derived from alpha-myosin in co-culture with bone marrow derived dendritic cells.

Results Treatment with anti-CD8, but not anti-CD4, depleting antibodies rescues survival of *Pdcd1*^{-/-}*Ctla4*[±] mice. Furthermore, adoptive transfer of splenocytes from *Pdcd1*^{-/-}*Ctla4*[±] mice with myocarditis to *Rag1*^{-/-} recipient mice was sufficient to induce fatal myocarditis. Single cell RNA/TCR sequencing on the cardiac immune infiltrate of *Pdcd1*^{-/-}*Ctla4*[±] mice identified highly activated, clonal CD8+ T cells as the dominant cell population. The TCR-A cell line, the most clonal TCR identified in single cell TCR sequencing, activates NFAT, NFκB, and AP-1 reporters in response to the alpha-myosin epitope VIQYFASI. The TCR-B and TCR-C cell lines activate their reporters in response to the alpha myosin peptide DALL-VIQWNIRAFMGVKNWP, indicating that alpha-myosin is an autoantigen in this mouse model of ICI-myocarditis.

Conclusions Clonal, activated CD8+ T cells are critical for the development of ICI-myocarditis. Alpha-myosin is an autoantigen recognized by the most clonal cardiac CD8+ T cells. Efforts are currently underway to determine whether human TCRs derived from ICI-myocarditis samples recognize similar antigens. These studies are the first to identify a candidate autoantigen in ICI-myocarditis and may yield new insights into irAE pathogenesis.

Ethics Approval All animal experiments were in accordance with the VUMC Institutional Animal Care and Use Committee (IACUC), protocol # M2000067

<http://dx.doi.org/10.1136/jitc-2021-SITC2021.805>

806

PD-1 BLOCKADE AFFECTS INFLAMMATION AND METABOLIC FLEXIBILITY TO POTENTIALLY MEDIATE CARDIAC IMMUNE-RELATED ADVERSE EVENTS<http://dx.doi.org/10.1136/jitc-2021-SITC2021.806>

¹Steven Bronson*, ²Elizabeth Stirling, ²Brian Westwood, ²Pierre Triozzi, ²David Soto-Pantoja. ¹Wake Forest Health Science, Winston-Salem, NC, United States; ²Wake Forest Health Sciences, Winston-Salem, NC, United States

Background Immune checkpoint blockade (ICB) is now a mainstay of cancer therapy with success in extending the survival time in several cancers, including melanoma. Still, these modalities result in immune-related adverse events (irAEs), with approximately 80% of melanoma patients experiencing toxicity. IrAEs can lead to treatment discontinuation, contributing to mortality. In addition, one uncommon irAE with a high mortality rate is ICB-related myocarditis. In addition to myocarditis, ICB can also cause arrhythmias and heart failure. Currently, early markers to predict cardiotoxicity are unknown. During cardiac insult, cardiomyocyte metabolic flexibility results in metabolic reprogramming from fatty acid oxidation to glycolysis to overcome injury; however prolonged metabolic remodeling precedes most pathological alterations in the heart, suggesting that changes in metabolism may contribute to immunotherapy-related cardiac damage.

Methods Male C57BL/6 mice were injected with B16 melanoma cells. Once tumors reached 100 mm³, the animals were treated with three doses of anti-PD-1 antibody (200 µg IP). Echocardiograms were performed prior to necropsy using Vevo LAZR ultrasound to assess cardiac function. Bulk RNA sequencing (RNA-seq) and immunohistochemistry were performed on cardiac tissue. Single-cell RNA sequencing (scRNA-seq) was performed on human peripheral blood mononuclear cells (PMBCs) in patients treated with anti-PD-1 therapy.

Results Echocardiogram showed that anti-PD1 treatment attenuated stroke volume and increase heart rate compared to WT mice, suggesting that anti-PD1 treatment may be associated with changes in cardiac function. Histological examination showed no evidence of cardiac inflammation. RNA-seq was performed to further examine mechanisms of anti-PD1 therapy on the heart. Our data shows that over 230 genes were uniquely expressed in cardiac tissue of mice treated with anti-PD-1 therapy compared to isotype control. While no overt changes in immune infiltrate were seen, gene set enrichment analysis (GSEA) showed significant positive enrichment in chemokine receptor interactions with anti-PD-1 treatment potentially playing a role in the differentiation of cardiac, immune cell populations. Furthermore, gene enrichment was also observed among metabolic pathways. Interestingly, upregulation of PDK4 was observed in the hearts of animals treated with anti-PD1 antibody. PDK4 activation restricts cardiomyocyte metabolic flexibility during stress. scRNA-seq data from patient PBMCs also indicates an increase in PDK4 levels in the monocytic population after anti-PD1 treatment, suggesting that this protein may be regulated due to checkpoint blockade.

Conclusions Cardiac inflammation due to checkpoint blockade is implicated in ICB-myocarditis. However, RNA-seq data suggest that PD-1 therapy alters chemokine and metabolic pathways that may contribute to cardiac damage, suggesting potential early markers to identify cardiac irAEs.

Acknowledgements T32 from the Office of The Director, National Institutes of Health (T32-OD010957, SMB) (R21CA249349, DSP), an American Cancer Society Research Scholar Grant (133727-RSG-19-150-01-LIB, DSP)

807 IMMUNOTHERAPY RELATED ADVERSE EVENTS: A SINGLE CENTER EXPERIENCE

Wei Yang*, Julie Rowe, Sophia Lee, Jing Zhang, Mohammad Rahbar. *University of Texas @ Houston, Houston, TX, United States*

Background As the role of immune checkpoint inhibitors (ICIs) expands in many malignancies, including hepatocellular carcinoma (HCC), a better understanding of the predictors of immunotherapy-related adverse events (irAEs) is needed due to the complexity that ICIs add to patient care.¹⁻⁵

Methods We conducted a single-institution retrospective chart review for cancer patients of any type who received at least one ICI between January 2015 and December 2020. Demographic, social, cancer-related, laboratory, and treatment variables were collected, along with irAE data. Exploratory statistical analysis was performed to find predictors of increased irAEs.

Results A total of 342 patients were included in the study: 133 women and 209 men. Median age was 65 years. The most common cancers were lung (110, 32.07%), kidney (51, 14.87%), and HCC (43, 12.54%). All patients received at least one dose of ICI (table 1); 11 received combination ICIs. One hundred and two (26.53%) patients developed irAEs of any grade (table 2). Nineteen patients (5.56%) had a grade 3 or 4 irAE; 20 patients required systemic steroids. No biologics were used for the management of severe irAEs. Patients who received prior chemotherapy were less likely to develop irAEs (odds ratio [OR] = 0.42, $p = 0.0006$). A history of hyperthyroidism or hypothyroidism was associated with more irAEs ($p = 0.011$). Combination ICI led to more irAEs overall (OR = 2.91, $p = 0.043$), as well as grade 3 or 4 events (OR = 5.32, $p = 0.008$). A trend toward more grade 3 or 4 events occurred in HCC patient (OR = 2.78, $p = 0.06$). Older patients showed a trend toward more irAEs ($p = 0.08$). Worse peri-treatment renal function was associated with an increased risk of irAE (OR = 1.86, $p = 0.047$). A higher peri-treatment hemoglobin nadir was associated with a lower risk of irAE (OR = 0.45, $p = 0.07$). Several other variables had ORs or confidence intervals close to 1, including number of sessions of ICI and higher baseline AST.

Conclusions Prior chemotherapy, worse renal function, and thyroid dysfunction were associated with irAEs, whereas higher hemoglobin nadir was protective against irAE. Unlike the current literature, our study included a large number of HCC patients. The higher irAE incidence in our study could be associated with this higher number of HCC patients; however, further studies are needed.

Abstract 807 Table 1 Immune checkpoint inhibitors received

Therapy	No.	Percent
Nivolumab	200	58.31%
Pembrolizumab	137	39.94%
Ipilimumab	21	6.12%
Durvalumab	9	2.62%
Atezo	8	2.33%
Ipilimumab + Nivolumab	11	3.22%

Abstract 807 Table 2 irAE incidence

irAE	Count	Percent
Endocrine	43	12.54%
Gastrointestinal	33	9.62%
Skin	17	4.96%
Rheumatologyc	5	1.46%
Pulmonary	3	0.87%
Musculoskeletal	1	0.29%
Renal	1	0.29%
Eye	0	0.00%
CNS	0	0.00%
Cardiovascular	0	0.00%
Total with irAE	102	29.74%

REFERENCES

1. Brahmer JR, et al. Management of immune-related adverse events in patients treated with immune checkpoint inhibitor therapy: American Society of Clinical Oncology Clinical Practice Guideline. *JCO* 2018;**36**:1714–1768.
2. National Comprehensive Cancer Network. Management of Immunotherapy-Related Toxicities, 2021. https://www.nccn.org/professionals/physician_gls/pdf/immunotherapy.pdf.
3. Kartolo A, Sattar J, Sahai V, Baetz T, Lakoff JM. Predictors of immunotherapy-induced immune-related adverse events. *Curr Oncol* 2018;**25**:e403–e410.
4. Suresh K, et al. Pneumonitis in non-small cell lung cancer patients receiving immune checkpoint immunotherapy: incidence and risk factors. *Journal of Thoracic Oncology* 2018;**13**:1930–1939.
5. Colen RR, et al. Radiomics to predict immunotherapy-induced pneumonitis: proof of concept. *Invest New Drugs* 2018;**36**:601–607.

Ethics Approval The study involving retrospective review of patient records was approved under the Institutional Review Board. All records identifying the patient was kept confidential and, to the extent permitted by the applicable laws and/or regulations, were not be made publicly available. Patient names will not be supplied to third parties. A unique study number will be assigned to each patient. Study data stored electronically will be stored in a password-protected, encrypted computers. Paper study data will be maintained by the primary investigators in the locked research offices.

Consent N/A

<http://dx.doi.org/10.1136/jitc-2021-SITC2021.807>

808 **TERTIARY LYMPHOID STRUCTURE GENE SIGNATURE
DETECTED IN IMMUNE CHECKPOINT INHIBITOR-
ASSOCIATED RENAL IMMUNE RELATED ADVERSE
EVENT**

¹Jamie Lin*, ²Amanda Tchakarov, ¹Noha Abdel-Wahab, ³Houssein Safa, ¹Salah-Eddine Bentebibel, ⁴Maen Abdelrahim, ¹Cassian Yee, ¹Adi Diab, ¹Ala Abudayyeh. ¹The University of Texas MD Anderson Cancer Center, Houston, TX, United States; ²University of Texas Health Science Center, Houston, TX, United States; ³Albert Einstein College of Medicine, Montefiore Medical Center, Bronx, NY, United States; ⁴Houston Methodist Cancer Center, Houston, TX, United States

Background Tertiary lymphoid structures (TLSs) have been previously associated with ICI induced response in patients with cancer, but a commensurate observation has not been made in ICI associated immune related adverse events (irAEs). Acute interstitial nephritis (AIN) is the predominant lesion reported in patients with renal irAEs, but various etiologies can also trigger the development of AIN including non-ICI drugs (e.g. non-steroidal anti-inflammatory drugs, antibiotics, proton pump inhibitors, etc.), and it is unknown whether these mechanisms are similar. With increasing indications for ICIs in cancer therapy, there is a critical need to define immune pathways driving the emergence of irAEs. To address this critical knowledge gap, we performed gene expression profiling on ICI-AIN, drug-AIN, and control (non-AIN) kidney biopsy specimens.

Methods Total RNA extracted from ICI-AIN (n = 6), drug-AIN (n = 4), and control (n = 4) fixed formalin paraffin embedded archival kidney biopsy samples was analyzed by Nanostring nCounter PanCancer Immune Profiling Panel using NanoString nCounter FLEX Analysis System.

Results

Three comparisons were conducted: ICI-AIN vs control, drug-AIN vs control, and ICI-AIN vs drug-AIN. A total of 147 genes were differentially expressed in ICI-AIN vs control and the most differentially expressed genes were CXCL 9, 10, and 11. Similarly, cell marker gene expression signatures (GES) revealed significant upregulation of T and B cell markers in ICI-AIN vs control (P < 0.01) and ICI-AIN vs drug-AIN (T cell P < 0.05; B cell P < 0.01). Differences in T and B cell score were not detected in drug-AIN vs control. Since irAEs have been associated with anti-tumor efficacy, we investigated whether a TLS signature could be detected in ICI-AIN using a four GES (CD79A, MS4A1, LAMP3 and POU2AF1). The ICI-AIN group had significantly higher TLS score compared to both control and drug-AIN groups. Since several TLS signatures have been reported, we also calculated a 12-chemokine TLS GES which was also found to be statistically significant (P < 0.05). Th1 and Th17 cells have been associated with the formation of TLS, differential upregulation of Th1 associated genes but not Th17 associated genes were detected. Furthermore, differential expression IFN- γ and TNF signature was also observed in ICI-AIN group.

Conclusions This study is the first to demonstrate the presence of TLS immune signature in irAEs. Further investigations into the prognostic significance and strategies to uncouple ICI-associated anti-tumor benefits from ICI-induced irAEs should be explored.

Ethics Approval The study was approved by The University of Texas MD Anderson Cancer Center institution's Ethics Board, approval number PA16-1016

<http://dx.doi.org/10.1136/jitc-2021-SITC2021.808>

810

IMPACT OF IMMUNE-RELATED ADVERSE EVENT DEVELOPMENT ON OVERALL SURVIVAL IN HOSPITALIZED LUNG CANCER PATIENTS

Eric Olson*, Greg Russell, Jeffrey Lantz, Andy Dothard, Vanya Aggarwal, Thomas Lycan. Wake Forest Baptist Medical Center, Winston Salem, NC, United States

Background Immune-related adverse events (irAEs) are a unique characteristic of immune checkpoint inhibitors (ICIs) and can confer survival benefits. For example, melanoma patients who develop vitiligo as an irAE tend to have improved overall survival (OS), hypothesized to be due to molecular mimicry between similar antigens.^{1 2} Further analysis of the impact of irAEs on OS among real-world lung cancer patients is needed; this study addresses this need in a hospitalized population.³⁻⁵

Methods This single-center retrospective cohort study collected data on a subset of lung cancer patients who received > 1 dose of an ICI (nivolumab or pembrolizumab) between 6/1/18 and 2/1/20 (n=210) and who were subsequently hospitalized and received > 1 dose of systemic corticosteroids for any indication (n=97). Patients were stratified according to whether or not they developed irAEs at any point. Clinical factors for data collection included: comorbidities, irAE development (organ and grade), cancer stage, ICI cycles, biomarkers, progression, and survival. OS analysis was calculated from the first dose of ICI to date of death or last known follow-up. To assess significance, the log-rank approximation of the chi-square test was used.

Results Kaplan-Meier survival analysis revealed that patients who developed irAEs (n=28, median OS 14.9 months) did not have an association with increased median OS when compared to patients without irAEs (n=69, 8.7 months, p 0.072) (table 1). The subgroup of patients who developed either colitis or pneumonitis had an increased median OS (n=15, 41.3 months, p 0.049) compared to patients without irAEs. Patients who only experienced grade ≥ 3 irAEs (n = 20, median OS 17.0 months, p 0.095) did not show any OS difference compared to patients without irAEs. Patients who developed ≥ 2 irAEs of any grade (n = 7, median OS 17.0 months, p 0.22) did not show any OS difference as compared to patients without irAEs.

Abstract 810 Table 1 Results of irAE impact on median OS analysis

Groups (n)	Median Overall Survival (months)	P value
All irAE (28) vs no irAE (69)	14.9, 8.7	0.072
Colitis/Pneumonitis (15) vs no irAE (69)	41.3, 8.7	0.049
Grade ≥ 3 irAEs (20) vs no irAE (69)	17.0, 8.7	0.095
Multiple irAEs (7) vs no irAE (69)	17.0, 8.7	0.22

Conclusions Initial analysis shows that while generalized irAEs in this hospitalized lung cancer population were not significantly associated with OS change, patients who developed pneumonitis and colitis were associated with treatment response and increased OS. Patients could be developing an interaction between pneumonitis and lung cancer analogous to the interaction between vitiligo and melanoma via molecular mimicry, resulting in improved OS. Thus, certain organ-related irAEs may indicate an immune response to ICIs depending on the malignancy being treated, correlating with improved prognosis.

REFERENCES

- Bertrand A, Kostine M, Barnetche T, Truchetet M-E, Schaevebeke T. Immune related adverse events associated with anti-CTLA-4 antibodies: systematic review and meta-analysis. *BMC Med* 2015;**13**:211.
- Teulings H-E, Limpens J, Jansen SN, et al. Vitiligo-like depigmentation in patients with stage III-IV melanoma receiving immunotherapy and its association with survival: a systematic review and meta-analysis. *J Clin Oncol* 2015;**33**(7):773–81.
- Owen DH, Wei L, Villalona-Calero MA, et al. Impact of immune-related adverse events (irAE) on overall survival (OS) in patients treated with immunotherapy for non-small cell lung cancer (NSCLC). *J Clin Oncol* 2017;**35**(15_suppl):9080–9080.
- Haratani K, Hayashi H, Chiba Y, et al. Association of immune-related adverse events with nivolumab efficacy in non-small-cell lung cancer. *JAMA Oncol* 2018;**4**(3):374–8.
- Owen DH, Wei L, Bertino EM, et al. Incidence, risk factors, and effect on survival of immune-related adverse events in patients with non-small-cell lung cancer. *Clin Lung Cancer* 2018;**19**(6):e893–900.

Ethics Approval The study protocol was approved by Wake Forest Baptist Medical Center's institutional review board.

<http://dx.doi.org/10.1136/jitc-2021-SITC2021.810>

811

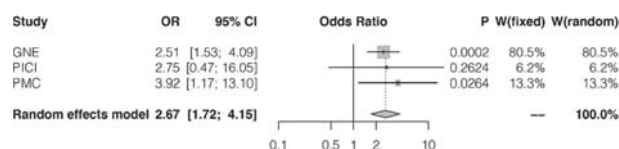
ALLELIC VARIATION IN HUMAN LEUKOCYTE ANTIGEN CLASS II GENES IS ASSOCIATED WITH PNEUMONITIS RISK IN CANCER PATIENTS TREATED WITH IMMUNE CHECKPOINT INHIBITORS

¹Ashis Saha, ²Christine Spencer, ¹Zia Khan, ¹Jonathan Carroll, ³Claudia Yanez Arellano, ¹Julie Hunkapiller, ²Nicholas Bayless, ²Leonardo Nissola, ⁴Roslyn Wallace, ¹Ira Mellman, ³Rajat Mohindra, ²Samantha Bucktrout, ⁴Shahneen Sandhu, ³G. Scott Chandler, ¹Christian Hammer*, ¹Christian Hammer. ¹Genentech, South San Francisco, CA, United States; ²Parker Institute for Cancer Immunotherapy, San Francisco, CA, United States; ³F. Hoffmann-La Roche, Basel, Switzerland; ⁴Peter MacCallum Cancer Centre, Melbourne, Australia

Background Immune-mediated adverse events (imAE) commonly occur in patients treated with immune checkpoint inhibitors (ICI), and pneumonitis is known to occur in 3–5% of patients treated with anti-PD-1 / PD-L1 antibodies.¹ Most cases are grade 1 or 2 events and can be treated with immunosuppression, but high-grade events occur in a minority of patients and can be fatal.² Since lung inflammatory phenotypes, including fibrotic idiopathic interstitial pneumonias and infectious pneumonias, were associated with allelic variation in Human Leukocyte Antigen (HLA) genes,^{3–4} we hypothesized that HLA variants might also be a risk factor for ICI-associated pneumonitis.

Methods Out of 1761 atezolizumab (anti-PD-L1) treated patients across nine Genentech (GNE) clinical trials with available whole-genome sequencing data, 72 (4.1%) developed pneumonitis (table 1). We inferred HLA genotypes using HLA-HD⁵ and performed an association study including 87 alleles with a carrier frequency of >2%. In order to confirm our results, and to test whether the association is generalizable to different classes of ICI, we genotyped two additional cohorts using an Illumina genome-wide SNP array (GSA v3), followed by HLA imputation using HIBAG⁶: (1) 20 ICI-treated cancer patients with pneumonitis and 20 matched controls without from a pilot study on the AEROSMITH trial from Parker Institute for Cancer Immunotherapy (PICI); (2) 15 ICI-treated melanoma patients with pneumonitis and 149 without from Peter MacCallum Cancer Centre (PMC) (table 1).

Results Two HLA class II alleles that are part of a common haplotype showed significant associations with pneumonitis risk after multiple testing adjustment (HLA-DRB1*15:01, HLA-DQA1*01:02), with HLA-DRB1*15:01 showing the strongest association ($p = 0.0002$, odds ratio (OR) = 2.51). No associations were identified in the control arms ($N = 1192$). In the PICI pilot cohort, HLA-DRB1*15:01 did not reach statistical significance in spite of a comparable OR ($p = 0.26$, OR = 2.75), but the allele was significantly associated with pneumonitis risk in the PMC cohort ($p = 0.03$, OR = 3.92). A meta-analysis across the three cohorts yielded a highly significant p -value of 1.2×10^{-5} (OR = 2.67, figure 1), suggesting that the association is generalizable across ICI. Importantly, the same class II haplotype was previously shown to be associated with diverse lung inflammatory, including fibrotic, phenotypes.^{3,4,7,8}



Abstract 811 Figure 1 Forest plot for HLA-DRB1*15:01 meta-analysis with ICI-associated pneumonitis. GNE, Genentech; PICI, Parker Institute for Cancer Immunotherapy; PMC, Peter MacCallum Cancer Centre; OR, odds ratio; CI, confidence interval; W, weight <http://dx.doi.org/10.1136/jitc-2021-SITC2021.811>

Conclusions In summary, our findings establish HLA class II allelic variation as a potential risk factor in ICI-associated pneumonitis, and future research is warranted to determine whether this genetic association can be refined according to specific clinical presentations.

REFERENCES

- Wang H, Guo X, Zhou J, Li Y, Duan L, Si X, et al. Clinical diagnosis and treatment of immune checkpoint inhibitor-associated pneumonitis. *Thorac Cancer* 2020;**11**:191–7.
- Naidoo J, Wang X, Woo KM, Iyriboz T, Halpenny D, Cunningham J, et al. Pneumonitis in patients treated with anti-programmed death-1/Programmed death ligand 1 therapy. *J Clin Oncol* 2016;**35**:709–17.
- Tian C, Hromatka BS, Kiefer AK, Eriksson N, Noble SM, Tung JY, et al. Genome-wide association and HLA region fine-mapping studies identify susceptibility loci for multiple common infections. *Nat Commun* 2017;**8**:599.
- Fingerlin TE, Zhang W, Yang IV, Ainsworth HC, Russell PH, Blumhagen RZ, et al. Genome-wide imputation study identifies novel HLA locus for pulmonary fibrosis and potential role for auto-immunity in fibrotic idiopathic interstitial pneumonia. *BMC Genet* 2016;**17**:74.
- Kawaguchi S, Higasa K, Shimizu M, Yamada R, Matsuda F. HLA-HD: An accurate HLA typing algorithm for next-generation sequencing data. *Hum Mutat* 2017;**38**:788–97.
- Zheng X, Shen J, Cox C, Wakefield JC, Ehm MG, Nelson MR, et al. HIBAG—HLA genotype imputation with attribute bagging. *Pharmacogenomics J* 2014;**14**:192–200.
- Voorter CEM, Drent M, Berg-Loonen EM van den. Severe pulmonary sarcoidosis is strongly associated with the haplotype HLA-DQB1*0602-DRB1*150101. *Hum Immunol* 2005;**66**:826–35.
- Furukawa H, Oka S, Shimada K, Sugii S, Ohashi J, Matsui T, et al. Association of human leukocyte antigen with interstitial lung disease in rheumatoid arthritis: a protective role for shared epitope. *PLoS One* 2012;**7**:e33133.

Ethics Approval Patients included in this study signed an optional Research Biosample Repository (RBR) Informed Consent Form (ICF) and provided whole blood samples. By signing the optional RBR ICF, patients provided informed consent for analysis of inherited and non-inherited genetic variation from whole blood samples. Ethics Committees (EC) and Institutional Review Boards (IRB) in each country and each study site for each clinical trial approved the clinical trial protocol, the main study ICF, and the RBR ICF.

<http://dx.doi.org/10.1136/jitc-2021-SITC2021.811>

Abstract 811 Table 1 Investigated cohorts

Cohort	ICI-associated pneumonitis		Treatment			
	yes	no	PD-L1	PD-1	CTLA4	PD-1 + CTLA-4
GNE	72	1689	1761	0	0	0
PICI	19	19	14	22	0	2
PMC	15	149	0	47	14	103
Total	106	1857	1775	69	14	105

812 **ERYTHEMA NODOSUM-LIKE TOXICITY IN AN IMMUNOTHERAPY TREATED PATIENT IS ACCOMPANIED BY OLIGOCLONAL MEMORY ACTIVATED CD4 T CELLS**

Xiaopeng Sun*, Margaret Axelrod, Yu Wang, Sanchez Violeta, Paula Gonzalez-Ericsson, Douglas Johnson, Justin Balko. *Vanderbilt University Medical Center, Nashville, TN, United States*

Background Immune checkpoint inhibitors (ICIs) are increasingly used to treat advanced malignancy but can be associated with immune related adverse events (irAE). Here we present a case report of a rare dermatologic toxicity occurring in a melanoma patient with isolated brain metastasis. After surgical resection, the patient was treated with ipilimumab (anti-CTLA-4) and nivolumab (anti-PD-1) combination therapy followed by single agent nivolumab with ongoing, excellent response. During nivolumab, the patient developed an erythema nodosum (EN)-like irAE. The condition resolved after potassium iodine treatment and nivolumab therapy was resumed. To understand the pathogenesis of this irAE, we examined samples from this patient's blood, brain metastasis and tissue biopsy of the EN toxicity.

Methods RNA and T cell receptor (TCR) sequencing on the patient's brain metastasis and site of irAE were performed. We also performed RNA sequencing on 3 non-ICI EN patients. RNA in situ hybridization (RNAish) for CD4, CD8 and granzyme B, and the most abundant TCR identified was conducted on the patient's site of toxicity. Single cell RNA/TCR sequencing was carried out on the patient's peripheral blood mononuclear cells (PBMC) at baseline, 3 weeks after ipilimumab and nivolumab combination therapy, during EN toxicity and after resolution.

Results RNAish showed that the most abundant TCR (20% of total TCR sequencing reads at the site of toxicity) colocalized with CD4 at the site of toxicity. According to CIBERSORT deconvolution, the site of toxicity had high memory activated CD4 T cells and low M2 macrophage infiltration, which is different from the brain metastasis and non-ICI-induced EN cases. Compared to non-ICI EN, the EN skin biopsy was also enriched for interferon response and inflammation related genes. In the peripheral blood, cytotoxic CD8 T cells clonally expanded during EN toxicity, accompanied by a decrease in naïve/memory CD4 T cells. The TCR repertoire in the site of toxicity did not overlap with that in the tumor or PBMC.

Conclusions We found oligoclonal memory activated CD4 T cells are enriched at the site of toxicity, suggesting their association with EN toxicity. The unique TCR repertoire, gene expression profile and immune cell composition at the site of toxicity could indicate that the EN toxicity is distinct from the anti-tumor immunity and analogous non-ICI autoimmunity. Future work will focus on determining the antigen for this irAE and determining its relevancy to other skin toxicities and EN autoimmune conditions.

Ethics Approval IRB 100178 and 161485

Consent Approval under IRB 100178

<http://dx.doi.org/10.1136/jitc-2021-SITC2021.812>

CD24Fc AMELIORATES IMMUNE-RELATED ADVERSE EVENTS WHILE PRESERVING ANTI-TUMOR THERAPEUTIC EFFECT

¹Mingyue Liu*, ¹Xu Wang, ¹Peng Zhang, ¹Juanjuan Su, ¹Xuexiang Du, ¹Yan Zhang, ²Yang Liu, ²Pan Zheng. ¹IHW/UMB, Baltimore, MD, United States; ²OncoC4, Inc., Rockville, MD, United States

Background Combination therapy with anti-CTLA-4 and anti-PD-1 mAbs has emerged as the most potent and durable cancer immunotherapy, yet it is associated with frequent and severe immune-related adverse events (irAEs).¹⁻² A largely unmet medical need is to reduce irAEs. The CD24–Siglec 10/G interaction is an emerging immune checkpoint that regulates inflammation caused by danger-associated molecular patterns (DAMPs).³⁻⁵ It is of great interest to investigate whether CD24Fc can ameliorate severe irAEs, the hallmark of which is a severe inflammatory state in multiple organs.

Methods We used a human CTLA-4 knock-in (Ctla4h/h) mice model that fully recapitulates human irAE in response to anti-PD-1 and anti-CTLA-4 antibodies to test if CD24Fc have therapeutic effect for irAE. We treated Ctla4h/h mice with Ipilimumab and anti-PD-1 Ab in conjunction with hIgFc or CD24Fc on day 10, 13, 16 and 19 after birth. The body weight was monitored over time, hematologic and histopathologic alterations were evaluated at 6 weeks of age. To evaluate the therapeutic effect of CD24Fc on ICIs induced tissue destruction, we performed histological analysis of internal organs and glands. Major organs were collected about 1 month after first treatment and fixed in 10% formalin, sectioned and stained with hematoxylin and eosin (H&E), and scored double blindly. To test whether CD24Fc immune modulation may interfere with the anti-tumor efficacy of the checkpoint inhibitors, we inoculated MC38 and B16-F10 tumor cells on Ctla4h/h mice, then treated with combination of Ipilimumab and anti-PD-1 Ab together with hIgFc or CD24Fc and monitored tumor growth.

Results We found that anti-CTLA-4 and anti-PD-1 therapy could induce growth retardation, anemia and severe inflammation in all organs examined. All of these adverse events were ameliorated by CD24Fc treatment. Moreover, in both tumor models tested CD24Fc modestly enhanced immunotherapeutic effect of anti-PD-1 and anti-CTLA-4 antibodies. CD24Fc treatment showed no effect on CD4+, CD8+ T cell or tumor associated macrophage (TAM) density intratumor. However, we observed significantly decreased Treg among CD4+T cells after CD24Fc treatment. CD24Fc treatment also decreased the TIM-3+ PD-1+ CD4+ and CD8+ T cells. These data suggest CD24Fc has the potential to optimize tumor microenvironment and augment antitumor immunity.

Conclusions Our data demonstrate that CD24Fc treatment ameliorates irAEs in multiple organs induced by combination of anti-CTLA-4 and anti-PD-1 Abs while modestly enhancing its anti-tumor activity, potentially by reducing the intratumor regulatory T cells and reverse exhaustion of tumor-infiltrating T cells.

REFERENCES

1. Wolchok JD, et al. Overall survival with combined nivolumab and ipilimumab in advanced melanoma. *N Engl J Med* 2017;**377**:1345–1356.
2. Larkin J, et al. Five-year survival with combined nivolumab and ipilimumab in advanced melanoma. *N Engl J Med* 2019;**381**:1535–1546.
3. Chen GY, Tang J, Zheng P, Liu Y. CD24 and Siglec-10 selectively repress tissue damage-induced immune responses. *Science* 2009;**323**:1722–1725.
4. Liu Y, Chen GY, Zheng P. CD24-Siglec G/10 discriminates danger- from pathogen-associated molecular patterns. *Trends Immunol* 2009;**30**:557–561.

5. Fang X, Zheng P, Tang J, Liu Y. CD24: from A to Z. *Cell Mol Immunol* 2010;**7**:100–103.

<http://dx.doi.org/10.1136/jitc-2021-SITC2021.813>

CUTANEOUS IMMUNE-RELATED ADVERSE EVENTS ARE PROTECTIVE OF MORTALITY IN PATIENTS TREATED WITH ANTI-PD1 AND ANTI-PDL1 THERAPY IN A MULTI-INSTITUTIONAL COHORT STUDY

¹Yevgeniy Semenov*, ²Kimberly Tang, ²Jayhyun Seo, ²Kerry Reynolds, ³Bruce Tiu, ⁴Thomas Le, ³Vartan Pahalyants, ²Neel Raval, ²Pearl Ugwu-Dike, ²Leyre Zubiri, ²Vivek Naranbhai, ⁵Alexander Gusev, ⁶Nicole LeBoeuf, ³Maryam Asgari, ⁴Shawn Kwatra. ¹Massachusetts General Hospital/Harvard Medical School, Boston, MA, MA, United States; ²Massachusetts General Hospital, Boston, MA, United States; ³Harvard Medical School, Boston, MA, United States; ⁴Johns Hopkins University, Baltimore, MD, United States; ⁵Dana Farber Cancer Institute, Boston, MA, United States; ⁶Dana Faber Cancer Institute, Boston, MA, United States

Background Immune checkpoint inhibitors (ICIs) have revolutionized cancer therapy over the last decade. Despite the efficacy of ICIs, immune-related adverse events (irAEs) occur in over a third of treated patients and can cause lasting morbidity and mortality.¹⁻³ Cutaneous irAEs (cirAEs) are the most frequently reported toxicities, occurring in 20–40% of treated patients. Though recent reports have investigated the prognostic significance of irAEs on cancer outcomes, little is known about the specific impact of cirAEs and their subtypes on cancer survival.⁴ In this landmark analysis, we present the first population-level study examining the influence of cirAE development following ICI therapy on the mortality of cancer patients.

Methods 7,008 patients who developed cirAEs after treatment with anti-programmed cell death receptor/ligand 1 (PD-1/PD-L1) therapy for malignant neoplasms of digestive organs, bronchus or lung, melanoma of skin, and urinary tract were identified through the TriNetX Diamond network along with 7,008 matched controls (table 1). The malignant neoplasms and cutaneous diagnoses for this study were identified from published literature and expert opinion.^{5 6} Looking at cutaneous eruptions within 6 months of the first instance of ICI administration, a 6-month landmark analysis using a Cox proportional hazards model was performed to determine the impact of cirAE on overall survival.

Results Presence of any cirAE (HR=0.695, p<0.0001), non-specific rashes (HR=0.704, p<0.0001), pruritus (HR=0.695, p<0.0001), drug eruption (HR=0.755, p=0.0013), and xerosis (HR=0.626, p=0.0013) were significantly protective of mortality using a Benjamini-Hochberg (BH) correction for multiple comparisons (table 2). Psoriasis (HR=0.703, p=0.0451) and lichen planus/lichenoid dermatitis (HR=0.511, p=0.0274) were nominally significant. Notably, though not reaching statistical significance, eczematous dermatitis (HR=0.612), vitiligo (HR=0.534), bullous pemphigoid (HR=0.524), and Grover's disease (HR=0.468) were associated with strong protective clinical effects. To explore the impact of landmark time on mortality, a sensitivity analysis was performed for cirAE onset within 3 months (HR=0.759, p<0.0001) and 9 months (HR=0.84, p<0.0001) of ICI initiation. A separate sensitivity analysis expanded to include all cancer types treated with ICI yielded similar results, with additional statistical significance reached for ICI-induced psoriasis (table 3).

Conclusions This is the first population-level study and largest analysis to date of the impact of cirAEs on mortality among patients with advanced cancer. With the exception of mucositis and hyperhidrosis, there was a strong clinically protective effect of cirAEs across all individual morphologies investigated. Our results demonstrate that cirAE development after ICI initiation is an important positive prognostic indicator of response to ICI therapy and patient survival.

Abstract 814 Table 1 Propensity score-matched baseline characteristics for patients treated with PD-1 or PL-L1 therapy

N	ICI with cirAE		ICI without cirAE		P-value
	7008		7008		
Age (years)	Mean	SD	Mean	SD	
Age at Index	68.2	11.2	68.3	11.1	0.7912
Gender	N	%	N	%	
Male	3972	56.7	3961	56.5	0.8513
Female	3036	43.3	3044	43.4	0.8915
Unknown	0	0	10	0.14	0.0016
Race and Ethnicity	Mean	%	Mean	%	
White Non-Hispanic	1549	22.10	1571	22.40	0.6551
Black Non-Hispanic	129	1.84	116	1.66	0.4021
Asian Non-Hispanic	17	0.24	10	0.14	0.1775
Hispanic or Latino	111	1.58	77	1.10	0.0125
Cancer Type	Mean	%	Mean	%	
Digestive organs	956	13.64	937	13.37	0.6387
Bronchus and lung	3993	56.9	3996	57.02	0.9592
Melanoma of skin	1300	18.55	1288	18.38	0.7939
Urinary tract	1306	18.64	1244	17.75	0.1746
Ill-defined, other secondary and unspecified sites	5399	77.04	5396	76.99	0.952

Abstract 814 Table 2 Association between cutaneous eruptions and survival

Cutaneous Diagnosis [‡]	N	Hazard Ratio	P-value*
Hyperhidrosis	281	1.381	0.0797
Mucositis	563	1.161	0.2068
Dermatomyositis	105	0.93	0.7894
Maculopapular eruption	230	0.845	0.3625
Erythroderma	247	0.769	0.1697
Drug eruption and non-specific drug reaction	1075	0.755	0.0013
Hyperkeratosis	39	0.707	0.4867
Rash and other non-specific eruption	3163	0.704	<0.0001
Psoriasis	299	0.703	0.0451
Pruritus	1694	0.695	<0.0001
Xerostomia	163	0.671	0.1301
Xerosis	441	0.626	0.0013
Eczema and Atopic Dermatitis	72	0.612	0.1467
Vitiligo	100	0.534	0.0929
Pemphigoid	32	0.524	0.3281
Lichen Planus	97	0.511	0.0274
Grover's disease	18	0.468	0.2768
Any cutaneous diagnosis	7008	0.778	<0.0001

[‡]Cutaneous diagnoses were identified based on published literature and expert opinion.

*Benjamini-Hochberg p-value of significance = 0.0013.

[‡]Cutaneous diagnoses were identified based on published literature and expert opinion.

*Benjamini-Hochberg p-value of significance = 0.0013.

Abstract 814 Table 3 Association between cutaneous eruptions and survival

Cutaneous Diagnosis [‡]	N	Hazard Ratio	P-value*
Dermatomyositis	128	1.405	0.1917
Mucositis	694	1.112	0.3398
Hyperhidrosis	322	1.063	0.697
Maculopapular eruption	264	0.951	0.7777
Lichen Planus	113	0.849	0.5988
Drug eruption and non-specific drug reaction	1194	0.83	0.028
Erythroderma	295	0.79	0.1833
Rash and other non-specific eruption	3557	0.769	<0.0001
Hyperkeratosis	48	0.741	0.5026
Pruritus	1901	0.737	<0.0001
Xerosis	499	0.658	0.0025
Xerostomia	228	0.63	0.0328
Eczema and Atopic Dermatitis	83	0.628	0.1633
Psoriasis	336	0.581	0.0005
Grover's Disease	21	0.481	0.2993
Vitiligo	103	0.458	0.0285
Pemphigoid	35	0.264	0.0207
Any cutaneous diagnosis	7975	0.805	<0.0001

[‡]Cutaneous diagnoses were identified based on published literature and expert opinion.

*Benjamini-Hochberg p-value of significance = 0.0025.

‡Cutaneous diagnoses were identified based on published literature and expert opinion.

*Benjamini-Hochberg p-value of significance = 0.0025.

REFERENCES

1. Puzanov I, Diab A, Abdallah K, et al. Managing toxicities associated with immune checkpoint inhibitors: consensus recommendations from the Society for Immunotherapy of Cancer (SITC) Toxicity Management Working Group. *J Immunother Cancer* 2017;**5**(1):1–28. doi:10.1186/s40425-017-0300-z.
2. Brahmer JR, Lacchetti C, Schneider BJ, et al. Management of immune-related adverse events in patients treated with immune checkpoint inhibitor therapy: American society of clinical oncology clinical practice guideline. *J Clin Oncol* 2018;**36**(17):1714–1768. doi:10.1200/JCO.2017.77.6385.
3. Phillips GS, Wu J, Hellmann MD, et al. Treatment outcomes of immune-related cutaneous adverse events. *J Clin Oncol* 2019;**37**(30):2746–2758. doi:10.1200/JCO.18.02141.
4. Petrelli F, Grizzi G, Ghidini M, et al. Immune-related adverse events and survival in solid tumors treated with immune checkpoint inhibitors: a systematic review and meta-analysis. *J Immunother*. 2020;**43**(1):1–7. doi:10.1097/CJI.0000000000000300.
5. Wongvibulsin S, Pahalyants V, Kalinich M, et al. Epidemiology and risk factors for the development of cutaneous toxicities in patients treated with immune checkpoint inhibitors: A United States population-level analysis. *J Am Acad Dermatol*. Published online 2021:1–10. doi:10.1016/j.jaad.2021.03.094.
6. Kalinich M, Murphy W, Wongvibulsin S, Pahalyants V, et al. Prediction of severe immune-related adverse events requiring hospital admission in patients on immune checkpoint inhibitors: study of a population level insurance claims database from the USA. *J Immunother Cancer*. 2021;**9**(3):e001935. doi: 10.1136/jitc-2020-001935. PMID: 33789879; PMCID: PMC8016099.

Ethics Approval Study utilized de-identified data from a multi-institutional registry and is exempt from IRB approval.

<http://dx.doi.org/10.1136/jitc-2021-SITC2021.814>

815

SINGLE-CENTER RETROSPECTIVE COHORT OF ALL PATIENTS SUSPECTED TO HAVE IMMUNOTHERAPY-MEDIATED DIARRHEA AND COLITIS

Vanya Aggarwal*, Ella LePage, Andrew Fauchoux, Hiral Patel, Gregory Russell, Eric Olson, Jared Rejeski, Thomas Lycan. *Wake Forest School of Medicine, Winston-Salem, NC, United States*

Background Immune-mediated diarrhea or colitis (IDC) is a potentially serious adverse event which can occur in up to 10% of patients receiving an immune checkpoint inhibitor (ICIs), but not all episodes of diarrhea among these patients are immune-mediated.¹ There is a paucity of research regarding the diagnosis and management of this common symptom among patients receiving an ICI.

Methods We collected retrospective clinical data for all patients who received at least one dose of an ICI for any cancer diagnosis (n=2,120) and subsequently underwent a diagnostic workup for acute diarrhea with stool testing for either *C. difficile* or a gastrointestinal pathogen panel (n=223) at any point between 1/1/13 to 3/17/21. We compared patients who had IDC “ruled out” to those who had confirmed IDC using Fisher's exact test for categorical variables and either independent samples t-test or Wilcoxon two-sample tests for interval variables. The Kaplan-Meier method was used to estimate progression-free and overall survival time. A two-sided alpha of 0.05 was utilized in determining which relationships might be significant.

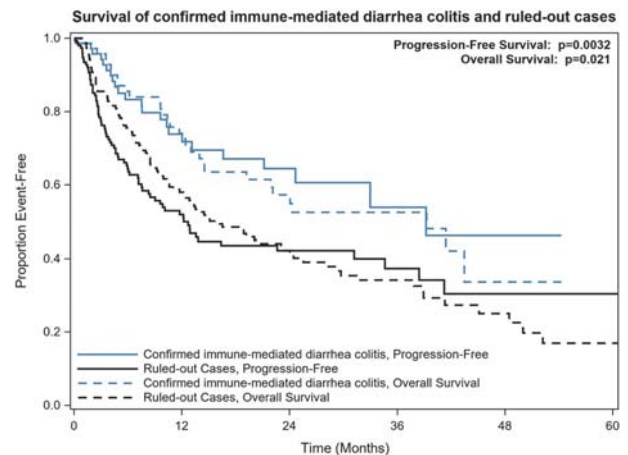
Results Thirty-seven percent had ICIs deferred upon symptom onset, and 28% received systemic steroids. Patients receiving an ICI who developed diarrhea were 2.14x more likely to have a different etiology for their symptoms (n=152, 68%) than IDC. Patients who had IDC ruled out were more likely to be female (47%, p 0.029) and have at least one comorbidity (93%, p 0.028). Patients with confirmed IDC were more likely to have peptic ulcer disease (4%, p 0.031), to have received ipilimumab (24%, p<0.0001) or >1 ICI concurrently (23%, p<0.001), and to have a shorter time since last dose of immunotherapy to onset of symptoms (12 vs. 26 days, p <0.0001). There were no differences in age, race, ethnicity, prior cancer therapies, types of other comorbidities, symptoms, presence of other adverse events, number of ICI cycles prior to symptom onset, or performance status. Progression-free survival was longer among patients with confirmed IDC (p 0.003). Overall survival was longer among patients with confirmed IDC (p 0.021) (figure 1).

Conclusions Diarrhea is often due to another etiology besides IDC, especially among patients who have onset of symptoms over 2 weeks after receiving an ICI other than ipilimumab. If ipilimumab or two ICIs are used concurrently, it is warranted to have increased suspicion for IDC especially with rapid progression of symptoms. This dataset provides additional evidence that confirmed IDC may be associated with prolonged progression-free and overall survival.

REFERENCE

1. Wang Y, Zhou S, Yang F, et al. Treatment-related adverse events of PD-1 and PD-L1 inhibitors in clinical trials: a systematic review and meta-analysis. *JAMA Oncol* 2019;5(7):1008–1019. doi:10.1001/jamaoncol.2019.0393

Ethics Approval The study was approved by Wake Forest Baptist Health Ethics Board, approval number #IRB00044126.



Abstract 815 Figure 1 Survival of confirmed IDC and ruled-out cases

<http://dx.doi.org/10.1136/jitc-2021-SITC2021.815>

SELECTIVE IMMUNE SUPPRESSION USING INTERLEUKIN-6 BLOCKADE IN IMMUNE RELATED ADVERSE EVENTS

¹Faisal Fa'ak*, ²Chrystia M. Zobniw, ²Maryam Buni, ²Linda Lu, ²Adewunmi Falohun, ²VanAnh Trinh, ²Muhammad Osama Awiwi, ²Khaled M Elsayes, ²Kaysia Ludford, ¹Maya Dimitrova, ¹Sabina Sandigursky, ³Amy Cunningham-Bussel, ³Jeffrey A. Sparks, ³Osama Abu-Shawar, ⁴Uma Thanarajasingam, ⁴Ashley M. Zeman, ⁵Rafee Talukder, ⁵Namrata Singh, ⁵Sarah H. Chung, ⁵Petros Grivas, ²May Daher, ²Ala Abudayyeh, ⁶Daniel Johnson, ²Maria Suarez-Almazor, ³Osama E. Rahma, ¹Jeffrey S. Weber, ²Jean Tayar, ²Adi Diab, ²Noha Abdel-Wahab. ¹Laura and Isaac Perlmutter Cancer Center, Mineola, NY, United States; ²The University of Texas MD Anderson Cancer Center, Houston, TX, United States; ³Brigham and Women's Hospital and Harvard Medical School, Boston, MA United States; ⁴Mayo Clinic, Rochester, NY United States; ⁵University of Washington School of Medicine, Seattle, WA United States; ⁶Louisiana State University Health Sciences Center, New Orleans, LA United States

Background Managing immune-related adverse events (irAEs) has become a critical challenge with the increasing implementation of immune-checkpoint inhibitors (ICIs) in cancer treatment. IrAEs may cause treatment interruption or discontinuation, the rate of which is higher with multi-agent ICI regimen needed to overcome resistant tumor microenvironment. Herein, we describe our clinical experience using interleukin-6 receptor antagonists (IL-6RA) to manage irAEs in cancer patients receiving ICIs.

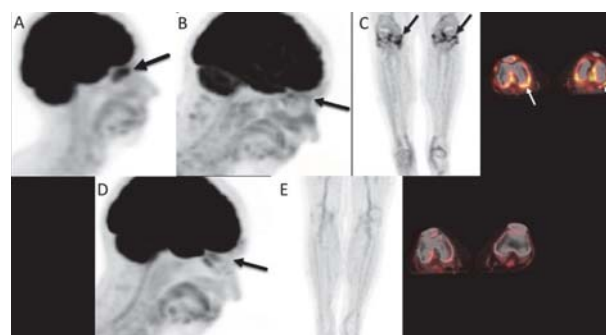
Methods We conducted a retrospective, multi-center study to evaluate the safety and efficacy of IL-6RA for irAE management. Eligible patients were identified from the institutional databases (pharmacy records, tumor registries, oncology and specialty clinic records for diagnosis and management of irAEs). The primary objective was assessing changes in irAE symptoms. The secondary objective was assessing overall response rate (ORR) before and after IL-6RA treatment.

Results A total of 81 patients received an IL-6RA (tocilizumab or sarilumab); median age was 66 years, 41% were females, 70% received single-agent anti-PD-1 and 23% received nivolumab plus ipilimumab. Cancer types were primarily melanoma (44%), genitourinary cancer (37%), and lung cancer (8.6%). Indications for using IL-6RA were inflammatory arthritis (74%), polymyalgia rheumatica (6%), myositis/myocarditis/myasthenia gravis (5%) encephalitis (5%), and 1% each with pneumonitis, colitis, hepatitis, central nervous system vasculitis, oral mucositis, and flare of pre-existing myasthenia gravis, psoriasis, and Crohn's disease. Notably, 83 % of patients received corticosteroids as first-line therapy, and 29% received disease-modifying antirheumatic drugs, without improvement. After initiation of IL-6RA, improvement of irAEs was observed in 78% after a median of 2.1 months. Of evaluable patients with inflammatory arthritis, the median clinical disease activity index (CDAI) at IL-6RA initiation was 28, indicating high disease activity, and dropped to 6 after treatment, indicating low disease activity. The median CRP level at IL-6RA initiation was 59.5 mg/L and dropped to 1.5 mg/L within 10 weeks of treatment. Seventy-two patients tolerated IL-6RA, and nine stopped treatment due to side effects. Thirty-eight patients were evaluated for tumor response by RECIST 1.1 criteria; the ORR was 58% prior to IL-6RA and 66% after treatment. Of 21 evaluable melanoma patients, the ORR was 62% prior to IL-6RA compared to 71% after treatment (figure 1).

Conclusions Our study demonstrated that targeting IL-6R could be an effective approach to mitigate autoimmunity while maintaining and possibly boosting tumor immunity. Clinical trials are currently evaluating the safety and efficacy of tocilizumab in combination with ICIs in patients with melanoma,

non-small cell lung cancer, and urothelial carcinoma (NCT04940299, NCT03999749).

Ethics Approval The study was approved by The University of Texas MD Anderson Cancer Center intuition's Ethics Board, approval number PA19-0089



Abstract 816 Figure 1 A patient with sinonasal malignant melanoma involving the ethmoid air cells. (A) Baseline maximum intensity projection (MIP) PET image at 1 month before initiation of ICI (ipilimumab and nivolumab) shows avid FDG uptake of the tumor at the ethmoid air cells (arrow). (B) MIP PET image at 7 months after ICI initiation shows resolution of the FDG uptake at the site of the tumor, consistent with complete response. (C) Concurrent MIP PET and corresponding fused PET-CT images 7 months after initiation of ICI show avid radiotracer uptake at the knee joints, suggestive of arthritis. (D) MIP PET image at 10 months after concomitant therapy with IL6R antagonist and nivolumab shows persistent absence of hypermetabolic radiotracer activity at the paranasal sinuses, consistent with complete response. (E) Concurrent MIP PET and corresponding fused PET-CT images show physiologic radiotracer uptake at the knee joints, consistent with resolving arthritis.

<http://dx.doi.org/10.1136/jitc-2021-SITC2021.816>

817

ACTIVATED OSTEOARTHRITIS FOLLOWING IMMUNE CHECKPOINT INHIBITOR TREATMENT: AN OBSERVATIONAL STUDY

¹Pankti Reid*, ²David Liew, ³Rajshi Akruwala, ⁴Anne Bass, ⁴Karmela Chan. ¹University of Chicago Medical Center, Chicago, IL, United States; ²University of Melbourne, Parkville VIC, Parkville VIC, Australia; ³SUNY Downstate Medical Center, New York, NY, United States; ⁴Hospital for Special Surgery, Weill Cornell, Chicago, IL, United States

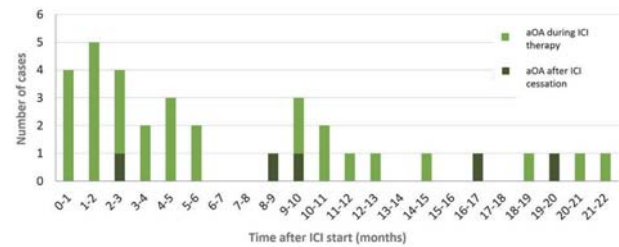
Background Immune checkpoint inhibitors (ICIs) have revolutionized cancer therapy but can result in toxicities, known as immune-related adverse events (irAEs), due to a hyperactivated immune system. ICI-related inflammatory arthritis has been described in literature, but herewith we introduce and characterize post-ICI activated osteoarthritis (ICI-aOA).

Methods We conducted a multi-center, retrospective, observational study of patients with cancer treated with ICIs and diagnosed with ICI-aOA by a rheumatologist. ICI-aOA was defined by (1) an increase in non-inflammatory joint pain after ICI initiation, (2) in joints characteristically affected by osteoarthritis and (3) lack of inflammation on exam. Cases were graded using the CTCAE (Common Terminology Criteria for Adverse Events) V6.0 rubric for arthralgia. RECIST (Response evaluation criteria in solid tumors) V1.1 (v.4.03) guidelines determined tumor response. Results were analyzed using Chi-squared tests of association and multivariate logistic regression.

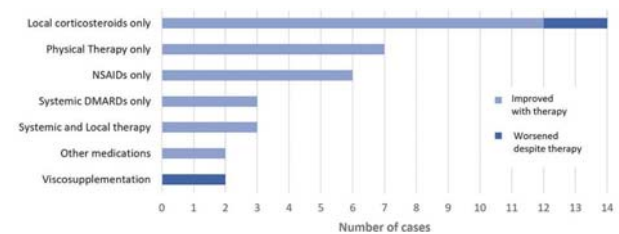
Results Thirty-six patients had ICI-aOA with mean age at time of rheumatology presentation of 66 years (51–81yrs). Most patients had metastatic melanoma (10/36, 28%) and had received a PD1/PDL1 inhibitor monotherapy (31/36, 86%) with 5/36 (14%) combination therapy. Large joint involvement (hip/knee) was noted in 53% (19/36), small joints of hand 25% (9/36), and spine 14% (5/36). Two-thirds (24/36) suffered multiple joint involvement. Three of 36 (8%) had CTCAE grade 3, 14 (39%) grade 2 and 19 (53%) grade 1 manifestations. Symptom onset ranged from six days to 33.8 months with median of 5.2 months after ICI initiation; 5 patients suffered ICI-aOA after ICI cessation (0.6, 3.5, 4.4, 7.3 and 15.4 months after ICI cessation) (figure 1). Most common form of therapy was intra-articular corticosteroid injections only (15/36, 42%) followed by NSAIDs only (7/36, 20%) (figure 2). Twenty patients (56%) experienced other irAEs, with rheumatic and dermatologic being the most common. All three patients with high-grade ICI-aOA also had another irAE diagnosis at some point after ICI initiation.

Conclusions ICI-aOA should be recognized as an adverse event of ICI immunotherapy. Early referral to a rheumatologist can facilitate the distinction between ICI induced inflammatory arthritis from post-ICI mechanical arthropathy, the latter of which can be managed with local therapy that will not compromise ICI efficacy.

Ethics Approval Collection of patient data was approved by local Institutional Review Boards at respective institutions: Hospital for Special Surgery in New York (HSS IRB # 2017–1898), University of Chicago in Chicago, Illinois (IRB150837) and Austin Health in Melbourne, Victoria, Australia (HREC/18/Austin/102).



Abstract 817 Figure 1 Incidence of ICI-aOA (activated osteoarthritis after immune-checkpoint inhibitor) ranged from the first month after ICI initiation up until month 22 after ICI initiation, with most cases occurring in the first 6 months after start of ICI. Five of 36 patients experienced ICI-aOA after ICI cessation (0.6, 3.5, 4.4, 7.3 and 15.4 months after ICI cessation), corresponding to presentation after ICI initiation as follows: 2.0, 9.6, 19.1, 8.7 and 16.1 months after ICI initiation, respectively (as denoted in darker color). ICI: Immune-checkpoint inhibitor, NSAIDs: Non-steroidal anti-inflammatory drugs, DMARDs: Disease modifying anti-rheumatic drugs



Abstract 817 Figure 2 Therapeutic option most used was local or intra-articular corticosteroid therapy, followed by conservative management with physical therapy only then NSAIDs. Most patients experienced improvement in signs and symptoms with treatment. ICI: Immune-checkpoint inhibitor, NSAIDs: Non-steroidal anti-inflammatory drugs, DMARDs: Disease modifying anti-rheumatic drugs

<http://dx.doi.org/10.1136/jitc-2021-SITC2021.817>

Machine Learning, Artificial Intelligence, and Computational Modeling

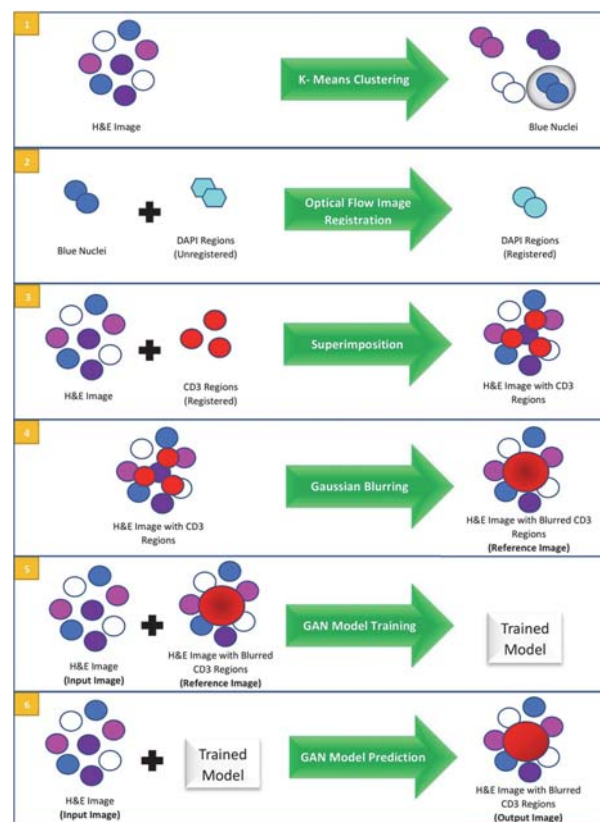
818 USING DEEP LEARNING APPROACHES WITH MIF IMAGES TO ENHANCE T CELL IDENTIFICATION FOR TUMOR -AUTOMATION OF INFILTRATING LYMPHOCYTES (TILS) SCORING ON H&E IMAGES

¹Abu Bakr Azam*, ²Yu Qing Chang, ¹Matthew Leong Tze Ker, ³Denise Goh, ³Jeffrey Chun Tatt Lim, ³Mai Chan Lau, ³Benedict Tan, ¹Lihui Huang, ³Joe Yeong, ¹Yiyu Cai. ¹Nanyang Technological University, Singapore, Singapore; ²Royal College of Surgeons in Ireland, Dublin, Ireland; ³A*Star Singapore, Singapore, Singapore

Background Examining Hematoxylin & Eosin (H&E) images using brightfield microscopes is the gold standard of pathological diagnosis as it is an inexpensive method and provides basic information of tumors and other nuclei. Complementary to H&E-stained images, Immunohistochemical (IHC) images are crucial in identifying tumor subtypes and efficacy of treatment response. Other newer technologies such as Multiplex Immunofluorescence (mIF) in particular, identifies cells such as tumor infiltrating lymphocytes (TILs) which can be augmented via immunotherapy, an evolving form of cancer treatment. Immunotherapy helps in the manipulation of the host immune response and overcome limitations like the PD-1 (Programmed Cell Death-1) receptor induced restrictions on TIL production. If the same biopsy specimen is used for inspection, the higher order features in H&E images can be used to obtain information usually found in mIF images using Convolutional Neural Networks (CNNs), widely used in object detection and image segmentation tasks.

Methods As shown in (figure 1), firstly, a novel optical flow-based image registration paradigm is prepared to co-register H&E and mIF image pairs, aided by adaptive color thresholding and automated color clustering. Secondly, generative adversarial networks (GANs) are adapted to predict TIL (CD3, CD45) regions. For this purpose, a unique dataset is ideated and used in which a given single channel mIF image, e.g., a CD3 channel mIF image is superimposed on the corresponding H&E image. Primarily, the Pix2Pix GAN model is used to predict CD3 and/or CD45 regions.

Results The intensity-based image registration workflow is fast and fully compatible with the given dataset, with an increase in evaluation metric scores after alignment (table 1). Furthermore, this study would be the first implementation of optical flow as the registration algorithm for pathological images. Next, the use of the special dataset not only reduces penalization during the training of the Pix2Pix model, but also helped in gaining repeatable results with high scores in metrics like structural similarity index measure and peak-signal to noise ratio, with minimal effects on location accuracy (table 2 and table 3).



Abstract 818 Figure 1 Proposed workflow

Abstract 818 Table 1 Image registration metrics

Method	Before Registration (mean)	After Registration (mean)
SSIM	0.591	0.778
PSNR	7.319	13.255
Correlation Ratio	0.192	0.330

Abstract 818 Table 2 CD3 negative regions examples

Sn No	Given Image	Reference and Predicted Image Heat Maps	Reference Image	Registered CD3 Regions
1				
2				

Abstract 818 Table 3 CD3 positive regions examples

Sn No	Given Image	Reference and Predicted Image Heat Maps	Reference Image	Threshold CD3 Regions
1				
2				

Conclusions This multi-modal pathological image transformation study could potentially reduce dependence on mIF and IHC images for TILs scoring, reducing the amount of tissue and cost needed for examination, as its information is derived directly from inexpensive H&E images automatically – ultimately develop into a pathologist-assisted tool for TILs scoring. This would be highly beneficial in facilities where resources are relatively limited.

Ethics Approval The Agency of Science, Technology and Research, Singapore, provided approval for the use of control tissue materials in this study IRB: 2020 112

<http://dx.doi.org/10.1136/jitc-2021-SITC2021.818>

819

RADIOMIC MARKERS ASSOCIATED WITH CLINICAL BENEFIT IN ADVANCED UVEAL MELANOMA PATIENTS WITH RADIOGRAPHIC PROGRESSION ON TEBENTAFUSP

¹Volkan Beylrigil, ²Laura Collins, ¹Lawrence Schwartz, ¹Thomas Eche, ¹Binsheng Zhao, ¹Richard Carvajal, ²Shaad Abdullah, ¹Volkan Beylrigil*, ¹Laurent Dercle. ¹Columbia University Medical Center, New York, NY, United States; ²Immunocore, Abingdon, United Kingdom

Background Tebentafusp, a bispecific fusion protein consisting of affinity-enhanced T cell receptor targeting a gp100 derived peptide fused to anti-CD3 effector, has shown overall survival (OS) benefit in untreated metastatic uveal melanoma (mUM). The OS benefit derives from all RECIST response categories, even progressive disease (PD). In Ph2 trial of previously treated mUM (NCT02570308), one-third (35%) of 48 evaluable patients with best response of PD had ctDNA reduction (≥ 0.5 log reduction) and longer OS (median 16.9 months) compared to the group without ctDNA reduction (median OS 8.5 months).

Methods 34 of 127 mUM patients from Ph2 trial¹ were selected based on best response of PD and no ctDNA reduction (Group A, n=17) or 0.5 log ctDNA reduction (Group B, n=17). One patient per group were excluded due to poor image quality or limited CT/MRI sequences. Tumor lesions were manually segmented on CT and MRI. Radiomics features were extracted at baseline and Week-8 (first assessment). The objective was to use unsupervised machine-learning to develop two signatures using 16 features to classify the two groups. The per-patient analysis signature (n=32) combined 8 volumetric features on CT-scan at baseline and change by Week-8. The per-lesion analysis signature (n=148) combined 4 features (volume and 3 radiomics features previously associated with outcome to checkpoint immunotherapy in cutaneous melanoma) at two timepoints using CT and MRI. Performance was evaluated using area under the receiver operating characteristic curve (AUC).

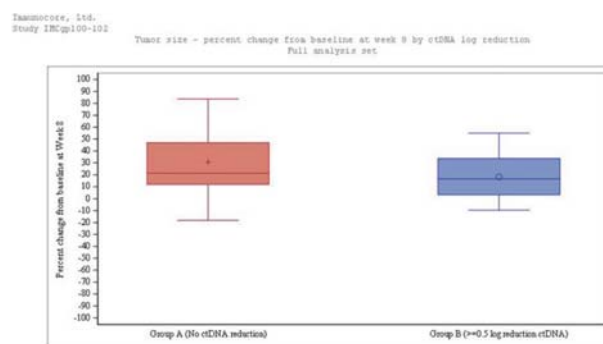
Results The median OS for Groups A and B were 8.5 and 16.9 months, respectively. In the per-patient analysis, a volumetric signature classified patients into the groups with AUC 0.71 (95%CI: 0.53–0.90) with 63% specificity and 81% sensitivity at the optimal threshold (0.57). In the per-lesion analysis, a radiomic signature reached an AUC of 0.70 (95%CI: 0.58–0.81) with 66% specificity and 74% sensitivity at the optimal threshold (0.53). Group B had lower baseline tumor lesion volume (AUC=0.65), distinct baseline tumor heterogeneity (AUC=0.66), and distinct change in tumor heterogeneity by week 8 (AUC = 0.66/0.69 on CT/MRI).

Conclusions A radiomic analyses of a subset of PD patients was able to predict Group B, patients with ctDNA reduction and longer OS, at a patient and lesion level. The strongest radiomic predictor by CT/MRI was decrease on treatment in tumor heterogeneity. Confirmation in a larger dataset of these signatures is needed to identify which patients may be benefiting from tebentafusp despite radiographic progression.

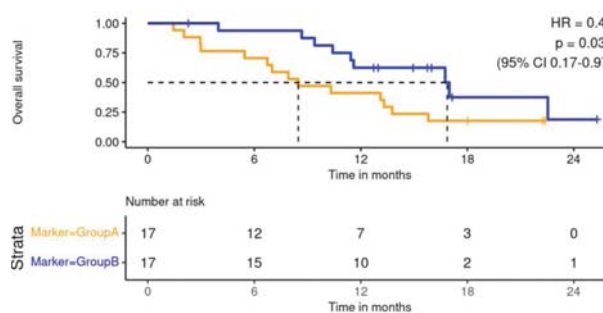
Trial Registration NCT02570308

REFERENCE

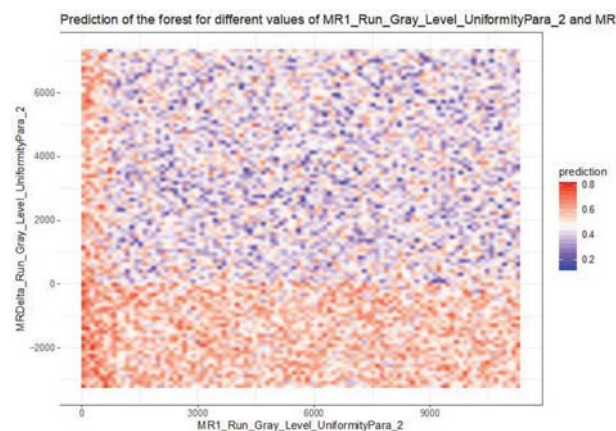
1. Sacco JJ, Carvajal R, Butler MO, et al. A phase (ph) II, multi-center study of the safety and efficacy of tebentafusp (tebe) (IMCgp100) in patients (pts) with metastatic uveal melanoma (mUM). *Ann Oncol* 2020;**31**:S1442–S1143.



Abstract 819 Figure 1 Percent change in tumor measurement from baseline at week 8 per independent review committee by Group A and B



Abstract 819 Figure 2 Kaplan-Meier plot comparing overall survival rates in group A and group B patients



Abstract 819 Figure 3 Blue color represents a high probability of the patient being in Group A while red color indicates high probability of being in Group B

<http://dx.doi.org/10.1136/jitc-2021-SITC2021.819>

**MACHINE LEARNING SIGNIFICANTLY IMPROVES
NEOANTIGEN-HLA PREDICTIONS UTILIZING > 26,000
DATA POINTS FROM THE PACTIMMUNETM DATABASE**

Vinnu Bhardwaj*, Amin Momin, Jonathan Johnston, Elizabeth Speltz, Tyler Borrman, Stefanie Mandl, Olivier Dalmás, Zheng Pan, Ashish Kheterpal, Eric Stawiski. *PACT Pharma, Inc, South San Francisco, CA, United States*

Background PACT Pharma has developed a state-of-the-art approach to validate predicted neoepitopes (neoEs) and their cognate T cell receptors (neoTCRs) by capturing neoepitope-specific T cells from peripheral blood. This neoTCR discovery and validation process is being applied in clinical trial (NCT03970382) evaluating personalized neoTCR-T cell therapy to treat patients across eight solid tumor types. Extensive pre-, on- and post-treatment data related to this trial has been accumulated in the PACTImmune Database (PIDB) which represents a growing data asset for patient-specific tumor immunogenicity in solid tumors. Here we present a specific use case of applying machine learning (ML) to significantly improve neoE-HLA predictions and further model anticipated improvements of TCR capture as a direct consequence.

Methods PACT has developed capabilities for high-throughput manufacturing of single polypeptide (comPACT protein) which consists of the predicted neoE peptide together with Beta-2-Microglobulin and the HLA heavy chain. comPACT molecules are considered successfully produced when protein yields reach concentrations >1 μ M. Data used for this study consisted of >26000 neoE-HLA predictions for 62 different HLA alleles. We applied ML to learn patterns that are predictive of neoE-HLAs that can be successfully produced as comPACTs, using scikit-learn and XGBoost. Data was first split into training and testing data. Models were trained on training data and model hyperparameters were tuned using 5-fold cross validation (5xCV). The performance of the models during 5xCV and on test data was measured using the area under the receiver operating characteristic curve (AUC). We additionally performed experimental prospective validation of the models. To do this, 603 neoE-HLAs (from 7 previously unseen cancer samples) were selected for comPACT production using netMHCpan4.1 and the newly trained models.

Results The mean AUC for the 5xCV of the selected models ranged from 0.75 to 0.86 depending upon the HLA allele (SD <0.05 for every model). The AUC on the test data ranged from 0.75 to 0.92 (median = 0.85). Prospective validation resulted on average in a 22% higher success rate (range 11%–39%) using the new models as compared to the netMHCpan4.1 predictions. This is expected to result in increased capture of neoepitope-specific CD8+ T cells as the PIDB indicates that 3.2% of the successful comPACTs result in validated neoTCRs.

Conclusions PIDB based ML predictions of neoE-HLAs led to a significant increase in TCR-capturing comPACT success rates. Because of this work, it is predicted both neoE-specific CD8+ T cell capture and actionable neoTCR options will increase per patient.

<http://dx.doi.org/10.1136/jitc-2021-SITC2021.820>

821

MACHINE LEARNING MODELS CAN QUANTIFY CD8 POSITIVITY IN LYMPHOCYTES IN MELANOMA CLINICAL TRIAL SAMPLES

¹Benjamin Glass*, ¹S Adam Stanford-Moore, ¹Diksha Meghwal, ¹Nishant Agrawal, ¹Mary Lin, ¹Cyrus Hedvat, ²George Lee, ²Scott Ely, ¹Michael Montalto, ¹Ilan Wapinski, ²Vipul Baxi, ¹Andrew Beck. ¹PathAI, Boston, MA, United States; ²Bristol Myers Squibb, Princeton, NJ, United States

Background An accurate histological characterization of immune cells in the tumor microenvironment is essential for developing novel immune oncology targeted therapies and can assist in guiding patient treatment decisions. However, immune phenotyping is subject to challenges of manual scoring and inter-pathologist scoring variability. To support pathologist-scored immune phenotyping across tumor types, we are developing machine learning (ML)-based models that can identify and quantify CD8+ lymphocytes within the stromal and parenchyma regions of tumors from non-small cell lung cancer, renal cell carcinoma, breast cancer, gastric cancer, head and neck squamous cell carcinoma, urothelial carcinoma, and melanoma. Here, we focus on the ML model for melanoma showing recent results for ML-based identification and quantification of CD8+ lymphocytes and concordance with manual pathologic assessment in data derived from clinical trials.

Methods ML algorithms were developed to quantify CD8+ lymphocytes in melanoma using 200 samples from a commercial dataset containing both primary and metastatic melanoma cases. Models were trained using the PathAI research platform on digitized whole slide images (WSI) stained for CD8 using clone C8/144b (Dako), and annotations were provided by the PathAI network of expert pathologists. Training included identification of slide artifacts, parenchyma, cancer stroma, and necrosis, as well as CD8+ lymphocytes and other CD8- cell types. Examples of melanin, such as pigmented macrophages, were added to non-CD8+ cell types. To evaluate the performance of the ML model, model-predicted CD8+ counts were compared to a consensus count from five independent pathologists for representative regions (“frames”) using the Pearson correlation. This was done in 112 held-out test frames from 90 WSI baseline samples from three clinical trials of immunotherapy treatment in individuals with metastatic melanoma. Inter-pathologist agreement among the five pathologists was also calculated.

Results ML-based quantitation of CD8 positivity in lymphocytes showed high concordance with manual pathologist consensus counts. In frames validation of CD8+ counts on the test set of WSI, there was high correlation between the ML model and pathologist consensus counts ($r=0.92$ [95% CI 0.88–0.94]). This correlation was comparable to the agreement among the five expert pathologists ($r=0.88$ [95% CI 0.85–0.91]).

Conclusions ML model-predicted CD8+ cell counts are highly concordant with pathologist scores on WSI samples from melanoma-focused clinical trials. These data demonstrate the capability of AI-powered digital pathology for accurate and reproducible quantitation of CD8+ lymphocytes in clinical trial samples, contributing to improved evaluation of the tumor microenvironment and targeted development of therapeutics.

<http://dx.doi.org/10.1136/jitc-2021-SITC2021.821>

GRAPHITE: UNSUPERVISED GRAPH EMBEDDINGS APPROACH TO MULTIPLEX IMMUNOFLUORESCENCE IMAGE EXPLORATION REVEALS NEW INSIGHTS INTO NSCLC AND HNSCC TUMOR MICROENVIRONMENT

¹Michael Surace*, ²Helen Angell, ²Christopher Innocenti, ²Zhenning Zhang, ²Isabelle Gaffney, ²Andreas Spitzmüller, ²Khan Baykaner, ²Balaji Selvaraj, ¹Medimmune Inc., Gaithersburg, MD, United States; ²AstraZeneca, Baldock, United Kingdom

Background Predictive biomarkers for response to IO therapies remain insufficient. Although multiplex immunofluorescence has the potential to provide superior biomarkers, the information garnered from these studies is frequently underleveraged. Due to the large number of markers that must be analyzed (6 - 40 +), and the complexity of the spatial information, the number of hypotheses is large and must be tested systematically and automatically. GraphITE (Graphs-based Investigation of Tissues with Embeddings) is a novel method of converting multiplex IF image analysis results into embeddings, numerical vectors which represent the phenotype of each cell as well as the immediate neighborhood. This allows for the clustering of embeddings based on similarity as well as the discovery of novel predictive biomarkers based on both the spatial and multimarker data in multiplex IF images. Here we demonstrate initial observations from deployment of GraphITE on 564 commercially-sourced NSCLC and HNSCC resections stained with a multiplex IF panel containing CD8, PDL1, PD1, CD68, Ki67, and CK.

Methods 4 µm FFPE tumor sections were stained with CD8, PDL1, PD1, CD68, Ki67, and CK at Akoya Biosciences using OPAL TSA-linked fluorophores and imaged on a Vectra Polaris. Images were analyzed by Computational Biology (AstraZeneca). Graphs were built by mapping each cell in the mIF image as a node, using the X, Y coordinates and connecting nodes with edges according to distance. 64-dimensional embeddings were generated using Deep Graph InfoMax (DGI).¹ Embeddings are downprojected to 2 dimensions using UMAP.² Details are available in the preprint of the GraphITE methods manuscript.³

Results A single downprojection was developed using embeddings from 158 HNSCC and 406 NSCLC cases. 60–80 distinct clusters were observed, some of which contained embeddings from both indications and others which were exclusive to one indication. Exclusive clusters describe tissue neighborhoods observed only in one indication. Drivers of cluster exclusivity included increased cell density in HNSCC as compared to NSCLC both in PD-L1- tumor centers with few infiltrating lymphocytes as well as in PD-L1- macrophage-dominated neighborhoods. HNSCC and NSCLC embeddings were more colocalized in PD-L1+ tumor centers and in tumor stroma with high CD8+ or CD68+ immune cell content and high PD-L1+ expression.

Conclusions This study demonstrates the utility and potential of the GraphITE platform to discriminate between and describe both unique and common neighborhood-level features of the tumor microenvironment. Deploying GraphITE across multiple indications effectively leverages spatial heterogeneity and multimarker information from multiplex IF panels.

REFERENCES

1. Veličković P, Fedus W, Hamilton WL, Liò P, Bengio Y, DevonHjelm R. Deep Graph Infomax. 2018. arxiv:1809.10341 [stat.ML].
2. McInnes L, Healy J, Melville J. UMAP: Uniform manifold approximation and projection for dimension reduction. 2020; arxiv:1802.03426 [stat.ML].
3. Innocenti C, Zhang Z, Selvaraj B, Gaffney I, Frangos M, Cohen-Setton J, Dillon LAL, Surace MJ, Pedrinaci C, Hipp J, Baykaner K. An unsupervised graph

embeddings approach to multiplex immunofluorescence image exploration bioRxiv 2021.06.09.447654; doi: <https://doi.org/10.1101/2021.06.09.447654>

Ethics Approval The study was approved by AstraZeneca.

<http://dx.doi.org/10.1136/jitc-2021-SITC2021.822>

823

SPATIAL ANALYSIS OF TUMOR-INFILTRATING LYMPHOCYTES CORRELATES WITH THE RESPONSE OF METASTATIC COLORECTAL CANCER PATIENTS TREATED WITH VACTOSERTIB IN COMBINATION WITH PEMBROLIZUMAB

¹Tae Won Kim*, ²Keun-Wook Lee, ³Joong Bae Ahn, ⁴Young Suk Park, ⁵Gahee Park, ⁵Kyunghyun Paeng, ⁵Chan-Young Ock, ⁶Hyejoo Park, ⁶Jiyeon Ryu, ⁶Bitna Oh, ⁶Bo-Kyoung Kim, ⁶Sunjin Hwang, ⁶Ki Baik Hahm, ⁶Seong-Jin Kim. ¹Asan Medical Center, University of Ulsan College of Medicine, Seoul, Korea, Republic of; ²Seoul National University Bundang Hospital, Seoul National University College of Medicine, Seoul, Korea, Republic of; ³Yonsei Cancer Center, Yonsei University College of Medicine, Seoul, Korea, Republic of; ⁴Samsung Medical Center, Sungkyunkwan University School of Medicine, Seoul, Korea, Republic of; ⁵Lunit Inc., Seoul, Korea, Republic of; ⁶MedPacto, Inc., Seoul, Korea, Republic of

Background Previously, we presented a promising anti-tumor efficacy (ORR: 16%, mOS: 15.8 months, RECIST) of the combination of vactosertib, a potent and selective TGF- β receptor I, and pembrolizumab (vac+pem) in patients with microsatellite stable metastatic colorectal cancer (MSS mCRC, MP-VAC-204 study). Recent reports showed immune-excluded TIL located in stroma would be closely related to TGF- β signature, which may harbor the primary resistance of pembrolizumab. In this study, we performed an exploratory biomarker analysis of TIL resided in either intra-tumoral or stromal area in pathology slides, and we hypothesized that spatial features of TIL would correlate with the response of vac+pem.

Methods Pathology slides stained with H&E were obtained from 31 patients at baseline and 14 patients at cycle 2 in MSS mCRC patients in MP-VAC-204 study. For spatial TIL analysis, we applied an artificial intelligence -powered H&E analyzer, named Lunit SCOPE IO, which automatically detects TIL, tumor and stroma. It calculates the proportion of immune phenotype consists of inflamed, as high TIL density inside tumor area, or immune-excluded, as high TIL density in stroma in whole-slide images. Additionally, PD-L1 and CD8 were stained using multiplex immunohistochemistry to validate immune phenotype assessed by Lunit SCOPE IO.

Results At baseline, the proportion of immune-excluded area (immune-excluded score, IES) was positively correlated with the density of CD8-positive cells in stroma area measured by mIHC (coefficient = 0.349), but it was not related to the density of PD-L1-positive cells (coefficient = -0.226). Area under receiver operating characteristics to predict the responder as partial response by RECIST v1.1 by IES and PD-L1 were 0.741 and 0.528. The overall response rate of vac+pem in the patients with high IES > 42.3% was 25% (4 out of 16), while no response was observed in those with low IES (0 out of 15). Overall survival (OS) of vac+pem was significantly prolonged in those with high IES > 42.3% compared to low IES (median OS: not reached versus 6.8 months, $P = 0.0097$), but it was not different according to PD-L1 level. After treatment of vac+pem, while IES was decreased regardless of treatment response, the proportion of inflamed area was increased in the responders ($N=3$) but decreased in the non-responders ($N=11$).

Conclusions Immune-excluded score which reflects TGF- β -driven TIL exclusion into stroma is correlated with anti-tumor response of vac+pem in MSS mCRC. Further investigation on spatial TIL analysis as a potential biomarker should be warranted. (Clinical trial information: NCT03724851)

<http://dx.doi.org/10.1136/jitc-2021-SITC2021.823>

HIGH QUALITY NEOANTIGENS ARE IMMUNOEDITED IN LONG-TERM PANCREATIC CANCER SURVIVORS

¹Zachary Sethna*, ²Marta Łuksza, ¹Luis Rojas, ³Kevin Soares, ⁴Joanne Leung, ¹Jayon Lihm, ¹David Hoyos, ¹Anton Dobrin, ¹Rajya Kappagantula, ¹Alvin Makohon-Moore, ⁵Amber Johns, ⁵Antony Gill, ¹Masataka Amisaki, ¹Pablo Guasp, ¹Abderezak Zebboudj, ⁴Rebecca Yu, ⁴Adrienne Kaya Chandra, ⁴Zagaa Odgerel, ¹Michel Sadelain, ¹Erin Patterson, ¹Christine Iacobuzio-Donahue, ¹Benjamin Greenbaum, ¹Vinod Balachandran. ¹Memorial Sloan Kettering Cancer Center, New York, NY, United States; ²Tisch Cancer Institute at Mount Sinai, New York, NY United States; ³Memorial Sloan Cancer Center, New York, NY, United States; ⁴Memorial Sloan Kettering, New York, NY United States; ⁵The Kinghorn Cancer Centre, Darlinghurst, Australia

Background Cancer immunoeediting predicts that T cells selectively kill tumor cells expressing immunogenic mutations (neoantigens) resulting in less immunogenic clones to outgrow in tumors.¹ Although established through longitudinal studies of how tumors evolve in immune-proficient and -deficient mice,¹ ² whether the human immune system naturally targets neoantigens to edit tumors, and the principles that identify the edited neoantigens, remains unclear.

Methods To investigate if immune selective pressures on neoantigens alter how human tumors evolve, we longitudinally studied how 70 human pancreatic ductal adenocarcinomas (PDACs) - a poorly immunogenic cancer largely presumed to not be subject to immunoeediting - evolved over 10 years. We use exome sequencing, neoantigen identification, and clonal reconstruction to compare how primary PDACs evolve to recurrence in rare long-term PDAC survivors previously shown to have more immunogenic tumors³ (n = 9 patients, n = 9 primary, 22 recurrent tumors), to short-term survivors with less immunogenic primary tumors (n = 6 patients, n = 6 primary, 33 recurrent tumors). To identify immunogenic “high quality” neoantigens, we use neopeptide-T cell functional assays and computational modeling to extend and apply a previously developed neoantigen quality model^{3 4} by predicting high quality neoantigens as arising from amino acid substitutions with sufficient antigenic distance from cognate wild-type peptides to differentially bind the MHC or activate a T cell.

Results Compared to short-term survivors, we observe that long-term survivors evolve fewer recurrent tumors with longer latency, and distinct tissue tropism. To evaluate if differential immune pressures explained these differences, we discover that despite longer times to evolve, long-term survivors evolve genetically less heterogeneous tumors with fewer clones, fewer nonsynonymous mutations, and fewer neoantigens. To identify if high quality neoantigens are selectively edited in recurrent tumors of long-term survivors, we observe that neoantigens with greater antigenic distance (“less self”) are more depleted in primary and recurrent tumors of long- compared to short-term survivors. Furthermore, we find that long-term survivors evolve markedly fewer new neoantigens of strikingly lower quality, to indicate clones with high quality neoantigens are immunoeedited.

Conclusions We submit longitudinal evidence that the human immune system naturally edits neoantigens in PDAC. Furthermore, we present a model that describes how cancer neoantigens evolve under immune pressure over time, with implications for cancer biology and therapy. More broadly, our results argue that immunoeediting is a fundamental cancer suppressive mechanism that can be quantified to predict tumor evolution.

Acknowledgements This work was supported by NIH U01 CA224175 (V.P.B.), a Stand Up to Cancer Convergence Award (B.D.G, V.P.B.), a Damon Runyon Clinical Investigator Award

(V.P.B), and the Avner Pancreatic Cancer Foundation (A.J, A. G). Services by the Integrated Genomics Core were funded by the NCI Cancer Center Support Grant (P30 CA08748), Cycle for Survival, and the Marie-Josée and Henry R. Kravis Center for Molecular Oncology.

REFERENCES

1. Shankaran V, et al. IFN γ and lymphocytes prevent primary tumour development and shape tumour immunogenicity. *Nature* 2001;**410**:1107–1111.
2. Matsushita H, et al. Cancer exome analysis reveals a T-cell-dependent mechanism of cancer immunoeediting. *Nature* 2012;**482**:400–404.
3. Balachandran VP, et al. Identification of unique neoantigen qualities in long-term survivors of pancreatic cancer. *Nature* 2017;**551**:512–516.
4. Łuksza M, et al. A neoantigen fitness model predicts tumour response to checkpoint blockade immunotherapy. *Nature* 2017;**551**:517–520.

Ethics Approval This study was performed in strict compliance with all institutional ethical regulations and approved by the institutional review boards of Memorial Sloan Kettering Cancer Center (MSK), the Garvan Institute of Medical Research, and the The Johns Hopkins Hospital (JHH). We obtained informed consent from all patients.

<http://dx.doi.org/10.1136/jitc-2021-SITC2021.824>

825 HIGH-DIMENSIONAL IMAGE CYTOMETRY REVEALS SPATIALLY ORGANIZED TUMOR-IMMUNE MICROENVIRONMENT IN HEPATOCELLULAR CARCINOMA

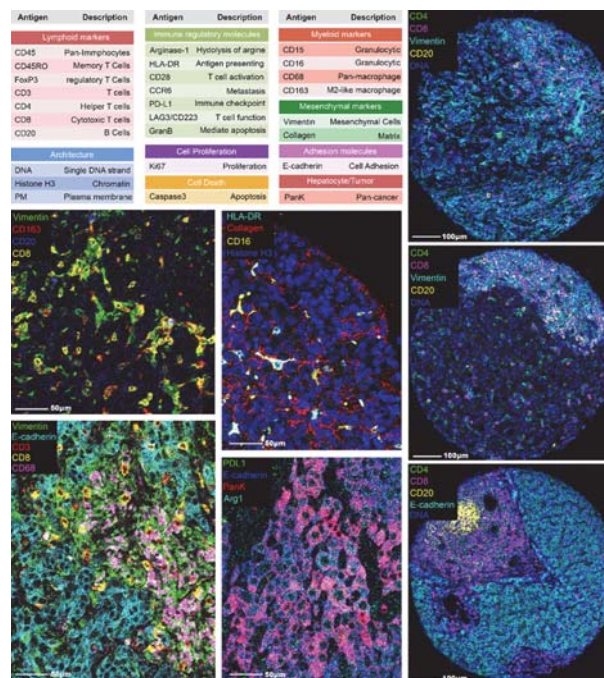
Haoyang Mi*, Aleksander Popel, Mark Yarchoan. *Johns Hopkins University Baltimore, MD, United States*

Background Structured and spatial-nuanced interactions between components in tumor microenvironment (TME) regulates the efficacy of anti-tumor regimens. Insights into this orchestrated behavior in therapeutic responders and non-responders will facilitate immunotherapies. High-multiplex imaging and spatial statistics enable deep profiling of TMEs by simultaneous arraying cell phenotypes and locations. In this study, we quantified the landscape of TMEs from neoadjuvant cabozantinib and nivolumab administered locally advanced hepatocellular carcinoma (HCC) biospecimen.

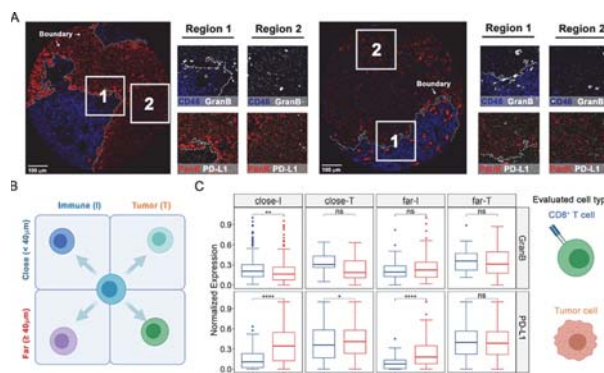
Methods 14 patients with HCC were treated with the combination of cabozantinib and nivolumab through the Johns Hopkins Sidney Kimmel Comprehensive Cancer Center. Among them, 12 patients (5 responders + 7 non-responders) underwent successful margin negative resection and are subjects to tissue microarray (TMAs) construction containing 37 representative tumor region cores. Using the TMAs, we performed imaging mass cytometry (IMC) with a panel of 27-cell lineage and functional markers (figure 1). All multiplexed images were then segmented to generate a single-cell dataset that enables (1) tumor-immune compartment analysis and (2) cell community analysis based on graph-embedding technology. Results from these hierarchies are merged to response-associated biological process patterns.

Results Image processing on 37 multiplexed images discriminated 59,453 cells and then clustered into 17 cell types. Multi-level spatial quantification revealed distinct TME arrangements across cores from responders (R) and non-responders (NR): compartment analysis showed that at immune-tumor boundaries from NR, PD-L1 level on tumor cells is significantly higher than remote regions; however, Granzyme B level is lower (figure 2B). We also identified the proximity of CD8+ T cells to a subset of macrophages – Arginase 1hi CD163- macrophages (hazard macrophage) and CD4+ T cells, is a prognostic biomarker to neoadjuvant therapy (figure 3A and 3B). In-depth cell community analysis extracted cell-cell interaction networks based on spatial proximity. Next, hierarchical clustering grouped all networks with similar components (cell types) into 8 community categories (CC). Using graph-embedding and correlation test, we observed that in NR, macrophage-enriched CC (MCC) and lymphocytes-enriched CC (LCC) are strongly communicating with tumor CC; whereas in R, such communications were weakened by the engagement between MCC and LCC (figure 3C).

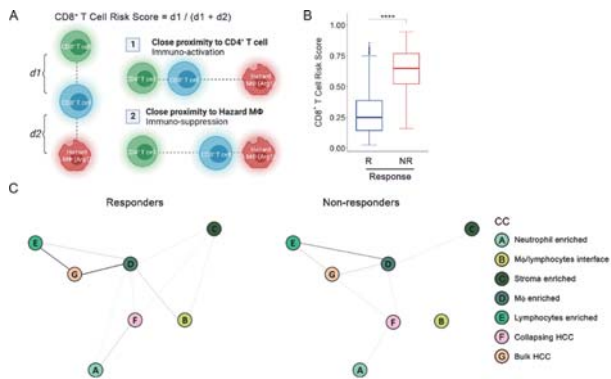
Conclusions In conclusion, we employed an unbiased, quantitative spatial analysis to determine how tumor and immune components interact in responding and nonresponding HCC tumors. Based on our results, four immune-regulating factors are derived and summarized as a communication landscape (figure 4). The proposed framework represents a novel application of multiplexed imaging in translational medicine and has potential in initialization and validation of computational immuno-oncology models.



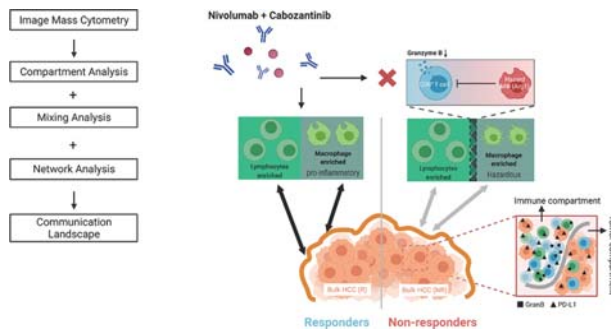
Abstract 825 Figure 1 A panel of 27 markers was used to stain the hepatocellular carcinoma tumor region cores and processed using IMC. The marker names and descriptions are included



Abstract 825 Figure 2 (A) Color overlays of lineage proteins covering Pan-Keratin and CD45 (rainbow) and functional markers covering PD-L1 and Granzyme B (white) in whole tissue core and subregions. (B) and (C) Protein expression analytical strategy. For compartmentalized cores, functional marker expressions on target cells were examined adjacent and remote to tumor-immune border and truncated to treatment response criteria for comparisons



Abstract 825 Figure 3 (A) Diagram of CD8+ T cell RiskScore. Denote each CD8+ T cell to its nearest hazard macrophages as d1 and to its nearest CD4+ T cell as d2, thus the RiskScore is formally computed by taking the proportion of d2 to the combined distance of d1 and d2. (B) RiskScore on per-cell basis for responders and non-responders. (C) Cell community communication maps in tumor microenvironment associated with responders and non-responders



Abstract 825 Figure 4 The synergistic anti-tumor immunity of macrophages and lymphocytes favors cabozantinib and nivolumab; immune function regulators (i.e., GranB and PD-L1) were upregulated throughout the immune compartment in non-responders; close proximity to hazard macrophages and distance away from CD4+ T cells associate with poorer effector function of CD8+ T cells

Acknowledgements The authors acknowledge financial support from Bristol-Myers Squibb, Exelixis, the National Cancer Institute Specialized Program of Research Excellence (SPORE) in Gastrointestinal Cancers (P50 CA062924), the Passano Foundation, the National Institutes of Health (Grant No. U01CA212007 and R01CA138264) and Emerson Collective Cancer Research Fund (640183).

Ethics Approval The studies involving human participants were reviewed and approved by Institutional Review Board of the Johns Hopkins Medical Institutions.

Consent Written informed consent for participation was not required for this study in accordance with the national legislation and the institutional requirements.

<http://dx.doi.org/10.1136/jitc-2021-SITC2021.825>

ESTABLISHING THE PRECLINICAL/TRANSLATIONAL PK/PD RELATIONSHIP FOR BT7480, A NECTIN-4/CD137 BICYCLE TUMOR-TARGETED IMMUNE CELL AGONIST™ (BICYCLE TICA™)

¹Hitesh Mistry, ¹Fernando Ortega, ¹Fernando Ortega, ²Johanna Lahdenranta, ²Punit Upadhyaya, ²Kristen Hurov, ²Phil Jeffrey, ¹Christophe Chassagnole*, ¹Physiomics plc, Oxford, United Kingdom; ²Bicycle Therapeutics, Lexington, MA, United States

Background A new class of modular synthetic drugs, termed *Bicycle* tumor-targeted immune cell agonists (*Bicycle* TICAs), based on constrained bicyclic peptides has been developed as agonists of immune costimulatory receptors in cancer therapeutics.¹ One example is BT7480 which binds simultaneously to Nectin-4 on tumor cells and CD137 on primed immune cells with activation (agonism) of CD137 being dependent on co-ligation of Nectin-4.

Methods *In vitro* CD137 reporter activity and cytokine secretion data were generated using *Bicycle* TICAs including BT7480. These *Bicycle* TICAs could display a concentration-dependent activation (e.g. CD137 activation increases IFN-gamma production) reaching a maximal activity, which then decreases as the drug concentration increases.² We developed a mathematical model to analyse this behaviour. We also modelled plasma and tumor pharmacokinetics of BT7480 in CT26-Nectin-4 tumor-bearing mice. A two-compartment model described the drug plasma profile after intravenous dosing and the tumor profile was described by a one effect compartment model. A tumor growth inhibition model for BT7480 was used to describe the preclinical data by placing the model within a mixed effect framework to estimate the population model parameters, i.e., tumor size at time 0 and tumor size growth rate, and to predict the parameter values for each mouse. We assessed how the tumor growth rate values correlate with the immune system markers collected.

Results We assessed the predictions of the *in vitro* model against the experimental observations and found that the position of the turning point could be predicted from the dissociation constants (Kd's). The combined BT7480 pharmacokinetic model shows that the elimination rate from plasma is faster than that from the tumor. We hypothesized that this results from BT7480 binding to Nectin-4 in the tumor. Also, we found that the level of tumor infiltrating CD8+ T-cells fully captures the treatment effect of BT7480 on tumor growth. Therefore, we established a likely causal link: from pharmacokinetic/dose to CD8+ T-cell infiltration changes and ultimately to tumor growth inhibition.

Conclusions A PK/PD modelling framework was developed that predicts preclinical biomarker level and tumor growth inhibition in response to changes in the BT7480 dose and dosing schedule. In addition, plasma and tumor drug concentration levels can be associated with the target concentration estimated using *in vitro* data.² Namely, the product of the square-root of the two target Kds is likely to be the free drug concentration at which maximal activity of the trimer [T-Cell—BT7480—Tumor-Cell] is achieved.

REFERENCES

1. Upadhyaya P. Anticancer immunity induced by a synthetic tumor-targeted CD137 agonist. *Journal for ImmunoTherapy of Cancer* 2021;9:e001762.
2. Perelson AS. Receptor clustering on a cell surface. III. theory of receptor cross-linking by multivalent ligands: description by ligand states. *Mathematical Biosciences* 1981;53:1–39.

<http://dx.doi.org/10.1136/jitc-2021-SITC2021.826>

STREAMLINING DESIGN OF SAFE AND EFFECTIVE TCR THERAPIES WITH AI

¹Mikolaj Mizera*, ¹Anna Sanecka-Duin, ¹Maciej Jasiński, ¹Paulina Król, ¹Giovanni Mazzocco, ¹Victor Murcia Pieńkowski, ²Alexander Myronov, ¹Iga Niemiec, ¹Piotr Skoczylas, ¹Sławomir Stachura, ¹Piotr Stępnik, ¹Daniel Wojciechowski, ¹Łukasz Grochowalski, ¹Oskar Gniewek, ¹Jan Kaczmarczyk, ¹Agnieszka Blum. ¹Ardigen, Krakow, Poland, Cracow, Poland; ²Ardigen, Krakow, Poland; Faculty of Mathematics and Information Science, Warsaw University of Technology, Warsaw, Poland, Kraków, Poland

Background Adoptive cell therapies with T lymphocytes expressing engineered T cell receptors (TCRs) are one of the most promising approaches to cancer therapy.¹ However, the experimentally driven development of novel TCR therapies is limited by the enormous biological variability of peptide: Human Leukocyte Antigen:TCR (pHLA:TCR) complexes. The in silico methods hold the promise to streamline the discovery of novel TCR therapies by reducing costs and time of laboratory research. In particular, the prediction of TCR binding to a target antigen, as well as the prediction of TCR off-target toxicity² can provide useful insights supporting the development of safe therapies. We aimed at the development of an experimentally validated AI model of pHLA:TCR binding that will help to prioritize and reduce the number of in vitro assays necessary to discover novel TCRs for cancer therapies.

Methods The limiting factor of successful pHLA:TCR binding modeling is data availability and completeness of TCR characterization. To address this issue, we are building an oncological pHLA:TCR database with paired alpha and beta chain TCR sequences. We are collecting and sequencing tumor and normal samples from 100 cancer patients, as part of an observational clinical trial. Those data are then screened with the Ardigen's ArdImmune Vax platform^{3 4} to select immunogenic epitopes. T cells that bind those epitopes are subsequently sorted and used to generate TCR sequencing data at single-cell resolution. We use data-driven and simulation-based models to extract insights about the dynamics of a pHLA:TCR system to predict the binding probability and explain the inference made by the model.

Results We optimized our data collection pipeline for the cost-efficient acquisition of a large oncological pHLA:TCR dataset. These data will enable us to build efficient models to streamline the development of TCR therapies against cancer. We benchmarked our modeling approach for pHLA:TCR binding against existing solutions⁵⁻⁷ on publicly available data. We also show how focus on model explainability facilitates the detection of model inconsistency of uncertain predictions by expert inspection. Our toxicity assessment solution² extends the applicability of our system to the prediction of TCR safety profile.

Conclusions The presented work shows perspectives and limitations of AI-aided TCR therapy development. We present results for our pHLA:TCR binding model, a TCR-toxicity-screening solution, and the study design of our observational clinical trial. Our growing database of pHLA:TCR interactions will enable us to develop highly predictive pHLA:TCR binding models, in particular for oncological targets.

Acknowledgements We acknowledge funding through the project "Creating an innovative AI-based (Artificial Intelligence) IN SILICO TECHNOLOGY TCRact to launch a NEW SERVICE for designing and optimizing T-cell receptors (TCR) for use in cancer immunotherapies" cofunded by European Regional Development Fund (ERDF) as part of Smart Growth Operational Programme 2014–2020.

REFERENCES

1. Farkona S, Diamandis EP, Blasutig IM. Cancer immunotherapy: the beginning of the end of cancer? *BMC Med* 2016;**14**:73. PMID: PMC4858828.
2. Murcia Pienkowski VA, Mazzocco G, Niemiec I, Sanecka-Duin A, Krol P, Myronov O, Skoczylas P, Kaczmarczyk J, Blum A. Off-target toxicity prediction in cellular cancer immunotherapies [Internet]. *Cytotherapy*. 2021;596. Available from: <http://dx.doi.org/10.1016/s1465324921004229>.
3. Stępnik P, Mazzocco G, Myronov A, Niemiec I, Gruba K, Skoczylas P, Sanecka-Duin A, Drwal M, Kaczmarczyk J. AI-augmented design of effective therapeutic cancer vaccines and adoptive cell therapies. *Journal For Immunotherapy Of Cancer*. Bmc Campus, 4 Crinan St, London N1 9xw, England; 2019.
4. Mazzocco G, Niemiec I, Myronov A, Skoczylas P, Kaczmarczyk J, Sanecka-Duin A, Gruba K, Król P, Drwal M, Szczepanik M, Pyrc K, Stępnik P. AI aided design of epitope-based vaccine for the induction of cellular immune responses against SARS-CoV-2. *Front Genet*. 2021;**12**:602196. PMID: PMC8027494.
5. Weber A, Born J, Rodriguez Martínez M. TITAN: T-cell receptor specificity prediction with bimodal attention networks. *Bioinformatics*. 2021;**37**(Suppl_1):i237–i244. PMID: PMC8275323.
6. Springer I, Besser H, Tickotsky-Moskovitz N, Dvorkin S, Louzoun Y. Prediction of specific TCR-peptide binding from large dictionaries of TCR-Peptide Pairs. *Front Immunol* 2020;**11**:1803. PMID: PMC7477042.
7. Jurtz VI, Jessen LE, Bentzen AK, Jespersen MC, Mahajan S, Vita R, Jensen KK, Marcatili P, Hadrup SR, Peters B, Nielsen M. NetTCR: sequence-based prediction of TCR binding to peptide-MHC complexes using convolutional neural networks [Internet]. Available from: <http://dx.doi.org/10.1101/433706>

<http://dx.doi.org/10.1136/jitc-2021-SITC2021.827>

828

QUANTIFYING PERIVASCULAR IMMUNE CELLS IN THE STROMA OF HUMAN TRIPLE NEGATIVE BREAST TUMORS USING DEEP LEARNING SPATIAL ANALYTICS

¹Anna Juncker-Jensen, ¹Nicholas Stavrou*, ²Mohammed Moamin, ¹Mate Nagy, ²Richard Allen, ²Angela Cox, ²Claire Lewis. ¹NeoGenomics, Aliso Viejo, CA, United States; ²University of Sheffield, Sheffield, United Kingdom

Background The spatial organization and density of the immune infiltrate in the tumor microenvironment, referred to as immune contexture, can yield information relevant to prognosis and prediction of response to immunotherapy in cancer. Specifically, a distinct subset of tumor-associated macrophages (TAMs) accumulate around blood vessels where they stimulate tumor angiogenesis and limit tumor responses to frontline anti-cancer therapies like irradiation and chemotherapy.

Methods In this study we leveraged the NeoGenomics MultiOmyx Multiplex Immunofluorescence platform alongside artificial intelligence (AI) based quantitative image analysis. This AI platform was ultimately used to investigate the distribution of perivascular (PV) TAMs, CD4+ and CD8+ T cells, and CD4+FOXP3+ regulatory T cells (Tregs) of 40 human triple negative breast carcinomas (TNBCs), and how this changed following neoadjuvant chemotherapy. During the multiplexing phase, eleven rounds of paired antibody staining were performed in sequence on tumor sections. After each round of staining, high resolution images were captured for regions of interests (ROIs) selected by a pathologist. We used AI models to segment and classify cells for each biomarker and classify regions as tumor cell islands (TCIs) or stroma. First, each nucleus was segmented out using a convolutional neural network combined with watershed thresholding on the DAPI (diamidino-2-phenylindole) immunofluorescent image. From the resulting nuclear segmentation mask, a pixel dilation on cells classified as non-tumor was employed to generate a cellular segmentation mask. A list of neighbours within a specified distance for each cell was generated by radially expanding from the cellular segmentation mask. Finally, cell neighbour information was combined with the marker expression information to quantify the cell clusters of interest.

Results We discovered that in the PV areas, up to 30% of PD1-LAG3-CD3+CD8+ T cells formed direct contact with both CD163+TIM3+ TAMs and CD4+FOXP3+ Tregs. Furthermore, these immune cell triads preferentially accumulated in the PV stroma regions. It is likely that close interaction with immunosuppressive TAMs and Tregs would suppress the function of T cells as they enter the PV region to reach the TCIs.

Conclusions Using an advanced analytics platform, we invented a new method to quantify clusters of cells within various regions of a tumor section. Using this platform, we detected specific immune cell triads, the frequency and location of which could correlate with the efficacy of T-cell based immunotherapies in TNBC. These analyses will enable further investigation of numerous complex cell interactions in TMEs.

<http://dx.doi.org/10.1136/jitc-2021-SITC2021.828>

829

SPATIAL ARRANGEMENT AND DENSITY OF TUMOR-INFILTRATING LYMPHOCYTES (TILS) PREDICTS RESPONSE TO IMMUNOTHERAPY IN HEAD AND NECK SQUAMOUS CELL CARCINOMA PATIENTS

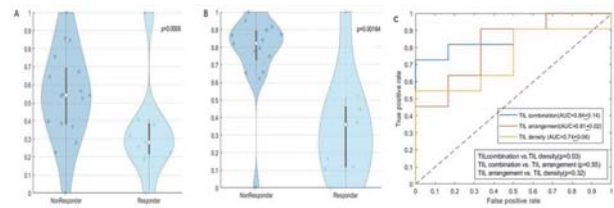
¹Reetoja Nag*, ¹Germán Corredor, ¹Vidya Viswanathan, ¹Pingfu Fu, ²James Lewis Jr, ¹Jay Wasman, ³Theodoros Teknos, ¹Monaliben Patel, ³Quintin Pan, ¹Anant Madabhushi.
¹Case Western Reserve University, Cleveland, OH, United States; ²Vanderbilt University Medical Center, Nashville, TN, United States; ³University Hospitals, Cleveland, OH, United States

Background Anti-PD-1 immunotherapies (IOs) have robust clinical benefit in a subset of head and neck squamous cell carcinoma (HNSCC) patients and is considered as a standard of care option in the recurrent/metastatic setting.¹ Previous studies showed association of higher number of lymphocytes and density of tumor-infiltrating lymphocytes (TILs) with better survival probability and prognosis in HNSCC patients.²⁻³ In this study, we evaluate whether the spatial interplay between TILs with surrounding nuclei and TIL density from digitized H&E-stained slides was associated with better immunotherapy response in HNSCC patients.

Methods Whole slide images (WSIs) from 43 HNSCC patients treated with IO at University Hospitals, Cleveland were selected. Response to immunotherapy was defined as per RECIST v1.1.⁴ Computerized algorithms identified and built clusters for nuclei of TILs and TIL density and spatial arrangement of the clusters was quantified using network graph-metrics. To assess the predictive ability of the combination of spatial arrangement and density features of TILs, a cross-validation scheme was used as follows: at each iteration, the dataset was randomly split into training (60%) and validation sets (40%). The Wilcoxon method selected top two features in the training set, then used to train a Naïve Bayes classifier to differentiate between responders and non-responders. Next, the classifier was applied to the validation set and its performance was evaluated by computing the area under the curve (AUC) for the receiver operating characteristic (ROC) curve. This process was repeated 250 times. For comparison, the same cross-validation procedure was used on (1) TIL arrangement and (2) TIL density features.

Results Figure 1(A) and 1(B) show the violin plots corresponding to the two selected top features across the cross-validation iterations for responders and non-responders. Figure 1(C) illustrates the average ROC curves for the three assessed models and corresponding AUC. The average AUCs for the model based on combination (TIL arrangement + TIL density), TIL arrangement and TIL density only yielded an average AUCs of 0.84 ± 0.14 , 0.81 ± 0.02 and 0.74 ± 0.06 respectively. After DeLong assessment of the ROC curves, significant difference was found for TIL combination vs. TIL density ($p=0.03$) whereas no significant difference was found for TIL combination vs. TIL arrangement ($p=0.55$).

Conclusions We present a predictive model based on image biomarkers i.e. spatial interplay between TILs and surrounding nuclei along with TIL density in order to distinguish HNSCC patients responding and not responding to immunotherapy. The model based on TIL combination performed better in comparison to only TIL density.



Abstract 829 Figure 1 (A) Violin plot for topmost feature 1 selected by Wilcoxon test (Feature selected from number of clusters surrounding a specific cluster type) (Responder vs. Non-responder $p=0.0006$). (B) Violin plot for topmost feature 2 selected by Wilcoxon test (Feature selected from the intersected area from the cell clusters formed from the centroids of the cell clusters) (Responder vs. Non-responder $p=0.00016$) (C) Average receiver operating characteristic curves for the 3 assessed models i.e. TIL combination (AUC= 0.84 ± 0.14), TIL arrangement (AUC= 0.81 ± 0.02) and TIL density (AUC= 0.74 ± 0.06). Significant difference between the ROC curves i.e. TIL combination vs. TIL density ($p=0.03$), TIL combination vs. TIL arrangement ($p=0.55$), TIL arrangement vs. TIL density ($p=0.32$)

REFERENCES

- Patel RR, Vladimir EB, Augustyn A, et al. De-intensification of therapy in human papillomavirus associated oropharyngeal cancer: a systematic review of prospective trials. *Oral Oncol* 2020;**103**:104608. <https://doi.org/10.1016/j.oraloncology.2020.104608>.
- Lilja-Fischer JK, Eriksen JG, Georgsen JB, et al. Prognostic impact of PD-L1 in oropharyngeal cancer after primary curative radiotherapy and relation to HPV and tobacco smoking. *Acta Oncol* 2020;**59**(6):666–672. <https://doi.org/10.1080/0284186X.2020.1729407>.
- Peled M, Onn A, Herbst RS. Tumor-infiltrating lymphocytes—location for prognostic evaluation. *Clin Cancer Res* 2019;**25**(5):1449–1451. <https://doi.org/10.1158/1078-0432.CCR-18-3803>.
- Therasse P, Arbuuck SG, Eisenhauer EA, et al. New guidelines to evaluate the response to treatment in solid tumors. *J Natl Cancer Inst* 2000;**92**(3):205–16. <https://doi.org/10.1093/jnci/92.3.205>

<http://dx.doi.org/10.1136/jitc-2021-SITC2021.829>

830

ARTIFICIAL INTELLIGENCE-POWERED SPATIAL ANALYSIS OF TUMOR-INFILTRATING LYMPHOCYTES REVEALS IMMUNE-EXCLUDED PHENOTYPE RELATED TO APOBEC SIGNATURE AND CLONAL EVOLUTION OF CANCER

¹Chan-Young Ock*, ¹Sanghoon Song, ¹Gahee Park, ²Changhee Park, ¹Soo Ick Cho, ¹Seunghwan Shin, ¹Yoojoo Lim, ¹Wonkyung Jung, ¹Heon Song, ¹Jeongun Ryu, ¹Minuk Ma, ¹Seonwook Park, ¹Sergio Pereira, ¹Donggeun Yoo, ¹Kyunghyun Paeng. ¹Lunit Inc., Seoul, Korea, Republic of; ²Seoul National University Hospital, Seoul, Kosovo, Republic of

Background Little is known about bridging clonal heterogeneity into the resistance of immune checkpoint inhibitors (ICI). Recent reports showed that excluded tumor-infiltrating lymphocytes (TIL) into stroma assessed by an artificial intelligence (AI)-powered spatial TIL analyzer, Lunit SCOPE IO, was related to loss-of-heterozygosity of HLA genes which would be one of crucial resistance pathways of ICI.¹ In the current study, we hypothesized that Immune-excluded phenotype called by Lunit SCOPE IO would be related to clonal heterogeneity resulted from genome-wide accidents during early carcinogenesis which may cause an improper targeting of TIL for diverse clones with multiple genomic aberrations.

Methods For spatial TIL analysis, we applied Lunit SCOPE IO¹ which automatically detects TIL and segmentizes cancer area and stroma, then it classified Immune phenotype of 1 mm²-sized grid in H&E image. Inflamed score or Immune-excluded score were defined as the proportion of Inflamed phenotype, which is high intra-tumoral TIL density, or Immune-excluded phenotype, which is exclusively high TIL density only in stroma, within a whole-slide image, respectively. We evaluated the correlation of Immune phenotype with APOBEC mutational signature by single-base substitution (SBS) signature 2 and/or SBS13,² whole-genome doubling, and subclonal genome fraction which reflects intra-tumoral heterogeneity,³ and clusters of T cell receptor (TCR) repertoire⁴ derived from previous reports of The Cancer Genome Atlas (TCGA), consists of 7,467 tumor samples from 22 cancer types.

high IS (spearman rho = 0.279), but it was not increased in those with high IES (spearman rho = -0.0595).

Conclusions There is a significant correlation between distinct TIL deposition in stroma, or Immune-excluded phenotype, with APOBEC-attributed clonal expansion of cancer, without proper expansion of TCR repertoire.

REFERENCES

- Ock CY, Park C, Paeng K, Yoo D, Kim S, Park S, Lee SH, Mok T, Bang YJ. Artificial intelligence-powered spatial analysis of tumor-infiltrating lymphocytes reveals distinct genomic profile of immune excluded phenotype in pan-carcinoma. *Cancer Res* 2021;**81**(Supp 13):1908.
- Alexandrov LB, Kim J, Haradhvala NJ, Huang MN, Tian Ng AW, Wu Y, Boot A, Covington KR, Gordenin DA, Bergstrom EN, Islam SMA, Lopez-Bigas N, Klimczak LJ, McPherson JR, Morganella S, Sabarinathan R, Wheeler DA, Mustonen V, PCAWG Mutational Signatures Working Group, Getz G, Rozen SG, Stratton MR, PCAWG Consortium. The repertoire of mutational signatures in human cancer. *Nature* 2020;**578**(7793):94–101.
- Taylor AM, Shih J, Ha G, Gao GF, Zhang X, Berger AC, Schumacher SE, Wang C, Hu H, Liu J, Lazar AJ, Cancer Genome Atlas Research Network, Cherniack AD, Beroukhir R, Meyerson M. Genomic and functional approaches to understanding cancer aneuploidy. *Cancer Cell* 2018;**33**(4):676–689.e3.
- Zhang H, Liu L, Zhang J, Chen J, Ye J, Shukla S, Qiao J, Zhan X, Chen H, Wu CJ, Fu YX, Li B. Investigation of antigen-specific T-Cell receptor clusters in human cancers. *Clin Cancer Res* 2020;**26**(6):1359–1371.

<http://dx.doi.org/10.1136/jitc-2021-SITC2021.830>

Abstract 830 Table 1 Correlation between immune phenotype and clonal evolution of cancer [* Median (95% confidence interval)]

		Immune-excluded score (Lunit SCOPE IO)	Inflamed score (Lunit SCOPE IO)	Immune cytolytic activity (GZMA and PRF1)
APOBEC mutational signature (SBS2 and/or SBS13)	No*	29.4% (2.94-74.4%)	17.3% (0.61-81.4%)	6.56 (3.85-9.50)
	Yes*	37.8% (5.62-77.5%)	15.8% (0.54-75.9%)	6.89 (3.85-9.63)
	Fold change	+26.0%	-8.67%	+5.03%
	P	< 2.2 x 10 ⁻¹⁶	0.00315	6.71 x 10 ⁻⁸
Whole genome-doubling	No*	29.1% (2.96-72.9%)	18.1% (0.64-80.5%)	6.71 (3.87-9.62)
	Yes*	38.3% (4.84-79.4%)	14.2% (0.74-2%)	6.73 (3.85-9.44)
	Fold change	+31.6%	-21.5%	+2.98%
	P	< 2.2 x 10 ⁻¹⁶	< 2.2 x 10 ⁻¹⁶	0.486
Subclonal genome fraction (intra-tumoral heterogeneity)	= Median*	27.2% (2.61-71.2%)	16.5% (0.45-80.2%)	6.44 (3.66-9.40)
	> Median*	38.0% (4.95-78.5%)	16.4% (0.53-77.2%)	6.91 (3.85-9.69)
	Fold change	+39.7%	-0.61%	+7.30%
	P	< 2.2 x 10 ⁻¹⁶	0.419	< 2.2 x 10 ⁻¹⁶

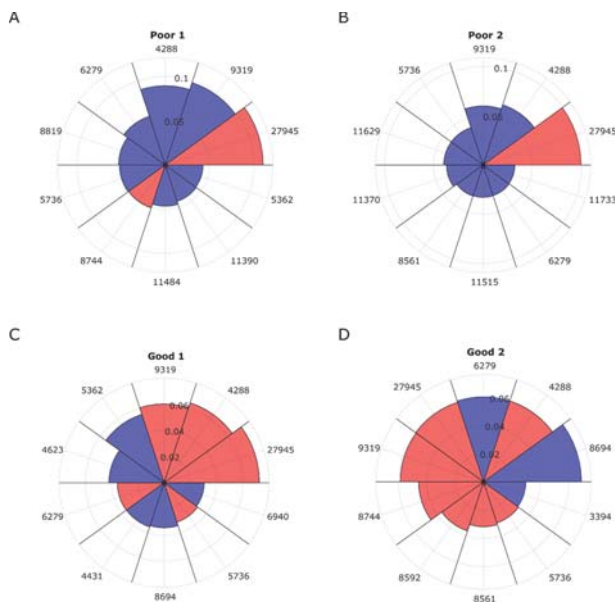
Results In the TCGA pan-carcinoma database, APOBEC mutational signature was significantly correlated with increased ratio of cancer stroma to cancer epithelium (median 0.866 vs 1.19, fold change +37.4%), and increased TIL density in cancer stroma (median 558 vs 764 / mm², fold change +36.9%), but it was not correlated with intra-tumoral TIL density (median 63 vs 59 / mm², fold change -6.3%). Interestingly, Immune-excluded score (IES) called by Lunit SCOPE IO was positively correlated with APOBEC mutational signature as well as expression levels of APOBEC1, APOBEC3A, and APOBEC3B, whole-genome doubling, and subclonal genome fraction, respectively, while Inflamed score (IS) or immune cytolytic activity (GZMA and PRF1 expressions) was negatively or not significantly correlated to those variables (table 1). TCR repertoire was expanded in the tumor samples with

831 EXACT SHAPLEY VALUES FOR EXPLAINING COMPLEX MACHINE LEARNING BASED MOLECULAR TESTS OF CHECKPOINT INHIBITORS: POTENTIAL UTILITY FOR PATIENTS, PHYSICIANS, AND TRANSLATIONAL RESEARCH

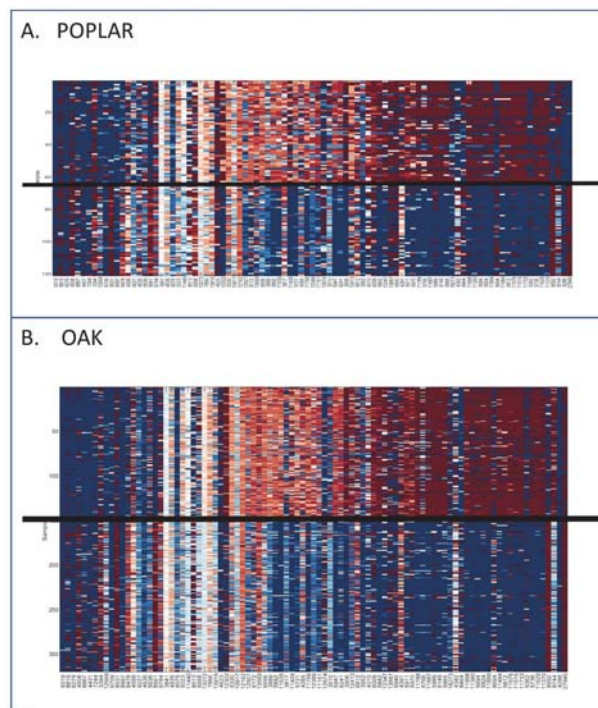
¹Heinrich Roder*, ¹Lelia Net, ²Joanna Roder, ¹Thomas Campbell, ³Mark McClelland, ⁴Wei Zou, ⁴Minu Srivastava, ⁴David Shames, ¹Laura Maguire, ¹Robert Georgantas III. ¹Biodesix, Boulder, CO, USA; ²Biodesix, Inc., Boulder, CO, USA; ³Former employee of Genentech, South San Francisco, CA, USA; ⁴Genentech, South San Francisco, CA, USA

Background Modern machine learning (ML) models based on highly multivariate attribute sets (e.g. unbiased -omics data) can be very successful at generating clinically useful predictions, but at the price of less transparency in how individual attributes are used to make those predictions. In short, ML test algorithms tend to be "black boxes". Shapley values (SVs)¹ describe the relative importance of the attributes used within a multivariate test to the generation of the test result for an individual patient.² While typically the calculation of SVs is computationally prohibitive, our ML architecture permits the generation of SVs for large patient cohorts. In this study, we evaluate SVs for the Anti-PD-L1 Response Test (ART), that was shown in independent validation to predict outcomes for patients treated with atezolizumab,³ for the POPLAR Ph2 and OAK Ph3 studies of non-small cell lung cancer (NSCLC) patients.^{4 5}

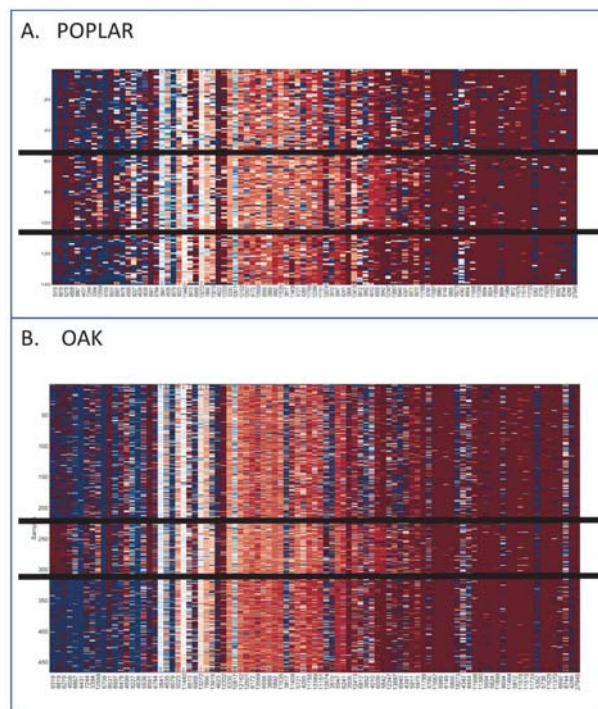
Methods ART results, Good or Poor had been produced for 262 patients in POPLAR (NCT01903993) and 786 patients in OAK (NCT02008227). Exact SVs were generated for each pretreatment serum sample for each of the 93 attributes (proteomic features) used in the test. The distribution of SVs across the cohort was investigated to assess the relative importance of each feature to test classification. Subgroups of patients with similar patterns of SVs were identified using t-sne plots and ML methods in the POPLAR cohort and validated in the OAK cohort.



Abstract 831 Figure 1 Radar plots illustrating the values of the 10 most important SVs for test classification generation for two samples classified as poor (A and B) and two samples classified as good (C and D). Positive SVs are shown in red and negative SVs are shown in blue



Abstract 831 Figure 2 Heatmaps of the SVs for samples classified as poor showing two subgroups (top and bottom, separated by horizontal line) with different patterns of SVs for (A) POPLAR and (B) OAK



Abstract 831 Figure 3 Heatmaps of the SVs for samples classified as good showing three subgroups (top, middle, and bottom, separated by horizontal lines) with different patterns of SVs for (A) POPLAR and (B) OAK

Results The SV distributions showed that the features influencing ART classification most were similar in both POPLAR and OAK. The relative importance of features to test classification differed between patients (figure 1), but subgroups of patients within test classification groups showed similar patterns of SVs (figures 2 and 3). Such patient subgroups, identified within POPLAR, were also found in the OAK cohort and were associated with differences in outcome and/or differences in patient characteristics.

Conclusions SVs can explain how complex ML-based tests combine molecular attributes to produce individual patient results. Exact SVs can be obtained for certain ML architectures used in molecular test development, revealing the overall relative importance of attributes used in such molecular tests. Subgrouping of patients with the same test classification by different patterns of SVs is possible. This may reveal different biologies contributing to a Good or Poor phenotype and inform translational studies.

Trial Registration ClinicalTrials.gov NCT01903993 and NCT02008227

REFERENCES

1. Shapley L. A value for n-person games. *Contributions to the Theory of Games*. 1953;2.28:307–317.
2. Roder J, Maguire L, Georgantas R, Roder H. Explaining multivariate molecular diagnostic tests via Shapley values. *BMC Med Inform Decis Mak* 2021;21(1):211.
3. Kowanetz M, Leng N, Roder J, et al. Evaluation of immune-related markers in the circulating proteomic and their association with atezolizumab efficacy in patients with 2L+ NSCLC. *J Immunother Cancer* 2018;6(Suppl1):114.
4. Fehrenbacher L, Spira A, Ballinger M, et al. Atezolizumab versus docetaxel for patients with previously treated non-small-cell lung cancer (POPLAR): a multicentre, open-label, phase 2 randomised controlled trial. *Lancet* 2016;387(10030):1837–1846.
5. Rittmeyer A, Barlesi F, Waterkamp D, et al. Atezolizumab versus docetaxel in patients with previously treated non-small-cell lung cancer (OAK): a phase 3, open-label, multicenter randomized controlled trial. *Lancet* 2017;389(10066):255–265.

Ethics Approval The OAK study that was done in 194 academic medical centers and community oncology practices across 31 countries worldwide. The study was done in full accordance with the guidelines for Good Clinical Practice and the Declaration of Helsinki. All patients gave written informed consent. The POPLAR trial was done at 61 academic medical centers and community oncology practices across 13 countries in Europe and North America. The study was done in full accordance with the guidelines for Good Clinical Practice and the Declaration of Helsinki. Protocol (and modification) approval was obtained from an independent ethics committee for each site. Patients gave written informed consent.

<http://dx.doi.org/10.1136/jitc-2021-SITC2021.831>

832

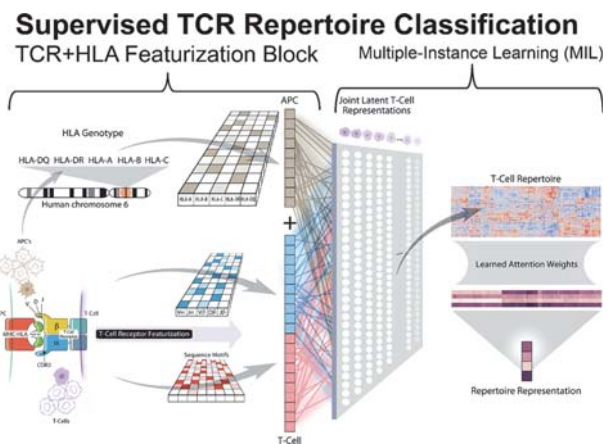
DEEP LEARNING REVEALS PREDICTIVE SEQUENCE CONCEPTS WITHIN IMMUNE REPERTOIRES TO IMMUNOTHERAPY

¹John-William Sidhom, ¹John-William Sidhom, ¹John-William Sidhom*, ²Petra Ross-Macdonald, ²Megan Wind-Rotolo, ¹Andrew Pardoll, ¹Alexander Baras. ¹Johns Hopkins University School of Medicine, Baltimore, MD, USA; ²Bristol Myers Squibb, Princeton, NJ, USA

Background Checkpoint inhibition (CPI) has changed the landscape of how oncologists treat advanced cancer^{1–6}; while there has been tremendous promise of immunotherapy, most patients do not respond to treatment.⁶ Biomarker development has grown as the field attempts to better select patients that may benefit from immunotherapy as well as further understand effective use of CPI in cancer.^{7–10} One area of interest has been studying the T-cell response through TCR-sequencing, allowing for characterization of the antigenic determinants of response.^{10–12} However, much of the work has been limited to characterizing the quantitative aspects of the TCR repertoire. Here, for the first time, we query whether there are TCR sequence concepts (i.e. motifs) that are predictive of response to immunotherapy.

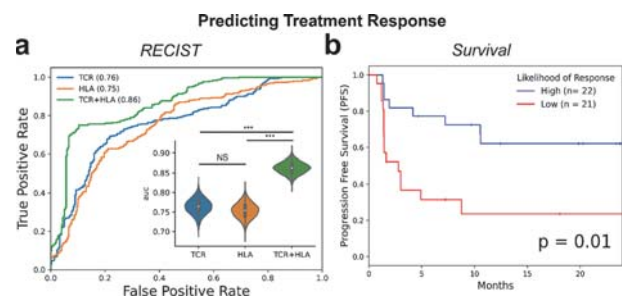
Methods We employ DeepTCR,¹³ a previously described set of deep learning algorithms, to search for sequence concepts in pre-treatment tumor samples that are predictive of effective immunotherapy in CheckMate 038 (NCT01621490), a clinical trial of CPI. We fit DeepTCR's multiple instance TCR repertoire classifier (figure 1) to predict response (via RECIST) in this cohort and assess not only the predictive performance of the model but insights into an effective antigen-specific T-cell response during CPI.

Results When applying DeepTCR to predict response, a joint representation of TCR repertoire with HLA background of the patient outperformed models that used TCR sequence or HLA genotype information alone (figure 2a). This model's predictions of likelihood to respond to treatment also significantly stratified progression free survival in this cohort of patients (figure 2b). For more qualitative descriptions of the TCR repertoire that defined an effective immune response, we used DeepTCR's variational autoencoder (VAE) to construct an unsupervised representation of the TCR sequences and highlighted the most predictive sequences for responders (blue) and non-responders (red) (figure 3 a,b). We noted that not only are the distributions within responders and non-responders multi-modal, but these multiple modes are shared between patients. When comparing the predictive signature in pre- vs post-treatment repertoires, we noted that while the responder signature remained constant over the course of treatment, the non-responder signature demonstrated changes in the TCR sequence space (figure 3 c,d).



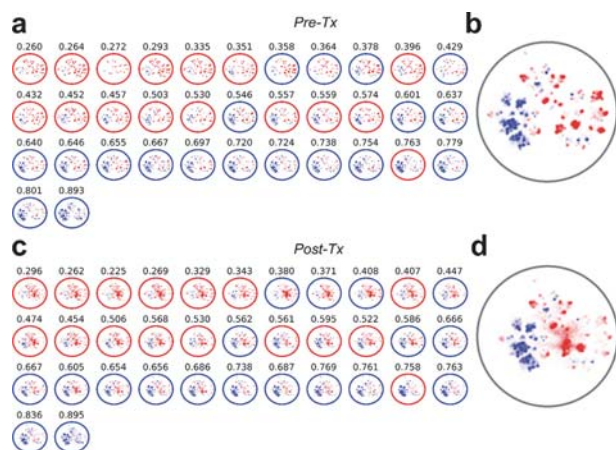
Abstract 832 Figure 1 DeepTCR's multiple instance learning repertoire classifier

We expand on previous work by modifying the DeepTCR Featurization block to incorporate the HLA background within which a given collection of TCRs were observed within. The HLA background of a sample/individual is provided to the neural network in a multi-hot representation that is re-represented in a learned continuous embedding layer and concatenated to the continuous learned representation of the TCR. As previously described, we implement a multi-head attention mechanism to make sequence assignments to concepts within the sample. The number of concepts in the model is a hyperparameter, which can be varied by the user depending on the heterogeneity expected in the repertoires. Of note, this assignment of a sequence to a concept is done through an adaptive activation function that outputs a value between 0 and 1, allowing the network to put attention on the sequences that are relevant to the learning task. When taking the average of these assignments over all the cells in a repertoire, this results in a value within the neural network that directly corresponds to the proportion of the repertoire that is described by that learned concept. These proportions of concepts in the repertoire are then sent into a final traditional classification layer.



Abstract 832 Figure 2 Repertoire classification in pre-treatment TIL. (A) Pre-treatment tumor biopsies were collected and TCR-Seq was performed from 43 patients enrolled in the CheckMate-038 (parts 2–4) clinical trial where they were either treated with anti-PD1 monotherapy (9 patients) or anti-PD1+ anti-CTLA combination therapy (34 patients) and followed for radiographic response to therapy via RECIST v1.1. Complete Responders and Partial Responders (CRPR) were denoted as responders to therapy while Stable Disease and Progressive Disease (SDPD) were denoted as non-responders to therapy. Receiver Operating Characteristics (ROC) Curves were created for predicting response (complete response, partial response) to immunotherapy given either TCR, HLA, or TCR+HLA information to the supervised repertoire classifier (100 Monte-Carlo simulations with train size: 37, test size: 6). Bootstrap analyses (5000 iterations) were performed to construct

confidence intervals (CI) around AUC values and assess differences in model performance, in which each AUC per sampling was compared in a paired manner across the three models designed above. The null hypothesis of two models exhibiting equivalent performance was rejected if the bootstrap difference did not cross 0. (***) : 99.9% CI). (B) The likelihood of response generated by the TCR+HLA model was dichotomized into "High" and "Low" using the median predicted value in this cohort (taken over the MC test sets and averaged per sample) and the Kaplan-Meier (KM) curves were shown for progression free survival (PFS), log-rank p-value = 0.005.



Abstract 832 Figure 3 Pre vs post-treatment TCR repertoire

In order to provide a descriptive understanding of the T-cell response in responders and non-responders in the CheckMate-038 clinical trial, we sought to characterize the distribution of the TCR repertoire in this cohort of patients. Data from CheckMate-038 were used to train a VAE on all sequence data (incorporating TCR+HLA information) in a sample and class agnostic fashion. The distribution of responders and non-responders repertoires were visualized via UMAP of the unsupervised VAE featurization. In order to visualize the distribution of the highly predictive TCR sequences, a per-sequence prediction value was assessed following each MC simulation on the TCRs within the independent test set, assigning the probability that a given TCR had a responder signature. Over the 100 MC simulations, each sequence in the cohort is assigned multiple prediction values that are averaged over all simulations to serve as a consensus predicted value for each sequence in this cohort of patients. Top 10% of sequences in responders and non-responders were selected and visualized over the entire cohort and on a per-sample basis where edge color denotes the ground truth label of the sample (non-responder = red, responder = blue) and average predicted likelihood taken over MC simulations to respond to treatment shown above each patient's distribution. For each pair of pre/post treatment repertoires, the repertoire-level prediction was compared for pre vs. post treatment across all trained models and the top 10% of predictive sequences in the 35 paired pre/post repertoires were visualized across all paired samples (a & c) as well as over the entire cohort (b & d). (blue = most predictive of response, red = least predictive of response)

Conclusions Taken together, these findings highlight the utility of deep learning to identify sequence features of TCR repertoire under the influence of immunotherapy and note that the pre-existing antigenic response is a key predictor of response

to treatment and the maintenance of this antigenic response is a hallmark of clinical benefit.

REFERENCES

- Sharma P, Allison JP. (2015). The future of immune checkpoint therapy. *Science* **348**(6230):56–61.
- Topalian SL, Drake CG, Pardoll DM. (2015). Immune checkpoint blockade: a common denominator approach to cancer therapy. *Cancer cell* **27**(4):450–461.
- Pardoll DM. (2012). The blockade of immune checkpoints in cancer immunotherapy. *Nature Reviews Cancer* **12**(4):252–264.
- Hodi FS, O'Day SJ, McDermott DF, Weber RW, Sosman JA, Haanen JB, ... Urba WJ. (2010). Improved survival with ipilimumab in patients with metastatic melanoma. *New England Journal of Medicine* **363**(8):711–723.
- Robert C, Thomas L, Bondarenko I, O'Day S, Weber J, Garbe C, ... Wolchok JD. (2011). Ipilimumab plus dacarbazine for previously untreated metastatic melanoma. *New England Journal of Medicine*, **364**(26):2517–2526.
- Topalian SL, Hodi FS, Brahmer JR, Gettinger SN, Smith DC, McDermott DF, ... Sznol M. (2012). Safety, activity, and immune correlates of anti-PD-1 antibody in cancer. *New England Journal of Medicine* **366**(26):2443–2454.
- Snyder A, Makarov V, Merghoub T, Yuan J, Zaretsky JM, Desrichard A, ... Chan TA. (2014). Genetic basis for clinical response to CTLA-4 blockade in melanoma. *New England Journal of Medicine* **371**(23):2189–2199.
- Rizvi NA, Hellmann MD, Snyder A, Kvistborg P, Makarov V, Havel JJ, ... Chan TA. (2015). Mutational landscape determines sensitivity to PD-1 blockade in non-small cell lung cancer. *Science* **348**(6230):124–128.
- Van Allen EM, Miao D, Schilling B, Shukla SA, Blank C, Zimmer L, ... Garraway LA. (2015). Genomic correlates of response to CTLA-4 blockade in metastatic melanoma. *Science* **350**(6257):207–211.
- Sidhom JW, Bessell CA, Havel JJ, Kosmides A, Chan TA, Schneck JP. (2018). ImmunoMap: a bioinformatics tool for T-cell repertoire analysis. *Cancer immunology research* **6**(2):151–162.
- Riaz N, Havel JJ, Makarov V, Desrichard A, Urba WJ, Sims JS, ... Chan TA. (2017). Tumor and microenvironment evolution during immunotherapy with nivolumab. *Cell* **171**(4):934–949.
- Anagnostou V, Bruhm DC, Niknafs N, White JR, Shao XM, Sidhom JW, ... Velculescu V E. (2020). Integrative tumor and immune cell multi-omic analyses predict response to immune checkpoint blockade in melanoma. *Cell Reports Medicine* **1**(8):100139.
- Sidhom JW, Larman HB, Pardoll DM, Baras AS. (2021). DeepTCR is a deep learning framework for revealing sequence concepts within T-cell repertoires. *Nature communications* **12**(1):1–12.

Ethics Approval CheckMate 038 (NCT01621490) is a BMS-sponsored, multi-center, institutional-review-board-approved, phase 1 biomarker study of nivolumab, ipilimumab, and nivolumab in combination with ipilimumab in patients with advanced melanoma.

<http://dx.doi.org/10.1136/jitc-2021-SITC2021.832>

833

A SCALABLE DEEP LEARNING FRAMEWORK FOR RAPID AUTOMATED ANNOTATION OF HISTOLOGIC AND MORPHOLOGIC FEATURES FROM LARGE UNLABELED PAN-CANCER H&E DATASETS

David Soong*, David Soong, David Soong, Anantharaman Muthuswamy, Clifton Drew, Nora Pencheva, Maria Jure-Kunkel, Kate Sasser, Hisham Hamadeh, Suzana Couto, Brandon Higgs. *Genmab, Plainsboro, NJ, USA*

Background Recent advances in machine learning and digital pathology have enabled a variety of applications including predicting tumor grade and genetic subtypes, quantifying the tumor microenvironment (TME), and identifying prognostic morphological features from H&E whole slide images (WSI). These supervised deep learning models require large quantities of images manually annotated with cellular- and tissue-level details by pathologists, which limits scale and generalizability across cancer types and imaging platforms. Here we propose a semi-supervised deep learning framework that automatically annotates biologically relevant image content from hundreds of solid tumor WSI with minimal pathologist intervention, thus improving quality and speed of analytical workflows aimed at deriving clinically relevant features.

Methods The dataset consisted of >200 H&E images across >10 solid tumor types (e.g. breast, lung, colorectal, cervical, and urothelial cancers) from advanced disease patients. WSI were first partitioned into small tiles of 128 μ m for feature extraction using a 50-layer convolutional neural network pre-trained on the ImageNet database. Dimensionality reduction and unsupervised clustering were applied to the resultant embeddings and image clusters were identified with enriched histological and morphological characteristics. A random subset of representative tiles (<0.5% of whole slide tissue areas) from these distinct image clusters was manually reviewed by pathologists and assigned to eight histological and morphological categories: tumor, stroma/connective tissue, necrotic cells, lymphocytes, red blood cells, white blood cells, normal tissue and glass/background. This dataset allowed the development of a multi-label deep neural network to segment morphologically distinct regions and detect/quantify histopathological features in WSI.

Results As representative image tiles within each image cluster were morphologically similar, expert pathologists were able to assign annotations to multiple images in parallel, effectively at 150 images/hour. Five-fold cross-validation showed average prediction accuracy of 0.93 [0.8–1.0] and area under the curve of 0.90 [0.8–1.0] over the eight image categories. As an extension of this classifier framework, all whole slide H&E images were segmented and composite lymphocyte, stromal, and necrotic content per patient tumor was derived and correlated with estimates by pathologists ($p < 0.05$).

Conclusions A novel and scalable deep learning framework for annotating and learning H&E features from a large unlabeled WSI dataset across tumor types was developed. This automated approach accurately identified distinct histomorphological features, with significantly reduced labeling time and effort required for pathologists. Further, this classifier framework was extended to annotate regions enriched in lymphocytes, stromal, and necrotic cells – important TME contexture with clinical relevance for patient prognosis and treatment decisions.

<http://dx.doi.org/10.1136/jitc-2021-SITC2021.833>

834 A ROBUST DEEP LEARNING APPROACH FOR PRECISELY SEGMENTING CELLS IN MULTIPLEX TISSUE IMAGES

¹Daniel Winkowski, ¹Jeni Caldara, ¹Brit Boehmer, ²Regan Baird*. ¹Visiopharm, Westminster, CO, USA; ²Visiopharm Corp, Roanoke, VA, USA

Background Multiplex images are becoming pivotal in tissue pathology because they provide positional location and multi-dimensional phenotype of every cell. The heterogeneity of cells, morphologies, and densities makes the identification of the millions of cells in a tissue slice challenging. There is an urgent need for a robust, yet flexible, algorithm to automatically demarcate each cell that accurately defines cellular boundaries. We have developed a method to extend a DL nuclear identification algorithm beyond the nucleus and to the outer boundary of the cell using biological signals from multiplex panels.

Methods All image analysis was performed in the Visiopharm image analysis platform. Three human observers provided ground truth (GT) annotations by outlining cells in predefined areas each containing ~30 cells in six different images from two different multiplex instruments: mIF = 8-plex via Vectra Polaris from Akoya and IMC = 13-plex via Hyperion from Fluidigm. Images were subsequently segmented by different AI methods: Machine Learning Nuclear Detection (ML), Deep Learning Nuclear Detection (DL), and DL that incorporates biological signals (DL+). Each set of computer-generated annotations was compared to GT using common evaluation metrics DICE, Precision and Sensitivity.

Results Overall, we found a high degree of concordance between the computer-generated and human annotations (DICE = 0.73 ± 0.08 , $n=12$) and between imaging modalities (mIF: 0.76 ± 0.07 ; IMC: 0.71 ± 0.08 ; $n=6$). Comparison of DICE scores for the AI methods indicated a superior delineation of cell boundaries using the DL+ method (DL+: 0.79 ± 0.07 ; ML: 0.74 ± 0.08 ; DL: 0.74 ± 0.03). Precision, which compares true vs false positive annotated regions to GT, was also high for all images (0.77 ± 0.11) (mIF: 0.76 ± 0.10 ; IMC: 0.78 ± 0.11). Sensitivity, which compares true positives vs false negative annotated regions GT, was also high for all images (0.77 ± 0.09) (mIF: 0.76 ± 0.09 ; IMC: 0.79 ± 0.09).

Conclusions We developed a flexible DL based strategy that enables the most comprehensive segmentation of cells in multiplex tissue images. Each AI approach shows a high concordance with segmentation annotations from human observers as measured by the industry standards DICE, Precision and Sensitivity. The DL+ method did achieve the highest DICE score indicating a more accurate delineation of cell boundaries. Expectedly, precision and sensitivity metrics are similar between all methods while DICE Coefficient better accounts for the annotations at the cell edge. The DL+ cell segmentation algorithm will yield an improved accuracy when phenotyping cells in downstream analysis as the precise biomarker composition is more accurately contained within each cell.

<http://dx.doi.org/10.1136/jitc-2021-SITC2021.834>

Microbiome and Other Environmental Factors

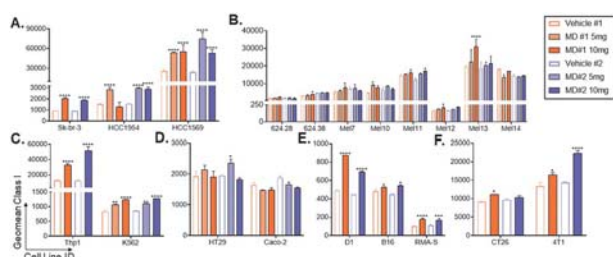
835 HARNESSING THE MICROBIOTA TO INCREASE RESPONSE RATES TO IMMUNOTHERAPY

¹Valentina Ferrari*, ²Alessia Melacarne, ³Francesca Algieri, ²Maria Rescigno. ¹Humanitas University, Milan, Italy; ²Humanitas Clinical and Research Center, Pieve Emmanuele, Italy; ³Postbiotica, Pieve Emmanuele, Italy

Background Tumor cell clearance by cytotoxic T lymphocytes (CTL) requires expression of relevant antigens on HLA Class I molecules on the surface of tumor cells. Reduced levels of HLA Class I expression is a common method of immune escape, as it hampers tumor-specific CTLs' ability to detect, recognize, and eliminate tumor cells. Recent data have shown that gut microbiota have a major impact on the clinical response to immune checkpoint inhibitors (ICIs), which could be due to a direct effect on malignant cells. Our hypothesis is that microbiota can influence the immune response by altering HLA Class I expression on tumor cells.

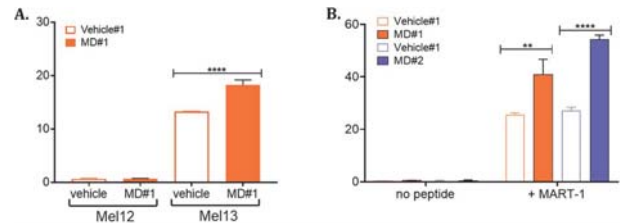
Methods To investigate the ability of bacteria-based products to upregulate HLA Class I expression, we tested two different proprietary microbial derivatives (MDs) on multiple murine and human tumor primary and immortalized cell lines from various tissues, including: breast, myeloid, melanoma, and colon. We next examined if the change in HLA expression was functional by measuring activation levels and cytotoxic capacity of MART-1-specific CTLs following tumor cell treatment with MDs. Lastly, we administered MDs intra-peritoneally in 4T1-bearing Balb/c mice to sensitize 4T1 tumors to combination treatment with anti-PD-1 ICI.

Results Our results to date show that *in vitro* treatment with MDs can upregulate surface HLA, albeit not uniformly across all tumor types, with breast and myeloid tumor cells showing the largest increase across the cell lines tested (figure 1). The MD-dependent HLA increase subsequently boosted CTL recognition of tumor cells without increasing background reactivity. The increased CTL degranulation correlated to the tumor cells' increased surface HLA expression and was consistent whether the antigen was endogenous (5% increase, $p < 0.0001$, figure 2A) or added exogenously (15%–30% increase, $p < 0.01$ and $p < 0.0001$ figure 2B). In combination with anti-PD-1 *in vivo*, MD treatment significantly abrogated tumor growth when compared to anti-PD-1 combined with the vehicle control ($p < 0.0001$, figure 3A) and tumors harvested from MD-treated mice expressed higher levels of MHC Class I compared to the vehicle control cohort ($p < 0.05$, figure 3B). Additionally, splenocytes from MD-treated mice showed increased recognition of 4T1 tumor cells when re-challenged *in vitro* (10% increase in $CD8^+41BB^+$ cells, $p < 0.0001$, figure 3C).

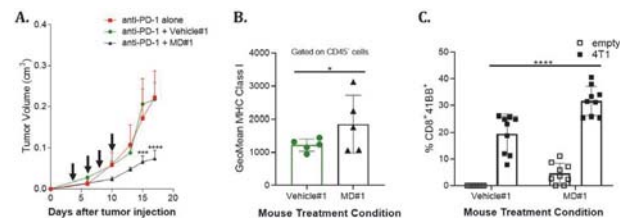


Abstract 835 Figure 1 Class I surface expression after MD treatment. (A) breast (B) colon (C) melanoma and (D) myeloid human cancer cell

lines were incubated with 5 (light bars) or 10 (dark bars) mg/mL MD#1, MD#2, and 10 mg/mL respective vehicle control (empty bars). (E) and (F) were treated with 10 mg/mL (dark bars) MD#1, MD#2, or respective vehicle controls (empty bars). After 48 hours, HLA Class I (A-D), H-2k^b (E), and H-2k^d (F) surface expression was measured by flow cytometry. Experiments repeated at least in duplicate. Statistical analysis by 2-way ANOVA, * $p < 0.05$, ** $p < 0.01$, *** $p < 0.001$, **** $p < 0.0001$.



Abstract 835 Figure 2 Antigen-specific CTL activation. Tumor cells were pre-treated for 48 hours with 10 mg/mL vehicle or MD, then washed and co-cultured for 5 hours with MART-1 specific CTL. A) primary HLA-A2⁺ melanoma cells that are negative (Mel12) or positive (Mel13) for the MART-1 antigen, and B) Thp1 loaded or not with MART-1 peptide. $CD8^+CD107a^+$ cells measured by flow cytometry. Experiments repeated in triplicate, statistical analysis by two-way ANOVA.



Abstract 835 Figure 3 *In vivo* treatment with MD. Fifteen 6-week-old Balb/c mice were subcutaneously inoculated with 1.5×10^5 4T1 tumor cells and divided into 3 treatment groups on day 3 based on equivalent tumor size. Mice were treated with 250 μ g microbial derivatives (MD#1) or vehicle control (vehicle #1) in combination with anti-PD-1 (200 μ g; clone 29F.1A12) starting on day 3 and continued every other day for a total of 4 injections (black arrows). (A) Tumor measurements were taken every other day using a caliper and volume calculated using the formula: tumor volume = (length x width²) ÷ 2 (B) 2×10^5 splenocytes were co-cultured 1:1 with 4T1 tumor cells *in vitro* and T cell activation (percent $CD8^+41BB^+$) was measured by flow cytometry. Experiment repeated in duplicate, statistical analysis by 2-way ANOVA (* $p < 0.05$, ** $p < 0.01$, *** $p < 0.001$, **** $p < 0.0001$).

Conclusions Our results thus far confirm that our proprietary MDs can increase HLA expression on tumor cells, and that this can lead to increased recognition by antigen-specific CTL both *in vitro* and *in vivo*. This suggests that MDs could be explored in combination with ICIs to enhance clinical anti-cancer immune responses.

<http://dx.doi.org/10.1136/jitc-2021-SITC2021.835>

836

MURINE FECAL MICROBIOTA TRANSFER MODELS COLONIZE HUMAN MICROBES SELECTIVELY AND REVEAL TRANSCRIPTIONAL PATHWAYS ASSOCIATED WITH RESPONSE TO NEOADJUVANT CHECKPOINT INHIBITORS

¹Fyza Shaikh*, ¹Joell Gills, ²Fuad Mohammad, ³James White, ²Courtney Stevens, ²Hua Ding, ²Juan Fu, ²Ada Tam, ²Richard Blosser, ²Tatianna Larman, ²Jarushka Naidoo, ²Patrick Forde, ²Sudipto Ganguly, ²Franck Housseau, ²Drew Pardoll, ²Cynthia Sears. ¹Johns Hopkins School of Medicine, Baltimore, MD, USA; ²Johns Hopkins University School of Medicine, Baltimore, MD, USA; ³Resphera, Baltimore, MD, USA

Background Human gut microbial species found to associate with clinical responses to immune checkpoint inhibitors (ICIs) are often tested in murine models using fecal microbiota transfer (FMT), wherein tumor responses in recipient mice may recapitulate human responses to ICI treatment. However, many FMT studies have reported only limited methodological description, including identification of colonizing species associated with murine outcomes, details of murine cohorts, and statistical methods. Thus, the reproducibility and robustness of ICI murine models remain uncertain.

Methods To investigate gut microbial species that impact ICI responses, we performed human to germ-free (GF) mouse FMT using pre-treatment stools from a pathologic lung cancer responder (R) and a pathologic lung cancer non-responder (NR) after neoadjuvant anti-PD-1 and anti-CTLA4 treatment, followed by implantation of the mice with syngeneic tumors and anti-PD-L1 treatment. Cohorts of GF mice varied by sex, age and syngeneic cell line implanted. To identify relevant microbes, murine tumor progressors (MT-P) and non-progressors (MT-NP) to anti-PD-L1 were classified based on tumor growth curves, 16S rRNA sequencing of human and mouse stools was performed, and data was statistically corrected for mouse characteristics using a generalized linear model. RNA sequencing was performed to assess transcriptional changes in murine tumors.

Results R-FMT mice yielded a greater anti-tumor response in combination with anti-PD-L1 treatment compared to NR-FMT, although the magnitude varied depending on the mouse cell line, sex, and individual experiment. Microbiota analysis revealed a shared presence of the most highly abundant taxa between the human inocula and mice, however low abundance human taxa colonized mice more variably after FMT. Multiple *Clostridium* species correlated with tumor outcome in individual anti-PD-L1-treated R-FMT mice. RNAseq analysis revealed differential expression of T cell and NK cell-related pathways in responding tumors, irrespective of FMT source, and enrichment of these cell types were confirmed by immunohistochemistry.

Conclusions This study identifies several human intestinal microbial species that may play a role in clinical responses to ICIs and suggests attention to biological variables is needed to improve reproducibility and limit variability across experimental murine models.

Ethics Approval All studies in this abstract have been approved by Johns Hopkins University Animal Care and Use and Johns Hopkins Medicine Institutional Review Board.

<http://dx.doi.org/10.1136/jitc-2021-SITC2021.836>

837

PRELIMINARY INSIGHTS INTO THE IMPACT OF TUMOR MICROBIOME IN HEAD AND NECK SQUAMOUS CELL CARCINOMA

¹Vidhya Karivedu*, ²Rebecca Hoyd, ³Caroline Wheeler, ¹Sachin Jhavar, ¹Priyanka Bhateja, ¹Marcelo Bonomi, ³Daniel Spakowicz. ¹The Ohio State University Wexner Medical Center, Columbus, OH, USA; ²The Ohio State University College of Medicine, Columbus, OH, USA; ³The Ohio State University, Columbus, OH, USA

Background Head and neck squamous cell carcinoma (HNSCC) is a heterogeneous set of distinct malignancies. Recognized prognostic factors rely on clinical and biological features, consisting mainly of stage, site of disease, performance status, comorbidities, smoking history and human papilloma virus (HPV) status. However, patients clustered by these parameters still differ in their clinical behavior and therapy response. The impact of the tumor microbiome on human disease has been explored and discussed extensively. Evaluating the tumor microbiome is a promising new approach that could be used as a prognostic and predictive tool in HNSCC, with the potential for improved treatment options and better clinical outcomes.

Methods We utilized The Cancer Genome Atlas (TCGA) database to obtain RNA sequencing (RNAseq) data to identify microbes in HNSCC samples. We utilized ExoTIC, "Exogenous sequences in Tumors and Immune cells," a tool recently developed by Spakowicz et al. ExoTIC takes raw RNAseq reads and carefully aligns them to both human and non-human reference genomes to identify low-abundance microbes. We performed Cox proportional hazards regression to identify the microbes associated with overall survival (OS), controlling for age, stage, and smoking status.

Results We evaluated 498 RNAseq samples from TCGA (table 1). ExoTIC identified 5838 microbes including bacteria, viruses and fungi, of which 330 were statistically associated with OS. Interestingly, 20% (n=100) of samples had HPV virus which was significantly associated with improved OS (HR 0.59, CI 0.4–0.9, p<0.01). There were also several other viruses and bacteria associated with significantly improved OS.

microbial profile of HNSCC subtypes with clinical outcomes retrospectively and prospectively.

<http://dx.doi.org/10.1136/jitc-2021-SITC2021.837>

Abstract 837 Table 1 Patient characteristics of TCGA dataset

Overall	
n	498
Age (mean (SD))	61.08 (11.92)
Sex = male (%)	366 (73.3)
Cancer Stage (%)	
Stage I	19 (3.9)
Stage II	94 (19.4)
Stage III	102 (21)
Stage IV	270 (55.7)
Primary Site (%)	
Oral cavity	108 (21.6)
Oropharynx	74 (15)
Hypopharynx	9 (1.8)
Larynx	111 (22.2)
Other	196 (39.3)
Vital Status = Deceased (%)	218 (43.7)

Conclusions We found the presence of certain microbes in tumor biopsies statistically correlated with OS in HNSCC patients. This supports further study into the presence and correlation of specific microbes with tumor subsite and outcomes. Assessing individual characteristics of a HNSCC subtype with its particular microenvironment (e.g., microbes) can lead to personalized treatment insights and improved outcomes. Our future research will validate and correlate the

838

THE ROLE OF MICROBIOTA IN METASTATIC BRAIN TUMORS

Sarah Johnson, Golnaz Morad*, Nadim Ajami, Jennifer Wargo, Matthew Wong, Matthew Lastrapes. *UT MD Anderson Cancer Center, Houston, USA*

Background Despite the substantial advances in the treatment of systemic cancer, brain metastases are still responsible for significant morbidity and mortality, necessitating a better understanding of the mechanisms underlying this disease. Microbiota has emerged as a significant hallmark of cancer. Our group and others have demonstrated a prominent role for gut and intratumoral microbiota in tumorigenesis, tumor immunity, and response to treatment. However, the role of microbiota in brain metastasis is poorly understood. We hypothesize that distinct microbial communities can alter the immune microenvironment in the brain and modulate the different steps of brain metastasis formation.

Methods To explore the role of microbiota in brain metastasis, we evaluated the gut and oral microbial signatures in brain metastasis patients through shotgun metagenomics sequencing. Furthermore, we conducted mechanistic *in vivo* studies in which the gut microbiota was depleted in conventionally raised mice using a broad-spectrum non-absorbable antibiotic regimen. Subsequently, melanoma tumor cells were injected intracranially to evaluate the effect of gut microbiota depletion and associated immune changes on tumor growth. Tumor growth was measured through *in vivo* bioluminescent imaging and histology. Peripheral and tumor immune profiling was conducted through flow cytometry and immunohistochemistry.

Results Our clinical studies demonstrated the enrichment of distinct bacterial and viral taxa within the gut and oral microbiota in brain metastasis patients. Depletion of the gut microbiota in mice decreased tumor growth in the brain. Evaluation of the peripheral and tumor immune profiles suggested the underlying mechanisms to involve alterations in the circulating cytokine profiles and an increase in anti-tumor T cell activity.

Conclusions Our clinical studies suggest the association of distinct microbial communities with brain metastasis. Our pre-clinical findings demonstrate that the absence of gut microbiota can modulate the regulation of T cell activity to induce an anti-tumor response in the brain. Further studies, currently in progress, will determine the mechanistic role of dysbiotic microbiota and distinct microbial communities in this process.

Acknowledgements This work was supported by the National Institute of Health (1F32CA260769-01).

<http://dx.doi.org/10.1136/jitc-2021-SITC2021.838>

MICROBIOTA-SPECIFIC T FOLLICULAR HELPER CELLS DRIVE TERTIARY LYMPHOID STRUCTURE FORMATION AND ANTI-TUMOR IMMUNITY IN COLORECTAL CANCER

Abigail Overacre-Delgoffe*, Hannah Bumgarner, Anthony Cillo, Ansen Burr, Justin Tometich, Amrita Bhattacharjee, Tullia Bruno, Dario Vignali, Timothy Hand. *University of Pittsburgh, Pittsburgh, PA, USA*

Background Colorectal cancer (CRC) is one of the most common and deadly cancers in the US, and the survival rate for advanced cases is poor. While immunotherapy has revolutionized cancer treatment, CRC remains largely unresponsive, with only ~6% of patients responding to anti-PD1. Specific microbiome signatures are associated with anti-PD1 response in melanoma patients; however, the underlying mechanism remains unclear. While the microbiome in cancer patients has been extensively studied, the endogenous immune response to these microbes and the subsequent effects on cancer immunity remain unstudied. Most microbes reside within the gut, and bacteria that adhere to the intestinal epithelium can stimulate bacteria-specific immune responses. Therefore, we hypothesized that the microbiome, especially adherent, immunogenic bacteria, may support anti-tumor immunity through activation of local microbiota-specific T cells.

Methods Using a carcinogen-induced mouse model of CRC, we sought to determine the impact of microbiome modulation on the anti-tumor immune response. We colonized tumor-bearing mice with *Helicobacter hepaticus* (Hhep) and assessed tumor burden, survival, and immune infiltration. Lymphocytes were isolated from the tumor and surrounding tissue when tumors were terminal (12 weeks). We utilized TCR transgenic mice and MHC class II tetramers to track the spatial and transcriptional Hhep-specific T cell response through 5' single cell RNAseq, flow cytometry, and spectral immunofluorescence.

Results Hhep colonization in tumor-bearing mice led to decreased tumor burden and significantly improved survival. Interestingly, colonization induced activation of Hhep-specific T follicular helper cells (TFHs) that supported formation of mature peri- or intra-tumoral tertiary lymphoid structures (TLS). The presence of TLS led to increased infiltration of cytotoxic lymphocytes (T and NK cells) within the tumor core. Surprisingly, the anti-tumor response was dependent on CD4+ T and B cells but not CD8+ T cells. Using TFH KO mice, we found that Hhep-specific CD4+ T cells were both necessary and sufficient to drive TLS maturation and anti-tumor immunity.

Conclusions Here, we demonstrate that addition of a single bacterial species after tumor formation leads to a reduction in CRC tumor burden and increased survival through TLS maturation. This microbiome-dependent remodeling of the tumor microenvironment is driven by Hhep-specific TFH cells that are both necessary and sufficient for tumor control, demonstrating for the first time that microbiota-specific T cells contribute to anti-tumor immunity. Overall, these findings suggest that microbiome modulation and the subsequent microbiota-specific CD4+ T cell response may represent a new variety of immunotherapies for cancers that remain resistant to checkpoint blockade.

<http://dx.doi.org/10.1136/jitc-2021-SITC2021.839>

Novel Single-Agent Immunotherapies

840

A THERAPEUTIC HUMANIZED ANTI-CARCINOMA MONOCLONAL ANTIBODY (MAB) CAN ALSO IDENTIFY IMMUNOSUPPRESSIVE REGULATORY T (TREGS) CELLS AND DOWN REGULATE TREG-MEDIATED IMMUNOSUPPRESSION

¹Kwong Tsang, ¹Massimo Fantini*, ²Christopher Cole, ²Christina Annunziata, ¹Philip Arlen.
¹Precision Biologics, Inc., Bethesda, MD, USA; ²NCI, NIH, Bethesda, MD, USA

Background NEO-201 is an IgG1 mAb reactive against many different human carcinomas expressing the NEO-201 antigen, but not against most normal epithelial tissues. NEO-201 can mediate antitumor activity against tumor cells through multiple mechanisms such as antibody-dependent cellular cytotoxicity (ADCC), complement dependent cytotoxicity (CDC), and blockade of the CEACAM5/CEACAM1 immune checkpoint inhibitory pathway. In addition to solid tumors, the NEO-201 target has also been found on human hematopoietic cells. Flow cytometry analysis has demonstrated that 98.9% of CD15+ granulocytes and about 4.6% of CD4+ T cells were positive for NEO-201 staining. No binding was observed with NEO-201 with respect to B cells, NK cells, monocytes, or CD8+ T cells and a majority of CD4+ T cells. This study was designed to characterize the subset of NEO-201+ binding CD4+ T cells and to evaluate the reactivity of NEO-201 to this subset of hematopoietic cells.

Methods Phenotypic analysis of PBMCs from healthy donors and cancer patients were performed by flow cytometry. Reagents used for flow cytometry were antibodies against human CD4, CD127, CD25, CD15s, FOXP3, CD39, CD73 and anti-NEO-201 mAb. Functional assays were performed using a flow cytometry based on CDC assay. Treg cells, isolated from 3 healthy donors using the EasySep™ Human CD4 +CD127lowCD25+ Regulatory T (Treg) Cell Isolation Kit were used as target cells.

Results Flow cytometry analysis revealed that NEO-201+CD4 + T cells were also CD25+/CD127-/FOXP3+/CD15s+ in human PBMCs from both healthy donors and cancer patients. NEO-201 also binds to CD4+/CD25+/CD127-/Foxp3+/CD15s+ cells in Treg cells isolated from human PBMCs using a commercial isolation kit. NEO-201+CD4+ T cells were also CD25+/CD127-/FOXP3+/CD39+. In addition, NEO-201 mAb can kill these isolated Treg cells through CDC.

Conclusions This study demonstrated that the small subset of NEO-201+CD4+ T cell in human PBMCs are highly suppressive Treg cells and NEO-201 can be used as a novel marker to identify functionally suppressive Treg cells. Furthermore, NEO-201 can kill Treg cells through CDC, presenting an opportunity for therapeutic intervention to increase anti-tumor immunity.

Ethics Approval The study was conducted according to the guidelines of the Declaration of Helsinki and approved by the Institutional Review Board of National Institutes of Health (NIH). All subjects gave their informed consent for inclusion before they participated in the study. PBMCs from healthy volunteer donors were utilized under the appropriate Institutional Review Board approval (protocol code NCT00001846, first approved Nov 4, 1999; latest update 11/10/2020). PBMCs from cancer patients were utilized under the appropriate Institutional Review Board approval (protocol code NCT03476681, first approved 03/26/2018; latest update 01/08/2020).

Consent Informed consent was obtained from all subjects involved in the study.

<http://dx.doi.org/10.1136/jitc-2021-SITC2021.840>

841 TARGETING THE INTERSECTION OF IMMUNOLOGY AND REDOX BIOLOGY: THERAPEUTIC POTENTIAL OF AN ANTI-THIOREDOXIN ANTIBODY

Gabriella Willman, Max Davidson, Carolina Trkulja, Owe Orwar, Sachin Bhat*. *Oblique Therapeutics AB, Göteborg, Sweden*

Background Human Thioredoxin 1 (Trx1) was initially discovered as Adult T cell Leukemia Derived Factor (ADF) that is capable of inducing IL-2R/Tac (CD25) in T and NK cells.¹ Serum Trx1 levels have been correlated to incidence and severity of disease in melanoma patients² and elevated serum Trx1 levels have been reported in hepatocellular carcinoma³ and pancreatic cancer.⁴ In contrast to extracellular Trx1, the role of intracellular Trx1 in redox biology is extensively studied (reviewed in 5). The role of Trx1 as a cytokine in regulating immune cells is less well explored. In order to understand the role of Trx1 in cancer immunology and evaluate the potential of anti-Trx1 monoclonal antibody (mAb) as a therapeutic, anti-Trx1 mAbs were generated and evaluated.

Methods mAbs against full length human Trx1 were generated in mice using standard immunization protocol. The antibodies were tested for their binding affinity to human Trx1 and cross-reactivity with mouse Trx1 using sandwich ELISA method. mAbs were screened for their ability to neutralize hTrx1 in a functional assay where naïve human CD4+ cells were polarized to differentiate into T regulatory cells (Tregs). Effects of the mAbs in vivo were tested in a mouse syngeneic tumor model as well as a tumor model in humanized mice.

Results Five unique mAbs were extensively characterized in in vitro and in vivo models. All five mAbs bound hTrx1 with high affinity with an EC50 of < 1 nM in a sandwich ELISA assay. To develop a screening assay for anti-Trx mAbs, the ability of exogenously added Trx1 to increase the level of expression of CD25 on human naïve peripheral CD4+ cells activated with anti-CD3 and anti-CD28 antibodies and polarized with TGFβ1 and IL-2 was assessed. Trx1 increases the level of expression of CD25 on CD4+CD25+ cells as well as CD4+CD25+FOXP3+ cells. In this Treg polarization assay, four of the five anti-Trx mAbs showed a statistically highly significant effect in reducing the % CD4+CD25+ as well as CD4+CD25+FOXP3+ cells within viable cells. In addition, there was a dramatic reduction in the expression levels of CD25 and FOXP3 in the respective cell populations. The ability of these antibodies to modulate immune cells within the tumor microenvironment and have an anti-tumor effect in a syngeneic model (using a mouse cross-reactive antibody) and a humanized mouse tumor model was investigated. Results from these studies will be presented.

Conclusions We describe a novel immunomodulator pathway in tumor immunology.

Acknowledgements We acknowledge Proteogenix for production of Trx mAbs, Aquila Biomedical for screening Trx mAbs in Treg polarization assay and Champions Oncology for running tumor models.

REFERENCES

1. Yutaka *et al.* (1989). *EMBO J* **8**(3):757–765.
2. Wang *et al.* (2015). *Oncolmmunology* **4**(9):e1027471.
3. Miyazake *et al.* (1998). *Biotherapy* **11**:277–288.
4. Nakamura *et al.* (2000). *Cancer Detect Prev* **24**:53–60.
5. Collet JF, Messens J. (2010). *Antioxidants & Redox Signaling* **13**(8):1205–1216.
6. Mougiakakos *et al.* (2011). *Blood* **17**(3):857–861.

<http://dx.doi.org/10.1136/jitc-2021-SITC2021.841>

842

EXOSOME MEDIATED REPROGRAMMING OF TUMOR ASSOCIATED MACROPHAGES BY EXOASO-STAT6 FOR THE TREATMENT OF HEPATOCELLULAR CARCINOMA (HCC)

Sushrut Kamerkar*, Charan Leng, Kelvin Zhang, Olga Burenkova, Su Chul Jang, Samuel Kaser, Tong Zi, Kyriakos Economides, Timothy Soos, Dalia Burzyn, Sriram Sathyanarayanan. *Codiak Biosciences, Cambridge, MA, USA*

Background Tumor associated macrophages (TAMs) play a critical role in tumor immunosuppression and resistance to immune checkpoint blockade. Reprogramming 'M2' TAMs to a proinflammatory 'M1' phenotype by selectively silencing M2 phenotype-driving transcription factors, such as STAT6, is a promising strategy to relieve TAM-induced immunosuppression. We have developed exoASO-STAT6™, an investigational therapeutic candidate consisting of exosomes loaded with anti-sense oligonucleotides (ASOs) targeting STAT6. By leveraging the TAM tropism of exosomes, exoASO-STAT6™ is the first systemically administered exosome designed to selectively silence STAT6 in TAMs. Preclinical biodistribution studies demonstrated that the liver is the main organ targeted by exoASO after intravenous (IV) dosing.

Methods We evaluated the translational potential of exoASO-STAT6 to treat hepatocellular carcinoma through pharmacokinetics (PK), pharmacodynamic (PD) and anti-tumoral efficacy studies in preclinical models, as well as computational analysis of human HCC datasets.

Results PK/PD were evaluated in naïve mice dosed IV with a single dose of exoASO-STAT6. PK analysis showed that the STAT6-ASO is rapidly cleared from plasma. Retention of the ASO in liver was dose-dependent and observed for at least 21 days. exoASO-STAT6 induced significant Stat6 mRNA knock-down (KD) in liver tissue with maximum KD at day 7 (70% KD at the 30 ug dose). IV administration of exoASO-STAT6 in an orthotopic, CPI resistant HCC model attenuated tumor growth and induced complete remission of tumor lesions in 50% of mice, while combination therapy with anti-PD1 antibodies further enhanced anti-tumor activity (75% complete remissions). Gene expression and histological analysis of the liver showed effective remodeling of the tumor microenvironment including a significant increase in interferon and cytotoxic T-cell gene signatures and iNOS expression. PD studies were also performed in cynomolgus monkeys that demonstrated a dose-dependent and durable silencing of STAT6 mRNA (50% and 31% at 1- and 3- weeks post-dose, respectively). STAT6 knockdown correlated with a reduction in STAT6 target genes, IL4R and EGR2, confirming modulation of the STAT6 pathway. Finally, we identified a STAT6 macrophage transcriptional signature and show high expression in human HCC tumors, both in immune cell-rich and TAM-rich/CD8 T-cell low tumors that correlates with worse survival.

Conclusions In summary, we demonstrate that exoASO-STAT6 has a durable PK/PD profile in the liver of several species and potent antitumoral efficacy in a preclinical model of HCC. Furthermore, we identify an inverse correlation between the STAT6 macrophage signature and survival in human HCC tumors. Altogether our data support the systemic administration of exoASO-STAT6 as a promising therapy for liver cancer.

Ethics Approval

For Mice Mice were maintained and treated at the animal care facility of Codiak Biosciences in accordance with the regulations and guidelines of the Institutional Animal Care and Use

Committee (CB2017-001). Animal housing and experimental procedures (mice) were conducted according to the French and European Regulations and the National Research Council Guide for the Care and Use of Laboratory Animals and Institutional Animal Care and Use Committee of Oncodesign (Oncomet) approved by French authorities (CNREEA agreement N° 91). For cynomolgus monkeys: All animals were maintained and treated at the animal care facility of Altasciences in compliance with the Animal Welfare Act and recommendations set forth in the Guide for the Care and Use of Laboratory Animals (National Research Council 2011).

<http://dx.doi.org/10.1136/jitc-2021-SITC2021.842>

DEVELOPMENT AND ENGINEERING OF HUMAN SIALIDASE FOR DEGRADATION OF IMMUNOSUPPRESSIVE SIALOGLYCANS TO TREAT CANCER

Li Peng*, Lizhi Cao, Sujata Nerle, Robert LeBlanc, Abhishek Das, Sandip Shelke, Autumn Turner, Jenny Che, Zakir Siddiquee, Hui Xu, Lihui Xu, Wayne Gatlin, James Broderick. *Palleon Pharmaceuticals, Waltham, MA, USA*

Background Sialoglycans, a type of glycans with a terminal sialic acid, have emerged as a critical glyco-immune checkpoint that impairs antitumor response by inhibiting innate and adaptive immunity. Upregulation of sialoglycans on tumors has been observed for decades and correlates with poor clinical outcomes across many tumor types. We previously showed that targeted desialylation of tumors using a bifunctional sialidase x antibody molecule, consisting of sialidase and a tumor-associated antigen (TAA)-targeting antibody, has led to robust single-agent efficacy in mouse tumor models. In addition to tumor cells, most immune cells present substantially more abundant sialoglycans than non-hematological healthy cells, which may also contribute to immunosuppression. Therefore, we studied the impact of immune cell desialylation and evaluated the therapeutic potential of a newly developed sialidase-Fc fusion (Bi-Sialidase), which lacks a TAA-targeting moiety and consists of engineered human neuraminidase 2 (Neu2) and human IgG1 Fc region, in preclinical mouse tumor models.

Methods The first generation Neu2 variant was further optimized to improve titers and stability to construct Bi-Sialidase. Bi-Sialidase's desialylation potency and impact on immune responses were studied *in vitro* using various human immune functional assays, including T-cell activation, allogeneic mixed lymphocyte reaction, antibody-dependent cellular cytotoxicity, macrophages polarization/activation, neutrophil activation, and peripheral blood mononuclear cell (PBMC) cytokine release assays. We evaluated its antitumor efficacy in mouse tumor models. Bi-Sialidase's safety profile was characterized by conducting rat and non-human primate (NHP) toxicology studies.

Results The optimized Bi-Sialidase achieved a titer of 2.5 g/L from a 15-day fed-batch Chinese hamster ovary cell culture; in contrast, the wild-type and first-generation Neu2 had no production or a low titer (<0.1 g/L) under similar conditions, respectively. We demonstrated that Bi-Sialidase led to dose-dependent desialylation of immune cells and potentiated T-cell immunity, without impacting NK, macrophage, or neutrophil activation by desialylating immune cells. Activated and exhausted T cells upregulated surface sialoglycans and Bi-Sialidase-mediated desialylation reinvigorated exhausted-like T cells as measured by IFN γ production. Bi-Sialidase treatment also enhanced DC priming and activation of naïve T cells by desialylating both T cells and DCs. Furthermore, Bi-Sialidase showed single-agent antitumor activity in multiple mouse tumor models, including MC38, CT26, A20, and B16F10. Importantly, Bi-Sialidase did not cause cytokine release in human PBMC assays and was tolerated to up to 100 mg/kg in rats and NHPs, demonstrating a wide safety margin.

Conclusions Bi-Sialidase with an optimized Neu2 offers a novel immunomodulatory approach to enhancing T-cell immunity by desialylating immunosuppressive sialoglycans for cancer treatment.

<http://dx.doi.org/10.1136/jitc-2021-SITC2021.843>

844

A TRISPESIFIC ROR1 X CD3 T CELL ENGAGER MEDIATES IN VITRO TUMOR CELL KILLING AND IN VIVO TUMOR ERADICATION

Bithi Chatterjee*, Daniel Snell, Daniel Snell, Christian Hess, Matthias Brock, Fabio Spiga, Alexandre Simonin, Tea Gunde, Stefan Warmuth, Christopher Weinert, Nicole Bassler, Niels Kirk, Nina Schumacher, Dana Mahler, Yasemin Yaman, Bettina Bommer, Giorgio Gambino, Noreen Giezendanner, Benjamin Kuettner, Naomi Flueckiger, Robin Heiz, Sandro Wagen, Dania Diem, Julia Zeberer, David Urech. *Numab Therapeutics, Wädenswil, Switzerland*

Background Receptor tyrosine kinase-like orphan receptor 1 (ROR1) is expressed on a variety of difficult to treat solid and hematological malignancies. Several therapeutic concepts targeting ROR1 are currently in clinical studies, including antibody-drug conjugates (ADCs), chimeric antigen receptor engineered T cells, as well as a bispecific T cell engager. In contrast to ADCs, T cell engagers have the capacity to induce tumor cell depletion irrespective of tumor cell mitotic activity. For the therapy of ROR1 expressing tumors, we engineered a T cell engager with prolonged half-life to support convenient administration schemes.

Methods NM32-2668, a ROR1-targeting T cell engager with prolonged serum half-life was engineered by joining three humanized rabbit antibody variable region (Fv) fragments specific for ROR1, CD3 ζ , and serum albumin, into our tri-specific scMATCHTM3 format. Each Fv fragment was stabilized using the ζ -capTM technology. NM32-2668 was tested in assays for specific tumor lysis, induction of T cell proliferation, and cytokine release. These studies were performed using human T cells co-cultured with tumor cell lines and human tumor samples expressing various levels of ROR1. In vivo xenograft mouse studies were conducted using a human mantle cell lymphoma model in NCG mice engrafted with human PBMCs.

Results Here we report the design and the promising preclinical activity of the scMATCHTM3 ROR1/CD3/hSA T cell engager NM32-2668 in vitro and in vivo. Importantly, we demonstrate potent and specific cytotoxic activity in the sub-nanomolar range on tumor cell lines expressing different levels of ROR1. NM32-2668 also mediates ROR1 dependent T cell activation and cytokine release. We observe robust tumor cell killing activity of NM32-2668 over an extended time period and at multiple ratios of effectors to targets in a real time imaging-based cytotoxicity assay. This molecule also mediates T cell proliferation in response to target cell binding. NM32-2668 mediates in vitro lysis of CLL patient tumor cells, T cell activation, and cytokine release, with minimal IL-6 involvement. In an in vivo mantle cell lymphoma model (Jeko-1) engrafted with human PBMCs, we observe tumor regression and eradication.

Conclusions Collectively, these data demonstrate robust anti-tumor efficacy by NM32-2668, a scMATCHTM3 ROR1/CD3/hSA. Our results demonstrate that NM32-2668 promotes ROR1 dependent T cell activation and proliferation, as well as T cell-mediated tumor cell lysis. The activity of NM32-2668 has the potential to provide significant benefit to patients with ROR1+ malignancies on a convenient dosing schedule. We intend to rapidly progress NM32-2668 to clinical development.

<http://dx.doi.org/10.1136/jitc-2021-SITC2021.844>

A COLONY STIMULATING FACTOR 1 RECEPTOR-BLOCKING BIFUNCTIONAL PROTEIN SIMULTANEOUSLY TARGETS TUMOR-ASSOCIATED MACROPHAGES AND EXHAUSTED T CELLS FOR THE TREATMENT OF TRIPLE-NEGATIVE BREAST CANCER<http://dx.doi.org/10.1136/jitc-2021-SITC2021.845>

¹Pandelakis Koni*, ¹Hung-Kai Chen, ²Yao-Wen Chang, ¹Huey-Wen Hsiao, ¹Chih-Lun Hsiao, ¹Jing-Yi Huang, ²Ju-Pei Chen, ²Muh-Hwa Yang. ¹*Elixiron Immunotherapeutics, Taipei City, Taiwan, Province of China*; ²*National Yang Ming Chiao Tung University, Taipei City, Taiwan, Province of China*

Background Tumor-associated macrophages (TAMs) are a significantly-poor prognostic factor for patients with triple-negative breast cancer (TNBC). The tumor microenvironment of TNBC features highly-infiltrating TAMs that contribute to tumor progression and metastasis. Therefore, TAM-targeted immunotherapies are recognized as a potential approach for treating TNBC. However, depleting TAMs alone by use of monoclonal antibodies against colony-stimulating factor 1 receptor (CSF1R) was insufficient to cause substantial tumor control. Recent studies revealed that interleukin-10 (IL-10) can directly activate terminally-exhausted CD8+ T cells to boost anti-tumor activity. We set forth to investigate whether a combination of anti-CSF1R antibody with a half-life-extended IL-10-Fc fusion protein (IL-10-Fc) may enhance anti-tumor immunity, and whether synergistic effects could be achieved with bifunctional antibody forms.

Methods Antibodies and recombinant proteins were produced in-house. In vitro CSF1R activity was evaluated by Western blot analysis of CSF1-mediated CSF1R phosphorylation and monocyte proliferation assays. In vitro IL10 activity was evaluated by MC/9 cell proliferation and CD8 T cell activation assays. 4T1 mouse breast tumor studies were performed at the National Yang Ming Chiao Tung University (Taiwan). Other tumor model studies employed the services of Crownbio (China). Methods of RNAseq analysis of 4T1 tumor masses included Cibersort, gene set enrichment analysis (GSEA) and immune gene signature score analysis.

Results Co-treatment with a recombinant human IL-10-Fc protein significantly improved the anti-tumor efficacy of anti-mouse CSF1R antibody in a mouse CT26 colon tumor model. It was then hypothesized that a better synergistic effect could be achieved by a bifunctional anti-mouse CSF1R-IL-10 fusion protein (anti-mCSF1R-IL-10), to allow targeted-delivery of IL-10 to CSF1R-positive-TAM-rich tumor microenvironments. Indeed, anti-mCSF1R-IL-10 showed greatly increased anti-tumor efficacy in both EMT-6 and 4T1 mouse models of breast cancer. Consistent with the in vivo efficacy, gene expression profiling revealed an enhanced intratumoral interferon-gamma signature by treatment with anti-mCSF1R-IL-10 as compared to either anti-mCSF1R or IL-10-Fc alone. An anti-human CSF1R-IL-10 (hCSF1R-IL-10) was also constructed using a newly-produced anti-human CSF1R antibody and tested in cell-based functional assays, demonstrating that anti-hCSF1R-IL-10 could both inhibit CSF1-dependent cell growth and activate tumor-infiltrating T cells isolated from tumor biopsies of triple-negative breast cancer patients. Further validation of this bifunctional form will be presented.

Conclusions Our findings provide a potential strategy for simultaneously targeting TAM and exhausted T cells to potentiate anti-tumor immunity for treatment of triple-negative breast cancer.

Ethics Approval The studies were approved by the institutional animal care and use committee of National Yang Ming Chiao Tung University; approval numbers 1081025 and 109060.

846 **PRE-CLINICAL VALIDATION OF A FLT3L-FUSION PROTEIN FOR DENDRITIC CELL EXPANSION AND ANTI-TUMOR EFFICACY**

Michelle Kuhne*, Hamlet Chu, Sarah Ng, Christopher Clarke, Brian Carr, Manuel Baca, Magdeleine Hung, Mark Nagel, Alexandre Ambrogelly, Nicholas Wilson. *Gilead Sciences, San Francisco, USA*

Background The ligand for the receptor tyrosine kinase FMS-like tyrosine kinase 3 (FLT3) plays an important role in hematopoiesis. FLT3 signaling is required for the differentiation and expansion of dendritic cells. In the context of cancer immunity, the conventional dendritic cell subtype 1 (cDC1) are required for the generation of tumor-specific T cell responses in mouse preclinical models. In human tumors cDC1 are often underrepresented in the tumor microenvironment, supporting the hypothesis that therapeutically increasing their number via FLT3 pathway stimulation has the potential to promote T cell-mediated anti-tumor efficacy.

Methods GS-3583 is a fusion protein composed of the extracellular domain (ECD) of human FLT3 ligand (FLT3L) combined with a modified fragment crystallizable (Fc) region of human IgG4. GS-3583 was designed to induce cDC1 expansion and subsequently promote tumor-reactive T cell priming, activation and recruitment into the tumor microenvironment. To evaluate the therapeutic efficacy of FLT3 stimulation in vivo, a mouse surrogate mGS-3583 was designed using the ECD of mouse FLT3L fused to an engineered mouse IgG2a Fc with attenuated binding to mouse FcγRs.

Results mGS-3583 bound to recombinant mouse FLT3 with an estimated affinity of 15 nM, and to mouse FLT3-expressing cells with an EC50 of 0.15 nM. In vivo, mGS-3583 showed single agent dose-dependent tumor growth inhibition (TGI) in tumors that correlated with peripheral and intratumoral cDC1 expansion. In tumors with no initial immune infiltration, mGS-3583 led to an influx of T cells into the tumors. In addition to single agent efficacy, mGS-3583 combined effectively with programmed cell death protein (ligand)-1 (PD(L)-1) pathway blockade.

Conclusions In vivo expansion of dendritic cells can convert uninfamed (cold) tumors to immunologically active (hot) tumors and initiate productive anti-tumor immune responses. These findings support the development of GS-3583 as a promising candidate for cancer immunotherapy.

<http://dx.doi.org/10.1136/jitc-2021-SITC2021.846>

PHARMACOKINETICS AND PHARMACODYNAMICS OF GS-3583 IN CYNOMOLGUS MONKEYS

Michelle Kuhne*, Hamlet Chu, Christopher Clarke, Brian Carr, Manuel Baca, Magdeleine Hung, Mark Nagel, Alexandre Ambrogelly, Nishanathan Rajakumaraswamy. *Gilead Sciences, San Francisco, USA*

Background The ligand for the receptor tyrosine kinase FMS-like tyrosine kinase 3 (FLT3) plays an important role in hematopoiesis. FLT3 signaling is required for the differentiation and expansion of dendritic cells. In the context of cancer immunity, the conventional dendritic cell subtype 1 (cDC1) are required for the generation of tumor-specific T cell responses in mouse preclinical models. In human tumors cDC1 are often underrepresented in the tumor microenvironment, supporting the hypothesis that therapeutically increasing their number via FLT3 pathway stimulation has the potential to promote T cell-mediated anti-tumor activity.

Methods GS-3583 is a fusion protein composed of the extracellular domain of human FLT3 ligand (FLT3L) combined with a modified fragment crystallizable (Fc) region of human IgG4. GS-3583 was designed to induce cDC1 expansion and subsequently promote tumor-reactive T cell priming, activation and recruitment into the tumor microenvironment. The pharmacokinetics (PK) and pharmacodynamics (PD) of GS-3583 has been characterized in a 4-week repeat dose GLP study in cynomolgus monkeys at doses ranging from 0.3 to 10 mg/kg. GS-3583 was given as an intravenous injection.

Results Immunophenotyping analysis of peripheral blood cells from GS-3583 treated monkeys demonstrated a non-dose-dependent expansion of cDC1 and cDC2 populations. The peak expansion for cDC1 and cDC2 occurred at Day 8 to Day 15. At peak, there was a 160-fold relative increase in cDC1 and 150-fold increase in cDC2 at the highest dose tested. There were dose-dependent increases in the exposure (AUC and C_{max}) of GS-3583. GS-3583 was well-tolerated with no mortality or adverse clinical signs.

Conclusions The administration of GS-3583 leads to increases in cDC1 and cDC2 populations. It was well tolerated at the maximal dose tested with no adverse clinical signs. Further clinical development of GS-3583 is warranted.

<http://dx.doi.org/10.1136/jitc-2021-SITC2021.847>

848 **NOVEL SMALL MOLECULE HPK1 INHIBITOR PCC-1 INDUCES STRONG ANTI-TUMOR ACTIVITY**

¹Sanjib Das, ¹Sravan Mandadi*, ¹Jagmohan Saini, ¹Sachin Chaudhari, ¹Ameya Deshpande, ¹Murugan Chinnappattu, ¹Malini Bajpai, ¹Priyanka Pangre, ¹Varada Potdar, ¹Megha Marathe, ¹Pooja Sawant, ¹Atul Akarte, ²Chandrasekhar Misra, ¹Subhadip Das, ¹Anuj Singh, ¹Avratanu Das, ¹Pandurang Lambade, ¹Chaitanya Tirumalasetty, ¹Raju Patole, ¹Nilanjana Biswas, ¹Vikas Karande, ¹Heta Shah, ¹Dayanidhi Behera, ¹Nagaraj Gowda, ¹Pravin Iyer. ¹Glenmark Pharmaceuticals Limited, Navi Mumbai, India; ²Glenmark Pharmaceuticals, Navi Mumbai, India

Background Hematopoietic progenitor kinase 1 (HPK1, MAP4K1), is a negative regulator of T and B cell receptor signaling.^{1 2 3} A strong anti-tumor immunogenic response and tumor rejection was observed in mice with HPK1 gene knocked out.³ Treatment of HPK1 kinase dead mice with immune check-point blockers (ICBs) demonstrated enhanced tumor growth inhibition.³ Hence, HPK1 is an attractive therapeutic strategy for immuno-oncology based treatment in cancers. In comparison to our previous HPK1 small molecule inhibitor, PCC,⁴ we present here a differentiated novel HPK1 inhibitor, PCC-1 with good anti-T cell kinases selectivity and stronger anti-tumor efficacy in CT26 tumor model. In addition, using the syngeneic model of MC38 expressing human PD-L1, we present for the first time, the combination efficacy of a HPK1 inhibitor with the clinical ICB, Atezolizumab.

Methods Intuitive medicinal chemistry complemented by structure-based drug design was used to identify & develop potent inhibitors of HPK1 with optimal kinase selectivity, PK and in vivo efficacy profile. The SAR efforts were guided by biochemical assays, functional read-outs and primary human in vitro T-cell activation assays. In vivo target engagement and pharmacodynamic data was generated using CT26 and MC38-hPD-L1 tumor models.

Results PCC-1 has sub-nanomolar HPK1 inhibition potency and strong target engagement resulting in pSLP76 inhibition, enhanced anti-tumor cytokine production of IL-2 and/or IFN-gamma in Jurkat cells, human PBMCs and human whole blood. PCC-1 also demonstrated nanomolar potency in inducing a complete reversal of PGE2 or adenosine mediated immunosuppression. Oral dosing of PCC-1 as a single agent, induced strong tumor growth inhibition (TGI) in the syngeneic model of CT26 and MC38-hPD-L1 tumor models. Combination of PCC-1 with anti-CTLA4 in CT26 tumor model induced significantly greater TGI than anti-CTLA4 alone. Moreover, as a first, the combination of PCC-1 with clinical ICB, Atezolizumab in MC38-hPD-L1 induced enhanced rejection of tumors. These results strongly suggest PCC-1 as a promising candidate for HPK1 inhibition and as a combination partner with ICBs in clinic.

Conclusions PCC-1 is a novel, orally active HPK1 inhibitor that demonstrates excellent stand-alone efficacy and enhances current immunotherapy efficacy. Further evaluation of PCC-1 is ongoing to advance towards clinic.

Acknowledgements We thank Dnyaneshwar Dahale, Sanjay Patale, Sandip Patil, Vidya Kattige, Jiju Mani, Namrata Singh, Ekta Kashyap, Sandeep Thorat, Pankaj Jain and Pramod Sagar for their contributions to the project

Trial Registration N/A

REFERENCES

1. Kiefer F, et al. *The EMBO Journal* 1996.
2. Hu, et al. *Genes and Development* 1996.
3. Sawasdikosol, Burakoff. *eLife* 2020;**9**:e55122.
4. Sachin S Chaudhari, et al. Poster#1709, AACR Annual Meeting April-May 2021.

Ethics Approval The studies involving animals have obtained ethics approval from Institutional Animal Ethics Committee (IAEC), The Committee for the Purpose of Control and Supervision of Experiments on Animals (CPCSEA), New Delhi, India, GRC/IAEC/472/2020-1. Participants of the studies have given informed consent before taking part.

<http://dx.doi.org/10.1136/jitc-2021-SITC2021.848>

849

RESTORE T CELL ENGAGER PLATFORM DEPLETES MDSC IN PARALLEL WITH ANTIGEN-SPECIFIC SOLID TUMOR CYTOTOXICITY

Sterling Eckard*, Bianca Rojo, Li Mei, Alberto Ponce, Patrick Chun, Victoria Smith. *Amphivena Therapeutics, South San Francisco, CA, USA*

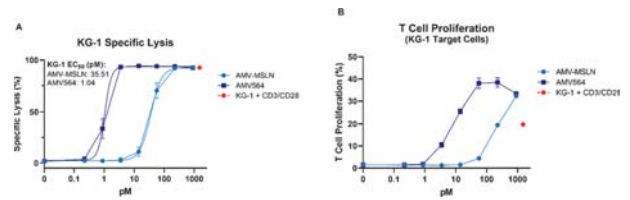
Background Amphivena's ReSTORE T cell engager platform produces tunable, potent, and selective molecules that mitigate immune suppression while also directly targeting tumor cells. The core function of this platform utilizes AMV564, a clinically active molecule that has been shown in a phase 1 study to selectively deplete myeloid-derived suppressor cells (MDSC) and produce clinical responses in cancer patients (NCT04128423).¹ Increased levels of MDSC in cancer patients correlate with reduced overall survival, as MDSC suppressive factors impair T cell activation and anti-tumor immunity. With the addition of unique target-specific VHH domains to the AMV564 core, new platform molecules can be engineered with additional functionality to selectively target tumor-specific antigens.

Methods Cell lines, primary human cells, and patient samples were analyzed using flow cytometry with appropriate marker panels including directly labeled AMV564 (phycoerythrin) and labeled anti-AMV564 antibodies. T cell cytotoxicity assays were conducted using primary human T cells and target cells (3:1 ratio) for 72 hours. Biophysical characterization was performed using standard techniques with SDS-PAGE gels, analytical SEC, and Octet analysis.

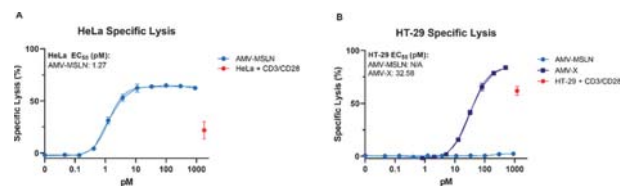
Results We have engineered a stable and potent T cell engager platform that targets both MDSC and tumor cells (figure 1). The tumor antigen potency relative to MDSC cytotoxicity is tunable, allowing design flexibility. We demonstrate that ReSTORE molecules expressing a variety of VHH domains can effectively mediate a cytolytic synapse with KG-1 target cells, which represent MDSC in in vitro assays due to their CD33 expression level and myeloid differentiation state (figure 2A).² Our platform molecules act as robust T cell agonists while maintaining selectivity with minimal activation-induced cell death (AICD) compared to positive controls (CD3/CD28) and demonstrate dose-dependent enhancement of cytolytic activity (figure 2B). Molecules with targets ranging from tumor targets to antiviral epitopes have been developed, and they maintain potent and selective T cell-dependent cytotoxicity against cells expressing the target antigen (figure 3A). New targets can be engineered to accommodate desired potency, and bivalent design yields selectivity (figure 3B). In all cases, these molecules significantly inhibit cancer cell growth in a dose dependent manner.



Abstract 849 Figure 1 ReSTORE platform molecules are bivalent and trispecific. The core function of each molecule targets MDSC (M) while activating and expanding T cells (T). By adding unique VHH domains, these molecules gain the ability to target specific tumor antigens (R) and direct specific tumor cell killing.



Abstract 849 Figure 2 Cytotoxicity assay using primary T cells demonstrates 'core' potency of platform molecules on the CD33-expressing KG-1 cell line. Core potency can be engineered to allow appropriate dosing for TME saturation while maintaining selectivity (2A). T cell proliferation exceeds positive control (CD3/CD28) across expected clinical dose range while maintaining selectivity and T cell viability (2B).



Abstract 849 Figure 3 Bivalent VHH affinity can be engineered to increase or decrease potency depending on the specific target while maintaining selectivity. AMV-MSLN lead demonstrates potent cytotoxic effects on MSLN-high HeLa cells (3A). The same AMV-MSLN molecule does not target MSLN-low HT-29 cells. AMV-X binds a non-MSLN surface antigen on HT-29, demonstrating the potency and specificity of ReSTORE molecules (3B).

Conclusions The clinically validated MDSC-depleting core of the ReSTORE platform molecules allow targeting of specific antigens associated with a variety of solid and hematologic tumor indications. This antigen-specific cytotoxicity of cancer cells occurs in parallel with control of the immunosuppressive MDSC.

REFERENCES

- Niharika B Mettu, Alexander Starodub, Sarina Anne Piha-Paul, Raghav Muhsin Abdul-Karim, Gabriel Tinoco, Michael Rahman Shafique, Victoria Smith, Christina Baccei, Patrick Youngwhan Chun. Results of a phase 1 dose-escalation study of AMV564, a novel T-cell engager, alone and in combination with pembrolizumab in patients with relapsed/refractory solid tumors. *J Clin Oncol* **39**,2021 (suppl 15; abstr 2555).
- Sterling Eckard, Aurelien Sarde, Li Mei, Curtis Ruegg, Patrick Chun, Victoria Smith. Abstract 528: MDSC suppress the T cell repertoire and contribute to a pathologic cytokine milieu in cancer patients. *Cancer Res* July 1 2021 (81) (13 Supplement) 528; DOI: 10.1158/1538-7445.AM2021-528

<http://dx.doi.org/10.1136/jitc-2021-SITC2021.849>

850

DUAL BLOCKADE OF THE EP2 AND EP4 PGE2 RECEPTORS WITH TPST-1495 IS AN OPTIMAL APPROACH FOR DRUGGING THE PROSTAGLANDIN PATHWAY

¹Brian Francica*, ¹Justine Lopez, ¹Anja Holtz, ¹Dave Freund, ²Dingzhi Wang, ¹Amanda Enstrom, ¹Sam Whiting, ¹Chan Whiting, ¹Thomas Dubensky, ¹Tempest Therapeutics, Berkeley, CA, USA; ²MUSC, Charleston, SC, USA

Background Prostaglandin E2 (PGE2) is a bioactive lipid produced by tumor cells that drives disease progression through stimulating tumor proliferation, enhancing angiogenesis and suppressing immune function in the TME.¹ PGE2 is also a mediator of adaptive resistance to immune checkpoint inhibitor therapy via the upregulation of cyclooxygenase-2 (COX-2). While the role of PGE2 signaling in cancer is clear, how best to inhibit PGE2 for cancer treatment remains under investigation. Inhibition of COX-1 and/or COX-2 has shown promising results in observational studies and meta-analyses, but inconsistent results in prospective studies. PGE2 signals through four receptors, EP1-4, that are variably expressed on tumor and immune cells and have distinct biological activities. The EP2/EP4 receptors signal through cAMP and drive pro-tumor activities, while EP1/EP3 receptors signal through calcium flux and IP3 and drive immune activation and inflammation. While COX-2 and single EP inhibitors continue to be developed, the nature of PGE2 signaling supports our rationale to inhibit PGE2 by dual antagonism of the pro-tumor EP2/EP4 receptors, while sparing the pro-immune EP1/EP3 receptors.

Methods We utilized human and murine whole blood to perform in vitro characterization of PGE2/inhibitor activity. In vivo, CT26 tumors and APCmin/+ mice were used to model CRC and measure immune endpoints.

Results In mouse and human whole blood assays, dual blockade of EP2 and EP4 receptors with TPST-1495 reversed PGE2-mediated suppression of LPS induced TNF- α , while EP4 receptor antagonists were unable to block suppression at higher PGE2 concentrations. Similarly, in murine and human T cells in vitro, TPST-1495 inhibited PGE2-mediated suppression, resulting in a significant increase of IFN- γ production in response to stimulation with cognate peptide Ag. In vivo, TPST-1495 therapy alone also significantly reduced tumor outgrowth in CT26 tumor bearing mice, correlated with increased tumor infiltration by NK cells, CD8+ T cells, AH1-specific CD8+ T cells, and DCs. The induced NKp46+CD4-CD8- cell population appeared to have an important role in TPST-1495 efficacy, as significant anti-tumor activity was observed in murine models lacking T Cells, particularly CT26 tumor-bearing RAG2-/- mice. TPST-1495 monotherapy demonstrated a decrease of both the intestinal tumor size and number in Adenomatous Polyposis (APCmin/+) mice, as compared to a single EP4 antagonist.

Conclusions TPST-1495 is a potent inhibitor of PGE2 mediated immune suppression and is currently being evaluated in an ongoing Phase 1 first-in-human study (NCT04344795) to characterize PK, PD, safety, and to identify a recommended phase 2 dose for expansion cohorts in key indications and biomarker selected patients.

REFERENCE

1. Zelenay S, van der Veen AG, Böttcher JP, et al. Cyclooxygenase-dependent tumor growth through evasion of immunity. *Cell* 2015;**162**(6):1257–70. doi: 10.1016/j.cell.2015.08.015

<http://dx.doi.org/10.1136/jitc-2021-SITC2021.850>

HARNESSING INNATE IMMUNITY IN CANCER THERAPIES: THE EXAMPLE OF NATURAL KILLER CELL ENGAGERS

Olivier Demaria, Eric Vivier*, Marie Vetizou, Audrey Blanchard Alvarez, Guillaume Habif, Cécile Bonnafous, Sivan Bokobza, Agnès Represa, Benjamin Rossi, Luciana Batista, Constance Vagne, Sabrina Carpentier, Stéphanie Cornen, Ariane Morel, Ivan Perrot, Yannis Morel, Laurent Gauthier. *Innate Pharma, Marseille, France*

Background Most immunomodulatory approaches have focused on enhancing T-cell responses, with immune checkpoint inhibitors, chimeric antigen receptor T cells or bispecific antibodies. Although these therapies have led to exceptional successes, only a minority of cancer patients benefit from these treatments, highlighting the need to identify new cells and molecules that could be exploited in the next generation of immunotherapy. Given the crucial role of innate immune responses in immunity, harnessing these responses opens up new possibilities for tumor control. Antibody engineering provides us with great opportunities to induce synthetic immunity and to optimize the biological functions of innate immune cells, in particular by boosting the capacity of Natural Killer (NK) cells to kill tumor cells directly and to stimulate T-cell responses indirectly.

Methods In order to leverage the advantages of harnessing NK cell effector functions, we used our Antibody-based NK cell Engager Therapeutics (ANKET) molecular platform¹ and designed a new generation of molecules that can engage activating receptors NKp46 and CD16, the IL-2R β chain and a tumor antigen in a single tetra-specific molecule (ANKET4). The variant of interleukin-2 (IL-2v) integrated in the ANKET4 molecule is unable to bind the α -subunit of its receptor to limit regulatory T cell activation and IL-2R α -mediated toxicity.

Results In vitro, ANKET4 provides proliferation and activation signals targeted to NK cells and induces primary human NK cell cytolytic activity and the secretion of cytokines and chemokines only after binding to the tumor target. In mouse models of both invasive and solid tumors, ANKET4 induced NK cell proliferation and accumulation at the tumor bed, and had a higher anti-tumor efficacy than approved therapeutic antibodies targeting the same tumor antigen. Mechanistically, transcriptomic analysis and in-vivo studies revealed that the geometry of the ANKET4 molecule including NKp46, CD16 and IL-2 receptor binding moieties on the same molecule was essential for its strong activity which results from a synthetic cooperativity between immunoreceptor tyrosine-based activation motif (ITAM) and cytokine signaling pathways. In non-human primates, CD20-directed ANKET4 resulted in sustained CD20+ B-cell depletion with minimal systemic cytokine release and no clinical sign of toxicity.

Conclusions Tetra-specific ANKET4 thus constitutes a technological platform combining the induction of NK cell proliferation and effector functions with a manageable safety profile, supporting its clinical development for next-generation cancer immunotherapies.

REFERENCE

- Gauthier L, Morel A, Anceriz N, Rossi B, Blanchard-Alvarez A, Grondin G, *et al.* Multifunctional natural killer cell engagers targeting NKp46 trigger protective tumor immunity. *Cell* 2019;**177**(7):1701–13 e16.

Ethics Approval Primary immune cells were purified from buffy coats from healthy donors obtained from Etablissement Français du Sang (EFS, Marseille) with written consent from each volunteer. All mouse experiments were performed in

accordance with the rules of the Innate Pharma ethics committee and were approved by the Ministère de l'Enseignement Supérieur, de la Recherche et de l'Innovation – France (APAFIS# 19272). All non human-primate procedures were conducted according to European guidelines for animal care and use for scientific purposes (Directive 63-2010, "Journal Officiel des Communautés Européennes", L276, September 22, 2010) and according to CEA institutional guidelines. The study was approved by the local ethical committee under the number A18_080 and by the French Administration (APAFIS#20525-2019050616506478 v1)

<http://dx.doi.org/10.1136/jitc-2021-SITC2021.851>

852 **TRIFUNCTIONAL NKP46/CD16A-NK CELL ENGAGER TARGETING CD123 OVERCOMES ACUTE MYELOID LEUKEMIA RESISTANCE TO ADCC**

¹Laurent Gauthier*, ²Angela Virone-Oddos, ²Angela Virone-Oddos, ²Jochen Beninga, ¹Benjamin Rossi, ²Céline Nicolazzi, ²Céline Amara, ¹Audrey Blanchard-Alvarez, ¹Nicolas Gourdin, ²Jacqueline Courta, ²Alexandra Basset, ¹Franceline Guillot, ¹Gwendoline Grondin, ²Hélène Bonnevaux, ²Anne-Laure Bauchet, ¹Ariane Morel, ¹Yannis Morel, ²Marielle Chiron, ¹Eric Vivier. ¹Innate Pharma, Marseille, France; ²Sanofi, Vitry sur-Seine, France

Background There is a clear need for targeted therapies to treat acute myeloid leukemia (AML), the most common acute leukemia in adults. CD123 (IL-3 receptor alpha chain) is an attractive target for AML treatment.¹ However, cytotoxic antibody targeting CD123 proved insufficiently effective in a combination setting in phase II/III clinical trials.² T-cell engagers targeting CD123 displayed some clinical efficacy but were often associated with cytokine release syndrome and neurotoxicity.³ Interest in the use of NK cells for therapeutic interventions has increased in recent years, as a potential safer alternative to T cells. Several NK-cell activating receptors, such as CD16a, NKG2D, and the natural cytotoxicity receptors NKp30 and NKp46, can be targeted to induce antitumor immunity. We previously reported the development of trifunctional NK-cell engagers (NKCEs) targeting a tumor antigen on cancer cells and co-engaging NKp46 and CD16a on NK cells.⁴

Methods We report here the design, characterization and pre-clinical development of a novel trifunctional NK cell engager (NKCE) targeting CD123 on AML cells and engaging the activating receptors NKp46 and CD16a on NK cells. The CD123 NKCE therapeutic molecule was engineered with humanized antibodies targeting NKp46⁴ and CD123.⁵ We compared CD123-NKCE and a cytotoxic ADCC-enhanced antibody (Ab) targeting CD123, in terms of antitumor activity in vitro, ex vivo and in vivo. Pharmacokinetic, pharmacodynamic and safety profile of CD123-NKCE were evaluated in non-human primate (NHP) studies.

Results The expression of the high affinity Fc gamma receptor CD64 on patient-derived AML cells inhibited the ADCC of the Ab targeting CD123 in vitro and ex vivo, but not the antitumor activity of CD123-NKCE. CD123-NKCE had potent antitumor activity against primary AML blasts and AML cell lines, promoted strong NK-cell activation and induced cytokine secretion only in the presence of AML target cells. Its antitumor activity in mouse model was greater than that of the comparator antibody. Moreover, CD123-NKCE had strong and prolonged pharmacodynamic effects in NHP when used at very low doses, was well-tolerated up to high 3 mg/kg dose and triggered only minor cytokine release.

Conclusions The data for activity, safety, pharmacokinetics, and pharmacodynamics provided here demonstrate the superiority of CD123-NKCE over comparator cytotoxic antibody, in terms of antitumor activity in vitro, ex vivo, in vivo, and its favorable safety profile, as compared to T-cell therapies. These results constitute proof-of-principle for the efficacy of CD123-NKCE for controlling AML tumors in vivo, and provide consistent support for their clinical development.

REFERENCES

1. Ehninger A, Kramer M, Rollig C, *et al.* Distribution and levels of cell surface expression of CD33 and CD123 in acute myeloid leukemia. *Blood Cancer J* 2014;**4**:e218.
2. Montesinos P, Gail J, Roboz GJ, *et al.* Safety and efficacy of talacotuzumab plus decitabine or decitabine alone in patients with acute myeloid leukemia not eligible

for chemotherapy: results from a multicenter, randomized, phase 2/3 study. *Leukemia* 2021;**35**(1):62–74.

3. Uy GL, Aldoss I, Foster MC, *et al.* Flotetuzumab as salvage immunotherapy for refractory acute myeloid leukemia. *Blood* 2021;**137**(6):751–762.
4. Gauthier L, Morel A, Anceriz N, *et al.* Multifunctional natural killer cell engagers targeting NKp46 trigger protective tumor immunity. *Cell* 2019;**177**(7):1701–13.
5. Jin L, Lee EM, Ramshaw HS, *et al.* Monoclonal antibody-mediated targeting of CD123, IL-3 receptor alpha chain, eliminates human acute myeloid leukemic stem cells. *Cell Stem Cell* 2009;**5**:31–42.

<http://dx.doi.org/10.1136/jitc-2021-SITC2021.852>

853

ACTM-838: A MICROBIAL-BASED IMMUNOTHERAPY THAT DELIVERS COMBINATION IL-15 + ENGINEERED STING TO TUMOR-RESIDENT APCs AFTER IV DOSING IN T-CELL EXCLUDED SOLID TUMORS

¹Haixing Kehoe*, ¹Alexandre Iannello, ¹Keith Cheung, ¹Bret Peterson, ²Marie Marotel, ¹Sara Tribble, ¹Hailey He, ²Jonathan Hodgins, ²Michele Ardolino, ¹Christopher Rae, ¹Christopher Thanos, ¹Laura Glickman. ¹Actym Therapeutics, Inc, Berkeley, CA, USA; ²University of Ottawa, OHRI, Ottawa, Canada

Background In a metastatic setting, systemically-administered therapies that overcome the immunosuppressive tumor micro-environment to promote T-cell recruitment and T-cell cytolytic function will be required to elicit durable anti-tumor immunity. To accomplish this, the STACT (S. Typhimurium-Attenuated Cancer Therapy) platform was developed. STACT is a live bacterial product that has been highly modified using precision genome editing for the following properties: (1) enhanced tolerability after IV dosing, (2) tumor-specific enrichment, (3) phagocytosis by tumor-resident antigen-presenting cells (APCs) with a lack of epithelial cell infectivity, (4) multiplexed genetic cargo delivery, and (5) attenuation of bacterial pathways that impair CD8+ T-cell function. An extensive screening campaign was performed to identify ideal encoded immunomodulatory payload combinations delivered by STACT for efficacy against T-cell excluded tumors.

Methods Chromosomal edits to the STACT platform strain were made using PCR. A panel of immunomodulatory proteins, including cytokines, type I interferon (IFN)-inducing factors, co-stimulatory receptors, checkpoint antibodies and TGFβR-Fc decoys were tested for combinatorial potency using STACT. An engineered STING (eSTING) was designed through an extensive protein engineering campaign to identify optimal variants. Combinations were evaluated in primary human APCs using in vitro functional assays, where STACT IL-15Rα-IL-15 (IL-15) + eSTING (ACTM-838) emerged as a lead candidate. ACTM-838 was then evaluated in multiple murine tumor models for therapeutic efficacy and mechanism, as well as tolerability in rodents and primates after systemic administration.

Results Combinatorial target profiling led to the discovery of ACTM-838, a STACT encoding IL-15 + eSTING. In vitro, ACTM-838 payloads synergistically produced high levels of type I IFN and T-cell recruitment and activation factors from primary human APCs. In vivo, ACTM-838 demonstrated a high degree of complete tumor responses that were entirely CD8+ T-cell dependent. In an autochthonous breast cancer model that lacks any significant lymphocyte infiltrate, ACTM-838 was able to uniformly enrich in each spontaneous lesion to high levels after IV dosing and resulted in significant CD8 + T-cell infiltration. In primates, ACTM-838 was well-tolerated, rapidly cleared, and elicited minimal cytokine response after IV dosing.

Conclusions ACTM-838 is a highly attenuated, precision genome-engineered bacterial immunotherapy that delivers IL-15 + eSTING to phagocytic APCs of the solid tumor micro-environment after systemic administration. In preclinical studies, ACTM-838 promotes CD8+ T-cell mediated tumor clearance in T-cell excluded tumors and elicits durable anti-tumor immunity, and is well tolerated in primates. Based on these data, ACTM-838 was nominated for clinical development and has entered cGMP manufacturing and IND-enabling studies.

Ethics Approval All animals were used according to protocols approved by an Institutional Animal Care and Use Committee

and maintained in specific pathogen-free conditions in a barrier facility.

<http://dx.doi.org/10.1136/jitc-2021-SITC2021.853>

SGN-B7H4V, A NOVEL, INVESTIGATIONAL VEDOTIN ANTIBODY-DRUG CONJUGATE DIRECTED TO THE T CELL CHECKPOINT LIGAND B7-H4, SHOWS PROMISING ACTIVITY IN PRECLINICAL MODELS

¹Elizabeth Gray*, ¹Angela Epp, ¹Michelle Ulrich, ¹Disha Sahetya, ¹Kelly Hensley, ¹Julie Hahn, ¹Sean Allred, ¹Jane Haass, ¹Katie Snead, ¹Sasha Lucas, ¹John Gosink, ²Rogely Boyce, ¹Esther Trueblood, ¹Piper Treuting, ¹Chris Frantz, ¹Alyson Smith, ¹Jason Schrum, ¹Natalya Nazarenko, ¹Shyra Gardai. ¹Seagen, Inc., Bothell, WA, USA; ²Beechy Ridge ToxPath LLC, Clay, WV, USA

Background SGN-B7H4V is a novel, investigational vedotin antibody drug conjugate (ADC) directed to B7-H4, a member of the B7 family of immune checkpoint ligands. B7-H4 expression is elevated on a variety of solid tumors including breast, ovarian, and endometrial tumors.¹ SGN-B7H4V is composed of a fully human IgG1 anti-B7-H4 monoclonal antibody (mAb) conjugated to the microtubule disrupting agent monomethyl auristatin E (MMAE) via a protease-cleavable peptide linker. SGN-B7H4V is designed to bind and internalize the immune checkpoint ligand B7-H4/ADC complex from the surface of malignant cells and release the cytotoxic payload MMAE. This "vedotin" drug linker system has been clinically validated by multiple ADC programs, including brentuximab vedotin, enfortumab vedotin, and polatuzumab vedotin.²⁻⁴ Here, we characterize the target antigen B7-H4 and evaluate SGN-B7H4V activity in preclinical models.

Methods B7-H4 expression was characterized by RNA expression and immunohistochemistry across multiple solid tumor types. The ability of SGN-B7H4V to kill B7-H4-expressing tumor cells in vitro and in vivo in a variety of xenograft tumor models was also evaluated. Finally, the tolerability of SGN-B7H4V was assessed in rodent and non-human primate toxicology studies.

Results Immunohistochemistry confirmed expression of B7-H4 across multiple solid tumor types, including ovarian and breast tumors. In vitro, upon binding to SGN-B7H4V, the immune checkpoint ligand B7-H4 was rapidly internalized and delivered the cytotoxic payload MMAE. Moreover, SGN-B7H4V killed B7-H4-expressing tumor cells in vitro by MMAE-mediated cytotoxicity, antibody-dependent cellular cytotoxicity (ADCC), and antibody-dependent cellular phagocytosis (ADCP). In vivo, SGN-B7H4V demonstrated strong anti-tumor activity in multiple xenograft models, including ovarian and breast cancer models. Activity was observed in models with both uniformly high and heterogeneous expression of B7-H4, consistent with robust bystander activity of vedotin ADCs. Finally, SGN-B7H4V was tolerated in both rat and non-human primate (NHP) toxicology studies at doses consistent with approved vedotin ADCs.

Conclusions B7-H4 is a promising ADC target expressed by several solid tumor types. SGN-B7H4V demonstrates robust anti-tumor activity in preclinical models through multiple potential mechanisms and is tolerated in rat and NHP toxicity studies. Altogether, these data support further evaluation of SGN-B7H4V in a planned, first-in-human phase 1 clinical study.

Acknowledgements We would like to thank Kellie Spahr for conjugation support and Martha Anderson for in vivo biology support.

REFERENCES

1. Leong SR, Liang WC, Wu Y, Crocker L, Cheng E, Sampath D, *et al.* An anti-B7-H4 antibody-drug conjugate for the treatment of breast cancer. *Mol Pharm* 2015;**12**(6):1717–29. Epub 2015/04/09. doi: 10.1021/mp5007745. PubMed PMID: 25853436.
2. Rosenberg JE, O'Donnell PH, Balar AV, McGregor BA, Heath EI, Yu EY, *et al.* Pivotal trial of enfortumab vedotin in urothelial carcinoma after platinum and anti-programmed death 1/programmed death ligand 1 therapy. *J Clin Oncol* 2019;**37**(29):2592–600. Epub 2019/07/30. doi: 10.1200/JCO.19.01140. PubMed PMID: 31356140; PubMed Central PMCID: PMC.
3. Senter PD, Sievers EL. The discovery and development of brentuximab vedotin for use in relapsed Hodgkin lymphoma and systemic anaplastic large cell lymphoma. *Nat Biotechnol* 2012;**30**(7):631–7. Epub 2012/07/12. doi: 10.1038/nbt.2289. PubMed PMID: 22781692.
4. Tilly H, Morschhauser F, Bartlett NL, Mehta A, Salles G, Haioun C, *et al.* Polatuzumab vedotin in combination with immunochemotherapy in patients with previously untreated diffuse large B-cell lymphoma: an open-label, non-randomised, phase 1b-2 study. *Lancet Oncol* 2019;**20**(7):998–1010. Epub 2019/05/19. doi: 10.1016/S1470-2045(19)30091–9. PubMed PMID: 31101489.

Ethics Approval All animal studies were conducted in accordance with protocols reviewed and approved by the Institutional Animal Care and Use Committee at Seagen or the external testing facility that conducted the studies.

<http://dx.doi.org/10.1136/jitc-2021-SITC2021.854>

DEVELOPMENT OF A NOVEL ANTI-MULTIPLE MYELOMA CHIMERIC ANTIGEN RECEPTOR T CELL THERAPY

Chuck Hay*, Mary Faber, Kemi Adeyanju, Jeffrey Medin. *Medical College of Wisconsin, Wauwatosa, WI, USA*

Background Multiple myeloma is a cancer of plasma cells, wherein the plasma cells begin outgrowing and even suppressing the growth of normal hematopoietic-lineage cells in the blood marrow. It is estimated that nearly 35,000 new cases of multiple myeloma will be diagnosed each year, and over 12,000 individuals will die from multiple myeloma in 2021. The current overall 5-year survival rate of 54% stresses the need for alternative treatment strategies. A chimeric antigen receptor T cell (CAR-T) therapy that targets multiple myeloma surface proteins may have the potential to improve this survival rate.

Methods A commonly associated multiple myeloma antigen was selected, and the extracellular domain of the protein was expressed in an Expi293 cell culture system. The multiple myeloma protein was expressed with and purified by a Hisx6 tag. The purified protein was used to pan a specific scFv phage display library that was generated uniquely for our lab from multiple blood donors. Several clones were identified and sequenced. One clone was selected and verified to be capable of binding the multiple myeloma antigen via ELISA. This anti-multiple myeloma scFv was then subcloned into CAR-T plasmids. This is a second-generation CAR-T using a 4-1BB co-stimulator domain and a CD3 ζ intracellular signaling domain was used for this therapy. Further, a cell-fate control gene, LNGFR Δ Tmpk, was added to the plasmid to combat potential graft versus host disease. CAR-T and lentivirus (LV) plasmids were transfected into HEK cells to produce anti-multiple myeloma CAR-T LV.

Results The anti-multiple myeloma CAR LV was transduced into HEK cells and titered via qPCR, which showed the LV prep produced 3.1E8 IU/ml. qPCR also showed there to be 0.407 vector copies per cell on average when using an MOI of 3. Our CAR-T LV was then used to transduce Jurkat cells at an MOI of 3. Using anti-Fab and anti-protein L antibodies, the transduced cells were shown to be expressing the anti-multiple myeloma CAR-T by flow cytometry. After confirming successful transduction and expression, transduced Jurkats (and controls) were co-cultured with multiple myeloma cell lines and incubated for 24 hours. ELISA testing for IFN- γ was performed on the resulting supernatants; specific engagement was demonstrated.

Conclusions These results show that our anti-multiple myeloma CAR is successfully expressed and is functional. Our future goal is to successfully transduce our anti-multiple myeloma CAR LV into primary T cells and test for functionality in these cells before transitioning into in vivo models.

<http://dx.doi.org/10.1136/jitc-2021-SITC2021.855>

INBRX-106: A NOVEL HEXAVALENT ANTI-OX40 AGONIST FOR THE TREATMENT OF SOLID TUMORS

Emily Rowell*, Heather Kinkead, Elisabeth Torretti, Bryan Becklund, Florian Sulzmaier, William Crago, Kyle Jones, John Timmer, Quinn Deveraux, Brendan Eckelman, Analeah Heidt. *Inhibrx, Inc., La Jolla, CA, USA*

Background OX40 is a co-stimulatory receptor enriched on immune cells in the tumor microenvironment. OX40 agonism promotes anti-tumor responses, both singly and in combination with checkpoint inhibitors. The cognate OX40 ligand, OX40L, is a trimeric protein that activates robust signaling through clustering. INBRX-106 is a novel hexavalent OX40 agonist that has been rationally designed to optimize target clustering and provide superior agonism to previously explored bivalent entities, leading to more potent anti-tumor activity.

Methods INBRX-106 is a homodimer, each half comprising three identical humanized, camelid single-domain antibody binding domains targeting OX40 linked end-to-end, and fused to an effector-enabled human IgG1 constant domain (Fc). Due to lack of rodent cross-reactivity, a valency, affinity and activity-matched murine surrogate, Hex-C04, was generated for the purpose of preclinical modeling. Hex-C04 contains an mIgG2a effector enabled Fc, the mouse isotype most analogous to the activity of human IgG1. The activity and potency of INBRX-106 and Hex-C04 were evaluated in functional in vitro T-cell assays, and the anti-tumor efficacy of Hex-C04 was evaluated alone or in combination with PD-1 blockade across a number of syngeneic tumor models.

Results INBRX-106 binds specifically to OX40 with a sub nanomolar apparent affinity, without blocking the binding of its ligand OX40L. In vitro, cross-linking by INBRX-106 rapidly induces loss of OX40 surface expression in addition to driving receptor signaling. In primary T-cell assays, INBRX-106 is more potent than a bivalent comparator antibody, inducing greater upregulation of activation markers, cytokine production and proliferation. This costimulatory activity exhibits a bell-shaped dose-response curve, with maximal activity occurring at receptor occupancies of 30–100%. In vivo, tumor growth control by Hex-C04 also follows a bell-shaped dose response curve. Rapid loss of OX40 is observed in vivo as well, with both the degree and duration of OX40 loss dependent on C_{max} and exposure. Hex-C04 demonstrated strong single-agent activity across a variety of preclinical tumor models including models that do not respond to a PD-1/PD-L1 checkpoint inhibitor, and this activity was improved in combination with a PD-1 blocking antibody.

Conclusions Preclinically, INBRX-106 significantly outperforms bivalent antibodies in co-stimulatory capacity and anti-tumor activity. On the weight of this data, Inhibrx Inc. has initiated a first-in-human Phase 1 trial of INBRX-106 as a single agent or in combination with Keytruda® (pembrolizumab). The complex relationship between dose, OX40 target modulation and activity indicate the importance of integrating preclinical data sets with emerging clinical data to make informed decisions regarding INBRX-106 dose and schedule.

Trial Registration NCT04198766

Ethics Approval The care and use of all animals were reviewed and approved by the IACUC committees of Explora BioLabs and Molecular Diagnostic Services and conducted in accordance with AAALAC regulations.

<http://dx.doi.org/10.1136/jitc-2021-SITC2021.856>

SELECTIVE TREG DEPLETION IN SOLID TUMORS WITH ALD2510, A NOVEL HUMANIZED CD25-SPECIFIC, IL-2 SPARING MONOCLONAL ANTIBODY

¹Jemila Houacine, ²Anne Marie-Cardine, ¹Aude Le Roy, ³Jérôme Giustiniani, ¹Riad Abes, ⁴Anne-Sophie Chrétien, ⁴Stéphane Fattori, ⁴Laurent Gorvel, ²Armand Bensussan, ⁴Daniel Olive, ¹Arnaud Foussat*. ¹Alderaan Biotechnology, Paris, France; ²INSERM U976, Paris, France; ³Inserm U955, Créteil, France; ⁴Inserm UMR1068, Institut Paoli Calmettes, Marseille, France

Background Regulatory T cells (Tregs) inhibit immune responses in solid cancers using cell-cell contacts and anti-inflammatory cytokine release. Also, due to high and constitutive levels of IL2Ralpha chain (CD25) expression, Tumor infiltrating (TIL)-Tregs cells preferably consume local Interleukin-2 (IL2), thus depriving conventional T cells from IL2-induced activation and proliferation. Therefore, the selective depletion of TIL-Tregs using therapeutic antibodies targeting CD25 represents a promising strategy to unleash tumor-specific immune responses in solid cancers.

Methods CD25 expression was evaluated by flow and mass cytometry on T-cell subsets from tumor biopsies collected in patients with various solid cancers (Breast, Endometrial and Cervix). ALD2510 potency was demonstrated in vitro and in vivo in human CD25 Knock-In huGEMM (huCD25-KI) MC38-bearing mice and in CD34+ humanized NSG mice grafted with human cancer cell lines (MDA-MB-231 and HT29).

Results In tumor biopsies, CD25 is highly and homogeneously expressed by TIL-Tregs, while being much less expressed by only a fraction of conventional CD4+ T cells and barely expressed by TIL-CD8+ cells. This confirms CD25 as the most selective marker to target TIL-Tregs in cancer patients. In vitro, ALD2510 shows potent ADCC and ADCP as well as strong Treg depletion capacity. Importantly, CD8+ and CD4+ conventional T cells are not impacted by ALD2510 even after activation confirming ALD2510 ability to selectively deplete Tregs. Accordingly, ALD2510 neither blocks IL-2 binding to CD25 nor inhibits IL-2 induced proliferation of activated T cells. In CD34+-humanized mice, ALD2510 efficiently depletes human Tregs but spares conventional T cells. Also, in the MC38 model in huCD25-KI mice, ALD2510 shows a strong anti-tumor activity as a single agent with 60% overall tumor growth inhibition together with massive Treg depletion 7 days after a single administration. In addition, combination of ALD2510 with anti-PD1 leads to complete tumor regression and strong activation of conventional T cells. Importantly, Basiliximab, a CD25-specific IL-2 blocking antibody, although efficient at depleting Treg cells, did not impact tumor growth, thus demonstrating that the IL-2 sparing feature of ALD2510 is critical to elicit anti-tumour response in vivo.

Conclusions This preclinical data package supports CD25 as a potent and selective Treg marker allowing Tregs depletion while sparing conventional T cells. In this context, ALD2510, a novel humanized CD25-specific and IL-2 sparing antibody presents all the required attributes for selective and efficient TIL-Tregs depletion, making it a promising drug candidate to treat a broad range of solid tumor patients.

Ethics Approval The studies involving human material were approved by the ethical committee "Comité de Protection des Personnes Sud Méditerranée" under approval numbers 1362 and 1048. All participants gave informed consent before taking part.

<http://dx.doi.org/10.1136/jitc-2021-SITC2021.857>

858

TILKINE-2: A NOVEL BEST-IN-CLASS TUMOR INFILTRATING LYMPHOCYTE (TIL) TARGETING ENGINEERED IL-2 WITH SUPERIOR PRE-CLINICAL EFFICACY AND SAFETY FOR IMMUNOTHERAPY OF CANCER

Sreerupa Challa, Jonathan Carnino, Andrea Umana, Yuesheng Li, Jing Xu, Lingyun Rui, Yao-Te Hsieh*. *Cugene, Waltham, MA, USA*

Background High-dose Interleukin-2 is the earliest FDA-approved immunotherapy for metastatic melanoma and renal cell carcinoma. Unfortunately, its application is limited due to its short half-life and severe toxicity at the therapeutic dose. To limit systemic toxicity, tumor-targeting antibody-based delivery of IL-2 has been developed, however with poor outcomes. We here deploy a novel strategy to deliver IL-2 to the tumor microenvironment by binding to Tumor-Infiltrating Lymphocytes (TILs). TILKine-2 is a recombinant bifunctional protein comprised of an antibody directed against TILs (TILAb) fused to an engineered IL-2, which simultaneously revives and expands antigen-primed exhausted T cells. The IL-2 portion of TILKine-2 was engineered to have improved tolerability, slower receptor-mediated clearance, and prolonged half-life.

Methods Target binding of TILKine-2 was evaluated by cell-free and cell-based methods. In vitro functional characterization was performed using human peripheral blood mononuclear cells (PBMCs). Pharmacokinetics (PK), pharmacodynamics (PD), and anti-tumor activity of murine TILKine-2 surrogate (TILKine-2s) were evaluated in various syngeneic models. The safety and immune cell activation of TILKine-2 were assessed in non-human primates (NHPs).

Results Structure-based design and activity-guided fine-tuning resulted in an optimized IL-2 variant that was fused to TILAb to generate TILKine-2. TILKine-2 demonstrated TIL-target antigen binding and blocking activity with sub-nM potency. TILKine-2 has a binding activity abolished to IL-2R α and fine-tuned to IL-2R $\beta\gamma$. In PBMCs, TILKine-2 potently induced intracellular signaling and cell proliferation in IL-2R $\beta\gamma$ dominant effector CD8+T and NK cells along with IFN- γ secretion. In vivo, TILKine-2 displayed significantly prolonged half-life with sustained proliferation, expansion, and Granzyme B expression on CD8+T and NK cells. Notably, the effects were more pronounced in the tumor than periphery, leading to massive immune hot tumors. Consequently, TILKine-2s exhibited robust anti-tumor primary and memory response in both cold and hot tumor models (MC38, CT26, B16F10, PAN02). Furthermore, TILKine-2s demonstrated superior and synergistic anti-tumor efficacy compared to TILAb alone, engineered IL-2 alone, or their combination, with 100% tumor regression resulting in ~80% tumor free mice in MC38 and Pan02 models. In NHPs, TILKine-2 preferentially induced memory CD8+T, total CD8+T, and NK cell expansion. TILKine-2 was safe and well-tolerated in NHPs with no notable changes in body weight, temperature, clinical pathology, or signs of vascular leakage after repeated dosing.

Conclusions By targeting TILs, TILKine-2 demonstrated robust anti-tumor efficacy by preferentially inducing proliferation, expansion, and activation of intra-tumoral lymphocytes while reducing systemic toxicity and improving therapeutic window. In conclusion, TILKine-2 is a promising therapeutic agent for clinical development.

Ethics Approval For mouse studies, the practices and procedures used were reviewed and approved by Brandeis University IACUC committee (Protocol #22001). For monkey

studies, the practices and procedures used were in accordance with the safety and Quality Assurance guidelines set out in the Guideline for Experiments document of Kunming Biomed International (KBI-01-GEv2.0).

<http://dx.doi.org/10.1136/jitc-2021-SITC2021.858>

TUNING THE TUMOR MICROENVIRONMENT BY REPROGRAMMING TREM1+ MYELOID CELLS TO UNLEASH ANTI-TUMOR IMMUNITY IN SOLID TUMORS

Nadine Jahchan*, Hanna Ramoth, Vladi Juric, Erin Mayes, Shilpa Mankikar, Ranna Mehta, Mikhail Binnewies, Subhadra Dash, Rachael Palmer, Joshua Pollack, Joshua Rudolph, Pamela Canaday, Linnea Haegglom, Carlos Santamaria, Xiaoyan Du, Leonard Reyno, Kevin Baker, Linda Liang. *Pionyr Immunotherapeutics, San Carlos, CA, USA*

Background The tumor microenvironment (TME) often contains high levels of suppressive myeloid cells that contribute to innate checkpoint inhibitor (CPI) resistance. Pionyr's Myeloid Tuning approach involves altering the composition and/or the function of myeloid cells in the TME. Myeloid reprogramming alters the function of immunosuppressive myeloid cells to acquire an immunostimulatory phenotype. Triggering receptor expressed on myeloid cells-1 (TREM1) is an immunoglobulin superfamily cell surface receptor enriched on tumor-associated myeloid cells. To investigate the potential of TREM1 modulation as an anti-cancer therapeutic strategy, Pionyr developed an afucosylated humanized anti-TREM1 monoclonal antibody termed PY159 and characterized it in pre-clinical and translational biomarker assays described below.

Methods PY159 responses in human whole blood and dissociated primary tumor cells in vitro were evaluated by flow cytometry and measurement of secreted cytokines and chemokines by MSD. TREM1 expression in human tumors was validated by scRNAseq, flow cytometry, and immunohistochemistry (IHC). In vivo efficacy and pharmacodynamic studies of a surrogate anti-mouse TREM1 antibody, termed PY159m, were evaluated using syngeneic mouse tumor models, either as a single-agent or in combination with anti-PD-1. To select tumor types and patients most likely to benefit from PY159 therapy, Pionyr developed qualitative and quantitative monoplex and multiplex IHC assays that detect TREM1 expression levels in human tumor tissues.

Results PY159 treatment in vitro induced signaling, upregulated monocyte activation markers, and induced proinflammatory cytokines. In human tumors, TREM1 was detected on tumor-associated neutrophils, tumor-associated macrophages, and monocytic myeloid-derived suppressive cells. The surrogate PY159m anti-mouse TREM1 antibody exhibited anti-tumor efficacy in several syngeneic mouse tumor models, both as single-agent and in combination with anti-PD-1. Screening for TREM1 expression in tumor tissues demonstrated that TREM1+ tumor associated myeloid cells were highly enriched in the TME of multiple solid tumor indications. The monoplex and multiplex IHC assays offered insights into the localization of TREM1+ myeloid cells and their spatial relationship with other immune cells present in the TME to determine what immune composition will be more favorable for response to PY159 therapy.

Conclusions Collectively, the available nonclinical data support PY159 as a TREM1 agonist that reprograms myeloid cells and unleashes anti-tumor immunity. PY159 safety and efficacy are currently being evaluated in first-in-human clinical trial (NCT04682431) involving select advanced solid tumors patients resistant and refractory to standard of care therapies alone and in combination with a CPI. The TREM1 IHC assay is successfully being used on FFPE archival tumor tissues from enrolled patients to determine TREM1 expression levels.

<http://dx.doi.org/10.1136/jitc-2021-SITC2021.859>

THE ANTI-TUMOR ACTIVITY OF HSP-90 THERAPEUTIC CANCER VACCINE (AST-021P) COMBINE WITH TLR2/3 AGONIST IN A MMTV-NEU TRANSGENIC MODEL

¹Jinho Kang, ²Eunkyo Joung, ³Hunwoo Shin, ⁴Byung cheol Ahn, ⁴Eunjung Jung, ³Hun Jung*, ¹Kyong Hwa Park. ¹Korea University College of Medicine, Seoul, Korea, Republic of; ²Aston Sci. Inc, Seoul, Korea, Republic of; ³Aston Sci. Inc., Seoul, Korea, Republic of; ⁴CHA Vaccine Institute, Seoul, Korea, Republic of

Background AST-021p, which is derived from HLA class II binding epitopes of human HSP90 protein, is an investigational therapeutic cancer vaccine for the malignant neoplasms. AST-021p is designed to demonstrate the immunologic efficacy by activating antigen-specific CD4+ Th1 cell in humans. Due to their ability to link the innate with the adaptive immune response, Toll-like receptor (TLR) agonists are highly promising as adjuvants in vaccines against life-threatening and complex diseases such as cancer, AIDS and malaria. In this study, AST-021p was investigated to evaluate the immunogenicity and tumor growth inhibitory effect under the condition of combining with various immune adjuvants derived from TLR agonists, using in-vivo model.

Methods Three different agonists of TLR (TLR-4, TLR-2/3, TLR-7/8) were assigned to investigate the immunogenicity in each group (4 FVB mice/group, total 4 groups). AST-021p was intradermally injected 3 times with different TLR-agonists and the immunogenicity was assessed from mouse splenocyte by HSP90-specific IFN- γ ELISpot method. We also examined the efficacy of AST-021p and selected TLR-agonist in MMTVneu Tg mice (4 mice/group, conducted twice and A total 8 mice was assigned to each group). The combination of AST-021p and TLR-2/3 agonist (AST-021p plus TLR-2/3 agonist) was injected 3 times every 10 days to mice followed by inoculated mouse mammary cancer cell line. The tumor volume change and immunogenicity were evaluated.

Results The most effective TLR-agonist as a potent immune adjuvant was a TLR-2/3 agonist (L-pampoTM, supplied by CHA Vaccine Institute). In MMTV-Neu transgenic mice, AST-021p (100 μ g) plus TLR-2/3 agonist significantly enhanced immunogenicity by increasing up to 130 ± 10 HSP-90 epitope specific T cells per 1×10^5 splenocytes ($P < 0.001$). AST-021p plus TLR-2/3 agonist also showed higher tumor growth inhibitory effect (170 ± 108 mm³) on post-implantation 35th day by suppressing mouse mammary cancer cell line (5 \times 105)-derived tumor growth, compared with a TLR-2/3 agonist alone (1031 ± 450 mm³).

Conclusions Combination regimen of AST-021p and TLR-2/3 agonist (as immune adjuvant) demonstrated significant immunogenicity and tumor prevention effect in in-vivo study. These data supported the clinical study of AST-021p combined with TLR-2/3 agonist as active immune adjuvant in certain tumor types, and phase 1/2 clinical program would be expected to be initiated.

Acknowledgements Not applicable

Trial Registration Not applicable

REFERENCES

1. Cserrmely P, Schnaider T, Soti C, Prohaszka Z, Nardai G. The 90-kDa molecular chaperone family: structure, function, and clinical applications. A comprehensive review. *Pharmacol Ther* 1998;79,129–168.
2. Wang H, Lu M, Yao M, Zhu W. Effects of treatment with an Hsp90 inhibitor in tumors based on 15 phase II clinical trials. *Mol Clin Oncol* 2016;5,326–334.
3. Ramalingam S, Goss G, Rosell R, Schmid-Bindert G, Zaric B, Andric Z, Bondarenko I, Komov D, Ceric T, Khuri F. A randomized phase II study of ganetespib, a heat shock protein 90 inhibitor, in combination with docetaxel in second-line therapy of advanced non-small cell lung cancer (GALAXY-1). *Ann Oncol Off J Eur Soc Med Oncol* 2015;26,1741–1748.

Ethics Approval All experimental procedures involving mice were performed with the guidance protocols approved by the Institutional Animal Care and Use Committee of Korea University (IACUC, Approval number: KOREA-2019-129)

Consent It is not an abstract containing sensitive or identifiable information.

<http://dx.doi.org/10.1136/jitc-2021-SITC2021.860>

REPROGRAMMING REGULATORY T CELLS (TREG) USING A MALT1 INHIBITOR FOR CANCER THERAPY

¹Peter Keller*, ¹Irina Mazo, ¹Yun Gao, ¹Vijayal Reddy, ¹Francisco Caballero, ¹Sam Kazer, ²Amina Fu, ²Yi Sun, ³Dannah Miller, ³Roberto Gianani, ⁴James Marvin, ⁵Bret Stephens, ⁶Gregory Beatty, ²Russell Jenkins, ²Ulrich Von Andrian, ⁷Daniel Krappmann, ²Thorsten Mempel. ¹*Monopteros Therapeutics, Boston, MA, USA*; ²*Harvard Medical School, Boston, MA, USA*; ³*Flagship Biosciences, Broomfield, CO, USA*; ⁴*University of Utah, Salt Lake City, UT, USA*; ⁵*Rincon Biosciences, Salt Lake City, UT, USA*; ⁶*University of Pennsylvania, Philadelphia, PA, USA*; ⁷*Helmholtz Zentrum, Munich, Germany*

Background MALT1 protease is a promising target in aggressive lymphomas¹, and two phase 1 clinical trials in hematological cancers are ongoing (NCT03900598, NCT04876092). More recently, MALT1 protease inhibition was also shown to reprogram regulatory T cells (Treg) in solid tumors, causing them to lose their immunosuppressive function and secrete interferon-gamma (IFN).² Changes in Treg metabolism in the tumor microenvironment (TME) may account for their destabilization and selective susceptibility to reprogramming in tumor tissue.^{3 4 5} While strong MALT1 inhibition can cause Treg depletion in blood and induce autoimmune toxicity,⁶ a therapeutic window for a differentiated MALT1 inhibitor that reprograms destabilized Treg in the TME before affecting Treg in healthy tissue may exist.² MPT-0118 is an orally dosed MALT1 inhibitor developed to reprogram destabilized Treg in the TME without causing autoimmune symptoms. A Phase 1/1b dose-escalation and cohort-expansion clinical trial evaluating MPT-0118 is underway (NCT04859777).

Methods Human xenograft models of lymphoma were used to assess the direct activity of MPT-0118 on MALT1-dependent (but not MALT1-independent) hematologic tumors. Effects of MPT-0118 on solid tumors were determined in syngeneic cancer models. Human and mouse tumor tissues were evaluated for Treg reprogramming by *in situ* hybridization or flow cytometry. Patient-derived organotypic tumor spheroids were assessed for immune-mediated cell killing. Studies in rodents and dogs assessed pharmacokinetics (PK) and safety.

Results MPT-0118 was selective and effective in preventing growth of aggressive MALT1 protease-dependent lymphomas. Beyond direct activity on hematologic malignancies, MPT-0118 also increased anti-tumor immune responses as single-agent or in combination with anti-PD-1 in syngeneic tumor models that are otherwise unresponsive to immune checkpoint blockade (ICB). MPT-0118-treated syngeneic tumors showed an increase in IFN-secreting Treg, associated with decelerated tumor growth. PK studies reveal that MPT-0118 has a high volume of distribution, and effective inhibitor concentrations are reached in the murine tumors upon oral dosing. The drug candidate caused tumor-associated Treg to produce IFN without changing the frequency of Treg circulating in the blood. *Ex vivo*, MPT-0118 induced Treg reprogramming in tumors resected from patients with colorectal and endometrial cancers and cell killing in spheroids derived from patients with colorectal cancer.

Conclusions The MALT1 inhibitor MPT-0118 is a clinical candidate for treating MALT1-expressing lymphomas and Treg-infiltrated solid tumors. MPT-0118 exploits the therapeutic opportunity presented by destabilized Treg in the TME. Treg reprogramming represents a novel strategy with the potential to improve responses to ICB therapy in a broad range of solid tumors.

REFERENCES

1. Nagel D, Spranger S, Vincendeau M, Grau M, Raffegerst S, Kloos B, Hlahla D, Neuenschwander M, Peter von Kries J, Hadian K, Dörken B, Lenz P, Lenz G, Schendel DJ, Krappmann D. Pharmacologic inhibition of MALT1 protease by phenothiazines as a therapeutic approach for the treatment of aggressive ABC-DLBCL. *Cancer Cell* 2012 December 11; **22**(6):825–37.
2. Di Pilato M, Kim EY, Cadilha BL, Prüßmann JN, Nasrallah MN, Seruggia D, Usmani SM, Misale S, Zappulli V, Carrizosa E, Mani V, Ligorio M, Warner RD, Medoff BD, Marangoni F, Villani AC, Mempel TR. Targeting the CBM complex causes Treg cells to prime tumours for immune checkpoint therapy. *Nature* 2019 June; **570**(7759):112–116.
3. Lim SA, Wei J, Nguyen TM, Shi H, Su W, Palacios G, Dhungana Y, Chapman NM, Long L, Saravia J, Vogel P, Chi H. Lipid signalling enforces functional specialization of Treg cells in tumours. *Nature* 2021 March; **591**(7849):306–311.
4. Zappasodi R, Serganova I, Cohen IJ, Maeda M, Shindo M, Senbabaoglu Y, Watson MJ, Leftin A, Maniyar R, Verma S, Lubin M, Ko M, Mane MM, Zhong H, Liu C, Ghosh A, Abu-Akeel M, Ackerstaff E, Koutcher JA, Ho PC, Delgoffe GM, Blasberg R, Wolchok JD, Merghoub T. CTLA-4 blockade drives loss of Treg stability in glycolysis-low tumours. *Nature* 2021 March; **591**(7851):652–658.
5. Overacre-Delgoffe AE, Chikina M, Dadey RE, Yano H, Brunazzi EA, Shayan G, Horne W, Moskovitz JM, Kolls JK, Sander C, Shuai Y, Normolle DP, Kirkwood JM, Ferris RL, Delgoffe GM, Bruno TC, Workman CJ, Vignali DAA. Interferon- γ drives Treg fragility to promote anti-tumor immunity. *Cell* 2017 June 1; **169**(6):1130–1141.e11.
6. Martin K, Junker U, Tritto E, Sutter E, Rubic-Schneider T, Morgan H, Niwa S, Li J, Schlapbach A, Walker D, Bigaud M, Beerli C, Littlewood-Evans A, Rudolph B, Laisney M, Ledieu D, Beltz K, Quancard J, Bornancin F, Zamurovic Ribrioux N, Calzascia T. Pharmacological inhibition of MALT1 protease leads to a progressive IPEX-Like pathology. *Front Immunol* 2020 April 30; **11**:745.

<http://dx.doi.org/10.1136/jitc-2021-SITC2021.861>

**DECTIN-2, A NOVEL TARGET FOR TUMOR
MACROPHAGE REPROGRAMMING IN CANCER
IMMUNOTHERAPY**

¹Justin Kenkel*, ¹Po Ho, ²Sameera Kongara, ¹Karla Henning, ¹Cindy Kreder, ¹Jess Nolin, ¹Steven Chapin, ¹Marcin Kowanetz, ¹Michael Alonso, ¹Shelley Ackerman, ²Edgar Engleman, ¹David Dornan. ¹Bolt Biotherapeutics, Redwood City, CA, USA; ²Stanford University, Palo Alto, CA, USA

Background Tumor-associated macrophages (TAMs) are an abundant immune cell population in most cancers that support tumor progression through their immunosuppressive effects. We discovered that TAMs express the pattern recognition receptor Dectin-2 (Clec4n/CLEC6A), an activating C-type lectin receptor (CLR) that binds to high-mannose glycans on fungi and other microbes and induces protective immune responses against infectious disease. Dectin-2 is selectively expressed by myeloid cells, and upon ligation mediates enhanced phagocytosis, antigen processing and presentation, and proinflammatory cytokine production. Given these properties, we evaluated the therapeutic potential of targeting Dectin-2 using naturally derived ligands. We also generated human Dectin-2-targeted agonistic antibodies capable of robustly activating immunosuppressive "M2" or TAM-like macrophages.

Methods Dectin-2 expression was assessed by flow cytometry, immunohistochemistry, and using public databases. Mouse and human monocytes were differentiated into macrophages using recombinant cytokines or tumor-conditioned media, and stimulation was measured following overnight incubation with Dectin-2 ligands or antibodies. Mouse tumor cell lines were implanted into syngeneic hosts and mice were treated with mannan derived from *S. cerevisiae* via IT or IV administration.

Results Dectin-2 gene expression is minimal in normal human tissues but elevated across many tumor types, including breast, colon, lung, and kidney cancers. Dectin-2 is strongly expressed by macrophages differentiated *in vitro* and on primary TAMs. The fungal Dectin-2 ligand mannan stimulated proinflammatory cytokine production (e.g. TNF α) and costimulatory molecule expression (e.g. CD86) by macrophages in a Dectin-2-dependent manner. Treatment of tumor-bearing mice with mannan mediated tumor regression in multiple syngeneic tumor models, with high rates of tumor clearance in the MB49 bladder cancer model. These effects were Dectin-2 dependent, as efficacy was not observed when a Dectin-2-blocking antibody was co-administered or in knockout mice lacking Dectin-2 signaling components. Furthermore, depletion of either macrophages or T cells impaired efficacy, suggesting that Dectin-2-stimulated TAMs augment anti-tumor T cell responses. Based on these data, we developed novel Dectin-2 targeted agonist antibodies capable of activating human "M2" or TAM-like macrophages *in vitro* to produce an array of proinflammatory cytokines and chemokines akin to tumor-destructive "M1" macrophages.

Conclusions The data presented demonstrate the therapeutic potential of targeting Dectin-2 using natural ligands or agonistic antibodies as a novel pan-cancer approach for myeloid cell-directed tumor immunotherapy.

Ethics Approval All animal studies were performed in accordance with Institutional Animal Care and Use Committee (IACUC)-approved protocols.

<http://dx.doi.org/10.1136/jitc-2021-SITC2021.862>

IN VITRO AND IN VIVO STUDIES ESTABLISH DUOBODY[®]-CD3xB7H4 AS A NOVEL DRUG CANDIDATE FOR THE TREATMENT OF SOLID CANCERS

Louise Koopman*, Laura Smits-de Vries, Frederikke Lihme Egerod, Sebastiaan Wubben, Mischa Houtkamp, Stefanie De Poot, Madelon Paauwe, Edward van den Brink, Andrea Gorlani, Dennis Verzijl, Kate Sasser, Esther Breijl. *Genmab, Utrecht, Netherlands*

Background The immune checkpoint protein B7H4 is expressed on malignant cells in various solid cancers, whereas its expression is highly restricted in normal tissue. B7H4 is therefore an attractive target for a CD3 bispecific antibody (bsAb) therapeutic. Moreover, its expression is reported to be inversely correlated with PD-L1. Here, we describe the pre-clinical characterization of two B7H4-targeting CD3 bsAbs with different CD3 affinities, supporting the selection of our clinical lead, DuoBody-CD3xB7H4 (GEN1047).

Methods B7H4 protein expression in patient-derived samples was determined by immunohistochemistry. Controlled Fab-arm exchange of an Fc-silenced B7H4 antibody with two Fc-silenced CD3 ϵ -binding antibodies generated two CD3xB7H4 bsAbs that differ in CD3 binding affinity by approximately 30-fold. In vitro T-cell mediated cytotoxicity, T-cell activation, and cytokine release were assayed using cocultures of B7H4-expressing tumor cells and healthy donor T cells. Nonclinical safety (NCS) of the two CD3xB7H4 bsAbs was assessed in cynomolgus monkeys, and antitumor activity of the clinical lead in vivo was tested in a patient-derived xenograft (PDX) screen in mice with a humanized immune system (HIS).

Results B7H4 protein expression was confirmed in tumor biopsies from multiple indications, including breast, ovarian and lung cancer. Both bsAbs induced target-specific and dose-dependent tumor cell kill in vitro. Maximal kill and T-cell activation were comparable for both variants, although the potency of the high CD3 affinity bsAb was higher. However, production of inflammatory cytokines at comparable effective concentrations (IC₉₀) was lower for the low CD3 affinity bsAb. Single dose NCS studies in cynomolgus monkeys showed that both CD3xB7H4 bsAbs were well-tolerated. A dose-dependent increase in plasma cytokines IL-6 and MCP-1 2 hours after dosing was observed only with the high CD3 affinity bsAb. Based on these findings, the low CD3 affinity bsAb was selected for follow-up studies and named DuoBody-CD3xB7H4 (GEN1047). DuoBody-CD3xB7H4 demonstrated antitumor activity in vivo in a PDX screen in HIS mice. Repeated dosing of DuoBody-CD3xB7H4 in cynomolgus monkeys confirmed an acceptable safety profile up to the maximal dose tested (30 mg/kg).

Conclusions These studies describe the preclinical development of DuoBody-CD3xB7H4, a bsAb that induces T-cell mediated cytotoxicity of B7H4-positive tumor cells, which may provide an alternative therapeutic modality in the immune-oncology space for patients with solid cancers.

Ethics Approval Animal experiments were performed according to the guidelines of the Institutional Animal Care and Use Committee (IACUC) and in accordance with the regulations of the Association for Assessment and Accreditation of Laboratory Animal Care (AAALAC). NCS studies were conducted at Citoxlab (Evreux, France) and Charles River Laboratories (Trarant, UK) in accordance with the European Convention for the Protection of Vertebrate Animals Used for Experimental and Other Scientific Purposes (Council of Europe).

<http://dx.doi.org/10.1136/jitc-2021-SITC2021.863>

864

IDENTIFICATION OF A NOVEL ALLOSTERIC ORAL CBL-B INHIBITOR THAT AUGMENTED T CELL RESPONSE AND ENHANCED NK CELL KILLING IN VITRO AND IN VIVO

Jun Kuai*, Yingzhi Bi, Yilin Qi, Deborah Conrady, Rajiv Govindaraj, Graham Hone, R Aldrin Denny, Ken Carson, Geraldine Harriman, Fang Wang. *HoSpot Therapeutics, Boston, MA, USA*

Background Immunotherapies aiming to boost anti-tumor cell responses in cancer patients has been proven successful by checkpoint inhibitors targeting PD1 or CTLA-4, but the majority of cancer patients do not garner durable benefit. Co-stimulation through the CD28 pathway is one potential approach to maximize the benefits of immunotherapies. The E3 ubiquitin ligase Cbl-b (casitas b-lineage lymphoma proto-oncogene b) has been established as a master negative regulator of T-cells and NK cells and plays an important role in immune suppression. Genetic ablation of Cbl-b or functional inactivation of its E3 ligase activity in mice resulted in CD8 T-cell-mediated rejection of primary tumors in several mouse models. Based on the overwhelming evidence supporting the role of Cbl-b in immune suppression, targeting Cbl-b with small molecule inhibitors is attractive for cancer immunotherapy.

Methods Cbl-b is activated by tyrosine kinases and undergoes a large conformational change from closed inactive form to open active form. Historically, it had been difficult to identify inhibitors of Cbl-b. Through the utilization of our proprietary SpotFinder platform, a druggable phosphoregulatory pocket was identified in the inactive form of Cbl-b. Learnings from the platform allowed for the development of screening assays utilizing specifically designed protein constructs. Assays were developed to identify inhibitors that bind to the hotspot and lock Cbl-b in its inactive form.

Results Here we report on a member of our lead series of inhibitors, a low nanomolar potent inhibitor identified via application of our SpotFinder platform. This inhibitor binds to the inactive form of Cbl-b, its binding mode in the identified hotspot confirmed by co-crystal structures. It inhibits the phosphorylation of Cbl-b by kinases, inhibits the E3 ligase activity of Cbl-b, promotes cytokine release and enhances T cell proliferation well as NK cell activation and killing. In vivo, our CBL-B inhibitors efficaciously augmented the T cell response in anti-CD3 treated mice.

Conclusions We herein demonstrated the validation of our proprietary SpotFinder platform via the prediction and drugging of a regulatory hotspot on an important immune oncology target that has to date been very difficult to drug.

<http://dx.doi.org/10.1136/jitc-2021-SITC2021.864>

IOSH2 EXERTS POTENT ANTI-TUMOR ACTIVITY BY BLOCKING LILRB1/2 AND KIR3DL1 RECEPTOR SIGNALING

¹Osiris Marroquin Belaunzaran, ¹Anahita Rafiei*, ¹Anil Kumar, ¹Marco Gualandi, ¹Magdalena Westphal, ¹Lorenz Vogt, ¹Sean Smith, ²Michael Curran, ¹Christoph Renner. ¹ImmunOs Therapeutics AG, Schlieren, Switzerland; ²The UTD MD Anderson Cancer, Houston, TX, USA

Background To develop novel anti-cancer therapeutics we have used a reverse rational approach and searched for human HLA class I molecules known to induce autoimmunity and long-term lasting viral control as a surrogate marker for potential anti-cancer activity. HLA-B*27 or HLA-B*57 are well known genetic factors associated with superior control of viral infections (e.g. HIV and HCV) through processes related to both adaptive and innate immunity. Here we demonstrate that the expression of an optimised HLA-B57-Fc fusion protein (iosH2) exerts anti-tumor efficacy through its multimodal inhibition of LILRB1/2 and KIR3DL1 receptors.

Methods iosH2 was produced by stable expression in CHO cells and purified by standard chromatography techniques. Interaction and competition studies were performed using Bio-Layer Interferometry, ELISA, and cell-based assays. Analysis of LILRB1/2 downstream ITIM signaling was assessed using an automated western blot system. Functional cell-based assays including in vitro polarization and phagocytosis of macrophages, T cell and NK cell assays were assessed using live-cell imaging. In vivo efficacy studies were performed using syngeneic and humanized mouse models of cancer.

Results iosH2 binds with nanomolar affinity to LILRB1/2 and KIR3DL1, and blocks HLA-G and ANGP1L's binding to LILRB1/2. iosH2 reduces ITIM downstream signalling including phosphorylation of SHP1/2 and promotes conversion from M2 to M1 macrophage phenotype resulting in enhanced tumor cell phagocytosis in vitro. In addition, iosH2 increases T and NK cell cytotoxicity in co-cultures with cancer cell lines. In vivo efficacy studies demonstrate therapeutic efficacy in syngeneic C38 colon cancer mice and in BRGSF-HIS humanized PDX NSCLC mice in concert with reduction of pro-tumorigenic cytokines.

Conclusions iosH2 binds to LILRB1/2 and KIR3DL1, restores immune effector cell function in vitro and demonstrates anti-tumor activity in diverse in vivo mouse models. iosH2 is a first-in-class multi-functional agent that promotes key components of the innate and adaptive immune system leading to profound anti-tumor activity. Clinical development is underway and a phase I trial in preparation.

Ethics Approval 1. Animal housing and experimental procedures were conducted according to the French and European Regulations and the National Research Council Guide for the Care and Use of Laboratory Animals^{7–8}. The animal facility is authorized by the French authorities (Agreement N° B 21 231 011 EA). All animals procedures (including surgery, anesthesia and euthanasia as applicable) used in the current study (200269/ACT1 C38 SC/Ethical protocol: ONCO 1) were submitted to the Institutional Animal Care and Use Committee of Oncodesign (Oncomet) approved by French authorities (CNREEA agreement N° 91). 2. Animal welfare for this study complies with the UK Animals Scientific Procedures Act 1986 (ASPA) in line with Directive 2010/63/EU of the European Parliament and the Council of 22 September 2010 on the protection of animals used for scientific purposes. All experimental data management and reporting procedures were in

strict accordance with applicable Crown Bioscience UK Guidelines and Standard Operating Procedures.

<http://dx.doi.org/10.1136/jitc-2021-SITC2021.865>

RBN-2397, A NOVEL, POTENT, AND SELECTIVE PARP7 INHIBITOR, INDUCES TUMOR-INTRINSIC TYPE I INTERFERON RESPONSES AND ADAPTIVE IMMUNITY IN PRECLINICAL MODELS AND PATIENT TUMORS

¹Kristy Kuplast-Barr*, ¹Kristy Kuplast-Barr, ²Melissa Johnson, ²Manish Patel, ³Timothy Yap, ²Gerald Falchook, ⁴Patricia LoRusso, ¹Ryan Abo, ¹Chang Liu, ¹Erika Manyak, ¹Lisa Cleary, ¹Viviana Bozon, ¹Sudha Parasuraman, ¹Heike Keilhack, ¹Kristen McEachern. ¹Ribon Therapeutics, Inc, North Cambridge, MA, USA; ²Sarah Cannon Research Institute, Nashville, TN, USA; ³MD Anderson Cancer Center, Houston, TX, USA; ⁴Yale University School of Medicine, New Haven, USA

Background PARP7 is a mono-ART that is upregulated in response to cellular stress (e.g., viral infection, cigarette smoke), and suppresses the Type I interferon (IFN) response following cytosolic nucleic acid sensing. RBN-2397 is a first-in-class PARP7 inhibitor, inducing cancer cell autonomous and immune stimulatory effects in preclinical models through enhanced Type I IFN signaling in cancer cells. Moreover, RBN-2397 induces CD8 T cell-dependent tumor-specific immune memory in an immunocompetent mouse cancer model.¹ RBN-2397 is currently being tested in an ongoing Phase I clinical study (NCT04053673).² Here we aimed to compare biomarker results from preclinical models and patient samples.

Methods In preclinical models, interferon-stimulated gene (ISG) expression was assessed by qPCR, NanoString, or ELISA. Plasma CXCL10 from patients was measured by MSD while ISG expression in PBMCs was measured by NanoString. Baseline and on-treatment patient tumor biopsies were analyzed by NanoString, CD8/GZMB IHC, and MIBI-TOF to characterize immune changes in the tumor microenvironment.

Results RBN-2397 potently restored tumoral Type I IFN signaling in preclinical models as demonstrated by increases in ISGs, namely CXCL10, which were not observed in non-tumor tissue (e.g. spleen, PBMCs). In peripheral blood from patients treated with RBN-2397, neither plasma nor PBMC CXCL10 increased more than 2-fold over baseline. Expression of 42 ISGs was not consistently induced in a dose-dependent manner in PBMCs. However, in tumor types of interest (e.g. cancers of the upper aerodigestive tract), CXCL10 expression increased 1.5 to 8-fold, with similar effects observed for a subset of ISGs in 5 evaluable paired biopsy samples. Confirming preclinical studies [1], up to 8-fold increases in CD8 T cell infiltration along with induction of granzyme B expression were observed in 4 of 5 paired patient tumor biopsies by immunohistochemistry. Using the MIBI-TOF technology, we observed up to 50-fold increases in intratumoral activated T cells as well as monocytes and M1 macrophages, most strikingly in two NSCLC patients.

Conclusions Inhibition of PARP7 with RBN-2397 restores tumor-intrinsic Type I IFN signaling in preclinical models leading to enhanced adaptive immunity, resulting in CD8 T cell-dependent durable tumor regressions. These observations are mirrored in samples from patients treated with RBN-2397 in that pharmacodynamic effects of RBN-2397 were preferentially observed in tumor tissue relative to the periphery, including an increase in immune infiltration into the tumor microenvironment. These data provide evidence for induction of an adaptive immune response and confirm the tumor-intrinsic, immunomodulatory mechanism of action of RBN-2397 in patients.

REFERENCES

1. Gozgit, *et al.* PARP7 negatively regulates the type I interferon response in cancer cells and its inhibition triggers antitumor immunity. *Cancer Cell* 2021; In press.
2. Falchook, *et al.* A first-in-human phase 1 study of a novel PARP7 inhibitor RBN-2397 in patients with advanced solid tumors. *ASCO* 2021; oral presentation.

<http://dx.doi.org/10.1136/jitc-2021-SITC2021.866>

867 TRITAC-XR IS AN EXTENDED-RELEASE T CELL ENGAGER PLATFORM DESIGNED TO MINIMIZE CYTOKINE RELEASE SYNDROME BY REDUCING CMAX IN SYSTEMIC CIRCULATION

Kathryn Kwant*, Sony Rocha, Katrina Stephenson, Maria Dayao, Subramanian Thothathri, Rose Banzon, Wade Aaron, Golzar Hemmati, Evan Callihan, Timothy Yu, Jessica O'Rear, Eric Bragg, Willis Kwong, Hubert Situ, Avneel Hundal, Stephen Yu, Taggra Jackson, Kevin Wright, Yinghua Xiao, Linh To, Richard Austin, Bryan Lemon, Holger Wesche, S Jack Lin. *Harpoon Therapeutics, South San Francisco, CA, USA*

Background CD3-targeted T cell engagers are potent anti-tumor therapies, but their development often requires management of cytokine release syndrome (CRS). Subcutaneous dosing is a promising strategy to reduce CRS, but its application is limited by its increased immunogenicity risks. Subcutaneous dosing is hypothesized to mitigate CRS by reducing the maximum drug concentration (C_{max}) and preserve efficacy by maintaining the same minimum drug concentration (C_{min}) as intravenous dosing. A T cell engager designed to be dosed intravenously but engineered to mimic the PK properties of subcutaneous dosing could alleviate CRS without increasing immunogenicity.

Methods TriTAC-XR molecules are engineered T cell engager prodrugs that become slowly activated in systemic circulation. This extended-release mechanism results in a slow build-up of circulating active drug, similar to subcutaneous dosing, and extends drug exposure to enable longer dosing intervals. The prodrug was engineered by adding a peptide mask and protease-cleavable linker to the N-terminus of a TriTAC, a constitutively active and half-life extended T cell engager. The mask binds to the anti-CD3 ϵ domain and prevents T cell binding. Upon cleavage by systemic proteases, active T cell engager is released. Binding was assessed using ELISA on recombinant CD3 ϵ protein and using flow cytometry on primary T cells. T cell engager function was assessed using T cell-dependent cellular cytotoxicity (TDCC) assays with resting human T cells. Safety and efficacy were modeled in non-human primates.

Results TriTAC-XR had markedly reduced binding to recombinant CD3 ϵ protein and to primary T cells as well as reduced potency in functional TDCC assays compared to its unmasked active drug. In cynomolgus monkeys, TriTAC-XR had significantly attenuated cytokine production while maintaining comparable pharmacodynamic effects as a non-masked active drug. The ratio of C_{max} to C_{min} for the active TriTAC-XR was significantly smaller than a non-masked control.

Conclusions TriTAC-XR is activated in a time released manner by systemic proteases to minimize differences between the C_{max} and C_{min} of systemic active drug. This mechanism is different from other protease-activated T cell engager prodrugs that are only activated by tumor-associated proteases. Compared to canonical T cell engagers, TriTAC-XR is expected to improve safety by reducing CRS and to provide convenience by extending dosing intervals.

<http://dx.doi.org/10.1136/jitc-2021-SITC2021.867>

OVERALL SURVIVAL ON TEBENTAFUSP IN METASTATIC UVEAL MELANOMA (MUM) ACROSS THE RANGE OF TUMOR GP100 EXPRESSION LEVELS

Emma Leach*, Sarah Stanhope, Revashnee Naidoo, Shaad Abdullah, Laura Collins, Koustubh Ranade. *Immunocore, Abingdon, UK*

Background Tebentafusp is a TCR–anti-CD3 bispecific fusion protein that targets melanoma-expressed gp100 antigen and has shown survival benefit in a randomized phase 3 trial in 1L patients with metastatic uveal melanoma.^{1 2} In phase 2 and 3 trials (NCT02570308, NCT03070392) enrolling late-stage mUM patients, we explored associations between gp100 expression in the tumor and pharmacodynamic response and clinical outcomes on tebentafusp.

Methods 2L+ (NCT02570308) or 1L (NCT03070392) HLA-A*02:01+ mUM patients were treated weekly with 68mcg tebentafusp after intra-patient dose escalation. Archival or fresh tumor biopsies were obtained prior to dosing. Expression of baseline gp100 was determined by immunohistochemistry (IHC) and RNAseq analysis (2L+ only) in up to 118 (2L+) and 187 (1L) samples. RNAseq analysis was used to evaluate association between baseline mRNA levels of gp100 and T cell infiltration and activation after 3 doses of tebentafusp (n=35). Serum samples (n=118, 2L+ only) collected at baseline and on-treatment were analyzed for ctDNA. An H-Score quantified tumoral gp100 protein expression. gp100 H score or mRNA levels were cut at the lowest quartile to identify gp100 low patients.

Results Distribution of gp100 protein by IHC was similar in both studies with median H-Scores of 170 (IQR 60–260) (2L+) and 155 (IQR 68–229) (1L). Over 70% of samples had \geq 50% gp100+ tumor cells at any intensity. gp100 H-scores were similar in archival and fresh tumor biopsies. High baseline gp100 mRNA levels were associated with \sim 2-fold increased CD3 and CD8 cell infiltration on tebentafusp compared to little or no change in the gp100 low group. There was greater T cell activation in the gp100 mRNA high group as demonstrated by induction of IFN α (fold change in gp100 high=2.5 p=0.00005), IFN γ signatures (FC in gp100 high=5.7 p=0.00004) and cytotoxic genes GZMB (FC high=4.6 p=0.000006) and PRF1 (FC high=2.4 p=0.00051) compared to little or no activation in the gp100 mRNA low group. Tumor shrinkage (TS) and overall survival (OS) > 12 months were observed in low and high gp100 H-score subgroups (table 1), and a RECIST partial response was observed at very low gp100 (H-score 11). ctDNA reduction on tebentafusp was also observed across the range of gp100 expression levels.

OS and ctDNA reduction—were observed across the range of gp100 expression levels.

Trial Registration NCT02570308, NCT03070392

REFERENCES

- Middleton MR, McAlpine C, Woodcock VK, *et al.* Tebentafusp, a TCR/Anti-CD3 bispecific fusion protein targeting gp100, potently activated antitumor immune responses in patients with metastatic melanoma. *Clin Can Res* 2020;**26**:5869–5878.
- Sacco JJ, Carvajal R, Butler MO, *et al.* A phase (ph) II, multi-center study of the safety and efficacy of tebentafusp (tebe) (IMCgp100) in patients (pts) with metastatic uveal melanoma (mUM). *Ann Oncol* 2020;**31**:S1442-S1143.

Ethics Approval The institutional review board or independent ethics committee at each center approved the trial. The trial was conducted in accordance with the Declaration of Helsinki and the International Conference on Harmonization Good Clinical Practice guidelines.

<http://dx.doi.org/10.1136/jitc-2021-SITC2021.868>

Abstract 868 Table 1 TS and OS in gp100 high and gp100 low patient groups

Clinical Trial	gp100 Group (H score IHC)	TS	OS
		(% with tumor reduction)	(% survival >12 months)
1L (NCT03070392)	gp100 high	38%	49%
	gp100 low	43%	50%
2L+ (NCT02570308)	gp100 high	48%	58%
	gp100 low	32%	61%

*P>0.05 for all high vs low (lowest quartile H score) comparisons within each trial.

Conclusions High gp100 expression was associated with the acute pharmacodynamic response to tebentafusp including greater T cell infiltration and activation in the tumor microenvironment. However, clinical outcomes on tebentafusp—TS,

869

LOCALLY ADMINISTERED IMMUNOTHERAPY SELF-DELIVERING RNAI PH-762 RESULTS IN ABSCOPAL CLEARANCE OF UNTREATED DISTAL TUMORS, SUGGESTING SYSTEMIC IMMUNE RESPONSE, IN A MURINE HEPATOCARCINOMA MODEL

Benjamin Cui^{ffo*}, Melissa Maxwell, Dingxue Yan, Brianna Rivest, James Cardia, Simon Fricker. *Phio Pharmaceuticals, Marlborough, MA, USA*

Background The development of locally administered immune checkpoint inhibition (ICI) holds potential promise for enhanced activity and decreased systemic toxicity, but such an approach is challenging with the available ICI antibodies. We have previously shown that the intratumoral (IT) delivery of PH-762, a self-delivering RNAi compound targeting PD-1 based on proprietary INTASYL™ technology, can significantly inhibit tumor growth associated with changes in the immune cell population in the tumor microenvironment towards an anti-tumor phenotype. We present data showing that IT administration of PH-762 not only inhibits local tumor growth but can also elicit an abscopal effect in distal untreated tumors. The *in vivo* efficacy and *in vitro* mechanism of action support the generation of a PH-762 driven systemic anti-tumor immune response. Therefore, ICI using INTASYL is an alternative to antibody drugs for immunotherapy.

Methods To assess *in vivo* efficacy, Hepa1-6 cells were implanted subcutaneously into the flanks of C57BL/6J mice. Vehicle (PBS) or murine targeting PH-762 (mPH-762) were administered IT on Days 1, 4, 7, 10 and 14. To determine an abscopal effect cells were also implanted into the opposite flank but left untreated. Tumor volumes and body weights were recorded. In addition, *in vitro* mechanism of action studies were performed with CD3-stimulated human pan T cells. PD-1 mRNA knockdown was assessed by qRT-PCR; PD-1 protein expression by flow cytometry; and T cell function by cytokine release.

Results Treatment with IT administered mPH-762 significantly inhibited tumor growth compared with vehicle treated control tumors. Furthermore, the growth of the untreated bilateral tumor was significantly reduced with 80% of these tumors showing complete regression. Mechanism of action studies showed potent and durable silencing of PD-1. Increased release of IFN- γ , CXCL10, and IL-6 and suppression of IL-10 release were indicators of an enhanced immune response.

Conclusions These data show that silencing PD-1 with IT administration of mPH-762 not only inhibits growth of treated tumors but elicits an abscopal effect leading to cure of distal tumors. This data and other recently published data showing evidence of a specific antitumor immune response in a tumor rechallenge model after prior treatment with INTASYL compounds, demonstrate the desired systemic immune response can be obtained with local administration of PH-762. INTASYL represent an alternative to antibody therapy for IT checkpoint blockade with potential for improved efficacy and reduced systemic toxicity which will be investigated in an upcoming clinical trial.

<http://dx.doi.org/10.1136/jitc-2021-SITC2021.869>

870 **TARGETING GCN2 KINASE-DRIVEN STRESS RESPONSE
INACTIVATION TO RESTORE TUMOR IMMUNITY IN
METASTATIC TRIPLE NEGATIVE BREAST CANCER**

¹Hariprasad Vankayalapati, ¹Kyle Medley, ¹Zhaoliang Li*, ¹Dongqing Yan, ²David Bearss, ¹Alana Welm, ¹Huntsman Cancer Institute, Salt Lake City, UT, USA; ²University of Utah, Salt Lake City, UT, USA

Background Patients with PD-L1-positive metastatic triple-negative breast cancers (mTNBC) who have been treated with atezolizumab+nab-paclitaxel had a clinically meaningful overall survival extension of 9.5 months compared to nab-paclitaxel alone, although overall survival in overall population was not statistically significant. Unlike many other cancers, immunotherapy for breast cancer has had limited success, due to the fact that there are very few T cells in the tumor microenvironment of mTNBC patients. Identifying ways to boost immunotherapy responses could change the paradigm of mTNBC, a disease still difficult to treat. The highly proliferative nature of tumor cells, along with infiltration of myeloid cells into the tumors, leads to depletion of nutrients such as functional/natural amino acids. This metabolically stressful milieu causes activation of nutrient stress pathways, autophagy, and repressed immune responses. A key mediator of this nutrient stress pathway is a cytoplasmic Ser/Thr protein kinase called General Control Nonderepressible 2 (GCN2), also called EIF2AK4. GCN2 switches on following reduction of amino acids, and its activity results in T cell inactivation, T cell death, regulatory T cell expansion, and the potentiation of myeloid-derived suppressor cells (MDSCs).

Methods We have developed and synthesized a series of novel small molecule immunotherapeutic agents that reversibly bind to GCN2 kinase, competitively block the ATP site, and elicit pharmacological responses in immune cells and in breast cancer cells.

Results GCN2 cell-free kinase binding, kinome selectivity, pGCN2, pEIF2 α , ATF-4 phosphorylation inhibition assays were performed. We confirmed on-target efficacy and tested the potency of our lead GCN2 inhibitor HCI-1046. HCI-1046 demonstrated potent activity, with an IC₅₀ of 36 nM in inhibiting GCN2 kinase and exhibited cellular efficacy with an IC₅₀ of 0.1 to 1.0 μ M range. Our preliminary results support the hypothesis that the inhibition of GCN2 reinstates anti-tumor immunity and blocks tumor progression in breast cancer models. In vivo PK studies of HCI-1046 in rodents showed excellent PK properties; 55% oral bioavailability, low clearance, and >5 hour half-life.

Conclusions Thus, HCI-1046 is nominated as a pre-clinical agent. Additional data regarding evaluation of the effects of HCI-1046 on the MDSC-suppressive function on T cells using ELISpot assays with breast cancer patient samples, and mouse model efficacy studies will be discussed.

REFERENCES

1. Ekiz HA, Lai SA, Gundlapalli H, Haroun F, Williams MA, Welm AL. Inhibition of RON kinase potentiates anti-CTLA-4 immunotherapy to shrink breast tumors and prevent metastatic outgrowth. *Oncoimmunology* 2018;**7**(9):e1480286.
2. Toogood PL. Small molecule immuno-oncology therapeutic agents. *Bioorg Med Chem Lett* 2018;**28**(3):319–329.
3. Ravindran R, Loebbermann J, Nakaya HI, Khan N, Ma H, Gama L, Machiah DK, Lawson B, Hakimpour P, Wang YC, Li S, Sharma P, Kaufman RJ, Martinez J, Pulendran B. The amino acid sensor GCN2 controls gut inflammation by inhibiting inflammasome activation. *Nature* 2016;**531**(7595):523–527.
4. Brazeau JF, Rosse G. Triazolo[4,5-d]pyrimidine derivatives as inhibitors of GCN2. *ACS Med Chem Lett* 2014;**5**(4):282–3.

<http://dx.doi.org/10.1136/jitc-2021-SITC2021.870>

871

CONSTRUCTION AND EVALUATION OF INTERLEUKIN 3 (IL3)-ZETAKINE REDIRECTED CYTOLYTIC T CELLS FOR THE TREATMENT OF CD123 EXPRESSING ACUTE MYELOID LEUKEMIA

Rebecca Moeller*, Julian Scherer, Sadik Kassim. *Vor Biopharma, Cambridge, MA, USA*

Background Acute Myeloid Leukemia (AML) is an aggressive bone marrow malignancy, characterized by the presence of leukemic blasts in the peripheral blood of patients. Poor AML prognoses¹ are largely attributable to high rates of disease relapse, of which CD123+ leukemic stem cells (LSCs) are the primary cause.²⁻³ CD123, the alpha-chain of the IL3 cytokine receptor,⁶ has been identified as a favorable therapeutic AML target, overexpressed in both LSCs and blasts.⁴⁻⁵ We sought to direct T cells to CD123+ AML cells via cell surface tethered IL3 (termed "IL3-zetakine").⁷ The use of a zetakine instead of a chimeric antigen receptor (CAR) construct enables structure-guided site-directed mutagenesis to increase binding affinity and alter target cell signaling without detrimental T cell hyperactivation.

Methods Zetakine constructs were designed using IL3 sequences bound to a transmembrane domain and intracellular costimulatory and CD3z signaling domains. The constructs were transduced into Jurkat cells with lentiviral vectors (LVV). T cell activation via CD69 expression was assessed via flow cytometry of sorted IL3 zetakine-positive Jurkat cells after co-culture with MOLM13 AML cells. Lead constructs were selected based on initial transduction percentage and activation response. In vitro functionality of each IL3 zetakine was tested with LVV transduced primary T cells by flow cytometry.

Results Zetakine constructs yielded a wide range of transduction percentages in Jurkat cells (0 – 98%) prior to sorting. In co-cultures with CD123+ MOLM13 AML cells, Jurkat cells expressing wildtype IL3 constructs lacking a costimulatory domain induced the highest level of CD69 expression (18.7% CD69+ T cells) in an antigen-specific manner (5.3-fold increase of CD69+ T cells over those cultured with MOLM13 CD123KO cells). The K110E mutant IL3 was reported to exhibit a 40-fold increased affinity over wildtype,⁸ but it showed no detectable zetakine function. However, additional mutant IL3 zetakines increased Jurkat cell activation up to 5.8-fold. Antigen-specific increases in CD69, as well as CD25, surface expression were also observed with zetakine-transduced primary T cells co-cultured with MOLM13 cells, in addition to target cell killing comparable to antibody-based CD123CAR T-cells.

Conclusions This work establishes IL3 zetakines as a viable alternative to traditional CD123-targeted CAR constructs. Structure-guided IL3 zetakine mutants with altered affinity and activation profiles will further our understanding of CD123-specific cytotoxicity modulation without inducing acute T cell hyperactivation and exhaustion. These results indicate the ability of IL3 zetakine-expressing T cells to kill CD123-expressing AML cells and illustrate the potential of this novel class of therapeutics.

REFERENCES

1. Ganzel C, et al. Very poor long-term survival in past and more recent studies for relapsed AML patients: the ECOG-ACRIN experience. *American journal of hematology* 2018;10.1002/ajh.25162.
2. Shlush LI, et al. Tracing the origins of relapse in acute myeloid leukaemia to stem cells. *Nature* 2017;547(7661):104–108.
3. Hanekamp D, Cloos J, Schuurhuis GJ. Leukemic stem cells: identification and clinical application. *International Journal of Hematology* 2017;105(5):549–557.

4. Bras AE, et al. CD123 expression levels in 846 acute leukemia patients based on standardized immunophenotyping. *Cytometry part B: Clinical Cytometry* 2019;96(2):134–142.
5. Sugita M, Guzman ML. CD123 as a therapeutic target against malignant stem cells. *Hematology/Oncology clinics of North America* 2020;34(3):553–564.
6. Mingyue S, et al. CD123: a novel biomarker for diagnosis and treatment of leukemia. *Cardiovascular & Hematological Disorders-Drug Targets* 2019;19(3):195–204.
7. Kahlon KS, et al. Specific recognition and killing of glioblastoma multiforme by interleukin 13-zetakine redirected cytolytic T cells. *Cancer Res* 2004;64(24):9160–6.
8. Bagley CJ, et al. A discontinuous eight-amino acid epitope in human interleukin-3 binds the alpha-chain of its receptor. *J Biol Chem* 1996;271(50):31922–8.

<http://dx.doi.org/10.1136/jitc-2021-SITC2021.871>

872 **PD1 X TGFBR2 AND CD5 X TGFBR2 BISPECIFICS SELECTIVELY BLOCK TGFBR2 ON TARGET-POSITIVE T CELLS, PROMOTE T CELL ACTIVATION, AND ELICIT AN ANTI-TUMOR RESPONSE IN SOLID TUMORS**

Gregory Moore*, Suzanne Schubbert, Christine Bonzon, Kendra Avery, Rumana Rashid, Erik Pong, Lukasz Ochyl, Alex Nisthal, Seung Chu, James Ernst, John Desjarlais. *Xencor, Inc., Monrovia, CA, USA*

Background TGFbeta production by solid tumors and their microenvironment is a major mechanism used by tumors to avoid immunosurveillance. Blockade of TGFbeta has been shown to promote an anti-tumor response; however, systemic blockade of TGFbeta has also been associated with toxicity. We hypothesized that a T cell-targeted TGFbR2 bispecific antibody could selectively block the suppressive activity of TGFbeta on T cells and enhance their anti-tumor activity while avoiding toxicity associated with systemic blockade.

Methods We engineered bispecific antibodies that simultaneously engage PD1 (activated) or CD5 (pan T) and block TGFbR2 using Xencor's XmAb[®] platform. The anti-TGFbR2 arm was tuned for optimal activity by introducing affinity-modulating amino acid substitutions. The activity of TGFbR2 bispecifics was evaluated in vitro using a signaling assay to measure phosphorylated SMAD (pSMAD) by flow cytometry with exogenous TGFbeta in unactivated and activated PBMC. In vivo activity was evaluated by monitoring the engraftment of human PBMC in NSG mice (huPBMC-NSG). Anti-tumor activity was assessed in huPBMC-NSG mice engrafted with established human cancer cell lines.

Results TGFbR2 bispecifics were confirmed to bind PD1 or CD5 and block binding of TGFbeta to TGFbR2. In vitro, we found that T cells from serum-deprived PBMC exhibited robust induction of pSMAD in response to TGFbeta, and TGFbR2 bispecifics selectively inhibited pSMAD induction in target-positive T cells as demonstrated by over a 100-fold potency increase compared to an untargeted anti-TGFbR2 control. Additionally, we saw an enhancement of potency when evaluating activity in target-high T cells versus target-low or -negative immune cells. Intriguingly, CD5-targeted TGFbR2 bispecifics allowed for the targeting of a broader population of T cells compared to PD1-targeting while still conferring potent selectivity against target-negative cells. In vivo, treatment of huPBMC-NSG mice with TGFbR2 bispecifics promoted superior T cell engraftment. Furthermore, TGFbR2 bispecific treatment of huPBMC-NSG mice containing established MDA-MB-231 triple-negative breast cancer tumors promoted an anti-tumor response that was augmented with PD1 blockade.

Conclusions PD1 x TGFbR2 and CD5 x TGFbR2 bispecific antibodies were engineered to selectively block TGFbR2 on target-positive T cells and evaluated in vitro and in vivo. These observations are compelling and suggest that development of these bispecifics is warranted for the treatment of human malignancies.

<http://dx.doi.org/10.1136/jitc-2021-SITC2021.872>

**873 S-531011, A NOVEL ANTI-HUMAN CCR8 ANTIBODY:
ANTI-TUMOR RESPONSES THROUGH DEPLETION OF
TUMOR-INFILTRATING CCR8-POSITIVE TREGS**

¹Ryohei Nagai*, ¹Morio Nagira, ¹Wataru Nogami, ¹Michinari Hirata, ¹Azumi Ueyama, ¹Mai Yoshikawa, ²Naganari Ohkura, ²Hisashi Wada, ¹Yoji Nagira. ¹Shionogi and Co., Ltd., Osaka, ID, Japan; ²Osaka University, Osaka, Japan

Background Regulatory T cells (Tregs) are suppressive immune cells required for the maintenance of immune homeostasis, but tumor-infiltrating Tregs are known to suppress the antitumor immune system and promote tumor progression. Therefore, selective reduction of tumor-infiltrating Tregs is anticipated to reinvigorate antitumor immunity without inducing autoimmunity. S-531011 is a novel anti-human IgG1 antibody targeting human CCR8 (C-C motif chemokine receptor 8) which is selectively expressed in tumor-infiltrating Tregs, with both in vitro antibody dependent cellular cytotoxicity (ADCC) against CCR8-expressing cells and neutralizing activity against CCL1-CCR8 signaling. Here, to evaluate antitumor activities and safety aspects of S-531011, we conducted non-clinical pharmacology studies of S-531011 using human CCR8 knock-in (KI) mice and human tissues.

Methods S-531011 was administrated to CT26WT tumor-bearing hCCR8-KI mice, and the effect on the presence of tumor-infiltrating CCR8+ Treg and tumor growth were evaluated. We also investigated the antitumor efficacy of S-531011 in combination with anti-mouse PD-1 antibody. Next, human lung cancer tissues and human NK-cells were co-cultured, and the ex vivo ADCC against tumor-infiltrating Tregs by S-531011 was verified. We also incubated human peripheral blood-derived mononuclear cells (PBMC) from healthy individuals with S-531011 to investigate the effects on the proportion of Tregs in human PBMC.

Results Intravenous administration of S-531011 to CT26WT tumor-bearing hCCR8-KI mice significantly reduced tumor-infiltrating CCR8+ Tregs and markedly suppressed tumor growth. Furthermore, the combined therapy of S-531011 with anti-mouse PD-1 antibody showed greater anti-tumor effect than monotherapy without any apparent side effects. Ex vivo ADCC studies using human lung cancer tissues and FCM analysis of CCR8 expression in tumor-infiltrating Tregs suggested that most of the tumor-infiltrating CCR8+ Tregs were depleted by S-531011. On the other hand, S-531011 didn't reduce Tregs in human PBMC.

Conclusions S-531011 is a promising drug which has a strong antitumor effect by depleting tumor-infiltrating CCR8+ Tregs, as a not only monotherapy but also combination therapy with other immune checkpoint inhibitors.

Ethics Approval The present study was approved by the Institutional Ethics Committee of Osaka University Hospital (approved number: 13266-15) and Shionogi Co., Ltd. (approved number: 021-003). Animal studies were approved by the Institutional Animal Care and Use Committee (approved number: S20093D, S20197D and S20198D).

<http://dx.doi.org/10.1136/jitc-2021-SITC2021.873>

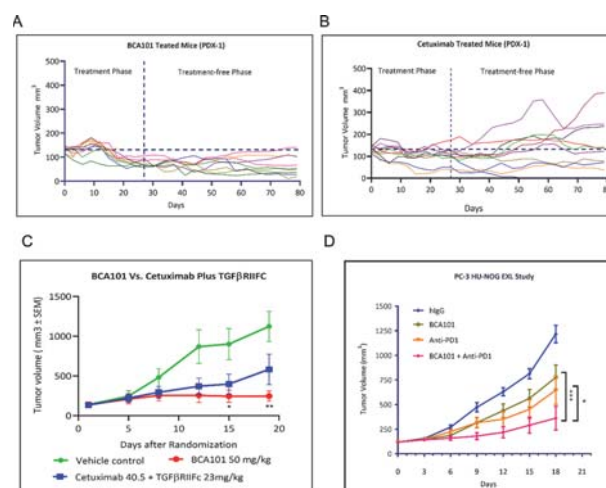
DEVELOPMENT OF BCA101, A BIFUNCTIONAL ANTIBODY CAPABLE OF SIMULTANEOUSLY DISABLING EGFR AND TGF β SIGNALING, AS NOVEL SINGLE-AGENT IMMUNOTHERAPY

¹Srinivas Reddy Boreddy*, ¹Reshmi Nair, ¹Arindam Banerjee, ¹Anshu Kuriakose, ¹Prashant Kumar Pandey, ¹Chaitali Dey, ¹Meena Shri, ¹Shruthi Rao, ¹Bhadravathi Marigowda Shivakumar, ²Moni Abhram Kuriakose, ²Ram Bhupal Reddy, ²Amritha Suresh, ³Praveen Reddy Moole, ¹Usha Bughani, ⁴Seng-Lai Tan, ¹Pradip Nair. ¹Biofusion Therapeutics Limited, Bangalore, India; ²Mazumdar Shaw Medical Center, Bangalore, India; ³Biocon Biologics Limited, Bangalore, India; ⁴Bicara Therapeutics Limited, Cambridge, MA, USA

Background Given the pleiotropic functions of transforming growth factor-beta (TGF β), current approaches to targeting systemic TGF β will likely lead to suboptimal clinical activity and/or undesirable effects. Epidermal growth factor receptor (EGFR) is one of the most extensively validated tumor-associated antigens. Bicara Therapeutics has developed a novel bifunctional fusion protein, composed of a monoclonal antibody against EGFR and an extracellular domain of human TGF β receptor II (TGF β RII). We demonstrate BCA101 has the potential to improve anti-tumor response by leveraging the cooperativity between EGFR and TGF β signaling pathways while restricting TGF β neutralization to EGFR-expressing tissues.

Methods Functional neutralization of TGF β by BCA101 was demonstrated by several in vitro assays which assessed TGF β -dependent epithelial to mesenchymal transition (EMT), cell invasion, inducible Treg differentiation, as well as allogeneic immune responses in tumor cell/immune cell coculture assays. In vivo, the anti-tumor efficacy of BCA101 was determined in tumor xenograft mouse models, using either human tumor cell lines or patient-derived tumor cells (PDX), as well as in a humanized mouse model.

Results In vitro, we showed BCA101 is capable of simultaneously binding EGFR and TGF β 1 with a significantly higher affinity for EGFR. The incorporation of the TGF β RII "trap" did not sterically interfere with the ability of BCA101 to bind EGFR, inhibit cell proliferation or mediate antibody-dependent cellular cytotoxicity (ADCC). Relative to cetuximab, BCA101 showed improved ability to reverse EMT and preserve ADCC activity. In tumor cell/immune cell co-culture assays, BCA101 increased production of proinflammatory cytokines associated with T and NK cell activation and suppressed VEGF release. Further, BCA101 inhibited differentiation of inducible Treg and displayed an immuno-potentiating profile in the BioMAP[®] TME model. In vivo, biodistribution studies showed that BCA101 localized to tumor tissues in xenograft mouse models, with comparable kinetics as cetuximab. TGF β in tissues was neutralized to about 90% at 10 mg/kg of BCA101 while equimolar doses of TGF β RII receptor inhibited TGF β in tumors by around 50%, confirming improved tumor localization with BCA101. In PDX models derived from head and neck cancer squamous cell carcinoma patients, BCA101 exerted sustained antitumor effect and delayed tumor growth compared to cetuximab. Finally, BCA101 improved the anti-tumor activity of PD1 blockade therapy in humanized HuNOG-EXL mice bearing PC-3 xenografts (figure 1).



Abstract 874 Figure 1

BCA101 shows superiority over cetuximab in animal models. (A) & (B). Patient derived xenograft (PDX) models. Patient derived tumors were engrafted into female NOG mice. Once tumor reached about 130 mm³, mice were randomized into control and test groups. Test group mice were treated with either BCA101 (A) or cetuximab (B), thrice a week (i.p), whereas control animals received placebo alone. Mice were treated for 27 days followed by a treatment-free phase until Day 79. Tumor volumes and mice weight were recorded twice a week. (C). BCA101 inhibits FaDu tumor xenograft growth (CDX) in vivo. Nude mice were implanted with FaDu cells on flanks. Once tumor reached about 100 mm³, mice were randomized (n=7) and treated with six doses of test compounds, BCA101 and cetuximab. Tumor volume and mice weight were recorded twice a week. (D). BCA101 and anti-PD1 combination studies in hu-NOG-EXL humanized animal model. PC-3 cells were implanted into flank of Hu-NOG-EXL humanized mice and randomized into control and test groups once tumors reached about 120 mm³. Test group mice were treated with cetuximab or BCA101, intraperitoneally for 6 doses. Anti-PD1 antibody (pembrolizumab) was administered intraperitoneally at a dose of 10 mg/kg with a dosage schedule of every fifth-day for 5 doses (Q5Dx5). Statistical analysis for panel (C) & (D) was performed using repeated measures two-way ANOVA followed by Bonferroni's multiple comparison test. Significance was indicated by * = p value \leq 0.05, ** = p value \leq 0.01 and *** = p value \leq 0.001. Tumor volumes are presented as Mean \pm SEM.

Conclusions These results support the clinical development of BCA101 as a targeted immunotherapy with the potential to induce improved anti-tumor response with a wider therapeutic window, either as a monotherapy or in combination with immune checkpoint blockade therapy.

Acknowledgements We acknowledge Mazumdar Shaw Center for Translational Research for providing the human tissues used for the PDX studies. We thank Syngene International for conducting the PDX and humanized mice studies at their vivarium. We thank Dr. Sreesha Srinivasa for providing suggestions and feedback at the early stages of this project.

REFERENCES

1. Bedi A, Chang X, Noonan K, Pham V, Bedi R, Fertig EJ, Considine M, Califano JA, Borrello I, Chung CH, Sidransky D, Ravi R. Inhibition of TGF- β enhances the in vivo antitumor efficacy of EGF receptor-targeted therapy. *Mol Cancer Ther* 2012;**11**:1–11.
2. Yegodayev KM, Novoplansky O, Golden A, Prasad M, Levin L, Jagadeeshan S, Zorea J, Dimitstein O, Joshua B-Z, Cohen L, Khrameeva E, Elkabets M. TGF-Beta-activated cancer-associated fibroblasts limit cetuximab efficacy in preclinical models of head and neck cancer. *Cancers* 2020;**12**:1–17.

Ethics Approval Mice were maintained as per the regulations of Committee for the Purpose of Control and Supervision of Experiments on Animals (CPCSEA), Government of India and Association for Assessment and Accreditation of Laboratory Animal Care (AAALAC) guidelines. All animal experiments were approved by institutional ethical committee and performed under approved protocols. For PDX model, head and neck cancer patient samples were obtained from Mazumdar Shaw Medical Foundation, Bengaluru, India after appropriate approvals were obtained from institutional ethical committee: NHH/MEC-RC2016-404

<http://dx.doi.org/10.1136/jitc-2021-SITC2021.874>

875 **AL009, A FUSION PROTEIN AND MULTI-SIGLEC
INHIBITOR, REPOLARIZES SUPPRESSIVE MYELOID CELLS
AND POTENTIATES ANTI-CANCER EFFECTS**

Sam Nalle*, Helen Lam, Ling Leung, Spencer Liang, Daniel Maslyar. *Alector, South San Francisco, CA, USA*

Background Sialic acid-binding immunoglobulin-type lectins (Siglecs) are a family of cell surface receptors expressed predominantly on myeloid cells that function to promote immune tolerance. Tumors increase the expression of sialic acid glycans and co-opt the immunosuppressive effects of Siglecs, driving tumor resident immune cells toward a cancer permissive phenotype. Due to the overlapping expression profile of Siglec family members on myeloid cells, targeting multiple Siglecs is required for robust efficacy. Here, we present data on AL009, an engineered Siglec-9 extracellular domain-Fc fusion molecule that acts as a sialic acid trap and repolarizes suppressive myeloid cells to activate an anti-cancer immune response.

Methods The ability of AL009 to competitively block various Siglec-Fc fusion proteins was assessed using cultured human myeloid-derived suppressor cells (MDSCs). MDSC repolarization was analyzed by flow cytometry. MDSCs were co-cultured with activated CD8+ T cells with and without exposure to AL009 and functionally assessed for T-cell activation by flow cytometry and ELISA. In vivo tumor models, including the MC38 and E0771 murine syngeneic subcutaneous models and the B16F10 intravenous lung metastasis model, were used to assess AL009 engineered with a murine Fc (AL009m).

Results AL009 competitively blocks the ability of at least 5 inhibitory Siglec family members to bind their corresponding sialic acid ligands. When incubated with MDSCs, AL009 promotes CD163 and CD206 downregulation and induces proinflammatory chemokine secretion, consistent with a repolarization effect. Further, AL009 potently relieves MDSC suppression of T cells in a co-culture system. In the MC38 and E0771 murine syngeneic subcutaneous tumor models, AL009m inhibits tumor growth as a monotherapy and in combination with the checkpoint inhibitor anti-PD-L1. In addition, AL009m combines with the tumor antigen targeting antibody TRP-1 in the B16F10 intravenous lung metastasis model to reduce tumor burden.

Conclusions AL009 represents a novel approach to targeting the myeloid cell compartment in oncology by directly repolarizing myeloid cells without cell depletion or limiting the targeting to specific suppressive subpopulations. AL009 has the potential to address tumors that are unresponsive or refractory to standard immunotherapies. These data support further development of AL009 in the clinic with IND enabling studies ongoing.

<http://dx.doi.org/10.1136/jitc-2021-SITC2021.875>

876

INTRATUMORAL ADMINISTRATION AND LOCAL RETENTION OF IL-2/IL-12 FUSION PROTEINS DRIVE A POTENT SYSTEMIC ANTI-TUMOR IMMUNE RESPONSE

¹Mehta Naveen*, ¹Bohong Li, ²Dane Wittrup, ¹Patrick Baeuerle, ¹Jennifer Michaelson. ¹Cullinan Amber Corp., Cambridge, MA, USA; ²MIT, Cambridge, MA, USA

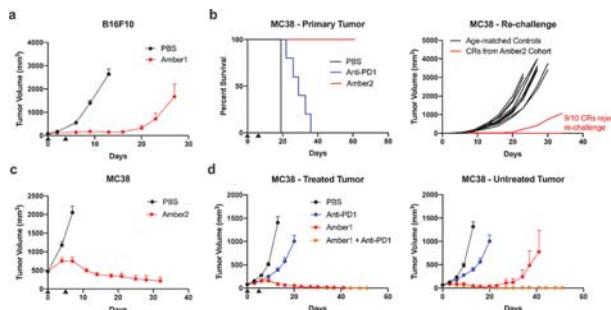
Background IL-2 and IL-12 synergistically trigger the stimulation and proliferation of T and NK cells to mediate anti-tumor immunity. Although aldesleukin, a high-dose IL-2 intravenous (IV) infusion regimen, has been approved for the treatment of melanoma and renal cell carcinoma, adoption has been hindered by frequent grade 3 and 4 severe adverse events. No IL-12 therapy has been approved yet due to toxicity. Cullinan Amber is developing a fusion protein that uniquely combines in one polypeptide both IL-2 and IL-12 with a collagen-binding domain to reduce toxicity and increase efficacy following intra-tumoral (IT) administration via retention in the tumor microenvironment.

Methods Proteins were expressed in HEK293 cells. Collagen binding was measured by ELISA. IL-2 and IL-12 bioactivity was evaluated by CTLL-2 proliferation and HEK-Blue IL-12 reporter cells. In vivo studies were conducted in B16F10, MC38, and CT26 syngeneic tumor models. Systemic Amber construct concentrations were determined by ELISA.

Results "Amber" constructs, comprised of IL-2, IL-12, and a collagen-binding domain, were produced and confirmed to retain bioactivity. B16F10 tumor-bearing mice injected with Amber IT had systemic Amber levels <5% as compared to mice administered the same dose IV. When IL-2/IL-12 fusion proteins lacking a collagen-binding domain were injected IT in B16F10-bearing mice, 60% of mice needed to be euthanized due to severe body weight loss, while Amber-treated mice did not lose body weight. In the checkpoint-refractory B16F10 and MC38 models, Amber demonstrated 95% tumor growth inhibition (figure 1a) and 100% CRs (figure 1b), respectively. 90% of the mice cured of their primary MC38 tumors were protected from re-challenge (figure 1b). Notably, 70% CRs were observed in the MC38 model even after a single-dose treatment of Amber. Similar data was obtained in the CT26 model. Amber treatment of mice bearing large 500 mm³ MC38 tumors resulted in dramatic tumor shrinkage (figure 1c). In mice bearing two MC38 tumors, only one of which was treated IT, 100% of treated tumors and 90% of distal untreated tumors were eliminated when Amber was combined with an anti-PD1 antibody (figure 1d), demonstrating a robust abscopal response.

Conclusions The use of collagen-binding domains for tumor retention enables the safe and effective delivery of IL-2 and IL-12 in a single multifunctional molecule. Taken together, the preclinical data suggests that Amber constructs may show robust single-agent activity in clinical trials against checkpoint-refractory tumors with minimal toxicity, as well as the potential to significantly deepen anti-tumor responses in combination with checkpoint inhibitor therapy.

<http://dx.doi.org/10.1136/jitc-2021-SITC2021.876>



Abstract 876 Figure 1 Efficacy of amber constructs in syngeneic tumor models

877

PSGL-1 BLOCKING ANTIBODIES REPOLARIZE TUMOR ASSOCIATED MACROPHAGES, REDUCE SUPPRESSIVE MYELOID POPULATIONS AND INDUCE INFLAMMATION IN THE TUMOR MICROENVIRONMENT, LEADING TO SUPPRESSION OF TUMOR GROWTH

¹Phuong Nguyen*, ¹Jessica Ritter, ¹Mohammad Zafari, ¹Denise Manfra, ¹Veronica Komoroski, ¹Brian O'Nuallain, ¹Ryan Phennicie, ¹Kevin Kauffman, ¹Dominika Nowakowska, ¹Joe Wahle, ¹Steve Sazinsky, ²Michael Brehm, ¹Igor Feldman, ¹Tatiana Novobrantsseva. ¹Verseau Therapeutics, Bedford, MA, USA; ²UMass Medical School, Worcester, MA, USA

Background Suppressive myeloid cell populations in the tumor microenvironment (TME) are associated with worse survival of cancer patients and low effectiveness of T cell checkpoint inhibitors. Recently, several early clinical trials have produced positive data for therapies aimed at repolarizing immunosuppressive myeloid populations in the TME. One new macrophage repolarizing target, PSGL-1 (P-selectin glycoprotein ligand-1), is expressed at high levels on suppressive tumor-associated macrophages (TAMs) and *in vitro* differentiated M2 macrophages. PSGL-1 has been shown to have an immunomodulatory activity, which includes its role in maintaining an immunosuppressive macrophage state.

Methods To assess the ability of PSGL-1 antibodies to convert macrophages and the tumor microenvironment from an immunosuppressive toward a pro-inflammatory state, we employed *in vitro* primary macrophage and multi-cellular assays, *ex vivo* patient-derived tumor cultures, and a humanized mouse PDX model.

Results We have determined that our lead anti-PSGL-1 antibody repolarized M2-like macrophages to a more M1-like state both phenotypically and functionally as assessed in primary *in vitro* macrophage assays. Transcriptomics profiling of M2c macrophages showed that the anti-PSGL-1 antibody upregulated TNF-alpha/NF-kB and chemokine-mediated signaling, while downregulating oxidative phosphorylation, fatty acid metabolism and Myc signaling pathways, consistent with a broad M2-to-M1 shift of the macrophage state. Furthermore, these repolarized M1-like macrophages enhanced the inflammatory response in complex multi-cellular assays. Pre-clinical efficacy of the anti-PSGL-1 antibody was demonstrated using *ex vivo* cultures of fresh patient-derived tumors that preserve the cellular heterogeneity of the TME. Anti-PSGL-1 increased production of inflammatory cytokines and chemokines involved in immune activation of the TME and T cell recruitment. Lastly, our lead anti-PSGL-1 antibody also showed *in vivo* anti-tumor effect in a humanized mouse PDX model of melanoma. The antibody suppressed tumor growth to a significantly greater degree compared to anti-PD-1. At the cellular and molecular levels, the anti-PSGL-1 treatment led to a more enhanced inflammatory microenvironment, including a reduced M2:M1 macrophage ratio, and an increase in systemic pro-inflammatory mediators. Compared to anti-PD-1 monotherapy, anti-PSGL-1 alone and in combination with anti-PD-1 increased the fraction of effector CD8+ T cells among the infiltrating T cells. Significant combination effects of anti-PSGL-1 plus anti-PD-1 were seen at the cellular and molecular levels within the tumor tissue, the spleen, and peripheral blood.

Conclusions The data presented here provide biological and mechanistic support for clinical testing of antibodies targeting PSGL-1 for the treatment of cancer.

Ethics Approval All legal and ethical requirements were met with regards to the humane treatment of animals described in

the study. The animal study was conducted in compliance with IACUC PROTO202000042 and the institutional assurance certification of the University of Massachusetts Medical School. The University of Massachusetts Medical School is fully accredited by AAALAC and has an Animal Welfare Assurance on file with the Office of Laboratory Animal Welfare (OLAW).

<http://dx.doi.org/10.1136/jitc-2021-SITC2021.877>

878 NOVEL MICROBIAL IMMUNOTHERAPY APPROACH FOR THE TREATMENT OF BLADDER CANCER

¹Nicholas Glanville, ¹Tobi Oke, ²Sonia Domingos-Pereira, ²Lenka Polak, ²Denise Nardelli-Haeffliger, ¹Livija Deban*. ¹Prokarium Ltd, London, UK; ²Centre Hospitalier Universitaire Vaudois, Lausanne, Switzerland

Background Microbial immunotherapy, in the form of intravesical *Bacillus Calmette-Guérin* (BCG), is the standard-of-care for non-muscle invasive bladder cancer (NMIBC). BCG therapy is associated with significant side-effects, high disease recurrence and progression rates, and product supply shortages, leaving a significant unmet medical need for bladder cancer patients.^{1 2} We sought to establish the preclinical safety and efficacy of live-attenuated *Salmonella enterica* Typhi strain ZH9 (Δ aroC, Δ ssaV) as a novel microbial immunotherapy.

Methods Therapeutic efficacy of intravesical ZH9 was established in the murine orthotopic, syngeneic MB49 bladder tumor model. Tumor-bearing animals were treated with a single intravesical dose of ZH9 or OncoTice BCG and long-term survival comparisons were evaluated by log-rank (Mantel-Cox) test. ZH9 interaction with urothelial cancer cells was investigated using in vitro invasion assays and flow cytometry staining for intracellular *Salmonella* common antigen (CSA-1) and propidium iodide for cell death. Local immune responses were analyzed by flow cytometry staining of disaggregated mouse bladders.

Results Mice treated with a single intravesical dose of ZH9 2 days after MB49 tumor inoculation demonstrated significant survival benefit compared to vehicle treated (median survival 49.5 vs. 31 days, $p=0.003$) and BCG treated animals (median survival 49.5 vs. 27.5 days, $p<0.001$). A second, stringent model setup with intravesical treatment 4 days after tumor inoculation showed significant efficacy of ZH9 versus vehicle and BCG (median survival 30 vs. 20.5 ($p=0.003$) and 23.5 ($p=0.025$) days, respectively). Surviving ZH9 treated animals demonstrated 100% protection from tumor take following repeated intravesical challenge with MB49 tumor cells, suggesting lasting anti-tumor immunity resulting from ZH9 treatment. In vitro, intracellular flow cytometry in human (UMUC3, T24, RT4, 5637) and mouse (MB49) urothelial cancer cell lines showed that ZH9 invaded and induced cell death in all cell lines. In vivo, a single treatment with intravesical ZH9 resulted in strong cellular immune responses characterized by recruitment of monocytes, NK cells, CD4+ and CD8+ T cells, and dendritic cells with an activated, cross-presenting (Ly6C+, CD103+) phenotype. Intravesical ZH9 resulted in a greater magnitude and duration of immune cell recruitment in the urothelium compared to a single equivalent dose of intravesical BCG.

Conclusions Live-attenuated *Salmonella* strain ZH9 demonstrated a significant survival benefit over the standard-of-care OncoTice BCG in an orthotopic bladder cancer model. ZH9 demonstrated direct tumour cell killing in vitro and induction of robust cellular immune responses in vivo. Preclinical studies indicate significant therapeutic potential of intravesical ZH9 as a novel microbial immunotherapy in bladder cancer.

REFERENCES

1. Liu Y, Lu J, Huang Y, Ma L. Clinical spectrum of complications induced by intravesical immunotherapy of *Bacillus Calmette-Guérin* for bladder cancer. *J Oncol* 2019 March 10;2019:6230409.
2. vanRhijn BW, Burger M, Lotan Y, *et al.* Recurrence and progression of disease in non-muscle-invasive bladder cancer: from epidemiology to treatment strategy. *Eur Urol* 2009 September;56(3):430–42.

Ethics Approval The studies were conducted under approval from Pennsylvania State College of Medicine Institutional Animal Care and Use Committee approval number 47682, or with approval of the Cantonal Veterinary Office of Canton de Vaud, Switzerland.

<http://dx.doi.org/10.1136/jitc-2021-SITC2021.878>

879

**A PROMISING CANCER IMMUNOTHERAPY TARGET:
NOVEL FULLY HUMAN AGONIST ANTIBODIES AGAINST
THE HUMAN T-CELL COSTIMULATORY RECEPTOR CD27**

Thierry Guillaudeux*, Yulia Ovechkina, Shaarwari Sridhar, David Jurchen, David Peckham, Emily Frazier, Eric Tarcha, Shawn Iadonato. *Kineta, Inc., Seattle, WA, USA*

Background CD27 is a member of the TNF receptor superfamily and plays a critical role in T-cell activation by providing a costimulatory signal. CD27 signaling enhances T-cell proliferation, activation and differentiation of effector and memory T cells and therefore promotes cytotoxic T cell (CTL)-based anti-tumor immunity.¹ Agonistic stimulation of CD27 is a promising cancer immunotherapy approach to boost specific T cell driven anti-tumor responses.

Methods In this study, we generated a series of 147 fully human monoclonal anti-CD27 antibodies and tested their agonist properties to stimulate T cell activation.

Results Using a NF- κ B reporter Jurkat cell line, we evaluated in vitro the ability of anti-CD27 antibodies to induce CD27 receptor activation. With this assay, five antibodies have been selected for their agonist properties. When combined with suboptimal T cell receptor (TCR) stimulation, agonist antibodies induced CD27 receptor activation with an EC50 of 1–5 μ g/mL. We also used human peripheral blood T cells to characterize the CD27-mediated costimulatory effects of agonist antibodies in combination with TCR stimulation. Our anti-CD27 monoclonal antibodies boosted T cell proliferation and induced IL-2 and TNF α secretion only in a presence of TCR engagement. Moreover, CD27 agonists induce strong T cell proliferation in a Mixed Lymphocyte Reaction. CD27 antibodies were shown to bind human and cynomolgus monkey CD27 with a KD value of 5–20 nM as determined by BioLayer Interferometry, but do not bind to mouse CD27. In vivo experiments are currently ongoing to demonstrate the efficient anti-tumor activity of the selected CD27 agonist antibodies in different mice tumor models.

Conclusions In conclusion, we have developed and successfully selected efficient fully human immuno-stimulatory agonist CD27 mAbs as a promising cancer immunotherapy.

REFERENCE

1. Hendriks J, Xiao Y, Borst J. CD27 promotes survival of activated T cells and complements CD28 in generation and establishment of the effector T cell pool. *J Exp Med* 2003; **Volume 198**, Number 9:1369–1380.

<http://dx.doi.org/10.1136/jitc-2021-SITC2021.879>

**TETRAVALENT, BISPECIFIC INNATE CELL ENGAGER
AFM24 ENHANCES MACROPHAGE MEDIATED TUMOR
CELL PHAGOCYTOSIS**

Sheena Pinto*, Susanne Wingert, Jens Pahl, Armin Beez, Sabrina Purr, Uwe Reusch, Arndt Schottelius, Joachim Koch. *Affimed GmbH, Heidelberg, Germany*

Background Enabling innate immunity holds promise to provide a treatment option for patients suffering from various kinds of malignancies. Innate cell engagers (ICE[®]) derived from the ROCK[®] (redirected optimized cell killing) platform have demonstrated to induce antibody dependent cellular cytotoxicity (ADCC) and phagocytosis (ADCP) via bivalent targeting of a unique epitope on CD16A of NK cells and macrophages, respectively. Previously published preclinical and clinical data of ICE[®] molecules show promising efficacy and safety as monotherapy, as a combination therapy with immuno-oncology drugs such as PD-1/PD-L1, and in combination with adoptive NK cell transfer. AFM24 is a tetravalent bispecific epidermal growth factor (EGFR)- and CD16A-binding ICE[®] for enhanced targeting and killing of EGFR+ tumor cells currently in clinical development. In contrast to approved EGFR-targeting antibodies, AFM24 does not inhibit the signaling pathway of the EGFR but utilizes this receptor merely as an "anchor" to direct NK cells and macrophages to attack tumor cells via ADCC and ADCP.

Methods ADCP assays were performed with monocyte-differentiated macrophages from healthy donor PBMCs. Target tumor cells were labelled and co-cultures with macrophages, AFM24 and control antibodies. FACS analysis and live-cell imaging (IncuCyte[®]) were used to measure ADCP events.

Results We show that AFM24 enhances macrophage mediated tumor cell phagocytosis i.e., ADCP of tumor cell lines with varying levels of EGFR expression and irrespective of EGFR signaling pathway mutations. The ability of AFM24 to enhance ADCP was further demonstrated in patient-derived xenograft cell lines from various EGFR+ tumor indications. Assays with myeloid-derived suppressor cells, natural killer cells and other immune modulators were designed to address the activity of our ICE[®] in the context of the suppressive nature of the tumor microenvironment.

Conclusions We report the ability of our ICE[®] to enhance ADCP, which might be instrumental to their efficacy, especially in tumors enriched with macrophages. In addition, due to its novel mechanism of action, AFM24 may overcome limitations of existing EGFR-targeting agents, such as dose limiting toxicity, and/or intrinsic or acquired resistance of the tumor. Consequently, AFM24 may be a potential future treatment option for a wide spectrum of patients including those that do not respond or are resistant to current EGFR-directed therapies that inhibit the signaling pathway.

<http://dx.doi.org/10.1136/jitc-2021-SITC2021.880>

881 **ENHANCED ANTIBODY-MEDIATED PHAGOCYTOSIS AND ANTIBODY-MEDIATED CELL CYTOTOXICITY USING TETRAVALENT, BISPECIFIC INNATE CELL ENGAGERS (ICE[®]) IN 3D SPHEROIDS**

Sheena Pinto*, Savannah Jackson, Julia Knoch, Christian Breunig, Arndt Schottelius, Joachim Koch. *Affimed GmbH, Heidelberg, Germany*

Background The redirected optimized cell platform (ROCK[®]) enables the generation of customizable innate cell engagers (ICE[®]) of varying valency, affinity, and pharmacokinetic profiles. Preclinical and clinical studies have demonstrated the advantage and unique features of this first-in-class ICE[®] antibodies across a multitude of cancers and its differentiation to monoclonal antibodies. ICE[®] are tetraivalent, bispecific antibodies that bivalently bind to a unique epitope on CD16A, which is selectively expressed on natural killer (NK) cells and macrophages, while the other domains target a tumor antigen. In addition to promoting antibody-dependent cellular cytotoxicity (ADCC) of NK cells, ICE[®] can also promote tumor targeting of macrophages eventually inducing antibody-dependent cellular phagocytosis (ADCP).

Methods ADCP and ADCC assays were performed using monocyte-differentiated macrophages and NK cells derived from healthy donor PBMCs. Target tumor lines and patient-derived xenograft line-derived spheroids were labelled and co-cultured with macrophages or NK cells. Live-cell imaging (IncuCyte[®]) was used to measure ADCP and ADCC events.

Results We show that ICE[®] molecules can enhance ADCP of tumor cells mediated by various functional/phenotypic subsets of macrophages derived from in vitro differentiation of human monocytes. ICE[®]-induced ADCP of tumor target cells was seen across different macrophage subtypes (M1 and M2). We further investigated the expression of immune-suppressive checkpoint programmed death-ligand 1 (PD-L1) on macrophages upon ICE[®] treatment that could be a key anti-tumor molecule within the suppressive tumor microenvironment. Based on patient-derived xenograft line-derived spheroids (3D) generated from primary tumor samples of patients suffering from various malignancies, we could demonstrate robust ADCC and ADCP mediated by NK cells and macrophages, respectively.

Conclusions ICE[®] molecules are able to mount robust NK cell- and macrophage-mediated anti-tumoral innate immune responses. This combined immune activity has the potential to not only fight tumor cells directly but also to initiate a full immune response comprised of innate and adaptive components of the immune system.

<http://dx.doi.org/10.1136/jitc-2021-SITC2021.881>

**SELECTIVE AFFINITY-ENHANCED T CELL RECEPTOR
BISPECIFIC TARGETING OF KRAS G12D NEOANTIGEN
DRIVEN CANCERS**

¹Andrew Whale*, ¹Andrew Poole, ²Vijaykumar Karuppiyah, ³Annabelle Hartt, ⁴Jaafar Haidar, ¹Sylvie Moureau, ⁴Aimee Bence Lin, ³Marc Van der Kamp, ⁴Gregory Plowman, ¹Annelise Vuidepot, ¹David Cole, ¹Chandramouli Chillakuri. ¹Immunocore Ltd, Abingdon, UK; ²Immunocore, Abingdon, UK; ³Bristol University, Bristol, UK; ⁴Lilly, New York, NY, USA

Background KRAS is the most frequently mutated oncogene, yet mutant KRAS has historically been a challenging target for conventional small molecule drug development. Tumour specific neoantigen peptides derived from KRAS are presented by cell surface human leucocyte antigens (HLA) and form a class of shared, tumour-specific antigens that are attractive targets for immunotherapy.

Methods A T cell clone that specifically recognizes the most common KRAS G12D mutant presented as a peptide in the context of HLA-A*11:01 was isolated from healthy donor PBMCs. The affinity of the respective T cell receptor (TCR) was enhanced by phage display and the x-ray crystal structures of the affinity-enhanced TCR bound to HLA presenting mutant KRAS G12D and wildtype (KRAS WT) peptides were solved. We used structural, biochemical, and computational approaches to investigate the molecular interactions underlying TCR selectivity for mutant KRAS G12D. Finally, the high affinity TCR was engineered into a soluble T cell engaging ImmTAC (Immune mobilizing monoclonal TCR Against Cancer) molecule, IMC-KRAS-G12D, and in vitro cell-based assays were performed to evaluate its potency and selectivity.

Results The affinity of the engineered TCR was enhanced by a million-fold and demonstrated remarkable ability to distinguish between KRAS G12D and KRAS WT peptide presented by HLA-A*11:01. X-ray crystal structures demonstrate that TCR binding is almost identical between KRAS G12D and KRAS WT despite a binding affinity difference of >4000 fold. The mutant residue G12D is buried into the HLA peptide binding groove and acts as a secondary anchor, making it inaccessible to the TCR. Thermodynamic analysis of TCR-HLA interaction combined with molecular dynamics simulations indicates a novel mechanism of peptide selectivity, mediated by an indirect energetic mechanism driven by an induced fit in the peptide upon TCR binding. In functional assays, this molecular differentiation translated into biological specificity with IMC-KRAS-G12D mediating T cell activation in response to cells pulsed with or expressing KRAS G12D but not KRAS WT. Furthermore, IMC-KRAS-G12D was able to redirect T cell cytotoxicity towards target KRAS G12D presenting colon cancer cells, while sparing normal colon epithelial cells.

Conclusions We developed a high affinity TCR bispecific with exquisite specificity towards a common shared neoantigen, KRAS G12D, that is a relevant therapeutic target in a wide range of cancers. These findings reveal a novel molecular mechanism for TCR selectivity for a neoantigen that differs from self-antigen by only a single amino acid, with attendant implications for therapeutic development.

<http://dx.doi.org/10.1136/jitc-2021-SITC2021.882>

883

AN ANTI-CARCINOMA MONOCLONAL ANTIBODY (MAB) NEO-201 CAN ALSO TARGET HUMAN ACUTE MYELOID LEUKEMIA (AML) CELL LINES IN VITRO

¹Alessandra Romano*, ¹Nunziatina Parrinello, ¹Sara Marino, Enrico La Spina¹, ²Massimo Fantini, ³Philip Arlen, ²Kwong Tsang, ¹Francesco Di Raimondo. ¹Università di Catania, Catania, Italy; ²Precision Biologics, Inc., Bethesda, MD, USA; ³Precision Biologics, Inc., Bethesda, MD, USA

Background NEO-201 is an IgG1 mAb targeting variants of CEACAM5/6 and has demonstrated tumor sensitivity and specificity in epithelial cells. Functional analysis has revealed that NEO-201 can engage innate immune effector mechanisms including ADCC and CDC to directly kill tumor cells expressing its target. A recent Phase 1 clinical trial at the NCI has determined both safety and recommended Phase 2 dosing. We have also seen the expression of the NEO-201 target on hematologic cells, specifically Tregs and neutrophils. Due to epitope being expressed both on malignant epithelial cells as well as several hematologic cells, we designed this study to explore the reactivity of NEO-201 against hematological neoplastic cells in vitro.

Methods Phenotypic analysis was conducted by flow cytometry. Cell lines used were six AML (HL60, U937, MOLM13, AML2, IMS-M2 and OCL-AML3), two multiple myelomas (MM) (OPM2, MM1.S), two acute lymphoblastic leukemia (ALL) (SUP-B15, RPMI8402) and four mantle cell lymphoma (MCL) (Jeko-1, Z138, JVM2 and JVM13). Markers used for flow cytometry analysis were CD15, CD45, CD38, CD138, CD14, CD19 and NEO-201. Functional analysis was performed by evaluating the ability of NEO-201 to mediate ADCC activity against AML cell lines using human NK cells as effector cells.

Results 5 of 6 AML cell lines tested bind to NEO-201 and the% of positive cells were 47%, 99.5%,100%,100% and 97.8% for HL60, U937, MOLM13, AML3 and IMS-M2, respectively. The% of positive cells in the two MM cell line were 99% and 18% for OPM2 and MM1.S, respectively. NEO-201 binding was not detected in the two ALL and the four MCL cell lines tested. Functional analysis has demonstrated that NEO-201 can mediate ADCC activity against the AML cell line (HL60) tested.

Conclusions This study demonstrates that NEO-201 mAb's target is expressed in most of the AML cell lines tested in vitro. In addition, we have shown it can mediate ADCC activity against HL60 cells (AML). Together, these findings provide a rationale for further investigation of the role of NEO-201 in AML as well as MM, further exploring patient PBMCs and bone marrow samples.

<http://dx.doi.org/10.1136/jitc-2021-SITC2021.883>

ENGINEERED TOXIN BODY MEDIATED DEPLETION OF TIGIT EXPRESSING IMMUNE CELLS FOR CANCER IMMUNOTHERAPY

<http://dx.doi.org/10.1136/jitc-2021-SITC2021.884>

Elizabeth Saputra, Garrett Cornelison, Jennifer Mitchell, Karia Williams, Andrea Mendiola, Rachael Orlandella, John Majercak, Joseph Dekker, Chris Moore, Swati Khanna*. *Molecular Templates Inc., Austin, TX, USA*

Background TIGIT (T cell immunoreceptor with Ig and ITIM domains) is an exciting novel target for immuno-oncology which functions as an immune checkpoint on multiple immune cell types including memory CD8+, CD4+ Treg, and memory CD4+ cells. TIGIT upregulation on tumor infiltrating lymphocytes (TILs) has been observed in multiple cancer types and contributes to an immunosuppressive tumor microenvironment (TME). Interestingly, TIGIT is commonly co-expressed with PD-1 on Tregs in the TME, tumor antigen specific CD8+ T cells and CD8+ TILs, leading to weakened anti-tumor immune responses.¹⁻² To date, TIGIT inhibiting monoclonal antibodies (mAb) have shown little activity as a monotherapy in clinical and preclinical studies.³⁻⁴ Therefore, current clinical trials are now focused on combining TIGIT mAbs with known commercial PD-1 or PD-L1 mAbs. A TIGIT-specific engineered toxin body (ETB) represents a wholly new approach to targeting TIGIT expressing cells including those co-expressing TIGIT and PD-1.

Methods ETBs targeting TIGIT were designed to deplete TIGIT-expressing TILs, including Tregs, directly in the TME. ETBs are proteins that consist of an antibody fragment genetically fused to a proprietary de-immunized (DI) form of the Shiga-like toxin A subunit (SLTA). These proteins are specific for a cell surface receptor, and function through triggering rapid internalization upon binding, followed by an enzymatic and irreversible termination of ribosomal protein synthesis resulting in cellular apoptosis. Here we provide proof of concept for ETBs as a novel modality for the depletion of TIGIT-expressing immune cells.

Results TIGIT-targeting ETBs exhibit potent in vitro cytotoxicity of TIGIT over-expressing cell lines (IC₅₀<1nM). These ETBs also lead to apoptotic depletion of ex vivo TIGIT-expressing regulatory T cells (Tregs) from healthy donors. In mixed culture assays, TIGIT ETBs increase the proliferation of TIGIT negative T cells by depleting TIGIT-expressing T cells.

Conclusions Studies to assess pharmacodynamics and efficacy of TIGIT targeting ETBs using a double knock-in (TIGIT and PD-1) mouse tumor model are ongoing, but these early proof of concept in vitro data support the hypothesis that ETBs can deplete TIGIT positive immune cell populations including those co-expressing PD-1. It is possible that targeted TIGIT inhibition through ETB-induced cell death could tip the balance towards tumor regression by eliminating this novel checkpoint (and TIGIT/PD-1 co-expression) at the level of the TME.

REFERENCES

1. Jinhua X, Ji W, Shouliang C, Liangfeng Z. Expression of immune checkpoints in T cells of esophageal cancer patients. *Oncotarget* 2016;**7**(39):1–10.
2. Blessin NC, Simon R, Kluth M, Fischer K, et al. Patterns of TIGIT expression in lymphatic tissue, inflammation and cancer. *Dis Markers* 2019;**2019**:1–13.
3. Johnston RJ, Comps-Agrar L, Hackney J, Yu X, et al. The immunoreceptor TIGIT regulates anti-tumor and antiviral CD8(+) T effector function. *Cancer Cell* 2014;**26**(6):923–927.
4. Bendell JC, Bedrad P, Bang Y-J, LoRusso P, et al. Phase Ia/Ib dose-escalation study of the anti-TIGIT antibody Tiragolumab as a single agent and in combination with atezolizumab in patients with advanced solid tumors. Proceedings: AACR Annual Meeting 2020; April 27–28, 2020 and June 22–24, 2020; Philadelphia, PA.

885

TARGETING FPR2 AS A NOVEL APPROACH FOR IMMUNOTHERAPY IN PANCREATIC CANCER FEMALE PATIENTS - STUDIES OF SEXUAL IMMUNE DIMORPHISM IN THE TUMOR MICROENVIRONMENT

Dhifaf Sarhan*, Fei He, Ahmed Calandigary, Enana Malki, Carlos Fernández Moro, Marina Kaisso, Peter Olofsson-Sahl, Marit Melssen, Matthias Löhr, Mikael Karlsson, Rainer Heuchel. *Karolinska Institutet, Stockholm, Sweden*

Background Immunotherapy for pancreatic cancer (PC) is inefficient due to a highly immune-suppressive tumor microenvironment (TME) orchestrated by myeloid suppressor cells, which limit the infiltration and function of cytotoxic immune cells. We have evidence that accumulation of a subpopulation of myeloid cells in human pancreatic lesions is associated with immune-exclusive tumor phenotype and effector T cell exhaustion by mechanisms involving the G-coupled protein receptor formyl peptide receptor 2 (FPR2), exclusively in women. We hypothesize that female FPR2+ myeloid cells in tumors induce immune exhaustion and contribute to immune-cold tumor phenotype.

Methods To test our hypothesis, we first investigated the FPR2 RNA and protein expression in PC transcriptomic data and in murine and human PC tissues. Further, in vitro cytokine differentiated, alternatively tumor conditioned myeloid cells (TCM) were co-cultured with T cells to mimic their interaction in the TME. In vivo, PC cells were injected subcutaneously in FPR2 WT and KO mice to study tumor progression and the immune landscape in male vs. female mice. Later, human myeloid cells were treated with FPR2 agonists and antagonists to study the interaction mechanisms in detail.

Results We found high FPR2 expression in tumor compared to healthy tissues and higher in women compared to men. In mice and human, FPR2+ myeloid cells were associated with immune cold-exclusive and cold-ignored tumor phenotype in women and men, respectively. Notably, analysis in PC and other gastrointestinal (GI)-tract cancers revealed a significant association of FPR2 expression and poor survival only in women, emerging the potential impact of sex factors in the TME. Such sexual dimorphism in the TME was associated with T cell exhaustion apparent by high expression of TIM3 and PD1. In vitro, FPR2-agonist treated myeloid-suppressive cells induced TIM3 and PD1 expression in T cells specifically in female T cells. However, a significant repression of TIM3 and a trend of PD1 expression was observed in T cells when interacting with FPR2-inhibited or -deficient myeloid cells. Finally, tumor progression was significantly slower in FPR2 KO female mice compared to WT and male FPR2 WT and KO mice.

Conclusions In this study, we have shown that sex differences are involved in shaping the TME in PC, where sexual dimorphism is still a largely unknown area allowing novel personalized/sex-specific immunotherapies. We found that FPR2 is highly involved in T cell exhaustion and can potentially be a therapeutic target for immunotherapy in women developing PC and other GI-tract cancers.

Ethics Approval The study was approved by the regional ethics review board in Stockholm (Dnr2020-06587 and Dnr2013.977-31.1) and the Swedish Board of Agriculture and regional ethical committee (10681-2020).

<http://dx.doi.org/10.1136/jitc-2021-SITC2021.885>

TARGETING VSIG4, A NOVEL MACROPHAGE CHECKPOINT, REPOLARIZES SUPPRESSIVE MACROPHAGES WHICH INDUCES AN INFLAMMATORY RESPONSE IN PRIMARY CELL IN VITRO ASSAYS AND FRESH HUMAN TUMOR CULTURES

Steve Sazinsky*, Phuong Nguyen, Mohammad Zafari, Ryan Phennicie, Joe Wahle, Veronica Komoroski, Kathryn Rooney, Craig Mizzoni, Boris Klebanov, Denise Manfra, Jessica Ritter, Igor Feldman, Tatiana Novobrantseva. *Verseau Therapeutics, Bedford, MA, USA*

Background VSIG4 (V-set immunoglobulin-domain-containing 4) is a B7 family related protein with known roles as a complement receptor involved in pathogen clearance as well as a negative regulator of T cell activation by an undetermined mechanism.¹⁻³ VSIG4 is expressed in tumor associated macrophages (TAMs) with exquisite specificity. In cancer, increased expression of VSIG4 has been associated with worse survival in multiple indications, including non-small cell lung cancer, multiple myeloma, ovarian cancer, and glioma, suggesting an important role in tumor immune evasion.³⁻⁶ Based upon computational analysis of transcript data across thousands of primary cancer and normal tissue samples, we hypothesized that VSIG4 has an important regulatory role in promoting M2-like immune suppressive macrophages in the tumor microenvironment, and that targeting VSIG4 via a monoclonal antibody could relieve VSIG4-mediated macrophage suppression by repolarizing TAMs to an inflammatory phenotype capable of coordinating an anti-tumor immune response.

Methods The ability of anti-VSIG4 antibodies to repolarize M2-like macrophages and induce T cell activation was assessed in vitro and ex vivo, by measuring production of inflammatory mediators. *In vitro* assays were performed primarily with M-CSF plus IL-10 driven monocyte-derived M2c macrophages from healthy donors. *Ex vivo* assays were performed with fresh, patient-derived tumor samples in culture. To determine whether targeting VSIG4 can lead to an anti-tumor effect *in vivo*, syngeneic mouse models were dosed with anti-mouse VSIG4 antibodies and characterized for changes in tumor volume and immune cell populations.

Results In *in vitro* and *ex vivo* assays anti-VSIG4 antibodies repolarize M2 macrophages and induce an immune response culminating in T cell activation. Targeting VSIG4 upregulates pro-inflammatory cytokines in M2c macrophages, as well as upregulates pro-inflammatory myeloid-derived cytokines and T cell-derived cytokines in M2c macrophages co-cultured with autologous T cells in the presence of staphylococcal enterotoxin B (SEB) activation. To assess targeting VSIG4 in a relevant translational model, fresh, patient-derived tumor samples were treated *ex vivo* with anti-VSIG4. Across multiple tumor types, anti-VSIG4 treatment resulted in a significant upregulation of cytokines involved in TAM repolarization and T cell activation, and chemokines involved in immune cell recruitment, at levels greater than observed by treatment with anti-PD-1 or a clinical macrophage repolarizing agent (anti-ILT-4). *In vivo*, tumor growth inhibition is observed in syngeneic mouse models dosed with anti-mouse-VSIG4 alone and in combination with anti-PD-1.

Conclusions Taken together, these data suggest that VSIG4 represents a promising new target capable of stimulating an anti-cancer response via multiple key immune mechanisms.

REFERENCES

1. van Lookeren Campagne M, Verschoor A. Pathogen clearance and immune adherence "revisited": immuno-regulatory roles for CRIg. *Semin Immunol* 2018;**37**:4-11.
2. Xu S, Sun Z, Li L, Liu J, He J, Song D, Shan G, Liu H, Wu X. Induction of T cells suppression by dendritic cells transfected with VSIG4 recombinant adenovirus. *Immunol Lett* 2010;**128**(1):46-50.
3. Liao Y, Guo S, Chen Y, Cao D, Xu H, Yang C, Fei L, Ni B, Ruan Z. VSIG4 expression on macrophages facilitates lung cancer development. *Lab Invest* 2014;**94**(7):706-715.
4. Roh J, Jeon Y, Lee A, Lee S, Kim Y, Sung C, Park C, Hong J, Yoon D, Suh C, Huh J, Choi I, Park C. The immune checkpoint molecule V-set Ig domain-containing 4 is an independent prognostic factor for multiple myeloma. *Oncotarget* 2017;**8**(35):58122-58132.
5. Xu T, Jiang Y, Yan Y, Wang H, Lu C, Xu H, Li W, Fu D, Lu Y, Chen J. VSIG4 is highly expressed and correlated with poor prognosis of high-grade glioma patients. *Am J Transl Res* 2015;**7**(6):1172-1180.
6. Byun J, Jeong D, Choi I, Lee D, Kang M, Jung K, Jeon Y, Kim Y, Jung E, Lee K, Sung M, Kim K. The significance of VSIG4 expression in ovarian cancer. *Int J Gynecol Cancer* 2017;**27**(5):872-878.

Ethics Approval All legal and ethical requirements were met with regards to the humane treatment of animals described in the study. The animal study was conducted in compliance with CRL IACUC under IACUC No. 1033.

<http://dx.doi.org/10.1136/jitc-2021-SITC2021.886>

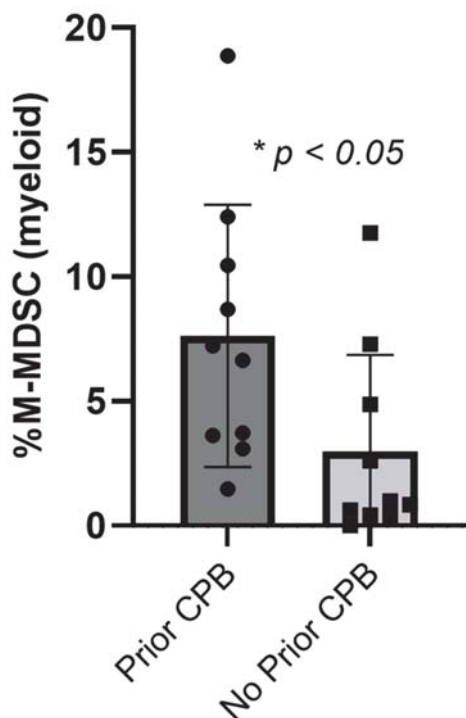
887

REPOLARIZATION OF T CELLS BY AMV564 IN PATIENTS PROGRESSING ON CHECKPOINT BLOCKADE

Victoria Smith*, Sterling Eckard, Bianca Rojo, Patrick Chun. *Amphivena Therapeutics, Inc., South San Francisco, CA, USA*

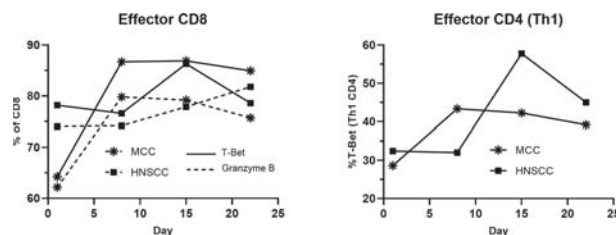
Background MDSC produce numerous immune-suppressive factors and are associated with poor outcomes across different cancers. They are frequently elevated in patients experiencing inadequate benefit from checkpoint blockade and there is a crucial need for therapies for this patient population. MDSC are recruited from bone marrow in response to both tumor signaling and T cell activation, and their accumulation in tumors and lymphatics can limit the potential benefits of immunostimulatory therapies. AMV564 is a bivalent T cell engager that selectively depletes MDSC. In a phase 1 study, pharmacodynamic analyses revealed significant depletion of MDSC, T cell activation, expansion of the T cell repertoire and an IFN-gamma-dominant cytokine profile with comparatively limited IL6 induction.¹ Monotherapy activity including a confirmed RECIST complete response was observed. The clinical and pharmacodynamic profiles of AMV564 are being further evaluated in specific patient cohorts, including patients progressing on checkpoint blockade.

M-MDSC after T Cell Activation



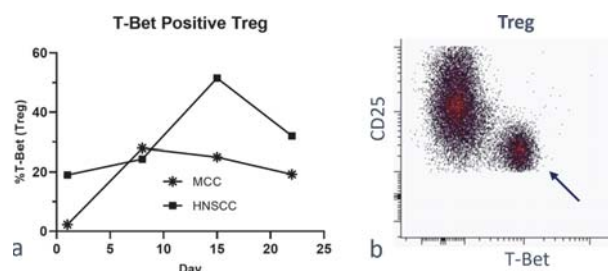
Abstract 887 Figure 1

Significantly higher induction of M-MDSC is apparent in patients previously receiving checkpoint blockade (CPB) after T cell activation by AMV564.



Abstract 887 Figure 2

Treatment with AMV564 promotes increases in effector CD8 and CD4 T cells in patients previously treated with CPB (examples shown are Merkel cell carcinoma (MCC) and head and neck squamous cell carcinoma (HNSCC)).



Abstract 887 Figure 3

Th-1 like repolarization of Treg is apparent in patients previously treated with CPB (MCC, HNSCC examples) after treatment with AMV564 (a). Example CD25 low and T-Bet high cells in HNSCC patient (arrow, b).

Methods In a phase 1b expansion study (NCT04128423), patient cohorts with cancers more likely to include actionable tumor antigens were selected for treatment with AMV564, with most patients representing checkpoint treatment failures. An additional cohort of patients included heterogeneous tumor types stratified by tumor mutation burden (TMB) score from circulating tumor DNA. Pharmacodynamic analyses including direct immunophenotyping (flow cytometry) of T and myeloid cell compartments in peripheral blood were performed on patients treated with AMV564 (15 μ g daily for 10 of 21 days by subcutaneous injection).

Results Changes in myeloid and T cell profiles consistent with the pharmacodynamic signature of AMV564 were observed in patients receiving AMV564 despite one or more prior lines of checkpoint blockade therapy. Notably, both high baseline MDSC and elevated induction of MDSC after T cell activation were apparent (figure 1). Control of MDSC by AMV564 was associated with increases in both effector CD8 and CD4 T cells (figure 2). Extremely elevated levels of regulatory T cells were often observed: after treatment with AMV564, a Th-1-like repolarization of these cells was apparent, often associated with reduction in CD25 (figure 3).

Conclusions Treatment with AMV564 yielded substantial reductions in MDSC and favorable polarization of CD8 and

CD4 T cells, including Th1-like polarization of Treg. This signature was apparent in patients previously treated with checkpoint inhibitors, despite strong induction of MDSC in response to T cell activation, and high baseline levels (>20%) of Treg.

Trial Registration NCT04128423

REFERENCES

1. Smith V, Eckard S, Rettig MP, *et al.* AMV564, a bivalent, bispecific T-cell engager, depletes myeloid derived suppressor cells and activates T cells in cancer patients. *Cancer Res* 2020;**80**(16 Supplement):5699.

Ethics Approval This study was approved by the Institutional Review Board (IRB) or Independent Ethics Committee (IEC) at each participating institution (including Ohio State University, MD Anderson Cancer Center, Duke University, University of California Los Angeles, Advent Health, Christ Hospital). All participants gave informed consent for samples used to generate pharmacodynamic data. No sensitive or identifiable information is included.

<http://dx.doi.org/10.1136/jitc-2021-SITC2021.887>

AN INTEGRATIVE APPROACH TO OPTIMIZE A SYNTHETIC EPHA2/CD137 AGONIST: BALANCING POTENCY, PHYSIOCHEMICAL PROPERTIES, AND PHARMACOKINETICS TO ACHIEVE ROBUST ANTI-TUMOR ACTIVITY

Punit Upadhyaya*, Gemma Mudd, Kristen Hurov, Johanna Lahdenranta, Elizabeth Repash, Julia Kristensson, Kevin McDonnell, Philip Brandish, Phil Jeffrey, Nicholas Keen. *Bicycle Therapeutics, Lexington, MA, USA*

Background CD137 (4-1BB) is a resurging target in immunotherapy after the first generation of monoclonal antibodies were limited by hepatotoxicity¹ or lack of efficacy.² A new generation of CD137 agonists are now in clinical development but they exclusively utilize large molecules derived from recombinant technology and are associated with long circulating terminal half-lives.^{3–6} Unlike checkpoint inhibition where complete saturation of the receptors drives the reversal of immunosuppression, intermittent target engagement that reflects the physiological context of T cell co-stimulation may be more appropriate for a CD137 agonist.⁷ Bicyclic peptides or *Bicycles* are a class of small (MW~2kDa), highly constrained peptides characterized by formation of two loops cyclized around a symmetric scaffold. To develop a differentiated tumor antigen dependent CD137 agonist for treating EphA2 expressing solid tumors, we integrated structure activity relationship (SAR) data from biochemical binding studies and in-vitro and in-vivo models to understand the relationship between exposure, target engagement and preclinical efficacy.

Methods Over 150 different EphA2/CD137 tumor-targeted immune cell agonists (*Bicycle* TICAs) were synthesized by linking *Bicycle*[®] binders to EphA2 to those binding CD137.⁸ The molecules were assessed in vitro using a CD137 reporter assay and by measuring cytokine production from primary human PBMC in tumor cell co-cultures. The pharmacokinetics were evaluated in rodents using Phoenix WinNonlin. The in vivo activity was determined in syngeneic mouse tumor models by measuring tumor growth kinetics and using tumor immune cell and transcriptional profiling by IHC and NanoString.

Results Evaluation of the *Bicycle* TICAs in co-culture assays with EphA2-expressing tumor cell lines and Jurkat reporter cells overexpressing CD137 or human PBMCs demonstrated that constructs bearing two CD137 binding *Bicycles* to one EphA2 binding *Bicycle* (1:2 format) were more potent than the 1:1 format.⁸ Several *Bicycle* TICAs with amino acid substitutions to the EphA2 binding *Bicycle* maintained sub-nanomolar potency in-vitro and exhibited a plasma terminal half-life (t_{1/2}) in rodents ranging from 0.4 and 4.0 h. Modifications that conferred aqueous solubility of greater than 10 mg/mL were considered suitable for further development. Treatment of MC38 tumors in immunocompetent mice with this series of molecules demonstrated that low MW *Bicycle* TICAs with sub-nanomolar potency and a t_{1/2} of ~1 h in mouse maintained target coverages necessary to produce robust modulation of the tumor immune microenvironment and tumor regression.

Conclusions A differentiated EphA2-dependent CD137 agonist was developed that exploits intermittent rather than continuous exposure for robust anti-tumor activity.

REFERENCES

1. Segal NH, Logan TF, Hodi FS, *et al.* Results from an integrated safety analysis of urelumab, an agonist anti-CD137 monoclonal antibody. *Clin Cancer Res* 2017;**23**(8):1929–1936.

2. Segal NH, Aiwu RH, Toshihiko D, *et al.* Phase I study of single-agent utomilumab (PF-05082566), a 4-1BB/CD137 agonist, in patients with advanced cancer. *Clin Cancer Res* 2018;**24**(8):1816–1823.
3. Chester C, Sanmamed MF, Wang J, Melero I. Immunotherapy targeting 4-1BB: mechanistic rationale, clinical results, and future strategies. *Blood* 2018;**131**(1):49–57.
4. Hinner MJ, Aiba RSB, Jaquin TJ, *et al.* Tumor-localized costimulatory T-cell engagement by the 4-1BB/HER2 bispecific antibody-anticalin fusion PRS-343. *Clin Cancer Res* 2019;**25**(19):5878–5889.
5. Claus C, Ferrara, C, Xu W, *et al.* Tumor-targeted 4-1BB agonists for combination with T cell bispecific antibodies as off-the-shelf therapy. *Sci Transl Med* 2019;**11**(496):eaav5989.
6. Eskiocak U, Guzman W, Wolf B, *et al.* Differentiated agonistic antibody targeting CD137 eradicates large tumors without hepatotoxicity. *JCI Insight* 2020;**5**(5): e133647.
7. Mayes PA, Hance KW, Hoos A. The promise and challenges of immune agonist antibody development in cancer. *Nat Rev Drug Discov* 2018;**17**:509–27.
8. Upadhyaya P, Lahdenranta J, Hurov K, *et al.* Anticancer immunity induced by a synthetic tumor-targeted CD137 agonist. *J Immunother Cancer* 2021;**9**:e001762.

<http://dx.doi.org/10.1136/jitc-2021-SITC2021.888>

DUOBODY®-CD3x5T4 INDUCES EFFICIENT T-CELL ACTIVATION AND KILLING OF PATIENT-DERIVED HEAD AND NECK CANCER CELLS IN VITRO AND EX VIVO

¹Rieneke van de Ven*, ¹Sonja Ganzevles, ¹Myrthe Veth, ²Patrick Franken, ²Esther Breijl, ¹Ruud Brakenhoff, ²Kristel Kemper. ¹Amsterdam UMC, VU University Medical Center, Amsterdam, Netherlands; ²Genmab, Utrecht, Netherlands

Background 5T4, also known as trophoblast glycoprotein, is expressed in many solid cancers, including non-small cell lung cancer, triple-negative breast cancer, bladder, esophageal, prostate, uterine and head and neck squamous cell carcinomas (HNSCCs). DuoBody-CD3x5T4 is a CD3 bispecific antibody that efficiently induces T-cell mediated cytotoxicity of 5T4-positive tumor cells. Currently, DuoBody-CD3x5T4 is being evaluated in a first-in-human clinical trial (NCT04424641) in solid cancers in partnership between Genmab and AbbVie. In this study we explored the preclinical mechanism-of-action of DuoBody-CD3x5T4 in vitro and ex vivo, using HNSCC as a case study.

Methods 5T4 protein expression in HNSCC tumor specimens was determined by immunohistochemistry (IHC) and flow cytometry. T-cell mediated cytotoxicity and T-cell activation induced by DuoBody-CD3x5T4 were studied in co-cultures of healthy donor T cells and patient-derived HNSCC cell lines in vitro. Lastly, the capacity of DuoBody-CD3x5T4 to activate tumor-infiltrating lymphocytes (TILs) was analyzed in freshly dissociated 5T4-expressing HNSCC tumor specimens ex vivo.

Results IHC analysis confirmed expression of 5T4 in HNSCC oral biopsies, including specimens from primary tumors, recurrent tumors and lymph node metastases. Patient-derived HNSCC cell lines (n=22) demonstrated 5T4 expression on the plasma membrane, ranging from 10,000 - 61,000 5T4 molecules per cell. Moreover, 5T4 expression was evident on EGFR+CD45- tumor cells in single-cell suspensions from freshly dissociated HNSCC biopsies, independent of the tumor site. DuoBody-CD3x5T4 demonstrated potent, target-dependent cytotoxicity in vitro in co-cultures of healthy donor T cells and patient-derived HNSCC cell lines across the range of 5T4 expression levels tested. Tumor cell kill was associated with CD4+ and CD8+ T-cell activation and granzyme B secretion. Importantly, DuoBody-CD3x5T4 induced potent activation of autologous TILs in single-cell suspensions from freshly dissociated HNSCC biopsies. Notably, T-cell activation (as assessed by expression of CD69, CD25 and CD137) was also observed in PD-1+ TILs, suggesting that DuoBody-CD3x5T4 was able to engage antigen-experienced T cells in the tumor microenvironment. In this autologous assay, preliminary data showed that 5T4-expressing HNSCC tumor cells were specifically eradicated.

Conclusions 5T4 was broadly expressed in HNSCC cell lines, tumor biopsies and primary tumor cell suspensions. DuoBody-CD3x5T4 activated healthy donor T cells in co-cultures with patient-derived HNSCC cell lines, resulting in secretion of granzyme B and efficient tumor cell kill. In single-cell suspensions from freshly dissociated 5T4+ HNSCC biopsies, DuoBody-CD3x5T4 activated autologous CD4+ and CD8+ TILs, including PD-1+ TILs. This dataset adds to the preclinical evidence for targeting 5T4-expressing solid cancers with DuoBody-CD3x5T4.

Ethics Approval Written informed consent was obtained from all patients from whom fresh tumor biopsies were used for research, as part of the HNcol protocol at the Department of Otolaryngology|Head and Neck Surgery of Amsterdam UMC

(VUmc) as approved by the Institutional Review Board (2008.071|A2016.035). Archival FFPE specimens were used for scientific research in agreement with the medical ethical guidelines described in the Code of Conduct for Proper Secondary Use of Human Tissue of the Dutch Federation of Biomedical Scientific Societies (Federa) in accordance with the Declaration of Helsinki and after Biobank approval (BUP2019-74).

<http://dx.doi.org/10.1136/jitc-2021-SITC2021.889>

890

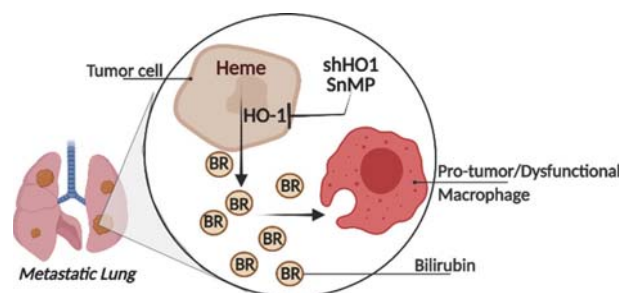
MANIPULATION OF EPITHELIAL-TO-MESENCHYMAL TRANSITION REVEALS METASTATIC BREAST CANCERS SUPPORT IMMUNE SUPPRESSION VIA HEME METABOLISM

Michelle Williams*, Sabrina Hafeez, Jessica Christenson, Nicole Spoelstra, Jill Slansky, Jennifer Richer. *University of Colorado Anschutz Medical Campus, Aurora, CO, USA*

Background Oncogenic epithelial-to-mesenchymal transition (EMT) enhances triple negative breast cancer (TNBC) aggressiveness and immune suppression. To identify alternative immunotherapy targets for metastatic TNBC, we reversed EMT in mesenchymal-like human TNBC and mouse mammary carcinoma models by restoring the micro-RNA-200c. This approach identified several tumor cell metabolizing enzymes with potential immune modulatory functions such as heme oxygenase-1 (HO-1). HO-1 converts heme to bilirubin, an established immune suppressor in other diseases that has never been tested as such in cancer. We **hypothesize** that tumor cell-HO-1 activity and subsequent bilirubin secretion enhance TNBC metastasis by supporting a pro-tumor immune microenvironment (figure 1).

Methods We tested the impact of tumor cell-HO-1 and bilirubin on macrophage immune suppression and efferocytic capacity (engulfment of dead tumor cells) using qRT-PCR, flow cytometry and live cell imaging. Human and mouse macrophages were analyzed after treatment with exogenous bilirubin or bilirubin-depleted conditioned medium collected from tumor cells treated with tin mesoporphyrin (SnMP), an enzymatic HO-1 inhibitor. Primary tumor growth and lung metastatic burden were observed in syngeneic mice harboring HO-1 depleted 66Cl-4 mammary tumors (shRNA). Breast cancer specimens were analyzed via CIBERSORT to predict immune cell abundance in patients with high versus low levels of heme metabolism genes.

Results Macrophages cultured with conditioned medium from tumor cells treated with the HO-1 inhibitor SnMP demonstrated a 35–65% decrease in immune suppressive genes (*Arg1*, *Cd274*, *Tgfb1*) compared to those treated with control conditioned medium. This effect was rescued by exogenous treatment with 2.5 μ M bilirubin. Direct bilirubin treatment enhanced macrophage PD-L1 mRNA and protein expression by at least 6-fold. In contrast, bilirubin decreased expression of macrophage efferocytosis genes (*Mertk*, *Tyro3*) by at least 50%, resulting in decreased efferocytic capacity. To test whether bilirubin supports tumor progression via modulation of macrophages, we evaluated tumor growth and metastasis after tumor cell-HO-1 depletion. While mice with shHO1 tumors had enhanced primary tumor growth compared to those with shCnt tumors, HO-1 depletion decreased lung metastatic capacity. Although immune cell infiltration and activation is currently underway in this mouse model, CIBERSORT analysis revealed that breast cancer specimens with high levels of heme metabolism genes have a predicted increase in M2 macrophage presence.



Abstract 890 Figure 1 Project model

Heme oxygenase-1 (HO-1) breaks down heme into immune modulatory products such as bilirubin (BR). We demonstrated that tumor cell-secreted BR may enhance TNBC lung metastasis by supporting macrophage immune suppression and dysfunction. This can be blocked by genetic (shRNA) or pharmacologic (SnMP) inhibition of HO-1 in TNBC cells. Figure made with biorender.com.

Conclusions Tumor cell-HO-1 may support immune cell suppression and dysfunction during breast cancer metastasis via bilirubin. Since HO-1 inhibitors including SnMP are FDA approved for treatment of other diseases, these findings could rapidly be translated to provide an additional immunotherapy for metastatic TNBC.

<http://dx.doi.org/10.1136/jitc-2021-SITC2021.890>

**S-531011, A NOVEL ANTI-HUMAN CCR8 ANTIBODY:
ANTIBODY SCREENING AND EVALUATION OF
BIOLOGICAL PROFILES**

¹Mai Yoshikawa*, ¹Yoji Nagira, ¹Morio Nagira, ¹Tetsuya Yoshida, ¹Shinpei Yoshida, ¹Tetsuyoshi Soh, ²Hisashi Wada, ²Naganari Ohkura, ¹Tatsuya Takahashi. ¹*Shionogi and Co., Ltd., Osaka, Japan*; ²*Osaka University, Osaka, Japan*

Background Regulatory T cells (Tregs) are involved in tumor progression and inhibition of anti-tumor immune responses by promotion of immunological tolerance in the tumor microenvironment. On the other hand, Treg cells in peripheral blood are also essential role in preventing autoimmunity and uncontrolled inflammation. So, selective control of tumor infiltrating Treg cells might be an attractive approach of immune-oncology therapies without disrupting their systemic anti-inflammatory functions. Here, we focused on CCR8 (C-C motif chemokine receptor 8) as a target molecule which was selectively and highly expressed on tumor-infiltrating Tregs and developed a novel anti-human CCR8 specific antibody.

Methods We immunized mice with human CCR8 by our original immunization method which could strongly induce antibodies for membrane proteins, and then constructed hybridoma cells. Anti-human CCR8 (human CCR4 as a negative control) binding assay and human CCL1-CCR8 neutralizing assay were simultaneously performed by using supernatants of hybridoma cells to isolate human CCR8 specific strong-neutralizing antibodies. After humanization and affinity maturation of some selected clones, we selected our lead antibody by binding specificity, neutralizing activity, antibody dependent cellular cytotoxicity (ADCC) and thermodynamic stability as index.

Results We rapidly induced human CCR8 specific antibodies in mouse with our unique immunization methods and constructed thousands of hybridomas secreting anti-human CCR8 antibodies. We also successfully humanized some of lead antibodies which show high affinity and specificity and isolated novel anti-human CCR8 specific humanized antibody S-531011 as our development antibody after affinity maturation. S-531011 selectively recognizes human CCR8 on the surface of tumor-infiltrating Tregs and shows strong ADCC. While human CCL1 is known as a dominant ligand of CCR8 which binds extracellular loop2 and N-terminal of CCR8, S-531011 recognizes similar epitopes and effectively neutralizes CCL1-CCR8 signaling. Furthermore, S-531011 also shows favorable blood kinetics in vivo and potently inhibits tumor growth in tumor bearing human CCR8 knock-in mouse model.

Conclusions We develop S-531011, a novel anti-human CCR8 humanized antibody which could selectively recognize and deplete tumor infiltrating Tregs. Based on our pre-clinical data, S-531011 has strong anti-tumor effect and we expect that it might be a potent novel tumor immuno-therapeutic agent with fewer side effect.

Ethics Approval The present study was approved by the Institutional Ethics Committee of Osaka University Hospital (approved number: 13266-15). Animal studies were approved by the Institutional Animal Care and Use Committee (approved number: S20192D, S20197D and S20198D).

<http://dx.doi.org/10.1136/jitc-2021-SITC2021.891>

892

ABL503 (TJ-L14B), PD-L1X4–1BB BISPECIFIC ANTIBODY INDUCES SUPERIOR ANTI-TUMOR ACTIVITY BY PD-L1-DEPENDENT 4–1BB ACTIVATION WITH THE INCREASE OF 4–1BB+CD8+ T CELLS IN TUMOR MICROENVIRONMENT

¹Uijung Jung, ¹Jaehyoung Jeon, ¹Shinai Lee, ²Hyung-Seung Jin, ¹Youngkwang Kim, ¹Eunsil Sung, ¹Hyunjoo Kim, ¹Yangmi Lim, ¹Jonghwa Won, ³Zhengyi Wang, ³Wenqing Jiang, ¹Jaeho Jung, ¹Gihoon You*. ¹ABL Bio Inc., Seongnam, Korea, Republic of; ²Asan Medical Center, Seoul, Korea, Republic of; ³I-Mab Biopharma, Shanghai, China

Background PD-(L)1 inhibitor has revolutionized cancer treatment, but there are unmet clinical needs for PD-(L)1 inhibitor-resistant/refractory patients. Activation of T cells in tumor microenvironment by 4-1BB agonist antibodies is one of the promising approaches to complement the current limitation of PD-(L)1 inhibitors. Although 4-1BB is a promising target for immunotherapy, clinical studies using 4-1BB agonist antibodies showed systemic immune cell activation resulting in dose-limiting hepatotoxicity. We generated ABL503 (TJ-L14B), a bispecific antibody that combines PD-(L)1 blockade and PD-L1-dependent 4-1BB agonistic activity by binding both PD-L1 and 4-1BB to limit unwanted toxicities while exerting a potent anti-tumor efficacy. Here, we reported the pre-clinical properties of ABL503 (TJ-L14B) in various studies.

Methods The activity of ABL503 (TJ-L14B) was characterized and evaluated in 1) PD-1 and 4-1BB signaling reporter cells cocultured with various tumor cells and PBMCs, 2) hPD-L1/h4-1BB knock-in mice implanted with MC38 tumor expressing different level of hPD-L1, 3) patient-derived lung cancer organoids cocultured with autologous PBMCs, and 4) PBMCs from healthy donors to measure cytokine release.

Results Functional evaluation of ABL503 (TJ-L14B) indicates the activation of 4-1BB signaling was solely dependent on engagement of hPD-L1 expressed on immune cells as well as on tumor cells, pointing to pivotal roles of PD-L1 on both immune cells and tumor cells for the activity of ABL503 (TJ-L14B). In vivo anti-tumor activity of ABL503 (TJ-L14B) across different hPD-L1 levels showed prominent anti-tumor effect with significantly increased number of CD8+ cells and 4-1BB+ cells in the tumor. This anti-tumor activity was correlated with the proliferation (Ki-67+) of CD8+ T cells in the tumor microenvironment. Ex vivo assays utilizing patient-derived lung cancer organoids revealed that ABL503 (TJ-L14B) exhibits superior tumor-killing activity than that by benchmark PD-L1 antibody, Atezolizumab. In addition, cytokine release assay demonstrated that ABL503 (TJ-L14B) did not induce non-specific pro-inflammatory cytokine release by human PBMCs.

Conclusions Our data indicate that PD-L1 and 4-1BB dual targeting bispecific antibody, ABL503 (TJ-L14B), shows potent 4-1BB agonistic activity and anti-tumor effect in a PD-L1-dependent fashion concomitant with 4-1BB+/CD8+ T cell activation and proliferation to overcome limitations of PD-(L)1-targeted therapy while minimizing the risk of peripheral toxicity. The phase 1 clinical trial in the U.S. is currently ongoing in patients with locally advanced or metastatic solid tumors (NCT04762641).

<http://dx.doi.org/10.1136/jitc-2021-SITC2021.892>

893

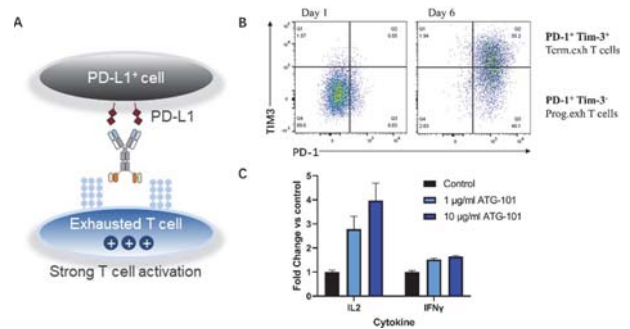
ATG-101, A NOVEL PD-L1/4-1BB BISPECIFIC ANTIBODY, AUGMENTS ANTI-TUMOR IMMUNITY THROUGH IMMUNE CHECKPOINT INHIBITION AND PDL1-DIRECTED 4-1BB ACTIVATION

¹Hui Yuwen, ¹Tengteng Li, ¹Yijing Ren, ²Dirk Hoenemann, ³Jay Mei, ³Bo Shan, ³Bing Hou*. ¹Shanghai Antengene Corporation Limited., Shanghai, China; ²Antengene Pty Ltd, Melbourne, Australia; ³Antengene Corporation Co., Ltd., Shao xing, China

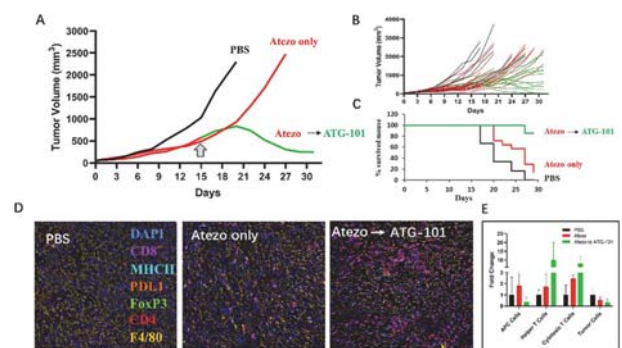
Background Programmed death-ligand 1 (PD-L1) and programmed cell death protein 1(PD-1) blockade therapy has revolutionized the treatment landscape of malignancies. However, only a minority of patients are anticipated to experience a deep and durable response. In addition, successful therapeutic agonism of 4-1BB, a promising co-stimulatory immunologic target, has been limited by major safety concerns of hepatotoxicity or suboptimal agonistic potency. ATG-101, a novel PD-L1/4-1BB bispecific antibody, was designed to activate 4-1BB positive T cells in a PDL1-crosslinking dependent manner and to effectively treat tumors without on-target-off-tumor liver toxicity (figure 1).

Methods ATG-101 was developed by introducing lower affinity 4-1BB scFv into a human IgG1 PD-L1 monoclonal antibody. The N297A mutation on CH2 abolishes the binding capacity to most FcγRs but retains the binding to FcγRn. A series of in vitro and in vivo studies were performed to evaluate the potency, safety and specific mechanism of action.

Results ATG-101 simultaneously binds to 4-1BB and PD-L1 with higher affinity to PD-L1, and potently activates 4-1BB positive T cells when crosslinked by PD-L1 positive cells. Upon crosslinking, ATG-101 also activates PD1+TIM3+ exhausted T cells in vitro, suggesting a potential in reversing T-cell dysfunction and exhaustion (figure 1). ATG-101 shows potent anti-tumor activities in various animal models, including h4-1BB humanized mice bearing MC38 colon cancer, PD(L)1 blockade insensitive B16F10 melanoma and EL4 lymphoma, with no body weight loss observed. To evaluate ATG-101 efficacy in tumors progressing after anti-PD(L)1 treatment, mice bearing MC38 tumors were treated with anti-PDL1 initially to achieve tumor growth inhibition, and half of the mice switched to ATG-101 upon disease progression, the other mice continuing with anti-PD-L1 treatment. ATG-101 induced potent tumor growth inhibition and tumor regression in anti-PDL1-resistant tumors and prolonged survival. Flow cytometry and multiplex IHC staining of tumor samples from mice treated with ATG-101 or control suggest that ATG-101 increases the infiltration, proliferation and activation of CD8+ T cells (figure 2), the infiltration of natural killer T cells and the CD8+/Treg ratio in TILs. In a 4-week GLP toxicity study in cynomolgus monkey, up to 100mg/kg repeated doses of ATG-101 were well tolerated with no hepatotoxicity observed. **Conclusions** ATG-101 demonstrated significant anti-tumor activity in various tumor models including those progressing on anti PD(L)1 treatment. Good safety and PK/PD properties has been demonstrated in preclinical in vivo models. A phase I, multicenter, dose-escalating clinical trial evaluating ATG-101 in patients with solid tumors and hematologic malignancies is ongoing.



Abstract 893 Figure 1 ATG-101 conditionally activates exhausted T cells. (A) Mechanism of action of ATG-101 (B) Exhausted T cells were induced by CD3+T cells cultured with anti-CD3/CD28 beads for 6 days. The percentage of terminally exhausted T cells (PD-1+Tim-3+) and progenitor exhausted T cells (PD-1+Tim-3-) were increased on Day6 (C) With the presence of PD-L1 positive cells, ATG-101 induced the IL2 and INF-γ secretion by exhausted T cells.



Abstract 893 Figure 2 Potent in vivo efficacy of ATG-101. (A) Representative MC38 tumor growth curve for individual mice treated with PBS (black), 10mpk atezolizumab (Atezo) only (red) or mice initially treated with 10mpk atezolizumab and switched to 13mpk ATG-101 upon disease progression (red-green); the arrow indicates the day switching Atezo to ATG-101; (B) MC38 tumor growth curve for all individual mice treated with PBS (black, n=6), atezolizumab only (red, n=14), and atezolizumab initially before switching to ATG-101 upon disease progression (red-green, n=14) ; (C) Survival data of mouse shown in (B); (D) Representative images for multiplex IHC staining of tumor samples collected from mouse from (B). (E) Quantitative analysis of TILs shown in (D). Compared with PBS group or atezo-only group, ATG-101 significantly increased the infiltration of T cells in the tumor microenvironment. MHCII: APC Cells, CD4+ CD8-: Helper T Cells, CD4-CD8+: Cytotoxic T Cells, CD4- CD8- F4/80- PDL1+: Tumor Cells.

Ethics Approval The protocol and any amendment(s) or procedures involving the care and use of animals in this study were reviewed and approved by the Institutional Animal Care and Use Committee (IACUC) of CrownBio or Innostar prior to execution with an AUP number or IACUC approval number for each animal study. During the study, the care and use of animals were conducted in accordance with the regulations of the Association for Assessment and Accreditation of Laboratory Animal Care (AAALAC). All studies were conducted following an approved IACUC protocol. AUP NO.:2004-12-1465, 2004-12-1000; IACUC approval number: IACUC-2021-M-003

<http://dx.doi.org/10.1136/jitc-2021-SITC2021.893>

THE BISPECIFIC INNATE CELL ENGAGERS AFM13 (CD30/CD16A) AND AFM24 (EGFR/CD16A) INCREASE THE FRACTION OF TUMOR TARGET-RESPONSIVE NK CELLS AND BOOST SERIAL KILLING

¹Chiara Zambarda*, ¹Karolin Guldevall*, ¹Chiara Zambarda, ¹Karolin Guldevall, ²Christian Breunig, ¹Damien Touleec, ¹Jacopo Fontana, ²Sheena Pinto, ²Jens Pahl, ²Susanne Wingert, ²Joachim Koch, ¹Björn Önfelt. ¹KTH Royal Institute of Technology, Solna, Sweden; ²Affimed GmbH, Heidelberg, Germany

Background The use of bispecific natural killer (NK) cell engagers has emerged as a successful strategy for immune cell activation and killing of tumor cells through antibody-dependent cellular cytotoxicity (ADCC). Among these, tetravalent, bispecific innate cell engagers (ICE[®]) with specificity for the activating receptor CD16A selectively triggering innate responses from NK cells or macrophages represent the most clinically advanced concept. The CD30/CD16A specific ICE[®] AFM13, has shown efficacy in patients with CD30+ lymphomas as monotherapy¹ and combination therapy with checkpoint inhibitors² and most recently in combination with adoptive NK cell therapy.³ The EGFR/CD16A specific ICE[®] AFM24, targeting a variety of solid tumors like colorectal, or lung cancer with a unique mode of action independent of EGFR signaling inhibition, is currently evaluated in an ongoing Ph1/2a clinical study.

Methods We used a microchip-based screening with single cell resolution⁴ to elucidate the dynamic responses of individual NK cells towards tumor target cells upon treatment with AFM13 or AFM24.

Results We found that AFM13 and AFM24 mediated potent activation of NK cells, leading to increased responsive cytotoxic NK cells and significantly increased the number of NK cells that exerted engagement with multiple target cells rendering these NK cells serial killers. Strikingly, bispecific ICE[®] molecules triggered stronger cytotoxic responses compared to monoclonal antibodies. One suggested strategy to boost killing by NK cells is to use molecular inhibitors or protein constructs that prevent shedding of CD16.⁵ However, previous results have shown that this can lead to impaired detachment from target cells, reducing the capacity for an individual NK cell to form serial contacts to target cells.⁶ We observed that the elevated NK cell killing induced by ICE[®] molecules was largely conserved when cells were treated with the shedding inhibitor Batimastat. Analysis of the functional dynamics of NK cells revealed that inhibition of CD16 shedding prevented NK cell detachment from target cells, resulting in cell cluster formation. This might strongly impact targeting of distant tumor cells by an individual NK cell thus limiting its anti-tumoral activity.

Conclusions In conclusion, we show that both AFM13 and AFM24 increase the fraction of tumor-target responsive NK cells and boost serial killing of target cells by individual NK cells. Based on these data, ICE[®] molecules can be characterized as potent anti-tumoral agents leveraging the enormous potential of NK cells while maintaining crucial features of NK cell biology.

Acknowledgements We thank members of the Önfelt lab for their valuable help and feedback.

REFERENCES

1. Sawas A, Elgedawe H, Vlad G, Lipschitz M, Chen P-H, Rodig SJ, *et al.* Clinical and biological evaluation of the novel CD30/CD16A tetravalent bispecific antibody (AFM13) in relapsed or refractory CD30-positive lymphoma with cutaneous presentation: a biomarker phase Ib/IIa study (NCT03192202). *Blood* 2018;**132**(Supplement 1):2908–2908.

2. Bartlett NL, Herrera AF, Domingo-Domenech E, Mehta A, Forero-Torres A, Garcia-Sanz R, *et al.* A phase 1b study of AFM13 in combination with pembrolizumab in patients with relapsed or refractory Hodgkin lymphoma. *Blood* 2020. *Blood* 2020;**136**(21):2401–2409.
3. Kerbauy LN, Marin ND, Kaplan M, Banerjee PP, Berrien-Elliott MM, Becker-Hapak M, *et al.* Combining AFM13, a bispecific CD30/CD16 antibody, with cytokine-activated blood and cord blood-derived NK cells facilitates CAR-like responses against CD30+ malignancies. *Clin Cancer Res Epub* 2021.
4. Guldevall K, Brandt L, Forslund E, Olofsson K, Frisk TW, Olofsson PE, *et al.* Microchip screening platform for single cell assessment of NK cell cytotoxicity. *Front Immunol* 2016;**7**:119.
5. Romee R, Foley B, Lenvik T, Wang Y, Zhang B, Ankarlo D, *et al.* NK cell CD16 surface expression and function is regulated by a disintegrin and metalloprotease-17 (ADAM17). *Blood* 2013;**121**(18):3599–608.
6. Srpan K, Ambrose A, Karampatzakis A, Saeed M, Cartwright ANR, Guldevall K, *et al.* Shedding of CD16 disassembles the NK cell immune synapse and boosts serial engagement of target cells. *J Cell Biol* 2018;**217**(9):3267–83.

Ethics Approval This work was performed with NK cells from healthy anonymous blood donors, which requires no ethical permit according to local regulations.

<http://dx.doi.org/10.1136/jitc-2021-SITC2021.894>

**DISCOVERY OF A SAFER 4-1BB AGONIST BY
TARGETING A MEMBRANE-PROXIMAL EPITOPE
COMBINED WITH BISPECIFIC-MEDIATED CROSS-
BRIDGING**

¹Andy Tsun*, ²Tianhang Zhai, ³Xiaoni Miao, ⁴Weifeng Huang, ³Chao Wang, ³Yifeng Xu, ³Zhijun Yuan, ³Tao Wang, ⁴Shuang Dai, ⁴Shaogang Peng, ³Tuling Pang, ³Wenchao Jiang, ³Yuhua Huang, ³Yuefeng Zou, ³Yingda Xu, ³Joanne Sun, ³Xinjiang Gong, ²Bin Li. ¹*Biotheus Inc, Zhuhai, China*; ²*Shanghai Institute of Immunology, Department of Immunology and Microbiology, Shanghai Jiao Tong University School of Medicine, Suzhou, China*; ³*Biotheus Inc, Zhuhai, China*; ⁴*Biotheus (Suzhou) Co., Ltd., Suzhou, China*

Background Checkpoint inhibitors towards cytotoxic T-lymphocyte protein 4 (CTLA-4) and programmed cell death protein 1 (PD-1) have paved the way for a new frontier of anti-cancer therapies that modulate our pre-existing immune system to fight against malignancies. 4-1BB is a tumor-necrosis superfamily member expressed on NK and T cells, that acts as a co-stimulatory receptor to improve effector/memory responses towards tumors. Early efforts have focused on the generation of agonist antibodies towards 4-1BB that relied on Fc-mediated cross-linking to cluster and induce receptor downstream signaling, but has led to liver- and immune-related toxicities. We have discovered a PD-L1 x 4-1BB bispecific that exhibits conditional agonist activity in the presence of PD-L1 with better safety features.

Methods vHH binders to PD-L1 and 4-1BB were generated from immune libraries derived from camelids and selected via yeast display. Antibody screening was carried out by protein-protein interaction analysis and cell-based binding. Target-related activity was confirmed using luciferase reporter assays. Primary immune cells were also tested for T cell activation via the detection of IL-2 and IFN γ secretion. PD-L1-mediated 4-1BB activation via cross-bridging was carried out using target cells expressing PD-L1 co-cultured with effector cells. X-ray crystallography was conducted to resolve the binding sites of both the anti-PD-L1 and anti-4-1BB vHHs. Both tumor efficacy and safety assessment were tested in human knockin mice.

Results The 4-1BB binder of PM1003 was found to interact with the CRD4 domain of 4-1BB, as determined by X-ray crystallography. Binding to this domain does not affect the binding between 4-1BB and its ligand 4-1BBL. The anti-PD-L1 vHH binds to an epitope on PD-L1 that overlaps with the binding region of PD-1, and is thus effective in disrupting the interaction between PD-1 and PD-L1. Using luciferase reporter assays and primary cell assays we found the PM1003 could activate 4-1BB in the context of PD-L1-mediated cross-bridging. Data from human 4-1BB and PD-L1 knockin mice also showed that PM1003 could effectively control tumor growth without observing any toxicity signals.

Conclusions PM1003 is a safe and efficacious bispecific antibody that blocks PD-L1 and concurrently activates 4-1BB receptor. An antibody with mild activity was selected directed against the CRD4 domain of 4-1BB to elicit effective potency while minimizing potential toxicity issues. This was reflected in our results. Thus, PM1003 is a potential next generation therapeutic antibody in the IO space that combines and synergizes two independent signaling pathways to control tumor growth.

<http://dx.doi.org/10.1136/jitc-2021-SITC2021.895>

Nursing/Pharmacy

896

**FIGHTING THE WAR AGAINST COVID-19:
ADMINISTRATION OF BAMLANIVIMAB (BAM) OR
BAMLANIVIMAB + ETESIVIMAB (BAM + E); A
COOPERATIVE EFFORT BETWEEN A COMMUNITY
CANCER CENTER AND AN URGENT CARE (UC) FACILITY**

¹Patrick Skeffington, ²Robert Aisenberg, ¹Janice Dallacosta*, ¹Ian Donaghy, ²Dani Hackner, ²Kelly Houde, ¹Kathy Moraes, ¹Annemarie Santos. ¹Southcoast Centers for Cancer Care, Fairhaven, MA, USA; ²Southcoast Health, Fall River, MA, USA

Background Goal of the Massachusetts DPH is to ensure equitable distribution of BAM to the most vulnerable at risk of poor outcomes from COVID-19 and to communities with the highest incidences of COVID-19. Hospitals should allocate available doses in a manner consistent with this guidance: 1. Patients who meet the EUA criteria; a lottery system will be used if supply is exceeded 2. Patients with comorbidities (high risk) tend to have worse outcomes when infected with SARS-CoV-2 3. BAM was approved under an EUA for the treatment of mild to moderate COVID-19 for those at high risk of progressing to severe disease (revoked 4/16/21). 4. BAM + E combo was approved under an EUA for the same patients and criteria, Southcoast Health entered into this relationship with DPH to provide this service to the southeastern MA population.

Methods Patients identified based on algorithm using Social Vulnerability Index (SVI) and EUA criteria RNs screened cases for positive criteria using lottery priority and SVI Pulmonologists consented appropriate patients, ordered infusions, routed cases for final scheduling within window of treatment Experienced nursing staff from various Southcoast departments treated up to 6 patients per day Oncology pharmacies are uniquely experienced to prepare monoclonal antibodies (MABS) such as BAM and BAM + E Due to proximity of the Oncology pharmacy to the UC Center, pharmacy reviewed, prepared and delivered infusions to UC once patient was assessed by RNs

Results First 152 cases: 7.2% inpatient admissions within 14 days 13.8% ED/UC visits within 14 days 2% inpatient admissions in 28 days 5.9% ED/UC visits within 28 days Two deaths during initial 152 cases.

Conclusions Cooperative effort between the Cancer Center and Urgent Care led to positive outcomes for local COVID-19 patients. Southcoast demonstrated a 6% hospital admission rate for COVID-19 patients in the MAB program versus 26% admission rate overall for COVID-19 patients.

Acknowledgements Thanks to our colleagues at the University of Rhode Island College of Pharmacy for their support with the poster

<http://dx.doi.org/10.1136/jitc-2021-SITC2021.896>

Other

897 **INFUSION EPISODE-RELATED BENEFITS OF PEMBROLIZUMAB Q6W DOSING SCHEDULE FOR PATIENTS WITH MELANOMA TREATED IN THE ADJUVANT AND METASTATIC SETTINGS IN THE UNITED STATES (US)**

¹Raquel Aguiar-Ibanez*, ²Emilie Scherrer, ²Dmitri Grebennik, ³Anvi Khandelwal, ³John Cook, ³Shalini Bagga, ³Baanie Sawhney, ⁴Scott Soefje. ¹Merck Canada Inc., Toronto, Canada; ²Merck and Co., Inc., Kenilworth, NJ, USA; ³Complete Health Economics Outcomes Resea, North Wales, PA, USA; ⁴Mayo Clinic, Rochester, NY, USA

Background A new dosing schedule for pembrolizumab (400 mg every six weeks (Q6W)) received accelerated FDA approval in 2020 across all approved adult indications. The Q6W dosing schedule provides an opportunity to reduce the number of infusions required over the treatment course, thereby decreasing time and costs for health care providers, patients and their caregivers. This study quantified the potential infusion episode-related benefits of pembrolizumab Q6W regimen for the treatment of patients with melanoma in the adjuvant and metastatic settings in the US.

Methods An Excel-based tool was developed to quantify the infusion episode-related time and cost of using pembrolizumab Q6W compared to available nivolumab dosing regimens (Q4W/Q2W) to treat patients with melanoma in the adjuvant and metastatic settings from the patient, caregiver, provider, and payer perspectives. The number of infusion visits, time and costs were estimated considering a hypothetical infusion center. Time-related inputs were based on a survey of patients, physicians and nurses; cost-related inputs were obtained from published sources. Sensitivity analyses were performed to assess the robustness of results. Additional analyses assessed the impact of using alternative regimens with different frequencies of administration.

Results Based on the tool, pembrolizumab Q6W reduced the number of infusion visits (31%), time at the infusion center (41%) and chair time (31%) in total, over one year, versus nivolumab Q4W. Because fewer visits are needed, travel time is estimated to decrease by 31%. The infusion-related direct and indirect costs borne by patients and caregivers are projected to decrease by \$1,095 and \$2,272, respectively over a treatment course. For a typical US infusion center treating 169 melanoma patients per week over a 1-year period, using pembrolizumab Q6W rather than nivolumab Q4W is estimated to reduce the number of infusions by 2,729 (31% reduction) for a total of 3,802 fewer hours of infusion chair time, allowing the infusion center to increase patient capacity by up to 45% using currently available resources. Time and cost savings are more prominent when comparing with nivolumab Q2W: 5,757 fewer infusion events (66% reduction) and 8,062 less hours of chair time, which would increase the patient capacity by 2.9 times.

Conclusions Utilizing pembrolizumab Q6W to treat patients with melanoma in the US is expected to substantially reduce the number of infusion visits and associated chair time required over the duration of treatment, reducing the time and monetary burden for patients and their caregivers. Additionally, it may also improve system capacity.

<http://dx.doi.org/10.1136/jitc-2021-SITC2021.897>

INTRATUMORAL ADMINISTRATION OF NL-201, AN ALPHA-INDEPENDENT IL-2/15 RECEPTOR AGONIST, INHIBITS THE GROWTH OF BOTH INJECTED AND UNINJECTED TUMORS IN PRECLINICAL MODELS

Laurie Tatalick, Kevin Yu, Justin Huard*, Justin Huard, Marianne Riley, Ryan Swanson, Carl Walkey. *Neoleukin Therapeutics, Inc., Redmond, WA, USA*

Background NL-201 is a potent, selective, and long-acting computationally designed alpha-independent agonist of the IL-2 and IL-15 receptors that is being developed as an immunotherapy for cancer. Intravenous NL-201 administration is active in numerous pre-clinical tumor models. Here, we report data demonstrating favorable tolerability, pharmacokinetics, and antitumor activity of NL-201 after intratumoral (IT) administration in syngeneic murine tumor models.

Methods Mice were implanted with syngeneic colorectal tumors in a single tumor (right flank) or bilateral tumor model (right and left flank). Once tumors were established, mice were randomized to receive IT or intravenous (IV) NL-201, or IV vehicle as control. Tumor volumes (mm³) and bodyweights were measured twice weekly, and mice were monitored for abnormal clinical signs. Blood samples were collected at pre-specified time points, and serum was analyzed for NL-201 concentration using a ligand-binding assay. Toxicokinetic parameters were determined using a non-compartmental model consistent with the IT and IV routes. Animals were sacrificed if tumor sizes reached 2000 mm³ or if body weight loss was >20%. In the bilateral tumor models, surviving tumor-free animals from both the IT and IV treatment arms were rechallenged with tumor cells after a washout period to assess antitumor immune responses.

Results IT NL-201 demonstrated dose-dependent antitumor activity and was well tolerated based on a lack of clinical observations and body weight changes at doses up to 10 µg/mouse. Comparable antitumor activity was observed in mice receiving 3 µg/mouse NL-201 via IV or IT routes, but reduced systemic exposure and better tolerability were observed after IT administration. The estimated absolute bioavailability following 3 µg/mouse IT administration was 19.4%–66.5% of the NL-201 IV exposure. In the bilateral tumor model, IT NL-201 resulted in significant antitumor activity in both the treated and untreated tumors. Surviving animals from both IT and IV groups in which the initial tumors regressed rejected engraftment of the same tumor cell line upon rechallenge.

Conclusions IT NL-201 administration resulted in dose-dependent antitumor activity in both injected and uninjected tumors while demonstrating markedly reduced systemic exposure and improved tolerability compared to systemic administration at equivalent dose levels. Rechallenged animals failed to develop tumors, demonstrating durable tumor-specific immunity after IT NL-201 treatment. Results of this study support planned clinical investigation of IT NL-201 administration to increase NL-201 concentrations in accessible lesions.

Ethics Approval This study was approved by the Institutional Animal Care and Use Committee (IACUC) of CrownBio.

<http://dx.doi.org/10.1136/jitc-2021-SITC2021.898>

Regulatory, Financial, and Access Considerations

899

POPULATION COVERAGE OF HLA-A*02:01, *02:05, *02:06 ACROSS SELECTED CANCER TYPES IN THE UNITED STATES

Nashita Patel*, Charlotte Carroll, Ken Culver, Shibani Pokras. *GlaxoSmithKline, Brentford, London, UK*

Background GSK is investigating an autologous TCR T-cell therapy for solid tumors that recognizes the cancer testis antigen, NY-ESO-1, presented on the cancer cell surface by specific HLA-A*02 sub-types. The aim of this study was to estimate the number of patients in the US in 2020 with HLA-A*02 genotype subtypes HLA-A*02:01, 02:05, 02:06 across selected cancer types (invasive lung, ovarian, gastric, esophageal, invasive and in-situ bladder and multiple myeloma), accounting for racial variation.

Methods This study was carried out in three parts utilizing three national datasets. 1. The prevalence of each cancer type was estimated by race utilizing prevalence rates from US Surveillance, Epidemiology, and End Results (SEER) 1975–2018 data.¹ 2. The US population coverage for the specific HLA-A*02 subtype (%) by race in 2020, was estimated utilizing Hardy Weinberg Principles and allele frequencies extracted from the allele frequency net database (US National Marrow Donor Program (NMDP) population only).² 3. The estimated population coverage for the specific HLA-A*02 subtype expression (%) by cancer subtype, was calculated using US Census (2019) data.³ For the purpose of this analyses, single race population estimates were used. Race was categorized as ‘White’, ‘Black’, ‘Asian/Pacific Islander’, ‘Native American’ and ‘Other’. The Hispanic population was included as a proportion of each category, where appropriate. Limitations include the seven assumptions underlying Hardy-Weinberg equilibrium, which were met, and the assumption that the NMDP, SEER and US Census data are reflective of the US population. Predictive and prognostic clinical characteristics including histological subtypes were not accounted for in this analysis.

Results Across selected cancer types, the most prevalent race category was White, reflecting the racial distribution of the US (table 1). Of these cancer types, multiple myeloma and invasive gastric cancer are represented by the lowest proportion of White patients and the highest proportion of Black patients. Results of the HLA sub-type distribution by race are presented in the table below. The overall proportion of patients who are HLA-A*02:01, *02:05 or *02:06 positive is estimated to be between 41.7% (multiple myeloma) and 45.8% (invasive and in-situ bladder) in the US accounting for the racial variations in each cancer type of interest.

Conclusions The proportion of patients with specific HLA-A*02 subtypes is similar across selected cancers, accounting for racial variation in the US. Racial variation by cancer type is an important consideration when estimating the size of eligible populations for T-cell therapies requiring specific HLA-A*02 histocompatibility.

Abstract 899 Table 1 Proportion of patients who are HLA-A*02:01, *02:05, or *02:06 positive by race and cancer subtype

Cancer type	Estimated US 25-year prevalence by cancer type in 2020, n	Racial distribution by cancer type, %*	Estimated distribution by race of HLA*02:01, *02:05 and *02:06 subtypes in the overall US population, %	Estimated overall proportion of HLA-A*02:01, *02:05 and *02:06 positive population accounting for racial variation, n (%)
Invasive lung	431,833	80.0% White, 7.8% Black, 2.7% Asian/ Pacific Islander, 0.0% Native American, 9.5% Other	HLA *02:01: 43.6% White, 21.9% Black, 18.8% Asian/ Pacific Islander, 40.3% Native American, 35.9% Other	189,557 (43.9)
Invasive & in-situ bladder	528,415	85.4% White, 3.7% Black, 1.5% Asian/ Pacific Islander, 0.0% Native American, 9.4% Other	HLA *02:05: 2.5% White, 3.5% Black, 1.1% Asian/ Pacific Islander, 1.4% Native American, 3.4% Other	241,970 (45.8)
Multiple myeloma	117,986	73.4% White, 14.8% Black, 2.0% Asian/ Pacific Islander, 0.0% Native American, 9.7% Other	HLA *02:06: 2.1% White, 0.1% Black, 8.1% Asian/ Pacific Islander, 11.7% Native American, 4.7% Other	49,177 (41.7)
Invasive ovarian (Female only)	149,911	83.0% White, 4.5% Black, 3.1% Asian/ Pacific Islander, 0.0% Native American, 9.3% Other	HLA *02:05: 2.5% White, 3.5% Black, 1.1% Asian/ Pacific Islander, 1.4% Native American, 3.4% Other	67,419 (45.0)
Invasive gastric	92,800	73.8% White, 10.0% Black, 6.5% Asian/ Pacific Islander, 0.0% Native American, 9.7% Other	HLA *02:06: 2.1% White, 0.1% Black, 8.1% Asian/ Pacific Islander, 11.7% Native American, 4.7% Other	39,061 (42.1)
Invasive oesophageal	37,200	88.6% White, 4.7% Black, 1.7% Asian/ Pacific Islander, 0.0% Native American, 9.8% Other	HLA *02:06: 2.1% White, 0.1% Black, 8.1% Asian/ Pacific Islander, 11.7% Native American, 4.7% Other	16,912 (45.5)

*White' includes US NMDP European Caucasian, North American Amerindian, Middle Eastern or North Coast of Africa. 'Black' includes US NMDP African, African American pop 2, Black South or Central American or Caribbean Black. 'Asian/ Pacific Islander' includes US NMDP Chinese, Filipino, Japanese, Korean, South Asian Indian, South East Asian, Hawaiian, Other Pacific Islander or Vietnamese. 'Native American' includes Alaskan Native or Aleut or American Indian South or Central America. 'Other' includes Caribbean Hispanic, Hispanic South or Central American or Mexican or Chicano. SEER, Surveillance, Epidemiology, and End Results.

Acknowledgements

Funding GlaxoSmithKline

REFERENCES

- Howlander N, Noone AM, Krapcho M, Miller D, Brest A, Yu M, Ruhl J, Tatalovich Z, Mariotto A, Lewis DR, Chen HS, Feuer EJ, Cronin KA (eds). SEER Cancer Statistics Review, 1975–2018, National Cancer Institute. Bethesda, MD, [https://seer.cancer.gov/csr/1975_2018/], based on November 2020 SEER data submission, posted to the SEER web site, April 2021 (Accessed July 2021).
- Gonzalez-Galarza FF, McCabe A, Santos EJ, Jones J, Takeshita LY, Ortega-Rivera ND, Del Cid-Pavon GM, Ramsbottom K, Ghattaraya GS, Alfirevic A, Middleton D, Jones AR. Allele frequency net database (AFND) 2020 update: gold-standard data classification, open access genotype data and new query tools. *Nucleic Acids Res* 2020;**48**:D783–8.
- U S Census Bureau (2011). ACS demographic and housing estimates. [https://data.census.gov/cedsci/table?q=United%20States&q=0100000US&tid=ACSDP1Y2017.DP05&vintage=2017&layer=state&cid=DP05_0001E] (Accessed July 2021).

<http://dx.doi.org/10.1136/jitc-2021-SITC2021.899>

Tumor and Stromal Cell Biology

900

DEPLETING NON-CANONICAL, CELL-INTRINSIC PD-L1 SIGNALS INDUCES SYNTHETIC LETHALITY TO SMALL MOLECULE DNA DAMAGE RESPONSE INHIBITORS IN AN IMMUNE INDEPENDENT AND DEPENDENT MANNER

¹Anand Kornepati*, ¹Clare Murray, ¹Barbara Avalos, ¹Cody Rogers, ²Kavya Ramkumar, ¹Harshita Gupta, ¹Yilun Deng, ¹Zexuan Liu, ¹Alvaro Padron, ¹Ratna Vadlamudi, ¹Eloise Dray, ¹Weixing Zhao, ¹Patrick Sung, ²Lauren Byers, ¹Tyler Curiel. ¹University of Texas Health Science Center San Antonio, San Antonio, TX, USA; ²UT MD Anderson, San Antonio, TX, USA

Background Tumor surface-expressed programmed death-ligand 1 (PD-L1) suppresses immunity when it engages programmed death-1 (PD-1) on anti-tumor immune cells in canonical PD-L1/PD-1.¹ Non-canonical, tumour-intrinsic PD-L1 signals can mediate treatment resistance²⁻⁶ but mechanisms remain incompletely understood. Targeting non-canonical, cell-intrinsic PD-L1 signals, especially modulation of the DNA damage response (DDR), remains largely untapped.

Methods We made PD-L1 knockout (PD-L1 KO) murine transplantable and human cell lines representing melanoma, bladder, and breast histologies. We used biochemical, genetic, and cell-biology techniques for mechanistic insights into tumor-intrinsic PD-L1 control of specific DDR and DNA repair pathways. We generated a novel inducible melanoma GEMM lacking PD-L1 only in melanocytes to corroborate DDR alterations observed in PD-L1 KO of established tumors.

Results Genetic tumor PD-L1 depletion destabilized Chk2 and impaired ATM/Chk2, but not ATR/Chk1 DDR. PD-L1KO increased DNA damage (γ H2AX) and impaired homologous recombination DNA repair (p-RPA32, BRCA1, RAD51 nuclear foci) and function (DR-GFP reporter). PD-L1 KO cells were significantly more sensitive versus controls to DDR inhibitors (DDRi) against ATR, Chk1, and PARP but not ATM in multiple human and mouse tumor models in vitro and in vivo in NSG mice. PD-1 independent, intracellular, not surface PD-L1 stabilized Chk2 protein with minimal Chk2 mRNA effect. Mechanistically, PD-L1 could directly complex with Chk2, protecting it from PIRH2-mediated polyubiquitination. PD-L1 N-terminal domains Ig-V and Ig-C but not the PD-L1 C-terminal tail co-IP'd with Chk2 and restored Chk1 inhibitor (Chk1i) treatment resistance. Tumor PD-L1 expression correlated with Chk1i sensitivity in 44 primary human small cell lung cancer cell lines, implicating tumor-intrinsic PD-L1 as a DDRi response biomarker. In WT mice, genetic PD-L1 depletion but not surface PD-L1 blockade with α PD-L1, sensitized immunotherapy-resistant, BRCA1-WT 4T1 tumors to PARP inhibitor (PARPi). PARPi effects were reduced on PD-L1 KO tumors in RAG2KO mice indicating immune-dependent DDRi efficacy. Tumor PD-L1 depletion, likely due to impaired DDR, enhanced PARPi induced tumor-intrinsic STING activation (e.g., p-TBK1, CCL5) suggesting potential to augment immunotherapies.

Conclusions We challenge the prevailing surface PD-L1 paradigm and establish a novel mechanism for cell-intrinsic PD-L1 control of the DDR and gene product expression. We identify therapeutic vulnerabilities from tumor PD-L1 depletion utilizing small molecule DDRi currently being tested in clinical trials. Data could explain α PD-L1/DDRi treatment resistance. Intracellular PD-L1 could be a pharmacologically targetable treatment target and/or response biomarker for selective DDRi alone plus other immunotherapies.

REFERENCES

1. Topalian SL, Taube JM, Anders RA, Pardoll DM. Mechanism-driven biomarkers to guide immune checkpoint blockade in cancer therapy. *Nat Rev Cancer* **16**:275–287, doi:10.1038/nrc.2016.36 (2016).
2. Clark CA, et al. Tumor-intrinsic PD-L1 signals regulate cell growth, pathogenesis and autophagy in ovarian cancer and melanoma. *Cancer* 0258.2016 (2016).
3. Gupta HB et al. Tumor cell-intrinsic PD-L1 promotes tumor-initiating cell generation and functions in melanoma and ovarian cancer. *1*, 16030 (2016).
4. Zhu H, et al. BET bromodomain inhibition promotes anti-tumor immunity by suppressing PD-L1 expression. *Cell Rep* **16**:2829–2837, doi:10.1016/j.celrep.2016.08.032 (2016)
5. Wu B, et al. Adipose PD-L1 modulates PD-1/PD-L1 checkpoint blockade immunotherapy efficacy in breast cancer. *Oncimmunology* **7**:e1500107, doi:10.1080/2162402X.2018.1500107 (2018)
6. Liang J, et al. Verteporfin inhibits PD-L1 through autophagy and the STAT1-IRF1-TRIM28 signaling axis, exerting antitumor efficacy. *Cancer Immunol Res* **8**:952–965, doi:10.1158/2326-6066.CIR-19-0159 (2020)

<http://dx.doi.org/10.1136/jitc-2021-SITC2021.900>

901

BACILLUS CALMETTE-GUERIN CAN SUBVERT PATIENTS ANTITUMOR IMMUNE RESPONSE BY DOWNREGULATING HLA-I EXPRESSION ON CANCER CELLS

¹Mathieu Rouanne*, ²Julien Adam, ¹Camelia Radulescu, ¹Diane Letourneur, ¹Severine Mouraud, ¹Delphine Bredel, ¹Anne-Gaelle Goubet, ³Tuan Zea Tan, ¹Amelie Bigorgne, ⁴Michael Dussiot, ¹Lambros Tselikas, ¹Sandrine Susini, ¹François-Xavier Danlos, ¹Roman Chabanon, ¹Nicolas Signolle, ¹Anna Schneider, ⁵Sophie Vacher, ⁵Ivan Bieche, ¹Thierry Lebret, ¹Yves Allory, ¹Jean-Charles Soria, ⁶Jean Paul Thiery, ¹Laurence Zitvogel, ¹Aurelien Marabelle. ¹Gustave Roussy, New York, NY, France; ²Hopital Paris Saint Joseph, Paris, France; ³Cancer Institute Singapore, Singapore, Singapore; ⁴Institut Imagine, Paris, France; ⁵Curie Institute, Paris, France; ⁶Singapore Cancer Institute, Singapore, Singapore

Background Patients with high-risk non muscle-invasive bladder cancer (NMIBC) frequently relapse after standard BCG immunotherapy and have a dismal outcome after progression to muscle-invasive bladder cancer (MIBC).^{1 2} The mechanisms of tumor resistance to such immunotherapy remain elusive.

Methods We performed functional assays of fresh human bladder tumors mixed with BCG, reinforced with in vitro experiments and in situ transcriptomics analyses together with immune profiling by immunohistochemistry (IHC) in a cohort of T1 NMIBC pre- and post BCG therapy.

Results We found two distinct patterns of BCG-induced immune subversion. In the first pattern, intracellular infection by live BCG was associated with HLA-I loss and epithelial-to-mesenchymal transition characteristics. Mechanistically, LC3-GFP reporter cell line showed a significant induction of autophagy upon BCG exposure. HLA-I deficient tumors displayed a myeloid immunosuppressive microenvironment together with an upregulation of autophagy-related genes, and dismal outcome. Conversely, HLA-I+ BCG-treated tumors generated a Th1 type of immune response associated with an upregulation of exhaustion markers. Such patients had a very favorable outcome upon radical surgery.

Conclusions We surmise that HLA-I expression in bladder cancers does not result from immunoediting but rather from HLA-I molecules endocytosis related to autophagy induction in infected cancer cells. Cancer cells HLA-I scoring by immunohistochemistry staining can be easily implemented by pathologists in routine practice to stratify future bladder cancer patient treatment strategies.

REFERENCES

1. Pietzak EJ, Zabor EC, Bagrodia A, *et al.* Genomic differences between "primary" and "secondary" muscle-invasive bladder cancer as a basis for disparate outcomes to cisplatin-based neoadjuvant chemotherapy. *Eur Urol* 2019;**75**(2):231–239.
2. Patrick J Hensley, Kelly K Bree, Matthew T Campbell, *et al.* Progression of disease after BCG therapy: refining patient selection for neoadjuvant chemotherapy before radical cystectomy. *J Urol* 2021 June 29;101097JU000000000000001943.

Ethics Approval Our study obtained ethics approval from the Foch Hospital Ethics Committee (IRB00012437). All the participants gave informed consent before taking part.

Consent We surmise that HLA-I expression in bladder cancers does not result from immunoediting but rather from HLA-I molecules endocytosis related to autophagy induction in infected cancer cells. Cancer cells HLA-I scoring by immunohistochemistry staining can be easily implemented by pathologists in routine practice to stratify future bladder cancer patient treatment strategies.

<http://dx.doi.org/10.1136/jitc-2021-SITC2021.901>

COMPREHENSIVE MULTI-OMICS META-ANALYSIS OF PANCREATIC CANCER MOUSE MODELS AND HUMAN PDAC DATA SETS IDENTIFIES UNIQUE CANCER-ASSOCIATED FIBROBLAST SUBSETS

¹Candace Wai Sze Lei*, ¹John Holt, ¹Brianna Flynn, ²Richard Barrett, ¹Pratha Budhani, ¹Mohanapriya Kamalakannan, ¹Ruby Wasti, ¹Lucinda Thiede, ¹Joshua Tagore, ¹Jessica Potts, ¹Jacqueline Larouche, ¹Marie Marcher, ¹Xiaoyun Liao, ¹Sarah O'Brien, ¹Abhishek Kashyap, ¹Jeanine Pignatelli, ¹Kang Liu, ¹Joseph Tumang, ¹Emily Corse, ³Ben Stanger, ²Ellen Pure, ¹Varenka Rodriguez DiBlasi. ¹Boehringer Ingelheim, Ridgefield, CT, United States; ²University of Pennsylvania School of Veterinary Medicine, Philadelphia, PA, United States; ³University of Pennsylvania Perelman School of Medicine, Philadelphia, PA, United States

Background Pancreatic ductal adenocarcinoma (PDAC) is resistant to many available therapies including immunotherapy because of its highly complex tumor microenvironment (TME). PDAC TME consists of a significant proportion of stromal cells, such as endothelial cells, perivascular cells, and cancer-associated fibroblasts (CAFs). Recent work indicates how CAFs can orchestrate the crosstalk cancer and immune cells, and contribute to many aspects of tumor progression, including angiogenesis, senescence, and inflammation. Recent studies based on scRNA-seq have increased understanding of CAF heterogeneity in PDAC in both human and genetically engineered mouse models (GEMMs) is of high interest. To understand the translatability of GEMMs in the setting of PDAC, we conducted a thorough scRNA-seq meta-analysis on CAFs across GEMMs and PDAC human samples. Hereafter, we characterized CAFs multi-dimensionally based on transcriptional, chromatin accessibility, and spatial profiles. Finally, we suggested certain transcription factors may be regulatory drivers of heterogeneous CAF phenotypes in both human and GEMMs.

Methods We collected publicly available and internally generated scRNA-seq data of PDAC CAFs from human and mouse. After dataset alignment and label transfer, we conducted differential expression analysis across CAF subsets to characterize myofibroblasts (myCAFs) and other CAF subsets of interest. Bioinformatically, we further interrogated CAF heterogeneity in terms of regulatory potential of transcription factors, gene set enrichment, and functional state transition. Complemented by epigenomic assessment, we investigated chromatin accessibility and transcription factor binding availability on the single-cell level. Finally, to investigate the TME organization and spatial neighborhood of cell-to-cell interaction, we explored potential functional differences across location and transcriptional changes of CAF subsets by spatial transcriptomics.

Results We found that myofibroblasts (myCAFs) make up a substantial proportion of the CAF population, in both human and mouse TME. In a combination of transcriptional profiling, chromatin accessibility assessment, and spatial transcriptomics, we elucidated potential functional and phenotypic differences within myCAF population and compared to other CAF subsets in the TME. While myofibroblasts are traditionally described as matrix remodeling related, heterogeneity in myofibroblasts may suggest additional roles played by this specific subset. In addition, CAFs in human and mouse share similarities, in terms of transcriptional profiles and phenotypes. The use of GEMMs facilitates our understanding of CAF heterogeneous behavior and phenotypes in the PDAC TME.

Conclusions Here, we presented a comprehensive overview of CAF heterogeneity in mouse PDAC models and human datasets. Our observations highlight molecular differences in CAFs, which facilitates our understanding on PDAC stromal

microenvironment and translatability in GEMMs in imitating human TME.

<http://dx.doi.org/10.1136/jitc-2021-SITC2021.902>

903

HUMAN CANCER-ASSOCIATED FIBROBLAST SUBSETS CAN PREDICT IMMUNE CHECKPOINT RESPONSE IN HEAD AND NECK CANCER PATIENTS

¹Diana Graves*, ²Aleksandar Obradovic, ³Michael Korner, ³Yu Wang, ³Sohini Roy, ³Yaomin Xu, ⁴Adam Luginbuhl, ⁴Joseph Curry, ³Michael Gibson, ³Paula Hurley, ⁵Ravindra Uppaluri, ²Charles Drake, ²Andrea Califano, ³Young Kim. ¹Vanderbilt University, Antioch, TN, United States; ²Columbia University, New York City, NY, United States; ³Vanderbilt University Medical Center, Nashville, TN, United States; ⁴Thomas Jefferson University, Philadelphia, PA, United States; ⁵Dana Farber Cancer Institute, Boston, MA, United States

Background Use of anti-PD-1 immune checkpoint inhibitors (ICI) is currently the first line therapy for recurrent/metastatic head and neck squamous cell carcinoma (HNSCC), but critical work remains in identifying factors guiding resistance mechanisms.¹⁻² While recent studies have specifically implicated cancer-associated fibroblasts (CAFs) as potential mediators of immunotherapy response, the immunoregulatory role of CAFs in head and neck cancer has not been thoroughly explored.³⁻⁵

Methods To determine if there are changes in cell populations associated with anti-PD-1 therapy in head and neck cancer patients, we performed high dimensional single-cell RNA sequencing (scRNA-SEQ) from a neoadjuvant trial of 50 advanced-stage head and neck squamous cell carcinoma (HNSCC) patients that were treated with the anti-PD-1 therapy, nivolumab, for the duration of one month. Tumor specimens were analyzed pre- and post-treatment with single-cell RNA sequencing performed on 4 patients as well as bulk RNA sequencing on 40 patients. Matched scRNA-SEQ data was analyzed using the Algorithm for the Reconstruction of Accurate Cellular Networks (ARACNe) and Virtual Inference of Protein-activity by Enriched Regulon (VIPER) bioinformatic analysis platform to determine TME cells that correlated with response and resistance to nivolumab.⁶ For CAF functional studies, surgical tumor specimens were processed and enriched for CAF subtypes, and these were co-cultured with T cells from peripheral blood and tumor infiltrating lymphocytes.

Results We identified 14 distinct cell types present in HNSCC patients. Of these 14 cell types, the fibroblast subtype showed significant changes in abundance following nivolumab treatment. We identified 5 distinct clusters of cancer-associated fibroblast subsets (HNCAF-0, 1, 2, 3, and 4) of which, two clusters, HNCAF-0 and HNCAF-3 were predictive of patient response to anti-PD-1 therapy. To determine the significance of these CAF subsets' function, we isolated HNCAF-0/3 cells from primary HNSCC tumor specimens and co-cultured with primary human T cells. Analysis by flow cytometry showed that HNCAF-0/3 reduced TGF β -dependent PD-1+TIM-3+ exhaustion of T cells and increased CD103+NKG2A+ resident memory phenotype and cytotoxicity to enhance overall function.

Conclusions To our knowledge, we are the first to characterize CAF heterogeneity within the head and neck TME and show direct immunostimulatory activity of CAFs. Our findings demonstrate the functional importance of CAF subsets in modulating the immunoregulatory milieu of the human HNSCC, and we have identified clinically actionable CAF subtypes that can be used as a biomarker of response and resistance in future clinical trials.

Trial Registration NCT03238365

REFERENCES

1. Ferris RL, Blumenschein Jr G, Fayette J, Guigay J, Colevas AD, Licitra L, Harrington K, Kasper S, Vokes EE, Even C, *et al.* Nivolumab for recurrent squamous-cell carcinoma of the head and neck. *N Engl J Med* 2016;**375**:1856–1867.

2. Seiwert TY, Burtneis B, Mehra R, Weiss J, Berger R, Eder JP, Heath K, McClanahan T, Lunceford J, Gause C, *et al.* Safety and clinical activity of pembrolizumab for treatment of recurrent or metastatic squamous cell carcinoma of the head and neck (KEYNOTE-012): an open-label, multicentre, phase 1b trial. *Lancet Oncol* 2016;**17**:956–965.
3. Dominguez CX, Muller S, Keerthivasan S, Koeppen H, Hung J, Gierke S, Breart B, Foreman O, Bainbridge TW, Castiglioni A, *et al.* Single-cell RNA sequencing reveals stromal evolution into LRRC15(+) myofibroblasts as a determinant of patient response to cancer immunotherapy. *Cancer Discov* 2020;**10**:232–253.
4. Feig C, Jones JO, Kraman M, Wells RJ, Deonaraine A, Chan DS, Connell CM, Roberts EW, Zhao Q, Caballero OL, *et al.* Targeting CXCL12 from FAP-expressing carcinoma-associated fibroblasts synergizes with anti-PD-L1 immunotherapy in pancreatic cancer. *Proc Natl Acad Sci U S A* 2013;**110**:20212–20217.
5. Kieffer Y, Hocine HR, Gentric G, Pelon F, Bernard C, Bourachot B, Lameiras S, Albergante L, Bonneau C, Guyard A, *et al.* Single-cell analysis reveals fibroblast clusters linked to immunotherapy resistance in cancer. *Cancer Discov* 2020;**10**:1330–1351.
6. Obradovic A, Chowdhury N, Haake SM, Ager C, Wang V, Vlahos L, Guo XV, Aggen DH, Rathmell WK, Jonasch E, *et al.* Single-cell protein activity analysis identifies recurrence-associated renal tumor macrophages. *Cell* 2021;**184**:2988–3005.

Ethics Approval Patients provided informed consent for this work. All experimental procedures were approved by the Institutional Review Board of Vanderbilt University Medical Center (IRB: 171883).

<http://dx.doi.org/10.1136/jitc-2021-SITC2021.903>

904

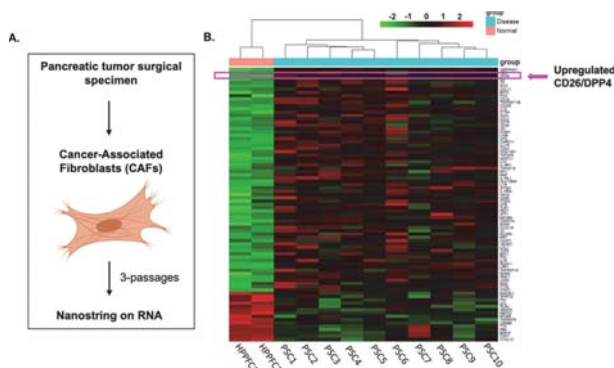
REPURPOSING CD26 (DPP4) INHIBITORS TO ENHANCE IMMUNOTHERAPY RESPONSE IN PANCREATIC DUCTAL ADENOCARCINOMA

¹Maggie Phillips*, ¹Michael Ware, ¹Cameron Herting, ²Thomas Mace, ¹Shishir Maitheh, ¹Juan Sarmiento, ¹Bassel El-Rayes, ¹Chrystal Paulos, ¹Megan Wyatt, ¹Gregory Lesinski, ¹Emory University, Atlanta, GA, USA; ²OSUMC, Columbus, OH, USA

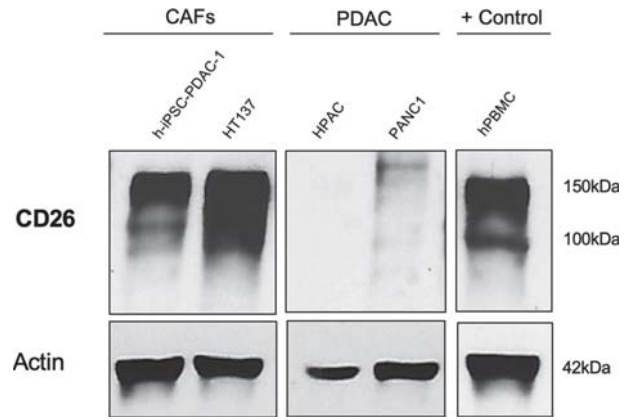
Background Pancreatic ductal adenocarcinoma (PDAC) is refractory to immunotherapy due in part to cellular cross-talk with cancer associated fibroblasts (CAFs). These interactions shape the microenvironment in a manner that is profoundly immunosuppressive. Our group is identifying novel targets in the PDAC stroma that can be manipulated to enhance immunotherapy efficacy. We hypothesize dysregulation of the serine protease, CD26/DPP4 in PDAC contributes to the limited efficacy of immunotherapy. Further, we posit targeting CD26 enzymatic activity using inhibitors that are FDA-approved for adult patients with Type 2 Diabetes Mellitus can enhance the efficacy of immunotherapy in PDAC.

Methods Primary CAFs isolated from patient PDAC resection specimens under an IRB-approved protocol, were subject to NanoString analysis.¹ CD26 protein expression was measured in primary and immortalized CAFs and PDAC cells by immunoblot, flow cytometry and immunofluorescence, while ELISA detected soluble CD26. For in vivo efficacy, luciferase-expressing KPC-tumor cells were implanted orthotopically in the pancreas of immune-competent C57BL/6 mice. Bioluminescence imaging (BLI) confirmed established tumors and mice were randomized to sitagliptin (75 mg/kg in drinking water, CD26/DPP4 inhibitor), anti-PD-L1 Ab (200 ug 2x/week), or both combined for 3 weeks. Controls received vehicle or isotype control Ab. BLI utilized to track tumor progression and tissues harvested for analysis at study endpoint (day 18 of treatment).

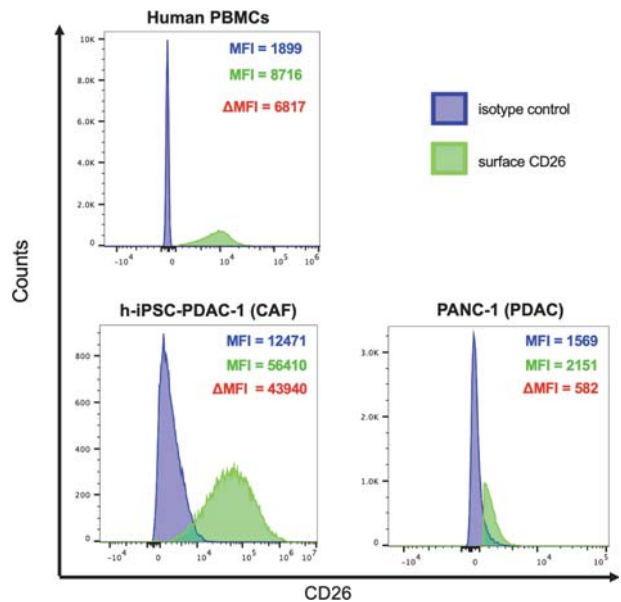
Results NanoString analysis identified CD26/DPP4 as significantly upregulated in RNA transcripts from primary CAFs vs. fibroblasts from normal pancreas (figure 1). We confirmed abundant CD26 expression on patient-derived CAFs and immortalized CAF cell lines, however, lower CD26 expression was observed on human PDAC cell lines (HPAC, PANC-1) by immunoblot, flow cytometry and immunofluorescence (figure 5).



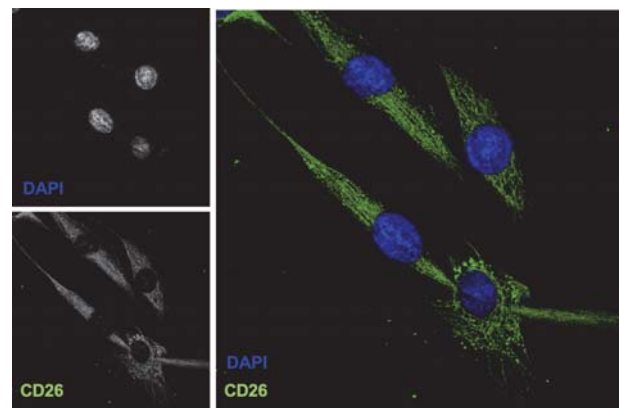
Abstract 904 Figure 1 (A) Schema for analysis of transcript from n=10 primary CAFs (PSC) from PDAC patients vs. normal human pancreatic fibroblasts (HPPFC) via NanoString nCounter PanCancer Immune Profiling Panel. (B) Heat map of gene expression with upregulate DPP4 or CD26 transcript detected. Adapted from Mace et al., 2016.



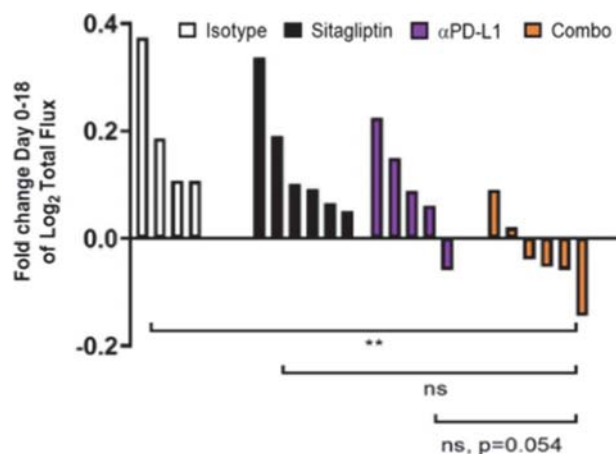
Abstract 904 Figure 2 Validation of CD26 protein expression in human PDAC-derived CAF and PDAC cell lines by immunoblot analysis



Abstract 904 Figure 3 Analysis of surface human CD26 expression in PBMCs, PDAC-derived CAFs (h-iPSC-PDAC-1), and PDAC cells (PANC-1) by flow cytometry. Histograms representing human surface CD26 expression



Abstract 904 Figure 4 Immunofluorescence analysis of CD26/DPP4 cellular localization in a human PDAC-derived CAF cell line



Abstract 904 Figure 5 Combined Sitagliptin and PD-L1 blockade in a murine orthotopic model of PDAC. Fold change in tumor volume, determined by BLI, comparing baseline (Day 0 of treatment) to Day 18 of treatment. Each bar represents fold change in BLI determined tumor volume for each animal

Conclusions Our results are the first to describe CD26 expression on PDAC-derived CAFs and indicate that sitagliptin augments anti-tumor activity of anti-PD-L1 in PDAC tumor-bearing mice. Our ongoing work will provide insight into specific immune cell populations responsible for efficacy of immunotherapy in murine models of PDAC, and the role of CD26 in various cellular compartments within the PDAC microenvironment.

REFERENCES

1. Mace TA, Shakya R, Pitarresi JR, Swanson B, McQuinn CW, Loftus S, Nordquist E, Cruz-Monserrate Z, Yu L, Young G, Zhong X, Zimmers TA, Ostrowski MC, Ludwig T, Bloomston M, Bekaii-Saab T, Lesinski GB. IL-6 and PD-L1 antibody blockade combination therapy reduces tumour progression in murine models of pancreatic cancer. *Gut* 2018;**67**(2):320–32.

<http://dx.doi.org/10.1136/jitc-2021-SITC2021.904>

FASN PREVENTS IMMUNOGENICITY OF IRRADIATED GLIOBLASTOMA BY INHIBITING ER STRESS

Mara De Martino*, Camille Daviaud, Claire Vanpouille-Box. *Weill Cornell Medicine, New York, NY, USA*

Background Glioblastoma (GBM) is the most aggressive and incurable adult brain tumor. Radiation therapy (RT) is an essential modality for GBM treatment and is recognized to stimulate anti-tumor immunity by inducing immunogenic cell death (ICD) subsequent to endoplasmic reticulum (ER) stress. However, RT also exacerbates potent immunosuppressive mechanisms that facilitate immune evasion. Notably, increased de novo lipid synthesis by the fatty acid synthase (FASN) is emerging as a mechanism of therapy resistance and immune escape. Here, we hypothesize that RT induces FASN to promote GBM survival and evade immune recognition by inhibiting ER stress and ICD.

Methods To determine if lipid synthesis is altered in response to RT, we first assessed FASN expression by western blot (WB) and lipid accumulation by BODIPY staining in murine (CT2A and GL261) and human (U118) GBM cell lines. Next, FASN expression was blocked in CT2A cells using CRISPR-Cas9 or an inducible shRNA directed against *Fasn* to evaluate ICD and ER stress markers by ELISA, WB, and electron microscopy. Finally, CT2AshFASN cells or its non-silencing control (CT2AshNS) were orthotopically implanted and FASN knockdown was induced by feeding the mice with doxycycline. The immune contexture was determined by *in situ* immunofluorescence (n=3/group). Remaining mice were followed for survival (n=7/group).

Results We found that *in vitro* irradiation of GBM cells induces lipid accumulation in a dose-dependent fashion; an effect that is magnified over time lasting at least 6/7 days. Consistent with these findings, FASN expression was upregulated in irradiated GBM cells. Confirming the role of FASN, RT-induced accumulation of lipids was reverted when GBM cells were incubated with a FASN inhibitor. Next, we found that FASN ablation in CT2A cells induces mitochondria disruption and was sufficient to increase the expression of the ER stress makers BIP and CHOP. Along similar lines, shFASN enhances the secretion of the ICD markers HMGB1, IFN-beta and CXCL10 in irradiated CT2A cells. *In vivo*, CT2AshFASN tumors presented increased infiltration of CD11c+ cells and CD8+ T cells, consistent with prolonged mice survival (56 days vs. 28 days for CT2AshNS). Importantly, 43% of CT2AshFASN-bearing mice remained tumor-free for more than 70 days, while none of the CT2AshNS-bearing mice survived.

Conclusions Altogether, our data suggest that FASN-mediated lipid synthesis is an important mechanism to prevent ER stress, ICD, and anti-tumor immune responses in GBM. While much work remains to be done, our data propose FASN as a novel therapeutic target to overcome immunosuppression and sensitize GBM to immunotherapies.

<http://dx.doi.org/10.1136/jitc-2021-SITC2021.905>

906

IMMUNOGENOMIC EVALUATION OF CLEAR CELL RENAL CARCINOMA UNCOVERS HK3 AS A MYELOID SPECIFIC METABOLIC ENZYME

¹Bradley Reinfeld*, ¹Matthew Madden, ¹Melissa Wolf, ²Agi de Cubas, ²Scott Haake, ²Rachel Hongo, ¹Margaret Axelrod, ²Jackie Bader, ³Aleksandar Obradovic, ¹Dalton Greenwood, ²Xiang Ye, ⁴Justin Balko, ²Katy Beckermann, ⁵Benjamin Vincent, ²Brian Rini, ³Charles Drake, ²Jeffrey Rathmell, ²W Rathmell. ¹Vanderbilt University School of Medicine, Nashville, TN, USA; ²Vanderbilt University Medical Center, Nashville, TN, USA; ³Columbia University Medical Center, New York City, NY, USA; ⁴Vanderbilt University Medical Center, Nashville, TN, USA; ⁵University of North Carolina, Chapel Hill, NC, USA

Background Glucose fixation is a hallmark clear cell renal carcinoma (ccRCC).¹⁻² Our group has shown unique metabolic enzyme utilization between malignant cells and infiltrating cells. Additionally, we uncovered the glycolytic nature of tumor infiltrating myeloid cells.³ Therefore, we decided to investigate the role of the hexokinase isoforms (HK1,2/3, GCK, and HKDC1) in the ccRCC tumor microenvironment (TME).

Methods For this study, we performed immunogenomic analyses across ccRCC samples available via The Cancer Genome Atlas (TCGA).⁴⁻⁵ Additionally, we examined the expression of hexokinases in the neoadjuvant VEGF inhibitor setting⁶ as well as correlation to a poor prognostic macrophage subset.⁷ Our group also performed single cell-ATAC seq on methocult cultures to further characterize the metabolic features of hematopoiesis. We additionally implemented qPCR on magnetically sorted bone marrow as well as myeloid cell culture to further interrogate the role of HK3 in macrophage biology and in situ RNA hybridization (RNA-ISH) to describe the subpopulation of HK3+ cells in the ccRCC TME.

Results Gene set enrichment analysis confirmed HK1/2's role in anabolic metabolism. GCK was barely detectable in these samples while HKDC1 expression decreased in ccRCC tumors. Intriguingly, patients with elevated expression of HK3 had an enrichment of interferon gamma response signature. In our evaluation of the TCGA, only HK3 expression correlated with poor outcome in ccRCC. CiberSortX demonstrated that HK3 expressing tumors correlated with the presence M2 macrophages while other HK family enzymes had marginal association with immune infiltrate. HK3 was the only hexokinase found to be significantly elevated with neoadjuvant pazopanib treatment in addition to being enriched in ccRCC patients with high levels of poor prognostic macrophages. RNA-ISH confirms HK3 expression is limited to myeloid cells in ccRCC tumors. The myeloid specific nature of HK3 is supported by transcript analysis from MC38 tumors, and qPCR on mouse bone marrow. Myeloid specificity for HK3 isoform expression is not restricted to malignancy; HK3 is one of a handful of genes that define myeloid identity from scATAC sequencing of in vitro differentiated CD34+ hematopoietic stem cells. Our ongoing in vitro studies indicate that M1 polarization (+LPS/IFN γ) increases expression of HK1/2/3, consistent with the anabolic phenotype of activate macrophages. However, stimulation with IFN γ alone only elevates the expression of HK3.

Conclusions HK3 is a myeloid specific interferon gamma responsive gene, whose expression imparts poor prognosis for ccRCC cancer patients, while HK1/HK2 contribute significantly to the glucose uptake/pseudohypoxic phenotype seen throughout the ccRCC TME.

Acknowledgements N/a

Trial Registration N/A

REFERENCES

1. Courtney KD, *et al.* Isotope tracing of human clear cell renal cell carcinomas demonstrates suppressed glucose oxidation in vivo. *Cell metabolism* 2018;**28**(5):793–800.e2.
2. Linehan WM, *et al.* The metabolic basis of kidney cancer. *Cancer Discov* 2019;**9**(8):1006–1021.
3. Reinfeld BJ, *et al.* Cell-programmed nutrient partitioning in the tumour microenvironment. *Nature* 2021.
4. Ricketts CJ, *et al.* The cancer genome atlas comprehensive molecular characterization of renal cell carcinoma. *Cell reports* 2018;**23**(1):313–326.e5.
5. Creighton CJ, *et al.* Comprehensive molecular characterization of clear cell renal cell carcinoma. *Nature* 2013;**499**(7456):43–49.
6. Wood CG, *et al.* Neoadjuvant pazopanib and molecular analysis of tissue response in renal cell carcinoma. *JCI Insight* 2020;**5**(22).
7. Obradovic A, *et al.* Single-cell protein activity analysis identifies recurrence-associated renal tumor macrophages. *Cell* 2021;**184**(11):2988–3005.e16.

Ethics Approval This clinical trial [in Reference 6] was approved by the IRBs at the University of Carolina at Chapel Hill (Office of Human Research Ethics) and MD Anderson (Office of Human Subjects Protection), and the research was conducted according to the Declaration of Helsinki principles. All participants provided written informed consent before the initiation of any research procedures. The studies were conducted in accordance with the guidelines approved by the Institutional Review Board (IRB) protocols, AAAO5706 and AAAA9967, respectively. Patients provided consent prior to taking part in the study. This is the clinical data take from the study in reference 7. All other studies referenced in the above abstract were conducted in accordance with the Declaration of Helsinki principles under a protocol approved by the Vanderbilt University Medical Center (VUMC) Institutional Review Board (protocol no. 151549). Informed consent was received from all patients before inclusion in the study by the Cooperative Human Tissue Network at VUMC. This is the clinical data take from the study in reference 3 and 7. All mouse procedures were performed under Institutional Animal Care and Use Committee (IACUC)-approved protocols from VUMC and conformed to all relevant regulatory standards. The mouse protocol ID is 19000125

<http://dx.doi.org/10.1136/jitc-2021-SITC2021.906>

MODULATION OF TUMOR IMMUNOGENICITY BY DNA METHYLATION OF IMMUNE SYNAPSE GENES IN CANCERS

Imene Hamaidi*, Anders Berglund, Matthew Mills, Ryan Putney, James Mule, Sunjune Kim. *H. Lee Moffitt Cancer Center and Research Institute, Tampa, FL, USA*

Background Cancer immunotherapy represents a major paradigm shift in cancer care. Despite such breakthrough, majority of cancer patients remains refractory to existing immunotherapeutic modalities highlighting the inherent capacity of tumors to escape immunosurveillance mechanisms. Frequently, cancer cells utilize the epigenetic machinery to silence tumor suppressors or activate oncogenes for survival and proliferation. Likewise, tumor cells might employ the epigenetic reprogramming of immune-related pathways to evade the immune system. Methylation is one of the major epigenetic mechanisms modulating gene transcription. Thus, we investigated the methylation profile of both co-stimulatory and immune checkpoint genes in cancer.

Methods Data from The Cancer Genome Atlas (TCGA) were used for methylation profiling and RNA-sequencing analysis. Twenty-six epithelial cancer cell lines with more than 3 mock and three 5-azacitidine-treated samples were selected for analysis from the GSE57342 dataset. t-distributed stochastic neighbor embedding (t-SNE) was calculated using 247 probes for the selected 20 genes across all TCGA samples. t-SNE analysis was performed on 8,186 solid tumors and 745 normal adjacent tissues for methylation levels for all probes. For principal component analysis, first and second principal components were used to represent the overall methylation status for 8,931 tumor and normal samples in the TCGA database. Survival analyses were retrieved from a prior publication.¹

Results We found that methylation profile of immune synapse genes is distinct in tumor versus normal adjacent tissue. Interestingly, our results demonstrate hypermethylation of co-stimulatory genes such as CD40 and hypo-methylation of immune checkpoint genes such as HHLA2 and PDL1 across multiple tumor types in comparison with the normal adjacent tissue. In addition, an inverse correlation between methylation and gene expression was manifest among tumor and normal adjacent tissue, confirming the epigenetic mechanism of gene suppression by gene methylation. Furthermore, we observed a reversal of hypermethylation of the co-stimulatory genes including CD40 by the demethylating agent 5-azacytidine in the data set of 26 epithelial cancer cell lines. Finally, we found that that hypomethylation of co-stimulatory genes within the immune synapse correlates with functional T cell recruitment to the tumor microenvironment and is followed by a favorable clinical outcome in melanoma patients.

Conclusions Our finding unveils methylation of immune synapse genes as a crucial driver of the immune evasive phenotype of cancer cells. Notably, identification of actionable targets to restore tumor immunogenicity is an attractive strategy in combination with immune checkpoint blockade.

Acknowledgements This work was supported by NIH grant K08 CA194273, the Immunology Innovation Fund, an NCI Cancer Center Support grant, (P30-CA076292), the Miriam and Sheldon G. Adelson Foundation, and the Moffitt Foundation.

REFERENCE

1. Liu J, Lichtenberg T, Hoadley KA, Poisson LM, Lazar AJ, Cherniack AD, Kovatich AJ, Benz CC, Levine DA, Lee AV, Omberg L, Wolf DM, Shriver CD, Thorsson V, Cancer Genome Atlas Research N, Hu H. An integrated TCGA pan-cancer clinical

data resource to drive high-quality survival outcome analytics. *Cell* 2018;**173**(2):400–16 e11.

<http://dx.doi.org/10.1136/jitc-2021-SITC2021.907>

908

**HUMANIZED MODEL FOR ASSESSMENT OF THERAPIES
TARGETING EITHER LYMPHOID OR MYELOID
COMPARTMENT: ENHANCED EVALUATION OF CLINICAL
RELEVANCY & TRANSLATABILITY**

¹Florence Renart-Depontieu, ¹Gaëlle Martin, ¹Chloé Beuraud, ²Poonam Yakkundi, ²Angus Sinclair, ³Morgane Denis, ³Léa Magadoux, ³Elsa Kress, ³Charles Dumontet, ⁴Ludovic Bourre, ⁴Dean Campbell, ⁴Astrid Doerner, ¹Patricia Isnard-Petit, ¹Alexandre Fraichard, ¹Yacine Cherifi, ¹Kader Thiam*. ¹genOway, Lyon, France; ²IGM Biosciences, Mountain View, CA, USA; ³Antinéo, Lyon, France; ⁴Crown Bioscience, Paris, France

Background The breakthrough of immunotherapies has unleashed new hope and new success for cancer therapy. However, the choice of a preclinical model is one of the main challenges as they are important for evaluation of translatability to help support testing in clinical studies, including potential efficacy and tolerability of immunotherapies during preclinical development. The development of mouse models featuring a human immune system (HIS) provides new paths for the investigation of the efficacy of immunotherapies in preclinical models engrafted with human tumors. Although these models provided a breakthrough in the assessment of immune targeting agents, they also come with a few significant caveats. These include: a lack of a mature human myeloid compartment in the mouse, and a short life span of the model when this compartment is promoted at non-physiological levels via the over-expression of human cytokines. Here, we report a novel mouse model (BRGSF-HIS), featuring functional human lymphoid and myeloid compartments. The human immune response of this model was assessed through examination of the immune cells composition in the tumor microenvironment (TME), and its ability to respond to biologics known to trigger cytokine release syndrome (CRS).

Methods BRGSF (balb/C Rag2^{-/-}, IL2Rg^{-/-}, SIRPaNOD and Flt3^{-/-}) is a highly immunodeficient mouse, with reduced murine myeloid cells, which allows long term CD34⁺ HSC-engraftment and development of human lymphoid and myeloid compartments (human CD141⁺ and CD1c⁺ DC subsets, CD123⁺ pDC, CD14⁺ monocytes), in blood, spleen and bone marrow. The engraftment is stable for over twelve months with no side effects. The effect of exogenous human Flt3 ligand (Flt3L) on the composition of TME in A549 model, and an anti-CD3 antibody (OKT3)-induced CRS, were assessed.

Results Exogenous human Flt3L significantly and transiently increased the proportion of human myeloid cells. This can be recalled by continuous dosing of Flt3L. Assessment of tumor immunobiology in A549 model, showed increased tumor-infiltrating T-cells (mainly CD8⁺ T-cells) and myeloid cells, while tumor-infiltrating NK cells were decreased. The presence of myeloid cells provides a new opportunity for assessment of myeloid targeted therapies, as proven using pDC-depleting antibodies. OKT3 administration resulted in CRS symptoms including a temperature drop, body weight loss and a change in serum cytokine levels. Symptoms were mitigated upon administration of tocilizumab, suggesting the contribution of the myeloid compartment in the response observed.

Conclusions These data demonstrate that BRGSF-HIS mice support development of functional human myeloid cells and that this mouse model enables preclinical evaluation of cancer immunotherapy in vivo.

<http://dx.doi.org/10.1136/jitc-2021-SITC2021.908>

909

DIFFERENTIATION SUBGROUPS WITHIN LKB1-DEFICIENT LUNG CANCER INFLUENCE BOTH THE IMMUNE EXCLUSION PHENOTYPE AND CELLULAR COMPOSITION OF THE IMMUNE MICROENVIRONMENT

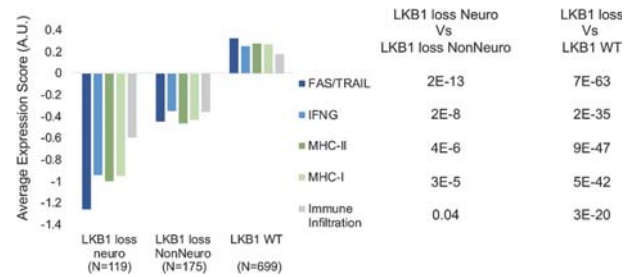
¹Jacob Kaufman*, ²Doug Cress, ²Theresa Boyle, ¹David Carbone, ³Neal Ready, Kris Wood. ¹Ohio State University, Columbus, OH, USA; ²Moffitt Cancer Center, Tampa, FL, USA; ³Duke University Medical Center, Chapel Hill, NC, USA

Background LKB1 (STK11) is a commonly disrupted tumor suppressor in NSCLC. Its loss promotes an immune exclusion phenotype with evidence of low expression of interferon stimulated genes (ISG) and decreased microenvironment immune infiltration.^{1 2} Clinically, LKB1 loss induces primary immunotherapy resistance.³ LKB1 is a master regulator of a complex downstream kinase network and has pleiotropic effects on cell biology. Understanding the heterogeneous phenotypes associated with LKB1 loss and their influence on tumor-immune biology will help define and overcome mechanisms of immunotherapy resistance within this subset of lung cancer.

Methods We applied multi-omic analyses across multiple lung adenocarcinoma datasets^{2 4-6} (>1000 tumors) to define transcriptional and genetic features enriched in LKB1-deficient lung cancer. Top scoring phenotypes exhibited heterogeneity across LKB1-loss tumors, and were further interrogated to determine association with increased or decreased markers of immune activity. Further, immune cell-types were estimated by Cibersort to identify effects of LKB1 loss on the immune microenvironment. Key conclusions were confirmed by blinded pathology review.

Results We show that LKB1 loss significantly affects differentiation patterns, with enrichment of ASCL1-expressing tumors with putative neuroendocrine differentiation. LKB1-deficient neuroendocrine tumors had lower expression of Interferon Stimulated Genes (ISG), MHC1 and MHC2 components, and immune infiltration compared to LKB1-WT and non-neuroendocrine LKB1-deficient tumors (figure 1). The abundances of 22 immune cell types assessed by Cibersort were compared between LKB1-deficient and LKB1-WT tumors. We observe skewing of immune microenvironmental composition by LKB1 loss, with lower abundance of dendritic cells, monocytes, and macrophages, and increased levels of neutrophils and plasma cells (table 1). These trends were most pronounced among tumors with neuroendocrine differentiation, and were concordant across three independent datasets. In a confirmatory subset of 20 tumors, plasma cell abundance was assessed by a blinded pathologist. Pathologist assessment was 100% concordant with Cibersort prediction, and association with LKB1 loss was confirmed (P=0.001).

Conclusions We conclude that tumor differentiation patterns strongly influence the immune microenvironment and immune exclusion characteristics of LKB1-deficient tumors. Neuroendocrine differentiation is associated with the strongest immune exclusion characteristics and should be evaluated clinically for evidence of immunotherapy resistance. A novel observation of increased plasma cell abundance is observed across multiple datasets and confirmed by pathology. Causal mechanisms linking differentiation status to immune activity is not well understood, and the functional role of plasma cells in the immune biology of LKB1-deficient tumors is undefined. These questions warrant further study to inform precision immuno-oncology treatments for these patients.



Abstract 909 Figure 1 Immune-associated Gene Expression Profiles Affected by Neuroendocrine Differentiation within LKB1-Deficient Lung Adenocarcinomas. Gene expression profiles corresponding to five immune-associated phenotypes are shown with bars indicating average GEP scores for tumors grouped according to LKB1 and neuroendocrine status as indicated. P-values represent results from Student's T-test between groups as indicated.

Abstract 909 Table 1 LKB1 Loss Affects Composition of Immune Microenvironment. Values indicate log10 P-values comparing LKB1-loss to LKB1-WT tumors. Positive (red) indicates increased abundance in LKB1 loss. Negative (blue) indicates decreased abundance.

	TCGA	Moffitt	Affy Array
B cells naive	3.5	-0.2	-0.1
B cells memory	-0.4	-0.5	-0.8
Plasma cells	15.6	16.9	6.8
T cells CD8	0.6	1	0
T cells CD4 naive	0.9	-0.4	-0.3
T cells CD4 memory resting	-1.2	0.3	-0.3
T cells CD4 memory activated	0	0.9	0.7
T cells follicular helper	3	2.7	-0.2
T cells regulatory (Tregs)	-1.5	-0.5	0
T cells gamma delta	-0.6	-2.1	-0.7
NK cells resting	1.5	1.1	1.8
NK cells activated	2.3	0.8	-0.5
Monocytes	-2.7	-1.7	-2.1
Macrophages M0	0	-0.2	-0.2
Macrophages M1	-3.9	-2.3	-2.4
Macrophages M2	-5	0.1	-5.1
Dendritic cells resting	-6	-4.7	-5.2
Dendritic cells activated	2.7	0.8	0.3
Mast cells resting	-3.9	-4.4	-5.9
Mast cells activated	0	-0.1	0.3
Eosinophils	-0.1	-0.7	-0.8
Neutrophils	3.9	8.4	2.4

Acknowledgements This work was funded by SITC AZ Immunotherapy in Lung Cancer grant (SPS256666) and DOD Lung Cancer Research Program Concept Award (LC180633).

REFERENCES

- Skoulidis F, Byers LA, Diao L, et al. Co-occurring genomic alterations define major subsets of KRAS-mutant lung adenocarcinoma with distinct biology, immune profiles, and therapeutic vulnerabilities. *Cancer Discov* 2015;**5**:860-77.
- Schabath MB, Welsh EA, Fulp WJ, et al. Differential association of STK11 and TP53 with KRAS mutation-associated gene expression, proliferation and immune surveillance in lung adenocarcinoma. *Oncogene* 2016;**35**:3209-16.
- Skoulidis F, Goldberg ME, Greenawalt DM, et al. STK11/LKB1 mutations and PD-1 inhibitor resistance in KRAS-mutant lung adenocarcinoma. *Cancer Discovery* 2018;**8**:822-835.
- Cancer Genome Atlas Research Network. Comprehensive molecular profiling of lung adenocarcinoma. *Nature* 2014;**511**:543-50.

5. Chitale D, Gong Y, Taylor BS, *et al.* An integrated genomic analysis of lung cancer reveals loss of DUSP4 in EGFR-mutant tumors. *Oncogene* 2009;**28**:2773–83.
6. Shedden K, Taylor JM, Enkemann SA, *et al.* Gene expression-based survival prediction in lung adenocarcinoma: a multi-site, blinded validation study. *Nat Med* 2008;**14**:822–7.

<http://dx.doi.org/10.1136/jitc-2021-SITC2021.909>

OVEREXPRESSION OF MIR-155-5P CAN UPREGULATE ANTIGEN PROCESSING AND PRESENTATION PATHWAY VIA TARGETING TAPASIN

Yuan Wang*, Maria-Filotei Lazaridou, Chiara Massa, Barbara Seliger. *Institute of Medical Immunology, Halle (Saale), Germany*

Background Dysregulation of major histocompatibility complex (MHC) class I antigen processing and presentation machinery (APM) components in the tumor as one main molecular mechanism of immune escape leading to deactivation of T cell immune surveillance could be due to post-transcriptional regulation via immune-modulatory microRNAs (miRNA). It is now well established from a variety of studies that several miRNAs could effectively modulate the expression of some MHC class I APM components in tumors. Tapasin is an important APM molecule involved in the association of MHC class I with transporter associated with antigen processing (TAP) and peptide loading. Since so far no detailed investigation of the post-transcriptional regulation of tapasin exists, the aim of this study is to identify and functionally characterize miRNAs targeting tapasin in melanoma.

Methods Using miRNA trapping by RNA in vitro affinity purification (miTRAP) and in silico as well as small RNA sequencing, miRNAs will be identified, which bind to the 3'untranslated region (3' UTR) of tapasin. Dual-luciferase assays will be performed to determine to bind of the miRNA. In silico analysis was performed to predict the effect of miRNAs on the survival of melanoma patients in correlation to tapasin. RT-qPCR, Western blot, flow cytometry, and other functional assays were performed after transfecting miRNA mimics in three melanoma cell lines.

Results Using the combination strategy of miTRAP and RNA seq we identified miR-155-5p to bind to the 3'UTR of tapasin, which was further confirmed by in silico analysis and dual-luciferase reporter assay. Transfection of miR-155-5p mimics demonstrated that miR-155-5p upregulate tapasin protein level, which was accompanied by an upregulation of the MHC class I (HLA-ABC) surface expression. Simultaneously, in several different types of cancer, including melanoma, the expression of miR-155-5p is significantly positively correlated with the patient's survival and HLA-A protein.

Conclusions Our data revealed for the first time a positive role of miR-155-5p in the posttranscriptional regulation of tapasin in melanoma and provide further insights into the miR-155-5p-mediated induction of HLA-ABC surface expression. This might lead to a better T cell response, avoidance tumor cell escape, improvement of patients' survival and thus might be a potential therapeutic target.

Acknowledgements The work was supported by a grant from the DKH (BS).

<http://dx.doi.org/10.1136/jitc-2021-SITC2021.910>

IMMUNE PROFILING REVEALS ENRICHMENT OF DISTINCT IMMUNE SIGNATURES IN HIGH-RISK ORAL POTENTIALLY MALIGNANT DISORDERS

¹Chai Gan*, ¹Bernard Kok Bang Lee, ²Shin Hin Lau, ³Thomas George Kallarakkal, ³Zuraiza Mohamad Zaini, ⁴Rosnah Binti Zain, ²Hans Prakash Sathasivam, ⁵Joe Poh Sheng Yeong, ⁶Natalia Saveljeva, ⁶Gareth Thomas, ⁷Christian Ottensmeier, ³Hany Ariffin, ¹Sok Ching Cheong, ¹Kue Peng Lim. ¹Cancer Research Malaysia, Subang Jaya, Malaysia; ²Institute for Medical Research, Kuala Lumpur, Malaysia; ³University of Malaya, Subang Jaya, Malaysia; ⁴MAHSA University, Jenjarom, Malaysia; ⁵Institute of Molecular Cell Biology, Singapore, Singapore; ⁶University of Southampton, Southampton, UK; ⁷University of Liverpool, Liverpool, UK

Background Patients with oral potentially malignant disorders (OPMD) having moderate or severe oral epithelial dysplasia (OED) have a greater risk of developing oral squamous cell carcinoma (OSCC) compared to mild OED with an odds ratio of 2.4.¹ The involvement of specific immune cell types associated with malignant transformation have been reported, giving rise to clinical trials in immunoprevention. However, the immune landscape of OPMD remains understudied. In this study, we aimed to elucidate the immune landscape of high-risk OPMD by transcriptomic profiling for the identification of potential immunoprevention strategy.

Methods Histological evaluation was performed on hematoxylin and eosin (H&E)-stained tissues to investigate the differences of lymphocyte infiltration in benign lesions (n=16), high-risk OPMD consisted of moderate and severe OED (n=46) and early-stage OSCC (n=6). Formalin-fixed paraffin-embedded tissue sections of selected cases from each sample type were subjected to RNA sequencing. Weighted-gene-correlation network analysis (WGCNA) was used to identify key gene modules expressed in specific disease type.² The immune landscape of high-risk OPMD was elucidated by the enrichment of immune signatures using single-sample gene set enrichment analysis.^{3–5} The response of high-risk OPMD to anti-PD1 treatment was predicted by the detection of T-cell-inflamed condition.⁶ Validation was performed by multiplex immunofluorescent (mIF) staining.

Results Our H&E evaluation showed that lymphocyte infiltration into the epithelial was seen in 80% of high-risk OPMD and early-stage OSCC, compared to 9% of benign lesion. Gene modules identified from WGCNA analysis revealed that genes involved in immune-related pathways were overexpressed in high-risk OPMD and in early-stage OSCC when compared to benign lesion, but unchanged between high-risk OPMD and early-stage OSCC. We further demonstrated that immune signatures representing lymphocyte infiltration, MHC-I antigen presentation and cytotoxic immune responses were enriched in high-risk OPMD, indicating the presence of immune surveillance. High-risk OPMD can be grouped into the T-cell-inflamed and non-immune reactive subtypes. The T-cell-inflamed subtype is enriched with T cells, interferon signaling and PD-1/PD-L1 immune checkpoint proteins, suggesting that these lesions may be amenable to anti-PD1 treatment. Meanwhile, the non-immune reactive subtype demonstrated low enrichment in signatures for immune cell infiltration, indicating a need of intervention to induce lymphocyte infiltration. Using mIF staining, we observed an increase of CD45+ immune cell population expressing PD-L1 in high-risk OPMD.

Conclusions Immune surveillance is a prominent feature of high-risk OPMD. However, different subsets of high-risk OPMD exist, suggesting a need of different immunoprevention approaches to prevent disease progression which warrants further investigation.

Acknowledgements This study was supported and funded by the Global Challenge Research Fund by the Medical Research Council, UK (MR/P024351/1) and Cancer Research Malaysia. We thank the Ong Heng Tiang & Ong Sek Pek Foundation for scholarship sponsorship.

REFERENCES

1. Iocca O, Sollecito TP, Alawi F, *et al.* Potentially malignant disorders of the oral cavity and oral dysplasia: a systematic review and meta-analysis of malignant transformation rate by subtype. *Head Neck* 2020;**42**:539–55.
2. Langfelder P, Horvath S. WGCNA: an R package for weighted correlation network analysis. *BMC Bioinformatics* 2008;**9**:559.
3. Subramanian A, Tamayo P, Mootha VK, *et al.* Gene set enrichment analysis: a knowledge-based approach for interpreting genome-wide expression profiles. *Proc Natl Acad Sci U S A.* 2005;**102**:15545–50.
4. Chen YP, Wang YQ, Lv JW, *et al.* Identification and validation of novel microenvironment-based immune molecular subgroups of head and neck squamous cell carcinoma: implications for immunotherapy. *Ann Oncol* 2019;**30**:68–75.
5. Thorsson V, Gibbs DL, Brown SD, *et al.* The immune landscape of cancer. *Immunity* 2018;**48**:812–30.
6. Ayers M, Lunceford J, Nebozhyn M, *et al.* IFN-gamma-related mRNA profile predicts clinical response to PD-1 blockade. *J Clin Invest* 2017;**127**:2930–40.

Ethics Approval The use of clinical specimens in this study has been approved by the Medical Ethics Committee, Faculty of Dentistry, University of Malaya [DF OS1624/0073(L)], and The National Medical Research Register, Malaysia [NMRR-16-1764-32566 (IIR)].

<http://dx.doi.org/10.1136/jitc-2021-SITC2021.911>

912

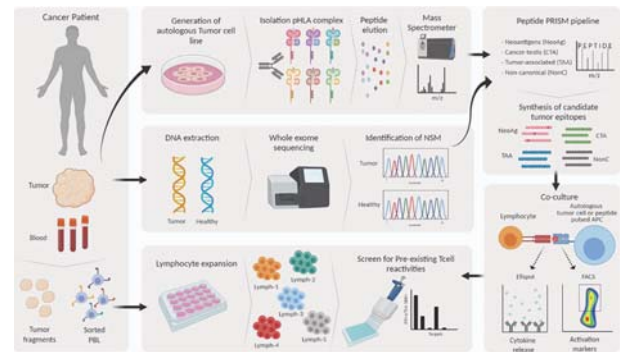
PREFERENTIAL RECOGNITION OF NEOANTIGENS OVER NON-CANONICAL PEPTIDES IN CANCER PATIENTS

¹Maria Lozano-Rabella*, ¹Andrea Garcia-Garjjo, ¹Jara Palomero, ²Florian Erhard, ³Juan Martín-Liberal, ¹Ignacio Matos, ⁴Jared Gartner, ⁴Steven Rosenberg, ⁵Michael Ghosh, ¹Francesc Canals, ⁶August Vidal, ⁷Josep Maria Piulats, ⁶Xavier Matias-Guiu, ¹Irene Braña, ⁸Eva Muñoz, ¹Elena Garralda, ²Andreas Schlosser, ¹Alena Gros. ¹Vall d'Hebrón Institute of Oncology (VHIO), Barcelona, Spain; ²Julius-Maximilians-University Würzburg, Würzburg, Germany; ³Institut Català d'Oncologia (ICO), Barcelona, Spain; ⁴National Cancer Institute (NCI), National Institutes of Health, Bethesda, MD, USA; ⁵University of Tübingen, Interfaculty Institute for Cell Biology, Tübingen, Germany; ⁶Bellvitge University Hospital, Barcelona, Spain; ⁷Catalan Institute of Oncology (ICO), Barcelona, Spain; ⁸Vall d'Hebron Hospital, Barcelona, Spain

Background Despite recent advances in exome and RNA sequencing to identify tumor-rejection antigens including neoantigens, the existing techniques fail to identify the vast majority of antigens targeted by tumor-reactive cells. A growing number of studies suggest that HLA-I peptides derived from non-canonical (nonC) open reading frames or derived from allegedly non-coding regions can contribute to tumor immunogenicity. Here we use proteogenomics to identify personalized candidate canonical and non-canonical tumor-rejection antigens and to evaluate their contribution to cancer immune surveillance in patients.

Methods Whole exome sequencing was performed to identify the non-synonymous somatic mutations (NSM) and immunopeptidomics to identify the HLA-I presented peptides (pHLA) in 9 patient-derived tumor cell lines (TCL). Peptide-PRISM proteogenomics pipeline was used to identify both canonical and non-canonical pHLA, including those derived from NSM in coding regions. All peptides containing mutations and derived from either cancer-testis (CTA) or tumor-associated antigens (TAA) were selected as candidate tumor antigens. For nonC peptides, an immunopeptidomics healthy dataset containing several tissues and HLA-allotypes was used to eliminate those derived from normal ORFs and select nonC peptides preferentially expressed in tumor cells (nonC-TE). The selected candidate peptides were synthesized, pulsed onto autologous APCs and co-cultured with tumor-reactive ex vivo expanded lymphocytes to assess immune recognition (figure 1).

Results NonC-TE peptides were identified in all TCL studied, ranging from 0.5% to 5.4% of the total HLA-I presented peptides (n= 506). As described previously, 5'UTR were the main source. Of note, the tumor type did not have an impact on the frequency of presented nonC peptides, but rather the presence of HLA-A*11:01 and HLA-A*03:01 was a major determinant. T cell responses were detected against at least 13/33 putative neoantigens, 2/24 CTA and 2/61 TAA. On the contrary, none of the 471 nonC-TE candidate peptides tested thus far, including one containing a NSM were able to elicit a recall immune response. Nevertheless, T cells recognizing at least 3 of them were detected through in vitro sensitization of non-autologous PBMCs.



Abstract 912 Figure 1 Workflow diagram

Tumor biopsies and blood samples are obtained from cancer patients (left panel). Patient-derived tumor cell lines are generated in vitro, the peptides presented on HLA molecules are further isolated and analyzed in a mass-spectrometer (top panel). Whole exome sequencing (WES) from matched tumor and healthy tissue is performed to identify the non-synonymous somatic mutations (NSM) (middle panel). Peptide-PRISM proteogenomics pipeline combines the information from the immunopeptidomics data and WES to identify pHLA sequences from both canonical and non-canonical candidate tumor antigens (top right panel). Lymphocyte populations either TILs or sorted PBMCs are expanded and further screened for pre-existing T cell responses (bottom panel) against the candidate epitopes by co-culturing the T cells with peptide-pulsed autologous APC. The recognition is assessed by measuring IFN γ release by elispot and the upregulation of activation surface markers by FACS (bottom right panel).

Conclusions Our results show that although HLA-I nonC peptides were frequently presented in all TCLs studied and they can be immunogenic, neoantigens derived from mutations in canonical coding regions were preferentially recognized by tumor-reactive lymphocytes, suggesting T cells targeting the latter are primed more efficiently. The identification of mutated nonC antigens using whole genome sequencing to identify mutations in non-coding regions warrants further examination. Still, the specificity of many tumor-reactive TILs remains unknown.

Ethics Approval "This study was approved by the "Comité de Ética de Investigación con Medicamentos del Hospital Universitario Vall d'Hebron" institution's Ethics Board; approval number PR(AG)537/2019."

<http://dx.doi.org/10.1136/jitc-2021-SITC2021.912>

A MURINE GASTRIC CANCER YTN16 MODEL FOR THE RATIONAL DESIGN OF COMBINATION IMMUNOTHERAPY

Koji Nagaoka*, Changbo Sun, Yukari Kobayashi, Kazuhiro Kakimi. *The University of Tokyo Hospital, Tokyo, Japan*

Background Although Immune checkpoint blockade (ICB) has changed the standard of care of cancer, ICB monotherapy is largely ineffective in patients with solid cancer. Therefore, the rational combination of ICB with other treatment modalities is warranted. We have recently established chemically induced gastric cancer cell line YTN16, transplantable in immune-competent mice,¹ and showed that inhibition of FGFR4 signaling suppressed the YTN16 tumor growth. We also demonstrated the depletion of IL-17-producing T cells in YTN16 tumors enhanced the anti-tumor effects of anti-PD-1 treatment.² In this study, we identified the neoantigens of YTN16 to monitor the dynamics of tumor-specific CD8⁺ T cells in response to combination immunotherapy.

Methods Whole-exome and transcriptome sequencing analyses were performed to identify missense mutations. As a result, candidate neoepitopes were predicted as follows; FPKM \geq 25, variant allele frequency in RNAseq \geq 0.04, IC50 of NetMHCpan \leq 250nM, EL rank of NetMHCpan \leq 0.5 and presentation percentile of MHCflurry \geq 0.5.

Results Exome sequencing identified 3,347 missense mutations in the YTN16 tumor. We synthesized 11 candidate neoepitope peptides and screened their reactivity to YTN16-reactive CD8⁺ T cell lines established from YTN16-rejected mice by ICB. Out of 11 peptides, five peptides (3 neoantigens, m(mutated)Cdt1, mScarb2 and mZfp106) induced IFN γ production in YTN16-reactive CD8⁺ T cells. MHC class I dimer assay identified these three neoantigen-specific T cells in YTN16 tumors. Anti-CTLA-4, but not anti-PD-1 increased neoantigen-specific T cells and completely eradicated tumors. Adoptive transfer of neoantigen-reactive CD8⁺ T cell lines and therapeutic vaccines of DCs pulsed with neoantigen short or long peptides inhibited YTN16 growth. Neoantigen-specific TCRs were cloned from neoantigen-reactive CD8⁺ T cell lines and retrovirally transduced to activated CD8⁺ T cells. TCR-transduced T cells killed YTN16 in vitro and adoptive transfer of TCR-transduced T cells showed anti-tumor effects. These results indicated that these three neoantigens were de fact neoantigens.

Conclusions We identified three neoantigens that induced CD8⁺ T cell response with anti-tumor effects in YTN16. Thus, YTN16 is a well-characterized murine gastric cancer model for rational design and optimization of combination immunotherapy.

REFERENCES

1. Yamamoto M, Nomura S, Hosoi A, Nagaoka K, Iino T, Yasuda T, Saito T, Matsushita H, Uchida E, Seto Y, Goldenring JR, Kakimi K, Tatematsu M, Tsukamoto T. Established gastric cancer cell lines transplantable into C57BL/6 mice show fibroblast growth factor receptor 4 promotion of tumor growth. *Cancer Sci* 2018;**109**(5):1480–1492.
2. Nagaoka K, Shirai M, Taniguchi K, Hosoi A, Sun C, Kobayashi Y, Maejima K, Fujita M, Nakagawa H, Nomura S, Kakimi K. Deep immunophenotyping at the single-cell level identifies a combination of anti-IL-17 and checkpoint blockade as an effective treatment in a preclinical model of data-guided personalized immunotherapy. *J Immunother Cancer* 2020;**8**(2):e001185.

<http://dx.doi.org/10.1136/jitc-2021-SITC2021.913>

LOSS OF LKB1 IS ASSOCIATED WITH RESISTANCE TO IFN-GAMMA AND T CELL KILLING IN NON-SMALL CELL LUNG CANCER

¹Alexandre Reuben*, ¹Peixin Jiang, ¹Hui Nie, ¹Ana Galan Cobo, ¹Minghao Dang, ¹Yu Qian, ¹Meredith Frank, ¹Emily Blitz, ²Haifa Hamdi, ³Warren Denning, ¹Monique Nilsson, ¹Alissa Poteete, ¹Li Shen, ¹Qi Wang, ¹Irene Guijarro, ¹Keri Nichols, ¹Roohussaba Khairullah, ¹Jiexin Zhang, ¹Ferdinandos Skoulidis, ¹Jing Wang, ¹Linghua Wang, ¹John Heymach. ¹MD Anderson, Houston, TX, USA; ²Kiromic Biopharma, Houston, USA; ³BMS, Houston, USA

Background KRAS-mutant non-small cell lung cancers (NSCLC) have exhibited unique response patterns to immunotherapy based on their co-occurring mutations. Patients harboring KRAS & STK11/LKB1 co-mutations (KL) have experienced shorter progression-free and overall survival compared to those with only KRAS mutations (K). Despite their limited responses, KL tumors exhibit a tumor mutational burden comparable to their K counterparts, suggesting the presence of additional mechanisms impairing antigen-specific responses. Accordingly, here we investigated the role of the MHC I antigen processing and presentation pathway in KL tumors.

Methods TCGA lung adenocarcinoma (LUAD) data were investigated for changes in expression of HLA molecules and chaperones involved in antigen processing and presentation. In mice, we performed single cell RNA sequencing of resected LKR13 K and KL tumors to evaluate changes in the tumor microenvironment and intrinsic differences in tumor antigen processing machinery. In vitro experiments were performed using the ovalbumin antigen to evaluate changes in antigen-specific T cell responses.

Results Expression of HLA-A ($p < 0.0001$), -B ($p < 0.0001$), -C ($p < 0.0001$), and beta2-microglobulin (B2M, $p < 0.0002$) was downregulated in KL tumors from TCGA, as were expression of the TAP1 ($p < 0.001$) and TAP2 ($p < 0.001$) transporter associated with antigen processing subunits. LKR13 KL tumors exhibited similar patterns with lower H2-k1 ($p < 0.0001$), H2-d1 ($p < 0.0001$), B2m ($p < 0.0001$), Tap1 ($p < 0.0001$) and Tap2 ($p < 0.0001$). As a result, LKR13 KL were resistant to recognition ($p < 0.005$) and killing (56.9% K versus 7.8% KL) by OT-I T cells. Decreased expression of IFN-gamma-regulated genes such as PSMB8 ($p < 0.001$), PSMB9 ($p < 0.0001$), PSMB10 ($p < 0.001$), CIITA ($p < 0.0001$), NLRC5 ($p < 0.0001$), IFNGR1 ($p < 0.0001$), and IFNGR2 ($p < 0.0001$) was also noted in KL tumors. Accordingly, KL tumors were unresponsive to exogenous IFN-gamma stimulation, maintaining repression of surface H2-Kb and resistance to T cell recognition ($p < 0.05$) and killing (12.8% K versus 4% KL). Expression of T cell chemokines and receptors CXCR3 ($p < 0.0001$), CXCL9 ($p < 0.0001$), and CXCL10 ($p < 0.0001$) was also repressed, potentially contributing to the lack of T cell infiltration in KL tumors.

Conclusions KRAS-mutant tumors harboring STK11/LKB1 alterations have an immunosuppressed phenotype and resistance to PD-1/PD-L1 inhibitors. Our findings provide evidence that these alterations are associated with markedly reduced antigen presentation and resistance to T cell killing, responsiveness to IFN-gamma stimulation, and impaired production of T cell chemokines, providing mechanistic insights into this immunosuppressed phenotype that could help guide the development of new therapeutic strategies for enhancing anti-tumor immunity.

<http://dx.doi.org/10.1136/jitc-2021-SITC2021.914>

MOLECULAR CHARACTERIZATION OF AXL IN SOLID TUMOR MALIGNANCIES USING REAL-WORLD DATA

¹Han Si*, ¹Maria Jure-Kunkel, ¹Nora Pencheva, ¹Steven Xu, ¹Brandon Higgs, ¹Kate Sasser, ¹Hisham Hamadeh, ²Phaedra Agius, ²Kristina Grigaityte. ¹Genmab Inc, Rockville, MD, USA; ²Tempus Labs, Inc, Chicago, IL, USA

Background The receptor tyrosine kinase AXL is aberrantly expressed in many cancer types and associated with epithelial-to-mesenchymal transition (EMT), poor prognosis, and therapy resistance. To better understand the expression of this gene across specific disease subtypes, correlated pathways, and how certain therapies potentially modulate AXL expression, we investigated real-world clinical and molecular data across five solid tumor types before and after chemotherapy or immune checkpoint inhibitor (CPI) therapy.

Methods Whole transcriptome and exome sequencing were derived from patient tumor specimens obtained either prior to treatment or following chemotherapy or CPI therapies. RNA reads were mapped using STAR and data was normalized using transcripts per million. DNA reads were mapped using Novoalign and variants were called using Freebayes and Pindel. Clinical data was curated from multiple sources, QC'd and deidentified according to standard protocols. Five diseases were included: non-small cell lung cancer (NSCLC, n=1181), ovarian cancer (OV, n=300), urothelial carcinoma (UC, n=140), pancreatic ductal adenocarcinoma (PDAC, n=942), and skin cutaneous melanoma (SKCM, n=157). PD-L1 positivity was defined as $\geq 1\%$ tumor cells with PD-L1 immunohistochemical staining at any intensity.

Results AXL mRNA levels were highest in PDAC followed by NSCLC, SKCM, UC and OV. Within OV, AXL expression levels were higher in tumors pre-treated with chemotherapy relative to untreated. For other tumor types, chemotherapy or CPI pre-treated tumors had AXL mRNA levels comparable to untreated tumors. Copy number amplifications of AXL were rare across all tumor types (<3%) and did not associate with mRNA expression. Distinct molecular subtypes in several cancers displayed relatively high AXL mRNA levels, including the mesenchymal subtype in OV and the stromal rich subtypes in PDAC. AXL levels also correlated with an EMT mRNA signature across all tumors ($\rho=0.67$). Further, higher AXL expression was associated with PD-L1 positivity in NSCLC, UC and PDAC ($p<0.01$), but not OV where only a few tumors were PD-L1 positive. Oncogenic KRAS mutations were associated with higher AXL expression in NSCLC and PDAC ($p<0.001$) and lower AXL expression in OV ($p=0.01$). Loss of KDM6A, known to induce tumorigenesis in PDAC, was associated with higher AXL expression in PDAC ($p<0.01$). Loss-of-function mutations in ARID1A, previously implicated as CPI sensitizing, were associated with lower AXL mRNA levels in OV tumors ($p<0.001$).

Conclusions Analyses of real-world mRNA datasets showed that AXL was upregulated in specific tumor and treatment settings as well as in patient populations with specific mutations and disease subtypes. Findings here should be validated with independent datasets.

<http://dx.doi.org/10.1136/jitc-2021-SITC2021.915>

IMMUNE LANDSCAPE AT THE INVASION FRONT OF SURGICALLY RESECTED ORAL SQUAMOUS CELL CARCINOMAS SHOWS SIGNIFICANT ASSOCIATIONS WITH DISEASE SPECIFIC SURVIVAL

¹Jebrane Bouaoud*, ²Frank Rojas Alvarez, ³Lucas Michon, ¹Nicolas Gadot, ⁴Sylvie Lantuejoul, ²Auriol Tamegnon, ²Mei Jiang, ²Shanyu Zhang, ²Pandurengan Renganayaki, ⁵Philippe Zrouba, ⁶Jean-Philippe Foy, ¹Karène Mahtouk, ⁶Chloé Bertolus, ²Edwin Roger Parra Cuentas, ¹Pierre Saintigny. ¹Cancer Research Center of Lyon, University of Lyon, France; Centre Leon Berard, Lyon, France, Lyon, France; ²MD Anderson Cancer Center, Houston, TX, USA; ³Centre Leon Berard, Lyon, France; ⁴Cancer Research Center of Lyon, University of Lyon, France; Centre Leon Berard, Lyon, France; Université Grenoble Alpes, Grenoble, France, Lyon, France; ⁵Centre Leon Berard, Lyon, France, Lyon, USA; ⁶Cancer Research Center of Lyon, University of Lyon, France; Sorbonne Université, Hôpital Pitié-Salpêtrière, Assistance Publique des Hôpitaux de Paris, Paris, France, Lyon, France

Background Oral squamous cell carcinomas (OSCC) prognosis remains poor. While AJCC TNM 8th edition has slightly improved patients' stratification with regard to prognostic, innovative approaches to are still needed. As in other tumor types, tumor immune microenvironment (TiME) might represent an opportunity to improve prognostic assessment.

Methods TiME landscape of 47 HPV-negative OSCC was analyzed using multiplex immunofluorescence (mIF). Markers for tumor cells (PanCK), tumor infiltrating lymphocytes (CD3, CD8), macrophages (CD68), inhibitory (PD-1, PD-L1, TIM3, LAG3, VISTA) or stimulatory (OX40, ICOS) immune checkpoints (ICP) were studied. Regions of interest (ROI), 5 in the tumor core and 5 at the invasion front, were subjected to cell markers identification and quantification (scoring) as well as tissue compartmentalization to divide them in tumor-epithelial and tumor-stroma compartments, respectively. A total of 20 cell phenotypes were defined based on previous work (CK+, CK+PD-L1+, CD3+, CD3+CD8+, CD3+PD-1+, CD3+CD8+PD-1+, CD3+PD-L1+, CD3+CD8+PD-L1+, CD3+PD-L1+PD-1+, CD3+CD8+PD-L1+PD-1+, CD68+, CD68+PD-L1+, CK+OX40+, CD3+VISTA+, CD3+ICOS+, CD3+LAG3+, CD3+OX-40+, CD3+TIM3+). Results were correlated with clinical features including disease-specific survival (DSS) using the Kaplan-Meier method and a multivariate Cox model. A multivariate general linear model (GLM) was built to test the specific association of each variable with a given cell density by correcting the possible confusion due to other variables.

Results Immune cells densities were significantly higher overall in the stroma. The intra-tumor stroma showed a significant enrichment of in CD3+PD-1+ T cells compared to peri-tumor stroma. None of the clinical or pathological (resection margin, tumor stage, lymph node invasion, perineural invasion) was significantly associated with DSS. In contrast, the following cell phenotypes in the tumor invasion front were strongly associated with a poor DSS, including CD3+PD-L1+ (P-value= 0.004), CD3+PD1+PD-L1+ (P-value= 0.02) and CD3+OX40+ (P-value= 0.02) T cells as well as CD3+CD8+PD-1+ (P-value= 0.048), CD3+CD8+PD-L1+ (P-value= 0.008) and CD3+CD8+PD1+PD-L1+ (P-value= 0.01) cytotoxic T cells. In the tumor core, CD68+PD-L1- macrophages (P-value= 0.06) were marginally associated with better DSS. Using a GLM, we found that tumor from smoker-drinker patients and/or with pN+, were significantly more infiltrated by PD-1- and/or PD-L1-positive immune cells. On the other hand, floor of mouth and gingiva-mandibular OSCC were significantly less infiltrated than others.

Conclusions The prognostic value of PD-1+ and/or PD-L1+ cells in the invasion front of resected OSCC was remarkable, underlying the importance of this area when studying the TiME. Incorporating TiME analysis in the invasion front may improve prognostic evaluation of patients treated for OSCC, especially in the context of immunotherapy.

Acknowledgements This study was supported by a strategic alliance between the Translational Molecular Pathology-Immunoprofiling las (TMP-IL) at the Department Translational Molecular Pathology, the University of Texas MD Anderson Cancer Center and the Université Claude Bernard Lyon, Centre de Recherche en Cancérologie de Lyon and the Department of Translational Medicine, Centre Léon Bérard, Lyon, France. The authors would acknowledge ITMO Cancer 2020, "Formation à la Recherche Fondamentale et Translationnelle en Cancérologie" (JB); CLARA 2020 "Soutien à la mobilité des jeunes chercheurs en oncologie, N° CVPPRCAN000198" (JB); Fondation de France 2020 "Aide à la mobilité international de médecins et pharmaciens, N° 00112162" (JB); Ligue contre le cancer 2021, comité de Saône-et-Loire (PS); 2017-INCa-DGOS-Inserm_12563: INCA SIRIC-LYriCAN INCa-DGOS-Inserm_12563 (PS)

Ethics Approval The study was conducted in accordance with all applicable laws, rules, and requests of French and European government authorities. Written informed consent was obtained from all patients and the study was approved by the Centre Leon Bérard institutional review board (Lyon, France). Samples were obtained from the CRB Centre Léon Bérard (n°BB-0033-00050) which is quality certified according NFS96-900 French standard and ISO 9001 for clinical trials.

Consent Written informed consent was obtained from all patients and the study was approved by the Centre Leon Bérard institutional review board (Lyon, France)

<http://dx.doi.org/10.1136/jitc-2021-SITC2021.917>

**DOXYCYCLINE REGULATABLE β -CATENIN
DEMONSTRATES INDUCIBLE IMMUNE EVASION IN A
MELANOMA GEM MODEL**

¹Alexandra Cabanov, ²Stefani Spranger, ¹Thomas Gajewski, ¹Alexandra Cabanov*,
³Elen Torres-Mejia. ¹University of Chicago, Chicago, USA; ²Koch Institute, Massachusetts
Institute of Technology, Ragon Institute, Cambridge, MA, USA; ³Koch Institute, Ragon
Institute, Cambridge, MA, USA

Background Lack of response to checkpoint blockade immunotherapy has been linked to a deficiency of immune cell infiltration within the tumor microenvironment (TME). One demonstrated mechanism sufficient for the non-T cell inflamed TME is tumor cell-intrinsic activation of the β -catenin signaling pathway. Using genetically engineered mouse models (GEMMs), tumors constitutively expressing active β -catenin lack a robust endogenous T cell infiltrate and fail to respond to immunotherapies. In support of these mouse studies, human melanoma metastases with increased active β -catenin signaling exhibit decreased numbers of tumor infiltrating Batf3-driven cDC1 and CD3+ T cells. However, whether temporal activation and inactivation of β -catenin within the same developing tumor would alter immune cell infiltration is not known.

Methods A model was created in which tamoxifen-regulated Cre-recombinase mediates BRAFV600E oncogene activation and PTEN tumor suppressor gene deletion as well as expression of a doxycycline regulatable reverse transactivator. Upon administration of doxycycline via the drinking water to these animals, a non-degradable form of nuclear β -catenin becomes expressed. Immunofluorescence assays were performed assessing the β -catenin expression status in the tumor cells as well as immune cell infiltration within the TME. Additionally, immunotherapy efficacy experiments were performed.

Results We observed that administration of doxycycline to these animals drove expression of an active form of nuclear β -catenin. Activation of nuclear β -catenin resulted in a 2-fold decrease in the overall CD3+ T cells infiltration into the TME. Moreover, this decrease in immune infiltration also resulted in loss of anti-PD-L1 + anti-CTLA-4 therapy efficacy. We next performed studies assessing the kinetics with which β -catenin levels diminish upon doxycycline removal. Switching animals to regular drinking water resulted in rapid reduction of nuclear β -catenin levels, including 50 percent reduction after two days of doxycycline removal and almost complete reduction of nuclear β -catenin after four days.

Conclusions We describe a novel mouse model in which we induce autochthonous melanoma tumors in mice along with inducible expression of a non-degradable, nuclear β -catenin modulated by doxycycline in the drinking water. Activation of β -catenin signaling in melanoma tumors resulted in reduction of immune cells in the TME as well as loss of checkpoint blockade immunotherapy efficacy. This activation can be rapidly reversed by removing doxycycline, allowing for future studies evaluating the consequences of turning off β -catenin once it has already driven a non-T cell-inflamed TME.

Acknowledgements This work was supported by the Wissler Fellowship from the University of Chicago (SS) K99/R00 (NCI; SS), and R35CA210098 (TG).

<http://dx.doi.org/10.1136/jitc-2021-SITC2021.918>

919

TEGAVIVINT REDUCES THE IMMUNOSUPPRESSIVE MACROPHAGE PHENOTYPE IN A PRECLINICAL CO-CULTURE MODEL OF THE NON-SMALL CELL LUNG CANCER TUMOR MICROENVIRONMENT

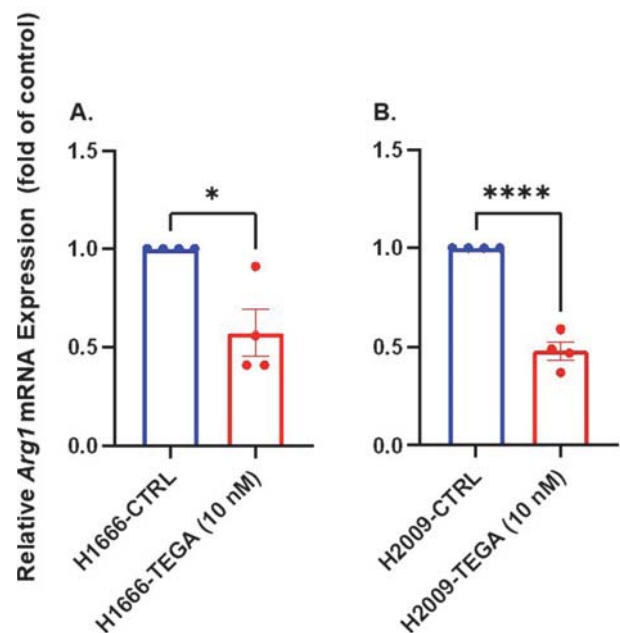
¹Raghav Chandra*, ¹Josiah Flaming, ¹Aiden Nguyen, ¹Michael Peyton, ¹Amit Das, ¹Boning Gao, ²Steven Horrigan, ¹Rolf Brekken, ¹John Minna. ¹University of Texas Southwestern Medical Center, Dallas, TX, USA; ²Iterion Therapeutics, Houston, TX, USA

Background Activation of the Wnt/ β -catenin pathway in non-small cell lung cancer (NSCLC) is associated with tumor growth and metastasis. Activation of this pathway in tumor cells may also modulate the immune tumor microenvironment (TME) by polarizing macrophages into an immunosuppressive M2-like phenotype. We tested whether treatment of co-cultures of human NSCLC cells, cancer-associated fibroblasts (CAFs) and macrophages with Tegavivint (Iterion Therapeutics), a novel compound that targets TBL1 to inhibit β -catenin function that is in early-phase clinical trials, altered the phenotype of mouse macrophages in vitro.

Methods Our prior work testing a large panel of patient-derived NSCLC lines in co-cultures of CAFs and mouse bone marrow-derived macrophages (BMDMs) demonstrated that individual NSCLC lines reproducibly generated several macrophage phenotypes, one of which was immunosuppressive (high expression of Arginase-1). We prepared co-cultures of NSCLC cells (H1666 and H2009) (70%), human CAFs (25%) and mouse BMDMs (5%) and demonstrated conversion to the macrophage high Arginase-1 immunosuppressive phenotype by monitoring quantitative expression of mouse genes with qRT-PCR. Expression of β -catenin protein relative to GAPDH by Western blot was determined before and after treatment with Tegavivint (10 and 20 nM). Co-cultures were treated with Tegavivint (10 nM) for 48 and 72 hours and qRT-PCR for mouse macrophage-specific genes reflecting an immunosuppressive M2-like or an inflammatory, immunostimulatory M1-like phenotype (Arginase-1 and iNos, respectively) was performed. Positive controls consisted of stimulation of macrophages with IL-4 and LPS (to generate M2-like and M1-like phenotypes, respectively). Cytotoxicity assays (MTS and crystal violet) to determine the IC₅₀ of Tegavivint were performed on NSCLC and macrophage cells.

Results Tegavivint IC₅₀ values for NSCLCs were 17–40 nM. At 10 nM, Tegavivint had no cytotoxic effect on macrophages. Treatment with Tegavivint decreased NSCLC expression of β -catenin by ~30–40%. When co-cultures of NSCLCs, human CAFs, and mouse BMDMs were treated with 10 nM Tegavivint, we found that macrophage expression of Arginase-1 was significantly inhibited at 48 and 72 hours of treatment (figure 1).

Conclusions Tegavivint, at pharmacologically achievable doses and concentrations that have little or no cytotoxic effect on NSCLCs or macrophages, decreases tumor cell β -catenin expression, and reduces the immunosuppressive macrophage phenotype (reduced macrophage Arginase-1 expression) induced by co-cultures of patient-derived NSCLCs and CAFs. These preclinical data set the stage for future clinical translation of Tegavivint as a NSCLC therapeutic in combination with immunotherapy approaches.



Abstract 919 Figure 1

Tegavivint reduces Arginase-1 mRNA expression from macrophages co-cultured with CAFs and H1666 (A) and H2009 (B) patient-derived NSCLC cell lines after 72-hour treatment. *: $p < 0.05$, ****: $p < 0.0001$.

Acknowledgements Supported by P50 CA070907 and Physician-Scientist Institutional Award from the Burroughs Wellcome Fund (TARDIS Fellowship)

<http://dx.doi.org/10.1136/jitc-2021-SITC2021.919>

920

A SINGLE-CELL SPATIALLY RESOLVED MERFISH MAP OF THE COLORECTAL TUMOR IMMUNE MICROENVIRONMENT

¹Colles Price*, ²Jonathan Chen, ³Karin Pelka, ⁴Sherry Chao, ¹Jiang He, ⁵Genevieve Boland, ¹George Emanuel, ⁶Nir Hacohen. ¹Vizgen, Cambridge, MA, United States; ²MGH, Cambridge, MA, United States; ³Broad Institute, Cambridge, MA, United States; ⁴Harvard University, Cambridge, MA, United States; ⁵Harvard Medical School, MGH, Cambridge, MA, United States; ⁶MGH, Harvard Medical School, Cambridge, MA, United States

Background Understanding the tumor microenvironment (TIME) requires more than just a catalog of cell types and gene programs. It is critical to see the spatial organization of the cells and where they form multicellular interaction networks. Here we present a single-cell spatially resolved transcriptomic analysis of human mismatch repair deficient (MMRd) and proficient (MMRp) colorectal cancer (CRC) specimens. High tumor mutational burden MMRd tumors are known to have an immune response characterized by higher cytolytic T cell infiltrates compared to MMRp tumors, making them an ideal system for spatial single-cell profiling and understanding how the immune-driven programs differ between these tumors.

Methods MERFISH is a massively multiplexed single molecule imaging technology which can simultaneously capture and measure the quantity and distribution of hundreds to thousands of RNA species within single cells across a tissue.¹ We designed a MERFISH library of over 450 genes including genes important to proliferation, apoptosis, immune signaling, immune cell type pathways and other critical pathways in CRC. Patient samples were obtained commercially or through Massachusetts General Hospital. Samples were hybridized with the designed MERFISH library and stained with a cell boundary marker to delineate cells across the tissue. We performed unsupervised clustering to identify cell types and we explored calculated spatial statistics to characterize how the cell type distribution varied between MMRd and MMRp tumors. We identified the cellular composition of each tumor, including immune and stromal cells, and the spatial distribution of these cell types.

Results Using MERFISH, we were able to readily identify all cell types and states previously discovered by single-cell RNA sequencing² in intact patient specimens, thus providing an accurate map of the cellular composition and spatial organization of these cells in the tumor microenvironment. Of note, previously predicted multicellular interaction networks² appeared as spatially organized structures in the tissue and were distinct in MMRd versus MMRp tumor specimens. Our data provide a richness of concrete hypotheses about which cells are working together and how these cells function cooperatively, which will be critical in advancing immunotherapy in these immunologically distinct types of colorectal cancer.

Conclusions Here we present a single-cell resolved spatial map of the cell types and states in the tumor microenvironment of MMRd and MMRp cancer. This will aid the development of future immunotherapies for CRC patients.

REFERENCES

1. Chen KH, Boettiger AN, Moffitt JR, Wang S, Zhuang X. RNA imaging. Spatially resolved, highly multiplexed RNA profiling in single cells. *Science* 2015;**348**:AAA6090.
2. Pelka K, Hofree M, Chen J, Sarkizova S, Pirl JD, Jorgji V, et al. Multicellular immune hubs and their organization in MMRd and MMRp colorectal cancer. *BioRxiv* 2021;426796.

Ethics Approval All samples not commercially purchased were collected in accordance with IRB protocol DF/HCC IRB 02-240.

<http://dx.doi.org/10.1136/jitc-2021-SITC2021.920>

921

COMPARISON OF PI3K/AKT/MTOR PATHWAY PROFILES AMONGST THREE IMMUNE PHENOTYPES CLASSIFIED BY ARTIFICIAL INTELLIGENCE-POWERED H&E ANALYZER IN NON-SMALL CELL LUNG CANCER

¹Hyung-Gyo Cho*, ²Grace Lee, ¹Hye Sung Kim, ³Sanghoon Song, ³Kyunghyun Paeng, ³Chan-Young Ock, ¹Young Kwang Chae. ¹Northwestern University, Feinberg School of Medicine, Chicago, IL, USA; ²Northwestern University, Chicago, IL, USA; ³Lunit Inc., Seoul, Korea, Republic of

Background The phosphatidylinositol 3-kinase (PI3K)/Akt/mechanistic target of rapamycin (mTOR) pathway plays a significant role in both tumorigenesis and progression of disease in non-small cell lung cancer (NSCLC).¹ Increased activation of the pathway, whether in tumor or immune cells, results in an immunosuppressive tumor microenvironment.² Therefore, we looked into how this pathway differs in three distinct NSCLC immune phenotypes.

Methods Lunit SCOPE IO (Lunit, Seoul, Republic of Korea), a deep learning-based hematoxylin and eosin (H&E) image analytics tool, identifies lymphocytes and quantifies lymphocyte density within the cancer epithelium (CE-Lym), stroma (CS-Lym), and combined area (C-Lym). We applied Lunit-SCOPE IO to H&E-stained tissue images of 965 NSCLC samples from The Cancer Genome Atlas (TCGA). Tumors in the lowest tertile of C-Lym were labeled as *immune-desert*, and the remaining tumors were classified as *inflamed* and *immune-excluded* according to the median of the ratio of CE-Lym to CS-Lym. Utilizing RNA-sequencing data from TCGA, gene set enrichment analysis (GSEA) was conducted to analyze the differences in mTORC1 and PI3K/Akt/mTOR signaling between the subtypes.³ We obtained mutational data related to the PI3K/Akt/mTOR pathway from cBioPortal to compare the ratio of functional mutations between the immune phenotypes.⁴

Results The mTORC1 signaling gene set was consistently enriched in *immune-excluded*, whether compared to *inflamed* ($p_{adj} < 0.01$, normalized enrichment score [NES]: 2.3) or *immune-desert* ($p_{adj} < 0.01$, NES: 1.6). However, PI3K/Akt/mTOR signaling gene set enrichment did not show statistically significant differences between the immune phenotypes. Within the three immune phenotypes, we analyzed three functional mutations: *PIK3CA*, *PTEN*, and *Akt1* (figure 1). Of the total 112 samples showing the functional mutations of the PI3K/Akt/mTOR pathway, 53 were *immune-excluded*, 31 *inflamed*, and 28 *immune-desert*. The relation between mutation frequency and the immune subtypes was significant ($X^2(2) = 11.1979$, $p < .01$). The *immune-excluded* was more likely than the other subtypes to have functional PI3K/Akt/mTOR mutations.

	Inflamed	Excluded	Desert
PIK3CA	17 / 64 (26.6%)	33 / 64 (51.6%)	14 / 64 (21.9%)
PTEN	13 / 49 (26.5%)	21 / 49 (42.9%)	15 / 49 (30.6%)
AKT1	2 / 3 (66.7%)	0 / 3 (0%)	1 / 3 (33.3%)
3-immune phenotype	31 / 112 (27.7%)	53 / 112 (47.3%)	28 / 112 (25.0%)

Abstract 921 Figure 1 The landscape of functional mutation and immune phenotypes regarding PI3K/Akt/mTOR pathway

Conclusions The three tissue phenomic subtypes showed different PI3K/Akt/mTOR pathway profiles, with *immune-excluded* having the most mutation samples and the greatest

enhancement of mTORC1 signaling gene set. Likewise, tissue H&E based tumor microenvironment classification by Lunit SCOPE IO can be applied to other hallmark pathways and tumor types, and such further investigation of the tumor microenvironment can provide insights into novel therapeutic avenues.

REFERENCES

1. Tan AC. Targeting the PI3K/Akt/mTOR pathway in non-small cell lung cancer (NSCLC). *Thorac Cancer* 2020;**11**(3):511–8.
2. O'Donnell JS, Massi D, Teng MWL, Mandala M. PI3K-AKT-mTOR inhibition in cancer immunotherapy, redux. *Semin Cancer Biol* 2018;**48**:91–103.
3. Liberzon A, Birger C, Thorvaldsdóttir H, Ghandi M, Mesirov JP, Tamayo P. The molecular signatures database hallmark gene set collection. *Cell Systems* 2015;**1**(6):417–25.
4. Cerami E, Gao J, Dogrusoz U, Gross BE, Sumer SO, Aksoy BA, et al. The cBio cancer genomics portal: an open platform for exploring multidimensional cancer genomics data. *Cancer Discov* 2012;**2**(5):401–4.

<http://dx.doi.org/10.1136/jitc-2021-SITC2021.921>

922

A NOVEL AUTOTAXIN INHIBITOR, IOA-289, MODULATES TUMOR, IMMUNE AND STROMAL CELL FUNCTION AND HAS MONOTHERAPY ACTIVITY IN FIBROTIC CANCER MODELS

<http://dx.doi.org/10.1136/jitc-2021-SITC2021.922>

¹Marcel Deken, ¹Karolina Niewola, ²Elisa Matas-Rico, ³Ragini Medhi, ³Alan Carruthers, ³Anne Cheasty, ⁴Olivier Peyruchaud, ³Amy Fraser, ³Pritom Shah, ⁵Wouter Moolenaar, ¹Lars van der Veen, ¹Michael Lahn, ¹Zoe Johnson*. ¹IONCTURA SA, Genève, Switzerland; ²Málaga University, Málaga, Spain; ³CRUK-TDL, Cambridge, UK; ⁴INSERM U1033, Lyon, France; ⁵NKI, Amsterdam, UK

Background Autotaxin (ATX) is a secreted glycoprotein that hydrolyzes lysophosphatidylcholine (LPC) to lysophosphatidic acid (LPA). The expression of both ATX and LPA is elevated in most solid tumors and plasma. LPA signaling directly modulates tumor cell function and contributes to the development of the fibrotic tumor microenvironment, a mechanism by which tumors evade host immunity and impairs response to therapy. IOA-289 is a potent, orally available autotaxin inhibitor which is being developed as a novel treatment of solid tumours burdened with a high degree of fibrosis.

Methods Inhibition of ATX activity in human plasma was determined by measuring reduction in LPA species as quantified by LC-MS/MS. In vitro activity on biomarkers of fibrosis was assessed using the BioMAP screen and fibroblast cell cultures. T cell migration was measured using 48-well chemotaxis chambers. PK/PD studies were performed following a single oral dose of IOA-289 in mice, and plasma LPA was used as a PD biomarker. In vivo efficacy was studied in two models of breast cancer, 4T1 and E0771. Bioinformatics used TCGA and GTEX publicly available datasets.

Results IOA-289 inhibits plasma LPA18:2 with an IC₅₀ of 36nM, with similar results for other LPA species. IOA-289 inhibited fibrosis relevant factors in the BioMAP phenotypic screen, including sIL-6, MCP-1, αSMA, collagen-III, and sVEGF. In further studies, IOA-289 inhibited the secretion of PAI-1 and IL-6 by stimulated fibroblasts. LPA and cancer cell conditioned media inhibited T cell chemotaxis in vitro and the effect was overcome in the presence of IOA-289. The efficacious human dose of IOA-289 was determined following PK/PD studies using plasma LPA as a biomarker of response to ATX inhibition. In vivo studies showed that IOA-289 inhibited metastasis of 4T1 cells, enhanced the infiltration of T cells into 4T1 s.c. implanted tumors and prevented the growth of primary, orthotopically implanted E0771 tumors. Bioinformatics analysis demonstrated elevated ATX expression in pancreatic cancer (PDAC), and PDAC patient plasma showed a correlation of ATX levels with CA-19-9.

Conclusions The ATX/LPA pathway represents a novel target for anti-cancer therapy with actions on the tumor, immune cell and stromal environment. IOA-289 is a highly potent and selective inhibitor of ATX with demonstrated monotherapy activity in cancer models. Based on the mechanism of action we are investigating combinations of IOA-289 with chemotherapy, immunotherapy and novel agents in ongoing preclinical studies. An acceptable safety and PK profile support the clinical development of IOA-289 which is currently in a phase I clinical trial.

Ethics Approval The 4T1 study was approved by The University Claude Bernard Lyon 1 Ethics Board; approval number DR2014-38 (vM). The E0771 study was reviewed and approved by the Institutional Animal Care and Use Committee of the contract research organization (Covance, Ann Arbor, MI, USA), an AAALAC International accredited program.

923

HEDGEHOG SIGNALING DRIVES EPITHELIAL-TO-MESENCHYMAL TRANSITION, IMMUNE EVASION, AND ANTI-PD-1 RESISTANCE THROUGH COORDINATED UPREGULATION OF WNT LIGANDS AND PGE2 SYNTHESIS

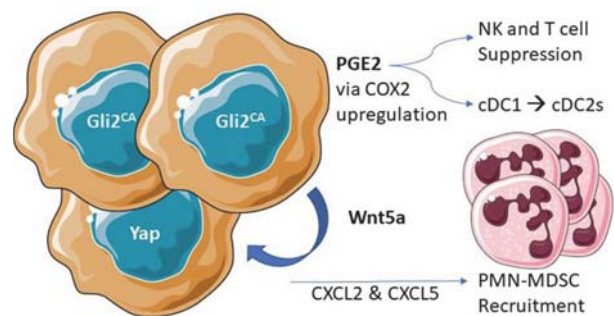
¹Nicholas DeVito*, ²Michael Sturdivant, ¹Balamayooran Theivanthiran, ¹Y-Van Nguyen, ¹Michael Plebanek, ¹Brent Hanks. ¹Duke University Medical Center, Durham, NC, USA; ²University of North Carolina, Chapel Hill, NC, USA

Background Immunotherapy resistance has been correlated with epithelial-to-mesenchymal transition (EMT),^{1, 2} however our understanding of tumor-intrinsic mechanisms driving this immune evasive phenotype is lacking. We have previously shown that Wnt ligands are upregulated in anti-PD-1 resistant melanomas,³ and postulated that upstream transcriptional regulation of select EMT pathways may underpin these findings. The hedgehog signaling (HH) transcription factor Gli2 promotes EMT.

Methods Gli2 was constitutively activated (Gli2^{CA}) in a BRAF^{V600E}PTEN^{-/-} murine cell line via an N-terminal truncating mutation and silenced using CRISPR-Cas9. Multi-parameter flow cytometry and RNAseq was utilized to evaluate the impact of Gli2 on the tumor immune microenvironment. Anti-PD-1 resistance studies were performed in Gli2^{CA} and control tumors. Bioinformatics studies were conducted using the melanoma TCGA and Hugo et al databases.²

Results We found upregulation of Gli2 targets in patients with anti-PD-1-refractory metastatic melanoma as well as in an autochthonous BRAF^{V600E}PTEN^{-/-} melanoma model after escape from anti-PD-1. RNAseq and Western blot studies demonstrated Gli2^{CA} to promote EMT and Wnt ligand production in addition to upregulated COX2 in BRAF^{V600E}PTEN^{-/-} melanoma. This finding was reversed by genetic ablation and pharmacologic inhibition of Gli2, implicating a previously undescribed role for Gli2 in modulating COX2. These data were consistent with a notable correlation between a Gli2 signature and a prostaglandin synthesis signature in human melanoma TCGA database. Flow cytometry analysis showed exclusion of cytolytic T and NK cells, a shift from cDC1s to cDC2s, and enhanced MDSC recruitment in Gli2^{CA} tumors. Consistent with these findings, whole tumor RNAseq of Gli2^{CA} tumors demonstrated a decrease in *Cd3e*, *Prf1*, and *Xcr1* with a concomitant increase in *Cxcl1*, *Cxcl2*, *Ccl2*, *Ptgs2*, and *Arg1* relative to control tumors. RNAseq of FACS-sorted DCs from Gli2^{CA} tumors demonstrated a loss of cDC1-associated genes including *Xcr1*, *Wdfy4*, and *Clec9a* compared to DCs derived from control tumors. In-line with our previous results showing that Wnt5a promotes MDSC recruitment in a Yap-dependent manner,⁴ we found that Yap inhibition or Wnt5a deletion in the BRAF^{V600E}PTEN^{-/-}Gli2^{CA} cell line diminished MDSC-recruiting chemokines. Further consistent with these findings, Gli2^{CA} tumors resist anti-PD-1 antibody therapy.

Conclusions Our data demonstrates that the HH transcription factor Gli2 drives the development of a tolerogenic tumor microenvironment unfavorable to anti-PD-1 immunotherapy by coordinating the upregulation of Wnt ligand expression and prostaglandin synthesis (figure 1). We propose that HH gene signatures are worthy of further study as a guide for selecting Wnt ligand and prostaglandin inhibitors in future immunotherapy studies.



Abstract 923 Figure 1 Gli2 in tumors promotes Wnt and prostaglandin signaling, generating an immunosuppressive microenvironment

Acknowledgements The authors would like to acknowledge the Duke Cancer Institute Flow Cytometry Core.

REFERENCES

1. Bagaev A, et al. Conserved pan-cancer microenvironment subtypes predict response to immunotherapy. *Cancer Cell* 2021.
2. Hugo W, et al. Genomic and transcriptomic features of response to anti-PD-1 therapy in metastatic melanoma. *Cell* 2016;**165**(1):35–44.
3. DeVito NC, et al. Pharmacological Wnt ligand inhibition overcomes key tumor-mediated resistance pathways to anti-PD-1 immunotherapy. *Cell Rep* 2021;**35**(5):109071.
4. Theivanthiran B, et al. A tumor-intrinsic PD-L1/NLRP3 inflammasome signaling pathway drives resistance to anti-PD-1 immunotherapy. *J Clin Invest* 2020;**130**(5):2570–2586.

<http://dx.doi.org/10.1136/jitc-2021-SITC2021.923>

THE SPATIAL HIERARCHY OF PRIMARY AND RECURRENT MEDULLOBLASTOMA TUMOR ECOSYSTEMS

¹Laura Donovan, ²Bei Hopkins, ¹Ben Draper, ¹Rivani Shah, ²Kristin Roman, ²Bethany Remeniuk*. ¹UCL, London, UK; ²Akoya Biosciences, Marlborough, MA, USA

Background Medulloblastoma recurrence occurs in approximately 30% of patients and is universally fatal, presenting one of the most significant unmet clinical challenges in pediatric oncology. It is now clear that medulloblastomas are complex ecosystems, evolving under selective pressure from their micro-environment and cell of origin. Different tumor-immune cell interactions, including, but not limited to, tumor-infiltrating lymphocytes and various tumor suppressive myeloid cell populations, significantly hamper effective treatment strategies for primary, metastatic, and recurrent tumors. Recurrent medulloblastomas are rarely biopsied making biological material for interrogation scarce. Research has assumed that recurrent and primary medulloblastoma tumors have similar biological composition and therefore will respond to the same therapeutic regimens, however, therapies designed using primary biopsies, but tested in Phase I/II trials on children with recurrent disease, have been largely unsuccessful. We hypothesize that there are select immunosuppressive population differences within primary vs. recurrent tumor microenvironments (TME) that need to be elucidated in order to improve treatment modalities and outcomes in pediatric patients.

Methods Using Akoya's MOTiFTM PD-1/PD-L1 Panel: Auto Melanoma Kit, the staining protocol was adapted for optimal staining performance on human brain tissue. Following this, 24-formalin-fixed, paraffin embedded pediatric medulloblastoma samples (primary and recurrent biopsies from 12 patients) were stained for the following markers on the Leica BOND RX. Multispectral images were acquired using the Vectra Polaris, and five regions of interest selected on each image. An analysis algorithm was developed using inForm tissue analysis software, and samples were batch processed and data exported. Cell counts, densities, and spatial parameters were generated using the R-script package phenoptrReports to produce outputs of the image analysis data.

Results Following spectral unmixing and autofluorescence isolation, no signal crosstalk was observed. The average signal intensity counts for all markers was found to be within the recommended ranges of 10–30, with a coefficient of variation of $\leq 15\%$, indicating successful and consistent staining of the medulloblastoma samples. Comparison between primary vs. recurrent tissues revealed distinctive spatial differences between immune-tumor cell interactions.

Conclusions We have demonstrated successful adaptation of the MOTiF PD-1/PD-L1 Melanoma panel kit in conjunction with the Phenoptics workflow to support examination of the TME in patient-matched primary and recurrent pediatric medulloblastoma tumor biopsies. Our study provides the first insight into distinctive spatial interactions between primary vs. recurrent tissues, which may improve strategies to comprehend cancer progression, immune surveillance, and ultimately the development of rational, targeted therapeutics based on the differences between the tumor compartments and their immune-microenvironment.

Ethics Approval Ethical approval obtained by Brain UK, ref: 20/008. All participants gave consent to use of their material.

<http://dx.doi.org/10.1136/jitc-2021-SITC2021.924>

925

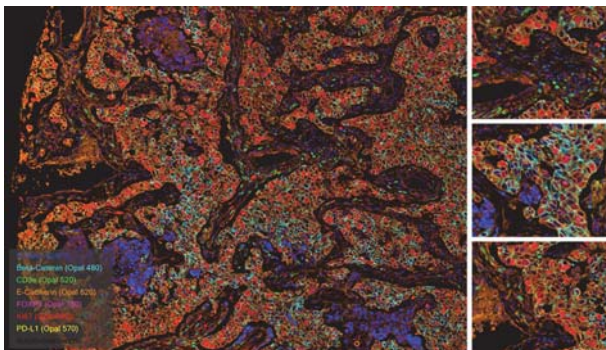
UTILIZING MULTIPLEX IMMUNOFLOUORESCENCE TO EXPLORE THE EPITHELIAL-MESENCHYMAL TRANSITION IN BREAST, OVARIAN CANCERS

Danielle Fails*, Michael Spencer. *Fortis Life Sciences, Montgomery, TX, USA*

Background Epithelial-mesenchymal transition (EMT) is instrumental during embryonic development—assisting in extensive movement and differentiation of cells. However, during metastasis and tumorigenesis, this process is hijacked. The disruption of this developmental process, and subsequent acquisition of a mesenchymal phenotype, has been shown to increase therapeutic resistance and often leads to poor prognosis in breast cancer.¹ Using bioinformatic resources and current clinical data, we designed a panel of biomarkers of value to specifically observe this epithelial/mesenchymal transition.

Methods Human breast cancer FFPE tissue samples were stained with Bethyl Laboratories IHC-validated primary antibodies, followed by Bethyl HRP-conjugated secondary antibodies, and detected using Akoya Opal™ Polaris 7-color IHC kit fluorophores (Akoya Biosciences [NEL861001KT]). The panel consisted of beta-Catenin, E-Cadherin, Ki67, CD3e, PD-L1, and FOXP3. Antibody staining order was optimized using tissue microarray serial sections, three slides per target, and stained in either the first, third, or sixth position via heat-induced epitope retrieval (HIER) methods. Exposure time was maintained for all three slides/target and cell counts, signal intensity, background, and autofluorescence were analyzed. The final optimized order was then tested on the breast cancer microarray in seven-color mIF. Whole slide scans were generated using the Vectra Polaris® and analyses performed using InForm® and R® Studio.

Results Two integral EMT targets, E-Cadherin and beta-Catenin, were used to observe a key occurrence in this transition. Under tumorigenic circumstances, when released from the complex they form together (E-cadherin-B-catenin complex), Beta-catenin can induce EMT. This disjunction/activation of EMT can be seen in the invasive ductal carcinoma below (figure 1). The disorganized E-cadherin cells are in direct contrast to normal, non-cancerous cells in similar tissue. Total CD3e cell counts were down (2%), with 35% cells restricted to the stroma vs. the 1% seen intra-tumorally. Coupled with the elevated presence of Ki67 (10%), a level of rapid cancer growth and potential metastasis (Invasive Ductal Carcinoma Grade II) can be observed.



Abstract 925 Figure 1 Invasive ductal carcinoma, grade II stained with a 6-plex mIF panel designed to show the epithelial-mesenchymal transition

Conclusions The presence of EMT in breast cancers is often indicative of a poor prognosis, so the need for reliable markers is imperative. E-Cadherin and beta-Catenin are both up-and-coming clinical targets that can serve to outline this transition within the tumor microenvironment. By utilizing these markers in mIF, closer spatial examination of proteins of interest can be achieved. The application of this mIF panel has the potential to provide invaluable insights into how tumor infiltrating lymphocytes behave in cancers exhibiting the hallmarks of EMT.

Acknowledgements We would like to acknowledge Clemens Deurrschmid, PhD, Technical Applications Scientist Southeast/South Central, Akoya Biosciences for his assistance with image analysis.

REFERENCES

1. Horne HN, Oh H, Sherman ME, *et al.* E-cadherin breast tumor expression, risk factors and survival: pooled analysis of 5,933 cases from 12 studies in the breast cancer association consortium. *Sci Rep* 2018;**8**:6574.

<http://dx.doi.org/10.1136/jitc-2021-SITC2021.925>

926

IMMUNE PROFILING OF KEAP1-DEFICIENT NSCLC: DEVELOPMENT OF THERAPEUTIC STRATEGIES TO OVERCOME RESISTANCE TO IMMUNOTHERAPY

Ana Galan-Cobo*, Yu Qian, Fuduan Peng, Daniel McGrail, Fahao Zhang, Xiang Zhang, Edwin Parra, Minghao Dang, Saxon Rodriguez, Alexandre Reuben, Ignacio Wistuba, Ferdinandos Skoulidis, Linghua Wang, John Heymach. *UT MD Anderson Cancer Center, Houston, TX, USA*

Background In LUAD, KEAP1 is the third most common tumor suppressor and loss-of-function mutations in KEAP1 commonly co-occur with STK11/LKB1 and KRAS mutations. KEAP1 protein that regulates the degradation of the antioxidant transcription factor NRF2. The role of STK11/LKB1 mutations in immunotherapy resistance has been characterized, however the mechanistic understanding of KEAP1 deficiency in shaping LUAD phenotype and therapy response is still very limited. Recent clinical data has been reported suggesting that mutations in STK11/LKB1 and KEAP1 are strongly associated with immune checkpoint blockade resistance in LUAD, particularly those with KRAS mutations. Nevertheless, the biology of KEAP1-deficient tumors and the immune suppression mechanisms are to be characterized.

Methods We have first validated response to anti-PD1 treatment in vivo using subcutaneous murine models, and performed a deep profiling and characterization of tumor microenvironment (TME) heterogeneity of KRAS-mutant (K) and LKB1 (KL), and/or KEAP1 deficient (KK and KLK) tumors using single-cell RNA sequencing (scRNA-seq) and multiplex staining. Data from pre-clinical models has been used to survey the immune genomic data available from the MD Anderson ICON study (a cohort of early stage lung cancer untreated 148 resected tumors) and TCGA lung cohorts to further validate our findings.

Results While K tumors showed significant response to anti-PD1 treatment, KEAP1 loss completely impaired therapeutic response to this immunotherapy. KEAP1-deficient tumors were characterized by low immune infiltration while displayed an enrichment of cancer associated fibroblasts (CAFs) and endothelial cells. scRNA-seq data indicated a significant reduction of T cell infiltration, in particularly, CD8 and NK T cells, pronounced decreased of B cell population and a marked M2 macrophages polarization. Likewise, IHC and multiplex analysis of CD3 and F4/80 markers confirmed these previous findings. In TCGA lung cancer cohort, CD8B expression was dramatically decreased while MIF (macrophage migration inhibitory factor) was upregulated in KK compared to K LUADs tumors, and expression of KEAP1 inversely correlated with CD163, ARG2 and IL10, which are mainly secreted by macrophages. Concordantly, KEAP1-deficient pre-clinical tumors showed a significant upregulation of MIF expression and secretion, and CRISPR-Cas9 deletion of MIF dramatically impaired in vivo tumor growth in KK and KLK but not in K or KL models.

Conclusions These findings indicate that loss of KEAP1, alone or in combination with STK11/LKB1 alterations, unfavorably reprograms TME. These changes appear to be mediated at least in part through MIF upregulation, providing a potential therapeutic strategy for overcoming KEAP1-dependent resistance to immunotherapy.

<http://dx.doi.org/10.1136/jitc-2021-SITC2021.926>

WILMS TUMOR REVEALS DNA REPAIR GENE HYPER-EXPRESSION IS LINKED TO LACK OF IMMUNE INFILTRATION

¹Emily Higgs*, ²Riyue Bao, ¹Ken Hatogai, ¹Thomas Gajewski. ¹University of Chicago, Chicago, IL, USA; ²University of Pittsburgh, Pittsburgh, PA, USA

Background A T cell-rich tumor microenvironment has been associated with improved clinical outcome and response to immune checkpoint blockade therapies in several adult cancers. Understanding the mechanisms for lack of immune cell infiltration is critical for expanding immunotherapy efficacy in the clinic. To gain new insights into the mechanisms of poor tumor immunogenicity, we turned to pediatric cancers, which are generally unresponsive to checkpoint blockade.

Methods RNAseq and clinical data were obtained for Wilms tumor, rhabdoid tumor, osteosarcoma, and neuroblastoma from the Therapeutically Applicable Research to Generate Effective Treatments (TARGET) database, and adult cancers from TCGA. Using an 18-gene tumor inflammation signature (TIS) representing activated CD8+ T cells, we identified genes significantly anti-correlated with the signature. Immunofluorescence was performed on metastatic melanoma samples for CD8, MSH2, and the tumor cell marker SOX10, and analyzed for relationship to anti-PD-1 efficacy.

Results Among the four pediatric cancers, we observed the lowest TIS scores in Wilms tumor. Wilms tumors demonstrated significantly lower T cell inflammation signatures than matched normal kidney samples, other pediatric tumor samples, and adult kidney tumor samples. Pathway analysis identified multiple types of DNA repair were upregulated in Wilms tumor and a score generated from the top 50 DNA repair genes strongly anti-correlated with TIS. This striking negative association was also observed in most adult tumor types. The anti-correlation was found to be independent of tumor mutation burden, suggesting that high expression of DNA repair pathway machinery may restrict tumor immunogenicity by mechanisms beyond prevention neoantigen accumulation. MSH2 was one of the top DNA repair genes identified from the Wilms tumor analysis and was confirmed to have a strong anti-correlation with TIS in melanoma samples from TCGA. Immunofluorescence from an independent cohort of metastatic melanoma patients revealed a significant negative correlation between CD8+ T cell numbers and MSH2+ SOX10+ tumor cell numbers. Additionally, non-responders to anti-PD-1 immunotherapy had significantly higher numbers of MSH2+ SOX10+ tumor cells than responders.

Conclusions Increased tumor expression of DNA repair genes is associated with a less robust immune response in Wilms tumor, and this was also observed in the majority of TCGA tumor types. Surprisingly, the negative relationship between DNA repair score and TIS remained strong across TCGA when correcting for mutation count, indicating a potential role for DNA repair genes outside of preventing the accumulation of mutations. Strategies targeting DNA repair pathways could be considered as new therapeutic interventions to transform non-T cell-inflamed tumors into immune-responsive tumors.

Ethics Approval The study obtained ethics approval under IRB protocol 15-0837.

<http://dx.doi.org/10.1136/jitc-2021-SITC2021.927>

928

A TRANSLATIONAL APPROACH TO CATALOG PANCREATIC CANCER HETEROGENEITY USING SPATIAL GENOMICS IN LARGE PATIENT COHORTS FOR TARGET VALIDATION AND RATIONAL COMBINATION SELECTION

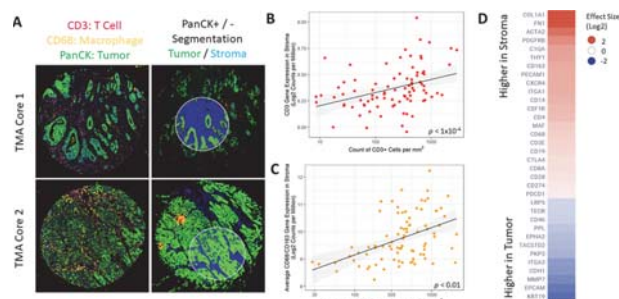
Omar Jabado*, Li Fan, Patricia Coutinho de Souza, Angelo Harris, Arturo Chaparro, Mohammed Qutaish, Han Si, Jan-Hermen Dannenberg, Kate Sasser, Suzana Couto, Mark Fereshteh. *Genmab, Princeton, NJ, USA*

Background Pancreatic ductal adenocarcinoma (PDAC) is an aggressive cancer with short overall survival; the standard of care (SoC) is chemotherapy. Immunotherapies in development aim to remodel the stroma by depleting immunosuppressive cell types or using T-cell redirection to kill tumor cells. To date, none of these methods have improved overall survival beyond SoC. Next generation immunotherapies that employ histopathology and molecular subtyping¹ for target and patient selection may succeed. Here we leverage a spatial transcriptomics platform (Nanostring Digital Spatial Profiling, DSP) to reveal molecular signaling in tumoral and stromal cells in 57 PDAC patients using tumor microarrays (TMAs). This approach is rapid and clinically relevant as molecular and histology data can be easily bridged.

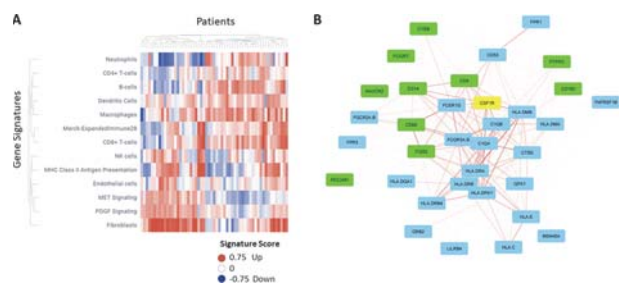
Methods TMAs generated from surgical resection tissue were commercially sourced. DSP was performed using the CTA RNA panel (1,800 target genes) using PanCK fluorescence for tumor/stroma segmentation. In parallel, slides were chromogenically stained for T-cells (CD3) and macrophages (CD68/CD163). Differential gene expression, gene signature and gene co-expression network analysis was performed using linear models in R.^{2,3}

Results Differential gene expression analysis and correlation to IHC confirmed the DSP platform successfully profiled tumor and stromal compartments (figure 1). Immune cell signatures⁴ and pathway analysis revealed a heterogeneous stromal environment. Using a fibroblast gene signature derived from single-cell RNAseq⁵ we found fibroblast density was positively correlated to PDGFR signaling and MHC-II expression but negatively correlated to B, CD4+ T and neutrophil cell levels (figure 2a). This finding supports the idea that atypical antigen presentation in cancer associated fibroblasts (CAFs) may be exploitable for immunotherapies.⁶ We constructed a co-expression network from in-situ stromal gene expression and used it to identify receptors coordinately expressed with the immunosuppressive macrophage marker CSF1R as a bispecific antibody partner (figure 2b).⁷ Classical macrophage markers were identified but also receptors with lesser-known functions in macrophages (TIM3/HAVCR2, FPR3, MS4A6A, LILRB4). Surveying target pairs in this method allows rapid, patient-specific confirmation in serial TMA sections with singleplex IHC or RNAscope.

Conclusions In this study we were able to recapitulate known PDAC biology using very small samples of primary tumors. The combination of TMAs and DSP enables a rapid validation of targets and hypothesis generation for bispecific pairings. Further analysis of untreated (n=14) and post-adjuvant chemotherapy (n=26) patients using RNA DSP, IHC and bulk RNA-seq is under way. Results from this cohort will enable an integrated histopathology and molecular approach to developing next-generation immunotherapies.



Abstract 928 Figure 1 Segmentation strategy and validation of DSP (A) PanCK, CD68 and CD3 staining from two representative tumor cores; (B, C) correlation of gene transcripts in stroma to cell counts from chromogenic staining; (D) heatmap of selected genes differentially expressed in tumor and stroma (n=57 patients).



Abstract 928 Figure 2 Exploration of the stromal compartment in PDAC TMAs. (A) Heatmap of selected cell type and gene signatures from gene expression in the stroma, color represents single sample enrichment score using GSVA method; (B) a gene co-expression subnetwork in the stroma centered on CSF1R, edge thickness represents strength of correlation, green nodes have evidence for cell surface expression based on proteomic profiling.⁷

REFERENCES

- Collisson EA, Bailey P, Chang DK, Biankin AV. Molecular subtypes of pancreatic cancer. *Nat Rev Gastroenterol Hepatol* 2019 April;**16**(4):207–220.
- Ritchie ME, Phipson B, Wu D, Hu Y, Law CW, Shi W, Smyth GK (2015). “limma powers differential expression analyses for RNA-sequencing and microarray studies.” *Nucleic Acids Research* **43**(7):e47.
- Hänzelmann S, Castelo R, Guinney J (2013). “GSVA: gene set variation analysis for microarray and RNA-Seq data.” *BMC Bioinformatics* **14**,7.
- Charoentong P, Finotello F, Angelova M, Mayer C, Efremova M, Rieder D, Hackl H, Trajanoski Z. Pan-cancer immunogenomic analyses reveal genotype-immunophenotype relationships and predictors of response to checkpoint blockade. *Cell Rep* 2017 January 3;**18**(1):248–262.
- Tirosh I, Izar B, Prakadan SM, Wadsworth MH 2nd, Treacy D, Trombetta JJ, Rotem A, Rodman C, Lian C, Murphy G, Fallahi-Sichani M, Dutton-Regester K, Lin JR, Cohen O, Shah P, Lu D, Genshaft AS, Hughes TK, Ziegler CG, Kazer SW, Gaillard A, Kolb KE, Villani AC, Johannessen CM, Andreev AY, Van Allen EM, Bertagnolli M, Sorger PK, Sullivan RJ, Flaherty KT, Frederick DT, Jané-Valbuena J, Yoon CH, Rozenblatt-Rosen O, Shalek AK, Regev A, Garraway LA. Dissecting the multicellular ecosystem of metastatic melanoma by single-cell RNA-seq. *Science* 2016 April 8;**352**(6282):189–96.
- Elyada E, Bolisetty M, Laise P, Flynn WF, Courtois ET, Burkhart RA, Teinor JA, Belleau P, Biffi G, Lucito MS, Sivajothi S, Armstrong TD, Engle DD, Yu KH, Hao Y, Wolfgang CL, Park Y, Preall J, Jaffee EM, Califano A, Robson P, Tuveson DA. Cross-species single-cell analysis of pancreatic ductal adenocarcinoma reveals antigen-presenting cancer-associated fibroblasts. *Cancer Discov* 2019 August;**9**(8):1102–1123.
- Bausch-Fluck D, Hofmann A, Bock T, Frei AP, Cerciello F, Jacobs A, Moest H, Omasits U, Gundry RL, Yoon C, Schiess R, Schmidt A, Mirkowska P, Härtlová A, Van Eyk JE, Bourquin JP, Aebersold R, Boheler KR, Zandstra P, Wollscheid B. A mass spectrometric-derived cell surface protein atlas. *PLoS One* 2015 April 20;**10**(3):e0121314.

Ethics Approval Specimens were harvested from unused tissue after a surgical tumor resection procedure. A discrete legal consent form from both hospital and individuals was obtained by the commercial tissue vendor BioMax US for all samples analyzed in this abstract. All human tissues are collected under HIPPA approved protocols.

Consent Written informed consent was obtained from the patient for publication of this abstract and any accompanying images. A copy of the written consent is available for review by the Editor of this journal.

<http://dx.doi.org/10.1136/jitc-2021-SITC2021.928>

DISSECTING INTRATUMORAL IMMUNE ORGANIZATION: DEFINING THE COMPARATIVE CELLULAR COMPOSITION OF TERTIARY LYMPHOID STRUCTURES T-CELL SUPPORTIVE ANTIGEN PRESENTING NICHES IN RENAL TUMORS

Caroline Jansen*, Ewelina Sobierajska, Rachel Greenwald, Jennifer Carlisle, Patrick Mullane, Nataliya Prokhnevskaya, Maria Cardenas, Mehmet Bilen, Adeboye Osunkoya, Viraj Master, Haydn Kissick. *Emory University, Decatur, GA, USA*

Background Tumor infiltrating T-cells have a prognostic benefit in many tumor types,^{1–8} and we recently sought to determine whether the level of T-cell infiltration into renal tumors predicts clinical outcomes. In our recent publication,⁹ we showed that patients with high of CD8 T-cell infiltration have improved progression free survival (PFS). Further, we found that this T-cell response is supported by TCF1+ stem-like CD8 T-cells, which reside within dense regions of closely clustered antigen presenting cells within the tumor. Interestingly, aggregations of immune cells have also been described in other tumor types and termed ‘tertiary lymphoid structures’ (TLS), which are typically defined as B-cell-dominant aggregates, containing high endothelial venules and reactive germinal centers.^{10–12} Together, these findings raise several important questions, which we explore here—(1) what additional cell types comprise these niches?⁹ and (2) how are these niches similar to or different from TLS?

Methods Tumor tissue was collected from patients with renal tumors undergoing surgery at Emory University Hospital. Intraoperative tumor samples were analyzed by flow cytometry, RNA sequencing, immunofluorescence, and immunohistochemistry. Immunofluorescence data was analyzed using our custom quantitative analysis pipelines, which allows for delineation of cell type and location, cell-cell distance, and density of cellular aggregation.

Results The proportion of CD8 T-cells infiltration human renal tumors varied widely, consistent with our previous reports.⁹ TCF1+ stem-like CD8 T-cells were identifiable by both flow cytometry and immunofluorescence and resided in dense antigen presenting niches. Quantitative immunofluorescence revealed the location of aSMA+ fibroblasts within tumor tissue, in relation to antigen presenting niches, and in tumors with many infiltrating T-cells. Pathologist scored hematoxylin and eosin-stained slides were delineated TLS+ or TLS-. Quantitative immunofluorescence imaging analysis revealed the detailed composition of tumor infiltrating immune cell populations and the contrasting cellular organization in TLS as compared to in antigen presenting niches.

Conclusions As we have shown CD8 T-cell infiltration to predict PFS in renal tumors and that antigen presenting niches containing stem-like cells maintain the anti-tumor T-cell response,⁹ it is critical to understand the additional cell types present in these niches and to understand how these niches relate to previously described phenomena of immune organization, such as TLS.^{10–12} This mechanistic understanding of the anti-tumor immune response represents an opportunity to inform development of enhanced prognostic tools and innovative therapeutic possibilities.

REFERENCES

1. Azimi F, *et al.* Tumor-infiltrating lymphocyte grade is an independent predictor of sentinel lymph node status and survival in patients with cutaneous melanoma. *J Clin Oncol* 2012;**30**(21):2678–83. Epub 2012/06/20. doi: 10.1200/jco.2011.37.8539. PubMed PMID: 22711850.

- Galon J, *et al.* Type, density, and location of immune cells within human colorectal tumors predict clinical outcome. *Science* 2006;**313**(5795):1960–4. Epub 2006/09/30. doi: 10.1126/science.1129139. PubMed PMID: 17008531.
- Mlecnik B, *et al.* Integrative analyses of colorectal cancer show immunoscore is a stronger predictor of patient survival than microsatellite instability. *Immunity* 2016;**44**(3):698–711. Epub 2016/03/18. doi: 10.1016/j.immuni.2016.02.025. PubMed PMID: 26982367.
- Pagès F, *et al.* Histopathologic-based prognostic factors of colorectal cancers are associated with the state of the local immune reaction. *J Clin Oncol* 2011;**29**(6):610–8. Epub 2011/01/20. doi: 10.1200/JCO.2010.30.5425. PubMed PMID: 21245428.
- Pagès F, *et al.* Immune infiltration in human tumors: a prognostic factor that should not be ignored. *Oncogene* 2009;**29**:1093. doi: 10.1038/onc.2009.416.
- Peranzoni E, *et al.* Macrophages impede CD8 T cells from reaching tumor cells and limit the efficacy of anti-PD-1 treatment. *Proceedings of the National Academy of Sciences of the United States of America* 2018;**115**(17):E4041–E50. Epub 2018/04/11. doi: 10.1073/pnas.1720948115. PubMed PMID: 29632196.
- Savas P, *et al.* Single-cell profiling of breast cancer T cells reveals a tissue-resident memory subset associated with improved prognosis. *Nat Med* 2018;**24**(7):986–93. Epub 2018/06/27. doi: 10.1038/s41591-018-0078-7. PubMed PMID: 29942092.
- Tosolini M, *et al.* Clinical impact of different classes of infiltrating T cytotoxic and helper cells (Th1, th2, treg, th17) in patients with colorectal cancer. *Cancer Res* 2011;**71**(4):1263–71. Epub 2011/02/10. doi: 10.1158/0008-5472.Can-10-2907. PubMed PMID: 21303976.
- Jansen CS, *et al.* An intra-tumoral niche maintains and differentiates stem-like CD8 T cells. *Nature* 2019;**576**(7787):465–70. doi: 10.1038/s41586-019-1836-5.
- Dieu-Nosjean MC, *et al.* Tertiary lymphoid structures in cancer and beyond. *Trends Immunol* 2014;**35**(11):571–80. Epub 2014/12/03. doi: 10.1016/j.it.2014.09.006. PubMed PMID: 25443495.
- Goc J, *et al.* Characteristics of tertiary lymphoid structures in primary cancers. *Oncimmunology* 2013;**2**(12):e26836. Epub 2014/02/06. doi: 10.4161/onci.26836. PubMed PMID: 24498556; PMCID: PMC3912008.
- Sautes-Fridman C, *et al.* Tertiary lymphoid structures in the era of cancer immunotherapy. *Nature reviews Cancer* 2019;**19**(6):307–25. Epub 2019/05/17. doi: 10.1038/s41568-019-0144-6. PubMed PMID: 31092904.

Ethics Approval Samples are collected under an approved IRB protocol (The Urological Satellite Specimen Bank at Emory University, IRB00055316). All patients provided informed consent.

Consent Samples are collected under an approved IRB protocol (The Urological Satellite Specimen Bank at Emory University, IRB00055316). All patients provided informed consent.

<http://dx.doi.org/10.1136/jitc-2021-SITC2021.929>

FIBROBLAST ACTIVATION PROTEIN ALPHA EXPRESSION IN TUMOR STROMA AND ITS ASSOCIATION WITH IMMUNO-REGULATORY CIRCUITS ACROSS EPITHELIAL TUMORS

¹Anton Kraxner*, ¹Franziska Braun, ¹Wei-Yi Cheng, ¹Marta Canamero, ¹Emilia Andersson, ²Suzana Vega Harring, ¹Sebastian Dziadek, ¹Ann-Marie Broeske, ¹Maurizio Ceppi, ¹Volker Teichgraber, ¹Jehad Charo. ¹Roche/Genentech, Basel, Switzerland; ²Exact Sciences, Genf, Switzerland

Background Carcinoma associated fibroblasts (CAFs) play important roles in modulating tumor development and prognosis through biochemical and biomechanical signals, but also through their immuno-modulatory characteristics. Fibroblast activation protein alpha (FAP), a serine protease with selectively high expression on CAFs, may be an ideal target for therapeutic intervention, including cancer immunotherapy. Therefore, a thorough understanding of FAP expression, but also immune cell composition and especially their interaction is key to optimally inform drug development and patient enrichment strategies.

Methods Formalin-fixed paraffin embedded tissue specimens comprising 253 primary tumors and 277 metastatic lesions were included in this study. Tumor sections were analyzed by digital immunohistochemistry (IHC) to assess tumor-stroma composition, FAP content and immune cell infiltration, complemented by transcriptomic analyses.

Results Across different types of epithelial tumors, FAP was detected by digital IHC in the tumor-associated stroma at a low to moderate proportion and with heterogeneous distribution patterns. Primary tumors in breast and lung cancer demonstrated a higher median FAP content (6.5% and 6.6% area coverage, respectively) compared to renal cell carcinoma (0.2% area coverage), which was confirmed on mRNA expression level. Median FAP levels were similar between primary and metastatic lesions in most tumor types except for renal cancer, for which FAP levels were significantly increased in metastasis lesions (3.3% area coverage). FAP content positively correlated with the density of FoxP3 positive regulatory T cells, but indication and tissue type specific differences were observed. Transcriptomic analysis revealed that both stroma-richness as well as higher FAP content were positively correlated with macrophage and dendritic cell gene signatures. However, while a higher stromal content was associated with signatures related to endothelial cells and preadipocytes, higher FAP content showed a stronger correlation with regulatory T cells. These findings are suggestive of a distinct biological role of FAP positive stroma in human tumors.

Conclusions FAP-targeted therapy is a promising strategy to optimize accumulation and action of anti-cancer drugs in the tumor microenvironment, potentially leading to more specific and effective therapies. Our study further elucidates the role of FAP by providing a comprehensive and granular landscape of FAP content in primary and metastatic tumor lesions derived from the same patient population and its association with immune cell composition. Future studies aim to elucidate the complex and dynamic interplay between malignant, stromal and immune cell populations in both temporal and spatial contexts and how that contributes to outcome in cancer immunotherapy.

<http://dx.doi.org/10.1136/jitc-2021-SITC2021.930>

931

LINC RNA MALAT1 REGULATED SERPINB6B SIGNALING SUPPRESSES PYROPTOSIS AND GOVERNS BREAST CANCER DORMANCY REACTIVATION AND THROUGH IMMUNE EVASION

Dhiraj Kumar*, Filippo Giaccotti. *UT MD Anderson Cancer Center, Houston, TX, USA*

Background Metastatic relapse is the major causes of mortality in patients with cancer and occur due to metastatic reactivation of dormant tumor cells. Early dissemination of tumor cells undergoing a protected period of dormancy in the target organs potentially explains this prevalent clinical behavior.¹⁻⁴ Long non-coding RNAs (lncRNAs) are involved in various biological processes and diseases. Malat1 is one of the most abundant and highly conserved nuclear lncRNAs and have shown the associated with metastasis and serving as a predictive marker for various tumor progression.⁵ However, the correlation of tumor intrinsic lncRNAs in regulation of tumor dormancy and immune evasion is largely unknown.

Methods Using an in vivo screening platform for the isolation of genetic entities involved in either dormancy or reactivation of breast cancer tumor cells, we have identified Malat1 as a positive mediator of metastatic reactivation.⁴ To dissect the functional role of Malat1 in metastatic reactivation, we developed a clean Malat1 knockout (KO) model using paired gRNA CRISPR-Cas9 in metastatic murine syngeneic breast cancer. As proof of concept we also used inducible knock-down system under in vivo models. To delineate the immune microenvironment, we used single cell RNA-seq, ChIRP-seq, multicolor flowcytometry, RNA-FISH, and coculture experiments.

Results Our data revealed that deletion of Malat1 induces dormancy and attenuated the metastatic colonization resulting in long-term survival of syngeneic mice model. In contrast, over-expression of Malat1 leads to metastatic reactivation of dormant breast cancer cells. Interestingly, 4T1-Malat1 KO dormant breast cancer cells exhibit metastatic outgrowth in T cells defective mice. Our single-cell RNA-seq and multicolor flowcytometry evaluation reveal enhanced T cells and reduced neutrophils proportions in mice with Malat1 KO cells. This indicates a critical role of immune microenvironment via Malat1-dependent immune evasion. Additionally, Malat1 KO inhibits cancer stemness properties. Similarly, RNA-seq and ChIRP-seq data suggest that KO of Malat1 hampers immune evasion and downregulates metastasis associated genes including Serpins and Wnts. Additionally, our data strongly suggests that Malat1 KO cells persists as non-proliferative dormant cells in lung due to CD8+ T cell-umpired immune activity. Interestingly, rescue experiments suggest that Malat1 or Serpinb6b protects T cell-induced cell death and induces dormancy re-awakening thereby rescue the metastatic potential of 4T1 Malat1 KO cells. Combination of Malat1 ASO with double immune checkpoint inhibitors greatly affects the metastatic outgrowth in breast cancer.

Conclusions Taken together, our studies demonstrate that tumor intrinsic Malat1 regulates Serpinb6b that eventually controls immune evasion and promote dormancy metastatic reactivation.

Acknowledgements NGS data generated was supported by Core grant CA016672(ATGC) and NIH 1S10OD024977-01 award to the ATGC. Single cell RNA sequencing data was supported by the CPRIT Single Core grant RP180684. The Advanced Cytometry & Sorting Core Facility is supported by NCI P30CA016672.

REFERENCES

1. Arun G, Diermeier S, Akerman M, *et al.* Differentiation of mammary tumors and reduction in metastasis upon Malat1 lncRNA loss. *Genes Dev* 2016 January 1;**30**(1):34–51.
2. Filippo G Giaccotti. Mechanisms governing metastatic dormancy and reactivation. *Cell* 2013 November 7;**155**(4):750–764.
3. Gao H, Chakraborty G, Lee-Lim AP, *et al.* The BMP inhibitor Coco reactivates breast cancer cells at lung metastatic sites. *Cell* 2012b;**150**:764–779.
4. Gao H, Chakraborty G, Lee-Lim AP, *et al.* Forward genetic screens in mice uncover mediators and suppressors of metastatic reactivation. *Proc Natl Acad Sci U S A* 2014 November 18;**111**(46):16532–16537.
5. Huang D, Chen J, Yang L, *et al.* NKILA lncRNA promotes tumor immune evasion by sensitizing T cells to activation-induced cell death. *Nat Immunol* 2018;**19**:1112–1125.

<http://dx.doi.org/10.1136/jitc-2021-SITC2021.931>

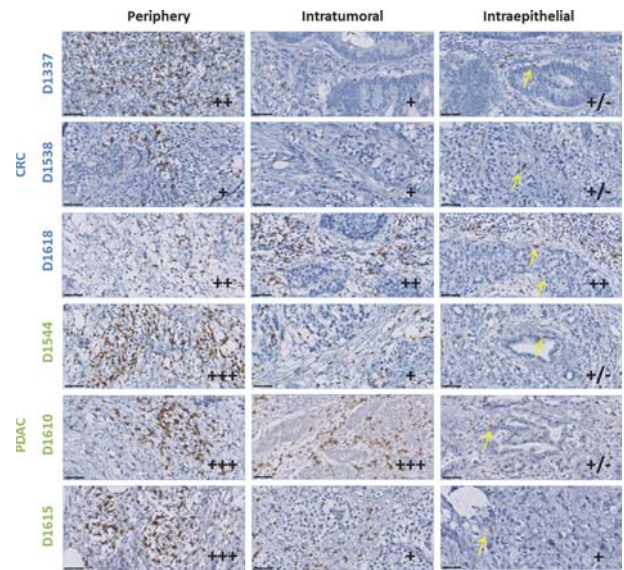
933 IMMUNE INFILTRATES DIFFERENCES BETWEEN CENTRAL AND PERIPHERY REGIONS OF COLORECTAL AND PANCREAS ADENOCARCINOMAS

¹Andreia Maia*, ¹Joana Lérias, ²Luis Miguel Borrego, ³Markus Maeurer, ³Mireia Castillo-Martin. ¹Champalimaud Centre for the Unknown, Lisbon, Portugal; ²CEDOC, Chronic Diseases Research Center, Lisbon, Portugal; ³Champalimaud Foundation, Lisbon, Portugal

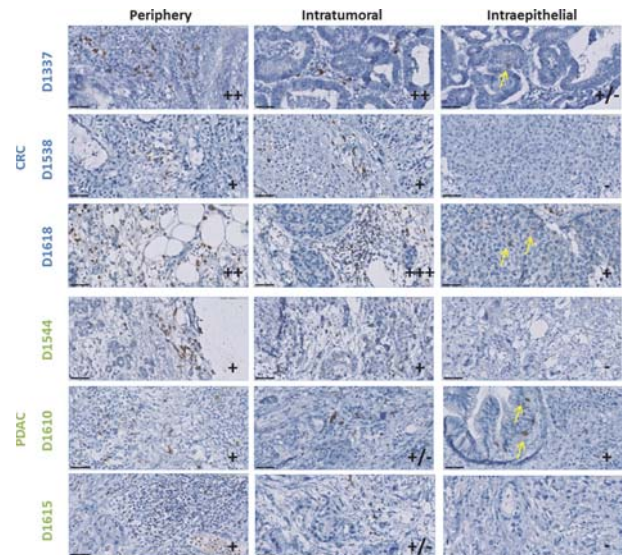
Background The tumor microenvironment (TME) is a complex system, where malignant cells co-exist and communicate with immune and non-immune cells.¹ This interaction orchestrates an immune response that regulates and recruits other immune cells that may either promote cancer growth or mediate tumor regression.² The number and spatiotemporal distribution of tumor-infiltrating lymphocytes (TILs) in the TME, as well as NK cells, have been correlated with favorable prognosis in patients with colorectal cancer or pancreatic adenocarcinomas (CRC and PDAC).³⁻⁵ A more detailed analysis of the TME landscape composition will help to understand which specific areas will give rise to immune cells with clinically relevant anti-cancer-directed responses and could be preferentially expanded for immunotherapy using tumor-infiltrating NK cells.

Methods Fresh CRC (n=6) and PDAC (n=6) tumor specimens were obtained within 20 minutes after surgery. A certified GI pathologist collected central and periphery tumor regions. From each region, half of the specimen was used for immunophenotypic analysis, the other half was cultured with IL-2 (1000 IU/mL) for 12 days. Immunophenotyping was performed using CD45, CD19, CD3, CD4, CD8, CD56, CD16, and LiveDead marker by flow cytometry at days 0, 6, and 12. Parallel formalin-fixed paraffin-embedded blocks were generated and analyzed by immunohistochemistry (IHC) for CD8 and CD56.

Results The immuneprofile of the tumor center and periphery is different both in CRC and PDAC. The mean percentages of B-cells, T-cells (CD4⁺ and CD8⁺ T-cells) and NK cells (CD56^{bright} CD16⁻ and CD56⁺ CD16⁺) of tumor regions are presented in figure 1) are more abundant in the TME and formed larger clusters than NK cells (figure 2). The majority of NK cells were found in the stroma however, in some cases, NK cells were located within the malignant epithelium.



Abstract 933 Figure 1 Representative IHC images of CD8⁺ T-cells in different regions: stroma (periphery and intratumoral) and intraepithelial of both CRC (n=3) and PDAC (n=3). Semi-quantitative analysis of CD8⁺ T-cells (from negative (-) to high numbers (+++)). Yellow arrows point to intraepithelial CD8⁺ T-cells. Scale bar corresponds to 50 µm.



Abstract 933 Figure 2 Representative IHC images of CD56⁺ NK cells in different regions: stroma (periphery and intratumoral) and intraepithelial of both CRC (n=3) and PDAC (n=3). Semi-quantitative analysis of CD56⁺ NK cells (from negative (-) to high numbers (+++)). Yellow arrows point to intraepithelial CD56⁺ NK cells. Scale bar corresponds to 50 µm.

Abstract 933 Table 1

Tumor	Mean %	CD19 ⁺ B-cells	CD3 ⁺ T-cells	CD4 ⁺ T-cells	CD8 ⁺ T-cells	NK cells	CD56 ^{bright} CD16 ⁻	CD56 ⁺ CD16 ⁺	
CRC	Central	Day 0	6.0	68.4	35.0	27.2	9.6	33.3	31.7
		Day 6	4.5	84.5	42.8	31.6	5.0	41.5	22.9
		Day 12	0.7	87.3	46.3	32.3	8.8	67.8	20.9
	Peripheric	Day 0	9.5	73.5	33.9	31.5	4.5	27.7	38.8
		Day 6	6.2	75.2	33.4	24.6	6.9	41.7	20.7
		Day 12	2.1	84.9	48.8	25.0	6.9	65.6	10.3
PDAC	Central	Day 0	15.4	65.8	30.5	31.3	9.4	6.1	54.9
		Day 6	5.3	84.3	47.7	29.1	3.8	26.0	30.1
		Day 12	0.5	91.1	52.4	31.9	5.4	55.7	17.6
	Peripheric	Day 0	12.6	75.4	37.2	34.5	2.7	11.1	54.2
		Day 6	4.5	88.3	48.5	34.0	2.7	35.6	22.1
		Day 12	1.8	87.0	50.2	29.3	6.8	49.6	12.9

Representation of percentage of immune cells in the central and periphery tumor regions of both CRC and PDAC tissues. The mean percentage of B-cells, T-cells (including CD4⁺ and CD8⁺-T-cells) and NK cells (including CD56^{bright} CD16⁻ and CD56⁺ CD16⁺ subpopulation) during *ex vivo* expansion (day 0, day 6 and day 12) are represented from the different regions of both CRC (n=6) and PDA (n=6).

Conclusions Our data in this small set of specimens show that TME immune cells in central and periphery tumor regions present different phenotypes in both tumor types. The tumor periphery exhibits a stronger infiltration with TIL and NK

cells as compared to the center. We also observed that immune cells are in close physical contact with tumor cells since they were identified inside the malignant epithelium in some specimens. NK-cells and particularly TIL close to cancer cells may be preferentially harvested to obtain improved anti-cancer-directed NK or TCR alpha-beta-directed immune cell products for active immunotherapy.

Acknowledgements The authors would like to thank the Champalimaud Foundation Biobank of the Champalimaud Centre for the Unknown for anonymously releasing tissue specimens.

Trial Registration N/A

REFERENCES

1. Giraldo NA, Sanchez-Salas R, Peske JD, Vano Y, Becht E, Petitprez F, Validire P, Ingels A, Cathelineau X, Fridman WH, *et al.* The clinical role of the TME in solid cancer. *Br J Cancer* (2019);**120**:45–53.
2. Li L, Yu R, Cai T, Chen Z, Lan M, Zou T, Wang B, Wang Q, Zhao Y, Cai Y. Effects of immune cells and cytokines on inflammation and immunosuppression in the tumor microenvironment. *Int Immunopharmacol* (2020);**88**:106939.
3. Lianyuan T, Dianrong X, Chunhui Y, Zhaolai M, Bin J. The predictive value and role of stromal tumor-infiltrating lymphocytes in pancreatic ductal adenocarcinoma (PDAC). *Cancer Biol Ther* (2018);**19**:296–305.
4. Idos GE, Kwok J, Bonthala N, Kysh L, Gruber SB, Qu C. The prognostic implications of tumor-infiltrating lymphocytes in colorectal cancer: a systematic review and meta-analysis. *Sci Rep* (2020);**10**:3360.
5. Zhang S, Liu W, Hu B, Wang P, Lv X, Chen S, Shao Z. Prognostic significance of tumor-infiltrating natural killer cells in solid tumors: a systematic review and meta-analysis. *Front Immunol* (2020);**11**:1–11.

Ethics Approval This study was approved by the Champalimaud Foundation Ethics Committee and by the Ethics Research Committee of NOVA Medical School of NOVA University of Lisbon; approval number 56.

Consent Written informed consent was obtained from the patient for publication of this abstract and any accompanying images. A copy of the written consent is available for review by the Editor of this journal.

<http://dx.doi.org/10.1136/jitc-2021-SITC2021.933>

BIOLOGICAL MECHANISMS IN THE DIFFERENT ETIOLOGIES OF MERKEL CELL CARCINOMA PATIENTS: POLYOMAVIRUS OR UV EXPOSURE

¹Domenico Mallardo*, ¹Giosuè Scognamiglio, ²Khrystyna North, ¹Mariaelena Capone, ²Michael Bailey, ³Luigi Scarpato, ²Sarah Church, ¹Gabriele Madonna, ²Jason Reeves, ¹Marcello Curvietto, ¹Marilena Tuffanelli, ¹grazia d'angelo, ¹Ester Simeone, ¹Lucia Festino, ¹Vito Vanella, ¹Claudia Trojaniello, ¹Maria Grazia Vitale, ¹Salvatore Tafuto, ¹Corrado Caracò, ¹Anna Maria Annicciello, ¹Nicola Normanno, ¹Maurizio Di Bonito, ²Sarah Warren, ¹Paolo Ascierto. ¹Istituto Nazionale Tumori IRCCS Pascale, Naples, Italy; ²NanoString Technologies, Seattle, WA, USA; ³Istituto Nazionale Tumori IRCCS Pascale, Naples, Italy

Background Merkel cell carcinoma (MCC) is a rare and aggressive skin cancer with neuroendocrine features, and it is associated with elevated mortality. The pathogenesis is associated with presence of clonally integrated Merkel cell polyomavirus (MCPyV) or ultraviolet light (UV) exposure.¹ The MCPyV causes up to 80% of MCC tumors in North America and Europe.²⁻⁴ Recently immunotherapy is having good results,⁵ the phase 2 trial JAVELIN Merkel 200 indicated that treatment with Avelumab (PDL1 inhibitor) in patients with metastatic MCC pre-treated have a meaningful long-term survival outcomes respect chemotherapy. Moreover, ORRs were highest in patients with high TMB that were also MCPyV-, PD-L1+ or had a greater CD8+ T cell density at the invasive margin.⁶ In this study, we investigated the biological signatures in patients with MCPyV or not.

Methods From April 2011 to June 2018, we collected retrospectively 50 FFPE (Formalin-Fixed Paraffin-Embed) from 37 patients with metastatic MCC and 13 tissues from a secondary metastatic site. All patients have appropriately signed informed consent. We performed an immunohistochemistry assays (IHC) for MCPyV and PDL1. In addition, through the NanoString GeoMx DSP (Digital Spatial Profiling), we analysed 11 patients (6 MCPyV+; 5 MCPyV-) with cutaneous metastasis using a 44-plex antibody cocktail. For each slide we selected three different areas: Intratumoral, extratumoral and tumour border, in each area we selected CD4+ and CD8+ cells in 4 different ROIs (Region of Interest). Statistical analysis was performed via Bonferroni correction, $P < 0.05$ was considered statistically significant for median stratification.

Results The DSP analysis showed that the tumour border cells have an overexpression of IDO respect intratumoral area (adj. $p < 0.01$). Instead, extratumoral area of MCPyV- patients have a higher expression of B7-H3 respect MCPyV+ as well as FOXP3 is higher in the tumour border of MCPyV+ patients and EpCAM in the intratumoral area ($p < 0.05$). PDL1 is overexpressed in MCPyV+ CD4+ cells respect CD8+ ($p < 0.05$). The IHC assay shown that viral status does not change in multiple metastases and PDL1 is elevated in the tumour border ($p < 0.05$).

Conclusions In this retrospective study, our preliminary data shown that tumour edge have an important role in the modulations of immune infiltrate and patients with Merkel cell polyomavirus could have a different pathway of immunosuppression compared to patients with non-virus related etiology. Further investigations are needed to get additional information.

Acknowledgements The study was supported by the Institutional Project "Ricerca Corrente" of Istituto Nazionale Tumori IRCCS Fondazione "G. Pascale" of Napoli, Italy.

REFERENCES

1. Kaae J, Hansen AV, Biggar RJ, *et al.* Merkel cell carcinoma: incidence, mortality, and risk of other cancers. *J Natl Cancer Inst* 2010 June 2;**102**(11):793–801.
2. Feng H, Shuda M, Chang Y, *et al.* Clonal integration of a polyomavirus in human Merkel cell carcinoma. *Science* 2008 February 22;**319**(5866):1096–100.
3. Gameski KM, Warcola AH, Feng Q, *et al.* Merkel cell polyomavirus is more frequently present in North American than Australian Merkel cell carcinoma tumors. *J Invest Dermatol* 2009 January;**129**(1):246–8.
4. Goh G, Walradt T, Markarov V, *et al.* Mutational landscape of MCPyV-positive and MCPyV-negative Merkel cell carcinomas with implications for immunotherapy. *Oncotarget* 2016 January 19;**7**(3):3403–15.
5. Bichakjian CK, Olencki T, Aasi SZ, *et al.* Merkel cell carcinoma, version 1.2018, NCCN Clinical Practice Guidelines in Oncology. *J Natl Compr Canc Netw* 2018 June;**16**(6):742–774.
6. D'Angelo SP, Bhatia S, Brohl AS, *et al.* Avelumab in patients with previously treated metastatic Merkel cell carcinoma: long-term data and biomarker analyses from the single-arm phase 2 JAVELIN Merkel 200 trial. *J Immunother Cancer* 2020 May;**8**(1):e000674.

Ethics Approval The study was approved by internal ethics board of the Istituto Nazionale Tumori IRCCS Fondazione "G. Pascale" of Napoli Italy, approval number of registry 33/17 OSS.

Consent Written informed consent was obtained from the patient for publication of this abstract and any accompanying images. A copy of the written consent is available for review by the Editor of this journal.

<http://dx.doi.org/10.1136/jitc-2021-SITC2021.934>

935 **ATTRACTION OF IMMUNE CELLS BY HEAD AND NECK
CANCER CELL LINES AND PRIMARY TUMOR-
CONDITIONED SUPERNATANTS**

Tara Muijlwijk*, Naomi Remkes, Jos Poell, René Leemans, Ruud Brakenhoff, Rieneke van de Ven. *Cancer Center Amsterdam, Amsterdam UMC, Amsterdam, Netherlands*

Background Head and neck squamous cell carcinomas (HNSCC) are classified in human papillomavirus (HPV)-positive and HPV-negative tumors. In general, HPV-negative HNSCC are genetically characterized by many chromosomal gains and losses.¹ Previously, we and others identified a HPV-negative subgroup with few or absent copy number alterations (CNA-silent), and a more favorable prognosis.²⁻³ Tumors with low copy number changes have generally been associated with high immune infiltration scores,⁴ but for CNA-silent versus CNA-high HPV-negative HNSCC such data are lacking. In this study we aim to unravel by functional assays immunological differences between HPV-negative and HPV-positive HNSCC, as well as between CNA-silent and CNA-high HPV-negative HNSCC. We analyzed the immune cell subsets attracted by HNSCC cell lines and by tumor-conditioned supernatants.

Methods Eight HNSCC cell lines (3 HPV-positive, 3 HPV-negative CNA-high, 2 HPV-negative CNA-silent) and 24-hour supernatants of thirteen HNSCC biopsies were used to characterize their ability to attract immune cells in a transwell migration system. A chemokine mixture was used as a positive control, while medium alone was used to determine spontaneous migration. Peripheral blood mononuclear cells (PBMCs) of various healthy donors were plated in the upper compartment and after six hours the transwell migration was quantified by flow cytometry.

Results Most HNSCC cell lines induced migration of monocytes, B cells and CD4+ T-cells up to maximal 12%, whereas CD8+ T-cells and conventional dendritic cells (cDCs) were not attracted, irrespective of the donor. Notably, one HPV-negative CNA-silent cell line induced significantly more migration compared to the negative control and other cell lines. Tumor-conditioned supernatants promoted immune cell migration with no apparent differences between tumor sites or HPV-status. Remarkably, up to 31% of monocytes migrated to these supernatants, 9x more than the chemokine control. Also cDC migration was induced, whereas lymphocytes were not attracted.

Conclusions HNSCC cell lines induced monocyte, B-lymphocyte and CD4+ T-lymphocyte migration, whereas tumor-conditioned supernatants attracted monocytes and cDCs only. No difference in immune cell attraction between HPV-positive and -negative HNSCC was observed. Interestingly, one HPV-negative CNA-silent cell line induced robust immune cell migration. Currently we perform a comprehensive chemokine analysis to explain the observed migration. The noted lack of CD8+ T-cell attraction may explain why current treatments with PD-1 inhibitors are effective in only a minority of HNSCC patients. Our data could provide a means to identify patients who might most likely respond to immune checkpoint blockade and to find clues to improve CD8+ T-cell attraction.

REFERENCES

1. Leemans CR, Snijders PJF, Brakenhoff RH. The molecular landscape of head and neck cancer. *Nat Rev Cancer* 2018;**18**:269–82.
2. Smeets SJ, Brakenhoff RH, Ylstra B, van Wieringen WN, van de Wiel MA, Leemans CR, *et al*. Genetic classification of oral and oropharyngeal carcinomas identifies subgroups with a different prognosis. *Cell Oncol* 2009;**31**:291–300.
3. Cancer Genome Atlas N. Comprehensive genomic characterization of head and neck squamous cell carcinomas. *Nature* 2015;**517**:576–82.

4. Davoli T, Uno H, Wooten EC, Elledge SJ. Tumor aneuploidy correlates with markers of immune evasion and with reduced response to immunotherapy. *Science* 2017;**355**.

Ethics Approval Written informed consent was obtained from all patients from whom fresh tumor biopsies were used for research, as part of the HNcol protocol at the Department of Otolaryngology|Head and Neck Surgery of Amsterdam UMC (VUmc) as approved by the Institutional Review Board (2008.071|A2016.035). Buffy coats, with written consent from the donors, were purchased from the Dutch blood bank (Sanquin) and used to isolate PBMC.

<http://dx.doi.org/10.1136/jitc-2021-SITC2021.935>

STROMAL REMODELING REGULATES DENDRITIC CELL ABUNDANCE IN THE TUMOR MICROENVIRONMENT

¹Athanasios Papadas*, ¹Gauri Deb, ¹Adam Officer, ²Chelsea Hope, ²Philip Emmerich, ¹Alexander Cicala, ¹Joshua Wiesner, ¹Garrett Arauz, ²Adam Pagenkopf, ²Kristina Matkowskyj, ²Dustin Deming, ³Katerina Politi, ⁴Scott Abrams, ¹Olivier Harismendy, ¹Fotis Asimakopoulos. ¹UCSD, La Jolla, CA, USA; ²UW-Madison, Madison, WI, USA; ³Yale, New Haven, CT, USA; ⁴Roswell Park, Buffalo, NY, USA

Background Stimulatory dendritic cells (SDC), enriched within the Batf3-DC lineage (also known as conventional type 1 DC, cDC1), engage in productive interactions with CD8+ effectors along tumor-stroma boundaries. This puzzling pattern of T-cell-DC localization has been interpreted as "tumor-exclusion", limiting anti-tumor immunity. To understand this paradox, we hypothesized that dynamic matrix remodeling at the invasive margin generates unique activation and cell-fate cues critical for Batf3-DC homeostasis.

Methods We studied immunocompetent tumor models of lung carcinoma, breast carcinoma, melanoma and multiple myeloma. For mechanistic experiments, we generated novel Vcan-targeted models through CRISPR-Cas9 targeting. We delineated DC subsets through multi-parametric flow cytometry and tumor immune contexture through mass cytometry. Batf3-DC cellular models included MutuDC1940 immortalized DC and iCD103 primary cells. TCGA data were mined for human validation.

Results We find that CD8+ T cells massively infiltrate tumor matrices undergoing robust matrix proteoglycan versican (VCAN) proteolysis, an essential organ-sculpting modification in development and adult tissue-plane forging. Across 7591 samples from 20 TCGA cancer types, a significant-positive correlation between VCAN substrate expression and Batf3-DC score was observed, suggesting that the VCAN pathway may regulate Batf3-DC across several cancer types. Experimental Vcan depletion in the tumor microenvironment was detrimental for Batf3-DC. Batf3-DC abundance was restored through the VCAN N-terminal fragment (matrikine) versikine, physiologically generated through ADAMTS protease activity in remodeled stroma. In addition to Batf3-DC expansion, versikine resulted in G-MDSC contraction as well as the emergence of an atypical innate lymphoid (NK/ILC1) subset expressing cytotoxicity receptors, low IFN γ and robust pro-survival GM-CSF. Despite broad intratumoral IRF8 induction (10-100-fold), adoptive transfer of pre-DC into versikine-replete microenvironments did not influence their differentiation choice between Batf3-DC and cDC2. Instead, versikine delivered a distinct Batf3-DC activation signal characterized by non-TLR maturation as well as downregulation of TGF β and Wnt signaling. In vivo, versikine promoted Batf3-DC abundance through NK cells but independently of stromal TLR2 or CD44. Versikine sensitized immune-evasive tumors to STING agonist immunotherapy in a Batf3-DC dependent manner and promoted antigen-specific CD8+ responses. Versikine-DC signatures correlated with CD8+ T cell scores in human lung cancers.

Conclusions We demonstrate that dynamic extracellular matrix remodeling controls Batf3-DC abundance in the tumor microenvironment. N-terminal proteolysis of the matrix proteoglycan versican (VCAN), releases a bioactive fragment (matrikine), versikine, that is remarkably necessary and sufficient for Batf3-DC accumulation. Versikine orchestrates a multi-lineage network that regulates Batf3-DC activation and survival at matrix-remodeling interfaces. Therapeutic

harnessing of matrix-Batf3-DC cross-talk sensitizes immune-evasive tumors to immunotherapy.

Acknowledgements We acknowledge support by the National Cancer Institute (R01CA252937 and U01CA196406), the American Cancer Society (127508-RSG-15-045-01-LIB), the Leukemia and Lymphoma Society (6551-18), the UW Trillium Myeloma Fund and the Robert J. Shillman Foundation.

Ethics Approval Laboratory animal work was performed under IACUC-approved protocols #M5476 and #S19109 in the University of Wisconsin-Madison and University of California, San Diego respectively.

<http://dx.doi.org/10.1136/jitc-2021-SITC2021.936>

937

ADVANCED UNDERSTANDING OF THE TUMOR MICROENVIRONMENT WITH MULTIPLEX ANALYSIS: AN AUTOMATED 7-COLOR MULTIPLEX ASSAY USING AKOYA'S OPAL TECHNOLOGY

¹Bhavika Patel*, ¹Stephanie Allen, ¹Tania Eliseeva, ²Najiba Mammadova, ²Agnes Haggerty, ¹Navi Mehra. ¹HTL Clinical, Boulder, CO, USA; ²Akoya Biosciences, Menlo Park, CA, USA

Background Immunotherapy and precision medicine are rapidly developing approaches to cancer therapy. Biomarkers that detect the tumor and tumor microenvironment allow for the development of strategies that accelerate the development of treatments that enhance a patient's immune system. Akoya's MOTiF™ PD-1/PD-L1 Panel is a validated, multiplex immunoassay enabling detection of the 6 most clinically relevant immuno-oncology and spatial markers: PD-1, PD-L1, FoxP3, CD8, CD68, and PanCK. This panel provides unparalleled quantitative data for pre-clinical and translational IO research.

Methods The MOTiF™ PD-1/PD-L1 Panel was used to stain normal and tumor lung tissues. Stained slides were analyzed using the InForm® and Visiopharm® image analysis platforms.

Results We introduce the workflow and image analysis solutions using InForm® and Visiopharm® software to provide robust, quantifiable data.

Conclusions This data provides insight into the innate and adaptive immune environment for targeted design of new immunotherapies. These new targeted immunotherapies could potentially improve efficacy and reduce toxicity.

<http://dx.doi.org/10.1136/jitc-2021-SITC2021.937>

STUDY OF THE TUMOR MICROENVIRONMENT OF ORAL SQUAMOUS CELL CARCINOMA USING MULTIPLEX IMMUNOFLOUORESCENCE AND IMAGE ANALYSIS APPROACHES

¹Frank Rojas*, ²Jebrane Bouaoud, ¹Edwin Parra, ²Pierre Saintigny, ¹Auriol Tamegnon, ¹Mei Jiang, ³Shanyu Zhang, ¹Pandurengan Renganayaki, ⁴Lucas Michon, ²Nicolas Gadot, ²Sylvie Lantuejoul, ⁴Philippe Zrounba, ²Jean-Philippe Foy, ²Karene Mahtouk, ²Chloe Bertolus. ¹MD Anderson Cancer Center, Houston, TX, USA; ²University Claude Bernard Lyon, Lyon, France; ³MD Anderson Cancer Center, Houston, TX, USA; ⁴Centre Leon Berard, Lyon, France

Background Head and Neck Squamous Cell Carcinoma is the 8th leading cancer worldwide and it is associated with significant morbidity and mortality.¹⁻² Tumor microenvironment (TME) is dynamic and it plays an important role in head and neck carcinogenesis.³⁻⁴ Cytotoxic T-cells, immune checkpoint molecules such as programmed cell death 1 (PD-1), its ligand (PD-L1), and other checkpoints molecules have been described in these tumors.¹⁻³ This study aimed to characterize the TME of oral squamous cell carcinoma (OSCC) and compare with their pathology features.

Methods Four microns thickness consecutive slides from representative OSCC (N=46) cases were stained and analyzed using 11 biomarkers (CK, CD3, CD8, CD68, PD1, PDL1, LAG3, TIM3, ICOS, VISTA, OX40) placed in two multiplex immunofluorescence panels to characterize the TME. For image analysis, the samples were divided in tumor, stroma and peritumoral compartment. Co-expression of markers (cell phenotypes) were analyzed as densities by mm² in each compartment. For PD-L1 expression by malignant cells (CK+PD-L1+) we set up a cutoff of positive case as \geq than 1%. Cell phenotypes were correlated with anatomopathological information retrieved from records such as tumor size, margin status, stage and perineural, lymphovascular, and bone invasion among others. Statistical analyses and plots were performed using SPSS and Graphpad prism8 software packages.

Results We found significant higher cell density for CK+PDL1+ (P= 0.038), CD3+PDL1+ (P= 0.027), CD3+CD8+PDL1+ (P=0.040) in female patients compared with the male population. Interestingly, smaller tumor size (\leq median, 25mm) showed higher densities of CD3+ (P= 0.006), CD3+CD8+ (P= 0.007), CD3+PDL1+ (P= 0.037), CD3+CD8+PDL1+ (P= 0.016), CD3+ICOS+ (P= 0.036), CD3+VISTA+ (P= 0.001), CD68+ (P= 0.001) and CD68+PD-L1+ (P= 0.008) than large tumors. Additionally, high cell density CD3+OX40+ (P= 0.011) was observed in tumors without margin invasion and high cell density for macrophages CD68+ (p= 0.005) in tumors without bone invasion. In ulcerative and infiltrative tumor pattern we observed higher cell density of CD3+PDL1+ (P= 0.020), CD3+CD8+PDL1+ (P=0.006) and CD3+OX40+ (P= 0.022) than non-ulcerate and no infiltrative pattern. Lastly, 58.7% of cases were PDL1+.

Conclusions Our findings of a diminished immune response in larger tumors might be correlated to their potential role in tumor aggressiveness and progression. Furthermore, high cell density of macrophages on tumor bone invasion may suggest an immune suppressive M2 response supported by the presence of PDL1+ expression. All these results can be the first approach for the development of a treatment based of immune interception.

Acknowledgements This study was supported by a strategic alliance between the Translational Molecular Pathology-Immunoprofiling lab (TMP-IL) at the Department Translational Molecular Pathology, the University of Texas MD Anderson

Cancer Center and the Université Claude Bernard Lyon, Centre de Recherche en Cancérologie de Lyon and the Department of Translational Medicine, Centre Léon Bérard, Lyon, France. The authors would acknowledge ITMO Cancer 2020, "Formation à la Recherche Fondamentale et Translationnelle en Cancérologie" (JB); CLARA 2020 "Soutien à la mobilité des jeunes chercheurs en oncologie, N° CVPPRCAN000198" (JB); Fondation de France 2020 "Aide à la mobilité international de médecins et pharmaciens, N° 00112162" (JB); Ligue contre le cancer 2021, comité de Saône-et-Loire (PS); 2017-INCa-DGOS-Inserm_12563: INCa SIRIC-LYriCAN INCa-DGOS-Inserm_12563 (PS)

REFERENCES

1. Cohen EEW, Bell RB, Bifulco CB, Burtneß B, Gillison ML, Harrington KJ, *et al.* The society for immunotherapy of cancer consensus statement on immunotherapy for the treatment of squamous cell carcinoma of the head and neck (HNSCC). *J Immunother Cancer* 2019;**7**(1):184.
2. Bouaoud J, Foy JP, Tortereau A, Michon L, Lavergne V, Gadot N, *et al.* Early changes in the immune microenvironment of oral potentially malignant disorders reveal an unexpected association of M2 macrophages with oral cancer free survival. *Oncoimmunology* 2021;**10**(1):1944554.
3. Mei Z, Huang J, Qiao B, Lam AK. Immune checkpoint pathways in immunotherapy for head and neck squamous cell carcinoma. *Int J Oral Sci* 2020;**12**(1):16.
4. Yokota T, Homma A, Kiyota N, Tahara M, Hanai N, Asakage T, *et al.* Immunotherapy for squamous cell carcinoma of the head and neck. *Jpn J Clin Oncol* 2020;**50**(10):1089–96.

Ethics Approval The study was conducted in accordance with all applicable laws, rules, and requests of French and European government authorities. Written informed consent was obtained from all patients and the study was approved by the Centre Leon Bérard institutional review board (Lyon, France). Samples were obtained from the CRB Centre Léon Bérard (n°BB-0033-00050) which is quality certified according NFS96-900 French standard and ISO 9001 for clinical trials.

<http://dx.doi.org/10.1136/jitc-2021-SITC2021.938>

939

**AUTOCRINE/PARACRINE FACTORS IN CANCER
ASSOCIATED FIBROBLASTS DRIVE
IMMUNOSUPPRESSION THROUGH IMPAIRED MYELOID
CELL FUNCTIONS**

Nikita Sharma*, Priya Govindaraju, Shermineh Bradford, Yarong Wang, Brianna Flynn, Candace Wai Sze Lei, Varenka Rodriguez Di Blasi, Jeanine Pignatelli, Kang Liu, Emily Corse, Abhishek Kashyap. *Boehringer Ingelheim Pharmaceuticals, Ridgefield, CT, USA*

Background Cancer associated fibroblasts (CAFs) promote tumorigenesis by secreting immunosuppressive cytokines, stimulating angiogenesis, and supporting the growth of tumor cells. Through their interactions with immune cells, CAFs are known to directly impact the functionality of T cells and macrophages. However, CAF interaction with dendritic cells (DCs) and DC progenitor cells and its impact on DC function is relatively understudied and was the main focus of this study.

Methods Two types of coculture systems were used in this study. For the human system, fibroblasts from lung squamous cell carcinoma (LUSC) were cocultured with MUTZ3 cells (hematopoietic progenitor cells) in the presence of DC differentiation stimuli, sometimes followed by DC maturation stimuli. For the mouse coculture system, activated (YPSC-c) and inactivated (PSC-b) pancreatic stellate cells (PSCs) were isolated from the pancreas of C57BL/6 mice by the density gradient method and co-cultured in the presence of bone marrow cells in the presence of DC differentiation and maturation stimuli. For human tumor antigen processing and cross presentation assay MART1 peptide (10mer and 20mer) was used.

Results Co-culture of human and murine hematopoietic progenitor cells with fibroblasts (human LUSC CAFs and murine PSC results in decrease in differentiation and maturation of DCs. DCs differentiated and matured in the presence of fibroblasts have impaired ability to process and present tumor antigen to T cells. In the presence of PSC fibroblasts DC differentiation from murine bone marrow cells is skewed more towards MDSC and macrophages. In contrast to inactivated PSC-b, activated PSC-c influence DC differentiation in a contact dependent manner. Furthermore, PSC-b and PSC-c show transcriptionally distinct signatures which translate to unique secretory profiles as measured by Luminex. Analysis of the conditioned media from the coculture demonstrated that PSC-c secrete (among others) CXCL1, IL6, and CCL5 chemo/cytokines. These and other factors may play an important role in mediating fibroblast induced suppression of DC differentiation from monocytes.

Conclusions Our study demonstrates that cancer associated fibroblasts, or their precursors directly impact DC differentiation and antigen presentation via cytokines that could be targeted therapeutically to improve DC expansion and activity in the tumor microenvironment.

<http://dx.doi.org/10.1136/jitc-2021-SITC2021.939>

940

TARGETING DKK1 TO REVERSE IMMUNOSUPPRESSIVE MACROPHAGES AND ENHANCE PD-1 BLOCKADE THERAPY IN GASTRIC CANCER

¹Tao Shi*, ¹Yipeng Zhang, ¹Yue Wang, ¹Yunfeng Pan, ¹Hanbing Wang, ¹Yuting Luo, ¹Kaijie Liang, ²Fangcen Liu, ¹Qin Liu, ¹Keying Che, ³Xuan Wang, ¹Lixia Yu, ¹Baorui Liu, ¹Jia Wei. ¹The Comprehensive Cancer Centre of Drum Tower Hospital, Medical School of Nanjing University and Clinical Cancer Institute of Nanjing University, Nanjing, China., Nanjing, China; ²Pathology Department, Affiliated Drum Tower Hospital to Medical School of Nanjing University, Nanjing, China, Nanjing, China; ³The Comprehensive Cancer Centre of Nanjing Drum Tower Hospital, Clinical College of Nanjing Medical University., Nanjing, China

Background Gastric cancer (GC) is a highly heterogeneous and immunosuppressive cancer type with poor prognosis. Current immunotherapies like immune checkpoint blockade (ICB) have very modest therapeutic effect in GC patients, reflecting urgent need for exploring new immunotherapeutic targets.

Methods IHC and mRNA analysis of 384 patients from Drum Tower Hospital Cohort and 1192 patients from other databases were performed to investigate Dickkopf-1 (DKK1) expression and local immune status. The MFC-challenged subcutaneous and abdominal dissemination GC models were established, and the impact of DKK1 blockade on gastric tumor immune microenvironment (TIME) and anti-tumor responses was explored by flow cytometry and RNA sequencing. In vivo immune cell-depletion GC models were constructed to further assess the function of DKK1 on different immune cell types. RAW264.7 and mouse bone marrow derived macrophages (BMDMs) were employed to analyze DKK1 modulation on macrophages in vitro by Cytometric Bead Array, flow cytometry and western blot.

Results In present study, we found high DKK1 expression is associated with poor overall survival and worse immune status in GC patients. DKK1 blockade could improve gastric TIME, including increased accumulation and activation of CD8+ T cells and NK cells, and trigger an effective anti-tumor response both in subcutaneous and abdominal dissemination GC models. DKK1 directly induces macrophages towards an immunosuppressive phenotype, while the TIME improvement and tumor reduction depend on the reversion of immunosuppressive macrophages mediated by DKK1 blockade. Furthermore, combined inhibition of PD-1 and DKK1 could achieve superior anti-tumor effect on GC models.

Conclusions Thus, our work identifies a new role of DKK1 to induce immunosuppressive TIME through macrophage modulation, and reveals DKK1 to be a novel and promising immunotherapeutic target for GC.

Ethics Approval The collection and analysis of tumor tissue sections were approved by the Ethics Committee of Nanjing University Medical School Affiliated Drum Tower Hospital (2021-324-01). All animal experiments were approved by the Institutional Animal Care and Use Committee of Drum Tower Hospital (approval number: 2020AE01064).

<http://dx.doi.org/10.1136/jitc-2021-SITC2021.940>

STROMAL CELL SIALYLATION SUPPRESSES T CELLS IN INFLAMMATORY TUMOUR MICROENVIRONMENTS: A NEW TUMOUR STROMAL CELL IMMUNE CHECKPOINT?

¹Oliver Treacy*, ¹Hannah Egan, ¹Kevin Lynch, ¹Niamh Leonard, ²Kim De Veirman, ²Karin Vanderkerken, ¹Laurence Egan, ¹Thomas Ritter, ³Aisling Hogan, ⁴Keara Redmond, ¹Janusz Krawczyk, ¹Sean Hynes, ⁴Emma Kerr, ⁴Philip Dunne, ¹Michael O'Dwyer, ¹Aideen Ryan. ¹National University of Ireland, Galway, Galway, Ireland; ²Vrije Universiteit Brussel, Brussels, Belgium; ³Galway University Hospital, Galway, Ireland; ⁴Queen's University Belfast, Belfast, UK

Background Immunosuppressive tumour microenvironments (TME) reduce the effectiveness of immune responses in cancer. Non-haematopoietic mesenchymal stromal cells, precursors to cancer-associated fibroblasts (CAFs), dictate tumour progression by enhancing immune cell suppression. Sialic acids, which exist as terminal sugars of glycans (known as sialoglycans), are highly expressed on cancer cells and hyper-sialylation of glycans is known to promote immune evasion in cancer. Sialoglycans are recognized by sialic acid-binding immunoglobulin-like lectins (Siglecs), a family of immunomodulatory receptors, which are analogous to the immune checkpoint inhibitor PD-1.¹ The role of sialylation in stromal cell-mediated immunosuppression, however, is unknown. Using models of solid (colorectal cancer - CRC) and haematological (multiple myeloma - MM) stromal-rich tumours in both mouse and human, the aim of this study was to investigate if stromal cell sialylation contributes to enhanced immunosuppression in the TME.

Methods Flow cytometric analysis of sialic acid expression was performed initially on bone marrow-derived stromal cells isolated from healthy human donor bone marrow aspirates, from wild-type Balb/c mice or from 5T33 multiple myeloma mice. Stromal cells were also isolated and expanded from colorectal cancer patient tumour biopsies (CAFs) with matched controls isolated from tumour-adjacent non-cancerous tissue (normal-associated fibroblasts - NAFs) or from whole blood from primary multiple myeloma bone aspirates. Informed consent was obtained from all patients prior to sampling. Immunosuppression assays were performed using these stromal cells with or without exposure to the tumour cell secretome from the mouse and human CRC cell lines CT26 or HCT116 and HT29, respectively, co-cultured with either murine lymphocytes or healthy human donor-derived peripheral blood mononuclear cells (PBMCs).

Results Our results showed that tumour conditioned stromal cells have increased levels of sialyltransferase gene expression, $\alpha 2,3/\alpha 2,6$ -linked sialic acid and Siglec ligands. Co-culture assays revealed that CAFs induced significantly higher frequencies of Siglec 7 and Siglec 9-expressing CD8 T cells, as well as Tim-3 and PD-1-expressing CD8 T cells, compared to NAFs. Inhibition of sialyltransferase activity using the inhibitor 3FAXNeu5Ac reversed these CAF-induced effects. Interestingly, sialyltransferase inhibition had no observed effects on T cells co-cultured with NAFs.

Conclusions These results demonstrate that targeting stromal cell sialylation can reverse immune cell suppression and reactivate exhausted T cells. These novel data support a rationale for the assessment of stromal cell sialylation and Siglec ligand expression in order to better stratify patients for immunotherapeutic combination treatments that aim to reactivate exhausted T cells in stromal-enriched tumour microenvironments.

Acknowledgements The authors would like to thank the Blood Cancer Network of Ireland Biobank for providing bone marrow aspirates.

REFERENCE

1. Gray MA, Stanczak MA, Mantuano NR, Xiao H, Pijnenborg JFA, Malaker SA, Miller CL, Weidenbacher PA, Tanzo JT, Ahn G, Woods EC, Läubli H, Bertozzi CR. Targeted glycan degradation potentiates the anticancer immune response in vivo. *Nat Chem Biol* 2020;**16**:1376–1384.

Ethics Approval Colorectal tumor and adjacent normal mucosal tissue were obtained from patients undergoing colon tumor resection at University Hospital Galway under an ethically approved protocol (Clinical Research Ethics Committee, Ref: C.A. 2074). Samples were collected and isolated by the Blood Cancer Network of Ireland under an ethically approved protocol. Written informed explicit consent was obtained from all patients prior to sampling. Mice were housed and maintained following the conditions approved by the Animals Care Research Ethics Committee of the National University of Ireland, Galway (NUIG) and procedures were conducted under individual and project authorisation licenses from the Health Products Regulatory Authority (HPRA) of Ireland or from the Ethical Committee for Animal Experiments, Vrije Universiteit Brussel (license no. LA1230281, 16-281-6).

<http://dx.doi.org/10.1136/jitc-2021-SITC2021.941>

942

THE TUMOR MICROBIOME CORRELATES WITH RESPONSE TO IMMUNE CHECKPOINT INHIBITORS IN RENAL CELL CARCINOMA

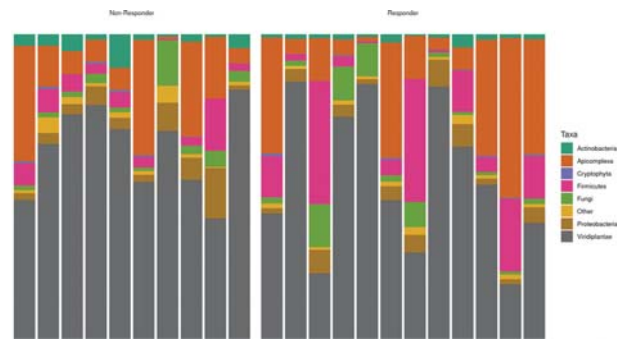
Caroline Wheeler*, Yuanquan Yang, Daniel Spakowicz, Rebecca Hoyd, Mingjia Li. *The Ohio State University Comprehensive Cancer Center, Columbus, OH, USA*

Background Immune checkpoint inhibitor therapy, or ICI, is currently the most successful treatment option for patients with renal cell carcinoma (RCC). However, only 20% of patients have a durable response,¹ driving a significant need to improve treatment outcomes. The tumor microbiome has recently been shown to play a role in chemotherapy-based treatment outcomes, but, to our knowledge, no study has explored its role in response to ICIs.²⁻⁴

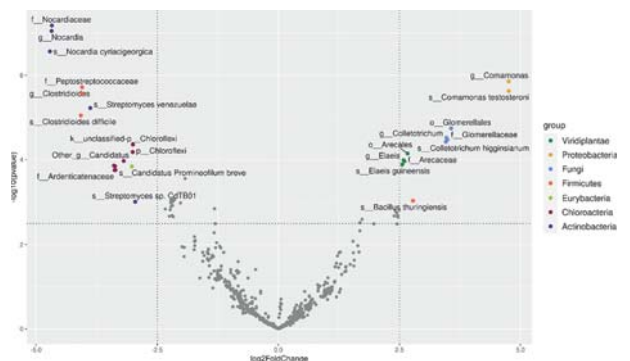
Methods Tumor samples were collected from 22 patients with RCC as a part of the Total Cancer Care program at The Ohio State University Comprehensive Cancer Center. Raw RNA-seq reads from these biopsies, as well as data on the responses to ICI therapy were collected. Response evaluation was based on RECIST v1.1 criteria with complete or partial response, or stable disease classified as "Responders," and progressive disease classified as "Non-responders". The RNA-seq reads were processed through a pipeline developed by the Spakowicz lab, known as ExoTIC (Exogenous sequences in Tumor and Immune Cells), to carefully identify exogenous sequences.^{5,6} Reads that don't align to the human reference genome are meticulously filtered of (1) common laboratory contaminants, (2) taxa that inversely correlate with input RNA quantity, and (3) taxa commonly found in the negative controls of microbiome experiments. DESeq2 was used to perform a differential abundance analysis on the comparison groups at every taxonomic level.

Results The 22 patients with RCC range from 22 to 74 years of age at diagnosis, are 72.7% male, and 54.5% responded to ICIs. Exogenous taxa are identified in the tumor RNAseq, including bacteria, fungi, and viruses (figure 1). Within the tumors responsive to immunotherapy, there was found to be a significant enrichment of certain microbial species, including *Bacillus thuringiensis*, *Comamonas testosteroni*, *Colletotrichum higginsianum*, and *Elaeis guineensis*. Comparatively, the cohort of non-responsive tumors was found to have a significant enrichment of *Candidatus Promineofilum breve*, *Clostridioides difficile*, *Nocardia cyriacigeorgica*, *Streptomyces* sp. CdTB01, and *Streptomyces venezuelae* (figure 2).

Conclusions We found that prior to ICI treatment the tumor microbiome of patients with RCC whose tumors responded to immunotherapy vary from those that did not respond to treatment. This implies that a therapeutic target to modify the tumor microbiome to improve treatment outcomes. Future research will evaluate whether these correlations are causally associated with outcomes and will evaluate their effect on the tumor microenvironment including immune cell infiltration.



Abstract 942 Figure 1 Relative abundances of exogenous taxa found in tumor RNAseq are shown in a stacked bar plot



Abstract 942 Figure 2 Differential abundance analysis of taxa found within tumor RNAseq data by the exotic pipeline. Colored points represent significantly (pvalue < 0.05) enriched taxa with a high (>2.5) fold-difference in abundance between the groups

Acknowledgements The authors acknowledge the support and resources of the Ohio Supercomputing Center (PAS1695).

REFERENCES

1. Ciccarese C, Di Nunno V, Iacovelli R, Massari F. Future perspectives for personalized immunotherapy in renal cell carcinoma. Expert opinion on biological therapy. Taylor & Francis. 2017;**17**(9):1049–1052.
2. Geller LT, Barzily-Rokni M, Danino T, Jonas OH, Shental N, Nejman D, Gavert N, Zwang Y, Cooper ZA, Shee K, Thaiss CA, Reuben A, Livny J, Avraham R, Frederick DT, Ligorio M, Chatman K, Johnston SE, Mosher CM, Brandis A, Fuks G, Gurbatri C, Gopalakrishnan V, Kim M, Hurd MW, Katz M, Fleming J, Maitra A, Smith DA, Skalak M, Bu J, Michaud M, Trauger SA, Barshack I, Golan T, Sandbank J, Flaherty KT, Mandinova A, Garrett WS, Thayer SP, Ferrone CR, Huttenhower C, Bhatia SN, Gevers D, Wargo JA, Golub TR, Straussman R. Potential role of intratumor bacteria in mediating tumor resistance to the chemotherapeutic drug gemcitabine. *Science* 2017 September 15;**357**(6356):1156–1160. PMID: 28912244.
3. Nejman D, Livyatan I, Fuks G, Gavert N, Zwang Y, Geller LT, Rotter-Maskowitz A, Weiser R, Mallel G, Gigi E, Meltzer A, Douglas GM, Kamer I, Gopalakrishnan V, Dadosh T, Levin-Zaidman S, Avnet S, Atlan T, Cooper ZA, Arora R, Cogdill AP, Khan MAW, Ologun G, Bussi Y, Weinberger A, Lotan-Pompan M, Golani O, Perry

- G, Rokah M, Bahar-Shany K, Rozeman EA, Blank CU, Ronai A, Shaoul R, Amit A, Dorfman T, Kremer R, Cohen ZR, Harnof S, Siegal T, Yehuda-Shnaidman E, Gal-Yam EN, Shapira H, Baldini N, Langille MGI, Ben-Nun A, Kaufman B, Nissan A, Golan T, Dadiani M, Levanon K, Bar J, Yust-Katz S, Barshack I, Peeper DS, Raz DJ, Segal E, Wargo JA, Sandbank J, Shental N, Straussman R. The human tumor microbiome is composed of tumor type-specific intracellular bacteria. *Science* 2020 May 29;**368**(6494):973–980.
4. Poore GD, Kopylova E, Zhu Q, Carpenter C, Fraraccio S, Wandro S, Kosciolk T, Janssen S, Metcalf J, Song SJ, Kanbar J, Miller-Montgomery S, Heaton R, McKay R, Patel SP, Swafford AD, Knight R. Microbiome analyses of blood and tissues suggest cancer diagnostic approach. *Nature* 2020;**579**(7800):567–574. PMID: 32214244.
 5. Malalur, Pannaga, Mo, Xiaokui, Hoyd, Rebecca, Hays, John, Carbone, David, Spakowicz, Daniel. Investigating intra-tumor microbes, blood microbes, and CEA for development of non-invasive biomarkers in colorectal cancer. *Journal of Clinical Oncology* 2021;**39**(15_suppl): 3551–3551.
 6. Malalur PG, Mo X, Hoyd R, Carbone DP, Spakowicz D. Intra-tumoral microbes and overall survival in colorectal cancer patients. *Journal of Clinical Oncology* 2020;**38**(15_suppl):4083–4083.

Ethics Approval Data were obtained through an IRB-approved Honest Broker protocol (2015H0185) supporting the Total Cancer Care protocol 2013H0199.

<http://dx.doi.org/10.1136/jitc-2021-SITC2021.942>

943

3D IN VITRO TUMOR MODEL PLATFORM RAPIDLY ASSAYS IMMUNOTHERAPY EFFICACY WITH HIGH CONTENT IMAGING AND DOWNSTREAM PHENOTYPIC CHANGES WITH FLOW CYTOMETRY AND CYTOKINE ANALYSIS

¹Bin Xue, ²Julia Schuler*, ¹Christopher Harrod, ¹Kolin Hribar. ¹Cypre Inc, San Francisco, CA, USA; ²Charles River Discovery Research Service, Freiburg, Germany

Background Cancer immunotherapy represents a burgeoning new direction for oncology therapeutic innovation, with the principal thesis of activating one's own immune system to irradiate cancer as opposed to the injection of foreign cytotoxic agents like chemotherapy. The first generation of checkpoint inhibitors unleash cytotoxic T cells to locate and kill their tumor target, however, only a small subset of patients (e.g. ~30% of NSCLC patients¹) respond favorably. In order to advance the next generation of immunotherapy to the clinic, we critically need models which more accurately represent the immunosuppressive tumor microenvironment (TME).

Methods Here, we describe a novel 3D in vitro tumor model platform which engineers the tumor, stromal, and immune cell compartments of the TME in an extracellular matrix hydrogel (VersaGel²) and a high throughput 96-well format. The system has been extensively tested across multiple solid tumor indications, such as colorectal, lung, pancreatic, breast, and others. Specifically for this study, we utilized NSCLC PDX cells from the Charles River compendium and cocultured with human dermal fibroblasts (HDF) and PBMCs to study the effects of checkpoint inhibitor monoclonal antibodies, Pembrolizumab (anti-PD1) and Atezolizumab (anti-PDL1), on T cell infiltration and T cell-mediated killing using high content imaging. Supernatants were analyzed for cytokines and the 3D models were subsequently digested for flow cytometry.

Results The 3D models demonstrated varying degrees of T cell infiltration and killing capacity across PDX in a dose-dependent manner to checkpoint inhibitors, and the inclusion of fibroblasts played a critical role in further modulating response. Moreover, the data revealed clinically-relevant levels of CD3+, CD4+, and CD8+ T cell subpopulations and cytokine secretions such as IFN-gamma.

Conclusions These data suggest a novel 3D model platform for assaying immunotherapeutic efficacy as well as its mechanism of action in the context of the TME. Future studies will include applying this novel platform to additional tumor models and screening multiple forms of immunotherapy – such as small molecules, biologics, and cell and gene therapy – in drug discovery, preclinical testing, and precision medicine.

REFERENCES

1. Haslam A, Prasad V. Estimation of the percentage of US patients with cancer who are eligible for and respond to checkpoint inhibitor immunotherapy drugs. *JAMA Netw* 2019;**2**(5):e192535.
2. Hribar KC, Wheeler CJ, Bazarov A, Varshneya K, Yamada R, Buckley P, Patil CG. A simple three-dimensional hydrogel platform enables ex vivo cell culture of patient and PDX tumors for assaying their response to clinically relevant therapies. *Mol Canc Ther* 2019;**18**(3):718–725.

<http://dx.doi.org/10.1136/jitc-2021-SITC2021.943>

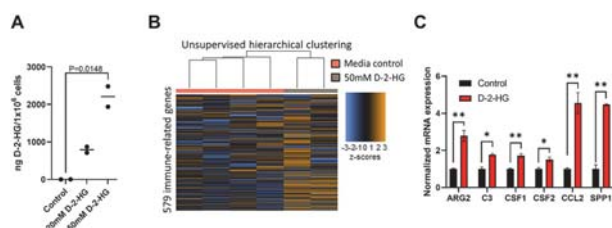
944

FIBROBLASTS AS PARACRINE TARGETS OF THE ONCOMETABOLITE D-2-HG IN THE IDH1-MUTANT CHOLANGIOCARCINOMA TUMOR MICROENVIRONMENT

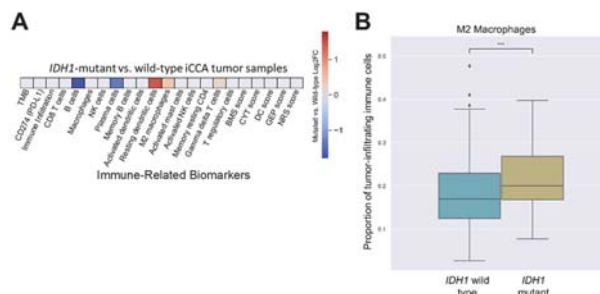
¹Daniel Zabransky*, ²Prerna Jain, ³Kabir Mody, ²Sherif El-Refai, ¹Elizabeth Jaffee, ¹Mark Yarchoan. ¹Sidney Kimmel Comprehensive Cancer Center at Johns Hopkins, Baltimore, MD, USA; ²Tempus Labs Inc., Chicago, IL, USA; ³Mayo Clinic, Jacksonville, FL, USA

Background Cholangiocarcinoma (CCA) is an aggressive malignancy of the biliary tract that carries an unfavorable prognosis. Recurrent, hotspot mutations in the IDH1 gene are found in 10–20% of CCAs and can be targeted with mutant IDH1 inhibitors, though objective responses leading to a reduction in tumor size are rare.^{1,2} Mutant IDH1 has neomorphic enzymatic activity that results in the production of the oncometabolite D-2-hydroxyglutarate (D-2-HG).³ D-2-HG promotes biliary tumor formation through cancer cell-intrinsic effects,^{4–6} but D-2-HG can also act as a paracrine factor released by IDH1-mutant cancer cells into the tumor microenvironment to promote tumor growth through non-cell intrinsic mechanisms.⁷ We have performed studies to determine the paracrine effects of D-2-HG on fibroblasts to further examine the CCA tumor microenvironment.

Methods To determine if fibroblasts are paracrine targets of D-2-HG in the CCA TME, we treated LX-2 hepatic stellate fibroblast cells with 0–50mM exogenous D-2-HG and utilized liquid chromatography-mass spectrometry to quantify the amount of intracellular D-2-HG. D-2-HG treated LX-2 fibroblasts and controls were then examined for changes in gene expression across 579 immune-related genes using the Nanostring platform. In partnership with Tempus, bulk RNA sequencing of IDH1-mutant (N=52) and wild type (N=403) CCA patient tumor samples was performed and CIBERSORT was used for deconvolution of gene expression data to define tumor-infiltrating immune cell populations.



Abstract 944 Figure 1 D-2-HG induces gene expression changes in fibroblasts. (A) Mass-spec analysis of intracellular D-2-HG levels in LX-2 fibroblasts treated with control or D-2-HG containing media. (B) Gene expression patterns for 579 immune-related genes in the Nanostring Human Immunology V2 panel for LX-2 cells treated with control media (pink) or 50mM D-2-HG (gray) for 48 hours. D-2-HG treated cells have a distinct gene expression pattern as indicated by unsupervised hierarchical clustering. (C) Normalized mRNA expression for selected genes in LX-2 cells treated with control (black) or 50mM D-2-HG (red) containing media reveal upregulation of multiple genes that may alter the tumor immune microenvironment in CCA (*P<0.05, **P<0.01).



Abstract 944 Figure 2 The infiltrating immune cell populations in IDH1-mutant CCA. (A) RNA sequencing data from IDH1-mutant and wild-type CCA tumor samples was deconvoluted with CIBERSORT to define tumor-infiltrating immune cell populations. Cell populations with significant increases or decreases (Mann-Whitney U test, p<0.01) are plotted in a color spectrum to represent Log2FC in IDH1-mutant vs. wild-type tumors. (B) Box plot of the proportion of tumor-infiltrating immune cells identified as M2 macrophages in IDH1 wild-type (turquoise) and IDH1-mutant (gold) patient tumor samples (**P<0.001).

Results Intracellular D-2-HG was increased in LX-2 cells treated with exogenous D-2-HG compared to controls (figure 1A). D-2-HG treated fibroblasts showed significant changes in immune-related gene expression with significant increases in expression of genes involved in immunometabolism, TLR signaling, and inflammasome signaling—as indicated by unsupervised hierarchical clustering (figure 1B). The most upregulated gene in D-2-HG-conditioned LX-2 fibroblasts is SPP1 (figure 1C). We further identified that human IDH1-mutant CCA samples have a unique tumor immune microenvironment (figure 2A) and a significantly higher number of infiltrating M2 macrophages compared to wild-type controls (figure 2B).

Conclusions D-2-HG significantly alters gene expression in hepatic stellate cells, precursors to cancer-associated fibroblasts in CCA.⁹ The most upregulated gene in D-2-HG conditioned fibroblasts was SPP1, which has been implicated in the recruitment and polarization of immunosuppressive M2 macrophages leading to decreased antitumor immunity.^{10–12} Interestingly, our analyses of resected human CCA samples showed that the IDH1-mutant CCA tumor immune microenvironment is characterized by an increase in M2 macrophages. Further study of how D-2-HG dysregulates fibroblast gene expression and affects tumor-infiltrating immune cell populations is warranted.

REFERENCES

- Crispo F, Pietrafesa M, Condelli V, Maddalena F, Bruno G, Piscazzi A, *et al.* IDH1 targeting as a new potential option for intrahepatic cholangiocarcinoma treatment-current state and future perspectives. *Molecules* 2020;**25**. doi:10.3390/molecules25163754.
- Abou-Alfa GK, Macarulla T, Javle MM, Kelley RK, Lubner SJ, Adeva J, *et al.* Ivosidenib in IDH1-mutant, chemotherapy-refractory cholangiocarcinoma (ClarIDHy): a multicentre, randomised, double-blind, placebo-controlled, phase 3 study. *Lancet Oncol* 2020;**21**:796–807.

3. Waitkus MS, Diplas BH, Yan H. Biological role and therapeutic potential of IDH mutations in cancer. *Cancer Cell* 2018;**34**:186–195.
4. Du X, Hu H. The roles of 2-Hydroxyglutarate. *Front Cell Dev Biol* 2021;**9**:651317.
5. Ma S, Jiang B, Deng W, Gu Z-K, Wu F-Z, Li T, et al. D-2-hydroxyglutarate is essential for maintaining oncogenic property of mutant IDH-containing cancer cells but dispensable for cell growth. *Oncotarget* 2015;**6**:8606–8620.
6. Saha SK, Parachoniak CA, Bardeesy N. IDH mutations in liver cell plasticity and biliary cancer. *Cell Cycle* 2014;**13**:3176–3182.
7. Böttcher M, Mouggiakakos D. Immunometabolic regulation of anti-tumor T-cell responses by the oncometabolite d-2-Hydroxyglutarate. *Immunometabolism* 2019;**1**. doi:10.20900/immunometab20190007.
8. Friedrich M, Bunse L, Wick W, Platten M. Perspectives of immunotherapy in isocitrate dehydrogenase-mutant gliomas. *Curr Opin Oncol* 2018;**30**:368–374.
9. Ma L, Wang L, Khatib SA, Chang C-W, Heinrich S, Dominguez DA, et al. Single-cell atlas of tumor cell evolution in response to therapy in hepatocellular carcinoma and intrahepatic cholangiocarcinoma. *J Hepatol* 2021. doi:10.1016/j.jhep.2021.06.028
10. Zhang Y, Du W, Chen Z, Xiang C. Upregulation of PD-L1 by SPP1 mediates macrophage polarization and facilitates immune escape in lung adenocarcinoma. *Exp Cell Res* 2017;**359**:449–457.
11. Psallidas I, Stathopoulos GT, Maniatis NA, Magkouta S, Moschos C, Karabela SP, et al. Secreted phosphoprotein-1 directly provokes vascular leakage to foster malignant pleural effusion. *Oncogene* 2013;**32**:528–535.
12. Wei J, Marisetty A, Schrand B, Gabrusiewicz K, Hashimoto Y, Ott M, et al. Osteopontin mediates glioblastoma-associated macrophage infiltration and is a potential therapeutic target. *J Clin Invest* 2019;**129**:137–149.

Ethics Approval This study was approved by the Johns Hopkins Hospital IRB: IRB approval number CR00023377.

<http://dx.doi.org/10.1136/jitc-2021-SITC2021.944>

Late-Breaking Abstracts

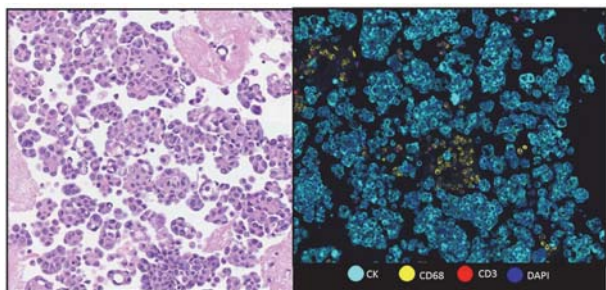
Biomarkers, Immune Monitoring, and Novel Technologies

945

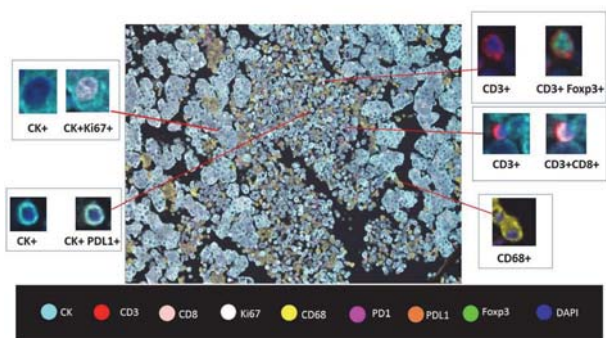
CHARACTERIZATION OF THE IMMUNE LANDSCAPE OF MALIGNANT PLEURAL EFFUSION COMPOSITION FROM PATIENTS WITH METASTATIC BREAST CARCINOMA: A PILOT STUDY

Caddie Dy Laberiano*, Edwin Parra, Qiong Gan, Heladio Ibarguen, Shanyu Zang, Esther Yoon. *The University of Texas MD Anderson Cancer Center, Houston, TX, USA*

Background Breast cancer(BC) is the second most common cause after lung cancer of malignant pleural effusions(MPEs),in approximately one third of all MPEs.Although,MPEs are relatively easy to be collated are still not well characterized in their cellular compositions. This opens new avenues to characterize the cellular milieu comprising the MPE, as it has the potential to be highly informative about mutational markers and immune response –ultimately guiding targeted therapy and predicting therapeutic outcomes with their study. The proposed study will characterize immune landscape of the cellular composition of MPE from patients with metastatic breast carcinoma and characterize their relationship with clinicopathologic features in these patients.



Abstract 945 Figure 1 Comparison between the cell block in H-E and mIF expression CK, CD68 and CD3



Abstract 945 Figure 2 Composite image in mIF expressing 8 markers. In higher magnification is possible to observe the co expression of CK+Ki67+, CK PDL1, CD3+Foxp3+ and CD3+CD8+

Abstract 945 Table 1 Results: cell phenotypes in percentage in the six cases analyzed

	EST01	EST02	EST03	EST04	EST05	EST06
Total CK+ (n/mm2)	82.06	1.64	5.73	85.18	69.93	91.43
CK+PD-L1+ (n/mm2)	0.18	45.22	7.57	0.11	0.29	0.03
CK+Ki67+ (n/mm2)	16.64	4.23	3.57	14.01	11.49	4.69
Total CD3+ (n/mm2)	0.71	43.63	28.39	0.74	0.43	0.36
CD3+CD8+ (n/mm2)	10.24	6.84	8.27	14.02	32.63	24.14
CD3+PD-1+ (n/mm2)	0.49	1.23	1.42	3.74	1.05	0.69
CD3+PD-L1+ (n/mm2)	0.00	0.01	0.00	0.00	0.00	0.00
CD3+Ki67+ (n/mm2)	3.90	0.87	0.11	3.74	9.47	7.59
CD3+CD8+Ki67+ (n/mm2)	0.00	0.06	0.00	0.00	7.37	3.45
CD3+CD8+PD-1+ (n/mm2)	0.00	0.00	0.05	1.87	0.00	0.00
CD3+FOXP3+CD8- (n/mm2)	42.44	2.09	4.86	11.68	11.58	5.52
Total CD68+ (n/mm2)	15.15	7.23	1.00	9.00	14.28	2.48
CD68+PD-L1+ (n/mm2)	0.00	0.00	0.00	0.04	0.00	0.00
Total Cells (n/mm2)	4526.05	6888.64	12681.85	5370.87	4750.26	6370.19
Area of analysis (n/mm2)	6.36	6.50	6.40	5.39	4.67	6.39

Abstract 945 Table 2 Clinical data of the six patients. L: left . R: right , BR : Breast cáncer, CRC: Colorrectal cáncer, NE: No evaluable , IDC : Invasive ductal carcinoma , CT: chemotherapy and BT : biotherapy

	EST01	EST02	EST03	EST04	EST05	EST06
AGE	43	89	78	47	46	42
FAMILY HISTORY	Maternal aunt and grandmother BC	Mothers, siblings(CRC), maternal aunt (BC)	Mother and cousin(BC)	Maternal grandmother (BC)	Maternal grandmother (BC)	Mother (BC)
TUMOR SIZE IN OX	NE	L: 1.5cm R: 5.5 cm	Multicentric(1.3 cm right, 0.8 cm left)	13.5 cm	4.1 cm	R: 1.5 cm L: 10.5 cm
HISTOPATHOLOGY	IDC with mucinous features, G2	L: IDC(grade I) R: R: with lobular features; grade 2/3	BC with ductal and lobular features	IDC grade 3	IDC grade 3	R: IDC
TREATMENT	CT/BT	L: mastectomy+LND R: mastectomy +CT/ BT	bilateral mastectomies CT/BI	Neoadjuvant CT+ mastectomy	Neoadjuvant CT+ mastectomy	R: mastectomy+ adjuvant CT L: mastectomy+adjuvant CT
STAGE	pT4C	R: pT3 L: pT1c	pT1	pT4d	pT3	R: pT3c; L: T3
METASTASIS	Extensive	No	Liver	No	No	No
SURVIVAL AFTER THE MPE COLLECTION	Less than 1 month	27 month +	11 months* 3 months*	3 months	Less than 1 month	5 months
ER IN PRIMARY TUMOR	50%	R: 100%; L: negative	R: 100%; L: 90%	50%	Negative	R: negative; L: 50%
PR IN PRIMARY TUMOR	45%	R: 20%; L: negative	R: 100%; L: 90%	0%	Negative	R: negative; L: negative
HER2 IN PRIMARY TUMOR	3+	R: 3+; L: unknown	R: negative; L: 3+	Negative	Negative	R: 2+; L: negative

* Last appointment of the patient.

Methods Five microns thickness paraffin cell pellet blocks from six cases randomly selected of breast carcinoma MPE were stained using a quantitative multiplex immunofluorescence(mIF) panel containing 8 markers against pancytokeratin (CK), PD-L1, PD-1, CD3, CD8, Foxp3, CD68, Ki67, and DAPI (figure 1). Representative regions of interest were scanned using a multispectral scanner (Vectra Polaris) in high magnification (20x) to capture different cell populations. Markers co-expression were processed and analyzed using a quantitative image analysis software (InForm). The final results were obtained as absolute number of cells from each phenotype and were characterized with clinicopathologic features.

Results We analyzed and stained six breast cancer MPE cases with previously optimized and validated mIF panel for formalin fixed and paraffin embedded (FFPE) tumor tissues against CK, CD3, CD68, CD8, Foxp3, Ki67, PD1 and PD-L1 (figure 2). The median cellular density was 5870.53 cells. Median for each marker: CK+ was presented in 75.9% (between malignant cells and reactive mesothelial cells) in these cells the expression of Ki67 was 8% and PD-L1+ was present in 0.2%.CD3+ was 0.72% and being the cytotoxic T-cells CD3+CD8+ was 12.13% of these cells and it expression for CD3+PD1+ was in 1.14% without concomitant expression for PD-L1. The median of the macrophages CD68+ was 8.1% of the total cells (table 2).

Conclusions mIF is a promising tool to study diverse corporal effusion from different origin. Although more studies are needed, this new perspective can help us to resolve some clues and possible prognosis in advanced stages of BC.

REFERENCE

1. Nicholas D T, Matthew A. S. Diagnosis and Management of Pleural Metastases and Malignant Effusion in Breast Cancer. En: Kirby I B, Edward M C, V. Suzanne K, William J. G. The Breast (Fifth Edition); Elsevier; 2018. P 934.

<http://dx.doi.org/10.1136/jitc-2021-SITC2021.945>

Cellular Therapies

946 STANDARDIZED TRANSCRIPTIONAL PROFILING FOR OPTIMIZING CELLULAR THERAPIES: A MULTI-CENTER PICI-NANOSTRING COLLABORATION

¹Sarah Church*, ¹Christina Bailey, ¹Sarah Warren, ²Lisa Butterfield. ¹NanoString Technologies, Seattle, WA, USA; ²Parker Institute, San Francisco, CA, USA

Background The field of cellular therapy remains one of the most promising areas for the development of new cancer treatments. To further these improvements, it is imperative to broadly understand cell therapy products at the molecular level and to identify factors that contribute to their efficacy. NanoString and the Parker Institute for Cancer Immunotherapy (PICI) have established a ground-breaking collaboration to characterize up to 1,000 apheresis and cellular therapy infusion products with the primary goal to dissect and study molecular pathways that correlate with optimal cellular therapies.

Methods Using a large and diverse sample cohort collected from eight PICI network Cell Therapy Centers the team will aim to study gene expression profiles (GEP) that correlate with optimal apheresis and downstream cellular products, identifying biomarkers and signatures for clinical response or toxicity and further explore unique cancer-specific and shared characteristics that make an optimal and effective chimeric antigen receptor (CAR) T cell. As shown here, this first of its kind study will include samples that target dozens of different antigens covering both primary and metastatic hematological and solid tumors. Samples will be characterized using the standardized set of genes included in the nCounter CAR-T Characterization Panel and will measure essential components of CAR-T including: metabolic fitness, phenotype, TCR diversity, toxicity, activation, persistence, exhaustion and cell typing along with individual transgene expression.

Results Presented here are initial questions that will be asked as part of this study. Meta-analysis will be performed as an aggregated set of data and individual site-specific analysis. Data will further be analyzed across individual cancer types, target types, outcome and manufacturing conditions as examples. We anticipate this information will prove useful across many aspects of the development, manufacturing and clinical applications for cellular therapies and further hypothesize that these findings will promote the understanding of pathways affecting safety and efficacy that may help optimize the therapy.

Conclusions The project is anticipated to begin Fall of 2021 with work continuing in phases through 2022 with periodic data reports to be shared through scientific conferences. All data and findings will be made publicly available to the scientific community through PICI's Cancer Data and Evidence Library analysis platform (CANDEL).

<http://dx.doi.org/10.1136/jitc-2021-SITC2021.946>

Checkpoint Blockade Therapy

947

**RECOMBINANT MYXOMA VIRUS MC509-N1
DEMONSTRATES ANTITUMOR EFFICACY AS
MONOTHERAPY AND IN COMBINATION WITH IMMUNE
CHECKPOINT INHIBITORS**

¹Enkhtaivan Gansukh*, ²Tommy Alain, ¹Tae-Geuk Kim, ¹Ye-Na Namgung, ¹Ka-Yeon Son, ¹Yeo-Jin Jeong, ¹Yeon-Sook Lee. ¹*Virocure Inc, Seoul, Korea, Republic of*; ²*University of Ottawa, Ottawa, Canada*

Background There are several obstacles to effective cancer immunotherapy including the heterogenic immune profile and the state of the tumor microenvironment. Oncolytic virotherapy provides an opportunity to overcome some of these limitations through high viral replication and the expression of therapeutic transgenes (TGs) within the tumor tissue. Myxoma virus (MYXV) belongs to the family of Poxviridae and represents a potent oncolytic virus and a safe platform as this virus is non-pathogenic in any hosts apart from lagomorphs. Importantly, MYXV has a high capacity of encoding for multiple TG payloads. Here we engineered MC509-N1, a novel double-encoding transgenes (TG1 and TG2) oncolytic MYXV designed for intravenous (IV) injection. The therapeutic TG1 acts to modify and remodel the immune state of the tumor microenvironment, and TG2 allows for prolonged self-evasion from the host immune defense.

Methods Transgenes expression upon infection was detected by ELISA and by flow cytometry. To determine anticancer efficacy, syngeneic B16F10 melanoma or MC38 colorectal cancer-bearing C57BL/6 mice were injected with MC509-N1 intratumorally or IV with or without immune checkpoint inhibitor (ICI). Tumor growth and survival was monitored after treatment and the immune profile within the tumor microenvironment was analyzed by flow cytometry. Mice cured of their tumors from the original treatment were rechallenged with primary tumor cells to examine anticancer immunity.

Results Cells upon infection with MC509-N1 were found to express both transgenes at high levels and stimulate downstream mechanisms. Importantly, the engineering of both transgenes did not affect MC509-N1 infectivity and productivity as compared to wild-type MYXV. Intratumoral injections of MC509-N1 effectively suppressed tumor growth and improved overall survival of both syngeneic cancer models. Furthermore, MC509-N1 therapy effectively modulated the immune profile within the tumor microenvironment, especially the ratio between tumor infiltrated CD8+ cytotoxic T cells and CD4+FoxP3+ T regulatory cells. In addition, IV injections of MC509-N1 showed improved inhibition of tumor growth compared to wild type MYXV. The combination therapy of MC509-N1 with the ICI anti-PD-L1 further promoted inhibition of tumor growth as demonstrated by higher rate of complete regression and improved survival rate. Furthermore, rechallenge experiments revealed that this combination regimen established specific anticancer immune memory and protected from cancer recurrence.

Conclusions Our results demonstrate that the novel engineered MC509-N1 exhibits potent anticancer efficacy, adequately modulates the immune state of the tumor microenvironment, and acts synergistically to eliminate cancer in combination with ICI.

<http://dx.doi.org/10.1136/jitc-2021-SITC2021.947>

Clinical Trials Complete

948

FINAL RESULTS FROM AIPAC: A PHASE IIB COMPARING EFTILAGIMOD ALPHA (A SOLUBLE LAG-3 PROTEIN) VS. PLACEBO IN COMBINATION WITH WEEKLY PACLITAXEL IN HR+ HER2- MBC

¹Hans Wildiers*, ²Luc Dirix, ³Anne Armstrong, ⁴Eveline De Cuyper, ⁵Florence Dalenc, ⁶Steven Chan, ⁷Frederik Marme, ⁸Carolina Pia Schröder, ⁹Jens Huober, ¹⁰Peter Vuylsteke, ¹¹Jean-Philippe Jacquin, ¹²Etienne Brain, ¹³Sherko Kümmel, ¹⁴Zsuzsanna Pápai, ¹⁵Christian Mueller, ¹⁵Christelle Brignone, ¹⁵Frederic Triebel. ¹University Hospitals Leuven; Department of General Medical Oncology and Multidisciplinary Breast Centre, Leuven, Belgium; ²GZA Ziekenhuizen campus Sint-Augustin, Oosterveldlaan, Belgium; ³The Christie NHS Foundation Trust, Manchester, UK; ⁴AZ Sint-Jan Brugge-Oostende AV, Ruddershove, Belgium; ⁵Institut Claudius Regaud (Institut Claudius regaud- Institut Universitaire du Cancer – Oncopole), Toulouse, France; ⁶Nottingham Cancer Clinical Trials Team, Nottingham, UK; ⁷National Center for Tumor Diseases (NCT), Heidelberg, Germany; ⁸University Medical Center Groningen, Groningen, Netherlands; ⁹Universitätsfrauenklinik Ulm, Ulm, Germany; ¹⁰CMSE UCLouvain, CHU UCL NAMUR Site Ste-Elisabeth, AND University of Botswana, Uccle, Belgium; ¹¹Institut de Cancérologie de la Loire, Saint Priest en Jarez, France; ¹²Institut Curie –Hôpital René Huguenin, Saint-Cloud, France; ¹³KEM | Evang. Kliniken Essen-Mitte, Essen, Germany; ¹⁴MH Egészségügyi Központ Onkológiai, Budapest, Hungary; ¹⁵Immupet, Berlin, Germany

Background Eftilagimod alpha (efti; IMP321) is a soluble LAG-3 protein (LAG-3Ig) that binds to a subset of MHC class II molecules and mediates activation of antigen-presenting cells followed by CD8 T-cells. Weekly paclitaxel is a standard of care chemo-regimen after failure of endocrine-based therapy for metastatic breast carcinoma (MBC). AIPAC (Active Immunotherapy PAClitaxel) investigated the addition of efti to weekly paclitaxel in these patients (pts).

Methods This placebo-controlled, double-blinded, 1:1 randomized phase IIB trial enrolled pts with measurable disease, HR+ HER2- MBC after endocrine-based therapy. Pts received paclitaxel (80 mg/m² IV on D1, D8, D15) + efti (30 mg) or placebo on D2, D16 (every 2 weeks) for up to 24 weeks following efti/placebo for up to 52 weeks. The primary endpoint (EP) was progression-free survival (RECIST1.1) by BICR. Secondary EPs included overall survival (OS), PFS (local read), overall response rate (ORR), biomarker, quality of life. Exploratory EPs included univariate/multivariate analyses.

Results 227 pts were randomized (Jan2017-Jul2019). All except 1 received ≥ 1 treatment and were included in the full analysis set [efti (n=114); placebo (n=112)]. Data cut-off was 14May2021 (min. follow-up= 22 months). Median age was 60 yrs with ECOG 0 in 61.5%. 91.6% had visceral disease. Pts were mostly endocrine resistant (84%) and partially pre-treated with CDK4/6 inhibitors (44.2%). Post-study treatment was similar. Median OS was 20.4 (95% CI: 14.3-25.1) months in the efti group vs. 17.5 (95% CI: 12.9-21.9) in the placebo group. HR was 0.88 (95%CI: 0.64-1.19; p=0.197). In predefined univariate analyses, younger pts, low baseline monocytes and luminal B showed significant/clinically meaningful improvement in OS (table 1).

Efti increased PBMC/T cell (CD4/CD8) count vs. placebo, correlating with improved OS (Spearman Rho=0.6, p=0.02 for CD8 T cells). In a whole population multivariate cox regression model, increasing BMI and prior treatment with CDK4/6 were independent significant poor prognostic markers for PFS and OS.

TEAEs leading to discontinuation were similar at 5.3%(efti) & 6.3%(placebo). PFS (Primary EP) and safety were reported at SABCs 2020 (Abstract#132).

Abstract 948 Table 1 Overall survival by subgroups at final analysis

OS / population	Overall	<65 yrs of age	Low monocytes (<250/ μ l)	Luminal B
Events % (N/N)	72.5 164 /226	72.8 107/147	70.2 33/47	83.1 69/83
Efti group – median (months); [95% CI]	20.4; [14.3-25.1]	22.3; [15.3-29.6]	32.5; [18.2-NA]	16.8; [9.9-24.9]
Placebo group median (months); [95% CI]	17.5; [12.9-21.9]	14.8; [10.9-18.5]	12.9; [7.5-20.4]	12.6; [10.2-17.3]
HR [95% CI]; p-value	0.88 [0.64-1.19]; 0.197	0.66 [0.45-0.97]; 0.017	0.44 [0.22-0.88]; 0.008	0.67 [0.41-1.08]; 0.049

Conclusions Efti added to paclitaxel led to a non-significant 2.9 months median OS increase in HR+ HER2- MBC pts after endocrine-based therapy. Effects were significant in pts <65yrs, with low monocytes and more aggressive disease (luminal B). Efti increased circulating CD4/CD8 T cells, which significantly correlated to improved OS. Weekly paclitaxel + efti should be further investigated in MBC.

Trial Registration The trial identifiers are IMP321-P011 (code for sponsor), 2015-002541-63 (EudraCT) and NCT02614833 (ClinicalTrials.gov).

Ethics Approval The study was approved by relevant ethic committees and institutional review boards.

<http://dx.doi.org/10.1136/jitc-2021-SITC2021.948>

949

FIRST-IN-HUMAN STUDY OF THE FIRST ACID PH-SENSITIVE AND RECYCLING CTLA-4 ANTIBODY THAT PRESERVES THE IMMUNE TOLERANCE CHECKPOINT TO AVOID IMMUNOTHERAPY-RELATED ADVERSE EVENTS IN CANCER PATIENTS

¹Tianhong Li*, ²Mei Tang, ³Karen Kelly, ³Hui Amy Chen, ³Stacy Joo, ⁴Imaan Khan, ⁴Nicole Do, ⁴Raymond Toumou, ⁴Dan Chen, ⁴Yang Liu, ⁴Pan Zheng. ¹University of California at Davis, Sacramento, CA, USA; ²Berman Cancer Institute at GBMC, Baltimore, MD, USA; ³UC Davis Comprehensive Cancer Center, Sacramento, CA, USA; ⁴OncoC4, Inc., Rockville, MD, USA

Background CTLA-4 is the first immune checkpoint target for cancer immunotherapy. However, the clinical benefit of targeting CTLA-4 has been limited by suboptimal doses and early discontinuation due to immunotherapy-related adverse events (irAE). Our preclinical studies suggest that acid pH-sensitive anti-CTLA-4 antibodies that preserve CTLA-4 recycling and avoid lysosomal degradation are more effective for immunotherapy but largely devoid of immunotherapy-related adverse events (irAE) [1-6]. To test this new hypothesis in human, we initiated first-in-human study evaluating the safety and tolerability of ONC-392 in patients with advanced solid tumors.

Methods ONC-392-001 Part A is a dose finding study of ONC 392, IV infusion, Q3W. Patients (pt) with advanced solid tumors who had progressed to standard of care cancer therapies with ≥ 1 measurable tumor were enrolled. Inpatient dose-escalation were performed for 4 doses (0.1, 0.3, 1.0 and 3.0 mg/kg) and 6 pts for the final dose of 10.0 mg/kg. The primary endpoints are the safety and tolerability of ONC-392 for identifying recommended Phase II dose (RP2D).

Results Ten pts have received 2-11 cycles of ONC-392 treatment at dose levels ranging from 0.1 to 10 mg/kg. Pt characteristics: median age 62 (range 43-81), female/male: 7/3, White/Asian/Black: 6/3/1. Tumor types: 4 ovarian, 4 NSCLC, 1 cervical and 1 GE junction cancer. Prior line of treatment: 2-7. Six pts were in 10 mg/kg dose level and received 2-4 doses of the drug as of this writing. None of the 10 pts experienced dose limiting toxicity (DLT) or Gr 3-4 adverse events (AEs) in DLT period. The RP2D for ONC-392 monotherapy is 10 mg/kg. After the DLT period, 1 patient developed Gr 3-4 elevated amylase/lipase at 10 weeks after 4 cycle of 10 mg/kg. No other treatment-related severe AE was observed. Among eight evaluable pts, 7/8 (87.5%) had stable disease (SD) after three cycle of treatment, and beneficial clinical efficacy activities was observed in 3/8 (37.5%) pts. Among them, a stage 4B ovarian cancer patient had stayed in treatment for 30 weeks till disease progression, and 2/2 evaluable PD(L)-1 antibody-refractory NSCLC patients were either eligible for surgery or had significant tumor shrinkage.

Conclusions ONC-392 monotherapy is well tolerated with very low irAE rate. The RP2D for ONC-392 monotherapy is 10 mg/kg. The acid pH-sensitive anti-CTLA-4 mAb that preserves CTLA-4 recycling and avoids lysosomal degradation was safe and well tolerated. Our work paves the way for significant increase of drug exposure to reach full immunotherapeutic potential of CTLA-4 targeting.

Acknowledgements The study is sponsored by OncoC4, Inc with the support of NCI SBIR grant R44CA250824.

Trial Registration NCT04140526

REFERENCES

1. Du X, et al. Uncoupling therapeutic from immunotherapy-related adverse effects for safer and effective anti-CTLA-4 antibodies in CTLA4 humanized mice. *Cell Res* 2018;**28**(4):433-447.

2. Du X, et al. A reappraisal of CTLA-4 checkpoint blockade in cancer immunotherapy. *Cell Res* 2018;**28**(4):416-432.
3. Liu Y, Zheng P. How does an anti-CTLA-4 antibody promote cancer immunity? *Trends Immunol* 2018;**39**(12):953-956.
4. Zhang Y, et al. Hijacking antibody-induced CTLA-4 lysosomal degradation for safer and more effective cancer immunotherapy. *Cell Research* 2019;**29**(8):609-627.
5. Liu Y, Zheng P. Preserving the CTLA-4 checkpoint for safer and more effective cancer immunotherapy. *Trends Pharmacol Sci* 2020;**41**(1):4-12.
6. Zhang P, et al. Mechanism- and immune landscape-based ranking of therapeutic responsiveness of 22 major human cancers to next generation anti-CTLA-4 antibodies. *Cancers (Basel)*, 2020;**12**(2):284.

Ethics Approval This study obtained ethic approval from WIRB with Study #20193108. All participants gave informed consent before taking part of the study.

Consent N/A.

<http://dx.doi.org/10.1136/jitc-2021-SITC2021.949>

FINAL ANALYSIS: PHASE 1B STUDY INVESTIGATING INTRATUMORAL INJECTION OF TOLL-LIKE RECEPTOR 9 AGONIST VIDUTOLIMOD ± PEMBROLIZUMAB IN PATIENTS WITH PD-1 BLOCKADE-REFRACTORY MELANOMA

¹John Kirkwood*, ²Yousef Zakharia, ¹Diwakar Davar, ³Elizabeth Buchbinder, ⁴Theresa Medina, ⁵Adil Daud, ⁶Antoni Ribas, ⁶Bartosz Chmielowski, ⁷Jiaxin Niu, ⁸Geoffrey Gibney, ⁹Kim Margolin, ¹⁰Anthony Olszanski, ¹¹Inderjit Mehmi, ¹²Takami Sato, ¹³Montaser Shaheen, ¹⁴Luping Zhao, ¹⁴Hong Liu, ¹⁴Heather Kelley, ²George Weiner, ¹Jason Luke, ¹⁴Dmitri Bobilev, ¹⁴Arthur Krieg, ¹⁴James Wooldridge, ²Mohammed Milhem. ¹University of Pittsburgh Medical Center, Pittsburgh, PA, USA; ²University of Iowa, Iowa City, IA, USA; ³Dana-Farber Cancer Institute, Boston, MA, USA; ⁴University of Colorado Denver, Aurora, CO, USA; ⁵University of California San Francisco, San Francisco, CA, USA; ⁶University of California Los Angeles, Los Angeles, CA, USA; ⁷Banner MD Anderson Cancer Center, Gilbert, AZ, USA; ⁸Georgetown Lombardi Comprehensive Cancer Center, Washington, DC, USA; ⁹City of Hope, Duarte, CA, USA; ¹⁰Fox Chase Cancer Center, Philadelphia, PA, USA; ¹¹The Angeles Clinic and Research Institute, Los Angeles, CA, USA; ¹²Thomas Jefferson University, Philadelphia, PA, USA; ¹³University of Arizona, Tucson, AZ, USA; ¹⁴Checkmate Pharmaceuticals Inc., Cambridge, MA, USA

Background There are limited therapeutic options for patients with progressive disease (PD) on or after PD-1-blocking antibody therapy. Vidutolimod (CMP-001) is a first-in-class, immunostimulatory virus-like particle containing a CpG-A Toll-like receptor 9 (TLR9) agonist. This phase 1b study evaluated the safety and clinical activity of intratumoral vidutolimod with and without pembrolizumab in patients with refractory melanoma.

Methods This two-part, open-label, multicenter, phase 1b study (NCT02680184) enrolled adults with histologically confirmed metastatic or unresectable cutaneous melanoma who had stable disease after ≥ 12 weeks or PD on anti-PD-1 treatment, measurable disease per RECIST v1.1, ECOG PS 0/1, and ≥ 1 lesion accessible for intratumoral injection. Part 1 evaluated vidutolimod + pembrolizumab and Part 2 evaluated vidutolimod monotherapy. Key objectives included assessment of safety and clinical activity, and exploratory analyses were performed on available tumor biopsies using immunohistochemistry and RNAseq.

Results At data cutoff (August 17, 2021), 159 patients had enrolled in Part 1 and 40 patients in Part 2. The median age was 64 years in Part 1 (range, 30-90) and 68 years in Part 2 (range, 30-89). Most patients had PD as their last response to prior anti-PD-1 therapy (Part 1, 93.1%; Part 2, 80.0%). Grade 3/4 treatment-related adverse events (TRAEs) occurred in 37.1% of patients treated with vidutolimod + pembrolizumab and in 22.5% of patients treated with vidutolimod monotherapy. No treatment-related deaths occurred. Based on the efficacy data presented in Table 1, vidutolimod polysorbate 20 (PS20) A was selected for further development as this formulation in combination with pembrolizumab had a best objective response rate (ORR; RECIST v1.1) of 23.5%, with a median duration of response (DOR) of 25.2 months. Vidutolimod monotherapy had an ORR of 20.0%, with a median DOR of 5.6 months. Exploratory translational analyses identified association of unique biomarkers with response among patients with T cell-inflamed versus non-T cell-inflamed tumors at baseline.

Abstract 950 Table 1 Safety and clinical activity of vidutolimod ± pembrolizumab

	Part 1: Vidutolimod + Pembrolizumab (Dose Escalation and Expansion)			Part 2: Vidutolimod Monotherapy
	Intention-to-Treat Population n=159	Vidutolimod PS20 A + Pembrolizumab n=98	Vidutolimod PS20 B + Pembrolizumab n=61	Vidutolimod n=40
Safety*				
TRAE grade 3, n (%)	55 (34.6)	37 (37.8)	18 (29.5)	9 (22.5)
TRAE grade 4, n (%)	4 (2.5) [†]	3 (3.1)	1 (1.6)	0
TRAE grade 5, n (%)	0	0	0	0
Clinical Activity				
Best ORR per RECIST v1.1, % (95% CI)	18.9 (13.1-25.8)	23.5 (15.5-33.1)	11.5 (4.7-22.2)	20.0 (9.1-35.6)
Best ORR, including postprogression responders, % (95% CI)	23.3 (16.9-30.6)	27.6 (19.0-37.5)	16.4 (8.2-28.1)	22.5 (10.8-38.5)
Responders, n (%)				
Complete response	8 (5.0)	7 (7.1)	1 (1.6)	0
Partial response	22 (13.8)	16 (16.3)	6 (9.8)	8 (20.0)
Postprogression partial response	7 (4.4)	4 (4.1)	3 (4.9)	1 (2.5)
Median DOR, months (95% CI)	19.9 (9.5-NE)	25.2 (8.7-NE)	11.4 (5.4-19.9)	5.6 (3.1-NE)

NE, not estimable; PS20 A, vidutolimod formulation with polysorbate 20 at 0.01%; PS20 B, vidutolimod formulation with polysorbate 20 at 0.00167%.

*Patients are reported for their highest-grade TRAE only.

[†]Grade 4 TRAEs were alanine aminotransferase increased, aspartate aminotransferase increased, blood creatine phosphokinase increased, hypotension, and platelet count decreased (n=1 [0.6%] each).

Conclusions Promising clinical activity was observed with vidutolimod + pembrolizumab and vidutolimod monotherapy in patients with PD-1 blockade-refractory melanoma. A manageable safety profile was observed. The DOR with vidutolimod + pembrolizumab was substantially longer than with vidutolimod monotherapy. Clinical studies to confirm the efficacy of vidutolimod + PD-1 blockade in patients with previously untreated unresectable/metastatic melanoma (phase 2/3, NCT04695977) or PD-1 blockade-refractory melanoma (phase 2, NCT04698187) are ongoing.

Acknowledgements This work was supported by Checkmate Pharmaceuticals. Medical writing assistance was provided by Steffen Biechele, PhD (ApotheCom, San Francisco, CA, USA), and funded by Checkmate Pharmaceuticals.

Trial Registration NCT02680184

Ethics Approval This study was approved by the WCG-WIRB; WIRB approval tracking number: 20152597.

<http://dx.doi.org/10.1136/jitc-2021-SITC2021.950>

Clinical Trials in Progress

951

A PHASE 1 FIRST IN HUMAN STUDY OF ADENOVIRALLY TRANSDUCED ANTI-HER2 CAR MACROPHAGES IN SUBJECTS WITH HER2 OVEREXPRESSING SOLID TUMORS: PRELIMINARY SAFETY, PHARMACOKINETICS, AND TME REPROGRAMMING DATA

¹Kim Reiss*, ²Yuan Yuan, ³Debra Barton, ³Amy Ronczka, ³Daniel Cushing, ³Michael Klichinsky, ³Sascha Abramson, ³Rehman Qureshi, ³Thomas Condamine, ⁴Elizabeth Dees. ¹University of Pennsylvania, Philadelphia, PA, USA; ²City of Hope Comprehensive Cancer Center, Duarte, CA, USA; ³Carisma Therapeutics, Springfield, NJ, USA; ⁴UNC, Chapel Hill, NC, USA

Background CT-0508 is an autologous monocyte-derived pro-inflammatory macrophage cell product engineered with Ad5f35 to express an anti-HER2 CAR. In pre-clinical studies CT-0508 was safe and effective. This abstract contains preliminary results from the first-in-human experience with CAR macrophages (CAR-M).

Methods This First-In-Human Phase 1, multi-center, open-label study is evaluating the safety, tolerability, manufacturing feasibility, pharmacokinetics and mechanism of action of CT-0508 in 18 subjects with advanced solid tumors overexpressing HER2 who have progressed on prior therapies, including HER2 targeted therapies if indicated.

Patients receive four doses of filgrastim for monocyte mobilization prior to apheresis. CT-0508 CAR-M is manufactured from autologous apheresis products and delivered as a cryopreserved cell product. Group 1 subjects enter an intra-patient fractionated dose escalation regimen, receiving CT-0508 on D1, D3 and D5, followed by Group 2 subjects who receive CT-0508 on D1. There is no preparative chemotherapy prior to CT-0508 infusion.

Pre and post treatment biopsies and blood samples are collected to investigate correlates of safety, serum cytokines and chemokines, pharmacokinetics, TME modulation, and induction of an adaptive anti-tumor immune response.

Results To date, two subjects have been treated with CT-0508 (esophageal adenocarcinoma and extrahepatic cholangiocarcinoma). Patient product was successfully manufactured, CT-0508 treatment was well tolerated, with no dose limiting and no major organ toxicities observed.

One subject experienced Grade 2 CRS on Day 3 which resolved on the same day.

Grade 3 AEs included anemia (present at baseline for both subjects) and lymphopenia (present at baseline in one subject). One subject experienced one SAE of Grade 4 tumor bleeding which was unrelated to CT-0508, 88 days after the last infusion.

CAR-M were transiently detected in the peripheral blood following each infusion, demonstrating rapid egress from the periphery into tissues within hours. Transient cytokine/chemokine elevations were observed (peak: 2 hours, back to baseline at 48 hours). Single cell RNAseq analysis of dissociated tumor tissue samples (pre-treatment, day 8 and week 4) demonstrated dynamic TME reprogramming, with recruitment of inflammatory innate immune cells and naïve T cells at day 8, and significant CD8+ T cell infiltration, activation, and proliferation at week 4.

Conclusions CT-0508 has been administered to two subjects thus far, exhibiting safety, good tolerability, T cell repertoire modulation, and reprogramming of the TME consistent with

the induction of anti-tumor immunity. The study continues to recruit patients and updated data will be presented.

Trial Registration NCT04660929

REFERENCE

1. Klichinsky M, Ruella M, Shestova O, *et al.* Human chimeric antigen receptor macrophages for cancer immunotherapy. *Nat Biotechnol* 2020;**38**(8):947–953.

Ethics Approval Ethics approvals have been obtained from the clinical sites enrolling patients: the University of Pennsylvania (844106/IORG0000029), the University of North Carolina and City of Hope Comprehensive Cancer Center (20201732/IORG0000432).

<http://dx.doi.org/10.1136/jitc-2021-SITC2021.951>

952

PHASE II TRIAL OF AV-GBM-1: DENDRITIC CELL VACCINE PULSED WITH LYSATE ENRICHED FOR AUTOLOGOUS TUMOR-INITIATING CELL ANTIGENS IN THE TREATMENT OF PATIENTS WITH NEWLY DIAGNOSED GLIOBLASTOMA

¹Daniela Bota*, ²David Piccioni, ³Christopher Duma, ⁴Renato LaRocca, ⁵Santosh Kesari, ⁶Mehrdad Abedi, ⁵Jose Carrillo, ⁷Robert Aiken, ¹Frank Hsu, ¹Xiaotang Kong, ¹Thomas Taylor, ⁸Candace Hsieh, ⁸Gabriel Nistor, ⁸Robert Dillman. ¹University of California Irvine, Orange, CA, USA; ²UCSD, San Diego, CA, USA; ³Hoag Hospital, Newport Beach, CA, USA; ⁴Norton Cancer Center, Louisville, KY, USA; ⁵John Wayne Cancer Institute, Santa Monica, CA, USA; ⁶UC Davis, Sacramento, CA, USA; ⁷Rutgers Cancer Center, New Brunswick, NJ, USA; ⁸AVITA Biomedical, Inc, Irvine, CA, USA

Consent n/a

<http://dx.doi.org/10.1136/jitc-2021-SITC2021.952>

Background Standard therapy of glioblastoma (GBM), which includes maximum safe resection, concurrent radiation therapy and temozolomide chemotherapy (RT/TMZ) followed by maintenance TMZ, is associated with poor overall survival (OS). Adding treatment with AV-GBM-1, a vaccine consisting of autologous dendritic cells (DC) pulsed with autologous tumor antigens (ATA) may improve OS. A multi-center phase II clinical trial was conducted to determine feasibility, safety, and efficacy of AV-GBM-1.

Methods Key eligibility criteria for tumor collection were clinical suspicion of newly diagnosed GBM and age 18 to 70 years at the time of surgery. Prior to starting RT/TMZ, key eligibility criteria for intent-to-treat-with-AV-GBM-1 enrollment were: (1) primary GBM confirmed, (2) successful GBM cell culture, (3) collection of sufficient numbers of monocytes (MC) by leukapheresis, (4) Karnofsky Performance Status 70 or greater and (5) plan to treat with concurrent RT/TMZ. AV-GBM-1 was manufactured during RT/TMZ. Interleukin-4 and granulocyte-macrophage colony stimulating factor (GM-CSF) were used to differentiate MC into DC. AV-GBM-1 consists of autologous DC incubated with ATA from the lysate of irradiated GBM cells grown in serum-free media with factors that favor the survival and proliferation of stem cells and early progenitor cells. After recovery from RT/TMZ, over six months patients received up to 8 subcutaneous injections of AV-GBM-1 admixed with 500 µg GM-CSF. The primary objective was to determine if OS was 75% or higher 14.6 months from ITT enrollment, which ended January 2020. The minimum follow-up at the time of analysis was 15.2 months. Secondary endpoints included progression-free survival (PFS) from ITT enrollment and from the first injection.

Results Success rates for cell cultures and sufficient monocyte collections were both 97%. AV-GBM-1 was manufactured for 60/60 (100%). 57 patients received 392 injections; 68% received all 8. The primary adverse events (AE) attributed to AV-GBM-1 were local injection site reactions (16%) and flu-like symptoms (10%). Progression-free survival (PFS) from ITT enrollment is 10.3 months, about 50% longer than reported in four randomized trials with comparable standard therapy arms. PFS from the first injection is 8.3 months, which is 51% and 107% longer than reported in two randomized trials with comparable standard therapy arms. OS was 72% at 12 months, but dropped to 54% at 14.6 months; median OS is 16.0 months.

Conclusions Patient-specific AV-GBM-1 was reliably manufactured and distributed for administration. AV-GBM-1 produced minimal toxicity. PFS was very encouraging but did not translate into OS, perhaps because of discontinuation of treatment after 8 months.

Trial Registration [Clinicaltrials.gov NCT03400917]

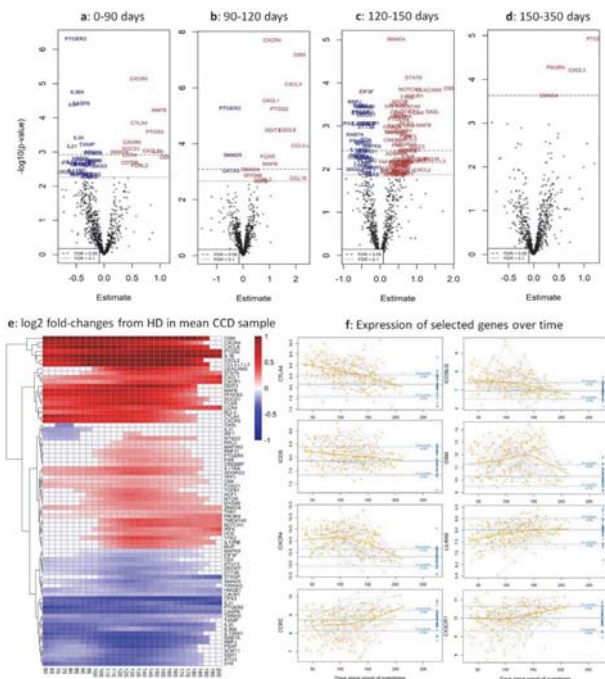
Ethics Approval Western IRB, approval number 20182582

953

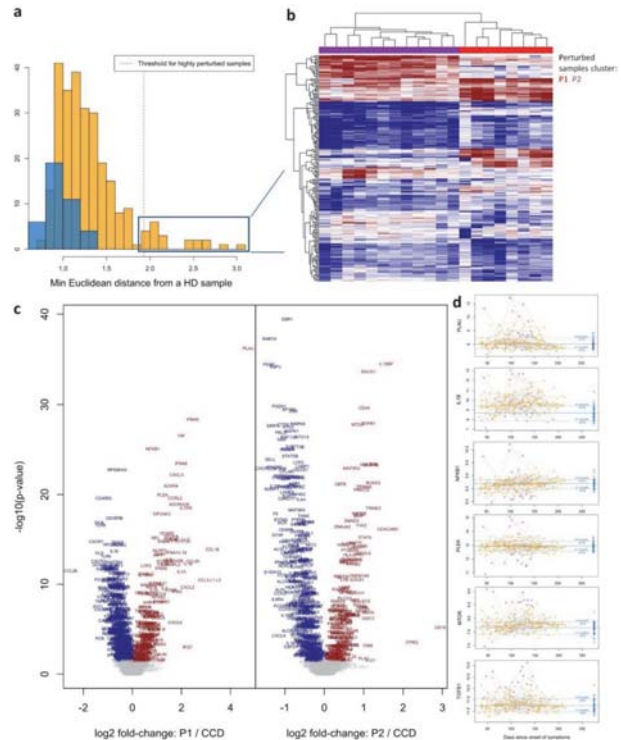
TRANSCRIPTIONAL ANALYSIS OF LEUKOCYTES FROM COVID CONVALESCENT DONORS REVEALS PERSISTENT ACTIVATION OF THE INNATE AND ADAPTIVE IMMUNE SYSTEM

¹Mallikarjuna Gedda, ²Patrick Danaher*, ¹Lipei Saho, ¹Martin Ongkeko, ¹Leonard Chen, ¹Mame Thiolye Sall, ¹Opal Reddy, ²Christina Bailey, ²Amy Wahba, ²Inna Dzekunova, ¹Valeria De Giorgi, ¹Robert Somerville, ¹Jin Ping, ¹Kamille West, ¹Sandhya Panch, ¹David Stroncek. ¹National Institutes of Health, Bethesda, MD, USA; ²NanoString, Seattle, WA, USA

Background Coronavirus disease 2019 (COVID-19) results in robust but dysregulated acute immune response characterized by pro-inflammatory cytokine production and T-cell exhaustion, but little is known concerning immune response following recovery. We assessed immune function in convalescent plasma donors (CCD) who had recovered from COVID-19. **Methods** The cellular immune response and T-cell receptor (TCR) diversity in CCD was investigated using the nCounter host response and TCR diversity panels. 270 CCD and 40 healthy donor (HD) blood samples collected 11 to 193 days after diagnosis were analyzed. The CCD samples were from 162 donors, 69 donated more than once. All HD donated only once.



Abstract 953 Figure 1 Longitudinal trends in CCD gene expression. **a-d**: Differential expression results in HD vs. 4 time windows of CCD. Genes with FDR < 0.1 are labeled; **e**: average CCD log₂ fold-changes from HD over time. Color is only given for times where the Loess regression is different from the mean HD with $p < 0.05$; **f**: longitudinal results for selected genes. Orange lines connect CCD samples over time. Blue lines show inner 95% quantiles of HD samples



Abstract 953 Figure 2 CCD with more severe departure from HD gene expression. **a**: CCD samples (in orange) were scored for perturbation from the mean HD (in blue), and 21 highly perturbed sample subsets emerged; **b**: clustering of the 21 highly perturbed patients. The dendrogram was cut to define two groups. **c**: volcano plots comparing expression in P1 (left) and P2 (right) vs. CCD; **d**: longitudinal trends of selected genes perturbed in P1 and P2

Results Many genes were differentially expressed for months following infection. Analysis of samples collected 0 to 90 days post-diagnosis found that 19 of 773 genes were differentially expressed among CCD and HD (FDR < 0.05) (figure 1a). At 90 to 120 days, 120 to 150 and >150 post-diagnosis, 13, 58 and 4 genes were differentially expressed respectively (FDR < 0.05) (figures 1b-d). At 120 to 150 days the differentially expressed genes included those in Treg differentiation, type III interferon signaling and chemokine signaling pathways. 76 genes were differentially expressed at least once during the time windows described above. (Figure 1e). Among CCD, the expression of CTLA-4, ICOS, ICOSLG, OSM and CXCR4 were initially elevated but fell to HD levels at the end of the study period. The expression of LILRA6, CCR2 and CX3CR1 increased or remained elevated throughout (figure 1f).

A subset of samples departed notably from the average trend. The transcriptome of each CCD sample was scored by its similarity to the mean transcriptome of HD samples. This analysis revealed 21 CCD samples from 19 unique donors

were highly perturbed from HD samples (figure 2a). Among these highly perturbed samples 80% were collected > 90 days post-diagnosis. The perturbed samples clustered into two groups, labelled P1 and P2 (figure 2b) and displayed dysregulation of distinct gene sets (figures 2c, 2d). The P1 were characterized by increased expression of genes in myeloid inflammation, type 1 interferon and innate immune signaling pathways, lower COVID antibody levels and increased T-cell receptor diversity. P2 were characterized by highly up-regulated CD44, BCL2, TGFB1, IL18BP, IL27RA, and IL11RA.

Conclusions Immune dysregulation in CCD continues at least 6 months post-infection. Some CCDs experienced marked transcriptional changes which may be the result of COVID-19 reactivation and could be responsible for long-haul syndrome.

Acknowledgements N/A

Trial Registration NCT04360278

REFERENCES

N/A

Ethics Approval N/A

Consent N/A

<http://dx.doi.org/10.1136/jitc-2021-SITC2021.953>

CLINICAL RESULTS FROM A PHASE I DOSE ESCALATION STUDY IN TREATMENT-NAÏVE EARLY STAGE PROSTATE CANCER PATIENTS WITH ORCA-010, A POTENCY ENHANCED ONCOLYTIC REPLICATION COMPETENT ADENOVIRUS

¹Tereza Brachtlova, ²Allan Abramovitch, ³Jonathan Giddens, ⁴Peter Incze, ⁵Kenneth Jansz, ⁴Richard Casey, ⁶Victor van Beusechem, ¹Wenliang Dong*. ¹ORCA Therapeutics BV, Den Bosch, Netherlands; ²Urology and Male Infertility Clinic, Scarborough, Canada; ³Jonathan Giddens Medicine Professional Corp, Brampton, Canada; ⁴The Fe/Male Health Centres, Oakville, Canada; ⁵G. Kenneth Jansz Medicine Professional Corp, Burlington, Canada; ⁶Amsterdam University Medical Center, Amsterdam, Netherlands

Background Oncolytic adenoviruses have proven to be clinically promising immunotherapeutic agents for the treatment of cancer. Besides the direct anti-tumor activity of oncolytic adenoviruses, their ability to create a favorable microenvironment for the action of the host immune system against unique cancer cell determinants and a non-compromised host immune system are recognized as a key factors in successful oncolytic cancer treatment.

Considering the role of the host immune system, treatment-naïve patients with early stage localized prostate cancer were enrolled in a phase I trial with ORCA-010. Here we report on the safety of intratumoral administration of ORCA-010 and present an interim analysis of the clinical and immunological responses observed.

Methods Treatment-naïve prostate cancer patients with localized disease (stage I or II) were treated with a single intratumoral administration of ORCA-010 in a phase I dose escalation study. Nine patients in three dose escalation cohorts (1E11, 1E12 or 1.5E12 viral particles/administration) were treated based on a 3+3 design with a 1-year follow-up period.

The primary study objectives include the safety profile of intratumoral administration of ORCA-010. Secondary objectives include 1) evaluation of the biological activity and antitumor efficacy of intratumoral administration of ORCA-010; 2) to evaluate potential antitumor immune responses and 3) to assess shedding of ORCA-010.

Results Nine patients with localized prostate cancer have been treated with a single intratumoral administration of ORCA-010. The safety profile demonstrated excellent tolerability and safety of ORCA-010 treatment with no DLTs reported. Treatment related adverse events observed in all patients were limited to transient grade I and grade II adverse events.

Shedding analyses demonstrated active replication of ORCA-010 post administration and a viremia peak was observed in all patients within 1 week post administration. Coinciding with the viral load, free PSA increased significantly post treatment and returned to under 10 ng/mL 1-2 months post administration. Preliminary analyses of the MRI data of the low dose cohorts demonstrated a significant reduction of prostate size 6 months post treatment in patients with significantly enlarged prostates prior to treatment.

Conclusions Intratumoral administration of ORCA-010 in treatment-naïve prostate cancer patients demonstrated an excellent safety profile, with no DLTs observed and transient grade I and II adverse events. Preliminary analyses of the data demonstrate viral replication post administration, encouraging initial anti-tumor activity and a prostate size reduction in prostate cancer patients with enlarged prostates.

Trial Registration NCT04097002

Ethics Approval The study was approved by Advarra institutional review board IRB#00000971 and patients completed an ICF prior to enrollment into the study.

<http://dx.doi.org/10.1136/jitc-2021-SITC2021.954>

955

**CORE1: PHASE 2, SINGLE ARM STUDY OF CG0070
COMBINED WITH PEMBROLIZUMAB IN PATIENTS WITH
NON MUSCLE INVASIVE BLADDER CANCER (NMIBC)
UNRESPONSIVE TO BACILLUS CALMETTE-GUERIN (BCG)**

¹Roger Li, ²Gary Steinberg, ³Donald Lamm, ⁴Ed Uchio, ⁵Vignesh Packiam, ⁶Ashish Kamat, ⁷Michael Chisamore, ⁸John McAdory, ⁹Paola Grandi, ¹⁰Jee-Hyun Kim, ¹¹James Burke*.
¹Moffitt, Tampa, FL, USA; ²NYU, New York, NY, Canada; ³BCG Oncology, Phoenix, AZ, USA; ⁴UCI, Irvine, CA, USA; ⁵University of Iowa, Iowa City, IA, USA; ⁶University of Texas MD Anderson, Houston, TX, USA; ⁷Merck, Wheaton, IL, USA; ⁸CG Oncology, Irvine, CA, USA

Background CG0070, an oncolytic vaccine available as an intravesical therapy, is a serotype 5 adenovirus engineered to express GM-CSF and replicate in tumor cells with mutated or deficient RB (which results in increased of the transcription factor E2F). The CG0070 mechanism of action includes direct cell lysis in conjunction with immunogenic cell death which is enhanced in the presence of GM-CSF. In an initial phase 1 study as well as a subsequent phase 2 study, an overall CR rate of ~62% and a CR at 12 months (m) of 29% have been observed in patients with high risk NMIBC previously treated with BCG. Intravenous Pembrolizumab was recently approved by the FDA for patients with BCG-unresponsive CIS (with or without papillary tumors) with an overall complete RR of 41% and a 12m CR rate of ~20%. This phase 2 study (NCT04387461) will assess the potential synergy of the two agents in the treatment of BCG-unresponsive NMIBC.

Methods 35 patients with BCG-unresponsive CIS with or without concurrent Ta or T1 disease will be treated with intravesical (IVE) CG0070 at a dose of 1x10¹² vp in combination with pembrolizumab at a dose of 400 mg IV q6 weeks. CG0070 will be administered weekly x 6 as induction followed by weekly x 3 maintenance instillations at 3, 6, 9, 12, and 18m. Patients with persistent CIS or HG Ta at 3 m may receive re-induction with weekly x 6 CG0070. Pembrolizumab will be administered up to 24m. Assessment of response will include q 3m cystoscopy with biopsy, urine cytology, CTU/MRU, and mandatory bladder mapping biopsies at 12m.

Results The primary endpoint is CR at 12 m. Secondary endpoints will include CR at any time, progression free survival, duration of response, cystectomy free survival and the safety of the combination. Correlate assessments will include changes in the TME, systemic immune induction, viral replication and transgene expression. Baseline expression of PD-L1, coxsackie adenovirus receptor, E2F transcription factor as well as anti-adenovirus antibody titer will be correlated with tumor response. At this time the first 5 patients demonstrates 100% 3 m CR. Treatment related AE have been limited to transient grade 1-2 urinary frequency (3 patients) and grade 1 bladder spasm, hematuria, painful urination, thyroiditis, and flu-like symptoms (one patient/each). No grade 3, 4, 5 AE or SAE were observed.

Conclusions The study is currently enrolling. Preliminary safety and efficacy data on 8 patients will be available by November 2021

Trial Registration NCT04387461

Ethics Approval IRB: CG2003C

<http://dx.doi.org/10.1136/jitc-2021-SITC2021.955>

RETIFANLIMAB (INCMGA00012) IN PATIENTS WITH RECURRENT MSI-H OR dMMR ENDOMETRIAL CANCER: RESULTS FROM THE POD1UM-101 STUDY

¹Dominique Berton, ²Patricia Pautier, ³Domenica Lorusso, ⁴Christine Gennigens, ⁵Laurence Gladieff, ⁶Anna Kryzhanivska, ⁷Sulabha Ranganathan, ⁷Chuan Tian, ⁷Nawel Bourayou, ⁸Ignace Vergote*. ¹GINECO and Institut de Cancérologie de l'Ouest (ICO), Centre René Gauducheau, Saint-Herblain, France; ²GINECO and Institut Gustave-Roussy, Villejuif, France; ³Fondazione Policlinico Universitario Agostino Gemelli IRCCS and Catholic University of Sacred Heart, Rome, Italy; ⁴University Hospital (CHU) of Liège, Liège, Belgium; ⁵GINECO and Institut Claudius Regaud IUCT Oncopole, Toulouse, France; ⁶Regional Clinical Oncology Center, Ivano-Frankivsk, Ukraine; ⁷Incyte Corporation, Wilmington, DE, USA; ⁸University Hospitals Leuven, Leuven Cancer Institute, Leuven, Belgium

Background Management of patients with recurrent endometrial cancer after failure on platinum-based therapy remains a clinical challenge. Retifanlimab (INCMGA00012) is an investigational humanized immunoglobulin G4 monoclonal antibody against programmed cell death 1 (PD-1). We previously reported encouraging results from a preplanned interim analysis in patients with microsatellite instability-high (MSI-H) recurrent endometrial cancer treated with retifanlimab in POD1UM-101 [1]. Here, we provide top-line results from the full cohort of patients in the POD1UM-101 study.

Methods Eligible patients have histologically proven, unresectable recurrent MSI-H or deficient mismatch repair (dMMR) endometrial cancer (per local testing), ECOG PS ≤1, disease progression during or following 1 to ≤5 prior systemic treatments, measurable disease (per RECIST v1.1), and are naïve to prior immune checkpoint inhibitors. MSI-H and dMMR status were centrally confirmed using PCR and IHC, respectively. Patients receive retifanlimab 500 mg every 4 weeks for up to 2 years. The primary study endpoint is safety. Confirmed best overall response and duration of response (DOR) were evaluated by independent central review (ICR) using RECIST v1.1.

Results As of July 6, 2021, 76 patients with centrally confirmed MSI-H (65 [85.5%]) or dMMR (11 [14.5%]) endometrial cancer had received ≥1 dose of retifanlimab; median age was 67.0 (49–88) years, 70 (92.1%) had endometrioid histology, 67 (88.2%) had metastatic disease, and 61 (80.3%) had visceral metastases. Sixty-eight (89.5%) patients had prior surgery or procedure, 54 (71.1%) patients were treated with radiotherapy, and 75 (98.7%) patients had received prior systemic therapy for advanced disease (33 [43.4%] received ≥2 prior systemic therapies for advanced disease). Median retifanlimab exposure was 7.4 (0.03–23.0) months. At data cutoff, 2 (2.6%) patients completed treatment and 30 (39.5%) were on treatment. Grade ≥3 treatment emergent AEs (TEAEs) occurred in 33 (43.4%) patients, including 10 (13.2%) with anemia and 7 (9.2%) with an immune-related AE (nephritis, n=2; autoimmune hepatitis, hepatitis, myositis, rash, and pneumonitis, n=1 each). There were no treatment-related AEs with fatal outcome. Centrally confirmed objective responses were observed in 33 (43.4%) patients (95% CI, 32.1–55.3), with 11 (14.5%) complete and 22 (28.9%) partial responses. Of the 33 patients with objective response, 25 (75.8%) had DOR for ≥6 months; median DOR was not reached. Median follow-up time for response was 8.4 (range, 1.9–28.3) months.

Conclusions Retifanlimab was well tolerated and demonstrated encouraging antitumor activity in patients with pretreated recurrent MSI-H or dMMR endometrial cancer, consistent with that achieved with other PD-1 therapies.

Acknowledgements This study is sponsored by Incyte Corporation (Wilmington, DE).

Trial Registration ClinicalTrials.gov NCT03059823, EudraCT 2017-000865-63

REFERENCE

1. Berton-Rigaud D, et al. *J Immunother Cancer* 2020;**8**(Suppl 3):A164–A165 [Abstract 268].

Ethics Approval This study was approved by institutional review boards or independent ethics committees in Belgium (Aan de Commissie Medische Ethiek University Hospitals Leuven [CEC: S62335]; Ethics Committee of Hospital-Faculty University of Liège [LEC: 2019/48]); Bulgaria (Ethics Committee for Clinical Trials, Sofia [RA: IAL-24443/08.06.2017; CEC: □□-80/08.06.2017]); Finland (HUS Tutkimuseettiset toimikunnat Biomedicum Helsinki [RA: KLnro 124/2019]); France (CPP Île-de-France X Hôpital, Aulnay-sous-Bois cedex [RA: MED MSA NAT-2019-08-00080; CEC: CN-RIPH 19.02.17.56415/CPP 27-2019]); Germany (Ethik-Kommission der Albert-Ludwigs-Universität Freiburg, Freiburg [RA: 3102/012; EC: 506/18]; Ethics Committee at the Technical University of Dresden, Dresden [RA: 3102/012; EC: EK 4854 AB]; Ethics Committee of the State of Berlin, Berlin [RA: 3102/012; EC: 17/0411 EK 12/15]); Italy (Comitato Etico del Policlinico Gemelli Fondazione Policlinico Universitario "Agostino Gemelli", Roma (RM) [no approval number issued by RA or EC]; Comitato Etico IRCCS di Candiolo, Candiolo-TO [no approval number issued by RA or EC]); Latvia (Ethics Committee for Clinical Research at Development Society of Pauls Stradins Clinical University Hospital, Riga [no approval number issued by RA or EC]); Lithuania (Lithuanian Bioethics Committee, Vilnius [no approval number issued by RA or EC]); Poland (Komisja Bioetyczna przy Uniwersytecie Medycznym, Poznań [RA: UR.DBL.474.0350.2017; CEC: 622/17]); Spain (Comité de Ética de Investigación con Medicamentos, Madrid Centro Actividades Ambulatoria [RA: 17-073 (Locator: 2VK42NE57D); CEC: 17/211]); Ukraine (Ethical Committee at Prykarpatsky Regional Clinical Oncology Center of Ivano-Frankivsk Regional Rada, Ivano-Frankivsk [no approval number issued by RA or EC]); United States (IntegReview IRB, Austin, TX [no approval number issued by IRB]; The University of Texas MD Anderson Cancer Center Institutional Review Board, Houston, TX [no approval number issued by IRB]).

<http://dx.doi.org/10.1136/jitc-2021-SITC2021.956>

NKTR-255+CETUXIMAB IN PATIENTS WITH SOLID TUMORS: INTERIM SAFETY AND EFFICACY RESULTS FROM THE PHASE 1B DOSE-ESCALATION STUDY

¹Mehmet Altan*, ²Amita Patnaik, ³Minal Barve, ⁴Lara Dunn, ⁵Patrick Cobb, ⁶Ari Rosenberg, ⁷Sunil Sharma, ⁸Ammar Sukari, ⁹Manish Patel, ¹⁰Xiaoli Wang, ¹⁰Haijun Ma, ¹⁰Neha Dixit, ¹¹Wildaliz Nieves, ¹⁰Christie Fanton, ¹⁰Sue Currie, ¹⁰Zachary Lee, ¹⁰Mario Marcondes, ¹⁰Johnathan Zalevsky, ¹⁰Mary Tagliaferri, ¹²Assuntina Sacco. ¹The University of Texas MD Anderson Cancer Center, Houston, TX, USA; ²South Texas Accelerated Research Therapeutics (START), San Antonio, TX, USA; ³Mary Crowley Cancer Research Center, Dallas, TX, USA; ⁴Memorial Sloan Kettering Cancer Center, New York, NY, USA; ⁵St. Vincent Frontier Cancer Center, Billings, MT, USA; ⁶University of Chicago, Chicago, IL, USA; ⁷HonorHealth Research Institute, Scottsdale, AZ, USA; ⁸Karmanos Cancer Center, Detroit, MI, USA; ⁹University of Minnesota Medical Center, Rochester, MN, USA; ¹⁰Nektar Therapeutics, San Francisco, CA, USA; ¹¹Nektar Therapeutics, San Francisco, CA, USA; ¹²University California San Diego, La Jolla, CA, USA

Background NKTR-255 is an investigational IL-15R α -dependent, polymer-conjugated, recombinant human IL-15 agonist designed to provide sustained pharmacodynamic (PD) responses without the need for daily dosing. NKTR-255 engages all IL-15 receptor binding complexes to expand, proliferate and activate natural killer (NK) and CD8+ T-cells. This Phase 1b/2 trial (NCT04616196) evaluates NKTR-255 +cetuximab in highly refractory patients with head-and-neck squamous cell carcinoma (HNSCC) or colorectal cancer (CRC).

Methods Successive cohorts received escalating doses of NKTR-255 (q3w) +cetuximab (250mg/m² < sup >2</sup> weekly), 1 week after a loading dose of cetuximab alone. Safety (CTCAEv5.0; MTD/recommended Phase 2 dose [RP2D]) and efficacy (RECISTv1.1) were measured. PK/PD analyses were conducted, including assessment by flow cytometry/plasma cytokine analysis. Fold-change was calculated as treatment over baseline for NKTR-255 (baseline=1).

Results As of August 15, 2021, 12 patients had received ≥ 1 dose of NKTR-255+cetuximab; (37–70 years; 92% male; HNSCC n=4, CRC n=8; NKTR-255 1.5 μ g/kg n=7, NKTR-255 3.0 μ g/kg n=5). Patients had received a median 3.5 lines of prior therapy for metastatic disease. 11 patients had no response to the most recent prior therapy. Of the 12 patients, seven remain on treatment, with five not yet reaching first scan. RP2D has not yet been reached; dose escalation is ongoing.

10 patients experienced an AE; one G5 AE occurred (due to progression). Seven patients reported NKTR-255-related AEs (all G1-2, except one G3 [which resolved in 24 hours]). Any-cause AEs in $\geq 20\%$ were acneiform dermatitis, fatigue, and infusion-related reaction.

Treatment-induced transient changes in inflammatory cytokines, including IFN γ , MCP-1 and IL-6, at 1.5 μ g/kg (n=3) peaked 4 hours post-infusion and resolved by 24-48 hours. Mean T_{1/2} of NKTR-255 (1.5 μ g/kg dose, first cycle) was 27.8 hours.

Dose-dependent expansion of NK and CD8+ T-cells was observed in peripheral blood. For NK cells, mean peak fold-change was ~4-fold and ~6-fold, and for CD8+ T-cells was ~2-fold and ~3-fold (1.5 μ g/kg and 3 μ g/kg dose levels, respectively). NK and CD8+ T-cells demonstrated increased Ki67+ proliferative ability.

As of August 15, four patients in the 1.5 μ g/kg NKTR-255 dose cohort were response-evaluable: one CRC patient (4 prior metastatic treatment lines) reported a confirmed PR (~52%) after 3 cycles; two HNSCC patients reported SD.

Conclusions NKTR-255 was biologically active and led to expansion and proliferation of NK and CD8+ T-cells. Early dose-escalation data suggest that NKTR-255+cetuximab is safe and tolerable with preliminary anti-tumor activity. Updated data will be presented. NKTR-255, alone and in combination with daratumumab and rituximab, is also being evaluated in liquid tumors.

Acknowledgements The authors thank the patients and their families involved in the trial.

Trial Registration NCT04616196

Ethics Approval The study was approved by site IRBs.

Consent N/A

<http://dx.doi.org/10.1136/jitc-2021-SITC2021.957>

958

BNT211: A PHASE I/II TRIAL TO EVALUATE SAFETY AND EFFICACY OF CLDN6 CAR-T CELLS AND VACCINE-MEDIATED IN VIVO EXPANSION IN PATIENTS WITH CLDN6-POSITIVE ADVANCED SOLID TUMORS

¹Andreas Mackensen*, ²Christian Koenecke, ³John Haanen, ⁴Winfried Alsdorf, ⁵Alexander Desuki, ⁵Eva Wagner-Drouet, ⁶Daniel Heudobler, ⁷Peter Borchmann, ⁸Erol Wiegert, ⁹Catrine Schulz, ⁹Benjamin Rengstl, ⁹Liane Preussner, ⁹Oezlem Tuerci, ⁹Ugur Sahin. ¹University Hospital Erlangen, Erlangen, NE, Germany; ²Hannover Medical School, Hanover, Germany; ³Netherlands Cancer Institute, Amsterdam, Netherlands; ⁴University Medical Center Eppendorf, Hamburg, Germany; ⁵University Medical Center Mainz, Mainz, Germany; ⁶University Hospital Regensburg, Regensburg, Germany; ⁷University Hospital of Cologne, Cologne, Germany; ⁸Bexon Clinical Consulting, Upper Montclair, USA; ⁹BioNTech SE, Mainz, Germany

Background BNT211 is a chimeric antigen receptor (CAR)-T cell product candidate that targets the tumor specific antigen Claudin-6 (CLDN6). Preclinical studies demonstrated that combining these engineered cells with a CAR-T cell Amplifying RNA Vaccine (CARVac) leads to in vivo expansion of adoptively transferred CAR-T cells, resulting in their improved persistence and functionality.

Methods This first-in-human, open label, multi-center trial involves a bifurcated 3+3 design with separate CLDN6 CAR-T cell dose escalations (single flat-dose) for monotherapy (part 1) and the combination with CARVac (part 2) based on 3 dose levels (DL). In part 2, CARVac is applied every 3 weeks starting at day 4 post transplantation including a one-step intra-patient dose escalation. Patients with CLDN6-positive relapsed or refractory solid tumors without further standard treatment options and ECOG 0 or 1 are eligible for recruitment.

Results As of July 23rd 2021, 8 patients have been treated. DL1 of part 1 has been completed, while dosing of part 1 DL2 and part 2 DL1 is ongoing. One patient with cancer of unknown primary was treated with a dose below DL1 in combination with CARVac; the underlying diseases of the other 7 treated patients were testicular, ovarian and endometrial cancer as well as soft-tissue sarcoma. No acute or dose-limiting toxicities and no serious adverse events related to the drug product have been reported. Manageable cytokine release syndrome (CRS, grade 1-2, the latter managed with Tocilizumab) without any signs of neurotoxicity have been observed in both patients of part 1 DL2. Only transient and moderate elevations of IL-6 and CRP serum levels occurred in remaining patients. Notably, administration of CARVac resulted in transient flu-like symptoms resolving within 24h. Analysis of CAR-T cell frequency in peripheral blood revealed robust engraftment followed by decline after day 17. Further expansion was noted in two patients with liver metastases accompanied by elevated levels of ALT, AST and AP, while total bilirubin was not affected. First tumor assessment 6 weeks after transplantation available for 5/8 patients revealed 4 SD (3 transitioned into PD after an additional 6-18 weeks) and 1 PD. Strikingly, three patients showed initial tumor shrinkage according to RECIST1.1 (reduction of target sum: -18%, -21% and -27%).

Conclusions CLDN6 CAR-T cells +/- CARVac show a favorable safety profile at doses tested and encouraging signs of efficacy. Updated data from open cohorts and especially for combination with CARVac will be presented.

Acknowledgements BNT211-01 is funded by BioNTech Cell & Gene Therapies GmbH.

Trial Registration ClinicalTrials.gov: NCT04503278

REFERENCES

N/A

Ethics Approval Ethics & Institutional Review Board approvals were obtained from the respective participating countries prior to initiation of the trial.

Consent N/A

<http://dx.doi.org/10.1136/jitc-2021-SITC2021.958>

SAFETY AND ANTI-TUMOR ACTIVITY OF TCR-ENGINEERED AUTOLOGOUS, PRAME-DIRECTED T CELLS ACROSS MULTIPLE ADVANCED SOLID CANCERS AT LOW DOSES – CLINICAL UPDATE ON THE ACTENGINE® IMA203 TRIAL

¹Martin Wermke*, ²Apostolia-Maria Tsimberidou, ³Ali Mohamed, ⁴Andrea Mayer-Mokler, ⁵Arun Satelli, ⁶Carsten Reinhardt, ²Dejka Araujo, ⁴Dominik Maurer, ²George Jr Blumenschein, ⁵Harpreet Singh, ⁶Jason Luke, ⁴Kerstin Guenther, ³Mamta Kalra, ⁷Manik Chatterjee, ⁴Norbert Hilf, ⁴Regina Mendrzyk, ³Steffen Walter, ³Stephen Eck, ⁸Tobias AW Holderried, ⁵Toni Weinschenk, ²Van Morris, ⁹Winfried Alsdorf, ⁵Cedrik M Britten. ¹University Hospital Dresden, Dresden, Germany; ²MD Anderson Cancer Center, Houston, TX, USA; ³Immatics US, Inc., Houston, TX, USA; ⁴Immatics Biotechnologies GmbH, Tuebingen, Germany; ⁵Immatics N.V., Tuebingen, Germany; ⁶University of Pittsburgh, Pittsburgh, PA, USA; ⁷University Hospital Wuerzburg, Wuerzburg, Germany; ⁸University Hospital Bonn, Bonn, Germany; ⁹University Med. Center Hamburg-Eppendorf, Hamburg, Germany

Background Adoptive cell therapy demonstrated significant clinical benefit in patients with hematological malignancies but results in most solid tumors have been less encouraging so far.

In the IMA203 trial we are treating advanced solid cancer patients utilizing TCR-engineered T cells (TCR-T) directed against an HLA-A*02-restricted peptide derived from the highly prevalent cancer testis antigen PRAME. This target was selected due to homogenous expression and exceptionally high target peptide density per tumor cell (assessed by quantitative mass spectrometry), two features we hypothesize to be critical determinants of anti-tumor activity in TCR-T trials.

Methods This ongoing first-in-human, dose escalation, multi-indication trial enrolls HLA-A*02:01- and PRAME-positive recurrent and/or refractory solid cancer patients, who failed all available standard treatments. Eligible patients undergo leukapheresis and an autologous TCR-T product is manufactured. After lymphodepletion with fludarabine and cyclophosphamide, T cells are infused, followed by low-dose IL-2. The primary objective of the trial is to assess the safety and tolerability of IMA203. Secondary objectives are to evaluate the anti-tumor activity and pharmacodynamics using molecular and immunological methods.

Results As of August 15, 2021, 16 heavily pre-treated patients received IMA203 T cells across multiple escalating dose levels (DL). Absolute IMA203 doses infused ranged from 0.08 to 0.81×10^9 transduced CD8 T cells per patient, which to our knowledge did not lead to anti-tumor responses in other TCR-T trials. Treatment-emergent adverse events after IMA203 infusion were transient and manageable. Most common events were expected cytopenias (G1-4), CRS and ICANS (both G1-2) and 1 DLT in DL2 (reported earlier). All evaluable patients (N=12) achieved disease control (i.e. best overall response: stable disease [SD] or partial response [PR]) and 6 patients demonstrated PRs according to RECIST1.1 with 2 of these PRs being confirmed. While all 3 patients treated at DL1 (median dose: 0.11×10^9) experienced SD, a PR was observed in 6/9 patients treated beyond DL1 (median dose: 0.30×10^9). Responses were seen in patients with synovial sarcoma (N=3), malignant melanoma (N=2) and head and neck cancer (N=1). Robust engraftment of T cells was observed in all patients and tumor infiltration by TCR-modified T cells was demonstrated in patients with evaluable on-treatment biopsies.

Conclusions To our knowledge IMA203 is the first TCR-T product candidate that induced frequent tumor responses across multiple solid cancers using transduced T cells at doses below 1 billion and has a manageable safety profile. The next

step is to assess response rates at higher dose levels and durability of responses.

Trial Registration NCT03686124

Ethics Approval The study was approved by the institutional review board/ethics committee as required for each participating site.

<http://dx.doi.org/10.1136/jitc-2021-SITC2021.959>

RANDOMIZED MULTICENTER STUDY OF NEOADJUVANT CHEMORADIATION THERAPY (CRT) ALONE OR IN COMBINATION WITH PEMBROLIZUMAB IN PATIENTS WITH RESECTABLE OR BORDERLINE RESECTABLE PANCREATIC CANCER

¹Osama Rahma*, ²Mathew Katz, ³Todd Bauer, ⁴Brian Wolpin, ⁵Chee-Chee Stucky, ⁵Tanios Bekaii-Saab, ⁶Rawad Elias, ⁴Andressa Dias-Costa, ⁴Jonathan Nowak, ⁴Lenahan Patrick, ³Gina Petroni, ⁴Stephanie Dougan, ³Craig Slingluff. ¹Dana-Farber Cancer Institute, Boston, MA, USA; ²MD Anderson Cancer Center, Houston, TX, USA; ³University of Virginia, Charlottesville, VA, USA; ⁴Dana-Farber/Harvard Cancer Center, Boston, MA, USA; ⁵Mayo Clinic, Phoenix, AZ, USA; ⁶Hartford Healthcare Cancer Institute, Hartford, CT, USA

Background Pancreatic cancer (PC) is a challenging target for immunotherapy due to its immune-suppressive microenvironment. Neoadjuvant chemoradiation (CRT) can increase the presence of tumor-infiltrating lymphocytes (TILs). We hypothesized that the combination of CRT and pembrolizumab can further expand and activate TILs.

Methods Patients with resectable or borderline resectable PC were randomized 2:1 to the investigational treatment (Arm A) of pembrolizumab 200mg IV every 3 weeks concurrently with CRT (capecitabine 825 mg/m² orally twice daily and radiation 50.4 Gy in 28 fractions over 28 days) or CRT only (Arm B) prior to surgical resection. The primary endpoints were safety and difference in TILs density between Arm A and B assessed using multiplexed immunofluorescence on resected tumor specimens. As a correlate analysis, single cell RNA-sequencing (scRNA-seq) was performed to quantify gene expression in T cells from tumors and peripheral blood, and to track expanded T cell clonotypes in these compartments (n=4 patients Arm A; n=3 patients Arm B). The study was amended after enrollment of 37 patients to allow FOLFIRINOX prior to CRT, given changes in standard of care.

Results 37 patients were enrolled (24 Arm A, 13 Arm B). After neoadjuvant therapy, 13 patients had unresectable disease (9 on A, 4 on B), and 24 patients underwent surgery and were evaluable for the TILs primary endpoint (17 arm A, 7 arm B). The mean difference (A-B) in CD8+ T cell density was 36 cells/mm² (95% CI -85 to 157, stdev 130) (p 0.48). Additional analysis did not show significant differences in activated cytotoxic T cells, regulatory T cells, M1- or M2-like polarized macrophages, or granulocytes. The median recurrence free survival (RFS) was 18.2 months on Arm A and 14.1 on Arm B (p 0.41). Overall survival was 27.8 months on Arm A and 24.3 on Arm B (p 0.68) with a median follow up of 2.2 years. The most common grade 3 treatment-related toxicities were lymphopenia reported in 29% on Arm A and 31% on Arm B, respectively followed by diarrhea in 8% on Arm A attributed to CRT. scRNA-seq revealed clonal expansion and expression of co-inhibitory markers among TIL subsets.

Conclusions The combination of CRT and pembrolizumab is safe. Preliminary analysis shows that the addition of pembrolizumab to CRT has minimal effects on intratumoral densities of TILs and other immune cell populations. Single cell transcriptome analyses enable in-depth characterization of the functional responses of T cells to pembrolizumab in the setting of CRT.

Acknowledgements This study was funded by Merck

Trial Registration NCT02305186

Ethics Approval The study was conducted at 6 sites: University of Virginia, Dana Farber Cancer Institute, MD Anderson Cancer Center (MDACC), Mayo Clinic, Hartford Healthcare Cancer Center, and University of Miami. Written informed

consent was provided by the study participants and the protocol was approved by the relevant local IRBs in each site.

<http://dx.doi.org/10.1136/jitc-2021-SITC2021.960>

PRELIMINARY RESULTS OF A PHASE 2 STUDY OF INTRATUMORAL ADMINISTRATION OF BO-112 WITH PEMBROLIZUMAB IN PATIENTS WITH ADVANCED MELANOMA THAT HAVE PROGRESSIVE DISEASE ON ANTI-PD-1-BASED THERAPY

¹Iván Márquez Rodas*, ²Philippe Saiag, ³Luis de la Cruz Merino, ⁴Caroline Dutriaux, ⁵Juan Rodríguez-Moreno, ⁶Caroline Robert, ⁷Ana Arance, ⁸Eduardo Castañón Álvarez, ⁹Pablo Cerezuela-Fuentes, ¹⁰Henry Montaudie, ¹¹Miguel Sanmamed, ¹²María González Cao, ¹³Julie Charles, ¹⁴María Pilar López Criado, ¹⁵Alfonso Berrocal, ¹⁶Enrique de Miguel, ¹⁷Elisa Funk-Brentano, ¹⁸Sorilla Prey, ¹⁹Roberto Huertas, ²⁰Delvys Rodríguez Abreu, ²¹Eva Muñoz Cousezo, ²²Juan Martín-Liberal, ²³Javier Sánchez López, ²⁴Helena Escuin-Ordinas, ²⁵Marisol Quintero, ²⁶Sonia Maciá, ²⁷Marya Chaney, ²⁸Stephane Dalle. ¹Hospital Universitario Gregorio Marañón, Madrid, Spain; ²Hôpital Ambrois Pare, Paris, France; ³Hospital Universitario Virgen Macarena, Sevilla, Spain; ⁴Hôpital Saint-André, Bourdeaux, France; ⁵Hospital Universitario Sanchinarro-Clara, Madrid, Spain; ⁶Hôpital Gustave Roussy, Villejuif-Paris, France; ⁷Hospital Clinic Barcelona, Barcelona, Spain; ⁸Clínica Universidad de Navarra, Madrid, Spain; ⁹Hospital Clínico Universitario Virgen de Murcia, Murcia, Spain; ¹⁰Centre Hospitalo-Universitaire de Nice, Nice, France; ¹¹Hospital Universitari Dexeus, Barcelona, Spain; ¹²Centre Hospitalier Universitaire Grenoble, Grenoble, France; ¹³MD Anderson, Madrid, Spain; ¹⁴Hospital General Universitario de Valenc, Valencia, Spain; ¹⁵Hôpital Saint-André Bourdeaux, Bourdeaux, France; ¹⁶Hospital Universitario Insular de Gran C, Las Palmas de Gran Canaria, Spain; ¹⁷Hospital General Universitario Vall d'He, Barcelona, Spain; ¹⁸Catalan Institute of Oncology (ICO), Barcelona, Spain; ¹⁹Highlight Therapeutics, Valencia, Spain; ²⁰Merck and Co., Inc, Kenilworth, NJ, USA; ²¹Hôpital Lyon Sud, Lyon, France

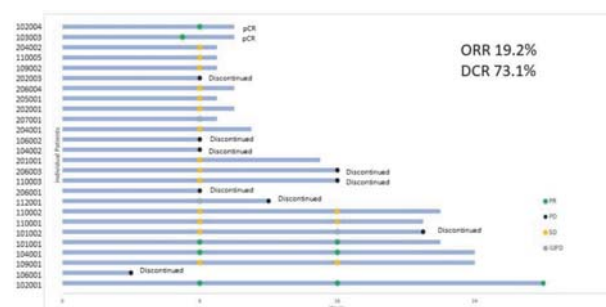
Background Intratumoral immunotherapies are being tested in different solid tumors. They trigger local and systemic responses.¹⁻² BO-112 is a double stranded RNA nanoplexed with polyethyleneimine (PEI), which mimics a viral infection and mobilizes the immune system.

In preclinical models and in a first in human clinical trial BO-112 activated dendritic cells, induced CD-8 infiltration, apoptosis and enhancement of immunogenic cell death and achieved an objective response in 2 out of 10 patients with melanoma with primary resistance to antiPD-1.³⁻⁴

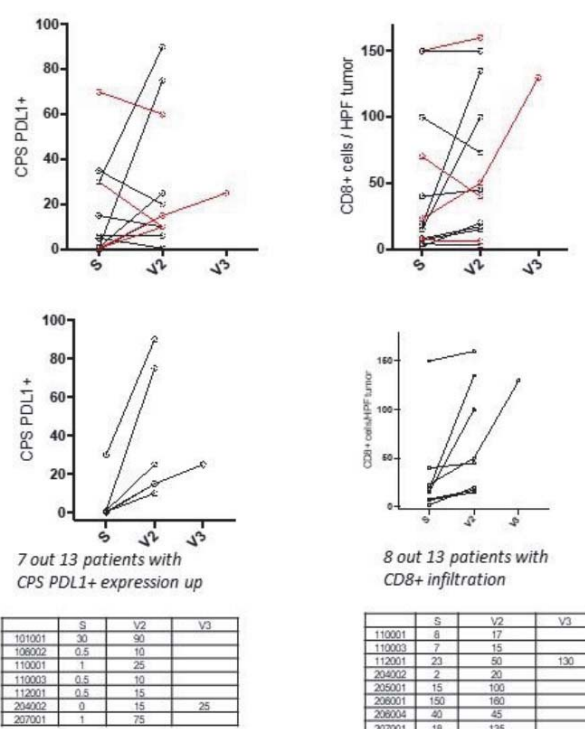
Methods In this phase 2 study, BO-112 plus pembrolizumab is evaluated in patients with advanced melanoma, who have developed progressive disease while on or within 12 weeks after anti-PD1/PD-L1 based therapy (either as first line or as adjuvant treatment). BO-112 is administered intratumorally once weekly in 1 to 8 tumor lesions, total dose 1 to 2 mg, for the first 7 weeks and thereafter every three weeks; pembrolizumab 200 mg is administered intravenously every three weeks. Overall response rate (ORR) is analyzed as primary endpoint by independent reviewer. Secondary objectives include disease control rate (DCR), duration of response and progression free survival (PFS); response assessment is done by RECIST 1.1 and iRECIST; in addition, CD-8 and PD-L1 IHC, NGS, itRECIST and radiomics signatures are prospectively assessed. Key eligibility criteria include cutaneous or mucosal melanoma with known BRAF status; at least one lesion RECIST 1.1 measurable and amenable for IT injection. Enrollment has been completed on 26th August.

Results With 26 evaluable patients with a first response assessment, seven have progressive disease (PD), five have partial response (PR) and fourteen patients show stable disease (SD). Preliminary ORR is 19.2% and DCR is 73.1% at week 8. Three patients with PR at week 8 have undergone a second assessment at week 16, with further decrease in sum of diameters (SOD) in both injected and non-injected lesions. Three out of five patients with SD and a second assessment maintain SD, showing a decrease in SOD in two cases (figure 1). In addition, two patients with only skin lesions have a pathological complete response. CD8 and PD-L1 have increased in 8

and 7 out of 13 patients with paired biopsies, being related with clinical benefit (figure 2).



Abstract 961 Figure 1 Swimmer plot, efficacy data for evaluable patients undergoing at least one response assessment



Abstract 961 Figure 2 Immunohistochemistry data for CPS and CD8 data from paired biopsies

Conclusions Despite these data being preliminary, there is a trend for benefit in terms of ORR and also in long lasting stable diseases. BO-112 is able to increase PD-L1 expression in tumor cells and increase CD8-T cell infiltrates.

Acknowledgements Merck, Pivotal SLU, Quibim radiomics, Pangaea laboratories, all participating sites and patients
Trial Registration NCT04570332

REFERENCES

- Aznar MA, Pannelles L, Perez-Olivares M, et al. Immunotherapeutic effects of intratumoral nanoplexed poly I:C. *J Immunother Cancer*. 2019 May 2;7(1):116.
- Hamid O, Ismail R, Puzanov I. Intratumoral immunotherapy-update 2019. *The Oncologist* 2020;25:e423-438.
- Márquez-Rodas I, Longo F, Rodríguez-Ruiz M, et al. Intratumoral nanoplexed poly I:C BO-112 in combination with systemic anti-PD-1 for patients with anti-PD-1-refractory tumors. *Sci Transl Med* 2020 Oct 14;12(565):eabb0391.

4. Kalbasi A, Tariveranmoshabad M, Hakimi K, Kremer S, *et al.* A. Uncoupling interferon signaling and antigen presentation to overcome immunotherapy resistance due to JAK1 loss in melanoma. *Sci Transl Med* 2020 Oct 14;**12**(565):eabb0152.

Ethics Approval The study obtained ethics approval by Spanish Health Agency (AEMPS), on 11th December 2020, and French Health Agency (ANSM) on 27th January 2021; study obtained approval from two Ethics Committee: Vall D’Hebron, Barcelona, Spain on 7th December 2020 (number 467), and Centre Léon Bérard, Lyon, France, CPP 20.11.10.38825 on 11th February 2021.

For each study patient, written informed consent is obtained prior to any protocol-related activities. As part of this procedure, the principal investigator or one of his/her associates must explain orally and in writing the nature, duration, and purpose of the study, and the action of the study drug in such a manner that the patient is aware of the potential risks, inconveniences, or adverse effects that may occur. They should be informed that the patient may withdraw from the study at any time. They will receive all information that is required by the regulatory authorities and ICH guidelines. The ICF has been signed by the patient and a copy provided to them.

Consent N/A

<http://dx.doi.org/10.1136/jitc-2021-SITC2021.961>

Combination Immunotherapies

962

INTEGRATIVE IMMUNOMICS HIGHLIGHT THE IMMUNOMODULATORY IMPACT OF NEOADJUVANT CHEMOTHERAPY AND IMMUNE-BASED TREATMENTS IN RESECTED NON-SMALL-CELL LUNG CANCER

Stephanie Schmidt*, Younghee Lee, Cheuk Leung, Lorenzo Federico, Heather Lin, Annikka Weissferdt, Apar Pataer, Hitoshi Dejima, Alejandro Francisco-Cruz, Frank Rojas, Luisa Solis, Edwin Parra, Monika Pradhan, Haiping Guo, William William, Alexandre Reuben, Humam Kadara, Ignacio Wistuba, Jianjun Zhang, Stephen Swisher, Ara Vaporciyan, Marcelo Negrao, Christopher Bristow, Timothy Heffernan, Chantale Bernatchez, Jack Lee, John Heymach, Boris Sepesi, Don Gibbons, Cara Haymaker, Tina Cascone. *The University of Texas MD Anderson Cancer Center, Houston, TX, United States*

Background How neoadjuvant chemo-immunotherapy modulates tumor immune composition and response is not completely understood. We interrogate immunomodulation of neoadjuvant platinum-based chemotherapy (C), nivolumab (N), and N-plus-C (NC) and their connections to therapeutic efficacy in resected non-small cell lung cancer (NSCLC) by integrating immunomic data from the Immunogenomic Profiling of NSCLC (ICON) study and NEOSTAR trial cohorts.

Methods In NEOSTAR (NCT03158129), patients with stage I-III A (single N2) resectable NSCLC (AJCC7th) received N (3 mg/kg IV, D1,15,29); patients with stage IB(\geq 4cm)-III A (single N2) resectable NSCLC received NC (N 360 mg IV plus C, D1,22,43 for 3 cycles, every 3 weeks) before surgery; major pathologic response (MPR) was the primary endpoint. In ICON, patients with stage IB(\geq 4cm)-III A resectable NSCLC received C before surgery. Surgically resected tumor samples underwent immune profiling via flow cytometry (n=16,13,9 for C,N,NC), immunohistochemistry (IHC;n=0,18,14), and multiplexed immunofluorescence (mIF;n=28,16,10). Treatment-associated immunomodulation and associations with therapeutic efficacy were analyzed using: 1) a shared nearest neighbors-based network we developed linking measurements across datasets; 2) MetaCyto, a specialized cytometry analysis method for identifying cell subsets by clustering.

Results We holistically explored the immunomic data by integration across cohorts. Through hierarchical regression of the integrated data, we determined the overall effect of a given treatment controlling for the presence or absence of the other treatment.

We examined C's effects across all cohorts controlling for N. Across all patients, regardless of MPR, C is associated with immunosuppression, increasing PD1+ T cell (CD45+CD3+) populations: regulatory (CD4+CD25+FOXP3+), helper (CD4+), and effector (CD8+) (effect size(ES):1.48,1.61,1.26; $q<0.05$). C also decreases proliferative (Ki67+) populations: helper and effector T cells as well as NK (CD45+CD3-CD56+) cells (ES:-1.27,-1.43;-1.36; $q<0.05$). In patients without MPR (i.e., non-responding patients), immunosuppression appears heightened by increased Ki67+ regulatory T cells (ES:1.86; $q<0.05$).

Conversely, we examined N's effects across all cohorts controlling for C. Across all patients, regardless of MPR, N is associated with immune activation, increasing ICOS+ T cell populations: regulatory, helper, and effector (ES:1.29,1.29,1.47; $q<0.05$). Comparing N and NC reveals that adding C may drive exhaustion by increasing TIM3+ regulatory, helper and effector T cells (ES:1.16,1.17,1.23;

$q<0.05$), an effect more pronounced in non-responding patients (ES:1.31,1.33,1.35; $q<0.05$).

Conclusions We report the first integrated examination of the immunomodulatory effect of neoadjuvant C and N. C is associated with immunosuppression while N with immune activation; together, N appears to lessen C's suppressive effects. Incorporation of transcriptomics into this integrated network of flow cytometry, mIF, and IHC immune profiling data is ongoing to augment translational insights for neoadjuvant chemo/immunotherapies.

<http://dx.doi.org/10.1136/jitc-2021-SITC2021.962>

The number next to the author indicates the page number, not the abstract number.

- Aamdal Elin, A416
Aamdal Steinar, A416
Aanur Praveen, A569
Aaron Wade, A908
Abate-Daga Daniel, A206
Abbadessa Giovanni, A433, A465, A483, A511, A550, A581, A636
Abbas Abdulraouf, A167
Abbasi Saqib, A318
Abbot Stewart, A128
Abbott Charles, A21, A22, A83, A88
Abdel-Wahab Noha, A845, A853
Abdel-Wahab Omar, A807
Abdelrahim Maen, A754, A761, A845
Abdullah Shaad, A568, A576, A857, A909
Abdullahi Wazir, A773
Abdulrahman Ziena, A41
Abed Afaf, A73
Abedi Mehrdad, A357, A358, A359, A361, A362, A1001
Abes Riad, A898
Abo Ryan, A907
Abraham Christopher, A428
Abramovitch Allan, A1004
Abrams Scott, A982
Abramson Sascha, A114, A148, A152, A1000
Abrantes Mario, A773, A775
Abreu Delvys Rodríguez, A1011
Abu-Shawer Osama, A853
Abudayyeh Ala, A252, A845, A853
Abujarour Ramzey, A126
Abukharma Hasan, A516, A520
Ackbarali Tariqa, A663
Ackerman Shelley, A817, A819, A903
Acklam Francis, A271
Acs Andreas, A201
Acuff Nicole, A511, A636
Adam Julien, A409, A945
Adam Stanford-Moore S, A859
Adamik Juraj, A695
Adamo Vincenzo, A25
Adams III Homer, A525
Adams Julian, A230
Adams Lexy, A571
Adams Micki, A42
Adams Zoe, A341
Adewoye Adebeye, A507, A508
Adeyanju Kemi, A896
Adeyemi Frances, A240
Adkins Douglas, A385, A468
Adoke Kasimu, A10
Adolacion Jay R, A199
Adotevi Olivier, A373
Agarwal Neeraj, A544
Agarwal Yash, A769
Agaugué Sophie, A558, A592
Agensky Laura, A468
Ager Casey, A793
Aggarwal Charu, A485
Aggarwal Vanya, A846, A852
Aggen David, A425
Aghajanian Carol, A381
Aghlara-Fotovat Samira, A225
Agius Phaedra, A961
Agmon Eran, A192
Agrawal Amit, A788
Agrawal Kriti, A706
Agrawal Nishant, A859
Aguar Vladimir Galvão de, A535
Aguar-Ibanez Raquel, A941
Aguilar Brenda, A133
Aguilar Laura, A427
Aguilar-Cordova Estuardo, A427
Aguilera Todd, A442
Aguirre Andrew, A670
Ahani Elnaz, A233
Ahlenstiel Golo, A552
Ahmad Shamaila Munir, A813
Ahmadi Tahamtan, A525, A546, A821
Ahmed Rafi, A434
Ahn Byung cheol, A901
Ahn Joong Bae, A82, A861
Ahn Myung Ju, A465
Ahn Myung-Ju, A485
Ahn Sae Jeong, A751
Ahn Sebastian, A585
Ahnert Jordi Rodon, A584
Aiken Robert, A357, A358, A359, A361, A362, A1001
Aisenberg Robert, A940
Aix Santiago Ponce, A491, A493, A546
Ajami Nadim, A879
Akagi Keiko, A788
Akarte Atul, A889
Akbay Esra, A632
Akce Mehmet, A434
Akhavne Neal, A53
Akruwala Rajshi, A854
Aksoy Murat, A59
Al-Rajabi Raed, A372
Al-Sulaiti Asma, A111
Alahmadi Asrar, A257
Alain Tommy, A996
Alaiwi Sarah Abou, A257
Alamgeer Muhammad, A577
Alban Tyler, A340
Albregues Jean, A108
Alcantar-Orozco Erik, A438
Alcazer Vincent, A719
Aldea Mihaela, A308
Alden Stephanie, A336
Aldrin Denny R, A905
Alese Olatunji, A434
Alessi Joao Victor, A74, A336
Alfaro Alejandro, A190, A191
Alfaro Alex, A418
Algazi Alain, A417
Algieri Francesca, A876
Alhalabi Omar, A259
AlHomsy Mohammed Ussama, A767
Alice Wang Y, A651
Alilou Mehdi, A44
Alimzhanov Marat, A792
Allan David, A181
Allen Alexander, A203
Allen Carter, A715
Allen Clint, A513
Allen Donald, A64
Allen Heather, A824
Allen Richard, A867
Allen Stephanie, A983
Allevato Michael, A631
Allison James, A379, A842
Allison Patrick, A625
Allory Yves, A945
Allred Sean, A818, A895
Almeciga Ingrid, A800
Almudhar Niran, A125
Alonso Guzman, A731
Alonso Marta, A307, A772, A776
Alonso Michael, A817, A819, A903
Alsaraby Ayat, A432
Alsdorf Winfried, A1008, A1009
Altan Mehmet, A304, A482, A1007
Alteber Zoya, A272
Altioek Soner, A616, A709, A794
Altman-Sharoni Efrat, A144
Alvarado Diego, A833
Alvarez Audrey Blanchard, A892
Álvarez Eduardo Castañón, A1011
Alvarez Frank Rojas, A962
Alvarez-Rodríguez Rubén, A209, A210
Alvarez-Rodríguez Ruben, A573
Alves Stephen, A303
Amaishi Yasunori, A113
Amara Céline, A893
Ambrogely Alexandre, A887, A888
Ambrose Christine, A170
Amech Samuel, A607
Amisaki Masataka, A862
Amit Ido, A713
Amit Inbar, A732
Amit OZA, A380
Ammari Samy, A300
Amoor Rafet, A221
Amrate Amele, A483, A550
Amritkar Amit, A199
An Annie, A348
An Erin, A136
An Ruifang, A460
An Xiaoyu, A753
An Xingyue, A199
An Zhiqiang, A327
An Zili, A128
Anand Banmeet, A475
Anand Puneet, A817, A819
Anang Nana-Ama, A631
Anant Shrikant, A372
Anaparthi Naishitha, A80, A91
Andersen Mads, A807
Andersen Mads Hald, A813
Anderson Ana, A277, A670
Anderson Courtney, A185
Anderson Kristin, A590
Anderson Nicholas, A152
Anderson Paul, A456
Anderson Randy, A454
Andersson Emilia, A94, A976
Andersson Jourdan, A240
Anderton Kate, A583
Ando Yuta, A131
Andoni Alma, A46
Andrade Lucas Ferrari de, A126
Andre Thierry, A398
Andreasen Haley, A615
Andrejeva Gabriela, A282
Andresen Thomas, A641
Andresen Thomas Lars, A806
Andreu-Vieyra Claudia, A577
Andrews David, A231
Andrews Lawrence, A274

- Andrian Ulrich Von, A244, A902
 Andrianopoulos Emanuelle, A188
 Andrianova Lana, A562
 Andriole Gerald, A453
 Andrulis Irene, A178
 Andtbacka Robert, A501
 Andtbacka Robert HI, A415
 Angeles Christina, A674
 Angelides Steven, A349
 Angell Helen, A46, A860
 Angevin Eric, A308
 Angus Andreina Garcia, A142
 Anniciello Anna Maria, A980
 Annunziata Christina, A881
 Anoka Janice, A452
 Ansell Stephen, A503
 Anselmo Dylan, A48, A65
 Ansstas George, A428
 Antonacio Fernanda, A62
 Antonia Scott, A665
 Antonio Chiocca E, A427
 Anzar Irantz, A416
 Aparicio Ana, A259
 Apolloni Laura, A787
 Apollonio Giulia, A16
 Apostolaki Angeliki, A42, A68
 Appleman Leonard, A374, A378
 Appleton Kathryn, A305
 Aquino-Michaels Keston, A671
 Aragon Anabel Ramirez, A205
 Arakelian Tsolere, A805
 Aramaki Takahiko, A251
 Arance Ana, A1011
 Arance Ana Maria, A422
 Arathoon Robert, A306
 Araujo DeJka, A1009
 Arauz Garrett, A982
 Archaya Luna, A318
 Ardila Connie, A736
 Ardolino Michele, A894
 Arellano Claudia Yanez, A847
 Arens Ramon, A805
 Ares Luis Paz, A396, A483
 Argus Elvira, A132, A155
 Arieta Christina, A212
 Ariffin Hany, A957
 Arkenau Hendrik-Tobias, A555
 Arlen Philip, A881, A925
 Armstrong Anne, A997
 Armstrong Michael, A532
 Arnold Julie, A787
 Arnoux Fanny, A489
 Aroldi Francesca, A538, A539
 Aronin Alexandra, A825
 Aronov Alexander, A123
 Arora Asrhi, A108
 Arranz Jose, A378
 Arrieta Oscar, A25
 Artandi Steven, A803
 Artru Emilie, A766
 Arvindam Upasana Sunil, A667
 Ascierito Paolo A, A581
 Ascierito Paolo, A27, A257, A332, A576, A980
 Asgari Maryam, A850
 Ashburn Ted, A542
 Ashcraft Kathleen, A655
 Asher Nethanel, A556
 Asimakopoulos Fotis, A982
 Asmellash Senait, A30, A33
 Assad Hadeel, A505
 Assi Hikmat, A735
 Asuelime Grace, A131
 Atieh Anas, A275
 Atkins Michael, A446
 Atkinson Victoria, A417
 Attig Sebastian, A579
 Atwal Sumandeep, A562
 Au Qingyan, A2, A58
 Audigier-valette Clarisse, A489
 Auer Julia, A542
 Aufiero Kristen, A363
 Aung Sandra, A417
 Aung Thazin, A258
 Ausejo-Mauleon Iker, A307, A776
 Austin Richard, A908
 Avalos Barbara, A944
 Avery Bill, A748
 Avery Kendra, A726, A736, A822, A913
 Avichzer Jasmine, A825
 Avila Kim, A632
 Avvaru Chai, A428
 Awad Mark, A74, A268, A336, A515
 Awivi Muhammad Osama, A853
 Axelrod Margaret, A842, A848, A951
 Aycock Jeff, A573
 Ayers Mark A, A391
 Azad Arun, A511
 Azad Nilofer, A20, A533, A566
 Azam Abu Bakr, A855
 Azevedo Ricardo De, A622
 Azoulay-Alfaguter Inbar, A173
 Azuma Hisaya, A510
 Baakili Adyb, A433, A581
 Babiker Hani, A368
 Baca Manuel, A887, A888
 Bachelet Ido, A823
 Bader Andreas, A127
 Bader Jackie, A951
 Badin Firas, A494
 Baek Eunhye, A440
 Baek SeungJae, A440
 Baere Thierry De, A300
 Baeuerle Patrick, A918
 Baffa Raffaele, A240
 Bagga Shalini, A941
 Bahary Nathan, A371
 Bahce Idris, A700
 Bahjat Rena, A822
 Bahleda Rastilav, A382
 Bahrke Sven, A816
 Bai Haiyan, A261, A321, A789
 Bai Jane, A407
 Bai Lu, A128
 Bai Yuxian, A400
 Bailey Christina, A995, A1002
 Bailey Jenna, A211
 Bailey Kelly, A682
 Bailey Michael, A27, A980
 Bailey Shania, A450
 Bailey Stefanie, A234
 Baird Regan, A875
 Bajaj Gaurav, A525, A821
 Bajaj Pawan, A386
 Bajpai Malini, A889
 Bajwa Gagan, A173
 Bak Martin, A641, A806
 Baker Amy, A205, A572
 Baker Kevin, A900
 Bakhit Charles, A726
 Bakker Alice, A738
 Balachandran Vinod, A862
 Balaji Aanika, A253
 Balar Arjun, A547
 Balasubramanian Priya, A240
 Baldini Capucine, A409, A562
 Balko Justin, A264, A342, A791, A842, A848, A951
 Balko Kelly, A636
 Ball Michael, A148
 Ballesteros-Merino Carmen, A417
 Balleyguier Corinne, A382
 Ballot Elise, A373
 Bampton Daryn, A366, A367
 Banaszak Katarzyna, A786
 Bandinelli Pierre-Alain, A301
 Banerjee Arindam, A915
 Banerjee Hridesh, A668, A720
 Banerjee Susana, A398
 Bang Kathy, A18, A804
 Bang Yung-Jue, A530
 Bannister Brianna, A625
 Banzon Rose, A908
 Bao Lei, A553
 Bao Leyuan, A210
 Bao Riyue, A972
 Bao Xuanwen, A443
 Bar Jair, A323
 Barajas Brook, A117
 Barak Reut, A732
 Baranda Joaquina, A372, A553, A562
 Baras Alexander, A872
 Barata Pedro, A318
 Barbash Olena, A654
 Barber Daniel, A721
 Barber Glen, A795
 Barbiro Inbal, A508
 Barbour Mark, A271
 Barboy Oren, A713
 Barbu Emilia, A516, A520
 Barca Taylor, A128
 Bárcena-Varela Marina, A653
 Barchan Karin, A785
 Bardelli Geraldine, A240
 Bardot Stephen, A452
 Bargou Ralf, A536
 Barkal Amira, A283
 Barlesi Fabrice, A489
 Barlow Norman, A726, A736
 Barnes Bryan, A482
 Baronas April, A833
 Barone Francesca, A427
 Barone Sierra, A45
 Barré Patricia, A489
 Barrón Feliciano, A25
 Barrera Luis, A165
 Barretina-Ginesta Maria-Pilar, A398
 Barrett Richard, A946
 Barrett Ronald, A738
 Barrette Benoit, A325
 Barrichello Adriana, A74, A336
 Barry III Clifton, A721
 Barry Vivian, A606
 Barshesht Yiftah, A756
 Barsoumian Hampartsoum, A407, A604
 Barte Eric, A207
 Bartha Gabor, A83, A88
 Bartkowiak Todd, A45
 Barton Debora, A1000
 Barve Minal, A435, A439, A511, A563, A1007
 Basak Nandini Pal, A40

- Basak Sayantani, A101
 Basar Rafet, A183
 Bashir Babar, A425, A510
 Bass Anne, A854
 Basset Alexandra, A893
 Bassett Phil, A401
 Bassler Nicole, A885
 Basso Andrea, A485
 Basu Subham, A91
 Bates Breanna, A590
 Bath Natalie, A401
 Batista Luciana, A892
 Batty Kathleen, A395
 Bauchet Anne-Laure, A893
 Bauer Todd, A569, A576, A1010
 Bauernfeind Franz-Georg, A502
 Baum Scott, A538
 Bauman Jessica, A488, A525
 Bauman Julie, A468
 Baumhauer Annette, A555
 Bautista Wynona, A749
 Bautzova Tereza, A287
 Baxi Vipul, A420, A859
 Baxter Dawn, A518
 Bay-Jensen Anne-Christine, A24
 Baykaner Khan, A860
 Bayless Nicholas, A847
 Bayley Erin, A53
 Bazhenova Lyudmila, A591
 Bearss David, A911
 Beasley Georgia, A538, A685
 Beatty Gregory, A902
 Beatty Matthew, A206, A418, A419
 Beaumont Kristin, A90, A338, A651
 Bechard David, A514, A534
 Becher Oren, A307
 Bechter Oliver, A550
 Beck Andrew, A859
 Becker-Hapak Michelle, A200
 Beckermann Kathryn, A454, A760
 Beckermann Katy, A951
 Beckford Denis, A619, A620
 Beckhove Philipp, A324
 Becklund Bryan, A12, A897
 Bedard Philippe, A402
 Bedford Mark, A654
 Bedi Nikita, A22
 Beechem Joseph, A57
 Beeler Kristina, A99
 Beez Armin, A922
 Behera Dayanidhi, A889
 Behrens Carmen, A632
 Behshad Elham, A247
 Beijnum Judy van, A808
 Bejar Rafael, A712
 Bekaii-Saab Tanios, A548, A1010
 Belaunzaran Osiris Marroquin, A906
 Belette Allison, A254
 Bell Diana, A788
 Belli Carmen, A503
 Bello Maria Giovanna Dal, A257
 Belousova Natalya, A351, A792
 Belvin Marcia, A735
 Ben Tran, A456
 Ben-Mayor May, A732
 Benatar Tania, A127
 Bendell Johanna, A512, A519, A527
 Bender Jim, A418, A419
 Bender Lewis, A533, A566
 Beninga Jochen, A893
 Benjamin Jonathan, A548
 Benlahrech Adel, A600
 Benner Brooke, A399
 Bennouna Jaafar, A483
 Benson Micah, A198, A215
 Bensussan Armand, A898
 Bentebibel Salah-Eddine, A845
 Bentley Keith, A820
 Bentzen Amalie, A322
 Bera Kaustav, A44
 Berciano-Guerrero Miguel-Ángel, A422
 Berezhnoy Alexey, A735
 Bergamaschi Laura, A1
 Bergen Jeroen Van, A805
 Berger Adam, A571
 Berger Allison, A505
 Berger Raanan, A823
 Berger Trisha, A234
 Berglund Anders, A795, A952
 Berhani-Zipori Orit, A172, A230
 Berichel Jessica Le, A713
 Beringer Audrey, A782
 Berlin Jordan, A368
 Bernabe Reyes, A493
 Bernard Antoine, A325
 Bernard Brady, A103
 Bernard Kok Bang Lee , A957
 Bernatchez Chantale, A183, A186, A199, A1013
 Bernett Matthew, A736, A822
 Bernstein Howard, A166, A224
 Berrien-Elliot Melissa, A200
 Berrocal Alfonso, A422, A1011
 Berry William, A374, A378
 Bersanelli Melissa, A257
 Berthe Julie, A46
 Bertolet Genevieve, A604
 Bertolus Chloé, A962
 Bertolus Chloe, A984
 Berton Dominique, A398, A1006
 Bertozzi Carolyn, A803
 Bescop Clément Le, A301
 Besien Koen Van, A130
 Besse Benjamin, A308, A394, A483
 Bessette Paul, A746
 Best Andrew, A114
 Betts Gareth, A401
 Beuraud Chloé, A782, A953
 Beury Daniel, A220
 Beusechem Victor van, A1004
 Beutner Karl, A76, A81, A522
 Beviglia Lucia, A809
 Bexon Alice, A452, A537
 Beylergil Volkan, A857
 Bezman Natalie, A226
 Bhadra Rajarshi, A768
 Bhadri Vivek, A395
 Bhagchandani Sachin, A801
 Bhagwati Niyati, A492
 Bhandarkar Vidit, A326
 Bhanu Krithikaa, A622
 Bhanu Krithikaa Rajkumar, A652
 Bharanikumar Ramit, A76
 Bhardwaj Nina, A90, A338, A360, A363, A651, A807
 Bhardwaj Vinnu, A858
 Bharmal Murtuza, A658, A660
 Bhat Arun, A128
 Bhat Sachin, A882
 Bhateja Priyanka, A878
 Bhatia Shailender, A574, A658, A689
 Bhatia Vinona, A426
 Bhatt Rupal, A188
 Bhattacharjee Amrita, A880
 Bhattacharjee Arindam, A175
 Bhutkar Arjun, A711
 Bi Yingzhi, A905
 Bialas Arkadiusz, A799
 Bian Zhen, A227
 Biancotto Angelique, A308
 Bicak Ece, A515, A551
 Bice Tristan, A318
 Bieche Ivan, A945
 Biesova Zuzana, A243
 Bigner Darell, A770
 Bigorgne Amelie, A945
 Bilen Mehmet, A975
 Bilic Sanela, A563
 Bilusic Marijo, A516
 Binder Bhavneet, A309
 Binnewies Mikhail, A900
 Birkbak Nicolai, A32
 Birstler Jen, A67
 Bishop Andrew, A410
 Bissinger Stefan, A324
 Biswas Nilanjana, A889
 Björgvinsdóttir Unnur Jóna, A806
 Bjordahl Ryan, A126, A180, A208
 Blackmer Trillium, A56
 Blagovic Katarina, A166
 Blaj Cristina, A614
 Blakemore Stephen, A2
 Blanc-Durand Félix, A308
 Blancas-Mejia Luis, A745
 Blanchard-Alvarez Audrey, A893
 Blanchfield Lori, A39
 Blando Jorge, A46
 Blankenstein Thomas, A104, A239, A531
 Blarcom Thomas Van, A290
 Blasberg Ronald, A649
 Blaser Bradley, A715
 Blasi Varenka Rodriguez Di, A985
 Blatt Sarah, A711
 Blaukat Andree, A351, A792
 Blinman Prunella, A484
 Bliss Zachery, A78
 Blitz Emily, A960
 Bloodworth Jeffrey, A319
 Bloomstein Joshua, A675
 Blosser Richard, A877
 Blouch Kristin, A423, A482
 Bloy Norma, A309
 Bluhm Julia, A104
 Blum Agnieszka, A866
 Blum Lisa, A819
 Blum Robert, A126
 Blumenschein George, A465
 Blumenschein George Jr, A1009
 Blumenthal Daniel, A114, A148
 Bluvshstein Olga, A732
 Bobilev Dmitri, A999
 Bockorny Bruno, A509, A563
 Boda Akash, A622, A793
 Bodd Monica, A665
 Boehmer Brit, A875
 Boes Marianne, A643
 Bogaert Liz, A817, A819
 Bohan Phillip Kemp, A571
 Bohat Ritu, A584
 Bojczuk Paul, A690
 Bokobza Sivan, A892

- Boland Genevieve, A670, A965
 Boland Genevive, A684
 Boland Nadthakarn, A243
 Bolanos-Ibarra Kristian, A131
 Bolen Joseph, A512
 Bollampalli Arjun Reddy, A219
 Boller Emily, A658
 Bolotin Diana, A580
 Bommareddy Praveen, A538, A539, A577, A580
 Bommer Bettina, A885
 Bonaventura Paola, A719
 Bondarenko Igor, A390
 Bone Jennifer, A375
 Boni Valentina, A422
 Bonini Chiara, A111
 Bonito Maurizio Di, A980
 Bonnafous Cécile, A892
 Bonnans Caroline, A327
 Bonnevaux Hélène, A893
 Bono Johann De, A374, A378, A448, A449, A455, A535
 Bonomi Marcelo, A878
 Bonzon Christine, A726, A736, A822, A913
 Boorjian Stephen, A452
 Borbath Ivan, A550
 Borchmann Peter, A1008
 Boreddy Srinivas Reddy, A915
 Borghaei Hossein, A664
 Borji Mehdi, A84
 Boroughs Angela, A226
 Borrego Luis Miguel, A978
 Borriello Frank, A174
 Borrman Tyler, A858
 Bos Remco, A232
 Bosson Nicolas, A287
 Bota Daniela, A357, A358, A359, A361, A362, A1001
 Botticelli Andrea, A257
 Bouaoud Jebrane, A962, A984
 Boucher Justin, A115
 Bouchlaka Myriam, A284, A294, A299
 Bouffard Amanda, A234
 Boulos Rasha, A719
 Bourayou Nawel, A1006
 Bourguignon Jérémie, A287
 Bourin Clotilde, A351, A792
 Bourre Ludovic, A953
 Bove Peter, A809, A810
 Bowden Michaela, A316
 Bowles Tawnya, A538
 Bowyer Samantha, A577
 Boyce Rogely, A895
 Boyd Kelli, A606
 Boyd-Kirkup Jerome, A498
 Boyer Arnaud, A489
 Boyer James, A833
 Boyer Michael, A391, A484
 Boyle Sean, A21, A22, A83, A88
 Boyle Theresa, A954
 Bozkus Cansu Cimen, A360, A807
 Bozon Viviana, A907
 Brück Patrick, A579
 Braña Irene, A958
 Brachtlova Tereza, A1004
 Bradford Shermineh, A985
 Bradley John, A766
 Brady Mallory, A198
 Bragg Eric, A908
 Brahmachary Manisha, A550
 Brahmandam Archana, A117
 Brahmer Julie, A320, A353
 Brain Etienne, A997
 Brakenhoff Ruud, A932, A981
 Brambilla Marta, A16
 Bramhecha Yogesh, A380
 Brana Irene, A526
 Brandenberger Ralph, A159
 Brandish Phil, A2
 Brandish Philip, A824, A931
 Brant Boris, A756
 Branthoover Holly, A418, A419
 Brard Caroline, A382
 Bratos Raquel, A381
 Braubach Oliver, A56, A334
 Braud Filippo De, A16
 Braun David, A84, A684
 Braun Franziska, A976
 Bray Mark, A519
 Bredel Delphine, A409, A945
 Brehm Michael, A919
 Breij Esther, A904, A932
 Brekken Rolf, A632, A964
 Breman Eytan, A118, A154
 Brennan Aoife, A532
 Brennan Mary Jane, A377
 Bressi Jerome, A126
 Breunig Christian, A923, A938
 Brewer Rachel, A283
 Brewis Neil, A602, A792
 Briante Raffaella, A306
 Brickman Nurit, A172
 Brideau Emily, A176
 Bridgeman John, A209, A210
 Bridgeman John S, A189
 Bridgen Devin, A175
 Brignone Chrystelle, A997
 Brink Edward van den, A904
 Bristow Christopher, A1013
 Britten Cedrik M, A1009
 Brlic Paola Kucan, A275
 Broad Robyn, A407
 Brock Matthias, A885
 Brockman Asa, A45
 Brocq Michelle Le, A210
 Brodbeck Jens, A606
 Broderick James, A884
 Brodtkin Heather, A744, A747, A752
 Brody Mary, A128
 Brody Rachel, A338, A360, A651
 Broeske Ann-Marie, A94, A976
 Brohl Andrew, A402
 Bronson Steven, A843
 Brookhouser Nicholas, A126
 Broom Wendy, A796
 Brose Marcia, A381
 Brough Douglas, A513
 Brown Brian, A653
 Brown Christine, A133
 Brown Jason, A749
 Brown Kathlynn, A648
 Brown Michael, A366, A367, A770
 Brown Myles, A728
 Brown Richard, A368
 Bruchez Marcel, A698
 Bruderer Roland, A99, A370
 Bruin Linda de, A383
 Brune Patrick, A535, A558, A592
 Brungs Daniel, A577
 Bruno Tullia, A682, A880
 Brycman Nurit, A230
 Brysting Josephine, A218
 Brzózka Krzysztof, A799
 Brzozka Krzysztof, A786
 Bu Xia, A728
 Buchbinder Elizabeth, A999
 Bucher Christoph, A731
 Bucktrout Samantha, A847
 Backup Mark, A713
 Budhani Pratha, A946
 Budhu Sadna, A108, A596, A634, A649
 Bueno Orlando, A476
 Buetz Christen, A636
 Buffet Renaud, A301
 Bugaj Marta, A786
 Bughani Usha, A915
 Buhandler Boaz, A230
 Bui Lynne, A809, A810
 Bui Nam, A395
 Bukhalid Raghida, A820
 Bulliard Yannick, A115, A145
 Bullock Andrea, A397, A509
 Bullock Caroline, A215
 Bullock Timothy, A694
 Bumgarner Hannah, A880
 Bunch Brittany, A616, A709, A794
 Bunchbinder Elizabeth, A417
 Buni Maryam, A853
 Buravenkov Vitaliy, A823
 Burchard Paul, A311
 Buren Luxuan, A123
 Burenkova Olga, A883
 Burg Sjoerd van der, A41, A383
 Burga Rachel, A176
 Burge Matthew, A366, A367
 Burgess Melissa, A574
 Burgher Blake, A78, A86, A89
 Burkard Nathaniel, A50
 Burke Aiden, A621
 Burke James, A456, A1005
 Burke Krista, A247
 Burman Poromendro, A310, A317
 Burnett Madison, A590
 Burns Andrew, A126
 Burr Ansen, A880
 Burrack Adam, A687
 Burris Howard, A559
 Burtness Barbara, A688
 Burvenich Ingrid, A349
 Burzyn Dalia, A883
 Busch Stephanie, A211
 Busse Antonia, A531
 Bustamante Mariana, A557
 Buti Sebastiano, A257
 Butler Marcus, A417, A423, A568
 Butt Omar, A428
 Butterfield Lisa, A95, A96, A695, A995
 Buuren Marit Van, A212
 Byers Lauren, A944
 Byford Alan, A303
 Bykova Katrina, A736, A822
 Byrd David, A689
 Byrd Kaelan, A764
 Byrne Katelyn, A603
 Caballero Francisco, A902
 Cabanov Alexandra, A963
 Cabanski Christopher, A370
 Cabral Crystal, A268
 Cadzow Louise, A198, A215
 Caffaro Carolina, A636

- Cafferata Allison, A688
 Caffrey Thomas, A683
 Caglevic Christian, A390
 Cahoon Jason, A221
 Cai Beilei, A591
 Cai Chufan, A691
 Cai Na, A735
 Cai Yiyu, A855
 Cai Yueqi, A835
 Calandigary Ahmed, A927
 Calareso Giuseppina, A16
 Caldara Jeni, A875
 Caldwell Charles, A55
 Calhoun Susan, A740
 Califano Andrea, A947
 Califano Joseph, A631
 Callahan Margaret, A540
 Callihan Evan, A908
 Calloud Sébastien, A287
 Calnan Conor, A215
 Calvo Emiliano, A531, A536, A546, A555
 Calvo Katherine, A270
 Camblin Adam, A165
 Campbell Carly, A2
 Campbell Dean, A953
 Campbell Kerry, A699
 Campbell Matthew, A259, A454
 Campbell Thomas, A30, A33, A47, A870
 Campesato Luis Felipe, A596
 Campian Jian, A428
 Campigotto Federico, A606
 Camps Marcel, A805
 Campton Daniel, A64
 Canaday Pamela, A900
 Canalda Adria-Jaume Roura, A645
 Canales Josue, A752
 Canals Francesc, A958
 Canamero Marta, A557, A976
 Candace Wai Sze Lei, A985
 Candelli Andrea, A119
 Candidate Caitlyn Miller, A803
 Cañete Guillermo Herrador, A772
 Canevari Silvana, A461
 Canoll Peter, A100
 Canter Robert, A675
 Canton David, A417
 Cantone Nico, A800
 Cao Lizhi, A884
 Cao María González, A1011
 Cao Subing, A365
 Cao William Wei, A120
 Cao Xuezi, A632
 Capitini Christian, A221
 Capoccia Benjamin, A282
 Capone Mariaelena, A27, A332, A980
 Capone Stefania, A441
 Cappuzzo Federico, A394
 Caracó Corrado, A27, A332, A980
 Carbone David, A323, A423, A954
 Carcereny Enric, A386
 Cardenas Maria, A669, A686, A779, A975
 Cardia James, A910
 Cardona Andrés, A25
 Carey Craig, A504
 Carrillo Jose, A362
 Carlino Matteo, A417, A552
 Carlisle Jennifer, A975
 Carlsson Erick, A714
 Carlsson Malin, A567
 Carnino Jonathan, A899
 Caro Nydia, A591
 Carpenter Elizabeth, A571
 Carpentier Sabrina, A892
 Carr Brian, A413, A606, A887, A888
 Carr Steven, A684
 Carrancio Soraya, A117
 Carrillo Jose, A357, A358, A359, A361, A1001
 Carrington Mary, A338
 Carroll Charlotte, A943
 Carroll Jonathan, A847
 Carron Emily, A147
 Carruthers Alan, A967
 Carson Ken, A905
 Carson William, A399, A714, A715
 Carstensen Laura Stentoft, A806
 Carter Brett, A304
 Carter Jo, A368
 Caruana Ignazio, A696
 Carvajal Richard, A568, A857
 Casal Guzman Alonso, A536
 Casartelli Chiara, A257
 Cascone Tina, A186, A1013
 Casey Kerry, A565
 Casey Richard, A1004
 Cassard Lydie, A409
 Cassier Philippe, A567
 Castano Ana, A582
 Castano Zafira, A219
 Castelli Chiara, A1
 Castillo Alyssa, A706
 Castillo Paul Del, A548
 Castillo-Martin Mireia, A978
 Castro Gilberto de, A62, A390, A391, A488
 Castro Henry, A539, A580
 Casucci Monica, A111
 Catania Vanessa, A721
 Catcott Kalli, A820
 Catherine Pietanza M, A391, A488
 Cathomen Toni, A8
 Catino Annamaria, A257
 Caudell David, A11
 Caushi Justina, A310, A317, A353, A693
 Caux Christophe, A719
 Cavalcante Ludimila, A643
 Cavalcanti Ernesta, A27
 Cavallo-Fleming Julie-Ann, A651
 Cave Judith, A572
 Ceccarelli Jake, A418, A419
 Cedres Susana, A491
 Cejas Paloma, A728
 Cemerski Saso, A749
 Ceppi Maurizio, A11, A94, A557, A976
 Cerezuela-Fuentes Pablo, A1011
 Cerf Emilie, A438
 Cervantes Andrés, A546
 Cervesi Julie, A301
 Cervini Amanda, A461
 Cha Edward, A544
 Chabanon Roman, A945
 Chablani Priyanka, A659
 Chacon Alexander, A311, A618, A705
 Chae Young Kwang, A29, A79, A254, A292, A555, A661, A966
 Chai Jitian, A217
 Chai-Ho Wanxing, A577, A580
 Chaib Mehdi, A710
 Chain Robert, A143
 Chajut Ayelet, A825
 Chakraborty Mala, A181
 Chalifa-Caspi Vered, A230
 Challa Sreerupa, A899
 Chambless Lola, A45
 Chamourin Maité, A48, A65
 Champiat Stéphane, A534
 Champiat Stephane, A514, A535
 Chan Ivan, A123, A137, A159
 Chan Karmela, A854
 Chan Li-Chuan, A622
 Chan Steven, A997
 Chan Timothy, A340, A807
 Chan Tze, A539
 Chandra Adrienne Kaya, A862
 Chandra Raghav, A964
 Chandrakasan Shanmuganathan, A779
 Chandrasekaran Ramya, A284, A299
 Chaney Marya, A435, A439, A464, A1011
 Chang Chia-Ming, A285
 Chang Chia-Wei, A126
 Chang Ching-Wei, A101
 Chang Christie, A713
 Chang Hewitt, A704
 Chang Jane, A660
 Chang Jui-Ying, A722
 Chang Kai-Hsin, A203
 Chang Shu Ching, A103
 Chang Tzu-Pei, A832
 Chang Wen-Chung, A135
 Chang Yao-Wen, A886
 Chang Yu Qing, A855
 Chantzoura Eleni, A144
 Chao Bo, A505
 Chao Mark, A554
 Chao Sherry, A965
 Chao Yee, A389
 Chaparro Arturo, A973
 Chaparro-riggers Javier, A290
 Chapin Brian, A379
 Chapin Steven, A817, A819, A903
 Chapkin Robert, A761
 Chapuis Aude, A204
 Chaput-Gras Nathalie, A300, A308, A409
 Charap Andrew, A338
 Chariau Paul, A635
 Charlene Liao X, A327
 Charles Julie, A1011
 Charo Jehad, A94, A976
 Charoentong Pornpimol, A41
 Charpentier Maud, A286
 Chassagnole Christophe, A865
 Chatani Praveen, A177, A680
 Chatterjee Bithi, A885
 Chatterjee Gourab, A60
 Chatterjee Manik, A1009
 Chauchet Xavier, A287
 Chaudhari Sachin, A889
 Chaudhary Surendra, A494
 Chaudhri Apoorvi, A244
 Chaussabel Damien, A111
 Chauvin-Fleurence Cynthia, A210
 Chavez Brandy, A768
 Chawla Kanika, A226
 Chawla Sant, A395
 Che Jenny, A884
 Che Keying, A986
 Chean Borom, A221
 Cheasty Anne, A967
 Chee Chen, A511
 Cheema Tooba, A542
 Cheever Mac, A462
 Cheikh Bassem Ben, A334

- Chekmasova Alena, A240
 Chelighem Safia, A627
 Chelvanambi Manoj, A797
 Chen Ada, A280
 Chen Alex, A745
 Chen Amy, A815
 Chen Benchao, A471
 Chen Benjamin, A316, A420
 Chen Chao-Hsien, A248, A622, A798
 Chen Chen, A228
 Chen Christine, A126
 Chen Clark, A180
 Chen Dan, A998
 Chen Diana (Qiusheng), A492
 Chen Dongping, A466
 Chen Fangyuan, A708
 Chen Fei, A84
 Chen Guang, A486, A523
 Chen Helen, A20
 Chen Heyu, A327
 Chen Hui Amy, A998
 Chen Hung-Kai, A886
 Chen Jacky, A178
 Chen Jerry, A745
 Chen Jia, A748
 Chen Jian, A397, A405
 Chen Jinguo, A570
 Chen Jo-Pai, A722
 Chen Jonathan, A670, A965
 Chen Ju-Pei, A886
 Chen Junjie, A622
 Chen Leonard, A1002
 Chen Liqing, A636
 Chen Lihong, A824
 Chen Mary, A619, A620
 Chen Mei, A303
 Chen Min, A706
 Chen Na, A288, A313, A783
 Chen Nianyong, A466
 Chen Peng, A638
 Chen Qian, A490
 Chen Richard, A21, A22, A83, A88
 Chen Sheryl, A569
 Chen Shih-Hsun, A290
 Chen Shuming, A312
 Chen Tianling, A408
 Chen Wei, A746
 Chen Wenbin, A443
 Chen Xianhui, A121, A145
 Chen Xiaocheng, A297
 Chen Xiaozhong, A466
 Chen Yaqing, A460
 Chen Yian Ann, A206
 Chen Yidong, A321
 Chen Yiwen, A584
 Chen Yu-Wei, A760
 Chen Yu-Zhong, A355
 Chen Yuan, A584
 Chen Zhendong, A479
 Chen Zhouxiang, A351
 Chenchik Alex, A77
 Cheng Chao, A674
 Cheng Michael, A35
 Cheng Phil, A597
 Cheng Serena, A52
 Cheng Wei-Yi, A94, A976
 Cheng Xiaobin, A443
 Cheng Xiaofei, A443
 Cheng Ying, A389, A488
 Cheong Sok Ching, A957
 Cherifi Yacine, A782, A953
 Cherniack Andrew, A74
 Chesney Jason, A538
 Cheuk Adam, A153, A171
 Cheung Alexander, A704
 Cheung Keith, A894
 Chew Jennifer, A91
 Chheda Milan, A428
 Chhum Sotheavy, A114
 Chianese-Bullock Kimberly, A421
 Chiang Jun Ding, A91
 Chick Robert, A571
 Chielewski Stefan, A786
 Chiffolleau Elise, A245
 Childs Richard, A181
 Chillakuri Chandramouli, A924
 Chilukuri Lakshmi, A335
 Chin Mike, A746
 Ching Keith, A768
 Chinnapattu Murugan, A889
 Chion-Sotinel Isabelle, A151
 Chiron Marielle, A308, A893
 Chisamore Michael, A440, A529, A632, A1005
 Chiu Joanne WY, A485
 Chiu Kevin, A658, A660
 Chmielewski Stefan, A786, A799
 Chmielowski Bartosz, A538, A553, A573, A999
 Cho Benjamin, A155
 Cho Byoung, A488
 Cho Byoung Chul, A390, A391, A499
 Cho Daniel, A546
 Cho Hyun-Jun, A764
 Cho Hyung-Gyo, A966
 Cho Jaeyong, A440
 Cho Soo Ick, A869
 Cho Soonweng, A280
 Cho Sukjoo, A254
 Choi Eun Ji, A138
 Choi Hyejin, A634
 Choi John, A724
 Choi Jungwon, A146
 Choi Seungtaek, A259
 Chojnowski Grace, A366, A367
 Chollate Sowmya, A553
 Chong Esther, A727
 Choo Su Pin, A97
 Chou Ching-Heng, A160
 Chou Hung-Yen, A500
 Chou Yung-Chih, A622
 Choueiri Toni, A257, A447
 Chow Andrew, A108
 Chow Chi-Wan, A186
 Chow Laura, A462, A530, A542
 Chrétien Anne-Sophie, A898
 Christensen Esben, A806
 Christenson Jessica, A933
 Christians Arne, A47
 Christopher Garcia K, A614
 Chrobak Ken, A200
 Chu Gina, A768
 Chu Hamlet, A887, A888
 Chu Hui-Yi, A126, A147
 Chu Philip, A147
 Chu Seung, A913
 Chun Brie, A103, A431
 Chun Chau Lawrence Cheung, A97
 Chun Patrick, A890, A929
 Chung Alexander, A501
 Chung Christine, A468
 Chung Donjun, A715
 Chung Hyun, A530
 Chung Hyun Cheol, A440
 Chung Sarah H, A853
 Chunyk Allison, A831
 Church Candice, A322
 Church Sarah, A613, A980, A995
 Chuvin Nicolas, A719
 Chyung Yung, A563
 Ciaramella Giuseppe, A165
 Cicala Alexander, A982
 Ciccolini Joseph, A382
 Cichocki Frank, A172, A180
 Cieniewicz Brandon, A218
 Cieri Nicoletta, A684
 Cieslewicz Michael, A397, A405
 Cifuentes Anokhi, A243
 Cillo Anthony, A682, A880
 Cinamon Guy, A275
 Cinay Gunce, A121
 Cindass Jessica, A571
 Cirauqui Beatriz, A463
 Clancy Trevor, A416
 Clara Joseph, A181
 Clark Kristopher, A583
 Clarke Christopher, A887, A888
 Clarke Jeffrey, A665
 Clarke Raedun, A126
 Cleary Lisa, A907
 Clergeaud Gael, A641
 Clerre Diane le, A151
 Clever Jared, A218
 Cleyrat Cédric, A211
 Clifton Guy, A571
 Cline Mark, A11
 Clouson Andrew, A367
 Clynes Raphael, A553
 Coaña Yago Pico de, A567, A831
 Coarfa Cristian, A248
 Cobb Dustin, A136
 Cobb Laura, A134
 Cobb Patrick, A1007
 Cobo Ana Galan, A960
 Cochran Jennifer, A803
 Codó Paula, A502
 Codde Rebecca, A132
 Coffin Robert, A538, A539, A580
 Cohen Daniel, A420
 Cohen Ezra, A463, A469, A553, A631
 Cohen Frederick, A107
 Cohen Heather, A2
 Cohen Merav, A713
 Cohen Roger, A515, A553
 Cohen Sherri, A230
 Cohn Allen, A381
 Coholan Lindsey, A165
 Cojocarú Gady, A272
 Cole Anna, A9, A237, A737
 Cole Christopher, A881
 Cole David, A924
 Coleman Niamh, A21
 Colen Rivka, A25
 Colette DIB, A308
 Colevas Dimitrios, A22, A577
 Colletti Nicholas, A198
 Colliander Anna, A641, A806
 Collichio Frances, A577, A580
 Collignon Aurélie, A65
 Collignon Aurelie, A48
 Collins Kimberly, A64
 Collins Krystle, A431

- Collins Laura, A600, A857, A909
 Collins Zachary, A372
 Collinson-Pautz Matthew, A240
 Colomba Emeline, A382
 Colombo Chiara, A1
 Colombo Mario Paolo, A16
 Colonna Catherine, A621
 Combeau Cecile, A308
 Condamine Thomas, A148, A1000
 Conejo-Garcia Jose, A95, A96
 Cong Xini, A35
 Conlin Alison, A103, A430
 Conner Michael, A690
 Conrad Valerie, A103
 Conrady Deborah, A905
 Conroy Jeffrey, A78, A86, A89
 Cons Laura, A287
 Conter Henry, A374, A378
 Conway Jake, A728
 Cooch Neil, A481, A812
 Cook John, A941
 Cook Katherine, A646
 Cooper Aaron, A226
 Cooper Jeremy, A64
 Cooper Matthew, A200
 Copeland Ron, A516
 Copeland Ronald, A599
 Copik Alicja, A716, A718
 Cordero Jose, A476
 Cordes Lisa, A513
 Cordes Ulrik, A187
 Corey Daniel, A218
 Corey Lawrence, A218
 Corigliano Ellie, A482
 Corn Paul, A259, A379
 Cornelson Garrett, A926
 Cornen Stéphanie, A892
 Coronella Julia, A132, A155
 Corredor Germán, A868
 Corrie Pippa, A573
 Corse Emily, A946, A985
 Cortés Javier, A364
 Cortellini Alessio, A257, A545
 Cortez Angelica, A604
 Cortez Czrina, A108
 Cortez-Retamozo Virna, A636
 Coss Christopher, A706
 Costa Amanda, A165
 Costa Andreia, A211
 Costa Maria Jose, A327
 Costantini Dominique, A394
 Costello Brian, A540
 Cote Shaun, A563
 Cotteaux-Lautard Christelle, A489
 Cotugno Gabriella, A441
 Coughlin Caroline, A703
 Couillault Coline, A315, A622
 Coukos George, A461
 Courta Jacqueline, A893
 Couselo Eva Muñoz, A1011
 Cousineau Isabelle, A267
 Couto Suzana, A546, A874, A973
 Cova Agata, A331
 Covert Markus, A192
 Covington Maryanne, A247
 Coward Jermaine, A457
 Cowen Benjamin, A652
 Cox Angela, A867
 Cox Bryan, A637
 Coy Jesse, A764
 Crago William, A751, A897
 Craig Andrew, A205
 Cranert Stacey, A132, A155
 Crawford Jeffrey, A665
 Crawford Jeremy, A160
 Creasy Caitlin, A199
 Crespin Athéna, A301
 Cress Doug, A954
 Crew Linda, A833
 Cripe Timothy, A537
 Cristescu Razvan, A391, A485
 Crochiere Marsha, A397, A405
 Crocker Andrea, A833
 Cron Kyle, A671
 Croom-Perez Tayler, A716
 Crosby Shadarra, A410
 Croteau Nicole, A495
 Crow Ailey, A59
 Cruz Payton De La, A36, A758
 Cruz Sylvia, A675
 Csiki Ildiko, A481
 Csiszovszki Zsolt, A72
 Cubas Agi de, A951
 Cuentas Edwin Parra, A788
 Cugno Chiara, A111
 Cugola Fernanda Rodrigues, A126
 Cui Ang, A593
 Cui Dan, A625
 Cui Lei, A800
 Cui Linda, A721
 Cui Yufei, A225
 Cuiffo Benjamin, A910
 Cuk Katarina, A579
 Culey Georgia, A48, A65
 Cullen Cody, A135
 Cultrara Christopher, A231
 Culver Ken, A943
 Cummings Richard, A800
 Cunha Fernando, A62
 Cunningham Rachel, A402
 Cunningham-Bussel Amy, A853
 Curiel Tyler, A249, A261, A321, A789, A944
 Curigliano Giuseppe, A398, A503, A550
 Curran Michael, A248, A315, A350, A622, A652, A759, A788, A793, A798, A906
 Currie Sue, A67, A1007
 Curry Joseph, A947
 Curti Brendan, A415, A540
 Curvietto Marcello, A980
 Cushing Daniel, A1000
 Cusumano Zachary, A520, A599
 Cutsem Eric Van, A433, A559
 Cuyper Eveline De, A997
 Ćwiertnia Grzegorz, A799
 Cwirla Steven, A738
 Cyprus Garrett, A12
 Cyranowski Salvador, A645
 Czerniak Bogdan, A259
 Czerwinski Debra, A803
 D'Alessio Antonio, A545
 D'Alise Anna Morena, A441
 D'Amico Leonard, A462
 D'Andrea Gabriela, A528
 d'angelo grazia, A27, A332, A980
 D'Angelo Sandra, A424
 Dabbagh Karim, A598
 Dabovic Kristina, A475
 Dadali Tulin, A268
 Daher May, A853
 Dahut Madeline, A757
 Dahut William, A450
 Dai Junqiang, A372
 Dai Nan, A490
 Dai Shuang, A939
 Dai Xiaomeng, A443
 Daigneault Tina, A828
 Dailey Thomas, A126
 Dalac-Rat Sophie, A538
 Dalenc Florence, A997
 Daley Jessica, A682
 Dallacosta Janice, A940
 Dalle Stephane, A300, A1011
 Dalmas Olivier, A858
 Damelin Marc, A820
 Danaher Patrick, A57, A1002
 Danesi Hassan, A407
 Dang Hao, A701
 Dang Minghao, A788, A960, A971
 Daniel Dylan, A735
 Daniel Jeannie, A559
 Danielczyk Antje, A741, A816
 Danielpur Liron, A732
 Daniels Ella, A257
 Daniels Gregory, A415, A417, A573, A577, A580
 Danlos François-Xavier, A300, A945
 Danlos Francois-Xavier, A409
 Dannenberg Jan-Hermen, A973
 Dao Tram, A182
 Daria Deidre, A710
 Daris Mark, A131
 Darmon Audrey, A771
 Darst Russell, A77
 Darwech Malik, A200
 Das Abhishek, A884
 Das Amit, A964
 Das Avratanu, A889
 Das Sanjib, A889
 Das Subhadip, A889
 Dash Subhadra, A900
 Daud Adil, A417, A553, A999
 Dauki Anees, A413
 Davar Diwakar, A503, A999
 Dave Rutwij, A606
 Daveri Elena, A331
 Daviaud Camille, A950
 David Amram Ben, A230
 David Eyal, A713
 David Tai Wai Meng, A97, A656
 Davidson Max, A882
 Davies Sarah, A145
 Davila Marco, A115, A703
 Davis Craig, A484
 Davis Hugh, A833
 Davis Thomas, A268, A504, A515, A551
 Davis Zachary, A180, A208
 Dayao Maria, A908
 Daza Jorge, A651
 Dea Steven, A88
 Dean Bayli DiVita, A262, A594
 Dean John, A200
 Deb Gauri, A982
 Deban Livija, A920
 Debnath Neha, A257
 Deboeve Nathaniel, A105
 DeCillis Arthur, A504, A515
 Dee Mike, A200
 Dees Elizabeth, A1000
 Deforges Jules, A777
 Dejima Hitoshi, A1013

- Deken Marcel, A967
 Dekker Joseph, A926
 Delafontaine Brant, A559
 Delaite Patricia, A441
 Delgoffe Greg, A109, A194, A673, A691, A697, A698, A707, A774
 Dellinger Kristen, A233
 Delston Rachel, A282
 Demaria Olivier, A892
 Demaria Sandra, A286, A589
 DeMario Mark, A212
 Dembrow Daniel, A213
 Demers Brigitte, A433, A550, A581
 Demin Oleg, A296
 Deming Dustin, A982
 DeMuth Peter, A167, A582
 Deng Liang, A724
 Deng Min, A638
 Deng Shibing, A371
 Deng Simai, A405
 Deng Yilun, A249, A261, A789, A944
 Dengel Karen, A461
 Dengel Lynn, A421
 Deniger Drew, A240
 Denis Fabrice, A394
 Denis Morgane, A953
 Denning Warren, A960
 Dent Rebecca, A364
 Deol Suprit, A817
 Deola Sara, A111
 DePeaux Kristin, A707, A774
 DePietro Paul, A78, A86, A89
 Depil Stephane, A719
 Depinho Ronald, A622
 Derclé Laurent, A857
 Derhovanessian Evelynna, A451, A579
 Dermime Said, A19, A767
 Deronic Adnan, A785
 Desai Anjali, A523
 Desai Keyur, A420
 Desbois Melanie, A740
 Deshmukh Kiran, A131
 Deshpande Ameya, A889
 Deshpande Amit, A792
 Desjarlais John, A726, A736, A822, A913
 Desland Fiona, A713
 Desnoyer Jill, A598
 DesRochers Tessa, A305
 Desselle Ariane, A245
 Desuki Alexander, A1008
 Detjen Katharina, A34
 DeTomaso David, A226
 Devarakonda Srinivas, A507
 DeVault Victoria, A787
 Devenport Martin, A246, A500
 Deveraux Quinn, A12, A897
 DeVito Nicholas, A343, A685, A968
 Dey Chaitali, A915
 Dey Joyoti, A633
 Deymar Simon, A11
 Dhainaut Maxime, A653
 Dhamsania Rohan, A779
 Dhar Arindam, A423
 Dhodapkar Kavita, A434
 Dhodapkar Madhav, A434
 Dholaria Bhagirathbhai, A475
 Dhupar Rajeev, A122, A708
 Diab Adi, A67, A845, A853
 Diamond Akiva, A257
 DiAndreth Breanna, A131
 Diao Peng, A458
 Dias-Costa Andressa, A1010
 Diaz Fulvio, A749
 Diaz Gabriela, A211
 Diaz Juan, A726, A822
 Dicker Adam, A323
 Dickey Andrea, A495
 Dickhoff Chris, A700
 Diede Scott, A417
 Dieffenthaler Thomas, A716
 Diem Dania, A885
 Diem Kurt, A218
 DiFiglia Andrea, A169
 Diggs Laurence, A721
 Dijk Marc Van, A144, A216, A432
 Dikshit Anushka, A101
 Dillman Robert, A357, A358, A359, A361, A362, A1001
 Dillon Christopher, A768
 Dillon Patrick, A363
 Dillon Stacey, A39
 DiMascio Leah, A498
 DiMatteo Darlise, A247
 Dimitrios Colevas A, A52, A468
 Dimitrov Dimiter, A171
 Dimitrova Maya, A853
 Ding Hua, A877
 Ding Jian, A185, A214
 Ding Kai, A708
 Ding Lina, A316
 Ding Sheng, A290
 Ding Ying, A553
 Dinh Huyen, A284, A294, A299
 Dinowitz Nathan, A230
 Dinter Teresa, A711
 Dirix Luc, A997
 Dirksen Anouk, A820
 Divakar Prajan, A258, A270
 Dixit Neha, A1007
 Dixit Vaishali, A633
 Dixon Kate, A208
 Djuretic Ivana, A607, A746
 Do Khanh, A569
 Do Nicole, A998
 Dobrin Anton, A142, A862
 Doerner Astrid, A953
 Doger Bernard, A386, A486, A550
 Domingo Christine, A155
 Domingo-Musibay Evidio, A573
 Domingos-Pereira Sonia, A920
 Dominguez Ana Lucia, A183
 Dominik Pawel, A290
 Donaghy Ian, A940
 Donahue Christine, A690
 Donahue Renee, A6, A513, A570, A612
 Donald Harvey R, A553
 Donaldson Ian, A401
 Dong Chunbo, A632
 Dong Juan, A276
 Dong Lauren, A634
 Dong Qi, A120
 Dong Wenliang, A1004
 Dong Yongcheng, A471
 Donio Michael, A282
 Donne Romain, A653
 Donovan Laura, A969
 Dooley Kevin, A601
 Doran Shawn, A768
 Dorigo Oliver, A380
 Dornan David, A817, A819, A903
 Doroshow Deborah, A548
 Dosunmu Ololade, A527
 Dothard Andy, A846
 Dougan Stephanie, A1010
 Dougherty Sean, A840
 Dowal Louisa, A268
 Dower William, A738
 Dowlati Afshin, A397, A505
 Doxie Deon, A434
 Dragovich Matthew, A726
 Drake Charles, A947, A951
 Drakes Dylan, A167
 Dranitsaris George, A512
 Draper Ben, A969
 Draper David, A298
 Dray Eloise, A944
 Dredge Keith, A366, A367
 Drenberg Christina, A699
 Drew Clifton, A874
 Drobinski Patryk, A24
 Droin Nathalie, A409
 Drouin Marion, A245
 Druta Mihaela, A424
 Druyts Eric, A339
 Du Bingfan, A820
 Du Dongliang, A206
 Du Karrie, A130
 Du Xiaoyan, A900
 Du Xuexiang, A246, A849
 Du Yangchun, A462
 Duan Fei, A379
 Duan Tao, A398
 Dubensky Thomas, A891
 Dudek Łukasz, A799
 Dudek Agata, A786
 Dudek Arkadiusz, A505
 Dudley Mark, A401
 Duffy Christine, A510
 Dufort Fay, A824
 Dugan Greg, A11
 Dugast Anne-Sophie, A219
 Dugopolski Caroline, A198
 Duke William, A807
 Duma Christopher, A357, A358, A359, A361, A362, A1001
 Dumbrava Ecaterina, A503, A507, A508
 Dummer Reinhard, A536, A597
 Dumontet Charles, A953
 Dunbar Zerick, A717
 Duncan Meghan, A549
 Dunn Gavin, A428, A812
 Dunn Lara, A468, A1007
 Dunn Robert, A735
 Dunn Zachary, A121
 Dunne Philip, A987
 Duong Ellen, A344, A711
 Dupont Christopher, A542
 Duque Sandra Chica, A387, A389
 Durand Justine, A829
 Düring Maria, A429
 Duska Linda, A562
 Dussiot Michael, A945
 Dutcu Corina, A381
 Dutriaux Caroline, A1011
 Dutta Lea, A381
 Dutzar Benjamin, A745
 Duvall Jeremy, A820
 Dwivedi Sanyog, A14
 Dwyer Connor, A207, A237
 Dwyer Jessica, A427

- Dwyer Karen, A472
 Dykema Arbor, A317
 Dzekunova Inna, A1002
 Dziadek Sebastian, A94, A976
 Dziadziusko Rafal, A394
 Dziedzic Katarzyna, A799
 Dzimitrowicz Hannah, A655
- Easton Rachael, A518
 Eberle Kirsten, A683
 Eberlein Jens, A119
 Eberst Lauriane, A382
 Ebrahimzadeh Walead, A380
 Eche Thomas, A857
 Eck Stephen, A1009
 Eckard Sterling, A890, A929
 Eckelman Brendan, A12, A751, A897
 Eckels Phillip, A240
 Economides Kyriakos, A601, A796, A883
 Ecsedi Matyas, A204
 Ecsedy Jeffrey, A102
 Edeline Julien, A387
 Edmonds Nicole, A363
 Edri Avishay, A172, A230
 Edukulla Ramakrishna, A576
 Edwards Robin, A420
 Edwin Roger Parra Cuentas , A962
 Egan Hannah, A987
 Egan Laurence, A987
 Egan Nicholas, A584
 Egeblad Mikala, A108
 Egerod Frederikke Lihme, A904
 Eggenschwiler Corinne, A536
 Egmond Sylvia van, A41
 Ehrhart Jared, A616, A709, A794
 Eickhoff Jens, A318, A377
 Eigentler Thomas, A502
 Einstein David, A188
 Eisenberg Seth, A122, A708
 Eitas Timothy, A820
 Eivazi Araz, A736
 Eiznhamer David, A543
 El-Anbari Mohammed, A111
 El-Hajjar Mikal, A617
 El-Khoueiry Anthony, A509, A533, A566
 El-Rayes Bassel, A20, A434, A779, A948
 El-Refai Sherif, A991
 Elboudjwarej Emon, A413
 Eleftheriadou Ioanna, A424
 Elemento Olivier, A309
 Elenko Eric, A512
 Elghonaimy Eslam, A442
 Elhalel Dranitzki Michal Michal, A825
 Elias Rawad, A1010
 Eliseeva Tania, A983
 Ellard Susan, A398
 Eller Ann-Kathrin, A579
 Ellert-Miklaszewska Aleksandra, A645
 Ellingsen Espen, A416
 Ellmark Peter, A567, A595, A785, A831
 Elloul Sivan, A219
 ElNaggar Adam, A507, A508
 Elon Yehonatan, A323
 Eloriaga Jonathan, A716
 Elrod Ashley, A305
 Elsayes Khaled M, A853
 Ely Scott, A420, A859
 Enamekhoo Hamid, A318, A377, A538
 Emancipator Kenneth, A7
 Emanuel George, A965
- Emmenegger Urban, A374, A378
 Emmerich Philip, A982
 Engelhard Victor, A54
 Engleman Edgar, A903
 Enoki Tatsuji, A71
 Enstrom Amanda, A891
 Epp Angela, A895
 Epps Heather Van, A818
 Epstein Michael, A205, A572
 Erbe Amy, A50, A67, A628, A629
 Erhard Florian, A958
 Erman Mustafa, A488
 Ernst James, A913
 Esch Amanda, A60
 Eschle Benjamin, A277
 Escobedo Erik, A727
 Escriou Guillaume, A300
 Escudier Bernard, A376
 Escuin-Ordinas Helena, A1011
 Espinosa Enrique, A568
 Esposito Assunta, A27
 Esquibel Vanessa, A454
 Estornes Yann, A719
 Ettestad Brianna, A667
 Ettinger David, A320
 Eurich Katrin, A36
 Evans Chris, A401
 Evans Elizabeth, A464
 Evans Jeff, A576
 Evans Mererid, A467
 Evaristo Cesar, A8
 Even Caroline, A465
 Evrard Béangère, A245
 Exley Mark, A231
 Eyquem Justin, A142
- Fa'ak Faisal, A853
 Faber Mary, A896
 Faber Matthew, A822
 Fahey Thomas, A130
 Fails Danielle, A970
 Faivre Thea, A441
 Fakh Marwan, A368, A441
 Falahat Rana, A795
 Falchook Gerald, A510, A511, A527, A542, A907
 Falk Martin, A502
 Falohun Adewunmi, A853
 Fält Anette, A567
 Fan Jean, A428, A435, A439
 Fan Jieqiong, A662
 Fan Li, A973
 Fan Xuejun, A640
 Fan Yanying, A123
 Fan-Port Michelle, A522
 Fang Chengyuan, A436, A437
 Fang Juntao, A97
 Fang Weijia, A443, A445
 Fang Xianfeng, A246
 Fanning Philip, A463, A469, A530
 Fanny Manoussa, A748
 Fantin Valeria, A606
 Fantini Massimo, A881, A925
 Fanton Christie, A1007
 Faraji Farhoud, A631
 Faramand Rawan, A703
 Farber Charles, A484
 Færch Sandra, A187
 Farhane Siham, A300
 Farhi Ronit, A823
 Faries Mark, A415, A571
- Farkas Adam, A90, A338, A651
 Farrar Michael, A345
 Fathi Mohsen, A199
 Fattori Stéphane, A898
 Faucheux Andrew, A852
 Federico Lorenzo, A186, A1013
 Fedoriw Andrew, A654
 Fehniger Todd, A200, A428
 Fei Cong, A387, A389
 Fei Qi, A297
 Feig Barry, A410
 Feils Arika, A67, A628
 Feinberg Bruce, A591
 Felder Mildred, A628, A629
 Feldman Hope, A105
 Feldman Igor, A919, A928
 Felices Martin, A473, A667
 Feliciano Josephine, A263, A320
 Felip Enriqueta, A386, A391, A394, A422, A485
 Feliu Waldo Ortuzar, A509
 Felt Kristen, A74
 Fend Laetitia, A777
 Feng Jun, A226
 Feng Qin, A654
 Feng Xudong, A796
 Feng Yan, A490
 Feng Zheng, A92
 Fereshteh Mark, A973
 Fereydouni Mohammad, A233
 Ferlin Walter, A287
 Fernández Moro Carlos, A927
 Fernald Anthony, A319
 Fernandez Aileen, A258
 Fernandez Iago Pinal, A570
 Fernandez-Penas Pablo, A417
 Fernandez-Perez Antonio, A126
 Ferré Pierre, A507, A508
 Ferrando-Martinez Sara, A435, A439
 Ferrara Roberto, A16
 Ferrari Valentina, A712, A876
 Ferrario Cristiano, A374, A378
 Ferreira Carolina, A624
 Ferrer Michaela, A727
 Fessenden Timothy, A711, A801
 Fessler Jessica, A671
 Festino Lucia, A27, A332, A980
 Fettes Petra, A536
 Feucht Judith, A142
 Feun Lynn, A415
 Fiaz Rana, A486, A523
 Fields Hannah, A712
 Fields Paul, A103
 Fieschi-Meric Jacques, A48, A65, A489
 Fietkau Rainer, A355
 Figenshau Robert, A453
 Figg Jack, A262
 Figg John, A594
 Fighini Mariangela, A331, A461
 Figueiredo Marxa, A586
 Figueredo Rene, A617
 Figueroa Elizabeth, A240
 Filbert Erin, A422
 Filbin Mariella, A307
 Filderman Jessica, A797
 Filetti Marco, A257
 Filipovic Aleksandra, A512
 Finckenstein Friedrich Graf, A486, A523
 Finn Jessica, A59
 Finocchiaro Giovanna, A485
 Finotello Francesca, A41

- Fischer Birgitt, A597
 Fischer Nicolas, A287
 Fischman Sharon, A732
 Fiset Stephan, A380
 Fisher Fernando, A131
 Fisher George, A370
 Fisher Terrence, A464
 Fitzgerald John, A169
 Fitzgerald Kelly, A596
 Fix Samantha, A183
 Flårdh Maria, A567
 Flament Anne, A438
 Flaming Josiah, A964
 Flammar Anne-Laurent, A108
 Flechner Anke, A741, A816
 Flechtner Jessica, A268, A515, A551, A787
 Fleener Catherine, A553
 Fleming Gini, A508
 Fleming-Trujillo Erica, A319
 Fletcher Graham, A519
 Fleury Devan, A60
 Fleury Michelle, A185, A214
 Flies Dallas, A516, A599
 Fling Steven, A322, A462
 Floquet Anne, A382
 Florentin Maria, A177
 Flores Catherine, A262, A594
 Flores Mike, A94
 Florin Lawrence, A556
 Floudas Charalampos, A513
 Flowers David, A241
 Fluck Michael, A502
 Flueckiger Naomi, A885
 Flynn Brianna, A946, A985
 Flynn Patrick, A764
 Flynn Peter, A138
 Fnu Tenzin Passang, A672, A779
 Foley Colleen, A176
 Foley-Comer Adam, A825
 Foloppe Johann, A777
 Foltz Jennifer, A428
 Fong Lauren, A126
 Fong Lawrence, A453, A485, A704
 Fong Peter, A374, A378
 Font Laura Falceto, A262, A594
 Font-Tello Alba, A728
 Fontaine Danielle, A815
 Fontana Jacopo, A938
 Ford Rhodes, A673
 Forde Patrick, A320, A353, A877
 Forero-Torres Andres, A503, A818
 Forget Marie Andree, A186
 Forget Marie-Andrée, A183
 Forgie Alison, A463, A469, A530
 Forman Stephen, A133, A135
 Formenti Silvia, A309, A763
 Forsberg Matthew, A221
 Forssmann Ulf, A546, A821
 Forster Martin, A386, A572
 Foster Amber, A464
 Foster Mark, A200
 Foster Martin, A205
 Foti Jamie, A268
 Foukakis Theodoros, A364
 Fountzilas Christos, A542, A543
 Fousek Kristen, A599, A739, A757
 Foussat Arnaud, A898
 Fox Bernard, A93, A417, A631
 Fox Floyd, A472
 Fox Ray, A294
 Foy Jean-Philippe, A962, A984
 Foy Teresa, A211
 Fraichard Alexandre, A953
 Fraile Jon Zugazagoitia, A258, A493
 Franceschetti Tiziana, A201
 Francesco Maria Emilia Di, A793
 Francica Brian, A891
 Francis Connor, A262, A594
 Francisco-Cruz Alejandro, A1013
 Franco Lina, A773, A775
 Franiak-Pietryga Ida, A631
 Frank Meredith, A186, A960
 Frankel Jason, A453
 Frankel Nicholas, A125
 Franken Patrick, A932
 Fransén Marieke, A700
 Frantz Chris, A895
 Frascóni Teresa Maria, A696
 Fraser Amy, A967
 Fraser Christopher, A773, A775
 Fraune Christoph, A104
 Frazier Emily, A921
 Frederick Josh, A569
 Frederickson Andrew, A339
 Freeman Gordon, A244, A277, A728
 Frendeus Bjorn, A777
 Frenel Jean-Sebastien, A382
 Frenkel Masha, A272
 Frentzas Sophia, A457
 Fresquez Joseph, A788
 Freund Dave, A891
 Frey Alan, A779
 Frey Benjamin, A355
 Fricker Simon, A910
 Fridland Stanislav, A79
 Friedlander Philip, A363
 Friedlander Sharon, A505
 Friedman Claire, A335
 Friese Christina, A187
 Frisch Andrew, A109, A194
 Fritsch Edward, A684
 Fritz Jacqueline, A132
 Frizell Sara, A831
 Frohna Paul, A535, A558, A592
 Fromm George, A615
 Fromond Claudia, A394
 Fu Amina, A902
 Fu Jingxin, A728
 Fu Juan, A679, A877
 Fu Pingfu, A44, A868
 Fu Qihan, A443
 Fu Siqing, A511, A516, A519
 Fu Yali, A525
 Fu Yang-Xin, A632, A835
 Fucikova Jitka, A589
 Fueyo Juan, A640, A776
 Fujimoto Junya, A186
 Fumet Jean-David, A373
 Fun Lee Victor Ho, A328
 Funk-Brentano Elisa, A1011
 Funkner Fatma, A502
 Furness Andrew, A572
 Furqan Muhammad, A546
 Fury Matthew, A565, A577
 Fyfe Susanne, A397, A405
 Gabbasov Rashid, A148, A152
 Gabitova Linara, A114, A148
 Gabra Hani, A632
 Gabelow Grant, A131
 Gad Nayra, A484
 Gadgeel Shirish, A484
 Gadgeel Shirish M, A391
 Gadkari Rishali, A817, A819
 Gadot Nicolas, A962, A984
 Gaertner Bjoern, A129
 Gaffney Isabelle, A860
 Gagnon John, A226
 Gaidarova Svetlana, A126
 Gainer Marcus, A125
 Gainor Justin, A530, A563
 Gaipl Udo, A355
 Gajewski Thomas, A319, A330, A347, A354, A671, A963, A972
 Galan-Cobo Ana, A971
 Galarreta Marina Ruiz de, A653
 Galbraith David, A2
 Galetta Domenico, A257
 Galetto Roman, A151
 Galezowski Michal, A786
 Gall John Le, A573
 Gallant Caroline, A80
 Galli Giulia, A16
 Galluzzi Lorenzo, A309, A589, A763
 Galon Jerome, A48, A65
 Galsky Matthew, A90, A338, A651
 Galvao Vladimir, A514, A526, A534, A555
 Galvez Carlos, A838
 Gamber Kevin, A47
 Gambino Giorgio, A885
 Gamboa Luis, A143
 Gameiro Sofia, A635
 Gan Chai, A957
 Gan Hui, A511
 Gan Lu, A563
 Gan Qiong, A993
 Ganapathy Karthik, A91
 Gandara David, A495
 Gandhi Saumil, A604
 Gane Edward, A481
 Ganesh MS, A40
 Ganguly Sudipto, A877
 Gannon Hugh, A198
 Gansukh Enkhtaivan, A996
 Ganta Teja, A257
 Ganthous Lucy, A825
 Ganti Apar Kishor, A422
 Ganzzevs Sonja, A932
 Ganzinelli Monica, A16
 Gao Bo, A457, A552
 Gao Boning, A964
 Gao Jianjun, A259
 Gao Rui, A295, A827
 Gao Shuang, A78, A86, A89
 Gao Xin, A454
 Gao Yun, A902
 Garassino Marina, A16, A331
 Garassino Marina Chiara, A391
 García-Moure Marc, A776
 Garcia Myrna, A249, A261, A789
 Garcia Stephane, A489
 Garcia-Barros Monica, A651
 Garcia-Garijo Andrea, A958
 Garcia-Moure Marc, A307
 Gardai Shyra, A895
 Gardberg Anna, A800
 Gardner Humphrey, A527
 Garelik Brigid, A523
 Garon Edward, A423, A485
 Garon Edward B, A391

- Garralda Elena, A503, A514, A535, A536, A546, A550, A555, A958
 Garralda Ellena, A534
 Gartner Jared, A177, A958
 Gartrell Robyn, A100
 Garty Guy, A100
 Gascoyne Duncan, A600
 Gasmil Billel, A108
 Gaspar Miguel, A602
 Gasparetto Cristina, A476
 Gassart Aude De, A535, A558, A592
 Gastman Brian, A363, A462, A573
 Gatlin Wayne, A884
 Gatt Moshe Etzion, A476
 Gaud Nilesh, A799
 Gaudernack Gustav, A416
 Gaughan Elizabeth, A363, A421
 Gausdal Gro, A632
 Gauthier Kelsey Sivick, A280, A614
 Gauthier Laurent, A892, A893
 Gauthy Emilie, A118
 Gauttier Vanessa, A245
 Gavigan Julie-Ann, A636
 Gavrielatou Niki, A258
 Gavvovidis Ioannis, A239, A531
 Gay Jason, A652
 Gaynor Katie, A824
 Gaynor Richard, A212
 Ge Moyer, A126, A180
 Geanon Daniel, A338, A651
 Gedda Mallikarjuna, A1002
 Geffen Yona, A172, A230
 Gehrke Jason, A165
 Geiger Jessica, A462
 Geiger Tamar, A199
 Geisler Lukas, A34
 Gelb Tara, A2
 Gellert Johanna, A741, A816
 Gemmill Robert, A708
 Genßler Sabrina, A597
 Genestie Catherine, A382
 Geng Yanan, A295, A827
 Gennart Isabelle, A118
 Gennigens Christine, A1006
 Genova Carlo, A257
 Genova Gianfranco Di, A368
 Gentile Angela, A129
 Gentzler Ryan, A840
 Geoghegan Eileen, A619, A620
 Georgantas III Robert, A870
 Georgantas Robert, A30, A33
 George Daniel, A655
 George Mariam, A807
 George Tad, A64
 Gerber Scott, A705
 Geroges Nermin, A110
 Gerhardt Lara, A617
 Germain Ronald, A603
 Gerralda Elena, A731
 Geschwindt Ryan, A559
 Gettinger Scott, A486
 Getz Gad, A234
 Geva Ravit, A569
 Gewurz Benjamin, A728
 Ghamande Sharad, A380
 Ghanem Paola, A263, A320
 Ghani Sofia, A225
 Gharavi Robert, A505
 Ghatage Prafull, A380
 Ghatak Payel, A792
 Gherardini Pier Federico, A370
 Ghezali Lamia, A489
 Ghigo Clément, A558
 Ghiringhelli François, A373, A382
 Ghiringhelli Francois, A494
 Ghodduji Majid, A132
 Ghonime Mohammed, A143
 Ghosh Arnab, A807
 Ghosh Chandra, A637
 Ghosh Michael, A958
 Giaccone Giuseppe, A394
 Giambalvo Raffaella, A602
 Giamo Vincent, A78, A86, A89
 Gianani Roberto, A55, A902
 Giancotti Filippo, A977
 Giangarra Valeria, A80
 Giannakis Marios, A670
 Giannarelli Diana, A27
 Giavridis Theodoros, A142
 Gibas Agnieszka, A786
 Gibbons Don, A53, A186, A304, A1013
 Gibbs John, A505
 Gibney Geoffrey, A573, A999
 Gibson Jackson, A238
 Gibson Michael, A468, A947
 Giddens Jonathan, A1004
 Gielniewski Bartłomiej, A645
 Giese Rachel, A596
 Giesecke Yvonne, A34
 Giezendanner Noreen, A885
 Giffon Thierry, A740
 Gigoux Mathieu, A108, A807
 Giladi Amir, A713
 Giladi Moshe, A756
 Gilbert Jonathan, A175
 Gilchrist Mark, A826
 Giles Francis, A643
 Gilham David, A118, A154, A438
 Gill Antony, A862
 Gillenwater Heidi, A477
 Gillig Marc, A221
 Gillison Maura, A515, A788
 Gills Joell, A877
 Gilmour Cassandra, A276, A340
 Giobbie-Hurder Anita, A402, A427
 Giorgi Valeria De, A1002
 Girard Luc, A632
 Girardi Marianna, A786
 Girault Isabelle, A394, A829
 Girgis Natasha, A749, A828
 Giusti Raffaele, A257
 Giustiniani Jérôme, A898
 Gjerci Brikena, A124
 Gjini Evisa, A728
 Gladieff Laurence, A1006
 Gładysz Mirosława, A799
 Glaich Ohad, A823
 Glanville Nicholas, A920
 Glass Benjamin, A859
 Glenn Sean, A78, A86, A89
 Glickman Laura, A894
 Glisson Bonnie, A468
 Głowniak-Kwitek Urszula, A799
 Gluza Karolina, A786
 Gnad-Vogt Ulrike, A502
 Gniewek Oskar, A866
 Go William, A522
 Golas Aniela, A799
 Goddard Audrey, A37, A408
 Goebeler Marie-Elisabeth, A536
 Goebeler Marie-Luise, A531
 Goepfert Ryan, A788
 Gogas Helen, A523
 Goh Denise, A656, A855
 Gokgoz Nalan, A178
 Gokhale Prafulla, A247, A277
 Golas Aniela, A786
 Gold Maiké, A579
 Goldberg John, A542
 Goldberg Zelanna, A39, A529
 Goldrath Ananda, A688
 Goldstein David, A366, A367
 Goldstein Joel, A833
 Goletz Christoph, A741, A816
 Gollob Jared, A633
 Golshadi Masoud, A551
 Gomes Bruno, A11, A557
 Gomez-Manzano Candelaria, A640, A776
 Gomez-Pinillos Alejandro, A505
 Goncz Edward, A203
 Gondela Andrzej, A786
 Gong Kan, A490
 Gong Xinjiang, A939
 Gontcharova Viktoria, A110, A486
 Gonzales Marissa, A694
 Gonzalez Louis, A3, A459, A526
 Gonzalez Marina, A502
 Gonzalez-Cao Maria, A422
 Gonzalez-Ericsson Paula, A791
 Gonzalez-Ericsson Paula, A264, A342, A848
 Gonzalgo Mark, A452
 Gooding Hayley, A271
 Gorbokon Natalia, A104
 Gordley Russell, A125
 Gordon Judi, A56
 Gordon Michael, A408, A509
 Gorlani Andrea, A904
 Gorvel Laurent, A898
 Gosink John, A895
 Gosling Jennifa, A107
 Gosselin Alice, A433, A581
 Gottardo Raphael, A590, A689
 Gottschalk Rebecca, A830
 Gottschalk Stephen, A160
 Goubet Anne-Gaelle, A945
 Gouble Agnès, A151
 Gouill Steven Le, A535
 Gouin Kenneth, A763
 Goulding John, A126
 Gourdin Nicolas, A893
 Gourley Lindsey, A426
 Govero Jennifer, A200
 Govindan Sindhu, A40
 Govindaraj Rajiv, A905
 Govindaraju Priya, A985
 Gowda Nagaraj, A889
 Gowri Shankar K, A40
 Goyal Rakesh, A578
 Goyal Subir, A20
 Grötzingler Carsten, A34
 Grabbe Stephan, A579
 Graddis Tom, A284, A294, A299
 Gradinaru Cristian, A602
 Graham Donna, A559
 Graham Julie, A462
 Graham Philippa, A451
 Graham Rachel, A452
 Grandgenett Paul, A683
 Grandi Paola, A456, A1005
 Granja Jeff, A226

- Grant Courtney, A271
 Grant James, A427
 Grant Joy, A126, A129
 Grant Michael, A572
 Grauslund Jacob, A807
 Graves Diana, A678, A947
 Gravis Gwenaëlle, A374
 Gray Elin, A73
 Gray Elizabeth, A895
 Grebennik Dmitri, A941
 Green Jordan, A235
 Greenbaum Benjamin, A862
 Greenberg Philip, A590, A696
 Greenplate Allison, A45, A335
 Greenwald Rachel, A975
 Greenwald Shirley, A825
 Greenwood Dalton, A951
 Greer Emily, A619, A620
 Gregory Mark, A57
 Greillier Laurent, A489, A494
 Grell Peter, A514, A534
 Greten Tim, A721
 Griffioen Arjan, A808
 Grigaitis Nicole, A773, A775
 Grigaityte Kristina, A961
 Grignani Giovanni, A574
 Griswold Anthony, A703
 Gritsch Simon, A427
 Grivas Petros, A660, A853
 Grob Jean-jaques, A574, A577
 Grochowalski Łukasz, A866
 Groff Brian, A126
 Groisberg Roman, A565
 Gromeier Matthias, A770
 Gromke Tanja, A536
 Gronchi Alessandro, A1
 Grondin Gwendoline, A893
 Groot Anne de, A337
 Groot Eleanor De, A240
 Gros Alena, A69, A958
 Grose Mark, A415
 Grosh William, A421
 Gross Jane, A830, A831
 Gross John, A609
 Gross Neil, A788
 Grossman Joseph, A509
 Grossman Noam, A732
 Grot Brian, A742
 Gru Alejandro, A54
 Gruber Joshua, A498
 Grudzinski Joseph, A624
 Gruijl Tanja de, A46, A232, A700
 Gryaznov Sergei, A725
 Grynberg Shirly, A556
 Gschweng Eric, A209
 Gu Shengqing, A728
 Guadagnoli Marco, A156, A157
 Guadagnolo Ashleigh, A410
 Gualandi Marco, A906
 Guan Shanhong, A463, A469
 Guan Siyu, A498
 Guan Wei, A490
 Guasp Pablo, A862
 Gubens Matthew, A485
 Gubin Matthew, A622
 Güç Esra, A600
 Gucalp Ayca, A431
 Gudgeon Chelsea, A39
 Guenther Kerstin, A1009
 Guerretaz Lisa, A138
 Guerriero Jennifer, A644
 Guest Ryan D, A189
 Guha Prajna, A637
 Gui Jiang, A674
 Gui Xun, A327
 Guida Michele, A574
 Guijarro Irene, A960
 Guillaudeau Thierry, A291, A921
 Guillot Franceline, A893
 Guldevall Karolin, A938
 Gulley James, A6, A450, A513, A570, A612
 Gullo-Brown Johnni, A768
 Gumber Sanjeev, A779
 Gumin Joy, A640
 Guminski Alexander, A395
 Gunasekaran Muthukumar, A25
 Gunde Tea, A885
 Gundurao Smitha, A128
 Gunesch Justin, A173
 Gunzburg Jean De, A301
 Guo Chao, A123, A159
 Guo Charles, A259
 Guo Haiping, A1013
 Guo Jing, A662
 Guo Matthew, A253, A263
 Guo Nancy, A349
 Guo Taylor, A730
 Guo Xuan, A169
 Gupta Aditi, A596
 Gupta Akshita, A420
 Gupta Amit, A44
 Gupta Harshita, A249, A261, A321, A944
 Gupta Hersh, A74
 Gupta Mamta, A188
 Gupta Manish, A821
 Gupta Priyanka, A818
 Gupta Shilpa, A569
 Guren Tormod, A416
 Gurney Howard, A374, A447
 Gururajan Murali, A768
 Gusev Alexander, A850
 Gutierrez Dario, A185, A214
 Gutierrez Martin, A485, A516, A520
 Guyot Valérie, A151
 Guzik Brian, A427
 Guzik Pawel, A786
 Guzman Kelly, A616, A709, A794
 Guzman Wilson, A748
 Haack Beatrice, A597
 Haake Markus, A536, A597
 Haake Scott, A951
 Haanen John, A212, A446, A1008
 Haass Jane, A895
 Habib Nagy, A545
 Habib Robert, A545
 Habif Guillaume, A892
 Hackett Adrian, A543
 Hackett Michael, A726, A736
 Hackner Dani, A940
 Hacohen Nir, A593, A670, A684, A965
 Haden Kathleen, A421
 Hadrup Sine, A322
 Haefliger Simon, A486
 Haegglblom Linnea, A900
 Hafeez Sabrina, A933
 Hagen Tom Van, A417
 Hagerbrand Karin, A785
 Haggerty Agnes, A983
 Haggstrom Daniel, A525
 Hahn Ki Baik, A82, A861
 Hahn Julie, A895
 Haidar Fatima, A674
 Haidar Jaafar, A924
 Hailu Astar, A172, A230
 Haimovich Rotem, A823
 Haines Eric, A824
 Halbert Brian, A188
 Hale Diane, A571
 Hales Russell, A263
 Hall Amy, A418
 Hall Evan, A540, A689
 Hall Jason, A226
 Hall Leslie, A247
 Hall MacLean, A418, A419
 Hall Richard, A840
 Halldórsdóttir Hólfríður Rósa, A806
 Halldórsdóttir Hólfríður, A641
 Halle Joern-Peter, A351, A792
 Hallmeyer Sigrun, A415
 Halmos Balazs, A492
 Ham Mina, A499
 Hamadeh Hisham, A874, A961
 Hamaidi Imene, A952
 Hamburger Agnes, A131
 Hamdi Haifa, A960
 Hamel Steven, A713
 Hamid Omid, A501, A518, A519, A520, A568, A573, A576
 Hamieh Mohamad, A142
 Hamil Alexander, A200
 Hamilton Erika, A459
 Hammer Christian, A847
 Hammerich Linda, A34
 Hammers Hans, A454
 Hammond Edward, A366, A367
 Hammond Russell, A833
 Hamon Pauline, A388, A713
 Han Booyeon, A705
 Han Chuanhui, A632
 Han Fei, A334
 Han Guangchun, A654
 Han Hyunsil, A565
 Han Jian, A375
 Han Jichang, A674
 Han Min Guk, A623
 Han Seungryel, A138
 Hanayama Rikinari, A743
 Hance Kenneth, A690
 Hancock Bryan, A126
 Hand Timothy, A880
 Hanifi Arezoo, A58
 Hanin Neta Zilony, A823
 Hank Jacquelyn, A628
 Hankin Amy, A450
 Hanks Brent, A343, A685, A968
 Hann Christine, A320
 Hanna Ann, A264
 Hanna Diana, A533, A566
 Hannes Susan, A212
 Hansen Aaron, A540
 Hansen Dennis, A807
 Hansen Gwenn, A107
 Hansen Ulla, A322
 Haond Christophe, A48, A65
 Haradvala Nicholas, A234
 Harati Hagit, A556
 Harb Wael, A368, A371
 Harding Taylor, A81
 Harel Michal, A199, A323

- Haria Dhvani, A598
 Hariri Robert, A169
 Harismendy Olivier, A982
 Harjanto Dewi, A212
 Harrabi Ons, A815
 Harrant Alexander, A134
 Harriman Geraldine, A905
 Harring Suzana Vega, A94, A976
 Harrington Kevin, A463, A467, A469, A538, A539
 Harris Angelo, A973
 Harris William, A433
 Harrison Helen, A824
 Harrod Christopher, A990
 Hart Matthew, A261
 Harter Patrick, A597
 Hartl Christina, A324
 Hartley Genevieve, A622, A798
 Hartman John, A665
 Hartman Zachary, A647
 Hartt Annabelle, A924
 Hartung Evelyn, A816
 Haruna Sanusi, A10
 Hasan Md Faqrul, A716, A718
 Hasanov Elshad, A49, A259
 Hashmi Haroon, A240
 Haskett Scott, A165
 Hassan Hariz, A555
 Hassanzadeh-Kiabi Nargess, A736
 Hassel Jessica, A568, A576, A579
 Hasselbalch Hans, A807
 Hatfield Steven, A749
 Hathaway Emma, A402
 Hatogai Ken, A354, A972
 Hatori Ryo, A91
 Haubner Sascha, A142
 Hauke Ralph, A422
 Hav Monirath, A59
 Hawinkels Lukas, A701
 Hawkins Bob, A209
 Hawkins Robert, A189, A210, A573
 Hay Chuck, A896
 Hay Joanne, A271
 Haydock Mark, A749
 Haydon Andrew, A366, A367, A417, A577
 Hayes Madeline, A45
 Haymaker Cara, A105, A186, A199, A439, A1013
 Hazard Sebastien, A2
 Hazenoot Monique, A150, A156, A157
 He Fei, A927
 He Hailey, A894
 He Jiang, A965
 He Jianhua, A606
 He Kai, A486
 He Kewen, A604
 He Kun, A564
 He Shui, A577
 He Shuyang, A169
 He Si-si, A355
 He Xinrong, A288, A313, A783
 Heatherton Kara, A637
 Heaton Alexa, A50
 Hecht Andrew, A225
 Hecht Markus, A355
 Heck Mackenzie, A629
 Hedge Shweta, A315
 Hedvat Cyrus, A859
 Hedvat Michael, A726
 Heeg Maximilian, A688
 Heeke Christina, A187
 Heese Lauren, A240
 Heffernan Timothy, A1013
 Hegde Shweta, A622
 Hegde Shwetha, A248
 Hegde Venkatesh, A788
 Hegewisch-Solloa Everado, A651
 Heichinger Christian, A557
 Heidt Analeah, A12, A751, A897
 Heininen-Brown Mari, A46
 Heinrich Bernd, A721
 Heinzerling Lucie, A502
 Heiz Robin, A885
 Hekim Can, A345
 Hellebust Anne, A64
 Hellequin Louis, A287
 Hellmann Matthew, A67, A353, A485, A488
 Helmlinger Gabriel, A176
 Helsel Eugene, A138
 Helsen Christopher, A127
 Heltemes-Harris Lynn, A345
 Helwig Christoph, A494
 Hemmati Golzar, A908
 Hempel Silvana, A579
 Henau Olivier De, A108
 Henault David, A325
 Hendrickson Eleanore, A768
 Hendrickson Ronald, A142
 Hengel Shawna, A818
 Henning Karla, A817, A819, A903
 Hensel Jonathan, A190, A191, A418
 Hensler Michal, A589
 Hensley Kelly, A818, A895
 Herati Ramin, A335
 Herbst Roy, A485
 Herbst Roy S, A391
 Herman Courtney, A110, A188
 Hermes Alexander, A91
 Hernandez Andrea, A225
 Hernandez Ivan, A809, A810
 Hernandez Reinier, A624
 Hernandez Richard, A504, A515
 Hernandez Robert, A3, A526
 Hernandez-Aya Leonel, A568
 Hernandez-Ruiz Sharia, A632
 Herrera Alex, A503
 Herrera-Hernandez Loren, A452
 Herring Kris, A665
 Herrman Marissa, A128
 Herting Cameron, A434, A948
 Hess Christian, A885
 Hessel Harald, A46
 Hester Danubia, A318
 Hettich Michael, A11
 Heuchel Rainer, A927
 Heudobler Daniel, A1008
 Hexner Elizabeth, A461
 Hey Amalie, A187
 Heyen Jonathan, A290, A768
 Heymach John, A53, A186, A304, A632, A960, A971, A1013
 Hickeron Annelies, A571
 Hickey John, A192, A193
 Hickingbottom Barbara, A553
 Hicklin Dan, A752
 Hicklin Daniel, A744, A747
 Hickman Alexandra, A54
 Hicks Kristin, A635
 Hieber Kate, A55
 Hiebsch Ronald, A282
 Higgs Brandon, A546, A874, A961
 Higgs Emily, A330, A347, A354, A671, A972
 Highfill Steven, A153
 Hilf Norbert, A1009
 Hilgers Werner, A394
 Hill Andrew, A577
 Hill Craig, A729
 Hill Jonathan, A702
 Hill Victoria, A177
 Hinck Andrew, A774
 Hinderlie Peter, A667
 Hirata Michinari, A914
 Hiret Sandrine, A494
 Hirsch Fred, A25
 Hirschhorn Daniel, A108
 Hirsle Lea, A275
 Histed Alex, A749
 Hivroz Claire, A142
 Hjelmeland Anita, A168
 Ho Chi-Sing, A70
 Ho Po, A817, A903
 Ho Vincent, A807
 Ho William, A440, A578
 Hobbs Gabriela, A807
 Hoch Ute, A67
 Hodgins Jonathan, A894
 Hoefges Anna, A50, A628
 Hoelzlwimmer Gabriele Gabriele, A94
 Hoenemann Dirk, A241, A638, A936
 Hofe Eric von, A130
 Hoff Olivia, A794
 Hoffman David, A476
 Hoffmeyer Eric, A134
 Hofmeister Robert, A185, A214
 Hofree Matan, A670
 Hogan Aisling, A987
 Hohmann Anja, A215
 Hoimes Christopher, A257
 Holay Nisha, A613
 Holderried Tobias AW, A1009
 Holgado Esther, A364
 Holland Aliya, A108, A596
 Holland Chris, A568, A576
 Holland Pamela, A39
 Hollingsworth Michael, A683
 Höllt Thomas, A41
 Holmkvist Petra, A777
 Holmström Morten Orebo, A813
 Holmstrom Morten, A807
 Holt John, A946
 Holt Sann, A157
 Holt Sanne, A150, A156
 Holtz Anja, A891
 Holzer Tatjana, A8
 Hominal Stéphane, A489
 Homs Mohammed Ussama Al, A19
 Hone Graham, A905
 Hong David, A407, A526
 Hong Emping, A18, A219, A804
 Hong Kyu, A327
 Hong Peter, A146
 Hong Ruey-Long, A722
 Hong Seung Pyo, A254
 Hongo Rachel, A951
 Hoos Axel, A423
 Hoover Maegan, A219
 Hope Chelsea, A982
 Hopkins Bei, A58, A969
 Hopkins Benjamin, A651
 Horinouchi Hidehito, A391
 Hormigo Adilia, A360
 Horn Lucas, A599, A739, A757

- Horowitz Amir, A90, A338, A651
 Horowitz Nina, A192, A193, A228
 Horrigan Steven, A964
 Horsey April, A247
 Horst Edward van der, A243
 Horton Brendan, A326, A354, A692
 Horton Holly, A185, A214
 Horton Janet, A365
 Hosking Martin, A126, A129, A208
 Hostetter Daniel, A143
 Hotard Michelle, A240
 Hou Bing, A241, A638, A936
 Hou Jiakai, A584, A654
 Houacine Jemila, A898
 Houde Kelly, A940
 Hourigan Christopher, A270
 Housseau Franck, A877
 Housseau Frank, A310
 Hout David, A495
 Houtkamp Mischa, A904
 Hovig Eivind, A416
 Howat Will, A91
 Hoyd Rebecca, A878, A988
 Hoyer Robert, A484
 Hoyos David, A862
 Hrach Heather, A773, A775
 Hribar Kolin, A990
 Hruska Matthew, A472
 Hsiao Chih-Lun, A886
 Hsiao Huey-Wen, A886
 Hsieh Candace, A357, A358, A359, A361, A362, A1001
 Hsieh Rodney Cheng-En, A622, A798
 Hsieh Yao-Te, A899
 Hsu Chiun, A387
 Hsu Frank, A357, A358, A359, A361, A1001
 Hsu Jingmei, A130
 Hsu Melinda, A320
 Hsu Michael, A130
 Hsu Wen-Hao, A622
 Hu Chunhong, A466
 Hu Hong-Ming, A93
 Hu James, A566
 Hu Shenshen, A729
 Hu Shuiqing, A632
 Hu Yun, A604
 Hu-Lieskovan Siwen, A553
 Hua Jing, A702
 Huan Jian, A384
 Huang Alexander, A335
 Huang Chao, A587
 Huang Hui, A351, A639, A810
 Huang Huiling, A460
 Huang Jianguo, A211
 Huang Jiayi, A428
 Huang Jie, A381
 Huang Jing-Yi, A886
 Huang Lihui, A855
 Huang Lingkang, A7, A364
 Huang Qing, A458
 Huang Ruiqi, A387, A389, A400
 Huang Tao, A327
 Huang Weifeng, A217, A939
 Huang Ying, A683
 Huang Yuhua, A939
 Huang Zhaoliang, A288, A313, A783
 Huard Justin, A745, A942
 Hubbard Charley, A787
 Hubbard Gregory, A345
 Hubensack Martina, A792
 Huber Christoph, A731
 Huber Martin, A549
 Huber Veronica, A331
 Huberty Fanny, A118, A154
 Hubner Richard, A389
 Huertas Roberto, A1011
 Huff Anne, A424
 Huffman Janel, A126
 Hughes Brett, A729
 Hugues Stéphanie, A287
 Huh Sung Jin, A462
 Hui Rina, A391
 Huijbers Elisabeth, A808
 Hull Caroline, A221
 Hund Stephanie, A42, A68
 Hundal Avneel, A908
 Hunder Naomi, A426
 Hundt Matthias, A809, A810
 Hung Magdeleine, A887, A888
 Hung Mien-Chie, A622, A642
 Hung Shao-Hsi, A244
 Hunkapiller Julie, A847
 Hunt Kelly, A410
 Hunt Thomas, A240
 Huober Jens, A997
 Hurley Paula, A947
 Hurov Kristen, A2, A865, A931
 Hurton Lenka, A240
 Husain Amreen, A819
 Huse Morgan, A142
 Hussain Abraham, A751
 Huynh Lyna, A52
 Hwang Jesse, A619, A620
 Hwang Joyce, A655
 Hwang Jun-Eul, A440
 Hwang Sunjin, A82, A861
 Hwang Wei-Ting, A461
 Hwang Yu-Kyeong, A138
 Hwu Patrick, A95, A96, A183, A199, A244, A584, A654
 Hydrose Shreena, A19
 Hynes Sean, A987
 Hyngstrom John, A415, A417, A571
 Iacobuzio-Donahue Christine, A862
 Iadonato Shawn, A291, A921
 Iannello Alexandre, A894
 Iannotti Nicholas, A422
 Ibarquén Heladio, A993
 Ibbett Paul, A144
 Ibekwe Ugochi, A240
 Ibitokou Samad, A132
 Iche Marina, A535
 Igoshin Oleg, A225
 Iheke James, A841
 Ihrie Rebecca, A45
 Iida Masafumi, A599
 Ijsselsteijn Marieke, A41
 Ikeguchi Alexandra, A568
 Ilano Arielle, A704
 Im Seock-Ah, A364
 Imedio Esteban Rodrigo, A451
 Imun Maria, A131
 Imus Cyr De, A211
 In Gino, A538
 Inchakalody Varghese, A19, A767
 Incze Peter, A1004
 Inderberg-Suso Else-Marit, A416
 Ingham Matthew, A533, A566
 Ingram Davis, A410
 Ingram Piers, A498
 Inman Brant, A547
 Innamarato Patrick, A418
 Innocenti Christopher, A860
 Iorgulescu Bryan, A84, A265, A277, A684
 Irish Jonathan, A45
 Irmeier Rebecca, A257
 Irvine Darrell, A593, A750, A769, A801
 Isa Douglas, A225
 Isacco Laura, A766
 Isakoff Steven, A548
 Isambert Nicolas, A491, A494
 Iserentant Hannes, A118, A154
 Isgrò Maria Antonietta, A27
 Islam Farah, A205
 Islam Marwa, A609
 Ismail Nesreen, A744, A747, A752
 Isnard-Petit Patricia, A782, A953
 Ito Takahiro, A472
 Ivanidze Jana, A130
 Iyer Archana, A142
 Iyer Pravin, A889
 Izraeli Avi, A230
 Izzo Kaitlyn, A203
 Jaafar Bennouna, A550
 Jabłońska Justyna, A799
 Jabado Omar, A973
 Jachetti Elena, A16
 Jack Lin S, A908
 Jackson Bryan, A407
 Jackson Donald, A636
 Jackson Katherine, A311
 Jackson Savannah, A923
 Jackson Taggra, A908
 Jacob Eyal, A323
 Jacob Jose, A83
 Jacobs Miriam, A385
 Jacqmin Philippe, A731
 Jacquemont Celine, A426
 Jacques-Hespel Celine, A154
 Jacquin Jean-Philippe, A997
 Jaderberg Magnus, A396, A491
 Jaekel Anika, A741, A816
 Jaffee Elizabeth, A991
 Jaganathan Kowshik, A40
 Jagasia Madan, A486, A523
 Jahchan Nadine, A900
 Jæhger Ditte, A641
 Jæhger Ditte Elisabeth, A806
 Jahnmatz Peter, A51
 Jain Michael, A703
 Jain Prerna, A991
 Jain Sumiti, A132
 Jaiswal Ashwin, A315
 Jakobsen Martin, A32
 Jakub James, A571
 Jamal-Hanjani Mariam, A205, A572
 Jamboretz Kate, A159
 James Nicole, A36, A758
 Jan Max, A234, A807
 Jana Jessica, A194
 Janc James, A729
 Jang Bum Sup, A623
 Jang Myoung Ho, A499
 Jang Su Chul, A601, A796, A883
 Jang Sung Woong, A146
 Janku Filip, A21, A512, A514, A532, A534
 Jann Henning, A34
 Jannin Camille, A300

- Jansen Caroline, A669, A686, A975
 Jansz Kenneth, A1004
 Jarvis Maria, A225
 Jasiński Maciej, A866
 Jason (Ping-Yen) Huang , A285
 Jaume Clémence, A48, A65
 Jayaprakash Priyamvada, A622, A652
 Jazaeri Amir, A183, A225, A523
 Jeager Ellen, A318
 Jean-Jacques Grob, A550
 Jeffrey Phil, A865, A931
 Jelinic Petar, A364
 Jenkins Kurt, A748
 Jenkins Russell, A902
 Jensen Christina, A23, A24
 Jensen Shawn, A417, A631
 Jeon Byeongwook, A630
 Jeon Donghwan, A802
 Jeon Jaehyoung, A935
 Jeong Jieun, A633
 Jeong Yeo-Jin, A996
 Jeun Eun-ji, A146
 Jewell Andrea, A398
 Jewell Rachel, A311, A618, A705
 Jhavar Sachin, A878
 Ji HaYeun, A101
 Ji Hongkai, A310, A317, A353, A693
 Ji Niannian, A261
 Ji Zhicheng, A310, A317, A353, A693
 Jia Ying Joey Lee Joe Yeong Li Wen Justina Nadia
 Lee Lit-Hsin Loo Jiahui Dong, A657
 Jiajia Zhang, A310
 Jian Dan, A490
 Jian Fei, A753
 Jiang Bo, A479, A788
 Jiang Feng, A351, A639
 Jiang Haixia, A295
 Jiang Hao, A436, A437
 Jiang Hong, A640
 Jiang Jun, A384
 Jiang Mei, A962, A984
 Jiang Peixin, A186, A960
 Jiang Peng, A728
 Jiang Pengfei, A120
 Jiang Wenchao, A939
 Jiang Wenqing, A730, A935
 Jiang Yizhou, A189, A573
 Jiang Yue, A117
 Jiang Zhi-Gang, A243
 Jimeno Antonio, A523, A569
 Jin Chunshan, A288, A783
 Jin Feng, A463, A466, A469, A530
 Jin Hyung-Seung, A935
 Jin Lei, A218
 Jin Moonsoo, A130
 Jin Ping, A153
 Jin Steven, A818
 Jin Su-Han, A355
 Jin Xiaoping, A288, A313, A457, A460, A466,
 A471, A783
 Jindal Sonali, A379
 Jo Gyeong Seok, A811
 Job Bastien, A409
 Jochems Caroline, A513
 Joerger Autumn, A794
 Johannes Kellsey, A615
 Johanns Tanner, A428, A812
 Johansen Lisa, A569
 Johansson Mortensen Rasmus Erik, A813
 John PARK, A581
 John Weroha S, A548
 John Wherry E, A274, A335
 Johns Amber, A862
 Johnson Brendan, A11
 Johnson Corey, A200
 Johnson Dan, A578
 Johnson Daniel, A853
 Johnson Douglas, A257, A568, A842, A848
 Johnson Evan, A51
 Johnson Jeremiah, A801
 Johnson Laura, A377
 Johnson Melissa, A423, A435, A439, A483, A501,
 A515, A525, A526, A527, A537, A565, A907
 Johnson Omar, A140
 Johnson Parker, A748
 Johnson Sarah, A879
 Johnson Zoe, A967
 Johnston Jonathan, A858
 Joly Florence, A398
 Jonas Oliver, A585
 Jonasch Eric, A454
 Jones Amber, A168
 Jones Dallas, A134
 Jones Emma, A46
 Jones Jeremy, A548
 Jones Katherine, A708
 Jones Kyle, A897
 Jones Philip, A793
 Jonjic Stipan, A275
 Joo Stacy, A500, A998
 Jordan SILVA, A604
 Jørgensen Matilde Smærup, A806
 Jørgensen Mia Aaboe, A813
 Joshi Ira, A225
 Joshi Prarthana, A738
 Joshua Anthony, A378, A448, A449, A455, A540
 Joung Eun-kyo, A811, A901
 Joung Julia, A234
 Joyce Peter, A583
 Ju Andrew, A621
 Ju David, A131
 Ju Yawen, A563
 Juckett Mark, A473
 Judge Sean, A675
 Juergens Rosalyn, A488
 Jun Susie, A226
 Junca Alba Gonzalez, A125
 Juncker-Jensen Anna, A867
 June Carl, A140
 Jung Eunjung, A901
 Jung Hun, A811, A901
 Jung Jaeho, A730, A935
 Jung Uijung, A935
 Jung Wonkyung, A869
 Jungels Christiane, A535
 Junghus Fred, A777
 Jurchen David, A921
 Jure-Kunkel Maria, A546, A821, A874, A961
 Jürgensmeier Juliane, A408
 Juric Dejan, A397, A505
 Juric Vladi, A900
 Justin Seah Yong Hock, A97
 Kabakibi Ayman, A200
 Kacena Katherine, A425
 Kaczanowska Sabina, A220
 Kaczmarczyk Jan, A866
 Kadara Humam, A1013
 Kadia Tapan, A474
 Kahler Katharina, A538
 Kahn Roy, A825
 Kaisso Marina, A927
 Kaitlynn Allen E, A160
 Kaka Quincy, A602
 Kakimi Kazuhiro, A71, A608, A676, A959
 Kalabus James, A12
 Kalaitidou Milena, A209, A210
 Kalaitzidis Demetrios, A143
 Kaldjian Eric, A64
 Kalimuddin Shirin, A656
 Kallarakkal Thomas George, A957
 Kallin Daniel, A212
 Kalofonou Foteini, A257
 Kalra Mamta, A173, A1009
 Kam Ngar Woon, A328
 Kamalakannan Mohanapriya, A946
 Kamat Ashish, A456, A1005
 Kamaz Baransel, A807
 Kamb Alexander, A131
 Kamber Dominique, A99
 Kamer Iris, A323
 Kamerkar Sushrut, A883
 Kamermans Alwin, A232
 Kamińska Bożena, A645
 Kamp Marc Van der, A924
 Kamphorst Alice, A338, A388, A653
 Kampta Kyle, A312
 Kan Qingsheng, A479
 Kanbour Aladdin, A19
 Kancharla Aravind, A249
 Kandalaft Lana, A461
 Kandiah Vinitha, A700
 Kane Lawrence, A668, A720
 Kanellopoulou Chrysi, A247
 Kang Jinho, A901
 Kang Lin, A169
 Kang Mi Hyun, A623
 Kang Yoon-Koo, A433
 Kanherkar Riya, A126
 Kann Michael, A234
 Kannan Madhavi, A70
 Kansagra Ankit, A476
 Kao Hsiang-Fong, A722
 Kapil Ansh, A392
 Kapilashrami Kanishk, A247
 Kaplan Rosandra, A220
 Kapoor Gurpreet, A424
 Kappagantula Rajya, A862
 Karande Vikas, A889
 Karantza Vassiliki, A364
 Karasic Thomas, A559
 Karaszewska Boguslawa, A390
 Kardosh Adel, A442
 Kari Suresh, A261, A321
 Karivedu Vidhya, A878
 Karki Keshav, A754
 Karlin Lionel, A476
 Karlsson Mikael, A927
 Karnes Jeffrey, A452
 Karnik Rahul, A633
 Karrison Theodore, A659
 Karsdal Morten, A23, A24
 Karupiah Vijaykumar, A924
 Karydis Ioannis, A467
 Karzai Fatima, A450, A513
 Kasahara Kazuo, A391
 Kaseb Ahmed, A49
 Kaser Samuel, A796, A883
 Kashyap Abhishek, A946, A985
 Kashyap Arun, A282

- Kasi Anup, A372
 Kask Angela Shaulov, A462
 Kaspers Jorn, A232
 Kassambara Alboukadel, A489
 Kassim Sadik, A124, A912
 Kästner Marion, A579
 Kasturi Vijay, A376
 Katirae Layla, A91
 Katopodis Andreas, A731
 Katsor Anna-Maria, A91
 Katumba Ruth, A428
 Katz Mathew, A1010
 Katz Steven, A637
 Kauffman Kevin, A919
 Kaufman Howard, A750
 Kaufman Jacob, A954
 Kaufmann Johanna, A778
 Kaufmann Roland, A579
 Kaur Varinder, A421
 Kaur-Lally Satwinder, A205
 Kaushik Garima, A4
 Kazer Sam, A902
 Kazmi Syed, A442
 Ke Danxia, A407
 Keam Bhumsuk, A463, A469
 Kedei Noemi, A721
 Keefe Aidan, A126
 Keegan Joshua, A174
 Keel Melody, A456
 Keen Nicholas, A2, A824, A931
 Keenan Bridget, A704
 Kehler Patrik, A741, A816
 Kehoe Haixing, A894
 Keilhack Heike, A907
 Keler Tibor, A833
 Kelleher Eugene, A820
 Keller Peter, A902
 Kelley Heather, A999
 Kelley Robin, A704
 Kelly Andrea, A547
 Kelly Geoffrey, A338, A651
 Kelly Karen, A500, A998
 Kelton Christie, A351
 Kempen Paul, A806
 Kemper Kristel, A932
 Kendra Kari, A714, A715
 Kenigsberg Ephraim, A713
 Kenkel Justin, A817, A903
 Kennedy Audrey, A573
 Kennedy Barry, A380
 Kennedy Philippa, A667
 Kennedy-Darling Julia, A56
 Kepley Christopher, A233
 Kern Nadja, A751
 Kerr Emma, A987
 Kerzeli Iliana, A416
 Kesari Santosh, A357, A358, A359, A361, A362, A1001
 Keshari Ravi, A13
 Keskin Derin, A684
 Keung Emily, A410
 Keyt Bruce, A740
 Khairullah Roohussaba, A186, A960
 Khalil Mariam, A240
 Khalili Jahan, A826
 Khan Aly, A76, A81
 Khan Imaan, A998
 Khan Javed, A153, A171
 Khan Zia, A847
 Khandelwal Anvi, A941
 Khanna Swati, A926
 Khanolkar Rahul, A600
 Khare Sonal, A70
 Khatrar Mithun, A176
 Khatwani Nikhil, A674
 Khaw Melissa, A208
 Kheterpal Ashish, A858
 Kheterpal Meenal, A580
 Kho Abel, A838
 Khrizman Polina, A562
 Khulaifi Moza Al, A111
 Khushalani Nikhil, A577
 Kidder Koby, A227
 Kieback Elisa, A104, A239, A531
 Kiefel Helena, A598
 Kiemle-Kallee Joachim, A514, A534
 Kilari Deepak, A318
 Kile Quinlan, A667
 Kim Albert, A428
 Kim Betty, A622
 Kim Bo-Kyoung, A82, A861
 Kim Dae Won, A439
 Kim Eric, A453
 Kim Eun Ji, A138
 Kim Hansol, A138
 Kim Hye Sung, A966
 Kim Hyunjin, A160
 Kim Hyunjoo, A935
 Kim In Ah, A623
 Kim Isaac, A103
 Kim Jae-Sung, A630
 Kim Jaegil, A424, A482
 Kim Jee-Hyun, A1005
 Kim Jeong Min, A138
 Kim Joel, A713
 Kim Johnovan, A742
 Kim Joseph, A498
 Kim Kyeongmin, A706
 Kim Kyung-Hoon, A606
 Kim KyungMann, A67
 Kim Leeseul, A29, A292, A661
 Kim Min Jeong, A254
 Kim Minsoo, A705
 Kim Peter, A195
 Kim Richard, A435, A439
 Kim Sean, A57
 Kim Seong-Jin, A82, A861
 Kim Sojung, A106, A213
 Kim Soo Jung, A630
 Kim Sung-Bae, A364
 Kim Sungjune, A952
 Kim Susan, A117
 Kim Tae Min, A530
 Kim Tae Won, A82, A861
 Kim Tae-Geuk, A996
 Kim Tae-Jin, A630
 Kim Taewan, A440
 Kim Teresa, A689
 Kim Won Seog, A530
 Kim Yeonhee, A477
 Kim Yoonyi, A811
 Kim Young, A677, A678, A947
 Kim Youngkwang, A935
 Kim Youngmi, A57
 Kim Yusun, A138
 Kim-Schulze Seunghee, A651
 King Catherine, A316
 King Emma, A467
 Kinkead Heather, A12, A751, A897
 Kinong Jennifer, A768
 Kirby Kenneth, A231
 Kirillova Natalia, A189
 Kirk Niels, A885
 Kirketerp-Møller Nikolaj, A187
 Kirkwood John, A95, A96, A576, A999
 Kirwin Katherine, A601, A796
 Kish Jonathan, A591
 Kissick Haydn, A669, A686, A779, A975
 Kitch Lacey, A370
 Kivimae Saul, A626
 KjÅr Lasse, A807
 Klaeger Susan, A684
 Klamann Irina, A557
 Klapholz Max, A277
 Klar Kathrin, A536, A597
 Klebanoff Christopher, A528
 Klebanov Boris, A928
 Klein Pamela, A306
 Klein Roger, A78, A86
 Klein Vanessa, A324
 Klein-Goldberg Anat, A756
 Kleinpeter Patricia, A777
 Klempner Samuel, A426
 Kleschenko Yuliya, A243
 Klichinsky Michael, A114, A148, A152, A1000
 Kliger Yossef, A272
 Klopp-Savino Sofia, A727
 Kluesner Mitchell, A229
 Kluger Harriet, A422
 Knickerbocker Aron, A732
 Knoch Julia, A923
 Knochelmann Hannah, A207, A237, A737
 Knorr David, A528
 Knott Simon, A763
 Knox JoAnne, A473
 Knudsen Trine, A807
 Ko Andrew, A370
 Ko Myat, A649
 Kobayashi Yukari, A71, A608, A676, A959
 Kobie Julie, A391, A485
 Koblisch Holly, A247
 Kobzik Lester, A77
 Koch Joachim, A922, A923, A938
 Kodysh Julia, A360
 Koenecke Christian, A1008
 Koguchi Yoshinobu, A103, A431
 Koh Young Jun, A499
 Kohler Jessica, A212
 Kolling Fred, A674
 Komoroski Veronica, A919, A928
 Kong Xiang-Tang, A361
 Kong Xiao-Tang, A357, A358, A359, A362
 Kong Xiaotang, A1001
 Kongara Sameera, A903
 Koni Pandelakis, A886
 Konopka Elizabeth, A625
 Koopman Louise, A904
 Kooreman Nigel, A809, A810
 Kooshki Mitra, A293
 Kopetz Scott, A522
 Korangy Firouzeh, A721
 Koren Lilach, A756
 Kornbluth Jacki, A221
 Kornepati Anand, A261, A321, A789, A944
 Korngold Ana, A240
 Koropatnick James, A617
 Korrer Michael, A611, A677, A947
 Korth Christopher, A512
 Kosaka Yoko, A764
 Koseoglu Secil, A267, A702

- Kotani Hiroshi, A115
 Kotanides Helen, A619, A620
 Kotecki Nuria, A531, A559
 Koth Jason, A91
 Kothambawala Tasnim, A740
 Kotsiou Eleni, A205
 Kotturi Maya, A740
 Koukos Aristeidis, A806
 Kowalski Dariusz M, A390, A391
 Kowalski Karen, A371
 Kowalski Karey, A484
 Kowanetz Marcin, A817, A819, A903
 Kozłowska Anna, A132
 Król Paulina, A866
 kraehenbuehl Lukas, A108
 Kramer Gero, A448, A449, A455
 Kranz Lena, A579
 Krappmann Daniel, A902
 Krauss Juergen, A502
 Krawczyk Janusz, A987
 Kraxner Anton, A94, A976
 Kraynak Jeffrey, A589
 Krebs Matthew, A386
 Kreder Cindy, A817, A903
 Kress Elsa, A953
 Kret Patryk, A786
 Krieg Arthur, A999
 Krige David, A368, A467
 Krimm Michael, A735
 Krishna Sri, A177, A680
 Krishnamoorthy Mithunah, A617
 Krishnan Sunil, A622
 Krisky David, A427
 Kriedte Timothy, A459
 Kristeleit Rebecca, A559
 Kristensson Julia, A824, A931
 Kroemer Alexander, A721
 Kroeninger Tessa, A452
 Kroep Judith, A383
 Kroger Benjamin, A728
 Krueger Sarah, A625
 Kruger Ryan, A654
 Kruisbeek Ada, A232
 Krumpoch Megan, A625
 Kruse Megan, A363
 Kryukov Gregory, A215
 Kryzhanivska Anna, A1006
 Kuś Kamil, A799
 Kuai Jun, A905
 Kubo Kaori, A71
 Kubota Kaoru, A390
 Kudaba Iveta, A390
 Kudchadkar Ragini, A577
 Kudirka Romas, A817, A819
 Kueberuwa Gray, A189, A209, A210
 Kuettner Benjamin, A885
 Kühnle Marie-Cristine, A451, A555
 Kuhlenkamp Alexandra, A201
 Kuhne Michelle, A413, A887, A888
 Kuizon Carmelle, A262
 Kujawa Maciej, A786
 Kulangara Karina, A68
 Kulkarni Meghana, A527
 Kulp Samuel, A706
 Kumar Anil, A906
 Kumar Dhiraj, A977
 Kumar Rajesh, A171
 Kumar Sandeep, A396
 Kumar Sanjay, A183
 Kumar Shaji, A475
 Kumar Shreya, A586
 Kumar Sushant, A279
 Kumaravel Subhashree, A761
 Kummar Shivaani, A554, A569
 Kümmel Sherko, A364, A997
 Kundu Pratima, A809, A810
 Kunwar Pratima, A106, A213
 Kuo Cheng-Fu, A133
 Kuo Tracy, A815
 Kuo Yi-Chiu, A133
 Kuplast-Barr Kristy, A907
 Kuppuraju Meghna, A143
 Kurd Nadia, A290
 Kuriakose Anshu, A915
 Kuriakose Moni Abhram, A915
 Kuryk Lukasz, A396, A491
 Kush Debra, A492
 Kushihara Yoshihiro, A676
 Kushnir Anna, A778
 Kwan Byron, A818
 Kwant Kathryn, A908
 Kwatra Shawn, A850
 Kwatra Vineet, A395
 Kwek Kon Yew, A457
 Kwong Willis, A908
 Kyriakopoulos Christos, A318, A377
 Laar Emily Van, A664
 Laberiano Caddie Dy, A993
 Labiano Sara, A307, A772, A776
 Lacey Simon, A461
 Lachance Kristina, A658
 Lackner Rudy, A515
 Lacroix Ludovic, A308
 Ladd Alden, A165
 Laethem Jean-Luc van, A567
 LaFramboise William, A95, A96
 Laghouati Salim, A409
 Lagkadinou Eleni, A525, A546, A821
 Laguerre Brigitte, A374, A378
 Laguna Ignacio Garrido, A371
 Lahana Carole, A452
 Lahav Coren, A323
 Lahdenranta Johanna, A2, A865, A931
 Laheurte Caroline, A373
 Lahn Michael, A967
 Lahr Walker, A687
 Lai Joey, A552
 Lai Stephen, A788
 Laino Andressa, A569
 Lajoie Scott, A176
 Lake Andrew, A267
 Lake Jessica, A134
 Lakhani Nehal, A425, A459, A529, A530, A565
 Lakins Matthew, A602
 Lako Ana, A728
 Lakshmiipathi Shwetha, A110, A188
 Laktionov Konstantin K, A390
 Lal Ashwin, A13
 Lal Prabha, A127
 Lal Preeti, A598
 Lam Helen, A917
 Lam Hubert, A787
 Lam Sam, A284, A294, A299
 Lam Vincent, A320
 Lam Wei-Sen, A485
 Lamb Lawrence, A168
 Lamba Nayan, A265
 Lambade Pandurang, A889
 Lambert Graeme, A221
 Lamberti Giuseppe, A74, A257, A336
 Lambrechts Marc, A494
 Lamm Donald, A456, A1005
 LaMothe Robert, A198
 Lampa Michael, A636
 Lan Yan, A639
 Lancaster Kelly, A820
 Lance Cowey C, A417
 Lancker Griet Van, A562
 Landers Gregory, A485
 Landgren Ola, A703
 Lang Cara, A677, A678
 Lang Frederick, A640
 Lang Jinyi, A444
 Lang Joshua, A377
 Langan David, A106
 Langer TJ, A418, A419
 Langermann Solomon, A516, A520, A599
 Langfitt Deanna, A160
 Langley Emma, A742
 Langley Meghan, A176
 Langone Francesca, A441
 Lankford Amy, A513
 Lantuejoul Sylvie, A962, A984
 Lantz Jeffrey, A846
 Lapinski Philip, A298
 Laporte Jason, A637
 Lapurga Gabriella, A714, A715
 Lapuyade Nicole, A735
 Lara-Mejia Luis, A25
 Lاراio Jenny, A654
 Larman Tatianna, A877
 LaRocca Renato, A357, A358, A359, A361, A362, A1001
 LaRoche Dominic, A651
 Larouche Jacqueline, A946
 Larsen Brian, A70
 Larsen Thomas, A807
 Larson Madeline, A134
 Larson Rebecca, A234
 LaRue Amanda, A708
 Lashuk Kanstantsin, A150, A585
 Laspidea Virginia, A307, A776
 Lassahn Katy, A305
 Lassoued Wiem, A450
 Lastrapes Matthew, A879
 Lau Denise, A81
 Lau Mai Chan, A656, A855
 Lau Sabina, A598
 Lau Shin Hin, A957
 Lauer Jeffrey, A800
 Lauveson Carina Nava, A696
 Laux Douglas, A580
 LaVallee Theresa, A370
 Lavi Erez, A823
 Law Travis, A234
 Lawler Sean, A427
 Lawrence Cheung Chun Chau, A656
 Lawrence David, A205
 Lawrence Donald, A573
 Lawrence Marissa, A35
 Lazar Alexander, A410
 Lazaridou Maria-Filothei, A956
 Lazetic Sasha, A123, A137, A159
 Le Dung, A441
 Le NgocDiep, A428, A435, A439
 Le Thomas, A850
 Le Xiuning, A788
 Leś Marcin, A799
 Lea Spencer, A622, A793, A798

- Leach Emma, A600, A909
 Leary Alexandra, A382
 Lebas Louisiane, A489
 Lebbe Celeste, A300, A502, A574, A577
 Lebid Andriana, A679
 LeBlanc Robert, A884
 LeBlanc Thomas, A665
 LeBoeuf Nicole, A850
 Lebret Thierry, A945
 Leca Vanina, A489
 Lecalve Benjamin, A154
 Lederer James, A174
 Leduc Sophie, A151
 Lee Adrian, A708
 Lee Arthur, A817, A819
 Lee Benjamin, A267, A702
 Lee Bo Ram, A630
 Lee Brian, A338, A651
 Lee Byung Ha, A428, A435, A439
 Lee Chen-Ting, A125
 Lee Dae Ho, A492
 Lee Daniel, A136
 Lee David, A704
 Lee Derrick, A125
 Lee Dong-Uk, A29, A292
 Lee Dooyoung, A625
 Lee Eudocia Quant, A427
 Lee Eun-Sol, A138
 Lee Gary, A125
 Lee George, A420, A859
 Lee Grace, A966
 Lee Hae-youn, A146
 Lee Hee Jun, A135
 Lee Hye Lim, A811
 Lee Jack, A304, A1013
 Lee Jae-Lyun, A499
 Lee Jared, A225
 Lee Jeeyun, A440
 Lee Jenny, A467, A577
 Lee Jihyun, A146
 Lee Jina, A598
 Lee Jong-Seok, A485
 Lee Joo Han, A630
 Lee Joon Sang, A308
 Lee Joon Sange, A550
 Lee Keun-Wook, A82, A440, A530, A861
 Lee Michael, A37
 Lee Patrice, A644
 Lee Percy, A105
 Lee Sae Bom, A115
 Lee Sandra, A95, A96
 Lee Seoho, A671
 Lee Seung Hyun, A630
 Lee Shinai, A935
 Lee Sophia, A844
 Lee Sungkyu, A197
 Lee Sunyoung, A49
 Lee Sylvia, A486, A523, A689
 Lee Tani-Ann, A742
 Lee Tom, A126, A129, A147, A180
 Lee Wen-Hua, A131
 Lee Yeon-Sook, A996
 Lee Yong, A651
 Lee Yong Hee, A78, A86, A89
 Lee Younghee, A1013
 Lee Yuchi, A18, A804
 Lee Zachary, A1007
 Leedom Tom, A200
 Leelatian Nalin, A45
 Leemans René, A981
 LeFace Drake, A226
 Legler Michelle, A563
 Legrand Margaux, A287
 Lehmann Frédéric, A438
 Leibovich Bradley, A452
 Leick Mark, A234
 Leidner Rom, A553
 Leierer Melanie, A579
 Leinert Patrick, A334
 Leinert Wm Pat, A334
 Leire Emma, A572
 Leisegang Matthias, A239
 Leishman Andrew, A583
 Leitheiser Christopher, A824
 Lemar Hadia, A137, A159
 Lemaster Jourdain, A106
 Lemech Charlotte, A366, A367, A457
 Lemeque charlotte, A511
 Lemon Bryan, A908
 Leng Charan, A883
 Lenkala Divya, A212
 Leo Eugen, A104, A531, A536, A597
 Leon Ivanna, A190
 Leon Michael, A57
 Leonard John, A464
 Leonard Niamh, A987
 Leonard Shannon, A219
 Leone Biagio Eugenio, A331
 Leoni Guido, A441
 Leow Wei Qiang, A656
 LePage Ella, A852
 Lérias Joana, A978
 Leser Ulf, A34
 Lesinski Gregory, A20, A434, A779, A948
 Leskowitz Rachel, A461
 Leslie Isla, A539
 Lesniak Jan, A392
 Lesser Glenn, A293
 Letourneur Diane, A409, A945
 Leung Cheuk, A1013
 Leung Cheuk Hong, A304
 Leung Irene, A726, A736
 Leung Joanne, A862
 Leung Ling, A917
 Levell Julian, A800
 Levenets Iana, A786
 Levenets Oleksandr, A786
 Leventhal Matthew, A807
 Leveque-ElMouttie Lucie, A366, A367
 Levesque Mitchell, A597
 Levi Jelena, A52
 Levin Itay, A732
 Levin Liron, A230
 Levin Mattias, A785
 Levine Zurit, A272
 Levisetti Matteo, A468, A749
 Levitin Natalie, A732
 Levitsky Victor, A396, A491
 Levy Benjamin, A320
 Levy Emily, A181
 Levy Eric, A21, A22, A83, A88
 Levy Irit Carmi, A823
 Levy Ronald, A803
 Levy-Efrati Liron, A823
 Lewin Anne, A316
 Lewis Claire, A867
 Lewis Dixie, A473
 Lewis Jeff, A304
 Lewis Jr James, A868
 Lewis Karl, A532
 Lewis Valerae, A410
 Ley Jessica, A385
 Leyton Claudia Kettlun, A604
 Leyvraz Serge, A568
 Lhuillier Claire, A286
 Li Anlong, A415
 Li Bai, A387, A389
 Li Baiyong, A288, A313, A457, A460, A466, A471, A783
 Li Biao, A408
 Li Bin, A939
 Li Bo, A632
 Li Bochong, A918
 Li Chen, A742
 Li Chuck, A131
 Li Gongbo, A115
 Li Guiling, A460
 Li Hai, A817
 Li Henry, A348, A753
 Li Huiyu, A632, A835
 Li Jian Ming, A779
 Li Jing, A259, A544
 Li Lei, A827
 Li Lixin, A501
 Li Mengxia, A490
 Li Michelle, A809, A810
 Li Min, A815
 Li Mingjia, A988
 Li Robin, A22, A83
 Li Roger, A1005
 Li Rong, A460
 Li Shamin, A57
 Li Shuqiang, A84, A593, A684
 Li Shuyin, A330
 Li Siyu, A565
 Li Taibo, A317, A693
 Li Tao, A444
 Li Tengting, A936
 Li Tianhong, A500, A998
 Li Tony, A704
 Li Wei, A171
 Li Wendy, A405
 Li Xiang, A682
 Li Xiangming, A636
 Li Xiaoguang, A632
 Li Xin, A641
 Li Xin Tong, A374, A378, A448, A449, A455
 Li Xinzhong, A479
 Li Yongjin, A391
 Li Yuesheng, A899
 Li Yunmin, A667
 Li Yunxia, A460
 Li Yuzhi, A460
 Li Zhang Kathryn Allaire Fan Zenghua, A704
 Li Zhaoliang, A911
 Li Zhenhua, A587
 Li Zhiyuan, A217
 Li Zhuoning, A142
 Li Ziyi, A728
 Li Zujun, A462
 Lian Kaixia, A348, A753
 Liang Hao, A436, A437
 Liang Jin Hua, A728
 Liang Kaijie, A986
 Liang Linda, A900
 Liang Qing, A619, A620
 Liang Spencer, A917
 Liang Xiaofang, A584
 Liao Wenjia, A602
 Liao Xiaoyun, A946

- Licitra Lisa, A465
 Liddle Ashley, A407
 Liebig Inga, A579
 Liebling Ian, A653
 Liebner David, A424
 Liechty Kirstin, A522
 Lierop Marie-José Van, A232
 Liew David, A854
 Ligon Keith, A427
 Lihm Jayon, A862
 Lillard Kate, A64
 Lillie Tom, A368, A467
 Lillquist Jay, A833
 Lim Emerson, A508
 Lim Hoyong, A138
 Lim James, A667
 Lim Jeffrey, A656
 Lim Jinback, A811
 Lim Kiat Hon, A97
 Lim Klothilda, A728
 Lim Kue Peng, A957
 Lim Min, A432
 Lim Tony, A656
 Lim Xinru, A656
 Lim Yangmi, A935
 Lim Yoojoo, A869
 Lima Cibelle, A410
 Limagne Emeric, A373
 Lin Aimee Bence, A924
 Lin Fu-Yang, A625
 Lin Heather, A252, A410, A1013
 Lin Jamie, A252, A845
 Lin Jianxin, A390
 Lin John, A796
 Lin Kai-Wen, A408, A413
 Lin Lanjia, A554
 Lin Mary, A859
 Lin Qin, A466
 Lin Quan, A401, A407
 Lin Shaojun, A466
 Lin Sharon, A198, A215
 Lin Shiaw-Yih, A186
 Lin Steven, A622
 Lin Tun Tun, A550
 Lin Yi, A522
 Lin-Liu Yvonne, A74
 Linch Mark, A378, A451
 Lind Charlotte Lybek, A429
 Lind Evan, A764
 Lindblad Katherine, A653
 Lindenbergh Pieter, A142
 Lindpaintner Klaus, A35
 Lindquist Kevin, A290
 Lindqvist Eva, A785
 Lindsay James, A74
 Lindsley R, A807
 Linehan David, A705
 Lineker Dimitry, A787
 Linnette Gerald, A422
 Ling Chen, A387, A389
 Ling Xiaodong, A436, A437
 Lippa Blaise, A625
 Lips Erin, A36
 Liron Itay, A823
 Lischke Timo, A741, A816
 List Catrin, A535
 Litten Jason, A138
 Litterman Adam, A226
 Littlewood Peter, A786, A799
 Littrell Joshua, A42
 Liu Arthur, A622, A759
 Liu Baorui, A986
 Liu Bei, A207
 Liu Bin, A801
 Liu Cailian, A108
 Liu Chang, A907
 Liu Chunxiao, A642
 Liu Dongyan, A682
 Liu Edwin, A131
 Liu Fang, A343, A685
 Liu Fangcen, A986
 Liu Fanlong, A443
 Liu Frances, A125
 Liu Glenn, A377
 Liu Hao, A247
 Liu Hong, A999
 Liu Jiangyue, A145
 Liu Jin, A656
 Liu Jingxia, A385
 Liu Kang, A946, A985
 Liu Ke, A736, A822
 Liu Lan, A563
 Liu Linda, A516, A520
 Liu Lixia, A136
 Liu Longchao, A632
 Liu Lulu, A443
 Liu Mingyue, A246, A849
 Liu Phillip, A247, A633
 Liu Qin, A986
 Liu Qinying, A248, A315
 Liu Shuaitong, A724
 Liu Sophia, A84
 Liu Tianbing, A77
 Liu Tianshu, A400
 Liu Xiajuan, A835
 Liu Yanfang, A446
 Liu Yang, A246, A500, A564, A849, A998
 Liu Yanyan, A601
 Liu Yong, A389
 Liu Yuan, A20, A227, A779
 Liu Yun, A638
 Liu Zexuan, A944
 Liu Zhida, A632
 Livak Kenneth, A84, A684
 Lizée Gregory, A244
 Ljung Lill, A785, A831
 Lledo Lester, A461
 Llewellyn Ryan, A290
 Llosa Nicolas, A609
 Lo Kin-Ming, A639
 Lobb Roy, A170
 Locke Darren, A56
 Locke Frederick, A115, A703
 Locke Susan, A665
 Lockey Timothy, A160
 Lockyer Heather, A495
 Lodie Tracey, A172, A230
 Loesch Barbara, A201
 Loferer Hannes, A324
 Logothetis Christopher, A259, A379
 Loh Lauren, A284, A299
 Loh Texia, A284, A299
 Lohmueller Jason, A122
 Löhr Matthias, A927
 Loizeaux James, A268
 Lonz Caroline, A438
 Long Georgina, A540
 Long Henry, A728
 Long Yan, A186
 Lontos Konstantinos, A109
 Loo Christopher, A764
 Loon Karlijn van, A808
 Lopes Gilberto, A390, A391
 Lopez Alejandra, A280
 Lopez Angelica, A50
 López Criado María Pilar, A1011
 López Javier Sánchez, A1011
 Lopez Juanita, A525
 Lopez Justine, A891
 Loquai Carmen, A579
 Lorens James, A632
 Lorigan Paul, A576
 Lorigan Paul C, A189
 Lorincz Orsolya, A72
 Lörks Verena, A579
 Lorusso Domenica, A1006
 LoRusso Patricia, A514, A525, A530, A534, A535, A546, A569, A907
 Lostes Maria, A536
 Loter Lorraine, A147
 Lotze Michael, A107, A375, A708
 Loughhead Scott, A166, A224
 Love J, A326
 Love Ruschelle, A726
 Low Jenny, A656
 Low Simon, A828
 Lowery Frank, A177, A680
 Lowinger Timothy, A820
 Lowy Israel, A565
 Lozac'hmeur Ariane, A522
 Lozano-Rabella Maria, A958
 Lu Changzheng, A835
 Lu Dan, A147, A543, A681, A832
 Lu Emily, A213
 Lu Hongtao, A295, A827
 Lu Linda, A853
 Lu Sen, A443
 Lu Wenyun, A230
 Lu Yen-Ta, A285
 Lu Ying, A417
 Lu Yong-Chen William, A680
 Lucas Anthony, A128
 Lucas Ashly, A830, A831
 Lucas Sasha, A895
 Ludford Kaysia, A853
 Ludwig Dale, A619, A620
 Luedde Tom, A34
 Luft Alexander, A485
 Luginbuhl Adam, A947
 Luison Elena, A331
 Lujambio Amaia, A653
 Luke Jason, A425, A532, A543, A568, A580, A729, A999, A1009
 Luke Raymond, A401
 Luketich James, A122, A708
 Luksza Marta, A862
 Lule Sevda, A796
 Luly Kathryn, A235
 Lum Lotus, A341
 Luna Xenia, A681, A832
 Luo AAngela Luondrew, A819
 Luo Angela, A819
 Luo Dayong, A479
 Luo Hao, A490
 Luo Jiamin, A490
 Luo Jingqin, A428
 Luo Qianyun, A53, A788
 Luo Xingbo, A458
 Luo Xuerui, A400
 Luo Ying, A466

- Luo Yuan, A838
 Luo Yunxiu, A466
 Luo Yuting, A986
 Lupo Kyle, A139
 Lutz Emi, A711
 Lutzky Jose, A577, A580
 Lv Dongqing, A497
 Lv Huilai, A587
 Lv Jiahua, A444
 Lycan Thomas, A846, A852
 Lyle John, A22, A83
 Lyman Jaclyn, A370
 Lynam Reena, A468
 Lynce Filipa, A644
 Lynch Alia, A840
 Lynch Kevin, A54, A638, A987
 Lynch Michael, A114
 Lynn Patricia, A698
 Lyon Kenyon, A147
 Lyu Xiabing, A743
- Ma Bo, A3, A459, A526
 Ma Brigitte, A519
 Ma Chi, A721
 Ma Haijun, A1007
 Ma Hu, A355
 Ma Hua, A485
 Ma Jianqun, A436, A437
 Ma Jing-Tyan, A327
 Ma Li, A356
 Ma Mark, A833
 Ma Minuk, A869
 Ma Weijie, A257
 Ma Xiaopeng, A387
 Ma Yuk Ting, A387
 Maccalli Cristina, A111, A767
 MacDonald Lisa, A380
 Mace Emily, A651
 Mace Thomas, A706, A948
 Macedo Chelsie, A12, A751
 Macedo Mariana De, A62
 MacFarlane Alexander, A699
 Machado Daniel, A740
 Macherla Shravanti, A257
 Machiels Jean-Pascal, A463, A469
 Maciá Sonia, A1011
 Mack Philip, A25
 Mackensen Andreas, A1008
 Mackert Jessica, A293
 Maclean Kirsteen, A60
 MacMullan Melanie, A121
 Macri Mary, A363
 Madabhushi Anant, A44, A868
 Madakamutil Loui, A592
 Madala Hanumantha Rao, A748
 Madan Rashna, A372
 Madan Ravi, A450, A513, A516
 Maddage Christopher, A247
 Madden Matthew, A951
 Madonna Gabriele, A27, A332, A980
 Maeurer Markus, A978
 Magadoux Léa, A953
 Magen Assaf, A388, A713
 Maguire Laura, A30, A33, A870
 Mah In Kyoung, A606
 Mahabhashyam Suresh, A729
 Mahadevan Daruka, A356, A509
 Mahalingam Devalingam, A397, A555
 Mahipal Amit, A512
 Mahlakoiv Tanel, A169
- Mahler Dana, A885
 Mahmood Sajid, A126
 Mahmood Syed, A533, A566
 Mahmoodi Amir, A723
 Mahmutovic Adela, A54
 Mahoney Kathleen, A408
 Mahtouk Karène, A962
 Mahtouk Karene, A984
 Mai David, A140
 Mai Haiqiang, A466
 Maia Andreia, A978
 Maier Daniela, A510
 Maine Chloe, A572
 Maiolino Piera, A27
 Mairesse Maelle, A592
 Maithel Shishir, A20, A434, A948
 Maitra Anirban, A186
 Majercak John, A926
 Majumdar Anish, A779
 Majumder Biswanath, A13
 Majumder Pradip, A13
 Makhanov Michael, A77
 Maki Izumi, A113
 Makker Vicky, A381
 Makkouk Amani, A128
 Makohon-Moore Alvin, A862
 Makowski Liza, A710
 Maleki Saman, A617
 Malhotra Kanam, A243
 Malhotra Ritu, A40
 Malinauskas Jenna, A81
 Malinge Pauline, A287
 Malissen Nausicaa, A713
 Malki Enana, A927
 Malkoun Richard, A489
 Malkova Natalia, A748
 Mallardo Domenico, A27, A257, A332, A980
 Mallet William, A817, A819
 Malli Naniye, A820
 Mallow Crystal, A464
 Malmberg Karl-Johan, A338
 Maloney David, A522
 Maloney Michael, A224
 Maltez Vivien, A603
 Mamdani Hirva, A435, A439
 Mamlouk Omar, A252
 Mammadova Najiba, A983
 Mammen Andrew, A570
 Mamuye Admasu, A475
 Mancini Kevin, A268, A504, A515
 Mandadi Sravan, A889
 Mandelboim Ofer, A275
 Mandeli John, A360
 Mandl Stefanie, A858
 Manesse Mael, A60
 Manfra Denise, A919, A928
 Mangarin Levi, A108, A649, A807
 Manglaviti Sara, A16
 Manglik Rushil, A13
 Mangsbo Sara, A416
 Mani Monisha, A107
 Manimaran A, A40
 Manirad Vanna, A372
 Maniyar Rachana, A649
 Manja Sanjana, A224
 Manjarrez Kristi, A529
 Manjula BV, A40
 Mankikar Shilpa, A900
 Manlusoc Marigold, A740
 Manne Sasikanth, A274, A335
- Manos Michael, A402, A728
 Mansilla-Soto Jorge, A142
 Manso Luis, A562
 Mansour Mena, A22
 Mant Andrew, A417
 Manting Erik, A232
 Mantooth Siena, A281, A650
 Manu Michell, A450
 Manuel Trigo Jose, A493
 Manyak Erika, A907
 Manzo Teresa, A696
 Manzoni Alessandro, A27
 Mapes Brandon, A70
 Mar Nataliya, A378
 Marabelle Aurélien, A300, A308
 Marabelle Aurelien, A382, A409, A514, A534, A535, A945
 Marathe Megha, A889
 Marcelo Kathrina, A788
 Marcenaro Emanuela, A338
 Marchand Jean-Baptiste, A777
 Marcher Marie, A946
 Marchetti Paolo, A257
 Marco-Sanz Javier, A776
 Marcondes Mario, A1007
 Marcus Butler, A550
 Mardilovich Katerina, A401
 Mardiros Armen, A522
 Marelli Bo, A639
 Margetts Jane, A389
 Margolin Kim, A415, A999
 Margossian Steven, A468
 Marie-Cardine Anne, A898
 Marijse Jerome, A154
 Marin Jose Flavio, A62
 Marina Neyssa, A511
 Marincola Francesco, A162, A164
 Marino Sara, A925
 Markel Gal, A556
 Markovska Angela, A643
 Markus Tegan, A240
 Marme Frederik, A997
 Marneth Anna, A807
 Marotel Marie, A894
 Marquez Eladio, A308
 Marquez Karl, A155
 Marquez-Solorzano Natalie, A126
 Marron Thomas, A257, A363, A388, A481, A484, A713, A729
 Marrone Kristen, A263, A320, A353, A729
 Marsh Henry, A833
 Marshall Amy, A461
 Marszalek Joseph, A652
 Martin-Liberal Juan, A958
 Marte Jenn, A513
 Marte Jennifer, A450
 Martel Maritza, A431
 Martens Alexander, A597
 Martens Andrew, A200
 Martensson Linda, A777
 Martin Aaron, A131, A149
 Martin Amber, A224
 Martin Anne-Marie, A423
 Martin Gaëlle, A782, A953
 Martin Juliette, A719
 Martin Lainie, A461
 Martin Maureen, A338
 Martin Patricia, A550
 Martin William, A337
 Martin-Liberal Juan, A1011

- Martinaite Evelina, A813
 Martinetti Antonia, A16
 Martinez Aitziber Buqué, A309, A589, A763
 Martinez Alonzo, A505
 Martinez Anthony, A500
 Martinez Javier, A772
 Martinez Salomon, A18
 Martinez Solomon, A804
 Martinez-Morilla Sandra, A258
 Martino Mara De, A950
 Martins Andrew, A570
 Martomo Stella, A543, A681, A832
 Marvin James, A902
 Marx Sascha, A427
 Mary caroline, A245, A829
 Masakyan Reed, A144
 Masi Gianluca, A387
 Masia Ricard, A267, A702
 Maslyar Daniel, A917
 Masrourpour Fatemeh, A604
 Massa Chiara, A956
 Massard Christophe, A382, A409
 Massarelli Erminia, A484, A542
 Massey Christopher, A624
 Master Viraj, A669, A686, A975
 Masternak Krzysztof, A287
 Mata Helena Verdaguer, A389
 Mata Melinda, A173
 Matas-Rico Elisa, A967
 Mathew Divij, A335
 Mathew Grace, A410
 Mathew Rebecca, A111
 Mathewson Nathan, A427
 Mathias Melissa, A565
 Mather Mary, A200
 Matias-Guiu Xavier, A69, A958
 Matissek Stephan, A267
 Matkowskyj Kristina, A982
 Matlawski Tina, A461
 Matos Ana de, A773, A775
 Matos Ignacio, A958
 Matosevic Sandro, A139, A158, A182, A834
 Matsumoto Noriko, A251
 Matsumura Haruka, A251
 Matthies Derek, A462
 Mauch Cornelia, A576
 Maul Julia-Tatjana, A536
 Mauldin Ileana, A54, A363, A421
 Maura Francesco, A703
 Maurer Deena, A370
 Maurer Dominik, A1009
 Maurer Mark, A39
 Maurin Mathieu, A142
 Maurus Daniel, A579
 Maus Marcela, A234
 Maxwell Melissa, A910
 Mayer-Mokler Andrea, A1009
 Mayes Erin, A900
 Mayo Michele, A633
 Mazieres Julien, A489
 Mazo Gregory, A724
 Mazo Irina, A902
 Mazurek Jolanta, A799
 Mazzeo Laura, A16
 Mazzocco Giovanni, A866
 Mbofung Rina, A126, A584
 McAdory John, A456, A1005
 McAfee Megan, A204
 McAlpine Cheryl, A401, A407
 McAlpine Indrawan, A768
 McArdel Shannon, A219
 McArthur Heather, A103
 McCarthy Brian, A212
 McCarthy Derrick, A185
 McCarthy Elizabeth, A704
 McCarthy Patrick, A571
 McCarty Erin, A64
 McClain Ethan, A200
 McClelland Mark, A30, A33, A870
 McClory Rena, A83
 McConnell Emma, A602
 McCully Michelle, A568
 McCutcheon Krista, A327
 McDaniel Lee, A21, A22, A88
 McDermott David, A188, A376, A454
 McDonald Alexander, A349
 McDonnell Kevin, A824, A931
 McEachern Kristen, A907
 Mcelvain Michele, A131
 Mcewan Brigid, A143
 McFarland Jesse, A723
 McGee Grace Helen, A626
 McGee Jonathan, A212
 MCGovern Karen, A102
 McGrail Daniel, A186, A971
 McGregor Kim, A5, A495
 McGuire Michael, A648
 Mclvaine Elizabeth, A544
 McIntosh Olivia, A709
 McKay Hannah, A3, A459
 McKay Zachary, A770
 McKean Meredith, A425, A511, A529, A542, A561, A563
 McKenzie Jodi, A584
 McLaughlin Megan, A748
 McLaughlin Rene, A156, A157
 McMahan Catherine, A830, A831
 McMahan Frank, A495
 McMahan Sheri, A513
 McMiller Tracee, A312
 McNeel Douglas, A377, A624, A802
 McPherson Rhoanne, A271
 McQuillan Nicholas, A100
 McWhirter Sarah, A614
 Meagher Michael, A160
 Means Gary, A39
 Meda Shirisha, A212
 Medcalf Amanda, A138
 Medhi Ragini, A967
 Medin Jeffrey, A896
 Medina Theresa, A999
 Medley Kyle, A911
 Medrano Ruan, A334
 Meehan Robert, A569
 Meghwal Diksha, A859
 Mehanna Nezar, A634
 Mehla Kamiya, A683
 Mehmi Inderjit, A999
 Mehra Navi, A983
 Mehra Ranee, A484
 Mehran Reza, A105
 Mehrazin Reza, A90, A338, A651
 Mehta Amit, A129, A147
 Mehta Amitkumar, A503
 Mehta Anita, A644
 Mehta Ranna, A900
 Mei Jay, A638, A936
 Mei Li, A890
 Meier Friedegund, A576
 Meier Roland, A472
 Meij Pauline, A383
 Meijers Wouter, A842
 Meinecke Lina, A392
 Mekhail Tarek, A484
 Melacarne Alessia, A876
 Melandri Daisy, A205
 Melero Ignacio, A536, A546, A577
 Mellacheruvu Dattatreya, A88
 Mellinger Staci, A430, A431
 Mellman Ira, A847
 Melrose Jennifer, A817, A819
 Melson John, A840
 Melssen Marit, A927
 Melton Zea, A290
 Melucci Alexa, A311, A618, A705
 Mempel Thorsten, A902
 Menas Fatima-Zohra, A433, A465
 Menchel Brett, A114
 Mender Ilgen, A725
 Mendiola Andrea, A926
 Mendrzyk Regina, A1009
 Meneveau Max, A54
 Menezes Lavita, A538
 Meng Hongxue, A436
 Meng Robin, A465, A483
 Meng Zhiqiang, A387
 Meniawy Tarek, A511
 Menk Ashley, A194, A707
 Menon Vilas, A100
 Mensali Nadia, A416
 Mentzer Michaela, A625
 Merad Miriam, A388, A713
 Merazga Zohra, A749, A828
 Merchan Jaime, A537, A729
 Mercier Isabelle Le, A215, A766
 Merghoub Taha, A108, A353, A596, A634, A649, A724, A807
 Merhi Maysaloun, A19, A767
 Merino Amy, A224
 Merino Luis de la Cruz, A1011
 Merle Philippe, A389
 Merritt Elliot, A651
 Meseck Marcia, A360
 Messersmith Wells, A371, A530
 Messina Cristina, A423
 Messing Mark, A381
 Mestiri Sarra, A767
 Met Özcan, A813
 Metts Jonathan, A190
 Meulen Jan ter, A176
 Meyer Christian, A566
 Meyer Clifford, A728
 Meyer Larissa, A183
 Meyer Nicolas, A300
 Meza Miguel, A126
 Mi Haoyang, A863
 Miao Hui, A384
 Miao Xiaoniu, A939
 Michael Kesi, A35, A268
 Michaelson Jennifer, A918
 Michalik Kinga, A786, A799
 Michel Adam, A596
 Michelet Xavier, A144, A216, A432
 Michels Judith, A382
 Michels Tillmann, A324
 Michelson Glenn, A519
 Michon Lucas, A962, A984
 Micklem David, A632
 Middleton Jen, A572
 Middleton Mark, A538, A539, A576

- Miederer Matthias, A579
 Miele Matthew, A142
 Mielinis Paulius, A80
 Miest Tanner, A452
 Migden Michael, A577, A580
 Miguel Enrique de, A1011
 Miguel Maria, A555
 Miguel Maria de, A536
 Mihalciou Catalin, A417
 Mihara Kenichiro, A113
 Mikkelsen Tarjei, A226
 Milani Pamela, A83
 Milaszewski Madison, A268
 Milberg Oleg, A569
 Milde Ronny, A324
 Miles David, A368
 Milhem Mohammed, A538, A999
 Milla Marcos, A636
 Miller Christine, A702
 Miller Dannah, A55, A902
 Miller Ebony, A687
 Miller Jeffrey, A180, A473, A667
 Miller Karen, A401
 Miller Peter, A56
 Miller Richard, A729
 Miller Rowan, A398
 Miller Sarah, A473
 Milling Lauren, A801
 Mills Matthew, A952
 Mills-Chen Laura, A833
 Millward Carl, A548
 Millward Michael, A73
 Milo Jay, A42, A68
 Milosevic Slavoljub, A201
 Milowsky Matthew, A547
 Min Bokyung, A138
 Mineno Junichi, A71, A113
 Mineo Brittany, A81
 Minna John, A632, A835, A964
 Minnar Christine, A635
 Minne Lien van der, A383
 Minns Hanna, A100
 Miranda Kayla, A760
 Miranda Noel de, A41, A701
 Miriyala Jaya, A615
 Mirza Amer, A18, A804
 Mishima Yuji, A251
 Mislang Anna, A457
 Misra Chandrasekhar, A889
 Mistry Akshitkumar, A45
 Mistry Hitesh, A865
 Mistry Sejal, A56
 Mita Alain, A498, A553, A555
 Mita Monica, A498
 Mitchell Duane, A594
 Mitchell Jennifer, A926
 Mitchell Joylise, A604
 Mitchell Kyle, A53, A186
 Mitchell Tara, A559
 Mittelbronn Michel, A597
 Mittendorf Elizabeth, A644
 Mitzel-Rink Heidrun, A579
 Mixson Lori, A547
 Mizera Mikolaj, A866
 Mizrahi Karin, A823
 Mizzoni Craig, A928
 Mo Xiaofei, A662
 Moamin Mohammed, A867
 Mobasher Mehrdad, A729
 Mobley Bret, A45
 Mock Jee-Young, A131
 Mockel-Tenbrinck Nadine, A8
 Mody Kabir, A991
 Moeller Rebecca, A912
 Mohamed Ali, A173, A1009
 Mohamed Yehia, A49
 Mohammad Fuad, A877
 Mohammad Helai, A654
 Mohan Suruchi, A111
 Mohanasundaram M, A13
 Mohankumar Kumaravel, A754, A761
 Mohanty Suchismita, A226, A306
 Moharana Kedar, A805
 Mohindra Rajat, A847
 Mohr Peter, A502
 Mohsen Reyad, A19
 Moine Valéry, A287
 Moisan Jacques, A351, A792
 Moiset Gemma, A150, A156, A157
 Mojadidi Michelle, A209
 Mok Tony SK, A390, A391
 Molina Julian, A522
 Moller Anne-Sophie, A396, A491
 Moller Mecker, A417
 Molnar Levente, A72
 Molvi Zaki, A807
 Momin Amin, A858
 Momin Noor, A326
 Moniz Raymond, A468, A749, A828
 Monk Bradley, A523
 Monohan Gregory, A476
 Montalto Michael, A859
 Montaudie Henry, A1011
 Monteiro Natalie, A58
 Montler Ryan, A175
 Monville Florence, A489
 Moodley Devapregasan, A702
 Mookhtiar Kasim, A279
 Moole Praveen Reddy, A915
 Moolenaar Wouter, A967
 Moon Yong Wha, A197
 Mooney Jill, A511, A636
 Mooradian Meghan, A841
 Moore Chris, A926
 Moore Ginger, A262
 Moore Gregory, A726, A913
 Moore Lindsay, A166
 Mootien Jennine, A205
 Moquin Deanna, A42
 Mora Alessandro, A543
 Morad Golnaz, A879
 Moraes Kathy, A940
 Moram Sritha, A628
 Morarity Branden, A687
 Morawski Aaron, A516, A520
 Moreau Leanié, A627
 Morel Ariane, A892, A893
 Morel Yanniss, A892, A893
 morello Aurore, A829
 Moreno Irene, A536
 Moreno Victor, A398, A546
 Moreno-Nieves Uriel, A228
 Morgan Duncan, A326, A692
 Morgan Jessica, A306
 Moriarity Branden, A229
 Morreau Hans, A701
 Morris Charles, A438
 Morris Kristin, A744, A747, A752
 Morris Shannon, A547
 Morris Van, A1009
 Morris Zachary, A628, A629
 Morriss Julia, A84
 Morrow Brittany, A622, A652
 Morrow Michelle, A602
 Morrow Zachary, A814
 Mortales Christie, A745
 Mortensen Joachim, A23
 Moser Justin, A509
 Mosher Rebecca, A820
 Moshiri Ata, A689
 Moskowitz Darrian, A216, A432
 Moslehi Javid, A842
 Mota Ines, A286
 Motaghed Mona, A233
 Mott Frank, A304
 Mou Haibo, A445
 Moudgil Tarsem, A93
 Moujaber Tania, A552
 Mourad Severine, A300
 Mouraud Severine, A409, A945
 Moureau Sylvie, A924
 Mourey Loic, A374, A378
 Moutafi Myrto, A258
 Moxon Nicole, A430, A431
 Moy Lily, A303
 Moy Terence, A625
 Moynihan Kelly, A593, A607, A746
 Mtchedlidze Nino, A794
 Mu Libing, A246
 Muñoz Eva, A538, A958
 Muñoz-Couselo Eva, A364
 Muchhal Umesh, A726, A736
 Mudd Gemma, A824, A931
 Mudri Sherri, A39
 Mueller Christian, A386, A997
 Mueller Sebastian, A99
 Mueller Steffen, A778
 Muijlwijk Tara, A981
 Muik Alexander, A546, A821
 Muir Alexander, A691
 Muise Eric, A303
 Mukherjee Arnab, A243
 Mukherjee Elina, A682
 Mukherjee Rinee, A390
 Mukherjee Sarbajit, A441
 Mukherjee Sudip, A225
 Mulcahy Mary, A397
 Mule James, A795, A952
 Mule Matthew, A570
 Mullally Ann, A807
 Mullane Patrick, A975
 Mullenix Alyssa, A125
 Müller Verena, A579
 Mullinax John, A190, A191, A418
 Mulvaney Kelly, A372
 Mundry Clara, A683
 Mundy Renee, A576
 Munkhbat Ariunaa, A204
 Munnik Sabrina de, A156, A157
 Munoz-Olaya Jose, A792
 Munson Paul, A695
 Murad John, A135
 Muroyama Yuki, A335
 Murphy Michael, A833
 Murray Clare, A261, A789, A944
 Murray Evan, A84
 Murray Joseph, A253, A263, A320
 Murray Ryan, A165
 Murter Benjamin, A668, A720
 Murthy Pranav, A375

- Musenge Faith, A165
Musher Benjamin, A498
Mustafa Dana, A41
Mutez Virginia, A719
Muthuswamy Anantharaman, A874
Myers Jeffrey, A788
Myers John, A571
Myint Han, A516, A520, A599
Myronov Alexander, A866
- Na Deukhae, A623
Nabhan Salah, A527
Nadia Lee Li Wen Justina, A656
Nadolski Gregory, A461
Nag Reetoja, A868
Nagai Ryohei, A914
Nagaoka Koji, A71, A608, A676, A959
Nagel Mark, A887, A888
Nager Andrew, A768
Nagira Morio, A914, A934
Nagira Yoji, A914, A934
Nagrial Adnan, A552
Nagy Mate, A2, A867
Naidoo Jarushka, A253, A353, A877
Naidoo Revashnee, A600, A909
Naik Shruthi, A452
Naing Aung, A25, A435, A439, A514, A534, A540, A561
Nair Pradip, A915
Nair Reshmi, A915
Nair Smita, A770
Najjar Yana, A553
Nakajima Jun, A71, A608
Nakajima Kanto, A251
Nakamura Norihiro, A251
Nakashima Hiroshi, A427
Nalle Sam, A917
Nam Dong Hyun, A822
Nam Hyeong Jin, A138
Namgung Ye-Na, A996
Nampe Daniel, A131
Nangle Leslie, A727
Naniong MarkVic, A165
Nanna Alex, A219
Naqa Issam El, A95, A96
Naqash Abdul Rafeh, A257
Naradikian Martin, A131
Naranbhai Vivek, A850
Nardelli-Haefliger Denise, A920
Nasarre Cecile, A708
Nascimento Ellen, A62
Nash Amanda, A225
Nasrah Nicole, A578
Nassar Amin, A257
Nassif Elise, A410
Natarajan Arvind, A110, A188
Nathan Paul, A568
Nathenson Michael, A424
Natoli Ed, A833
Nava Daniel de la, A307, A776
Navarrete Natalie, A147
Navarro Alejandro, A493
Navarro Fabio, A21, A83
Naveen Mehta, A918
Navenot Jean-Marc, A401, A407
Navia Susan, A580
Nawaz Sidra, A205
Nazarenko Natalya, A895
Nazaretyan Samvel, A126
Nazari Fereshteh, A821
- Ndoye Babacar, A809
Ndubaku Chudi, A614
Neal Carly, A200
Nebelitsky Eugene, A625
Nebhan Caroline, A257
Needels Michael, A738
Neev Guy, A823
Neff-LaFord Haley, A818
Negrao Marcelo, A53, A186, A1013
Nehil Michael, A203
Nejati Reza, A699
Nelson David, A316
Nelson Lauren, A461
Nelson Megan, A516, A520
Nelson Michelle, A830, A831
Nenclares Pablo, A539
Nerle Sujata, A884
Neskey David, A207
Nesline Mary, A78, A86, A89
Net Lelia, A30, A33, A870
Neuberg Donna, A684
Neuhoefer Patrick, A803
Neves Adriana Turqueti, A201
Newell Evan, A57, A689
Newman Matthew, A764
Newsom Alysha, A452
Newton Katy, A205, A572
Neyton Stéphanie, A245
Nezi Luigi, A696
Ng Dean, A740
Ng Eric, A522
Ng Felicia, A46
Ng Kenneth, A341
Ng Sarah, A887
Ng Stanley, A832
Nghiem Paul, A322, A658
Nguyen Aiden, A964
Nguyen Cindy, A787
Nguyen Cokey, A145
Nguyen Hanh, A736
Nguyen Huong, A55
Nguyen Kim, A344
Nguyen Linh, A218
Nguyen Michelle, A226
Nguyen Ngan, A548
Nguyen Phuong, A919, A928
Nguyen Quynh-Nhu, A604
Nguyen Quynhanh, A688
Nguyen Teresa, A640
Nguyen Thuy, A118
Nguyen Tuan, A67
Nguyen Vy, A87
Nguyen Y-Van, A968
Ni Irene, A746
Nichols Garrett, A547
Nichols Helen, A666
Nichols Kerri, A960
Nichols Paige, A452
Nicholson Benjamin, A748
Nicola Massimo Di, A550
Nicolai Christopher, A614
Nicolazzi Céline, A893
Nido Elizabeth del, A663
Nie Chenpan, A348
Nie Hui, A960
Niedziejko Paulina, A786
Nielsen John Rømer, A429
Nielsen Maria Juul, A187
Nielsen Tyler, A5, A495
Nielson Nels, A243
- Niemiec Iga, A866
Nieto Jordan, A60
Nieves Wildaliz, A1007
Nieves-Rosado Hector, A720
Niewola Karolina, A967
Nijenhuis Cynthia, A212
Nikitin Benjamin, A103
Nikulina Nadya, A56
Nilsson Anneli, A595, A831
Nilsson Monique, A960
Nimmerjahn Falk, A597
Nimrod Guy, A732
Ning Jianfang, A180
Nirschl Christopher, A744, A747, A752
Nishie Toshikazu, A71
Nishimoto Kevin, A128
Nishino Mizuki, A74
Nissola Leonardo, A847
Nisthal Alex, A913
Nistor Gabriel, A357, A358, A359, A361, A362, A1001
Nitsch William, A91
Nitya-Nootan Thanyashanthi, A127
Niu Jiaxin, A538, A999
Niu Xiaofeng, A295
Nogami Wataru, A914
Nolan Garry, A192
Nolin Jess, A819, A903
Norman Patrick, A30, A33
Norman Teleen, A549
Normanno Nicola, A27, A332, A980
Normington Karl, A35
North Khrystyna, A613, A980
Northcott Josette, A21, A22
Northcutt Adam, A47
Nouraein Shirin, A225
Novello Silvia, A492
Novicoff Wendy, A840
Novik Amit, A272
Novobrantseva Tatiana, A919, A928
Nowak Jonathan, A1010
Nowakowska Dominika, A919
Nowogrodzki Marcin, A786
Nunns Harry, A58
Nuti Shanthi, A7
Nyesiga Barnabas, A785
- O'Brien Kelly, A240
O'Brien Sarah, A946
O'Brien Shane, A654
O'Connell Kyle, A637
O'Connor Alissa, A306
O'Day Steven, A509
O'Donnell Timothy, A90
O'Donnell-Tormey Jill, A370
O'Dwyer Michael, A987
O'Farrell Aoife, A631
O'Hara Mark, A370
O'Hayer Kevin, A559
O'Keefe Bridget, A417
O'Malley David, A523
O'Neil Jennifer, A549
O'Neill Grainne, A371
O'Nuallain Brian, A919
O'Rear Jessica, A908
O'Reilly Eileen, A370
O'Rourke Jason, A126
O'Shaughnessy Joyce, A365
O'Shea Anne, A571
O'Donnell Rebekah, A748

- O'Hagan Ronan, A748
O'Neil Jennifer, A748
O'Neill Thomas, A833
O'Toole Caitlin, A748
Oaknin Ana, A398
Obejero-Paz Carlos, A810
Obenaus Matthias, A104, A239, A531
Oberholzer Jose, A225
Oberoi Honey, A502
Oberoi Honey Kumar, A503
Obiedat Akram, A275
Obradovic Aleksandar, A947, A951
Obrocea Mihail, A725
Ocando Alonso Villasmil, A176
Occhipinti Mario, A16
Ochsenreither Sebastian, A502
Ochyl Lukasz, A913
Ock Chan-Young, A82, A861, A869, A966
Odegard Valerie, A426
Odeh Osaruese, A787
Odgerel Zagaa, A862
Odier Luc, A489
Oduro Jennifer, A104
Oehm Petra, A579
Oelke Mathias, A106, A213
Oesterreich Steffi, A708
Officer Adam, A982
Ofoedu Jennifer, A602
Ofran Yanay, A732
Ogasawara Ken, A477
Ogonek Justyna, A201
Ogorek Mateusz, A786
Oh Bitna, A82, A861
Oh Do-Youn, A440
Oh Sang Cheul, A440
Oh Sangmi, A721
Oh Yeonjoo, A211
Oh Youjin, A254
Ohkura Naganari, A914, A934
Ohri Rachit, A221
Ohtani Yumi, A148, A152
Okamoto Sachiko, A71, A113
Oke Amogh, A145
Oke Tobi, A920
Olagunju Damilola, A111
Olah Marta, A100
Old Matthew, A715
Oldridge Derek, A335
Oliva Jacqueline Lizabeth, A105
Oliva Marc, A502
Olivares Emarco, A240
Olive Daniel, A535, A558, A898
Olive Marion, A48, A65
Oliveira Giacomo, A353, A684
Oliwa Madisson, A644
Oliyarasi M, A40
Øllegaard Trine, A32
Olmedo Maria Eugenia, A493
Olmo Brook, A190
Olofsson-Sahl Peter, A927
Ols Michelle, A176
Olson Brian, A20
Olson Eric, A846, A852
Olson Walter, A421
Olsson-Brown Anna, A538, A539
Olszanski Anthony, A505, A533, A543, A566, A999
Omokoko Tana, A579
Oneto Jose Mejia, A395, A723
Önfelt Björn, A938
Ongkeko Martin, A1002
Onimus Kenneth, A110, A188
Onkar Sayali, A682
Ooi Chiahuey, A557
Oosting Sjoukje, A463, A469
Opalenik Susan, A842
Opheim Zach, A615
Ophir Eran, A272
Oppelt Peter, A385, A453
Opyrchal Mateusz, A363
Orcurto Angela, A486
Orentas Rimas, A171
Orlandella Rachael, A926
Orloff Marlana, A576
Orlowski Robert, A381
Ornstein Moshe, A318, A454
ORourke Jason, A129
Orpilla Nicole, A97
Orr Kristin, A547
Ortega Fernando, A865
Ortiz-Otero Nerymar, A66
Orwar Owe, A882
Osorio Nahum Puebla, A407
Ossendorp Ferry, A805
Osta Erica, A321
Ostertag Eric, A132, A155
Ostrowski Adam, A556
Osunkoya Adeboye, A975
Oswald Eva, A150, A585
Othman Ahmed, A413
Ott Patrick, A542, A684
Ottensmeier Christian, A467, A957
Otto Raik, A34
Ou Kevin, A238
Ouspenskaia Tamara, A234
Outters Pernelle, A489
Ouyang Yong (Stella), A209
Ovechkina Yulia, A921
Overacre-Delgoffe Abigail, A880
Overman Michael, A441, A663
Oweida Ayman, A627
Owen Dwight, A257, A706
Owonikoko Taofeek, A542
Oyasu Miho, A740
Oyer Jon, A768
Ozay Emrah Ilker, A166, A224
Ozsoy Melih, A758
Paauwe Madelon, A904
Pabla Sarabjot, A78, A86, A89
Pacheco Jennifer, A838
Pachhal Sagarika, A619, A620
Pachynski Russell, A453
Paci Angelo, A382
Packiam Vignesh, A1005
Packiasamy Juliet, A52
Packiriswamy Nandakumar, A452
Padalia Zinkal, A143
Padel Thomas, A392
Padilla Oscar, A100
Padrón Álvaro, A261
Padron Alvaro, A249, A789, A944
Paeng Kyunghyun, A861, A869, A966
Paes Wayne, A583
Page David, A103, A430, A431
Pagenkopf Adam, A982
Pahalyants Vartan, A841, A850
Pahl Jens, A922, A938
Pai Sara, A468
Paidhungat Madan, A735
Paik Sang-Min, A138
Paillon Noémie, A142
Pal Sumanta, A376, A544
Palcza John, A485
Palena Claudia, A599, A739, A757
Palermo Miguel, A125
Pales Peter, A72
Palka Kevin, A385
Palmer Rachael, A900
Palomares Karina, A126
Palombella Vito, A267, A702
Palomero Jara, A69, A958
Palová Lenka, A541
Palti Yoram, A756
Pan Hongming, A400
Pan Ke, A584
Pan Quintin, A868
Pan Yijia, A126, A129, A147
Pan Yunfeng, A986
Pan Zheng, A858
Panageas Katherine, A108
Panch Sandhya, A1002
Pande Anuja, A648
Pandey Prashant Kumar, A915
Pandit Rajay, A12, A751
Pandite Lini, A3, A459, A526
Pang Tuling, A939
Pang Xinghua, A288, A313, A783
Pangre Priyanka, A889
Paniagua Melisa Angela, A199
Panisello Carla, A69
Pant Shubham, A397, A439, A553
Pantya Katalin, A72
Papa Sophie, A486
Papadas Athanasios, A982
Papadopoulos John, A259
Papadopoulos Kyriakos, A507, A508, A519
Papai Zsuzsanna, A451
Pápai Zsuzsanna, A997
Papanicolau-Sengos Antonios, A450
Papastoitis Gregory, A750
Papp Eniko, A477
Pappalardo Angela, A782
Pappas Danielle, A746
Parakh Sagun, A484
Parasuraman Sudha, A907
Pardoll Andrew, A310, A317, A353, A679, A693, A872
Pardoll Drew, A877
Paria Biman, A177
Parikh Anup, A202
Parikh Neilesh, A177, A680
Paris Sebastien, A604, A771
Park Areum, A146
Park Changhee, A869
Park Gahee, A861, A869
Park Heedong, A146
Park Hyejoo, A82, A861
Park Hyo-Hyun, A811
Park Hyung Soon, A499
Park Hyunsil, A632
Park Jong Chul, A469, A542
Park Joseph, A807
Park Kyong Hwa, A901
Park Minjeong, A146
Park Miso, A133
Park Robin, A372
Park Seonwook, A869
Park Soo, A712
Park Terrence, A746
Park Yeon Hee, A364

- Park Young Suk, A82, A861
 Parkhurst Maria, A202, A680
 Parnell Erinn, A2, A58
 Parpaleix Aurelien, A409
 Parra Edwin, A53, A410, A971, A984, A993, A1013
 Parrinello Nunziatina, A925
 Pascarella Stephanie, A569
 Pastor Danielle, A516
 Pastor Fernando, A307
 Pastore Desa Rae, A279
 Pataer Apar, A1013
 Patel Arpita, A615
 Patel Bhavika, A983
 Patel Chirag, A679
 Patel Ekta, A549, A748
 Patel Hinal, A205
 Patel Hiral, A852
 Patel Jeegar, A543, A681, A832
 Patel Manish, A397, A462, A501, A510, A537, A569, A907, A1007
 Patel Manishkumar, A651
 Patel Minesh, A368
 Patel Monaliben, A868
 Patel Nashita, A943
 Patel Ravi, A628
 Patel Roma, A423
 Patel Sandip, A484, A522, A554, A562
 Patel Shil, A601, A796
 Patel Shreenal, A205
 Pathan Nuzhat, A371
 Patiño-García Ana, A776
 Patil Deepak, A132
 Patil Pradnya, A44
 Patnaik Amita, A507, A508, A529, A544, A1007
 Pato Aviad, A172, A230
 Patole Raju, A889
 Patrick Lenehan, A1010
 Pattali Rithu, A203
 Patterson Colleen, A833
 Patterson Erin, A862
 Patterson Troy, A214
 Patton Thomas, A44
 Paulos Chrystal, A9, A207, A237, A737, A948
 Paulus Astrid, A494
 Pautier Patricia, A382, A1006
 Pavisic Jovana, A100
 Pavlakis Nick, A366, A367, A484
 Pavlov Dmitri, A484
 Pavuluri Bhavana, A9
 Pawar Vivek, A660
 Paz Anastasia, A823
 Paz Keren, A275
 Paz Rom, A756
 Paz Suzanne, A727
 Paz-Ares Luis, A486, A491, A493
 Peach Matthew, A37, A408, A621
 Pearson Cecelia, A819
 Pecker Iris, A825
 Peckham David, A921
 Peddi Parvin, A430
 Pedersen Ayako Wakatsuki, A813
 Pedersen Gitte, A87
 Pedersen Jesper, A32
 Pedersen Katrina, A441
 Pedersen Morten, A87
 Pederzoli-Ribeil Magali, A748
 Pedro Kyle, A176
 Pegliasco Hervé, A489
 Peguero Julio, A386, A470
 Peiser Leanne, A117, A477
 Pejovic Tanja, A380
 Peled Amnon, A172, A825
 Pelka Karin, A670, A965
 Pelletier Sandy, A325
 Peltz Lindsay, A68
 Pencheva Nora, A546, A874, A961
 Peng Fuduan, A971
 Peng Kah Whye, A452
 Peng Kah-Whye, A537
 Peng Li, A884
 Peng Qian, A458
 Peng Shaogang, A217, A939
 Peng Stanford, A39, A529
 Peng Weiyi, A225, A584, A654
 Peng Zeyu, A833
 Pengam Sabrina, A245
 Pennell Nathan, A44
 Pennella Eduardo, A454
 Pentsova Elena, A429
 Peoples George, A571
 Pepi Ryan, A219
 Perales-Puchalt Alfredo, A481, A812
 Peralta Eigen, A147
 Peralta Ronal, A697
 Perdomo-Ortiz Carolina, A531
 Pereira Daniel, A282
 Pereira Sergio, A869
 Perera Jason, A76, A81, A522
 Perets Ruth, A569
 Perez Cesar, A462
 Perez Diego de Miguel, A25
 Perez Edith, A819
 Pérez José Trigo, A502, A546
 Perez-Villaruel Patricio, A191, A795
 Perini Rodolfo, A446, A447
 Perk Timothy, A52
 Perlewitz Kelly, A430
 Pernarrieta Elise, A287
 Perol Maurice, A489
 Perreault Claude, A201
 Perrin Florence, A690
 Perrone Federica, A1
 Perrot Ivan, A892
 Peter Jack St, A775
 Peters Joann, A481, A812
 Peters Solange, A492
 Peterson Blake, A714
 Peterson Bret, A894
 Peterson Christine, A25
 Petroni Gina, A1010
 Petroni Giulia, A309, A763
 Pettaway Curtis, A379
 Peyruchaud Olivier, A967
 Peyton Michael, A632, A964
 Pfaff Kathleen, A74
 Pfeffer Katie, A778
 Pfeiffer Shannon, A370
 Phadnis Milind, A372
 Pham Helene, A511
 Phani Veeranki S, A658
 Phelps Mitch, A706
 Phennicie Ryan, A919, A928
 Philbert IP, A127
 Philip Anite, A19
 Phillips Craig, A291
 Phillips Maggie, A948
 Phung Shee Kwan, A667
 Piatek Agnieszka, A786
 Picard Lea, A221
 Piccione David, A361
 Piccioni David, A357, A358, A359, A362, A1001
 Picton Lora, A614
 Pierkowski Victor Murcia, A866
 Pienta Kenneth, A468, A749
 Pieper Alexander, A628
 Pierini Stefano, A148
 Pierre Vadryn, A561
 Pignatelli Jeanine, A946, A985
 Piha-Paul Sarina, A426, A532, A559
 Pikiel Joanna, A398
 Pilanc-Kudlek Paulina, A645
 Pillai Manon, A189
 Pillarisetty Venu, A689
 Pilon-Thomas Shari, A190, A191, A206, A418, A419, A795
 Pinato David, A257, A545, A559
 Ping Jin, A1002
 Pinheiro Elaine, A303
 Pinsker Marina, A605
 Pinto Peter, A450
 Pinto Sheena, A922, A923, A938
 Piovesan Dana, A280
 Pipp Frederic Christian, A792
 Pirasteh Ali, A318
 Pires Michelle, A149
 Pirzkall Andrea, A538, A539, A580
 Pisano William, A427
 Pitzka Christina, A8
 Piulats Josep, A374, A378, A568
 Piulats Josep Maria, A69, A958
 Pizzutilo Pamela, A257
 Placa Chris La, A68
 Planchard David, A308, A409, A492
 Plebanek Michael, A343, A685, A968
 Plesa Gabriela, A461
 Plimack Elizabeth, A447
 Ploeg Manon van der, A701
 Plowman Gregory, A924
 Plummer Ruth, A398, A545, A572
 Poczka Aleksandra, A799
 Poda Zohar, A823
 Podkowa Adrian, A786
 Poehlein Christian, A374, A378, A448, A449, A455
 Poell Jos, A981
 Pogacnik Javier Salgado, A442
 Poh Yeh-Chuin, A165
 Poholek Amanda, A673
 Poirier Nicolas, A245, A394, A829
 Poitevin Yves, A287
 Poitras Michael, A277
 Poklepovic Andrew, A580
 Pokras Shibani, A943
 Polak Lenka, A920
 Polasek Melissa, A547
 Polaske Nathan, A103
 Poleszak Katarzyna, A645
 Politi Katerina, A982
 Pollack Joshua, A900
 Pollan Sara, A58
 Pollard Jack, A308
 Polonskaya Zhanna, A681, A832
 Polovina Anya, A751
 Polusani Srikanth, A261
 Polyak Dina, A226
 Pommeret Fanny, A382
 Pommey Sandra, A267
 Pomponio Rob, A550
 Ponath Paul, A306
 Ponce Alberto, A890
 Ponce Francisco, A68

- Ponce Jordi, A69
 Pong Erik, A913
 Pongtornpipat Praechompoo, A738
 Pons Jaume, A463, A469, A530, A815
 Pontini Guillemette, A287
 Poole Aleksandra, A359
 Poole Andrew, A924
 Poon Edmund, A602
 Poot Stefanie De, A904
 Popel Aleksander, A863
 Popis Martyna, A144
 Porta Camillo, A376
 Posch Alex, A68
 Posner Marshall, A462, A547
 Post Leonard, A297
 Potdar Varada, A889
 Poteete Alissa, A960
 Pothuri Bhavana, A398
 Potluri Hemanth, A624
 Potts Jessica, A946
 Pousa Antonio López, A386
 Powdery John, A548, A549
 Powell Daniel, A461
 Powell Eric, A61
 Powell Mark, A368
 Powell Steven, A537
 Powers Amy, A122, A708
 Powers Janine, A107
 Powles Thomas, A447
 Poy Florence, A800
 Prabha Amritha, A40
 Pradhan Monika, A1013
 Prakash BV, A40
 Prasad Rishika, A622
 Prelaj Arsel, A16
 Prendergast Jillian, A35
 Prenen Hans, A559
 Presler Marc, A241, A821
 Presley Carolyn, A257, A304
 Presta Leonard, A306
 Preussner Liane, A1008
 Prey Sorilla, A1011
 Pribadi Mochtar, A126, A129, A147
 Price Colles, A965
 Price Jessica, A504, A515
 Priceman Saul, A135, A238
 Prickett Todd, A177
 Prieto Peter, A311, A618, A705
 Primack Benjamin, A176
 Princiotta Michael, A337
 Prinzi Natalie, A574
 Probst Peter, A284, A294, A299
 Prochazkova Michaela, A153
 Prokhnivska Nataliya, A669, A686, A975
 Proscurshim Igor, A505
 Proto Claudia, A16
 Protopopova Marina, A820
 Provencher Diane, A380
 Pruthi Raj, A547
 Psyri Amanda, A523
 Ptacek Jason, A59
 Pu Yu, A490
 Puc Janusz, A130
 Pucilowska Joanna, A103
 Puebla-Osorio Nahum, A604
 Pulini Jennifer, A574
 Punnonen Juha, A18, A804
 Purbhoo Marco, A432
 Pure Ellen, A946
 Puri Kamal, A294, A299
 Puri Sonam, A554
 Puro Robyn, A282
 Purr Sabrina, A922
 Putney Ryan, A952
 Puzanov Igor, A363, A417, A542, A543, A729
 Pyke Rachel, A21, A22, A88
 Qayyum Aliya, A49
 Qi Jing, A726, A822
 Qi Jingjing, A651
 Qi Yilin, A905
 Qian Chengyuan, A490
 Qian Hong, A479
 Qian Yu, A960, A971
 Qiao Qi, A625
 Qin Guozhong, A639
 Qin Haiyan, A599, A739, A757
 Qin Haiying, A220
 Qin Jim, A117
 Qin Juan, A842
 Qin Shuyang, A311, A618, A705
 Qin Tianxin, A466
 Qiu Huawei, A748
 Qiu Jing, A155
 Qiu Yangsheng, A295, A827
 Qu Song, A466
 Qu Tailong, A288
 Qu Yujie, A303
 Qu Yun, A121
 Quayle Steve, A468, A749, A828
 Quemeneur Eric, A777
 Quezada Sergio, A205, A572
 Quibell Martin, A583
 Quinkhardt Juliane, A579
 Quintero Marisol, A1011
 Quintini Gianluca, A502
 Quiroga Dionisia, A715
 Quoix Elisabeth, A394
 Quong Andrew, A60
 Qureshi Rehman, A1000
 Qutaish Mohammed, A973
 Rabadan Raul, A100
 Rabeau Audrey, A409
 Rabinovich Brain, A792
 Rabinowitz Joshua, A230
 Radford Maluki, A257
 Radonic Teodora, A700
 Radulescu Camelia, A945
 Radzimierski Adam, A786
 Rae Christopher, A894
 Rafail Stavros, A407
 Rafie Salomeh, A308
 Rafiei Anahita, A906
 Rahbar Mohammad, A844
 Rahm Osama, A370
 Rahma Osama, A402, A1010
 Rahma Osama E, A853
 Rahman Justin, A727
 Rahman Nafees, A159
 Raimondo Francesco Di, A925
 Raitman Irene, A169
 Rajakumaraswamy Nishanathan, A888
 Rajakumaraswamy Nishanthan, A413
 Rajamanickam Venkatesh, A103
 Rajan Arun, A570
 Rajapakshe Kimal, A248, A793
 Rajapurkar Satyajit, A654
 Rajashekar M, A40
 Rakhmievich Alexander, A50, A628, A629
 Ram Sripad, A61
 Ramaiya Nikhil, A257
 Ramalingam Suresh, A546
 Ramchurren Nirasha, A322
 Ramelot Nancy, A118, A154
 Ramelyte Egle, A536
 Ramirez Megan, A818
 Ramkumar Kavya, A944
 Ramlau Rodryg, A492
 Ramos Carlos, A105
 Ramos Hilario, A830, A831
 Ramos Ilyssa, A148
 Ramos-Hernandez Natalia, A482
 Ramoth Hanna, A900
 Ramouz-Charpentier Raana, A48, A65
 Rampal Raajit, A807
 Ramsingh Giri, A554
 Ramsland Aubrianna, A319
 Rana Hemlata, A169
 Ranade Koustubh, A600, A909
 Randolph Hecht J, A522
 Randolph Sophia, A463, A469, A530
 Randolph William, A569
 Ranganathan Sulabha, A1006
 Rangwala Fatima, A3, A459, A526
 Rangwala Reshma, A454
 Ranti Daniel, A651
 Rao Rachita, A40
 Rao Shruthi, A915
 Raoult Thibault, A300
 Rasco Drew, A501, A507, A508
 Rashid Asif, A49
 Rashid Rumana, A726, A736, A822, A913
 Rasmussen Kayla, A629
 Rasmussen Luke, A838
 Rathmell Jeffrey, A951
 Rathmell W, A951
 Rau Mary, A191
 Rauch Kaitlyn, A727
 Raulet David, A614
 Raulf Nina, A545
 Rausch Matthew, A267
 Raval Neel, A850
 Ravetch Jeffrey, A528
 Ravichandar Jayamary Divya, A598
 Ravindranathan Sruthi, A672, A779
 Ravn Ulla, A287
 Rawi Ahmed Al, A410
 Ray Adrian, A625
 Ray Maryannick Le, A489
 Ray Satyajit, A177
 Rayannavar Vinayak, A768
 Rayford Austin, A632
 Raymon Heather, A138
 Raynor Jackson, A687
 Raza Afsheen, A19, A767
 Razak Albiruni, A566
 Razmara Aryana, A675
 Read Scott, A552
 Ready Neal, A665, A954
 Reagan Patrick, A569
 Real Ronaldo de, A338, A651
 Reardon David, A247, A277, A427
 Reck Martin, A391
 Reckner Monica, A452, A537
 Recondo Gonzalo, A74
 Reddy Bobby, A739
 Reddy Opal, A1002
 Reddy Ram Bhupal, A915
 Reddy Vijay, A279

- Reddy Vijayapal, A902
 Redman Jason, A513, A612
 Redmond David, A108, A807
 Redmond Keara, A987
 Redmond William, A103, A430, A431, A626
 Reebye Vikash, A545
 Reed Daniel, A840
 Rees Mark, A60
 Reeves Jason, A980
 Reeves Melissa, A341
 Reger Robert, A181
 Regev Aviv, A234, A670
 Rehani Peter, A50
 Rehn Matilda, A777
 Reid Jack, A204
 Reid Kayla, A115, A703
 Reid Pankti, A854
 Reijmers Rogier, A119
 Reilley Matthew, A553
 Reimers Melissa, A453
 Reinfeld Bradley, A951
 Reinhardt Carsten, A1009
 Reiss Kim, A1000
 Reiss Neria, A823
 Reiter Lukas, A99, A370
 Rejeski Jared, A852
 Rekdal Oystein, A589
 Remaily Bryan, A706
 Remeniuk Bethany, A58, A969
 Remkes Naomi, A981
 Remy-Ziller Christelle, A777
 Ren Ning, A642
 Ren Yijing, A936
 Ren Zhenggang, A389
 Ren Zhenhua, A835
 Renart-Depontieu Florence, A953
 Renganayaki Pandurengan, A962, A984
 Rengstl Benjamin, A1008
 Renken Stephanie, A451, A579
 Renner Christoph, A906
 Rennert Paul, A170
 Renouf Daniel, A402
 Repáraz David, A653
 Repash Elizabeth, A824, A931
 Represa Agnès, A892
 Rescigno Maria, A876
 Resseguier Noémie, A489
 Reszka-Blanco Natalia, A625
 Rettig Michael, A428
 Retz Margitta, A374
 Reuben Alexandre, A53, A186, A788, A960, A971, A1013
 Reuda Antonio, A523
 Reusch Uwe, A922
 Reuss Joshua, A253
 Reyes Amalia Rivera, A207
 Reyes Christopher, A183
 Reyes Ryan, A249, A261
 Reyes-Uribe Patricia, A114
 Reyno Leonard, A900
 Reynolds Kerry, A841, A850
 Rezvan Ali, A199
 Rezvaya Alexandra, A824
 Rhee Paul, A440
 Rheindorf Daniela, A8
 Rhodes Terence, A538
 Rhunke Leo, A535
 Ribas Antoni, A999
 Ribeiro Jennifer, A36, A758
 Ribrag Vincent, A503
 Ricca Jacob, A108
 Ricciardi Toni, A363
 Ricciuti Biagio, A74, A257, A336
 Rice David, A105
 Rice Meghan, A652
 Rice Rachel, A35
 Rich Jeani, A418
 Richard Françoise, A287
 Richard Guilhem, A337
 Richards Allison, A418
 Richards Jon, A415
 Richardson Debra, A459
 Richardson Vanitra, A132
 Richer Jennifer, A933
 Richly Heike, A536
 Richter Anne, A8
 Richter Emilia, A561
 Richter Maximilian, A132, A155
 Richtig Erika, A502
 Rickli Sarah, A826
 Ricordel Charles, A491
 Riddell Stanley, A689
 Riemer Pamela, A34
 Riese Richard, A532
 Rifman Julia, A172, A230
 Rightmyer Steven, A30, A33
 Rigopoulos Angela, A349
 Riley Marianne, A942
 Rimm David, A59, A258
 Rinaldi Stephanie, A787
 Rini Brian, A376, A447, A663, A760, A951
 Rini Francesca, A1
 Rinsurongkawong Vadeerat, A304
 Rinsurongkawong Waree, A304
 Rios Joshua, A613
 Rios Peter, A225
 Rios-Doria Jonathan, A247
 Rioth Matthew, A568
 Ripp Jacob, A372
 Rischin Danny, A577
 Rittenhouse Natalie, A673
 Ritter Gerd, A596
 Ritter Jessica, A919, A928
 Ritter Thomas, A987
 Rivadeneira Dayana, A109, A691, A698, A774
 RIVERA Guillermo Rangel, A9, A207, A237, A737
 Rivest Brianna, A910
 Rivoltini Licia, A1, A331
 Rizzuto Gabrielle, A108
 Robbins Paul, A177, A202, A573, A680
 Robbrecht Debbie, A550
 Robert Caroline, A300, A1011
 Robert Coleman J, A778
 Roberts Zachary, A573
 Roberts Zachary J, A189
 Roberts-Thomson Emily, A519
 Roberts-Thomson Rachel, A417
 Robinet Gilles, A394
 Robinson Brian, A779
 Robinson Gain, A303
 Robinson Joe, A205
 Robinson Jonathan, A199
 Robles-Carrillo Liza, A716
 Robson Mark, A528
 Rocha Sony, A908
 Rochestie Sarah, A481, A812
 Rochlin Kate, A168
 Rockow-Magnone Shayna, A476
 Rocnik Jennifer, A800
 Rodón Jordi, A505
 Rodas Iván Márquez, A1011
 Roder Heinrich, A30, A33, A870
 Roder Joanna, A30, A33, A870
 Roderburg Christoph, A34
 Rodig Scott, A74, A402, A427, A684, A728
 Rodon Jordi, A371, A498
 Rodríguez-Abreu Delvys, A422
 Rodríguez-Moreno Juan, A1011
 Rodríguez-Ruiz María, A536
 Rodríguez-Vida Alejo, A550
 Rodríguez Cristina, A468
 Rodríguez DiBlasi Varenka, A946
 Rodríguez Moreno Juan Francisco, A486
 Rodríguez Nicole, A736
 Rodríguez Saxon, A971
 Rodríguez-Abreu Delvys, A391
 Rodríguez-Lopez Karla, A447
 Roe Caroline, A45
 Roelands Jessica, A701
 Roelli Patrick, A91
 Roemeling Reinhard von, A349
 Roey Erik Van, A78, A86, A89
 Rogacki Maciej, A799
 Rogers Amber, A205
 Rogers Bruce, A625
 Rogers Cody, A944
 Rogers Paul, A126, A180, A208
 Rognoni Lorenz, A46
 Roguev Assen, A125
 Rohaan Maarje, A212
 Rohrberg Kristoffer, A525
 Rojas Frank, A984, A1013
 Rojas Luis, A862
 Rojo Bianca, A890, A929
 Roland Christina, A410
 Rolfo Christian, A25, A494
 Rolig Annah, A626
 Rollins Meagan, A687
 Roman Kristin, A58, A969
 Romano Alessandra, A925
 Romano Emanuela, A374
 Romeo Margarita, A381
 Romero Pedro, A338
 Romine Kyle, A764
 Ronczka Amy, A1000
 Rooney Kathryn, A928
 Root Charlotte, A625
 Roozen Inge, A383
 Rösemann Roman, A555
 Rosén Anna, A785
 Rose Daniel, A626
 Rose Peter, A523
 Roselli Emiliano, A115
 Rosen David, A18, A804
 Rosen Lee, A368, A543
 Rosen Neal, A634
 Rosenberg Ari, A1007
 Rosenberg Marisa, A407
 Rosenberg Steven, A177, A195, A202, A680, A958
 Rosenthal Katherine, A509
 Rosete Rodnie, A740
 Ross Camidge D, A484
 Ross Douglas, A5, A495
 Ross John, A749, A828
 Ross Miranda, A543
 Ross Theresa, A176
 Ross-Macdonald Petra, A872
 Rossetti Renata, A206
 Rossi Benjamin, A892, A893
 Rossi Jacopo de, A136

- Rossi John, A218, A545
 Rossi Moira Pinzan, A144
 Roth Iris, A690
 Roth Jack, A186
 Rotondi Marco, A151
 Rotondo Salvatore, A169
 Rottey Sylvie, A371, A531
 Rouanne Mathieu, A945
 Rouleau Etienne, A308
 Roumieux Marie, A489
 Rouseva Valentina, A169
 Rovis Tihana Lenac, A275
 Rowe Julie, A844
 Rowell Emily, A897
 Rowinsky Eric, A498
 Roxburgh Patricia, A386
 Roy Ananya, A446
 Roy Aude Le, A898
 Roy Severine, A300
 Roy Sohini, A678, A947
 Roy Vivek, A475
 Rozelle Dan, A2
 Rozenblatt-Rosen Orit, A670
 Rubas Werner, A626
 Rubinstein Mark, A207
 Rubinsteyn Alexander, A360
 Rudnick Jenny, A729
 Rudolph Joshua, A900
 Rudqvist Nils-Petter, A622
 Ruf Benjamin, A721
 Ruffner Katherine, A463, A469
 Ruggieri Amanda, A20, A434
 Rui Eugene, A768
 Rui Lingyun, A899
 Ruiz-Juarez Bryan, A145
 Rupar Mark, A247
 Ruskin Susan, A590
 Russell Greg, A846
 Russell Gregory, A852
 Russell Luke, A537
 Russell Stephen, A537
 Russo Alessandro, A25
 Russo Giuseppe Lo, A16
 Rutherford Erica, A598
 Ruthinda Cleopatra, A627
 Rutkowski Piotr, A574
 Ruzich Janet, A430
 Ryan Aideen, A987
 Ryan Aileen, A363
 Ryan Declan, A11
 Rytlewski Julie, A477
 Ryu Heeju, A57
 Ryu Jeongun, A869
 Ryu Jiyeon, A82, A861
 Ryu Min Hee, A440
 Ryu Min-Hee, A550
 Rzepecka Justyna, A271
- Saad Mariam, A96
 Saba Nabil, A468
 Sabath Niv, A272
 Sabharwal Simran, A18, A804
 Sacco Assuntina, A1007
 Sacco Joseph, A538, A539, A568
 Saccomano Nicholas, A644
 Sacher Adrian, A423
 Sachse Richard, A514, A534
 Saddawi-Konefka Robert, A631
 Sade-Feldman Moshe, A684
 Sadelain Michel, A142, A862
- Saeed Anwaar, A257, A372
 Saeed Azhar, A372
 Saeedi Arash, A584
 Saenz Javier, A245
 Saetersmoen Michelle, A142
 Safa Houssein, A845
 Safe Stephen, A754, A761
 Safi Barroq, A792
 Safina Brian, A817, A819
 Saggese Matilde, A572
 Sagi Yael, A605
 Sagiv-Barfi Imit, A803
 Saha Ashis, A847
 Saha Sunandan, A176
 Sahebjam Solmaz, A559
 Sahetya Disha, A895
 Sahin Ugur, A451, A555, A579, A821, A1008
 Şahin Uğur, A525, A546
 Saho Lipei, A1002
 Sahu Avinash Das, A728
 Sai Kiran Solingapuram, A11
 Saiag Philippe, A1011
 Saini Avneesh, A740
 Saini Jagmohan, A889
 Saintigny Pierre, A962, A984
 Sakai Shunsuke, A721
 Sakellariou-Thompson Donastas, A183
 Salahudeen Ameen, A70
 Salama April, A576, A655
 Saleem Imran, A539
 Saleem Rao, A581
 Salek-Ardakani Shahram, A290
 Salinas Emily, A321
 Säll Anna, A785
 Sall Mame Thioye, A1002
 Salmeron Andres, A744, A747, A752
 Salmon Ruth, A211
 Salojin Costa, A800
 Salome Berengere, A338, A651
 Saltman David, A495
 Salvary Vanessa, A133
 Samson Adel, A538
 Sanabria Angelica, A12, A751
 Sanborn Rachel, A503
 Sanchez Katherine, A430
 Sanchez Violeta, A264, A342, A791
 Sanchez-Jauregui Paloma, A796
 Sanchez-Martin Marta, A66, A102
 Sanda Martin, A686
 Sandberg Mark, A131
 Sanders Melinda, A264, A342, A791
 Sanderson Joseph, A401
 Sandhu Shahneen, A847
 Sandigursky Sabina, A853
 Sands Arthur, A107
 Sandy Peter, A527
 Sane Abhay, A13
 Sanecka-Duin Anna, A866
 Sanford Nina, A442
 Sangalang Emma, A815
 Sangaletti Sabina, A16
 Sankaran Preethi, A312
 Sankaran Satish, A40
 Sanmamed Miguel, A536, A1011
 Sannasardo Zachary, A191
 Santamaria Carlos, A900
 Santana-Davila Rafael, A530
 Santegoets Saskia, A41
 Santillana Sergio, A425
 Santone Gabriella, A515, A551
- Santoro Armando, A550, A562
 Santoro Stephen, A226
 Santos Annemarie, A940
 Saputra Elizabeth, A926
 Saraiya Megha, A46
 Sardesai Niranjan, A481, A812
 Sarhan Dhifaf, A927
 Sarker Debashis, A545
 Sarkozy Clementine, A503
 Sarma Ganapathy, A817, A819
 Sarmiento Juan, A434, A948
 Sarnaik Amod, A206, A418, A419, A573
 Sasmal Sujit, A786
 Sasser Kate, A874, A904, A961, A973
 Sassi Monica, A572
 Sasson Yehezkel, A732
 Sastry Jagannadha, A788
 Satelli Arun, A1009
 Sater Houssein Abdul, A450
 Sathasivam Hans Prakash, A957
 Sathyanarayanan Sriram, A796
 Sathyanarayanan Sriram, A601, A883
 Sato Ai, A309
 Sato Takami, A568, A999
 Sato Yasuyoshi, A71
 Satpayev Daulet, A128
 Sauer Amy, A407
 Sauer John-Demian, A814
 Saumyaa Saumyaa, A228
 Savardekar Himanshu, A714, A715
 Savelyeva Natalia, A957
 Savi Chris De, A633
 Sawant Pooja, A889
 Sawhney Baanie, A941
 Saxena Mansi, A360, A363
 Sayehli Cyrus Michael, A536
 Sazinsky Steve, A919, A928
 Sbarrato Thomas, A489
 Scally Christopher, A410
 Scarfo Irene, A234
 Scarpato Luigi, A980
 Scarselli Elisa, A441
 Schäfer Tina, A597
 Schad Sara, A108, A807
 Schadendorf Dirk, A550
 Schaich Katharina, A150
 Schaller Kristin, A134
 Schalper Kurt, A258
 Schantz Laura Von, A785
 Scharping Nicole, A673, A688, A707
 Schatz Jonathan, A703
 Scheel Birgit, A502
 Schellenberg Samuel, A661
 Schendel Dolores, A201
 Scherer Julian, A124, A912
 Scherrer Emilie, A339, A941
 Scheuenpflug Juergen, A92
 Scheuplein Vivian, A104, A239, A531
 Schiffer-Mannioui Cecile, A151
 Schlabach Michael, A198, A215
 Schlehuber Lisa, A165
 Schlom Jeffrey, A6, A513, A570, A599, A612, A635, A739, A757
 Schloss Charles, A374, A378, A448, A449, A455
 Schlosser Andreas, A958
 Schmid Peter, A364
 Schmidt Alexander, A201
 Schmidt Emily, A401
 Schmidt Emmett, A381, A417
 Schmidt Guenter, A392

- Schmidt Mark, A103
 Schmidt Michael, A750
 Schmidt Stephanie, A1013
 Schmierer Maggie, A114
 Schmitt Andreas, A205
 Schmitt-Bormann Beate, A502
 Schnabel Catherine, A356
 Schneider Anna, A945
 Schneiders Famke, A700
 Schoenfeld Adam, A486
 Schoffski Patrick, A526
 Schottelius Arndt, A922, A923
 Schröder Carolina Pia, A997
 Schröder David, A108
 Schreiber Robert, A334, A607
 Schreiber Taylor, A3, A615
 Schroeder Martin, A473
 Schrum Jason, A895
 Schubbert Suzanne, A913
 Schubert-Wagner Christine, A536, A597
 Schuchter Lynn, A422
 Schuda Lily, A604
 Schueller Olivier, A543
 Schuetze Scott, A424
 Schuler Julia, A150, A585, A990
 Schuler Martin, A536
 Schultz Lena, A831
 Schulz Catrine, A1008
 Schulze Isabell, A108, A634
 Schumacher Nina, A885
 Schumacher Ton, A607, A746
 Schumann Christian, A492
 Schwabe Christian, A413
 Schwarck-Kokarakis Doreen, A579
 Schwartz Brian, A279
 Schwartz Cynthia, A666
 Schwartz Lawrence, A857
 Schwartz Myron, A388, A713
 Schwarz Emily, A399, A715
 Schwarzenberger Paul, A363, A488
 Schweickert Patrick, A280
 Schweickhardt Rene, A792
 Schweitzer Brock, A5, A495
 Scoazec Jean-Yves, A300, A308
 Scognamiglio Giosuè, A980
 Sclan Erwan Le, A735
 Scott Andrew, A349
 Scott Chandler G, A847
 Scott Charles, A231
 Scott Fiona, A349
 Screever Elles, A842
 Seager RJ, A78, A86, A89
 Searles Tyler, A674
 Sears Cynthia, A877
 Sebra Robert, A338, A651
 Seebach Frank, A565
 Seery Virginia, A188
 Segal Robert, A556
 Segerer Felix, A46
 Seibel Tobias, A502
 Seidel Ronald, A828
 Seidel-Dugan Cindy, A747, A752
 Seite Margaux, A829
 Seitz Rob, A5, A495
 Seiwert Tanguy, A468
 Sekhavati Farzad, A392
 Sela Itamar, A323
 Seliger Barbara, A956
 Sell Jenny, A417
 Selvaraj Balaji, A860
 Semenov Yevgeniy, A841, A850
 Semmrich Monika, A777
 Sender Lennie, A739
 Seo Jayhyun, A841, A850
 Sepesi Boris, A53, A105, A186, A1013
 Serganova Inna, A649
 Serie Daniel, A35
 Sers Christine, A34
 Sethi Dhruv, A176
 Sethna Zachary, A862
 Seto Anna, A408
 Setta Rebecca, A417
 Sette Jessica, A583
 Severgnini Mariano, A402, A427
 Sexton Steven, A203
 Sezen Duygu, A604
 Sfakianos John, A90, A338, A651
 Sfeir Nour, A48, A65
 Shafaattalab Sanam, A131
 Shaffer Donald, A636
 Shaffer Jami, A715
 Shafique Michael, A484
 Shah Amishi, A259
 Shah Heta, A889
 Shah Manish, A441
 Shah Neil, A454
 Shah Parin, A186
 Shah Payal, A461
 Shah Pritom, A967
 Shah Riddhishkumar, A655
 Shah Rivani, A969
 Shahar Michal, A605
 Shaheen Monaster, A417
 Shaheen Montaser, A422, A571, A999
 Shahor Moshe, A230
 Shaik Jahangheer, A516, A520
 Shaikh Fyza, A877
 Shainheit Mara, A515, A551
 Shaked Yuval, A323
 Shames David, A30, A33, A870
 Shamimi-Noori Susan, A461
 Shan Bo, A638, A936
 Shan Ming, A482
 Shang Limin, A287
 Shang Olive, A56
 Shankar Sadhna, A574
 Shanker Anil, A717
 Shankles Brooke, A540
 Shantzer Lindsey, A840
 Shao Lipei, A153
 Shapira-Frommer Ronnie, A556
 Shapiro Geoffrey, A544, A644
 Shapiro Irina, A432
 Sharabi Andrew, A631
 Sharei Armon, A166, A175, A224
 Sharma Bijaya, A74
 Sharma Keerti, A562
 Sharma Manish, A507, A508, A512, A544
 Sharma Nikita, A985
 Sharma Padmanee, A379
 Sharma Shruti, A131
 Sharma Sunil, A1007
 Sharon Elad, A20, A402
 Sharon Ofer, A323
 Sharp Leslie, A773, A775
 Shasha Carolyn, A689
 Shaver Laura, A127
 Shaw Pamela, A820
 Shaxted Jenna, A70
 Shay Jerry, A725
 Shea Joanne, A461
 Shearman Mark, A203
 Shedlock Devon, A132, A155
 Shek Dmitrii, A552
 Sheladia Piyush, A577
 Sheldon Brenna, A704
 Shelke Sandip, A884
 Shen Bo, A355
 Shen Gang, A355
 Shen Li, A960
 Shen Lianjun, A120
 Shen Lin, A400
 Shen Yuyi, A817, A819
 Shen Zhirong, A387, A389, A400
 Sheng Qinsong, A443
 Sheng Yeong Joe Poh, A957
 Sheng Zhen, A730
 Shenker Sol, A198, A215
 Sher Christian, A654
 Sheth Rahul, A225
 Shi Chaomei, A636
 Shi Lei, A227, A297
 Shi Leilei, A584, A654
 Shi Stephanie, A768
 Shi Tao, A986
 Shi Wen, A523
 Shi Yang, A400
 Shi Yaoyao, A240
 Shields Anthony, A441, A553
 Shields Jacqueline, A167
 Shiers Jason, A583
 Shifeng Mao, A454
 Shim Byoung Yong, A440, A499
 Shimoni Chen, A823
 Shin Dong Ho, A640
 Shin Hunwoo, A811, A901
 Shin John, A516
 Shin June, A228
 Shin Jung Hyu, A811
 Shin Sang Joon, A499
 Shin Seunghwan, A869
 Shinde Vaishali, A505
 Shiong Patrick Soon, A739
 Shirai Keisuke, A674
 Shiraishi Mamoru, A251
 Shirinbak Soheila, A126, A129
 Shirley Liu X, A728
 Shivakumar Bhadravathi Marigowda, A915
 Shlanksy-Goldberg Richard, A461
 Sholevar Cyrus, A675
 Sholl Lynette, A336
 Shore Neal, A374, A448, A449, A455, A456
 Shorr Jolene, A553
 Shoustari Alexander, A396, A568, A576
 Shpektor Diana, A477
 Shrestha Bishwas, A129
 Shrestha Niraj, A200
 Shrestha Rupesh, A761
 Shri Meena, A915
 Shroff Sanjana, A338, A651
 Shuga Joe, A91
 Shui Irene, A339
 Shukor Syukri, A515, A551
 Shum Elaine, A520, A553
 Shumilov Anatoliy, A46, A392
 Shuptrine Casey, A615
 Si Han, A961, A973
 Sia Christine, A601
 Sicheva Marisella Panduro, A267
 Siddiqi Noor, A822

- Siddiquee Zakir, A884
 Siddiqui Bilal, A379
 Sidhom John-William, A872
 Siefker-Radtke Arlene, A67, A259
 Sigal Michael, A34
 Signolle Nicolas, A945
 Signorelli Diego, A16
 Sikaroodi Shohreh, A126
 Sikorski Julian, A579
 Silk Ann, A577
 Sills William, A11
 Silva Andrea, A224
 Silva Jordan Da, A771
 Silva Saulo, A62
 Silva Suresh De, A615
 Silverman Rachel, A447
 Silvestre Nathalie, A777
 Silvio Gutkind J, A631
 Sim Janet, A815
 Simantov Ronit, A172
 Simeone Diane, A522
 Simeone Ester, A27, A332, A980
 Simmons Jessica, A818
 Simmons Julissa, A240
 Simmons Randi, A294
 Simon Aaron, A631
 Simon Ronald, A104
 Simonin Alexandre, A885
 Sims Jennifer, A731
 Sinclair Angus, A740, A953
 Singh Anuj, A889
 Singh Harpreet, A1009
 Singh Hema, A280
 Singh Jasmine, A56
 Singh Jay, A742
 Singh Latika, A303
 Singh Namrata, A853
 Singh Preeti, A271
 Singh Ranjeet, A13
 Singh Sanjay, A640
 Singh Satwinder Kaur, A232
 Singh Shalini, A379
 Singhi Eric, A304
 Singhi Naina, A689
 Singletery Will, A119
 Sinha Pragya, A788
 Sinigaglia Laura, A545
 Sinnaeve Justine, A45
 Sipe Laura, A710
 Siso Silvia, A796
 Siteni Silvia, A725
 Situ Hubert, A908
 Siu Lilian, A518, A526, A533, A566
 Sivakumar Pallavur, A211
 Sivan Ayelet, A671
 Sjöstrand Maria, A142
 Skala Melissa, A50
 Skeffington Patrick, A940
 Skłodowski Kamil, A99, A370
 Skoczylas Piotr, A866
 Skokos Dimitris, A565
 Skoulidis Ferdinands, A960, A971
 Skov Vibe, A807
 Slane Katie, A453
 Slansky Jill, A933
 Slay Ravaen, A622, A788
 Slingluff Craig, A54, A363, A421, A1010
 Sloas Chris, A152
 Slowinski Jacob, A629
 Smerdou Cristian, A772
 Smethurst Dominic, A2
 Smith Alyson, A895
 Smith Aubrey, A9, A207, A237, A737
 Smith Carolyne, A166
 Smith Ernest, A464
 Smith Jenessa, A226
 Smith Karin Enell, A567, A595
 Smith Kellie, A310, A317, A353, A693
 Smith Kelly, A421
 Smith Robina, A507, A508
 Smith Sarah, A165
 Smith Sean, A906
 Smith Victoria, A890, A929
 Smitheman Kimberly, A654
 Smothers James, A690
 Smutske Inese, A625
 Smythe Kimberly, A689
 Snead Katie, A895
 Snell Daniel, A885
 Snick Jacques Van, A596
 Snyder Alexandra, A485
 Snyder Gail, A614
 Snyder Kristin, A208
 Snyder Michael, A88
 Soares Kevin, A862
 Sobczyk Monika, A606
 Sobierajska Ewelina, A686, A975
 Sodergren Mikael, A545
 Soefje Scott, A941
 Sofjan Katri, A198, A215
 Soh Tetsuyoshi, A934
 Sohn Joohyuk, A364
 Sohoni Sagar, A640
 Soikes Raul, A349
 Sokac Mateo, A32
 Sokolovska Anna, A532
 Soliman Hatem, A542
 Solis Luisa, A632, A1013
 Soloff Adam, A122, A708
 Solomon Isaac, A427
 Somaiah Neeta, A410, A424
 Somanchi Srinivas, A138
 Somarakis Antonios, A41
 Somerville Robert, A1002
 Somma Alexander, A613
 Sommerhalder David, A501, A511
 Sommermeyer Daniel, A201
 Somogyi Eszter, A72
 Son Ka-Yeon, A996
 Son Mi kwon, A630
 Sondak Vernon, A95, A96
 Sondel Paul, A50, A67, A628, A629
 Sónego Fabiane, A782
 Song An, A327
 Song Eurim, A146
 Song Hannah, A153
 Song Haocan, A257
 Song Heon, A869
 Song Kun, A460
 Song Sanghoon, A869, A966
 Song Yong, A496
 Song Yuang, A607
 Sonke Gabe, A212
 Sonntag Donna, A221
 Soong David, A874
 Soos Timothy, A883
 Sorbo Maria Rosaria Del, A441
 Sorensen Rick, A37, A408
 Soria Ainara, A502
 Soria Jean-Charles, A409, A945
 Soriano Ferdie, A280
 Sorrentino Antonio, A332
 Sorrentino Jessica, A365
 Sosman Jeffrey, A729, A838
 Soto-Pantoja David, A293, A646, A843
 Southard Jackson, A593
 Souza Fabricio, A390
 Souza Patricia Coutinho de, A973
 Sowinska Marta, A786
 Spakowicz Daniel, A878, A988
 Spalding Duncan, A545
 Spalinskas Rapolas, A91
 Sparks Jeffrey A, A853
 Sparks Jessica, A155
 Spartz Ellen, A687
 Speltz Elizabeth, A858
 Spencer Christine, A847
 Spencer Kristen, A559, A562
 Spencer Michael, A970
 Spencer Tom, A240
 Spezzano David, A51
 Spiegelman Dan, A628
 Spiga Fabio, A885
 Spigel David, A510
 Spille Jeremy, A495
 Spina Enrico La, A925
 Spinner William, A401
 Spira Alexander, A269, A519
 Spitler Kristen, A115
 Spitzmüller Andreas, A46, A860
 Spoelstra Nicole, A933
 Spranger Stefani, A326, A344, A692, A711, A801, A963
 Spreafico Anna, A519, A542
 Squifflet Pierre, A530
 Sridhar Shaarwari, A921
 Sridhar Sriram, A46
 Srimuninnimit Vichien, A390
 Srinivasamani Anupallavi, A248, A315, A622
 Srinivasan Sangeetha, A395, A723
 Srivastava Minu, A30, A33, A870
 Sępiak Piotr, A866
 Stachura Sławomir, A866
 Stadler Walter, A659
 Stadtmauer Edward, A476
 Stafford Ryan, A327
 Stagg John, A267
 Stanfield Jessica, A290
 Stanger Ben, A946
 Stanhope Sarah, A600, A909
 Stanko Dominika, A786
 Stanley Amanda, A366, A367
 Stanton Sasha, A430
 Starobinets Hanna, A787
 Stauff Charles, A778
 Stavrou Nicholas, A867
 Stawiski Eric, A858
 Stawowczyk Marcin, A778
 Steele Miranda, A375
 Steelman Scott, A766
 Stegen Spoukje van der, A142
 Stegmeier Frank, A198, A215
 Stein Mark, A515, A553
 Steinberg Gary, A337, A1005
 Steinberg Seth, A513
 Steiner Madeline, A622
 Steiner Philipp, A744, A747, A752
 Steinke Seema Mehta, A253
 Steklov Mikhail, A154
 Stemmer Salomon, A569

- Stephen Hodi F, A95, A96, A402, A728
 Stephens Bret, A902
 Stephenson Katrina, A908
 Steuer Conor, A462
 Steuert Zoe, A744, A747, A752
 Stevens Aaron, A365
 Stevens Christina, A247
 Stevens Courtney, A877
 Stevenson Cheri, A820
 Stewart Kai, A234
 Stewart Morag, A766
 Stewig Blair, A728
 Stinchcombe Thomas, A665
 Stinson Susanna, A606
 Stirling Elizabeth, A293, A646, A843
 Stoeckius Marlon, A91
 Stoeckle Michael, A378
 Stoff Ronen, A556
 Stone Sarah, A276
 Storkus Walter, A95, A96, A797
 Stovroff Merrill, A721
 Stowman Anne, A54
 Štrajbl Marek, A732
 Strange Chad, A105
 Strauss James, A395, A408, A532, A537, A554
 Strauss Julius, A6, A513
 Streicher Howard, A95, A96, A402
 Strickland Justin, A268
 Strickler John, A426
 Strobl Stefan, A555
 Strojny Izabela, A799
 Stromhaug Kari, A684
 Stromnes Ingunn, A687
 Stroncek David, A153, A1002
 Stuckey Jacob, A800
 Stucky Chee-Chee, A1010
 Sturdivant Michael, A968
 Sturm Gregor, A41
 Su Juanjuan, A849
 Su Lihe, A170
 Su Yapeng, A590
 Suarez Lauren, A106, A213
 Suarez Magdalia Rodgers, A590
 Suarez-Almazor Maria, A853
 Subbiah Vivek, A395, A544, A554, A562
 Subramaniam Dharmalingam, A372
 Subramanian Kas, A241
 Subramanian Shyam, A176
 Subramanyam Varun, A721
 Subudhi Sumit, A379
 Suchindran Sunil, A424
 Sudol Sylwia, A786
 Sugiura Ayaka, A842
 Sugizaki Maiko, A113
 Sukari Ammar, A468, A486, A515, A523, A1007
 Sukumaran Sujita, A209
 Sullivan Jenna, A744, A747, A752
 Sullivan Kristin, A316
 Sullivan Peter, A171
 Sullivan Ryan, A200, A508, A569, A841
 Sultan Hussein, A607
 Sulur Giri, A486, A523
 Sulzmaier Florian, A12, A751, A897
 Sun Changbo, A608, A959
 Sun Dawei, A295, A827
 Sun Joanne, A939
 Sun Jun, A827
 Sun Kathryn, A401
 Sun Mengzhu, A287
 Sun Ming, A584
 Sun Steven, A714
 Sun Sunny, A766
 Sun Weijing, A372
 Sun Xiaopeng, A264, A842, A848
 Sun Yang, A704
 Sun Yi, A902
 Sun Yuan, A364
 Sun Zhaoyu, A430, A431
 Sundstedt Anette, A785, A831
 Sung Eunsil, A935
 Sung Patrick, A944
 Sunshine Joel, A235
 Sunwoo John, A22, A52, A192, A193, A228
 Suo Liye, A252
 Superville Daphne, A341
 Sura Sneha, A269
 Surace Michael, A46, A860
 Suresh Amritha, A915
 Suri Anish, A749, A828
 Suri Prerna, A212
 Suru Aditya, A609
 Susini Sandrine, A945
 Sussman Jeffrey, A571
 Sussman Kelly, A616
 Sussman Tamara, A257
 Suva Mario, A427
 Svane Inge, A813
 Sveinbjornsson Baldur, A589
 Svensson Carolin, A777
 Swanson Ryan, A592, A745, A942
 Swarbrick Martin, A786
 Swatler Julian, A645
 Sweezy David, A165
 Sweis Randy, A319, A569, A671
 Swirski Mateusz, A786
 Swisher Stephen, A1013
 Sykrova Martina, A210
 Symeonides Stefan, A555
 Szalontay Luca, A100
 Szeremeta-Spisak Joanna, A786
 Szeto Julia, A689
 Sznol Mario, A422
 Szymczak-Workman Andrea, A668
 Ta Hieu, A276, A340
 Tabachnikova Alexandra, A713
 Tabakman Rinat, A825
 Tabrizi Azita, A327
 Tabriziad Maryam, A128
 Tabuena-Frolli Siena, A68
 Tachiki Lisa, A658
 Tacke Frank, A34
 Tacner Zachary, A773, A775
 Tadjalli-Mehr Keyvan, A544
 Tae Yang Desmond Hung, A328
 Tafrova Juliana, A778
 Tafuto Salvatore, A980
 Tagliaferri Mary, A1007
 Tagore Joshua, A946
 Tai-Hsien, A94
 Taib Nassiba, A767
 Tak Paul, A427
 Takacs Istvan, A451
 Takahashi Shunji, A71
 Takahashi Tatsuya, A934
 Takahashi Toshiaki, A488
 Talbot Thomas, A545
 Talleur Aimee, A160
 Talukder Rafee, A853
 Tam Ada, A609, A877
 Tam Arvin, A147
 Tam Stanley, A176
 Tamegnon Auriole, A962, A984
 Tamir Ami, A825
 Tamir Ayala, A556
 Tamir Liat, A825
 Tamzalit Fella, A142
 Tan Adrian, A724
 Tan Aik Choon, A95, A96
 Tan Alan, A425
 Tan Antoinette, A365
 Tan Benedict, A656, A855
 Tan Cindy, A306
 Tan Daniel Weng, A371
 Tan Fangya, A355
 Tan Seng-Lai, A915
 Tan Thuan Tong, A656
 Tan Tira, A511
 Tan Tuan Zea, A945
 Tan Yan, A458
 Tan Yening, A132, A155
 Tanaka Miho, A341
 Tanaka Tiffany, A712
 Tanda Enrica Teresa, A574
 Tang Chad, A259
 Tang Hao, A420
 Tang Kimberly, A841, A850
 Tang Lily, A827
 Tang Mei, A500, A998
 Tang Szu-Yu, A768
 Tangirala Raghuram, A799
 Taniguchi Cullen, A622
 Tanne Antoine, A216
 Tannir Nizar, A67, A259
 Tannous Elie, A842
 Tanos Tamara, A557
 Tarcha Eric, A291, A921
 Tarhini Ahmad, A95, A96
 Tasker Sybil, A778
 Tatalick Laurie, A942
 Tatt Lim Jeffrey Chun, A855
 Taube Janis, A353
 Tavares Amy, A582
 Tawbi Hussein, A339
 Tay Joshua, A228
 Tayar Jean, A853
 Taylor Brandie, A342
 Taylor David, A611
 Taylor Matthew, A381
 Taylor Sarah, A80
 Taylor Thomas, A357, A358, A359, A361, A362, A1001
 Tazhibi Masih, A100
 Tchaicha Jeremy, A176
 Tchakarov Amanda, A252, A845
 Tchakov Ilian, A545
 Teer Jamie, A418, A419
 Tegtmeier Kyle, A838
 Teichgraber Volker, A976
 Teige Ingrid, A777
 Teknos Theodoros, A868
 Tenn-McClellan Austin, A107
 Tenney Daniel, A420
 Teplitz Kyla, A64
 Teppaz Geraldine, A245
 Teppaz Geraldine, A829
 Terheyden Patrick, A502
 Ternette Nicola, A583
 Terrett Jonathan, A143
 Testori Marco, A46

- Teunisse Bram, A805
 Tevetnitsky Vadim, A246
 Tewari Alok, A728
 Texier Matthieu, A409
 Texier Matthieuu, A300
 Thépénier Virginie, A245
 Thaddeus Beck J, A371
 Thagesson Mia, A785
 Thakkar Dipti, A498
 Thalhauser Craig, A821
 Thalhofer Colin, A175
 Thanarajasingam Uma, A853
 Thanos Christopher, A894
 Thaxton Jessica, A207
 Thebault Pamela, A325
 Theilhaber Joachim, A550, A636
 Theiss Noah, A94
 Theivanthiran Balamayooran, A343, A685, A968
 Thekkat Pramod, A247
 Theodosakis Nicholas, A841
 Thepenier Virginie, A829
 Thiam Kader, A782, A953
 Thibaudin Marion, A373
 Thiede Lucinda, A946
 Thierry Jean Paul, A945
 Thin Tin Htwe, A360, A651
 Thisted Thomas, A243
 Thistlethwaite Fiona, A531, A572
 Thistlethwaite Fiona C, A189
 Thomas Alexandra, A293, A646
 Thomas Gareth, A957
 Thomas Jacob, A533, A566
 Thomas Joshua, A820
 Thomas Justin, A706
 Thomas Lawrence, A833
 Thomas Martine, A189
 Thomas Matthew, A467
 Thomas Paul, A160
 Thomas Sajeve, A417, A523, A573
 Thomas Sunil, A218
 Thomas Susan, A779
 Thompson John, A553, A689
 Thompson Reid, A45
 Thorlacius-Ussing Jeppe, A23, A24
 Thorne Stephen, A774
 Thornton Dan, A176
 Thorpe Jerill, A477
 Thosar Sanjana, A698
 Thothathri Subramanian, A908
 Tian Chuan, A574, A1006
 Tian Hongyu, A327
 Tian Linjie, A516
 Tian Mengxi, A125
 Tian Yang, A587
 Tian Ziqiang, A587
 Tiberti Silvia, A696
 Tidwell Rebecca, A379
 Tien Tracy, A656
 Tighe Robert, A185, A214
 Timmer John, A12, A751, A897
 Timmerman Robert, A442
 Timofeevski Sergei, A768
 Timothy Marissa, A425
 Timothy O, A360
 Tina Cheng, A550
 Tine Brian Van, A424
 Tinker Anna, A398
 Tipping Alex, A401
 Tirrell Steve, A66
 Tirumalasetty Chaitanya, A889
 Tiu Bruce, A841, A850
 Tjon Emily, A268, A515, A551
 To Linh, A908
 Toader Dorin, A820
 Tocheva Anna, A651
 Todenhoefer Tillman, A374, A378
 Toglia Daphne, A826
 Tognetti Marco, A99, A370
 Toh Han Chong, A97
 Tokatlian Talar, A131
 Toke Eniko, A72
 Tokheim Collin, A728
 Toland Grant, A68
 Tolaney Sara, A67
 Tolcher Anthony, A408, A501, A520, A561
 Toledo-Warshaviak Dora, A131
 Tollefson Matthew, A452
 Toma Alessandro De, A16
 Tomczak Katarzyna, A105
 Tomei Sara, A111
 Tometich Justin, A880
 Tompers Dennie, A684
 Toney Nicole, A6, A612
 Tong Carmen, A583
 Tong Min, A132, A155
 Tong Zhen, A133
 Tong Zhou, A443, A445
 Tonon Laurie, A719
 Topalian Suzanne, A312, A322
 Tordesillas Leticia, A206
 Torok Molly, A706
 Torre Claudia Palomino La, A132
 Torres David, A240
 Torres Keila, A410
 Torres-Dominguez Lino, A775
 Torres-Mejia Elen, A326, A344, A692, A963
 Torretti Elisabeth, A897
 Torrez Dulgeroff Laughing Bear, A819
 Toschi Luca, A483
 Toth Jozsef, A72
 Toufiq Mohammed, A111
 Toullec Damien, A938
 Toumou Raymond, A998
 Townsend Madeline, A644
 Tozzo Effie, A766
 Tracy Sean, A345
 Trager James, A123, A137, A159
 Traina Tiffany, A431
 Trajanoski Zlatko, A41
 Tran Michelle, A90, A651
 Tran Quan, A228
 Tran Steven, A838
 Traugh Nicole, A728
 Treacy Daniel, A766
 Treacy Oliver, A987
 Tremblay Jack, A176
 Treuner Kai, A356
 Treuting Piper, A895
 Tribble Sara, A894
 Triebel Frederic, A386, A470, A997
 Triggs Daniel, A427
 Trigo Perez Jose Manuel, A398
 Trillò Giusy, A27
 Trillo-Tinoco Jimena, A316, A420
 Trinh Alex, A48, A65
 Trinh VanAnh, A853
 Triozzi Pierre, A293, A646, A843
 Tripathi Abhishek, A729
 Triplett Aleata, A683
 Triplett Todd, A613
 Trkulja Carolina, A882
 Troast Dawn, A625
 Trojaniello Claudia, A27, A332, A980
 Trojer Patrick, A800
 Trombetta Sergio, A286
 Troncoso Leanna, A713
 Trowe Torsten, A413
 Troy Jesse, A665
 Trueblood Esther, A895
 Trujillo Jonathan, A347
 Trumpfheller Christine, A224
 Truntzer Caroline, A373
 Tsai I-Fang, A285
 Tsai Katy, A417, A538, A580
 Tsai Pei-Fang, A126
 Tsai Randy, A712
 Tsai Yo-Ting, A6, A612
 Tsang John, A570
 Tsang Kwong, A881, A925
 Tsao Anne, A105, A664
 Tsao Li-Chung, A647
 Tsao Tsu-Shuen, A94
 Tsarovsky Noah, A629
 Tselikas Lambros, A300, A945
 Tseng Hubert, A155
 Tseng Kuo-fu, A835
 Tsimberidou Apostolia, A509
 Tsimberidou Apostolia-Maria, A1009
 Tsoi Kim, A178
 Tsukerman Pini, A275
 Tsun Andy, A217, A939
 Tu Nhan, A115
 Tu Xiaoxuan, A445
 Tubo Noah, A198
 Tucker Matthew, A760
 Tuerci Oezlem, A555, A1008
 Tufa Dejene, A134
 Tuffanelli Marilena, A332, A980
 Tuininga Katie, A180
 Tumala Brunda, A200
 Tumang Joseph, A946
 Turajlic Samra, A205, A572
 Turcott Paul, A212
 Turcotte Simon, A325
 Türeci Özlem, A451, A525, A546, A579
 Tureci Özlem, A821
 Turk Mary, A674
 Turka Laurence, A219
 Turkekul Mesruh, A80
 Turkoz Mustafa, A128
 Turna Hande Z, A390, A391
 Turner Autumn, A884
 Turner Darryl, A271
 Turner Gail, A211
 Turner Scott, A606
 Twardowski Przemyslaw, A509, A515
 Twitty Christopher, A417
 Twumasi-Boateng Kwame, A419
 Twyffels Laure, A118
 Tyagi Ethika, A752
 Tyan Kevin, A402
 Tykocinski Mark, A825
 Tykodi Scott, A689
 Tyler Samantha, A727
 Tze Ker Matthew Leong, A855
 Tzeng Stephany, A235
 Uchio Ed, A456, A1005
 Uddin Shahab, A19, A767
 Ueyama Azumi, A914

- Ugwu-Dike Pearl, A841, A850
 Uhl Christopher, A231
 Uhlenbroich Sandra, A824
 Ulahannan Susanna, A397, A510, A548
 Ulge Umüt, A540
 Ulrich Michelle, A895
 Umana Andrea, A899
 Umana Pablo, A224
 Upadhyay Madhav, A224
 Upadhyaya Punit, A865, A931
 Uppal Karan, A18, A804
 Uppaluri Ravindra, A947
 Urba Walter, A103, A431
 Urbonas Liudvikas, A824
 Urech David, A885
 Utikal Jochen, A579
 Uttard Alex, A820
 Uyttingco Cedric, A91
 Uyttenhove Catherine, A596
- Vacher Sophie, A945
 Vad Nikhil, A588
 Vadlamudi Ratna, A321, A944
 Vaena Daniel, A507, A508
 Vagne Constance, A892
 Vahdat Linda, A528
 Vahrenhorst Dominik, A502
 Vaickus Lou, A397
 Vainer Gilad, A7
 Vaishampayan Ulka, A505, A554
 Vakil Aesha, A590
 Vakkasoglu Ahmet, A828
 Vaknin Ilan, A507
 Valamehr Bahram, A126, A208
 Valamehr Bob, A129, A147, A180
 Valanparambil Rajesh, A686
 Valdera Franklin, A571
 Valdes-Albini Frances, A548
 Vale Nolan, A195
 Valentin Emmanuel, A535, A558
 Vallacchi Viviana, A1, A331
 Valladeau-Guilemond Jenny, A719
 Vallera Daniel, A473
 Vanasse Gary, A176
 VandenBerg Tracy, A198
 VandenHeuvel Sabrina, A629
 Vanderkerken Karin, A987
 VanderWalde Ari, A538
 Vandewalle Thomas, A394
 Vandross Andrae, A549
 Vanegas Alejandro, A658
 Vanella Vito, A27, A257, A332, A980
 Vangsgaard Sara, A806
 Vankayalapati Hariprasad, A911
 Vanpouille-Box Claire, A100, A950
 Vaporciyan Ara, A186, A304, A1013
 Varadarajan Navin, A199, A584
 Varas Laura, A785
 Varga Andreea, A409
 Varga Matthew, A5, A495
 Varma Rajat, A736
 Varshavsky Asya, A699
 Varterasian Mary, A532
 Vasanth K, A40
 Vashishtha Anshu, A413
 Vashist Neha, A597
 Vasileva Elena, A296
 Vasselli James, A732
 Vasseur Bérangère, A394
 Vathiotis Ioannis, A258
- Vaz Victor, A74, A336
 Vázquez Patricia Claudio, A229
 Veatch Joshua, A689
 Veen Lars van der, A967
 Veeranki Phani, A660
 Veerapathran Anand, A110, A188
 Veiga Gael Clergeaud, A806
 Veillon Remi, A494
 Veire Benton, A91
 Veirman Kim De, A987
 Veiseh Omid, A225
 Velcheti Vamsidhar, A44
 Velez Diana, A212
 Velghe Amelie, A118
 Vella Jennifer, A674
 Vellano Christopher, A652
 Vemulapalli Vijetha, A268, A515
 Ven Rieneke van de, A46, A932, A981
 Veneris Jennifer, A398
 Venhaus Ralph, A363
 Venkataraman Jagadish, A70
 Venkatesh Divya, A807
 Venkatesh Hrishi, A345
 Venkatesulu Bhanu, A622
 Venugopal Indu, A648
 Verdegaal Els, A383
 Vergani Barbara, A331
 Vergote Ignace, A1006
 Verma Svena, A649, A807
 Vermond Sophie, A150, A156, A157
 Vermeris Michael, A134
 Verschraegen Claire, A532, A580
 Verzijl Dennis, A904
 Verzoni Elena, A376
 Vesely Matthew, A59
 Vessoni Alex, A200
 Veth Myrthe, A932
 Vetizou Marie, A892
 Vethrus Sylvia, A491
 Vey Norbert, A535
 Vezean Remus, A218
 Viandier Alizée, A287
 Viari Alain, A719
 Vicier Cécile, A535
 Victor Anja, A561
 Vidal August, A69, A958
 Vidal Gregory, A5
 Vignali Dario, A274, A682, A880
 Vignali Paolo, A673, A707
 Vijayakumar Suma, A19
 Vilar-Sanchez Eduardo, A622
 Vilardo Monika, A68
 Villella Jeannine, A380
 Vincent Benjamin, A951
 Vincent Krystal, A201
 Vincent Melanie, A397, A405
 Violeta Sanchez, A848
 Violle Benjamin, A118
 Virone-Oddos Angela, A893
 Visintin Alberto, A268
 Visser Marten, A383
 Viswanathan Vidya, A868
 Vitale Laura, A833
 Vitale Maria Grazia, A27, A332, A980
 Viteri Santiago, A394
 Vitoc Vlad, A725
 Vitry Fabien, A301
 Vivancos Ana, A69
 Vivat Valerie, A800
 Vivier Eric, A892, A893
- Vlaming Marijn, A156, A157
 Vogelzang Nicholas, A454
 Vogler Isabel, A451, A579
 Vogt Lorenz, A906
 Vohra Anmol, A137
 Vohra Nasreen, A621
 Voillet Valentin, A590
 Volgina Alla, A247
 Völker Timo, A555
 Volodin Alexandra, A756
 Voloshin Tali, A756
 Vonderheide Robert, A370
 Voong Khinh Ranh, A263
 Voss Martin, A447
 Voss Tiffany, A604
 Vowell Katie, A690
 Vowinckel Jakob, A370
 Vrabel Maura, A650
 Vreeland Timothy, A571
 Vries Helga E de, A232
 Vries Laura Smits-de, A904
 Vu Sallyann, A748
 Vu Trang, A706
 Vugmeyster Yulia, A494
 Vuidepot Annelise, A924
 Vuylsteke Peter, A997
- Wabitsch Simon, A721
 Wada Hisashi, A914, A934
 Wagen Sandro, A885
 Wagenaar Timothy, A636
 Wages Nolan, A54
 Wagner Thomas, A571
 Wagner-Drouet Eva, A1008
 Wahba Amy, A1002
 Wahle Joe, A919, A928
 Wai Sze Lei Candace, A946
 Waight Jeremy, A690
 Wainber Zev, A512
 Wainberg Zev, A370
 Walcheck Bruce, A208
 Waldes Jana, A544
 Walker Nigel, A280
 Walkey Carl, A592, A745, A942
 Walkser Dan, A91
 Wall Valerie, A284, A294, A299
 Wallace Roslyn, A847
 Waller Edmund, A672, A779
 Walravens Ann-Sophie, A118
 Walter Kimberly, A548
 Walter Steffen, A173, A1009
 Walters Ian, A533, A566
 Walters Matthew, A280
 Walunas Theresa, A838
 Wan Gang, A444
 Wan Hong, A530, A815
 Wanderley Carlos Wagner, A62
 Wang Beatrice, A740
 Wang Bingxia, A505
 Wang Carole, A290
 Wang Cathy, A240
 Wang Chao, A939
 Wang Chensu, A593
 Wang Chun-Chieh, A622
 Wang Danyang, A443
 Wang Danyi, A92
 Wang Ding, A368, A569
 Wang Dingzhi, A891
 Wang Dong, A490
 Wang Erxuan, A479

- Wang Fang, A905
 Wang George, A681
 Wang Haitao, A355
 Wang Hanbing, A986
 Wang Hao, A384
 Wang Hong, A351, A639
 Wang Hongbo, A180
 Wang Hsin, A735
 Wang Jennifer, A259
 Wang Jessie, A348
 Wang Jiahu, A724
 Wang Jian, A638
 Wang Jianxiang, A478
 Wang Jiao, A158
 Wang Jing, A21, A22, A295, A460, A960
 Wang Jingyuan, A475
 Wang Juan, A321
 Wang Judy, A511, A512, A519, A527
 Wang Lei, A66, A102, A425
 Wang Li, A276, A338, A340, A460, A651
 Wang Linghua, A654, A788, A960, A971
 Wang Lingyang, A171
 Wang Lixia, A548
 Wang Max, A457, A471
 Wang Minjing, A229
 Wang Nianfei, A479
 Wang Pin, A121
 Wang Ping, A120
 Wang Qi, A960
 Wang Qifeng, A444
 Wang Rui, A511, A550
 Wang Ruipeng, A213
 Wang Ruoxi, A407
 Wang Seunggho, A630
 Wang Shuhua, A779
 Wang Steve, A247
 Wang Steven, A132
 Wang Suming, A397, A405
 Wang Tao, A120, A939
 Wang Wei-Lien, A410
 Wang Weilin, A387
 Wang Xiaoli, A1007
 Wang Xiaoqing, A728
 Wang Xiaoxu, A679
 Wang Xiaoyuan, A436, A437
 Wang Xinan, A74
 Wang Xinhua, A297
 Wang Xinxin, A120
 Wang Xu, A849
 Wang Xuan, A986
 Wang Xueting, A8
 Wang Xueyin, A131
 Wang Yan, A462
 Wang Yarong, A985
 Wang Yi, A444, A724
 Wang Ying-Chih, A338, A651
 Wang Yinghong, A257
 Wang Yiyang, A109, A194
 Wang Yu, A678, A848, A947
 Wang Yuan, A956
 Wang Yuan-Shuo, A338
 Wang Yue, A384, A986
 Wang Yunfei, A183, A244, A584, A654
 Wang Yupeng, A109, A691
 Wang Zhen, A496
 Wang Zhengyi, A730, A935
 Wang Zhiyong, A631
 Wang Zhongmin, A288, A313, A783
 Wangen Rose, A473
 Wani Khalida, A410
 Wapinski Ilan, A859
 Ward Christine, A505
 Ward John, A379
 Ware Brandon, A207, A237, A737
 Ware Michael, A9, A434, A779, A948
 Wargo Jennifer, A410, A879
 Wargowski Ellen, A377
 Warlick Erica, A473
 Warmuth Stefan, A885
 Warren Michael, A267
 Warren Sarah, A27, A332, A980, A995
 Washburn Newell, A375
 Wasiuk Anna, A833
 Wasko Kevin, A203
 Wasley Mark, A604
 Wasman Jay, A868
 Wasti Ruby, A946
 Waterhouse Nigel, A367
 Watnick Jing, A397, A405
 Watnick Randolph, A397, A405
 Watson Geoffrey, A561
 Watson McLane, A707, A774
 Watt Amy, A185
 Watts Brittany, A68
 Watzl Carsten, A221
 Wayne Saville M, A395
 Weaver Kyle, A45
 Webb Lindsay, A185, A214, A351, A792
 Webber Beau, A229, A687
 Weber Jeffrey, A423
 Weber Jeffrey S, A853
 Weber Matthew, A825
 Webster-Carrion Andrea, A100
 Wechsler Erin, A588
 Wedekink Florian, A597
 Wege Henning, A387
 Wei Caimiao, A371
 Wei Hong-Jian, A100
 Wei Jia, A986
 Wei Lu, A632
 Wei Spencer, A842
 Weiß Lisa, A816
 Weichert Jamey, A624
 Weickhardt Andrew, A540
 Weide Benjamin, A597
 Weidlick Jeff, A833
 Weimholt Cody, A453
 Weinberg Andrew, A175, A613
 Weinberg Uri, A756
 Weiner George, A999
 Weinert Christopher, A885
 Weinschenk Toni, A1009
 Weirather Jason, A728
 Weis-Banke Stine Emilie, A813
 Weisdorf Daniel, A473
 Weisel Katja, A476
 Weisenburger Thomas, A579
 Weisenfeld Neil, A91
 Weishaupt Carsten, A502
 Weiss Leslie, A155
 Weiss Mia, A395
 Weiss Sarah, A422
 Weissferdt Annika, A186
 Weissferdt Annikka, A105, A1013
 Weissman Irving, A283
 Weller Sven, A641
 Welliver Tim, A463, A469
 Wells Adrian, A110, A188
 Welm Alana, A911
 Welsch Dean, A652
 Welsh James, A407, A604
 Welters Marij, A41
 Wen Lee Justina Nadia Li, A97
 Wen Patrick, A427
 Weng Tan Daniel Shao, A485
 Weng Winnie, A413
 Wengenmayer Peter, A502
 Wenham Robert, A523
 Wennerberg Erik, A589
 Wentzel Kristopher, A544
 Werchau Doreen, A785
 Wermke Martin, A531, A535, A1009
 Wesa Amy, A4
 Wesche Holger, A908
 Wescott Elizabeth, A791, A842
 Wesolowski Robert, A542, A715
 West John, A83, A88
 West Kamille, A1002
 Westphal Magdalena, A906
 Westwood Brian, A843
 Wetzko Katrin, A535
 Weyl Emmanuel, A272
 Whale Andrew, A924
 Whalen Corey, A542
 Whalen Giles, A533, A566
 Whang Michael, A159
 Wharton Keith, A60
 Wheeler Caroline, A878, A988
 Whelan Sarah, A107
 Whidden Mark, A548
 White Andrew, A27, A332, A613
 White James, A877
 White Kerry, A702
 Whiteley Erik, A159
 Whiting Chan, A891
 Whiting Sam, A891
 Whitman Darbie, A284, A294
 Whitman Eric, A417
 Whitney Megan, A664
 Wichmann Christian, A349
 Widegren Magnus, A799
 Widger Jenifer, A833
 Wiedenmann Bertram, A34
 Wiegert Erol, A452, A537, A1008
 Wiesner Joshua, A982
 Wiklund Erik Digman, A396
 Wiklund Peter, A90, A338, A651
 Wildiers Hans, A997
 Wilhelm Emmanuelle, A245
 Wilhem Emmanuelle, A829
 Wilky Breelyn, A509
 William Josette, A58
 William William, A1013
 Williams Alyssa, A705
 Williams Blake, A738
 Williams Chakita, A665
 Williams Eloise, A572
 Williams Jaspar, A226
 Williams John, A133
 Williams Karia, A926
 Williams Leila, A198, A215, A584, A654
 Williams Michelle, A788, A933
 Williams Nikki, A450
 Williams Stephen, A80, A91
 Williamson Stephen, A372
 Willis Sophie, A46
 Willman Gabriella, A882
 Willumsen Nicholas, A23, A24
 Wilmes Gwen, A176
 Wilson Adam, A646

- Wilson Casey, A282
Wilson Jonathan, A800
Wilson Nathaniel, A259
Wilson Nicholas, A887
Wilson Rosalind, A395
Wilson Sabine, A557
Wilson Taylor, A160
Wimalasingham Akhila, A562
Wind-Rotolo Megan, A420, A684, A872
Winer Ira, A562
Wingert Sabine, A221
Wingert Susanne, A922, A938
Winkeler Crystal, A47
Winkler Kevin, A134
Winkler Michelle, A350, A622
Winkowski Daniel, A875
Winston William, A744, A747, A752
Wirth Lori, A468
Wischhusen Jörg, A536, A597
Wise Scott, A298
Wise-Draper Trisha, A580
Wistuba Ignacio, A53, A186, A410, A632, A971, A1013
Wistuba-Hamprecht Kilian, A597
Witsuba Ignacio, A663
Witt Luke, A749
Wittrup Dane, A918
Wittrup K, A326, A711, A750, A769
Witty Alec, A129, A147
Wo Serena, A818
Wojciechowski Daniel, A866
Wojcik John, A420
Wolchok Jedd, A108, A596, A634, A649, A724, A807
Wolf Alex, A766
Wolf Melissa, A951
Wolf Natalie, A614
Wolf Steven, A665
Wolff Robert, A370, A439
Wollerton Francisca, A792
Wolpe Stephen, A809, A810
Wolpin Brian, A1010
Wolter Ralf, A531
Won Ji Yeong, A440
Won Jonghwa, A935
Wong Ada Hang-Heng, A355
Wong Hing, A200
Wong Jenna, A356
Wong Jonathan, A128
Wong Karrie, A198, A215
Wong Kenneth, A735
Wong Lu-Min, A131
Wong Matthew, A879
Wong Maurice, A35
Wong Oi Kwan, A297
Wong-Rolle Abigail, A270
Wongthida Phonphimon, A820
Wood Kris, A954
Woodman Morgan, A36, A758
Woodman Scott, A199
Woods Jared, A427
Woodson Elizabeth, A547
Wool Assaf, A272
Wooldridge James, A999
Worden Francis, A468
Workman Creg, A274
Worst Michelle, A304, A664
Worth Alison, A148
Worth Angela, A413
Wright Deborah, A144
Wright Gus, A761
Wright Kevin, A908
Wrocklage Christopher, A198, A215
Wrong Andrew, A548
Wu Catherine, A84, A353, A684
Wu Cheng-Chia, A100
Wu Christina, A434
Wu Dehua, A466
Wu Elise, A269, A666
Wu Guixian, A497
Wu Hui, A165
Wu Jianming, A208
Wu Kevin, A476
Wu Lan, A170
Wu Lei, A444
Wu Lingying, A460
Wu Ren-Chin, A622
Wu Victoria, A631
Wu Xiao, A523
Wu Xikun, A387, A389
Wu Yaping, A430, A431
Wu Yi-Long, A390, A391
Wu Zhihao, A295, A827
Wubben Sebastiaan, A904
Wucherpfennig Kai, A126, A427
Wulff-Burchfield Elizabeth, A318
Wunder Jay, A178
Wyant Timothy, A732
Wyatt Megan, A9, A207, A237, A737, A948
Wynn Richard, A247
Wypych Joe, A110
Wyrebeek Przemyslaw, A786
Xella Agata, A133
Xia Bairong, A460
Xia Collin, A833
Xia Dennis, A288, A313, A471, A783
Xia Michelle, A471
Xia Xu, A288, A313, A783
Xia Yu, A457, A460, A466
Xiang Jenny Zhaoying, A724
Xiao Dongmei, A766
Xiao Lianchun, A49, A259
Xiao Weihong, A788
Xiao Yinghua, A908
Xie Congying, A389
Xie Jingjing, A327
Xie Ming-Hong, A123, A137, A159
Xie Sunny, A417
Xie Yingtian, A728
Xie Zhiliang, A706
Xin Yanzhong, A436, A437
Xing Yan, A548
Xiong Yanli, A490
Xu Caiyue, A335
Xu Chunxiao, A351, A792
Xu Chunyu, A225, A584, A654
Xu Gege, A35
Xu Haiyan, A303
Xu Han, A131
Xu Hui, A884
Xu Jing, A899
Xu Lihui, A884
Xu Mingfang, A490
Xu Rui-Hua, A466
Xu Stacey, A127
Xu Steven, A961
Xu Tianlei, A198
Xu Xiangmin, A443
Xu Xiaoting, A384
Xu Yanzhao, A587
Xu Yaomin, A947
Xu Yifeng, A939
Xu Yingda, A939
Xu Zhiwen, A727
Xue Bin, A990
Xue Li, A551
Yackoubov Dima, A172, A230
Yadav Deepak, A742
Yadav Vinod Yadav, A625
Yaghoobi Vesal, A258
Yahalom Galit, A323
Yakkundi Poonam, A740, A953
Yalavarthi Sireesha, A351, A792
Yamaguchi Yukiko, A238
Yaman Yasemin, A885
Yamano Tomoyoshi, A743
Yamazaki Takahiro, A309, A589
Yan Dingxue, A910
Yan Dongqing, A911
Yan Gaoshu, A458
Yan Shu, A308
Yana Jess, A698
Yanamandra Ananta, A788
Yanez Adrienne, A542
Yang Becky, A606
Yang Bi-Huei, A126
Yang Bin, A633
Yang Bitna, A138
Yang Eun hee, A630
Yang Gengjie, A247
Yang Hai, A704
Yang Hee Jung, A146
Yang Hongying, A460
Yang James, A202
Yang James Chih-Hsin, A485, A488
Yang Jason, A135
Yang Jing, A39
Yang Liangpeng, A604
Yang Muh-Hwa, A886
Yang Ning, A724
Yang Qidi, A81
Yang Se Hwan, A428
Yang Shuai, A145
Yang Tao, A753
Yang Wei, A844
Yang Wenjing, A290
Yang Xiaodong, A442
Yang Xiaoyun, A408
Yang Xue (Cher), A128
Yang Xueqin, A490
Yang Yan-ou, A247
Yang Yi, A656
Yang Yingnan, A436, A437
Yang Yuanfan, A770
Yang Yuanquan, A988
Yang Zhenhuang, A584
Yang Zhifen, A162, A164
Yao Chunmei, A479
Yao Lu, A132
Yao Melissa, A653
Yao Xue, A834
Yao Zhifang, A466
Yaomin Xu, A678
Yap Timothy, A563, A907
Yarbro John, A710
Yarchoan Mark, A20, A481, A863, A991
Yarinsky Jacob, A709
Yarka Clare, A209

- Yavuz Betul Gok, A49
 Ye Chun Jimmie, A704
 Ye Fei, A257
 Ye Jianfeng, A632
 Ye Xiang, A951
 Yearley Jennifer, A364
 Yee Andrew, A476
 Yee Cassian, A252, A584, A845
 Yee Nathan, A395, A723
 Yegnasubramanian Srinivasan, A353
 Yeh Elizabeth, A708
 Yeh Wen-I, A126
 Yen Chia-Jui, A465
 Yeong Joe, A97, A656, A855
 Yerov Oleg, A748
 Yeung Andy, A746
 Yeung Kristin, A749
 Yeung Tsz-Lun, A639
 Yeung Yik Andy, A607
 Yi Dae Gwan, A146
 Yi Hyoju, A146
 Yi John, A365
 Yi Ping, A606
 Yi Ping Cheng, A37, A408
 Yi Yanhua, A640
 Yigit Burcu, A216, A432
 Yim Leon, A692, A711
 Yin Manli, A120
 Yin Wenjie, A120
 Yin Yifeng, A91
 Yingst Ashley, A134
 Yinmeng (Amy) Yang, A165
 Yong Lin-Kin, A240
 Yoo Donggeun, A869
 Yoo Kyung Jin, A615
 Yoon Esther, A993
 Yoon Won-Hee, A552
 Yoon Yi Na, A630
 Yoseph Rami, A680
 Yoshida Shinpei, A934
 Yoshida Tetsuya, A934
 Yoshikawa Mai, A914, A934
 Yossef Rami, A177
 You Benoit, A382
 You Gihoon, A935
 You Xiaoli, A494
 You Yun, A687
 Young Lauren, A165
 Young Ng Cedric Chuan, A656
 Young Paul, A452
 Young Samuel, A54
 Young Stephen, A280
 Yu Bin, A115
 Yu Changpu, A818
 Yu Danni, A67
 Yu Dihua, A642
 Yu Evan, A374, A378, A448, A449, A455
 Yu Jia Xin, A370
 Yu Kevin, A942
 Yu Lanfang, A445
 Yu Lianbo, A399
 Yu Lixia, A986
 Yu Ming, A101
 Yu Rebecca, A862
 Yu Stephen, A908
 Yu Timothy, A908
 Yu Xianzhong, A571
 Yu Zhiya, A177
 Yuan Jessica, A56
 Yuan Jianda, A485
 Yuan Mu, A479
 Yuan Ying, A400
 Yuan Yuan, A1000
 Yuan Zhijun, A939
 Yuet Amy, A475
 Yuki Yuko, A338
 Yun Nari, A499
 Yung Bryan, A631
 Yuraszcek Theresa, A241
 Yuwen Hui, A241, A936
 Zaboli Shiva, A606
 Zabransky Daniel, A991
 Zacharakis Nikolaos, A680
 Zacharek Sima, A569
 Zacharoulis Stergios, A100
 Zafari Mohammad, A919, A928
 Zafra Christina Zuch de, A818
 Zagorska Anna, A786
 Zagorulya Maria, A326, A692
 Zaharoff David, A281, A650
 Zahi Sarah, A489
 Zaid Jessica, A742
 Zaidi Mohammad, A434, A779
 Zain Jasmine, A503
 Zain Rosnah Binti, A957
 Zaini Zuraiza Mohamad, A957
 Zajic Stefan, A424
 Zakharia Yousef, A318, A999
 Zakharian Michael, A395, A723
 Zalacain Marta, A772
 Zalcman Gérard, A301
 Zalcman Gerard, A409
 Zalevsky Johnathan, A1007
 Zamarin Dimitriy, A335
 Zambarda Chiara, A938
 Zang Dae Young, A440
 Zang Miao, A465, A483
 Zang Shanyu, A993
 Zangl Luke, A628
 Zapata Francisco, A284, A299
 Zappasodi Roberta, A649, A807
 Zar Gul Abdul Rehman, A19
 Zarour Hassane, A423
 Zastawna Magdalena, A786
 Zatarra Ghadeer, A7
 Zauderer Maurice, A464
 Zavadovskaya Marianna, A37, A408, A606
 Zawadzka Magdalena, A799
 Zayed Hany, A529
 Zazrin Hadas Aharoni, A823
 Zebboudj Abderezak, A862
 Zeberer Julia, A885
 Zehnin Michael, A732
 Zeidan Stephanie, A516, A520
 Zellander Amelia, A231
 Zeman Ashley M, A853
 Zemer-Tov Efrat, A756
 Zeng Veronica, A726
 Zeng Yu, A427
 Zeng Zexian, A728
 Zha Dongxing, A315
 Zha Zhengyu, A642
 Zhai Qianting, A306
 Zhai Tianhang, A939
 Zhai Yifan, A474, A478
 Zhang Abigail Tianai, A427
 Zhang Anli, A632, A835
 Zhang Bingqing, A101
 Zhang Boyang, A310, A317, A353, A693
 Zhang Cheng Cheng, A327
 Zhang Christie, A749
 Zhang Danhui, A588
 Zhang David, A225
 Zhang Dong, A351
 Zhang Fahao, A971
 Zhang Guoliang, A443
 Zhang Hangyu, A443, A445
 Zhang Hongyi, A632
 Zhang Jiajia, A317, A353, A693
 Zhang Jianjun, A53, A105, A186, A304, A1013
 Zhang Jiexin, A960
 Zhang Jinfeng, A436, A437
 Zhang Jing, A844
 Zhang Jinhui, A827
 Zhang Juan, A400
 Zhang Kate, A203
 Zhang Kelvin, A601, A796, A883
 Zhang Keman, A276, A340
 Zhang Li, A390, A614
 Zhang Luquan, A436, A437
 Zhang Michelle, A66, A102
 Zhang Ningyan, A327
 Zhang Pei, A387
 Zhang Peng, A849
 Zhang Ping, A771
 Zhang Pingye, A488
 Zhang Pinping, A306
 Zhang Qianfei, A721
 Zhang Qingyuan, A400
 Zhang Ruyi, A445
 Zhang Sen, A561
 Zhang Shanyu, A962, A984
 Zhang Shengle, A78, A86, A89
 Zhang Shiheng, A490
 Zhang Shihong, A204
 Zhang Simo, A88
 Zhang Tian, A655
 Zhang Tuo, A724
 Zhang Wubing, A728
 Zhang Xiang, A971
 Zhang Xiaokui, A169
 Zhang Xinlian, A712
 Zhang Xinyue, A321
 Zhang Xu, A100
 Zhang Yan, A132, A155, A246, A849
 Zhang Yao, A662
 Zhang Yi, A728
 Zhang Yingying, A165
 Zhang Yipeng, A986
 Zhang Yiwei, A415
 Zhang Yu-an, A636
 Zhang Yuchen, A434
 Zhang Yue, A171
 Zhang Yueli, A842
 Zhang Yun, A400
 Zhang Zhenning, A860
 Zhang Zhenqing, A217
 Zhang Zhiguo, A100
 Zhang Zhikai, A832
 Zhang-Hoover Jie, A303
 Zhao Bin, A391
 Zhao Binsheng, A857
 Zhao Chen, A270, A570
 Zhao Dawen, A293
 Zhao Fan, A749
 Zhao Liang, A490
 Zhao Luping, A999
 Zhao Peng, A443
 Zhao Weixing, A944

Zhao Xiaoning, A280
 Zhao Yanding, A674
 Zhao Yingying, A132
 Zhao Zeguo, A142
 Zhao Zhen, A713
 Zheng Dayong, A436, A437
 Zheng Grace, A226
 Zheng Jia, A348, A753
 Zheng Pan, A246, A500, A564, A849, A998
 Zheng Wei, A436, A437
 Zheng Xiufen, A617
 Zheng Yi, A443
 Zheng Ying, A679
 Zhigarev Dmitry, A699
 Zhong Li, A490
 Zhong Tingting, A288, A313, A783
 Zhou Alice, A428
 Zhou Chenhao, A642
 Zhou Chensheng, A316
 Zhou Jian-Guo, A355
 Zhou Juying, A384
 Zhou Matthew, A817, A819
 Zhou Nicolas, A105
 Zhou Qinjie, A516, A520
 Zhou Xi, A589
 Zhou Xueyuan, A792
 Zhou Yiting, A457
 Zhou You, A200
 Zhou Yu 'Jerry', A768
 Zhu Hongyu, A384
 Zhu Jingru, A779
 Zhu Jun, A338, A651
 Zhu Xi-xu, A496
 Zhu Xudong, A443, A445
 Zhu Yi, A826
 Zhu Zhou, A371
 Zi Tong, A601, A796, A883
 Ziblat Andrea, A354
 Ziccheddu Bachisio, A703
 Zieba Adam, A185, A214
 Zilberberg Jenny, A231
 Zimolag Eliza, A786
 Zitvogel Laurence, A300, A945
 Zobniw Chrystia M, A853
 Zolotarjova Nina, A247
 Zondag Gerben, A805
 Zong Hailing, A56
 Zorde-Khvaleyevsky Elina, A825
 Zou Wei, A30, A33, A870
 Zou Yuefeng, A939
 Zoutendijk Iris, A805
 Zrounba Philippe, A962, A984
 Zubiri Leyre, A841, A850
 Zucchetti Andres, A142
 Zuchowicz Karol, A786
 Zuck Meghan, A294, A299
 Zuniga Luis, A18, A804
 Zuo Haoxiao, A232
 Zuris John, A203

Key and Abbreviations:

"A" refers to the page number.

- Adoptive immunotherapy A106, A110, A114, A127, A139, A167, A172, A174, A176, A180, A182, A183, A186, A187, A188, A189, A190, A191, A193, A195, A197, A198, A199, A201, A202, A203, A204, A205, A211, A212, A215, A216, A220, A221, A228, A233, A237, A239, A240, A418, A419, A432, A486, A572, A573, A640, A680, A696, A716, A737, A743, A958, A995, A1000, A1008, A1009, 97, 101, 104, 118, 130, 157, 162, 164, 166, 169, 171, 172, 174, 175, 176, 177, 178, 179, 181, 184, 185, 186, 187, 189, 190, 191, 192, 193, 200, 201, 204, 205, 209, 210, 215, 220, 223, 225, 226, 384, 385, 400, 458, 543, 544, 610, 651, 668, 688, 708, 714, 912, 946, 951, 958, 959
- Angiogenesis A797, A808, 762, 773
- Antibody A169, A208, A429, A471, A472, A484, A503, A554, A592, A595, A604, A620, A636, A647, A679, A727, A731, A732, A816, A819, A881, A886, A898, A908, A921, A925, 159, 197, 397, 441, 443, 456, 474, 524, 563, 566, 575, 590, 606, 617, 650, 699, 703, 704, 781, 784, 840, 845, 857, 867, 879, 883
- Antibody A998, A1002, 949, 953
- Antigen presenting cells A213, A224, A227, A286, A395, A611, A625, A635, A683, A685, A686, A695, A708, A710, A711, A712, A723, A756, A770, A799, A804, A814, A887, A894, A956, A975, A982, A985, A997, A1000, 202, 211, 214, 264, 367, 581, 595, 605, 654, 657, 658, 667, 680, 682, 683, 684, 695, 726, 739, 764, 769, 779, 846, 853, 910, 929, 936, 939, 948, 951
- Autoimmunity A252, A753, 236, 724
- B cell A54, A453, A538, A778, A880, 47, 423, 506, 747, 839
- Bioinformatics A45, A72, A76, A360, A584, A593, A673, A682, A717, A874, A957, A965, A972, 38, 65, 68, 334, 554, 564, 644, 653, 689, 833, 911, 920, 927
- Bioinformatics A995, A1013, 946, 962
- Biomarkers A3, A36, A37, A34, A48, A53, A55, A57, A61, A78, A80, A99, A101, A103, A316, A357, A380, A397, A405, A423, A551, A556, A771, A855, A860, A868, A869, A878, A907, A911, A976, A983, A984, A993, A995, A1005, A1011, 3, 31, 32, 29, 41, 46, 48, 50, 54, 70, 72, 90, 92, 94, 292, 331, 353, 369, 375, 390, 521, 526, 740, 818, 822, 829, 830, 837, 866, 870, 930, 937, 938, 945, 946, 955, 961
- Bispecifics A473, A568, A576, A749, A828, A865, A909, A922, A923, A924, A929, A931, 444, 538, 546, 720, 793, 826, 868, 880, 881, 882, 887, 888
- CAR T cells A117, A119, A136, A146, A149, A477, A582, A912, A995, A1008, 106, 108, 127, 137, 140, 449, 552, 871, 946, 958
- Carcinogenesis A811, A952, 776, 907
- Checkpoint blockade A4, A247, A253, A254, A257, A262, A268, A276, A277, A301, A305, A309, A311, A317, A319, A320, A324, A325, A326, A328, A334, A338, A340, A341, A343, A344, A347, A351, A353, A368, A374, A376, A377, A378, A386, A415, A416, A417, A430, A433, A440, A451, A455, A465, A470, A471, A472, A474, A475, A478, A481, A484, A486, A491, A502, A503, A505, A507, A510, A513, A514, A515, A518, A519, A532, A534, A537, A538, A540, A544, A549, A551, A554, A555, A556, A559, A562, A568, A571, A572, A573, A576, A579, A612, A902, A909, A929, A997, A998, A1000, A1001, A1004, A1005, A1006, A1007, A1008, A1009, A1010, A1011, 94, 226, 331, 332, 333, 334, 335, 336, 346, 347, 349, 350, 351, 352, 359, 367, 369, 370, 375, 381, 382, 383, 396, 397, 398, 400, 402, 416, 420, 421, 422, 423, 425, 435, 440, 441, 443, 445, 447, 450, 453, 456, 458, 462, 473, 474, 476, 477, 480, 483, 484, 485, 488, 489, 500, 502, 505, 506, 509, 513, 519, 521, 524, 525, 526, 529, 531, 538, 542, 543, 544, 546, 549, 582, 861, 868, 887, 948, 949, 951, 952, 954, 955, 956, 957, 958, 959, 960, 961
- Coinhibition A197, A510, A647, 185, 480, 617
- Costimulation A219, A224, A235, A481, A514, A534, A595, A611, A616, A625, A628, A634, A686, A711, A720, A725, A731, A743, A750, A770, A773, A775, A792, A897, A905, A921, A931, A1008, 208, 211, 222, 453, 484, 502, 566, 581, 586, 595, 598, 604, 658, 683, 692, 697, 703, 714, 721, 739, 742, 744, 757, 856, 864, 879, 888, 958
- COVID and Immunotherapy A432, A472, A655, A940, A941, A1002, 400, 443, 625, 896, 897, 953
- Cytokine A4, A9, A34, A114, A117, A137, A175, A185, A219, A220, A224, A225, A231, A235, A305, A316, A326, A343, A368, A417, A433, A465, A502, A514, A519, A534, A540, A556, A586, A592, A596, A600, A607, A614, A626, A629, A635, A636, A711, A717, A720, A731, A737, A739, A742, A744, A745, A746, A747, A748, A749, A750, A752, A753, A758, A769, A773, A775, A786, A799, A800, A805, A811, A828, A853, A882, A889, A894, A902, A912, A918, A921, A942, A953, A1007, 4, 9, 29, 104, 106, 128, 165, 173, 208, 209, 211, 212, 218, 222, 281, 292, 303, 319, 342, 383, 402, 435, 473, 484, 489, 502, 509, 526, 556, 563, 567, 571, 578, 584, 596, 599, 605, 606, 683, 689, 692, 703, 708, 710, 713, 715, 716, 717, 718, 719, 720, 721, 723, 724, 729, 738, 742, 744, 752, 764, 765, 770, 776, 793, 816, 841, 848, 853, 861, 871, 876, 879, 898, 908, 957
- Dendritic cell A205, A286, A357, A358, A359, A361, A362, A386, A470, A527, A555, A571, A582, A594, A603, A611, A624, A625, A631, A632, A683, A685, A686, A695, A706, A710, A711, A712, A723, A724, A743, A770, A793, A800, A814, A819, A884, A887, A920, A950, A975, A981, A982, A985, A997, A999, A1001, A1011, 193, 264, 331, 332, 333, 335, 336, 359, 440, 495, 525, 542, 552, 565, 574, 581, 594, 595, 601, 602, 654, 657, 658, 667, 678, 682, 683, 684, 695, 696, 714, 739, 758, 765, 779, 784, 843, 846, 878, 905, 929, 935, 936, 939, 948, 950, 952, 961
- Epidemiology A658, A841, 628, 804
- Epigenetics A584, A635, A667, A673, A764, A767, A795, A952, 554, 605, 638, 644, 734, 736, 760, 907
- Extracellular vesicles/exosomes A601, A683, A796, A883, 572, 654, 761, 842
- Gene expression A21, A34, A78, A80, A84, A91, A100, A101, A105, A117, A199, A202, A229, A233, A325, A326, A365, A416, A423, A477, A491, A502, A633, A654, A667, A673, A682, A695, A727, A728, A754, A761, A772, A794,

- A845, A907, A948, A957, A965, A966, A972, A991, A995, A1002, A1005, 19, 29, 70, 72, 76, 83, 91, 92, 96, 106, 187, 190, 216, 220, 302, 303, 339, 382, 390, 449, 462, 473, 603, 624, 638, 644, 653, 667, 699, 700, 725, 732, 741, 759, 808, 866, 904, 911, 920, 921, 927, 944, 946, 953, 955
- Glycoproteomics A982, 936
- Granulocyte A343, A814, A1002, 319, 779, 953
- Immune adjuvant A167, A231, A235, A237, A395, A428, A505, A527, A532, A607, A611, A626, A629, A630, A650, A731, A739, A750, A754, A756, A769, A770, A774, A795, A798, A800, A802, A803, A805, A894, A901, A941, 157, 218, 222, 223, 367, 396, 476, 495, 500, 578, 581, 596, 599, 600, 620, 703, 710, 721, 725, 726, 738, 739, 743, 760, 763, 765, 767, 768, 770, 853, 860, 897
- Immune contexture A3, A34, A45, A48, A57, A61, A105, A309, A326, A423, A613, A632, A670, A763, A770, A867, A874, A929, A950, A957, A962, A966, A975, A976, A981, A982, A983, 3, 29, 38, 41, 50, 54, 96, 285, 303, 390, 583, 602, 641, 733, 739, 828, 833, 887, 905, 911, 917, 921, 929, 930, 935, 936, 937
- Immune monitoring A1, A4, A47, A48, A55, A57, A76, A81, A101, A103, A270, A309, A359, A360, A365, A373, A377, A379, A416, A428, A481, A502, A515, A541, A551, A556, A612, A811, A812, A814, A846, A854, A881, A901, A929, A953, A965, A981, A983, A995, A1000, A1002, A1005, 1, 4, 40, 41, 48, 50, 68, 73, 92, 94, 250, 285, 333, 334, 339, 346, 350, 352, 382, 396, 453, 473, 485, 510, 521, 526, 582, 776, 777, 779, 810, 817, 840, 860, 887, 908, 920, 935, 937, 946, 951, 953, 955
- Immune suppression A37, A45, A55, A66, A76, A101, A139, A220, A227, A253, A317, A319, A325, A338, A341, A343, A360, A395, A496, A590, A596, A600, A606, A609, A616, A618, A625, A632, A633, A652, A654, A667, A676, A683, A684, A685, A695, A704, A705, A707, A710, A720, A727, A766, A768, A772, A786, A791, A793, A798, A803, A813, A853, A867, A869, A875, A879, A881, A882, A884, A889, A890, A891, A898, A905, A926, A927, A929, A933, A940, A948, A950, A952, A962, A969, A983, A984, A985, A990, 32, 38, 48, 58, 68, 92, 130, 209, 214, 237, 293, 295, 302, 314, 317, 319, 334, 367, 467, 561, 567, 571, 577, 580, 586, 588, 595, 602, 603, 622, 624, 638, 647, 654, 655, 657, 667, 676, 677, 679, 682, 692, 699, 735, 737, 741, 752, 756, 758, 763, 768, 778, 816, 828, 830, 834, 838, 840, 841, 843, 848, 849, 850, 857, 864, 884, 885, 887, 890, 896, 904, 905, 907, 917, 924, 937, 938, 939, 943
- Immune tolerance A76, A623, A625, A678, A683, A685, A704, A707, A869, A884, A898, A902, A905, A952, A985, 68, 593, 595, 649, 654, 657, 676, 679, 830, 843, 857, 861, 864, 907, 939
- Immune toxicity A76, A125, A225, A252, A253, A254, A257, A317, A362, A377, A415, A750, A760, A838, A840, A841, A843, A844, A845, A846, A848, A853, A854, A908, A942, A953, A995, 68, 116, 212, 236, 237, 238, 239, 293, 336, 350, 381, 721, 731, 802, 803, 804, 806, 807, 808, 810, 812, 816, 817, 867, 898, 908, 946
- Immunoscore A855, A972, 818, 927
- Inflammation A1, A225, A252, A311, A343, A395, A453, A618, A651, A677, A708, A723, A747, A753, A756, A770, A782, A797, A799, A803, A804, A805, A813, A814, A843, A875, A951, A953, A957, A972, A976, A982, A985, A1002, 1, 212, 236, 287, 319, 367, 423, 588, 621, 648, 680, 695, 718, 724, 726, 739, 749, 762, 764, 768, 769, 770, 778, 779, 806, 834, 906, 908, 911, 927, 930, 936, 939, 953
- Leukemia/Lymphoma A117, A137, A216, A270, A432, A471, A472, A473, A474, A475, A477, A478, A503, A505, A613, A633, A764, A775, A912, A925, A995, 106, 128, 205, 250, 400, 441, 443, 444, 445, 447, 449, 450, 474, 476, 583, 603, 734, 744, 871, 883, 946
- MDSC A343, A397, A405, A609, A616, A623, A630, A637, A652, A678, A706, A710, A793, A798, A803, A804, A890, A911, A917, A929, A977, A985, 319, 369, 375, 580, 586, 593, 600, 607, 622, 649, 678, 682, 758, 763, 768, 769, 849, 870, 875, 887, 931, 939
- Metabolism A182, A194, A199, A237, A311, A471, A609, A643, A652, A667, A673, A685, A691, A694, A695, A696, A697, A698, A707, A720, A793, A843, A933, A950, A951, 171, 183, 187, 223, 287, 441, 580, 613, 622, 638, 644, 657, 663, 666, 667, 668, 669, 670, 679, 692, 758, 806, 890, 905, 906
- Microbiome A301, A532, A814, A876, A878, A879, A880, A988, 278, 500, 779, 835, 837, 838, 839, 942
- Monocyte/Macrophage A45, A55, A114, A219, A220, A227, A233, A283, A311, A324, A325, A341, A361, A379, A545, A599, A600, A609, A623, A633, A644, A647, A670, A678, A682, A695, A704, A705, A706, A708, A709, A710, A723, A724, A727, A756, A763, A793, A798, A804, A813, A814, A819, A860, A867, A875, A883, A886, A894, A906, A907, A917, A920, A922, A923, A927, A933, A951, A953, A962, A964, A965, A969, A981, A985, A986, A1000, 38, 48, 104, 208, 209, 214, 220, 261, 287, 301, 302, 317, 335, 352, 515, 570, 571, 580, 593, 603, 614, 617, 641, 649, 653, 667, 676, 677, 678, 680, 681, 682, 695, 696, 699, 726, 733, 758, 763, 769, 778, 779, 784, 822, 828, 834, 842, 845, 853, 865, 866, 875, 878, 880, 881, 885, 890, 906, 908, 917, 919, 920, 924, 935, 939, 940, 951
- Myeloid cells A45, A114, A220, A227, A283, A324, A325, A343, A379, A453, A478, A609, A611, A630, A633, A644, A652, A670, A685, A704, A706, A708, A710, A711, A724, A727, A793, A798, A804, A813, A819, A860, A867, A883, A886, A890, A906, A911, A917, A920, A925, A929, A933, A953, A975, A981, A982, A985, A1000, 38, 104, 209, 214, 261, 301, 302, 319, 352, 423, 450, 580, 581, 600, 603, 614, 622, 641, 657, 676, 678, 680, 682, 683, 696, 699, 758, 763, 769, 778, 784, 822, 828, 842, 845, 849, 865, 870, 875, 878, 883, 887, 890, 908, 929, 935, 936, 939, 951
- Neoantigens A21, A71, A110, A186, A195, A197, A202, A205, A212, A240, A268, A353, A357, A358, A359, A360, A361, A373, A418, A419, A481, A486, A515, A551, A572, A573, A580, A583, A607, A680, A684, A689, A693, A767, A805, A807, A828, A924, A958, A959, 19, 64, 101, 174, 184, 185, 190, 193, 201, 226, 248, 327, 331, 332, 333, 334, 335, 346, 384, 385, 453, 458, 485, 521, 543, 544, 550, 553, 578, 651, 655, 661, 665, 736, 770, 772, 793, 882, 912, 913
- NK/NKT cell A55, A123, A125, A137, A138, A139, A169, A172, A174, A180, A182, A193, A203, A208, A216, A219, A221, A228, A229, A235, A328, A338, A432, A433, A465, A473, A507, A541, A612, A614, A636, A651, A667, A675, A690, A716, A717, A731, A732, A739, A757, A773, A775, A778, A824, A875, A880, A891, A905, A906, A920, A986, A1007, 48, 113, 116, 128, 129, 130, 159, 162, 164, 169, 171, 181, 191, 197, 205, 208, 210, 215, 216, 222, 305, 314, 400, 402, 435, 444, 477, 510, 582, 584, 606, 621, 638, 646, 662, 688, 689, 703, 704, 710, 727, 742, 744, 747, 789, 834, 839, 850, 864, 865, 878, 940, 957
- Pediatric tumors A100, A136, A190, A220, A643, A682, A772, A969, A972, 91, 127, 178, 209, 613, 653, 741, 924, 927
- Post-translational modifications A505, A654, 476, 624
- Proteomics A91, A99, A199, A359, A612, 83, 90, 187, 333, 582
- Radiotherapy A100, A227, A259, A429, A496, A604, A620, A621, A623, A624, A625, A626, A628, A629, A630, A763, A771, A950, A1010, 91, 214, 241, 397, 467, 575, 590, 591, 593, 594, 595, 596, 598, 599, 600, 733, 740, 905, 960
- Regulatory T cell (Treg cell) A4, A48, A279, A317, A324, A491, A503, A519, A603, A623, A630, A669, A679, A720, A724, A731, A732, A752, A763, A774, A867, A875, A880, A881, A882, A898, A902, A925, A926, A929, A953, A993, A1002, A1011, 4, 41, 257, 293, 301, 462, 474, 489, 574, 593, 600, 640, 650, 692, 696, 703, 704, 723, 733, 743, 828, 834, 839, 840, 841, 857, 861, 883, 884, 887, 908, 945, 953, 961
- RNA A80, A81, A84, A101, A175, A199, A202, A212, A224, A270, A365, A416, A451, A502, A545, A579, A794, A910, A956, A965, A972, A977, A988, A995, A1002, A1008, A1011, 72, 73, 76, 92, 165, 187, 190, 201, 211, 250, 339, 382, 421, 473, 515, 549, 759, 869, 910, 920, 927, 931, 942, 946, 953, 958, 961
- Solid tumors A4, A9, A34, A36, A45, A53, A57, A61, A78, A80, A99, A103, A105, A107, A114, A125, A127, A136, A138, A139, A167, A169, A172, A176, A182, A183, A185, A186, A187, A188, A189, A190, A191, A193, A197, A198, A201, A202, A203, A205, A208, A211, A213, A215, A216, A220, A224, A227, A228, A237, A239, A240, A247, A253, A254, A257, A259, A262, A274, A276, A281, A301, A305, A309, A311, A316, A319, A320, A324, A325, A326, A338, A341, A344, A365, A368, A377, A380, A397, A398, A405, A417, A433, A465, A471, A481, A484, A486, A491, A496, A502, A503, A505, A510, A513, A514, A515, A518, A519, A534, A540, A541, A544, A545, A549, A551, A554, A555, A556, A559, A562, A568, A573, A576, A583, A586, A590, A591, A593, A594, A595, A603, A609, A612, A616, A625,

- A630, A631, A633, A635, A636, A637, A640, A643, A644, A647, A650, A651, A658, A665, A667, A668, A670, A678, A680, A682, A683, A684, A690, A691, A694, A698, A704, A709, A710, A717, A721, A722, A723, A724, A737, A746, A748, A750, A752, A754, A758, A760, A761, A766, A768, A769, A770, A772, A773, A774, A776, A779, A793, A794, A796, A798, A800, A803, A804, A808, A816, A819, A824, A840, A841, A846, A859, A865, A867, A874, A876, A879, A883, A886, A889, A890, A891, A894, A897, A902, A906, A907, A908, A910, A911, A917, A918, A920, A922, A923, A924, A931, A933, A942, A950, A951, A962, A965, A966, A975, A981, A983, A985, A987, A991, A995, A998, A999, A1000, A1004, A1005, A1006, A1007, A1008, A1009, 4, 9, 29, 31, 38, 46, 50, 54, 70, 72, 90, 94, 96, 98, 104, 116, 118, 127, 129, 130, 157, 159, 162, 166, 171, 172, 173, 174, 175, 176, 177, 178, 179, 181, 185, 186, 189, 190, 191, 193, 197, 200, 202, 204, 205, 209, 211, 214, 215, 223, 225, 226, 232, 237, 238, 239, 241, 243, 253, 255, 259, 278, 281, 285, 287, 292, 295, 296, 301, 302, 303, 314, 317, 320, 339, 342, 350, 353, 369, 370, 375, 383, 402, 435, 441, 453, 456, 458, 462, 467, 473, 474, 476, 480, 483, 484, 485, 488, 489, 502, 509, 510, 513, 515, 519, 521, 524, 525, 526, 529, 531, 538, 544, 546, 553, 556, 561, 562, 564, 565, 566, 574, 580, 582, 586, 595, 600, 601, 603, 605, 606, 607, 610, 613, 614, 617, 620, 621, 628, 636, 638, 639, 641, 649, 651, 653, 654, 655, 662, 663, 666, 670, 676, 681, 682, 689, 693, 694, 695, 696, 708, 717, 719, 721, 723, 725, 729, 731, 732, 735, 737, 738, 739, 741, 742, 743, 745, 748, 758, 759, 761, 763, 765, 768, 769, 773, 781, 784, 789, 803, 804, 810, 821, 826, 828, 833, 835, 838, 842, 845, 848, 849, 850, 853, 856, 861, 865, 866, 867, 869, 870, 875, 876, 878, 880, 881, 882, 888, 890, 898, 905, 906, 917, 920, 921, 929, 935, 937, 939, 941, 944, 946, 949, 950, 951, 954, 955, 956, 957, 958, 959
- Stem cell/cancer-initiating cell A344, A357, A358, A361, A362, A1001, 320, 331, 332, 335, 336, 952
- Surfaceome A771, 740
- Surgery A379, A453, A631, A650, A1010, 352, 423, 601, 620, 960
- Systems biology A45, A311, A584, A593, A603, A631, A670, A682, A865, A869, 38, 287, 554, 564, 574, 601, 641, 653, 826, 830
- T cell A4, A9, A21, A45, A48, A54, A55, A57, A71, A72, A81, A84, A101, A103, A106, A107, A110, A117, A119, A127, A136, A146, A149, A167, A174, A175, A176, A183, A185, A186, A187, A189, A190, A191, A194, A195, A197, A198, A201, A202, A204, A205, A211, A212, A213, A215, A216, A219, A224, A225, A227, A231, A237, A239, A240, A247, A268, A270, A274, A276, A279, A305, A311, A316, A317, A324, A325, A326, A328, A338, A340, A341, A344, A353, A365, A368, A373, A379, A380, A386, A418, A419, A433, A450, A451, A453, A465, A472, A477, A486, A503, A507, A510, A513, A519, A538, A540, A541, A551, A555, A559, A568, A572, A573, A576, A579, A580, A582, A583, A590, A592, A595, A600, A601, A603, A604, A607, A611, A612, A613, A614, A618, A624, A626, A628, A629, A630, A632, A640, A643, A651, A652, A653, A654, A668, A669, A670, A673, A676, A677, A679, A680, A684, A686, A689, A690, A691, A693, A694, A696, A697, A698, A704, A705, A707, A710, A711, A720, A721, A725, A727, A731, A732, A737, A743, A745, A746, A748, A749, A752, A761, A763, A766, A770, A771, A773, A774, A775, A778, A786, A792, A795, A802, A803, A804, A805, A811, A812, A813, A828, A841, A848, A855, A859, A860, A865, A867, A879, A880, A881, A882, A884, A886, A889, A890, A891, A897, A898, A901, A905, A907, A908, A909, A911, A912, A920, A921, A924, A926, A927, A929, A931, A950, A952, A953, A958, A959, A965, A969, A975, A977, A986, A990, A993, A997, A999, A1002, A1007, A1008, A1009, A1010, A1011, 4, 9, 19, 38, 41, 47, 48, 50, 64, 65, 73, 76, 92, 94, 97, 98, 101, 106, 108, 118, 127, 137, 140, 157, 164, 165, 166, 172, 173, 174, 175, 177, 178, 179, 183, 184, 185, 186, 189, 190, 192, 193, 200, 201, 202, 204, 205, 208, 211, 212, 214, 218, 223, 225, 226, 232, 248, 250, 253, 255, 257, 281, 287, 292, 293, 301, 302, 303, 305, 314, 316, 317, 320, 327, 339, 342, 346, 352, 353, 359, 384, 385, 402, 420, 421, 423, 435, 443, 449, 458, 474, 477, 480, 483, 489, 506, 509, 510, 521, 525, 529, 538, 543, 544, 546, 549, 550, 552, 553, 561, 563, 566, 571, 572, 574, 575, 578, 581, 582, 583, 584, 588, 594, 596, 598, 599, 600, 602, 610, 613, 621, 622, 623, 624, 639, 640, 641, 644, 647, 648, 650, 651, 655, 658, 661, 662, 663, 665, 666, 668, 669, 670, 676, 677, 679, 682, 683, 692, 693, 697, 699, 703, 704, 708, 714, 716, 717, 719, 720, 723, 732, 733, 735, 739, 740, 742, 743, 744, 747, 752, 757, 760, 767, 768, 769, 770, 776, 777, 778, 793, 804, 812, 818, 821, 822, 826, 828, 838, 839, 840, 841, 843, 845, 848, 849, 850, 856, 857, 860, 864, 866, 867, 868, 870, 871, 878, 879, 882, 884, 885, 887, 888, 905, 907, 908, 912, 913, 920, 924, 929, 931, 940, 943, 945, 948, 950, 953, 957, 958, 959, 960, 961
- T cell lineages A4, A48, A57, A101, A186, A197, A237, A317, A326, A365, A432, A603, A613, A669, A684, A686, A710, A720, A814, A875, A911, A975, A1010, 4, 41, 50, 92, 174, 185, 223, 293, 303, 339, 400, 574, 583, 640, 655, 658, 682, 692, 779, 834, 870, 929, 960
- Targeted therapy A117, A136, A137, A139, A167, A169, A176, A186, A213, A235, A239, A247, A281, A317, A328, A376, A380, A429, A446, A452, A453, A472, A473, A475, A477, A503, A510, A518, A519, A537, A544, A554, A559, A562, A572, A580, A609, A620, A632, A633, A634, A635, A638, A640, A643, A644, A647, A650, A653, A725, A747, A754, A761, A779, A782, A803, A813, A816, A819, A841, A865, A886, A890, A901, A905, A907, A908, A911, A912, A920, A921, A924, A925, A931, A933, A950, A991, A1000, A1004, A1005, A1009, 106, 127, 128, 130, 157, 159, 166, 174, 202, 222, 225, 232, 259, 293, 305, 349, 353, 397, 416, 422, 423, 443, 444, 447, 449, 474, 480, 488, 489, 505, 513, 524, 529, 531, 543, 550, 580, 590, 602, 603, 604, 605, 608, 610, 613, 614, 617, 620, 623, 697, 718, 725, 732, 748, 749, 768, 778, 781, 784, 804, 826, 845, 849, 860, 864, 866, 867, 870, 871, 878, 879, 882, 883, 888, 890, 905, 944, 951, 954, 955, 959
- TLR A343, A502, A555, A611, A626, A637, A721, A802, A803, A804, A814, A819, A999, A1011, 319, 473, 525, 581, 596, 607, 693, 767, 768, 769, 779, 784, 950, 961
- Tumor antigens A71, A72, A106, A110, A119, A125, A186, A189, A197, A201, A202, A204, A213, A224, A231, A239, A240, A360, A377, A395, A416, A451, A481, A486, A510, A515, A572, A573, A579, A583, A607, A611, A612, A653, A680, A683, A684, A689, A693, A743, A749, A754, A771, A774, A795, A807, A811, A812, A816, A819, A828, A865, A881, A901, A912, A924, A925, A958, A959, A1008, A1011, 64, 65, 97, 101, 108, 116, 174, 177, 185, 189, 190, 192, 202, 211, 218, 225, 226, 334, 350, 367, 382, 421, 453, 458, 480, 485, 543, 544, 549, 553, 578, 581, 582, 623, 651, 654, 655, 661, 665, 714, 720, 725, 740, 743, 760, 772, 776, 777, 781, 784, 793, 826, 840, 860, 871, 882, 883, 912, 913, 958, 961
- Tumor evasion A4, A119, A183, A195, A202, A262, A286, A319, A325, A326, A338, A347, A538, A540, A616, A625, A631, A651, A653, A654, A670, A684, A685, A695, A698, A705, A720, A745, A757, A761, A791, A795, A807, A828, A869, A884, A901, A921, A933, A948, A950, A951, A952, A956, A963, A966, A972, A982, 4, 108, 172, 184, 190, 243, 264, 295, 302, 303, 314, 322, 506, 509, 586, 595, 601, 621, 623, 624, 641, 655, 657, 667, 670, 677, 692, 716, 727, 732, 756, 760, 772, 793, 830, 843, 860, 879, 890, 904, 905, 906, 907, 910, 918, 921, 927, 936
- Tumor infiltrating lymphocytes (TILs) A4, A9, A45, A48, A55, A57, A61, A71, A80, A84, A101, A103, A105, A107, A110, A175, A176, A182, A183, A186, A187, A188, A189, A191, A193, A194, A195, A197, A198, A199, A202, A205, A215, A219, A225, A227, A228, A235, A237, A274, A276, A277, A279, A305, A311, A317, A324, A325, A326, A328, A334, A338, A344, A351, A353, A360, A368, A380, A416, A418, A419, A450, A453, A486, A491, A538, A540, A572, A573, A580, A583, A595, A599, A604, A624, A625, A626, A630, A632, A633, A638, A651, A652, A653, A667, A668, A669, A670, A673, A675, A676, A679, A680, A684, A689, A690, A693, A694, A697, A698, A705, A707, A711, A720, A723, A724, A731, A737, A744, A745, A747, A752, A761, A766, A768, A770, A771, A774, A776, A778, A786, A791, A792, A793, A795, A797, A798, A803, A804, A811, A828, A855, A860, A865, A867, A868, A869, A875, A880, A882, A886, A887, A891, A894, A897, A901, A909, A921, A926, A950, A951, A953, A958, A962, A963, A966, A975, A976, A981, A985, A993, A996, A1005, A1010, 4, 9, 38, 41, 48, 50, 54, 64, 72, 76, 92, 94, 96, 98, 101, 165, 166, 171, 172, 174, 175, 176, 177, 179, 181, 183, 184, 185, 186, 187, 190, 193, 204, 208, 212, 214, 215, 222, 223, 253, 255, 256, 257, 281, 287, 293, 301, 302, 303, 305, 309, 314, 320, 326, 327, 334, 342, 353, 382, 384, 385, 420, 423, 458, 462, 506, 509, 543, 544, 550, 553, 566, 570, 575, 594, 595, 596, 600, 602, 603, 608, 621, 622, 623, 638, 639, 640, 641, 644, 646, 647, 650, 651, 655, 661, 662, 665, 666, 669, 670, 677, 679, 683, 692, 695, 696, 703, 708, 715, 716, 718, 723, 732, 735, 737, 739, 740, 743, 745, 747, 752, 756, 757, 758, 760, 762, 763, 768, 769, 776, 793, 818, 822, 826, 828, 829, 830, 834, 839, 841, 845, 846, 850, 853, 856, 860, 868, 879, 884, 905, 906, 908, 912, 917, 918, 921, 929, 930, 935, 939, 945, 947, 955, 960

Tumor microenvironment A4, A34, A37, A45, A47, A48, A53, A54, A55, A57, A66, A80, A81, A84, A91, A100, A101, A105, A123, A139, A182, A183, A186, A187, A194, A211, A220, A225, A227, A228, A270, A281, A286, A305, A311, A316, A317, A319, A324, A325, A326, A328, A334, A338, A341, A343, A344, A347, A351, A360, A365, A368, A379, A397, A405, A416, A417, A423, A450, A453, A502, A538, A540, A549, A580, A583, A584, A586, A590, A593, A595, A596, A599, A600, A603, A604, A606, A609, A611, A613, A616, A623, A624, A630, A632, A633, A635, A637, A638, A644, A651, A652, A653, A654, A667, A668, A670, A673, A675, A676, A677, A679, A682, A683, A684, A685, A690, A691, A696, A697, A698, A705, A707, A708, A709, A710, A711, A717, A720, A721, A724, A727, A739, A742, A744, A750, A752, A754, A757, A760, A761, A763, A768, A770, A771, A772, A774, A778, A791, A792, A793, A794, A795, A797, A798, A800, A803, A804, A811, A813, A859, A860, A867, A869, A874, A875, A879, A880, A882, A883, A886, A889, A890, A891, A894, A897, A902, A907, A910, A911, A918, A921, A926, A927, A933, A948, A951, A953, A962, A963, A964, A965, A966, A969, A972, A975, A976, A977, A981, A982, A983, A984, A986, A987, A988, A990, A991, A993, A996, A999, A1000, A1007, A1010, A1011, A1013, 4, 29, 32, 38, 40, 41, 46, 47, 48, 50, 58, 72, 73, 76, 83, 91, 92, 96, 113, 130, 171, 172, 174, 175, 183, 200, 209, 212, 214, 215, 250, 259, 264, 281, 287, 292, 293, 295, 301, 302, 303, 305, 309, 314, 317, 319, 320, 322, 326, 334, 339, 342, 352, 369, 375, 382, 383, 390, 420, 423, 473, 506, 509, 519, 550, 553, 554, 556, 561, 564, 566, 567, 570, 571, 574, 575, 577, 580, 581, 583, 586, 593, 594, 600, 602, 603, 605, 607, 608, 614, 621, 622, 623, 624, 638, 639, 641, 644, 646, 647, 648, 650, 653, 654, 655, 657, 662, 663, 668, 669, 670, 677, 679, 680, 681, 682, 683, 689, 692, 693, 696, 699, 710, 713, 715, 721, 723, 725, 727, 731, 732, 733, 737, 739, 740, 741, 743, 747, 756, 757, 758, 759, 760, 762, 763, 765, 768, 769, 776, 778, 821, 822, 828, 830, 833, 834, 838, 839, 841, 842, 845, 848, 849, 850, 853, 856, 861, 866, 869, 870, 876, 879, 884, 885, 890, 904, 906, 908, 917, 918, 919, 920, 921, 924, 927, 929, 930, 931, 935, 936, 937, 938, 940, 941, 942, 943, 944, 945, 947, 950, 951, 957, 960, 961, 962

Tumor stroma A47, A48, A55, A57, A343, A395, A538, A613, A616, A652, A670, A709, A742, A773, A794, A860, A867, A869, A875, A901, A907, A948, A975, A976, A977, A982, A983, A987, A990, A991, 40, 41, 48, 50, 319, 367, 506, 583, 586, 622, 641, 681, 713, 742, 759, 822, 828, 830, 834, 860, 866, 904, 929, 930, 931, 936, 937, 941, 943, 944

Vaccine A72, A167, A224, A227, A231, A358, A359, A360, A361, A362, A377, A415, A416, A450, A451, A452, A481, A513, A515, A537, A551, A571, A579, A604, A607, A611, A612, A624, A628, A629, A655, A724, A802, A805, A807, A808, A811, A812, A813, A814, A828, A901, A959, A982, A1001, A1008, 65, 157, 211, 214, 218, 332, 333, 334, 335, 336, 350, 381, 382, 420, 421, 422, 453, 483, 485, 505, 521, 542, 549, 575, 578, 581, 582, 594, 598, 599, 625, 696, 767, 770, 772, 773, 776, 777, 778, 779, 793, 860, 913, 936, 952, 958